Proceedings of the 36th International Symposium on Automation and Robotics in Construction (ISARC 2019)

May 21-24, 2019 Fairmont Banff Springs Hotel Banff, AB, Canada

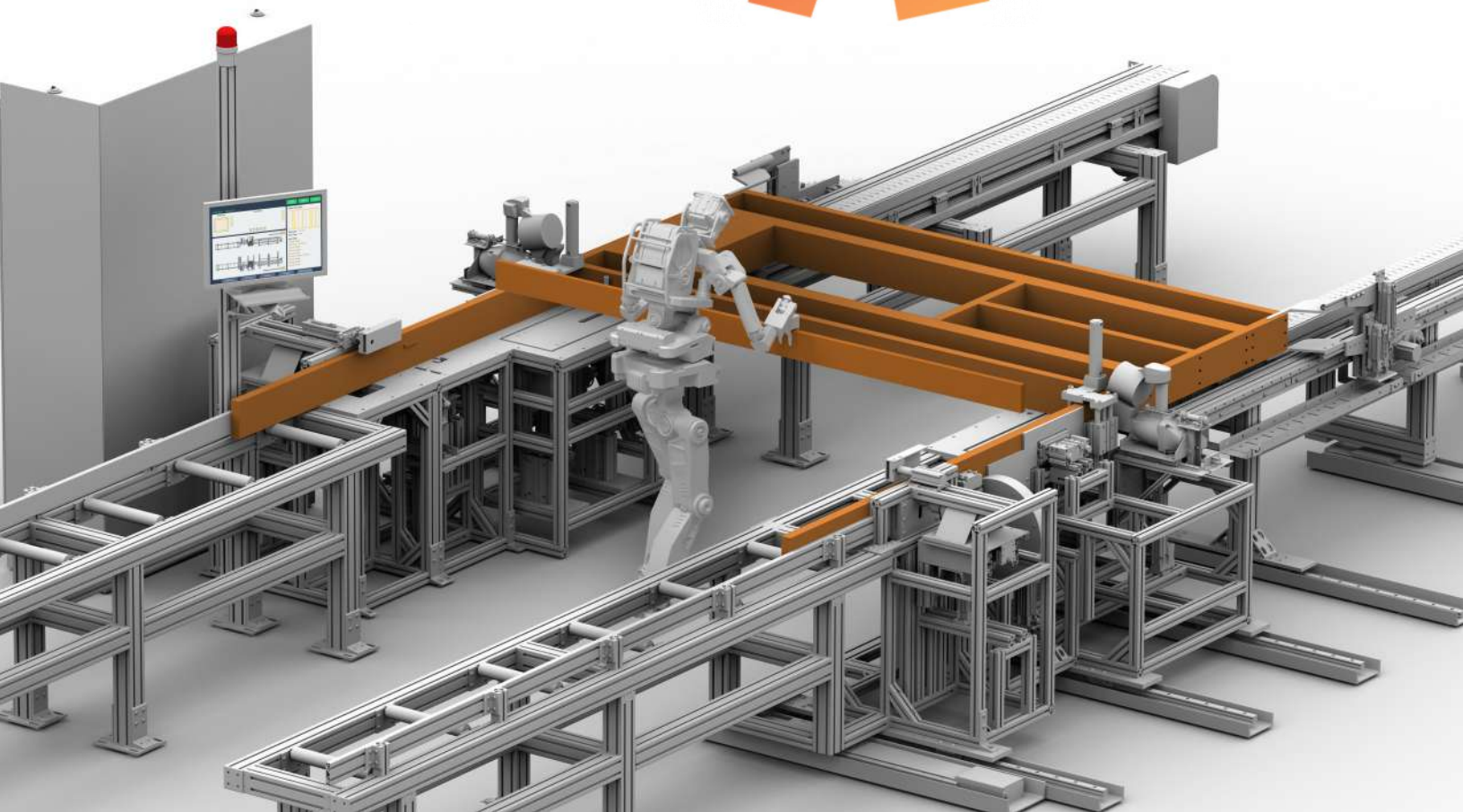

Editor

Dr. Mohamed Al-Hussein, University of Alberta

ISBN 978-952-69524-0-6

©The International Association for Automation and Robotics in Construction (IAARC)

Organized by

University of Alberta (Edmonton, Alberta, Canada)

Hosted by

University of Alberta at the
Banff Fairmont Springs (Banff, Alberta, Canada)

Supported by

Western Economic Diversification Canada
Diversification de l'économie de l'Ouest Canada
Canada

ALBERTA INNOVATES

MODULAR BUILDING INSTITUTE

AUTODESK

ALL WEATHER WINDOWS

DIRTT Build better.

SEMA SOFTWARE

LAFAETE LOCAÇÃO DE EQUIPAMENTOS

CPCI.ca

ROCKWOOL

GROUP OF INNOVATIVE SOLUTIONS
GIS INTERNATIONAL TECHNOLOGY LLC

Conference Chairs

Dr. Mohamed Al-Hussein

PROFESSOR,
UNIVERSITY OF ALBERTA

Chair

Dr. Ahmed Bouferguene

PROFESSOR,
UNIVERSITY OF ALBERTA

Co-chair

Dr. Ying Hei Chui

PROFESSOR,
UNIVERSITY OF ALBERTA

Co-chair

Dr. Rafiq Ahmad

ASSISTANT PROFESSOR,
UNIVERSITY OF ALBERTA

Co-chair

Prof. Yaowu Wang

PROFESSOR,
HARBIN INSTITUTE OF
TECHNOLOGY

Co-chair

TABLE OF CONTENTS

A Decision Tool to Simulate the Concurrent Interdependencies Between Multi-DFX Techniques in Machine Design Conflict Resolution 1
Anas Itani, Rafiq Ahmad and Mohamed Al-Hussein

Robotic Technologies in Concrete Building Construction: A Systematic Review 10
Marwan Gharbia, Alice Yan Chang-Richards and Ray Zhong

The Effectiveness of Virtual Reality in Safety Training: Measurement of Emotional Arousal with Electromyography 20
Sheng Xu, Qingqing Ni and Qiang Du

3D Posture Estimation from 2D Posture Data for Construction Workers 26
Yantao Yu, Heng Li and Xincong Yang

A Low-Cost and Smart IMU Tool for Tracking Construction Activities 35
Xincong Yang, Fenglai Wang, Heng Li, Yantao Yu, Xiaochun Luo and Ximei Zhai

An Investigation into the Effects of Deposition Orientation of Material on the Mechanical Behaviours of the Cementitious Powder and Gypsum Powder in Inkjet 3D Printing 42
Pshtiwan Shakor, Shami Nejadi and Gavin Paul

BIM-based Takt-Time Planning and Takt Control: Requirements for Digital Construction Process Management 50
Juergen Melzner

Automated Unit Price Visualization Using ArcPy Site Package in ArcGIS 57
K. Joseph Shrestha and H. David Jeong

Real-time Tracking for Intelligent Construction Site Platform in Finland and China: Implementation, Data Analysis and Use Cases 62
Jianyu Zhao, Jinyue Zhang and Olli Seppänen

Identifying Moderation Effect between Project Delivery Systems and Cost Performance 69
Hyosoo Moon, Hyun-Soo Lee, Moonseo Park and Bosik Son

Designing a Reliable Fiducial Marker Network for Autonomous Indoor Robot Navigation 74
Bharadwaj Mantha and Borja Garcia de Soto

Designing a Development Board for Research on IoT Applications in Building Automation Systems 82
Markus Hans Schraven, Carlo Guarnieri Calo Carducci, Marc Axel Baranski, Dirk Müller and Antonello Monti

Optimal Laser Scan Planning for As-Built Modeling of Plant Renovations Using Mathematical Programming 91
Eisuke Wakisaka, Satoshi Kanai and Hiroaki Date

Automatic Generation of the Vertical Transportation Demands During the Construction of High-Rise Buildings Using BIM 99
Keyi Wu, Borja Garcia de Soto, Bryan T. Adey and Feilian Zhang

Standard Closed-Circuit Television (CCTV) Collection Time Extraction of Sewer Pipes with Machine Learning Algorithm 107
Xianfei Yin, Yuan Chen, Ahmed Bouferguene, Hamid Zaman, Mohamed Al-Hussein, Randy Russell and Luke Kurach

Implementation Framework for BIM Adoption and Project Management in Public Organizations 114
Giuseppe Miceli Junior, Paulo C. Pellanda and Marcelo de Miranda Reis

Classification and Exemplary BIM Models Development of Design Changes 122
Jia-Rui Lin, Yu-Cheng Zhou, Jian-Ping Zhang and Zhen-Zhong Hu

Multi-objective Optimization Analysis for Selective Disassembly Planning of Buildings 128
Benjamin Sanchez, Christopher Rausch, Carl Haas and Rebecca Saari

Construction and Usage of Three-dimensional Data for Road Structures Using Terrestrial Laser Scanning and UAV with Photogrammetry 136
Satoshi Kubota, Chiyuan Ho and Kotaro Nishi

Cartesian Points Visualization in Game Simulation for Analyzing Geometric Representations of AEC Objects in IFC 144
Jiansong Zhang, Yunfeng Chen, Rui Liu and Luciana Debs

The Benefits of and Barriers to BIM Adoption in Canada 152
Yuan Cao, Li Hao Zhanga, Brenda McCabe and Arash Shahi

On the Estimation of Resonance Frequencies of Hydraulically Actuated Systems 159
Manuel Pencelli, Renzo Villa, Alfredo Argiolas, Marta Niccolini, Matteo Ragaglia, Paolo Rocco and Andrea Maria Zanchettin

Predicting Bridge Conditions in Ontario: A Case Study 166
Maedeh Taghaddos and Yasser Mohamed

Automated Mathematical-Based Design Framework for The Selection of Rigging Configuration 172
Seyed Mohammad Amin Minay Hashemi, Sanghyeok Han, Jacek Olearczyk, Ahmed Bouferguene, Mohamed Al-Hussein and Joe Kosa

An Analysis of the Problems of BIM-Based Drawings and Implementation During the Construction Document Phase 179
Yije Kim and Sangyoon Chin

Identification of the Structural State in Automated Modular Construction 187
Aparna Harichandran, Benny Raphael and Abhijit Mukherjee

A Conversation-based System for School Building Inspections 194
Hao-Yung Chan, Liang-Yuan Liu and Meng-Han Tsai

Enabling BIM for Property Management of Existing Buildings Based on Automated As-is Capturing 201
Ralf Becker, Elisa Lublasser, Jan Martens, Raymond Wollenberg, Haowei Zhang, Sigrid Brell-Cokcan and Jörg Blankenbach

Impact of 5G Technology on IoT Applications in Construction Project Management 209
Varun Kumar Reja and Koshy Varghese

Context-Realistic Virtual Reality-based Training Simulators for Asphalt Operations 218
Faridaddin Vahdatikhaki, Armin Kassemi Langroodi, Denis Makarov and Seirgei Miller

Generating Generic Data Sets for Machine Learning Applications in Building Services Using Standardized Time Series Data 226
Florian Stinner, Yingying Yang, Thomas Schreiber, Gerrit Bode, Marc Baranski and Dirk Müller

Developing Personalized Intelligent Interior Units to Promote Activity and Customized Healthcare for Aging Society 234
Rongbo Hu, Amir Kabouteh, Katja Pawlitza, Jörg Güttler, Thomas Linner and Thomas Bock

A Representative Simulation Model for Benchmarking Building Control Strategies 242
Alexander Kümpel, Florian Stinner, Bastian Gauch, Marc Baranski and Dirk Müller

Accurate Position Control for Hydraulic Servomechanisms 250
Manuel Pencelli, Renzo Villa, Alfredo Argiolas, Gianni Ferretti, Marta Niccolini, Matteo Ragaglia, Paolo Rocco and Andrea Maria Zanchettin

The Automation of the Softer Side of Smart City: a Socio-Semantic Roadmap 258
Tamer El-Diraby, Alain Zarli and Mohamed El-Darieby

Factors Affecting the Performance of 3D Thermal Mapping for Energy Audits in a District by Using Infrared Thermography (IRT) Mounted on Unmanned Aircraft Systems (UAS) 266
Yu Hou, Lucio Soibelman, Rebekka Volk and Meida Chen

Evaluating the Performance of e-Construction Tools in Highway Resurfacing Projects 274
Dhaivat Patel, Roy Sturgill, Gabriel Dadi and Timothy Taylor

Evaluating Risk Response Strategies on Construction Projects Using a Fuzzy Rule-Based System 282
Seyed Hamed Fateminia, Nima Gerami Seresht and Aminah Robinson Fayek

A Review of Data-Driven Accident Prevention Systems: Integrating Real-Time Safety Management in the Civil Infrastructure Context 289
Amin Assadzadeh, Mehrdad Arashpour, Ali Rashidi, Alireza Bab-Hadiashar and Sajad Fayezi

Augmented Reality-Enabled Production Strategy Process 297
Hala Nassereddine, Dharmaraj Veeramani and Awad Hanna

Chatbot System for Data Management: A Case Study of Disaster-related Data 306
James Yichu Chen, Meng-Han Tsai, Cheng-Hsuan Yang, Hao-Yung Chan and Shih-Chung Kang

Integrating Hardware-In-the-Loop Simulation and BIM for Planning UAV-based As-built MEP Inspection with Deep Learning Techniques 310
Kai Wang and Jack C.P. Cheng

A Review of Social, Physiological, and Cognitive Factors Affecting Construction Safety 317
Sahel Eskandar, Jun Wang and Saiedeh Razavi

Automatic Classification of Design Conflicts Using Rule-based Reasoning and Machine Learning—An Example of Structural Clashes Against the MEP Model 324
Ying-Hua Huang and Will Y. Lin

Augmented Reality and Deep Learning towards the Management of Secondary Building Assets 332
Alessandra Corneli, Berardo Naticchia, Alessandro Cabonari and Frédéric Bosché

Assessing Digital Information Management Between Design and Production in Industrialised House-Building – A Case Study 340
Henrik Eriksson, Marcus Sandberg, Jani Mukkavaara, Gustav Jansson and Lars Stehn

Platforms for Enabling Flexibility at Two Construction Companies 348
Henrik Eriksson and Ellinor Emilsson

A Study of Kinetic Façade Modelling Performance Using Virtual Reality 356
David Panyaa, J.H. Seo, H.J. Park, W.J. Lee and Seungyeon Choo

A Basic Study on Methodology of Maintenance Management Using MR 360
T. Kim, J. Jeong, Y. Kim, H. Gu, S. Woo and S. Choo

Process Modelling in Civil Infrastructure Projects: A Review of Construction Simulation Methods 368
Maryam Al-Kaissy, Mehrdad Arashpour, Sajad Fayezi, Ali Akbarnezhad and Baabak Ashuri

Optimizing Site Layout Planning Utilizing Building Information Modelling 376
Abhishek Raj Singh, Yash Patil and Venkata Santosh Kumar Delhi

Hyperspectral Imaging for Autonomous Inspection of Road Pavement Defects 384
Mohamed Abdellatif, Harriet Peel, Anthony G Cohn and Raul Fuentes

Inference of Relevant BIM Objects Using CNN for Visual-input Based Auto-Modeling 393
Jinsung Kim, Jaeyeol Song and Jin-Kook Lee

Predicting Safety Hazards Among Construction Workers and Equipment Using Computer Vision and Deep Learning Techniques 399
Mingzhu Wang, Peter Kok-Yiu Wong, Han Luo, Sudip Kumar, Venkata-Santosh Kumar Delhi and Jack Chin-Pang Cheng

The Design of Building Management Platform Based on Cloud Computing and Low-Cost Devices 407
Li-Te Huang, Yi-Yang Chiu and Ying-Chieh Chan

Spatial Information Enrichment using NLP-based Classification of Space Objects for School Bldgs. in Korea 415
Jaeyeol Song, Jinsung Kim and Jin-Kook Lee

Towards Automated HVAC Controls Commissioning: Mechanisms to Identify Temperature and Flow Related Functions of AHU Components 421
Raghuram Sunnam, Semiha Ergan and Burcu Akinci

A Chatbot System for Construction Daily Report Information Management 429
Jehyun Choa and Ghang Lee

Supporting Deconstruction Waste Management through 3D Imaging: A Case Study 438
Yujie Wei, Akash Pushkar and Burcu Akinci

Text Detection and Classification of Construction Documents 446
Narges Sajadfar, Sina Abdollahnejad, Ulrich Hermann and Yasser Mohamed

Holonic System for Real-Time Emergency Management in Buildings 453
Berardo Naticchia, Leonardo Messi, Massimiliano Pirani, Andrea Bonci, Alessandro Carbonari and Lucia Cristina Tolve

Grasped Element Position Recognition and Robot Pose Adjustment during Assembly 461
Kepa Iturralde, Taku Kinoshita and Thomas Bock

Adaptive Haptically Informed Assembly with Mobile Robots in Unstructured Environments 469
Pradeep Devadass, Sven Stumm and Sigrid Brell-Cokcan

Integrating Earthwork Ontology and Safety Regulations to Enhance Operations Safety 477
Alhusain Taher, Faridaddin Vahdatikhaki and Amin Hammad

Combining Deep Learning and Robotics for Automated Concrete Delamination Assessment 485
Evan McLaughlin, Nicholas Charron and Sriram Narasimhan

Web-Based Job Hazard Assessment for Improved Safety-Knowledge Management in Construction 493
Emad Mohamed, Parinaz Jafari, Estacio Pereira, Stephen Hague, Simaan Abourizk and Rod Wales

Leading Safety Indicators: Application of Machine Learning for Safety Performance Measurement 501
Parinaz Jafari, Emad Mohamed, Estacio Pereira, Shih-Chung Kang and Simaan Abourizk

Towards the Ontology Development for Smart Transportation Infrastructure Planning via Topic Modeling 507
Jin Zhu and Sudipta Chowdhury

Automated Detection of Urban Flooding from News 515
Farzaneh Zarei and Mazdak Nik-Bakht

Adaptive Automation Strategies for Robotic Prefabrication of Parametrized Mass Timber Building Components 521
Oliver David Krieg and Oliver Lang

Semantic Network Analysis as a Knowledge Representation and Retrieval Approach Applied to Unstructured Documents of Construction Projects 529
Rodrigo Rodrigues Aragao and Tamer El-Diraby

Digital Fabrication and Crafting for Flexible Building Wall Components: Design and Development of Prototypes 537
Nzar Naqeshbandi and Paulo Mendonça

As-is Geometric Data Collection and 3D Visualization through the Collaboration between UAV and UGV 544
Pileun Kim, Jisoo Park and Yong Cho

Web-based Deep Segmentation of Indoor Point Clouds 552
Zehuan Chen, Erzhuo Che, Fuxin Li, Michael Olsen and Yelda Turkan

Ontology for Logistics Requirements on a 4D BIM for Semi-Automatic Storage Space Planning 560
Jan Weber, Jana Stolipin, Markus König and Sigrid Wenzel

Integrating Social Sustainability in Value Stream Mapping: Panelized Post-Disaster Temporary Housing Case Study 568
Miguel Mora, Burcu Akinci and Luis Alarcón

An Experimental Investigation of the Integration of Smart Building Components with Building Information Model (BIM) 578
Kereshmeh Afsari, L. Florez, Emily Maneke and Mahdi Afkhamiaghda

Semantic Segmentation of Sewer Pipe Defects Using Deep Dilated Convolutional Neural Network 586
Mingzhu Wang and Jack C.P. Cheng

Information Exchange Process for AR based Smart Facility Maintenance System Using BIM Model 595
Suwan Chung, Soonwook Kwon, Daeyoon Moon, K.H. Lee and J.H. Shin

A Framework Development for Mapping and Detecting Changes in Repeatedly Collected Massive Point Clouds 603
Sanghyun Yoon, Sungha Ju, Sangyoon Park and Joon Heo

Development of the Simulator for Carrying a Lifted Load in Large Plant Construction 610
Yoshihito Mori, Masaomi Wada, Sayuri Maki and Satoshi Tsukahara

Digital Twinning of Existing Bridges from Labelled Point Clusters 616
Ruodan Lu and Ioannis Brilakis

Improved Tag-based Indoor Localization of UAVs Using Extended Kalman Filter 624
Navid Kayhani, Adam Heins, Wenda Zhao, Mohammad Nahangi, Brenda McCabe and Angela Schoellig

Live Data Visualization of IoT Sensors Using Augmented Reality (AR) and BIM 632
Worawan Natephra and Ali Motamedi

An Image Augmentation Method for Detecting Construction Resources Using Convolutional Neural Network and UAV Images 639
Seongdeok Bang, Francis Baek, Somin Park, Wontae Kim and Hyoungkwan Kim

A New UAV-based Module Lifting and Transporting Method: Advantages and Challenges 645
Jin Ouk Choi and Dong Bin Kim

Time-Warping: A Time Series Data Augmentation of IMU Data for Construction Equipment Activity Identification 651
Khandakar M. Rashid and Joseph Louis

Comparative Study of Experienced and Inexperienced Operators with Auto-controlled Construction Machine 658
Takeshi Hashimoto and Kenichi Fujino

Design, Modelling and Simulation of Novel Hexapod-Shaped Passive Damping System for Coupling Cable Robot and End Effector in Curtain Wall Module Installation Application 665
Meysam Taghavi, Taku Kinoshita and Thomas Bock

Computer Vision Techniques in Construction, Operation and Maintenance Phases of Civil Assets: A Critical Review 672
Shuyuan Xu, Jun Wang, Xiangyu Wang and Wenchi Shou

Monitoring and Alerting of Crane Operator Fatigue Using Hybrid Deep Neural Networks in the Prefabricated Products Assembly Process 680
Xiao Li, Hung-Lin Chi, Wenfeng Zhang and Geoffrey Qiping Shen

Automatic Floorplan Generation of Living Space for Simulating a Life of an Elderly Resident Supported by a Mobile Robot 688
Can Jiang and Akira Mita

Infographics on Unmanned Dozer Operation 696
Shigeomi Nishigaki and Katsutoshi Saibara

Formulation of the Optimization Problem of the Cyber-Physical Diagnosis System Configuration Level for Construction Mobile Robots 704
Alexey Bulgakov, Thomas Bock and Tatiana Kruglova

Ontology-Based Knowledge Modeling for Frame Assemblies Manufacturing 709
Shi An, Pablo Martinez, Rafiq Ahmad and Mohamed Al-Hussein

Measuring and Positioning System Design of Robotic Floor-tiling 716
Tianyu Liu, Huixing Zhou, Yanan Du and Jianping Zhao

3D Human Body Reconstruction for Worker Ergonomic Posture Analysis with Monocular Video Camera 722
Wenjing Chu, Sanghyeok Han, Xiaowei Luo and Zhenhua Zhu

Dispersed Cyber-Physical Coordination and Path Planning Using Unmanned Aerial Vehicle 730
Alexey Bulgakov, Daher Sayfeddine, Thomas Bock and Sergei Emelianov

Design and Development of Drill-Resistance Sensor Technology for Accurately Measuring Microbiologically Corroded Concrete Depths 735
Nicolas Giovanangeli, Lasitha Piyathilaka, Sarath Kodagoda, Karthick Thiyagarajan, Steve Barclay and Dammika Vitanage

A Real-Time 4D Augmented Reality System for Modular Construction Progress Monitoring 743
Zhiyang Lin, Frank Petzold and Zhiliang Ma

Development of an Eye- and Gaze-Tracking Mechanism in an Active and Assisted Living Ecosystem 749
Alexander Liu Cheng, Nestor Llorca Vega and Galoget Latorre

Improvement of Automated Mobile Marking Robot System Using Reflectorless Three-Dimensional Measuring Instrument 756
Takehiro Tsuruta, Kazuyuki Miura and Mikita Miyaguchi

A Mask R-CNN Based Approach to Automatically Construct As-is IFC BIM Objects from Digital Images 764
Huaquan Ying and Sanghoon Lee

Using Scan-to-BIM Techniques to Find Optimal Modeling Effort; A Methodology for Adaptive Reuse Projects 772
Mansour Esnaashary Esfahani, Ekin Eray, Steven Chuo, Mohammad Mahdi Sharif and Carl Haas

Primitive Fitting Using Deep Geometric Segmentation 780
Duanshun Li and Chen Feng

Employing Simulated Annealing Algorithms to Automatically Resolve MEP Clashes in Building Information Modeling Models 788
Hsieh-Chih Hsu and I-Chen Wu

Application of Virtual Reality in Task Training in the Construction Manufacturing Industry 796
Regina Barkokebas, Chelsea Ritter, Val Sirbu, Xinming Li and Mohamed Al-Hussein

Improving the Quality of Event Logs in the Construction Industry for Process Mining 804
Liyuan Chen, Seokyoung Kang, Shahin Karimidorabati and Carl Haas

Applying an A-Star Search Algorithm for Generating the Minimized Material Scheme for the Rebar Quantity Takeoff 812
Shen Chang, Ruei-Shiue Shiu and I-Chen Wu

Using BIM and Sensing Mats to Improve IMU-based Indoor Positioning Accuracy 818
Chia-Hsien Chen and I-Chen Wu

Assessment of Work Efficiency of HMD Viewing System for Unmanned Construction Work 824
Genki Yamauchi, Takeshi Hashimoto and Shin'Ichi Yuta

Using Virtual Reality Simulation for Optimizing Traffic Modes Toward Service Level Enhancements. 831
Firas Habbal, Fawaz Habbal, Abdallah Al Shawabkeh, Abdulla Al Nuaimi and Ammar Safi

PPEs Compliance Technology to Legalize the Automated Monitoring of Safety Standards 838
Fawaz Habbal, Firas Habbal, Abdulla Al Nuaimi, Anwaar Al Shimmari, Ammar Safi and Tala Abhushuqair

Use of Finite Element Analysis for the Estimate of Freezing & Maintenance Phase of Indirect & Direct Artificial Ground Freezing of Proposed Frozen Silt Mat, an Alternative of Timber Mat 846
Ghulam Muhammad Ali, Mohamed Al-Hussein and Ahmed Bouferguene

DEM-based Convolutional Neural Network Modeling for Estimation of Solar Irradiation: Comparison of the Effect of DEM Resolutions 854
Jae Heo, Jaehoon Jung, Byungil Kim and Sanguk Han

Direct-Write Fabrication of Wear Profiling IoT Sensor for 3D Printed Industrial Equipment 862
Nuwan Munasinghe, Lewis Miles and Gavin Paul

Developing Responsive Environments based on Design-to-Robotic-Production and -Operation Principles 870
Henriette Bier, Turkuaz Nacafi and Erik Zanetti

An Approach to Enhance Interoperability of Building Information Modeling (BIM) and Data Exchange in Integrated Building Design and Analysis 876
Troy Nguyen and Elvis Amoah

Impact of BIM on Electrical Subcontractors 884
Anoop Sattineni and Bradley Brock

Analytic Hierarchy Process as a Tool to Explore the Success Factors of BIM Deployment in Construction Firms 897
Shunming Liang, I-Chen Wu, Zheng-Yun Zhuang and Chin-Wen Chen

3D Modeling Approach of Building Construction based on Point Cloud Data Using LiDAR 906
Byeongjun Oh, Minju Kim, Chanwoo Lee, Hunhee Cho and Kyung-In Kang

New System Form Design Process Using QFD and TRIZ 913
Changsu Lee, Dongmin Lee, Hunhee Cho and Kyung-In Kang

Automated Clash Resolution of Rebar Design in RC Joints using Multi-Agent Reinforcement Learning and BIM 921
Jiepeng Liu, Pengkun Liu, Liang Feng, Wenbo Wu and Hao Lan

Automated Localization of a Mobile Construction Robot with an External Measurement Device 929
Selen Ercan, Sandro Meier, Fabio Gramazio and Matthias Kohler

Analysis of the Perceptions of Beneficiaries and Intermediaries on Implementing IPD in Indian Construction 937
V. Paul C. Charlesraj and Vatsala Gupta

Modelling Traffic Conditions on Fuel Use and Emissions of On-road Construction Equipment 945
Khalegh Barati and Xuesong Shen

Distributed Coordination and Task Assignment of Autonomous Tandem Rollers in Road Construction Scenarios 953
Patrick Wolf, Thorsten Ropertz, Alexander Matheis, Karsten Berns and Peter Decker

Indoor Visualization Experiments at Building Construction Site Using High Safety UAV 961
Tomohiro Narumi, Shigeru Aoki and F. Muramatsub

Using Serious Games in Virtual Reality for Automated Close Call and Contact Collision Analysis in Construction Safety 967
Olga Golovina, Caner Kazanci, Jochen Teizer and Markus König

Impact of BIM on Field Pipeline Installation Productivity Based on System Dynamics Modeling 975
Lijuan Chen, Peixin Shi and Qinglin Wu

Trajectory Prediction of Mobile Construction Resources Toward Pro-active Struck-by Hazard Detection 982
Daeho Kim, Meiyin Liu, Sanghyun Lee and Vineet R. Kamat

Automated Monitoring of Physical Fatigue Using Jerk 989
Lichen Zhang, Mohsen Mutasem Diraneyya, Juhyeong Ryu, Carl Haas and Eihab Abdel-Rahman

A Real-time Path-Planning Model for Building Evacuations 998
Farid Mirahadi and Brenda McCabe

Development of an Earthmoving Machinery Autonomous Excavator Development Platform 1005
Rauno Heikkilä, Tomi Makkonen, Ilpo Nishanen, Matti Immonen, Mikko Hiltunen, Tanja Kolli and Pekka Tyni

Construction Data-Driven Dynamic Sound Data Training and Hardware Requirements for Autonomous Audio-based Site Monitoring 1011
Yiyi Xie, Yong-Cheol Lee, Tallis Huther Da Costa, Jongyoon Park, Jayati H Jui, Jin Woo Choi and Zhongjie Zhang

Applying Kanban System in Construction Logistics for Real-time Material Demand Report and Pulled Replenishment 1018
Ningshuang Zeng, Xuling Ye, Xiaofeng Peng and Markus König

Simulating Wood-framing Wall Panel's Production with Timed Coloured Petri Nets 1026
Fabiano Correa

Spatial Efficacy of Respiration Monitoring using Doppler Radars for Personalized Thermal Comfort Assessment 1034
Wooyoung Jung and Farrokh Jazizadeh

BIM-based Automated Design Checking for Building Permit in the Light-Frame Building Industry 1042
Harish Narayanaswamy, Hexu Liu and Mohamed Al-Hussein

Schedule Quality Assessment for nD Models using Industry Foundation Classes 1050
Ashok Kavad, Rahul Dharsandia, Abdelhady Hosny and Mazdak Nik-Bakht

A Mixed VR and Physical Framework to Evaluate Impacts of Virtual Legs and Elevated Narrow Working Space on Construction Workers' Gait Pattern 1057
Mahmoud Habibnezhad, Jay Puckett, Mohammad Sadra Fardhosseini and Lucky Agung Pratama

Experiencing Extreme Height for The First Time: The Influence of Height, Self-Judgment of Fear and a Moving Structural Beam on the Heart Rate and Postural Sway During the Quiet Stance 1065
Mahmoud Habibnezhad, Jay Puckett, Mohammad Sadra Fardhosseini, H. Jebelli, Terry Stentz and Lucky Agung Pratama

Applying Eye Tracking in Virtual Construction Environments to Improve Cognitive Data Collection and Human-Computer Interaction of Site Hazard Identification 1073
Xuling Ye and Markus König

Optimizing the Usage of Building Information Model (BIM) Interoperability Focusing on Data Not Tools 1081
Elvis Amoah and Troy Nguyen

Digital Terrain Modeling Using AKAZE Features Derived from UAV-Acquired, Nadir and Oblique Images 1091
Hyojoo Son, Hyunsoo Kim and Changwan Kim

Deep-Learning for Occupancy Detection Using Doppler Radar and Infrared Thermal Array Sensors 1098
Milad Abedi and Farrokh Jazizadeh

Towards Mobile Projective AR for Construction Co-Robots 1106
Siyuan Xiang, Ruoyu Wang and Chen Feng

Implementing Collaborative Learning Platforms in Construction Management Education 1114
Ralph Tayeh, Fopefoluwa Bademosi and Raja R.A. Issa

Quantifying Remoteness for Construction Projects Using Nighttime Satellite Imagery and Machine Learning 1121
Pouya Zangeneh, Hesam Hamledari and Brenda McCabe

BIM-based Decision Support System for Concrete Formwork Design 1129
Roman Romanovskyi, Leonardo Sanabria Mejia and Ehsan Rezazadeh Azar

Deep Learning Detection for Real-time Construction Machine Checking 1136
Bo Xiao and Shih-Chung Kang

A Comparison of TLS-based and ALS-based Techniques for Concrete Floor Waviness Assessment 1142
Nisha Puri and Yelda Turkan

Comparison of Virtual Communication Environment for Remote BIM Model Review Collaboration 1149
Tzong-Hann Wu, Feng Wu, Shih-Chung Kang and Hung-Lin Chi

Efforts to Unmanned Construction for Post-disaster Restoration and Reconstruction 1155
Shigeo Kitahara, Yasushi Nitta and Shigeomi Nishigaki

Service Level Evaluation of Florida's Highways Considering the Impact of Autonomous Vehicles 1163
Amirsaman Mahdavian, Alireza Shojaei and Amr Oloufa

Study of Construction-Oriented Structural Connectors for a Temporary Bridge 1171
Yao-Yu Yang, Chia-Ming Chang, Shih-Chung Kang and Fang-Yao Yeh

Through-Wall Object Recognition and Pose Estimation 1176
Ruoyu Wang, Siyuan Xiang, Chen Feng, Pu Wang, Semiha Ergan and Yi Fang

Schedule Uncertainty Analysis System Framework to Manage and Allocate Historical Data for Industrial Construction Project 1184
In Seok Yoon, Hyun-Soo Lee, Moonseo Park, Jin Gang Lee and Sang Sun Jung

A Methodology for Indoor Human Comfort Analysis Based on BIM and Ontology 1189
Weiwei Chen, Keyu Chen, Vincent J.L. Gan and Jack C.P. Cheng

Pavement Crack Mosaicking Based on Crack Detection Quality 1197
Yeo-San Yoon, Seongdeok Bang, Francis Baek and Hyoungkwan Kim

VBUILT: Volume-based Automatic Building Extraction for As-Built Point Clouds 1202
Mustafa Khalid Masood, Akash Pushkar, Olli Seppänen, Vishal Singh and Antti Aikala

Robotic Fabrication of Nail Laminated Timber 1210
Hakim Hasan, Anish Reddy and Andrew Tsayjacobs

Design of a Robotic Software Package for Modular Home Builder 1217
Cheng-Hsuan Yang, Tzong-Hann Wu, Bo Xiao and Shih-Chung Kang

Implementation of an Augmented Reality AR Workflow for Human Robot Collaboration in Timber Prefabrication 1223
Ondrej Kyjanek, Bahar Al Bahar, Lauren Vasey, Benedikt Wannemacher and Achim Menges

Case Study on Mobile Virtual Reality Construction Training 1231
Mario Wolf, Jochen Teizer and J.H. Ruse

Simulating Extreme Points of Crane by Robot Arm in Virtual Reality 1238
Kn-Lin Chen, King-Ho Tsang, Yao-Yu Yang and Shih-Chung Kang

Development of Classification Model for the Level of Bid Price Volatility of Public Construction Project Focused on Analysis of Pre-Bid Clarification Document 1245
Yeeun Jang, June Seong Yi, Jeongwook Son and Jeehee Lee

Construction Payment Automation through Smart Contract-based Blockchain Framework 1254
Han Luo, Moumita Das, Jun Wang and Jack C.P. Cheng

Government Open Data and Sensing Data Integration Framework for Smart Construction Site Management 1261
Chiu-Ming Lee, Wei-Liang Kuo, Tzu-Jan Tung, Bo-Kai Huang, Shu-Hsiang Hsu and Shang-Hsien Hsieh

Review of BIM-centered IoT deployment: State of the Art, Opportunities, and Challenges 1268
Mehrzad Shahinmoghadam and Ali Motamedi

Automatic Key-phrase Extraction to Support the Understanding of Infrastructure Disaster Resilience 1276
Xuan Lv, Seyed Ahnaf Morshed and Lu Zhang

Artificial Intelligence Techniques to Support Design and Construction 1282
Atefeh Mohammadpour, Ebrahim Karan and Somayeh Asadi

Frequency Sweep Based Sensing Technology for Non-destructive Electrical Resistivity Measurement of Concrete 1290
Sathira Wickramanayake, Karthick Thiyagarajan, Sarath Kodagoda and Lasitha Piyathilaka

3D Printing Architectural Freeform Elements: Challenges and Opportunities in Manufacturing for Industry 4.0 1298
Marjo Niemelä, Anqi Shi, Sara Shirowzhan, Samad Sepasgozar and Chang Liu

Teaching Robots to Perform Construction Tasks via Learning from Demonstration 1305
Ci-Jyun Liang, Vineet Kamat and Carol Menassa

Applying Augmented Reality Technique to Support On-site Rebar Inspection 1312
Hao-Wei Hsu and Shang-Hsien Hsieh

Developing a Workflow for Cloud-based Inspection of Temporary Structures in Construction 1319
Chang Liu, Sara Shirowzhan and Samad M.E. Sepasgozar

Towards Rule-Based Model Checking of Building Information Models 1327
Christoph Sydora and Eleni Stroulia

Smart Construction Monitoring for Disaster Prevention Based on Spatial Information and GNSS/USN/IoT 1334
Sangho Yeon and Chunhum Yeon

A Decision Tool to Simulate the Concurrent Interdependencies Between Multi-DFX Techniques in Machine Design Conflict Resolution

A. Itani[a], R. Ahmad[b], and M. Al-Hussein[c]

[a,c] Department of Civil and Environmental Engineering, University of Alberta, Canada
[b]Department of Mechanical Engineering, University of Alberta, Canada
E-mail: aitani@ualberta.ca, rafiq.ahmad@ualberta.ca, malhussein@ualberta.ca

Abstract –

The overall performance of a life-cycle phase under investigation can be improved if Multi-Design for X (MDFX) technique's design guidelines are applied concurrently. However, the complexity of selecting MDFX techniques at the conceptual and detailed design stages during machine development can increase by uncertain and imprecise knowledge about the MDFX interdependencies. For many industrial companies, alleviating the design decision complexity at these stages can have a positive impact on the industry's competitive market. Therefore, it becomes crucial to have a robust MDFX tool embedded with conflict resolution in valuing potential applications to justify their cohesion. Some limitations on the compatibility between MDFX remain a challenge. The unresolved challenge is how the information contained within MDFX can be organized such that the implications of design decisions are proactively evaluated and implemented. To address this challenge, an efficient decision tool for applying MDFX in the conceptual and detailed machine design development phases is proposed. In this paper, the relative importance of DFXs guidelines and the essence of the interactions that arise between them are also studied. Also, a matrix model with multi-layers to simulate the interactions between MDFX is suggested to resolve the conflict of experts' opinion and aggregates the decision criteria layers into a single output. The proposed decision tool was applied in a machine design case study and shows its effectiveness in the decision-making process by eliminating MDFX negative interactions and aiding the designer in shaping the optimal machine design with less development cost and time.

Keywords –

Multi-Design for X (MDFX); life-cycle cost; conceptual and detailed design stage; conflict resolution; multi-layers.

1 Introduction

The implementation of MDFX in concurrent engineering machine design can result in contradictory and conflicting conclusions and recommendations for the designer's design-making process. Several independent studies have started to investigate and analyze these contradicting interactions by using various frameworks developed by Watson that can quantify the MDFX usefulness by design phase [9]. They concluded that MDFX, depending on where they are implemented during the machine development process, have a varying impact threshold. Whereas Willcox and Sheldon realized that the implementation of Design for Assembly methodology is most useful at the conceptual stage [10]. Because the tool component analysis is the main part of the methodology, it is preferred during the machine detailed design stage. The DFA analysis tool is an unreliable tool to be utilized during the conceptual machine stage because the design details required to undergo the analysis are not available at this stage. Hence, if the analysis tool is not effective at the conceptual design stage, then the alternative will be the benefits that the design guidelines of a specific DFX provide. So, to minimize the machine redesign possibilities and reduce the cost/time of this activity, the analysis tool should consider the importance of DFX guidelines.

Some research was undertaken to investigate how to tackle the conflicting implementation guidelines of MDFX. Thurston suggests a methodology to model the design decision results on the interval of a machine life-cycle [8]. A framework was developed to facilitate the decision-making process through ranking the design alternatives and calculating design trade-offs. In engineering design, it is a powerful analysis tool for decision making where multiple criteria and objectives exist. Unfortunately, for most applications, this method is very complicated and extensively time-consuming for designers in small to medium-sized organizations. If this ranking method is adopted to classify the design

guidelines, it would be unnecessarily tedious because the model used by Thurston is to some extent more complicated to implement than what is required for this application. A simpler and faster method for trade-off analysis between MDFX is to implement a matrix approach. Meerkamm concludes that if MDFX techniques are to be utilized in a problem context, then their design guidelines will often contradict and constrain the design output [4]. Consequently, as explained by Watson et al., finding an optimal solution is becoming a difficult task for designers [9]. As the design guidelines tend to be the DFX toolbox's most flexible aspect, they accurately indicate the nature of the DFX interactions and links between them and their concurrent interdependencies in ultimately finding an optimal design solution.

It is important to evaluate the application of MDFX in machine design development comprehensively. But due to the absence of information in the conceptual machine stage, problems and conflicts can arise when MDFX techniques are employed. This is because of a lack of information and vague objectives, which interfere with the designer's ability to evaluate design decision alternatives precisely. Decisions that emerge from applying one DFX technique seem to be good for one phase of the machine life cycle but can conflict with other life cycle phases. The designer should oversee the concurrent effects of the decision-making process in machine design. If the previous decisions are based on inaccurate information, the following design stages will be affected significantly. The application of MDFX techniques in machine design development requires effective decision support systems. In view of this, a decision support tool that simulates the concurrent interdependencies between MDFX techniques during the conceptual machine design stage is proposed in this paper.

2 Methodology

The methodology presented in this section is based on Watson et al.'s model that uses a weighted matrix method to exploit the interactions between MDFX [9]. The matrix method is extended to simulate the concurrent interdependencies between MDFX. The model output provides three useful indices. The first one indicates major areas of potential conflict occurring between the compared MDFX. The second illustrates how the value of a specific guideline is modified when interacting with the competing DFX guidelines. And the third is measuring the DFX techniques in terms of time metrics to estimate and reliably verify DFX interactions and design decisions comprehensively.

2.1 Procedure of the matrix

The methodology for assessing and ranking the DFX's competing design guidelines requires six distinct tasks to be undertaken. These tasks are described in the flowchart presented in Figure 1.

2.2 Task 1: Determine DFX overall weight using the analytical hierarchy process (AHP) method

The first task involves selecting and calculating the overall relative importance (weight) of the chosen DFX techniques. This can be achieved by calculating the weight of each DFX technique separately with respect to the design criteria, and then by combining them in an AHP model developed by Saaty to determine their relative importance in machine conceptual and detailed design stages [6]. In general, the relative importance of a DFX technique varies as to where and when it can be applied during the machine development process [1]. He concludes that the area where a DFX technique can be utilized is defined by company and customer requirements, production capabilities, and industry orientations, in addition to other considerations.

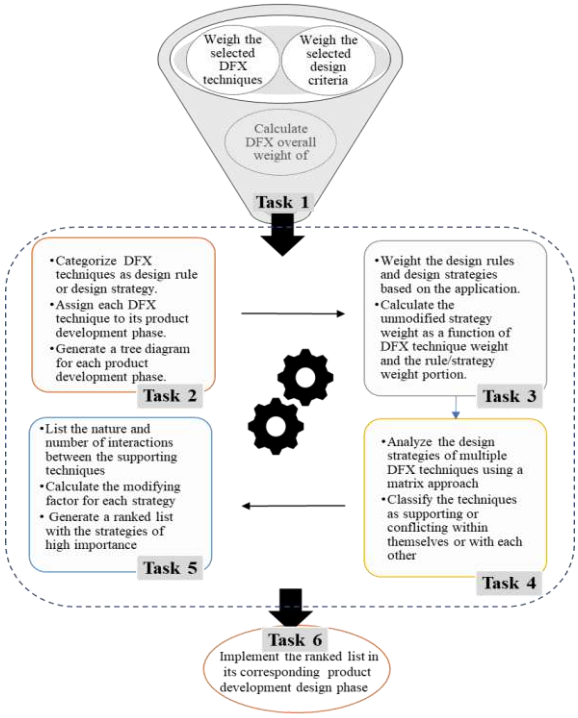

Figure 1. Multi-DFX techniques matrix model flow chart

The product design specification (PDS) must be formulated at the beginning of the project based on the statement of needs prior to any design activity, as shown

in Figure 2. Thus, it acts as the governor for the total design activity model, because it revolves around the boundaries of each design stage for any machine.

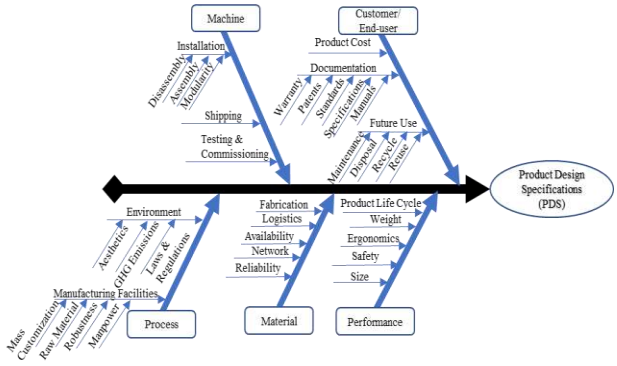

Figure 2. Product design specification (PDS).

The PDS forms a progressive, evolutionary, and extensive written document that evolves in consideration of the final machine characteristics. The PDS is then translated into design criteria that are followed by the design team, and as such, each design criterion will be associated with one or multiple DFX techniques that can satisfy its requirements. By adapting the total life-cycle cost/time method developed by Lukasz and Tomasz, the design team can successfully estimate each DFX technique's effect with respect to the other, and those values will be an indicator as to how much each DFX can reduce the development life-cycle overall cost and time [2].

DFX techniques are weighted with respect to each design criterion to generate an overall general normalized importance weight W_{DFXG} with a total value of 1. From that, the time required for each design activity T_{DFXG} can be derived under a certain DFX. This weighting factor will then be adopted in the general model for conceptual and detailed design stages. The weighting in the AHP model must rely on the designer's experience and intuition. W_{DFXG} and T_{DFXG} are calculated using Equation (1) and (2), respectively, as follows:

$$W_{DFXG} = \frac{Cost\ x}{Cost\ T} \quad (1)$$

Where,
$Cost_x$= The cost of life-cycle area x
$Cost_T$= The combined cost of the life-cycle

$$T_{DFXG} = W_{DFXG}\ x\ T_t \quad (2)$$

Where,
T_{DFXG}= The allocated time for a specific DFX in days

T_t= The total time for the design activity in days

2.3 Task 2: Generate tree diagram to classify DFX design guidelines

In this section, the machine development process is categorized, and the hierarchical level of the DFX technique design guidelines is established. Watson, Radcliffe et al. proved that if DFX decision analysis tools are utilized during conceptual and detailed machine design stages, they could improve the design performance significantly [9]. They also concluded that most DFX techniques fail to give what is expected because they merely provide the designer with directions on how and when the design rules can be implemented.

Pugh's Total Design Activity Model is used to describe the machine development process [5]. The model phases are 1) user need; 2) machine specification; 3) conceptual design; 4) detail design; 5) manufacture; and 6) and sales. Though design activities might not always have to occur concurrently in the sequence outline by Pugh, his machine development model provides a detailed structured procedure of all the stages required. Table 1 contains some design guidelines examples which are the most applicable for machine design development process extracted from the Design for Assembly (DFA) methodology [2].

Table 1. DFA guidelines per design stage

Specification	• Standardize a machine's style. • Establish the machine design specification.
Concept Design	• Reduce the number of parts and components. • Eliminate machine features that do not have any tangible value to the customer. • Standardize a machine's style. • Using new materials and technologies. • Rational machine design by modules and product families.
Detailed Design	• Design multi-functional parts. • Developing the machine features that facilitate the positioning. • Avoid costly clamping systems.
Manufacture	• Simplicity. • Adapted tolerances. • Consideration of process-related design guidelines.

The second task in constructing the model is to organize the DFX technique design guidelines into a decision tree using a hierarchical structure. Each DFX technique consists of primary and secondary design guidelines called design rules and design strategies, respectively. The tree diagram consists of three levels where the first level is associated with the general DFX tool under study, the second level is associated with

DFX design rules, and the third level is associated with DFX design strategies. Table 2 contains an example of the hierarchical tree using the DFA guidelines during the detailed design phase [2].

Table 2. DFA detailed design stage guidelines

Design Rules	Design Strategies
Reduce the number of parts and their types	Reduce unstandardized fasteners. Eliminate parts that function as connectors and conduits. Design multi-function parts. Do not follow piece-part producibility guidelines.
Eliminate physical adjustments	Reduce the number of physical parts between the machine input and output functions. Relocate critically related part surfaces close together. Implement kinematic design procedures and principles.
Ensure adequate clearance and unrestricted vision	Ensure adequate clearance for hands, tools, and subsequent process. Ensure that the vision of the operation is not restricted or compromised.
Minimize re-orientations	Minimize the necessity for reorientations during and after parts installation.

2.4 Task 3: Determining the weightings levels of the guidelines

The third task requires that the DFX technique design rules and strategies be weighted. Regarding the weighting levels, they are determined in each phase, which gives the designer a general design overview of the machine development process. The design rules weighting, W_{TR}, is determined independently, regardless of the design strategies number (on a scale of 1 to 10). While the design strategies weighting, W_{PS}, is determined in proportion to the design rule it corresponds to on a scale of 1 to 10, such that the total weight summation under design rules is equal to 1. The total weight of each design strategy, W_{TS}, is calculated using Equation (3) by multiplying the DFX technique overall weight, the design rule total weight, and the design strategy proportional weight. Thus, the total weight of each design strategy can fluctuate between 0 and 1. While the time required for each design strategy, T_{TS}, is calculated in days using Equation (4) by multiplying the strategy calculated weight from Equation (3) by the allocated time for the selected DFX divided by the summation of strategies weight for the selected design phase.

$$W_{TS} = W_{DFXG} \times W_{TR} \times W_{PS} \quad (3)$$

$$T_{TS} = \frac{T_{DFXG} \, x \, W_{TS}}{\sum_{i=0}^{n} W_{TS}} \quad i=0,1,2\ldots. n \quad (4)$$

2.5 Task 4: Identifying interactions and links between guidelines

The fourth task involves determining the interactions and links between the strategies and reporting them inside the matrix model. The severity of any conflicts can be measured from these interactions. The matrix model can be utilized to compare multiple numbers of strategies from MDFX techniques. However, the process of finding each relationship between strategies can become tedious and time consuming for MDFX guidelines. It is assumed that not more than four DFX tools and a maximum number of ten strategies per phase should be adopted in the model.

Table 3. Strategies comparison values

R Values	Description
+ 1	Two or more strategies interact positively.
+0.5	One strategy supports positively the other in a broader scope.
0	No interaction occurs between the design strategies.
-0.5	One strategy supports negatively the other in a broader scope.
-1	Two or more strategies interact negatively.

From the matrix model, it is possible to pinpoint any conflict between two strategies to alert the designer that special consideration should be in place when dealing with them. This is done using the conflict index, CI, which quantifies the severity of the conflict. When a negative interaction occurs, the equation to calculate the conflict index is employed. The conflict index constant is calculated using Equation (5) as follows:

$$CI = W_{TS} \times W_{TS'} \times R \quad (5)$$

if CI < -10 then conflict must be examined.

Where,

$W_{TS'}$ = Total weight of compared strategy

R = The comparison value for the two design strategies, as shown in Table 3.

2.6 Task 5 & 6: Generating the ranked list of DFX strategies

The fifth task involves calculating the overall value ($\square_{TS}$) of a design strategy considering strategies weight and their interactions with each other. The main process is based on the assumption that each design strategy has a total weighted value (W_{TS}) and interactions with other strategies adjust this. The prime factor is a function of the comparison index and the compared guideline weight. By summing the prime value over all the DFX interactions, a global scaler is determined. Equations (6) & (7) calculate the overall value ($\square_{TS}$) as follows:

$$\square_{TS} = W_{TS} (1 + \delta \square) \quad (6)$$

$$\square_{TS} = W_{TS} \left(1 + \sum \frac{(W_{TS'} \, x \, R \, x \, S)}{100}\right) \quad (7)$$

Where,

$$S=\frac{15}{W_{TS}} \quad \text{if } W_{TS'}>W_{TS} \text{ and } R<0 \qquad (8)$$
$$S=1 \quad \text{else}$$

Where,
δ □ =the total prime factor overall strategies and DFX techniques
S = the scaler
15 = Number of DFX techniques being researched
100 =scaling factor

In Equation (8), the scaler considers the instances when a low weight design strategy conflicts with a high weight one. Having determined the total strategy value, a ranked list can be configured to be implemented in the machine development. Any design strategies that have a negative total value should be ignored because if adopted, then it may lead to a life-cycle performance reduction due to its conflicting correlations with other strategies. After generating the ranked list, the redundant design strategies within the competing DFX will be removed to save time and to eliminate design repetition. However, if both design strategies match each other in the core objective, then the lesser time duration will be selected.

3 Validation Case Study

In this section, the focus of the case study will revolve around a part of the multi-function bridge machine prototype which is the nailing carriage in its conceptual design stage, as shown in Figures 3 and 4.

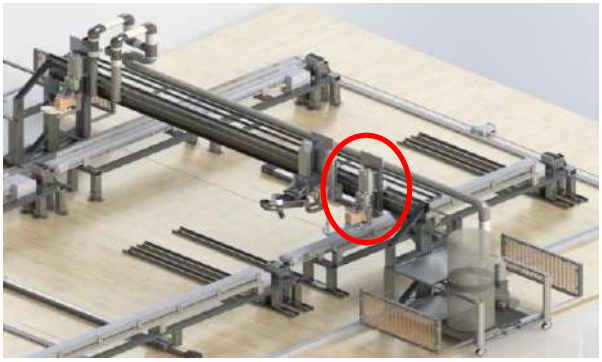

Figure 3. 3D model of multi-function bridge prototype

As the carriage at this stage is primarily a research tool, it is assumed that there would be a maximum amount of flexibility and testability within the variability of the experimental parameters. It also meant that a simple and unique machine would be designed. As the carriage will be operating in a large area with extreme precision at a controlled speed, it is apparent that the geometry and versatility of the carriage are considered as a major design criterion. It is also apparent that because the vertical force loads are so small, any part stresses would be negligible.

Figure 4. Nailer carriage detailed view

From the PDS, the carriage to be designed is to accommodate multiple configurations of interchangeable tools, such as a nailer, stapler, and screwdriver. This operational requirement results in the device being partially disassembled and re-assembled after each operation and for different sheathing configurations. Regarding parts service life, it is expected that no major parts should fail throughout the device's life. The final requirement is that the device is to be designed and manufactured within a very limited budget. The detailed technical information of the machine development is excluded from this paper for patentability and commerciality of the machine. Instead, some of the case study design related issues are discussed in broad terms. The timeline to complete the carriage conceptual design was 60 calendar days. These days are distributed on all 15 DFX techniques in accordance with their global weighting results.

DFA Design rules and strategy weights by product development phase							
Product Development Phase	Design Rules	W_{DFXG}	W_{TR}	Design Strategies	W_{TS}	W_{TS}	T_{TS}
Concept Design	1- Minimize the number of parts (Types & Count).	0.08	10	1- Minimize the number of parts and levels of assembly.	0.3	0.24	0.39
				2- Minimize the number of components and subassemblies.	0.3	0.24	0.39
				3- Reduce product complexity.	0.2	0.16	0.26
				4- Eliminate any product features that do not add value to the customer.	0.1	0.08	0.13
				5- Design multi-function parts.	0.1	0.08	0.13
	2- Increase product modularity.		8	1- Design products from modular subassemblies so that modules can be scheduled, built and tested independently.	0.4	0.26	0.42
				2- Standardize by common components, processes and methods to reduce costs across the whole system.	0.6	0.38	0.63
	3- Ensure base part design.		10	1- The product must has a suitable base part on which the rest of the assembly can be built.	0.6	0.48	0.78
				2- Maximize process yields between base and at each workstation for the whole assembly system.	0.4	0.32	0.52
	4- Aim for sequential assembly design.		8	1- Design the product to be built up in layers.	0.4	0.26	0.42
				2- Components can be added from above and located positively.	0.4	0.26	0.42
				3- Reduce the tendency to move during subsequent motions or steps.	0.2	0.13	0.21
	5- Minimize the need for reorientations during assembly.		2	1- Minimize the need for reorientations during assembly.	1	0.16	0.26

Figure 5. Design for assembly design rules and strategies for the conceptual stage

DFDA Design rules and strategy weights by product development phase							
Product Development Phase	Design Rules	W_{DFXG}	W_{TR}	Design Strategies	W_{TS}	W_{TS}	T_{TS}
Concept Design	1- Improve the products structure for disassembly.	0.05	10	1- Subdivide the product into manageable subassemblies.	0.5	0.25	1.19
				2- Minimize the number of components and subassemblies.	0.5	0.25	1.19
				3- Standardize the products style.	0	0.00	0.00
	2- Improve the disassembly planning.		2	1- A void long disassembly paths.	1	0.10	0.48

Figure 6. Design for disassembly design rules and strategies for the conceptual stage.

This to allocate time for each DFX technique and to study the effect of utilizing the proposed methodology in the time management of design activities.

Table 4. DFX global weighting results with their time allocations in the conceptual design stage

Global Weighting Associated with DFX in relation to each design criterion in Conceptual Design Phase	W_{DFXG}	T_{DFXG}
Design for Cost (DFC)	0.228	13.66
Design for Manufacturing (DFM)	0.125	7.49
Design for Assembly (DFA)	0.083	4.96
Design for Variety (DFV)	0.087	5.20
Design for Quality (DFQ)	0.087	5.23
Design for Six Sigma (DFSS)	0.051	3.06
Design for Disassembly (DFDA)	0.048	2.86
Design for Reliability (DFR)	0.058	3.51
Design for Testability (DFT)	0.038	2.29
Design for Maintainability (DFMAI)	0.033	1.96
Design for Robustness (DFRO)	0.036	2.14
Design for Mass Customization (DFMC)	0.025	1.51
Design for Sustainability (DFS)	0.044	2.66
Design for Network (DFN)	0.033	2.00
Design for Environment (DFE)	0.024	1.46

In this case, 15 DFX techniques fall under the scope of the conceptual design stage with their global weighting associated with the PDS that was calculated by adopting the AHP model. Table 4 summarizes the results where the total summation of all DFX weighting is equal to 1 and where each DFX has a time allocation associated with it. In this paper, two DFX techniques were selected from the list to demonstrate the model functionality: Design for Assembly (DFA) and Design for Disassembly (DFDA). The DFA technique selected was developed by Boothroyd and Dewhurst [2]. The methodology has been refined and upgraded to provide a realistic and reliable design analysis tool with set of guidelines that are presented in a structured format. The tool follows the same basic procedures to analyze for manual, automatic and robotic assembly with different input data tables for the various processes. For this project, the manual assembly method is adequate. The designed machine would encounter assembly and re-assembly process on a regular basis. This process has a substantial effect on how the design guidelines are interpreted and rated. A team of researchers developed the DFDA technique adopted in this case study at the Manchester Metropolitan University ([7], [11]). The developed technique purpose is focused on the disassembling process to facilitate reconfiguration. Figures 5 and 6 contains the list of design rules and strategies for conceptual design machine development phases for both DFA and DFD techniques. Since two DFX techniques are being investigated, only one decision matrix for the conceptual machine development phase is selected for the demonstration of the comparison and ranking process. Figure 7 shows the conceptual design comparison matrix for DFA versus DFDA highlighting the guidelines interactions.

Conceptual Design	DFDA Strategies	Subdivide the product into manageable subassemblies.	Minimize the number of components and subassemblies.	Standardize the products style.	Avoid long disassembly paths.			
DFA Strategies	W_{TS}	0.25	0.25	0.00	0.10			
Minimize the number of parts and levels of assembly.	0.24	0.5	1	0	0	0.0038	0.24	9
Minimize the number of components and subassemblies.	0.24	0.5	1	0	0	0.0038	0.24	9
Reduce product complexity.	0.16	0	0	0.5	0	-	0.16	11
Eliminate any product features that do not add value to the customer.	0.08	0	0	0	0	-	0.08	16
Design mult-function parts.	0.08	0	0	0	0.5	0.0005	0.08	15
Design products from modular subassemblies so thatmodules can be scheduled, built and tested independently.	0.26	1	0	0	0	0.0025	0.26	4
Standardize by common components, processes and methods to reduce costs across the whole system.	0.38	0	0	0.5	0	-	0.38	2
The product must has a suitable base part on which the rest of the assembly can be built.	0.48	0	0	-0.5	0	-	0.48	1
Maximize process yields between base and at each workstation for the whole assembly system.	0.32	0	0	0	0.5	0.0005	0.32	3
Design the product to be built up in layers.	0.26	0.5	0	0	0.5	0.0018	0.26	5
Components can be added from above and located positively.	0.26	0	0	0	0.5	0.0005	0.26	6
Reduce the tendency to move during subsequent motions or steps.	0.13	0	0	0	0.5	0.0005	0.13	13
Minimize the need for reorientations during assembly.	0.16	0	0	-0.5	0	-	0.16	11
		0.0062	0.0048	- 0.0005	0.0052	δV		
		0.25	0.25	-	0.10		VT	
		7	8	17	14			Ranking

Figure 7. DFA vs DFDA comparison matrix.

4 Results and Discussion

As highlighted in the matrix shown above in Figure 7, two design strategies have conflicted, so special consideration must be in place to resolve this conflict before they the ranking procedure starts. However, the conflict occurs, in this case, is when the designer simultaneously attempts to minimize the need for reorientation during assembly while attempting to standardize the machine during disassembly. It is assumed that the arising conflict could be ignored, subject to further investigation, as the conflict index slightly exceeds the threshold value of ten.

Figure 8 summarizes the ranking of the strategies in descending order based on their respective total value. After analyzing the results, the designer can eliminate from the ranked list the strategies that are repeated or have the same core objective, while the strategies with the same ranking order can be implemented concurrently in the design process to emphasize their relatively equal importance.

Figure 9 summarizes the modifications after the designer has conducted the analysis. If both selected DFX techniques were to be applied in standalone mode, then after several design iterations they will conflict, which would lead to a machine redesign. The redesign process is a costly and time-consuming activity, and by applying this methodology, the designer can avoid the pitfall of such activity.

If the designer is to apply DFA with 4.96 days and DFDA with 2.86 days independently then the total time required for both will be 7.82 days. However, if they are applied together, the redundant design strategies between the two and the conflicted area will be removed and adjusted before initiating the design activity. Thus, reducing the total time to 6.63 days with a difference of 1.19 days.

Some observations were concluded after applying the matrix model in the case study mentioned above such as if the value of the conflict index constant exceeds a value of negative ten, then it can be declared that a conflict of substantial consequences has occurred, and some considerations are required to resolve it. This conflict can be resolved and avoided by implementing some tactics as follows:

1. If the conflict index constant is close to ten, then the resulted conflict could be ignored and eliminated on the basis that it will create a down weight effect on the other design strategies in the ranked list.
2. Develop and integrate a design methodology after examining the conflict-specific details to decrease the negative interaction areas between strategies—this is very useful in areas where partial conflict has been spotted ($CI \leq -10$).
3. The matrix model ranking function will eliminate any two design strategies that have a large total value difference, and it will eliminate negative values too.

The weighting procedure of any parameter may sometimes be a subjective process, as two different designers may weigh the same guideline differently. This difference comes from the usage circumstances, the experience, and interpretation of the designers as to what the guideline means. However, these differences will not give the user a misleading result because the guidelines are interpreted according to the designer's understanding.

That said, future work will be required to extend the applicability of the decision tool in the DFX trade-off analysis with respect to cost and quality to provide a better understanding of client needs while controlling the machine lifecycle. Moreover, the future development of this methodology will be required to cover the other phases of the machine lifecycle (e.g., embodiment design, manufacturing, and sales).

DFA and DFDA Strategies in Conceptual Design Stage Ranking List Summary	Ψ_{TS}	Ranked List	T_{TS}
The product must has a suitable base part on which the rest of the assembly can be built.	0.48	1	0.78
Standardize by common components, processes and methods to reduce costs across the whole system.	0.38	2	0.63
Maximize process yields between base and at each workstation for the whole assembly system.	0.32	3	0.52
Design products from modular subassemblies so thatmodules can be scheduled, built and tested independently.	0.26	4	0.42
Design the product to be built up in layers.	0.26	5	0.42
Components can be added from above and located positively.	0.26	6	0.42
Subdivide the product into manageable subassemblies.	0.25	7	1.19
Minimize the number of components and subassemblies.	0.25	8	0.39
Minimize the number of parts and levels of assembly.	0.24	9	0.39
Minimize the number of components and subassemblies.	0.24	9	1.19
Reduce product complexity.	0.16	11	0.26
Minimize the need for reorientations during assembly.	0.16	11	0.26
Reduce the tendency to move during subsequent motions or steps.	0.13	13	0.21
Avoid long disassembly paths.	0.10	14	0.48
Design mult-function parts.	0.08	15	0.13
Eliminate any product features that do not add value to the customer.	0.08	16	0.13
Standardize the products style.	0.00	17	0.00

Figure 8. DFA vs DFDA strategies ranking list in the conceptual design stage (before analyzing).

DFA and DFDA Strategies in Conceptual Design Stage Ranking List Summary	Ψ_{TS}	Ranked List	T_{TS}
The product must has a suitable base part on which the rest of the assembly can be built.	0.48	1	0.78
Standardize by common components, processes and methods to reduce costs across the whole system.	0.38	2	0.63
Maximize process yields between base and at each workstation for the whole assembly system.	0.32	3	0.52
Design products from modular subassemblies so thatmodules can be scheduled, built and tested independently.	0.26	4	0.42
Design the product to be built up in layers.	0.26	5	0.42
Components can be added from above and located positively.	0.26	6	0.42
Subdivide the product into manageable subassemblies.	0.25	7	1.19
Minimize the number of components and subassemblies.	0.25	8	0.39
Minimize the number of parts and levels of assembly.	0.24	9	0.39
Reduce product complexity.	0.16	10	0.26
Minimize the need for reorientations during assembly.	0.16	10	0.26
Reduce the tendency to move during subsequent motions or steps.	0.13	12	0.21
Avoid long disassembly paths.	0.10	13	0.48
Design mult-function parts.	0.08	14	0.13
Eliminate any product features that do not add value to the customer.	0.08	15	0.13

Figure 9. DFA vs DFDA strategies ranking list in the conceptual design stage (after analyzing).

5 CONCLUSION

Engineering design is an iterative process of solution generation and evaluation. It requires a designer to take a forward-thinking and a look ahead approach when finalizing a solution. In a dynamic environment, a concurrent application of MDFX techniques during the design process can be organized into multiple stages in which both evaluation and decision are needed. The main theme of this paper was to present the need for a tool that can reliably estimate and verify the time/benefits of applying MDFX in a harmonized way in machine design. As a result, a decision support tool that can aid the designer in the decision-making process when MDFX are utilized will be required. The main feature of a design decision simulation tool is to enable designers to foresee and explore lifecycle consequences during the machine design. Also, to provide a structured workflow specifying how and when MDFX techniques can be applied with the ability to quantify the arising conflict that may occur between them. The tool's fundamental core is based on the information contained within the DFX guidelines, which may be classified as either a design strategy or rule so their interactions can be examined explicitly. Thus, the generation of a ranked list can be integrated in a time-effective and strategic manner, thereby shrinking the machine design time by at least 15%. As demonstrated, the MDFX decision tool can be implemented to serve as a generative decision system that proactively aids the designer in the decision-making process.

6 ACKNOWLEDGMENTS

The authors would like to acknowledge the financial support of the Natural Sciences and Engineering Research Council of Canada (NSERC).

7 REFERENCES

[1] Ahmad, R., Lahonde, N., and Omhover, J. F. (2014). "Game Methodology for Design Methods and Tools Selection." *Journal of Learning Design*, 7(1), 1-9.

[2] Boothroyd, G. and Dewhurst, P. (1989). "Product Design for Assembly." *Boothroyd Dewhurst Inc.* Wakefield, USA.

[3] Lukasz, M. and Tomasz, N. (2007). "Dfx Platform-a Holistic Approach to Design Concepts Evaluation." Guidelines for a Decision Support Method Adapted to NPD Processes, 21-22.

[4] Meerkamm, H. (1994). "Design for X - A Core Area of Design Methodology." *Journal of Engineering Design*, S (2), 145-163.

[5] Pugh, S. (1991). "Total design: Integrated methods for successful product engineering."

[6] Saaty, T. L. (2008). "Decision making with the analytic hierarchy process*." International journal of services sciences*, 1(1), 83-98.

[7] Simon, M., Fogg, B., and Chambellant, F. (1992). "Design for Cost-Effective Disassembly." *Technical Report* DDRnRl.

[8] Thurston, D. (1991). "A Formal Method for Subjective Design Evaluation with Multiple Attributes." *Research in Engineering Design*, 3 (2), 105-122.

[9] Watson, B., Radcliffe, D., & Dale, P. (1996). "A meta-methodology for the application of DFX design guidelines." *In Design for X* (pp. 441-462). Springer, Dordrecht.

[10] WILCOX, M., and Sheldon, D. (1993). "How the design team in management terms will handle the DFX tools." *In Proceedings of the 9th International Conference on Engineering Design* (pp. 875-881).

[11] Zhang, 'B., Simon, M., and Dowie, T. (1993). "Initial Investigation of Design Guidelines and Assessment of Design for Disassembly." *Technical Report*, DDRTR03, Aug (pp. 17-19).

Robotic Technologies in Concrete Building Construction: A Systematic Review

M. Gharbia[a], A.Y. Chang-Richards[a], and R.Y. Zhong[b]

[a]Department of Civil and Environmental Engineering, University of Auckland, New Zealand
[b]Department of Industrial and Manufacturing Systems Engineering, University of Hong Kong, Hong Kong
E-mail: mgha253@aucklanduni.ac.nz, yan.chang@auckland.ac.nz, zhongzry@hku.hk

Abstract –

Several researchers have worked in the field of implementing robotics technology in concrete building construction, after the first attempt in the 1980s in Japan. Various motivations such as the shrinking labor population, the aging of skilled workers, and the construction safety issues have promoted the development of such technologies. However, the future visionary on how construction robots can transform the concrete building construction sector is still not solid nor well structured.

What really needs to be changed? What types of construction activities can be taken by automated robotic technologies, as opposed to manpower or skilled worker? To answer these questions, the systematic review reported in this paper seeks to evaluate and synthesize empirical findings on the use of robotic technologies in concrete building construction.

A systematic search of Scopus, Web of Science, IEEE, and Engineering Village databases was conducted, and 48,200 documents were targeted. By applying the inclusion and exclusion criteria, 48,149 records were excluded, and the remaining 51 records were assessed for eligibility and included in the qualitative synthesis. The systematic review shows that researchers in the USA played a leading role on robotics in concrete building construction, followed by Germany and Switzerland. The robotics application and techniques have been largely used on-site and targeted low-rise buildings. The robotic technologies that have been popular in literature included 3D printers, and swarm robotics. Most of the papers have proposed a limited novel structural design, without introducing innovative construction material. Even though the direct and indirect construction activities related to formwork, steel reinforcement, and concreting can be replaced and thus eliminated, the horizontal RC elements still cannot be built on-site without supports. Moreover, rapid prototyping found to be the best robotic design for the purpose of building construction through utilizing manipulator robots.

Keywords –

Concrete buildings; Robotics in construction; Freeform construction; Future of construction.

1 Introduction

The fundamental principles in building construction have not yet substantially changed, since the Romans invented concrete about 100 BC [1]. Later, concrete is still considered globally as the primary material for construction. According to a recent report by the Cement Sustainability Initiative (CSI) [26], concrete is the second most consumed substance after water, with around 10 billion tonnes of concrete are manufactured globally in every year. Consequently, concrete has been the focus in several investigations into robotically fabricated, geometrically complex, non-standard loadbearing constructions [2].

The building construction industry has not been a favourable field for the application of robotic technologies, however, various motivations such as the shrinking labour population, the aging of skilled workers, and the construction safety issues have promoted the development of robotic construction systems [3]. The United Nations world population prospects in 2015 indicated that global population is expected to grow by 34% by 2050 compared to 2014, which will reach 6.5 billion people in 2050 or about two-thirds of the global population [4]. In accordance, the rising in population is expected to growth the necessity for new buildings.

Meanwhile, the building construction process has been characterized as simple and systematic; depending on formwork systems and skilled labour to build any type of concrete structural element [5]. The current construction methodologies used in structural concrete buildings are completely dependent on manual techniques that are slow, expensive, and non-coordinated [27]. Moreover, the main obstacles for the

introduction of robotics within the building construction industry are the variability of the construction processes and the complex conditions of the construction environment [6].

Many building construction activities have the potential to be executed by implementing the robotic technologies techniques [7]. However, adapting new technologies necessitates several special properties of high payload, reliability, and wide workspace to be achieved [8]. In addition, many robots will work in the same task, in which path planning on site would be complicated [9]. As explained by Scott et al. (2011), human construction differs from construction by robots as it involves some sort of pre-defined high-level plan and in some regard is independent from the environment [10].

Several researchers have worked in the field of implementing robotic technologies in building construction, after the first attempt in the 1980s in Japan [2]. While some autonomous construction robots have been developed, they can only be applied to simple tasks to support human workers [9]. An example of such approaches is the Big-Canopy, which is the world's first automated construction system for building a precisely defined concrete structure in Japan [11]. Nevertheless, the degree of intelligence exhibited by commercially-available robots is still deemed very limited, as robots are currently deployed only in a small subset of possible applications with low level of localization accuracy [12, 31].

If robotic technologies could truly be implemented in construction, they would certainly have the potential to improve measures like its speed and efficiency, as well as enabling construction in settings where it is difficult or dangerous for humans to work such as working at heights, in extra-terrestrial environments and disaster areas [13, 32, 33]. In this context, this paper aims to review existing studies in this field, to investigate how the robotic technology can be implemented in the concrete building construction. To overcome the existing constraints and limitations, the ongoing research will examine construction activities with a potential to be executed by robotic technologies, functionality of the robots, and the interaction between humans and robots.

The remainder of the paper is structured as follows. Section 2 introduces the background of the research, followed by the methodology of using a systematic review. Section 4 and 5 detail the results and discussion. Finally, the paper concludes with the guidelines for future research.

2 Background of the study

2.1 Early attempts

Despite the recent advances in adoption of robotic technologies in the construction industry, the architectural processes which demand a high degree of geometric freedom remain largely labour intensive and manual [19]. This is due to the inherent difficulties in robotizing the current implementation of such processes coupled with the lack of alternate technologies [2].

In the last three decades some Japanese construction companies have attempted to remedy the shortage of skilled labour in building construction by resorting to automation [20]. Khoshnevis et al. (2006) categorized the current robotic technologies in concrete building construction in accordance to the Japanese companies. The first one uses single task robots that can replace simple labour activities at the construction sites. The second category consists of fully automated systems that can construct steel reinforced concrete buildings using prefabricated components [11].

So far, the application of robots is feasible only if it generates a value-adding effect. According to Hack et al. 2014, the centralised fully automated Japanese construction systems failed to do so, as they merely tried to automate the existing construction processes. They only focused on the elimination of human labour from the building site, without considering the complexity of the building process. Hence, Hack suggested that some innovated construction processes need to be developed first, to specifically address the strengths of robots to be applied where they actually outperformed humans and conventional construction [14].

2.2 Present attempts

The Chinese Huashang Tengda company in Beijing has recently claimed to 3D print an entire 400 m2 two story villa 'on-site' in 45 days uses a unique process allowing to print an 'entire house' in 'one go'. This is by erecting the frame of the house including steel reinforcements and plumbing pipes conventionally, and then ready-mix concrete extruded over the frame and around the rebars using a novel nozzle design and 3D printer [15].

The WinSun decoration design engineering company worked jointly with architectural and structural design companies such as Gensler, Thornton Tomasetti, and others to build an office building for the Dubai Future Foundation with a technique similar to contour crafting, in which wall elements are manufactured from extruded prismatic bodies [30]. One more technology known as WASP (World's Advanced Saving Project) has focused on using Additive

Manufacturing technologies to build "zero-mile homes" that utilize on-site materials to build houses in places where it is hard to find access to construction materials [16].

In despite of presently attempted, the current construction is in need for large scale 3D printers to build complex geometric shapes on projects where construction time, cost, and quality are the predominant and determining success criteria [17]. In accordance, a novel approach for 3DCP technology for on-site construction, named CONPrint3D, is currently being developed at the TU Dresden, Germany, which intends to bring 3DCP directly into the building sites [15]. In addition, Skanska is a construction company that recently has utilized advancements in the area of additive manufacturing by printing unique cladding for the Bevis Marks building in London [16].

2.3 Future visionary

A comparison by Helm et al. (2012) between the usages of robotic technologies in building site with other industries, revealed that the construction sector has been rather slow to adopt such innovative technologies with most tasks on a building site still carried out using manual methods [18]. As stated by Hwang, et al. (2005), the present state of automation and robotic technologies are not sufficient to economically replace skilled labour, thus suggested that the construction industry needs to think "out of the box" and seek alternatives to existing fabrication and assembly processes [19].

Howe at el. (2000) had a different view, when proposed to study the possible applications of robotic technologies to traditional methods because they are the most familiar to us, while the feasibility of automating the entire construction site would be dependent on need and would occur gradually. At the same time, Howe confirmed that there are many problems need to be overcome first in order to develop usable robotics in the building construction [20].

It has been furtherly explained by Choi et al. (2005) that in a field of construction work, the content of work and working material are frequently changeable, thus construction robot needs several special properties of high payload, safety, reliability, and a wide workspace [21]. Thus, a collaboration between conventional tools, humans and robots, and standard concrete pumps is required to transfer the actual structural mass, while the robot could unlock the inherent potential of concrete to take any desired shape by building complex formwork in high resolution [14].

The new paradigm brings a host of new topics into the forefront of robotics in construction research. These topics have been neglected in the past by researchers inspired by the old paradigm, and therefore there is a backlog of research problems to be solved. This systematic review has been performed to respond to this research gap, and by using its results to develop a comprehensive framework. The methodological approach of the systematic review is outlined in the next section.

3 Research methodology

To provide a robust investigation on the applications of robotic technologies in the concrete building construction, a systematic review approach was adopted. In comparison with a conventional literature review, a systematic review applies an explicit, rigorous, reproducible, and auditable methodology for evaluating and interpreting all available research relating to a particular research question, topic area, or phenomenon of interest [22].

A systematic review originates from the need to overcome the shortcomings of a single facet approach which is often adopted in a literature review, by representing the bigger picture by combining discrete pieces and synthetizing results in an organized way [23]. Additional benefits also include that researchers can summarize existing evidence about a phenomenon, identify gaps in current research, and provide grounds to position or support new ideas and hypotheses [24].

The review has been undertaken in distinct stages as shown in Figure 1, including the development of review protocol, the identification of inclusion and exclusion criteria, searching for relevant studies, critical appraisal, data extraction, and synthesis. In the rest of this section, we describe the detail of these stages and the methods used.

3.1 Protocol development

The protocol for the systematic review has been developed in accordance with the Preferred Reporting Items for Systematic Reviews and Meta-Analyses (PRISMA) guidelines [28]. This protocol specified the research questions, search strategy, inclusion, exclusion and quality criteria, data extraction, and methods of synthesis.

3.2 Research question

The aim of the systematic review is to locate relevant existing studies based on the research question of 'What type of robotic technologies have been in use in the concrete building construction industry?', to report the evidence in a way that clear conclusions with regard to further research to be drawn [29]. For the purposes of this paper, the systematic review shall provide a theoretical basis for understanding to what extent the topic of robotic technologies is being

addressed in concrete buildings construction.

3.3 Inclusion and exclusion criteria

Studies were excluded if their focus, or main focus, was not related to robotics in construction or if they did not present empirical data. Furthermore, the research question is concerned with concrete building, therefore, studies that focused on other building construction were excluded. Studies were eligible for inclusion in the review if they presented empirical data on robotics in concrete building construction and passed the minimum quality threshold (see Section 3.5). The systematic review included research studies published up to and including 2018. Only studies written in English, clearly describe its methodology, completed and concluded were included.

3.4 Data sources and search strategy

The search strategy included electronic databases. Of Scopus, Web of Science, IEEE, and Engineering Village. Figure 1 shows the systematic review process and the number of papers identified at each stage.

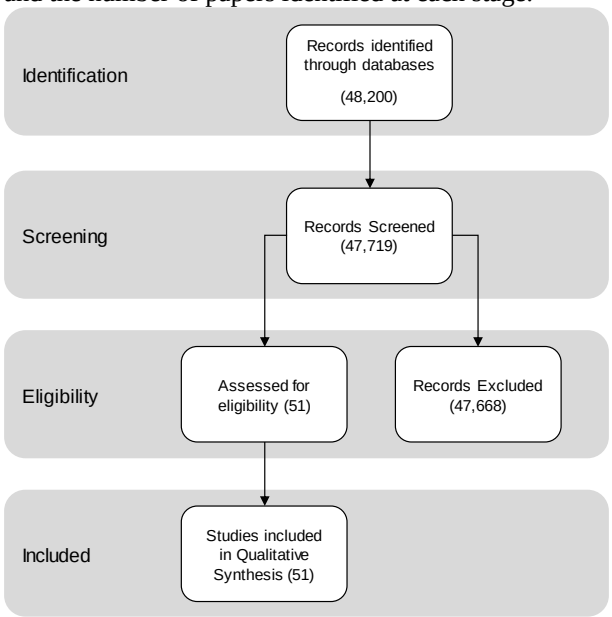

Figure 1. Flowchart of systematic review process. (PRISMA flow diagram [28])

In the identification stage, the titles, abstracts, and keywords of the articles in the included electronic databases and were searched using search term of (robot* AND construction)". These keywords are widely-known for their use in research articles. Excluded from the search were editorials, prefaces, article summaries, interviews, news, reviews, correspondence, discussions, comments, reader's letters and summaries of tutorials, workshops, panels, and poster sessions. This search strategy resulted in a total of 48,200 documents. Of total number of documents (n = 47,719), 1,020 were book sourced, 15,646 journals, and 31,053 were resulted from a conference proceeding source.

At screening stage, duplicates were removed as well as papers from undefined or trade publications resources. At this stage, 481 articles were excluded after removing duplicates as well as papers from undefined or trade publications resources. However, it was not always obvious whether a study was, indeed, an empirical one. Therefore, all studies that indicated some form of experience with robotics in construction were included. At eligibility stage, studies were excluded if their main focus was not robotics in on-site building construction. As a result, 51 primary studies were included for the detailed quality assessment.

3.5 Quality assessment

The methodological quality of the eligible selected studies was critically appraised using a set of screening questions adopted from the Critical Appraisal Skills Programme (CASP) [25]. A summary of the questions used to assess the quality of these studies is presented in Table **1**. The tool provides a guide for appraising qualitative research to consider if the results of the study are valid, what the results are, the benefits of the results, and the tool has been used in a range of reviews. Taken together, these questions provided a measure of the extent to which we could be confident that a particular study's findings could make a valuable contribution to the review. Each of the 9 questions was graded on scale of (YES = 1, NO = 0), and only question 1 was used as the basis for including or excluding a study.

Table 1. Quality appraisal questions

	Screening Questions
Q1	Research: Is the paper based on research
Q2	Aim: Was the aim of the research clear?
Q3	Method: Was the research methodology used appropriate?
Q4	Design: Did the study design address the aims of the research?
Q5	Data analysis: Was the data analysis sufficiently rigorous?
Q6	Findings: Are the findings clearly stated?
Q7	Gaps: Have gaps in the literature been clearly identified?
Q8	Acceptance: Can I accept these findings as true?
Q9	Value: Can I apply these findings to my own work?

The results of the quality assessment are shown in Figure **2**. Because only research papers were included in

this review, all included studies were rated as yes on the first screening question, in addition, they all had a clear statement of the aims of the research as well as appropriate research methodology. While the number of negative answers was three for each criterion of research methodology, study design and findings acceptance. Furthermore, the data analysis did not seem sufficiently rigorous for four of the studies. The highest numbers of negative answers were 17, and 19 as it has been noticed that the findings were not well described, and gaps in the literature were often not identified.

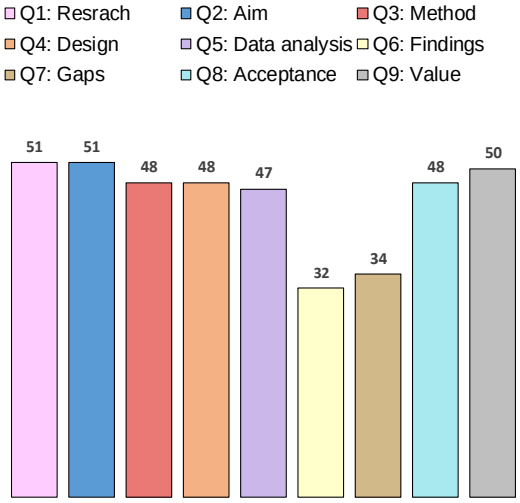

Figure 2. Quality appraisal summary results (out of total number of articles: 51)

3.6 Data extraction

During this stage, data was extracted from each of the 51 primary studies included in this systematic review according to a predefined extraction form (see Figure 3). This form enabled to record full details of the articles under review and to be specific about how each of them addressed the research question. All data from all primary studies were extracted by the authors in consensus meetings. The aims, settings, research methods descriptions, findings, and conclusions, as reported by the authors of the primary studies, were tabulated in Microsoft Excel.

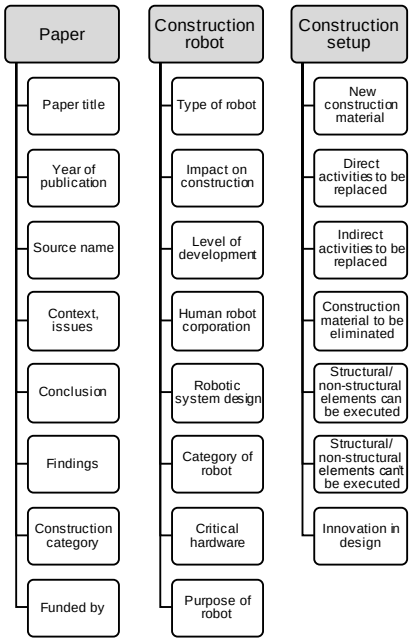

Figure 3. Data extraction

3.7 Peer assessment

The first two authors sat together and went through the titles of all studies that resulted from identification stage, to determine their relevance to the systematic review. At the eligibility stage, the abstracts were divided among the first two authors and the third author in such a way that each abstract was reviewed by two researchers independently of each other. All disagreements were resolved by discussion that included all three researchers, before proceeding to the final stage. Each of the 51 studies that remained was assessed independently by the authors, according to quality assessment procedure.

4 Results

4.1 Publishing framework

The chronological distribution of articles in Figure 4 indicated for a growing interest in performing research related to the subject. 6 papers have been published from 2000 to 2005 and 9 papers from 2006 to 2011. While the period from 2012 to 2018 accounted for the most published papers of 36 number. The analysis results demonstrate that there is a substantial increase in the number of literature during the last 6 years. This would indicate for a promising established research area in concrete building construction.

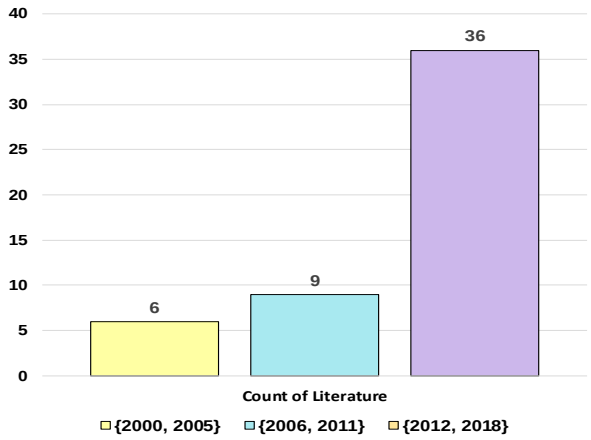

Figure 4. Chronological Distribution of publications (total number of articles: 51)

Furthermore, Figure 5 shows the number of publications according to the different country for each of the authors. When comparing the geographical distribution of the total number of 51 papers, USA and Germany are ahead of all others. However, by filtering out only the 23 articles of highly related studies to the review topic, research on the subject has been dominated by authors from USA, and France. While, focusing on the 4 extremely related studies revealed that authors from Switzerland are leading the topic.

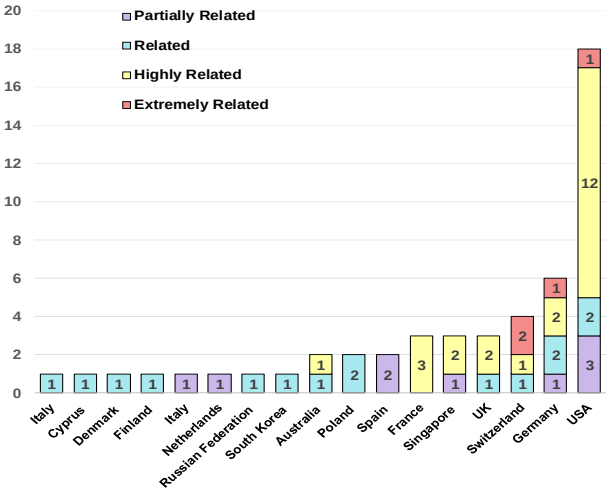

Figure 5. Geographical distribution of publications (total number of articles: 51)

4.2 Implementation on a construction site

The construction applications and techniques for the outcome are mainly on-site and related to the robotic technologies of 3D printers, automated building construction system, and swarm robotics construction system (see Figure 6). In context, 57% from the proposed technologies have targeted low rise building projects and 35% focused on low to medium rise buildings, while only 8% could target the medium to high rise building category. This could indicate that adapting most of the studies for the 3D printing technology, has resulted in a major limitation to target high rise building construction.

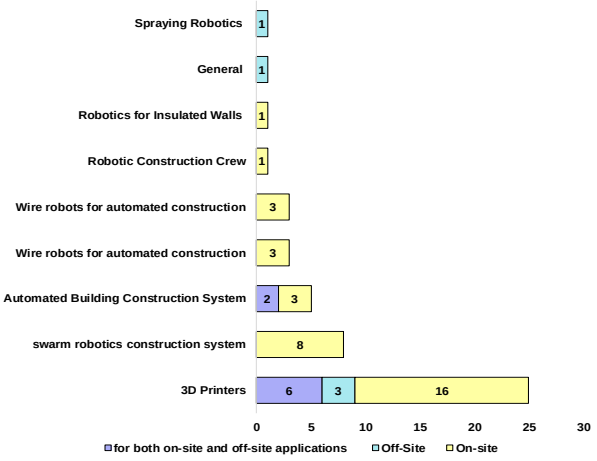

Figure 6. Construction robots' types & application (total number of articles: 51)

In parallel, Figure 7 shows that most of the researched robotic technologies were found to be either under development or conceptual. At the same time, their implementation in concrete building construction is challenging. Only 10% from the proposed topics were classified as developed technologies, and merely 8% could be implemented in a construction site.

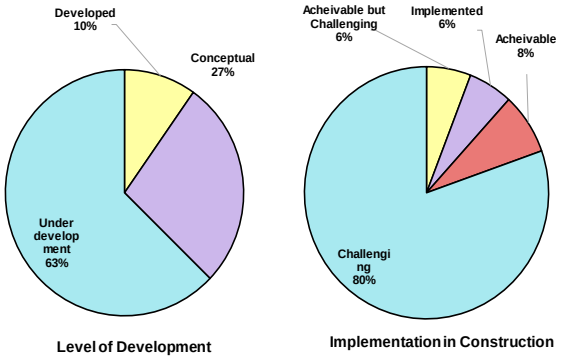

Figure 7. Robotics technologies level of development and implementation in construction

Concerning the reasons behind proposing such technologies, nearly 70% of the papers shared the same goal of enhancing the concrete building construction efficiency. While construction in space, besides proposing new construction technologies have attracted almost 20% from the authors. The remaining papers were interested in the construction in disaster or

hazardous areas, as well as reducing the accident rate. (See Table 2).

Table 2. Purpose of the robotic technologies (total number of articles: 51)

Purpose of the robotic technology	Number of paper
Construction in disaster areas	1
Reducing high accident rate	2
Construction in a constrained/ hazardous environment	2
New construction technology	5
Construction in space	5
Greater efficiency	36

4.3 Innovation in construction material and structural design

As illustrated in Figure 8, 53 % of the papers proposed a limited novel structural design and 29% projected a complete novel design proposal, while the remaining 18% adopted the conventional structural design for the construction of concrete structures. Concerning the innovation in construction material, the researchers could not introduce novel material to the construction, however they have focused on finding alternatives to replace the conventional ready-mix concrete and steel reinforcement.

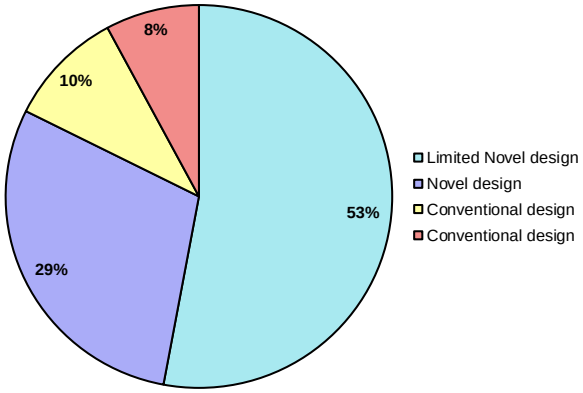

Figure 8. Innovation in structural design

As presented in Figure 9, 45% of the papers considered mesh wire as an alternative to reinforcement rebar, and around 79% from the total literature proposed polymer based material and cementitious material to replace the ordinary cement. While mortar mix, intelligent concrete blocks, and ultra-high-performance concrete found to be the new alternatives to conventional concrete mix.

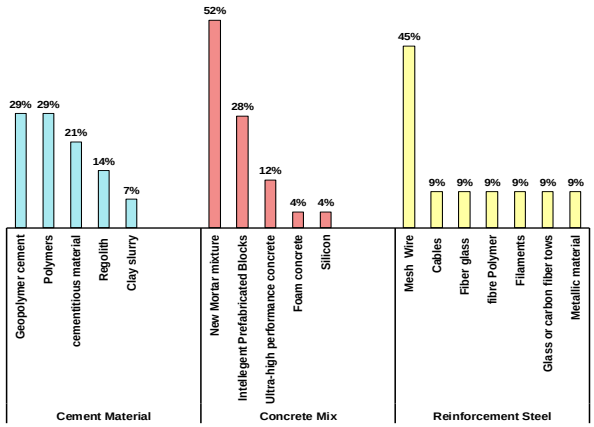

Figure 9. Alternative construction material

4.4 Impact on building construction activities

Formwork fixing and striking, steel rebar fixing, and concrete pouring and curing are the main direct construction activities could be replaced by the proposed robotic technologies. The major indirect construction activities that could be eliminated comprise ready-mix concrete delivery to site, formwork fabrication, steel rebar fabrication, and material handling by cranes and manually (see Figure 10). This would have a huge impact not only on the overall productivity of the construction activities, but also on the entire efficiency of the concrete building construction. The proposed construction technologies will not depend on plywood, formwork systems and scaffolding to build any concrete structural element.

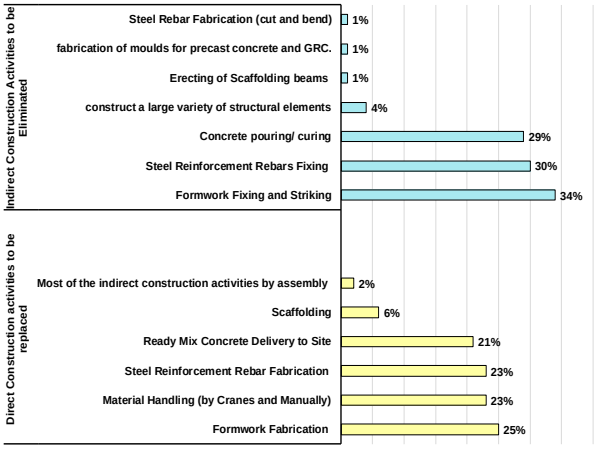

Figure 10. Impact on construction activities

Regarding the applicability of the construction robotics to build all the structural concrete elements, 93% of the literature claimed that their proposed technologies can build vertical RC elements on-site, while 4% suggested pre-casting and assembly, and only 3% proposed a full solution to construct all RC elements on-

site for one story building. The same studies claimed to build vertical RC elements have shown incapability of their proposed technologies regarding the construction of horizontal RC elements on-site, unless they were temporary supported during the construction or pre-casted and assembled by cranes.

4.5 Construction robotic features

Different types of robotic systems have been adopted through the literature, however, rapid prototyping and self-assembly found to be the most appropriate systems for the purpose of concrete building construction (see Table 3). This outcome is in line with the results in 4.2 construction applications and techniques.

Table 3. Robotic system

Robotic system design/ programme	% of literature
VR-assisted virtual prototyping	2%
Multi-robot construction and assembly	2%
Automated assembly systems	2%
Generic, versatile mobile robotics system	4%
Cartesian motions	6%
Self-organized construction	8%
Controlled assembly	8%
Self-assembly	12%
Rapid prototyping	56%

In terms of the construction robotic category, 63% from the studies considered manipulator robots for their proposed technologies, and around 15% adopted the collective construction robot category (see Figure 11). This is in consonance with rapid prototyping and self-assembly systems, in addition to the results in 4.2. Furthermore, nozzle, manipulator arm, and multiple mobile robots were the most critical hardware components for such robotic categories.

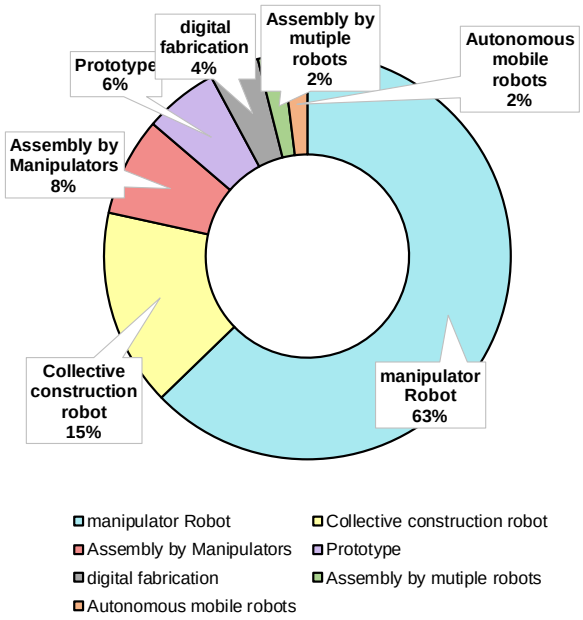

Figure 11. Category of construction robot

5 Discussion

Most of the present attempts to implement robotic technologies in concrete building construction were focusing on freeform construction for vertical RC elements, in the aim of improving the building construction efficiency and reducing the dependency on formwork.

The concrete building industry is currently in need for numerous researches to alter the conventional building process, by thinking out of the box in terms of innovating structural design and construction material. Moreover, lessons should be learned from the past attempts in the last three decades to robotize the building construction sector. Consequently, the future visionary is necessary for a systematic approach to increase efficiency in this type of research. An example for such visionary can be found in few innovative researches adapted the swarm intelligence for building construction by self-assembly.

Despite that the aim of this research is solely for concrete building construction, some other industries have attracted the researchers. Around 40% from the explored papers have been interested in building construction in extra-terrestrial environment. Their researches are mainly funded by the National Aeronautics and Space Administration (NASA), in addition to Kennedy Space Center Swamp Works and the Office of Naval Research in the USA, as well as the European Space Agency (ESA).

In this context, new research questions should concentrate on what could be altered within the

construction process or the robotic technologies, to construct a complete building structure on-site. What type of concrete building structures should be targeted in the future researches, to overcome the present obstructions?

6 Conclusion

The review demonstrates that the research on robotic technologies in concrete building construction is still in its infancy, and thus is characterized to be under development and mostly challenging to be implemented. The literature all points that conventional methods for building construction proved to be inefficient, and the construction industry can innovate towards improved health and safety and time and cost savings.

The systematic review shows that the researchers in the USA played a lead role in researching robotics in concrete building construction, followed by Germany and Switzerland. The robotics application and techniques have been largely used on-site and targeted low-rise buildings. The robotic technologies that have been popular in literature included 3D printers, and swarm robotics. Most of the papers have proposed a limited novel structural design, without introducing novel construction material. Even though the direct and indirect construction activities related to formwork, steel reinforcement, and concreting can be replaced and thus eliminated, the horizontal RC elements still cannot be built on-site unless they were supported. Moreover, rapid prototyping found to be the best robotic design for the purpose of building construction through utilizing manipulator robots.

While the application of robotics in construction has limitations that need to be acknowledged, research for innovative robotic technologies to be adapted in the construction appears as an emergent approach. Collaboration in research across all the segmented disciplines such as architecture, engineering, building, computer science, would be an essential element for developing a related research area and also for deepening and widening research area dimensions and domain. Future research should also focus on the different types of barriers behind implementing the robotic technologies in the construction field.

Acknowledgement

This systematic review was completed as part of the first author's PhD research and is funded by the Dean's Discretionary Doctoral Scholarship, University of Auckland.

References

[1] Asprone D. and Auricchio F. 3D printing of reinforced concrete elements: Technology and design approach. *Construction and Building Materials*, 165: pp. 218-231, 2017.

[2] Kumar S. and Hack N. Design, development and experimental assessment of a robotic end-effector for non-standard concrete applications. *Proceedings of the 2017 IEEE International Conference on Robotics and Automation (ICRA))*, pages 1707 - 1713, Singapore, 2017.

[3] Chu B. and Jung K. Robot-based construction automation: An application to steel beam assembly (Part I). *Automation in Construction*, 32: 46-61, 2013.

[4] United Nations, Department of Economic and Social Affairs, Population Division. World Population Prospects: The 2015 Revision, Key Findings and Advance Tables. On-line: http://www.un.org/en/development/desa/publications/world-population-prospects-2015-revision.html, Accessed: 02/09/2018.

[5] Panda B. and Paul S.C. Additive manufacturing of geopolymer for sustainable built environment. *Journal of Cleaner Production*, 167: pp. 281-288, 2018.

[6] Martinez S. and Jardon A. Building industrialization: Robotized assembly of modular products. *Building Industrialization*, 28(2): pp. 134-142, 2008.

[7] Parker L. *Collective manipulation and construction*, volume 1. Springer Handbook of Computational Intelligence, Berlin, Heidelberg, 2015.

[8] Jung K. and Kim D. Development of the gripping control algorithm for wire-suspended object in steel construction. *Proceedings of the 24th International Symposium on Automation and Robotics in Construction (ISARC)*, pages 151-155, India, 2007.

[9] Terada Y. and Murata, S. Automatic modular assembly system and its distributed control. *International Journal of Robotics Research*, 27(3-4): 445-462, 2008.

[10] Scott D. and Pan Y. Smart beacons and their application to distributed multi-robot construction tasks. *Proceedings of the 16th IASTED International Conference on Robotics and Applications*, pages 1-8, Canada, 2011.

[11] Khoshnevis B. and Hwang D. Mega-scale fabrication by Contour Crafting. *International Journal of Industrial and Systems Engineering*, 1(3): 301-320, 2006.

[12] Magnenat S. and Philippsen R. Autonomous construction using scarce resources in unknown

environments. *Autonomous robots*, 33(4): 467-485, 2012.

[13] Petersen, K. and Nagpal R. TERMES: An autonomous robotic system for three-dimensional collective construction. In *Proceedings of the International Conference on Robotics Science and Systems, RSS*, pages 257-264, United States, 2011.

[14] Hack, N. and Lauer W.V. Mesh-mould: Robotically fabricated spatial meshes as reinforced concrete formwork. *Architectural Design*, 84(3): 44-53, 2014.

[15] Nematollahi B. and Xia M. Current progress of 3D concrete printing technologies. *Proceedings of the 34th International Symposium on Automation and Robotics in Construction (ISARC)*, pages 260-267, Taiwan, 2018.

[16] Camacho D.D. and Clayton P. Applications of additive manufacturing in the construction industry - A prospective review. *Proceedings of the 34th International Symposium on Automation and Robotics in Construction (ISARC)*, pages 246-253, Taiwan, 2018.

[17] Teizer J. and Blickle A. Large scale 3D printing of complex geometric shapes in construction. *Proceedings of the 33rd International Symposium on Automation and Robotics in Construction (ISARC)*, pages 948-956, United States, 2016.

[18] Helm V. and Ercan S. Mobile robotic fabrication on construction sites: DimRob. *Proceedings of the 2012 IEEE/RSJ International Conference on Intelligent Robots and Systems*, pages 4335-4341, Portugal, 2012.

[19] Hwang D. and Khoshnevis B. An innovative construction process-contour crafting (CC). *Proceedings of the 22nd International Symposium on Automation and Robotics in Construction (ISARC)*, pages 246-253, Italy, 2005.

[20] Howe A. and W Howe J. Applying construction automation research to extraterrestrial building projects. *Proceedings of the 30th International Conference on Environmental Systems*, France, 2000.

[21] Choi H.S. and Han C.S. Development of hybrid robot for construction works with pneumatic actuator. *Automation in Construction*, 14(4): 452-459, 2005.

[22] Oates B. J. and Capper G. Using systematic reviews and evidence-based software engineering with masters students. *Proceedings of the 13th International Conference on Evaluation and Assessment in Software Engineering (EASE)*, UK, 2009.

[23] Cooper H. The Integrative Research Review: A Systematic Approach Sage Publications: Beverly Hills. *Educational Researcher*, 15(8): 17-18, 1986.

[24] Dyba T. and Kitchenham B.A. Evidence-based software engineering for practitioners. *IEEE Software*, 22(1): 58-65, 2005.

[25] Brún C. *Critical Appraisal*, volume 1. Wiley - Blackwell, Oxford, UK, 2009.

[26] The Cement Sustainability Initiative (CSI). Cement Industry Energy and CO2 Performance; Getting the Numbers Right (GNR). On-line: http://wbcsdcement.org/pdf/GNR%20dox.pdf, Accessed: 16/11/2018.

[27] Balaguer C. and Abderrahim M. FutureHome: An integrated construction automation approach. *IEEE Robotics and Automation Magazine*, 9(1): pp. 55-66, 2002.

[28] Moher D. and Shamseer L. Preferred reporting items for systematic review and meta-analysis protocols (PRISMA-P) 2015 statement. *Systematic reviews*, 4(1): pp. 1-9, 2015.

[29] Denyer D. and Tranfield D. Producing a systematic review. *The Sage Handbook of Organizational Research Methods*, 1(1): pp. 671-689, 2009.

[30] Stuart-Smith R. Behavioural production: Autonomous swarm-constructed architecture. *Architectural Design*, 86(2): pp. 54-59, 2016.

[31] Feng C. and Xiao Y. Vision guided autonomous robotic assembly and as-built scanning on unstructured construction sites. *Automation in Construction*. 59: 128-138, 2015.

[32] Liang CJ. and Kang SC. RAS: a robotic assembly system for steel structure erection and assembly. *International Journal of Intelligent Robotics and Applications*. 1(4): 459-476. 2017.

[33] Yang Y-Y. and Chang C-M. Framework of Automated Beam Assembly and Disassembly System for Temporary Bridge Structures. *Proceedings of the 35th International Symposium on Automation and Robotics in Construction (ISARC)*, pages 230-235, Germany, 2018.

The Effectiveness of Virtual Reality in Safety Training: Measurement of Emotional Arousal with Electromyography

S. Xu[a, b], Q. Ni[c], and Q. Du[a]

[a] School of Economics and Management, Chang'an University, China
[b] National Centre of International Research on Digital Construction and Management for Transport Infrastructure along the Belt and Road Initiative, China
[c] School of Civil Engineering, Chang'an University, China
E-mail: sheng.xu@chd.edu.cn, Q.Du@163.com

Abstract –

The improvement of safety performance of construction workers heavily lies in safety training and great improvement has been achieved in training technology, training materials and training organisation. Currently, the form of training and induction based on traditional lectures and workshop studies has been innovated and enriched by digital and e-learning technologies and applications, such as immersive visualization techniques like Virtual Reality (VR), Augmented Reality (AR) and game engines. The visualization techniques allowed workers to enhance their safety capabilities by playing the safety training game in virtual scenarios. However, the validation of its effectiveness was measured with either self-reported questionnaire or the improvement in safety performance and productivity. This research proposed a framework to directly validate the effectiveness of virtual reality in safety training by measuring the degree of emotional arousal with electromyography (EMG). Specifically, the degree of inducement of fear was measured during safety trainings with pictures, videos and VR. The higher degree of fear was induced, the more effective the safety training was. In this way, this research provided a novel approach to prove the effectiveness of the immersive visualization techniques and a possible framework to further identify important personal and environmental factors of safety training process.

Keywords –

Virtual Reality; Safety Training; Emotional Arousal; Electromyography

1 Introduction

Safety training and education is an important issue in construction safety management. Because of the massive amount of new construction, large groups of new workers come into the construction industry without proper skills or enough experience. Migrant workers are common worldwide. In China, most Chinese on-site workers used to do agricultural jobs, and the number of migrant workers in the construction industry has increased by more than 1 million per year. Less than 7% of them attended vocational training programs. Senior technicians accounted for less than 0.3% of all workers, compared to 20%~40% in developed countries. The US construction sector provided 7% of all employment in the workforce but accounted for 20% of worksite fatalities [1]. According to statistics, there were more than two million Hispanic workers in the construction industry in the U.S., and those Hispanic workers also had the highest injury and fatality rates [2]. Human errors and unsafe behaviours contribute greatly to accidents [3], Garrett and Teizer [4] pointed that previous research showed human factors accounted for 90% of all accidents in complex industries with high risks. Furthermore, inexperienced workers are more likely to perform unsafe behaviour and cause accidents.

Currently, the form of training and induction based on traditional lectures and workshop studies has been innovated and enriched by digital and e-learning technologies and applications, such as accident simulations in Building Information Modelling (BIM) systems, and other immersive visualisation techniques, such as Virtual Reality (VR), Augmented Reality (AR) and game engines [5-7]. The variety of training schemes does not only transfer essential knowledge to workers, it also guarantees the attainment of certain task proficiency that is required to prepare workers for real-work task settings [8], as well as to instil a positive danger/risk-sensitive attitude and safety climate in the workplace [9, 10].

It is well recognised that VR technologies are effective in enhancing construction safety training programs, however, the amount and mechanisms of the improvement brought by VR to safety training have not

been fully explored and measured with objective index other than self-reported questionnaire surveys. Therefore, this research proposed a possible explanation of the enhancement of VR safety training, and an approach to measure the effectiveness of VR safety training.

2 Literature Review

2.1 VR Applications in Construction Safety Training

The literature review identifies a variety of training approaches and techniques for construction safety. There is a long history of using classroom-based studies to upskill the construction workforce. The improvement of knowledge, attitude and self-reported practice followed by a one-hour classroom study, was evidenced by Sokas [11]. Tailored classroom training programs were also applied to 2700 training construction workers working on a railway project, which revealed positive effects, such as that workers were more likely to handle materials safely [12]. The conventional safety training takes the form of classroom teaching, and is tedious, difficult to understand and memorize, and has unsatisfying influence on performance improvement. In recent years, the form of classroom training programs has been enriched. A series of studies have made their efforts to improve safety training, for example, the peer-led training programs, which believed the interventions of co-workers could improve the learning outcomes [13]; the encouragement of verbal communications on safety between supervisors and workers [14]; the localisation of safety training materials for Hispanic workers [15] and narrative simulations, and improved toolbox training programs that are delivered by workmates or trained foremen [16]. Foremen, peers and unions help with safety performance through safety leadership and communication [17], and they improve the safety climate, which has a social influence on construction workers. It has to be noted, however, that classroom-based training was stereotyped, as its form may not be effectively conducive to motivating learners, and the uniform teaching manner may not take the learner disparity into account.

With the emergence of innovative Information Communication and Technology (ICT) applications, construction practitioners and researchers have started to shed light on technology-assisted training paradigms. To gain hands-on skills and practical experience with a shorter training turnaround, it is preferable that traineeships should be more task-oriented and available for both on and off-the-job options. Because it makes more sense to justify workers performance, potential hazards and causation factors in real-time working contexts. To facilitate a more task-oriented, context-aware and customisable training environment, innovative visualisation manners such as Virtual Reality (VR), Augmented Reality (AR), Mixed Reality (MR) and Building Information Modelling (BIM) have been formulated and researched [18]. The rationale of VR, AR, MR and BIM is that these technologies make use of computer graphic representations (e.g., agent-based avatars, virtual/ augmented task instructions and clues, etc.) to create a virtual but immersive space where real-life scenarios can be replicated for trainees to experience and make sense of risks. Traditional safety training with texts and few graphical elements were difficult to be understood, especially by low literacy novice workers. On-the-job training engaging hands-on experience could be more efficient [19] but time-intensive, expensive, and potentially hazardous [20]. To help low-literacy construction workers who may have linguistic and understanding problems at work [14, 21], Lin et al. [19] developed a game-engine based VR serious game which can offer visual representations that remind unsafe conducts; Le et al. [5] proposed an online VR training framework for multiple students to perform role-playing construction safety training with communications within groups and social interactions; Behzadan and Kamat [22] presented an innovative pedagogical tool that adopting remote videotaping, AR, and ultra-wideband (UWB) to better link virtual objects to the real world. One of the advocating evidences is the expedited process of developing complex procedural skills required to operate construction heavy equipment on modern, large scale complex infrastructure projects [7]. Overall, the motivation of safety training can also be intervened by ICT paradigms. For this purpose, one of the proffered research directions is that ICT applications should interface with real-life task scenarios that are often dynamic, complicated and varied.

2.2 Possible Explanations of Effective VR Training

The advantages of using VR in education and training are related to its ability to enable students to interact with each other within virtual three-dimensional (3D) environments. Intuitive sense about the learning subjects can also be developed by interacting with the objects, related messages and signals in the virtual environment. Different from the conventional education and training approaches, such as the utilizations of static pictures or two dimensional (2D) drawings, VR's visual representation allows more degrees of freedom (DoFs) to be integrated. Compared to conventional training methods, ICT innovations for training was reported to be more conducive to development of short-term memory, emotional arousal, attention maintenance,

confidence enhancement [23, 24], information retention, and various essential cognitive mechanisms that underpin workers' kinesthetic and psychomotor abilities [25]. Therefore, it was suggested that the future of construction safety education should incorporate VR/AR technologies into the pedagogy.

Psychologically, a possible explanation of the advantages of VR/AR technologies in safety training might be related to the emotional memory enhancement effect. It was used for the phenomenon that events or materials loaded with emotional information are more likely to be retained in individual memory and have a higher recall accuracy compared with neutral events or materials [26]. This effect can be found no matter whether emotional words, emotional pictures or emotional films are used, or whether they are used in recognition tests, free recall or clue recall [27, 28]. Previous studies have found that the enhancement effect of emotional memory is mainly affected by the arousal level of emotional stimulation, and highly aroused emotional stimulation can get priority attention and thus be processed preferentially [29]. Therefore, no matter emotional pictures or emotional words, highly aroused emotional stimulation has better memory effect. Individuals' fear stimulation is a rapid automatic processing, so as to quickly deal with threats.

In construction safety research, the effects of emotional arousal have been recognised [30, 31]. The assessment of emotions of accidents was included in workers' judgement of construction accidents' likelihood and severity [32], and negative emotions from previous experience could lead to the decision of avoid risky behaviour [33]. Furthermore, while positive emotions in learning could lead to higher levels curiosity, interest, and desire to improve performance, research also showed that negative emotions could arise extrinsic motivation to avoid failure [34], lead to better engagement in learning [35]. Lang [36] proposed limited capacity model of motivated mediated message processing (LC4MP) to explain the relationship between emotion and learning motivation.

Fear is an emotion closely related to evolution. It can stimulate workers' defense mechanism and help human survival and adapt to the environment. The formation and expression of fear is activated by the brain regions including the amygdala, anterior cingulate gyrus and the frontal cortex [37, 38]. The use of event-related potential methods can help the study find the neural basis of emotional infection. It is a research method with high time precision, which can help researchers discover a cognitive processing process and reflect the time course of emotional infection. It can record multiple brain components induced by emotions. The occurrence time, amplitude intensity and brain area of these components will be important indicators reflecting the processing of cognitive emotions. Different components represent different psychological cognitive processes, including P200 and P300. P200 is an early positive component, the peak is located after the stimulus is presented to the left and right, and the scalp is in the forehead or the occipital region [39-41]. P200 peak can be used to reflect the emotional valence (or, pleasure) and arousal of the information (or strength). P300 is related to attention, identification, decision, memory, etc. [42, 43].

However, existing measurement of fear are by means of electroencephalography (EEG), electro-cardio (ECG) and galvanic skin response (GSR), and it was difficult for the portable devices of the measurement of these indicators to be adequately accurate (medical level) and instantaneous enough to capture the spontaneous reaction of fear. On the other hand, electromyography (EMG) signals are perfect to measure real time responses if the responses include muscle motions. Portable devices on the open market to accurately measure EMG are also easily accessible. Therefore, this research used EMG which could be measured accurately with a wristband and be recorded instantaneously.

3 Pilot Study

3.1 Experiment Design

3.1.1 Participants

In the pilot study, university students were recruited as participants, including 9 graduate students in Construction Management major, out of which there were five female students and four male students.

3.1.2 Measuring Devices

An episode of VR safety training material for construction workers on Fall-from-Height was mounted with HTC Vive and displayed to each participant.

Electromyography signals were measured with DTing Gesture Control Wristband, which is in the world's first easy-start gesture-controlled robot series. The wristband is able to detect users' gesture behaviour, including forearm movement, hand gesture and finger force. In this research, put around the wrist, it is able to capture the signals with pollicis. The surface electromyography (sEMG) signal, gyoroscope signal, accelerometer signal and more related signals are fused to recognize gestures in high precision.

Heart rates were measured with Polar H10 heart rate sensor because it monitors heart rate more accurate and adaptable and connect heart rates to cellphones by Bluetooth simultaneously. Pictures of the wristband and heart rate sensor were shown in Figure 1.

Figure 1. DTing Gesture Control Wristband (left) and Polar H10 heart rate sensor (right)

3.1.3 Measurement approach

The purpose of the pilot study was to determine if the EMG devices could reveal the instantaneous muscle tensions caused by fear during VR trainings on the prevention of fall-from-heights and to adjust the experiment design for a larger scale of experiments on diverse students to determine the effect of personal factors on training effects.

The participants wore the HTC VIVE headset and watch a small episode of safety training material on fall from height. Meanwhile, they also wore DTing wristband on their left or right wrist (according to their free will) and Polar H10 heart rate sensor around their chest. The wristband recorded the changes in electromyography on their pollicis instantaneously and the signals were uploaded to an application to process them with an Android device. Then it could be exported to Matlab and be further processed and mapped graphically. Polar H10 heart rate sensor recorded their heart rate changes and could also be exported to Microsoft Excel for further analysis.

Follow up questions for reviewing and sharing feelings during VR training were asked and discussed with every participant. However, those questions and discussion topics were not pre-determined in the pilot study, but along a broad spectrum of their after-test feelings and possible suggestions.

3.2 Results and discussions

The pilot study revealed that the EMG devices had successfully captured muscle tensions in the pollicis, as shown in Fig. 2. A group of peaks could be observed at almost the same time at the moment of falling in the VR training.

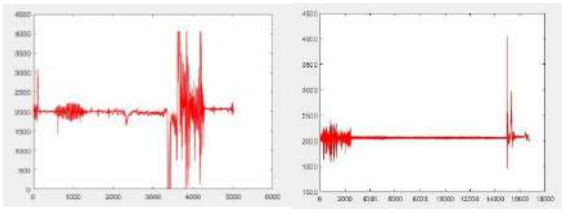

Figure 2. Examples of sudden muscle tensions in pollicis captured by DTing Wristband

However, some participants could be used to the VR trainings after repetitive experiments. Fig. 3 (left) showed that after three trials, the same participants as Fig. 2 (left) showed little tension during the training.

Females and males reacted very different. All female students showed muscle tension to a certain degree at their first trials and reported that VR trainings had raised their fear in the after-test discussions. However, two out of four male students showed little muscle tension and reported “not very scary” in the after-test discussions. Fig. 3 (right) showed a male participant barely tensioned throughout the training, except for the adjustment of his handset at the beginning.

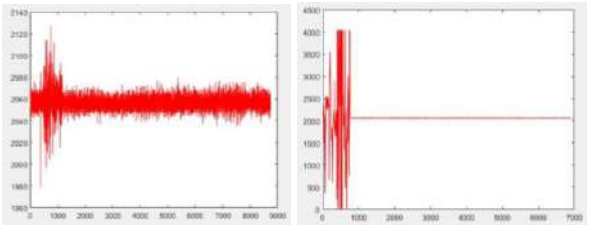

Figure 2. Examples of participants showed little tension during the training after three repetitive trials (left) and from the beginning (right)

The pilot study revealed that several improvements need to be addressed in the experiment design. First of all, the tension of fear could be in different muscles with different participants. Some participants reported tension in the wrist, feeling they “need to grasp something”, and others reported tension in their thighs, feeling that they “could hardly stand straight” and “got cold feet”. Approaches to fix this problem may be providing gesture control bands around the thighs as well as the wrist.

Secondly, the unrelated muscular tensions should be identified and filtered out from tensions caused by fear. Participants could use their pollicis to adjust their HTC VIVE headset and handset, or tensions caused by taking the test, or any other reasons. Fig. 3 shows the signals of a participant feeling tension throughout the training. It would be necessary to filter the actual signals caused by fear of the falling in VR training. Approaches to fix this problem may include developing a filtering algorithm to process the signals, excluding the handset in experiencing the falling to avoid unnecessary muscle tensions and using time stamps to determine the beginning of the signals possibly caused by the falling animation, and so on.

Thirdly, a structured survey should follow up right after the VR training to better review the EMG signals and determine participants’ training effectiveness. As in the pilot study, the follow-up discussion helped the researchers to better understand participants’ reactions to the training materials.

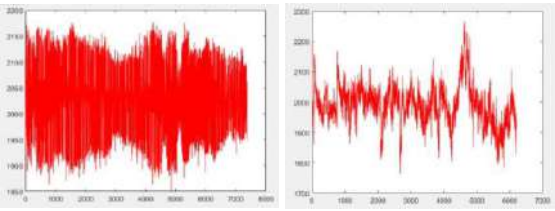

Figure 3. Signals of a participant feeling tension throughout the training.

4 Conclusions

This research tried to validate the effect of VR in construction safety trainings and provide a possible explanation for the advantage of VR training. This research measured the EMG showing muscle tensions of participants watching a piece of VR-based fall-from-height training material with a gesture control wristband. The pilot study confirmed that some participants showed muscle tensions on their pollicis when they experienced falling in the VR training, which indicated that VR-based trainings could raise fear in participants and the fear could improve the effectiveness of training because of the emotional arousal. However, the pilot study also showed that a lot of improvements should be made to the experiment design to provide trustworthy and insightful results.

References

[1] Lavy S., Aggarwal C. and Porwal V. Fatalities of Hispanic Workers: Safety Initiatives Taken by U.S. Construction Companies to Address Linguistic and Cultural Issues. *International Journal of Construction Education and Research*, 6(4): 271-284, 2010.

[2] Menzel N. N. and Gutierrez A. P. Latino worker perceptions of construction risks. *Am. J. Ind. Med.*, 53(2), 179–187, 2010.

[3] Reason J. *Human error*. New York: Cambridge University Press, 1990.

[4] Garrett J. W. and Teizer J. Human Factors Analysis Classification System Relating to Human Error Awareness Taxonomy in Construction Safety. *Journal of Construction Engineering and Management* 135(8): 754-763.

[5] Le Q. T., Pedro A. and Park C. S. A Social Virtual Reality Based Construction Safety Education System for Experiential Learning. *Journal of Intelligent & Robotic Systems*, 79(3-4): 487-506, 2015.

[6] Li H., Chan G. and Skitmore M. Visualizing safety assessment by integrating the use of game technology. *Automation in Construction*, 22: 498-505, 2012.

[7] Hou L., Chi H. L., Utiome E. and Wang X. Y. Cooperative and Immersive Coaching to Facilitate Skill Development in Construction Tasks. *Cooperative Design, Visualization, and Engineering, Cdve* 20169929: 371-377, 2016.

[8] Hou L., Chi H.-L., Tarng W., Chai J., Panuwatwanich K. and Wang X. A framework of innovative learning for skill development in complex operational tasks. *Automation in Construction*, 83: 29-40, 2017.

[9] Shin M., Lee H.-S., Park M., Moon M. and Han S. A system dynamics approach for modeling construction workers' safety attitudes and behaviors. *Accident Analysis & Prevention*, 68: 95-105, 2014.

[10] Choudhry R. M. Behavior-based safety on construction sites: A case study. *Accident Analysis & Prevention*, 70: 14-23, 2014..

[11] Sokas R. K., Jorgensen E., Nickels L., Gao W. and Gittleman J. L. An Intervention Effectiveness Study of Hazard Awareness Training in the Construction Building Trades. *Public Health Reports*, 124 (4_suppl1): 161-168, 2009..

[12] Bena A., Berchialla P., Coffano M. E., Debernardi M. L. and Icardi L. G. Effectiveness of the training program for workers at construction sites of the high-speed railway line between Torino and Novara: Impact on injury rates. *American Journal of Industrial Medicine*, 52(12): 965-972, 2009.

[13] Williams, Q., M. Ochsner, E. Marshall, L. Kimmel and C. Martino. The Impact of a Peer-Led Participatory Health and Safety Training Program for Latino Day Labourers in Construction. *Injury Prevention*, 16: A235-A235, 2010.

[14] Andersen LP, Karlsen IL, Kines P, et al. Social identity in the construction industry: implications for safety perception and behaviour, *Construction Management and Economics*, 33(8): 640-652, 2015.

[15] Evia C. Localizing and Designing Computer-Based Safety Training Solutions for Hispanic Construction Workers. *Journal of Construction Engineering and Management*, 137(6), 452-459, 2011.

[16] Kaskutas V., Buckner-Petty S., Dale A. M., Gaal J. and Evanoff B. A. Foremen's intervention to prevent falls and increase safety communication at residential construction sites. *American Journal of Industrial Medicine*, 59(10): 823-831, 2016.

[17] Jeschke K. C., Kines P., Rasmussen L., Andersen L. P. S., Dyreborg J., Ajslev J., Kabel A., Jensen E. and Andersen L. L. Process evaluation of a Toolbox-training program for construction foremen in Denmark. *Safety Science*, 94: 152-160, 2017.

[18] Bosche F., Abdel-Wahab M. and Carozza L. Towards a Mixed Reality System for Construction Trade Training. *Journal of Computing in Civil Engineering*, 30(2), 2016.

[19] Pedro A., Le Q.T., Park C.S., Framework for Integrating Safety into Construction Methods Education through Interactive Virtual Reality. *J. Prof. Issues Eng. Educ. Pract*. 142 (2): 04015011, 2015.

[20] Wang X., Dunston P.S., A user-centered taxonomy for specifying mixed reality systems for AEC industry. *J. Inf. Technol. Constr. (ITcon)*, 16 (29): 493–508, 2011.

[21] Lin K.-Y., Lee W., Azari R. and Migliaccio Giovanni C. Training of Low-Literacy and Low-English-Proficiency Hispanic Workers on Construction Fall Fatality. *Journal of Management in Engineering*, 34(2): 05017009, 2018.

[22] Behzadan A.H., Kamat V.R. Enabling discovery-based learning in construction using telepresent augmented reality, *Automation in Construction.* 33: 3–10, 2013.

[23] Sacks R., Perlman A., Barak R., Construction safety training using immersive virtual reality, *Construction Management and Economics*, 31 (9): 1005–1017, 2013.

[24] Juang J., Hung W., Kang S., SimCrane 3D+: A crane simulator with kinesthetic and stereoscopic vision, *Adv. Eng. Inform.* 27 (4): 506–518, 2013.

[25] Bhandari, S. and Hallowell M. R. Emotional Engagement in Safety Training: Impact of Naturalistic Injury Simulations on the Emotional State of Construction Workers. *Journal of Construction Engineering and Management*, 143(12), 2017.

[26] Hamann S. Cognitive and neural mechanisms of emotional memory. *Trends in Cognitive Sciences*, 5(9): 394-400, 2001.

[27] Kensinger EA, Corkin S. Memory enhancement for emotional words: Are emotional words more vividly remembered than neutral words? *Memory and Cognition*, 31: 1169- 1180, 2003.

[28] Talmi D, Schimmack U, Paterson T, et al. The role of attention and relatedness in emotionally enhanced memory. *Emotion*, 7: 89-102, 2007.

[29] Kern RP, Libkuman TM, Otani H, et al. Emotional stimuli, divided attention, and memory. *Emotion*, 5: 408-417, 2005.

[30] Fassbender E., Richards D., Bilgin A., Thompson W. F., and Heiden W. VirSchool: The effect of background music and immersive display systems on memory for facts learned in an educational virtual environment. *Comput. Educ.*, 58(1), 490–500, 2012.

[31] Tixier A. J. P., Hallowell M. R., Albert A., van Boven L., and Kleiner B. M. Psychological antecedents of risk-taking behavior in construction. J. Constr. Eng. Manage., 140(11): 04014052, 2014.

[32] Bechara A., Damasio H., and Damasio A. R. Emotion, decision making and the orbitofrontal cortex. *Cereb. Cortex*, 10(3): 295–307, 2000.

[33] Slovic P., and Peters E. Risk perception and affect. *Curr. Dir. Psychol. Sci.*, 15(6): 322–325, 2006.

[34] Pekrun R., Elliot A. J., and Maier M. A. Achievement goals and achievement emotions: Testing a model of their joint relations with academic performance. *J. Educ. Psychol.*, 101(1): 115–135, 2009.

[35] Chung S., Cheon J., and Lee K. W. Emotion and multimedia learning: An investigation of the effects of valence and arousal on different modalities in an instructional animation. *Instruct. Sci.*, 43(5): 545–559, 2015.

[36] Lang A. Using the limited capacity model of motivated mediated message processing to design effective cancer communication messages. *J. Commun.*, 56(S1): S57–S80, 2006.

[37] Feinstein J. S., Adolphs R, Damasio A., and Tranel D. The human amygdala and the experience of fear. *Current Biology*, 21(1): 34-38.

[38] Admon R., Lubin G., Stern O., Rosenberg K., Sela L., Ben-Ami H. et al. Human vulnerability to stress depends on amygdala's predispositon and hippocampal plasticity. *Proceedings of the National Academy of Sciences*, 106(33): 14120-14125, 2009.

[39] Carretie L., Mercado F., Tapia M., and Hinojosa J. A. Emotion, attention and the "negativity bias" studied through event-related potentials. *International Journal of Psychophysiology*, 41: 75-85, 2001.

[40] Thomas S. J., Johnstone S. J. and Gonsalvez C. J. Event-related potentials during emotional Stroop task. *International Journal of Psychophysiology*, 63131: 22I-231, 2006.

[41] Sergei, A., Alexei, N. G. and Julius, K. Categorization of unilaterally presented emotional words: an ERP analysis. *Acta Neurobiological Experiment*, 60: 17-28, 2000.

[42] Maguire M., Brier M. R and Moore P. S. et al. The influence of perceptual and semantic categorization on inhibitory processing as measured by the N2-P3 response. *Brain and Cognition*, 71: 19G-203, 2009.

[43] Briggs K. E. and Martin F. H. Affective picture processing and motivational relevance arousal and valence effects on ERPs in an oddball task. *International Journal of Psychophysiology*, 72: 299-306, 2009.

3D Posture Estimation from 2D Posture Data for Construction Workers

Y. Yu[a] , H. Li[a], and X. Yang[a]

[a]Department of Building and Real Estate, The Hong Kong Polytechnic University, HKSAR, China
E-mail: yt.yu@connect.polyu.hk, xincong.yang@outlook.com, heng.li@polyu.edu.hk

Abstract –
Construction workers' behaviour is important for safety, health and productivity management. Workers' 3D postures are the data foundation of their behaviours. This paper established a preliminary 3D posture dataset of construction tasks and provided a 3D posture estimation method based on 2D joint locations. The results showed that the method could estimate 3D postures accurately and timely. The mean joint error and estimation time of each frame were 1.10 cm and 0.12 ms respectively. This method makes it possible to estimate construction workers' 3D postures from construction site images and contributes to a data-based construction workers' behaviour management.

Keywords –
Posture estimation; Construction worker; Behavior management

1 Introduction

Construction workers' behavior is an important factor in construction management. Construction workers' behavior is closely related to safety, health and productivities. More than 80% of construction accidents are related to workers' unsafety behaviors [1]. In addition, working behaviors, especially working postures, durations and work-rest schedules, are closely related to musculoskeletal disorders, which are very common in construction workers and have caused extremely negative effects on construction workers' health [2,3]. Finally, construction workers' motions, such as the number of production cycles, can also effect the labor productivity [4]. Therefore, it is important to understand construction workers' behaviors for better performance.

Construction workers' posture data provides a foundation for working behavior analysis. For safety management, working postures could help to identify unsafe behaviors and prevent safety accidents [5,6]. For health and sustainability of construction workers, posture data could help to assess the workloads of different working tasks and mitigate the risk of fatigue and injuries [7,8]. For labor productivity, posture data has been used for working/rest status identification for evaluating work efficiency [9]. The studies have demonstrated the importance of workers' posture data in construction management. However, considering the complexity of construction site environments and the dynamics of construction motions, the posture data collection methods used in previous methodologies cannot support effective behavior-based management due to the inaccurate data, uncomfortableness or limitations on indoor working environments.

This study aims to provide a 3D posture data collection method for construction workers, which (1) could provide 3D joint locations, (2) has no limitation on working environments and (3) doesn't require any wearable sensors and thus will not lead to uncomfortableness of workers. The method could provide the data foundation of posture-based behavior analysis and management for individualized unsafe behavior identification, ergonomic assessments and productivity evaluation.

2 Related work

2.1 Previous posture data collection method in construction industry

There are mainly four categories of objects on construction sites, namely human, materials, machines and environment. For materials and machines, tracking technologies such as radio frequency identification and global positioning system have been widely used [10,11]. For environments, laser scanning techniques were used to collect 3D point data for building construction site model [11]. This section mainly focuses on the approaches for collecting the motion data of construction workers.

Manual observation was commonly-used to collect construction workers' joint angle data for ergonomic assessments [12,13]. Manual observation method usually classifies joint angles in to different categories, such as 0-30 degree, 30-60 degree and 60-90 degree. The results of manual observation depend heavily on the observers' experiences and subjective judgement, thus is not accurate enough. In addition, the manual observation cannot collect data continuously from the whole construction site, thus cannot support timely management [14].

Inertial measurement units (IMUs) have been widely used to collect construction workers' posture data. If attached to the key joints, IMU sensors could provide the three-axis rotation angle of each body segments, which could be used to calculate the 3D joint location if given the length of each body segment [15]. Based on the 3D posture data collected with IMU, previous studies have tried to detect construction workers' unsafe behaviour [16], identify awkward postures [15] and estimate productivity [17]. The main disadvantage of IMU, however, is the requirement of attaching IMU sensors to the human body, which may interfere workers' performance. In addition, such sensors may not be suitable for prolonged usage because they may lead to discomfort [14,18].

Motion capture systems (e.g., the VICON system, OptiTrack and Optotrak) are commonly used in laboratories for 3D motion capture and analysis. To capture motion data, an examiner needs to set up multiple cameras in a laboratory and then put reflective markers on the designated locations of an individual's body. The system estimates the 3D position and movement trajectory of each marker based on the signals of the reflective markers captured by the cameras. The reported accuracy of the VICON system is as high as 2 mm [19]. In construction industry, motion capture systems have been applied to collect 3D joint locations for the detailed biomechanical analysis of working postures. However, since these motion capture systems require the installation of at least 4 cameras within 10 m from the attached reflective markers on the body of target workers in order to capture the whole-body posture, it is impractical to use on construction sites [20].

Depth cameras provides a non-invasive method for 3D posture data collection. Depth camera can provide more information than ordinary 2D cameras [21]. There are mainly two kinds of depth cameras, stereo camera and infrared camera. A stereo camera infers the 3D structure of a scene from tow images from different viewpoints. If applied on construction workers, the method could be used to construction the 3D skeletons with 2D images [22]. Infrared cameras could infer the depth of each RGB pixels and provide 3D skeleton based on machine learning networks [5]. However, as for the application on real construction sites, a search of the relevant products (e.g. ZED, Realsense D435 and Kinect) yielded that depth cameras cannot provide accurate 3D joint locations over a long distance. In addition, the infrared cameras cannot provide accurate depth information in outdoor environments due to the interference of sunlight on infrared signals.

RGB cameras are the most common-seen cameras in daily life. Considering the widely use and low cost of RGB cameras, pervious research has tried to identify construction workers posture motions or cameras based on RGB camera [6,23,24]. The methods successfully recognized construction workers from site pictures and classified postures into squatting, standing or walking. However, these methods could only get 2D joint information from the images, which cannot support 3D posture analysis for accurate behaviour recognition or ergonomic analysis.

In summary, above posture data collection methods have the following limitations if applied on construction sites: (1) intrusiveness: sensor-based methods may make the workers feel uncomfortable and even interfere working performance; (2) possible poor performance on construction sites: depth cameras may not provide accurate 3D pose estimation results over long distances in outdoor environments; (3) the lack of 3D results: 3D poses could provide better support for behaviour-based management. Recent progresses in computer vision provide possible solutions for the above limitations. The following is a review on related computer vision algorithms.

2.2 Pose estimation in computer vision

Pose estimation is a classical problem in computer vision. With the development of deep learning, the performance of pose estimation algorithms has been enhanced a lot [25]. The pose estimation algorithms focus on mainly two tasks: 1) 2D pose estimation, which aims to evaluate 2D joint locations from RGB images, 2) 3D pose estimation, which aims at inferring the depth of each joint based on 2D joint locations. The 2D pose estimation algorithms, open pose [26], has been successfully applied on construction sites to estimate 2D construction postures, which worked well even over long distances or when some parts of the body were obstructed [27]. 3D pose estimation algorithms, however, performed not very well when applied in estimating the postures of construction workers. The gaps are 1) previous 3D pose dataset for training the 3D pose estimation algorithms are mainly

daily life postures, such as sitting, taking and calling, which differ a lot with the postures of the construction workers, and 2) the structures and parameters of the algorithms are not suitable for estimating the 3D postures of construction workers.

3 Research aim and contribution

Considering above research gaps and limitations, this study tries to develop 3D pose estimation algorithm that is suitable for the postures of construction workers. The method could estimate the 3D joint locations based on RGB images in near real time. This method makes it possible to continuously collect 3D pose data from construction site videos and contributes to 3d-pose-data-based behavior management, such as identifying unsafe behavior postures, estimating joint workloads and assessing labor productivity.

4 Methodology

This study aims to train a 3D pose estimation according to 2D pose with transfer learning [25]. To reach the aim, a 3D database of the postures in construction tasks was firstly built, then a deep learning network was trained based on the dataset.

4.1 Establish the training database

The training dataset includes the 3D joint location data of construction tasks and the corresponding 2D joint locations. A laboratory experiment was performed to establish the dataset with an IMU system (3-Space™ Wireless 2.4GHz DSSS, OH, USA).

4.1.1 Collecting 3D posture data

Participants: A healthy male graduate student, aged 27 years, was recruited to perform a simulated plastering task in a laboratory.

Equipment: The participant was required to wear the IMU system to collect 3D posture data. The IMU sensor has an accuracy of 1° and an frequency of 50 Hz [28]. The IMU system includes 13 IMU sensors. They were tightly tied to the head, chest, back, waist, upper arms, forearms, thighs and shanks.

Simulated plastering task: After putting on the IMU sensors, the participant was instructed to perform a simulated plastering task. The participant mimiced the motion of plastering an area of 5 meters width and 2 meters height. To calibrate the IMU system before the task, the paricipant was requried to stand with both feet closed together and both arms stretched out to the sides and held parallel to the ground to form a T shape.

4.1.2 Data processing

The results of the IMU system were 1397 frames of postures. The data was stored in a BVH file, which includesdthe three-axis rotations of each body segments in each frame. The 3D joint locations were calculated based on the three-axis rotations angles and the length of each body segment with Denavit-Hartenberg matrix [29].

Then the 2D joint locations were calculated based on the 3D joint locations with projection matrix. The generated 2D joint locations are related to the location of the camera. In this study, given the hip joint as the origin, the spherical coordinate of the camera is (0°, 75°, 20 m).

4.1.3 Dataset structure

The dataset includes input dataset and target dataset. The input dataset is a matrix with 1397 rows and 48 columns. Each row stores the 3D Cartesian coordinates of 16 joints (head, neck, chest, waist, trunk, central hip, bilateral shoulders/elbows/wrists/hips/knees/ankles). The target dataset is matrix with 1397 rows and 32 columns. Each row stores the 2D Cartesian coordinates of the 16 joints.

For training and testing the algorithms, the dataset was divided into two parts. 1000 rows were randomly selected from the input dataset and target dataset respectively to form the training dataset. The rest rows of the input dataset and target dataset were used for testing the performance of the algorithm.

4.2 Network architecture

The network is composed of several basic network unit. Each unit includes a linear layer and an RELU layers. The linear layer aims to increase the dimensions of the input data to ensure the depth of the networks. The RELU layer next to the linear layer could add non-linearities to the deep neural networks [30]. The residual connections could improve generalization performance and reduce training time [25]. Figure 1 shows the network architecture.

The complexity of the network is decided on the width of linear layers and the numbers of the basic network units. Complex network could increase the accuracy but is prone to overfitting and computationally expensive. In the experiments, various combinations of the width of linear layers and the numbers of the basic network units were tested to decide the proper complexity.

In addition, batch normalization, dropout and max-norm constraints were applied to prevent overfitting and speed up training. Batch normalization allows us to use larger learning rates to accelerate the learning process [31]. Dropout randomly drops components from a layer of neural network, and thus could prevent overfitting and improve the generalization performance [32]. Max-norm constraints enforce an absolute upper bound on the norm of the weight of every neuron, which helps to prevent overfitting.

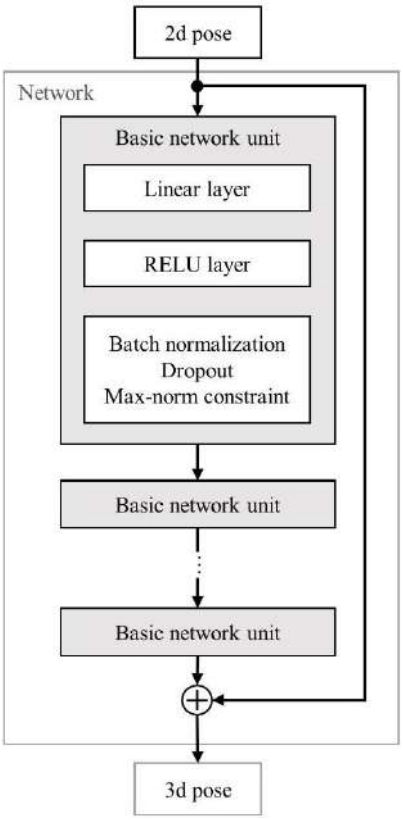

Figure 1. The convergence of training loss (learning rate = 10^{-3}, batch size = 32)

5 Experiment and results

The aim of the experiment is to decide the proper network complexity and the weights of every nodes in the network. In the following training process, the loss function is defined as mean-squared loss and optimized with Adam algorithm [33]. The dropout rate is 0.5. The max-norm constraint is 1.

5.1 Network complexity

As aforementioned, the complexity of the network has a great influence on the network performance. This experiment aims to find the proper network complexity. We change the depth and width of the network through edit the number of basic units (2, 3, 4) and the number of nodes in each linear layer (512, 1024, 2048). As a result, nine different networks were generated. They were trained based on the training dataset, and the accuracy was tested on the testing dataset. In this experiment, the initial learning rate was set as 1e-4, and the batch size was set as 32. Each network was trained for 400 epochs. Table 1 provides the comparison of the performance of the nine networks.

Table 1. The comparison of the performance of different network structures

No. of basic units	No. of layer nodes	Training loss	Test error [cm]	Testing time [ms/frame]
2	512	376.99	24.77	0.09
3	512	78.29	7.76	0.09
4	512	37.67	7.64	0.10
2	1024	29.18	7.16	0.09
3	1024	21.11	5.42	0.09
4	1024	16.09	5.39	0.10
2	2048	13.89	3.46	0.10
3	**2048**	**9.52**	**3.23**	**0.11**
4	2048	8.65	3.42	0.12

Table 1 compares the nine networks according to training loss, testing error and testing time. Training loss represents the final value of loss function. A smaller training loss is preferable. The trained network was then used to estimate the 3D joint locations according to the inputs data in the test database. The estimation results were then compared with the target data. The testing error is defined as the mean of the distances between the estimated 3D location and the target 3D locations of the 16 joints. The last column of Table 1 is the time spent on estimating the 3D joint locations in one frame.

Based on the comparison of the nine networks in Table, it could be found that the increasing the width and depth of the network could significantly decreases the training loss and the testing error. The network with three basic units and 2048 nodes of each layer was selected for the lowest testing error.

5.2 Training the network

Learning rate and batch size decide the step and direction of the training loss decrease, thus are important for the convergence of the loss function. This experiment tried different combinations of learning rate and batch size for training loss convergence and low testing error. Based on the comparison of different network structures in section 5.1, the network with three basic units and 2048-node-layers were used in this

experiment. The combination of different learning rates (1e-3, 1e-4, 1e-5) and different batch sizes (2, 4, 8, 16, 32, 64, 128, 256, 512) were tested. Table 2, Table 3 and Table 4 show the comparison of training loss, testing error and testing time for each

Table 2. The comparison of the training loss with different learning rates and batch sizes

LR* / BS**	10^{-3}	10^{-4}	10^{-5}
2	155.02	2348.89	9583.45
4	50.81	85.68	7113.02
8	19.60	42.38	6772.76
16	7.92	23.43	6494.98
32	**5.44**	13.76	6175.47
64	10.11	9.52	5783.18
128	12.71	8.87	6016.59
256	21.66	9.44	6953.94
512	36.92	116.06	8243.36

*LR represents learning rate.
** BS represents batch size.

Table 3. The comparison of the test error with different learning rates and batch sizes

LR / BS	10^{-3}	10^{-4}	10^{-5}
2	62.53*	118.41	169.39
4	4.88	11.25	153.75
8	2.51	5.55	148.94
16	1.44	3.99	142.30
32	**1.10**	3.61	134.36
64	2.76	3.23	125.55
128	3.60	2.87	126.82
256	7.60	2.80	136.83
512	24.46	16.61	150.19

*The unit is cm.

Table 4. The comparison of the testing time with different learning rates and batch sizes

LR / BS	10^{-3}	10^{-4}	10^{-5}
2	0.53*	0.53	0.53
4	0.31	0.31	0.31
8	0.20	0.20	0.20
16	0.14	0.14	0.14
32	0.12	0.11	0.11
64	0.11	0.11	0.11
128	0.10	0.10	0.10
256	0.09	0.09	0.09
512	0.09	0.09	0.09

*The time spent in estimating 3D posture of one frame of 2D posture. The unit is ms.

According to Table 2 and Table 3, both the training loss and testing error reached the minimum when the learning rate was 10^{-3} and the batch size was 32. Table 4 shows that the above combination is also time-saving. In addition, Figure 2 shows the process of training loss convergence under above learn rate and batch size.

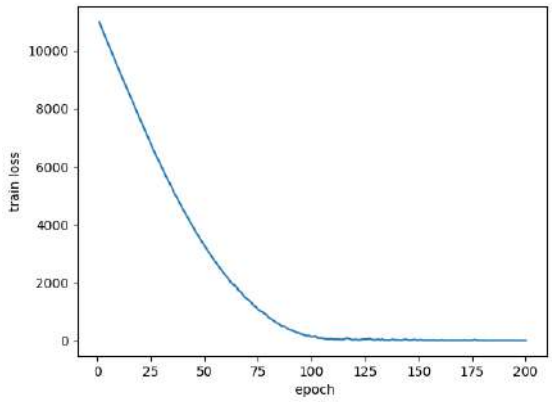

Figure 2. The convergence of training loss (learning rate = 10^{-3}, batch size = 32)

5.3 Testing the results

To this end, the network with 3 basic units, 2048-node-layers, and trained learning rate = 10^{-3}, batch size = 32 was selected. Table 5 shows the mean error of each joints. The mean error of all the joints is 1.10 cm, and the standard deviation is 0.45 cm.

Table 5. The comparison of the performance of different network structures

Joint	Mean error [cm]	Standard deviation [cm]
Waist	0.27	0.28
Right hip	0.46	0.30
Right knee	1.25	1.07
Right ankle	1.51	1.27
Left hip	0.46	0.25
Left knee	1.05	0.99
Left ankle	1.55	1.61
Chest	0.52	0.32
Neck	0.91	0.52
Head	0.94	0.50
Left shoulder	1.08	0.66
Left elbow	1.38	0.78
Left wrist	1.54	0.81
Right shoulder	0.99	0.63
Right elbow	1.60	0.78

Right wrist	2.16	1.08
Mean	1.10	0.45

Figure 3 is the histogram of the mean error of the joints in each frame. The maximum error is about 3.0 cm. Most of the errors are between 0.5 cm and 1.5 cm. The mean error is 1.10 cm, and the standard deviation is 0.45 cm.

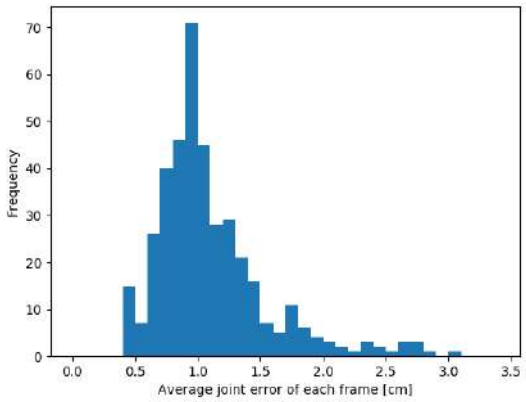

Figure 3. The histogram of the mean error of the joints in each frame

Figure 4 is an intuitive presentation of the estimation results. It could be found that the estimation postures are nearly the same with the ground truth.

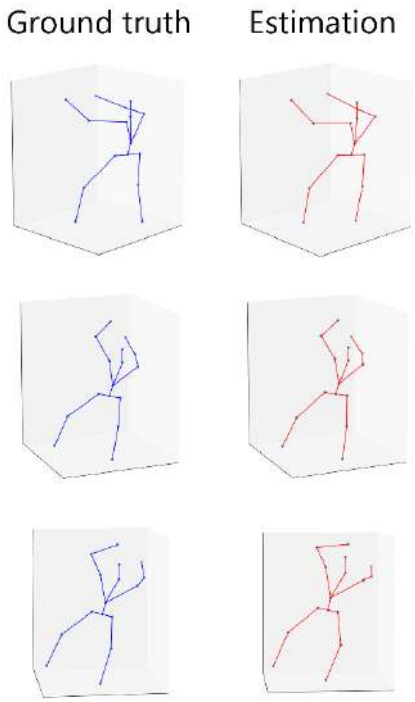

Figure 4. The estimated 3D postures and the ground truth data

6 Discussion

3D postures of construction workers are very important to safety, health and productivity management. This method provides a 3D posture estimator based on workers' 2D postures. The results show that the method could provide accurate 3D posture estimations in nearly real time. The latency time for testing one frame on a GTC 1080Ti GPU was 0.12 ms. The mean error of each joint was 1.10 cm. The accuracy was significantly improved compared with previous computer vision 3D pose estimation methods in construction industry, the mean joint error of which was 3.5 cm [34].

Compared with previous motion capture methods in construction industry, the proposed method was non-intrusive and could work well in outdoor environments. In addition, if combined with 2D posture estimation programs, such as Open Pose [35], the method could make it possible to collect construction workers' 3D postures continuously and timely, providing the data foundation for behavior-based safety, health and production management.

The method has the following limitations and could be improved in the future. First of all, the training dataset is not large enough. The dataset used in this study only includes the postures of one participant during plastering, which may limit the generalization

performance of the method. In future, a more diversified training database should be established, which includes the posture data of different construction tasks collected from participants of different heights, weights and BMIs.

Secondly, the 2D postures were generated from 3D posture based on projection matrix. In the current study, only one projection view was used. In the following studies, the 2D postures generated in different views could be used to train the 3D posture estimation method, so that it could be more applicable on construction sites.

Finally, the current study aims to estimate 3D postures from 2D postures. Future studies could try to combine it with 2D posture estimation method from RGB images, so that the 3D postures could be directly inferred from construction site videos or images.

7 Conclusion

Construction workers' posture data provides the foundation for working behavior analysis, such as unsafe behavior identification, ergonomic assessment and labor production evaluation. This paper established a preliminary 3D posture dataset of construction tasks and provided a 3D posture estimation method based on 2D joint locations. The results showed that the method could estimate 3D postures accurately and timely. The mean joint error and estimation time of each frame were 1.10 cm and 0.12 ms respectively. This method makes it possible to estimate construction workers' 3D postures from the images of construction sites and contributes to a data-based construction workers' behavior management.

References

[1] H.W. Heinrich, D. Petersen, N. Roos, Industrial accident prevention: a safety management approach, McGraw-Hill, Tokyo, 19800070280614.

[2] J. Seo, M. Moon, S. Lee, Construction Operation Simulation Reflecting Workers' Muscle Fatigue, in: Computing in Civil Engineering, American Society of Civil Engineers, Reston, VA, 2015: pp. 515–522. doi:10.1061/9780784479247.064.

[3] D. Wang, F. Dai, X. Ning, Risk Assessment of Work-Related Musculoskeletal Disorders in Construction: State-of-the-Art Review, Journal of Construction Engineering and Management. 141 (2015) 04015008. doi:10.1061/(ASCE)CO.1943-7862.0000979.

[4] S.P. Dozzi, S.M. Abourizk, Productivity in Construction, Institute for Research in Construction, National Research Council, Ottawa, ON, Canada, 19930662211340.

[5] Y. Yu, H. Guo, Q. Ding, H. Li, M. Skitmore, An experimental study of real-time identification of construction workers' unsafe behaviors, Automation in Construction. 82 (2017) 193–206. doi:10.1016/j.autcon.2017.05.002.

[6] L. Ding, W. Fang, H. Luo, P.E.D. Love, B. Zhong, X. Ouyang, A deep hybrid learning model to detect unsafe behavior: Integrating convolution neural networks and long short-term memory, Automation in Construction. 86 (2018) 118–124. doi:10.1016/j.autcon.2017.11.002.

[7] Y. Yu, X. Yang, H. Li, X. Luo, H. Guo, Q. Fang, Joint-Level Vision-Based Ergonomic Assessment Tool for Construction Workers, Journal of Construction Engineering and Management. 145 (2019) 04019025. doi:10.1061/(ASCE)CO.1943-7862.0001647.

[8] X. Yan, H. Li, A.R. Li, H. Zhang, Wearable IMU-based real-time motion warning system for construction workers' musculoskeletal disorders prevention, Automation in Construction. 74 (2017) 2–11. doi:10.1016/j.autcon.2016.11.007.

[9] X. Luo, H. Li, X. Yang, Y. Yu, D. Cao, Capturing and Understanding Workers' Activities in Far-Field Surveillance Videos with Deep Action Recognition and Bayesian Nonparametric Learning, Computer-Aided Civil and Infrastructure Engineering. 34 (2019) 333–351. doi:10.1111/mice.12419.

[10] H. Guo, Y. Yu, M. Skitmore, Visualization technology-based construction safety management: A review, Automation in Construction. 73 (2017) 135–144. doi:10.1016/j.autcon.2016.10.004.

[11] S.M.E. Sepasgozar, P. Forsythe, S. Shirowzhan, Evaluation of Terrestrial and Mobile Scanner Technologies for Part-Built Information Modeling, Journal of Construction Engineering and Management. 144 (2018) 04018110. doi:10.1061/(ASCE)CO.1943-7862.0001574.

[12] W.P. Neumann, R.P. Wells, R.W. Norman, J. Frank, H. Shannon, M.S. Kerr, A posture and load sampling approach to determining low-back pain risk in occupational settings, International Journal of Industrial Ergonomics. 27 (2001) 65–77. doi:10.1016/S0169-8141(00)00038-X.

[13] M. Otsuka, T. Nishimura, A. Seo, K. Doi, Relationship between Work Position and Physical Work Load during Insertion of Pin Connectors(Theory and Methodology), Journal of Japan Industrial Management Association. 61 (2010) 275–283.

https://ci.nii.ac.jp/naid/10027761503/en/.

[14] E. Valero, A. Sivanathan, F. Bosché, M. Abdel-Wahab, Musculoskeletal disorders in construction: A review and a novel system for activity tracking with body area network, Applied Ergonomics. 54 (2016) 120–130. doi:https://doi.org/10.1016/j.apergo.2015.11.020.

[15] J. Chen, J. Qiu, C. Ahn, Construction worker's awkward posture recognition through supervised motion tensor decomposition, Automation in Construction. 77 (2017) 67–81. doi:10.1016/j.autcon.2017.01.020.

[16] H. Jebelli, C.R. Ahn, T.L. Stentz, Fall risk analysis of construction workers using inertial measurement units: Validating the usefulness of the postural stability metrics in construction, Safety Science. 84 (2016) 161–170. doi:10.1016/j.ssci.2015.12.012.

[17] A. Alwasel, M. Nahangi, C. Haas, E. Abdel-Rahman, Level-of-Expertise Classification for Identifying Safe and Productive Masons, in: Computing in Civil Engineering 2017, 2017. doi:10.1061/9780784480823.043.

[18] A. Golabchi, S. Han, J. Seo, S. Han, S. Lee, M. Al-Hussein, An Automated Biomechanical Simulation Approach to Ergonomic Job Analysis for Workplace Design, Journal of Construction Engineering and Management. 141 (2015) 04015020. doi:10.1061/(ASCE)CO.1943-7862.0000998.

[19] VICON Motion Capture System, (2018). https://www.vicon.com (accessed April 18, 2018).

[20] J. Hicks, Preparing your data for OpeinSim 3.3, National Center for Simulation in Rehabilitation Research (NCSRR), US. (2018). https://simtk-confluence.stanford.edu:8443/display/OpenSim33/Preparing+Your+Data (accessed December 24, 2018).

[21] C. Liu, S. Shirowzhan, S.M.E. Sepasgozar, A. Kaboli, Evaluation of Classical Operators and Fuzzy Logic Algorithms for Edge Detection of Panels at Exterior Cladding of Buildings, Buildings. 9 (2019) 40. doi:10.3390/buildings9020040.

[22] M. Liu, S. Han, S. Lee, Tracking-based 3D human skeleton extraction from stereo video camera toward an on-site safety and ergonomic analysis, Construction Innovation. 16 (2016) 348–367. doi:10.1108/CI-10-2015-0054.

[23] X. Luo, H. Li, D. Cao, Y. Yu, X. Yang, T. Huang, Towards efficient and objective work sampling: Recognizing workers' activities in site surveillance videos with two-stream convolutional networks, Automation in Construction. 94 (2018) 360–370. doi:10.1016/j.autcon.2018.07.011.

[24] H. Zhang, X. Yan, H. Li, Ergonomic posture recognition using 3D view-invariant features from single ordinary camera, Automation in Construction. 94 (2018) 1–10. doi:10.1016/j.autcon.2018.05.033.

[25] J. Martinez, R. Hossain, J. Romero, J.J. Little, A simple yet effective baseline for 3d human pose estimation, ArXiv Preprint ArXiv:1705.03098. (2017).

[26] Z. Cao, T. Simon, S.-E. Wei, Y. Sheikh, Realtime Multi-Person 2D Pose Estimation using Part Affinity Fields, CVPR2017. (2016). http://arxiv.org/abs/1611.08050.

[27] X. Yan, H. Li, C. Wang, J. Seo, H. Zhang, H. Wang, Development of ergonomic posture recognition technique based on 2D ordinary camera for construction hazard prevention through view-invariant features in 2D skeleton motion, Advanced Engineering Informatics. 34 (2017) 152–163. doi:10.1016/j.aei.2017.11.001.

[28] Yost Labs, 3-Space™ Sensors, Yost Labs. (2017). https://yostlabs.com/3-space-sensors/ (accessed April 19, 2018).

[29] G. Legnani, F. Casolo, P. Righettini, B. Zappa, A homogeneous matrix approach to 3D kinematics and dynamics — I. Theory, Mechanism and Machine Theory. 31 (1996) 573–587. doi:10.1016/0094-114X(95)00100-D.

[30] V. Nair, G.E. Hinton, Rectified Linear Units Improve Restricted Boltzmann Machines, in: Proceedings of the 27th International Conference on International Conference on Machine Learning, Omnipress, USA, 2010: pp. 807–814. http://dl.acm.org/citation.cfm?id=3104322.3104425.

[31] S. Ioffe, C. Szegedy, Batch Normalization: Accelerating Deep Network Training by Reducing Internal Covariate Shift, (2015). http://arxiv.org/abs/1502.03167.

[32] N. Srivastava, G. Hinton, A. Krizhevsky, I. Sutskever, R. Salakhutdinov, Dropout: A Simple Way to Prevent Neural Networks from Overfitting, J. Mach. Learn. Res. 15 (2014) 1929–1958. http://dl.acm.org/citation.cfm?id=2627435.2670313.

[33] D.P. Kingma, J. Ba, Adam: A Method for Stochastic Optimization, (2014). http://arxiv.org/abs/1412.6980.

[34] Y. Yu, H. Li, X. Yang, W. Umer, Estimating Construction Workers' Physical Workload by Fusing Computer Vision and Smart Insole Technologies, in: 2018 Proceedings of the 35th ISARC, International Association for Automation and Robotics in Construction, Berlin, Germany, 2018: pp. 1212–1219. doi:10.22260/ISARC2018/0168.

[35] Z. Cao, G. Hidalgo, T. Simon, S.-E. Wei, Y. Sheikh, OpenPose: Realtime Multi-Person 2D Pose Estimation using Part Affinity Fields, (2018). http://arxiv.org/abs/1812.08008.

A Low-Cost and Smart IMU Tool for Tracking Construction Activities

X. Yang[a,b,*], F. Wang[a], X. Zhai[a], H. Li[b], Y. Yu[b], and X. Luo[b]

[a]School of Civil Engineering, Harbin Institute of Technology, Harbin, China
[b]Department of Building and Real Estate, The Hong Kong Polytechnic University, Hong Kong
E-mail: xincong.yang@outlook.com, fl-wang@hit.edu.cn, xmzhai@hit.edu.cn, yt.yu@connect.polyu.hk, heng.li@polyu.edu.hk, eric.xiaochun.luo@polyu.edu.hk

Abstract –

Real-time activity monitoring is becoming one of the most significant technologies on construction sites because it can be applied to a variety of management problems, such as productivity formula and safety monitoring. However, current monitoring technologies are limited to recognizing postures in an ideal environment rather than dealing with the ambient occlusion and people-intensive situations on real construction sites. Therefore, this study develops a low-cost, non-intrusion and portable tool system in order to trace and track construction activities on complex and crowed construction sites. This system is composed of wireless sensors and a smart algorithm. Each sensor consists of an inertial measurement unit, a communication sensor (bluetooth low energy sensor) and several environmental sensors, which broadcasts the identification, acceleration, palstance and environmental measurements at a constant frequency. Since the dimension of the sensor is only 20 x 15 x 2 mm, it can be easily attached or screwed on to the hand tools as well as integrated with power tools. When a laptop or cell phone receives from these sensors, the construction activities are derived by the artificial intelligence algorithm in a timely manner, providing an visual posture monitoring as well as an automatic record of project progress. In the end, practical experiments of a concrete vibrator and a hammer prove the feasibility and effectiveness of the proposed IMU-based tool tracing and tracking system.

Keywords –

Inertial measurement unit; Construction tools; Activity recognition; Non-intrusive; Low-cost

1 Introduction

Construction is a typical labor-intensive industry that a variety of construction assignments are accomplished manually, such as wood formwork, bar bending and tying, concrete pouring, etc. Therefore, the on-site construction activity is one of the critical resources contributing to the construction project performance, and its effective control and management is always considered as a key to success [1]. By tracking workers-on-foot and construction heavy equipment, near-misses, collisions and safety risks can be prevented and alleviated [2], dangerous and awkward postures can be detected and alarmed [3], productivity can be measured in a timely and quantitative manner [4-6], etc.

The main obstacle for automated construction activity control and management is the real-time activity tracking. State-of-the-art technologies, including computer vision, wearable sensor, etc., which are available for on-site motion tracking, are emerging; however, the installation or monitoring process is intrusive and the effectiveness is seriously affected by complicated environment, such as none-line-of-sight effect due to ambient occlusions and multipath effect by signal reflection.

The purpose of the present study is to develop a smart and low-cost IMU-based tool system and test the feasibility for on-site activity tracking. The research introduced the novel concept and established the framework of the proposed system at first, developed a general prototype and an effective algorithm for construction works using cyclic patterns, and finally, conducted a pilot study to validate the system [7].

2 Background

The conventional way to monitor construction activities is human inspection, which is still the popular at the present time. An inspector roams around the site at regular intervals, the records the observation and draws a daily or weekly report. Once awkward or dangerous postures are recognized, the inspector send alarms and prevent further damage to the health and safety of workers. This is a commendable achievement, but it requires full time observation, which is impossible

and inefficiency for such a large field as construction site [8].

In the recent times, cutting-edge sensors are introduced to evaluate the spatial-temporal activities in the construction industry by attaching inertial and biomechanical sensors on human body segments [9]. The earliest instruments for linear posture detection are tapes and goniometer, and further progress is the advent of electromyographic devices (EMG) that using the muscle strength to access the movement and rotation. However, these devices are only used in clinical environments as they are tedious and intrusive to deploy [10]. With the emergence and development of micro-electro-mechanical system (MEMS), the device measuring the inertial properties of objects becomes small while the accuracy, robustness and quick response are improved dramatically, which is called inertial measurement unit (IMU). Nowadays, commercial IMU is usually made up of a tri-axis gyroscope and a tri-axis accelerometer (6-axis IMU), and a tri-axis magnetometer (9-axis IMU), enabling the measurement of acceleration, angular velocity, and magnetic field [11]. Scholars have applied this technology to detect awkward postures to prevent musculoskeletal disorders [3, 12, 13], near-misses and hazards are also recognized automatically and analyzed to assess the potential risks [14].

Another popular way to monitor construction activities is by computer vision, which can be briefly categorized into three types according to their instruments: monocular, binocular and depth cameras [1]. Compared with sensor-based activity monitoring, CV-based methods are visual and insightful, enabling to record various information, not only workers but also associated contexts [15]. At the beginning, computer vision is used to localize construction resources, including manpower, excavators, cranes, etc., providing a picture of space use on sites [16], predicting the proximity conflicts [17, 18]. After that, with the advent of deep learning techniques, motion recognition and tracking is available that specific body skeleton can be extracted from images or videos. Scholars then transform the technology into monitoring construction activities [19-21]. Risky and dangerous behaviors, such as falling from heights, not wearing a hat or personal protective equipment, hazardous materials, etc. are identified by cameras.

The pros of sensor-based human posture detection contain direct and simple measuring principle, high accuracy and frequency, as well as low latency and cost. However, the cons of this detection are also distinct that the deployment is tedious and intrusive as people are prone to suffer from discomfort and motion restriction by the attached sensors. What's more, the privacy issue of monitoring the personal data also exacerbates the problem. On the other hand, the considerable advantages CV-based human posture detection consist of non-intrusion into normal construction activities, easy deployment, remote monitoring, tremendous potential for artificial intelligence. Nevertheless, some disadvantages hinder the wide applications in practice. A primary disadvantage of CV-based human posture detection is the legal issue of intrusion of privacy that employees may object to being filmed under constant surveillance. Another disadvantage is the cost. As construction sites are always huge, high-resolution cameras are required, added by the instruments for transmission, compression and storage, it is expensive to purchase and keep the detection algorithms upgraded all the time. The third disadvantage is the non-line-of-sight (NLoS) effect due to ambient occlusions that CV-based detection performs badly without direct observations. What's more, the illumination and transparency of exposed environment also have an adverse impact on the detection. Other disadvantages, such as low accuracy and high latency or frame loss, weaken the applicable ability in construction industry as well.

Either sensor-based or CV-based human posture detection has exposed their weaknesses in literature and practice. This research therefore proposes a novel approach that leveraging the location and posture of a hand tool or power tool to detect the corresponding human postures by a single MEMS-IMU [22, 23]. This creative conceptual approach is not only a positive solution of personnel concerns and privacy that employees are not working under immediate surveillance, but also a non-intrusive and marker-less solution of human posture detection.

3 Framework for tracking construction activities by tools

This is an insightful conception that the way human beings make and use tools is perhaps what sets us apart more than anything else. In turn, tools also have positive impacts on our evolution. Workers in modern industries are always carry out their jobs with the assistance of valuable tools.

Construction is a typical labor-intensive industry that a variety of construction assignments are accomplished manually. To improve the productivity and ensure the safety, diverse tools are designed and adopted on constriction sites, containing hand tools (tape measure, torpedo level, screwdriver, wrench, trowel, hammer, coping saw, etc.), as well as power tools (circular saw, drill. jig saw, orbit sander, angle grinder, etc.) in Figure 1.

Figure 1. Common hand and power tools can be integrated with an IMU sensor

Thus, for these kinds of jobs using various assistant tools, the motions of tools apparently describe the detailed process of construction activities. For example, the trajectory of concrete vibrator suggests the area of concrete consolidation after pouring; the angular rotation of screwdriver indicates the effects of workers on the connection of reinforcement bars. The data of tools therefore not only suggest the status of construction activities, but also work as an event data recorder that record the associated information during specific events. When an accident happens, the information can be collected for analysis, to identify the status before, during and after the accident.

The schematic model for this tool-based construction activity monitoring is illustrated in Figure 2. To monitor the construction activities, manual assignments are transformed into tool motions at first. For example, the acceleration of tools indicates the workload at the construction stage; the velocity and angular velocity (palstance) exposes the mobile characteristics of workers; and position, rotation of tools provides a relative reference of the postures of workers. Then the construction regulations, standards, or codes are represented by tool rules. By comparing the tool data and these rules, it is a quantitative way to determine whether the actual construction activity is in conformity to the existing strict regulations [24].

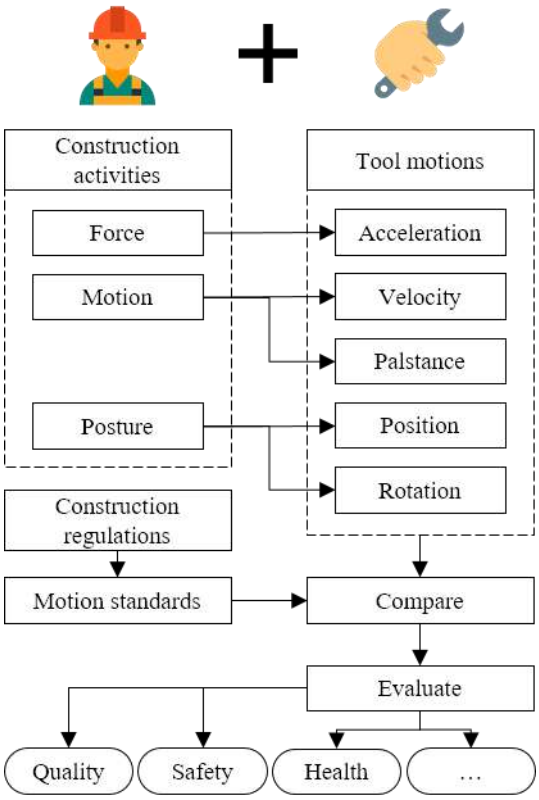

Figure 2. Schematic model for the IMU tool system

4 Data collection method

Various methods can be considered for the implementation of the framework for tracking the construction activities on-site. Among the current cutting-edge technologies, electro-mechanical system inertial measurement units (MEMS-IMUs) are economic and easy-handling.

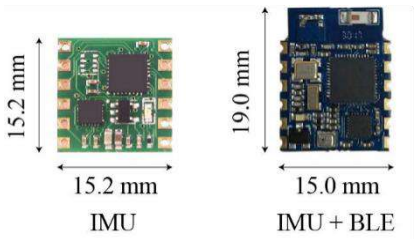

Figure 3. IMU and IMU+BLE sensors to collect tool data

As shown in Figure 3, the sensors are quite small and light, which can be integrated with power tools or installed on hand tools. This simple deployment ensures the non-intrusion during the construction stage.

These sensors are able to collect acceleration and angular velocity as a tri-accelerometer and a tri-gyroscope are imbedded in. Therefore, the task diagram

of IMU sensors is described in Figure 4. The IMU starts with measuring acceleration and angular velocity, and the calibrate each other according to the earth model. The adjusted acceleration is integral to produce velocity, and integral twice to generate displacement. Meanwhile the calibrated angular velocity is then integral to obtain the rotation and orientation at each time interval. By differential operation, the angular velocity can extract the angular acceleration as well. Noted that the magnetometer is more sensitive to tiny changes in direction, 9-axis is more common in applications as the measurement of magnetic field improve the accuracy significantly by calibrating at a high frequency.

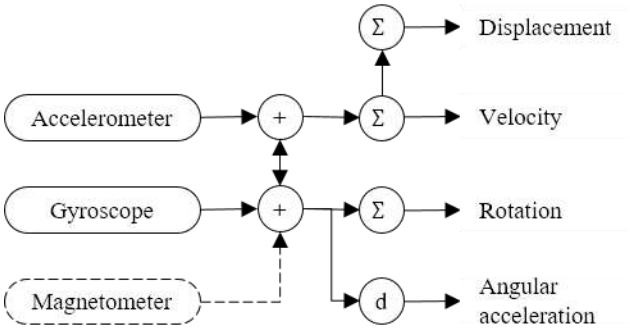

Figure 4. Task diagram of IMUs

The kinematics of a rigid body like a tool is composed of translation and rotation. This research only focuses on the rotation component as it produces considerable impacts on bar connections. Although the initial data collected by MEMS-IMU is in Euler angle form, here the orientation is represented in quaternion form which is simple and efficient in transforming computation. Thus, a rotation around axis $\boldsymbol{n}$ with an angle of θ is represented by

$$\boldsymbol{Q} = \left[\cos\left(\frac{\theta}{2}\right), \sin\left(\frac{\theta}{2}\right)\boldsymbol{n}\right] = [q_0, q_1, q_2, q_3] \tag{1}$$

While the orientation $\boldsymbol{R}$ is denoted by

$$\boldsymbol{R} = [0, \boldsymbol{r}] = [0, r_1, r_2, r_3] \tag{2}$$

The corresponding differential function is written by

$$\frac{\mathrm{d}\boldsymbol{Q}}{\mathrm{d}t} = \frac{1}{2}\boldsymbol{Q} \otimes \boldsymbol{\omega}_{\mathrm{nb}}^{\mathrm{b}} \tag{3}$$

where $\boldsymbol{\omega}_{\mathrm{nb}}^{\mathrm{b}} = [\omega_x \quad \omega_y \quad \omega_z]^{\mathrm{T}}$, refers to the angular velocity of each axis. And the matrix form of formula can be represented by

$$\begin{bmatrix} \dot{q_0} \\ \dot{q_1} \\ \dot{q_2} \\ \dot{q_3} \end{bmatrix} = \begin{bmatrix} 0 & -\omega_x & -\omega_y & -\omega_z \\ \omega_x & 0 & \omega_z & -\omega_y \\ \omega_y & -\omega_z & 0 & \omega_x \\ \omega_z & \omega_y & -\omega_x & 0 \end{bmatrix} \begin{bmatrix} q_0 \\ q_1 \\ q_2 \\ q_3 \end{bmatrix} \tag{4}$$

As the MEMS-IMU measures the angular velocity at a constant frequency, the iteration formulation is

$$\boldsymbol{Q}(t+1) = (\boldsymbol{I}\cos\frac{2\Delta\theta}{2} + \Delta\boldsymbol{\Omega}\frac{\sin\frac{2\Delta\theta}{2}}{\Delta\theta})\boldsymbol{Q}(t) \tag{5}$$

where $\Delta\boldsymbol{\Omega} = \begin{bmatrix} 0 & -\Delta\theta_x & -\Delta\theta_y & -\Delta\theta_z \\ \Delta\theta_x & 0 & \Delta\theta_z & -\Delta\theta_y \\ \Delta\theta_y & -\Delta\theta_z & 0 & \Delta\theta_x \\ \Delta\theta_z & \Delta\theta_y & -\Delta\theta_x & 0 \end{bmatrix}$, refers to the direct output of MEMS-IMU, $\Delta\theta = \sqrt{\Delta\theta_x^2 + \Delta\theta_y^2 + \Delta\theta_z^2}$ is the total changes of angular velocity.

The initial quaternion is determined be the transformation matrix from the earth frame to the sensor body frame, which is represented by

$$\begin{aligned} \boldsymbol{C}_{\mathrm{n}}^{\mathrm{b}} &= [\boldsymbol{c_1}, \boldsymbol{c_2}, \boldsymbol{c_3}] \\ \boldsymbol{c_1} &= \begin{bmatrix} q_0^2 + q_1^2 - q_2^2 - q_3^2 \\ 2(q_1q_2 + q_0q_3) \\ 2(q_1q_3 - q_0q_2) \end{bmatrix} \\ \boldsymbol{c_2} &= \begin{bmatrix} 2(q_1q_2 - q_0q_3) \\ q_0^2 - q_1^2 + q_2^2 - q_3^2 \\ 2(q_2q_3 + q_0q_1) \end{bmatrix} \\ \boldsymbol{c_3} &= \begin{bmatrix} 2(q_1q_3 + q_0) \\ 2(q_2q_3 - q_0q_1) \\ q_0^2 - q_1^2 - q_2^2 + q_3^2 \end{bmatrix} \end{aligned} \tag{6}$$

At the same time, $\|\boldsymbol{Q}\| = 1$ that each quaternion of rotation and orientation is normalized.

Although the integral approach appears to be accurate in theory, random noise, signal bias, etc. accumulates overtime. To improve the robustness and accuracy of rotation measurement, acceleration and magnetic field data collected by accelerometer and magnetometer are fused to orientation estimation by gyroscopes as well. Given a specific construction field, the direction of gravity and magnetic field are known. An orientation of the sensor frame relative to the earth frame is therefore calculated by comparing the measurement by gyroscope and by accelerometer and magnetometer.

If the rotation quaternion relates the earth frame to the sensor body frame is denoted by $\boldsymbol{q}_{\mathrm{e}}^{\mathrm{b}}$, the expected measurement of acceleration and magnetic field in the earth frame is denoted by $\boldsymbol{d}^{\mathrm{e}}$, meanwhile these in the sensor body frame measured in real-time is represented by $\boldsymbol{s}^{\mathrm{b}}$. The fusion of acceleration data and magnetic field data is modeled as an optimization problem. The objective function is

$$f(\boldsymbol{q}_{\mathrm{e}}^{\mathrm{b}}, \boldsymbol{d}^{\mathrm{e}}, \boldsymbol{s}^{\mathrm{e}}) = \boldsymbol{q}_{\mathrm{e}}^{\mathrm{b}*} \otimes \boldsymbol{d}^{\mathrm{e}} \otimes \boldsymbol{q}_{\mathrm{e}}^{\mathrm{b}} - \boldsymbol{s}^{\mathrm{b}} \tag{7}$$

To approximate to the minimum of the objective function, the corresponding gradient of the objective function is written by

$$\nabla f\left(\boldsymbol{q}_{\mathrm{e}}^{\mathrm{b}}, \boldsymbol{d}^{\mathrm{e}}, \boldsymbol{s}^{\mathrm{e}}\right) = \boldsymbol{J}^{\mathrm{T}}\left(\boldsymbol{q}_{\mathrm{e}}^{\mathrm{b}}, \boldsymbol{d}^{\mathrm{e}}\right) f\left(\boldsymbol{q}_{\mathrm{e}}^{\mathrm{b}}, \boldsymbol{d}^{\mathrm{e}}, \boldsymbol{s}^{\mathrm{e}}\right) \quad (8)$$

where $\boldsymbol{J}$ is the Jacobian matrix.

For acceleration data,

$$\boldsymbol{s}^{\mathrm{e}} = [0 \quad 0 \quad 0 \quad 1] \quad (9)$$

$$f\left(\boldsymbol{q}_{\mathrm{e}}^{\mathrm{b}}, \boldsymbol{a}^{\mathrm{e}}, \boldsymbol{s}^{\mathrm{e}}\right) = \begin{bmatrix} 2(q_1 q_3 - q_0 q_2) - a_x \\ 2(q_0 q_1 + q_2 q_3) - a_y \\ (1 - 2q_1^2 - 2q_2^2) - a_z \end{bmatrix} \quad (10)$$

$$\boldsymbol{J}\left(\boldsymbol{q}_{\mathrm{e}}^{\mathrm{b}}, \boldsymbol{a}^{\mathrm{e}}\right) = \begin{bmatrix} -2q_2 & 2q_3 & -2q_0 & 2q_1 \\ 2q_1 & 2q_0 & 2q_3 & 2q_2 \\ 0 & -4q_1 & -4q_2 & 0 \end{bmatrix} \quad (11)$$

For magnetic field,

$$\boldsymbol{s}^{\mathrm{e}} = [0 \quad s_x \quad 0 \quad s_z] \quad (12)$$

$$f\left(\boldsymbol{q}_{\mathrm{e}}^{\mathrm{b}}, \boldsymbol{m}^{\mathrm{e}}, \boldsymbol{s}^{\mathrm{e}}\right) = \begin{bmatrix} 2s_x(0.5 - q_2^2 - q_3^2) + 2s_z(q_1 q_3 - q_0 q_2) - m_x \\ 2s_x(q_1 q_2 - q_0 q_3) + 2s_z(q_0 q_1 + q_2 q_3) - m_y \\ 2s_x(q_0 q_2 + q_1 q_3) + 2s_z(0.5 - q_1^2 - q_2^2) - m_z \end{bmatrix} \quad (13)$$

$$\boldsymbol{J}\left(\boldsymbol{q}_{\mathrm{e}}^{\mathrm{b}}, \boldsymbol{a}^{\mathrm{e}}\right) = [\boldsymbol{J_1}, \boldsymbol{J_2}, \boldsymbol{J_3}, \boldsymbol{J_4}]$$

$$\boldsymbol{J_1} = \begin{bmatrix} -2s_z q_3 \\ -2s_x q_3 + 2s_z q_1 \\ 2s_x q_2 \end{bmatrix}$$

$$\boldsymbol{J_2} = \begin{bmatrix} 2s_z q_3 \\ 2s_x q_2 + 2s_z q_0 \\ 2s_x q_3 - 4s_z q_1 \end{bmatrix} \quad (14)$$

$$\boldsymbol{J_3} = \begin{bmatrix} -4s_x q_2 - 2s_z q_0 \\ 2s_x q_1 + 2s_z q_3 \\ 2s_x q_0 - 4s_z q_2 \end{bmatrix}$$

$$\boldsymbol{J_4} = \begin{bmatrix} -4s_x q_3 + 2s_z q_1 \\ -2s_x q_0 + 2s_z q_2 \\ 2s_x q_1 \end{bmatrix}$$

In this research, acceleration, angular velocity and magnetic field data are available, 9-axis MEMS-IMU algorithms is therefore applied to fuse and combine these data for compensating distortion, filtering erroneous data and smoothing. The fundamental way to accomplish this goal is Kalman filter.

Consider the spatial-temporal characteristics of a construction tool is a state vector that contains a series of variables. The model assumes that the true state at current time t is evolved from the state at the previous time t - 1. This discrete-time linear stationary model without control loop can be represented by

$$\boldsymbol{x}_t = \boldsymbol{\Phi} \boldsymbol{x}_{t-1} + \boldsymbol{\Gamma} \mathbf{w}_{\mathrm{t}-1} \quad (15)$$

where x is the state vector, $\boldsymbol{\Phi}$ refers to the state transition matrix, $\boldsymbol{\Gamma}$ is the control matrix of noises, $\mathbf{w} \sim \boldsymbol{\mathcal{N}}(\mathbf{0}, \mathbf{W}_{\mathrm{t}})$ represents the process noise that is assumed to be generated from a zero mean multivariate normal distribution $\boldsymbol{\mathcal{N}}$ with covariance $\mathbf{W}_{\mathrm{t}}$.

Concurrently, the measurement process is:

$$\boldsymbol{z}_t = \mathbf{H} \boldsymbol{x}_t + \mathbf{v}_{\mathrm{t}} \quad (16)$$

where H is the observation matrix and $\mathbf{v} \sim \boldsymbol{\mathcal{N}}(\mathbf{0}, \mathbf{V}_{\mathrm{t}})$ is the observation noise that drawn from a zero mean Gaussian distribution $\boldsymbol{\mathcal{N}}$ with covariance $\mathbf{V}_{\mathrm{t}}$.

5 Pilot study and results

As shown in Figure 5, IMU sensors can be deployed on the surface of a wrench, a hammer, etc. By tight connection, the data collected is according to the location of sensors, that is to say, the crucial axis for analysis is determined by the position and relation between sensor deployment and the core motion space.

Figure 5. Deployment of IMU sensors

The MEMS-IMU sensor tested here required extra battery support, and the chip is named JY901. The weight is 40 g and the size is less than 2 cm^2, almost non-intrusive when used.

Assume a wrench is adopted to apply torque to turn a screw for connection. Wireless MEMS-IMU is the device collecting the data of the combination wrench, providing a quantitative assessment of turning. In addition, a rubber mallet is also tested to conduct a wood work, requiring a softened strike with a positive drive.

In Figure 6, the curves of raw data revealed the turning process by a wrench rotating around y-axis. It could be seen that the turning job appears to be cyclic in much the same way as a wave with various frequencies. By integral operation, the rotation angle of turning process was shown in Figure 7. The cyclic pattern was more apparent that each cycle ranged from 0 to 90 degree at the begging time for applying torque, and then decreased to the initial position for the next cycle. In this experiment, 22 cycles were counted and the total rotation angle of turning was around 1442 degree, that means the screw has been turned for 4 circles. While the actual rotation was 1620 degree, and the relative measurement error was 10.99%.

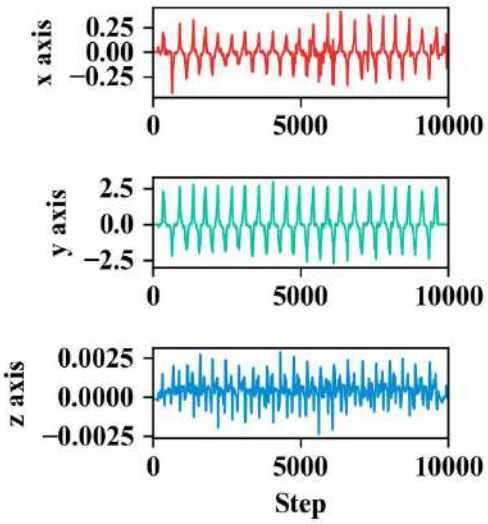

Figure 6. Angular velocity of turning collected by MEMS-IMU

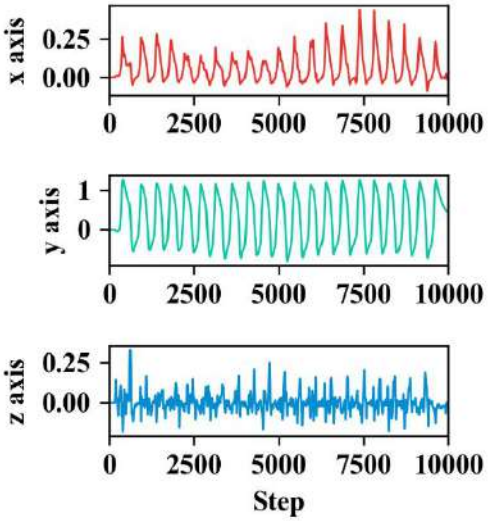

Figure 7. Rotation of turning collected by MEMS-IMU

On the other hand, the angular velocity of hammering process in Figure 8 exposed another kind of cyclic patterns. Here, x-axis was the rotation axis that the rubber mallet was held to hit on the objective panel. The extreme values of palstance were much higher than those of turning process. At the same time, the rotation angle of hammering was also larger as shown in Figure 9. The process begun with hanging on the mallet at the rotation angle of zero, then fell down as the rotation angle raised up to around 90 degrees. However, the measurement of highest rotation angles in each cycle was not accurate that the obtained value was more than 143 degrees. The error was unacceptable at this moment, which required to be improved in the future.

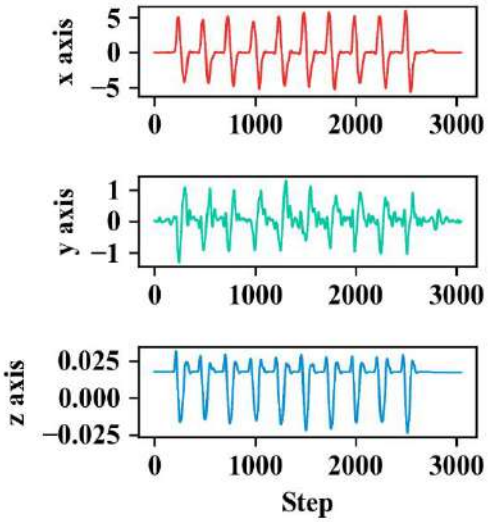

Figure 8. Angular velocity of hammering collected by MEMS-IMU

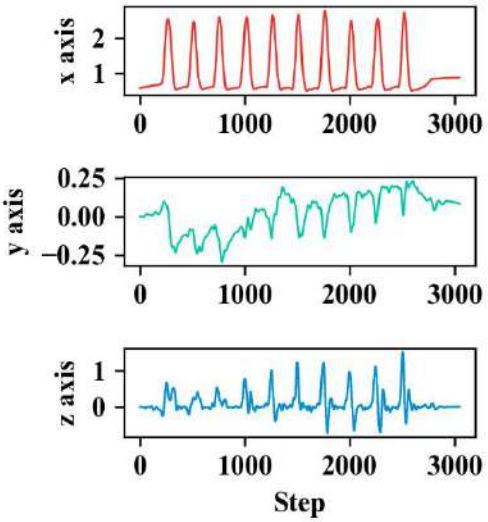

Figure 9. Rotation of hammering collected by MEMS-IMU

By comparing the different cyclic patterns from these two preliminary experiments, the extracted raw data clearly revealed the spatial-temporal characteristics of the different construction activities. Although the data was not so accurate because the current MEMS-IMU algorithm enlarged the cumulative errors over time, these two pilot studies have shown the potential of the proposed IMU-based tool system for monitoring the construction activities in a timely and automated manner.

6 Conclusion

This study proposed a feasible solution to monitor the construction activities without intrusions by collecting and analyzing the IMU data of hand tools used in the construction processes. Two simple experiments validated the novel concept and the preliminary framework. However, further developments were required in the future research, containing the reduction of random errors and cumulative errors and the pattern recognition for various tools and activities.

References

[1] Lee, Y.-J. and M.-W. Park, 3D tracking of multiple onsite workers based on stereo vision. *Automation in Construction*, 2019. 98: p. 146-159.

[2] Golovina, O., J. Teizer, and N. Pradhananga, Heat map generation for predictive safety planning: Preventing struck-by and near miss interactions between workers-on-foot and construction equipment. *Automation in Construction*, 2016. 71: p. 99-115.

[3] Chen, J., J. Qiu, and C. Ahn, Construction worker's awkward posture recognition through supervised motion tensor decomposition. *Automation in Construction*, 2017. 77: p. 67-81.

[4] Hui, L., M.-W. Park, and I. Brilakis, Automated Brick Counting for Facade Construction Progress Estimation. *Journal of Computing in Civil Engineering*, 2015. 29(6): p. 04014091.

[5] Sacks, R., R. Navon, and E. Goldschmidt, Building project model support for automated labor monitoring. *Journal of computing in civil engineering*, 2003. 17(1): p. 19-27.

[6] Navon, R. and E. Goldschmidt, Can labor inputs be measured and controlled automatically? *Journal of Construction Engineering and Management*, 2003. 129(4): p. 437-445.

[7] Hajdasz, M., Flexible management of repetitive construction processes by an intelligent support system. *Expert Systems with Applications*, 2014. 41(4): p. 962-973.

[8] Navon, R. and R. Sacks, Assessing research issues in automated project performance control (APPC). *Automation in Construction*, 2007. 16(4): p. 474-484.

[9] Luinge, H.J. and P.H. Veltink, Measuring orientation of human body segments using miniature gyroscopes and accelerometers. *Medical and Biological Engineering and Computing*, 2005. 43(2): p. 273-282.

[10] Valero, E., et al., Musculoskeletal disorders in construction: A review and a novel system for activity tracking with body area network. *Applied Ergonomics*, 2016. 54: p. 120-130.

[11] Seel, T., J. Raisch, and T. Schauer, IMU-based joint angle measurement for gait analysis. *Sensors*, 2014. 14(4): p. 6891-6909.

[12] Valero, E., et al., Analysis of construction trade worker body motions using a wearable and wireless motion sensor network. *Automation in Construction*, 2017. 83: p. 48-55.

[13] Yan, X., et al., Wearable IMU-based real-time motion warning system for construction workers' musculoskeletal disorders prevention. *Automation in Construction*, 2017. 74: p. 2-11.

[14] Jebelli, H., C.R. Ahn, and T.L. Stentz, Fall risk analysis of construction workers using inertial measurement units: Validating the usefulness of the postural stability metrics in construction. *Safety Science*, 2016. 84: p. 161-170.

[15] Fang, Q., et al., Computer vision aided inspection on falling prevention measures for steeplejacks in an aerial environment. *Automation in Construction*, 2018. 93: p. 148-164.

[16] Tomé, A., et al., Space–use analysis through computer vision. *Automation in Construction*, 2015. 57: p. 80-97.

[17] Kim, D., et al., Remote proximity monitoring between mobile construction resources using camera-mounted UAVs. *Automation in Construction*, 2019. 99: p. 168-182.

[18] Akinci, B., et al., Formalization and automation of time-space conflict analysis. *Journal of Computing in Civil Engineering*, 2002. 16(2): p. 124-134.

[19] Yang, J., Z. Shi, and Z. Wu, Vision-based action recognition of construction workers using dense trajectories. *Advanced Engineering Informatics*, 2016. 30(3): p. 327-336.

[20] Seo, J., et al., Computer vision techniques for construction safety and health monitoring. *Advanced Engineering Informatics*, 2015. 29(2): p. 239-251.

[21] Gong, J., C.H. Caldas, and C. Gordon, Learning and classifying actions of construction workers and equipment using Bag-of-Video-Feature-Words and Bayesian network models. *Advanced Engineering Informatics*, 2011. 25(4): p. 771-782.

[22] Li, H., et al., Automated classification of construction site hazard zones by crowd-sourced integrated density maps. *Automation in Construction*, 2017. 81: p. 328-339.

[23] Yang, X., et al., Location-based measurement and visualization for interdependence network on construction sites. *Advanced Engineering Informatics*, 2017. 34: p. 36-45.

[24] Eastman, C., et al., Automatic rule-based checking of building designs. *Automation in construction*, 2009. 18(8): p. 1011-1033.

An Investigation into the Effects of Deposition Orientation of Material on the Mechanical Behaviours of the Cementitious Powder and Gypsum Powder in Inkjet 3D Printing

P. Shakor[a], S. Nejadi[a], and G. Paul[b]

[a]Center for Built Infrastructure Research, School of Civil and Environmental Engineering, University of Technology Sydney, Australia
[b]Centre for Autonomous Systems, School of Mechanical and Mechatronic Engineering, University of Technology Sydney, Australia
E-mail: pshtiwan.shakor@student.uts.edu.au, {shami.nejadi, gavin.paul}@uts.edu.au

Abstract –

Three-Dimensional Printing (3DP) is widely used and continues to be rapidly developed and adopted, in several industries, including construction industry. Inkjet 3DP is the approach which offers the most promising and immediate opportunities for integrating the benefits of additive manufacturing technic into the construction field. The ability to readily modify the orientation angle that the printed material is deposited is one of the most advantageous features in a 3DP scaffold compared with conventional methods. The orientation angle has a significant effect on the mechanical behaviours of the printed specimens. Therefore, this paper focuses on printing in different orientations somehow to compare various mechanical properties and to characterise a selection of common construction materials including gypsum (ZP 151) and cement mortar (CP). The optimum strength for the gypsum specimens in compression and flexural strength was observed in the (0° and 90°) and (0°) in the X-Z plane, respectively. According to the experimental results, the compression and flexural strength for ZP 151 are recorded at (11.59±1.18 and 11.78±1.19) MPa and 15.57±0.71 MPa, respectively. Conversely, the highest strength in compression and flexural strength are observed in the (90°) and (0°) degrees in the X-Z plane for the cement mortar, respectively. Moreover, it has been discovered that the compression and flexural strengths for CP are recorded as 19.44±0.11 MPa and 4.06±0.08 MPa, respectively. In addition, the dimensional effect for various *w/c* ratio has been monitored and examined.

Keywords –

Inkjet 3DP; cement mortar (CP); gypsum (ZP 151); mechanical strength; dimensional precision.

1 Introduction

Generally, the most common method in civil engineering is to cast in place or use precast procedures to construct structural members. These structural members are cast using different materials such as concrete, and masonry [10], [12] and [16]. Given the ever-increasing need for speed, quality and tailored design in the construction industry and due to the advances in rapid prototyping, the procedures for constructing structural members need to be rethought and upgraded [18].

Owing to the earlier studies, three main techniques for the 3DP powder-bed process have been recognized [14], i) selective binder (cement) activation, ii) binder jetting and iii) selective paste intrusion, respectively [22] [17]. These process could be monitored via the online vision sensor to control the slurry printing process [26]. The selective binder activation is the process that is used in this paper, which is usually known as powder-bed printing (binder/inkjet printing) [19] [23].

Inkjet printing is a layer-by-layer procedure to complete the entire scaffold using the powder-based materials and an activator such as water, Figure (1).

In inkjet 3DP, there are many limitations while printing the objects. For example, [28] discussed a few limitations in the 3DP such as binder selection, powder reactions, post-processing bed manipulations and de-powdering. One of the major limitations in 3DP is the orientation angle which has been discussed in earlier studies for the plastic and poly-jet materials [25].

In the following subsections, the mechanical strength of the recommended powder (ZP 151) and the modified powder (CP) have been monitored and compared. Moreover, the printed element has been examined within the different inclined rates for different angles. Nevertheless, the maximum compressive strength has been obtained for (CP) and (ZP 151). For the flexural strength, the highest results that have been observed for both (CP) and (ZP 151) are reported. Finally, the conclusions about the experimental study are presented and the future works are discussed.

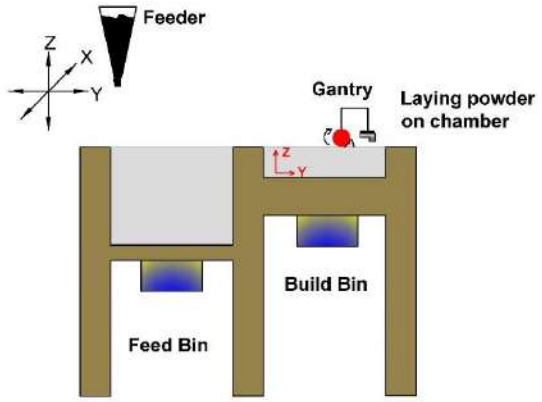

Figure 1. Schematic depiction of the powder-bed printing technique in inkjet 3D printing.

2 Materials and Specimens Preparation

2.1 Materials Composition

According to 3DSystems manual [2], the ZP151 contains (80-90%) of calcium sulphate hemihydrate ($CaSO_4 \cdot 1/2H_2O$). Moreover, Zb 63 is an aqueous solution and known as a binder, which has a high water content and humectant with the density of 1g/cm^3 [1].

In the previous study, [23] it has been found that the water/cement ratio (*w/c)* or (binder/powder) ratio can be determined by using Equation (1). The volume of a drop of binder will be measured according to the enveloped volume of powder in the build chamber of the printer.

$$Sat_{level} = \frac{V_b}{V_{EnvPowder}} \qquad (1)$$

Where Sat_{level} is saturation level (*w/c*), V_b is the volume of the binder, and $V_{envpowder}$ the volume of the enveloped powder on the build chamber (build bin).

The alternative mix that has been used for printing contains as a percentage of total weight are 67.8% of Calcium Aluminate Cement (CAC) ranging sieve (75-150μm), 32.2% of Ordinary Portland Cement (OPC) and 5% of fine sand. Figure (2) shows the histogram and curve of the density distribution of the custom-made and recommended materials versus particle size.

Figure (3) shows the modified mixing powder (cement mortar CP), which replaces the ZP 151. It is noted that the mixing process has been completed using a Hobart mixer at a speed of 1450 RPM.

Moreover, the homogeneity and consistency of the powder materials are crucial factors that must be controlled when in pursuit of superior resolutions and results. Therefore, the speed of the mixer and the time of mixing are considered as a major contributor to the homogeneity of the powder and production of better quality 3DP objects.

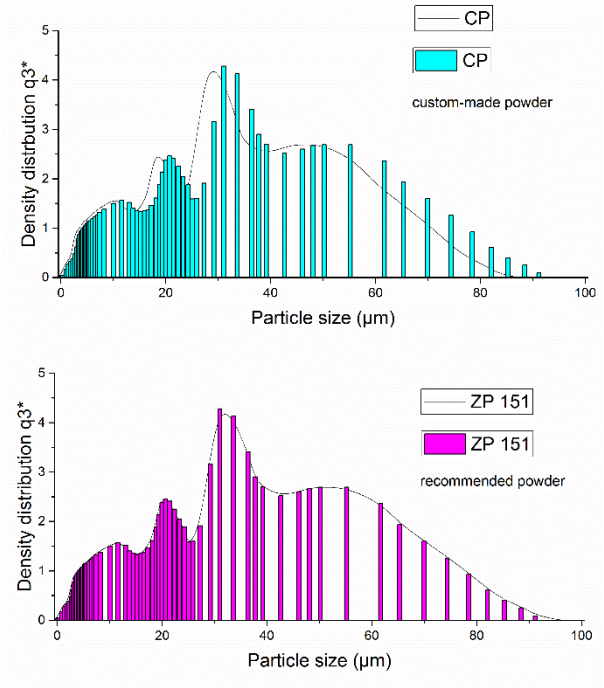

Figure 2. Histogram and curve of particle size distributions of ZP 151 and CP (custom-made) powder. *q3 is the unit standing for the density distribution of the total particles.

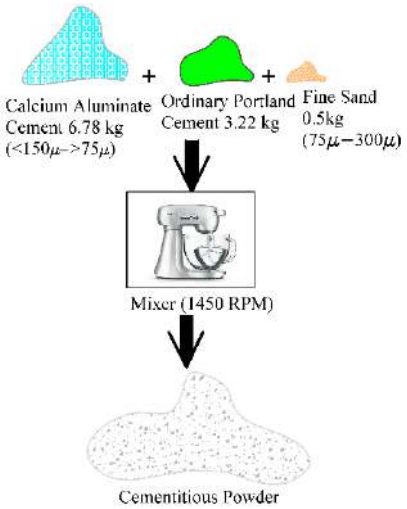

Figure 3. Schematic illustration of the process for preparing cementitious powder.

In addition, the optimum saturation level (*w/c*) of the binder for 3DP specimens has been reported [7]. According to the report, the highest saturation level is (S170C340) (Shell=170, Core=340), determined by Equation (1), which produces the highest result for the mechanical strength in 3DP specimens. The saturation level of the modified powder (S170C340) is equivalent to (*w/c*=0.52) in the manual mixing process for the cement mortar (CP) and (*w/c*=0.46) for the gypsum (ZP 151). The materials' chemical composition have been presented in Table (1).

Table 1. Chemical constituent percentages of the main materials in CP

Chemical Constituent % of Calcium Aluminate Cement			
Al_2O_3	CaO	SiO_2	Fe_2O_3
≥ 37.0	≤ 39.8	≤ 6.0	≤ 18.5
Chemical Constituent % of Ordinary Portland Cement (General Purpose)			
Cement Clinker	$CaCO_3$	$CaSO_4.2H_2O$	Clinker Kiln dust
>92%	0-7.5%	3-8%	0-2.5%

2.2 Specimen Preparation

The (ZP 151) has been directly placed into the 3DP (ProJet 360). However, the modified mix was prepared by a 20L Hobart mixer. The mixing procedure has been conducted in a dry mix state. Then, the prepared mix powder is placed into the inkjet 3D printer to print the mortar specimens. A Shimadzu load cell (AGS-X 50kN, Japan) testing machine was used to perform the mechanical tests at room temperature of (22±2°C) with a humidity level in the range of (60±10) %.

Different orientation angles have been used to print the specimens (0, 30, 37.5, 45, 90)°. These angles have been selected because the halfway point of (0° and 90°), are the angle 45°. Commonly most of the shear rupture happens in concrete were between 0° and 45° [11]. Therefore, this paper focused on these angles between 0° to 45°. Figure (4) schematically shows the specimens with different orientation angles of print. Table (2) presents the name of the tests, numbers of samples, and CAD dimensions for both materials specimens

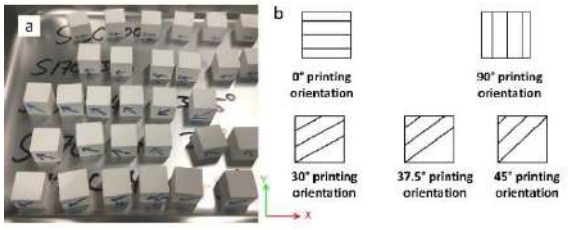

Figure 4. (**a**) Real-world images of the 3DP cubes in (0°,30°,37.7°,45°,90°) orientation (**b**) Drawing of 3DP cubes in (0°,30°,37.7°,45°,90°).

3 Experimental Program

To determine the mechanical properties of the 3DP specimens, all the samples were designed in SolidWorks software as an STL file. Figure (5) shows the cubic samples in different orientation angles, which are printed at (0°, 30°, 37.5°, 45°, 90°). It also shows the orientation angle of prepared specimens with regard to the X, Y, Z plane in the 3DSystems software. A mould (20×20×20), (167×17×7) mm used for casting the comparison, samples. All of the samples for compressive, and flexural strength tests have been prepared in a similar process.

The orientation angles in 3DP can be used in inkjet printing to create different geometries, optimize the mechanical strength of structure parts and optimize the number of layers to print an object.

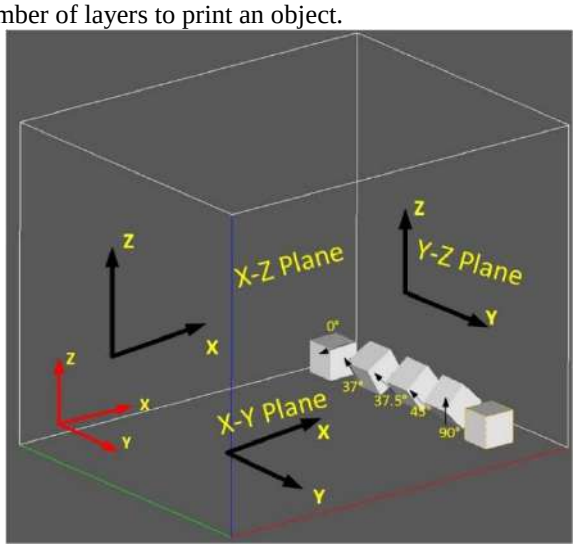

Figure 5. An illustration of the cube to be printed in different orientation angles according to X-Z plane.

Table (2) shows the type of tests, number of samples, and CAD drawing dimensions of the printing parameters.

Table 2. Tests with respect to the numbers and dimensions

Tests	**No. of Samples**	**CAD Dimensions (mm)**
Compression test	36	20×20×20
Three-point bending test	36	167×17×7
Dimensional accuracy	10	20×20×20

3.1 Testing and loading procedures

All the specimens have been tested using the universal testing machine (50 kN) with different rates of speed.

3.1.1 Effect of Dimensional Accuracy

The most vital features that distinguish the powder-based (inkjet) 3DP from the conventional casting method are the accuracy and dimensional precision of 3DP. Figure (6) shows the printed samples (cube and prism), which have been printed by inkjet 3DP: (a) left is mortar (CP) and (a) right is gypsum (ZP 151). Dimensions of the specimens have been measured by digital callipers with an accuracy of 0.01 mm and for the height, it has been used MeasumaX with an accuracy of ±0.04mm. Ten samples were used for the effects of dimensional accuracy test.

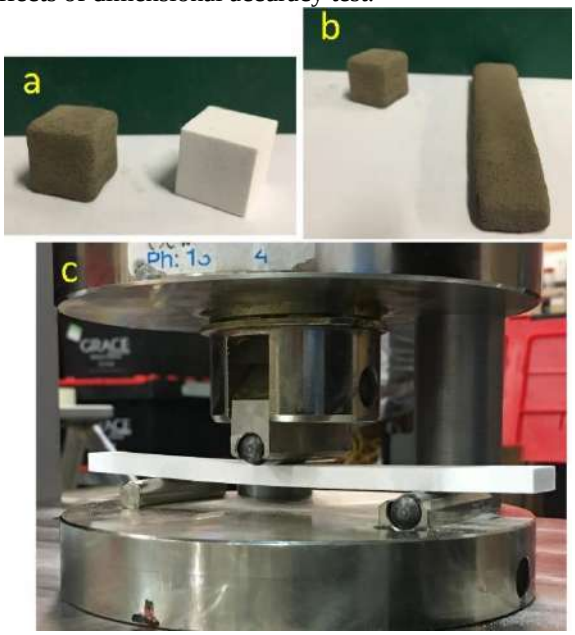

Figure 6. (a) 3DP cubic samples for CP and ZP 151, (b) 3DP cubic and prism CP sample, (c) 3DP prism gypsum while testing for three-point bending test.

3.1.2 Compressive Strength Test

One of the common factors that can be used to assess the durability of the concrete and mortar is its compressive strength [6]. Thus, the compression strength test has been performed for the 3DP samples according to the ASTM standard [6]. A total of 36 samples have been tested including 3 samples for each of orientation angles. The speed rate of the loading in the test was 0.833 kN/sec.

3.1.3 Flexural Strength Test

The specimens for the flexural strength test were prepared according to the ASTM standard [7]. A total of 36 samples have been printed using the manual mix, including 3 samples prepared for each orientation angle. The speed rate of the loading in the test was 426 N/min.

3.1.4 Post-Processing Procedure

The curing and post-processing procedures are crucial to produce robust 3DP elements. After the element is printed, it should be kept for a minimum of 2 hours inside the build chamber of the printer so it can dry. According to the study of Feng et al. [8], specimens should be left for a further three hours to dry in an oven at 60°C after drying inside the build chamber. This leads to accelerating the solidifications and incremental stiffness of the gypsum scaffold (ZP 151). For that reason, the three hours curing in the oven has been implemented for ZP 151.

Curing of CP has been monitored using different trials and tests at the vitro. Accordingly, before and after curing in the water, CP has been drying at 60°C, results in higher compression strength in the CP specimens.

4 Results and Discussion

4.1.1 Effect of Dimensional Accuracy

The major advantage of the inkjet 3DP technique is a fabrication of structural components with complicated geometries without implementing costly formwork. The most vital aspect that distinguishes the inkjet (powder-based) 3DP from conventional casting method is the precision of printing. Figure (7) shows the results of the dimensional accuracy for the green cubic sample (green part) for the CP materials. Note that "green part" means a specimen that has been removed from the build chamber (build bin) prior to any post-processing.

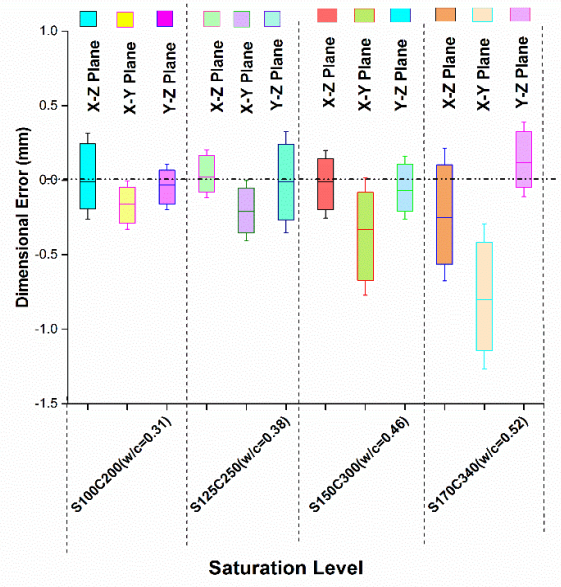

Figure 7. The relationship between dimensional accuracy and saturation level (*w/c*) for printed green cube CP specimens (CAD 20×20×20mm),

printed by ProJet CJP (304 nozzles). (Note: the box is the mean ±standard deviation, and the whisker is ±minimum and maximum).

The dimensional error can be found using Equation (2):

$$D_{error} = D_{printed} - D_{CAD} \quad (2)$$

Where D_{error} is a dimensional error, $D_{printed}$ is an actual printed dimension, and D_{CAD} is a CAD dimension.

Figure (7) also shows that in general the dimensional accuracy increases as the *w/c* is reduced for all planes. However, in the X-Y plane, a significant amount of undesirable deviation in the dimensional precision can be observed. These are lower than the nominal (CAD dimensions) that due to the inaccuracy of the printhead nozzle and closeness of the nozzles. This inaccuracy could lead overlapping and collision of the binder when it drops on the powder. Another reason is the chemical and physical characterization of the powder-to-binder and the ability of the powder for drop penetration. In addition, the printhead located on the fast axis rails which have a high rate movement. This can be counted as another important factor in the contribution of the accuracy of dimensions. The gantry holds all binder supply system, which is located on the fast axis rails in the printer.

4.1.2 Compressive Strength Test

In the previous study conducted by Shakor et al. [19], the porosity and voids in the cubic samples were investigated. The findings and optimum saturation level have been used in this paper to print and prepare all the scaffolds at the same saturation levels.

Figure (8) shows the porosity of the specimens versus the *w/c* ratio, where the highest saturation level (*w/c*) resulted in a reduction of the porosity percentage for both powders (CP) and (ZP 151). According to the study of Popovics et al. [15], the relationship between *w/c* ratio and porosity can be described by Equation (3);

$$p = 0.001a + \frac{w/c}{w/c+1/G} \quad (3)$$

Where p is the total porosity for the fresh cement, a is the air content by volume, G is specific gravity of cement and *w/c* is a water/cement ratio by mass. Consequently, an increase in *w/c* ratio means an increase in porosity of the sample, and resulted in a reduction in strength of the sample. However, this equation cannot be applied to the 3DP cementitious powder (CP) or gypsum (ZP 151). The printing of (CP) and (ZP 151) is completed in a layer-by-layer process. This technique is totally different from the manual mix process, which involves mixing the powder with water within one batch and vibrating it in the casting mould. The process of printing and post-processing applications has various effects on the mechanical properties and durability of the printed object. For example, the hygroscopic of the powder and electrostatic charge on the surface of the powder has a significant influence on the capability of powder to absorb moisture from the air. This leads to an increase in the cohesion and a reduction in the flowability of the powder. Additionally, this property in the powder would affect the size of the specimen and change the mechanical properties of the specimen as well.

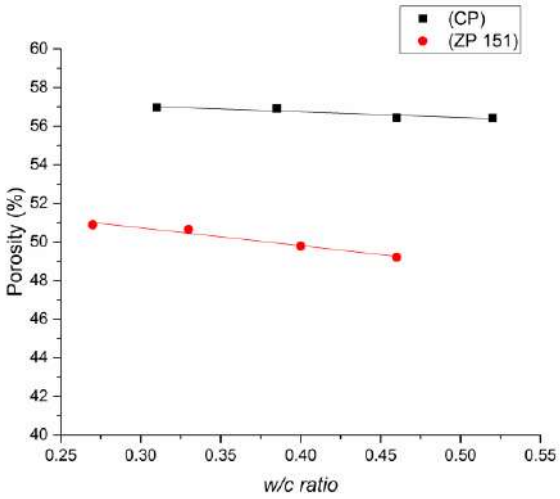

Figure (8) Relationship between porosity and w/c ratio for the mortar and gypsum printed scaffold.

Figure (9) illustrates the compressive strength of the specimen for the saturation level of S170C340. This saturation level is equal to a *w/c* of 0.52 in CP and 0.46 in ZP 151 using for all orientation angle. Accordingly, it shows the orientation angle of (90°) gives the highest value (19.44±0.11 MPa) for CP after curing in an oven for 3 hours before and after wet curing, and a 7-day curing in water. This value is enough to build a structural member, which is cured only for 7-day. According to ACI code, a 7-day cure is counted as a 65% of the strength of mortar or concrete [3], while the compressive strength of mortar or concrete increases to about 99% strength in 28-day.

On the other hand, ZP 151 has recorded the highest result with an orientation angle of (0°) and (90°), i.e. when the printhead is parallel to the *x*-axis the highest result was recorded. This result matches with results reported by Asadi-Eydivand et al. [5]. However, this investigation needs further study to assess specimens in all three planes and axes. In addition, the rotating and changing scale of the specimens also needs further examination.

It is clear from the experimental results that the printing orientation angle has a major impact on the mechanical strength of the specimens, particularly in the cement mortar specimens. As shown in Figure (9) the printing orientation of (90°) has recorded the highest value of compressive strength which means the perpendicular directions has the optimum strength in the X-Z plane for cement mortar. However, the results for gypsum are slightly different since both angles (0° and 90°) could obtain maximum compressive strength. The results of the two angles are very similar to each other with

differences in the decimals range. Thus, it is highly recommended to print in the orientation angle of 90° for CP to achieve the highest compressive strength with concern to the flexural strength, which explaining in the following subsection.

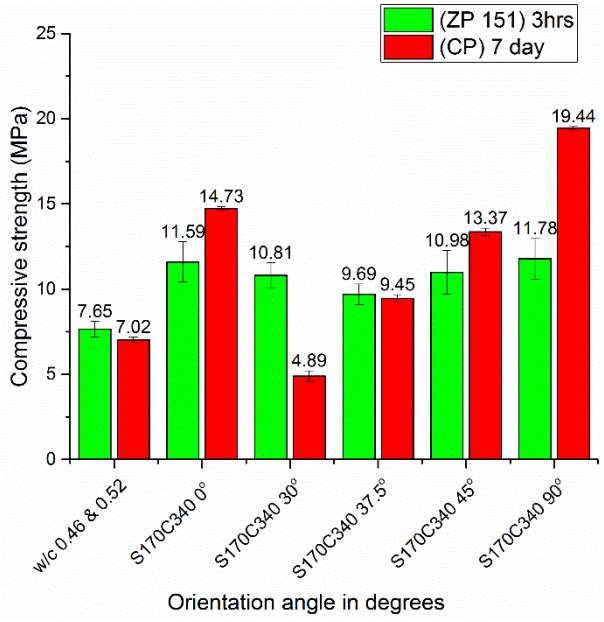

Figure (9) Compressive strength results for the ZP 151 cubes and CP cubes (average ±standard deviation).

The halfway point between 0° and 45° is the angle 22.5° on the plane and is the most critical place for a crack in the concrete sample to begin. In this study, the angle 30° is the closest angle to 22.5° and is the reason for the emergence of a lower mechanical strength specifically in the cement mortar specimens. Further investigations are needed to check the results in different angles, e.g., 22.5° and 67.5°. The procedure used in this study is similar to a study conducted by [27], where tests were performed at a 22.5° angle for concrete blocks with dimensions (454×371)mm. However, the test results are quite different since the samples prepared in [27], were blocks joined by mortar, and not one continuous layer. Another reason is that the size, dimensions and properties of the materials are different which each have a significant impact on the outcomes of "orientational angle" results. Hence, the whole printed specimens are made from mortar and have a continuous longitudinal layer without the interruption of block joints. Therefore, the results would be different from conventional blocks.

4.1.3 Flexural Strength Test

Three-point bending tests have been conducted to evaluate the flexural strength of the printed gypsum and cement mortar specimens. Figure (10) shows that in general, the flexural strength in gypsum is higher than the cement mortar specimens. According to the ACI code [4], the flexural strength of concrete is about 10% to 20% of the compressive strength result. Likewise, the result of CP in flexural strength after 7-day shows that the measured flexural strength is about 14% of compressive strength. Moreover, this could be due to the medium of the specimens, type, sizes, the volume of the particle size and duration of the curing.

Figure (10) shows flexural strength results quite opposite to the compressive strength result of both materials. As shown in Figure (9) the highest result is in CP specimens. However, in Figure (10) the results of the ZP 151 show higher values than the CP specimens. Previous studies have proved that using gypsum leads to an increase in bending and tensile strength [9]. The high percentage of lime content in fly ash with a high ratio of gypsum (1%), leads to a dramatic increase in the tensile strength [9]. Therefore, gypsum is acting as a flexible material and has great flexibility compared to the cement materials. In an earlier study by Lewry et al. [13], it has been proven that the reaction of water to plaster (gypsum), which is similar to the material ZP 151, with a 0.6 *w/c* ratio could gain about 12.2 MPa. This result is quite close to the manual mix of ZP 151 with *w/c* ratio of 0.46 in this study, which is 14.23 MPa. However, post-processing and purity of the materials have a significant effect on the result of the bending strength of gypsum materials.

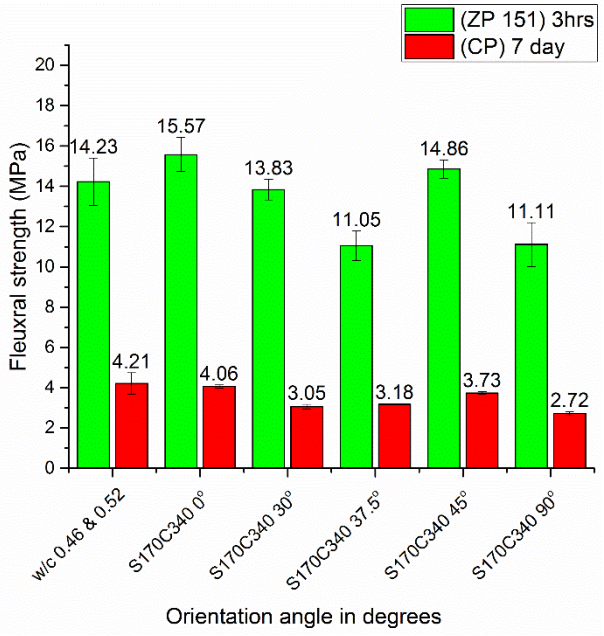

Figure (10) Flexural strength results for the ZP 151 cubes and CP cubes (average ±standard deviation).

Furthermore, the result for the printed ZP 151 and CP samples are important due to the highest bending

strength recorded at the orientation angle of 0°. Meanwhile, the manual mix of CP in bending strength is slightly higher than the printed angle 0°. Therefore, the present study, the printing for the CP in the 0° and 90° are optimum angles to print for construction members because of the highest results achieved for compressive strength at angle 90° and highest results achieved for bending strength at angle 0°. This could be improved by adding reinforcement and later used for façade and cladding of the building [21] [24] [20].

5 Conclusion

3DP cubic and prism specimens have been printed with ZP 151 and CP materials. These specimens have been printed in different orientation angles to obtain better mechanical properties. In this paper, the dimensional accuracy for the CP printed specimens in the various *w/c* ratio (saturation levels) has been scrutinized and discussed. The results show that the *x*-*y* plane always has smaller dimensions than the other planes, this is due to the printhead direction, which is parallel to the *x*-axis and perpendicular to the *y*-axis. The printhead nozzles are too close and adjacent to each other and most probably the liquid binder overlapping and collide when dropping the droplet at high speeds. The other reasons could be due to the high capability of penetration of the water (binder) into the powder. Moreover, the dimensional accuracy is mostly decreased and highly variable while the *w/c* increases as a result of spreading high volumes of the water through the printhead. Particularly, spreading water in the *y*-axis is less than in the *x*-axis, which is perpendicular to the printhead, and vice-versa in the parallel direction (X-axis).

Furthermore, this study has investigated the effect of orientation angle on the printed structural members using CP (mortar) and ZP 151 (gypsum). The results show that this is an important factor that needs to be taken into consideration in the future studies of 3DP. The most appropriate orientations are 90° and 0° degrees for the strongest bending and compression strengths, respectively. In addition, this study is conducted to check the height of the printhead, number of the nozzles and spreading of the water (binder) while the printhead is moving on the powder bed and dripping water droplets at a fast speed. However, the effects of temperature and medium curing needs to be studied in detail for different powder types.

Acknowledgement

The authors would like to thank A/Prof. Anne Gardner and staff at the civil engineering laboratory for their support at the University of Technology Sydney. The authors would also like to gratitude to Kerneos Australia Pty Limited to provide CAC.

References

[1] 3DSystems, ZB63 Safety Data Sheet, 2012.
[2] 3DSystems, ZP151 Powder Safety Data Sheet, 2013.
[3] ACI308R-01, Standard Guide to Curing Concrete, 2001.
[4] A.c.i. ACI330R-01, Guide for Design and Construction of Concrete Parking Lots, 2001.
[5] M. Asadi-Eydivand, M. Solati-Hashjin, A. Farzad, N.A. Abu Osman, Effect of technical parameters on porous structure and strength of 3D printed calcium sulfate prototypes, Robotics and Computer-Integrated Manufacturing 37 (2016) 57-67.
[6] ASTMC39, 39, Standard test method for compressive strength of cylindrical concrete specimens, ASTM International (2001).
[7] ASTMC293/C293M, 293 Standard Test Method for Flexural Strength of Concrete (Using Simple Beam With Center-Point Loading), ASTM Standard (2002).
[8] P. Feng, X. Meng, J.-F. Chen, L. Ye, Mechanical properties of structures 3D printed with cementitious powders, Construction and Building Materials 93 (2015) 486-497.
[9] A. Ghosh, C. Subbarao, Tensile strength bearing ratio and slake durability of class F fly ash stabilized with lime and gypsum, Journal of Materials in Civil Engineering 18 (1) (2006) 18-27.
[10] H. Haroglu, Investigating the structural frame decision making process, © Hasan Haroglu, 2010.
[11] N.M. Hawkins, Simplified shear design of structural concrete members, Transportation Research Board, 2005.
[12] K.S. Kumar, P. Premalatha, K. Baskar, G.S. Pillai, P.S. Hameed, Assessment of Radioactivity in Concrete Made with e-Waste Plastic, Journal of Testing and Evaluation 46 (2) (2017) 1-6.
[13] A.J. Lewry, J. Williamson, The setting of gypsum plaster, Journal of Materials Science 29 (23) (1994) 6085-6090.
[14] D. Lowke, E. Dini, A. Perrot, D. Weger, C. Gehlen, B. Dillenburger, Particle-bed 3D printing in concrete construction – Possibilities and challenges, Cement and Concrete Research (2018).
[15] S. Popovics, J. Ujhelyi, Contribution to the concrete strength versus water-cement ratio relationship, Journal of Materials in Civil Engineering 20 (7) (2008) 459-463.
[16] M. Rashidi, R.S. Ashtiani, J. Si, R.P. Izzo, M. McDaniel, A Practical Approach for the Estimation of Strength and Resilient Properties of Cementitious Materials, Transportation Research Record (2018) 0361198118769900.
[17] P. Shakor, S. Nejadi, 3D Printed Concrete Evaluations by Using Different Concrete Mix Designs, Recent Trends in Engineering and

Technology, Bangkok, Thailand, 2017.
[18] P. Shakor, S. Nejadi, G. Paul, S. Malek, Review of Emerging Additive Manufacturing Technologies in 3D Printing of Cementitious Materials in the Construction Industry, Frontiers in Built Environment 4 (85) (2019).
[19] P. Shakor, S. Nejadi, G. Paul, J. Sanjayan, A Novel Methodology of Powder-based Cementitious Materials in 3D Inkjet Printing for Construction Applications Sixth International Conference on the Durability of Concrete Structures, Whittles Publishing, Leeds, UK, 2018.
[20] P. Shakor, S. Nejadi, G. Paul, J. Sanjayan, A. Nazari, Mechanical Properties of Cement-Based Materials and Effect of Elevated Temperature on 3-D Printed Mortar Specimens in Inkjet 3-D Printing, ACI Materials Journal 116 (2) (2019).
[21] P. Shakor, S. Pimplikar, U. Ghare, Techno-Commercial aspects of use of glass fibre in construction industry, Advances and Trends in Engineering Materials and their Applications, Advanced Engineering Solutions (Ottawa, Canada) Montreal, Canada, 2011.
[22] P. Shakor, J. Renneberg, S. Nejadi, G. Paul, Optimisation of Different Concrete Mix Designs for 3D Printing by Utilizing Six Degrees of Freedom Industrial Robot, 34th International Symposium on Automation and Robotics in Construction, Automation in Construction, Taipei, Taiwan 2017.
[23] P. Shakor, J. Sanjayan, A. Nazari, S. Nejadi, Modified 3D printed powder to cement-based material and mechanical properties of cement scaffold used in 3D printing, Construction and Building Materials 138 (2017) 398-409.
[24] P.N. Shakor, S. Pimplikar, Glass fibre reinforced concrete use in construction, Int. J. Technol. Eng. Syst 2 (2) (2011).
[25] M. Sugavaneswaran, G. Arumaikkannu, Modelling for randomly oriented multi material additive manufacturing component and its fabrication, Materials & Design (1980-2015) 54 (2014) 779-785.
[26] S. Sutjipto, D. Tish, G. Paul, T. Vidal-Calleja, T. Schork, Towards Visual Feedback Loops for Robot-Controlled Additive Manufacturing, in: J. Willmann, P. Block, M. Hutter, K. Byrne, T. Schork (Eds.), Robotic Fabrication in Architecture, Art and Design 2018, Springer International Publishing, Cham, 2019, pp. 85-97.
[27] J.A. Thamboo, M. Dhanasekar, Behaviour of thin layer mortared concrete masonry under combined shear and compression, Australian Journal of Structural Engineering 17 (1) (2016) 39-52.
[28] B. Utela, D. Storti, R. Anderson, M. Ganter, A review of process development steps for new material systems in three dimensional printing (3DP), Journal of Manufacturing Processes 10 (2) (2008) 96-104.

BIM-based Takt-Time Planning and Takt Control: Requirements for Digital Construction Process Management

J. Melzner[a]

[a]W. Markgraf GmbH & Co KG, Germany
E-mail: juergen.melzner@gmx.de

Abstract –

Continuous and robust process planning is contrary to the different goals of project participants in the construction business. The aim of holistic building process management must be to optimize the overall process by streamlining individual processes. Lean management methods are increasingly being used to harmonize building processes. For this purpose, especially the method of takt time planning and takt control is appropriate. Building information modeling (BIM) is another promising way to promote a collaborative planning and construction process. BIM is generally understood as a virtual 3D model of a project with additional information. In order to be able to use the synergies of the two methods, the requirements, framework conditions, and goals of the two methods must be coordinated so that the added value of information for process planning can be used. The parallel application of lean construction methods and BIM can create added value that leads to productivity gains. In established BIM applications, the product (e.g., building) is planned as optimally as possible. However, the production process is not sufficiently considered. This is where lean construction methods are used to optimize the process. This article describes synergies through the combination of both methods and defines the requirements for a new BIM use case, "takt time planning and takt control." The presented concept is prototypically tested on a hotel tower project and the benefits and requirements are discussed.

Keywords –

Lean Construction; Process planning; Construction Management; Building Information Modeling

1 Introduction

A paper of the ISARC 1993 starts with the paragraph "The chronic problems of construction are well-known: low productivity, poor safety, inferior working conditions, and insufficient quality" [1]. Although this statement from more than 25 years ago could describe many of today's construction projects, little seems to have changed since then. Low productivity is one of the biggest challenges facing the construction industry nowadays.

Many studies show that the productivity of the construction industry has not increased in recent years compared to that of other industries. While other manufacturing industries have increased their productivity by more than 20% in the last 20 years, productivity in the construction industry has increased by only about 4%. These considerations raise the question of whether other industries are better at realizing the opportunities of digitization than the construction industry.

The construction industry is facing a change. Digitization is pervading more and more sectors of the industry. The implementation of digitization projects requires a strong standardization for business processes as well as for products and components.

Building Information Modeling is seen as the driver of digitization in construction. All relevant information in a construction project will be mapped into a consistent data model. Thereby an improvement in the achievement of the project goals in the dimensions dates, costs and quality is to be achieved. However, the industry has not been able to increase productivity to nearly the same level as other manufacturing industries. With the aim of increasing productivity, lean management methods are increasingly being adapted in the construction industry. Lean Construction and Building Information Modelling, at first glance, are two independent methods whose evolution has been shaped by different perspectives.

This paper describes two methods currently most promising in construction management to increase productivity, occupational safety and quality. Lean Construction methods and BIM are internationally used methods in construction. However, the combination of both methods lacks framework conditions to enable a digital exchange of building data especially for the takt-

time planning application. Therefore, the minimum requirements will defined in the paper.

2 Problem Description and Objective

Ineffective processes not only lead to a loss of time, but also to wastage of various resources. Not fully used or misdirected resources lead to rising costs during operation, indicating flawed planning and reduced values. Studies in the United States, Great Britain and Scandinavia have shown that wastage in the building construction process is very high:

- 30% of the construction work must be repeated to produce appropriate quality,
- 10% of material assets get lost due to wastage and disorder, and
- only 40–60% of the performance is efficiently used in construction activities [2].

The complex process of construction project planning depends on many parameters and the quality of construction schedules is highly related to the engineers´ knowledge. The initial schedule includes, in most cases, only the basic information about the planned construction. The pieces of basic information are the approximate start and end dates of the different trades. Detailed schedules with linked activities to represent the dependencies between activities are in most cases missing [3].

Software applications relieve users from routine tasks. However, the shortcomings of present software tools, which are currently used for construction process management, include the separate generation of the building information model and the construction process model.

The successful implementation of projects requires a structured and effective communication between all stakeholders. The increasing development of BIM tools has to be evaluated concerning their situational suitability of information exchange in construction projects. Construction projects are generally characterized by a large number of stakeholders such as construction companies, architects, planners, and representatives of regulatory bodies.

In order to gather the relevant information in a BIM process, information pertaining to who, when, how, and which has to be identified and provided. The buildingSMART propagated a method to define such exchange requirements is the Information Delivery Manual (IDM) (ISO 29481). The objectives of IDM are meant to standardize the information needed for specific-use cases in the BIM process. This manual defines the requirements for data exchange for all participants, including software providers.

An IDM targets both BIM users and solution providers and consists of three main parts- process map, exchange requirements, and functional parts. The process map describes the flow of activities for a specific process e.g., cost estimation. It improves the understanding of configuration of activities, the involved actors, the required information, and the consumed and produced information (Figure 1).

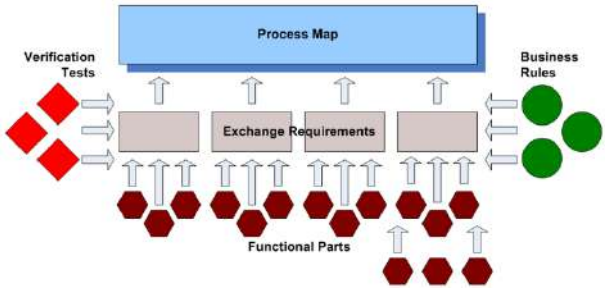

Figure 1. BIM-based lean construction production model [4]

The exchange requirements are a set of information that needs to be exchanged to support a specific business requirement at a particular stage of a project. An exchange requirement represents the connection between process and data. It applies the relevant information defined within an information model to fulfil the requirements of an information exchange. Finally, the functional parts are units of information used by solution providers to support an exchange requirement [4].

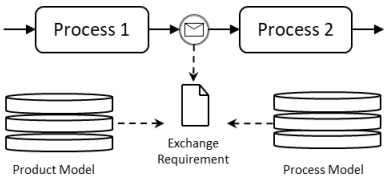

Figure 2. Scheme of Exchange Requirements

This paper describes the requirement of the BIM process to facilitate takt-time planning for a building information model.

3 Background

3.1 Building Information Modeling

The core of BIM-based project management is an integral digital building data model. The aim of the Building Information Model is to combine complex and heterogeneous data from the project participants into a consistent database. The flow of data between project

participants and project phases is best handled digitally in a Common Data Environment (CDE). The current projects are largely concerned with the digital product model and less with the processes surrounding a construction project, even if the BIM vision focuses on process-related project execution.

Digitalization in the construction industry and the application of modern information technologies offer a great potential to improve construction safety and health in the planning phases. According to Eastman et al. [5], "BIM is one of the most promising developments in architecture, engineering, and construction (AEC) industries. With the BIM technology, an accurate virtual model of a building can be digitally constructed." The BIM-based risk management, clash detection, cost estimation, and 4D simulation have now become established features to support construction project management [6]. It supports the design through all its phases until the project is completed, and also allows better analysis and control than existing manual processes [7].

Building Information Modeling (BIM) represents a promising development in the architecture, engineering and construction industries. With this method, accurate building models can be digitally displayed. It supports the design through all its phases till the project is completed and allows better analysis and control than existing manual processes.

3D-model-based clash detection, risk management, cost estimation and 4D animation have become established methods to make construction management more efficient [8]. The use of BIM for construction project planning offers many other advantages [9].

3.2 Lean Construction Management

A production system is based on fundamental principles, standards, methods, and tools. It describes the standardized way of working and organizing companies according to lean principles. The goal of Lean Management in the construction industry is to avoid waste, to focus on the customer, and to increase the added value of its product. So far, the application scenarios used in the construction industry have focused predominantly on analogous processes for planning and controlling construction [10]. The inherent focus of Lean Construction's production system is on the process level, system control, and process-based organizational design.

It is clear from these statements that the two methods have different modes of operation. The Building Information Model represents the product and the Lean Construction Method describes the process

Building Information Modeling (BIM) and Lean Construction are two different methods of improving the construction process originally developed by different stakeholders with different goals. Over the past decade, both methods have begun to spread fast in practice.

Recently, however, it has come to be realized that these two methods have considerable synergy and that it is advantageous to implement them together. In view of this, there is an increasing need to sensitize BIM users to Lean principles and methods as well as Lean users to the BIM project workflows.

3.3 Synergies

A combination of the BIM and Lean methods can generate synergies if the two methods are harmonized. On closer inspection, it can be seen that the two methods are complementary in many target images, but the approaches and modes of action are different. A detailed study examining BIM applications and lean processes was conducted by Sacks et al. a. and showed 56 interactions of both methods [11]. In order to realize the synergies of the two methods, concrete intersections have to be identified.

4 Methodology

This research contributes to the improvement of construction process planning by using the information of a Building Information Model to develop a takt-time plan according to lean construction principles.
In this research, two main data sources are needed for construction process planning. Information about the building including all objects and quantities will be delivered via a Building Information Model (BIM). Second, information about the processes is needed. The process information will be derived from the process model database. The major parts of the proposed framework are shown in Figure 3.

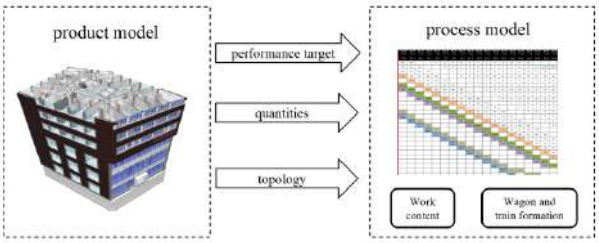

Figure 3. BIM-based lean construction production model

Decision-making in construction management is commonly based on empirical knowledge, because it is not easy to evaluate different execution strategies by using traditional scheduling methods. Although the

number of possible solutions is limited by numerous constraints, the remaining possible execution strategies are almost unlimited. However, they are influenced in terms of production technique and production costs due to different constraints [12].

The objective of this approach is to integrate basic and methodical knowledge of construction management into the model. In order to achieve this objective, four steps need to be defined:

1. Capture the relevant requirement from users point of view,
2. Describe this requirement within a model,
3. Develop abstract solutions by using empirical knowledge and
4. Implement the solutions by adapting them for a specific project.

Building components are represented in an object-oriented context in this work. Accordingly, objects belong to a class with their individual properties. Furthermore, building information models contain geometric data about the material, location, weight and other properties. The building structure is hierarchical. The building is structured in floors, groups of objects (e.g., walls, slabs) and individual objects. Objects must be uniquely identifiable.

5 Use case: Takt-time planning

5.1 BIM-Lean Integration

How can the two methods, Lean Construction and BIM, be combined on a practical level? Lean Construction is operationalized through application-oriented methods. An essential method in construction is the takt-time planning aimed at reducing the size of batches to simplify the control of construction processes. The way to a Lean Construction takt-time planning can be sustainably supported by the consistent and reliable information provided by BIM-based project handling.
The basis of the timing of the construction process is a precise reflection of the performance target. The performance target is guaranteed in the BIM project by a model-based calculation of the construction work. The content of the model-based calculation is the spatially separated quantities and service items and their combination with effort and performance values. Further calculation bases from the product model are - for example, the building topology to derive a zoning for the building. These data can be incorporated directly into the takt-time planning from basic quantities or used as a control entity for plausibility calculations. The link between the production processes and the objects of the building information model enables the simulation of execution strategies and their return to a harmonized production schedule.

5.2 Product Model

The input data for the generation of the schedule are project-specific data generated from the building information model. This model provides the building with specific input data e.g., building objects, hierarchical order, and quantities.

Building components are represented in an object-oriented context in this work. Accordingly, objects belong to a class with their respective properties. Building information models contain the geometric data about the material, location, weight, and other properties. The building structure is hierarchical. The building is structured in floors, groups of objects (e.g., walls, slabs, rooms) and individual objects. Objects must be uniquely identifiable (Figure 4). In the model-based cost calculation phase, every single object will be calculated.

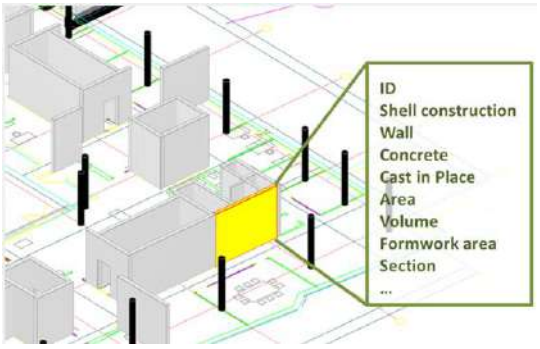

Figure 4. Definition of the building structure

In the cost calculation process, the individual costs of the part services are already determined for every single object. This includes, for example, the costs of wages, materials, and equipment. In the following, this object-oriented cost calculation allows these component and room-specific values to be used as a basis for process planning.

The described preparation process from modelling the building and determining the component-specific costs provides the information needed in the following multi-level process planning.

5.3 Takt-time planning process

Takt-time planning is one of the most used methods in the Lean Construction context. The German word "Takt" means "beat". In this context, it means the processes on the site follow a standardized takt developed in the following eight steps (Figure 5).

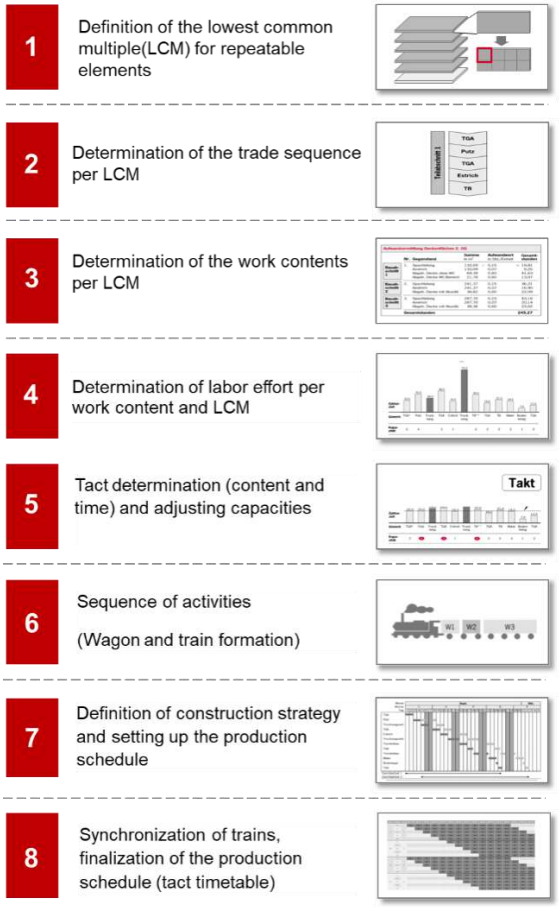

Figure 5.Takt-time planning workflow

In order to determine the exchange requirements with regard to process planning, the eight steps must be examined with regard to the following criteria:

- **Who** is requesting?
- **Why** is this information important to exchange?
- **When** is the information needed?
- **What** information supports the request?
- **To Whom**? Actor that fulfills the information need.

In the first step of the workflow is the analysis of the lowest common multiple (LCM) (Figure 6). Projects with a high repetition factor on similar construction stages are well-suited for takt-time planning. In this case, all services of internal works for a LMC have to be calculated at once and multiplied by the repetition factor.

With the traditional method of process planning, steps 1–4 involve considerable effort. All information must be gathered together from different documents e.g., tender specifications, and expert reports (Figure7).

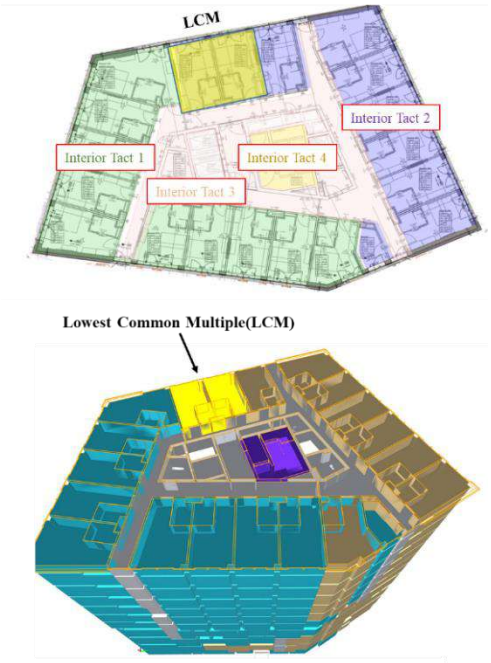

Figure 6.Visualization of interior takt areas on a 2D-plan (on the top) and BIM-Model (below) with the lowest common multiple.

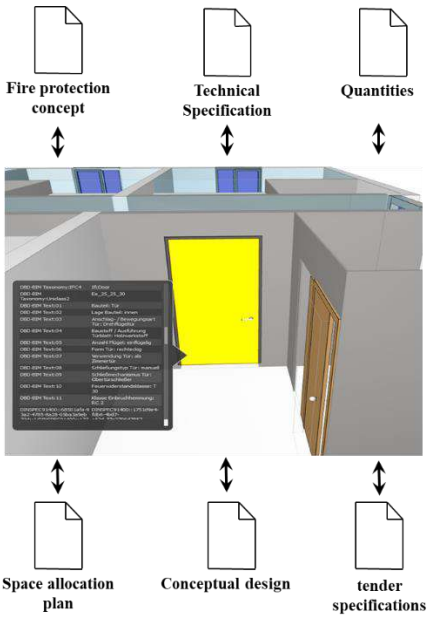

Figure7. Sources of information for building specifications

In BIM-based process planning, the information for steps 1–4 is generated directly from the BIM-model. However, the questions raised before must be addressed.

Who is requesting? <<Process planner>> According

to a uniform classification system such as OmniClass.

Why? Process planning according to Lean Construction methods requires detailed information on the performance and structure of the building.

When? The information is transferred after the technical description of the elements before the work preparation.

What information? A set of attributes are the minimum requirement for the process (Table 1).

Table 1. Minimum requirement for process attributes for rooms

Attributes	Attributes
ID	Ceiling surfaces
Component type	Floor area
Classification	Floor
Room number	Construction phase
Length, Width, Height	Takt number
Ceiling height	Process code
Structural height	Costing code
Wall surfaces	

To Whom? <<Architect>> According to a uniform classifications system such as OmniClass.

In step 5, the previously calculated workload must be adjusted to the set takt time (e.g., one week). This happens through the variation of different parameters. This includes the shifting of services within the interior work train, adjusting the number of employees (Figure 8).

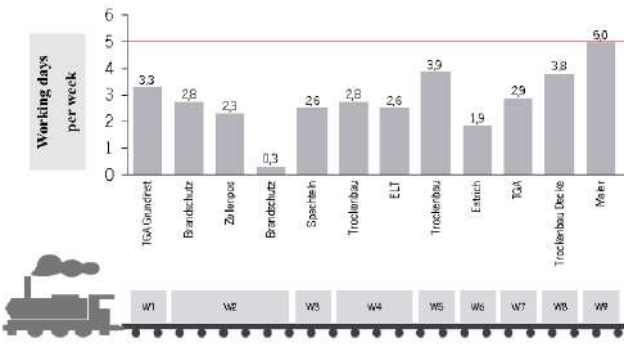

Figure 8. Takt adjustment

Work packages can be grouped together in one wagon if there is a no collision. Such a grouping can be seen in the picture 8 wagon "W2". There, three trades together become a wagon because with simultaneous execution no mutual influence is to be expected.

The first resulting Step 6 is a train of trades to complete the work. Now you can change the construction process by changing the construction strategy. For example, the number of trains and the direction of the construction work flow can be varied. In the proposed framework, the effects can be analysed directly on a 4D model. Figure 9 shows a 4D-takt-time sequence of shell construction work. The wagons "W1"- concrete walls - and "SL1"- concrete slabs - alternate floor by floor between the construction sections. Through this sequencing of work, an optimal use of resources is ensured.

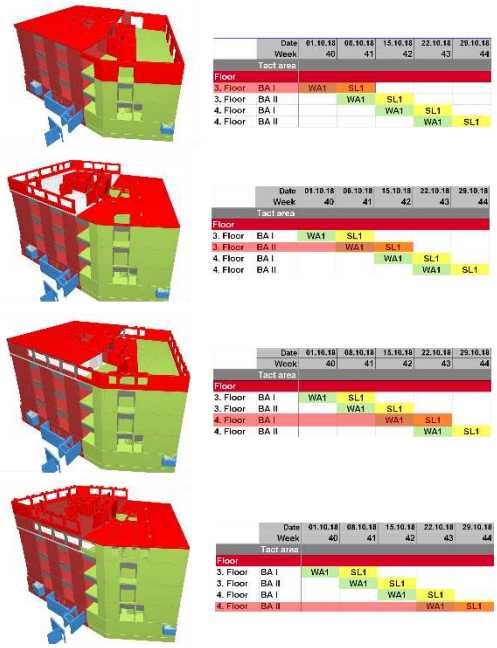

Figure 9. 4D-takt time sequence

6 Results

The following investigations are presented using the example of a real construction project. An object-oriented 3D building information model of a 17-story hotel building was selected for the case study. The hotel building has 220 guest rooms. The 3D model represents all the structural elements of the concrete shell structure such as foundations, beams, walls, columns, and slabs. Furthermore, the model includes all rooms with their specific attributes to determine the interior work processes. The building model contains approximately 55000 objects (Figure 10). The objective of this study was to determine the practical benefits and limitations of the developed system.

The benefit for a process planner is the developed querying function that automatically determines the quantities and labour hours from the model and calculates the duration for each of the planned activities. The developed semi-automated takt-time planning approach has been found to assist the workflow and quality during construction process planning. However, there are some current limitations and challenges. The

framework requires a comprehensive knowledge of the construction processes and its subsequent activities. The gathering of all the necessary input information is a crucial point when generating quality results. While activities related to concreting work were investigated, further investigations have to be done in developing process templates for the major construction works. In order to make use of the full potential of the method, the IDM with all elements must be described in further work.

Figure 10. BIM-Model for evaluations

7 Conclusions

BIM and Lean Construction are promising methods to improve construction processes. Until now, these methods used to be developed and applied separately. Linking the methods may create currently undiscovered benefits. However, finding an effective way to join both methods is difficult. First, this work has determined the minimum information requirements for process-oriented project planning using BIM.

It initially demonstrates the application of an Information Delivery Manual (IDM), specially the exchange requirements to determine the standard attributes that are necessary for takt-time planning.

By using digital building information models, construction processes can be planned in detail. Both the planning and the execution processes are, thus, holistically considered and coordinated. The next development steps are the further expansion of the method for more Lean methods and the integration of the takt control in the framework. Thus, the planned processes with actual site data are evaluated.

References

[1] Koskela L. Lean Production in Construction. *Proceedings of the 10th ISARC*, pages 47-54, Houston, USA, 1993.

[2] Egan J. *Rethinking Construction*, London, 1998.

[3] Hollermnann S. *An object-oriented approach to knowledge-based project planning*. Bauhaus-Universität Weimar, Ph.D. thesis, 2016.

[4] BuildingSMART International User Group http://iug.buildingsmart.org, Accessed: 28/01/2019.

[5] Eastman C., Teicholz P., Sacks R., and Liston K. *BIM Handbook: A Guide to Building Information Modeling for Owners, Managers, Designers, Engineers, and Contractors*, volume 2. John Wiley & Sons, 2011.

[6] Hartmann T., van Meerveld H., Vossebeld N. and Adriaanse A. Aligning building information model tools and construction management methods, *Automation in Construction*, vol. 22, pages 605–613, 2012.

[7] Melzner J., Teizer J., Zhang S. and Bargstädt H.-J. Objektorientierte sicherheitstechnische Planung von Hochbauprojekten mit Hilfe von Bauwerksinformationsmodellen“, Bauingenieur, Vol. 11, pages 471-479, 2013.

[8] Hardin B. *BIM and Construction Management: Proven Tools, Methods, and Workflows, Wiley, Indianapolis*, 2009.

[9] Hartmann T., Gao J. and Fischer M. Areas of Application for 3D and 4D Models on Construction Projects. *Journal of Construction Engineering and Management*, 134 (10), pages 776–785, 2008.

[10] Sitzberger R., Ditandy J. and Wolf R. End-to-End Projektmanagement: Mehr Transparenz und Stabilität in Bauprojekten. *Jahresausgabe Bauingenieur*, pages127-129, 2018/19.

[11] Sacks R., Koskela L., Dave B. A. and Owenet R. Interaction of lean and building information modeling in construction. Journal of Construction Engineering and Management, 136(9), pages 968-980, 2010.

[12] Melzner J., Hollermann S., Elmahdi A., Le Ha Hong, and Bargstädt H.-J. Pattern-Based Process Modeling for Construction Management. *Proceedings of the 14th International Conference on Computing in Civil and Building Engineering (14th ICCCBE)*, Moscow State University of Civil Engineering, 2012.

Automated Unit Price Visualization Using ArcPy Site Package in ArcGIS

K.J. Shrestha[a] and H.D. Jeong[b]

[a]Department of Engineering, Engineering Technology, and Surveying, East Tennessee State University, USA
[b]Department of Construction Science, Texas A&M University, USA
E-mail: shresthak@etsu.edu, djeong@arch.tamu.edu

Abstract –

State Departments of Transportation (DOTs) in the U.S. have an increasing amount of digital data from various sources. One such set of data is structured unit price data collected from bid lettings. Such data contain unit prices of thousands of bid items from hundreds of projects every year. While state DOTs have such data from over a decade-long period, utilizing such data has been challenging because of the lack of automated analytical and visualization methodologies and tools to generate meaningful and actionable insights. This study develops an automated methodology to quickly and accurately generate color-coded visualization maps representing unit price variation across a geographical region. It uses Inverse Distance Weighted (IDW) technique that is based on the Tobler's First Law of Geography. The law states that points closer together in space are more likely to have a similar value than points that are farther away. The methodology is automated using ArcPy site package in ArcGIS. It imports unit price data from preformatted spreadsheets and boundary maps from existing ArcGIS shape files to generate unit price maps. The tool and the visualizations are expected to aid state DOTs in generating and communicating meaningful insights for making data-driven decisions. It can be used to investigate areas with higher unit prices for various items which can aid state DOTs in identifying potential causes of higher unit prices such as lack of competition and lack of sources of materials (e.g. quarry) in nearby locations.

Keywords –

Geographic-Information-System; Unit-Price-Visualization; Spatial-Analysis; Bid-Price-Estimating; Construction-Market

1 Introduction and Background

Computing accurate cost estimates for highway construction projects is a never ending challenge faced by state Department of Transportation (DOT) engineers. Estimating accurate construction costs is especially challenging in early phases of the project when a limited amount of information is available. Some of the major factors affecting construction costs and its accuracies include project location, project size, project type, and market inflation. State DOTs collect a large amount of data that can be used to improve the construction estimation accuracies. While project size, type, and market inflation can be represented easily using numerical or categorical variables to account for construction cost variations, accounting for the location factor is more challenging. The spatial information collected by state DOTs coupled with computational tools such as ArcGIS can be used to account for the spatial variation of construction costs. A methodology for such process is described in a previous paper by the authors [1]. Although such methodology has been developed, adaptation of such methodology is likely to be hindered by complications in its implementation. Thus, there is a need to develop a tool to automate such spatial analysis to ease its implementation. This paper discusses a tool that is developed to automatically generate and import relevant data and create a unit price map that can be used as a visual communication tool about the construction market across a geographical region and to generate unit price estimates that account for the spatial variation.

2 Prior Studies

The location of a construction project is one of the most important factor affecting the project's productivity, and costs [2,3]. Those effects are a result of the cost for hauling materials, mobilizing equipment, and other site conditions. Other potential reasons that affect the construction costs across a geographical region include the level of competition in the construction market and local regulations such as minimum wage rates. Highway contractors tend to limit their projects in a certain region to remain competitive.

Similarly, the availability of limited space for construction and state DOTs' desire to complete projects faster in populated areas can significantly increase the construction costs in urban areas. Thus, accounting for the spatial factor is a must for accurate cost estimating. However, current practices have been very limited to partial accounting for such spatial effects on construction costs. For example, Iowa DOT uses an average unit prices from across the state to generate estimates for new construction projects [4]. Using the statewide average unit prices basically ignores the effect of spatial variations in the construction costs. In other cases, experienced engineers tend to account for the location factor based on their experience with previous projects. Several organizations have developed location adjustment factors to address this issue. This includes ENR city indexes and RS Means location factors [5,6]. However, those indexes provide data for a limited number of cities and are not necessarily focused on heavy civil construction projects and hence might be of little use for state DOTs' estimation purposes. A previous study by the authors developed a new methodology to account for spatial variation of construction costs across a geographical region by utilizing historical bid data and ArcGIS [1]. Similarly, another study by Zhang [7] also developed GIS based method to adjust construction cost estimates by project location. Another study utilized spatial interpolation method to understand housing and commercial establishment market [8]. However, while the methodologies are powerful, the implementation of such methodologies is challenging for state DOTs' day to day use because of the lack of automation and complexity in manually utilizing such methodologies. Thus, there is a need to develop a tool to automate the methodology to develop unit price maps of bid items which can be used to communicate and account for the spatial variation of the unit prices across a geographical region.

3 Limitations of Prior Studies

While some studies have attempted to solve the issue, the biggest challenge to communicate and account for spatial variation of construction costs in actual practice by state DOT estimators is the lack of automation. While researchers may be able to utilize advanced data analytics to prove the applicability of innovative techniques, such methods are rarely used in actual practice by state DOTs. State DOT employees have limited time and are not necessarily familiar with statistical and visualization theories and computer applications. This study tackles this challenge by developing an automated script that utilizes Python-based ArcPy Site Package developed by Environmental Systems Research Institute (ESRI) for ArcGIS.

4 ArcGIS and ArcPy Site Package

The ArcGIS is a powerful mapping and analytical platform developed by ESRI [9]. While powerful, it can also be complicated and time consuming to manually conduct spatial analysis using ArcGIS – especially when such analysis includes multiple steps and are to be performed by those who are not very familiar with the software. Thus, ESRI has developed an ArcPy Site Package to automate spatial data analysis, data conversion, data management, and map development [10]. The site package is based on Python programing language that is widely used for statistical analysis, text mining, as well as general purpose programming. This study utilizes the ArcPy Site Package to automate the unit price map development.

5 Framework for Automated Unit Price Visualization

The automated unit price visualization framework can be divided into four components (Figure 1): a) database preparation, b) base map preparation, c) unit price map development, and d) unit price estimation.

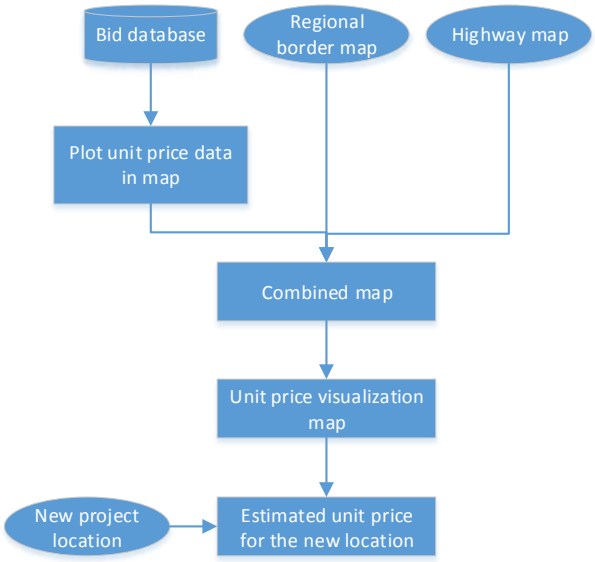

Figure 1. Automated unit price visualization methodology

5.1 Database Preparation

State DOTs have collected digital structured bid data for years. This database consists of historical project information such as the project location and bid data that include the unit prices of various bid items. The project information database can include data such as project ID, contract ID, project description, winning bid

(or contractor), and project location coordinates. The bid database can consist of the project ID that the bid data belongs to, item IDs of all bid items for a given project, and quantities and unit prices of various bid items.

5.2 Base Map Preparation

The geographical maps of the state border lines and highway maps are the two mapping components required for the unit map preparation. The border map becomes a boundary within which the color-coded visualization map will be developed based on the unit prices of items at various locations. The highway maps make it easier to comprehend the visual data points indicating the locations of the projects in respect to the highways.

5.3 Unit Price Map Development

In this step, first, the project data and bid data are combined to generate a list of unit prices of a bid item of interest and coordinates of the project locations where the bid item was used. The data are then plotted in an ArcGIS map to indicate exact project locations and unit prices of the bid item at those locations. Then, the unit price data are interpolated using the Inverse Distance Weighted (IDW) method to generate a map showing the estimated unit prices of the bid item of interest in any location within a boundary map.

5.3.1 Inverse Distance Weighted (IDW) Method

The IDW method is based on the Tobler's First Law of Geography. The law states that points closer together in space are more likely to have a similar value than points that are farther away [11]. Mathematically, the law can be expressed as:

$$p_j = \frac{\sum_{i=o}^{n} \frac{p_i}{d_{ij}}}{\sum_{i=o}^{n} \frac{1}{d_{ij}}} \qquad (1)$$

In this equation (1), p_j is the estimated unit price of the bid item in a new project (j) location, p_i indicates a unit price of the same bid item from a past project (i), and d_{ij} indicates the distance between the past project location and the new project location. Thus, given the locations of the past and new projects and the unit prices of the item of interest in all the past projects, the unit price of the item for the new project location can be estimated.

5.4 Unit Price Estimation

Once the unit price visualization map is developed, estimators can input the location of a new project and obtain an estimated unit price for the location based on the IDW technique.

6 Results

The researchers collected historical bid data from the Montana Department of Transportation (MDT) in Excel format. The most important datasets relevant to this study were the project information and bid item datasets for all the projects awarded from 2010 to 2014. These datasets were imported in MS Access database program to enable generating customized data quickly for only the bid item of interest for select year or range of years by combining the two datasets. The data generated from the query was exported and saved as a comma separated values. Table 1 shows a sample unit price data generated for the bid item 4020368 (emulsified asphalt CRS-2P). This item is one of the largest items in terms of total dollar value accounting for $120,350,573 in the projects included in the database and is also one of the most frequently used items.

This data is read by a python script and a new shape file capable of storing location and unit prices of the bid items is programmatically developed. This shape file is combined with a Montana state boundary map and a highway map obtained from MDT's GIS division. This intermediate map is shown in Figure 2.

Table 1. Sample unit price data for item 4020368 (emulsified asphalt CRS-2P)

Latitude	Longitude	Unit Price	Project ID
48.43666667	-104.4969444	654.26	1196
48.02916667	-115.3302778	658	1257
45.88305556	-111.87	463	791
45.88305556	-111.87	463	790
46.32666667	-112.745	510	834
47.48805556	-111.1813889	925	463
46.36472222	-113.3725	465	845
46.36472222	-113.3725	465	844

47.16111111	-114.86	598	964

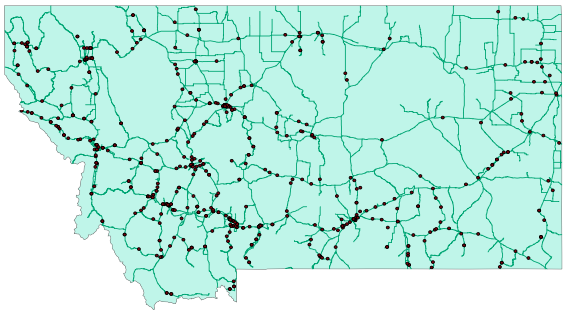

Figure 2. Montana state border map and highway map with project locations.

Finally, a color-coded interpolation map indicating unit prices of the bid items throughout the state is developed as a new shape file and combined with the maps. Figure 3 shows a unit price map generated for the bid item 402020368: emulsified asphalt CRS-2P per ton. The unit prices of the item vary from as low as $125 to as high as $3,500. The red color indicates higher unit prices while the blue color indicates lower unit prices.

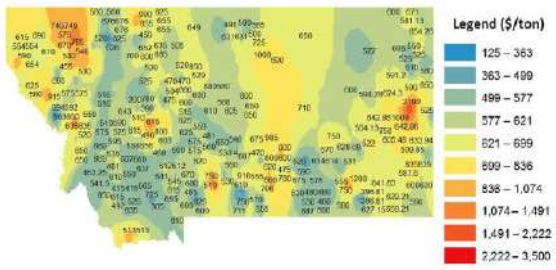

Figure 3. Unit price map for emulsified asphalt CRS-2P per ton

7 Discussion

The automated unit price visualization tool developed in this study enables estimators to easily develop unit price maps of desired bid items. This tool can be used to get insights about the market condition across a geographical region aiding state DOTs to identify areas with higher construction costs. Such insights can direct state DOT estimators to further investigate the reasons behind the higher construction costs and develop strategic plans to potentially reduce construction costs. Further, this highly detailed cost information about the regional construction market enables estimators to determine more accurate construction cost estimates by accounting for the spatial effect that is otherwise challenging to address. This tool also offers a higher granularity than any other location factors that are currently available to state DOT estimators.

8 Future Research

Currently this tool has two separate components: a) generating the required data from the master database containing all the project level and bid level information and b) unit price map generation based on the data generated from the previous component. While both steps are automated, those steps are isolated and hence they need to be executed separately. A future tool should combine those two components into a single coherent system. This can potentially be achieved by using the database such as ArcSDE where the required data are extracted systematically using programmatically generated dynamic Structured Query Language (SQL) queries. Further, the current Python based tool does not have a Graphical User Interface (GUI). Adding a user friendly GUI will make it even easier for the implementation of the tool for unit price map generation as well as estimation purposes.

Current tool is more focused on automating the visual unit map development. Current Python scripts enable estimators to develop a unit price map of one bid item at a time. This function can be further enhanced to develop a more sophisticated tool that possibly takes all bid items of a new project as input to generate unit price maps for all bid items at once. Thus, such tool can be used to effectively generate the total construction cost estimate of a new project.

Finally, the current tool serves as a powerful visualization tool. However, the tool only accounts for the spatial factor and ignores other factors such as project type. Such factors may be incorporated in the future tool by using pre-filtered data only from the projects of the same type to generate a more precise unit price map.

9 Conclusion

This study developed a tool to automate the unit price map generation process using the bid data collected by state DOTs. This tool enables estimators to utilize their own data for construction market analysis, visually communicating the market information, and develop bid item price estimates that can be used to develop construction cost estimates. The automation and ease of utilizing the tool will aid in implementation of the powerful unit price development methodology that might otherwise be a complicated process for DOT estimators.

10 References

[1] Jain D, Shrestha J, Jeong D. Spatiotemporal Visualization of Major Cost Items in Highway Construction in Iowa 2014.

[2] Erickson R, White K. Description of Federal Highway Administration's National Highway Construction Cost Index, 2011.

[3] Ghosh A, Lynn R. DOD Area Cost Factors (ACF) 2014.

[4] Iowa Department of Transportation (IADOT). Cost Estimating Database Details 2012.

[5] Grogan T. What Drives ENR's Cost Indexes. Engineering News-Record 2008.

[6] RSMeans Engineering Staff. RSMeans Building Construction Cost Data 2016. 74th edition. RS Means; 2015.

[7] Zhang S. Validation of Geographically Based Surface Interpolation Methods for Adjusting Construction Cost Estimates by Project Location 2014:1–13. doi:10.1061/(ASCE)CO.1943-7862.0000850.

[8] Montero JM, Larraz B. Interpolation methods for geographical data: Housing and commercial establishment markets. Journal of Real Estate Research 2011;33:233–244.

[9] Environmental Systems Research Institute (ESRI). About ArcGIS | Mapping & Analytics Platform n.d. https://www.esri.com/en-us/arcgis/about-arcgis/overview (accessed December 19, 2018).

[10] Environmental Systems Research Institute (ESRI). What is ArcPy?—Help | ArcGIS for Desktop n.d. http://desktop.arcgis.com/en/arcmap/10.3/analyze/arcpy/what-is-arcpy-.htm (accessed December 13, 2018).

[11] Eberly S, Swall J, Holland D, Cox B, Baldridge E. Developing Spatially Interpolated Surfaces and Estimating Uncertainty. 2004.

Real-time Tracking for Intelligent Construction Site Platform in Finland and China: Implementation, Data Analysis and Use Cases

Jianyu Zhao[a], Jinyue Zhang[b], and Olli Seppänen[a]

[a]Department of Civil Engineering, Aalto University, Finland
[b]Tianjin University-Trimble Joint Laboratory for BIM, Tianjin University, China
E-mail: jianyu.zhao@aalto.fi, jinyuezhang@tju.edu.cn, olli.seppanen@aalto.fi

Abstract –

Production control, especially lean construction approaches, has necessitated the needs of eliminating waste onsite. Though the collaborative methods such as Location-Based Management System (LBMS) and Last Planner System (LPS) have proven the improvement of productivities, the process of data collection has still remained manual, which could result in inaccuracy and incompletion. Automatically locating workers has been proposed to enable a method for production control in construction projects onsite. Thus, a platform is sought where an easy and passive tracking system is designed to enhance the production control processes.

In recent years, Finland is experiencing crucial transition from traditional production to digitalization formation while China has been a model where massive construction takes place as cities are expanding over the economic booming. The extensive building activities require a smooth and automated tracking system that can control and manage resources onsite to monitor in real time and examine the productivities more efficiently. This paper presents case studies in Finnish and Chinese construction sites where the proposed real-time tracking system was implemented, and the tracking data were analyzed for purposes of operations management. The model combines Bluetooth Low Energy (BLE) technology and 3G/4G network as connection methods, and explores the movements and time information of workers onsite, aiming to establish an intelligent construction site platform, which can be used for managing resource flow within lean principles in Finland and China.

Keywords

real-time tracking, production control, construction, China, Finland, case studies

1 Introduction

Complexity and hazard in construction sites are not uncommon where coordinating and managing onsite resources such as labor, material and tools with high efficiency is usually challenging [1]. To overcome poor site management performance and improve the workflow in construction, production control has been introduced and developed over years from the perspective of lean construction including Last Planner System (LPS) [2], Location-Based Management System (LBMS) [3] and their integration [4]. The approaches have tested many applications and they are expected to contribute positively to plan and control production scenarios [5] where waste reduction and project duration elimination can be realized through production control and forecasting [6]. However, the data collected onsite depend on manual work of information input, which requires substantial amount of time and resources and could lead to errors and inaccuracy [7]. Thus, it is reasonable to believe that current stages of production control based on manual collection of data have not reached the full potential of site management [8].

In recent years huge amount of construction activities have witnessed the growth of the construction industry in China [9]. However, the risks of project delays, quality defects, low customer satisfaction, etc. have been a series of obstacles that Chinese construction firms have to face [10]. In China, the comprehension and application of lean approaches have still remained in early stages and studies of lean methods in construction are also rare [11]. On the other hand, Finland has been actively piloting lean methods in construction. For example, meetings and data collections were organized by Skanska Finland to execute LPS phase scheduling and define Locations Breakdown structure in addition to tasks and logic in 2010 [3]; I.S Mäkinen Oy as a Finnish turnkey contractor specialized in cruise ship cabin refurbishment

applied Takt Time planning in a project to shorten project duration and improve productivity [12]. Those applications have seen the enhancement of production control in construction, but the difficulties of manual data collection during the process are revealed at the same time [13]. Thus, China and Finland can be good candidates to test the real-time platform under different degrees of lean methods applied and to see if a standardized tracking platform could be developed to unify country-specific requirements (e.g. China and Finland) and enable the potentials of automation of real-time onsite monitoring in construction.

There are many mature tracking methods that have been tested in construction industry with a goal to promote transition from traditional management which is heavily rely on manual work towards more intelligent onsite monitoring system where automation plays an important role of utilizing the input information [14]: (1) Lin et al. suggested a tracking system to support analyzing laborers' behaviors using ZigBee technology[15]; (2) Costin et al. used radio frequency identification (RFID) technology for construction resource filed mobility and status monitoring in a high-rise renovation project [16]; (3) Cheng et al applied Ultra-wideband (UWB) for automated task-level activity analysis [17]. However, among those technologies, Bluetooth-based system are examined to offer high degree of simplicity thanks to its ease of installation [18]. Olivieri et al. (2017) proposed a prototype where Bluetooth Low Energy (BLE) technology was applied to track workers, materials and tools from the perspective of production control [19]. Furthermore, Zhao et al. (2017) implemented the system in a laboratory test and proposed the possible use case scenarios [20]. However, no tracking data have been analyzed for visualization of worker's daily movement or the visualization results from the tracking can be shown to back up the proposed use cases in practice.

Aiming to solve the gaps of lacking data visualization results from the proposed tracking system and visualization-based use cases, we implemented the model on both Finnish and Chinese cases using the standardized procedures; then we gathered, analyzed and visualized the data from a random selected worker to examine his/her daily movement in all cases; at last we proposed the potential use cases based on the visualization results suitable for both Finnish and Chinese scenarios. The paper is focused to answer the following research questions:

1. How to implement the proposed real-time tracking system following standardized procedures in Finland and China?
2. How is the data visualization of randomly selected tracking worker in the case studies based on the proposed system?
3. What are the use cases of this real-time tracking system according to the results of data analysis and visualization?

2 Methods

2.1 Description of the model

Olivieri et al. (2017) have explored the requirements and solutions of the real-time tracking model within the scope of production control using BLE technology [19]. This paper followed the same infrastructure of the system, tried to generate the data visualization and suggest the use case scenarios according to the results.

Figure 1 illustrates how this real-time tracking model works in reality. The model is featured with gateways, beacons and a cloud storage. Gateways are Raspberry pies that are fixed at different places in construction sites, and beacons are portable that can be carried or tagged to track workers, materials and tools. Beacons passively transmit Bluetooth signals to gateways and gateways can determine the relative locations onsite by calculating the signal strength received from the beacons (link 1, 2 and 3). The gateways are connected with WIFI or dongles that uses 3G or 4G mobile network to be able to connect to cloud storage. The cloud processes the incoming data, apply algorithms and logics in production control, visualizes the information, and displays the updates of time and location details of the tracking resources in real time (link 4 and 5). Thus, the data visualization results can serve the purpose of onsite management and monitoring.

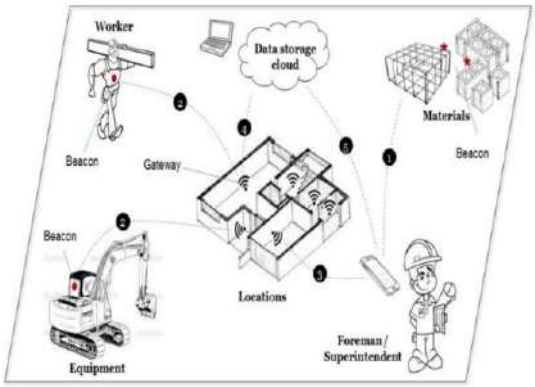

Figure 1. Proposed real time tracking scheme in construction site [19]

2.2 Implementation of the system in Finland and China

Case studies were scheduled one in Finland and one in China. For the Finnish case study, a residential renovation project was selected; for the Chinese case study, the onsite mechanical, electrical and plumbing (MEP) installation project was selected. We aimed to differentiate the project types and countries in our cases so we can test if the model can be applied in different forms and places with a standardized instruction and guidance. In our research, we aim to invest a platform as inexpensive as possible and still obtain holistic visualization information based on our light-weighted and easy implementation onsite. The cost for tracking gateways is 55 euro each and beacons for 4 euro each. Table 1 shows the case study description.

Table 1. Case studies description

Case	*Companies participated*	*Tracked objects and beacon distribution*	*Number of gateways*	*Total cost of the system*
Case 1. Renovation project in Finland	Renovation company	10 beacons to workers and 2 to foremen;	10 gateways onsite;	598 Euro
Case 2. Office building in China	MEP subcontractor	5 beacons to MEP workers; 1 beacons to onsite equipment	5 gateways onsite	299 Euro

2.2.1 Case 1. Residential renovation project in Finland.

The jobsite is located in Helsinki, Finland where we put 10 gateways and the warehouse for material delivery is located in Vantaa, Finland where we put 2 gateways. The renovation building is 3 floors where we put 1 gateway at entry in ground floor, 4 gateways in first floor covering each apartment, and 5 gateways in second floor with 1 additional one in the corridor. Figure 2 shows the simplified jobsite floor with gateways marked. The initial system setup time onsite is 6 hours with a few hours per week for maintenance. However, during the tracking period, the onsite conditions (e.g., gateway connections and locations) did not change, thus making the system maintenance work easy and convenient.

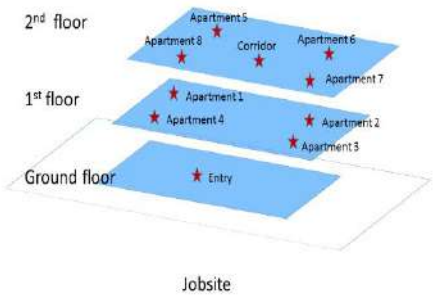

Figure 2. Real time tracking case study floor plan in case 1

2.2.2 Case 2. MEP installation project in China

We selected an entire floor in an office building of around 1500 square meters (open space with length of 50 meters times width 30 meters) to test the same tracking system. The jobsite is located in ShiJiaZhuang, a city that is about 100 kilometers from the capital Beijing. The tracking system monitored the work process of mechanical, electrical and plumbing jobs. Apart from case 1, 4 gateways were placed at each corner of the floor facing northeast, northwest, southeast and southwest. 1 gateway was placed in the middle closed to the entry of that floor. The setup time for the system onsite is 7 hours with approximate 2 hours per week to ensure the gateway connectivity stays valid. Figure 3 lists a floor plan of the jobsite with gateways installed.

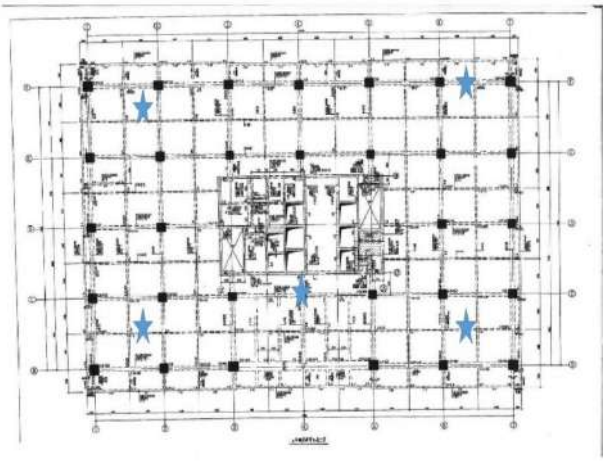

Figure 3. Real time tracking case study floor plan in case 2

2.2.3 Case selection and standardized instruction

We aimed to provide a standardized instruction for installation and implementation of the system onsite so

that we could overcome the country-specific requirement in practice and make the system function well regardless the construction site location. We selected Finland and China as a pilot places for testing because we wanted to see if the real-time tracking system serving the purpose of lean construction can be successfully implemented in these countries where one started to apply lean construction actively for many years [3][12] while the other still remained reluctant to explore the lean approaches [11]. Thus, it would be beneficial to see if the real-time tracking system under the scope of lean construction philosophy, because of its easy installation and automation data collection, can promote the process of applying lean methods in countries that are at the early stage.

We standardized the guidance of installation and instructions of workers in both case studies in order to promote the universal solution of onsite system implementation despite of the location or country selected. The general system implementation processes are: (1) determine the number of gateways and beacons needed; (2) configure file images into each gateway and activate beacons; (3) register beacons with predefined work type (e.g. plumber 1) in the tracking system; (4) onsite gateway installation and mark the gateway location precisely in the floor plan; (5) notify the workers of the tracking process and obtain their consents. (6) Tracking begins.

2.2.4 Data analysis and visualization

The raw data in the cloud storage display thousands of recorded time intervals, which contains information including the tracking carrier (e.g. plumber 1), location, start time, end time and the time duration. Thus, the raw data is very fragmented and hard to comprehend. We filtered out large time intervals such as overnight durations, aggregated them based on site location and visualized the daily movement of tracking workers. The results are especially useful for proposed applications of use cases in different scenarios. To illustrate the movement of workers, the details of random selected workers and time are listed in table 2.

Table *2*. Random selected worker for tracking

Case	*Random selected worker*	*Selected date*
Case 1. Renovation project in Finland	Carpenter 2	June 5th
Case 2. Office building in China	Plumber 4	January 22nd

3 Results

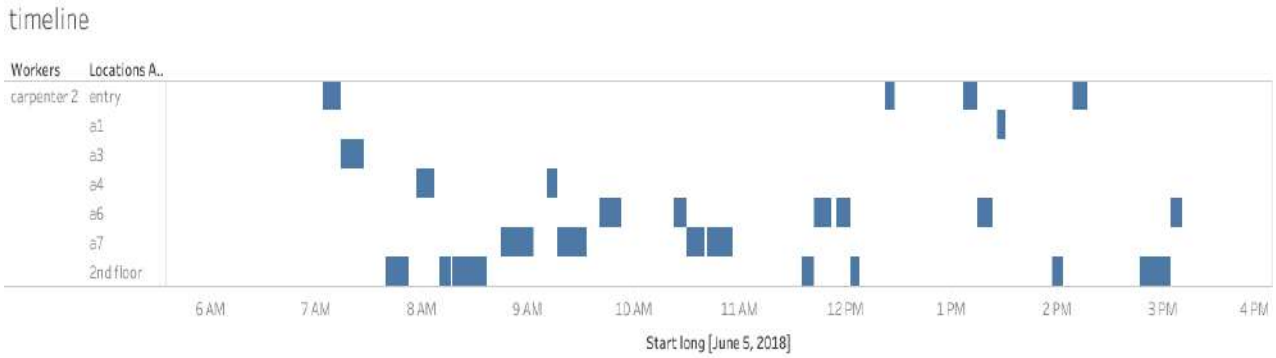

Figure 4. Movement visualization of tracking result for carpenter 2 on June 5th in Finnish case

3.1 Visualization result for the Finnish case

Figure 4 demonstrates the real movement line of the selected worker in Finnish case on June 5th. The horizontal axis indicates the timeline, and the vertical axis shows the location details of the time from 6am to 4pm. In the figure, a1 to a7 are the apartment numbers.

From the figure, we can see that the worker entered jobsite at 7:44 am and left jobsite at 3:05pm. The worker spent his/her first 10 minutes near the entry area and he/she actually first started at the work-related place (e.g. apartment a3) at 7:14am. He/she probably had a lunch break between 11am and 11:30am, and possibly had several coffee breaks between 9:50am to 10:20am and between 12:40 pm and 1:05 pm outside of the jobsite. Since the worker stayed at the second floor the most time during the tracking period, it is reasonable to think that he/she did the most work in the area (especially apartment a6 and a7).

3.2 Visualization result for the Chinese case

We executed the visualization process following the same method and obtained the results for the random selected worker daily movement in Chinese case as in Figure 5.

The horizontal axis indicates the timeline details from 6am to 12pm. The worker did not spent time in northeast area so the system automatically filtered out that location in the figure.

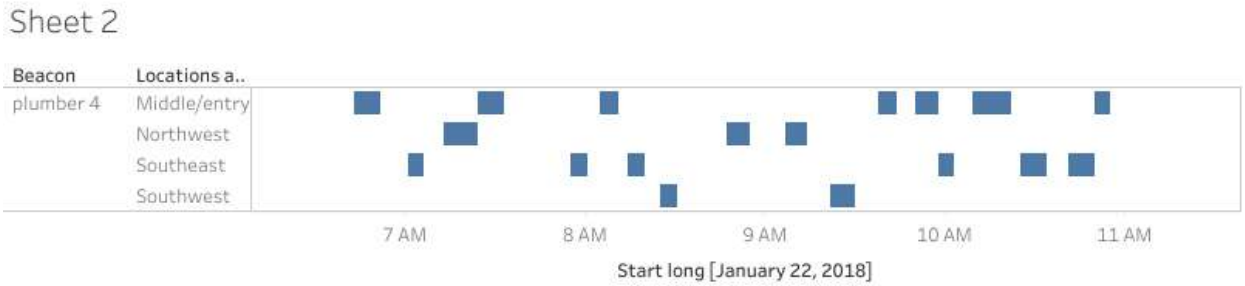

Figure 5. Movement visualization of tracking result for plumber 4 on January 22nd in Chinese case

We can see the plumber entered the jobsite at 6:43am and left the tracking floor at 10:56am. The visualization figure indicates the scattered movement for the worker onsite while in schedules they are typically expected to finish a task in one location before moving to another. This corresponds to our assumption of existence of potential construction waste in jobsite.

3.3 Use case proposal based on visualization

Zhao et al (2018) has suggested several use cases based on real-time tracking system for monitoring the movement of workers in construction sites [21]. However, the paper has not connected the proposed use cases with the actual data visualization results so that no real-life results have yet backed up those use cases. Because of this, we explored the use cases based on the data visualization to promote the underlying tracking system into more practical level.

3.3.1 Waste detection and value-adding activities

Based on the visualization figures, the movement line of a worker can be displayed. It is clear to see how much time the worker has spent in different locations including entry area and offsite. For both cases in Finland and China, workers have spent quite much time in entry area, which would be a notable factor to result in waste on the jobsite. Though it is difficult to judge accurately if a worker has wasted time in the work areas, the waste level in terms of time spent on entry and offsite is obvious and worth noticing for site managers.

Waste level is tied with value-adding activities, which is an important use case for lean construction applications. In figure 4 and 5, the tracking visualization has indicated that the second floor areas in Finnish case and the southeast area in Chinese case are the main workplaces that the laborers performed their jobs. Thus, by aggregating the time durations that workers spent on workplaces to compare with total time of the day spent onsite would be a good use application to explore the value-adding level of the workers.

3.3.2 Safety control

The visualization helps with jobsite safety control in an efficient way. Since the visualization results are classified by location in vertical axis and time in horizontal axis, it is easy to apply safety control in the specified jobsite areas. For example, if southeast area in the Chinese case was alerted as an access-restricted place, it is straightforward for site managers to check whether or not and how many times the workers have entered the area and how much time they spent there. Since the beacons associated with carriers send signals passively to gateways, notifications can be sent to management and worker themselves in real time.

4 Discussion

4.1 Location-based tracking data visualization improvement

Figure 4 and 5 visualized the selected workers' movements in one day based on location and time information from the system. In vertical axis the locations were listed without real-life connections with each other. For instance, in Finnish case, the carpenter first entered the entry then moved to apartment a3 and the movement line connected both ends in the figure. However, it cannot give the information that the workers have necessarily passed through apartment in between. For better visualization experience in future research, 3D approaches are recommended to enable the logics and pathways between tracking locations. BIM applied in construction would be a good candidate to be integrated in the real-time tracking system.

4.2 Value-adding activity determination

Time spent on entry area or outside of jobsite during worktime can be determined as waste or non-value-adding time. However, it is of difficulties to define the amount of value-adding time even if the workers are detected in the workplaces during the worktime. In further studies, the data visualization process can be linked with workers' updated schedule for better recognition of value-adding activities onsite. If a worker is scheduled in a place for his/her work, the time spent in that workplace and captured by the real-time tracking system is more likely to be value-adding activities onsite.

4.3 System limitation and country-specific requirement

To make the tracking system function, gateways need to be connected with internet and power throughout the period. This could be challenging for construction jobsites equipping with all necessary supporting devices. Besides the system limitation, country-specific requirement is also important to observe. For instance, in Finland, it is by law required to get workers' explicit consents of tracking and labor union needs to give a pass too. In China, onsite device safety protection is needed from stealing when the tracking gateways are exposed in the open space. Internet connecting stability is another matter to ensure the usability of the system in China

4.4 Comparison discussion for future studies

The BLE real-time tracking scheme has been successfully implemented in both Finnish and Chinese construction environment and the data results were good for visualization. Compared with the Chinese case, the gateway placement in Finland is denser and in apartment-specific level in contrast of floor level. This provides an interesting perspective when it comes to the optimal gateway tracking placement strategy corresponded to different requirement of detail level of tracking. Furthermore, the visualization analysis can be executed in future study where the workflow and logistic flows can be researched as combination by tracking multiply onsite resources, therefore meaningful metrics such as utilization rate, uninterrupted presence of workers at work location, and material moving times in the building can be calculated and compared in Finland and China for its productivity and waste level of construction projects.

5 Conclusion

The paper has provided a set of standardized guidance and instructions on onsite implementation of BLE technology based real time tracking system. The model follows the principle of production control in construction under the scope of lean approaches, aiming to improve the productivity and decrease the waste onsite.

The case studies were scheduled for actual construction projects in Finland and China, providing time and location information that is recorded in real-time automatically in the system for data analysis. Furthermore, the paper presented the data results by visualizing the movement path of randomly selected workers in both cases. The visualization backs up the two proposed use cases in practice where waste detection can contribute to identifying the value-adding activities onsite and safety control uses can prevent men from entering the restricted areas. The contribution of the research is developing a light-weighted and low-cost tracking system, suitable for multiply construction projects, to seamlessly obtain movement and time information and provide managerial implication to workers and site managers. In future research and the further development of the system, the model is expected to enhance resource flows in construction and automate the management process in a smart and effortless way.

References

[1] Tah, J. H. M., and V. Carr. "Towards a framework for project risk knowledge management in the construction supply chain." Advances in Engineering Software 32.10-11 (2001): 835-846.

[2] Ballard, H. G. (2000) The last planner system of production control (Doctoral dissertation, University of Birmingham).

[3] Seppänen, O., Ballard, G., & Pesonen, S. (2010). The Combination of Last Planner System and Location-Based Management System. Lean Construction Journal.

[4] Seppänen, O., Modrich, R. and Ballard, G. (2015) Integration of last planner system and location-based management system. In 23rd Annual Conference of the International Group for Lean Construction. Perth, Australia. 29-31.

[5] Kala, T., Mouflard, C., & Seppänen, O. (2012, December). Production control using location-based management system on a hospital construction project. In 20th Annual Conference of the International Group for Lean Construction, San Diego, California, USA (p. 039).

[6] Seppänen. O, Evinger. J and Mouflard. C. (2014): Effect of the location-based management system on production rates and productivity, Construction Management and Economics, DOI: 10, 1080/01446193, 2013,853881

[7] Grau, D., Abbaszadegan, A., Tang, P., Ganapathy, R., & Diosdado, J. (2014). A combined planning and controls approach to accurately estimate, monitor, and stabilize work flow. In Computing in Civil and Building Engineering (2014) (pp. 105-112).

[8] Vieira, G. G., Varela, M. L. R., Putnik, G. D., Machado, J., & Trojanowska, J. (2016). Integrated platform for real-time control and production and productivity monitoring and analysis.

[9] Wang, Y., Sun, M., Wang, R., & Lou, F. (2015). Promoting regional sustainability by eco-province construction in China: A critical assessment. Ecological indicators, 51, 127-138.

[10] Gao, S., & Low, S. P. (2014). The Last Planner System in China's construction industry—A SWOT analysis on implementation. International Journal of Project Management, 32(7), 1260-1272.

[11] Li, S., Wu, X., Zhou, Y., & Liu, X. (2017). A study on the evaluation of implementation level of lean construction in two Chinese firms. Renewable and Sustainable Energy Reviews, 71, 846-851.

[12] Heinonen, A., & Seppänen, O. (2016). Takt time planning in cruise ship cabin refurbishment: lessons for lean construction. In Proc. 24th Ann. Conf. of the Int'l. Group for Lean Construction, IGLC, Boston, MA, USA.

[13] Rios, F. C., Grau, D., Assainar, R., Ganapathy, R., & Diosdado, J. (2015). Stabilizing craft labor workflow with instantaneous progress reporting. In 23rd Annual Conference of the International Group for Lean Construction, IGLC 2015. The International Group for Lean Construction.

[14] Nath, T., Attarzadeh, M., Tiong, R. L., Chidambaram, C., & Yu, Z. (2015). Productivity improvement of precast shop drawings generation through BIM-based process re-engineering. Automation in Construction, 54, 54-68.

[15] Lin, P., Li, Q., Fan, Q., and Gao X. (2013). Real-time monitoring system for workers' behavior analysis on a large-dam construction site. International Journal of Distributed Sensor Networks, 9(10), 509423.

[16] Costin, A, Pradhananga, N., and Teizer, J. (2012). Leveraging passive RFID technology for construction resource field mobility and status monitoring in a high-rise renovation project. Automation in Construction, 24, 1-15

[17] Cheng, T., Teizer, J., Migliaccio, G. C., and Gatti, U. C. (2013). Automated task-level activity analysis through fusion of real time location sensors and worker's thoracic posture data. Automation in Construction, 29, 24-39

[18] Park, J., Marks, E., Cho, Y. K. and Suryanto, W. (2016) Performance test of wireless technologies for personnel and equipment proximity sensing in work zones. Journal of Construction Engineering and Management, 142(1), 04015049

[19] Olivieri, H., Seppänen, O. and Peltokorpi, A. (2017) Real-time tracking of production control: requirements and solutions. In: Proc. Lean & Computing in Construction Congress (LC3), Vol. 1 (CIB W78), Heraklion, Greece.

[20] Zhao, J., Olivieri, H., Seppänen, O., Peltokorpi, A., Badihi, B. and Lundstrom, P. (2017) Data Analysis on Applying Real Time Tracking in Production Control of Construction (in press). 2017 International Conference on Industrial Engineering and Engineering Management (IEEM).

[21] Zhao, J., Seppänen, O., Peltokorpi, A., Olivieri, H., & Badihi Olyaei, B. (2018). Real-time resource tracking on construction site: implementation practice and use cases in different projects. In 17th International Conference on Computing in Civil and Building Engineering (pp. 449-456). Tampere, Finland: Suomen rakennusinsinöörien liitto RIL.

Identifying Moderation Effect between Project Delivery Systems and Cost Performance

H. Moon[a], H.-S. Lee[a], M. Park[a], and B. Son[b]

[a] Department of Architecture and Architectural Engineering, Seoul National University, South Korea
[b] Department of Architectural Engineering, Namseoul National University, South Korea
E-mail: axis1106@gmail.com

Abstract –

This study was performed to identify the theoretical attribution of project type that moderates the impact of project delivery systems on cost performance. Previous studies have used direct relationship analysis to evaluate the project performance (e.g., the relationship between PDS and its cost performance, or the relationship between project type and cost performance). These analyses can cause inconsistent results and need to be analyzed in a single model. To combine the relationships between influential factors on cost performance, a causal model (i.e., moderation model) was suggested. The objective of this study is to develop a moderation model and test the statistical significance of moderation effect between PDS and cost performance. As a preliminary study, we established a simple moderation model and examine the moderation effect of project type. To test the model, 134 public sector projects completed between 1998 and 2013 in South Korea were utilized. The dataset consists of both Design-Build and Design-Bid-Build projects which are the most prevalent delivery systems. Even though the preliminary test results were not statistically significant, we can suggest the better way to understand the causal relationship moderated by project type between PDSs and their cost performance. This study is expected to provide the theoretical basis of the mechanism by which PDS impact cost performance, help project participants to select PDS by considering moderating effects in specific project types, and evaluate PDS appropriately in terms of cost performance.

Keywords –

Cost management; Project delivery system; Design-build(DB); Design-bid-build(DBB); Cost performance; Change order; Project type; Moderation effect

1 Introduction

Evaluating project delivery system (PDS) in terms of cost performance has been conducted by comparing two prevalent methods: design–build (DB) and design–bid–build (DBB) [1-5]. Until the end of 1990s, most studies had concluded that DB outperforms the traditional DBB delivery systems in all aspects (e.g., cost, time, quality, safety and so on) [1-3]. However, adverse results have emerged in terms of cost performance since the early part of 2000s [4-7]. They found that DB is superior to DBB in terms of project schedule, however, cost performance is uncertain and debatable up to date. According to the previous studies, the reason why the comparison results are inconsistent depends on project type and dataset [7-8]. The explanation about the inconsistent results have been arbitrary without any theoretical basis.

To deal with this problem, causal model that explains the mechanism by which PDS cost effects operate should be needed. In research design, mediators and moderators are necessary to solve complex and unsettled problems in theory development [9]. Identifying and quantifying the mediators and moderators are useful in making contributions to the body of knowledge and both variables are the focus of research design in many situations [10]. Moderation is a causal model that postulates “when” or “for whom” an independent variable most strongly (or weakly) causes a dependent variable, while mediation is explains the process of “why” and “how” a cause-and-effect happens [10-12].

For the first step applying these theoretical basis, we [13] identified and quantified a mediation effect between project delivery systems and cost performance through bidding characteristics (e.g., bid price, the number of bidders). The study suggests that the previous studies of evaluating PDS cost performance could be improved when the bidding characteristics are considered. As a second phase, we explored a moderation effect that affect the causal relationship

between PDSs and their cost performance.

The objective of this study is to develop a moderation model and test the statistical significance of moderation effect. As a preliminary study, we developed a simple moderation model and the test of the significance. The goal of this study is to identify the theoretical attribution of project type that moderates the impact of project delivery systems on cost performance. We use the same dataset as in the previous study [13], also the same cost performance metric (i.e., change order rate) is used. With the results, the current study can provide the theoretical basis on the reason why the cost performance comparison of PDSs is inconsistent.

2 Related Work

This section describes literature reviews related with the moderation effect and the influence of project type on the causal relationship between PDSs and their cost performance. Moderators is defined as a third variable that modifies a causal effect, an association between two variables X and Y is said to be moderated when its size or sign depends on a third variable of set of variables [14-15]. Moderation is also known as interaction. Moderation analysis is typically examined by testing for interaction between moderator and X in a model of Y [15]. In construction management discipline, studies on moderation effects have been rarely conducted [9, 16-17].

Yang et al [17] tested the moderating effect of project type by conducting a two-way ANOVA when examining the relationship between knowledge management and project performance. A number of studies indicate that project type affects cost performance [2, 7, 8, 18-21]. We assume that PDS cost performance varies depending on the project type.

3 Preliminary Moderation Model

As a preliminary model, we postulated a simple moderation model

Models were categorized to conceptual and statistical diagram. Conceptually, the moderation model is depicted in the form of a conceptual diagram in Figure 1. The diagram represents a process in which the effect of PDS on change orders is influenced or dependent on project type, as reflected by the arrow pointing from project type to the line from PDS to change order.

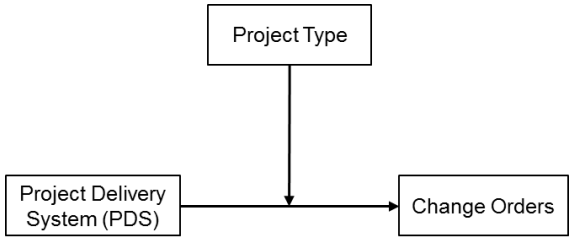

Figure 1. Moderation Model as a Conceptual Diagram

The conceptual diagram is very different in form from its corresponding statistical diagram, which represents how such a model is set up in the form of an equation. As is described in figure 2, the statistical diagram corresponding to this conceptual model requires not two but three antecedent variables, and project type is one of those antecedent.

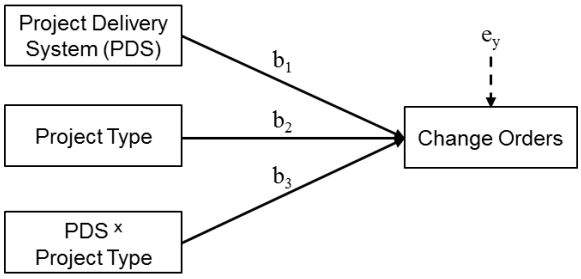

Figure 2. Moderation Model as a Statistical Diagram

Statistically, moderation effect is conducted by testing for interaction between project type(M) and PDS(X) in a model of change orders(Y). With evidence that X's effect on Y is moderated by M, we then quantify and describe the contingent nature of the association or effect by estimating X's effect on Y at various values of the moderator, an exercise known as probing an interaction. Equation (1) shows the standard multiple linear regression model. " b_3 " represents interaction role between PDS and project type.

$$Y = b_{01} + b_1\mathrm{X} + b_2\mathrm{M} + b_3\mathrm{XM} + e_\mathrm{y} \quad (1)$$

The moderation effect is interpreted depending on both the statistical significance and the sign of b_3[22]. If the model result of b_3 is statistically significant. The association between PDS and change orders is various depending on project type (i.e., moderator).

4 Experiment and Results

The developed moderation model is being applied to the construction project of 134 samples from the same dataset of the previous work. Samples are categorized to three project types (i.e., residential building, non-residential building, and road civil work) where the sample sizes are evenly distributed. Table 1 shows the descriptive statistics of change orders according to project types. To examine the effect of moderator, two-way ANOVA was conducted. The results is shown in Table 2.

Table 1. Descriptive statistics of project types

Dependent var.	Project type (M)	N	Mean	S.E.
Change order rate (Y)	Building(residential)	41	13.936	2.753
	Building(non-residential)	49	10.304	2.236
	Civil(road)	44	19.151	2.919

Table 2. Results of two-way ANOVA

Variable	Sum of Squares	df	Mean Square	F	p
PDS (X)	349.185	1	349.185	1.431	.234
Project type (M)	1415.473	2	707.736	2.901	.059
PDS*Project type (XM)	725.054	2	362.527	1.486	.230
Error	31231.363	128	243.995		

According to the test results, the interaction effect (XM) of PDS and project type is not significant (p value > 0.05). Figure 3 shows the moderation effect (i.e., interaction effect) of PDS and project type on change orders.

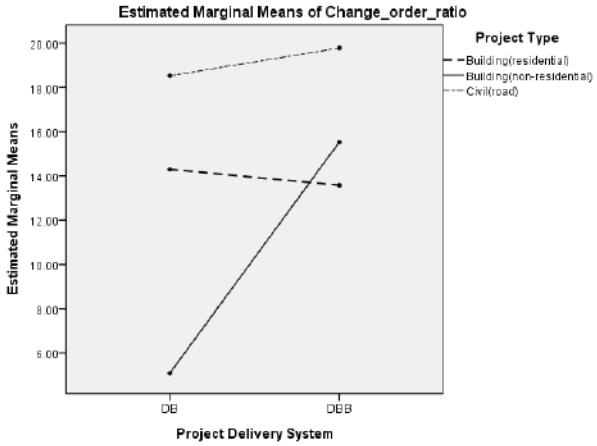

Figure 3. Moderation effect of PDS and project type on change orders

The slopes of non-residential building and civil projects intersect each other in a cross, then the main effect of PDS appears wherever it is, and wherever it is

reversed. That is, the main effect of the independent variable (i.e., PDS) does not consistently appear, and other results appear depending on mutual combinations with other variables. In this case, the model results show the dis-ordinal interaction.

5 Conclusions

A simple moderation model as a preliminary study was proposed to examine that project type moderates the impact of PDSs on their cost performance. This study is expected to provide a better understanding of the mechanism by which PDS impact cost performance, help project participants to select PDS by considering moderating effects in specific project types, and evaluate PDS appropriately in terms of cost performance. The academic contribution of the current study is to theoretically identify project type as a moderator using empirical data.

Regarding the limitations of this study, partial projects were selected from the original database, various combinations of project type should be applied to validate the moderation model. Also, value engineering costs for improvement were not considered because of data limitations.

For the further studies, conditional process model that integrates mediating effect and moderating effect in a single model could be developed. That is, moderated mediation and mediated moderation model considering project characteristics and bidding characteristics simultaneously need to be applied. Those models are to be expected to enhance the explanation the inconsistent evaluating results of PDS performance comparison.

Acknowledgement

This work was supported by the Technology Innovation Program (10077606, To Develop an Intelligent Integrated Management Support System for Engineering Project) funded by the Ministry of Trade, Industry & Energy (MOTIE, Korea).

References

[1] Bennett, J., Pothecary, E., and Robinson, G. Designing and building a world-class industry: The University of Reading design and build forum report. Centre for Strategic Studies in Construction, Univ. of Reading, UK., Rep. No. ISBN 0704911701, 1996.

[2] Konchar, M. and Sanvido, V. Comparison of U.S.Project Delivery Systems. J. Constr. Eng. Manage., 124:435-444, 1998.

[3] Molenaar, K., Songer, A., and Barash, M. Public-sector design/build evolution and performance. J. Manage. Eng., 15(2), 54–62. 1999.

[4] Ibbs, C. W., Kwak, Y., Ng, T. and Odabase, A. M. Project Delivery Systems and Project Change: Quantitative Analysis. J. Constr. Eng. Manage., 129:382-387, 2003.

[5] Minchin, R. E., Li, X., Issa, R. R., and Vargas, G. G. Comparison of Cost and Time Performance of Design-Build and Design-Bid-Build Delivery Systems in Florida. J. Constr. Eng. Manage., 139(10), 04013007. 2013

[6] FHwA (U.S. Department of Transportation, Federal Highway Administration). Design-build effectiveness study. 2006. Online: http://www.fhwa.dot.gov/reports/designbuild/designbuild.pdf, Accessed: 22/06/2016

[7] Chen, Q., Jin, Z., Xia, B., Wu, P., and Skitmore, M. Time and Cost Performance of Design-Build Projects. J. Constr. Eng. Manage., 142(2):04015074, 2016.

[8] Asmar, M. E., Hanna, A. S., and Loh, W. Quantifying performance for the integrated project delivery system as compared to established delivery systems. J. Constr. Eng. Manage., DOI: 10.1061/(ASCE)CO.1943-7862.0000744, 04013012-1-13, 2016.

[9] Xiong, B., Skitmore, M. and Xia, B. A critical review of structural modeling applications in construction research, J. Automat. Constr., 49 (2015) 59–70, 2015.

[10] Baron, R.M. and Kenny, D.A. The moderator–mediator variable distinction in social psychological research: conceptual, strategic, and statistical considerations, J. Pers. Soc. Psychol. 51 (6): 1173-1182, 1986.

[11] Kraemer, H. C., Wilson, G T., Fairburn, C. G. and Agras, W. S. Mediators and moderators of treatment effects in randomized clinical trials. Archives of General Psychiatry, 59, 877–883, 2002.

[12] Frazier, P. A., Tix, A. P. and Baron, K. E. Testing moderator and mediator effects in counselling psychology. Journal of Counselling Psychology, 51, 115–134, 2004.

[13] Moon, H., Kim, K., Williams, T. P., Lee, H., Park, M., Son, B. and Chun, J. Modeling of identifying mediator effects between project delivery systems and cost performance. In Proceedings of the 35th ISARC, pages 578-585, Berlin, Germany, 2018.

[14] Wu, A. D. and Zumbo, B. D. Understanding and Using Mediators and Moderators. Social Indicators Research, 87, 367-392, 2008.

[15] Heyes, A. F. Introduction to mediation, moderation, and conditional process analysis: a regression-based approach, Guilford Press, New York, 2013.

[16] Aibinu, A. A. and Al-Lawati, A. M. Using PLS-SEM technique to model construction organizations' willingness to participate in e-bidding, J. Automat. Constr., 19(2010), 714-724, 2010.
[17] Yang, L., Chen, J. and Wang, H., Assessing impacts of information technology on project success through knowledge management practice, doi:10.1016/j.autcon.2011.06.016, J. Automat. Constr., 22 (2012) 182–191, 2012.
[18] Jahren, C. T., and Ashe, A. M. Predictors of cost overrun rates. J. Constr. Eng. Manage., 116(3):548-552, 1990.
[19] Gkritza, K., and Labi, S. Estimating cost discrepancies in highway contracts: multistep econometric approach. J. Constr. Eng. Manage., 134(12): 953-962, 2008.
[20] Love, P. E. D. Influence of Project Type and Procurement Method on Rework Costs in Building Construction Projects. J. Constr. Eng. Manage., 128(1):18-29, 2002.
[21] Liu, B., Huo, T., Liang, Y., Sun, Y., and Hu, X. Key Factors of Project Characteristics Affecting Project Delivery System Decision Making in the Chinese Construction Industry: Case Study Using Chinese Data Based on Rough Set Theory. J. Prof. Issues Eng. Educ. Pract., 05016003, 2016.
[22] Cohen, J., Cohen, P., West, S. and Aiken, L. S. Applied Multiple Regression/Correlation Analysis for the Behavioral Sciences. Lawrence Erlbaum Associates, Inc., New Jersey, 2002.

Designing a Reliable Fiducial Marker Network for Autonomous Indoor Robot Navigation

B. R. K. Mantha[a] and B. Garcia de Soto[b,c]

[a]S.M.A.R.T. Construction Research Group, Division of Engineering, New York University Abu Dhabi (NYUAD), Abu Dhabi, UAE
[b]S.M.A.R.T. Construction Research Group, Division of Engineering, New York University Abu Dhabi (NYUAD), Abu Dhabi, UAE
[c]Department of Civil and Urban Engineering, New York University (NYU), Tandon School of Engineering, USA
E-mail: bmantha@nyu.edu, garcia.de.soto@nyu.edu

Abstract –

Automation and robotics offer significant potential to address some of the challenges faced by facility managers to efficiently operate and maintain indoor building environments. Previous efforts have focused on deploying mobile service robots for scheduled and periodic tasks such as monitoring, inspecting, and collecting data. Localization and navigation are two of the fundamental capabilities required for any robotic system to accomplish these periodic tasks successfully. Most of the existing approaches for achieving semi/fully autonomous indoor mobile robot navigation either require dense instrumentation of the physical space (e.g., Bluetooth beacons) or are computationally burdensome (e.g., Simultaneous Localization And Mapping). To address these issues, the authors previously developed localization, navigation, and drift correction algorithms based on cost-effective and easily-reconfigurable fiducial markers (e.g., AprilTags). However, these algorithms were based on context-specific assumptions regarding the marker characteristics, sensor capabilities, and environmental conditions. This study comprehensively investigates the design characteristics of a fiducial marker network localization system to achieve autonomous mobile indoor navigation. A generalized framework in the form of a process flow chart is proposed that is agnostic of indoor building environment application, marker category, robot, and facility type. That is, the proposed framework can be used to systematically to design the desired robot, required sensors, and create the optimal marker network map. The feasibility of the proposed approach is explained with the help of a facility management related example. The outcomes of this study can be generally applicable to any mobile robot, building type (e.g., office), and application (e.g., construction progress monitoring).

Keywords –

Autonomous Robot Navigation; Fiducial Markers; Indoor Localization; and Facility Management

1 Introduction

Recent advancements in technology have given rise to the use of intelligent robots for several service applications. Some of the examples of deployed indoor robotic systems for professional and domestic service applications include museum guide robots [1], hotel butler robots [2], vacuum cleaning robots [3], and surveillance robots [4]. As per a report published by the International Federation of Robotics in 2018, the annual growth rate in service robots is about 21% [5]. In addition, Baeg et al. [6] emphasized the significance, usability, and the potential of service robots for everyday activities. It can thus be reasoned that intelligent robots will soon be ubiquitous and there is a strong need to explore the potential of robots to improve autonomy in the operation and utilization of today's buildings.

Two of the fundamental capabilities robots need to possess to enable such autonomy are localization (i.e. identify and orient their location in the physical environment) and navigation (i.e. direct to the respective locations of interest). Previous approaches and methods either require dense instrumentation (e.g., bluetooth beacons) of the physical environment (i.e., significant upfront costs, suffer from low accuracy (e.g., wireless local area network), or made application-specific assumptions (e.g., marker-based systems). To address the limitations of existing studies, the authors propose a general framework for marker-based localization and navigation systems in the form of a process flowchart that is agnostic of the indoor building environment application, marker category, robotic platform, and facility type. The proposed framework is general, not domain specific, and can be used for several single and

swarm indoor robotic system applications. The use and feasibility of the proposed framework are illustrated with the help of several built environment examples.

In the context of this paper, localization is defined as the robot's ability to identify its current location in a given indoor environment setting [7]. For example, a robot being able to recognize that its location is in room 201, or knowing its location and orientation in the global coordinate reference system. The robot's navigation can be briefly defined as the robot's ability to plan a course of action to reach the destination location while accurately localizing itself in its frame of reference at strategic locations [7].

Several indoor localization and navigation techniques have been explored previously. Literature suggests that every method has advantages and limitations. Some of the previous approaches explored for robot localization include Wireless Local Area Network (WLAN), Ultra-Wide Band (UWB), Bluetooth, Cameras, and Lasers. Wi-Fi is an economical solution because most of the existing infrastructure consists of wireless nodes required for localization. However, it suffers from a significant error in localization accuracy [8,9]. Bluetooth based localization tends to be expensive, time-consuming and also have space constraints because of the requirement of wireless infrastructure deployment indoors [8,10]. Similarly, UWB-based systems require a large number of receivers making it inconvenient and infeasible (due to space constraints) indoors [11,12].

Laser scanner based techniques eliminate the need to instrument the physical space but they are highly expensive, sensitive to obstructions and require high computational capabilities [1,13-17]. To summarize, common disadvantages affecting a majority of the reviewed methods include low accuracy, significant upfront investments, high computational requirements and complex instrumentation of the indoor environment.

Vision-based methods using fiducial or natural markers are particularly immune to the disadvantages mentioned above. This is because, markers offer high accuracy in estimating the relative three-dimensional pose in an environment, require relatively less computing capabilities, are cost-effective, and are easy to install [18-20]. In addition, fiducial markers can store virtual information regarding a multitude of things such as information regarding physical location (e.g., room number), emergency evacuation directions, indoor navigational information, and inspection-related data regarding building systems helpful for facility managers [14]. Feng and Kamat [14] demonstrated how markers having virtual information and navigational directions can help humans navigate indoors.

To take this further, Mantha et al. [21] showed that the virtual location information (for localization), navigational direction (for navigation), and 3D pose estimates (for drift correction) can be used to achieve autonomous behavior of the mobile robot. However, this was just a proof of concept which used a specific type of robotic platform, camera, marker type, marker size, and facility type which cannot be generally applicable to other scenarios or built environment applications.

1.1 Importance of the Research

Robots have become increasingly pervasive in our day to day lives, with global experts predicting that intelligent robots will soon be ubiquitous [22]. Baeg et al. [6] emphasized the usability of service robots for everyday activities. Building Service Robots have numerous advantages such as a) high productivity: can perform tasks significantly faster without getting tired (e.g., laying bricks) [23], b) improve safety: can work in harsh and unsafe environments where humans are unwilling or unable to work (e.g., gas pipe inspection) [24], c) reduce cost: cheaper than human counter parts (e.g., it is very cheap to deliver items in hospitals/hotels with robots) [2, 25], d) improve quality: robots can be more precise and accurate than humans (e.g., structural monitoring) [24], e) provide better quality of life: can help the people with restricted mobility or handicaps with several mundane tasks (e.g., help blind people navigate indoors) [26]. The demand for Building Service Robots is also reflected in the exponential increase in the venture capital investment in robotics [27]. More importantly, the world robotics executive summary released in 2016 estimates around 23 billion USD in sales for the professional service robot installations between 2016 and 2019. In addition, a study published by McKinsey shows that the price of these robotics systems continues to drop (almost halved), whereas, the labor costs have consistently increased [28].

Thus, there is a strong need to investigate the potential of these systems, especially for facility management applications. Most of the existing service robotic systems still rely on expensive sensors, computationally intensive methodologies and complex instrumentation for semi and fully autonomous navigation. In addition, these systems are particularly disadvantageous for temporary or one-time applications such as air quality assessment, retrofit decision making, occupant schedule detection, and structural health monitoring [21]. On the contrary, marker-based systems offer significant potential since they are easily reconfigurable, cost-effective (can be printed on paper), and computationally efficient [14].

Different types of markers have been developed and studied in the recent past. For example, Xu and McCloskey [29] developed a 2D barcode-based localization system. Though this is an economical solution when compared to the previous alternatives, 2D systems fail to provide 3D orientation information. This

is particularly important for successful indoor robot navigation. Olson [20] developed AprilTags that can be printed on a regular paper but have the capability to determine 3D relative pose information.

Feng and Kamat [14] used these markers for indoor wayfinding applications. Furthermore, Babinec et al. [19] showed how a mobile robot can be localized using planar markers. Extending this further, Mantha et al. [21] used these markers for mobile robot navigation. However, all these aforementioned methods were just proof of concepts with context-specific assumptions regarding marker size, marker placement, and camera type. On the other hand, several other studies focused on improving individual marker characteristics such as successful detection rate, performance of the detection algorithm, size of the marker, and camera configurations. For example, Romero-Ramirez et al. [18] compared the speed performance of detecting different markers such as ArUco, Chili tags, AprilTags, and ArToolKit+. Lundeen et al. [30] compared the accuracy performance of different marker sizes, relative marker camera distances, and its relevance to the operation of an autonomous robotic excavator. However, none of the aforementioned studies, nor other existing studies, integrate, investigate, and identify the appropriate selection of marker networks for autonomous indoor robot navigation. That is, none of these studies establish a procedure to determine the optimal marker network design characteristics (e.g., marker camera configurations) based on a given set of inputs (e.g., facility type, and application objectives).

Thus, the objective of this research is to develop a general framework that can be used by facility managers or stakeholders to identify optimal camera marker network design characteristics based on different inputs (e.g., application objectives). The proposed framework is applicable to single or multiple robotic systems with and without constraints such as performance speed, occlusions, and lighting conditions. The feasibility of the proposed framework is explained in detail with the help of a facility management related example involving a variety of robotic platforms and marker types.

2 Proposed Framework

The framework is divided based on four main roles namely facility manager, real building, robot, and markers of the whole camera marker network design process for the autonomous robotic navigation. Each of these directly or indirectly influence, possess or are responsible for certain tasks and/or actions. Figure 1 shows the proposed framework including each of the aforementioned roles, their tasks, actions, processes, and sub processes. The different tasks of the proposed framework are illustrated using the example of ambient robotic data collection presented by Mantha et al. [21]. It has to be noted that for simplicity and easier understanding of the reader, tasks are described as sub sections of each role rather than in the chronological order of the process flow shown in Figure 1.

2.1 Facility Manager

One of the important roles of this framework is the facility manager who is responsible to define the objectives pertaining to the application context and the corresponding inputs. The objectives can be derived from the targeted action or intended tasks that need to be performed. In the example considered, the objective is to monitor ambient parameters in buildings. Therefore, the intended action is to gather data regarding ambient parameters such as temperature, relative humidity, and lighting, and compare it with the standard parameter range or the occupant preferences. Other relevant inputs can be the locations in the building and the frequency at which the data needs to be collected.

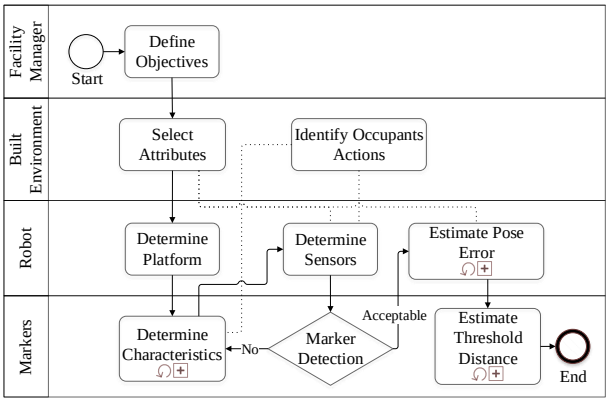

Figure 1. Design of marker network map for autonomous indoor robotic navigation.

2.2 Built Environment

Service robotic systems are designed to navigate in the built environment and perform the assigned tasks. Hence the built environmental attributes along with the users (or occupants) actions will significantly influence the design parameters of the robotic navigation system (marker network system in the context of this paper). Each of these categories is described below in detail.

2.2.1 Select Attributes

Attributes primarily represent the physical properties and characteristics of the built environment such as facility type, floor plans, equipment, surface geometry, flooring type, thermal zones, lighting, acoustics, and other services. In the previous ambient parameter monitoring example discussed at the beginning of section 4, some of the relevant attributes can be indoor temperature, relative humidity, light intensity, sound levels, and indoor air quality.

2.2.2 Identify Occupants Actions

Occupants are users of the built environment who directly or indirectly interact with the robotic systems. Though this task is not part of a technical process flow as can be seen in Figure 1, this can impact the characteristics of the markers (i.e., marker placement in particular) and determination of sensors (e.g., camera in this case) on the robot. Thus, identifying occupant actions is important as they have the potential to impact the successful accomplishment of the goals and objectives. Some examples of the behaviors and actions of the occupants include their movement, schedule, use of the built environment, and routine. In the example case considered, occlusions due to occupant movement and their interaction with these systems to provide feedback in the form of a questionnaire regarding their preferences are some of the most important factors to be considered. Further details regarding the significance of occlusions is described in the marker placement section of this paper.

2.3 Robot

In the context of this paper, three important tasks that encompass the role of an indoor robot are the type of platform, sensors (e.g., camera for detecting markers), and navigation performance (e.g., error accumulation). Though other elements such as task allocation, path planning, and motion planning for task execution are critical, they are not considered in the scope of this study and hence are not elaborated. However, interested readers are referred to [30,31] for further information.

One of the other considerations which did not receive much attention in the past is the cybersecurity implications of these intelligent autonomous agents [32]. This is particularly important in this case because of the potential human-robot collaboration and the accessibility of these robotic systems in these facilities. It has to be noted that the cyber threats are not just limited to data breaches but can cause some serious safety concerns to the infrastructure and the occupants [33,34]. So, with the increasing popularity of artificial intelligence enabled autonomous mobile robots, it is necessary to keep a check on the cybersecurity aspects, safety standards, and risk assessment of the robot chosen.

2.3.1 Determine Platform

As the name suggests, the goal of this step is to determine the ideal robotic platform based on the defined objectives (refer to section 4.1). The classification of robots can be dependent on several things such as the type of work, mechanical structure, or morphology [35]. Here, the goal is to determine the mechanical structure of the robot whether it is a mobile robot with wheels, legs, wings, tracks, or any other existing automated platform. In the example application, since the mobile robot needs to collect data and get occupant feedback, a mobile robot with wheels and a display platform for interaction might be ideal. Though a legged locomotion-based robot might also serve the purpose, a mobile robot with wheels might outpace the legged robots and can be more efficient (faster) in collecting data.

2.3.2 Determine Sensors

Though several sensors will be required on the robot, in the context of this paper, the sensor (camera) for the purpose of localization and pose estimation is discussed. One of the advantages of marker-based pose estimation systems is that they do not require expensive cameras. The type of cameras available on mobile phones these days can be used. Typically, most of the robotic systems come with a built-in camera. These cameras are of sufficient quality to be used for the purpose of marker-based localization and pose estimation [18].

2.3.3 Estimate Pose Error

One of the most important factors that have a direct impact on whether the robot will successfully navigate to desired locations or not, is the relative pose error accumulation of the robot. This is because there is always a difference between the robot's actual and ideal pose. It is important to estimate this at regular intervals and rectify it accordingly. Relative pose between camera and marker can be determined by a total of six components, three of which correspond to translation (e.g., x, y, and z) and three of which correspond to the rotation (e.g., roll, pitch, and yaw angles). This is represented in the form of a homogenous transformation matrix (H) in which R (3*3) denotes a rotation matrix and T (3*1) denotes a translation matrix (Eq. 1). However, depending on the type of application, only some of these six components might be required. For example, in case of ambient data collection, only the lateral distance (distance between the camera and the marker) is extracted and hence the pose error is estimated only using the variance of this parameter with respect to the ground truth values.

$$H = \begin{matrix} R11 & R12 & R13 & Tx \\ R21 & R22 & R23 & Ty \\ R31 & R32 & R33 & Tz \end{matrix} \quad (1)$$

Where,
H is part of the Homogeneous transform matrix
R (3∗3): Rotation matrix
T (3∗1): Translation matrix

A generalized procedure of the sub process for estimating the pose error is shown in Figure 2. First, assume a zero yaw angle (as shown in Figure 3) and determine the camera marker distance range. That is, the minimum and maximum lateral distance between the marker and the camera (i.e., robot) to be able to detect the marker. Then, identify the ideal marker to camera distance to maximize the allowable error accumulation

based on the environmental attributes and robotic platform. Further discussion regarding the reason for maximizing the allowable error is provided in section 4.4.3. If further optimization is required for the pose error, relative camera marker orientation can be varied to achieve the same. Though it might seem counter-intuitive, it is possible that a non-zero yaw angle (e.g. -15 degrees) gives better results than a zero yaw angle [30].

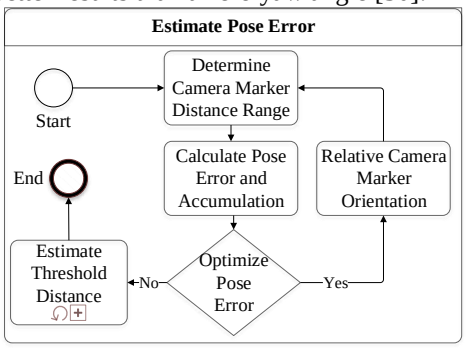

Figure 2. Sub-process to estimate pose error

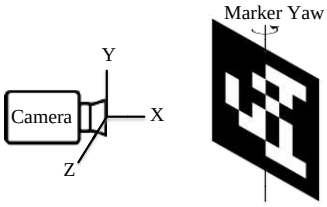

Figure 3. An illustration of marker yaw

For example, in the case of ambient robotic data collection, the robot's ideal path is along the centerline of the corridor to maximize allowable drift as shown in Figure 4. This is because, if the robot's ideal path is closer to the wall, the allowable drift accumulation will be very less (compared to the robot's path being on the centerline of the corridor) to avoid the robot colliding with the wall. The allowable drift accumulation, in this case, will be less than half the width of the corridor considering the width of the robot.

2.4 Markers

A fiducial marker is an artificial landmark with prescribed geometry and features to distinguish itself from the naturally occurring objects and other markers. The detection is usually done by capturing videos of markers using optical cameras and subsequently analyzing the image to determine the relative camera marker pose [30].

Unique fiducial markers are required to be placed at strategic locations along the navigational path of the robot (e.g., corridors, entrances to rooms, etc.) to form a Marker Network Map (MNM). These markers will act as landmarks, and the strategic locations can be the end of the corridors, the intersection of hallways, and entrances to the rooms. A graphical network G = {N, E} can then be generated where N represents nodes representing locations of markers and E represents edge links connecting these nodes (e.g., corridors and stairs). The network formed henceforth can be used to determine the optimal paths in the building and subsequently for the autonomous navigation of the robots. The subsections below provide further discussion regarding different marker characteristics (e.g., type and placement), detection of markers (e.g., placement), and threshold marker distance (i.e., maximum distance between two consecutive markers).

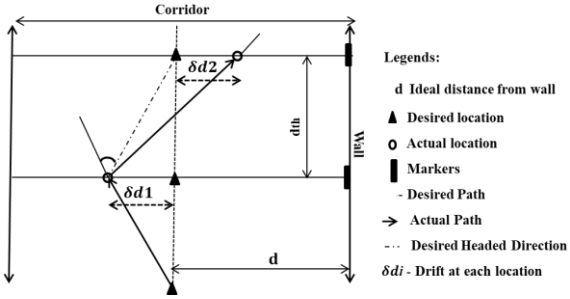

Figure 4. Illustration of drift accumulation and marker to marker distance for an indoor mobile robot (adapted from [21])

2.4.1 Determine Characteristics

At this stage, the building attributes are known and the robotic platform was chosen. This section describes the selection process for different marker characteristics.

Type, Size, and Library Size

One of the significant factors that drive the selection of the marker type and size is the error tolerance range and the type of pose requirements for the intended application based on the identified objectives. Several different types of markers were developed and studied by researchers such as planar markers, 2D bar codes, ARToolKit, BinARyID, AprilTags, ArUco, and ChiliTags [18,20,36,37]. Some of these markers are shown in Figure 5. Based on the accuracy, detection, and library sizes, ArUco and AprilTags are currently the best for marker detection [18,30].

The marker library (or dictionary) size is the number of unique markers available in chosen given marker type. For example, AprilTags have more than 4,000 unique codes, whereas ARTags have about 2,000 [20]. Therefore, it is important to check for the size of the library for the chosen marker to ensure that it meets the corresponding application before proceeding further (Figure 6). That is, estimate the number of unique markers required for the type of application and compare it with the available marker size. For example, in the monitoring example, the number of unique markers is approximately equal to the

number of distinct notable locations (e.g., in front of a room, end of the corridors, and elevators) along with other possible places where data needs to be collected inside the building.

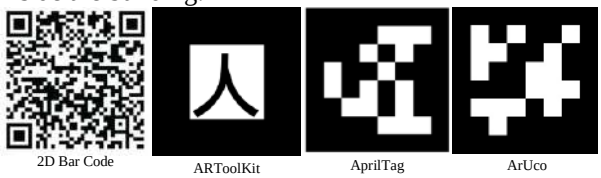

Figure 5. Different types of markers

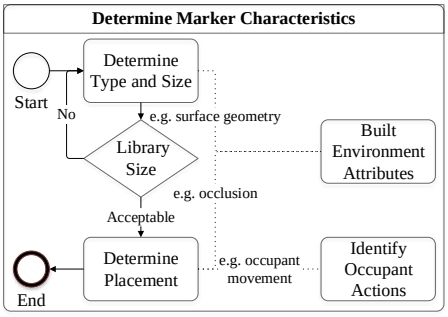

Figure 6. Sub process to determine marker characteristics

In addition, some of the built environment attributes such as surface geometry can influence the marker type and size selection. For example, if the built environment does not have planar surfaces, then larger size planar markers cannot be used because of field-of-view issues in the detection of the markers. In the ambient data collection example, the facility type is buildings with mostly planar surfaces, limited number of locations, and require relative 3D pose requirements. Thus, it is reasonable to assume that AprilTags are suitable because they are planar markers, have a decent library size, and can be used for determining 3D relative pose [20].

Placement

Different marker placement techniques such as wall mounted, ceiling mounted, and floor mounted have been explored for built environment settings [21,38,39]. However, it has to be noted that each of these methods has their own advantages and disadvantages depending on the built environment attributes such as ceiling heights, occlusions, and occupant actions such as occupant movement.

Floor mounted markers have shown promising results in a structured industrial/warehouse setting where Kiva robots manage the entire storage area of the warehouse [39]. Horan et al. [40] used a tape-based path sensing method for mobile indoor robot navigation. A similar study was performed by the National Institute of Standards and Technology (NIST), in which additional boundary markers were introduced along with the tape line [38]. However, the aforementioned floor based marker mounting techniques would suffer from frequent wear and tear in an unstructured building environment with frequent occupant movement. Ceiling mounted marker-based techniques were explored in warehouses as an alternative to the laser triangulation method [38]. However, in the context of ambient data collection, Mantha et al. [21] suggested that the ceiling heights (especially near the atrium areas) might have a significant effect on the pose estimation of the robot. Hence a wall mounted technique is ideal in this scenario or a combination of wall and ceiling mounted if multiple cameras placed on the robot.

2.4.2 Marker Detection

The immediate next step after selecting the marker characteristics is to develop a corresponding marker detection algorithm. In general terms, the marker detection algorithm works as follows. First, images are captured at a very high rate and are analyzed for the presence of a marker. This process is called segmenting. Second, the computer decodes the information from the markers in the form of 1s and 0s and determines the unique identification of the marker by cross-referencing (matching) with the library of markers. Further details regarding the detection algorithm can be found in [14,18].

Two of the important factors to be considered in the marker detection are false positive and false negative rates. False positive rate implies the rate of falsely reporting the existence of a marker in the captured image when there is no marker present in reality. On the contrary, false negative implies that there is a marker present in the image but the algorithm does not detect the maker. It is particularly important to check these rates before finalizing the marker type and size. Though the comparison of rates sometimes depends on the library size, an acceptable rate can be anything less than 0.1% [20,42]. If these rates are not acceptable, it is recommended to alter the aforementioned categories until desired results are obtained.

2.4.3 Estimate Threshold Distance

At this stage, the robot's camera can detect markers (landmarks), localize itself in the built environment, and navigate based on the relative pose. Since there will be errors accumulated along the navigational path as discussed previously (for e.g., as shown in Figure 4), it is necessary to place the markers at strategic locations to rectify the errors and ensure the robot reaches its next intended destination without drifting too much (e.g., colliding with the wall as shown in Figure 4). So, in addition to placing markers at the locations of interest, additional markers need to be placed along the way.

The objective of this specific task is to determine the threshold distance (d_{th}) between any two successive markers. That is, determine the maximum distance

between two consecutive markers along the navigational path of the robot. This is a result of the maximum allowable drift of the robot and hence a direct measure of the camera marker distance and drift accumulation pattern of the robot. To calculate the threshold distance, several robot runs should be performed to estimate the distance the robot will travel with an allowable drift (less than or equal to the maximum possible drift). The threshold distance is the minimum of these distances travelled for that particular case. Figure 7 shows the representative flowchart of the sub-process estimate threshold distance. This is subject to change depending on different factors such as flooring type (e.g. wheeled robot) and payload (e.g. drones). It has to be noted that the density of the markers and threshold marker to marker distance are inversely proportional. The density of the markers is basically the number of markers per area (e..g., m^2) or length (e.g., running meter). So, higher the threshold distance, lesser the density.

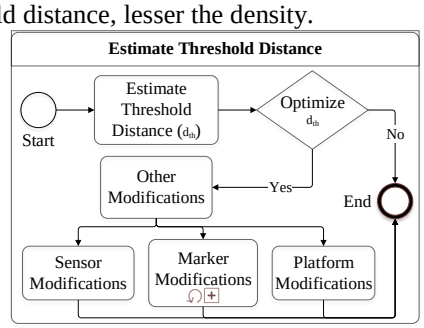

Figure 7. Sub process to estimate threshold distance

If d_{th} needs to be optimized, then the following modifications to the existing system such as a) sensors (on robot), b) markers, and c) platform (robot) can be explored. For example, multiple cameras (e.g. pointing in different directions as shown in [43]) instead of a single camera can be used to overcome occlusions and avoid more frequent placement of markers. 3D markers (i.e., multiple planar markers in the shape of a book used as a benchmark marker in [43]) can also be explored to improve visibility, optimize pose error, and subsequently optimize threshold distance. Further to that, multiple small markers instead of a single big marker can also be used to achieve the same. Finally, platform changes (e.g., other wheel types) can also be explored to optimize the error accumulation and hence d_{th}.

3 Conclusions and Future Work

A generalized framework to design a reliable fiducial marker network for autonomous indoor robotic navigation is proposed. The framework is general and can be applied to different robotic platforms operating in the built environment. Four key roles affecting the design process such as facility manager, built environment, robot, and markers are identified. The corresponding tasks and actions by these key roles that influence the marker network design characteristics such as marker type, size, library size, environmental attributes, occupant actions, robotic platform, camera marker configurations, threshold marker to marker distance are established and described in detail. In addition, four process flow diagrams are proposed that describe a step by step procedure of the proposed theoretical framework. The feasibility of the proposed framework is explained with the help of a real-world built environment example. That is by relating each of the integral task elements in the framework with an autonomous mobile robotic data collection case study. Future work aims to design two different marker network systems using AprilTags and ArUco for autonomous navigation of a specific robotic platform (e.g. Turtlebot3) in a real-world setting. The objective is to compare and analyze different design and performance factors such as threshold distance, marker density, error accumulation, optimal camera and marker configurations. Results of this study are generally applicable to any indoor robot, building type (e.g., office, retail), and application (e.g., environmental data collection). Other potential applications include construction progress monitoring, on-site worker safety identification, and real-time inventory management.

References

[1] Burgard W., Cremers A. B., Fox D., Hähnel D., Lakemeyer G., Schulz D., Steiner W., and Thrun S. (1998). The interactive museum tour-guide robot. In *AAAI*, Madison, Winsconsin, USA (pp. 11-18).

[2] Boltr (2018) Relay delivers to hospitality savioke.com Accessed: 04/01/2019.

[3] iRobot (2019) Robot Vacuums www.irobot.com Accessed: 09/01/2019.

[4] SDR (2019) Tactical Surveillance Robots sdrtactical.com Accessed: 09/01/2019.

[5] IFR (2018) Executive Summary World Robotics ifr.org Accessed: 09/01/2019

[6] Baeg S. H., Park J. H., Koh J., Park K. W., and Baeg M. H. (2007) Building a smart home environment for service robots based on RFID and sensor networks. In *ICCAS'07* (pp. 1078-1082). IEEE.

[7] Levitt T. S., and Lawton D. T. (1990) Qualitative navigation for mobile robots *Artificial intelligence*, *44*(3), 305-360

[8] Kriz P., Maly F., and Kozel T. (2016) Improving indoor localization using bluetooth low energy beacons. *Mobile Information Systems*.

[9] Youssef M., Abdelnasser H., Robertson P., Puyol M., Grand E. L., and Bruno L. (2018) Enabling landmark-based accurate and robust next generation

indoor LBSs. In *ACM SIGSPATIAL* (pp. 401-403).
[10] Raghavan A. N., Ananthapadmanaban H., Sivamurugan M. S., and Ravindran B. (2010) Accurate mobile robot localization in indoor environments using Bluetooth. *ICRA*(pp4391-4396)
[11] Du P., Zhang S., Chen C., Alphones A., and Zhong W. D. (2018) Demonstration of a Low-complexity Indoor Visible Light Positioning System Using an Enhanced TDOA Scheme. *IEEE Photonics Journal*
[12] Montañés J., Rodríguez A., and Prieto I. S. (2013) Smart indoor positioning/location and navigation: A lightweight approach. *IJIMAI*, 2(2), 43-50.
[13] Chow J. C., (2018) Drift-Free Indoor Navigation Using Simultaneous Localization and Mapping of the Ambient Heterogeneous Magnetic Field. *arXiv* 1802.06199
[14] Feng C., and Kamat V., (2012) Augmented reality markers as spatial indices for indoor mobile AECFM applications. In *CONVR* (pp. 235-24).
[15] Habib M. (2007) "Robot Mapping and Navigation by Fusing Sensory Information." *INTECH*.
[16] Thrun S., Burgard W., and Fox D., (2005) Probabilistic Robotics. *MIT Press*.
[17] Bar-Shalom Y., Li X., and Kirubarajan T. (2004) Estimation with applications to tracking and navigation: theory algorithms and software. *John Wiley and Sons.*
[18] Romero-Ramirez F., Muñoz-Salinas R., and Medina-Carnicer R. (2018) Speeded Up Detection of Squared Fiducial Markers. *IVC*, pp. 38–47 (46)
[19] Babinec A, Jurišica L, Hubinský P, Duchoň F. (2014) Visual localization of mobile robot using artificial markers. *Procedia Engineering*. 96:1-9.
[20] Olson E., (2011) AprilTag: A robust and flexible visual fiducial system. *ICRA*, pp. 3400-3407
[21] Mantha B., Menassa C., Kamat V. (2018) Robotic data collection and simulation for evaluation of building retrofit performance. *AIC*. pp 88-102 (92).
[22] Pinto J., (2016) Intelligent robots will be everywhere automation.com Accessed: 09/01/2019
[23] Sklar J. (2015) Robots lay three times as many bricks as construction workers, technologyreview.com Accessed: 09/01/2019
[24] Liu B., Luk F., Tong Y., Chan, (2011) Application of service robots for building NDT inspection tasks *Industrial Robot*, Vol. 38 Issue 1 pp. 58 - 65
[25] Aethon (2017) Autonomous Mobile Robots and Tracking Solutions aethon.com Accessed: 9/1/2019.
[26] Azenkot S., Feng C., and Cakmak M. (2016) Enabling building service robots to guide blind people a participatory design approach *HRI* (3-10).
[27] The Robot Report (2017) "2016 best year ever for funding robotics startup companies robotreport.com Accessed: 09/01/2019
[28] Tilley (2017) Automation, robotics and the factory of the future mckinsey.com Accessed: 09/01/2019
[29] Xu W., and McCloskey S. (2011) 2D Barcode localization and motion deblurring using a flutter shutter camera *IEEE WACV* (pp. 159-165).
[30] Lundeen K., Dong S., Fredricks N., Akula M., Seo J., Kamat V. (2016) Optical marker-based end effector pose estimation for articulated excavators. *AIC* (65) pp 51-64.
[31] Mantha B., Menassa C., Kamat V. (2017) Task Allocation and Route Planning for Robotic Service Networks in Indoor Building Environments. *JCCE*. 31(5):04017038.
[32] Mantha B., and Garcia de Soto B., (2019) Cyber security challenges and vulnerability assessment in the construction industry. *CCC (Abstract Accepted)*
[33] Greenberg (2017) Watch Hackers Hijack Three Robots for Spying and Sabotage https://www.wired.com/ Accessed: 29/01/2019
[34] RBR (2012) Robots Vulnerable to Hacking roboticsbusinessreview.com Accessed: 29/01/2019
[35] ISO (2012) Robots and robotic devices — Vocabulary iso.org Accessed: 29/01/2019
[36] Bonnard Q., Lemaignan S., Zufferey G., Mazzei A., Cuendet S., Li N., Özgür A., Dillenbourg P., (2013) Chilitags 2: Robust Fiducial Markers for Augmented Reality and Robotics http://chili.epfl.ch/software .
[37] V.A. Knyaz, R.V. Sibiryakov, (1998) The Development of New Coded Targets for Automated Point Identification and Non-contact Surface Measurements, 3D Surface Measurements, *IAPRS*, 23(5) pp. 80–85.
[38] Shneier M., and R. Bostelman (2015) Literature review of mobile robots for manufacturing, *NIST*, nist.gov Accessed: 23/01/2019.
[39] Röhrig C., C. Kirsch, J. Lategahn, M. Müller, L. Telle (2012) Localization of autonomous mobile robots in a cellular transport system *Eng Lett* 20 (2).
[40] Horan B., Z. Najdovski, T. Black, S. Nahavandi, P. Crothers, OzTug (2011) mobile robot for manufacturing transportation, *SMC* pp. 3554–3560.
[41] Gomes, A., Pinto, A., Soares, C., Torres, J. M., Sobral, P., & Moreira, R. S. (2018, March). Indoor Location Using Bluetooth Low Energy Beacons. In World Conference on Information Systems and Technologies (pp. 565-580). Springer, Cham.
[42] Bergamasco F., Albarelli A., & Torsello A. (2013). Pi-tag: a fast image-space marker design based on projective invariants. *MVA*, *24*(6), 1295-1310.
[43] Feng C., Kamat V., and Cai H. (2018) Camera marker networks for articulated machine pose estimation. *AIC 96*, pp:148-160.

Designing a Development Board for Research on IoT Applications in Building Automation Systems

M.H. Schraven[a], C. Guarnieri[b], M.A. Baranski[a], D. Müller[a] and A. Monti[b]

[a]Institute for Energy Efficient Buildings and Indoor Climate, Germany
[b]Institute for Automation of Complex Power Systems, Germany
E-mail: mschraven@eonerc.rwth-aachen.de, cguarnieri@eonerc.rwth-aachen.de

Abstract

Recent advances in the development of Internet-of-Things (IoT) devices have enabled researchers to apply such on building automation systems (BAS). Especially in existing BAS, one big challenge is the diversity of communication methods. In such systems, gateways are required to connect various devices. However, while there are very few IoT-gateways able to interface a wide variety of common sensors and actuators, those often implicate high costs, entailing inacceptable investments for larger field tests.

To overcome this issue, we prototyped a low-cost plug-and-play and freely programmable IoT-gateway, which supports common analog signal interfaces like 0-10 V or 0-20 mA current loop, and digital ones via RS-485 serial communication. The gateway is based on the ESP32-PICO-KIT development board, a fully functional board with a microcontroller and embedded WiFi. Accordingly, we enhanced this board by adding custom-designed peripherals and developing the required firmware for acquiring sensor data and driving actuators.

In order to validate the functionality of the interfaces, we conducted an experimental test series. The experiments comprise measurements of inputs and outputs for either the IoT-gateway or the connected sensors and actuators. The results show an average relative error for analog interfaces of 7 %, hence being sufficient for building automation applications. The RS-485 was successfully tested with a Modbus RTU slave device.

Therefore, the prototyped IoT-gateway is directly applicable to both analog and Modbus-based sensors and actuators, shows acceptable errors in analog readings and can be manufactured at a relatively low price, facilitating test benches containing several plug-and-play gateways.

Keywords –

IoT, Gateway, Building Automation, Wireless Communication, ESP32

1 Introduction

In Germany, potential energy savings due to building automation system (BAS) improvements estimate roughly 20 % [1]. Additionally, in existing non-residential buildings, wireless IoT devices constitute a promising resource to enable BAS without causing high expenses due to elaborate cable installations. However, the beneficial installation of radio-based devices only applies if the configuration effort is not as high as in conventional systems on the other hand. Furthermore, local wired automation systems are well-known and widely adopted due to their reliability. However, there is no comprehensive study on a real BAS yet, which is completely operated via IoT devices. Hence, our research is focussed on the stability and properties of such systems utilizing several IoT devices.

When investigating IoT applications in BAS, the most cost-efficient approach is to use an existing infrastructure. Instead of exchanging sensors and actuators, gateways can be used. With BAS often comprising sensors and actuators with various communication interfaces, there are only few IoT-gateways directly applicable to all these devices. Some of the most popular communication interfaces used are 0-10 V and 0-20 mA analog signal transmission and bus-based communication e.g. via Ethernet, BACnet, LON, KNX and Modbus [2]. Some examples for multi-communication gateways are the BASremote at a price of 350 € [3], the EWIO-9180-M at 425 € [4], the UCM-316 at 325 € [5] and the WISE-4470-S250 at 400 € [6]. All these examples are rather edge controllers than decentral plug-and-play IoT-gateways. These edge controllers imply high costs when used for each sensor and actuator individually or limit one to research activities on decentralized summarized data processing. By contrast, already available open-source platforms like Controllino, PiXtend and UniPi Neuron, just to name a few, prove to be still expensive or not versatile enough for single transducer interfacing.

We thus identified the need to design an IoT-gateway

that features only the necessary characteristics to enable IoT on single devices without causing inacceptable costs.

The rest of this paper is structured as follows: Chapter 2 starts with the deduction of requirements for the IoT-gateway, followed by a detailed description of the electronic design as well as the software implementation. In chapter 3, the conducted test series is described; chapter 4 summarizes the validation results and discusses the purchase cost. Finally, chapter 5 concludes with a summary and future possible improvements.

2 System requirements and design

From our experience with designing and operating BAS, we define the following properties for the IoT-gateway as mandatory requirements to allow for an accurate operation of BAS. These properties were mainly derived by the current technical building equipment, which was planned and used by the Institute for Energy Efficient Buildings and Indoor Climate for their new test hall.

- Timescale – Due to fluid and thermal inertia, but also delay of moving actuators, we suggest a physical and interpretation delay of maximum 1 s.
- Storage – Since the gateway will be connected to a wireless or local area network with constant access to online database storage systems, a limited internal storage capacity is requested for buffering purposes.
- Interfaces – For a start, we focus on analog signals and serial communication and thus omit the Ethernet-based communication. The gateway shall at least support 0-10 V signals, 0-20 mA signals and communication over RS-485.
- Resolution – Actuators such as valve actuators, volumetric flow controllers or pumps commonly receive their values in percent. Therefore, the analog output should at least resolve integer values ranging from 0-100, which represents a resolution of at least 7 bit (2^7 = 128 discrete values). Analog inputs are often used to receive signals from temperature sensors like resistance temperature detectors (RTDs) and negative temperature coefficient (NTC) thermistors. Assuming a range of 140 K, the gateway should at least read for one decimal, resulting in a minimum resolution of 11 bit (2^{11} = 2048 discrete values).
- Network connection – The gateway requires a way to connect to a local area network or the internet, e.g. via WiFi.
- Time tagging – For some control applications, it is necessary to tag each data measurement with a synchronized time. Hence, the IoT-gateway should offer a chronometric and time-reading possibility.
- Software development – In order to test different configuration setups, local or agent-based control strategies, remote service and maintenance concepts as well as different security and encryption functionalities, the gateway needs to be freely programmable. As Python is the most frequently used programming language at our institute, we require Python language support for our gateway.
- Power supply – The gateway should connect to existing sensors and actuators that are often supplied with industrial voltage level of 24 Vdc.

We use the ESP32-PICO-KIT [7] as a base for our IoT-gateway. The ESP32-PICO-KIT is a relatively cheap system on a chip by Espressif, yet providing solutions to several of the defined requirements. A detailed overview is presented in Table 1. ESP32-PICO-KIT properties

Table 1. ESP32-PICO-KIT properties [7]

Feature/requirement	ESP32-PICO-KIT
Timescale (physical, interpretation delay)	0.1 ~ 1 s
Storage	520 KB SRAM
Interfaces/resolution	12 bit ADC (0-1.1 V), 8 bit DAC (0-3.3 V), UART TTL (serial)
Network	WLAN/Bluetooth
Time tagging	RTC (internal real time clock) + NTP (network time protocol)
Software	Micropython support
Power	5 Vdc, 3.3 Vdc

2.1 Electronic Design

From Table 1, we can derive the required adjustments:

- Power supply voltage level,
- 0-10 V reading and writing voltage level,
- 0-20 mA current to voltage and voltage to current conversion and
- UART to RS-485 conversion.

2.1.1 Power Conversions

The IoT-gateway will be connected to 24 Vdc. As the ESP32 runs on a nominal power of 5 Vdc, we use a low dropout voltage regulator (LDO) to provide the requested conversion while being able to supply a current up to 1.5 A. Due to the 5 V operation, the ESP32 cannot provide a voltage output up to 10 V. Therefore, we also use a 10 V voltage reference (VREF), which serves as the upper reference for the 0-10 V output loop. The sensors/actuators and the IoT-gateway share the same ground.

2.1.2 0-10 V Input

As shown in Table 1, the ESP32 has a 12 bit ADC with an input voltage range of 0-1.1 V. This range has to be mapped to a sensor output ranging from 0-10 V.

The easiest and most cost-efficient solution to reduce voltage to a specific range is a voltage divider circuit (see Figure 1). This circuit converts the input signal according to Equation (1). Since the ESP32 ADC input impedance is not provided by the manufacturer, an operational amplifier (OPA) in buffer configuration is used as precaution to decouple the voltage divider from the ADC, thus avoiding measurement errors due to load effects.

$$V_{ADC} = V_{in} \cdot \frac{R_{13}}{R_{14} + R_{13}} \quad (1)$$

As the ESP32 is a low-cost device, its ADC is not of the best quality. It is only assumed to be linear in a range of 100 mV to around 950 mV [8]. Therefore, we selected the resistors so that input voltages of 0-10 V match ADC input voltages of 0-0.91 V. Note, that this reduces the effective resolution of originally 12 bit to about 3400 discrete values, which is still considerably higher than the required 11 bit resolution.

2.1.3 0-20 mA Input

The 0-20 mA input current loop requires a conversion from current to voltage so that the ADC can read its value. The easiest solution is to use a single resistor providing a voltage following Ohm's law (see Equation (2)). Again, we add a buffer to decouple the load resistor R_3 from the ADC and select the resistor so that the ADC input voltages match 0-0.91 V for input currents of 0-20 mA.

$$V_{ADC} = I_{in} \cdot R_3 \quad (2)$$

2.1.4 0-10 V Output

The DAC of the ESP32 has a maximum output voltage of 3.3 V. In order to achieve higher output voltages, this voltage has to be amplified. For this purpose, we use a rail-to-rail OPA in non-inverting amplifier configuration, as shown in Figure 2. By adapting the resistor values, the gain, and hence the output voltage is adjustable, as long as it is below the power supply. The OPA drains a current of just 160 µA, allowing to be powered with a high precision voltage reference (see Section 2.1.1). Whilst the internal voltage supply of the ESP32 is 3.3 V, the DAC may output maximum voltages of 3.2 V. Adopting a conservative approach, we select the resistors to map the DAC output voltage of 0-3.15 V to an output voltage of 0-10.1 V. Because this output is used to control actuators, the output voltage must exceed 10 V, for instance to ensure that the actuator is actually capable of fully closing a valve. The resistor values can be derived by Equation (3). Regarding the effects on the final resolution, the safety margin causes a negligible loss of 12 discrete values.

$$V_{out} = V_{DAC} \cdot \left(1 + \frac{R_{11}}{R_{10}}\right) \quad (3)$$

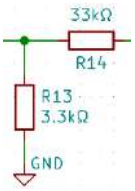

Figure 1. Voltage divider circuit of our IoT-gateway, transfers 0-10 V to 0-0.91 V

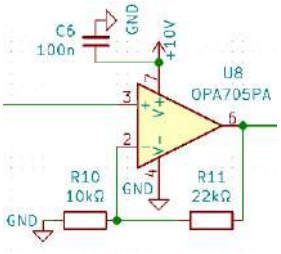

Figure 2. Voltage amplifier circuit of our IoT-gateway, amplifies 0-3.15 V to 0-10.1 V

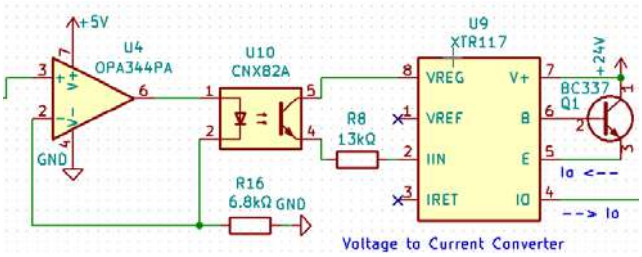

Figure 3. Current loop driver of our IoT-gateway, converts 0-3.15 V to 0-21 mA

2.1.5 0-20 mA Output

We realize voltage to current conversion by resorting to the XTR117 by Texas Instruments, a commercial precision current driver that can be configured both in true and live zero configurations at a very low cost. Since both the DAC and the XTR117 share the same ground, the driving block is isolated from the control block by means of an optocoupler. However, since the relation between the current flowing in the diode and photo-generated current in the bipolar junction transistor is non-linear, the linear control on the former does not result in an equally linear control of the latter. The circuit illustrated in Figure 3 follows the characteristic described in Equation (4), which we derived by measuring the driver current for different values of control voltage.

$$I_{out} = \mathrm{a} \cdot {V_{DAC}}^{b} \quad (4)$$

2.1.6 UART TTL to RS-485 Conversion

The Universal Asynchronous Receiver Transmitter (UART) interface is an interface used to transfer serial data asynchronously. The asynchronous communication does not require a clock signal but rather expects a start and an end of a transferred message [9]. On the ESP32, the UART runs on 5 V. A further difference is the line driver, which converts single ended UART signal to a bi-directional differential signal resulting in two data lines, Data A and Data B. The signals for RS-485 usually range between +/- 1.5 V [9]. For the signal conversion, we use a commercially available UART to RS-485 converter, which also features automatic flow control. Without automatic flow control, a digital control signal is required, in order to assign one line the for communication, as it is not possible to transfer data over both reading and transmitting line at the same time. This, in particular, complicates timing the communication, hence we decided to use a module with automatic flow control.

2.1.7 Reference Voltage Calibration

The ADC and DAC lack quality in terms of linearity that are mainly due to noise and varying reference voltages between different microcontrollers. Hence, we perform an automatic ADC and DAC calibration by calculating two points used for linear interpolation.

A reference voltage for the ESP32 is set, emitted and redirected to two ADC pins, after the voltage is reduced to 1/3 and 2/3 of the reference voltage, respectively. With this construction, the ADC is calibrated. Afterwards, the DAC redirects its output to an ADC pin, reading the provided voltage from the DAC.

2.1.8 Low-Pass Filter

Input and output stages are low pass filtered using first order RC filters to reduce the noise. The adopted bandwidth of 15 Hz is selected to allow all signals in timescales down to 1 s without significant delays and attenuations.

2.1.9 Summary

The ESP32-PICO-KIT is expanded by adding a 24 Vdc power conversion, 5 circuits for each of the individual communication interfaces and a calibration circuit. Figure 4 depicts a view of our finished prototype. The schematic and Printed Circuit Board (PCB) layout can be examined on the publicly available GitHub repository [10].

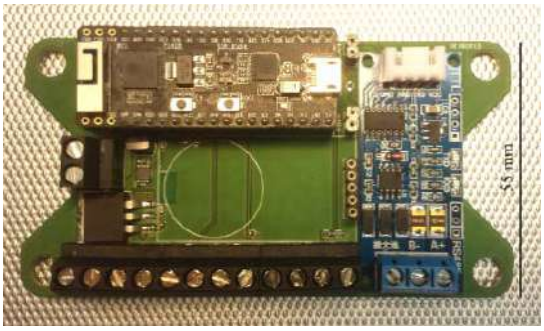

Figure 4. Assembled IoT-gateway PCB prototype from our defined requirements

2.2 Software Design

We programmed the firmware in Python code. However, the microcontroller could also be programmed with other languages like Arduino or C++. The storage space on the ESP32 is limited, therefore we use Micropython, which is a lean Python implementation and was especially developed for microcontrollers [11]. Because the basic Micropython firmware does not allow for setting a reference voltage, we used the LoBo Micropython implementation, that is freely available on GitHub [12]. The GitHub page also contains some instructions on how to flash the firmware onto the ESP32 (we use the esptool for flashing the firmware and ampy to transfer files over serial connection). Following the instructions, the ESP32 accommodates a file system, so the software can be written with any Python programming environment or plain text editor and be transferred onto the ESP32.

When booting the ESP32 with Micropython firmware, two files, boot.py and main.py, are always executed one after the other. The following sections explain the individual parts of the software in more detail.

2.2.1 Main.py

In this file, an instance of the board class is created. All functions, which are used for addressing the analog signal transmissions and Modbus communication, are implemented within the board class. The functions may be called from the instance within a Python shell that is available on the ESP32 when e.g. connecting via serial connection.

2.2.2 Board.py

The board.py is the main file for interfacing the different communication interfaces and provides the corresponding functions. In this file, a class “board” is defined. All parameters are stored within the class object. The following methods are available:

- __init__(self): This function is called when creating an instance of the board class. Parameters are

fetched from the parameters.py and assigned to the attributes. In addition, the ADC and DAC pins for 0-10 V input and output as well as 0-20 mA input and output are assigned. After this, a Modbus instance is created. Finally, the methods for setting a reference voltage and executing the calibration are called.

- set_ESP_referenceVoltage(self): This function sets the reference voltage to the predefined pin (in our case IO27, see schematic [10]).
- calibrate(self): This function calls the ADC and DAC calibration.
- calibrate_adc(self): In this function, the ADC regression parameters are calculated and slope and intercept are returned.
- calibrate_dac(self): In this function, the ADC regression parameters are calculated and slope and intercept are returned.
- Four methods for either ADC or DAC conversions between digital and voltage values: This allows an incremental and consistent calculation for the reading and writing functionalities, but also requires to define the ADC and DAC characteristic at least once.
- Four methods for either reading or writing analog voltages and currents: The reading and writing methods contain the relations described in chapter 2.1.
- Modbus-related functions are callable by the Modbus instance.

2.2.3 Parameters.py

This file contains all predefined parameters. E.g.:

- Pin numbers
- Predefined digital and voltage values for calibration
- Parameters of the relations described in chapter 2.1.
- Modbus-related parameters: Definition of the physical serial port and other specific parameters like the baudrate of the connected device, the Modbus slave address and register lengths.

2.2.4 Modbus

For Modbus, the modules uModbusSerial.py, uModbusFunctions.py and uModbusConst.py are available. These files are slightly adjusted versions of the uModbus package for Micropython [13]. The uModbusSerial.py being the main file provides a class with standard reading and writing functionalities for registers and coils. Our changes mostly concern reading the UART interface.

2.2.5 Summary

The software implementation features a board class that provides the interfacing methods for reading and writing analog voltages and currents as well as receiving and sending Modbus signals. At current state, no automatic sensing or control and logging routines are implemented. When booting the ESP32, a “board” instance is created. This board instance is used via console from serial connection. Modbus-specific functions were taken from the Micropython uModbus module. Parameters may be accessed and changed in the parameters.py module. The complete software implementation is available in the GitHub repository [10].

3 Test series

In order to validate the functionality of the interfaces, a test series is conducted. For the validation of analog reading and writing, we use a test setup consisting of a Programmable Logic Controller (PLC) and terminals for 0-10 V input and output as well as 0-20 mA input and output. With these terminals, it is possible to provide constant voltages and currents or read those generated by the IoT-gateway. We validate the RS-485 interface with a Modbus RTU slave device – an electric valve actuator [14]. The Modbus protocol works with digital values stored in registers and coils; a description of the Modbus registers is provided by the manufacturer [15]. Table 2 provides an overview of the used testing hardware components.

Table 2. Test series hardware

Tested gateway interface	Testing device
-	CX5130 (PLC)
0-10 V input	EL4008
0-10 V output	EL3008
0-20 mA input	EL4018
0-20 mA output	EL3048
RS-485	LM24A-MOD

3.1 Setup

We investigate the analog reading and writing functionality by providing predefined voltages and currents with either the PLC terminal or the IoT-gateway and measuring the corresponding value on the other side. For 0-10 V, we therefore varied the voltage with a step width of 0.5 V, for 0-20 mA we used 1.0 mA steps. Accordingly, we compared the IoT-gateway’s signal to the terminal’s signal. Because of noise, the signal may vary at equal conditions. Therefore, we read 1000 samples and calculate the average value.

The Modbus communication is validated by simply writing a set point to a register, waiting for the actuator to move and reading its corresponding actual value afterwards. We wrote on register 1 a value of 2500 and 7500 and read the related value on register 5. Register 1

is related to the positional set point, which ranges from 0-10000, where 10000 corresponds to 100 %. Register 5 reads the actual position, again ranging from 0-10000.

3.2 Calibration issues

With the proposed calibration method, the ADC and DAC results show severe deviations from expected. However, the problems with noise and accuracy due to different reference voltages are known issues to the manufacturer of the ESP32, Espressif, that provide in their own software development kit and programming guide some useful calibration functions that depend on the internal reference voltage.

For chips produced after the beginning of 2018, the internal reference voltage is measured and directly fused to each chip and hence the calibration can be automated easily. Since the chips of our ESP32-PICO-KITs were produced in 2017, their reference voltage cannot be read directly from the chip. Therefore, in order to use the calibration functions provided by Espressif, we measured the reference voltage and calculated slope and intercept for the linear regression. The calibration functions by Espressif lead to results that are more accurate; consequently, we use their calibration method over our two-point regression. The next section gives an overview of the validation results with this calibration applied.

4 Results and Discussion

The validation results for 0-10 V input and output are summarized in Figure 5, Figure 6 illustrates the corresponding results for 0-20 mA input and output. Table 3 summarizes the maximum and average deviations for the analog communication.

Even with the calibration functions given by Espressif, the results show significant errors for both small voltage and current values. On the one hand, the internal ADC characteristic typically exhibits a negative offset of almost 75 mV that results in the impossibility of reading any value below that threshold, i.e. approximately 750 mV and 1.5 mA for the voltage input interface and the current one respectively. On the other hand, the DAC characteristic shows an offset of almost 300 mV, thus resulting also in this case in a reduced effective range.

With regard to control purposes, the DAC should always be able to apply a zero voltage; besides that, the DAC deviations are probably negligible, since, in many applications, control algorithms rather rely on differences between set and actual values to produce a specific output for an actuator, for instance in case of simple proportional–integral–derivative (PID) control. On the contrary, the ADC readings should be accurate and hence improved on the whole range. This, for instance, applies in case of cascaded PID control where different single sensor errors could add up to significant gain errors. However, the minimum range limitation rather affects actuator position feedback, as e.g. temperature or humidity sensors normally operate far from the minimum of the range. Besides that, following the example of simple PID control, the sensor data acquisition inaccuracy would lead to a different gain, but would not change the general behavior. In order to fully evaluate the limitations for BAS operation, a detailed study is required addressing specific criteria like cyclic communication times, packet size, delays et cetera to guarantee the system's controllability.

At this stage, excluding the error below the 20 % of the input/output range, maximum absolute errors are 0.08 V and 0.16 mA, respectively, which shows that the device is usable for operating with standard voltages 2-10 V and standard currents 4-20 mA for control purposes.

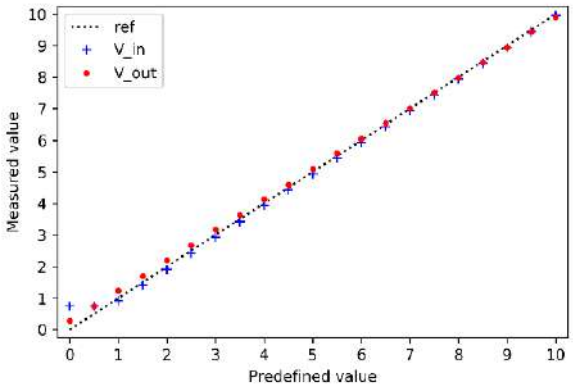

Figure 5. Validation of 0-10 V input and output

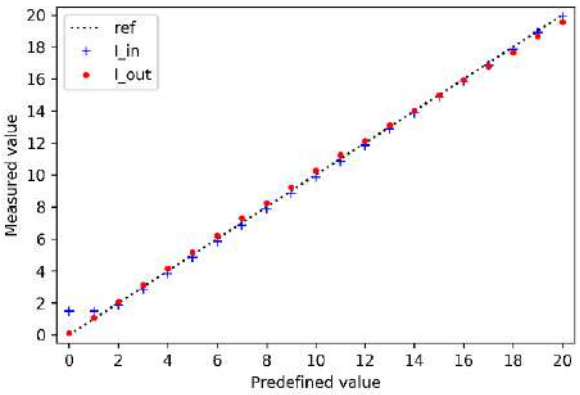

Figure 6. Validation of 0-20 mA input and output

Table 3. Analog relative (e_r) and absolute (e_a) maximum, minimum and average errors

Interface	0-10|2-10 V in	0-10|2-10 V out	0-20|4-20 mA in	0-20|4-20 mA out
	[%]	[%]	[%]	[%]
$e_{r,max}$	49.5|4.19	48.6|10.1	50.0|3.88	7.64|4.32
$e_{r,min}$	0.42|0.42	0.36|0.36	0.53|0.53	0.77|0.77
$e_{r,avg}$	4.35|1.45	6.39|2.43	4.29|1.44	2.76|2.32
	[V]	[V]	[mA]	[mA]

$e_{a,max}$	0.75|0.08	0.29|0.20	1.5|0.16	0.46|0.46
$e_{a,min}$	0.04|0.04	0.03|0.03	0.11|0.11	0.08|0.12
$e_{a,avg}$	0.11|0.07	0.12|0.09	0.22|0.14	0.21|0.24

For the Modbus device set point of 2500, we read a value of 2501, for 7500 we read 7502 on register 5. Modbus is a digital communication, hence not causing any deviations. The very small deviations may occur due to the accuracy of the actuator position.

From the validation results, we conclude following assertions:

- Due to varying internal voltages between different ESP32 modules, the proposed calibration method did not show the desired improvement on the ADC and DAC accuracy. A different method should be proposed in the future to calibrate the conversions between analog and digital values automatically.
- Within the range of 2-10 V and 4-20 mA, the IoT-gateway was able to read analog voltages and currents at an average error of 1.45 % and 1.44 %, respectively. The maximum deviation amounted to 4.19 %. In the same range, writing of analog voltages and currents accounted for average errors of 2.43 % and 2.32 %, respectively. The maximum deviations for writing amounted to 10.1 %. For smaller voltages and currents, the ADC is not able to dissolve them. This issue should be addressed in the future, since reading the actual value accurately is important when calculating a specific output. The writing functionality yielded an acceptable accuracy.
- The PLC terminal EL3048 has an input impedance of about 85 Ω. The current output loop was tested with different loads and showed that a maximum load of 250 Ω can be handled. Further research on input impedances of BAS devices is necessary to assure a general suitability for BAS applications.
- Communication via RS-485 was tested with a Modbus device. The set point register was written and the actual value register read with success. Very small deviations occurred, probably due to the electric motor accuracy.
- The IoT-gateway transmitted signals within 1 s for all tested interfaces.

The technical requirements are met. However, one question remains: How much does this multi-gateway cost compared to the commercially available devices?

4.1 Prices

With the assumption, that a larger field test would require around 50-100 IoT-gateways, we examine the prices for all used components. Figure 7 shows the cost distribution: except for the RS-485 converter, all component prices are fetched from www.mouser.de [16].

This diagram shows that the ESP32-PICO-KIT costing 8.73 € accounts for almost half of the total costs. The circuits for 0-10 V in- and output as well as 0-20 mA input are equally distributed with costs of about 1 € each, the RS-485 module falling little behind with 1.18 €. Because of the high precision reference voltage for the OPA705, the power supply costs 4.34 € and thus causes the second highest costs in total. Since the OPA705 is the only part in need of 10 V, this design should be revised in order to further reduce the costs. However, this component could also help utilizing and improving an automated ADC calibration. The current output loop yields the fourth highest costs and should be revised as well, in order to allow for devices with higher input impedances. The total component price is 23.57 €.

In addition to the components, the PCBs have to be produced and all parts have to be assembled. The costs for 100 PCBs including assembly and shipping account for roughly 400 € corresponding to 4 € per piece. In total, the purchasing costs for one IoT-gateway at quantities of 100 amount to about 28 €. From a vendor's perspective, this price could obviously be reduced by purchasing the components in larger amounts or entering special contracts with manufacturers. However, aside from researching aspects, a single-gateway would probably be more suitable for industrial BAS applications.

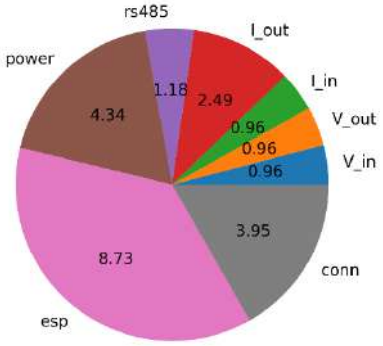

Figure 7. Cost distribution of the IoT-gateway; costs per gateway in € for 100 pieces ordered

5 Summary and Conclusion

In this paper, we designed an IoT-gateway for research on applications in BAS. From our experience, we derived technical requirements for an IoT-gateway in BAS applications. More specifically, we defined:

- Timescales for physical and interpretation delay
- Storage and resolution requirements
- Commonly used signal transmission interfaces
- Software requirements
- Network and time-tagging requirements

- Common industrial power supply in BAS

Utilizing the ESP32-PICO-KIT as a base module satisfies several of the defined requirements such as network connection and time-tagging abilities, ADC and DAC functionalities with appropriate resolution or enough storage capacity for buffering purposes. In order to provide the required interfaces, we designed the additionally necessary peripheral circuits accordingly to allow for analog as well as bus-based communication via RS-485. The ESP32 is a freely programmable WiFi controller; the software addressing all interfaces was written in Micropython, however, it could be programmed with different languages either.

To validate the designed circuits for the different communication interfaces, a test series was conducted comparing target values to measured values. In the validation, analog readings showed severe issues when reading very small values. The average relative errors were around 4.3 %. The analog writing functionality resulted in deviations that were higher than the deviations in reading. In BAS, control algorithms often use differences between set and actual values to calculate an output, hence we conclude that the reading functionality requires improvement. However, further investigations should aim for specifying the exact limitations for BAS operation. Besides that, the analog writing functionalities require small changes in order to at least ensure reaching both upper and lower limit. Additionally, the current output loop is only able to produce a current for devices with resistances up to 250 Ω. For RS-485, we successfully tested a Modbus device. This interface could also be utilized to realize BACnet communication. Further development should focus on extending the firmware and testing BACnet support. In general, the technical requirements could be met showing some restrictions.

Additional improvements include logging routines and streaming of measurement results over WiFi as well as the implementation of control loops.

As regards purchase costs, the total costs amount to roughly 28 €, hence being far below comparable IoT-gateways like a shielded Raspberry Pi with a retail price of 100 €, a Controllino at 200 € or edge controllers at 300-400 €.

6 Acknowledgement

We thank the ERDF for their financial support.

References

[1] Lonmark Deutschland e.V. Energieeffizienz automatisieren, Aachen, 2011.

[2] MeGA, Marktstudie, Marktstudie Gebäudeautomation, Schweiz, 2012.

[3] Control Consultants Inc. BASR-8M. On-line: https://controlconsultantsinc.com/basr8m-contemporary-controls-bas-remote-master-6-universal-io-2-relay.html, Accessed: 04/01/2019

[4] Arigo Software EWIO-9180-M. On-line: https://www.arigo-software.de/de/shop/110910.html, Accessed: 04/01/2019.

[5] Monotaro UCM-316. On-line: https://www.monotaro.com/p/0040/5912/, Accessed: 04/01/2019.

[6] EK3OT WISE-4470-S250. On-line: https://ekzot.com.ua/product/wise-4470-s250/, Accessed: 04/01/2019.

[7] Espressif ESP32-PICO-KIT Getting Started Guide. On-line: https://docs.espressif.com/projects/esp-idf/en/latest/get-started/get-started-pico-kit.html#, Accessed: 07/01/2019.

[8] Espressif ESP32 Datasheet. On-line: https://www.espressif.com/sites/default/files/documentation/esp32_datasheet_en.pdf, Accessed: 07/01/2019.

[9] FTDI Ltd. What is UART? On-line: https://www.ftdichip.com/Support/Documents/TechnicalNotes/TN_111%20What%20is%20UART.pdf, Accessed: 07.01.2019.

[10] RWTH-EBC AixOCAT. On-line: https://github.com/RWTH-EBC/IoT-Gateway/, Accessed: 31/01/2019.

[11] Damien George Micropython. On-line: https://micropython.org/, Accessed: 07/01/2019.

[12] Loboris Micropython for ESP32. On-line: https://github.com/loboris/MicroPython_ESP32_psRAM_LoBo, Accessed: 04/01/2019.

[13] uModbus. On-line: https://github.com/pycom/pycom-modbus/tree/master/uModbus, Accessed: 04/01/2019.

[14] Belimo LM24A-MOD. On-line: https://www.belimo.eu/pdf/e/LM24A-MOD_datasheet_en-gb.pdf, Accessed: 04/01/2019.

[15] Belimo Modbus-Register Description. On-line: https://www.belimo.ch/pdf/e/AirWater_Modbus-Register_en.pdf, Accessed: 04/01/2019.

[16] Mouser Electronics Inc. https://www.mouser.de, Accessed: 30/01/2019.

Optimal Laser Scan Planning for As-Built Modeling of Plant Renovations Using Mathematical Programming

E. Wakisaka[a], S. Kanai[b], and H. Date[b]

[a]Shinryo Corporation, Japan
[b]Hokkaido University, Japan
E-mail: wakisaka.ei@shinryo.com, kanai@ssi.ist.hokudai.ac.jp, hdate@ssi.ist.hokudai.ac.jp

Abstract –

In recent years, terrestrial laser scanners have been introduced to enable efficient as-built modeling. Since heating, ventilating, and air conditioning facilities often include many pipes and ducts packed into small spaces, it is difficult to manually determine optimal scanner placements that can capture their surfaces with high accuracy and quality and with few occlusions.

To solve this problem, we propose an optimal scan planning method based on mathematical programming that uses a coarse 3D model obtained from structure-from-motion as prior knowledge of the objects to be scanned. Integer programming enables us to identify optimal scanner locations that maximize scan coverage while satisfying general scan constraints. The proposed method can outperform experienced operators in terms of scan coverage and modeling accuracy. In addition, we extend our original method to address additional objectives and constraints encountered in practice, such as ensuring full scan coverage, minimizing travel time, and guaranteeing point cloud registration. We also confirm our methods' effectiveness via computer simulations.

Keywords –

Laser scanning; scan planning; Structure-from-motion; Next-best-view; As-built; Plant renovation

1 Introduction

Recently, increasing numbers of building facility renovations are being conducted in the heating, ventilating, and air conditioning (HVAC) industry. Laser scanning with terrestrial laser scanners (TLSs) is being used to reconstruct as-built three-dimensional (3D) models of these facilities, enabling shorter survey periods and in-depth construction planning. To reconstruct such 3D models to the precision required for renovation, the TLSs must be positioned appropriately and the scanning process must consider several different objectives and constraints. First, with a TLS, the scanning error depends on the scanning range and the incidence angle between the scanning beam and the surface to be scanned [1]. Second, the acceptable level of scanning error can vary for different parts of the facility depending on the scan's purpose. Finally, the aim is to maximize the scan coverage, with as few occlusions as possible, while respecting the first and second constraints.

Currently, however, the TLS positions are generally determined manually by experienced operators, so there is no guarantee that the scanner placements will satisfy the above scanning objectives and conditions.

To deal with these issues, in this paper, we propose a new optimal laser scan planning method for TLSs that utilizes a coarse 3D model reconstructed via a structure-from-motion (SfM) technique as prior knowledge. It uses integer programming to find optimal scanner placements that maximize scan coverage while satisfying the beam incidence angle and scanning range constraints. We also propose ways to address three further objectives and constraints encountered in practice: providing full scan coverage, minimizing travel time to increase scanning efficiency, and guaranteeing point cloud registration. To achieve this, we develop three extensions to the original method. Finally, we evaluate our methods' effectiveness via experiments and computer simulations.

2 Related Work

In the reverse engineering and robotics fields, the problem of automatically determining optimal sensor placements and measurement sequences is known as the *next-best-view* (NBV) problem [2]. NBV problems can be divided into two types: ones with prior knowledge about the objects to be scanned and ones without. It is known that better sensor placements can be found in the former case [3] than in the latter.

Several NBV problem studies have considered optimal laser scan planning problems involving prior knowledge. Soudarissanane et al. [4] and Ahn et al. [5]

proposed scanner placement estimation methods that maximize the building's measurable wall length using greedy methods, based on 2D drawings of the building's interior and exterior. However, since their methods treat scanner placement as a simple two-dimensional (2D) optimization problem, it is difficult to ensure the scanner placements provide sufficient scan coverage, minimizing occlusions, when applied to scanning plant facilities involving complex, 3D structures with TLS.

Turning now to 3D optimization approaches, Kitada et al. [6] and Zhang et al. [7] proposed methods for deriving optimal scanner placements that maximize scanned surface coverage. These apply integer programming [6] or full search [7] to a 3D model of the building's exterior, but they do not consider the beam incidence angle and scanning range constraints. In addition, these studies did not compare the optimal scanner placements found by their algorithms with those determined by experienced operators in terms of scanning efficiency and quality for as-built modeling.

In our previous study [8], we also proposed a method of solving the optimal TLS planning problem that uses the mesh model representation of an SfM model as prior knowledge. Our method formulates the problem of maximizing the number of measurable surfaces while satisfying the incidence angle and scanning range constraints as a 0–1 integer programming problem, deriving the optimal scanner placements from its solution. However, this method cannot provide full scan coverage, minimize travel time, or guarantee point cloud registration.

To address these issues, in this paper, we extend our previous approach [8] so as to derive the additional scan positions needed for full scan coverage, optimize the scan sequence to minimize travel time, and generate scanner placements that guarantee point cloud registration.

3 Planning Optimal Scans Using Mesh Models And Integer Programming

3.1 Algorithm Overview

In this section, we provide a brief overview of our previous planning algorithm [8]. As shown in Figure 1, the first step is to generate a coarse 3D SfM model from photos of the facility to be modeled. Next, since the required scan quality can differ substantially depending on the area and construction type, we assign a "scan significance level" to each region to specify the quality needed, which is later used to determine the constraint level. Each of the SfM model's surfaces is assigned one of three scan significance levels: *high*, *medium*, or *low*.

During the second step (Figure 2) the space enclosing the SfM model is decomposed into a set of

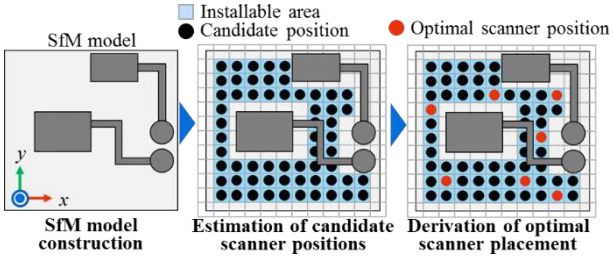

Figure 1. Outline of our optimal scan planning algorithm based on mesh-based integer programming

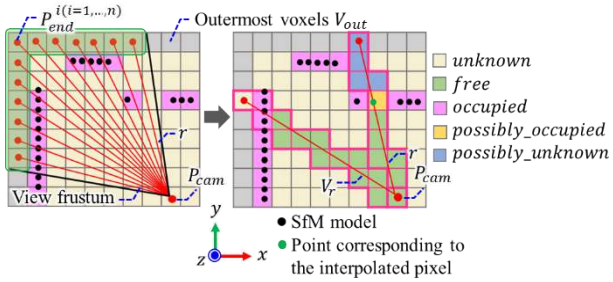

Figure 2. Spatial occupancy classification

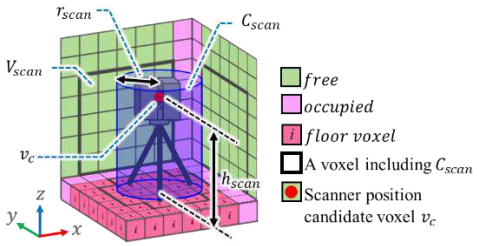

Figure 3. Candidate scanner positions

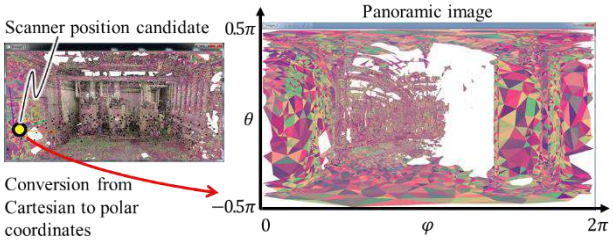

Figure 4. Rendering of an SfM model's surfaces as a panoramic image

voxels with a spatial resolution of l_v, and any voxels that include one of the SfM model's surfaces have their space occupancy attributes set to *occupied*. Next, rays are cast from each camera position toward the centroid of the outermost voxel P_{end} included in that camera's view frustum. Based on these results, the space occupancies of the remaining voxels are set to one of the remaining three types: *free*, *possibly_occupied*, and *possibly_unknown*. Then, as shown in Figure 3, based

on the voxels' space occupancy classifications, a set of candidate scanner positions v_c is extracted from the voxel space enclosing the SfM model.

The final step is to reduce the optimal scan planning problem to a 0–1 integer programming problem. First, we calculate the observation matrix $A = \{a_{v_c,f}\}$, where $a_{v_c,f}$ indicates whether surface f of the SfM model is visible from scanning position v_c. To efficiently determine the visibility, we render the sections of each surface of the SfM model in different colors on a spherical image generated from v_c (Figure 4). Then, surface f is visible if the color used to render it remains in the image produced by the graphics processing unit (GPU). If f also satisfies the incidence angle and scanning range conditions, it is labeled as *observable* $(a_{v_c,f} = 1)$. By repeating this process for all $v_c \in V_c$, we can generate the observation matrix A.

Finally, we derive the optimal scanner placements by integer programming, where the indicator variables represent whether or not a scanner should be placed at v_c. Here we use the Numerical Optimizer [9] package, with the branch and bound algorithm.

3.2 Performance

We compared the performance of our original method with that of experienced operators for a room containing a machine acting as a heat source (12.1 × 14.1 × 4.6 m^3) in terms of the number of scans, scan coverage ratio, modeling accuracy, and processing time. The scanning conditions and threshold constraint values were as shown in Tables 1 and 2, respectively. The optimal laser scanner positions found by both methods are shown in Figure 5.

These results confirm that the proposed method yielded higher scan coverage than the human operator could achieve. The geometric errors in the point cloud-based model captured with the optimal scanner positions were less than 5 mm, sufficient for practical use, while those in the model captured using the operator's placements were more than 7 mm and it is too high for the model to be useful. Furthermore, our method was able to generate optimal scanner positions in only a few minutes, giving it a significant advantage for use in practical scanning tasks.

4 Addressing Practical Constraints

4.1 Issues and Resolutions

Unfortunately, several issues still remain when applying the original optimal scan planning algorithm (Section 3) in practice, namely the following.

- When scanning complex facilities, the use of 2D candidate scanner positions, with the scanner placed at a constant height on a tripod, means that un-scanned SfM model surfaces often remain near ceilings, regardless of the scanner positions used.
- Since the sequence in which the scans are performed does not affect the coverage or scan quality, the sequence used is left to the operator's judgment. However, when scanning large-scale facilities, it is difficult for unskilled operators to move from one position to the next efficiently without getting lost.
- Since no constraints are imposed on the overlaps between point clouds from different scans, the scanner positions generated do not necessarily ensure point cloud registration.

Table 1. Scanning parameters

Parameter	Value
Scanner height (h_{scan})	1.4 m
Scanner base radius (r_{scan})	0.3 m
Vertical field of view	320°
Horizontal field of view	360°
Vertical and horizontal scan pitch	0.072°

Table 2. Scanning constraints

Constraint	Scanning significance level		
	High	Medium	Low
Max. incidence angle	45°	90°	90°
Min. scan range	0.3 m	0.3 m	0.3 m
Max. scan range	5.0 m	8.0 m	20.0 m

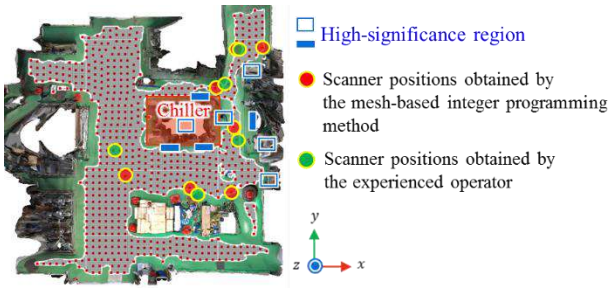

Figure 5. Scanner positions in a room with a machine-based heat source

To address these issues, in this study, we extend our original method in the following ways, then evaluate the effectiveness of these extensions in computer simulations.

1. We formulate an additional planning problem using integer programming to derive additional and optimal 3D scanner placements that can achieve full scan coverage with the minimum number of scans.

2. We formulate an optimal scan ordering problem, deriving the shortest distance needed to travel among the scanner positions from an instance of the *traveling salesman problem*.
3. We formulate scan planning as a constraint satisfaction problem to derive optimal scanner placements that guarantee point cloud registration.

4.2 Full-Coverage Scan Planning Algorithm

4.2.1 Generating Additional Scanner Positions

First, based on the constraints given in Table 2, we define a view frustum (Figure 6) such that the viewpoint is located at the centroid f_u of the unmeasured surface, with the view direction directed toward the surface's normal vector n_i, the vertical and horizontal fields of view being $2\theta_\alpha$, and the *near* and *far* planes being d_{min} and d_{max}, respectively. Then, *free* or *possibly_occupied* voxels whose centroids are included in the view frustum are extracted as additional candidate scanner positions $v_s \in V_{scanner}$.

4.2.2 Checking Visibility and Generating the Observation Matrix

As with the original method [8], we formulate the problem of planning additional scans as a 0–1 integer programming problem. Therefore, we again need to generate an observation matrix $B = \{b_{f_u,v_s}\}$, where b_{f_u,v_s} indicates whether or not the un-scanned surface f_u is observable from scanning position v_s.

To efficiently evaluate these element values, we generate spherical images of the SfM model's surfaces as seen from each position v_s as before, labeling each surface as *observable* $(b_{f_u,v_s} = 1)$ or *unobservable* $(b_{f_u,v_s} = 0)$ using pixel-wise visibility checks and scan quality checks that consider the beam incidence angle and scan range. By repeating this process for all $v_s \in V_{scanner}$, we can generate the observation matrix B.

4.2.3 Generating Additional Scanning Positions

Using the observation matrix B (Section 4.2.2), we formulate the additional scanner placement problem as the following 0–1 integer programming problem.

$$\left|\begin{array}{ll} \underset{z_{v_s}}{\text{minimize}} & \sum_{v_s \in V_s} z_{v_s}(1 + \alpha h_{v_s}) \quad (1)\text{-}1 \\ \text{subject to} & \sum_{v_s \in V_{scanner}} b_{f_u,v_s} z_{v_s} \geq 1 \ (f_u \in F_u) \quad (1)\text{-}2 \\ & z_{v_s} \in \{0,1\} \ (v_s \in V_s) \quad (1)\text{-}3 \end{array}\right.$$

Here, the terms are defined as follows:
$v_s \in V_s$: a candidate additional scanning position,
$f_u \in F_u$:an unmeasured triangular SfM model surface,

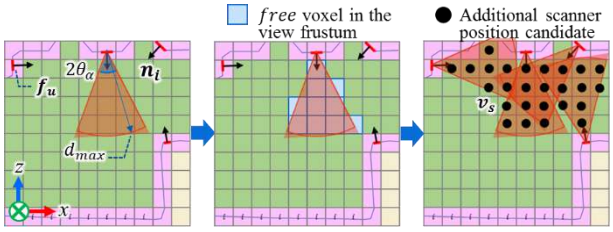

Figure 6. Generating additional scanner position candidates

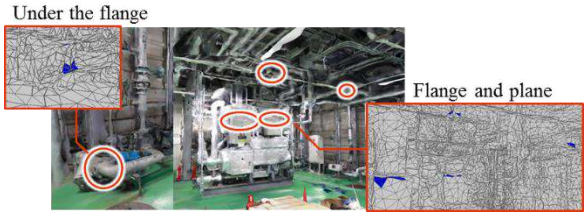

Figure 7. Distribution of the unmeasured high-significance surfaces

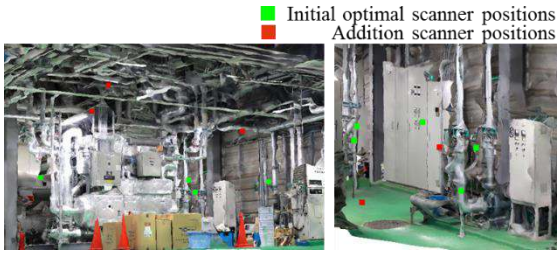

Figure 8. Distribution of additional scanner positions

$$z_{v_s} = \begin{cases} 1 & \text{if } v_s \text{ is used as a scanning position,} \\ 0 & \text{if } v_s \text{ is not used as a scanning position,} \end{cases}$$

$$x_f = \begin{cases} 1 & \text{if } f \text{ is measured,} \\ 0 & \text{if } f \text{ is not measured,} \end{cases}$$

and

h_{v_s}: z coordinate of v_s.

Here, the objective function (Equation (1)) aims to minimize both the number of additional scan positions and their z-coordinates, so lower v_s positions will tend to be selected as additional scan locations.

Finally, we derive the solution to this optimization problem by integer programming. The centroids of the voxels v_s for which $z_{v_s} = 1$ are adopted as additional scanning positions, and added to the set of scanner positions Z_{opt} derived in Section 3.

4.2.4 Results

We applied the above algorithm for planning additional scans to the room used for the previous evaluation (Section 3.2). Figure 7 shows the high-significance surfaces that could not be measured using only the previous scanner positions. The parameters and

constraints were as before (Tables 1 and 2, respectively).

Here, 2,258 additional candidate scanner positions v_s were considered, from which the proposed algorithm extracted the five positions shown in Figure 8. These included several high locations, needed to scan several pipes installed near the ceiling. We were able to confirm that the scan coverage reached 100% with these additional scanner positions added. The time required to solve the optimization problem was 9.6 min, which is reasonable for on-site planning.

The TLS unit used for these experiments weighed 9.8 kg, and its body was 170 mm wide, 286 mm deep, and 286 mm high. This made it difficult to position at the heights required on a tripod due to instability. Therefore, for these additional scans, another laser scanner would be needed that is smaller, lighter, and has a tripod capable of greater extension.

4.3 Optimal Scan Ordering Algorithm

4.3.1 Estimating the Passable Areas

First, the areas of the SfM model through which the operator can travel are extracted using the voxels' space occupancy attributes (Section 3.1).

This is achieved by approximating the shape of a human body as a closed cylinder C_{human} with a radius of r_{human} (Figure 9), and determining the minimum connected voxel set V_{human} that can include C_{human}. As shown in Figure 9, if the ratio of the area of the projected floor voxels (M) to that of V_{human} projected along the z-axis (N) is greater than the threshold value τ_{place}, the floor voxel is classified as *passable*. This condition can be represented as

$$M/N \geq \tau_{place}, \tag{2}$$

where we set $\tau_{place} = 0.80$ in this paper.

4.3.2 Constructing the Path Graph

Generating the optimal scan ordering that achieves the shortest possible travel distance among the given scanner positions can be formulated as an instance of the traveling salesman problem. In this problem, the costs, namely the distances $dist_{i,j}$ between pairs of scanner positions i, j, have to be evaluated and assigned. With this in mind, we construct candidate operator routes as path graphs.

First, as shown in Figure 10, the passable voxels are projected onto a horizontal plane and the centroids of passable voxels are designated as nodes, with pairs of adjacent nodes connected by edges. Then, the set of optimal scanner positions Z_{opt} is projected onto this horizontal plane and the closest nodes are regarded as the scanner nodes. Finally, the shortest path between each pair of scanner nodes, i.e., the path that minimizes

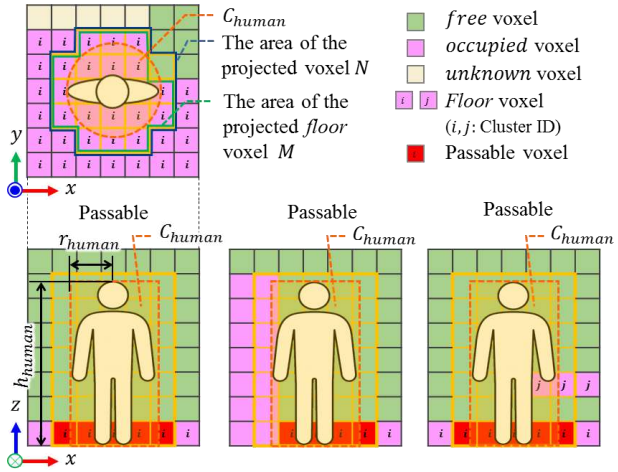

Figure 9. Estimating passable area

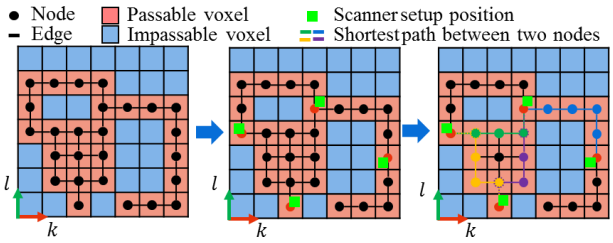

Figure 10. Constructing path graph

the distance between them, is evaluated using Dijkstra's algorithm. Here, the distances between scanner nodes are calculated in terms of the Manhattan distance. This enables us to define all the distances $dist_{i,j}$ between pairs of scanner nodes.

4.3.3 Calculating the Shortest Path and Optimal Scanning Order

The optimal scan ordering problem can be formulated as the following traveling salesman problem.

$$\text{minimize}_{x_{i,j}} \quad \sum_{i \in V_{opt}} \sum_{j \in V_{opt}} dist_{i,j}\, x_{i,j} \tag{3}\text{-1}$$

$$\text{subject to} \quad \sum_{j \in V_{opt}} x_{i,j} = 1 \left(\forall i \in V_{opt}\right) \tag{3}\text{-2}$$

$$\sum_{i \in V_{opt}} x_{i,j} = 1 \left(\forall j \in V_{opt}\right) \tag{3}\text{-3}$$

$$y_i - y_j + (n-1)x_{i,j} \leq n-2 \quad \left(\forall i, j \in V_{opt} \setminus \{1\}, i \neq j\right) \tag{3}\text{-4}$$

$$x_{i,j} \in \{0,1\} \left(\forall i, j \in V_{opt}\right) \tag{3}\text{-5}$$

Here, the terms are defined as follows:
$i \in V_{opt}$: a scanner node,
$x_{i,j} = \begin{cases} 1 & \text{if the path traverses from nodes } i \text{ to } j, \\ 0 & \text{otherwise,} \end{cases}$

$dist_{i,j}$: the distance from nodes i to j,
and
y_i: a dummy variable.

Finally, we can solve this optimization problem using integer programming.

4.3.4 Results

We used the above scan ordering optimization algorithm to plan the scanning sequence for the machine room example considered in Sections 3.2 and 4.2.4. The eight scanner nodes shown in Figure 11 had previously been derived using the original method [8]. Here, the numbers indicate scanner position IDs. In this case, since the entrance and exit were located at the lower left of the room, this was selected as the start point S, and a route derived that started and ended at *S*. For this experiment, we used $r_{human} = 0.3$ m and $h_{human} = 1.6$ m.

The optimal route is shown in Figure 11. Conducting the scans in the order $S \rightarrow 1 \rightarrow 5 \rightarrow 7 \rightarrow 6 \rightarrow 4 \rightarrow 3 \rightarrow 2 \rightarrow S$ gave us a minimum travel distance of 35.1 m. Constructing path graph process (Section 4.3.2) took 309 s, and the optimization process (Section 4.3.3) took 0.4 s, meaning this approach could also be used for on-site scan planning.

Being able to calculate such optimal routes could be very helpful in practice, as it could enable unskilled operators to complete scans efficiently without getting lost.

4.4 Planning Optimal Scans that Guarantee Point Cloud Registration

4.4.1 Problem Setting

Point cloud registration is the process of aligning overlapping scanned points or point clouds with common target markers. It is essential to ensure point cloud registration in laser scanning to create as-built models, so we must generate scanning plans that guarantee point cloud registration. In this paper, we simplify this problem by using target markers to assist with point cloud registration when planning the scans.

In particular, we enforce the following two constraints to enable point cloud registration.

1. As shown in Figure 12, at least two common target markers must be visible from any two different scanner positions.
2. The registration graph must be fully connected. This graph defines the scanning positions as nodes, and has edges between positions that satisfy Condition 1.

Here, the proposed scanner placement method only attempts to satisfy Condition 1 because it is almost satisfied during the scanning of an open room with plenty of planes. Conversely, when aligning plurality of rooms, second Condition 2 must be satisfied. Therefore, we plan to deal with Condition 2 in the future.

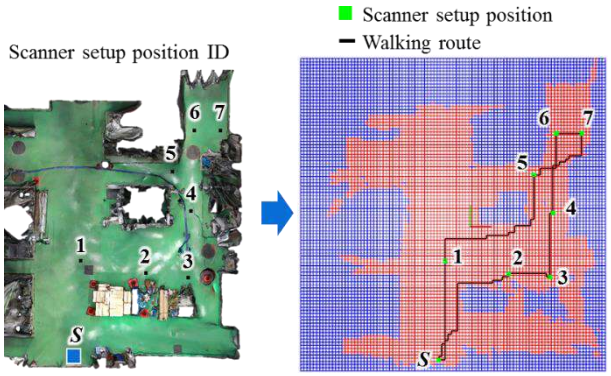

Figure 11. Shortest route and scanning order

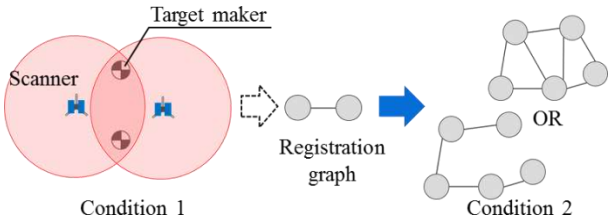

Figure 12. Conditions required to create a point cloud registration graph

4.4.2 Selecting Planar Regions

First, the operator interactively designates planar areas in the SfM model as target markers, and assigns each one a marker ID.

4.4.3 Checking Visibility and Generating the Registration Matrix

Again, our approach is similar to that used for the original method [8]. First, we construct an observation matrix $A = \{a_{i,f}\}$ describing whether or not the surface f can be observed from the candidate scanner position i, in the same way as in Section 3.1.

In addition, we also calculate the registration matrix $G = \{g_{i,j}\}$ describing whether or not given pairs of scanner positions i, j enable registration between their point clouds. Here, we first calculate the marker observation matrix $E = \{e_{i,m}\}$ describing whether or not marker m can be observed from scanner position i. Next, as shown in Figure 13, if the marker plane f_m passes the pixel-wise visibility check (Section 4.2.2) then it is labeled as *visible*. If f_m also satisfies the incidence angle and scanning range conditions given in Equations (4) and (5), it is labeled as *observable*.

$$ang\{l(f_m, i), \boldsymbol{n_f}(f_m)\} < \theta_m \quad (4)$$

$$d_{mmin} < dist(f_m, i) \leq d_{mmax} \quad (5)$$

$$f_m / F_M \geq \tau_m \quad (6)$$

Then, as described in Equation (6), if the ratio of observable plane elements f_m to the complete set of plane elements F_M constituting the marker is larger than τ_m, we set $e_{i,m}$ to 1, i.e., observable.

Next, we calculate the inner product of the row vectors $\boldsymbol{e_i}$ and $\boldsymbol{e_{i'}}$ in the marker observation matrix E, which correspond to the i-th and i'-th scanner positions. When $\boldsymbol{e_i} \cdot \boldsymbol{e_{i'}} \geq 2$, the point clouds scanned at these two positions have at least two markers in common, so point cloud registration is possible and we set $g_{i,i'} = 1$:

$$g_{i,i'} = \begin{cases} 1 \text{ if } & \boldsymbol{e_i} \cdot \boldsymbol{e_{i'}} \geq 2, \\ 0 \text{ if } & \boldsymbol{e_i} \cdot \boldsymbol{e_{i'}} < 2. \end{cases} \quad (7)$$

4.4.4 Generating Optimal Scanner Placements that Allow for Registration

Using the registration matrix G (Section 4.4.3), we can generate optimal scanner placements that ensure point cloud registration as follows.

$$\begin{aligned}
&\underset{x_f, z_i}{\text{maximize}} && \sum_{f \in F} x_f && (8)\text{-}1 \\
&\text{subject to} && \sum_{i \in V_c} z_i \leq T && (8)\text{-}2 \\
& && \sum_{i \in V_c} a_{i,f} z_i \geq x_f \ (\forall f \in F) && (8)\text{-}3 \\
& && \sum_{i \in V_c} z_i z_{i'} g_{i,i'} \geq 1 \ (\forall i' \in V_c) && (8)\text{-}4 \\
& && z_i \in \{0,1\} \ (\forall i \in V_c) && (8)\text{-}5 \\
& && x_f \in \{0,1\} \ (\forall f \in F) && (8)\text{-}6
\end{aligned}$$

Here, the terms are defined as follows:
$i \in V_c$: a candidate scanning position,
$f \in F$: a triangular surface with high significance in the SfM model,
T: the upper limit on the number of scans,

$$z_i = \begin{cases} 1 & \text{if position i is adopted,} \\ 0 & \text{if position } i \text{ is not adopted,} \end{cases}$$

$$x_f = \begin{cases} 1 & \text{if } f \text{ is measured,} \\ 0 & \text{if } f \text{ is not measured,} \end{cases}$$

$$a_{i,f} = \begin{cases} 1 & \text{if } f \text{ is observable from } i, \\ 0 & \text{if } f \text{ is not observable from } i, \end{cases}$$

and

$$g_{i,i'} = \begin{cases} 1 & \text{if positions } i \text{ and } i' \text{are aligned,} \\ 0 & \text{if positions } i \text{ and } i' \text{ are not aligned.} \end{cases}$$

In the formulation of 4.2 and 4.3, as the objective function and constraints can be expressed as linear functions, 4.2 and 4.3 can be handled as an integer programming problem. Therefore, an optimal solution can be derived through the simplex method. In contrast,

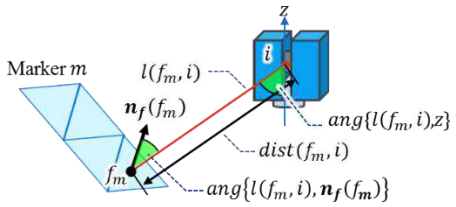

Figure 13. Checking the visibility of the surface f_m containing the marker

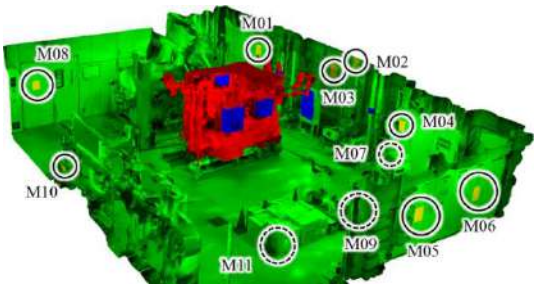

Figure 14. Planes selected as target markers

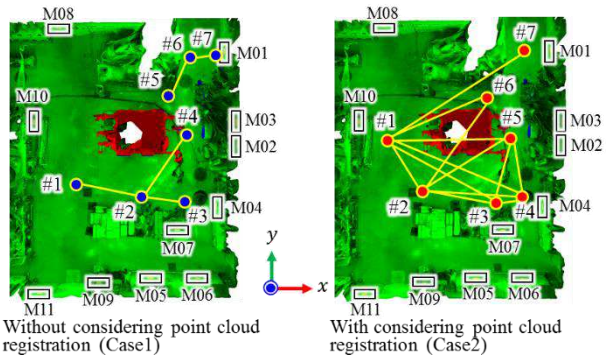

Figure 15. Scanner position pairs that enable point cloud registration

as the registration constraint in the formulation of 4.4 needs to be expressed by a quadric function, it cannot be handled as an integer programming problem. Therefore, we treat it as a constraint satisfaction problem, and derive a solution using tabu search, which is a metaheuristic [10], [11]. This algorithm solves the problem of minimizing total penalty for the violation of each constraint. Because this algorithm is an approximate solver, even if there is no solution that satisfies all constraints, we can derive a solution that satisfies the constraint to the maximum possible extent.

Finally, the scanner positions i for which $z_i = 1$ were added to the set of optimal scanning positions Z_{opt}.

4.4.5 Results

We again applied the algorithm to the machine room used in our previous evaluations (Sections 3.2, 4.2.4, and 4.3.4). As shown in Figure 14, eleven planes were

chosen as being representative of the given area, excluding the floor, and were selected as target markers. The same parameters and conditions were used as before (Tables 1 and 2). In addition, since the target markers had to be scanned with high precision, the conditions for Equations (4) and (5) were taken to be $\theta_m = 45°, d_{mmin} = 0.3\ m, d_{mmax} = 10.0\ m,$ and $\tau_m = 0.8$.

We compared the scanner placements obtained by the proposed method (Case 2) with those obtained via the original integer programming method (Section 3) that does not consider registration, with $T = 7$ (Case 1).

The resulting scanner placements are shown in Figure 15. The scan coverage of the high-significance areas was 85.0% in Case 2, which was 3.2% lower than in Case 1 (88.2%). We also confirmed that the proposed scanner setup (Case 2) yielded a fully-connected registration graph, with every point cloud pair including at least two markers that were visible from both clouds and it being possible to connect all the point clouds to each other by a sequence of registrations. By contrast, in Case 1, the registration graph was not fully connected and the scanner positions were divided into two connected components, making it impossible to register point clouds in different components.

5 Conclusions

In this paper, to ensure that the laser scans used for as-built modeling are sufficiently complete, efficient, and reliable for use in plant renovation, we have proposed three optimal scan planning methods that extend our original method.

First, we confirmed that we could achieve 100% scan coverage using the additional scanner positions generated by our extended planning method. Next, we confirmed that we could derive the scan order that minimized the total travel distance using our scan ordering method. Finally, we confirmed that the scanner positions generated by our registration-aware method ensured that every pair of point clouds included at least two markers that were visible from both clouds and that all the point clouds could be connected via a sequence of registrations.

In future work, we plan to introduce conditions on the scan overlap to ensure global registration in the optimal scan planning problem, and also to develop a navigation system that can present the scanner setup positions without requiring any survey instruments.

References

[1] Soudarissanane S., Lindenbergh R., Menenti M. and Teunissen P. Incidence angle influence on the quality of terrestrial laser scanning points, *International Archives of ISPRS*, 183–188, 2009.

[2] Scott W.R., Roth G. and Rivest J.F. View planning for automated three-dimensional object reconstruction and inspection, *ACM Computing Surveys (CSUR)*, 35(1):64–96, 2003.

[3] Munkelt C., Kühmstedt P. and Denzler J. Incorporation of a-priori information in planning the next best view, *International Archives of ISPRS*, XXXVI-5, 37–42, 2006.

[4] Soudarissanane S. and Lindenbergh R. Optimizing terrestrial laser scanning measurement set-up, *International Archives of ISPRS*, XXXVIII-5/W12, 127–132, 2011.

[5] Ahn J. and Wohn K. Interactive scan planning for heritage recording, *Multimedia Tools and Applications*, 1–21, 2016.

[6] Kitada Y., Dan H. and Yasumuro Y. Optimization scenario for 3D-scanning plans of outdoor constructions based on SFM, *Proceedings of CONVR 2015*, 65–68, 2015.

[7] Zhang C., Kalasapudi V. S. and Pingbo T. Rapid data quality oriented laser scan planning for dynamic construction environments, *Advanced Engineering Informatics*, 30(2):218–232, 2016.

[8] Wakisaka E., Kanai S. and Date H. Optimal laser scan planning of terrestrial laser scanner for as-built modeling of HVAC Systems, *Journal of the Japan Society for Precision Engineering*, 84(8):738–745, 2018.

[9] Numerical Optimizer. Online: https://www.msi.co.jp-/nuopt/. Accessed: 13/12/2018.

[10] Nonobe K. and Ibaraki T. a tabu search approach for the constraint satisfaction problem as a general problem solver, *European Journal of Operational Research*, 106:599–623, 1998.

[11] Nonobe K. and Ibaraki T. An improved tabu search method for the weighted constraint satisfaction problem, *INFOR* 39:131–151, 2001.

Automatic Generation of the Vertical Transportation Demands During the Construction of High-Rise Buildings Using BIM

K. Wu[a,b], B. García de Soto[c,d], B.T. Adey[a], and F. Zhang[b]

[a] Institute of Construction and Infrastructure Management, ETH Zurich, Switzerland
[b] School of Civil Engineering, Central South University, China
[c] Division of Engineering, New York University Abu Dhabi (NYUAD), UAE
[d] Department of Civil and Urban Engineering, Tandon School of Engineering, New York University (NYU), USA
E-mail: keyi-wu@hotmail.com, garcia.de.soto@nyu.edu, adey@ibi.baug.ethz.ch, zfl@csu.edu.cn

Abstract –

The explosion of high-rise building projects has increased the awareness on the importance of the planning and management of vertical transportation systems (i.e., tower cranes, construction elevators and concrete pumps). Although researchers have made beneficial efforts in several aspects of vertical transportation systems (e.g., optimal design capacities and layouts), the estimation of demands on vertical transportation systems (i.e., the quantity of construction resources associated with location, trip date and vertical transportation mode) has not been fully integrated. Currently, this process is still done manually. Building information modeling (BIM) provides the possibility to automate this process, decreasing the time it takes to gather that information and reducing errors associated with manual collection and quantification. This paper proposes a BIM-based framework to generate the vertical transportation demands during the construction of high-rise buildings. It consists of six parts: (1) determine the vertical transportation information of building materials, (2) generate the vertical transportation information of temporary construction materials, (3) link the project schedule with construction materials, (4) generate the vertical transportation information of construction workers, (5) determine the vertical transportation mode for construction materials, and (6) generate the vertical transportation demands. A prototype tool, in the form of an add-in using Revit API, has been developed to demonstrate the functionality of the proposed framework through testing the BIM model of a 36-story high-rise building. The findings show that the framework allows to exploit BIM to generate the information needed to determine the vertical transportation demands quickly and effortlessly.

Keywords –

BIM; Vertical transportation demands; Vertical transportation systems; High-rise buildings

1 Introduction

In recent years, the number and height of high-rise buildings have increased significantly [1]. According to the Council on Tall Buildings and Urban Habitat (CTBUH) [2], the total number of 200-meter-plus buildings in the world was 263 in 2000. This number increased to 1,319 in 2017, a 402% increase from 2000. The average height of the world's 100 tallest buildings increased from 285 meters in 2000 to 372 meters in 2017, a 31% increase.

The vertical transportation of resources required in construction projects is becoming increasingly important, especially in the case of high-rise buildings [3]. During the construction of high-rise buildings, there are not only more resources to be transported, but also transportation distances are longer, making the vertical transportation efficiency an important factor when considering the progress of construction projects [1]. For this reason, vertical transportation systems, including tower cranes, construction elevators and concrete pumps (Figure 1), are attracting more and more attention from both academia and industry.

Figure 1. Tower cranes and concrete pumps used in the early stages of the construction of a high-rise building (source: the authors)

Some researchers have made beneficial efforts in several aspects of vertical transportation systems, such as optimal design capacities [1] [3] [4] and layouts [6] [7] [8]. These studies require vertical transportation demands (i.e., the quantity of construction resources (e.g., weight and volume of materials, number of workers) associated with location, trip date and vertical transportation mode) as the basis for analysis and calculation. However, a main challenge is to obtain the required information because the current estimation process is still being done manually, making this process time consuming, tedious, and prone to errors [1] [9].

As a rapidly developing digital technology in the AEC industry, building information modelling (BIM), has made it possible to solve some of the above problems due to its rich information stored (e.g., quantity and location of building elements), with the potential of automating the estimation process [10] [11]. Some researchers have made beneficial attempts to estimate the vertical transportation demands using BIM. In their research, the quantity, weight, dimension, coordinate and level of building elements in the BIM model were extracted to determine the load and destination of each transportation for tower cranes [4] [9] [12]. Each building element was categorized according to its material under the same family name and associated with schedule information [4] [9]. In order to estimate the vertical transportation demands of temporary construction materials, formwork and scaffolding were created in the BIM model [9]. However, these studies still have some application limitations. First, manually creating temporary construction materials is inefficient, it has been showed that the total modelling time doubles or more according to previous project experience [14]. Second, the researchers have not yet developed a method to link the objects explicitly according to their characteristics due to the discrepancy between the model break down structure in the BIM model and the work break down structure in the project schedule [13]. Although some BIM tools, such as Autodesk Navisworks, can link project schedule information with building elements semi-automatically [5], they are still inconvenient due to the need to create the corresponding collection of building elements in the BIM model according to tasks in the project schedule. Third, construction workers have a greater impact on the transportation performance of construction elevators than construction materials [1], nevertheless, construction workers are difficult to capture in the BIM model, and have not been included yet in the previous studies. Fourth, there is a variety of vertical transportation modes (e.g., tower crane, construction elevator, and concrete pump) to be used in high-rise building construction, the researchers have not yet allocated transportation resources to different vertical transportation modes available.

In order to address these limitations, this paper proposes a BIM-based framework to generate the vertical transportation demands during the construction of high-rise buildings. The remainder of the paper is organized as follows. First, each part of the framework is explained in detail. Subsequently, an example is tested using a prototype tool to validate this framework. Furthermore, the benefits and limitations of the framework are discussed. Finally, conclusions and ongoing work are provided.

2 Proposed Framework

Based on the use of BIM authoring tools (e.g., Autodesk Revit), a framework to generate the vertical transportation demands is proposed (Figure 2). It consists of the following six parts: (1) determine the vertical transportation information of building materials, (2) generate the vertical transportation information of temporary construction materials, (3) link the project schedule with construction materials, (4) generate the vertical transportation information of construction workers, (5) determine the vertical transportation mode for construction materials, and (6) generate the vertical transportation demands. These six parts are explained in the following subsections.

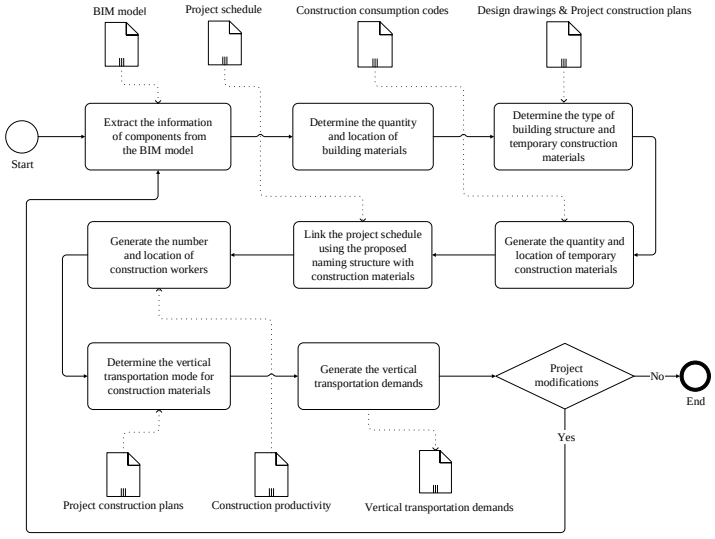

Figure 2. A BIM-based framework to generate the vertical transportation demands

2.1 Part 1: Determine the vertical transportation information of building materials

In Part 1, the information of components is extracted from the BIM model, including building elements (ID number, category (e.g., columns, walls, beams, slabs, stairs), type (e.g., rectangular beam, special-shaped beam), floor, material property (e.g., material quality, density) and dimension (e.g., height, length, width)), building areas (ID number, floor and area), and building levels (ID number, level and elevation). This information is used to determine the quantity (i.e., weight and volume) and location of building materials, and to gather the information required to generate the vertical transportation information of temporary construction materials in the next part.

2.2 Part 2: Generate the vertical transportation information of temporary construction materials

During the construction of high-rise buildings, the quantity of temporary construction materials (i.e., formwork and scaffolding) to be transported is large. It becomes critical when deciding vertical transportation cycle-time [15]. Part 2 is to generate the vertical transportation information of temporary construction materials, including quantity and location.

In the construction industry, there are existing construction consumption codes to estimate the quantity of temporary construction materials. For example, according to the consumption code [16], the quantity of formwork is based on the type (e.g., rectangular beam, special-shaped beam, lintel) and dimension (e.g., height, length, width) of building elements to be constructed, as well as the type of formwork to be used (e.g., bamboo plywood formwork with steel shoring). Similarly, the quantity of scaffolding is based on the building structure type (e.g., frame structure, shear wall structure), building height and area, as well as the type of scaffolding to be used (e.g., steel pipe scaffolding). In this part, the construction consumption codes are used. Figure 3 shows the process to estimate the quantity of temporary construction materials using the consumption codes. It consists of three steps. First, obtain the information required by the consumption codes from the BIM model and project construction documents (i.e., design drawings and project construction plans). Then, determine the unit quantity of the corresponding items in the consumption codes according to the information obtained, including the unit quantities of formwork for different building elements and the unit quantities of scaffolding for different building areas. Finally, calculate the quantity of temporary construction materials. Meanwhile, the location of temporary construction materials is determined from that of corresponding building elements (in the case of formwork) and building areas (in the case of scaffolding). Through using the BIM model and applicable consumption codes, the vertical transportation information of temporary construction materials is generated without creating them directly in the BIM model.

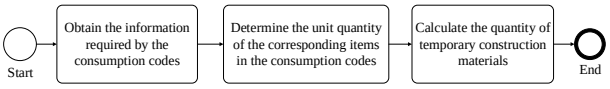

Figure 3. Process to estimate the quantity of temporary construction materials

2.3 Part 3: Link the project schedule with construction materials

Part 3 is to link the information from the project schedule (i.e., start and finish dates) with construction materials. This information will be used to quantify the number of construction workers and determine the trip date of construction materials and workers in the subsequent parts (Part 4 and Part 6).

The work break down structure of the project schedule typically has four levels (Figure 4 (a)), including sub-projects (e.g., foundation, main structure,

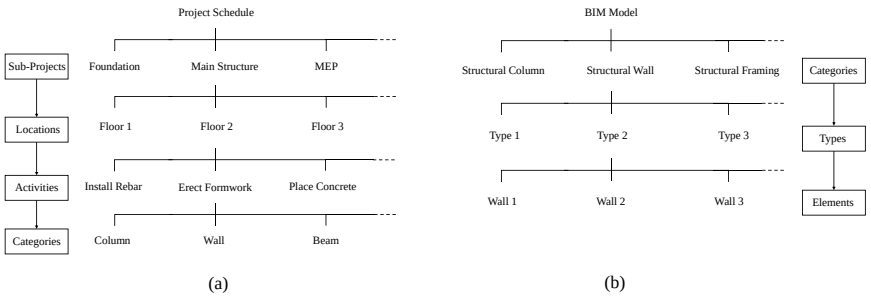

Figure 4. Work break down structure of the project schedule (a) and model break down structure of the BIM model (b)

MEP), locations (e.g., floors), activities (e.g., install rebar, erect formwork, place concrete), and categories (e.g., column, wall, beam). While the BIM model is generally broken into three levels (Figure 4 (b)), with categories, types, and elements. The discrepancy between the work break down structure in the project schedule and the model break down structure in the BIM model, leads to considerable time and efforts spend in matching and linking construction tasks and building elements [13]. To address that, a naming structure for tasks of the project schedule is proposed, as shown in Figure 5.

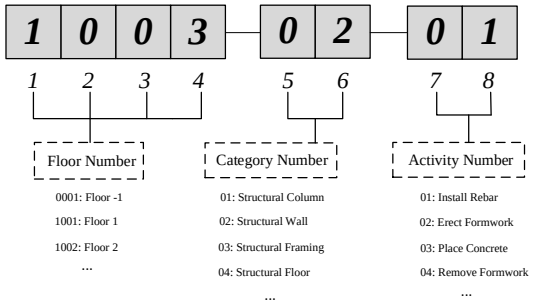

Figure 5. Proposed naming structure for tasks of the project schedule

The naming structure consists of three parts, namely (1) floor number, (2) category number, and (3) activity number. The floor number indicates the location of tasks. The category number is defined based on building element categories in the BIM model. The activity number represents the work scope of tasks. For example, a task with a "1003-02-01" name, as shown in Figure 5, means (read backwards) installing rebar for the structural walls in floor 3. According to this information, the task links all the structural wall rebar located on floor 3, meanwhile, the construction workers installing the structural wall rebar will also be connected in Part 4.

2.4 Part 4: Generate the vertical transportation information of construction workers

Ensuring that construction workers can be transported to destination floors on time, has a great influence on the construction progress, in some cases, it is more critical than transporting construction materials [1] [17]. Therefore, having a good understanding on the vertical transportation demands of construction workers is very important. In Part 4, the number and location of construction workers are generated.

The number of construction workers are calculated based on the quantity of construction materials, the duration of tasks (i.e., start and finish dates), and the construction productivity (Equation (1)).

$$N = \frac{Q}{(F - S + 1) \times P} \quad (1)$$

Where, N represents the number of construction workers per day for a given task; Q indicates the quantity of construction materials, with units depending on the type of materials (e.g., rebar (kg), formwork (m^2), concrete (m^3)); S and F are the start and finish dates, respectively, of the task evaluated; and P, namely the construction productivity, refers to the construction quantity per worker per day (e.g., for concrete: m^3/worker/day). For example, if the concrete volume of a structural column is 17.5 m^3, the start and finish dates of placing concrete are the same day, and the construction productivity is 35 m^3/worker/day, the construction worker number, using Equation (1), is 0.5. Meanwhile, the construction worker location is determined based on that of the column. The total number of construction workers required at a given date and location will be aggregated in Part 6.

2.5 Part 5: Determine the vertical transportation mode for construction materials

In the construction of high-rise buildings, different types of construction materials are usually transported through specific vertical transportation modes, for example, rebar is generally transported using tower cranes. But in some cases, some types of construction materials may also use different vertical transportation modes, for instance, concrete is usually transported by concrete pumps, but sometimes tower cranes are also used to lift it using concrete buckets. Therefore, Part 5 is to determine the vertical transportation modes for all construction materials taking into account actual planning defined by the project team.

Figure 6 shows the process to specify the vertical transportation modes to be used for different construction materials. It consists of the following three steps: (1) select the material to be transported (e.g., rebar, formwork, concrete); (2) choose the location to which the material will be transported (e.g., floor 1, floor 2, floor3); and (3) specify the vertical transportation mode to be used (e.g., tower crane, construction elevator, concrete pump).

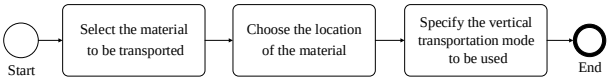

Figure 6. Process to specify the vertical transportation modes to be used for different construction materials

Table 1. Quantity output of construction resources using different vertical transportation modes

Vertical transportation mode	Quantity output		
	Material weight	Material volume	Worker number
Tower crane	✓		
Construction elevator	✓	✓	✓
Concrete pump		✓	

2.6 Part 6: Generate the vertical transportation demands

After the implementation of Part 1 through Part 5, the quantity, location, trip date, and vertical transportation mode of different construction resources have been determined. In Part 6, this information is compiled to display the vertical transportation demands for each type of vertical transportation systems. If there are any modifications to the project, the vertical transportation demands will be regenerated according to the updated BIM model and construction documents.

In general, the transportation volume of vertical transportation systems is limited by their loading capacities and space constraints. For tower cranes, the loading capacity is the main limiting factor. With respect to construction elevators, cages impose constraints on the dimensions of the object being transported, hence, construction elevators are limited by both the loading capacity and space constraint simultaneously. Concrete pumps are different from the above two types of vertical transportation systems since their transportation volume is based on the volume of concrete transported per hour. Thus, the quantity output of materials to be transported by tower cranes is weight, that of materials to be transported by construction elevators is weight and volume, that of materials to be transported by concrete pump is volume, and workers are output by number (Table 1).

3 Example

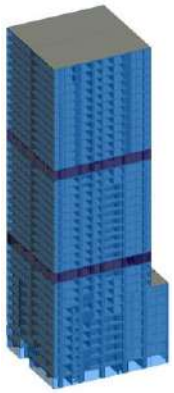

Figure 7. 3D view of the BIM model used in the example

A BIM model developed using Autodesk Revit 2017 [18] was used to test the proposed framework. The BIM model consists of a 36-story high-rise building with a height of 149.6 meters (Figure 7), which contains columns, walls, beams, slabs, stairs, wall finishes, doors, windows and glass curtain walls. For simplicity, the MEP system was excluded. The rebar information was generated using the Glodon software (GGJ 2013) [19]. Based on the framework, a prototype tool was developed in C# by using Revit API [20]. A database containing 14 tables was created using MySQL [21] (Figure 9), it can be divided into 4 parts, the blue table information (i.e., “Building Element”, “Building Area”, and “Building Level”) was from the BIM model, the green table information (i.e., “Consumption Code”, “Construction Productivity”, and “Formwork Content) was from the construction codes, the yellow table information (i.e., “Project Schedule”, “Vertical Transportation Mode”, “Formwork Type”, “Scaffolding Type”, and “Building Characteristic”) was from the project construction documents, and the red table information (i.e., “Formwork”, “Scaffolding”, and “Construction Worker”) was from the generated information. A use interface (Figure 8) was developed to determine the formwork type (i.e., bamboo plywood formwork with steel shoring), building structure type (i.e., frame-shear wall structure), scaffolding type (i.e., steel pipe scaffolding) and vertical transportation mode (e.g., tower crane, construction elevator, concrete pump) used for construction materials. Microsoft Project was used to develop the project schedule. The vertical transportation demands were generated as the Microsoft Excel files (Figure 10 to Figure 14).

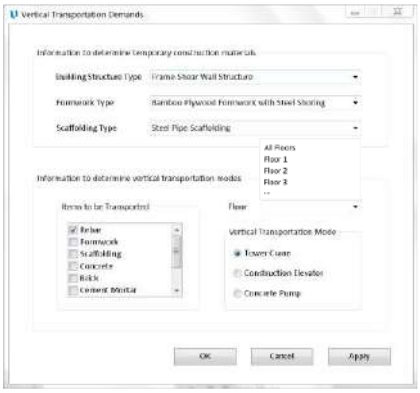

Figure 8. Developed user interface

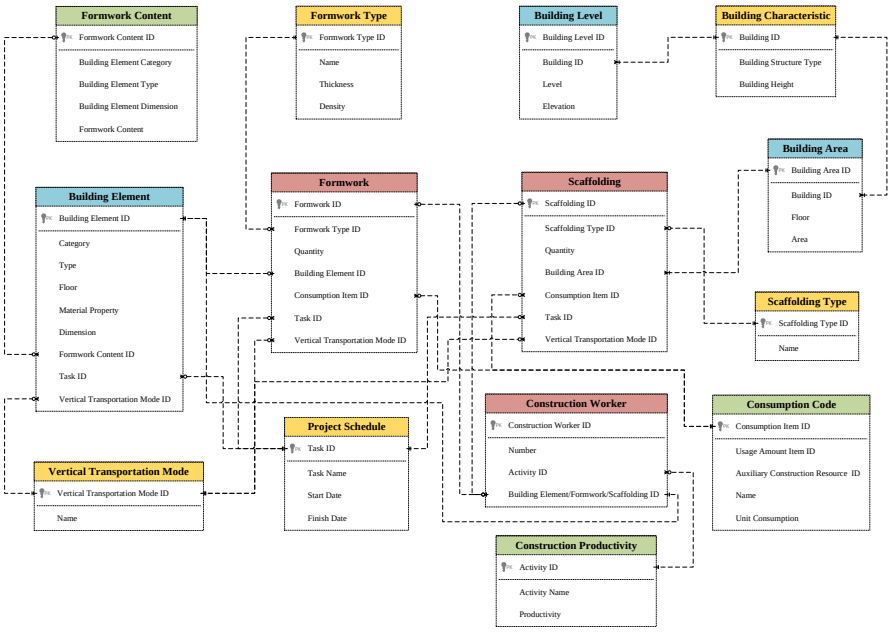

Figure 9. Database model diagram of the prototype tool

Figure 10 through Figure 14 show the vertical transportation demands for different types of vertical transportation systems. The horizontal, longitudinal and vertical axes represent the trip date, location and transportation volume, respectively. They provide valuable information for the project team. For example, this information shows that the maximum transportation weight of 765,871.43 kg for tower cranes occurs on May 24, 2015 and it is transported to floor 1 (Figure 10); the maximum transportation weight for construction elevators is 411,943.68 kg (139,232 kg to floor 4 and 272,711.68 kg to floor 19) on October 18, 2015 (Figure 11); the maximum transportation volume for construction elevators is 385.61 m³ to floor 8 on August 22, 2015 (Figure 12); the maximum transportation volume to be transported using concrete pumps is 615.57 m³ to floor 24 on October 22, 2015 (Figure 13); 238 construction workers (the maximum number) take construction elevators to floor 2, 3, 8, 16 and 21 on October 5, 2015 (Figure 14). With the information generated, the maximum transportation demands for different types of materials can also be obtained. For example, the maximum transportation weight for rebar is 142,613.59 kg (May 24, 2015/floor 1) and the maximum transportation weight of formwork is 176,658.9 kg (August 2, 2015/floor 10).

In addition to the obvious maximum transportation demands, the different trends can also be analyzed from the results. For example, different phases can be defined by the project manager based on the requirements for different transportation modes. When looking at the number of construction workers using construction elevators per day (Figure 15), from May 24 to August 20, 2015, the number of construction workers gradually rises to 149, this period could be defined as Phase 1. From August 21 to December 28, 2015, the number of construction workers starts to exceed 150, with the peaks over 200, this period could be defined as Phase 2. From December 29, 2015, the number quickly drops below 100, after that, the utilization remains stable, this period could be defined as Phase 3. The number and type of construction elevators to be used can be adjusted for each phase.

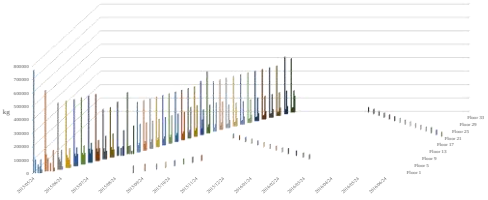

Figure 10. Output showing the vertical transportation demands (kg) to be transported by tower cranes

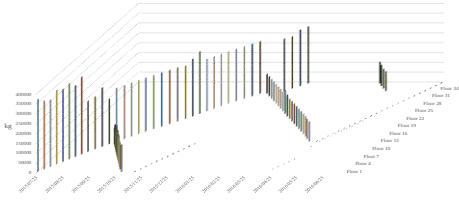

Figure 11. Output showing the vertical transportation demands (kg) to be transported by construction elevators

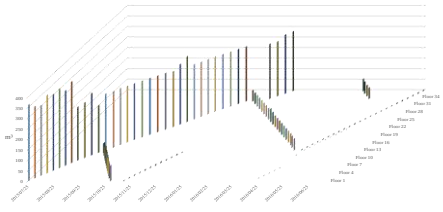

Figure 12. Output showing the vertical transportation demands (m³) to be transported by construction elevators

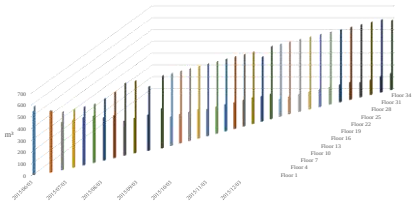

Figure 13. Output showing the vertical transportation demands (m³) to be transported by concrete pumps

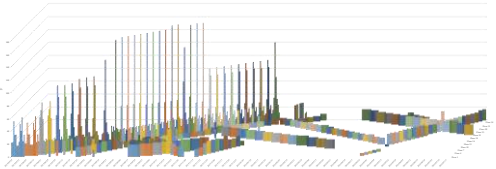

Figure 14. Output showing the vertical transportation demands (No. of workers) to be transported by construction elevators

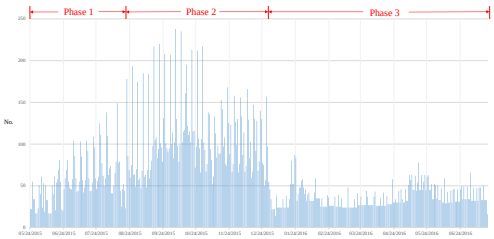

Figure 15. Output showing the number of workers to be transported by construction elevators per day

4 Discussion

This study is beneficial to the information collection of vertical transportation resources, and it makes three main improvements to the existing literature. First, the information of temporary construction materials is automatically generated without creating them directly in the BIM model (i.e., the design information model), as well as that of construction workers, which greatly enhance the efficiency of the collection process. Second, the proposal of the naming structure for tasks in the project schedule breaks the information barriers between BIM model and project schedule, making no additional manual operation is required for their interoperability so that reducing the unnecessary duplication of work and the loss of information. Third, the demands on multiple vertical transportation modes (i.e., tower crane, construction elevator and concrete pump) are generated simultaneously, not just one mode, allowing the project team to easily plan and manage the overall vertical transportation systems for achieving the global optimal solution. At the same time, the framework provides a dynamic aspect, generated results can be easily adjusted to account for changes.

This framework provides a promising solution to automate the generation process of vertical transportation demands during the construction of high-rise buildings, however, there are limitations yet to be addressed. First, it is common to use some floors as temporary storage spaces in the construction of high-rise buildings, hence, it is necessary to account for the transportation of resources between floors. Second, the framework does not consider the issue of transporting construction waste produced during construction down due to the amount of construction waste is not negligible in high-rise building construction. Third, it is normal to use permanent elevators when construction elevators have to be removed before finishing building enclosure work, which would reduce the demands on construction elevators, so the permanent elevator should be included as a vertical transportation mode. Ongoing research is carried out by the authors for addressing these limitations to make the framework more practical and valuable.

5 Conclusion

The boom in the construction of high-rise buildings creates some new challenges, such as the planning and management of vertical transportation systems. It also indirectly puts forward new requirements for the speed and accuracy of the vertical transportation demand collection. This paper proposes a BIM-based framework to automatically generate the vertical transportation demands, integrating the construction codes and project construction documents. The framework has been validated through an example project consisting of a 36-story high-rise building using a developed prototype tool. From the application of the proposed framework, the construction materials and workers needed by different types of vertical transportation systems were obtained quickly and effortlessly, greatly reducing the collection time. The generated three-dimensional graphs clearly show the quantity, location, and date of different vertical transportation demands, they can be utilized by the project team during the planning and management of

vertical transportation systems (e.g., determine vertical transportation period time). The current framework is at an early stage, it is expected to make the estimation on vertical transportation demands faster and more accurate by expanding and extending this basic framework. Ongoing work is conducted to address the limitations mentioned above.

References

[1] Park, M., Ha, S., Lee, H.-S., Choi, Y.-K., Kim, H. and Han, S. Lifting demand-based zoning for minimizing worker vertical transportation time in high-rise building construction. *Automation in Construction*, 32(4):88–95, 2013.

[2] Council on Tall Buildings and Urban Habitat. CTBUH year in review: tall trends of 2017. Online: http://www.skyscrapercenter.com/year-in-review/ 2017, Accessed: 16/11/2018.

[3] Shin, Y., Cho, H. and Kang, K.-I. Simulation model incorporating genetic algorithms for optimal temporary hoist planning in high-rise building construction. *Automation in Construction*, 20(5):550–558, 2011.

[4] Marzouk, M. and Abubakr, A. Decision support for tower crane selection with building information models and genetic algorithms. *Automation in Construction*, 61:1–15, 2016.

[5] Wang, W.-C., Weng, S.-W., Wang, S.-H. and Chen, C.-Y. Integrating building information models with construction process simulations for project scheduling support. *Automation in Construction*, 37(6):68-80, 2014.

[6] Abdelmegid, M.A., Shawki, K.M. and Abdel-Khalek, H. GA optimization model for solving tower crane location problem in construction sites. *Alexandria Engineering Journal*, 54(3):519–526, 2015.

[7] Lee, D., Lim, H., Cho, H. and Kang, K.-I. Optimization of luffing-tower crane location in tall building construction. *KICEM Journal of Construction Engineering and Project Management*, 5(4):7–11, 2015.

[8] Huang, C., Wong, C.K. and Tam, C.M. Optimization of tower crane and material supply locations in a high-rise building site by mixed-integer linear programming. *Automation in Construction*, 20(5):571–580, 2011.

[9] Wang, J., Zhang, X., Shou, W., Wang, X., Xu B., Kim, M.J. and Wu, P. A BIM-based approach for automated tower crane layout planning. *Automation in Construction*, 59:168–178, 2015.

[10] Borrmann, A., Hochmuth, M., König, M., Liebich, T. and Singer, D. Germany's governmental BIM initiative – Assessing the performance of the BIM pilot projects. In *Proceedings of the 16th International Conference on Computing in Civil and Building Engineering*, pages 871–878, Osaka, Japan, 2016.

[11] Wu, K., García de Soto, B., Zhang, F. and Adey, B.T. Automatic generation of the consumption for temporary construction structures using BIM: applications to formwork. In *Proceedings of the 35th International Symposium on Automation and Robotics in Construction*, Berlin, Germany, 2018.

[12] Irizarry, J. and Karan, E.P. Optimizing location of tower cranes on construction sites through GIS and BIM integration. *Journal of Information Technology in Construction*: 17:351–366, 2012.

[13] Park, J. and Cai, H. Automatic construction schedule generation method through BIM model creation. In *Computing in Civil Engineering 2015*, pages 620–627, 2015.

[14] Monteiro, A. and Poças Martins, J. A survey on modeling guidelines for quantity takeoff-oriented BIM-based design. *Automation in Construction*, 35:238-253, 2013.

[15] Wang, J., Liu, J., Shou, W., Wang, X. and Hou L. Integrating building information modelling and firefly algorithm to optimize tower crane layout. In *Proceedings of the 31st International Symposium on Automation and Robotics in Construction and Mining*, Sydney, Australia, 2014.

[16] Hunan Construction Engineering Cost Management Station. *Consumption code of construction engineering in Hunan province of China*. Hunan Science and Technology Press, Changsha, 2014. (in Chinese)

[17] Jung, M., Moon, J., Park, M., Lee, H.-S., Joo, S.U. and Lee, K.-P. Construction worker hoisting simulation for sky-lobby lifting system. *Automation in Construction*, 73:166–174, 2017.

[18] Autodesk, Inc. Revit, building design and construction software. Online: https:// www.autodesk.com/education/free-software/revit, Accessed: 16/11/2018.

[19] Glodon. GGJ, Rebar calculation software. Online: http://www.glodon.com/product/introduction.aspx ?c=5&Pid=247&attribute=24&model=31, Accessed: 16/11/2018.

[20] Autodesk, Inc. Autodesk developer network. Online:http://usa.autodesk.com/adsk/servlet/index? siteID=123112&id=2484975, Accessed: 16/11/2018.

[21] Oracle Corporation. MySQL community edition. Online:https://www.mysql.com/downlads/ Accessed: 16/11/2018.

Standard Closed-Circuit Television (CCTV) Collection Time Extraction of Sewer Pipes with Machine Learning Algorithm

X. Yin[a], Y. Chen[a], A. Bouferguene[b], H. Zaman[c], M. Al-Hussein[a], R. Russell[d], and L. Kurach[d]

[a] Department of Civil and Environmental Engineering, University of Alberta, Canada
[b] Campus Saint-Jean, University of Alberta, Edmonton, Canada
[c] Waste Management, City of Edmonton, Canada
[d] EPCOR Drainage Services, Edmonton, Canada
E-mail: xianfei@ualberta.ca, ychen10@ualberta.ca, ahmedb@ualberta.ca, hamid.zaman@edmonton.ca, mohameda@ualberta.ca, RRussell@epcor.com, LKurach@epcor.com

Abstract –
Closed circuit television (CCTV) is probably one of the most important technologies that is used by municipalities in order to monitor the structural and operational condition of sewer pipes. To be useful, CCTV video footage needs to be collected according to standards, which make such an operation, time consuming especially when pipes have operational issues like debris or tree roots. In this respect, developing benchmarks for data collection can be an important source of information that can improve the efficiency of future surveying campaigns. Computer simulation is an effective method for improving the efficiency of maintenance work schedules. However, CCTV collection data consists of abundant noise (waiting time or defect inspection time) due to the characteristics of pipes in different structural or operational conditions. For example, crawlers equipped with CCTV cameras could be blocked by deposits or serious structural issues in the pipe, which would cost some waiting time for the crawler to proceed with the inspection. In order to extract the standard CCTV collection time, excluding waiting time and defect inspection time a machine learning based approach is proposed in this work in the form of an algorithm commonly known as the Random Sample Consensus (RANSAC). This algorithm is developed to clean the data automatically, arriving at a function of CCTV collection time with two variables (i.e., length of pipe segment and number of taps in the pipe). The results can be fed into a simulation model to imitate the CCTV collection work in future research.

Keywords –
CCTV; Sewer pipes; Time extraction; RANSAC

1 Introduction

The sewer system plays an important role as a type of municipal infrastructure that has a significant influence on the efficiency and quality of our lives. However, the pipes that make up a sewer system undergo deterioration due to aging, external force, excessive demand, and other factors. [1]. This deterioration poses a great challenge for municipal maintenance departments since the maintenance is time-consuming and heavily dependent on capital investment and operating costs. To perform an efficient and quality sewer maintenance job, closed-circuit television (CCTV) is commonly adopted as the pipe condition inspection technique [2–4]. The wide usage of CCTV for pipe inspection has been driven by many practical reasons the most important of which being safety since this monitoring procedure does not require man entry [2]. Furthermore, since the videos are stored on appropriate media, they not only can be visualized for the purpose of inspection or comparison with other techniques (e.g., laser-based system, ultrasonic-based sensors and ground penetrating radar [5]) but more importantly they can serve as accurate historical data.

The CCTV collection process will be discussed in the next section. For this research, it should be noted, we only consider the time period that starting at the beginning of the video to the end. The objective of this research is to extract the standard CCTV collection time, excluding all waiting time, idle time, and other time delays in the collection process. The results can be fed into a simulation model to perform schedule optimization, which is the next stage of our research. In addition, the extracted standard CCTV collection time can be viewed as a benchmark for the CCTV collection process. Management decision can be derived for each

of the CCTV collection job in the perspective of time efficiency. For example, CCTV collection time within in new developed neighborhood should be align to the standard CCTV collection time; while it could be slower in older neighborhood theoretically considering the deterioration of the pipe, since more defects may cause more waiting time.

2 CCTV Collection Process

CCTV operators travel to inspect sewer pipes at the assigned locations as per the schedule set up by the municipal maintenance department. In general, before beginning the video collection phase, the pipes to be inspected are cleaned in advance by means of flushing equipment, in order to eliminate deposits and obstacles in the pipes which in turn ensures that the conditions for data collection are acceptable [6,7]. Following flushing activities, operators begin set-up work for CCTV data collection on the ground. The setup includes adjustment of a remotely controlled robot equipped with a specialized television camera. Next the camera begins to record a video for the observed pipe from the start point. In the process, the operators need to adhere to standards such as those described in National Association of Sewer Service Company (NASSCO) in order to obtain quality information that can be accurately analyzed later in the process. For instance, four primary categories of pipe defects are listed based on the pipeline assessment and certification program (PACP) [8]: that is, (i) structural defects, (ii) operation and maintenance defects, (iii) construction defects, and (iv) miscellaneous defects. While collecting the video, the technologist controlling data acquisition can decide to spend more time on serious defect such as those referred to as pipe broken or substantial deposits. The total CCTV collection time can be derived by means of Equation (1),

$$Time_n = a \bullet L_n + b \bullet T_n + W_n + C + \varepsilon_n \quad (1)$$

where $Time_n$ represents the total CCTV collection time for pipe segment, n; L_n is the length of the pipe segment; T_n is the number of taps of this pipe segment; W_n is the total waiting time, which may include the time for inspection of severe defects, adjustment of camera, etc.; C is the fixed time for the CCTV collection process, which may include time for equipment setup and other routine processes; and ε_n is an error representing the uncertainties regarding this process.

From a theoretical viewpoint, if there are no serious defects or other accidents that hinder the CCTV collection process observed in one pipe, a CCTV collection time can be generally described in Equation (2),

$$Time_n = a \bullet L_n + b \bullet T_n + C + \varepsilon_n \quad (2)$$

The waiting time is eliminated in this equation. $Time_n$ is denoted as standard CCTV collection time. The data points that contain waiting time are the noisy points that we want to exclude. The standard CCTV collection time extraction is conducted by the RANSAC algorithm, which will be described in the next section.

3 RANSAC Model

In order to extract the standard CCTV collection time, this research applies the Random Sample Consensus (RANSAC) algorithm to clean the raw data automatically. RANSAC, proposed by Fischler & Robert in 1981, is a non-deterministic approach to use the smallest initial dataset to determine the parameters of a model, then repeat the process until it reaches the predefined criterion [9]. Unlike linear regression using least-squares estimation, which seeks to minimize the distance from all the data points to the fitted function, RANSAC model searches for the best fitted function without considering the outliers (see Figure 1). From Figure 1. we can see that the solid line constructed by the RANSAC algorithm is better at describing the trend for all five points than the dotted line developed by least-square estimation. The outlier is called a noise point in this scenario, and it is these noise points that are supposed to be eliminated in constructing this regression model.

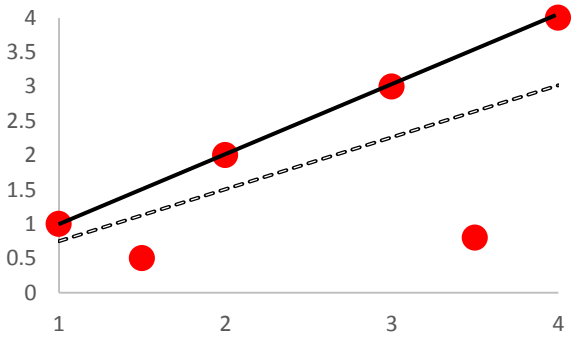

Figure 1. Comparison of least-square estimation and RANSAC.

The mechanism of the RANSAC algorithm is presented in Figure 2. The algorithm starts with selecting X points (where X = number of independent variables + 1). For instance, two points are needed to fit a line (2-dimensional problem) while three points are needed to fit a panel (3-dimensional problem). From Equation (2), we know that the extraction of the standard CCTV collection time is a problem with two independent variables, namely, the length of the pipe segment associated with video (L), and the number of taps within the pipe segment (T). Therefore, three points

need to be selected for each iteration. An objective function (Y_i) can be formed based on the selected points. Then, the Euclidean distance of each point to the objective function is calculated. A threshold (t) should be selected in order to decide whether the point is an inlier or an outlier. If the distance is within the threshold, it is an inlier; otherwise, it is an outlier. The number of inliers (N_i) should be counted and compared with the N_{i-1} (i.e., the greatest number of inliers among all the historical iterations). If the N_{i-1} is bigger, we save the N_{i-1} as N_i, and Y_{i-1} as Y_i. Otherwise, we update the N_i and Y_i accordingly. The process is repeated until the predetermined number of iterations (N) is reached. As for the number of iterations (N), it can be calculated by means of Equation (3) [10].

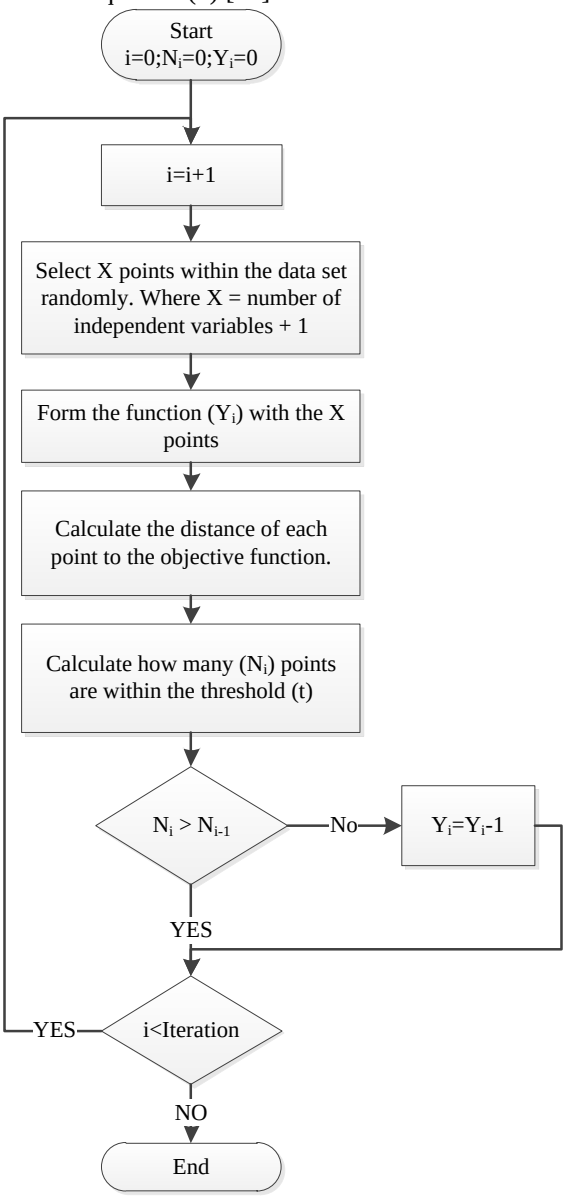

Figure 2. Flow chart of RANSAC algorithm.

$$1-p=(1-\lambda^X)^N \Rightarrow N \geq \frac{\log(1-P)}{\log(1-\lambda^X)} \quad (3)$$

where X is the number of points needed to construct the objective function; N is the number of iterations; P is the probability that at least one of the objective functions built in all N iterations is constructed by X inliers; and λ is the inlier ratio, which can be calculated using Equation (4). Although a priori it is an unknown ratio, it can be updated during the algorithm progress [11].

$$\lambda = \frac{Inliers}{Inliers + Outliers} \quad (4)$$

Considering the probabilistic nature of the RANSAC algorithm, the parameters (e.g., a and b) of the objective function will vary from one time to another if the algorithm runs multiple times. Therefore, the mathematical expectation of each parameter can be calculated from a large number of run-times of the algorithm. The mathematical expectation of the parameters will be used to form the objective function for the convenience of constructing the simulation model in the future research.

4 Case study

4.1 Data description

The data used in this research was collected by EPCOR Drainage Services, which is responsible for the operation and maintenance of the sewer infrastructure in Edmonton, Canada. For each pipe segment, the data is provided in two formats (two types of files), namely, Microsoft Access (.mdb), and video file (.mp4). The video duration (in seconds) and length of pipe segment surveyed (in meters) can be retrieved from the Access database directly. The number of taps is counted by a count query (combining all kinds of code associate with taps, such as Breaking-In/Hammer, Factory-made, Saddle, etc.) in the database in order to derive the total number of taps in a given pipe segment. Other attributes associated with the pipe segment can be derived from the Access database as well, such as the number of defects, location, and material type. The CCTV video serves as the validation function; that is to say, it is used to check the validity of the data recorded in the Access database either through manual viewing and analysis of the CCTV footage or by means of algorithms. In this research, we consider three attributes— video duration (s), length of pipe segment (m), and number of taps. 540 data records are fed into the RANSAC model to capture the relationship described in Equation (2) by excluding

any data records that contain forms of waiting time as described above.

4.2 Results and findings

As discussed in section 3, three parameters need to be determined for the RANSAC model: the number of points needed to form the candidate objective function (X), the number of iterations (N), and the threshold (t). In this case, X = 3 since there are two independent variables in this model, as per Equation (2). The lower boundary of the number of iterations, meanwhile, can be calculated from Equation (3). Considering the positive correlation between the number of iterations and the probability of obtaining the optimal results, along with the size of the dataset and CPU processing time, an iteration number of 100,000 was selected. As for the threshold, several experiments were conducted with different values of t (see Fig 3).

From Figure 3, we can see that the objective function can be plotted as a plane in a 3D space. The video duration (time) increases with an increase in the length of pipe segment (L), and number of taps (T), a finding which aligns with reality, since an increase in either the length of pipe segment or the number of taps will increase the CCTV collection time. The red dots represent the pipe segments classified as inliers; that is to say, these pipes are in good condition since there are no severe defects or other accidents that would lead to significant waiting time during the inspection process. Similarly, the blue dots represent the pipe segments that are classified as outliers, which means that these inspections must have been delayed by some extenuating circumstances (either sever defects within the pipe or other accidents such as equipment failure). The inliers and outliers are tabulated in Table 1.

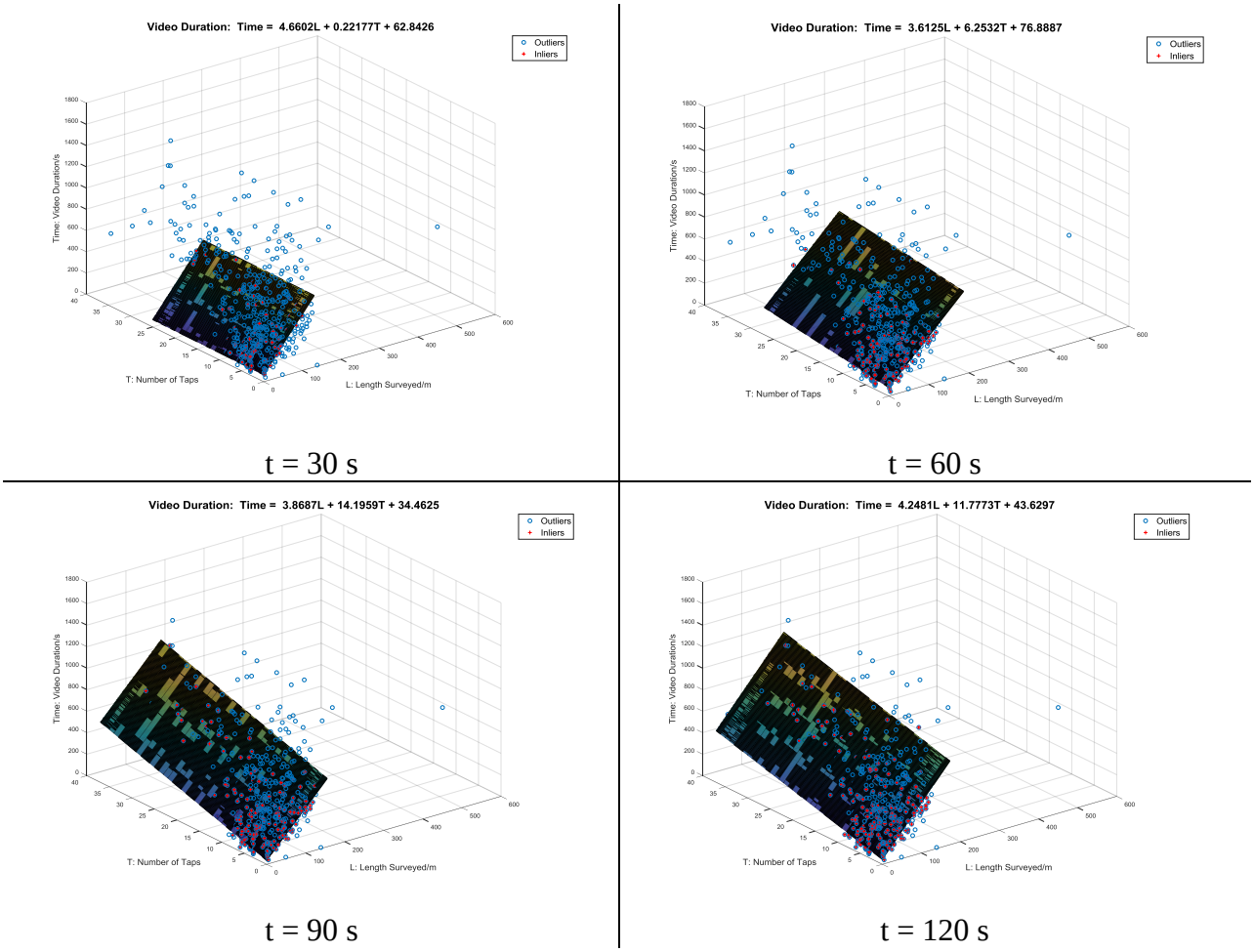

**Note that the red dots are the inliers (within the threshold) and the blue dots are outliers (outside of the threshold).*

Figure 3. Results of RANSAC model with different values of threshold (t)

Table 1. Number of inliers and outliers at different thresholds.

Threshold	30 s	60 s	90 s	120 s
Inliers	130	217	285	335
Outliers	410	323	255	205

Comparing the results in Figure 3 and Table 1, we can see that, as the value of the threshold grows, the number of inliers shows an increasing trend. The information in Figure 3 and Table 1 can be interpreted as follows: with the relaxation of the conditions, the number of pipe segments classified as being in good condition increases. A box-plot can be plotted based on the inliers at the four threshold values, along with the original video duration in the original 540 data (see Fig 4). Obviously, the original dataset has the highest median video duration, while the dataset has the lowest video duration when the threshold is set at the lowest value (30 s). The medians of the last three scenarios (t = 60 s, t = 90 s, and t = 120 s) do not vary significantly compared with the variation between the first two scenarios (t = 30 s and t = 60 s). Similar relationships for the 75th quantile of the video duration in the box-plot can be observed. The threshold selection is subjective due to the nature of this algorithm. Although a smaller threshold ensures that all the inliers are classified correctly, it may lead to the loss of points that should have been classified as inliers in reality. On the contrary, if the threshold is greater, it may include points that should have been classified as outliers in reality. Identifying the optimal tradeoff between accuracy and completeness in this threshold selection process requires several experiments and statistical analysis at the same time. Ultimately the threshold of 60 s was selected, as it contains the inliers that take part in around 40% of the total data points, which is aligned with the empirical judgment from the dataset.

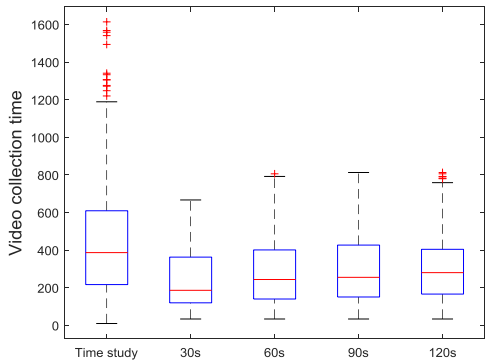

Figure 4. Box-plot of video durations of inliers in four scenarios, along with original dataset.

As discussed in Section 3, due to the probabilistic nature of the RANSAC algorithm, multiple runs are needed to capture the distribution of the three parameters (a, b and C) in Equation (2). Figure 5. shows the results of 500 runs of the RANSAC algorithm with the threshold of 60 s. Parameters a and b are both fitted with triangular distribution, with the mathematical expectation of 3.84 and 8.34 separately. Parameter C conforms to the uniform distribution with an expectation of 54.56. Therefore, the objective function can be summarized as $Time_n = 3.84 \bullet L_n + 8.43 \bullet T_n + 54.56$. The statistical analysis can be interpreted as follows: for one meter of pipe segment in good condition, it takes 3.84 s to finish the CCTV collection process; if there is one tap present within the pipe segment, it takes 8.43 s to finish the inspection; the fixed duration for the CCTV collection process is 54.56, which may include equipment setup time, camera adjustment time, and other routine processes. With the function derived from the RANSAC model, theoretical video collection time can be calculated with the two inputs (L and T). A histogram (see Figure 6.) can be constructed to show the performance of the RANSAC model by comparing the distribution of video collection time of the original data (inliers) and the theoretical results calculated from the RANSAC model. We can see from Figure 6 that the two histograms are largely co-terminous, which means that the results from the model are quite close to reality.

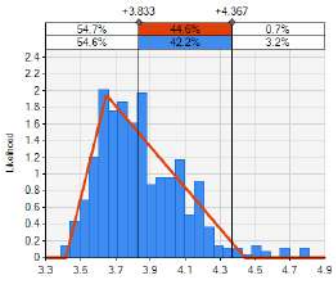

Parameter a: Triangular distribution; Expectation (a) = 3.84

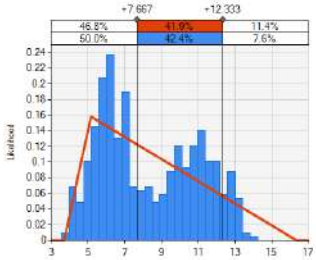

Parameter b: Triangular distribution; Expectation (a) = 8.34

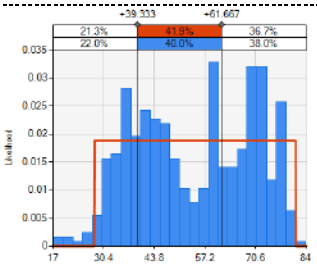

Parameter c: Uniform distribution; Expectation (a) = 54.56.

Figure 5. Results of the parameters in RANSAC model.

This function can be fed into a simulation model to model the CCTV collection process. In addition, it can be used as a classifier to distinguish whether or not a given pipe segment being inspected by CTTV is in good condition.

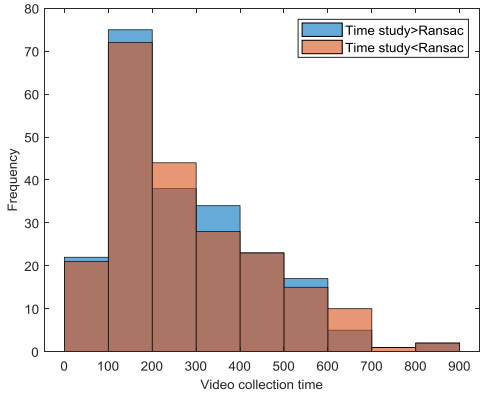

Figure 6. Histogram of RANSAC model and original time study.

5 Conclusion

Exclusion of noisy data is the objective of this research, so the RANSAC algorithm is utilized to exclude all data points that contain noise of any form. The CCTV collection process is summarized as a background of this study. Followed by the interpretation of the RANSAC model, focusing on the mechanism of the algorithm and the implementation process. Three key parameters need to be determined based on the nature of the problem and the authors' subjective judgment, namely, the number of points needed in order to form the candidate objective function (X), the number of iterations (N), and the threshold (t). A case study was performed to show the application of the RANSAC algorithm. Five hundred-forty data records collected by EPCOR Drainage Services were utilized to build the model, leading to a linear function that describes the relationship among CCTV collection time (Time), length of pipe segment (L), and number of taps (T). The results can be used in a simulation model to simulate the CCTV collection process in future research.

Acknowledgments

We gratefully acknowledge the financial support of the Natural Sciences and Engineering Research Council of Canada (CRDPJ 503647-16).

References

[1] R. Wirahadikusumah, D.M. Abraham, T. Iseley, R.K. Prasanth, Assessment technologies for sewer system rehabilitation, Autom. Constr. 7 (1998) 259–270. doi:10.1016/S0926-5805(97)00071-X.

[2] R. Navab-Kashani, L.F. Gay, A. Bayat, Productivity Improvement of Sewer CCTV Inspection through Time Study and Route Optimization, J. Constr. Eng. Manag. 138 (2013) 51–60. doi:10.1061/(ASCE)CO.

[3] J.C.P. Cheng, M. Wang, Automated detection of sewer pipe defects in closed-circuit television images using deep learning techniques, Autom. Constr. 95 (2018) 155–171. doi:10.1016/J.AUTCON.2018.08.006.

[4] M. Der Yang, T.C. Su, Segmenting ideal morphologies of sewer pipe defects on CCTV images for automated diagnosis, Expert Syst. Appl. 36 (2009) 3562–3573. doi:10.1016/j.eswa.2008.02.006.

[5] O. Duran, K. Althoefer, L.D. Seneviratne, State of the art in sensor technologies for sewer inspection, IEEE Sens. J. 2 (2002) 73–81. doi:10.1109/JSEN.2002.1000245.

[6] H. Zaman, A. Bouferguene, M. Al-Hussein, C. Lorentz, Improving the productivity of drainage operations activities through schedule optimisation, Urban Water J. (2017). doi:10.1080/1573062X.2015.1112409.

[7] H. Zaman, A. Bouferguene, M. Al-Hussein, C. Lorentz, Framework for Modeling On-Site Productivity of Preventive Maintenance Activities for Wastewater Collection Systems, J. Infrastruct. Syst. (2015). doi:10.1061/(asce)is.1943-555x.0000252.

[8] National Association of Sewer Service Company (NASSCO), Pipeline assessment and certification program (PACP), 2015.

[9] M. a Fischler, R.C. Bolles, Random sample consensus: A paradigm for model fitting with applications to image analysis and automated

cartography, Commun. ACM. 24 (1981) 381–395. doi:10.1145/358669.358692.

[10] M.S. Altaf, A. Bouferguene, H. Liu, M. Al-Hussein, H. Yu, Integrated production planning and control system for a panelized home prefabrication facility using simulation and RFID, Autom. Constr. 85 (2018) 369–383. doi:10.1016/j.autcon.2017.09.009.

[11] R. Raguram, J. Frahm, M. Pollefeys, A Comparative Analysis of RANSAC Techniques Leading to Adaptive Real-Time Random Sample Consensus, in: Eur. Conf. Comput. Vis., Berlin, 2008: pp. 500–513. doi:https://doi.org/10.1007/978-3-540-88688-4_37.

Implementation Framework for BIM Adoption and Project Management in Public Organizations

G. Miceli Junior [a] and P.C. Pellanda [a], and M.M. Reis [a]

[a] Defense Engineering Graduate Program, Military Institute of Engineering
E-mail: gmicelijr@uol.com.br, pcpellanda@ieee.org, marceloreis@ime.eb.br

Abstract –

The arrival of Building Information Modelling (BIM) platforms to the Architecture, Engineering and Construction (AEC) markets and companies has led to a significant increase in efficiency in this economy sector. However, many AEC companies try to implement BIM as a normal or incremental change or improvement in technology rather than as a technological paradigm shift that radically affects most organizational processes, which may hinder a successful adoption of BIM with a deployment of its full potential. This paper aims to present a basic BIM framework amenable to ensure a successful BIM adoption in public organizations, particularly adapted to the Brazilian federal government. Based on a literature review, we propose to split the factors into three main groups: project development procedures, model development procedures and public governance policies. Some processes were studied in order to infer which of them is necessary for a successful BIM adoption. A BIM implementation is expected to be a success only if all main groups of factors are well defined and the established goals for each of them are reached. We also describe results of two concept proofs related to actual cases of BIM processes implementation, with extensive changes in product and governance management processes. Main results show that any BIM adoption should consider the close relation among model management, product management and governance management groups. All these groups should be contextualized in the environment of any public organization.

Keywords – BIM adoption; Collaborative Design; Building Information Modelling; Public Works.

1 Introduction

The current main paradigm for project process managing is the Building Information Modelling (BIM). It can be defined as a set of associated technologies, processes and policies to produce, communicate and analyse constructive models, enabling the stakeholders to collaboratively design, build and operate a facility [1-2]. It has been successfully implemented around the world, becoming a common practice in many countries and internal markets, whether public or private.

However, while the adoption of BIM is commonly related to significant increases in efficiency, many public organizations are unaware that BIM is primarily a process change that depends on a well-defined action plan to be successfully implemented.

This work aims to develop a management framework for BIM adoption in Brazilian public organizations, which encompasses all main factors that could guarantee an optimized implementation process.

This paper is organized in five sections besides this introduction: Section 2, with a literature review on BIM adoption and all factors related to a successful BIM implementation; Section 3 with the management framework enunciation; Section 4 with the description of two concept proofs in two different public organizations in Brazil; and a conclusion with the main remarks about results.

2 Literature review

2.1 BIM adoption in public organizations

Many countries around the world have adopted BIM. The United States is believed to be one of the pioneering countries for BIM adoption, and several of USA public-sector organizations in different government levels have established BIM programs, set up BIM goals, begun implementation roadmaps and created BIM standards [3].

Apart the USA, many European and Asian countries have been implementing BIM successfully. Noteworthy is the United Kingdom, which published its family of PAS 1192 standards - in revision and transformation processes to international standard ISO 19650 [4;5]. Studies on BIM adoption in public environments can also be highlighted, for example, in Sweden, Finland, Norway and Singapore [6].

BIM has been implemented in Brazilian public

organizations since 2010, when the first state action with public results took place with the development of an initial version of a BIM component library for state program "Minha Casa Minha Vida" [7;9]. Several public and state organizations have been implementing BIM in their project processes; most adopted use cases have been quantification take-off, 4D planning and geometric modeling of civil engineering projects.

Experiences in contracting BIM projects have been developed in southern Brazilian states, with accurate BIM mandates with guidelines for projects to be contracted by the state government. The technical evaluation of the companies' proficiency and the level of development of their projects have been carried out with the analysis of IFC models with automated routines of code checking [7].

In an operational point of view, Brazilian Army has improved real estate management quality by using the Unified System of Works Process (from the Portuguese expression "Sistema Unificado do Processo de Obras", whose acronym is OPUS), a technology information and communication system developed by its Directorate of Civil Works. OPUS is described as an integration of specialized Enterprise Resource Planning (ERP) software with construction building information models, created for supporting built environment lifecycle management including buildings and assets related to AEC [8-9].

2.2 Management factors

One can try to figure out the factors that influence a good BIM adoption in public environments. In this work, these factors will be classified into three groups of actions, described below and illustrated in Figure 1.

- Model management actions, referring to building information models utilization in process management and all related specifications, including the BIM adoption effort in organizations;
- Product management actions, referring to product adequacy to client technical specifications and its compliance with deadlines and costs; design and construction methodologies conducted by related teams are also included in this group;
- Public governance management actions, which submits any and all project effort to auditing rules and all necessary and legal internal and external governance and auditing rules.

2.3 Model management

All tasks on this group refer to the growing influence and impact of BIM in project process, from its implementation in company to supervision of all day-to-day procedures. Building information model (BIModel) turns into the principal database of any architecture or engineering project:

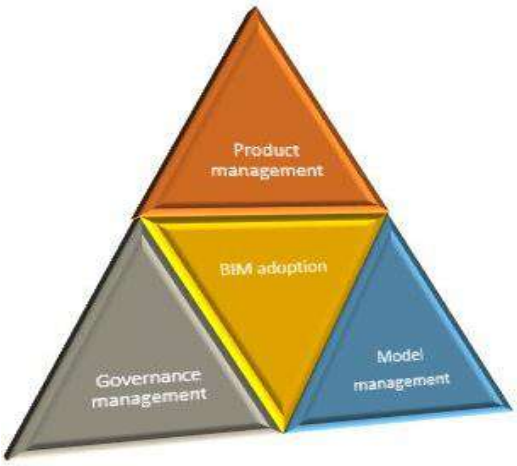

Figure 1. Management groups in BIM adoption

- Employer Information Requirements (EIR), sometimes called "BIM mandate" or "BIM manual": document where the contractor declares what they are after when they ask for BIM [5].
- A BIM Execution Plan (BEP), with an identification of the objectives and the goals of the implementation process in answer to the EIR desired by the organization, as well of the definition of all supporting infrastructure needed. This phase can be split in two parts: one pre-contractual BEP before procurement, containing the project implementation plan, its schedule, all information modelling and collaboration goals, as well the main milestones of the project information design creation; and a post-contractual BEP, beyond pre-contractual BEP, it still encompasses all project management processes description and to all methods and procedures that will be followed, as well as all solutions to be employed in implementation, including software, hardware, cloud and network solutions [5;11].
- A Project Execution Plan (PEP), with all necessary guidelines for good work of professionals. It encompasses all guidelines that make BIM workflow possible: modelling, file linking, work sharing, work sets, interoperability between programs and collaboration among professionals, information exchange. It also regulates all deliverables that would be produced (e.g. quantity take-offs, model templates, model views, annotations, sheets and model standards) [11-12].
- The modelling process itself, that is always related to a cyclic design process with high BIM tool interoperability and broad collaboration among professionals. It encompasses all development process with intense BIModel creation under BEP

and the PEP directives.

Generally, the three first steps described above are developed by consulting companies specialized in BIM implementation. It involves generally a knowledge transfer agreement contract, which may or may not cover the sale of software licenses, modelling software training or in-company support.

The modelling process of all disciplines and the related federated BIModel is always developed by the project team, along with product management and great participation and aid of the team of BIM champions.

2.4 Product management

Product management is related to project development and all stages that form part of it. Under this group task, client's technical demands and needs must be considered for the development of the project. It also includes all the documents that regulate them, such as sustainability analyses, budgeting and scheduling rules, works supervision standards and its compliance with performance, operation and quality organizational standards.

Although there are different definitions and standards for which project phases exist, the phases generally follow a sequence. In England, for example, there are six design phases: brief, concept, definition, design, build and commission, handover and closeout, followed by maintenance and proper use [5].

On the other hand, Brazilian standards divides project effort in a design preparation phase, including feasibility studies, preliminary and specific data collection and location definition; and a technical design development phase, including draft development and construction design itself.

2.5 Governance management

In general, a public organization must always be accountable for its actions and expenditures, so BIM adoption processes must take it into account. In this group are included all effort of the public organization for public hiring processes, personnel admission and accountability principles, guaranteeing compliance to public administration principles.

Unlike the other two groups, governance management activities are not sequential, but all of them interfere the entire project process. A summary of some important governance tasks that ensure a good project development and BIM deployment in given in the following:

- Demand of the organization direction for starting a new project;
- Requirements definition for project development, cost and schedule management;
- Provision of all conditions for project team to develop the project (budget prediction and authorization for bidding);
- Definition of bidding processes for services and public process to select professionals necessary to enable the satisfactory development of the product;
- Monitoring and supervision of project development and the construction model;
- Definition of bidding process for contract award;
- Bidding process itself and contract award;
- Construction contract inspection and follow up;
- Commissioning;
- Handover and close.

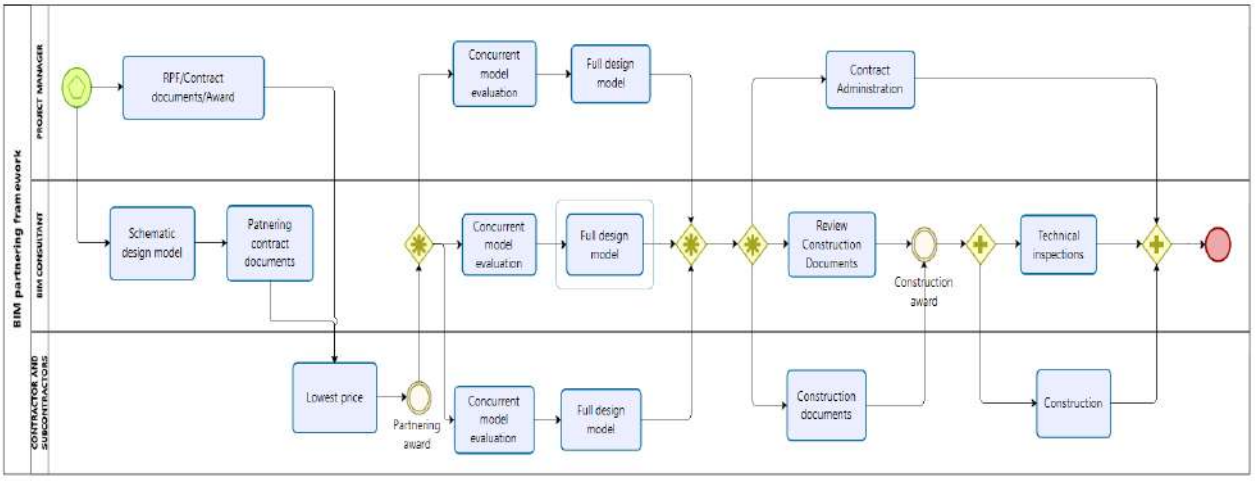

Figure 2. Partnering framework for public construction projects (adapted from [6])

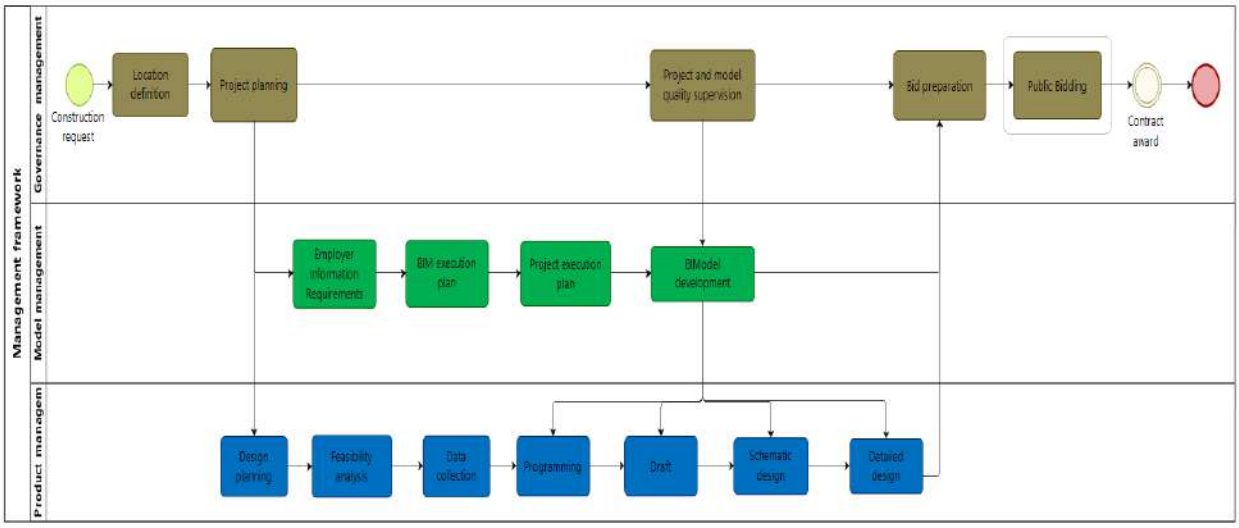

Figure 3. Framework proposition, with all three management groups.

With respect to BIM implementation in public environments, Porwal and Hewage [4] define a BIM partnering framework for public construction projects, in opposition to traditional methods of procurement where design and construction processes are separated.

A broad integration between product management and model management activities is suggested from Figure 2. Unfortunately, in some countries, Brazil included, there is little legal support for non-Design-Bid-Build (DBB) bidding and procurement process, so most BIM public projects, if not all of them, follow DBB pattern.

3 Framework map process

Once all management groups have been described, one must organize them in order to reflect an acceptable sequence for the framework. In its representation in Figure 3, it is assumed that the public institution has not yet implemented BIM or that an unsuccessful implementation has been initiated.

First action was the decision of the authority responsible for construction of the work, followed by site location definition according to feasibility studies of the project.

Next phase, within the governance axis, represented in brown boxes, is project planning. This is an important phase because it directs all of project's upcoming planning efforts. It must provide all conditions for both BIM deployment and project development to occur with minimal disruption, avoiding design rework.

In this way, all efforts to acquire the necessary resources - hardware, software, new network solutions, CDE, contract auxiliary services - topographic and geotechnical surveys, demolition teams, and hire professional and technical personnel must be initiated. All processes must be conducted according to well-defined bidding documents that have undergone prior legal analysis.

Only from this moment, after all contract awards, model and product management have their main actions. Any unplanned service may put design and project development in risk.

Model management efforts, represented in green boxes in Figure 3, are initially defined by the client in the EIR. They are then best developed in the BEP, which describes all implementation efforts and procedures of all work processes, and in the PEP, which encompasses all information regarding to day-to-day work conducted by the professionals since the very beginning of design development.

Product management phases, represented in blue boxes in Figure 3, however, are directly linked to project development, beginning with its planning, following the feasibility analysis, data collection and design programming.

At all stages of model and product management, there must be supervision of engineers, architects, and managers who are able to oversee the developed products - designs, models and their deliverables -, as well as to manage all contracts related to project.

A careful preparation of all tender documentations, where all bid conditions are given, is mandatory for a good public bidding. Any lack of data could make the bidders request for further information, and then, causing delays in tender documentation openings.

At the end of tender preparation, bidding process should be launched, usually on an on-line platform for government acquisitions. Tender process continues until contract award.

4 Concept proofs

Two concept proofs are presented, each one in a distinct public organization responsible for military work projects. Both projects have a profile of defense and public safety, which began to be developed within the framework of two recent BIM deployments.

Each experiment refers to public works projects focused on strategic and control areas that are currently being developed. Organizations are expected to tender both construction by DBB contracting process.

4.1 Concept proof 1 (CP1)

The first experiment is a project that will be built in an area of about 20,000 m^2 with a constructed area on a plot of about 28,000 m^2, from a demand of Organization A, currently considered one of the references in BIM adoption in Brazilian public service. Due to project order of magnitude, a specific BIM adoption became necessary.

Since project beginning, there was a rigid delivery schedule that was accompanied by the project management team and the client, with strict delivery deadlines. Thus, construction is formed by a building with five floors, being them underground, ground and three floors.

Programming studies and draft development were then developed over several meeting cycles, considering all necessary terrain and geotechnical surveys, predicted area for each office based on their organizational requirements and all expected mechanical and electrical equipment needed for the involved complex operation.

Since project initiation, a room was separated for the team, which worked collaboratively on a shared network even with development of the initial drafts in Autodesk AutoCAD.

BIM implementation in project office started to be conceived from this moment to optimize collaborative work within the project process, obtaining all necessary means - personnel and technologies - to guarantee its success, by bidding processes and professional selection processes, always with legal approval of a federal attorney:

- Personnel: personnel selection process were initiated, in which civil engineers, electricians and mechanics as well as architects were hired. A good knowledge in BIM software was mandatory, though most of them had only some prior knowledge;
- Hardware: fixed workstations were acquired in three different biddings, with necessary configuration for collaborative work and the building information model's development.
- Software: through a specific bidding process, new software licenses were acquired to enable model development by all professionals;
- Computer networks: there was no assembly of a new network with support to the high flow of information, dedicated to the project; new computers were connected to the existing administrative network;
- BIM Consultancy: through a bidding process, a BIM consultancy was also contracted, whose mission was the technology transfer as a progressive process of BIM implementation, involving development of a BEP, component library development and all necessary software training and support for adequate design development.

After consultancy contract award, diagnostic meetings between the consultant and office representatives were then held for the development of a BEP. The target was set so that, at the end of the project, the management procedures and all project professionals would evolve from the "pre-BIM" stage to stage 2, when BIM collaboration procedures is totally based in BIModels [1].

BEP contained general guidelines for template and file development, file naming, component material creation, as well as shared parameters creation. Components were then developed at the same time the design was being developed, according to the professionals – engineers and architects – needs.

The first implementation activities had as first case uses to be developed the design authoring, 3D coordination, cost estimation and phase planning, 4 out of the 25 BIM uses described by [12], so that the technical requirements, budget development and schedule planning were directly linked from beginning of the design.

It was from the preliminary phase that the concepts of construction information modeling developed a greater synergy with project management, where a maximum of 14 professionals were involved in model and design development.

Based in BEP, a Common Data Environment (CDE) was created within existing organization network, where all professionals developed their model designs, obeying a previous norm of file and model naming. Because of the organizational security requirements, the use of cloud-based CDE, as well as any cloud communication platforms, has been strictly banned.

Geometric coordinates were shared from the design beginning, either through work sets or through model links to a federated model. For each main discipline in the first-level partition around federated model, a discipline model was created; second-level subdivisions were then linked to each discipline model, as shown in the scheme of Figure 4.

IFC (Industry Foundation Classes) was interoperability standard for communication between suite software and interference detections. However, in cases where software offered few interoperability resources or did not have versions that could be IFC-compatible, DXF file format was then used: DXF drawings were created from design models and then they were read by the applications. BEP predicted these interoperability guidelines.

The collaboration and interoperability procedures made clash detection much easier and more efficient. Compatibilization routines were realized in a daily basis, and clashes were solved as soon as they were discovered. Team communication was done personally in the team room in short reunions all the time or through a message platform where all design decisions and interference resolutions were recorded.

In general, design development expanded from design programming (still with CAD files) to schematic and detailed design completely developed using BIM software. Once design had a minimum maturity, 4D planning and cost estimation, based in Brazilian cost databases, evolved quantity take-offs and specific budgets provided by qualified suppliers.

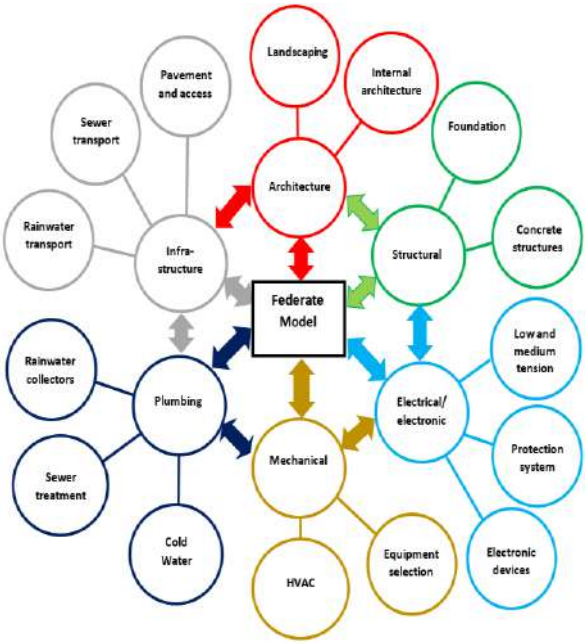

Figure 4. Coordination scheme for CP1

4D planning was carried out initially in MS Project, following a defined process. As quantity take-offs were extracted from all discipline models, predecessors and successors were defined for all tasks for project Gantt chart, for future work progress visualization using Autodesk Navisworks.

Budget development was based in take-offs extracted from discipline models and calculation reports extracted from engineering software. There was no direct interface of BIM authoring tools and the budget development software adopted by the organization. Although budget process was constantly error-prone, an experienced planner revised project budget and schedule all the time.

Currently, detailed design is near to completion. Client seeks from federal agencies the money needed to bid and contract the project.

4.2 Concept proof 2

The second experiment describes BIM implementation in organization B, conducted differently from the first experiment.

In 2016, BIM usage became mandatory for all professionals. Before that, only some professionals have had an interest in applying BIM in their workflow, with initial training in geometrical modelling and information management. These pioneer professionals, called internally “BIM team”, have already used some BIM processes in their workflow in the development of three simple proofs of concepts.

It was then necessary to contract an outsourced consultancy through a specific bidding and procurement process, in order to gain knowledge on BIM processes.

Implementation had as main aim technology the transfer of technology from outsourced consultants to BIM team. At the end of 24 months and three proofs of concept, which involves design, construction and operation of a building, the team would be responsible for disseminating knowledge obtained to all other design teams and professionals in other sections.

The consultants also had another aim: meet all information requirements for a new CDE that would provide interoperability between BIM models, data and related databases. It would play a similar role to construction and operational management that OPUS already plays in Brazilian Army.

Hardware in organization B – workstations in general – is at least three years aged. The last software acquisition was four years ago, when 2015 Autodesk Building Design Suite was installed in all computers.

Professionals working at organization B are generally high skilled, partially because of specific scope of all projects which are developed there. They have been working in organization at least for 10 years.

To meet organization demands, a broader BEP was developed by the consultants, encompassing several use cases related to design, construction and operation. BIM implementation would then last two years from contract award but would also include future tasks for the next eight years.

First concept proof conducted by organization B is currently in progress – an operational update of a 1000 m2 and four floors design, aiming to improve

operational project in order to allow the installation of other specific electronic equipment. At that time, it became necessary to update terrain and geotechnical survey of the construction area; based on new organization needs, new architectural and operational requirements were developed.

Until beginning of BIM implementation, there has not much difference between product development flow from organizations A and B, beginning with programming based in strict organizational needs, preliminary studies, work planning, design and project development, scheduling and budget development in order to start future procurement process.

With BIM implementation, design development has shifted from a sequential process to a matrix collaborative process in which all professionals started to participate. BIM team itself has been developing construction components and architectural and engineering templates for their own use, following BEP with the consultants aid and supervision.

Design process became then under a "development-analysis-discussion meeting-design" revision cycle. Coordination meeting were held at the end of each design phase with participation of the BIM team, their managers and their clients by videoconference. The meetings have been used for solving design decisions, for deciding about project cost estimate (based in preliminary BIM models) and discussing the next steps of the project.

Until now, lack of modern engineering software imposes DXF and proprietary file formats as preferred interoperability standard. On the other hand, all files and models follow a strict organization in network, separated by design phase and design discipline. All models also follow a collaboration scheme, where each team professional is responsible for only one design model, as showed in Figure 5.

Nowadays, although project is still in draft phase, with development of the first discipline models following Figure 5 scheme, information regarding to 4D planning, quantity take-off and operation have been added to federate model. Budget planner has got access to all design models since programming phase, with which he already develops construction site simulations, budget estimates and the first schedule forecasts.

Expectation in the future is to use acquired software suite at full potential, including Dynamo procedures for enhancing it in structural and MEP designs. Only after reaching this milestone, acquisition of more modern architecture and engineering BIM tools would happen, considering in-depth study of consultants team.

What one must have in mind is that the presented framework contains only general procedures. All its procedures must be detailed in depth, considering all organizational culture and public environment constraints involved.

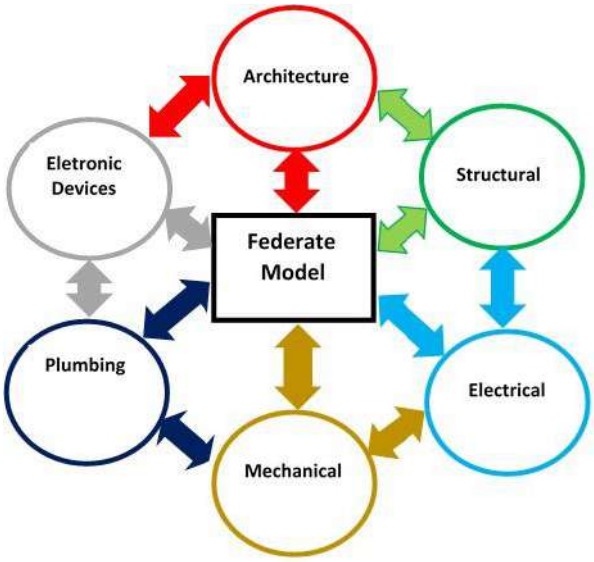

Figure 5. Coordination scheme for CP2

5 Conclusions

The aim of this article was to develop a conceptual structure that would contain all main factors that would guarantee an optimized development of a construction project with the use of BIM.

Conceptual structure can be divided into three groups: model management, product management, and governance management. Each group has a defined sequence: while model and product management follow a strict sequence of processes, governance management includes all public administration processes, without which other two groups cannot be developed.

In general, BIM implementations described in both CP followed the framework described in Figure 3. Public administration processes permeate all product and model processes.

In summary, three described groups constitute parts of a suggested tri-axial conceptual structure where each axis has a deep relationship with each other, so that a harm of one of the axes compromises project management in some way.

One can remark that BIM has already been adopted in both organizations A and B. However, it was totally based in software acquisition and basic training, not considering characteristics of product and management organization processes.

Any BIM implementation should then consider the "tri-axial relationship" among model management group, product management group and governance management group, so that each group procedure be contextualized to the public and organizational

environment.

References

[1] Succar, B. Building information modelling framework: A research and delivery foundation for industry stakeholders. *Automation in Construction* 18:257-275, 2009.

[2] Eastman, C. Teicholtz, P. Sacks, R. Liston, K. *BIM Handbook: A guide to building information modeling for owners, managers, designers, engineers, and contractors*. John Willey & Sons Inc., New Jersey, 2008.

[3] Porwal, A. and Hewage, K.H. Building Information Modeling (BIM) partnering framework for public construction projects. *Automation in Construction* 31:204-214. 2013

[4] PAS 1192-2:2013. *Specification for information management for the capital & delivery phase of construction projects using BIM.* British Standards Institution, London, 2013.

[5] ISO 19650-2. *Delivery phase of assets.* International Standards Organization, Geneva, Switzerland. (in development).

[6] Gu, N., London.K. Understanding and facilitating BIM adoption in the AEC industry. *Automation in Construction* 19:988-999, 2011

[7] Cunha, J.M.F. and Silva, R.F.T. The experience of the State of Santa Catarina, Brazil, in bidding a BIM project. In *4th BIM International Conference*, pages 67-68, São Paulo, Brazil, 2016.

[8] Kassem, M. Mohamad Kassem: "Strategy for the diffusion of BIM in Brazil". On-line: http://www.makebim.com/2016/08/31/mohamad-kassem-strategy-for-the-diffusion-of-bim-in-brazil/?lang=en, Accessed: 27/03/2017.

[9] Nascimento, A.F. Miceli Jr, G. and Pellanda, P.C. Built environment lifecycle management by using large-scale BIM: a Brazilian Army case study. In *4th BIM International Conference*, pages 49-50, São Paulo, Brazil, 2016.

[10] Won, J and Lee, G. How to tell if a BIM Project is successful: a goal-driven approach. *Automation in Construction* 69:34-43,2016.

[11] Holzer, D., *The BIM managers handbook: guidance for professionals in Architecture, Engineering and Construction*. John Willey & Sons Inc., New Jersey, 2016.

[12] Pennsylvania State University. BIM project execution planning guide, version 2.1. The Computer Integrated Construction Research Program at the Pennsylvania State University.

Classification and Exemplary BIM Models Development of Design Changes

J.R. Lin[a,*], Y.C. Zhou[b], J.P. Zhang[a], and Z.Z. Hu[a]

[a]Department of Civil Engineering, Tsinghua University, China
[b]College of Civil Engineering, Tongji University, China
E-mail: lin611@tsinghua.edu.cn, zhouyucheng98@qq.com, zhangjp@tsinghua.edu.cn, huzhenzhong@tsinghua.edu.cn

Abstract –

Detection of design changes is essential for collaboration and version management in the design process of buildings. However, current detection methods based on Building Information Modeling (BIM) usually cause unreliable or meaningless results. This is because most of the current researches look at the question from a data change view, which sometimes is meaningless from a designer's view. To overcome this problem, this paper first classifies and identifies meaningful design changes from a designer's view, and develops exemplary BIM models of typical design changes. In this paper, categories of data changes are divided into property data, appearance data and relationship data, and design changes are classified into instance level, type level and model level from a designer's view. The test of two BIM tools (Autodesk BIM360 and IFCdiff) with developed BIM models shows that the detection results for changes at instance level are perfect while detection results for type and model level still need to be further improved. This work contributes a new view and classification method of design changes, and also sets up a baseline model database for further development and validation of relevant methods and tools.

Keywords –

Design Changes; Classification; Building Information Modeling (BIM); Exemplary Model Database; Validation

1 Introduction

The design process of Architecture, Engineering and Construction (AEC) is complex. It includes a lot of iterative work and involves multidisciplinary design work that can be done sequentially, concurrently or in parallel [1] .Changes of a project are inevitable, which can occur from multi-source in any time, and have extensive impact [2]. Accordingly, ensuring the accuracy and consistency of data after sharing and emerging is significant, which raises the requirement of detection of design changes. Building Information Modeling (BIM) is widely used for building lifecycle management. However, current methods for design change detection of BIM models are still not perfect.

Generally, current methods are mainly based on comparing all properties of each instance in BIM models one by one, which is not always meaningful for designers. For example, exchanging the location of two columns that have the same properties should not be detected as a design change in spite of changes of location. To contribute to the development and validation of detection, this paper classifies and identifies meaningful design changes from a designer's view, and develops exemplary BIM models of typical design changes.

This paper is structured as follows. Section 2 reviews the related works and analyses some existing detection methods. Section 3 lists all possible design changes by classifying it by different categories and levels. Section 4 uses exemplary BIM models developed to test some BIM tools and summarizes their results. Finally, section 5 concludes this paper's contribution.

2 Literature Review

Design changes in the BIM model has been extensively studied by researchers. These research works included the management of design changes by versioning Industry Foundation Classes (IFC) models [3] or IFC extension [4], improving design coordination [5], quantifying the design change time ripple effect [6], and assessing impacts of construction change orders [7]. Even though these researches made design changes to be managed and evaluated more effectively, few works focused on the definition and classification of meaningful design changes from a designer's view.

The most common method used for detecting design changes between two BIM models is based on the ID (e.g. GlobalId in IFC file or ElementId in Autodesk Revit) and comparing all properties between two instances, which is adopted in the above references and most commercial BIM platforms such as Autodesk Revit, Navisworks, etc..

However, ID is unstable sometimes, which will lead to wrong and unnecessary detection results. Meanwhile, its detection results are not always meaningful. For example, exchanging the location of two same columns will be detected as a change by this method, but that is a meaningless change for designers actually.

Daum, S. and A. Borrmann [8] proposed an approach for detecting equivalences in datasets of the Industry Foundation Classes (IFC), which based on a geometrical matching and semantic comparison method. This approach is independent of ID, which means the detection can be completed even IDs are not reliable. Nevertheless, meaningless results will still be detected by this method.

Shi, X., et al. [9] proposed a content-based automatic comparison approach for IFC files. This approach will construct a hierarchical structure for both files and then use an iterative bottom-up procedure to compare them. However, the test results of detecting changes in some cases such as exchanging location of two same columns and deleting and recreating a same beam are still not perfect.

In summary, most of the current methods only look at the problem from a data change view, while ignore the designers' view. To overcome this problem, the design changes should be carefully reviewed and classified.

3 Classification of Design Changes

As an open BIM model data representation standard, IFC defines an express based entity-relationship model consisting of several hundred entities organized into an object-based inheritance hierarchy [10]. And in Autodesk Revit, the data in a document consists primarily of a collection of elements [11], where each element has many properties. It can be seen that BIM models can be described by instances (objects), which consist of many properties.

Design change detection is usually between an old and a new files (documents). Previously, design changes can be divided into 3 change types from a data change view as follows.

- Added. An instance is created in the new file.
- Deleted. An instance is deleted in the old file.
- Modified. An instance exists in both old and new file but its properties has been changed.

However, it is not enough to simply classify design changes as the above three types. Because that may lead to meaningless results and the results can be further optimized. To address this issue while ensuring all the changes can be properly identified from a data change view, this paper firstly divides data changes of BIM into three categories, namely, property data, appearance data and relationship data. Then, all possible design changes are classified into three levels, instance level, type level, and model level respectively from a designer's view.

3.1 Categories of Data Changes

The data changes of BIM can be divided into three categories as follows.

- Property data: represents instances' properties, such as parameters or other user specified attributes.
- Appearance data: represents instances' 3D appearance, such as the geometry and location.
- Relationship data: represents the relationship between two instances, such as the relationship that a wall hosts a door.

As for property data, the possible changes are:

1. Added. Add a new property of an instance.
2. Deleted. Delete an existing property of an instance.
3. Value Modified. Modify a property's value.
4. Name Modified. Modify a property's name.
5. Order Changed. Change the order of some properties of an instance.

As for appearance data, the possible changes are:

1. Added. Add a new geometry of an instance.
2. Deleted. Delete an existing geometry of an instance.
3. Geometry Modified. Modify a geometric shape of an instance.
4. Transformation Modified. Modify a transformation property of an instance. Such as scaling, translation and rotation.
5. Representation Method Modified. Change the way of representation of a geometry. Such as converting a solid model to a surface model.

As for the relationship data (assuming that the order of relationships is meaningless), the possible changes are:

1. Added. Add a new relationship between two instances.
2. Deleted. Delete an existing relationship between two instances.
3. Instance Modified. Modify property data of a relationship instance.
4. Relationship Modified. Modify a relationship between two instances, e.g. change the relationship between A and B to A and C.

3.2 Levels of Design Changes

The possible data changes given above should be identified as least at the instance level. Thus, adding and deleting properties of an instance should be identified as changing an instance, so as modifying some properties of an instance (Left part of Figure 1). However, for meaningful and optimal identification results, the

perspectives of type level and model level are required.

From the perspective of type level, the changing of instances may be caused by changing of a type (or family type in Revit) of the instances. For example, the geometric changes of multiple instances caused by changing the geometry of the type that all the instances inherit from should be correctly detected (Middle part of Figure 1), which can reduce the detection results and make the results more meaningful.

From the perspective of model level, data changes or modification of instances may be meaningless sometimes. For example, exchanging the location of two same columns should not be identified as a change, so as deleting a beam and recreating a same one (Right part of Figure 1). Besides, modification of the elevation of a Level may result in a large number of changes in related instances. So identifying the source of the change is better than just detecting the changed related instances, and that will contribute to more meaningful results. Changes from the perspective of these three levels are illustrated in Figure 1.

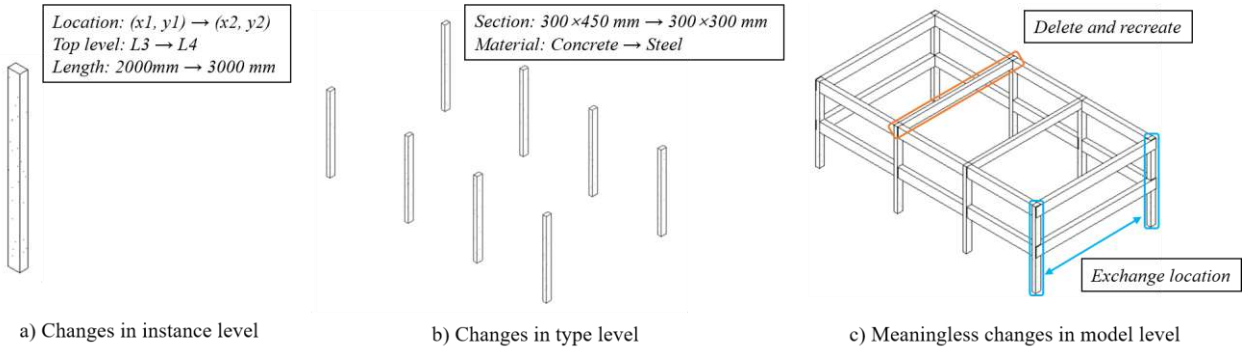

Figure 1. Design changes from perspective of instance level, type level and model level

4 Exemplary Models and Case Study

4.1 Exemplary BIM Models

Since there is no public available database for testing and verifying current design change detection methods, this research develops 11 simple BIM models according to the changes described in section 3. In these changes, added or deleted in all types of data are combined to facilitate test. And the order change of property data and representation method change of appearance data are ignored in this paper. Meanwhile, type level design changes and meaningless design changes at model level are also embedded in the developed BIM models. Detailed information of these models are shown in Table 1, and their screenshots are shown in Figure 2.

Table 1. The detailed information of exemplary BIM models

Model Name	Category of Data change [a]	Level of Design Change	Description of Changes	Meaningful [b]
M1	-	-	The origin model	-
M1_All-A	Added in P, A and R	Instance	Add 2 beams and 2 columns (new category)	O
M1_All-D	Deleted in P, A and R	Instance	Delete 2 beams and 4 columns	O
M1_All-DA(M)	Deleted and then added in P, A and R	Model	Delete 2 beams and 4 columns and recreate them	X
M1_A-MG	Geometry modified in A	Instance	Modify the sectional dimensions of 2 beams	O
M1_A-MG(T)	Geometry modified in A	Type	Modify the section of family of a beam from 400×800 to 800×400	O
M1_A-ML	Location modified in A	Instance	Modify the location of 4 columns and 2 beams	O
M1_A-ML(M)	Location modified in A	Model	Exchange the location of 2 pairs of columns and 1 pair of beams	X
M1_P-MV	Value modified in P	Instance	Modify a parameter (COMMENTS) in a beam	O
M1_R-MI(M)	Instance modified in R	Model	Modify the elevation of a level (Level3)	O
M1_R-MR	Relationship modified in R	Instance	Modify the top level of 4 columns	O

[a] P, A, R means property data, appearance data, relationship data respectively.
[b] O and X means the change is meaningful and meaningless respectively.

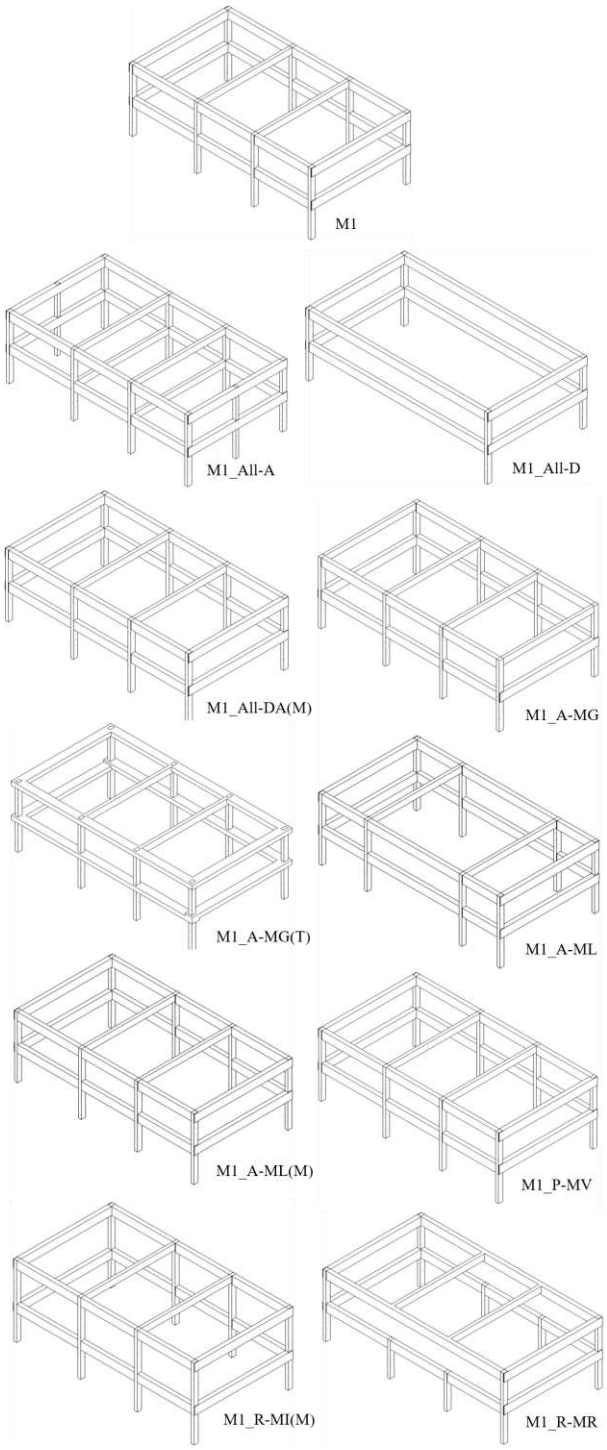

Figure 2. Exemplary BIM models

It is apparently that the model named M1 has 8 columns and 10 beams, and the changes from M1 to any other model can be used as a test case for design change detection methods. A repository contains these exemplary BIM models and their detailed description are established on GitHub. Each model has a .rvt and .ifc file (the contents of the files in these two different formats are the same). The link address is: https://github.com/smartaec/Design-Change-BIM-Models.

4.2 Test of Related Systems

This paper selects Autodesk BIM360 and the IFCdiff [9] to verify their accuracy of detection (according to the file format they support, BIM360 uses the .rvt files while the IFCdiff uses the corresponding .ifc files).

The ideal test results are all changes at instance level are detected. Meanwhile, for changes at type level, the source of changes should be detected instead of the direct results. And for changes at model level, the results should be that nothing has changed because changes in these cases are meaningless.

4.2.1 Test Result of Autodesk BIM360

BIM360 has the correct results for all test cases of changes at instance level, but its results for type and model level are incorrect. The screenshots of detection results in M1_A-MG(T) and M1_All-DA(M) using BIM360 are shown in Figure 3.

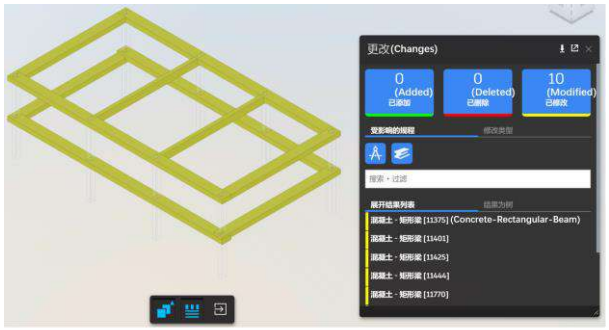

a) M1_A-MG(T)

b) M1_All-DA(M)

Figure 3. The detection result of M1_A-MG(T) and M1_All-DA(M) by BIM360.

In Figure 3 a), 10 modified changes are detected. 8 beams of them are changed in section size while other 2

beams are changed in volume because of the affect in geometry of joint. Actually, the only change is the change of the section dimension of a family of beam from 400×800 to 800×400 mm, which is a change at type level. However, BIM360 detected the changes of the affected 8 beams but doesn't identified that the family of these beams has changed. So, BIM360 is not as good as we expected.

In Figure 3 b), 6 added and 6 deleted changes are detected. The actual operations in this model are delete 6 components and recreate 6 same one. And the ground truth from a designer's view is that nothing has changed since these changes are meaningless. So, BIM360 cannot handle the model level changes properly now.

4.2.2 Test Result of IFCdiff

Similar to BIM360, IFCdiff has correct results for all test cases of changes at instance level and incorrect results for type level. But for changes at model level, its results are better than BIM360. The screenshots of detection results in M1_A-MG(T) and M1_All-DA(M) using IFCdiff are shown in Figure 4 (the output of IFCdiff is text).

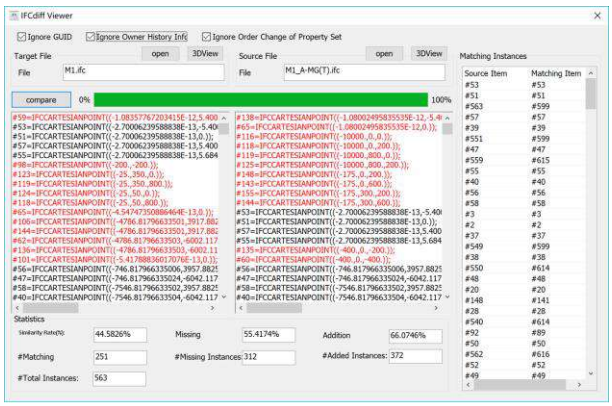

a) M1_A-MG(T)

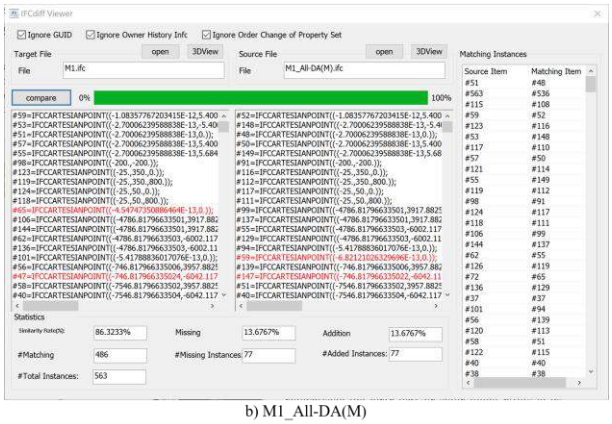

b) M1_All-DA(M)

Figure 4. The detection result of M1_A-MG(T) and M1_All-DA(M) by IFCdiff.

In IFCdiff, the similarity rate (%) is defined as the rate of the number of identical instances between File A (the target file) and File B (the source file) divided by the total number of instances in File A (both files have been removed redundant instances), i.e.

$$\text{Similarity}(A,B)(\%) = \frac{|A \cap B|}{|A|}.$$

In Figure 4 a), File A (i.e. M1) has 563 instances and File B (i.e. M1_A-MG(T)) has 623 (251+372) instances. The number of matching, missing and addition are 251, 312 and 372 respectively. From the result of BIM360, 10 of 18 components have been changed, about 44.44% (8/18) of the components have not changed. So, the similarity rate 44.58% given by IFCdiff is reasonable. But it also cannot identified that the family of these beams has changed from the perspective of the type level. Therefore, IFCdiff cannot handle type level changes properly.

In Figure 4 b), the similarity rate is 86.3% and the added and deleted rates are both 13.6%. In contrast, the test result of BIM360 is 6 added and 6 deleted. It can be inferred that the added or deleted rate is about 33.3% (6/18) detected by BIM360. Thus, the result of IFCdiff is a bit better than BIM360 but still not perfect.

In the authors' opinion, the reason why test result of IFCdiff is better than BIM360 in the latter case is IFCdiff can ignore changes of GlobalId, Owner History, etc. when comparing two instances. In the latter case, the deleting and recreating same instances are equivalent to updating their ID, so IFCdiff will detect less changes. But for the former test case, there is no essential difference between IFCdiff and BIM360 when detecting changes at type level, so neither can give a perfect result.

4.3 Summary of Test Results

According to the results of the case study and analysis, Table 2 summarizes the correctness of the two tools.

Table 2. The detection results of BIM360 and IFCdiff using developed exemplary models

Model Name	BIM360	IFCdiff
M1_All-A	O	O
M1_All-D	O	O
M1_All-DA(M)	X	*
M1_A-MG	O	O
M1_A-MG(T)	X	X
M1_A-ML	O	O
M1_A-ML(M)	X	*
M1_P-MV	O	O
M1_R-MI(M)	X	X
M1_R-MR	O	O

○ means the result is correct (only this means passed the test).
X means the result is not completely correct.
⋆ means the result is not completely correct but better than X.

It can be seen from the Table 2 that both BIM360 and IFCdiff can passed tests when detecting changes at instance level but cannot deal with type and model level changes now. Meanwhile, the detection results of IFCdiff for changes at model level are better than BIM360, since IFCdiff will get fewer changed results when detecting meaningless changes.

5 Conclusion

This paper proposes a new view and classification method of design changes, and also sets up a baseline model database for further development and validation of relevant methods and tools. Three categories of data changes (property data, appearance data and relationship data) and 3 levels of design changes (instance level, type level and model level) are considered, and corresponding exemplary BIM models are developed. Then, this paper selects Autodesk BIM360 and IFCdiff to verify their accuracy of design change detection. The results show that both BIM360 and IFCdiff can detect changes at instance level well but cannot handle type and model level changes properly.

This work reveals current problems in design change detection and introduces new method on classification of design changes. Meanwhile, this paper first sets up an exemplary BIM model database of design changes, which can be used as baseline data for the validation of future methods and tools for design change detection.

Acknowledgements

This work was supported by the National Key R&D Program of China (No. 2018YFD1100900) , the Beijing Natural Science Foundation (No. 8194067), the Beijing Municipal Science and Technology Project (No. Z181100005918006), the Young Elite Scientists Sponsorship Program by China Association for Science and Technology (No. QNRC2016001) and the Tsinghua University-Glodon Joint Research Centre for Building Information Model (RCBIM).

References

[1] Nour, M. and K. Beucke. Object versioning as a basis for design change management within a BIM context. In *International Conference on Computing in Civil and Building Engineering (ICCCBE-XIII)*, pages 147–152, Nottingham, UK, 2010.

[2] Motawa, I.A., et al. An integrated system for change management in construction. *Automation in Construction*, 16(3): 368–377, 2007.

[3] Jaly-Zada, A. and W. Tizani, Design Change Management Based on Versioning the IFC Models. In *16th International Conference on Computing in Civil and Building Engineering*, 520–526, Osaka, Japan, 2016.

[4] Jaly-Zada, A., C. Koch and W. Tizani. IFC Extension for Design Change Management. In *32nd CIB W78 Conference 2015*, 328-335, Eindhoven, Netherlands 2015.

[5] Kim, H. and F. Grobler, Design Coordination in Building Information Modeling (BIM) Using Ontological Consistency Checking. *Computing in Civil Engineering (2009)*, 410–420. ASCE, https://doi.org/10.1061/41052(346)41, 2009.

[6] Moayeri, V., O. Moselhi and Z. Zhu, BIM-based model for quantifying the design change time ripple effect. *Canadian Journal of Civil Engineering*, 44(8): 626–642, 2017.

[7] Likhitruangsilp, V., T.N. Handayani and N. Yabuki, A BIM-Enabled Change Detection System for Assessing Impacts of Construction Change Orders. In *17th International Conference on Computing in Civil and Building Engineering*, Tampere, Finland 2018.

[8] Daum, S. and A. Borrmann. Enhanced Differencing and Merging of IFC Data by Processing Spatial, Semantic and Relational Model Aspects. In *23rd International Workshop of the European Group for Intelligent Computing in Engineering*, Kraków, Poland, 2016.

[9] Shi, X., et al., IFCdiff: A content-based automatic comparison approach for IFC files. *Automation in Construction*, 86: 53–68, 2018

[10] Wikipedia. Industry Foundation Classes. Online: https://en.wikipedia.org/wiki/Industry_Foundation_Classes, Accessed: 12/12/2018.

[11] Autodesk, Element Class. On-line: http://www.revitapidocs.com/2018.1/eb16114f-69ea-f4de-0d0d-f7388b105a16.htm, Accessed: 12/12/2018.

Multi-objective Optimization Analysis for Selective Disassembly Planning of Buildings

B. Sanchez[a], C. Rausch[a], C. Haas[a], and R. Saari[a]

[a]Department of Civil and Environmental Engineering, University of Waterloo, Canada
E-mail: b2sanche@uwaterloo.ca, chris.rausch@uwaterloo.ca, chaas@uwaterloo.ca, rebecca.saari@uwaterloo.ca

Abstract –

Adaptive reuse has the potential to maximize the residual utility and value of existing assets through green design methods such as selective disassembly planning. Studies in the field of selective disassembly for adaptive reuse of buildings are scarce and there is no evidence of established methodologies and/or analysis for the optimization of the environmental and financial benefits. In this paper we provide a framework for the multi-objective analysis to obtain several effective selective disassembly plans through the combination of different deconstruction methods. The analysis is delineated in terms of the physical, environmental, and economic constraints of the deconstruction methods per building component. Then, a weighted multi-objective optimization analysis is incorporated to generate the set of noninferior solutions that minimizes environmental impacts and building cost. For adaptive reuse of buildings, the methods described in this study can be used to improve the project outcomes according to specific goals and constraints (e.g. environmental, economic, technical).

Keywords –

multi-objective optimization, selective disassembly, adaptive reuse, Circular Economy, green design.

1 Introduction

Adaptive reuse of buildings plays a key role in the transition from a resource-based economy and towards a Circular Economy (CE) in the construction industry. Adaptive reuse has the potential to maximize the residual utility and value of existing assets by "giving them new life" through green design methods, such as selective disassembly planning. Adaptive reuse is considered a disruptive practice in the current capital project delivery model for the renewal of today's built environment [1,2]. Therefore, the field of green design methods for buildings is still underdeveloped in comparison to other industries such as automotive, textile, and manufacturing. In particular, the studies in the field of selective disassembly for adaptive reuse of buildings are scarce and, to the knowledge of the authors, there is no evidence of established methodologies and/or analyses for the optimization of environmental and financial benefits. The aim of this study is to develop the framework for a multi-objective optimization analysis for the selective disassembly planning of an existing asset through the combination of different deconstruction methods. The analysis is carried out in terms of the physical, environmental, and economic constraints of the deconstruction methods per building component. The Sequential Disassembly Planning for Buildings (SDPB) method, presented in previous studies [3,4], is used in order to generate the optimized disassembly plans for retrieving single or multiple targeted components. The SDPB method is extended with the purpose of including more than one deconstruction method per component. Finally, a weighted multi-objective optimization analysis is incorporated to generate the set of noninferior solutions that minimizes environmental impacts and building costs.

The study shows that different complete disassembly plans exist for all the possible combinations. The possible combinations are driven by the deconstruction methods per component, as well as the dismantling interdependence. For adaptive reuse of buildings, the proposed study can be used to improve the project outcomes according to specific goals and constraints (e.g. environmental, economic, technical). The implementation of this approach could improve the decision-making process for adaptive reuse building projects by adding comprehensive quantitative analysis towards resource optimization. This study provides a better understanding of the management of the multiple variables involved in the process of selective disassembly for adaptive reuse in order to improve the project performance.

2 Background

Over the last two decades, environmental concerns have driven the research of construction projects' life cycle performance towards a holistic approach to

sustainability [5-8]. In this matter, several studies have recognized the importance of the End of Life (EoL) stage in existing buildings, and the opportunity of their adaptive reuse as a superior alternative in terms of CE [3,9,10]. However, for the capital project delivery in a CE framework, there is a lack of science-based, user-friendly, and generic methods to: 1) improve adaptive reuse project outcomes, 2) develop appropriate planning for closed-loop cycle construction, and 3) plan for the optimization of the benefits of adaptive reuse.

2.1 Green Design Methods for Adaptive Reuse of Buildings

In previous work, the important role of green design methods and deconstruction planning methods in the adaptive reuse process of buildings has been discussed [3]. Green design methods are intended to reduce environmental cost and increase economic benefits over the entire product or service lifecycle [11]. Examples of green design methods are design for assembly, supply chain management, Product Recovery Management (PRM), Life Cycle Assessment (LCA), design for disassembly, design for remanufacture, and disassembly sequence planning.

In the field of design for disassembly and deconstruction for buildings, improvements can be achieved by considering future disassembly of building elements at the planning stage of new buildings [12]. Studies have investigated the optimization of the economic performance of the deconstruction and recovery processes of EoL buildings by using mixed-integer and binary linear programming [13,14]. Despite the advances in the area of building deconstruction planning, only a few studies have developed deconstruction planning methods for the adaptive reuse of existing assets. Sanchez and Haas [3] developed the first-in-its-class selective disassembly sequence planning method for adaptive reuse of buildings. The method seeks to minimize environmental impact and cost of the selective disassembly of building components to retrieve, based upon physical, environmental, and economic constraints. As an extension of this work, Sanchez, Rausch, and Haas [4] developed a multiple-target sequential disassembly planning model for buildings, as well as a novel approach for deconstruction programming for adaptive reuse of buildings.

2.2 Multi-objective Optimization Analysis for Selective Disassembly

According to Revelle & Whitlach [15], the goal of multi-objective optimization analysis is to quantify the degree of conflict among objectives. The conflict between objectives originates when a strategy that is optimal with respect to one objective may be nonoptimal for another. Therefore, the concept of optimality may be inappropriate for a multi-objective analysis. Instead of searching for an optimal or the best overall solution, the goal of a multi-objective analysis is to define the set of solutions for which no other better solutions exist for the objectives of interest. This set of solutions is well known with the name of noninferior solutions or Pareto frontier. An important characteristic when dealing with a multi-objective analysis is that each objective is measured in different units. In other words, the units are incommensurable. At the end of the analysis, the decision makers have the responsibility of choosing the appropriate solution from the set of noninferior solutions.

The multi-objective optimization analysis for this study deals with managing environmental and economic resources in the process of selective dismantling of an existing asset. We might seek to evaluate environmental quality and economic efficiency trade-offs along the deconstruction process. For this study, one of the objective functions seeks to minimize the amount of environmental impacts due to the discarded parts during the selective dismantling process of a building, that might involve the total or partial disassembly of multiple buildings' subsystems. Depending on the approach of the overall analysis, the user can select a specific environmental impact of interest, such as Global Warming Potential (GWP), Primary Energy Demand (PED), and Water Consumption (WC). The second objective function seeks to minimize the overall cost of deconstruction works. The conflict or trade-off between the mentioned objectives is found in the incommensurable differences between the environmental value and removal cost of different selective disassembly plans for components.

2.3 The Knowledge Gap

The field for improving the inefficiencies inside the process of adaptive reuse of buildings through the implementation of green design methods, such as selective disassembly planning and PRM, is still underdeveloped in comparison to other industries (e.g. automotive, textile, and manufacturing). The purpose of this study is to describe a methodology for optimizing the environmental and financial performance of the selective disassembly planning process for adaptive reuse of buildings. A multi-objective optimization analysis is key to finding several effective selective disassembly plans for the adaptive reuse of an existing asset through the combination of different deconstruction methods.

3 Methodology

The proposed methodology for a multiple objective optimization analysis is incorporated into the framework of selective deconstruction project planning by using

BIM-based phase planning presented in a previous work [4]. First, the Sequential Disassembly Planning for Buildings (SDPB) method is used to generate the optimized disassembly plans for retrieving single or multiple target components from a given building's assembly, and according to the adaptive reuse design. The SDPB method optimizes disassembly plans in terms of the physical, environmental, and economic constraints per building component and by using just one deconstruction method per building component, which is "selective disassembly". Once the disassembly plans are ready, more deconstruction methods per component are included in the next stage of the analysis. The other deconstruction methods included are "selective demolition" and "perfect disassembly". At the end, a weighted multi-objective optimization analysis is implemented to generate the set of noninferior solutions that minimizes a specific environmental impact and the building cost (see Figure 1). After finding the set of noninferior solutions for a given disassembly plan, the decision makers can select the alternative that is more aligned to the objectives of the overall project and they can continue with the next stages of the deconstruction planning, in order to estimate the final cost and total duration. As shown on Figure 1, this becomes an iterative process whereby if the project needs are not fulfilled, the adaptive reuse design should be changed by the designers.

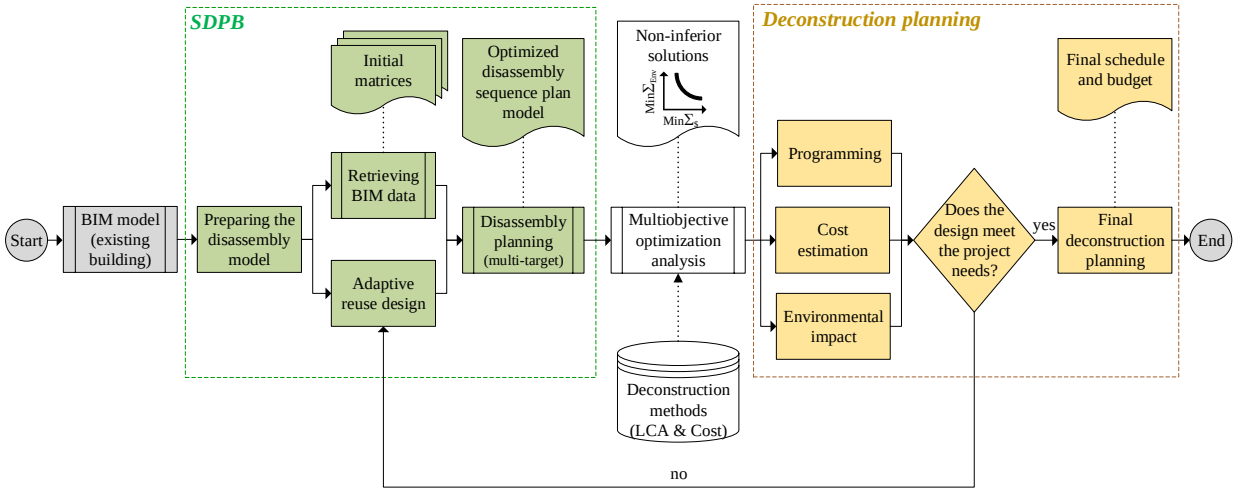

Figure 1. Multiple objective optimization analysis for selective deconstruction project planning

3.1 The Disassembly Sequence Plan Model for Adaptive Reuse of Buildings

This study is built on previous works related to selective disassembly planning for adaptive reuse [3,4]. First, the authors developed the SDPB single-target disassembly sequence plan model which is an inverted tree that contains a minimum set of parts that must be removed before retrieving a target component. A part *p*, in this case, can be a component *c* (building component) or a fastener *f* (building connection). Root nodes in the inverted tree represent target components, leaf nodes represent parts that constrain the target components, and the links between them represent constraints. A constraint can be physical, or functional. The SDPB method for creating a single-target selective disassembly model for buildings gets parts from the Disassembly Graph (DG) model, arranges and orders the parts in levels, and adds the parts to the inverted tree [3,16]. Finally, the approach uses expert rules to improve solution quality, minimize graph complexity, and reduce searching time for finding optimized disassembly sequence plans [3,11,16]. In a subsequent study, the authors extended the SDPB method to multiple-target selective disassembly of building components, and also provide the programming of deconstruction works.

Figure 2 shows as an example the multi-target SDPB for a building assembly subset which was part of an adaptive reuse project of the "Engineering 2" (E2) building at the University of Waterloo campus. Figure 2 shows the 57-part assembly model under study. The SDPB method creates optimized single-target disassembly sequences for the targeted components c_7 and c_{13}. For Figure 2, the best direction for removing components c_7 and c_{13} is $+x$ direction. Figure 2 also shows a multiple-target disassembly plan (inverted tree) for components c_7 and c_{13}. For the disassembly plan in Figure 2, n_t are the number of targeted components; and n_c, n_f, and n_p are the number of components, fasteners, and parts in the disassembly plan, respectively.

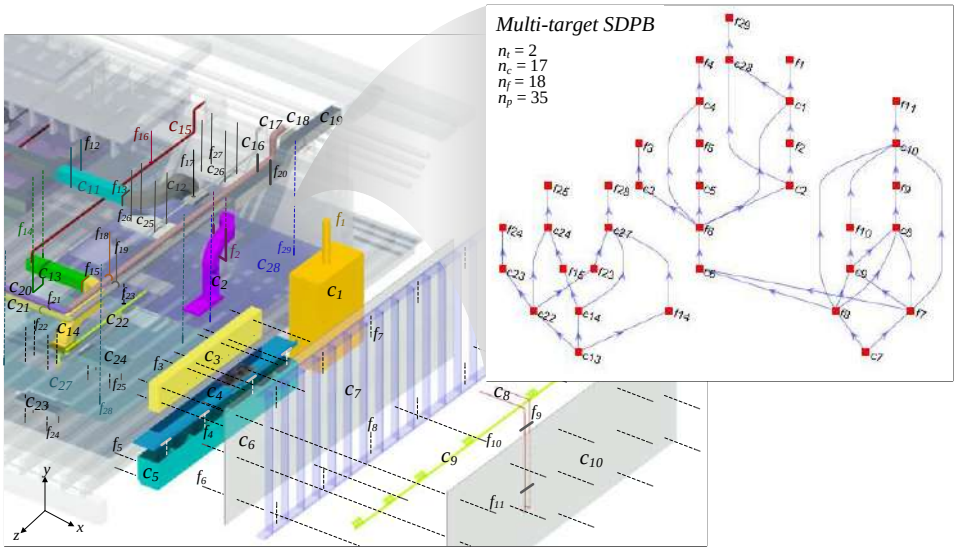

Figure 2. Automated generation of the multiple-target SDPB for components c_7 and c_{13}

3.2 Deconstruction Methods per Building Component

For the proposed approach in this study, it was necessary to estimate the environmental and economic information related to the deconstruction methods included for the multi-objective optimization analysis. The environmental data for building components includes the LCA of selected environmental impacts for each component j ($j=1,\ldots,J$) meant to be part of the same assembly. The LCA system boundaries and limitations were determined according to the most common current practices for buildings and in accordance with a full cradle-to-grave life cycle analysis as in previous studies [3]. The Environmental Impacts EI^a, *where* $a \in A$, were: 1) Global Warming Potential (GWP) in kilograms of carbon dioxide equivalent (kg CO_2 eq) and 2) Primary Energy Demand (PED) in Mega Joules (MJ). The phases included in the LCA were production stage, construction stage, and End-of-Life (EoL). According to Schultmann & Sunke [17] the operational stage of an LCA cannot be assigned to a building component or material separately. Fortunately, the sustainability of disassembly plans should theoretically not differ based on the building use phase, assuming they support the same functions. Three different deconstruction methods m ($m=1,\ldots,M_j$) were analysed for the EoL stage per building component: 1) selective demolition, 2) destructive disassembly, and 3) perfect disassembly. Therefore, the LCA, LCA_{jm}^{a}, of a specified environmental impact a of a building component j in deconstruction method m is calculated according to Equations (1)-(3).

$$LCA_{jm}^{a} = EI_{jm}^{a,production} + EI_{j}^{a,construction} + EI_{jm}^{a,EoL} \quad (1)$$

$$EI_{jm}^{a,production} = EI_{jm}^{a,raw\ materials\ supply} + EI_{j}^{a,transport} + EI_{jm}^{a,manufacturing} \quad (2)$$

$$EI_{j}^{a,construction} = EI_{j}^{a,transport} + EI_{j}^{a,installation\ process} \quad (3)$$

Selective demolition is defined in this methodology as being synonymous with the destruction of components and connections. The EoL treatment for selective demolition is based on average US construction and demolition waste treatment methods and rates, including an avoided burden approach for recycling processes, credit for average energy recovery rates on materials' incineration, and impacts associated with landfilling of materials [18]. The LCA for selective demolition was calculated per component using the commercial 6D BIM software Revit® and Tally®.

Destructive disassembly is defined in this methodology as the disassembly of components and connections in a manner which preserves their physical integrity. As a simplification for the LCA of destructive disassembly, the results of selective demolition were used with a reduction of 80% of the production stage for raw materials supply and manufacturing, assuming that disassembled components could be reused with only minor refurbishments being made [19].

For estimating the LCA for destructive disassembly, the avoided environmental burden of the recycling processing was neglected from the selective demolition LCA calculations since destructive disassembly does not presume the recycling of the recovered components. Perfect disassembly in this approach is defined as the disassembly of building parts with extreme care in order to warrant their direct reuse (i.e., complete physical and

functional utility). The LCA for perfect disassembly assumes 100% reduction of the production stage for raw materials supply and manufacturing from the selective demolition LCA. These simplifications were made to accelerate the process of calculating LCA per building component and also due to technical limitations of the LCA software Tally® employed in this research. Further investigations are required in order to make these calculations more accurate and representative. Therefore, the environmental impact EI^a of the LCA production stage for a building component j with an associated deconstruction method m (m=*selective demolition*, *destructive disassembly*, *perfect disassembly*) is calculated according to Equations (4)-(6):

$$EI_{j,sel.demolition}^{a,production} = EI_{j,sel.demolition}^{a,raw\ materials\ supply} + EI_{j}^{a,transport} + EI_{j,sel.demolition}^{a,manufacturing} \quad (4)$$

$$EI_{j,destruct.disassembly}^{a,production} = EI_{j,destruct.disassembly}^{a,raw\ materials\ supply} + EI_{j}^{a,transport} + EI_{j,destruct.disassembly}^{a,manufacturing} \quad (5)$$

$$EI_{j,perfect\ disassembly}^{a,production} = EI_{j}^{a,transport} \quad (6)$$

Where:

$$EI_{j,destruct.disassembly}^{a,raw\ materials\ supply} = \left(EI_{j,sel.demolition}^{a,raw\ materials\ supply}\right)0.2 \quad (7)$$

$$EI_{j,destruct.disassembly}^{a,manufacturing} = \left(EI_{j,sel.demolition}^{a,manufacturing}\right)0.2 \quad (8)$$

Similarly, the environmental impact EI^a of the LCA EoL stage is calculated according to Equations (9)-(11):

$$EI_{sel.demolition}^{a,EoL} = EI^{a,demolition} + EI^{a,transport} + EI^{a,waste\ processing} + EI^{a,disposal} + EI^{a,recovery\ \&\ recycling\ potential} \quad (9)$$

$$EI_{destruct.dissasembly}^{a,EoL} = EI^{a,deconstruction} + EI^{a,transport} \quad (10)$$

$$EI_{perfect\ \ dissasembly}^{a,EoL} = EI^{a,deconstruction} + EI^{a,transport} \quad (11)$$

The economic data for building components j' includes the information related to the budgeting (bare cost) C associated with the three deconstruction methods m described above. The cost information for destructive disassembly was retrieved from the national database RSMeans®. The data recovered from this database is considered representative for the scope of this study (i.e., the building market in North America). Nevertheless, further investigations should be done in order to adjust the fluctuations of the suggested prices due to particularities of the local economies of the building location. Even though RSMeans® contains the prices for a wide variety of construction activities, in the matter of deconstruction activities such as selective deconstruction, selective demolition, and building refurbishment, the estimations are limited to only a few options according to the most common trends in the construction industry. RSMeans® was therefore used for estimating the building cost for the destructive disassembly per building component, and adjustment factors of 0.65 and 1.35 for estimating the selective demolition and the perfect disassembly costs, were used respectively. This is just a rough approximation of the cost variation between conventional demolition and deconstruction/disassembly of building components [20]. The cost estimations in this study do not include salvaged material resale value for simplification purposes. As part of future research, the assumptions used for estimating the LCA and deconstruction cost should be refined. Therefore, the cost C associated with each deconstruction method m for a building component j is defined as:

$$C_{j,m} = c_{j,m}^{materials} + c_{j,m}^{labor} + c_{j,m}^{equipment} \quad (12)$$

The developed form of Equation (12) for the deconstruction methods m are:

$$C_{j,destruct.disassembly} = c_{j,destruct.disassembly}^{materials} + c_{j,destruct.disassembly}^{labor} + c_{j,destruct.disassembly}^{equipment} \quad (13)$$

$$C_{j,sel.demolition} = \left(C_{j,destruct.disassembly}\right)0.65 \quad (14)$$

$$C_{j,perfect\ disassembly} = \left(C_{j,destruct.disassembly}\right)1.35 \quad (15)$$

3.3 Multi-objective Optimization Analysis for Selective Disassembly

Several methodologies have been devised to portray a multi-objective optimization analysis. For the purposes of this study, we used the weighted method of multi-objective optimization that boasts widespread use among engineers and is acknowledged as the oldest multi-objective solution technique [15]. The multi-objective optimization problem in this study is to minimize the environmental impact LCA^a, as well as the total cost C for the selective deconstruction of a building assembly. Depending on the approach of the overall analysis, the user can select a specific environmental impact of interest. For each building component j (j=*1,…,J*) that is part of the final disassembly sequence plan calculated by the SDPB, one of the three different deconstruction methods m (m=*1,…,*M_j) established in the previous section could be applied. Each deconstruction method has an associated environmental impact EI^a and building cost C. Therefore, the two objective functions have been formulated as follows.

$$Minimize\ Z_1 = \sum_{j=1}^{J}\sum_{m=1}^{M_j} LCA_{jm}^{a} \quad (16)$$

$$Minimize\ Z_2 = \sum_{j=1}^{J}\sum_{m=1}^{M_j} C_{jm} \quad (17)$$

According to the multi-objective weighted method, the objective functions must be combined into a single-objective function, or grand objective function, by multiplying each objective function by a weight w_n and adding them together. For minimization objectives the grand objective function is multiplied by -1 to change its sense to a maximization. The weight is a variable whose value will change systematically during the solution process. The resulting grand objective function is:

$$Maximize\ Z^G = -w_1 \sum_{j=1}^{J} \sum_{m=1}^{M_j} LCA_{jm}^a - w_2 \sum_{j=1}^{J} \sum_{m=1}^{M_j} C_{jm} \quad (18)$$

Subject to:

$$\sum_{j=1}^{J} \sum_{m=1}^{M_j} x_{jm} = 1 \qquad j = 1, \dots, J \quad (19)$$

$$\sum_{k=1}^{K} w_k = 1 \qquad k = 1, \dots, K \quad (20)$$

$$x_{jm} \in (0,1) \qquad j = 1, \dots, J; m = 1, \dots, M_j \quad (21)$$

Where:

- j building component of a building assembly, $j=1,\dots,J$,
- m deconstruction method for a building component, $m=1,\dots,M_j$,
- a type of environmental impact, $a=1,\dots,A_{jm}$,
- k associated weighting factor, $k=1,\dots,K$,
- LCA_{jm}^a LCA for an environmental impact a of a building component j in deconstruction method m
- C_{jm} total cost for deconstruction of a building component j in deconstruction method m
- w_k value of the associated weighting factor k
- x_{jm} decision variable

$$x_{jm} = \begin{cases} 1, & \text{if comp. } j \text{ ends in deconstr. } m \\ 0, & else \end{cases}$$

The grand objective function (18) will generate the set of noninferior solutions for the multi-objective optimization problem. Constraints (19) ensure that every deconstruction method is processed once. Constraints (20) ensure that every weighting factor is processed once. Constraints (21) define the decision variable $x_{jm} \in \{0,1\}$ as binary.

4 Preliminary Experiments

For the process described in Figure 1, BIM was used as the main digital platform for the preliminary experiments. The E2 assembly building example in Figure 2 is used to demonstrate our approach for a multi-objective optimization analysis for selective disassembly planning for buildings. The software used for this purpose was Matlab®. Once the disassembly plan DSPB is ready, the weighted multi-objective optimization analysis for deconstruction methods is implemented to generate the set of noninferior solutions that minimizes a specific environmental impact (GWP) and the building cost. Table 1 summarizes the result of the calculations, and Figures 3 and 4 displays in a graphical way the noninferior solutions founded with the proposed approach.

Table 1. Set of noninferior solutions for the SDPB of components c_7 and c_{13}

k	w_1	w_2	Solution	GWP (Kg CO_2 eq)	Deconstr. Cost ($USD 2018)
1	1.0	0.0	A	120	$2,955
2	0.9	0.1	B	121	$2,930
3	0.8	0.2	C	135	$2,856
4	0.7	0.3	D	144	$2,833
5	0.6	0.4	E	330	$2,507
6	0.5	0.5	F	640	$2,117
7	0.4	0.6	G	844	$1,900
8	0.3	0.7	H	981	$1,876
9	0.2	0.8	I	1,930	$1,462
10	0.1	0.9	J	2,080	$1,430
11	0.0	1.0	K	2,199	$1,423

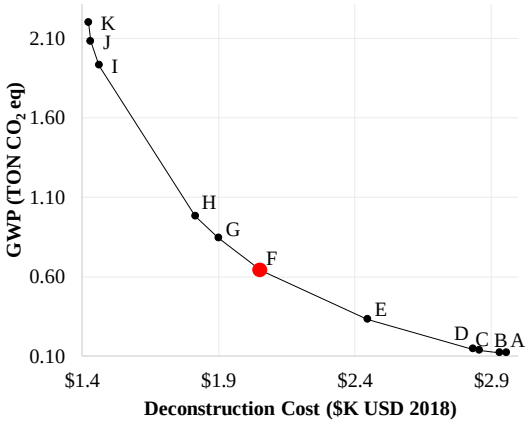

Figure 3. Pareto frontier for minimizing the Global Warming Potential and deconstruction cost of the SDPB for components c_7 and c_{13} by using different deconstruction methods

The result of the case study shows that the different deconstruction methods per building component influence the environmental and economic cost of the selective deconstruction process. The solution A represents the eco-friendlier option because it is the one which reduces its negative environmental loads as represented by GWP. In contrast, the solution K represents the most cost-effective option because it minimizes the cost for the deconstruction of the building

assembly. The points in between are intermediate points that balance the negative environmental load and building cost according to the weighting factors defined by the user. Potential weighting factors determine solutions that are part of the Pareto frontier. This method is thus an effective approach to generate a set of non-inferior solutions for multiple objectives in the selective deconstruction planning of buildings. In the end, the decision makers have the responsibility of choosing the most appropriate solution from the set of non-inferior solutions, according to the specific adaptive reuse building project goals. The methodology described in this study is an effective and user-friendly tool for practitioners and decision makers to perform a multi-objective analysis based on scientific and holistic life-cycle techniques.

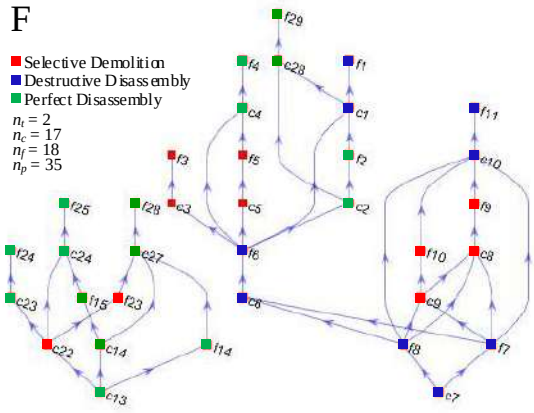

Figure 4. Graphic representation of the noninferior solution "F" for the SDPB of components c_7 and c_{13}

5 Conclusions

Adaptive reuse has the potential to maximize the residual utility and value of existing assets through green design methods, such as selective disassembly planning. Green design methods are used to reduce environmental impacts and to increase economic benefits over the entire product or service lifecycle. However, the field of green design methods for buildings is still underdeveloped in comparison to other industries such as automotive, textile, and manufacturing. Attending the aforementioned need, the aim of this study is to develop a multi-objective optimization analysis framework for the selective disassembly planning of an existing asset through the combination of different deconstruction methods. The analysis is carried out in terms of the physical, environmental, and economic constraints of the deconstruction methods per building component. The SDPB method presented in previous studies is used in order to generate the optimized disassembly plans for retrieving target components. The SDPB method was extended with the purpose of including more than one deconstruction method per component. At the end, a weighted multi-objective optimization analysis is incorporated to generate the set of noninferior solutions that minimizes environmental impacts and building cost.

This study demonstrates that there is a considerable environmental and economic savings potential along the selective deconstruction planning for adaptive reuse of existing assets. During the process of selective deconstruction planning the designers have to wisely evaluate the environmental and economic cost of the building components to deconstruct and the deconstruction methods to apply. In this way, it is possible to maximize the net benefits of the selective deconstruction of a building. Even though the main objective of this study is focus in the optimization of selective disassembly planning for adaptive reuse of buildings, emphasis is placed on the potential for reusing the recovered building components through the proposed selective disassembly methods. It is well known that reuse of components is the best EoL alternative in terms of sustainability due to the amount of environmental benefits embedded. As demonstrated in the case study, the recovery of building components through selective disassembly increases the building cost but it decreases considerably the negative net environmental loads (emissions to the atmosphere, energy demand, water depletion, etc.). Other potential environmental benefits of deconstruction are: decreased disturbance to the site (its soil, ground cover, and vegetation), conserved landfill space, reduction in material mass sent to landfill, conservation of natural resources by reused materials replacing new building materials (this allows the regeneration rate of natural resources to be faster than the depletion rate), and decreased air-borne lead, asbestos, and nuisance dust at and around the job site [20].

The major contribution of this work is the development of an integrated decision-making methodological framework for the adaptive reuse design process, encompassing the optimization of the environmental impacts as well as the building cost through the deconstruction processes. In contrast, the past research efforts focused mainly on suggesting qualitative and quantitative approaches for the entire deconstruction of a building asset with a fixed deconstruction programming of activities that do not capture the issues of customized selective deconstruction processes.

A number of methodologies have been devised to portray the noninferior set among conflicting objectives in engineering problems. For the purposes of this study, we use the weighted method of multi-objective optimization that has widespread use among engineers.

The final goal is to generate the set of noninferior solutions by the appropriate technique. Based in previous studies in the field of selective disassembly planning for buildings, the proposed approach has been demonstrated to be a strong and efficient way to generate comprehensive information about the best available choices for the selective deconstruction of a building asset. This method represents an affordable tool for the decision makers along the deconstruction process for the adaptive reuse of an existing building.

This study has demonstrated the technical affordability of applying the proposed methodology with a reasonably level of complexity and accuracy. The tools and methods that are part of the workflow in the proposed approach, such as the SDPB method, 6D BIM modeling, RSMeans® databases, and Tally® LCA analysis, are available in the market and they are specialized tools for buildings with simplified procedures in order to keep the overall analysis in a reasonable range of complexity. The evidence suggests that in the future all these tools and methods will be continuously developed in order to make them more efficient, simple, and reliable. The proposed study represents an advance on the integration of diverse technologies in the fields of deconstruction building planning, virtual building modelling, environmental assessment, and cost performance of adaptive reuse building projects.

Acknowledgement

The authors would like to thank the Energy Council of Canada (ECC) and the Waterloo Institute for Sustainable Energy (WISE), and the National Council of Science and Technology (CONACYT) of Mexico for providing support for this research paper.

References

[1] Sanchez B and Haas C. Capital project planning for a circular economy. Constr Manage Econ 2018;36(6):303-12.

[2] Geissdoerfer M, Savaget P, Bocken NMP and Hultink EJ. The Circular Economy A new sustainability paradigm? J Clean Prod 2017;143:757-68.

[3] Sanchez B and Haas C. A novel selective disassembly sequence planning method for adaptive reuse of buildings. Journal of Cleaner Production 2018;183:998-1010.

[4] Sanchez B, Rausch C and Haas C. Deconstruction programming for adaptive reuse of buildings. Automation in Construction 2019; Submitted in September 2018, (under review).

[5] Blengini GA and Di Carlo T. The changing role of life cycle phases, subsystems and materials in the LCA of low energy buildings. Energy Build 2010;42:869-80.

[6] Ortiz O, Castells F and Sonnemann G. Sustainability in the construction industry: A review of recent developments based on LCA. Constr Build Mater 2009;23:28-39.

[7] Chastas P, Theodosiou T and Bikas D. Embodied energy in residential buildings-towards the nearly zero energy building: A literature review. Build Environ 2016;105:267-82.

[8] Anderson JE, Wulfhorst G and Lang W. Expanding the use of life-cycle assessment to capture induced impacts in the built environment. Building and Environment 2015;94:403-16.

[9] Langston C, Wong FKW, Hui ECM and Shen L. Strategic assessment of building adaptive reuse opportunities in Hong Kong. Build Environ 2008;43:1709-18.

[10] Teo EAL and Lin G. Building adaption model in assessing adaption potential of public housing in Singapore. Build Environ 2011;46:1370-9.

[11] Smith S, Hsu LY and Smith GC. Partial disassembly sequence planning based on cost-benefit analysis. J Clean Prod 2016;139:729-39.

[12] Gorgolewski M. Designing with reused building components: Some challenges. Build Res Inf 2008;36:175-88.

[13] Aidonis D, Xanthopoulos A, Vlachos D and Iakovou E. On the optimal deconstruction and recovery processes of end-of-life buildings. 2008.

[14] Xanthopoulos A, Aidonis D, Vlachos D and Iakovou E. A planning optimisation framework for construction and demolition waste management. International Journal of Industrial and Systems Engineering 2012;10:257-76.

[15] Revelle CA and Whitlach EE. Civil and environmental systems engineering. Upper Saddle River, N.J.: Prentice Hall PTR, 1996.

[16] Smith S, Smith G and Chen W-. Disassembly sequence structure graphs: An optimal approach for multiple-target selective disassembly sequence planning. Adv Eng Inf 2012;26:306-16.

[17] Schultmann F and Sunke N. Energy-oriented deconstruction and recovery planning. Build Res Informat 2007;35:602-15.

[18] KT Innovations, thinkstep, Autodesk. Tally. 2018.

[19] Sára B, Antonini E and Tarantini M. Application of life-cycle assessment (LCA) methodology for valorization of building demolition materials and products. 2001;4193:382-91.

[20] Coelho A and de Brito J. Economic analysis of conventional versus selective demolition—A case study. Resources, Conservation and Recycling 2011;55:382-92.

Construction and Usage of Three-dimensional Data for Road Structures Using Terrestrial Laser Scanning and UAV with Photogrammetry

S. Kubota[a], C. Ho[a], and K. Nishi[a]

[a]Faculty of Environmental and Urban Engineering, Kansai University, Japan
E-mail: skubota@kansai-u.ac.jp

Abstract –

In road maintenance, it is necessary to construct an environment that manages three-dimensional data and maintenance information for its effectivity and efficiency. The primary objective of this research is to support road maintenance work using three-dimensional data by combining point cloud data of terrestrial laser scanning and unmanned aerial vehicles (UAV) with photogrammetry. For on-site surveying, the limitations have been clarified. The first limitation is based on site circumstances. Passengers and cars use the road being surveyed during measurements. There are few berms and little space for setting a terrestrial laser scanning. In addition, locations where instruments can be placed are limited. It is difficult to perform the number of measurements necessary for acquiring point cloud data. The second limitation is the measurement range, given the specifications of the instrument functionality for pavement surveys. The experimental results indicate that the high-density measurement range is restricted to within an approximately 10-m radius.

Based on these limitations, the upside of a slope or a landform is surveyed using a camera mounted on a UAV. Point cloud data for these objects are constructed using photographs with SfM technology. SfM data and terrestrial laser scanning data are combined because three-dimensional data for bridge sides and lower works cannot be constructed. To evaluate the accuracy of three-dimensional data, we compare the three-dimensional data with its design conditions. The inaccuracy for the bridge is an effective length of 12 mm and an effective width of 19 mm and the three-dimensional data describes the structure of the bridge with high accuracy.

The three-dimensional data for the road structures could be used to develop a road maintenance management system that accumulates data and refers to the inspection results and repair information in three dimensions.

Keywords –

Point Cloud Data; Terrestrial Laser Scanning; Unmanned Aerial Vehicle; Road

1 Introduction

Roads must be safe and maintained in good condition. Maintenance management is an essential operation that must be carried out effectively for maintaining, repairing, and rehabilitating roads. If large-scale damage occurs to a road in an urban area and it cannot be used, many aspects of life may be affected. Thus, it is important to protect roads from large-scale damage and to carry out road maintenance in order to maintain services for the public. In addition, it is necessary to accumulate information produced during the entire life cycle of a road in order to analyze problems and solutions within a temporal sequence and to maintain roads strategically and effectively. In Japan, much road infrastructure was built over fifty years ago. Due to progressive deterioration in road infrastructure, ensuring proper maintenance of overall facilities to avoid potential problems is currently an important issue. In particular, in order to avoid or reduce substantial loss, deal with an emergency, prevent damage, perform emergency disaster control, and carry out disaster recovery, road administrators must maintain roads more efficiently. In current maintenance work, road administration facilities are represented on a two-dimensional map, which is not suitable for pothole repair, inspection, or annual overhaul. Locating and analyzing a position can be difficult when using such a map.

In road maintenance, it is necessary to construct an environment that manages three-dimensional data and maintenance information. A road management system comprises functions for planning, design, construction, maintenance, and rehabilitation of roads. A fundamental requirement of such a system is the ability to support the modeling and management of design and construction

information, and to enable the exchange of such information among different project disciplines in an effective and efficient manner.

Engineers should be able to use three-dimensional data not only for virtually reviewing the design of a facility, but also for analyzing building operations and performance. Three-dimensional data tend to be applied to a particular phase of a construction project. Using three-dimensional data will thus improve the efficiency of operations and maintenance.

Dense point cloud data were generated using three and over pictures which taken same points [1], [2]. Agarwal et al. and Frahm et al. were constructed three-dimensional city by automated reconstruction [3], [4]. The three-dimensional point cloud data are constructed on the basis of the Structure from Motion (SfM) range-imaging technique of photogrammetry using video camera data. The accuracy of three-dimensional model by SfM were evaluated by several researches [5]. And, the generated point cloud data which measured the objects from several measurement points are integrated for representing the accurate objects. The integration method of point cloud data is iterative closest point method (ICP) [6], globally consistent registration method of terrestrial laser scan data using graph optimization [7], curve matching [8], [9], and automated registration using points curve [10].

The primary objective of this research project is to propose a road maintenance framework using three-dimensional point cloud data. A point cloud is a collection of data points defined by a given coordinate system. In a three-dimensional coordinate system, for example, a point cloud may define the shape of some real or created physical system. Terrestrial laser scanning [1], [2], and [3] and photogrammetry technologies are used to survey road structures. In road maintenance work, a mobile mapping system (MMS) is used, which generates point cloud data. In this research project, terrestrial laser scanning and photogrammetry by an unmanned aerial vehicle (UAV) are used. Three-dimensional data for the Shiraito Highland Way in Japan are constructed using point cloud data generated by terrestrial laser scanning. Shiraito Highland Way is approximately 10 km in length, and its elevation varies between 1000 m and 1400 m. The measuring range of terrestrial laser scanning on a road varies from approximately 10 m to 100 m. Point cloud data are combined using coordinate points. In addition, the data are used for road maintenance, taking into consideration data size and accuracy. Road maintenance information can be referenced at any three-dimensional point in the point cloud data. PhotoScan Professional (Agisoft) is used for SfM. This paper evaluates the accuracy of the usage of point cloud data by laser scanning and photogrammetry for road maintenance. For example, this method can be used to check potholes and surface irregularities on pavement that can be easily and quickly confirmed by management.

2 Usage of Terrestrial Laser Scanner and Photogrammetry of UAV Camera

There are a number of survey methods for constructing three-dimensional data using laser imaging detection and ranging (Lidar; laser profiler), laser-based photogrammetry, mobile mapping system, terrestrial laser scanning, and photogrammetry using a camera by UAV. Combining these survey methods according to site situations and structures enables surveys of civil infrastructure and construction of three-dimensional point cloud data. It is necessary to understand the characteristics and specifications of the specific measurement instruments and choose suitable point cloud data for a use case for a road maintenance site. In this research project, terrestrial laser scanning and UAV-based photogrammetry are used for usage scenes as shown in Figure 1.

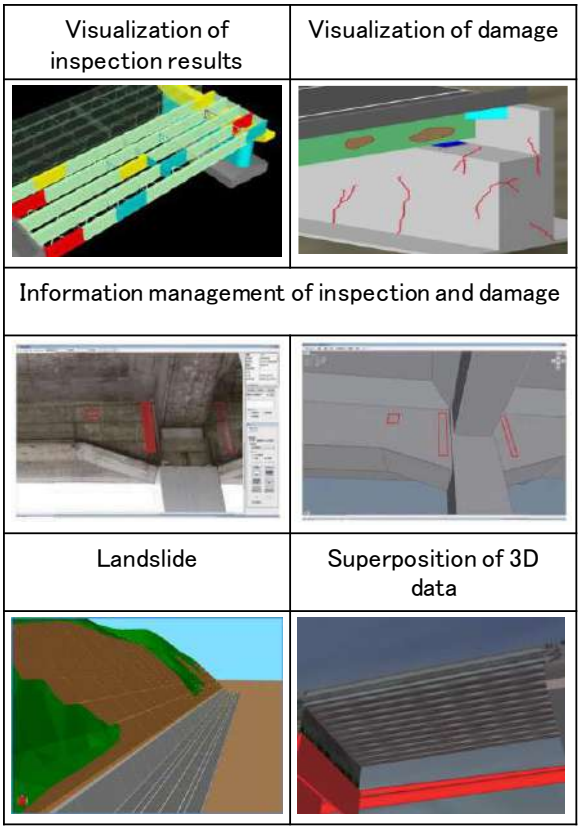

Figure 1. Usage scenes of three-dimensional data

2.1 Usage of Terrestrial Laser Scanner

A terrestrial laser scanner is set on a ground surface,

and the laser component illuminates objects. A laser beam is reflected, and a return-beam detection device records two-way travel time, calculating the distance between the scanner and the object. As a result, point cloud data for an observed object are generated. When using terrestrial laser scanning, it is important to choose a location where the instrument can be set up easily. It is usually advantageous to overlook and survey the location when setting up the instrument.

Table 1 Characteristics of point cloud data by TLS and UAV photogrammetry

	Terrestrial Laser Scanner	UAV photogrammetry
Survey cost (time)	Expensive, but portable	Less expensive and small size
Measurement range	Narrow area	Wide area
Visible area	Visible area from point of terrestrial laser scanning	UAV flight area
Invisible area	Superior surface cannot be measured	Overhang area cannot be measured
Accuracy	A few millimeter	Depends on SfM software
Density of points	Extremely high	High
Distribution	Non-uniform	Depends on SfM software
Angle	10 to 90 degrees	Approximately 90 degrees
Measurement of edge	Exactly	Potentially inaccurate
Measurement of surface	Including noise	Including noise
Measurement of structure	Side surface can be measured	All surfaces can be measured
Noise	Including noise	Including noise
Reflected data	*xyz* coordinates value of local coordinate	*xyz* coordinates value of plane rectangular coordinate system

2.2 UAV Platform Camera

Point cloud data are generated by aerial photogrammetry using photographs or a video-output camera on a UAV. The data are generated using a SfM process [4], [5], and [6]. The characteristics of terrestrial laser scanning and UAV photogrammetry are represented in Table 1. They are analyzed with respect to time cost, measurement range, visible area, invisible area, accuracy, density, distribution, angle, measurement of edge, ground, and structure, noise, and enabled data.

3 Survey and Construction of Three-dimensional Data

Terrestrial laser scanning and UAV photogrammetry technologies are used to survey and generate road structures. Three-dimensional point cloud data for the Shiraito Highland Way in Karuizawa Village, Kitasaku County, Nagano Prefecture, Japan, are used.

In this paper, usage of point cloud data for road maintenance is proposed. If a road administrator possesses point cloud data for a MMS, the data are used for road maintenance. Usage of terrestrial laser scanning is more efficient for surveying narrow areas to check for cracks and holes in the pavement of a road. In the case of a landslide on the side of a road, using terrestrial laser scanning to survey the upside of a slope can be difficult. The reason is that terrestrial laser scanning has limitations for measuring the upside of a landform or slope occluded by such objects as trees or other vegetation and by the angle of incidence of the scanner.

3.1 Construction of Landform Data

Therefore, the upside of a slope or a landform is surveyed using a camera mounted on a UAV. Point cloud data for such objects are constructed using photographs employing SfM technology. Figure 2 depicts SfM data and laser scanning data for a slope. The point cloud data are constructed by combining SfM data with laser scanning data corresponding to 5000 random points between those data, as depicted in Figure 2. The constructed three-dimensional data were superposed for grasping the difference in temporal sequences. The data of 2017 and 2018 were used. The difference was calculated and represented using difference analysis function of Cloud Compare software as shown in Figure3. The lack of soil in slope was represented using blue color and was used for understanding the shape of cross section.

A terrestrial laser scanner is set on a ground surface, and the laser component illuminates objects. A laser beam is reflected, and a return-beam detection device records two-way travel time, calculating the distance between the scanner and the object. As a result, point cloud data for an observed object are generated. When

using terrestrial laser scanning, it is important to choose a location where the instrument can be set up easily. It is usually advantageous to overlook and survey the location when setting up the instrument.

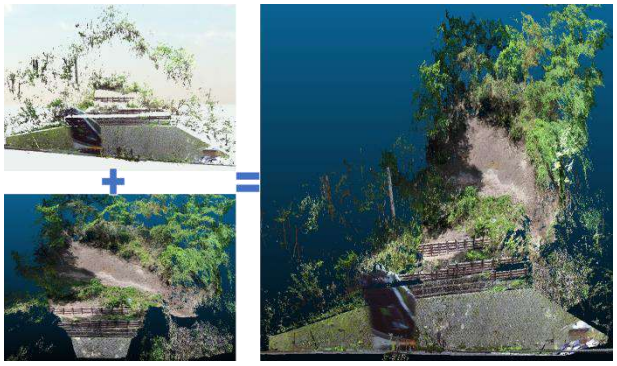

Figure 2. Fusion of three-dimensional point cloud data acquired by terrestrial laser scanning and UAV photogrammetry on slope

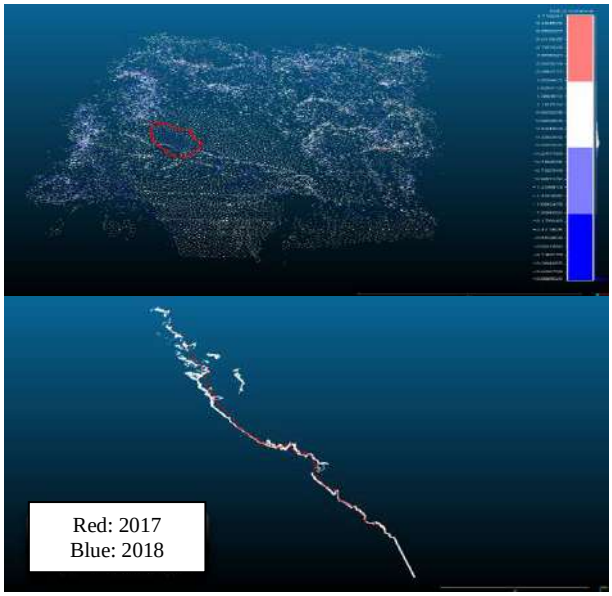

Figure 3. Difference of cross section in temporal sequences

3.2 Limitations for On-site Survey

According to the results of an on-site survey, limitations have been discovered. The first limitation is based on site circumstances. Passengers and cars pass by on the road being surveyed during measurement. There are few berms and little space for setting a terrestrial laser scanning, given the high slope on the Shiraito Highland Way. In addition, locations where instruments can be set are limited. Therefore, it is difficult to perform a number of measurements for acquiring point cloud data. It is necessary to pay attention to surveyors and instruments, and to determine measurement range and accuracy for the set of circumstances.

The second limitation is measurement range, given the specifications of instrument functionality for pavement surveys. According to experimental results, high-density measurement range is restricted to within an approximately 10-m radius, as depicted in Figure 4. It is necessary to perform a number of plural measurements for surveying wide-range pavement data. Figure 5 shows the three-dimensional data of road surface connected the thirteen laser scanning data of 10 m radius. The reference points such as trees and guard rails were set for data fusion. The data have about 300 m length and 208,375,900 points.

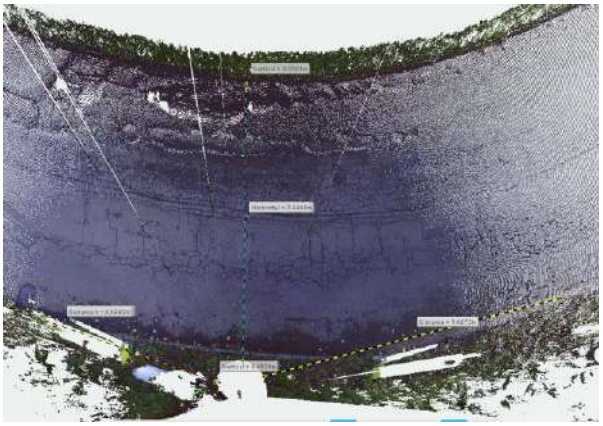

Figure 4. Point cloud data on road surface

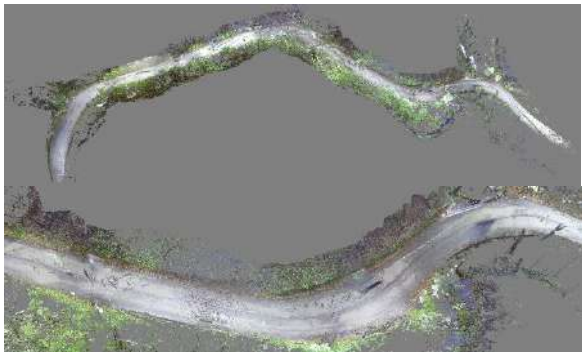

Figure 5. Three-dimensional data of road surface

3.3 Construction of Bridges

To construct the three-dimensional data for the upper and lower part of bridges, UAV aerial photogrammetry and terrestrial laser scanning measurements were performed for the Kashii River (Izumisano City) and Kimyuji River (Sennan City) in the south of Osaka Prefecture in November 2017. During the UAV aerial photogrammetry, the UAV flew at an altitude of 30 m, the movie was converted into pictures, and SfM processing was performed with PhotoScan to construct the three-dimensional data.

Figures. 6 and 7 depict examples of data fusion of terrestrial laser scanning and SfM data acquired by a UAV using the same method as described above.

Figure 6. Data fusion of terrestrial laser scanning and UAV in road and bridge

Figure 7. Data fusion of terrestrial laser scanning and UAV on a bridge

4 Accuracy Evaluation of Three-dimensional Data

4.1 Accuracy of UAV Photogrammetry Data

The accuracy of UAV photogrammetry data and constructed three-dimensional data were evaluated by assigning absolute coordinates from the global navigation satellite system survey to the three target points as reference points, and four verification points were used as shown in Figure 8. The accuracy is validated using root mean squared error with *xy* plane and altitude of *z* coordinate. RMSE is calculated using the true coordinate measured by GNSS (Pentax G3100-R2B) and point clouds. The root mean square error was 0.272 m in the *xy* direction and 0.261 m in the *z* direction (Table 2). Because the wind was strong at the time of the measurements, the fact that the aircraft and the camera were not stable affected the accuracy. For the terrestrial laser scanning, we targeted the Megata Bridge in Kashigawa River and the Warazuhata Bridge in Kinyuji River, the feature points of multiple-point group data measured from six places bridges from five places were matched, and thinning processing was applied to obtain one data point.

Figure 8. Target setting points

Table 2. Accuracy verification results for SfM data

Inaccuracy (m)	*xy* direction	*z* direction
Point A	0.199	0.349
Point B	0.232	0.082
Point C	0.414	0.211
Point D	0.185	0.120
Average	0.258	0.191
Root mean squared error	0.272	0.216

Table 3. Accuracy verification results for fusion data

Inaccuracy (m)	*xy* direction	*z* direction
Point A	0.035	0.033
Point B	0.011	0.009
Point C	0.010	0.008
Point D	0.043	0.047
Average	0.025	0.024
Root mean squared error	0.029	0.029

4.2 Accuracy of Fusion Data

The three-dimensional point cloud data obtained by SfM are measured from the air, and SfM data and terrestrial laser scanning data are combined because three-dimensional data for bridge sides and lower works cannot be constructed. The accuracy of terrestrial laser scanning data is higher than that of SfM data, and therefore duplicate SfM data are deleted before combining. According to Cloud Compare, we can combine 50,000 characteristic points for each type of data with reference to each other type of data and describe the side and bottom works of bridges that could not be acquired by UAV aerial photogrammetry as three-dimensional data. The fusion data of Warazuhata Bridge were evaluated by root mean squared error in Table 3. The root mean squared error was 0.029 m in the *xy* direction and 0.029 m in the *z* direction. It

represents high accuracy of the three-dimensional data combined by terrestrial laser scanning data and UAV photogrammetry data. To evaluate the accuracy of three-dimensional data, we compare the point cloud data of the Warazuhata Bridge with its design conditions. The bridge length is 22.20 m and its width is 4.00 m, whereas the bridge length from the point cloud data is 22.212 m and its width is 4.019 m. Therefore, the inaccuracy for the bridge is an effective length of 12 mm and an effective width of 19 mm (Figure 9) and the three-dimensional point cloud data describes the structure of the bridge with high accuracy.

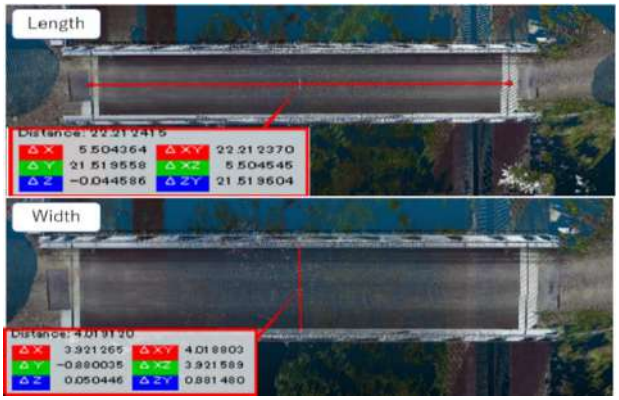

Figure 9. Length and width based on the combined point cloud data for Warazuhata Bridge

5 Proposal of Road Maintenance Information System Using Three-dimensional Data

The three-dimensional point cloud data for the road pavement surface and the bridge could be used to develop a road maintenance management system that accumulates data and refers to the inspection results and repair information in three dimensions.

An information system for road maintenance is proposed in this research project. This chapter discusses the information system, which uses point cloud data based on the definition of an information system.

By definition, an information system collects, processes, transfers, and utilizes information in its own domain. Figure 10 depicts the definition of a road maintenance information system using point cloud data.

A road maintenance system was considered based on the definitions within an information system. The road maintenance system can link inspection results and recondition information with the point cloud data for display, storage, and reference, facilitating the management of road cracks and areas for repair. In future work, point cloud data will be used to identify changes in the shape and condition of damage through spatial and temporal management.

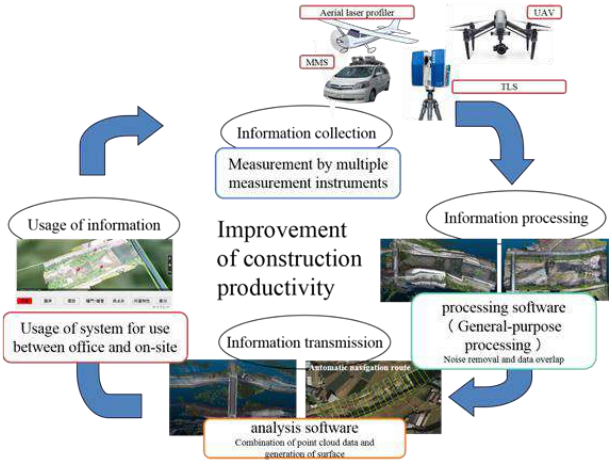

Figure 10. Definition of road maintenance system

5.1 Information Collection

Point cloud data for road infrastructure are collected using terrestrial laser scanning and UAV-based photogrammetry. In addition, maintenance and operation data, such as for inspection, rehabilitation, and repair, are collected on-site for the system.

5.2 Information Processing

Point cloud data generated by terrestrial laser scanning contain noise data concerning trees and vegetation on a road. In information processing, such objects should be removed in order to represent road structures accurately. terrestrial laser scanning's survey range is confined to the visible range and the scan range of the scanner; therefore, it contains blind spots that are not represented by the point cloud data cloud. Accordingly, surveyors need to move the scanner to multiple locations across a number of points in time. UAVs can acquire photographs or videos in-flight. Such visual records are used for SfM software and translated point cloud data. In addition, the point cloud data are colorized for visualization.

5.3 Information Transmission

Terrestrial laser scanning and UAV-based photogrammetry each have distinct characteristics with respect to survey time cost, scan range, and accuracy. Wide area and high precision point cloud data are generated by combining each set of data units. In addition, in this process, structural members and surface data, such as a triangulated irregular network, are extracted and generated in accordance with the purpose of usage. Furthermore, it is also possible to compare

two different temporal data units for analysis.

5.4 Usage of Information

In this research project, instead of a surface model, point cloud data are used for road maintenance. A road maintenance information system is proposed, which has functions for detecting cracks and superimposing photographs based on point cloud data. In addition, a function is needed for reflecting inspection and repair events that have been represented on a two-dimensional map displayed on a smart device onto three-dimensional point cloud data on-site.

In the road maintenance system, the inspection result and repair information can be linked with three-dimensional point cloud data and displayed, stored, and referenced. It is easy to detect road cracks and spots in need of repair, as depicted in Figure 10. In addition, it is possible to determine changes in shape and damage using temporal management of point cloud data.

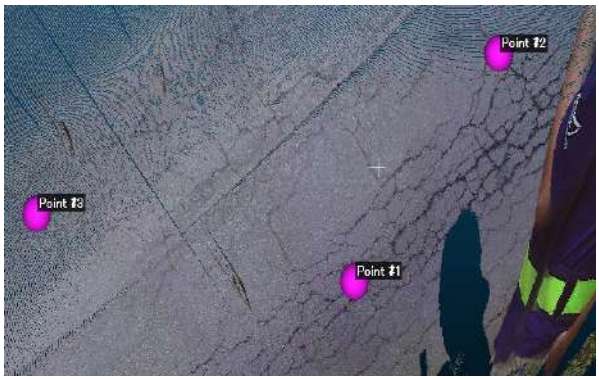

Figure 11. Repair information linked with three-dimensional point cloud data

6 Conclusion

In this research project, point cloud data for road infrastructure have been surveyed using terrestrial laser scanning and UAV photogrammetry for road maintenance. For on-site surveying, the limitations of these methods have been clarified. The first limitation is based on site circumstances. Passengers and cars use the road being surveyed during measurements. There are few berms and little space for setting a terrestrial laser scanning, given the high slope on the road. In addition, locations where instruments can be placed are limited. Therefore, it is difficult to perform the number of measurements necessary for acquiring point cloud data. The surveyors, instruments, and measurement range and accuracy of the conditions should be considered. The second limitation is the measurement range, given the specifications of the instrument functionality for pavement surveys. The experimental results indicate that the high-density measurement range is restricted to within an approximately 10-m radius. Thus, multiple measurements must be taken for surveying wide-range pavement data. Based on these limitations, in this work, the upside of a slope or a landform is surveyed using a camera mounted on a UAV. Point cloud data for these objects are constructed using photographs with SfM technology. SfM data and laser scanning data are used for slopes. The point cloud data are constructed by combining SfM data with laser scanning data corresponding to 5000 random points between these data.

References

[1] Furukawa, Y. and Ponce, J., Accurate, dense, and robust Multiview stereopsis, *IEEE Transactions on Pattern Analysis and Machine Intelligence*, 32(8), pp. 1362-1376, 2010.

[2] Hirschmuller, H., Stereo processing by semiglobal matching and mutual information, *IEEE Transactions on Pattern Analysis and Machine Intellingence*, 3(2), pp. 328-342, 2008.

[3] Agarwal, A., Snavely, N., Simon, I., Seitz, S. and Szeliski, R., Building Rome in a day, *ICCV09*, pp. 72-79, 2009.

[4] Frahm, J.M., Fite-Georgel, P., Gallup, D., Johnson, T., Raguram, R., Wu, C., Jen, Y.H., Dunn, E., Clipp, B., Lazebnik, S. and Pollefeys, M., Building rome on a cloudless day, *ECCV10*, pp. 368-381, 2010.

[5] Remondino, F., Del, P.S., Kersten, T.P. and Troisi, S., Low cost and open source solutions for automated image orientation – a critical overview, *Lecture Notes in Computer Science*, 7616, pp. 40-54, 2012.

[6] Besl, P. J. and McKay, H. D., "A method of registration of 3-D shapes," *IEEE Transaction Pattern Analysis and Machine Intelligence*, Vol. 14, No. 2, pp. 239-256, 1992.

[7] Pascal, W. H., Wegner, J. D. and Schindler, K., "Globally consistent registration of terrestrial lase scans via graph optimization," *ISPRS Journal of Photogrammetry and Remote Sensing*, Vol. 109, pp. 126-138, 2015.

[8] Grune, A. and Akca, D. "Least squares 3D surface and curve matching," *ISPRS Journal of Photogrammetry and Remote Sensing*, Vol. 59, pp. 151-174, 2005.

[9] Yang, B. and Zang, Y., "Automated registration of dense terrestrial laser-scanning point clouds using curves," *ISPRS Journal of Photogrammetry and Remote Sensing*, Vol. 95, pp. 109-121, 2014.

[10] Yang, B., Dong, Z., Liang, F. and Liu, Y., "Automated registration of large-scale urban scene point clouds based on semantic feature points

curves," *ISPRS Journal of Photogrammetry and Remote Sensing*, Vol. 113, pp. 43-58, 2016.

[11] Tanaka, S., Imai, R., Nakamura, K., Kubota, S. and Umehara, Y. Research on Method for Generating River Cross-Section Using Airbone Laser. In *Proceedings of Civil Engineering Conference in the Asian Region*, pages 1-12, Hawaii, USA, 2016.

[12] Tanaka, S., Nakamura, K., Imai, R., Kubota, S. and Sakurai, J. Design Data Generation System for Progress Control of Working Form. In *Proceedings of Civil Engineering Conference in the Asian Region*, pages 1-12, Hawaii, USA, 2016.

[13] Tien, K-K., Tien, P-H., and Ko, W-T. The Integration of an Unmanned Aerial Vehicle (UAV) and a Laser Scanner and its Application in the 3D Modeling of an Historical Building. *Science and Technology Reports of Kansai University*, 60:33-42, 2018.

[14] Kubota, S. and Kawai, Y. River Maintenance Management System Using Three-dimensional UAV Data in Japan. *ISPRS Annals of the Photogrammetry, Remote Sensing and Spatial Information Sciences*, IV-2/W1:93-98, 2016.

[15] Kubota, S., Kawai, Y., and Kadotani, R. Accuracy Validation of Point Clouds of UAV Photogrammetry and its Application for River Management. The International Archives of the Photogrammetry, Remote Sensing and Spatial Information Sciences, XLII-2-W6: 195-199, 2017.

[16] Tanaka, S., Tsuji, M., Ito, T., Kubota, S., Imai, R., and Nakamura, K. Surveying and Utilization of Three-dimensional Data on Civil Infrastructures Using Terrestrial Laser Scanner and Unmanned Aerial Vehicle. In *Research Report of Information Processing Society of Japan*, 2015-IS-134(4), pages 1-6, Tokyo, Japan, 2017 (in Japanese).

Cartesian Points Visualization in Game Simulation for Analyzing Geometric Representations of AEC Objects in IFC

J. Zhang,[a] Y. Chen[a], R. Liu[b], and L. Debs[a]

[a]School of Construction Management Technology, Purdue University, U.S.A.
[b]M.E. Rinker, Sr. School of Construction Management, University of Florida, U.S.A.
E-mail: zhan3062@purdue.edu, chen428@purdue.edu, liurui@ufl.edu, ldecresc@purdue.edu

Abstract –

Industry foundation classes (IFC) is widely accepted as a promising standard for building information modeling (BIM). IFC data can be processed with many open toolkits such as IfcOpenShell and java standard data access interface (JSDAI), which greatly supports BIM research and technology development. However, IFC data is not intuitive and requires training to understand it fully. As the core of almost any IFC data, understanding geometric representation is critical in most BIM research and technology development. The official IFC schema specifications provide detailed explanations of entities and attributes in IFC, which are helpful for gaining such understanding. However, understanding the explanations in the specifications requires certain knowledge and background. To facilitate an easier understanding of IFC data and to promote a wider adoption of IFC-based BIM, in this paper, an interactive visualization of the formation of fundamental 3D representations of a selected architecture, engineering, and construction (AEC) object was created in game simulation in a first-person view. The interactive simulation can help people gain understanding of 3D geometric formation and representation in IFC in an intuitive and speedy manner, which is expected to achieve retention of such knowledge comparable to or better than the conventional way of reading the specifications. The visualization was tested by 14 volunteers in comparison to reading the IFC schema specifications. A survey based on the experiment showed that the game simulation-based visualization was significantly easier to understand and took significantly less time to understand comparing to reading the specifications.

Keywords –

BIM; IFC; Geometric Information; AEC Objects; Game Simulation; Visualization; Cartesian Points

1 Introduction

Building information modeling (BIM) is a "data rich digital representation cataloging the physical and functional characteristics of design and construction" [1]. It is expected to serve as "a shared knowledge resource for information about a facility forming a reliable basis for decisions during its life-cycle from inception onward" [2]. Since its inception BIM has been used for various purposes such as 3D coordination, 4D modeling, design reviews, as-built conditions modeling, structural analysis, energy analysis, cost estimation, sustainability evaluation, lighting analysis, and asset management [3]. For each of these purposes there are multiple (if not many) software applications to use, which benefited project stakeholders by reducing errors, time, and cost, improving quality, safety, profitability, and facilitating collaborations [4]. BIM applications are intended to be interoperable by definition, meaning that these applications should be able to "exchange information and to use the information that has been exchanged" [5]. However, a seamless interoperability between BIM applications is far from reality. Information missing and information inconsistency is not uncommon when BIM is exported from one application and imported into another. Even BIM applications from the same software provider may not have fully seamless interoperability [6] [7]. Such a lack of BIM interoperability costed the architecture, engineering, and construction (AEC) industry $15.8 billion annually [8].

In North America, the adoption of BIM in the AEC industry increased from 28% in 2007 to 71% in 2012 and is continuing to increase [4]. With the increased adoption of BIM, the lack of interoperability between BIM applications is only becoming a bigger problem, as was evidenced by a survey of contractors which showed that almost half (46%) of contractors with heavy software use considered the need of improving BIM interoperability to be of high/very high importance [4].

Standardization is one potential solution for BIM interoperability. Two main standardization efforts are industry foundation classes (IFC) and the CIMSteel Integration Standards Version 2 (CIS/2) [9]. While CIS/2 focuses on exchangeable data representation and information modeling for structural steel type of projects [10], the IFC standard is designed to be able to represent any type of building construction projects. IFC is an open and neutral data standard that is registered as an international standard ISO 16739 [11]. IFC has been widely accepted as the most promising data standard to solve BIM interoperability. IFC is dominating BIM research in academia and almost all main BIM software applications claimed to be compatible with IFC (i.e., through exportation and/or importation). Since its inception in 1997, IFC has been going through eight main release versions (IFC1.0, IFC1.5, IFC2.0, IFC2x, IFC2x2, IFC2x3, IFC2x3_TC1, IFC4) and is still under development towards IFC5, which is planned to extend to represent not only building projects but also infrastructure projects such as roadways and bridges. It stimulated a national trend in the U.S. towards civil integrated management (CIM) which is about implementing the same life cycle information management idea of BIM from vertical building projects to horizontal infrastructure projects [12]. Therefore IFC is attracting great attention in all sectors from academia, industry, and government. Some familiarity and understanding of IFC data is gradually becoming necessary for practitioners in the AEC industry, therefore IFC contents are entering the curriculum of construction education and training.

In spite of the openness of IFC standard, data instance files using IFC schema are not directly understandable like a bar chart. As of the current version IFC4, the IFC schema includes more than 750 entities and more than 350 types [13]. Each entity has its own specifications that define its attributes and allowed value assignments to the attributes. In an effort to limit the size of IFC instance files, cross referencing is used ubiquitously where one entity instance can refer to another entity instance as the value of one of its attribute. It takes a certain level of training to understand IFC data, and the learning curve is not steep. For example, in a graduate level class taught by the first author, it took a significant portion of a lecture's time to explain the intricacies of the IFC data.

Geometric information is an essential part of any BIM data, and it is a critical part of any IFC data files. Entity instances that represent geometric information can take a significant portion of an IFC instance file. For example, "in the 'Duplex Apartment' IFC data published by buildingSMARTalliance of the National Institute of Building Sciences [14], more than 71.6% (27,866 out of 38,898) of the entities were directly used for representing geometric information." [15]. Therefore, IFC data cannot be fully understood without understanding its geometric information representations.

Cartesian points are the most fundamental elements for representing geometric information in IFC data, they play critical roles in the interchange of information between as-built model and as-design model, and from as-design model to advanced visualization platforms such as game simulation and virtual reality platforms. To help understand geometric representations using Cartesian points in IFC data, the authors proposed the use of a new game simulation-based interactive visualization. The remaining sections of this paper describe the background of this visualization technique, the details of an example using this visualization and its testing results and analysis.

2 Background

This background section introduces background knowledge in game simulation, industry foundation classes (IFC), and Cartesian points in IFC.

2.1 Game Simulation

The concept of game simulation is a combination of the concept of game and the concept of simulation. The key elements of a game are rules and goals, interaction and feedback, challenge and strategies, and motivation and fun [16] [17]. The key elements of a simulation are model of reality, abstract concepts, interaction, experiment, decisions from a specific angle of view, and purposeful testing [17]. Therefore interactions from a specific role or angle of view is an essential element of a game simulation. Game simulation has been shown to be an effective teaching tool, based on the two assumptions that "practice improves one's ability to perform" and "simulations provide students with opportunities to practice making management decisions in a safe environment" [18].

Game simulation has been widely used in AEC research to help with construction engineering and management education [17][19], architectural design review [20] [21] [22], mechanical, electrical, and plumbing (MEP) design and analysis [23], facility management [24] [25], constructability and productivity analysis [26], and construction operation/safety training [27] [28].

There are multiple game engines available off-the-shelf such as Unity3D, Unreal Engine, and CryENGINE. Game simulations using these game engines may well use information from BIM especially geometric information, through intermediate format transfers such as FBX and OBJ files. Cartesian points lay the foundation of geometric information representation in these formats. For example, Figure 1 shows the starting section of an OBJ file that represents the geometry of a bent wood

plank. While the lines starting with # indicate comments, each line that starts with a "v" is representing the x,y,z coordinates of one Cartesian point.

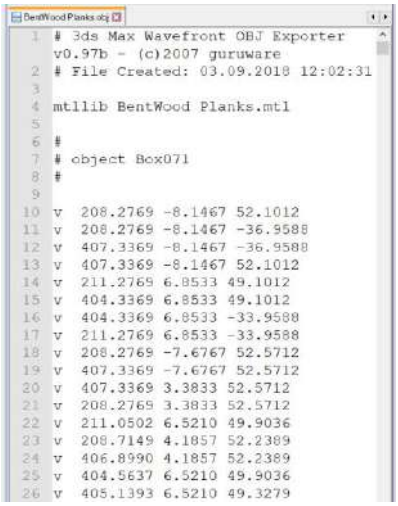

Figure 1. Starting section of an OBJ file

2.2 Industry Foundation Classes

Industry foundation classes (IFC) is an open and neutral data standard for building and construction industry data, and it is registered as ISO 16739 since the IFC4 version [29]. IFC data files can be using one of three main formats - .ifc, .ifcXML, and .ifcZIP, which are the default, XML represented, and compressed formats, respectively. The default and XML represented formats are mainly used in BIM research, especially the default .ifc format. Because it is based on the STEP physical file structure which is according to another international standard ISO10303-21. There are many open sourced utilities that can be used to directly read/write .ifc files, such as IfcOpenShell, java standard data access interface (JSDAI), and IFC++.

In the IFC schema, entities and attributes of the entities are used to represent concepts and relations between or properties of concepts, respectively. For example, *IfcWallStandardCase* is an entity to represent a standard wall concept. The second attribute of *IfcWallStandardCase*, *OwnerHistory* is used to represent the relation between the standard wall and an owner history entity that is used to represent all history and identification related information of the standard wall. The third attribute of *IfcWallStandardCase*, *Name* is used to represent the name property of the standard wall. In the instantiated data files using the IFC schema, cross referencing is used between one entity instance and another to represent the relations between entity instances. For example, Figure 2 shows the partial view of an IFC instance file where six cross references were highlighted.

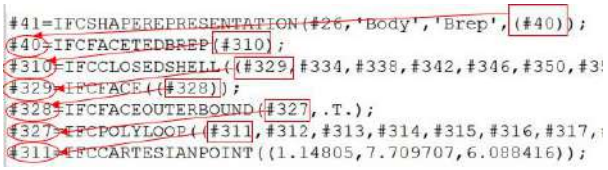

Figure 2. An example partial IFC instance file

Geometric information is an important part of an IFC model. The mechanism for representing geometric information in IFC is based on an international standard ISO 10303-42 [11]. In spite of the standardization of the geometric representation, the geometric data in an IFC file is not intuitively understandable. One reason is the varieties of geometric representations in IFC, such as "Body" and "Axis" [30]. Another reason is the complexities within each type of geometric representation. For example, the solid model of a "Body" can be represented by "Swept Solids" "Boolean Results" or "Brep Bodies." [31]. "Swept Solids" use the solid sweeping technic to form a 3D representation, i.e., planar bounded surfaces swept along a defined direction. "Boolean Results" take the union or intersection between two solids to define a new solid. "Brep Bodies" use boundary representations to represent a 3D shape where each boundary representation is a surface element. The IFC data in Figure 2 was using the "Brep Bodies" 3D geometric representation, which can be seen from the use of the entity *IfcFacetedBrep*. The *IfcClosedShell* is an entity to represent the 3D shape. Figure 3 summarizes the path from the *IfcClosedShell* to the lowest-level element *IfcCartesianPoint*. The boundaries of this *IfcClosedShell* are represented by multiple occurrences of *IfcFace*. The boundaries of the *IfcFace* are defined by *IfcFaceOuterBound*, whose boundaries, in turn, are defined by *IfcPolyLoop*. Finally, the definition of the *IfcPolyLoop* is achieved by using multiple occurrences of *IfcCartesianPoint*.

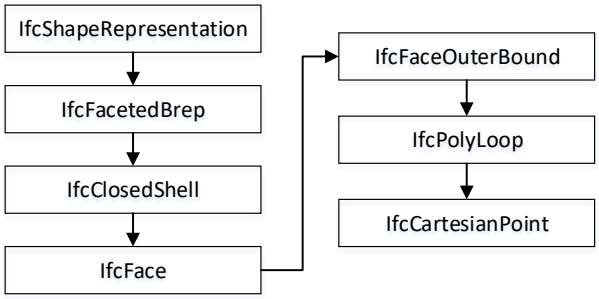

Figure 3. Summary of the pathway of a Brep geometric representation in IFC

2.3 Cartesian Points in IFC

In spite of the variety of ways of representing geometric information in IFC, they all reduce to Cartesian points in the end. Therefore the understanding of Cartesian points is the key to the understanding of geometric information in IFC. Such an understanding is also important to the collective use of IFC model with other models such as as-built models [32], which can be collected using various sensing technologies such as laser scanning [33] and image sensing [34]. One classic use of as-built models together with as-designed models in IFC is to monitor the progress of construction, where matching Cartesian points from as-built point clouds and IFC data need to be performed manually and/or algorithmically [34] [35].

In the future use of robotics both in a built environment and in the construction of a built environment, the geometric information carried by an IFC model could foreseeably play critical roles. For example, IFC models have already been used in researching and developing indoor robotic navigation algorithms [36] [37]. IFC models have also been proposed to guide the use of robotic systems to automatically construct different types of structures such as concrete structure [38], masonry structure and prefabricated steel structure [39].

Due to the importance of geometric information representation in IFC, it is desirable to incorporate its introduction to modern AEC curriculum. In fact, in the first author's graduate level class titled "automation in construction management," a 3-hour lecture is designated to the introduction of BIM with a focus on IFC. There are also homework assignments, quizzes, and exams to enforce students' learning. However, such a devotion of time and efforts is not practical for all learners, especially for casual learners who just need to grasp a basic understanding of IFC data without too much detail. Unfortunately, IFC data was not designed this way. For example, Figure 4 shows partial data instances of an IFC file that represents a cone frustum-shaped bridge pier. All entity instances in Figure 4 except for the last one are representing Cartesian points, and the last entity instance is representing a poly loop that is defined using all the shown Cartesian points that are above it. It is not intuitively clear how these Cartesian points form the poly loop and it is not clear either where the poly loop fits in the cone frustum shape, even if a visualization of the cone frustum shape is given (Figure 5).

3 Proposed Method

To help casual learners grasp how Cartesian points were used to form and represent a 3D shape in IFC data, the authors propose a new interactive visualization method based on game simulation. Such method is also useful for serious learners to quickly grasp the idea before they go deeper in learning the details.

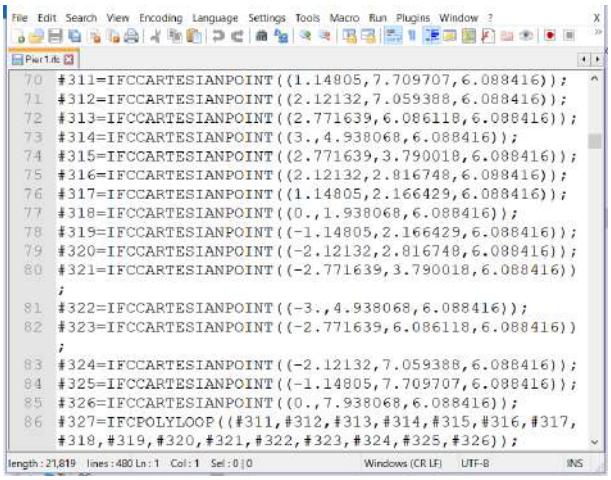

Figure 4. Cartesian points data from the geometric representation of a cone frustum shape in IFC

Figure 5. Visualization of a cone frustum shape

As shown in Figure 6, the proposed method uses an elemental cube to represent a Cartesian point and a colored line to represent a relation between one Cartesian point and another. In the time dimension, the Cartesian points and their connected relations are visualized one by one, following a sequence dictated by the order of these Cartesian points in the original structured IFC data instance file. This visualization can be observed from a first-person view, a third-person view, or any arbitrary angle of view as defined. The view can also be changed in real-time based on learners' preferences.

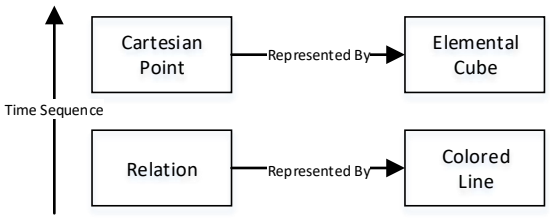

Figure 6. Proposed Cartesian point visualization method

4 Preliminary Experimental Testing

To test the effectiveness of the proposed method, a preliminary experiment was conducted by implementing the game simulation-based visualization of the cone frustum-shaped bridge pier object shown in Figure 5. The Cartesian points that represent the geometric information of the cone frustum shape were extracted manually from the source IFC instance file. The Unity3D game engine was used to implement the visualization based on the proposed method. The background was set to be an arbitrary white ground and a default blue sky. The visualization was created following a first-person view that can be adjusted in real-time based on the position and head orientation of the virtual observer. Figure 7 to Figure 10 show snapshots of the visualization during different stages of the game simulation, namely, the first Cartesian point, the first poly loop, side faces, and the completed shape. It can be seen that the virtual observer was observing from different angles of view in these snapshots.

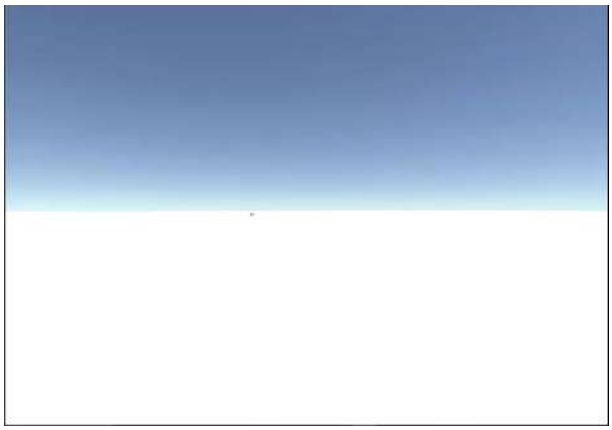

Figure 7. Visualization of the first Cartesian point in a cone frustum shape

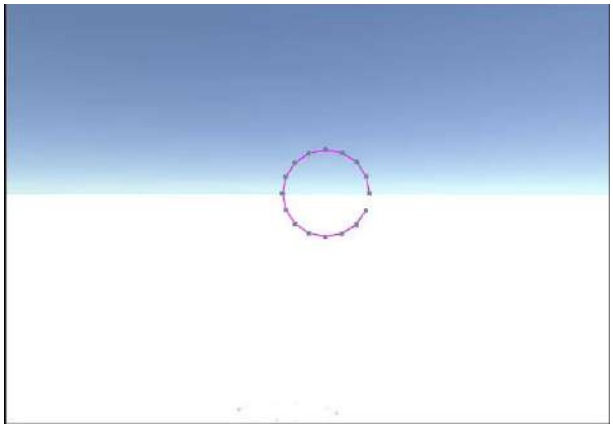

Figure 8. Visualization of the first poly loop in a cone frustum shape

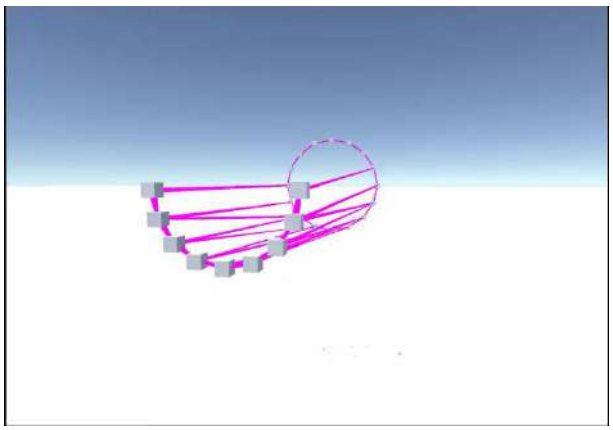

Figure 9. Visualization of side faces formed by Cartesian points in a cone frustum shape

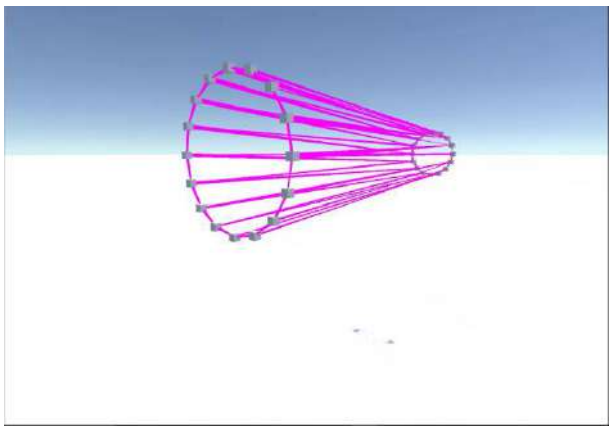

Figure 10. Visualization of the complete cone frustum shape formed by Cartesian points

The implemented visualization was tested by 14 graduate students at Purdue University and University of

Florida, who all have some research experience in BIM (Table 1). The game simulation was given to the participants together with and in comparison with an explanation material based on IFC specifications. Half of the students were asked to start with the game-based simulation, and then move to the written explanation material; the other half of the students were asked to start with the written explanation material, and then move to the game-based simulation to reduce the effect of multiple-treatment interference with the results. The explanation material included: (1) an explanation of the goal, (2) visualization of the cone frustum shape (Figure 5), (3) geometric representation of the cone frustum shape in raw IFC data (Figure 2; Figure 4), and (4) official explanations of the entities by buildingSMART.

Table 1. Participants' information

BIM research experience	Number of Participants
1 Year or Less	4
1-2 Years	4
2-3 Years	2
3 Years and above	4

5 Experimental Results and Discussion

The experimental results were shown in Table 2. The scale levels are: 1-Very difficult, 2-Difficult, 3-Neutral, 4-Easy, 5-Very easy. The maximum score, minimum score, and mean score for the easiness of understanding of the written explanation material were 3, 1, and 1.79, respectively. The maximum score, minimum score, and mean score for the easiness of understanding of the game simulation-based visualization were 5, 3, and 4.00, respectively. The game simulation-based visualization was much easier to understand than the written explanation material and the difference was significant at 99.9% confidence level based on paired t-test. The time taken to understand the written explanation material had a maximum, minimum, and mean values of 1,680(s), 225(s), and 545.89(s), respectively. The time taken to understand the game simulation-based visualization had a maximum, minimum, and mean values of 480(s), 80(s), and 130.37(s), respectively. It took much less time to understand the game simulation-based visualization than that in understanding the written explanation material and the difference was significant at 99.9% confidence level.

Some comments received during the test were: (1) the written explanation material was difficult to understand because of the needed background knowledge, (2) a slower speed in the visualization would make it easier to follow and understand, (3) the explanation material could be used to complement the visualization, and (4) adding audio to the visualization would make learners' understanding even easier.

Table 2. Easiness of understanding results

	Explanation material			Game simulation-based visualization		
	min	mean	max	min	mean	max
Easiness of understanding	1	1.79	3	3	4.00	5
Time taken to understand (*s*)	225	545.89	1,680	80	130.37	480

6 Conclusion

With the fast development and adoption of building information modeling (BIM), the demand in learning industry foundation classes (IFC) data – the ISO registered data standard of BIM, is increasing. In this paper, the authors proposed the use of a new method to help people learn the formation of geometric representations using Cartesian points in IFC data. The new method is based on game simulation technology and visualizing the Cartesian points and relations between the points in sequence. The new method was evaluated in a preliminary test where a cone frustum-shaped bridge component represented in IFC was presented using the method to 14 test participants. At the same time a written explanation of the same knowledge was provided to the participants. Collected results showed that the game simulation-based visualization was significantly easier to understand and took significantly less time to understand comparing to reading the explanation material.

7 Contributions to the Body of Knowledge

This paper contributes to the body of knowledge in that it is the first time that game simulation in first person view was used to help with understanding of geometric representation of IFC data with a focus on Cartesian points and the comparative effects were tested with respect to a written explanation material in a quantitative manner.

8 Limitations and Future Work

Two main limitations are acknowledged. In spite of the novelty of the proposed method, the test was only conducted on one shape and with a limited set of participants. More testing on more shapes and participants are needed to make the results more robust. The test was only conducted on first-person view, how other angles of views affect the understanding need to be further explored. In future work, the authors plan to extend the test to cover more shapes, more participants, and more angles of views.

9 Acknowledgements

The authors would like to thank the National Science Foundation (NSF). This material is based on work supported by the NSF under Grant No. 1745374. Any opinions, findings, and conclusions or recommendations expressed in this material are those of the author and do not necessarily reflect the views of the NSF.

References

[1] General Service Administration (GSA). BIM guide overview. GSA BIM Guide Series 01. Online: http://www.gsa.gov/portal/getMediaData?mediaId=226771, Accessed: 31/12/2018.

[2] National Institute of Building Sciences (NIBS). National BIM standard-United States. Online: https://buildinginformationmanagement.files.wordpress.com/2011/06/nbimsv1_p1.pdf, Accessed: 31/12/2018.

[3] Kreider, R., Messner, J. and Dubler, C. Determining the frequency and impact of applying BIM for different purposes on projects. In *Innovation in AEC Conference*, pages 1-10, University Park, Pennsylvania, U.S.A., 2010.

[4] McGraw-Hill Construction. The business value of BIM for construction in major global markets: How contractors around the world are driving innovation with Building Information Modeling. Online: https://www.academia.edu/11605146/The_Business_Value_of_BIM_for_Construction_in_Major_Global_Markets_How_Contractors_Around_the_World_Are_Driving_Innovation_With_Building_Information_Modeling, Accessed: 31/12/2018.

[5] Institute of Electrical and Electronics Engineers (IEEE). *IEEE standard computer dictionary: a compilation of IEEE standard computer glossaries.* Institute of Electrical and Electronics Engineers, New York, U.S.A., 1990.

[6] Aldegeily, M., Zhang, J., Hu, Y. and Shao, X. From architectural design to structural analysis: a data-driven approach to study building information modeling (BIM) interoperability." In *Proceedings of 54th ASC Annual International Conference*, pages 537-545, Minneapolis, MN, USA. 2018.

[7] Ren, R., Zhang, J. and Dib, H.N. BIM interoperability for structural analysis. In *Proceedings of ASCE Construction Research Congress 2018*, pages 470-479, New Orleans, LA, USA. 2018.

[8] Gallaher, M.P., O'connor, A.C., Dettbarn JR., J.L. and Gilday, L.T. *Cost analysis of inadequate interoperability in the U.S. capital facilities industry*. NIST Publication GCR 04-867. NIST, Gaithersburg, MD, U.S.A., 2004.

[9] Isikdag, U., Aouad, G., Underwood, J. and Wu, S. Building information models: a review on storage and exchange mechanisms. In *Proceedings of 24th W78 Conf. & 5th ITCEDU Workshop & 14th EG-ICE Workshop, Bringing ITC Knowledge to Work*, pages 135-144, Maribor, Slovenia, 2007.

[10] Eastman, C. and Wang, Frank. Comparison of steel detailing neutral format (SDNF) and CIMsteel Version 2 (CIS/2). In *Proceedings of Structures Congress 2004*, pages 1-8, Nashville, Tennessee, USA. 2004.

[11] Laud, A. Interoperability between IFC's (ISO 16739) and ISO 15926. Online: http://iringtoday.com/wordpress/wp-content/uploads/2012/01/IFCs-and-ISO-15926.pdf, Accessed: 31/12/2018.

[12] O'Brien, W.J., Sankaran, B., Leite, F.L., Khwaja, N., Palma, I.D.S., Goodrum, P., Molenaar, K., Nevett, G. and Johnson, J. *NCHRP Research Report 831: Civil integrated management (CIM) for departments of transportation*, Volume 2. Transportation Research Board, Washington, DC, USA, 2016.

[13] Cheng, J.C.P., Deng, Y., Das, M. and Anumba, C. Evaluation of IFC4 for the GIS and green building domains. In *Proceedings of Computing in Civil and Building Engineering*, pages 2216-2223, Orlando, Florida, USA, 2014.

[14] East, E.W. Common building information model files and tools. Online: http://www.nibs.org/?page=bsa_commonbimfiles&hhSearchTerms=%22common+and+BIM+and+file%22, Accessed: 1/1/2019.

[15] Zhang, J. Towards systematic understanding of geometric representations in BIM standard: an empirical data-driven approach. In *Proceedings of ASCE Construction Research Congress*, pages 96-105, New Orleans, LA, USA, 2018.

[16] Prensky, M. The Motivation of gameplay or, the REAL 21st century learning revolution. Online: http://www.marcprensky.com/writing/Prensky%20-%20The%20Motivation%20of%20Gameplay-OTH%2010-1.pdf, Accessed: 1/1/2019.

[17] Nikolic, D. *Evaluating a simulation game in construction engineering education: The Virtual Construction Simulator 3*. Ph.D. Dissertation, The Pennsylvania State University, University Park, Pennsylvania, USA, 2011.

[18] Buck, W. A competitive business ethics simulation game. *Developments in Business Simulation and Experiential Learning*, 42:155-163, 2015.

[19] Dib, H., Adamo-Villani, N. and Issa, R. A GIS-based integrated information model to improve building construction management: design and initial evaluation. In Proceedings of CONVR 2011, pages 769-781, Weimar, Germany, 2011

[20] Yan, W., Culp, C. and Graf, R. Integrating BIM and gaming for real-time interactive architectural visualization. *Automation in Construction*, 20(2011): 446-458, 2011.

[21] Heydarian, A., Carneiro, J., Gerber, D., Becerik-Gerber, B., Hayes, T. and Wood, W. (2015). Immersive virtual environments versus physical built environments: A benchmarking study for building design and user-built environment explorations. *Automation in Construction*, 54(2015):116-126, 2015.

[22] Alghamdi, A., Sulaiman, M., Alghamdi, A., Alhosan, M., Mastali, M. and Zhang, J. Building accessibility code compliance verification using game simulations in virtual reality. In *Proceedings of 2017 ASCE Intl. Workshop on Comput. in Civ. Eng.*, pages 262-270, Seattle, WA, USA, 2017.

[23] Shen, Z., Jiang, L., Grosskopf, K. and Berryman, C. Creating 3D web-based game environment using BIM models for virtual on-site visiting of building HVAC systems. *In Proceedings of Construction Research Congress 2012*, West Lafayette, IN, USA, 2012.

[24] Shi, Y., Du, J., Lavy, S. and Zhao, D. A multiuser shared virtual environment for facility management. *Procedia Engineering*, 145 (2016):120–127, 2016.

[25] Bucarelli, N., Zhang, J. and Wang, C. Maintainability assessment of light design using game simulation, virtual reality and brain sensing technologies. In *Proceedings of ASCE Construction Research Congress*, pages 378-387, New Orleans, LA, USA, 2018.

[26] Aldafaay, M., Zhang, J. and Oh, J. Visualizing the constructability of a steel structure using building information modeling and game simulation. In *Proceedings of International Conference on Maintenance and Rehabilitation of Constructed Infrastructure Facilities (2017 MAIREINFRA)*, Seoul, South Korea, 2017.

[27] Mastali, M. and Zhang, J. Interactive highway construction simulation using game engine and virtual reality for education and training purpose. In *Proceedings of 2017 ASCE Intl. Workshop on Comput. in Civ. Eng.*, pages 399-406, Seattle, WA, USA, 2017.

[28] Yu, Y., Zhang, J. and Guo, H. (2017). Investigation of the relationship between construction workers' psychological states and their unsafe behaviors using virtual environment-based testing. In *Proceedings of 2017 ASCE Intl. Workshop on Comput. in Civ. Eng.*, pages 417-424, Seattle, WA, USA, 2017

[29] BuildingSMART. IFC overview summary. Online: http://www.buildingsmart-tech.org/specifications/ifc-overview/ifc-overview-summary, Accessed: 12/01/2019.

[30] Geiger, A., Benner J. and Haefele, K.H. *Generalization of 3D IFC building models*. M. Breunig et al. (eds.), 3D Geoinformation Science, Lecture Notes in Geoinformation and Cartography, 19-35, Springer International Publishing, Switzerland, 2015.

[31] BuildingSMART. IfcShapeRepresentation. Online: http://www.buildingsmart-tech.org/ifc/IFC2x3/TC1/html/ifcrepresentationresource/lexical/ifcshaperepresentation.htm, Accessed: (Aug. 1, 2017).

[32] Akinci, B. and Boukamp, F. Representation and integration of as-built information to IFC based product and process models for automated assessment of as-built conditions. In *Proceedings of the 19th ISARC*, pages 543-548, Washington, U.S.A, 2002.

[33] Atasoy, G., Tang, P., Zhang, J. and Akinci, B. Visualizing laser scanner data for bridge inspection. In Proceedings of 27th ISARC, pages 390-399, Bratislava, Slovakia, 2010.

[34] Yang, J., Park, M.W., Vela, P.A. and Golparvar-Fard, M. Construction performance monitoring via still images, time-lapse photos, and video streams: Now, tomorrow, and the future. *Advanced Engineering Informatics*, 29(2015): 211-224, 2015.

[35] Golparvar-Fard, M., Peña-Mora, F. and Savarese, S. (2015). Automated progress monitoring using unordered daily construction photographs and ifc-based building information models. *Journal of Computing in Civil Engineering*, 29(1): 04014025, 2015.

[36] Lin, Y., Liu, Y., Gao, G., Han, X., Lai, C.Y. and Gu, M. The IFC-based path planning for 3D indoor spaces. *Advanced Engineering Informatics*, 27(2): 189-205, 2013.

[37] Taneja, S., Akinci, B., Garrett, J.H. and Soibelman, L. Transforming IFC-based building layout information into a geometric topology network for indoor navigation assistance. In *Proceedings of International Workshop on Computing in Civil Engineering 2011*, pages 315-322, Miami, Florida, U.S.A., 2001.

[38] Davtalab, O., Kazemian, A. and Khoshnevis, B. Perspectives on a BIM-integrated software platform for robotic construction through contour crafting. *Automation in Construction*, 89(2018):13-23, 2018.

[39] Tibaut, A., Rebolj, D. and Perc, M.N. Interoperability requirements for automated manufacturing systems in construction. *Journal of Intelligent Manufacturing*, 27(1): 251-262, 2016. Jqbmgx

The Benefits of and Barriers to BIM Adoption in Canada

Y. Cao[a], L. H. Zhang[a], B. McCabe[a], and A. Shahi[a]

[a]Department of Civil and Mineral Engineering, University of Toronto, Canada
E-mail: ayuan.cao@mail.utoronto.ca, lihao.zhang@mail.utoronto.ca, brenda.mccabe@utoronto.ca, arash.shahi@utoronto.ca

Abstract –

The adoption of Building Information Modelling (BIM) has influenced the traditional methods of planning, design, construction and operation of a physical asset. Organizations in Canada have adopted BIM to improve designs, foster stakeholder collaboration, and facilitate construction processes. To understand the extent of BIM adoption and implementation in the industry, the University of Toronto Building Tall Research Centre conducted two annual BIM surveys. The 2018 survey, which was conducted in collaboration with tBIMc, focused on the Greater Toronto Area. In 2019, the survey was expanded nation-wide with support from Canada BIM Council, BuildingSMART Canada, and local BIM chapters. In this paper, the results of the 2019 nation-wide survey are presented and benchmarked against those in the 2018 survey. An in-depth discussion of the perceived benefits of and barriers to adopting BIM in Canada are also provided. This study serves as one of the milestones of the BIM transition process in Canada and aims to present a detailed view of the role that BIM plays in the future of the industry.

Keywords –

Building Information Modelling; BIM; survey; benefits; barriers; benchmark;

1 Introduction

In the past decades, the construction sector has been seeking alternatives to enhance efficiency during project design, planning and construction phases from the traditional project delivery [1]. As a result, Building Information Modelling (BIM) is gaining interest in the building industry. BIM can be defined as the process of creating, managing and utilizing the shared digital representation of physical and functional aspects of any built asset by project stakeholders [2]. BIM can be a reliable basis for decision-making throughout the lifecycle of the asset [2].

Recognizing the prominent values of BIM, the implementation and uptake of BIM around the world have gained great momentum over the last decade. Leading countries have developed specific strategies and mandatory requirements for BIM adoption. An overview of global BIM implementations in terms of degree of regulatory mandate over the past 5 years is illustrated in Figure 1, where the size of the circle that represents each country is proportional to its population.

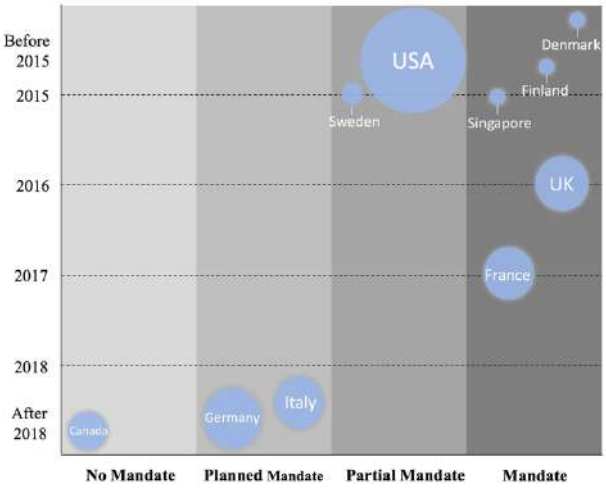

Figure 1. Global BIM Implementation Overview

Denmark was one of the earliest adopters of BIM in the world. They first mandated BIM for public projects in 2007 and extended the requirement to all projects in 2011 [3]. Similarly, Finland, Singapore, United Kingdom (UK) and France successfully mandated the full deployment of BIM in 2012, 2015, 2016 and 2017 respectively [3]. United States of America (USA) and Sweden represent partial BIM mandates, where BIM use was mandated only in certain regions and by specific government authorities [4]. Italy and Germany have specified plans to mandate BIM in 2019 and 2020, respectively [3].

In comparison to the aforementioned countries, Canada has neither an in-place BIM mandate nor clear national plans to implement BIM, and appears to be lagging behind the global trend of BIM adoption [5]. To better understand the extent of BIM adoption and implementation in the Canadian architecture,

engineering, and construction (AEC) industries as well as the issues in the current BIM adoption, the Second Annual BIM Survey was conducted in 2019 as a continuation of the First Annual BIM Survey in 2018 [6,7]. In collaboration with Canada BIM Council, BuildingSMART Canada, and local BIM chapters, the survey was disseminated across Canada and over 300 respondents participated this year. In this study, major findings obtained from the Second Annual BIM Survey are presented, along with benchmark analyses for the 2018 survey. The contribution of this study is to provide a holistic perspective of the adoption and implementation of BIM in Canada, with emphasis on the perceived benefits and barriers in the AEC industry.

2 Benefits of and Barriers to BIM Adoption

Compared to traditional project delivery methods, BIM brings many benefits and opportunities in the various project phases, namely, project design, construction and operation [1]. Major benefits identified in the project design phase include clash detection, enhanced visualization, cost estimation, design simulation, and automated code compliance checking [8,9,10]. During construction, BIM facilitates scheduling, activity sequencing, progress tracking, site safety assessment, and site logistics planning [11,12]. For the project operation phase, facility managers benefit from the information stored in the BIM database when performing space planning, facility maintenance, and refurbishment [13,14]. Finally, improved collaborations among stakeholders throughout the project life cycle can be achieved by adopting BIM [15,16,17].

Despite the numerous benefits and opportunities of BIM implementation, barriers and challenges were identified in previous research, which can be categorized into five major aspects, including technical, legal, cultural, financial and managerial [18]. Regarding BIM technologies, pertinent technical problems such as software compatibility were still unsolved. Some of the legal issues that hinder the adoption of BIM include stakeholders' liabilities on the accuracy and quality of data embedded in BIM models [5]; lack of regulations or guidelines on resolving any dispute that might arise due to BIM implementation [18]; intellectual property rights issues such as model ownership, copyright and authorization of model usage [19]. Cultural issues associated with BIM adoption that are most frequently mentioned by researchers include resistance to change and inadequate coordination among project stakeholders [18]. Financial barriers refer to the high initial investment in BIM technology [20], and the uncertain rate of return on investment [21]. Managerial barriers mainly come from the lack of confidence in BIM by management in an organization due to significant changes required in design phase workflow, project delivery methods [22], as well as software and hardware [23].

Successful implementation of BIM requires users to understand the values and issues associated with the technology, such that benefits can be reaped, and barriers can be eliminated. In addition, support and guidance from government bodies and related organizations would further speed up the adoption process [18].

3 BIM Surveys

To understand the status quo, barriers, and trends of BIM adoption in the AEC industry, several countries and organizations have conducted BIM surveys over the last decade.

3.1 Global BIM Surveys

In 2011, UK published its First National BIM Survey for understanding BIM adoption and implementation in the country. The National Building Specification (NBS), in collaboration with the Royal Institute of British Architects and the UK BIM Task Force, has been the main driving force for designing, collecting, and analyzing the surveys. Eight national reports have been published by NBS. The style and design of the UK national surveys questions were varied and adjusted throughout the years. For instance, the 2011 and 2012 national survey comprised a comprehensive list of questions, but the result analyses were relatively simple and straight-forward [24,25]. From 2013 onwards, the questions were categorized into sections, namely, BIM Experience, BIM and Government, as well as Attitudes toward BIM. In addition, more in-depth analyses and discussions on the survey results were included [26]. Simple comparisons with previous years' results were provided in the 2014, 2015 and 2016 BIM reports, and trends were identified [27,28,29]. Due to the launch of the UK's national BIM mandate in 2016, the main focus of the 2017 survey was shifted to examine the organizational engagement level of BIM implementation in the industry [30]. The latest 2018 NBS survey was similar to the previous one, with the emphasis on understanding the effect of government mandates and associated strategies [31].

In addition to the national BIM reports, NBS conducted two international BIM surveys in 2013 and 2016. Along with UK and Canada, New Zealand and Finland participated in the 2013 international survey while Denmark, Japan, and Czech Republic took part in 2016. There were only 78 and 127 respondents from Canada in the 2013 and 2016 international BIM surveys. The structure and design of the surveys were similar to the national surveys but significantly fewer questions were included in the international ones. Only common

and applicable questions were selected, and benchmark analyses among participating countries were presented in the two international BIM reports [32,33].

3.2 Local BIM Survey

In 2017-18, and in collaboration with the Toronto BIM Community (tBIMc), researchers from the University of Toronto Building Tall Research Centre conducted the First Annual BIM Survey to analyze BIM adoption in the Greater Toronto Area (GTA). Questions in the UK survey were adopted to facilitate benchmark analyses [7]. More than 250 respondents participated in the survey and a complete report of the key findings from the first annual survey was published in April of 2018 [6,7]. This survey serves as the baseline for BIM implementation in the Canadian market. As a pilot study, the first BIM survey was well-received by industry professionals and the results provided useful benchmarking indicators for future studies.

4 Second Annual BIM Survey

The Second Annual BIM Survey was a continuation effort. The goal of the 2019 survey was to collect a comprehensive understanding of BIM implementation from coast to coast in Canada.

The majority of questions for the Second Annual BIM Survey were adopted from the first survey with a few additional questions related to BIM application across Canada. An overview of the survey questions is presented in Table 1. Many of these questions had subsections, resulting in over 100 individual questions. The survey was structured into three sections: General Information, BIM Experience, and, Resources and Future of BIM. The demographics, background, and company information of the respondents were collected in section 1. Then, participants were asked to share their BIM experiences, such as the level of familiarity with BIM technology, the functionality of BIM, and perceived benefits and barriers for adopting BIM in project workflow. Finally, insights and opinions on BIM resources and the future trend of the construction industry were gathered in the last section.

Table 1. Overview of Survey Questions

Section 1: General Information
1. Which of these better explains your main role?
2. Years you been working in your discipline?
3. What is your age?
4. In what province is the office you primarily work?
5. In what city are you currently working?
6. How would you describe your organization type?
7. How many employees are there in your organization?
8. Where is your organization doing most work?
9. Which project types have you participated last year?
10. How familiar are you with BIM?
11. Which statements best describes your organization?
Section 2: BIM Experience
12. Ever involved in the following projects last year?
13. Level of confidence in BIM knowledge and skills?
14. What is your opinion on BIM-related beliefs?
15. Have you ever adopted BIM for projects?
16. What % of projects have you used BIM last year?
17. Number of parties you share BIM with per project?
18. What are your thoughts on Open BIM?
19. Which tools did you mainly use last year?
20. What do you use BIM for?
21. What are the main barriers to using BIM?
22. What is your opinion on the BIM benefits below?
Section 3: Resources and Future of BIM
23. Which sources of BIM information will you use?
24. Which Canadian BIM resources are you aware of?
25. How likely are the technologies to have significant influence on the industry over the next 10 years?

The Second Annual BIM Survey was first opened in October 2018 at a Toronto BIM Community event and closed in late February of 2019. The survey was promoted via social media channels and online platforms. It was also distributed through CANBIM and buildingSMART networks, Canada's two national BIM organizations. To further increase the number of participants for the survey, quick response (QR) cards that linked to the online survey were disseminated to AEC professionals across Canada. As Canada is bilingual, the survey was offered in both French and English.

5 Results and Discussions

In this section, an overview of the survey demographics will first be presented. The perceived benefits and barriers are identified from the survey and discussed in detail. Benchmarking analyses of the 2019 survey against the 2018 survey is also presented.

5.1 Demographics

The demographics of respondents for the Second Annual BIM Survey are shown in Figure 2. Of the 398 responses received, more than half (64%) are from Ontario (ON), perhaps because the survey was first launched and promoted in Ontario. Also, the BIM community in the Greater Toronto Area is very active

compared to other metropolitan centres in Canada. Response rates from Alberta (AB), British Columbia (BC), Quebec (QC) and outside of Canada are at 15%, 8%, 5%, and 5% respectively. A few industry professionals from Nova Scotia, Manitoba and Saskatchewan participated in the survey. For the scope of this paper, only responses from the top four participating provinces, namely, ON, AB, BC, and QC are included in the following discussions.

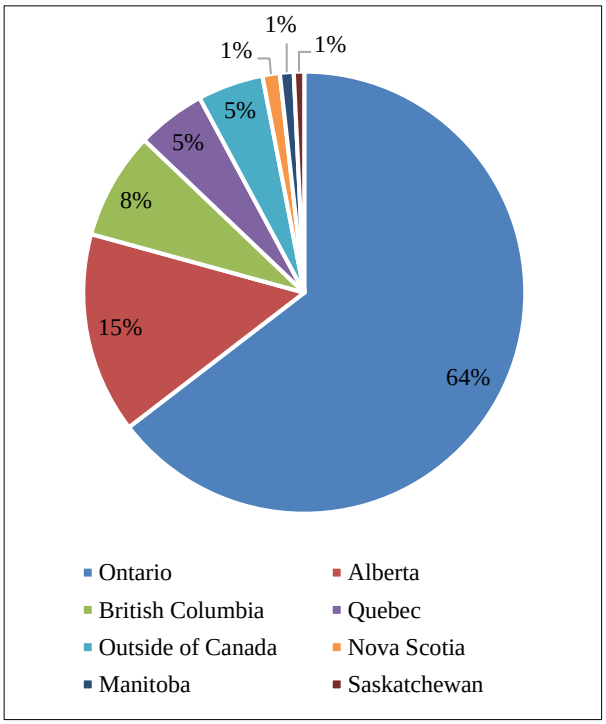

Figure 2. Demographics of 2019 Survey

5.2 Perceived Benefits of BIM Adoption

Question 22 focused on the perceived benefits of using BIM, where respondents were asked to agree or disagree with the statement that adopting BIM can:

- BN1: Improve visualization
- BN2: Bring cost efficiency
- BN3: Enable international collaboration
- BN4: Increase profitability
- BN5: Increase speed of delivery
- BN6: Enable new types of project

Figure 3 indicates over 80% of respondents agree that adopting BIM can bring visualization benefits (BN1). Second to visualization is the cost efficiency (BN2) that BIM can potentially provide in a project, especially if BIM is implemented with the support of all project stakeholders. The benefits from BN3 to BN6 also received over 50% agreement, whereby respondents generally agree with the perceived benefits of BIM.

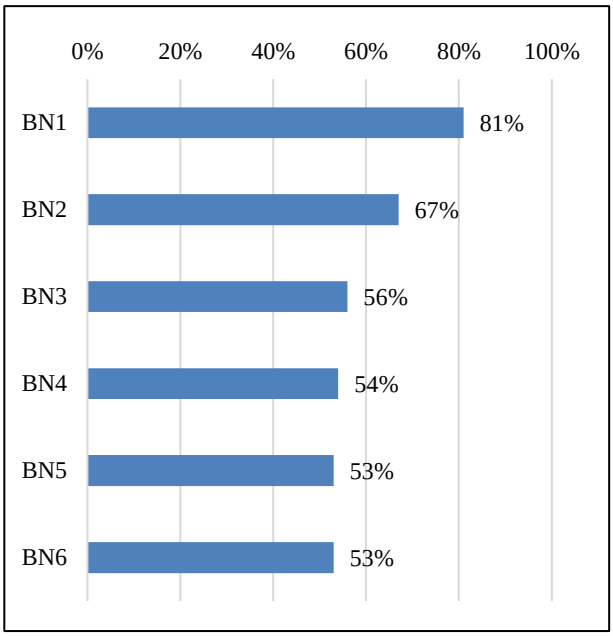

Figure 3. Overall Perceived Benefits of Respondents

Based on the demographics of respondents, Analysis of Variance (ANOVA) was adopted to analyze the differences among the four provinces with the $p<0.05$ threshold for rejecting the null hypothesis. ”Strongly Agree” and “Agree” were coded as “1” and “Unsure”, “Disagree” and “Strongly Disagree” were coded as “0”. Table 1 shows the P-values that were output when ANOVA tests were run for the six perceived benefits. All benefits (BN1-BN6) have P-values over 0.05, which means that there was no statistically significant difference towards the perception of the six BIM benefits among the four provinces. This shows a positive sign for the industry as the various benefits of BIM adoption are consistently perceived by different regions across Canada.

Table 1. P-Values for the Six Benefits

	BN1	BN2	BN3	BN4	BN5	BN6
P	0.447	0.673	0.766	0.594	0.792	0.680

5.2.1 Comparison of 2018 and 2019 Perceived Benefits in GTA Only

BIM users and non-users were identified in both years: BIM users are those who have used or currently use BIM on projects, and non-users are those who have basic BIM knowledge but do not use BIM on a regular basis [7]. Responses from the GTA region in 2019 were compared

to respondents in 2018, across the six identified benefits as shown in Figure 4. Comparison of 2018 and 2019 GTA Surveys, users have stronger beliefs than non-users such that users' experience provides better insights into the perceived benefits for adopting BIM in projects, workflow, and industry. Three benefits (BN1, BN2, and BN4) are well-perceived (over 80% agreement) by BIM users in both 2018 and 2019 surveys. Non-users generally have an increase in beliefs in the perceived benefits, except for visualization (BN2). However, the slight drop in visualization is not significant. The general increase in understanding for BIM benefits for users and non-users shows promising results for the future of the AEC industry.

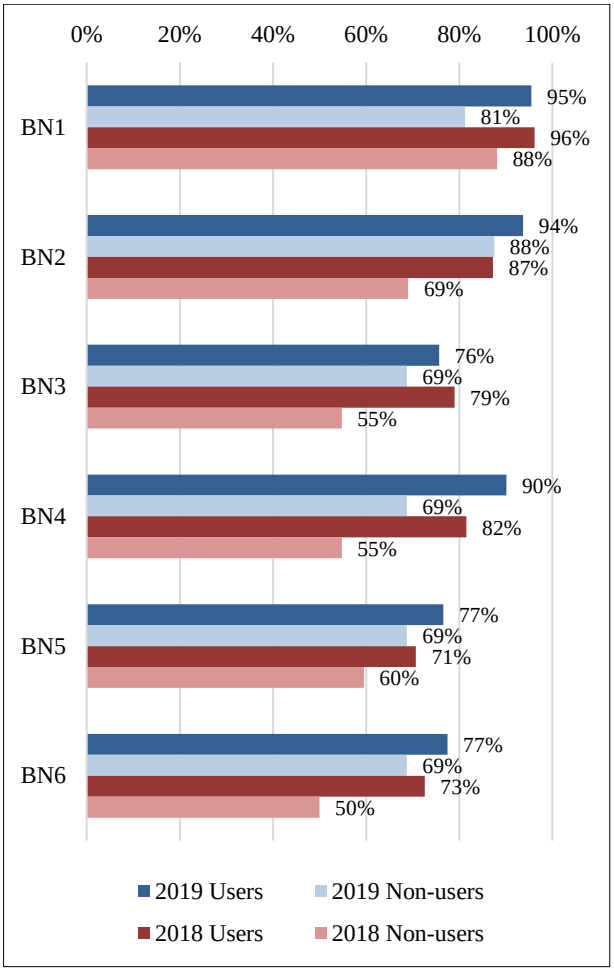

Figure 4. Comparison of 2018 and 2019 GTA Surveys

5.3 Perceived Barriers to BIM Adoption

Question 21 examined the barriers to BIM adoption. Respondents were asked to select the barriers they encountered from a list:

- BR1: Resistance to change
- BR2: Lack of knowledge/skill
- BR3: Software learning curves
- BR4: Lack of training
- BR5: Lack of mandate
- BR6: No client demand
- BR7: Lack of collaboration/cooperation
- BR8: Legal issues
- BR9: Doubts on return on investment
- BR10: Lack of perceived benefits

Based on the responses, top barriers to BIM adoption in ON, AB, BC, and QC are presented in Figure 5. Resistance to change (BR1) is the number one barrier throughout four provinces, which might imply that the local construction industry is ready for BIM implementation but there are still a lot of people refusing to embrace the technology. Lack of knowledge/skill (BR2) is another common barrier identified to BIM adoption. It was interesting to see that this barrier is more prominent in BC and QC comparing to AB and ON. In terms of software learning curves (BR3) and lack of training (BR4), the responses from BC, AB, and QC are rather close at around 50%. The results from ON for BN3-BN5 were significantly lower than the rest provinces, which might indicate that there are comparatively more software training opportunities available and more support from public authorities towards BIM adoption in Ontario.

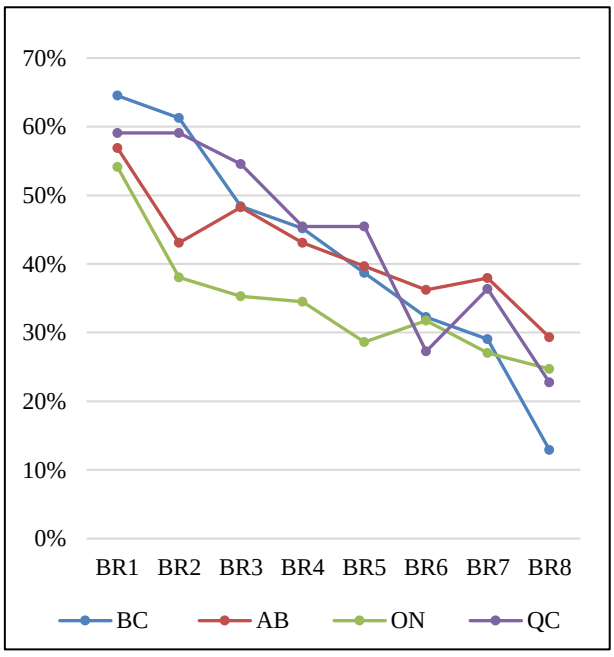

Figure 5. Comparison of Perceived Barriers in ON, AB, BC, and QC

In addition, around 30% of respondents agreed on the barriers of lack of client demand (BR6) and lack of collaboration/ cooperation (BR7). This indicates that joint efforts from the government, project stakeholders and clients are important but not crucial to ensuring BIM adoption. Lastly, legal issues (BR8), including ownership, liability, and licensing, are considered as a greater barrier in AB, ON and QC compared to BC.

5.3.1 Comparison of 2018 and 2019 Perceived Barriers in GTA Only

Top barriers to BIM adoption in GTA are presented in Figure 6. Comparing the barriers identified in 2018 and 2019, a growing trend in BIM adoption can be identified in the GTA region. In 2019, significantly more respondents are able to see the benefits of BIM and fewer are having doubts on the Return on Investment (ROI) of implementing BIM comparing to 2018. Even though a lack of mandate is perceived to be less of a barrier in 2019, industry professionals are seeing more demand from clients (as indicated by the reduction in No Client Demand) and starting to develop their own BIM Execution Plan within their company. With wider BIM implementation in the GTA region this year, barriers including lack of training, software learning curves and resistance to change are becoming more prominent.

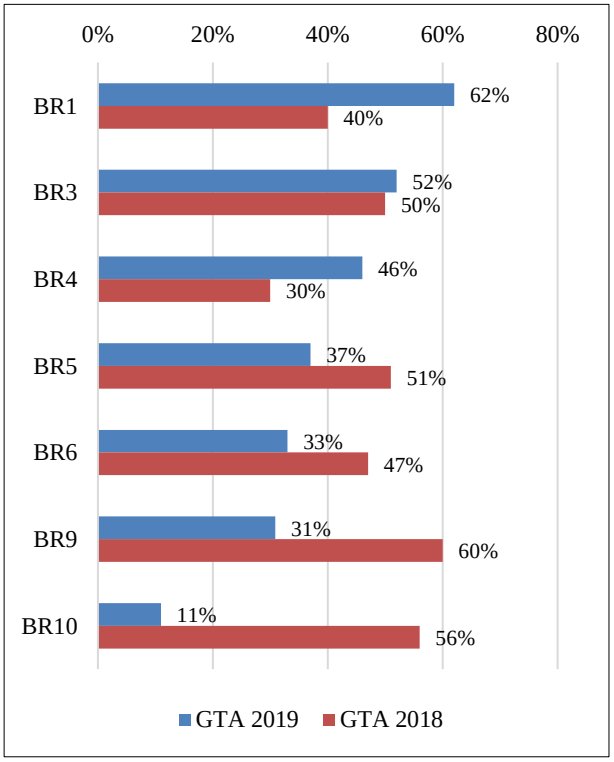

Figure 6. Comparison of 2018 and 2019 GTA Surveys

6 Conclusion and Future Work

Understanding the local and national barriers to innovation and new technologies can help streamline the adoption process. This paper first reviewed the global status of BIM implementation, worldwide initiatives on BIM surveys as well as some of the potential benefits and barriers in BIM adoption in literature reviews. Local BIM survey initiatives including the First Annual BIM Survey in GTA and the Second Annual BIM Survey in Canada were introduced in detail. The goal of the surveys was to capture and document the adoption status of BIM in the Canadian AEC industry.

In this paper, special attention was paid to the perceived benefits and barriers to BIM implementations. The complete survey results and analysis for the Second Annual BIM Survey will be published online at the Building Tall Research Centre (buildingtall.utoronto.ca) and tBIMc (tbimc.ca) websites. This BIM survey initiative will be repeated on an annual basis in the future to identify and monitor the trend of the BIM adoption in Canada, which serves as a milestone in the BIM transition process in the Canadian AEC industry.

Acknowledgement

The authors gratefully acknowledge the support of the National Science and Engineering Council of Canada (NSERC) Grant, the Residential Construction Council of Ontario (RESCON) and Qoo Studios grant CRDPJ 530550-18.

This work was undertaken through University of Toronto's Building Tall Research Centre.

References

[1] Volk R., Stengel J. and Schultmann F. Building Information Modeling (BIM) for existing buildings – Literature review and future needs. *Automation in construction, 38*: 109-127, 2014.

[2] British Standard Institution. Building Information Modelling – Information Delivery Manual: Methodology and Format. London, UK, 2016.

[3] McAuley B., Hore A. and West R. BICP Global BIM Study – Lessons for Ireland's BIM Programme. Construction IT Alliance Limited, 2017.

[4] Tahrani S., Poirier E. A., Aksenova G. and Forgues D. Structuring the adoption and implementation of BIM and integrated approaches to project delivery across the Canadian AECO industry: Key drivers from abroad. In *Proceedings of the Construction Specialty Conference of the Canadian Society for Civil Engineering*, pages 059:1-10, Vancouver, Canada, 2015.

[5] Smith P. BIM implementation – global strategies. *In*

Proceedings of the Creative Construction Conference, pages 482-492, 2014.

[6] McCabe B., Shahi A. and Zhang L. H. *1st Annual BIM Report 2018 for the Greater Toronto Area*. University of Toronto, Canada, 2018.

[7] Zhang L. H., McCabe B., Shahi A., Cozzitorto C and De Berardis P. Benchmarking Building Information Modelling in the Greater Toronto Area. In *Proceedings of the Canadian Society for Civil Engineering Annual Conference*, Fredericton, New Brunswick, 2018.

[8] Gu N. and London K. Understanding and facilitating BIM adoption in the AEC industry. *Automation in construction*, *19*(8): 988-999, 2010.

[9] Eastman C., Teicholz P., Sacks R. and Liston K. *BIM handbook: A Guide to Building Information Modeling for Owners, Managers, Designers, Engineers and Contractors*. John Wiley & Sons, New Jersey, 2011.

[10] Greenwood D., Lockley S., Malsane S. and Matthews J. Automated compliance checking using building information models. *In Proceedings of the Construction, Building and Real Estate Research Conference of the Royal Institution of Chartered Surveyors*, Paris, France, 2010.

[11] Bryde D., Broquetas M. and Volm J. M. The Project Benefits of Building Information Modelling (BIM*). International Journal of Project Management*, 31(7): 971-980, 2013.

[12] Grilo A. and Jardim-Goncalves R. Value Proposition on Interoperability of BIM and Collaborative Working Environments. *Automation in Construction*, 19(5): 522-530, 2010.

[13] Becerik-Gerber B., Jazizadeh F., Li N. and Calis G. Application Areas and Data Requirements for BIM-enabled Facilities Management. *Journal of Construction Engineering and Management*, 138(3): 431-442, 2011.

[14] Codinhoto R., & Kiviniemi A. BIM for FM: a Case Support for Business Life Cycle. In *Proceedings of the International Conference on Product Lifecycle Management*, pages 63-74, Berlin, Germany, 2014.

[15] Singh V., Gu N. and Wang X. A Theoretical Framework of a BIM-based Multi-disciplinary Collaboration Platform. *Automation in Construction*, *20*(2): 134-144, 2011.

[16] Shen W., Hao Q., Mak H., Neelamkavil J., Xie H., Dickinson J. and Xue H. Systems Integration and Collaboration in Architecture, Engineering, Construction, and Facilities Management: A Review. *Advanced engineering informatics*, *24*(2): 196-207, 2010.

[17] Shafiq M. T., Matthews J. and Lockley S. A study of BIM collaboration Requirements and Available Features in Existing Model Collaboration Systems. *Journal of Information Technology in Construction, 18*: 148-161, 2013.

[18] Sardroud J. M., Mehdizadehtavasani M., Khorramabadi A. and Ranjbardar A. Barrier Analysis to Effective Implementation of BIM in the Construction Industry. In *Proceedings of 35th International Symposium on Automation and Robotics in Construction.* Berlin, Germany, 2018.

[19] Ghaffarianhoseini A., Tookey J., Ghaffarianhoseini A., Naismith N., Azhar S., Efimova O. and Raahemifar K. Building Information Modelling (BIM) uptake: Clear benefits, understanding its implementation, risks and challenges. *Renewable and Sustainable Energy Reviews*, *75*: 1046-1053, 2017.

[20] Hardi J. and Pittard S. If BIM is the solution, what is the problem? A review of the benefits, challenges and key drivers in BIM implementation within the UK construction industry. *Journal of Building Survey, Appraisal & Valuation*, *3*(4): 366-373, 2015.

[21] Azhar S. Building information modeling (BIM): Trends, benefits, risks, and challenges for the AEC industry. *Leadership and management in engineering*, *11*(3): 241-252, 2011.

[22] Makelainen T., Hyvarinen J., Peura J. and Ronty J. Strategies, Guidelines and Project Level Leadership as Methods for BIM Practices in Transition. In *Proceedings of the 19th CIB World Building Congr*ess, Brisbane, Australia, 2013.

[23] Mihindu S. and Arayici Y. Digital construction through BIM systems will drive the re-engineering of construction business practices. In *Proceedings of the International Conference Visualisation*, page 29–34, London, UK, 2008.

[24] NBS. *National BIM Report 2011*. RIBA Enterprises, Newcastle, UK, 2011.

[25] NBS. *National BIM Report 2012*. RIBA Enterprises, Newcastle, UK, 2012.

[26] NBS. *National BIM Report 2013*. RIBA Enterprises, Newcastle, UK, 2013.

[27] NBS. *National BIM Report 2014*. RIBA Enterprises, Newcastle, UK, 2014.

[28] NBS. *National BIM Report 2015*. RIBA Enterprises, Newcastle, UK, 2015.

[29] NBS. *National BIM Report 2016*. RIBA Enterprises, Newcastle, UK, 2016.

[30] NBS. *National BIM Report 2017*. RIBA Enterprises, Newcastle, UK, 2017.

[31] NBS. *National BIM Report 2018*. RIBA Enterprises, Newcastle, UK, 2018.

[32] NBS. *International BIM Report 2013*. RIBA Enterprises, Newcastle, UK, 2013.

[33] NBS. *International BIM Report 2016*. RIBA Enterprises, Newcastle, UK, 2016.

On the Estimation of Resonance Frequencies of Hydraulically Actuated Systems

M. Pencelli [a], R. Villa [b], A. Argiolas [a], M. Niccolini [a], M. Ragaglia [a], P. Rocco [b], and A. M. Zanchettin [b]

[a] Yanmar Research and Development Europe, Viale Galileo 3/A, 50125, Firenze, Italy
[b] Politecnico di Milano, DEIB, Piazza L. Da Vinci 32, 20133, Milano, Italy.

E-mail: manuel_pencelli@yanmar.com, alfredo_argiolas@yanmar.com, matteo_ragaglia@yanmar.com, marta_niccolini@yanmar.com, renzo.villa@polimi.it, andreamaria.zanchettin@polimi.it, paolo.rocco@polimi.it

Abstract –

A common problem when operating heavy hydraulic machines consists in low-frequency resonance phenomena that significantly limit the bandwidth of the closed loop position control. The interest in this topic is further motivated by the fact that the usage of traditional dynamic models of hydraulic actuators usually leads to the identification of very high-frequency resonances. This paper tries to explain the origin of low-frequency resonances by analysing the kinematic coupling between hydraulic actuators and structural links that can be found in typical hydraulically actuated machines. A novel formula for the identification of such resonance frequencies is derived. A realistic simulation environment is used to identify the resonance frequencies corresponding to different load masses and link lengths. Finally, the identified frequencies are compared to the results obtained using the two formulas, showing the superior accuracy of the newly proposed approach with respect to the traditional one.

Keywords –

Hydraulic systems, Hydraulic actuators, Motion Control

1 Introduction

Hydraulic actuation systems are characterized by multiple convenient features (namely high power density, reliability, and relatively low maintenance cost) that make them particularly fit to several application domains. Not by chance these actuators are the most widespread in the construction and earthworks machinery sector [1,2], in the mining industry [3], and also in the agriculture and forestry field [4]. In spite of the aforementioned advantages, hydraulic actuators are typically affected by low-frequency resonance phenomena. In addition, these resonances are further exacerbated by the large masses and inertias typically characterizing the components of a hydraulically actuated machine. Unfortunately, these resonance phenomena significantly limit the performance and the overall bandwidth of any possible closed loop control systems [5]. In order to address this problem, several control strategies have been proposed, that aim at suppressing the oscillations caused by these resonances [6,7,8]. Machine design solutions have also been proposed. For instance, in [9] the authors increase the resonance frequency (thus minimizing the resulting oscillations) by properly sizing the hydraulic cylinders and by computing the optimal distribution of the inertias along the kinematic chain of the machine.

Even though a significant effort has been spent trying to limit the effects of these low-frequency resonances, very few research contributions focusing on the explanation of these phenomena can be found. Some contributions suggest that the origin of these low-frequency resonances may lie in the variation of the oil compressibility [10], that in turn can be triggered by the presence of air contaminating the fluid [11].

Nonetheless, one of the most interesting aspects of these resonance phenomena consists in their incoherence with respect to the classical dynamic equations of the generic hydraulic servomechanism, whose manipulation usually results in the identification of very high resonance frequencies. Starting from this observation, our work tries to explain the low-frequency resonance phenomena from an alternative point of view. As a matter of fact, traditional formulations of the dynamic model of the hydraulic actuator represent the load as a point mass simply acting in either compression or traction on the actuator itself, while in a generic hydraulically powered machine (e.g. an excavator) hydraulic actuators are connected to the links they move

through rotational joints. By explicitly taking into account the geometry of the connection (and consequently, the configuration-dependent nature of the mechanical load), it is possible to refine the dynamic model of the hydraulic actuator and to develop a suitable formula for the estimation of the smallest resonance frequency. The proposed approach was tested in simulation on a 1-DoF system modelled using MATLAB's SimHydraulics Toolbox. Results confirm that the proposed formulation of the resonance frequency is coherent with respect to the behavior of the simulated system.

This paper is organized as follows. Section 2 describes the classical model of a hydraulic servo-mechanism, while Section 3 introduces a more realistic model, characterized by a non-trivial coupling between the actuator and the load. For both systems the transfer function between the valve control signal and a mechanical quantity (either the cylinder's stroke or its linear velocity) is provided, together with a formula for the computation of the smallest resonance frequency. Then, Section 4, shows a comparative analysis between the frequency values obtained with a realistic simulator and the ones computed using the aforementioned formulas. Finally, conclusions and future development are discussed in Section 5.

2 Hydraulic cylinder with a rigidly connected load

In this section the standard model of a symmetric hydraulic actuator connected to a load mass is briefly recalled (see Figure 1).

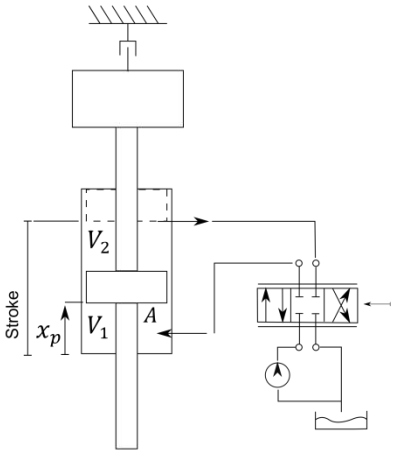

Figure 1. Hydraulic system with compressive load.

More specifically, after the derivation of the dynamical equations, the transfer function between the piston velocity and the valve control signal is presented, together with a rough estimation of the first resonance frequency of the system.

2.1 Hydraulic model

In order to derive the piston equation, we assume that:

- the oil is characterized by a finite compressibility defined by the nominal Bulk Modulus β;
- the thermal expansion of the oil is considered negligible;
- the oil density ρ is the same in the two chambers;
- the fluid losses to the external environment are negligible;
- the internal leakage q_L is proportional to the chambers pressure drop: $q_L = C_L(p_1 - p_2)$;
- the valve electro-mechanical dynamic is considered negligible.

Under these assumptions and according to [12], ρ can be considered equal to its nominal value ρ_0:

$$\rho = \rho_0 \left[1 + \frac{1}{\beta}(p_i - p_r)\right] \cong \rho_0 \tag{1}$$

(where p_i is the i-th chamber pressure and p_r is the initial pressure of the fluid). Therefore, the mass conservation equations for the cylinder chambers can be written as follows:

$$q_1 - q_L = \dot{V}_1 + \frac{V_1}{\beta}\dot{p}_1 \tag{2}$$

$$q_L - q_2 = \dot{V}_2 + \frac{V_2}{\beta}\dot{p}_2 \tag{3}$$

where p_i is the i-th chamber pressure and q_i is the i-th in/out volume flow rate. The two chamber volumes are given by:

$$V_1 = V_0 + Ax_p \tag{4}$$

$$V_2 = V_0 - Ax_p \tag{5}$$

where A is the piston area, x_p is the piston displacement and V_0 is the nominal chamber volume, computed when x_p corresponds to half of the cylinder's stroke.

Since the piston is symmetric the pressure drop

$\Delta p_m = p_1 - p_2$ can be considered as a state variable. Furthermore, by defining $q_m = q_1 = q_2$ and given the supply pressure p_p, the valve orifice equation can be written as follows:

$$q_m = \frac{K_v}{2} u \sqrt{\frac{p_p - p_m}{\rho_0}} \cong \frac{K_v}{2} u \sqrt{\frac{p_s}{\rho_0}} \tag{6}$$

where K_v is the discharge coefficient and u is the valve control signal. The overall hydraulic equation is then obtained as:

$$\frac{V_0}{\beta} \Delta \dot{p}_m = K_v u \sqrt{\frac{p_p}{\rho_0}} - 2A\dot{x}_p - 2C_L \Delta p_m \tag{7}$$

where C_L is the internal leakage coefficient. Finally, the resulting hydraulic force is given by:

$$F_p = A \Delta p_m \tag{8}$$

2.2 Mechanical equation

The mechanical equation is derived by considering a load mass rigidly connected to the piston rod:

$$(M_p + M_l)\ddot{x}_p + (D_p + D_l)\dot{x}_p + F_d = A\Delta p_m \tag{9}$$

where M_p (M_l) is the mass of the piston (load), D_p (D_l) is the damping coefficient of the piston (load), and F_d is a disturbance force (e.g. gravitational force).

2.3 Transfer function

By gathering the masses and the damping coefficients together in the terms M and D, respectively, it is possible to linearize equation (9) in a small neighborhood of the following equilibrium point:

$$x_p = 0 \quad \dot{x}_p = 0 \quad u = 0$$

This way, we obtain the following transfer function between the piston velocity and the control signal:

$$\frac{V_p(s)}{U(s)} = \frac{K_v \frac{\beta A}{V_0 M} \sqrt{\frac{p_p}{\rho_0}}}{s^2 + \left(2\frac{\beta}{V_0} C_L + \frac{D}{M}\right) s + 2\frac{\beta}{V_0 M}(A^2 + C_L D)} \tag{10}$$

Equation (10) represent a second order system whose resonance frequency can be roughly computed by simply neglecting the internal leakages ($C_L = 0$):

$$f_n = \frac{1}{2\pi} \sqrt{\frac{2\beta A^2}{M V_0}} \tag{11}$$

Notice that in case of a standard asymmetric piston the above relation slightly changes in:

$$f_n = \frac{1}{2\pi} \sqrt{\frac{2\beta}{M} \left(\frac{A_1^2}{V_{01}} + \frac{A_2^2}{V_{02}}\right)} \tag{12}$$

where A_1 and A_2 are the bottom-side and rod-side piston areas, respectively.

3 Hydraulically actuated mechanism

The above formulation clearly does not represent a system characterized by a non-trivial coupling between the actuator and the load. The case-study of this paper is indeed the 1-D.o.F. system shown in Figure 2, which is more similar to a real-world scenario (e.g. an excavator link).

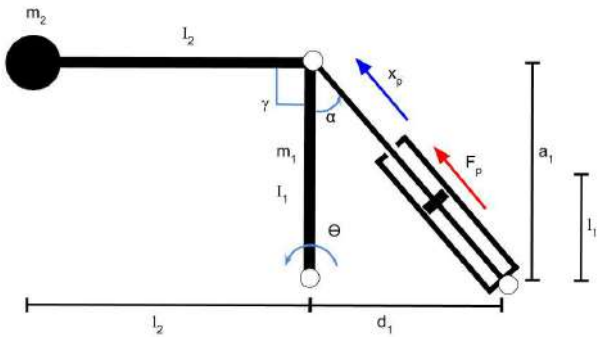

Figure 2. 1-D.o.F. hydraulically actuated mechanism

In this section we start by presenting the non-linear dynamical equations of the system, then we select a proper working point and, finally, we obtain the linearized model.

3.1 Kinematics

In order to retrieve the model as a function of the cylinder displacement, we can apply the cosine formula to the a_1-d_1-x_p triangle (see Figure 2):

$$\theta = \text{acos}\left(\frac{a_1^2 + d_1^2 - x_p^2}{2a_1 d_1}\right) = f_\theta(x_p) \quad (14)$$

3.2 Mechanical dynamics

The mechanical balance of the system can be obtained by assuming the piston mass and inertia to be negligible. Given these assumptions, the mechanism is equivalent to a 2-Link planar robot, where angle γ corresponds to the second DoF. Consequently, the dynamic of the mechanism can be computed according to [13]. In particular, given all the geometrical parameters shown in Figure 2 and defining m_i and I_i as the mass and the inertia momentum of the i-th link, the following equation is obtained:

$$B_1\ddot{\theta} + B_2\ddot{\gamma} + C_1\dot{\theta}\dot{\gamma} + C_2\dot{\gamma}^2 + G = \tau_1 \quad (15)$$

where:

$$B_1 = m_1 l_1^2 + I_1 + m_2 a_1^2 + m_2 l_2^2 + 2m_2 a_1 l_2 \cos(\gamma) + I_2 \quad (16)$$

$$B_2 = m_2 l_2^2 + m_2 a_1 l_2 \cos(\gamma) + I_2 \quad (17)$$

$$C_1 = -2m_2 a_1 l_2 \sin(\gamma) \quad (18)$$

$$C_2 = -m_2 a_1 l_2 \sin(\gamma) \quad (19)$$

$$G = m_1 g l_1 \cos(\theta) + m_2 g\, a_1 cos(\theta) + m_2 g l_2 \cos(\gamma + \theta) \quad (20)$$

and τ_1 is the equivalent torque provided by the hydraulic actuator:

$$\tau_1 = d_1 \cos(\alpha)\, F_p = d_1 \cos(\alpha)\, A \Delta p_m \quad (21)$$

A simpler formulation of the previous equations can be obtained by assuming:

- $I_1 = I_2 = 0$
- $m_1 = 0$
- $\gamma = {}^{\pi}/_{2}$ (fixed)

As a result, the dynamic equation reduces to:

$$m_2(a_1^2 + l_2^2)\ddot{\theta} + m_2 g a_1 \cos(\theta) - m_2 g l_2 \sin(\theta) = \tau_1 \quad (22)$$

Finally, the hydraulic dynamics is obtained according to Equation (7).

3.3 Linearized model

To compute the linearized model, the working point defined by $\theta_0 = \pi/2$ is considered. It is also useful to define the following quantities:

$$\delta x_p = x_p - x_{p_0} \quad (23)$$

$$\delta p_m = \Delta p_m - \Delta p_{m_0} \quad (24)$$

$$\delta u = u - u_0 \quad (25)$$

where:

$$x_{p_0} = \sqrt{a_1^2 + d_1^2} \quad (26)$$

$$\Delta p_{m_0} = \frac{m_2 g l_2}{d_1 \cos(\alpha_0)\, A} \quad (27)$$

$$u_0 = \frac{2C_L}{K_v}\sqrt{\frac{\rho_0}{p_p}}\Delta p_{m_0} \quad (28)$$

$$\alpha_0 = \text{atan}\left(\frac{d_1}{a_1}\right) \quad (29)$$

Moreover, the linear dependence of joint angle θ on piston displacement x_p can be defined as follows:

$$\theta = f_\theta\left(x_{p_0}\right) + \left.\frac{df_\theta}{dx_p}\right|_{x_{p_0}} \delta x_p = = f_\theta\left(x_{p_0}\right) + n_\theta \delta x_p \quad (30)$$

$$\dot{\theta} = n_\theta \delta \dot{x}_p \quad (31)$$

$$\ddot{\theta} = n_\theta \delta \ddot{x}_p \quad (32)$$

Therefore, the linearized mechanical equation is given by:

$$m_2(a_1^2 + l_2^2) n_\theta \delta \ddot{x}_p - m_2 g l_2 n_\theta \delta x_p - m_2 g l_2 \text{f}\left(x_{p_0}\right) = A d_1 \cos(\alpha_0)\, \delta p_m \quad (33)$$

and the linear hydraulic equation is:

$$\frac{V_0}{\beta}\delta \dot{p}_m = K_v\sqrt{\frac{p_p}{\rho_0}}\delta u - 2A\delta \dot{x}_p - 2C_L \delta p_m \quad (34)$$

3.4 Transfer function

Similarly to the previous case, it is possible to retrieve the transfer function of the linearized dynamics between the piston displacement and the valve control signal:

$$\frac{X_p(s)}{U(s)} = \frac{\mu}{Ks^3 + Fs^2 + Qs - H} \quad (35)$$

where:

$$K = \frac{V_0}{\beta} m_2 (a_1^2 + l_2^2) n_\vartheta \quad (36)$$

$$F = 2C_L m_2 (a_1^2 + l_2^2) n_\vartheta \quad (37)$$

$$Q = 2d_1 \cos(\alpha_0) A^2 - m_2 g l_2 n_\vartheta \frac{V_0}{\beta} \quad (38)$$

$$H = 2C_L m_2 g l_2 n_\vartheta \quad (39)$$

$$\mu = d_1 \cos(\alpha) 2AK_v \sqrt{\frac{p_p}{\rho_0}} \quad (40)$$

In addition, by neglecting the internal leakage ($C_L = 0$), it is possible to simplify the denominator, obtaining the following transfer function between the piston speed and the valve control signal:

$$\frac{V_p(s)}{U(s)} = \frac{\mu}{Ks^2 + Q} \quad (41)$$

Therefore, the resonance frequency can be estimated by:

$$f_n = \frac{1}{2\pi}\sqrt{\frac{K}{Q}} = \\ = \frac{1}{2\pi}\sqrt{\frac{2d_1 \cos(\alpha) A^2 - m_2 g l_2 n_\vartheta \frac{V_0}{\beta}}{\frac{V_0}{\beta} m_2 (a_1^2 + l_2^2) n_\vartheta}} \quad (42)$$

4 Numerical Simulations

In order to better understand the effect of the joint connected load, several simulations have been performed. In this section, the results of these simulations are presented and compared to the results of the previously explained formulas.

For this purpose, a realistic simulator has been developed in MATLAB/Simulink environment, using the SimHydraulics toolbox [14]. More specifically, the parameters of an off-the-shelf double-acting asymmetric cylinder and the ones of a commercial 4/3 valve have been considered. In addition, the mechanical system shown in Figure 2 has been reproduced. Finally, the pump behavior was assumed to be ideal, meaning that the supply pressure p_p was always constant. The simulations have been performed by feeding the valve with a sine sweep-shaped control signal and varying the load mass m_2 and the link length l_2 for a total of 40 different configurations. Then, resonance frequencies have been identified by analyzing the spectrum of the resulting cylinder's speed signal. As far as the "rigidly connected load" case is concerned, f_n is computed according to equation (11). For the sake of clarity, we replaced mass m_2 with an equivalent mass, computed on the basis of the average static load "sensed" by the hydraulic cylinder. In this way, we were able to incorporate in a single inertial parameter the effects of both m_2 and l_2. Figure 3 shows how the resonance frequency changes with respect to different load masses. Moreover, for each load mass value, five different link lengths have been considered. On the other hand, Figure 4 shows the dependency of the resonance frequency with respect to different link lengths. In this case, eight different values of load mass have been considered for each link length value. In both cases the identified frequencies are displayed in red, while the computed ones are pictured in blue. As expected, given the same load mass (link length), the resonance frequency tends to decrease as the link length (load mass) increases.

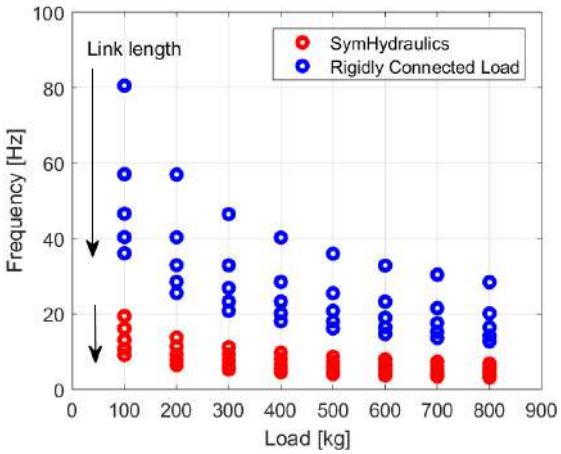

Figure 3. Resonance with varying load mass and rigidly connected load

Nevertheless, it is clear that the estimated resonance frequencies f_n computed according to equation (11) are significantly higher with respect to the corresponding identified frequencies. To this regard, Figure 5 and Figure 6 show the comparison among the identified frequencies and the ones computed according to equation (42). Clearly, the proposed formula is significantly more accurate than the traditional one. In addition, these results demonstrate how the kinematic coupling between the load and the actuator affects the natural frequencies of this system. Indeed, by means of Root Mean Square Error the following results are obtained:

$$RMSE_{rigid} = 23.4900\ rad/s$$

$$RMSE_{joint} = 0.0635\ rad/s$$

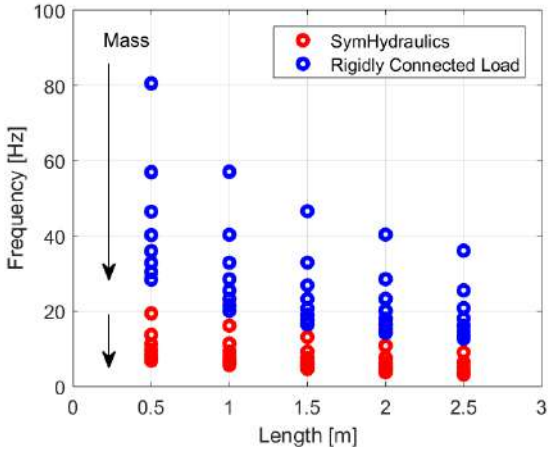

Figure 4. Resonance with varying length and rigidly connected load

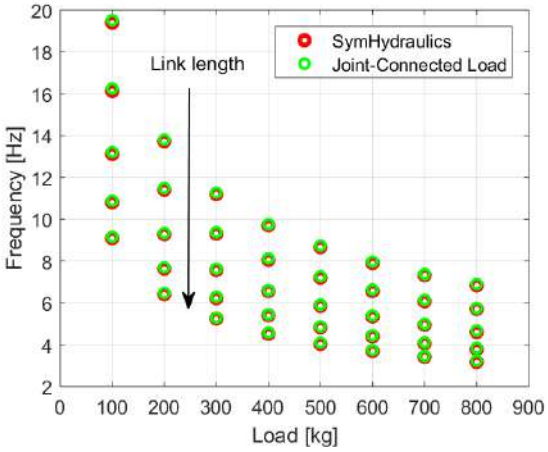

Figure 5. Resonance with varying mass and joint-connected load

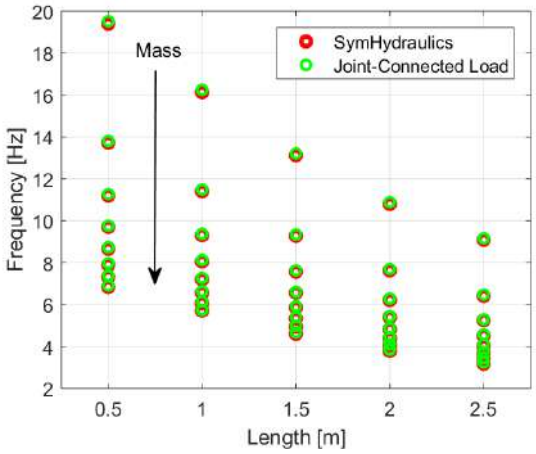

Figure 6. Resonance with varying link length and joint-connected load

5 Conclusions

This paper presents a study carried out on a hydraulic actuation system with the aim to achieve a better understanding of the causes of the low frequency resonances affecting the system. Starting from very simple models of the actuator and the load which it is connected to, the transfer function between the valve control signal and a mechanical quantity was computed and a formula to retrieve the resonance frequency was derived. Then, a more complex system characterized by a non-trivial coupling between the load and the hydraulic cylinder was considered. Once again, the model of the system was retrieved and, after linearization, a more complex formula for the estimation of the resonance frequency was computed.

Finally, a simulation environment of the joint-connected load was developed and several simulations were performed in order to obtain, via spectral analysis, an accurate estimation of the resonance frequencies corresponding to different load masses and link lengths. These estimated frequencies were compared to the results obtained using the two formulas, showing how critical is the impact of the kinematic coupling on the natural frequency of this kind of systems.

As far as future developments are concerned, the formula for the resonance estimation can be furtherly improved by taking into account the asymmetry of the hydraulic actuator and a more detailed description of the valve dynamics. To this regard, a promising solution could be represented by the adoption of object-oriented modelling strategies and tools [15], which allows to easily implement custom models such as the ones showed in [16].

References

[1] Hutter M., Leemann P., Stevsic S., Michel A., Jud D., Hoepflinger M., Siegwart R., Figi R., Caduff C., Loher M. and Tagmann S. "Towards optimal force distribution for walking excavators". In *International Conference on Advanced Robotics (ICAR)*, pages 295-301, Istanbul, Turkey, 2015.

[2] Tanzini M., Jacinto-Villegas J. M., Filippeschi A., Niccolini M., and Ragaglia M. "New interaction metaphors to control a hydraulic working machine's arm". In *IEEE Symposium of Safety and rescue Robotics (SSRR)*, pages 297-303, Lausanne, Switzerland, 2016.

[3] Corke P., Roberts J., Cunningham J. and Hainsworth D. "Mining Robotics". *Springer Handbook of Robotics*, Springer, Berlin, Heidelberg, 2008.

[4] Billingsley J., Visala A. and M. Dunn, "Robotics in Agriculture and Forestry" *Springer Handbook of Robotics*, Springer, Berlin, Heidelberg, 2008.

[5] Merritt H. E., *Hydraulic Control Systems*, John Wiley & Sons Inc, New York, 1967.

[6] Park J. Y. and Chang P. H. "Vibration control of a telescopic handler using time delay control and commandless input shaping technique" *Control Engineering Practice*, 12(6): 769-780, 2003

[7] Singh S. "The state of the art in automation of earthmoving" *ASCE Journal of Aerospace Engineering*, 10, 1997.

[8] Singhose W. E., Porter L. J. and Seering W. P. "Input shaped control of a planar gantry crane with hoisting" In *Proceedings of American Control Conference*, pages 97-100, Albuquerque, NM, USA, 1997.

[9] Yoo S., Park C. G., Lim B., Lee K. I. and Park F.C. "Bandwidth Maximizing Design for Hydraulically Actuated Excavators," *Journal of Vibration and Control*, 16(14): 2109–2130, 2010.

[10] Ding G., Qian Z. and Pan S. "Active vibration control of excavator working equipment with ADAMS" In *International ADAMS User Conference*, 2000

[11] Sakama S., Tanaka Y. and H. Goto "Mathematical model for bulk modulus of hydraulic oil containing air bubbles" *Mechanical Engineering Journal*, 2(6), 2015.

[12] Manring N. D. *Hydraulic Control Systems*, John Wiley & Sons Inc, New York, 2005.

[13] Siciliano B., Sciavicco L., Villani L. and G. Oriolo, *Robotics: Modelling, Planning and Control*, Springer, London, 2009.

[14] Simscape Fluids™ (formerly SimHydraulics®), 2019, Online: https://www.mathworks.com/products/simhydraulics.html.

[15] Fritzson P., *Principles of Object-Oriented Modeling and Simulation with Modelica 2.1*, Wiley Press, 2004.

[16] Pencelli M., Villa R., Argiolas A., Ferretti G., Niccolini M., Ragaglia M., Rocco P. and A.M. Zanchettin, "Accurate dynamic modelling of hydraulic servomechanism," In *Design Automation and Test in Europe Conference*, 2019.

Predicting Bridge Conditions in Ontario: A Case Study

M. Taghaddos[a] and Y. Mohamed[a]

[a] Department of Civil & Environmental Engineering, University of Alberta, Canada
E-mail: taghaddo@ualberta.ca, yasser.mohamed@ualberta.ca

Abstract –
Maintenance and repair of bridges represent significant costs in provincial and municipal government budgets. Prediction of bridge conditions can help managers in annual cost estimating and budget allocation. To assess Bridge Condition Index (BCI), each bridge component must be inspected every two years, tested if it is required, and rated. Bridge condition can be affected over time by different attributes such as material, structure, location, and use. This paper presents a study conducted to model and predict BCI based on a historical dataset of 2803 bridges in Ontario from 2000 to 2014. The paper describes the work related to data collection, cleaning and transformation. In addition, a comparison of the cross-validation performance of alternative BCI prediction models is presented and discussed.

Keywords –
Bridge maintenance; Bridge Condition Index (BCI); Prediction model; Cluster; Data analysis

1 Introduction

Bridges are essential infrastructures which are commonly used in transportation networks, and it is vital for them to function up to the acceptable level during their service life. However, to keep their functionality acceptable maintaining them and the corresponding cost is unavoidable. In the United States, the annual cost of rehabilitation is $7 billion [3]. To optimize the functionality of bridge infrastructure, continuous bridge access must be balanced with repair and maintenance costs as well as safety consideration [1]. Early identification of deterioration and following repairs enable decision makers to expedite the maintenance significantly with a lower cost and minimum disruption [4].

Continues bridge assessment can improve the maintenance of structure since it can accurately determine the structure condition, provide condition factor for load rating calculation, find the main reason of any deterioration and finally, determine appropriate rehabilitation process and corresponding budget [4]. Current tests for identifying bridge conditions are costly and time-consuming. Hence, a cost and time effective model for predicting bridge condition is beneficial from the budget allocation perspective.

The objective of this paper is to develop a framework to forecast the bridge condition for the future using historical data. Various prediction models are implemented and compared, and the best one is selected.

The advantages of the proposed approach are:

1. Enables managers to prioritize the bridges based on the level of urgent action required in a time and cost effective manner before formal assessments are conducted.
2. Helps to prioritize the expensive and invasive tests for the upcoming years.
3. Benefit ministries to proportionally allocate budget for repair and maintenance in advance.
4. Enable managers to evaluate different maintenance- scenarios over time to choose the best strategy.

2 Bridge Condition Index

One tool that can assist in the management of highway structure is Bridge Condition Index (BCI). BCI was developed based on two factors of the extent/severity factor Sf and element factor Ef, which both can have values between 1 to 10. Development of this index is entitled to High-Point Rendel and Taywood Engineering [5]. This index serves as a principle of resource allocation within a network [6] and can be helpful in various purposes naming [5]:

- It is an indication of a change in condition state over a period of time for the entire or part of the bridge
- By considering the entire bridge over a long period of time, the level of provided funding can be assessed to recognize its adequacy to keep the stock in a steady state
- By considering applied funding, BCI and type of material, the best and the most economic material of construction in the long run, can be assessed in each area
- By considering the level of funding and the BCI, it might be possible to achieve an

indication for the performance of agents who are responsible to take corrective actions.

Aside from these advantages, BCI has its own constraints in its applicability, such as [5]:

- BCI is not an indicator for the functionality of a bridge from a traffic point of view
- Safety is not a primary concern in BCI

Finally, since BCI is widely used in different countries including Canada, this paper considers BCI as a representative factor for the bridge conditions.

3 Case Description

The Ministry of Ontario adopted the BCI measurement system to evaluate the conditions of the bridge [7]. They inspected and assessed all bridges (2803 bridges) in Ontario from 2000 to 2014. In each inspection, experienced engineers and inspectors followed Ontario's Structure Inspection Manual (OSIM) which provides inspection procedures in great details. To identify maintenance procedure, they assess each bridge component comprehensively, such as barriers, sidewalks, deck asphalt, expansion joints, beams, pier cap, pier column, bearings, soffits, wingwall, and abutment. They performed a detailed visual inspection by checking the general condition of bridges, assessing components of each bridge, looking for any potential problem and reporting any safety issue (if there is any). Four common bridge test methods are used in the assessment.

1. External test using ultrasonic and magnetic particle tests, to identify hidden cracks in the structure.
2. Steel fatigue test using ultrasonic to identify cracks where steel parts are connected (it is common in older steel bridges).
3. Internal test using small samples for the test in the lab.
4. Bridge load capacity test with a driving special truck loaded with concrete blocks while instruments are attached to the bridge and record the movement to find the weight that bridge can safely carry at one time [7].

After scoring the bridge based on the BCI system, they assess the score according to Table 1 [7]. The Ministry of Ontario uses an innovative technology of rapid bridge replacement. In this method, crews lift the old bridges in a few hours and replace them with the new ones which are built nearby. Examples of this technology include Toronto 401 off-ramp bridge at Yorkdale Shopping Centre (2012), Ottawa - Island Park (2007) and Hamilton Aberdeen Bridge (2010) [7].

Table 1. The bridge condition index

BCI	condition	Maintenance
70-100	Good	Is not required in the next 5 years
60-70	Fair	Is required in the next 5 years
<60	Poor	required in the next year

4 Data mining

4.1 Explaining data set

This data set contains 2803 records for bridges in Ontario. Each record contains name, exact location, longitude, latitude, structural system (e.g. slab, beam/girder or frame), material, year built, last major and minor rehabilitation years, details of spans and measured BCI since the year 2000.

4.2 Proceeding data preparation

Preparing data is one of the most important parts of data mining problems. In this case study, data mining is a major consideration. Most of Bridge Condition Indexes are measured on a bi-yearly basis, meaning data organization is crucial. Many classification algorithms consider the gap years between measurements as "missing values," which is not true in this study because the measurements are not taken on an annual basis. To overcome this misperception, the BCIs are sorted chronologically based on the year in which they were measured and then assigned sequential numbers. One record is illustrated as an example in Table 2, which was then transformed into Table 3.

Table 2. Original dataset of one record for BCI

Year	2013	2012	2011	2010	2009	2008
BCI	88	-	89.9	-	96.2	-

Table 3. Transformed dataset of one record for BCI

Year	BCI1(BCI)	BCI2	BCI3
BCI	88	89.9	96.2

Many bridges have only minor or major rehabilitation, which affects the BCI. Although the better approach is to capture both, since the majority of bridges only have one type of rehabilitation, it will increase the missing data to a great extent. Therefore, it is decided to take the most recent rehabilitation (regardless of the type, either major or minor). Data

cleaning is coded in R [8], an open-source statistical environment.

4.3 Feature Selection

Feature selection is an essential step in machine learning, particularly in big data. Many gathered variables are irrelevant to the classification, and its relevancy is unknown unless tested [9]. Most importantly, using large feature sets data, slows down algorithms [9] and decreases its accuracy when numbers of utilized attributes are more than optimal [10]. Hence, from the practical perspective selecting small and possibly minimum feature set is highly desirable [9]. This problem considered a minimal optimal problem [11], which has been studied for several years to reduce the feature set. Although using more attributes may result in better accuracy, the model is hard to interpret, and overfitting is more likely. One of the feature selection methods is called wrapper, which finds the best combination of features (subset). Boruta feature selection is a wrapper built based on random forest algorithm. Its algorithm is coded in R- an open source statistical environment in a package called Boruta [8]. It helps find the most important attributes or recognize unimportant ones. This package iteratively compares the importance of each feature with the importance of shadow attributes, that is initiated by shuffling original dataset [9]. Then, those attributes that are significantly better than shadow attributes are confirmed; otherwise, they will be dropped. This process continues until the maximum run occurs or only the confirmed attributes are left. If the former one occurs, it is called Tentative. Hence, the user can increase the number of runs or decrease p-value. To calculate the importance measure of an attribute, first the loss of accuracy of classification for all trees of the forest (that have this attribute) is calculated separately. This loss of accuracy is the result of the random disposition of attribute values between objects. Then the importance measure would be the result of dividing the average loss by its standard deviation [9]. Although it has some deficiencies, it is a useful tool since it can count the fluctuations of the mean accuracy loss among trees in the forest [9].

In order to conduct the Boruta selection algorithm, first the dataset is cleaned, similar attributes were removed, and derived attributes are mutated. The result of this algorithm is shown in Figure 1. Based on this selection feature algorithm, the previous measure BCI (CI2) has the most crucial role in the prediction of bridge condition. Furthermore, different feature selection methods such as subset selection, forward and backward methods as well as filtering method (single factor analysis to evaluate the prediction power of each attribute) are also conducted. All these feature selection methods confirm that the most effective attribute is the most recent BCI.

Hence, the features that have importance value greater than 15 are selected for prediction model which are BCI2, BCI3 (the two recent BCI), the year of most recent rehab and age. Adding more attributes such as longitude and latitude (which implicitly is in the country), material or category, not significantly change the accuracy of the models. It is important to note that different models are conducted based on the result of other feature selection algorithms, namely subset selection, forward, backward, filter and Boruta selection (as each feature selection algorithm suggests a different set of attributes). Although all of them are common in BCI2, the Borouta model is the best based on its performance, hence, proposed.

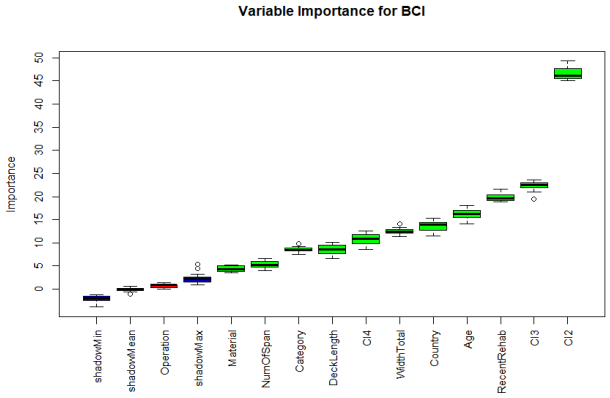

Figure 1. Boruta selection algorithm

4.4 Prediction Model

In this case study, in order to predict the BCI, different numerical prediction algorithms are conducted. Each model is tested in a cross-validation test. Then, the results are compared to choose the best one.

4.4.1 Model Development

The first step in developing the framework is to export the cleaned data from R [8] in a spreadsheet, which is the input for RapidMiner Studio as the Data-Mining Software [12] (Its graphical environment eases its usage for data mining users). As Figure 2 shows, linear regression, KNN, neural network, support vector machine, and random forest are modelled.

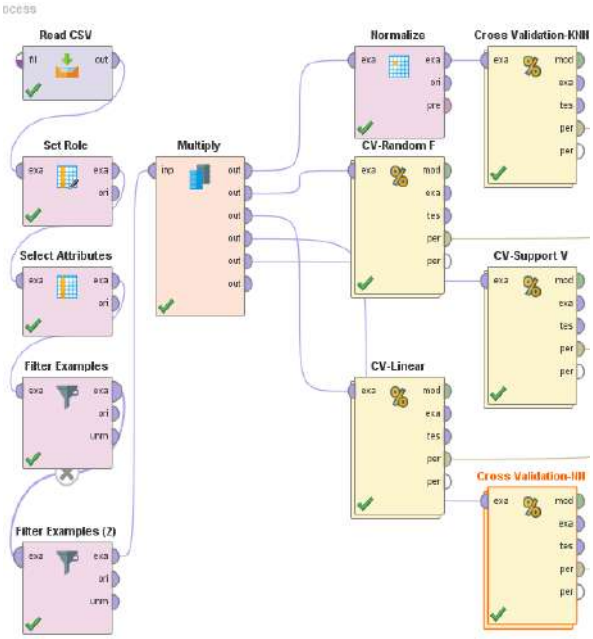

Figure 2. Classification model development

4.4.2 Linear Regression (LR)

In this classification, the relationship between attributes and target attribute is defined with a linear predictor function and their unknown parameters of this function are calculated from training dataset. Table 2 shows the statistical results of this model.

The formula to calculate the upcoming BCI for the next two years will be as equation 1.

$$Next\ BCI = 0.823 \times BCI2 - 0.075 \times BCI3 + 0.08 \times Year\ of\ Most\ Recent\ Rehab - 0.024 \times Age - 139.854 \quad (1)$$

In this equation, BCI is the predicted Bridge Condition Index for the next year, BCI2 and BCI3 are two formers measured BCIs for the past years. Year of the most recent rehab is the previous year of rehabilitation (either minor or major) and Age is the current year minus the year built of the bridges.

4.5 K-Nearest Neighborhood (KNN)

K-Nearest Neighbour (KNN) is a lazy classification algorithm based on the instances. The mechanism of this method is by calculating the distance for each instance from other instances and assigning them to a class based on k-nearest point. There are different equations for calculation distances such as Manhattan or Euclidian distance. In this study, Euclidian distance is used to measure. David William Aha studied KNN in his doctoral dissertation (1990) and suggested normalizing the values of each feature before applying the model [13]. That is because KNN is sensitive to the scale of data and if they have a different scale, the effect of bigger attributes may neutralize the value of small attributes. Finding the best K in the KNN method can be achieved by try and error as there is no precise rule for this purpose.

4.6 Neural Network (NN)

Artificial Neural Network (ANN or NN) is a data-driven model which is trained iteratively from a random state to estimate target value. This algorithm tries to mimic brain behaviour to learn through neurons. The neurons receive signals from other neurons through the links from the previous layer, which may strength or weaken through weights. When the signal excitation reaches to a certain extent, the neurons will react and fire. However, it is not clear what happens inside this algorithm completely as it is called a black box engine. NN is not depended on the distribution or probability; hence, is considered as a universal approximator [14]. It can be used for both classification (which is well known for it) and regression. It is important to note that by the iterative process, the algorithm finds the weights in a way that can minimize the error.

4.7 Support Vector Machine (SVM)

It is a supervised learning classification model that analyses data for classification or regression analysis. SVM finds the algorithm that had the best and well-separated categories with the clear gap (as wide as possible) between the classes, which increase the probability of a new sample to belong to only one group. Generally, in this algorithm, the wider the margin, the lower the generalization error [15].

4.8 Random Forest (RF)

Random forest is based on the idea of a random selection of features to generate trees. It is an ensemble learning method based on numerous decision trees in training. This algorithm can be used for classification or regression, and the predicted output will be the mode of the classes or mean of prediction, respectively [16, 17].

4.9 Model Selection and Comparison

To select the best model, the first step is to test the accuracy of the model. If there is an extremely big data set, the best practice is to use half of the data for training and the rest for testing. However, usually, data-limitation is a common problem. Thus, it is important to find the best approach for dividing the dataset into training and testing sets. That is crucial because if all data is used in training, although the model is highly accurate, the performance of the model facing new

unseen input is highly unknown (validity). On the other hand, if a small

portion of data is utilized for training, the model will not be precise enough. Cross-validation is a tool to overcome this difficulty by dividing data to n folds." The technique of cross-validation usually is recommended as a better test of the model because of the well-known bias induced by testing the predictive validity of a model on the same data that were used to estimate its parameters" [18]. Hence, by cross-validation, we can use all of the data-set in the model. Table 4 shows the error comparison of classifiers by cross-validation test.

Based on Table 5, the relative error of support vector machine is the lowest, root mean squared error of the random forest is the lowest, and correlation of random forest is the highest among all prediction models. However, statistically, there is not a meaningful difference in the accuracy of these models based on statistical t-test with alpha 0.05. Therefore, it is better to find the model which has the smallest range for the error. For this purpose, the box plot of accuracies, based on root mean square error is plotted in Figure 3.

As Figure 3 shows, although the ranges do not vary too much, support vector machine, KNN (K=4) and neural network have a relatively wider range. Based on Figure 3, the author recommends using random forest prediction model, which has a relatively denser box-plot, or linear regression because of its simplicity.

Table 4. Statistics of Linear Regression Model

attribute	coefficient	std. Error	std. Coefficient	Tolerance	t-stat	p-value	code
BCI2	0.823	0.031	0.818	0.288	26.847	0.000	****
BCI3	−0.075	0.031	−0.074	0.286	−2.414	0.016	**
Most Recent Rehab	0.080	0.010	0.126	0.995	8.028	0.000	****
age	−0.024	0.010	−0.042	0.868	−2.484	0.013	**
(Intercept)	−139.854	20.059	NaN	NaN	−6.972	0.000	****

Table 5. Error comparison of classifiers

Classifier	Root Mean Squared Error	Relative Error	Correlation
KNN(K=2)	4.511 +/- 0.758	3.29% +/- 0.35%	0.749 +/- 0.090
KNN(K=3)	4.292 +/- 0.614	3.26% +/- 0.30%	0.772 +/- 0.069
KNN(K=4)	4.178 +/- 0.705	3.22% +/- 0.39%	0.783 +/- 0.079
KNN(K=5)	4.169 +/- 0.688	3.21% +/- 0.36%	0.784 +/- 0.076
LR	4.092 +/- 0.821	3.24% +/- 0.79%	0.807 +/- 0.083
RF	3.947 +/- 0.806	2.91% +/- 0.36%	0.810 +/- 0.091
NN	4.092 +/- 0.821	3.24% +/- 0.79%	0.807 +/- 0.083
SVM	4.203 +/- 0.878	2.19% +/- 0.32%	0.799 +/- 0.086

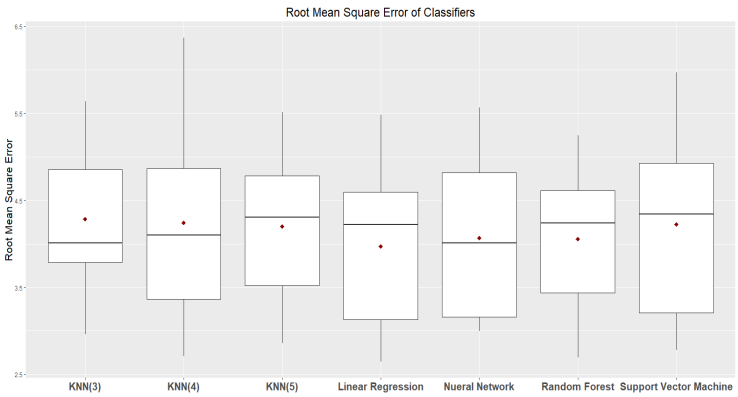

Figure 3. Root Mean Square Error comparison of classifiers

5 Conclusion

Annually, Maintenance and repair of bridges impose significant costs to municipalities. Having a good prediction of bridge conditions can help to recognize the bridges that need an urgent repair, or require repair in a short interval of time. This can be highly beneficial for governments for budget allocation and sequencing the maintenance operation. Furthermore, it can be helpful for planners in order to have a targeted bridge inspection.

This study is based on the historical data of the Municipality of Ontario to find a predictive model for bridge condition index. After feature selection, four prediction models are assessed, namely, linear regression, random forest, neural network, KNN and support vector machine. Then, based on the corresponding accuracy between these models, random forest and support vector machine are suggested. As the study shows, this model can predict the next BCI with 97% accuracy having two former BCIs, age and the year of most recent rehabilitation. By annual update of the database, the suggested framework can enhance further to achieve better accuracy. If the historical data is available, this model can be conducted for a different location.

6 Limitation

The scope of this study is limited to develop a prediction model for BCI and excludes improvement of measurement in BCI experiment or incorporating safety in BCI. This model is not also for selecting the type of material or any design specification of the bridges.

7 References

[1] NEWMAN J. Concrete Repair Strategies, Essentials of Concrete Investigations. Institution of Engineers of Ireland, Dublin, 2003.

[2] Federal Highway Administration. Delivering Infrastructure for America's Future. US Department of Transportation, Washington DC 2002.

[3] Sánchez-Silva M, Frangopol DM, Padgett J, Soliman M. Maintenance and operation of infrastructure systems. Journal of Structural Engineering. 2016 Jun 2;142(9): F4016004.

[4] Pearson-Kirk D. The benefits of bridge condition monitoring. In Proceedings of the Institution of Civil Engineers-Bridge Engineering 2008 Sep (Vol. 161, No. 3, pp. 151-158). Thomas Telford Ltd.

[5] Das PC, editor. Management of highway structures. Thomas Telford; 1999.

[6] Chase SB, Adu-Gyamfi Y, Aktan AE, Minaie E. Synthesis of national and international methodologies used for bridge health indices. United States. Federal Highway Administration; 2016 May 1.

[7] Ontario Ministry of Transportation, Bridge repairs, Online:http://www.mto.gov.on.ca/english/highway-bridges/ontario-bridges.shtml, Accessed: 12/04/2018

[8] Team RC. R: A language and environment for statistical computing, 2013.

[9] Kursa MB, Rudnicki WR. Feature selection with the Boruta package. Journal of Statistical Software. 2010 Sep 16;36(11):1-13.

[10] Kohavi R, John GH. Wrappers for feature subset selection. Artificial intelligence. 1997 Dec 1;97(1-2):273-324.

[11] Nilsson R, Peña JM, Björkegren J, Tegnér J. Consistent feature selection for pattern recognition in polynomial time. Journal of Machine Learning Research. intelligence. 1998 Aug;20(8).

[12] Cooil, B., Winer, R., & Rados, D. Cross-Validation for Prediction. Journal of Marketing Research, 24(3), 271-279, 1987.

Automated Mathematical-Based Design Framework for The Selection of Rigging Configuration

S.M.A.M Hashemi[a], S. Han[a], J. Olearczyk[b], A. Bouferguene[b], M. Al-Hussein[b], J. Kosa[c]

[a]Department of Building, Civil and Environmental Engineering, Concordia University, Canada
[b]Department of Civil and Environmental Engineering, University of Alberta, Canada
[c]NCSG Engineering Ltd., Canada
E-mail: seyedmohammadamin.minayhashemi@mail.concordia.ca, sanghyeok.han@concordia.ca, jaceko@ualberta.ca, ahmed.bouferguene@ualberta.ca, malhussein@ualberta.ca, joe.kosa@ncsg.com

Abstract –

Modularization in construction involves erection of large and heavy prefabricated modules at the job site. Modules, especially in industrial plants, are required to be lifted without any tilted angles vertically and horizontally to prevent applying bending moments to the lifting lugs and structural components. Configuration of rigging elements, which are the link between the crane hook and the module, plays a vital role in the load distribution to the rigging components. In practice, designing a rigging assembly to ensure safe and successful lifts is a time-consuming and tedious process relying heavily on guesswork, especially when the module's center of gravity is offset. In addition, the pitch angle of the module remains unknown until it is lifted, thus raising safety issues regarding the failure of rigging components. To overcome these limitations, this paper proposes a mathematical-based design framework which consists of: (1) collecting the module information; (2) designing a preliminary configuration by selecting the rigging components from the database; (3) Optimizing the number, size and capacity of the rigging components selected for the preliminary configuration in order to ensure that positions of module and spreader bars are set on parallel lines without tilted angles; and (4) reporting the list of used rigging components and visualizing their configuration as the output. To validate this framework, this paper uses a case study which designs the optimal rigging configuration for a 4-point pick module based on the inventory availability.

Keywords –

Crane rigging; Automation; Center of gravity offset

1 Introduction

Modularization is a growing trend in construction thanks to its efficiency in terms of time and cost. In industrial plants, the off-site constructed modules can typically be classified as pipe racks, cable trays and building modules [1]. These modules may have up to 16 lifting points. Once transported to the job site, the modules are lifted from the pick points to their set points. In order to prevent applying bending moments to the lifting lugs and structural components of the module, the modules are required to be lifted vertically and maintained in a horizontal position during the lift. Slinging arrangement of the rigging assembly determines how the load is distributed from the lifting lugs of the module to the crane's hook.

Anderson [2] enumerated three possible slinging arrangements of 4-point pick modules as they are shown in Figure 1.

In Figure 1-a, 4 shackles and 4 slings are used to transfer the load directly from the lifting lugs to the crane's hook. The alignment of the lifting lugs is important in this configuration. Each of them must be in plane towards the COG. Otherwise, according to the supplier's manual, a reduction in the capacity of the shackles might be needed based on the angle the shackles make with the slings to which they are attached [3]. It is recommended to design the lifting lugs, shackles, and slings in a way that two of them are able to carry the entire load due to possible differences in the angles between the slings and horizon when the COG is offset [2]. Sam [4], presented a spreadsheet to analyze and calculate the sling loads for this slinging arrangement with consideration of the variations in the COG location. Similar rigging configuration is used when the object is lifted from the bottom with vertical slings used to transfer the lifting points above the object. However, lifting from the bottom has the risk of instability especially when the object's COG is too high. Longman and Freudenstein [5] suggested an analytical necessary and sufficient criterion for Liapunov stability or asymptotic stability for the 4-point pick lift from below the load's COG. They defined an expression for the margin of stability in which the disturbance forces caused by crane hook motion during the lift can be tolerated.

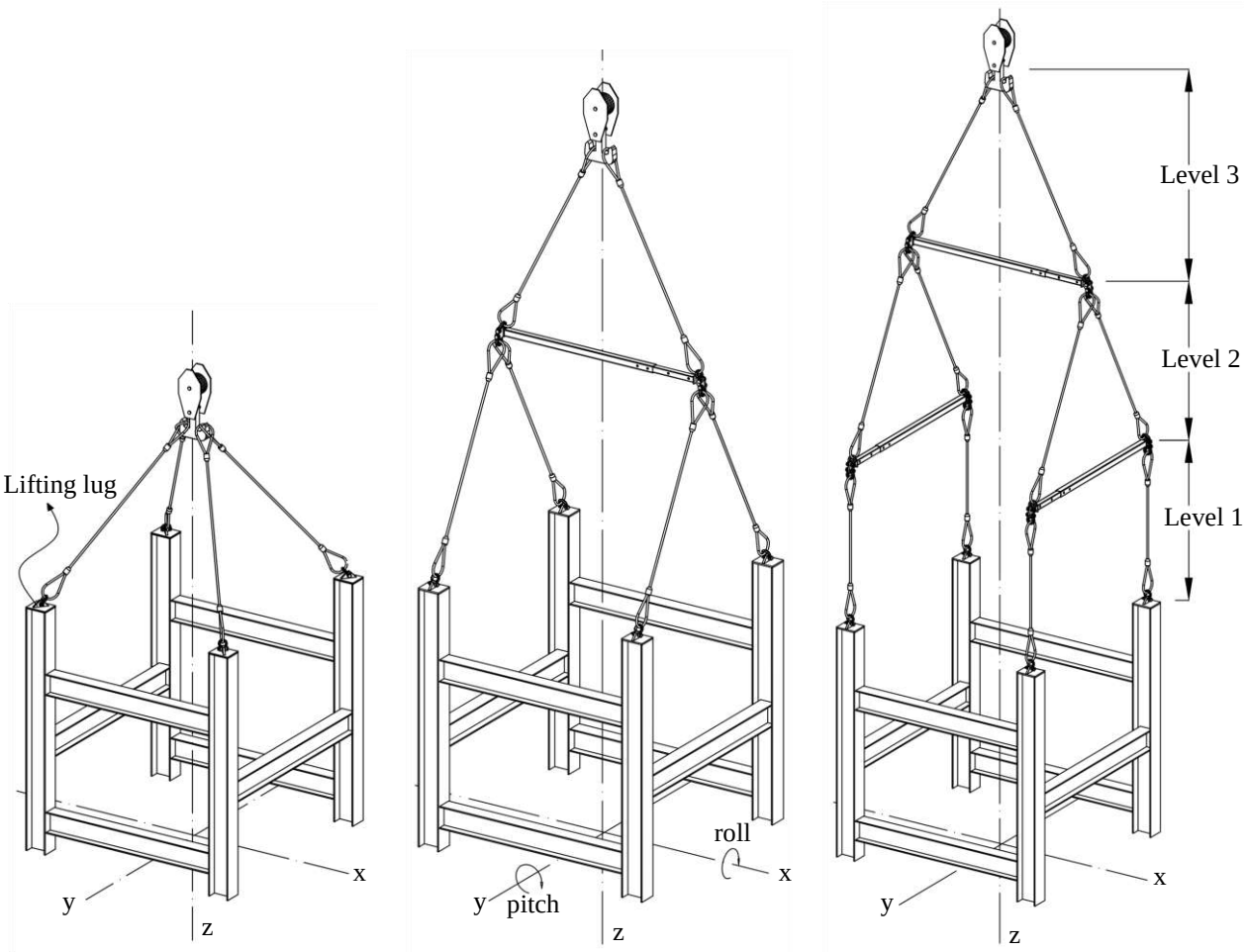

Figure 1-a Figure 1-b Figure 1-c

Figure 1. Three different slinging arrangements for a 4-poit pick module

In Figure 1-b, 8 shackles, 6 slings, and a spreader bar are used to first transfer the load from the lifting lugs to the spreader bar and from there to the crane's hook. The lifting lugs orientation needs to be along the y-axis of the module. In order to level up the module, the length of slings needs to be adjusted when the COG is offset. Regardless of the length of slings below the spreader bar, all of the slings will take the load [2].

In Figure 1-c, 16 shackles, 10 slings and 3 spreader bars are rigged in three levels. At the first level, the load is transferred vertically from the lifting lugs to two spreader bars along the y-axis of the module. From the second level to the crane's hook is virtually the same as Figure 1-b. When the COG is offset, in order to prevent the module from rolling and pitching (rotating around the x and y-axis of the object) the length of slings needs to be adjusted at the second and third level respectively. Needless to say, among the aforementioned slinging arrangement the latter is the only one that can ensure a vertical lift.

Operating two cranes and manipulating the length of their hoist lines could also be proposed as a way to control the pitch angle of the lifted module. However, operating a single crane is associated with a lower risk in comparison with operating two cranes or more. Thus, the lifting process is commonly accomplished by a single-crane operation unless the module, like vessels, necessitates vertical orientation at the set point [6]. In other words, it is not justifiable to add another crane only to have better control of the angle of lifted object considering the higher cost and risk of using more than one crane. In this regard, Chen et al [7] suggested a numerical model for manipulating the pitch angle of twin-hoisted objects with one crane. In their model, they adjust the length of the hoist lines of the boom and auxiliary jib to reach to the required pitch angle for the object during the lift. However, this model cannot be used to prevent the lifted object from rolling. In addition,

the available capacity of the crane becomes more limited when crane's auxiliary jib is used which is necessary for their model.

Designing the rigging assembly is a time-consuming and tedious process relying heavily on guesswork, especially when the COG is offset and sling length adjustment is required. When a module is not level after being lifted due to a wrong guess about the required sling length, the assembled rigging components need to be unrigged and adjusted again which leading to waste of time and decrease in productivity. In this respect, this paper presents a mathematical-based design framework which automates the design of the rigging assembly for 4-point pick modules. To ensure a vertical lift the third mentioned slinging arrangement is considered

2 Methodology

2.1 Overview

As it was mentioned earlier, if the Module's COG is offset in order to level up the module and spreader bars the length of slings needs to be adjusted at different levels of the rigging assembly. To compensate the offset toward y-axis of the module the two slings at the second level and on the opposite side of the COG are lengthened. Similarly, to compensate the offset toward x-axis of the module the sling at the third level and on the opposite side of the COG is lengthened. Lengthening the sling at the first level of rigging assembly is not desired since the spreader bars remain inclined.

As there are no slings with exact required lengths, the specified required length is made up using a standard sling and a number of shackles in chain. Each shackle has a specific inside length published in the supplier's manual. The question is: How many and what size of shackles should be used to reach the required amount of increase to the length of the slings. Added shackles have to meet the capacity requirement based on the sling they are attached to.

The research implements an automated design framework, written in C# language within Microsoft.Net framework. To find the angle of the forces acting upon the rigging components and also to find the required amount of increase to the length of slings, Wolfram Mathematica kernel is called within the code to solve a system of 12 nonlinear equations. Having the forces calculated, the framework selects the appropriate rigging elements from the Microsoft Excel database to which it is bound. The calculations are done in two perpendicular 2D planes of the rigging assembly (i.e. xz and yz).

As shown in Figure 2, the algorithm starts off by collecting the module information. In the next step, a preliminary rigging assembly is designed in which the module's COG is assumed to be at its center. Then by considering the COG offset and based on the calculations at the second and third level, the number, size, and capacity of the rigging components selected for the preliminary design are optimized to ensure that the module and spreader bars are maintained in a horizontal position during the lift. Finally, as the output, a list of used rigging components and the used percentage capacity of them, total height and weight of rigging assembly and the configuration figure in two 2D views is reported.

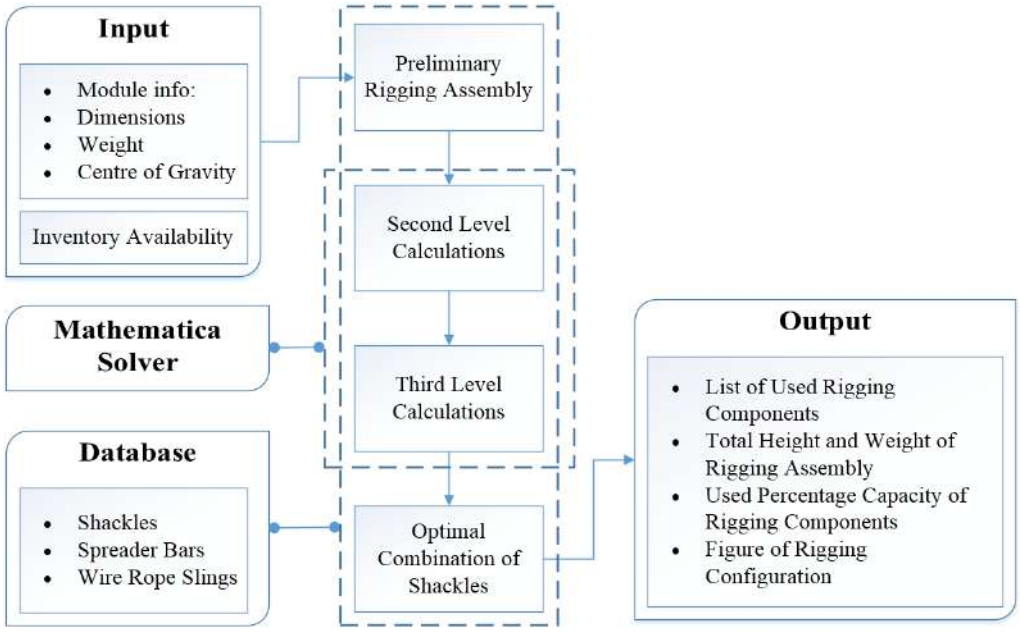

Figure 2. The framework algorithm

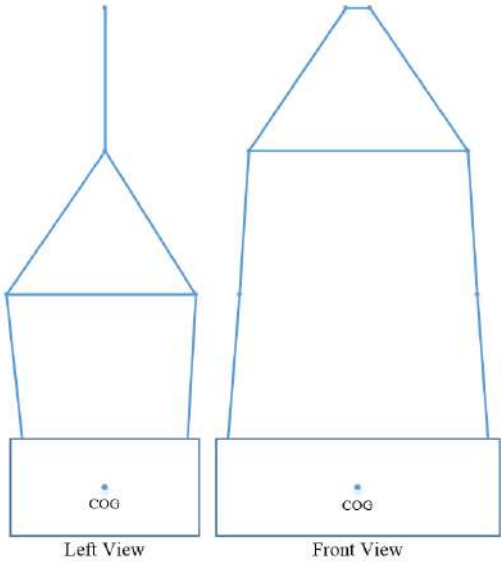

Figure 3. Left and front view of the rigging assembly for a 4-point pick module

2.2 Preliminary design

To design the preliminary rigging assembly, it is assumed that the module's COG is at its center. This will result in a symmetrical design in two perpendicular planes of the rigging configuration (Figure 3). The inclined lines in the figure represent the slings and the shackles they are attached to. The horizontal lines stand for the spreader bars except the top one in the front view which is the hook. Calculating the angles and in consequence, the forces acting upon the rigging components is straightforward due to the symmetrical configuration. Typically, the span of adjustable spreader bars has the intervals of one foot. Compared to the span of lifting lugs a shorter or longer spreader bar could be selected. This deviation in span will result in a non-vertical lift. In this case, the first four slings above the module, that are called drop slings, are lengthened to decrease their offset angle to the vertical line. The minimum acceptable offset angle is used as an input of the framework.

Based on the required capacity the minimum acceptable rated capacity is selected for each of the rigging components.

2.3 Second level calculations

The second level calculations are aimed at finding the angles between the slings and spreader bars and also calculating the required amount of increase to the slings when the COG offset is taken into consideration.

In either case shown in Figure 4, in order that the equilibrium conditions are satisfied the common point of inclined dashed red lines have to land on the vertical one. That is because the module's weight and the reaction force of the crane hoist lines to the hook is acting upon the vertical line; so the extensions of the inclined slings

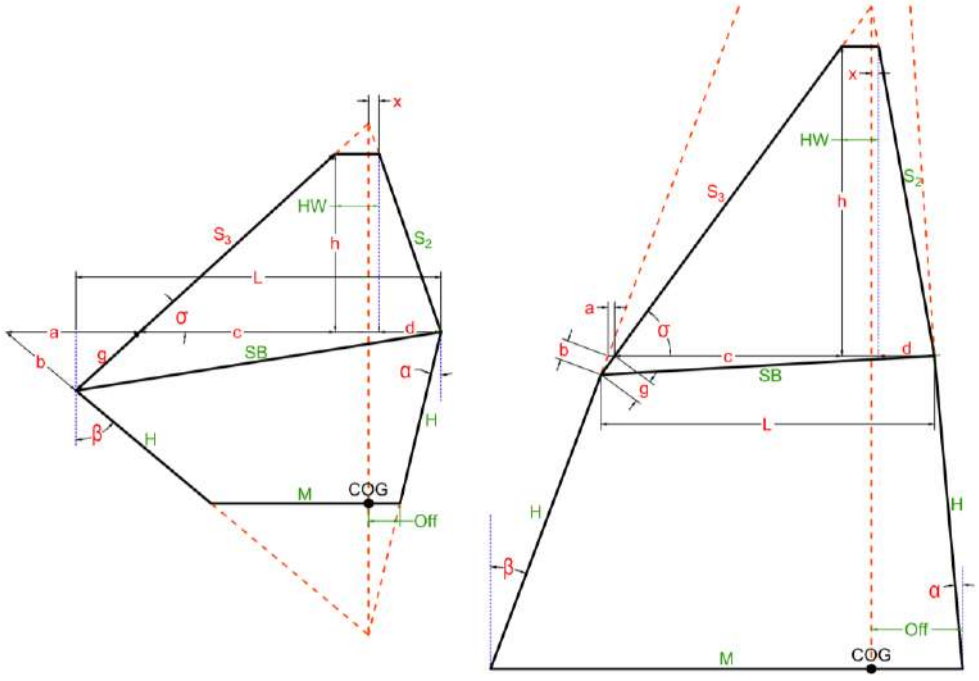

Figure 4. Schematic figure of rigging assembly when the spreader bar is longer (left figure) or shorter (right figure) than the distance between the lifting lugs

need to meet each other on the vertical line. To have a horizontal module, the spreader bar has a slight inevitable slope when the spreader bar and the module are unequal in length.

In Figure 4 (left) when the spreader bar is longer than the width of the module, there are 12 unknown variables, shown in red, which can be determined by solving a system of 12 nonlinear equations. The known and unknown variables are as follows:

Known variables: $\mathrm{HW}, M, \mathrm{Off}, \mathrm{SB}, \mathrm{S}_2, H$

HW: Width of the hook which is zero for the second level calculations.

M: Module width.

Off: The distance from the COG to the closer lifting lug in yz plane.

SB: Spreader bar length.

S_2: The total length of the sling and the shackles to which it is connected at the second level.

H: The total length of the drop sling and the shackles to which it is connected.

"HW", "ML" and "Off" are inputs of the framework. "SB", "S_2" and "H" are collected from the preliminary design.

Unknown variables: $x, \mathrm{S}_3, g, a, b, c, d, h, \alpha, \beta, \sigma, L$ as shown in Figure 4.

Where the equations are:

$$\mathrm{S}_2{}^2 = h^2 + d^2 \quad (1)$$
$$\mathrm{S}_3{}^2 = h^2 + c^2 \quad (2)$$
$$x/d = (\mathrm{HW} - x)/c \quad (3)$$
$$\mathrm{Off}/(H \operatorname{Sin}\alpha) = (\mathrm{M} - \mathrm{Off})/((H + b) \operatorname{Sin}\beta) \quad (4)$$
$$\mathrm{Off}/(x + d) = (\mathrm{M} - \mathrm{Off})/(a + c + \mathrm{HW} - x) \quad (5)$$
$$H \operatorname{Cos}\alpha = (H + b) \operatorname{Cos}\beta \quad (6)$$
$$b \operatorname{Cos}\beta = g \operatorname{Sin}\sigma \quad (7)$$
$$\mathrm{S}_3 \operatorname{Cos}\sigma = c \quad (8)$$
$$a = b \operatorname{Sin}\beta + g \operatorname{Cos}\sigma \quad (9)$$
$$L^2 + (g \operatorname{Sin}\sigma)^2 = \mathrm{SB}^2 \quad (10)$$
$$L = g \operatorname{Cos}\sigma + c + \mathrm{HW} + d \quad (11)$$
$$x + d = \mathrm{Off} + H \operatorname{Sin}\alpha \quad (12)$$

In Figure 4 (right), when the spreader bar is shorter than the width of the module equations 9 and 12 need to be replaced by the following two equations:

$$a + b \operatorname{Sin}\beta = g \operatorname{Cos}\sigma \quad (13)$$
$$x + d + H \operatorname{Sin}\alpha = \mathrm{Off} \quad (14)$$

And finally, when the length of spreader bar and the width of the module are the same, the value of a, b, g, α, β are equal to zero and S_3 is found using the following formula:

$$S_3 = \sqrt{\frac{(\mathrm{HW} - \mathrm{SB})^2(\mathrm{SB} - 2\mathrm{off}) + \mathrm{SB} \times S_2^2}{\mathrm{SB}}} \quad (15)$$

In any case, the required amount of increase (RAI) to the sling at the second level and on the opposite of the COG is equal to:

$$\mathrm{RAI} = \mathrm{S}_3 + g - \mathrm{S}_2 \quad (16)$$

That is, in fact, the difference between the length of two slings used above the spreader bar. In order to maintain the consistency at each level of the rigging configuration, identical slings are used and the required difference is made up by a chain of shackles.

After finding the unknown variables, the angles between the slings and spreader bars are calculated accordingly. Having the required capacity for each rigging component, the minimum acceptable rated capacity is selected from the database. If the COG is extremely offset, the angle of slings above the spreader bar will be very acute which increases the compression forces and bending moments applied to the spreader bar. In that case, there might not be any available spreader bar for the required capacity. So the next available longer sling will be selected for the slings above the spreader bar to increase the angle and decrease the required capacity.

2.4 Third level calculations

Similar to the second level calculations, the aforementioned system of equations is solved to find the RAI. However, some of the parameters have a different definition from their counterparts in the second level calculations.

M: Module length

Off: the distance from the COG to the closer lifting lug in xz plane.

S_2: The total length of the sling and the shackles to which it is connected at the third level.

H: the total height of the rigging assembly below the third level.

The rest of the parameters and equations are defined exactly the same as those in the second level calculations.

2.5 Optimal combination of shackles

In order to make up the optimal length with a chain of shackles, the goal function is defined as follows:

$$\mathrm{RAI} - \sum_{i=1}^{N} n_i d_i \leq 0 \quad (17)$$

Where:

RAI: The required amount of increase which calculated in the second and third level calculations.

N: The total number of shackles available with different size. Only those shackles which meet the capacity requirement based on the sling they are attached to.

n_i: The number of shackles i used in the chain.

d_i: The inside distance of shackle i.

This classic linear optimization problem is solved with a customized function using the Microsoft Solver

Table 1. The designed and used rigging components of rigging assembly on each level

	As Designed				As Used			
	Description	Required Capacity	Rated Capacity	Used Capacity	Description	Required Capacity	Rated Capacity	Used Capacity
Shackles attached to the lifting lugs	1-3/8 in (35 mm)	12.27 ton	13.5 ton	90.89%	1-3/4 in (44 mm)	12.27 ton	25 ton	49.08%
Drop slings	Ø1-1/4 in x 20 ft (Ø32 mm x 6.10 m)	27,052 lbs (12.27 ton)	30,000 lbs (13.61 ton)	90.17%	Ø2 in x 20 ft (Ø51 mm x 6.10 m)	27,051 lbs (12.27 ton)	74,000 lbs (33.57 ton)	36.56%
Spreader bars at level 2	NC-6L 14-24 @18 ft (5.49 m)	48,764 lbs (22.12 ton)	52,600 lbs (23.86 ton)	92.71%	NC-6L 14-24 @19 ft (5.79 m)	48,764 lbs (22.12 ton)	63,000 lbs (28.58 ton)	77.40%
Slings at level 2	Ø1-3/8 in x 15 ft (Ø35 mm x 4.57 m)	30,841 lbs (13.99 ton)	36,000 lbs (16.33 ton)	85.67%	Ø1-3/4 in x 20 ft (Ø44 mm x 6.10 m)	29,370 lbs (13.32 ton)	56,000 lbs (25.40 ton)	52.45%
Spreader bar at level 3	NC-8 18-31 @25 ft (7.62 m)	87,140 lbs (39.53 ton)	112,600 lbs (51.07 ton)	77.39%	NC-8 18-31 @25 ft (7.62 m)	87,140 lbs (39.53 ton)	112,600 lbs (51.07 ton)	77.39%
Slings at level 3	Ø2 in x 20 ft (Ø51 mm x 6.10 m)	56,100 lbs (25.45 ton)	74,000 lbs (33.57 ton)	75.81%	Ø2 in x 30 ft (Ø51 mm x 9.14 m)	51,755 lbs (23.48 ton)	74,000 lbs (33.57 ton)	69.94%
RAI at level 2	12.42 in (32.5 cm)				10.66 in (27.08 cm)			
RAI at level 3	18.38 in (46.69 cm)				12.62 in (32.05 cm)			
Total height	54 ft (16.46 m)				70 ft 6 in (21.49 m)			
total weight	4,414 lbs (2.00 ton)				5,591 lbs (2.54 ton)			

Foundation library.

3 Case study

In order to validate the framework, the rigging assembly design of a 4-point pick module is taken into consideration as a case study. The following described module has been successfully lifted and erected in one of the NCSG Crane & Heavy Haul Corporation's projects. The module has 45 ft. (13.72 m) length, 17 ft. 7 in (5.36 m) width and 15 ft. 1 in (4.59 m) height. The lifting lugs of the module which are located at its bottom make a 25 ft. 2 in (7.67 m) by 17 ft. 7 in (5.36 m) rectangle. The module's COG is offset by 1 ft. 6 in (0.46 m) and 1 ft. (0.29 m) from the center of the rectangle towards x and y-axis of the module respectively. Thus, sling length adjustment is needed at the second and third levels of the rigging configuration. As the lifting lugs are at the bottom of the module, the length of the drop slings is needed to be greater than the module height. This is added to the design framework as a constraint. The rigging assembly is designed by the proposed framework and is compared to what was actually used on the job site. Table 1 represents the designed and used rigging components of rigging assembly on each level. As it is clear in the table, the design with the proposed framework is more efficient as the total height and weight of the automatically designed rigging assembly are 23.31% and 21.05% less than manually designed one respectively. In order to increase the length of slings at level 2 of the rigging configuration, a combination of one 25-ton and one 13.5-ton shackle is added to make up a chain with 12.25 in (31.12 cm) length. Similarly, a combination of one 55-ton and one 35-ton shackle is added to the slings at level 3 to increase the length of the sling by 18.25 in (46.36 cm). In the manually designed rigging assembly, one 55-ton shackle has been added to both second and third level to increase the length of slings by 10.5 in (26.67 cm). The designed shackles for the lifting lugs might not be suited in term of size. In that case, larger shackles could be replaced after completion of the design to match the size of lifting lugs.

4 Summary and future research

In this paper, a mathematical based design framework is presented which automates the selection of rigging assembly for 4-point pick modules. The framework collects the module information and calculates the required capacity for each rigging component using a mathematical-based solver and selects the most suitable rigging components from the database. The final

designed assembly ensures a vertical lift while the module and spreader bars are maintained horizontal during the lift. This results in a safe and time efficient lift in contrast to the current practice which is time-consuming and relies heavily on guesswork especially when the COG is offset.

This paper uses a case study in order to validate the practicality of the proposed framework. The case study proves that the automatically designed lift study is more efficient in terms of: total height and weight of the rigging assembly, inventory list of rigging components and detailed position of them.

The presented methodology is applicable to modules with 4 lifting points. In future research, the framework should be developed in order to automate the rigging assembly design for modules with more lifting points. As an instance, the rigging assembly for a module with 16 lifting points consists of 5 levels of rigging configuration which includes at least 270 rigging components [1]. This increases the complexity of the rigging system exponentially. In that respect, automation in rigging assembly design could be highly beneficial for large modules with more than 4 lifting points.

5 Acknowledgments

The authors would like to show their gratitude to the Natural Sciences and Engineering Research Council of Canada (NSERC) and NCSG Crane & Heavy Haul Corporation who supported this research.

References

[1] Westover L., Olearczyk J., Hermann U., Adeeb S., and Mohamed Y. Analysis of rigging assembly for lifting heavy industrial modules. *Canadian Journal of Civil Engineering*, 41(6), 512-522, 2014.

[2] Anderson J. K. *Rigging Engineering Basics*, 1(1), ITI Bookstore, Woodland, Washington 98674, 2013.

[3] The Crosby Group LLC. *Crosby General Catalogue*. 2801 Dawson Rd., Tulsa, OK 74110, 2017.

[4] Sam M. T. Offshore Heavy Lift Rigging Analysis Using Spreadsheet. *Practice Periodical on Structural Design and Construction*, 14(2), 63-69, 2009.

[5] Longman R.W. and Freudenstein, F. Stability Analysis of Lifting Rigs—Part 1: Necessary and Sufficient Conditions. *Journal of Engineering for Industry*, 97(2), 532-536, 1975.

[6] Han S., Hasan S., Bouferguene A., Al-Hussein M., and Kosa J. An integrated decision support model for selecting the most feasible crane at heavy construction sites. *Automation in Construction*, *87*, 188-200, 2018.

[7] Chen P., Zhuang Z., Chang C. and Kang S. A Numerical Model for the Attitude Manipulation of Twin-Hoisted Object. In *Proceedings of the 35th ISARC*, pages 211-215, Berlin, Germany, 2018.

An Analysis of the Problems of BIM-Based Drawings and Implementation During the Construction Document Phase

Y. Kim[a] and S. Chin[b]

[a]Department of Convergence Engineering for Future City, Sungkyunkwan University, Korea
[b]School of Civil, Architectural Engineering, and Landscape Architecture, Sungkyunkwan University, Korea
E-mail: dlwpek@skku.edu, schin@skku.edu

Abstract –

As construction projects become larger and more complex and the amount of information increases, the necessity of introducing BIM becomes bigger and the importance of BIM-based drawing extraction is also increasing. In particular, the construction document (CD) stage draws and documents the subjects determined from the project planning stage so that actual construction can be possible. Therefore, information management and drawings using BIM in the CD stage have a great impact on the design, construction, and maintenance stages. However, in practice, the BIM results in the CD stage do not include all the necessary information in the construction stage, and the practical use of the drawings extracted from BIM is low.

To solve this problem, this study first analyzed the current status and level of BIM-based drawings in the CD stage by investigating projects that apply BIM in the Korean construction market. Next, the limitations and problems of BIM-based drawings are analyzed from a practical perspective by experts using the Delphi method. Finally, based on the results, methods to improve BIM-based drawings and work efficiency are discussed.

The results of this study can be interpreted based on how the BIM is perceived in different country. However, this study analyzes the current status and problems of BIM applications from general and practical perspectives. It will contribute to further activation of BIM in the architecture, engineering, and construction (AEC) industry if BIM-based drawing standards are established based on this study and follow-up studies are conducted on the development of quality and consistency review models for BIM-based drawings.

Keywords –

BIM; BIM-based drawings; Construction documents; Construction drawings; Construction document phase

1 Introduction

1.1 Research Background and Purpose

As construction projects become larger and more complex and the amount of information increases, two-dimensional (2D) based drawing information systems are switching to three-dimensional (3D) building information modeling (BIM) based information systems [5][11][17]. However, even with this change, drawings remain as a contract standard or legal unit; hence, creating and managing drawings in a BIM-based information system is important [4][7][9]. In particular, the construction document (CD) stage draws and documents the subjects determined from the project planning stage so that actual construction can be possible. Therefore, information management and drawings that use BIM in the CD stage largely affect the design, construction, and maintenance stages. However, in practice, an inefficient and limited collaborative environment exists among the participants, and the BIM results in the CD stage do not include all the necessary information in the construction stage [1][3][10].

To solve this problem, our laboratory has researched rational methods to extract drawings from BIM in the CD stage and investigate the consistency between the BIM results and design drawings in the CD stage. As part of this study, this paper presents the analysis results of our previous works.

First, we analyzed the current status and level of BIM-based drawing in the CD stage according to the construction work and drawing types by investigating an actual BIM application project in the Korean construction market. Second, we analyzed the limitations and problems in BIM-based drawings from the practical viewpoint of experts using the Delphi method. Finally, from the analyzed results, methods to improve BIM-based drawings and work efficiency are discussed.

The results of this study may be different depending on how BIM is implemented in each country. However,

this study aimed to analyze the current status and problems of the BIM application process from a general and practical perspective. If a BIM-based drawing standard is established and follow-up studies on the quality of drawings and development of a consistent review model are carried out according to the results of this study, it would help enable the automation of drawing extraction and verification in the CD stage using BIM. Therefore, the results of this study will strengthen the BIM-based design process and further promote the activation of BIM in the architecture/engineering /construction (AEC) industry.

1.2 Research Scope and Method

In this paper, we present the necessity and direction of BIM-based drawing plans by discussing the analysis of actual practical problems and the current situation regarding BIM-based drawing works in the CD stage.

To investigate the current status of the BIM-based drawings, actual drawings and BIM performance reports of three office buildings where BIM was applied in public construction projects in Korea were analyzed. In addition, a survey among experts was conducted using the Delphi method to analyze the problems and limitations of BIM-based drawings. The Delphi method statistically and systematically analyzes survey results using two or more questionnaires provided to an expert group in a specific field of expertise [6][12]. This is an efficient method for analyzing results when empirical evidence is lacking or when objective data collection is difficult [6][12]. Therefore, in the present study, two surveys and interviews were conducted with 10 design experts and five construction engineers who are experienced in BIM-based drawings in the CD stage. In the first survey and interview, the problems and limitation factors of BIM-based drawing-extraction works from a practical viewpoint were derived. The second survey, which applied a five-point scale (very low: 1 point to very high: 5 points) on the drawing-hindrance factors obtained from the first survey, was carried out to analyze the average values and stability (standard deviation/calculated average). From this analysis, we verified the severity and reliability of BIM-based drawing-hindrance factors.

2 Literature Review

Despite the advantages of using BIM and its major technological advances, BIM has not been fully established in the Korean construction industry because of practical problems and limitations [5]. In particular, as the necessity for effective linkage between BIM and existing 2D drawings in the design-process stage has increased, studies on the problems of introducing BIM into the design process and development plan of BIM-based drawings have been carried out. According to literature reviews, the problems of extracting drawings using BIM can be divided into the following three categories:

1. Inevitable additional work

- In BIM, additional information should be supplied to the first automatically generated drawing to complete the drawing [2][4][9][10][19].

2. Limitations of drawing representation according to the level of details

- The level of details expressed by a BIM model does not reach the level of existing drawings [2][3][10][19].

3. Slow working speed

- If the level of details is increased to that of existing 2D drawings, the modification and creation of the BIM model become slow [2][10].

To solve these problems, Chae and Lee [2] developed alternative solutions for the problems of existing drawing-representation methods using Korean and American cases when introducing BIM to architectural drawings. They also suggested an improvement plan for drawing licensing and delivery efficiency that are applicable to the Korean construction industry. In addition, Oh et al. [17] proposed the need for a BIM-based integrated design system to solve problems such as data loss, communication difficulties, and poor work efficiency resulting from the use of different BIM-based software among designers in the design stage. Lee and Jeon [11] also suggested a BIM-based integrated design process to improve the inefficient drawing-generation process due to institutional constraints. Kwon and Jo [9] proposed the development direction of 2D electronic drawing standards for effective introduction of BIM-based drawings.

Studies were also made on specific BIM software. Song and Jeon [18] classified the main functions provided by the Revit BIM software and conducted a survey on architectural design offices relative to the user perception of the BIM process and the current status and problems of BIM design works. Lee, Jeong, and Oh [10] compared the method of applying Revit to construction drawings of wall-type apartments with the existing 2D-based work method to analyze the additional work required and the work efficiency of BIM-based construction drawings. Cho and Lee [3] verified the possibility of printing the working-design drawings to the same level as those that used existing computer-aided design (CAD) systems when printing drawings using Revit.

To maximize the efficiency of BIM, Kim et al. [8]

developed an automatic 2D drawing program at the level of design development (DD) stage. Studies on the automatic generation of BIM-based drawings mainly focused on drawings for licensing at the DD level and extraction of shop drawings for production of specific materials. Zaki [19] developed a parametric model for automatic generation of shop drawings and detailed quotations for block walls in BIM. Manrique et al. [15] proposed a parametric and BIM-based automatic extraction of detailed drawings (FRAMEX) for wood members. Liu et al. [13] presented a solution that can automatically extract the layout configuration and material-cutting plan for a light residential building using BIM.

Previous studies related to BIM-based drawings presented methods to improve the efficiency of BIM drawing by deducing the problems that arise from a specific construction work field (referred to as "work type") or specific BIM software. However, research on the problems and application in the CD stage has been insufficient. Studies have been conducted on the extraction of drawings in the DD stage or shop drawings for product fabrication; however, no studies on BIM-based drawing automatic generation have investigated drawing extraction in the CD stage. Therefore, the present study aims to analyze the practical problems and limitations of BIM-based drawing works from a practical point of view, instead of focusing on the specific construction or software problems in the CD stage.

3 Analysis of current status of BIM-based drawings

3.1 Application of BIM-based drawings by work type

To investigate the current status and level of BIM-based drawings in the CD stage in terms of the construction work type and to identify the problems of each type, actual drawings and BIM performance reports of three office buildings, which are public construction projects in Korea, were analyzed. The analyzed work types were architecture, structure, machine equipment, electricity, and fire protection where BIM was applied during the CD and construction stages in the three cases.

3.1.1 Architecture and structure

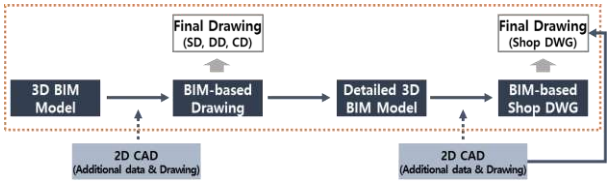

Figure 1. Current status of BIM-based drawings in the field of architecture and structure

In the architectural and structural work cases, BIM-based drawing work was performed using a 3D BIM model. Here, depending on the drawing type, additional 2D CAD work or 2D CAD drawings were performed. Extracting the drawings in the schematic design (SD), DD, and CD stages and the shop drawings during the construction stage could be possible.

3.1.2 Machine equipment

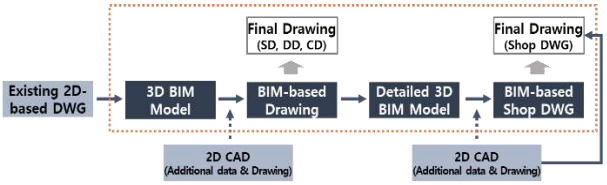

Figure 2. Current status of BIM-based drawings in the field of machine equipment

In the machine equipment case in the Korea AEC industry, the 3D BIM model was constructed from existing 2D CAD drawings, and the constructed model was processed using BIM, if necessary. Similar to the architectural and structural works, during the BIM-based drawing, extracting the drawings in the SD, DD, and CD stages and the shop drawings in the construction stage was possible, depending on the drawing type, using additional 2D CAD works or 2D CAD drawings. However, implementation of the BIM-based drawing work was low during the design stage.

3.1.3 Electricity and fire protection

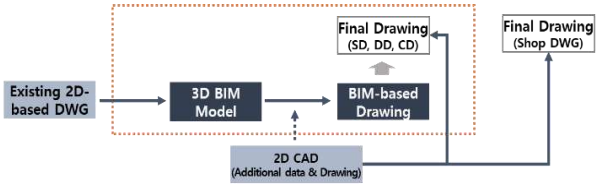

Figure 3. Current status of BIM-based drawings in the field of electricity and fire protection

In the electricity and fire protection work cases, similar to the machine work, the 3D BIM model was constructed from existing 2D CAD drawings, and the constructed model was processed using BIM, if necessary. During the BIM-based drawing, depending on the drawing type, extracting the drawings in the SD, DD, and CD stages was possible by performing additional 2D CAD works or 2D CAD drawings. In the shop drawings in the construction stage, 2D CAD drawings were utilized in most cases.

3.2 Utilization of BIM-based drawing according to drawing type: Architecture and structure

The level of utilization of a BIM-based drawing is different according to the work type. For the architecture and structure work types, the BIM model was not built according to the 2D CAD drawings, but the BIM-based drawing was performed after the BIM model was developed.

On this basis, this section presents our analysis of the BIM-based drawing extraction methods according to the drawing type of the architectural and structural works. The BIM-based drawing extraction result in the CD stage according to the three drawing methods is listed in Table 1.

Table 1. BIM-based drawing methods according to the drawing type

Classification	Drawing method
① BIM	Extraction of drawings from BIM
② BIM + CAD	Additional 2D CAD work on the BIM-extracted drawings
③ CAD	Drawing using CAD

3.2.1 Architecture

In the architectural work cases, 10% of the drawings were extracted from BIM, 54% of the drawings were completed by additional 2D CAD works on the BIM-extracted drawings, and 36% of drawings were CAD drawings. In other words, according to the characteristics of each drawing, 64% BIM-based drawing work was performed, and 36% was performed using CAD (Table 2). The drawing-extraction methods for each type of drawing were classified as listed in Table 3.

Table 2. Current status of the BIM-based drawing methods: Architecture

Classification	Percentage (%)		Note
① BIM	10	64	BIM utilization
② BIM + CAD	54		
③ CAD	36	36	CAD utilization
Total	100	100	-

Table 3. Drawing method according to the type of drawing: Architecture

Classification	Drawing type
① BIM	Floor plan, elevation, main section, window section, etc.
② BIM + CAD	Plot plan, plan drawing, enlarged plan, enlarged cross-section, plane/elevation details, etc.
③ CAD	Site planimetric map, interior material finish schedule, other detailed drawings, etc.

3.2.2 Structure

In the case of structural works, 10% of the drawings were BIM-extracted drawings, 44% were completed by additional 2D CAD works on the BIM-extracted drawings, and 46% were CAD drawings. In other words, 54% of BIM-based drawing work was performed, and 46% was performed using CAD (Table 4). Compared with the architectural works, the utilization rate of the CAD drawings was relatively high. The drawing-extraction methods in each drawing type are classified as listed in Table 5.

Table 4. Current status of BIM-based drawing methods: Structure

Classification	Percentage (%)		Note
① BIM	10	54	BIM utilization
② BIM + CAD	44		
③ CAD	46	46	CAD utilization
Total	100	100	-

Table 5. Drawing method according to the type of drawing: Structure

Classification	Drawing type
① BIM	Structure plan, column center plan, structure cross section, etc.
② BIM + CAD	Enlarged structure plan, Enlarged column center, partial structure cross section, etc.
③ CAD	Structure general items, schedule, detailed drawings, etc.

4 Limitations and problems of BIM-based drawing from a practical perspective

From the analysis of the BIM-based drawing applications discussed in Section 3, the problems and limitations of the BIM-based drawing-extraction work in the CD stage were investigated. For this purpose, the BIM model and the extracted drawings from the BIM project were analyzed. In addition, a survey using the Delphi method was conducted twice from 10 design experts and five construction engineers who were experienced in BIM-based drawings in the CD stage. In the first survey and interview, the problems and limitation factors of the BIM-based drawing-extraction works from a practical viewpoint were obtained. To verify the severity and reliability of each item in the drawing-inhibition factors obtained from the first survey, the average and stability (standard deviation/calculated average) of each item were analyzed through the second survey, which applied a five-point scale (very low: 1 point to very high: 5 points). Thus, the present study verified the severity and reliability of the BIM-based drawing-hindrance factors. The limitations and problems of the BIM-based drawing obtained in this process from the practical viewpoint are described in the next section.

4.1 Functional problems in BIM software

Because of the functional limitations of the detailed expressions of BIM-based drawings using the BIM software, cases arise where drawings created using 2D CAD are used as they are, or drawing elements extracted from the BIM model are used after being modified using the BIM software (Table 6).

Table 6. Results of the Delphi analysis of the limitations or problems: 1

Limitations or problems	Average	Standard deviation	Stability
Inevitable additional work	4.60	0.49	0.107
Functional limitations for detailed drawings of BIM software	3.20	0.75	0.234

The plan and cross sections of the delivered architectural and structural works of the three analyzed projects were created from the BIM drawing-extraction method (Tables 3 and 5). From the analysis results of extracting the expression elements in each drawing using the following two methods, extracting approximately 75% of the architectural plan without additional work using BIM was made possible. In the structural cross section, 80% of the drawing elements could be generated by additional work using BIM (Table 7).

- Method 1: Automatic extraction
  - Elements that can be used as drawing elements without additional work after extraction from the BIM model
  - Examples: grid, architectural wall, window, elevator, etc.
- Method 2: Additional work
  - Elements that require additional work after extraction from the BIM model
  - Examples: leader line, structural wall, parking lamp, equipment-related facility, etc.

Table 7. BIM-based drawing element-extraction method

Drawing type		BIM-based drawing-work method according to element (%)		
		Automatic extraction	Additional work	Total
Architecture	Plan	75	25	100
	Section	56	44	100
Structure	Plan	60	40	100
	Section	20	80	100

4.2 Differences in the application and utilization level of BIM according to work type

Participant collaboration and integrated management among works are the main purpose and greatest advantage of utilizing BIM [4][14][16]. However, because the utilization level of BIM-based drawings among works is different (as discussed in Section 3), limitations exist in integrating project management using BIM-based drawings. In particular, in the mechanical, electrical, and plumbing (MEP) field, which corresponds to machine equipment, electricity, and fire-protection work types, the capacity of the BIM model was approximately three times larger than that of the architecture or structure type. In addition, restrictions on the drawing work in the CD stage appeared because a detailed model was not determined. Furthermore, the participant ability to perform BIM was lower than that in the architectural and structural works. Therefore, BIM was performed by the service supplier, and utilization of the BIM model was low. In the MEP case, fitting and route changes frequently occurred at the construction site. Hence, confidence on the pre-verification using BIM was lacking. Because according to the contract, the specialized company was not responsible for the quantity, it did not empathize with the need to confirm the interference and to calculate an accurate quantity in advance using BIM.

Table 8. Results of the Delphi analysis on the limitations or problems: 2

Limitations or problems	Average	Standard deviation	Stability
Different utilization level of drawing according to work	4.60	0.49	0.107
Determination of MEP detailed model (design plan) at construction stage	4.60	0.49	0.107
Lack of ability of participants to perform BIM	4.50	0.50	0.111
MEP BIM model capacity size	4.40	0.66	0.151

4.3 Process and institutional issues

Problems are encountered in using BIM-based drawings from the process and institutional perspectives (Table 9). When a public organization that makes an order (owner) requests a delivery form based on existing 2D drawings and the criteria and guidelines of the delivery form of the BIM drawing and BIM-based drawing are not specified, delivering and utilizing the drawings extracted from the BIM are difficult. In particular, when a professional subcontractor who performs practical construction work participates in the construction stage, new design plans and decisions are often made, such as capacity to construct and interference. The resulting modification in the BIM model and the drawings represent considerable hindrance factors in BIM-based drawing-extraction work. In addition, when the service cost is not clearly specified according to the BIM work and application scope, BIM is passively utilized, resulting in a low BIM application effect.

Table 9. Results of the Delphi analysis on the limitations or problems: 3

Limitations or problems	Average	Standard deviation	Stability
Frequent design changes	4.60	0.49	0.107
Request delivery of 2D CAD form drawings (double drawing work)	4.10	1.22	0.298
Lack of criteria and guidelines for BIM-based drawings	3.80	0.40	0.105
Lack of BIM service costs due to low-cost bidding	3.40	0.80	0.235

5 Discussion

In this section, the factors that must be considered for promoting the use of BIM in the construction industry and improving the efficiency of BIM-based drawing work using the current status of BIM-based drawing works (Section 3) and analysis of actual problems

(Section 4) are discussed.

5.1 Establishment of a standard BIM delivery process

Establishing a standard BIM delivery process is necessary by standardizing the roles and responsibilities of each participant in each step of a BIM application project. Therefore, the BIM work system should be evolved into a system centered on the design and construction practitioners, rather than on the BIM-specialized service companies, by improving the drawing and delivery standards using BIM in the CD stage that serve as the BIM guidelines for practitioners.

5.2 Development of drawing templates

As presented in Sections 3 and 4, cases arise where some 2D CAD drawings are used or elements extracted from BIM are used as drawing elements through additional work in the BIM-based drawing-extraction process. Therefore, defining the minimum essential expression element for each drawing is necessary through the following: 1) considering the work efficiency from a practical viewpoint, 2) classifying and presenting the elements utilizing 2D CAD drawings and the elements that use the BIM model, and 3) gradually reducing the range of 2D CAD utilization factors that require unnecessary additional work. In addition, BIM-based drawing templates for each design stage should be developed so that the drawing-extraction work can be efficiently performed according to the work method in the BIM environment.

5.3 Automation of quality inspection and drawing extraction

The drawings extracted from BIM should be automatically updated when the BIM model is used. However, when the drawing element is not automatically extracted during the drawing extraction, additional works should follow. Therefore, examining the consistency between the BIM model and drawings is necessary. If the drawing elements in each drawing are defined and reviewed by classifying the extraction method for each element, the quality of the drawing (as well as the consistency), can be examined. Thus, if a checklist for the extraction method of each drawing type can be derived (and software can automatically check it), quality inspection and drawing-extraction automation will be possible.

6 Conclusion

This paper has presented the analysis results of previous works as part of a study to develop a rational method of deriving CD stage drawings using BIM and a model for examining the quality and consistency of the drawings derived from BIM.

First, we analyzed the current status and level of BIM-based drawing in the CD stage by investigating an actual BIM project case in the Korean construction market (Section 3). As a result, the level of utilization of BIM-based drawings in terms of the construction work type was different. The level and method of utilization according to the drawings also varied depending on the characteristics of the drawing and efficiency of the work.

Second, the limitations and problems of the BIM-based drawing works were derived from a practical viewpoint using the Delphi method involving experts. The derived limitations and problems can be categorized into the following three characteristics: 1) functional issues of the BIM software, 2) difference in the BIM application and utilization level in terms of the construction work type, and 3) process and institutional issues. The limitations and problem factors of each item were analyzed by applying a five-point scale. All stability values were 0.5 or less; therefore, the validity and reliability were determined.

Application of the results of this study may be different depending on the implementation in each country. However, this study is significant because it analyzed the current status and problems of the BIM application process from a general and practical perspective. In addition, stimulating BIM utilization in the AEC industry and improving the work efficiency of BIM-based drawings are possible if follow-up studies are conducted by considering the work environment and reality according to the status and problem analysis results. These studies should include the following: 1) establishment of standard BIM delivery process, 2) development of BIM-based drawing templates, and 3) automation of BIM drawing quality inspection and BIM-based drawing extraction.

Acknowledgement

This research was supported by a grant (18AUDP-B127891-03) from the Architecture & Urban Development Research Program funded by the Ministry of Land, Infrastructure and Transport of the Korean government.

A part of this work was also supported by the National Research Foundation of Korea (NRF) grant funded by the Korea government (MSIT) (No. 2018R1A2B6003564).

References

[1] Arayici, Y., Fernando, T., Munoz, V., and Bassanino, M. Interoperability specification

development for integrated BIM use in performance based design. *Automation in Construction*, 85, 167-181, 2018.

[2] Chae, K.S. and Lee, G. A study on the problems and the measurements for improving representations and drafting methods of architectural drawings by adopting BIM. *Transactions of the Architectural Institute of Korea*, 27(10), 67-74, 2011.

[3] Cho, Y.S. and Lee, H.W. A study on the possibility of 2D design drawing implementation by Revit Architecture. *Journal of Korea Academy Industrial Cooperation Society*, 14(10), 5243-5250, 2013.

[4] Eastman, C., Teicholz, P., Sacks, R., and Liston, K. *BIM Handbook: A Guide to Building Information Modeling for Owners, Managers, Designers, Engineers and Contractors.* John Wiley & Sons, 2011.

[5] Ghaffarianhoseini, A., Tookey, J., Ghaffarianhoseini, A., Naismith, N., Azhar, S., Efimova, O., and Raahemifar, K. Building information modelling (BIM) uptake: Clear benefits, understanding its implementation, risks and challenges. *Renewable and Sustainable Energy Reviews*, 75, 1046-1053. 2017.

[6] Hallowell, M.R. and Gambatese, J.A. Qualitative research: Application of the Delphi method to CEM research. *Journal of Construction Engineering and Management*, 136(1), 99-107, 2009.

[7] Kazaz, A., Acıkara, T., Ulubeyli, S., and Koyun, H. Detection of architectural drawings errors in 3 dimension. *Procedia Engineering*, 196, 1018-1025, 2017.

[8] Kim, I.H., Lee, M.J., Choi, J.S., and Kim, G.T. Development of an application to generate 2D drawings in automation using Open BIM technologies. *Korean Journal of Computational Design and Engineering*, 21(4), 417-425, 2016.

[9] Kwon, O.C. and Jo, C.W. A study on the improvement of 2D digital drawing standards considering the paradigm shift to BIM. *Journal of the Architectural Institute of Korea Planning & Design*, 24(5), 49-57, 2008.

[10] Lee, J.C., Jung, J.H., and Oh, H.O. Work efficiency analysis of BIM based structural drawing. *Journal of the Architectural Institute of Korea Structure & Construction*, 29(6), 21-28, 2013.

[11] Lee, J.H. and Jun, H.J. A study on the adaptability of BIM-based integrated building design process in domestic architectural design firms. *Journal of Korean Institute of Interior Design*, 16.6: 19-27, 2007.

[12] Linstone, H.A. and Turoff, M. (Eds.). *The Delphi Method* (pp. 3-12). Reading, MA: Addison-Wesley, 1975.

[13] Liu, H., Singh, G., Lu, M., Bouferguene, A., and Al-Hussein, M. BIM-based automated design and planning for boarding of light-frame residential buildings. *Automation in Construction*, 89, 235-249. 2018.

[14] Liu, Y., Van Nederveen, S., and Hertogh, M. Understanding effects of BIM on collaborative design and construction: An empirical study in China. *International Journal of Project Management*, 35(4), 686-698, 2017.

[15] Manrique, J. D., Al-Hussein, M., Bouferguene, A., and Nasseri, R. Automated generation of shop drawings in residential construction. *Automation in Construction*, 55, 15-24. 2015.

[16] Migilinskas, D., Popov, V., Juocevicius, V., and Ustinovichius, L. The benefits, obstacles, and problems of practical BIM implementation. *Procedia Engineering*, 57, 767-774, 2013.

[17] Oh, M., Lee, J., Hong, S.W., and Jeong, Y. Integrated system for BIM-based collaborative design. *Automation in Construction*, 58, 196-206, 2015.

[18] Song, K.M., John, Y.S., and Song, K.M. A comparative analysis on BIM usage between Korean & USA architectural firms regarding effective design process. *Journal of Digital Design*, 12(4), 523-533, 2012.

[19] Zaki, T. *Parametric Modeling of Blockwall Assemblies for Automated Generation of Shopdrawings and Detailed Estimates using BIM.* Thesis for Masters of Science in Construction Management, The American University, Cairo, 2016.

Identification of the Structural State in Automated Modular Construction

A. Harichandran[a,b], B. Raphael[a], and A. Mukherjee[b]

[a]Building Technology and Construction Management Division, Indian Institute of Technology Madras, India
[b]Department of Civil Engineering, Curtin University, Bentley, WA 6102, Australia
E-mail: aparnaharichandran@gmail.com, benny@iitm.ac.in, abhijit.mukherjee@curtin.edu.au

Abstract –

Automated construction involves complex interactions between machines and humans. Unless all possible scenarios involving construction and equipment are carefully evaluated, it may lead to failure of the structure or may cause severe accidents. Hence monitoring of automated construction is very important and sensors should be deployed for obtaining information about the actual state of the structure and the equipment. However, interpreting data from sensors is a great challenge. In this research, a methodology has been developed for monitoring in automated construction. The overall methodology involves a combination of traditional model-based system identification and machine learning techniques. The scope of this paper is limited to the machine learning module of the methodology. The efficacy of this approach is tested and evaluated using experiments involving the construction of a steel structural frame with one storey and one bay. The construction is carried out by a top-to-bottom method. During the construction of the frame, 99 base cases of normal operations are involved. 158 base cases of possible failures have been enumerated. Failure cases involve, for example, certain lifting platforms moving faster than others, improper connections of joints, etc. Strain gauges and accelerometers are installed on the structure and the data from these sensors are used to determine possible failure scenarios. Preliminary results indicate that machine learning has good potential for identifying activities and states in automated construction.

Keywords –

Structural Monitoring, System Identification, Machine Learning, Automated Construction Monitoring

1 Introduction and Background

The construction industry is one of the oldest and biggest industries in the world. Diffusion of the latest technology is difficult in construction compared to other industries due to diverse parties and uncertainties involved in construction projects. Development of construction technologies is highly influenced by the innovative technologies in other fields. Introduction of robotics and automation in construction is inevitable due to advantages such as improvement of productivity, reliability and quality, enhancement of working conditions, safety, component standardization, workforce simplification and savings in lifecycle cost as well as labour cost [1].

Automating the construction processes involves a lot of complexities in micro-level details. Machines cannot anticipate certain conditions which may look obvious to a human being. This may lead to either failure of the structure being constructed or severe accidents or both. Hence monitoring of automated construction is of paramount importance.

2 Automated Monitoring of Construction

Sensors are widely used for automated monitoring of constructed structures as well as structures under construction. In structural health monitoring, constructed structures are measured to check for the presence of defects or reserve capacity [2]–[4]. Construction activities are being monitored for ensuring various requirements such as safety practices [5], the productivity of the workers [6] and the progress of the work [7]–[9]. Sensor-based monitoring to ensure the stability of the structure is rarely studied. Cho *et al*. used strain measurements to predict the conditions of collapse for scaffolding structures using machine learning [10]. This method requires an accurate model of the scaffolding as input, which might not be available in most of the construction sites. Other than temporary structures, there are cases of monitoring of construction of high-rise buildings. Choi *et al*. studied column shortening effects of high-rise buildings with wireless strain sensing system in real-time [11]. The sensors are embedded in the column while it is being constructed. Measurements with the sensors and transferring the measured data through a wireless sensor network are automated through this system. However, from the monitored column shortening data the managers have to

take appropriate corrective actions manually.

It is evident from various examples discussed above, that conventional method of construction can be improved with an automated monitoring system. For ensuring safety and reliable operations, an automated monitoring system is a necessity for automated construction. The degree of automation which can be attained in construction depends on to the extent to which micro-activities can be automated. This also depends on how well the control information is collected and coordinated to achieve overall monitoring of the entire structure. However, Sensor-based monitoring of safety and stability of an entire structure being constructed is not well explored yet.

3 System Identification in Construction

Automated construction requires rigorous monitoring to ensure the safety and stability of the structure. Appropriate sensors at optimum locations on the system will give necessary data about the system. The main research question is: How do you make sense of data from the monitoring system to take decisions about the construction process? For this, the actual state of the structure being constructed has to be identified. This can be achieved by System Identification.

System Identification appears to be a promising methodology which can be adopted for monitoring of automated construction. This methodology is widely adopted in various fields of engineering, especially for structural health monitoring in civil engineering [12]–[15]. The measurements from already existing structures are used for assessing their condition by system identification. Various methods for identifying the state of the constructed facilities are discussed in detail in a report published by ASCE in 2011[16]. However, the possibility of applying system identification in monitoring automated construction and stability of the structure being constructed has been not explored so far. Successful interpretation of measured data is highly dependent on the measurement system as well. In order to gain maximum useful information with minimal cost, the measurement system has to be systematically designed.

Most of the well-established system identification methods in construction require models or prior information about the structure. But in ongoing construction, the structure changes continuously. In this context, a rigorous approach free of models would be much more appropriate for monitoring. Machine learning techniques which are entirely data-driven opens up a possibility here.

A machine learning technique, Support Vector Machine (SVM) is proven to be successful in solving various complex construction management problems and acts as an efficient support system for decision making[17]–[22]. With careful selection of parameters, SVM gave better identification of construction activities compared to conventional system identification methods from strain sensing data [8].

4 Objective

The overall objective of this research is to develop a framework based on system identification which can be used to monitor automated construction of a structural frame. Conventional model-based system identification methods, as well as model-free approaches based on machine learning, were explored for this task. However, this paper focuses only on a machine learning based framework for monitoring. In particular, the feasibility of using support vector classification is explored. More complex deep learning models such as convolutional neural networks will be studied in the future. The machine learning module will eventually be integrated with conventional system identification techniques in order to develop a hybrid strategy that is most effective for the task of automated construction monitoring.

5 Methodology

The methodology adopted in this research involves experiments and data analytics. A prototype of an automated construction system was developed and experiments were conducted in controlled settings.

Figure 1. The partially constructed structural frame on the automation system

The automated construction methodology adopted in this study follows a top to bottom method of

construction [23]. In this method, the structural frame for the roof is constructed first and the lower part is constructed sequentially by adding one module of a column at a time, followed by the coordinated lifting of the finished structure. The advantage of this type of construction is that all the activities are performed at the ground level and heavy equipment such as tower cranes are not needed. Currently, the coordinated lifting operation is automated, whereas the connection of modules of the members is done manually. Higher levels of automation are planned for the future.

The structural frame used in this study consists of circular pipe sections with couplers as connectors (Figure 1). The scaled model of a one bay one storey structural frame has six columns (Figure 2 and 3). The automation system consists of 6 lifting machines at each column position (Figure 1). Each individual machine in the system has 2 ton lifting capacity.

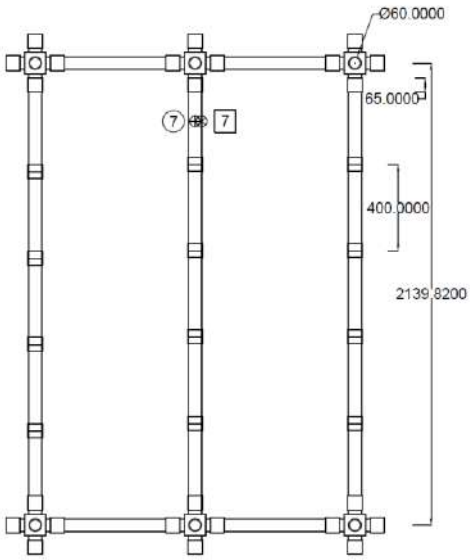

Figure 2. Front view of the structural frame with the location of sensors (All dimensions are in mm)

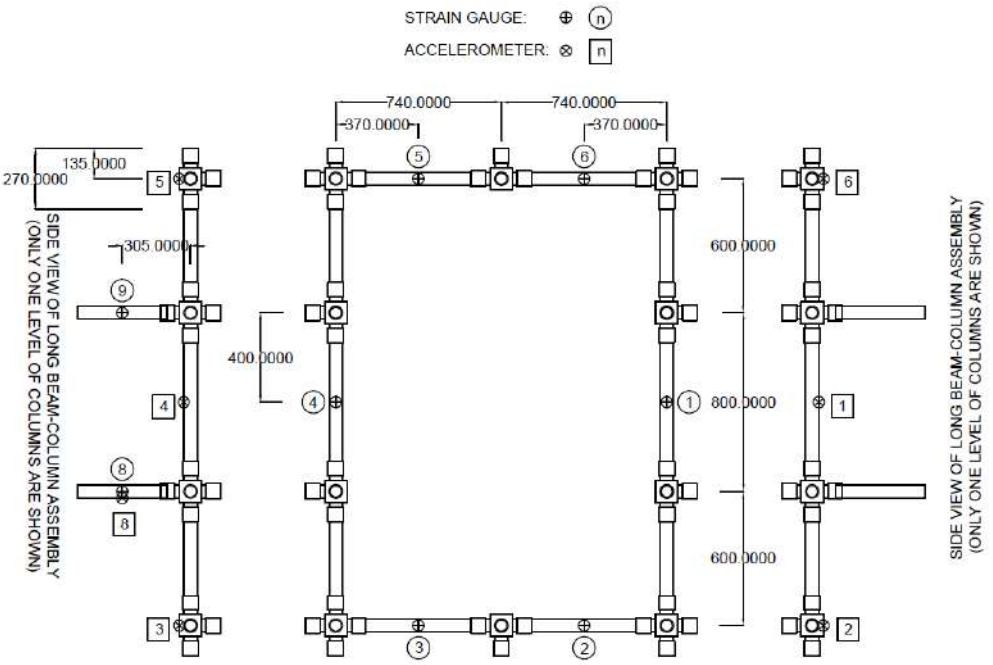

Figure 3. Plan of structural frame with the location of sensors (all dimensions are in mm)

6 SVM based framework for Monitoring Automated Construction

To monitor the state of the structure being constructed and the construction operations, a machine learning based monitoring framework is adopted in this study (Figure 4). This involves two major steps, training and predictions. During the training phase, the automated construction of the structural frame is carried out in controlled conditions within the limits of technical feasibility. Measurements from various sensors deployed in the structure are collected

continuously during the automated construction process. The measured signals are analysed and features for recognising the patterns are extracted. The patterns of measurements (PTij) recorded during the tests for each combination of measurement location (i) and operating condition (j) are used to train the algorithm. This involves patterns of measurement during normal operating conditions as well as failure conditions. SVM identifies each operation state by binary classification. The data corresponds to the operation to be identified is labelled as positive class and all other operations are labelled as negative class. In linear classification, the function or discriminant which separates the classes will be a hyperplane. The equation of the discriminant is obtained by maximizing margin, which is the distance between the nearest data points from either class to the surface.

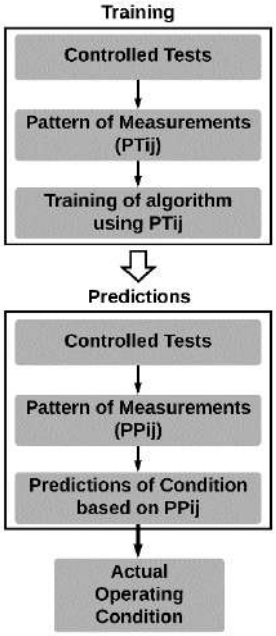

Figure 4. Machine learning based **system identification methodology**

Then controlled tests are performed and measurements are recorded (PPij). Based on the training data set, the algorithm will predict the operating condition.

7 Experimental Validation

Accelerometers (AM) and strain gauges (SG) are placed on the structure for measuring the vibration and strain during automated construction. The locations of sensors are shown in Figure 2 and 3. Totally 9 strain gauges and 8 accelerometers are deployed on the structure. 6 strain gauges are placed on the top of beam members at midspan and 3 strain gauges are placed on the top-level column modules at mid-height. 120-ohm linear strain gauges with 5 mm gauge length are used for the study. Monoaxial piezoelectric accelerometers are used for vibration monitoring. It has a measurement range of -5 g to +5 g with 1000 mv/g sensitivity. 4 out of 8 piezoelectric accelerometers are placed under the universal joints at each corner, 2 are placed under the long beams at midspan and rest of the 2 are placed on first level columns at mid-height.

First, the structure is constructed in perfect lifting conditions without errors in the assembly. Later, various failure criteria such as differential settlement and overturning are systematically introduced. Table 1 shows all the normal operating conditions and potential failure conditions involved in the construction of a one bay one storey structural frame with 5 levels of column modules. There are totally 257 cases of operation involved in constructing the structural frame in the current configuration with the automation systems developed. However, only a limited number of cases can be tested experimentally.

Considering the symmetry of the structure and practical operating conditions, the cases which have to be experimentally tested is limited to 70 without losing major details. The wired sensors are placed at the first level of the beam and column assembly in the current set of experiments. Hence connection of the beam assembly is not tested in this stage. Future experiments in which wireless communication strategy is used, the beam assembly will also be tested. While testing the failure cases, faulty conditions which will lead to potential failure of the structure during construction will be incorporated. Then the automated construction is continued and measurements will be taken. If we introduce a faulty condition, for example, an improper connection between modules of a column member, the pattern of strain and vibration will be different compared to the patterns of measurements corresponding to normal operation cycle.

The measurements taken during normal as well as failure cases will be analysed to arrive at features to train the algorithm. Each case of operation is repeated 6 times. 5 sets of data are used for training and 1 set of data is used for prediction. Starting time, ending time and duration of each operation is recorded manually in a time tracking excel sheet. Results of prediction are compared with this recorded data. The accuracy of prediction is calculated as a percentage of the total number of data points classified. Linear SVM classifier with an error penalty value 10 is used for this study.

Table 1. Total normal operating conditions and failure conditions in the automated construction

Sl. No.	Cases	Conditions of Operation	Number of Cases
	NC	Normal Operating Conditions	
1	NC1	Connection of Beam Assemblies	2
2	NC2	Coordinated Lifting of Finished Structure	7
3	NC3	Lowering of Supports	30
4	NC4	Addition of Column modules	30
5	NC5	Lifting the support until it takes the load	30
		Total Number of Normal Cases	99
	FC	Failure Conditions	
1	FC1	Non-contact of Supports after adding Column modules	30
2	FC2	Support moving faster during Co-ordinated Lifting	42
3	FC3	Improper Connection of Column modules	36
4	FC4	Improper Connection of Beam modules	40
5	FC5	Accidental Loading on the structure	10
		Total Number of Failure Cases	158
		Total Number of Cases	257

More than 50 operations are involved in the construction of a structural frame in 3 different levels of assembly by top to bottom automated construction method. This paper shows the classification of 3 different operation states. The idle state is the condition when the machine is switched on and the constructed structure is supported by all lifting supports, but no other construction activity is going on. This state gives the ambient vibration readings of the constructed structure. The normal coordinated lifting of finished structure (NC2) is the lifting of the constructed structure equally by all lifting supports for the assembly of next level of column modules beneath it. The failure condition considered is one of the supports moving faster during coordinated lifting (FC2). If this condition continues beyond a certain time, it leads to the overturning of the structure. The failure conditions are tested carefully in such a way that it will never be extended until the actual failure of the structure.

The data is acquired at a sampling frequency of 200 Hz. Millions of data points are generated from each experiment. Observing the pattern of strain and vibration measurements, average (AV) and standard deviation (SD) over moving time windows are found to be suitable features for recognizing the pattern of measured signals. In order to capture the change in pattern during sub activities, measurement data corresponds to each operation at each location is divided into 3 time windows and AV and SD are calculated for each part. These features are used to train the algorithm. Results of the study are discussed in the next section.

8 Results and Discussion

Six different parameters (3 AV values and 3 SD values) at each measurement location are used for training the algorithm. The algorithm is trained to identify three different scenarios; i) idle condition and a normal operating condition, ii) a normal operating condition and a failure condition and iii) a failure condition and idle condition. The prediction results are summarized in Table 2.

It is interesting to see that, just by using the SD of accelerometers, the algorithm can predict all operations with 100% accuracy. This will help us reduce the number of sensors used for monitoring. SD is a strong parameter for pattern recognition from vibration data. However, SD could not give good results with strain data while identifying Idle and FC2. This might be due to the small number of data points in support moving faster condition as it is a severe failure case which cannot be extended for a long-time during experiments. AV is not a reliable parameter as it might not give good results in all conditions. All the cases selected here for classification has average acceleration reading close to zero. In fact, including AV in certain cases might not even influence the prediction results.

Among the measurement type, vibration is more useful in accurate prediction. Strain data sometimes get affected by a minor level difference in the structural

frame, temperature or defect in the deployment of the sensor. In terms of prediction accuracy, the best results are obtained for separation between normal and failure cases (NC2 and FC2) among all the three cases. The clearly differentiating pattern over time ensures best predictions irrespective of parameters used.

Table 2. Prediction results for normal and failure conditions. Each column reporting the percentage of accuracy corresponds to a specific combination of features and the type of measurement

Operations Classified	Percentage of accuracy						
	AV and SD of AM and SG	AV of AM and SG	SD of AM and SG	AV of AM	SD of AM	AV of SG	SD of SG
Idle and NC2	100	83.33	100	50	100	66.67	83.33
NC2 and FC2	100	100	100	50	100	100	100
Idle and FC2	100	83.33	100	50	100	66.67	66.67

9 Conclusions

Automated construction of a structure has to be monitored continuously and accurately. Sensor data have to be appropriately interpreted to take control actions during automated construction. The challenge of making sense of a large amount of sensing data can be achieved by system identification methods. These methods have been used in structural health monitoring applications. Automated monitoring of a structure using this methodology has not been explored. Most of the conventional system identification methods in construction are limited by the prior information required to apply it. Data-driven techniques in machine learning are one of the best possibilities for addressing these limitations. Machine learning techniques such as SVMs have been proven to be capable of solving complex problems in construction. However, the quality of sensor data collected drives the performance of these methods.

Results from the present study show that an SVM based framework for monitoring automated construction is feasible. In the current set of experiments, the framework has a prediction accuracy of 100% with appropriate parameters for training. Depending on the type of measurement and operation, training parameters (features) have to be selected appropriately. Standard deviations of measurement data over moving time windows have been found to be very effective in accurate prediction. Among the measurement types, vibration is found to be more useful than strains.

Research is currently in progress on the use of more sophisticated machine learning models such as convolutional neural networks. Formulation of a robust framework for automated construction monitoring which combines a conventional system identification methodology with machine learning techniques is also in progress.

Acknowledgement

Authors wish to extend their sincere gratitude to all the faculties, staff members and project interns at Structural Engineering Laboratory, Building Automation Laboratory and Civil Engineering Department Fabrication Facility, IIT Madras for their unparalleled help and support in fabrication, installation and instrumentation required for the project. The doctoral research of the first author is supported by the scholarship from the Ministry of Human Resource Development (MHRD), Government of India. The project is funded by the Department of Science and Technology (DST), Government of India through the grand DST/TSG/AMT/2015/234.

References

[1] Castro-Lacouture D. Construction Automation. In *Springer Handbook of Automation,* Nof S. Y., Ed. Springer, pages 1063–1078, 2009.

[2] Zhang Y. and Bai L. Rapid structural condition assessment using radio frequency identification (RFID) based wireless strain sensor. *Automation in*

Construction, 54:1–11, 2015.

[3] Alavi A. H., Hasni H., Lajnef N., Chatti K., and Faridazar F. An intelligent structural damage detection approach based on self-powered wireless sensor data, *Automation in Construction*., 62:24–44, 2016.

[4] Spencer Jr B. F., Ruiz-Sandoval M., and Kurata N. Smart sensing technology for structural health monitoring. In *Proceedings of 13th World Conference on Earthquake Engineering*, Vancouver, 2004.

[5] Kim S. H., Ryu H. G., and Kang C. S., Development of an IoT-Based Construction Site Safety Management System. In *Proceedings of International Conference on Information Science and Applications*, pages 617–624, Hong Kong 2018.

[6] Aryal A., Ghahramani A., and Becerik-Gerber B. Monitoring fatigue in construction workers using physiological measurements. *Automation in Construction*., 82:154–165, 2017.

[7] Soman R. K. *Automated Monitoring of Launching Girder Operations Using Wireless Sensor Network*. Masters Thesis, Indian Institute of Technology Madras, 2016.

[8] Harichandran A., Raphael B., and Varghese K. Inferring Construction Activities from Structural Responses Using Support Vector Machines. In *Proceedings of 35th International Symposium on Automation and Robotics in Construction (ISARC 2018)*, pages 324–331, 2018.

[9] Soman R. K., Raphael B., and Varghese K. A System Identification Methodology to monitor construction activities using structural responses, *Automation in Construction*,75:79-90, 2017.

[10] Cho C., Kim K., Park J., and Cho Y. K., Data-Driven Monitoring System for Preventing the Collapse of Scaffolding Structures. *Journal of Construction Engineering and Management*, 144(8): 4018077, 2018.

[11] Choi S. W., Kim Y., Kim J. M., and Park H. S. Field monitoring of column shortenings in a high-rise building during construction, *Sensors (Switzerland)*, 13(11):14321–14338, 2013.

[12] Goulet J.-A., Texier M., Michel C., Smith I. F. C., and Chouinard L. Quantifying the Effects of Modeling Simplifications for Structural Identification of Bridges, *Journal of Bridge Engineering*, 19(1):59–71, 2014.

[13] Pasquier R., Angelo L. D., Goulet J.-A., Acevedo C., Nussbaumer A., and Smith I. F. C. Measurement, Data Interpretation, and Uncertainty Propagation for Fatigue Assessments of Structures, *Journal of Bridge Engineering*, 21(5):4015087, 2016.

[14] Pai S. G. S., Nussbaumer A., and Smith I. F. C. Comparing Structural Identification Methodologies for Fatigue Life Prediction of a Highway Bridge. *Frontiers in Built Environment*, 3:1–15, 2018.

[15] Robert-Nicoud Y., Raphael B., and Smith I. F. System Identification through Model Composition and Stochastic Search. *Journal of Computing in Civil Engineering*.19(3):239–247, 2005.

[16] Çatbaş F. N., Kijewski-Correa T., and Aktan A. E. *Structural Identification (St-Id) of Constructed Facilities.* American Society of Civil Engineers (ASCE), Structural Engineering Institute (SEI) 2011.

[17] Saitta S., Raphael B., and Smith I. F. C. Data mining techniques for improving the reliability of system identification. *Advanced Engineering Informatics*, 19(4):289–298, 2005.

[18] Lam K. C., Palaneeswaran E., and Yun Yu C. A support vector machine model for contractor prequalification. *Automation in Construction*., 18(3):321–329, 2009.

[19] Wauters M. and Vanhoucke M. Support Vector Machine Regression for project control forecasting. *Automation in Construction*, 47:92–106, 2014.

[20] Cheng M. Y., Peng H. S., Wu Y. W., and Chen T. L. Estimate at completion for construction projects using evolutionary support vector machine inference model. *Automation in Construction*., 19(5):619–629, 2010.

[21] Kargul A., Glaese A., Kessler S., and Günthner W. A. Heavy Equipment Demand Prediction with Support Vector Machine Regression Towards a Strategic Equipment Management. *International Journal of Structural and Civil Engineering Research*,6(2):137–143, 2017.

[22] Alwasel A., Sabet A., Nahangi M., Haas C. T., and Abdel-Rahman E., Identifying poses of safe and productive masons using machine learning. *Automation in Construction*, 84:345–355, 2017.

[23] Raphael B., Rao K. S. C., and Varghese K. Automation of modular assembly of structural frames for buildings. In *Proceedings of the 33rd International Symposium on Automation and Robotics in Construction (ISARC 2016), Auburn, USA*, pages 412–420, 2016.

A Conversation-based System for School Building Inspections

H.-Y. Chan[a], L.-Y. Liu[a], and M.-H. Tsai[a]

[a]Department of Civil and Construction Engineering, National Taiwan University of Science and Technology, Taiwan
E-mail: d10705005@mail.ntust.edu.tw, liangyuanfukumu@gmail.com, menghan@mail.ntust.edu.tw

Abstract –

This research aims to develop a conversation-based system for school building safety inspections. The safety of school buildings requires routine and additional post-disaster inspections. However, the inspections are often complicated due to various timings and sets of checkpoints for different situations. In addition, the traditional paperwork process is not convenient for assessors to add additional images for detailed descriptions. Moreover, managers may face the inefficiency of grasping situations from numerous paper reports. To solve these problems, we developed a chatbot to notify, guide, and assist assessors to complete safety inspections, and a dashboard for managers to consume reports in order to determine whether further assessments or retrofits are required. In this research, we digitalized the process of safety inspections and developed a chatbot to notify and guide the assessors to complete their tasks. When an earthquake occurs, the chatbot notifies the assessor if the intensity scale of the earthquake meets the school building's safety threshold. The chatbot then guides the assessor to complete the inspection. The assessor may interact with the chatbot for further instructions and upload pictures of damaging. The system collects the reports from all schools, analyzes the data, and displays via the dashboard we designed for the managers which enables the managers to efficiently and correctly consume the reports for making decisions. The conversation-based system provides an effective interface for reducing the inefficiency of school buildings' inspections, featuring automatic notifications for assessors, a conversation-based interface for guiding assessors to accomplish inspections, the integration of intuitively concatenating the whole process of inspections, the acceptability of multimedia for lowering possibility of inspection mistakes, and the view of data visualization for decision supporting of the manager.

Keywords –

Conversation-based system; Building safety inspection; Decision support; Chatbot; Data visualization

1 Introduction

The earthquake occurrence is quite frequent in Taiwan since Taiwan is located on the circum-Pacific seismic zone. The annual average number of earthquakes recorded from 1991 to 2004 increased to 18,649, of which approximately 1,047 were felt [1]. Despite the common occurrences of earthquakes, the majority barely causes bare damage to buildings and infrastructure. However, there were some destructive earthquakes, such as the magnitude-7.3 Chi-Chi Earthquake in 1999, which destroyed nearly half of the school buildings in Central Taiwan, and eventually damaged over 600 school buildings [2].

Due to the frequent occurrences of earthquakes in Taiwan, the Ministry of Education has ordered all public schools to establish "safety inspection task forces" for evaluating the seismic resistance of existing school buildings [3]. The safety inspection task force of each school is composed of the principal, the president of the parents' association, the director of general affairs, and other staffs of the school. Besides routine inspections once a year, additional inspections on irregular bases are required, especially after the occurrences of disasters including earthquakes that meet the critical safety thresholds. Based on the results of inspections, the managers who make decisions of budget allocation determine how to allocate resources for school building repairing.

The number and spatial complexity of school buildings make it tedious for assessors to repeat the inspections multiple times on different buildings. In addition, paperwork restricts forms of reporting inspections; multimedia such as images and videos are hardly accepted even though they provide richer information about building damages. Moreover, such numerous paper-form reports hinder managers to grasp the situation of potential damage. Currently, the

evaluations are paperwork and cover at least 20 checkpoints. Also, the members of safety inspection task forces usually do not have expertise in structural or civil engineering. The process of inspections may be quite a burden to the assessors, and the results may not completely illustrate the building damages to the managers.

The evolution of information and communications technology (ICT) has enhanced developments in communications and electronic devices. Wireless protocols and techniques make it possible to connect to the Internet regardless of time and location. In addition, electronic devices are smaller and more powerful than in the past; nowadays, people can access, process, and produce information online via smartphones at anytime and anywhere. Electronic devices are adapted to constructions problems to eliminate the difficulty due to paperwork; for example, iSafe, an iPad application, improves day-to-day practices and management of safety inspections, and allows consistent data collection that can eventually be used to aid the development of advanced safety and health data analysis techniques [4]. However, despite the popularity of smart devices to access the web, traditional designs of user interfaces are not ideal for the reduced size of the screen and keyboards of smart devices [5]. Graphic user interfaces designed for tablets may not fit with smartphones, which are more popular than tablets [6].

On the other hand, the growing popularity of smartphones has triggered the growth of messaging applications. The number of people using messaging applications has surpassed the number of people using social networks since 2015 [7]. Such a phenomenon has promoted chatbots as a new trending solution for trivial problems in people's life and work. Recently, chatbots are widely used in several areas, including economic, medical, and disaster management [8].

For construction projects, most chatbots are aimed to assist the management of work sites. Some chatbots are adapted to assist scheduling future works and remind managers to fulfill scheduled daily tasks; for example, ConBot, a construction site data assistant produced by Botmore Technology in the UK [9], and SafeTrack, developed by Talania Ltd in New Zealand [10], allows workers and managers to submit daily reports and information of accomplished works via dialogue. In addition, there are other chatbots that focus on site safety issues, such as Workplace Safety Bot, a chatbot developed by the Robust Tech House of Singapore, which allows users to report hazards easily and broadcasts safety reminders to users [11].

Chatbots have lower resistance than smartphone applications for users because of the needless of additional downloads and installations. It is not necessary for users to download any additional application which may occupy storages of devices. Only adding chatbots to contact lists is required for acquiring services. For most messaging applications, adding chatbots to contact lists is equivalent to adding true people. Also, conversations can be opened simply to offer specific services. Since chatbots are based on dialogue interface, users don't need extra efforts to be familiar with how to use the services. By contrast, it takes more time for users to learn how to use smartphone applications.

According to an online survey report [12], chatbots outperformed applications in the following five benefits categories: quick answers to simple questions, getting 24-hour service, quick answers to complex questions, ability to easily register a complaint, and getting detailed/expert answers. The detailed survey results are listed in Table 1. The percentages represent the proportion of respondents who associate the category with communication with business.

Table 1. Comparison of the top five benefits of chatbots which are associated with communication with business

Category	Chatbot(%)	Application(%)
Quick answers to simple questions	69	51
Getting 24-hour service	62	54
Quick answers to complex questions	38	28
Ability to easily register a complain	33	24
Getting detailed / expert answers	28	27

In conclusion, the convenience to access and capability to interact with users have made chatbots a new and feasible solution to integrate smart devices to all fields. Such benefits of chatbots make it a feasible solution to the complication of inspections, the inconvenience of the paperwork process, and the inefficiency of management for Taiwan's school building safety inspections.

2 Objectives

This research aims to reduce the complication of safety inspections, the inconvenience of the paperwork process, and the inefficiency of management. The safety inspections are often complicated due to various timings and sets of checkpoints for different situations. In addition, the traditional paperwork process is not convenient for assessors to add additional images for detailed descriptions. Moreover, managers may face the inefficiency of grasping situations from numerous paper reports.

In this research, we developed a system to solve the problems above. The system uses a chatbot as an interface to notify, guide, and assist assessors to accomplish safety inspections, and a dashboard as the other interface for managers to consume reports in order to determine whether further assessments or retrofits are required. The developed system includes the following features:

1. **Automatic notification** for notifying the assessor to accomplish inspections after earthquakes if the safety threshold of the school is reached.
2. **Conversation-based interface** for guiding the assessor to accomplish inspections in a non-professional-friendly way.
3. **Integrated tool** for concatenating receiving notifications and the inspections task in a single tool or application in order to improve the intuitiveness of the whole inspection process.
4. **Acceptability of multimedia** for allowing the assessor upload images or videos for showing damages directly in order to lower the possibility of mistakes in inspections.
5. **Data visualization** for decision supporting of the manager in order to enhance the quality and accuracy of budget allocation for building retrofit.

3 Methodology

In this research, we digitalized the process of safety inspections and developed a conversation-based system to notify and guide the assessors to accomplish their tasks. The system includes 3 modules: (1) the notification module, (2) the conversation module, and (3) the display module. The system architecture is illustrated in Figure 1. All 3 modules connect to the database, storing data including intensity scale thresholds of areas, assessors' contact information of schools, earthquake records, and inspection reports. The notification module and the conversation module interacts with assessors in the form of the chatbot we developed. The display module is accessed via web browsers by managers.

The notification module is activated by receiving earthquake information when an earthquake occurs. The intensity scale of each area is considered when selecting critical schools to announce safety inspections. The system looks up in the database to select the schools which locate at areas of which intensity scale thresholds are reached and sends notifications for safety inspections to the registered assessors of the schools via instant messaging applications in the form of the chatbot.

The conversation module interacts with the assessor via the instant messaging application in the form of the chatbot. The assessor starts a new inspection after receiving the notification from the chatbot. The chatbot guides the assessor to complete the pre-designed checkpoints in the inspection. The assessor may interact with the chatbot for further instructions and upload pictures of damaging. The chatbot collects the inspection, confirms the content with the assessor, and submits the inspection to the system. The system stores the inspection reports in the database.

The display module manages the dashboard for managers to check out the status of inspections via web browsers. The display module reads the inspection reports from all critical schools, analyzes the data, and displays via the dashboard we designed for the managers which enables the managers to efficiently and correctly consume the reports for making decisions.

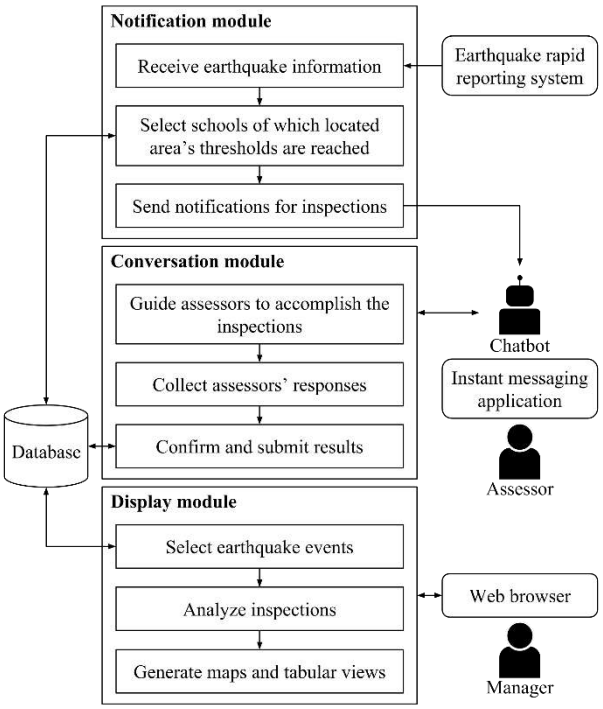

Figure 1. The system's architecture

3.1 Notification Module

The major task of the notification module is to inform the assessors whose schools locate in areas having higher intensity scales when an earthquake occurs. The procedure is illustrated in Figure 2. The notification module, connecting to the system's database, digitalizes the process of determining which schools require inspections and send notifications to the registered assessors of those schools, reducing the time of checking schools' thresholds and notifying assessors manually. The direct notifying messages sent to assessors' messaging applications are accomplished by the chatbot in their contact list as if they are sent by real people; the assessors may start the inspections smoothly by replying the chatbot when they receive the messages without

switching to another application, improving the intuitiveness from receiving notifications to starting inspections.

When an earthquake occurs, the system receives the information including the center, the magnitude, and intensity scales of different areas. The notification module determines the areas which are critical by the intensity scale threshold of each area which is defined by experts considering the sensitivity of the area. The schools in the critical areas will be selected to announce safety inspections after the earthquake. Notifications are then sent by the chatbot via instant messaging applications. The assessors' messaging application accounts are bind with their schools when they add the chatbot to their contact lists initially. After the critical schools are selected, the notification module sends instant messages to announce the assessors of the critical schools for accomplishing safety inspections. For the schools that do not locate in critical areas, the notification module does not send messages to the schools' assessors since such schools do not require inspection.

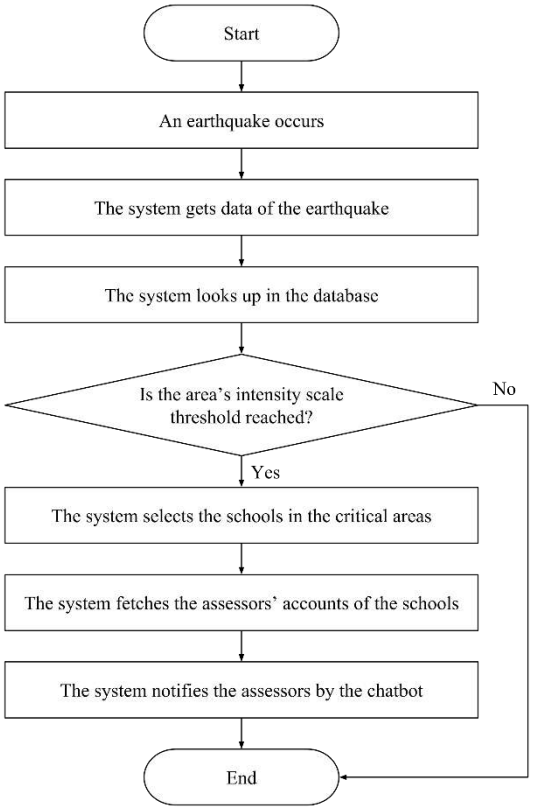

Figure 2. The process of the notification module

3.2 Conversation Module

The major task of the conversation module is to interact with assessors in the form of conversation in order to lower difficulties of assessors accomplishing the inspection. The procedure is shown in Figure 3. Since most assessors do not have expertise in structural or civil engineering, they may not be capable of accomplishing the complicated and tedious inspection checkpoints efficiently and correctly. The conversation module interacts with assessors with the chatbot, making inspections similar to having conversations with real people. The module guides assessors to accomplish the inspections, replacing the traditional paper-based procedure which lacks guidance for the non-professional assessors. The module also accepts multimedia file sent from assessors to the chatbot for clearer reports of damages, reducing the potential mistakes of inspection.

The assessors start the inspection by sending commands in text messages to the chatbot when receiving notifications. The chatbot asks assessors "questions" referring to the pre-designed inspection checkpoints. The inspection checkpoints are divided into 4 categories: overview, about indoor facilities, about outdoor facilities, and about facilities in corridors. The categories are set by roughly dividing building facilities. Assessors are allowed to start the inspection from anyone of the 4 categories. They answer the questions sequentially in the form of sending messages to the chatbot. They may pause in the inspection and continue accomplishing the remaining checkpoints later at any time they want since the conversation module manages the process of filling out the checkpoints; data of filled checkpoints will not be lost. In addition, assessors are allowed to send images and videos as if they are having conversations with real people via messaging applications. The chatbot collects the multimedia files as the answers to the checkpoints. The chatbot summarizes the contents into a message after accomplishing the inspection and presents it to the assessor for final confirmation. If modifying is required, the assessor may select the checkpoints to be modified and correct the answers. Finally, after the corrections are accomplished and confirmed, the system saves the results to the database.

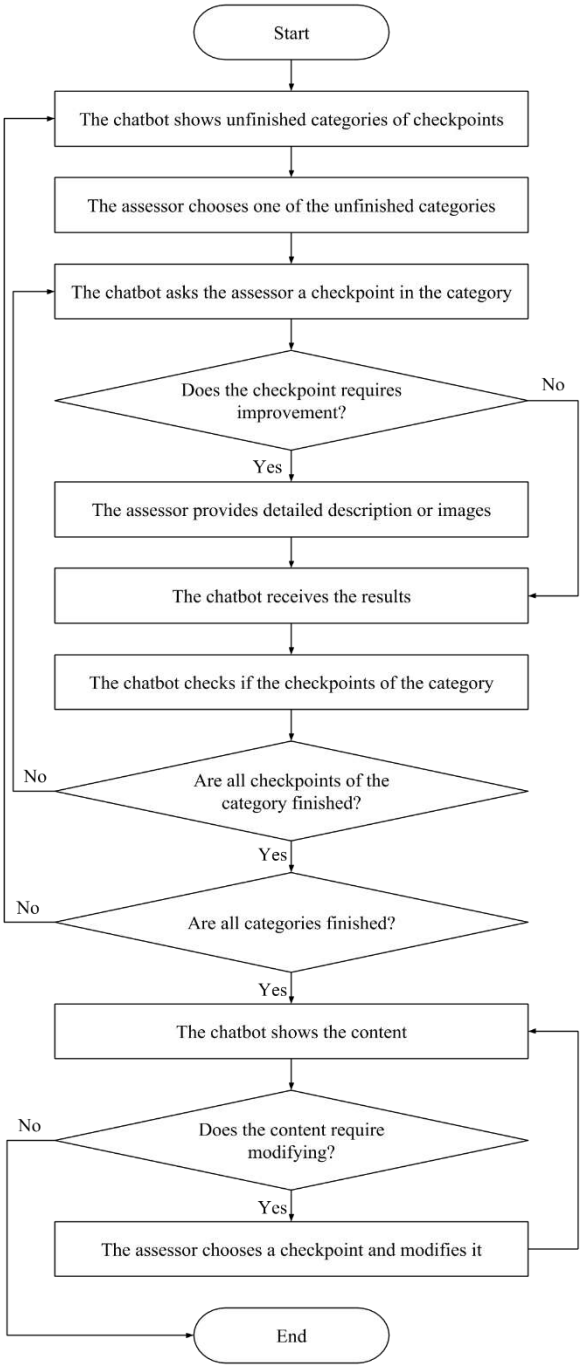

Figure 3. The process of the conversation module

3.3 Display Module

The major task of the display module is to demonstrate the results of the inspections by visualization in order to lower the inefficiency and difficulty for the managers to consume the data for making high-quality decisions. The procedure is illustrated in Figure 4. Managers need to grasp the situation of school building damages after an earthquake occurs and determine the budget allocation for building retrofit. The display module assists managers in selecting digitalize reports, analyzing the reports, and visualizing the results for decision support.

The dashboard is designed to access with web-browsers. The dashboard is composed of an interactive map showing the number of expected reports and a list of detailed inspection reports that are actually accomplished. First, managers select one of the earthquake events on the dashboard. Next, the system retrieves the reports of the selected earthquake event from the database and then shows them on the dashboard. The map demonstrates the number of critical schools in the areas by coloring them, while the tabular view lists all schools and their reports. By clicking one of the areas on the interactive map, reports of schools in that specific areas will be filtered and highlighted to emphasize the severe levels. Finally, managers consume and utilize the information shown on the dashboard to make decisions about allocating budgets and resources to retrofit the damaged school building.

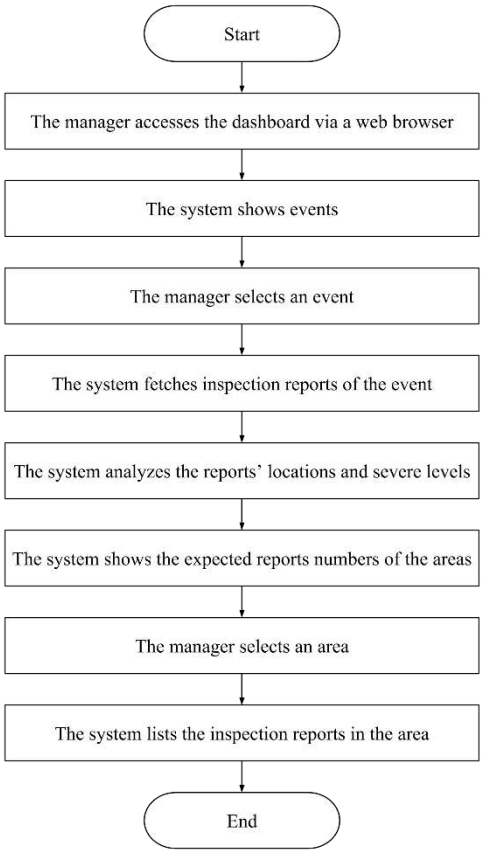

Figure 4. The process of the display module

4 Implementation

We implemented the conversation-based system as a

chatbot via LINE, a commonly used messaging application in Taiwan. LINE Messaging API provides various types of messages include confirming button and accepts multimedia as users' responses [13]. These features are utilized in our developed system. Flask, a micro web framework written in Python [14], is used for implementing the system as an HTTP service to control the process of interaction with LINE Messaging API and host the web-based dashboard. The web-based dashboard is constructed using HTML/CSS/JavaScript in order to be accessed via any web browser.

Screenshots of part of the chatbot are shown in Figure 5. The chatbot interacts with assessors using diverse formats of messages provided by LINE Messaging API. The system informs assessors to start inspections after an earthquake occurs. The assessor selects one of the question categories and starts to fill in the report. Entire questions are displayed as confirming buttons. If the assessor selects "no problem", the next item for inspection will popup sequentially; if "require improvement" is chosen, the chatbot will be switched into input mode. The assessors are allowed to make detailed descriptions in text or with multimedia. After accomplishing the inspection, the system summarizes the current contents and presents it to the assessor for final confirmation. If modifying is required, the assessor may select the items to be modified and correct the answers. After the corrections are accomplished and confirmed, the system saves the results to the database.

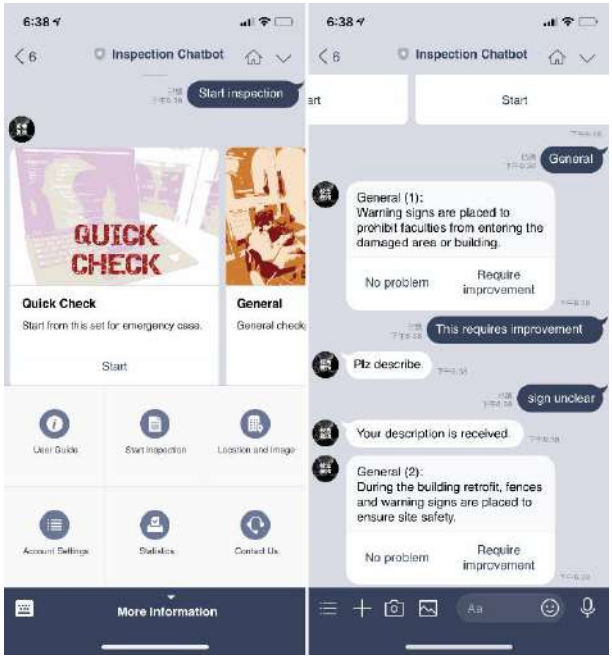

Figure 5. Screenshots of the chatbot

The dashboard for managers is shown in Figure 6. The dashboard is web-based and composed of an interactive map and a tabular list. The managers first select an earthquake event using the select bar, and then by clicking a district on the map, inspection reports of schools related to the earthquake event in the district will be listed with links to detailed results. The color demonstrates the severe level of each school according to the inspection records; the more checkpoints fail in the inspection, the darker the color of the report is. By clicking on one of the links to a specific detailed result, the result will be shown as in Figure 7. By default, only the items reported to be "require improvement" and their descriptions are displayed in the detailed result.

Figure 6. A screenshot of the dashboard

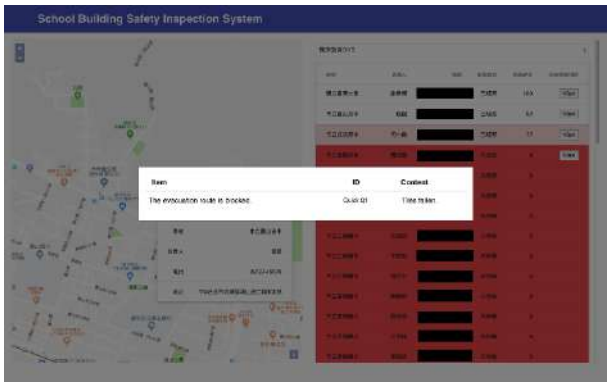

Figure 7. A screenshot of the dashboard after clicking on one of the inspection report for more details

5 Conclusions

In this research, we digitalized the process of safety inspections and developed a conversation-based system for notifying and guiding the assessors to accomplish their tasks. The system includes the notification module, the conversation module, and the display module. The notification module is activated by receiving earthquake information when an earthquake occurs and sends

notifications for safety inspections to the registered assessors of the schools via instant messaging applications. The conversation module interacts with the assessor via the instant messaging application in the form of a chatbot which guides the assessor to complete the pre-designed checkpoints in the inspection. The display module reads the inspection reports from all critical schools, analyzes the data, and displays via the dashboard for the managers. The research provides a conversation-based solution to reduce the complication of safety inspections, the inconvenience of the paperwork process, and the inefficiency of management. The developed system features automatic notifications for notifying assessors, a conversation-based interface for guiding the non-professional assessors to accomplish inspections, the integration of intuitively concatenating receiving notifications and the inspections task, the acceptability of multimedia to show damages directly without possibility of mistakes, and the view of data visualization for decision supporting of the manager in order to enhance the quality and accuracy of budget allocation.

In future work, to improve our developed system and enhance managers' efficiency of grasping information, interviews with the managers for evaluating the design of the dashboard is required. Also, techniques of natural language processing may be adapted to analyze text in inspection reports in order to obtain more accurate severe levels of the inspection reports, which may support the managers determine the budget allocation. In addition, techniques of image recognition may be adopted to find damages from assessors' uploaded images automatically and reduce the time for managers to check the images manually. Furthermore, to obtain the accurate positions of building damages, a method to clearly describe the positions is required. Although by utilizing interactive image messages of LINE, assessors may report the positions of damages by clicking on an image of the site plan, the scale of images and the process of inspections require further discussions.

6 Acknowledgment

This work was financially supported by the Taiwan Building Technology Center from The Featured Areas Research Center Program within the framework of the Higher Education Sprout Project by the Ministry of Education in Taiwan. The authors are grateful to Mr. Hung-Kai Kung, Mr. Cheng-Yu Ho, Mr. Chun-Mo Hsieh, and Prof. Yun-Cheng Tsai of National Taiwan University for their assistance in the development of the system.

References

[1] Central Weather Bureau. FAQ for Earthquake. On-line: https://www.cwb.gov.tw/V7e/knowledge/encyclopedia/eq000.htm, Accessed: 07/01/2019

[2] Chuang, M.-C., Liao, E., Lai, V. P., Yu, Y.-J. and Tsai, K.-C. Development of PISA4SB for Applications in the Taiwan School Building Seismic Retrofit Program. *Procedia Engineering*, 14:965–973, 2011.

[3] The Ministry of Education, Taiwan. Safety checklist of a school building, An official document, 2012. On-line: http://public.hlc.edu.tw/index_dt_web.asp?i=13985, Accessed: 31/01/2019.

[4] Lin, K.-Y., Tsai, M.-H., Gatti, U. C., Lin, J. J.-C., Lee, C.-H. and Kang, S.-C. A user-centered information and communication technology (ICT) tool to improve safety inspections. *Automation in Construction*, 48:53–63, 2014.

[5] Griol, D., Molina, J.M. and Callejas, Z. A proposal for the development of adaptive spoken interfaces to access the web. *Neurocomputing*, 163:56–68, 2015.

[6] StatCounter. Desktop vs Mobile vs Tablet Market Share Worldwide. On-line: http://gs.statcounter.com/platform-market-share/desktop-mobile-tablet, Accessed: 20/01/2019

[7] BI Intelligence. Messaging apps are now bigger than social networks. On-line: https://www.businessinsider.com/the-messaging-app-report-2015-11, Accessed: 03/07/2018

[8] Tsai, M.-H., Chen, J. Y. and Kang, S.-C. Ask Diana: A Keyword-Based Chatbot System for Water-Related Disaster Management. *Water*, 11(2):234, 2019.

[9] Botmore Technology. CONBOT - Digital Assistant. On-line: http://www.botmore.co.uk/, Accessed: 18/03/2019

[10] Talania. SafeTrack. On-line: https://botdirectory.net/solutions/talania-chat-works-chatbot-solutions/, Accessed: 18/03/2019

[11] Robust Tech House. Workplace Safety Chatbot. On-line: https://singaporechatbots.sg/workplace-safety-chatbot/, Accessed: 18/03/2019

[12] Drift, SurveyMonkey Audience, Salesforce, and myclever. The 2018 State of Chatbots Report: How Chatbots Are Reshaping Online Experiences. On-line: https://www.drift.com/blog/chatbots-report/, Accessed: 20/01/2019

[13] LINE Corporation. Messaging API. On-line: https://developers.line.biz/en/docs/messaging-api/overview/, Accessed: 01/01/2019

[14] Ronacher, A. Flask. On-line: http://flask.pocoo.org/, Accessed: 01/01/2019

Enabling BIM for Property Management of Existing Buildings Based on Automated As-is Capturing

R. Becker[a], E. Lublasser[b], J. Martens[a], R. Wollenberg[a], H. Zhang[b], S. Brell-Cokcan[b], and J. Blankenbach[a]

[a]Geodetic Institute and Chair for Computing in Civil Engineering & Geo Information Systems, RWTH Aachen University, Germany
[b]Individualized Production in Architecture, RWTH Aachen University, Germany
E-mail: ralf.becker@gia.rwth-aachen.de, jan.martens@gia.rwth-aachen.de, raymond.wollenberg@gia.rwth-aachen.de, blankenbach@gia.rwth-aachen.de, lublasser@ip.rwth-aachen.de, zhang@ip.rwth-aachen.de, brell-cokcan@ip.rwth-aachen.de

Abstract –

Digitization and automation in construction are increasing particularly due to the establishment of Building Information Modelling (BIM). The models of BIM contain geometric as well as semantic information. The level of abstraction ranges from coarse models up to detailed modeled technical components of the buildings. So far, BIM has been developed and used for the planning and construction phase of the building's lifecycle. In order to fully use the benefits of BIM also for the operation and refurbishment phase, BIM models need to provide a reliable data basis of the as-built and respectively the as-is situation. However, up to now many properties have neither been planned nor constructed using BIM, at times not even digital planning information is available. Therefore, the digital model must be created from the real world.

The author's research proposes the development of an automated as-is capturing process of existing buildings as well as the data integration into BIM as a basis for property management. Suitable capturing techniques have been analyzed. Up to now, these techniques and the subsequent data transfer are still characterized by lots of manual work. Accelerating this process requires methods for the automation of data segmentation, classification and the modeling process. Conventional data capturing techniques such as laser scanning measure only visible surfaces. However, knowledge about inbuilt materials, constructional layers or thickness of e.g. walls is also important for optimized planning and utilization.

This paper summarizes the results of a joint research project in cooperation with a property management company.

Keywords –

Building Information Modeling, BIM, Automation and Robotics, Data Sensing, Computing

1 Introduction

For property management of buildings such as facility management (FM) a vast amount of data about functional, technical, descriptive as well as commercial aspects is needed. These are geometric data (e.g. for space management, the thickness of walls) or semantic data (e.g. fire ratings or the material of the walls). In many disciplines worldwide, digitization and automation are on the rise. In construction, a main aspect of digitization is the Building Information Modelling (BIM). During the past years BIM has been more and more introduced into the planning and construction phase of buildings. However, the planned situation usually differs to the built situation. Furthermore, BIM models of existing buildings often do not exist. In the following sections we discuss the requirements, techniques and steps for creating a suitable as-is model for the maintenance respectively operation phase of a building for the purposes of property management.

For development of such models, the following topics have been identified relevant: BIM systematics like as-is-terminology, level of development for BIM objects, computer aided facility management, data filtering and exchange. For each topic the paper gives a general overview based on state of the art literature and proposes additional systematics with focus on not yet met FM demands. Furthermore, capturing technologies and modeling systematics for the captured data are discussed. Here, experimental evaluation as well as concepts for a proposed modeling approach are added to a review of the current state of the art. Thereby, first results of the research project are described. Generally, the project is focused on two aspects – the integration of

geometrical information as well as semantic information using available scanning techniques. The overall objective of the project is the development of an automated as-is capturing process for existing buildings as well as the data integration into BIM. The resulting BIM model shall be the foundation for the property management. This paper focuses on the aspect of the integration of geometrical information.

2 As-built vs. as-is BIM

BIM models should not only serve as a planning tool but also for managing tasks over the whole lifecycle of buildings. However, BIM is still an upcoming paradigm. Up to now, it is most frequently used in the earliest stage of the lifecycle, the planning phase [1]. Nevertheless, the operation phase is the longest lifecycle phase of a building. Consequently, extending BIM for use in this phase requires the introduction of additional BIM model specifications [2–4].

If BIM is also used for the facility operation it is crucial to keep the underlying model updated even after construction [5]. Currently, most existing buildings are not documented using BIM due to their planning and construction date before the rise of this method. The consequence is the necessity of creating digital models for existing building structures. In research journals, literature and professional's magazines these models, which represent the current geometric and semantic conditions, are called as-built or as-is models. Often the differentiation between as-built and as-is is not always clear. Therefore, we propose definitions to differentiate between these two terms.

[6] show in their literature review the different possibilities of creating as-built models with and without having an as-planned model. We hold the view that the existence of an as-planned BIM should be the fundamental characteristic for differentiation between an as-is and an as-built model. The as-built model arises during or after the construction phases by updating the as-planned model due to the observed accordances or differences between the actual as-built situation and the as-planned model. The as-is model in contrast represents a model which has been created from an existing in-use building, for which no reliable planning documents exist.

In particular, this means that an as-built modelling process takes place during or immediately after the BIM-supported construction phase. In between construction steps, it is also possible to get information about hidden building elements, such as the arrangement of concrete reinforcement layers. In contrast, the as-is modelling process describes the goal of creating the model of an existing in-use building. This scenario limits the possibilities of capturing information especially about hidden building elements. The fact that the building is in use and equipped with multiple (mobile) assets leads to more difficult conditions for data capturing.

3 Level of development (LOD)

With their Building Information Modeling Protocol Exhibit in 2008 the American Institute of Architects (AIA) established the levels of development (LOD) for describing the level of completeness to which a model element is developed [7]. In the updated document "Project Building Information Modeling Protocol Form" the AIA defines the LOD 500: "The Model Element is a field verified representation in terms of size, shape, location, quantity and orientation. Non-graphic information may also be attached to the Model Elements." [8]. BIMforum, the American chapter of buildingSMART, used these LODs to develop the Level of Development Specification Guide [9]. In general, this specification framework supports the design process by providing tools for a collaborative work environment. This guide serves as a communication tool for the standardized definition of the contents required in the design phase, in order to make them available to all project participants in a standardized way.

Within the LOD level system, LOD 500 can be considered as the as-built LOD. Figure 1 and 2 are depicting LODs and associated BIM lifecycle phases: planning LODs in green and as-built LOD in yellow.

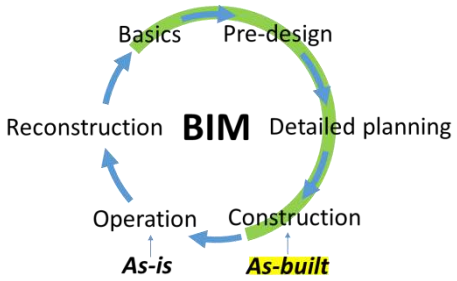

Figure 1. As-is and as-built BIM in lifecycle

Figure 2. The different LODs of a precast structural column out of the LOD Spec. Guide, extended by a self-made illustration of LOD500.

LOD500 should represent the geometric verification e.g. by a laser scan. [9]

LOD 500 marks the conclusion of the planning and construction phases by representing in general the geometric update of the as-planned model after the building's construction.

In our research, we develop a specification framework for existing buildings without existing planning and construction models. There is no need to define stepwise requirements for building elements as during the planning phase. Rather, the challenge is to filter the relevant data out of an existing building. Therefore, we developed the level of as-is documentation (LOAD), which is described in the next section.

4 Level of as-is-documentation (LOAD)

Before making use of the benefits of BIM in operation, the data required for the BIM applications has to be defined. BIMForum developed a framework (Level of development specification guide [9]) for specifying BIM model contents with standardized specifications for planning and construction. Due to the fact that it is hardly possible to use these frameworks for an as-is documentation (see section 2) we present the level of as-is documentation (LOAD).

The LOAD is divided into three parts. The first part is the level of as-is geometry (LOAG) representing the specification for geometric requirements. The level of as-is information (LOAI) defines requirements for semantic data, which focus on the attribution of model elements. The last part is the level of accuracy (LOA), which has been contributed by the U.S. Institute of Building Documentation and defines the tolerance for the geometric deviation between reality and BIM model [10].

4.1 Level of as-is geometry (LOAG)

The LOAG is structured into four increments of ten beginning with LOAG10 and extending to LOAG40. The LOAG10 represents the simplest version of a building element, usually a one or two-dimensional one. The LOAG20 serves for describing the optimized bounding box (OBB) of a building element. For many applications, only the OBB of building elements is needed, e.g. for the management of available spaces. The LOAG30 and LOAG40 are geometric representations of higher detail, where the step from LOAG30 to LOAG40 requires a higher modelling effort. In figure 3 the LOAGs of columns are shown. The LOAG30 is modelled with an idealized constant profile, whereas the LOAG40 represents the highest geometric depth of detail, most closely to a true-to-deformation model.

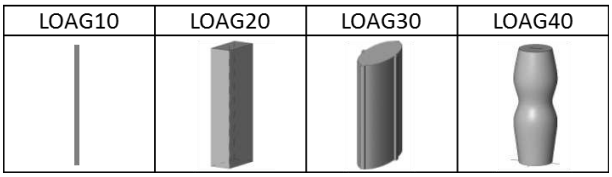

Figure 3. The four LOAGs of a column.

4.2 Level of as-is information (LOAI)

In contrast to the LOAG structure, the LOAI is non-hierarchical and represents semantic requirements related to attribute sets. These attributes refer to the different applications of the BIM model. The actual selection of required semantic attributes depends on the specific use case. When transferring data, proprietary formats do not cover all data interfaces. In such cases, the open standard format Industry Foundation Classes (IFC) [11] has been identified as best practice. The IFC documentation already provides a minimum quantity of different attributes, which can be attached to building elements in a standardized way. These attributes are organized in different property sets. For example, walls have the property set Pset_WallCommon, with the attributes of this property set being "Reference, Status, Acoustic Rating, Fire Rating, Combustible, Surface Spread Of Flame, Thermal Transmittance, Is External, Extended To Structure, Load Bearing and Compartmentation". For adding new attributes from the IFC documentation, so-called custom property sets can be created. Such custom property sets allow for the description of any arbitrary information, though their non-standardized way may limit their interpretation.

4.3 Level of Accuracy (LOA)

The U.S. Institute of Building Documentation provides the LOA in the USIBD Level of Accuracy (LOA) Specification Guide [10]. The LOA is structured into five levels, LOA10 to LOA50, with accuracy requirements increasing at each level.

Table 1. Levels of Accuracy defined by USIB

Level	Upper Range	Lower Range
LOA10	User defined	5cm *
LOA20	5cm *	15mm *
LOA30	15mm *	5mm *
LOA40	5mm *	1mm *
LOA50	1mm *	0 *

*specified at the 95 percent confidence level.

It is important to understand that the LOA Spec. Guide differentiates between different types of accuracy.

- *Measured Accuracy:* Standard deviation range that is required from the final measurement.
- *Represented Accuracy:* Standard deviation range that is required once the measurements are processed into a model.
- *Absolute Accuracy:* Standard deviation related to a given reference frame (e.g. whole building, floor or object)
- *Relative Accuracy:* Standard deviation related not to a fixed superior datum, but within an object´s region.

Consequently, it becomes possible to choose different LOAs for specific object types or regions. The following example shows how to use the different accuracies. For a Computer Aided FM (CAFM) project, a model with low accuracy for the global position of a building asset is sufficient, but the asset itself should be captured and stored with a high accuracy. It means that the absolute accuracy requirements for an asset are low (e.g. LOA10), but for the relative accuracy are much higher (e.g. LOA30). Thus, a suitable measurement technique has to be chosen due to the needed LOA. E.g., mobile laser scanning reaches only minor absolute accuracies (up to multiple decimeters) but – with some systems – relative accuracies within one centimeter can be achieved.

5 BIM for Property Management

In comparison to design and construction, the operation phase is the longest phase in a buildings' lifecycle. The pre-operation phases design, detailed planning and construction take about 2-5 years. In contrast to this, a building is in operation for a minimum of 20 years [12]. The main task during the operation phase is the FM , as it ensures the maintenance and value preservation of the building. CAFM systems store FM-related building data and allow for a methodized access to this data. Hence, it can be used for management of inventory documentation, spaces, contracts, energy, sustainability and other tasks that require assessing, controlling and maintaining building data [13].

For setting up these CAFM systems, BIM is capable of providing the database, since a building information model is in particular a unified information base and a location-aware model of building assets attached with information [14]. Furthermore, the data of a BIM model can be transferred to the CAFM application, such that time-consuming and error-prone efforts on manual data input can be bypassed, ultimately improving the final data's quality[15]. The automatic transfer mechanism data updates, e.g. in the case of reconstruction or renovation [16]. For these purposes, Gnanarednam et al. [17] present suitable data exchange formats such as the IFC and the Construction-Operations Building information exchange (COBie).

Apart from the synergies between BIM and CAFM, there are advantages to creating BIM models of existing structures, such as the reduction of errors to minimize risks for reconstruction [2] or the use of BIM models for building performance simulations [18]. In principle, this framework is a synthesis of encountered challenges and lessons learned from the presented case study. The framework proposes questions for identifying important data and ensuring interoperability between the different interfaces.

The mentioned literature in context of BIM and FM focus on setting up BIM models for aspects of FM during the planning phase [5,12,16,17]. They show significant benefits of the data exchange from BIM to a FM system. However, research on setting up BIM models in the later lifecycle phase is scarce and does not highlight the workflows of capturing and organizing on-site data for the BIM model [19]. Instead they propose the use of floor plans [15], which are often not representative of the actual state of the property situation.

For FM software applications several exchange formats haven been developed. COBie [20] was developed by the buildingSMART alliance and focuses on providing information about type and location of assets. For identifying and maintaining the asset, it defines requirements for identification tags and typecasting as well as for needed information about e.g. installation date, warranty and scheduled maintenance. COBie attributes can be added to model elements in BIM software. The associated standard exchange format is a spreadsheet application file with data organized in different sheets. Another standard for defining attributes for the use of CAFM are BIM profiles of CAFM-Connect [21]. The aim of CAFM-Connect is to grant interoperability between different software which are in use throughout the whole lifecycle management of buildings. The recently released BIM profile is CAFM-Connect 3.0, which delivers a framework for classifying documents, space usage and building components. This framework uses IFC as a programming platform for documenting FM relevant data. The attributes of the IFC entities are filtered and extended with additional attributes in the BIM profiles. Research already observed that there might be a lack of utilities in COBie to satisfy CAFM information requirements. Progress can be made by utilizing IFC for that purposes [17].

5.1 Data filtering and exchange

For proper usability of CAFM systems, great amounts of as-is information with high LOAD content not only need to be stored with the help of BIM but also

have to be filtered to allow for a user-friendly FM operation or for sufficient exchange with other stakeholders. Thereby FM can make use of general BIM concepts for restricting models into partial-, aspect- or submodels such as the Information Delivery Manual (IDM) methodology developed by buildingSMART [22,23]. The IDM defines standardized exchange of information in several steps by participants and the coordinator in form of a handbook. The purpose of the IDM process is to filter the essential information for a partial model to generate the Model View Definition (MVD) and to establish an exchange requirement (ER). Thereby all participants of the different sectors agree on a certain communication. Based on the ER, automatic data management can be developed which will positively affect the interoperability of any collaboration [23].

One of the key components of the IDM process is the capturing of workflows with the participants. BuildingSMART refers to the method of Business Process Model and Notation (BPMN) as a guideline for the design of graphical Process Map documentation. The BPMN uses a flowchart and a column division to describe the overall process with the tasks of the various participants, as well as when and which data needs to be exchanged [22,24].

6 Data capturing techniques

For getting information about the actual geometric state of buildings, one common method today is the use of terrestrial laser scanning for data capturing. Different studies identified terrestrial laser scanning as a valid and popular method [2,25]. Multiple scan positions are registered to each other and the point cloud of the captured area will be processed. Another scan method is mobile laser scanning. Mobile laser scanning uses the simultaneous localization and mapping (SLAM) algorithm for continuous scanning [26]. This leads to enormous time saving during on-site capturing. The downside is a decreased accuracy. In this project, one goal was to find easy-to-use scanners, which provide fast data capturing. They should guarantee a sufficiently high accuracy while at the same time being rather affordable. Thus, we evaluated BLK360 from Leica [27], an easy to use low cost terrestrial laser scanner and mobile laser scanner ZEB-Revo RT from Geoslam [28].

First part of the evaluation of the two scanners was an accuracy check. In case of BLK360 we compared a single as well as a multiple scan setup. The reference laser scanning instrument for this evaluation was VZ-400 from RIEGL [29], a high accuracy surveying instrument. We calculated cloud-to-cloud distances, the minimized sum of distances between points of two point clouds, using the software CloudCompare [30]. The distances distribution classified in LOAs is shown in table 2.

Table 2. Relative distribution of cloud-to-cloud distances in single scan and multi scan scenario

Level of Accuracy	Single Scan	Multi Scan
LOA50 (0-1mm)	19.39%	15.83%
LOA40 (1mm-5mm)	54.23%	44.18%
LOA30 (5mm-15mm)	22.13%	33.29%
LOA20 (15mm-5cm)	4.25%	7.71%

The results show that 94.75% (single scan position) and 92.29% (multi scan position) of the distances achieve the requirements of LOA30 (or better), while only 4.25% and 7.71%, respectively, do not. Hence, we decided that the BLK360 could fulfil the accuracy requirements of LOA30. For the Zeb Revo we present initial investigations. For a simple visual analysis, we superimposed two point clouds, one captured with BLK360 and one captured with Zeb Revo (Figure 4).

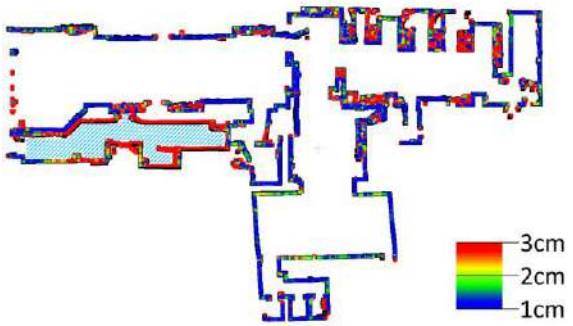

Figure 4. Point to point distances. Colored – Zeb Revo. Black (underlaid) – BLK360.

The colored points (enlarged for presentation) represent the point cloud surveyed with Zeb Revo. The colorization depends on the deviations to the point cloud captured with BLK360. Deviations here represent to the absolute accuracy. Apart from the highlighted corridor the deviations were almost everywhere below 1 cm. The scan of the corridor was drifting (absolute accuracy here appx. 10 cm). Nevertheless, we found out that there was overall a relative accuracy according to LOA30 (5-15mm).

We validated BLK360 to be accurate enough for retrofits requiring a LOA30 (absolute and relative accuracy). The ZEB-Revo RT shows a good relative accuracy but in a given reference frame the absolute accuracy is up to multiple decimetres. Therefore, we decided to use this technique when a fast but not too accurate survey is needed.

7 Automation in modelling

The captured laser point clouds generated by the equipment described in the section before are then used as the basis for the modeling process. Common suitable building information modeling software accompanies much manual work. However, with manual modeling being a time-consuming and costly process, automation in modeling would save much time and money.

Automation takes different forms which can roughly be divided into modeling aids and partial or even full reconstruction methods. Modeling aids are mostly concerned with solving specific tasks without necessarily reconstructing geometry. Such methods could include techniques for point cloud alignment, filtering or the extraction of features. These can ease both, manual and automated modeling processes. Despite contributing to the modeling process, the aforementioned methods have in common that they are neither meant for nor capable of fully reconstructing building geometry. Fully automated methods aim to fill this gap requiring at most only minimal user input. In fact, a detailed review of the various steps required for automated modelling has been outlined in [31,32].

In context of the project's tasks, we investigated various strategies used during the automated reconstruction process, which can be categorized into preprocessing and segmentation methods.

Preprocessing is generally used as an optional step and aims to simplify and ease subsequent steps. Point cloud denoising, axis-alignmend and downsampling in particular are most illustrative of this issue, as each of these methods addresses common problems present in raw point cloud data. Denoising is usually performed through use of filters which are already known from image analysis like the bilateral filter [33] and are meant to mitigate the effect of outliers in the point cloud. Usually, this effect helps segmentation algorithms to extract sharper point clouds segments, however in case of low-quality data denoising can be absolutely mandatory. Not only does denoising help to improve the data's visual quality, it also eases the software supported manual modeling process. Point cloud axis alignment addresses the problem of incorrectly aligned point clouds and is best applied to man-made structure with dominant rectangular geometry. Similar to denoising, alignment methods simplify manual modeling, reorienting point clouds in a way that their major walls are oriented along the global coordinate system axes. Despite this benefit appearing to be marginal from a user perspective, it offers a significant benefit to automated methods. Voxel-, supervoxel- and octree-based data structures [34,35] which are being used for downsampling or fast neighborhood lookups are themselves axis-aligned. They are thus more compact and offer better performance for axis-aligned point clouds.

With the former steps offering ways of cleaning up point clouds, they generally fall into the category of modeling aids, but as mentioned earlier, they also have a notable impact on segmentation algorithms. Segmentation and feature extraction methods in particular stand in close relation with them, as both usually involves octrees or voxelgrids for neighborhood lookups and deliver more precise results for denoised point clouds. Commonly extracted features include structure indicators such as linearity, planarity and scatter values and surface normals. Structure indicators are particularly useful for extracting features such as edges. Figure 4 illustrates the results of feature line segmentation. Such methods lend themselves to the category of semi-automated modeling aids, as they create geometry meant for guiding manual modeling.

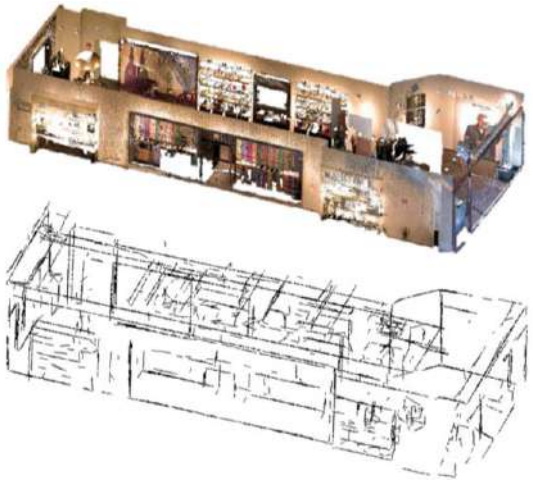

Figure 4. Top: Laser scan (ceiling removed for visibility). Bottom: Simplified model based on extracted feature lines.

In terms of plane segmentation, in other contributions [36,37] normal estimations and the RANSAC paradigm has been applied. Both help estimate local planes oriented along surface in point clouds. The extracted planes can directly be used to extract wall and floor segments, thus letting these methods fall into the category of fully automated reconstruction methods.

Figure 5. Point cloud segmentation for planar segments. Left: Input point cloud. Center:

Outlines of detected plane surfaces. Right: Exploded view, the single points being mapped to their respective plane

Figure 5 shows, how a successful plane extraction can lay out the foundation for this step. Other creative methods involve the removal of extracted planes as a preliminary step to detecting and reconstructing pipes [38].

8 Conclusions and Outlook

Within this paper we presented first results of our research concerning the needed requirements, techniques and steps for creating a suitable as-is BIM model for the maintenance respectively operation phase. Future work will now focus on detailing and optimizing the capabilities of the presented techniques and workflows. For data capturing e.g. in-depth investigation in the field of mobile laser scanning and the reachable accuracies are intended. Furthermore it should be researched in how far a point to point distance calculation is representative to verify accuracy in a real survey scenario where multiple scans get registered.

Automated modelling methods still offer much potential not only for reconstructing geometry, but also deriving semantic information. Future work with previously described techniques will involve a combined approach which will most certainly lead to a more robust segmentation with less outliers and improved performance. With the current approaches being capable of e.g. associating point cloud regions to detected planes, going beyond geometry-based point cloud analysis becomes an intriguing possibility. Traditional texture analysis techniques employed in the field of image analysis are well-established and, in combination with machine learning, have led to solid results in the fields of object recognition and classification [39]. Applying these techniques with respect to point cloud colour information for identifying, segmenting and classifying surfaces to derive additional semantic information, seems quite intriguing.

Another perspective would be a survey on how automated methods are capable of dealing with input data of varying quality. Further investigations with mobile scanning devices would prove interesting, especially when it comes to techniques for denoising the data and comparing automatically reconstructed models of capturing devices with varying accuracies.

Either way, with capturing techniques becoming more accurate and inexpensive and automated methods becoming less reliant on user interaction while at the same time providing more detailed and semantically rich results, the BIM process for capturing the as-is state of existing buildings will grow more attractive and more popular in the future. Furthermore, the described strategies for the implementation of as-is geometry information into the BIM context will now be used for implementing semantic as-is information alike. Both aspects will then be combined to allow efficient property management of existing buildings based on a reliable geometric and semantic data basis.

References

[1] Klein L., Li N. and Becerik-Gerber B. Imaged-based verification of as-built documentation of operational buildings. *Automation in Construction*, 21(23):161–171, 2012.

[2] Volk R., Stengel J. and Schultmann F. Building Information Modeling (BIM) for existing buildings — Literature review and future needs. *Automation in Construction*, (38):109–127, 2014.

[3] Becker R., Falk V., Hoenen S., Loges S., Stumm S., Blankenbach J., Brell-Cokcan S., Hildebrandt L. and Vallée D. BIM – Towards the entire lifecycle. *International Journal of Sustainable Development and Planning*, 13(01):84–95, 2018.

[4] Stumm S., Schwan P., Becker R., Lublasser E., Blankenbach J., Vallée D., Hildebrand L. and Brell-Cokcan S. Towards Life Cycle Complete BIM, in: *34th International Symposium on Automation and Robotics in Construction*, Berlin, Germany, 2017.

[5] Arayici Y., Onyenobi T. and Egbu C. Building Information Modelling (BIM) for Facilities Management (FM). *International Journal of 3-D Information Modeling*, 1(1):55–73, 2012.

[6] Pătrăucean V., Armeni I., Nahangi M., Yeung J., Brilakis I. and Haas C. State of research in automatic as-built modelling. *Advanced Engineering Informatics*, 29(2):162–171, 2015.

[7] The American Institute of Architects AIA Document E202, 2008.

[8] The American Institute of Architects Guide, Instructions and Commentary to the 2013 AIA Digital Practice Documents, 2013.

[9] BIMForum LOD Spec 2017 Part I: For Building Information Models, 2017.

[10] USIBD Level of Accuracy Specification Guide, 2nd ed., 2016.

[11] buildingSMART IFC Overview summary. Online: http://buildingsmart-tech.org/specifications/ifc-overview, Accessed: 06/12/2018.

[12] Kensek K. BIM Guidelines Inform Facilities Management Databases: A Case Study over Time. *Buildings*, 5(3):899–916, 2015.

[13] May M. CAFM-Handbuch: IT im Facility Management erfolgreich einsetzen, Springer Vieweg, Wiesbaden, 2013.

[14] Teicholz P. BIM for Facility Managers, John Wiley & Sons, Inc., Hoboken, 2013.
[15] Kelly G., Seginson M. and Lockley S. BIM for Faciltiy Management: A review and case study investigating the value and challenges, in: *Proceedings of the 13th Inernational Conference on Construction Applications of Virutal Reality*, London, UK, 2013.
[16] Matějka P., Kosina V., Tomek A., Tomek R., Berka V. and Šulc D. The Integration of BIM in Later Project Life Cycle Phases in Unprepared Environment from FM Perspective. *Procedia Engineering*, 164:550–557, 2016.
[17] Gnanarednam M. and Jayasen H. Ability of BIM to satisfy CAFM Information Requirements, in: *The Second World Construction Symposium*, pages 12–21, Colombo, Sri Lanka, 2013.
[18] Pinheiro S., Wimmer R., O'Donnell J., Muhic S., Bazjanac V., Maile T., Frisch J. and van Treeck C. MVD based information exchange between BIM and building energy performance simulation. *Automation in Construction*, 90:91–103, 2018.
[19] Sattenini A., Azhar S. and Thuston J. Preparing a building information model for facility maintenance and management, in: *28th International Symposium on Automation and Robotics in Construction*, Seoul, Korea, 2011.
[20] East B. The COBie Guide. Online: https://nibs.org/?page=bsa_cobieguide, Accessed: 23/04/2018.
[21] CAFM Connect. Online: https://cafm-connect.org/, Accessed: 06/12/2018.
[22] Borrmann A., König M., Koch C., Beetz J. Building Information Modeling, Springer Vieweg, Wiesbaden, 2015.
[23] Gürtler M., Baumgärtel K. and Scherer R. Towards a Workflow-Driven Multi-model BIM Collaboration Platform, in: *16th Working Conference on Virtual Enterprises*, Albi, France, 2015.
[24] Kalderén B. Information Delivery Manual Guide to Components and Development Methods. Online: http://iug.buildingsmart.org/idms/development/IDMC_004_1_2.pdf, Accessed: 06/12/2018.
[25] Anil E.B., Akinci B. and Huber D. Representation Requirements of As-Is Building Information Models Generated from Laser Scanned Point Cloud Data, in: *28th International Symposium on Automation and Robotics in Construction*, Seoul, Korea, 2011.
[26] Riisgaard S., Blas M.R. SLAM for Dummies: A Tutorial Approach to Simultaneous Localization and Mapping. Online: https://ocw.mit.edu/courses/aeronautics-and-astronautics/16-412j-cognitive-robotics-spring-2005/projects/1aslam_blas_repo.pdf, Accessed: 08/05/2018.
[27] BLK360. Online: https://lasers.leica-geosystems.com/eu/de/blk360.
[28] Zeb-Revo RT. Online: https://geoslam.com/zeb-revo-rt/, Accessed: 06/12/2018.
[29] Riegl VZ-400. Online: http://riegl.com/nc/products/terrestrial-scanning/, Accessed: 06/12/2018.
[30] CloudCompare. Online: https://danielgm.net/cc/, Accessed: 06/12/2018.
[31] Loges S. and Blankenbach J. Von der texturierten Punktwolke zum as-built BIM. *Terrestrisches Laserscanning 2016*:23–25, 2016.
[32] Loges S. and Blankenbach J. As-built Dokumentation für BIM - Ableitung von bauteilorientierten Modellen aus Punktwolken, in: *Photogrammetrie - Laserscanning - optische 3D-Messtechnik Beiträge der Oldenburger 3D-Tage 2017*, pages 290–298, Oldenburg, Germany, 2017.
[33] Digne J. and Franchis C. de The Bilateral Filter for Point Clouds. *Image Processing On Line*, 7:278–287, 2017.
[34] Papon J., Abramov A., Schoeler M. and Worgotter F. Voxel Cloud Connectivity Segmentation - Supervoxels for Point Clouds, in: *2013 IEEE Conference on Computer Vision and Pattern Recognition*, pages 2027–2034, Portland, OR, USA, IEEE, 2013.
[35] Blasonea G., Cavallib M., Marchib L. and Cazorzia F. Monitoring sediment source areas in a debris-flow catchment using terrestrial laser scanning. *CATENA*, 123:23–26, 2014.
[36] Fischler M. and Bolles R. Random Sample Consensus: A Paradigm for Model Fitting with Applications to Image Analysis and Automated Cartography. *Readings in Computer Vision*:726–740, 1987.
[37] Oehler B., Stueckler J., Welle J., Schulz D. and Behnke S. Efficient Multi-resolution Plane Segmentation of 3D Point Clouds, in: *Proceedings of the 4th International Conference on Intelligent Robotics and Applications*, pages 145–156, Aachen, Germany, 2011.
[38] Czerniawski T., Nahangi M., Walbridge S. and Haas C. Automated Removal of Planar Clutter from 3D Point Clouds for Improving Industrial Object Recognition, in: *33rd International Symposium on Automation and Robotics in Construction*, Auburn, Alabama, 2016.
[39] Liang Y., Gong W., Pan Y., Li W. and Hu Z. Gabor Features-Based Classification Using SVM for Face Recognition, in: *Second International Symposium on Neural Networks*, pages 118–123, Chongqing, China, 2005.

Impact of 5G Technology on IoT Applications in Construction Project Management

V. K. Reja[a] and K. Varghese[a]

[a] Department of Civil Engineering, IIT Madras, India
E-mail: varunreja7@gmail.com, koshy@iitm.ac.in

Abstract –

IoT based platforms are enhancing decision-making capabilities in many sectors. The impact of IoT in construction has not been significant because of the unstructured nature of the process and the project-based approach to construction. Further, the technology platforms available today do not support high data flow from distributed locations as required for construction. However, it is anticipated that the use of IoT in construction will increase significantly when standards such as 5G are implemented for widespread usage. The first objective of this paper is to identify the potential usage of IoT technology for various construction project processes based on the PMBOK framework for construction. Several works on the applications of IoT which have been published are reviewed, and a framework for construction domain is proposed. The second objective is to identify and discuss the barriers raised by connectivity issues within this framework and influence of 5G technology in overcoming this barrier is elaborated. A comparative quantitative analysis of sample processes is presented to show the potential advantage that 5G technology will bring over 4G with the help of an example.

Keywords –

IoT, 5G, Digital Construction, Wireless Technology, Connectivity in Construction

1 Introduction

IoT is one of the disruptive technologies in recent years which have brought groundbreaking improvement to commercial, consumer, industrial and infrastructure applications. IoT based platforms can gather data to make the decision-making process faster and more efficient. IoT has brought significant change in operations and decision making in several sectors such as manufacturing, healthcare, agriculture, energy, etc. Unlike construction, these sectors involve repetitive processes mostly in a closed working environment which makes the adoption of this technology.

On the other hand, the construction sector is different as it involves complexities like unstructured processes, erratic work environment, and remote construction sites. Construction is also a highly fragmented as well as a multi-disciplinary industry. Therefore, the adoption of IoT in construction will require significant effort in ensuring appropriate changes at policy, technology and project implementation.

In construction, the technology succession planning has not been managed well. Woodhead suggests the construction industry needs to undergo a pivotal shift to digitized processes to make the project delivery process cost-effective. Companies that don't embrace this shift will not be able to ensure sustained business growth due to significant productivity losses [1].

The process of digitalization has brought with it an improvement in many domains including productivity, agility, innovation, consumer experience, quality, costs and revenue [2]. Even though there have been significant advancements in construction techniques, materials, automation of the worksite, scheduling techniques and collaborative platforms like BIM, concerns have been expressed on the resistance to adopting such technology in the construction sector.

The applications of IoT are vastly spread across all domains. Although other sectors are integrating it into their everyday process, the construction industry is lagging in adopting an IoT eco-system. A recent study by Burger identifies several areas for application of construction projects such as remote operation, supply replenishment, construction tools and equipment tracking, equipment servicing and repair, remote usage monitoring, augmented reality (AR), Building Information Modelling (BIM), predictive maintenance, progress monitoring, construction safety & quality monitoring [3].

Woodhead stated that construction companies which are using IoT for decision-making process are using it more as a point-based model for solutions to some of their problems and not developing an ecosystem for all-around integrated business decision support [1]. For

example, an IoT based early warning system was proposed by Ding et al. for safety management in an underground construction project in China [4]. Another application is of an IoT enabled BIM platform (MITBIMP) by Zhong at el. to achieve real-time visibility and traceability in prefabricated construction [5]. There are many such examples of specific applications of IoT in construction in the field of quality, safety, inventory management, etc.

In spite of proven advancement in IoT technology, there remain certain barriers in IoT implementation. These include connectivity issues, such as high latency, low speeds, and large connection density. There are also technological issues such as presently used ERP systems which lack tools for integration of IoT in their design.

Applications of IoT in construction today are scattered, and due to the remoteness of sites and work locations, there are connectivity barriers. Hence with these capabilities of IoT which can revolutionize construction, an IoT framework specific to construction appears to be the need of the hour. Further, the shortcomings due to connectivity standards to that framework should be addressed for smooth implementation. Therefore, this paper attempts to:

1. Identify the potential usage of IoT technology for through a holistic framework which encompasses various processes of a construction project.
2. Identify and discuss the barriers raised by connectivity issues within this framework and the influence of 5G technology in overcoming these barriers.

This paper is broadly divided into three sections; the first section describes the potential applications of IoT platforms in construction management based on the established PMBOK framework. The second section proposes a layered structure of IoT ecosystem for construction and explains in detail about the various layers. The third section of this paper highlights the benefits that 5G standard of connectivity can bring to address the existing barriers and challenges in the implementation of IoT technology. This discussion will emanate from a general context of IoT technology but will move on to focus on the construction sector in particular. In the final section, the conclusions and future implications of this study are presented.

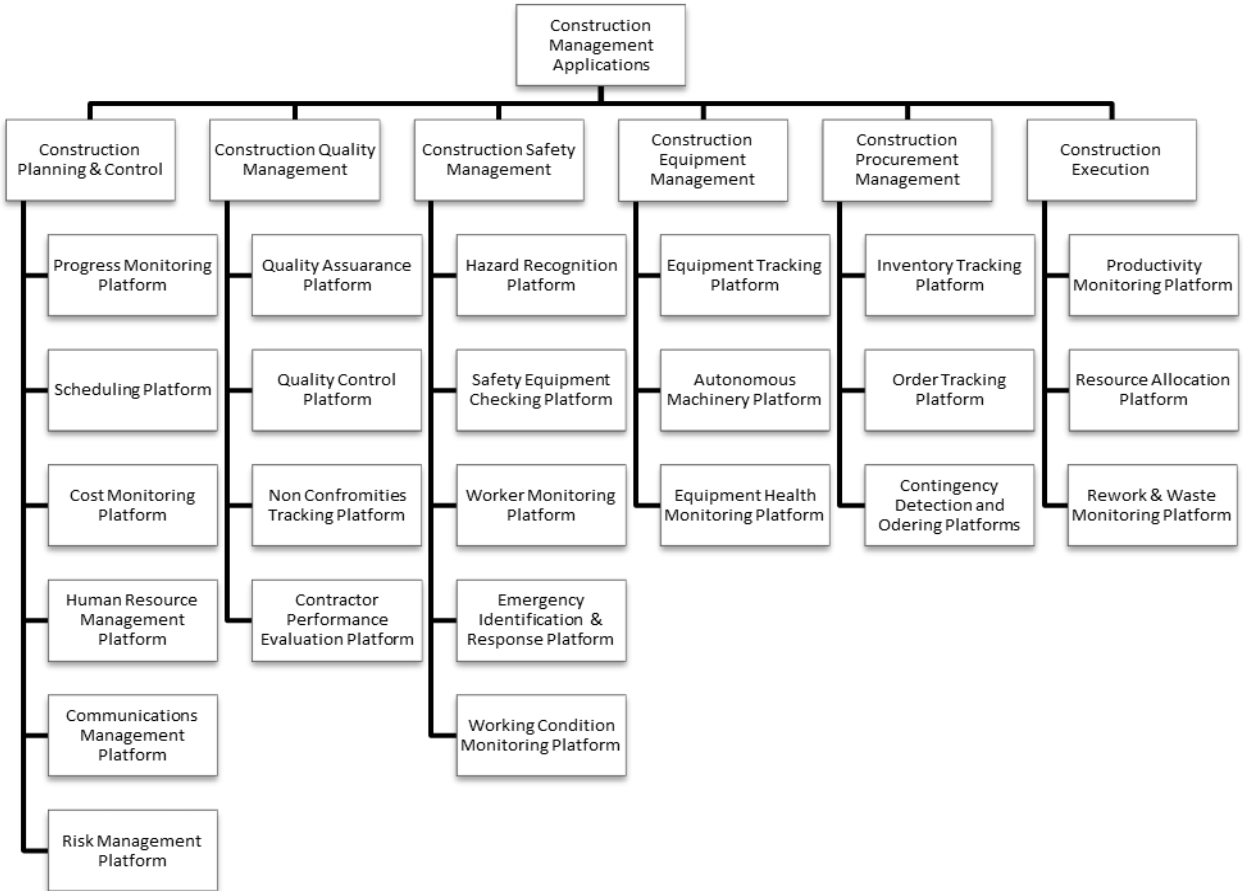

Figure 1. Applications of IoT platforms in construction phase of a project

2 Framework of IoT Application in Construction

For proposing a holistic framework for construction processes, this paper adopts the widely accepted PMI-PMBOK framework for project management. The PMBOK framework has been developed with the inputs from numerous project management professionals and covers all the essential processes required for construction under eh following six categories [6].

1. Construction Planning & Control
2. Construction Quality Management
3. Construction Safety Management
4. Construction Equipment Management
5. Construction Procurement Management
6. Construction Execution

Figure 1 shows the few of the applications for which IoT platforms can be installed to facilitate these areas in the construction phase of the project. There can be many more applications depending on the characteristics of the project.

Each of these platforms can be embedded in a different type of data collecting devices. Example, a progress monitoring platform can be embedded in imaging devices, bar codes, RFID tags or even laser scanners. A study from MIT on construction safety by Bernal et al. demonstrated application of various sensors to monitor a worker's health, the worker's vest and jacket can be embedded with many sensors to monitor the working conditions [7]. Similarly, data can be obtained from installing sensors in worker's shoes, helmet, etc. These data can be stored in the company's database and can be accessed for monitoring by the safety team; they can identify dangerous situations and can alert the worker, worker's team or site supervisor. A GPS based sensor can be used for tracking and collecting information on equipment.

2.1 Structure of an IoT Ecosystem

Figure 2 represents a proposed network outline for the flow of data for Integrated IoT applications on construction sites. A construction project can have *n* numbers of sites where execution is going on simultaneously. Within these sites, there can be *m* number of processes or activities going on. The integrated IoT system will capture data for all the departments (m*n data types); hence there should be a combined embedded system of sensors, actuators and other IoT things fitted for each processing environment. The sensors for the respective departments capture the needed information, and this data can be accessed by the concerned department or the management staff in the project office to facilitate decision making.

Figure 3 illustrates a proposed structure of IoT Ecosystem for decision making in construction management. The Integrated IoT in projects can be enabled by five layers which connect with one and another sequentially to form IoT platforms.

2.1.1 Physical Layer or Sensing Layer

It is the bottom-most layer which consists of the devices that capture or senses the information. This layer is also called the perception layer as it perceives the data from the environment [8]. These devices consist of several sensors, actuators, RFIDs, mobile devices, etc. which forms a network of things.

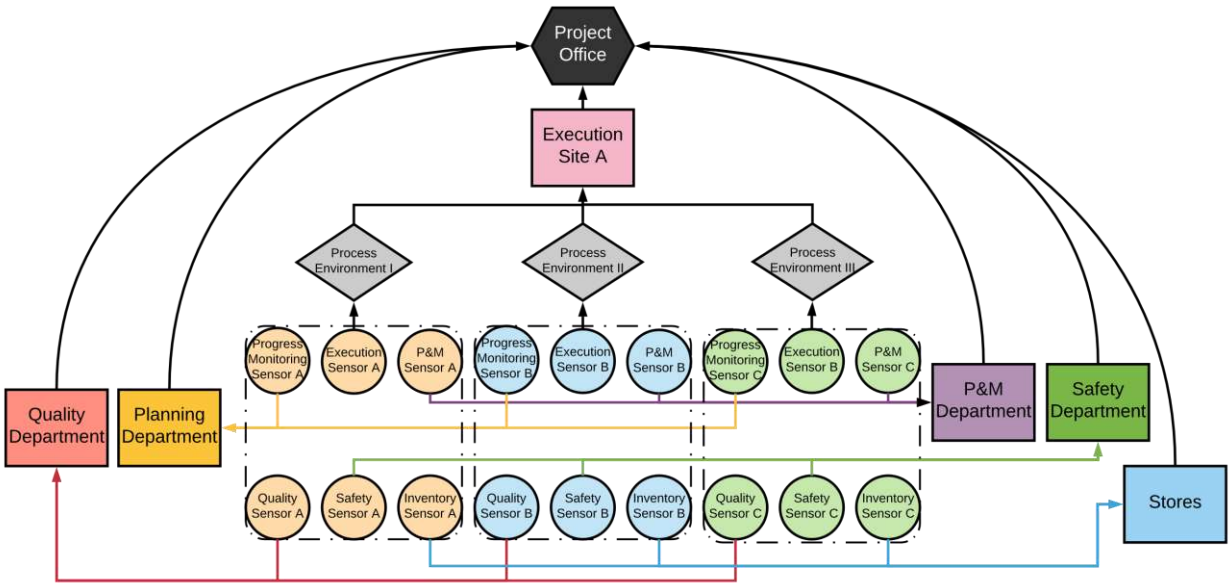

Figure 2. A proposed network outline for data flow for integrated IoT application on construction sites

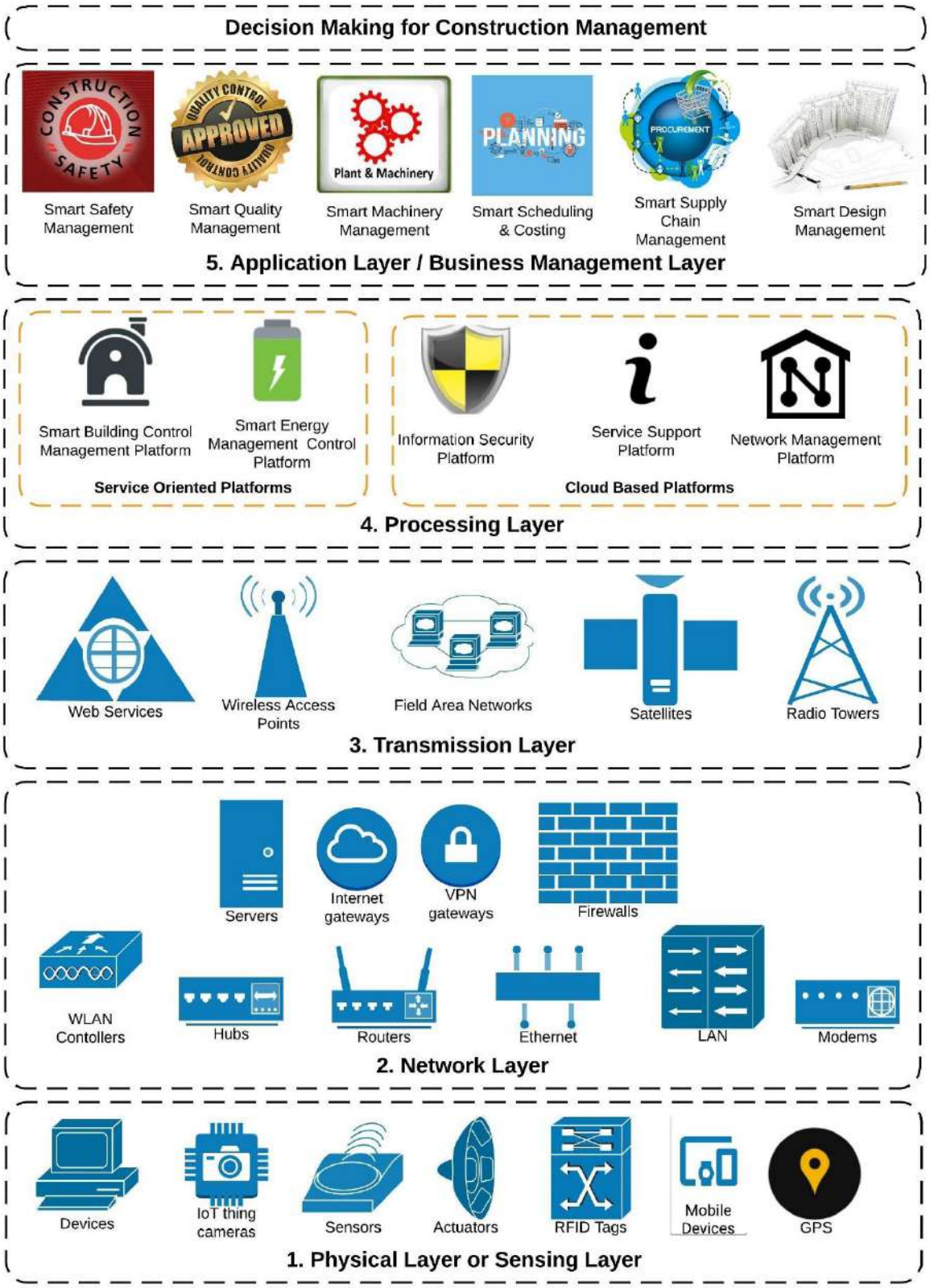

Figure 3. A proposed structure of IoT ecosystem for construction project management decision making

These can be of two types, static and mobile. In a construction project environment, these can be placed anywhere in the site, inside offices, integrated with the machinery, in the hands of site engineer or elsewhere from where it can capture valuable data. These things are connected directly or indirectly to the IoT network after signal conversion and processing. These devices form nodes of the network. In the sensing layer, the nodes are subject to different constraints such as energy limitation, the reliability of wireless medium, security, and privacy [9].

2.1.2 Network Layer

The network layer is one of the two sublayers of the connectivity layer which comprises the local networks of routers, hubs, LAN controllers, servers and other necessary network forming devices. This layer acts as the interface between nodes and the internet. The nodes or things are connected to the gateways present in this layer. The VPN gateway serves as a jurisdiction to the nodes under it and assigns a local address to them in a local area network. IPv6 is commonly adopted for addressing IoT nodes. From that point data flows through a proxy server if internet access is required and then to a web socket in the next layer. When these nodes are needed to interact with each other, or they are transmitting data, they send it to destination nodes. The data first must be transferred to the local network and then if the intended destination is outside the local network, then it is sent through internet gateways.

2.1.3 Transmission Layer

The transmission layer is the second sub-layer of the connectivity layer. This layer acts as interphase between the network and cloud platforms when the data is stored and analyzed. It focuses on end-to-end communication and provides features including reliability, congestion avoidance, and guaranteeing that packets will be delivered in the same order that they were sent [10].

2.1.4 Processing Layer or Cloud Layer

This layer consists of backend services like analytics and cloud computing. Here, the analog data from the devices is converted into a format that is easy to read and analyze. These analysis algorithms can be based on machine learning, artificial intelligence or neural networks. Combining cloud computing with service-oriented architecture (SOA) could provide an efficient middleware for IoT supporting a high level of heterogeneity and flexibility [9].

Additionally, it provides information about the usage of IoT products and handles issues related to the quality of service within operations revealing which device generates problems, revealing data patterns and trends and providing reports and analysis of anomalies [9].

2.1.5 Application Layer or Business Management Layer

The application layer includes people and businesses for collaboration and decision making based on the data derived from IoT computing. It can be merged with the company's ERP system as well as can be made available to the different departments as mobile applications to access data set customizable standards for various activities and make timely changes if necessary. It can include options for auto-actuation or manual actuation for critical machinery works.

3 Shortcomings of IoT in Construction

Usually, construction sites are in remote areas, and their company offices are in cities, constant communication is required between the various workforces within site to the site office as well as site office to home-office and offices of other stakeholder involved in the projects that are located away from the vicinity. Due to limitations in network performance at various places, the connectivity and communications get disrupted in the work environment.

Even in construction sites, basic IoT systems which are meant only for data transfers generally fall short of the expectations as they are not able to provide enough speed and lower latency to undergo primary tasks. Below are a few examples where unnecessary delay causes due to network issues: -

- Data transfer between parties taking longer than expected
- Remote meetings voice and video delay maybe halted
- A significant delay in voice conferencing allowing users to talk over one another
- ERP system resulted in timeouts if remotely accessed
- Slow loading of website and platforms and longer wait time to load or download things

The number of 'things' involved in IoT network is large, so it is much different from a computer network, as the number of nodes increases the complexity of the network increases. In IoT ecosystems, the sensors, actuators and other gadgets are dependent on the responsiveness of the system or network to work effectively. Gerber validates that high latency means delayed responsiveness, and with that comes the inability of things to function to their full capacity [10]. Some IoT systems are designed to respond in case of emergencies, and delayed responsiveness can result in life or deaths. Example: - A delayed response of an actuator intended to close the valve at a certain temperature can result in overheat or even an explosion.

Also working with unmanned machinery in hostile environment needs real-time precision and speed, with present-day network specifications it is not possible to deliver these critical tasks with reliability.

IoT devices usually run on batteries or are self-powered, so they save energy by switching over to energy saving mode, this intern reduced the performance and impacts in slower speeds. Therefore, a low power low latency solution is required [13].

The current system architecture was not designed with IoT in mind. Many systems with their current architecture cannot handle the traffic caused by millions of IoT devices [14]. In construction, most companies are dependent on an Enterprise Resource Planning (ERP) System for project management. These systems have become standard and process designed based on them. For adapting IoT architecture, ERP platforms need to be reconfigured and redesigned. They need an upgrade for the technology which bonds the Layer 1, 2 and 3 of data collection and transmission with the layers 4 and 5 of data analysis and application. (Refer to Figure 3). Though the initial cost of installing an IoT ecosystem is high for small and medium level firms and these firms, need to understand the long-term benefits in decision making and process improvements they will get at later stages.

Additionally, there is an exponential rise in the trend of the number of IoT devices worldwide, and it is expected to rise. Various studies have been conducted to forecast the number of IoT devices, the results of one such study BY Statista estimates that by 2025 almost 76 billion IoT devices will be connected to the internet which is almost three times the devices connected in 2018 [15].

Therefore, combining all these factors there is a critical need for the upgradation of the IoT components and the connectivity skeleton to be able to sustain and meet the growing demand of the future. It is anticipated that the upcoming 5G technology can handle the three connectivity issues, i.e., data traffic, latency, and data transfer issues.

4 Wireless Connectivity: 5G

The International Mobile Telecommunications (IMT) framework of standards is set by the International Telecommunications Union (ITU) for mobile telephony. ITU issued the IMT-Advanced specifications in 2008 as a requirement for the 4G standard. Now, with the growing need of technology upgrade ITU have set a benchmark as IMT-2020 specifications issued in 2017 for the 5G standard.

The 5G technology is divided into three categories based on usage [14]:-

1. **Enhanced Mobile Broadband Service (eMBB):** It will be used for data-driven applications requiring high data rates across a wide coverage area which will enable platforms for immersive VR and AR applications, 360-degree streaming and Ultra HD video.
2. **Ultra-Reliable Low Latency Communication (URLLC):** This is the second phase of 5G which will have strict requirements on latency and reliability for mission-critical communications, such as autonomous vehicles or the tactile internet.
3. **Massive Machine Type Communication (mMTC):** It will be used for supporting many devices in a small area, which may only send data sporadically such as IoT use cases.

4.1 4G Vs. 5G: Head to Head Comparison

Figure 4 shows a comparison of chief KPIs of 4G (IMT-Advanced) and 5G (IMT-2020) network.

This paper uses the theoretical values of KPIs obtained in a test environment for the 5G and 4G networks; these values can be different than what users practically get depending on the quality of network they are connected to and the connection density.

Some of these KPI's are discussed below in detail.

1. **Very Low Latency:** Reduced latency of the 5G standard is expected to be about 1ms, in that case, construction firms can now hope for real-time operations for autonomous machinery used in critical remote tasks. 4G has a latency of about 30-50ms.
2. **Improved throughput:** Throughput refers to the ratio of data transmitted in a unit time. It is expected that 5G can handle the throughput of

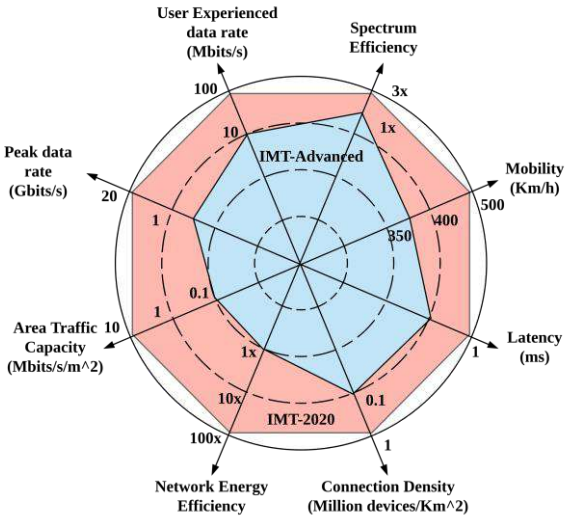

Figure 4. A quantitative comparison of KPIs of 4G and 5G standards (Source: IMT-2020, Network High Level Requirements)

about 10Gbps per connection in comparison to 100Mbps by 4G. That means downloading and uploading speed will be up to 100 times faster. Sometimes having a high-speed network isn't always beneficial especially when it consumes high power, therefore, 5G will phase in new devices like 'Category M1' and 'Narrow Band (NB-IoT)' which will enable lower-power, battery-driven devices as well as far-reaching coverage for remote locations and penetration deep into buildings [16]. These devices will be working on mMTC Technology.

3. **High User Mobility & Improved Reliability:** The eMBB technology of 5G is expected to enhance user mobility up-to 500km/h in moving vehicles, heavy construction machinery. High-quality data at high mobility will allow construction firms to collaborate on various platforms. eMBB will provide broadband access everywhere which will facilitate enhanced connectivity making remote area coverage more reliable.
4. **High user density:** 5G will be able to handle the connection density up-to 1 million connections per square kilometer compared to ten thousand devices by 4G. It is necessary because of the exponential rise in the number of IoT devices per square kilometer. Also, in large construction sites located in cities, where the density of things rises these 5G networks will be able to handle the load smoothly with its Massive-IoT enabling technology.

4.2 Comparative Analysis: Construction Progress Monitoring

Construction managers work under enormous pressure of delivering projects on time, and they tend to monitor schedules more closely and strictly for making better as well as timely decisions. Due to the development of IoT technology, automated daily progress monitoring systems have become a possible (Refer to Figure 1) and as well as necessary tools for managers. Also, BIM platforms require the data to be centralized in a remote server for two reasons, firstly for the collaborative decision making by all the stakeholders and secondly for saving the on-site costs of installing a local server and investing in additional human resource to maintain it. Hence there is a critical need for safe and efficient data transfer mechanism.

Pushkar conducted a study for masonry activity of construction, though this can be easily extended to other construction activities [17]. The data acquisition was made using the commercially available stereo camera as a video file as a part of the input to the planning department, and the setup is as the one describes in Figure 2.

The videogrammetry data size generally depends on the resolution of the video captured and the frame rate but is usually in the range of Gigabytes to Terabytes of data per day. Here is a small piece of time calculation, for the above scenario, the resolution of the camera was set to 720p, and the frame rate was 30fps. Following was the data obtained,

$$Size\ of\ 1164\ frame\ video = 1.3\ GB \quad (1)$$

Converting the frames into the duration captured using frame rate, Therefore

$$Size\ of\ 39\ sec\ video = 1.3\ GB \quad (2)$$

Hence, $$Size\ of\ 1{-}minute\ video = 2\ GB \quad (3)$$

Considering that the Camera captures a one-minute video every 30 minutes cycle, for an 8-hour work day, we will require 16 cycles of data capturing (first video captured after 30 minutes from the start).

$$Total\ Data\ to\ be\ captured\ per\ day = 2\ GB * 16\ cycles = 32\ GB \quad (4)$$

Considering the user experience data rates for the transmission of data, over a 4G network the speed is 10 Mbits/s

$$Time\ to\ transfer\ 1GB\ Data = 13.33\ Minutes \quad (5)$$

Over a 5G network, expected speed is 100 Mbits/s

$$Expected\ Time\ to\ transfer\ 1GB\ Data = 80\ sec \quad (6)$$

*1 Megabit= 0.125 Megabyte

**1 Megabyte = 1000 Gigabyte

The speed being ten times faster can save up to 12 minutes per GB of data transmitted. So, with our single camera, the previous calculation 32GB of data is being transferred to the cloud server in a day then a 5G network can save about 6.4 hours of data transmission time.

Table 1. Time savings for data transfer for multiple cameras

Description	Number of stereo Cameras Collecting data simultaneously									
	1	2	3	4	5	6	7	8	9	10
Data Generated for 1 day (GB)	32	64	96	128	160	192	224	256	288	320
Uploading Time over 4G Network (hours)	7.1	14.2	21.3	28.4	35.5	42.7	49.8	56.9	64.0	71.1
Uploading Time over 5G Network (hours)	0.7	1.4	2.1	2.8	3.6	4.3	5.0	5.7	6.4	7.1
Time Savings (Hours)	6.4	12.8	19.2	25.6	32.0	38.4	44.8	51.2	57.6	64.0

Considering a construction site with ten stereo cameras and daily progress monitoring scenario, we get

the results of time savings as shown in Table 1. Results show that instead of 71 hours the 5G network can transfer the same data over the cloud in 7 hours which will help construction managers to get the analyzed results as a report the next morning itself.

As demonstrated in Figure 2 construction sites consist of many activities going parallelly, there will be many sensors capturing the data simultaneously. The amount of data obtained will be huge, even the BIM files which are to be sent over the cloud for processing are of considerable size and takes time for uploading through the different layers of IoT structure as shown in Figure 3. The 5G data speeds can help us to save a considerable amount of time in data transfer and hence resulting in timely decision making.

If sensors are placed for real-time monitoring purpose over a 5G network, the latency will be in the order of 1ms, which is equivalent to the real-time scenario, whereas using a 4G network gives a latency of 30-50ms. The 5G network is expected to provide more reliability than a 4G network, so the data packets will not be lost during the transmission which sometimes results in an erroneous or incomplete data while processing.

This speed of data transmission, lower latency, availability to bear high connection density makes the 5G network more efficient and reliable than the present 4G network. It can result in a considerable amount of savings in time and cost by facilitating timely decision making.

5 Conclusion

Implementation and effective use of IoT in the construction environment will not be an easy task. Within the next ten years, IoT networks will face prominent challenges because the networks will denser, more complex and heavily loaded than today. The continuous evolvement of IoT is needed along with developing and embracing new paradigms as it should continue to meet consumer and enterprise expectation and mission-critical applications in the coming future. However, a properly planned map to its deployment will smoothen the transition of the construction industry into the IoT ecosystem.

One of the challenges is the need for a faster, reliable, robust connectivity network. 5G implementation can be one of the technological upgrades to overcome these issues. The future connectivity standards will focus on improvement in connection density to handle the massive number of IoT devices, pervasive coverage to reaching challenging locations, low-power consumption and reducing network complexity. These technological challenges if dealt with planned and proper approach will make an ambient environment for wide-scale 5G adoption. In addition to this, the governments and private players should join hands to understand the economic growth the 5G standard can bring and should work closely for all the necessary technological upgradation necessary.

IoT has prospects to be the backbone of the construction industry, and therefore, there is a significant need to understand and address the challenges and barriers in IoT implementation and usage to foresee a future where IoT will be embedded as a ubiquitous tool to support the businesses and projects.

The future research can be focussed upon the applications of IoT in construction management that have been proposed in this paper. These applications will collect data from numerous resources and will have to integrate it collaboratively for better decision making. The five layers of IoT are the backbone to any IoT platform, and each has a high potential for exploration and improvement. The data processing capabilities using cloud computing and tools such as AI and Machine learning have shown a significant trend in usage and are a potential area of research to make IoT further useful for decision making.

References

[1] Woodhead R., Stephenson P., and Morrey D., "Digital construction: From point solutions to IoT ecosystem," *Autom. Constr.*, vol. 93, no. October 2017, pp. 35–46, 2018.

[2] Almada-lobo F., "Six benefits of Industrie 4.0 for businesses Control Engineering," 2017. [Online].Available:https://www.controleng.com/articles/six-benefits-of-industrie-4-0-for-businesses/. [Accessed: 04-Dec-2018].

[3] Burger R.,"How The Internet of Things is Affecting the Construction Industry," 2018. [Online].Available:https://www.thebalancesmb.com/how-internet-affects-the-construction-industry-845320. [Accessed: 03-Dec-2018].

[4] Ding L. Y. *et al.*, "Real-time safety early warning system for cross passage construction in Yangtze Riverbed Metro Tunnel based on the internet of things," *Autom. Constr.*, vol. 36, pp. 25–37, 2013.

[5] Zhong R. Y. *et al.*, "Prefabricated construction enabled by the Internet-of-Things," *Autom. Constr.*, vol. 76, pp. 59–70, 2017.

[6] PMI, *Construction Extension to the PMBOK® Guide*. 2016.

[7] Bernal G., Colombo S., Al Ai Baky M., and Casalegno F., "Safety++: Designing IoT and Wearable Systems for Industrial Safety through a User Centered Design Approach," *Int. Conf. PErvasive Technol. Relat. to Assist. Environ.*, pp.

163–170, 2017.

[8] Duan R., Chen X., and Xing T., "A QoS architecture for IOT," *Proc. - 2011 IEEE Int. Conf. Internet Things Cyber, Phys. Soc. Comput. iThings/CPSCom 2011*, pp. 717–720, 2011.

[9] Abdmeziem M. R., Tandjaoui D., and Romdhani L., "Architecting the internet of things: State of the art," *Stud. Syst. Decis. Control*, vol. 36, no. July, pp. 55–75, 2016.

[10] Gerber A., "Connecting all the things in the Internet of Things – IBM Developer," *IoT 101*, 2018.[Online].Available:https://developer.ibm.com/articles/iot-lp101-connectivity-network-protocols/. [Accessed: 10-Dec-2018].

[11] "IoT (Internet of Things) Data Analytics Platform | Comarch IoT," *IoT Analytics Platform*.[Online].Available:https://www.comarch.com/iot-ecosystem/iot-connect/iot-analytics-platform/. [Accessed: 10-Dec-2018].

[12] "Why It's Important to Improve Your Network Latency | Independents Fiber Network," *Independent Fiber Networks*.[Online]. Available: http://www.ifnetwork.biz/resources/blog/why-it's-important-improve-your-network-latency. [Accessed: 10-Dec-2018].

[13] "A Solution to Latency in IoT Devices | IEEE Innovation at Work," *IEEE Innovation at Work*, 2016.[Online].Available:https://innovationatwork.ieee.org/latency-solution-in-iot-devices/. [Accessed: 10-Dec-2018].

[14] Akins B., "Internet of Things and Solving Latency For an Instantaneous World," *Electric Energy T&D Magzine*, 2016.[Online]. Available: https://electricenergyonline.com/energy/magazine/985/article/Internet-of-Things-and-Solving-Latency-For-an-Instantaneous-World.htm. [Accessed: 10-Dec-2018].

[15] Statista, "IoT: number of connected devices worldwide 2012-2025 | Statista," 2016. [Online]. Available:https://www.statista.com/statistics/471264/iot-number-of-connected-devices-worldwide/. [Accessed: 03-Dec-2018].

[16] "5G - Connection Density-Massive IoT and So Much More | CIO," *CIO*. [Online]. Available: https://www.cio.com/article/3235971/internet-of-things/5g-connection-density-massive-iot-and-so-much-more.html.[Accessed:10-Dec-2018].

[17] Pushkar A., "Development of framework for automated progress monitoring of construction project," MS Thesis 2018.

Context-Realistic Virtual Reality-based Training Simulators for Asphalt Operations

F. Vahdatikhaki[a], A. Kassemi Langroodi[a], D. Makarov[a], and S. Miller[a]

[a] Department of Construction Management and Engineering, University of Twente, The Netherlands
E-mail: f.vahdatikhaki@utwente.nl, a.kassemilangroodi@utwente.nl, d.makarov@utwente.nl, s.r.miller@utwente.nl

Abstract -

Asphalt operations are equipment-intensive, highly-coordinated, and context-sensitive. To ensure high-quality asphalt, operators need to be mindful of, among others, the degree of compaction required/achieved, temperature of the asphalt mixture, its cooling rate, other equipment, and the supply logistics. However, the current training program for the operators of asphalt equipment is inadequate because (1) the training heavily depends on the use of actual equipment for the training and because of the cost/safety risks involved in using actual equipment, novice trainees do not get enough opportunity to develop the required skills; and (2) given the sensitivity of the asphalt operations to the environment, the type of the asphalt mixture, logistics, etc., it is very difficult to allow trainees become sensitized to all the influential parameters in a limited time provided for the practical training.

In recent years, Virtual Reality (VR) based training simulators are employed to help train operators in a safe environment. However, scenarios used in the construction simulators are mostly hypothetical. The context of operation in these scenarios is static and devoid of dynamism common in a construction site. This is a major oversight, particularly in highly-collaborative asphalt operations. Therefore, it seems crucial to better represent the actual work context in the training simulators. Given the myriad of parameters involved in the asphalt operations, designing a training scenario based on pure modeling is very challenging.

This research proposes an approach for developing a training simulator based on the data collected from actual asphalt operations. The collected data will be analyzed and translated into a training simulator that can better capture the interaction between various operators of asphalt operations. A prototype is developed and a case study is conducted to demonstrate the feasibility of the proposed approach. It is shown that actual data can be used to effectively generate realistic training scenarios.

Keywords -

Virtual Reality; Context-realistic; Operator Training; Asphalt operations

1 Introduction

Hot mixed asphalt (HMA) is the dominant material of choice for road construction all over the world. However, the quality of HMA is very sensitive to the construction operations [1]. For HMA to be of desirable quality, the compaction must be executed over a limited period when the asphalt is within a certain temperature window, which depends on the type of the mix. Compaction below and above this temperature window results in suboptimal quality [2,3]. Therefore, operators of asphalt operation equipment (i.e., paver and compactor) need to be aligned with one another. Additionally, operators need to be able to process a wide range of information (e.g., the temperature of the asphalt, the number of desired and achieved compaction, the speed of pavers, the movement of compactors, etc.) to be able to deliver a high-quality operation. This requires a high degree of coordination and operational skills.

Operators of asphalt construction equipment go through rigorous training before they are certified to work on the site. However, there are several limitations that compromise the effectiveness of the current training programs. First and foremost, since the practical training with the equipment is expensive, trainees may not have the chance to sufficiently train with actual equipment for work in different types of operations. Second, given the sensitivity of the HMA quality to multitude of environmental (e.g., weather), design (e.g., type of mix), and operational (e.g., the size of the team) parameters, the current training programs cannot sensitize the trainees to all the influential parameters in a limited time provided for the practical training.

Virtual Reality (VR) based training simulators have been used in other industries (e.g., aviation) to address the very same problems. The construction industry has also started to use VR for training in recent years [4,5]. These simulators can considerably reduce the cost and

risks involved in on-equipment training[6]. However, to the best of the authors' knowledge, a comprehensive training simulator for asphalt operation is missing. Besides, the available construction simulators (dominantly focusing on excavators and cranes) mainly focus on the dexterity and equipment handling skills of the operators. Accordingly, a lion share of the developers' attention is placed on the graphical fidelity and realistic kinematics of the equipment. While very important, this steers the focus away from capturing the realistic context of the training. In other words, the current simulators place the trainee in a mostly isolated and static site where the trainee can move freely and unhindered. For a highly collaborative work such as asphalt operations, this is a major oversight because operators need to perform the tasks in view of many peripheral parameters about the operation of other equipment, the behavior of the asphalt layer, and weather condition. For instance, when considering the trajectories of other compactors in the team, what could have been an optimal path for a single compactor may become very unsafe or inefficient in tandem compaction. Additionally, since the focus is too much on kinematics, many other aspects of physics in the simulators are left out. Current simulators use theoretical principles to develop the physics of the scene. Even though these theoretical principles are very effective, they are normally simplified and can hardly account for the complex interaction between the behavior of the of the asphalt layer, the type of the mix, weather condition, and the compaction regime. Capturing this complex interaction through physics-based modeling is very difficult.

Recent advancements in sensing technologies and Internet of Things (IoT) allow for the collection of a wide range of data about various aspects of actual construction sites. The authors have previously indicated the potentials of using various types of sensors to track and monitor asphalt operations [7]. The collected data from actual site capture various aspects of the context of asphalt operations that are not represented in the current hypothetical training scenes. This includes the context-specific cooling rate of the asphalt as well as the movement and motions of all the equipment in the asphalt operation team. It is argued that these data can be used to reconstruct the actual asphalt operations in a VR environment. Because the virtualized scene incorporates several elements of the operational context, the training scene created in this fashion is expected to be more realistic in terms of fidelity to the context. Trainees can use these simulators to become more sensitized to the collaborative nature of asphalt operations and to delicacies involved around compaction at the right temperature.

The authors have previously proposed a generic framework for data-driven context-realistic training simulator for construction operations [8]. However, the previous work of the authors is generic and not focused on a specific operation. Besides, the previous work of the authors assumed that most of the feedback about the performance of trainees is provided at the end of the session. This is a limitation because novice trainees and early-stage learners can benefit from mid-training guidance to build up competency about the development of compaction strategy.

Therefore, the primary objective of this research is to present an approach for developing an asphalt-specific training simulator using the previously presented framework for context-realistic training simulators. In this research work, the focus is placed on asphalt operation and the generic framework is retrofitted to adapt to the requirements of training simulators for asphalt operations. In particular, the paper extends the previous work of the authors to incorporate mid-training guidance targeted at novice and early-stage learners.

The layout of the paper is as follows: first, the proposed approach is presented. Next, the implemented prototype and case study is introduced. Finally, the conclusions and future work of the research is presented.

2 Proposed Approach

Figure 1 shows the overview of the proposed approach for the generation of context-realistic training simulators for asphalt operations, focusing on mid-training guidance. As stated in Section 1, this framework is retrofitted from the generic framework presented in the previous work of the authors [8] to customize the training simulators for the purpose of asphalt operations.

A training simulator focusing on the asphalt operation should be able to sensitize trainees to the importance of compacting asphalt at the right temperature. Given the complexity involved in simulating the behavior of asphalt on the construction site, the application of context-realistic simulators seems to be appropriate and helpful. The proposed approach has four main steps, namely, data collection, context generation, scene reconstruction, and context-based feedback.

2.1 Data Collection

During the data collection step, all the relevant data for the representation of the context of asphalt operation need to be collected. The context of asphalt operation is defined as the combination of environment, mobile equipment, and behavior of the asphalt.

In recent years, many municipalities and provincial government of large cities provide either the 3D models of their jurisdictions or the essential data needed for the reconstruction of 3D models. For instance, CityGML models of many major cities are now publicly available [9,10]. These models can be used to represent the

environment of the actual construction sites in the VR.

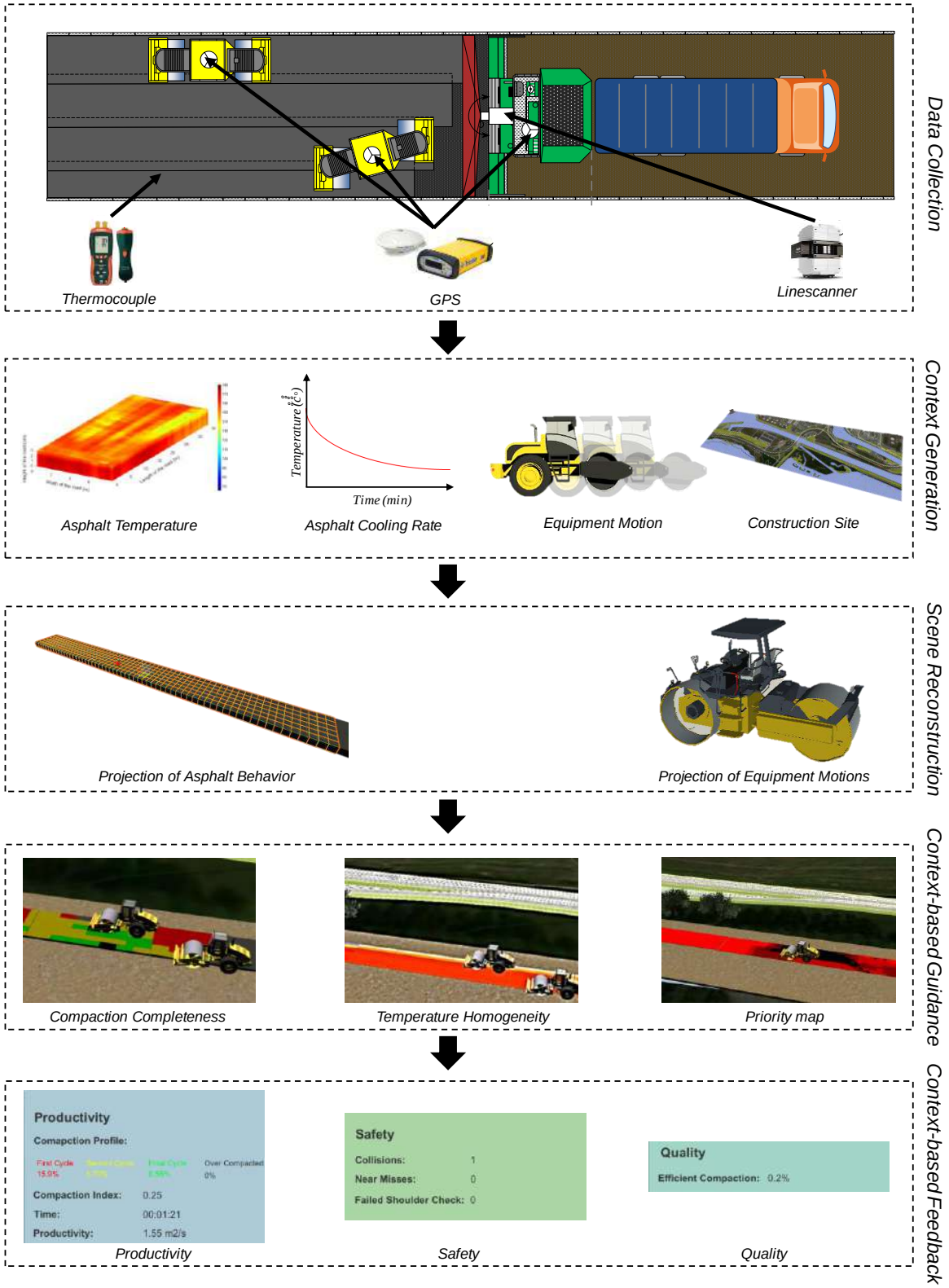

Figure 1. Overview of the proposed approach for context-realistic asphalt operation training simulators

For tracking mobile equipment, Global Positioning System (GPS) can be used. Since the kinematics of pavers and rollers are rather simple, 2D tracking is enough for representing mobile equipment in the VR scene. GPS rovers can be installed on each equipment. The data collected from GPS rovers can later be projected to the local coordinate of the VR scene. As for the asphalt behavior, the proposed simulator only focuses on the temperature of asphalt and the cooling rate. These two pieces of information indicate the temperature of the asphalt layer (at surface and core) and the rate at which it cools down. These data are critical for effective compaction and they are sensitive to various parameters such as weather condition, layer thickness, logistics, and type of asphalt mix, which makes them context-sensitive.

The previous work of the authors provides a comprehensive account of how this data can be collected from asphalt operations [1,7]. However, for the completeness, a brief description will be provided here.

The surface temperature of the laid asphalt mixture is collected using linescanner mounted at the rear of the paver, as shown in Figure 1. The width of the asphalt layer is split into several points and the temperature of each point is measured. By synchronizing GPS and linescanner data, the surface temperature data is geo-referenced. To be able to determine the cooling rate of asphalt, a set of thermocouples in combination with infrared camera are used to continuously measure the core and surface temperature of the asphalt layer at a fixed location. It should be noted that the cooling rate of the asphalt is not a constant value but rather a non-linear function, as shown in Figure 1.

2.2 Context Generation

Using the continuous stream of core and surface temperatures at the fixed location (i.e., the output of the thermocouples) and the initial surface temperature of different parts of the asphalt mat (i.e., the output of linescanner), we can interpolate the core temperature of the asphalt at any other points on the mat. With all the measured and calculated data, the 3D temperature contour of the asphalt mat and the cooling curve of the asphalt at the core and surface can be determined. These two types of data can be fed into the simulator to realistically represent the thermal behavior of asphalt in the context. Since this behavior is extracted from actual construction sites, the asphalt behavior captures the complex causal relationships that impact the thermal behavior of asphalt (e.g., weather condition, layer thickness, type of asphalt mix, etc.) without requiring to model these relationships mathematically.

Another element of context in asphalt operation training simulator is the 3D model of the site. As stated before, the data required for 3D modeling of the site can be extracted from public data (e.g., CityGML). Depending on the Level of Detail (LoD) of the available data, the 3D model may need some adjustment such as draping and minor geometric adjustment. Also, additional pieces of information such as new buildings and underground utilities can be extracted from relevant asset information models such as Building Information Models (BIM). Asset information models can be incorporated into CityGML model using available tools for BIM and GIS integration (e.g., Infraworks [11]).

The final element of context in the simulators is motions of different pieces of equipment. For this element, GPS data need to be corrected. Authors have previously presented an approach for enhancing the quality of the location data [12].

2.3 Scene Reconstruction

In the next phase of the proposed approach, the context data and the 3D model of the site need to be integrated. Game engines can be used for this purpose. The first step in this phase is to import the 3D model of the site into the game engine. In many cases, when the 3D model is imported into the game engine, the native coordinate system is distorted. If this happens, the 3D model needs to be re-scaled and re-positioned. This process is explained in the previous work of the authors [12].

The next step in this phase is data synchronization. Depending on the used sensors, different types of data have different resolution and frequency. To improve the consistency of the scene, it is best to unify the update rate of different types of data and align the timeframe across all the data. This can be done through averaging the data and interpolation.

Upon the completion of data synchronization, temperature, cooling rate, and mobility data should be integrated into the scene. Figure 2 presents an overview of how these types of data are integrated into the VR scene. As shown in Figure 2A, the first step is to translate the latitude and longitude data coming from GPS to the local coordinate of VR scene, using the method explained in the previous work of the authors [8]. Since pieces of equipment used in the asphalt paving operations have rather simple kinematics (i.e., 1 controllable degree of freedom for transitional movements), the project time-stamped coordinate data can be linked to a single point hinged to the 3D model of the equipment at the same location where GPS rover was installed on the actual equipment.

To incorporate the temperature ($T_{x,y}$) and cooling rate (dT/dt) data into the scene, first, the geo-location of each data point needs to be projected to the local coordinate of the VR scene, similar to the previous step. Then, the 3D model of the asphalt layer needs to be discretized into a grid, as shown in Figure 2b. Since the data collected by

linescanner, i.e., red dots in Figure 2b, (1) are not necessarily projectable into a uniform grid and (2) have a very high update rate that may render the VR scene very slow if they are supposed to be used as is, the grid size in the VR scene is determined by human modeler. Then, by intersecting the coordinates of the temperature data ($IT_{x,y}$) with the user-defined grid and applying interpolation the initial temperature of each cell of the asphalt layer in VR scene ($IT_{i,j}$) is determined. In the VR scene, each cell becomes visible only when it collides with the paver for the first time (i.e., when it is placed on the mat on actual site). From that moment, the temperature cools down according to the measured cooling rate.

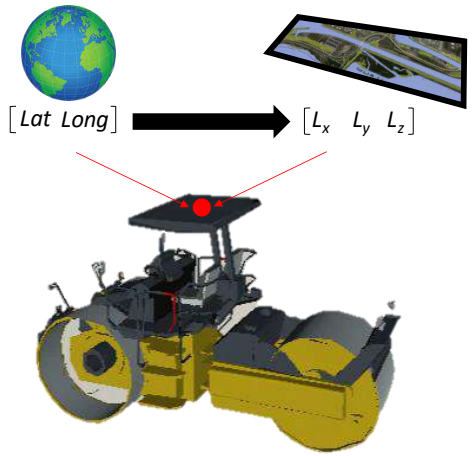

(a) GPS data integration

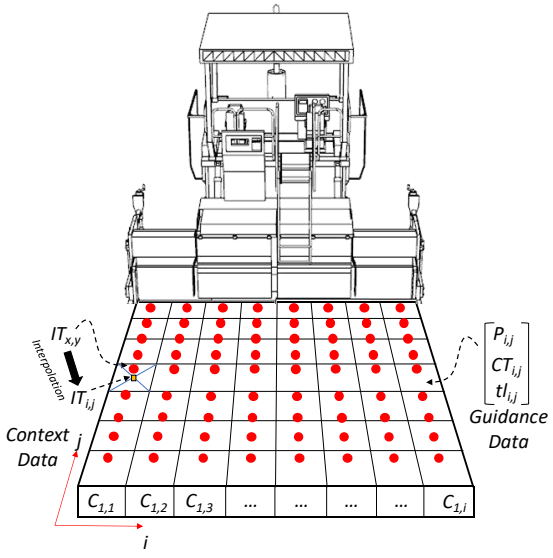

(b) Linescanner data integration

Figure 2. Overview of the proposed approach for context-realistic asphalt operation training simulators

2.4 Context-based Guidance

Upon the integration of data in the VR scene, the next step is to develop a guidance mechanism inside the scene. The guidance is supposed to help trainees (particularly novice learners) develop better compaction strategies by observing the behavior of the asphalt and the impact of decisions made on the site. To this end, three types of guidance are provided to the trainees: (1) compaction completeness, (2) temperature homogeneity, (3) proximity, and (4) compaction priority map. These three types of guidance are provided on-demand, meaning that the trainee can choose which of the three types of guidance he/she wants to see on the main screen and which one of the guidance types he/she wants to see in small side windows. More experienced trainees can choose not to use any of the guidance types at all.

Compaction completeness measures the number of times each cell in the grid is subject to compaction ($P_{i,j}$), as shown in Figure 2b. This index is calculated by counting the number of times the drum of the trainee-operated roller collides (i.e., come to contact) with each cell. This type of guidance is displayed through the use of a color coding scheme. This means that based on the required number of compaction, which is a function of the type of the asphalt and the thickness of the layer, different colors in the spectrum of dark red to dark green indicates the number of compaction achieved at each cell. Also, the cells that are over-compacted can be indicated by changing the color to black. The user uses this guidance to (1) evaluate his completed work and (2) devise a plan for compacting the reminder of work.

Temperature homogeneity guidance displays the current temperature of each cell. As shown in Figure 3, this is done by considering (1) the initial temperature of the cell and (2) the simulation time (t) passed from the moment each cell is placed on the mat.

The cooling curve of the asphalt, which is generated at the end of the data gathering phase, is used to determine the current temperature of each cell at each frame of the VR scene ($CT_{i,j}$). Similar to the compaction completeness index, the temperature of the cell can be visualized using a color coding scheme. Trainees can use this form of guidance to determine whether or not a cell is still within a compactable temperature zone and how much time there is before a cell becomes too cold for compaction.

Proximity guidance indicates the distance of the trainee-operated equipment to other pieces of equipment. Additionally, when the trainee-operated equipment become hazardously close to any other equipment/workers in the scene, a warning is generated. The trainee can use this guidance to become sensitized to situation awareness required for safe execution of the job.

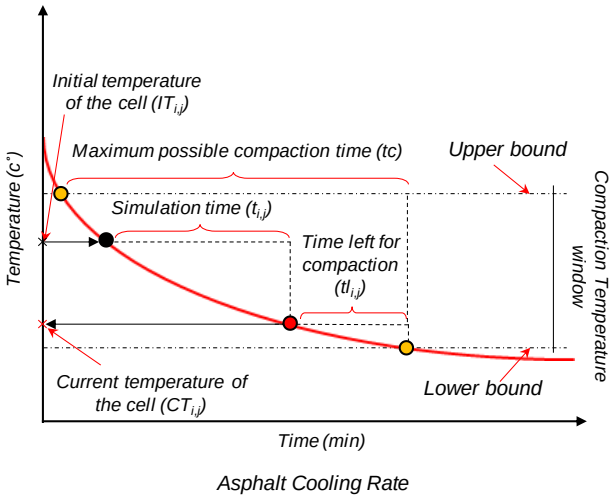

Figure 3. Calculation of the current temperature of each cell based on the initial temperature and the cooling rate

The last type of guidance that can be provided to the trainee is the compaction priority map. While the previous two guidance types merely indicate the state of asphalt layer in terms of compaction and temperature, the priority map tries to combine the two state data into guidance about how compaction of different parts of the asphalt needs to be prioritized. In order to generate the priority map, two parameters are considered. The first parameter is the time left for the compaction of a cell. As shown in Figure 3, this is determined by calculating the time left to the lower bound of compaction temperature window ($tl_{i,j}$) for each cell at every frame of the VR scene. The second parameter is the number of compaction achieved so far for each cell ($P_{i,j}$). These two parameters are translated to a priority index using Equations 1 to 3.

$$R_{i,j} = CP_{i,j} \times TP_{i,j} \quad (1)$$

$$CP_{i,j} = \begin{cases} \frac{PD - P_{i,j}}{PD} & PD \geq P_{i,j} \\ 0 & PD < P_{i,j} \end{cases} \quad (2)$$

$$TP_{i,j} = \begin{cases} 0 & tl_{i,j} > t_c \\ \frac{t_c - tl_{i,j}}{t_c} & 0 < tl_{i,j} \leq t_c \\ 0 & tl_{i,j} = 0 \end{cases} \quad (3)$$

Where:

$R_{i,j}$ =*Priority of cell i and j*
$CP_{i,j}$ =*Compaction priority of cell i and j*
$TP_{i,j}$ =*Temperature priority of cell i and j*
PD =Desired number of compaction
$P_{i,j}$ = *Compaction achieved at cell i and j*
tc= Maximum possible compaction time
$tl_{i,j}$ = *Time left for compaction of cell i and j*

The priority value ($R_{i,j}$) is displayed using a color coding scheme in the spectrum of light to dark red, corresponding to high and low priorities. Trainees can use this form of guidance to plan the compaction path.

2.5 Context-based Feedback

The next phase in the proposed approach is to provide relevant feedback to trainees, i.e., after the training session is completed. Feedback helps trainees better pinpoint areas of attention in their practices. Additionally, feedbacks and the metrics used to assess the performances of the trainees can help track the progress of the trainees throughout the training program. Based on the scope, feedbacks can be categorized in 3 classes: (1) productivity-related, (2) safety-related, and (3) quality-related. Productivity-related feedback measure the overall compaction time, proportion of under, adequately, and over compacted cells, average compaction, and productivity. Safety-related feedback indicates the number of collision with other objects/equipment, the near misses, and failed shoulder checks (i.e., if VR goggle is used). Finally, quality-related feedback measures the ratio of cells that have been properly compacted within the compaction temperature window to the overall asphalt area.

3 Implementation and Case Study

To demonstrate the feasibility of the proposed approach case study is conducted. The case study is built upon the previous case study presented by the authors [8]. For completeness, the description of the case study is repeated in this paper.

The data collected from a surface rehabilitation of a part of a highway (A15) near Rotterdam is used. The collected data included the GPS of the paver and two compactors and the temperature/cooling of the asphalt. The principles explained in the earlier work of the authors are used for data collection [1].

The 3D model of the site is generated using Infraworks and Unity 3D, as explained the previous work of the authors [12]. The data collected from linescanner and GPS rovers are integrated with the asphalt cells and the 3D model of equipment, respectively.

The scene is designed so that one trainee can operate one of the rollers in the scene. Depending on the purpose of the training, the trainee can decide to be the leader or follower in the compaction process. The details of the two possible scenarios and how they are implemented in the scene can be found in the previous work of the authors.

As stated in Section 1, the main focus of the paper is to generate mid-training guidance to the trainees. Therefore, the principles explained in Section 2.4 is implemented in the VR scene. Figure 4 shows different types of mid-training guidance that trainees will receive.

As shown in this figure, the discretization of asphalt into cells can help provide easy guidance to the trainees. Also, the dangerous proximity of the trainee-operated equipment to other equipment is warned using the highlights in the real-time proximity indicator.

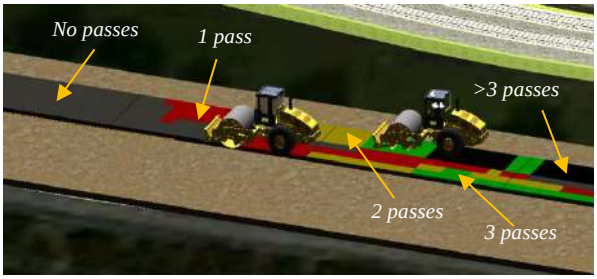

(a) Compaction guidance

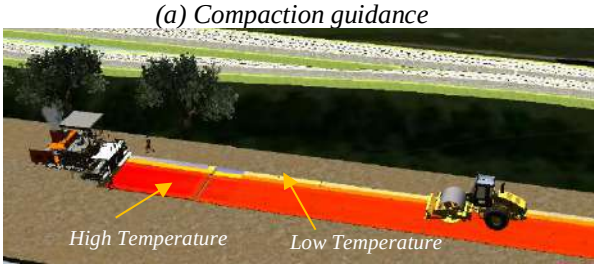

(b) Temperature homogeneity guidance

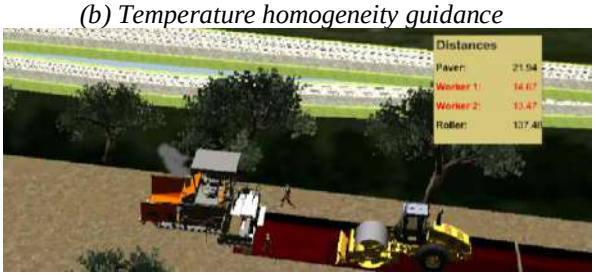

(c) Proximity guidance

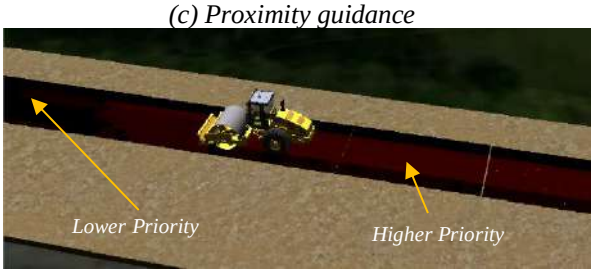

(d) Compaction priority map

Figure 4. Overview of different types of mid-training guidance that can be provided to the trainees in the context-realistic training simulators

4 Conclusions and Future Work

In this paper, an approach for the generation of context-realistic training simulators for paving operation was presented. A generic framework developed by the authors was tailored to the specific characteristics of paving operations. Additionally, special focus was placed on the incorporation of mid-training guidance for early stage learners. A case study was conducted to demonstrate the feasibility of the proposed approach based on actual data collected from a paving operation.

The result of the case study indicated that the actual data collected from paving operations can be easily used to generate context-realistic training simulators. It is shown that a variety of real-time calculations can be applied to provide early-stage learners with various types of guidance. These mid-training guidance can be used by trainees to hone the skills required for developing compaction strategies faster.

While the results are promising, the positive impact of mid-training guidance on the development of compaction skills needs to be validated in a case study with a group of actual trainees. This would be the future focus of this research.

4.1 References

[1] Makarov D.S. Vahdatikhaki F. Miller S.R. Dorée A.G. A Methodology for Real-Time 3D Visualization of Asphalt Thermal Behaviour During Road Construction, In *Proceedings of Advances in Informatics and Computing in Civil and Construction Engineering*, Chicago, the U.S, 2019: pp. 797–804.

[2] Delgadillo R. Bahia H.U. Effects of Temperature and Pressure on Hot Mixed Asphalt Compaction: Field and Laboratory Study, *Journal of Materials in Civil Engineering*. 20:440-448, 2008.

[3] Willoughby K.A. Mahoney J.P., Pierce L.M. Uhlmeyer J.S., Anderson K.W. Construction-Related Asphalt Concrete Pavement Temperature and Density Differentials, Transportation Research Record: *Journal of the Transportation Research Board*, 1813:68–76, 2002.

[4] Machine simulators for education - Tenstar Simulation. Online: https://www.tenstarsimulation.com/en/ Accessed: 16/1/2019.

[5] CM Labs Simulations. Online: https://www.cm-labs.com/, Accessed: 16/1/2019.

[6] Dunston P.S. Proctor R.W. Wang X. Challenges in evaluating skill transfer from construction equipment simulators, *Theoretical Issues in Ergonomics Science*. 15:354–375, 2014.

[7] Makarov D.S. Miller S.R. Dorée A.G. Developing a real-time process control system for asphalt paving and compaction, in: *Proceedings of CROW Infradagen 2016*, 2016.

[8] Vahdatikhaki F. El-Ammari K. Kassemi Langroodi A. Miller S. Hammad A. Dorée A. Framework for Context-Realistic Construction Equipment Training Simulators, *Automation in Construction*. (Accepted with modifications), 2019.

[9] City of Montreal. Online:

http://donnees.ville.montreal.qc.ca/ Accessed: 16/1/2019.

[10] City of Rotterdam. Online: https://www.rotterdam.nl/werken-leren/3d/ Accessed: 16/1/2019.

[11] InfraWorks. Online: https://www.autodesk.com/products/infraworks/overview. Accessed: 16/1/2019.

[12] Vahdatikhaki F. Hammad A. olde Scholtenhuis L.L. Miller S.R. Makarov D. Data-Driven Scenario Generation for Enhanced Realism of Equipment Training Simulators, in: *Proceedings of 6th CSCE/CRC International Construction Specialty Conference*, 2017.

Generating Generic Data Sets for Machine Learning Applications in Building Services Using Standardized Time Series Data

F. Stinner[a], Y. Yang[a], T. Schreiber[a], G. Bode[a], M. Baranski[a], and D. Müller[a]

[a] RWTH Aachen University, E.ON Energy Research Center, Institute for Energy Efficient Buildings and Indoor Climate, Germany
E-mail: fstinner@eonerc.rwth-aachen.de

Abstract –

Machine Learning Algorithms (ML) offer a high potential with low manual effort to discover appropriate energy efficiency measures for buildings. Although many building automation systems (BAS) record a high amount of data, technical systems such as boilers provide only a few data points per building. However, machine-learning algorithms require training based on a sufficient number of instances of a technical system in order to enable cross-building use.

In contrast to electrical systems, few data sets of actual operation of thermal systems are publicly available. Since 2012, the monitoring system in our test object has continuously provided threshold-based data with a maximum resolution of 1 minute. We monitor the plants, energy consumption and comfort parameters with 9239 data points in total. In this paper, we show how our published data set from this building is structured. In order to facilitate the use of ML, each data point receives a uniform label according to a previously developed approach.

Since the documentation of ML data sets varies in the building sector, we show an approach to standardize data sets with special datasheets for thermal systems to provide sufficient information for application of ML.

We use the Brick Schema, a unified ontology standard for the description of topology in buildings, which is part of the future ASHRAE Standard 223P. We couple this with an approach we developed for the structured labeling of data points in buildings.

We show how to semi-automatically generate physical models based on an open-source Modelica library from this ontology-based model. We show that the models, enriched with real time series data and data sheets, are in good agreement with the measured data.

Finally, we show with an ML example that our approach based on Brick Schema and Modelica is able to deliver ML compliant data sets.

Keywords –
Standardized data sets; Machine Learning; Simulation; Modelica; Building Energy Systems

1 Introduction

Machine Learning Algorithms (ML) are increasingly finding their way into building energy systems (BES) in order to increase the systems' energy efficiency. One application of ML algorithms in BES is the optimization of the control system. Further applications are the modelling and prediction of behavior of energy systems or energy consumption [1]. They can support the normalization of metadata of data points [2] or fault detection [3]. Since different disciplines use the term "data point" differently, we use the following definition, which we derived from the use in building automation (BA): a data point is an information carrier that continuously provides information about a state. The use cases and methods for the application of ML in energy technology are manifold. [4] and [5] give an overview for the application of supervised learning in energy systems.

Each data point receives a label in the building, the so-called data point identifier. Therefore, there is no common standard or exchange format for data point identifiers for all buildings. This leads to the fact that applications in the building are not or only with difficulty transferable to other buildings. Thus for ML, most time series from BES are unstructured.

However, a large amount of structured data is required for the development and application of most ML use cases in BES. These data should be retrieved from as many different systems as possible, so that a comparison with different building types is possible [6]. Some technical system types exist only in small numbers within a building, e.g. often there is only one heat pump in a

building. In order to develop special classification applications for these technical systems, a clearly sufficient number of structured time series is necessary.

[7] shows an approach to structure or classify data points of BA in 22 classes. In practice, the data points in BA have a higher differentiation.

Published data sets on buildings or building operation originate mainly from the electrical monitoring [8][9] or the comfort [10]. If the operation in thermal systems is covered, then mainly in 15-minute samples [11][12] or for special applications, such as air handling units [6] or subways [13]. The 15-minute rate is not sufficient to reflect the technical monitoring in control as described in VDI 6041 [14].

In existing simulative approaches for virtual data sets, models of buildings were used to generate a virtual data set for the comparison of building consumption [15] or synthetic data for Non-intrusive Load Monitoring (NILM) were produced [16].

For the testing and benchmarking of ML algorithms, it has become standard practice to use test data sets. According to [17], developers and users of ML approaches need a precise description of the data sets in order to interpret them correctly. The existing approaches for the description of building datasets provide information for a limited number of use cases. In particular, the data sets do not describe the difficulties of data collection or data application. [17] developed a comprehensive questionnaire for describing ML data sets. However, the use of BES data in ML algorithms requires more information that is special. Therefore, in our questionnaire, we added suitable questions and removed unsuitable questions for BES in [17].

Physical simulation models can supplement existing data or multiply existing time series with variants of technical systems for the application of ML. For example, simulations support different operating conditions of a wide range of technical systems. However, the creation of such simulation models is a very time-consuming process, and the reuse of existing data point identifiers can significantly reduce this effort.

Here, the use of a unique machine-readable data point identifier is necessary. There are currently countless standards and norms that promise universal descriptiveness of building data. However, no standard can support all requirements for the simple creation of simulation models of BES. Building Information Modeling (BIM) with IFC4 could help here. However, IFC4 describes only few tags in the description of metadata for data points [18] and, in a survey conducted by the German Architects' Association [19], only 12% of the respondents used BIM in projects at all. The approach for naming and which we described in [20], together with the Brick Schema [21] which will be included in the future ASHRAE Standard 223P [22], fulfils the requirements for simulation and ML.

However, to the best of our knowledge, there is no combined approach for real-life and simulated time series data for the training of supervised learning algorithms for classification of rare time series in BES.

In this paper, we show how to standardize real time series data sets in building energy system (BES) with a unique machine-readable data point identifier for usage in Machine Learning (ML). We propose a questionnaire for BES that a data set provider should fill out to support the use for ML practitioners. We show that our developed toolchain can extract information from data point identifiers and use it for the semi-automated creation of a simulation model. We also present how our toolchain can create a simulated data set of rare time series in the BES. In a use case, we demonstrate how ML applications can use our simulated data set for the classification of rare time series in BES. We point out whether the developed approach is suitable for application in ML.

2 Standardized data sets for timeseries data

2.1 Questionnaire for Time Series Data Sets in Building Energy Systems

In order to standardize the description of data sets, we defined a set of questions that an owner of data sets, who intends to publish the sets, should answer. We used an existing approach [17] and added questions suitable for BES. We want to make a user aware of the obstacles in the use of the data set.

The main aspects of these questions are as follows:

- Motivation for data set creation.
- Data set composition
- Data collection process
- Data preprocessing
- Data set distribution
- Data set maintenance
- Legal & ethical considerations

The static or dynamic boundary conditions under which the data was recorded helps the user of ML in BES. This is one question of the questionnaire: “What information (static and dynamic) can be given about the system(s) in which the data was recorded?”

The structure and design of the BES has a high influence on the energy efficiency of the individual components. It is not only decisive which components in what dimension the BES contains, but also their actual connection plays an important role. A graph-based system offers the possibility to map the topology of data points and facilities. The topology offers the possibility that e.g. all data points of a special plant are searchable.

An insight into the influences of connected systems is thus conceivable. Related questions are therefore as follows: "Are relationships between instances made explicit in the data? Are schemas of the technical equipment included? Is there a representation of the schemas as a graph model?"

Time series data often have gaps or are not complete. Therefore, we have added questions to this questionnaire in the section "Data Collection Process": "How many gaps are in the data set? How can a user of the dataset recognize them?"

As the full questionnaire is very extensive, readers may refer to the corresponding Github repository for the complete questionnaire (https://github.com/RWTH-EBC/JUDO).

2.2 Just Unified Data set for building Operation (JUDO)

The building selected for this paper is the E.ON ERC main building in Aachen, Germany. It has a variety of different energy systems, providing a representative example of the building landscape. The energy systems include, among others, a combined-heat and power unit, a boiler, a geothermal field with 41 boreholes and comprehensive monitoring, a chiller, a sorption system, facade ventilation units, concrete core activation, underfloor heating, radiators. The zones of the building include offices, seminar rooms, computer rooms, workshops and laboratories. This data set contains different usage behavior of different systems at different times. More information about the building and the operation strategy of the building can be found in [23].

We added information about the dimensions of the BES and the connection of the systems with the Brick Schema to this dataset. We also provided instructions on how to interpret the data in the data set. The dataset includes all existing data points of the selected plants. This includes, for example, all status messages, valve positions and set points. Therefore, the data set shows the overall picture of the operation of the plants.

For the first standardized data set, we selected the time series of 765 data points of 31 technical devices in four representative months. Each of these months represents one of the four seasons. The name of this data set is JUDO (Just Unified Data set for building Operation) and is available at https://github.com/RWTH-EBC/JUDO.

This set includes the data points sorted by technical system (Table 1) and types (Table 2).

Table 1. Data points in JUDO sorted by technical system (main examples)

Technical System	Number of Data Points
Geothermal field	221
Heat Pump	181
Glycol cooler	68
Heat Exchanger	57
Concrete Core Activation	56
Boiler	29
Combined Heat and Power	26
Chiller	8

Table 2. Data points in JUDO sorted by data point type (main examples)

Data point type	Number of Data Points
Command	240
Temperature sensors	189
Status	81
Alarm	65
Volume Flow	58
Position	26

3 Process overview of generating generic simulated data sets

The whole process of generating Modelica simulation models from an ontology-based model (BrickModel) is a tool-chain of various special-purpose tools. Figure 1 shows the various steps of the process. First, a user fills out an Input Data File. Based on this file, a tool called BuToOn creates a brick model and a data property file, in which the user has the possibility to enter further information. At the same time, the tool BouGen determines the time series data for the boundaries of the model. OnWithData creates a common Brick model for all inputs. OnToMo converts the Brick model into a Modelica model.

The whole toolchain is written in Python. The subsystems of the simulation models are taken from the open source Modelica library Aixlib [24].

In the following, we describe the underlying data schema approaches of the toolchain and describe the toolchain itself.

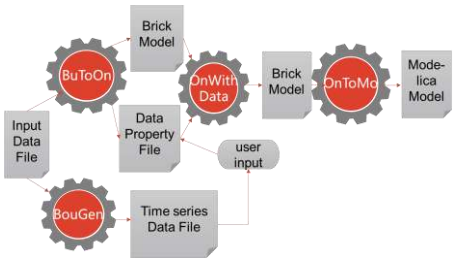

Figure 1. Process of generating Modelica simulation models from an ontology-based model

3.1 Used approaches

3.1.1 BUDO Schema

In this work, data points named by "buildings unified data point naming schema for operation management" (BUDO) [20] are used for the modelling. A BUDO key consists of several parts as shown in Figure 2. Each part provides a hierarchy level for the topology model and the corresponding simulation model. Information in system, subsystem, subsubsystem, medium/position and type of the BUDO key can be extracted to determine entity types in BrickModel.

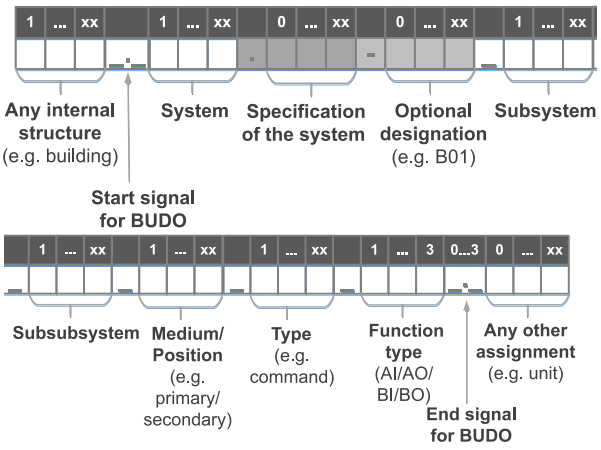

Figure 2. Structure of BUDO Key

3.1.2 BrickModel

The BrickModel is based on the Brick Schema developed by Balaji et al (2018) [21]. Figure 4 displays a sample of Brick's class hierarchy. Two classes of Brick are important for BrickModel: Equipment and Point. However, Brick can only describe which components are connected, but falls short in describing more detailed positions of the individual components, for example whether the primary or secondary side of a heat pump is connected to another equipment. In addition, the Modelica language uses connectors between two components. In order to describe the physical connection between equipments more precisely and meet the requirements of Modelica, we developed another class named Port to complement this ontology. One definition of these three important classes is as follows.

- Equipment: "Physical devices designed for specific tasks controlled by points belonging to it. E.g., light, fan, AHU" [21].
- Point: "Points are physical or virtual entities that generate time series data. Physical points include actual sensors and setpoints in a building, whereas virtual points encompass synthetic data streams that are the result of some process which may operate on other time series data, e.g. average floor temperature sensor" [21].
- Port: Ports represent the boundary and the physical connector of physical devices and store related static design data such as nominal mass flow.

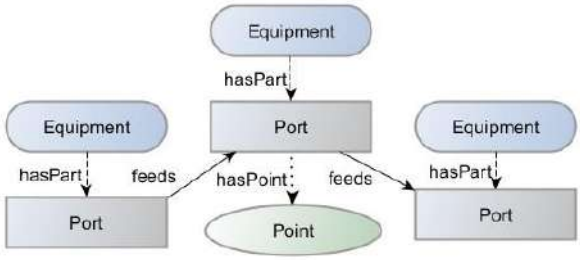

Figure 3. Information Concepts in BrickModel

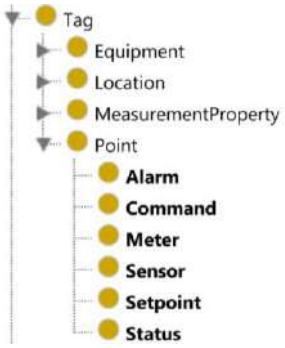

Figure 4. A subset of the Brick hierarchy [21]

As shown on the left side of Figure 5, we defined ports for heat flows, flows, electric currents, weather, equipment, comfort, transfer to rooms, control and fuels. Ports for heat flow are the most used in this work. Primary and secondary ports define the physical position of ports. In addition, we defined several data properties, which represent the design data of equipments and devices. On the right side of Figure 5, there is a subset of the data property hierarchy.

Data properties such as nominal mass flow, nominal temperature and nominal pressure difference are defined,

which can be used to set corresponding parameters required in Modelica simulation model. Furthermore, relationships in Brick connect the different entities in the building and describe the physical topology. Table 3 summarizes the definitions of relationships used in BrickModel. Figure 3 demonstrates how relationships connect entities of different classes with each other in BrickModel.

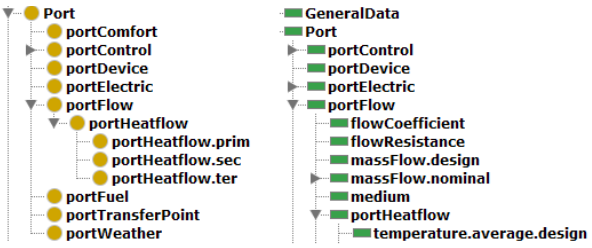

Figure 5. A subset of the port class and data property hierarchy

Table 3 List of the used Brick relationships and their definition

Relationship (Inverse)	Definition	Endpoints
hasPart (isPartOf)	A has some component or part B (typically mechanical)	Equip./Port Equip./Equip.
hasPoint (isPointOf)	A is measured by or is otherwise represented by point B	Equip./Point Port/Point
feeds (isFedBy)	A "flows" or is connected to B	Port/Port

3.2 Generating the BrickModel

The starting point for the workflow is manually gathering information and storing them in an Excel file. In addition, users can choose to specify the period of the time series and the data points they want to integrate into the Modelica simulation model.

If the user has filled out the Input Data File, BuToOn generates a BrickModel. The first generated BrickModel still lacks some information required by the Modelica simulation model. Therefore, BuToOn generates a data property file at the same time. The user has to input corresponding parameter values for the Modelica Model in this file. A tool named BouGen extracts the corresponding data from the time series data set and writes them into a file readable by Modelica. For the requested period, the time series database provides the corresponding time series for each data point and BouGen stores them in a Modelica-compatible format.

The tool OnWithData combines the Brick Model from BuToOn with the additional information from the data property file and the generated files of the time series data from BouGen and creates a BrickModel from all previous information.

3.3 Transformation To Modelica model

In the final step, the tool OnToMo extracts the information of the BrickModel and generates the corresponding Modelica model. We developed this tool using a code templating tool (CoTeTo) [25] and the SPARQL Protocol And RDF Query Language (SPARQL) [26].

The approach to generate Modelica code is template-based. CoTeTo supports the template engine Mako [27] that allows users to predefine templates for the corresponding Modelica code and conveniently store templates for each Modelica module in a separate template document.

SPARQL queries specify constraints and patterns of triples, and traverse the BrickModel to return those that match. Table 4 shows two examples of extracting information from BrickModel.

The first example demonstrates a SPARQL query for searching an instance of class Pump. The query searches in BrickModel for instances that match the triple pattern and return them.

The second example shows the extraction of the physical topology of the model, which is used to connect the modules. The existence of the Port class provides sufficient connection information for Modelica. This query returns the port, which is fed by the specified pump port as result.

After extracting information from BrickModel, the toolchain generates the Modelica simulation model.

Table 4. SPARQL Query Examples

```
SELECT ?instance
WHERE {?instance rdf:type brick:Pump.}
```

```
SELECT ?port
WHERE {
ex:BL-4120_._HX-H03_PU-M02_WS.H.SEC_PH
bf:feeds ?port.}
```

4 Modelling Use Case

To prove the functionality of the tool-chain, several use cases are developed based on the main building of E.ON Energy Research Center. In total, 13 simulation models, 244 modules and 211 connections between modules were established and 2153 lines of Modelica code were automatically generated. In this section, only one selected use case is illustrated: a heat pump system with real time series data. As shown in Figure 6, the heat pump system consists of one heat pump and four

temperature sensors. Figure 7 shows the corresponding Modelica model. During the modelling process, our developed approach transforms and connects all the modules automatically and correctly. In addition, this model successfully integrates time series data of temperature and mass flow from a database as boundary conditions. Moreover, for the control of the heat pump, the time series data of the electrical power of the compressor are integrated into the model of the heat pump. The heat pump does not provide a control signal. This creates uncertainty if the signal integrated into the model will affect the real behaviour.

Figure 8 compares the simulated and actual measured return water temperatures of the condenser side of the heat pump. The blue curves are the simulation results and the green curves represent the measured data. It is obvious that the simulated data of the heat pump model are in good agreement with the measured data, although there are still occasional deviations. The Root Mean Square Error (RMSE) of the return temperature on the condenser side is 1.414 K and the Normalized Root Mean Square Error (NRMSE) amounts to 0.086. For the evaporator side, the return temperature reaches a RMSE of 2.040 K and a NRMSE of 0.156.

We use this model to generate more rare time series for a classification approach. For this purpose, we scale the power and mass flows of the heat pump shown here.

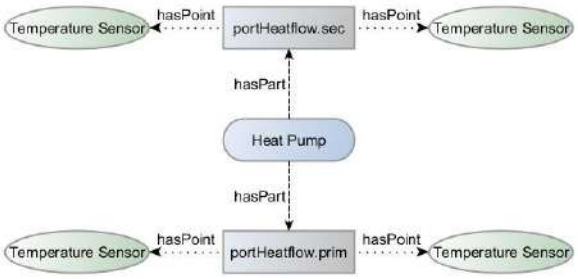

Figure 6. BrickModel structure of a heat pump system

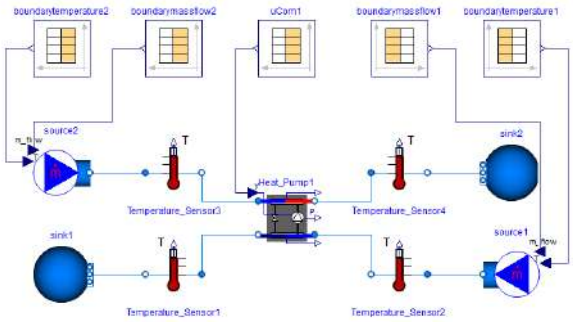

Figure 7. Modelica simulation model of a heat pump system

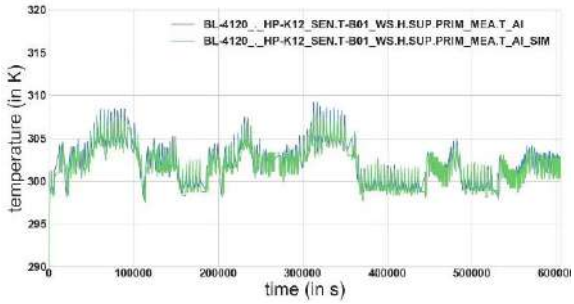

Figure 8. Comparison of simulation result with measured data of heat pump return water temperature on condenser side. Corresponding to Temperature_Sensor4 in Figure 7

5 Classification Use Case

In this section, we demonstrate how generated data sets can be used to train algorithms for classification of real time series classification. We train ML classifiers with both real and generated data points. For this purpose, two heat pump temperature time series (T_HP.Cond, T_HP.Evap) are generated with the model illustrated in Figure 7. We used the following further classes from real measurements:

- room air temperatures (T_AIR)
- temperature of concrete core activation in room automation (T_RA_CCA)
- temperature of concrete core activation in distribution (T_DIST_CCA)
- façade ventilation units in room automation (T_RA_FVU)

Due to the small temperature difference, the flow and return of the CCA and FVU data points are combined in one class in each case. The final data set contains the following data points:

- 180 samples from each T_HP.Cond and T_HP.Evap
- 340 samples from T_AIR
- 76 samples from T_RA_CCA
- 120 samples from T_ DIST_CCA
- 100 samples from T_RA_FVU

Each sample consists of the data point's label and time series data of one month. The used time series have a resolution of one minute. We detect and eliminate outliers with hampel filter [31].

For the training of the classifiers except of heat pump, we split the data set into 70% training data and 30% testing data. We extract six statistical features, following the recommendations published in [28]. We have also sorted out time series that did not have any usable statistical characteristics. We apply nine of the most suitable classifiers for real world classification problems

according to, using the implementations provided by scikit-learn [29]. In Figure 9, we present the classification scores of the algorithms when applied to the test data set.

Four out of the nine algorithms reach more than 70 % classification accuracy [30]. The best performing classifier is "Gradient Boosting" with 80.7% top score.

For the second test case, we use 10 real temperature measurements from both T_HP.Cond and T_HP.Evap to our test data set. Figure 10 shows the classification done by classifiers. "AdaBoost" classifier correctly assigned 9 of 10 of T_HP.Cond and 8 of 10 T_HP.Evap.

We conclude that the training of classification algorithms with simulated data also has a high potential for data point mapping in modern building automation systems. However, for a robust application in building automation further investigations are necessary.

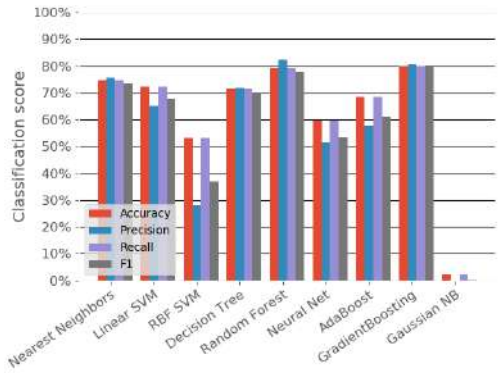

Figure 9. Scores of nine selected classifiers trained with 70 % of the real data set and tested with 30 % of it

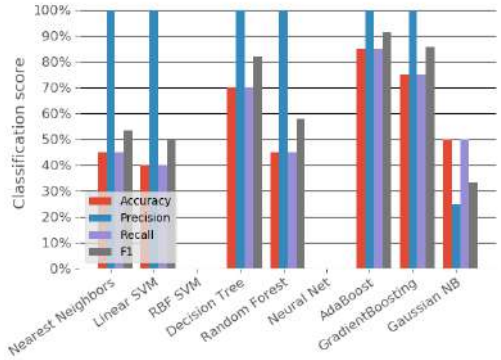

Figure 10. Scores of nine selected classifiers trained with simulated data sets and tested with real data sets of Temperatures of Heat Pump

6 Conclusion

In this paper, we presented a data set extracted from the real operation of a multifunctional building with various energy plants, the Just Unified Data set for building Operation (JUDO). We extended a special questionnaire for Machine Learning (ML) users with specific questions for Building Energy Systems (BES) and filled it in for JUDO. This questionnaire can be used for further data sets from BES. Consequently, we named the data set with a labelling schema for building data (BUDO). In future, we provide a Brick model of this.

We were able to show that our developed toolchain can semi-automatically generate simulation models using the standardized data point identifiers of time series data sets from the operation of BES. Finally, the toolchain creates an ML-compatible simulation data set. An extension to arbitrary periods and facilities of this and other buildings is possible.

We were able to apply this approach to the ML application of data classification. The current approach showed first good results but there is still a great need for research. We expect that a combination with calibration methods could increase the automation and accuracy of the approach. We will expand the considered technical facilities so that we can simulate a wider field of BES. We will extend the existing data set of currently 765 data points by further data points. We also consider an automatic generation of the currently required static information of the technical equipment from data sheets.

7 Acknowledgements

The authors would like to acknowledge the financial support of the German Federal Ministry of Economic Affairs and Energy promotional reference 03SBE0006A.

8 References

[1] Deb C, Zhang F, Yang J, Lee SE, Shah KW. A review on time series forecasting techniques for building energy consumption. Renewable and Sustainable Energy Reviews 2017;74:902–24.

[2] Koh J, Balaji B, Akhlaghi V, Agarwal Y, Gupta R. Quiver: Using Control Perturbations to Increase the Observability of Sensor Data in Smart Buildings; 2016.

[3] Benndorf GA, Wystrcil D, Réhault N. Energy performance optimization in buildings: A review on semantic interoperability, fault detection, and predictive control. Applied Physics Reviews 2018;5(4):41501.

[4] Wei L, Tian W, Silva EA, Choudhary R, Meng Q, Yang S. Comparative Study on Machine Learning for Urban Building Energy Analysis. Procedia Engineering 2015;121:285–92.

[5] Molina-Solana M, Ros M, Ruiz MD, Gómez-Romero J, Martin-Bautista MJ. Data science for

building energy management: A review. Renewable and Sustainable Energy Reviews 2017;70:598–609.
[6] Fierro G, Pritoni M, AbdelBaky M, Raftery P, Peffer T, Thomson G et al. Mortar: An Open Testbed for Portable Building Analytics. In: The 5th ACM International Conference on Systems for Built Environments (BuildSys '18); 2018.
[7] Fütterer J, Kochanski M, Müller D. Application of selected supervised learning methods for time series classification in Building Automation and Control Systems. Energy Procedia 2017;122.
[8] Kolter JZ, Johnson MJ. REDD: A Public Data Set for Energy Disaggregation Research. In: SustKDD 2011; 2011.
[9] Barker S, Mishra A, Irwin D, Cecchet E, Shenoy P, Albrecht J. Smart*: An Open Data Set and Tools for Enabling Research in Sustainable Homes. In: SustKDD12; 2012.
[10] Abrol S, Mehmani A, Kerman M, Meinrenken CJ, Culligan PJ. Data-Enabled Building Energy Savings (D-E BES). Proceedings of the IEEE 2018;106(4):661–79.
[11] Babaei T, Abdi H, Lim CP, Nahavandi S. A study and a directory of energy consumption data sets of buildings. Energy and Buildings 2015;94:91–9.
[12] Miller C, Meggers F. The Building Data Genome Project: An open, public data set from non-residential building electrical meters. Energy Procedia 2017;122:439–44.
[13] Wang Y, Feng H, Qi X. SEED: Public Energy and Environment Dataset for Optimizing HVAC Operation in Subway Stations; 2013.
[14] Verein Deutscher Ingenieure. VDI 6041 - Facility-Management - Technisches Monitoring von Gebäuden und gebäudetechnischen Anlagen; 2017.
[15] Nikolaou T, Skias I, Kolokotsa D, Stavrakakis G. Virtual Building Dataset for energy and indoor thermal comfort benchmarking of office buildings in Greece. Energy Build. 2009;41(12):1409–16.
[16] Henriet S, Simsekli U, Richard G, Fuentes B. Synthetic Dataset Generation for Non-intrusive Load Monitoring in Commercial Buildings. In: Proceedings of the 4th ACM International Conference on Systems for Energy-Efficient Built Environments. New York, NY, USA: ACM; 2017, 39:1 - 39:2.
[17] Gebru T, Morgenstern J, Vecchione B, Vaughan JW, Wallach H, Daumeé H III et al. Datasheets for Datasets; 2018.
[18] Bhattacharya A, Ploennigs J, Culler D. Short Paper: Analyzing Metadata Schemas for Buildings: The Good, the Bad, and the Ugly. In: Proceedings of the 2nd ACM International Conference on Embedded Systems for Energy-Efficient Built Environments. 2821674: ACM; 2015, p. 33–34.
[19] Reiß & Rommerich. Bericht zum Thema Building Information Modeling (BIM): Bundesweite Befragung der Mitglieder der Architektenkammern der Länder; 2017.
[20] Stinner F, Kornas A, Baranski M, Müller D. Structuring building monitoring and automation system data. In: REHVA, editor. The REHVA European HVAC Journal - August 2018; 2018, p. 10–15.
[21] Balaji B, Bhattacharya A, Fierro G, Gao J, Gluck J, Hong D et al. Brick Metadata schema for portable smart building applications. Appl. Energy 2018;226:1273–92.
[22] Haynes A. ASHRAE's BACnet Committee, Project Haystack and Brick Schema Collaborating to Provide Unified Data Semantic Modeling Solution. ATLANTA, BERKLEY, CA and RICHMOND, VA; 2018.
[23] Bode G, Fütterer J, Müller D. Mode and storage load based control of a complex building system with a geothermal field. Energy and Buildings 2018;158:1337–45.
[24] Müller D, Lauster M, Constantin A, Fuchs M, Remmen P. AixLib - An Open-Source Modelica Library within the IEA-EBC Annex 60 Framework. In: BauSim 2016; 2016, p. 3–9.
[25] Nytsch-Geusen C, Inderfurth A, Kaul W, Mucha K, Rädler J, Thorade M et al. Template based code generation of Modelica building energy simulation models. In: Proceedings of the 12th International Modelica Conference, Prague, Czech Republic, May 15-17, 2017. Linköping University Electronic Press; 2017, p. 199–207.
[26] Prud'hommeaux E, Seaborne A. SPARQL query language for RDF 2007.
[27] Bayer M. Mako Templates for Python. [January 02, 2019]; Available from: https://www.makotemplates.org/.
[28] Fernández-Delgado M, Cernadas E, Barro S, Amorim D. Do We Need Hundreds of Classifiers to Solve Real World Classification Problems? J. Mach. Learn. Res. 2014;15(1):3133–81.
[29] Pedregosa F, Varoquaux G, Gramfort A, Michel V, Thirion B, Grisel O et al. Scikit-learn: Machine Learning in Python 2011.
[30] Nanopoulos A, Alcock R, Manolopoulos Y. Feature-based Classification of Time-series Data: Information Processing and Technology. In: Mastorakis N, Nikolopoulos SD, editors. Commack, NY, USA: Nova Science Publishers, Inc; 2001, p. 49–61.
[31] Pearson R, Neuvo Y, Astola J, and Gabbouj M. Generalized hampel filters. EURASIP Journal on Advances in Signal Processing, 2016(1):115, 2016.

Developing Personalized Intelligent Interior Units to Promote Activity and Customized Healthcare for Aging Society

R. Hu[a], A. Kabouteh[a], K. Pawlitza[a], J. Güttler[a], T. Linner[a], and T. Bock[a]

[a]Chair of Building Realization and Robotics, Technical University of Munich, Germany
E-mail: rongbo.hu@br2.ar.tum.de, amir.kabouteh@br2.ar.tum.de, katja.pawlitza@br2.ar.tum.de, joerg.guettler@br2.ar.tum.de, thomas.linner@br2.ar.tum.de, thomas.bock@br2.ar.tum.de

Abstract –

The world's population is aging at an unprecedented pace. Aging society is not only a severe crisis in the developed world such as Germany and Japan, but also a rigorous challenge in emerging economies such as China. Many age-related diseases are fostered by the lack of physical, cognitive, and social activities. Increasing the activity level has many benefits for the elderly and can improve their independence. The research project REACH (funded by European Union's Horizon 2020 Research and Innovation Program under grant agreement No. 690425) aims to develop a service system that will turn clinical and care environments into personalized modular sensing, prevention, and intervention systems that encourage the elderly to become healthy through activities (e.g., physical, cognitive, socializing, personalized food, etc.). As a core research partner, the Chair of Building Realization and Robotics at Technical University of Munich developed a series of Personalized Intelligent Interior Units (PI²Us), which are a special type of smart furniture, that materialize the REACH concepts and functionality seamlessly into the different REACH use case settings. Specifically, the design and functions of the PI²Us, which consist of the PI²U-SilverArc, PI²U-MiniArc, PI²U-Bed, and PI²U-iStander, will be described in detail. In addition, a modular apartment integrating all PI²Us and key technologies in REACH is designed and simulated to create a total interior living and care environment for elderly users. Due to its modularity, parts of the apartment can be easily adapted and rapidly deployed in different REACH use case settings in four European countries, which will then help the REACH consortium execute a series of testing activities. In conclusion, this research project provides a systematic and innovative example for the world to mitigate the impact of aging society.

Keywords –

Aging society; Assistive technology; Personalized Intelligent Interior Units; Physical and cognitive activities; Sensing technology

1 Background

The world's population is aging at an unforeseen rate. Aging society is a crisis that is experienced all around the globe, including developed countries such as Germany and Japan, and emerging economies such as China. For instance, the health expenditure in the EU is expected to rise by 350% by 2050 compared to an economic growth of only 180% in the same timeframe [1]. The Directorate General for Economic and Financial Affairs reported that the provision of long-term care (LTC) in particular will pose an increasing challenge to the sustainability of public finances in the EU, due to an aging population [2]. Evidently, many age-related diseases are fostered by a lack of physical, cognitive, and social activities. Increasing the level of activity has many benefits for the elderly and can improve their level of independence [3]. Therefore, the project REACH represents a solution that seeks to protect elderly citizens against loss of function and a decline in ability to independently perform Activities of Daily Living (ADLs), which ultimately lead to entering LTC. REACH will allow European industries, including small- and medium-sized enterprises, to capitalize on the European high-tech knowhow, make Europe a world leader in prevention technologies, services, and underlying healthcare ICT platforms, and meanwhile tackle the ultimate crisis of rising healthcare expenditures.

2 Introduction to REACH

REACH stands for Responsive Engagement of the Elderly promoting Activity and Customized Healthcare.

With a project duration of four years, it is a cross-disciplinary, multi-partner, EU-funded research project that develops the future generation of technologies and services for a value-based and prevention-oriented health care system. The key elements and concepts of REACH will be explained as follows.

2.1 Objectives and the consortium

In the project REACH, an experimental, cross-disciplinary sensing-monitoring-intervention system is developed that can be placed in an unobtrusive way in various care settings and living environments of elderly citizens. The system aims at 1) using a variety of sensors to detect specific vital signs, behavioral patterns, and health status; 2) predicting future health status, risks or events; and 3) anticipatorily providing a series of customized health products and services that support and promote physical activities. As a result, the Healthy Life Years (HLY) of the elderly would be increased, and their time spent in LTC facilities would be reduced. The REACH consortium consists of six research partners who serve as the scientific backbone of the project; seven industry partners who undertake various tasks from sensor and rehabilitation device development, to ICT platform integration, standardization support, and business model generation; and four application partners who take on the real-world deployment of the technologies developed in REACH in their exemplary care environments [4].

2.2 Touchpoints and Engine concept

As a major achievement of the first project year, the REACH consortium developed the "Touchpoints and Engine" concept as a comprehensive solution of REACH's system architecture. It further guides the detailed structural relation between the subsystems of REACH. With the "Touchpoints and Engine" concept, REACH´s product-service-system architecture is divided into six manageable research and development clusters: four Touchpoint (TP) clusters (in other words, work groups each focusing on a specific topic within the project, including TP1: Personal Mobility Device, TP2: Active Environment, TP3: Socializing & Nutritional Monitoring/Intervention, and TP4: Gaming & Training System) that represent tangible connections between users (e.g., seniors, caregivers, physicians, etc.) and the REACH system; one "Engine" cluster which is a cloud-based digital platform serving as the brain of the project; and one "Interface" cluster which is composed of a set of means that allow the TPs and other products and services to interact with the Engine. Each cluster is associated with a dedicated and independent development team coming from the project consortium members (see Figure 1).

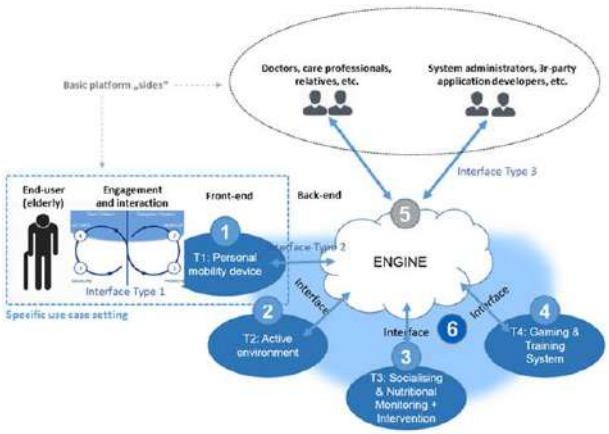

Figure 1. "Touchpoints and Engine" concept in REACH

3 Personalized Intelligent Interior Units

The Personalized Intelligent Interior Unit (PI²U) is a special type of smart furniture that seamlessly integrates the REACH concepts and functionality into the different REACH use case settings. This paper focuses on a series of PI²Us developed by the project team in TP2 (i.e., the "Active Environment" work group of the project). The relevant PI²Us include PI²U-SilverArc, PI²U-MiniArc, PI²U-Bed, and PI²U-iStander.

3.1 PI²U-SilverArc

The PI²U-SilverArc was developed for the use in a large kitchen or dining space (e.g., a community kitchen). It offers an interactive projection area in the kitchen, where recipes and games can be displayed. It also has a foldaway projection area where a training program can be displayed (see Figure 2). The round shapes, wood material, and bright colors give the PI²U-SilverArc a warm and inviting appearance.

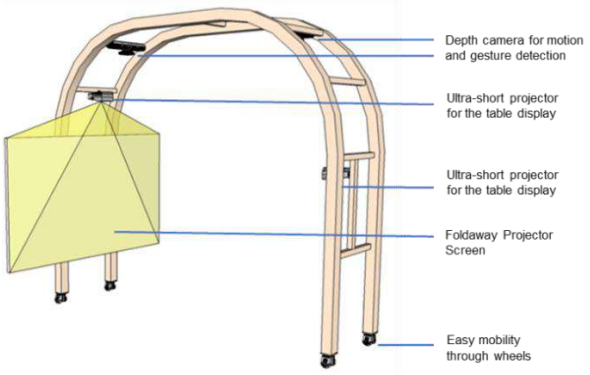

Figure 2. Preliminary design of the PI²U-SilverArc

The design of the PI²U-SilverArc cannot be directly converted into a prototype. For example, the material of the prototype and the final product differ substantially. After evaluation, it was decided that MayTec's modular aluminum profile system is suitable for building the prototypes (maytec.com.de). MayTec offers a wide range of modular profiles, accessories, and different connection possibilities. Simple changes can readily be made after the first test by using the aluminum profile system. Furthermore, in order to lower the costs, the curves were omitted in the prototypes because they mainly serve an aesthetic function and are not necessary for the testing.

Figure 3 shows in detail how the technical equipment is integrated into the prototype. An ultra-short projector is fixed above the projection screen. It was purposely decided against a mounting under the projection area, since the dust load for the projection lens would increase. Depth cameras are attached to a sliding system so that their positioning can be adjusted.

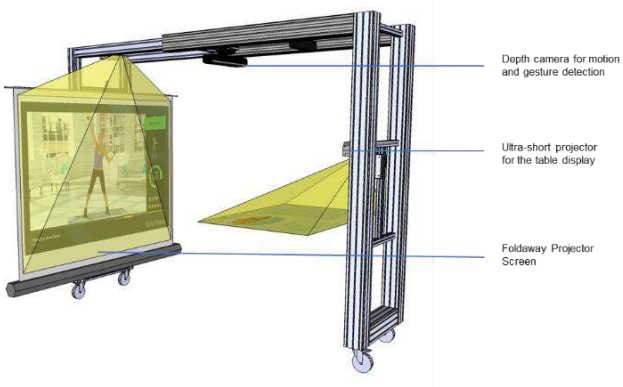

Figure 3. Prototypical version of the PI²U-SilverArc

3.2 PI²U-MiniArc

The PI²U-MiniArc can be considered as a flexible and smaller variant of the PI²U-SilverArc, which is designed to assist in the training and moving of the elderly who are in hospital or live in smaller apartments. An ultrashort projector can project the user interface on its foldaway table or on a separate table as needed. In addition, a motion-sensing camera (Microsoft Kinect) is integrated to detect the user's gestures, enabling the interactive gaming function. There is another projector on top of the device that can project extra information onto a wall. This prototype is equipped with wheels and thus is mobile. Figure 4 and Figure 5 respectively demonstrate the preliminary design and the final prototypical version of the PI²U-MiniArc.

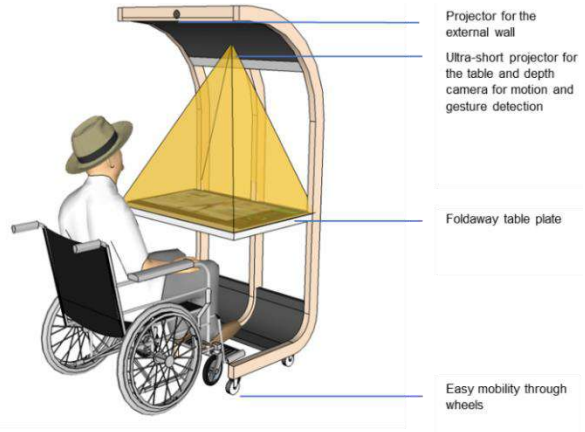

Figure 4. Preliminary design of the PI²U-MiniArc

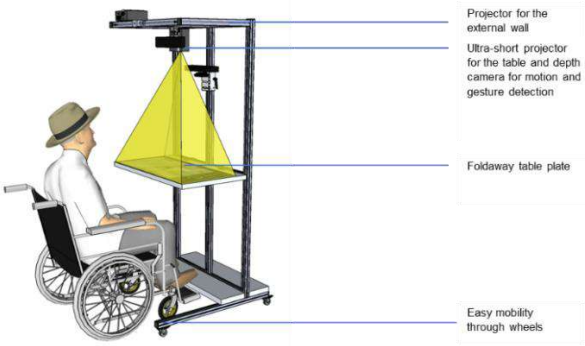

Figure 5. Prototypical version of the PI²U-MiniArc

3.3 PI²U-Bed

As shown in Figure 6, the first design of the PI²U-Bed resembles a normal bed for private use. A special feature is an arc-shaped frame that covers the entire length of the bed, which allows for an easy integration of sensors and technologies such as a thermal camera for breath detection and a projector for the bed. The height of the bed can be adjusted. On the one hand, this feature makes it possible for the caregivers to work at a height that is comfortable for their torsos. On the other hand, the lowest height of the bed facilitates the transfer of the patient from the bed to other functional units such as a wheelchair. The bed can be set to both a sitting and a vertical position. The sitting position allows the bed to support the patient and the nurse in many tasks such as eating, while the vertical position is especially apt for patients in an Intensive Care Unit (ICU) who must perform the transfer from lying to vertical position. The passive standing that is enabled by a standing frame aims to improve respiratory function and cardiovascular fitness, increase the levels of consciousness, functional

independence, and psychological well-being, and reduce the risk for delirium and the adverse effects of immobility [5].

In order to adapt the bed system to each patient's needs, a modular docking system was integrated into the design. Modules providing additional functions such as a toilet, physical training, transfer, and mobility can dock at different positions in the frame of the bed and are symmetric and self-guided. For example, with the Leg-curl Training Module (see Figure 6), the patient can rest on their abdomen and use their legs to move the weight up and down. Training muscles is important to the performance of daily tasks.

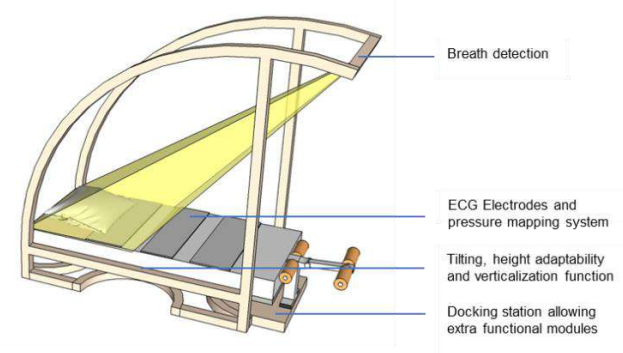

Figure 6. Preliminary design of the PI²U-Bed

To validate the concept of the PI²U-Bed, a prototype was planned and built. Figure 7 shows the final design of the PI²U-Bed prototype that was manufactured.

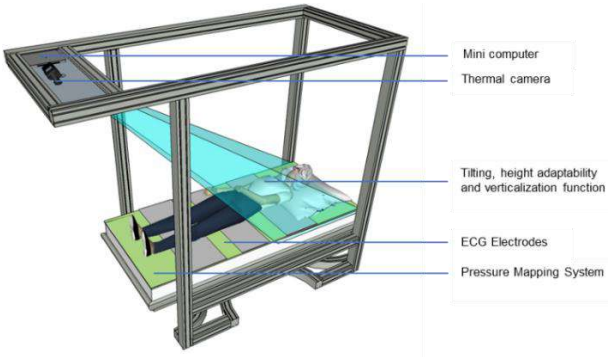

Figure 7. Prototypical version of the PI²U-Bed

3.4 PI²U-iStander

The PI²U-iStander is designed to activate the physical and mental activity of people of old age whose daily activity level has reduced. It is used to prevent elderly people from falling and provides effective support for cognitive processes through the combination of physical and cognitive exercises. Due to its flexibility and reasonable size, the system can be easily deployed in spaces such as living rooms and bedrooms (see Figure 8). The device is equipped with a mechanism to assist the elderly user to stand up and to perform movement exercises of the ankles, knees, and hip joints. A special corset and a seat ensure safety during the exercises that strengthen the back and abdominal muscles by lifting the legs. It also allows the user to maintain a safe, upright standing position and perform balance exercises as well as exercises where the upper body parts are activated using the ActiveLife gaming platform (see Figure 9) [6].

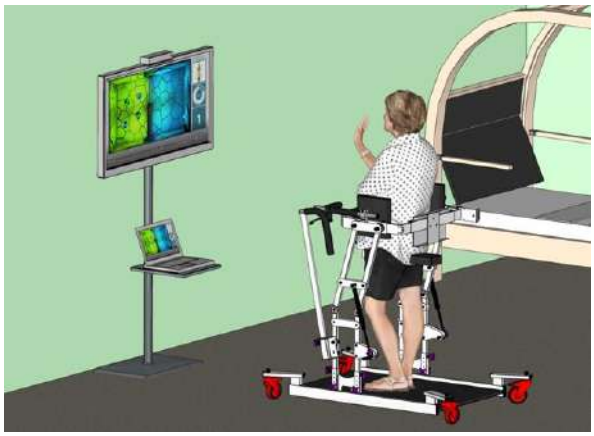

Figure 8. ActivLife system deployed in a bedroom environment

Figure 9. PI²U-iStander (Image: Alreh Medical)

3.5 Major sensing, monitoring, and analysis activities using the PI²Us

As mentioned in the previous section, the project team in TP2 developed a series of Personalized Intelligent Interior Units (PI²Us), which are a special type of smart furniture that materialize the REACH concepts and functionality seamlessly into the different REACH use case settings. The PI²Us consist of the PI²U-SilverArc, PI²U-MiniArc, PI²U-Bed, and PI²U-

iStander. The PI²U prototypes are manufactured, currently deployed, and tested for major, sensing, monitoring, and analysis activities in REACH in the laboratory of the Chair of Building Realization and Robotics (BR2) at Technical University of Munich (TUM) (see Figure 10).

Figure 10. The prototypes of various PI²Us (e.g., PI²U-SilverArc, PI²U-MiniArc, PI²U-Bed, and PI²U-iStander) deployed and tested in the laboratory

The electrocardiogram (ECG) sensors, which are embedded in the PI²U-Bed, will provide the medical staff with data regarding the patient's heart activity during the sleeping period. Additionally, this aspect can support the early detection aspect of the REACH project. Figure 11 presents the sensor integration on the PI²U-Bed, which resulted in the ECG measurement signals in the second image (Figure 11 middle). In order to implement such sensors, flexible plastic material was used to improve patient comfort and measurement (Figure 11 right). The ECG implementation uses two electrodes to produce the ECG signal.

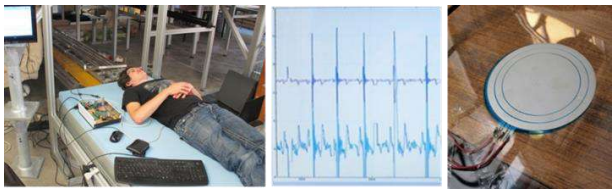

Figure 11. Testing of the ECG sensors on the PI²U-Bed

An important issue when considering an immobile patient's care is the prevention and management of pressure ulcers or decubitus. In order to implement the early detection and prevention aspects of REACH in the PI²U-Bed, it was decided to integrate a pressure-sensing mattress. This mattress monitors the peak pressure points of a person lying on the bed. Using this data, the REACH Engine can monitor peak pressure points and inform the care personnel for repositioning the patient before they develop decubitus. This sensor provides other functions as well. Using this sensor, a breath frequency monitor mainly for patients sleeping on their abdomens (see Figure 12) as well as a micro-mobility monitor are currently under implementation. Additionally, the project team is currently investigating the possibility of monitoring heart rate.

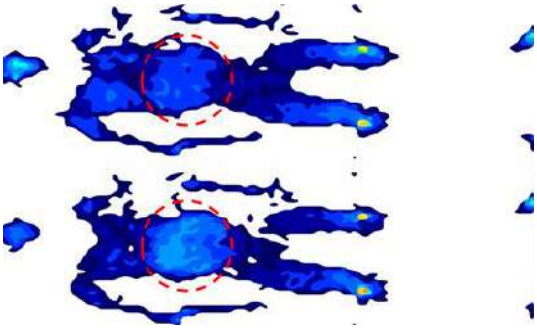

Figure 12. Pressure change on diaphragm when inhaling and exhaling (generated by the pressure-sensing mattress)

The thermal camera targets two major objectives: 1) breath frequency monitoring over the nostrils during sleep on the back, and 2) body temperature detection/monitoring over the eyes (see Figure 13 and 14). In the first implementation of these modules in TUM's laboratory, the results showed the following: breath frequency monitoring is possible and implemented via the nostrils and that the body temperature monitoring is implemented (monitoring the body temperature via the eyes is, naturally, only possible before the patient goes to sleep). There is a small limitation regarding the implemented prototype; due to the resolution of the current thermal camera, it is only possible to monitor these factors in a range of approximately 50cm distance from the patient's face. As a result, the thermal camera must either be mounted at the appropriate distance to the face, or the thermal camera must be replaced with a higher quality camera.

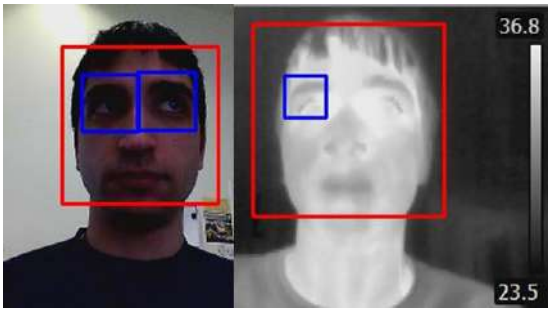

Figure 13. Eye following and body temperature measurement

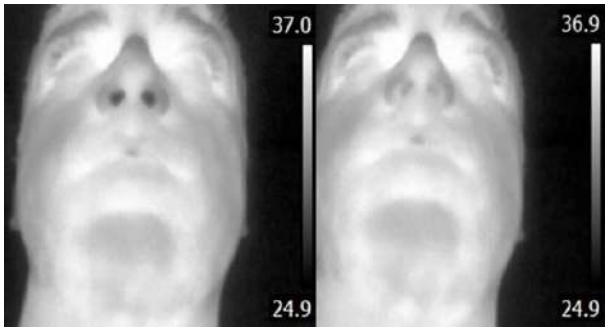

Figure 14. Respiration rate monitoring and body temperature measurement

The Kinect sensors, integrated into the PI²U-MiniArc and PI²U-SilverArc, are used for gesture recognition by considering the hand motions from the user side (see Figure 15). The Kinect was programmed by using the standard libraries from Microsoft. Therefore, it is necessary to continue with Microsoft Windows as the operating system since the libraries of the Kinect are not compatible with other operating systems. The control program of the Kinect gesture recognition was programmed using visual studio and was developed separately from the Graphical User Interface (GUI). Furthermore, the software development of the mounted Kinect on the PI²U-MiniArc is finalized including the adjustability for recognizing gesture at two different distances (i.e., standing table surface and sitting table surface).

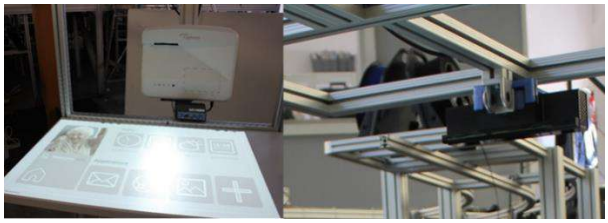

Figure 15. User interface and Kinect sensor in the PI²U-MiniArc

Designed and implemented as “battery-based” and “plug-and-play”, the stand-up counting sensor is mounted on the Alreh Medical device in a specific way, so that the clinical certificate of the device will not be undermined (see Figure 16). This sensor counts the number of "stand-up" events and transfers this count to a local server via WiFi. In addition, this sensor is implemented with consideration of its exceptionally low power consumption. With the implemented battery, it will run for more than three months without the need for recharging the battery.

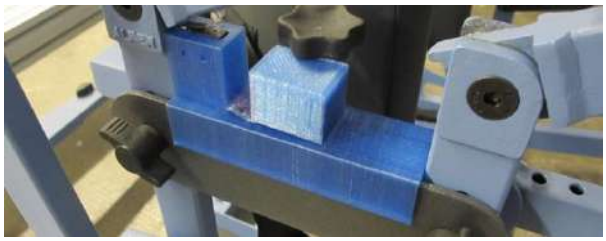

Figure 16. Stand-up counter embedded in the PI²U-iStander

It is planned to implement an activity sensing system for the Alreh Medical device (see Figure 17). This activity sensing system will be fused with the current gaming interface of the Alreh Medical device in order to enable lower body interactions with the games. In the first trial, the electromyography (EMG) sensing was implemented and tested. EMG is an electrodiagnostic medicine technique for evaluating and recording the electrical activity produced by the muscles. This was planned to serve as the controller interface for the legs allowing the user to steer a training or rehabilitation game via gestures (e.g., by the Kinect sensor) and leg movements. After the initial implementations and tests in TUM’s laboratory, the results showed immense amounts of noise when reading the EMG signal over the clothes. As a result, the project team planned to change the approach with the sensor electrodes and read the user activity from different sensors (e.g., touch sensors as previously mentioned). Afterwards, such inputs can be used to steer a training or rehabilitation game via foot gestures. Additionally, it will implement early detection, monitoring, and activation for the elderly.

Figure 17. Activity monitoring sensors used in the PI²U-iStander

Currently, the overall testing of the PI²Us was successful. Based on the feedback from the testing, the PI²Us will be further revised and eventually resemble the proposed furniture design. After the early prototype testing of functionality and the first data collection, TUM proposed a design of a modularized apartment integrating all PI²Us and key technologies in REACH’s four TPs to create a total interior living and care environment for elderly users. This design demonstrates the comprehensive REACH platform and can be adapted and implemented partially or entirely to different use case settings in an easy and rapid manner.

4 The REACH Apartment integration and simulation

As mentioned in the previous section, the project team in TP2 developed a series of Personalized Intelligent Interior Units (PI²Us), which are a special type of smart furniture, that materialize the REACH concepts and functionality seamlessly into the different REACH use case settings. The PI²Us consist of PI²U-SilverArc, PI²U-MiniArc, PI²U-Bed, and PI²U-iStander. Based on the current outcomes from four TPs, TUM designed a modularized apartment integrating all PI²Us and key technologies in REACH to create a complete interior living and care environment for elderly users (see Figure 18).

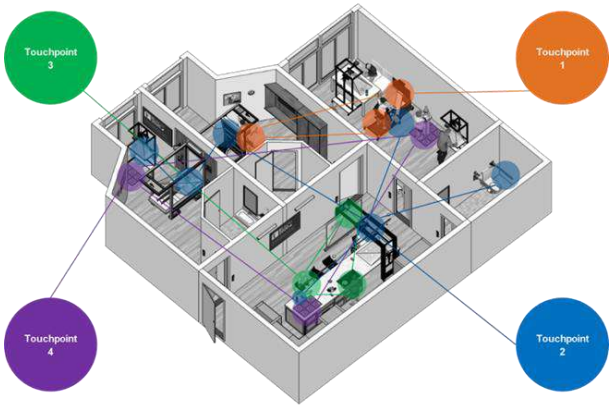

Figure 18. Technologies from four Touchpoints (TPs) distributed and integrated in the REACH apartment

Adopting barrier-free design principles, the apartment consists of a community kitchen, an activity room, and two patient rooms. In these living spaces, the Alreh Medical rehabilitation devices in TP1, smart furniture in TP2, socialized nutrition solutions in TP3, and gaming/training devices in TP4 are seamlessly integrated to create a comprehensive experience of the REACH platform for the users. Due to its modularity, parts of the apartment can be easily adapted and rapidly deployed in different REACH use case settings in four European countries, which will then help the REACH consortium execute a series of testing activities.

4.1 The community kitchen

The community kitchen serves as a key space for one of the most important daily activities – cooking and eating. It provides an ideal application space for technologies, particularly from TP3 (i.e., the "Socializing & Nutritional Monitoring/Intervention" working cluster of the project). The elderly users of the community kitchen can cook and eat together with the help of state-of-the-art technologies. As shown in Figure 19, the PI²U-SilverArc (or alternatively PI²U-MiniArc) will project an interactive cooking table allowing the elderly to cook in a smart and interactive way. Furthermore, the elderly in the kitchen are encouraged to use a series of smartphone apps. In addition, healthy and customized food developed by Biozoon [7] will be provided to the elderly who use the kitchen. As a result, the elderly are expected to become more socially active and nutritionally healthy through using the community kitchen.

Figure 19. Simulation of the community kitchen

4.2 The activity room

One of the major research goals of the REACH project is to promote the activity level of elderly people. Therefore, the activity room provides a flexible space for the elderly to become more physically and mentally active. In this room, the ActivLife gaming platform and the PI²U-iStander training device (developed by Alreh Medical), the PI²U-MiniArc in both table mode and mobile mode, and the Playware Moto Tiles (moto-tiles.com) will be implemented to provide the elderly with an active environment to improve their physical and mental health (see Figure 20).

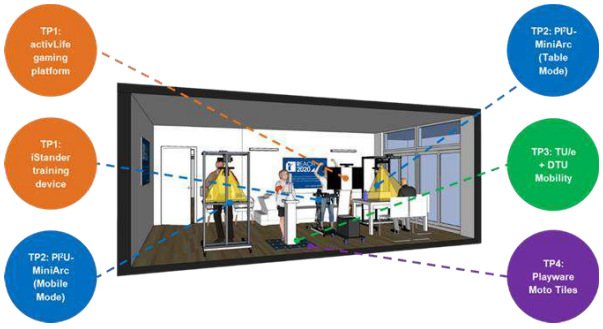

Figure 20. Simulation of the activity room

4.3 The patient rooms

In the patient room, the elderly can independently live, exercise, and play cognitive games using the PI²U-

MiniArc. Meanwhile, when the patient is resting on the PI²U-Bed, the bed can monitor the user's body temperature and respiration rate by using a thermal camera, the body pressure can be measured using the Pressure Mattress, and ECG data can be monitored by using ECG sensors on the bed (see Figure 21).

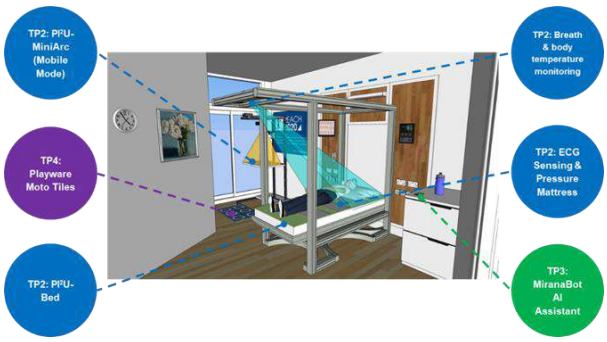

Figure 21. Simulation of the patient room type A

Figure 22 shows a variant of the patient room, in which the PI²U-Bed rises to a vertical position, helping the user stand up easily and transfer into a PI²U-iStander with or without the help of a caregiver. The PI²U-iStander serves as a training device for standing up as well as a mobility device to help the user move to other areas easily (e.g., bathroom, kitchen, activity room, etc.).

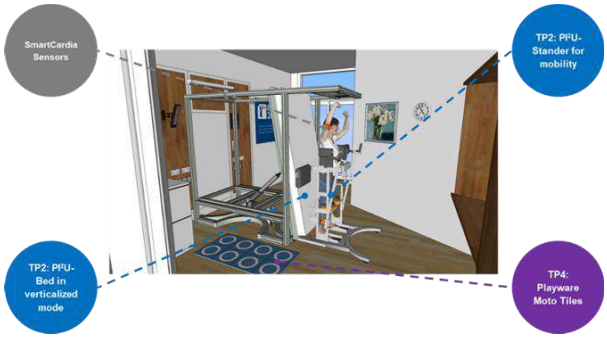

Figure 22. Simulation of the patient room type B

5 Conclusion

In this paper, the overall information of the REACH project as well as the detailed designs of the PI²Us and their prototypes are reported. The PI²U-SilverArc has two interfaces that can be adapted to any large kitchen. Training programs and culinary recipes can be played on the interfaces. The PI²U-MiniArc is a smaller and more mobile version of the PI²U-SilverArc. Both PI²Us aim to increase the social inclusion of their users. The PI²U-Bed is a patient bed which can assist the patient and caregivers in various daily tasks. With the PI²U-iStander and the ActivLife gaming platform, the elderly can safely train their leg muscles without the risk of fall and train the upper body with ease and comfort. Furthermore, the main testing, sensing, monitoring, and analysis activities using the PI²U prototypes are smoothly undertaken in TUM's laboratory. Based on the functionality validation of the PI²Us, a comprehensive REACH apartment design integrating all PI²Us and technologies of REACH is proposed, which can later be adapted and implemented partially or entirely to different use case settings. As of writing this paper, the testing in TUM's laboratory is performed mainly with young healthy individuals. The usability and performance of these devices will be further validated by elderly testing persons, and the results will be revealed in subsequent experiments and research.

Acknowledgements

This project has received funding from the *European Union's Horizon 2020 research and innovation programme* under grant agreement No 690425. The authors would like to thank all partners of the REACH consortium for their contributions to the presented work. Furthermore, the authors would like to express their gratitude to Mr. Andreas Bittner, Ms. Charlie Zhao, and Dr. Katharina Langosch for their support in this project.

References

[1] Espinoza, J. Europe's Failing Health. http://www.wsj.com/articles/SB10001424052748704893604576200724221948728, Accessed: 03/01/2019.

[2] Lipszyc, B., Sail, E., and Xavier, A. Long-term care: need, use and expenditure in the EU-27. *Directorate General Economic and Monetary Affairs*, European Commission, 2012.

[3] McPhee, J. S., French, D. P., Jackson, D., Nazroo, J., Pendleton, N., & Degens, H. Physical activity in older age: perspectives for healthy ageing and frailty. *Biogerontology*, 17(3): 567-80, 2016.

[4] Bock, T. REACH: Responsive Engagement of the Elderly promoting Activity and Customized Healthcare. *Gerontechnology*, 16(3): 125–128, 2017.

[5] Stiller, K., & Phillips, A. Safety aspects of mobilising acutely ill patients. *Physiotherapy Theory and Practice*, 19: 239-257, 2003.

[6] Kozak, D., Burgermeister, S., De Chassey, J. D. B., Naefb, A., Maringue, A., & Dietrich, D. A functionality, safety and validity study of innovative REACH devices. *Gerontechnology*, 16(3): 181-188, 2017.

[7] Biozoon. On-line: https://biozoon.de/en/, Accessed: 03.01.2019.

A Representative Simulation Model for Benchmarking Building Control Strategies

A. Kümpel[a], F. Stinner[a], B. Gauch[a], M. Baranski[a], and D. Müller[a]

[a]Institute for Energy Efficient Buildings and Indoor Climate, E.ON Energy Research Center, RWTH Aachen University, Germany
E-mail: akuempel@eonerc.rwth-aachen.de, fstinner@eonerc.rwth-aachen.de

Abstract –

To increase the energy efficiency of building energy systems, many control strategies have been investigated in recent years. Researchers apply control strategies to different building energy systems in order to evaluate their performance. However, the scientific community lacks a commonly accepted reference building model and evaluation criteria.

In this paper, we therefore propose a simulation-based benchmark to rate different control strategies for building energy systems. Based on identified requirements for benchmarking, we design a building model on which researchers can apply different control strategies and compare them with each other. The building consists of five different rooms and an energy system with several heat and cold generators. A concrete core activation and a central air-handling unit with additional decentralized cooling and heating registers supply each room individually. To benchmark a control strategy, the model calculates the consumed energy, the primary energy costs and the indicators of indoor air quality. We apply the benchmark to two different control strategies. The benchmark provides reproducible quantitative assessments of the performance of the tested control strategies. The diversity of the energy system as well as the individual air-conditioning of the rooms allow complex and sophisticated control strategies to demonstrate their potentials.

Keywords –

Building control strategies; Building automation; Benchmark; Modelica

1 Introduction

In the last decades, plenty of control strategies, e.g. Model Predictive Control (MPC), Fuzzy Logic Control, Neuronal Network Control and Cyber-physical control [1], promised to increase the efficiency of building energy systems in order to reduce CO_2 emissions and energy consumption [2]. To evaluate the developed control strategies, many researchers compare the developed control strategy with a standard control strategy such as On/Off control, PID control [3] or an ideal controller [4]. They point out the achieved savings with the newly developed control strategy in comparison to the standard one. However, the scientific community lacks a commonly accepted model for benchmarking control strategies. The controlled energy systems as well as the reference control differ in almost all case studies. Thus, the calculated performance or relative energy savings for newly developed control strategies are not comparable with each other.

The focus of this work is the design of a building model including its energy system that serves as the core of a benchmark for control strategies in the building domain. Additionally, we propose evaluation criteria in order to rate the achieved performance. We implement the designed building in the modeling language Modelica in order to provide a simulation based benchmark.

1.1 Related Work

To rate the performance of a controller, researchers commonly use criteria like the IAE (integral of time-multiplied absolute value of error) or the ISE (integral squared error), especially in control theory or PID tuning [5]. Nevertheless, other criteria are of greater importance in the building sector. DIN EN ISO 50001:2011 [6] defines benchmarking as a process of analyzing and comparing power data of comparable activities with the aim to compare the energy-based power data. Besides the energy consumption, criteria like carbon emissions, indoor air quality [7] or operation costs [8] are research topics. Recent work focuses on methods to benchmark the operation of a building based on the above-mentioned evaluation criteria. Borgstein et al. [9] present static, dynamic and statistical methods in order to calculate the energy consumption of non-residential buildings. Du et al. [4] developed an exergy-based method to calculate the theoretical minimal energy consumption to compare it with the energy consumption of the tested controller. However, all methods lack a specified building model, which other developers could use to rate their control strategy and compare them with each other.

Sänger et al. [10] suggest an approach to tackle this

problem: they developed a toolchain for benchmarking control strategies. Within the toolchain, the user can select different building types and create a control strategy. The control strategy consists of different combinable blocks and modules (e.g. hysteresis). However, the proposed toolchain does not support complex and advanced control strategies (e.g. MPC).

2 Benchmark Model

Benchmarking is a method frequently used in the information technology (IT) to quantify the performance of a computer, central processing unit (CPU) or graphics processing unit (GPU). According to Gray [11], domain-specific benchmarks are needed that are tailored to the system to be tested. For instance, a benchmark in the IT domain is not directly applicable to a benchmark for building control strategies. Nevertheless, Gray defined four general key criteria for a domain-specific benchmark, which we will transfer to the building controller domain:

- Relevant
- Portable
- Scalable
- Simple

Relevant means that the benchmark calculates relevant criteria (e.g. performance or price in the IT domain). A benchmark is portable if it is applicable to different systems. Additionally, the benchmark must be scalable to large and small computer systems in the IT domain. Finally, the benchmark has to be understandable (simple). [11]

In building domain, a relevant benchmark has to include typical building operations and measure the performance of the system in a relevant unit, e.g. energy consumption. Portable means in our use case that the benchmark is applicable to different control strategies. A scalable benchmark allows the evaluation of controllers of different size or complexity. To be understandable, the controller decisions have to lead to reasonable reactions in the performance measurement.

2.1 Benchmark Requirements

A benchmark for building control strategies should fulfill the above-mentioned criteria. To provide portability and scalability, we developed a simulation-based benchmark. In contrast to a real-life experiment, a simulation can produce reproducible boundary conditions, e.g. weather or occupancy, and is often executable at a lower price. In order to develop an understandable (simple) benchmark, we design the building model based on standards and real-life data.

In general, a benchmark measures the performance of a specific task, e.g. the needed time for mathematical operations. The complexity of the task has a major impact on the meaningfulness of the benchmark. For instance, measuring millions of instructions per second cannot point out the potential of a multi-core CPU in comparison to a single-core CPU [11].

Transferred to our case, controlling the building and its energy system is part of the tasks the controller needs to solve. The task's difficulty and thus the complexity of the building needs to be sufficiently high: a simple task could be solved with a sufficient accuracy even by poor control strategies. For instance, a building has less optimization potential, if its building energy system (BES) includes only an electric heater without any heat storage. Another example for a simple system is a room that has low requirements regarding the thermal comfort.

A simple benchmark system will not identify the potentials of sophisticated and advanced control strategies. Therefore, the complexity of the energy system as well as the requirements for thermal comfort need to reach a certain level. However, the complexity of the system must not exceed an engineer's understanding to create an understandable/simple benchmark.

2.2 Building Type

In general, buildings can be divided into residential and non-residential buildings. Residential buildings account 75 % of the net floor area and consume 68 % of the total final energy use in buildings in Europe [12]. The energy systems of European residential buildings are often simple and often provide only heat. Non-residential buildings contain a higher amount of different energy generation and distribution components including heating, cooling, ventilation, and air-conditioning (HVAC), which makes them more interesting for the benchmark.

In Europe, 28 % of the area of non-residential buildings belong to wholesale and retail buildings, 23 % offices, 17 % educational buildings, 11 % hotels and restaurants, 7 % hospitals, 4 % sport facilities and 11 % other buildings [12]. In our opinion, wholesale/retail buildings and offices are most relevant because of their large percentage. Furthermore, the advantage of offices are standards concerning the area and climate comfort. Offices usually consist of several rooms with heating, cooling and air conditioning. Thus, their energy system provides the necessary complexity for our purposes. Additionally, office rooms have high disturbances, e.g. changing internal gains due to occupancy and solar radiation, especially if there is a high share of glass in the facades. The disturbances set a difficult task to the controller in order to keep the set-point temperatures and humidity in a certain range.

Therefore, we chose an office building as the building type for the benchmark model.

2.3 Building Physics

The building model should consist of typical rooms in order to be relevant and understandable. In contrast to a real building, the number of rooms needs to be smaller in order to achieve a scalable and simple benchmark. If the number of rooms exceeds, it would take a lot of work and time to apply a control strategy to the benchmark.

The ASR A1.2 [13] describes different room types and their typical area, usage and number of persons. We consider large-scale office rooms as open-plan office rooms and both single offices and small multi-person office rooms as shared offices rooms. Conference rooms are special regarding the space requirements and occupancy. The fluctuating occupancy leads to high changes of the internal gains. Additionally, the set-point temperatures and humidity can vary during the day, e.g. if the room is empty for some hours.

Further room types that are common in office buildings are hallways, stairways, toilets, entrances and storage rooms. Due to the short time a person stays in these rooms, the climate comfort is less relevant, and the internal gains are approximately constant. Hence, we do not include any of these rooms.

In order to provide rooms with different comfort requirements, temperature levels and internal gains, we added a workshop and a canteen to the benchmark building. Workshops and canteens require, due to emissions, a high ventilation rate, which makes them interesting for our benchmark.

All in all, the benchmark building consists of five different rooms with typical specifications for the selected room type:

- Open plan office
- Shared office
- Conference room
- Canteen
- Workshop

Each room has different requirements regarding usage, energy demand and comfort. Figure 1 shows the floor plan. The dimensions of the rooms are based on ASR A1.2 [13]. The height of the rooms is three meters.

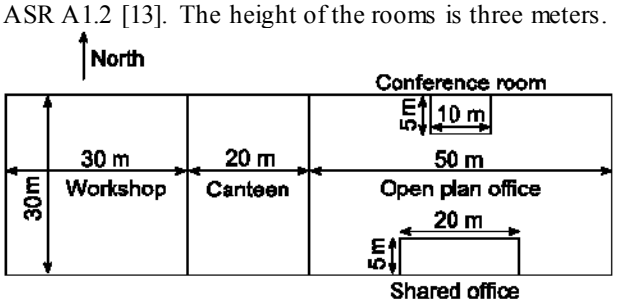

Figure 1. Floor plan of the benchmark model

2.4 Building Energy System

The energy system aims to heat, cool and ventilate the building in order to achieve a comfortable climate in the rooms. The energy system of our model should contain typical components to be relevant and understandable. Additionally, the energy system should cover the requirements concerning its complexity. Figure 2 illustrates the designed energy system. In the following, we describe the design of the energy system.

Each of the five rooms of the benchmark building contains a ventilation unit with heating and cooling registers in order to supply the room with conditioned air. A central air-handling unit (AHU), which consists of a heater, cooler and humidifier, supplies the decentralized ventilation unit. Additionally, each room can be heated and cooled by a concrete core activation (CCA).

In order to supply the concrete core activation, the air-handling unit and the decentralized ventilation units with heat and cold, the energy system provides hot water at two temperature levels (high temperature and low temperature) and cold water at one temperature level. A boiler and a combined heat and power unit (CHP) produce heat at the high temperature level. The CHP offers an efficient simultaneous electricity and heat production, but its operation is bounded by minimal on and off times. In contrast, the boiler can be switched on and off faster to respond to a changing demand more dynamically. Both the CHP and the boiler are supplied with gas.

A central element of the energy system is a heat pump. The heat pump produces low temperature heat as well as cold for the cold-water supply. A geothermal field as well as an outside air heat exchanger with a fan serve as a heat source. The geothermal field provides a constant temperature (13 °C) whereas the outside temperature fluctuates. Thus, depending on the outside temperature, using the geothermal field or the outside air as a heat source is more efficient.

The geothermal field and the outside air can be used for free cooling as well; if there is only a small cold demand, the building can be cooled without using the heat pump. Additionally, the outside air serves as a heat sink for the heat pump.

In order to decouple the heat/cold generation and the consumption, the system contains one storage at each temperature level. The high temperature and low temperature heat storage can be used at two temperature levels; both can be supplied by either the heat pump or the CHP and boiler. The three storages allow a flexible operation of the heat/cold generators, thus predictive control algorithms could show their potentials.

Besides the thermal generators and consumers, the benchmark building contains electrical components. The CHP and a photovoltaic system (PV) produce electricity. The produced electricity can be fed into the grid or used

for the building operation. Electrical consumers in the building are the heat pump, the air-handling unit, fans, pumps and all appliances inside the building such as computers and lights. The electrical consumption of the energy system is directly influenced by the control actions, whereas the consumption of the appliances inside the building is based on the occupant behavior (see section 2.5).

We dimensioned the heat/cold generators and consumers as well as the piping network according to DIN EN 12831 [14]. In a first step, we need to define the placement of the building. We chose the region 12 around the city Mengen in Germany because of the unsteady weather with higher temperature peaks in comparison with other regions of the DIN EN 12831. Based on the weather conditions, we determine the heat demand according to DIN EN 12831. The static heat demand for the whole building amounts to 94.5 kW. In order to use a night set back, which allows the reduction of the room temperature to 15 °C, an additional heating power of 139.7 kW is needed for reheating the building.

The calculated cooling demand is 166.7 kW according to DIN V 18599-2 [15] and DIN V 18599-10 [16]. The concrete core activation and the ventilation units cover equal shares of the cooling demand.

Based on the calculated demands, the pipe and air duct diameters can be specified according to DIN EN 10255 [17]. According to Laasch et al. [18], we assume a maximum water flow velocity of 2 m/s in the pipes and a maximum air flow velocity of 4 m/s in the air ducts.

Based on the heating and cooling demand, we defined the power of the boiler, CHP, heat pump and outside air heat exchanger.

The photovoltaic system fills half of the roof area and the power of the AHU fans is assumed to be 3 kW/(m³/s) [19, 20]. Table 1 lists the power levels of the components. The electrical power of the 24 pumps are in the range of 75 W up to 4700 W.

The storages allow decoupling heat/cold generation and consumption. In order to provide a flexible and predictive use, we dimension very large storages. The two heat storages are able to cover the heat demand for the reheating of the building. Each heat storage has a volume of 22 m³. The cold storage can cover the maximum cold demand for three hours and has a volume of 46 m³.

In summary, the energy system consists of 30 valves, 24 pumps, a central ahu and the components boiler, CHP, heat pump and outside air heat exchanger with a fan that have to be controlled.

Table 1. Power of the components

Component	Power in kW
Boiler	19.9 – 66.2 (thermal)
CHP	46 (thermal), 26 (elect.)
Heat Pump	96.6 – 193.2 (thermal)
Chiller	67 – 235 (thermal $\Delta T = 15$ K)
PV	112.5 (elect.)
AHU Fan	10.1 (elect.)

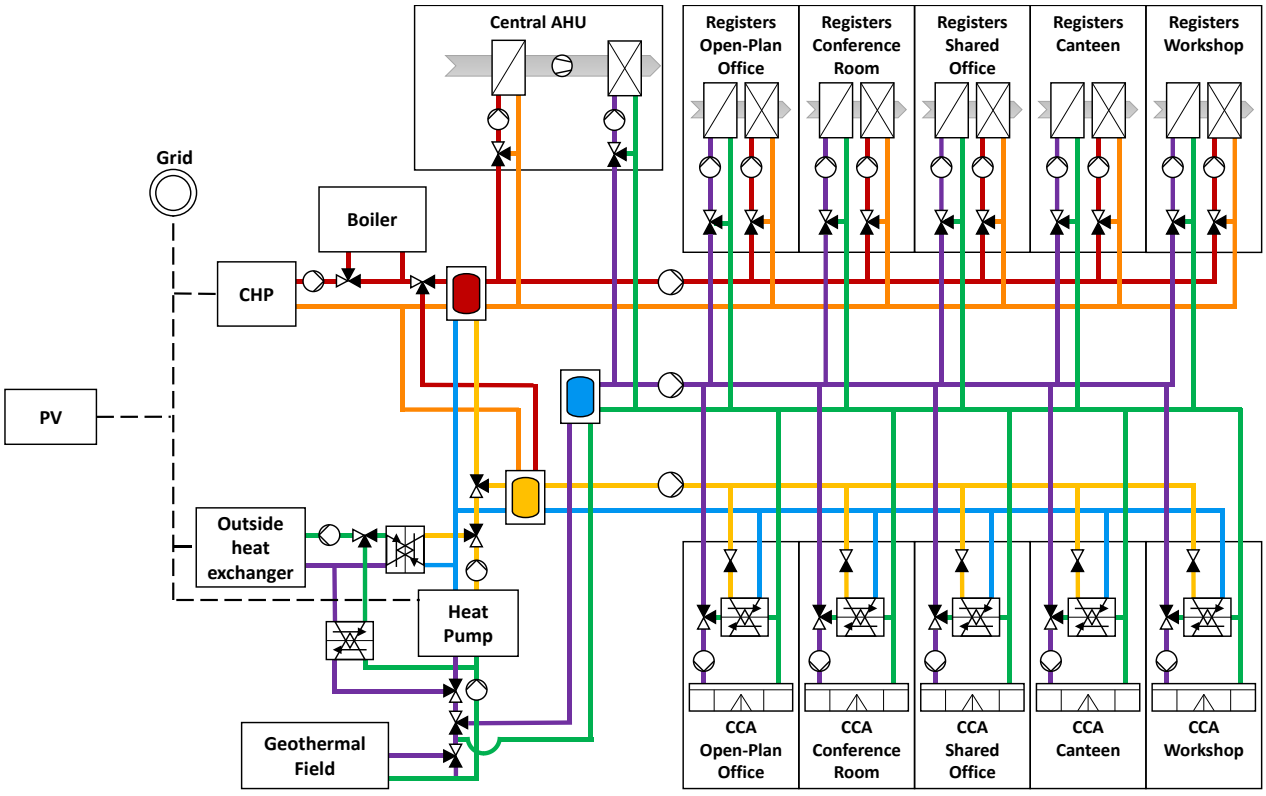

Figure 2. Energy system of the benchmark building model

2.5 Internal Gains

Internal gains are emitted heat caused by occupants and electrical appliances such as lighting and computers. Fluctuating internal gains challenge the controller to reach given set-point temperatures. Hence, we define varying occupancy profiles for each of the five rooms of the benchmark building. We assume five days per week with eight hours working time. In Germany, the absence of an employee per year is 20 days due to holidays [21] and 14.6 days due to illness [22]. We calculate the presence for each day with a probability distribution based on holiday and illness. The start time for the open plan office and the shared office is between 8:00 and 9:00 am, for the canteen between 8:45 and 9:15 am and for the workshop between 6:00 and 6:15 am. The arrival of each employee is random within the start times. The conference room is used randomly on an hourly basis. Figure 3 shows the resulting occupancy profiles for one exemplary day.

To calculate the produced heat of the occupants, we assume an activity level according to DIN EN ISO 7730 [23] of 2 met in the workshop and 1.2 met in the other rooms. The clothing level is 1 clo for all rooms and occupants. The resulting heat amounts to 209 W per occupant in the workshop and 125 W per occupant in the other rooms.

Based on the occupancy profiles, we calculate the electrical internal gains. In accordance with [24], we assume an illumination of 400 lx for the open plan office, the shared office and the conference room, 350 lx for the canteen and 500 lx for the workshop. Based on the floor area and an assumed luminosity of 95 lm/W [25], the lighting power amounts to 5684 W for the open plan office, 210 W for the conference room, 420 W for the shared office, 2210 W for the canteen and 4737 W for the workshop. Lights switch on if at least one person is present.

Laptops (20 W) and screens (30 W) cause further internal gains. We assume that laptops and screens are on if the associated employee is present. In the conference room, there are no screens available.

The power demand in the canteen is estimated in accordance with Renggli and Horbaty [26]. We add the minimum power for cooking (0.15 kWh/guest) to the power for cleaning (0.09 kWh/guest) and divided the result by the mean duration of stay (0.875 h). Since the study of Renggli and Horbaty is from the year 1992, we reduced the power consumption for cooking and cleaning by 22 percent. This value corresponds to the efficiency increase from class D to A [27]. The final power consumption in the canteen is 213 W/guest. In the workshop, we assume a power consumption of 200 W/employee for using tools.

We assume that the total consumed electrical power is converted to heat.

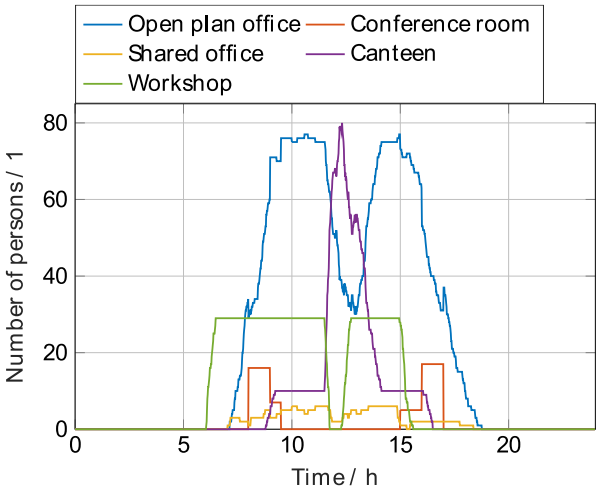

Figure 3. Occupancy profile of the building for one exemplary day

2.6 Weather

To set a difficult task to the controllers, the weather needs to have high fluctuation in order to disturb the energy system by a changing temperature and solar radiation. To achieve this, we use weather data from the city Mengen in Germany. In order to keep the execution time of the benchmark small, we need to reduce the simulation period as simulating a whole year would last more than one day. Thus, we reduce the total simulation period to eight weeks, using two characteristic weeks in winter, spring, summer and autumn, respectively. The characteristics of the eight weeks are high fluctuations in temperature, solar radiation and wind velocity. The start and end temperature, solar radiation and wind velocity of each week is adjusted so that the resulting weather profile is continuous. Figure 4 shows the resulting temperature profile.

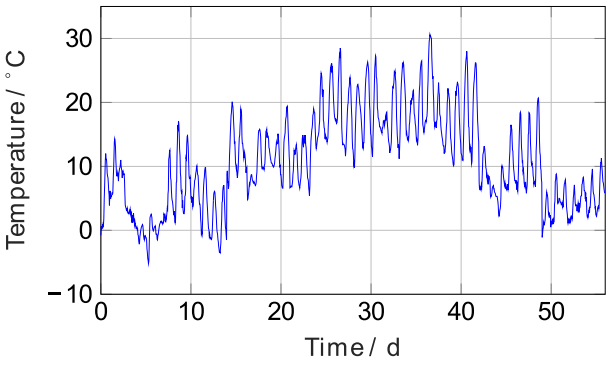

Figure 4. Outdoor temperature profile for the simulation period

2.7 Evaluation Criteria

The evaluation criteria are a basic part of the benchmark. To rate a control strategy, the benchmark model calculates the frequently used criteria comfort, energy consumption and energy costs.

The control of a building aims to provide a certain comfort to the user. Thus, the comfort is a key factor in building control strategies that we include in the benchmark. To rate the thermal comfort, Fanger [28] defined the predictive mean vote (PMV), which divides the comfort level into seven groups (hot, warm, slightly warm, neutral, slightly cool, cool, cold). Since each person's sense of comfort is different, the predicted percentage dissatisfied (PPD) shows a statistical distribution of the PMV. To rate the thermal comfort, the benchmark calculates the PMV and PPD.

Furthermore, the benchmark calculates the total final energy. The final energy consumption includes the gas and the electricity from the grid. The power fed into the grid is calculated as a negative energy purchase.

Besides the energy consumption, the energy costs for operating a building are vitally important; a highly energy efficient control strategy will rarely be implemented if it leads to uneconomical high costs. Thus, the benchmark needs to consider the operating costs of the energy system.

The energy system of the benchmark building uses electricity and gas. We define the price based on the electricity and gas market in Germany. According to a pricing list of the energy provider Werl [29], we split the electrical tariff into a high-rate tariff and a night tariff. The high-rate tariff is 29 ct/kWh and active between 6:00 am and 10:00 pm. The night rate is 19 ct/kWh. The two different tariffs enable a more cost-efficient operation by producing and storing heat and cold at night.

According to [30], the produced electricity of the CHP can be sold at a price of 12.34 ct/kWh. If the produced electricity is consumed by the building, a surcharge of 4 ct will be paid. The selling price of the produced electricity of the photovoltaic system is set to 10.5 ct/kWh. Based on [31], we assume a gas price of 6.09 ct/kWh.

3 Results and Discussion

We implemented the developed building and its energy system in the modeling language Modelica [32]. Modelica is an object orientated language and thus is suitable for modeling complex energy systems. The benchmark model is published in the open source library AixLib [33]. To simulate the benchmark model, we used the software Dymola.

3.1 Benchmarked Control Strategies

We apply the benchmark to two different control strategies to evaluate the meaningfulness of the benchmark. The control strategies are not optimized to be particularly energy or cost efficient. They should rather demonstrate the benchmark and serve as a first reference.

The first control that we apply to the benchmark is a basic control. The basic control has a heating and cooling mode with a fixed set-point temperature for the ventilation units and the concrete core activation. The mixing and throttling valves in the ventilation units and in the concrete core activation (CCA) are controlled by PID-controllers. All heat and cold generators have fixed flow temperature set points. Additionally, two-point controllers switch the heat pump, boiler and CHP on and off depending on the storage temperatures. The air-handling unit and all pumps operate at nominal power.

The second control is a night tariff control. It aims to decrease the electricity costs. The heat pump operates only at night trying to load the heat and cold storage. Additionally, the air-handling unit is switched off at night (between 10 pm and 6 am) to further reduce the electricity consumption. All other components are controlled in the same way as in the basic control.

3.2 Results

Figure 5 shows the total energy consumption and the operation cost for the two benchmarked control strategies. Further, Figure 5 shows the mean PPD and absolute mean PMV values. The mean PPD and PMV values do not allow a detailed analysis of the comfort. Nevertheless, the mean values represent the comfort level in general. Smaller values for the PPD, PMV as well as the energy consumption and operational costs indicate a better control of the benchmark building.

The basic control consumes 3.7 GJ energy and produces 16800 € costs. The thermal comfort reaches a high level with a mean PPD of 6.3 % and an absolute mean PMV value of 0.25.

In contrast, the night rate control saves around 42 % energy (2.16 GJ) and 46 % (9100 €) of the operational costs. However, the thermal comfort decreases in comparison to the basic control. This is caused by using the heat pump only at night. The heat pump is not always able to charge the cold storage at night. This leads to higher room temperatures in periods with high internal gains caused by high outdoor temperatures and solar radiation. Therefore, the thermal comfort is smaller for the night rate control than for the basic control.

The results show that the developed benchmark provides a standardized evaluation of control strategies. The complexity of the designed energy systems provides a wide range of different control options leading to different energy consumption, costs and thermal comfort.

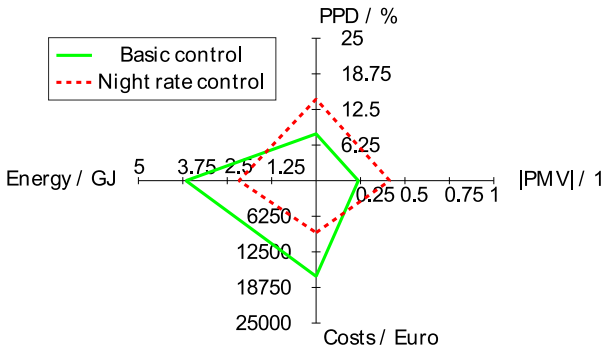

Figure 5. Results of the two benchmarked control strategies

Thus, the benchmark model is able to figure out the potentials of efficient and performant control strategies. In our example, the basic control reaches higher thermal comfort but less energy efficiency compared to the night rate control. However, figuring out which control performs better in total depends on the prioritization: a building operator would prefer the night rate control whereas occupants would prefer the basic control.

A disadvantage of the benchmark model is its complexity caused by the high number of actuators, which leads to a high effort to apply a control strategy.

Further, a benchmark holds the risk of overfitting. A control strategy could be tailored to the benchmark so that it only achieves good results in this benchmark. Applied to other systems, such a control could lead to low control performance. To avoid this problem, we suggest developing a bunch of different building models as standardized benchmark systems.

Furthermore, benchmarking control strategies based on standardized building models leads to comparable results. With a growing number of applied control strategies, the benchmark could become more and more useful.

4 Conclusion

In this paper, we presented a simulation-based benchmark model to rate the performance of different controllers and control strategies in the building energy domain. The core of the benchmark is a specially designed office building. The building consists of five representative rooms and an energy system with various heat and cold producers. The complexity of the system offers a high range of operating modes. Thus, the energy system sets a challenging task to the controller. Therefore, the benchmark is able to investigate the potential of advanced and efficient control strategies in comparison to other control strategies.

We applied the benchmark to two simple control strategies in order to evaluate the usefulness of the developed benchmark system. The first control strategy is a simple mode-based control in combination with PID control. The second control strategy extends the first one by exploiting a night rate. The benchmark model calculates higher costs and energy consumption for the basic control in comparison to the night rate based control. By contrast, the average comfort is higher in the basic control. As a conclusion, the benchmark is able to point out strengths and weaknesses of the tested control strategies.

Further work aims to improve the evaluation criteria. Besides, the energy consumption, costs and thermal comfort, the carbon emissions as well as the electricity consumption of the control algorithm itself could be considered. Additionally, a standardized criterion that combines all other criteria in one value could facilitate the rating of different control strategies.

5 Acknowledgement

We gratefully acknowledge the financial support provided by the BMWi (Federal Ministry for Economic Affairs and Energy), promotional reference 03SBE006A. We would further like to thank our project partners Werkkraft GmbH.

References

[1] M. Schmidt and C. Åhlund, “Smart buildings as Cyber-Physical Systems: Data-driven predictive control strategies for energy efficiency,” *Renewable and Sustainable Energy Reviews*, vol. 90, pp. 742–756, 2018.

[2] A. Afram and F. Janabi-Sharifi, “Theory and applications of HVAC control systems – A review of model predictive control (MPC),” *Building and Environment*, no. 72, pp. 343–355, 2014.

[3] X. Lü, T. Lu, M. Viljanen, and C. J. Kibert, “A new method for controlling CO2 in buildings with unscheduled opening hours,” *Energy and Buildings*, vol. 59, pp. 161–170, 2013.

[4] Z. Du, X. Jin, X. Fang, and B. Fan, “A dual-benchmark based energy analysis method to evaluate control strategies for building HVAC systems,” *Applied Energy*, no. 183, pp. 700–714, 2016.

[5] K. J. Åström and T. Hägglund, *PID controllers: theory, design, and tuning*: Instrument society of America Research Triangle Park, NC, 1995.

[6] *Energiemanagementsysteme*, DIN EN ISO 50001:2011, 2011.

[7] J. Laverge, N. van den Bossche, N. Heijmans, and A. Janssens, “Energy saving potential and repercussions on indoor air quality of demand

controlled residential ventilation strategies," *Building and Environment*, vol. 46, no. 7, pp. 1497–1503, 2011.

[8] W. Surles and G. P. Henze, "Evaluation of automatic priced based thermostat control for peak energy reduction under residential time-of-use utility tariffs," *Energy and Buildings*, vol. 49, pp. 99–108, 2012.

[9] E. H. Borgstein, R. Lamberts, and J.L.M. Hensen, "Evaluating energy performance in non-domestic buildings: A review," *Energy and Buildings*, no. 128, pp. 734–755, 2016.

[10] F. Sänger, K. Klimke, and J. Jungwirth, Eds., *Toolchain zur Bewertung von Regelstrategien im Gebäudebereich*, 2014.

[11] J. Gray, *Database and Transaction Processing Performance Handbook*.

[12] M. Economidou *et al.,* "Europe's buildings under the microscope. A country-by-country review of the energy performance of buildings," *Buildings Performance Institute Europe (BPIE)*, pp. 35–36, 2011.

[13] "Raumabmessungen und Bewegungsflächen: ASR A1.2," in *Technische Regeln für Arbeitsstätten*, 2017.

[14] *Heizsysteme in Gebäuden*, DIN EN 12831 Bbl 1:2008-07, 2008.

[15] *Energetische Bewertung von Gebäuden*, DIN V 18599-2:2016-10, 2018.

[16] *Energetische Bewertung von Gebäuden*, DIN V 18599-10:2011-12, 2016.

[17] *Rohre aus unlegiertem Stahl mit Eignung zum Schweißen und Gewindeschneiden*, DIN EN 10255:2004 + A1:2007, 2007.

[18] T. Laasch and E. Laasch, *Haustechnik: Grundlagen - Planung - Ausführung,* 13th ed. Wiesbaden: Springer Vieweg, 2013.

[19] *Raumlufttechnik*, VDI 3803, 2018.

[20] *Energetische Bewertung von Gebäuden - Lüftung von Gebäuden*, DIN EN 16798-3, 2017.

[21] "Arbeitszeit der Arbeitnehmer: § 3 ArbZG," in *Arbeitszeitgesetz*.

[22] TK Presse & Politik, *Fehlzeiten: Fehltage nach Berufsfeldern*. [Online] Available: https://www.tk.de/tk/service/infografiken/fehlzeiten/215980. Accessed on: Sep. 11 2018.

[23] *Ergonomie der thermischen Umgebung*, DIN EN ISO 7730:2006-03, 2006.

[24] Bundesanstalt für Arbeitsschutz und Arbeitsmedizin, "Beleuchtung: ASR A3.4," in *Technische Regeln für Arbeitsstätten*, 2011.

[25] Osram, *Powerbrik LED*. [Online] Available: https://www.osram.de/ls/ecat/mit%20opaler%20Abdeckung%20aus%20PC-POWERBRIK%20LED-Feuchtraumleuchten-Innenleuchten/de/de/GPS01_2822280/PP_EUROPE_DE_eCat/ZMP_1219720/.

[26] U. Renggli and R. Horbaty, "Energieverbrauch in gewerblichen Küchen," Bundesamt für Konjunkturfragen, Bern, Feb. 1992. [Online] Available: http://www.energie.ch/energie/bfk/ravel/13D.pdf. Accessed on: Sep. 17 2018.

[27] *Delegierte Verordnung (EU) Nr. 1059/2010 der Kommission*, 2010.

[28] P. O. Fanger, "Thermal comfort. Analysis and applications in environmental engineering," *Thermal comfort. Analysis and applications in environmental engineering.*, 1970.

[29] Stadtwerke Werl GmbH, *Bedingungen und Preise zum Nachstrom-Sonderabkommen N und NV*. [Online] Available: https://www.stadtwerke-werl.de/_Resources/Persistent/bac22ff5b429ed89cee20367033c8bca94bab3ac/Preisblatt_NNV_%202018_01.pdf. Accessed on: 20.09.18.

[30] *Gesetz für die Erhaltung, die Modernisierung und den Ausbau der Kraft-Wärme-Kopplung: KWKG*, 2015.

[31] Statistisches Bundesamt, "Preise: Daten zur Energiepreisentwicklung," Jul. 2018.

[32] *Modelica—A unified object-oriented language for system modeling and simulation*: Springer, 1998.

[33] D. Müller, M. Lauster, A. Constantin, M. Fuchs, and P. Remmen, "AixLib-An Open-Source Modelica Library within the IEA-EBC Annex 60 Framework," in *BauSIM 2016*, 2016, pp. 3–9.

Accurate Position Control for Hydraulic Servomechanisms

M. Pencelli[a,b], R. Villa[b], A. Argiolas [a], G. Ferretti[b], M. Niccolini[a], M. Ragaglia[a], P. Rocco[b] and A. M. Zanchettin[b]

[a]Yanmar R&D Europe S.r.l
[b]Politecnico di Milano
E-mail: manuel_pencelli@yanmar.com, renzo.villa@polimi.it

Abstract -

A common problem when operating heavy hydraulic machines consists in the inability of performing accurate motion. In the last few years the development of non-linear control techniques and the production of increasingly more accurate and cheaper hydraulic drives induced a steadily growing interest towards the development of controlled hydraulic systems. Clearly, this interest is also motivated by the possibility to exploit the huge power density, which is an intrinsic feature of hydraulic systems. This paper specifically focuses on the development of several position control schemes, whose aim is to guarantee accurate motion of a standalone hydraulic servomechanism. By relying on an experimentally validated mathematical model of the servomechanism itself, different control schemes have been synthesized and the resulting control performances have been verified and compared together.

Keywords -

Hydraulic systems, Hydraulic actuators, Motion Control

1 Introduction

Nowadays the vast majority of high performance servomechanisms is composed by electrical servomechanisms. Nevertheless, hydraulic actuation systems are characterized by multiple convenient features (namely high power density, reliability, and relatively low maintenance cost) that make them particularly fit to several application domains, like for instance: construction and earthworks machinery [1, 2], mining industry [3], agriculture and forestry [4]. Typically, hydraulic servomechanisms are controlled either manually by human operators opening and closing valves, or by using heavily approximated linear controllers.

Specifically in case of linear controllers, obtaining accurate motion of such kind of servomechanisms is a quite complex task, mainly due to the highly non-linear dynamics describing the behaviour of valves, and to high parametric uncertainty affecting the mathematical models of the different system components. Given this situation, the resulting motion is often characterized either by very low accuracy and repeatability or by a limited bandwidth of the closed loop system due to a rather conservative design in order to ensure stability. Despite the mentioned problems, linear controllers are still implemented for hydraulic servomechanism [5] because of their simplicity and the consolidated well-known theoretical background [6].

However, recent research developments in the field of non-linear control finally allowed to overcome some of the aforementioned limitations and to guarantee reasonably good performance. Among these non-linear control strategies, Sliding Mode Control (SMC) is probably the most widespread solution when dealing with hydraulic actuators [7, 8]. More recently, in [9] a 1^{st}-order SMC scheme was applied to control a 1-DoF hydraulic crane, while in [10] a 2^{nd}-order SMC scheme for the same system was proposed. Dynamic switching functions have been introduced in [11] and also adaptive SMC laws have been proposed [12, 13] in order to improve the robustness of the controller of an hydraulic motor. Finally, a comprehensive discussion of the various application of SMC to hydraulic systems is given in [14], while alternative approaches based on backstepping [15] and cascaded adaptive control [16, 17, 18, 19] have also been proposed.

With respect to the mentioned scientific literature, the main contribution of this work consists in an experimentally-based comparative evaluation of the performance levels of an advanced P-PI linear controller and an approximated 1^{st}-order SMC, both applied on a standalone hydraulic servomechanisms. First, the paper details the development and the validation of the mentioned control strategies aiming. Then, a comparative evaluation of the performance of the proposed control strategies is discussed. In particular, starting from a previously validated dynamic model of a generic hydraulic servomechanisms [20], a linear cascade control with static compensation of the dead-zone and a 1^{st}-order SMC have been synthesized. The tracking performance of time-varying reference signals of the SMC scheme has been improved by introducing a model-based feed-forward action. In addition, the high frequency chattering (caused by the SMC action) has been reduced by approximating the discontinuity inside the SMC law with a sigmoid function. Finally, the performance of the different closed-loop control systems have been tested on an experimental test-bench.

The paper is organized as follows. Section 2 briefly introduces the dynamic model of the hydraulic servomechanism, while Section 3 describes the linear controller scheme synthesized on the basis of the linearized dynamic model. Then, Section 4 details the development of the proposed SMC schemes and Section 5 shows the experimental validation of all the proposed control schemes and discusses the performance levels achieved by each solution. Finally, conclusions and future developments are presented in Section 6.

2 Hydraulic Servomechanism Model

The dynamic model of the generic hydraulic servomechanism used as a basis to develop the proposed control algorithms is defined as follows:

$$\begin{cases} \dot{x}_p = \dot{x}_p \\ \ddot{x}_p = \frac{1}{M}[A_1 P_1 - A_2 P_2 - f_r(\dot{x}_p) - D\dot{x}_p - \zeta \dot{x}_p^2 - Mg] \\ \dot{P}_1 = \frac{\beta}{V_1(x_p)}(Q_1 - A_1 \dot{x}_p) \\ \dot{P}_2 = \frac{\beta}{V_1(x_p)}(-Q_2 + A_2 \dot{x}_p) \end{cases} \tag{1}$$

$$Q_1 = \begin{cases} c_1(P_p - P_1) - c_2(P_1 - P_t) & d_z^- < x_v < d_z^+ \\ k_1^+(x_v)\frac{\pi}{4}\frac{d^2 x_v^2}{\sqrt{1-x_v^4}}\sqrt{\frac{2}{\rho}(Pp - P_1)} & x_v \geq d_z^+ \\ -k_1^-(x_v)\frac{\pi}{4}\frac{d^2 x_v^2}{\sqrt{1-x_v^4}}\sqrt{\frac{2}{\rho}(P1 - P_t)} & x_v < d_z^- \end{cases} \tag{2}$$

$$Q_2 = \begin{cases} c_3(P_p - P_2) - c_4(P_2 - P_t) & d_z^- < x_v < d_z^+ \\ k_2^+(x_v)\frac{\pi}{4}\frac{d^2 x_v^2}{\sqrt{1-x_v^4}}\sqrt{\frac{2}{\rho}(Pp - P_2)} & x_v \geq d_z^+ \\ -k_2^-(x_v)\frac{\pi}{4}\frac{d^2 x_v^2}{\sqrt{1-x_v^4}}\sqrt{\frac{2}{\rho}(P_2 - P_t)} & x_v < d_z^- \end{cases} \tag{3}$$

where:

- x_p, $\dot{x}_p$, $\ddot{x}_p$: hydraulic cylinder position, velocity and acceleration, respectively;
- M: mass of the mechanical load;
- A_1, (A_2): bottom(rod)-side chamber internal surfaces;
- V_1, (V_2): bottom(rod)-side chamber internal volumes;
- P_1, (P_2): bottom(rod)-side chamber internal pressures;
- $f_r(\cdot)$: Coulomb friction function;
- D: viscous friction coefficient;
- ζ: dynamic pressure loss coefficient;
- g: gravitational constant;
- β: mineral oil bulk modulus;
- Q_1: flow rate from tank to bottom-side chamber;
- Q_2: flow rate from rod-side chamber to tank;
- c_i: valve static pressure loss coefficients;
- P_p: pump pressure;
- P_t: tank pressure;
- x_v: valve PWM, acting as control signal;
- $k_1^{\pm}(\cdot)$, ($k_2^{\pm}(\cdot)$): bottom(rod)-side chamber valve opening function2;
- d: valve orifice diameter;
- ρ: mineral oil density;
- d_z^-, d_z^+: valve negative and positive dead-zones.

A more detailed discussion of the dynamic model (along with its experimental validation) can be found in [20].

3 Linear Controller

In this Section a linearized version of the previously introduced dynamic model is given, allowing to synthesize a linear control scheme.

3.1 Dynamic Model Linearization

Starting from equations (1)-(3), the linearized model can be computed. The equilibrium point has been chosen by considering the valve opening outside of the deadzone region and by taking the middle position of the cylinder as working point:

$$\begin{aligned} &\overline{x}_v < d_z^- \quad \vee \quad \overline{x}_v > d_z^+ \\ &\overline{x}_p = \frac{{x_p}^{MAX} - x_{p\,min}}{2} \\ &\overline{V}_1 = A_1 \overline{x}_p, \quad \overline{V}_2 = A_2 \overline{x}_p \end{aligned} \tag{4}$$

consequently, the following set of linear equation is obtained:

$$\begin{pmatrix} \delta\ddot{x}_p \\ \delta\dot{P}_1 \\ \delta\dot{P}_2 \end{pmatrix} = \begin{pmatrix} \frac{-(D+2\zeta\dot{x}_p)}{M} & \frac{A_1}{M} & \frac{-A_2}{M} \\ \frac{-\beta A_1}{\bar{V}_1} & \frac{\beta\lambda_1}{\bar{V}_1} & 0 \\ \frac{\beta A_2}{\bar{V}_2} & 0 & \frac{-\beta\lambda_2}{\bar{V}_2} \end{pmatrix} \begin{pmatrix} \delta\dot{x}_p \\ \delta P_1 \\ \delta P_2 \end{pmatrix} + \begin{pmatrix} 0 \\ \frac{\beta\lambda_3}{\bar{V}_1} \\ \frac{-\beta\lambda_4}{\bar{V}_2} \end{pmatrix} \delta x_v \tag{5}$$

where $\lambda_1, \lambda_2, \lambda_3, \lambda_4$ are the linearization coefficients of the valve:

$$\begin{aligned} \delta q_1 &= \lambda_1 \delta P_1 + \lambda_3 \delta x_v \\ \delta q_2 &= \lambda_2 \delta P_2 + \lambda_4 \delta x_v \end{aligned} \tag{6}$$

Finally, the state space formulation can be turned into the corresponding transfer function between the valve opening and the cylinder velocity:

$$F(s) = \frac{\delta \dot{x}_p(s)}{\delta x_v(s)} = k_f \frac{\tau_1 s + 1}{(\tau_2 s + 1)(s^2/\omega^2 + 2Ds/\omega + 1)} \tag{7}$$

and the transfer function between the valve opening and the cylinder position can be obtained by simply integrating the cylinder velocity:

$$G(s) = \frac{\delta x_p(s)}{\delta x_v(s)} = \frac{F(s)}{s} \tag{8}$$

3.2 Controller Block Scheme

After linearization of the dynamic model, the cascaded control scheme has been developed (see Figure 1). A proportional-integral (PI) controller with anti-windup block was chosen for the inner velocity loop, while a pure proportional (P) controller was selected for the outer position loop. On the top left part of the digram it is possible to see a derivative block that outputs a velocity feed-forward term that helps improving tracking performance. On the other hand, since a direct measure of the cylinder velocity is not available, another derivative block is needed in order to indirectly compute $\dot{x}_p$. Clearly, each derivative block is equipped with a tunable low pass filter in order to ensure that the transfer function of the complete system is proper. Moreover, the filter inside the feed-forward derivative block ensures that the control action is not too aggressive, while the one on the measurement line mitigates the effect of the noise. Finally, the saturation blocks ensure that the value of the valve opening stays inside the admissible range $[-1,\ +1]$, while the "*sig*" block contains the dead-zone compensation function $sig\,(u)$, defined as:

$$sig\,(u) = d_z^- + \frac{d_z^+ - d_z^-}{1 + e^{-\eta u}} \tag{9}$$

in order to avoid chattering of the controlled variable. For the sake of completeness, to tune the control gains it is sufficient to neglect the effect of the non-linear blocks and to apply the Bode criterion to both the internal velocity loop and to the external position one.

4 Sliding Mode Controller

The parametric uncertainties and the intrinsic high non-linearities of hydraulic systems can greatly deteriorate the performances of classical linear controllers, especially when the state configuration of the system is far from the linearization point. For this reason SMC can be a suitable alternative for the realization of an accurate position control. In this Section, after a brief overview of the SMC theory is given and the control law adopted for our system is presented and. Finally, the condition that guarantees the overall stability of the closed loop is discussed.

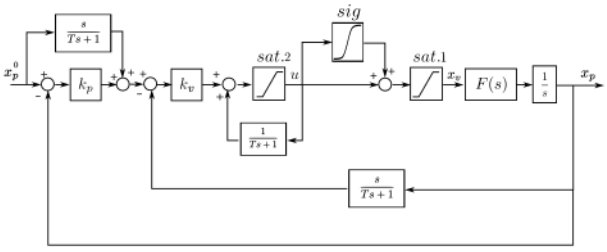

Figure 1. P-PI cascaded control scheme with anti-windup, feed-forward and dead-zone compensation.

4.1 Sliding mode control overview

The main properties of SMC are the robustness with respect to both external disturbances and parametric uncertainties, and the capability to constrain the system state within a specific a-priori defined state subspace. This subspace is called "sliding surface" and it is defined by:

$$S = \{\mathbf{x} : \sigma(\mathbf{x}) = 0\} \tag{10}$$

where $\mathbf{x} \in R^n$ is the state vector of a given system and $\sigma(\mathbf{x}) : R^n \rightarrow R$ is the sliding variable, a function properly defined in order to achieve the desired performances. Given a generic non-linear SISO system with bounded state:

$$|\dot{x}_i| < U_i, \quad |x_i| < Ub_i, \quad x_i \in \mathbf{x} \tag{11}$$

Lyapunov's theory can be used in order to compute a control signal that forces the state movement on S:

$$V(\mathbf{x}) = \frac{1}{2}\sigma(\mathbf{x})^2 > 0, \quad \dot{V}(\mathbf{x}) = \dot{\sigma}\sigma \tag{12}$$

Usually, by making proper manipulation, the first derivative of the sliding variable can be expressed as a function of the control variable:

$$\dot{\sigma} = \dot{\sigma}(u) \tag{13}$$

Then, by choosing the following discontinuous control law:

$$u = k_s sign(\sigma) \tag{14}$$

with a sufficiently large k_s, it's possible to guarantee $\dot{V} < 0$.

Note that the 1^{st}-order sliding mode is characterized by a discontinuous control law. When the system reaches the

sliding surface, a chattering phenomenon on the control variable will be triggered at an ideally infinite frequency. This fact entails a very intense use of the control variable and determines the presence of undesired vibrations on the overall system, that can also damage physical components. These phenomena can be reduced, either by approximating the sign function or implementing an higher order SMC.

4.2 A different formulation of the model

In order to design a proper control law, a different formulation of the model has been adopted. Ignoring momentarily deadzone and internal leakages, the valve model can be written as follows:

$$\Phi_1 = S(\nu)\lambda_1^+\sqrt{Pp - P1} + S(-\nu)\lambda_1^-\sqrt{P_1 - P_t} \quad (15)$$

$$\Phi_2 = S(-\nu)\lambda_2^-\sqrt{Pp - P2} + S(\nu)\lambda_2^+\sqrt{P_2 - P_t} \quad (16)$$

$$\lambda_1^- = k_1^-(x_v)\frac{\pi}{4}d^2\sqrt{2/\rho} \quad \lambda_1^+ = k_1^+(x_v)\frac{\pi}{4}d^2\sqrt{2/\rho} \quad (17)$$

$$\lambda_2^- = k_2^-(x_v)\frac{\pi}{4}d^2\sqrt{2/\rho} \quad \lambda_2^+ = k_2^+(x_v)\frac{\pi}{4}d^2\sqrt{2/\rho} \quad (18)$$

$$\nu = f(x_v) = \frac{x_v^2}{\sqrt{(1 - x_v^4)}}sign(x_v) \quad (19)$$

where $S(\nu)$ is the Heaviside step function. Therefore, the flow rates can be expressed as $Q_1 = \Phi_1\nu$ and $Q_2 = \Phi_2\nu$. Also, a new state vector can be defined:

$$\mathbf{z}^t = \begin{pmatrix} e & \dot{e} & P_1 & P_2 \end{pmatrix} = \begin{pmatrix} z_1 & z_2 & z_3 & z_4 \end{pmatrix} \quad (20)$$

where $e = {x_p}^0 - x_p$ and $\dot{e} = \dot{x}_p^0 - \dot{x}_p$ are the position and speed tracking errors, respectively. By defining the following quantities:

$$H_1 = \frac{A_1\Phi_1}{V_1(x_p)} + \frac{A_2\Phi_2}{V_2(x_p)} \quad H_0 = \frac{A_1^2}{V_1(x_p)} + \frac{A_2^2}{V_2(x_p)} \quad (21)$$

z_2 can be expressed as a function of the hydraulic force first derivative:

$$z_2 = \frac{\dot{F}_p}{\beta H_0} - \frac{H_1}{H_0}\nu + \dot{x}_p^0 \quad (22)$$

Finally, the new formulation is obtained by writing (1) with respect to the new state vector:

$$\begin{cases} \dot{z}_1 = \frac{1}{\beta H_0}\dot{F}_p - \frac{H_1}{H_0}\nu + \dot{x}_p^0 \\ \dot{z}_2 = \frac{1}{M}[F_{loss}(\dot{x}_p^0 - z_2) - A_1 z_3 + A_2 z_4 + g + \ddot{x}_p^0] \\ \dot{z}_3 = -\frac{\beta}{V_1(x_p^0 - z_1)}A_1(\dot{x}_p^0 - z_2) + \frac{\beta}{V_1(x_p^0 - z_1)}\Phi_1\nu \\ \dot{z}_4 = -\frac{\beta}{V_2(x_p^0 - z_1)}A_2(\dot{x}_p^0 - z_2) - \frac{\beta}{V_2(x_p^0 - z_1)}\Phi_2\nu \end{cases} \quad (23)$$

where $F_{loss}(\dot{x}_p) = f_r(\dot{x}_p) - D\dot{x}_p - \zeta\dot{x}_p^2$.

4.3 Evaluation of the control law

The design of the control law starts with the definition of a proper sliding variable and a candidate Lyapunov function. A common choice is:

$$\sigma(\mathbf{z}) = C_1 z_1 + z_2, \quad V(\mathbf{z}) = \frac{1}{2}\sigma(\mathbf{z})^2 \quad (24)$$

In order to ensure $\dot{V}(\mathbf{z}) < 0$ the aforementioned control law can be used:

$$\nu = k_s sign(\sigma) \quad (25)$$

Unfortunately with the current experimental set-up the measure of z_2, which depends on $\dot{x}_p$, is not available. However at the increasing of C_1, the dependency of $\sigma(\mathbf{z})$ of z_2 becomes negligible, therefore the time derivative of $V(\mathbf{z})$ can be written as:

$$\dot{V}(\mathbf{z}) = \sigma(z_1)\left[-\frac{C_1 H_1}{H_0}\nu + \frac{C_1\dot{F}_p}{\beta H_0} + C_1\dot{x}_p^0\right] \quad (26)$$

and the control law changes into:

$$\nu = k_s sign(z_1) \quad (27)$$

The numerical value of k_s is computed accordingly to the absolute upper bound of the hydraulic force time derivative(UB_{dF_p}) and reference velocity ($UB_{\dot{x}_p^0}$).

$$k_s > \frac{H_0}{H_1}\left[\frac{UB_{dF_p}}{\beta H_0} + UB_{\dot{x}_p^0}\right] \quad (28)$$

The maximum speed achievable by the load depends on the supply pressure and it can be set as the upper bound of the reference speed. Also both UB_{dF_p} and $UB_{\dot{x}_p^0}$ can be estimated by several simulations of the validated model, as suggested in [21].

In addition, control law (27) can be improved by adding feed-forward and proportional actions:

$$\nu = k_p z_1 + k_s sign(z_1) + \frac{H_0}{H_1}\dot{x}_p^0 \quad (29)$$

therefore the condition on the time derivative of the candidate Lyapunov function becomes:

$$\sigma(z_1)\left[-\frac{H_1}{H_0}(k_p z_1 + k_s sign(z_1)) + \frac{UB_{dF_p}}{\beta H_0}\right] < 0 \quad (30)$$

In order to compute k_s the worst case can be considered. More specifically, the value of the control signal ν is minimum when the proportional action tends to zero ($z_1 \approx 0$), thus the condition on k_s can be re-written as follows:

$$k_s > \frac{UB_{dF_p}}{\beta H_1} \quad (31)$$

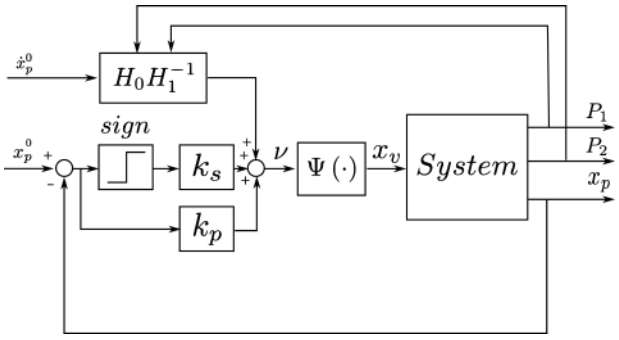

Figure 2. Sliding mode control scheme with proportional term, feedforward model based and sigmoid

Figure 3. Hydraulic test-bench.

By using the proposed control law (29) a less stringent condition has been retrieved:

$$\frac{UB_{dF_p}}{\beta H_1} \leq \frac{H_0}{H_1}\left[\frac{UB_{dF_p}}{\beta H_0} + UB_{\dot{x}_p^0}\right] \tag{32}$$

Consequently, smaller values of k_s can be adopted and in general smaller oscillations can be induced with respect to the ones determined by control law (27) .

Furthermore, the introduction of the proportional term and of the model-based feed-forward action entails a faster time response and an improvement of the dynamic tracking performances.

Moving to the dead-zone, its effect can be considered by means of a further condition on k_s. In particular, with reference to the worst case, the following condition must be always satisfied:

$$k_s > max\{|f(d_z^+)|, |f(d_z^-)|\} \tag{33}$$

Moreover, in order to reduce the undesired oscillations, triggered by the presence of the $sign(\cdot)$, a sigmoid approximate function is usually adopted:

$$sign(x) \approx sig(x) = -1 + \frac{2}{1 + e^{-\epsilon x}} \tag{34}$$

Finally, once ν is computed, it is possible to find the corresponding valve opening by directly inverting function f:

$$x_v = \Psi(\nu): \quad f(\Psi(\nu)) = \nu \tag{35}$$

The result is a smooth control action at the price of a partial loss in terms of robustness and accuracy (see [21]). Nevertheless, as shown in the next discussion, this choice does not significantly compromise the overall tracking performance.

5 Experimental Validation and Performance Analysis

In this Section the experimental validation platform is described, experimental results are presented, and, finally, the performance levels achieved by each control solution are compared together.

5.1 Hydraulic Test-bench

The hydraulic test-bench used to test the proposed control schemes is pictured in Figure 3. The system is composed by two independent hydraulic servomechanisms. The rod-side of each cylinder is rigidly connected to the load, which consists in a plate (constrained by vertical motion guides) on top of which it is possible to load a generic weight. More in detail, the test-bench comprises:

- 2 asymmetric hydraulic cylinders: one with a traction load and one with a compression load;
- 2 directional valves with 4 ways and 3 positions;
- 1 hydraulic pump powering the entire system;
- pressure relief valves to ensure operational safety;
- 2 linear potentiometers that measure the position of each cylinder;
- 5 pressure sensors installed at the outlet of the pump and inside the four chambers of the two cylinders;
- 2 load cells installed between the rod side and the plate.

5.2 Experimental Validation - Linear Controller

The control scheme pictured in Figure 1 has been tuned in the following way:

$$k_p = 1, \quad k_v = 0.108, \quad T = 0.002, \quad \eta = 50 \tag{36}$$

All the transfer functions have been discretized using the Backward Euler method and the experiments have been

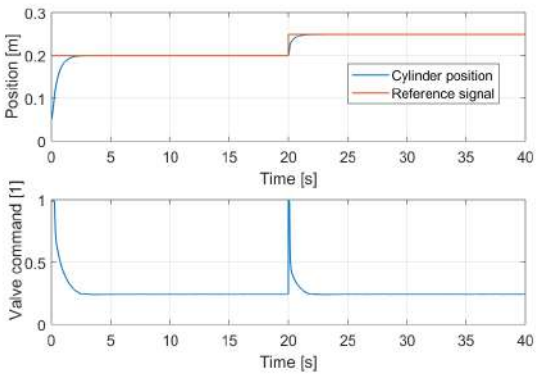

Figure 4. Linear Controller: response to step set-point.

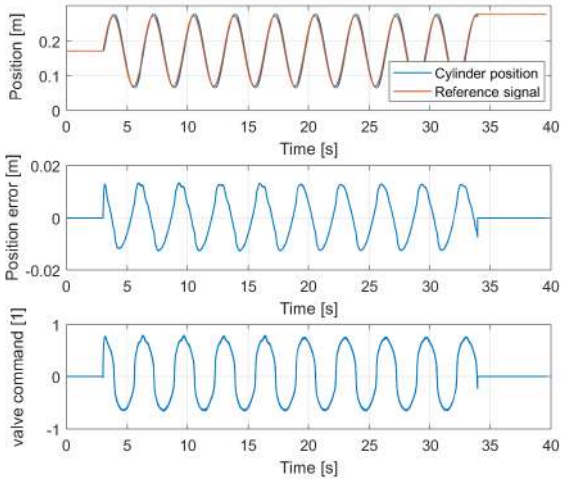

Figure 5. Linear Controller: response to sine reference signal.

performed on the actuator with a compression load mass of 282 kg.

Figure 4 show the system responses to a step set-point. The control action is not affected by any chattering and the system converges to the desired set-point value without oscillating.

On the other hand, Figure 5 shows the results of a tracking experiment during which a sinusoidal reference signal is sent to the control system. The control action seems not to be affected by significant chattering phenomena. Nevertheless, the not completely accurate compensation of the valve dead-zone determines a relevant tracking error, that reaches up to 13.4 *mm* where the sign of the speed changes.

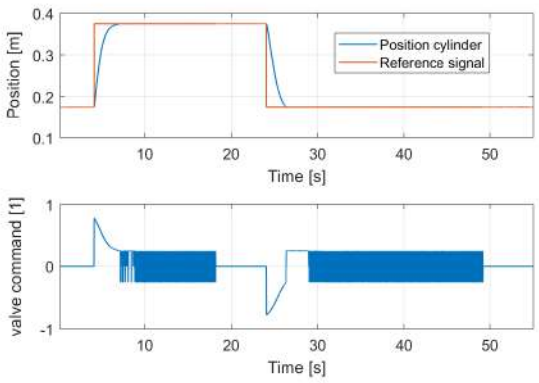

Figure 6. SMC: response to step reference signal.

5.3 Experimental Validation - SMC

At first, a simplified version of SMC law (29) was implemented in the hydraulic test-bench:

$$\nu = k_p(x_p^0 - x_p) + k_s sign(x_p^0 - x_p) \tag{37}$$

with:

$$k_p = 4.5 \quad k_s = 0.067 \tag{38}$$

The response to a step set-point is shown in Figure 6. The system is able to converge to the imposed set-point with zero static error. Nevertheless, as soon as the state reaches the sliding surface, the control variable starts to chatter at high frequency.

In order to improve the dynamic tracking performance, the feed-forward term was added to equation (37):

$$\nu = k_p(x_p^0 - x_p) + k_s sign(x_p^0 - x_p) + \frac{H_0}{H_1}\dot{x}_p^0 \tag{39}$$

In addition, to simplify the implementation, the following assumptions have been made:

$$\frac{H_0}{H_1} \approx \frac{A_1}{\Phi_1}, \quad k_1^+ = 0.052, \quad k_1^- = 0.045 \tag{40}$$

Figure 7 shows the response of the system to a sinusoidal reference signal. After the initial peak, the position error rapidly decreases with a maximum of 3.3 *mm*. The chattering phenomenon of the valve opening is still visible. To remove these undesired oscillations, the final SMC law (29) was implemented choosing $\epsilon = 4000$.

Figure 8 shows the response of the complete SMC law to a trapezoidal set-point profile, while Figure 9 shows the response to a sinusoidal reference signal. In both cases, we can see that good performance in terms of position error are achieved (maximum tracking error on sine signal is equal to 6.4 *mm*) and that the use of the approximating sigmoid function enforces a smooth control action, without any significant chattering.

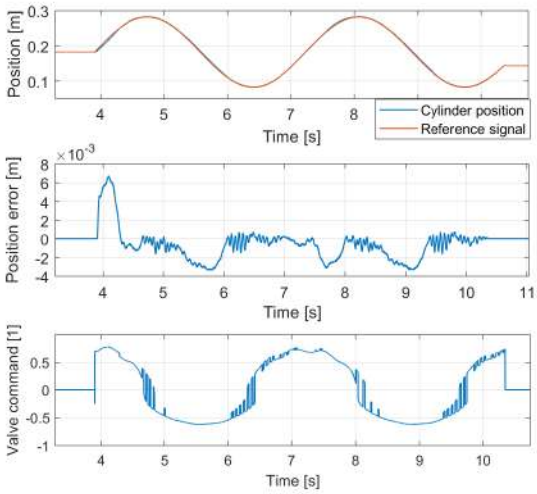

Figure 7. SMC with feedforward: response to sine reference signal.

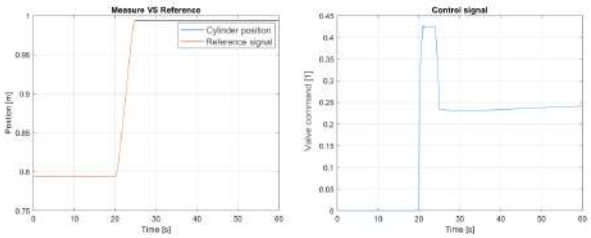

Figure 8. SMC with feed-forward and sigmoid: response to trapezoidal set-point profile.

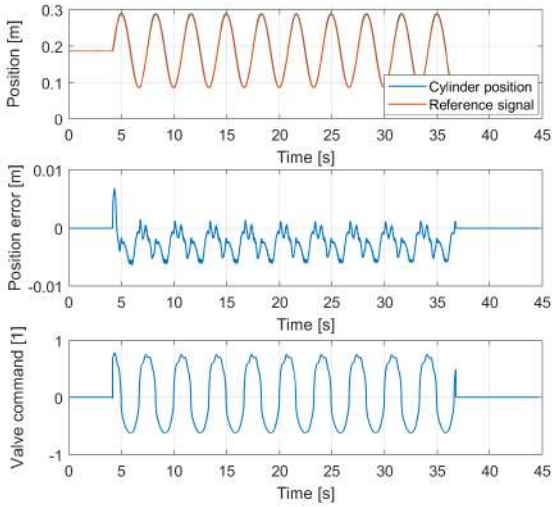

Figure 9. SMC with feed-forward and sigmoid: response to sine reference signal.

5.4 Comparative Evaluation of Performance

Generally, we can state that the linear controller is able to achieve good static performance, but it also entails poor tracking capabilities. Moving to the classical SMC controller, this solution is able to guarantee the best performance both in steady-state and in tracking, but the control action is heavily affected by chattering. Finally, the introduction of the feed-forward term and of the sigmoid approximating function allows to eliminate the chattering problem, without significantly undermining the performance in terms of both convergence time and tracking error.

6 Conclusions and Future Developments

This paper describes the research activities leading to the development of several position control schemes for a standalone hydraulic servomechanism. Starting from a previously validated mathematical model of the hydraulic actuator, several control laws have been synthesized and validated on an real system. Various experiments have been performed in order to verify the performance of each control schemes with respect to both step set-points and sinusoidal reference signals. Experimental results suggest that the SMC schemes (both the classical one and the one with sigmoid approximation) are able to guarantee better performance with respect to the linear cascade control scheme. Moreover, the intrinsic robustness of the SMC strategy leads to a high level of accuracy of the closed loop system.

As far as future developments are concerned, at first a decentralized position control system for an hydraulic manipulator will be designed on the basis of the SMC schemes here discussed. Then, possible alternatives in terms of control strategies will also be evaluated, like for instance the SuperTwisting algorithm (which is an example of 2^{nd}-order SMC) [22], and the linear control with adaptive compensation of the dead-zone [23].

References

[1] M. Hutter, P. Leemann, S. Stevsic, A. Michel, D. Jud, M. Hoepflinger, R. Siegwart, R. Figi, C. Caduff, M. Loher, and S. Tagmann. Towards optimal force distribution for walking excavators. In Advanced Robotics (ICAR), 2015 International Conference on, pages 295–301, July 2015.

[2] M. Tanzini, J. M. Jacinto-Villegas, A. Filippeschi, M. Niccolini, and M. Ragaglia. New nteraction metaphors to control a hydraulic working machine's arm. In IEEE Symposium of Safety and rescue Robotics (SSRR), 2016.

[3] Peter Corke, Jonathan Roberts, Jock Cunningham, and David Hainsworth. Mining Robotics, pages 1127–1150. Springer Berlin Heidelberg, Berlin, Heidelberg, 2008.

[4] John Billingsley, Arto Visala, and Mark Dunn. Robotics in Agriculture and Forestry, pages 1065–1077. Springer Berlin Heidelberg, Berlin, Heidelberg, 2008.

[5] Mohieddine Jelali and Andreas Kroll. Hydraulic servo-systems: modelling, identification, and control. 01 2003.

[6] Torben Andersen, Michael Hansen, Henrik Pedersen, and Finn Conrad. Comparison of linear controllers for a hydraulic servo system. Proceedings of the JFPS International Symposium on Fluid Power, 2005, 01 2005.

[7] Y. Liu and H. Handroos. Technical //note sliding mode control for a class of hydraulic position servo. Mechatronics, 9(1):111 – 123, 1999.

[8] M. Jerouane and F. Lamnabhi-Lagarrigue. A new robust sliding mode controller for a hydraulic actuator. In Proceedings of the 40th IEEE Conference on Decision and Control (Cat. No.01CH37228), volume 1, pages 908–913 vol.1, 2001.

[9] S. Aranovskiy and C. Vazquez. Control of a single-link mobile hydraulic actuator with a pressure compensator. In 2014 IEEE Conference on Control Applications (CCA), pages 216–221, Oct 2014.

[10] Carlos Vazquez, Stanislav Aranovskiy, Leonid Freidovich, and Leonid Fridman. Second order sliding mode control of a mobile hydraulic crane. In Decision and Control (CDC), 2014 IEEE 53rd Annual Conference on, pages 5530–5535. IEEE, 2014.

[11] Rui Tang and Qi Zhang. Dynamic sliding mode control scheme for electro-hydraulic position servo system. Procedia Engineering, 24(Supplement C):28 – 32, 2011.

[12] Cheng Guan and Shanan Zhu. Adaptive time-varying sliding mode control for hydraulic servo system. In ICARCV 2004 8th Control, Automation, Robotics and Vision Conference, 2004., volume 3, pages 1774–1779 Vol. 3, Dec 2004.

[13] Cheng Guan and Shuangxia Pan. Adaptive sliding mode control of electro-hydraulic system with nonlinear unknown parameters. Control Engineering Practice, 16(11):1275 – 1284, 2008.

[14] Lasse Schmidt. Robust Control of Industrial Hydraulic Cylinder Drives - with Special Reference to Sliding Mode- & Finite-Time Control. PhD thesis, Aalborg Universitet, 2014.

[15] Mohammad Reza Sirouspour and Septimiu E Salcudean. Nonlinear control of hydraulic robots. IEEE Transactions on Robotics and Automation, 17(2):173–182, 2001.

[16] Mauro André Barbosa Cunha, Raul Guenther, Edson R. De Pieri, and Victor Juliano De Negri. Design of cascade controllers for a hydraulic actuator. International Journal of Fluid Power, 3(2):35–46, 2002.

[17] Mauro André Barbosa Cunha, Raul Guenther, and Edson R. De Pieri. A fixed cascade controller with an adaptive dead-zone compensation scheme applied to a hydraulic actuator. Control 2004, Bath, United Kingdom, 2004.

[18] Mauro André Barbosa Cunha and Raul Guenther. Adaptive cascade control of a hydraulic actuator with an adaptive dead-zone compensation. In ABCM Symposium Series in Mechatronics, volume 2, pages 385–392, 2006.

[19] Leandro dos Santos Coelho and Mauro André Barbosa Cunha. Adaptive cascade control of a hydraulic actuator with an adaptive dead-zone compensation and optimization based on evolutionary algorithms. Expert Systems with Applications, 38(10):12262–12269, 2011.

[20] Manuel Pencelli, Renzo Villa, Alfredo Argiolas, Gianni Ferretti, Marta Niccolini, Matteo Ragaglia, Paolo Rocco, and Andrea Maria Zanchettin. Accurate dynamic modelling of hydraulic servomechanisms. In Design, Automation and Test in Europe (DATE), 03 2019.

[21] Leonid Fridman Yuri Shtessel, Christopher Edwards and Arie Levan. Sliding mode control and observation. Springer, 2014.

[22] T. Gonzalez, J. A. Moreno, and L. Fridman. Variable gain super-twisting sliding mode control. IEEE Transactions on Automatic Control, 57(8):2100–2105, Aug 2012.

[23] Mauro André Barbosa Cunha, Raul Guenther, and Edson R. De Pieri. A fixed cascade controller with an adaptive dead-zone compensation scheme applied to a hydraulic actuator. Control 2004, Bath, United Kingdom, 2004.

The Automation of the Softer Side of Smart City: A Socio-Semantic Roadmap

T. E. El-Diraby[a], A. Zarli[b], and M. E. El-Darieby[c]

[a] Department of Civil and Mineral Engineering, University of Toronto, Canada
[b] R2M Solution, France
[c] Software Systems Engineering, University of Regina, Canada
E-mail: tamer@ecf.utoronto.ca, alain.zarli@r2msolution.com, mohamed.el-darieby@uregina.ca

Abstract –

We present a roadmap for guiding public officials on establishing platforms for citizen empowerment in the smart city. The proposed roadmap is not a technical architecture. Rather, a set of paradigms, guidelines and references to advanced technology approaches that can support building a technical architecture. We start from the perspective that the smart city architecture is not a venue for services, but a domain of innovation. We advocate encouraging citizen science to co-create new solutions—in contrast to engaging them to inform them or to evaluate solutions developed by professionals. We advocate giving equal attention to structured and unstructured data analysis. We also encourage the adoption of adaptable data orchestration tools to help navigate and organize the complexity of city data. Finally, we provide an outlook on the future trends (such as Blockchain and cognitive computing) in urban systems decision making.

Keywords –

Smart city; Citizen science; Socio-semantic analysis

1 Introduction

Traditionally, cities take a *control-room approach, to* centrally manage and optimize urban systems. The target is to develop and use technical operational policies that can make cities more sustainable, efficient, comfortable and enjoyable (de Waal & Dignum 2017). This is a *service-user model*, where citizens are considered as subjects, or, at best, customers. However, the concept of e-citizen is far more transformative. First, a smart city effectively tracks and is highly responsive to its citizens' opinions, behavior and objectives. Support for behavior changes can be the most valuable resource for meeting the challenges of climate change and sustainability. This is because there is a limit to the extent of possible efficiency gains that smarter hardware can achieve. In contrast, a limited savings in energy at the individual level, if adopted by the crowds, will provide effective and lasting impact. Engaging citizens can help find the best approaches to support such behaviour change. For example, what incentives can be offered to citizens to encourage the use of public transit, what new technologies or motivations for energy saving can be implemented.

Second, and more importantly, we should move citizens from a reactive role of service-recipients to co-creator of policies. In post-modernist planning theories, knowledge is distributed with citizens possessing equally valid knowledge to that of professionals. The role of planners is not to decide, but rather to seek and actualize multiple knowledge(s) to support transformative decision making. Collaborative planning approaches span four major categories (Linnenluecke et al. 2017): predictive (using forecasting); adaptive (adjusting to changing conditions); visionary (generating alternatives); and transformative planning (co-creation of solutions). Transformative planning is not limited to the idea of co-creation and harnessing community knowledge. It aims to empower communities, promote social learning/ innovation and foster behavior change.

We aim to provide a high-level map for 1) the issues that should be considered in developing a socially-savvy e-city platform, and 2) illustrate the value, relevance and interactions between available enabling technologies. It is expected that a city manager or a director of capital projects will use the map as a benchmark or a starting point for scoping an actionable policy for engaging citizens, collating their input and supporting their collective deliberations and innovation.

We present here a set of requirements and an initial architecture for augmenting sensor data about the physical city systems with that of people: their views, needs, ideas. The objective is to establish a repository of data for the access, use and analytics of (unstructured) data in the context of smart city.

2 The Smart City

The complexity of the fusion of data about the physical systems (attributes of the infrastructure) with that of its citizen (input, views, ideas) is not limited to computational issues, but, more fundamentally, to the very definition of a smart city. Pardo and Nam (2011) view a smart city from three perspectives: i) a mandatory technological perspective with a general reference to smart hardware and information technology tools.; ii) citizen creativity perspective that considers the role of citizens in using and generating smart city data; and iii) an institutional dimension that refers to cooperation of societal institutions with governments to co-develop policies and decisions. These three perspectives corresponds to the terms Digital City, Knowledge City and Smart Community, respectively.

In a departure from the control-room approach, citizens and civic organizations are empowered to use digital technologies to create solution to advance city systems. They not only have the right to a share of decision making powers, but also an equal right to being the source of knowledge and innovation—technical and otherwise. Examples of this approach has inspired several new applications and concepts: citizen sensor networks, DIY-citizenship (Ratto and Boler 2014), tactical urbanism (Lydon and Garcia 2015) or hackable city-making (de Waal et al. 2017). Such state-of-the-art practices use interactive citizen science for pooling citizen knowledge across all phases of city management including data collection, selecting amongst proposed alternatives, definition of the problems to consider, generating solutions, initiation of decision making, and monitoring actual implementations. This infuses more democracy into decision making, harness social innovation and allow citizens to act as agents of change.

In fact cities of the future are described to be "*territories with high capability for learning and innovation, which is built-in the creativity of their population, their institutions of knowledge creation, and their digital infrastructure for communication and knowledge management*" (Komninos 2006). The co-creation of knowledge by citizens and institutions is in fact "*continuous creation, sharing, evaluation, renewal and update of knowledge*" (Ergazakis 2004).

2.1 Collaborative Social Innovation

Several recent initiatives showcase that a paradigm shift towards citizen science in urban areas is viable and valuable—for example, Hackerspace (with 1330+ physical sites); include Network of 'Science Shops': scientific research in cooperation with citizens and local and national civil society organizations; DESIS-network: over 30 design labs supporting 'social innovation towards sustainability'; Global Ecovillage Network: network of 500 ecovillages; and Transition Towns: 450 grassroots community initiatives working on "local resilience". These advocate using sensing tools to enhance perception of environmental conditions (ex, Extreme Citizen Science); diffusion of solution and implementation tools (ex. Citizen Cyberlab); creating new sets of data (ex. Mapping for Change); provide open access to data (ex. DataShare); collection of idea (ex. IdeaConnection); taking collective actions (ex. Hacking the City). These efforts entwine electronics, media and humans, into co-agents in data and knowledge-production and decision-taking (Parikka, 2011).

2.2 Data Challenges for the Smart City

Smart city data is categorized into structured and unstructured data. Structured data follows a formal pre-defined data model and typically relates to physical and technology data—for example sensor and camera data or vehicle location. Unstructured data does not adhere to specific models. Unstructured data such as social media and popular media contents or citizen reviews is a fundamental input to any socio-technical analysis of smart city systems. This makes unstructured data more essential to citizen science, because it helps in understanding user needs and in customizing data delivery to them. For example, structured data can be used to define patterns of use of autonomous vehicles (AV) to support predicting traffic volumes or to correlate electric vehicles travel patterns to determine best location for electric charging stations. Unstructured data can be used to represent citizen willingness to support efficient mobility and energy usage; best means to operate an AV system or fix a broken pipe.

In general, one of the main challenges for serving data to citizens is the manipulation of data (especially the unstructured), due to the following challenges:

Complexity: The complexity of issues to consider in any urban decision is increasing. For example, Lambert et al. (2011) developed a model to prioritize major civil infrastructures projects. It included the following fourteen indicators: create employment, reduce poverty, improve connectivity and accessibility, increase industrial/agricultural capacity, improve public services and utilities, reduce corruption/improve governance, increase private investment, improve education and health, improve emergency preparedness, improve refugee management, preserve religious and cultural heritage, improve media and information technology, increase women's participation and improve environmental and natural resource management.

Multidisciplinary analysis: In addition to complexity, the issues are multidisciplinary. For example, considering the scope of assessment knowledge, Kabir and Khan (2013) enumerated 300 different possible issues for analysis. They span seven classes (each class is

followed by the number of related issues): hydrological resource systems (68), potable and wastewater (54), transportation (56), bridges (58), buildings (33), underground infrastructures (11) and urban systems (21).

Subjectivity: many of these issues are quite subjective in nature. To help quantify the assessment, a variety of quantification approaches have been developed (Hoogmartens et al. 2014), including life cycle analysis (LCA), life cycle costing (LCC) and cost–benefit analysis (CBA). Domain-specific methods were further explored, including environmental LCA (eLCA), social LCA (sLCA), financial LCC (fLCC), environmental LCC (eLCC), full environmental LCC (feLCC), societal LCC (sLCC), financial CBA (fCBA), environmental CBA (eCBA) and social CBA (sCBA).

3 The Proposed Architecture: Overview

The proposed roadmap aims to maximize the contribution of smart city systems (hardware and data) to empower citizens to lead innovation and knowledge generation within the city. The focus is on the know-how dimensions, which spans the creation of platforms to enable data management, processing, protection, visualization and analytics. It is out of scope for this roadmap to consider the know-why dimension, which models and understands the externalities that impact the development and effective management of smart city, including economic, legal, political, social and ethical issues. Also out of scope is the know-what dimensions which focuses on developing policies to create technical and process-based standards, and skill development and training (Cuquet et al 2017).

A high-level map that describes the main elements relevant to a typical smart city architecture is shown in Figure 1. Raw active data is ingested, curated and archived in long-term storage. Then data is catalogued and metadata and context information are extracted and used to tag/ annotate data. This enables searching through the "data lake." This workflow can be divided into detailed lower-level workflows that span each step; for example data upload and ingestion requires its own sub-workflow and User Interface.

The main pillars in the proposed map are as follows:

- The acquisition and ingestion of intrinsic data. Securing access to diversified and easy to use data. That is, the data has a higher value if it can be fused with other relevant data.
- Computational services. Much like an API or an "app store", this pillar offers citizens services to process data. Here, we assume that a citizen or a decision maker is using such data to create new products or conduct certain analyses.
- Modeling Pillar. Much like IFC (industry foundation classes), we need formalized models of data: rules that describe their behaviors, and basic relationships between datasets. How does the available data cohere to each other and how does the data relate to typical city analyses. Such conceptual models of data will require technical expertise, which is not easily available to citizens. For example, creating a bridge between IoT raw data and BIM-based software will enable users to access and develop a large number of applications without having to manipulate the technical architectures of this data (such as understanding IFC). Still, a savvy user can use the bridge to generate higher order models—without worrying about interoperability between the two data models.

4 Pillar 1: Data Acquisition

We identify below a set of challenges for acquiring smart city data and suggestions for possible solutions based on recent advances in data management approaches.

4.1 Data Heterogeneity

Establishing meaningful data from a multitude of structured and unstructured data will remain a challenge. For example, how to make sense and integrate CCTV data, with sensor data with citizen data. While ontologies can be very effective in handling this, their static nature will limit their ability to be exhaustive. Different types of tools were proposed to solve this problem:

Fact-finding platforms such as YAGO2 contains 350, 000 classes, 10 million entities and 120 million facts extracted automatically from online sources, with an accuracy of 95% (Hoffart et al. 2013).

Linked data and distributed stream computing help manage the high-variety and high-volume data within high-velocity activities (Hasan and Curry 2014). The combination of linked data tools and stream computing tools with machine learning tools will facilitate the semantic coupling of know-how knowledge with real time data. This creates a realm of self-improving data models and associated learning/analytics needed to support spot decision making (Curry et al. 2013).

Edge computing: Decision-embedded analytics that have real-time access to big data will facilitate in-network and in-field analytics (called edge-computing). In conjunction with enterprise-level analytics, these tools are poised to create higher levels of customization (for example, which driverless car is best choice for each commuter), real-time operational (what are the best evacuation routes for each commuter in the case of emergency), and even new business models (for example, carbon tax refunds based on usage of energy within/outside home)

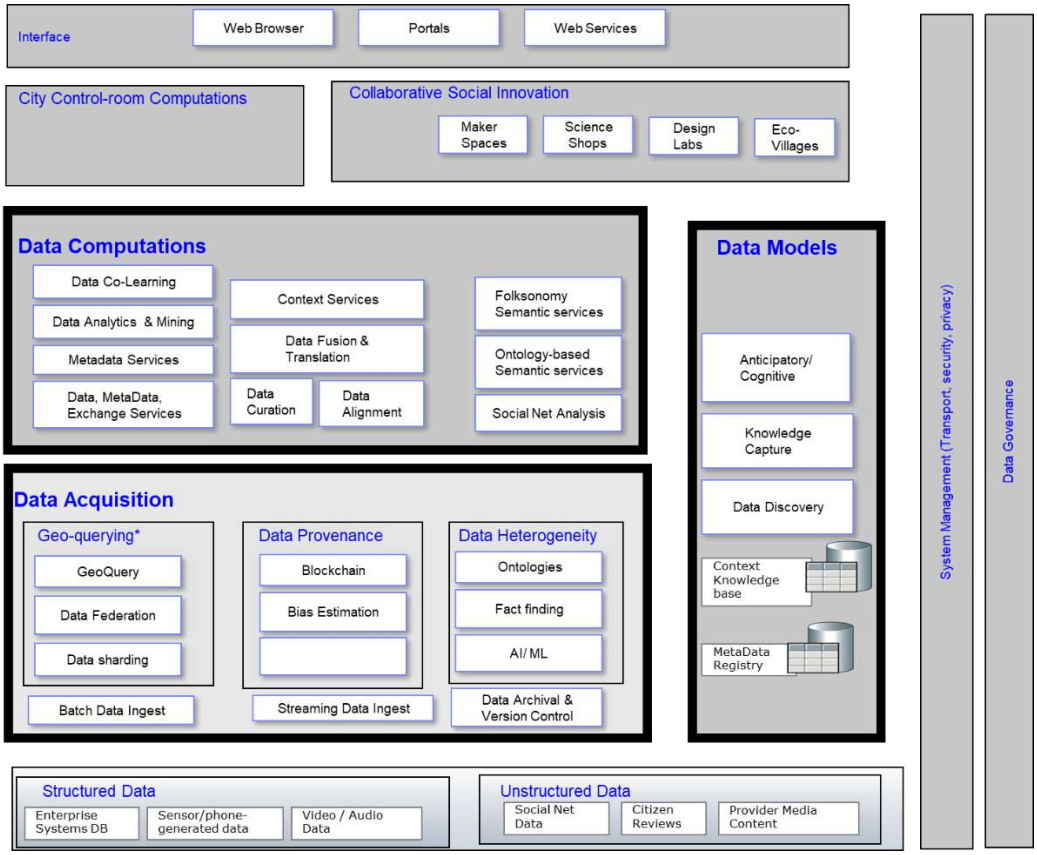

Figure 1. Overview of the proposed roadmap

4.2 High-Performance Data Access

Access can be provided by customizable and intelligent sharding of the data streams based on application and infrastructure requirements. Technologies such as Apache Kafka already provides an ability to shard relative to the memory capacity of the system conducting the analysis. Two of the key challenges that must be addressed by any smart city architecture are contextualization and federation.

The architecture needs to enable and include a process of contextual sharding. A set of intelligent mechanisms at the network edge are required to understand specific applications. This ranges from understanding their data structures to identifying access rights to specific users.

Another challenge is data federation. How to accommodate data query and retrieval functionality from multiple individual platforms. MicroELement (MEL) is a simplified software used to describe a basic IoT computation (Ranjan et al. 2018):

1. MicroServices: functionalities deployed/migrated across different infrastructures (e.g., Docker) available across Cloud, Edge, and Things layers;
2. MicroData: contextual information about i) devices, protocols for collecting and sharing data, ii) the specific type of data (e.g., temperature, vibration, pollution) it needs to process, and iii) data management steps, such as storage and access rules.
3. MicroComputing: executing analysis tasks based on historic and real-time data through tools such as NoSQL, stream processing, batch processing, etc.);
4. MicroActuator: interfaces with actuator devices for changing or controlling object states in the IoT.

MEL will need to expose a uniform programmatic interface (APIs) to models and analytics, hence, reducing the barriers to data ingestion. The new federated API suite may utilize the Apache Spark SQL API to benefit from its existing interoperability features, in addition to other Apache libraries such as Samza and Kafka. The API must be lightweight, and enable integration with services supported by other vendors.

4.3 Data Provenance

Traditional data provenance techniques require collection and transmission of large data volumes, which is impractical for IoT applications that warrant sub-second decision making and data processing latency. Hence, new techniques are required which can reduce and enhance the efficiency of provenance and metadata

collection, recording, and transmission. Understanding how provenance relationships can be derived from IoT data processing activities is a challenge, as precedence relationships identifying which output was a consequence of an inputs may be difficult to establish.

One possible opportunity is to develop IoT data provenance technique based on Blockchain's Distributed Ledger Technology (DLT) to record lifecycle activities on data as it travels through the IoT ecosystem. Another hard challenge to solve will be to develop provenance techniques than can verify complying with data privacy regulation such as GDPR (Berberich & Steiner 2016). Undertaking GDPR compliance for statically held data (e.g. user information) can be easier to manage, however extending this to a dynamic data stream (which may be context dependent) remains a challenge. Another challenge is when IoT deployments involve more than one vendor. Finally, the authenticity of data and protecting it against organized campaigns is important. The roadmap recommends investing in technology to detect and eliminate misinformation and bias (amplified through the viral nature of social media) using algorithms like WSARE (What's Strange About Recent Events) and platforms such as SwiftRiver (Yu et al. 2016).

4.4 Access Control

It is important to identify application actors: Information flows between actors is modelled as message passing. Such messages are to be stated explicitly along with identification of the content of such messages. This makes it possible to discover which actors have access to information items necessary for answering provenance use case questions.

Of equal important is to map out actor interactions. This is a network of data items, users with access to them, and platform components processing them.

Finally, identify knowledgeable actors. Any actor that has access to an information item is known as a knowledgeable actor. The team will associate every information item (within a use case) with an actor. For each, the necessary provenance functionality is to be set. When an information has not been exposed in the interactions between actors through message exchanges, use cases (in data management system) must be revised.

4.5 Geo-Distributed Cross-Querying

In smart city applications, there is a need to curate data based on its geo-location. The challenge is to design multi-query planning algorithms that can not only map queries to different parts of an IoT infrastructure but also map that to the requirements of data analytics applications. The algorithms are required to also optimize end-to-end QoS associated with the query plan, to improve resource utility and meet users' SLAs. Existing geo-distributed querying systems were designed for managing only static data. They neither consider heterogeneous processing infrastructure, nor execute queries using standard heterogeneous models (e.g., stream processing, NoSQL, SQL, batch processing).

Event Processing Language (EPL) can enhance the performance of existing geo-distributed querying systems, EPL can limit the query data size to guarantee real-time processing. Hence, EPL has been used in majority of stream process platform such as Apache Spark, Kafka, Flink and Esper. Similar to SQL, however, one of the core limitations of EPL-based querying approaches is that they cannot handle heterogeneous data stored across multiple types of storage platforms and/or programmed using multiple types of storage and analytics programming models.

A more dynamic approach is to find data linkage through bottom-up discovery of association patterns. New tools such as blockmodeling (part of network analysis techniques) allow a platform to detect data clusters. Studying the patterns of repeated clusters can help discover and designate a set of data templates: a set of typical heterogeneous data that can be seen as complementary. This can span both the semantic and structured data. Machine learning approaches can also be very effective in this regard.

5 Pillar 2: Computation and Generation of New Knowledge

The computation pillar aims to create a bottom-up environment to foster collaborative analysis and re-mixing of data through collaboration between citizen scientists. This pillar spans the following features.

- Data representation: Structure and represent the data to facilitate multiple modalities (i.e. different models of data logic), exploiting the redundancy of different data sources.
- Data translation: Interpret data from one modality to another, i.e., a translator allows the modalities to interact with each other for enabling data exchange.
- Data alignment: bridges among modalities.
- Data fusion: integrate data from different domains
- Data co-learning: transfer modality knowledge between users.

The following are some relevant approaches to support bottom-up analyses of city systems:

5.1 Citizen Sensor Networks

Scientists and engineers are already providing interactive cloud-based models to help users (with limited or no technical background) to learn, conduct or study the use of some of these assessment methods. This

can cover purely technical issues such as environmental modelling; visualization systems through interactive 3D modelling and GIS maps; and even tools to help connect mental models with quantitative system dynamics (Voinov et al. 2016). Examples includes (Evers al. 2016): stakeholder participation in developing an agent based model to profile social values; and modelling through role playing games (Haase et al. 2013); enhance acceptability of environmental models (Wassen et al., 2011); and environmental models validation (Newig et al., 2008). Kishita et al. (2016) developed a review of scenario generation for sustainability analysis, which is very relevant to supporting citizen science.

5.2 Gaming

Gaming has been used to help in recruiting and sustaining participants. Evolving as a venue for interactive co-creation, games galvanize partnerships and provide opportunities for peer-to-peer learning. They are also some of the best tools to study "choice molecules" (action-outcome combinations) especially when non-linearities make it hard to communicate system features and reactions in conventional learning and dialogue processes (de Suarez et al. 2012).

Cases for the use of games in co-creating and studying alternative futures include, for example, the game "Paying for Predictions". It helps in risk assessment in relation to resource shortages and disaster management in light of climate change. "Ready!" is a game that uses narrative to help identify solutions to environmental problems. The Rockefeller "Resilience game" addresses the disconnection between decisions and actions: government or communities not following options selected. The game "Before the Storm" generates decisions as players think through the various options that may be available to them when a particular disaster strikes. "Upstream, Downstream" game promotes consensus building and social learning through providing players with the ability to assign risks based on individual views. Through repeated reviews by all, a better collective understanding of risk can emerge. The game "Dissolving Disasters" considers choices in the context of changing probability of, say, rainfall. It is designed to rush players into decision making. Later, players are given time to reflect on the problem, and, more importantly, the decision making process.

5.3 Application Orchestration

An IoT application is typically expressed as a collection of multiple self-contained data analysis activities (e.g., MEL). These activities are orchestrated to execute in a specific order with specific rules that respond to user requirements. To realize a dynamic environment for citizens to collaborate on creating new knowledge, there is a need for platforms that can enable application orchestration, including the following:

- Choosing storage and analytics programming models (e.g., stream processing, batch processing, NoSQL) and data analysis algorithms to seamlessly execute in highly distributed and heterogeneous IoT;
- Dynamically detecting faults across multiple parts of the IoT infrastructure;
- Dynamically managing data, and software available in "Things, Edge and Cloud" layers driven by IoT.

6 Pillar 3: Modelling

Established models (such as IFC, for example) add context and structure to data. Such models represent the best means by which technical experts can communicate their knowledge to citizens in an indirect way. Because such models are limited to the data level, they allow users to benefit from the basic rules embedded in the data model, but, at the same time, they do not mandate specific analysis approach on the users. They act as connectors and check-system on data. This is similar to the IFC-BIM relationship. Users can be very innovative in their programming of BIM without worrying about the basics of data structures (they are served through IFC)

Using flexible data structures foster social learning. The proposed roadmap advocate balancing the top-down approach of data standards with a bottom-up discovery means. For example, the roadmap advocate using ontologies (formalized and programmed conceptual model) and, at the same time, using folksonomies (ad hoc, bottom-up and loose model of concepts).

On the long term, lifelong Machine Learning is a central paradigm in smart city systems. How to discover knowledge based on smart search, conduct intelligent analysis, and constantly re-train algorithms based on newly found knowledge. Recent trends in Transfer Learning and multitask learning are task-specific and domain-agnostic (Liu 2017). Such smartness is rooted and supported by the surge in synthesis research and the advancement of knowledge capture and representation tools. Synthesis is a type of inferential reasoning that recursively integrates inductive thinking (combine observations into a larger model) with deductive analysis (examining the consistency of a general model to real cases). Emphasis in recent years is focused on automating the inductive part given the mushrooming number of models in all domains.

6.1 Knowledge Capturing and Representation

Thanks to amazing advancement in semantic systems/ algorithms, the field of knowledge acquisition and representation has evolved into extensive and efficient levels. Probase (and its successor Microsoft

Concept Graph) is a probabilistic taxonomy (with 5.4 million concepts) that constantly assesses the typicality of knowledge using probabilities, which in turn is used to support probabilistic reasoning (Zang et al. 2013). YAGO2 is an informatics ontology based on WordNet and Wikipedia YAGO2 contains 10 million entities and 120 million facts, which were extracted automatically from Wikipedia, GeoNames, and WordNet. YAGO2 stores extraction rules in text files, which allows easy extension without changing source code. Human assessment of facts in YAGO2, showed that it achieved an accuracy of 95% (Hoffart et al. 2013). Freebase was a scalable graph database used to structure general human knowledge. The data in Freebase could be collaboratively created, structured, and maintained by people and software. Freebase provided automatic suggestion to help the user enter new knowledge. It was replaced by Googl's Knowledge Graph, which contains 70 billion facts!

Open Information Extraction (OPEN IE) is a protocol for extracting a large number of relations from arbitrary text on the Web without specifying the targets to be extracted (Fader et al. 2011). KnowItAll is a scalable and domain-independent system that uses OPEN IE for extracting facts from the Web in an unsupervised manner. It ran for four days on a single machine and extracted over 50 000 facts (Etzioni et al. 2004).

6.2 Cognitive and Anticipatory Computing

One of the most promising technologies in citizen science is cognitive computing. It refers to computers learning how to complete tasks traditionally done by humans. The focus is on finding patterns in data, carrying out tests to evaluate the data validity. A key technology in this regards is natural language generation (NLG). NLG is not like traditional natural language process (NLP) systems. NLG tools are able to transform unstructured data into readable summaries with synthesis of key takeaways. Advanced NLG offers traceability: why the system chose to communicate in a particular manner. Bots (a short name for software robots) are used for live chat with customers. Story Engine is a program that can read through unstructured data and summarize conversations, including the ideas discussed, the frequency of the communication and the mood of the speakers. Interestingly, some newspapers are starting to use some of these Bots to summarize sport events based on transcripts of commentators' speech.

The next frontier is anticipatory/assistive computing. In this regards, the computer moves from reacting to explicit commands into understanding implicit queries and anticipating questions and actions. Bot help search engines exploit big data analytics to infer similar/related strings of searches/questioning by other users (Reed et al. 2012). They exploit advances in inductive (logic) programming, which is predicated on finding solutions to problems/queries in the same manner humans would do through predicting next steps and inductively collating related facts from the web. Some of the most successful and sophisticated examples of Bots that deploy cognitive and anticipatory computing include Apple's Siri, Amazon's Alexa, Microsoft's Cortana, and Google's Google Home and Facebook Messenger. These and IBM's Watson apply deep learning for superior knowledge acquisition and representation. .

7 Discussion

Our aim here was not to build a technical architecture for smart city and citizen science applications. Rather, collate and organize relevant paradigms, governance issues and analysis approaches into a roadmap that can guide cities in developing the technical architecture. We advocated that smart city architecture has to balance the use of structured and unstructured data. They also have to be able to provide processed data and means to process data. A user, based on their technical agency can have the choice of using either approach. One of the main technical roles for a smart city architecture is in providing computational services (apps) that enables users to mix and match data analyses to produce new original contribution. Another significant contribution is to provide users with basic models that can create minimal and meaningful structure to data. This can include data models and ontologies or folksonomies.

The proposed architecture places special attention to machine learning and cognitive computing. These are very promising approaches in enabling smarter and easier analyses and, at the same time, customize the access, delivery and usage of data (including BigData) to user profiles.

References

[1] Berberich, M., & Steiner, M. (2016). Blockchain Technology and the GDPR-How to Reconcile Privacy and Distributed Ledgers. *Eur. Data Prot. L. Rev.*, *2*, 422.

[2] Brownill, S., & Parker, G. (2010). Why bother with good works? The relevance of public participation(s) in planning in a post-collaborative era. *Planning Practice and Research*, 25, 275–282.

[3] Cuquet, M., Fensel, A., & Bigagli, L. (2017, June). A European research roadmap for optimizing societal impact of big data on environment and energy efficiency. In *Global Internet of Things Summit (GIoTS), 2017* (pp. 1-6). IEEE.

[4] Curry, E., O'Donnell, J., Corry, E., et al. (2013). Linking building data in the cloud: Integrating cross-domain building data using linked data. *Advanced Engineering Informatics*, 27, 206–219

[5] de Suarez, J. M., Suarez, P., Bachofen, C., Fortugno, N., Goentzel, J., Gonçalves, P. and van Aalst, M. (2012). *Games for a new climate: experiencing the complexity of future risks*. Pardee Center Task Force Report.

[6] de Waal, M., & Dignum, M. (2017). The citizen in the smart city. How the smart city could transform citizenship. *Info. Technology*, *59*(6), 263-273.

[7] de Waal, M., de Lange, M., and Bouw, M. 2017. The Hackable City. Citymaking in a Platform Society. *AD Architectural Design* 87, 1, 50–57.

[8] Ergazakis, M., Metaxiotis, M., & Psarras, J. (2004). Towards knowledge cities: conceptual analysis and success stories. *Journal of Knowledge Management*, *8*(5), 5–15 (Emerald Group Publishing Limited).

[9] Etzioni O, Cafarella M, Downey D, Kok S, Popescu A, Shaked T, Soderland S, Weld D, and Yates A. (2004). Web-scale information ex-traction in KnowItAll: (Preliminary results). *13th Int. Conf. World Wide Web*, May 2004, pp.100-110.

[10] Fader A, Soderland S, Etzioni O. (2011). Identifying relations for open information extraction. *Conf. on Empirical Methods in Natural Language Processing*, Jul. 2011, pp.1535-1545.

[11] Hasan, S., & Curry, E. (2014). Thematic event processing. *15th international middleware conference on-middleware'14*, ACM Press, New York, NY, pp 109–120

[12] Hoffart J, Suchanek F. M, Berberich K., and Weikum G. (2013). YAGO2: A spatially and temporally enhanced knowledge base from Wikipedia. *Artificial Intelligence*, 194: 28-61.

[13] Hoogmartens, R., Van Passel, S., Van Acker, K., & Dubois, M. (2014). Bridging the gap between LCA, LCC and CBA as sustainability assessment tools. *Environmental Impact Assessment*, 48, 27-33.

[14] Kabir, S., and Khan, N. E. A. (2013). Water sensitive urban design: Dhaka City. *2nd International Workshop on Design in Civil and Environmental Engineering*, 16.

[15] Kishita, Y., Hara, K., Uwasu, M., & Umeda, Y. (2016). Research needs and challenges faced in supporting scenario design: a literature review. *Sustainability Science*, *11*(2), 331-347.

[16] Komninos, N. (2006). The architecture of intelligent cities: integrating human, collective and artificial intelligence to enhance knowledge and innovation. *IE*

[17] Lambert, J.H., Karvetski, C.W., Spencer, D.K., Sotirin, B.J., Liberi, D.M., Zaghloul, H.H., Koogler, J.B., Hunter, S.L., Goran, W.D., Ditmer, R.D. and Linkov, I. (2011). Prioritizing infrastructure investments in Afghanistan with multiagency stakeholders and deep uncertainty of emergent conditions. *Infrastructure Systems*, 18(2), 155-166.

[18] Lee, J. H., Hancock, M. G., & Hu, M. C. (2014). Towards an effective framework for building smart cities: Lessons from Seoul and San Francisco. *Tech. Forecasting & Social Change*, *89*, 80-99.

[19] Linnenluecke, M. K., Verreynne, M. L., de Villiers Scheepers, M. J., and Venter, C. (2017). A review of collaborative planning approaches for transformative change towards a sustainable future. *Cleaner Production*, 142, 3212-3224.

[20] Liu, B. (2017). Lifelong machine learning: a paradigm for continuous learning. *Frontiers of Computer Science*, 11(3), 359-361.

[21] Lydon, M. and Garcia, A. 2015. *Tactical urbanism short-term action for long-term change*. Island Press, Washington, D. C.

[22] Newig, J., Haberl, H., Pahl-Wostl, C., and Rothman, D. S. (2008). Formalised and non-formalised methods in resource management—knowledge and social learning in participatory processes: an introduction. *Systemic Practice and Action Research*, 21(6), 381-387.

[23] Pardo, T. A., & Nam, T. (2011). Smart city as urban innovation: focusing on management, policy and context. *Proceeding of the 5th International Conference on theory and Practice of Electronic Governance* (pp. 185–194). New York: ACM.

[24] Parikka, J. (2011). *Media nature. The materiality of information technology and electronic waste*. Open Humanities Press.

[25] Ranjan, R., Rana, O., Nepal, S., Yousif, M., James, P., Wen, Z., ... & Villari, M. (2018). The Next Grand Challenges: Integrating the Internet of Things and Data Science. IEEE Cloud Computing, 5(3), 12-26.

[26] Ratto, M. and Boler, M. 2014. DIY citizenship?: critical making *and social media*. The MIT Press, Cambridge, MA.

[27] Reed, D., Larus, J. R., and Gannon, D. (2012). Imagining the future: Thoughts on computing. *Computer*, 45(1), 25-30.

[28] Voinov, A., Kolagani, N., McCall, M. K., Glynn, P. D., Kragt, M. E., Ostermann, F. O., and Ramu, P. (2016). Modelling with stakeholders–next generation. *Enviro. Model. & Software*, 77, 196-220.

[29] Wassen, M. J., Runhaar, H., Barendregt, A., and Okruszko, T. (2011). Evaluating the role of participation in modeling studies for environmental planning. *Enviro. Planning B*, 38(2), 338-358.

[30] Yu, R., Qiu, H., Wen, Z., Lin, C., and Liu, Y. (2016). A survey on social media anomaly detection. *ACM SIGKDD Explorations Newsletter*, 18(1), 1-14.

[31] Zang L. J., Cao C, Cao Y. N. et al. (2013). A survey of commonsense knowledge acquisition. *Computer Science and Technology*, 28(4): 689-719. DOI 10.1007/s11390-013-1369-6

Factors Affecting the Performance of 3D Thermal Mapping for Energy Audits in a District by Using Infrared Thermography (IRT) Mounted on Unmanned Aircraft Systems (UAS)

Y. Hou[a], L. Soibelman[a], R. Volk[b], and M. Chen[a]

[a]Sonny Astani Department of Civil and Environmental Engineering, University of Southern California, USA
[b]Institute for Industrial Production, Karlsruhe Institute of Technology, Germany
E-mail: yuhou@usc.edu, soibelman@usc.edu, rebekka.volk@kit.edu, meidache@usc.edu

Abstract –

Infrared Thermography (IRT) is a widely used non-destructive method for energy audits. However, plenty of research indicates that the performance of passive thermography is influenced by the method of data collection. Unmanned Aircraft Systems (UAS) has been successfully employed for conducting RGB photogrammetry, but the data collected from an infrared thermal camera and an optical camera differ from one another. The infrared Thermal camera usually has a lower display resolution, is more likely influenced by ambient condition, and is limited to the distance between camera and objects. UAS is being utilized for reducing the time and complexity of data collection and for capturing detailed thermal images on large areas like university campuses or entire city districts. Meanwhile, it is important to investigate the impacts of factors such as camera angle, flight patterns, and overlap of pictures when auditing energy of a group of buildings within a district. This paper introduces the preliminary results of a study that tested factors that affect 3D thermal mapping by using a UAS. To measure the performance of mapping, this research compared the quality of rendered images generated from a mapping model constructed by drone acquired data with images acquired directly from a thermal camera. The efficiency of different UAS flying configurations were investigated. The investigation showed that the adjustment of flying configurations can improve the quality of rendered images for energy audits, even though rendered images were not as high-quality as images captured directly from a thermal camera.

Keywords –

Thermal mapping; Unmanned aircraft system (UAS); Flying configurations; Energy audits

1 Introduction

Energy audit has been used to reduce energy loss from buildings and distribution networks for many years. There are plenty of ways in auditing energy loss, including simulation methods, data-driven methods, and Infrared Thermography methods (IRT)[1][2]. Infrared Thermography (IRT), as a non-destructive approach, has been widely utilized for both a quantitative type of approach [3][4] and a qualitative type of approach[5]. However, IRT is influenced by the different approaches for data collection. In general, there are two types of approaches to collecting data for IRT, including Active Thermography and Passive Thermography[6][7][8]. Active Thermography employs an external stimulus to produce an extreme thermal difference (heating or cooling) between the objects and the environment. These approaches can detect hidden defects in detail, but they assume that auditors are fully aware of positions of potential thermal anomalies. Therefore, active approaches cannot be adopted effectively when auditing a whole district. On the contrary, passive thermography does not rely on man-made stimuli. Passive thermography concentrates on observing thermal patterns based on the temperature values and is influenced by weather and thermal emissivity.

Automated fly-past survey is referred as Unmanned Aircraft System (UAS), known as drones, with mounted thermal cameras. Firstly, UAS is flexible to collect thermal information from different angles and different altitudes.[9] Secondly, UAS not only can capture images horizontally, obliquely, and vertically from different angles around a building, but also can fly at a lower altitude and fly through two buildings to capture fine details. Finally, UAS can reduce time and labor. To date, UAS based IRT has been one of the most popular methods used in energy audits. New products, for example, allow the deployment of dual cameras to capture RGB images and thermal images at the same time

from the same angle and altitude. The main issue is that thermal camera's resolution is not as high as optical camera's resolution resulting in a lower quality 3D model generated by photogrammetry mapping.

Although UAS based IRT can reduce the time and complexity of data collection, and capture detailed images throughout a whole district, there remained serval problems in terms of drone flying configurations and efficiency. Additionally, auditing a single building differed from auditing a group of buildings within a district. It was crucial to investigate the impacts of factors such as camera angle, flight patterns, and pictures overlap when auditing energy of a group of buildings within a district. To explore factors affecting the performance of 3D thermal mapping for energy audits by using Infrared Thermography (IRT) mounted on Unmanned Aircraft Systems (UAS), this study proposed a method for testing different combinations of flying configurations and for comparing the results derived from those different combinations. The comparisons were based on quality and efficiency, and different factors' influences were analyzed. The following sections will present the proposed research method, the results, the discussion and conclusions.

2 Research Method

2.1 Architecture of Research Method

This study has three parts, Data Collection[10]; 3D Mapping; and Data Analysis and Comparison. In the first stage, different drone flying configurations in terms of flight patterns (vertical grid, horizontal grid and mesh grid), camera angles (90 and 45 degrees), and the percentage of image overlap (90% and 85%) were tested over a district. In the second stage, the features of every image were detected and used to reconstruct a 3D model. Due to several well-established commercial 3D reconstruction software programs, this process is effortless to implement. In the last stage, all 3D models based on different flying configurations were ranked. The ranking criteria compares the images rendered from 3D models and terrestrial images captured on site at the same time when flying the drone. The rendered images consist of points so relative points can be projected onto captured images. For thermal models and thermal images, points contain the temperature data, and so do the images. Temperature errors can distinguish the performance of different flying configurations. The workflow is shown in Figure 1. Each stage will be introduced in detail in the following paragraphs.

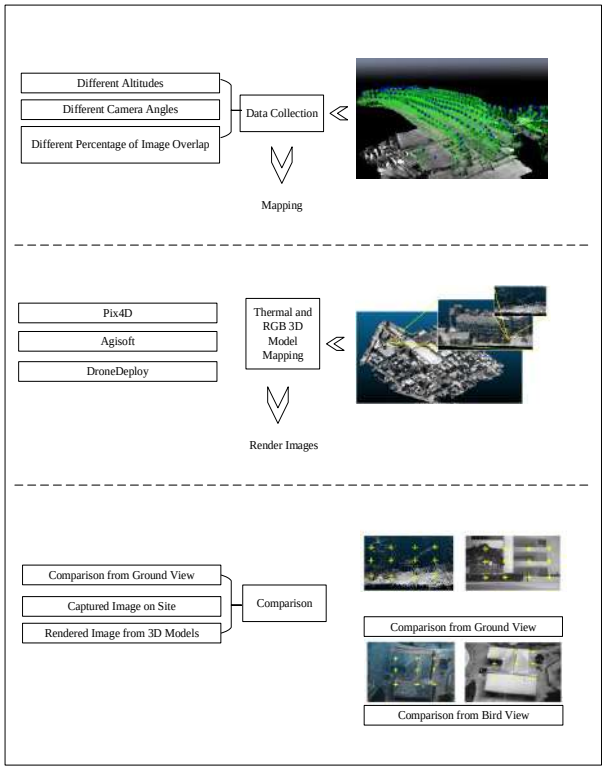

Figure 1. Workflow of research method

2.2 Data Collection

The Unmanned Aircraft System (UAS) used in this study is shown in Figure 2. The UAS consists of three parts: the main body, the data collection system, and the controller. The main body consists of an aircraft and a gimbal. The DJI M600, an industrial level drone, was deployed in this research. Gremsy T3 was the gimbal connecting the camera to the drone. It can horizontally and continuously yaw 360 degrees, has a vertical pitch from positive 90 degrees to negative 135 degrees, and can roll positive and negative 45 degrees. The gimbal can also connect to data collection system. One thermal camera, FLIR DUO Pro R was used in the data collection system. This camera can provide at the same time both a high-resolution featuring thermal image and a high-definition color image in a single integrated package. The data format is known as Radiometric JPEG. This file format contains both thermal and visible data in a single file. The resolutions of visible sensors and thermal sensors are 4000*3000 and 640*512 respectively. An additional benefit of this product is that absolute temperature can be read from its thermal images. The final part of this whole system is the controller. The controller can both remotely operate an aircraft for flight patterns, gimbal for angles, and cameras for data collection.

(1) Gimbal - Connection to DJI M600; (2) Gimbal - Frame for Camera; (3) FLIR DUO Pro R – Visible Lens Barrel; (4) FLIR DUO Pro R – IR Lens Barrel; (5) FLIR DUO Pro R – Electric Wires; (6) FLIR DUO Pro R – Integration Cable; (7) FLIR DUO Pro R – GPS Antenna Cable; (8) FLIR DUO Pro R – USB Cable.

Figure 2. Cameras setup for the deployed unmanned aircraft system

The most significant part in the data collection stage was to test different flying configurations. In this study, different flight patterns (vertical grid, horizontal grid and mesh grid), camera angles (90 and 45degrees), and percentage of image overlap (90% and 85%) were tested.

There are a great number of software programs which can be used for data collection. The available software programs are compared with each other in Table 1. However, not all software can be used to support both a drone systemand a camera system. In this study, DIJ GS Pro were used.

2.3 Visible and Thermal 3D Mapping

Due to the overlaps between two pictures, common feature points in different pictures can match with each other. To find common feature points, two widely used methods, Scale-Invariant Feature Transform (SIFT) and Speeded-up Robust Features (SURF) has been introduced. This process is called finding correspondence. To filter incorrectly matched points, Random Sample Consensus (RANSAC) is responsible for removing the outliers. After enough common feature points obtain their matches, the Location Determination Problem (LDP) can be solved and the positions of points can be determined in space. This technique for reconstructing 3D points from two-dimensional image sequences is called Structure from Motion (SfM)[11]. There are plenty of well-established commercial software programs for 3D reconstruction, including Pix4D, Agisoft, and DroneDeply [6] that implement this approach. In this study, Pix4D was used because of its ability to process both RGB and thermal images and to merge RGB and thermal models

Table 1. Comparison of data collection software

Designed by	Operated on IOS System	Operated on Android System	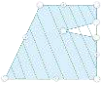 Plan Mapping	Circular	Peripherical Mapping	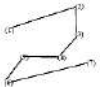 Waypoint Route	360 Degree Panorama
Pix4D Capture	Yes	Yes	Yes	Yes	No	No	No
DIJ GS Pro	Yes	No	Yes	Yes	No	Yes	No
Drone Deploy	Yes	Yes	Yes	No	No	No	No
Drone Harmony	No	Yes	Yes	Yes	Yes	Yes	No
Hangar360	Yes	No	No	No	No	No	Yes
Drone Blocks	Yes	No	Yes (by coding)	Yes (by coding)	No	Yes (by Coding)	Yes (by Coding)

2.4 Data Analysis and Comparison

After images collected through different flying configurations and processed by mapping, different 3D models with different flying configurations were obtained. In this stage, all constructed 3D models can be tested and ranked to determine which UAS flying configurations are the superior ones to audit energy loss.

In this study, data collected with UAS was compared with data captured by terrestrial thermal camera. Temperature values can change over time, however, each flight took less than 15 minutes, a span of time that does not allow temperature values change dramatically. After each flight, cameras have been immediately utilized as a stationary equipment to capture a thermal image close to

a selected building (less then 12m) facing selected façade and windows. Shown in Figure 3 (a), this picture was captured by thermal camera. Meanwhile, this selected viewing position and the same camera parameters were recorded. These setting then can be used to create a virtual camera with the same viewing position in a given 3D mapping model related to the flight to render an image from the model. Shown in Figure 3 (b), this is a rendered image from the thermal model. In order to measure the performance of mapping, quality of rendered images generated from a 3D mapping model, and captured images from a thermal camera were compared. Every point in (b) had color information representing temperature values. The criterion of comparison was to calculate the differences and errors between points in rendered images, illustrated by yellow crosses in (b), and related pixel in captured images, illustrated by yellow crosses in (a).

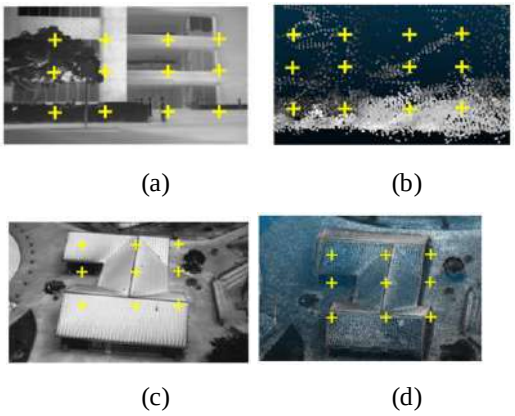

(a) (b)

(c) (d)

Figure 3. Cameras setup for unmanned aircraft system

One case of comparison was facing façade and windows shown in Figure 3 between (a) and (b). Another case was facing the roof system. In the second case, capturing extra images on site were not necessary. The images that were captured from drone view could be directly employed, shown in Figure 3 is a captured thermal image (c) and a rendered thermal image (d). The same comparison was also conducted for the second case.

To calculate the differences and errors between two images, two mathematical approaches were used being Mean Squared Error (MSE) and Structural Similarity Measure (SSM). Shown in equation (1) and equation (2).

$$MSE = \frac{1}{mn}\sum_{i=0}^{m-1}\sum_{j=0}^{n-1}[I(i,j) - K(i,j)]^2 \quad (1)$$

$$SSIM(x,y) = \frac{(2\mu_x\mu_y + c_1)(2\sigma_{xy} + c_2)}{(\mu_x^2 + \mu_y^2 + c_1)(\sigma_x^2 + \sigma_y^2 + c_2)} \quad (2)$$

MSE checks difference of every two relative pixels in two images. It squares these differences, sums them up and divides the sum of squares by the total number of pixels in the images. An MSE of value 0 indicates that two pictures are perfectly identical. The greater the value of MSE is, the more errors rendered pictures create. However, MSE simply compares the distance between pixel intensities. There is a need to compare the structural information of images. The SSIM method can perceive changes in small sub-samples, whereas MSE estimates the perceived errors in the entire images. In equation two, (x, y) indicates the $N \times N$ sub-window in each image, and SSIM can be calculated on various windows of an image. The SSIM value can range between -1 and 1, where 1 represents perfect identicality.

3 Case Study

IRT for energy audits usually has a requirement for a minimum indoor and outdoor temperature difference. The required temperature difference between indoor and outdoor for energy audits using IRT should be at least 10 °C (18 °F)[12]. In order to meet this requirement, we conducted our case study on a university campus in Boston, USA. According to the *105 CMR 410.00: Minimum Standards of Fitness for Human Habitation* published by Massachusetts Department of Public Health [13], regulation requires indoor temperatures of at least 64 °F at night and 68 °F during the day from September 15th to June 15th. During the data acquisition for our case study in Boston the outdoor temperature was 30.2 °F at 7:00 AM and 43 °F at 10:00 AM when we conducted the research.

In this case study, we tested 3 different factors, flight patterns, camera angles, and overlap of images. Due to the complexity of this study, we tested vertical grid (parallel to north-south direction), horizontal grid (parallel to east-west direction) and their combination mesh grid in the area for flight patterns factor, 90 degrees (facing the ground) and 45 degrees (to the horizon) for camera angle factor, and 90% and 85% for the overlap of images. Table 2 shows the 8 flight configurations that were implemented in this study

In table 2, Number of calibrated images indicates how many images were calibrated to create 3D mapping. The pictures which were not calibrated and did not match with other images did not contribute to the creation of 3D points and meshes. 2D key points features were extracted from images by using SIFT or SURF as was explained in the research method above. 3D points were matched to 2D key points and indeed contributed to the creation of 3D models. The reprojection error referring to the image distance between a projected point and a measured one was introduced to quantify how closely an estimate of a 3D point recreates the point's true projection.[14]

Table 2. Summary of different flight configuration

Session	Flight Pattern	Camera Angle	Front Overlap	Side Overlap	Number of Calibrated Images	Number of 2D Key points Observations for Bundle Block Adjustment	Number of 3D Points for Bundle Block Adjustment	Mean Reprojection Error [pixels]	Abbreviation
1	Horizontal Grid	45	90	65	505 out of 512 images calibrated (98%)	418410	121473	0.208	45-h
2	Vertical Grid	45	90	65	590 out of 592 images calibrated (99%)	490601	142500	0.209	45-v
3	Complete Mesh Grid	45	90	65	1099 out of 1104 (99%)	935059	274080	0.198	45-com
4	Complete Mesh Grid	45	85	65	884 out of 887 images calibrated (99%)	734397	224810	0.191	45-com-85
5	Horizontal Grid	90	90	65	539 out of 651 images calibrated (82%)	237600	77236	0.205	90-h
6	Vertical Grid	90	90	65	560 out of 644 images calibrated (86%)	214038	70300	0.216	90-v
7	Complete Mesh Grid	90	90	65	946 out of 1295 images calibrated (73%)	371617	123600	0.207	90-com
8	Complete Mesh Grid	90	85	65	720 out of 1040 images calibrated (69%)	263227	90663	0.195	90-com-85

4 Result and Discussion

Two cases for comparison were created for each flying session as demonstrated on Table 2. One was facing doors and windows and the images were captured by a camera from a fixed location on the ground as shown in Figure 4 (a). The left image was a rendered image, and the right one was a camera captured image. Therefore, there was only one scenario for doors and windows.

For the other case the flight acquired data facing the roof with 90 degrees and 45 degrees camera angles. The camera captured images were direct bird view images. Two 3D models were reconstructed with all 90-degree images and all 45-degree images, each of those two models produced four rendered images two with 90-degrees and two with 45-degrees by the use of model based virtual cameras. The two 90-degree rendered images from models were compared to a 90-degree camera captured image and the same was done for the 45-degree rendered images from models. Due to the camera angle, the visual perception of the camera captured images was totally different between 90 degrees and 45 degrees. This was also the reason for the cross comparison of both scenarios. The images shown in Figure 4, (b) is for 45 degrees camera, while (c) is for 90 degrees camera. The left ones are rendered images and the right ones are camera captured pictures in both (b) and (c). The rendered images in (b) and (c) are both from a model reconstructed from all 45-degree images. A comparison of two rendered images from a model reconstructed using all 90-degree images with two camera captured images were also conducted, but they are not shown here.

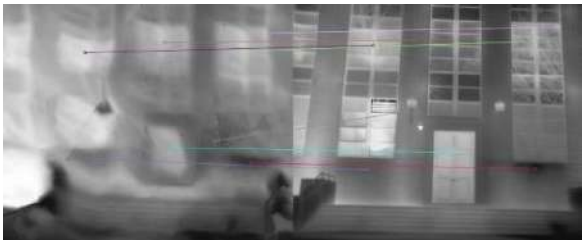

(a) Comparison of façade case

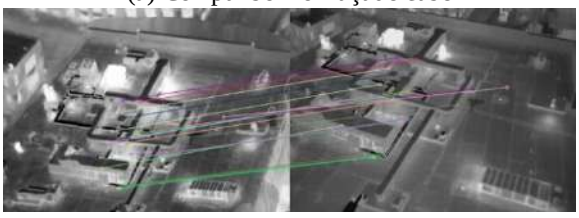

(b) Comparison of roof system case – 45-degree scenario

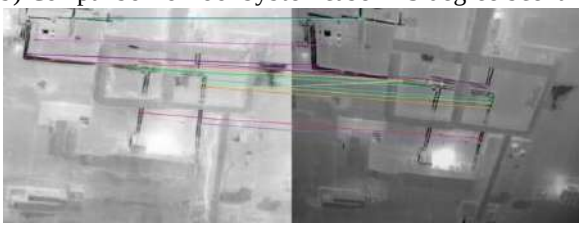

(c) Comparison of roof system case – 90-degree scenario

Figure 4. Illustration of match points between

camera captured pictures and rendered pictures

In Figure 4, the solid lines illustrate the match points between rendered images and captured images. Match points, MSE, and SSIM were calculated and plotted in Figure 5. The legend in Figure 5 refer to the *abbreviations* on table 2. Average and standard deviation of flying session 1-4 and flying session 5-8 in different comparisons are calculated and shown on the top bar charts. According to Figure 5 (a), two roof system scenarios created more numbers of match points than door and windows scenario. As for those two roof system scenarios, a model reconstructed by a flight camera angle of 45 degrees can create more numbers of match points in its rendered images than a model generated by a flight camera angle of 90 degrees can in both scenarios. Average numbers of match points in 90-degree and 45-degree rendered images from a model with a flight camera angle of 45 degrees (session 1-4) are 958.250 and 1055.250 calculated based on the captured images taken by a 90-degree camera and on a 45-degree camera respectively, while those numbers are 547.500 and 706.500 in rendered images from a model with a flight camera angle of 90 degrees (session 5-8). More match points indicate that rendered images have a better performance in terms of capturing control points. To test color rendering performance and structure similarity performance, MSE and SSIM are introduced in Figure 5 (b) and (c). According to Figure 5 (b), rendering images from a model with a 90-degree flight camera angle (session 5-8) performed worse than rendering images from a model with a 45-degree flight camera angle (session 1-4) in all scenarios in terms of capturing color information, because they had higher MSE scores. In Figure 5 (b), the session *"45-h"* where the flight camera angle was 45 degree, and the flight pattern was horizontal obtained a rendering image in façade scenario whose MSE was 3497.17159. This abnormal score is bigger than the average score plus standard deviation which should be considered an outlier. In Figure 5 (c), rendered images from a model reconstructed by all images with a 90-degree flight camera angle performed better than rendered images from a model with a 45-degree flight camera angle in both two roof system scenarios because of the higher SSIM scores. However, it was entirely different in scope for façade scenarios. Rendering images from a model with a 45-degree flight camera angle obtained 0.641 for average score of all flight patterns, which is higher than 0.593 average score obtained by rendering images from a model with a 90-degree flight camera angle.

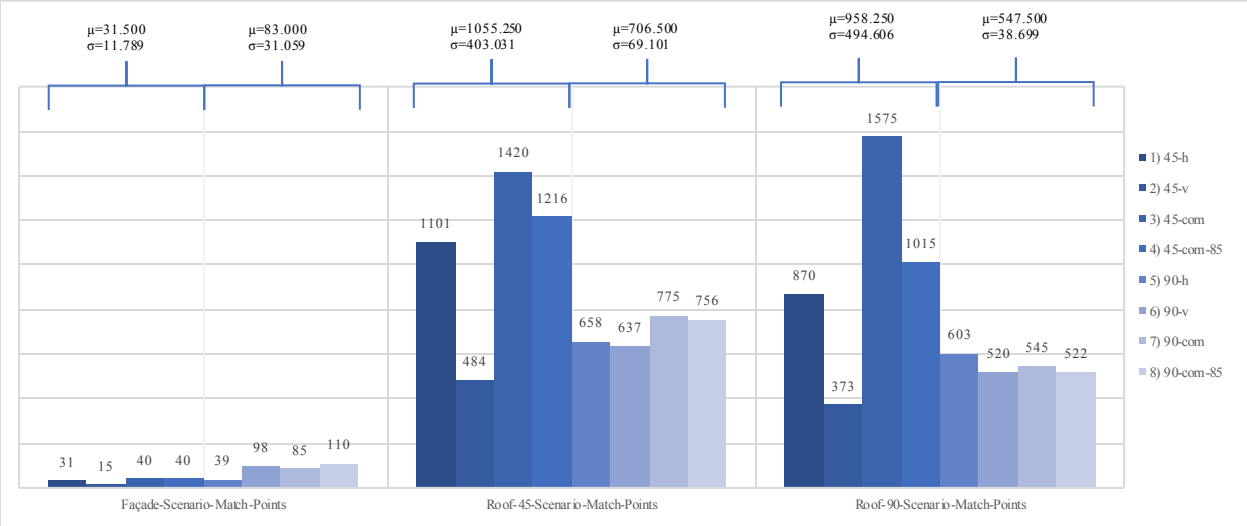

(a) Key points

Figure 5. Statistics of match points, MSE, and SSIM for different flying configurations

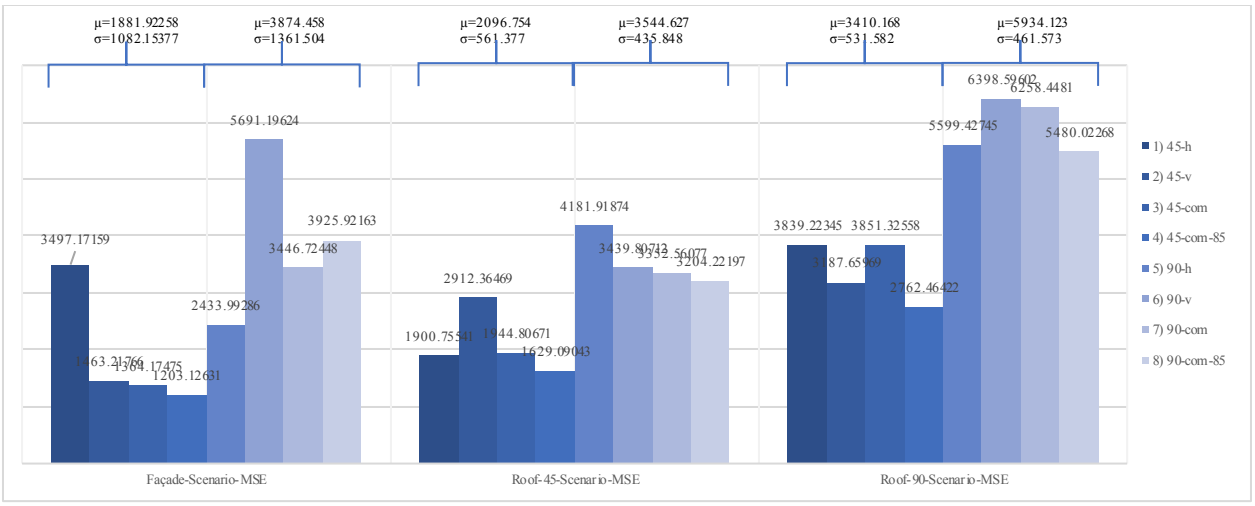

(b) MSE

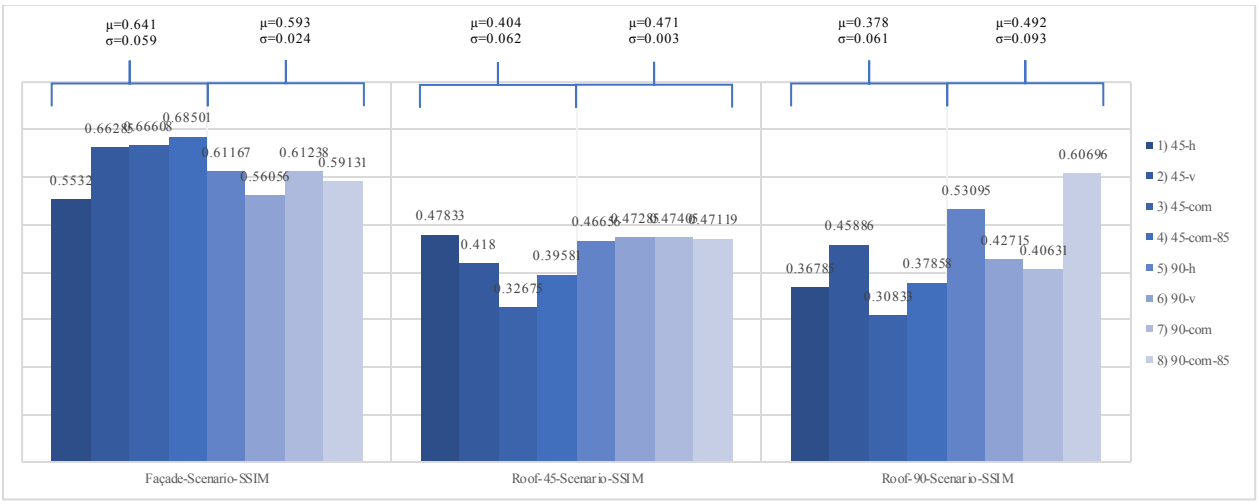

(c) SSIM

Figure 5. Statistics of match points, MSE, and SSIM for different flying configurations (continued)

Not only can flight angles have an influence on the performance, but also the flight patterns and the image overlaps. According to Figure 5 (b) and (c), mesh grid flight patterns can result in lower MSE and higher SSIM than a monotonous grid which can only have vertical or horizontal lines. However, as for the image overlaps, in this study, higher image overlaps (90 %) not always performed better than lower image overlaps (85%). More thermal images do not contribute to a better reconstruction of a 3D thermal model. Some thermal images cannot be calibrated and matched to each other. Observation in Figure 6 also confirmed this statement. There are holes on the roof system in a point cloud model no matter how much the images overlap. Different types of roof systems have different influences on performance. As the pix4D software manual mentioned, water surfaces, snow, and sand have almost no or little visual content due to its large uniform areas. Roofs of buildings may have versatile color in RGB images but may have monotonous thermal values, which means the color of roofs will be monotonous in thermal images. Those large uniform areas can result in a sparse point cloud model. Shown in Figure 6, there was some equipment on the left roof in Figure 6 (a). Thus, sufficient points could be created. However, less points could be created on the right roof in Figure 6 (a). Figure 6 (b) is a mesh model fitted from a point cloud model.

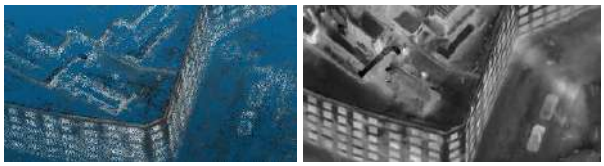

(a) (b)

Figure 6. Thermal point cloud model and mesh model

5 Conclusions

UAS has been introduced into a great number of research fields. It also has been utilized to capture energy loss from a single building. However, to audit energy loss from a group of buildings in a district and to create a 3D thermal model for infrastructure use are still challenges in terms of the efficiency and performance. Methodologically, different drone flying configurations in terms of flight patterns (vertical grid, horizontal grid and mesh grid), camera angles (90 and 45 degrees), and the percentage of image overlap (90% and 85%) were tested over a group of buildings in a district in this study.

Empirically, a flight camera angle of 90 degrees could capture more details on the roof system, whereas a flight camera angle of 45 degrees is more suitable for capturing details on façades. Also, more images could obtain a perfect 3D model. According to the result in this study, A flight angle of 90 degrees does exceed a flight angle of 45 degrees on roof case, and a flight angle of 45 degrees outperform a flight angle of 90 degrees on façade case in terms of structure similarity performance. As for color rendering, a flight angle of 90 degrees has a disappointing performance in both roof and façade cases. Indeed, mesh flight patterns are suggested over single grid patterns. As for the overlap of images, more thermal images might introduce more outliers. The algorithms can have difficulties in reconstruction. Additionally, no matter how many images are utilized, it is hard to create a 3D thermal model for a flat roof system which has large uniform areas. If both RGB and thermal images can be captured from the same angles and altitude, a detailed 3D model can be created by high resolution RGB images, and thermal textures can then be projected on top of the 3D model. This is the next factor's influence on efficiency and performance 3D Thermal Mapping we plan to explore.

Reference

[1] O. Friman *et al.*, "Methods for Large-Scale Monitoring of District Heating Systems Using Airborne Thermography Methods for Large-Scale Monitoring of District Heating Systems using Airborne Thermography," vol. 52, no. 52, pp. 5175–5182, 2014.

[2] S. Zhou, Z. O'Neill, and C. O'Neill, "A review of leakage detection methods for district heating networks," *Appl. Therm. Eng.*, vol. 137, no. April, pp. 567–574, 2018.

[3] P. A. Fokaides and S. A. Kalogirou, "Application of infrared thermography for the determination of the overall heat transfer coefficient (U-Value) in building envelopes," *Appl. Energy*, vol. 88, no. 12, pp. 4358–4365, 2011.

[4] E. Barreira, R. M. S. F. Almeida, and J. M. P. Q. Delgado, "Infrared thermography for assessing moisture related phenomena in building components," *Constr. Build. Mater.*, vol. 110, pp. 251–269, 2016.

[5] E. Lucchi, "Applications of the infrared thermography in the energy audit of buildings: A review," *Renew. Sustain. Energy Rev.*, vol. 82, no. May 2017, pp. 3077–3090, 2018.

[6] T. Rakha and A. Gorodetsky, "Review of Unmanned Aerial System (UAS) applications in the built environment: Towards automated building inspection procedures using drones," *Autom. Constr.*, vol. 93, no. January, pp. 252–264, 2018.

[7] A. Kylili, P. A. Fokaides, P. Christou, and S. A. Kalogirou, "Infrared thermography (IRT) applications for building diagnostics: A review," *Appl. Energy*, vol. 134, pp. 531–549, 2014.

[8] E. Lucchi, "Applications of the infrared thermography in the energy audit of buildings: A review," *Renew. Sustain. Energy Rev.*, vol. 82, no. November 2017, pp. 3077–3090, 2018.

[9] M. Fox, S. Goodhew, and P. De Wilde, "Building defect detection: External versus internal thermography," *Build. Environ.*, vol. 105, pp. 317–331, 2016.

[10] R. Bai, J. Zhao, D. Li, and W. Meng, "A new technique of camera calibration based on X-target," *Commun. Comput. Inf. Sci.*, vol. 97 CCIS, no. PART 1, pp. 39–46, 2010.

[11] J. L. Schonberger and J.-M. Frahm, "Structure-From-Motion Revisited," *IEEE Conf. Comput. Vis. Pattern Recognit.*, 2016.

[12] FLIR Systems, "An informative guide for the use of thermal imaging cameras for inspecting buildings, solar panels and windmills. THERMAL IMAGING GUIDEBOOK FOR BUILDING AND RENEwABLE ENERGy APPLICATIONS Content," *Guid B.*, p. 68, 2011.

[13] Massachusetts Department of Public Health, "105 CMR 410.000: Minimum Standards of Fitness for Human Habitation (State Sanitary Code, Chapter II)," *J. Exp. Psychol. Gen.*, vol. 136, no. 1, pp. 23–42, 2007.

[14] H. Richard and A. Zisserman, *Multiple View Geometry in computer vision*. Cambridge University Press, 2003.

Evaluating the Performance of e-Construction Tools in Highway Resurfacing Projects

D.G. Patel [a], R. Sturgill[b], G.B. Dadi[a], and T.R.B. Taylor[a]

[a]Department of Civil Engineering, University of Kentucky, United States
[b]Kentucky Transportation Center, University of Kentucky, United States
E-mail: dgpa223@uky.edu, roy.sturgill@uky.edu, gabe.dadi@uky.edu, tim.taylor@uky.edu

Abstract -

Interest in integrating E-construction in highway construction projects has increased in recent years due to reductions in staffing and resources across Departments of Transportation (DOTs) and initiatives from the Federal Highway Administration (FHWA). Specifically, the addition of e-construction methods offers a boost in efficiency and safety in highway resurfacing jobs. E-ticketing, Paver Mounted Thermal Profiling, and Intelligent Compaction were incorporated on resurfacing projects in the state of Kentucky. Using GPS and GIS technology tied with electronic report-out systems, a fleet tracking system traces haul routes, travel times, and tonnage. The addition of paver mounted thermal profilers that allow for remote monitoring of temperatures, and intelligent compaction offers the ability to monitor roller patterns and track the overall compaction effort. The contribution of this manuscript is to document recent advancements, lessons learned, and evaluate their effectiveness compared to traditional inspection practices. Future work discussed include the possibility of combining these technologies into a singular interface for easier integration into the industry.

Keywords –

E-Construction; E-Ticketing; Paver Mounted Thermal Profiling; Intelligent Compaction

1 Introduction

Ground-breaking technological advancements over the past decades have drastically changed individuals' lives. Today, gadgets such as smart phones, personal computers, and tablets are providing a wide range of services in an economical and efficient manner. Industries around the world have made significant changes to adopt to these technologies to improve efficiency and safety, and reduce operating costs. The highway construction industry in the United States has been slower to adopt technology and thus opportunities to improve efficiency and safety in its operations exist. In addition, the industry is facing staffing reductions both in the field and management levels. The labor force is decreasing partially due to a cultural change of young adults wanting higher education and desiring white-collar jobs. Management staffing is seeing a reduction because people are being pulled by the booming private construction industry. Due to the staffing reductions, DOT personnel are being forced to do more work with fewer resources. A study produced by the National Cooperative Highway Research Program (NCHRP) reported that, "DOTs are managing larger roadway systems with fewer in-house staff than they were 10 years ago. For the 40 DOTs that responded to the survey, between 2000 and 2010 state-managed lane-miles increased by an average of 4.10%, whereas the number of full-time equivalents (FTEs) decreased by 9.68% [1]."

The Federal Highway Administration (FHWA) and Departments of Transportation (DOTs) are looking to incorporate e-Construction practices and advanced technologies into their workforce to improve overall efficiency and reduce workload on the personnel. E-Construction is defined as "The creation, review, approval, distribution, and storage of highway construction documents in a paperless environment [2]." These processes can include electronic submission and approval of documents, and real-time management of documents through electronic devices [2]. E-Construction has been heavily promoted by the FHWA through the Every Day Counts (EDC) model that looks to rapidly deploy proven yet underutilized innovations in the highway construction industry [3]. E-Construction was first promoted in EDC-3 in the year 2013, and since then, many DOTs have collaborated to share their e-Construction practices through webinars and peer exchange reports [2]. The addition of e-Construction and other advanced technologies can help maintain high quality and service in highway construction.

One specific area of the industry that can be drastically improved through the addition of technology is asphalt paving inspections. The collection of delivery tickets, monitoring of pavement temperatures, and

tracking roller operations all fall under this activity, and is typically done by a DOT inspector. This crucial activity that can impact the long term performance of the pavement is often given little attention due to insufficient staffing levels, and the DOT inspectors having to cover multiple projects at once due to the short paving windows. Incorporating technologies such as e-Ticketing, Paver Mounted Thermal Profiling, and Intelligent Compaction can assist the inspectors improve productivity and document project records.

The three technologies discussed herein have been promoted by many DOTs and were recently tested in two pilot projects by the Kentucky Transportation Cabinet. The goal of this manuscript is to document the results, discuss the lessons learned for industry practitioners, and discuss the possibilities of combining these separate technologies into a singular interface for easier use and integration into the industry.

2 Background

Two resurfacing projects in the state of Kentucky were chosen as pilots to evaluate the effectiveness of the technologies. The study was coordinated with the Kentucky Transportation Cabinet (KYTC) District 7's staff to use the technology complimenting the typical duties of the inspectors. Although a typical highway resurfacing job includes many activities such as traffic control, plant operations, milling, paving, striping etc. For simplicity and a better control of the study, the focus is solely on the paving operations which included ticket handling, tracking mat temperatures, and monitoring roller operations. The data collection during the study included ticket receipt and acceptance; tracking theoretical tonnage; monitoring asphalt temperatures behind the paver, in the screed, and in the hopper; and tracking temperatures at breakdown and roller passes. The data collection was completed both through the traditional manner and through the technologies. The traditional manner included collecting data the way that the inspectors would traditionally. Simultaneously, the same data was collected using the technologies that were being tested during the pilots. The results were then compared for accuracy of the technology data, and the time savings that come with incorporating technology.

2.1 Electronic Ticketing (E-Ticketing)

The process of manually collecting delivery tickets from delivery trucks is an outdated practice that exposes the inspectors to many safety hazards. Whether it is walking adjacent to traffic, climbing the side of the trucks to collect the tickets, or working near moving equipment, the inspectors face many safety challenges while conducting this simple task that can easily be computerized. E-ticketing technology exists that can collect the same information electronically allowing for inspections that are safer and more efficient.

E-Ticketing was promoted by the FHWA in the EDC-4 model as an e-Construction method that can be collaborative and mutually beneficial to both the contractor and the DOT [2]. Additionally, the technology was initially successfully incorporated in highway construction by IowaDOT. In 2015, IowaDOT began the transition to have a completely paperless construction management operation to improve efficiency. The agency used GPS and GIS technologies to trace haul routes, report yield tonnages, and record travel times [4]. In 2016, Iowa achieved a major milestone of 100% paperless processes on a construction project [4]. The implementation of e-Ticketing can be a significant time saver, as it can provide a way for the inspectors to track material deliveries remotely from a safe location.

2.2 Paver Mounted Thermal Profiler

Traditionally, highway construction inspectors have used hand-held infrared thermal cameras/guns to ensure proper pavement temperatures and to identify isolated areas in the mats [5]. Paver mounted thermal profilers provide real time tracking of the temperatures of the entire mat. An infrared temperature monitoring system can be installed on the back of the paver capable of providing a continuous record of mat temperatures throughout the project [5].

This technology has been used by DOTs across the country, and Texas was an early adopter. In 2012, TxDOT implemented Pave-IR as a standard test method into its HMA specifications [6]. The current specification requires the contractor to use a "thermal imaging system" as defined in test procedure Tex-244-F in the Standard Specifications for Construction and Maintenance of Highways, Streets, and Bridges [7]. Thermal imaging has also been promoted by the FHWA as a technology to enhance quality control on asphalt pavements [8]. This technology provides a way to track the mat temperatures in real time, on site and remotely, allowing more efficient inspections and the ability to inspect multiple projects concurrently.

2.3 Intelligent Compaction

Intelligent compaction (IC) technology is available to improve quality control during the compaction phase of paving projects. IC rollers are equipped with GPS devices, infrared temperature trackers, accelerometers, and on-board LED screens that display roller movement in real time. These devices track roller movements, temperatures at breakdown, and record the Intelligent Compaction Measurement Values (ICMV) [9]. Currently, two forms of IC rollers are available in the industry. The Original Engineering Manufacture (OEN) is installed

directly from roller vendor's factory, whereas the IC retrofit can be installed on select roller models [9].

From 2008 to 2010, 13 DOTs participated in a FHWA, Transportation Pooled Fund (TPF) study that tested and evaluated IC technologies in multiple field pilots [10]. The results of the study showed that IC can be an effective way to track roller passes, and asphalt surface temperatures [10]. Being able to track the roller passes and temperatures can assist the roller operators to improve uniform compaction of the mat. Additionally, the technology enriches projects records for the DOTs to look at if pavement defects are noticed during the life cycle of the road.

3 Methodology

3.1 E-ticketing

E-ticketing technology works during the construction phase of a project to improve project efficiency and safety by going paperless. For the two pilot projects, EarthWave Technologies based out of Indianapolis, IN were contracted to set up an e-Ticketing system. EarthWave provided GPS transponders for all equipment that was to be used during the projects. All transponders could be tracked on EarthWave's online system called FleetWatcher. Additionally, this interface allowed all parties to view delivery tickets electronically, and view cycle times during operations.

A Geo-Fence called a Static GeoZone around the perimeter of the project site and a smaller Geo-Fence around the paver and haul trucks called a Mobile GeoZone were established by the contractor. When the GPS transponders entered or exited the static GeoZone, the system showed that as the trucks entering or leaving the project site, which could be used to control deliveries and reduce wait times in front of the paver. When the GPS transponders entered or exited the mobile GeoZone, the system showed that as the time at which the load was dumped from the truck into the paver.

Each e-ticket would have the same crucial information that is found on traditional tickets such as: Ticket Number, Ticket Data/Time, Material Name, Cumulative Tons, Net Tons, and Dump Coordinates. All e-Tickets for the project could be accessed on the FleetWatcher website, and in the field through the FleetWatcher app.

Throughout the projects, the traditional tickets were collected by the inspectors, and the ticket information was recorded in the field along with the time it took to retrieve the individual tickets. The same information was then retrieved from FleetWatcher, and the time required for this activity was also recorded. The conventional and the technology information was then compared for data accuracy and time savings.

In addition to measuring the accuracy of the data and time savings, electronic tickets can be used to calculate theoretical tonnages in a more efficient and safe manner. The theoretical tonnage is a crucial calculation that the inspectors perform to estimate the amount of asphalt mix that should be used over a certain paved distance. This value is then compared to the cumulative tons given on the delivery tickets to confirm if the crews are paving according to the specifications, and to ensure that material is not being wasted along the process. The theoretical tonnage calculation is given be Equation 1:

$$Theoretical\ Tonnage(tons) = Mix\ Density\left(\frac{lb.}{sy.in.}\right) \times Pavement\ Thickness(in.) \times \frac{1(sy.)}{9\ (sf.)} \times Pavement\ Width(ft.) \times Pavement\ Length\ (ft.) * \frac{1\ (ton)}{2000(lb.)} \quad (1)$$

In Equation 1, the pavement length is calculated from the dump coordinates on the e-Tickets. To calculate the theoretical tonnage, the distance between a dump location and the starting point, or between two dump locations is estimated using the "measure" tool in Google Earth. This distance is then used in Equation 1, along with the other factors which are found in the specifications to estimate the yield tons for the paved surface. This value can then be compared to the cumulative tons delivered to track project productivity.

3.2 Pave-IR

As mentioned previously, the Pave-IR system provides real time temperature tracking of the entire mat. For the pilots, MOBA Automation installed thermal cameras on the back of the pavers to track the mat temperatures at placement. Unfortunately, due to communication issues between the contractor and the technology vendor, no cameras were placed over the hopper, or the screed to track the temperatures of the dumped load. The installed infrared cameras displayed the mat temperatures in real time on LED screens mounted on the pavers for the crews to look for cold spots and take immediate measures if necessary. Additionally, the thermal recordings of the mat are directly uploaded to a MOBA Cloud, or they are stored on a USB storage drive for remote areas without sufficient cellular signals.

For the study, the mat temperatures at various locations were recorded using a temperature gun periodically throughout the projects. Following project completion, the same thermal recordings were retrieved from the MOBA Cloud, and the manually recorded temperatures were compared to the Pave-IR temperatures to assess the accuracy of the data. This technology allows the inspectors to monitor and inspect paving projects remotely and cover multiple projects at the same time in

an efficient manner. Additionally, this allows the DOTs to review pavement temperatures at a later date if failures are noticed on the road.

3.3 Intelligent Compaction

Prior to the pilot projects, Sitech Solutions were contracted to setup an Intelligent Compaction system for the study. Two breakdown rollers were retrofitted with the Intelligent Compaction technology that could track roller movements, temperatures at breakdowns, and record the ICMV. A LED screen mounted on the roller shows real time tracking of roller passes which can assist the roller operator achieve uniform compaction of the entire mat.

During the pilots, the roller movement and the temperatures at breakdown were tracked periodically by the inspector to ensure proper compaction. The IC system on the roller, recorded the same information electronically and displayed it on Sitech's web-interface called VisionLink. This system displays information such as, temperatures, roller passes, and ICMV on a GIS-based map. Following project completion, manual data and IC data was compared for accuracy. IC provides similar benefits to Pave-IR in that it allows the inspectors to cover multiple projects at once, and it provides continuous project record to review if a failure is noticed in the pavement.

4 Results

4.1 E-ticketing

When comparing the accuracy of the data collected electronically by FleetWatcher to the traditional tickets, it was found that the data aligned perfectly for following categories: Truck Number, Mix Design, Ticket Number, Net Tons, and Cumulative Tons. A small sample of the collected data is shown in Table 1 where the "conventional" data was gathered from physical tickets, and the "technology" data was recorded through FleetWatcher. Although Table 1 shows a small sample of data collected during a single shift of one project, it is representative for all 75 load delivery tickets.

Improving inspector safety was one of the main driving factors behind conducting this study. As mentioned earlier, highway construction inspectors face many hazards while collecting delivery tickets. Activities such as walking adjacent to traffic, climbing the side of dump trucks, and working next to heavy equipment exposes the inspectors to unnecessary risks. The data from the projects shows that the time to acquire the traditional tickets was significantly longer than through FleetWatcher. Additionally, data retrieval through e-ticketing could be done in a safe environment away from the hazards. During this shift, a total of 19 tickets were collected from delivery trucks. It took the inspector approximately 54 minutes to collect the 19 paper tickets. In comparison, the same data was retrieved from FleetWatcher in just 18 minutes. Additionally, the data from FleetWatcher was retrieved in the inspector's truck, which eliminated the hazards from physically collecting paper tickets.

E-Ticketing provides a way to calculate theoretical tonnages in a more safe and efficient manner. It is important to note that the calculated theoretical tons rarely match with the cumulative tons delivered to the project site due to the many errors and uncertainties that are present in construction projects. However, huge differences between the values can indicate that the pavement is too thin, too thick, or material loss along the process. Several theoretical tonnage calculations were performed using the dump coordinates recorded by FleetWatcher, and the information given in the specifications. Table 2 shows the results of the calculations. Many accurate estimations were calculated throughout the study, and the KYTC inspectors assigned to the projects confirmed that the theoretical tonnages calculated followed the trends noticed in the field.

To further investigate differences, a theoretical tonnage was calculated for each load delivery and compared to the values on the ticket. With the

Table 1. Data Alignment, Date: 07/05/2018

Data	Truck Number	Mix Design	Ticket Number	Net Tons	Cumulative Tons
Conventional	CB25	CL4.S.38 A 76	868794	25.72	51.30
Technology	CB25	CL4.S.38 A 76	868794	25.72	51.30
Conventional	PR10	CL4.S.38 A 76	868807	26.06	103.48
Technology	PR10	CL4.S.38 A 76	868807	26.06	103.48
Conventional	H98	CL4.S.38 A 76	868811	25.30	155.13
Technology	H98	CL4.S.38 A 76	868811	25.30	155.13

Table 2. Theoretical Tonnage

Date	Approx. Dist. (ft.)	Lane Width (ft.)	Thickness (in.)	Density (lb./Sy.In.)	Theoretical Tons	Cumulative Tons
7/2/2018	3205.49	14	1.25	110	342.81	381.60
7/3/2018	3219.49	14	1.25	110	344.31	358.88
7/6/2018	7634.74	14	1.25	110	816.49	801.26
7/7/2018	6954.59	14	1.25	110	743.79	754.44

Table 3. Paired Samples T-Test

Pair	Mean	Std. Deviation	Std. Error Mean	t	df	p(2-tailed)
Theoretical - Actual	-0.710	20.810	2.403	-.296	74	0.768

corresponding nature of the data, a paired samples t-test will unveil whether there are any statistical differences between the theoretical and actual ticket loads. The results of the paired samples t-test are reported in Table 3. The null hypothesis of a paired samples t-test is that the true mean difference is zero with the alternative hypothesis being that the true mean differences are not zero. The high p-value of 0.768 indicates that the null hypothesis cannot be rejected and that the true mean difference is zero. Practically speaking, there is no significant difference between the theoretical and actual ticket tonnage. Thus, while differences are expected from a variety of error sources, the theoretical tonnage calculation embedded in the e-ticketing software is effective at reporting accurate quantities for these projects.

4.2 Pave-IR

Utilizing Pave-IR proved to be an effective way of tracking pavement temperatures throughout the projects. During the paving operations, it was noticed that the real time display of mat temperatures on the LED screens allowed the crews to quickly patch any cold spots that were noticed. Concerning data accuracy, it was found that the temperatures that were physically collected during the operations using an infrared gun were well aligned with the temperatures recorded using Pave-IR. Figure 1 is a screen shot of the Pave-IR interface that shows a continuous recording of mat temperatures throughout the paving operations. Table 4 provides the field recorded temperatures and the Pave-IR temperatures, and it can be seen that the percent differences between the two methods are almost insignificant. Although the Pave-IR data shown here is a small sample, it is representative of the data collected across the two pilots for the study.

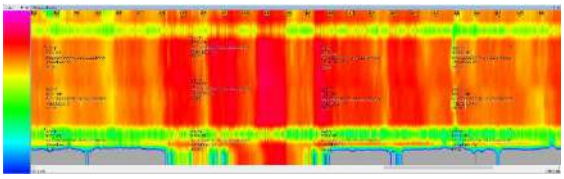

Figure 1. Pave-IR Interface

In addition to data accuracy, retrieving data from Pave-IR was much more efficient and eliminated the need for the inspector to be physically present at the project site. Project records were improved through Pave-IR as well since it provided an electronic cloud storage of the data in comparison to the traditional method where the temperatures were written down in inspector notes.

4.3 Intelligent Compaction

Of the three technologies tested during the study, Intelligent Compaction was the least successful in terms of data accuracy and improving project efficiency. Poor

Table 4. Temperature Alignment, Date: 07/02/2018

Data	Lat.	Long.	Avg. Mat Temp (◦F)	Percent Difference (%)
Conventional	38.403	-84.567	297.33	0.78
Technology	38.403	-84.566	299.67	
Conventional	38.0417	-84.567	290.00	1.78
Technology	38.042	-84.567	295.27	
Conventional	38.0396	-84.570	293.00	1.12
Technology	38.04	-84.570	296.33	

communication between the parties lead to no data being collected for one of the pilots. The data that was collected by the IC rollers did not align with the manually recorded data. Figure 2 is a screen shot of the temperature data displayed on VisionLink. It shows that over 95% of the temperatures at breakdown were below 200ºF. Figure 3 shows the manually recorded temperatures at breakdown. It can be seen that the actual temperatures were between 200-250ºF or above 250ºF. The data range on VisionLink was customized to provide a better visual understanding through the screenshot. The average temperature at breakdown captured through IC was approximately 160ºF.

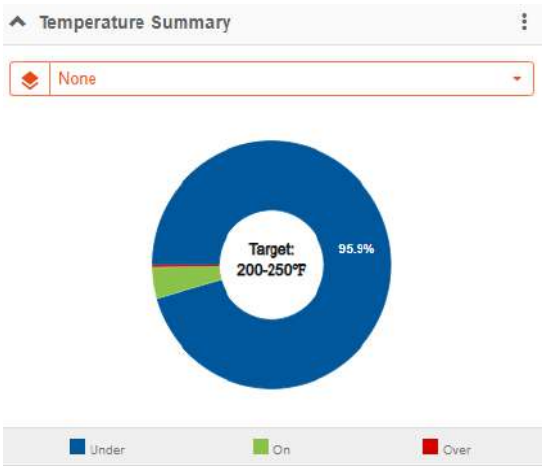

Figure 2. Temperature Summary, VisionLink

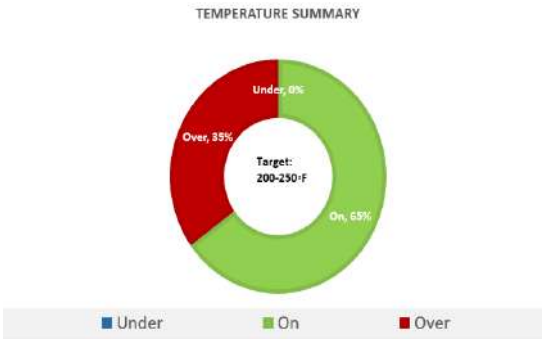

Figure 3. Temperature Summary, Manual

Inconsistent results were also noticed when comparing the roller pass counts between the IC and manually collected data. Figures 4 and 5 respectively show the pass count data as displayed on VisionLink, and the manually recorded pass counts. Similar to the temperatures, the pass counts recorded by IC were also significantly lower than what was noted in the field.

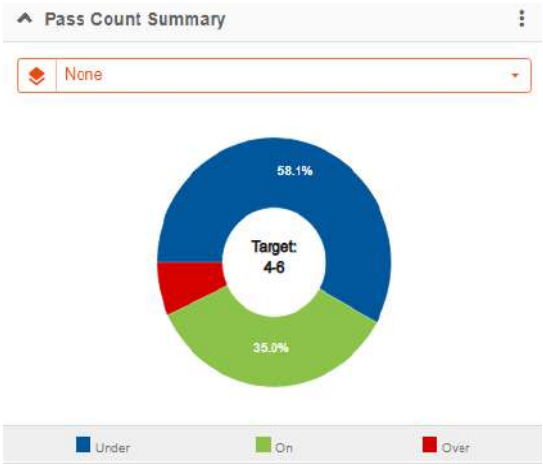

Figure 4. Pass Count Summary, VisionLink

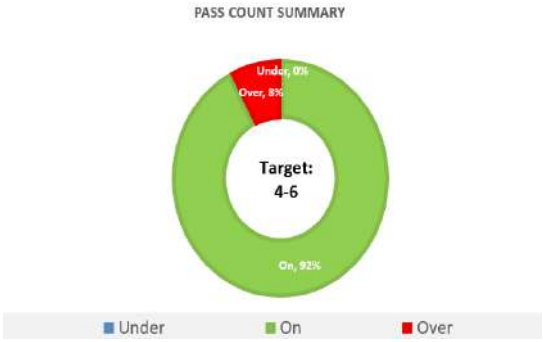

Figure 5. Pass Count Summary, Manual

Although Intelligent Compaction did not perform up to the expectations during this study, it has proved to be useful in other cases. The inconsistent data collected by the technology could have been caused by improper setup of the technology, miscommunication between the parties, and many other uncertainties that are present during construction projects.

5 Lessons Learned

The technologies discussed in this manuscript are still relatively new in the highway construction industry and the case study revealed many important lessons to take away for future use. First thing to note about all three technologies is that the most important step is to ensure that all aspects are setup prior to the project starting. There were many issues encountered throughout the project that showed lack of preparation by both the contractor and the technology vendors.

One major issue encountered with the e-ticketing technology was the setup of the Static GeoZone. As discussed previously, the purpose of this GeoZone was to record the time when the trucks arrived at the project site, in order to reduce wait times. However, the contractor

failed to setup the GeoZone around either of the project sites and therefore no data was recorded in this category. Another crucial issue encountered with e-ticketing was that some of the trucks being used for deliveries did not have GPS transponders installed. Without the GPS transponders, the mobile GeoZone could not be utilized and thus dump times for those trucks were not recorded.

Regarding the paver mounted thermal profiler, the contracts stated that infrared cameras were to be setup on the paver, on top of the hopper, and on top of the screed. However, only the back of the paver cameras were successfully installed for both of the pilots. This was a huge loss for the study because seeing the temperatures in the hopper and screed could be one way to monitor effective workflows and future pavement failures. Further, the technology vendor was unsuccessful in providing access information for the online MOBA interface to the stakeholders prior to project startup, which delayed data analysis.

Finally, Intelligent Compaction had the most issues during the pilot projects. Lack of communication between the parties led to no IC data being collected from one of the pilots. The data that was retrieved was not consistent with the field findings. The contractor played a part in this due to the rushed schedule of the project, and the lack of transparency with the other stakeholders.

In general, most of the issues encountered during this study could have been solved easily through having open communication between the parties. If used properly, these technologies can benefit all stakeholders involved in the projects, but the parties must be willing to collaborate and change their attitudes towards technology to take full advantage of these tools.

6 Future Work

Veta is a standardized software for the use and analysis of Intelligent Compaction and Infrared (IR) technologies. This map-based tool can be used to view and analyze geospatial data that can be imported from IC machines and MOBA, Pave-IR scanners. This software is required in the AASHTO PP81-70 specifications and most DOT IC specifications. Additionally, Veta has been promoted by the pooled fund study TPF-5 (334) "Enhancements to the Intelligent Construction Data Management System (VETA) and Implementation." The goal behind this pooled fund study is to "provide a platform for states to engage in discussions and to share information to assist with moving these technologies to the next levels [11]." The collaboration and funding between 16 DOTs from the pooled fund is continuously enhancing the VETA software for easier implementation into the industry.

Although, this tool provides a great, singular platform to analyze IC and IR data, it has yet to incorporate e-ticketing. Having a fleet tracker and electronic documentation system would allow VETA to be the ideal software for tracking paving projects. Having a singular software that tracks all three technologies, would increase accessibility, and ease of use. The three technologies combined can have a tremendous impact on highway construction projects in the United States by boosting project efficiency and safety of the highway inspectors. Finally, contractors and equipment vendors would be more open to incorporating these technologies if they only have to manage one system rather than three different technologies.

7 Conclusions

According to the comparisons between the manually collected data and the electronic data, the technologies shows great potential in improving the efficiency of paving projects and improving project safety. For e-ticketing, and Pave-IR the results support the accuracy of the data as well as the time savings that come with the incorporation of technology into the work place. Although Intelligent Compaction did not perform up to the expectations for this particular case study, it has been successfully used by other DOTs and has shown great potential in improving project records and efficiency of roller operations.

This manuscript presents the application of three technologies which, if used properly can result in much safer and efficient paving projects. Having a strong and healthy culture of collaborating and partnering would significantly help further implement these technologies in the highway construction industry. E-ticketing can eliminate paper, enhance project records for all stakeholders and maintain safer projects. Pave-IR can increase the life of the pavement by providing instant detection of cold spots during the paving operations and also reducing maintenance costs. Lastly, Intelligent Compaction shows great potential of improving project records, and increasing pavement life by allowing consistent compaction during construction. Combining these technologies into a singular interface where all stakeholders can monitor project progress, and store project records will allow further implementation of technology in highway construction.

As the industry faces personnel reductions and resources, technologies such as the ones discussed here will have to be utilized as they offer a way to maintain quality and service on paving operations.

8 Acknowledgements/Disclaimer

The authors wish to thank the Kentucky Transportation Cabinet and its contractors, and the Kentucky Transportation Center for funding this work

under KYSPR 18-554. Any mention of technology providers/vendors/manufacturers in this manuscript is strictly for informative purposes only and not intended to be an endorsement by KYTC, KTC, or the authors.

References

[1] Taylor, T. and Maloney, W. 2013 "Forecasting highway construction staffing requirements." NCHRP Synthesis 450, Washington, D.C.

[2] "e-Construction and Partnering: A Vision for the Future."Online: https://www.fhwa.dot.gov/innovation/everydaycounts/edc_4/epartnering.cfm, Accessed: 01/02/2019.

[3] "About Everyday Count (EDC)." Online: https://www.fhwa.dot.gov/innovation/everydaycounts/about-edc.cfm, Accessed: 01/02/2019.

[4] "E-Ticketing Show Promise of Speeding Process and Improving Accuracy at Asphalt Job Sites." Online: http://www.transportationmatters.iowadot.gov/2015/12/eticketing-show-promise-ofspeeding-process-and-improving-accuracy-at-asphalt-job-sites.html. Accessed: 01/02/2019.

[5] Wen, H., Muench S. T., Chaney S. L., Littleton K., and Rydholm T., "Recommendations for extending asphalt pavement surface life within Washington State," (in English), Tech Report 2016.

[6] Stephen S., Thomas, S., "Statewide Implementation of Pave-IR in the Texas Department of Transportation," Tech Report, 2012.

[7] "Standard Specification for Construction and Maintenance of Highways, Streets, and Bridges." Online:ftp://ftp.dot.state.tx.us/pub/txdot-info/des/spec-book-1114.pdf. Accessed:01/02/2019.

[8] "Technologies to Enhance Quality Control on Asphalt Pavements (R06C)." Online: https://www.fhwa.dot.gov/goshrp2/Solutions/RiskManagement/R06C/Rapid_Technologies_to_Enhance_Quality_Control_on_Asphalt_Pavements/PDF, Accessed: 01/02/2019.

[9] Transtec Group, "Intelligent Compaction and Infrared Scanning Field Projects with Consulting Support," Tech Report, 2018.

[10] "Summary of Intelligent Compaction for HMA/WMA Paving." Online: https://www.fhwa.dot.gov/construction/ictssc/pubs/hif13053.pdf, Accessed: 01/02/2019.

[11] "NRRA: Phase I Enhancement to the Intelligent Construction Data Management System (Veta) and Implementation (Pooled Fund)." Online: http://dotapp7.dot.state.mn.us/projectPages/pages/projectDetails.jsf?id=18028&type=CONTRACT, Accessed: 01/02/2019.

Evaluating Risk Response Strategies on Construction Projects Using a Fuzzy Rule-Based System

S.H. Fateminia[a], N.G. Seresht[a], and A.R. Fayek[a]

[a]Hole School of Construction Engineering, Department of Civil and Environmental Engineering, University of Alberta, Canada
E-mail: fateminia.h@ualberta.ca, geramise@ualberta.ca, aminah.robinson@ualberta.ca

Abstract –

The development and implementation of risk response strategies contributes to effective risk management processes in construction organizations. Risk response strategies need to be developed and implemented as follows: first, all possible risk responses for each given risk event of a project are identified; next, each risk response is evaluated to determine its effectiveness; then, for each risk event of the project, the optimal risk response is identified and implemented; and finally, the risk events and responses are consistently monitored. The existing literature confirms that there is a lack of research on evaluation criteria for risk responses, making it difficult to determine their effectiveness. This paper presents research that fills this gap by developing a way to evaluate the effectiveness of risk response strategies using a fuzzy rule-based system (FRBS) that consists of three inputs and one output. The inputs of the FRBS are the affordability and the achievability of risk responses and the controllability of risk events; the output is the effectiveness of the risk response. The application of fuzzy ranking methods instead of crisp ranking methods allows the model to mimic three human attitudes towards risk: risk averse, neutral, and risk taking. The proposed model lays the foundation for an automated evaluation of risk response strategies and provides a decision support tool for experts in the field.

Keywords –

Risk management; risk response; fuzzy logic; FRBS

1 Introduction

Risk management is vital for achieving business objectives on construction industry projects. Current trends in the construction industry are towards bigger and more complex projects, which can result in a greater amount of risks and uncertainties [1]. These risks can cause failures in terms of cost overruns, schedule delays, environmental damages, and fatal injuries. In general, risk management processes include identification, qualitative analysis, quantitative analysis, risk response planning, and monitoring and control [2]. First, risk events need to be identified and documented. These risk events should be analyzed by qualitative methods so they can be prioritized based on probability and impact. Next, quantitative risk analysis must be performed to model the combined effects of randomly occurring risk events and to develop a synthesized view of the overall effects of risk events on the project. Then, risk responses should be identified, evaluated, and implemented to mitigate occurrence probability and/or the negative impacts of risk events. Finally, the overall effectiveness of the risk management process needs to be monitored, reviewed, and controlled on a regular basis. The effectiveness of the risk response is the extent to which the risk events' probabilities and/or impacts are reduced as a result of implementing the risk responses.

A large amount of the research on risk management acknowledges the importance of risk response planning [3]. Hillson [4] argues that identifying and analyzing risks and uncertainties is clearly vital for the risk management process, as it is not possible to address risks that are not identified or that are poorly analyzed. Risk response planning is considered an important step for effective risk management; it is a process that is complementary to risk identification and analysis; and without risk response planning, only limited benefits can be had from the risk management process [4]. Risk response strategies need to be developed and implemented as follows: first, all possible risk response strategies for each given risk event of the project are identified. Next, each risk response strategy is evaluated to determine its effectiveness. Then, for each risk event, the optimal risk response strategy is identified and implemented. Finally, the risk events and the response strategies are consistently monitored.

Although some researchers have developed optimization-based methods for selecting an optimal set of risk responses [5], the application of these methods on real projects can be a complex and costly process due to

the effort and amount of data that are required. Moreover, these models account for only a limited number of criteria, namely time, cost, and quality, which can lead to the selection of risk responses that are cost effective but unfeasible in terms of technology, environment, and achievability. Optimization-based approaches have low transparency (i.e., they operate in such a way that it is not easy for others to see what actions are performed) during the process of selecting the optimal set of risk responses. Employing approaches with the ability to address the abovementioned weak points can result in more realistic, applicable, and feasible risk responses—a fuzzy ruled-based system (FRBS) is just such an approach. The existing literature confirms that there is a lack of research on evaluation criteria for risk response strategies, making it difficult to determine their effectiveness. The objectives of this paper are to (1) identify appropriate criteria for evaluating risk responses; (2) develop an FRBS to determine the effectiveness of risk responses; and (3) develop a fuzzy ranking method for selecting the most effective risk responses.

This paper is organized as follows. First, a brief literature review of risk management and risk response planning in construction projects is presented, followed by a discussion about the application of fuzzy logic methods in the risk management process. Second, evaluation criteria for risk responses are identified and an FRBS is developed for determining the effectiveness of risk responses; a fuzzy ranking method is then applied to rank the risk responses based on their effectiveness (determined by the FRBS) on construction projects. Third, a hypothetical example is provided to illustrate the proposed framework. Finally, conclusions are presented and future extensions of the current research are discussed.

2 Overview of Risk Response Evaluation and Selection Approaches

Risk response planning involves reducing the negative impact and probability of occurrence of risk events to ensure project success. Identified risk responses need to be evaluated, and the optimal risk response needs to be implemented for each risk event. Several researchers have developed decision support systems for evaluating and selecting risk responses using different approaches, including the trade-off approach [4, 6, 7], the zonal-based approach [8, 9], mathematical modeling and optimization [5, 3, 10–13], and a combination of these approaches and fuzzy logic [14].

The trade-off approach makes trade-offs between parameters—such as cost, time, and quality—that are either risk event-related or risk response-related in order to evaluate a set of risks. Kujawski [6] makes trade-offs that account for a project's objective requirements and project stakeholders' subjective preferences. Risk responses are selected based on the cost of implementing each risk response compared with the probability of project success when the risk response is implemented. Hillson [4] argues that the effectiveness of proposed risk responses must be assessed based on appropriateness (i.e., the correct level of risk response according to the severity of the risk event, ranging from a crisis response to a "do nothing" response), affordability (i.e., the cost effectiveness of the risk response), achievability (i.e., how realistically achievable or feasible the risk response is, either technically or in terms of a respondent's capability and authority), agreement (i.e., the consensus and commitment of stakeholders), and allocation (i.e., the responsibility of and accountability for implementing the risk response). Qazi et al. [7] develop a model for selecting a set of optimal risk responses by measuring the impacts of different combinations of risk responses on the objective function of a project. In zonal-based approaches, two-dimensional diagrams are applied to assess the regions of the risk responses using one of two common assessment tools: (1) a matrix that features different factors in a two-dimensional diagram and (2) a two-axis graph that maps risk responses based on the values of the two dimensions.

Using an optimization-based approach, Fan et al. [5] suggest a model for assessing the effectiveness of risk responses based on three criteria: risk event controllability, risk response costs, and project characteristics. Kayis et al. [10] employ five heuristic algorithms to minimize the cost of implementation within the constraints of the implementation budget and acceptable risk effects for new product development. Zhang and Fan [11] maximize the sum of estimated risk response effects (i.e., they reduce the expected loss of the risk event) after risk response strategy implementation using a method for selecting risk responses with an integer linear programming (ILP) model. Zhang [12] uses an ILP model that accounts for the cost of implementation and the determined budget for risk responses. Wu et al. [13] propose a multi-objective decision-making model for the selection of risk responses that minimize total expected losses, total expected schedule delays, and total expected quality reduction. An optimization model is used to minimize expected time loss, expected cost loss, and expected quality loss. To calculate the coefficients of the objective function, a fuzzy analytic hierarchy process (FAHP) is employed as a technique to guide the risk analysts [14].

3 Developing the Risk Response Evaluation and Selection Approach

In order to develop the proposed FRBS for the evaluation of risk responses, appropriate evaluation

criteria are identified, which are the inputs of the FRBS. The output of the FRBS is the effectiveness of the risk responses. Based on the output of the FRBS, the risk responses are then ranked using a fuzzy ranking method that allows the model to mimic the three human attitudes towards risk: risk averse, neutral, and risk taking.

3.1 Evaluating Risk Responses: Identifying Inputs and Outputs

This study uses three criteria to evaluate risk responses: affordability of the risk response, achievability of the risk response, and controllability of risk events. These criteria make up the three inputs of the FRBS, and its output is the effectiveness of the risk response strategy. There is a positive correlation between the controllability of a risk event and the effectiveness of its risk response. For example, even if you implement a risk response with high affordability and high achievability, the risk response will not be effective in addressing a risk event with low controllability. Therefore, the FRBS developed for the evaluation of risk responses needs to evaluate both risk events and their identified risk responses in order to identify the most effective risk responses. Subjective system variables (evaluation criteria) are represented by triangular fuzzy membership functions, which are commonly used in engineering applications.

Affordability refers to the cost-effectiveness of risk responses, where the amount of time, effort, and money spent on addressing a risk should not exceed the available resources for implementing risk responses. One way to measure the cost-effectiveness of risk responses is to use the risk reduction leverage (RRL) factor, which can be calculated by converting the impact of the risk event into a monetary value (for example, the cost of delay and/or the cost of negative impacts on quality) [4]. RRL represents the ratio of the increase in risk event exposure to the cost of risk response implementation. RRL can be calculated by dividing the difference between the risk responses' cost impacts before and after implementation by the implementation cost (see Equation (1)) [4].

$$RRL = \frac{(\text{Cost Impact})_{\substack{before \\ response}} - (\text{Cost Impact})_{\substack{after \\ response}}}{\text{Cost of response}} \quad (1)$$

Hillson [4] proposes that responses with high effectiveness in terms of affordability should have RRL values above 20. Responses with medium effectiveness have RRL values ranging from 1 to 20, and RRL values of less than 1 can be labelled as having low effectiveness (i.e., they are ineffective) because their implementation cost is more than what they might save later. Thus, the fuzzy membership functions for affordability are defined as low (less than 1), medium (between 1 and 20), and high (more than 20).

Achievability refers to the feasibility of a risk response in terms of three considerations: the technical complexity of the proposed risk response, the capability of the respondent, and the authority of respondent [4]. According to Fan et al. [5], the complexity of a risk response may stem from technical obstacles, political obstacles, limited access to information, or conflict resolution obstacles. Three fuzzy membership functions of achievability can be defined, namely low, medium, and high achievability.

Miller and Lessard [15] define *controllability* as the likelihood that the probability of occurrence of a risk event can be changed. This criterion describes the nature of the risk situation. Risk events with a low degree of controllability include occurrences such as natural disasters, while risk events with a high degree of controllability are caused by scheduling and budget problems. The latter can be addressed more effectively than the former by implementing an identified risk response [5]. Although the controllability value of a risk event is the same for all of its related risk responses, this criterion can be used to ascertain whether risk responses meet the threshold for effectiveness, which can be determined by risk decision makers. As with affordability and achievability, controllability can be categorized into three fuzzy membership functions, namely low, medium, and high.

3.2 Evaluating Risk Responses Using an FRBS

An FRBS is a methodology for modeling human logical thinking and decision-making. These systems use membership functions and fuzzy rules to make a decision [16]. An FRBS can be developed with either data or expert judgments using one of the few approaches proposed in the literature. Fuzzy c-means (FCM) clustering can be employed when there is access to historical data [17]. Expert judgments can be applied to develop an FRBS when historical data is unavailable [18, 19]. In this paper, the FRBS for the evaluation of risk responses is developed using expert judgments. The membership functions of three inputs and one output are determined based on documented literature using MATLAB® R2018b.

In this paper, a Mamdani fuzzy inference system is used to develop an FRBS for the evaluation of risk responses; by delivering fuzzy outputs, the Mamdani inference system facilitates the use of different defuzzification methods for fuzzy ranking. The membership functions of affordability are determined by RRL values between 0 and 20 as recommended by Hillson [4]. Figure 1 shows the membership functions of affordability.

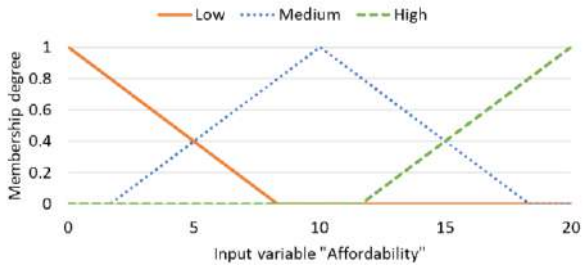

Figure 1. Membership functions of affordability

For the achievability and controllability membership functions, the three linguistic terms *low*, *medium*, and *high* are used, as illustrated in Figure 2 and Figure 3, respectively.

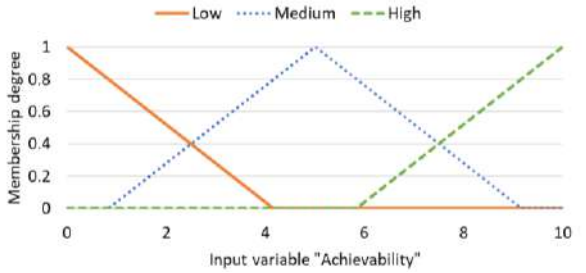

Figure 2. Membership functions of achievability

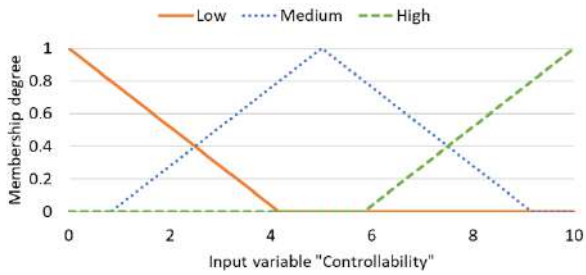

Figure 3. Membership functions of controllability

The membership function of the FRBS output (effectiveness) is also between 0 and 1, as shown in Figure 4.

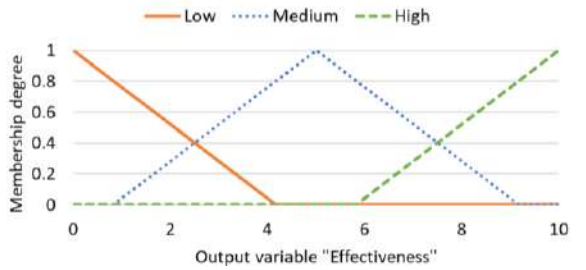

Figure 4. Membership functions of effectiveness

Fuzzy rules are defined as "if-then" rules. In this system, 27 if-then fuzzy rules are defined. Some of these rules are presented in Table 1.

Table 1. Fuzzy rules used in the FRBS

Rule	If			Then
	Affordability	Achievability	Controllability	Effectiveness
1	Low	Low	Low	Low
2	Low	Low	Medium	Low
3	Medium	Medium	Medium	Medium
4	Low	Medium	Medium	Medium
5	High	High	High	High
6	Medium	High	High	High

Figure 5 shows the three-dimensional curve that represents the mapping from inputs to output and the dependency of effectiveness on controllability and affordability.

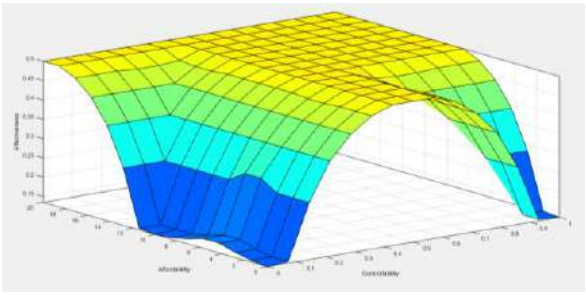

Figure 5. Three-dimensional representation of the proposed FRBS

3.3 Selecting Effective Risk Responses Using the Fuzzy Ranking Method

In the next step, the risk responses need to be ranked based on their effectiveness, so that the most effective risk response can be selected for each risk event. In order to solve decision-making problems, fuzzy ranking methods are commonly used, wherein the evaluation scores (i.e., effectiveness) of decision alternatives (i.e., risk responses) are represented by fuzzy membership functions [20, 21]. There are various fuzzy ranking methods discussed in the literature, the majority of which can be grouped into three categories based on the approaches they use to rank fuzzy numbers. The first category of fuzzy ranking methods includes those methods that rank fuzzy numbers based on their α-cuts at a pre-specified level of α [22]; thus, these methods change the fuzzy ranking problem into an interval ranking problem. The second category of fuzzy ranking methods includes those methods that use fuzzy distance measures to rank fuzzy numbers [23]. The third category

of fuzzy ranking methods includes those that rank the fuzzy numbers based on their defuzzified values [21]; these methods change the fuzzy ranking problem into a simple problem of ranking crisp numbers. The first two categories of fuzzy ranking methods (i.e., α-cut-based methods and fuzzy distance-based methods) usually require that fuzzy numbers be regularly shaped (e.g., triangular or trapezoidal fuzzy numbers) [21]. However, in this paper, the output of the FRBS (i.e., the effectiveness of the risk responses) is an irregularly shaped fuzzy membership function. Therefore, in this paper, the third category of fuzzy ranking methods (i.e., ranking methods based on the defuzzified value) is used to rank risk responses based on their effectiveness. To do this, the results of the FRBS need to be defuzzified. There are various defuzzification methods proposed in the literature; the smallest of maximum (SOM), largest of maximum (LOM), and center of area (COA) methods are commonly used in different engineering applications of fuzzy logic. Figure 6 presents the three aforementioned defuzzification methods implemented on a hypothetical example of risk response effectiveness. Moreover, Figure 6 also shows how different defuzzification methods can result in different defuzzified values for risk response effectiveness.

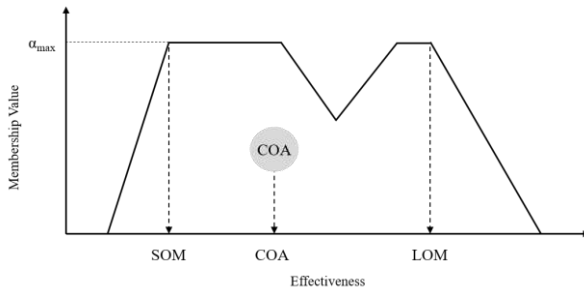

Figure 6. COA, SOM, and LOM defuzzification methods

When ranking risk responses based on the defuzzified value of their effectiveness, the use of different defuzzification methods can mimic different human attitudes towards risk. Ranking risk responses based on the results of the SOM method means that the decision maker considers the smallest maximum value of effectiveness for each risk response and ignores all other possible values for the effectiveness of the risk response (see Figure 6). Thus, ranking risk responses based on the results of the SOM method mimics a risk-averse attitude. In contrast, ranking the risk responses based on the results of the LOM method means that the decision maker considers the largest maximum value of effectiveness for each risk response and ignores all other possible values for the effectiveness of the risk response (see Figure 6). Thus, ranking the risk responses based on the results of the LOM method mimics a risk-taking attitude. The COA, on the other hand, determines the defuzzified value of effectiveness by taking into consideration all possible values of effectiveness for each risk response. Accordingly, ranking risk responses based on the results of the COA method mimics a neutral human attitude towards risk. In this paper, the three aforementioned defuzzification methods (i.e., SOM, LOM, and COA) are used to rank risk responses based on their effectiveness so that all three human attitudes towards risk can be mimicked in the selection of the most effective risk responses.

4 Hypothetical Example

In this section, a hypothetical example is presented to demonstrate how to use the proposed approach to evaluate the effectiveness of risk responses and select the most effective. Assume two risk events: (1) incomplete design and (2) operation interruption due to adverse weather conditions. The first risk event can be addressed by two possible risk responses: (1-1) outsourcing design to subcontractors or (1-2) employing professional design teams. To mitigate the second risk event, two risk responses are possible: (2-1) schedule compression using extra resources or (2-2) considering alternative construction methods, such as using precast materials. A number between 0 and 10 represents achievability (where 10 is high) and another number between 0 and 10 represents controllability (again, 10 is high); these numbers are determined for each risk response by expert judgment. The values for each criterion can be found in Table 2.

Table 2. The input values of each risk response and its related risk event

Risk Event	Risk Response	Affordability (RRL)	Achievability	Controllability
1	1-1	7.00	9.00	6.00
	1-2	12.00	5.00	6.00
2	2-1	7.00	6.00	2.00
	2-2	5.00	3.00	2.00

Since this hypothetical example is presented simply for illustrating the proposed approach, a limited number of risk factors are identified for risk response evaluation. In a real construction case study, a comprehensive list of risk factors such as environmental and safety risk factors may be considered for risk response evaluation. Table 3 shows the effectiveness values, which are based on the information in Table 2. The inputs are imported to the FRBS to evaluate the effectiveness of the risk responses. Crisp numbers representing the effectiveness of the risk responses are then predicted by the FRBS using three defuzzification methods (i.e., SOM, LOM, and COA) as discussed in Section 3.3 and the risk responses are ranked accordingly. Table 3 presents the effectiveness of the risk responses and their rankings for the two risk events.

Table 3. The effectiveness values of each risk response and its related risk event

Risk Response	Effectiveness					
	(SOM)	Rank	(LOM)	Rank	(COA)	Rank
1-1	8.50	1	10.00	1	6.95	1
1-2	4.10	2	6.00	2	5.00	2
2-1	0.00	-	2.00	2	3.74	2
2-2	0.00	-	2.50	1	3.92	1

Table 3 presents the most effective risk response for each of the two risk events as determined by three different defuzzification methods. The effectiveness value determined using the SOM defuzzification method mimics a risk-averse attitude; the LOM defuzzification method mimics a risk-taking attitude; and the COA defuzzification method mimics a neutral attitude towards risk. Although in this case study the rankings of the risk responses are similar for each of the three defuzzification methods, on real construction projects with numerous risk responses, rankings can be different for different defuzzification methods. Since higher effectiveness of risk responses is favorable, in the hypothetical example, risk responses 1-1 and 2-2 should be selected for risk events 1 and 2, respectively. As shown in Table 3, the values of effectiveness for risk responses 2-1 and 2-2 are equal to zero, which indicates neither of these two risk responses should be applied to risk event 2 if the risk response strategy is based on a risk-averse attitude. Moreover, as discussed in Section 3.1, risk responses can be rejected if their effectiveness is less than a threshold value that is determined by the decision maker. For instance, assuming an effectiveness value of 5 as the threshold for the risk responses' effectiveness, both risk responses for the second risk event (i.e., 2-1 and 2-2) are not acceptable in this case study (refer to Table 3). In this situation, new risk responses should be identified for the second risk event or its adverse effects on the project should be accepted.

5 Conclusions and Future Research

This paper presents a methodology for evaluating the effectiveness of identified risk responses by applying an FRBS that has three inputs as evaluation criteria and that produces the effectiveness of risk responses as an output.

The three inputs are the affordability of each risk response, the achievability of each risk response, and the controllability of related risk events. The FRBS uses the estimated crisp values of affordability, achievability, and controllability to evaluate the effectiveness of risk responses according to the rules developed based on experts' opinions. The output, which is a fuzzy set, is used as an input for three different fuzzy ranking methods, one based on SOM, one based on LOM, and one based on COG (COA), to determine the most effective risk response in terms of affordability, achievability, and controllability. Applying an expert-driven FRBS and fuzzy ranking methods can help automate the evaluation of risk response strategies, and this technique delivers an expert-level risk management tool to a non-expert in the field. The contributions of this paper are threefold: first, the appropriate criteria for evaluating risk responses are identified from the literature; second, an FRBS is developed to automate the evaluation of risk responses; and third, the application of different fuzzy ranking methods is proposed to mimic the risk-taking attitude of experts for risk response evaluation.

On construction projects, risk events are often dependent on one another; for example, the risk of precipitation is linked to the risk of excessive soil moisture in earthmoving operations. In order to develop a comprehensive risk response planning tool, interdependencies between different risk events need to be taken into consideration. In future research, the FRBS developed in this paper will be extended to capture these interdependencies and determine the most effective risk responses for each risk event, accounting for all risk events that affect a project throughout its life cycle.

6 Acknowledgments

This research is funded by the Natural Sciences and Engineering Research Council of Canada (NSERC)

Industrial Research Chair in Strategic Construction Modeling and Delivery (NSERC IRCPJ 428226–15), which is held by Dr. Aminah Robinson Fayek. The authors gratefully acknowledge the financial support provided by industry partners and NSERC through the Chair.

7 References

[1] Abdelgawad M. and Fayek A.R. Risk management in the construction industry using combined fuzzy FMEA and fuzzy AHP. *Journal of Construction Engineering Management, 136*(9):1028–1036, 2010.

[2] Project Management Institute. *Construction extension to the PMBOK guide.* Newtown Square, Pennsylvania, 2016.

[3] Ben-David I. and Raz T. An integrated approach for risk response development in project planning. *Journal of Operation Research Society,* 52(1):14–25, 2001.

[4] Hillson D. *Effective opportunity management for projects: Exploiting positive risk.* Marcel Dekker, New York, 2004.

[5] Fan M., Lin N. and Sheu C. Choosing a project risk-handling strategy: An analytical model. *International Journal of Production Economics*, 112(2):700–713, 2008.

[6] Kujawski E. Selection of technical risk responses for efficient contingencies. *Systems engineering*, 5(3):194–212, 2002.

[7] Qazi A., Quigley J., Dickson A. and Kirytopoulos K. Project complexity and risk management (ProCRiM): Towards modelling project complexity driven risk paths in construction projects. *International Journal of Project Management*, 34(7):1183–1198, 2016.

[8] Datta S. and Mukherjee SK. Developing a risk management matrix for effective project planning—An empirical study. *Project Management Journal*, 32(2):45–57, 2001.

[9] Piney C. Risk response planning: Selecting the right strategy. In *Proceedings of the fifth European project management conference*, 2002.

[10] Kayis B., Arndt G., Zhou M. and Amornsawadwatana S. A risk mitigation methodology for new product and process design in concurrent engineering projects. *CIRP Annals*, 56(1):167–170, 2007.

[11] Zhang Y. and Fan Z. An optimization method for selecting project risk response strategies. *International Journal of Project Management*, 32(3):412–422, 2014.

[12] Zhang Y. Selecting risk response strategies considering project risk interdependence. *International Journal of Project Management*, 34(5):819–830, 2016.

[13] Wu D., Li J., Xia T., Bao C., Zhao Y. and Dai Q. A multiobjective optimization method considering process risk correlation for project risk response planning. *Information Sciences*, 467:282–295, 2018.

[14] Nik E.R., Zegordi S.H. and Nazari A. A multi-objective optimization and fuzzy prioritization approach for project risk responses selection. In *Proceedings of the 2011 IEEE International Conference on Industrial Engineering and Engineering Management*, pages 889–892, Singapore.

[15] Miller R. and Lessard D. Understanding and managing risks in large engineering projects. *International Journal of Project Management*, 19(8):437–43, 2001.

[16] Fayek A.R. and Lourenzutti R. Introduction to fuzzy logic in construction engineering and management. In *Fuzzy hybrid computing in construction engineering and management. Ed. Fayek A.R.* Emerald Publishing Limited, Bingley, United Kingdom, 2018.

[17] Bezdek JC. *Pattern recognition with fuzzy objective function algorithms.* Plenum Press, New York, 1981.

[18] Khanzadi M., Nasirzadeh F. and Alipour M. Integrating system dynamics and fuzzy logic modeling to determine concession period in BOT projects. *Automation in Construction*, 22:368–376, 2012.

[19] Gerami Seresht N. and Fayek A.R. Dynamic modeling of multifactor construction productivity for equipment-intensive activities. *Journal of Construction Engineering Management*, 144(9):04018091, 2018.

[20] Sadeghi N., Fayek A.R. and Gerami Seresht N. A fuzzy discrete event simulation framework for construction applications: Improving the simulation time advancement. *Journal of Construction Engineering and Management*, 142(12):04016071, 2016.

[21] Chen S. J. and Chen S.M. Fuzzy risk analysis based on the ranking of generalized trapezoidal fuzzy numbers. *Applied Intelligence*, 26(1):1–11, 2007.

[22] Chen S.M. and Wang C.H. Fuzzy risk analysis based on ranking fuzzy numbers using α-cuts, belief features and signal/noise ratios. *Expert Systems with Applications*, 36(3):5576–5581, 2009.

[23] Cheng C.H. A new approach for ranking fuzzy numbers by distance method. *Fuzzy Sets and Systems*, 95(3):307–317, 1998.

A Review of Data-Driven Accident Prevention Systems: Integrating Real-Time Safety Management in the Civil Infrastructure Context

A. Assadzadeh[a], M. Arashpour[a*], A. Rashidi[b], A. Bab-Hadiashar[c], and S. Fayezi[d]

[a]Department of Civil Engineering, Monash University, Australia
[b]Department of Civil Engineering, Monash University, Malaysia
[c]School of Engineering, RMIT University, Australia
[d]Business and Economics Faculty Office
[*]E-mail: Amin.AssadzadehBirjandi@monash.edu, Mehrdad.Arashpour@monash.edu

Abstract –

Statistical reports point to the fact that civil infrastructure projects remain hazardous working environments. Despite the implementation of various safety procedures, the frequency and cost of work-related injuries are significant. Improvements in sensor technologies, wireless communication and processing power of computers as well as advancements in machine learning and computer vision are now enabling data-driven systems as effective safety barriers for accident prevention. In recent years, many researchers have studied various methods of leveraging technology to improve safety in civil infrastructure projects. However, previous investigations have not produced a thorough analysis of the practicality of those approaches. While considerable progress has been made in developing methods to improve construction safety, few studies have focused on implementation of data-driven real-time accident prevention systems to effectively minimize risk in the event where other safety measures have failed or been absent. Motivated to facilitate the development of such method, this paper carries out thorough analysis of the field and its trends, identifies research gaps, provides a discussion of recent advancements, and highlights future research directions to help researchers gain an up-to-date overview of the state-of-the-art and navigate through this domain efficiently.

Keywords –

Automation; Behavior related accidents; Building information modeling (BIM); Infrastructure sector; Construction safety management; Information Technology; Machine learning; Neural networks; Object detection; Risk analysis and control; Sensors

1 Introduction

Around 15% of occupational fatal accidents have occurred on construction sites across Australia, where construction only accounts for 5% of the workforce [1]. In the same year, United States construction fatalities alone amounted to 991 lives lost [2]. In the past decades, research on safety climate and culture, worker-oriented safety, safety management programs, hazard recognition and risk assessment, and applications of information technology in construction safety has led to improvements in overall safety performance [3]. However, the number of fatal and non-fatal accident injuries still remain significantly high in the construction industry.

Recent advancements in machine learning, computer vision, and increased affordability and processing power of advanced technologies have prompted researchers to work towards the development of data-driven accident prevention systems, adding a technology-driven safety layer to construction sites.

Given that safety is an ongoing issue on the construction site, the development of continuous safety monitoring systems has great potential to improve safety risk management. As described by Australia's Work Health and Safety Act (WHS), the risk management process involves identification hazards, assessing risks, controlling risks, and reviewing control measures [4], [5].

This paper provides a review of recent developments of data-driven accident prevention systems designed to improve construction safety. It reveals the trend of technologies and approaches being used, and discusses their potential applications, and identifies future research directions. As such, it can be used as a guide for researchers interested in this particular domain to study an up-to-date account of state-of-the-art research.

2 Review methodology

A methodological approach is employed to conduct a comprehensive review. Scopus was selected as the

database for the search, and the keywords such as construction safety management, machine learning, computer vision, sensors, information and communication technology, building information modeling and so on, were used for the initial search. The returned results are screened based on their title and abstract, and out of 982 documents, 118 were found to be relevant. To ensure a more comprehensive and thorough search, an explorative search was also carried out, leading to an additional 125 documents found, amounting to a database of 243 journal articles in total. Section 3 provides an overview of the selected articles, and critical review of the most relevant papers is carried out in section 4 of this study.

3 Analysis of the domain

The database of the selected papers cover articles published from 2006 to 2018. The number of relevant papers did not exceed 6 before the year 2012. In the past few years, however, the number of publications have risen significantly, due to increased interest in using sensor technologies and vision-based systems, wherein 2018 it nearly doubles to 78 publications. The analysis reveals that the United States, China, and South Korea are the top three countries contributing to the domain. Figure 1 shows the distribution of selected articles by year and country of affiliation.

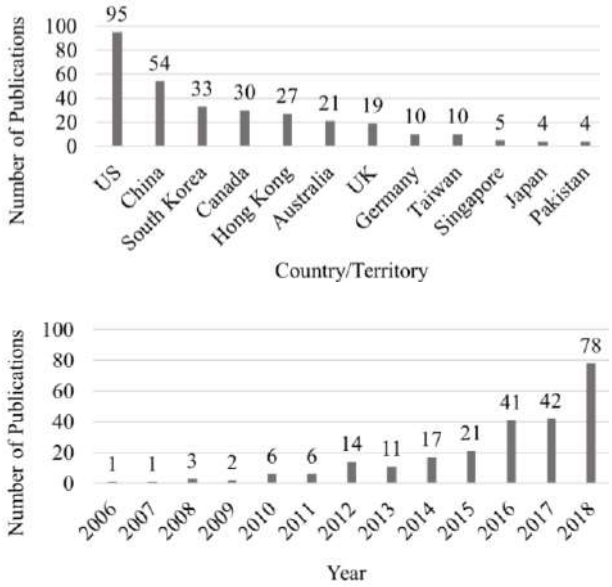

Figure 1. Distribution of articles by publication time, and country of affiliation

Table 1. Journals and the number of corresponding articles

Journal	Number of Appearances
Automation in Construction	93
Advanced Engineering Informatics	23
Journal of Computing in Civil Engineering	21
Journal Of Construction Engineering And Management	17
Safety Science	16
Visualization in Engineering	12
Sensors (Switzerland)	6
Engineering Construction And Architectural Management	4
Journal Of Management In Engineering	4

The selected studies include publications from more than 35 different journals. Table 1 lists the journals publishing more than four papers within the selected list of articles. Not surprisingly, Automation in Construction has contributed the most to this domain, with more than 38% of the papers being published in this journal. Other relevant journals include Advanced Engineering Informatics, Journal of Computing in Civil Engineering, Journal of Construction Engineering and Management, and Safety Sciences, each representing more than 15 papers in the selected database.

Based on the database of selected articles, co-publication of authors are analyzed using Gephi, an open source graph and network analysis software [6]. Figure 2 shows the network of the most prominent scholars, active in the domain.

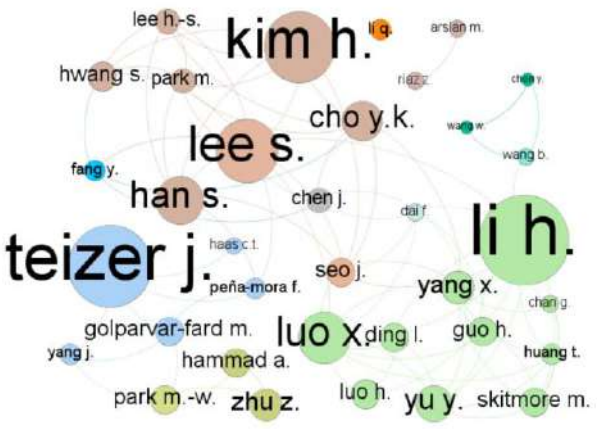

Figure 2. Network of the most influential scholars in the domain

4 Data-driven safety risk management

This section provides an overview of latest developments in data-driven accident prevention systems and discusses their relation to various steps of safety risk management as described by Australia's Work Health and Safety Act (WHS) [4], [7]. The following subsections cover the impact of such systems on identification of hazards, assessing risks, controlling risks and reviewing control measures.

4.1 Hazard identification

Hazard identification is the process of finding entities or situations that have the potential of causing harm. Developing data-driven systems for real-time hazard identification is a crucial step towards intelligent safety management. Three different approaches to hazard identification are discussed in this section. First, an indirect approach, which attempts to identify hazards by analyzing data from the construction site for anomalies that may be suggestive of an existing hazard. Second, identifying hazards as they directly relate to workers' behavior. And the last approach is to monitor the workplace for specific anticipated hazards.

4.1.1 Indirect hazard identification

Considering the dynamic nature of a construction site, regular safety inspections need to be carried out to ensure a hazard-free work environment. However, since inspections are often manually performed, it is not uncommon for newly appeared hazards to remain unidentified for a prolonged period of time, exposing workers of the site to risks of trip, fall, struck by falling objects, electrocution or other accidents. Continuous monitoring of the site can therefore immensely facilitate safety management. An innovative approach to automatically identify hazardous areas has been proposed by Kim et al. [8]. In this study, a real-time tracking system is used to identify potentially hazardous areas by comparing workers' actual path to their optimal routes. Location tracking is performed using an RFID-based Real-Time Location Tracking System (RTLS), where RFID tags are mounted on workers' hardhats. Upon testing the framework in a case study, it was found that 80% of the identified hazards by the system corresponded to real hazards such as material piles, openings, areas with inadequate electric wire protection, and areas with a lack of falling object protection.

Although RFID technology is used in various industries for tracking some entities, the rapidly changing nature of the construction sites and their complexity make effective use of RFID very challenging. RFID requires a direct line of sight for optimum accuracy, which is a condition hard to realize in construction. In addition, it requires installation of multiple tags and receivers which limit its practicality [9].

Ultra-wideband (UWB) is another radio frequency-based technology used for location tracking. UWB uses high-bandwidth radio pulses for communication, which makes it less susceptible to signal interferences. However, it still requires installation and maintenance of multiple tags and receivers [10].

Global Positioning System (GPS) has also been widely used to track workers' trajectories in construction sites in order to improve safety. For instance, Arslan et al. [11] demonstrated a prototype of a GPS-based system for identifying stay points, the intersection of multiple trajectories, and classifying the trajectory into running or walking. Such semantic enrichment of data using various data mining and machine learning techniques helps improve the decision-making process by providing insight on workers' behavior.

Vision-based systems as an alternative to other methods for tracking various entities on construction sites has recently attracted researchers' attention. Although still in early stages of development, vision-based systems have the advantage of not requiring installation of multiple tags, have lower costs, and are easier to maintain.

Park et al. [12] propose a vision-based method that uses videos obtained from ordinary 2D cameras, and employs detection and tracking algorithms in a hybrid system for tracking entities. However, the method is limited to tracking workers across video frames, and is unable to produce trajectories with respect to the workplace.

In another study, Konstantinou et al. [13] developed a framework for obtaining 3D trajectories using multiple camera views. The proposed method uses three sequentially activated matching techniques. The output of a 2D tracking method is first checked using a motion matching technique, followed by a geometry matching, and finally a template matching technique. In any step if a match is found, further checking is terminated, therefore significantly reducing the required computational power.

In a comparative study, Xiao et al. [14] evaluated the performance of a number of 2D vision-based tracking methods employed in the context of construction. Their study showed that although vision-based systems have promising potentials, many challenges such as occlusion, clutter, illumination, and scale variation need to be tackled for practical deployment of such systems.

Another innovative approach for identifying potential hazards based on real-time information obtained from construction site was proposed by Yang et al. [15]. They propose using wearable Inertial Measurement Unit sensors to analyze workers' gait abnormalities to identify potential fall hazards. In their experiment, subjects were asked to walk across a steel beam in a controlled

environment. There were two hazards placed along the beam, a slippery surface, and an obstacle. Upon analysis of data obtained from multiple subjects, it was found that the correlation between collective gait abnormality and presence of a hazard is significant. However, this study was limited to one dimension only. The extension of such method to two or three dimensions by taking advantage of location tracking methods as discussed above would provide valuable information that could be used for effective real-time hazard identification. Moreover, such spatio-temporal data enriched with information about gait pattern, activity, etc. can be used for further analysis.

4.1.2 Behavior-related accident precursors

Construction accidents are often directly related to the worker's behavior. In an investigation of identifying the root causes of accidents, Abdelhamid et al. [16] explained that accidents occur either due to the failure of workers in identifying hazards, workers deciding to proceed despite identification of hazardous condition or workers deciding to act unsafely regardless of work condition.

Real-time safety monitoring systems have great potential to be used as supplementary tools for safety supervision. Workers' disregard of hazards often manifests itself in lack of adequate personal protective equipment usage. Recent advancements in computer vision and machine learning provide powerful tools for object detection using images. For instance, Park et al. [17] used Histogram of Oriented Gradients along with Support Vector Machines to detect human bodies and hardhats, and by matching geometric and spatial relationship of the two, identify cases where the person is not using a hardhat.

Fang et al. [18] developed a method for monitoring appropriate usage of harness, anchoring and hardhats by steeplejacks. In the proposed method, cameras are installed inside the rooms and facing the windows where steeplejacks are to perform the aerial work on exterior walls. They use the Single Shot MultiBox Detector (SSD) algorithm, which uses Convolutional Neural Networks (CNNs), and reported precision and recall rates of higher than 90%.

In a similar study, Fang et al. [19] used Faster R-CNN, and a deep CNN model to identify workers not wearing a safety harness when working at height. Using automated safety inspections, safety managers can be notified of unsafe behaviors, and take appropriate action to mitigate the risks in a timely manner.

A different approach of identifying unsafe behaviors was proposed by Guo et al. [20] whereby they used depth cameras to identify various postures related to unsafe behavior. Various body angles obtained from the skeleton-based posture information are compared to an unsafe behavior database in order to identify postures that are suggestive of unsafe actions, such as jumping over a guardrail or dumping construction waste from higher levels.

Other forms of unsafe behavior leading to hazardous conditions include working under the influence of drugs or alcohol, working under a high level of fatigue or attempting a hazardous task with low relevant skill level. One example is the loss of balance possibly induced by the aforementioned factors. To address this issue, Umer et al. [21] developed a balance monitoring tool that uses wearable Inertia Measurement Units (IMUs) and fuzzy set theory to determine workers' balance performance by taking 20-second tests at different times of the day.

Monitoring physiological condition of workers using Physiological Status Monitors (PSMs) has also been explored [22]. Using these methods, metrics such as heart rate and breathing rate can be monitored, providing valuable information for identifying unsafe working conditions as they arise.

High levels of stress induced by schedule pressure or other factors may cause workers to act unsafely in certain conditions. Therefore, it is essential to provide a work environment, which is free of stress-producing conditions.

4.1.3 Workplace-related accident precursors

Certain hazards can be identified by monitoring the workplace for specific accident precursors. One example is site congestion. Congested working areas are more prone to accidents. Location tracking systems as discussed in section 4.1.1 can enable workplace analysis in terms of congestion. Zhang et al. [23] used GPS sensors attached to workers' hardhats to track their activity while working on cast-in-place concrete columns. The workspaces were then visualized in a BIM platform to identify conflicts among other work-zones or material handling paths.

Environmental factors of the site such as temperature, noise level, and pollutants are important workplace hazards that require constant monitoring. For instance, Riaz et al. [24] have proposed using wireless sensor networks for monitoring workplace temperature conditions, and integrating the system with a BIM platform for enhanced work and safety management.

Temporary structures on construction sites are another aspect requiring a thorough inspection to ensure all safety requirements are met. Safety inspection of scaffolds, for instance, is performed visually by the inspector and is a labor-intensive process. Cho et al. [25] proposed a system for real-time safety monitoring of the structure using strain sensors mounted on the scaffolds. With the aid of Finite Element Method (FEM) analysis, they develop a machine learning model to classify various states of the scaffolds such as over-loading, uneven settlement, and over-turning based on the data

obtained from the strain sensors.

Vision-based systems also have the potential to be used as an effective monitoring method to ensure worksite safety. Kolar et al. [26] explored using transfer learning and CNN-based models for detecting guardrails in images. Furthermore, an improved version of Faster R-CNN can be used for detecting workers and equipment in images of civil infrastructure projects [27].

Often in construction sites, workers are required to perform their task alongside heavy equipment in a shared working area and therefore are exposed to high risk of struck-by accidents. Developing proactive real-time alarm systems are another active area of research. In a recent study, Soltani et al. [28] developed a method, fusing computer vision based systems with real-time location systems to estimate the poses of excavators in three dimensions, using surveillance cameras installed on the construction sites as stereo-cameras.

Understanding task-specific accident precursors, and defining quantitative metrics for evaluation of unsafe behaviors or conditions will facilitate the development of effective real-time monitoring systems.

4.2 Risk Assessment

Assessing risks associated with the identified hazards requires consideration of how severe the consequences are if someone is exposed to the hazard, and how likely it is to occur. Data-driven systems facilitate the process of risk assessment and reduce the bias caused by the subjectivity of the analysis.

The context in which hazards appear and the co-occurrence of various hazards determine the severity and likelihood of risks. For instance, in the case of struck-by accidents, heavy equipment approaching a worker in a congested working area is more likely to cause an accident than one approaching worker spacious area. Similarly, the close proximity of a worker and equipment is more indicative of high risk if the worker is standing in the blind spot of the equipment. Seo et al. [29] developed a method to monitor struck-by accidents using computer vision. They propose using fuzzy inference for determining the safety level, based on risk factors such as congestion and proximity.

Evaluating safety and health risks associated with a given task is another important part of safety management. A number of studies have focused on methods of performing ergonomic analysis in a minimally intrusive way. The rapidly changing and complex nature of construction make reliable ergonomic assessment challenging. To address this issue, researchers have developed data-driven systems to quantitatively perform ergonomic risk analysis [30]. The outcome of such systems can be used to improve safety training, planning, and task design.

For instance, insole pressure sensors have been used to detect and classify awkward working postures. In a study, Nath et al. [31], using accelerometer and gyroscope sensors built-in in smartphones, and machine learning algorithms estimated duration and frequency of various activities. And by doing so evaluated the overexertion risk level associated with the task.

Vision-based systems have also been used to perform ergonomic risk assessment using posture analysis based on body angles. Golabchi et al. [32] proposed a framework for data collection, analysis, and visualization to facilitate ergonomic analysis. Vision-based techniques that utilize CNNs, to estimate 3D skeleton of the subject from 2D images for ergonomic assessment have also been reported.

Risk assessment is a crucial step in safety risk management. Therefore, development of effective automated safety monitoring systems requires the integration of data-driven risk assessment systems into the frameworks.

4.3 Control risks

Controlling risks, once identified and assessed, can be categorized into three levels based on their effectiveness. The most effective level of control is elimination [33]. Real-time safety monitoring systems facilitate elimination control by identifying newly appeared or unidentified hazards and informing safety managers or site supervisors, which will then take the necessary steps to eliminate the risks if applicable.

The second level of control includes substitution of the hazard with a safer alternative, isolating the hazard from people, or reducing the risks through engineering controls [34]. Safety will be enhanced by timely identification of hazards, and notification of the people in charge to take appropriate actions. In addition, real-time safety alarm systems that will notify the workers or equipment operators of danger can be considered as another form of engineering control, driven by data-driven monitoring systems.

The last level of control is aimed at reducing exposure to hazards. This level includes methods such as Personal Protective Equipment (PPE) and administrative controls. Proper usage of PPE is often overlooked on construction sites. Real-time monitoring systems provide a promising solution to continuous supervision of their appropriate utilization. The data obtained from real-time systems can also be used for trend analysis and evaluating safety culture at different work zones or various stages of the project. Thus, facilitating targeted administrative controls, and enhancing safety training quality.

4.4 Safety Control Measures

The last step in the safety risk management process refers to performing hazard identification, risk

assessment and controlling risks repeatedly to ensure appropriate control measures are taken at all times. Data-driven monitoring systems facilitate automation of the process. By continuously monitoring the workplace and workers' conditions, the automated safety risk management systems supplement human supervision to effectively prevent accidents at the construction site.

5 Discussion of Research Gaps

In this study, we have reviewed various aspects of safety risk management that can be improved using data-driven systems. This section identifies a number of research gaps and suggests future research directions.

1. At the current stage, most studies have focused on the development of monitoring systems that collect and process certain types of information from various entities at construction sites (e.g. workers' gait pattern, physiological state, workers' activity, workspace congestion, temperature, etc.). A desirable feature would be a framework for combining information obtained using various methods into an integrated system. The added dimensionality to the data can provide managers with valuable information. For example, a system that is able to detect safety violations can be extended to include more information such as where the violation has occurred, information about the subcontractor, environmental factors at that time (e.g. temperature), and information about the physiological conditions of the workers.
2. Near-miss events are important safety-leading indicators that are often left unreported and undocumented. Although frameworks, which facilitate the process of reporting near-misses and visualizing them through BIM have been proposed [35], the possibility of using real-time monitoring systems to identify and document near-misses automatically has not yet been fully explored.
3. Real-time monitoring systems create enormous amounts of data. Further domain specific studies, including Big Data Engineering and Data Analytics, are required to extract valuable information from data obtained from real-time monitoring systems, and explore their applications to construction safety [36][37].
4. Visualization of information obtained via real-time monitoring systems through BIM platforms can improve analysis, facilitate accessibility, and enhance communication and training. While some studies have explored the integration of wireless sensor networks with BIM [38], solutions that combine vision-based monitoring systems with BIM platforms have not been sufficiently explored.
5. Rapid advancements in the field of computer vision, and an abundance of cameras on construction sites create an exceptional opportunity for vision-based techniques to be used as effective monitoring systems in the industry. However, the majority of vision-based studies have evaluated their proposed algorithms on datasets that are proprietary to that project and are often small in size. Lack of publicly available large datasets for construction safety monitoring that can be used as benchmarks makes performance comparison of various algorithms difficult.
6. Further research in the identification of critical accident precursors as they relate to fall, struck-by, caught in or between, and electrocution, and detailed breakdown of each accident precursor by defining quantitative parameters to be monitored can accelerate the development of automated monitoring systems.

6 Conclusion

Developing sensor-based systems for improving construction safety has recently gained a considerable amount of attention. In particular, vision-based monitoring systems have become an active topic of research in construction. This study has provided an overview of recent advancements in the domain as they relate to safety risk management and mapped the area for future work.

Safety risk management as described by Safe Work Australia {4} includes four steps, identifying hazards, assessing risks, controlling risks, and reviewing control measures. The impact of data-driven systems on each aspect of the process, along with examples of various methods employed by researchers have been discussed. The reviewed studies cover a range of technologies and approaches being used. These include but are not limited to utilization of wireless sensor networks, RFID, UWB, IMUs (accelerometers and gyroscopes), and vision-based techniques for location tracking, gait analysis, object detection, activity recognition, ergonomic assessment, and so on for the development of data-driven accident prevention systems.

Data-driven systems can be used for automated continuous monitoring of construction sites. They can be used to proactively prevent accidents by notifying workers or equipment operators of an incoming hazard. Further, such systems can be used to notify safety managers or site supervisors of unidentified, or newly appeared hazards. As a result, necessary actions can be taken in a timely manner to prevent accidents.

The overview provided in this study can be used as a guide for researchers pursuing research on intelligent accident prevention systems. It is acknowledged that this review study is only limited to construction industry.

Future research effort should examine state-of-the-art techniques and technologies used in other sectors and consider their applicability to tackling construction safety challenges.

Acknowledgments

This work was supported by a Monash Infrastructure (MI) grant. The authors would also like to acknowledge the support of the industry partners of this research. Any opinions, findings, conclusions, and recommendations expressed in this paper are those of the authors and do not necessarily reflect the views of the industry partners or Monash Infrastructure (MI).

References

[1] P. Swuste, A. Frijters, and F. Guldenmund, "Is it possible to influence safety in the building sector?," *Saf. Sci.*, vol. 50, no. 5, pp. 1333–1343, 2012.

[2] O. S. and H. Administration, "Commonly Used Statistics." [Online]. Available: https://www.osha.gov/oshstats/commonstats.html.

[3] R. Jin *et al.*, "A science mapping approach based review of construction safety research," *Saf. Sci.*, vol. 113, pp. 285–297, 2019.

[4] S. W. Australia, "How to manage health and safety risks: code of practice," 2011. [Online]. Available: https://www.safeworkaustralia.gov.au/system/files/documents/1702/how_to_manage_whs_risks.pdf.

[5] M. Arashpour and R. Wakefield, "Developing an uncertainty analysis model for off-site building production," in *8th International Structural Engineering and Construction Conference: Implementing Innovative Ideas in Structural Engineering and Project Management, ISEC 2015*, 2015, pp. 1121–1125.

[6] S. H. Mathieu Bastian Mathieu Jacomy, "Gephi: An Open Source Software for Exploring and Manipulating Networks," *Proceedings of the Third International ICWSM Conference*. 2009.

[7] M. Arashpour, R. Wakefield, N. Blismas, and B. Abbasi, "Quantitative analysis of rate-driven and due date-driven construction: Production efficiency, supervision, and controllability in residential projects," *J. Constr. Eng. Manag.*, vol. 142, no. 1, 2016.

[8] H. Kim, H.-S. H.-S. Lee, M. Park, B. Chung, and S. Hwang, "Automated hazardous area identification using laborers' actual and optimal routes," *Autom. Constr.*, vol. 65, pp. 21–32, 2016.

[9] H.-S. Lee, K.-P. Lee, M. Park, Y. Baek, S. Lee, and K.-P. L. Hyun-Soo Lee Moonseo Park, Yunju Baek, SangHyun Lee, "RFID-based real-time locating system for construction safety management," *J. Comput. Civ. Eng.*, vol. 26, no. 3, pp. 366–377, 2012.

[10] I. Awolusi, E. Marks, and M. Hallowell, "Wearable technology for personalized construction safety monitoring and trending: Review of applicable devices," *Autom. Constr.*, vol. 85, pp. 96–106, 2018.

[11] M. Arslan, C. Cruz, A.-M. Roxin, D. Ginhac, and C. C. Muhammad Arslan Ana-Maria Roxin, Dominique Ginhac, "Spatio-temporal analysis of trajectories for safer construction sites," *Smart Sustain. Built Environ.*, vol. 7, no. 1, pp. 80–100, 2018.

[12] M.-W. M.-W. Park and I. Brilakis, "Continuous localization of construction workers via integration of detection and tracking," *Autom. Constr.*, vol. 72, pp. 129–142, 2016.

[13] E. Konstantinou and I. Brilakis, "Matching Construction Workers across Views for Automated 3D Vision Tracking On-Site," *J. Constr. Eng. Manag.*, vol. 144, no. 7, 2018.

[14] B. Xiao and Z. Zhu, "Two-Dimensional Visual Tracking in Construction Scenarios: A Comparative Study," *J. Comput. Civ. Eng.*, vol. 32, no. 3, 2018.

[15] K. Yang, C. R. Ahn, M. C. Vuran, and H. Kim, "Collective sensing of workers' gait patterns to identify fall hazards in construction," *Autom. Constr.*, vol. 82, pp. 166–178, 2017.

[16] J. G. E. T.S. Abdelhamid, "Identifying root causes of construction accidents," *J. Constr. Eng. Manag.*, vol. 126, no. 1, pp. 52–60, 2000.

[17] M.-W. M.-W. Park, N. Elsafty, and Z. Zhu, "Hardhat-Wearing Detection for Enhancing On-Site Safety of Construction Workers," *J. Constr. Eng. Manag.*, vol. 141, no. 9, 2015.

[18] Q. Fang, H. Li, X. Luo, L. Ding, H. Luo, and C. Li, "Computer vision aided inspection on falling prevention measures for steeplejacks in an aerial environment," *Autom. Constr.*, vol. 93, pp. 148–164, 2018.

[19] W. Fang, L. Ding, H. Luo, and P. E. D. Love, "Falls from heights: A computer vision-based approach for safety harness detection," *Autom. Constr.*, vol. 91, pp. 53–61, 2018.

[20] H. Guo, Y. Yu, Q. Ding, and M. Skitmore, "Image-and-Skeleton-Based Parameterized Approach to Real-Time Identification of Construction Workers'

Unsafe Behaviors," *J. Constr. Eng. Manag.*, vol. 144, no. 6, 2018.

[21] W. Umer, H. Li, W. Lu, G. P. Y. Szeto, and A. Y. L. Wong, "Development of a tool to monitor static balance of construction workers for proactive fall safety management," *Autom. Constr.*, vol. 94, pp. 438–448, 2018.

[22] U. C. Gatti, S. Schneider, and G. C. Migliaccio, "Physiological condition monitoring of construction workers," *Autom. Constr.*, vol. 44, pp. 227–233, 2014.

[23] S. Zhang, J. Teizer, N. Pradhananga, and C. M. Eastman, "Workforce location tracking to model, visualize and analyze workspace requirements in building information models for construction safety planning," *Autom. Constr.*, vol. 60, pp. 74–86, 2015.

[24] Z. Riaz *et al.*, "BIM and sensor-based data management system for construction safety monitoring," *J. Eng. Des. Technol.*, vol. 15, no. 6, pp. 738–753, 2017.

[25] C. Cho, K. Kim, J. Park, and Y. K. Cho, "Data-Driven Monitoring System for Preventing the Collapse of Scaffolding Structures," *J. Constr. Eng. Manag.*, vol. 144, no. 8, 2018.

[26] Z. Kolar, H. Chen, and X. Luo, "Transfer learning and deep convolutional neural networks for safety guardrail detection in 2D images," *Autom. Constr.*, vol. 89, pp. 58–70, 2018.

[27] W. Fang, L. Ding, B. Zhong, P. E. D. Love, and H. Luo, "Automated detection of workers and heavy equipment on construction sites: A convolutional neural network approach," *Adv. Eng. Informatics*, vol. 37, pp. 139–149, 2018.

[28] M. M. Soltani, Z. Zhu, and A. Hammad, "Framework for Location Data Fusion and Pose Estimation of Excavators Using Stereo Vision," *J. Comput. Civ. Eng.*, vol. 32, no. 6, 2018.

[29] J. Seo, S. Han, S. Lee, and H. Kim, "Computer vision techniques for construction safety and health monitoring," *Adv. Eng. Informatics*, vol. 29, no. 2, pp. 239–251, 2015.

[30] N. D. Nath, R. Akhavian, and A. H. Behzadan, "Ergonomic analysis of construction worker's body postures using wearable mobile sensors," *Appl. Ergon.*, vol. 62, pp. 107–117, 2017.

[31] N. D. Nath, T. Chaspari, and A. H. Behzadan, "Automated ergonomic risk monitoring using body-mounted sensors and machine learning," *Adv. Eng. Informatics*, vol. 38, pp. 514–526, 2018.

[32] A. Golabchi, X. Guo, M. Liu, S. Han, S. Lee, and S. AbouRizk, "An integrated ergonomics framework for evaluation and design of construction operations," *Autom. Constr.*, vol. 95, pp. 72–85, 2018.

[33] M. Arashpour, R. Wakefield, B. Abbasi, M. Arashpour, and R. Hosseini, "Optimal process integration architectures in off-site construction: Theorizing the use of multi-skilled resources," *Archit. Eng. Des. Manag.*, vol. 14, no. 1–2, pp. 46–59, 2018.

[34] M. Arashpour, Y. Bai, G. Aranda-mena, A. Bab-Hadiashar, R. Hosseini, and P. Kalutara, "Optimizing decisions in advanced manufacturing of prefabricated products: Theorizing supply chain configurations in off-site construction," *Autom. Constr.*, vol. 84, pp. 146–153, 2017.

[35] E. M. Xu Shen, "Near-Miss Information Visualization Tool in BIM for Construction Safety," *J. Constr. Eng. Manag.*, vol. 142, no. 4, 2016.

[36] M. Bilal *et al.*, "Big Data in the construction industry: A review of present status, opportunities, and future trends," *Adv. Eng. Informatics*, vol. 30, no. 3, pp. 500–521, 2016.

[37] M. Arashpour and G. Aranda-Mena, "Curriculum renewal in architecture, engineering, and construction education: Visualizing building information modeling via augmented reality," in *9th International Structural Engineering and Construction Conference: Resilient Structures and Sustainable Construction, ISEC 2017*, 2017.

[38] Z. Riaz, M. Arslan, A. K. Kiani, S. Azhar, and M. A. Zainab Riaz Adnan K. Kiani, Salman Azhar, "CoSMoS: A BIM and wireless sensor based integrated solution for worker safety in confined spaces," *Autom. Constr.*, vol. 45, pp. 96–106, 2014.

Augmented Reality-Enabled Production Strategy Process

H. Nassereddine[a], D. Veeramani[b], and A. Hanna[a]

[a]Department of Civil and Environmental Engineering, University of Wisconsin–Madison, USA
[b]Department of Industrial and Systems Engineering, University of Wisconsin–Madison, USA
E-mail: hnassereddin@wisc.edu, raj.veeramani@wisc.edu, ashanna@wisc.edu

Abstract –

Disruptive technologies offer avenues to significantly improve the performance of construction project delivery. While the construction industry is often labeled as conservative and unimaginative with regard to technology adoption, significant strides have been made in recent years – specifically, the use of Building Information Modeling (BIM) for information storage, distribution and communication, as well as Lean construction techniques such as production planning and control (PPC). While the implementation of these innovative technologies and practices individually improve project performance, integrating them together can provide still greater benefits. BIM is certainly useful, but it alone is not a satisfactory answer to the paradox: how does one design and visualize a 3D product in a 2D space? Augmented Reality (AR) is a disruptive technology that can help address this challenge. AR is both an aggregator of information and an information publishing platform which allows users a spectrum of capabilities to 1) passively view displayed information, 2) actively engage and interact with published content, and 3) collaborate with others in real time from remote locations. No extant research effort has comprehensively investigated the opportunities and benefits of the integrated use of AR, BIM, and Lean in the planning process to improve project performance. This paper addresses precisely this research gap. Using insights gained from real-world construction projects, this paper examines the current state of production strategy process (PSP) development – an integral part of PPC, identifies pain-points and opportunities for process re-engineering using AR, and develops an AR-enabled PSP future state.

Keywords –

Augmented Reality; Building Information Modeling; Lean Construction; Production Planning and Control; Production Strategy Process; Takt Time Planning

1 Introduction

The construction industry is poised for significant growth. [1] forecasts that by 2030 the global expenditure on construction and related activities will reach $15.5 trillion. While the construction industry is quintessentially a factor in the prosperity of nations, it is fraught with waste and inefficiencies. Since the 1960s, manufacturing, service, and other industries have steadily and significantly increased their level of productivity, and consequently realized improved quality and better profitability [2]. There are several factors that play into construction's stagnant productivity: its project-based nature prevents the same holistic improvement that a process-based manufactory can achieve; the supply chain in construction is not consistent and is constantly in flux; the industry operates at a high level of complexity; there is a high level of heterogeneity; and construction is subject to the whims of international markets [3]. Per [4], a single instance of rework can cost on average 10% of the total project cost (in the United States). The volume of waste in construction has been estimated at between 25% and 50% of total project cost. This figure stems from inefficient control of labor, materials, interactions between trades, and the site in general.

The information-intensive nature of construction projects is a significant contributor to inefficiencies and losses in the industry. Between $17 billion and $36 billion are lost annually due to omitted information when design documents are translated into construction documents. [5] noted that on average only 55% of work planned and promised to be completed each week was actually completed. Other studies that focus on construction efficiency have documented 25% to 50% waste in coordinating labor and management [6].

In an effort to respond to these issues, significant strides have been made over the past two decades to improve construction planning, collaboration, and integration. These methods include Lean Construction via Production Planning and Control (PPC) and Information and Communication Technologies via Building Information Modeling (BIM).

Both these initiatives are radical in and of themselves,

and their impacts on construction have been far reaching and documented by multiple researchers.

[7] analyzed possible interactions between 24 principles of Lean Construction and 18 BIM functionalities. They identified 54 points of direct interaction, 50 positive and only 4 negative. Their conclusion was that implementing BIM and Lean alongside each other was optimal, as the functionality of BIM improved Lean processes significantly.

[8] contended that traditional delivery systems, like Design-Bid-Build (DBB) preclude proper implementation of these innovative practices, and instead recommended the use of Integrated Project Delivery (IPD). IPD is a construction contracting approach which promotes trust, collaboration, team chemistry, team alignment and maximizes value – key support mechanisms for the implementation of innovation [9]–[11].

Construction leaders have recognized this need for innovation, and have taken measures to transform their operating procedures. These leaders have realized benefits that put them ahead of other competitors in the construction sector – which given the competitive nature of the industry is a distinct advantage [11]. Thus, in order to remain competitive and support further growth, companies must successfully innovate to the point that they differentiate themselves from their peers. Early adopters have already realized benefits and brought the industry along, but must now ask: what comes next? [12].

Researchers argue that disruptive technologies have the potential to significantly improve project performance. One such technology that is currently gaining increasing traction is Augmented Reality (AR).

This paper will explore the new frontier that AR offers to construction companies, and how these firms may best exploit it by leveraging existing innovations (BIM and Lean) in an AR space to improve and innovate PPC, specifically the Production Strategy process (PSP).

2 Research Objectives and Methodology

The principal objective of this paper is to propose a new, AR-Enabled Production Strategy Process (AR-PSP). Our approach to achieving this goal entails the completion of several sub-goals: (1) investigate via literature review and expert interviews the current state of PPC and BIM integration in the industry; (2) identify current challenges and choke points in the current state PPC; (3) identify leverage areas for the integration of AR; and (4) define an AR-Enabled PSP future state. The research tasks and outcomes are described in the remainder of this paper.

3 Background

The notion of innovative production philosophy originates in Japan in the 1950s with the Toyota Production System (TPS) [13]. [14] defines this philosophy as a management philosophy for manufacturing, as well as a method of enhancing corporate vitality which aims to totally eliminate waste and achieve the maximum possible quality with the shortest possible lead time. In the early 1990s, the term ‘Lean’ production was introduced to contrast with ‘mass’ production [15]. The operational prerogative of Lean is the reduction of waste and maximization of value, and as such it has quickly become popular in healthcare, service, administration, production development, and construction [13], [16].

Lean as applied to construction was first discussed by [13]. In 2000, Koskela explained that Lean construction projects should be viewed as production systems, with the output being the built product [17]. This departs from the traditional view, or the transformative view, in which construction production is performed through individual activities that transform inputs (raw materials) into output (built product). Koskela put forth the Transformation/Flow/Value (TFV) theory, which prescribes that construction be viewed as the transformation of resources (raw materials), flow of materials and people, and the creation of value. In this system, construction projects are considered temporary production systems, with three pillars: eliminate waste, collaborate, and optimize the value-added chain [17]. The crucial challenge to construction is the spatial and scheduling coordination of the vested parties and disciplines. As such, innovative PPC methods like Last Planner System and Takt Time planning have come to the fore.

3.1.1 Last Planner™ System

The Last Planner System (LPS) was initially developed by Glenn Ballard and Greg Howell as a PPC system to improve construction predictability and reliability by bringing ‘last planners’ forward in the process [18]. The last planner is the project party who is responsible for the control of operative tasks – typically trade foreman. As such, the LPS involves these foremen with general contractors, architects, and owner’s representatives to bring site knowledge and practical experience to the table, making plans more realistic [19]. LPS decentralizes management tasks and improves cooperative work [20]. There are four chronological phases to LPS, as follows [21]:

1. Master Scheduling is a front-end planning process that produces a schedule describing the work to be carried out over the project duration.
2. Phase Scheduling generates a schedule covering each project phase, such as foundation, structural frame,

overhead, in-walls, or finishing. In a collaborative planning setup, the project team defines these phases and their various activities and uses pull planning to schedule the activities backward from the milestones.
3. Lookahead planning is the first step in production control (i.e., executing the work) and it usually covers a six-week time frame. At this level, activities are broken down into the level of production processes, constraints are identified, operations are designed, and assignments are made ready.
4. Weekly work planning is the most detailed plan in the system, and covers the particulars of work to be performed each week.

3.1.2 Takt Time Planning

The traditional view of construction considers a project as a conglomeration of various tasks and focuses on optimizing the process by which each task transforms its inputs into outputs. The shortcoming of this view is its lack of consideration for the dynamics and interdependencies of construction tasks [22].

[23] stressed the importance of considering space as a resource when planning construction projects. One space planning method that has been previously explored by academicians and professionals is Takt-Time planning. Takt is a German word which means 'beat' or 'rhythm.' It is applied to Lean Production to establish flow [24]. Implementing Takt into processes prevents overproduction, reduces lead times and inventory, stabilizes processes, optimizes workflow, and improves production capacity [25].

Within Lean Construction, 'Takt Time' is the unit of time in which a product must be produced (i.e. supply rate) to match the rate at which the product is needed (i.e., demand rate) [26].

Takt-time planning thus breaks work down into individual, manageable, chunks and determines their demand and supply rates [27]. [28], [26], [29] presented various methodologies to implement takt-time planning in construction. The current study presents a generic framework for implementing Production Strategy through the synthesis of the aforementioned methods with existing practices via industry expertise.

3.1.3 Integration of Last Planner System and Takt Time Planning

As noted by [30], LPS does not presuppose any specific work structure. The authors indicated that work structuring happened before project control – i.e., before lookahead planning could occur. However, location-based work structures like Takt-Time planning have been successfully integrated with LPS. [31] demonstrated the complimentary nature of Takt-Time and LPS, noting that Takt-Time introduces a standard, continuous flow of work that the LPS then is able to control, and LPS allows the flow of work to remain when obstacles emerge and must be adapted to.

[32] added a stage to the LPS: Production Strategy. Its three principal goals are: 1) implementing sequence and flow analyses, 2) defining production areas, and 3) designing production using takt-time principles to achieve stable and predictable construction flows.

Production Strategy is the portion of the PPC which has the highest potential for AR integration given its high volume of information and necessary level of communication and understanding.

3.2 Building Information Modeling

BIM has transformed the traditional paradigm of construction industry from 2D-based drawing information systems to 3D-object based information systems [33], [34]. For more than a decade, BIM has been one of the most important innovation means to approach building design holistically, to enhance communication and collaboration among key stakeholders, to increase productivity, and to improve the overall quality of the final product [35]. BIM's greatest strength is its ability to represent in an accessible way the information needed throughout a project lifecycle, rather than being fragmented [36]. BIM serves as a shared knowledge resource for information about a facility, forming a reliable basis for decisions during its lifecycle from inception to commissioning and beyond [37].

3.3 Augmented Reality

In the context of this research, Augmented Reality (AR) is characterized as both an information aggregator and a data publishing and visualization platform. As such, it allows the user to 1) passively view displayed information, 2) actively engage and interact with published content, and 3) collaborate with others in real time from remote locations [38], [39].

AR's market share is anticipated to reach $63 billion by 2021 and has found application in many domains such as gaming, medical, military, and manufacturing [40]. [41] described AR as the bridge between digital and physical realities; a new information delivery paradigm which permits consideration of both physical and digital information simultaneously. [42] found that AR facilitates a more thorough understanding of project documentation, construction progress, and communication between stakeholders. [3] stated that AR has great potential to improve the scheduling software.

3.4 Cross-Pollination of AR, BIM, and Lean

[38], [42] have developed several frameworks and prototypes that support the integration of BIM and AR

using different platform (i.e., Head Mounted Displays, smartphones, etc.). [43] noted that BIM and AR have a direct relationship with what Koskela defined in 1992 as construction integrated by computer and automatization in construction. [8] highlighted the potential use of AR for collaborative planning to improve predictability and reduce waste. [3] developed a framework and a mobile application, AR4Construction that integrated BIM and AR with Lean Construction methods, particularly Location-Based Management System to support the efficient management of construction works on site. Most existing literature focuses on implementing AR on the construction site. Our research focuses earlier in the project delivery process, and explores opportunities for integrating AR with PPC, such that it is used before construction begins, particularly with the PSP.

4 Production Strategy Process Current State

Before embarking on any process re-engineering effort, it is important to gain a sound understanding of the current state of practice as this will allow those involved in the innovation initiative to develop a shared basis for the improvement [44]. As such, this section describes the five principal steps of the PSP as it currently stands, using the example of an IPD project. The current PSP is illustrated in Figure 1.

Step 0 – Prerequisites

Prior to the Production Strategy, the project team (including last planners) must have set the expectations for the project and identified the major milestones for the project in the Master Scheduling phase. The project team then must divide the project into phases (such as overhead, in-walls, exterior finishes). Each phase should contain a series of activities performed by different trade partners. In the Production Strategy level, the project team works together to develop a production plan for each phase using the following four steps:

Step 1 – Perform Sequence and Flow Analysis

The project team reviews the 2D construction drawings of each phase, identifies repeatable and non-repeatable work, agrees on the linear sequence of construction activities of the corresponding phase, determine flow and non-flow areas, and finally determines the direction of the flow (i.e., work to be performed from North to South, East to West, etc.). The output of this step is a set of 2D construction drawings highlighting the flow and non-flow areas and indicating the direction of the flow for each phase.

Step 2 – Gather Information

The General Contractor (GC) conducts one-on-one interviews with the Trade Partners individually. For each activity within the corresponding phase, the GC provides the last planner of the corresponding trade partner with the 2D construction drawings. The last planner is then asked to use color markers to highlight the 2D drawings and show how much work they can complete in one day based on their ideal crew size. This is referred to as daily production. The last planner uses the direction of the flow identified earlier for the corresponding phase as a reference to identify their daily production. The GC acts as a facilitator. A 2D color-up construction drawing will be created for each activity within this step. Color-up drawings are not quantity takeoffs, as they require the last planner to think about how the work will be performed, by whom, where and in what sequence [26]. The GC then asks the last planner from each trade partner to use the color-up drawings and divide their floor plan into production areas. The production area, also referred to as Takt area, is a collection of individual daily productions. For example, if the last planners are asked to develop one-week takt areas, then each area should include five days' worth of work (assuming conventional schedule), or five daily productions. It should be noted that the precise mechanism of determining takt time is beyond the scope of this research. One week is used as a threshold since it is consistent with the weekly work plan phase of the LPS. The output of this second phase is a set of 2D drawings with production areas for each activity assigned to the corresponding phase.

Step 3 – Develop common areas

The GC collects the individual 2D production areas drawings, overlays them and attempts to identify common areas. The objective is to develop common areas within which the scopes of work of all the different activities are balanced.

Step 4 – Define Production Strategy

Once common areas are determined by the GC, the GC will determine the scope of work for each trade in that area and identify which trade(s) will bottleneck. The objective is to balance workflow such that all trades finish their work in an area within takt time for that area. The workflows are balanced either by adjusting crew size and hours or by adjusting work area. This process should go through multiple iterations to produce a cohesive strategy.

Step 5 – Validate the Production Strategy

The GC circulates the initial production plan to trade partners for feedback, which is collected and used to inform updates and revisions. Once a working plan is agreed upon, it should be documented via a convenient mechanism (e.g., an Excel spreadsheet).

5 Challenges in the Current State and Augmented Reality Opportunities

As is evident from Section 4, PSP is information-dense, lengthy, and iterative. The lynchpin of this process are numerous sets of 2D construction drawings, which are the conventional means of communication

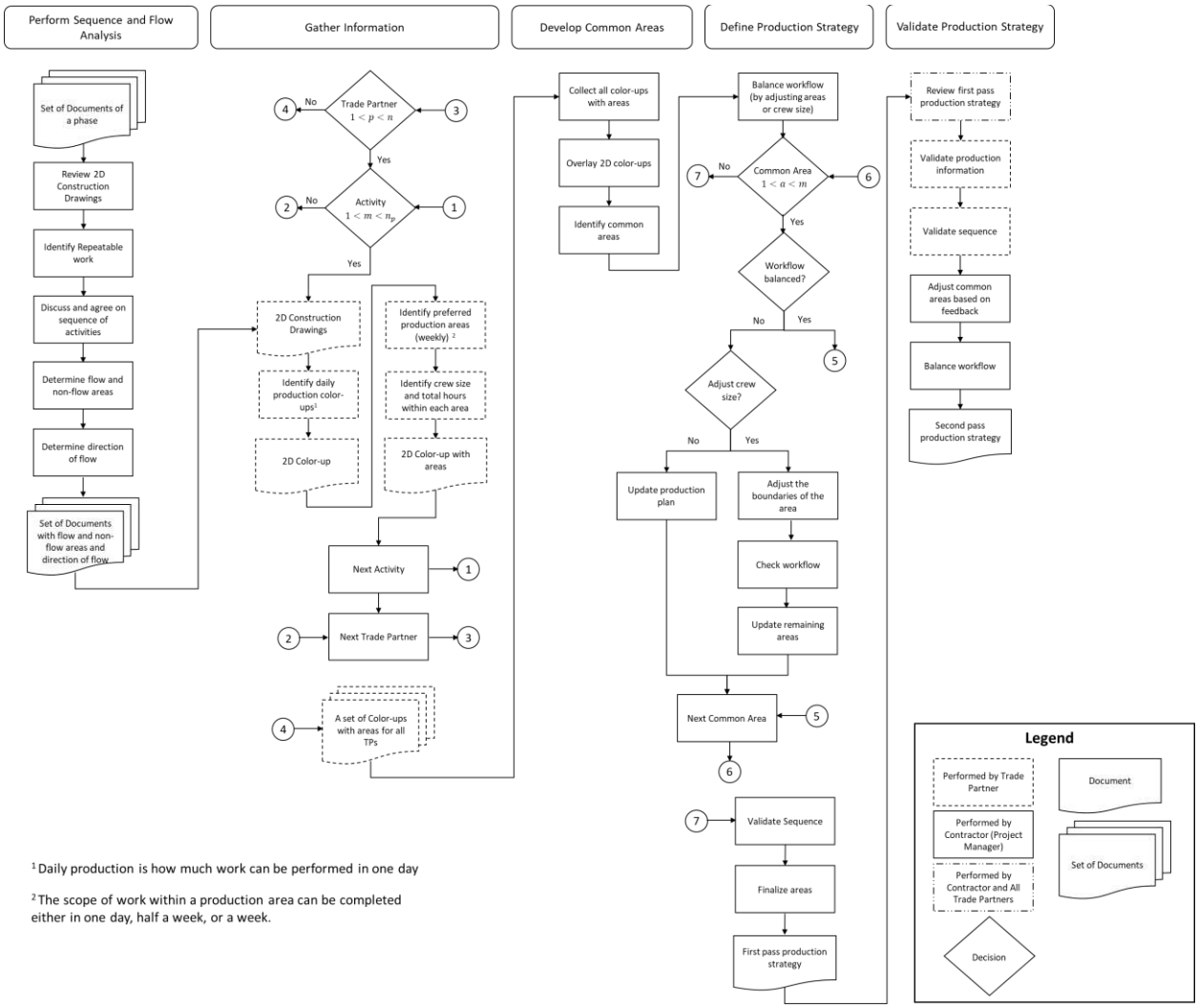

Figure 1. Current state of the production strategy process

between different contracting parties [45]. However, they present an individual view that is subject to individual interpretation [46]. Based on the 2D drawings, a last planner must visualize the built product, which will exist in 3D space. This presents a difficulty, as some information will not correctly translate (e.g., flat pipe vs. inclined pipe). Furthermore, another challenge that pertains to this phase is software diversity (i.e., 2D drawing packages may be prepared in numerous different CAD suites which are incompatible).

During the planning process, there is a lack of centralized information storage – necessary data is often stored in various forms (hard copy, spreadsheets, email chains, etc.) across different devices or locations.

As such, a challenge emerges in making sure last planners fully understand what work they are committing to.

Furthermore, the current process does not effectively consider safety, which should be a perspective from which the plan is validated.

In addition, this process requires project team to be available in the same space.

These challenges result in numerous iterations and mixed coordination of data, which ultimately increases the chances of miscommunications and associated non-valued added effort.

Opportunities to Integrate Augmented Reality:

Using augmented reality as the delivery mechanism for drawings and production information during the planning process has several advantages. First, it allows more advantageous use of BIM, as AR can operate in 3D space. Second, it creates a living single source of information, reducing miscommunication. This allows for an overall improvement in collaboration and communication, permits the last planner a better understanding of scope of work and as a result produces

more reliable commitments, allows for safety analysis in more real space, improves spatial cognition, and allows an iterative tracking system. According to [41] the use of AR eliminates the need to mentally translate two-dimensional information into the three-dimensional world, and elaborate that this improves the ability to absorb and interpret information which leads to better decision making, and tasks being executed faster and more efficiently. A study by [47] noted that AR eases information retrieval for those working in information-intensive environments, and increases the efficiency of the working processes through avoiding information overload. Finally, using AR facilitates standardization of the process to a single governing data point and citation.

6 AR-enabled Production Strategy Process Future State

We envision an AR-enabled PPC process in which the BIM model is used as the guide and chief reference for production strategy development. Thus, BIM is a precursor to implementing AR-PPC. The following five steps define the process by which AR-PPC can be implemented.

Step 1 – Perform Sequence and Flow Analysis

The project team:

1. collectively uses the 3D model as a guide and reference to visualize the corresponding construction phase(s) and its activities
2. interacts with the 3D model and selects repeatable work
3. interacts with the 3D model and collectively develops the sequence of activities and identifies potential safety hazards, thus improving the decision-making process in a collaborative environment
4. interacts with the 3D models and collectively discuss flow and non-flow areas
5. interacts with the 3D models and collectively assess the project and determine the direction of flow.

AR helps project participants from diverse trades better understand each other's scope and flow of work, facilitating better collaborative decision making. The output of this step is saved within the 3D model and accessible at any later point by the project team. This central information repository is more efficient than traditional methods, and provides additional transparency – all participants are provided the same information.

Step 2 – Gather Information

Last planners will be among the project team participants with access to the information generated in Step 1. Integration of BIM and AR allows 3D visualization of the scope of work, and improves visual understanding by providing an interactive solid model of the whole project. Within the augmented environment, the last planner:

1. selects to only visualize their scope of work
2. performs their daily production for the entire phase in a virtual environment, which in addition to generating 3D color-up drawings, will also create quantity takeoffs. The last planner can also investigate the space for any safety problems and adjust their daily production accordingly
3. creates production areas virtually. This allows the last planner to automatically visualize the scope of work within each area, obtain the total quantity of work to be installed, and input production information (such as labor hours, crew size, working days, constraints, etc.). This information can be easily retrieved by the last planner.

Each last planner can create their production areas and save them to the same source, allowing project managers to coordinate and check for trade clashes

Step 3 – Develop Common Areas

The GC retrieves the results of the last planner's work from step 2. Their production areas are overlaid, allowing visual creation of common areas.

Step 4 – Define Production Strategy

The GC, once common areas are developed, retrieves the production information that was input pertinent to each scope of work. This facilitates the performance of workflow balancing in an environment that updates in real-time, improving efficiency. AR thus acts as a decision support tool for the GC as they create the production strategy plan draft.

Step 5 – Validate Production Strategy

Once the first-pass production strategy is complete, the team meets in the augmented environment to review it. This greatly enhances collaboration, as it facilitates meetings that do not require co-location of participants, as well as changes that are visible in real-time to all parties.

The production plan created in AR can be used during project execution to visualize the work to be installed and to track performed work. Project Percent Complete could be then calculated more accurately and effectively.

In summary, AR has the potential to transform the current state of the PSP. It provides a common source of truth which enables a higher level of collaboration among the participants of the PSP when working in the same space or in remote locations. The AR-enabled PSP is a centralized reference that encompasses the different types of information used during the PSP. AR enables the users to interact with the built product in real-time, thereby enhancing visualization, space perception, and decision-making. The technology also allows last planners to identify potential safety hazards during planning and integrate safety more effectively into the production strategy.

7 Future Work

Based on the framework for an AR-enabled PSP that we have defined in this paper, we are developing a proof-of-concept application on a wearable display. Using BIM models from real-world construction projects, we are validating the reengineered future state PSP and the associated benefits.

8 Conclusions

Most literature which was reviewed focuses on the avenues to integrate AR into site operations (visualizing blueprints, safety, etc). However, this paper and research effort considers integrating AR into PPC, and specifically into the Production Strategy Process. A process map was presented which highlights the current state of the practice based on previous research and industry expertise. Challenges which exist in the current method were then presented, and opportunities to address these challenges via AR were explored.

Finally, a conceptual future state of the Production Strategy was described. The principal advantage that AR-enabled PSP has is its centralization of information and increased collaboration over traditional PSP.

9 Acknowledgements

This research was funded in part by The Boldt Company.

References

[1] PricewaterhouseCoopers. Global Construction 2030: A global forecast for the construction industry to 2030 Online: https://www.pwc.com/vn/en/industries/engineering-and-construction/pwc-global-construction-2030.html, Accessed: 12/01/2019.

[2] McKinsey&Co. The construction productivity imperative. Online: https://www.mckinsey.com/industries/capital-projects-and-infrastructure/our-insights/the-construction-productivity-imperative. Accessed: 12/01/2019.

[3] Ratajczak J., Schweigkofler A., Riedl M. and Matt D. Augmented Reality Combined with Location-Based Management System to Improve the Construction Process, Quality Control and Information Flow, *Advances in Informatics and Computing in Civil and Construction Engineering*, 2019.

[4] Forbes L. H. and Ahmed S. M. *Modern construction: lean project delivery and integrated practices*. CRC Press, Boca Raton, FL, 2011.

[5] Howell G. and Lichtig W., Lean Construction Opportunities Ideas Practices. Speech presented to the Cascadia LCI "Introduction to Lean Design" Workshop. Seattle, Washington, 2008.

[6] Modular Building Institute. Improving construction efficiency & productivity with modular construction, 2010.

[7] Sacks R., Radosavljevic M. and Barak R. Requirements for building information modeling based lean production management systems for construction, *Automation in Construction*, 19(5):641-655, 2010.

[8] Dave B., Koskela L., Kiviniemi A., Tzortzopoulos P. and Owen R., *Implementing lean in construction: lean construction and BIM*. Ciria, London, 2013.

[9] Dave B., Seppänen O. and Modrich R.-U., Modeling Information Flows Between Last Planner and Location Based Management System. *Production Planning and Control*, 2016.

[10] Fischer M., Ashcraft H., Reed D. and Khanzode A. *Integrating Project Delivery*. John Wiley & Sons, Inc., Hoboken, NJ, 2017.

[11] Sacks R., Korb S. and Barak R. *Building Lean, Building BIM: Improving Construction the Tidhar Way*. Routledge, 2017.

[12] Mossman A. Why isn't the UK construction industry going lean with gusto?, 2009.

[13] Koskela L., Application of the new production philosophy to construction, 1992.

[14] NPS. The New Production System. Online: http://www.nps-kenkyukai.jp/english/index.html, Accessed: 12/01/2019.

[15] Womack J. P., Jones D. T. and Roos D. *The machine that changed the world: the story of lean production*. Simon and Schuster, 1990.

[16] Tezel A. and Aziz Z. From conventional to IT based visual management: a conceptual discussion for lean construction, *Journal of Information Technology in Construction*. 22: 220–246, 2017.

[17] Koskela L. An exploration towards a production theory and its application to construction, 2000.

[18] Mossman A. Last Planner® 5 + 1 crucial & collaborative conversations for predictable design & construction delivery, 2013.

[19] Eilers H., Morrow M. and Parco W. Last Planner System and the Construction Project Schedule. *Association for the Advancement of Computing in Education*, 2016.

[20] von Heyl J. and Teizer J. Lean Production Controlling and Tracking Using Digital Methods. In *Proceedings of the 25th Annual Conference of the Int'l Group for Lean Construction*, pages 127–134, Heraklion, Greece, 2017.

[21] Hamzeh F., Ballard G. and Tommelein I. Rethinking Lookahead Planning to Optimize Construction Workflow, *Lean Construction Journal*, 2012.

[22] Ghosh S. and Reyes M., Production Planning Using Location Based Management and 'Takt' Time: A Postmortem and Premortem. In *Proceedings of the 53rd ASC Annual Int'l Conference*, 2017.

[23] Ballard G. and Howell G. What Kind of Production Is Construction? In *Proceedings of the 6th Int'l Annual Conference Int'l Group for Lean Construction*, 1998.

[24] Liker J. *The Toyota way: 14 management principles from the world's greatest manufacturer*. McGraw-Hill , New York, 2004.

[25] Haghsheno S., Binninger M., Dlouhy J. and Sterlike S. History and Theoretical Foundations of Takt Planning and Takt Control. In *Proceedings of the 24th Annual Conference of the Int'l Group for Lean Construction*, Boston, MA, 2016.

[26] Frandson A., Berghede K. and Tommelein I. Takt time planning for construction of exterior cladding. In *Proceedings of the 21st Annual Conference of the Int'l Group for Lean Construction*, Fortaleza, Brazil, 2013.

[27] Tommelein I. Collaborative Takt Time Planning of Non-Repetitive Work", In *Proceedings of the 25th Annual Conference of the International Group for Lean Construction*, Heraklion, Greece, 2017.

[28] Fiallo M. and Howell G. Using production system design and takt time to improve project performance. In *Proceedings of the 20th Annual Conference of the International Group for Lean Construction*, San Diego, CA, 2012.

[29] Yassine T., Bacha M. B. S., Fayek F. and Hamzeh F. Implementing takt-time planning in construction to improve work flow. In *Proceedings of the 22nd Ann. Conf. of the Int'l Group for Lean Construction*, 2014.

[30] Ballard G. and Tommelein I., Current Process Benchmark for the Last Planner System. *Lean Construction Journal*, 89, 2016.

[31] Frandson A., Berghede K. and Tommelein I. Takt-time planning and the last planner. In *Proceedings of the 22nd Ann. Conf. of the Int'l Group for Lean Construction*, 2014.

[32] Ebrahim M., Berghede K., Thomack D., Lampsas P., Kievet D. and Hanna A. A Framework of Five-Stream Production System for Megaprojects", In *Proceedings of the 25th Annual Conference of the International Group for Lean Construction*, Heraklion, Greece, 2017.

[33] Arayici Y., Coates P., Koskela L., Kagioglou M., Usher C. and O'Reilly K., Technology adoption in the BIM implementation for lean architectural practice. *Automation in Construction*, 20(2):189-195, 2011.

[34] BIM Alliance. BIM Alliance on BIM. Online: https://www.bimalliance.se/vad-aer-bim/bim-alliance-om-bim/, Accessed: 12/01/2019.

[35] Schweigkofler A., Monizza G. P., Domi E., Popescu A., Ratajczak J., Marcher C., Riedl M. and Matt D. Development of a Digital Platform Based on the Integration of Augmented Reality and BIM for the Management of Information in Construction Processes, *Product Lifecycle Management to Support Industry 4.0*, 540, 2018.

[36] Carlsén A. and Elfstrand O. Augmented Construction: Developing a framework for implementing Building Information Modeling through Augmented Reality at construction sites, 2018.

[37] Rossini F. L., Novembri G. and Fioravanti A. BIM and Agent-Based Model Integration for Construction Management Optimization", In *Proceedings of the 25th Annual Conference of the Int'l Group for Lean Construction*, Heraklion, Greece, 2017.

[38] Wang X., Love P. E. D., Kim M. J., Park C.-S., Sing C. and Hou L., A conceptual framework for integrating building information modeling with augmented reality. *Automation in Construction*, 34:37–44, 2013.

[39] Augmented Reality Gartner's Tech Definition", Online: https://www.gartner.com/it-glossary/augmented-reality-ar/, Accessed: 12/01/2019.

[40] Campbell M., Kelly S., Jung R. and Lang J., The State of Industrial Augmented Reality 2017, 2017

[41] Porter M. and Heppelmann J. Why Every Organization Needs an Augmented Reality Strategy. *Harvard Business Review*, 2017

[42] Meža S., Turk Ž. and Dolenc M. Measuring the potential of augmented reality in civil engineering. *Advances in Engineering Software*, 90:1–10, 2015.

[43] Calderon-Hernandez C. and Brioso X. Lean, BIM and Augmented Reality Applied in the Design and Construction Phase: A Literature Review. *International Journal of Innovation, Management and Technology*, 9(1):60–63, 2018.

[44] Sheperis C., Young J. S. and Daniels M. H., *Counseling research: Quantitative, qualitative, and mixed methods*. Pearson, Boston, MA, 2010.

[45] Ghaffarianhoseini A., Doan D., Zhang T. and Tookey J. Integrating augmented reality and building information modeling to facilitate construction site coordination", In *Proceedings of the 16th Int'l Conference on Construction Applications of Virtual Reality*, Hong Kong, 2016.

[46] Cory C. A. Utilization of 2D, 3D, or 4D CAD in construction communication documentation. In *Proceedings of the 5th Int'l Conference on Information Visualisation*, 2001.
[47] Chu M., Matthews J. and Love P. E. D. Integrating mobile Building Information Modelling and Augmented Reality systems: An experimental study. *Automation in Construction*, 85:305–316, 2018.

Chatbot System for Data Management: A Case Study of Disaster-related Data

J.Y. Chen[a], M. Tsai[b], C. Yang[c], H. Chan[b], and S. Kang[c]

[a] Department of Civil Engineering, National Taiwan University, Taiwan
[b] Department of Civil Engineering, National Taiwan University of Science and Technology, Taiwan
[c] Department of Civil and Environmental Engineering, University of Alberta, Canada
E-mail: yie@caece.net, menghan@gapps.ntust.edu.tw, chenghsuan@ualberta.ca, katrina.hyc@gmail.com, sckang@ualberta.ca

Abstract -

This research aims to explore the effectiveness of chatbot system for highly-complex data management. With the growing popularity of mobile devices, the conversational information technology (IT) service, such as chatbot, has permeated into our daily life. Conversation-based systems are now widely utilized for helping the user to access the data they need or control other devices more intuitively. Although lots of systems have been developed for personal assisting, such as Siri, Alexa, and so on, or customer services, seldom of them are used for data management. Therefore, this research will focus on exploring the application of chatbot system for the management of complex data. We used the disaster-related data and a chatbot system developed in the previous work as a case study. A one-year field test was conducted for figuring out the feasibility and effectiveness of chatbot system for data management. After the field test, we found that the number of users of the developed system was doubled within six months. The usage of the system increased approximately 2.5 times with six months. We also found that the users now rely on the chatbot system for their daily tasks. The results reveal that the chatbot system may be a promising direction for highly-complex data management due to its intuitive data accessing process.

Keywords –

Data Management; Conversational System; Chatbot

1 Introduction

Data management has always been a critical issue in the field of engineering. Recently, the fast development of the internet and high computational hardware bring the explosion of digital data. Around 2.5 exabytes of data are created each day in 2012 [1]. Therefore, how to effectively translate those massive amounts of data into the knowledge that can improve the decision-making and performance is essential and worth for detailed research. To deal with the massiveness and diversity of the data, many information technologies were developed within these years. For instance, the Lesson Learn Center proposed by Kang et al. provided all the historical disaster data in Taiwan for decision-makers' reference [2]. Terroso-Saenz et al. proposed an IoT platform for the management of energy data in 2019 [3]. Carmona et al. used the IoT technology in the data collection of the construction site for enhancing the productivity of constructions [4].

Although IT related systems have been developed, the user interface and the data retrieval approach of these systems seem unintuitive and inconvenient for users. Therefore, studies have recently started to focus on developing conversation-based systems [5, 6] by considering user involvement [7]. The Siri, Amazon Alexa, and Google are the most famous examples. Those conversational systems play the role of personal assistant that allows users to check the weather, traffic, email, and so on. Ko and Lin used a chatbot system as a virtual assistant for business card management [8]. Besides personal assisting, such systems are also widely utilized as customer services. For instance, Thomas and Gupta et al. both utilized the chatbot for the customer service for e-business [9, 10]. Despite that chatbots have been developed for different purposes, the application of the chatbot system in complex data management is rarely discussed.

2 Previous research

To explore the feasibility of applying the conversational system on data management, we developed a chatbot, named Ask Diana, for water-related disaster in 2018 [11]. Among different types of data, disaster-related data is one of the most difficult for managing due to its following characteristics [12]:

- large number of producers and consumers of information;
- time sensitivity of the exchanged information;
- various levels of trustworthiness of the information sources;
- lack of common terminology;
- combination of static and streaming data;
- heterogeneous formats, ranging from free text to XML and relational tables.

Ask Diana was designed as a keyword-based chatbot system for disaster data management. It consists of a disaster database, a user-intent understanding mechanism, and a mobile-based user interface (Figure 1). The system allows the disaster-related personnel to access the data they need through directly using inputting keywords. Building on a popular communication platform, LINE, also allows the user to forward the data to others easily.

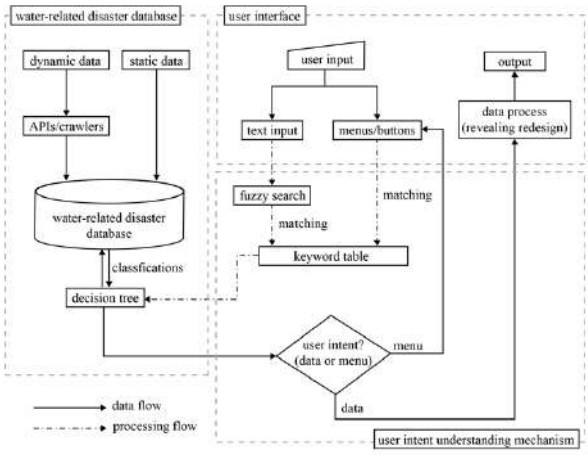

Figure 1. The system structure of Ask Diana [11]

Ask Diana improved data management of disaster data delivery process and allow decision-makers to access real-time disaster data by themselves. During emergency operation period, rapid response is essential. Decision-makers require real-time disaster data to make decisions. However, decision-makers are high-level government officials, who are not the first line operators who operate the disaster response system. Therefore, in real emergency operation process, decision-maker would ask their major supervisors to provide disaster data which required no emergency response personnel's judgement or confirmation. Then, the supervisors would ask emergency operators and their cooperation team to provide disaster data. After cooperation team fulfils the requirement, they would provide disaster data to operators. Operators would then deliver the data to major supervisors. Finally, the major operators would deliver the related information to decision-makers for further decision making. The delivery process is very time-consuming which would usually cost more than one hour. It may somehow make the disaster data hard to deliver in time.

Ask Diana was validated to have higher efficiency in disaster data retrieving through a six-month field test. Ask Diana has an easy user interface to allow user access to real-time disaster data by themselves. Therefore, decision-makers could require disaster data just by click Ask Diana's menu or input simple disaster keywords. Ask Diana would provide feedback in just seconds without long-time latency. The related personnel were thus willing to use Ask Diana for their daily tasks. Three hundred eighty-one users have used Ask Diana for disaster response activities. Twelve thousand seventy-eight using records were collected within six months (Figure 2).

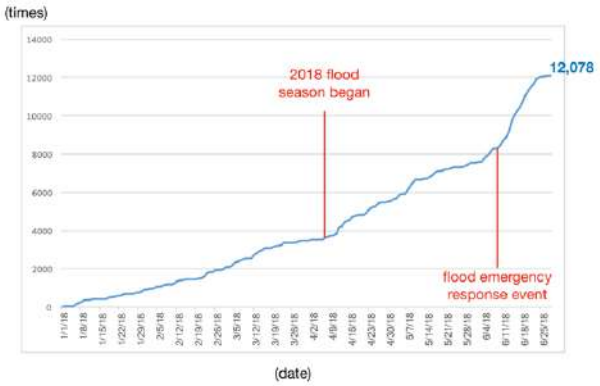

Figure 2. The user records of the field test [11]

3 Research Objectives

This research aims to explore the feasibility of utilizing the chatbot system on data management. A field test of utilizing the developed system into an actual field was conducted. The user's behaviours were all recorded for further analysis. After the field test, the advantages and the shortage of chatbot system for data management would be concluded.

4 Field Test

For feasibly test, we cooperated with the government of Taiwan (Water Hazard Mitigation Center) to have a six-month field test in our previous research. In this research, we extended the duration of the field test to one year for more detailed observation of the user behaviours. The background of the users and the usage of Ask Diana were all recorded for analysis.

Based on the user log, 790 users have added Ask Diana as their Line friend at the end of 2018. The number is doubled within only six months, which represents the

willing to using Ask Diana for their tasks is gradually increasing. Figure 2 illustrates the distribution of the registered user role. Among the 790 users, 95% are disaster response personnel, 2% are system developers, 2% are system managers, and 1% are decision-makers.

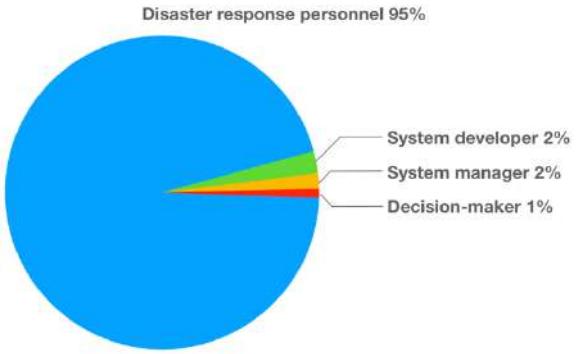

Figure 3. The distribution of the user role

Ask Diana collected totally 31,355 records from actual users within a year (Figure 3). The usage is around 2.5 times increasing compared with the first six months. In Figure 3, we can find that the usage will have a significant rising when major disasters happened.

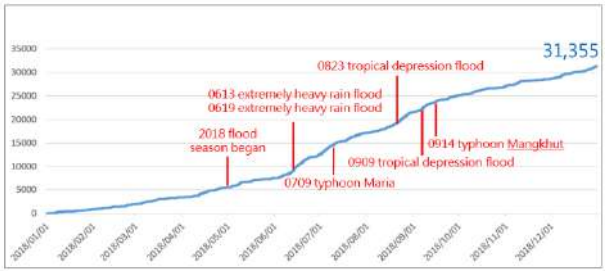

Figure 4. The cumulative usage graph of Ask Diana during Jan. 1st ,2018 to Dec. 31th, 2018

Besides the user logs, we also collected the user feedbacks during the field test. According to those feedbacks, three major comments were concluded:

1. Ask Diana provides an intuitive platform for the user to access data easily and efficiently. With the low threshold operation, the willing of the user to use it for actual disaster response activities were increased.
2. The keyword-based mechanism of Ask Diana did not allow the user to get the data through hierarchical questions. Therefore, they needed to provide Ask Diana with the keyword of the data specifically.
3. The user expected that Ask Diana could have some emotional responses. For example, when the user inputted "Hi Diana, I would like to know the flooding situations now," instead of just providing the flooding information, it will be better if Ask Diana can reply "Taipei is now having serious flooding, please keep your attention at any time!"

5 Conclusions

This research explored the feasibility and effectiveness of the chatbot system in data management. Through a long-term field test on disaster-related data with user feedbacks collected, we found that the chatbot system can have high performance and efficiency in data management, even for highly-complex data. Due to the intuitive operation process of chatbot system, the willing of the user to use such a system can be significantly increased. More discussions can be found in Ask Diana: A Keyword-Based Chatbot System for Water-Related Disaster Management [11]. However, as a chatbot system, the user will expect it to have a more human-like response with emotions. Also, for the complex data, the user may need to retrieve the data through hierarchical queries. In conclusion, the chatbot system can effectively be utilized for data management meanwhile provide an intuitive platform for users to access the data.

6 Acknowledgement

This research was supported by Taiwan's Ministry of Science and Technology (MOST) under contract 107-2119-M-011-002 & 108-2119-M-011-002. Also, Weather Climate and Disaster Research of National Taiwan University (NTU) and Water Resources Agency provided great support and enormous feedbacks in field application and user test. Prof. Yun-Cheng Tsai of NTU assistance in developing the system and conducting user tests.

References

[1] Brynjolfsson, E., & McAfee, A. (2012). Big Data: The Management Revolution. *Harvard Business Review*, (October), 1–12. https://hbr.org/2012/10/big-data-the-management-revolution. (Assessed: Mar. 22, 2019).

[2] Kang, S. C., Yang, C. C., Shiu, R. S. (2012). Lesson Learned Center. *Conference for Disaster Management in Taiwan*, Taipei, Taiwan.

[3] Terroso-Saenz, F., González-Vidal, A., Ramallo-González, A. P., & Skarmeta, A. F. (2019). An open IoT platform for the management and analysis of energy data. *Future Generation Computer Systems*, 92, 1066–1079. https://doi.org/https://doi.org/10.1016/j.future.2017.08.046.

[4] Carmona, A. M., Chaparro, A. I., Velásquez, R.,

Botero-Valencia, J., Castano-Londono, L., Marquez-Viloria, D., & Mesa, A. M. (2019). Instrumentation and Data Collection Methodology to Enhance Productivity in Construction Sites Using Embedded Systems and IoT Technologies. In I. Mutis & T. Hartmann (Eds.), *Advances in Informatics and Computing in Civil and Construction Engineering* (pp. 637–644). Cham: Springer International Publishing.

[5] Griol, D., Molina, J. M., Callejas, Z. (2015). A proposal for the development of adaptive spoken interfaces to access the web. *Neurocomputing*, 163, 56-68. https://doi.org/10.1016/j.neucom.2014.09.087.

[6] Kloeckner, K., Davis, J., Fuller, N. C., Lanfranchi, G., Pappe, S., Paradkar, A., … Wiesmann, D. (2018). Conversational IT Service Management. In *Transforming the IT Services Lifecycle with AI Technologies* (pp. 75–93). Cham: Springer International Publishing. https://doi.org/10.1007/978-3-319-94048-9_5.

[7] Lundkvist, A., & Yakhlef, A. (2004). Customer involvement in new service development: a conversational approach. *Managing Service Quality: An International Journal*, *14*(2/3), 249–257. https://doi.org/10.1108/09604520410528662.

[8] Ko, M.-C., & Lin, Z.-H. (2018). CardBot: A Chatbot for Business Card Management. In Proceedings of the 23rd International Conference on Intelligent User Interfaces Companion (pp. 5:1–5:2). New York, NY, USA: ACM. https://doi.org/10.1145/3180308.3180313.

[9] Thomas, N. T. (2016). An e-business chatbot using AIML and LSA. *2016 International Conference on Advances in Computing, Communications and Informatics, ICACCI 2016*, 2740–2742. https://doi.org/10.1109/ICACCI.2016.7732476.

[10] Gupta, S., Borkar, D., Mello, C. D. & Patil, S. (2015). An E-Commerce Website based Chatbot. *International Journal of Computer Science and Information Technologies*, 6(2), 1483–1485. https://doi.org/ijcsit20150602125.

[11] Tsai, M.-H., Chen, J. Y., & Kang, S.-C. (2019). Ask Diana: A Keyword-Based Chatbot System for Water-Related Disaster Management. Water, 11(2). https://doi.org/10.3390/w11020234.

[12] Hristidis, V., Chen, S.-C., Li, T., Luis, S., & Deng, Y. (2010). Survey of data management and analysis in disaster situations. *Journal of Systems and Software*, *83*(10), 1701–1714. https://doi.org/https://doi.org/10.1016/j.jss.2010.04.065.

Integrating Hardware-In-the-Loop Simulation and BIM for Planning UAV-based As-built MEP Inspection with Deep Learning Techniques

K. Wang[a] and J.C.P. Cheng[a]

[a]Department of Civil and Environmental Engineering, the Hong Kong University of Science and Technology, Hong Kong SAR
E-mail: kwangaw@connect.ust.hk, cejcheng@ust.hk

Abstract –

Unmanned Air Vehicles (UAVs) are increasingly used and have many potential applications in the architecture, engineering, and construction (AEC) industry. UAVs are now commonly controlled manually with an experienced survey engineer in field operation, but UAVs can also fly autonomously with the support of localization technologies such as simultaneous localization and mapping (SLAM). Autonomous flying of UAVs can reduce human effort and minimize human error. However, it requires careful flight path planning, active environment sensing, and effective obstacle avoidance techniques, especially where the built environment is complex and space is tight. Currently, algorithms flight path planning, object detection and obstacle avoidance are developed based on testing that involves actual Survey UAVs; this is not only time consuming but also expensive and hazardous in the sense that it may damage hardware and injury ground personnel if error-induced crashes occur. This paper presents a hardware-in-the-loop simulator which can simulate the behavior of a drone and generate synthetic images from the scene as datasets, detect and verify as-built MEP objects with a trained neural network, and generate point cloud data for validating as-designed BIM model with as-built BIM model in the future. The system architecture, operations, and performance of the developed simulator are discussed, followed by an illustrative example.

Keywords –

Automation; Flight Path Planning; Robotic Perception; Simulation; UAV

1 Introduction

Surveying using terrestrial laser scanners has been common practice in the AEC industry. Meanwhile, building information modeling [1] (BIM) has been increasingly required by both public and private sectors as a part of any building and infrastructure developments. As the more recent a design is, the higher level of details its digital 3D model will contain, and as-designed BIM models need to be validated against their as-built counterparts. For example, mechanical, electrical and plumbing (MEP) inspection of a tunnel traditionally requires inspectors to go inside the tunnel and use a terrestrial laser scanner to inspect and confirm coherence with the as-designed BIM model. This method normally requires much manpower, making it inefficient, time-consuming and risky. Some civil structures like tunnels and wastewater treatment plants can have hazardous volatile organic chemicals (VOCs) [2] which can lead to cancer and other medical problems. For another example, to conduct a bridge inspection, expensive high-energy laser scanners and a helicopter are often required. UAVs equipped with cameras, Lidar and/or other detection equipment are promising alternatives as they can collect point cloud data [3] and photogrammetry images [4] and generate 3D models for inspection and visualization.

Testing a physical survey UAV in a real-world environment can be dangerous, expensive and time-consuming. On April 28, 2017, the US Federal Aviation Administration (FAA) released a very detailed report on drone crash tests. The 107-page report was a joint research involving 23 academic institutions working together with the FAA with the aim to understand the risk and hazards (including possible injuries) of the system failure of a UAV. The objective is based on the FAA's research addressing seven questions: (1) What are the hazard severity criteria for a UAV collision (e.g. weight and kinetic energy)? (2) What is the severity of a UAV collision with aircraft on the ground? (3) What is the severity of a UAV collision with property on the ground? (4) What is the severity of a UAV collision with a person on the ground? (5) What are the characteristics of a UAV where it will not be a risk to an aircraft or person/property on the ground? (6) Can the severity of a UAV collision

with an aircraft or person/property on the ground be characterized into UAV categories and what would those categories look like? (7) How can UAV be designed so as to minimize the potential damage done during a collision? [5] In the study of human injuries due to loss of control of a UAV, Section 2.4.4 (Payload Loss Injury Applications) and Section 2.4.5 (Fire Injury Applications) of the report are the most relevant to our research interest: indoor UAV scanning application. In an indoor environment under the condition with no magnetic and wind interference, yet with low lighting and weak GPS signals, a UAV can still be prone to crashes even when the operator is an experienced pilot. Energy sources such as Lithium Polymer battery or Nitromethane mixed with methanol [6] (depending on the overall payload of the vehicle) may ignite upon ground collision, which poses danger to the ground operator. In addition, a survey UAV that carries high precision laser scanners, cameras, and/or various control and processing units on board are too expensive to be damaged. Even a single failure can result in a devastating crash. Therefore, designing a virtual environment close to the real environment for UAV simulation and training before testing a physical UAV on site is proposed in this framework.

Many simulators have been established in the fields of robotic research, computer vision, gaming technology. The UE4 [7] engine, for example, is considered a leading game engine among others such as Unity to provide many resources such as AAA-level realistic virtual environment, through its state-of-the-art shader and the recently improved ray tracing rendering technique. These photorealistic virtual environments can be used as a source for generating images for neural network training, such as training a convolutional neural network to detect objects. However, simulators like UE4 or Unity [8], despite the shader rich feature that they support, lack features such as predefined sensors models provided in the (robotics operating system) ROS [9] simulator.

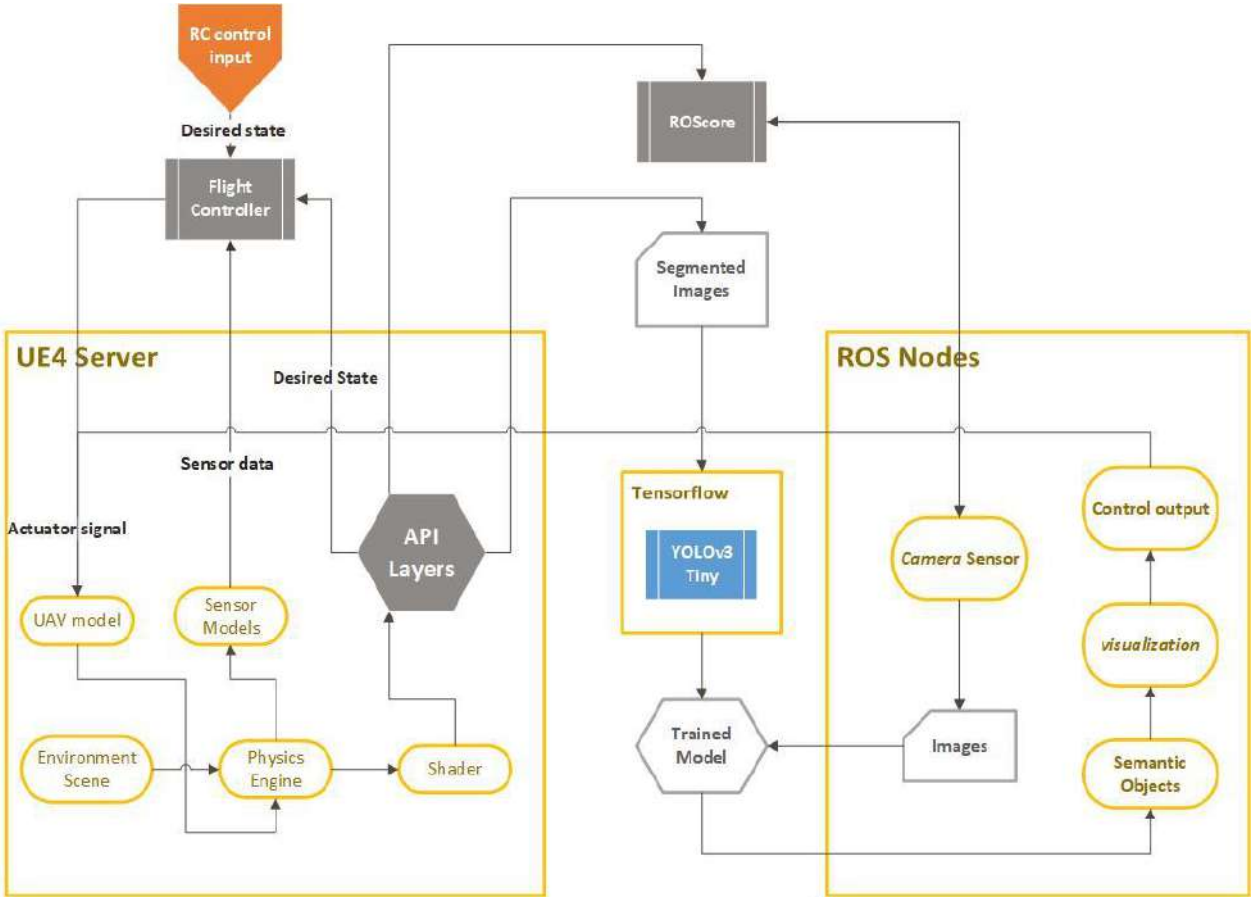

Figure 1. The developed framework for UAV planning using hardware-in-the-loop simulation and BIM technology

Section 2 illustrates the developed framework for UAV planning using hardware-in-the-loop simulation and BIM technology, which contains the following three major parts:

1. The creation of a high-fidelity simulation environment with MEP pipes models and connected flight controller in hardware-in-the-loop [10] mode.

2. The creation of ROS nodes that link the virtual Lidar from ROS to UE4 simulator and generate point cloud data and obstacle avoidance.

3. The creation of a perception system by training of a YOLO v3 [11] object detection neural network with pictures of MEP models.

Implementation details and results of these three parts will be presented separately in the followings.

2 Proposed Framework for UAV Planning Using Hardware-in-the-Loop Simulation and BIM

The proposed framework (as shown in Figure 1) starts where a radio control signal is passed from a radio controller to the virtual flight control module, which drives an actuator on the UAV. Gravity and weather information from the environment will then be sent to the physics engine to simulate the kinematics and return pose information of the UAV. The image API will then acquire high-fidelity images from the scene and compose a directory for neural network training, for the purpose of object detection. The ROS API layer will receive the vehicle pose and location information and via each ROS node for simultaneous localization and mapping, and trajectory planning.

2.1 Simulation Environment Setup

A MEP scene is focused in this study due to the complexity in geometry. The scene, which contains common MEP components such as pipes, elbows and supports, is generated in realistic visual effect using the UE4 engine. This virtual environment consists of MEP pipelines, both having similar object settings and made with appropriated UV to make it realistic. A virtual quadcopter is also created as an avatar to simulate a physical UAV with a weight of 3 kg. A physical flight controller is installed in hardware-in-the-loop mode, and we use a physical 9-channel radio controller which is plug in our server USB port to control the virtual quadcopter within the scene. The simulated environment is shown in Figure 2.

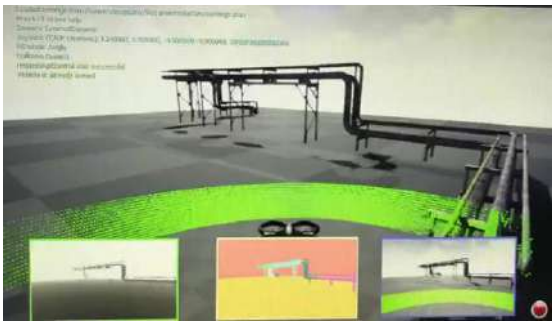

Figure 2. The simulation environment

2.2 Hardware-in-the-Loop simulation with Pixhawk Flight Controller

Hardware-in-the-loop simulation is a type of real-time simulation that are commonly used to test complex embedded system [12]. Figure 3 illustrated the relationship between the flight controller hardware and to the developed simulator.

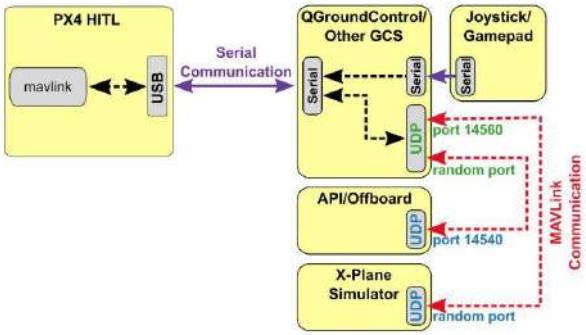

Figure 3. Connection between Pixhawk 4 and the developed simulator

Pixhawk 4 [13] is connected to the USB port of a server. Through the UDP port of the simulation engine, the flight controller can establish communication with the simulator and interact with the built-in physics sub-engine to send actuator signals, pass environment data (e.g. gravity, wind, atmospheric pressure, etc.), and update the real gyro and accelerometer sensors onboard the flight controller. In this way, the simulated environment can behave as close to the real environment as possible.

2.3 Training of an Object Detection Neural Network with YOLO v3 Tiny

The simulator has a Python API so that it can connect with Keras [14], a high-level deep learning

Python middleware that runs on top of Tensorflow [15], which we use for the neural network training (of xxx). There are numerous deep learning-based object detection architectures. YOLO (You Only Look Once) v3 Tiny [16] is used in this research because it is 100 times faster than Fast R-CNN [17] and it is a very small model, comprising only 9 convolutional layers, which is ideal where computational power is limited, such as what is available on the Nvidia TX2 [18] embedded unit. Darknet [19] is used as a trained deep architecture with trained YOLO weights. The training process consist of the following four steps.

1. Create a dataset which includes image classes of MEP models such as pipes, valves, industrial air conditioning units, fittings, water heating, etc. 2000 images are used as training set for each class.

2. Tag images via Visual Object Tagging Tool.

3. Batch and subdivision, using an input resolution of (416 x 416) with a batch of 64 and a subdivision of 3. (Note: values were chosen based on the maximum result achieved without CUDA [20] error.)

4. Train a model, weights will be given for every 100 epochs in Darknet. The result is shown in Table 1.

Table 1.

Input Resolution	416 x 416
Weights	YOLO v3-tiny-VM.cfg
Iterations	50,000
Average Loss	0.2103
Average IoU (%)	47.18%
mAP	62.39%

Finally, we will test the result of training by connecting this object detection network with our simulator via the Python API. MEP pipes are detected in the simulator as the simulated UAV flies, detects objects of interest, and marks their locations in the simulated scene in the virtual environment, as shown in Figure 4.

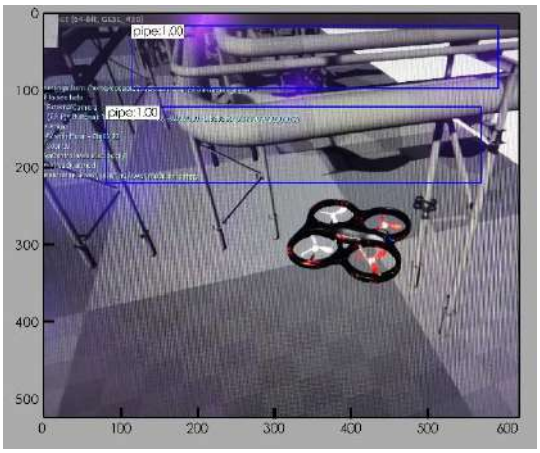

Figure 4. Detection with YOLO v3 Tiny

2.4 Generate Virtual Lidar Data with ROS and UE4

The virtual Lidar in the UE4 engine requires the implementation of two technologies: (1) ray tracing within the UE4 engine to have the visual effect of a laser beam, and (2) construction of virtual sensors within ROS via ROSbridge to publish the defined Lidar sensor reading from ROS to the listening port of the UE4 engine.

The parameters of the virtual Lidar in the simulator are configured in the same way as the RS-Lidar 32 with 32-channel laser, 640K points per second, +/- 15-degree FOV (vertical) and 360-degree FOV (horizontal). [21] The green line indicates the laser beam is generated, as shown in Figure 5 and Figure 6.

The acquired point cloud data will need to change the camera projection matrix with a Build Projection Matrix function, which computes a 4x4 matrix using FOV, width, height and near plane.

Figure 5. Virtual Lidar in the simulator

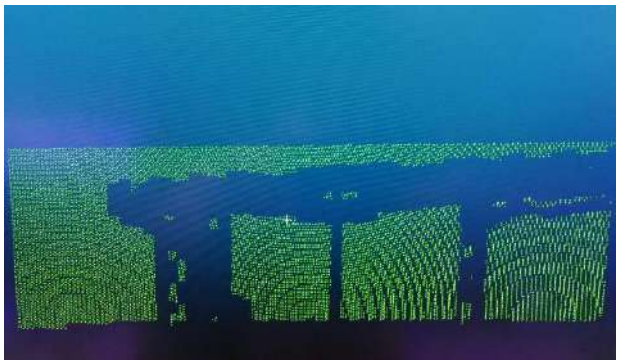

Figure 6. Point cloud visualization

3 Implementation and results

The proposed survey UAV is implemented with a DJI F350 chassis and a Nvidia TX2 embedded unit. The Nvidia Jetson TX2 features a Nvidia Denver dual-core and an ARM Cortex-A57 quad-core. TX2 also carries a 256-core Nvidia Pascal GPU with 8GB of RAM. The power consumption is only 7.5 watts. A stereo camera is incorporated for running a visual simultaneous localization and mapping (SLAM) [22] algorithm for the purpose of localization and obstacle avoidance. A 32-channel Lidar is also mounted on the system to generate some point cloud data. A Pixhawk flight controller with radio receiver is installed along with four electronic speed controllers and corresponding RC rotors. A 9-channel radio controller is used to control the UAV. The total weight of the system is approximately 3 kilograms with a 20K mAh Lithium Polymer battery.

Figure 6. UAV implementation

The stereo camera is a global shutter camera, which does not have an onboard IMU. It is calibrated using a checkerboard (shown in Figure 7) to calculate the intrinsic and extrinsic camera parameters with Pinhole model. With the calibrated stereo camera, we flew the UAV with a VINS SLAM algorithm running in TX2, and a circular trajectory is generated. The trajectory is visualized in Rviz as shown in Figure 8 and Figure 9.

Figure 7. Stereo Camera Calibration

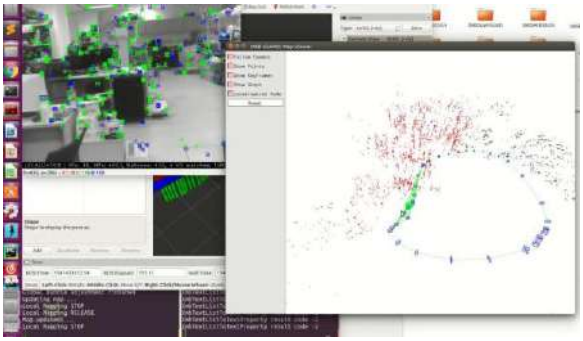

Figure 8. ORB SLAM in Rviz

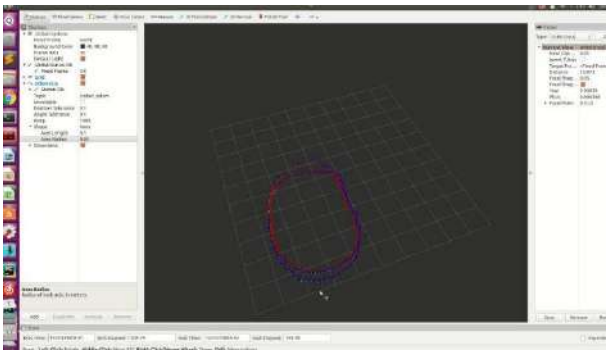

Figure 9. Trajectory in simulator

We also load the AirLib library from our simulator and deployed it on the TX2. The simulator uses the MavLinkCom component, which is a proxy architecture where a connection to the Pixhawk flight controller can be achieved via a serial or UDP port. The Pixhawk flight controller will send messages via MavLink, which allows the controller to be connected to the serial port of QGroundControl (QGC) [23]. We can control the UAV as a client to run on the TX2 meanwhile have it connected to our server with virtual simulation environment.

Running the VINS stereo algorithm along with the YOLO v3 Tiny object detection neural network gives a high load of computation. Usage statistics show that VINS uses roughly 60% of the processing power in the TX2.

4 Conclusion and Future Work

This paper presents a hardware-in-the-loop simulation, which can simulate the behavior of a UAV, generate synthetic images from the scene as datasets, detect and verify as-built MEP objects with a trained YOLO v3 neural network, and generate point cloud data for future as-designed BIM and as-built BIM validation. This demonstrates an effective way of testing the behavior of a UAV prior to live demo flight and blazes a trail toward implementing AI-based robotic inspectors in the AEC industry. Moreover, the capability of generating virtual point clouds in the simulation engine provides a low-cost way for verifying the trajectory of a survey UAV before actual UAV-based scanning takes place. This can simulate any missing point cloud region in the environment constructed with an as-designed BIM model.

The developed framework will be improved in the future. In particular, (1) the proposed framework has not been tested in a real industrial environment with MEP piping installed for field detection. Future tests at a plant room site with MEP components will be conducted. (2) A better stereo camera with IMU will be installed to give the VINs' SLAM performance a boost, potentially resulting in better localization and mapping. (3) A trajectory planning module will be developed on the system and further tested its stability with a motion capture system.

References

[1] Cheng, Jack CP, and Qiqi Lu. "A review of the efforts and roles of the public sector for BIM adoption worldwide." Journal of Information Technology in Construction (ITcon) 20.27 (2015): 442-478.

[2] Zhang, Qijun, et al. "Emission factors of volatile organic compounds (VOCs) based on the detailed vehicle classification in a tunnel study." Science of The Total Environment 624 (2018): 878-886.

[3] Wang, Qian, Jack Chin Pang Cheng, and Hoon Sohn. "Automatic Reconstruction of As-built BIM from Laser Scanned Data of Precast Concrete Elements for Dimensional Quality Assessment." Proceedings of the International Symposium on Automation and Robotics in Construction (ISARC). 2016.

[4] Colomina, Ismael, and Pere Molina. "Unmanned aerial systems for photogrammetry and remote sensing: A review." ISPRS Journal of photogrammetry and remote sensing 92 (2014): 79-97.

[5] Arterburn, David, et al. "FAA UAS Center of Excellence task A4: UAS ground collision severity evaluation, revision 2." (2017).

[6] Miller, Robert C., and Raymond M. Fuoss. "Electrolyte-Solvent Interaction. II. Quaternary Salts in Methanol-Nitromethane and Methanol-Benzene Mixtures." Journal of the American Chemical Society 75.13 (1953): 3076-3080.

[7] Qiu, Weichao, and Alan Yuille. "Unrealcv: Connecting computer vision to unreal engine." European Conference on Computer Vision. Springer, Cham, 2016.

[8] Haas, John K. "A history of the Unity game engine." (2014).

[9] Quigley, Morgan, et al. "ROS: an open-source Robot Operating System." ICRA workshop on open source software. Vol. 3. No. 3.2. 2009.

[10] Cai, Guowei, et al. "Design and implementation of a hardware-in-the-loop simulation system for small-scale UAV helicopters." Automation and Logistics, 2008. ICAL 2008. IEEE International Conference on. IEEE, 2008.

[11] Redmon, Joseph, and Ali Farhadi. "Yolov3: An incremental improvement." arXiv preprint arXiv:1804.02767 (2018).

[12] McDonnell, Rachel, Martin Breidt, and Heinrich H. Bülthoff. "Render me real?: investigating the effect of render style on the perception of animated virtual humans." ACM Transactions on Graphics (TOG) 31.4 (2012): 91.

[13] Meier, Lorenz, et al. "PIXHAWK: A micro aerial vehicle design for autonomous flight using onboard computer vision." Autonomous Robots 33.1-2 (2012): 21-39.

[14] Chollet, François. "Keras: The python deep learning library." Astrophysics Source Code Library (2018).

[15] Abadi, Martín, et al. "Tensorflow: a system for large-scale machine learning." OSDI. Vol. 16. 2016.

[16] Redmon, Joseph, and Ali Farhadi. "Yolov3: An incremental improvement." arXiv preprint

arXiv:1804.02767 (2018).

[17] Girshick, Ross. "Fast r-cnn." Proceedings of the IEEE international conference on computer vision. 2015.

[18] NVIDIA, "NVIDIA Jetson TX2 Module" Online: https://developer.nvidia.com/embedded/buy/jetson-tx2, Accessed: 31/01/2019

[19] Shafiee, Mohammad Javad, et al. "Fast YOLO: A Fast You Only Look Once System for Real-time Embedded Object Detection in Video." arXiv preprint arXiv:1709.05943 (2017).

[20] Kirk, David. "NVIDIA CUDA software and GPU parallel computing architecture." ISMM. Vol. 7. 2007.

[21] Schwarz, Brent. "LIDAR: Mapping the world in 3D." Nature Photonics 4.7 (2010): 429.

[22] Dissanayake, MWM Gamini, et al. "A solution to the simultaneous localization and map building (SLAM) problem." IEEE Transactions on robotics and automation 17.3 (2001): 229-241.

[23] MEIER, Lorenz. "MAVLink Micro Air Vehicle Communication Protocol-QGroundControl GCS." QGroundControl GCS [online] (2009).

A Review of Social, Physiological, and Cognitive Factors Affecting Construction Safety

S. Eskandar[a], J. Wang[b], and S. Razavi[c]

[a]Ph.D. Student, Department of Civil Engineering, McMaster University, Canada
[b]Assistant Professor, Department of Civil and Environmental Engineering, Mississippi State University, United States
[c]Associate Professor, Department of Civil Engineering, McMaster University, Canada
E-mail: eskandah@mcmaster.ca, jwang@cee.msstate.edu, razavi@mcmaster.ca

Abstract -

Safety improvement in construction remains a high priority due to the significant rate of accidents compared to other industries. Despite the ongoing multitude of safety studies and policy recommendations concerning the high rate of injuries and casualties in construction, the extent of damage sustained is still significant. Major research studies in construction safety are focused on identifying conditions and causal factors leading to near misses, incidents, and accidents. This paper aims to provide a review of such literature in construction safety from social and individual perspectives. Three major categories of construction safety factors, i.e., social, physiological, and cognitive factors, are synthesized, and the main findings in each category are presented. Implications of the findings are further discussed to guide the research and practice in construction safety management.

Keywords –

Construction; Safety; Social Factors; Physiological Factors; Cognitive Factors

1 Introduction

Improvement of safety in construction sites remains a vital concern due to the high rate of accidents compared to other industries [1, 2]. In addition to the high rate of injuries and casualties in construction industry, the complex and unpredictable nature of work is adding to the importance of safety improvement for construction sites [3]. Construction workplace safety has been extensively studied [4], and human unsafe behaviour and error were recognized as some of the direct causes of accidents [5-7]. Many research studies in construction safety are focused on identifying conditions and causal factors leading to near misses, incidents, and accidents, which in this paper will be classified to aid construction industry with the aim of improving safety. This paper provides a review of such literature in construction safety, aiming to clarify reasons leading to an unsafe act, from social and individual perspectives.

Through a systematic review of the literature, aiming to clarify reasons leading to an unsafe act, three major categories have been considered and studied in this research. Due to the connection and collaboration among workers and other construction personnel in construction sites, social factors have been viewed as one of the major categories to identify attributes related to accident occurrence. Furthermore, due to the demanding nature of construction work and the rough environment of its working place, physiological conditions of individuals are another set of factors discussed in this paper. In addition to social and physiological factors, cognition has been considered as another category of factors in construction safety, which relates to the way workers perceive information, think and decide. Therefore, the construction industry can benefit from a systematic review of social, physiological, and cognitive factors that have not been presented in the current body of knowledge.

In the following sections, a literature search for construction safety is presented and significant social, physiological, and cognitive factors extracted from the literature are discussed. Afterward, some discussions on the implications of findings in addition to the challenges and opportunities are presented.

2 Literature Search

In the search of representative factors influencing construction safety in each major category (i.e., social, physiological, and cognitive), keywords have been chosen based on the number of published papers. The number of the literature linked to each keyword was counted in order to see a distribution of the literature in each major categories. Figure 1 shows the number of the literature that appeared relevant to the subject in six different publishers (i.e., ASCE, Elsevier, Taylor and Francis, Springer, IEEE, American Psychological Association). These factors were reviewed in this paper to give readers a broader view while supporting the majority of research in construction safety.

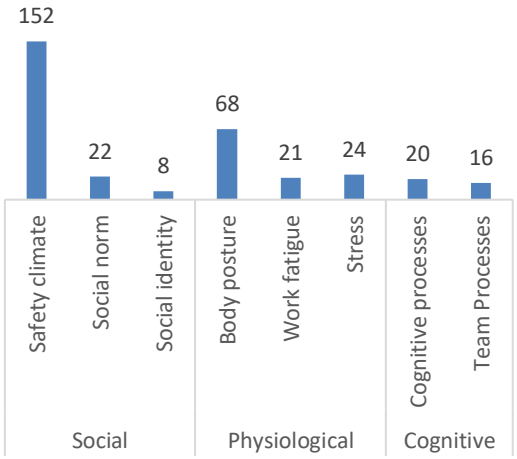

Figure 1. Distribution of the literature in each major categories of factor affecting construction safety

3 Social Factors

Safety in construction sites is not only related to the isolated act of workers, but also the social interactions resulted from the collaboration and communication among workers in such a dynamic environment. Therefore, investigating workers' safety behaviours from a social point of view has attracted researchers' attention. The following section will briefly present safety climate and social norm and identity as the social aspects of workers' safety behaviours.

3.1 Safety climate

Safety climate is defined as a subordinate of organizational climate and management commitment to safety, which determines workers' view toward safety in their workplace [8]. Safety climate has been considered as an effective component in the safe behaviour of construction workers [9] and is considered to have a higher impact on improving safety when compared to factors associated with workers experience (e.g., it is more practical to improve management commitments to safety instead of recruiting workers with more work experience) [10]. Therefore, understanding the factors contributing to the safety climate will have a positive outcome through the safe conduct of work in construction sites.

For measuring safety climate, Zohar in 1980 established an eight-factor model and concluded that a change in management attitudes and increased commitment are essential for safety in industrial workplaces [8]. In 1986, Brown & Holmes established a three-factor structure on an American sample of production workers for assessing safety climate [11]. Following the research conducted by Zohar [8] and Brown & Holmes [11], Dedobbeler & Blend [12] presented a two-factor model by using data on nine nonresidential construction sites in Baltimore, MD. The two selected factors for measuring safety climate were (a) management's commitment to safety and (b) workers' involvement in safety with the overall emphasis on management and workers' participation in safety matters.

Core components of safety climate approach have been identified as (a) safety priority, (b) safety supervision, training, and communication, (c) safety involvement, and (d) safety rules and procedures [13].

In addition to the identified factors in safety climate, the impact of five specific safety climate factors (i.e., safety management systems and procedures, management's commitment, safety attitudes, workmate influence, and employees involvement), and four other factors associated with workers' experience were investigated. The results indicated the higher impact of safety climate factors on improving safety when compared to workers' experience factors [10].

3.2 Social norm and social identity

The other social factor that has been considerably studied in the literature is the effect of social norms and social identities on workers' safety behaviour. This is due to the importance of social influence on construction worker's safety behaviour. [14] demonstrated the effect of social influence by adopting a virtual reality system in a hazardous situation. Social norm driven from co-workers and managers influences workers' safety behaviour and could be responsible for workers' unsafe act [15].

In social context, social identity theory explains that people categorize themselves and others into different social groups with specific group members' behaviour [16]. When a specific group identity is salient in an individual's mind, that person considers herself or himself as a representative of the group and is eager to align with group norms, which would affect her or his behaviour [17]. Choi et al. studied the role of social norm and social identity on construction workers' safety, and the chosen group identity included trade, workgroup, union, project, and company [18]. The results showed the strong influence that group norms have on personal standards since trade identity and workgroup identity were more prominent in construction workers' mind, as they identified themselves a representative of trade and workgroup. Consequently, workers' safety behaviour is more likely to be influenced by trade and workgroup norms. Project identity, however, was identified as the least relevant group among the construction workers. Therefore, workers' safety behaviour is not strongly affected under project managers' influence. The findings indicate that improvement in the project identity could enhance the relationship that the perceived management

norms have on workers' safety behaviour.

In [19] the effect of different cultural backgrounds and organizational structures on achievement from [18] was investigated. United States, Korea, and Saudi Arabia were chosen to study the impact of social norms (i.e., perceived management norms, perceived workgroup norms) and project identity on construction workers' safety behaviours in different settings. The results showed the lessening effect that project identity has on the relationship between social norms and safety behaviour in the U.S. and Korea. However, Saudi Arabia with a direct hiring system that leads to a strong project identity did not show an effective impact that project identity and social norms could have on safety behaviour (the reason recognized as the project manager did not show enough strictness to influence workers' safety behaviours).

In [20] the effects of three different safety management interventions on workers' safety behaviour along with three different site risks were investigated. The three safety management interventions, i.e., stricter management feedback, more frequent management feedback, and fostering workers' project identification were found effective for reducing incident rate. Based on the results, improving workers' project identification in moderate-risk site condition was recommended as the best policy as their risk acceptance would be aligned with their perceived management norms rather than workgroup norms. Also, in the low-risk site condition, rigorous management feedback is needed to see the improving results of other interventions.

4 Physiological Factor

Construction work is a physically demanding job, and a considerable number of workers go beyond the accepted and safe physiological level for manual work [21]. In addition to the physical demands of the work, workers' physical status can affect the safety and productivity in the work setting. Therefore, measuring and monitoring workers' physiological status can provide valuable information for safety in construction. Three major physiological aspects of construction workers, i.e., body posture, work fatigue, and stress, are identified from the literature and will be discussed in detail below [22-28].

Implementing new technologies for monitoring workers' unsafe actions and providing instructions on conducting safe activities have been suggested by Bernold and Guler [29]. For collecting data on workers' physical status, Lee et al. [30] investigated the applicability of wearable sensors on roofing crews. Data were collected during and after work hours for measuring heart rate, energy expenditure, metabolic equivalent, and sleep efficiency aiming to observe workers' physiological status and well-being. This study confirmed the feasibility of using wearable sensors for construction safety and individual health monitoring and management.

4.1 Body posture

Excessive physically demanding work such as manual material handling tasks in construction activities could lead to musculoskeletal injuries [31], which is a risk to workers' safety and health. To identify and locate unsafe postures of workers, Cheng et al. [32] presented an automatic remote monitoring approach focusing on bending postures. Different physical status such as heart rate and bending angle recorded using physical status monitoring (PSM) tools (BioHarness BT 1 and Equivital EQ-01) were synchronized with ultra-wideband (UWB) signal to give the accurate time and locations of unhealthy bending postures. Moreover, PSM tools were validated to be an effective tool for unobtrusive and remote monitoring and control tool to manage workers' health and safety [33].

4.2 Work fatigue

Analysing sleep deprivation and fatigue among construction workers showed the 8.9% increase in the risk of having an accident [34], and the construction industry needs to avoid fatigue especially for workers in higher risk that need priority in training and monitoring. In general, crewmembers are more prone to physical fatigue than machine operators and they routinely exceed acceptable levels of energy expenditure, oxygen consumption, and heart rate [35]. Among different occupation of crewmembers, Chang et al. [26] investigated work fatigue and physiological symptoms in order to identify occupations in need of more attention regarding health and safety. The scaffolders, steel fixers, and form workers were categorized as the most physically-demanding work groups, and scaffolders experienced the highest average heart rate during work hours. Furthermore, Techera et al. in [36] investigated a fatigue predictor model and showed that predictors vary by trades in a construction setting.

4.3 Stress

Job stress has been recognized as a risk factor in different industries that affect workers' health and safety [37-39]. Finance, inadequate personal time, and the nature of work have been recognized as the main source of daily stressors among construction workers [40]. Construction environment with a dynamic setting, complicated ongoing tasks, and various threatening hazards, shakes workers' stress level and their behaviour toward safety. Goldenhar et al.'s paper [41] investigated

the relationship between different job stressors (job-task demands, organizational stressors, and physical/chemical hazards and protection from them) and near misses among construction workers. Moreover, Leung et al. [42] conducted research to identify the relationship between job stressors (safety equipment, supervisor support, co-worker support, job control, and job certainty), physical stress (i.e., biological reactions), psychological stress (i.e., traumatizing experience), safety behaviour, and accident. The result showed that (1) having a job certainty, co-worker support, and safety equipment would result in decreased physical stress; (2) the level of psychological stress is predicted by supervisor support and lack of job certainty; (3) safety behaviour would be achieved by supervisor support and minimum physical stress; and (4) accidents could be prevented by safety behaviour.

5 Cognitive Factors

Understanding the way construction workers perceive information and decide to take a specific action is undoubtedly a critical way of discovering why an unsafe act has been chosen and how information collected by workers can affect their decisions. In this section, critical cognitive factors in the literature are discussed to better understand workers' cognition and its impact on safety in construction sites.

5.1 Cognitive processes

Knowing human error as the most frequent cause of accidents [5-7], different cognitive models in high-risk industries (e.g., nuclear plants [43], aviation [44], and mining [45]) have been developed to describe human cognition. For construction worker's unsafe behaviour, Fang et al. [46] proposed a cognitive model that contains stages of a construction worker cognitive process while encountering with a potential hazard, namely obtaining information, understanding information, perceiving responses, selecting response, and taking action.

As described in [5], an unsafe behaviour could be derived from a failure at any stage of cognition. In a construction setting, limitations in worker's senses due to unfavourable site conditions (e.g., loud noise or obstructed views) could prevent a worker from observing the hazards and consequently result in a failure in obtaining information [46]. Also, workers' lack of attention could prevent a worker from identifying an incident that leads to an accident [47]. Certain eye movements can represent the state of worker's attention and therefore be used to predict human error [48]. Furthermore, workers' selected response is likely to be influenced by the high production and coordination pressure rather than safe conduct of the job [46].

5.2 Team Processes

Team process is an essential factor for construction safety since a team can stop errors from happening and manage a situation that affects safety. The relationship between team members could help workers with learning and adopting safety behaviours. Moreover, from a resiliency perspective, the team recognizes, collaborates, and adjusts to unplanned events and manages to stabilize the situation [49]. Teamwork as a component of a team performance includes cognition, attitude, and behaviour leading to the dynamic processes of performance [50]. Team cognition is a cognitive activity happening at a team level and not individually [51], which has different dimensions, namely team mental model, transactive memory, group learning, shared team situation awareness, and strategic consensus [52]. Compatible environment, anticipation to balance workload, and instant information are essential for a team's cognition, performance, and safety in construction [49].

6 Concluding Remarks

This study presented significant factors affecting construction safety through a review of the literature in this realm from social, physiological, and cognitive viewpoints. Three major categories of construction safety factors, i.e., social, physiological, and cognitive factors, were synthesized to guide the research and practice in construction safety management.

It was identified that improvement in safety behaviours in construction site can be achieved by improving management commitment and engagement in safety programs. The study also presented that improving safety climate is more effective than paying attention to the individual's work experience. In a work setting, workers' safety behaviour is more likely influenced by the trade and workgroup norms rather than the project norm. Improving project identity to increase project managers' influence on workers' safety behaviour would be a solution to align workers safety behaviour with project manager attitude.

With high volume of manual and physical work in a construction, monitoring workers physical factors such as bending angle, heart rate, energy expenditure, and oxygen consumption can help manage and control workers physical status during working hours. Eliminating job stressors (i.e., safety equipment, supervisor support, co-worker support, job control, and job certainty) is another way of improving workers safety behaviour.

Studying individual cognition and team cognition is instrumental in understanding the reasons in taking an unsafe act. Different stages of cognition are important since a failure in any stage could lead to an accident.

Providing appropriate circumstances in favour of accurate cognition is essential to eliminate accidents.

7 References

[1] D. C. P. Ho, S. M. Ahmed, J. C. Kwan and a. F. Y. W. Ming, "Site safety management in Hong Kong," *Journal of Management in Engineering*, vol. 16, no. 6, pp. 34-42, 2000.

[2] P. Kines, L. Andersen, S. Spangenberg, K. Mikkelsen, J. Dyreborg and D. Zohar, "Improving construction site safety through leader-based verbal safety communication," *Journal of safety research*, vol. 41, no. 5, pp. 399-406, 2010.

[3] H. van der Molen, E. Koningsveld, R. Haslam and A. Gibb, "Ergonomics in building and construction: Time for implementation," *Applied Ergonomics*, vol. 36, p. 387–389, 2005.

[4] S. Silva, M. Lima and C. Baptista, "OSCI: an organisational and safety climate inventory," *Safety science*, vol. 42, no. 3, pp. 205-220, 2004.

[5] J. Reason, Human error, Cambridge university press, 1990.

[6] H. Heinrich, D. Petersen and N. Roos, "Industrial accident prevention," McGraw-Hill, New York, 1950.

[7] M. D. K. H. Chua and Y. M. Goh, "Incident Causation Model for Improving Feedback of Safety Knowledge," *Journal of Construction Engineering and Management*, vol. 130, no. 4, 2004.

[8] D. Zohar, "Safety climate in industrial organizations: theoretical and applied implications," *Journal of applied psychology*, vol. 65, no. 1, p. 96, 1980.

[9] S. Mohamed, "Safety climate in construction site environments," *Journal of construction engineering and management*, vol. 128, no. 5, pp. 375-384, 2002.

[10] Q. Zhou, D. Fang and X. Wang, " A method to identify strategies for the improvement of human safety behaviour by considering safety climate and personal experience," *Safety Science*, vol. 46, no. 10, pp. 1406-1419, 2008.

[11] R. Brown and H. Holmes, "The use of a factor-analytic procedure for assessing the validity of an employee safety climate model," *Accident Analysis & Prevention*, vol. 18, no. 6, pp. 455-470, 1986.

[12] N. Dedobbeleer and F. Béland, "A safety climate measure for construction sites," *Journal of safety research*, vol. 22, no. 2, pp. 97-103, 1991.

[13] C. Wu, X. Song, T. Wang and D. Fang, "Core dimensions of the construction safety climate for a standardized safety-climate measurement," *Journal of Construction Engineering and Management*, vol. 141, no. 8, p. 04015018, 2015.

[14] Y. Shi, J. Du, E. Ragan, K. Choi and S. Ma, "Social influence on construction safety behaviours: a multi-user virtual reality experiment," in *Construction Research Congress*, New Orleans, Louisiana, 2018.

[15] Y. Goh, C. Ubeynarayana, K. Wong and B. Guo, "Factors influencing unsafe behaviours: A supervised learning approach," *Accident Analysis & Prevention*, vol. 118, pp. 77-85, 2018.

[16] H. Tajfel, J. Turner, W. Austin and S. Worchel, "An integrative theory of intergroup conflict," Organizational identity: A reader, 1979, pp. 56-65.

[17] S. Haslam, D. Van Knippenberg, M. Platow and N. Ellemers, Social identity at work: Developing theory for organizational practice, Psychology Press, 2014.

[18] B. Choi, S. Ahn and S. Lee, "Construction workers' group norms and personal standards regarding safety behaviour: Social identity theory perspective," *Journal of management in engineering*, vol. 33, no. 4, p. .04017001, 2017.

[19] B. Choi and S. Lee, "Role of social norms and social identifications in safety behaviour of construction workers. II: Group analyses for the effects of cultural backgrounds and organizational structures on social influence process," *Journal of Construction Engineering and Management*, vol. 143, no. 5, p. 04016125, 2016.

[20] B. Choi and S. Lee, "An Empirically Based Agent-Based Model of the Sociocognitive Process of Construction Workers' Safety Behaviour," *Journal of Construction Engineering and Management*, vol. 144, no. 2, p. 04017102, 2017.

[21] T. Abdelhamid and J. Everett, "Physiological demands during construction work," *Journal of construction engineering and management*, vol. 128, no. 5, pp. 427-437, 2002.

[22] H. Kim, C. Ahn and K. Yang, "Identifying safety hazards using collective bodily responses of workers," *Journal of Construction Engineering and Management*, vol. 143, no. 2, p. 04016090, 2016.

[23] W. Umer, H. Li, G. Szeto and A. Wong, "Proactive Safety Measures: Quantifying the Upright Standing Stability after Sustained Rebar Tying Postures," *Journal of Construction Engineering and Management*, vol. 144, no. 4, p. 04018010, 2018.

[24] Y. Yu, H. Guo, Q. Ding, H. Li and M. Skitmore, "An experimental study of real-time identification of construction workers' unsafe behaviours," *Automation in Construction,* vol. 82, pp. 193-206, 2017.

[25] H. Jebelli and S. Lee, "Feasibility of Wearable Electromyography (EMG) to Assess Construction Workers' Muscle Fatigue," *In Advances in Informatics and Computing in Civil and Construction Engineering,* pp. 181-187, 2019.

[26] F. Chang, Y. Sun, K. Chuang and D. Hsu, "Work fatigue and physiological symptoms in different occupations of high-elevation construction workers," *Applied ergonomics,* vol. 40, no. 4, pp. 591-596, 2009.

[27] P. Basnet, S. Gurung, R. Pal, S. Kar and D. Bharati, "Occupational stress among tunnel workers in Sikkim," *Industrial psychiatry journal,* vol. 19, no. 1, p. 13, 2010.

[28] L. Goldenhar, N. Swanson, H. Jr, J.J., A. Ruder and J. Deddens, "Stressors and adverse outcomes for female construction workers," *Journal of occupational health psychology,* vol. 3, no. 1, p. 19, 1998.

[29] L. Bernold and N. Guler, "Analysis of back injuries in construction," *Journal of Construction Engineering and Management,* vol. 119, no. 3, pp. 607-621, 1993.

[30] W. Lee, K. Lin, E. Seto and G. Migliaccio, "Wearable sensors for monitoring on-duty and off-duty worker physiological status and activities in construction," *Automation in Construction,* vol. 83, pp. 341-353, 2017.

[31] E. Valero, A. Sivanathan, F. Bosché and M. Abdel-Wahab, "Musculoskeletal disorders in construction: A review and a novel system for activity tracking with body area network," *Applied Ergonomics,* vol. 54, pp. 120-130, 2016.

[32] T. Cheng, G. Migliaccio, J. Teizer and U. Gatti, "Data fusion of real-time location sensing and physiological status monitoring for ergonomics analysis of construction workers," *Journal of Computing in Civil engineering,* vol. 27, no. 3, pp. 320-335, 2012.

[33] U. Gatti, S. Schneider and G. Migliaccio, "Physiological condition monitoring of construction workers," *Automation in Construction,* vol. 44, pp. 227-233, 2014.

[34] R. Powell and A. Copping, "Sleep deprivation and its consequences in construction workers," *Journal of construction engineering and management,* vol. 136, no. 10, pp. 1086-1092, 2010.

[35] T. Abdelhamid and J. Everett, "Physiological demands of concrete slab placing and finishing work," *Journal of construction engineering and management,* vol. 125, no. 1, pp. 47-52, 1999.

[36] U. Techera, M. Hallowell, R. Littlejohn and S. Rajendran, "Measuring and Predicting Fatigue in Construction: Empirical Field Study," *Journal of Construction Engineering and Management,* vol. 144, no. 8, p. 04018062, 2018.

[37] T. Probst and T. Brubaker, "The effects of job insecurity on employee safety outcomes: Cross-sectional and longitudinal explorations," *Journal of occupational health psychology,* vol. 6, no. 2, p. 139, 2001.

[38] T. Rundmo, "Risk perception and safety on offshore petroleum platforms—Part II: Perceived risk, job stress and accidents," *Safety Science,* vol. 15, no. 1, pp. 53-68, 1992.

[39] A. Nakata, T. Ikeda, M. Takahashi, T. Haratani, M. Hojou, Y. Fujioka, N. Swanson and S. Araki, "Impact of psychosocial job stress on non-fatal occupational injuries in small and medium-sized manufacturing enterprises," *American journal of industrial medicine, ,* vol. 49, no. 8, pp. 658-669, 2006.

[40] R. Langdon and S. Sawang, "Construction Workers' Well-Being: What Leads to Depression, Anxiety, and Stress?," *Journal of Construction Engineering and Management,* vol. 144, no. 2, p. 04017100, 2017.

[41] L. M. Goldenhar, L. J. Williams and N. G. Swanson, "Modelling relationships between job stressors and injury and near-miss outcomes for construction labourers," *Work & Stress,* vol. 17, no. 3, pp. 218-240, 2003.

[42] M. Leung, Q. Liang and P. Olomolaiye, "Impact of job stressors and stress on the safety behaviour and accidents of construction workers," *Journal of Management in Engineering,* vol. 32, no. 1, p. 04015019, 2015.

[43] Y. Chang and A. Mosleh, "Cognitive modeling and dynamic probabilistic simulation of operating crew response to complex system accidents: Part 1: Overview of the IDAC Model," *Reliability Engineering & System Safety,* vol. 92, no. 8, pp. 997-1013, 2007.

[44] M. Byrne and A. Kirlik, "Using computational cognitive modeling to diagnose possible sources of aviation error," *The international journal of aviation psychology,* vol. 15, no. 2, pp. 135-155, 2005.

[45] S. Mohan and D. Duarte, "Cognitive modeling of underground miners response to accidents," in

Reliability and Maintainability Symposium, IEEE, 2006.

[46] D. Fang, C. Zhao and M. Zhang, "A Cognitive Model of Construction Workers' Unsafe Behaviours," *Journal of Construction Engineering and Management*, vol. 142, no. 9, p. 04016039, 2016.

[47] G. Manchi, S. Gowda and J. Hanspal, "Study on cognitive approach to human error and its application to reduce the accidents at workplace," *International Journal of Engineering and Advanced Technology (IJEAT)*, vol. 2, no. 6, pp. 236-242, 2013.

[48] S. Hasanzadeh, B. Esmaeili and M. Dodd, "Impact of Construction Workers' Hazard Identification Skills on Their Visual Attention," *Journal of Construction Engineering and Management*, vol. 143, no. 10, p. 04017070, 2017.

[49] P. Mitropoulos and B. Memarian, "Team processes and safety of workers: Cognitive, affective, and behavioural processes of construction crews," *Journal of Construction Engineering and Management*, vol. 138, no. 10, pp. 1181-1191, 2012.

[50] E. Salas, N. Cooke and M. Rosen, "On teams, teamwork, and team performance: Discoveries and developments," *Human factors*, vol. 50, no. 3, pp. 540-547, 2008.

[51] N. Cooke, J. Gorman, J. Winner and F. Durso, "Team cognition," *Handbook of applied cognition*, vol. 2, pp. 239-268, 2007.

[52] S. Mohammed, L. Ferzandi and K. Hamilton, "Metaphor no more: A 15-year review of the team mental model construct," *Journal of management*, vol. 36, no. 4, pp. 876-910, 2010.

Automatic Classification of Design Conflicts Using Rule-based Reasoning and Machine Learning—An Example of Structural Clashes Against the MEP Model

Y. Huang[a] and W.Y. Lin[b]

[a]Department of Civil and Construction Engineering, National Yunlin University of Science and Technology, Taiwan
[b]Department of Civil Engineering, Feng Chia University, Taiwan
E-mail: huangyh@yuntech.edu.tw, weiylin@mail.fcu.edu.tw

Abstract -

With the emergence of 3D technologies in a recent decade, BIM software makes it easy to detect those conflicts in the early stage of a project. Clash detection in BIM software is now a common task. Among those conflicts found by BIM software, however, a relatively high percentage belongs to 'pseudo conflicts'—which are permissible or tolerable, but BIM software does not reveal this information. Thus, currently BIM managers have to manually inspect every detected conflict to classify the type of conflict. Some researchers urged an automated process to facilitate this laborious process. This study implemented both a rule-based reasoning system and machine learning classifiers to help classify those BIM-detected conflicts. Preliminary testing results indicate that machine learning algorithms can achieve comparable results to a traditional rule-based system, but with much less costs and energy in developing.

Keywords –

Clash detection, Machine learning, Rule-based reasoning, BIM

1 Introduction

Generally, engineering designs are constructed and compiled by engineers of different professions, such as those in construction, structural engineering, and mechanical, electrical, and plumbing (MEP). Therefore, conflicts between different design disciplines are inevitable [1, 2]. Design conflicts are errors in which building components overlap in a certain space when various design plans are being compiled. Minor design conflicts often induce rework and cost increases, whereas severe conflicts may cause change orders, resulting in cost overruns, delays, and labour safety issues. Therefore, project performance will be substantially affected if design conflicts are not properly mitigated. [3].

The emergence of building information modelling (BIM) software in recent years has simplified design clash detection, with conflict or interference checking being basic functions of BIM software programs. Because resolving design conflicts is critical to project performance, combined with the popularity of BIM software, building codes in many countries have mandated the enforcement of clash detection in public projects [1]. For example, in the United Kingdom, a design team is mandated to perform clash detection every 1 to 2 weeks to ensure that engineering designs are fully coordinated and free of conflicts, thus reducing the likelihood of design changes occurring.

However, a discussion of effective methods to mitigate design conflicts and the use of BIM to assist in decision-making has been neglected in the literature [3]. Due to the existence of numerous engineering interfaces in a single project, BIM software can often easily detect hundreds of clashes, even for small-scale projects. BIM managers thus must examine and analyse each conflict manually. Some researchers have stated that although BIM software programs have excellent clash detection functions, the classification of detected clashes is still difficult, time-consuming, and costly, and thus an automated classification method is urgently required [1].

Because classifying clash types requires the input of experts with vast knowledge and experience, conventionally a rule-based expert system is often used for automated process development. However, rule acquisition when developing an expert system is time-consuming and laborious, and its prediction performance is usually limited by the number of rules. By contrast, supervised learning (i.e., machine learning) only requires the collection of sufficient cases and appropriate feature manipulation to quickly obtain required results. Furthermore, its accuracy increases continuously as the number of cases increases.

This study used the structural and MEP models of a construction project as an example, and implemented

three automated processes to classify those conflicts detected by BIM software using rule-based expert system, individual classifiers of supervised learning, and multiple classifiers of ensemble learning, respectively. Their performances in terms of predictive accuracy were then compared and evaluated. The results showed that the accuracy of the rule-based expert system was approximately 58% while 92% and 94% were acquired using individual classifiers and ensemble learning, respectively. This indicated that machine learning algorithms can achieve comparable results to a traditional rule-based system regarding conflict classification, but with much less costs and energy in developing.

2 Related Work

2.1 Spatial clashes

Wu [4] divided spatial conflicts into four categories: design conflicts, construction conflicts, damage conflicts, and congestion. Design conflict refers to spatial overlap between building components when different design teams develop their own designs. Wu also found that the existence of numerous interfaces among construction project participants is the main source of design conflicts. Researchers in another participatory action research project in the United Kingdom introduced a collaborative environment in a jointly designed large-scale, multistory construction project, and assisted the designers in avoiding design conflicts. However, more than 400 conflicts were still observed between the structural model and the MEP model [1]. The study revealed that although collaboration can decrease design conflicts, clash detection still remains a necessary process.

In summary, design collaboration does not prevent all conflicts; thus, clash detection and resolution are still necessary. Although most BIM software provide clash detection, classifying and resolving those detected clashes remain manual and difficult. The UK study [1] found that after performing clash detection, BIM managers need to classify types of those detected clashes, namely: (1) errors, which must be resolved; (2) pseudo clashes, which are permissible and does not require to be resolved; 3) deliberate clashes; and (4) duplicate clashes. Due to the considerable number of engineering interfaces, BIM software will produce substantial clash detection results, even for small-scale projects. BIM managers must go through the above-mentioned manual process. Since this process is highly mechanized, time-consuming, and costly, an automated classification method is urgently required; otherwise, the benefits of clash detection provided by BIM software will be reduced due to information overload [1]. Concluding remarks in those studies illustrated the necessity and importance of this study.

2.2 Machine learning in civil engineering

Machine learning is a computer science related to how machines can learn in a similar manner to humans. In machine learning, the process of human learning and adjustment is transferred to machines. According to whether or not the answers are provided during the training, machine learning has been usually identified as two categories: (1) Supervised learning：During training, answers (labels) are supplied to a question to provide the machine with the ability to recognize errors. This study applied this approach to train and test those classifiers; and (2) Unsupervised learning：No answers are provided to a question during training process; thus, the machine must find the answer itself. The expected results from this learning method are usually less accurate than those in supervised learning.

Machine learning has widely been used in numerous studies on civil engineering applications, such as for monitoring construction progress using 4D BIM, performing regulatory inspections using BIM, reconstructing 3D models using computer vision, and using static images to monitor constructability [5].

The development of machine learning algorithms involves five basic steps [6]: (1) Obtaining data required for training, analysing and selecting the features related to problem solving. (2) Choosing a performance metric. (3) Choosing a classifier and optimization algorithm (4) Evaluating the performance of the model; and (5) Tuning the algorithm. Once learning is completed, estimations can be performed by inputting new data into the algorithm. In most problem-solving tasks, the classifiers can be either linear or nonlinear models. The most common linear model is the linear regression model while non-linear models include the decision trees, k nearest neighbors (k-NN), support vector machine (SVM), and deep learning. However, due to problems having different domain-specific characteristics, it is nearly impossible for a single classifier to work well across all scenarios [7]. Besides, the performance may be dependent on the training and testing data, especially when the number of samples is not large enough. Therefore, it is highly suggested to compare the performance of different classifiers and select the best model for the domain problem.

Since the problem of identifying clash types in this study belongs a classification problem in machine learning, this study used non-linear models to implement individual classifiers and ensemble learning models.

3 Methodology

To evaluate the performance of the rule-based reasoning and machine learning algorithms on classification of clash types, this study developed a process of research methodology as shown in Figure 1. Section 3.1 and 3.2 describes the collection of clash cases and how we labelled the clash type by human experts. Section 3.3 introduced the implementation of the rule-based system, followed by Section 3.4 and 3.5 which detailed the training of single classifiers and multiple classifiers, respectively. Section 4 then provides the results of prediction by different methods using the testing dataset as well as the evaluation of their performance in terms of prediction accuracy。

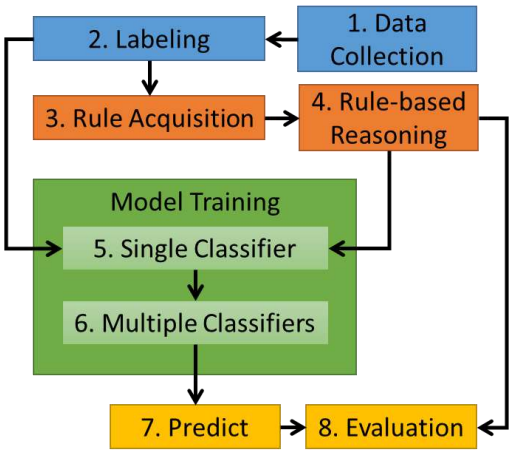

Figure 1. Process of research methodology

3.1 Data Collection

This study used a large shopping mall with nine floors above ground and four floors underground as a sample case. Three floors of the structure were extracted, and Autodesk Navisworks was employed for clash detection. To reduce the load of subsequent labelling process, this study only selected water supply pipelines within the MEP model against the structural model for clash detection. Figure 2 shows the clash detection report for models on the sixth floor . The table at the top shows the total number of clashes while the following table lists all details of each clash, including grid location, clash point, distance, and information about the two clashed items (e.g., item ID, layer, item name, and item type). In addition, two image icons are available. The image can also be viewed by clicking on the icon (Figure 3). Table 1 shows the statistics of the entire clash detection report including 415 structural clashes against flow segments such as pipes and fittings.

Figure 2. Illustration of the clash detection report produced by Autodesk Navisworks 2017

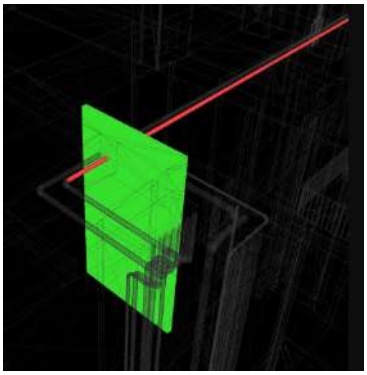

Figure 3. The snapshot of a clash produced by Autodesk Navisworks 2017

Table 1. Statistics of the clash detection report

	Pipes	Fittings	Total
Framings	153	25	178
Walls	155	68	223
Columns	1	1	2
Landings	12	0	12
Total	321	94	415

3.2 Labeling the Clash Types

After completing the clash detection report, the research team integrated the HTML-based clash report into a spreadsheet. Two senior engineers with experience in clash resolution were requested to classify the clash types. A column with a drop-down menu in the spreadsheet was provided for the experts to carry out labelling (Figure 4). This spreadsheet contains all the information in the clash detect report of Figure 2, including a hyperlink to view the clash image, as shown in Figure 3. The drop-down menu consists of four

options with intuitive common vocabulary: severe clashes, negligible clashes, legal interventions, and unknown. These four options were mapped to the four categories suggested in the literature: errors, pseudo clashes, deliberate clashes, and unknown, respectively. The research team also provided the experts with 2D CADs and 3D models of the building for their references.

The labeling process took approximately 10 days. Table 2 shows the summary of results by the two experts. After a detailed comparison was undertaken, 89 clashes were labelled with different answers by the two experts, accounting for approximately 20% of the total number of clashes. Therefore, the remaining 326 cases were used for subsequent analysis.

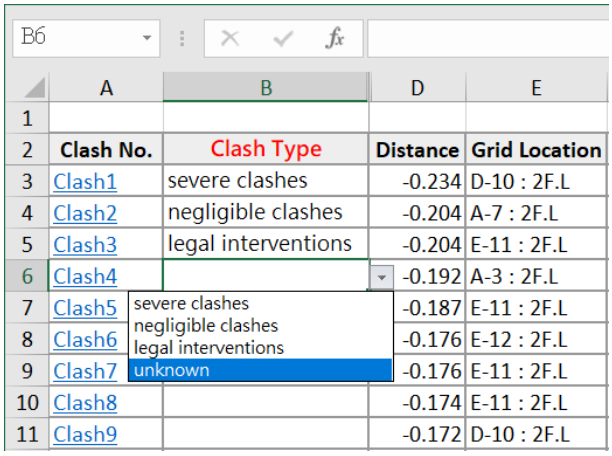

Figure 4. Spreadsheet-based clash detection report for labelling by human experts

Table 2. Statistics of training and testing data

Clash Type	Expert #	Expert #2
Serious clashes	159	208
Neglectable clashes	0	0
Legal intervenes	174	148
Unknown	82	59
Total	415	415

3.3 Rule-based reasoning

After obtaining the labelling results from the experts, the research team acquired 4 rules of clash type classification rules by interviewing the two experts as follows:

1. Beam rule: If the structural component of a clash is a beam, then the clash type is either a severe clash (i.e., error) or negligible clash (i.e., pseudo clash). Severe clashes located near two ends of the beam can affect structural safety, whereas negligible clashes do not affect structural safety but require perforation processing.
2. Column rule: If the structural component of a clash is a column, then the clash type must be a severe clash (i.e., an error).
3. Slab rule: If the structural component of a clash is a slab, then the clash type must be a legal intervention (i.e., a deliberate clash).
4. Wall rule: If the structural component of a clash is a wall and a load-bearing wall, the clash type must be a severe clash (i.e., an error); otherwise, it is a negligible clash.

Some rules involve complex spatial operations or require other supporting information to be processed. For example, the identification of clash position and wall type is required for Beam and Wall rules, respectively. The limited information provided in the report did not allow for corresponding calculations. Therefore, under a conservative consideration, this study simplified the aforementioned Beam and Wall rules as follows:

1. Simplified beam rule: If the structural component of a clash is a beam, then the clash type is a severe clash (i.e. errors).
2. Simplified wall rule: If the structural component of a clash is a wall, then the clash type is unknown.

Numbers in parentheses in Table 3 represent the numbers of clashes that are consistent with expert classification results. Because the simplified rule tends to be conservative, the prediction accuracy rate will be lower, especially for the Wall rule, which had an accuracy rate of only 15%, resulting in an overall classification accuracy of less than 60% (189/326).

A further modification was made to the Wall rule: “If the structural component of a clash is a wall, then the clash type is negligible (i.e., a deliberate clash).” This increases the overall accuracy rates to 87% (283/326). However, this modification may carry a potential risk of mis-classification

Table 3. Results of rule-based reasoning using simplified rules

Clash Type	Simp. beam rule	Column rule	Slab rule	Simp. wall rule	Total
Serious clashes	174 (154)	2 (2)			176 (156)
Neglectable clashes			12 (12)		12 (12)
Unknown				138 (21)	138 (21)
Accuracy	0.89	1.00	1.00	0.15	0.58

3.4 Feature selection and pre-processing for machine learning

As described in the literature review, the first step in developing a machine learning algorithm involves selecting features that are relevant to problem solving. In addition, because the development tool used in this study (i.e., scikit-learn) can only process numerical data, the nominal or text features must be coded as numerical features. Table 4 shows the selection and manipulation of each feature that we used for training machine learning algorithms. Among them, numerical features such as "Distance", "Floor-1", and "Floor-2" remain unchanged; "Clash Point" is the coordinate with a mixture of numbers and text and is separated into three numerical features, namely "Clash Point_x", "Clash Point_y", and "Clash Point_z"; As for "ItemType-1" and "ItemType-2", which are nominal features, one-hot encoding is performed separately, thus deriving six features as shown in Table 4.

In addition, to test whether the results of rule-based reasoning (see Section 3.3) contribute to the improvement of the prediction accuracy of the machine learning algorithm, another feature "Rule-Tag" was also added to label the result of the rule-based reasoning. Since this feature is nominal, one-hot encoding is also performed before the training process.

Table 4. Summary of feature selection and pre-processing

Original Feature	Data Type	Example Value	Revised Feature
Distance	numeric	-0.234	unchanged
Floor-1	numeric	2	unchanged
Floor-2	numeric	2	unchanged
Clash Point	text	x:-7370, y:-1171, z:24	Clash Point_x Clash Point_y Clash Point_z
ItemType-1	nominal	Pipes	{Pipes, Fittings}
ItemType-2	nominal	Framings	{Framings, Walls, Slabs, Columns}

3.5 Modeling by machine learning classifiers

The research team adopted a free software machine learning library, scikit-learn, as the implementation environment, which provides a rich set of tools for classification, regression and clustering using machine learning algorithms such as decision trees, SVM, k-NN, random forests, gradient boosting, k-means and DBSCAN. Researchers suggested that no single classifier can work well across all scenarios. Therefore, this study implemented three common single non-linear classifiers and three multiple classifiers of ensemble learning. We will evaluate the performances of those different classifiers later in Section 4.

Table 5 summarizes the manipulation of training classifiers by this study. In order to test and evaluate classifier performances, the research team randomly selected 30% of the entire 326 cases as testing dataset, i.e. 98 cases, while the rest of cases is further split into training and validation datasets with a proportion of 4:1 when applying k-fold cross-validation (k=5). For classifiers like kNN, SVM, Voting, the features of training dataset were standardized before the training process.

Table 5. Summary of machine learning manipulations

Measures	Description
Data splitting	7:3 (228 cases for training; 98 cases for testing)
Performance metric	Confusion matrix
Classifiers	Decision Tree, SVM, kNN, Voting, Bagging, Random Forest
Evaluation	k-fold cross-validation (k=5)

3.5.1 Single classifiers

1. Decision Tree

First, the research team implemented a classifier using decision tree algorithm with a maximum tree depth of 6 and a criterion of Gini impurity. Figure 5 shows its learning curves with the best f1-score of 0.92. Both the training and validation curves converge at a high prediction accuracy indicating the classifier doesn't under-fit the real situation. However, two curves converge with a large gap indicating the model may suffer from over-fitting.

2. K Nearest Neighbors (k-NN)

Next, a classifier using k-NN algorithm with 3 neighbors and a uniform weight. Figure 6 shows its learning curves with the best f1-score of 0.90. Both curves in Figure 6 also converge at a high prediction accuracy with a small gap indicating the classifier doesn't suffer from under-fitting, but a bit from over-fitting.

3. Support Vector Machine (SVM)

The last single classifier implemented in this study is using SVM algorithm with 1.0 penalty and a linear kernel. Figure 7 shows its learning curves with the best

f1-score of 0.90. Although the curves do not converge well as the previous two classifiers, its high prediction accuracy and small gap still indicate the classifier doesn't suffer from high variance nor high bias.

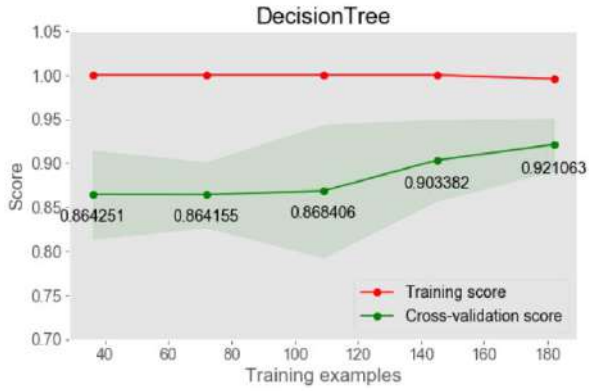

Figure 5. The learning curves of the classifier of a decision tree with a maximum depth of 6

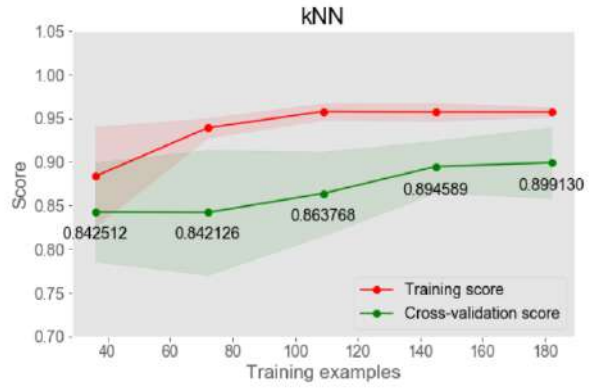

Figure 6. The learning curves of a k-NN classifier with 3 neighbors and a uniform weight

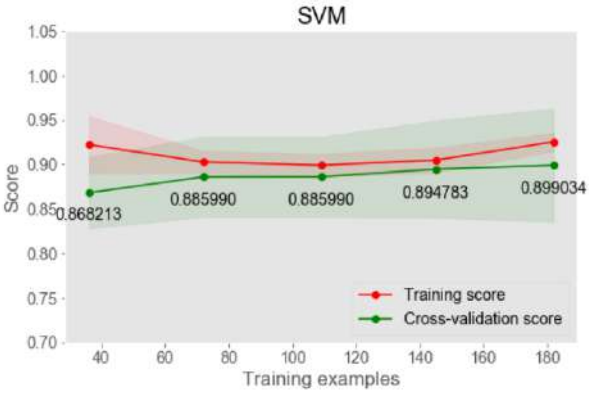

Figure 7. The learning curves of a SVM classifier with 1.0 penalty and a linear kernel

3.5.2 Multiple classifiers by ensemble learning

All single classifiers implemented previously have performed well in terms of prediction accuracy so the research team then moved forward to build up a set of classifiers following the principles of ensemble learning. The benefit of ensemble methods is to combine different classifiers into a multiple classifier that can often have a better predictive performance than each individual classifier alone. Those multiple classifiers implemented by this study include Voting classifier, Bagging classifier, and Random Forest classifier.

1. Voting

The first implemented ensemble learning algorithm is the Voting classifier, which combined three individual classifiers implemented previously, namely, a decision tree classifier, a k-NN classifier, and a SVM classifier, with a soft voting weight of 5:1:1, respectively.

Figure 8 shows its learning curves where both training and validation curves converge with a small gap at the best f1-score of 0.94 indicating the classifier doesn't suffer from under-fitting, but slightly over-fits.

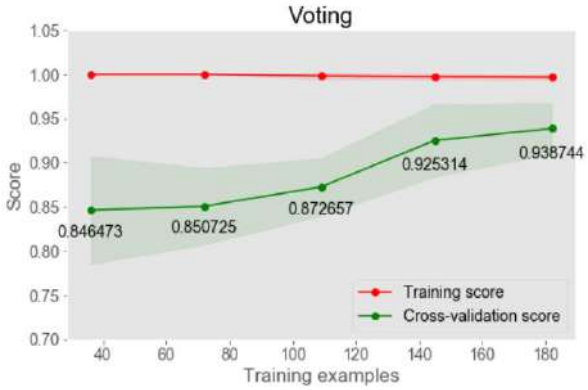

Figure 8. The learning curves of a Voting classifier combining a decision tree, k-NN, and SVM classifiers

2. Bagging

The research team then implement a Bagging classifier with 100 default estimators, where are decision tree classifiers. The learning curves shown in Figure 9 indicate that the classifier has gained a higher prediction accuracy (0.96) than any of previous classifiers. The convergence of both training and validation curves also indicates this classifier does not over-fit nor under-fit.

3. Random Forest

Finally, the research team implemented the commonest ensemble learning classifier, Random Forest,

with also 100 default estimators, or the decision trees. Figure 10 shows its learning curves with a very similar shape with the Bagging classifier.

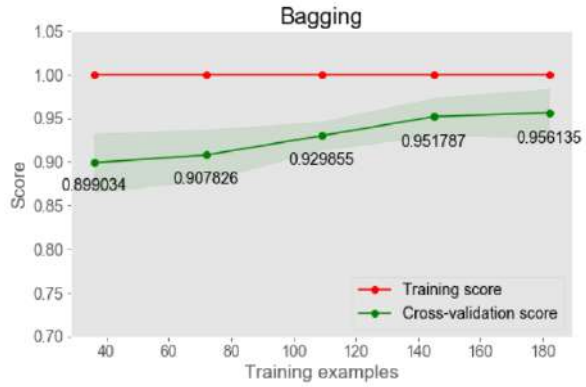

Figure 9. The learning curves of a Bagging classifier with 100 decision tree classifiers

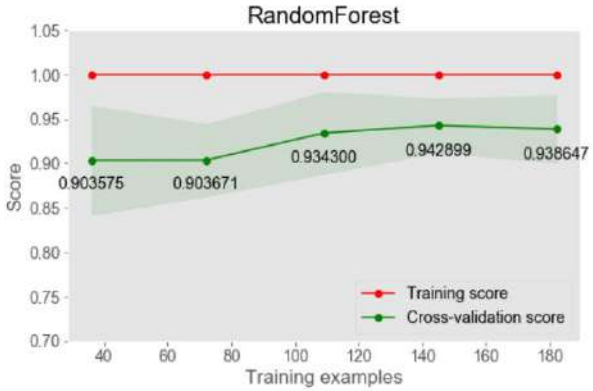

Figure 10. The learning curves of a Random Forest classifier with 100 decision tree classifiers

4 Results and Evaluation

In this section, the testing dataset of 98 cases is used to test the performance of those trained classifiers. The confusion matrix is adopted for the evaluation, which reports the counts of the true positive, true negative, false positive, and false negative predictions of a classifier, as shown in Figure 11. Three rates derived from the confusion matrix are recorded as the performance metric against all trained classifiers, including precision, recall, and f1-score, which are defined as in formulas (1), (2), and (3).

Besides those quantitative measurements, feature importance suggested by each classifier is also addressed to reveal which features explain more about the prediction results than others. Only the decision tree classifier and Bagging classifier are selected for evaluation.

		Predicted labels	
		True Positives (TP)	False Negatives (FN)
Actual labels		False Positives (FP)	True Negatives (TN)

Figure 11. The confusion matrix used to evaluate the performance of the trained classifiers

$$Precision = \frac{TP}{TP + FP} \quad (1)$$

$$Recall = \frac{TP}{TP + FN} \quad (2)$$

$$f1 - score = 2 * \frac{Precision * Recall}{TPrecision + Recall} \quad (3)$$

4.1 Results

Table 6 illustrate the testing results of 98 cases against the decision tree classifier with 6 levels. The average f1-score is 0.92 indicating a good predictive accuracy. Table 7 show the testing results of the bagging classifier with 100 decision trees. The average f1-score reaches an even better predictive accuracy of 0.94. Compared with the classification accuracy obtained by the rule-based reasoning, both classifiers can produce a much better predictive performance.

Table 6. Performance matrix of the decision tree classifier

	precision	recall	f1-score
Deliberate clashes	1	1	1.00
Errors	0.89	0.95	0.92
Unknown	0.78	0.58	0.67
Average	0.93	0.93	0.92

Table 7. Performance matrix of the Bagging classifier

	precision	recall	f1-score
Deliberate clashes	0.98	1.00	0.99
Errors	0.93	0.95	0.94
Unknown	0.80	0.67	0.73
Average	0.94	0.94	0.94

4.2 Evaluation

According to the confusion matrix of the decision tree classifier shown in Figure 12, none actual “errors” is classified as deliberate clashes or pseudo clashes, which provides a conservative prediction with a lower risk. In addition, the classifier filters out 42 “noises” (in

this case, deliberate clashes), accounting for 43% of all clashes from the original clash report, remaining only 57% to be inspected by human. Similarly, none actual "errors" is mis-classified by the Bagging classifier. The classifier also filters out 43% of clashes from the original clash report.

Figure 13 lists the top 6 features that have the higher importance to contribute the prediction results. Item type-1 "Framing" is the most discriminative feature in the dataset, which aligns with the result of rule-based reasoning in Section 3.3. Likewise, the feature importance suggested by the Bagging classifier presents a similar distribution to that by the decision tree classifier.

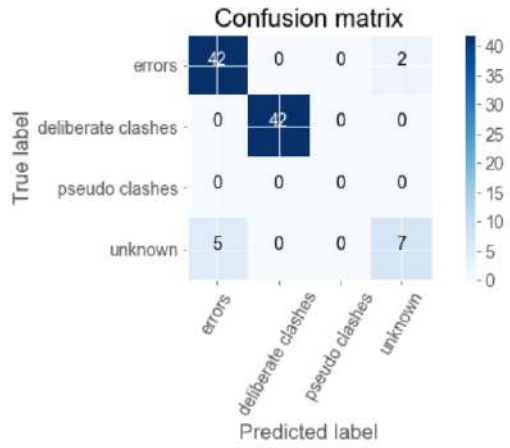

Figure 12. The confusion matrix of the decision tree classifier

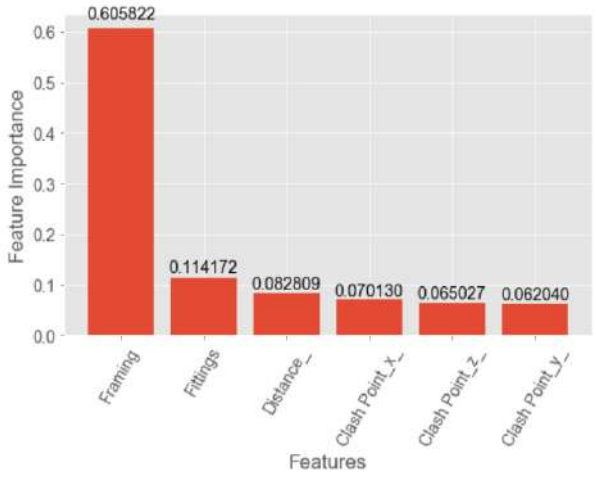

Figure 13. Feature importance suggested by the decision tree classifier

5 Conclusions

This study developed a tiny rule-based reasoning system to classify those conflicts detected by BIM software, which obtained a predictive accuracy of 58%. Then, both individual machine learning classifiers and multiple classifiers were also implemented to perform the same task. Preliminary testing results showed that both the decision tree classifier and 3 ensemble learning classifiers can obtain a much better predictive accuracy than the rule-based version.

However, the current model and its predictive performance can only be applied to this setting since the dataset used to train and test the machine learning classifiers only contains clashes between structural components and piping components. The dataset needs to be extended to include other MEP components, such as ducts, conduits, fire alarm devices, or lighting devices. Besides, most classifiers built in this paper have an over-fitting issue according to their learning curves. This could also be resulted from a relatively small number of training cases in our dataset. This limitation originates from that fact that labeling the dataset highly relied on human experts' experiences and labor work. All the mentioned issues remain to be solved in the future.

References

[1] E. A. Pärn, D. J. Edwards, Michael C.P. Sing, Origins and probabilities of MEP and structural design clashes within a federated BIM model, *Automation in Construction*, 85: 209-219, 2018.

[2] Lopez, R., et al., Design error classification, causation, and prevention in construction engineering. *Journal of Performance of Constructed Facilities*, 24(4): 399-408, 2010.

[3] J. Won, G. Lee. How to tell if a BIM project is successful: a goal-driven approach, *Automation in Construction*, 69: 34–43, 2016.

[4] Lin Y. C., Chou S. H. and Wu I. C. Conflict Impact Assessment between Objects in a BIM system. In *Proceedings of the 30th International Symposium on Automation and Robotics in Construction*, Montreal, Canada, 2013.

[5] H. Son, F. Bosche, C. Kim, As-built data acquisition and its use in production monitoring and automated layout of civil infrastructure: a survey, *Advanced Engineering Information*, 29 (2) (2015) 172–183.

[6] Raschka S. *Python Machine Learning*. Packt Publishing, Livery Place, 35 Livery Street, Birmingham B3 2PB, UK, 2015.

Augmented Reality and Deep Learning towards the Management of Secondary Building Assets

A. Corneli[a]*, B. Naticchia[a], A. Carbonari[a], and F. Bosché[b]

[a]Polytechnic University of Marche, DICEA, Ancona, Italy
[b] Heriot-Watt University, Edinburgh, UK
E-mail: a.corneli@pm.univpm.it; b.naticchia@univpm.it; alessandro.carbonari@staff.univpm.it; f.n.bosche@hw.ac.uk

Abstract -

The retrieval of as-is information for existing buildings is a prerequisite for effectively operating facilities, through the creation or updating of Building/Asset Information Models (BIM/AIM), or Digital Twins. At present, many studies focus on the capture of geometry for the modelling of primary components, overlooking the fact that many recurring actions need to be conducted on assets inside buildings. Furthermore, highly accurate survey techniques like laser scanning need long offsite processing for object recognition. Performing such process on site would dramatically impact efficiency and also prevent the need to revisit the site in the case of insufficient/incomplete data.

In this paper, an Augmented Reality (AR) system is proposed enabling inventory, information retrieval and information update directly on-site. It would reduce post-processing work and avoid loss of information and unreliability of data. The system has a Head-Mounted Display (HMD) AR interface that lets the technician interact hands-free with the real world and digital information contained in the BIM/AIM. A trained Deep Learning Neural Network operates the automatic recognition of objects in the field of view of the user and their placement into the digital BIM. In this paper, two uses cases are described: one is the inventory of small assets inside buildings to populate a BIM/AIM, and the second is the retrieval of relevant information from the AIM to support maintenance operations. Partial development and feasibility tests of the first use case applied to fire extinguishers, have been carried out to assess the feasibility and value of this system.

Keywords -

Augmented Reality, Building survey, Inventory, BIM, Facility Management.

1 Introduction

One of the biggest challenges in the construction industry today is information management both in the construction phase and in the operational phase [1, 2].

In fact, the retrieval of specific data during the lifecycle of buildings represents a high cost for all the stakeholders involved in this field [3, 4]. Today, facility maintenance contractors are paid to survey existing buildings in order to capture the as-built/as-is status. In these cases, owners would pay twice, once for the construction contractor to complete the documents at the end of construction and again for the maintenance contractor survey [1]. Moreover, as far as existing buildings are concerned, information is often not available nor updated, although data mirroring the current state (i.e. digital twin) are needed for further action. As a result, a building survey is usually necessary. A number of techniques and technologies are now in use, including EDM (Electronic Distance Measurement), GPS (Global Positioning System), 3D Laser scanner [5]. However, each of the aforementioned technologies requires further post processing of data in order to provide its interpretation. This may also require further site visits to acquire supplementary data.

Another aspect to take into consideration is how the information is stored after being collected. Since BIM is becoming an industry standard, Facility Management (FM) is expected to be based on information contained in an Asset Information model (AIM) populated from the BIM model. Information collected through a BIM process and stored in a BIM/AIM could be beneficial for a variety of FM practices: such as commissioning and closeout, quality control and assurance, energy management, maintenance and repair, and space management [6]. Furthermore, data modelling is often conducted manually. The automatic detection of objects types and the related automatic creation of the digital objects

would improve process efficiency and data reliability.

For the reasons stated above the objectives of this research are as follows:

- to decrease post-processing efforts thanks to the automation of some processes and smart human intervention on site;
- to reduce the time necessary to gather any piece of information;
- to collect data in in a BIM model by creating standard BIM objects with linked data including all information necessary for further operations.

The core innovation proposed in this research lays in the integration of several hardware and software innovations into one system architecture: Neural Networks, Mixed Reality (MR) and BIM. The proposed system develops efficient human-machine collaboration, employing MR as a powerful medium between the human, (cloud) computing facilities and the BIM data.

2 Literature review

In recent years there have been increasing efforts towards the automation of survey procedures. Technologies such as Laser Scanning and photogrammetry are very accurate but they also collect a vast amount of raw data that need to be interpreted. Solutions for semi-automatic survey of the environment have already been pursued:

- The Bonanni et al. [7] combine a robot, which employs a SLAM (Simultaneous Localization and Mapping) module for building up the map of the environment, and human input to provide spatial hints about entities of interest that must be included into the map. Solutions of this type still demand a lot of effort and long time to detect all the objects since the operator has to manually detect the object and enter its features.
- Adan et al. [8] resent a coloured 3D laser scanned point clouds algorithm that allows the location of doors. This system integrates the analysis of both geometry and colour provided by a calibrated set of 3D laser scanner and colour camera with the aim of detecting, localizing and sizing doors.
- The method proposed by Quintana et al. [9] regards a system for the detection of 'small components' in coloured point clouds acquired by a 3D laser scanner.
- Lu et al. [10] propose a recognition system composed of sub-systems for: (1) object recognition, based on a new neuro-fuzzy framework; (2) material recognition, based on image classification procedures and the trained texture library; (3) IFC BIM object generation, that automatically transforms recognized objects with materials information into complete BIM objects in IFC.

These studies focus on the automatic interpretation of collected data. Anyway, they still require post processing effort, such as the Adan [8] and the Quintana [9] studies, or they are way too complex to be effective during on site procedures, like the Bonanni's one.

As far as the support given by MR in maintenance operations is concerned some early experiments have already demonstrated the possibilities provided by the display of information on site. The numerous advantages in the use of MR towards the entire lifecycle of building is well described by Riexinger et al. [12]. Both this article and the one by Fonnet et al. [13] demonstrate the convenience in displaying information on site through holograms so as to help during the refurbishment of buildings. Practically, Ammari et al. [11] developed a system capable of showing holograms thanks to Augmented Reality (AR) and image tracking. The system is composed of a IFC XML database that makes it possible to display separated pieces of information if necessary. Hugo et al. [14] used Revit for the geometric and appearance features and Dynamo for a query of data transferred to Unity in XML format. Then they developed the MR environment in Unity and finally deployed into the Hololens a first attempt of holographic projection of a building three dimensions model at a small scale. Finally, Kopsida and Brilakis [15] present an evaluation of different methods that could be implemented for a marker-less mobile BIM -based AR solution for inspections. In conclusion they state that there are no efficient mobile AR solutions for on-site inspections and that other methods for marker-less AR, even if already introduced, have not yet been tested on construction sites.

As for the use of Neural Network (NN) and Augmented Reality together, Baek et al. [16] proposed a NN-based method for indoor localization. Their work is also motivated by the need to provide relevant information in FM applications.

While these works demonstrate the growing interest of the AEC industry in MR, many issues have still to be addressed: the proper scale of the visualization of building components in situ; accurate localization of the operator inside the building so as to automatically display relevant information; recognizing building assets without specific markers (visual markers or RFID tags); and providing an effective interface between MR headsets and BIM data.

In this paper we propose an architecture that combines some of the aforementioned techniques to allow operators effectively survey buildings for maintenance applications, with MR interface to the

BIM/AIM model, and automatic object detection supported by NN.

A significant challenge to the delivery of such system is the development of an effective approach to indoor user localization.

3 System Architecture

The system architecture supports both use cases previously defined and it can be divided into two main environments as shown in Figure 1:

- The Mixed Reality (MR) environment which is where the digital copies of the real objects are developed and/or manipulated while on siteThis includes an object recognition application (paragraph 5.2).
- The real environment which is represented by the building and the assets object of the survey, the operator and its whole equipment. The real environment is the place where the holograms are displayed and overlapped to it.

The MR environment is composed of the following components:

- BIM environment used to develop the initial building model. This digital twin of the real building will be enriched with the data from the survey.
- The MR environment, which is represented by the software Unity, that allows to develop applications for the MR tool. The scene inside Unity includes the building model imported and all the components necessary to make operations and have interactions between reality and digital information.
- The real environment on the other hand comprises the following elements:
- Microsoft Hololens which is the head-mounted display chosen to show the MR environment on site and to act as an interface between the digital world and the real world (operator and environment).
- On-site operator who is doing the survey wearing the Hololens.
- Neural Computer Stick-Movidius which is a neural computer stick that is specially designed for working with neural networks. In order to make the entire system usable on site the images are processed by this tool, as opposed to rely on cloud computation.
- Embedded PC- Raspberry which works as an interface between the Hololens and the Movidius, and as a hardware support for the latter.

The Hololens application created in Unity performs the following tasks:

1. it keeps track of the position of the gaze (the

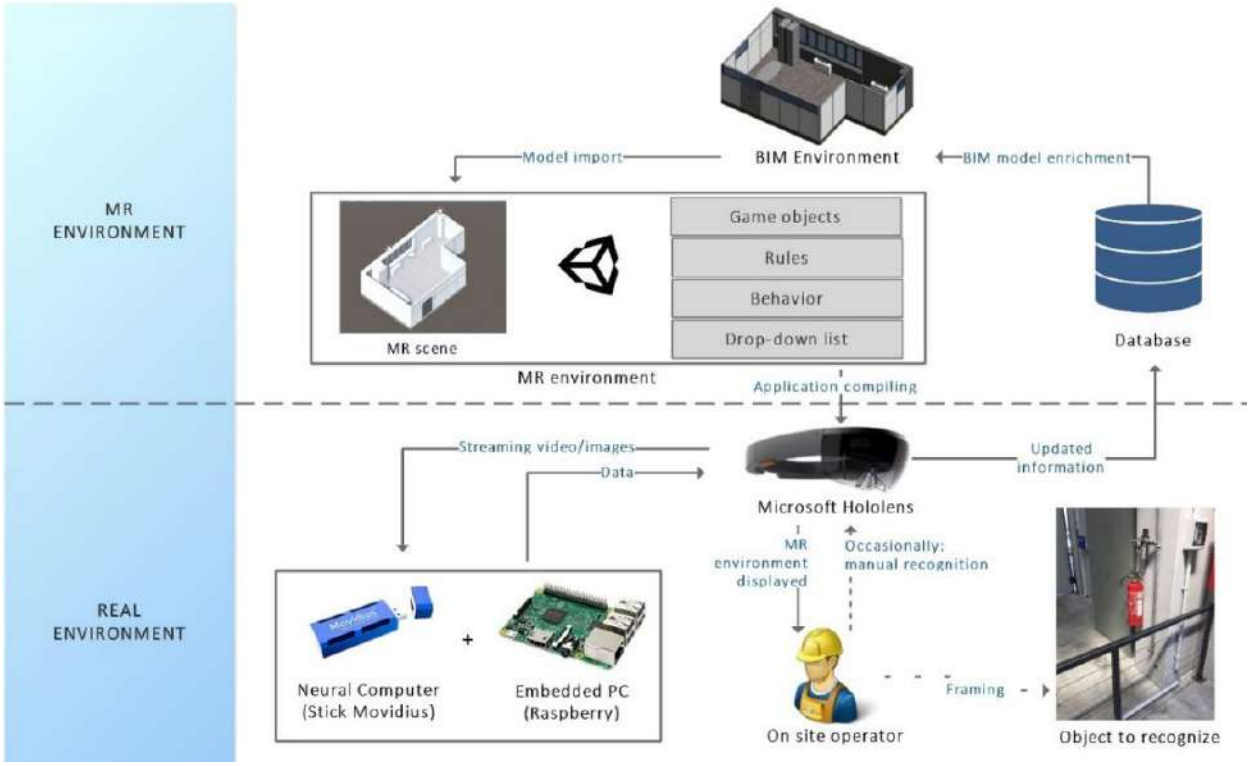

Figure 1. System architecture

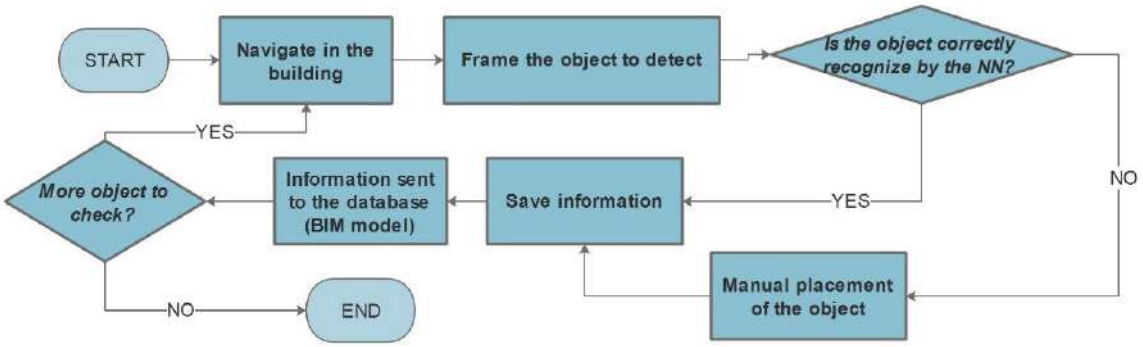

Figure 2. Assets inventory procedure

point the operator is looking at);
2. it sends the streaming video (or images) to the embedded pc;
3. it reads the information provided by the neural network;
4. it acts as interface for the user to manipulate digital objects, their placement in the BIM model.

4 Use cases

The previously explained architecture is specifically thought to be used in two different use cases: the inventory of secondary building assets ; and the support of maintenance operation through asset recognition and retrieval of information concerning selected objects.
These two use cases are discussed in the following paragraphs.

4.1 Assets inventory

The inventory is a costly operation [2] since it requires a large amount of money and thousands of man-hours for creating/updating information [3, 4] necessary for operating buildings. The system proposed aims to reach a certain level of automation in the process of data collection, especially compared to current inventory procedures that still require long post-processing [8].
For these reasons, the first use case aims to improve the efficiency of survey procedures as well as to lead to the automatic enrichment of BIM models.
The procedure proposed (Figure 2) with this system considers an operator wearing the MR head-mounted display and walking into the building for the first time. Once any asset (secondary component) to detect is framed by the MR device the image is sent in real time to the neural network which is trained to recognize a specific category of objects. The neural network sends back the label associated with the image (as an outcome of the recognition) and the coordinates of the position of the object (assessed from the drawing of a bounding box containing the element). These data allow the application to choose a specific object, among a predefined library, and to place it, as a hologram, into the real environment. In the case of incorrect or missing identification, the operator has still the possibility of manually placing the object, as a hologram, into the real world. All the data about the detected objects and their positions are transferred into a NoSQL Database so as to be available for future operations.
The procedure just explained will enable the operator to check real time the collected data and to modify them if necessary while on site. This will reduce the possibility of errors or of losing. AR will represent a valuable means to display the gathered information so as to interact with them on site. The operator and the application proposed will work in parallel leading to a higher efficiency in contrast with current methods where there is a prevalence of man-machine working in series. This use case has been partially developed as explained in section 5.

4.2 Maintenance operation support

The architecture proposed can also be valuable to support maintenance operations. Buildings contain a series of assets that need maintenance and which are subjected to regular inspection. Correct and immediate localization of objects requires time and it involves a greater possibility of error in complex buildings.
With the objects recognition system the procedure starts with the inspector walking around the facility with the head-mounted display. The application in the device sends continuously in real time the video of what the operator sees to the embedded system. Once the operator frames a component of interest, a pre-trained neural network in the embedded system performs an identification. The application

automatically shows the hologram of the object identified, with all its components, and asks for the information to additional show as holograms (e.g. procedures, check-lists, user manuals, usage data). The technician has the possibility to check information needed and to fill in forms at the end of operations. The information entered in the application is transferred to the FM database so as they can be consulted in case of further maintenance operations.

On one hand this procedure will ensure better performance on site, thanks to the possibility to show larger amounts of information on a digital device and directly related to the object. This will save time used to retrieve the useful information. On the other hand, the real time updating of data reduces the time necessary to fill in the database with this information and support the operators in preventing data loss. Furthermore the automatic localization on site is highly beneficial in case of buildings where the operator is working for the first time, or to avoid manual errors (e.g. wrong floor selection). Finally, this system would definitely provide support with new personnel since the MR allows to show detailed step-by-step procedures directly in their field of view.

5 Preliminary development

5.1 From BIM to Unity

Information from the BIM model necessary to create the proper MR scene. First, the geometry of the building is required to allow an accurate positioning of the secondary components. Secondly, component definition, parameters and details are needed to improve the accuracy of the location data. For instance, an object fire extinguisher has to be placed on wall surfaces, thus walls need to be sufficiently detailed. Materials too could be practical as it would make the vision more pleasant and realistic and it would help the operator in identifying surfaces and components.
In order to upload the BIM model into the Unity project the method chosen was to use the *.fbx* format. Importing such file directly into Unity without any other operation results in a loss of graphical information, so it is fundamental to do a second passage through 3D Studio Max so as to re-assign materials to objects. However, with this first method, non-graphical object information is not showed in Unity. The recognition system for inventory requires the geometry more than these non-graphical parameters. However, for the second use case, object parameters are necessary in order to update or consult data during operations. For this reason, further studies will be conducted on a new method to import non-graphical along with graphical object information, possibly by deploying a COBIe or IFC data parser.

Figure 3. Secondary element recognition embedded system

5.2 Recognition application

The recognition application will be developed in Unity, using the programming language C#. This application will carry out the following tasks:

1. to read and interpret the data about the position of the operator in the building, and therefore in its digital twin;
2. to send the streaming video to the embedded system;
3. to read the data from the recognition process (bounding box coordinates and object type);
4. to identify among a predefined library of objects the object type that matches the recognition response;
5. to locate the object in the right position according to the bounding box coordinates provided in the recognition response, the depth dimension provided by the mesh (that Hololens automatically does because the fire extinguisher owns a behavior for its positioning on walls);
6. to provide the possibility of modifying the object type or its position manually;
7. to provide the possibility of adding objects manually.

Tests on the insertion of doors and windows in the MR environment have been carried out.

5.3 Streaming video and data transfer Hololens – embedded system

The purpose of this system was to have the whole process performed on site. From the sending of the first piece of information, the video, up to the positioning inside the digital building of the

components, in the form of hologram, everything is carried out on site and real time (Figure 3). The communication protocol supporting the information flow for the recognition process from the Hololens to the embedded pc is defined as follows. In order to let the Hololens communicate with the Raspberry, a custom protocol over TCP/UDP is employed. This communication works through a local network and it is able to transfer both streaming video and data deriving from the recognition.

5.4 Neural Network

The recognition of small objects takes place by means of trained neural networks. The objectives of this recognition process are to identify the right type of object (e.g. fire extinguisher size), and locate it accurately within the frame ;

Several types of neural networks exist and the YOLO is the one chosen for this project, for the following reasons [17, 18]:

- the speed which is 45 frames per second; this means streaming video can be processed in real-time, with negligible latency of a few milliseconds.
- the one-step method for classification and localization of objects;
- the simultaneous prediction of multiple bounding boxes;
- the simultaneous prediction of multiple label confidence score;
- it is an open source solution.

In this project, a pre-trained YOLO is used. With this kind of neural networks, it is possible to re-train the last level of the network to detect the object of interest. The network needs a dataset of images to learn how to recognize the object of interest. The dataset features are explained in the following sub-section.

5.4.1 Dataset creation

The dataset to train the network to recognize a specific object should have specific features. With the aim of identifying only the right object, i.e. a fire extinguisher, the dataset will include at least one image for every existing type of fire extinguishers, so as to be able to recognize the fire extinguisher no matter the external appearance. As the dataset must include thousands of pictures, it will be made up of both original pictures and graphically re-edited photos as suggested by studies on dataset creation [19]. The process of editing the original photos is performed with the help of an augmentor software program available online.

The creation of the dataset involves labelling all the images, both with the bounding box around the object to be recognized and with the label assigned to it. YOLO requires a .txt file for each image with a line declaring the class and the bounding box coordinates (X,Y of the center and width and length).

The first goal was to recognize the object but next steps will handle the recognition of different fire extinguisher type. For this purpose, the distinctive components of the fire extinguisher need to be recognized separately. For instance, the pressure gauge helps in the identification of the extinguishing agent, the horn too is helpful in defying the type.

5.4.2 Neural Network training

A first training has been carried out using a tiny YOLOv2 pretrained with the COCO dataset.
YOLO requires some files to start training which are [17, 18]:

- total number of action classes (1 for our case);
- text file with the path to all frames which we want to train;
- text file with names of all action classes (fire extinguisher);
- the path to save trained weight files;
- a configuration file with all layers of YOLO architecture (described in Figure 2).
- pre-trained convolutional weights.

The value of filters in the configuration file of YOLO (.cfg file) for the second last layer is not arbitrary and depends on the total number of classes. The number of filters can be given by: filters=5*(5+number of classes). In order to start training the original .cfg file, the structure must be modified in its following features:

- batch=64, this means we will be using 64 images for every training step;
- subdivision=8, the batch will be divided by 8;
- classes=1, the number of categories we want to detect;
- filters=30, from the previous formula;

Figure 4. Training image type

Figure 5. Drawing the bounding box and labelling the object

- learning rate=0.001, advised by the developer of YOLO in order to avoid false minimum point.

After the training session, the new *.cfg* and weights files are created. The network automatically creates two groups of images, the former to train the network and the latter to test and validate it.

6 Tests and Results

First tests have been made about the training of the Neural Network. All these tests have been carried out on a computer in this preliminary phase.
The YOLO tiny v2 chosen has been trained with three different datasets in order to check if there was any improvement in the detection of fire extinguisher.
The three datasets are composed as follows:

- DATASET 1 (D1) =300 images, 75 (25%) original taken inside the Engineering Faculty premises (Polytechnic University of Marche), 225 (75%) obtained through the augmentation process;
- D1 added to DATASET 2 (D2) = 200 images, 50 (25%) original downloaded from Flickr (only images of fire extinguisher meeting the requirements expressed in the paragraph 5.4.1), 150 (75%) obtained with dataset augmentation;
- D1 and D2 added to DATASET 3 (D3) = 200 images, 50 (25%) original taken inside the Economic and Science Faculties (Polytechnic University of Marche), 150 (75%) come from the augmentation process.

For every dataset the images were divided into two groups, one for the training and one for the test, with the following splits: first dataset (D1) 260 training images and 40 testing images, second dataset (D1+D2) 429 training images and 71 testing images, third dataset (D1+D2+D3) 590 training images and 110 testing images. The kind of chosen images was similar for all the photos, close-up and with the object entire and placed in the center (Figure 4). In the test performed we worked using Visual Object Tagging

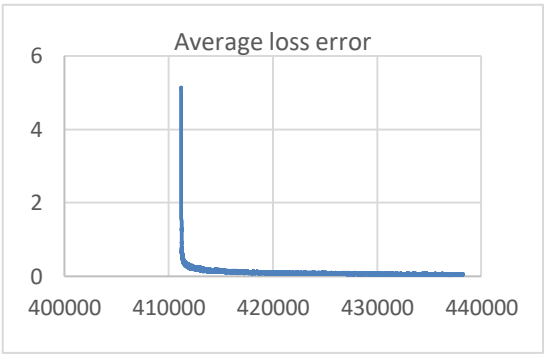

Figure 6. Decreasing of average loss error training 2

Tool for the manual drawing of the bounding box and for the assignment of the label (Figure 5).
The output of this process was a series of .txt file (one for every picture) containing the coordinates of the boxes and the category label (fire extinguisher in this case).
With the first dataset the training was stopped after 22100 iteration. For every training the choice of the weights was done extracting the indicators every 1000 iteration and then choosing the best one in the no longer decreasing area of the average loss error (Figure 6). The reached mean average precision (mAP) was 60,23% in the first case.
The second training counts 86700 iterations and in this case the mAP was 61,54%.
In the final training the number of iterations reached 26900 with a mAP of 62,81%.
The validation tests have been conducted for each of the three training sessions with the third training dataset of 110 photos. The results are displayed in Table 1. The percentage of fire extinguisher identified started from 38% and reached 45% with the latest training. the precision improved too because while in the first case 26 false positives occurred, in the latest case the number decreased to 14.

Table 1. Training results

	TR 1	TR 2	TR 3
N° of recognized fire extinguisher	42	44	50
N° of multiplied bounding box for one fire extinguisher	26	16	14

7 Conclusion and next steps

This research aims to provide a support to FM operations during the building lifecycle. The system proposed combines three different technologies: the AR, the BIM data model and Deep Learning, all in one embedded solution for on-site use. The two use cases described could improve their efficiency thanks to the

effective Human-Computer Interaction (HCI). First feasibility tests have been conducted related to the training of Neural Network and the recognition through the AR device. Further steps will be developed, starting from the increase of the number of images in the dataset so as to achieve a higher precision in the recognition process. Furthermore, after having reached a higher level of precision the new datasets will be developed for the recognition of precise type of fire extinguisher. Next steps will include also the full development of the AR interface and tests in a real environment.

References

[1] East E.W., Brodt W., 2007, BIM for Construction Handover, Journal of Building Information Modeling.

[2] Lee S., An H. & Yu J., 2012, An extension of the technology acceptance model for BIM-based FM, Construction Research Congress, 602-611.

[3] Keady R. A., 2013, Financial Impact and analysis of equipment inventories, Facilities Engineering Journal.

[4] Gallaher M.P., O′ Connor A.C., Dettbarn J.L. & Gilday L.T., 2004, Cost analysis of inadequate interoperability in the U.S. capital facilities industry, U.S. Department of Commerce Technology Administration, (NIST GCR 04-867).

[5] Arayici Y., 2010, Use of the 3D laser scanner technology in the Built Environment, in Geller, P.S. (Ed.), Built Environment: Design, Management, and Applications, Environmental Science, Engineering and Technology, Nova Science Publishers, New York, NY, 89-120.

[6] Burcin Becerik-Gerber, Farrokh Jazizadeh, Nan Li, and Gulben Calis, 2012, Application Areas and Data Requirements for BIM-Enabled Facilities Management, Journal of Construction Engineering and Management, Vol. 138, Issue 3.

[7] Bonanni, T. M. et al., 2013, Human-Robot collaboration for semantic labeling of the environment, Cognitive Cooperating Robots, pp. 1-25.

[8] Adán, A., Quintana, B., Prieto, S. A. & Bosché, F. (2018). Automation in Construction Door detection in 3D coloured point clouds of indoor environments. Automation in Construction, 85(October 2016), 146–166. https://doi.org/10.1016/j.autcon.2017.10.016

[9] Quintana B., Prieto S. A., Adán A. & Bosché F., 2017, Scan-to-BIM for small building components, Proceedings of the Joint Conference on Computing in Construction (JC3), Heraklion, Greece.

[10] Lu Q, Lee S, Chen L., 2018, Image-driven fuzzy-based system to construct as-is IFC BIM objects. Automation in Construction.; 92:68-87.

[11] AMMARI, Khaled El; HAMMAD, Amin, 2014, Collaborative BIM-based markerless mixed reality framework for facilities maintenance. In: Computing in Civil and Building Engineering, p. 657-664.

[12] Riexinger, Günther, et al., 2018, Mixed Reality for On-Site Self-Instruction and Self-Inspection with Building Information Models. Procedia CIRP, 72: 1124-1129.

[13] Fonnet, A., Alves, N., Sousa, N., Guevara, M.A., Magalhães, L., 2017, Heritage BIM integration with mixed reality for building preventive maintenance, 24º Encontro Português de Computação Gráfica e Interação (EPCGI), 1-7.

[14] Hugo S., Resende R., Breternitz M., 2018, Mixed reality application to support infrastructure maintenance. In: Young Engineers Forum (YEF-ECE), 2018 International. IEEE, p. 50-54.

[15] Kopsida, M., Brilakis, I., 2017, BIM Registration Methods for Mobile Augmented Reality-Based Inspection. In: eWork and eBusiness in Architecture, Engineering and Construction: ECPPM 2016: Proceedings of the 11th European Conference on Product and Process Modelling (ECPPM 2016), Limassol, Cyprus, 7-9 September 2016. CRC Press, p. 201.

[16] Baek, F., Ha, I., & Kim, H. (2019). Augmented reality system for facility management using image-based indoor localization. *Automation in Construction*, *99*(August 2018), 18–26. https://doi.org/10.1016/j.autcon.2018.11.034

[17] J. Redmon, S. Divvala, R. Girshick and A. Farhadi, "You Only Look Once: Unified, Real-Time Object Detection," 2016 IEEE Conference on Computer Vision and Pattern Recognition (CVPR), Las Vegas, NV, 2016, pp. 779-788.

[18] Shinde, S., Kothari, A., & Gupta, V. (2018). YOLO based Human Action Recognition and Localization. Procedia Computer Science, 133(2018), 831–838.

[19] Mas L. Q., Montserrat D., Allebach J., Delp E. J., 2017, Training Object Detection and Recognition CNN Models Using Data Augmentation, Electronic Imaging, Imaging and Multimedia Analytics in a Web and Mobile World 2017, pp. 27-36(10).

Assessing Digital Information Management Between Design and Production in Industrialised House-Building – A Case Study

H. Eriksson[a], M. Sandberg[a], J. Mukkavaara[a], G. Jansson[a], and L. Stehn[a]

[a]Department of Civil, Environmental and Natural Resources Engineering, Luleå University of Technology, Sweden
E-mail: henrik.2.eriksson@ltu.se, marcus.sandberg@ltu.se, jani.mukkavaara@ltu.se, gustav.jansson@ltu.se, lars.stehn@ltu.se

Abstract –

Managing digital information in construction is commonly described through Building Information Modelling (BIM), which advocates seamless chains of information, increased coordination between different actors and a life-cycle perspective on information management. However, low adoption outside the design phase entails that handling information in production is in many cases manual and paper-based, which increases vulnerability for upstream errors materialising downstream in production. Furthermore, issues with interoperability surround many areas when managing digital information. For industrialised house-builders, the transmitter and receiver of information are in many cases integrated within the same company or based on long-term collaboration. This affects their ability to manage information and utilise design information, which implies that their strategy for digital information management (DIM) might benefit from being addressed differently compared to more traditional BIM-based approaches. In this paper, we describe and discuss an implemented DIM-solution at an industrialised house-builder in order to address the benefits and challenges with DIM when managing information from design to production. The results imply that in order for several different functions within the company to reap benefits, a customised DIM-solution adapted after the company's specific needs is a well-suited approach forward to avoid sacrificing functionality when utilising design information.

Keywords –

Digital Information Management; Industrialised house-building; Information utilisation; Tailored interoperability; Building Information Modelling

1 Introduction

Utilisation of design information is crucial for planning and execution in production. The sequential nature in which a construction process is carried out poses however challenges for the continuity of the information flow, partly because different phases can be divided over longevity of time but also distributed amongst various actors with different responsibilities. Further complexity is added when these phases are carried out in a sprint-like manner where the previous ends as the sequent begin [1].

Paper-based documentation (e.g. printed drawings) constitutes the main container for generated design information during production. However, with the digital evolution, questions regarding its suitability as a main source to manage the amount of information generated during design has been raised [2]. Paper-based information is surrounded with limitation in regards to its lack of flexibility, meaning that changing prerequisites are difficult to address in production, partly due to information flowing unilaterally from design to production and rarely vice versa. Effects thereof can lead to vulnerability downstream in production when errors, or rather the rationale behind errors generated in design, are difficult to assess, and iterative bi-directional communication between design and production is rarely supported [3]. Most commonly, proposed solutions stress the importance of Building Information Modelling (BIM) to advocate seamless information management. BIM has for a long time been discussed as a solution to obtain information traceability and to minimise information losses over a building's life-cycle. However, there has been a concentration on the use of BIM during the design phase and less focus on BIM use during production [4]. In recent years, critical voices regarding BIM has also been raised, where the utopia of BIM as it is addressed today is being questioned [5]. Among identified challenges, interoperability stands out, both in its

occurrence found in literature and with various frameworks containing proposed solutions [6]. Commonly, open and globally standardised schemas such as Industry Foundation Classes (IFC) serves as the backbone to resolve issues linked to interoperability. There are however differences between construction companies in terms of their capability to handle information in a standardised way which could be connected to their level of industrialisation. In this paper, we discuss how industrialisation affects the need to conform to traditional BIM-approaches to resolve e.g. interoperability.

Increased industrialisation can be obtained by integrating otherwise sub-contracted activities into a controlled concept or moving value-adding activities upstream in the value chain (e.g. by moving on-site production to an off-site setting) [7]. This increases the use of pre-engineered solutions with standardised work procedures [8]. In a study, Johnsson [9] mapped core capabilities at four different case companies with various production strategies regarding pre-engineering, i.e., different levels of industrialisation. Companies with a full product offer (i.e. delivering turnkey buildings) and higher levels of pre-engineering exhibited core capabilities in areas wider spread along the construction value chain in comparison with more traditional project-based construction companies. This aligns well with the notion that industrialised house-builders tend to own or control a larger portion of the value chain, reaping the benefits of repetitiveness from pre-engineering and standardisation in several phases of construction.

It is argued that the benefits with BIM should be far greater within industrialised house-building in comparison with traditional construction [10]. Regardless of if this is true or false, when applying the lens of BIM as a tool for coordination and communication of digital information between different actors, this statement at least needs diversification to be adapted for the specific context of industrialised house-building [11]. Value chain control, pre-engineering of products and standardisation of work procedures, positively affects the possibility to manage information and presents an opportunity to assess information in a controlled environment [12] with less need for actors coordination. This is essential, as it implies that handling digital building information could benefit from being addressed differently compared to a more traditional BIM-approach. The software solutions and the work procedures determining how information is managed could be unique and tailored in that sense that they are adapted to the specific needs and circumstances visible at each company rather than there being a one-size-fits-all solution readily available off the shelf. It might also imply that challenges with managing digital building information are different within industrialised house-building compared to traditional construction. Furthermore, focusing on the notion of BIM, a single unified definition does not exist and the concept has different meanings depending on the situation or application. To avoid preconceptions, it was therefore in this paper deemed useful to broaden the perspective and address how information is being managed between design and production more generally.

The area of information management (IM) [13] describes how information is acquired from its sources to a format that can be distributed to those needing it until its disposal to an archive or to a trash bin. Although IM stems from the development of information technology as a managerial field of how organisations, for example, should get the best use of storage formats, ranging from early technology like punch cards and magnetic tapes to today's cloud services, it can still be of value to have a subfield named digital information management (DIM). In this subfield, we would specifically focus on IM based on digital technology. For construction, this would include BIM-tools with links that work as a glue [14] by enabling automation functionalities between different software. In this way, a sort of tailored interoperability between different IT-systems can be enabled, for communicating information between domains, such as design and production within construction companies. In this paper interoperability with BIM is exemplified in the specific context of industrialised house-building, but addressed using DIM.

There is a shortage of studies demonstrating the interplay between IT systems and work procedures linked to IM in construction, as well as studies reporting on the benefits and challenges of the tool implementations.

The purpose of this research is twofold, firstly to, through a case study approach, describe digital information management between design and production at an industrialised house-builder. This is exemplified through structures for information utilisation, a DIM-solution for linking software used in design and production, and how different departments have adapted their work procedures after implementing a DIM-solution. Secondly, the purpose is to discuss benefits and challenges with digital information management, from a perspective of flexibility in managing information and rigidity imposed by a digital solution. With the standpoint that flexibility and rigidity are opposing properties when managing information.

2 Research approach

This study was conducted as a single case study at an industrialised house-builder during the spring and fall of 2018. The research was explorative in the sense that no clearly demarcated research questions were set prior to

the study other than focusing on exploring digital information management between design and production. This influenced the course of the study, as gathered input guided the direction along the way. The main method for collecting data was through semi-structured interviews with representative persons with different insights into how information is managed and handled between design and production. The interviewees consisted of the project manager for implementing the DIM-solution at the case company; the head of the design department; an employee at the pre-production department with particular insights in the structures and systems within the DIM-solution; and finally, an employee from the production department with responsibility over integrating and managing the control system for machinery used in production. As a supplement to interviews, archival material, participation in a workshop, observations, and observed demonstrations by operators were used to collect data. In total, four interviews were conducted which lasted from circa 45 minutes to 1 hour and 30 minutes. Questions posed during interviews were mainly specific since facts rather than opinions were of interest. The first author transcribed the interviews verbatim. Since facts in regards to an already existing IT-solution was in focus, little regards were focused at interpreting the responses collected during the interviews and no thematic analysis were performed. The workshop was recorded with image and audio. Findings gathered from workshop notes as well as from reviewing the recording was later discussed in a separate meeting with key participants (said meeting was recorded and transcribed) and used to formulate a process map of the information flow from design to production. The process map was iterated back and forth until the case company deemed it representative for their process of managing information. Although the process map itself is excluded as a result from this paper, due to its size and level of detail, experiences thereof were used to compliment the interviews in the case description.

Determining the choice of case company was important for the purpose of the study. The case company, CC, is one of the leading actors on the Swedish market for industrialised house-building. CC offers customisation in each building project, not relying on a catalogue of pre-engineered buildings whilst maintaining a high level of standardisation in their work procedures for designing and producing buildings. CC regularly competes in tendering against construction companies which applies traditional building design processes and on-site production which means that narrowing the customer segmentation would affect CC's market position adversely. Mitigating the effects of adapting to customer requirements puts stress on how information must be managed in order to maintain efficient production. How CC balances pre-engineering, standardisation, and customisation whilst simultaneously controlling the construction value chain are therefore significant characteristics for this study.

In order to give a broad perspective on the many aspects which together forms contemporary experience on DIM within industrialised house-building, the case description has been allowed to take up the major part of this paper. The scarcity of published work with a similar focus or approach to describe information management between design and production for industrialised house-builders is also a reason for why this structure was deemed relevant.

3 Case CC

CC produces multi-family dwellings consisting of wooden-frame modules. They enter the construction process as early on as possible and takes full responsibility from the entrance to a completed building. The modules are manufactured off-site, elements, i.e. walls and slabs, are primarily based on pre-engineered components but the modules they form and the module's interrelated composition in a completed building are unique for each project.

Within CC, sales, design, purchasing, logistics, pre-production, factory-set production, and on-site assembly are all integrated departments. Their design process bears many resemblances with a more traditional construction design process in that different actors, e.g. architects, HVAC engineers, and structural engineers, both in-house and procured, has to be coordinated for each project due to the high level of customisation. The isolated tasks needed to be performed in order to complete a building design are however the same or very similar for each individual project. The pre-production department operates in midst of design and production, with a role to serve as a bridge between these two. Their main assignment is to feed information to production in the corresponding production sequence, acting as a funnel and a filter so that the right information gets delivered at the right time to production. In production, there are different production lines for elements which are later combined into modules, sequent work (i.e. electricity, HVAC, mounting etc.) is carried out by a skilled workforce in a one-piece takted flow. In conjunction with starting up a new production facility, CC initiated a project to digitally integrate their information management systems (DIM-solution) and exchanging printed paper drawings for a Manufacturing Execution System (MES) to display information in production. Previously, CC relied on physical deliveries of drawings and documentation used in production. The sheer size of their new production facility together with an aim for a decrease in takt-time rendered this approach infeasible.

The overarching aim with implementing a DIM-

solution was to reduce the amount of time passed from the point information was needed in production to when it could be retrieved, i.e. a solution primarily focusing on the needs of the operators in production. However, in order to facilitate utilisation of design information and obtain a broader perspective on DIM, work efforts and changes affecting many departments at CC were needed. In lieu of a strict top-down or bottom-up process, an interplay between adapting to the current way of working whilst simultaneously adapting this so it fits in a digital environment rendered CC to have more of a middle-out approach. Instead of buying an off-the-shelf software solution, CC decided to customise the solution on their own by integrating new and existing software. The implemented DIM-solution was mainly aimed at providing the factory-set production lines with digital information but derived functionality for supporting functions, such as purchasing and logistics, was also obtained.

The work procedures related to how information is managed and the system solution are interrelated with each other. DIM at CC is not fully automated, meaning that workers interact and adapt to the procedures stipulated by the system solution. It is therefore of importance to describe how work procedures are affected as well as describing the DIM-solution itself. This research did not partake in the actual development of any solutions, and at the time of this study, the DIM-project was in a start-up phase, meaning that functionality existed and was, for the most part, implemented but still in a run-in period.

3.1 Information structures for information utilisation

In order to utilise digital information generated during design, three separate but related information structures were identified during the course of this study.

3.1.1 Article-based information

In order to determine what articles (e.g. boards, studs, insulation etc.) are needed in production within a digital system, building information had to be broken down and sorted in an article database with a standardised nomenclature. At this stage, this is only done for information linked to elements such as slabs and different types of walls. The DIM-solution is prepared however to handle information related to e.g. installations (HVAC, electrical etc.) furnishing etc. Communicating defined article objects forms a vital part for information utilisation since it enables article identification along the entire information chain for different functions and departments. With information on an article level, customised bills-of-material (BOM) can be formed, readable to both man and machine. In this case, a BOM contains information about every article that together forms each element. This includes studs, noggins, boards, etc. with related metadata such as dimensions and type of material, but also relations between articles, elements, modules, levels, and buildings.

3.1.2 Sequence-based information

The second key aspect for utilising digital information was to incorporate the production sequence, hence attending to the aspect of in which order work procedures should be performed and when information is needed, thus enabling detailed planning and scheduling. The factory production sequence is ruled by the assembly sequence on the construction site. The key to deducting a corresponding factory production sequence is to work backward from building orientation onsite by modules to component assembly in elements production. This is possible as production is executed with a one-piece takted flow, meaning that production work is organised following one line of modules through the factory. Slabs follow the module sequence so that two slabs, forming the floor and ceiling of a module are completed prior to module assembly. The various types of walls used to enclose a module (inner, outer, apartment separating) facilitate that production of wall elements can be optimised so that as many similar walls are produced as a long wall segment, which later can be separated into different wall elements.

3.1.3 Operational-based information

After incorporating information in a sequence, the next step is to further enrich the data with information on work procedures and instructions on how they should be performed. Descriptions of standardised work procedures are communicated through Standardised Operation Sheets (SOS). The SOS documents describe in a step-by-step fashion accompanied with images what, how and why an operation should be performed. The idea of developing SOS is to enrich the knowledge of production by the use of experience. The novel approach is to link this information on parts level by incorporating it with the BOM, which entails a digital representation of what work procedure should be performed on an article. This is done automatically during design due to each article being defined and based on where a specific article is located in the element. When linking a particular work procedure to a particular article, detailed planning and resource allocation in production are enabled.

By addressing these structures and incorporating them into a DIM-solution, the ability to combine and digitally incorporate several functions and departments within the value chain enables a wide variety of information utilisation.

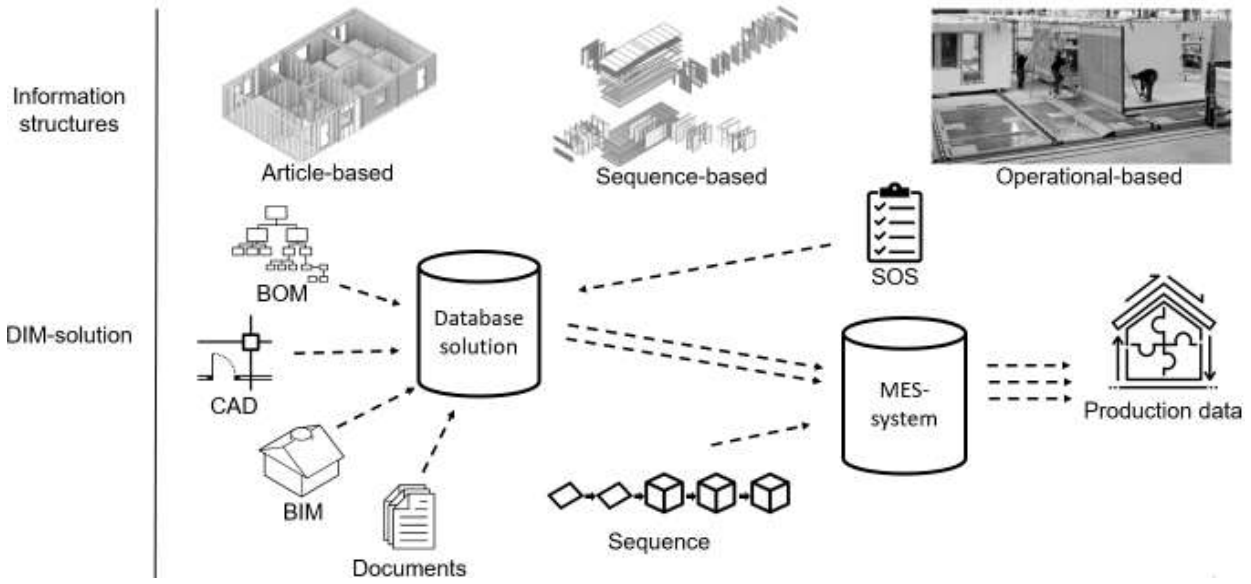

Figure 1. Illustration of information structures and DIM-solution

3.2 DIM-solution at CC

No suitable off-the-shelf IT-solution to accommodate presented needs at CC were found. Placed amidst between manufacturing and construction, CC's demands for a software solution for managing information are specific. Adapting to a proprietary solution had also in this case been associated with risk since a number of related systems would have had to change at once to make them interoperable with each other. Building design is performed using two different software applications. One of which is a BIM-software adapted for supporting element and module design within industrialised house-building, and one CAD-software for designing module features, e.g. kitchen layouts, wardrobes, etc. The latter is currently used for 2D-drawing. In production, an MES was introduced to track and document production data as the material is converted to finished modules along the production lines, as well as distributing the relevant information to the operators at each work-station. Their solution was to customise a database solution (DS) to operate as a link and a translator between the CAD/BIM-software's used in the design and the MES used in production. This was needed since interoperability between these is lacking. Functionality for digitally supporting sequence planning, as previously explained, was added as well. Figure 1 illustrates the different information structures as well as a schematic outline of the DIM-solution. The figure is illustrative in that sense that its purpose is to assist the reader by complementing the text provided in this paper rather than the other way around. As prime input to enable information utilisation, DS takes the bill-of-material (BOM) in a spreadsheet format from the BIM-software. Once imported into DS, a hierarchical structure is formed with parent-child relations for parts into elements, elements into modules, modules into floors and floors into buildings. Apart from structuring material, links to drawings from both CAD-software as well as additional documentation relevant for the project are created in DS. Models from the 2D-CAD-software lack possibility to trace each object on an article level, the generated drawings are however being funnelled through the database solution. In this case, the DIM-solution serves as an intermediary step to avoid printing drawings on paper. The generated links are semi-dynamic, meaning that it requires that the name and location of each file are syntactically correct in order with a standardised nomenclature and file system structure. The links are imported according to the right production sequence by the MES together with necessary additional documentation e.g. SOS, room data sheets etc. In this case, the MES is serving as a document manager for production, supplying production data in the right sequence to work station operators.

3.3 Impacts on work procedures

Implementing a DIM-solution affects how the workforce manages information, however, depending on the level of abstraction, the overarching process before and after the implementation of a DIM-solution has remained basically the same, albeit the processes are adapted to fit in a digital environment. These differences are highlighted in the following section, the headlines marked in bold are presented in a chronological (from a project perspective) order and an attempt to clarify the

utilisation of the DIM-solution between the different departments step-by-step has been made.

Design: As previously stated, building design follows a rigorously monitored and standardised process. In implementing the DIM-solution, the design department´s work procedures are adapted so that it affects where information is retrieved and in what form it is received and delivered, previously printed documents are now managed digitally. Templates for modules and parts from pre-engineered rules and dimensions generate information in relation to CAD and BIM-tools.

Pre-production: The most notable changes in work procedures is visible at the pre-production unit. Previously, upon completed building design, pre-production used to receive design information digitally from the design department and print, e.g. drawings and material lists on paper. A vital and time-consuming task was to sort and order drawings and documentation in sequence for production. As production is based on standardised work-procedures and split up on multiple stations, the number of drawings needed can be quite considerable. A single floor element can require around six different drawings to mediate all views necessary for each layer and work-operation. Apart from printing drawings and necessary additional information, pre-production also used to audit element drawings in search of non-frequent occurring articles, which are parts for structural rigidity, e.g. lifting posts. This operation was important to enable a high pace in production where time to review drawings in detail is limited. This was done by manually marking on the drawings to clarify for the right recipients in production. In time for production, pre-production previously physically delivered drawings and additional information to the logistics department. For pre-production, the tedious task of manually printing and auditing drawings for non-frequent occurring articles could be removed due to the DIM-solution. The objects formerly marked manually on drawings are now listed objects in a parts database. Manually sorting drawings in sequence and physically delivering drawings and enclosed documentation is also rationalised. The imposed change is first and foremost time saving (at least for pre-production), but since a manual audit of drawings can be considered error-prone in comparison with an automated solution, the quality and precision has also been positively affected. On the other hand, the time-consuming task of auditing drawings also served as an extra opportunity to detect errors made in design which are better off being discovered prior to, rather than during, on-going production.

Logistics and purchasing: Pre-production's main point of delivery is the logistics department, they receive information that they use to prepare and supply workstations with material. The material is cut-to-fit and kitted in the corresponding production sequence. Enhanced overview over the production sequence provided by the DIM-solution enables logistic preparations to be more on par with the flow of the production lines.

Purchasing takes place during an extended period in parallel with design, pre-production and almost up until production. The level on which the DIM-solution can be utilised is related to the overall progress in the project. Early on, prior to detailed design, purchase might need analogue documents (e.g. printed drawings or lists) and as information gets entered in the system, the possibility to utilise DIM increases. Previously, various articles e.g. timber used for studs and noggins and plaster boards was bought in bulk based on visual inspection of the stock. This ad-hoc approach to purchasing was made redundant when article based information was made available through a DIM-solution. The ability to retrieve tailored bills-of-material sorted by production sequence enables purchasing of smaller batches with the right material delivered more in sync with production.

Production: Just prior to production detailed planning and dividing of specific tasks on different operators working on the production lines take place. This could previously be done explicitly through markings on drawings. For production, the main difference after implementing a DIM-solution is related to how information is received and read. Where paper drawings previously were used, there is now monitors and portable display devices to communicate all information required for them to carry out their work. Through the monitors, linked documentation describing for example how the current work task is to be performed (SOS-sheet) and functionality to support reporting errors or deviations is also available. Detailed production planning previously performed by marking on a physical drawing are now performed by balancing the required operations with available operators aided by time studies for work operations in a spreadsheet distributed to all operators.

4 Discussion

Production in a one-piece takted flow requires that there is detailed knowledge on *what* needs to be done, *when* it should be done, and *how* a specific work procedure should be executed in order for production to run smoothly. DIM does not add the possibility of answering these questions, at CC these questions were already addressed prior to extending DIM. Adapting to how information should be managed digitally rather suggests that these questions need to continue being addressed in order for production to work properly. This is highlighted when assessing how element information is managed in relation to module information. The latter is not yet detailed enough to obtain the same level of

information utilisation, as individual objects cannot be queried within the system. This hinders, for example, purchasing from extracting information with the resolution needed to purchase off a customised BOM.

For CC, the opening of a new production plant spurred the initiative to rethink how information was managed and distributed from design to production. As side effects rather than their main objective, digitally integrating the systems for managing information enabled added functionality. Both in terms of ability to log production data for quality control and analysis, as well as a possibility to perform production simulations to verify constructability or to optimise resource allocation in the production line to name a few examples.

Different challenges exist which span over a wide range of perspectives. Moving information from humans to computers in an existing organisation requires workers to adapt to new procedures and routines. Enforcing a new system upon a workforce is, therefore, a considerable aspect to handle. Furthermore, a digital system exhibits less inertia when comparing it to managing paper-based information. In this case, inertia can be seen as the momentum needed to send or receive information between two entities (i.e. from computer to human, computer to computer, or human to human). This entails a following responsiveness when sending and retrieving information which presents itself as both part of the solution as well as an associated risk. In cementing a confined digital solution, the flexibility enabled by a skilled workforce, possible to adapt to whatever problem is presented, was decreased. Changed prerequisites which previously could be managed ad-hoc now requires implementation (adding of new functionality) in a system in order for the function as a whole to be maintained. The same responsiveness also implies that errors entering the system quickly spreads and affects both vertically and horizontally within the organisation. At CC, the DIM-solution is still dependent on a manual step being performed between design and pre-production, namely exporting and importing the BOM from the BIM-software to DS. The remaining steps are automated, provided that information is placed and named correctly. A side effect from this manual step is that some inertia is introduced to the system. In a practical sense, this means that information is compiled and audited by the design department before being pushed into DS instead of being pulled on demand by pre-production. To further the understanding of what role inertia plays in a digital IT-system is an interesting aspect for future studies. Balancing this inertia could serve as a strategy to mitigate risks associated with responsiveness in a semi-automated system for managing information where there is an interplay between a system, and the work-force operating the system.

At CC, a trade-off between the DIM-solution's flexibility and information quality was visible. This means that the enrichment (e.g. increased use of metadata to enable purchasing) and precision of information (e.g. reduced dependency on manual auditing) increased. Although no time studies have been conducted, by rationalising the time-consuming step with printing, auditing and physically delivering drawings in pre-production, there are also implications that the total expenditure of time for managing information has decreased. These preliminary benefits are achieved at the expense of increased rigidity in how information must be managed. Albeit these results are preliminary and this single case cannot be used to generalise, it is a noteworthy aspect that risks and constraints associated with managing information digitally needs to be assessed and weighed against the benefits rather than digitalisation being an end in itself.

At CC, the DIM-solution was tailored, meaning that CC avoided adapting to an off-the-shelf proprietary software solution and thus managed to better adapt their DIM-solution after the organisation rather than the other way around. This could be very important for already existing organisations striving towards digitising their information management and where a top-down process could be associated with risk since it might affect several parts of the organisation simultaneously. For industrialised house-building, it is reasonable to argue that adaptations and tailoring of DIM so it fits the existing organisation is required. In part, because they depend on technology-intensive manufacturing equipment to support automation in production to a higher degree than in comparison with traditional construction. Nailing portals, robots, and conveyors which are utilised in production are delivered from a wide range of suppliers and interoperability is not guaranteed. Machinery used in production is also often delivered as unique products to each customer due to spatial- or requirements adaptations at each industrialised house-builder, which makes reusing solutions for DIM between different industrialised house-builders complex. At CC, introducing an MES sorted out the interoperability between machinery in production. However, in order to broaden the perspective and better utilise design information to establish links between production, design and support functions such as logistics and pre-production, a tailored DIM-solution was required to avoid sacrificing functionality. The authors have not encountered such a solution readily available off-the-shelf, addressing similar needs as those presented at CC.

Owning or controlling the value chain [9] alleviates the threshold for successfully implementing a solution with a broader perspective on information management, spanning for instance over several departments within an organisation as exemplified in this paper with information being managed between design and

production. The system also encompasses a digital bi-directional link between design and production in comparison with the usual mono-directional link between different trades [1]. Results imply that utilising BIM-data for information management in the specific context of industrialised house-building could benefit from being addressed with a strategy adopted for the unique traits visible for these companies. Value chain control, or ownership, minimises the need for adapting to commonly proposed strategies to obtain system interoperability, such as open format schemas (IFC). This encompasses a wider solution space with the ability to choose optimal software solutions for each sub-department, not needing to worry about systems interoperability to the same extent since this could more easily be tailored alongside the solution itself.

5 Conclusion

This paper focuses on the (digital) information management between design and production in industrialised house-building. A case company was studied to describe and discuss benefits and challenges with implementation of a solution for digital information management (DIM). The main conclusions from this study are:

- Characteristics visible in industrialised house-building, such as value chain control and the possibility to standardise work procedures, affects how information can be managed compared to traditional construction.
- Effects thereof imply that a tailored solution, adapted for the specific company, as opposed to an off-the-shelf proprietary solution could be a viable way forward to extend information utilisation.

References

[1] I. D. Tommelein, D. Riley, and G. A. Howell, "Parade game - impact of work flow variability on succeeding trade performance," *J. Construcit. Eng. Manag.*, vol. 125, no. 5, pp. 304–310, 1999.

[2] R. Howard and B. C. Björk, "Building information modelling - Experts' views on standardisation and industry deployment," *Adv. Eng. Informatics*, vol. 22, no. 2, pp. 271–280, 2008.

[3] S. Alsafouri and S. K. Ayer, "Review of ICT Implementations for Facilitating Information Flow between Virtual Models and Construction Project Sites," *Autom. Constr.*, vol. 86, no. August 2016, pp. 176–189, 2018.

[4] J. D. Goedert and P. Meadati, "into Building Information Modeling," *Constr. Eng. Manag.*, vol. 134, no. 7, pp. 509–517, 2008.

[5] R. Miettinen and S. Paavola, "Beyond the BIM utopia: Approaches to the development and implementation of building information modeling," *Autom. Constr.*, vol. 43, pp. 84–91, 2014.

[6] R. Santos, A. A. Costa, and A. Grilo, "Bibliometric analysis and review of Building Information Modelling literature published between 2005 and 2015," *Autom. Constr.*, vol. 80, pp. 118–136, 2017.

[7] J. Lessing, L. Stehn, and A. Ekholm, "Industrialised house-building - Development and conceptual orientation of the field," *Constr. Innov.*, vol. 15, no. 3, pp. 378–399, 2015.

[8] G. Jansson and E. Viklund, "Advancement of platform development in industrialised building," *Procedia Econ. Financ.*, vol. 21, no. 15, pp. 461–468, 2015.

[9] H. Johnsson, "Production strategies for pre-engineering in house-building: Exploring product development platforms," *Constr. Manag. Econ.*, vol. 31, no. 9, pp. 941–958, 2013.

[10] F. H. Abanda, J. H. M. Tah, and F. K. T. Cheung, "BIM in off-site manufacturing for buildings," *J. Build. Eng.*, vol. 14, no. March, pp. 89–102, 2017.

[11] X. Li, P. Wu, and T. Yue, "Integrating Building Information Modeling and Prefabrication Housing Production Automation in Construction Integrating Building Information Modeling and Prefabrication Housing Production," *Autom. Constr.*, vol. 100, no. January, pp. 46–60, 2019.

[12] G. Jansson, H. Johnsson, and D. Engström, "Platform use in systems building," *Constr. Manag. Econ.*, vol. 32, no. 1–2, pp. 70–82, 2014.

[13] M. Hinton, *Introducing information management: the business approach*. Routledge, 2006.

[14] M. Madiajagan, "Interoperability in Component Based Software Development," *Proc. World Acad.*, vol. 2, no. 10, pp. 68–76, 2006.

Platforms for Enabling Flexibility at Two Construction Companies

H. Eriksson[a] and E. Emilsson[a]

[a]Department of Civil, Environmental and Natural Resources Engineering, Luleå University of Technology, Sweden
E-mail: henrik.2.eriksson@ltu.se, ellinor.emilsson@.com

Abstract –

Product platforms have proven to be an effective means for many industries, seeking to achieve front end variety based on back end commonality. Modular design with standardised interfaces, enabling reuse of components in derivative products over time, has been a success factor for i.e. automotive industry and other types of industries operating in a modify-to-order or configure-to-order supply chain. For construction companies who operate in an engineer-to-order, or even design-to-order supply chain, extensive and changing customer requirements must be managed and full product standardisation could, therefore, affect a company's market offer adversely depending on its market segmentation. In previous research, one key finding is that construction companies tending to a wider market segment could focus on standardising processes rather than products. Furthermore, previous research highlight the notion of process platforms as a subset within product family design, albeit, little research focus has been given to process platforms for construction companies. In this study, two construction companies are studied with the aim to describe their means for enabling a flexible product offer whilst maintaining a platform strategy. Findings shows that both companies have process platforms with explicit and implicit relations to product realisation and that standardised processes are a vital part in offering end product flexibility whilst maintaining a platform strategy. This study identifies the need for additional research to elaborate and generalise the relation between process platforms and product flexibility, and implies that theory linked to product platforms need to be developed in order to incorporate construction companies where full product standardisation is in conflict with their production strategy.

Keywords –

Industrialised house-building; Process platform; Process standardisation; Platform strategy

1 Introduction

Industrialisation in construction has gained attention and traction from both academia and construction companies [1]. By moving value-adding activities upstream in the construction value chain, through pre-engineering and off-site construction, a trade-off between flexibility and productivity can be evaluated and used to target specific customer segments [2]. An orientation towards increased industrialisation is often, for the Swedish market, motivated in research through low productivity for the construction industry in comparison with more traditional manufacturing industries [3] and therefore often proposed approaches have been suggested by glancing towards the same successful strategies which has been applicable for traditional manufacturing, e.g. automotive industry. Applicability of lean principles for industrialised house-building [4], [5] or adoption of product platforms has been among notable examples of such strategies, where the latter forms the basis for this paper.

A widely used description of a product platform is presented by Robertson & Ulrich [6] which defines it as *'the collection of assets that are shared by a set of products'* and that these assets can be divided into *components*, *processes*, *knowledge* and *people and relationship*. In essence, product platforms strive to offer customers products which exhibit front-end variety based on back-end commonalities, by altering the process of product development. The leap is from the development of unique one-off products to platforms where a family containing several variants shares some common assets. Through modularisation, i.e. dividing products into modules or chunks containing related components and standardising interfaces between these, the automotive industry has been and remain to be successful [7]. Jiao et al. [8] presented '*a holistic view of product family design and development'* based on axiomatic design [9] in which several platforms in between different domains accounts for all fundamental issues related to product realisation from a client perspective (front-end) to the entire supply chain (back-end). In related work, Jiao et al. [10] define

a process platform in a generic hierarchical structure as the combination of machining- and assembly operations required in combination with a corresponding product structure (raw material, parts, and subassemblies) to formalise an end product. Most of the subsequent studies including process platforms have adopted this view on its relation to explicit product realisation [11]–[13]. However, it is the authors' standpoint that a formally defined solution space for product realisation requires confined boundaries for the product definition, which is contradictive for construction companies which offer product flexibility through open design processes.

In a multiple case study by Johnsson [14], empirical findings were used to suggest that mainly companies *'who integrate the supply chain towards a specific market segment benefit fully from the platform concept'*, i.e. companies with a higher degree of product standardisation. Companies with a wider scope of customer segmentation could, whilst maintaining a platform strategy, focus on standardising processes rather than products. It is important to distinguish between two different types of processes and how they are being used in this paper, those with explicit or implicit relation to product realisation.

- **Explicit processes:** Machining operations, assembly operations, raw material treatment with direct connection to product realisation [10]
- **Implicit processes:** An umbrella-term for processes which indirectly aides product realisation, e.g. open design work, setup/preparation in production or following routines when managing information.

The purpose of this study is twofold, firstly to describe platforms at two construction companies with production strategies aimed at enabling flexible products. Secondly to discuss, whether the theoretical notion of process platforms, found in literature today, are applicable for house-builders where full product standardisation conflicts with their production strategy.

2 Related research

2.1 Distinguished characteristics of different construction companies

Construction companies can be differentiated according to their level of industrialisation, which partly depends on their use of pre-engineered solutions [14] and production methods [2]. A different but related take is the dividing on companies depending on how they manage their supply chain [15]. As buildings are rarely pre-produced and kept in stock based on a forecast, and product realisation often requires an engineering design phase to adapt to regulations or spatial conditions, the predominant production strategy for construction can be characterised as engineer-to-order [14]. Johnsson (ibid.) elaborates on this and distinguishes between different production strategies within the engineer-to-order context depending on the level of pre-engineering in the design phase. Engineer-to-stock represents a fully predefined product and design-to-order offers product flexibility through an open design process. Adapt-to-order is a middle ground between these two. This determines in what stage the customer enters where a fully defined engineer-to-stock-solution entails later client entrance.

There are various contextual interpretations available for the specifics related to the construction industry on this matter. Winch [16] proposes concept-to-order and design-to-order to distinguish between the difference visible between two standard forms of procurement, namely design-build (CTO) and design-bid-build (DTO). Segerstedt & Olofsson [15] differentiates between different production strategies based on the level of completed specifications upon client entrance, where building systems within engineer-to-order bases the pre-set specifications on current building codes and local regulations, leading to high flexibility in the end product. When buildings instead are completely specified upon client entrance, all that is left is for the client to select a variant. Regardless of terminology, the different strategies can be linked to the level of pre-engineering applied in product definition and realisation.

2.2 Platform use in construction

In this paper, platform use can be interpreted as an agreed upon strategy applied by a company, to gather, distribute and reuse pre-engineered solutions and standardised processes as well as actively working with managing, maintaining and utilising said solutions and processes. A prerequisite is that product or component pre-definition exists to some degree within the platform.

Applied to construction, the majority of studies available on platform development have inherited their product orientation from traditional manufacturing, focusing on either confining or defining the product within boundaries set by a product platform. Veenstra et al. [17] introduce a methodology for developing product platforms in the specific context of house-building in which a framework for defining a module based product architecture is presented. Jensen et al. [18], [19] similarly approach the construction industry by modularising the building system. In their work, different module variations with standardised interfaces and parameterised variables, i.e. length, width etc., produce an allowed solution space in which the product can be designed through a configurator.

In a case study, Bonev et al. [20] applies the holistic approach to product family design as suggested by Jiao

et al. [8] on a precast manufacturer and noted the interrelationship between reuse and commonality along the entire value chain. Furthermore, they highlight product platform deployment as a mean to retain flexibility whilst moving towards mass customisation, but argue simultaneously that a higher degree of predefinition during the engineering phase is inevitable for platform benefits. Thuesen et al. [21] made a study on success factors from a German housing platform and highlighted the importance of continuous learning, repetition, and standardisation through *'[…] long-term incremental and systematic innovation with a clear separation between the continuous development of and the production based on the platform'*. Standardisation of different house types available for the customer was particularly stressed.

construction company. The platforms are described as the collection of blueprints with technical solutions and documents or procedural descriptions aimed at guiding the design and production phases. Lessing [1] reinterprets the traditional platform concept and separates for industrialised house-builders between a technical platform and a process platform. Figure 1 depicts how the continuous interplay between both platforms are used to support a stream of projects as well as how experience is continuously fed back to each platform.

Even though no empirical data is presented to verify or in practice identify his exemplified process platform, it is proposed to contain processes beyond assembly operations or raw material treatment, i.e. beyond explicit product realisation. In his licentiate thesis, the process platform consists of modules where ICT (Information

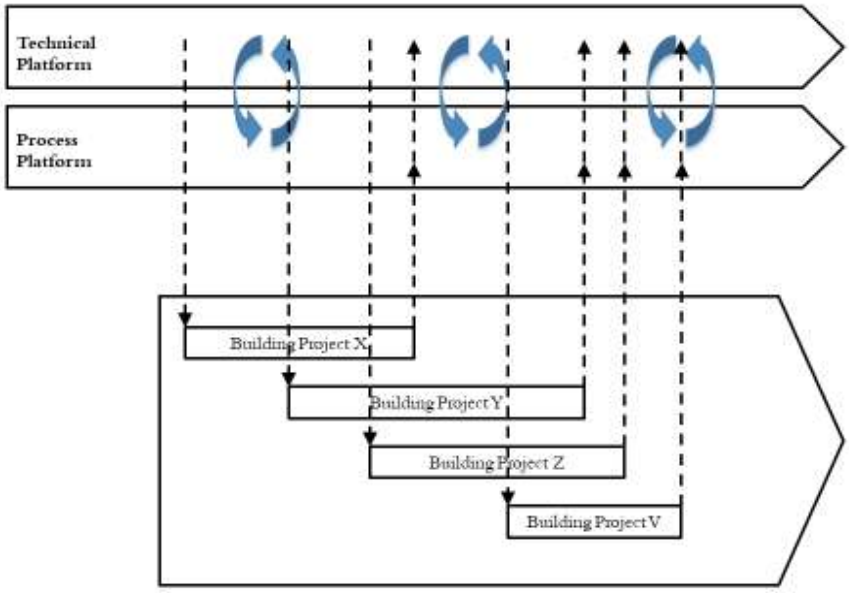

Figure 1. Process model for industrialised house building [1]

Jansson et al. [22] acknowledge the specific conditions visible for ETO construction companies in terms of managing the balance between commonalities and distinctiveness. Jansson et al. (ibid.) propose a platform model with support methods to manage distinctive project parameters. That case study identified all product platform assets described by Robertson and Ulrich [6], but the presented support methods for implicit product realisation focuses mainly on the design phase.

According to Styhre & Gluch [23], the platform serves as an object to facilitate knowledge sharing and accumulation. This knowledge management perspective on platforms is presented through a case study in a large

and Communication Technology), team collaboration and routines for integrating logistics for a reliable flow of material are some examples. In reviewing these platform-related studies applied for construction, the production process and its interrelatedness to a defined product are of essence when process platforms are addressed. Many elude the flexibility required or desired by certain actors in terms of their ability to adapt their end product after customer requirements, and there is a scarcity of studies which elaborates on how the process platform mediate end product flexibility.

3 Research approach

To meet the purpose addressed in this paper, two companies have been studied. The research was grounded in a literature review on process platforms and platform use in construction where the literature review highlighted the gap in the reviewed body of previous research which motivated the purpose of the study.

To collect empirical data, two different methods were used; interviews and study of archival material. Interviews were conducted with a representative person of each company who has insight and responsibility for the use and development of platforms. Each interview lasted approximately one hour and questions posed were mostly concise, focusing on facts linked to each company's product offer and platforms rather than opinions. Interviews were semi-structured, where follow-up questions were posed for clarity when deemed appropriate. Interviews were recorded and later transcribed verbatim for the analysis. Both authors participated during both interviews and were later responsible for transcribing one interview each. The archival material consisted of access to one of the participating company's (Alpha) intranet, where all documentation in regards to their platform is stored.

The descriptions of each company provided in the following section of this paper are based on empirical data and the idea is to provide insights into what kind of strategy each company applies, i.e. what their product offer is, as well as information regarding their platforms with particular focus on their process platforms. The empirical data was also used to identify explicit and implicit processes according to the definitions previously provided in this paper.

4 Companies Alpha and Beta

Two different companies has been examined, Alpha and Beta. Alpha is a Swedish multinational construction company that has construction projects in all main areas, including residential buildings, commercial buildings, roads, bridges, tunnels and more. The company is among the top biggest construction companies in Sweden and they are organised in regions as separated divisions all over the country.

Beta is an industrialised house-builder who uses modular technique to produce multi-family dwellings for the Swedish market. The company is mid-sized, family owned and an important actor on the market for multi-family dwellings as well as one of the leading actors applying industrialised methods in production.

Both companies apply industrialised methods to various degrees with the common traits that they both have adopted a platform strategy and they both gain a competitive advantage in offering product flexibility to their customers, albeit to various degrees in comparison to one and another.

4.1 Alpha

Alpha is what can be considered as a traditional construction company. They do both general contracts, turnkey contracts and project developments starting with a concept. Alphas main selling point is that they can develop and produce almost any kind of structure that the client has in mind. Alpha has almost no repetition of projects. In offering this variety, it is difficult to define Alpha as a single entity. This study is limited to the part of Alpha affiliated with design and production of multi-family dwellings.

4.1.1 Strategy

Alpha's main production strategy is either concept-to-order or design-to-order depending on contractual agreements (design-build respectively design-bid-build) [16].

For concept-to-order, Alpha can either procure an architect or do design in-house, depending on the client's wishes. Structural design is often performed in-house by Alpha's engineers, often in concrete or steel as Alpha is more experienced with these materials. Remaining disciplines, e.g. HVAC engineering is often procured. The construction process follows a traditional flow with tendering, design and construction. The projects are treated like small companies within the company. The design and engineering department work with several projects at one time. Construction is either done completely on-site or in combination with prefabricated walls or slabs produced off-site. Each project usually procures multiple subcontractors to work at the construction site.

Alpha previously offered a platform-based concept containing multi-family dwellings with a high degree of pre-engineering. Late adaptation to customer requirements and an inability to reduce production costs rendered the business unsuccessful and the project was cancelled. Alpha now has an affiliated subsidiary that offers platform-based engineer-to-stock concepts for housing.

To offer a very flexible product in a resource effective way, Alpha operates two main platforms on different abstraction levels. MP (Managing Platform), for managing a full project life-cycle from tendering to the maintenance phase, and CP (Construction Platform), for the design and construction phase.

4.1.2 Process platform

The main difference between the two used platforms is that the MP (Managing Platform) contains only support for the process of pursuing and controlling a project, while the CP (Construction platform) contains both

support for the design process and the technical solutions and decisions. Both platforms are easily accessible for all employees on the intranet home page.

The MP is used for all projects regardless of size and type, and supports the process of pursuing a project, but has no connection to technical components at all. The MP is divided into two parts, where the first part is aimed for upper management and is the same for all divisions. The second part is aimed at site managers downwards to all the white-collar worker positions and is division specific. The MP consists of mostly different kind of text documents, checklists, time planning sheets, and descriptions. It is organised around the different phases, specifying all the required activities, whose responsibility it is to realise them, comments, and supporting materials.

During the engineering process, the MP defines standardised steps mostly consisting of meetings where limits and responsibilities for the project are to be decided. There are many templates for meeting agendas, how the organisation and positions in the project should be set up, when and how important economic decisions should be made, what risks to consider and when to consider them, and how the engineering phase should support a later safe work environment in production. For the production phase, the MP is focused on quality control, what to consider in different situations, how and what to check to ensure that the projects are running well, and make sure laws, certifications and standards are followed.

The CP consists of descriptions, checklists, drawings, films and documents for both the design phase and construction phase. For the design phase, the CP consists of a collection of conceptual technical solutions. For each technical solution, there is a document describing the components and what to consider for each of them, and advice on how to avoid risks and mistakes that will lead to a lower quality product. Some of the advice is more conceptual, while some are detailed with given values or solutions. The conceptual technical solutions for different parts of a building are referred to as "standard construction parts", and most technical solutions prescribed by engineers are variations of these. There are ready made-drawings of standard construction parts complete with text for production that can be imported to a project drawing.

The design process is supported by the CP where there are predefined concept solutions that can either be used as they are or tweaked to fit the current project. These predefined concepts act as a base for the engineers to work from, but they are free to create their own solutions if it better fits their project. The CP also contains a great number of documents describing what is important to consider and why for different parts and concepts of a building, on both higher abstraction levels like the layers in a wall, and more concrete ones like the required measurements for garages. The designer also has access to documents that describe risks with different options and what can be considered to minimise these.

The CP has a dedicated chapter for standardised productions methods, that contains pictures, drawings, documents, links to manufacturers and instructional films. There are links between the standard construction parts and their corresponding standard construction method. For each construction method there are lists of prerequisites, "tips and tricks" from other employees, possibilities and risks described. The production methods described give room for adaptations to the project and describe how to create a quality structure rather than a specific one.

4.2 Beta

Beta integrates sales, design, manufacturing and on-site assembly within the firm as different departments and takes full client responsibility from client entrance to a finished building. Modules are manufactured off-site in one of two production plants and shipped to the construction site where they are assembled together. Both production plants have different production lines for wall elements and slabs which are later combined into modules; sequent work (i.e. electricity, HVAC, mounting etc.) is carried out by a skilled workforce in a one-piece takted flow.

Beta has a technical product related platform consisting of templates in their CAD-software with predefined technical solutions for e.g. planar elements or joints between two elements. Complementing the technical platform, there is linked related information for product realisation such as assembly operations, checklists etc. which forms a part of their process platform.

4.2.1 Strategy

Beta competes regularly for tenders with traditional contractors within their product offer, and balances between platform standardisation and product flexibility as one of their competitive advantages. Beta produces multi-family dwellings (tenancy and condominiums), hotels and student housing, but no single-family houses or row houses. Element standardisation from a parts library within a technical platform forms their basis for enabling off-site production in a factory setting. Repetitiveness in production must be high enough to enable specific workstations for each particular operation to be performed. This is especially important for the structural system forming the modules, i.e. wall elements and slabs. Each section of the production line is designed for a particular operational procedure, e.g. mounting layers of plasterboards, insulating etc. This can be done manually by a skilled workforce or fully automated by

machines, depending on where in the line or in what factory the operation takes place.

On the sequent volume line, after elements have been assembled to modules, work-tasks vary more according to the specifics of each module. Even though planar elements are highly standardised between different projects, compositional combinations of different modules are customised for each project. In that sense, the modules are not standardised objects, apart from in a few pre-defined concepts aimed at e.g. student housing which can be offered to clients. In doing so, Beta fulfils customer needs and requirements by offering product flexibility in regard to floor layout or module features. This requires a somewhat traditional design process where both in-house (e.g. structural engineers) and procured personnel (e.g. HVAC engineers) collaborate.

Beta operates mainly with an adapt-to-order engineering strategy based on their level of predefinition in their structural building system, which can be used to configure unique modules. The level of platform adaptation varies between and within different projects where certain project related subparts, e.g. a detached but adjacent building for laundry could be engineered design-to-order in accordance with an open design process based on customer requirements together with current norms and standards. Engineer-to-stock solutions, as in the case with conceptualised solutions for student housing exists as well.

Beta has *'preferred solutions'* in different aspects of defining or realising a building in which they know, based on experience, what works well and what doesn't. In operating a platform strategy, there are some *'non-negotiable'* limitations for product flexibility at Beta, i.e. the thickness on a slab separating two storeys, affecting the structural system.

4.2.2 Process platform

To alleviate the constraints inflicted by product standardisation in the technical platform, Beta has a process platform. Standardised processes for product realisation are mainly communicated through Standard Operating Sheets (SOS), but they could be any type of documentation which successfully can be used to illustrate how a certain task should be carried out, e.g. through a checklist. The collection of documentation capturing these standardised processes constitute the basis for Beta's process platform. Some SOS explain explicitly how to conduct a specific task, for example through a step by step guide with associated images, which are needed to perform a specific work operation.

There is however a large number of standardised processes which has no explicit connection to a specific product, these can instead have implicit relations to the realisation of a product. This can be exemplified by describing Beta's design process, which is aided by a tailored software system for visual planning. The broken-down processes needed to carry out a building design is to a large extent standardised and rigorously monitored in a system as the design progresses. What documentation or activity is required, who should deliver or perform it, when should it be delivered or performed and who is the recipient. These are formalised questions which are gradually being answered during the design process. The majority of all sub-processes in the design process are the same in each project, regardless of which building project is in focus.

There are also standardised processes for different departments at Beta, including supporting functions such as sales, logistics, and purchasing. The process of drafting a standardised process is in itself a standardised process, which is firmly grounded within the collegial community as they are regularly formed and updated.

The complete collection of process documentation for all departments is stored on a server in which the head of each department has the responsibility to update and maintain its own processes. According to the company respondent on the managerial level, both the technical platform and the process platform are equally important. Though that may be a view not entirely shared between everybody at Beta, it gives an insight into the perceived value of working with standardisation on both product and process level.

5 Analysis and discussion

The limited amount of empirical data collected should be assessed alongside the sparsely explored subject in focus of this research. Being a study with a qualitative analysis, the purpose is not to claim generalisability, but rather to provide insights into the subject at focus by providing experiences from these two construction companies. The possibility to access and study archival material in form of documentation of Alpha's process platform was a strength for the validity of the findings. It provided an additional perspective on the platform description by enabling the authors to examine the content and structure for themselves. On the other side, those insights could not be used to draw any conclusions regarding how the platform is actually implemented in projects. The access was however important to avoid misinterpretations during and after the interview, as the platform concept as discussed in research literature, was quite unfamiliar to the respondent at Alpha. No such clearly compiled documentation was available for the authors at case company Beta, where the respondent on the other hand is very knowledgeable in the field of product platforms from both a practical and a theoretical perspective.

Platforms at Alpha differs from the more traditional notion of product platforms mainly aimed at

manufacturing industries in that it contains fewer defined products and more processes. The concept of e.g. product family development is not aimed or well suited for describing platform use in a company like Alpha. According to Jiao et al. [8], the concept even implies a make-to-order or assemble-to-order production strategy. Alpha strives however towards increasing platform utilisation in which appropriate theoretical models could be useful.

At Beta, platform use is already firmly grounded within the company, and considering their level of component pre-engineering in their structural system and their production method, both a technical platform and a process platform forms a vital part of their knowledge base. Nevertheless, their use of open design processes to accommodate customer needs outside the boundaries of their platforms on a project basis is not sufficiently represented within the reviewed frame of platform-related theory.

At both companies, processes not explicitly related to the realisation of a specific product were identified. More than so, these were a formalised part of each company's platform. Probably most companies have formalised and standardised processes which could be argued to have an implicit relation to realising products, regardless of production strategy or type of business, for that matter. The question is how the theoretical notion of product platforms should incorporate or account for this? This study does not answer that question, but the results suggest that standardising processes with implicit relations to product realisation could be an important aspect of enabling product flexibility whilst maintaining a platform strategy. Product platforms is a strategy originally intended for businesses with fewer open design processes on a project basis compared to the companies Alpha and Beta. This suggests that theoretical frameworks, which accurately address these aspects, needs to be developed to fit within the existing body of platform-related theory.

At both companies, we saw both an interplay between a technical platform and a process platform as well as how parts from both platforms fed the stream of ongoing projects. This interplay was for instance manifested at Alpha when links between a pre-engineered part (e.g. a wall element) and associated documentation (e.g. checklists etc.) were established. At Beta the same interplay could be seen through the link between a pre-engineered part and the collection of associated SOS. A proposed update to the process model presented by Lessing [1] is that the process platform, not just the technical platform, is feeding each project. This is specifically highlighted and presented in Figure 2. The revised figure does not deepen the insights regarding the actual interplay between a technical and a process platform but it stresses the process platform's role in individual projects as important.

The platform model proposed by Jansson et al. [22] could also be used to incorporate findings presented in this paper, the implicit processes are arguably acting as support methods in product realisation at the two case companies. However, as a platform model, it too lacks the required granularity needed to depict how pre-engineered solutions and standardised processes actually interplay with each other and fit together within the

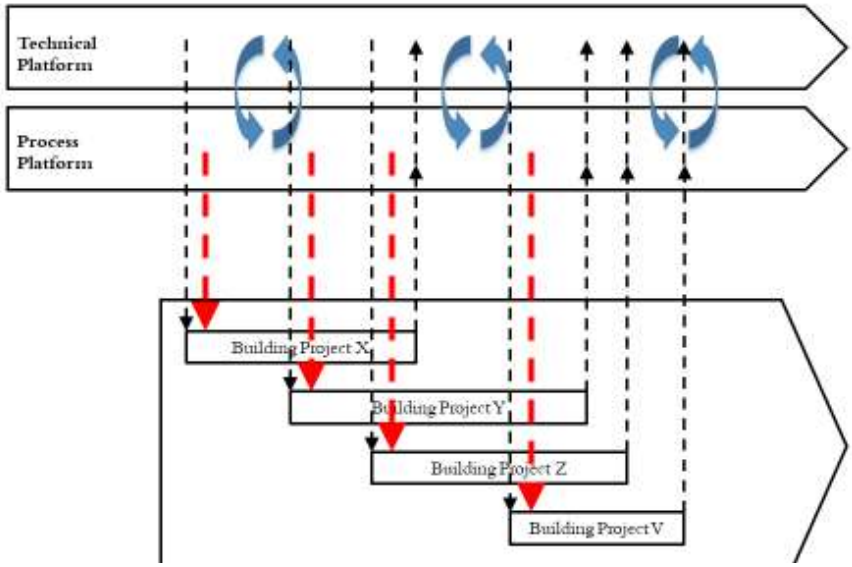

Figure 2. Process model for industrialised house building, revised from [1]

platform. Therefore, further studies are needed to elaborate on this interplay and provide data to identify what mechanisms are put to use within the platform as all subsets within a platform work together to offer flexibility whilst maintaining benefits from applying a platform strategy. An updated platform model should differentiate between mechanisms which are completely or partially dependent on open design processes from those mechanisms which are needed to handle pre-engineered solutions as this study suggest that this level of granularity is needed to establish the relevant processes, implicit and explicit, needed to accommodate product flexibility. Then it can be further developed and concretised to form the basis for a platform strategy better suited to companies like particularly Alpha.

References

[1] J. Lessing, *Industrialised House-Building*. Licentiate Thesis, Lund Institute of Technology, 2006.

[2] H. Jonsson and M. Rudberg, "Classification of production systems for industrialized building: A production strategy perspective," *Constr. Manag. Econ.*, vol. 32, no. 1–2, pp. 53–69, 2014.

[3] Miljödepartementet, "Till statsrådet och chefen för Miljödepartementet," *Sou 200760*, no. november 2005, 2007.

[4] A. Björnfot, "An Exploration of Lean Thinking for Multi-storey Timber Housing Construction-Contemporary Swedish practices and future opportunities," pp. 1–60, 2006.

[5] M. Höök and L. Stehn, "Applicability of lean principles and practices in industrialized housing production," *Constr. Manag. Econ.*, vol. 26, no. 10, pp. 1091–1100, 2008.

[6] D. Robertson and K. T. Ulrich, "Planning for Product Platforms," *Sloan Manag. Rev.*, vol. 39, no. 4, pp. 19–31, 1998.

[7] J. P. MacDuffie, "Modularity-as-Property, Modularization-as-Process, and 'Modularity'-as-Frame: Lessons from Product Architecture Initiatives in the Global Automotive Industry," *Glob. Strateg. J.*, vol. 3, no. 1, pp. 8–40, 2013.

[8] J. Jiao, T. W. Simpson, and Z. Siddique, "Product family design and platform-based product development: A state-of-the-art review," *J. Intell. Manuf.*, vol. 18, no. 1, pp. 5–29, 2007.

[9] N. P. Suh, "Axiomatic Design Theory for Systems," *Res. Eng. Des. - Theory, Appl. Concurr. Eng.*, vol. 10, no. 4, pp. 189–209, 1998.

[10] J. Jiao, L. Zhang, and S. Pokharel, "Process platform planning for variety coordination from design to production in mass customization manufacturing," *IEEE Trans. Eng. Manag.*, vol. 54, no. 1, pp. 112–129, 2007.

[11] F. Alizon, K. Khadke, H. J. Thevenot, J. K. Gershenson, T. J. Marion, S. B. Shooter, and T. W. Simpson, "Frameworks for product family design and development," *Concurr. Eng. Res. Appl.*, vol. 15, no. 2, pp. 187–199, 2007.

[12] L. L. Zhang and B. Rodrigues, *A Petri net model of process platform-based production configuration*, vol. 24, no. 6. 2013.

[13] J. Larsson, W. Lu, J. Krantz, and T. Olofsson, "Discrete Event Simulation Analysis of Product and Process Platforms: A Bridge Construction Case Study," *J. Constr. Eng. Manag.*, vol. 142, no. 4, p. 04015097, 2016.

[14] H. Johnsson, "Production strategies for pre-engineering in house-building: Exploring product development platforms," *Constr. Manag. Econ.*, vol. 31, no. 9, pp. 941–958, 2013.

[15] A. Segerstedt and T. Olofsson, "Supply chains in the construction industry," *Supply Chain Manag. An Int. J.*, vol. 15, no. 5, pp. 347–353, 2010.

[16] G. M. Winch, "Models of manufacturing and the construction process: The genesis of re-engineering construction," *Build. Res. Inf.*, vol. 31, no. 2, pp. 107–118, 2003.

[17] V. S. Veenstra, J. I. M. Halman, and J. T. Voordijk, "A methodology for developing product platforms in the specific setting of the housebuilding industry," *Res. Eng. Des.*, vol. 17, no. 3, pp. 157–173, 2006.

[18] P. Jensen, T. Olofsson, and H. Johnsson, "Configuration through the parameterization of building components," *Autom. Constr.*, vol. 23, pp. 1–8, 2012.

[19] P. Jensen, H. Lidelöw, and T. Olofsson, "Product configuration in construction," *Int. J. Mass Cust.*, vol. 5, no. 1, p. 73, 2015.

[20] M. Bonev, M. Wörösch, and L. Hvam, "Utilizing platforms in industrialized construction: A case study of a precast manufacturer," *Constr. Innov.*, vol. 15, no. 1, pp. 84–106, 2015.

[21] C. Thuesen and L. Hvam, "Efficient on-site construction: Learning points from a German platform for housing," *Constr. Innov.*, vol. 11, no. 3, pp. 338–355, 2011.

[22] G. Jansson, H. Johnsson, and D. Engström, "Platform use in systems building," *Constr. Manag. Econ.*, vol. 32, no. 1–2, pp. 70–82, 2014.

[23] A. Styhre and P. Gluch, "Managing knowledge in platforms: Boundary objects and stocks and flows of knowledge," *Constr. Manag. Econ.*, vol. 28, no. 6, pp. 589–599, 2010.

A Study of Kinetic Façade Modelling Performance Using Virtual Reality

D.S. Panya[a], J.H. Seo[a], H.J. Park[a], W.J. L[a], and S.Y. Choo[a]

[a]Department of Architecture, Kyungpook National University, South Korea
E-mail: davidpanya@yahoo.com, lelia004@naver.com, gpwls3143@gmail.com, wjee0306@naver.com, dadlchoo@gmail.com

Abstract –

Kinetic facades are dynamic building surfaces that manage light, ventilation, energy, or information. The programming of Kinetic facades require a vast technical expertise of building systems, materials and computer devices and constant alteration of models to examine till the desire purpose of the kinetic façade is achieved. There heavy dependence alterations to physical scale models to understand the systems performance. This paper focuses on a building a mechanical building skin that adjust to the sun path to harness solar energy while shading the building and considering unpredictable weather changes which is an inspiration from biomimicry architecture concepts derived from how leaves react to sunlight in nature rather the conventional fixed photovoltaic panels. Using rhino grasshopper plugin we design and find geometric forms representing panels that can optimally harness sunlight at different times of the day without disrupting sunlight from accessing the interior space though a radiation analysis that measures kilowatt hours per meter squared (Khpm2). The collection changes in panel elements of the façade in various position, orientation generated from Rhino grasshopper are then compiled into a sequence through unreal engines animation tool that can be triggered to move in relation to another object and function in the virtual world which simulates the animation of the system in relation to the suns position and intensity which becomes a virtual animated model. This animated virtual model created in the game engine can constantly be edited to improve performance through immersive experiential design and alterations of the forms generated in grasshopper. The task of simulating and designing models that are performance based is challenging and requires constant Adjustments. We explore the possibility of using a virtual reality model as a potential alternative for physical simulation models that require constant alterations to reach the desired design properties for complex kinetic motion facade.

Keywords –

Kinetic system, performance-based design, digital simulations, design considerations, simulation.

1 Introduction

Building facades perform various function such as such as ventilation, daylight management, interior providing convenience for users, energy saving and information display.

Recently, there has been an increase in the interest of users and designers in Kinetic facades as a solution to problems that arise in the buildings and cities. Technology has played an important role in innovation and increased performance of Kinetic facades to respond to climatic problems that could not be solved by the conventional static façade.

Computational simulation tools and 3D modelling grant designers the ability to creatively simulate and experiment on various forms, structures and materials, while considering environmental factors such as climate and use real time-data to design building skins that are intelligently perform required task such as improved daylighting, shading, displaying aesthetic information, and movement as required.

Kinetic facades combine mechanical electrical and often sensor devices into the building skin that creates the behavior of the building.

To achieve the desired results for kinetic façade design there various design decisions that need to be made from conceptualization to maintenance of the façade. As kinetic facades are complicated based on the task they are required to perform. Early decisions need to be explicit and precise as mistakes made from the early stages further get complicated in later stages of the design process and can lead to facades that perform below the required performance standard intended by the designer.[1]

Even though there has been a constant development of computational simulation and 3d modeling tools there are still limitations that hinder the creative expression and

innovation of kinetic facades such as motion simulation and user convenience experience. Previous researches conducted on Kinetic façade design presents that most users create physical scale models in early design stages to experiment and analyze design concepts and ideas. This can be a tedious process as physical models need to be constantly altered to achieve the desired result.

Virtual reality technology is a possible solution to test and analyze the performance of Kinetic models. Recently Game engines have be used to create various architectural projects and have become a pivotal tool for communication in the Architectural engineering construction (AEC) Industry. Functions such as real time rendering, lighting, shading, collision detection and animation are important for rapid prototyping and interaction of digital models that are dynamic in nature which allows users to make more efficient and accelerated decisions that could not be made through the means of physical models. Although Game engines are a beneficial tool for rapid prototyping of kinetic models, as a standalone game engines cannot perform required measurement of performance required. The required performance and expected behavior need to based on the modelling and climatic that are compatible with real world data

2 Background and Related Research

There has been a substantial amount of research concerning the geometric forms, technology, and fabrication of with little research allocated to the motion. A composition of multiple elements of a kinetic façade have to create a pattern that can remain in constant motion to achieve the required expected motion behavior.

It is not enough to see architecture or interpret it based on drawings; the experience of a built environment reveals the collection of all design decisions. Virtual reality has the potential to provide the AEC professional with the ability to experience the project designs before they are built. With benefits such as immersion and interaction that can be achieved at a higher level in virtual models than physical models. A research conducted by Siitonen used and compared a walk-through VR and an endoscope-photographing model method, and verified which one was better in manipulation, lighting and spatial reasoning capacity through visual observation of outcomes and interviews with participants with VR the most accepted tool. [2]

Game engines have a physics that is based on physical systems to provide approximate simulation, such as rigid body dynamics (including collision detection) that is important to the scope of this paper to simulate the motion of the geometry.

Dynamic animation in game engines allow the simulation of various assets in the game individually as required. They can act collectively or based on individual object oriented animations that collectively become a system patterned of motion.

Adaptive façade design aim at creating strategies for designing facades to respond to environmental conditions, various factors are to be considered but in this paper we focus on motion that can optimized to create shading for the building and harness sunlight at the same time. Adaptable architecture is described for the first time by Frei Otto as a system that is able to change of shape, location, utilization, or spaciousness.[3] The lighting and shading system of game engines allow the user to immersive experience kinetic with a high degree of realism.

Based on the typology classification by F. Otto Mechanical movements can always be reduced to basic types of movement: Rotation, Translation and a combination of the two. [4] Rotation was the selected motion to analyse in this paper.

For kinetic facades, the main considerations in delivering viable plans are automating and active arrangement with comprehension of kinematics, development of recreation, dependability and toughness are the keys to fruitful execution of kinetic elements in structures. These components are concurred by the greater part of the planners and designers when managing dynamic facades. Essentially, the behaviour of the simulation and kinetic motion patterns and what capability of the mechanical essential as the understanding will impact the expected execution of the kinetic facades.

In moving in the direction of utilizing the style and productivity of game engine shading functions, we asked "what can be a data generated comparable base to the virtual model? Furthermore, "What aspects of kinetic motion can be studies in a virtual model?" which presented the required tools for this research as Rhino grasshopper and unreal engine 4.

3 Methodology

3.1 Approach

The proposed experimental process of modelling and simulation considers two main factors that are important in the design for the scape of this research.

1. The optimization of the kinetic faced based on climatic data especially illuminance annual daylight of the interior space
2. Visualization of the kinetic system’s motion in virtual reality with special concentration on day light intensity and shading from the façade design which can be an immersive experience in virtual reality.

There are limitations to the function animation of geometry in game engine virtual spacey based on real world data. So in this paper we consider a simple vertical upward and downward motion of the building cladding to provide sunlight and shading to the interior space as required. Absolute prediction and mimicry of the behavior of kinetic motion of facades that can be applied to real world buildings in a game engine simulation is a challenge and most likely an ineffective method at the current time so the scope of this paper is limited to conceptual design decisions using the combination of data generated from an optimized model and animation functionality of VR game engines to create innovative design concepts and solutions. As seen in figure 1.

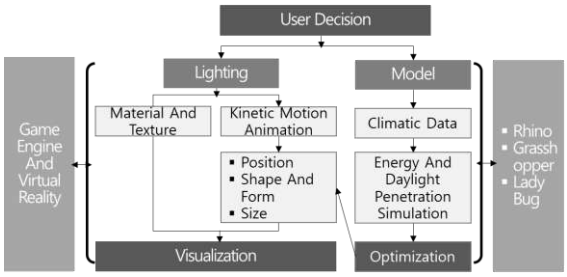

Figure 1. Overall Flow of Research

3.2 Kinetic façade optimization

The performance of the kinetic façade was measure using Ladybug grasshopper plugin. The cladding is a simple hanging cladding at the bottom and top of the curtain wall that shades the building as it rotates upwards and downwards. Both claddings rotated as a mirror of the cladding. Computing for multiple levels presented inconclusive results. So the simulation was conducted for a single floor. Four simulations where conducted in relation to motion. The Climatic data was real world data of Incheon, South Korea downloaded from an open source.

1. The Static mesh averaged 626.5 kWh/m2 and the annual daylight was concentrated around the windows of the space.
2. Introducing the cladding without any rotation the annual daylight averaged 783.9 kWh/m2 and the lighting concentration was even all across the space due to the replacement of windows with a curtain wall.
3. At rotation motion of 15 degrees of the cladding the annual daylight averaged 506.8 kWh/m2 and the lighting concentration was most concentrated at the rear end of the space.
4. At rotation motion of 20 degrees of the cladding the annual daylight averaged 469.9 kWh/m2 and the lighting concentration was generally dimmer than previous iterations.

Further simulations presented results that were either to bright or too Dim, which presented the acceptable range of rotation motion of the cladding to be from 0 degrees to 20 degrees. The annual daylight simulation was programed using the ladybug plugin as show in figure 2.

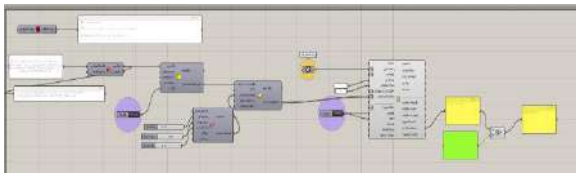

Figure 2. Ladybug grasshopper simulation using real world climatic data

3.3 Game Engine Animation system

The animation of the kinetic system in the game engine was created using a visual language system called blueprinting. The entire movement was controlled by the blueprint which remain constant through the entire simulation excluding the angle of rotation that needed to be changed after every run of the animation as seen in figure 3. Considering that the motion was purpose was to provide insight into the motion of the cladding, the simulation was ran at different the animation speeds and durations that are easily customizable after each animation run. Every cladding had its own animation blueprint which made the animation of every element independent and made it possible to run the animation of any single geometry possible when required

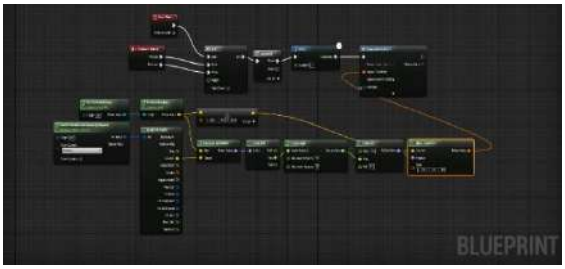

Figure 3. Rotation animation blueprint

3.4 Virtual Reality Experience

Through Virtual reality executables we were able to experience the lighting, shading and motion in immersive VR as seen in figure 4. And shading created by the kinetic motion of the cladding in real world scale and as a small scale model. Through virtual reality controls, aspects of the kinetic façade were edited or turned off to help the user understand how other movements can be changed. A limitation of this process was the complexity of the workflow that made it difficult to make changes to

the virtual simulation in real time.

Figure 4. Immersive VR experience of the Kinetic façade motion

4 Results and Assessment

The results of this proposed workflow that incorporates Rhino as a simulation tool and unreal engine as an immersive VR game toll presented the following results as seen in figure 5.

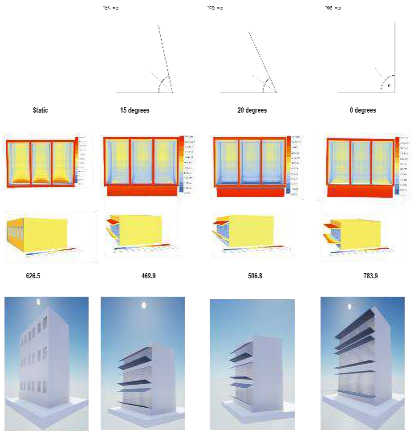

Figure 5. Results comparing the data and model of the Daylight simulation and Game VR motion

1. The game engine lighting and shading were consistent with performance simulation models which makes light and shading studies through the VR game engine effective and convenient.
2. The dynamic nature of the motion of the kinetics elements changed the level of lighting intensity in both the performance model and virtual space thereby altering the comfort of the space.
3. The Immersive animation conveyed the experience of the performance simulation explicitly compared to a third person view of the 3D model

5 Discussion and conclusion

The behavior if the kinetic of the kinetic motion that was required in this paper was simulated using a real world data compatible simulation tool which is an important as designers of kinetic structure must consider performance

The potential for game engine VR to be a toll for modelling complicated kinetic structures is possible but requires the user to have an in depth understanding of game engines or VR software which can make the process of integrating such method of modelling kinetic systems apprehensible for constant use.

VR game engines are potentially alternative modelling tools as any errors or mistakes enquired during the performance simulation in Rhino grasshopper were adjusted and re integrated into the animation blueprint which would have been a more complicated and tedious task in a physical model

We acknowledge that this research is basic in and simplified in in the demonstration of the convergence of performance based model and virtual models. Our Further research intends to address more complicated geometry, structures, mechanics and materialism

The proposed process can be an important way forward for designers to innovative create kinetic modes that perform based on real world data in a convenient workflow.

References

[1] Sharaidin K. and Salim F. Design Considerations for Adopting Kinetic Facades in Building Practice . New Design Concepts and Strategies - Volume 2 - eCAADe 30 , 2012.

[2] Sun L. Toshiki T. Tokuhara F. Nobuyoshi Y. Differences in spatial understanding between physical and virtual models. .Frontiuers of architectural Research. 2014

[3] Romano R. Aelenei L. Aelenei D. Mazzuchelli E.S. What is an Adaptive Façade, 2018.

[4] Sharaidin, M. Kinetic facades: towards design for environmental performance. Doctor of Philosophy (PhD), Architecture and Design, RMIT University.

Acknowledgements

This research is a basic research project funded by the Korean government (Future Creation Science Department) in 2016 and supported by the Korea Research Foundation. Assignment number: 2016R1A2B4015672.

This research was supported by a grant(19RDRP-B076268-06) from R&D Program funded by Ministry of Land, Infrastructure and Transport of Korean government.

A Basic Study on Methodology of Maintenance Management Using MR

T. Kim[a], J. Jeong[a], Y. Kim[a], H. Gu[a], S. Woo[b], and S. Choo[a]

[a]School of Architecture, Kyungpook National University, South Korea
[b]Department of Architecture, Kyungil University, South Korea
E-mail:thlouiskim@gmail.com, jjw6720@gmail.com, ye_d_@naver.com, ghm3186@naver.com, openbim@naver.com, choo@knu.ac.kr

Abstract -

Today, with the development of technology, various buildings can be constructed in the field of architecture, and the size and complexity of construction are increasing, and the life cycle of buildings is also increasing. As a result, the importance of technology and systems that can maintain and manage not only old buildings but also newly constructed complex buildings is emphasized in modern society. Therefore, in this study, we propose a methodology to improve the efficiency of utilizing MR in the visible aspect of the maintenance of buildings and try to find a way to improve the efficiency of the actual worker by verifying the feasibility of the methodology. The information obtained from the BIM model was uploaded to the MR device, confirming its effectiveness in terms of visibility. We have developed an add-in that can complement the interoperability problems such as data exchange and uploading through the data that can be obtained through the current limited BIM model. By integrating it with other technologies such as artificial intelligence in the future, It is expected that we will be able to fill in deficiencies other than the problems of visualization presented.

Keywords –

Maintenance; BIM(Building Information Modeling); MR(Mixed Reality); Efficiency

1 Introduction

1.1 Research Background and Purpose

The shape of architecture has changed according to the trend of the times. In the modern era, buildings were widely distributed in internationalist style, and buildings built at that time are still continuing and aging. Also, with the development of technology today, various buildings can be built in the field of architecture, and the size and complexity of construction are increasing, and the life cycle of buildings is also increasing. As a result, the importance of technology and systems that can maintain and manage not only old buildings but also newly constructed complex buildings is emphasized in modern society.

Considering the safety performance of the building at the time of construction, maintenance and maintenance of the building, maintenance and replacement of the structure during the lifecycle of the building, and improvement of the performance are performed according to the aging of the structural materials. Building Information Modeling (BIM) has been introduced to manage such a series of work efficiently, so that it can cover all phases of design - construction - maintenance. Based on the information generated through BIM model, Facility Management System, FMS) as basic data. In other words, when creating the BIM model, the information necessary for maintenance should also be input to the BIM model as attribute information. Based on the information, the FIM can be utilized actively. In spite of this technology, however, it is still difficult to establish a complete link between BIM information and FMS. Therefore, in the maintenance stage, it is based on the existing 2D drawings. Especially, when the lifecycle of construction materials is confirmed, BIM information is utilized for intuitive visualization. It depends on human eyes and 2D drawings.

In recent years, 'Microsoft' in the United States has introduced Mixed Reality (AR), which is a mixture of augmented reality (AR) that adds virtual information based on reality and augmented virtuality (AV) , MR) devices have been developed for 'Hololens' HMD (Head Mounted Display). In the field of construction, it is used as a tool to visualize parts that are difficult to understand in drawings and to help constructors understand them. Therefore, this study suggests a methodology that can improve the efficiency of utilizing the existing ineffective method in the maintenance of buildings, especially MR, in terms of visual aspect, and by verifying the feasibility of the methodology, I want to find a way to do that.

1.2 Scope and method of research

This study is a basic study to find a methodology for efficient operation using MR devices in the field of building maintenance. Therefore, this study limited the MEP(Mechanical Electrical and Plumbing) area in terms of visualization, which was especially difficult even in the inefficient way that has been done with the existing drawings in the maintenance process of the buildings. The flow of research is shown in Figure 1.

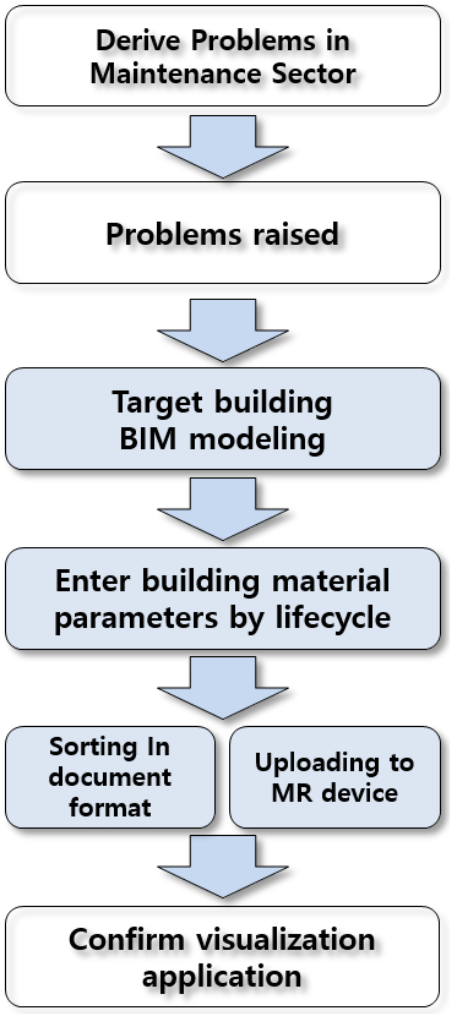

Figure 1. Flow of Study

First, the verification target building for method validation is modeled using BIM tool. After inputting attribute information such as life cycle to the completed MEP model, coloring is performed on the material in the BIM model so that efficient visualization can be performed by filtering according to the information required for maintenance. At the same time, data sorting is performed to increase the efficiency of actual workers by using information of materials according to attribute information. After the work as a BIM tool is completed, the BIM model is uploaded to the MR device and the verification step is performed in an actual 1:1 size AR model.

2 Background and Related Research

In Korea, since the approval of the use of buildings since 2013, the maintenance management system of existing buildings, which was maintained only by the unilateral intention of the owner or manager, is supplemented, and periodic maintenance and inspection of collective structures and multi-use building. Maintenance and inspection system of buildings is being implemented. [1] In the Building Act before the revision in 2012, owners or managers of buildings were legally required to maintain and manage buildings, land, and building facilities. However, the willingness of the relevant authorities to supervise and supervise the maintenance of such buildings was weak, the contents of the management check items are unclear, the maintenance reporting time and the report maker are not clear due to the use and size of the building, and the overall control system is lacking. [2] Since the current buildings are approved by the law, they are maintained and managed only by the unilateral will and intention of the owner and the manager. In the process of using after the completion, there is no specific regulation for the maintenance of the building, but it has not fulfilled the role of protection. [3]

In the United States, each state or city is operated as a form of each ordinance. Especially, evaluation items and criteria for the specific performance of the building are developed and maintained for the purpose of improving the specific performance of the building.

In the UK, maintenance and management are being carried out to build a healthy and comfortable residential complex based on HQI (Housing Quality Indicators) and to improve the quality of the residential level. This provides comprehensive and specific performance evaluation criteria by providing information on performance certification and standard setting related to residential buildings.

In Japan, the Architectural Standard Law, which introduces concrete and strengthened regular reporting systems at the government level, has been amended to take a more active attitude toward maintenance. As such, internationally, maintenance-related systems are approaching from a broad perspective, such as environment, energy, performance evaluation, and urban environment, from a futuristic point of view. However, in each country, improvement is being made in terms of the system by laws and regulations.

Through a series of efforts, the BIM technology

mentioned above is introduced to process the data generated during the construction process at once and utilize it throughout the life cycle of the building. However, this is also due to the various information required by various software functions, and several owners of BIM data are created, but there is a lack of a single integrated information system. [4] Even if the integrated BIM model is constructed to manage all information, there is still a lack of research on visualization of work such as supplementing and replacing aged building components in the maintenance field.

MR technology has been applied as a means to overcome the problems of visualization and has already been widely used in the field of architecture. 'MIDASI'T introduced a display house using VR (Virtual Reality) equipment and introduced a virtual reality in the field of architecture. The company called 'Urbanbase' developed the interior application using AR to maximize the visual effect thereby increasing the satisfaction of actual users. In addition, 'Hololens for Sketchup Viewer', developed by 'Trimble', improves the efficiency of work by showing MR parts to the contractor not only in MEP field but also in difficulties. However, there is not yet a methodology and research that utilize this in the maintenance field.

Figure 2. VR Display House from 'MIDASIT'(vr.midasitonline.com)

Figure 3. AR Interior System from 'Urbanbase'(https://urbanbase.com)

3 Target building analysis and BIM modeling

In this study, the building is one of the lectures within Kyungpook National University located in Daegu, Korea. The outline of the building is shown in Table 1 below.

Table 1. The Outline of Target Building

Type	Straight Type
Height	14.6 m
Each Floor Area	1278.5 ㎡
Floor	4
Long side/ Short side	70000mm/18800mm

This building is a building that has been over 20 years old since its completion and is in need of maintenance but not properly maintained. In particular, although the remodeling has been carried out twice in the past, there is no work to supplement the performance of the building such as elevator installation, rooftop solar panel installation, and structural aspects. Autodesk's Revit 2017 was selected as a tool to make this target building a BIM model. Revit is a BIM modeling tool that not only provides basic modeling but also has an embedded energy performance analysis program that can be used in many aspects of building performance in terms of maintenance.

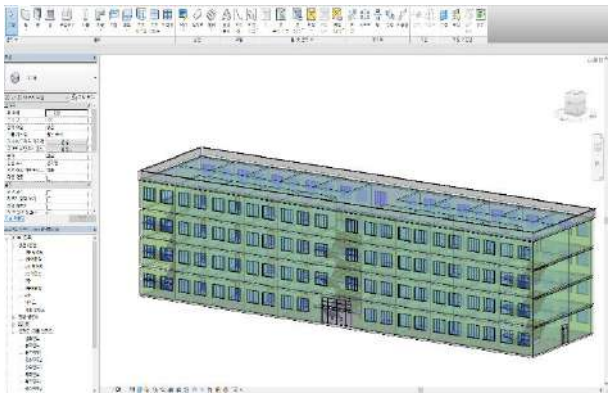

Figure 4. BIM Model of Target Building

The modeling level is defined as LOD 100 based on document E202TM-2008 and AIA Document G203TM-2013 document considering the level of visualization of the target object only in view of maintenance rather than accurate numerical information. In this document, LOD is used in combination with 'Level of Detail' and 'Level

of Development'. However, in order to prevent confusion, this study used 'LOD Development'. Contents are shown in the following Table 2. [5]

Table 2. Contents of LOD(Level of Development)

LOD	Contents
LOD 100 Conceptual	The type, volume, and type of mass are defined at the level of the planning task, and the area, height, volume, position, and orientation of the entire building are set.
L0D 200 Approximate Geometry	Space program, space plan and spatial relation are defined and main architectural general system is determined as conceptualized planning stage. The rough floor area, coverage ratio, floor area ratio, floor height, number of floors, main structure, envelope structure, facility system, etc. are planned
L0D 300 Precise Geometry	The LOD 200 is a step in which the outline of the building process is determined. The building system including the specific facility elements is determined, and all the building elements are modeled.
L0D 400 Fabrication	The size, shape, quantity, etc. of all systems determined as modeling steps for actual construction are modeled. All the elements related to construction, fabrication, and assembly are modeled, such as materials, structures, equipment, piping, and wiring.
LOD 500 As Built	The LOD 500 model is a completion model. The modeling data is the same as the actual building, and includes the entire maintenance/operation.

In this study, MEP, which is an architectural material to be confirmed in this study, is modeled only in the pipes(Plumbing) so that it can be visually and clearly seen at the same LOD level as the same BIM tool, and detailed piping is omitted and three main piping models are modeled.

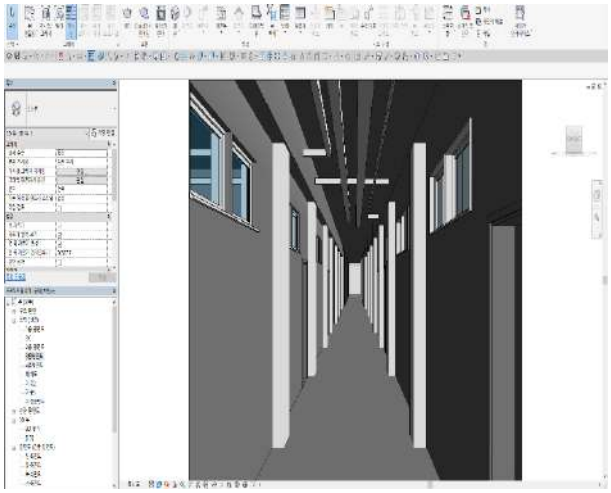

Figure 5. MEP(main pipes) Modeling by BIM

4 Experiment

The detailed experimental scenarios are as follows.

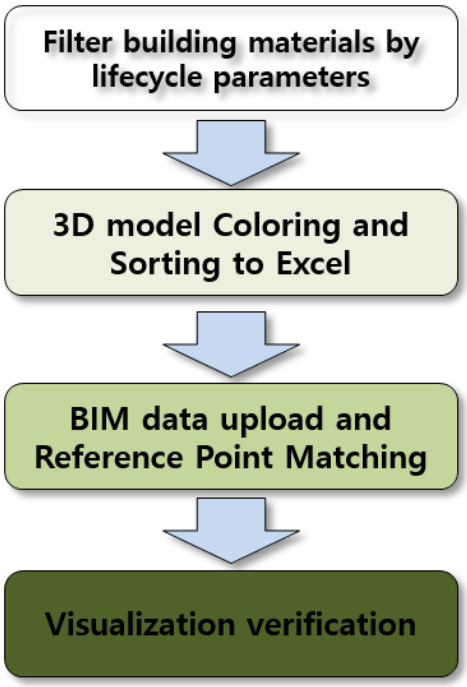

Figure 6. Experimental Scenario

In order to investigate the degree of deterioration of the main piping in Kyungpook National University 's

maintenance lecture, we firstly input the life cycle information of each pipe as a parameter in BIM. Also, the degree of replacement according to input parameters was filtered with different colors.

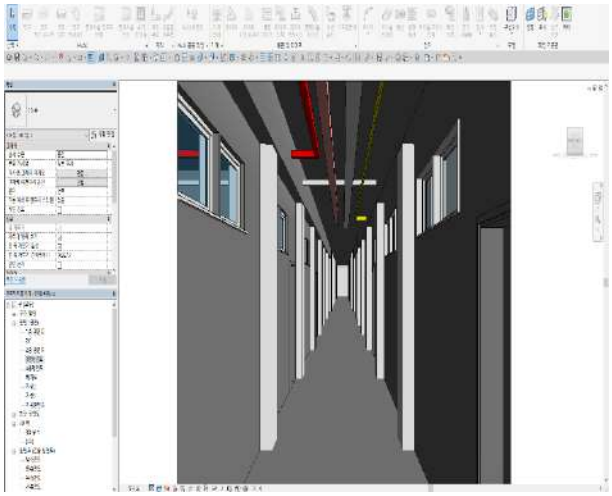

Figure 7. Coloring each Pipes by Life Cycle Parameter

In Revit, you can extract the filtered data using the input parameters according to the desired modeling material. Figure 7 shows data obtained by sorting the coloring data of the piping according to the life cycle into an Excel file.

	A	B	C	D	E	F
1	Name	Floor	Life Cycle	Construction	Coloring	
2	E02-MEP-Pipe01	E02-1	10 year	1990's		
3	E02-MEP-Pipe01	E02-1	10 year	1990's		
4	E02-MEP-Pipe01	E02-1	10 year	1990's		
5	E02-MEP-Pipe02	E02-1	15 year	1990's		
6	E02-MEP-Pipe02	E02-1	15 year	1990's		
7	E02-MEP-Pipe02	E02-1	15 year	1990's		
8	E02-MEP-Pipe03	E02-1	20 year	1990's		
9	E02-MEP-Pipe03	E02-1	20 year	1990's		
10	E02-MEP-Pipe03	E02-1	20 year	1990's		
11	E02-MEP-Pipe04	E02-1	25 year	1990's		
12	E02-MEP-Pipe04	E02-1	25 year	1990's		
13	E02-MEP-Pipe04	E02-1	25 year	1990's		
14	E02-MEP-Pipe05	E02-1	30 year	1990's		
15	E02-MEP-Pipe05	E02-1	30 year	1990's		
16	E02-MEP-Pipe05	E02-1	30 year	1990's		
17				Total number : 15		
18						
19	Name	Floor	Life Cycle	Construction		
20	E02-MEP-Pipe01	E02-2	10 year	1990's		
21	E02-MEP-Pipe01	E02-2	10 year	1990's		
22	E02-MEP-Pipe01	E02-2	10 year	1990's		
23	E02-MEP-Pipe02	E02-2	15 year	1990's		
24	E02-MEP-Pipe02	E02-2	15 year	1990's		
25	E02-MEP-Pipe02	E02-2	15 year	1990's		
26	E02-MEP-Pipe03	E02-2	20 year	1990's		
27	E02-MEP-Pipe03	E02-2	20 year	1990's		
28	E02-MEP-Pipe03	E02-2	20 year	1990's		
29	E02-MEP-Pipe04	E02-2	25 year	1990's		
30	E02-MEP-Pipe04	E02-2	25 year	1990's		

Figure 8. Sorting from BIM Parameter Data

When the modeling work using the BIM tool is finished, the BIM data is uploaded to the MR device Hololens. The experiment was carried out using 'BIM Holoview' which is a program to link BIM with Hololens. From the BIM Holoview homepage, create the user ID and upload the BIM model. After logging in with the same user ID in Hololens, you can view the uploaded BIM model as Viewer.

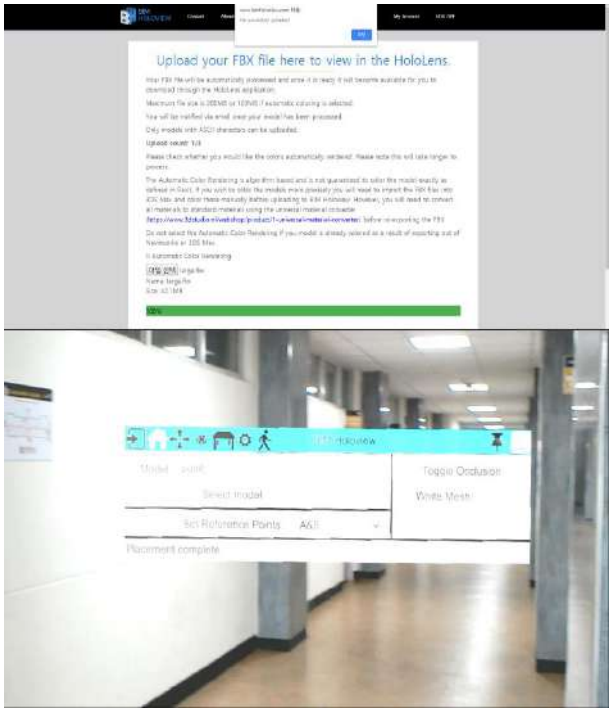

Figure 9. Uploading BIM Data to BIM Holoview

The operation of Hololens is simple. Speech recognition is possible and you can use a remote controller, but the function of clicking on the computer mouse is called 'Air Tap'. You can select it according to the point of sight by hitting your finger on Hololens screen. Another function is 'Bloom' which makes the windows on the screen disappear.

Figure 10. Gestures for Hololens(https://www.microsoft.com/en-us/hololens/)

Figure 11. Control the Hololens

A In this study, BIM data did not include any information other than life cycle parameters other than basic building information. BIM model can have location information and can contain a lot of information such as other energy performance, Time Data (meaning 4D), and Cost Estimate (meaning 5D).

However, as mentioned above, due to the limitation of interoperability in information exchange, only the data required in this study is omitted.

In this case, since the location data is not input, the Reference Point matching the existing BIM data should be prioritized with the Reference Point of the building on the actual Hololens.

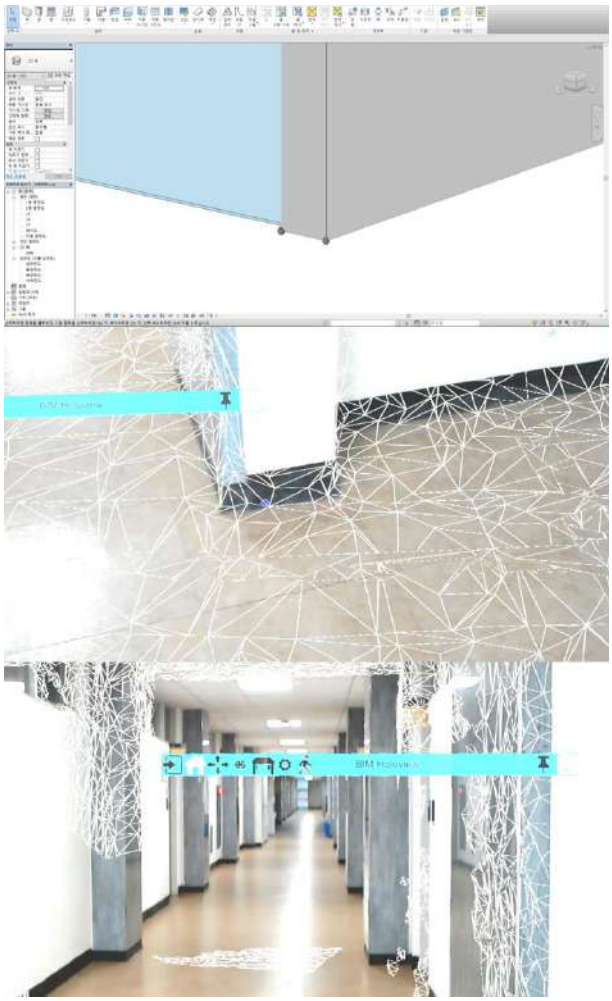

Figure 12. Matching the Reference Point

Then, the verification of the visualization to the MR device was performed based on the sorted Excel data.

5 Discussion

As described in Chapter 4, the BIM model in Hololens was viewed through the Viewer. In addition, the results of the coloring of the piping life cycle as a parameter were also confirmed.

However, the object information in the BIM model, that is, the wall as a wall-specific object and the slab as a slab-specific object, can not be recognized.

Hololens, which is the MR device used in this study, recognizes the wall and space itself in the MR device itself, but the object information of the BIM data disappears in the exporting process and does not reach the step of selecting or modifying the wall in the MR. However, it shows almost 100% synchronous rate, and it is confirmed that MEP which is the target of this study

can be utilized in the maintenance field through the model fitted according to the reference point, and that it is an efficient visualization methodology.

Figure 13. Verification of BIM-MEP model visualization through MR device

6 Conclusion

This study suggests a methodology to increase the efficiency between work during the maintenance and repair process according to the aging of the MEP in the maintenance stage of the building. Especially, it is a method to improve the work efficiency of the actual worker.

Based on the BIM model filtered through the BIM model, the method using the MR device was proposed. The model generated by BIM contains a lot of basic data and can manipulate the parameters to contain more data. However, at present technology level, there is a limit to bring all the data of BIM into MR device.

However, this study shows that it is possible to upload the location information of the desired material and the filtered data according to the life cycle to the MR device. Based on these results, it was confirmed that colorized materials were observed according to the life cycle. And compared to the method of replacing and repairing by relying on the existing 2D drawings, it was able to grasp the exact position, and it was possible to locate the piping of the MEP which was mainly installed in the ceiling duct, And confirmed the possibility of reducing manpower.

In the maintenance stage, the replacement and maintenance of the obsolete materials, which were limited in this study, are part of the maintenance and maintenance in various aspects is needed. If add-in is developed that can complement interoperability issues such as data exchange and uploading through the data obtained through the current limited BIM model, it will be possible to maintain and manage the performance of various buildings such as energy and safety. And it is expected that it will be able to fill deficiencies other than the problems of visualization presented in this study through fusion with various technologies such as artificial intelligence in the future.

Acknowledgements

This research was supported by a grant(19RDRP-B076268-06) from R&D Program funded by Ministry of Land, Infrastructure and Transport of Korean government.

This research is a basic research project funded by the Korean government (Future Creation Science Department) in 2016 and supported by the Korea Research Foundation. Assignment number: 2016R1A2B4015672

References

[1] Yoo Chul-Jong. A Study on Efficient Building Maintenance Plan – Focusing on the Importance Calculation of the Check Items – *Journal of the Architectural Institute of Korea Structure & Construction*, 31(9):3-10, 2015.

[2] Yoon Hyo-Jin. A Study on the Improvement of Building Maintenance System – Focusing on Comparison with Japanese Case. *Journal of the Korean Society of Civil Engineers*, 35(3):737-745, 2015.

[3] Yoo Hyo-Jin. A Study on Building Maintenance Institutionalization by Comparing with the Foreign Countries's cases. Journal of the Korean Society of Civil Engineers D, 31(6D):857-865, 2011.

[4] Choi Tae-Sook. Study on the Integrated Management System Configuration for Building Maintenance. *Journal of the Korean Society of Living Environmental System*, 22(5):696-704, 2015.

[5] AIA. AIA Document G203TM-2013, 2013.

[6] Iveta Pukite., Mg. sc., Ineta Geipele, Prof., Dr. oec. Different Approaches to Building Management and Maintenance Meaning Explanation. *Procedia Engineering*, 172:905-912, 2017.

[7] Ibrahim Motawa, Abdulkareem Almarshad. A knowledge-based BIM system for building maintenance. *Automation in Construction*, 29:173-182, 2013.

[8] Enrique Valero, Frederic Bosche, Alan Forster. Automatic Segmentation of 3D point clouds of rubble masonry walls, and its application to building surveying, repair and maintenance. *Automation in Construction*, 96:29-39, 2018.

[9] Xinghua Gao, Pardis Pishdad-Bozorgi. BIM-enabled facilities operation and maintenance: A review. *Advanced Engineering Informatics*, 39:227-247, 2019.

[10] C. Nzukam, A. Voisin, E. Levrat, D. Sauter, B. Iung. A dynamic maintenance decision approach based

on maintenance action grouping for HVAC maintenance costs savings in Non-residential buildings. *IFAC-PapersOnLine*, 50(1):13722-13727, 2017.

[11] Moshood Olawale Fadeyi. The role of building information modeling(BIM) in delivering the sustainable building value. *International Journal of Sustainable Built Environment*, 6(2):711-722, 2017.

[12] Lucy Linder, Damien Vionnet, Jean-Philippe Bacher, Jean Hennebert. Big Building Data – a Big Data Platform for Smart Buildings. *Energy Procedia*, 122:589-594, 2017.

[13] Gunther Riexinger, Andreas Kluth, Manuel Olbrich, Jan-Derrik Braun, Thomas Bauernhansl. Mixed Reality for On-Site Self-Instruction and Self-Inspection with Building Information Models. *Procedia CIRP*, 72:1124-1129, 2018.

[14] Jad Chalhoub, Steven K. Ayer. Using Mixed Reality for electrical construction design communication. *c*

[15] Danubia Bueno Espindola, Luca Fumagalli, Marco Garetti, Carlos E. Pereira, Silvia S.C. Botelho, Renato Ventura Henriques. A model-based approach for data integration to improve maintenance management by mixed reality. *Computer in Industry*, 64(4):376-391, 2013.

[16] Choo Seung-yeon, Lee Kweon-Hyoung, Park Sun-Kyoung. A Study on LOD(Level of Development) for Development of Green BIM Guidelines – Focused on Energy Performance Estimation -. *Journal of the Architectural Institute of Korea Planning & Design*, 28(6):37-47, 2012.

[17] Kim Tae-Hoon, Seo Ji-Hyo, Choo Seung-Yeon. An Energy Performance Comparison of University Lecture Facilities for Energy Saving Building Design. *Journal of the Architectural Institute of Korea Planning & Design*, 34(11):105-112, 2018.

[18] Sara Madureira, Ines Flores-Colen, Jorge de Brito, Clara Pereira. Maintenance planning of façade in current buildings. *Construction and Building Materials*, 147:790-802, 2017.

[19] P. Paulo, F. Branco, J. de Brito, A. Silva. BuildingsLife – The use of genetic algorithms for maintenance plan optimization. *Journal of Cleaner Production*, 121:84-98, 2016.

Process Modelling in Civil Infrastructure Projects: A Review of Construction Simulation Methods

M. Al-Kaissy[a], M. Arashpour[a*], S. Fayezi[b], A. Nezhad[c], and B. Ashuri[d]

[a]Department of Civil Engineering, Monash University, Australia
[b]Business and Economics Faculty Office, Monash University, Australia
[c]School of Civil Engineering, University of Sydney, Australia
[d]School of of Civil & Environmental Engineering, Georgia Tech, USA
[*]E-mail: maryam.alkaissy@monash.edu, mehrdad.arashpour@monash.edu

Abstract –

It is known that process simulation is a feasible solution to deal with real-world complexities and problems. Civil infrastructure in particular, is a complex system that can benefit from process simulation. This paper provides a critical overview of different simulation modelling paradigms used in construction to achieve better system performance. Three simulation paradigms of agent based modelling, discrete events simulation, and system dynamics are reviewed and their different applications, specifically in civil infrastructure are discussed. The paper then discusses the hybrid paradigms of agent based modelling with system dynamics, and agent based modelling with discrete event simulation, and how hybrid approaches have better capabilities to model complex problems occurring in civil infrastructure. Such modelling approaches, therefore, will improve overall efficiency of construction production.

Keywords –

Construction project planning, Infrastructure sector; Integrated and combined models; productivity and efficiency; Supply chain management

1 Introduction

When prototyping or experimenting with a civil infrastructure system is expensive or impossible, modelling is the best way of solving real world problems, which gives the privilege of optimizing systems prior to implementation [1]. Modelling includes the abstraction process, which is mapping a problem from the real world to its model in the world of models, analyzing and optimizing the problem, then mapping it back to the real system [2]. There are three levels of abstraction, based on the range of problems that are efficiently addressed with simulation modelling, High Abstraction "macro level", Middle abstraction "meso level", Low Abstraction "micro level". Table 1 generates a better understanding of the abstraction level concept and different modelling schema used for each abstraction. Considering an example, macro level traffic and transportation models may not consider individual vehicles or packets. Supply chains are being modeled at very different abstraction levels and they could be placed anywhere in middle to high abstraction range. Problems at the top of Table 1 are typically approached in terms of aggregate values, global feedbacks, trends, etc. Individual elements such as people, parts, products, vehicles, animals, houses are never considered there. Thus, considering how different modelling approaches correspond to abstraction; System dynamics dealing with aggregates is located at the highest abstraction level. Discrete event modelling is used at low to middle abstraction. As for agent based modelling, this approach is being used across all abstraction levels [2, 3]. Agents may model objects of very diverse nature and scale: at the micro level agents may be pedestrians or cars or robots, at the middle level they can be customers, at the macro level they can be competing companies.

The purpose of this paper is to discuss different simulation paradigms in civil infrastructure by focusing on Agent Based Modelling (ABM), Discrete Events Simulation (DES), and System Dynamics (SD). Furthermore, different applications of these approaches along with related advantages/disadvantages are presented. After that, the paper discusses Hybrid paradigms and enhanced modelling performance that can be achieved when combining more than one paradigm. A focus will be on Hybrid ABM-SD, and Hybrid ABM-DES. The paper concludes that agent based modelling is not a substitution to the other modelling paradigms, but a useful add-on that can be combined with system dynamics and discrete event simulation to achieve better results.

Table 1. Paradigms corresponding to different abstraction levels, and applications related to different abstraction level

Abstraction Level	Applications of Simulation modeling (Some of)	Paradigms
High Abstraction/ Macro level/ Strategic Level/ Less details	• Market Place & Competition • Population Dynamics • Manpower & Personnel • Ecosystems • Health Economics	ABM & SD
Medium Abstraction/ Meso level/ Tactical Level/ Medium details	• R&D project Management • Supply Chain • Waste Management • Transportation • Electrical Power Grid • Call Center • Emergency department	ABM & DES
Low Abstraction/ Micro level/ Operational Level/ More details	• Pedestrian movement • Warehouses • Factory floor • Automotive Control System • Computer Hardware	ABM & DES

2 Literature Review of Different Simulation Modelling

2.1 Agent Based Modelling (ABM)

ABM is a computer simulation technique that allows the examination of how system rules, and patterns emerge from the behaviours of individual agents [4]. There is no universally accepted definition for ABM, the primary reason is that researchers in literature are still arguing and discussing what kind of properties an object should have to earn to be called an "Agent" [2]. One of the widely accepted definitions provided by Wooldridge and Jennings, 'A self-contained program capable of controlling its own decision-making and acting based on its perception of its environment, in pursuit of one or more objectives' [5]. Nasirian, et al. [6] explain that Agent-based simulation is basically a model in which dynamic processes of agent interactions are simulated repeatedly over time as in SD, discrete event and other types of conventional simulations. An Agent Based simulation mostly consists of more than one agent interacting, that's why it is often called a multi-agent system, MAS, [7]. Agent- based models, ABMs or MASs, consist of a set of agents characterized by attributes, and interact with each other through the definition of pre-set rules in a given environment [8]. Agents produce output behaviour according to their interaction with each other and their environment and also by following their rules. Many scholars have tried to introduce properties for agents in ABM, [9] defines three properties for agents to be: Cooperative, Learning and Autonomous, and that every agent should possess two of three at least [10]. Pro- and re-activeness, spatial awareness, ability to learn, social ability, "intellect", etc. as described in [7] are some of the many properties of ABM. Aside from the different properties that define Agents, an important feature that distinguishes Agent Based Models from SD or DE is that they are essentially decentralized [2]; there is no such place in AB model where the dynamics of the system could be defined. Instead, the modeler defines behaviour at individual level, and the global behaviour emerges as a result of the many individuals interacting, each following its own behaviour rule, living together in some environment and communicating with each other and with the

environment [2]. The complexity of the ABM system arises from the interactions between different agents [11]. The main objective of the ABM simulation is to track the interactions of the agents in their artificial environment and understand processes through which global patterns emerge [12]. The number of applications to which ABM can be applied are endless due to its distributed and flexible computational power [13]. ABM is a suitable tool to describe the behaviour of complex systems as it serves a 'bottom-up' approach to seize the interactions between individual agents, recognizes each entity as heterogeneous rather than identical, and allows the agents to dynamically evolve and adapt [4]. Extremely complex behaviours can arise from repetitive and competitive interactions between agents enabled to be accounted by the computational power of computers [14]. And thus, ABM is progressively seen in more natural science and engineering purposes, though specific construction applications are more limited. Most recently, Son, et al. [15] have reviewed the use of ABM in construction research and noted its ability to deal with emergent behaviour in complex systems and the advantage that ABM might have over more reductionist approaches. Sawhney, et al. [16] reviewed the use of ABM in answering questions within complex construction systems. They conclude that by combining ABM with more traditional discrete event approaches, these systems can consider human factors that impact the construction site. The traditional approach adopted in studying and understanding construction models has been defined as a "central control" approach, in which the construction plan and schedule are created in advance based on defined resource and constraints [16].

2.2 Discrete Events Simulation (DES)

Discrete Events modelling origins back to 1960s by Geoffrey Gordon, who developed the existing idea of GPSS and brought about its IBM implementations [17]. Entities in DE are passive objects that represent people, parts, documents, they can be delayed, processed, seized and release resources, split, combined, etc. [18], defined the DE methodology as ''the modelling of a system as it evolves over time by a representation in which the state variables change only at a countable number of points in time''. Pidd [19], defined DE simulation as "An instant of time at which a significant state change occurs in the system". Simulation entities can be defined as the elements of the system being modeled and individually identified and processed [20]. Moreover, flow entities and resource entities need to be distinguished in simulation [21]. Flow entities, are usually referred to as (customer entity or temporary entity) and pass through a sequence of activities in a process, and interact with the resource entities (server entities or permanent entities). In contrast with resource entities, flow entities are identical to one another, in a sense that no physical attributes are required to define and distinguish them [22]. A flow entity only carries a time cell to track their arrival times, waiting times, and departure times at activities. The "transaction-flow world view" often provides the basis for discrete-event simulation. In this simulation view, a system is visualized as consisting of discrete units of traffic that move/flow from point to point in the system while competing with each other for the use of scarce resources. The units of traffic are sometimes called Transactions, giving rise to the phrase "transaction flow" [23]." Plentiful systems fit the previous description, which include many manufacturing, material handling, transportation, health care, civil, natural resource, communication, defense, and information processing systems, and queuing systems in general. A discrete-event simulation is one in which the state of a model changes at only a discrete, but possibly random, set of simulated time points. Two or more traffic units often have to be manipulated at one and the same time point. Such "simultaneous" movement of traffic at a time point is achieved by manipulating units of traffic serially at that time point. This often leads to logical complexities in discrete-event simulation because it raises questions about the order in which two or more units of traffic are to be manipulated at one time point. Discrete-event simulation has been recognized as a very useful technique to be taught to tertiary engineering students for the quantitative analysis of operations and processes that take place during the life cycle of a constructed facility [24, 25]. Construction planning is the most crucial, knowledge-intensive, ill-structured, and challenging phase in the project development cycle due to the complicated, interactive, and dynamic nature of construction processes [26, 27]. DES provides support to construction planning by predicting the future state of a real construction system following the creation of a computer model of the real system based on real life statistics and operations [28]. Simulation models for typical construction systems have been delivered as electronic realistic prototypes for engineers to experiment on, which eventually will lead to productive, efficient, and economical field operations.

2.3 System Dynamics (SD)

Developed in the early 1950s by an electrical engineer, Jay W, Forrester, defined System Dynamics as "the study of information-feedback characteristics of industrial activity to show how organizational structure, amplification (in policies), and time delays (in decisions and actions) interact to influence the success of the enterprise" [27]. Since then, definitions and applications

of System Dynamics have been widely studied both in literature and in practical life. Mathematically, a System Dynamics model is a system of differential equations [2]; it is a methodology to understand a specific, predefined- problem or complex problems that include changes over time through multiple feedback loops. System Dynamics uses feedback loops, stocks and flows to model the behavior of complex systems over time [29]. In real world, stocks are a representation of different processes such as, people, money, knowledge, material, etc. Also, real world processes interactions are represented by the flows between the different stocks, and the information that determines the values of the flows [2]. Specifically, feedback loops are closed chains of cause and effect links in which information about the result of actions is fed back to generate further action [30]. To describe the System Dynamics behavior accurately, it should be highlighted that the system is rising from two fundamental types of feedback loops; Negative loops showing goal-seeking behavior and represented with minus sign, and positive feedback loops, represented as plus sign, having the tendency to strengthen their input, leading to exponential growth or decay [31]. A positive feedback loop generates evolution or progression, not equilibrium as in a negative feedback loop [32]. System Dynamics abstracts from single events and entities and takes a comprehensive view concentrating on policies. To method an SD problem, one has to describe the system behavior as a number of interacting feedback loops, balancing or reinforcing. Once the feedback loop are structured and identified, they are translated to what is called stock-flow diagrams to enable simulations [31]. It is important to highlight that large-scale construction projects are extremely complex, highly dynamic, have multiple feedbacks and nonlinear relationships, and require both hard and soft data [31].That explains why System Dynamics can fulfill certain modelling requirements, especially for large-scale construction models. In general, the strength of SD lies in its ability to account for nonlinearity in dynamics, feedbacks and time delays [14], and thus, System Dynamics has been a widely successful tool applied to issues ranging from social, industrial and environmental to project management systems [33]. In construction management, System Dynamics is a widely used modelling tool; however, SD developments in the construction field focus on the characteristics of the traditional construction, or separate sub-systems [30]. A first simple SD model for general project management is developed by [32]. This model then modified for managing different project phases.

3 Analysis of Different Hybrid Paradigms

3.1 Hybrid ABM-SD Simulation

SD and ABM are two simulation methods used to investigate nonlinear social and socio-economic systems [29]. SD has difficulties in many situations and ABM might help to cope with these problems [34]. However, this does not mean that SD is a poorer methodology than ABM, most likely the field of SD is more mature than ABM, which is still in its infancy [35]. Schieritz and Milling [7] presented a comparison between ABM and SD characteristics and found some similarities between the two models. Both of them have the same aim, which is to search for principles underlying the dynamics of complex systems [11]. Lorenz and Jost [36] argued that combining two methodologies helps to be closer to reality as they can synchronize best-fit methods of different methodologies. Schieritz and Milling [7] showed that combining SD and ABM offers the strength of the two methodologies. Adding to that, they believe this combination reduces complexity of the model from the beginning. A hybrid paradigm approach has the advantage of allowing complex problems to be represented more naturally, which improve efficiency and enhance better communication with the simulation project developers [37]. Hybrid simulation involves the use of multiple simulation paradigms, and is becoming an increasingly common approach to modelling modern, complex systems [38]. ABM and SD are among the most important simulation methods available [34]. The idea of creating hybrid models consisting of ABM and SD has been started in the late 1990s. An integration of the two concepts can be successful when it allows for the combination of properties that are otherwise proprietary to a single concept [7]. To fruitfully design a hybrid ABM-SD model; firstly, the framework for this hybrid simulation has to be proposed. This aids construction modelers to combine ABM and SD to benefit the strengths of the two methodologies [29]. It is necessary to define whether a single simulation method or a hybrid ABM-SD simulation approach is needed to model the problem from the beginning, as every simulation method has limited capabilities. The selection of the simulation method replies on the problem type. One should determine the problem can be simulated by one of the ABM or SD, or a hybrid simulation approach is needed [29]. The next step is to define the modelling hierarchy “a top-bottom as in SD, or Bottom –up as in ABM”. Prior to defining the hierarchy, an important note should be highlighted; despite the growing interest in hybrid simulation, little guidance exists for modelers regarding the nature and variety of hybrid models [38]. They proposed three types of hybrid ABM-SD simulation classification including Integrated, Interfaced and Sequential. The

integrated class incorporates feedbacks between ABM and SD representing a continuous process. It means within the Interfaced class may be run in parallel where their outputs are combined as required to represent the desired output as a function of time. In the Sequential class, ABM or SD has to be run first and its output will then be fed to the next. And thus, to determine the hierarchy of the model, for the integrated class of hybrid simulation, SD and ABM can be in a higher or lower level in comparison to each other [38]. However, the SD model is in a higher level in comparison to ABM for the sequential class of hybrid simulation. The next step is to define Information flow path, which the created information passes from one model to another, SD to ABM or vice versa. Nasirzadeh, et al. [29] suggested that the defined path of information flow can be determined based on the purpose of modelling. For example, there is a mutual IFP between SD and ABM models for the integrated class of simulation. The following step is to determine the simulation type based on the modelling purpose. In the case that there is not any connection between ABM and SD models, an interfaced class will be selected. However, if there is an interaction between the two, an integrated or sequential class would be selected. In the case that the interaction is mutual, an integrated class is used. When this interaction is not mutual, a sequential class is used. The last step is to define the Interface variable; which is to determine what should be exchanged between SD and ABM. The variables whose values are changed or influenced by variables of the other model and the variables which influence the values of variables of other models during hybrid simulation are named as 'interface variables'. The interface variables pass data from one model to another in the integrated and sequential classes of hybrid simulation and act as a gate for the transition of data between the two models. So that, SD and ABM exchange data through running time of the hybrid model.

3.2 Hybrid DES-ABM Simulation Modelling

DES is widely accepted in the construction simulation literature as the default approach for modelling construction. Humans, machineries and organizations are modeled in ABM and activities and project environment modeled using DES. The agents' decisions are dependent on the variables in the DES simulation. DES is very established in construction simulation and can be easily adapted to allow interaction with an ABM model. The hybrid framework consists of discrete event simulation as the core, but heterogeneous, interactive and intelligent (able to make decisions) agents replace traditional entities and resources [37]. Many DES models can become more representative of the real world if entities are agents with the ability to adapt to changes in the model. Instead of using the simulation approaches individually, a hybrid DES-ABM simulation proposes framework to integrate unlimited behavioral activities, such as considerations in safety behavioral into construction activity planning. [37]. With further investigation into the relationships of the two modeling paradigms, in DES model, individual entities already exist; those entities can naturally become agents. The DES entities are however described as passive objects and the rules that drive the system are concentrated in the flowchart blocks. Hybrid DES-ABM is described as the process from the entity's viewpoint, thus decentralize "some of" the rules. Goh, et al. [37] describes the hybrid model in a simple manner as; the first component of the hybrid model is an ABM-DES model that analyzes a system in an individual level [39]. This component therefore produces data for the existing base case system, as well as, for systems to test strategic planning scenarios. The second component is the intelligent DES workflow-based that takes as inputs the incident data that is generated from the base case and scenarios. The DES model then combines the time-based input data, and compares the KPIs between the simulated scenarios [39].

4 Conclusion

Prior work has utilised different simulation approaches to model civil infrastructure processes [40, 41]. This paper reviews such simulation approaches. Some simulation techniques such as ABM allow the examination of how systems behave, and patterns emerge from the behaviours of individual agents. ABM is a suitable tool to describe the behaviour of complex systems as it serves a 'bottom-up' approach to seize the interactions between individual agents, recognizes each entity as heterogeneous rather than identical, and allows the agents to dynamically evolve and adapt. Researchers have reported on ABM's ability to deal with developing behaviour in complex construction systems and the advantage that ABM have over other approaches.

DES on the other hand, provides entities that are passive objects and represent people, parts, and documents. Entities can be delayed, processed, seized and released, split, and combined. DES provides support to construction planning by predicting the future state of a real construction system following the creation of a computer model based on statistics and operations. Applications of System Dynamics have been widely studied both in literature and in practical life. The strength of SD lies in its ability to account for nonlinearity in dynamics, feedback and time delays. Thus, SD has been a widely successful tool applied to large scale and complex construction projects. To sum

up, Table 2 shows advantages and disadvantages of using individual modelling paradigms.

Table 2. Comparision of Advantages and Disadvantages between the individual modeling approaches, DES, ABM, and SD

	DES	ABM	SD
Advantages	Easier to create a DES model	Absence of existing elements to be used, provides more flexibility to the modelers to model any scenario in any way they like Understanding the model logic is quite easier as the state-charts do not require simulation modelling knowledge to be understood	Ability to account for nonlinearity in dynamics, feedbacks and time delays
Disadvantages	Output elements had to be added to the model to improve the model performance Understanding the model logic can be difficult	Models are harder to create because no existing and built-in blocks can be used	Difficult in heterogeneous environments As the structure of the system tends to be fixed in SD, it is impossible to use it to study systems which tend to evolve through time

Moreover, the paper focuses on the hybrid modelling paradigms and resultant enhanced applications that can be achieved. The paper findings confirm that better modelling performance can be achieved using hybrid paradigms. A hybrid approach has the advantage of allowing complex problems to be represented more naturally, which improves efficiency and enhances modelling robustness. Hybrid simulation involves the use of multiple simulation paradigms, and is becoming an increasingly common approach to model modern and complex systems.

Acknowledgements

This work was supported by a Monash Infrastructure (MI) grant. The authors would also like to acknowledge the support of the industry partners of this research. Any opinions, findings, conclusions, and recommendations expressed in this paper are those of the authors and do not necessarily reflect the views of the industry partners or Monash Infrastructure (MI).

5 References

[1] M. J. I. J. o. S. Remondino, "Reactive and deliberative agents applied to simulation of socio-economical and biological systems," vol. 6, no. 12-13, pp. 11-25, 2005.

[2] A. Borshchev and A. Filippov, "From system dynamics and discrete event to practical agent based modeling: reasons, techniques, tools," in *Proceedings of the 22nd international conference of the system dynamics society*, 2004, vol. 22: Citeseer.

[3] M. Arashpour, E. Too, and T. Le, "Improving productivity, workflow management, and resource utilization in precast construction," in *9th International Structural Engineering and Construction Conference: Resilient Structures and Sustainable Construction, ISEC 2017*, 2017: ISEC Press.

[4] M. Watkins, A. Mukherjee, N. Onder, K. J. J. o. c. e. Mattila, and management, "Using agent-based modeling to study construction labor productivity as an emergent property of individual and crew interactions," vol. 135, no. 7, pp. 657-667, 2009.

[5] M. Wooldridge and N. R. J. T. k. e. r. Jennings, "Intelligent agents: Theory and practice," vol. 10, no. 2, pp. 115-152, 1995.

[6] A. Nasirian, M. Arashpour, and B. Abbasi, "Critical Literature Review of Labor Multiskilling in Construction," (in English), *Journal of Construction Engineering and Management*, Article vol. 145, no. 1, 2019, Art. no. 04018113.

[7] N. Schieritz and P. M. Milling, "Modeling the forest or modeling the trees A comparison of system dynamics and agent-based simulation," in *in Proceedings of the 21st International Conference of the System Dynamics Society*, 2003: Citeseer.

[8] M. Barbati, G. Bruno, and A. J. E. S. w. A. Genovese, "Applications of agent-based models for optimization problems: A literature review," vol. 39, no. 5, pp. 6020-6028, 2012.

[9] H. S. J. T. k. e. r. Nwana, "Software agents: An overview," vol. 11, no. 3, pp. 205-244, 1996.

[10] Z. Ren and C. J. J. A. i. C. Anumba, "Multi-agent systems in construction–state of the art and prospects," vol. 13, no. 3, pp. 421-434, 2004.

[11] S. E. J. S. P. Phelan and A. Research, "A note on the correspondence between complexity and systems theory," vol. 12, no. 3, pp. 237-246, 1999.

[12] M. Epstein and R. Axtell, "Growing artificial societies: Social science from the ground up," ed: Boston, MA, MIT Press, 1996.

[13] C. Molinero and M. J. A. i. C. Nunez, "Planning of work schedules through the use of a hierarchical multi-agent system," vol. 20, no. 8, pp. 1227-1241, 2011.

[14] D. D. Wu, X. Kefan, L. Hua, Z. Shi, D. L. J. T. F. Olson, and S. Change, "Modeling technological innovation risks of an entrepreneurial team using system dynamics: an agent-based perspective," vol. 77, no. 6, pp. 857-869, 2010.

[15] J. Son, E. M. Rojas, S.-W. J. J. o. c. e. Shin, and management, "Application of agent-based modeling and simulation to understanding complex management problems in CEM research," vol. 21, no. 8, pp. 998-1013, 2015.

[16] A. Sawhney, H. Bashford, K. Walsh, and A. R. Mulky, "Construction engineering and project management II: agent-based modeling and simulation in construction," in *Proceedings of the 35th conference on Winter simulation: driving innovation*, 2003, pp. 1541-1547: Winter Simulation Conference.

[17] G. Gordon, "A general purpose systems simulation program," in *Proceedings of the December 12-14, 1961, eastern joint computer conference: computers-key to total systems control*, 1961, pp. 87-104: ACM.

[18] W. KELTON, "Simulation modeling and analysis," ed: McGraw-Hill, New York. NY, 1982.

[19] M. Pidd, *Computer simulation in management science*. John Wiley & Sons, Inc., 1988.

[20] S. Xiang, M. Arashpour, and R. Wakefield, "Hybrid simulation modeling of hoist downpeak operations in construction sites," in *33rd International Symposium on Automation and Robotics in Construction, ISARC*, 2016, vol. 33, pp. 156-164, ISBN: 9781510829923.

[21] M. J. J. o. C. E. Lu and Management, "Simplified discrete-event simulation approach for construction simulation," vol. 129, no. 5, pp. 537-546, 2003.

[22] M. Arashpour, V. Kamat, Y. Bai, R. Wakefield, and B. Abbasi, "Optimization modeling of multi-skilled resources in prefabrication: Theorizing cost analysis of process integration in off-site construction," *Automation in Construction*, Article vol. 95, pp. 1-9, 2018.

[23] T. J. Schriber, D. T. Brunner, and J. S. Smith, "Inside discrete-event simulation software: how it works and why it matters," in *Proceedings of the 2014 Winter Simulation Conference*, 2014, pp. 132-146: IEEE Press.

[24] J. C. J. J. o. C. E. Martinez and Management, "Methodology for conducting discrete-event simulation studies in construction engineering and management," vol. 136, no. 1, pp. 3-16, 2009.

[25] M. Arashpour, A. Sagoo, D. Wingrove, T. Maqsood, and R. Wakefield, "Single capstone or multiple cornerstones? Distributed model of capstone subjects in construction education," in *Proceedings of 8th International Structural Engineering and Construction Conference, ISEC 2015*, 2015, pp. 971-976, DOI: 10.14455/ISEC.res.2015.27: ISEC Press.

[26] D. W. Halpin and L. H. Martinez, "Real world applications of construction process simulation," 1999, pp. 956-962: ACM.

[27] J. W. Forrester and J. Forrester, "Urban Dynamics. Waltham, MA. Pegasus Communications," ed: Inc, 1969.

[28] A. Nasirian, M. Arashpour, and B. Abbasi, "Multiskilled human resource problem in off-site construction," in *35th International Symposium on Automation and Robotics in Construction and International AEC/FM Hackathon: The Future of Building Things, ISARC 2018*, 2018: International Association for Automation and Robotics in Construction I.A.A.R.C).

[29] F. Nasirzadeh, M. Khanzadi, and M. J. I. J. o. C. M. Mir, "A hybrid simulation framework for modelling construction projects using agent-based modelling and system dynamics: an application to model construction workers' safety behavior," vol. 18, no. 2, pp. 132-143, 2018.

[30] S. Chritamara, S. O. Ogunlana, and N. J. C. I. Bach, "System dynamics modeling of design and build construction projects," vol. 2, no. 4, pp. 269-295, 2002.
[31] J. D. J. U. m. Sterman, Cambridge, MA, "System dynamics modeling for project management," vol. 246, 1992.
[32] G. P. Richardson and A. I. Pugh III, *Introduction to system dynamics modeling with DYNAMO*. Productivity Press Inc., 1981.
[33] F. Nasirzadeh, A. AFSHAR, and Z. M. KHAN, "System dynamics approach for construction risk analysis," 2008.
[34] L. Lättilä, P. Hilletofth, and B. J. E. S. w. A. Lin, "Hybrid simulation models–when, why, how?," vol. 37, no. 12, pp. 7969-7975, 2010.
[35] P. Hilletofth, T. Aslam, O.-P. J. I. J. o. N. Hilmola, and V. Organisations, "Multi-agent-based supply chain management: a case study of requisites," vol. 7, no. 2-3, pp. 184-206, 2010.
[36] T. Lorenz and A. Jost, "Towards an orientation framework in multi-paradigm modeling," in *Proceedings of the 24th International Conference of the System Dynamics society*, 2006, pp. 1-18: System Dynamics Society Albany, NY.
[37] Y. M. Goh, M. J. A. J. A. A. Ali, and Prevention, "A hybrid simulation approach for integrating safety behavior into construction planning: An earthmoving case study," vol. 93, pp. 310-318, 2016.
[38] C. Swinerd, K. R. J. S. M. P. McNaught, and Theory, "Design classes for hybrid simulations involving agent-based and system dynamics models," vol. 25, pp. 118-133, 2012.
[39] M. Fakhimi, A. Anagnostou, L. Stergioulas, and S. J. Taylor, "A hybrid agent-based and discrete event simulation approach for sustainable strategic planning and simulation analytics," in *Proceedings of the 2014 Winter Simulation Conference*, 2014, pp. 1573-1584: IEEE Press.
[40] M. Arashpour, M. Miletic, N. Williams, and Y. Fang, "Design for manufacture and assembly in off-site construction: Advanced production of modular façade systems," in *35th International Symposium on Automation and Robotics in Construction and International AEC/FM Hackathon: The Future of Building Things, ISARC 2018*, 2018: International Association for Automation and Robotics in Construction I.A.A.R.C).
[41] M. Arashpour, Y. Bai, V. Kamat, R. Hosseini, and I. Martek, "Project production flows in off-site prefabrication: BIM-enabled railway infrastructure," in *35th International Symposium on Automation and Robotics in Construction and International AEC/FM Hackathon: The Future of Building Things, ISARC 2018*, 2018: International Association for Automation and Robotics in Construction I.A.A.R.C).

Optimizing Site Layout Planning utilizing Building Information Modelling

A.R. Singh[a], Y. Patil[b], and V.S.K. Delhi[c]

[a]PhD candidate, Department of Civil Engineering, Indian Institute of Technology Bombay, India
[b]Undergraduate Student, Department of Civil Engineering, Indian Institute of Technology Madras, India
[c]Assistant Professor, Department of Civil Engineering, Indian Institute of Technology Bombay, India
E-mail: arsingh@iitb.ac.in, ce16b137@smail.iitm.ac.in, venkatad@iitb.ac.in

Abstract -

Site layout planning (SLP) is categorized as a non-deterministic polynomial time (NP) hard or complete class problem. Inefficient SLP can lead to congestion, safety conflicts and productivity reductions. Significant attention to the problem is evident in the field of construction management. A number of optimization routines and mathematical models are suggested in past research to reduce costs associated with improper layouts. However, such models are seldom adopted on real-life projects, where SLP is primarily carried out based on heuristics. The two significant inhibitors to the adoption of sophisticated approaches identified in this study are; lack of realism in the mathematical models and the significant effort involved in setting up the model for each construction site. These two inhibitors tend to reflect as reluctance on the part of the project teams to adopt SLP models. In the present study, the first inhibitor is addressed by incorporating realism into the mathematical model for SLP. The SLP is formulated as an optimization problem involving the reduction of transportation cost on construction site with associated constraints. Realism to the optimization model was brought through the modelled travel distances utilizing Building Information Modelling (BIM). Genetic Algorithm (GA) was used to optimize the objective function. The combined model thus incorporates all the site constraints in terms of travel paths as captured in the BIM model thus bringing in more realism into the SLP modelling. This work is preliminary work in developing a fully automated SLP process where the second inhibitor would also be addressed.

Keywords -

Site Layout Planning; Optimization; Building Information Modelling; Genetic Algorithm

1 Introduction

Research to address the problem of layout planning also exists in sectors like manufacturing, electronics, computer science and information technology and construction. The objectives to achieve and the constraints encountered are unique to the Architecture, Engineering and Construction (AEC) industry. The layout planning for a construction project starts at the initial phase of the project. The objectives during this phase are not limited to the identification of potential locations to accommodate temporary facilities (TFs) [1], finalizing the routes for vehicular movement [2] and selection of equipment [3]. Intertwined tasks brings more complexity to be handled while planning layouts for construction sites [4]. There exist literature where researchers have tried modelling SLP as a mathematical problem. Mathematical models too possessed the complexity and were referred to NP-Hard [5] and NP-Complete [6] class problems. Despite enormous research in the domain of layout planning, the AEC industry utilizes heuristics of the experienced stakeholders on the project for the purpose of SLP. Sometime the drawbacks of layout through experiential learning come to forth in the form of site congestion, restricted access, unnecessary vehicle movement, multiple handling of material etc. The mathematical approach existing in literature provides a segmental solution to the layout problem and lacks in capturing the realism of a construction site [7], [8]. Although the studies in the domain of layout planning have focused on developing a varied approach to tackle different objectives [7] and comparing the algorithms, adopted in the domain for the solution search [6]. This research in contrast presents an effort to understand the inhibitors to the adoption of existing mathematical models and approach. An evolution in the mathematical approach is also evident to make mathematical models closer to real site scenario; from discrete space layout planning problem to continuous space optimization [3] and from

adopting rectilinear distances, to generating actual paths for planning layout [9]. This research effort is focused on the latter and is a distinguish approach as it involves modelling of paths rather generating it algorithmically.

The existing research presents the adoption of BIM and simulation-based methods to benefit the SLP process through optimization approach. The approach established in this research presents a simple and dissimilar method by utilizing BIM, to bring realism to the mathematical model for SLP. The actual paths modelled for SLP to represent the manoeuvring paths of vehicles and the site personnel replaces the Euclidean and the Manhattan distances considered in existing literature. A test case is also demonstrated with an objective to minimize the transportation cost of material on construction site. The domain of layout planning for construction site has shown significant advancement and the approach developed in this study conform to the recent advancements in the area.

2 Site Layout Planning

The task of allocating space to TFs, material, site personnel and equipment can be referred as 'Site layout planning'. During the task, ensuring optimal usage of the available space is among the prime objectives to the stakeholders involved [10]. The task is part of the front-end planning of a construction project and has close interaction with other processes like scheduling, equipment selection and supply management [3]. The existing research in the domain has attempted the problem in ways like static site layout [11], dynamic site layout [12] and phase based site layout [9]. There have been attempts to model the site space utilizing girds, discrete site spaces and continuous site space [13]. These approaches of representing site space present the peers' desire to model construction scenario close to reality. The methods presented in the existing research have utilized different ways to map the site distances. Some studies have considered the Euclidean and Manhattan distances to replicate the site movements of vehicles and site personnel [14]. The depiction of rectilinear distances on the site may help in mathematical modelling of the construction site but are of no good as the resulted output of these models also lead to sub-optimal solutions. Although there exist rich literary resources to plan site layout efficiently, the construction site layout planning is attempted by the responsible stakeholders utilizing heuristics and the experiential learning gained over the years. The employed approach to layout planning sometimes leads to sub-optimal layouts for the construction site resulting in congestion, multiple handling of material and a rise in safety concerns. The adoption of available optimization routines and mathematical models is still not profound in the AEC industry and the reason can be contributed to the lack of representing actuality in the approach [15]. BIM and computer simulation has marked applicability for SLP and offered help to the planners to plan close to reality. There have been advancements in the mathematical modelling for site layout planning and the adoption of fuzzy sets to incorporate uncertainty has also been employed. Some studies have highlighted the interaction of SLP with the other planning process in very recent years [16], [17].

2.1 Advancements in Research of SLP

Mathematical models for layout planning exist from a long period, formulated as a single objective to optimize [18] and sometime multi-objectives are transformed to a single objective by assigning appropriate weights to individual objectives [19]. The literature has an intensive focus towards optimizing the sum of weighted distance represented as $\sum w*d$ [20]. The primary focus of the existing studies has been on smooth interaction between the facilities on construction site [21]. It is also a shift observed from macro-level planning for the site to micro-level planning, leaving the problem of site utilization partially addressed. The concern towards other objectives has also captured the interest of the construction management researchers. The objectives of the layout problems are both qualitative and quantitative. The factors like safety are addressed in layout optimization in both ways [20]. To address the objectives in an efficient manner that were unaddressed due to the uncertainties involved were approached through the simulation technique integrated with optimization [22]. A few BIM based approaches for layout optimization of the construction site are also evident in the studies of recent past. The shape of a temporary facility is one parameter that can affect the site layout decisions. The area of site locations have a tendency of getting changed as the progress of construction moves forward. There exist research to generate a freeform geometry of the locations and its transformation [23]. Studies have presented a necessity to have 'shortest paths' [23] on construction site and a few have highlighted to have 'actual paths' in consideration [9]. The utilization of BIM for planning site layouts collaboratively is another application of BIM integrated with Augmented Reality (AR). The research presented the users' behavior when subjected to AR enabled platform for planning SLP [24]. The concepts of BIM help in providing the required level of realism to the virtual model by leveraging it with the information. There are few studies highlighting the requirement of BIM for rule based checking system for planning site layouts. The rule based checking is to identify conflicts with the design of the permanent facility [10]. Apart from adopting BIM, the four

dimensional (4D) planning is also proposed in existing studies to replicate realistic site planning. These cases of 4D planning comprises of a three dimensional (3D) model integrated with the schedule of a construction project, and based on the generated 4D visualization of construction activities the SLP is carried out [8]. Moreover, to BIM, simulation and visualization aids; there exist efforts of researchers in the domain to generate paths on construction site for mobile cranes [25] and site personnel but sometime the computer generated paths may also be found infeasible to adopt.

The presented approach in this research combines the existing approach of SLP i.e. mathematical optimization and BIM. The BIM module of the study can be an add-on to the existing optimization models bringing them closer to the reality of the construction site.

3 BIM based Framework for SLP

The apparent utilization of BIM in the AEC industry has simplified the tasks of quantity take-off, detecting and resolving clashes, progress monitoring, asset management etc. This research highlights the potential of BIM for SLP. The BIM model of a hypothetical construction site has been developed and is detailed to a required level of detail (LOD). The LOD 300 model presented in Figure 3 is found apt for implementing the conceptual framework of this study. This detailed model acted as a supplement to the mathematical optimization module presented in section 3.1. The developed approach is depicted in Figure 1.

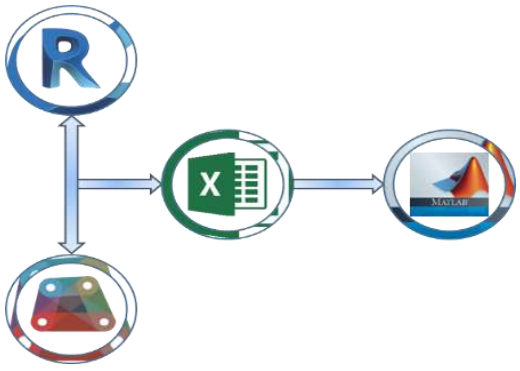

Figure 1. Interoperability Offered by BIM

The modelled site comprises of a reinforced concrete framed structure with isolated footings and a site area of 12385.42 square meters (sq.m.). The main structure has been divided into four quadrants marked in Figure 2.

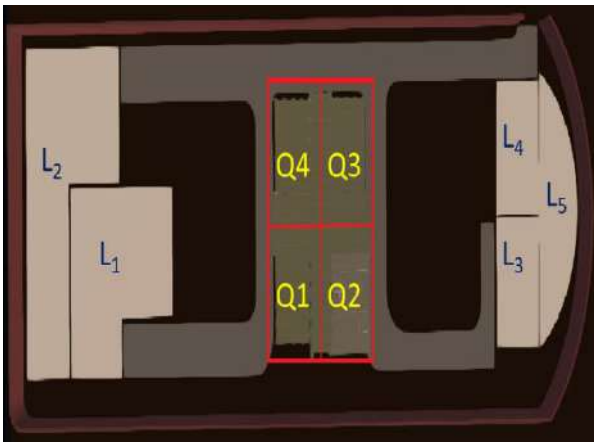

Figure 2. Top View of the Modelled Site

The locations to accommodate TFs, marked as L_1...L_5 in Figure 2 are identified and this represents a case of discrete SLP. It is assumed that the route planning for the construction site is in place and the movement of the vehicles for supporting construction is restricted to the planned paths. During the preparation of the 3D model for the main structure, the paths are modelled to the desired precision. The LOD 300 provided flexibility to takeoff the quantity with high accuracy through Dynamo 2.0, an add-in to Autodesk Revit.

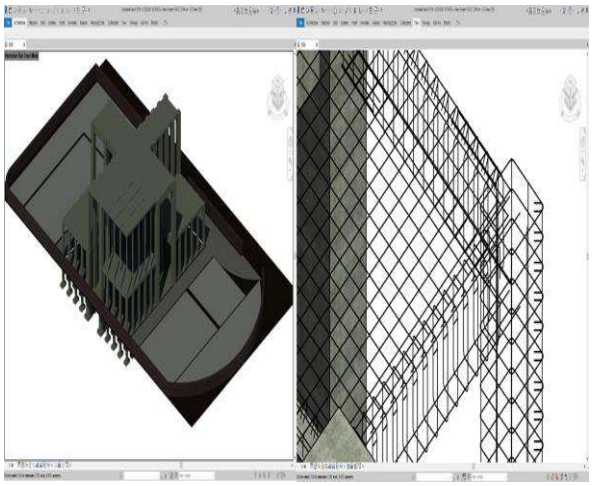

Figure 3. Construction Site Model (LOD 300)

The whole construction site elements are mapped utilizing the visual programming interface of the Dynamo. Figure 4 shows the mapped routes on the construction site joining the locations for temporary facilities and the quadrants of the main structure.

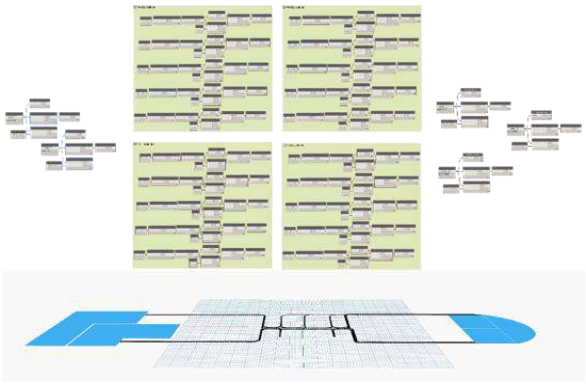

Figure 4. Dynamo Workspace and Preview

The length of the planned routes is extracted from the model and stored in location-distance (LD) matrix as shown in Table 1. The LD matrix is one input for the mathematical optimization module presented in this research.

The quantity takeoff for the required material (M) has been extracted for each quadrant (Q) utilizing Dynamo. The materials required for the modelled framed structure and its respective quantity is tabulated in Table 2. The muck quantity is taken as an approximate of 1.5 times the quantity of concrete required for the isolated footings. The quantities generated by Dynamo are in different SI units and are brought to a common measurement unit by required arithmetic operations.

Table 1. Location to Quadrant Distance

Quadrant / Location	Q1	Q2	Q3	Q4
	Distance in Meters			
L_1	175.8	215.6	220.5	176.7
L_2	186.7	228.1	227.3	166.4
L_3	204.0	164.2	163.1	206.6
L_4	243.5	199.5	195.2	239.2
L_5	242.2	201.0	153.1	210.7

The materials for which the quantity takeoff has been executed are Reinforcement Steel (M_1), Concrete (M_2), Pre-Engineered Steel Sections (M_3), Excavated Muck (M_4) and Shuttering Formwork (M_5). Data from five construction sites of similar area and are at an initial project phase have been acquired to identify the equipment requirement and the cost of operating the equipment. Table 3 highlights the equipment running cost and the maximum carrying capacity per trip.

Table 2. Quantity Takeoff from BIM Model

M \ Q		Q1	Q2	Q3	Q4
M_1	m^3	3.1	3.1	3.1	3.1
M_2	m^3	405.5	405.5	405.5	405.5
M_3	m^3	0.0	91.2	0.0	0.0
M_4	m^3	1459.8	1458.7	1458.2	1459.8
M_5	m^2	1900.2	1897.3	1894.1	1900.2

The trips are calculated utilizing the derived quantities and converting into an appropriate unit. The conversion has been done for M_1, M_2, M_3 and M_4 using the density of material as 7850 kg/m^3 [26], 2400 kg/m^3 [27], 7700 kg/m^3 [28] and 2000 kg/m^3 [29] respectively. The quantity of M_5 is transformed by adopting a value from the industry of 11.3 kg/m^2. The trips required for transporting the entire material to the construction site is shown in Table 4, and is calculated adopting the operable capacity of the appropriate equipment.

Table 3. Data from Field

Equipment	Rated Capacity	Operable Capacity	Cost Unit per Trip of Unit Meter
Transit Mixer	6 m^3	5 m^3	100
Mobile Crane	16 T	16 T	100
Dumping Truck	35 T	32 T	100

Table 4. Required Number of Trips

Material	Q1 Trips	Q2 Trips	Q3 Trips	Q4 Trips
M_1	2.0	2.0	2.0	2.0
M_2	82.0	82.0	82.0	82.0
M_3	0.0	44.0	0.0	0.0
M_4	92.0	92.0	92.0	92.0
M_5	2.0	2.0	2.0	2.0

The transit mixer is found suitable for material M_2 and likewise M_1, M_3 and M_5 are expected to be hauled by a mobile crane. The material M_4 is required to be transported from the execution site to a location for storage by a dumping truck. The excavated soil is stored for backfilling once the planned footings are installed.

Table 5. Transportation Cost Matrix

M \ Q	Q1	Q2	Q3	Q4
M_1	200.0	200.0	200.0	200.0
M_2	8200.0	8200.0	8200.0	8200.0
M_3	0.0	4400.0	0.0	0.0
M_4	9200.0	9200.0	9200.0	9200.0
M_5	200.0	200.0	200.0	200.0

The trip matrix and the cost unit matrix provided the transportation cost unit for materials (TCM) which is another input to the optimization module of this study. The TCM matrix is presented in Table 5. The TCM matrix is the product of cost unit per trip of equipment and the number of trips required to transport the material to the quadrants.

Once the inputs for the mathematical module are acquired, the SLP optimization approach is formulated. The approach adopted is developed to identify the position for storing the materials before transporting to the quadrants along with an objective of minimizing the transportation cost of the materials.

3.1 GA based Optimization for SLP

The adoption of GA for layout optimization is evident in the existing literature. The algorithm follows the criteria 'survival of the fittest' of natural evolution. This study adopts the algorithm to optimize the cost function formulated in equation 1.

$$\text{Min} \sum_{L=1}^{5}\sum_{M=1}^{5}\sum_{Q=1}^{4} \mathbf{C_{MQ}D_{LQ}X_{ML}} \qquad (1)$$

The objective function represents the transportation cost of materials from locations to the quadrants of the proposed main facility. The term C_{MQ} is the cost of transporting material (M) to quadrant (Q), D_{LQ} is the distance between the location (L) and the quadrant (Q) and X_{ML} represents the decision variable depicting the location of material 'M' at location 'L'. The decision variable is chosen as a Boolean variable, limiting its value to 0 or 1.

This research presents a case of constrained optimization where the above-mentioned cost function is minimized subjected to the constraints presented in equation 2 and 3.

$$\sum_{L=1}^{5} \mathbf{X_{ML}} = 1 \qquad \text{Where, } \{M=1,2,\ldots5\} \qquad (2)$$

$$\sum_{M=1}^{5} \mathbf{X}_{ML} = 1 \qquad \text{Where, } \{L=1,2,\ldots5\} \qquad (3)$$

The formulated constraints represent a case of an equal area site layout problem [30]. Here the locations are assumed to accommodate any temporary facility for storing material, irrespective of the area requirement. The constraint in equation 2 limits the allocation of one material to only one location and in equation 3 the restriction is upon the location to accommodate only one material.

This case of constrained optimization is dealt utilizing GA, and MATLAB® is used for running the algorithm. GA requires encoding of the desired parameter, and in this research, the binary encoding is employed. The working of GA starts with initializing a population, followed by performing operations and once the stopping criteria are met, GA provides the optimal value of the fitness function.

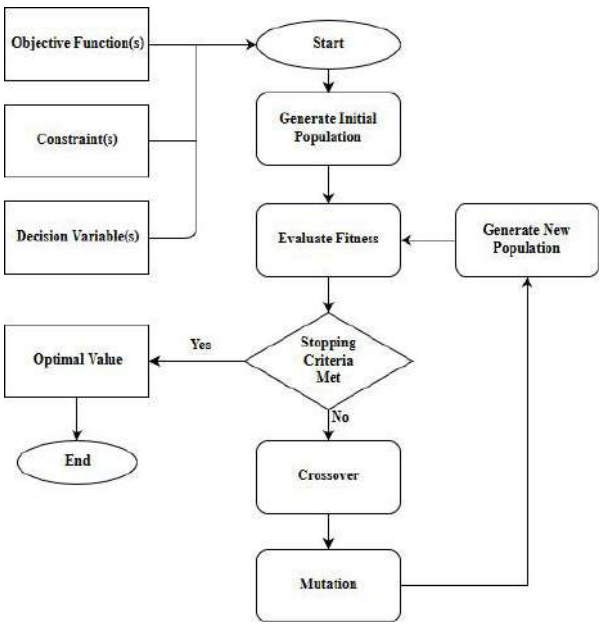

Figure 5. Adopted GA Flow Process

The results from GA are obtained at the parameter values [14] presented in Table 6. A minimum of ten trials are executed for every combination. The optimal results obtained from each combination are presented in Figure 6, Figure 7 and Figure 8.

Table 6. GA Parameters

Item	**Minimum**	**Intermediate**	**Maximum**
Initial Population	100	100	100
Crossover Rate	0.3	0.5	0.8
Mutation Rate	0.01	0.1	0.3

This study has not focused upon tuning up the GA parameters for achieving the optimal or the near-optimal results.

4 Results and Discussion

With the growing demand of BIM for AEC and being mandated on a number of construction projects, it could be anticipated that BIM models would exist for the projects in the near future. The present framework will mandate the creation of material flow paths in BIM models. The depiction of paths on the site model provided a clear view of the vehicular movement anticipated to happen on the modelled site. Whereas manoeuvring on the planned path is expected for safe site conditions, this exercise is expected to enhance safety on construction sites. The adoption of BIM has penetrated in the AEC industry for all phases of construction, but a few studies have highlighted its adoption for SLP. The present study details out the task of integrating BIM into the SLP process. The optimization model supplemented with realistic data of the site could result in better and realistic solutions.

The adoption of GA in this research is an outcome of the existing literature focused on evolutionary algorithm based SLP. The comparative analysis of GA with other evolutionary algorithms and some deterministic algorithms showed the suitability of GA for SLP. The results obtained from all three combinations of parameter set are presented in Figure 6, Figure 7 and Figure 8. The results show the variation in the convergence due to the parameter variation and in this study the ten trials with each parameter set provided an opportunity to understand the concept of near optimality.

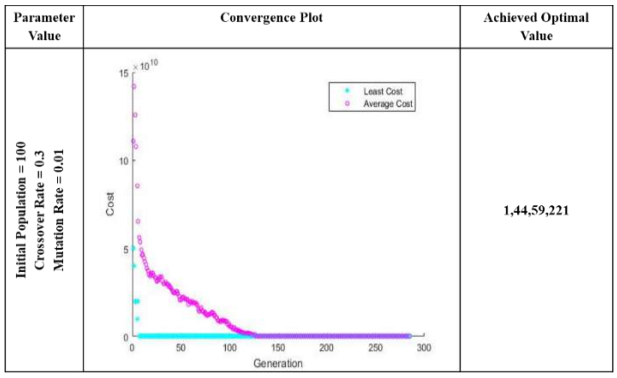

Figure 6. Convergence Plot at Crossover=0.3 and Mutation=0.01

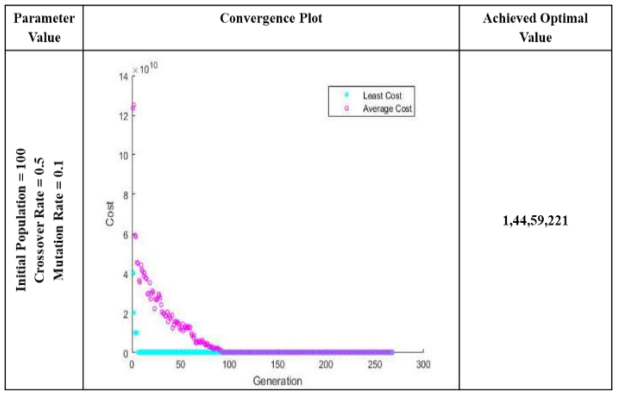

Figure 7. Convergence Plot at Crossover=0.5 and Mutation=0.1

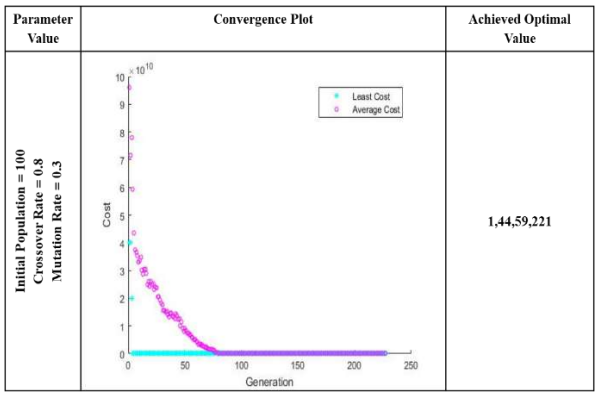

Figure 8. Convergence Plot at Crossover=0.8 and Mutation=0.3

The observation of the convergence plot revealed the effect of the tuned GA parameters and the difference in the plots is easily identifiable. The crossover rate and the mutation rate in Figure 6 reveal the delayed convergence in comparison to other plots in Figure 7 and Figure 8. Whereas the plot in Figure 7 depicts the early convergence due to a high mutation and crossover

in comparison to the mutation rate of 0.01 and crossover of 0.3, adopted as the minimum rate in this study. The convergence plot in Figure 8 also justifies the parameter values of GA by representing a mixed convergence i.e. uneven and early due to high crossover and mutation.

Ten trials with each combination allowed the researchers to verify no premature convergence of GA. The optimal value of cost resulted out to be 1,44,59,221 cost unit. The interpretation of the resulted GA output is presented in Table 7.

Table 7. GA Result Interpretation

Optimal Position	Interpretation	Achieved Optimal Cost Unit
$\begin{bmatrix} \mathbf{0} & \mathbf{1} & \mathbf{0} & \mathbf{0} & \mathbf{0} \\ \mathbf{1} & \mathbf{0} & \mathbf{0} & \mathbf{0} & \mathbf{0} \\ \mathbf{0} & \mathbf{0} & \mathbf{0} & \mathbf{1} & \mathbf{0} \\ \mathbf{0} & \mathbf{0} & \mathbf{1} & \mathbf{0} & \mathbf{0} \\ \mathbf{0} & \mathbf{0} & \mathbf{0} & \mathbf{0} & \mathbf{1} \end{bmatrix}$	M_2 at L_1 M_1 at L_2 M_4 at L_3 M_3 at L_4 M_5 at L_5	1,44,59,221

5 Limitation and Future Scope

The study is focused to bring the realism of the construction site to the mathematical approach for SLP. Close integration of BIM with mathematical optimization for the purpose of layout planning has been presented. The study is still under process and is supposed to bring more complexities to the formulation by including multi-objectives and constraints to be solved. The case of discrete layout can also be made continuous. A comparative study of Euclidean distances and the actual travel paths will also add to the understanding and will bring up the necessity of the presented approach. The parameter value optimization presented here is in brief, and further study may include adaptive parameters for GA. Simulation integrated optimization based studies are also expected to help the planners for SLP in an efficient way.

6 Conclusion

There have been attempts to make the process of SLP efficient. The past research optimization routines have received limited adoption in the AEC industry and this research highlights some of the inhibitors to the adoption. This study is an attempt to supplement the existing models with the realism of the construction site. It has been found that the technological advancements like BIM have the potential to promote the existing models by bringing actuality of the site to the mathematical models. In an attempt to do so, the researchers here have modelled a mathematical optimization problem and have presented a framework to integrate it with the available BIM tools. The interaction of the tools resulted in an optimal solution to the formulated problem of transportation on a construction site. The study presented the applicability of GA with this new approach of capturing site realism and thus have strengthened the existing literature of SLP on the other hand.

References

[1] K. El-Rayes and H. Said, "Dynamic Site Layout Planning Using Approximate Dynamic Programming," *J. Comput. Civ. Eng.*, vol. 23, pp. 119–127, 2009.

[2] K. Varghese and J. T. O'Connor, "Routing Large Vehicles on Industrial Construction Sites," *J. Constr. Eng. Manag.*, vol. 121, pp. 1–12, 1995.

[3] F. Sadeghpour and M. Andayesh, "The Constructs of Site Layout Modeling : An Overview," *Can. J. Civ. Eng.*, vol. 42, pp. 199–212, 2015.

[4] S. Razavialavi, S. Abourizk, and P. Alanjari, "Estimating the Size of Temporary Facilities in Construction Site Layout Planning Using Simulation," in *Construction Research Congress 2014*, 2014, pp. 70–79.

[5] R. Gholizadeh, G. G. Amiri, and B. Mohebi, "An Alternative Approach to A Harmony Search Algorithm for A Construction Site Layout Problem," *Can. J. Civ. Eng.*, vol. 37, pp. 1560–1571, 2010.

[6] A. Kaveh, M. Khanzadi, M. Alipour, and M. Rastegar Moghaddam, "Construction Site Layout Planning Problem Using Two New Meta-Heuristic Algorithms," *Iran. J. Sci. Technol. - Trans. Civ. Eng.*, vol. 40, pp. 263–275, 2016.

[7] H. Said and K. El-Rayes, "Optimizing Material Procurement and Storage on Construction Sites," *J. Constr. Eng. Manag.*, vol. 137, pp. 421–431, 2011.

[8] Z. Ma, Q. Shen, and J. Zhang, "Application of 4D for Dynamic Site Layout and Management of Construction Projects," *Autom. Constr.*, vol. 14, pp. 369–381, 2005.

[9] S. S. Kumar and J. C. P. Cheng, "A BIM-Based Automated Site Layout Planning Framework for Congested Construction Sites," *Autom. Constr.*, vol. 59, pp. 24–37, 2015.

[10] S. Zolfagharian and J. Irizarry, "Current Trends in Construction Site Layout Planning," in *Construction Research Congress*, 2014, pp. 1723–1732.

[11] A. W. A. Hammad, A. Akbarnezhad, D. Rey, and S. T. Waller, "A Computational Method for Estimating Travel Frequencies in Site Layout

Planning," *J. Constr. Eng. Manag.*, vol. 142, p. 04015102(1-13), 2016.
[12] P. P. Zouein and I. D. Tommelein, "Dynamic Layout Planning Using a Hybrid Incremental Solution Method," *J. Constr. Eng. Manag.*, vol. 125, pp. 400–408, 1999.
[13] C. Huang and C. K. Wong, "Optimisation of Site Layout Planning for Multiple Construction Stages with Safety Considerations and Requirements," *Autom. Constr.*, vol. 53, pp. 58–68, 2015.
[14] M. J. Mawdesley, S. H. Al-jibouri, and H. Yang, "Genetic Algorithms for Construction Site Layout in Project Planning," *J. Constr. Eng. Manag.*, vol. 128, pp. 418–426, 2002.
[15] E. M. M. O. A. Elgendi, "An Automated Dynamic Site Layout Planning System - A Case Study of Egypt," University of Salford, Salford, UK, 2016.
[16] J. Xu and X. Song, "Multi-Objective Dynamic Layout Problem for Temporary Construction Facilities with Unequal-Area Departments Under Fuzzy Random Environment," *Knowledge-Based Syst.*, vol. 81, pp. 30–45, 2015.
[17] J. Xu, S. Zhao, Z. Li, and Z. Zeng, "Bilevel Construction Site Layout Optimization Based on Hazardous-Material Transportation," *J. Infrastruct. Syst.*, vol. 22, pp. 1–16, 2016.
[18] A. Warszawski, "Layout and Location Problems-The Quantitative Approach," *Build. Sci.*, vol. 7, pp. 61–67, 1972.
[19] J. Michalek, R. Choudhary, and P. Papalambros, "Architectural Layout Design Optimization," *Eng. Optim.*, vol. 34, pp. 461–484, 2002.
[20] S. Razavialavi and S. M. Abourizk, "Site Layout and Construction Plan Optimization Using an Integrated Genetic Algorithm Simulation Framework," *J. Comput. Civ. Eng.*, vol. 31, p. 04017011 (1-10), 2017.
[21] C. K. Wong, I. W. H. Fung, and C. M. Tam, "Comparison of Using Mixed-Integer Programming and Genetic Algorithms for Construction Site Facility Layout Planning," *J. Constr. Eng. Manag.*, vol. 136, pp. 1116–1128, 2010.
[22] S. Razavialavi and S. Abourizk, "Genetic Algorithm – Simulation Framework for Decision Making in Construction Site Layout Planning," *J. Constr. Eng. Manag.*, vol. 143, p. 04016084 (1-13), 2017.
[23] I. Abotaleb, K. Nassar, and O. Hosny, "Layout Optimization of Construction Site Facilities with Dynamic Freeform Geometric Representations," *Autom. Constr.*, vol. 66, pp. 15–28, 2016.
[24] A. R. Singh and V. S. K. Delhi, "User behaviour in AR-BIM-based site layout planning," *Int. J. Prod. Lifecycle Manag.*, vol. 11, pp. 221–244, 2018.
[25] H. R. Reddy and K. Varghese, "Automated Path Planning for Mobile Crane Lifts," *Comput. Civ. Infrastruct. Eng.*, vol. 17, pp. 439–448, 2002.
[26] IS 1786:2008, "High Strength Deformed Steel Bars and Wires for Concrete Reinforcement." Bureau of Indian Standards, New Delhi, India, pp. 1–12.
[27] "Handbook on Concrete Mixes," New Delhi, India: Bureau of Indian Standards, 2001, pp. 103–122.
[28] IS 808:1989, "Dimensions for Hot Rolled Steel Beam, Column, Channel and Angle Sections." Bureau of Indian Standards, New Delhi, India, pp. 1–13.
[29] M. L. Trani, B. Bossi, M. Gangolells, and M. Casals, "Predicting Fuel Energy Consumption During Earthworks," *J. Clean. Prod.*, vol. 112, pp. 3798–3809, 2016.
[30] H. Li and P. E. D. Love, "Genetic Search for Solving Construction Site-Level Unequal-Area Facility Layout Problems," *Autom. Constr.*, vol. 9, pp. 217–226, 2000.

Hyperspectral Imaging for Autonomous Inspection of Road Pavement Defects

M. Abdellatif[a], H. Peel[a], A.G. Cohn[b,c], and R. Fuentes[a]

[a]School of Civil Engineering, University of Leeds
[b]School of Computing, University of Leeds, LS2 9JT, The United Kingdom
[c] Tongji University, China
E-mail: m.abdellatif@leeds.ac.uk, cnhap@leeds.ac.uk, ag.cohn@leeds.ac.uk, r.fuentes@leeds.ac.uk

Abstract –
Autonomous inspection of roads is gaining interest to improve the efficiency of road repair and maintenance. In this paper we will be showing the potential for using Hyper Spectral Cameras, HSC, to identify road defects. The key idea of this paper is that cracks in the road show the interior material of road pavement which have different chemical composition from the surface materials due to surface wear. Material changes of the road surface give rise to a spectral signature that can be easily detected in HSC images. This condition facilitates the detection of cracks and potholes, which can be difficult if working in the visible spectrum domain only. We report on experiments with a HSC to identify the road material changes and their association to cracks and potholes. A new metric is devised to measure the amount of metal oxides and associate its absence to the appearance of cracks. The metric is shown to be more discriminative than previous indicators in the literature.

Keywords –
Road crack detection; Pavement defect inspection; Hyperspectral Imaging; Autonomous road inspection.

1 Introduction

Detection of road cracks from images is difficult since cracks are dark, only have few features and hard to distinguish from road texture [1]. As a result, state of art road crack detection systems suffer from low recall and high false positive rates as reported by [2] [3]. Hyper Spectral Cameras, HSC, are considered in this paper in search for more discriminative clues for crack detection. HSC are used to measure typically spectral range of 350nm-2500nm which contains spectra beyond the human vision range (400nm-700nm). Hyperspectral imaging, though relatively expensive and developed mainly for satellite and scientific imaging, is now becoming affordable and can be exploited for city road monitoring. HSC can be used to identify changes of surface materials if it has a unique spectral signature. Our interest is to exploit HSC fitted on drones for road and infrastructure surface inspection to detect cracks and anomalies.

Hyperspectral imaging, HSI, has been used previously to classify road conditions from satellite images [4] [5] [6] [7] [8]. The research was intended to classify road conditions in general and the spatial resolution cannot detect road cracks or defects. Only few papers considered the detection of pavement cracks based on hyperspectral data [1] [9] [10]. In such case HSC were fitted on drones of low altitude flights to have higher spatial resolutions to enable observing cracks. The previous studies considered using descriptors of the spectrum such as the VIS2 (intensity difference between 830nm and 490nm-showing metal oxide content) and Short Wave Infra-Red, SWIR (Intensity difference between 2120nm and 2340 showing hydrocarbon content). The metrics measure the rise and decay of spectral response curve at the wavelength regions for metal oxides and hydrocarbon which usually characterizes road conditions. These metrics have also been linked [11] to the Pavement Condition Index, PCI, (A standard metric by ASTM D6433 and D5340, used to indicate the condition of road pavement and ranges 0-100) and is usually computed using visual surveys [5].

In this paper, a new spectral descriptor is proposed to describe the spectra of road pavement and, in particular, assist the search for cracks. New roads are mainly composed from minerals and hydrocarbons, while deteriorated roads show more metal oxides on their surfaces [5]. The regions sensitive to both metal oxides and minerals are shown in Figure 1. The hypothesis of this paper is that cracks have a different chemical composition as shown schematically in Figure 2 and therefore, present a unique spectral response. That response can be used to distinguish cracks from un-cracked road surface material. A novel metric is proposed to measure the content of metal oxides from the spectra and associate its depletion to the appearance of road anomalies or cracks.

This paper is structured as follows: The next section outlines the relevant work in road condition analysis using hyper-spectral imaging, then, the new algorithm is described in detail in section 3. The experiments and results on real road conditions are described and discussed in section 4, whilst conclusions are drawn in section 5.

2 Related Work

Hyper-Spectral Imaging, HSI has been used in space and satellite cameras for remote sensing and analysis of natural resources and several other forestry and agricultural applications [12]. Some applications have used HSI as a tool for detecting forgery in art work [13]. It have also been used for art work authentication and for crack detection in paintings [14]. There is currently an increasing interest in the application of HSC with UAV to monitor the conditions of city roads, see [12] for a review of UAV based sensors. A simple UAV system was described in [15] for application in forestry and agriculture.

Several basic problems are still inherent in the use of HSI and infra-red imagery. One is the need to measure the illumination colour, online rather than with a single measurement before using the sensor as is the current practice [16]. Another basic problem is blurred edges [12], since it severely affect the measurements due to spectral aberrations on edges and several studies have focused on de-blurring edges [17] [18].

Spectral mixing also occurs since one pixel of a satellite camera may represent more than five metres of different materials on earth. Hyperspectral un-mixing is useful for satellite images since it can improve the resolution and show different material contents. This effect is less significant when the camera is used at close range to surfaces. Hyperspectral images have been processed by super-resolution systems through different successful methods and reported to improve the spatial detection of target in typical 4 m resolution satellite images. [19] However, the issue of compromise between the spatial and spectral scale in hyperspectral imaging is critical and was the subject of extensive research in remote sensing [6] [20]. Table 1 summarizes the major works in the literature and their significant features. The table shows three categories of research namely: basic problems, physics-based solutions and pure learning approaches.

2.1. Physics-based approaches

Several spectral descriptors were developed in spectral and spatial domains for the classification and object detection in hyperspectral images [9] [18] [20] [21]. Approaches to associate the spectra of roads monitored from satellite with road conditions in general (not for crack detection) have been reported in [4] [10] . The simplest spectral descriptors were devised to measure the rise and decay of spectral response curves for road materials in the full spectral range of typical HSC that is (400nm-2500nm).

The spectral descriptors are known as VIS2 and SWIR ratios [10]. The ratios were used as metrics for a material with the following definition [8]:

$$VIS2_{Difference} = I_{\lambda=830nm} - I_{\lambda=490nm} \quad (1)$$

$$VIS2_{Ratio} = \frac{I_{\lambda=830nm}}{I_{\lambda=490nm}} \quad (2)$$

where I is the intensity of light and (lambda)is the wavelength in nanometer, nm. The ratio SWIR is defined as:

$$SWIR = I_{\lambda=2120nm} - I_{\lambda=2340nm} \quad (3)$$

It should be noted that the metric VIS2 is termed as a ratio in the literature, while it is mathematically a difference. Therefore, we preferred to define it as two metrics, namely the difference and the ratio.

The frequency domain has been exploited to derive spectral metrics. A spectral similarity measure was suggested [22] using the magnitude values of the first few low-frequency components for spectral signature. Harmonic analysis was also used to describe the spectral reflectance and recognize objects [23].

The design of a spectral descriptor requires a compromise between accuracy and simplicity. It seems that a precise descriptor is required, which is easy to compute and encapsulates all the precious information obtained from the camera spectra. This was highlighted in [6] where they discussed whether Hyperspectral imaging with huge number of spectral bands is really required rather than using a limited number of bands, in a multi-spectral imaging fashion, at a much reduced cost.

2.2 Pure learning approaches

Deep learning and convolutional neural networks have been used in a purely learning approach to identify features in both spectral and spatial domains. Classification from a training set, such as the work reported by [24] [25]. The work in this category is interesting, especially for unsupervised classification, since there is a limited set of labelled data for training in general. It is also challenging due to the huge computational complexity of deep learning added to the

Table 1: Summary of Relevant Work

Category	Authors	Description	Resolution
Basic	Li et al [17]	Deblurring and spectral segmentation for material identification	3.7m
Basic	Lanaras et al. [20]	Study of hyperspectral super resolution problem	3.7m
Basic	Khan et al.[16]	Illuminant estimation in Multispectral imaging	3.7m
Basic	Simoes et al.[19]	A formula for Hyperspectral image super resolution to improve spatial detection of satellite images	3.7 m
Physics-Based	Jengo et al. [9]	Road condition assessment and detecting potholes. Used VIS2 and SWIR ratios as indicators.	0.5 m
Physics-Based	Herold et al. [5]	Road condition mapping using UAV and report good correlation between VIS2 ratio and PCI	1m
Physics-Based	Noronha et al. [6]	Road extraction and pavement condition evaluation from HSI, Recommended using fewer bands for efficient discrimination	2.5- 4.0 m
Physics-Based	Mohammadi [8]	Road classification using several spectral description functions	4m
Physics-Based	Wang et al. [22]	Frequency analysis for HSI clasification and proposed spectral similarity measure as a spectral indicator	3.7m
Physics-Based	Khuwuthyakorn et al. [23]	used harmonic analysis for spectral affine invariant descriptor for HSI	3.7m
Physics-Based	Carmon et al.[4]	Map road skid resistance (friction) to spectrum indicators and mentioned problem of atmospheric correction	1m
Physics-Based	Liang [7]	Detailed study of spectral spatial feature extraction for HSI image classification	3.7m
Pure Learning	Gao et al. [24]	HSI classification using CNN + Multiple feature learning for better class labelling	3.7m
Pure Learning	Liu et al. [25]	Active Deep learning classification in HSI using weighted incremental dictionary algorithm	3.7m
Pure Learning	Zhao, W. and Du, S. [26]	Deep learning approach for dimensional reduction and feature extraction for classification	3.7m

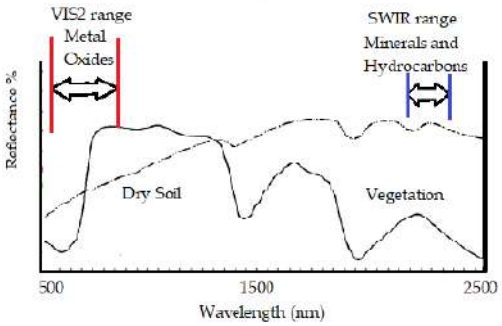

Figure 1: Spectral response and regions for describing pavements.

complexity of the spectral cube typical for HSI [26]. Feature mining had also been reported to learn discriminative features from datasets through feature selection and reduction methods [27].

3 The New Descriptor

A typical response curve from HSC is shown in Figure 1; the camera used is working in the Visible and Near Infra-Red, VNIR spectral range. That means the spectral range that can be of interest for road material change detection, and hence cracks, is the range showing metal and iron oxide in particular. The response in the VNIR range changes significantly for road based on age and wear as reported in several studies (e.g., [6] [8] [28]).

The main idea is explained schematically in Figure 2. The crack shows the internal pavement material which is different in composition from the road surface due to surface wear. The surface usually reflects light similar to metal oxides because of gravel pigments and loss of the bonding asphalt rich in hydrocarbon and oil.

In the previous work, only the intensity at two spectral bands was used to derive the VIS2 ratio. The new descriptor relies on the observation from Figure 3, that the slope is different between cracks and normal surfaces in the range 450-550nm. In this paper, the approximate line that represents the spectrum in the region between 450nm and 550nm is found. The slope, S, of a line is computed using the least squares method in the range [450nm - 550nm]. The angle of the line from the horizontal axis is then fond through the following equation:

$$\phi = \arctan(S) \qquad (4)$$

The reason to select the range (450nm-550nm) is that it is representing the change of metal oxides in response. It is observed in Figure 4 of the spectral response that this particular region is almost straight without curves. This justification is proved empirically through the experiments.

There is an assumption that the surfaces are clean because the spectral response depends on the surface condition. Fortunately, the weather in the UK is often rainy, which increases the probability that road surfaces will be clean from dust and other metal oxides that may impair the crack detection. The application for road inspection also requires low sensitivity to illumination colour because in real outdoor situations, the illumination colour will continually change. This issue will not be covered here and we will rely on measuring the illumination with the standard grey patch before measurement with the assumption that illumination is not changing after the calibration.

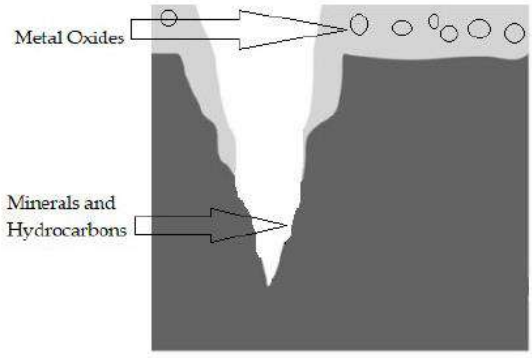

Figure 2: Schematic diagram showing the cross sectional view in a road pavement crack.

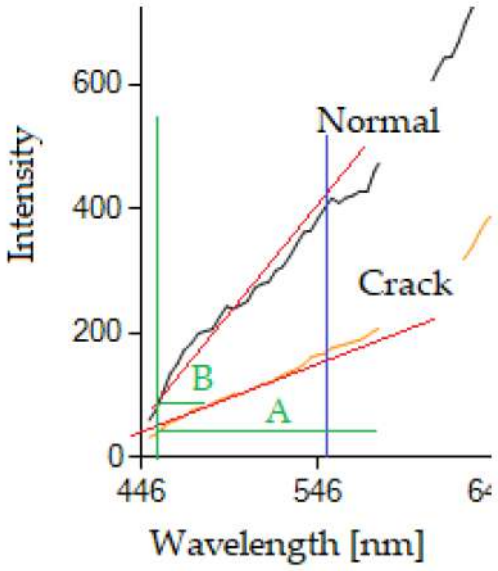

Figure 3: Method of computing the angle ϕ from spectral response.

4 Results

The hyperspectral camera used in this study is a Cubert (model S185) measuring in the range (450nm-950nm) across 125 channels and fitted with a lens of 23 mm focal length. The total image size is 1000*1000 pixels. With the optical system used, one pixel represent (0.5 * 0.5) mm area at one metre depth. The spectral range of the camera enables the measurement of the metal oxides sensitive spectra as shown in Figure 1.

Several experiments were conducted using the camera to view real cracks in paved roads and 3 sample

results are shown in Figure 4. The location of cracks are known in these experiments and both 'normal surface' and 'crack' pixels were randomly selected from identified areas. The images are shown on the left-hand side of Figure 4 and two square windows marked in the image, one for normal road surface and another for a crack region. The right-hand side curve shows the spectral response of both normal surface and crack reflection. The area used to capture the spectrum is fixed during this experiment to one pixel size.

It can be observed in Figure 4, that the crack reflection is less than the reflection from normal surface. It can also be observed that the slope of the spectrum in 450nm-550nm range is radically different from normal to crack surfaces. The angle - was computed using Equation 4, and shown in Figure 5 for regions of both cracks and normal surfaces for comparison.

It can be observed that the slope angle is lower for the crack regions than the surface regions of the pavements in most of the cases. The histograms of this angle computed for cracks and normal surfaces have very little overlap as shown in the right-hand side of Figure 5. However, for any given sample, the angle of slope of crack is always lower than that of road surface. This implies that a single threshold can be used to discriminate cracks from normal surfaces.

The VIS2 ratio was computed for the same sample set and is shown in Figure 6 as a ratio (Equation 2). The VIS2 difference (Equation 1) is also computed and shown in Figure 7. It is observed that the histograms are almost 80 % overlapping in Figures 6 and 7 compared to less than 20 % overlap in Figure 5.

5 Conclusions

Hyperspectral imaging is exploited in this paper to discover the defects and anomalies in road pavement. HSC has the potential to be useful for revealing the defects in infrastructure by observing the changes in spectral reflectance caused by different materials. A new metric was used in this study as an indicator for the change of material and was shown to be a good indicator representing the change of metal oxides in the spectral region 450nm-550nm. The angle of slope of the spectral line in this region, is shown to be better than the VIS2 metric. The angle of the slope utilizes more information from the spectral response than the previous VIS2 indicator. Exploiting more spectral information is good to improve the clues used to find material changes and hence associate this with cracks and potholes and even normal wear of the road surface. This finding may allow

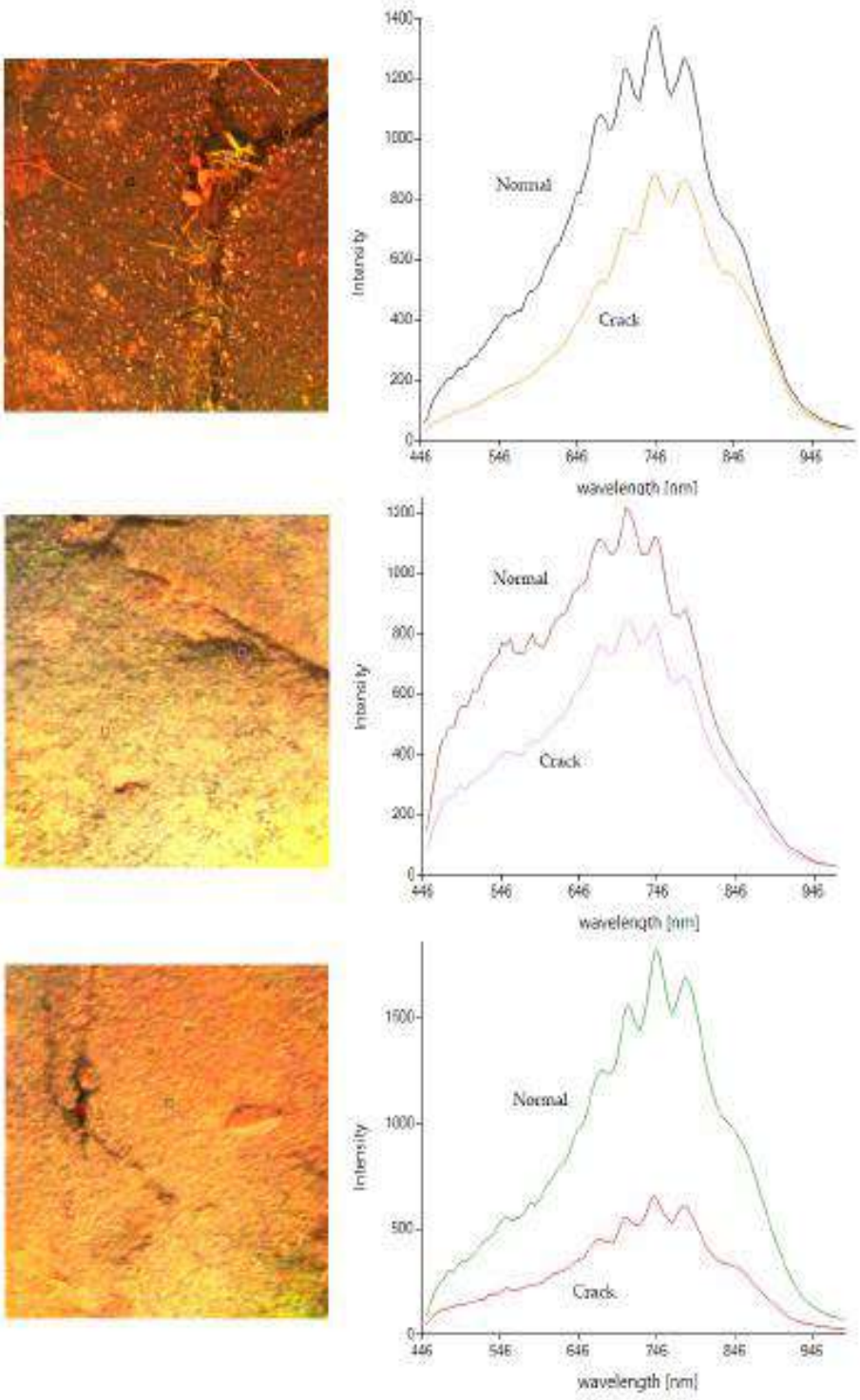

Figure 4: Sample HSC images of pavements (left) and their spectral characteristics (right) inside the regions marked by coloured squares in the HSC images.

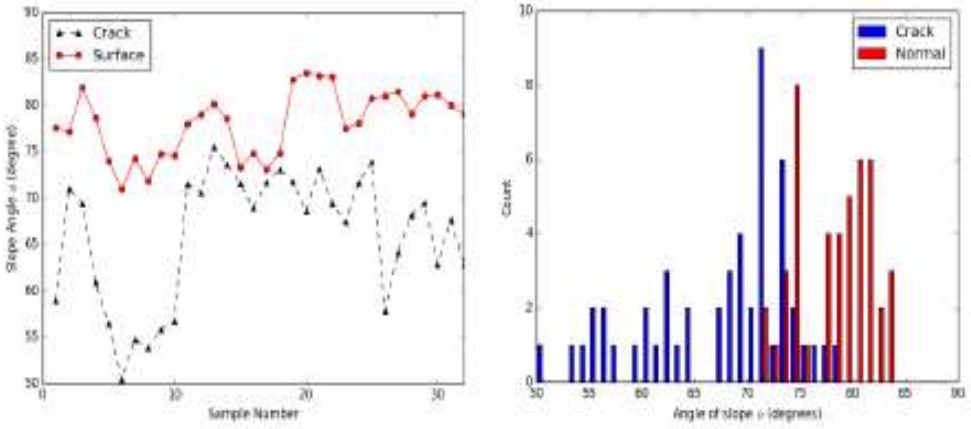

Figure 5: Proposed slope angle ϕ (Left) computed for Sample Pavement for crack and surface regions, and the histogram (Right)

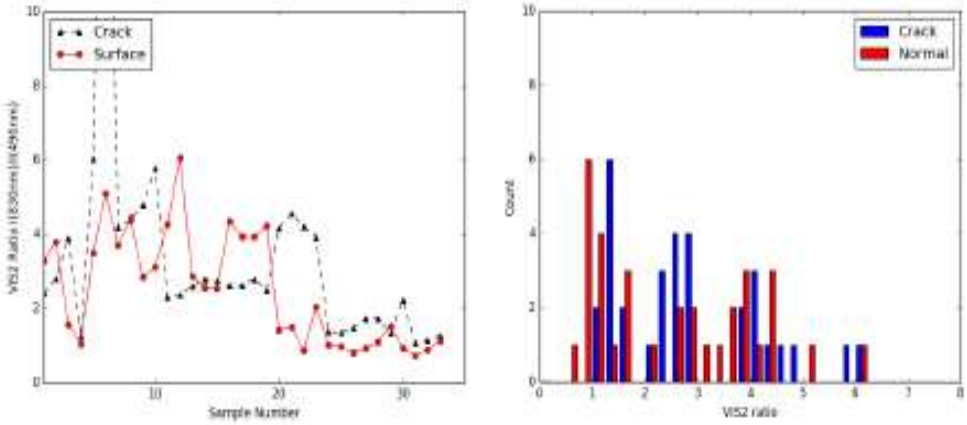

Figure 6: VIS2 Ratio (Left) computed for Sample Pavement for crack and surface regions and the histogram (Right)

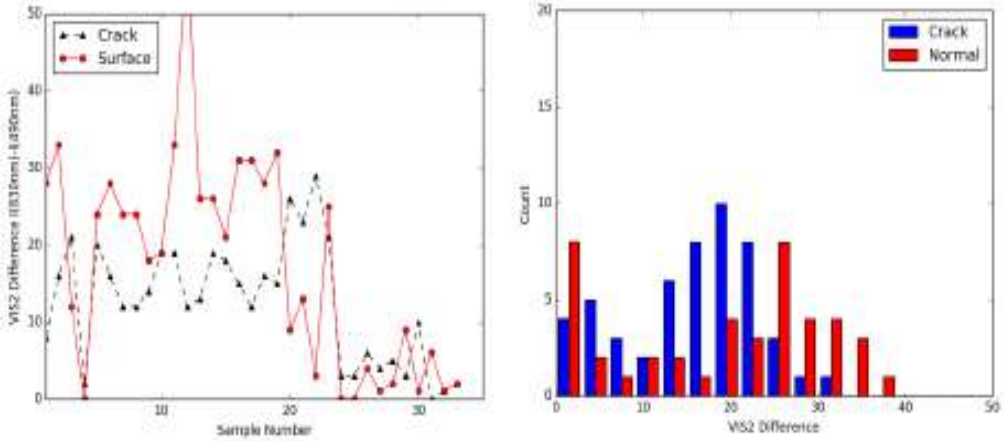

Figure 7: VIS2 Difference (Left) computed for Sample Pavement for crack and surface regions and the histogram (Right)

Aknowledgement

The authors gratefully acknowledge the financial support of the EPSRC under grant EP/N010523/1.

References

[1] M. Gavilan, D. Balcones, O. Marcos, D.F. Llorca, M.A. Sotelo, I. Parra, M. Ocana, P. Aliseda, P. Yarza, and A. Amirola. Adaptive road crack detection system by pavement classification. Sensors, 11(10):9628–9657, 2011.

[2] E. Aldea and S. Le Hegarat-Mascle. Robust crack detection for unmanned aerial vehicles inspection in an a-contrario decision framework. Journal of Electronic Imaging, 24, 2015.

[3] Y. Pan, X. Zhang, M. Sun, and Q. Zhao. Object-based and supervised detection of potholes and cracks from the pavement images acquired byUAV. International Archives of the Photogrammetry, Remote Sensing and Spatial Information Sciences - ISPRS Archives, 42(4W4):209–217, 2017.

[4] N. Carmon and E. Ben-Dor. Mapping asphaltic roads' skid resistance using imaging spectroscopy. Remote Sensing, 2018.

[5] M. Herold and Dar A. Roberts. Mapping asphalt road conditions with hyperspectral remote sensing. 01 2005.

[6] V. Noronha, M. Herold, D. Roberts, and M. Gardner. Spectrometry and hyperspectral remote sensing for road centerline extraction and evaluation of pavement condition. 2002.

[7] J. Liang. Spectral-spatial Feature Extraction for Hyperspectral Image Classification. PhD thesis, College of Engineering and Computer Science, The Australian National University, 2016.

[8] M. Mohammadi. Road Classification and Condition Determination Using Hyperspectral Imagery. ISPRS - International Archives of the Photogrammetry, Remote Sensing and Spatial Information Sciences, pages 141–146, July 2012.

[9] C.M. Jengo, J.D. Laveigne, and I. Curtis. Pothole Detection and Road Condition Assessment Using Hyperspectral Imagery. In ASPRS 2005 Annual Conference Baltimore, Marryland, USA, 2005.

[10] M. Herold, Roberts Dar A., O. Smadi, and Val Noronha. Road condition mapping with hyperspectral remote sensing. 2004.

[11] M. Herold, D. Roberts, V. Noronha, and O. Smadi. Imaging spectrometry and asphalt road surveys. Transportation Research Part C: Emerging Technologies, 16(2):153 – 166, 2008.

[12] T. Adao, J. Hruska, L. Padua, J. Bessa, E. Peres, R. Morais, and J.J. Sousa. Hyperspectral imaging: A review on uav-based sensors, data processing and applications for agriculture and forestry. Remote Sensing, 9(11):1110, 2017.

[13] A. Polak, T. Kelman, P. Murray, S. Marshall, D. Stothard, J.M. David, N. Eastaugh, and F. Eastaugh. Hyperspectral imaging combined with data classification techniques as an aid for artwork authentication. Cultural Heritage, 26:1 – 11, 2017.

[14] H. Deborah, N. Richard, and J.Y. Hardeberg. Hyperspectral crack detection in paintings. In 2015 Colour and Visual Computing Symposium (CVCS), pages 1–6, Aug 2015.

[15] C. Tsouvaltsidis, N. Zaid Al Salem, G. Benari, D. Vrekalic, and B. Quine. Remote Spectral Imaging Using A Low Cost UAV System. ISPRS - International Archives of the Photogrammetry, Remote Sensing and Spatial Information Sciences, 2015.

[16] H.A. Khan, J.B. Thomas, J.Y. Hardeberg, and O. Laligant. Illuminant estimation in multispectral imaging. Optical Society of America A, 2017.

[17] F. Li, M.K. NG, R.J. Plemmons, S. Prasad, and Q. Zhang. Hyperspectral image segmentation, deblurring, and spectral analysis for material identification. In Visual Information Processing, 2010.

[18] M. J. Khan, H. S. Khan, A. Yousaf, K. Khurshid, and A. Abbas. Modern trends in hyperspectral image analysis: A review. IEEE Access, 6:14118–14129, 2018.

[19] M. Simoes, J. Bioucas Dias, L. B. Almeida, and J. Chanussot. Aconvex formulation for hyperspectral image superresolution via subspace-based regularization. IEEE Transactions on Geoscience and Remote Sensing, 53(6):3373–3388, June 2015.

[20] C. Lanaras, E. Baltsavias, and K. Schindler. Hyperspectral super-resolution with spectral unmixing constraints. Remote Sensing, 9(11):1196, 2017.

[21] C. Mettas, K. Themistocleous, K. Neocleous, A. Christofe, K. Pilakoutas, and D. Hadjimitsis. Monitoring asphalt pavement damages using remote sensing techniques. In Third International Conference on Remote Sensing and Geoinformation of the Environment, volume 9535, 2015.

[22] K. Wang and B. Yong. Application of the frequency spectrum to spectral similarity measures. Remote Sensing, 8(4), 2016.

[23] P. Khuwuthyakorn, A. Robles-Kelly, and J. Zhou. Affine Invariant Hyperspectral Image Descriptors Based upon Harmonic Analysis, pages 179–199. Springer Berlin Heidelberg, 2011.

[24] Q. Gao, S. Lim, and X. Jia. Hyperspectral image classification using convolutional neural networks and multiple feature learning. Remote Sensing, 10(2), 2018.

[25] P. Liu, H. Zhang, and K.B. Eom. Active deep

learning for classification of hyperspectral images. IEEE Journal of Selected Topics in Applied Earth Observations and Remote Sensing, 10(2):712–724, Feb 2017.

[26] W. Zhao and S. Du. Spectral spatial feature extraction for hyperspectral image classification: A dimension reduction and deep learning approach. IEEE Transactions on Geoscience and Remote Sensing, 54(8):4544–4554, Aug 2016.

[27] X. Jia, B.C. Kuo, and M.M. Crawford. Feature mining for hyperspectral image classification. Proceedings of the IEEE, 101(3):676–697, March 2013.

[28] M. Herold and Dar A. Roberts. Spectral characteristics of asphalt road aging and deterioration: implications for remote-sensing applications. Applied Optics, 44(20):4327–4334, 2005.

Inference of Relevant BIM Objects Using CNN for Visual-input Based Auto-Modeling

J. Kim[a], J. Song[a], and J. Lee[a]

[a] Department of Interior Architecture and Built Environment, Yonsei University, South Korea
E-mail: wlstjd1320@gmail.com, songjy92@gmail.com, leejinkook@yonsei.ac.kr

Abstract –

This paper aims to propose an approach to inferring relevant BIM objects using techniques for recognition of design attributes and calculation of visual similarity using a deep convolutional neural network. Main objective is a visual-input based modelling approach to the automated building and interior design, and this paper represents a preliminary yet critical part of the process. While designing a building, it is important to consider requirements such strong constraints (e.g. regulations, a request for proposal) as well as relatively weak and qualitative constraints such as preference style of clients or users, design trend and etc. Building Information Modeling (BIM) enables to execute to check and review a building design according to the constraints. Until now there is no research that has focused on relatively qualitative and "soft" constraints such as preference or design trend. As a part of research on design supporting system for such "soft" constraints, this paper focuses on training deep learning models that recognize design attributes of BIM object, calculate visual similarity with other objects, and for visual-input based auto-modeling on BIM using the models. A deep convolutional neural network is utilized to extract a visual feature of the 3D object. The input data type for extracting feature data is a 2D rendering image of an object with a specific view and option. The target object is a chair. The feature data is used as input to training models inferring design attributes such as design style, seating capacity and sub-type of a chair and also calculating the visual similarity between objects. This models plays an important role of visual-input based automated modelling system.

Keywords –

Automated Modeling, Building Information Modeling (BIM); Design Attributes; Visual data; Visual similarity;

1 Introduction

In general, design problems have been known as "wicked problem [1]" that means ill-defined problem including complex and various requirement [2]. In particular, while designing a building, requirements include strong constraints such building permit regulations, a request for proposal (RFP) as well as relatively weak and qualitative constraints such as preference style of clients or users, design trend and etc.

Building Information Modeling (BIM) enables a computer to understand a building design model and execute to check and review and simulate the digital model with consideration of the above constraints [3]. Until now the researches have focused on relatively quantitative constraints (e.g. energy simulation [4], quantity take-off [5] and etc.), or strong constraints (e.g. rule-checking [6], in particular, indoor circulation [7] and space program [8]). It is true that consideration of such constraints is important as increasing the size of buildings [9] and changing standards of building performance.

In a high level of detailed design phase such as interiors, however, the relatively qualitative and "soft" constraints such as preference or design trend need to be considered as well. Nevertheless, research focusing on "soft" constraints using BIM has not been studied so far. As a part of research on design supporting system for such "soft" constraints, the ultimate goal of this study is to propose a BIM-based design approach using a deep learning model that can understand the design. The approach targets the visual representation of building design references, among other media representing such constraints. Traditionally, visual representation has been the role of important sources to analysis and understand architectural design [10].

As a preliminary study for the implementation of this approach, this paper explores the ways to combine deep learning-based model understanding design reference image or picture with BIM-based design. The scope of this paper is on training deep learning models that recognize design attributes of BIM object, calculate

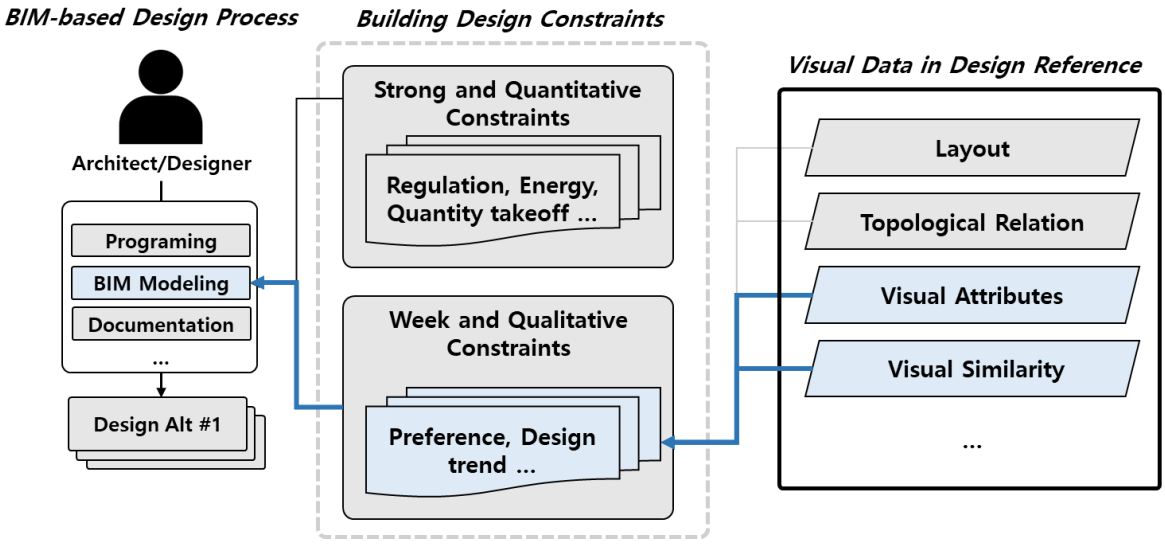

Figure 1. The scope of this paper for visual-input based modelling approach

visual similarity with other objects, and propose an approach to visual-input based auto-modeling on BIM using the models (Figure 1).

For training such intelligent models, this paper utilizes a deep convolutional neural network (CNN) model that showed the successful performance of understanding general object [11], context [12]and even design attributes of interior design object [13] on visual data. The pre-trained CNN model (VGGnet [14]) is used to extract visual feature map data from 2D rendering image of a design object. The feature map data is used as input data to train models recognizing design attributes of chair object (e.g. design style, seating capacity and sub-type). The results of recognition are used to query BIM object in BIM library as a semantic annotation. The feature map data is also used to calculate the visual similarity between objects for the similarity-based query.

2 Background

2.1 Reusing Design Objects in BIM-based Design Process

While solving design problems such as architectural, interior design and etc, the strategy based on generating possible design alternatives is generally adopted [15]. Since it is difficult to make a clear and explicit definition of the problem (“wicked problem”) [16] architects and designers compare, analyze and test the alternatives to reach a satisfactory answer.

Building information modeling (BIM) provides the advantages of rapidly generating design alternatives, evaluating and analyzing them. BIM supports the model-oriented design process, enabling integrated and automatic design tasks about as drawing, simulation, various review processes, and visualization with BIM model and related applications. BIM is derived from the idea that a building is considered as a spatial composition of the spatial composition of a set of parts [17]. In other words, determining which design elements will be utilized and how to combine them is an important process for BIM-based architectural design.

The Search accuracy of traditional keyword-based retrieval models, such as Boolean model, vector space model, or probabilistic model, has been often problematic because of the semantic ambiguity of terminologies in BIM documents and queries. The semantic ambiguity in BIM documents can be alleviated by using a domain ontology. As compared to the traditional metadata retrieval of BIM models, Ge Gao et. al. [18] present a way to search into the content of BIM models, which contains more information. It provides a way to customize their requirement specifically. Both accurate numerical value search and text search is supported A survey of the state of the art is beyond the scope of this paper. Instead, this section briefly reviews the most related studies associated with our work.

2.2 Deep Convolutional Neural Network for Extracting Visual Feature

Deep convolutional neural networks (CNN) is known as the most powerful method to extract a visual feature from pixel data of image [11]. For the feature extraction, stacked convolution filters and pooling filters are used

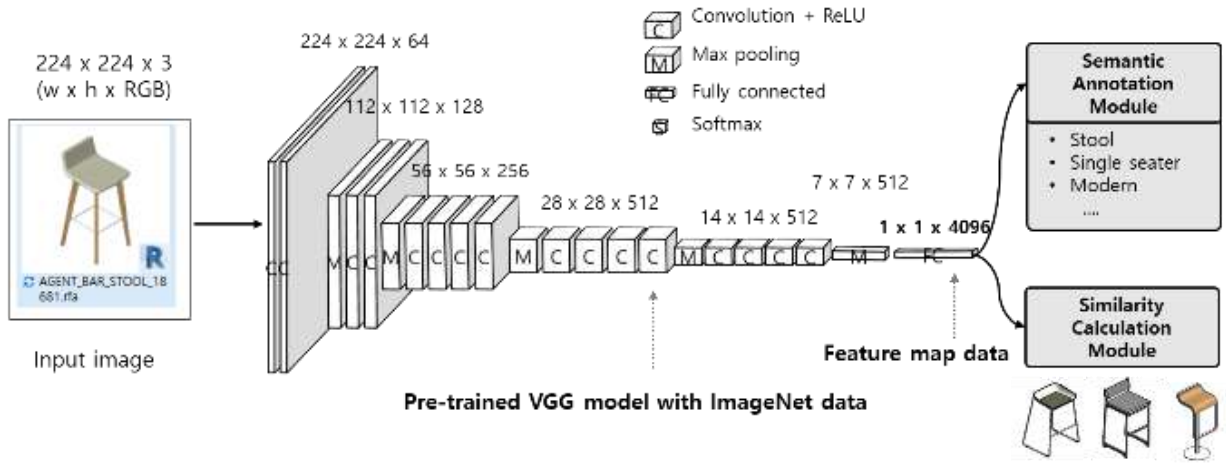

Figure 2. Extraction and utilization of feature map data to get semantic annotation and calculate similarity using VGG model [14]

(Figure 2.). These filters have a specific (n x n) size and are used to screen key pixel data as you scroll through the image to extract a simpler abstracted 'feature map'. The input images are converted to multi-dimensional vector values representing complex elements, such as points, lines, faces, shapes, color, and sizes. These feature map data can be used to train multi-class inference models with softmax algorithm [19] or support vector machine [20] and to find a visual similar one with the Euclidean distance or cosine angle distance [21]. A good model can extract meaningful visual feature. Such good models (e.g. VGG pre-trained with ImageNet [14]) and frameworks (e.g. Tensorflow [22]) are open to the public. The pre-trained model can be directly used to extract features of other images. In this paper, we utilize the pre-trained VGG model to extract visual feature data of BIM object.

3 Methodology

3.1 Approach

This paper proposes an approach to recommend a relevant collection of design objects using visual information from BIM objects. A collection of design objects means a set of objects that a user needs in the context of a particular design process. Metadata, geometry data, and topological relational data can be used when sorting a set of objects in the BIM library, but in this study, semantic annotation information and visual similarity information are only treated. The information of annotation is semantic string information that can be obtained from the shape. For example, when an image of a chair is given, string information such as category, sub-type, functional feature (e.g. armrests, backrest, wheel and etc.), the seating capacity, and even design styles can be inferred. The visual similarity means a degree of visual similarity between the shape of a target object and a shape of the others.

In this paper, the feature map data derived from 2D rendering image of BIM object is used to get semantic annotation and visual similarity information. To get 2D rendering images of BIM object, we develop the image generating module using rendering engine and API of BIM Tool. These images are input into the deep convolutional neural networks model [11] and the feature map data is generated. We utilize VGGnet [14] model that previously trained the ImageNet dataset as feature map extractor. It has been proven that the pre-trained model very well extracts important feature map of the image, and showed the high accuracy (93.2%) of image classification task with at ILSVRC challenge [14].

The feature map data are used as an input in two modules: 1) Semantic annotation module, 2) Similarity between objects calculation module. 2D images of objects are collected through the API of the BIM tool. The inference of semantic annotation information is executed using the softmax algorithm with, and the calculation of visual similarity is done using the Cosine angle distance. Through these two modules, the collection of related and visually similar objects can be recommended.

3.2 Extraction of Visual Feature from Object using CNN

In this study, the feature map data extracted from the 2D image is utilized as visual feature data of the 3D object. CNN model can extract the feature map data that means the abstraction of pixel data that is considered important in the image among the 3 channel (RGB color)

pixel data of the input2D image. We extract the featured 4096-dimensional vector value, using the VGG model pre-trained with ImageNet dataset. Images of 3D objects for input into the model are generated by the rendering engine of the BIM software. We collect the BIM object from public BIM object library such as BIMObject [23], Revitcity [24] and NBS National BIM Library [25]. We developed plug-ins using API to automatically generate such images from consistent and accurate view angles with specific rendering option. In this paper, two different views are used: 1) front view and 2) view of horizontal 45 degrees with vertical 60 degrees. There are no shadows but only shading and realistic color with line stroke. The results of extracted feature maps can be saved as an ASCII file, so the feature map data is stored in an external database or in property field of the BIM object. The feature is used for inferring the semantic information of the object and calculating visual similarity. Sections 3.3 and 3.4 describe methodology and calculatation results using feature map data, respectively.

3.3 Inferring Semantics Information of Object

We train the model inferring semantics information of BIM object using the softmax algorithm [26]. The softmax algorithm is the most popular function for inferring labeling of data. Softmax function takes an N-dimensional vector of real numbers and transforms it into a vector of a real number in the range (0,1). The outputs are marginal probabilities and therefore can be used for multiple-class classification.

The target object is a chair and the scope of semantic information includes a sub-type, seating capacity, a design style. There are other many design related attributes, but we adopt some attributes proposed by Kim et al [13]. The sub-type means conceptual and qualitative classification criteria according to function or shape. This paper covers a normal chair, stool, sofa and office chair. Seating capacity means how many seaters a chair has and this is seen as a quantitative property. The design style is a very qualitative feature that can be perceived differently according to culture, period, region and people. Therefore, this paper cover causal, classic and modern that can be seen as the simple and rough classification criteria of design style.

We use BIM seating object images that are generated from the BIM tool as well as real chair product images that are collected from the catalog. Finally, 250 images per class were collected, 20% of which are utilized for validating and 80% for training. Training model for the design style was conducted with only three detailed classes, so 750 images were utilized. While the others have four detailed classes, so 1000 images were utilized. Training is executed on the Tensorflow framework [22] that is the most useful to train machine learning model. Table 1 shows the results training of models. The accuracy of models training design style and sub-type is closed to 85%. On the other hand, the accuracy of model training seating capacity is relatively lower than others (closed to 75%).

Table 1. The results of training models to recognize design attributes of a chair object

Model	Class	Images	Training Accuracy
Seating capacity	Single 2-seaters 3-seaters 4-seaters	1000	75.2%
Design style	Casual Classic Modern	750	86.2%
Sub-type	Chair Sofa Stool Office chair	1000	85.1%

3.4 Calculating visual feature similarity with Cosine Angle Distance

The similarity is calculated through the cosine distance with vector feature maps. The cosine distance is the cosine value of the angle between two vectors, which the value is bound on the interval (-1~1). The correlation of distribution between random vectors may tend to get closer to zero as the dimensions of space increases. Therefore, the even small value of similarity become significant with growing dimension. Given two vectors of visual feature map, VF_a and VF_b on the n-dimensional space, and cosine similarity, $\cos(\theta)$, is represented as;

$$\cos(\theta) = \frac{\sum_{i=1}^{n} VF_{a,i} \times VF_{b,i}}{\sqrt{\sum_{i=1}^{n} VF_{a,i}{}^2} \times \sqrt{\sum_{i=1}^{n} VF_{b,i}{}^2}} \quad (1)$$

The resulting similarity ranges from −1 meaning exactly opposite, to 1 meaning exactly the same or a very similar one and with 0 indicating orthogonality (decorrelation). The feature map data is the positive number, so practical similarity value ranges from 0 to 1. Table 2 shows the examples of calculation of similarity between chair objects and the inferred semantic annotations. The target object is a famous stool and the

Table 2. The examples of inferring semantic annotation and calculating similarities between target and inputs objects using feature map data and cosine distance

	Target	Input #1	Input #2	Input #3	Input #4	Input #5
Image						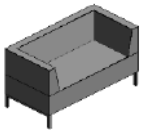
Similarity	-	88.9%	81.0%	66.6%	58.1%	51.6%
Seating capacity	Single	Single	Single	Single	Single	2-seaters
Sub-type	Stool	Stool	Stool	Chair	Stool	Sofa
Design style	Modern	Modern	Casual	Casual	Casual	Modern

input #1 is the same one, but slightly different sizes and width. The similarity between the above two is calculated as 88.9%. The input #2 is another stool with different color and detailed design (punched hole). The similarity between target and input #2 is calculated as 81.0% lower than the previous value. Input #3, 5 is not stool, but normal chair and sofa, respectively, and the similarity values are lower than 70%. The input #4 is a round stool, but the similarity value is relatively lower that the values of other stool.

4 Conclusion

As a preliminary study for the implementation of this approach, this paper explores the ways to combine deep learning-based model understanding design reference image or picture with BIM-based design. The scope of this paper is on training deep learning models that recognize design attributes of BIM object, calculate visual similarity with other objects, and propose an approach to visual-input based auto-modeling on BIM using the models. For training such intelligent models, this paper utilizes a deep convolutional neural network (CNN) model that showed the successful performance of understanding general object [11], context [12]and even design attributes of interior design object [13] on visual data. The pre-trained CNN model (VGGnet [14]) is used to extract visual feature map data from 2D rendering image of a design object. The feature map data is used as input data to train models recognizing design attributes of chair object (e.g. design style, seating capacity and sub-type). The results of recognition are used to query BIM object in BIM library as a semantic annotation. The feature map data is also used to calculate the visual similarity between objects for similarity-based query. This models plays an important role of visual-input based automated modelling system.

Acknowledgement

This work was supported by the National Research Foundation of Korea(NRF) grant funded by the Korea government(MSIT) (No. 2019R1A2C1007920).

References

[1] Rittel H.W. and Webber M.M., Wicked problems, *Man-made Futures*, 26(1):272-280, 1974

[2] Simon H.A., The structure of ill structured problems, *Artificial intelligence*, 4(3-4):181-201, 1973

[3] Eastman C., et al., *Book BIM handbook: A guide to building information modeling for owners, managers, designers, engineers and contractors*, John Wiley & Sons, 2011

[4] Schlueter A. and Thesseling F., Building information model based energy/exergy performance assessment in early design stages, *Automation in construction*, 18(2):153-163, 2009

[5] Monteiro A. and Martins J.P., A survey on modeling guidelines for quantity takeoff-oriented BIM-based design, *Automation in Construction*, 35(238-253, 2013

[6] Eastman C., et al., Automatic rule-based checking of building designs, *Automation in construction*, 18(8):1011-1033, 2009

[7] Lee J.-k., et al., Computing walking distances within buildings using the universal circulation network, *Environment and Planning B: Planning*

and Design, 37(4):628-645, 2010
[8] Lee J.-K., et al., Development of space database for automated building design review systems, *Automation in Construction*, 24(203-212, 2012
[9] Choi J., et al., Development of BIM-based evacuation regulation checking system for high-rise and complex buildings, *Automation in Construction*, 46(38-49, 2014
[10] Koutamanis A. and Mitossi V., Computer vision in architectural design, *Design Studies*, 14(1):40-57, 1993
[11] LeCun Y., et al., Deep learning, *nature*, 521(7553):436, 2015
[12] Karpathy A. and Fei-Fei L., Deep visual-semantic alignments for generating image descriptions, *Proceedings of the IEEE conference on computer vision and pattern recognition*, pages 3128-3137, 2015
[13] Kim J.s., et al., Approach to the Extraction of Design Features of Interior Design Elements using Image Recognition Technique, *Proceedings of the 23rd International Conference of the Association for Computer-Aided Architectural Design Research in Asia (CAADRIA) 2018*, pages 287-296, Beijing, China, 2018
[14] Simonyan K. and Zisserman A., Very deep convolutional networks for large-scale image recognition, *arXiv preprint arXiv:1409.1556*, 2014
[15] Cross N., *Book Designerly ways of knowing*, Springer, 2006
[16] Buchanan R., Wicked problems in design thinking, *Design issues*, 8(2):5-21, 1992
[17] Eastman C., An Outline of the Building Description System. Research Report No. 50, Institute of Physical Planning, Carnegie Mellon Univ., Pittsburgh, 1974
[18] Gao G., et al., A query expansion method for retrieving online BIM resources based on Industry Foundation Classes, *Automation in construction*, 56(14-25, 2015
[19] Szegedy C., et al., Rethinking the inception architecture for computer vision, *Proceedings of the IEEE conference on computer vision and pattern recognition*, pages 2818-2826, 2016
[20] Niu X.-X. and Suen C.Y., A novel hybrid CNN–SVM classifier for recognizing handwritten digits, *Pattern Recognition*, 45(4):1318-1325, 2012
[21] Qian G., et al., Similarity between Euclidean and cosine angle distance for nearest neighbor queries, *Proceedings of the 2004 ACM symposium on Applied computing*, pages 1232-1237, 2004
[22] Abadi M., et al., Tensorflow: Large-scale machine learning on heterogeneous distributed systems, *arXiv preprint arXiv:1603.04467*, 2016
[23] BIMObject: BIM Libarary. Online: https://www.bimobject.com/, Ascessed: 15/01/2019
[24] Revitcity:Public BIM library. Online: https://www.revitcity.com, Ascessed: 15/01/2019
[25] NBS National Bim Library. Online: https://www.nationalbimlibrary.com, Ascessed: 15/01/2019
[26] Dunne R.A. and Campbell N.A., On the pairing of the softmax activation and cross-entropy penalty functions and the derivation of the softmax activation function, *Proc. 8th Aust. Conf. on the Neural Networks, Melbourne*, pages 185, 1997

Predicting Safety Hazards Among Construction Workers and Equipment Using Computer Vision and Deep Learning Techniques

M. Wang[a], P. Wong[a], H. Luo[a], S. Kumar[b], V. Delhi[b], and J. Cheng[a]

[a]Department of Civil and Environmental Engineering, the Hong Kong University of Science and Technology, Hong Kong
b Department of Civil Engineering, Indian Institute of Technology Bombay, India
E-mail: mwangaz@connect.ust.hk, kywongaz@connect.ust.hk, han.luo@connect.ust.hk, sudip.k.m1997@gmail.com, venkatad@iitb.ac.in, cejcheng@ust.hk

Abstract –

The construction industry is one of the most hazardous industries suffering from a high on-site accident rate. A lot of safety hazards result from dynamic activities of construction workers and equipment. Therefore, tracking the location and motion of workers and equipment as well as identifying the interaction between them are crucial to preventing safety hazards on construction sites. Currently, with the extensive installation of surveillance cameras, computer vision techniques can be applied to process the videos and images captured on construction sites, which can be used to monitor site safety and to identify potential hazards. With the aim to predict and prevent the safety hazards among workers and equipment, this paper proposes a methodology to monitor and analyse the interaction between workers and equipment by detecting their locations and trajectories and identifying the danger zones using computer vision and deep learning techniques. First, workers and construction equipment are automatically located from cameras and classified by a deep region-based convolutional neural network (R-CNN) model. Then, the location and classification results are further processed by another CNN-based model to obtain trajectories of those objects. Based on the detection and trajectories, the spatial-temporal relationship between workers and equipment is analysed, from which the danger zones for the workers are identified and the corresponding safety alarms are generated. Experiments are conducted to demonstrate the capability of the proposed methodology for accurately identifying and predicting safety hazards among construction workers and equipment, which can contribute to the safety conditions on construction sites.

Keywords –

Computer vision; Construction site safety; Convolutional neural network (CNN); Deep learning; Object detection; Spatial-temporal relationship; Trajectory tracking.

1 Introduction

The construction industry is one of the most hazardous industries suffering from a high on-site accident rate. Between 2013 and 2017 in Hong Kong, the construction industry has reported the highest fatality rate among 11 industry sections in every year [1]. In particular, striking against or struck by moving objects has been ranked the top 3 highest number of industrial injuries out of 23 accident types [1]. These figures reflect that the construction industry has been significantly hazardous. Specifically, the dynamic characteristic of the construction site activities such as the movement of construction workers and equipment is one of the major causes for construction safety accidents, such as injury of workers due to the surrounding equipment. Therefore, monitoring the interaction among workers and equipment is essential to predict and prevent safety hazards on construction sites.

Currently, construction safety monitoring mainly relies on observing the real-time site conditions manually through on-site surveillance cameras. Early alerts of potential hazards are judged based on previous experiences and provided based on observations from the cameras. Such manual approaches are labor-intensive and error-prone considering the difficulty of monitoring through multiple cameras simultaneously. Human fatigue could lead to the ignorance of potential hazards, such as workers unconsciously approaching heavy equipment. Furthermore, the alerts based on personal experiences can be subjective or belated, leading to severe consequences. Therefore, a method capable of

automatically monitoring and predicting safety issues on construction sites is desired to reduce the resources and to improve the efficiency for safety monitoring.

Computer vision techniques are adopted to automatically process images or videos to assist with various human activities. In addition, deep learning techniques have been widely applied to facilitate computer vision tasks and achieved promising performance. The objective of this study is to automatically predict the safety hazards among construction workers and equipment through analyzing spatial-temporal interaction among workers and equipment using computer vision and deep learning techniques. In the rest of the paper, related works are reviewed in Section 2 and the proposed methodology is introduced in Section 3. Experiments and results are elaborated in Section 4, followed by conclusions and future work in Section 5.

2 Related Work

Previous studies for construction safety monitoring were reviewed. In particular, computer vision-based techniques for construction safety monitoring were categorized by [2] into three aspects.

The first category is object detection. Some researches detected workers and equipment by background subtraction algorithm [3], Histograms of Oriented Gradients (HOG) descriptor with Support Vector Machine (SVM) classifier [4], and Scale-Invariant Feature Transform (SIFT) [5]. The approach of SIFT in [5] segmented a wide range of objects on images covering workers, different kinds of equipment and materials. More recently, Fang et al. [6] used a region-based CNN framework named Faster R-CNN to detect workers standing on scaffolds. A deep CNN then classified whether workers are wearing safety belts. Those without safety belt appropriately harnessed were identified to prevent any fall from height. Adoption of deep learning was shown to achieve promising detection accuracy [6].

The second group of techniques is object tracking. Some studies adopted detection-based tracking method, where by definition newly detected objects either initialize new tracks or are mapped to existing tracks for identity maintenance over certain duration. The DeepSORT developed by [7] is a detection-based tracking model. Zhu et al. [8] used SIFT to extract visual features for detecting workers and equipment. Kalman Filter was then used to predict future movement with respect to past measurement. Another study by [9] detected workers and equipment based on HOG features, while their movement were tracked with Particle Filter. For construction site monitoring, deep learning has not been fully studied for target detection in many detection-based tracking approaches.

The third cluster is action recognition. For example, Ding et al. [10] combined CNN with Long-Short-Term-Memory (LSTM) to identify unsafe actions of workers, such as climbing ladders with hand-carry objects, backward-facing or reaching far. While safety hazards of workers were effectively identified, their method only captured single worker and multi-object analysis was not considered. On the other hand, Soltani et al. [11] used background subtraction to estimate posture of an excavator by individually detecting each of its three skeleton parts including dipper, boom and body. Although knowing the operating state of construction equipment would allow safety monitoring nearby, the influence of the equipment on the surrounding objects was not studied [11].

Overall, in terms of automated safety monitoring with computer vision techniques, previous studies focused on different parts accounting for the safety issues separately, such as identifying working status of construction equipment or tracking the movement of workers. There is a lack of an integrated analysis of the spatial-temporal interaction among workers and equipment considering the potential influences from different aspects. A robust mechanism that analyzes the spatial-temporal interaction among workers and equipment is desired for automated and real-time monitoring of on-site safety.

3 Methodology

In this study, an integrated approach is proposed for predicting safety hazards among construction workers and equipment using computer vision and deep learning techniques. The proposed approach involves three parts, as shown in Figure 1. First, images are extracted from videos, and construction workers and equipment in video frames are extracted by the detection model. Then, the detection results are imported into the second part. For construction equipment, the danger zone is identified

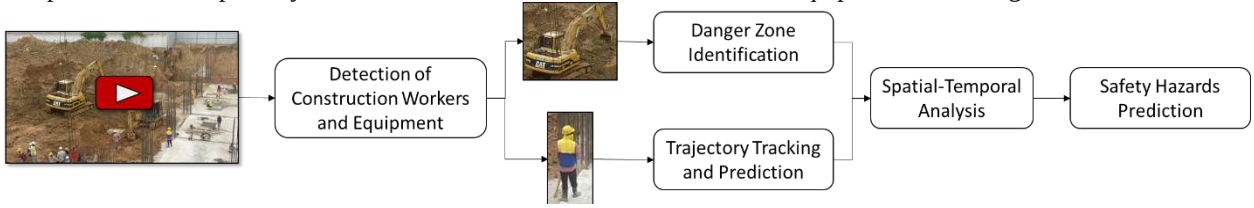

Figure 1. Overall workflow for predicting the safety hazards among construction workers and equipment

while for construction workers, the trajectory is tracked and predicted. By combining the identified danger zone and predicted trajectory, the spatial-temporal relationship among construction workers and equipment is analyzed. In the end, safety hazards are predicted based on the spatial-temporal relationship analysis.

3.1 Equipment and Worker Detection

The detection of equipment and workers are realized through Faster R-CNN, in view of its higher accuracy demonstrated by previous studies [12,13]. The architecture of Faster R-CNN includes (1) backbone network to extract image features; (2) region proposal generate (RPN) network for generating region of interest (ROI), and (3) classification network for producing class scores and bounding boxes for objects. Details of each part are introduced as follows.

3.1.1 Backbone Network

The backbone of the Faster R-CNN is used for feature extraction through a stack of convolution, activation, and max pooling layers. After pre-processing, each image is fed into the network as a three-dimensional array representing the pixel values on the RGB channels. In the beginning, a certain number of filters are assigned with random weights as initialization. During convolution, each filter slide across the input volume and the dot product between the filter and the corresponding image patch convolved is calculated and added with a bias value to obtain the convolution result. To add non-linearity to the network, the convolution result is fed into an activation function, for which rectified linear units (ReLU) is used in this study. After activation, max pooling is performed to reduce the dimension of feature maps by selecting the maximum value from each image patch covered by the filter and use the maximum value as the new feature value. Through setting the max pooling filter size and stride, the dimension of feature maps is down-sampled by a factor of 2 each time, such that the computational cost is reduced. A stack of convolution, ReLU and max pooling layers are performed to generate the feature maps, which are then fed into the RPN network for generating candidate ROIs (i.e. the potential regions with objects). As training the model from scratch is time-consuming and requires a large number of images, transfer learning is applied in this study as the low-level features of objects such as edges and corners are transferable among different datasets. Specifically, the weight of a model namely VGG16, which is pre-trained on another large dataset, is utilized to initialize the backbone network. The model is then fine-tuned with our dataset of construction equipment and workers such that high-level features (i.e. the characteristics of equipment and workers) are learned in the applied model.

3.1.2 RPN Network

The generated feature maps from the backbone network are passed through the RPN network which consists of a convolutional layer and a ReLU layer. The results are then fed into two parallel layers for label classification and bounding box regression. The class labels include foreground and background, indicating whether an object is contained in the region or not while the bounding box regression layer is used for refining the location of bounding boxes. In the beginning, a number of small windows, named anchors, with different sizes and aspect ratios are designed at each pixel location such that multi-scale features can be extracted. During the training, the class scores and the four coordinates of each bounding box are predicted for each anchor, after which the loss for both class scores and coordinates are computed. The number of anchors is reduced by non-maximum suppression (NMS) based on the foreground scores.

3.1.3 Classification Network

After obtaining the potential ROIs from the RPN, the regions on the feature maps corresponding to the ROIs are extracted through a crop pooling method. The extracted regions of the feature maps are reshaped and fed into the classification network, where two parallel layers are used for predicting the class labels with probability of each class and bounding boxes with more accurate locations. There are 7 classes included in this study including 5 types of equipment, the worker and the background. In the end, the loss of the predicted classes and the bounding boxes are computed based on the ground truth labels. The model weights are then updated by back-propagation during training process.

The layers of the three networks are combined together and the weights are trained in an end-to-end manner. After training the model on our dataset, the model is capable of detecting construction equipment and workers accurately during inference using the optimal trained weights.

3.2 Worker Trajectory Tracking

For trajectory tracking and prediction, the DeepSORT framework proposed by Wojke et al. [7] is used as our baseline because it demonstrated robustness of identity preservation upon arbitrary duration of occlusion. As a detection-based tracking framework, the worker detection results at a frame either initialize new tracks or are mapped to the most similar identities being tracked. Kalman Filter is used to predict future position of the target for position proximity matching. Apart from position constraint, identity assignment of the set of new detection also considers appearance similarity against the targets being tracked. Readers are referred to the original

publication for more detailed mathematical formulation of DeepSORT.

There are several parameters in DeepSORT that define its track management mechanism. Two of them are highlighted since their values are adapted to our site analytics. 'Lambda' controls the relative influence of position and appearance constraints in identity matching. For our analysis, Lambda is set as 0.5 for a complementary effect among these two factors. On one hand, construction sites tend to be crowded such that many workers may walk very close to others. Position proximity alone may make identity matching inaccurate when there are many candidates near a target. On the other hand, construction workers tend to have very similar appearance when wearing reflective vest and safety helmet, such that appearance may not explicitly distinguish multiple worker. Therefore, a balanced reliance among these two aspects is granted.

Another parameter 'Max_age' is set to be 200 frames in our study. This means that unique identity of a disappeared worker is remembered for 200 consecutive frames, during which it can be retrieved upon reappearance of the target. A long memory increases the computational burden for handling many targets, while a short memory leads to discontinuous trajectory history and subsequently inaccurate prediction of future trajectory. A 200-frames memory is considered reasonable for obtaining trajectory history. Acquiring complete trajectory history would support the prediction of future trajectory.

3.3 Worker Trajectory Prediction

Trajectory prediction for workers is based on the inference output from Kalman Filter used in DeepSORT. The translation of the 'foot' position of a target is considered, since it represents the area on which he/she walks. Therefore, the bottom center coordinate of a box is obtained by relating the corner coordinates with the width and height of a box. Since Kalman Filter only infers target movement at next timestamp, a mechanism is proposed to predict movement in a longer future. In particular, the future position of the 'foot' of a target (x_2, y_2) is linearly extrapolated with respect to its current position (x_1, y_1) and velocity:

$$x_2 = x_1 + (\alpha_x * \dot{x}) \quad (1)$$

$$y_2 = y_1 + (\alpha_y * \dot{y}) \quad (2)$$

where $\dot{x}$ and $\dot{y}$ are velocities along individual direction output by Kalman Filter, α_x and α_y are number of future frames for position prediction.

With the current and future positions, $P = (x_1, y_1)$ and $P' = (x_2, y_2)$, respectively, the predicted trajectory of a target is defined to be the directed line segment PP' pointing from P to P'. On the image plane, this trajectory line is represented by a linear equation, while the coordinates of P and P' define its boundary. An assumption is that targets tend to produce smooth motion within the inference period, like standing still or walking constantly with current velocities $\dot{x}$ and $\dot{y}$.

3.4 Definition of Danger Zone

When a construction equipment (e.g. excavator) is in its working state, there is an activity region around the construction equipment. There is a high potential of safety hazards when workers or other construction machines enter this activity region. In this study, this kind of activity region is defined as a danger zone.

For an excavator, the exact danger zone could be defined as a located circle in a real construction site, which is an ellipses when projected to 2-D images, based on danger parameters including the position (pos) of the excavator, the lengths (l), working directions (d) and ranges (r) of arms, the size (s) of its body, and other factors (o). An exact danger zone (edz) is defined in Equation (3)

$$edz = f(pos, l, d, r, s, o) \quad (3)$$

On a construction site with a working schedule for on-site machines, most danger parameters of a construction machine are deterministic during a certain time interval, such as the lengths, working directions and ranges of arms, and the size of the construction equipment. On the other hand, the location of the excavator is obtained from the bounding box coordinates through the equipment and worker detection model, as introduced in Section 3.1. With those danger parameters, the size of the danger zone around an excavator could be determined.

3.5 Spatial-Temporal Analysis

Safety status of each worker is categorized into 3 types, based on the geometric relationship between the predicted trajectory and danger zone. As shown in Figure 2, 'Normal' is marked if the starting point of a trajectory (current position) is outside any danger zone while the predicted trajectory does not touch any danger zone (e.g. T1, T6). 'Danger Now' is marked as long as the start point lies within a danger zone (e.g. T2, T3). 'Potential Danger' is marked if the start point is outside any danger zone while the predicted trajectory intercepts a danger zone at least once (e.g. T4, T5, T7).

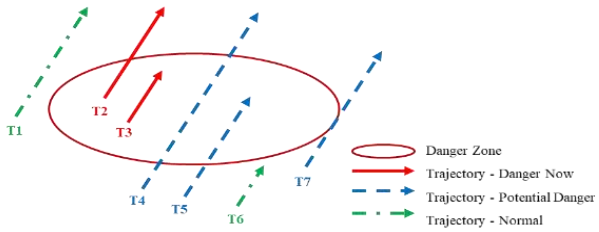

Figure 2. Examples of categorizing safety statuses based on predicted trajectory of a worker

The mathematical relationship between an ellipse and a straight line is derived to check for interception. Equation (4) and Equation (5) show the general forms of an ellipse and an infinite straight line on x-y plane respectively, while Figure 3 summarizes the notation of all related symbols.

$$\frac{(x-x_c)^2}{{r_x}^2}+\frac{(y-y_c)^2}{{r_y}^2}=1 \quad (4)$$

$$y=\frac{y_2-y_1}{x_2-x_1}*x+y_0 \quad (5)$$

$$\text{where, } y_0=y_1-\left(\frac{y_2-y_1}{x_2-x_1}\right)x_1 \quad (6)$$

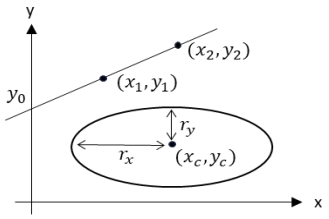

Figure 3. Notation for general representation of ellipse and straight line

A danger zone is centered at (x_c, y_c) with radiuses r_x and r_y. As for the predicted trajectory of a worker, an infinite straight line is defined by the current position as (x_1, y_1) and future position as (x_2, y_2). To find the intercept(s) between an ellipse and a straight line, Equation (4) and Equation (5) are solved simultaneously for x and y. After substitution, a quadratic equation is obtained, as shown in Equation (7).

$$Ax^2+Bx+C=0 \quad (7)$$

$$A=\frac{1}{{r_x}^2}+\frac{m^2}{{r_y}^2} \quad (8)$$

$$B=-\frac{2x_c}{{r_x}^2}+\frac{2m(y_0-y_c)}{{r_y}^2} \quad (9)$$

$$C=\frac{{x_c}^2}{{r_x}^2}+\frac{(c-y_c)^2}{{r_y}^2}-1 \quad (10)$$

$$m=\frac{y_2-y_1}{x_2-x_1} \quad (11)$$

The solution(s) to Equation (7), if any, correspond to the x-coordinate(s) at which the straight line intercepts the ellipse. The expression in Equation (12) is used to check whether interception exist. If $\Delta \geq 0$, the line either passes through the ellipse at two distinct points, or touches the ellipse at one point. In this case, Equation (13) provides the corresponding intercepted x-coordinate(s). If $\Delta < 0$, the line is always outside the ellipse.

$$\Delta=B^2-4AC \quad (12)$$

$$x^+=\frac{-B+\sqrt{\Delta}}{2A} \; and \; x^-=\frac{-B-\sqrt{\Delta}}{2A} \quad (13)$$

The key consideration when checking interception is that each trajectory is a definite segment spanning from the current to future position of the target. It is possible that the interception point(s) is/are outside the definite segment which is only a portion of its associated infinite line. Therefore, an additional condition is imposed to check whether the definite segment intercepts the ellipse. Table 1 illustrates the decision logic. In case of no interception at all, 'Normal' is assigned to a target (e.g. T1 in Figure 2). Otherwise, if the current position lies between the intercepted points, it lies within the danger zone and 'Danger Now' is assigned (e.g. T2, T3 in Figure 2). If the current position lies outside the zone while at least one of the intercepted point(s) is within the definite segment, the trajectory passes through the zone and 'Potential Danger' is assigned (e.g. T4, T5, T7 in Figure 2). Otherwise, the trajectory does not enter the zone at all and 'Normal' is assigned (e.g. T6 in Figure 2).

Table 1. Algorithm for assigning safety status based on worker trajectory and danger zone

If $\Delta < 0$:
Assign '*Normal*'
Else:
If $x_1 \in [x^-, x^+]$:
Assign '*Danger Now*'
Else if $x^- \in [x_1, x_2]$ or $x^+ \in [x_1, x_2]$:
Assign '*Potential Danger*'
Else:
Assign '*Normal*'

4 Experiments and Results

Experiments are performed to demonstrate the capability of the proposed methodology for automatically predicting safety hazards on construction sites through the analysis of spatial-temporal relationship between construction workers and equipment based on the captured images and videos from surveillance cameras. The spatial-temporal relationship is analysed based on two inputs: (1) the danger zone obtained from the detected location of the construction equipment and other

parameters, and (2) the predicted worker trajectory based on the historical trajectory records.

4.1 Experiment Dataset

Several videos captured from surveillance cameras on construction sites are collected and images are extracted from those videos. 2410 images containing 5 types of construction equipment (i.e. dump trucks, excavators, loaders, mixer trucks, and rollers) and construction workers are extracted and each image is annotated with ground truth labels and bounding boxes. 90% of the images are used for model training and validation while 10% are for model testing. In the end, the methodology is also applied on a new construction site video to demonstrate the real-time prediction of the hazards.

4.2 Experiment Implementation

The danger parameters of a construction equipment are assumed to be known in the experiment. Based on this assumption, the size of the danger zone around a construction equipment such as excavator is pre-defined. Then, the exact danger zones on a construction site are determined with the result of equipment detection, and the identified danger zones are used for spatial-temporal analysis.

Firstly, the architecture of the model for construction worker and equipment detection, as introduced in Section 3.1, is constructed using Pytorch, which is a common platform for implementing deep learning models. The model is trained using the annotated images for 40 epochs and the training loss is plotted to monitor the learning progress of the model. The model is evaluated using average precision (AP) for each class and the mean AP (mAP) for all the classes.

As for the worker trajectory prediction introduced in Section 3.3, α_x and α_y are both set to be 60 frames, such that for each target his/her position after 60 frames is inferred. This is a reasonable period because it predicts the target movement in the next 2 seconds, if considering a typical video with 30 frames per seconds. For safety monitoring on construction sites, 2-second movement prediction would allow identification of potential hazards.

4.3 Experiment Results and Analysis

The results include two parts – (1) the accuracy of equipment and worker detection; (2) the prediction results of safety hazard based on the analysis of spatial-temporal relationship among workers and equipment.

4.3.1 Accuracy of the detection model

The accuracy of the Faster R-CNN model on the testing dataset is summarized in Table 2. The model achieved high detection accuracy for both workers and construction equipment. The AP values of all the classes achieved at least 85% and even exceed 95% for most classes except for dump trucks, rollers and workers. With a mAP of 92.55%, the model is demonstrated to be promising for detecting workers and equipment accurately on the construction site.

Table 2. Accuracy of worker and equipment detection

Class Name	AP (%)	mAP (%)
Dump truck	85.12	
Excavator	95.94	
Loader	96.19	
Mixer truck	97.73	
Roller	86.91	
Worker	93.40	
		92.55

Nevertheless, as shown in Figure 4, the detection model tended to miss the excavator when its arm was not hanged horizontally, and those workers squatting or carrying objects. These cases could be attributed to our limited training dataset, which may not have covered a variety of view angles or human gesture. An enriched dataset would further enhance the detection accuracy.

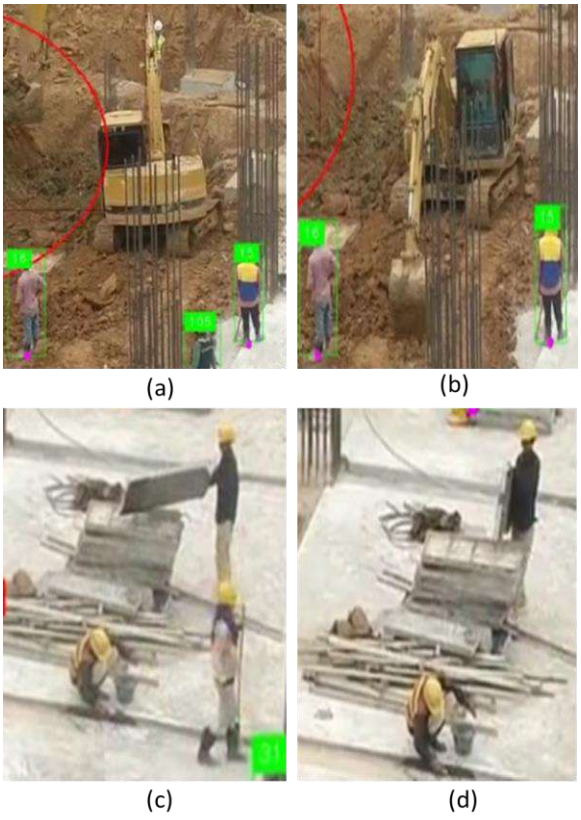

Figure 4. Examples of incorrect detection of equipment and workers

4.3.2 Accuracy of the spatial-temporal analysis

The detection model was applied on a construction site video to detect the equipment and workers. Trajectories of workers were also tracked and predicted. Danger zones were then defined to monitor safety statuses of workers based on spatial-temporal relationship among their trajectories and the danger zones. As shown in Figure 5, an ellipse around the excavator bounded a danger zone. In addition, historical trajectories of workers were displayed in purple, while their predicted trajectories after 60 frames were visualized as blue arrows. Safety statuses were then assigned to individual worker, based on the mathematical formulation in Section 3.5. Different safety statuses were categorized by colorized bounding boxes.

Figure 5. Examples of identified danger zones and different safety statuses of workers

The accuracy of assigning safety statuses is evaluated by Average Precision of Status (AP_{status}), as defined by Equation (14).

$$AP_{status} = \frac{TS}{TP} \tag{14}$$

where TS counts the number of workers assigned with true safety status, TP counts the number of detected workers as true positives from the detection model. In our experiment, assignment of safety statuses achieved an 87.45% AP_{status}. This suggests that our framework accurately revealed the safety status of individual worker against the danger zones. For example, in Figure 5, worker number 15 was alerted in red with 'danger now' since he lied within the danger zone, while worker number 16 was labelled in blue as 'potential danger' since he was about to enter the danger zone.

Nevertheless, dangerous conditions were sometimes not identified. As shown in Figure 6, red alerts were not issued even when workers 15 and 16 stood close to the excavator, possibly because the equipment was not detected and hence no danger zone was defined. Moreover, blue alert was not issued to the worker walking towards the operating area of excavator, possibly because he was occluded by other objects. These cases reflect that the accuracy of assigning safety status heavily relies on the performance of equipment and worker detection. The spatial-temporal analysis would be further supported with a more robust detection model and an enriched training dataset.

Figure 6. Examples of incorrect prediction of safety statuses

5 Conclusion and Future Work

Construction industry is reported to be the most hazardous with a high rate of accidents on construction site. There are various dynamic activities on construction sites such as the operation of various construction equipment and the movement of workers. The interaction between construction workers and equipment is one important reason resulting in on-site safety hazards. Therefore, to avoid potential safety hazards, it is necessary to monitor the working status of construction workers and equipment, and analyse the spatial-temporal interactions between them. Currently, on-site conditions are monitored and analysed manually from the surveillance cameras, which is labour-intensive and error-prone. Furthermore, the alerts for safety hazards may be subjective and belated, leading to severe consequences.

In this study, an integrated approach based on computer vision and deep learning techniques is proposed to predict safety hazards on construction site

through the spatial-temporal analysis of construction workers and equipment. Specifically, Faster R-CNN is first applied to detect construction workers and equipment from surveillance videos. Based on the detection results, danger zones of the construction equipment are identified while worker trajectories are tracked and predicted as well. Finally, the spatial-temporal interaction between the danger zone and the predicted worker trajectory is analysed, based on which the potential hazards are predicted and corresponding alerts are issued.

Experiments are performed with videos captured from surveillance cameras on construction sites to validate the capability of the proposed methodology. The detection model obtained high accuracy on detecting workers and equipment, with a mAP of 92.55% and AP values above 95% for most classes. As for the spatial-temporal analysis, the precision of assigning safety statuses to workers achieved 87.45%, based on which the safety hazard alerts are provided. The experiment results demonstrated that the proposed approach is capable of automatically predicting potential safety hazards through detecting construction workers and equipment, identifying danger zones, tracking and predicting worker trajectories, and analysing spatial-temporal interactions on construction sites. Even though there are still some negative examples in experiments, the overall experiment results demonstrate promising performance of the proposed integrated approach for predicting safety hazards among construction workers and equipment on construction sites. Future work will focus on exploring better methods to obtain danger zones around construction equipment and to improve the performance of the proposed approach.

References

[1] Occupational Safety and Health Statistics Bulletin, Hong Kong, 2018. https://www.labour.gov.hk/eng/osh/pdf/Bulletin2017.pdf (accessed February 4, 2019).

[2] J. Seo, S. Han, S. Lee, H. Kim, Computer vision techniques for construction safety and health monitoring, Adv. Eng. Informatics. 29 (2015) 239–251. doi:10.1016/j.aei.2015.02.001.

[3] S. Chi, C.H. Caldas, Automated Object Identification Using Optical Video Cameras on Construction Sites, Comput. Civ. Infrastruct. Eng. 26 (2011) 368–380. doi:10.1111/j.1467-8667.2010.00690.x.

[4] M. Memarzadeh, M. Golparvar-Fard, J.C. Niebles, Automated 2D detection of construction equipment and workers from site video streams using histograms of oriented gradients and colors, Autom. Constr. 32 (2013) 24–37. doi:10.1016/j.autcon.2012.12.002.

[5] H. Kim, K. Kim, H. Kim, Data-driven scene parsing method for recognizing construction site objects in the whole image, Autom. Constr. 71 (2016) 271–282. doi:10.1016/j.autcon.2016.08.018.

[6] W. Fang, L. Ding, H. Luo, P.E.D. Love, Falls from heights: A computer vision-based approach for safety harness detection, Autom. Constr. 91 (2018) 53–61. doi:10.1016/j.autcon.2018.02.018.

[7] N. Wojke, A. Bewley, D. Paulus, Simple online and realtime tracking with a deep association metric, in: Proc. - Int. Conf. Image Process. ICIP, 2018: pp. 3645–3649. doi:10.1109/ICIP.2017.8296962.

[8] Z. Zhu, M.W. Park, C. Koch, M. Soltani, A. Hammad, K. Davari, Predicting movements of onsite workers and mobile equipment for enhancing construction site safety, Autom. Constr. 68 (2016) 95–101. doi:10.1016/j.autcon.2016.04.009.

[9] Z. Zhu, X. Ren, Z. Chen, Integrated detection and tracking of workforce and equipment from construction jobsite videos, Autom. Constr. 81 (2017) 161–171. doi:10.1016/j.autcon.2017.05.005.

[10] L. Ding, W. Fang, H. Luo, P.E.D. Love, B. Zhong, X. Ouyang, A deep hybrid learning model to detect unsafe behavior: Integrating convolution neural networks and long short-term memory, Autom. Constr. 86 (2018) 118–124. doi:10.1016/j.autcon.2017.11.002.

[11] M.M. Soltani, Z. Zhu, A. Hammad, Skeleton estimation of excavator by detecting its parts, Autom. Constr. 82 (2017) 1–15. doi:10.1016/j.autcon.2017.06.023.

[12] S. Ren, K. He, R. Girshick, J. Sun, Faster R-CNN: Towards Real-Time Object Detection with Region Proposal Networks, IEEE Trans. Pattern Anal. Mach. Intell. 39 (2017) 1137–1149. doi:10.1109/TPAMI.2016.2577031.

[13] J.C.P. Cheng, M. Wang, Automated detection of sewer pipe defects in closed-circuit television images using deep learning techniques, Autom. Constr. 95 (2018) 155–171. doi:10.1016/j.autcon.2018.08.006.

The Design of Building Management Platform Based on Cloud Computing and Low-Cost Devices

L. Huang[a], Y. Chiu[a], and Y. Chan[a]

[a] Department of Civil Engineering, National Taiwan University, Taiwan

E-mail: r06521709@ntu.edu.tw, b04501041@ntu.edu.tw, ychan@ntu.edu.tw

Abstract -

Indoor environment monitor and control are important aspects of reducing building energy consumption and maintaining occupants' visual and thermal comforts. Previous research showed that the lots of buildings were not able to provide designed service level in the daily operation and the feedback from occupants showed that the predetermined service level sometimes did not match occupants' desire. However, most of existing buildings and residential buildings did not have building management systems that can systematically monitor the indoor environment, collect occupants' feedback, and fine-tune built-in control logic when the occupants' needs could not be met. An easy-to-build and easy-to-use build management system can help researchers, engineers, and occupants themselves to identify the issue.

The goal of this study was to develop a building management platform with the functions of indoor environment data collection (temperature, relative humidity, solar radiation, etc.), remote control (air conditioner, window, shading), occupants' feedback collection (set point, status of building components, etc.), and user interface for retrieving the data and modifying control logic. The platform was developed using Arduino-based and Raspberry Pi-based microcontroller board, low-cost sensors, 3D printing technology, and cloud computing technology. The stored data can serve for personal behavior/comfort analysis, components efficiency analysis, and advanced control logic development. This last part of this paper demonstrated the ability of the developed platform and exhibited the potential application. In the end, we provided further discussion about the potential challenges we might face when developing building management systems in other existing spaces/buildings.

Keywords –

Building Management Platform; Cloud Computing; Low-Cost Devices

1 Introduction

A considerable portion of energy consumptions in buildings are from satisfying occupant' needs and providing human-beings a better life. Researchers try to reduce the energy usages by setting up efficient automated control algorithms for building components such as lighting, shading, heating ventilation and air conditioning (HVAC) system using strategies. However, these newly developed control algorithms may sometimes cause displeased indoor environments since sometimes the algorithms were set too high or too low in an attempt to save more energy and occupants might have different thermal preferences. When occupants took the business on their own and took unexpected actions to control the indoor environment manually, it may result in interfering the designed energy-saving strategies and goals. For example, the HVAC system might experience a startup peak caused by occupants setting the set point too low during the cool down process from the initial state.

To overcome these issues, researchers are paying more and more attention to occupants' behavior and their reactions to automated control recently. One particular challenge of collecting occupants' feedback, is that most of the existing buildings do not have built-in building automation and management system. While the concept, some companies have been promoting intelligent building energy management systems for years[1], the market has not fully accepted these products because of its price and the installation labor works. For most of the prototypes in existence now, the installation and the system integration task are a laborious, ad-hoc process. Adding each new device/features into the building or zone requires a great deal of work. After getting the orders, the engineers must research that targeted buildings' characteristics, operation, protocols of existing devices in the buildings, determining how to integrate new components into the existing system, where to install, how to configure it and how to interface with it. On the other hand, the cost is usually one of the priorities for people when investing in a new system. An easy-to-build and easy-to-use building management system can help

researchers, engineers and occupants themselves identify the issue.

The goal of this research is to develop a building management platform in an existing space with the functions of indoor environment data collection (temperature, relative humidity, solar radiation, etc.), remote control (air conditioner, window, shading), occupants' feedback collection (set point, equipment status, etc.), and user interface for retrieving the data and deploying control logic interface.

2 Literature Review

Human's lifestyle is constantly changing along with the development of technology. In Teichroew [2]'s paper from 1971, they already started to talk about the importance of home automation. Murata [3] introduced a system that can control home computer, television, audio and video entertainment with verbal commands. Ryan [4] designed a system using cordless humidity sensors and temperature sensor to control the heater remotely by occupants. The smart building concept has become very more popular recently. Lots of researchers have started to investigate how to improve the energy efficiency of buildings and how to improve the indoor environment we live in.

To run a smart building systematically, a building management system (BMS) or a building energy management system (BEMS) is essential. Without a good building management system, it is hard for the building manager to find out the issues, for the devices to communicate with each other, and for occupants to provide feedback. Not to say, it would be very challenging for engineers to deploy newly developed control logic and to add new technology into an existing system. Building management system has been installed in more and more newly constructed buildings, especially after some researchers have pointed out that its potential for energy saving.

Rotger-Griful et al. [5] present a multi-modal building energy management system for capturing residential demand response. They set a testbed where they collected indoor environment data from sensors and power meters in order to analyze the occupant's demand response. According to the study, the energy saving potential of a building to be 7.4 MWh/year. Macarulla et al. [6] present the procedure of implementing a predictive control strategy in a commercial BEMS for boilers in buildings based on a neural network that turned on the boiler each day at the optimum time, according to the surrounding environment, to achieve thermal comfort levels at the beginning of the working day. The results showed that the implementation of predictive control in a BEMS for building boilers could reduce the energy required to heat the building by around 20% without compromising the user's comfort. However, as the introduction section points out, it is especially tricky for existing building/space regarding system integration and cost.

Low-cost developmental systems such as Arduino and Raspberry Pi are widely used for developing prototypes of smart building applications [7] since it is capable of serving as a data acquisition system and is also capable of being a controller [8].

Data collecting and monitoring is the core of a building energy management system, and lots of advanced control algorithms are relying on accurate and reliable data sources. Researchers tried to cut the cost of data collecting. Li et al. [9] developed a low-cost real-time data logger with PM sensor, an Arduino Nano ATmega328, and an XBee radio to measure particulate matter. Habibi et al. [10] developed a smart system prototype based on Arduino microcontroller which can obtain and monitor environmental data (light, sound pressure/mic, temperature, and humidity) in real-time. Jin [11] developed a similar system to monitor IEQ. Rajalingam and Malathi [12] used an Arduino system as a smart controller for home power management. Lovett et al. [13] present an approach minimized the cost of sensing by inferred performance metric (e.g., high CO2 levels may indicate poor ventilation). They designed a process for grouping sensor sets to capture energy events in buildings. While these techniques are being widely studies, the accuracy and reliability of these low-cost sensors have not thoroughly been studied.

Research communities and companies started from developing systems and interfaces that allow the occupants to control lighting, shading, and HVAC system remotely. Gill et al. [14] developed a home automation system based on ZigBee to control lighting system and radiator. Occupants can control the lights and the radiator through any device supporting Wi-Fi and Java. Piyare et al. [15] developed a Bluetooth based home automation on a Symbian OS mobile phone for controlling lamps remotely. Al-Ali et al. [16] developed a JAVA based home automation interface that can control lighting, fan, and oven through a local web page. Later on, the research scope was extended. Advanced automated control by analyzing sensors' feedback was studied and implemented. Kuo et al. [17] developed an automatic shading control system using photometer, 3D-printing component, and support vector machine algorithm for learning an individual's lighting preference. Cheng et al. [18] developed a satisfaction based Q-learning system which integrated lighting and blind control by gathering occupants' feedback. Tang et al. [19] used smartphone and light sensors to perform daylight harvesting while maintaining occupant desired light color. Compared to the original control mode, the power savings were up to 54.7%. Fewer studies were published

about the HVAC system since the system is generally more complicated, but it had huge energy saving potential. Rashid et al. [20] retrofitted the functionality of the HVAC system by using the existing distributed heating/cooling infrastructure in buildings to provide a low-cost centralized command and control mechanism namely. The paper targeted buildings in developing countries that lack the necessary infrastructure of a traditional HVAC system. The result showed it could save approximately 45% of the total energy consumption of the air conditioner (AC) on a day.

From reviewing past studies, we can find that the benefits brought by building management system are valuable. More and more researchers started to develop a low-cost smart control and monitor system and building management system for existing buildings. However, the integration of protocols from different appliances and different manufacturers has not been discussed. In the past, we usually control each component separately. While more and more studied indicated – HVAC system, lighting system, shading system, and window system are related and should be considered together in order to achieve [21].

Moreover, the impact of occupants' inputs and feedback were skimmed. This paper aims to address some of the issues mentioned and to present an overview of an integrated building management system that can facilitate further research about occupants behavior and advanced control.

3 Methodology

This section described the system we developed and the method we used to overcome the existing conditions. This system was specifically designed for the test space described in next session. The design plan was carried out according to the current situation and the characteristics of existing building components (HVAC system, lighting system, and shading system).

3.1 System Structure

Figure1 showed the overall system structure which included four groups: the user interface, the cloud platform, the processing units, and the sensors and controllers.

There were two types of front-end components in the structure, environmental sensors, and controlled objects. Sensors collected environmental conditions that helped the controllers to provide appropriate environmental control. Meanwhile, the collected data helped the researchers to understand the conditions when occupants provided certain feedback (i.e., interact with building components) and for other research purposes. Sensors installed for monitoring the indoor and outdoor environment include thermocouples, temperature sensors, humidity sensor, light sensors, illuminance sensors, and pyranometers, and so on. Extra sensors such as and pyroelectric infrared detectors (PIR) were for detecting occupancy, and infrared receivers were for capturing remote controllers' signals. In the developed system, there were two controlled objects – shading systems and mini-split air conditioner. In the future, its scope would be expanded to other common building components in the spaces.

The processing unit was the medium of sensors, controllers, and database. For gathering environmental data from sensors, we used two types of systems (sensors + processing unit) in this study. The low-cost ones were there for the targeted system and data collected through this system was directly used for control. The high-end sensors and processing unit (mainly DAQ system) were set up in order to validate the readings collected by low-cost sensors. Both systems were integrated into the overall system frame, and the data was sent to a cloud database.

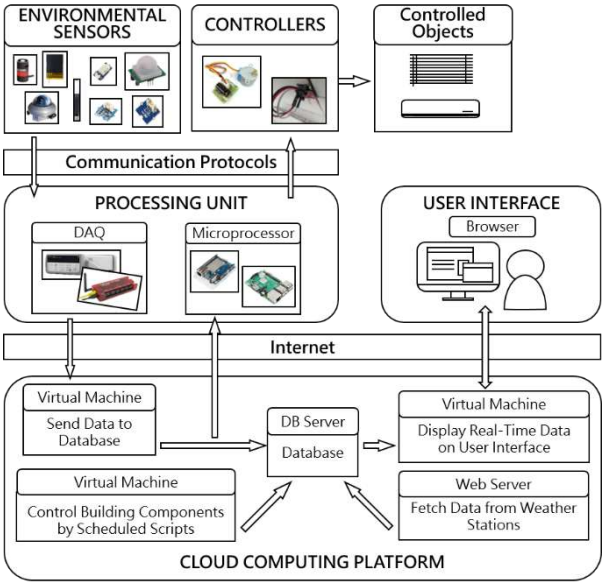

Figure 1. The overall system structure of developed building management platform

For low-cost data gathering, we chose Arduino and Raspberry Pi microcontroller boards as our processing unit. Both boards were capable of decoding communication protocols such as UART, I^2C, Modbus, and other communication protocols, which allowed better flexibility. Both boards supported Wi-Fi, which was critical to the existing space. Although communication through physical wires might be more reliable, it would increase the overall installation cost and workload. The data gathering program was running on

the boards directly. After gathering the reading from sensors, it sent POST requests with the readings to a cloud server running a custom database and PHP application.

High-end system's processing units consisted of several different data acquisition systems which connected to sensors with voltage outputs, current outputs, etc. Instead of installing a program into the packaged DAQ system, the data gathering was running on the cloud server which sent signals to communicate with the DAQ system while the DAQ system communicates with sensors through its internal protocol. The data collected by the cloud server were sent and stored in the database directly.

Some microprocessors served for control purpose. The details would be present in 3.2 and 3.3. The typical way to interact with components in daily life were kept while the occupants' action being recorded. The web-based user interface also allowed engineers and occupants control the system remotely and to set up more complicated control algorithm.

The user interface of our system is web-based. The website present real-time information such as temperature, humidity from weather stations and sensor data, components' status, and occupancy status. We can also download CSV data for a customized period from the website.

The cloud computing platform was the core of the system. It was set up on the cloud instead of on-site to increase the computational efficiency, and to save the cost and space and can be accessed by people with access right from anywhere. Tasks hosted by cloud computing platform include hosting database, hosting PHP server that passed data to the database, performing data gathering programs, fetching data from weather stations, hosting user interface websites, and running control scripts on the virtual machines. New control algorithms would be deployed from the cloud computing platform. The expandability of the platform would give us the flexibility to add more functions and to add more computational capacity to the system in the future.

3.2 Thermal Environment Control

The section describes how our system control the thermal environment for the targeted space according to occupants' actions or control algorithm commands while capturing occupants' feedback. The structure of how the system executes thermal environment control is shown in Figure2.

The air conditioner demonstrated, in this case, was a mini-split system. Typically, it was controlled by occupants through the factory remote controller. However, it did not keep when and the conditions when occupants took a control action. The developed system kept the original way to control and added a web-based user interface that allowed both users and system to control the air conditioner from outside of the space. The original factory controller communicated with air conditioner through infrared signals, so we installed an Arduino Yun microprocessor with infrared receiver right next to the air conditioner signal to capture and decode the infrared signal sent by the controller in order to record occupants' actions. The remote controller sent out a specially timed sequence of pulses to transmit data. The infrared sequence consisted of a set of marks and spaces referred to as a "frame" of data. The receiver captured the whole sequence and determined critical time intervals (space) to decode the set point temperature and wind speed the controller was trying to tell the air conditioner. For realizing the control from outside of the space, an infrared transmitter and a WEMOS D1 mini pro microprocessor with a built-in web server were set up and aimed to the receiver in order to pass the infrared signal according to users' command through the website instead of factory remote controller. One of the most challenging parts was to decode the signals before setup the extra receiver and transmitter. In order to differentiate from the signals sent from the factory remote controller and signals sent by the website, we altered the small part of the signal.

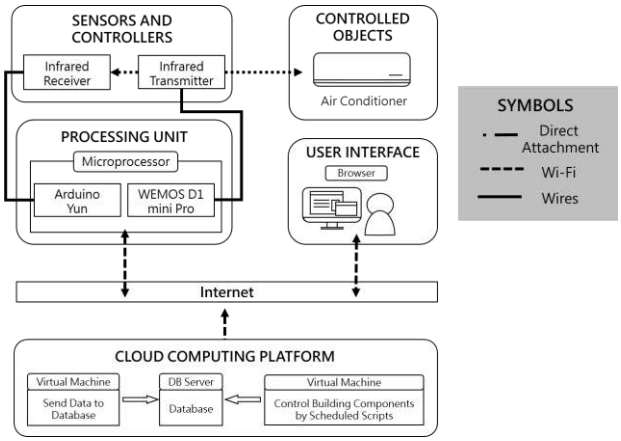

Figure 2. The system structure of thermal environment control

The user interface displayed the latest air conditioner temperature set point and wind speed. When changes were made, the code will swap out the characteristic time intervals to regenerate the corresponding infrared signal. It then emitted it through the infrared LED transmitter, and the signals were expected to be captured by the air conditioner and the Arduino Yun. After decoding and filtering the signal, the code on Arduino Yun then POST sensor reading to another web server on the cloud computing platform. The targeted website server would execute a PHP code that reads the information containing in the URL string and passed the sensor readings to the

database.

Other than establishing the ability to control from outside of space and gathering occupants' action records, we also deployed multiple thermocouples and other sensors to gather indoor environment data as described before, so we knew what the indoor environmental condition was when the occupants happened to take the actions. The beeper in the air conditioner was replaced with a blue LED to avoid the disturbance caused by automated control.

3.3 Shading Control

The targeted shading system in our study was Venetian blinds which controlled the amount of sunlight entering the environment and controlled the glare by its slats. Venetian blinds system consist of slats, gears, a fixed frame, a drawstring, and a rotating rod. The drawstring's function was for adjusting the height of the blinds. When released, the louver would cover the entire window. In this study, we fixed the blind's height to the full-covered position in order to reduce the complexity of the shading control system. The rotating rod's function was for adjusting the angle of the slats, which would also change the amount of sunlight entering the space. The slats angle was the primary control variable in this system.

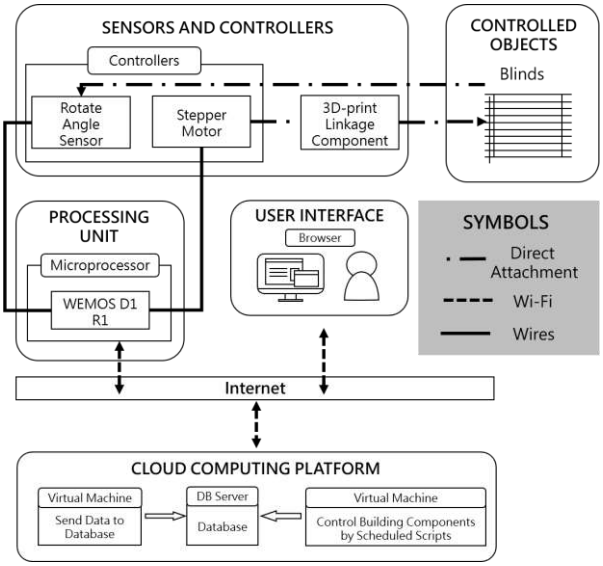

Figure 3. The system structure of shading control

Figure3 shows the system structure of shading control. We connected the rotating rod of the shades to a stepper motor by a customized 3D printed device. Then in the same WEMOS D1 R1 microprocessor, we installed an angle sensor and put it on top of the slats to measure the three axial displacements. The readings from the angle sensors were used to tell the stepper motor when to stop. The slats angle operation procedure is shown in Figure 4.

A web server was also hosted on this WEMOS D1 R1 board. By accessing the web server, the users and the system can control the shading system directly. When a command was sent, WEMOS D1 R1 would execute the code to trigger the motor, and it would stop when the slats reached the desired angle. At the same time, an URL containing the desired angle was POST to the cloud server. An infrared receiver was also installed, and programmed to couple with a remote controller and to provide another control option. Consequently, the shades can be controlled by either infrared signals or web commands.

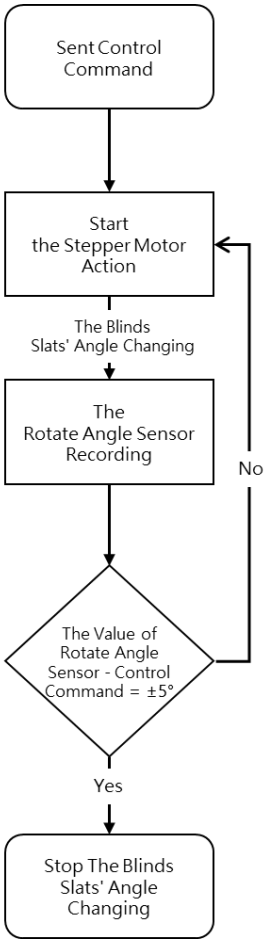

Figure 4. The slats angle operation procedure

4 Case Demonstration

In this section, we demonstrated the system's capabilities by deploying it into an existing space. The following session showcased the function of the current building management platform, the control implementation, and the environmental data and the occupants' feedback can be collected by the system.

4.1 Introduction The Testbed Environment

The testbed was set up in Taipei, Taiwan. The city is located 121 degrees east longitude and 25 degrees north latitude, with an average annual temperature of 23.6 °C and an average annual average relative humidity of 76%. The climatic conditions are classified into a subtropical monsoon climate, which means high temperature and rain in summer and warm and humid in winter than in the same latitude.

Figure 4 presents the configuration of the testbed. The size of the testbed was 6.1 m × 2.4 m × 2.6 m (length × width × height). The testbed had a door (90 × 200cm) and three windows on the west wall and three windows on the east wall. Each window is 110 × 90cm. The window to wall ratio for east wall and west wall is around 18.8%.

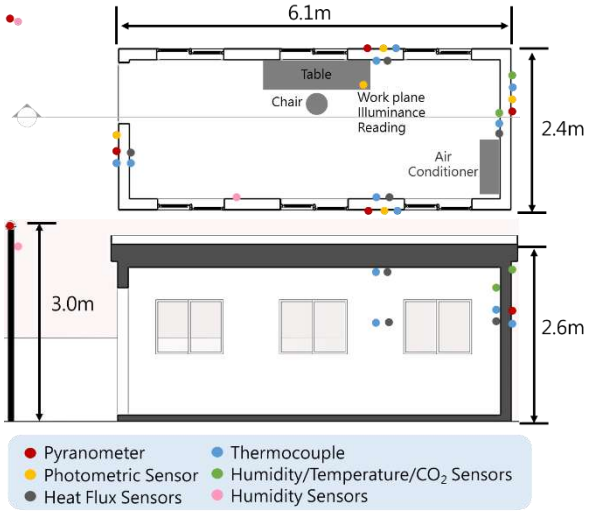

Figure 5. The Testbed Environmental Sensors Arrangement Position

The existing components targeted in this study were a split air conditioner and Venetian blinds. Only the west side of windows and blinds can be altered, while the shades on the east side were all closed during the experiments period in order to simulate the situation of a typical individual office. The table for the occupant was placed in front of the middle west window, and there was a photometric sensor to read work plane illuminance on the table.

We recruited several occupants to test the environmental comfort in the testbed. In order to observe the occupants' activities and actions, we maintained testbed's starting conditions similarly before the occupant entered the testbed by automated control. For this purpose, we set up a virtual machine program to execute the control sequence at 01:00 am every day, so the Venetian blinds would be fully open, and the air conditioner would be off when occupant entered the room. Before the test, we told the occupant that we gave him/her the full control of targeted building components.

4.2 Occupant's Behavior Related Thermal Comfort

We designed a test to gather occupants' response to the changes in the indoor environment and to demonstrate the system's capability to control from outside of the space. Figure 6 shows a comparison between a day with the air conditioner on (top) and a day with the air conditioner off (bottom). The vertical axis on the left side indicated the temperature, and the vertical axis on the right side indicated the passive infrared (PIR) sensor - value 0 indicates occupant was not there, value one indicates occupant was in the space. In the case with the air conditioner on, it was evident that the air conditioner is hunting the set point in comparison to the case with the air conditioner off – which has a smooth curve. Therefore, sometimes we do not need action response sensors to capture occupant behavior. The virtual sensor can be developed by analyzing the data.

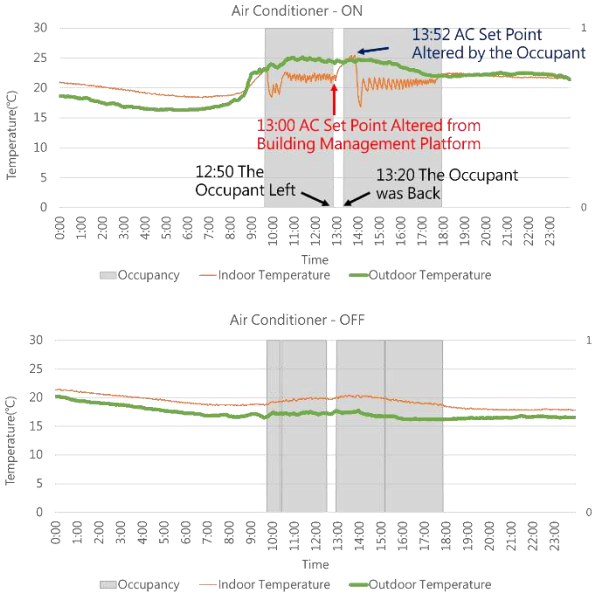

Figure 6. Occupant and Air Conditioner Interactions

The test process was to adjust the temperature setpoint while the ambient temperature is stable in order to recognize their thermal tolerance and to develop energy-saving strategies. Figure 6 (top) shows that the adjustment was sent at around 13:00 when occupant left for lunch but forgot to turn off the air conditioner. The system raised the set point by 4 degrees. The occupant was not happy about this adjustment. While when the occupant came back, the temperature set point of the air conditioner was not immediately adjusted, the occupant decided to lower the setpoint 30 minutes after entering the room. From the case where the air conditioner was off, we can find that the occupant's preferred temperature

range is approximately between 21 and 23 degrees. The energy-saving adjustment, unfortunately, caused the occupant discomfort and resulted in occupant's unexpected action by adjusting the set point to somewhere even lower than the set point before adjustment. The presented result was a compelling case that the control algorithm developer should pay attention to. It also demonstrated the importance of building management system and its remote control function.

4.3 Occupants' Behavior Related to Visual Comfort

This session demonstrates the capability of the system's shade adjustment and feedback from occupants. Figure 7 shows the results of shade status and occupant's behavior on a sunny day and a cloudy day. The vertical axis on the left is the illuminance level, and the vertical axis on the right is the slat angle. The gray block was the interval that the occupant was in the space.

In the sunny day case, the system read the report from weather prediction and knew that the day was sunny beforehand. It then adjusted the slat angle to 40 degrees in advance through the management platform before the occupant entered the testbed for capturing the occupant's reaction. Note that: the slat angle is zero degrees when the slat is horizontal, -70 degrees when it rotated towards the ground and 70 degrees when it rotated towards the sky.

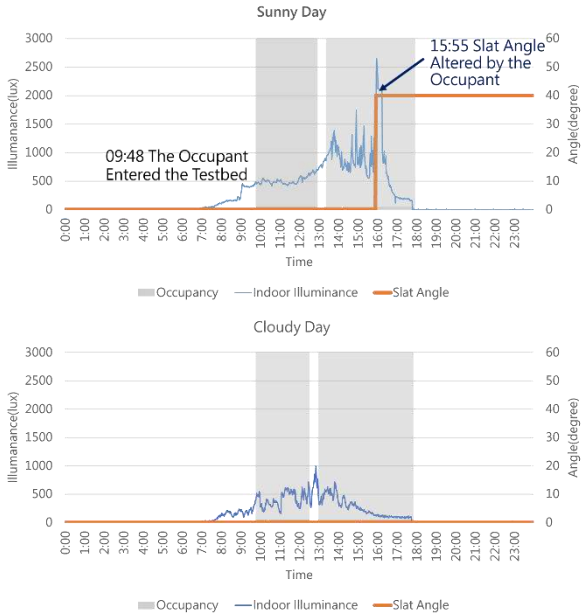

Figure 7. Occupant and Air Conditioner Interactions

From Figure 7, we knew that once the occupant entered the space, the occupant found that the indoor light is insufficient. The good news is that instead of turning on the light, this occupant chose to change the slat angle to 20 degrees. The occupant adjusted the slat angle again at 15:55 to reduce the amount of light coming in and maintain visual comfort because it is the time when direct light can transmit through the gap between the slats from what we found in Figure 7. Unfortunately, the sensor here was placed on the work plane instead of the vertical plane. It was a lesson learned from testing and can be used to adjust the set up for control.

5 Discussion

Although this system is designed to be easy to build and easy to use, there are still some challenges to overcome when adapting our system to other cases.

We need a knowledge base for setting up remote and automated control for different existing building components. There are many different types of building components with different communication protocols and different shapes, and the component with the same communication protocol might adopt different ways to decode the signal. For example, the infrared signals differ from one air conditioner to another air conditioner. 3D printed adapter for connecting step motors and rod also needs to be redesigned for different rod shape.

After all, we are looking forward to expanding our system to include more building components such as fans, stand-alone heaters, etc. The industry standard should be established in the future, and a more natural way to build accessories such as 3D printed adapter should be studied. We also need to find a more efficient way to deploy the control logic that requires less experiencing on programming.

6 Conclusion

We built a building management platform in an existing space to verify the feasibility and effectiveness of the overall system structure. The preliminary results and demonstration provided a crucial foundation for the subsequent implementation of intelligent systems and equipped a testbed that can be used for other behavior studies and control studies in the future.

The building management platform is composed of many different hardware devices and software services. The low-cost sensors and microprocessors were selected to reduce the implementing cost. The demonstration showed that the low-cost hardware devices could be used as a good terminal device for intelligent systems and carefully designed and commissioned devices could achieve good stability and accuracy. The low-cost concept would benefit buildings that are in the operation and maintenance phase, and make the system more acceptable in the market.

The concept of getting feedback from occupants can help the manager and research communities understand occupants' need better. The continuous monitor of the indoor environment can help the managers check if the building components such as air conditioner and the blind system can achieve designed service level. The cloud-based platform makes the commission process and other services more flexible.

In the past, the control of the building environment and the management and maintenance of building components strongly depend on the experience of the building managers, which usually led to an unnecessary waste of energy and increased the difficulty to deploy new control algorithms. This study showed that we have the potential to learn more and occupants and to run advanced energy saving control logic by introducing the cloud-based building management platform into the existing building space.

Acknowledgments

The work described in this paper was supported by a grant from the National Taiwan University and Ministry of Science and Technology, Taiwan (project no. MOST 108-2636-E-002-005).

References

[1] Manic, M., et al., Building Energy Management Systems: The Age of Intelligent and Adaptive Buildings. *IEEE Industrial Electronics Magazine*, 10(1): 25-39, 2016.

[2] Teichroew, Daniel, and H. Sayani, Automation of system building, in *datamation*. 1971. p. 25-30.

[3] Murata, et al., A Proposal for standardization of home bus system for home automation, *IEEE Transactions on Consumer Electronics*. 1983. p. 524-530.

[4] Ryan, J.L., Home automation. *Electronics & Communication Engineering Journal*, 1(4): 185-192, 1989.

[5] Rotger-Griful, S., U. Welling, and R.H. Jacobsen, Implementation of a building energy management system for residential demand response. *Microprocessors and Microsystems*, 55: 100-110, 2017.

[6] Macarulla, M., et al., Implementation of predictive control in a commercial building energy management system using neural networks. *Energy and Buildings*, 151: 511-519, 2017.

[7] Ali, A.S., et al., Open Source Building Science Sensors (OSBSS): A low-cost Arduino-based platform for long-term indoor environmental data collection. *Building and Environment*, 100(Supplement C): 114-126, 2016.

[8] Altaf Hamed, S. and A. Anand. Data acquisition and control using Arduino-Android platform: Smart plug. *2013 International Conference on Energy Efficient Technologies for Sustainability*. pages 241-244, 2013.

[9] Li, J., et al., Spatiotemporal distribution of indoor particulate matter concentration with a low-cost sensor network. *Building and Environment*, 127(Supplement C): 138-147, 2018.

[10] Habibi, S., Micro-climatization and real-time digitalization effects on energy efficiency based on user behavior. *Building and Environment*, 114(Supplement C): 410-428, 2017.

[11] Jin, Q., M. Overend, and P. Thompson, Towards productivity indicators for performance-based facade design in commercial buildings. *Building and Environment*, 57: 271-281, 2012.

[12] Rajalingam, S. and V. Malathi, HEM algorithm based smart controller for home power management system. *Energy and Buildings*, 131(Supplement C): 184-192, 2016.

[13] Lovett, T., et al., Designing sensor sets for capturing energy events in buildings. *Building and Environment*, 110: 11-22, 2016.

[14] Gill, K., et al., *A* zigbee-based home automation system, *IEEE Transactions on Consumer Electronics*. 2009. p. 422-430.

[15] R.Piyare and M.Tazil, Bluetooth based home automation system using cell phone, *IEEE 15th International Symposium on Consumer Electronics*. 2011.

[16] Al-Ali, A.R. and M. AL-Rousan, Java-based home automation system, *IEEE Transactions on Consumer Electronics*. 2004. p. 498-504.

[17] Kuo, T.-C., Y.-C. Chan, and A.Y. Chen, An Occupant-centered Integrated Lighting And Shading Control for Energy Saving and Individual Preferences, *ASCE International Workshop on Computing in Civil Engineering 2017*. 2017, American Society of Civil Engineers: Seattle, Washington. p. 207-214.

[18] Cheng, Z., et al., Satisfaction based Q-learning for integrated lighting and blind control. *Energy and Buildings*, 127: 43-55, 2016.

[19] Tang, S., et al., Development of a prototype smart home intelligent lighting control architecture using sensors onboard a mobile computing system. *Energy and Buildings*, 138: 368-376, 2017.

[20] Rashid, S.A., et al., Retrofitting low-cost heating ventilation and air-conditioning systems for energy management in buildings. *Applied Energy*, 236: 648-661, 2019.

[21] Sun, B., et al., Building energy management: Integrated control of active and passive heating, *cooling, lighting, shading, and ventilation systems*. 10(3): 588-602, 2013.

Spatial Information Enrichment using NLP-based Classification of Space Objects for School Bldgs. in Korea

J. Song[a], J. Kim[a], and J. Lee[a]

[a]Department of Interior Architecture and Built Environment, Yonsei University, Republic of Korea
E-mail: songjy92@gmail.com, wlstjd1320@gmail.com, leejinkook@yonsei.ac.kr

Abstract –

This paper presents an approach to classifying spatial categories of space objects using their textual properties in IFC data. As a standardized data format of building information, IFC enhances the data interoperability between the heterogeneous domain software. However, there are some problems that required information is omitted due to the technical translation error or mistake by users. The other problem is that some semantic information cannot be defined in the IFC data scheme. Manually checking and modifying this information requires an amount of time and labor. The intelligent information enrichment system can facilitate the application of BIM. In this regards, this research tried to address the interoperability problems with a machine learning-based method by automatically enhancing the semantic information of the BIM model. In this paper, we focused on the semantic enrichment of space objects by using textual data in the IFC. We implemented the NLP-based classification training model, which employs the word embedding techniques. As an early phase of research, this paper conducted training experiments with variable input properties, name and area of space, from space object in Korea school buildings. The accuracy of the classification model with a single feature (name) is measured at 85.9%, which is higher than multi feature (name and area). The suggested model can be expanded to more variable properties and target objects as a part of the semantic enrichment system.

Keywords –

Building information modeling (BIM), Spatial information enrichment, Natural language processing (NLP), Industry foundation classes (IFC)

1 Introduction

The adoption of building information modeling (BIM) contribute to enhancing the efficiency of architecture, engineering, and construction (AEC) industry by generating and managing building information with a computational model. BIM enables the automation of variable processes such as code compliance checking, design analyses [1]. Industry Foundation Class (IFC) standard supports the data interoperability of BIM, which aims to maximize the advantage of BIM.

However, several problems still remain in terms of practical applications of BIM. Some basic analysis processes can be driven by quantitative data from IFC, but the practical analysis requires more complex and domain-specific data that are not defined in IFC scheme. The semantic information required for specific analysis tasks can be easily obtained by a human who has domain-specific knowledge. Domain experts reason the semantic information about building objects using various types of data, such as text, images or quantity values. In order to intelligently automate these reasoning process by a computer, there have been some researchers to implement the automated information inference system. The research area, called semantic enrichment, addressed the interoperability of semantic BIM data by employing rule-based or machine learning methodologies [2, 5-8]. This research is also a part of them, which tried to implement the semantic enrichment system focusing on a space object instance. In this paper, we propose the utilization of textual values to intelligently inference the semantic information of space objects, as domain experts.

As machine learning and deep learning technology have been dramatically developed, natural language processing (NLP), which is sub-domain of artificial intelligence, also has made an amount of progress [3]. Machine learning-based NLP enables the computer to learn the semantic meaning of natural languages by itself. Word embedding technique helps to represent the semantic meaning of words in numerical vectors, which make a breakthrough in variable NLP tasks. In this research, the NLP techniques including word embedding are employed to implement the classification model. The approach to NLP-based feature generation and spatial category classification model are depicted in this paper. The results of training experiments with spaces in Korean school buildings are also described for validations. The overview of this research and scope of this paper are illustrated in Figure 1.

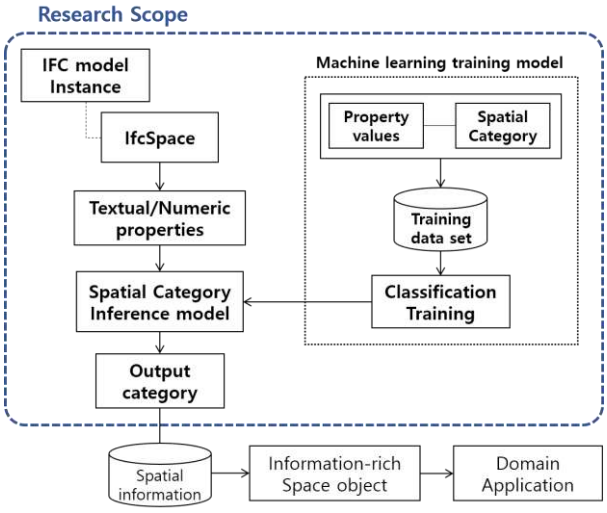

Figure 1. An overview of the suggested spatial information enrichment system and scope of this paper

2 Background

2.1 Semantic information of building objects for domain-specific application

As a standardized data specification, IFC is meant to support data interoperability between the different BIM platforms, however, there have been some studies reported practical problems of IFC [3]. Domain-specific applications require higher levels of semantic information and the required information is different for each domain task. Model View Definitions (MVDs) was suggested to define a subset of IFC required for domain-specific applications. However, MVD approach has a limitation on practical applications since it has to be defined respectively for every application.

Recent studies in code compliance checking, building analysis, and BIM model query tried to develop a system to supplement the semantic information. Solihin et al. suggested FORNAX platform for code compliance checking system, which supplements the semantic attributes of building objects with pre-defined FORNAX objects [5]. Lee et al. developed space database and mapping algorithms that provides the standard information of space object instances [6]. Belsky et al. proposed a Semantic Enrichment Engine for BIM (SEEBIM) which is a rule-based inference system for classifying components of bridge models [7].

Tanya and Rafael suggested machine learning-based inferencing method for semantic enrichment of space objects. Using the single features and pairwise features of space objects, the machine learning algorithm is trained to classify the type of room [2]. Koo et al. utilized support vector machines, which is one of the machine learning algorithms, to classify the building objects and check the semantic integrity of them [8]. These studies tried to switch the rule-based inference method into machine learning-based method, and showed the potential of the approaches.

2.2 Spatial category classification

Space is one of the critical elements in the computer-based information system for the concept design, construction process, and facility management process [5, 8]. As a functional element where human activities are performed, space is used as a unit of design or building analysis.

Traditional 2D CAD system only represents space object with surrounding physical objects and labels. BIM application is based on the objects-based modeling, which represents space object dependent on their

Table 1. Classification of spatial categories and training labels for Korean school buildings [11, 12]

Space use category	Training label	Space use category	Training label
Classroom	1. General classroom	General Use Facilities	13. School cafeteria
Laboratory Facilities	2. Laboratory room		14. Corridor
Office Facilities	3. School office		15. Lobby
	4. Principal's office		16. Toilet
	5. Counseling room		17. Parking lots
	6. Teacher's lounge	Support Facilities	18. Security office
Study Facilities	7. Library		19. Electric room
	8. Computer lab		20. Water tank room
Special Use Facilities	9. Gymnasium		21. Machine room
	10. Practice room	Health Care Facilities	22. Nursing room
	11. Audiovisual room		
	12. Multi-purpose room		

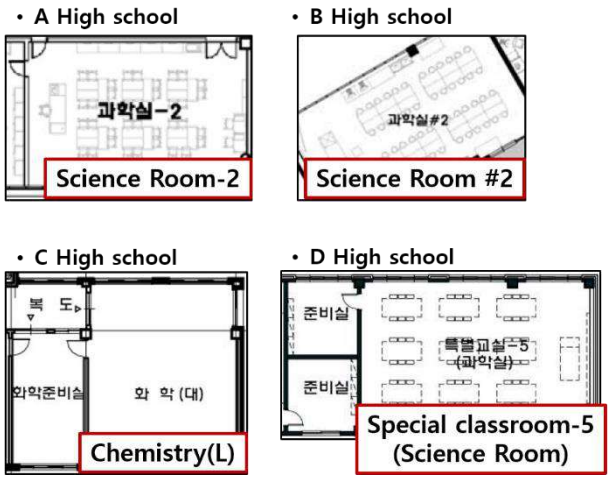

Figure 2. Examples of different naming convention for laboratory classroom

physical boundaries. This approach enables AEC industry stakeholders to manage and utilize required information of space objects.

Although, BIM provides rich-information about space objects, there are limitations on the interoperability of space objects in the domain application. Space instance can be classified differently, according to the applications. In some analysis, several spaces can be defined in a single zone, which is an aggregation of spaces. These characteristics hinder the utilization of space objects and their associated information. As an early phase of research to address the classification problems, we propose an approach to automated spatial category classification for space instance in the BIM model using machine learning algorithms. The motivation of this research is based on the research of Lee et al [6], which used space name data for classifying spatial categories.

3 Spatial categories classification of space objects for school buildings in Korea

The environmental comfort of educational facilities, which primarily depends on the building design, can affect the work or study productivity [10]. In this regards, many countries make efforts to establish more comfortable and effective facilities for both students and teachers. The Korean government also tries to improve the education environment with advanced facilities. The standard area for each student and classroom is specified in design regulations. In addition, the Korean ministry of education tried to introduce subject classroom system, which requires classrooms for each subject [11]. The design plans of school buildings have to follow these guidelines. In terms of subject classroom system, classifying the spatial categories of spaces is critical for the design and assessment of school building.

The fundamental features for spatial category classification is a name and area. The problem of utilization of name property is that the computer cannot understand the textual semantics of the space names written by different naming conventions. Figure 2 shows a simple example of naming convention problems. The floor plans of each project have a different naming convention for the same subject classroom.

In this paper, we focused on the functional usage of space object among the spatial categories. The classification of usage is listed in Table 1. Omniclass Table 13: Spaces by Function [12] and Classification system in Subject Class Operation Guidelines in Korea [11] are considered for the space classification system. The concept of high-level categories is borrowed from Omniclass and detailed training labels referenced the classification in Korean guidelines.

4 Development of NLP-based spatial category classification model

4.1 Property Extraction from IfcSpace object

The classification model in this research is based on a supervised learning method, which requires input features and corresponding label of objects. The input feature is a critical factor for machine learning since the model is trained to capture the patterns of input features and use the patterns for classification. The property values of IfcSpace objects are extracted for generating input feature of the usage classification model. The extracted property values of each IfcSpace instance object are expressed in a single vector as an input of the classification model.

Table 2. A list of IfcSpace properties

Attribute /Pset	Property name	IFC entity	Data type
Attribute	LongName	IfcLabel	String
	Name	IfcLabel	String
	GlobalId	IfcGolbally UniqueID	String
	Description	IfcText	String
	...	...	...
Property set	Department	IfcText	String
	Occupant	IfcText	String
	Area	IfcArea Measure	Numeric
	Unbounded Height	IfcLength Measure	Numeric
	...	...	...

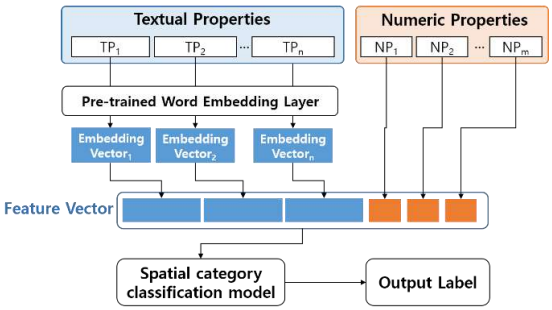

Figure 3. Feature extraction from space object properties

Table 2 shows a snippet list of IfcSpace properties. The IfcSpace object has attributes and property set which express the information of a space. Each property has a specific data type suitable for expressing the information. The feature generation is proceeded with converting property values in a suitable form. Numeric or Boolean data can be simply converted into input features. In order to translate textual data in a numeric form, word embedding techniques are applied. The details of utilization of word embedding are described in the next section. In this paper, we use the values of space name and area among the listed properties for classification.

4.2 Feature generation with NLP techniques

Neural network-based word embedding techniques become a prominent method for representing text data into the numeric form. In order to help the computer to understand and process the natural language, there have been variable methods to encode text in numeric format. The count-based representation approach has a limitation for representing the semantics of each word. Distributed representation makes a breakthrough by predicting the possibility of co-occurrence of words or phrases and encoding their features into vector format [13]. The concept of distributed representation is recently implemented with neural network-based models, which can handle the amount of text data. In this research, we obtained word vectors with word embedding model named fastText developed by Facebook's AI Research (FAIR) lab. The fastText model uses subword information for obtaining word vectors, which enables a model to represent the words that did not appear in the training data set [14].

We train the 100-dimensional word embedding model with 356,010 sentences from Korean Act sentences collected with an Open API data of National Law Information Center (law.go.kr). The 100-dimensional word vectors can be used for classification alone or concatenated with other numeric properties (Figure 3). Other numeric properties are obtained from the property value of given space object, with IFC parsing tool such as IfcOpenShell or it can be simply derived from the room schedule exported from BIM authoring tool. An approach to the explicit representation of relational properties such as connection, inclusion, adjacency is also another important issue for utilizing the information to machine learning or deep learning training.

4.3 Classification training and inference model

The classification model is implemented with a feed-forward network composed of three hidden layers. Each hidden layer contains 50 nodes respectively and the size of the output layer is 22 which is same as the number of output labels. ReLU (Rectified Linear Unit) function is used for activation function of each layer. The cross-entropy loss function and the stochastic gradient descent algorithm are employed to calculate the loss of training and optimize the model. The neural network model is implemented with the PyTorch framework [15]. The inference model makes an inference for new input data with a classifier of the trained model.

5 Training experiments and results

5.1 Training experiments

The training data set is collected from the best practice examples of educational facilities in Korea, provided by Education Facilities Research & Management Center (EDUMAC). EDUMAC provides design proposals of school buildings which include floor plans and space programs. In this research, 7 buildings are selected by the author, and 598 space data are collected for training. Training data is randomly separated in 80:20 ratio for training data and validation data, thus 478 spaces are used for training and 120 spaces are used for measuring the accuracy of trained data.

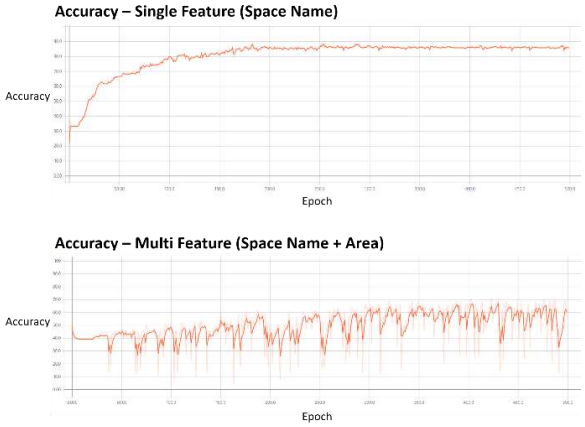

Figure 4. Training accuracy of each training

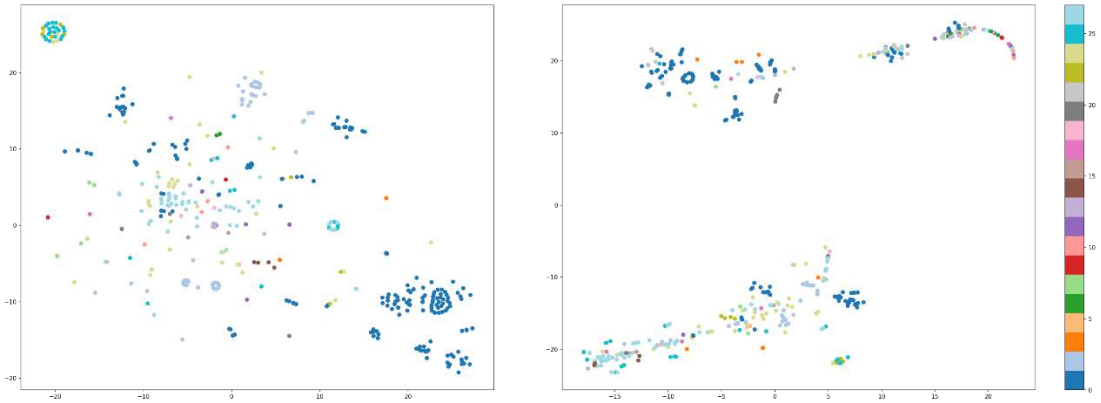

Figure 5. t-SNE Visualization of input feature vectors; Left: 100-dimensional vector (word embedding vector), Right: 101-dimensional vector (concatenated vector of word embedding and space area)

Training experiments are conducted with two scenarios. The first training is proceeded with a single feature, in this case, word embedding vectors of space name. In the second training experiment, the multi feature, which is a concatenated vector of word embedding vector and the value of the space area, are inputted to a training model. The training model and the number of training epoch are used for training, to compare the results.

5.2 Training results

The training results of each training model with 500 iterations are illustrated in Figure 4. Figure 4 illustrates the plot of training accuracy of single feature training model in the above graph and multi feature training model below. As shown in the above graph, there are no advances in training after 350 times of iteration for the single feature training result. The final training accuracy is measured by 85.9%. The training accuracy of second training experiment with multi feature is measured lower than the former one, measured to 60%. This result shows one single feature - space area in this case - can affect the training outcome by changing the input values and even produce worse results.

Figure 5 is a t-SNE (t-distributed Stochastic Neighbor Embedding) visualization [16] of input feature vectors. t-SNE visualization is a visualization tool for high dimensional data, which capture the similarity between the points and tries to express them in a lower dimension. By visualizing data in 2D or 3D space, the user can easily figure out the distributed pattern of data. In Figure 4, Left one is a 2D scatter plot of the 100-dimensional vectors with a single feature and the right one is the plot of 101-dimensional vectors with the multi feature. The color of dots represents the usage label of each observation. The clusters of data are more easily identified in left scatter plot than the right one. In other words, the computer can easily figure out the patterns and classify input observations of single feature vectors than multi feature.

This result can be attributed to the design plan of school building based on the unified spatial module. Most of the spaces in school buildings have a similar area and geometric feature regardless of functional features. They are partitioned to a certain size which is mostly based on the size of the general classroom. Whether the functional usage of space is laboratory classroom or teacher office, most of them have very similar, even almost the same, geometric features to the general classroom. In the training experiment from this research, the area value acts as a noise to lower classification accuracy since they cannot show the pattern to distinguish the usage. In the future work, other geometric properties and relational properties of space object can be appended to the input features for validation of the proposed approach.

6 Conclusion

This research proposes a spatial category classification method utilizing name and area of space objects. The spatial category classification is based on a neural network model, which use the word embedding techniques for processing textual data. The results of training experiments show that deep learning model can classify the space object by their name. However, deciding which properties to be utilized as training features is critical for training output.

The contribution of this research is to expand the utilization of textual data that is one of the important values for inferencing the semantic information of space object. In the proposed classification model, machine learning-based NLP techniques are employed, which can help the computer to understand the semantic meaning of natural languages. The machine learning-based model

can deal with the lexical problems, such as acronyms, omissions, which are difficult to handle in the rule-based algorithm.

This research could be expanded in terms of input features and target objects. Input features can be expanded with other textual data or numeric data. If there is more information about occupants or department of space, these textual properties could be converted into the feature vector of training models. Additionally, the other geometric properties and relational properties also can be applied to training. Utilization of variable properties are expected to be more independent to the requirements of input properties; Even if some information is missing in the BIM model, the trained model may infer the semantic information about the space objects. The target of the classification also can be expanded to variable objects including building itself.

Acknowledgement

This work was supported by the National Research Foundation of Korea(NRF) grant funded by the Korea government(MSIT) (No. 2019R1A2C1007920).

References

[1] Eastman, Chuck, et al. BIM handbook: A guide to building information modeling for owners, managers, designers, engineers and contractors. John Wiley & Sons, 2011.

[2] Bloch, T. and Sacks, R. Comparing machine learning and rule-based inferencing for semantic enrichment of BIM models. *Automation in Construction*, 256–272, 2018.

[3] Young, T., Devamanyu, H., Poria, S., and Cambria, E. Recent trends in deep learning based natural language processing. *IEEE Computational Intelligence Magazine*, 13(3), 55–75, 2018.

[4] Pazlar T. and Turk Z. Interoperability in practice: geometric data exchance using the IFC standard, *Journal of Information Technology in Construction* (*ITcon*), 13, Special issue Case studies of BIM use: 362-380, 2008.

[5] Solihin, W., Shaikh, N., Rong, X. and Lam, K. Beyond interoperability of building model a case for code compliance checking, 2004.

[6] Lee, J. K., Lee, J., Jeong, Y. S., Sheward, H., Sanguinetti, P., Abdelmohsen, S. and Eastman, C. M. Development of space database for automated building design review systems. *Automation in Construction*, 24: 203–212, 2012.

[7] Rafael, S., Ling, M., Raz, Y., Andre, B., Simon, D. and Uri, K. Semantic Enrichment for Building Information Modeling: Procedure for Compiling Inference Rules and Operators for Complex Geometry. *Journal of Computing in Civil Engineering*, 31(6): 4017062, 2017.

[8] Koo, B., La, S., Cho, N.-W. and Yu, Y. Using support vector machines to classify building elements for checking the semantic integrity of building information models. *Automation in Construction*, 98:183–194, 2019.

[9] Ekholm, A. and Fridqvist, S. A concept of space for building classification, product modelling, and design. *Automation in Construction*, 9(3): 315–328, 2000.

[10] da Graça, V. A. C., Kowaltowski, D. C. C. K. and Petreche, J. R. D. An evaluation method for school building design at the preliminary phase with optimisation of aspects of environmental comfort for the school system of the State São Paulo in Brazil. *Building and Environment*, 42(2): 984–999. 2007.

[11] Korean Educational Development Institute, Manual for subject classroom system 2018 – middle school, Research articles CRM 2018-146, 2018.

[12] OmniClass, OmniClass Construction Classification System, http://www.omniclass.org/, Accessed date: 30, January, 2019.

[13] Mikolov, T., Sutskever, I., Chen, K., Corrado, G.S. and Dean, J.: Distributed representations of words and phrases and their compositionality. *Advances in Neural Information Processing Systems*, 26: 3111-3119, 2013.

[14] Bojanowski, P., Grave, E., Joulin, A. and Mikolov, T. Enriching Word Vectors with Subword Information. *Transactions of the Association for Computational Linguistics*, 5: 135–146, 2017.

[15] PyTorch, Depp learning platform (2018) (https://pytorch.org/ accessed January 31, 2019)

[16] Maaten, Laurens van der and Geoffrey Hinton. Visualizing data using t-SNE. *Journal of machine learning research* 9: 2579-2605, 2008.

Towards automated HVAC controls commissioning: Mechanisms to identify temperature and flow related functions of AHU components

R. Sunnam[a,c] , S. Ergan[b], and B. Akinci[a]

[a]Department of Civil and Environmental Engineering, Carnegie Mellon University, Pittsburgh, PA – 15213, USA;
[b]Department of Civil and Urban Engineering, NYU Tandon School of Engineering, Brooklyn, NY – 11201, USA;
[c]stok, 945 Front Street, Suite B, San Francisco, CA – 94111, USA;
E-mail: rsunnam@cmu.edu, semiha@nyu.edu , bakinci@cmu.edu

Abstract

Commissioning (Cx) of heating, ventilating, air conditioning (HVAC) systems has emerged as an effective sustainable practice to ensure high performance of these systems during operation. According to a DOE report, HVAC systems used 62% of the energy consumed by buildings in the US in 2011. It was also reported that controls related issues resulted in wastage of 50% of the HVAC energy consumption in 2011 (around 10% of total building energy consumption). Incorrect implementation of controls is a very common issue that can be traced back to improper representation of design intent of controls in the sequence of operations (SOOs). SOOs are currently represented through textual narratives that cannot be completely and accurately interpreted for comparison against the implemented controls during Cx. As a result, incorrectly implemented controls may remain undiagnosed, resulting in inefficient operation, energy wastage or both.

Currently, there is no guideline that can be used to identify the information to be included in SOOs. ASHRAE GPC 36 provides SOOs for 13 AHUs and ASHRAE Guideline 13 provide one sample SOOs, but they both do not list specific information to be included in SOOs. OpenBuildingControl is a research project to automatically implement the SOOs from ASHRAE GPC36 and simulate them through Spawn of EnergyPlus (SOEP) simulation engine. Even with all these efforts, there is still a need for a generalizable approach for identifying the information to be included SOOs for any AHU configuration, including the ones not included in ASHRAE GPC36. This paper describes a generalized way of identifying information items to be listed in SOOs. This approach incorporates functional and topological reasoning mechanisms to identify all temperature and flow related control processes within an air handling unit (AHU) and all components that influence each control process in a generalized way, regardless of the configuration of specific AHU.

Keywords –

HVAC Controls Commissioning, HVAC Controls Design Intent, HVAC Controls Information Requirements, HVAC Sequence of Operations, Building Information Modeling

1 Introduction

Commissioning of heating, ventilating, air conditioning (HVAC) systems is a formal step by-step process of verifying that a building is designed, constructed, and operated according to an owner's project requirements. From the energy performance perspective, commissioning of HVAC systems is important to ensure that these systems are installed to meet the heating/cooling needs of interior spaces and use energy optimally. Traditional commissioning of HVAC systems verifies a given design through various project phases and ensures that the correct system components are installed and are operational according to design documentation.

The documentation of HVAC controls is traditionally done through textual narratives called, sequence of operations (SOOs). A previous study related to this research identified several categories of challenges in accurately interpreting the design intent of controls from these narratives [12]. The identified challenges were classified into five categories: 1. Missing controlling/controlled parameters; 2. Missing set points; 3. Missing control logic; 4. Inconsistent values from multiple information sources; and 5. Missing information items. Due to these challenges, it may not be possible to accurately interpret the design intent of HVAC controls for verification during commissioning. And HVAC controls, which are not commissioned properly, will

likely result in energy wastage, occupant discomfort or both.

This paper presents an approach to generate a customized list of all control processes related to air flow and air temperature within an AHU. Further, a list of all components that influence each control process that need to be described in SOOs is also generated to support commissioning. The reasoning mechanisms rely on a building information model (BIM) of a given AHU and identify all control processes related to air flow and air temperature using the types of sensors and actuators in the model. Further, the developed approach reasons with the inherent control function of components (like temperature controlling components, flow controlling components, etc.) and their topological sequence to identify all components that influence each control process. At the end, it outputs a checklist that states all control processes along with a list of all AHU components that influence each control process.

These reasoning mechanisms were implemented in a prototype that takes the BIM of an AHU as an input and generates a checklist of all temperature and flow related control processes with the AHU and all components that influence each control process. The paper provides the results of the initial experiments conducted over a case study project.

2 Background

The primary function of an AHU control system is to maintain ambient parameters of a space at pre-determined set points. These parameters such as temperature, flowrate, etc. controlled by an AHU are called controlled variables. A component like valve, damper, etc. that reacts to a signal is a controlled device. A series of actions, induced by controlled devices to manipulate controlled variables related to air or water, is called a control process. The role of controlled devices within a system depends on their inherent functionality. The roles of AHU components relevant to this study are - to enable movement of air/water through the system (flow-moving); to control the movement of air/water through the system (flow-controlling); and to enable transfer of energy between two different air/water streams in a system (energy-conversion). Each controlled device may also influence more than one control process within a system through its interactions with other system components. For example, a hot water pump next to a heating coil influences the control of hot water flowrate through the pump directly and indirectly influences the control of air temperature due to its interaction with the heating coil. This study emphasizes the interdependence of a component's inherent functionality and its impact on other control processes due to its topological relations relative to other components in the system. To ensure that the controls are accurately verified during commissioning, this information about each components' inherent functionality and indirect impact on other control processes needs to be captured in SOOs. The following sections summarize various points of departure for this study.

2.1 Previous research related to information requirements of HVAC SOOs

2.1.1 Standards and Guidelines

While no industry standard exists in identifying information requirements for HVAC SOOs, there are several guidelines published by ASHRAE that provide guidelines to generate SOOs.

ASHRAE Guideline 13, 2014 [2]:
Summary: This guideline provides suggestions in developing specifications for Direct Digital Controller (DDC) systems for HVAC control applications and provides guidance system architecture, input/output structure, communication, program configuration, system testing and documentation.
Gaps in standard/guideline: 1. This guideline does not assist mechanical designers in verifying the completeness of SOOs; 2. It does not guide mechanical designers to identify information items to be included in SOOs.

SOOs for common HVAC systems, ASHRAE, 2005[3]:
Summary: This document includes a set of 28 SOOs for various AHU configurations. Each SOOs has text version, control schematic diagram, object lists and control model summary for the AHUs.
Gaps in standard/Guideline: 1. It does not provide guidance about adapting the SOOs for other types of AHU configurations; 2. Only focuses on SOOs for AHUs and no other components of HVAC systems; 3. Does not provide guidance of testing the implemented controls based on these SOOs.

ASHRAE RP-1455 SOOs (ASHRAE GPC-36, 2018) [1]:
Summary: This specification contains a set of 13 SOOs for air distribution and terminal variable volume systems. The document contains: (a) list of hard-wired points; (b) control diagrams; (c) sequence of operations; (d) programming parameters, settings and variables for the systems.
Gaps in standard/guideline: 1. It does not provide information of the approach used to identify the information items represented in the document for extending the document to other types of systems; 2. It does not provide guidance for testing the implemented controls based on these SOOs; 3. The findings of this research project were not validated to be generalized.

2.1.2 Previous research studies

Several researchers acknowledged many challenges

involved in interpreting HVAC controls' design intent from SOOs and addressed various aspects of these issues. Using the Function-Behavior-Structure (F-B-S) framework proposed by [7], the information requirements of SOOs from the past research was categorized and summarized in Table 1. Examples of information items for each category of the F-B-S framework according to previous researchers are listed in bold in the second column in Table 1.

Table 1. Information requirements of SOOs based on Function-Behavior-Structure framework

Category	References
Functional requirements	**E.g.: Be time efficient, Provide comfort, etc.**
Static information items	[4] [9] [15] [16]
Behavioral requirements	**E.g.: Heat absorption rate, response time, etc.**
Run-time information items	[10] [11]
Energy performance related information items	[10] [11]
Structural requirements	**E.g.: Geometrically interconnected components, Logically and physically interconnected components, etc.**
Relational information items	[9] [13] [15]
Constraints and heuristic information items	[5] [8]

It is required that the SOOs narrate about all control processes and relevant controlled variables and controlled devices to clearly convey the controls' design intent. Currently, as there is no formal approach to identify all the information items to be included in the SOOs, the mechanical designers are unable to verify the completeness of SOOs effectively. Hence, there is a need for a generalized approach to identify all the information items to be included in SOOs of a given HVAC system to validate the completeness of SOOs. The following sections describe the proposed research approach and reasonings that were developed to address this need.

3 Research Approach

Since the reasoning mechanisms and data representation are interdependent, all data schemas that are currently used in the industry to represent HVAC controls design information were analyzed. Table 2 presents the coverage of data schemas to represent various controls related information items that were identified under each category listed in Table 1.

Table 2. Analysis various data schemas related to HVAC controls to represent SOOs related information items

	Information items identified under each category listed in Table 1	**IFC4***	**COBie***	**HVACie***	**BAMie***	**BRICK**	**EnergyPlus**	**gbXML***
Static information items								
1	Type of controlled variables / devices	X		X	X	X	X	X
2	Sensor unique id	X			X	X		
3	Component unique id	X		X	X		X	X
4	Control set points and schedules	X			X	X	X	X
5	Functional role of a controlled device							
Run-time information items								
1	Operation modes	X	X		X	X		
2	Control logic					X		
3	Sensor measurements and controlled device status					X	X	X
Energy performance related information items								
1	Design values for controlled variables						X	X
2	Efficiency and capacity	X		X	X		X	X
Relational information items								
1	Topological relationships	X		X	X	X		
2	Functional relationships						X	X
Constraints and heuristic information items								
1	Impact of components on all control processes							
2	Performance limitations						X	X

**IFC4 – Industry Foundation Classes 4; COBIE: Construction Operations Building Information Exchange; HVACie – HVAC Information Exchange; BAMie – Building Automation Modeling Information Exchange; gbXML – Green Building XML schema*

As can be driven from Table 2, none of the data schemas that are currently used in the industry represent all information items to be included in the SOOs to enable automated controls Cx. This study specifically focuses on identifying all components influencing each temperature and flow control process in an AHU. This can be achieved by determining the functional role of all controlled devices in the AHU. Although none of the data schemas can currently be used to represent the functional role of components within an AHU, reasoning with other static information items can help determine this. Other static information items required to be represented in HVAC SOOs are mostly represented by IFC4 and BAMie schemas. BAMie is a model view definition of the IFC4 schema, i.e. it is a sub-set of IFC4 schema. Hence, the reasoning mechanisms to identify the functional role of components were developed for an input file represented in IFC4 format. The subsequent sections present the vision and reasoning mechanisms that were developed.

3.1 Proposed Approach

The developed approach, which automates the process of determining the identification of components that directly or indirectly impact temperature and flow control processes in an AHU, consists of two major steps as shown in the shaded boxes in Figure 1. The approach takes an AHU represented in IFC4 format with all enumerations of sensor types and distribution system types as an input and outputs a list of all control processes and all components that directly and indirectly influence each control process. For example, the hot water heating coil in the AHU shown in Figure 3 directly influences supply air temperature and the hot water pump indirectly influences the air temperature by maintaining the hot water flow.

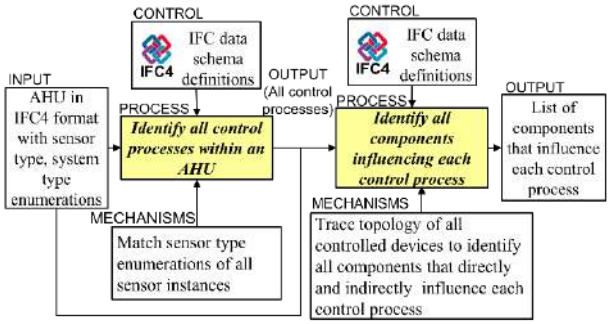

Figure 1. Proposed envisioned reasoning mechanisms

IFC4 schema has classes defined for sensors, controllers and different controlled devices. The two steps in the proposed approach rely on the sensor type enumerations, system type enumerations, component inherent functionalities and topological relationships of all components defined in the input IFC4 format file to identify each control process and components that directly and indirectly influence it. Figure 2 presents a flowchart showing the various reasonings that were developed in this study. The flowchart shows some sample results in bold-italics.

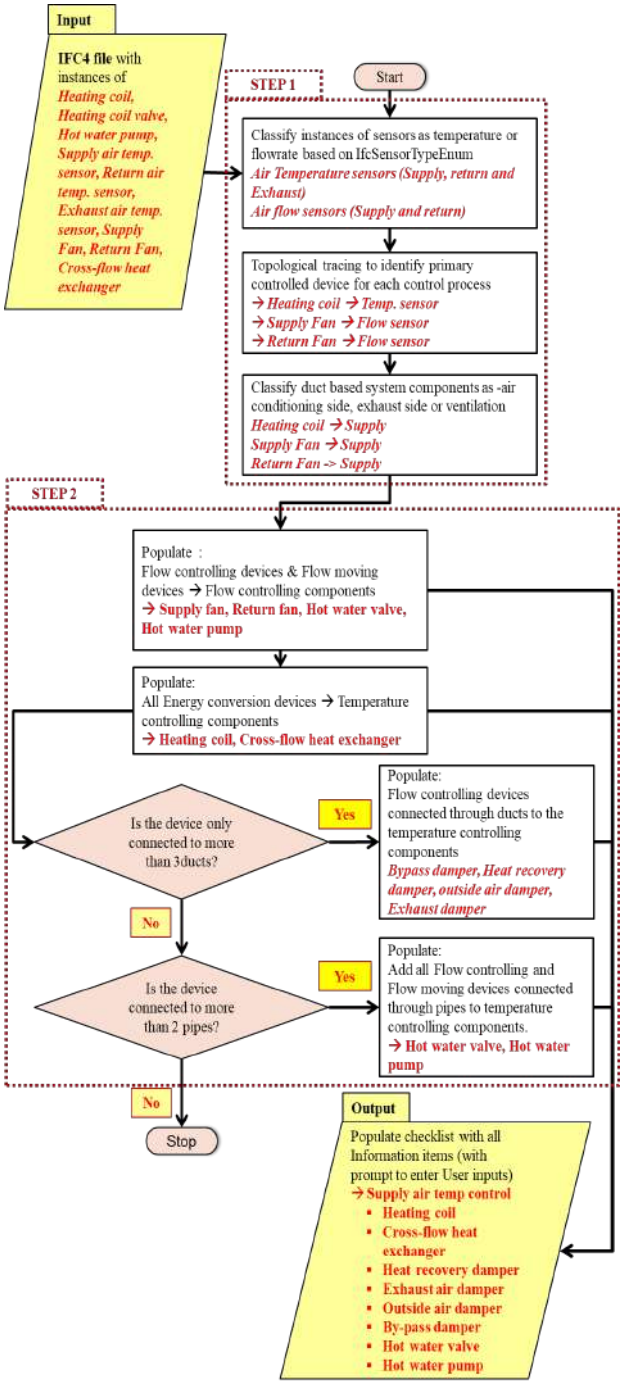

Figure 2. Flowchart showing the proposed reasoning mechanisms implemented in the prototype

Currently, many of the existing BIM authoring tools do not directly allow defining these enumerations. For the purpose of this study, enumerations of all components (IfcDistributionSystemTypeEnum, IfcFlowDirectionEnum and IfcSensorTypeEnum) within the testcase were manually populated. Figure 3 shows the AHU that was used as the test-case for this study.

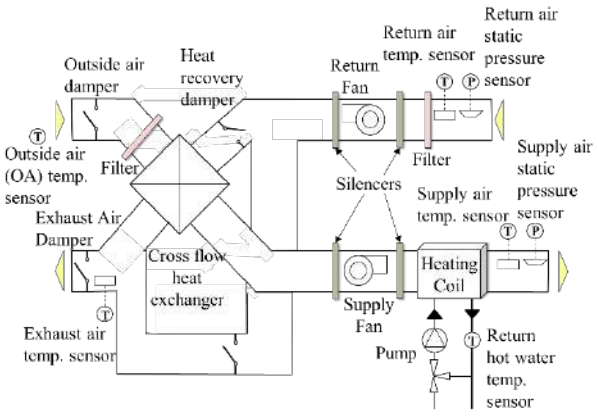

Figure 3. An AHU used as a test case for the study

3.1.1 Step 1: Identification of all temperature and flow related control processes

The first step in the proposed reasoning mechanisms is to identify all the control processes within the system. This step also involves the identification of the primary controlled devices influencing the control process and its relative location within the system to determine if it indirectly influences other control processes. For example, the supply air temperature sensor in the test case in Figure 3 is determined based on its sensor type enumeration (TEMPERATURESENSOR). Due to the relative location of the heating coil and the cross-flow heat exchanger occurring before the supply air temp sensor, it is determined to primarily impact supply air temperature control process. The reasonings are explained below:

Step 1a – Matching of sensor type enumerations for each sensor instance to identify control process types:

According to the principal of design for closed loop control systems, each control process uses the measurements from sensors at the end of a control sequence to send feedback to the controller about the controlled variable. The functioning of a controlled device is adjusted based on the feedback until the desired measurement is received from the sensor. Hence, knowing the types of sensors defined through the IfcSensorTypeEnum class helps in identifying the types of the control processes in a system. Since the scope of this study is limited to air temperature and flow related control processes, an instance of a sensor with FLOWSENSOR enumeration can be used to identify flow related control process and an instance of a sensor with TEMPERATURESENSOR enumeration can be used to identify temperature related control process. These two enumeration definitions for IfcSensorTypeEnum class are listed in Table 3.

Table 3. Enumerated item definitions for IfcSensorTypeEnum class relevant to this study in IFC4 schema

Enumeration	Definition	Reasoning
FLOWSENSOR	a device that senses or detects flow in a fluid	Match enumeration to flow control process
TEMPERATURE SENSOR	a device that senses or detects temperature	Match enumeration to temperature control process

Step 1b – Topological tracing to identify primary controlled devices associated with each sensor:

Further, knowing the topological location of the sensor with respect to other system components can help in identifying the specific control process, whose output is being measured using the sensors. This step involves tracing the sequence of AHU components to identify the energy conversion devices preceding temperature sensors and flow moving devices immediately preceding the flow/pressure sensors in an AHU. Since sensors can only measure the impact of preceding components in a control sequence, the proposed reasoning only looks for components preceding the sensors in a given AHU configuration. Also, all components are connected to each other through flow-fittings like ducts, pipes or cables. Since these flow-fittings do not directly influence the control processes, if a flow-fitting is directly preceding a sensor, the next preceding energy conversion device or flow moving device are identified respectively. The sequence of components in the AHU can be determined by the component's ports that connect to the adjacent component. IFC4 schema defines four different types of ports using IfcFlowDirectionEnum. Table 4 presents the definitions that were used in this study. SOURCE port corresponds to the outlet and the SINK port corresponds to the inlet of any component. The flow direction of air and thereby the sequence of AHU components is determined by the connections of source of a component to the sink of the adjacent component. For example, the supply air temperature sensor in Figure 3, has a duct connected to its source port. Further, the sink port of the heating coil is connected to the source port of the duct. Hence, the air flows through the heating coil to the duct to the sensor.

Table 4. Enumerated item definitions for IfcFlowDirectionEnum class in IFC4 schema

Enumeration	Definition	Reasonings
SOURCE	A flow source, where a substance flows out of the connection	Component connected to SOURCE port occurs prior in the sequence
SINK	A flow sink, where a substance flows into the connection	Component connected to SINK port occurs after in the sequence

Step 1c – Matching of distribution system enumerations and topological tracing to identify all control processes:

For each control process, once its type and the controlled devices primarily associated with it are determined, its context within the AHU (i.e., if it belongs to the supply side, return/exhaust side) is identified by matching the enumeration of the abstract class IfcDistributionSystem for each primary controlled device identified. This is required as the same type of control process can occur on the supply and the return side. For example, air flow is controlled by both the supply and return fans. All components that can be connected to ducts (since this study only involves AHU components) have three possible enumerations, based on the definitions in IfcDistributionSystemEnum. All control processes associated with components with AIRCONDITIONING or VENTILATION enumeration are classified as supply side control processes. All control processes with components with EXHAUST enumeration are classified as return / exhaust side control processes. Table 5 presents the enumerations for IfcDistributionSystemEnum class for duct-based systems used in this study.

Table 5. Enumerated item definitions for IfcDistributionSystemEnum class for duct-based systems in IFC4 schema

Enumeration	Definition	Reasonings
AIR CONDITIONING	Duct-based systems with this enumeration are meant to maintain temperature range within one or more spaces;	Match enumeration as supply side components
EXHAUST	Duct-based systems with this enumeration are meant to remove air from or more spaces;	Match enumeration as return / supply side components
VENTILATION	Duct-based systems with this enumeration are meant to either exchange or circulate outside air to spaces in a building;	Match enumeration as supply side components

3.1.2 Step 2: Identification of all components that influence each control processes

The second step of the reasoning mechanism is to identify all components that influence each identified control process in Step 1. This involves determining the inherent functionality of all components within the input IFC4 file through abstraction. For example, the supply fan is represented by an instance of IfcFan. The super-class of IfcFan is IfcFlowMovingDevice. All instances of sub-classes of IfcFlowMovingDevice influence flow related control processes based on the defined inherent functionality in IFC4 schema. Further, it is important to understand the interaction between control processes related to air flow and air temperature within an AHU. Temperature related control processes may involve direct heat transfer, air-to-air heat transfer or water/refrigerant-to-air heat transfer. While no additional components are involved for direct heat exchange, components that influence air temperature control for air-to-air and water/refrigerant-to-air heat exchange are identified through classification of component types and analyzing their configuration. The reasonings for step 2 are explained below:

Step 2a: Identification of inherent control functionality of all components through abstraction to associate with the identified control processes:

Inherent control functionality of HVAC components is defined at superclass level in IFC4 schema. Various control functionalities of components are defined as sub-classes for IfcDistributionFlowElement class. Instances of subclasses (e.g., IfcFan, IfcPump) of IfcFlowMovingDevice are used to define components that initiate the movement of fluids within an AHU. Instances of sub-classes (e.g., IfcDamper, IfcValve) of IfcFlowController are used to define components that regulate the flow of fluids through a system. All components that are instances of sub-classes of IfcFlowMovingDevice and IfcFlowControllingDevice define the occurrence of a device to control or enable flow of fluids through a system. All instances of sub-classes of IfcEnergyConversionDevice influence temperature related control processes based on their inherent functionality as defined in IFC4 schema. The other sub-classes of IfcDistributionFlowElement (e.g., IfcFlowFitting, IfcFlowTerminal, etc.) are not relevant for this study as their inherent functionality as defined by their abstract class do not influence air flow and

temperature within an AHU. Figure 4 shows the relevant class hierarchy at which the inherent functionality of various components can be determined.

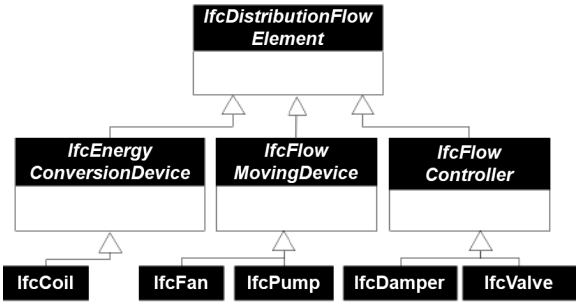

Figure 4. Subtypes of IfcDistributionFlowElement in the IFC4 schema relevant to this study

Step 2b: Identification of components influencing temperature control processes involving air-to-air heat transfer:

Air-to-air heat transfer resulting in air temperature related control processes can be identified based on the number of ducts connected to the instance of energy conversion device. Energy conversion devices can be classified as air-to-air heat transfer devices if they are connected to more than three ducts at their ports. The configuration of one air stream through an energy conversion device can have a maximum of three ducts – entering, leaving and exhaust (optional for pressure release). Hence, energy conversion devices with more than one air stream passing through them would have more than three ducts connected to them. Flow controlling devices immediately next to these air-to-air heat transfer energy conversion devices help modulate temperature of air. For example, the cross-flow heat exchanger in the test case modulates the flow air supply and return air streams. Dampers adjacent to the cross-flow heat exchanger are also used to control the supply and return air, but their purpose is to control the temperature by modulating air streams through a heat-exchanger.

Step2c: Identification of components influencing temperature control processes involving water/refrigerant-to-air heat transfer:

Water/refrigerant-to-air heat transfer resulting in temperature related control processes in an AHU can be identified if an energy conversion device is configured to be connected to a maximum of three ducts that correspond to one air stream and at least two pipes connected to it that correspond to one water or refrigerant stream. These correspond to an air stream and another stream of water/refrigerant through pipes. The first flow moving device and first flow controlling device connected to the pipe immediate after the water/refrigerant-to-air energy conversion device help modulate the temperature of air through the component. For example, the hot water heating coil in the test case enables water-to-air heat transfer to control the supply air temperature. The hot water valve and the hot water pump immediately next to the coil modulate to influence the control of temperature of air through the coil.

3.2 Prototype development and discussion

The described reasoning mechanisms were developed with the aim of identifying all temperature and flow related control processes within an AHU. Further all components that influence each control process are identified in a customized way through abstraction, classification and configuration analysis of each component. A prototype was developed with the proposed reasonings to identify the contextual functions of components in an AHU.

The prototype was created and the reasonings were verified using the test-case AHU shown in Figure 3 to see if it captured all the temperature and flow control processes and the components that directly and indirectly influence each identified control process. Table 6 presents the results identified by the prototype. Since no components precede the return air temperature sensor, no components were identified for the control process.

Table 6. Control processes and the components directly and indirectly influencing them identified by the reasoning mechanisms in the prototype

Control process identified	Components identified to directly and/or indirectly influence the control process
Supply air temp control	Heating coil, heat exchanger, heat recovery damper, outside air damper, by-pass damper, hot water valve, hot water pump
Return air temp control	-
Exhaust air temp control	Heat exchanger, outside air damper, heat recovery damper, by-pass damper
Supply air flow control	Supply fan, outside air damper
Return air flow control	Return fan, heat recovery damper, bypass damper, exhaust air damper

As a summary, reasoning mechanisms to identify components that directly and indirectly influence air temperature and flowrate in an AHU were developed and verified using a testcase. Future research in this study will focus on determining components that directly and indirectly influence other types of control processes within an AHU like humidity, CO2 level, etc.

4 Conclusion

This paper highlights the information items that need to be included in SOOs for HVAC systems based on the Function-Behavior\-Structure (FBS) ontology structure. FBS ontology structure is a proven robust descriptor of designs and designing process [7]. Reasoning mechanisms were developed based on function and structure ontology to identify temperature and flow related control processes within an AHU. Also, the components that influence each control process through abstraction, classification and their configuration analysis. Future research in this study will be extended to other control processes within an AHU such as humidity, CO2 level, etc. Also, future work will extend data schemas and reasoning mechanisms to enable automated extraction of all information requirements for HVAC SOOs identified in this paper.

References

[1] A. S. H. R. A. E. ASHRAE RP-1455: Advanced Control Sequences for HVAC Systems Phase I, Air Distribution and Terminal Systems. Online: http://www.taylor-engineering.com/downloads/guides/RP-1455%20Advanced%20HVAC%20Control%20Sequences%20for%20Airside%20Equipment.pdf, Accessed: 03/09/2019.

[2] A. S. H. R. A. E. Guideline 13: Specifying Direct Digital Control Systems. ASHRAE, Atlanta, GA, 2007.

[3] A. S. H. R. A. E. Guideline 36: High Performance Sequences of Operation for HVAC systems. ASHRAE, Atlanta, GA, 2015

[4] Balaji B., Bhattacharya A., Fierro G., Gao J., Gluck J., Hong D., Johansen A., Koh J., Ploennigs J., Agarwal Y., Berges M., Culler D., Gupta R., Kjæraard MB., Srivastava M., and Whitehouse K. Brick: Towards a unified metadata schema for buildings. In Proceedings of the 3rd ACM International Conference on Systems for Energy-Efficient Built Environments, pages 41-50, Palo Alto, CA, USA, 2016

[5] Bălan R., Cooper J., Chao K. M., Stan S., and Donca R. Parameter identification and model based predictive control of temperature inside a house. Energy and Buildings, 43(2): 748-758, 2011.

[6] Buildings Technologies Program, Energy Efficiency and Renewable Energy, U.S. Department of Energy. Buildings Energy Data Book. Online: http://buildingsdatabook.eren.doe.gov/docs/DataBooks/2011_BEDB.pdf, Accessed: 03/09/2019.

[7] Gero J. S., and Kannengiesser U. The function-behaviour-structure ontology of design. In An anthology of theories and models of design. Springer, London, 263-283, 2014.

[8] Leveson N. G., Heimdahl M. P. E., Hildreth H., & Reese J. D. Requirements specification for process-control systems. IEEE transactions on Software Engineering. 20(9): 684-707, 1994.

[9] Liu X., Akinci B., Garrett J. H., and Bergés M. Requirements for an Integrated Framework of Self-Managing HVAC Systems. In Proceedings of 2011 ASCE International Workshop on Computing in Civil Engineering, pages 802-809, Miami Beach, FL, USA, 2011.

[10] Pérez-Lombard L., Ortiz J., Coronel J. F., and Maestre I. R. A review of HVAC systems requirements in building energy regulations. Energy and buildings, 43(2): 255-268, 2011.

[11] Stenzel P, Haufe J., and Redondo J.N. Using a BIM flow for the design and operation of Building Energy Management Systems. In Proceedings of the 4th eeB Data Models workshop, pages 46-60, Nice, France, 2013.

[12] Sunnam R., Ergan S., and Akinci B. Challenges in Interpreting the Design Intent from HVAC Sequence of Operations to Assess the System Behavior: A case study. In Proceedings of the Computing in Civil and Building Engineering, pages 1465-1472, Orlando, FL, USA, 2014.

[13] Sunnam R., Ergan S., and Akinci B. Deviation analysis of the design intent and implemented controls of HVAC systems using sensor data: A Case Study. In Proceedings of the International workshop for Computing in Civil and Building Engineering, pages 223-231, Austin, TX, USA, 2015.

[14] Wetter M., Nouidui T. S., Lorenzetti D., Lee E. A., and Roth A. Prototyping the next generation energyplus simulation engine. In Proceedings of the 3rd IBPSA Conference, pages 27-29, Jeju island, South Korea, 2016.

[15] Yang X., and Ergan S. Processes, information requirements and challenges associated with corrective maintenance in relation to indoor air problem related work orders. In Proceedings of ISARC 2013 - 30th International Symposium on Automation and Robotics in Construction and Mining, Held in Conjunction with the 23rd World Mining Congress, pages 1119-1128, Montreal, Quebec, Canada, 2013.

[16] Zamanian M. K., and Pittman J. H. A software industry perspective on AEC information models for distributed collaboration. Automation in Construction, 8(3): Pages 237-248, 1999.

A Chatbot System for Construction Daily Report Information Management

J. Cho[a] and G. Lee[a]

[a]Department of Architecture and Architectural Engineering, University of Yonsei, South Korea
E-mail: jkun86@naver.com, glee@yonsei.ac.kr

Abstract –

Consistently updating, analyzing, and managing construction-related information is one of the key success factors in project management. Quite a few construction projects have recently started to utilize instant messaging (IM) applications such as Slack, WhatsApp, and WeChat as a communication channel among project participants to share daily construction information due to easy accessibility. However, general contractors are still required to manually extract and integrate the data from instant messages to compose daily reports. This is because the data inputted by subcontractors through IM applications are usually in an unstructured form and the IM application is not normally interoperable with the systems database especially developed for construction management. To solve this problem, this study proposes a chatbot-assisted construction daily report data management system. The chatbot in the proposed system collects and processes the required information through conversations with subcontractors, and automatically generates and shares a daily report for general contractors. A prototype system has been designed and implemented to prove the concept.

Keywords –

Construction daily report; Chatbot; Instant messaging application

1 Introduction

Consistently collecting and analyzing construction management related information, such as the schedule and cost, is very important for successful project results due to the inherent risks and uncertainty of the construction industry. Therefore, a systematic communication plan or process between the general contractor and subcontractors needs to be defined for efficient data collection.

However, it can be problematic if all participants do not utilize a unified communication channel or if a low level of technical understanding about the system prevents them from using it. Nevertheless, the use of everyday instant messaging (IM) applications at construction sites has been on the rise as a channel of information exchange. There are many advantages to using popular IM applications, such as interoperability with external systems, searching for information, and exchanging files.

In addition, chatbot technologies can be deployed. A chatbot is a service that provides a communication interface with users based on rules or artificial intelligence (AI). An AI-based chatbot answers based on the understanding the intentions of texts from users using natural language processing (NLP), while rule-based chatbot can answer only when detect predefined expressions[1]. When using chatbot technologies that understand intent and context from a user's utterances, and provide the necessary information through an interactive interface, there is the potential to support the user's efforts to collect and unify information. Therefore, this study presents a chatbot system model that collects construction daily report data through conversations with users, such as general contractors and subcontractors, and automatically generates daily report.

This paper is organized as follows. First, the requirements of the chatbot system are defined through the literature review. Then, the system architecture and dialog model for the two main functions of data extraction and report generation are explained. Finally, the functional feasibility was validated through the development of prototypes.

2 Literature Review

2.1 Limitations of Previous Studies on Construction Daily Report Systems

Many studies have suggested a system model for troubleshooting time-consuming and inefficient processes performed each day for collecting data and creating construction daily reports.

Russell et al. emphasized the importance of readily and reliably collecting data while presenting an early model of the computing system [2]. However, even with

the advantages of storing and utilizing information, the proposed early system model was not able to relieve the burden on the business because the manager still had to input all the information at construction field. In a case study lead by Yan-chyuan et al., a system model in which a daily report module extends its functionality by incorporating the estimation, pricing, and accounting system to enable cost management [3]. However, it was also not clearly defined for the main body to enter the necessary report data.

Subsequently proposed system models were designed to allow subcontractors to enter construction daily report data. The system model designed by Chin et al. would reduce a manager's tasks and enable plan-completion management by entering detailed level of work items by subcontractors [4]. More recently, a number of BIM-based cloud computing software programs, such as BIM360 and Procore, allow for effective construction project management by reflecting the system model explained above.

However, while this software provides strong management functionality, it has a major issue in that the systems require users to have a high level of technical understanding. Several factors, such as lack of education programs and low levels of subcontractor technical expertise, have been cited as the main cause of the problem with regards to using a unified platform [5].

2.2 Possibilities and Limitations in Current Use of IM Applications for Daily Report Information Collection

Recently, participants of quite a few construction projects have communicated using IM applications originally developed for nonbusiness purposes [6].

IM applications can provide better management capabilities when coupled with external management systems, such as a BIM-based construction management system explained above. However, due to the lack of connectivity, managers are currently required to spend additional time reformatting, integrating, and re-entering the same information.

This study proposes a "chatbot" as a solution to such redundant and manual data-input problems. In the construction domain, NLP has been mainly used for analysis of documentations for checking code compliance [7], retrieving similar project cases [8], and managing safety factors [9]. However, there are no studies utilizing NLP for construction daily report related data management.

In order to automatically manage information related to the construction daily report through communications with the chatbot, the specific model of the chatbot system needs to be designed to understand the messages from the users, to automatically extract the necessary information or store it in the database, and to automatically generate relevant documents for users.

3 Requirement and Coverage Definition of the System

3.1 Requirement of the System

The system requirements defined through the literature review are as follows:

1. The chatbot system should be able to extract the information related to the daily report from the messages or through the conversation with the chatbot and automatically store it in a linked database.
2. The chatbot system should be able to generate reports automatically based on information from the database.

With respect to the first requirement, it is necessary to define which types of information should be handled by this system. In this research, information types are defined based on prior research by Song [6]. Song has analyzed conversations that have taken place using IM applications on seven actual construction projects. Through the analysis, "date," "name of company," "types and number of labor," "types and number of equipment," and "work items" have been defined as primarily shared information types through IM applications. Figure 1 is an example message for daily reporting, including the five information types used in construction projects.

With respect to the second requirement, automatically created documents are defined as including "project name," "date," "total number of units per labor type," "total number of units per equipment type," and "work item list" as shown in Figure 2.

In order to calculate the total number of laborers and equipment used, the sum of the numbers entered by different subcontractors must be determined.

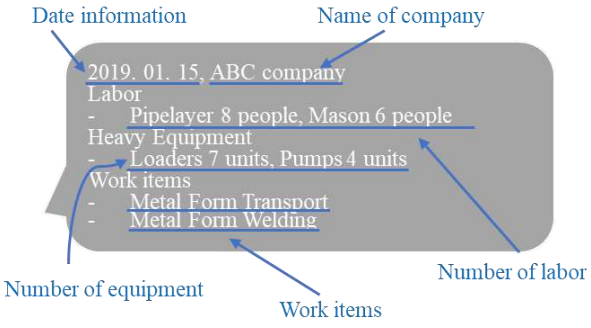

Figure 1. Mainly shared information types in an example user message for daily reporting

3.2 Coverage of the Defined Information Types in the System

In the case of labor and equipment, it has been determined that it is generally entered in a structure that follows the order of "type," "quantity," and "unit name," such as "Mason 6 people" in Figure 1. Therefore, in this study, a regular expression (regexp) approach is applied to detect the types "number of labor" and "number of equipment."

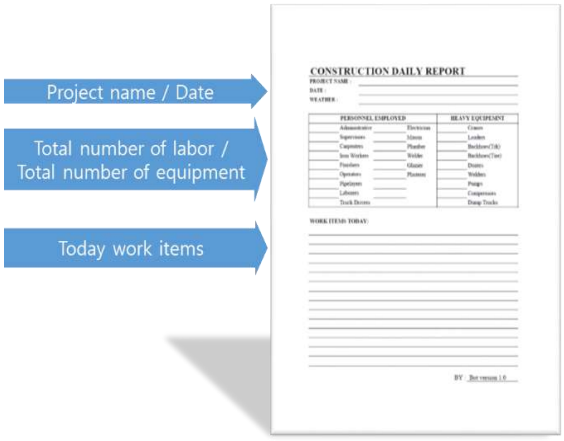

Figure 2. defined report format and included information types

In defining the regular expression for the "number of labor" and "number of equipment," because the detailed items of both types may vary depending on the breakdown structure applied, the items in Table 1 are temporarily defined as labor and equipment items that the system deals with.

Table 1. Temporary breakdown structure of labor and equipment covered by the chatbot system

Labor types		Equipment types
Carpenter	Electrician	Crane
Supervisor	Mason	Loader
Ironworker	Plumber	Backhoe
Glazier		Dozer
Operator		Welder
Pipelayer		Pumpcar
Truck driver		Compressor
Plasterer		Dump Truck

Individual input about work items for the day is designed to be made through a dialog with the chatbot because it is determined that a phrase about work items for the day follows a declaration expression such as "work item" in Figure 1 and is not entered in a structured form.

The architecture of the chatbot system to meet the defined requirements will be explained in the next section.

4 Design of the Chatbot System

The architecture of the system to meet the above requirements is designed as shown in Figure 3. This system consists of a web application, a chatbot module, and a back-end module that connects to IM applications.

The web application receives the text input from the user through the IM application and transfers it to the chatbot module. The chatbot module then analyzes the messages from the users and generates a responding sentence or call using several functions of the web application and utilizing the back-end module.

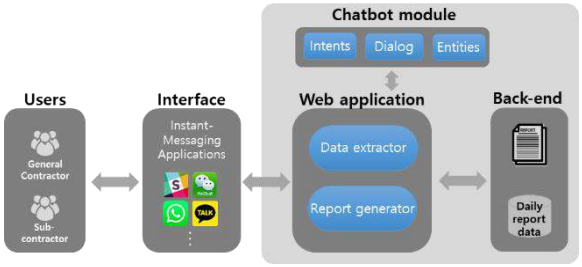

Figure 3. The architecture of the proposed system

The chatbot is an AI module based on Natural Language Processing (NLP) and it plays a role in understanding sentences that are received from users and then producing appropriate responses. The chatbot module is composed of "intent," "entity," and "dialog." Intent represents the purpose of the input by a user. All types of requests users made by users are defined as intent.. Entity means a term or object related to intent. Entity is used to provide a specific context for intent. Dialog is a branching conversation flow that defines responses to the defined intents and entities.

The web application consists of a "data extractor" and "report generator." Both modules are activated by function calls derived from the analysis results of chatbot modules.

The back-end system includes a database for storing extracted daily construction information obtained through message analysis and a file system for managing daily construction documents that are generated automatically upon user request.

In the following section, the design of the dialog model, intents, and entities for information input and report generation in the chatbot module are explained.

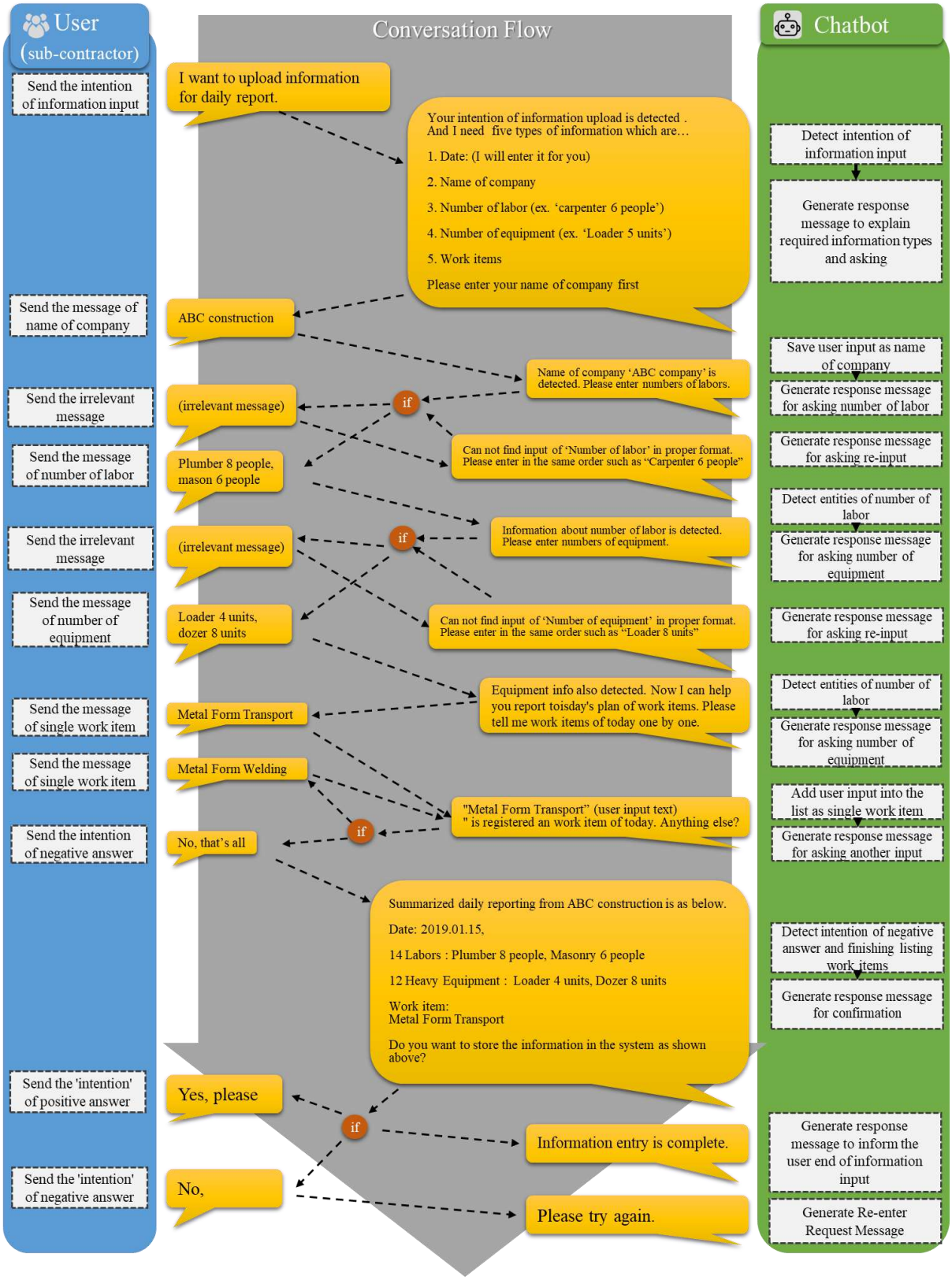

Figure 4. Dialog design for information input

The dialog model includes example messages between the user and the chatbot. Messages from the chatbot are generated by detecting one of the predefined "intents" and "entities" based on the context of the dialog.

4.1 Chatbot Module Design for Information Extraction

First, the dialog model for information extraction has been designed as illustrated in Figure 4.

The conversation begins with the chatbot detecting a message, representing the intention of the user to input information. Subsequent conversation flows are designed for chatbot to ask users for information in the order of labor, equipment, and work item. Finally, it is designed for the user to receive a final confirmation message generated by summarizing the information.

Table 2. Defined intents and examples of user utterances

Intent	Example expressions
Information input	"I want to upload information for the daily report" "Information input for daily report"
Positive answer	"Yes, please," "Great"
Negative answer	"No, it isn't," "No"

The types of intent to cover the dialog model defined above are given in Table 2. All the example expressions from users are necessary for the NLP training of the AI chatbot. The intent "information input" is designed to start a conversation process about information extraction with the chatbot. The "positive answer" and "negative answer" are designed for the confirmation step in the last part of dialog.

Table 3. Defined entities and value types

Entity	Value type	Structure description
Date	Patterns	Combination of year, month, and day
Name of company	Synonyms	Synonym from predefined list
Number of labor	Patterns	Combination of type, number of quantity, name of unit (Figure 5)
Number of equipment	Patterns	

The types of entity are defined in order to detect the types of information and extract them from the user messages as designed in Table 3. The remaining four information types were defined as "entities" for this dialog model, except for the non-structural form of work item mentioned previously.

The intent type "date" borrowed the most common form of structure, and the intent type "name of company" is defined as matching the text within a list of company names.

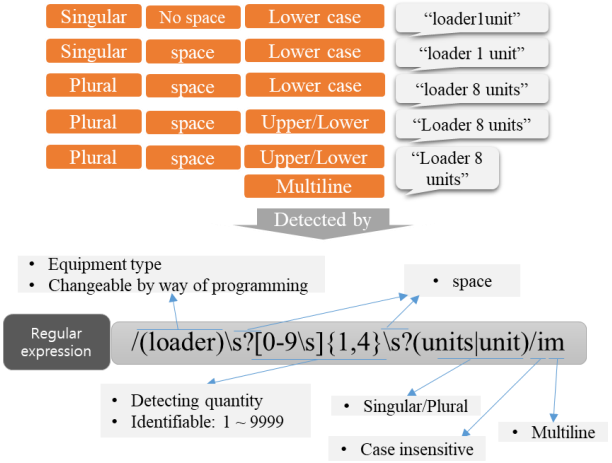

Figure 5. Designed regular expression approach for entity detection

Intent types "number of labor" and "number of equipment" takes the identical approach with regards to the pattern. Figure 5 describes the structure design of the regular expressions for recognizing the example text for the number of equipment. The pattern structure consists of "equipment type," "number of quantity," and "name of unit." The regular expression structure also includes consideration for "singular and plural form," "existence of space," "upper case and lower case," and "multiline" for the text from users.

Although Figure 4 explains the longest possible flow of conversation, based on the defined types of entities, it is also possible to have a scenario in which the chatbot module extracts all of the information for each of the four types from a single message sent by the user.

4.2 Chatbot Module Design for Report Generation

The dialog model for daily report generation has been designed as illustrated in Figure 6. The conversation begins with the chatbot detecting a message representing the intention of the user to request a document. Subsequent conversation flows are designed for the chatbot to ask for the user's e-mail address to send the generated document. The conversation is finished when the user receives an e-mail with the generated daily report.

This dialog model is designed for short conversations; only one type of intent "requiring document" is designed. Several example expressions, including the message

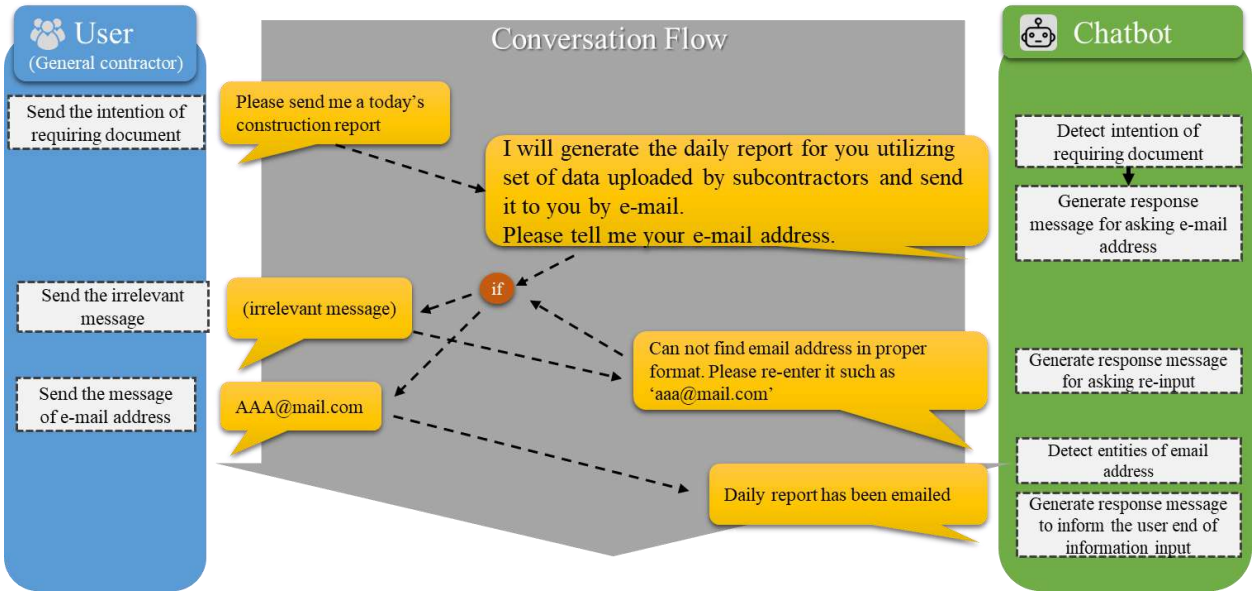

Figure 6. Dialog design for daily report generation

"Please send me today's construction report," are required for AI training as shown in Figure 6.

A single entity type is defined to obtain an e-mail address from a user in regular expression pattern.

It is also possible to skip this dialog in actual system implementation because once the system saves the email address, or has alternative information such as a phone number, the chatbot can automatically generate the documents and send them to the user on a regular basis at a defined time.

5 Prototype Implementation

5.1 Configuration of the Prototype System

A prototype of the proposed system as depicted in Figure 7 was developed to check the functional feasibility to determine how well it satisfies the requirements identified in the requirements analysis phase of system development.

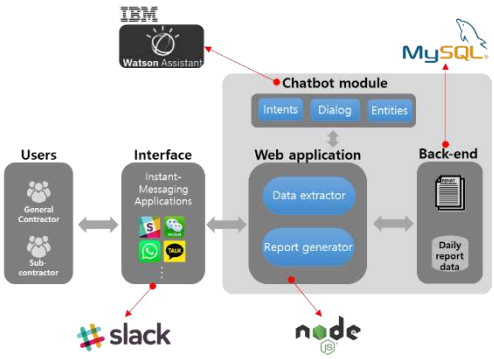

Figure 7. Configuration of the system prototype

First, the collaborative platform Slack, a well-established IM application, has been utilized for connecting users and the chatbot system.

The chatbot module has been implemented with Watson Assistant, which is an AI as a Service (AIaaS) provided by IBM for designing and implementing chatbots.

The web application has been implemented as a Node.js application. Node.js is an open source development platform for executing JavaScript code server-side. In the development of the Node.js web application, several packages shared through NPM (Node Package Manager) are included as dependencies of the system as explained in Table 4.

Table 4. Utilized packages for Node.js web application in the prototype

Name	Role
botkit	Integrating IM application and chatbot service
Express	Providing web application framework
Node-MySQL	Handling database
XLSL	Generating and updating excel file
Nodemailer	Sending e-mail

The "botkit" package has been utilized to integrate

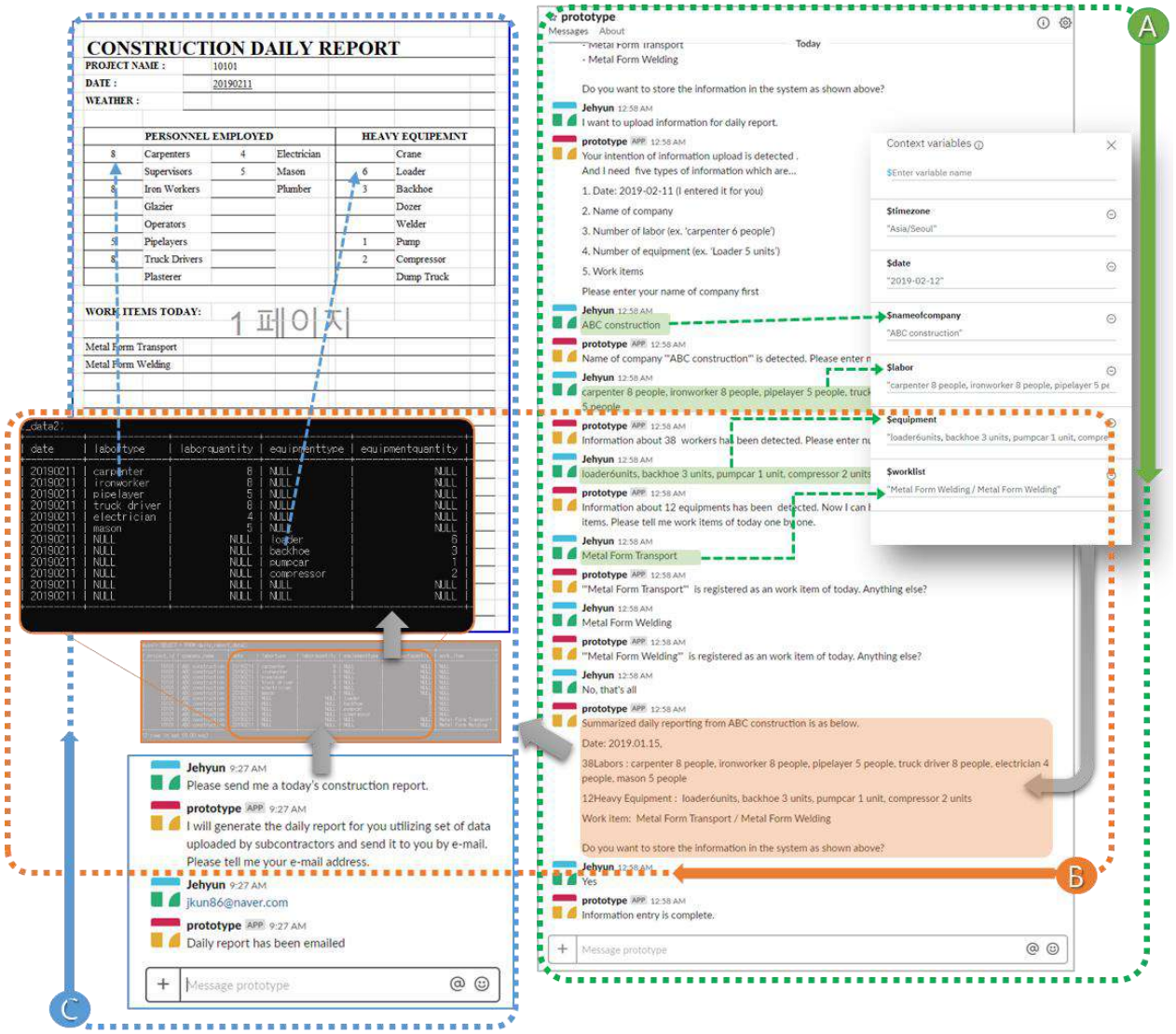

Figure 8. Implementation of the dialog models in the prototype system

the IM application and the chatbot service, which are Slack and Watson Assistant in the prototype. The "Express" package has been utilized for operating the server. The "Node-MySQL" package has been utilized for handling the database. The "XLSX" package has been utilized to generate and update the Excel file for the daily report. The "Nodemailer" package has been utilized to send emails to users.

The database system has been implemented with MySQL, which is a popular open source database.

5.2 Implementation of the Designed Dialog Model in a Prototype System

Data collection and automated report generation were tested using the prototype system based on predefined dialog models.

First, as depicted in area A of Figure 8, it is confirmed that, except for the "date" information, information related to the "name of company," "number of labor," "number of equipment," and "work items" was properly extracted from user messages, saved in the form of context variables during the process of conversation, and finally utilized for generating confirmation message.

Following this, as described in area B of Figure 8, user-confirmed data was parsed and stored by the web application as multiple rows in the database. In the case of "number of labor" and "number of equipment," quantity information was extracted and stored separately from the structured text such as "8" in the example "Carpenter 8 people,".

Finally, as shown in area C of Figure 8, a document was automatically generated by the web application by entering the information from the database into the

report's Excel form, which is predefined in advance when requested by the user.

5.3 Discussion

Through the experiments, the chatbot system has been identified as a functional and feasible system model that is expected to provide the following benefits:

- It can serve as a basis for enhancing management functions because IM application data is no longer volatile; it is now part of the system environment.
- This system model is beneficial to both user groups. The subcontractors do not require any special courses in the system input process, and the burden of data collection and documentation is reduced for the general contractors.

Nevertheless, the proposed system model has some problems to overcome at the current level.

- In the case of labor and equipment, the structure of text was borrowed from a previous study. However, for the "work items," because each subcontractor has a different work breakdown structure (WBS) and the text of the message is mixed with information about the work location in an unstructured form, it needs to incorporate a cognitive approach based on standardized WBS and LBS (Location Breakdown Structure).
- Due to the nature of the interactive interface, compared to the visual user interface, it is necessary to extend the dialog model in terms of convenience to meet various user scenarios. For example, it may be possible to modify only some of the total information entered, or to re-check the information entered.

6 Conclusion

This study presented a chatbot system model that automatically extracts information related to the construction work daily report exchanged in IM applications and automatically generates the construction daily report. The proposed system model includes a chatbot module, web application, and database. Several types of "intents" and "entities" are defined as needed for the conversation between users and the chatbot, along with dialog models. Detected information through the conversation between the user and chatbot could be utilized by the web application for data extraction and document generation using a database.

The prototype was developed and validated to determine whether the chatbot system can perform functions related to the requirements of data extraction and document generation.

The proposed system is expected to provide benefits for subcontractors in terms of ease of use and for general contractors with regards to reducing the effort to collect and document information. In addition, studies required for structural recognition of work items and functional range extensions for other management purposes, such as schedule and cost management, are further expected.

Acknowledgements

This work was supported by Institute for Information & communications Technology Promotion(IITP) grant funded by the Korea government(MSIT) (No.2017-0-00701(2nd year), Development of the Smart Field Platform for Planning and Managing Building Construction), grant (no. 19AUDP-B127891-03) from the Architecture and Urban Development Research Program funded by the Ministry of Land, Infrastructure, and Transport of the Korean Government and partially supported by the Graduate School of Yonsei University Research Scholarship Grants in 2017.

References

[1] Shridhar K. *Rule based bots vs AI bots. Online:* https://medium.com/botsupply/rule-based-bots-vs-ai-bots-b60cdb786ffa, Acessed: 2017, 03/22/2019.

[2] Russell A. D., Computerized daily site reporting, *Journal of Construction Engineering*, 119 (2):385-402, 1993.

[3] Shiau Y. and Wang W., Daily report module for construction management information system, *Proc. 20th Int. Symp. on Automation and Robotics in Construction*, 2003.

[4] Chin S., Kim K., and Kim Y.-S. J. J. o. c. i. c. e., Generate-select-check based daily reporting system, 19 (4):412-425, 2005.

[5] Construction M. H., "The Business Value of BIM for Construction in Major Global Markets." McGraw Hill Construction, Bedford, MA.," McGraw Hill Construction2014.

[6] Song T. S., "Extracting daily report information from text messages between the field managers," Master, Architecture & Architectural Engineering, Yonsei University, 2018.

[7] Zhang J. and El-Gohary N. M., Integrating semantic NLP and logic reasoning into a unified system for fully-automated code checking, *Automation in Construction*, 73:45-57, 2017/01/01/ 2017.

[8] Zou Y., Kiviniemi A., and Jones S. W., Retrieving similar cases for construction project risk management using Natural Language Processing techniques, *Automation in Construction*, 80:66-76, 2017/08/01/ 2017.

[9] Tixier A. J. P., Hallowell M. R., Rajagopalan B., and Bowman D., Automated content analysis for construction safety: A natural language processing system to extract precursors and outcomes from unstructured injury reports, *Automation in Construction*, 62:45-56, 2016/02/01/ 2016.

Supporting Deconstruction Waste Management through 3D Imaging: A Case Study

Y. Wei[a], A. Pushkar[a], and B. Akinci[a]

[a]Department of Civil & Environmental Engineering, Carnegie Mellon University, USA
E-mail: yujiew@andrew.cmu.edu, apushkar@andrew.cmu.edu, bakinci@cmu.edu

Abstract –

Conventional demolition approaches of razing a building at the end of its life-cycle generate a large amount of mingled debris, which is difficult to reuse and recycle. Compared to demolition, deconstruction involves disassembling a building systematically and it is a more environmentally friendly alternative. Recent research studies have focused on the transition from demolition to deconstruction to minimize the amount of generated waste and maximize the amount of recycling and reusing material. However, due to tight schedule requirements, extra labor cost, and the lack of drawings and design information, it is difficult for an owner to estimate the cost and duration of deconstruction ahead of time. 3D imaging technologies, such as laser scanning and image-based 3D reconstruction, provide an opportunity to obtain data about as-is conditions at a job site and hence can potentially help in identifying quantities of materials that will be recycled. Existing 3D imaging workflows have two primary limitations: visibility and appearance ambiguity. First, 3D imaging can only capture visible objects before a deconstruction process starts. Also, data captured before deconstruction or at different times during deconstruction can only include a subset of all building components. Second, building components with similar appearances can be made from different materials, resulting in misclassification and errors in quantity estimation. Only a few case studies have discussed how visibility and appearance ambiguity can affect the usage of 3D imaging in deconstruction waste management. In this paper, the authors aim to illustrate the application of 3D imaging during a small-scale deconstruction project in Pittsburgh. Specifically, the authors documented the waste generated during deconstruction manually and by using two different 3D imaging technologies: laser scanning and image-based registration. We then quantified the number of invisible objects and objects with ambiguous appearances at different stages of deconstruction. Through the comparison between the quantity takeoffs from 3D imagery and the ground truth, the paper aims at providing insights on the following questions: 1) How accurate are the quantity estimation and documentation of two 3D imaging technologies (laser scanning and imagery) compared to the actual waste generated? 2) Does 3D imaging capture all components of interest during deconstruction?

Keywords –

3D Imaging; Demolition; Deconstruction; Waste Management; Laser Scanning; Image

1 Introduction

The paper starts with an introduction of challenges encountered in deconstruction projects and review how previous research aimed to address these limitations.

1.1 Background

The demolition projects in the US generated over 547 million tons of demolition debris in 2015, which had tripled compared to the 170 million tons of debris in 2005 [1]. Over 30% of demolition debris had become landfill without being adequately recycled [2]. Demolition often generates mingled waste, which might contain hazardous materials, such as asbestos, lead, PCBs and medical waste [3]. With the concerns mentioned above, several researchers have proposed utilization of deconstruction instead of demolition to systematically disassemble a building into reusable components [4–7]. As governments all over the world publish stricter waste management and landfill regulations and guidelines, such as [8], deconstruction is becoming an important alternative to conventional demolition approaches.

Many barriers need to be overcome for a successful transition from demolition to deconstruction. For example, deconstruction projects often require a longer period and extra labor cost compared to demolition ones and such extra time and cost deter owners from adopting deconstruction approaches [9]. Deconstruction planning also requires a more accurate quantity takeoff than demolition. First, the feasibility of a deconstruction

project heavily depends on the value of salvaged material. Therefore, owners need an accurate quantity takeoff to support an economic assessment for a deconstruction project [10]. Second, deconstruction allows for preservation of a reusable component to maximize its value, such as keeping a reusable door rather than a 30-pound wood [11]. In a demolition project, waste quantity is usually estimated by using waste index inferred from historical data [12] and quantities from related deconstruction databases [13,14] of materials, which cannot satisfy the two requirements mentioned above.

Deconstruction projects also require prior knowledge of an existing building to facilitate planning and selection of disassembling procedures [10]. For example, a deconstruction project manager needs prior information of a building to estimate how long a project will take, how many workers are needed during deconstruction, and how much material can be recycled. However, as-built documents are often not available for buildings to be deconstructed. For example, 169 out of the 433 buildings demolished in Portland in 2016 had no as-built drawings information while the rest of buildings had drawings that were obsolete and hence were not reliable for deconstruction planning [15].

Another challenge when shifting from demolition to deconstruction is the need for detailed documentation of removed components. In a demolition project, the amount of recycled material is often measured by landfill diversion rate, which measures how much waste has been diverted from landfills and can be conveniently calculated using landfill receipts [16]. In comparison, documentation during deconstruction requires to record categories, quantities, and specifications of each component to support future recycling and potential tax reporting [5].

Several researchers have proposed many approaches, such as Building Information Model (BIM)-based deconstruction planning, reality capturing, and design for deconstruction, to address the limitations above [6,10,17]. The section below overviews these related research works and discusses their strengths and limitations.

1.2 Previous research

Previous research on obtaining information to support deconstruction waste management can be broadly categorized into two groups: 1) retrieving information from as-designed documents and 2) retrieving information from as-captured data. For instance, many researchers have been using Building Information Model (BIM) to facilitate the planning and waste management during demolition and deconstruction [5,6,17,18]. With an up-to-date BIM, it is convenient to generate an accurate quantity takeoff and a detailed deconstruction plan [19]. However, BIM is usually not available for most buildings to be deconstructed as mentioned in Section 1.1, which generates extra labor and time cost for manually creating a BIM for a deconstruction project.

Reality capturing through 3D imaging, such as laser scanning and RGB-D images, have become an active research topic in the Architectural, Engineering, and Construction (AEC) industries to capture the as-is status of a building [20]. For instance, Scan-to-BIM approaches that convert point clouds captured by a laser scanner to an integrated BIM are widely used for progress monitoring, as-designed and as-is comparison, and facility management [21–23]. Structure-from-Motion methods that reconstruct a 3D model from images are also well studied in the past ten years [24,25].

Previous case studies on using 3D imaging in deconstruction projects have focused on reconstructing a BIM from point clouds captured before deconstruction begins and generating quantity takeoffs from the reconstructed model [26,27]. However, many concerns exist about the possibility of using existing reality capturing approaches in deconstruction projects. The first concern is related to occlusion. For instance, Liu et al. reported that a data collection event with three laser scans for each room could only capture about 40% of the total components [28]. Most facility components are invisible due to occlusion before deconstruction begins, which will affect the completeness and accuracy of quantity estimation. While using progressively-captured data during deconstruction can possibly mitigate the occlusion problem, it raises new concern about the balance between data collection frequency and component coverage rate. Another issue is around identifying which 3D imaging technology would be more suitable for supporting deconstruction projects, especially due to the need for efficiency. This paper aims to provide insights on these issues through a case study of a deconstruction project.

2 A case study of using 3D imaging in a deconstruction project

Section 2 will first provide an overview of motivating problems associated with the case study, and then briefly introduce the project settings.

2.1 Problem statement

As mentioned in Section 1.2, existing reality capture approaches are faced with many challenges when used for deconstruction projects. This paper introduces the application of two types of 3D imaging - laser scan and imagery – in a small deconstruction project and examines the following questions in detail:

- Completeness: What portion of a building can be captured through 3D imaging at different stages of a deconstruction project and how will it affect the

quantity estimation?

- Quantity Estimation Accuracy: Can 3D imaging technologies provide accurate geometric information to support quantity estimation?
- What is the cost of using a 3D imaging in a deconstruction project, including labor hours, data collection, data processing, and data storage?

2.2 Project information

The case study was conducted on a two-story house job site with an area of 500 ft^2, consisting of a living room, a kitchen, a restroom, a bedroom, and two mechanical rooms. Figure 1 shows the exterior look of the building to be deconstructed.

Figure 1. The front view (left) and back view (right) of the building to be deconstructed

The goal of the deconstruction project is to reuse most structural and facility components in a new construction project, including but not limited to interior oak, roof panels, appliances, doors, windows, solar thermal systems, decking and lumbers. There are 125 groups of components to be recycled in total. Table 1 shows an example list of components.

Table 1. Example list of components to be recycled

Category	Components
Structure	Cypress plywood
	Cedar exterior cladding
	Laminated Veneer Lumber
	Structurally Insulated Panels
Doors and Windows	Fixed window
	Awning window
	Metal door frame
	Door wood
Appliances	Light fixtures
	Hand sink
	Solar photovoltaic panels
HVAC	Air diffuser
	Flex duct
	Insulated piping

The deconstruction of the building was mostly conducted manually with the help of a crane for lifting only. Since the building was designed for research purpose, it has a full set of design drawings and a 3D model, which provided useful information for pre-deconstruction planning. In the actual deconstruction process, the deconstruction team identified all components to be recycled from drawings and the 3D model first, created a detailed deconstruction plan, and then performed the actual disassembly. Figure 2 shows the interior disassembly plan for structural components. There are corresponding deconstruction plans for mechanical rooms, appliances, and exterior structural components respectively. A crew with about 20 students was involved in deconstruction activities. During deconstruction, once a component is removed from the building, the deconstruction team documents the component and uses the record as ground truth to evaluate the 3D imaging approaches discussed later.

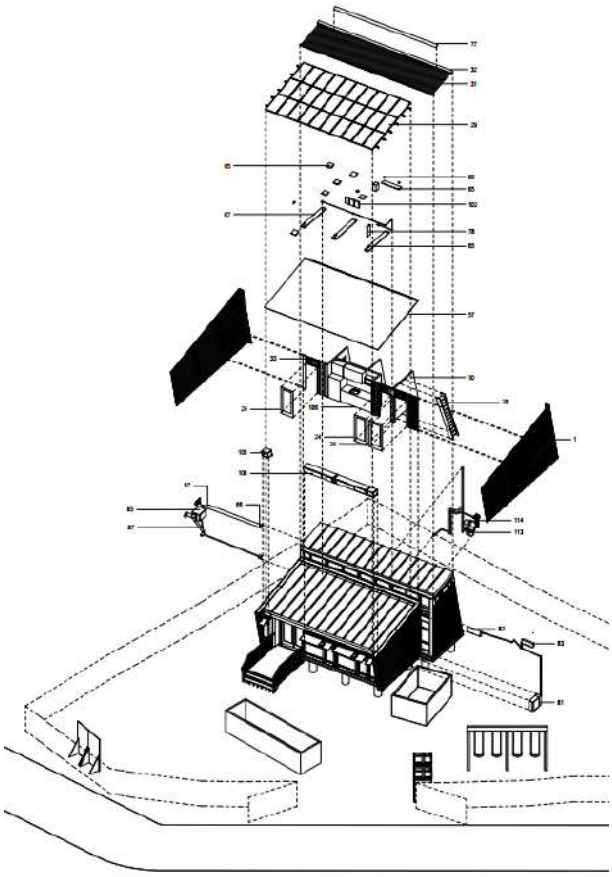

Figure 2. Interior disassembly plan for structural components (Figure generated from the 48-719 Architecture Design Studio: AECM UDBS course material taught at CMU during Fall 2018)

2.3 Application of 3D imaging technologies in the deconstruction project

Two 3D imaging technologies were used in this

project to collect data for the purpose of quantity estimation and documentation. One is terrestrial laser scanning which captures point clouds at different locations on site and the other one is unstructured images captured by cameras at fixed locations and hand-held cameras together. Below, we will introduce the details of how each technology was used in the deconstruction project.

2.3.1 Laser scanning

In this project, we used a Faro Focus3D S120 laser scanner to capture point clouds of the building. The laser scanner can capture 5 million points per scan with a view angle ranging from 0 to 360° horizontally and 30 to 330° vertically. In addition, the laser scanner also captures a panorama image to facilitate visualization and point cloud registration.

Figure 3. Point clouds captured at different times during the project: (a) before deconstruction, (b) after removing furniture and exterior walls, (c) after removing door and window frames, (d) after lifting the roof

Since laser scanning requires dedicated time for data collection to avoid possible occlusions from moving workers and equipment, we conducted 4 data collection events during the period of deconstruction, each consisting of 6-12 scans covering both interior and exterior of the building. The first scan event was conducted before deconstruction, the second was conducted right after removal of exterior panels, the third was after removal of door and window frames, and the fourth was after lifting of the roof. Figure 3 shows an example data captured from the laser scanner.

2.3.2 Imagery

Images captured by RGB-D cameras, DSLR cameras, and smartphones are also used for supporting deconstruction documentation. Before deconstruction began, we used an Intel Realsense D435 RGB-D camera to capture a set of images around the building. During deconstruction, two DSLR cameras were set up in the front of the building to record time-lapse image sequences. There were also 4-6 cameras moving around the job site to capture working progress and components being removed. At the end of the deconstruction project, there were more than 5,000 images available. Figure 4 shows example images captured during deconstruction.

Figure 4. Example images captured during deconstruction (Top: exterior; Bottom: interior)

2.4 From progressively-captured 3D imaging to quantity takeoff

The goal of using 3D imaging in a deconstruction project is to obtain a quantity takeoff consisting of important entries for cost estimation and activity planning, such as component categories, quantities, dimensions, materials, and recyclability. In this case study, we will focus on extracting categories and quantities from 3D imageries as a primary result. We used following methods to generate a component list and compared it with the manually-calculated ground truth. For laser scans, we manually identified and annotated objects in registered point clouds and measured their dimensions. Figure 5 shows an example of window frame annotations in the captured point cloud.

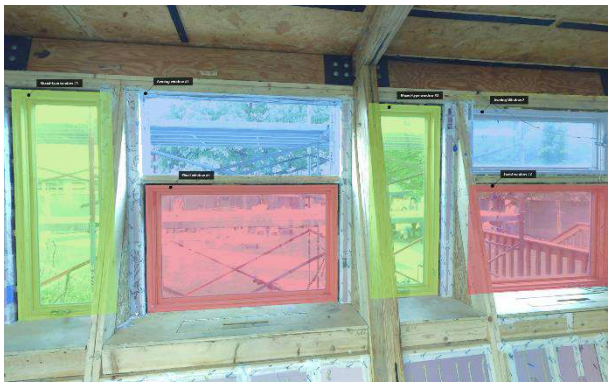

Figure 5. Component annotation from laser scans (red: fixed window, blue: awning window, green: mix-type window)

For images, since there are much more images (~5,000) compared to laser scans (6-12 scans per data collection), it is laborious to annotate objects on images to obtain the number of components. Therefore, for the purpose of evaluation only, we used the ground truth component information extracted from drawings to help identify objects presented on images. A component presented in the digital model is marked as found if at least one image captures the object on site. Similarly, a component presented in a digital model is marked as missing if there is no image captures the object. Figure 6 shows a concatenation of images covering all components of the mechanical room.

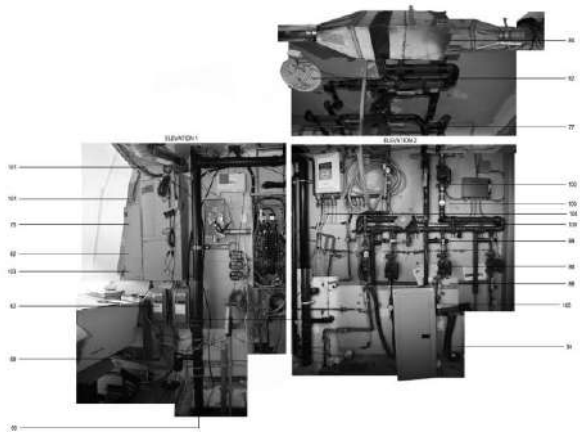

Figure 6. Components identified on images of the mechanical room (Numbers indicate the index in quantity estimation)

Table 2 below shows an example list of quantity takeoff in this case study. In the complete table, we also documented whether a component is recycled, labor hours for removing a component, and whether a component is seen on laser scans and images respectively. The quantity takeoff will be used for evaluation in the next section.

Table 2. Example list of a quantity takeoff

Component	Dimension	Quantity	MasterFormat
Hardwood boards	4’-4’’-2’’	9	061300
Plywood	4’-1’-3/4’’	3	061626
Door track	10’ - 10’’	4	083513
Glass door	8’-3’	1	081710
Structurally insulated panels	12’-9’	6	036866
Cabinets	2’-2’-1’	2	060000
Wash sink	-	1	-

3 Evaluations

In this section, we first define the metrics employed for evaluating the application of various 3D imaging approaches into a deconstruction project. Next, the results are analyzed to demonstrate the benefits and limitations of each 3D imaging technology.

3.1 Metrics

As mentioned in Section 2.1, this case study aims to address multiple concerns of using a 3D imaging approach in deconstruction projects, including completeness, capability of dimension measurement, labor time, and amount of data generated. Below we will talk about the metric used for the evaluation of each perspective.

- Completeness: The completeness of quantity estimation is defined as shown below where the number of identified components is calculated by counting the components that are captured during data collection and the number of total components is determined based on on-site documentation logs. We use the completeness to measure the accuracy of quantity estimation.

$$\text{Completeness} = \frac{\#\ of\ identified\ components}{\#\ of\ total\ components}$$

- The capability of dimension measurement: This metric indicates how well a 3D imaging approach supports dimension measurement, which is critical for quantity estimation. For example, if a user conducts a measurement on the captured data, obtaining a real-size measurement and an up-to-scale measurement that requires correction make a significant difference in quantity estimation.
- Time: We measured the time used for data collection, data processing, and component annotation to evaluate the efficiency of a 3D

imaging method.

- Amount of data generated: This metric measures the space needed to store the captured data.

In the primary experiments below, we ignore two important metrics for the moment: identifiability and dimension error. Identifiability indicates whether a 3D imaging method can distinguish objects with similar appearances. Since in this case study all components are annotated manually, we will leave the evaluation of identifiability after automating the quantity estimation process using 3D imaging. Also, for the metric dimension error which shows how much a measurement on length, area, or volume deviates from its ground truth, we will leave the evaluation for further experiments whose measurements are not performed manually.

3.2 Results and analysis

In this section, we will present the evaluation of two 3D imaging technologies using the metrics mentioned above. In our evaluation, we didn't include all the components listed in the as-designed documents. Small and unimportant components, such as woodscrews and assorted wires, are ignored when evaluating 3D imaging technologies. After selection, we have 1,041 components from 123 categories.

Table 3. Evaluation of using 3D imaging for quantity estimation in the deconstruction project

Metric	Laser Scanning		Imagery	Manual
Completeness	1	54%		
	2	19%	100%	100%
	3	11%		
	4	2%		
	Total	86%		
Dimension	Real-size		Up to a scale	Real-size
Data collection	16 hours		4.5 hours	48 hours
Annotation	20 hours		-	0 hour
Storage	13 GB		2.2TB	22kb

Table 3 shows the evaluation results for each 3D imaging technologies in comparison with documenting quantities manually. There are several interesting points worth discussing:

3.2.1 Completeness

The results indicate that with four laser scanning events, we can capture about 86% of the total components that need to be recycled. Specifically, the first data collection event consisting of 12 scans can only capture 54% of the components of interest, indicating that directly using scan-to-BIM approaches to estimate quantities is not very accurate.

Through inspection of the missing objects, we found that the incompleteness of data captured by laser scanning comes from two sources: 1) occlusions, 2) the temporal gap between two laser scans.

Occlusion refers to the problem that some components are invisible until other components are removed. The comparison between the completeness of the progressively-captured data and the one of data captured before deconstruction indicates that capturing data progressively during deconstruction can mitigate the occlusion problem. Figure 7 Metal studs behind the kitchen region are invisible in Scan 1 (left) but become visible in Scan 2 (right)shows how progressively captured data can address occlusions presented in a scene.

Figure 7. Metal studs behind the kitchen region are invisible in Scan 1 (left) but become visible in Scan 2 (right)

If an invisible object in a previous scan is removed before the next round of data collection, it will be missing in the quantity estimation. In our case study, there were 30 solar panels installed on the roof which cannot be captured by a terrestrial laser scanner in the first scan. After lifting the roof, these solar panels were removed between the third and the fourth scan, resulting in one of the primary errors in our quantity estimation.

In comparison, images captured by handheld cameras and time-lapse cameras can cover all objects of interest. Though in this case study we captured more imagery data than usual, the result shows that with enough crowd-sourced image data, it is possible to generate a complete quantity takeoff without missing components.

3.2.2 Dimension measurement

Point clouds intrinsically support measurements and can achieve a low dimension error of ~2-5 mm as reported in previous research [25]. Image-based approaches cannot provide the functionality of measurement unless all images are well calibrated, which limits its application in quantity estimation.

3.2.3 Time efficiency

Table 3 also shows the time used for data collection and annotation to obtain a quantity estimation. For data collection, we only counted the dedicated labor hours in our calculation. Therefore, crowd-sourced images captured during deconstruction activities require the least time to collect. However, when it comes to annotating objects to generate a quantity estimation, it is quite difficult for human beings to annotate over 5,000 images, which originates the need for either reconstructing a 3D model from images or recognizing components automatically. For point clouds, annotating objects manually also took a significant number of hours. Therefore, automation in identifying components of interest will benefit both laser scanning-based approaches and image-based approaches.

4 Conclusions

This paper presents a case study of using two different 3D imaging technologies to support quantity estimation and documentation in deconstruction projects. Through the evaluation of completeness, the capability of dimension measurement, and time efficiency, we highlighted the importance of capturing data progressively during deconstruction and automating the process of annotating components from 3D imaging data. In addition, despite that we have a deconstruction schedule, planning when and where to perform data collection is still challenging during deconstruction. It is necessary to develop an approach to plan progressively data collection events during deconstruction. Also, though imagery data covers all recyclable objects during deconstruction, the amount of data is enormous. Therefore, the next step of our study will be to develop an automated approach to process progressively-captured data from 3D imaging to support deconstruction planning and documentation.

5 Acknowledgement

We would like to acknowledge and thank Professor John Folan, all staffs and students participating in the course 48-719 Architecture Design Studio: AECM UDBS taught in Fall 2018 at Carnegie Mellon University for their help during deconstruction, data collection, and data analysis.

References

[1] Agency EP. *Sustainable Management of Construction and Demolition Materials*.; 2015. https://www.epa.gov/smm/sustainable-management-construction-and-demolition-materials#America.

[2] Consulting H. *Construction and Demolition Waste Status Report - Management of Construction and Demolition Waste in Australia*.; 2011. http://www.environment.gov.au/protection/waste-resource-recovery/publications/construction-and-demolition-waste-status-report.

[3] Valle D, Worth F. Construction Waste Management Database | Whole Building Design Guide. *Build Des*. 2008:5-6. https://www.wbdg.org/resources/construction-waste-management. Accessed October 19, 2018.

[4] Dantata N, Touran A, Wang J. An analysis of cost and duration for deconstruction and demolition of residential buildings in Massachusetts. *Resour Conserv Recycl*. 2005;44(1):1-15. doi:10.1016/j.resconrec.2004.09.001

[5] Akbarnezhad A, Ong KCG, Chandra LR. Economic and environmental assessment of deconstruction strategies using building information modeling. *Autom Constr*. 2014;37:131-144. doi:10.1016/j.autcon.2013.10.017

[6] Akinade OO, Oyedele LO, Bilal M, et al. Waste minimisation through deconstruction: A BIM based Deconstructability Assessment Score (BIM-DAS). *Resour Conserv Recycl*. 2015;105:167-176. doi:10.1016/j.resconrec.2015.10.018

[7] Kibert CJ, Chini AR, Languell J. *Deconstruction as an Essential Component of Sustainable Construction*.; 2001. https://www.irbnet.de/daten/iconda/CIB3122.pdf. Accessed January 27, 2019.

[8] *CONSTRUCTION AND DEMOLITION WASTE GUIDE-RECYCLING AND RE-USE ACROSS THE SUPPLY CHAIN*.; 2012. https://www.environment.gov.au/system/files/resources/b0ac5ce4-4253-4d2b-b001-0becf84b52b8/files/case-studies.pdf. Accessed March 8, 2019.

[9] Kibert CJ. *Sustainable Construction : Green Building Design and Delivery*. John Wiley & Sons; 2016.

[10] Rios FC, Chong WK, Grau D. Design for Disassembly and Deconstruction - Challenges and Opportunities. *Procedia Eng*. 2015;118:1296-1304. doi:10.1016/J.PROENG.2015.08.485

[11] Iacovidou E, Purnell P. Mining the physical infrastructure: Opportunities, barriers and interventions in promoting structural components reuse. *Sci Total Environ*. 2016;557-558:791-807. doi:10.1016/j.scitotenv.2016.03.098

[12] Llatas C. A model for quantifying construction waste in projects according to the European waste list. *Waste Manag*. 2011;31(6):1261-1276. doi:10.1016/j.wasman.2011.01.023

[13] Solís-Guzmán J, Marrero M, Montes-Delgado MV, Ramírez-de-Arellano A. A Spanish model for quantification and management of construction waste. *Waste Manag*. 2009;29(9):2542-2548. doi:10.1016/j.wasman.2009.05.009

[14] Yuan H, Shen L. Trend of the research on construction and demolition waste management. *Waste Manag*. 2011;31(4):670-679. doi:10.1016/j.wasman.2010.10.030

[15] Sustainability B of P and. *Oregon Deconstruction Program Report*.; 2017. www.exploredecon.com. Accessed January 27, 2019.

[16] Tchobanoglous G, Theisen H, Vigil SA, Alaniz VM. *Integrated Solid Waste Management: Engineering Principles and Management Issues*. Vol 949. McGraw-Hill New York; 1993.

[17] Cheng JCP, Ma LYH. A BIM-based system for demolition and renovation waste estimation and planning. *Waste Manag*. 2013;33(6):1539-1551. doi:10.1016/j.wasman.2013.01.001

[18] Eadie R, Browne M, Odeyinka H, McKeown C, McNiff S. BIM implementation throughout the UK construction project lifecycle: An analysis. *Autom Constr*. 2013;36:145-151. doi:10.1016/j.autcon.2013.09.001

[19] Volk R, Stengel J, Schultmann F. Building Information Modeling (BIM) for existing buildings - Literature review and future needs. *Autom Constr*. 2014;38:109-127. doi:10.1016/j.autcon.2013.10.023

[20] Wei Y, Kasireddy V, Akinci B. 3D imaging in construction and infrastructure management: Technological assessment and future research directions. In: *Lecture Notes in Computer Science (Including Subseries Lecture Notes in Artificial Intelligence and Lecture Notes in Bioinformatics)*. Vol 10863 LNCS. Springer, Cham; 2018:37-60. doi:10.1007/978-3-319-91635-4_3

[21] Xiong X, Adan A, Akinci B, Huber D. Automatic creation of semantically rich 3D building models from laser scanner data. *Autom Constr*. 2013;31:325-337. doi:10.1016/j.autcon.2012.10.006

[22] Anil EB, Tang P, Akinci B, Huber D. Deviation analysis method for the assessment of the quality of the as-is Building Information Models generated from point cloud data. *Autom Constr*. 2013;35:507-516. doi:10.1016/j.autcon.2013.06.003

[23] Bosché F, Ahmed M, Turkan Y, Haas CT, Haas R. The value of integrating Scan-to-BIM and Scan-vs-BIM techniques for construction monitoring using laser scanning and BIM: The case of cylindrical MEP components. *Autom Constr*. 2015;49:201-213. doi:10.1016/J.AUTCON.2014.05.014

[24] Chaiyasarn K, Kim T-K, Viola F, Cipolla R, Soga K. Distortion-Free Image Mosaicing for Tunnel Inspection Based on Robust Cylindrical Surface Estimation through Structure from Motion. *J Comput Civ Eng*. 2016;30(3):04015045. doi:10.1061/(ASCE)CP.1943-5487.0000516

[25] Golparvar-Fard M, Bohn J, Teizer J, Savarese S, Peña-Mora F. Evaluation of image-based modeling and laser scanning accuracy for emerging automated performance monitoring techniques. *Autom Constr*. 2011;20(8):1143-1155. doi:10.1016/j.autcon.2011.04.016

[26] Ge XJ, Livesey P, Wang J, Huang S, He X, Zhang C. Deconstruction waste management through 3d reconstruction and bim: a case study. *Vis Eng*. 2017;5(1):13. doi:10.1186/s40327-017-0050-5

[27] Marino E, Spini F, Paoluzzi A, et al. Modeling Semantics for Building Deconstruction. doi:10.5220/0006227902740281

[28] Liu X, Eybpoosh M, Akinci B. Developing As-Built Building Information Model Using Construction Process History Captured by a Laser Scanner and a Camera. In: *Construction Research Congress 2012*. Reston, VA: American Society of Civil Engineers; 2012:1232-1241. doi:10.1061/9780784412329.124

Text detection and classification of construction documents

Narges.Sajadfar[a], Sina.Abdollahnejad[a] , Ulrich.Hermann[b] , Yasser.Mohamed[a]

[a] Department of Civil and Environmental Engineering, University of Alberta, Canada
[b] PCL Industrial Management Inc., 5404 99th St., Edmonton, Alberta, Canada
E-mail: sajadfar@ualberta.ca, sabdolla@ualberta.ca, rhhermann@pcl.com, yaly@ualberta.ca

Abstract –
Large construction projects generate thousands of documents that require a careful management. The classification of documents is an important step in document management and control. Construction documents are generated in different formats, many of which are unstructured and contain drawings and images, which makes the task of document classification and control even more challenging. In this paper, a dataset of 5000 documents is used as a case study. Optical Character Recognition (OCR) bounding boxes are applied to extract text from the set of documents. In the next step, two classification methods are applied. One based on a predefined set of keywords and another based on deep learning long short-term memory (LSTM) network. The challenges of the proposed approaches are discussed in relation to OCR bounding box locations with different document layout and how to obtain a set of representative key words for each class. Initial results of the study are encouraging and show that OCR technique combined with text classification is a powerful method for construction documents' control and can reach an accuracy of 92%.

Keywords –
Construction document; Text detection; Classification; Data mining; Optical Character Recognition (OCR); Deep Learning

1 Introduction

Many construction documents are complex and include text, images and drawings, which represent a vital source of information and knowledge regarding a construction project.

Text in construction documents includes important information such as title and number, which can be used to manage and classify construction document. However, not all documents are digitized or machine readable. Therefore, we need to create an image file of any printed document for text analysis. In this case, text is presented as an image in the file. Then, we can use OCR software to convert the scanned text and image into a machine-readable document. Also, it is one of the most used extraction techniques for documents and images [1]. In this paper, the research of OCR in construction industry is reviewed. In the second step, text detection and classification of construction documents are described, then two classification methods are applied on the case study. First classification is based on a predefined set of keywords and the second one is based on deep learning long short-term memory (LSTM) network. Finally, we compared and analyzed the effectiveness of the two classification, and the research results are presented.

2 Related studies

The literature review shows that previous researchers used OCR in construction document for different purposes. Berkhahn et al., (2008) used OCR and Kohonen neural network in construction drawings, in order to extract information about the dimensions of construction parts and inscription texts. Their model checks out all the dimension line points and construction element points to extract the dimension number and text. However; the user needs to check the result and correct the errors [2]. Banerjee et al., (2016) used OCR system to hyperlink engineering drawing documents. They created a hyperlink based on the extracted information, as a result the engineers can quickly navigate between different files. They

achieved more than 94% accuracy on automatic hyperlinking [3]. Also, Banerjee et al., (2017) used OCR engine in (Architecture, Engineering & Construction) AEC industry drawing documents for detection of Elevation Datum (ED) name, and graphical shape of ED, also they used experimental analysis to validate the ED name. The result of their research shows they achieved overall accuracy of 95% for ED detection and accurate destination document text recognition [4]. Another research of Banerjee et al., (2017) used OCR engine for extraction of alphabetic code and text of reference document, for that purpose of creating automatic navigation among architectural and construction documents. Their result shows the OCR has more than 91% accuracy on character level recognition [5]. Seraogi et al., (2017) used OCR engine in AEC to find the correct orientation of the documents based on the information of extracted texts and graphical shapes. They used mixed text/image drawings as their case study and achieved more than 99% accuracy on automatic orientation [6]. Gupta et al., (2018) used OCR engine in AEC to extract the title of the documents. In their method, OCR engine is scanning the information table only to extract the title. Also, they used historical data to increase the accuracy of their model. However, the extracted title should be reviewed by user to achieve 100% accuracy [7].

3 Related software and applications

Several commercial software packages are using OCR technology to extract the document information. Procore is a construction project management software that is using OCR on pre-defined template to extract drawing number, drawing discipline and drawing title. Drawing block text should be on the bottom right of drawing with specific size and location, then the Procore can automatically pre-populate the fields [8]. Docparser is another software which is using OCR engine to extract the text from any document. The user must define the specific locations inside the document and rules to apply on the all documents. Then Docparser will train to find the location of each field. Finally, this software will extract the text from pre-defined location based on regular expressions and pattern recognition [9]. Microsoft Azure is a computer application which is using variety of technologies such as OCR engine for text analysis. It can extract the text from images and documents, which can be used for label recognition, key phrase extraction and enable searching. Microsoft Azure is also using computer vision algorithms for image classification. The user must provide the labeled images to train a custom vision algorithm and create a model, which can classify new images [10]. The biggest problem of existing software is that they are not suitable for documents with variety of templates and their accuracy will significantly decrease in such situations.

4 Methodology

4.1 Dataset preparation

10 different document types and 500 documents from each document type (in total 5000 documents) was selected for case study analysis. All documents were in PDF format, which should be converted to image format for the purpose of using OCR text detection. Adobe Acrobat Pro DC was used to convert PDFs to PNGs. Since the information we want to extract is usually on the first page of each document, only the first page of each document was selected for future text analysis.

4.2 Pre-processing steps for improving image quality

The case study includes different sizes of documents, with different qualities. The resolution of images should be at least 300 DPI for a better text detection result. The first step is to resize all the documents to A4 size (8.27*11.96 inch) which will affect the resolution of images. In the second step, *Matlab*'s image processing toolbox is used for improving the quality of images. It has different function and filters that can be applied to modify the images. *rgb2gray* filter is used to convert documents to grayscale images. *Imadjust* filter is applied to increases the contrast and brightness of the output image and

Median filter is used to remove the noise from the grayscale pictures [11]. Figure 1 shows an original image and the enhanced images using *Matlab*'s image processing toolbox.

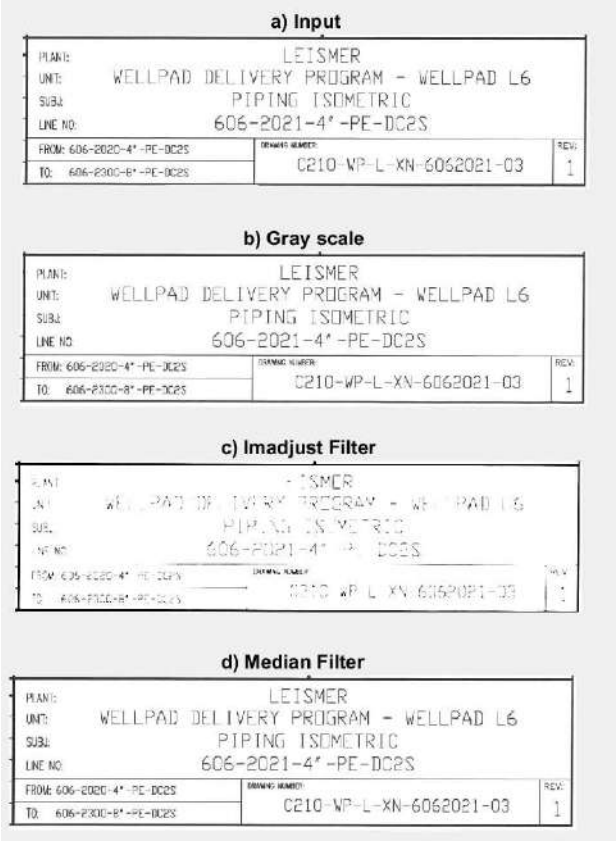

Figure 1: Original image and enhanced images using *Matlab* image processing

4.3 Layout analysis

Layout analysis such as page segmentation and region classification have an important role in text detection. Different regions such as texts, images, and tables should be identified in order to extract the text correctly. Layout analysis defines the possible location of text that needs to be extracted which can increase the OCR accuracy and extract more useful text from each document [12]. As figure 2 shows the dataset has different layouts which needs to classify to text and non-text segmentations.

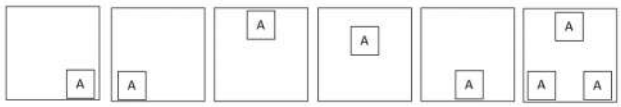

Figure 2: Possible locations of text in dataset

For the case study, connected component analysis was used to classify text and non-text segmentations. Non-text segmentation involves table, image, and lines. In the next step all the text segmentations will be processed through *Matlab*'s OCR in Computer Vision System Toolbox™. Figure 3 illustrates the layout analysis and text extraction in next section.

4.4 Text extraction from Construction Document

Different OCR engines were tested for text detection. The best result for case study was achieved via *Matlab* OCR in Computer Vision System Toolbox™. As figure 3 shows, the following steps were applied [13]:

- Resize the image if needed
- Binarize image (creates a binary image from image)
- Connected component analysis
- Detect text regions using MSER algorithm
- Remove non-text regions
- Provide region of interest (ROI) around the text
- Expand bounding boxes around words
- Dilate image to make letters thicker
- Apply OCR to find as much text as possible in no specific order, even if they are embedded in images.
- Store the detected text in text file format

Matlab OCR can provide the word confidence and character confidence for extracted result. To have a better accuracy, we only accept more than 80% confidence level.

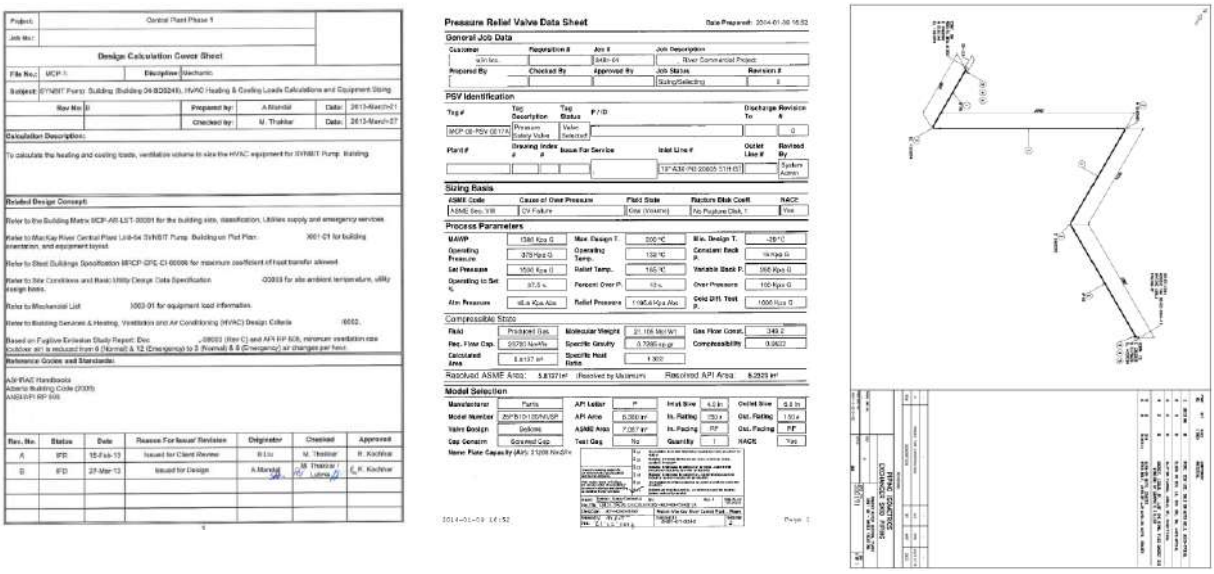

a) Text document b) Table document c) Drawing document

Figure 1. Document examples of the dataset

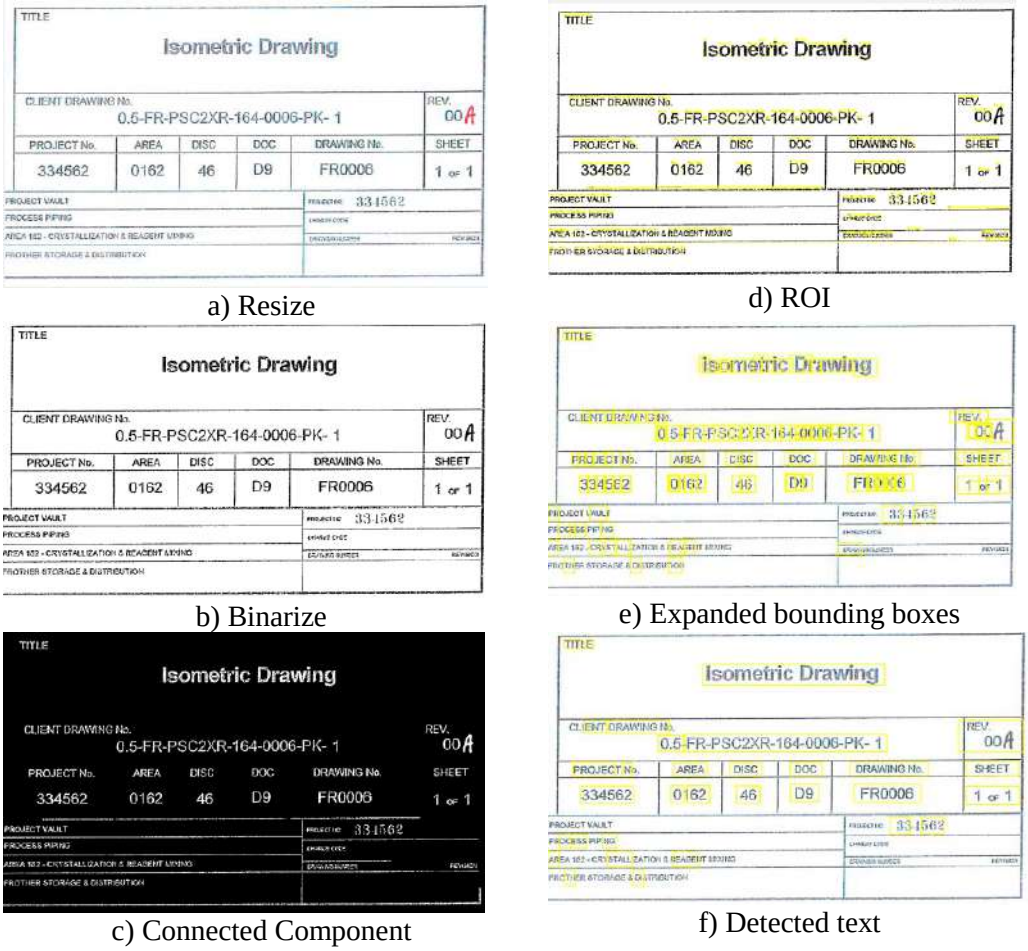

a) Resize

d) ROI

b) Binarize

e) Expanded bounding boxes

c) Connected Component

f) Detected text

Figure 4. Text extraction steps

4.5 Classification based on predefined set of keywords

In order to process text categorization, we need to provide a list of keywords before classification. The keywords can either be determined by experts in the specific domain of the application or based on historical documents. In case study experiment, we program a *Matlab* tool box to find the keywords in the text files and then assign the appropriate classes to the documents. Based on our case study experiment, we analyzed 5000 documents for text categorization from 3 different construction projects. The accuracy of classification is tested based on 100 documents for each class and it was between 73% to 85% for different classes. However, in this method each document can be assigned to more than one class since each document can contain the keywords of more than one class. The other challenge of this method is reliability of accuracy. The accuracy of classification for a new project that we do not have any samples is questionable. To increase the reliability of the pre-defined keywords, text mining was applied via *Matlab*'s Text Analytics Toolbox™. The purpose of this method is analyzing the most repeated words in each document type, and then unique words were added to the keywords, which can be another option instead of pre-defined keywords for any new project. In this step, the accuracy of classification has increased between 85% to 92%.

4.6 Classification based on deep learning long short-term memory (LSTM) network

Recurrent neural network (RNN) is a class of artificial neural network which is developed during the 1980s [14]. RNN is a repeating model of neural network with different loops to connect the previous information to the present task. When there is a gap between relevant information and output, the RNN is unable to connect the information. A long short-term memory (LSTM) network is a type of RNN which is designed to fill the gap and avoid the long-term dependency problem. LSTM network will take three decisions about the information: decide about the useless information which should be removed, decide about the new information which should pass to the next layer, and decide about the output of each layer [15]. Recently, LSTM is increasingly used to classify text data. Text data is naturally sequential, and LSTM can learn sequences from the training data [16]. Several researchers reported the high accuracy of their text classification result base on LSTM, such as [17], [18], [19]. We used *Matlab*'s Deep Learning Toolbox™ to test LSTM network with a word embedding layer on our dataset. The dataset was imported to the toolbox in .CSV format and it contains two columns: The first one is label of document types and the second column contains the text of each document. In the next step, each word converted to numeric sequences to be use as an input in LSTM network. The LSTM model was defined by hidden layers, and word embedding layer. Table 1. shows the architecture of LSTM network used in our case study. The training model partitioning is: 70% training, 15% validations, and 15% test observations. The maximum number of epochs is 10 and initial learn rate is 0.01. The validation accuracy of classification is between 75% to 83%.

Sequence input layer	1 dimension
Word Embedding Layer	100 dimensions and 87106 unique words
LSTM layer	180 hidden units
Fully connected layer	Number of classes, 10 layers
Softmax layer	softmax
Classification Output layer	Number of outputs, 10 classes
Loss function	Cross entropy

Table1. LSTM architecture

5 Results and conclusion

Document text detection and classification is a challenging task especially for construction documents which includes text, images and tables. The result of case study on construction documents confirmed that OCR is a feasible tool for text detection and the result of that can be used for classification of construction documents. We conducted experiments on large-scale datasets consisting of 5000 construction documents. The first classification was based on predefined set of keywords and most repeated words in each document. The accuracy of this classification was between 85% to 92%. The second classification

was based on LSTM network and the accuracy was between 75% to 83%. The evaluation demonstrated that predefined set of keywords has more accurate result. however, the layout of documents and texts should be analyzed in advance which is time consuming and expensive. LSTM has a better accuracy on new sets of data, and it does not require data analysis. The result of classification can improve if we can increase the accuracy of OCR text detection.

The paper shows that deep learning algorithms such as LSTM has potential benefit to be use in construction documents classification. However, other deep learning algorithms need to be tested. In this paper, we consider the experiments as preliminary result and more data and algorithm should be test in future research.

6 Acknowledgments

The authors would like gratefully to acknowledge the PCL company for providing case study material for this project and their support.

References:

[1] Zhang, J., Cheng, R., Wang, K., & Zhao, H. (2013, September). Research on the text detection and extraction from complex images. In *Emerging Intelligent Data and Web Technologies (EIDWT), 2013 Fourth International Conference on* (pp. 708-713). IEEE.

[2] Berkhahn, V., & Tilleke, S. (2008). Merging neural networks and topological models to re-engineer construction drawings. *Advances in Engineering Software*, *39*(10), 812-820.

[3] Banerjee, P., Choudhary, S., Das, S., Majumdar, H., Roy, R., & Chaudhuri, B. B. (2016, April). Automatic Hyperlinking of Engineering Drawing Documents. In *Document Analysis Systems (DAS), 2016 12th IAPR Workshop on* (pp. 102-107). IEEE.

[4] Banerjee, P., Das, S., Seraogi, B., Majumdar, H., Mukkamala, S., Roy, R., & Chaudhuri, B. B. (2017, November). Automatic Elevation Datum Detection and Hyperlinking of Architecture, Engineering & Construction Documents. In *2017 14th IAPR International Conference on Document Analysis and Recognition (ICDAR)* (Vol. 2, pp. 37-38). IEEE.

[5] Banerjee, P., Choudhary, S., Das, S., Majumder, H., Mukkamala, S., Roy, R., & Chaudhuri, B. B. (2017, November). A System for Creating Automatic Navigation among Architectural and Construction Documents. In *Document Analysis and Recognition*

[6] Seraogi, B., Das, S., Banerjee, P., Majumdar, H., Mukkamala, S., Roy, R., & Chaudhuri, B. B. (2017, November). Automatic Orientation Correction of AEC Drawing Documents. In *Document Analysis and Recognition (ICDAR), 2017 14th IAPR International Conference on* (Vol. 2, pp. 9-10). IEEE.

[7] Gupta, S., MuNherjee, J., Bhattacharya, D., Majumder, H., Roy, R., & Chaudhuri, B. B. An Efficient Approach for Designing Deep Learning Network on Title Block Extraction for Architecture, Engineering & Construction Documents. In Document Analysis Systems (DAS), 2018: 13th IAPR International Workshop on Document Analysis Systems (pp. 5-6) VIENNA, 5.

[8] Which fields can Procore automatically populate when uploading drawings? On-line: https://support.procore.com/faq/which-fields-can-procore-automatically-populate-when-uploading-drawings, Accessed: 25/01/2019.

[9] Extract Data From PDF: How to Convert PDF Files into Structured Data. On-line: https://docparser.com/blog/extract-data-from-pdf/, Accessed: 25/01/2019.

[10] What is Computer Vision? On-line: https://docs.microsoft.com/en-us/azure/cognitive-services/computer-vision/home, Accessed: 25/01/2019.

[11] Inglot, J. (2012). Advanced image processing with MATLAB.

[12] Antonacopoulos, A., Clausner, C., Papadopoulos, C., & Pletschacher, S. (2015, August). ICDAR2015 competition on recognition of documents with complex layouts-RDCL2015. In *Document Analysis and Recognition (ICDAR), 2015 13th International Conference on* (pp. 1151-1155). IEEE.

[13] Computer Vision System Toolbox. On-line: https://www.mathworks.com/help/vision/index.html, Accessed: 25/01/2019.

[14] Rumelhart, D. E., Hinton, G. E., & Williams, R. J. (1986). Learning representations by back-propagating errors. nature, 323(6088), 533.
[15] Sak, H., Senior, A., & Beaufays, F. (2014). Long short-term memory recurrent neural network architectures for large scale acoustic modeling. In Fifteenth annual conference of the international speech communication association.
[16] Chung, J., Gulcehre, C., Cho, K., & Bengio, Y. (2014). Empirical evaluation of gated recurrent neural networks on sequence modeling. arXiv preprint arXiv:1412.3555.
[17] Nowak, J., Taspinar, A., & Scherer, R. (2017, June). Lstm recurrent neural networks for short text and sentiment classification. In International Conference on Artificial Intelligence and Soft Computing (pp. 553-562). Springer, Cham.
[18] Rosander, O., & Jim, A. (2018). Email Classification with Machine Learning and Word Embeddings for Improved Customer Support.
[19] Tang, D., Qin, B., & Liu, T. (2015). Document modeling with gated recurrent neural network for sentiment classification. In Proceedings of the 2015 conference on empirical methods in natural language processing (pp. 1422-1432).

Holonic System for Real-Time Emergency Management in Buildings

B. Naticchia[a], L. Messi[a], M. Pirani[b], A. Bonci[b], A. Carbonari[a], and L.C. Tolve[a]

[a] Polytechnic University of Marche, DICEA, via Brecce Bianche n. 12, Ancona, Italy
[b] Polytechnic University of Marche, DII, via Brecce Bianche n. 12, Ancona, Italy
E-mail: b.naticchia@univpm.it, l.messi@staff.univpm.it, massimiliano.pirani@gmail.com, a.bonci@univpm.it, alessandro.carbonari@staff.univpm.it, l.c.tolve@pm.univpm.it.

Abstract –

Emergency management can benefit from advanced information and communication technology (ICT), since it can support officers in charge of emergency management to deal with urgent decision within a really short deadline. Further enhancement can derive from the application of holonic systems, which typically deal with the unexpected. In fact, unexpected events may prevent the application of emergency plans, e. g. evacuation of people outside of a building in fire through a network of pre-determined paths.

The holonic emergency management system, proposed in this paper, guarantees the shift to a contingent approach, leveraging the flexibility and adaptability to changing scenarios deriving from the holonic theory. Last but not least, the BIM integration provides all the building's topological information. Such a technology can exploit general data to automatically detect unconventional ways out and arrange rescue operations in real-time. The developed system has been applied to the fire safety management of a large building in a university campus. The BIM model of the case study has been imported in a game environment where an unconventional pathfinding has been experienced.

Keywords –

Holonic System; Emergency Management; Fire Safety; BIM.

1 Introduction

1.1 Building Management System

Building automation systems (BAS), also known as building management systems (BMS), denote a wide range of computerized building control systems, from special-purpose controllers, to standalone remote stations, to larger system including central computer stations. A BAS comprises several subsystems which are connected in various ways to form a complete system. The system has to be designed and engineered around the building itself to serve the services systems for which it is intended. Consequently, although the component parts used may be identical, no two systems are the same, unless they are applied to identical buildings with identical services and identical uses [1]. BMS, with their typical hierarchical structure, are usually able to reach their goals in an efficient way and with no faults, whereas they fail to stick to pre-determined targets in the presence of disturbances. In fact, traditional systems cannot pursue the assigned task if any unforeseen events occur. Their rigid structure makes it very difficult to tackle unexpected scenarios. As low-level modules have to consult higher hierarchy levels in case of a disturbance, their reactivity becomes weak. Furthermore, global decision-making is often based on obsolete information [2]. Building services include HVAC systems, electrical systems, lighting systems, fire systems, security systems and lift systems. In industrial buildings they may also include the compressed air, steam and hot water systems used for the manufacturing process [1].

In this paper, fire and security systems for the emergency management will be studied in depth in order to overcome the limits of the traditional BMS. Emergency management, since directly affects safety of people, represents a relevant issue in each phase of building lifecycle, from a foresighted design of buildings and infrastructures to the elaboration of emergency plans according to specific regulations. Emergency scenarios are even more relevant as case studies, if the high frequency of unexpected events affecting them is considered. The traditional approach to the emergency management is based on a deterministic forecast of main scenarios. The emergency plan resulting from them has a key role, although it does not consider the totality of possible scenarios. As a consequence, it is regardless of contextual, changing and unexpected events that may happen and seriously affect the effectiveness of emergency measures.The limits of such a knowledge-based approach are confirmed by several examples of

complications in the emergency operations. To name one, during the emergency response to the September 11, 2001 attack on the World Trade Centre, commanders on the scene were unable to communicate to '911' Public Service Access Points (PSAP) that people should evacuate the building [3]. As a result, PSAP operators complied with New York City's standard operating procedure for hi-rise fires and advised callers to stay in impacted buildings. The '911' system was inadequate for handling a major disaster and could not adapt to the emergency. The final death toll 2749 may have been substantially reduced if the PSAP's were adaptive in coping with the overload. Moreover, commanders trying to evacuate fire fighters from the north tower during the World Trade Centre disaster were seriously hampered by ineffective radio communications; the final death toll 343 of New York fire fighters may also have been substantially reduced if the system controlling the radio communications was also adaptive [3]. To name another example, the Grenfell Tower fire produced a high number of victims not only for technical reasons, due to the employment of a not proper cladding system and to a lack of separated fire boxes into the building, but also to a mistake in the emergency evaluation [4]. The "stay put" strategy, led by a tardive declaration of the situation as a major incident with the consequent delay of one hour in the evacuation process, has revealed as a fatal mistake in the rescue operations [4]. Furthermore, a traditional emergency plan does not facilitate the operational use. In fact, it remains as a plain-text document which is difficult to consult during an excited situation due to an oncoming danger. In other words, a way out plan hung on the wall cannot help incisively to find a viable exit route. The fire in the Rhode Island station club represents an example of how a not profound knowledge of the building in which people were located affected the evacuation process: a study has demonstrated that people did not use alternative ways out since they ignored their presence [5]. While the main exit doors were obstructed by the smoke presence, there were no indication to use alternative paths to escape from the building; therefore, the evacuation process was affected by a fatal delay [5].

Starting from this shortcomings, the current research proposes a contingent approach which exploits a BIM-based holonic technology to overcome the limits of the traditional BMS. The developed holonic management system integrates a building digital model, which provides all the necessary data for the real-time detection of ways out. This paper is organized as follows. Section 2 provides a description of the system architecture. Section 3 describes the Virtual Reality Platform. Section 4 provides a description of the Bayesian Selector. Section 5 describes the generation of Multi-Target Partial Plans for the considered case study. Section 6 provides a description of the Combiner and shows the simulations results. Section 7 is devoted to conclusion.

1.2 Holonic Theory

The holonic concept, which is the basis of holonic management systems, is the key enabler to tackle unexpected events and overcome the limits of the traditional BMS. The holonic theory was introduced in 1967 by Koestler [6] to explain the evolution of biological and social systems. Likewise, in the real world, where almost everything is at the same time a part and a whole, each holon can be part of another holon [2]. In fact, the word holon is the combination of "holos", which in Greek means "whole", and the suffix "on", which suggests a part [7], [8], [9]. In the manufacturing field, holons are autonomous and cooperative building blocks, since they can both control the executions of their own strategies and develop mutually acceptable plans [2]. Furthermore, holons consist of an information-processing part and often a physical-processing part [2], [7], [8]. The former is responsible for high-level decision making, collaborating and negotiating with humans and other holons, while the latter is a representative of its linked physical component and responsible for transferring decisions and instructions to it [7]. According to Koestler, a holonic system or holarchy is then a hierarchy of self-regulating holons that function (i) as autonomous wholes in supra-ordination to their parts, (ii) as dependent parts in subordination to control at higher levels, and (iii) in coordination with their local environment [2], [6], [9]. Therefore, holonic architecture combines high and predictable performance, which distinguishes hierarchical systems, with the robustness against disturbances and the agility typical of heterarchical systems [8]. In this way, systems' resilience is guaranteed. Holonic management systems, which have been successfully applied in the manufacturing field, can constitute a novel technology to tackle unforeseen scenario variations. Indeed, the autonomy and cooperation of their elementary units, the holons, makes it possible to avoid the rigid structure of hierarchical systems and therefore respond quickly to disturbances [2].

2 System Architecture

The architecture of the developed holonic system, depicted in Figure 1, supports fire emergency management and rescue operation, detecting the most effective way out. Its aim is not to substitute the actual approach foreseen by regulations, rather to enhance the standard emergency plan, detecting unconventional path to exit the building, if an unexpected event occurred. The architectural principles are shortlisted as follows:

- *Real-time effectiveness*: it must regard both the information flow and the decision making process.

Since the system is continuously evolving, especially in complex scenarios like emergencies, it is not feasible to represent all the changing status it assumes, in order to provide the proper solution to the occurring situations. Moreover, the response of the system must be sufficiently reactive in order to result effective to face the situations that are in place.

- *Proactive and unconventional problem solving*: on the basis of the information gathered in a real-time manner, the system, in order to be sufficiently resilient, must be capable to extract the information useful to reach its objectives also by general data, as well as to provide escape solutions with the employment of unconventional means.
- *Resilience*: the system must be reactive and adaptive to the new possible configurations that may occur, without compromising its primary function of managing the emergency scenario. Failure, interruptions, damages to the standard communication backbone systems, as well as injuries or obstructions to the usual evacuation means, must not impede the main objective of keeping people safe during emergencies.
- *Emergent cooperation*: the system architecture embodies the capability of the holons to cooperate in temporary associations, namely the holarchies, introducing the "emergent cooperation". This concept can be described using a metaphor: the behaviour of these agents is similar to the one belonging to the birds of a flock; no one is able to manage flock's shape and dimension, but everyone takes care of maintaining flock's trajectory, flock's speed and minimum distance from its fellows. Although no one of the birds has a complete view of the scene, the behaviour described above is the result of an "emergent collaboration". This kind of cooperation is not so onerous for birds because it is supposed to be integrated within their DNA and, therefore, instinctive. The same functioning characterizes the agents inside the developed architecture.

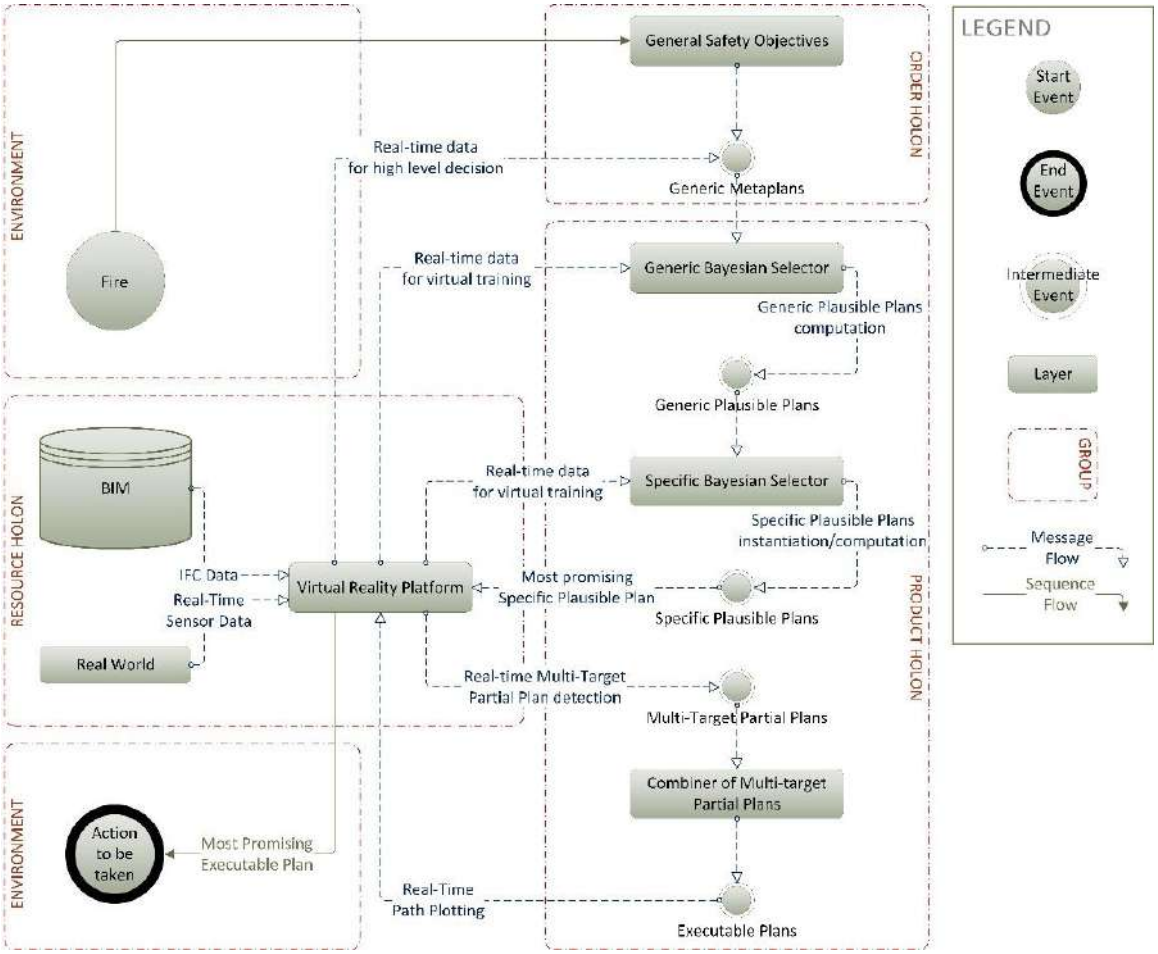

Figure 1. System architecture of the developed holonic management system

The system architecture in Figure 1 is composed by different layers interacting each other according to a publish/subscribe scheme, whose central concept is the notion of *topic*: each node/layer of the architecture subscribes and some other publishes information on the *topic*. In other words, the *topic* is simply the database content itself without intermediate language adapters: the unique language is the database language and its queries. Hence, the architecture layers behave like a human being that only subscribes to interesting events/information and publishes relevant events/information, which are specifically useful for the occurring situation, complying to the actual needs [10].

The different layers can be clustered by function according to the PROSA reference architecture [2], a conceptual architecture for manufacturing control, that has shown great potentialities to be applied also in different context. The acronym PROSA stands for *product-resource-order-staff architecture* and refers to the different types of holons. Three basic types of holons can be distinguished: product holons, resource holons, and order holons. Staff holons are optional and can be added to provide the other holons with expert knowledge [2]. In PROSA, the holons' physical part belongs to the world of interest, that is the part of reality which falls within a certain scope relevant for the application [8]. In Figure 1, the PROSA analogy is highlighted identifying resource, product and order holons. Finally, the environment is the real world scenario where the holons operate, namely the fire occurring and the countermeasures to be taken at the end of the elaboration process.

The highest architecture layers, namely the General Safety Objectives and the Generic Metaplans (see Figure 1), correspond to the order holon, which in the manufacturing system represents a task that needs to be executed, for example the delivery of a package [2]. The General Safety Objectives represents the always valid target: "Save all the people inside the building". As a consequence, the Generic Metaplans are triggered and fed with real-time data from the Virtual Reality Platform. The output of this elaboration are the general processes to be executed, which may be represented by the generic instruction "Stay in/go out" and are published to the following layer. Thanks to the generality of the high level setting, the resilience architectural principle is guaranteed and the resulting system is applicable for every building, without the need to configure it manually every time. This is a key feature that distinguishes the developed architecture from classic BMS.

3 Virtual Reality Platform

The Virtual Reality Platform (VRP) is the heart of the resource holon, which in the logistic context corresponds to resources like all transport means and material handling equipment [2]. In the developed system, the VRP is implemented using the Unity 3D game engine. It has been selected as the most suitable tool because of the following characteristics:

- high interoperability with other software, including the capability to integrate several functional mockups afferent to different engineering disciplines;
- presence of a physics engine that provides physical behaviour to the components of the scene, basically the correct acceleration and the affections by collisions, gravity and other forces, making the simulation of a great likelihood with the real world;
- possibility to introduce artificial intelligence by scripts, based on C# or Java programming languages, or by means of visual programming.

In other words, Unity 3D offers an extremely realistic environment to simulate a fire emergency scenario of the case study and building occupants' behaviour using artificial intelligence. The VRP constitutes a dynamic hub able to collect IFC data from BIM and real-time data from pervasive sensors distributed in the real world. The interconnection with the BIM software Autodesk Revit has been established through an IFC Loader, based on the IFCEngine DLL Library [11]. This component makes it possible to import contextual, geometrical, material properties from the BIM, once exported in IFC format. The interconnection with sensors, which has not been tested in this research step, is one of future developments. The technological solution to this issue is ASP.NET Core SignalR, an open-source library that simplifies adding real-time web functionality to apps. Real-time web functionality enables server-side code to push content to clients instantly [12]. The building digital model, coherently updated during the whole lifecycle, provides in real-time accurate topological information, that goes further beyond the static and poor information usually contained in emergency plans. In this environment, the Unity 3D asset A* Pathfinding Project Pro (A*PPP) [13], applying the A* algorithm, detects the most effective way out. If the usual escape route is obstructed by smoke, fire, collapsed building elements or other kinds of accidents, the A* algorithm can detect unconventional ways out through internal doors. Moreover, BIM is proposed not only as a comprehensive provider of the main building properties, but it is subjected to a proper semantic enhancement: some building elements can be exploited in an unusual way in respect of their main purpose and become evacuation means in an unconventional manner. This contribution appears even more relevant, if we consider the possibility to have random visitors inside building, affected by a poor awareness of the spatial distribution. As depicted in

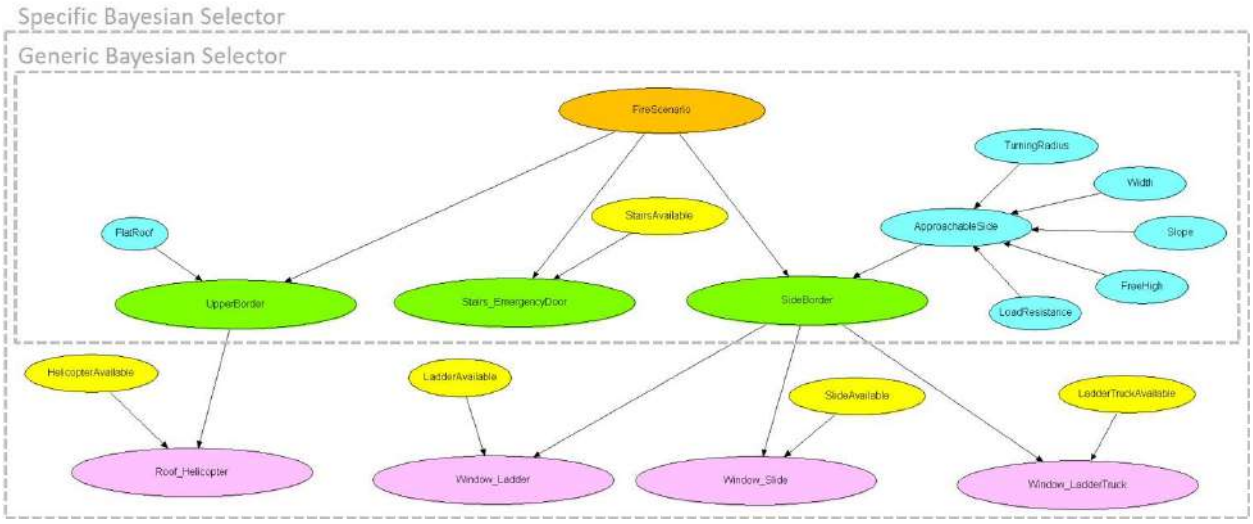

Figure 2. Bayesian Selector

Figure 1, the VRP acts as a collector of heterogeneous data and represents the proper environment where the required knowledge can be produced and published. In this way, real-time data are available for each subscribing layer of the architecture.

4 Bayesian Selector

The Bayesian Selector (BS) is conceived as the translation into a Bayesian network of an expert's knowledge. Bayesian networks, which constitute a powerful mean to represent phenomena affected by a high level of uncertainty, are a probabilistic graphical model that uses Bayesian inference for probability computations. They aim to model conditional dependence, and therefore causation, by representing conditional dependence by edges in a directed graph. Through these relationships, one can efficiently conduct inference on the random variables in the graph through the use of factors [14].

In the fire emergency management, the BS, fed by real-time data from the VRP, detects which strategy or plan is probabilistically the most effective to exit safely the building in fire. As shown in Figure 1Figure 2Figure 1, it is composed by a generic part and a specific one, respectively linked to Plausible Plans and Multi-Target Partial Plans. The Generic Bayesian Selector suggests the most effective preliminary escape strategy (called also Generic Plausible Plan) amongst those ones valid for any building. The Specific Bayesian Selector detects the most promising escape plan (called also Specific Plausible Plan), instantiated for the analysed building. All these layers, according to the PROSA analogy, constitute the product holon, which contains the knowledge on how instances of a specific task type (represented by order holons) can be executed by the resources [2].

4.1.1 Generic Bayesian Selector

The Generic Bayesian Selector subscribes data deriving from Generic Metaplan and is trained by real-time data published by the VRP; as output, the most effective Generic Plausible Plan is computed (see Figure 1). In details, when the "Fire Scenario" (see orange node in Figure 2) is activated by the alarm, the Bayesian network computes which Generic Plausible Plan (see green nodes in Figure 2) should be analysed in depth in order to find a viable exit route. The "generic" attribute means that the Generic BS is applicable for every building. As a matter of fact the green nodes in Figure 2 represent the possibilities to exit any building:

- "Stairs and Emergency Door" represents all the exit routes which exploit stairs and emergency doors. They comprise not only the standard exit route suggested by the emergency plan, but also alternative and unconventional ways out through internal doors connecting adjacent rooms.
- "Upper Border" and "Side Border" represent the building's frontiers where rescue teams could pick up and save endangered people. They comprise only the unconventional ways out, detected when an unexpected event voids the standard emergency plan.

Finally, blue nodes represent building's features (for example "Flat Roof", in Figure 2, stands for "Is the building's roof flat?") whereas yellow ones represent resource availability (for example "Stairs Available", in Figure 2, stands for "Are the building's stairs available/viable?").

4.1.2 Specific Bayesian Selector

The Specific Bayesian Selector integrates the generic one adding the Specific Plausible Plans (see purple nodes in Figure 2). It subscribes data deriving from Generic BS and is trained by real-time data published by the VRP. On the base of these data, the technology described in [15] and [16] is able to instantiate in real-time the Specific Plausible Plans for the emergency management of the considered building. As output, the most promising Specific Plausible Plan is detected (see Figure 1). In Figure 2, four Specific Bayesian Plans, instantiated for the building case study, are reported as examples:

- "Roof and Helicopter" which stands for "Lead people to the roof and pick up them by a helicopter";
- "Window and Ladder" which stands for "Lead all people to the window and pick up them by a normal ladder";
- "Window and Slide" which stands for "Lead all people to the window and use a slide";
- "Window and Ladder Truck" which stands for "Lead all people to the window and pick up them by a ladder truck".

5 Multi-Target Partial Plan

5.1 Description of the case study

In order to implement and test the developed architecture, the mixed-use building "Eustachio", located in Ancona (Italy), has been chosen. The building belongs to a major complex of edifices occupied by the Faculty of Medicine of Polytechnic University of Marche. This eight storeys-building presents a quite regular shape with two major blocks on the north and south side, containing spaces devoted to heterogeneous scopes: classrooms, scientific laboratories, administrative offices for students, a library, books storage rooms, services. The two main blocks are connected by two double stairwells, which present a separate reinforced concrete envelope that makes these parts separated from the block for seismic reasons. The choice has fallen on this edifice for its characteristic of public building with several uses that may involve variable flow of different people inside it: estimated between 100 and 2320 individuals and characterized by several age ranges and, more specifically, owning a different level of knowledge of the building. Finally, the presence of inflammable substances in several laboratories leads to simulate the fire scenario in this building, since this is one of the most common and disruptive emergency situation, often affected by unexpected events and mistakes in the management of the evacuation process.

a.

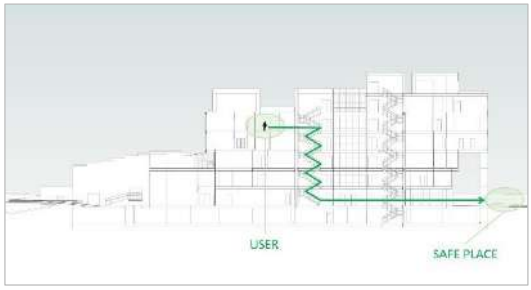

b.

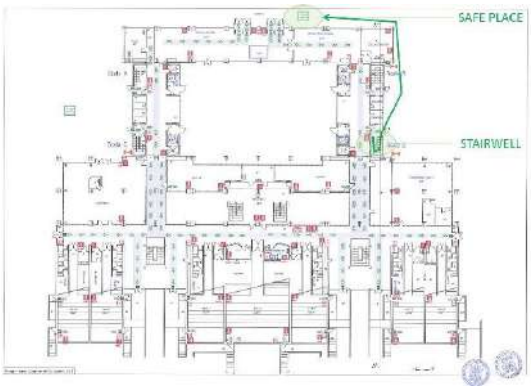

Figure 3. Example of exit route according to the Eustachio's emergency plan: section view (a.) and ground floor plan view (b.)

5.2 Strengths of the system

The traditional approach to the emergency management is based on a deterministic forecast of a finite number of main scenarios. Unfortunately, unexpected events could prevent the effectiveness of the pre-determined paths defined by the standard emergency plan. According to the Eustachio's one, as shown in Figure 3.a. and Figure 3.b.Figure 4, a user, in whatever floor he is, should reach the closest stairwell, go downstairs until the ground floor and, finally, exit the building. It may not be the best solution to run away from a building in fire, especially if an unforeseen event occurs and the usual escape route is unviable. In other words, the obstruction of a path by operators in charge of operation and maintenance or the collapse of non-structural components, like ceilings, may have tragic consequences during a fire. The developed holonic system detects alternatives and unconventional ways out in real-time, overcoming the limits of an a-priori plan. Hence, officers in charge of emergency management can benefit of the proposed system's computing capability and nimbly coordinate rescue operation.

5.3 Generation of Multi-Target Partial Plans

The developed holonic system, as mentioned before, can tackle unexpected events, providing in real-time unconventional paths outwards. More in details, the pathfinding, carried out in the VRP by means of the A* algorithm (see Section 3), detects the Multi-Target Partial Plans (see Figure 4). Given the most promising Specific Plausible Plan, the A*PPP detects automatically all the possible routes towards intermediate points. For example, assuming that the Bayesian Selector has classified "Window and Ladder Truck" as the most effective Specific Plausible Plan, the VRP by means of A*PPP provides the following Multi-Target Partial Plans:

- all the shortest paths (see blue lines in Figure 4) from the endangered user towards all the building's windows, assumed as intermediate points and identified by their GUID (Globally Unique Identifier);
- all the shortest paths (see red lines in Figure 4) from the rescue team, represented for example by the ladder truck, towards the building's windows.

6 The Role of the Combiner Unit

The Combiner of Multi-Target Partial Plans, along with the connected plans (see Figure 1), completes the product holon largely discussed in Section 4. The role of the Combiner is to find the fastest escape route outwards, composed of only one path for each of Multi-Target Partial Plan. Following the example discussed in Section 5 (see Figure 4), the Combiner detects the path composed by the fastest route that leads the user to that window which can be reached and approached in the shortest time by the ladder truck. The detected Executable Plan is then plotted into the VRP and notified both to the endangered user and the rescue team. In this way, both of them can act coordinately towards the same intermediate point, exploiting the emergent collaboration and speeding the rescue operation. Assuming the user and the rescue team starting moving at the same time, the rescue operation lasts as the slower one. For this application path data about Multi-Target Partial Plans are exported into Excel (see Figure 5) to be elaborated. Obviously this process can be automated within the VRP in order to directly detect the viable Executable Plan.

7 Conclusions

The holonic management system, described in this paper, improves the usual emergency management approach, supplying more updated and significant information and investigating unusual solutions for rescue purposes in case of unforeseen events. In fact, the connection with BIM and sensors from the real world provides, in real-time, building's topological information and contextual data. Furthermore, the resilient system, based on the holonic theory, makes it possible to tackle unexpected events by means of unconventional escape routes and support the standard rescue operations.

The developed system architecture, tested in a large mixed-use public building, shows its potentiality through the contribution given to officers in charge of emergency management. The detection of unconventional solutions in real-time helps, in an emergency scenario, to deal with urgent decision within a really short deadline.

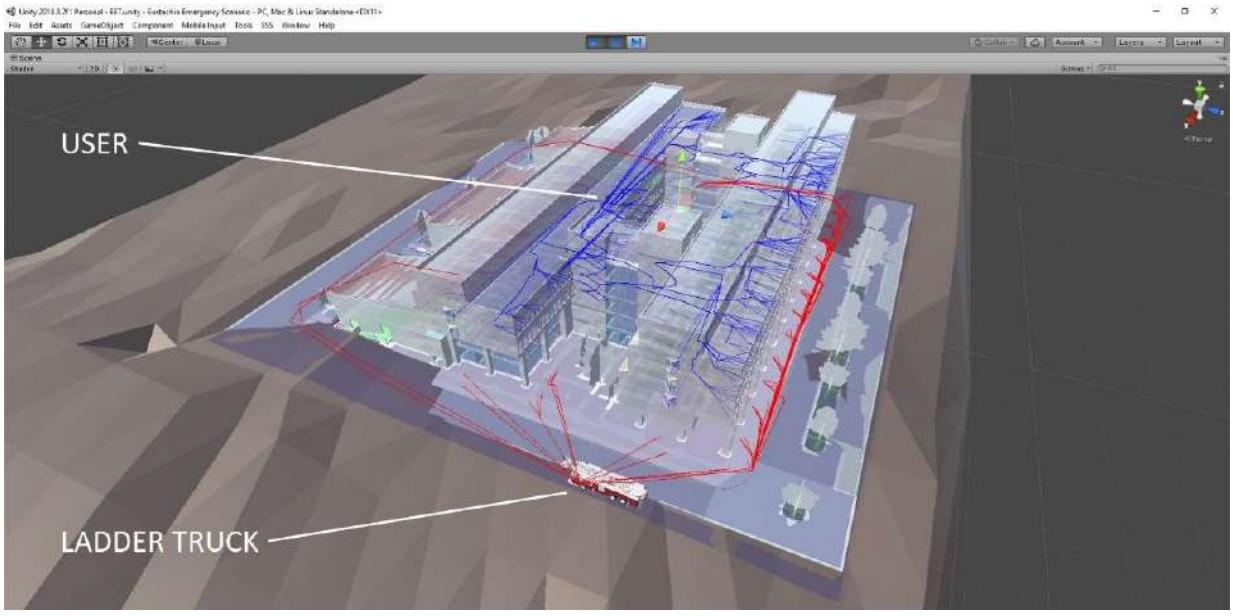

Figure 4. Generation of Multi-Target Partial Plans within the VRP using A*PPP

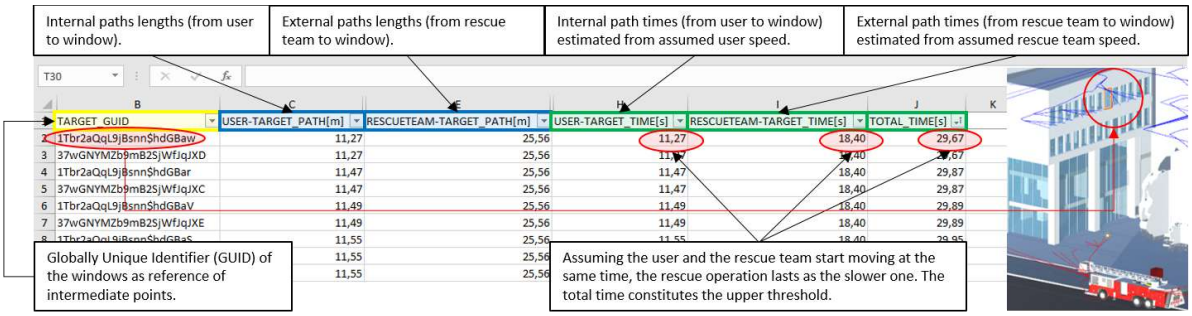

Figure 5. Processing in Excel of path data about the Multi-Target Partial Plans

Acknowledgments

This research work was supported by the EU funded project "ENergy aware BIM Cloud Platform in a COst-effective Building REnovation Context' — ENCORE" (H2020, Grant Agreement no. 820434).

References

[1] Wang, S. (2009). Intelligent buildings and building automation. Routledge, ISBN: 0-203-89081-7.

[2] P. Valckenaers, H. Van Brussel, Design for the Unexpected, From Holonic Manufacturing Systems towards a Humane Machatronics Society, Butterworth-Heinemann, 2016, ISBN: 978-0-12-803662-4.

[3] Ulieru, M., Worthington, Paul. (2006). Autonomic risk management for critical infrastructure protection. Integrated Computer-Aided Engineering. 13. 63-80, https://doi.org/10.3233/ICA-2006-13105.

[4] B. Lane, New Civil Engineer (4.6.2018), available online (last accessed 10.12.2018): https://www.newcivilengineer.com/latest/grenfell-expert-report-cites-catastrophic-flaws/10031720.article.

[5] W.L. Grosshandler, N. Bryner, D. Madrzykowski, and K. Kuntz. Report of the Technical Investigation of The Station Nightclub Fire. NIST NCSTAR 2, National Institute of Standards and Technology, Gaithersburg, Maryland, July 2005.

[6] Koestler A., The Ghost in the Machine. The Macmillan Company, Hutchinson, 1967, ISBN: 0-14-019192-5.

[7] L. Wang, Azadeh Haghighi, Combined strength of holons, agents and function blocks in cyber-physical systems, Journal of Manufacturing Systems, 2015, https://doi.org/10.1016/j.jmsy.2016.05.002.

[8] P. Verstraete, B. Saint Germain, K. Hadeli, P. Valckenaers, H. Van Brussel, On applying the PROSA reference architecture in multi-agent manufacturing control applications, Multiagent Systems and Software Architecture, Proceedings of the Special Track at Net.ObjectDays, 2006.

[9] A. Giret, V. Botti, Holons and Agents, Kluwer Academic Publishers, Journal of Intelligent Manufacturing, 2004, https://doi.org/10.1023/B:JIMS.0000037714.56201.a3.

[10] Bonci, A. & Pirani, M. & Longhi, S. (2017). A Database-Centric Framework for the Modeling, Simulation, and Control of Cyber-Physical Systems in the Factory of the Future. Journal of Intelligent Systems. 27, https://doi.org/10.1515/jisys-2016-0281.

[11] RDF Ltd., IFCEngine DLL Library, available online (last accessed 9.1.2019): http://www.ifcbrowser.com.

[12] Microsoft Corporation, Introduction to ASP.NET Core SignalR (25.04.2018), available online (last accessed 15.3.2019): https://docs.microsoft.com/it-it/aspnet/core/signalr/introduction?view=aspnetcore-2.2.

[13] A. Granberg, A* Pathfinding Project, available online (last accessed 9.1.2019): https://arongranberg.com/astar/#.

[14] D. Soni, Introduction to Bayesian Networks (8.6.2018), available online (last accessed 8.1.2019): https://towardsdatascience.com/introduction-to-bayesian-networks-81031eeed94e.

[15] Bonci, A. & Pirani, M. & Cucchiarelli, A. & Carbonari, A. & Naticchia, B. & Longhi, S. (2018). A Review of Recursive Holarchies for Viable Systems in CPSs. Proceedings of the 2018 IEEE 16th International Conference on Industrial Informatics (INDIN), 37-42, https://doi.org/10.1109/INDIN.2018.8472055.

[16] Bonci, A. & Pirani, M. & Carbonari, A. & Naticchia, B. & Cucchiarelli, A. & Longhi, S. (2018). Holonic Overlays in Cyber-Physical System of Systems. Proceedings of the 2018 IEEE 23rd International Conference on Emerging Technologies and Factory Automation (ETFA) 1240-1243, https://doi.org/10.1109/ETFA.2018.8502586.

Grasped Element Position Recognition and Robot Pose Adjustment during Assembly

K. Iturralde[a], T. Kinoshita[b], T. Bock[a]

[a] Chair of Building Realization and Robotics, Technical University of Munich, Germany
[b] Division of Human Mechanical Systems and Design, Graduate School of Engineering, Hokkaido University, Japan
E-mail: kepa.iturralde@br2.ar.tum.de

Abstract –

Upgrading building envelopes with fully prefabricated 2D modules requires high accuracy during the manufacturing process with tolerances lower than 1 mm. In the research described in this paper, computer designed and accurately manufactured objects have been assembled with robotic arms. However, in previous phases, it was detected that during the assembly process, the placement differed from the planned location due to undesired deviations of the object while being grasped and placed by the robotic tool. The experiments presented in this paper imply correcting this deviation by localizing the grasped object's position and recalculating the path and final pose of the assembly process. For localizing the deviated grasped object's location, an intermediate pose was planned. During this pose, the location of the grasped object was estimated by two different means. For the first solution, visual markers have been placed on a known corner of the objects and these have been recognized with a camera. For the second solution, the coordinates of the objects were measured by a digital theodolite. The location of the deviated object was calculated and compared to the planned location so the robot could divert from its original path. The measurable parameter in the experiments was the assembly accuracy. The results in the two experiments have been analyzed and compared. According to the results, the solutions could be implemented not only in the factory, but at on-site processes as well.

Keywords –

Deviation; Localization; Estimation; Adjustment

1 Introduction

The existing building stock's envelope capabilities need to be upgraded in order to achieve zero-energy consumption [1]. In an ongoing research project named BERTIM [2], timber based prefabricated 2D modules with embedded renewable energy sources (RES) are fixed onto existing building façades in order to improve the insulation of the building and generate energy. According to the objectives of the research project, these 2D modules should be fully prefabricated, which means that no rework should be necessary after fixing the modules onto the façade. As a consequence, on-site installation time is reduced. These fully prefabricated modules need to achieve waterproof and airtight conditions while ensuring fitting ducts [2]. This requires an accurate manufacturing of the modules with very low tolerances of up to 1 mm. In 2D module manufacturing with timber-frames, traditional off-site techniques [3] don't fulfil the demanded accuracy, where tolerances can reach up to 10 mm. In brief, current marketed processes are based on precut studs and beams, which are placed in a carpentry bench according to their position. Afterwards, studs and beams are nailed and the frame is compiled. In the next step, OSB boards are placed and nailed onto the timber-frame and, finally, the OSB boards are cut by a CNC bridge crane.

There are several reasons for such inaccuracies that were pointed out in previous phases of the research [3]. As a solution to these inaccuracies, it was proposed that all the objects of the prefabricated modules should be contoured in a CNC machine and then robotically assembled to create a façade module as shown in Figure 1. In this sense, there is experience in the manufacturing process of CNC routed timber objects [4]. Moreover, there are some experiences that link the design and the robot thanks to parametric design tools [5]. However, besides some exceptions [6], the assembly of studs and boards is mainly achieved manually. The robotic assembly of prefabricated modules is still a process which faces some challenges related to accuracy as well. The remainder of this paper is to define and test a solution related to overcome accuracy issues with the robotic assembly processes.

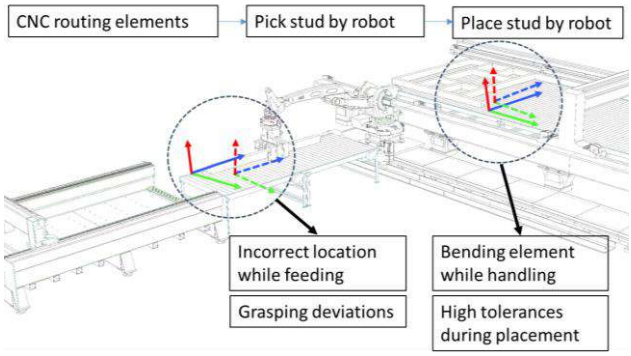

Figure 1. Scheme for a fully robotized assembly of prefabricated timber frames

In Figure 1 it is shown an scheme based on CNC routed elements that are robotically placed into an automated multi-function bridge for the assembly. In previous phases of the research, it was detected that deviations occur mainly while grasping and placing the timber elements by the robot.

2 Challenges of robotic assembly of fully prefabricated (timber-framed) modules

30 years ago, Kodama et al. [7] reported deviations during the grasping and placing of construction blocks while building a wall. These blocks were specially designed for facilitating the assembly process following the robot oriented design (ROD) concept [8]. However, the deviation of the wall built was considerable. Gambao et al.[9] also faced similar issues during the erection of a wall with robots during the ROCCO project. In more recent research projects, ordinary bricks were used to build parametrically designed walls. Bonwetsch [10] reported deviations of up to 10 mm compared to the desired location. Similar deviations happened in a research project that assembled timber profiles for building structures and, for this case, Willmann et all [6] suggested sensor feedback mechanisms in order to allocate the grasped object as well as the assembled module. In the researches explained by Willmann and Bonwetsch [6, 10], the objects to be assembled don't present any special joining system such as ROD, which in turns does not facilitate the allocation of the parts or elements with each other. On the other hand, some timber-framing machine builders offer the possibility of robotizing the assembly process of boards (not timber frame elements such as studs and mullions). However, as can be seen in reference [11], the grasped object tends to bend, which jeopardizes the exact placement of the object.

Therefore, it can be stated that the current robotic tools aren't as precise as desired in the assembly process of prefabricated modules. The accuracy of the robot's grasping is not guaranteed. This lack of precision increases especially when working in unstructured environments where the grasped objects aren't placed in a known location. Besides, the variety of design of the prefabricated modules hinders an automated programming of the robot's grasp and path planning.

During the research project explained in this paper, some tests were already achieved before [12]. A simulation was defined and some problems were intercepted (see also Figure 1):

- Incorrect placement of objects during feeding
- Deviations while grasping the objects
- In the case of some objects, especially boards, the object tends to bend and, therefore, the final position might not be adjusted
- Tolerances due to robotic arms calibration and accuracy during placing

As stated previously, it is necessary to recognize the location of the grasped or handled object to be assembled. In this sense, robotic assembly in construction can take advantage of concepts such as measurement assisted assembly (MAA). Maropoulos et al. [13] determined a solutions that enable a more predictive and flexible assembly process by using active tooling and closed loop control. This concept was mainly developed for complex and large-scale assembly processes such as in the aviation industry, but it can be used for the construction industry as well. Following these ideas, Druot et al. [14] applied the MAA for high accuracy aerospace assembly with robots with optimal results.

During the assembly process with robots, an adjustment of the robot's path is necessary. There is already literature where robots' paths can be adjusted depending on the feedback that the robot receives from different data acquisition and sensing devices and there are also some experiences in robotic assembly that can be found in the literature. Nottensteiner et al. defined a system to recognize objects and plan the assembly process by using two robotic arms [15]. In the research carried out by Feng et al. [16], markers were used for localizing objects and defining a plan for the assembly of parametrically designed walls. Finally, Lundeen et al. [17] used optical marker on top of the end effector to estimate the pose of articulated excavators.

2.1 Objective

The main research objective presented in this paper is to adjust the robotic assembly path depending on the location of the grasped element. Subsequently, the research question is if element location recognition and object path adjustment improve the deviations and displacements generated while grasping the object during

the assembly processes. The objective is to increase accuracy on the final pose for achieving the assembly of a timber-frame with CNC routed elements. For achieving that goal, it has been necessary to use visual systems that recognize the position of the grasped element and accordingly correct the deviation by adjusting the path of the robot.

3 Tests in laboratory environment

The works carried out during the experimentation phase consisted on assembling a mockup that resembled a timber-frame. The objects of the mock-up were made or fabricated by a 3D printer (German RepRap X400©) using PLA filament (Polylactide PLA from German RepRap ©) as an additive material. The objects were dovetailed as can be seen in Figure 2 in order to facilitate the placement by the robot.

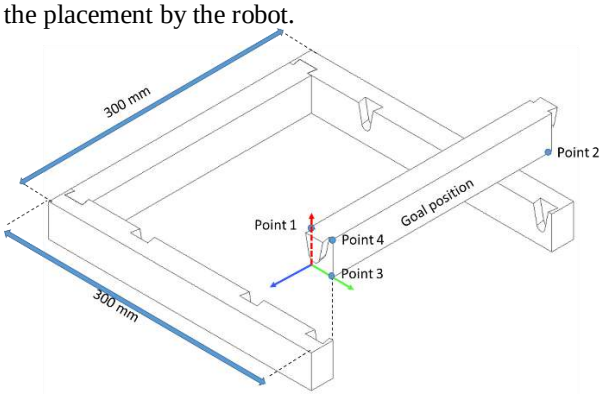

Figure 2. Prefabricated module mockup used for the assembly in laboratory environment experiments

The robot was placed in a referenced/known location with respect to the assembled module. The objects were also in known locations. The size of the mock-up was 300mm*300mm*35mm, which is about ten times smaller than a conventional prefabricated timber-frame module.

Figure 3. Assembly process carried out by the Kinova Jaco® robotic arm

The robot used for the assembly process was a Kinova Jaco® (six Degrees of Freedom) robotic arm (see Figure 3). It is noteworthy that the scale of the mock-up and the functionalities of the robot don't appear to reflect the reality of the assembly of the prefabricated module or that of the building industry. However, the materials and the robot used for the test reflect a worst-case scenario regarding deviations. On the one hand, the accuracy of the end-effector (hand type) of the Kinova Jaco® is not appropriate for grasping cubicle objects and, therefore, the deviations are considerable and appear exaggerated when compared to a gripper that is more adequate for such conditions. These "large" deviations are "good"; it is assumed that the robot and the mockup are suitable for this test and carrying out the adjustment of such grasping inaccuracies while picking and placing objects. In Table 1, the materials and devices used during the experimentation are defined.

Table 1. Equipment, materials and resources used

Computer processor	Intel CORE i7 8th Gen
Robotic arm	Kinova Jaco®
Controller	ROS
Path planning	MoveIt!
Camera	Logitech C170©
Digital theodolite	Leica 3D Disto©
Light source	LED lamp

The protocol for the experimentation follows a linear process. This linear process is included in a broader integrated workflow that spans from the data acquisition of the existing building to the assembly process of the prefabricated modules (it must be recalled that the prefabricated modules are conceived for building renovation [3]). The protocol for this experimentation starts by gathering the information that parametric software named Dynamo© [18] generates, which is a list with the coordinates of the location of each of the objects. In ROS-MoveIt! environment, the robot reads the list and plans the motion and starts executing the plan. During the execution of the planned operations, there is a pause in the path. This paused pose's objective is to facilitate the recognition of the location of the grasped element. Three tests were carried out during the experimentation phase. The first test was achieved without applying any deviation correction. The second test was achieved by the use of ArUco markers for localizing the grasped object's place. The third test was achieved by using a digital theodolite or total station for localizing the key point coordinates of the object. Each test was repeated five times. Once the grasped object's location was determined, the robot modified its position in order to get closer to the planned location of the object. All three tests finalized with a goal position where the location of the grasped object was measured in order to define the accuracy

obtained in each test. Four points were measured as it is shown in Figure 2 and Table 2: point 1, point 2, point 3 and point 4.

Table 2. Planned location for point 1, 2, 3, and 4(mm)

Name	Position X	Position Y	Position Z
Point 1	0.0	25.0	0.0
Point 2	0.0	25.0	37.5
Point 3	0.0	0.0	37.5
Point 4	-250.0	25.0	0.0

In all tests, the robot was positioned with respect to a reference coordinate, in other words, the position of the robot was independent of the location of the assembly module.

The deviation of positions is obtained by the equations as follows:

$$r_i = \sqrt{(x_{ni} - x_0)^2 + (y_i - y_0)^2 + (z_i - z_0)^2} \quad (1)$$

$$\bar{r} = \frac{\sum_{i=1}^{N} r_i}{N} \quad (2)$$

$$\sigma_k = \sqrt{\frac{\sum_{i=1}^{N} (r_i - \bar{r})}{N}} \quad (3)$$

where N is number of trials, (x_0, y_0, z_0) is the planned location and (x_i, y_i, z_i) is the accomplished location during the i number of trials. The accuracy of the test is shown by the equation as follows:

$$\delta_k = \sqrt{\frac{\sum_{i=1}^{N} r_i}{N}} \quad (5)$$

3.1 Test without any deviation correction

This experimentation was carried out in order to determine the benchmark or the "normal" capabilities of the robot. The protocol is a process without any iterative step as shown in Figure 4, and no correction or adjustment was applied.

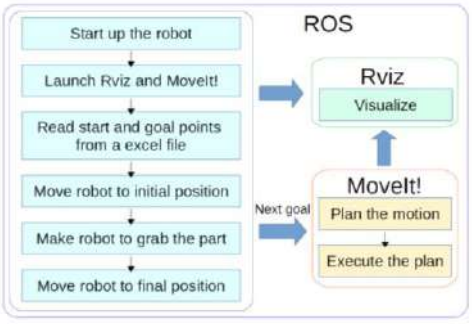

Figure 4. Protocol of the assembly process for the test without any deviation correction

The path planning and the grasping was determined in advance by the data generated for the parametric software. In Figure 5, the five different localitions of the object on the final pose of the robot are shown in red. In green, the planned location of the object are shown. In Table 3, the average point coordinates of the five different locations can be seen.

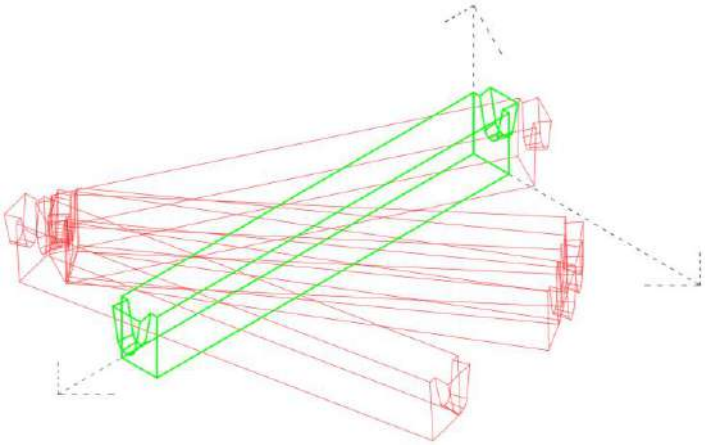

Figure 5. Goal position results without using any deviation adjustment

The results of the pose without any pose deviation, as expected, show a high deviation in comparison to the planned location of the object, where distances reach up to 136,86 mm in Point 2.

Table 3. Absolute location in the test without any deviation correction and distance from planned location (mm)

Name	Position X	Position Y	Position Z	Distance
Point 1	-65,20	-106,50	14,90	147,53
Point 2	-47,70	-94,10	-10,10	136,84
Point 3	-47,10	-93,00	-1,80	111,41
Point 4	-188,60	99,20	-22,60	98,93

As can be observed in Table 3, the results are considerably poor and impede the assembly of the mock-up with deviations higher than 100 mm. Therefore, these results show a worst-case scenario regarding deviations that need to be improved upon in the next two tests.

3.2 Test with Open CV and ArUco markers.

This test was based on the capabilities of Open CV [19] for recognizing the so-called ArUco markers. It states on their official website [19] "*OpenCV (Open Source Computer Vision Library) is an open source computer vision and machine learning software library*". In this test, two types of markers were used according to their functionality. First, a set of markers was placed onto the grasped element so that the pose of the center of it could be obtained if any of the markers were detected. The other marker was fixed on the working table as a reference for the coordinates of the robot and the

assembled module. The marker on the working table was used as a reference for the positioning.

During this test, an iterative step was defined in order to check and correct the deviation as explained in Figure 6. This iterative step improved the adjustment of the goal position. The camera was calibrated by using OpenCV and the chess board square placed in front of the Jaco robot. The corner of this square was used as a Reference coordinate, as it is shown in Figure 7.

The detection of the markers was not without issues e.g. it was affected by insufficient lighting. Furthermore, the occlusion of the markers caused the grasped object to not be recognized. When the markers were inclined too much away from the camera, it was difficult to detect them. In addition, z-axis flipping sometimes occurred [20]. This problem was prevented by using several markers and by accepting the majority decision.

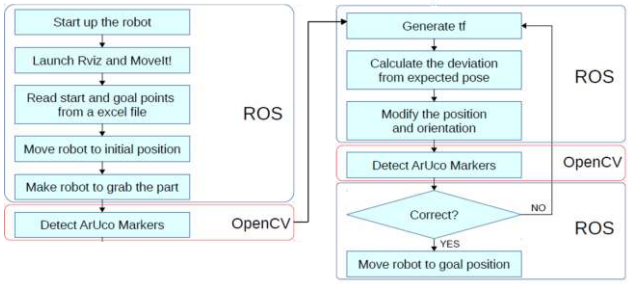

Figure 6. Protocol of the assembly process for the test with the ArUco markers

However, due to specific conditions such as grasped point or brightness, only one marker was detected and z-axis flipping was found to occur occurred.

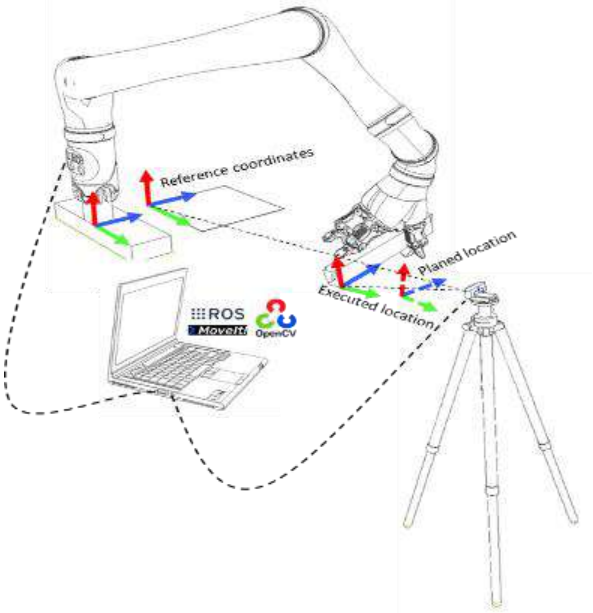

Figure 7. Scheme of the recognition of the grasped object by using the ArUco markers

In Figure 7, the scheme on the left shows the relative simplicity of the system. The camera needed to be placed on the point where the markers on the object and the reference marker can be seen at the same moment. The results; however, improve the final position location considerably.

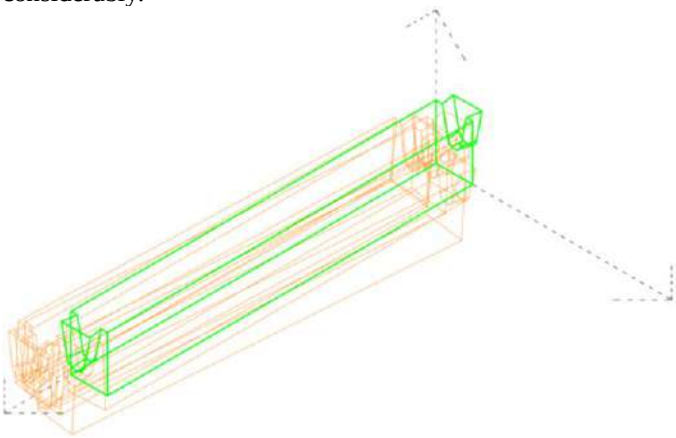

Figure 8. Goal position results using markers

In Figure 8, the five different locations of the object on the final pose of the robot are presented in orange. In green, the planned location of the object is shown.

Table 4. Absolute location in the test with the markers and distance from planned location (mm)

Name	Position X	Position Y	Position Z	Distance
Point 1	11,50	11,80	9,40	19,87
Point 2	11,40	10,10	1,90	40,24
Point 3	13,20	-10,30	28,20	19,15
Point 4	-238,10	18,10	-14,20	19,77

In Table 4, the results show deviations smaller than those that were presented in the test in sub-chapter 3.1. Similar to the test in sub-chapter 3.1, in Table 4, the average point coordinates of the five different locations are shown.

3.3 Test with the digital theodolite.

In this test, during the intermediate pose, the objects were recognized by localizing three points of the object. This test further requires that a human operator recognizes the location of the grasped object points by the Leica 3D Disto©.

During this test, an iterative step was defined as well as in the previous test, in order to check and correct the deviation as explained in Figure 9. In all five tests, the same three points of the element's corner were measured in the same order.

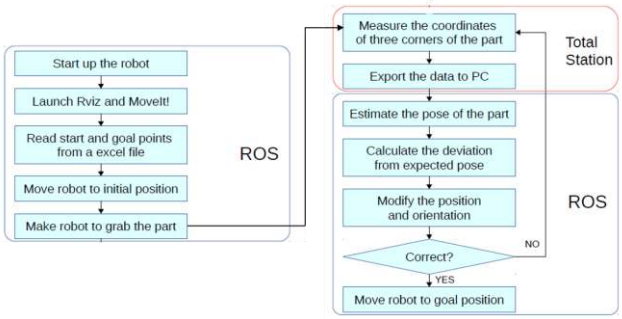

Figure 9. Protocol of the assembly process for the test with the digital theodolite

For calculating the necessary robotic pose adjustment depending on the element's position, a series of algorithms were used, which is explained as follows.

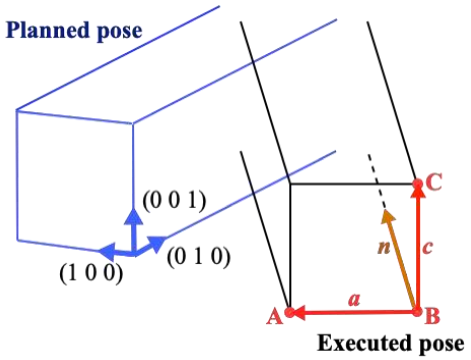

Figure 10. Deviation between the planned pose and the executed pose

From the three points (in Figure 10, A, B, and C), two vectors of the object were calculated ($\boldsymbol{a}$ = A − B, $\boldsymbol{c}$ =C−B). Then, the cross product of the two vectors was the same as the normal vector of them:

$$\boldsymbol{n} = \boldsymbol{a} \times \boldsymbol{c} \tag{6}$$

The unit vectors of the three vectors were calculated by dividing by the magnitude of themselves:

$$\boldsymbol{u}_a = \boldsymbol{a}/\|\boldsymbol{a}\| \tag{7}$$

$$\boldsymbol{u}_c = \boldsymbol{c}/\|\boldsymbol{c}\| \tag{8}$$

$$\boldsymbol{u}_n = \boldsymbol{n}/\|\boldsymbol{n}\| \tag{9}$$

Then, the following equation was established:

$$(\boldsymbol{u}_a \quad \boldsymbol{u}_n \quad \boldsymbol{u}_c) = \boldsymbol{R}_z\boldsymbol{R}_y\boldsymbol{R}_x \begin{pmatrix} 1 & 0 & 0 \\ 0 & 1 & 0 \\ 0 & 0 & 1 \end{pmatrix} = \boldsymbol{R}_z\boldsymbol{R}_y\boldsymbol{R}_x \tag{10}$$

where $\boldsymbol{R}_x$, $\boldsymbol{R}_y$, and $\boldsymbol{R}_z$ are the rotation matrices about x-, y-, and z-axis respectively. When the angles about each axis are α, β, and γ;

$$\boldsymbol{R}_z\boldsymbol{R}_y\boldsymbol{R}_x = \begin{pmatrix} C\beta C\gamma & S\alpha S\beta C\gamma - C\alpha S\gamma & C\alpha S\beta C\gamma + S\alpha S\gamma \\ C\beta S\gamma & S\alpha S\beta S\gamma + C\alpha C\gamma & C\alpha S\beta S\gamma - S\alpha C\gamma \\ -S\beta & S\alpha C\beta & C\alpha C\beta \end{pmatrix} \tag{11}$$

where $C\theta$ means $\cos\theta$; $S\theta$ means $\sin\theta$.

Thus, $\boldsymbol{u}_a$, $\boldsymbol{u}_n$, and $\boldsymbol{u}_c$ were defined as follows:

$$(\boldsymbol{u}_a \quad \boldsymbol{u}_n \quad \boldsymbol{u}_c) = \begin{pmatrix} u_{a_x} & u_{n_x} & u_{c_x} \\ u_{a_y} & u_{n_y} & u_{c_y} \\ u_{a_z} & u_{n_z} & u_{c_z} \end{pmatrix} \tag{12}$$

α, β, and γ were calculated by using the following equations:

$$\alpha = \tan^{-1}\left(u_{n_z}/u_{c_z}\right) \tag{13}$$

$$\beta = \tan^{-1}\left(-u_{a_z}/\sqrt{{u_{n_z}}^2 + {u_{c_z}}^2}\right) \tag{14}$$

$$\gamma = \tan^{-1}\left(u_{a_y}/u_{a_x}\right) \tag{15}$$

On the other hand, the coordinates of the center of the object P were calculated by the following equation:

$$\mathrm{P} = \mathrm{B} + (\boldsymbol{a} + \boldsymbol{c})/2 + l\boldsymbol{u}_n/2 \tag{16}$$

where l is the length of the object.

Then, the deviation of the position and orientation between the planned pose and the executed pose was obtained.

As shown in Figure 11, the robotic system is not complex. However, the interfaces with the digital theodolite were not robust and therefore time consuming.

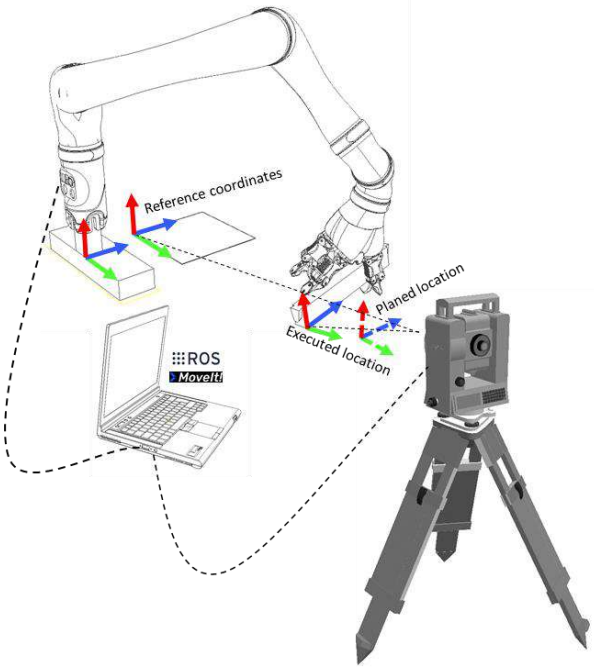

Figure 11. Scheme of the localization of coordinate recognition by using a digital theodolite

Similar to the test explained in sub-chapter 3.2, there were some issues while estimating the position of the grasped element. The points in this test were selected manually, and therefore the obtained coordinates were subject to errors.

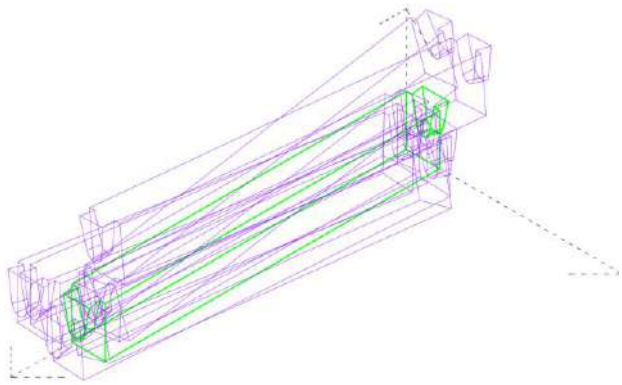

Figure 12. Goal position results by using digital theodolite

In Figure 12, the five different localizations of the object on the final pose of the robot are shown in purple. In green, the planned location of the object is presented. Table 5 shows the average point coordinates of the five different locations.

Table 5. Absolute location in the test with the digital theodolite (mm) and distance from planned location

Name	Position X	Position Y	Position Z	Distance
Point 1	-6,10	10,60	6,90	17,09
Point 2	-7,90	-18,60	40,70	44,43
Point 3	-6,40	6,00	43,80	10,80
Point 4	-254,40	26,00	5,40	7,04

3.4 Discussion

The results differ considerably during the three tests. On the first test (without any deviation adjustment), the final pose deviations are too high to accomplish any type of assembly tasks. On the two tests carried out with adjustment operations, the final localization of the object improves considerably, as an average, around 70 mm. The experiments achieved with the guidance of the markers show the best and most accurate results compared to the final desired location of the object. The tests achieved by the coordinate's localization with the digital theodolite present higher deviations than the results gathered with the ArUco markers.

Among the methods presented in this paper, the third test (recognition of coordinates) requires more attention from the human operator. However, it is not necessary to stick a marker on the object to be assembled which, in complex assembly processes where there are many parts, may be advantageous. Human-robot cooperation environments could benefit from this approach as the human worker could mark the necessary points. A specific interface for processing the data gathered with the digital theodolite and linking it with the ROS controller would reduce the time necessary to complete the processing.

Regarding the assembly of large-scale and bended objects such as plaster boards, the markers may be a better solution because the object moves while being handled. This means that the object recognition and its adjustment must be achieved once the object is close to the rest of the assembly.

The results show that, depending on the robotic system's accuracy, there should be consequences in the design of the objects to be assembled. This means that the openness of the joinery system in particular must be dependent on the accuracy of the robotic system. Therefore, in the timber-frame industry, it would be necessary to find the optimal CNC machining and routing geometries of the objects depending on the robot's assembly accuracy.

4 Conclusions

The main problems of assembly processes in fully or partially unstructured environments such as the prefabricated module industry are the inaccuracies associated with the picking and placing of objects. The grasping of objects typically requires structured environments and accurate grasping end-effectors. However, due to the variety of objects, shapes, sizes, and weights in the construction industry, this premise might not always be possible to achieve. In other words, due to the high variety of randomized products and objects in construction and particularly in building renovation, it is difficult to generate a fully structured environment. Therefore, the CNC machined elements of timber-frames need to be recognized before placing them in the module or in the construction site.

In the research outlined in this paper, two techniques have been tested for resolving such inaccuracies. As a conclusion, it can be stated that the objective of the research has been accomplished, which was to adjust the deviations of the grasped objects by recognizing their location. However, future work is necessary to create a more robust solution. Moreover, future experiments will be carried out using 3D laser scanners for localizing the grasped objects' deviations and linking the object with CAD or possibly BIM information.

The procedures executed in this research can be applied to the on-site installation of fully prefabricated modules as well. The pick and place prefabricated modules at the construction site is a task that could benefit from the methods described in this paper.

Acknowledgements

This project has received funding from the European Union's Horizon 2020 research and innovation programme under grant agreement No 636984.

The authors acknowledge the help provided by Mr. Ahmed Agha Osama (from the Chair of Building Realization and Robotics) and by Dr. Peter Wasmeier and the whole Chair of Geodesy of the Technical University of Munich.

References

[1] Santamouris, M., Innovating to zero the building sector in Europe: Minimising the energy consumption, eradication of the energy poverty and mitigating the local climate change, *Solar Energy*, 128, 61-94, 2016. https://doi.org/10.1016/j.solener.2016.01.021

[2] Lasarte, N., Chica, J. A., Gomis, I., Benito, J., Iturralde, K., Bock, T., Prefabricated Solutions and Automated and Digital Tools for the optimisation of a Holistic Energy Refurbishment Process. In *Proceeding of the 8th EESAP 1st ICAC* pages 125-140, San Sebastian, Spain, 2017. https://web-argitalpena.adm.ehu.es/pdf/UCPDF176683.pdf

[3] Iturralde, K., Linner, T., Bock, T. First Monitoring and Analysis of the Manufacturing and Installation Process of Timber Based 2D Modules for Accomplishing a Future Robotic Building Envelope Upgrading. In Proceedings of ISARC 2017, pages 65–73, Taipei, Taiwan, 2017. https://doi.org/10.22260/ISARC2017/0009

[4] Robeller, C., Konakovic, M., Dedijer, M., Pauly, M. and Weinand, Y., A Double-Layered Timber Plate Shell-Computational Methods for Assembly, Prefabrication, and Structural Design. In *Proceedings of Advances in Architectural Geometry*, pages 104-122. Zürich, Switzerland 2016. https://vdf.ch/advances-in-architectural-geometry-2016-e-book.html

[5] Braumann, J., Brell-Çokcan, S., Parametric Robot Control: Integrated CAD/CAM for Architectural Design. In *Proceedings of the 31st annual conference of the Association for Computer Aided Design in Architecture*, pages 242-251, Calgary, Canada, 2011. https://publications.rwth-aachen.de/record/658507

[6] Willmann, J., Knauss, M., Bonwetsch, T., Apolinarska, A.A., Gramazio, F. and Kohler, M., Robotic timber construction—Expanding additive fabrication to new dimensions, *Automation in construction*,61:16-23,2016. https://doi.org/10.1016/j.autcon.2015.09.011

[7] Kodama, Y., Yamazaki, Y., Kato, H., Iguchi, Y., Naoi. H., A robotized wall erection system with solid components, In *Proceedings of the 5th ISARC*, Pages 441-448. Tokyo, Japan 1988. https://doi.org/10.22260/ISARC1988/0052

[8] Bock, T., A Study on Robot-Oriented Construction and Building System. Ed: University of Tokyo, In: National Institute of Informatics, Tokyo, 1989.

[9] Gambao, E., Balaguer, C., Barrientos, A., Saltaren, R, Puente, E.A., Robot assembly system for the construction process automation, *In Proceedings of International Conference on Robotics and Automation*, pages 46-51, Albuquerque, USA, USA. http://ieeexplore.ieee.org/stamp/stamp.jsp?tp=&arnumber=620014&isnumber=13464

[10] Bonwetsch, T., Robotically assembled brickwork: manipulating assembly processes of discrete objects, PhD diss., ETH Zurich, 2015.

[11] Randek Zero labor. http://www.randek.com/en/wall-floor-and-roof-production-lines/zerolabor , On-line: 28/01/2019

[12] Iturralde, K. Bock, T., Integrated, Automated and Robotic Process for Building Upgrading with Prefabricated Modules, In *Proceedings of the 35th ISARC*, pages 340-347 , Berlin, Germany, 2018. https://doi.org/10.22260/ISARC2018/0048

[13] Maropoulos, P. G., Muelaner, J. E., Summers, M. D., Martin, O. C., A new paradigm in large-scale assembly—research priorities in measurement assisted assembly, *The International Journal of Advanced Manufacturing Technology*, 70(1-4), 621-633, 2014 https://doi.org/10.1007/s00170-013-5283-4

[14] Drouot, A., Zhao, R., Irving, L., Sanderson, D. and Ratchev, S., Measurement assisted assembly for high accuracy aerospace manufacturing, *IFAC-PapersOnLine*, 51(11), pp.393-398, 2018 https://doi.org/10.1016/j.ifacol.2018.08.326

[15] Nottensteiner, K., Bodenmueller, T., Kassecker, M., Roa, M.A., Stemmer, A., Stouraitis, T., Seidel, D. and Thomas, U., A complete automated chain for flexible assembly using recognition, planning and sensor-based execution. In *Proceedings of 47st International Symposium on Robotics*; pages 1-8, Munich,Germany 2016 https://ieeexplore.ieee.org/document/7559140

[16] Feng, C., Xiao, Y., Willette, A., McGee, W. and Kamat, V.R., Vision guided autonomous robotic assembly and as-built scanning on unstructured construction sites, *Automation in Construction*, 59, 128-138,2015. https://doi.org/10.1016/j.autcon.2015.06.002

[17] Lundeen, K.M., Dong, S., Fredricks, N., Akula, M., Seo, J. and Kamat, V.R., Optical marker‐based end effector pose estimation for articulated excavators, *Automation in Construction*, 65, 51-64, 2016. https://doi.org/10.1016/j.autcon.2016.02.003

[18] https://dynamobim.org/, Accessed: 28/01/2019

[19] Open Source Computer Vision Library, https://opencv.org/, On-line: 28/01/2019

[20] Oberkampf, D., DeMenthon, D.F. and Davis, L.S., Iterative pose estimation using coplanar feature points, *Computer Vision and Image Understanding*, 63(3), 495-511, 1996. https://doi.org/10.1006/cviu.1996.0037

Adaptive Haptically Informed Assembly with Mobile Robots in Unstructured Environments

P. Devadass[a], S. Stumm[a] and S. Brell-Cokcan[a]

[a]Chair for Individualized Production, RWTH Aachen University Germany
E-mail: office@ip.rwth-aachen.de

Abstract -

Robot assisted construction processes in the architectural domain which include assembly are uncommon due the size difference of the robot with respect the scale of the output. In order to extend the workspace of industrial robots, these can be mounted on top of a mobile platform. However industrial mobile robotics currently focuses on the utilization within clearly defined and structured production environments. Nevertheless, due to increasing product variety, a paradigm shift away from repetition of static task towards dynamic human robot collaboration is noticeable. Especially mobile robots face very specific challenges such as inaccuracy, dynamic on-site adaptability and predictability of whether the design is producible within the constraints of the robot. In this paper we discuss these challenges encountered due to onsite construction through a built project and illustrate the solution taken forward to address these challenges. In this research we propose a new methodology for on-site construction of non-standard components using mobile robots. The demonstrated project comprises of complex space frame timber system where every component of the structure is unique in its shape and size. For this we combine pre-planning of design with human-robot collaboration for on-site adaptation. The approach utilizes force torque sensors embedded within the robot in combination with haptic fiducials, in order to improving accuracy of the robotic fabrication and allow for human-robot collaboration within assembly. Employing the a-priori design knowledge the robot places the work-piece at the correct angle, while allowing for human adaptation of the path in order to increase accuracy. The paper illustrates the various optimization techniques developed to predict design manufacturability including potentially necessary adaptions. The research envisions a safe and automated large-scale construction methodology for complex systems and opens to new gateways for construction, allowing the collaboration between human workers and mobile robots within unstructured environments.

Keywords –

Mobile Robotics; Onsite Construction; Haptic Feedback; Re-informed design; Human-Robot Collaboration; Haptic Programming

1 Introduction

Low level automation is becoming common practice for pre-fabrication of building elements in construction industries. Simultaneously concepts from Industry 4.0 allow for more and more custom production specifically in fabrication of individualized elements. However, construction industry still struggles to develop effective techniques for onsite construction processes especially for assembly due to the limited working envelope of a stationary robot as well as limited adaptability in robotics in order to handle raw material with high tolerances. But with the advent of mobile robotics, the possibility of onsite construction seems promising. However, there are several factors which limit the use of these tools.

One critical factor is the design being developed independently of fabrication process constraints of these complex machines. Hence the designer does not realize the limitations of the fabrication setup while developing complex designs. This results in fabrication difficulties or even non-manufacturable designs. In a commercial practice, the designer typically sends the design directly to a fabricator, who tries to find quick solutions and intuitively fabricates by experience which results in a one-off solution for each design. But in case of mass production of individualized components an automated workflow is necessary. In the project developed by Aarhus School of Architecture, Israel Institute of Technology and the ETH Zurich [1], which has proved the value of integrating topology optimization for direct realization in the digital process. The research pavilion, 2011 of ICD Stuttgart further demonstrates the use of structural optimization for the full-scale fabrication of plated timber structures using bespoke robotic milling. Current robotic fabrication methods carried out at ETH Zurich under the Robotic Timber Construction group [2], as well as the Digital Urban Orchid by IAAC [3] achieve

similar output. However, these projects do not address the direct influence of fabrication process and its parameters towards the design, as well as the potential of a reciprocal relationship between fabrication and design. Similarly, the Wood Chip Barn project by Hooke Park [4] although harvesting the inherent structural form of the timber fail to automate the challenges of using a limited size robot for oversized workpieces (tree forks). At the time of writing, there are no existing design methods in timber construction where the machine and fabrication workspace parameters and its constraints are integrated into the digital design process which informs the design.

To overcome the gap between design and fabrication, we introduce a novel concept of design which is driven by a continuous production feedback and the integration of fabrication constraints. The fabrication constraints are addressed within the domain of robot's reachability for the given design. This methodology is demonstrated through 'The Twisted Arch' project (Figure.1). The potentials and limitations of each fabrication resource are analyzed through design and construction of a 1:1 scale prototype of complex space frame timber structures by employing a mobile robotic setup and a bandsaw cutting process for fabrication, as well as human robot collaborated assembly. The outcome of the research results in the creation of an intelligent computational program, which provides visual guidance for the user during the design process. The project was first introduced in [4].

Another critical factor to be considered while using mobile robots is the inaccuracies encountered due to the movement of the mobile platform which could be caused due to uneven floor, dirt, etc. This requires an additional element which compensates the accumulated errors of all elements in the structure. In our research, a construction feedback method is implemented where the inaccuracies of fabrication of each workpiece is automatically measured using haptic sensors and the errors are then compensated in the subsequent assembly of the structure. Thus, avoiding errors accumulation within the process establishing a continuous design and process feedback loop.

Figure 1. 'Twisted Arch' Project

2 Concept and Workflow

The general workflow and concept of our approach, as illustrated within Figure 2 based on our demonstrator project, consists of the following elements:

- Global Design (the overall structure to be fabricated)
- Assembly workspace analysis based on the global design ensuring reachability and collision free assembly, as well as structural stability
- Extraction of a single work pieces informed by the global design
- Fabrication workspace analysis to ensure manufacturability with feedback into the global design
- Execution of design to fabrication workflow with dynamic calibration resulting in feedback to the workpiece design
- Execution of design to assembly workflow with human-assisted adaption resulting in feedback to the global design

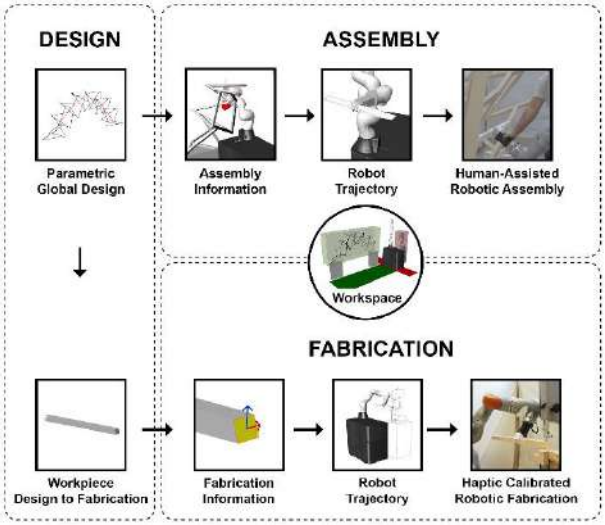

Figure 2. Process Overview

Within the following this workflow will be discussed in detail based on 'The Twisted Arch' project. Therefore, a first proof of concept is introduced, which illustrates the potential of bidirectional feedback between design, fabrication and assembly both in the context of work-piece fabrication as well as global structural design. Within [6] a first approach to transfer workspace constraints towards human-robot collaboration within assembly was introduced, specifically through the integration of constraint models within the robot controller and the term haptic programming was coined. The architectural impact of this workflow, with specific focus on the continuous design and process feedback loop, will be further discussed in section 10.

3 Global Design

The design of the prototype is based on a simple catenary arch comprising of a complex triangular space frame system made of timber elements. To test the process' influence on design, a complex timber space frame design connected by simple butt joints which follows a user-defined curve, is developed parametrically in a CAD environment. The parameters which include span, height, and offset of the catenary arch are optimized to test the workspace of the mobile robotic assembly process within the limits of structural stability of the design. The optimization in turn radically changes the space frame design and subsequently changes the length and angle of the cut of each element while still maintaining the configuration of the system. The maximum reach of the robot is verified to generate the working envelope and subsequently the robot's workspace. This data is continuously fed to the designer through custom visualization to make an informed choice for an ideal design. The entire interface is developed in the Rhinoceros3D and Grasshopper3D environment. The algorithms are custom plugins to check the functionality of the process developed by the authors. The design is initially simplified using the centerlines of the components and system for easier computation.

Another algorithm informs the design towards structural stability with the help of Karamba, a third-party plugin in grasshopper developed by Clemens Preisinger. The plugin integrates timber properties, in this case beech as part of the structural simulation. Irregularities like rot, cracks, etc. are not considered in process. The displacement of potential designs is then visualized to allow the designer to make an informed choice for the ideal design. The space frame is generated along the Cantenary arch allowing the design to choose different space frame variations, which are in turn used to generate solid geometries from the structural centerlines. Both algorithms simultaneously, inform the user to evaluate the design in terms of fabricability and structurally (Figure.3).

The design is evaluated every time to identify the non-manufacturable components through another iterative algorithm. The algorithm uses inverse kinematic solver, namely KUKA|prc [8], which checks for reachability, collisions, and singularities of the robot simulation. Nevertheless, after a series of optimization procedures, there are instances where the robot is still not able to manufacture the components (for example if the workpiece exceeds the fabrication limitations such as workpiece length, the angle of cut or a combination of both). The algorithm then highlights the geometries which cannot be manufactured in red. This visual illustration informs the designer whether the design can be fabricated or not, throughout the design process. The design can be continuously altered by the designer through quick modifications of the curve until all components are manufacturable. The designs generated are recorded and analyzed to understand deviation of the manufacturable design from the one intended by the designer.

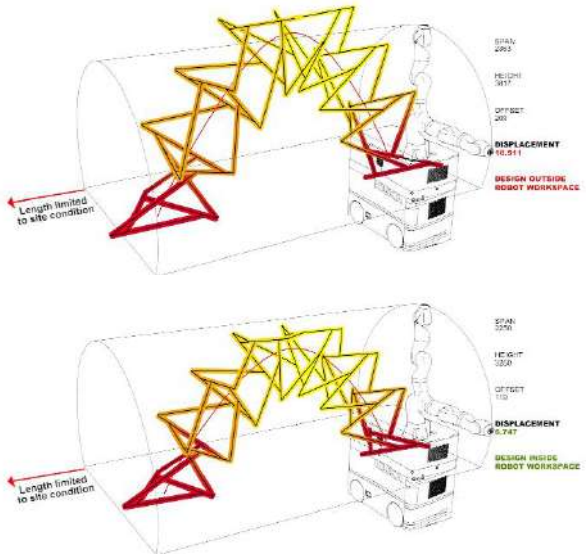

Figure 3. Optimization of the Design guided by the robotic workspace and structural constraints

This process establishes a new methodology in the field of architecture where every design decision is continuously informed and controlled by the parameters of fabrication. The process results in multiple options where every design is completely manufacturable but with slight modifications in its overall appearances from the one initially envisioned by the designer. The biggest drawback of this method is that the algorithm does not indicate which exact parameters are to be modified and by how much to achieve a manufacturable design. Although the constraints are identified and parameterized in this research, the next step is to develop an interface which would result in providing the above-mentioned feedback to the designer. The next steps are also to develop an algorithm to find the best suitable robot position, tool position and orientation of end-effector. This would result in an alternative approach where an optimal machine setup is generated based on the design created which otherwise would be a local solution for a given setup.

4 Workpiece: Design to Fabrication

After several iterations an optimized design is finalized, and an algorithm creates simple butt joinery between connecting components from the centerlines of the space frame system. Butt joinery is generally used to

connect two more timber pieces when the ends are cut flat at specific angles where they meet. The flat faces of the butt joints are fastened using timber screws. The butt joinery results in compound angles at certain connections due to complexity of the design. The sectional dimensions of the timber stock are 35x35mm. To avoid loss of the strength considering the limited sectional size of the timber, each timber component is restricted to only one connection at each end. The output from the algorithm is the final geometry which needs to be fabricated from the given stock material.

The length of each component is limited to a certain size depending on the maximum reach of the robotic arm or the robots working envelope. This is ensured to avoid collision between the timber material and the robotic arm or the environment. As the timber is gripped by the robot only at the center, the lengths of the timber pieces are limited to avoid extensive vibrations are the end of the stock material.

As the entire workflow is based on the centerline information and the local design (joinery) is automatically developed from it, this method allows transfer of the global design (timber framing drawing) made by another designer into the fabrication process. The centerlines of the connecting members in a design are required for the cad data.

5 Demonstrator Process Overview

Within the Twisted Arch project, the fabrication and assembly process flow consists of the following steps:

- Gripping of a square timber pieces from a supply station are manual handover.
- Optimization of the mobile robot's position towards the bandsaw with regard to reachability
- Haptic measurement adaption of the bandsaw plane to reduce the positioning error of the mobile platform
- Reorientation of the timber piece towards the bandsaw blade
- Cutting of the timber piece according to the compound angle
- Reorientation of the timber piece towards the band sawblade with the second side
- Cutting of the second side of the timber piece according to its compound angle
- Moving the piece away from the saw workstation
- Movement of the mobile platform towards the assembly station
- Movement of the cut timber piece towards the assembly position
- Manual adaption of the timber piece position to reduce inaccuracies
- Robot-assisted assembly
- Movement of the arm away from the assembly
- Movement of the mobile platform towards the bandsaw work station
- The assembly process is continued by retrieving the next timber piece.

6 Workspaces

The setup consists of a KUKA iiwa with 14kg payload and maximum reach of 840mm which has a gripper as an end effector, the robot is mount KUKA Mobile Robotic (KMR) platform, a standard workshop bandsaw with a maximum cutting depth of 110mm. Due to the limited reachability of the robot two boxes which provide the base on either ends of the arch at a raised height of 500mm is constructed.

The major challenge of using stationary robot is developing a successful robot path devoid any collisions. In this process the challenge is amplified due to continuous repositioning of the mobile robot base. For mobile robots a dynamic workspace is considered, unlike in stationary robots with a static workspace. The actual workspace is dependent on the setup and therefore requires the superposition of various workspaces, such as robot, fabrication, assembly workspace and its surrounddings taking into consideration within ever-changing and unstructured construction environments.

Before we begin to understand the fabrication and assembly processes, one needs to consider the setup and various workspaces involved in production (Figure.4). To comprehend and implement the parameter space within which fabrication and assembly can be successfully carried out, the effective workspace of each production resource (machine, tool, material) is analyzed. These analytical results are combined to create a process model that considers the interrelationship between all parts of the fabrication process. The fabrication workspace is a combination of robot, end effector (gripper) and tool workspace (bandsaw).

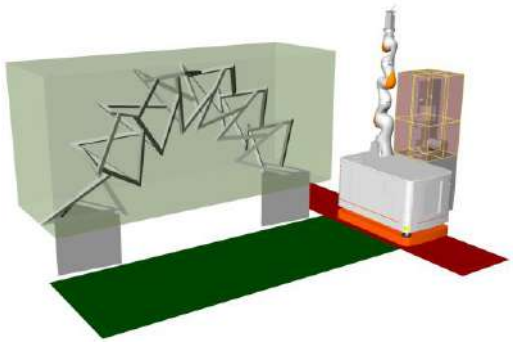

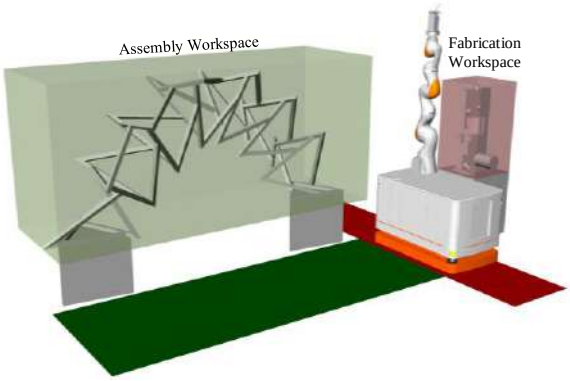

Figure 4. Workspaces

The robot workspace is the functional workspace which differs from working envelope of robot because the workspace takes the robots TCP (Tool Center Point) into account [7]. To determine the robot workspace an iterative algorithm is developed with the help of a genetic solver (namely Galapagos a Grasshopper3D plugin), which in turn generates some material and additional design constraints, such as timber section length and possible cutting angles. With the minimum and maximum reach known we can determine the three-dimensional robot workspace.

The bandsaw workspace can be described as a collection of robots TCP positions for cutting. The intersection of the robot with end-effector and bandsaw workspace defines the fabrication workspace. By establishing this fabrication workspace, it is easier to test the manufacturability of a component. Comparative studies are conducted between various robot and tool positions to understand their impact on the workspace.

The intersection of robot with end-effector with various TCP positions for assembly of all components in the prototype define the assembly workspace. The sequential assembly order of the timber components must be considered and understood so that the robot workspace does not collide with assembly workspace of the surrounding components. Each process is clearly defined by the boundaries of fabrication and assembly workspaces which are placed orthogonally to each other so that the mobile platform is allowed to freely operate to resolve reachability issues without any collisions.

7 Robot trajectory optimization for fabrication process

While manually cutting timber using a bandsaw, tremendous amount of forces is exerted by the bandsaw blade on the workpiece. Therefore, the workpiece is ensured to rest on the bandsaw table so that the forces are mostly absorbed by the table. This allows the fabricator to easily guide the workpiece at the required direction and angle without experiencing much of the forces. Similarly, while using the robot, in order to ensure least amount of forces are transferred to the robotic arm, the workpiece is required to rest on the bandsaw table during the cut (Figure.5). This prerequisite becomes a major robot trajectory challenge as the robot not only has to place the workpiece at the required orientation and position but also ensure the workpieces rests on the bandsaw table.

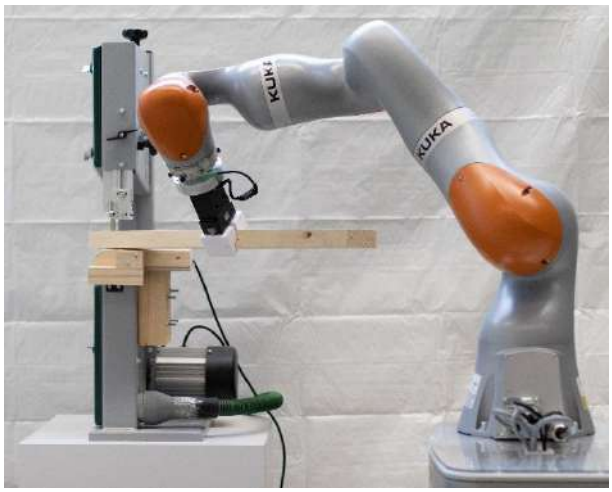

Figure 5. Resting the workpiece on the bandsaw table using the robot during fabrication

Hence, to achieve robot reachability for the above complex trajectory devoid of any collisions, a series of optimizations are executed. While using a stationary robot, a suitable gripping position from any of the four available directions of the workpiece is used to ensure reachability. Unfortunately, due to gripping and regripping of the workpiece every time for each cut of the workpiece, severe inaccuracies are encountered. To rest the workpiece on the bandsaw table, the workpiece geometry is rotated around the cutting surface until at least one edge (in case of compound angle cut) or a flat surface (in case of a simple angle cut) aligns with the table. However, in the current process to resolve this problem, we move the KUKA mobile platform, which in turn changes the base position of the KUKA iiwa and therefore enables different axis configuration in the robotic arm movement (Figure.6). This automatic optimization is conducted until a suitable trajectory is obtained which is free from collisions and well within the reach of the robot.

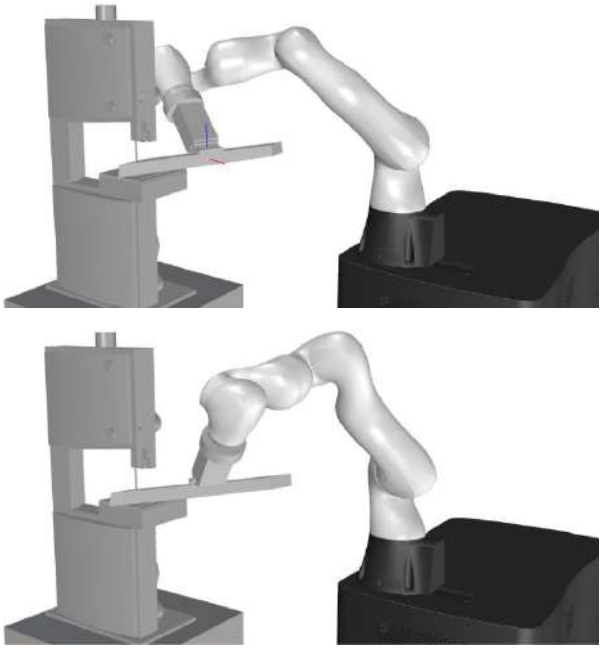

Figure 6. Optimizing the workpiece position to the robot and machine workspace

While the movement of the robotic arm is highly accurate the movement of the mobile platform is not. While it is possible to create a full map of the environment using the mobile platforms laser scanners this is however a very static process that does not allow for a dynamically changing environment as is often the case within construction. We compensate the inaccuracies within the process through haptic feedback for dynamic adaptivity on top of the statically planned fabrication process from design. In order to create dynamic adaptivity within the fabrication process, the robot is moved to a pre-calibrated position employing a haptic fiducial, before the cut is processed (Figure.7). Using the force torque sensors inbuilt in the robot, the robot dynamically calibrates the deviation between the haptic fiducial and the pre-calibrated position. By calculating this deviation, the cutting position is automatically updated to a corrected position in accordance with the real-world placement of the bandsaw thus providing an accurate cut. The pre-calibrated plane on the haptic fiducial serves as the primary reference point for the entire fabrication and assembly setup. All robot movements are referenced to it.

Without the haptic feedback for accuracy, the fabrication process observed an error over serval centimeters. The inaccuracies was inconsistent to evaluate as the mobile robot moved to various position depending the angle and size of the cut. But on an average the inaccuracies was found to be 20-30mm. With the haptic feedback the accuracy improved with an error less than 2.5mm.

Figure 7. Haptic Feedback using the custom built fiducial

8 Robot trajectory optimization for assembly process

Current workflows consider design informed fabrication the construction of complex assembly however requires more consideration for sequence planning as well as adaptation towards on-site deviations. Within assembly deviations between pre-planned design and real-world construction increase with every layer. Similar to fabrication, to resolve reachability issues during assembly the mobile platform is moved closer to the position of the component (Figure.8), however while creating the structure there are no available haptic fiducials on or closer to the prototype to increase the mobile platforms accuracy.

There are instances where the robot is still unable to reach the target position. Since the geometry plane is placed along the centreline of the geometry, we can rotate it into four different configurations which leads the robot gripping the part from 4 different directions. This also changes the robot's configuration while keeping the geometry in the same place. In order to compensate for these deviations, the robot connects the assembly component to the existing butt joint of its predecessor.

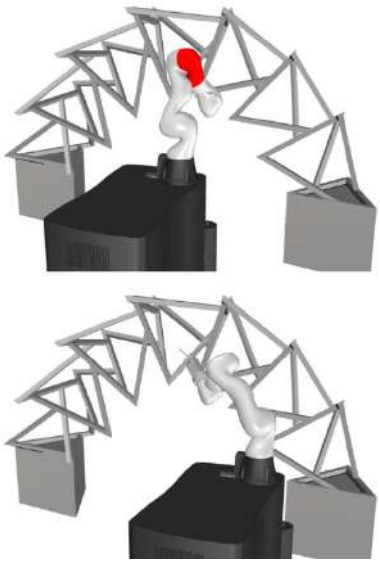

Figure 8. Optimizing the mobile robot position for reachability

However, the final assembly is conducted through human robot collaboration where the robot orients the workpiece in position while the human co-workers adapts the timber piece position in order to connect it correctly to the already fabricated space frame system (Figure.9). During assembly the robot is therefore set to an adaptive compliance mode, meaning the robot is in soft mode that allows the human co-worker to move the workpiece to a certain degree. If the deviations between planned target position and real-world position become too high the robot increases its stiffness and cannot be moved further of track. The components should be assembled in order so that they do not interfere with the assembly of its nearby components.

Figure 9. Human Robot Collaboration

9 The IDAA Framework

This leads to a reciprocal communication strategy between human co-worker and robot. This movement is easily guided by a user with its respective joinery to compensate the inaccuracies encountered during fabrication and transition, while simultaneously allowing the identification of construction errors that would lead to high deviations between design and assembly. The Production Immanent Design concepts of KUKA|prc which allow for a direct motion planning based on parametric design are therefore redefined and extended within the IDAA System, which was first introduced 2016 in [9] and further detailed in [5] for a stationary KUKA iiwa robot. However, within this paper the reciprocal relationship between the mobile platform and robotic arm movement is detailed.

In general, this system allows the integration haptic interaction primitives and concepts for dynamic configuration and path adaptation on-site, which is especially valuable for mobile robotics. The IDAA system does not rely on computer vision, which is unreliable in environments with dynamic lighting conditions but creates new means of communication between design and assembly through haptic feedback, not only for fully automated processes but also for human-robot collaboration.

Figure 10. Robotic Assembly

The design of adaption and control strategies can be challenging especial for users without expertise in robotics. In order to allow for the use of haptic feedback for adaptation in fabrication as well as assembly, or even extending these control strategies with other sensory input, a superposition between the geometrically planned

path and control strategy needs to be created.

Similar to skilled based robot programming [10] a catalogue of operations is created allowing the designer to link between geometric positioning and the execution of complex operations, such as dynamic recalibration of the robotic base frame at a haptic fiducial within fabrication. Such operations need to be accessible to designers but also create reusable descriptions of each operation. The IDAA Framework therefore allows for the extension of the operation catalogue in a combined approach the data interface to each operation is given by the geometric but localized path description, based on this the fitting control strategy can be chosen in a clearly defined setting.

1 Architectural Impact

The research illustrates how a single mobile robot can be resourcefully used for complex onsite construction processes and for multiple applications (including fabrication and assembly) and through efficient material handling in the 'Twisted Arch' project. Thus, demonstrating in what manner designers can thoughtfully develop design considering the parameters of the construction thereby yielding maximum efficiently from minimal resources. The research social impacts tangibly, by realizing the downsides of current technology and shows how human senses can be used sensibly for collaborative processes. Within the larger context of construction, the workflow establishes a new methodology in architectural design where the designer is always informed not only during design process but also during the construction process. One such example is the machinic inaccuracies encountered which is addressed through continuous designing and redesigning during the construction process. Thus, this methodology also allows the designer to have complete control throughout the process.

2 Synopsis

Within this work we illustrated the use of an adaptable mobile robot for onsite construction. By establishing a continuous design and process feedback loop the integration of a wide variety of fabrication and assembly tasks becomes, as well as individualized production becomes feasible. In order to make this approach applicable to other construction task further development is however necessary.

Within future work we will therefore focus on the automatic modelling of superimposed workspaces. By allowing for the representation and transfer of the necessary parameter space both from a production point of view as well as intended design adaptation can be optimized to adhere to the existing constraints from both viewpoints. While feedback from onsite production is possible this is still not fully integrated.

Furthermore, the used system is not suited for the rough environments of the construction site. The transfer to different systems and processes is still a major challenge and requires further research and development.

References

[1] Søndergaard, A.; Amir, O.; Eversmann, P.; Piskorec, L.; Stan, F.; Gramazio, F. and Kohler, M. 2016, "Topology Optimization and Robotic Fabrication of Advanced Timber Space-Frame Structures" Robotic Fabrication in Architecture,Art and Design, pp 190-203

[2] Willmann, J.; Knauss, M.; Bonwetsch, T.; Aleksandra Apolinarska, A.; Gramazio, F. and Kohler, M. 2015, "Robotic timber construction — Expanding additive fabrication to new dimensions." Automation in Construction. 61.

[3] Figliola, A. et.al. 2016. "Digital Urban Orchard: robotic manufacturing of complex shape." Advances in Architectural Geometry 2016

[4] Mollica, Z. and Self, M., 2016, 'Tree Fork Truss: Geometric Strategies for Exploiting Inherent Material Form' in Adriaenssens, S., Gramazio, F., Kohler, M., Menges, A. and Pauly, M. (eds.), Advances in Architectural Geometry 2016

[5] Stumm, S.; Devadass, P. and and Brell-Cokcan, S., 2018 'Haptic programming in construction' in the Construction Robotics Journal Volume 2, pp. 3-13

[6] Stumm, S. and Brell-Cokcan, S., 2018 'Haptic programming' in Robotic Fabrication in Architecture, Art and Design 2018, pp 44-58

[7] Aggarwal, Luv, 2016 "Reconfigurable Validation Model for Identifying Kinematic Singularities and Reach Conditions for Articulated Robots and Machine Tools" (2014). Electronic Theses and Dissertations. Geometry 2016, Zurich, p.138-153

[8] Braumann, J., and Brell-Cokcan, S., 2011 "Parametric Robot Control: Integrated CAD/CAM for Architectural Design." In Integration through Computation: Proceedings of the 31st Annual Conference of the Association for Computer Aided Design in Architecture (ACADIA), pp. 242-251.

[9] Stumm S, Braumann J, Brell-Cokcan Sigrid (2016) Human-machine interaction for intuitive programming of assembly tasks in construction. In: 6th CIRP conference on assembly technologies and systems (CATS) procedia CIRP 44, pp 269–274

[10] M. R. Pedersen, L. Nalpantidis, R. S. Andersen, C. Schou, S. Bøgh, V. Krüger, and O. Madsen. Robot skills for manufacturing: From concept to industrial deployment. Robotics and Computer-Integrated Manufacturing, 37:282 – 291, 2016.

Integrating Earthwork Ontology and Safety Regulations to Enhance Operations Safety

A. Taher [a], F. Vahdatikhaki [b], and A. Hammad [c]

[a]Concordia University, Concordia Institute for Information Systems Engineering, (CIISE), Canada
[b]University of Twente, Department of Construction Management and Engineering, The Netherlands
[c]Concordia University, Concordia Institute for Information Systems Engineering, (CIISE), Canada
E-mail: al_taher@encs.concordia.ca , f.vahdatikhaki@utwente.nl , hammad@ciise.concordia.ca

Abstract –

Safety in the construction industry remains a major challenge despite the technological advancements made in recent years. In recent years, ontologies are applied to give a formal structure to the knowledge in different domains. Ontologies also facilitate the integration of various domain knowledge and thus allow for better cross-functional developments (e.g., operator support systems that consider safety and productivity at the same time). The authors have previously developed a comprehensive Earthwork Ontology (EW-Onto). However, there has been no linkage between safety regulations and EW-Onto. Therefore, this research aims to: (1) develop a formal representation of earthwork safety regulations knowledge, and (2) integrate this knowledge with EW-Onto. A case study is developed to validate the integrated ontology. It is shown that the integrated ontology can be used to bridge the gap between high-level safety regulations and task-level instructions.

Keywords –

Earthwork; Ontology; Regulations; Safety

1 Introduction

Worker and equipment safety is a critical issue in the construction domain. Numbers from construction sites show that hazards in workzones affect projects at different levels. According to OSHA [1], in 2016, 21.1% of fatalities in the private industry are related to construction. Ignoring the safety rules, not following safety regulations, weather, and reckless equipment operators are the main factors that lead to accidents on construction sites. Accidents in construction sites are the main reason for the loss of life, which in turn affects schedules, productivity, costs, and the reputations of construction firms. In earthwork domain, excavation, especially trenches, are recognized as the most hazardous construction operation that can lead to serious accidents, such as cave-ins, toxic atmospheres, and falls [1]. *Job Hazard Analysis* (JHA) from OSHA [2], is a technique used for identifying, evaluating, and controlling these types of hazards. This technique is one of the different methods used for checking if the variables that are related to workers, tools, equipment, and the environment meet the associated regulations and rules. The data collected from construction sites using different technologies can enhance construction site productivity and safety. Moreover, combining human (e.g., workers, operators, designers, and coordinators) experience and best practices that are gained from previous similar projects is another method to avoid accidents in workzones. However, it is necessary to link the related hazards at the different levels of the project with other entities on the site (e.g., products, equipment, and the surrounding environment) in order to have better decision making. In recent years, ontologies are applied to give a formal structure to the knowledge in different domains. Ontologies also facilitate the integration of various domain knowledge and thus allow for better cross-functional developments (e.g., operator support systems that consider safety and productivity at the same time). The authors have previously developed a comprehensive Earthwork Ontology (EW-Onto). However, there has been no linkage between safety regulations and EW-Onto. Therefore, this research aims to: (1) develop a formal representation of earthwork safety regulations knowledge, and (2) integrate this knowledge with EW-Onto.

The rest of this paper is organized as follows: Section 2 discusses the related works on the safety regulations in construction. The methodology considering the different hazards in earthwork are presented in Section 3. Section 4 discusses the implementation of the ontology. Section 5 presents the conclusion and future work.

2 Related works

2.1 Safety Checking Methods and Techniques in Construction

Providing and performing safety procedures in workzones are a major factor for the success of the construction industry. These procedures should be followed by everyone involved in the business, which, in turn, saves lives and reduces the costs of business. Safety checking, which is the main part of safety management, aims to identify potential hazards before they occur on construction sites. Different methods and techniques are used to perform safety checks on construction workzones. The most efficient method is JHA, which defines the relationships between jobs, tools, workers, and the surrounding environment and provides a list of procedures and resources that are needed to prevent or reduce these hazards [2]. *Occupational Risk Assessment* (ORA) [3] is a process that is performed on the construction site to gather information from different sources to build better knowledge about hazards [4]. Check-list [5] technique is used to perform ORA on construction sites to define the safety issues at early stages of the work. Zhang, et al. [6] outlined a framework for early hazards identification in the construction model by integrating the *Building Information Model* (BIM) and safety regulations. Thus, the related hazards and the corresponding prevention procedures can be automatically identified and applied. 4D-BIM technologies connect the safety activities, construction planning, and visualizing the safety arrangements at any time [7]. Thus, the safety personnel and the designer with less knowledge about safety can use BIM-based friendly software to organize the *Safety Knowledge* (SK) and to improve occupational safety.

2.2 Ontological Modeling in Construction

Ontologies aim to represent the implicit knowledge in a domain in an explicit way through an organized structure of related concepts and relationships. Gruber [8] defined the ontology as "an explicit specification of a conceptualization."

Different studies use ontology and combine it with modeling techniques (e.g., BIM) [6][9]. Lee et al. [9] proposed an ontological approach for quantity take-off using BIM as a data source. The developed ontology is then used to infer the suitable items based on the estimated cost. Zhong et al. [10] provided an approach to integrate construction processes with regulation, which are related to quality compliance.

Zhang et al. [11] described an approach to store and re-use the safety management knowledge in construction. This approach links three main models, which are represented as ontology (i.e., product model, process model, and safety model). Ding et al. [12] proposed an approach to combine BIM with ontology to semantically organize construction risk knowledge. Wang and Boukamp [13] created a framework to improve access to the company's JHA. The framework uses the ontology to organize knowledge about activities, jobs' steps, and the related hazards.

Earthwork operations are a common part of construction projects. These operations include excavation, hauling, dumping, scraping, and grading. Earthwork operations account for 20% of the total cost of road building projects [14]. Using advanced information technologies in earthwork operations to improve safety and productivity is a major concern for researchers. Vahdatikhaki et al. [15] proposed the application of *a Multi-Agent System* (MAS) as a means to support fleet-level coordination for earthwork operations. Ontologies are one of the advanced technologies that have been used in construction to facilitate not only the human-to-human but also machine-to-machine communications by formalizing the information exchange scheme [16]. Taher et al. [16] proposed a framework to develop *Earthwork Ontology* (EW-Onto) to support and enhance the communication and data exchange between different stakeholders in earthwork projects.

2.3 Ontology Development Methodologies

The foundation Ontology (FO), also known as top-level or upper ontology, is an ontology that describes the most general terms across the domains. Zhou et al. [17] explained that certain studies might include some steps from the previous methodologies for developing their ontologies. In the 1990's, some methodologies for developing ontologies have been outlined. Skeletal methodology [18], and METHONTOLOGY [19] are examples of general methodologies used to build ontologies. IDEF5 is an ontology capture method and one of the Integrated DEFinition (IDEF) family languages that support the analysis and design of models [20]. Other methodologies or approaches are used to build the ontologies by re-using the existing ontologies or integrating two or more ontologies.

Description Logics (DL) is a language to formalize the knowledge representation that provides high-level descriptions of the world to be used in intelligent systems [21]. DL delivers syntax to describe the knowledge by expressions, which are built as atomic concepts, atomic roles and role constructors. DL is separated into three formalism components: Terminological Component (TBox), Assertion Component (ABox), and Role Axiom (RBox). TBox axioms describe the general properties of concepts and contain the intensional knowledge in the form of taxonomy or terminology such as concept inclusion. ABox axioms contain the assertional knowledge for specific individuals in the domain.

Whereas RBox refers to the properties of roles, such as role equivalence axioms and role inclusion [22].

3 Proposed Framework

The framework used to develop EW-SKB follows the approach of METHONTOLOGY for the following reasons: (1) it is application-independent and mature; (2) it is well-documented and has clear development activities; (3) it is based on the experience acquired from developing ontologies for many domains [19]; and (4) it has an integration step, which facilitates reusing EW-Onto as the main base of EW-SKB.

3.1 Main Steps to Develop EW-SKB

The best practices and knowledge in the earthwork domain and the related safety issues are used in EW-SKB development. Figure 1 illustrates the main phases of developing EW-SKB as explained in detail below.

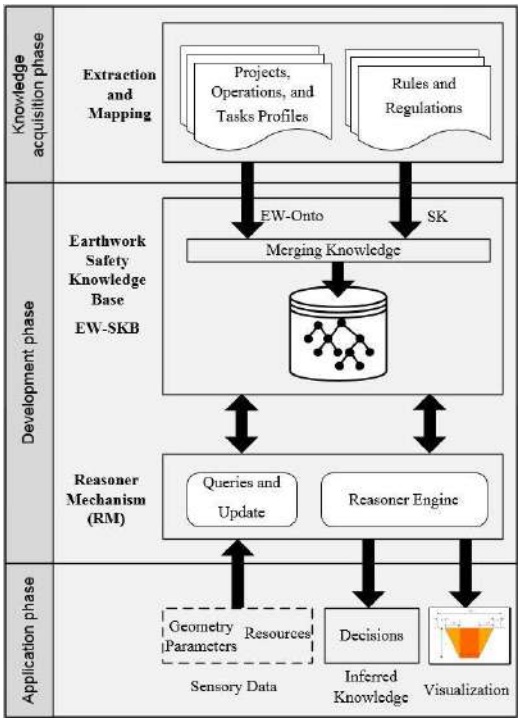

Figure 1. Proposed framework

3.1.1 Knowledge Acquisition Phase

The initial phase of the proposed framework, i.e., the knowledge acquisition phase, consists of defining the scope of the EW-SKB and defining concepts and taxonomies based on the requirements. The requirement data (e.g., terms and properties) are collected from various sources, such as textbooks and online resources (e.g., OSHA). EW-SKB should address the *Competency Questions* (CQ), such as: Why do we need to develop or extend the ontology? What are the domains and the scope of the ontology? Who are the users of the ontology? Answering these questions addresses parts of the requirements in the earthwork safety domain. Also, it helps to clarify what should be included in the developed ontology, and to which level of detail it should be developed. Furthermore, the basic concepts and relationships of EW-SKB structure is defined at this phase. The concepts, terms, properties, and instances are parts of the *Glossary of Terms* (GT). Developing the GT becomes easier when the specifications are clear.

3.1.2 Development Phase

In this phase, safety knowledge is added to the EW-Onto. SK includes the related concepts and relationships that link EW-Onto, related hazards, and related rules and regulations. The development phase includes the steps to add the SK to EW-Onto. The formalization of EW-SKB starts with transferring the conceptual model into the formal model using DL. Table 1 illustrates some examples of the conceptual components represented as terminology, assertion, and rules axioms, which define the concepts, individuals, and relationships, respectively. These components are added to the EW-Onto to link the concepts to soil types, product hazards, and equipment hazards. *The Reasoning Mechanism* (RM) or reasoner engine is the mechanism that represents the inferred knowledge and performing the queries over the explicit knowledge in the ontology. The RM checks the consistency of the developed ontology and validates the update of the relationships to ensure that there is no conflict.

3.1.3 Application Phase

This phase consists of any changes and updates of EW-SKB. The assumption here is that the ontology receives the sensory data from the site, including geometry data and resources data. Geometry data is more about the terrain model and the products (e.g., depth, width). Resources data includes data about the different types of resources in the earthwork domain including equipment (e.g., hoes, trucks), and materials (e.g., soil) from the workzones. The decisions are then generated based on the received data and the rules in EW-SKB. The visualization mechanism is not included in this paper and will be considered in future work.

3.2 Earthwork Related Hazards

In earthwork operations, there are a variety of hazards that affect the earthwork project at different levels. In this research, and as one of the main steps to map the concepts in the first phase, hazards in earthwork operations are classified into three main categories: material hazards, product hazards, and equipment hazards.

Table 1. Examples of TBox, ABox, and RBox components related to soil classification, product hazards, and equipment hazards

Axiom	Explanation	Examples
TBox	Express the terminological knowledge	SoilType_A, HazardWorkzone, ProtectionSystem, SlopingSystem, CaveIn, Path, Segment, Intersection, ExcavationZone, DumpingZone, IntersectionZone, WarningRange
ABox	Express the knowledge about the individuals	Soil1, Soil2, Workzone1, TrenchBox1, Slop1, Path1, Segment3, IntersectionPointT1, ExcavationZone
RBox	Describe the properties of the roles	hasStructure, hasTexture, hasType hasSiltAndClayPercentage, hasSoilType, hasHazard, hasSlopAngle, hasSpeed, hasLocation, hasCollisionWarning, hasToStop, hasDirection

It should be noted that products (e.g., trench) and materials (e.g., soil) are linked to each other. Product hazards are the result of the geometry of the product (e.g., length, width, and depth). Whereas, soil hazards are linked with the properties of the soil. Different actors who share and perform the processes and tasks (e.g., equipment operators, and on-feet workers) need to avoid hazards during the project at any level. To make the situations at the site more practical, the excavations and trenches are divided into workzones. Thus, each trench is composed of some workzones that may be different in their properties (e.g., soil type, depth, or other nearby workzones). Moreover, at each workzone, the tasks are performed by one individual or a team of different equipment and workers.

3.2.1 Material Hazards

In this research, and since the earthwork operations are linked to soil, the hazards related to soil are considered. These hazards are related to the different materials that are used in the project in different earthwork operations, such as cleaning and grabbing operations, excavation operations, and compaction operations. In some earthwork projects, explosive materials could be used in cleaning and grubbing operations, which affect the soil (e.g., the stability).

Soil classification plays a vital role in safety regulations, where each type of soil has its own structure and properties, which affect soil behavior under different circumstances. Soil classification can be obtained based on different values of the properties [23], which directly affect the stability of the excavation and the choice of suitable safety procedures and resources. OSHA standard number 1926 Subpart P Appendix A [24] provides examples of the guidelines that can be applied to classify the soil based on various properties. In EW-SKB, the quantitative properties are used to write the classification rules, which are: the structure of the soil (i.e., cohesive, granular, or granular cohesionless); the percentage of silt and clay in the soil, this percentage can be less or more than 15%; and the *Unconfined Compressive Strength value* (UCS), which is a result from the soil lab test and signifies the consistency and measures shear strength.

Different OSHA standard rules are translated to Semantic Web Rule Language (SWRL) to integrate them into the developed ontology. The next paragraph lists examples of SWRL in EW-SKB to classify the soil based on these quantitative properties. In addition, the pseudocode illustrates the logical steps to apply the rule. Soil classification is used to link to other rules related to the product hazards

Rule 1. This rule uses the structure of the soil, the clay percentage, and the UCS value to classify the soil and determine the soil texture.

Start
Input: The soil structure, the Silt and Clay percentage (scp), The value of (ucs)
Output: Soil classification, The soil texture
For each Soil sample **do**
If Soil has structure = "Cohesive" and scp > 15% and ucs >1.5 and **has** plasticity and **is** fissured
Set soil **has** type (A)
Set soil **has** texture (clay)
end if
end
End

Soil(?s)^hasStructure(?s,"Cohesive")^hasSiltAndClayPersentage(?s,?scp)^swrlb:greaterThan(?scp,0.15)^hasUnconfinedCompressiveStrengthValue(?s,?ucs)^swrlb:greaterThan(?ucs,1.5)^hasPlasticity(?s,true)^isFissured(?s,false)->Soil_Type_A(?s)^ hasType(?s,"A")^hasTexture (?s, "Clay")

3.2.2 Products Hazards

Products hazards describe the hazards that are linked to the final or intermediate outcomes of the processes and tasks, such as trenches, excavations, and holes. The focus here is on the trench-related hazards and how to improve the safety level in this type of earthwork.

OSHA rule number 1926.652, subpart P [25] is related to requirements for protective systems for

excavation. This clause specifies in general the rules related to trench shields. OSHA regulation (1926 Subpart P App B) [26] states the angle of slope for each type of soil. Based on these regulations, the following examples of SWRL rules link the workzones, the type of the earthwork operation, the type of the soil, the expected hazards, and how hazards can be avoided by performing certain procedures.

Rule 2. This rule checks the depth of the workzone. If the depth is more than 153 cm, then this workzone is classified as hazard workzone. The rule determines the type of hazard that this workzone has and which safety resources are needed to make it safer. As a result, the excavation operation is classified as hazard operation.

Start
Input: The workzone depth (d)
Type of the earthwork operation (exc)
Output: The potential hazard
The safety resource needed
Classification of the workzones
For each excavation operation **do**
For each workzone in the operation **do**
If d > 152 cm
Set workzone **has** hazard (CaveIn)
Set workzone **needs** safety resource (ProtectionSystem)
Set workzone **is** hazard workzone
Set excavation operation **has** hazard
end if
end
end
End

ExcavationOperation(?exc)^ProtectionSystem (?ps)^ CaveIn(?ca)^swrlb:greaterThan(?d,152)^has Depth (?w,?d)^hasWorkzone(?exc,?w)^Workzone(?w)-> hashazard(?w,?ca)^needSafetyResource(?w,?ps)^ HazardWorkzone(?w)^has (?exc, Hazard)

Rule 3. This rule classifies the earthwork operation based on the range of the depth and the soil type. If the depth of the operation in the range between 365 cm and 609 cm, and the soil type is A, then this operation is classified as hazard operation. The hazard type of this operation is Cave In hazard. Thus, this operation needs a safety procedure, which in this case is making a slop with 53˚.

Start
Input: The workzone depth (d), Type of Soil, and
Type of the earthwork operation (exc)
Output: The potential hazard, The safety procedure needed, Classification of the earthwork operation
For each excavation operation **do**
If d > 365 cm and < 609 cm and Soil Type = A
Set excavation operation **needs** safety procedure (Trench Slop)
Set excavation operation **needs** slop Angle 53˚
Set excavation operation **has** hazard (CaveIn)
Set excavation operation **is** hazard operation
end if
end
End

SlopingSystem(?ss)^Workzone(?w)^Excavation Operation(?exc)^hasWorkzone(?exc,?w)^ hasType (?s,"A")^CaveIn(?ca)^hasDepth(w,?d)^swrlb:greater Than (?d,365)^swrlb:lessThan (?d,609)^hasSoilType (?w,?s)^Soil(?s)-> needSafetyProcedure(?exc,?ss)^ needSlopAngle(?exc,53)^hashazard (?exc,?ca)^Hazard Operation (?exc)^has(?exc,Hazard)

The steps to identify the hazards in the earthwork workzones and equipment are illustrated in Figure 2. The algorithm considers the hazards in workzones, which are a combination of soil and product hazards.

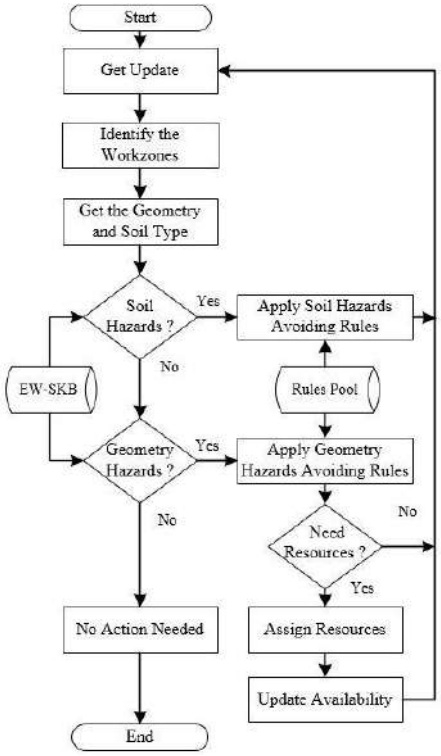

Figure 2. Material and product hazard identification

The steps begins with retrieving an update of a particular workzone. The type of workzone is identified (e.g., excavation or trench), followed by retrieving the geometry and soil type of the workzone. Then, the type of hazards are recognized based on applying the rules of the ontology. In the case that resources are needed to avoid the hazard (e.g., trench boxes), the assigned resources are used to update the availability of resources.

Then, an update is applied to ensure that the safety rules will not be triggered again.

3.2.3 Equipment Hazards

Several types of equipment (e.g., trucks, scrapers, dozers and hoes) are used in earthwork sites because of their ability to perform different tasks. These pieces of equipment are usually working together as a team to achieve the work. Equipment hazards could be called the operation hazards, where the risks are higher when several teams of equipment perform different tasks in parallel in a congested site. For equipment hazards, trucks are considered as sources of hazards when they are moving from one location to another. There are a variety of hazards related to trucks, which can increase the potential hazards of accidents and collisions, such as exceeding the maximum load or speed on roads and paths, and right-of-way regulations. Uncontrolled paths in construction sites pose high potential hazards to equipment and workers. Intersections have more complex traffic situations, which are influenced by a variety of safety rules, such as the permitted and prohibited directions and different priorities for equipment crossing the intersection at the same time. Moreover, the hazard level is raised when the equipment is operated by reckless drivers or poorly-trained operators. However, using a decision-support mechanism can help the operators in improving their safety.

Figure 3 illustrates how the hazards related to equipment are identified after retrieving the update of sensory data from the site.

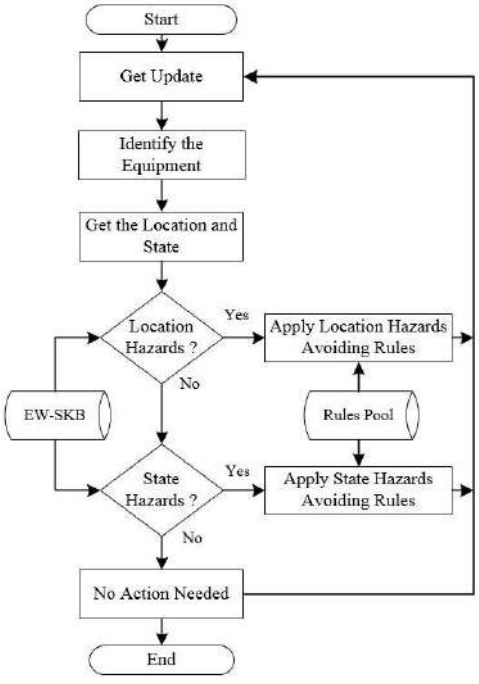

Figure 3. Equipment hazards identification

Generally, the equipment hazards are divided into two main categories, namely hazards related to equipment location and hazards related to the equipment state. Hazards related to equipment location are the result of changes in locations while the equipment is preforming a task (e.g., a truck or scraper moving between excavation and dumping area) or equipment relocation (e.g., a hoe moving from one workzone to another). Whereas the hazards related to the equipment state are the result of performing the tasks (e.g., a hoe swinging to the digging area). The hazards related to the equipment state are beyond the scope of this paper.

Data properties can obtain their values from sensors attached to the equipment (e.g., truck) and/or located on the paths and intersections. *locatedAt*, *movingFrom*, *goingTo*, *isOn*, *isUnder*, and *isToward* are object properties linked the individuals. Figure 4 shows a hazards situation where a group of three trucks performs their tasks (i.e., hauling and return from the dumping zones).

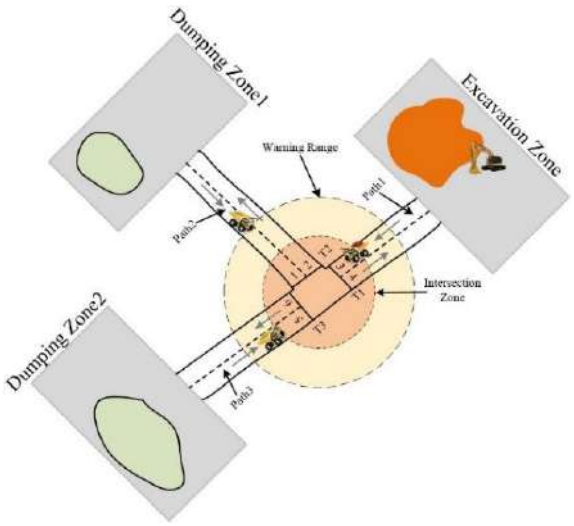

Figure 4. The case study scenario of the uncontrolled intersection

The trucks equipment are located near an uncontrolled intersection. This scenario simulates the hazards related to the equipment locations. Figure 4 shows the simulated scenario. Trucks on paths (1, 2, and 3) are moving in different directions. Each truck is labeled based on its direction and its path. SWRL is used to link the above-mentioned concepts with other concepts and entities in EW-Onto. SWRL is also used in EW-SKB to infer the safety decisions and create a safe driving environment, such as the right-of-way, sending a warning, order to stop, or order to slow down. The next SWRL rules are examples that formularize the knowledge about truck hazards at an uncontrolled intersection.

Rule 4. This rule illustrates an example of the orders that

trucks are received based on the situation of truck with the priority. In this rule, Truck1 has the priority, its direction is straight, and is located at the intersection. Thus, Truck3, which its direction is left receives the order to stop in case it is under the warning ranges.

Start
Input: The location, The direction, Truck name
Output: The order to stop or slow down
For each Truck do
If label = "Truck1" and location= isLocatedAt (IntersectionPointT1) and direction= "GoingStraight"
If label= "Truck3" and direction= "GoingLeft" and location =isUnder (Warning_Range)
Set Truck3 **has** Order (Stop)
end if
end if
end
End

Truck(?tr1)^hasLabel(?tr1,"Truck1")^isLocatedAt(?tr1, IntersectionPointT1)^hasDirection(?tr1,"GoingStraight")^Truck(?tr3)^hasLabel(?tr3,"Truck3")^hasDirection(?tr3,"GoingLeft")^isUnder?tr3,?wr)^Warning_Range(?wr) -> hasToStop(?tr3, true)

4 Implementation and Case Study

As mentioned in Section 1, EW-Onto is used as the main part of EW-SKB. In this paper, Protégé, 5.0.2 [27] is used to edit EW-Onto by adding the related concepts and relationships using a set of graphical plugins. Moreover, SWRL rules can be added and edited using Protégé. The verification is done by checking whether EW-SKB can answer the CQ or not. Furthermore, the consistency of EW-SKB is checked using a reasoner (HermiT reasoner). Figure 5 illustrates an example of using the reasoner engine based in Rule 1 to define the soil type.

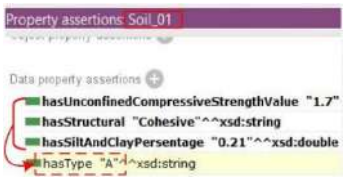

Figure 5. Reasoning engine result for soil classification

Thus, *Soil_01* is soil type A based on the values of this sample. Figure 6 provides examples of hazard related to workzone and excavation operation based on the Rules 2 and 3. Excavation-100-01 has inferred a hazard because it has an instance of workzone (i.e., Workzone001), and has soil type A.

A simulated case study is conducted to verify the developed implementation. As demonstrated in Figure 4 and based on Rule 4, Figure 7(a) shows the simulated scenario. Truck1 *isOn* Path1, and *isToward* the intersection. This truck gets the priority (*hasPriority: true*) because it is located in the intersection area and is loaded (*isLoaded: true*).

(a) (b)

Figure 6. Reasoning engine results for workzones (a) and for excavation operation (b)

The other trucks (Truck2 and Truck3) are ordered to stop or slow down. The messages to the other trucks are based on their locations and directions. For example, as shown in Figure 7(a), Truck1 is moving in a straight direction. Thus, Truck2 received the order to stop (*hasToStop=true*) as in Figure 7(b) and Truck3 received the order to slow down (*hasToSlow=true*) because its direction is also going straight (*hasDirection"GoingStright"*) as shown in Figure 7(c). Whereas the order will be changed to stop (*hasToStop=true*) if Truck3 direction is going left (*hasDirection" GoingLeft"*) as shown in Figure 7 (d).

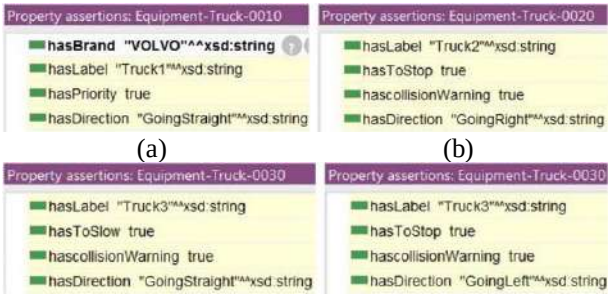

(a) (b)

(b) (d)

Figure 7. Reasoning engine results in EW-SKB for trucks at an uncontrolled intersection.

5 Conclusion and Future Work

In this paper, the previously developed earthwork ontology (EW-Onto), has been augmented by adding safety knowledge base (EW-SKB). EW-SKB is a combination of essential knowledge related to the safety issues in earthwork, which can contribute to improving safety decision-making. Knowledge associated with safety is integrated with EW-Onto to link the different concepts in EW-SKB. EW-SKB has the added value of integrating different entities (e.g., equipment, trench, and

soil) in construction sites with safety regulations. The potential benefits of the developed ontology are combined from the scalability nature and the automatic inferring decisions that can be taken based on data collected from actual projects. The future work will focus on developing an approach to visualizing the decisions and combining soil and sensor ontologies, which will add a more robust base to extend EW-SKB. Thus, more comprehensive representation of the concepts and relationships will be included in the resulting ontology.

References

[1] OSHA. Commonly used statistics, On-line: www.osha.gov/oshstats/commonstats.html, Accessed: 27/03/2018.

[2] Chao E. L. and Henshaw J. L. Job Hazard Analysis (JHA), OSHA Publication 3071(Revised). *Department of Labour, (OSHA)*, 2002.

[3] Pinto A., Nunes I. L. and Ribeiro R. A. Occupational risk assessment in construction industry–Overview and reflection. *Saf.Sci.*, 49(5): 616-624, 2011.

[4] Lu Y., Li Q., Zhou Z. and Deng Y. Ontology-based knowledge modeling for automated const. safety checking. Saf.Sci., 79: 11-18, 2015.

[5] Mattila M., Rantanen E. and Hyttinen M. The quality of work environment, supervision and safety in building const. *Saf.Sci.*, 17(4): 257-268, 1994.

[6] Zhang S., Teizer J., Lee J., Eastman C. M. and Venugopal M. Building information modeling (BIM) and safety: Automatic safety checking of construction models and schedules, *Auto. Const.*, 29: 183-195, 2013.

[7] Kiviniemi M., Sulankivi K., Kähkönen K., Tarja M. and Merivirta M. BIM-based safety management and communication for building construction., *VTT Rese. Notes 2597*, 2011.

[8] Gruber T. R. A translation approach to portable ontology specifications. *Knowledge acquisition*, 5(2): 199-220, 1993.

[9] Lee S., Kim K. and Yu J. BIM and ontology-based approach for building cost estimation. *Auto. Const.*, 41: 96-105, 2014.

[10] Zhong B., Ding L., Luo H., Zhou Y., Hu Y. and Hu H. Ontology-based semantic modeling of regulation constraint for automated construction quality compliance checking. *Auto. Const.*, 28: 58-70, 2012.

[11] Zhang S., Boukamp F. and Teizer J. Ontology-based semantic modeling of construction safety knowledge: Towards automated safety planning for job hazard analysis. *Auto. Const.*, 52: 29-41, 2015.

[12] Ding L., Zhong B., Wu S. and Luo H. Construction risk knowledge management in BIM using ontology and semantic web technology. *Safety Science*, 87: 202-213, 2016.

[13] Wang H. and Boukamp F. Ontology-based representation and reasoning framework for supporting job hazard analysis. *J.Comput.Civ.Eng.*, 25(6): 442-456, 2011.

[14] Smith S., Osborne J. and Forde, M. The use of a discrete-event simulation model with Erlang probability distributions in the estimation of earthmoving production. *Civ.Eng.Syst.*, 13(1): 25-44, 1996.

[15] Vahdatikhaki F., Langari, S. M., Taher A., El Ammari K. and Hammad A. Enhancing coordination and safety of earthwork equipment operations using Multi-Agent System. *Auto. Const.*, 81: 267-285, 2017.

[16] Taher A., Vahdatikhaki F. and Hammad A. Towards Developing an Ontology for Earthwork Operations. *ASCE*, 101-108, USA, 2017

[17] Zhou Z., Goh Y. M. and Shen L. Overview and Analysis of Ontology Studies Supporting Development of the Construction Industry. *J.Comput.Civ.Eng., 30(1)*, 2016.

[18] Uschold M. and Gruninger M. Ontologies: Principles, methods, and applications. *The knowledge engineering review*, 11(2): 93-136, 1996.

[19] Fernández-López M., Gómez-Pérez A. and Juristo N. Methontology: from ontological art towards ontological engineering. *AAAI Technical Report SS-97-06*, 33-40, 1997.

[20] Noran O. UML vs. IDEF: An Ontology-Oriented Comparative Study in View of Business Modelling. 674-682, 2004.

[21] Baader F. *The description logic handbook: Theory, implementation, and applications*, Cambridge University Press, 2003.

[22] Krötzsch M., Simancik F. and Horrocks I. A description logic primer. *arXiv preprint arXiv: 1201.4089*, 2012.

[23] Du H., Dimitrova V., Magee D., Stirling R., Curioni, G., Reeves H., Clarke B. and Cohn A. An ontology of soil properties and processes. 30-37, 2016.

[24] OSHA. Soil classification. On-line: www.osha.gov/pls/oshaweb/owadisp.show_document?p_table=STANDARDS&p_id=10931, Accessed: 25/4/2018.

[25] OSHA Trenching and Excavation Safety. *U.S.Department of Labour, OSHA*, 2015.

[26] OSHA Sloping and Benching. On-line: www.osha.gov/pls/oshaweb/owadisp.show_document?p_table=STANDARDS&p_id=10932, Accessed: 21/06/2018.

[27] Stanford U., Stanford centre for biomedical informatics research; The Protégé ontology editor. On-line: https://protege.stanford.edu/products.php, Accessed: 08/05/2018.

Combining Deep Learning and Robotics for Automated Concrete Delamination Assessment

E. McLaughlin[a], N. Charron[a], and S. Narasimhan[a]

[a]Department of Civil and Environmental Engineering, University of Waterloo, Canada
E-mail: em3mclau@uwaterloo.ca, ncharron@uwaterloo.ca, snarasim@uwaterloo.ca

Abstract –

Computer vision and robotics present tremendous opportunities for automating routine inspections of reinforced concrete bridges. One of the most critical aspects of these inspections is delamination assessment, as delaminations present immediate safety concerns due to falling concrete. Current methods of delamination assessment include hammer sounding and chain dragging, which are time consuming and difficult when accessibility is limited. Infrared technology presents an alternative method of assessing delaminations. In this work, a novel inspection method is proposed that uses an infrared camera combined with a convolutional neural network to automatically assess delaminations in infrared images. MobileNetV2 is implemented as an encoder with Deeplab V3 to perform pixel-wise segmentation in infrared images of delaminations.

The results show 74.5% mean intersection over union (mIoU) for predicting delaminated areas, which is comparable with the performance of this network architecture on benchmark data sets. Reviewing the predicted delamination areas also shows that the results accurately predict delamination locations, and accuracy limitations primarily exist in the fine outline details of the delamination. The automated delamination assessment method was also tested by mounting an upward facing thermal camera on a mobile ground robot to perform a bridge soffit inspection. The robotic scanning data set yielded a mIoU of 79.5% for delamination assessment. The increase in mIoU is likely due to the image data being better structured in the robotic images. This displays the ability to combine infrared imagery, convolutional neural networks, and unmanned mobile robots to meet case-specific accessibility needs for more accurate and time-efficient delamination assessment.

Keywords –

Convolutional neural network; Pixel-wise segmentation; automation; Delamination assessment; Bridge inspection

1 Introduction

Modern technologies in computer vision and robotics enable automation of routine tasks, with potential for improved efficiency in large-scale work. Routine concrete bridge inspection is one task where these technologies could provide great benefits [1]. In North America, there is demand for improved bridge inspections to more efficiently allocate the resources invested in bridge management. Routine inspections are performed by qualified inspectors following standardized guidelines (e.g., OSIM [2]). These inspections can be cumbersome and fraught with human error when access is limited due to long spans, water bodies, traffic conditions, and safety requirements. In addition, the results of routine inspections can be subjective and variable between inspectors [3].

One of the most important defects assessed during routine concrete bridge inspections is delamination. Concrete delamination can be described as a subsurface void in a concrete structure, which is caused by excessive internal stresses. The surface concrete next to the void is referred to as the delaminated concrete. Delaminations are critical, as they pose multiple safety hazards. The immediate hazard is that the mass of concrete below the void is likely to eventually fully detach and fall. This hazard is especially dangerous for bridges over high pedestrian or vehicular traffic areas.

In addition to being critical defects, delaminations are also one of the most difficult defects to assess during routine visual inspections because they are a subsurface defect that can seldom be detected by human vision. Currently, delaminations tend to be detected by manual process of hammer sounding or chain dragging to listen for hollow sounding concrete. These current sounding methods are time-consuming, inaccurate, and often not performed due to accessibility limitations. This makes delamination assessment a good candidate for an automated inspection method.

Infrared cameras combined with mobile robotic technologies present the opportunity for an efficient method of delamination assessment. The first step

towards developing this method is to use hand-held infrared cameras to assess delaminations. Delaminations can be identified in infrared images of concrete [4], as the delaminated concrete heats and cools at a different rate than the surrounding concrete. This occurs because the internal void acts as an insulating layer, making the delaminated concrete an independent, small mass [5]. This phenomenon makes delaminated areas often appear as a hot or a cold spot in an infrared image, depending on the time of day and environmental conditions. Detecting delaminations in infrared images is based on relative differences in thermal readings, so the absolute temperature of the delaminated areas is not critical for this study. Figure 1 shows examples of both hot and cold delaminations in infrared images of concrete bridge soffits.

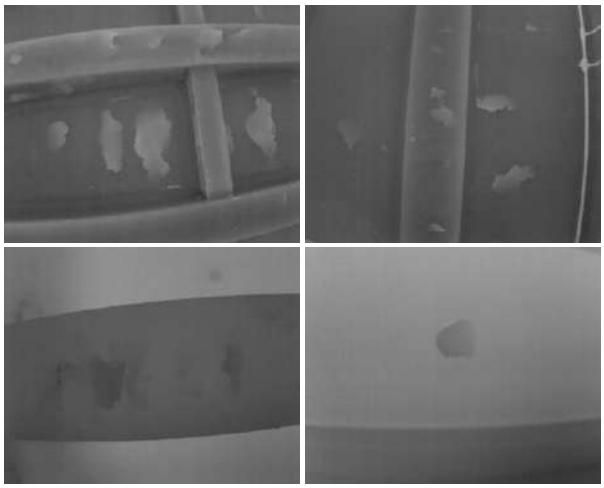

Figure 1. Examples of white-hot (top row) and black-cold (bottom row) delaminations in infrared images of concrete bridges.

Another advantage of using infrared cameras to detect delaminations is that this creates new possibilities for easy access to hard to reach bridge components. Many existing infrared cameras come in compact forms, ready to be mounted on an unmanned mobile robotic vehicle. This has the potential to eliminate many accessibility issues, as an infrared camera can be deployed on various vehicle types (aerial, ground, water) to account for the specific limitations of any bridge environment. For example, a bridge over water could have an upward facing infrared camera on a water vehicle to collect images. This proposed vision based infrared and robotic delamination assessment procedure provides a reasonable alternative in situations where traditional methods (e.g. hammer sounding) are not economically feasible due to special equipment and/or traffic control requirements.

Of all the advantages, perhaps the most useful advantage of using infrared imagery to assess delaminations is the ability to detect and localize the delaminations automatically using computer vision. In the computer vision community, there are two types of approaches that are used to automatically process image data for detecting objects of interest (delaminations being the objects of interest in this work): knowledge-driven methods and data-driven methods.

Knowledge-driven methods are based on the known characteristics of the object of interest. For example, this knowledge may include known colours and shapes of the objects of interest in the images. Knowledge based methods will often include human inputted rules for determining which features in images correspond to which objects. The second approach is data-driven methods, which rely on large quantities of labelled image data to train deep prediction networks. Once these networks have been trained to detect and localize the objects of interest based on the inputted data, they can then be used to detect and localize those objects on new data sets. These methods require large labelled data sets and significant processing resources to train the networks. Data-driven methods have become the method of choice for many computer vision based object recognition. These methods have consistently dominated computer vision competitions since a data-driven network first won the ImageNet challenge in 2012 [6].

For the assessment of concrete delaminations, knowledge-driven methods are difficult to implement successfully as delaminations have no definitive shape, and can show as a hot or cold area in the image depending on environmental conditions. This makes it difficult to determine a set of rules that will work across various delamination cases. Little research has been done to automatically assess delaminations using knowledge-driven methods, but some algorithms exist to automatically detect delaminations using a simple data-driven method (e.g., k-means clustering [7]). These existing methods are limited to specific bridge environments and often require some expert supervision.

Alternatively, convolutional neural networks (CNN) present an opportunity to use data-driven methods for fully automated detection. CNNs are considered state-of-the-art in computer vision as they currently dominate benchmarks such as [8], and can be leveraged to detect and localize objects of interest within images. Thus CNNs not only allow detection of images that show delaminations, but also provide the location of delaminated areas within each image. CNNs have yet to be applied to concrete bridge delamination assessment, but present a viable opportunity to improve upon existing results for delamination detection. This work proposes a CNN for semantic pixel-wise segmentation of delaminated areas within an infrared image of a reinforced concrete bridge.

The work presented herein can be divided into three main contributions. First, a versatile image labelling methodology is presented. This methodology fosters rapid pixel-wise labelling of concrete bridge defects in images to accelerate dataset building. Second, a novel approach is taken to concrete delamination detection and localization using infrared imagery combined with a convolutional neural network. Lastly, the described delamination detection methodology is demonstrated on a mobile ground robot. This final demonstration proves that the method presented herein can alleviate accessibility constraints in many bridge inspections. The methodology can be extended to aerial robots as well.

2 Related Works

Research work combining computer vision with concrete bridge inspection has primarily focused on automated crack detection and localization in visible spectrum images [9,10]. Some research has also been done on spall/delamination detection [11,12], but to a far lesser extent. With regards to delamination specifically, automated assessment via computer vision is still significantly limited. Since this work is focusing on delamination detection on concrete bridges using a CNN, this section will briefly present the work done to date on automated delamination detection as well as a the use of CNNs for general defect detection.

Automated detection of delaminations is fairly novel, as computer vision techniques applied to infrared imagery is required. Omar et al. [7] presented an automated procedure for detecting delaminations in concrete bridge decks using infrared thermography. They first created a thermal mosaic of the entire bridge deck from individual enhanced thermal images using a stitching algorithm. They then segmented the mosaic and identified objective thresholds using a k-means clustering method, to be able to identify delamination locations based on changes in heating patterns. This algorithm results in a condition map that effectively identifies delaminations within bridge decks.

A convolutional neural network (CNN) is a type of feed-forward neural network that utilizes the convolution operator in place of typical fully connected network layers. These CNNs are commonly applied to analyze inputs that have a grid-like data structure (e.g. pixel structure of images) [13]. Many practical computer vision applications require localization information within an image in addition to classification. Localization in this context means identifying which pixel areas in an image belong to a specific class (e.g., which pixels are part of a delamination). There are currently two CNN-based methods to achieve this: region based CNNs (R-CNN) and CNNs for semantic pixel-wise segmentation of images (semantic segmentation CNNs). R-CNNs improve on classification by adding a bounding box around the detected object to provide location information. Semantic segmentation CNNs provide structured grid-like data output, which provides pixel-level location accuracy within the image. Some researchers have begun to implement CNN algorithms for detection and/or localization of structural defects, and have shown promising results. However, much work is yet to be done for bridge inspections to incorporate the level of CNN technology that is currently available.

Region based CNNs (R-CNN) have been used more frequently than semantic segmentation CNNs. Cha et al. [14] developed a R-CNN algorithm for detecting cracks in high-resolution images. This method is computationally inefficient, as it uses a 256x256 pixel sliding window approach to classify each region as cracked/not cracked. The algorithm reported a high accuracy, but results were only tested on images of similar locations with a consistent background. This method was not proven to generalize to varying environments. Cha et al. [15] also used Faster R-CNN [16] for assessing five defect types (four types of steel defects and concrete cracking). This algorithm is efficient and showed promising test results for concrete cracks, but was limited to images of two bridges and a building complex. In addition, this study primarily focused on steel bridges rather than reinforced concrete bridges. Kim et al. [17] proposed a R-CNN as part of a complete bridge inspection solution. They used an unmanned aerial vehicle to collect images and combined it with a R-CNN for data processing and damage analysis. This work only studied visual images for crack assessment and did not investigate thermal defect analysis.

Zhang et al. [18] proposed a semantic segmentation CNN called CrackNet. CrackNet automates crack detection on 3D asphalt surfaces and maintains the shape of the original input image for pixel-wise classification/localization. This algorithm was successful for pixel-level detection of cracks but the results are only tested on asphalt. In addition, the algorithm is limited to crack labelling using 3D images from a high-quality PaveVision3D road inspection system. As a result, it is expected that this system cannot generalize to structural bridge inspections.

3 Methodology

The delamination assessment method proposed in this work uses a data-driven CNN for semantic pixel-wise segmentation. The first step to the proposed implementation is to collect a training data set large and diverse enough to provide high detection accuracy on a variety of concrete bridges. The following sections will

elaborate on the data collection and the labelling process. Finally, the implementation of the CNN will be presented in detail.

3.1 Image Data Set

A data-driven image segmentation approach is highly dependent on the size and quality of the image dataset provided. Therefore, collecting an adequate dataset to train, validate, and test a neural network is a critical step to the success of this method. There exist few public online data sets containing infrared images of delaminations, and no data sets where these images are labelled at a pixel-level to indicate delaminated areas. As a result, it is essential that a new infrared image data set be created and labelled appropriately.

The data set collected for this research consists of 500 infrared images taken of four reinforced concrete bridges in the cities of Kitchener and Waterloo, Ontario. The four selected bridges were in variable conditions. Images were taken at varying times of day, on different days, and under different weather conditions to ensure a variety in the data set. Of the 500 images, 261 contain some delamination, and 239 show no delamination in the concrete. All images were collected using a FLIR VUE Pro thermal camera. This camera can be mounted on small robots, including on unmanned aircraft systems, and can be remotely controlled. The camera has a 512x640 pixel resolution, and has a 7.5-13.5 micrometer spectral band. The images for this study were taken using the 'white hot' thermal camera setting (i.e., hot areas appear white in images, as shown in Figure 1).

The images that make up the dataset were collected in two ways: (1) manually and (2) automatically via unmanned ground robot. The manual method was used for the majority of the images in the dataset. In this case, the inspector held the camera. When the inspector suspected an area as delaminated, images were captured of that area using the FLIR camera phone application. The automatic image collection was done by mounting the FLIR camera in an upward facing configuration on a Husky unmanned ground robot (manufactured by Clearpath Robotics). Figure 2 shows this configuration including the robot and other sensors integrated into the system. This configuration allows the images to be captured at precise intervals and be synchronized with the other images taken on-board the robot. Furthermore, the exact position that the images were taken from can be determined based on the known coordinates of the robot.

The second collection method not only proves the additional benefits of integrating this defect detection method with other robotic sensors (e.g., GPS and visible spectrum cameras) but it also shows that this methodology can be used on any generic unmanned robot. As a result, this approach is suitable to address

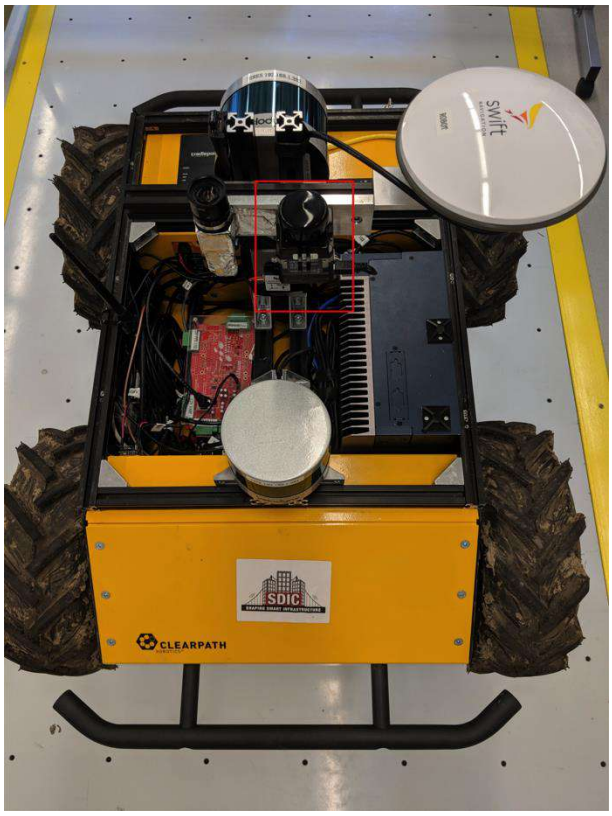

Figure 2. Husky unmanned ground vehicle with upward facing thermal camera.

the accessibility problems with delamination assessment by utilizing the mobility of aerial, ground, and surface robotics.

3.2 Image Labelling

To train the proposed CNN to detect objects in images at a pixel level, each training image needs all the pixels to be labelled as one of the classes. In this case, only two classes are used: (1) sound concrete, and (2) delamination. Semantic pixel-wise image labelling is a tedious task, even with only two classes. To help with the labelling, a labelling graphical user interface (GUI) was created using MATLAB [19]. The goal of this GUI is to be generic enough that it can be used to label image pixels for any number of defect types on concrete bridges. This GUI makes use of basic image processing techniques to provide an initial estimate of the defect locations, and then provides tools to manually fine-tune the labelling.

Figure 3 shows the process used to provide the initial estimate of the pixel labels, prior to manual editing. First the image is converted to grayscale. This is required as grayscale thresholding is used to generate the initial delamination segmentation estimate. Even though most of the images used for this dataset were

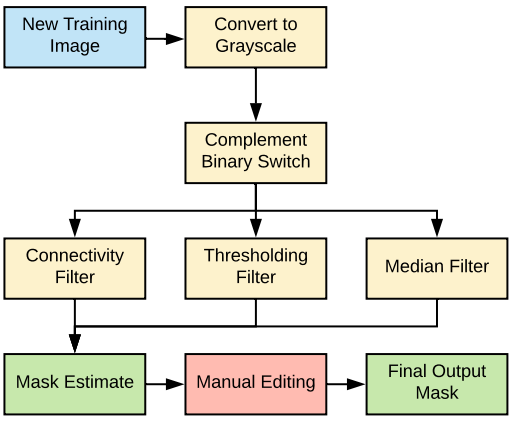

Figure 3. Flowchart of the image processing techniques used to simplify pixel-wise labelling.

collected in grayscale, this approach would generalize to any visible spectrum image or infrared images that use coloured heat gradients. The second step is to perform a complement binary switch (if required) to ensure the delamination consistently appears as back in the image mask. The three filters can then be applied including the thresholding, connectivity, and median filters. Each of these filters is applied using a sliding adjuster to allow easy editing of the three filters' sensitivities. Finally, a manual editing tool is used to remove unwanted areas or add missing areas.

Figure 4 shows the two main steps of the graphical interface for the image labeller. The top image shows the sliding filters. The bottom image shows the interface used for manually editing the initial mask.

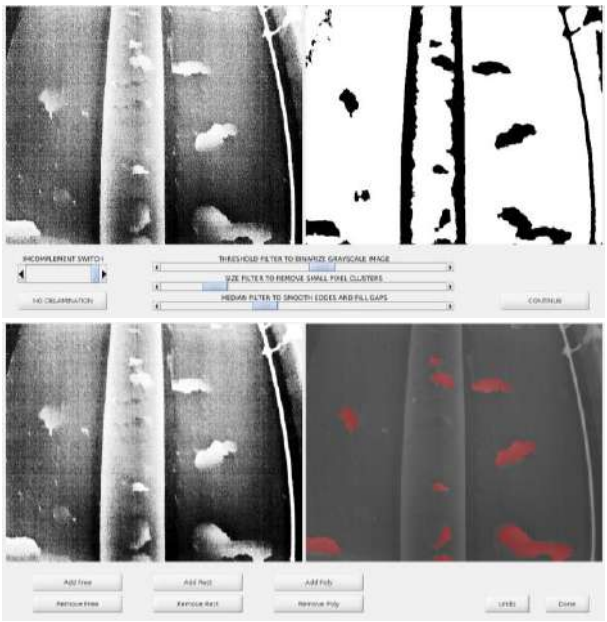

Figure 4. Image processing sliders to adjust delamination mask estimate (top) and GUI tools to manually adjust image mask (bottom).

These image processing techniques provide a good pixel-wise estimate of delaminated locations, but have several shortcomings. First, there tend to be other artifacts in the image that will be included during thresholding and cannot be removed by other filters. For example, girder edges tend to also heat/cool quicker than the surrounding concrete, giving them similar thermal patterns to a delaminated area. These edges are an example of an object requiring manual removal from the mask. Second, there can be some small gaps in the detected delamination area that cannot be fixed by the connectivity or median filters. This is an example of areas required to be manually added to the mask.

The described labelling approach allows for accurate, time-efficient labelling, which is necessary to be able to generate an adequate, well labelled data set. This approach has also been tested for labelling cracks, spalls, corrosion stains, and exposed reinforcement in concrete structures.

3.3 CNN Implementation

In order to properly assess delaminations in infrared imagery, both detection and pixel-level localization of the defect is required. In other words, it is not sufficient to say there is a delamination in the image, as the location of the delamination in the image is essential. The current state-of-the-art method for achieving this is a CNN algorithm. Many CNN algorithms exist to perform semantic pixel-wise segmentation, and often report exceptional results on standard segmentation data sets, such as Pascal VOC [8] or Cityscapes [20]. These datasets contain more classes, and more variable images compared to a dataset for delamination detection. Thus a similar quality of results should be expected when applied to delaminations, since the complexity of the data does not increase.

The network chosen for this application is MobileNetV2 [21] as a feature extractor with Deeplab V3 [22] to perform semantic pixel-wise segmentation. This network architecture was developed for mobile deployment, where time-efficiency is considered more important than accuracy. This is preferable as certain applications may benefit from real-time delamination assessment. For example, an inspector benefits more from real-time viewing of detected delamination locations on site than obtaining higher-resolution localization information about the exterior-boundary of the delaminated area.

The main building blocks of the network are from [21,22]. However, minor modifications were made to suit this specific application of this network to delamination assessment. The network input size is adjusted to be 512x640 to match the infrared image size. The last layer of the delamination prediction network is programmed to be a pixel-wise softmax activation layer,

which is given by the equation,

$$softmax(x)_i = \frac{\exp(x_i)}{\sum_{j=1}^{n} \exp(x_j)} \quad (1)$$

where x_i represents the network's calculated output score for a given class and n represents the number of classes [9]. In this case, $n = 2$ and the softmax activation is applied to predict each output pixel individually. This activation function restricts the output scores of each pixel to be between 0 and 1 so that the model can be trained using the categorical cross entropy (CCE) loss function, given by the equation,

$$J(\theta) = -\sum_{i=1}^{n} y_i \log(P(\theta)_i) \quad (2)$$

where θ represents the network weights, n is the number of possible classes, y_i is a binary classifier if the pixel does ($y_i = 1$) or does not ($y_i = 0$) belong to class i, and $P(\theta)_i$ is the network predicted likelihood that the pixel belongs to class i [9]. This combination of softmax output layer and CCE loss was used as it is generally considered best practice for multiple-class single-label classification. For this case it is also possible to use a sigmoid activation function with a binary cross entropy loss function, but this algorithm is intended to be scalable to include more defect classes in the future so the binary method was not preferred.

The network was trained using stochastic gradient descent [9], with a learning rate of 0.005, momentum of 0.9, and weight decay of 0.005/number of epochs. Image augmentation was used during training help prevent overfitting. Before each epoch, random transformations were applied to the training images only. These randomized image transformations include: flip horizontal, flip vertical, rotation, width and height shift, and zoom. This data augmentation ensured that the network would highly likely not see the exact same image twice during training.

4 Results

The collected 500 image data set was split into two main structures. The first structure consisted of randomly sorting the images into a 400 image training set, 50 image validation set, and 50 image test set. This yields a 80/10/10 dataset split. The second structure separated the images into a validation set consisting of images that were taken from the ground robot (Figure 2) under a bridge, and the training set consisted of all other images. This data split will be referred to as the robotic scanning split, where 62 images taken from a robot were used in the validation set and 436 of the remaining 438 images were used in the training set. Two images were left out to keep the number of training examples divisible by four (the desired batch size for this application).

The CNN algorithm for delamination assessment was reviewed for accuracy using the CCE loss (Equation 2) and mean intersection over union (mIoU) metrics. IoU is a common metric to compare segmentation results on benchmark datasets and is given by the equation,

$$IoU = \frac{TP}{TP + FP + FN} \quad (3)$$

where TP is true positives, FP is false positives, and FN is false negatives. In this application, positive is considered predicting a delamination and negative is considered predicting no delamination. CCE and mIoU were calculated and tracked at the end of each epoch for both the training and the validation set. Figure 5 shows the results of training on both dataset splits and Table 1 summarizes the final results.

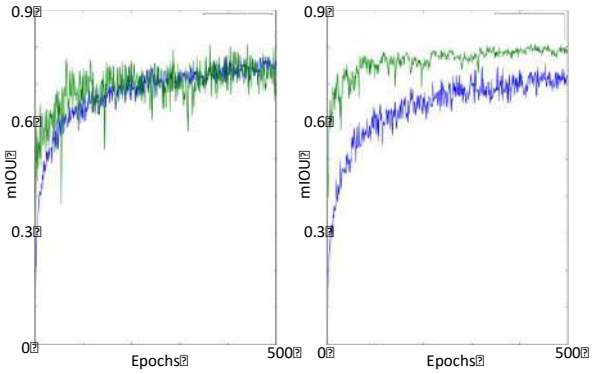

Figure 5. CNN results tracking mIoU during training for the 80/10/10 split (left) and robot scanning split (right). Blue represents training data and green represents validation data.

Table 1. Network Evaluation Metrics

Dataset	Split	CCE	mIoU
80/10/10	Train	0.0182	76.0%
	Val.	0.0163	72.7%
	Test	0.0169	74.5%
Robotic Scanning Split	Train	0.0166	71.1%
	Val.	0.0560	79.5%
Pascal VOC 2012	Benchmark	n/a	77.3% [8]

The results measured by CCE and mIoU show the network achieves comparable results for delamination assessment when compared to its performance on benchmark datasets. However, numbers cannot be compared to existing delamination assessment methods, as no fully automated methods exist on a similar infrared image dataset. To review the quality of the method, the output of the network was assessed on its

ability to predict delaminations for a typical inspection. Figure 6 shows delamination locations predicted by the network. The first three examples show results on images of bridge deck soffits that contain a various number of delaminated locations. The results show that the proposed methodology is capable of detecting nearly all delaminations, while avoiding false positives.

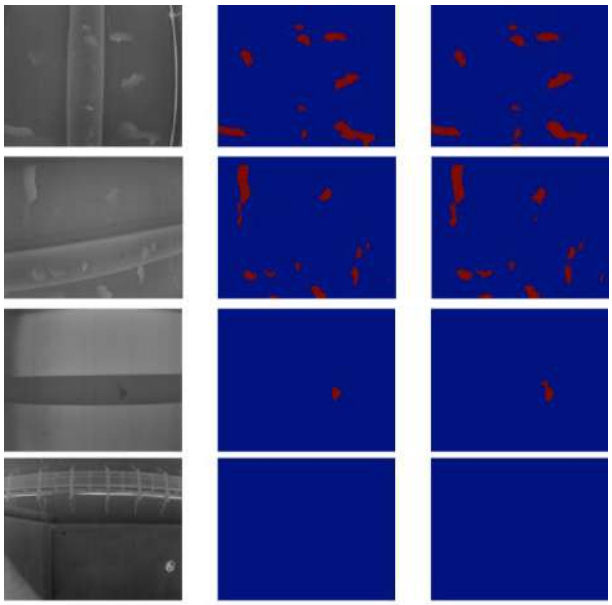

Figure 6. CNN example prediction results. Image (left), prediction (middle), true label (right).

The main source of error in these examples is the fine details. The edges of delaminations in the prediction are more rounded compared to the label, and small or thin delaminations are not well detected. This is a limitation based on the number of parameters used in the network and can be solved by adding more trainable parameters in the network. However, this limitation is not of great concern for concrete bridge inspection since precise knowledge of the delamination borders is not a requirement for bridge inspection. As discussed earlier, real-time visualization of the delamination assessment results is more valuable. In addition, traditional inspection procedures such as chain dragging and hammer sounding are not capable of precisely detecting edges and therefore this methodology is already a major improvement over current practice.

The fourth example in Figure 6 shows an example where there are a few potential areas that the network could falsely predict as a delamination. There is a scaffolding structure underneath the bridge, a small dark area and a small white area. In this case, the network successfully avoids false positives, showing that it has successfully learned some characteristics of a delamination and is not easily misled by similar artifacts.

It is also worth noting that the validation set of the robotic scanning split achieved the highest mIoU rating. This is most likely because the images taken by the robotic scan contained a large number of fairly clear delaminations. This is evidence that the quality of the image can influence the ability of the network to predict delamination locations.

5 Conclusion and Future Work

This work presents a novel automated concrete delamination assessment methodology using infrared imagery, robotics, and CNNs. A versatile pixel-wise defect labeler was first developed specifically for concrete bridge defects and was shown to help expedite the pixel-wise labelled image dataset creation. MobileNetV2 (Deeplab V3 implementation) was used to perform pixel-wise segmentation on infrared images of reinforced concrete bridges. This method was able to achieve high performance when evaluated on a data set of 500 infrared images by accurately detecting and locating delaminations under varying bridge environments. Quantitatively, the mIoU score for delamination assessment was shown to be comparable to what this network achieved on the Pascal VOC 2012 benchmark dataset. Qualitatively, the network was shown to predict delaminated areas correctly and avoid areas that have high potential to be classified as a false positive. The majority of the errors lowering the mIoU score are due to fine details around the edges of the delaminations which is of little concern to bridge inspections.

The network was also shown to be able to combine with a mobile ground robot (or any other unmanned mobile robotic platform). 62 images of a concrete bridge soffit and girder were taken by an upward facing compact infrared camera mounted on the robot and delaminated areas were predicted by the network. This test achieved high mIoU, which illustrates the ability of the delamination assessment network to integrate with robotic inspection. This is highly beneficial, as different unmanned robots can be used to accommodate specific accessibility limitations. Overall, this methodology presents significant improvements over state-of-the-art bridge inspection.

Future work will involve collecting a larger dataset to improve results, but a more complex network is likely not necessary as finer details are redundant for delamination assessment. In addition to more data, a quantitative comparison will be performed between the automated robotic assessment results and results from traditional sounding methods. Lastly, this methodology will be extended to other concrete bridge defects such as spalls, cracks, corrosion stains, and exposed reinforcing bar in visible spectrum images.

References

[1] Koch C., Georgieva K., Kasireddy V., Akinci B and Fieguth P. A review on computer vision based defect detection and condition assessment of concrete and asphalt civil infrastructure. *Advanced Engineering Informatics*, 29(2):196–210, 2015.

[2] Ministry of Transportation Ontario, St. Catharine's, ON. *Ontario Structural Inspection Manual (OSIM)*, 2008.

[3] Graybeal B.A., Phares B.M., Rolander D.D., Moore M. and Washer G. Visual inspection of highway bridges. *Journal of Nondestructive Evaluation*, 21(3):67–83, 2002.

[4] Yang X., Li H., Yu Y., Luo X., Huang T. and Yang X. Automatic Pixel-Level Crack Detection and Measurement Using Fully Convolutional Network. *Computer-Aided Civil and Infrastructure Engineering*, 33(12):1090–1109, 2018.

[5] Clemena G.G. and McKeel W.T. Detection of Delamination in Bridge Decks with Infrared Thermography. *Transportation Research Recorc No. 664, Bridge Engineering, Volume 1*, pages 180–182, 1978.

[6] Krizhevsky A., Sulskever I. and Hinton G.E. ImageNet Classification with Deep Convolutional Neural Networks. *Advances in Neural Information and Processing Systems (NIPS)*, 60(6):84–90, 2012.

[7] Omar T., Nehdi M.L. and Zayed T. Infrared thermography model for automated detection of delamination in RC bridge decks. *Construction and Building Materials*, 168(April):313–327, 2018.

[8] Everingham M., Van Gool L., Williams C.K.I., Winn J. and Zisserman A. The PASCAL Visual Object Classes (VOC) Challenge 2012. *International Journal of Computer Vision*, 88(2):303-338, 2010.

[9] Torok M.M., Golparvar-Fard M. and Kochersberger K.B. Image-Based Automated 3D Crack Detection for Post-disaster Building Assessment. *Journal of Computing in Civil Engineering*, 28(5):A4014004-1, 2014.

[10] Jahanshahi M.R., Masri S.F., Padgett C.W. and Sukhatme G.S. An innovative methodology for detection and quantification of cracks through incorporation of depth perception. *Machine Vision and Applications*, 24(2):227-241, 2013.

[11] German S., Brilakis I. and Desroches R. Rapid entropy-based detection and properties measurement of concrete spaling with machine vision for post-earthquake safety assessments. *Advanced Engineering Informatics*, 26(4):846-858, 2012.

[12] Adhikari R.S., Moselhi O. and Bagchi A. A study of image-based element condition index for bridge inspection. In *Proceedings of ISARC 2013 – 30th International Symposium on Automation and Robotics in Construction and Mining, Held in Conjunction with the 23rd World Mining Congress*, pages 345-356, Montreal, Canada, 2013.

[13] Goodfellow I., Benigo Y. and Courville A. *Deep Learning*. MIT Press, 2016.

[14] Cha Y.J., Choi W. and Büyüköztürk O. Deep Learning-Based Crack Damage Detecion Using Convolutional Neural Networks. *Computer-Aided Civil and Infrastructure Engineering*, 32(5):361–378, 2017.

[15] Cha Y.J., Choi W., Suh G., Mahmoudkhani S. and Büyüköztürk O. Autonomous Structural Visual Inspection Using Region-Based Deep Learning for Detection Multiple Damage Types. *Computer-Aided Civil and Infrastructure Engineering*, 33(9):731–747, 2018.

[16] Ren S., He K., Girshick R. and Sun J. Faster R-CNN: Towards Real-Time Object Detection with Region Proposal Networks. In *Advances in Neural Information Processing Systems 28*, pages 91–99, Montreal, Canada, 2015.

[17] Kim I.H., Jeon H., Baek S.C., Hong W. and Jung H.J. Application of crack identification techniques for an aging concrete bridge inspection using unmanned aerial vehicle. In *Sensors*, 18(6):1881, Basel, Switzerland, 2018.

[18] Zhang A., Wang K.C.P., Li B., Yang E., Dai X., Peng Y., Fei Y., Liu Y., Li J.Q. and Chen C. Automated pixel-level pavement crack detection on 3d asphalt surfaces using a deep-learning network. *Computer-Aided Civil and Infrastructure Engineering*, 32(10):805–819, 2017.

[19] MATLAB. Version 9.2.0 (R2017a). The MathWorks Inc., Natick, Massachusetts, 2017.

[20] Cordts M., Omran M., Ramos S., Rehfeld T., Enzweiler M., Benenson R., Franke U., Roth S. and Schiele B. The cityscapes dataset for semantic urban scene understanding. In *Proceedings of the IEEE Conference on Computer Vision and Patter Recognition (CVPR), Las Vegas, USA*, 2016.

[21] Sandler M., Howard A.G., Zhu M., Zhmoginov A. and Chen L.C. Mobile networks for classification, detection and segmentation. *CoRR*, abs/1801.04381, 2018.

[22] Chen L.C., Papandreou G., Schroff F. and Adam H. Rethinking atrous convolution for semantic image segmentation. *CoRR*, abs/1706.05587, 2017.

Web-Based Job Hazard Assessment for Improved Safety-Knowledge Management in Construction

E. Mohamed[a], P. Jafari[a], E. Pereira[a], S. Hague[a], S. AbouRizk[a], and R. Wales[b]

[a] Department of Civil and Environmental Engineering, University of Alberta, Canada
[b] Vice President, Ledcor Contractors Ltd., Canada
E-mail: ehmohame@ualberta.ca, parinaz@ualberta.ca, estacio@ualberta.ca, shague@ualberta.ca, abourizk@ualberta.ca, rod.wales@ledcor.com

Abstract –

An essential component of effective safety management systems is the identification and proactive mitigation of hazards through the completion of job hazard assessment (JHA). Aimed at identifying potential hazards and subsequently implementing controls that reduce the likelihood or severity of incidents, JHA is a manual process influenced by the experiences, specific expertise, and biases of safety practitioners, rendering the development of standard mitigation strategies difficult in practice. Due to factors including ineffective information storage and dissemination systems, knowledge management of JHA data remains a challenge in the industry. To overcome these limitations, this paper proposes and describes the development and application of a web-based JHA system designed to enhance JHA management efficiency by facilitating accessibility, interfacing, connectivity, and information-sharing between users during the completion of JHAs. By increasing and facilitating access to information, the proposed system can enhance the consistency of JHAs generated throughout the organization, while also ensuring that potential safety risks are not overlooked by less experienced or otherwise biased personnel. Project and safety managers validated the functionality of the proposed system; they indicated that the proposed system could enhance the efficiency and consistency with which JHAs were generated, resulting in the improvement of real practice. The proposed system's importance is described, and its approach is detailed.

Keywords –

Safety; Job Hazard Assessment; Web-Based; Knowledge Management

1 Introduction

The construction phase of many projects has multiple potential hazards associated with various activities and tasks [1]. Many researchers have aimed to understand, identify, and analyze the root cause of construction-site incidents with the goal of reducing or preventing occupational hazards. These research efforts can be divided into two categories, namely: pre-hazard (proactive) analysis, and post-hazard (reactive) analysis [2]. Whereas reactive analysis research focuses on mitigating future reoccurrence by analyzing incidents that have occurred , proactive analysis research focuses on preventing incidents through advanced construction planning by analyzing factors that may result in potential hazards (e.g., equipment, height, or space requirements) [2]. Planning for safety typically involves the identification of all potential hazards and the selection of corresponding safety measures through a pre-hazard analysis process [3]. Effective safety planning can prevent incidents and the injury of construction personnel, in turn reducing associated project costs and delays [3].

Job hazard analysis (JHA) is one of the most widespread safety management practices for proactive safety planning in construction [2]. The Occupational Safety and Health Administration (OSHA) recommends conducting JHAs to address hazards in the workplace, and to reduce injuries and illnesses [4]. By identifying all potential task-related hazards and suggesting the means to reduce or avoid them, JHAs can be an effective tool for examining workplace operations, establishing proper job procedures, and ensuring that all employees are properly trained [4]. If effectively performed, JHAs can result in fewer worker injuries and illnesses, safer and more effective work methods, reduced workers' compensation costs, and increased productivity [4].

As with many construction practices, efficient management of JHA data is critical for preventing errors

from reoccurring,[5] particularly when construction personnel lack sufficient experience, or are biased by the occurrence of prior incidents. A lack of safety knowledge has been reported as one of the main reasons for high incident rates in the construction industry [6]. In many circumstances, worksite fatalities are associated with the insufficient sharing and communication of required information [7]. The role of knowledge management in improving the performance of occupational health and safety systems has been analyzed in the academic literature [8][9], where sharing safety knowledge and experience has been found to improve safety performance. The traditional JHA process requires construction personnel to perform several tasks, including reviewing historical documentation and applying findings to activities on new construction projects [10][11]. While several research studies aimed at enhancing JHA practices have been conducted, none has addressed the inherent problem of knowledge-management in traditional construction JHA practice.

Due to varying site conditions, job constraints, and work environments, no construction project is truly identical to any other. JHAs must be continuously recompiled or re-performed [2][12][10]. While JHA knowledge from previous activities may be revisited for guidance, reviewing previous JHAs can be time-consuming, especially when the number of activities, their steps, and their associated hazards are significant [2]. Additionally, construction personnel creating JHAs must often review fragmented information across various references, such as safety regulations, incident records, best practices, and personal experiences [11]. As a result, the completion of JHAs is an error-prone, time-consuming task [13][10]. Furthermore, the inconsistent use of terminology, lack of detailed information, and inappropriate storage of data may result in knowledge being inadvertently omitted during the development of future JHAs, potentially even creating a false sense of security in documentation.

This paper proposes the design of a web-based system capable of addressing the knowledge management problem inherent to traditional JHA practice. This system uses a dual database approach that allows practitioners to quickly and easily combine pre-defined, task-level JHAs to best suit the specific needs of a project. Implemented as a web-based system, the proposed approach is capable of efficiently managing historical data, unifying JHA knowledge of various experts, facilitating the creation of new JHAs, and easily sharing JHA knowledge between workers.

2 Literature Review

The process of conducting JHAs (reviewed in [2], [4], [13], [14], and [15]) consists of three main stages, as detailed in Figure 1 and detailed as follows:

1. *Identification*: The identification of hazards is performed for a specific job or activity by segmenting the activity into a sequence of stages, resulting in the identification of all possible hazards that may occur during the work. Currently, construction personnel conducting JHAs rely on brainstorming sessions to identify steps within different construction jobs and to identify associated hazards [14].
2. *Assessment*: The assessment is carried out by evaluating the severity level and probability of all identified hazards.
3. *Mitigation and Control*: Strategies for mitigating or controlling hazards are identified and proposed.

Before beginning the job onsite, JHAs are typically read and explained to workers in a pre-task work meeting. To ensure that each worker is familiar with the hazards associated with each task as well as the proposed mitigation strategies, each participant may be required to acknowledge its content by signing a form [10]. Notably, JHAs may also be used by certain project teams or owners for legal purposes [10].

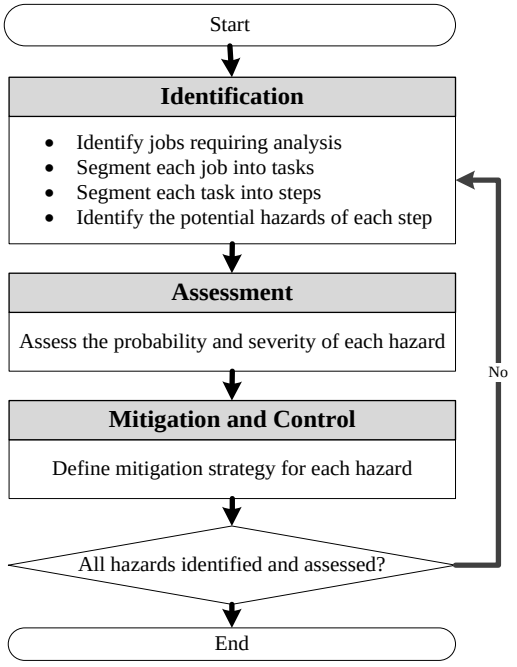

Figure 1. Traditional JHA process

2.1 Enhancing JHA Practices in Construction

Several studies have focused on automating the generation of JHAs. Chi et al. [12] presented a text-classification-based approach that analyzes construction safety documents and extracts safety approaches to automate the 'mitigation and control' step of JHAs. In a

separate study, Chi et al. [1] applied an ontology-based text classification to automate the matching of safe approaches identified from existing resources with unsafe scenarios to enhance the development of JHAs. Zhang et al. [10][13] used an ontological approach to capture, model, and connect safety management knowledge to building information models (BIM), enabling automated hazard analysis and safety task scheduling. An ontological approach was proposed by Wang et al. [2] for structuring knowledge regarding activities, job steps, and hazards to enhance access to safety information. Their approach includes an ontological reasoning mechanism for automatically identifying and selecting safety rules that apply to given activities.

Automated prediction of incident sites and activities associated with increased incident likelihood has been the focus of other studies. By linking the information between the CPM schedule and safety-recommendation databases, Bansal [3] introduced a geographic information system (GIS)-based, navigable 3D animation of safety planning for identifying sites and activities with an increased potential for incidents. A structured tool has also been developed for Construction Job Safety Analysis (CJSA) focusing on the identification of potential loss-of-control events for detailed staging of construction activities [15].The goal of this tool is predicting fluctuating safety risk levels and supporting safety-conscious planning and management.

Notably, while previous studies have attempted to automate the identification of hazards, none has focused on developing systems that enhance knowledge management in traditional JHA practice.

2.2 Management of Safety Knowledge

The importance of knowledge management in construction project safety has been extensively reported. By analyzing safety knowledge-sharing through social networks, Fang et al. [6] have examined how construction employees selected their social relations on the basis of safety knowledge. Finding that safety knowledge-sharing through social networks was a significant source of knowledge transfer, the authors concluded that safety education was more critical than tenure during the safety knowledge sharing process. Observing an influence of knowledge exchange systems on safety compliance, Gressgård [5] suggested that knowledge management and exchange systems are central for enhancing safety behavior, particularly in cases involving shift changes, varying working times, high-level subcontracting, and other factors that lead to nonsynchronous knowledge sharing.

Technologies focused on enhancing knowledge-sharing have also been proposed. Li et al. [7] investigated the ability of various technologies to share construction safety knowledge, finding that mobile apps, the Internet of Things (IoT), and Web 2.0 could provide promising solutions for the distribution of knowledge on construction sites. A conceptual, web-based safety knowledge management system designed to improve safety performance and productivity has been discussed by Kamardeen [9]. Similarly, Elzarka et al. [16] proposed a knowledge-based management system capable of integrating safety and schedule information to facilitate the inclusion of safety as an integral part of project planning and control. As an extension of this, a knowledge management tool for small and medium enterprises that allows users to easily aggregate and capitalize on information from various sources has also been developed [17]. Sherehiy and Karwowski [8] have proposed a knowledge management model for effective OSHE (occupational safety, health, and ergonomics) management, establishing knowledge as the central resource.

Although the studies mentioned above share similar objectives with this study (i.e., facilitating safety knowledge development and accessibility), none of these studies has formalized the traditional JHA in a way that can support efficient development, storage, and sharing of the JHAs in construction. A system designed to enhance knowledge management in JHA practice has yet to be developed.

3 System Design and Development

The proposed system is built on the concept of segmenting construction activities (which vary considerably from project-to-project) into a subset of repetitive tasks that can be combined to suit the specific requirements and needs of a particular construction job. Using this system, job-level JHAs are built by combining multiple segments, each containing various combinations of recurring task-level hazard assessments to suit the specific requirements of a project. This approach is expected to reduce the time and effort required to develop JHAs, decrease errors, and increase the consistency of JHAs throughout the organization.

An innovative feature of the system is its dual database design, which allows for the customization of JHAs in one database while ensuring existing knowledge is not lost during the customization process. Specifically, the *Template Database* generated by safety experts contains the entire table of tasks and associated steps, hazards, assessments, tools, and personal protective equipment (PPE), as well as all associated expert knowledge and experience. In contrast, the *JHA Database* contains modified JHAs specific for each project. Safety supervisors search the template database for the required job and pull the job to the JHA database,

where the JHA is adapted and modified for the specific conditions of the new project. Since the template database is anticipated to contain all information related to a task, modifications would simply involve the removal of unnecessary safety considerations (e.g., removal of grading considerations if work is to be completed on a flat surface).

3.1 System Architecture

An overview of the proposed JHA process is illustrated in Figure 2. The system's architecture is built using *Django* [18] and a *React & Redux* framework [19]. The system is built on a cloud-based *MySQL* database, which provides a centralized, reliable means of sharing and storing JHA knowledge that is accessible to users from various locations. JHA knowledge is stored on a server, and a standard web browser is used as a gateway to exchange JHA knowledge.

The web-based JHA system is implemented using an architecture composed of the following four logical layers: a user layer, an interface layer, an application layer, and a repository layer. Figure 3 depicts the system architecture and describes the various functional activities that are carried out within the JHA extranet.

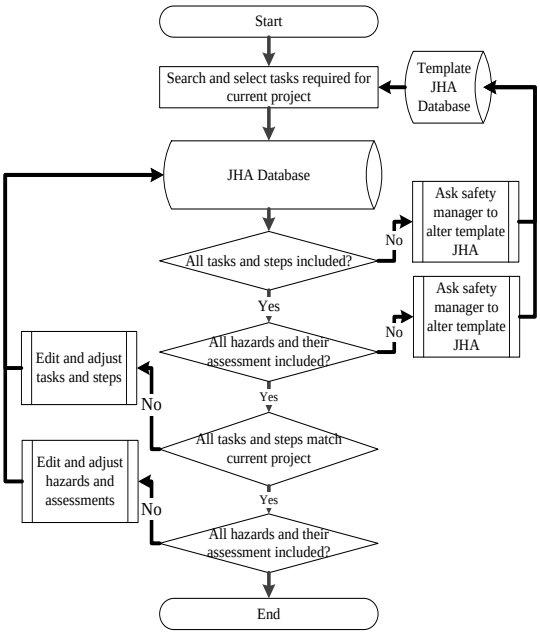

Figure 2. Proposed JHA process

The *user layer* (layer one) is installed on the user's machine and is connected to the server through the *interface layer* (layer two). The interface layer is, in turn, connected to the *repository layer* (layer four), with access to and control over the *information layer* (layer three) within the *MySQL* database, subject to access restrictions. The *interface layer* (layer two) lists the processes available to each user depending on their assigned access level. In the developed system, the following three access-levels are as follows: (1) a safety manager level, which has full access to the system; (2) a safety supervisor level, which can create, edit, view, and download a JHA but is unable to alter the template database; and (3) a worker level, which is limited to viewing and downloading existing JHAs in the system. In summary, the JHA safety knowledge is represented in the form of a relational model using *MySQL*. The relational model [20] defines a set of relations, describes the relationships between entities, and determines how these stored data interact.

3.2 System Development

The main development tools of the system include *React & Redux* [19], a *Django* REST framework (*D*RF) [18], and *MySQL*. The *D*RF connects to the database, which uses *Python* as the programming language. The database is initialized on *MySQL*. *React & Redux* uses *JavaScript* as a programming language. While *React & Redux* acts as the user interface, a cascading style sheet (CSS) layout is used to perform certain formatting functions of the user interface. *React & Redux* uses a built-in tool to connect the system's front end and back end, allowing a front end user to fetch data from the back end, and to push data to the back end.

4 Practical Application of the System

A simple, illustrative example is used to demonstrate the practical application of the proposed system. Involving the operation of an excavator on a construction site, the job is associated with the following three tasks: pre-operation, operation, and post-operation. To build a new JHA, a user logs into the system using the login interface (Figure 4). Once logged in, the user accesses the main dashboard of the system, which varies in appearance based on the user's access level (i.e., visibility of the various components will be affected by the user's access level). For example, the dashboard of a safety manager level user contains the (1) template database, which encompasses the tasks, steps, hazards, tools, and PPE tables; (2) JHA database, which contains all the JHAs of the various projects; and (3) the create button, which initiates the creation of a new JHA (Figure 5). The JHA database in the dashboard of a worker-level user, contrastingly, contains only the means to view and download existing JHAs.

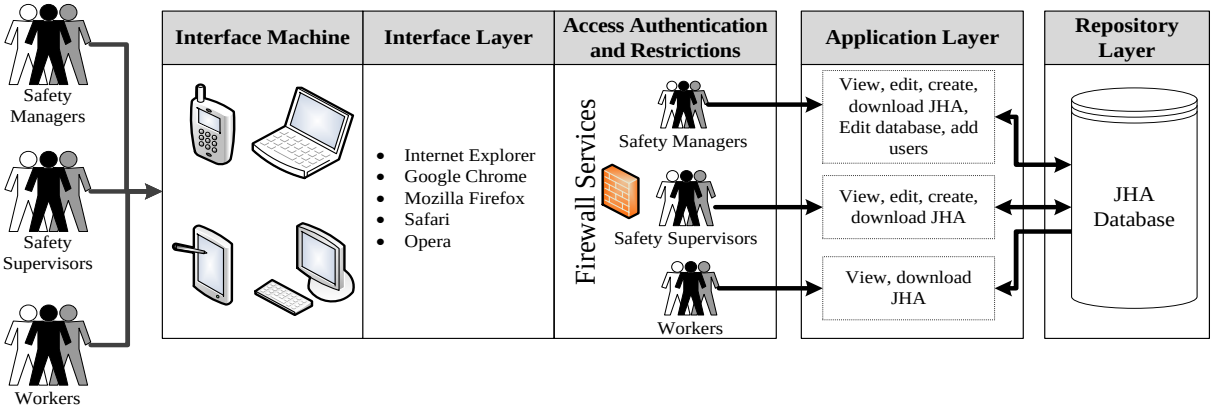

Figure 3. Structure of the JHA system

To initiate the creation of a new JHA, users click on the create button, which triggers the opening of a new window (Figure 6, *top*). This window contains eight tabs: general information, creators, editors, prerequisites, tasks, crew review, and approval tabs, which mimic the layout of a traditional JHA. Tasks are added to a job using the "Tasks" tab (Figure 6, *bottom*); importantly, only predefined tasks contained within the template database can be added to a job, ensuring that all JHAs are first populated with existing, standardized knowledge. Once the predefined tasks have been selected and imported from the template database into the JHA database, subcomponents can be adjusted according to the context of the current project (Figure 7). After all eight of the tabs have been finalized, the new JHA is created and stored in the database where it can be viewed, edited, and downloaded.

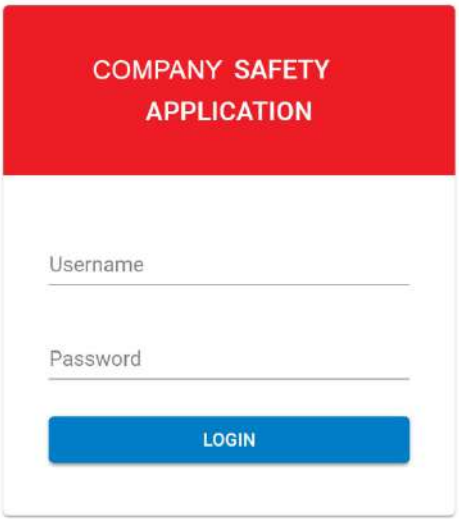

Figure 4. System login

5 System Evaluation

Subject matter experts assessed functionality and determined whether or not the proposed system had the potential to enhance JHA practices. A demonstration of the software was presented to safety managers who were then asked to provide feedback in an interview format. Specifically, they were asked (C1) if they found the system easy to use, (C2) if they thought the system would improve accuracy of generated JHAs, (C3) if the system would allow timelier access JHA knowledge, and (C4) if access to information was improved. All experts interviewed were pleased with the system functionality, indicating that it was straightforward, easy-to-use, and had the potential for improving current practices. Suggested improvements included adding a visualization component that could provide more intuitive insight regarding the number and severity of project-associated risks. In order to quantitatively assess the functionality of the system, the three experts (E1, E2, and E3) were asked to evaluate the system on Likert scale (1-5) where 1 means very low, 2 means low, 3 means medium, 4 means high, and 5 means very high. They were asked to evaluate the system based on the criteria listed above. Experts are not fully satisfied with the initial stage of the system. Future work will increase efficiency.

Table 1. Quantitative Evaluation of Expert Opinion

Criteria	E1	E2	E3	Average	Avg. %
C1	4	5	5	4.67	93.4%
C2	4	4	3	3.67	73.4%
C3	3	4	4	3.67	73.4%
C4	4	5	4	4.33	86.7%

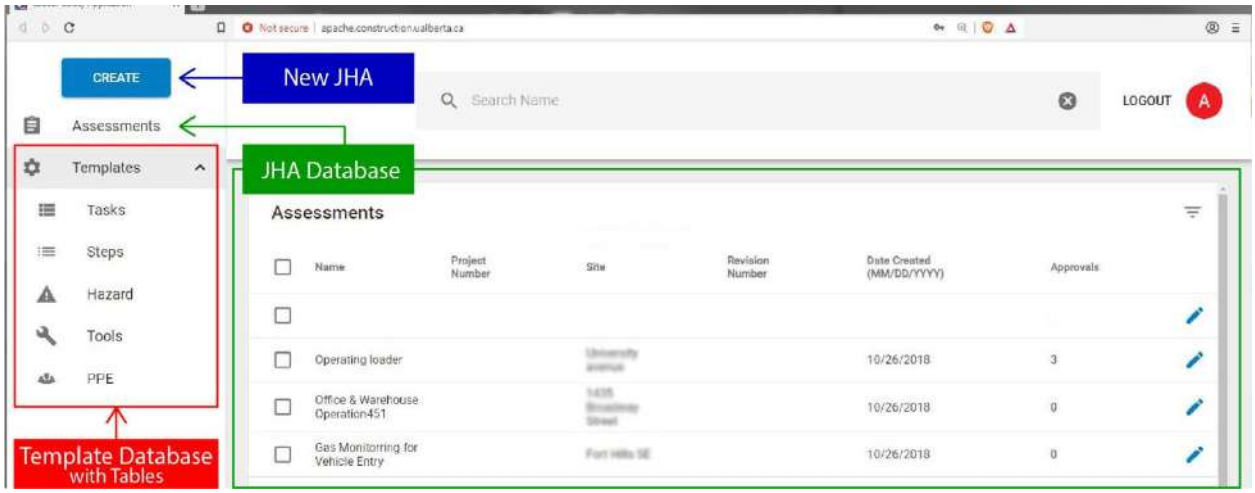

Figure 5. Main dashboard of the system

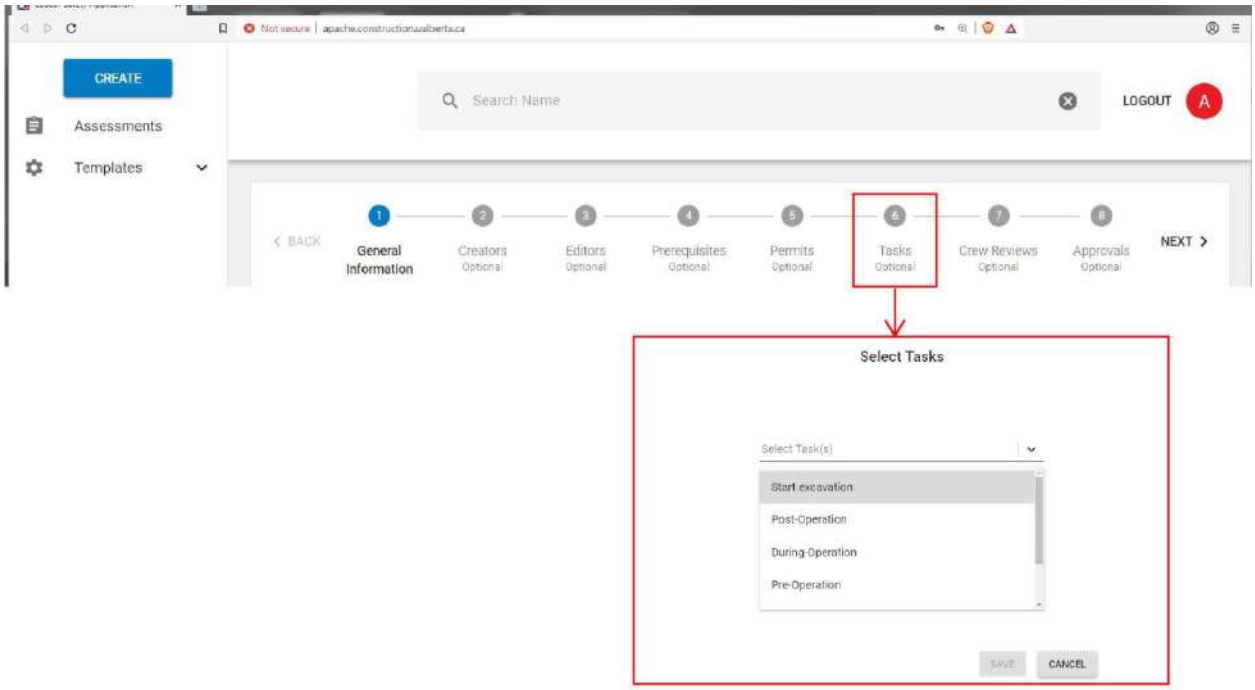

Figure 6. Components of the proposed system

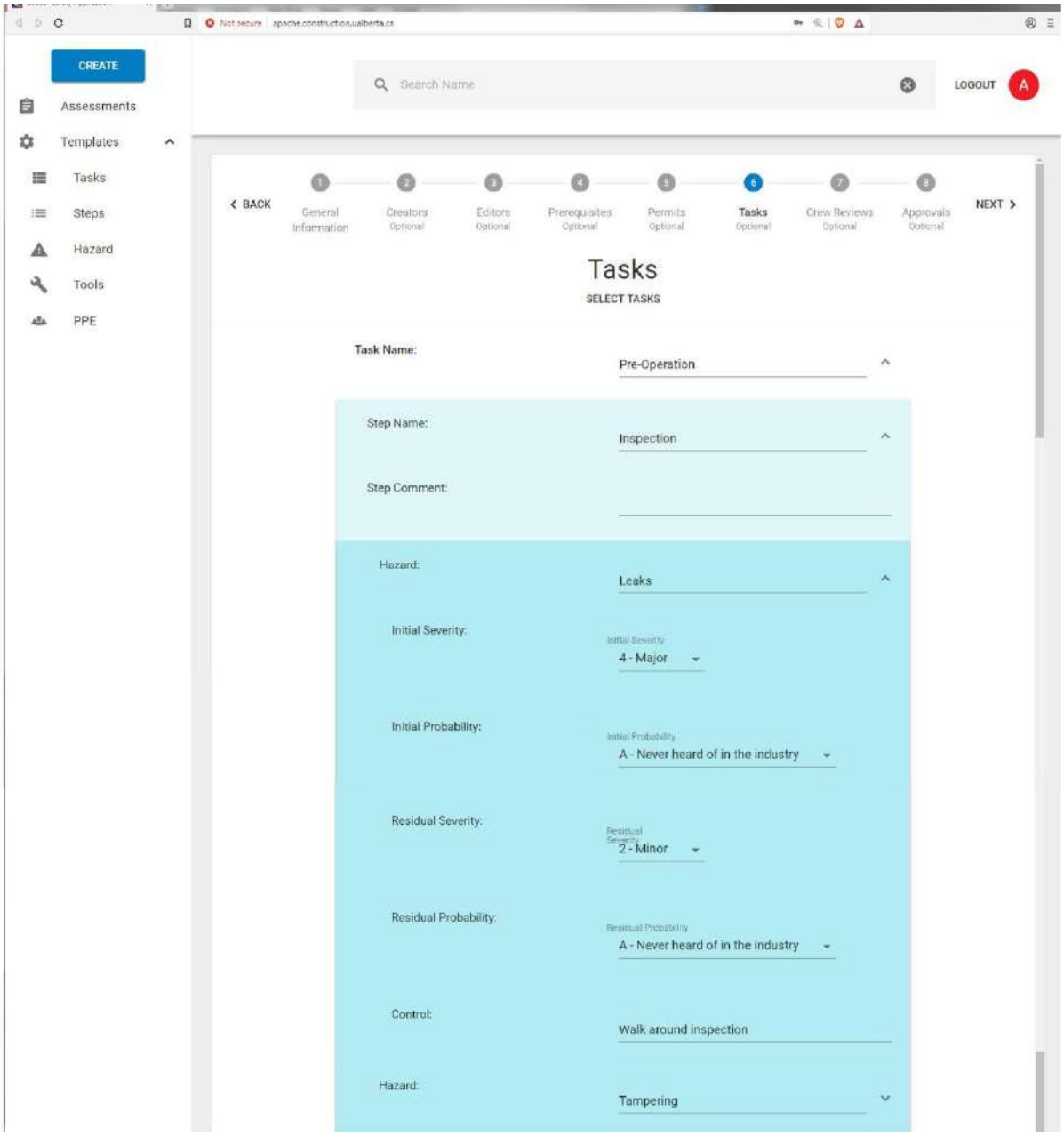

Figure 7. Hazard steps

6 Conclusion

JHA is a routine component of many proactive safety management systems in construction. Reliance on inconsistently-formatted and often fragmented information motivated the development of a web-based system. Using a dual database approach, the proposed system facilitates JHA creation, storage, and sharing. Subject matter experts found the preliminary version of the system capable of improving current practice. Future work may include the addition of graphics depicting the number and severity level of hazards, integration of the system with the project schedule to visualize the day-to-day hazard-levels, or development of text-mining algorithms. Currently, safety personnel have to search the template database to identify and assess hazards and their severity. Automation of these processes is suggested for future research. Automating the identification process is planned by applying some artificial intelligence techniques (such as case-based reasoning) to help the safety personnel easily identify and evaluate potential hazards based on current context

and historical information. Real project data will later be used to quantitatively evaluate the functionality, accuracy, and efficacy of the system.

7 Acknowledgments

This work was supported by the *Ledcor* Constructors Inc. through a Collaborative Research and Development (CRD) Grant (CRDPJ 492657) from the National Science and Engineering Research Council (NSERC) of Canada.

8 References

[1] Chi N., Lin K. and Hsieh S. Using ontology-based text classification to assist Job Hazard Analysis. *Advanced Engineering Informatics*, 28(4): 381–394, 2014.

[2] Wang H. and Boukamp F. Ontology-based representation and reasoning framework for supporting job hazard analysis. *Journal of Computing in Civil Engineering.* 25(6): 442–456, 2011.

[3] Bansal V. Application of geographic information systems in construction safety planning. *International Journal of Project Management*, 29 (1) 66–77, 2011.

[4] Chao E. and Henshaw J. Job hazard analysis, U.S. Department of Labor Occupational Safety and Health Administration. Online: https://www.osha.gov/Publications/osha3071.html , Accessed 11/11/2018.

[5] Gressgård L. Knowledge management and safety compliance in a high-risk distributed organizational system. *Safety and Health at Work*, 5(2): 53–59, 2014.

[6] Fang D., Huang J. and Fong P. Sharing construction safety knowledge through social networks. In *Proceedings of the CIB W099-Safety & Health in Construction, "Special Track 18th CIB World Building Congress,"* pages 215–226, Salford, UK, 2010.

[7] Li R., Chau K., Ho D., Lu W., Lam M. and H. Leung T. Construction safety knowledge sharing by Internet of Things, Web 2.0 and mobile apps: Psychological and new institutional economics conceptual analysis. In *Proceedings of the IOP Conference Series: Materials Science and Engineering*, pages 062042, 2018.

[8] Sherehiy B. and Karwowski W. Knowledge management for occupational safety, health, and ergonomics. *Human Factors and Ergonomics in Manufacturing & Service Industries.* 16(3): 309–319, 2006.

[9] Kamardeen I. Web-based safety knowledge management system for builders: A conceptual framework. In *Proceedings of the CIB W099 Conference,* Australia, 2009.

[10] Zhang S., Boukamp F. and Teizer J. Ontology-based semantic modeling of construction safety knowledge: Towards automated safety planning for job hazard analysis (JHA). *Automation in Construction.* 52: 29–41, 2015.

[11] Pedro A., Lee D., Hussain R. and Park C. Linked data system for sharing construction safety information. In *Proceedings of the ISARC Conference,* pages 121-127, Taipei, Taiwan, 2017.

[12] Chi N., Lin K., and Hsieh S. On effective text classification for supporting job hazard analysis. In *Computing in Civil Engineering,* pages 613–620, Los Angeles, California, US, 2013.

[13] Zhang S., Teizer J. and Boukamp F. Automated ontology-based job hazard analysis (JHA) in Building Information Modelling (BIM). In *Proceedings of CIB W099 International Conference on "Modelling and Building Health and Safety*, pages 78-81, Rotterdam Netherlands, 2012.

[14] Wang H., Boukamp F. and Elghamrawy T. Ontology-based approach to context representation and reasoning for managing context-sensitive construction information. *Journal of Computing in Civil Engineering*, 25(5): 331–346, 2011.

[15] Rozenfeld O., Sacks R., Rosenfeld Y. and Baum H. Construction job safety analysis. *Safety Science*. 48(4): 491–498, 2010.

[16] Elzarka H., Minkarah I. and Pulikal R. A knowledge-based approach for automating construction safety management. In *Proceedings of the 2nd International Conference on the Implementation of Safety and Health on Construction Sites*, pages 24-27, Hawaii, US, 1999.

[17] Fargnoli M., De Minicis M. and Di Gravio G. Knowledge management integration in Occupational Health and Safety systems in the construction industry. *International Journal of Product Development*, 14(1/2/3/4), pages 165-185. 2011.

[18] Christie T. *Django* REST framework, Home-*Django* REST Framework. Online https://www.django-rest-framework.org/, Accessed: 20/04/2018.

[19] Banks A. and Porcello E. Learning React: Functional web development with *React and Redux*, O'Reilly Media, Inc., 2017.

[20] Codd, Edgar F. 1970. "A Relational Model of Data for Large Shared Data Banks." *Communications of the ACM* 13 (6): 377–387.

Leading Safety Indicators: Application of Machine Learning for Safety Performance Measurement

P. Jafari[a], E. Mohamed[a], E. Pereira[a], S. Kang[a], and S. AbouRizk[a]

[a]Department of Civil and Environmental Engineering, University of Alberta, Canada
E-mail: parinaz@ualberta.ca, ehmohame@ualberta.ca, estacio@ualberta.ca, sckang@ualberta.ca, abourizk@ualberta.ca

Abstract –

Proactive approaches designed to prevent incidents before they occur are essential for achieving effective safety management. Emerging as an important component of proactive safety management, leading indicators are used to assess and control safety performance. With the aim of reducing the number or severity of worksite accidents, methods capable of predicting future safety performance using leading safety indicators have been developed. However, these methods have been developed for a specific set of leading indicators. This has substantially limited their application in practice, as leading indicators with the greatest impact on safety performance vary considerably between organizations and projects. An approach for predicting accident occurrence on construction sites that can be applied to any combination of leading indicators is proposed to address these limitations. Data used to develop the proposed approach were collected by a construction company from eight construction projects over a period of two years. Feature selection techniques were used to filter the original factors into the most critical subset, which were then used as inputs. Various supervised learning algorithms, namely support vector machine (SVM), logistic regression, and random forest, were then tested to determine which algorithm(s) yielded the highest prediction accuracy. The results demonstrate that the proposed procedure can be used for early recognition of potentially hazardous project characteristics and site conditions regardless of the number or type of leading indicators available within an organization. Research in this area is expected to facilitate the implementation of targeted safety management controls and to improve safety performance.

Keywords –

Safety Leading Indicators; Safety Management; Safety Performance; Machine Learning

1 Introduction

Safety leading indicators are an essential component of proactive safety management, providing valuable information regarding organizational safety performance [1]. Leading indicators, defined by Grabowski et al. [2], Hinze et al. [3], and Kjellén [4], are conditions, events, or measures antecedent to undesirable events that can be used to predict the occurrence of accidents, near misses, or any undesirable safety state. Measuring leading indicators allows practitioners to define a threshold value for metrics below which corrective actions should be taken, with the aim of reinstating the performance above the required level [5]. Accordingly, leading safety indicators have emerged as a more effective alternative than traditional lagging indicators, which are measured after the occurrence of an accident [5].

Safety professionals have contended that the careful selection, measurement, and mitigation of leading indicators can result in real improvements in practice [3]. Practical improvements are attributed to the ability of leading indicators to be linked causally and proactively with safety outcomes in terms of accidents [6]. Criteria for selecting useful leading indicators have been defined [7] and include validity, reliability, sensitivity, representativeness, openness to bias, and cost-effectiveness. Øien et al. [8] have expanded on this, indicating that successful safety indicators should also be measurable on a numerical scale, updated regularly, and reflect selected determinants of overall safety.

Because of the potential interactive effect associated with combining and analyzing various leading indicators, a comprehensive set of leading indicators is believed to provide the best predictive result [9]. Indeed, many researchers, including Garza et al. [10] and Hinze et al. [9], recommend that companies should use a combination of leading indicators to assess safety performance rather than depending on a single indicator. Furthermore, companies should consider indicators outside of the safety department that have been found to reliably predict safety performance, such as those

associated with project performance. While construction companies collect a liberal amount of project-performance data to track the overall performance of their projects, they struggle to make use of these data for safety performance assessment purposes.

A number of leading indicator-based methods capable of predicting safety performance have been reported in the literature. However, these methods have been developed using only a specific set of leading indicators. Accordingly, many of these methods are dependent on certain dataset types or formats, making it difficult for practitioners to generalize the application of these methods in practice.

This study proposes an approach capable of proactively assessing safety performance regardless of the number or type of leading indicators available to a specific construction organization or project. The first part of this work is published in [11] where the authors showed that project performance data collected by different departments can be used as inputs for creating machine learning algorithms for safety leading indicators. Using a machine-learning approach, the proposed methodology can be applied to any dataset. In this particular case, the dataset is collected for non-safety associated purposes (e.g., cost, quality, and schedule) to predict the occurrence (i.e., yes/no) of an accident. The proposed approach was used to assess the safety performance of an organization based on data collected from eight projects over a period of two years., Various measures not traditionally associated with safety performance (i.e., quality, cost, and schedule) were included in the analysis to demonstrate the adaptability of the proposed approach. The various machine-learning algorithms were compared.

2 Literature Review

While several theoretical safety leading indicator studies have been conducted [3, 5, 12], few construction companies have successfully implemented programs capable of monitoring safety leading indicators in practice. In cases where companies have implemented such systems, there is little information available in the literature detailing which specific leading indicators have been applied by these companies [9]. Several factors identified by the Construction Industry Institute (CII) and other academic researchers may explain why successful leading-indicator monitoring programs have yet to be widely used in practice (i.e., knowledge gaps).

2.1 Predictive Models in the Safety Domain

Previous investigators have suggested that personal protective equipment (PPE) and proactive detection-based strategies are not sufficient for facilitating a zero injury state [13] and that predictive models of safety performance may play a key role in bridging this gap [14]. Predicting and understanding anticipated changes in safety performance can assist organizations in developing accident mitigation strategies more efficiently and effectively. Indeed, Schultz [13] has demonstrated the ability of one company to reduce injury rates through the application of advanced and predictive analytics together with a growing safety dataset. A number of predictive models have been developed with the aim of proactively forecasting where and when workplace injuries will occur. Ghodrati et al. [14] built various models to predict construction safety outcomes at the macro level. They demonstrated that the number of companies in any liable earnings category predicted safety outcome as well as the number of claims and entitlement claims in all constructed models. They also found a positive and significant relationship between the number of companies in various liable earnings categories and the severity of associated occupational injuries. In another study, Esmaeili et al. [15] used principal component analysis and a linear prediction model to test the validity of risk attributes for predicting safety outcomes. Although their method was able to predict safety outcomes effectively, it was limited to small-scale projects. A Bayesian-network hybrid model has been proposed by Xia et al. [16], to holistically explore safety risk factors in construction projects and predict the probabilities of project safety states.

2.1.1 Machine Learning-Based Models

Machine-learning algorithms function by learning from historical data in a manner that easily complements expert opinion. Although machine learning has been used widely in construction research for more than two decades, its application in the field of construction safety remains limited [17]. Poh et al. [18] presented a machine-learning approach to develop leading indicators that classify construction sites by their safety risk. A machine-learning approach using occupational accident data was also used by Sarkar et al. [19] to predict occupational accident outcomes, such as injuries, near misses, and property damage. Although the results of the studies mentioned above demonstrate considerable promise, the specificity of the datasets that the researchers used to develop these methods renders the widespread application of these methods difficult in practice for organizations with dissimilar data; in particular, generalization is difficult for datasets related to project performance rather than safety performance.

3 Research Methodology

Figure 1illustrates the research methodology. This methodology is a standard data mining process, as

Table 1. Collected variables

Performance Category	Variable/Feature
General	Project ID, Contract Type, Report Date, Contract Change Order (CCO), Outstanding CCO, CCO Submitted to Date, Request for Information (RFI), RFI Submitted to Date, Open RFI
Cost	Original Budget, Re-Baseline Budget, Approved Changes, Revised Contract Value, Pending Changes, Forecast at Completion, Earned Value, Incurred Value, Outstanding Change %, Work Order CPI
Schedule	Work Order % Complete, Work Order SPI, Work Order HPI
Quality	Non-Conformance Report (NCR), Open NCR, Field Surveillance Report (FSR), FSR Submitted to Date, Open FSR.
Safety	(0-1) Years of Experience Direct Hours, (1-2) Years of Experience Direct Hours, (2-3) Years of Experience Direct Hours, (3-4) Years of Experience Direct Hours, +4 Years of Experience Direct Hours, Foreman Hours, Shift Hours, Exposure Hours, Accident

defined by Witten et al. [20]. First, data are collected and studied to determine if the dataset is suitable for further processing. Second, raw data are cleaned and prepared (i.e., removal of missing data and outliers) for input into machine-learning algorithms. Data cleaning and preparation attempts to address any empty fields in records, data entry errors, and instances where data have been collected in an ad hoc manner [21]. This step ensures that the machine-learning algorithms produce an ideal model with improved performance. Finally, various prediction models are developed, and their performances are evaluated.

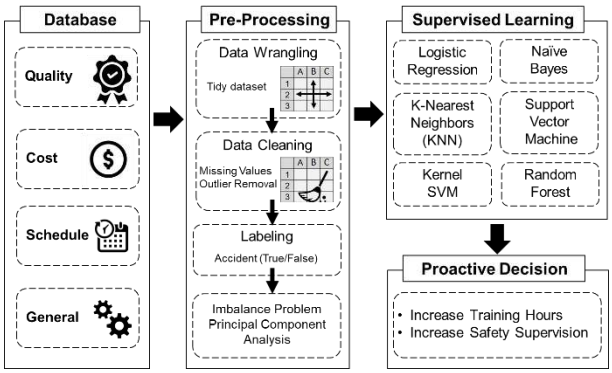

Figure 1. Research methodology

3.1 Data Collection

The dataset used in this research was obtained from a large construction company in Alberta, Canada, with a broad range of construction expertise including building, industrial, and infrastructure projects. The dataset, which encompassed eight industrial projects completed over two consecutive years (2016 to 2017), initially contained 123 biweekly records of each project's performance- (e.g., cost, schedule, and quality performance) and safety-related data (e.g., direct worker hours, foreman hours, shift hours, and accident occurrence). Biweekly accident records were associated with biweekly project performance- and safety-related data. More details about the definition of each of these features and integration of data from different departments is provided in [11]. A description of the variables collected is presented in Table 1.

3.2 Data Cleaning and Preparation

Features and variables that were not useful for this work were first removed. For example, three variables related to the budget and contract value (i.e., original budget, re-baseline budget, revised contract value) all provided similar information. Here, only one variable (re-baseline budget) was considered and kept. Second, missing values were removed or substituted by values that allowed for the development of the model while, at the same time, not adversely affecting model performance [20]. In this particular dataset, the value "Years of Experience Direct Hours" was missing in over 50% of the total records. Due to the limited number of data points, associated columns were removed. The features listed in Table 1 were filtered, resulting in a dataset of 23 features.

3.2.1 Data Labeling

Two labels were selected: (1) True, indicating an accident occurred in the worksite or (2) False, indicating no accident occurred.

3.2.2 Class Imbalance Problem

Machine-learning algorithms perform best when the number of observations is approximately equal in each class [20]. After data cleaning and feature selection, a total of 79 "no accident" and 23 "accident" cases were recorded. Random over-sampling techniques [22] were used to overcome the class imbalance and to reduce the negative impact this may have on algorithm performance.

3.2.3 Principal Component Analysis (PCA)

In machine learning, Principal Component Analysis (PCA) is useful for dimension reduction when analyzing high-dimensional datasets, reducing the number and increasing the independence of predictors [23]. Each principal component is a normalized principal component or linear combination of original variables. Based on the concept that principal components are orthogonal to each other (and correlation coefficients are all zero), PCA allows for the removal of multicollinearity in the features. In PCA, the first principal component is the one that captures the maximum variance of the data set. In other words, it determines the direction of the highest variability in the data.

Scatter plots and correlations between the independent variables are depicted in Figure 2. Of note, the highest correlation observed was between Shift Hours and Foreman Hours, (r=0.93; Figure 2). The results of PCA showed that PC1 explained 59% of the variability in the data set and that the first four principal components explained 90% of the variability in the dataset.

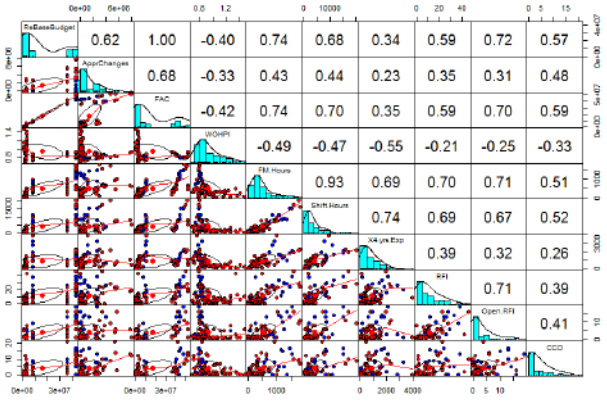

Figure 2. Correlation between independent variables

3.3 Model Generation

After the dataset was cleaned, various machine-learning models were generated and tested. In the current study, classification models were developed using the statistical package *R* [22]. While a large variety of classification models are available in the literature, this study selected models that (1) are widely used for investigating construction problems; (2) have been used in previous studies to predict safety performance and accident occurrence; and/or (3) are useful for modeling complex relationships. The models chosen include k-nearest neighbours (k-NN), logistic regression (LR), random forest (RF), support vector machine (SVM), Kernel support vector machine (KSVM), and Naïve Bayes.

4 Results

Model error is estimated using cross-validation or split validation, and often repeated several times [20]. In this study, the classification models were trained and validated using a 70/30 split validation approach, where the dataset was randomly divided into two parts used for (70%) training and (30%) testing purposes.

Models were evaluated and chosen based on several performance metrics derived from the confusion matrix (Table 2)[24]. These metrics include the following: *Recall*, which describes the probability of correctly predicting "True" relative to the total number of actual "True" and "False False" (FF) in the dataset [Eq. (1)]; *Precision* [Eq. (2)]; and *Accuracy*, which describe the probability correct predictions relative to the total number of predictions [Eq. (3)] [20]. These measures are commonly applied as performance indicators by researchers due to their straightforward interpretation.

Table 2. Description of confusion matrix

	Predicted False	Predicted True
Actual False	True False (TF)	False True (FT)
Actual True	False False (FF)	True True (TT)

$$Recall = TT/(TT + FF) \quad (1)$$

$$Precision = TT/(TT + FT) \quad (2)$$

$$Accuracy = (TT + TF)/(TT + FT + FF + TF) \quad (3)$$

Table 3. Summary of performance metrics of models

Table 3. Model performance

Model	Recall (%)	Accuracy (%)	Precision (%)
LR	71.4	93.5	100
KNN	85.7	87.0	66.6
SVM	57.1	87.0	80.0
Kernel SVM	28.5	80.6	66.6
NB	85.7	87.0	66.6
RF	57.1	87.0	80.0

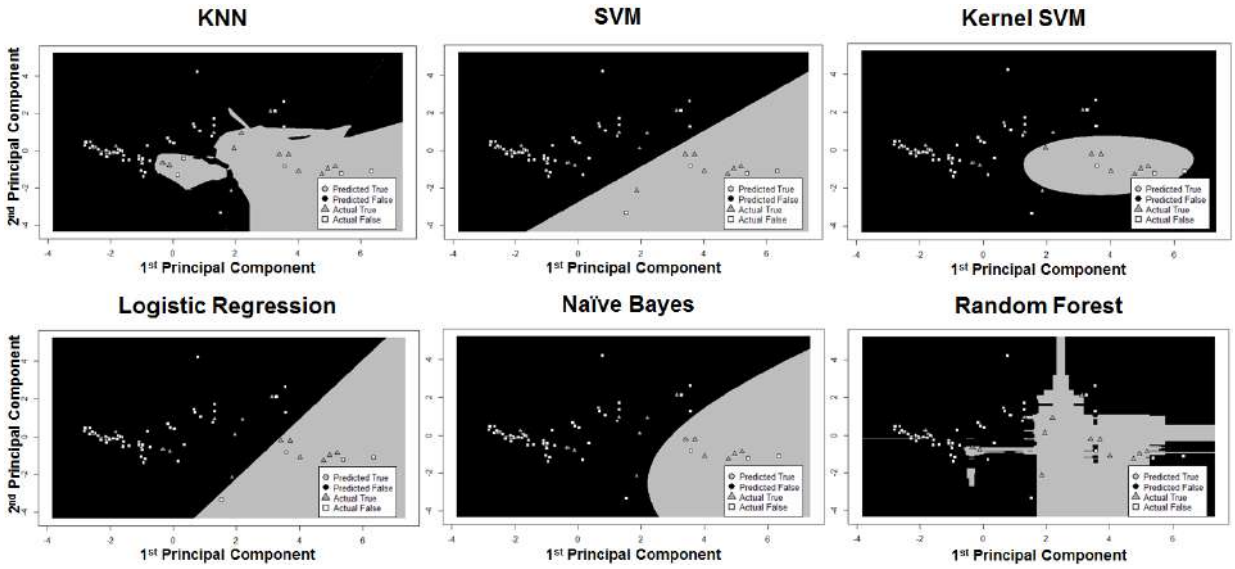

Figure 3. Hyperplanes and decision boundaries of different classifiers

Although *Accuracy* offers a simple measure of the overall performance of a model, it (1) does not consider the type of prediction errors being made and (2) does not consider the distribution (i.e., relative frequencies) of the classes.

Recall is considered the most suitable metric for selecting a model when there is a high cost associated with True/ False. For instance, in accident prediction, if an accident (True True) is predicted as no accident (True False), the consequence can lead to enormous costs for the company. For this reason, *Recall* is used to identify the best model in this study. Both KNN and Naïve Bayes classifiers were associated with the greatest *Recall*, indicating that these models were able to best predict the low-frequency class (in this case, accident occurrence).

Figure 3 visualizes the decision boundaries and the performance of the mentioned classification methods on a randomly selected subset of data. A dimension reduction algorithm (PCA) was applied to reduce the dimensions of the feature vector to two dimensions. As mentioned, the first PCA captures the highest amount of variance in the feature vector, and the second PCA is a component orthogonal to the first one. In Figure 3, as indicated in the legend, the gray and black areas represent proportions predicted by the classifier to be True (i.e., accident) or False (i.e., no accident), respectively. Gray triangles and white squares represent data points that are actually True or False, respectively.

5 Conclusion

While many research studies have been conducted investigating the impact of safety leading indicators on safety performance of construction sites, their use remains limited by certain practical challenges. Due to the approach in which the models were designed in particular, the implementation of prediction methods is often limited to a specific set of leading indicators.

This research study used a machine-learning approach to develop a model that can forecast safety performance from leading indicators regardless of the number or type of leading indicators available. First, the dataset is cleaned and pre-processed. Then, feature selection techniques are applied to reduce the dimensionality of the dataset and to identify the important features affecting safety performance. Finally, machine-learning algorithms are applied for training and validating purposes.

The method was tested using a dataset provided by a large construction company in North America. Out of 23 features, only 10 were found to have a notable influence on safety performance. After evaluation, Naïve Bayes (NB) and K-Nearest Neighbours (KNN) were found to be the best performing algorithms, achieving a *Recall* of 0.857.

Unlike previous studies, which have used theoretical or statistical approaches, this study has used a machine-learning approache to develop a safety performance prediction metric. The results of this study can be used by safety practitioners to (1) improve safety practices or (2) guide the allocation of resources towards monitoring indicators with the most influence on safety performance, saving organizations time and money. For future research, the authors suggest further segmenting the variables of safety (safety hours) with respect to weather conditions, overtime, or other impacting factors.

6 Acknowledgments

This work was supported. through a Collaborative Research and Development (CRD) Grant (CRDPJ 492657) from the National Science and Engineering Research Council (NSERC) of Canada.

References

[1] Reiman T. and Pietikäinen E. Leading indicators of system safety: Monitoring and driving the organizational safety potential. *Safety Science*, 50(10): 1993–2000, 2011.

[2] Grabowski M., Ayyalasomayajula P., Merrick J., Harrald J.R. and Roberts K. Leading indicators of safety in virtual organizations. *Safety Science*, 45 (10): 1013–1043, 2007.

[3] Hinze J., Hallowell M.R., Gibbons B., Green L., Trickel S. and Wulf D. *Measuring safety performance with active safety leading indicators* RS248-1. Construction Industry Institute, Austin, Texas, 2012.

[4] Kjellén U. The safety measurement problem revisited. *Safety Science*, 47(4): 486–489, 2009.

[5] Akroush N.S. and El-adaway I.H. Utilizing construction leading safety indicators: Case study of Tennessee. *Journal of Management in Engineering*, 33(5): 06017002, 2017.

[6] Guo B.H.W. and Yiu T.W. Developing leading indicators to monitor the safety conditions of construction projects. *Journal of Management in Engineering*, 32(1): 04015016, 2016.

[7] Hale A. Why safety performance indicators? *Safety Science*, 47(4): 479–480, 2009.

[8] Øien K., Utne I.B., and Herrera I.A. Building safety indicators: Part 1 – Theoretical foundation. *Safety Science*, 49(2): 148–161, 2011.

[9] Hinze J., Thurman S. and Wehle A. Leading indicators of construction safety performance. *Safety Science*. 51(1): 23–28, 2013.

[10] de la Garza J.M., Hancher D.E. and Decker L. Analysis of safety indicators in construction. *Journal of Construction Engineering and Management*, 124(4): 312–314, 1998.

[11] Mohamed E., Jafari P., Kang SC., Pereira E. and AbouRizk S. Leading indicators for safety management: understanding the impact of project performance data on safety performance. *In Proc., Canadian Society for Civil Engineering, 2019, Montreal, Canada*

[12] Hallowell M.R., Hinze J.W., Baud K.C., and Wehle A. Proactive construction safety control: Measuring, monitoring, and responding to safety leading indicators. *Journal of Construction Engineering and Management*, 139(10): 04013010, 2013.

[13] Schultz G. Using advanced analytics to predict and prevent workplace injuries. Online: https://ohsonline.com/Articles/2012/07/01/Using-Advanced-Analytics-to-Predict-and-Prevent-Workplace-Injuries.aspx, Accessed: 01/30/2019.

[14] Ghodrati N., Yiu T.W., Wilkinson S. and Shahbazpour M. A new approach to predict safety outcomes in the construction industry. *Safety Science*, 109(2018): 86–94, 2018.

[15] Esmaeili B., Hallowell M.R. and Rajagopalan B. Attribute-based safety risk assessment. II: Predicting safety outcomes using generalized linear models. *Journal of Construction Engineering and Management*, 141(8):04015022, 2015.

[16] Xia N., Zou P.X.W., Liu X., Wang X., and Zhu R. A hybrid BN-HFACS model for predicting safety performance in construction projects. *Safety Science*, 101: 332–343, 2018.

[17] TixierA.J.-P., Hallowell M.R., Rajagopalan B. and Bowman D. Application of machine learning to construction injury prediction. *Automation in Construction*, 69(2016): 102–114, 2016.

[18] Poh C.Q.X., Ubeynarayana C.U. and Goh Y.M. Safety leading indicators for construction sites: A machine learning approach. *Automation in Construction*, 93 (2018): 375–386, 2018.

[19] Sarkar S., Vinay S., Raj R., Maiti J. and Mitra P. Application of optimized machine learning techniques for prediction of occupational accidents. *Computers and Operations Research* (2018): 1-15.

[20] Witten I.H., Frank E., Hall M.A. and Pal C.J. *Data mining: Practical machine learning tools and techniques*, Morgan Kaufmann Publishers, Burlington, Massachusetts, 2016.

[21] Soibelman L. and Kim H. Data preparation process for construction knowledge generation through knowledge discovery in databases. *Journal of Computing in Civil Engineering*, 16(1) 39–48, 2002.

[22] R Core Team. R: A language and environment for statistical computing. Online: https://www.r-project.org/, Accessed: 01/30/2019.

[23] Abdi H. and Williams L.J. Principal component analysis. *Computational Statistics*, 2(2010): 433–459.

[24] Kuhn M. and Johnson K. *Applied predictive modeling*. Springer, New York, NY, 2013.

Towards the Ontology Development for Smart Transportation Infrastructure Planning via Topic Modeling

S. Chowdhury[a] and J. Zhu[b]

[a]Department of Civil and Environmental Engineering, University of Connecticut, 261 Glenbrook Road Unit 3037, Storrs, CT 06269-3037
[b]Department of Civil and Environmental Engineering, University of Connecticut, 261 Glenbrook Road Unit 3037, Storrs, CT 06269-3037
E-mail: sudipta.chowdhury@uconn.edu, jzhu@uconn.edu

Abstract
Media age has seen a huge amount of data flowing in from all directions, be it online news sources, social media, technical documents, and many more. There is a huge scope of these data sources for utilization in the transportation sector that can potentially improve the current practice of transportation infrastructure planning. In order to effectively capture, analyze, and utilize the information from various sources, ontologies are useful tools as they can provide clear and structured knowledge in the transportation domain. Majority of the existing transportation-related ontologies focus on traffic management and route planning. The objective of this paper is to initiate the development of an integrated ontology that can help with long-term planning and decision-making of transportation infrastructure by proposing a preliminary taxonomy in this domain. To this end, 20 transportation planning visionary documents published by government agencies were collected and analyzed using topic modelling techniques. Specifically, two topic modeling methods: Latent Dirichlet Allocation (LDA) and Non-negative Matrix Factorization (NMF) models were used to extract important and emerging concepts related to transportation infrastructure planning. Leveraging the important and emerging concepts, a preliminary taxonomy of transportation infrastructure planning was then developed and presented.
Keywords –
Smart Transportation infrastructure planning; Ontology; Taxonomy; LDA; NMF

1 Introduction

Ontology is a systematic description of entities with regards to their properties, relationship, and constraints expressed by axioms [1]. Due to its ability in promoting sharing of knowledge bases, knowledge organization, and interoperability among systems, ontologies have been used extensively in many domains and studies (e.g., disaster management, business modelling, disease management) [2-5].

The transportation research domain has long been benefitting from the application of ontologies. Ontologies are particularly fitting to handle the challenges arising from the large volume and variety of transportation related data (e.g., survey, sensor data) [6-7]. Majority of the ontologies developed in transportation research domain focus on trip planning [1, 8], trip disruption [9], traffic management [10-11], service monitoring [12], and urban freight transport problems [13, 14]. Despite the extensive use of ontologies in transportation research, to the best of the authors' knowledge, there is no scholarly work available in literature that directly focuses on an integrated ontology for transportation infrastructure planning. In many of the existing studies, transportation infrastructure planning had been considered as an auxiliary element towards other functions of transportation (e.g., see [15]). An assumption had been made in many of these studies that a desirable level of transportation infrastructure quality was already achieved for other transportation planning purposes such as trip planning, traffic management, and service monitoring. However, infrastructure is the foundation for realizing transportation functions. With the help of an integrated transportation infrastructure planning ontology, transportation infrastructure can be planned and managed in a more holistic way. Thus, transportation infrastructures can be better equipped to serve traffic demand, public safety, and social needs.

Transportation infrastructure planning can be defined as the process of making decisions concerning the potential changes required for transportation related infrastructures to improve the quality of life. Transportation infrastructure planning is a complex process. Without a structured ontology for information and knowledge management, there are major challenges in transportation infrastructure planning. First, transportation infrastructure planning documents and

publications from different sources may have different focus and use different structures and terminologies. For example, different agencies may have different definitions and metrics to assess transportation infrastructure performance. Therefore, it will be difficult to compare or integrate transportation infrastructure performance data and establish uniform baselines across different agencies. Second, a robust transportation infrastructure planning requires information from varied sources such as online news, social media, technical reports, and many more [5]. There is no way to effectively extract, analyze, and utilize the information from heterogeneous sources without a formal structure.

To address these challenges, the objective of this study is to initiate the development of an integrated ontology for transportation infrastructure planning. Such integrated ontology could help: (1) increase interoperability across different transportation infrastructure plans published by different governmental and non-governmental agencies at different levels; (2) facilitate the collection and analysis of data from various sources including social media (e.g., Twitter). Essentially, the ontology would help to build an integrated framework for smart transportation planning by incorporating data from different sources into a smart knowledge management and decision making system. It ultimately helps decision makers and planners to have a holistic approach to plan, build, and manage our transportation infrastructures.

As a first step in developing the ontology, a preliminary taxonomy for transportation infrastructure planning is proposed in this study via two topic modelling techniques: Latent Dirichlet Allocation (LDA) and Non-negative Matrix Factorization (NMF). The models have been used to extract important and emerging concepts related to transportation planning from 20 transportation planning documents. These concepts are then appropriately analysed and categorized to create a hierarchical taxonomy for transportation infrastructure planning.

2 Methodology

The methodology used to develop the preliminary taxonomy includes six steps. As shown in Figure 1, the first step was document collection, in which transportation planning related documents were collected.

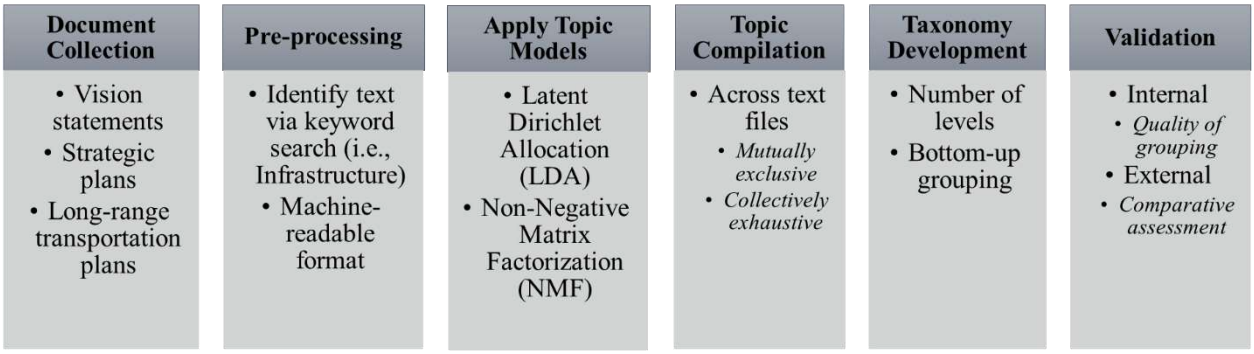

Figure 1. Taxonomy development steps

In the second step, useful texts were extracted from the collected documents and processed into a format that could be readily used for topic modelling. In the topic modelling step, two modeling techniques, i.e., LDA and NMF, were implemented on data extracted from each document to generate relevant topics. Then, different topics identified across all the documents were compiled and summarized in step four, i.e., topic compilation. The fifth step was taxonomy development, in which the structure of a preliminary transportation infrastructure planning ontology were developed. Finally, in step six, the proposed taxonomy was validated. Details of each of the steps in the proposed methodology are provided below.

2.1 Document Collection

As a first step, transportation planning documents were collected via a standard google search using key words such as transportation planning vision, transportation long-term plan, strategic transportation plan, etc. In total, 20 documents were identified through this process. These documents include transportation vision statements [13], long-range transportation plans [14], long-term regional transportation and land use plans [16-17], and many more. Majority of these documents were developed by state DOTs, while some were developed by legislative bodies at the city level. In some cases external consultants were assigned to provide support to develop such documents.

2.2 Pre-processing

Since transportation planning is such a broad term and covers many different aspects, the collected

documents in the first step are often times long-winded and hence, contain a variety of information that may not be directly pertinent to transportation infrastructure planning. Hence, data pre-processing was conducted by searching the keyword *"infrastructure"* within each document. Paragraphs with the keyword "*infrastructure*" in them were extracted from each document under the assumption that such texts were more apposite to the focus of this study. Separate text files were created for each document. These text files were then further processed to eliminate the possibility of encoding errors when they were read via *Python* for topic modelling. For example, all the apostrophe characters were removed from the text files before topic models were applied.

Table 1. A sample output of the application of topic models

Topic Model	Topic Example	Contexts (from "Invest in Transit 2018-2023 Regional Strategic Plan" [21])
Non-negative Matrix Factorization (NMF)	Funding, agencies, projects, state, local	• The agencies are ready to deliver more improvement projects, but more funding is required to do that. • The agencies have filled some of the funding gaps with short term fixes and by working with local governments and agencies. • If supported by a diversity of state, federal, and local funding commitments, it would empower agencies to improve the systems. • Agencies will be specific and transparent about funding needs and usage of funds. • RTAs Project Management Oversight office monitors the implementation of capital projects and found in its most recent report that 95 of state bond funded projects were tracking on time and 100 were on budget notwithstanding delays related to state funding. • Diversify and increase transit capital funding sources through state and local funding commitments of new revenue sources or expansions of existing revenues (e.g. gas tax). • The region will continue to seek federal funding and apply it to regionally and nationally significant projects. • The agencies have a track record of delivering on large capital project commitments.

2.3 Apply Topic Models

The processed data was then analyzed using topic modelling. Topic modelling is essentially a form of text mining that utilizes either unsupervised or supervised statistical machine learning techniques to identify patterns in structured or unstructured text [18]. It employs the process of similarity by clustering the words and identifying topics. Two topic modelling techniques: LDA and NMF were implemented in this study. LDA and NMF are two widely used topic modelling techniques. LDA is based on probabilistic graphical modelling while NMF relies on linear algebra [19-20]. While LDA and NMF have significantly different mathematical underpinnings, both techniques are capable of returning the most pertinent topics in a document. In this study, we used both techniques for analysis to ensure we capture all the important topics for transportation infrastructure planning. Before delving into detail about the mechanisms of LDA and NMF, it is important to clarify that in this study we ran topic models for each text files individually. Therefore, each text file generated is considered as a collection of *documents*. Here, *document* means a complete sentence (shown as one line in text files). The topic modeling results generated for each text file by both LDA and NMF were essentially based on the analysis of the collection of *documents* in each file. For better representation, from now on *document* in the text files will be referred to as "Single Line Source (SLS)" throughout this paper.

The mechanisms and implementation procedures of LDA and NMF are provided below. Machine learning library Scikit-learn was used in conjunction with Python to implement both LDA and NMF for identifying topics and their respective contexts [21].

2.3.1 Latent Dirichlet Allocation (LDA)

Let us suppose there are D SLSs in a text file with W words. Assuming K topics to discover, LDA was implemented as

Step 1: Randomly assign each word in $d \in D$ to one of the $k \in K$ topics

Step 2: Identify topic representations of all the SLSs and word distributions of all the topics.

Step 3: For each SLS $d \in D$:

- Go through each word $w \in W$
  - For each topic $k \in K$:
    - Compute the proportion of words in SLS $d \in D$ that are currently assigned to topic $k \in K = p(k|d)$
    - Compute the proportion of assignments to topic $k \in K$ over all SLSs that come from the word $w \in W = p(w|k)$
  - Reassign $w \in W$ to a new topic based on the probability $p(k|d) * p(w|k)$

Step 4: Repeat step 3 a large number of times to reach a steady state solution.

2.3.2 Non-negative Matrix Factorization (NMF)

Let us consider a nonnegative data matrix where each column of X corresponds to a SLS $d \in D$ and each row to a word $w \in W$. Each entry (m, n) in data matrix X represents the number of times the mth word appears in the nth SLS. Given such a matrix X with rank r, it can be factorized into two matrices V and H such that

$$X(:, n) \approx \sum_{k=1}^{r} V(:, k)\, H(k, n) \quad with\, V, H \geq 0$$

The goal is to find the best possible factorized matrixes that minimizes the following objective function

$$\underset{V,H\geq 0}{minimize} ||X - VH||^2$$

Since the weights in the linear combinations are nonnegative (i.e., $H \geq 0$), only the union of the sets of words defined by the columns of V can be used to reconstruct the original SLSs. Hence, the columns of V can be interpreted as topics.

The primary output of both LDA and NMF is a set of topics, each of which consists of a cluster of words. However, with only words in a topic, it is sometimes challenging to interpret or determine what each topic is about. This is non-trivial especially in ontology or taxonomy development as understanding of the context of each topic is crucial for better representation of the categories, properties, and relations among the data, concepts, and entities. Hence, in this study, not only the topics but also the context of each topic (i.e., SLSs that are the origins of each topic) are extracted and evaluated. A sample output of the topic models is provided in Table 1. This example shows one of the topics extracted from "Invest in Transit 2018-2023 Regional Strategic Plan" that provides a regional transit strategic plan for Chicago and Northeastern Illinois using NMF [22]. This topic covers a set of 5 words and the 8 SLSs. With the help of the contexts, it is evident that this topic is about the funding of transportation infrastructure projects. More specifically, the diversity of funding sources and transparent use of funding are the two focuses of this topic.

2.4 Topic Compilation

Due to the varying nature of collected files, a vast array of topics were generated. In this step, first, topics generated via LDA and NMF from each text file were compared and compiled. Then, topics identified across different text files were complied. Two criteria were used for topic compilation: mutually exclusive and collectively exhaustive. Mutually exclusive ensures that no topics were repeatedly counted and collectively exhaustive ensures that all the important topics identified were included.

2.5 Taxonomy Development

Taxonomy development step provides a preliminary solution about what concepts and/or factors impact and should be considered in smart transportation infrastructure planning. Moreover, successful implementation of this step can provide a hierarchical structure to organize different concepts and/or factors. A bottom-up approach was used in this step to develop the taxonomy using topic information generated in the previous step. For example, different hazards such as tornado, wildfire, and heatwave were included in the contexts of topics related to natural hazards and their impacts on transportation infrastructure. Therefore, these specific hazards were identified as the bottom-level entities and were grouped together at a higher level of the taxonomy under *natural risk*. Since there were other topics identified extensively discussing man-made hazards and their impacts on transportation infrastructure, "*natural risks*" and "*man-made risks*" were identified as two parallel concepts and grouped together under "*risk*" category in the taxonomy (see Figure 2 for details). In this study, four levels (i.e., level 0, level 1, level 2, level 3) in total were identified in the taxonomy to organize all the important information and concepts in a structured way. Level 3 is the lowest level with the finest level of granularity, followed by level 2, level 1, and finally level 0. It should be noted that caution needs to be taken in this step, as subjective judgement is required for appropriate grouping.

2.6 Validation

As the last step, both internal and external validation of the preliminary taxonomy were conducted. First, internal validation was conducted by the authors to ensure the quality of topic modelling and taxonomy development. The topics identified as well as the concept grouping structure were cross checked. Second, external validation was conducted by comparing the taxonomy with other existing studies. For example: *mobility* was a key topic captured across multiple documents and thus was identified as a concept related to service performance of transportation infrastructure in the proposed taxonomy.

In related transportation literature [23], *mobility* is used as one indicator of service quality of transportation infrastructure as well. Therefore, it was validated that *mobility* was properly grouped with other concepts that are relevant to *service quality* of transportation infrastructure under the *performance* domain in the proposed taxonomy.

3 Proposed Taxonomy

This section presents the preliminary transportation infrastructure planning taxonomy developed in this study. Figure 2 shows the first three levels in the taxonomy. Level 3 is not shown in Figure 2 due to the large magnitude of information. A sample representation of all the levels is demonstrated in Table 2 using the example of *risk* domain. The details of the proposed preliminary taxonomy are explained as follows, organized by the seven categories of concepts in Level 1:

Risk

A few documents explored the potential of *natural* and *man-made hazards* on transportation infrastructure and risks associated with them. Among the man-made hazards, traffic crashes were considered to be the most important source and hence, were investigated in detail. Apart from traffic crashes; hazmat spills, cyber-attacks, terrorism, etc. were also explored in several documents as potential man-made hazards that could have a detrimental effect on transportation infrastructure.

It was observed that natural hazards and their associated risks were given more importance compared to man-made hazards. A variety of natural hazards, such as wildfire, drought, heatwave, flooding, landslides, avalanches, storm surges, and earthquakes were extensively discussed and investigated for their threats to the transportation infrastructure (e.g., prolonged heat waves could increase the premature deterioration of infrastructure).

Utilization

Utilization refers to the utilization of transportation infrastructure in terms of the type and weight of vehicles using the infrastructure, and the usage frequency of infrastructures. The information of utilization has significant impacts on current and future transportation infrastructure planning. For example: in Georgia's statewide transportation plan [24], it highly emphasized that flow of freight in terms of weight, the type of vehicle most commonly used for freight transportation, and the usage of roads could provide useful insights into the infrastructure needs. Hence, *vehicle type*, *road usage*, and *vehicle weight* need to be carefully monitored. *Vehicle type* can refer to different classes of vehicles specified by The Federal Highway Administration (FHWA), *road usage* can refer to estimating Average Annualize Daily Traffic (AADT), and *vehicle weight* can refer to the maximum allowable weight that each class of vehicle can carry. *Vehicle type*, *road usage*, and *vehicle weight* can holistically provide useful information to maintenance requirement and frequency, as well as future needs of transportation infrastructures.

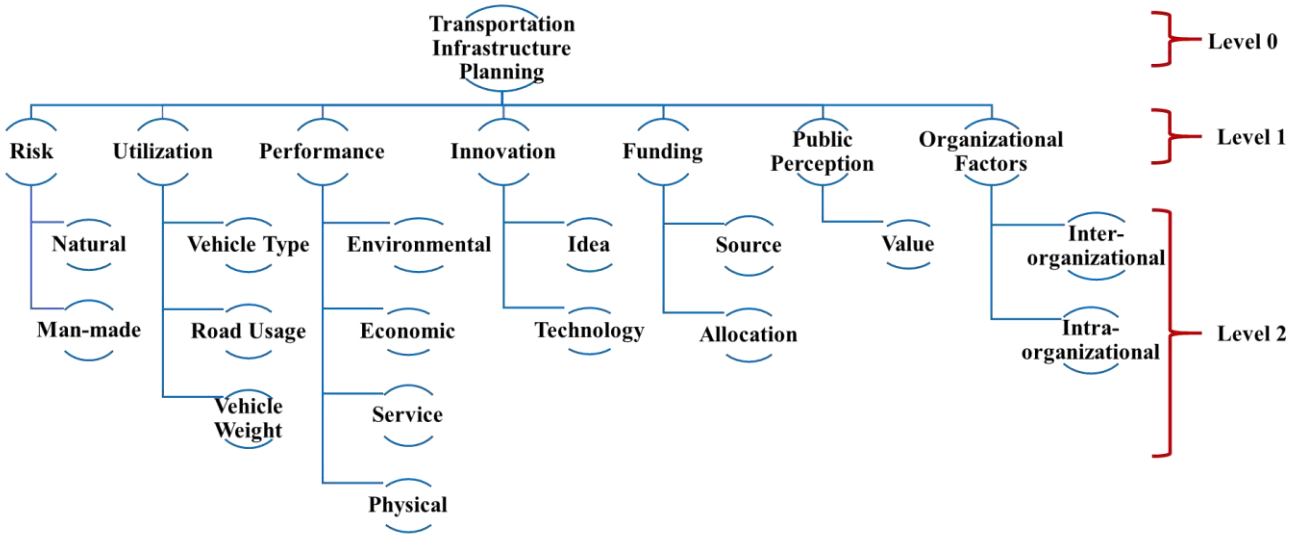

Figure 2. Illustrating the proposed transportation infrastructure planning taxonomy

Performance

Performance refers to the capability of current transportation infrastructures to fulfill the user needs.

Performance has been categorized into four classes in the proposed taxonomy, i.e., *environmental, economic, service*, and *physical*. In terms of *environmental* performance, different state DOTs or local legislative bodies provided different benchmarks such as air quality, water quality, greenhouse gas/carbon emission, and preservation of open space. Among them, greenhouse gas/carbon emission had been the focal point in majority of the documents that discussed the environmental performance of transportation infrastructures. With regards to *economic* performance, employment growth, supply chain and logistics reliability, inter-industry economic competition, etc. were identified as the major indicators for transportation infrastructure. *Service* performance is arguably the predominant measure of transportation infrastructure performance that was emphasized in almost all the documents. There were a number of transit service performance measures that had been discussed in detail such as ride quality, vehicle mobility, accessibility, intermodal coordination, transit security, connectivity, flexibility, and quality of transit fare system. On the other hand, service measures in terms of personal mobility such as walkability were also highlighted in a few documents. There were a few additional service measures that were not associated with transit but with quality of transportation infrastructure in general. For example, quality of road signs, quality of lightings, and coverage of emergency service patrol were discussed as indicators of transportation infrastructure quality in many documents. Finally, *physical* performance measures refer to the physical conditions of transportation infrastructures. *Physical* performance measures refer to the condition of transportation infrastructures such as bridge, culvert, airport, parking lots, rapid transit, heavy rail, and urban rail. The physical performance measures indicators can range from visual inspection ratings to complex performance index (e.g., pavement condition index (PCI)).

Innovation

Innovation has brought a lot of changes to today's transportation infrastructure. In the proposed taxonomy, innovation has been identified as an important concept in Level 1 and can be represented by two classes, i.e., *idea* and *technology*. *Idea* refers to new lines of thoughts to improve the quality of transportation system. For example, complete streets (i.e., streets that are designed and maintained to enable convenient and safe travel and access for all users regardless of modal choice) and greenway corridors (i.e., corridors that are specifically designed for recreational or pedestrian use ensuring environmental, wildlife habitat, and water resources benefits) are new and innovative ideas that were introduced in many of the documents to future-proof transportation infrastructure [17].

In terms of *technology*, it was found that automated and connected vehicles, novel data management framework, alternative fuel, alternative energy (e.g. solar power) etc. had been gaining attention and adopted widely across USA and hence, need to be exhaustively investigated regarding their impacts on transportation infrastructure planning and development. For example, with more electric vehicle on the road, there is a need to integrate the electric charging infrastructure development into transportation planning.

Funding

Funding was identified to be a critical factor in transportation planning. It is often challenging to acquire adequate funding to maintain and improve the existing transportation infrastructure, as well as to develop new infrastructure. Leveraging the information from topic modelling results, there are two level-2 concepts under funding: *source* and *allocation. Source* refers to the authorities and financial entities that provide money for transportation infrastructure related ventures. Three types of major sources were found from the documents, i.e., public, private, and public-private partnerships. *Allocation* refers to allocating the monetary funds to different areas or activities. For example, allocation of funding can be based on different levels of transportation development and improvement needs in different areas (e.g., rural, urban, or sub-urban). Allocation of funding could also be based on types and urgency of activities (e.g., preservation, modernization, or expansion). Different funding allocation rules might be applied to make sure the money is used in a most effective way to the most needed areas and activities.

Public Perception

Public perceptions and opinions are influencing transportation infrastructure more and more. One example found in the topic modelling result from this study is that, people (especially the younger generation) are becoming more conscious of the transportation choices they have and how these choices affect not only their lives but also the environment and society. They are becoming more aware of the detrimental effects of auto-dependency and want a transportation system that promote healthy living. Moreover, there is a growing consensus among the people that reducing auto-dependency help preserve the environment in many ways as well. Hence, it was observed from multiple documents that there had been a growing demand in recent years for developing and improving biking, hiking, and walking infrastructures. This phenomenon has been termed as *value* in the proposed taxonomy under public perception category. There are other types of public perceptions such as complaints that might affect transportation infrastructure planning, which were not captured in the

20 documents analysed in the current study. More documents will be included in the analysis to further develop the concept of public perception and its impacts on transportation infrastructure planning in future work.

Organizational Factors

Organizational factors relate to the culture of the transportation planning agencies (e.g., DOT) towards better management practices. These organizational factors greatly affect the adoption and implementation of any transportation planning policies and decision-making process behind. There are two major classes of organizational factors: *intra-organizational* and *inter-organizational* factors. *Intra-organizational* factors include an agency's commitment to not only improve internal communications and engagement processes, but also ensure that plans, programs, and projects are in line with its long term strategic goals. For example, San Francisco Municipal Transportation Agency's strategic plan emphasize that all agency plans, programs, and projects of the agency must be adjusted accordingly to fit the scope of the strategic plan [25].

On the other hand, *inter-organizational* factors refer to the collaboration and coordination attitude of transportation planning agencies with other transportation partners. A high level of coordination and collaboration among state government leaders, congressional delegation, land use planning governing bodies, industry stakeholders, tribes, non-profit organizations, and the general public were found to be significant in ensuring robust transportation infrastructure [e.g., 26].

Table 2. Sample construction of transportation planning taxonomy

Level 0	Level 1	Level 2	Level 3
Transportation infrastructure planning	Risk	Natural	Wildfire, drought, heatwave, flooding, landslides, avalanches, storm surges, earthquakes
		Man-made	Hazmat spills, cyber-attacks, terrorism, traffic crash

4 Conclusions

In order to develop an integrated ontology for transportation infrastructure planning, a taxonomy was proposed in this study as the first step. The transportation infrastructure planning taxonomy was developed using topic modelling techniques based on textual information from 20 transportation planning documents published by government agencies. The taxonomy and the ontology that will be built could potentially address the interoperability challenge of transportation plans at various levels and across different regions. In addition, they could provide a formalized structure to collect, organize, analyse, and utilize information from different sources to help transportation infrastructure planning. The ultimate goal of this study is to create a smart transportation infrastructure planning platform that can help planners to make informed infrastructure planning and management decisions using information and knowledge effectively with the help of the ontology.

The current study has several limitations. First, both the number and scope of documents included in the topic modelling analysis in this study are limited. For future study, the authors will collect more data from more sources, including online social media data to implement topic modelling and identify emerging concepts related to transportation infrastructure planning. The taxonomy will be further developed based on new concepts and information captured. Second, in order to grow the taxonomy proposed into an integrated ontology, more elements including attributes, relationships, rules, and restrictions of concepts will need to be investigated extensively in future studies.

Acknowledgement

The authors acknowledge the support received from U.S. DOT under its Transportation Infrastructure Durability Center (TIDC). The views expressed in this paper are those of the authors. The findings, conclusions or recommendations either inferred or specifically expressed herein do not necessarily indicate acceptance by US DOT.

5 References

[1] Houda, M., Khemaja, M., Oliveira, K., & Abed, M. (2010, May). A Public Transportation Ontology to Support User Travel Planning. In Research Challenges in Information Science (RCIS), 2010 Fourth International Conference on (pp. 127-136). IEEE.

[2] Babitski, G., Probst, F., Hoffmann, J., & Oberle, D. (2009). Ontology Design for Information Integration in Disaster Management. GI Jahrestagung, 154, 3120-3134.

[3] Wang, Z., & Lei, J. (2013, June). A Study of Spatial Information Sharing Model Based on Geological Hazard Domain Ontology. In Computational and Information Sciences (ICCIS), 2013 Fifth International Conference on (pp. 268-270). IEEE.

[4] Upward, A., & Jones, P. (2016). An Ontology for Strongly Sustainable Business Models: Defining an Enterprise Framework Compatible with Natural and Social Science. Organization & Environment, 29(1), 97-123.

[5] Chowdhury, S., Emelogu, A., Marufuzzaman, M., Nurre, S. G., & Bian, L. (2017). Drones for Disaster Response and Relief Operations: A Continuous Approximation Model. International Journal of Production Economics, 188, 167-184.

[6] Katsumi, M., & Fox, M. (2018). Ontologies for Transportation Research: A Survey. Transportation Research Part C: Emerging Technologies, 89, 53-82.

[7] Jain, G. V., Jain, S. S., & Parida, M. (2014). Public Transport Ontology for Passenger Information Retrieval. International Journal of Transportation Engineering, 2(2), 131-144.

[8] Corsar, D., Markovic, M., Edwards, P., & Nelson, J. D. (2015, October). The Transport Disruption Ontology. In International Semantic Web Conference (pp. 329-336). Springer, Cham.

[9] Bermejo, A. J., Villadangos, J., Astrain, J. J., & Cordoba, A. (2013). Ontology Based Road Traffic Management. In Intelligent Distributed Computing VI (pp. 103-108). Springer, Berlin, Heidelberg.

[10] Herzog, A., Jacobi, D., & Buchmann, A. (2008, September). A3ME-an Agent-based Middleware Approach for Mixed Mode Environments. In Mobile Ubiquitous Computing, Systems, Services and Technologies, 2008. UBICOMM'08. The Second International Conference on (pp. 191-196). IEEE.

[11] Benvenuti, F., Diamantini, C., Potena, D., & Storti, E. (2017). An Ontology-based Framework to Support Performance Monitoring in Public Transport Systems. Transportation Research Part C: Emerging Technologies, 81, 188-208.

[12] Anand, N., Yang, M., Van Duin, J. H. R., & Tavasszy, L. (2012). GenCLOn: An Ontology for City Logistics. Expert Systems with Applications, 39(15), 11944-11960.

[13] Bouhana, A., Zidi, A., Fekih, A., Chabchoub, H., & Abed, M. (2015). An Ontology-based CBR Approach for Personalized Itinerary Search Systems for Sustainable Urban Freight Tansport. Expert Systems with Applications, 42(7), 3724-3741.

[14] Malloy, D. P. (2015). Connecticut's Bold Vision for a Transportation Future. Available from https://www.ct.gov/dot/lib/dot/documents/dcommunications/ctdot_30_yr.pdf

[15] De Oliveira, K. M., Bacha, F., Mnasser, H., & Abed, M. (2013). Transportation Ontology Definition and Application for the Content Personalization of User Interfaces. *Expert Systems with Applications*, *40*(8), 3145-3159.

[16] MaineDOT. (2010). Statewide Long-Range Transportation Plan 2008 – 2030. Available from <https://www.maine.gov/mdot/publications/docs/plansreports/connectingmainefulldocument.pdf>

[17] City of Portland. (2018). 2035 Comprehensive Plan. Available from https://www.portlandoregon.gov/bps/2035-comp-plan.pdf

[18] Grimmer, J. (2010). A Bayesian Hierarchical Topic Model for Political Texts: Measuring Expressed Agendas in Senate Press Releases. Political Analysis, 18(1), 1-35.

[19] Khanzadeh, M., Chowdhury, S., Marufuzzaman, M., Tschopp, M. A., & Bian, L. (2018). Porosity Prediction: Supervised-learning of Thermal History for Direct Laser Deposition. Journal of manufacturing systems, 47, 69-82.

[20] Gillis, N. (2014). The Why and How of Nonnegative Matrix Factorization. Regularization, Optimization, Kernels, and Support Vector Machines, 12(257).

[21] Chowdhury, S., Khanzadeh, M., Akula, R., Zhang, F., Zhang, S., Medal, H., Marufuzzaman, M., & Bian, L. (2017). Botnet Detection Using Graph-Based Feature Clustering. Journal of Big Data, 4(1), 14.

[22] Regional Transportation Authority (2018). Invest in Transit 2018-2023 Regional Strategic Plan. Available from https://www.rtachicago.org/sites/default/files/documents/Invest%20in%20Transit%202018-2023%20Regional%20Strategic%20Plan%20ScreenView%20for%20Web.pdf

[23] Compares, T. F. (2003). Measuring Transportation: Traffic, Mobility and Accessibility. ITE journal, 73(10), 28-52.

[24] GDOT. (2007). 2005-2035 Georgia State-wide Transportation Plan. Available from http://www.dot.ga.gov/InvestSmart/Documents/SSTP/SWTPFinalReport.pdf

[25] San Francisco Municipal Transportation Agency. (2018). Strategic Plan. Available from https://www.sfmta.com/sfmta-strategic-plan

[26] NMDOT. (2015). The New Mexico 2040 Plan: NMDOT's Long Range, Multi-Modal Transportation Plan. Available from http://dot.state.nm.us/content/dam/nmdot/planning/NM_2040_Plan.pdf

Automated Detection of Urban Flooding from News

F. Zarei[a], and M. Nik-Bakht[a]

[a]Department of Building, Environment and Civil Engineering, Concordia University, Canada
E-mail: f_zaire@encs.concordia.ca, mazdak.nikbakht@concordia.ca

Abstract –
Although minor overflows do not cause a huge amount of loss; as the number of such overflows increases, the amount of water wasted, and the compound consequent challenges become considerable. Therefore, detecting overflows, investigating their cause root and resolving them in a timely manner are among new needs for infrastructure managers. This paper suggests a new method for detecting distributed water overflows by extracting the flood information (such as the date and location of the incident) from the news. As a case study, we crawled Montreal newspaper and news websites to detect the related news to urban flooding and their detailed information. We trained several classifiers to identify news relevant to flood. Our experiments illustrate that by applying mutual information method for feature selection and employing support vector machine (SVM) architecture as the classifier, relevant news can be detected with an accuracy (F-measure) of above 80%. Such actionable information can help infrastructure managers with a wide range of decisions from repair and maintenance of existing systems, to capacity evaluation for new designs.

Keywords –
Classification; Montreal newspaper; Urban Flooding; Water overflows

1 Introduction and background

Nowadays, anthropogenic climate change alters weather patterns with significant shifts in climate normal and extremes [1]. On the one hand, having more extreme events such as heavy rainfalls could lead to an increase in the risk of urban flooding. On the other hand, the aging infrastructure, encroachment on drainage canals, and reduced natural drainage introduce additional risk factors. Heavier rainfalls in aging infrastructure may generate urban flooding [2]. This is particularly increasing the frequency and magnitude of distributed incidence which is also known as compound effect.

At the same time, 'responsible citizenship' is an emerging phenomenon with several benefits such as citizen engagement, detecting public service performance and citizens 'priorities via feedbacks [3]. Reporting the civic complains in the media in recent years is supporting in this regard. In fact, it is a belief that citizens are inherently capable to solve their own problems at a higher level, collectively and collaboratively.

The citizens are enabled by resolving the urban issues to monitor, record and report the social problems together [4]. Several social media platforms such as Twitter, Instagram and complaint boards provide channels for the citizens to get engaged in different levels of problem solving and decision making. Using these platforms, citizens can take a photo from a civic phenomenon, add a comment, geotag, and share it. In fact, it is argued that citizens gain more awareness by the aid of these platforms and they can help the authorities to learn about the issues faster and more efficient. In [5], the authors use Deep Belief Network (DBN) and Long Short-Term Memory (LSTM) for detecting traffic accidents from social media data, specifically Twitter, and compared their results with the data of 15,000 loop detectors. It is concluded in this research that around 66% of the tweets which are relevant to the accidents are consistent with the facts about the accidents.

By using tweets, the authorities can gain a better understanding of the number of involved citizens with the issues and the intensity of problems [6]. In this regard, after the emergence of smart cities, it is attempted to apply new technologies and ideas to improve social, political and economic systems. It is aimed that such technologies could help the citizens to increase their level of participation in civic issues.

In [7], the authors provided a platform named "Citicafe". This platform has an exchangeable based interface to improve the citizen engagement by allowing direct messaging. It can help citizens to gather information related to their neighborhoods and report their problems. As another example, Indian government authorities collaborated with Twitter to launch "Twitter Seva" [8] whose goal is the enhancement of public service engagement by providing a platform for following complaints in a real-time manner. In this platform, the citizen interactions are limited to one

whose communicated since there are no chat interfaces.

Considering board range of events reported in social media, one of the high-level goals of our research work is to automatically detect the overflow incidents from people's inputs and also to communicate warning alarms. We need to study the source of any observed and reported on-the-ground water to know whether it is related to flood, overflows or pipe leakages.

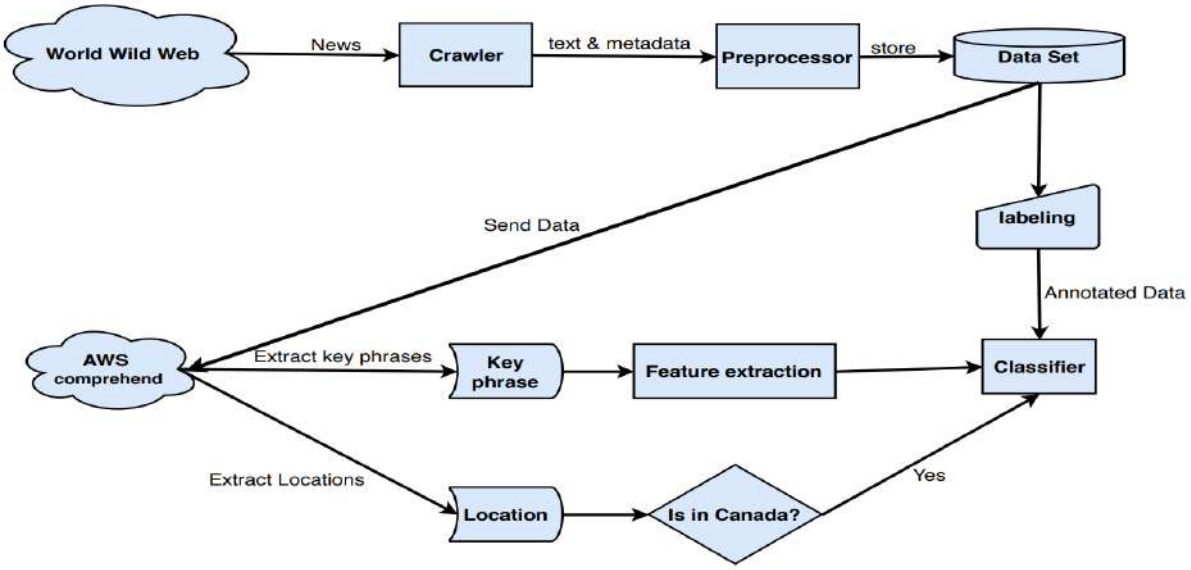

Figure 1. The architecture of the proposed method

In this regards, a binary classifier is required to categorize floods in a more specific context; from a nice rainy day to some serious failures. In the ideal case, not only we should be able to automatically detect flood spots in the city, but also we must detect the source and type of flood. In fact, we must be able to realize whether, with a high chance, it is a natural phenomenon or related to an infrastructure shortcoming.

With this aim, we collected and annotated news, and went through their content to find more related words. Considering co-occurrence of terms, we need to exclude the news which are not about water but include the terms which are normally used in discussing articles. On the first step, by searching the term "flood" on flood newspaper websites, we let the website's search engine to screen the news. Then, the obtained news was passed to Comprehend, which is Software as a Service (SaaS) provided by the amazon web services (AWS) [9]. Comprehend helped us to extract entities and key phrases from the news sentences. On the next step and after generating the relevant features manually, the required features for classification were selected by applying a mutual information method [10]. Having the features, Bayesian classifier (Naïve Bayes) [11], Meta algorithm (AdaBoost) [12], Decision tree (Id3) [13], Neural network (Multi-layer perceptron (MLP)) [14], Kernel estimation (KNN) [15] and Support vector machine (SVM) [16] classifiers were tested to label the news as relevant and irrelevant to the flood. Finally, the accuracy of the classifiers was evaluated in the sense of F-measures.

The remainder of this paper is organized as follows. The overall process flowchart of the proposed method is discussed in Section 2. Section 3 provides a discussion about the approach of crawling and also the data collection process. Applied feature extraction and feature selection approaches are explained in Section 4. In Section 5 the method of classification is provided. Section 6 presents the simulation and the obtained results, and finally, concluding remarks are provided at the end of the paper.

2 Proposed method

In this section, the entire flowchart of the proposed method will be discussed. As mentioned before, the main purpose of this work is detecting flood events in city of Montreal. In this regard, we concentrate on the flood-related news reported in Montreal newspapers. After gathering such news, the topic of each news article, which is a sentence, is considered as the input of the system. By using the Application Programming Interface (API) of the AWS, the existing name-entities and the key-phrases of the sentence are extracted. The news is considered irrelevant to our research if its extracted location is outside Canada. In such cases, the system goes to the next sentence. Otherwise, each word of the news article is searched in the provided word-list. If that word exists in the *i-th* place of the word-list, the

i-th element of the feature vector becomes 1 and remains zero otherwise. Next, the feature generator provides an appropriate matrix of data with their features for the classifier. Finally, the classifier decides whether the news is related to the flood. This procedure is represented in Figure 1.

3 Data extraction

3.1 Data collection

The applied dataset was selected from the most popular Montreal local English newspaper, "Montreal Gazette" [17]. In this regard, with the aid of search engine of this website, we filtered the news archive and selected the ones which contain the word "flood". On the next step and after such filtering, all the related news gathered into our database by building a crawler for this website in python.

3.2 Corpus construction

Once we crawled all the news form the mentioned newspaper, we had to reorganize the collected data in a format which is easy to use for our research purposes. The data of the gathered collection consist of 6 attributes including title, the body of the news, the category of the news, the date, the link, and the link of images.

3.3 Data annotation

In the next step, we assign a number to each sentence manually, which indicates the relevance of the news article. The news was divided into two categories named as relevant and irrelevant. The relevant news examples to the flood were labeled as '+1' and the irrelevant ones labeled as '-1'. "Leaky pipe floods Van Horne Ave., creates Sunday traffic woes" and "More than a year after floods, family of 7 will soon be homeless" are two examples for each group, respectively.

4 Feature extraction and feature selection

Feature extraction and feature selection are two important processes which should be done prior to classification to improve its accuracy and decrease its computational complexity. Therefore, feature selection has a considerable importance in the scope of this paper. The methodology of feature selection applied in this work can be explained in two main steps: keywords extraction, and filtering.

4.1 Keyword extraction

The main aim of this step is extracting the 'name entities' such as the locations and extracting key-phrases of each news article. The location of a news is important in this research since our goal is finding the place of flooding. We applied AWS Comprehend service to extract the locations mentioned in the news as well as their key phrases. Amazon Comprehend is a natural language processing (NLP) service that uses deep learning to find the meaning and insights in texts. The topic of news was the input of the Comprehend service and the output was the location and key phrases of the news. We consider these keywords as the features for the classification. However, not all the extracted keywords can be beneficial for the classification. Firstly, the features applied in classification must be able to discriminate the data. Moreover, some of the extracted features are redundant and can deteriorate the classifier. Therefore, the features need to be filtered prior to the classification. The way of filtering of the features is described in the next section.

4.2 Manual selection of related and unrelated key-phrases

In this step, we calculate the occurrence of each feature in our dataset. Then, those features which are not very common in our corpus are deleted from the list of features. These features are the ones whose occurrence is less than 5 times in sentences. After this reduction, we still need to reduce the features to the ones related to flooding. Hence, we were through the list and deleted the irrelevant features. Finally, an automatic feature selection method was applied to the list of remaining features to make the features ready for classification.

4.3 Automatic feature selection by applying mutual information

There are many different approaches for feature selection. In this work, we focus on the information-theory-based approach. This method has attracted the most attention since it can detect nonlinear correlations among the features. Mutual information is an important concept in information theory. It can evaluate the relevance between two random variables X and Y. In this paper, the mutual information of two variables $word\ (w)$ and $topic\ (t)$ is defined as below:

$$\boldsymbol{MI(w,t) = \log\big(P(w|t)\big) - \log\big(P(w)\big)}. \quad (1)$$

Here,

$$P(w|t) = \frac{\text{NDTW}}{Total\ number\ of\ Docs\ with\ the\ topic\ t}$$

$$P(w) = \frac{NDW}{Total\ number\ of\ Docs}$$

Here, NDTW stands for the number of documents with the topic t containing the word w and NDW stands for the number of documents containing the word w. We apply this method to select a subset of highly discriminant features. Hence, the features which have the capability of discriminating the data of different classes are selected.

5 Classification

In a typical supervised classification problem, the main goal is to train a classifier by using a dataset $U = \{(X^1, t^1), \dots, (X^n, t^n)\}$ of n labeled instances where each instance x^i is characterized by d features, i.e. $X = (X_1, \dots, X_d)$, and a label which indicates the class that it belongs to.

In this section, the main goal is to classify the news into 'related to the flood' and 'nonrelated to the flood'. Different applied classification methods are Naïve-Bayes classifier, AdaBoost, Id3, MLP and SVM. In the next section, the results of these classifiers are compared.

In order to evaluate the classifiers diagnostic tests were performed and three metrics were considered: precision, recall and F-measure.

$$precision = \frac{tp}{tp + fp}$$

$$Recall = \frac{tp}{tp + fn}$$

$$F_measure = 2.\frac{precision.recall}{precision + recall}$$

Here, *tp* is the number of data samples with the real label of positive which are labeled as positive by the machine. Furthermore, *tn* is the number of data samples with the real label of negative which are labeled as negative by the classifier. Similarly, *fp* is the number of data samples with the real label of negative which are labeled as positive by the machine. Finally, *fn* is the number of data samples with the real label of positive which are labeled as negative by the classifier.

6 Result and Evaluation

After search in "Montreal Gazette" newspaper data, the term "flood", 957 news items were found, started from September 16, 2009. This extracted news was manually labeled: 528 of them are labeled as relevant and 429 as irreverent.

By applying the feature extraction through Comprehend service and omitting the irrelevant features, the number of selected features for the classification was reduced to 98. In the next step and by applying the mutual information method, the number of features reduced to 50.

These features were passed to the classification agents whose results are reported in Table 1. For the evaluation, 10-fold cross validation was applied and precision, recall, and F-measure were calculated.

Table 1. Results of the classifiers

Classifiers	Precision	Recall	F-measure
Naïve Bayes	0.741	0.887	0.807
AdaBoost	0.711	0.932	0.805
Id3	0.707	0.887	0.787
MLP	0.697	0.870	0.774
KNN	0.751	0.859	0.801
SVM	0.762	0.832	0.824

The importance of precision and recall depends on the application. In some cases, having a higher precision is critical and in some other cases the recall has such importance. However, generally it is desired to consider both of them and evaluate the F-measure. Comparing the accuracy of the classifiers, it is seen that the SVM classifier classified the data more accurately. This is due to the characteristic of the SVM classifier that makes it a good choice for providing an adequate discrimination boundary for double class classification problems.

7 Demonstration of the results

After extracting the locations and finding the relevant news, results were encoded as colors and were visualized. Figure 2 presents number of news mentioned flooding in "Montreal Gazette" from 2009 to 2018. As seen, the number of sections in which flood is reported is increasing through the time. Also, the colors are getting more saturated which indicates the higher number of flood report in that area.

8 Conclusion

Detecting the small water overflows and finding their resources are important especially when the cause of water overflows is a malfunction of the infrastructure. In this work, we attempted to detect news about the flood as either a natural or a man-made phenomenon, reported in Montreal newspaper. In this regard, 4 classifiers were trained and the results were compared. In the end, we reached more than 80% accuracy in terms of the F-measure score, which belongs to the SVM classifier by applying mutual information method

for feature selection. The results of this research are useful for infrastructure managers who make decision about the maintenance of different infrastructure.

One of the main limitations of this work is that our corpus is quite small for the learning process since we just applied the text of one newspaper. Hence, more data sets should be applied to improve the performance of this work.

Following this work, we can use more properties from the website contents such as images of the news. In this work, we just classified the topic of the news. However, most of the news in the newspapers have images. Hence, by applying some image processing techniques, we can understand whether the news is related to the flood or not. By combing this results with the classifier results, we can increase the accuracy of the classification.

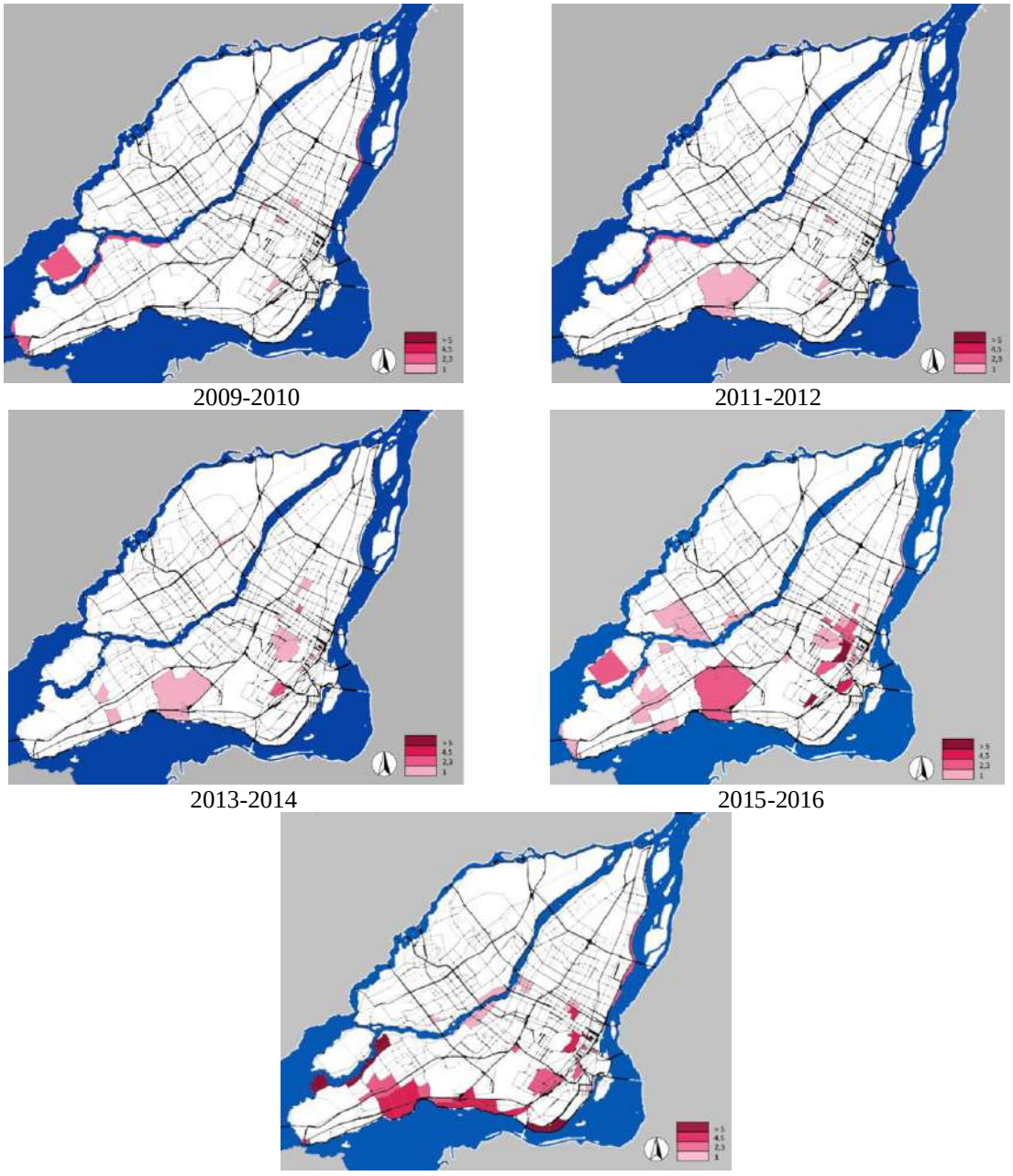

Figure 2. Number of flood reported in “Montreal Gazette” in different parts of Montreal

References

[1] IPCC (2013) Climate Change 2013: *The Physical Science Basis*. Stocker T, Qin D (Co-Chairs) Contribution to the Fifth Assessment Report of the Intergovernmental Panel on Climate Change. Working Group I Technical Support Unit, Switzerland.

[2] Markolf, S. A.; Hoehne, C.; Fraser, A.; Chester, M. V. & Underwood, B. S. Transportation resilience to climate change and extreme weather events – Beyond risk and robustness Transport Policy, 2019, 74, 174 - 186

[3] M. M. Skoric, Q. Zhu, D. Goh and N. Pang. 2015. Social media and citizen engagement: A meta-analytic review. New Media and Society, Sage Publishing.

[4] S. K. Prasad, R. Patil, S. Beldare, and A. Shinde. 2016. Civic complaint application under smart city project, International Journal of Advanced Computing and International Technologies, vol. 3, no. 2.

[5] Zhang, Z.; He, Q.; Gao, J. & Ni, M. A deep learning approach for detecting traffic accidents from social media data Transportation Research Part C: Emerging Technologies, 2018, 86, 580 – 596

[6] M. M. Skoric, Q. Zhu, D. Goh and N. Pang. 2015. Social media and citizen engagement: A meta-analytic review. New Media and Society, Sage Publishing.

[7] Atreja, S.; Aggarwal, P.; Mohapatra, P.; Dumrewal, A.; Basu, A. & Dasgupta, G. B. Citicafe: An Interactive Interface for Citizen Engagement 23rd International Conference on Intelligent User Interfaces, ACM, 2018, 617-628

[8] Twitter Seva https://blog.twitter.com/official/en_in/a/2016/the-ministry-of-communication-adopts-twitter-seva-in.html

[9] https://docs.aws.amazon.com/index.html#lang/en_us (accessed January 29, 2019)

[10] Bolón-Canedo V., Sánchez-Maroño N., Alonso-Betanzos A.A review of feature selection methods on synthetic data Knowledge and Information Systems, 34 (2013), pp. 483-519

[11] Webb, G. I., J. Boughton, and Z. Wang (2005). Not So Naïve Bayes: Aggregating One-Dependence Estimators. Machine Learning 58(1). Netherlands: Springer, pages 5-24.

[12] Rojas, R. (2009). AdaBoost and the super bowl of classifiers a tutorial introduction to adaptive boosting. Freie University, Berlin, Tech. Rep.

[13] Taggart, Allison J; DeSimone, Alec M; Shih, Janice S; Filloux, Madeleine E; Fairbrother, William G (2012). "Large-scale mapping of branchpoints in human pre-mRNA transcripts in vivo". Nature Structural & Molecular Biology. 19 (7): 719–721.

[14] R. Collobert and S. Bengio (2004). Links between Perceptrons, MLPs and SVMs. Proc. Int'l Conf. on Machine Learning (ICML).

[15] Nigsch F, Bender A, van Buuren B, Tissen J, Nigsch E, Mitchell JB (2006). "Melting point prediction employing k-nearest neighbor algorithms and genetic parameter optimization". Journal of Chemical Information and Modeling. 46 (6): 2412–2422.

[16] Fradkin, Dmitriy; and Muchnik, Ilya; "Support Vector Machines for Classification" in Abello, J.; and Carmode, G. (Eds); Discrete Methods in Epidemiology, DIMACS Series in Discrete Mathematics and Theoretical Computer Science, volume 70, pp. 13–20, 2006

[17] https://montrealgazette.com (accessed September 1, 2018)

Adaptive Automation Strategies for Robotic Prefabrication of Parametrized Mass Timber Building Components

O. D. Krieg[a] and O. Lang[a]

[a] Intelligent City Inc., Canada
E-mail: odk@intelligent-city.com

Abstract –

This paper presents applied research into automated and adaptive robotic prefabrication strategies for a generative platform design enabling mass customized, mass timber modular construction. The development is part of an ongoing effort by the company to bring a holistic approach of design-driven modular mass timber housing and advanced prefabrication techniques into the market of urban densification. The presented work is currently developed for the delivery of two mass timber housing projects with four and 12 storeys, the latter acting as a case study in this paper. In the first part, the paper explains the possibilities and challenges of large-scale robotic fabrication in timber construction as well as strategies for embedding robotics within a digital design workflow. The focus will be on the required change in the industry's design thinking for automation strategies to be effective. In the second part the development of an adaptable construction system suitable for robotic automation will be presented. We argue that while automation of conventional assembly steps might be suitable in some cases, the construction system, and ultimately the individual building parts, must be developed in reciprocity with the capabilities, or the design space, of the machine. The authors share their experience of the application of such an integrated process and its requirements towards the collaboration between, and the automation of, design, construction, engineering, and manufacturing. In its conclusion, the authors argue that a long overdue paradigm change in the architecture and building industry can only be achieved through the complete convergence of all disciplines.

Keywords –

Robotics; Prefabrication; Timber construction; Mass timber; Automation; Modular building; Computational design; Digital fabrication; Affordability; Platforms for life;

1 Introduction

Throughout human history wood has almost always played a dominant role as a building material. Its wide-spread availability in most climate zones, combined with the relative ease of shaping and processing the material allowed humans to develop and refine resourceful, resilient and adaptive construction techniques over thousands of years. In fact, many hundred-year old buildings in China, Japan and Europe are still standing today and prime examples of the creative and intricate constructions made from mostly linear elements.

The required labour and material knowledge for harvesting and processing trees led to a wide-spread but locally differentiated culture of timber fabrication. The interdependency of available materials, tools and culture is evident in the differences between structural systems and buildings throughout the world [1].

However, as the Industrial Revolution took hold of the building industry in the 19th century, it led to a shift from local knowledge and local fabrication to industrialized and globalized mass production, which also brought a shift from value-added products to value-engineered and standardized components [2]. The replacement of manual but customized processes with automated but standardized manufacturing also resulted in standardized construction systems still applied in various forms today. Although standardization brought the advantages of higher quality control and the economies of scale, standardized construction systems lacked geometric flexibility and therefore the ability to adapt to different internal and external conditions. With a dramatic increase in available energy, the focus shifted away from wood and towards the mass production of steel and concrete, which became the primary building material of an industrialized world.

Given the environmental challenges we are facing today, and the struggle for sustainable living and urban densification, it is clear that the future of building construction needs to be energy-efficient, adaptable, lightweight, multifunctional and prefabricated in factory environments. Although wood is one of the oldest

building materials, new engineered wood products such as Cross Laminated Timber (CLT) are answering to all of these criteria. Although wood in its natural occurrence exhibits a great range of variation in material characteristics [3], engineered timber has a high and controllable structural strength, a positive carbon footprint [4], and a very low embodied energy compared to other building materials [5, 6]. Moreover, its mostly localized availability makes the material particularly suitable for the development of sustainable construction methods with short transportation routes [7]. Lastly, its accessibility as a renewable resource makes wood a prime candidate for new design and manufacturing developments, and it comes to no surprise that the general interest in mid-rise and high-rise timber construction has grown significantly over the last decade. On the example of robotically prefabricated mass timber building components, the paper presents an approach to a new paradigm of a sustainable and digitally designed architecture.

2 Context

2.1 Systemic Innovation and Digital Design

The Industrialization initiated a paradigm change in the building industry that, although advantageous at first, proved to be a barrier in our post-industrialized world [8]. During the 19th and 20th century, design, engineering, manufacturing and construction became fragmented and compartmentalized into highly specialized and disconnected disciplines [9]. The result was a highly hierarchical model with specialized organizations that soon developed individual interests opposing each other, ultimately limiting the free movement of knowledge and slowing down innovation. This is particularly detrimental as innovation in architecture is highly dependent on many different disciplines. Research on innovation explains this interdependency with the term "systemic innovation", where multiple and interdependent industries need to change all their processes in order for innovation to take place [10]. Systemic innovation diffuses slowly in project-based industries such as the construction sector. When multiple organizations must act together in order to implement change, innovation is dependent on an interorganizational network [11].

The industry's ongoing resistance to innovation becomes evident in its spending on research and development. In Canada, construction accounted for 8.8% of the nation's 2014 Gross Domestic Product (GDP) while its R&D spending was at 0.06% of the GDP. By contrast, the manufacturing sector comprised 13% of the GDP while its R&D spending was at 3.91% of the GDP [12]. Productivity has lagged accordingly: in the U.S., construction labour productivity has barely gained 10% over the past 70 years, versus a 760% productivity increase in overall economic productivity during the same period. Even worse, for the past 50 years construction productivity has actually declined [8].

A good example for this slow change is the adaption of digital planning processes such as Building Information Modelling (BIM), which requires a multitude of organizations distributed across all hierarchies of the construction industry to employ the technology. And although BIM is slowly being implemented by companies and municipalities today, the rise of digital planning processes has been almost independent from developments of digital fabrication. While both industries have slowly been digitalized in the past decades, they are still within the same hierarchical and fragmented model with limited information exchange and flexibility [9].

While digitalized planning processes may allow for more complex shapes and potentially more adapted and performative buildings, they are still characterized by a traditional top-down design method, leaving questions of producibility and materiality for a later stage [13]. Designers and architects are usually uninformed about manufacturing capabilities, leading them to either overestimate or underestimate the possibilities [14]. This lack of information exchange not only causes higher planning costs through late changes in the design, but it also requires more time and effort for manufacturers [15]. Ultimately, design decisions can not be based on transparency and idea generation but are instead driven by assumed cost efficiencies and risk mitigation.

We argue that in order to truly advance architecture and the building industry, systemic innovation throughout the fields of design, material science, manufacturing and construction is necessary, ultimately leading to a reconceptualization of how architecture is designed, made and delivered, while avoiding the friction inherent in the conventional building industry of today. This is the basis of production immanent planning [16] where reciprocities between fabrication possibilities, materiality and the design process are enabled through interactive digital tools [17]. Only through the convergence of design and manufacturing, and a constant feedback between the disciplines, the true potentials of technological innovation, namely affordability, precision, quality and sustainability will be unlocked.

2.2 Robotics in Timber Construction

The renewed interest in timber construction goes hand in hand with digital fabrication tools such as CNC machines having become well established in the industry. But although most wood processing machines are speeding up typical processing steps, they are task-specific and reinforce the use of already known fabrication methods and construction systems.

Meanwhile, the automobile industry witnessed the introduction of industrial robots in the 1980s, which came together with new manufacturing paradigms such as mass customization [18]. During the 1990s, early exploration of large-scale robotics for automated on-site construction were carried out in Japan [19]. Although technical challenges of building-sized machines on construction sites, and the decline of the building economy proofed to be too big of a hurdle, robotics has again been explored in architectural research more recently [20]. To some extend, this renewed interest is due to the concept of the industrial robot constituting a very different approach. The main difference when compared to process-specific CNC machines is that industrial robots were designed as mass-produced, affordable, high quality and flexible machines. They serve as a generic platform on which different tools and functions can be attached. Their controls are easy to access and can be directly implemented with an adaptive, digital design and manufacturing process.

The potential of industrial robots in timber construction ultimately derives from their extended kinematic range and their adaptability to new fabrication processes, allowing for the development of more complex and differentiated building components [21]. This introduces a shift from machines being made for specific processes towards the building or component being viewed as a product. Following the pattern of innovation consequences during the Industrialization in the 19th and 20th century, technical innovation such as the implementation of industrial robots can have a large impact on the development of architectural design.

Ultimately, innovation in manufacturing techniques for architecture has to go hand in hand with a rethinking of how building systems are conceived. In order to take full advantage of the industrial robot's flexibility, the main focus has to lie in the development of a comprehensive, digital design-to-fabrication workflow with a direct transfer of machine data.

2.3 Potentials of Applied Research

Research in advanced robotic fabrication in timber construction has shown promising results in the reciprocal development of manufacturing processes, construction systems and architectural potentials. The fundamental difference to typical innovation in the construction industry lies in the bottom-up research methodology.

The roof of the Arch_Tec_Lab at ETH Zurich is an example for automation of complex assembly processes that would not be feasible with manual labour (fig. 1). The precise spatial positioning of wooden components requires a new kind of manufacturing process with high precision and without any additional formwork [22]. The roof was designed and developed by the Gramazio Kohler Research group in collaboration with a larger planning team. The roof is made from large wooden trusses that consist of small timber slats stacked together in an alternating manner [23]. Instead of continuous top and bottom cords the trusses are entirely made from short slats nailed together at different angles. The type of nailed connection, the position and order of assembly were all developed in conjunction with a new robotic manufacturing technology that is able to cut, position, attach and photograph in one sequence. The design space derived from this process was explored through the undulation of the roof, which ultimately changed the angle and nailing position of each of the over 94,000 connections.

Figure 1. Robotic assembly of large timber trusses for the ETH Zürich Arch_Tec_Lab. Source: ETH Zürich, Apolinarska 2016 [21]

The Institute for Computational Design and Construction at the University of Stuttgart is leading research for robotic fabrication methods for segmented timber shells. Here, the manufacturing technology is developed in conjunction with a computational design method to generate and control the geometry of each segment of a larger shell structure and output the required manufacturing data [24]. For the development of a construction system made from double-layered, hollow cassettes, the researchers employed industrial robots to precisely assemble and then format each component in a multi-step manufacturing process (fig. 2). The complexity of the manufacturing process and the customized shapes of each building element necessitates a digital design-to-fabrication method and is ultimately only possible because of the adaptability of the developed manufacturing system. This approach allowed the researchers to design extremely lightweight and efficient shell structures [24].

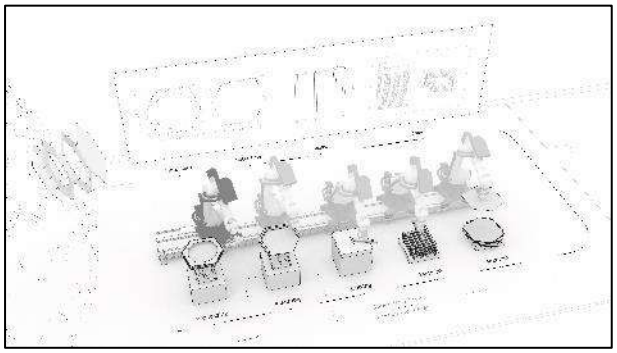

Figure 2. Robotic manufacturing process for hollow sandwich cassette panels. Source: ICD University of Stuttgart [22]

2.4 Project Aim and Application

Although industrial robots have size and weight restrictions that originally related to car manufacturing, the above examples show their potential application for the prefabrication of medium-scale building components for large-scale structures. They also show how adaptability can play an important role when developing a completely digital workflow in relation to the available machines and tools.

While traditional processing steps and construction systems have been developed in relation to human strength and size [1], so are newly available machines related to the size and weight of building elements, as well as to the dexterity required for assembly or processing. It can therefore be argued that the machine setup defines the design space of the manufacturing process as much as the material.

The authors have applied the approach of production-immanent planning in the development of a mass timber building system. The aim of this development is the careful application of innovative manufacturing techniques, and therefore bridging the gap between academia and practice. In this process, industrial robots are applied for additive processes in order to allow for the assembly of heavy, medium-sized elements into larger panels. The task of formatting those elements stays within the realm of standard CNC machines but is implemented within the digital design-to-fabrication workflow in order to allow for a direct output of machine data. This holistic approach to design and manufacturing not only streamlines the entire process but, more importantly, allows for an inherent flexibility and adaptability without additional complexities. In its application, the developed processes can combine the consistency and quality control of mass production with the variability and individuality of cultural and societal responses to the built environment. Only then can quality, performance, scalability and differentiation replace repetition and manual construction.

3 Methods

The development presented in this paper is situated within the context of the architecture and building industry's need for affordable, sustainable, customizable and qualitative urban living. Through an integration of design, architecture, manufacturing and off-site prefabrication, the authors are introducing a new paradigm in the construction industry: empowering people to live better and more sustainably with the help of highly digitalized design and fabrication processes.

While the manufacturing development is based on robotically assisted, complex assembly processes, it is also connected to a larger development effort of parametric design methods that allow for a product-design approach in architecture, incorporating the entire value chain from design to delivery of innovative buildings. The main motivation is not to build shapes that were otherwise not possible, but to develop the ability for a variable response on a consistent platform.

3.1 Platform-Based Design

In the context of manufacturing automation, the concept of platform-based design is one of the key factors for allowing architecture to embrace a product-oriented design approach incorporating fabrication, material, engineering and functionality. Platform-based design is an integration-oriented design approach for the systematic use of an underlying logic, system, or platform, for the development of complex products that share compatible hardware or software [25]. This allows to establish a general knowledge base on which variant forms of the same solution can be realised. It also directs the development of the design process towards a class of products that can have a variety of design solutions for customized requirements within a common framework [26]. While platform-based design has been an established and decade-old concept in many other industries such as car manufacturing, its application in the highly individualized construction industry has not yet been explored to a level that would satisfy the need for customization in relation to a building's context, owner and tenants. By developing a platform within a computational design framework, the focus lies on a high degree of variability in the design process.

The platform is based on the modularised or panelised prefabrication of mass timber building components that can be shipped and assembled on site. The main structural components are defined by their relationship to the modular framework, and their geometry is derived from a parametrically defined logic further explained in chapter 2.3. For the explanation of the building system and its robotic assembly the authors will focus on the floor panels, which can also be assembled into volumetric modules at a later stage in the process.

The platform can be described as a four-sided but not necessarily rectangular, panel made from two layers of smaller Cross Laminated Timber (CLT) panels that are interconnected with smaller Laminated Veneer Lumber (LVL) beams. This panel is later connected to a varying number of columns on site, which are placed on the axis of the panels' borders and intersect with the panels in a way that allows steel connectors to connect and ensure a continuous force-flow. The panels are further connected between each other with thin strips along their edges to form a structurally continuous slab and allow for lateral force transer. Connections to concrete cores or CLT shear walls are special cases for which specific details have been developed. While smaller CLT panels are chosen as the main structural element due to their global availability, the width of a panel is not necessarily constrained by shipping container dimensions as they can be transported vertically on trucks.

The exact arrangement of CLT panels within one floor panel, their width and length, and the number of columns to be connected to a specific panel is parametrically defined and derived from a 3D model that incorporates design intent and structural requirements (fig. 3). The panels and their shapes are generated in an algorithm taking into account all connection details that will lead to certain penetrations or cuts within the panels. Following the geometry of a boundary condition from a preceding digital design process, the design space is ultimately defined by transportation constraints, but generally between 25 ft and 53ft in length, and between 10 ft and 40 ft in width (fig. 4). This allows to accommodate studios as well as up to 3BR and double-storey apartments.

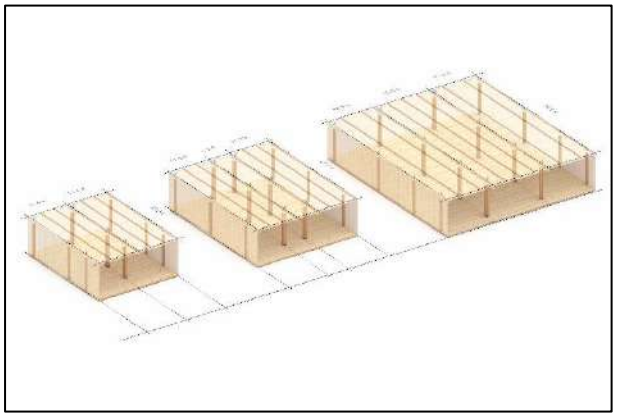

Figure 3. Visualisation of the parametric model adapting to the design space. The individual building elements populate the available space and obtain certain connection details through locators

3.2 Integrated Robotic Assembly

Timber is a great fit for modular construction due to its machinability and relatively low weight, meaning it can be more easily transported and assembled on site when compared to steel or concrete. Mass timber specifically, however, regardless of its structural and fire safety advantages compared to lightweight timber frame, is leaving the realm of human-scale building elements due to its weight and size, and therefore emphasizing the need for advanced manufacturing techniques. While many building materials and construction systems have been developed for the human scale and manual assembly, focusing on robotic processes allows for a reconceptualization of building element dimensions and weights. Most medium-sized mass timber elements are within the size and weight range of common industrial robots and therefore ideal for the introduction of automated and adaptive manufacturing. As a result, intersection points between human labour and robotic processes need to be carefully integrated.

The presented digital design process is developed in conjunction with appropriate manufacturing techniques and their possibilities: The arrangement of CLT panels and their connections were developed to be executed by similar but adapted robotic processing steps with offline programming. Contrary to traditional CAD/CAM processes where the geometry of the building element is imported into special software for machine code generation, the digital design-to-fabrication workflow developed by the authors generates machine code directly with the geometry. This seemingly complex digital connection between manufacturing and design is in fact easier as the geometry and meta-data of every building element is already parametrically generated, and all information can be further processed to generate the required machine code within one program.

The main development goal was to automate the process from CNC formatting to the assembly of the main structural components visualised in the previous chapter. Not only would this allow for an expedited assembly process but also reduce the complexity of manually measuring and laying out heavy timber elements. Instead, previously CNC-formatted timber elements are being handled by industrial robots, put into a measurably correct position and joined together. Robots are positioned on tracks parallel to either side of the panels in order to pick and place material as well as to connect elements with screws and nails (fig. 4). The size of the elements and the dimensions of the robotic manufacturing cell was developed in relation to the required design space. The manufacturing process is currently being implemented at the company's factory. First prototypes will be produced in the first half of 2019 and full manufacturing capacity will be expected by the end of the year.

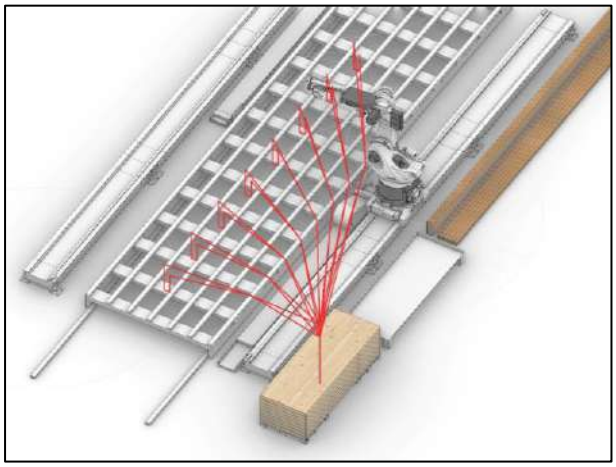

Figure 4: Diagrammatic overview of the robotic assembly process with the highlighted tool path of a robot for handling a stack of CLT panels during assembly

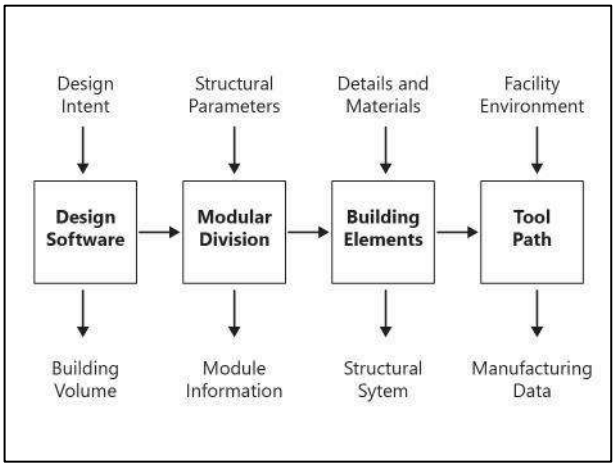

Figure 5. Flow chart of the design process towards the fabrication model. The early design model gets transferred to a modular division, its building elements and finally machine data

3.3 Parametric Design Process

The automatic generation of building components and manufacturing data is preceded by a digital design process that allows the exploration of different building designs within the design space of the construction system. In a digital design process, larger building volumes with up to 18 storeys are subdivided based on the requirements of the modular or panelised construction. After the subdivision, several structural parameters can be inserted in order to control the position of columns and concrete cores if necessary. The modular subdivision will adjust pass on the geometric information together with structural information in the form of locators. Each building group essentially acts as a data container, continuing to collect information as the digital process continues (fig. 5). When populated with all structural elements described in chapter 2.1, each element is already connected to information regarding its robotic assembly. In the case of the CLT panels, the assembly process can be stored depending on the overall size of a floor panel and the position of the CLT panel within it. Hence, each CLT panel has a certain number of geometric locations in its data model, along which the industrial robot will pick and place it in relation to the facility environment. These locations are previously defined and will result in tool path instructions for the robot. In the algorithm, all building elements of one building group will be processed simultaneously in order to export one file for the manufacturing process. A similar process is also created for the generation of CNC machining data before the assembly. The geometry of each building element is directly transferred into the necessary machining steps in order to cut the boundaries and penetrations of each CLT panel.

4 Result: High-Rise Modular Buildings

The platform-based design and manufacturing process has been developed to serve a multitude of urban infill developments ranging from 4 to 18 storeys, with sites ranging from 33 to 400 ft in width. To date, the platform has been tested on a dozen project proposals, six of which are currently in the design process. Among one of the first to showcase the platform in a real-life, large-scale application is a project called Corvette Landing (fig. 6)

Corvette Landing is a 12-storey mixed-use development designed to transition the still low-density single- and multi-family Township of Esquimalt BC, adjacent to Victoria. Planned and developed as an industry-first panelized and prefabricated mass-timber hybrid building, it seeks to combine the low carbon footprint with a high level of livability and expedited construction. The building is an affordable housing project to be Passive Haus certified in order to act as an example for adaptable, repeatable, scalable and sustainable condominium buildings.

Mass timber construction based on the building system described in this paper is applied from the second floor up. Around 150 panels will be prefabricated in the company's manufacturing facility specifically developed for this kind of application. On site, the panels and columns will connect to so-called concrete micro-cores necessary for lateral stability in this high seismic zone. As the elevators and stair cases are in an external, open courtyard, the concrete cores are only as big as a bedroom in this project.

The project received rezoning and development permit approval from the Township of Esquimalt due to its innovative character, green building strategy, and the

broken-up and terraced building volume. It passed the Review Board for Site Specific Regulation by the BC Housing Ministry's Building Safety Standard Branch in 2018 and will be one of the first mass timber high-rise housing projects in Canada. Start of construction is scheduled for 2019.

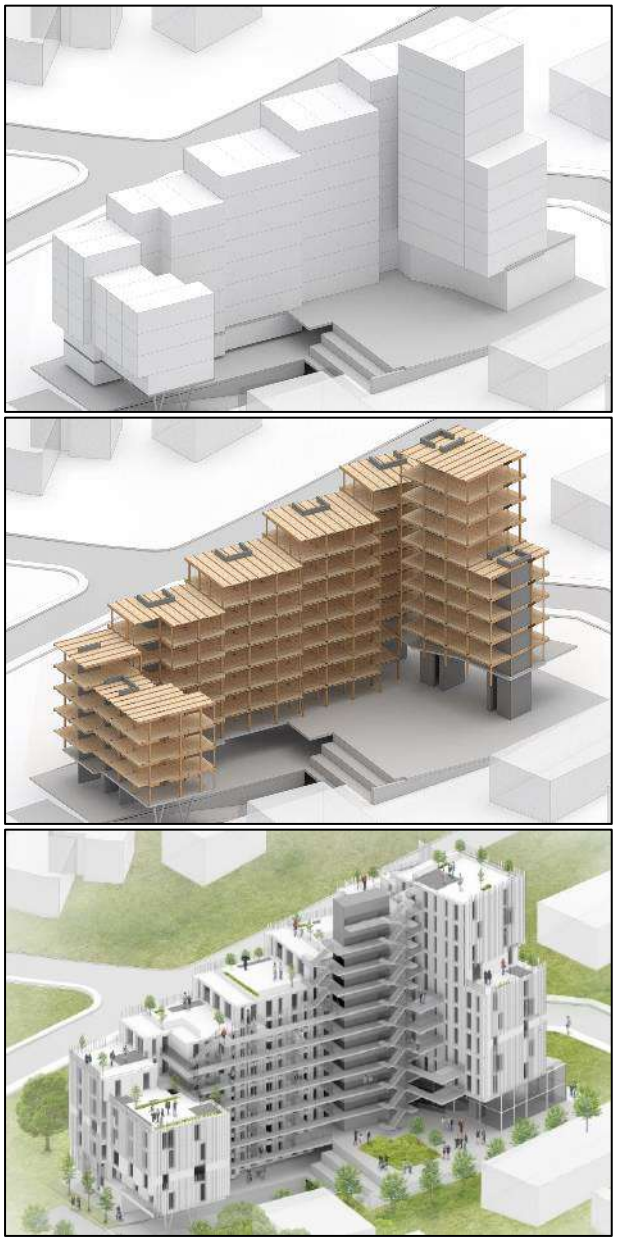

Figure 6. Visualisation of the modular layout (top) and the resulting construction system (bottom) for Corvette Landing. Each panel has a different geometry due to the setbacks, column positions and concrete cores

5 Conclusion

The development presented in this paper is a manifestation of a new paradigm in architecture and construction, converging design, material, structure and manufacturing. It enables the urgently needed transformative change of the urban housing sector towards a resilient urban densification and sustainable and livable future.

Mass timber construction most notably provides the opportunity to develop more adaptive and geometrically differentiated construction systems while still being realized with a certain economic efficiency. However, in order to adapt a construction system and its building parts to specific structural or architectural situations, a parametric design process and a direct and automated fabrication data generation is required.

We argue that in order for a paradigm shift to take place in the architecture and construction industry, already existing knowledge needs to be combined, calibrated and exchanged. A wholesale shift towards prefabricated buildings with mass timber components is challenging but possible. Collaboration across the spectrum of industry players will be necessary. The barriers to innovation run deep and cannot be solved by one actor alone.

6 Acknowledgements

The authors would like to thank their colleagues at LWPAC and Intelligent City as well as their consulting partners for their support in the development of the methods and results described in this paper. Part of this research and development was funded by the Industrial Research Assistance Program (IRAP) of the National Research Council Canada.

References

[1] Schindler C. Die Standards des Nonstandards. In *Graz Architecture Magazine*, 06:181-193, 2010.

[2] Correa D., Krieg O. D. and Meyboom A. Beyond Form Definition: Material informed digital fabrication in timber construction. In *Digital Wood Design*, Springer, Berlin, 2019.

[3] Dinwoodie J. M. *Timber: Its Nature and Behaviour*. E&FN Spon, London, 2000.

[4] Kolb J. *Systems in Timber Engineering: Loadbearing Structures and Component Layers*. Birkhäuser, Basel, 2008.

[5] Alcorn A. *Embodied Energy Coefficients of Building Materials*, Centre for Building Performance Research, Victoria University of Wellington, 1996.

[6] Gordon J. E. *Structures: Or Why Things Don't Fall*

Down, Da Capo Press, Boston, 2003.

[7] Krieg O.D., Schwinn T. and Menges, A. Integrative Design Computation for Local Resource Effectiveness in Architecture. In *Urbanization and Locality: Strengthening Identity and Sustainability by Site-Specific Planning and Design*, pages 123–143, Springer Science and Business Media, 2015.

[8] Barbosa F., Woetzel J., Mischke J., Ribeirinho M. J., Sridhar M., Parsons M., Betram N., and Brown S. *Reinventing Construction: A Route to Higher Productivity*. McKinsey & Company, McKinsey Global Institute, 2017.

[9] Kieran S. and Timberlake J. *Refabricating Architecture. How Manufacturing Methodologies Are Poised to Transform Building Construction*, McGraw-Hill, New York, 2004.

[10] Taylor J. E. *Three Perspectives on Innovation in Interorganizational Networks: Systemic Innovation, Boundary Object Change, and the Alignment of Innovations and Networks*. Stanford: Stanford University, 2006.

[11] Taylor J. E. and Levitt R. E. Inter-Organizational Knowledge Flow and Innovation Diffusion in Project-Based Industries. In *System Sciences HICSS'05 Proceedings of the 38th Annual Hawaii International Conference on System Sciences IEEE*, pages 1–10, 2005.

[12] The Conference Board of Canada. Provincial and Territorial Ranking, Business Enterprise R&D. http://www.conferenceboard.ca/hcp/provincial/innovation/berd.aspx. Accessed: 20/01/2019.

[13] Kimpian J., Mason J., Coenders J., Jestico D. and Watts S. Sustainably Tall: Investment, Energy, Life Cycle, in: *ACADIA 09: reForm() - Building a Better Tomorrow*, pages 130-143m Chicago, USA, 2009.

[14] Menges A. Morphospaces of Robotic Fabrication. In *Proceedings of the Robots in Architecture Conference*, pages 28-47, Springer, Vienna, 2012.

[15] Abdul-Rahman H., Chen W. and Yap Boon Hui J. Impacts of Design Changes on Construction Project Performance: Insights from a Literature Review. In *Proceedings of the 14th Management in Construction Research Association Conference 2015*, Kuala Lumpur, Malaysia, 2015.

[16] Brell-Çokcan S. and Braumann J. A New Parametric Design Tool for Robot Milling. In *Proceeding of the 30th Conference of the Association for Computer Aided Design in Architecture*, pages 357– 363, New York City, 2010.

[17] Schwinn T., Krieg O.D. and Menges A. Behavioral Strategies: Synthesizing Design Computation and Robotic Fabrication of Lightweight Timber Plate Structures. In Design Agency, Proceedings of the 34th ACADIA conference, pages 177-188, Los Angeles, 2014.

[18] Pine II B. J. Mass Customization: *The New Frontier in Business Competition*. Harvard Business School Press, Massachusetts, 1993.

[19] Cousineau L., and Nobuyasu M.: *Construction robots: the search for new building technology in Japan*. ASCE Publications, 1998.

[20] Bechthold M. The Return of the Future: A Second Go at Robotic Construction. In: *Architectural Design*, 80(4), 116-121, 2010.

[21] Menges A., Schwinn T. and Krieg O.D. Landesgartenschau Exhibition Hall. In *Interlocking Digital and Material Cultures*, pages 55-71, Spurbuchverlag, Baunach, 2015.

[22] Helm V., Knauss M., Kohlhammer T., Gramazio F. and Kohler M. Additive robotic fabrication of complex timber structures. In *Advancing Wood Architecture – A Computational Approach*, pages 29-44, Routledge, Oxford, 2016.

[23] Apolinarska A.A., Knauss M., Gramazio F. and Kohler M. The Sequential Roof. In *Advancing Wood Architecture – A Computational Approach*, pages 45-58, Routledge, Oxford, 2016.

[24] Krieg O. D., Bechert S., Groenewolt A., Horn R., Knippers J. and Menges A. Affordances of Complexity: Evaluation of a Robotic Production Process for Segmented Timber Shell Structures. In *Proceedings of the 2018 World Conference on Timber Engineering*, pages. 1-8, Seoul, Korea, 2018.

[25] Bailey B., Martin G. and Anderson T. *Taxonomies for the Development and Verification of Digital Systems*. Springer, New York, 2005.

[26] Jiao J. Simpson T.W. and Siddique Z. J. Product Family Design and Platform-Based Product Development: A State-of-the-Art Review. In *Journal of Intelligent Manufacturing*, 18(1):5-29, 2007.

Semantic Network Analysis as a Knowledge Representation and Retrieval Approach Applied to Unstructured Documents of Construction Projects

R.R. Aragao[a], and T.E. El-Diraby[b]

[a]Petrobras – Petróleo Brasileiro S.A., Brazil; University of Toronto, Canada (alumnum)
[b]Department of Civil & Mineral Engineering, University of Toronto, Canada
E-mail: r.aragao@petrobras.com.br, r.aragao@alum.utoronto.ca, tamer@ecf.utoronto.ca

Abstract –

Reusing knowledge from past projects is a critical task in construction, given the increasing complexity in such projects: numerous stakeholders, a multi-disciplinary domain, and multi-objectives besides the traditional ones such as cost and schedule. Unstructured data, such as progress reports and minutes, is a rich source of knowledge that can be revisited in projects as the contextual nature of documents permits describing the nuances of the interrelations and uniqueness of each project. However, texts are difficult to formalize in a way that the process of retrieval and analysis of relevant knowledge be automated using computers. In this paper, we present an innovative approach that encompasses formalization, retrieval, analysis, and reuse of knowledge from case studies of past construction projects. Assuming that energy is an objective, the cases are represented as a network of common concepts found in every project. The nodes are the concepts, and the links between them are established whenever there is an association between two concepts that affects the energy use in construction. Conversely, the comments of team members of a current project can also be captured and represented using the same standardized set of concepts. Using network analysis, we can retrieve the most relevant cases, which are similar to the current project, study the most important concepts, extract clusters of concepts, and capture the nuances of the cases in a more objective way. A concept map based on the literature and three case studies of past oil and gas projects are developed to undertake this approach. We evaluate the method by simulating the collaborative environment of one of the cases through the participation of ten volunteers in Green 2.0, an online media to discuss construction projects. At the end of the test, we perform a correlation between the networks of the test and the case study.

Keywords –

Knowledge retrieval and representation; Unstructured data; Network analysis; Blockmodeling; Construction management; Energy use

1 Introduction

The primary objective of this work is to utilize network theory to help formalize and consistently process unstructured data (mainly text) in construction management. The aim is to support capturing, retrieving and coordinating knowledge reuse during project deliberations. Documents and reports developed based on the input or deliberations of project stakeholders are a fundamental container and widely used means to capture construction knowledge. This fact is primarily due to the subjectivity of the domain. In general, planning and managing construction projects depend on the reuse of implicit knowledge and expertise gained in previous projects. The challenge is how we can capture and reuse knowledge contained in unstructured data developed by project stakeholders. How can one externalize the tacit knowledge contained in them? Doing so in an efficient manner has been increasingly becoming important due to the growing complexity of projects. First, due to the increase in the number of stakeholders who have to participate in decision making. Second, the increase in the number and diversity of decision criteria. For example, in addition to the traditional cost and schedule, project decision makers have now to consider additional issues such as environmental impacts as well as energy consumption. Third, compounding the challenges, many of the issues are contested—for example: how to identify and measure impacts on communities and sustainability.

Foundational approaches, such as rule-based expert systems and knowledge bases, have significant limitations in this milieu [1]. These limitations are due to the contextual nature of projects. Each project has

unique composition/attributes and boundary conditions, which influence the relevance and interpretation of rules as well as the ability to adapt them to the needs of the project context. Semantic models of knowledge, such as ontologies, provide a very suitable approach to handle such subjective and unstructured nature of knowledge [2]. However, the static nature of ontology has shortcomings [3]. This constraint, again, is due to the contextual nature of construction knowledge. More importantly, knowledge constructs (models) are "relativistic" as they depend on the judgment of stakeholders: it is typically quite difficult to achieve full (standardized) agreements between stakeholders.

Unstructured data, such as online discussions, minutes of meetings, e-mails, progress reports, and case studies have recently gained the attention of knowledge management (KM) practitioners [4,5]. This remark is because such corpus represents subjective knowledge in semantic forms. They are also, by default, context-sensitive. However, possibly, the most important advantage of using project text corpus as a source of knowledge is that they are the results of intense and critical dialogue between experts. Meetings transcripts, online discussions, e-mail threads, final reports and project case studies represent venues for knowledge exchange, conflict resolution, innovation, and consensus creation. Hence, it is not surprising that unstructured data are more informative than other sources.

Given that a good deal of the knowledge in the domain is textual, can using semantic network analysis be helpful? Instead of free text, typically used in case studies, can we build networks of project concepts and benefit from the traditional network analysis measures in enhancing the formality and objectivity of analyzing project knowledge? For example, what can we learn about a project if we study the centrality of, say, safety in its concept network? If two concepts, for instance, safety and excavation, are not linked in the concept network, does this reflect incomplete analysis?

In other words, the specific problem that this research project aims to address is that pure textual representation of project knowledge in the case studies may not be an optimal solution. First, the retrieval of such cases for future use can be inefficient. Typically, this would be done through a set of keywords recorded by the case developers or suggested by a content analysis algorithm. The automatically generated topics are suggested based on word frequencies and associations. This procedure, however, does not necessarily capture coherent or essential topics from a text corpus. While human tags (the manual categorization of the text in meaningful topics) are more superior, their standalone nature does not allow for capturing the interrelationships of case concepts. Furthermore, such tags are never optimal (they cannot cover all possible future needs). Second, it is difficult for upper management to conduct any formalized analytics using just a set of documents. Beyond the benefits of case reuse to guide new projects, cross-case analysis can detect trends, suggest and emphasize concept relationships (for a more detailed review of works published in this field, please see [6]).

Compared to other stages of the project life cycle, the construction phase has received the least attention from researchers [7]. This fact is mainly because of its limited contribution to the overall energy consumption of a project but, more importantly, it is the unique challenges of the construction stage. While the energy use in construction has been a topic of constant debate in academia [8,9], this scope falls much more under the umbrella of the construction knowledge management domain than energy efficiency or life cycle assessment. Hence, this research is not an energy assessment or a quantitative estimate of the energy use of the construction phase.

For such a subjective domain, learning from historical project cases can be very helpful. They map prior project conditions and their relationships to project performance (about energy); and document pitfalls, solutions, and lessons learned. The textual nature of these cases allows the user to contextualize the options and challenges of the project and gain a deeper understanding of the relevance of the listed best practices to a new project.

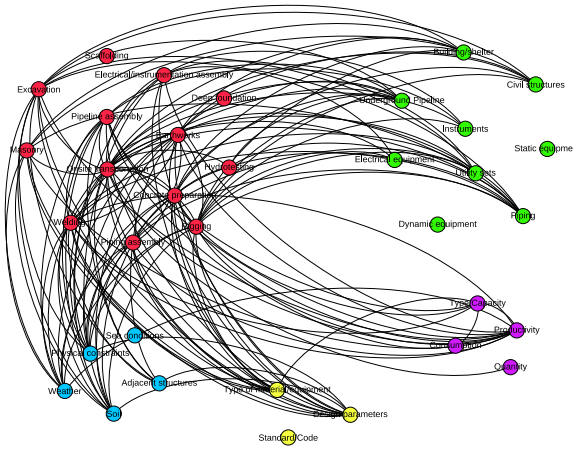

Figure 1. The concept network for one of the case studies developed in the research

The main objective of this research is to realize a system to use network theory to help formalize text corpus of project cases and, possibly, other documents to facilitate the externalization of tacit knowledge in an objective and reusable manner. The main contribution of this research is the creation of an approach that

formalizes the knowledge of projects embedded in unstructured data through transferring text into a network of concepts. In more specific terms, by using the formalized networks of concepts, the method can capture and reuse the knowledge from previous project cases to support the deliberations of the decision-making team during the construction planning of future projects.

The proposed system will permit stakeholders to collaborate, investigate, formalize, and capture the knowledge embedded in unstructured data to manage energy use in the construction phase of O&G projects.

2 Methodology

The proposed approach relies on the following scenario: using manual or automated means, the network of concepts of a current project is established. The network can be developed through semantic analysis of project documents or a summary report of a project, hopefully, developed by a group of collaborators. At the same time, during a retrieval process, the project team was able to find relevant cases that are similar to the current project. Figure 1 shows an example of the graph of a network of concepts of one of these case studies. The team then is interested in discovering (or externalizing) the most relevant knowledge constructs of this case. The goal is to help them sift through the complexity of the network: what are the concepts that have significant interaction within the current project. Alternatively, help them externalize and discover some of their implicit knowledge that the network captured for them. For that, they use a prior generic network built on the common sense knowledge of a group of experts. Blockmodeling, in this case, is used to rearrange this generic network into meaningful blocks that are easier to visualize and to interpret. A manager can work on comparing the blocks of several cases, the current project, and the generic network to study differences of patterns.

The main steps of the methodology are as follows:

a) Based on the literature review, we present a concept map, which is a simplified taxonomy of concepts associated with the energy use in construction. The proposed concept map guarantees the networks are always represented on the same base of concepts Figure 2.

b) We develop three case studies of past oil and gas projects in Brazil. In-depth semi-structured interviews of project team members are the main source of evidence of each case. A minimum number of participants should be interviewed until the authors reach the saturation of information, in which the information provided by the interviewees begin to repeat and therefore no additional interview is necessary [10]. The participants respond open-ended questions about the challenges, best practices, opportunities, and risks that affects or could affect the energy use during the construction phase. A profile of responses is generated for each interview. In each profile, the research team identifies keywords or expressions that semantically resembles the concepts from the base taxonomy (letter “a”). A relation or a link is established whenever there is a semantic association between two concepts that affects the energy use in the construction phase. These relations are transferred to an adjacency matrix, and a network of concepts is represented for each case study, such as the one in Figure 1. The procedure above permits to represent any case study as a network of concepts. Dealing with case studies as a formalized network of pre-established concepts allows us to apply several metrics and indexes to study them by using network analysis. For example, if the discussions or social interactions of members of a current project, such as an online discussion tool, are captured using the same procedure discussed in letter “b”, a QAP analysis [11] of the current and case networks offers an interesting retrieving method of similar past projects.

Supposing that the three case networks presented in this article were retrieved from a repository of cases using such alternative, now we want to compare the retrieved cases with a generic network, which does not reflect any specific project. Exploring the differences between project-driven cases and a general network can shed light on what relevant knowledge the past project has to offer so that it should be taken into consideration in the new project.

c) To collect the data for the generic network, we conduct an expert survey [6]. As opposed to the project-related cases, the survey is conducted to collect the common knowledge of the participants without any project in mind. To do so, we transform the 573 possible relations of the concept map in close-ended questions, divided them into fourteen online surveys and submit them to experts in the O&G field in Brazil. The questions are multiple choice, in which the answers follow an intensity rating scale: no effect/low effect/moderate effect/high effect, with each answer having a score from 1 to 4, respectively. As a criterion to create the relations in the generic network, we establish a link or tie between two concepts whenever the average of all responses for each question was greater than 2.5. Three examples of questions are listed below.

- Does excavation affect the energy use during the construction of utility systems?
- Does welding affect the energy use during the assembly of piping?
- Does weather affect the energy use of earthworks?

d) Once the data collection phase is concluded, we represent the survey answers as a three-mode generic network, in which the ties between the nodes of the same category are disregarded.

e) The steps below allow us to contrast the knowledge constructs between each case and the generic network, by using a three-mode generalized blockmodeling approach [12] to create a baseline (a blockmodel) from the generic network as follows:

- We pre-define the clusters of the construction activities based on their typical function in construction sites and our prior knowledge of the cases. This assumption increases the chance to find substantive blocks using the blockmodeling method.
- As an input for the blockmodeling, we define the number of clusters and the type of blocks allowed to form during the optimization. With the clusters of the activities and the constraints established beforehand, the algorithm attempts to reorder the remaining concepts in such a way that it fulfills the defined requirements.
- After running the blockmodeling with the constraints defined above for the generic network, we select the solution that provides the best interpretation. The status of generic network is assigned to the best solution.
- The adjacency matrix of the case networks are rearranged to fit the blockmodel obtained from the previous procedure. In this case, the interest is in the different blocks. The different blocks and their inter-relations are interpreted and compared with the baseline in the light of the case studies, and then these findings are reported.
- We introduce a block analogy index that quantitatively assesses the overall and the block-to-block similarities of the case-based networks. The less similar the case network is to the baseline, the more case-specific, contextual the project is.

Construction Activities		Systems		Factors	
1	Excavation	14	Civil structures	Design	
2	Deep foundation	15	Building/shelter	23	Type of material/equipment
3	Welding	16	Static equipment	24	Design parameters
4	Piping assembly	17	Underground pipeline	25	Standard/Code
5	Earthworks	18	Piping	Site characteristics	
6	Rigging	19	Electrical equipment	26	Soil
7	Concrete preparation	20	Instruments	27	Sea conditions
8	Electrical/instrumentation	21	Dynamic equipment	28	Weather
9	Pipeline assembly	22	Utility sets	29	Adjacent structures
10	Hydrotesting			30	Geographical location
11	Masonry			Resources	
12	Onsite transportation			31	Type/Capacity
13	Scaffolding			32	Consumption
				33	Productivity
				34	Quantity

Figure 2. The proposed concept map (taxonomy) of energy concepts

3 Results and Discussions

The results are presented in the following sections for the concept networks of projects A, B, and C, and the combined case. More details of the case studies can be found in [6]. The combined case is a Boolean sum of the three networks of cases, and is an attempt to produce a network that generically represents the three cases. Three analyses are presented: similarity, centrality-level, and blockmodeling. Detailed information for each analysis can also be found in [6].

3.1 Similarity of Networks

We used the concept of dissimilarity to develop a retrieving process. Two nodes have a dissimilarity equal to 1 (one) if they do not share any one of their neighbors. In contrast, they are structurally equivalent (or 100% similar) if the dissimilarity is 0 (zero) or, in other words, they share all their ties.

Using UCINET, we used the Quadratic Assignment Procedure (QAP) regression analysis to calculate the correlation coefficient and its respective p-value for each pair of networks. In the dissimilarity matrices, each cell of the matrix is the dissimilarity calculated for each pair of nodes of the original studied matrix). The dissimilarity is zero for the elements of the diagonal of the matrix, since each node is 100% similar to itself.

Table 1. Correlation coefficient of the dissimilarity matrices using QAP regression of the three case studies and two combined case networks

	Project A	Project B	Project C	Combined case 1	Combined case 2
Project A	1	0.516	0.309	0.720	0.695
Project B	0.516	1	0.333	0.690	0.728
Project C	0.309	0.333	1	0.502	0.433
Combined case 1	0.720	0.690	0.502	1	0.659
Combined case 2	0.695	0.728	0.433	0.659	1

Table 2 P-values of the similarity matrices using QAP regression

	Project A	Project B	Project C	Combined case 1	Combined case 2
Project A	0	0.0003	0.0003	0.0003	0.0017
Project B	0.0003	0	0.0003	0.0003	0.1310
Project C	0.0003	0.0003	0	0.0003	0.1060
Combined case 1	0.0003	0.0003	0.0003	0	0.0017
Combined case 2	0.0017	0.1310	0.1060	0.0017	0

Table 1. presents the correlation coefficient for each pair of the similarity matrices using the QAP regression

on UCINET. Each concept network has a similarity matrix. Since the correlation coefficient can assume any value between -1 and 1, the values in the diagonal are one because, indeed, the correlation between each matrix and itself is perfect. Nevertheless, the results of Table 1 must be carefully cross-checked with the p-values in Table 2. To be confident that a strong correlation exists between the structure of two networks, assuming a 95% confidence interval, the p-values in should be lower than 5% or 0.05, meaning that such correlation coefficient is statistically significant.

By analyzing the results, it is observed that the network of Project A correlates better with Project B when compared to Project C (0.516 against 0.309). This correlation probably exists because, although Project A and B have different logistics and environments, both construction projects are characterized by having a high volume of piping, static equipment, electrical/automation, and utility works. The correlations between the case studies are not so little that one can affirm the networks are not part of the same domain, but they are not high enough to be considered useless in dealing with different cases whose network representations are the same.

Regarding the combined cases, each one being an attempt to represent the three case studies generically, the results of Table 1 for the correlation coefficient were considered relatively satisfactory with some limitations [6].

3.2 Centrality Measures

Centrality measures are used to identify the most prominent nodes in the network. The structure of the concept networks suggests that the choice of the most suitable measure depends on the category of node. As the concept networks are directed, we opted to calculate the out-degree, which just considers the number of outward ties. The construction activities are in the intermediate layer of the network, and they serve as a bridge connecting the factors and the physical system; thus, betweenness is more appropriate to detect the more important construction activities. Regarding the systems, we considered not only the nodes with the highest degree, but also the degree of the nodes each node is connected to. In this sense, the in-eigenvector centrality is more indicated [10].

Table 3 presents the out-degree, betweenness, and in-eigenvector centralities for Project A. The table is truncated for the sake of saving space. Concerning the 13 construction activities, rigging (or material handling), onsite transportation, and scaffolding are the most central activities considering the betweenness centrality. These activities were cited several times by the respondents during the interview phase. However, no participant directly indicated the importance of these construction activities as being the most influential for the energy expenditure during construction. This fact could be better investigate by looking at their betweenness centrality. As a brownfield located in an existing industrial plant in full operation, the performance of this project was highly influenced by the numerous restrictions regarding access control, limited layout, and existing equipment or buried structures. These limitations ended up shaping the logistics of the construction, which is formed by the transportation of materials and workforce, material handling, and assembly/disassembly of scaffolds due to work at higher heights. Using the betweenness centrality permitted the research to elicit other influential activities other than the obvious energy-intensive ones, such as welding, excavation, deep foundation, and more.

Table 3. Out-degree, in-degree, betweenness, and in-eigenvector centralities for the network of Project A. The values are presented in descending order to highlight the most central activities/factors

Activities/factors	Out-degree	Betweenness	In-Eigenvector
Construction activities			
Rigging	9	73.261	0.363
Onsite transportation	8	28.152	0.246
Scaffolding	7	19.894	0.297
Welding	4	8.753	0.363
Masonry	9	6.673	0.066
Excavation	8	6.651	0.066
Physical systems			
Piping	0	0.000	1.000
Static equipment	0	0.000	0.964
Civil structures	0	0.000	0.938
Utility sets	0	0.000	0.860
Electrical equipment	0	0.000	0.654
Instruments	0	0.000	0.654
Design factors			
Design parameters	12	16.012	0.000
Type of material/equipment	9	0.000	0.000
Standard/Code	5	0.000	0.000
Site characteristics			
Geographical location	15	0.000	0.000
Adjacent structures	13	0.000	0.000
Soil	5	0.000	0.000
Resources factors			
Productivity	11	49.012	0.117

Type/Capacity	6	51.975	0.206
Consumption	6	4.000	0.117
Quantity	1	0.000	0.000

The out-degree of site characteristics, design and resources factors is the most appropriate centrality to highlight the most prominent factors. The schedule of this project was highly challenging, and the volume of activities provided by the design (scope) had a critical role: the larger the scope is, the higher the energy use. As such, the centrality analysis revealed that the node "design parameters" has the highest out-degree in the design category. Regarding site characteristics, the geographical location and adjacency structures have the highest out-degree. These two factors are closely related to the causes that affected the construction activities mentioned above (access control, limited layout, and the presence of buried structures).

Looking at the in-eigenvector measures of the physical systems, it was found that piping, static equipment, and civil structures were the most impacted systems concerning energy use. As a matter of fact, these four systems encompassed most of the scope of the project. In this regard, static equipment is a proxy for the five atmospheric storage tanks, which required large volumes of rigging, onsite transportation, scaffolding, and welding. Piping and utility systems are portrayed here because of the amount of piping assembly, which also involves welding and energy-intensive logistics. Finally, civil structures received a high in-eigenvector degree because of the works regarding excavation and deep foundation services for the tanks and other pieces of equipment.

3.3 Blockmodeling

To find a meaningful blockmodel for the generic network that can be compared with the networks of the case studies, four subgroups of activities are created according to a functional classification: logistics, heavy-duty equipment, structural civil works, and electro-mechanical assembly. Onsite transportation, rigging, and scaffolding are the three activities that best represent the logistics in construction sites. Excavation, earthworks, and pipeline assembly are characterized by demanding pieces of heavy-duty equipment, such as excavators, dozers, graders, and pipelayers. Structural civil works encompass deep foundation, concrete preparation, and masonry works. Finally, electro-mechanical assembly, which significantly differs oil and gas projects from other installations, is comprised of electrical/instrument assembly, piping, welding, and hydrotesting. In the optimization blockmodeling process, these four subcategories of activities are four pre-established clusters. Hence, the blockmodeling algorithm attempts to create blocks by permuting systems and factors to match the pre-specified clusters of activities, the required of blocks types and the constraints. Since the logistics, heavy-duty equipment, structural civil works, and electro-mechanical services have different characteristics, it is expected that the final optimized blocks capture clusters of meaningful knowledge constructs that are representative of the generic network.

Figure 3 brings the adjacency matrix of the generic network before and after the generalized blockmodeling. We can visualize the participants' perception with regards to the region of the factors vs. activities blocks (area "1"), as well as the "activities x systems" blocks (area "2"). Most importantly, through the figure, we observe how blockmodeling rearranged the nodes in a way that it is easier to interpret and simplify the network.

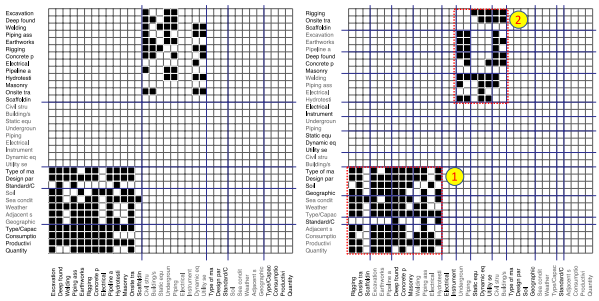

Figure 3. The three-mode adjacency matrix of the generic network before (left) and after (right) a generalized blockmodeling with twelve clusters [13]

Figure 4 (see [13] for enlarged pictures) brings the blockmodel in the form of the adjacency matrix for both the generic network of the survey and Project B. The results suggest Projects A and B have several features in common because many of their blocks diverge equally from the generic network. They have similarities even though the former is an industrial facility and the latter is an offshore LNG terminal.

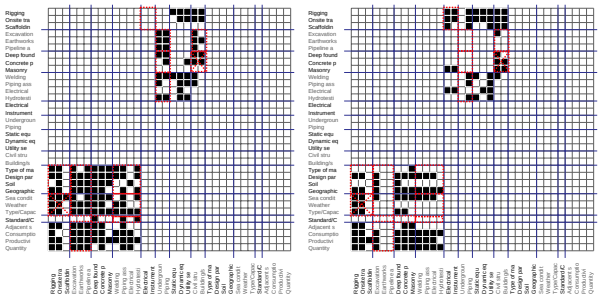

Figure 4. The three-mode adjacency matrix of the blockmodel of the baseline (left) and the rearranged Project B network (right) [13]

The main objective of the survey was to capture the general knowledge of the participants with no specific project in mind, which means that one should not expect the generic network to represent unusual relations and blocks that can potentially aggregate a meaningful knowledge. Conversely, comparing the differences between blocks can pinpoint what is so singular in the case study, and this information, along with the related context of the project, can be used in future projects.

The proposed method also includes the calculation of the average block analogy index $\bar{k}$ for each case-based network with the blockmodel obtained above as a baseline [6,13]. The smaller $\bar{k}$, the more the case-based network moves away from the baseline blockmodels, and therefore the more one can learn from the differences and the context of the past project embedded in a case network.

3.4 The Evaluation Approach

Since we introduced a new collaborative approach for energy-related processes in the construction phase, the best way to assess this research is through evaluation, not validation. Validation checks if a proposed model complies with internal specifications and if the results collected from the samples can be statistically generalized to the population. The validation would require a significant number of projects and a corresponding extensive database to conclude, which is out of the scope of this research.

To undertake the evaluation phase of this research, we conducted a test using Green 2.0, an online discussion media to discuss energy in construction [14]. We simulated the discussion environment of one of the cases studied in this research: Project A. Ten volunteers participated in the test: undergraduate and master's civil engineering students, construction managers, and a design engineer. The participants were educated in the case and asked to tag their comments based on the 34 concepts of the concept map. For each comment, the participants needed to choose the systems associated with their ideas, and, for each system, the factors that would influence the energy use of the corresponding construction activities. At least a triple of tags should be selected for each comment: one factor that influences at least one activity that is associated in turn to at least one system.

Since the test and Project A are based on the same case study, it is expected that both concept networks are similar. A correlation analysis between both networks can provide an internal validation for the proposed methodology to represent the network of the cases. We performed a QAP analysis and calculated the block analogy index $\bar{k}$ for the networks (the closer $\bar{k}$ is to 1, the more similar the networks are). The correlation factor found was 0.45 with a level of significance of 0.0002 (0.02%), and $\bar{k}$ was 0.51. Some of the factors that may have limited the results are the hypothetical nature of the test, the lack of experience of the students with O&G projects, and the time of the test.

Right after the test, we submitted an online questionnaire and conducted a focus group with the participants. In both evaluation methods, the participants assessed the concept map, the process of collaboration, the outcome of the test, and Green 2.0 as the interface. Overall, all the participants reported a high level of satisfaction with the four criteria. However, many commented on the difficulty of dealing with a limited number of tags. The issue of dealing with the tags may also have prevented from obtaining a better correlation/similarity between the networks.

4 Conclusion

Using unstructured data in a KM system has always been a problem in the construction domain. The industry struggles to deal even with intrinsic processes, such as documenting, historical productivity metrics, and benchmarking. In this sense, knowledge retrieval and representation methods such as lessons learned, case studies, and ontology have been widely used to improve the performance of projects. Nevertheless, these solutions have limitations regarding adaptability, applicability (capturing what is right for each project), documentation, and operation/maintenance (case studies and ontologies).

This research proposes a collaborative knowledge-based method to improve the use and management of unstructured data sources. It can be applied to the decision-making and planning processes related to energy management during the construction phase. Fundamentally, the proposed approach transfers text corpus into concept networks. A simplified taxonomy of factors, systems, and construction activities is used to capture the central concepts (to be used by the networks). The networks has edges (or links) set between the concepts (or nodes) that significantly affect energy use during the construction phase of a project.

The proposed method, as well as the system, can support the DM with better assumptions while providing a collaborative environment in which project teams can debate and co-investigate the best means to improve energy consumption during the construction phase.

Capturing knowledge from interviews, surveys and case analysis (the primary tools used in this work) is dependent on human interpretation, which may be subject to errors during the phases of profiling the answers and interpreting/collecting the relations. Despite its intrinsic disadvantages, the human interpretation allows for the exploration and detection of subtle relations in the participants' answers that are often difficult to perceive through other methods, such as surveys or questionnaires

[15,16]. The methodology to detect the relations cited above leads to semantically rich and contextualized knowledge, and the human interpretation is very effective in producing such outcomes.

Despite following a scientific procedure, detecting the relations from the case studies manually may be prone to errors. Future works can attempt to integrate automated knowledge retrieval tools to collect and represent the concept networks directly from the unstructured data generated in project environments.

Generalized blockmodeling has a significant number of parameters and constraints that influence the number of solutions. Although the number of inconsistencies in each solution is one of the most crucial parameters, each solution has to be manually interpreted before the one with the most substantive sense can be identified. Depending on the number of possibilities and solutions, this trial-and-error process may be overwhelmingly time-consuming. Therefore, the method to obtain blocks should be meticulously adapted to the needs of the study. For example, instead of using the four suggested clusters of activities, one can obtain a blockmodel from the three subcategories of factors of the concept map.

The analysis focused on the different types of blocks and the inconsistencies of each block to obtain valuable information regarding the case studies. Nevertheless, an alternative (and perhaps complementary) interpretation may be given to the opposite approach: What are the inconsistencies that have prevented blocks of the same type from being ideally equal? In addition, future works can attempt to implement semi-automated knowledge retrieval and representation tools to generate the cases and the networks.

References

[1] S.H. Liao, Expert system methodologies and applications-a decade review from 1995 to 2004, Expert Syst. Appl. 28 (2005) 93–103. doi:10.1016/j.eswa.2004.08.003.

[2] J. Read, Using Emoticons to reduce Dependency in Machine Learning Techniques for Sentiment Classification, in: ACL Student Res. Work., Association for Computational Linguistics, 2005: pp. 43–48. doi:10.3115/1628960.1628969.

[3] M. Park, K.W. Lee, H.S. Lee, P. Jiayi, J. Yu, Ontology-based construction knowledge retrieval system, KSCE J. Civ. Eng. 17 (2013) 1654–1663. doi:10.1007/s12205-013-1155-6.

[4] A. Singhal, Introducing the Knowledge Graph: things, not strings, Google. (2012). https://googleblog.blogspot.ca/2012/05/introducing-knowledge-graph-things-not.html (accessed October 2, 2017).

[5] M.P.I.I. MPII, YAGO: Overview, Max Planck Inst. Informatics. (2014). https://www.mpi-inf.mpg.de/departments/databases-and-information-systems/research/yago-naga/yago/#c10444 (accessed October 2, 2017).

[6] R.R. Aragao, Using Network Theory to Manage Knowledge from Unstructured Data in Construction Projects: Application to a Collaborative Analysis of the Energy Consumption in the Construction of Oil and Gas Facilities, University of Toronto, 2018. https://search.proquest.com/openview/6d484bda470e83a7a7c2134d831b50c0/1?pq-origsite=gscholar&cbl=18750&diss=y.

[7] M.M. Bilec, A Hybrid Life Cycle Assessment Model for Construction Processes, University of Pittsburgh, 2007.

[8] C.L. Saunders, A.E. Landis, L.P. Mecca, A.K. Jones, L.A. Schaefer, M.M. Bilec, Analyzing the practice of life cycle assessment: Focus on the building sector Saunders et al. Analyzing the practice of life cycle assessment, J. Ind. Ecol. 17 (2013) 777–788. doi:10.1111/jiec.12028.

[9] S. Junnila, A. Horvath, A.A. Guggemos, Life-Cycle Assessment of Office Buildings in Europe and the United States, J. Infrastruct. Syst. 12 (2006) 10–17. doi:10.1061/(ASCE)1076-0342(2006)12:1(10).

[10] R.R. Aragao, T.E. El-Diraby, Using network analytics to capture knowledge: Three cases in collaborative energy-oriented planning for oil and gas facilities, J. Clean. Prod. 209 (2019) 1429–1444. doi:10.1016/j.jclepro.2018.10.346.

[11] D. Krackhardt, Predicting with networks: nonparametric multiple regression analysis of dyadic data, Soc. Networks. 10 (1988) 359–381.

[12] P. Doreian, V. Batagelj, A. Ferligoj, Generalized Blockmodeling, 1st editio, Cambridge University Press, New York City, NY., 2005.

[13] R.R. Aragao, T.E. El-diraby, Using blockmodeling for capturing knowledge: The case of energy analysis in the construction phase of oil and gas facilities, Adv. Eng. Informatics. 39 (2019) 214–226. doi:10.1016/j.aei.2019.01.003.

[14] T. El-Diraby, T. Krijnen, M. Papagelis, BIM-based collaborative design and socio-technical analytics of green buildings, Autom. Constr. 82 (2017) 59–74. doi:10.1016/j.autcon.2017.06.004.

[15] E. Rice, I.W. Holloway, A. Barman-Adhikari, D. Fuentes, C.H. Brown, L. a. Palinkas, A Mixed Methods Approach to Network Data Collection, Field Methods. 26 (2014) 252–268. doi:10.1177/1525822X13518168.

[16] A. Marin, Are respondents more likely to list alters with certain characteristics? Implications for name generator data, Soc. Networks. 26 (2004) 289–307. doi:10.1016/j.socnet.2004.06.001.

Digital Fabrication and Crafting for Flexible Building Wall Components: Design and Development of Prototypes

N.F. Naqeshbandi[a] and P. Mendonça[a]

[a]Department of Architecture, University of Minho, Portugal
E-mail: nzarbandi@gmail.com, mendonca@arquitectura.uminho.pt

Abstract –

This research aims to explore and reflect the links between form, function, material and fabrication to develop and assemble more adjustable and flexible building walls. The interconnection of these main aspects of creation is particularly driven by the raising prominence of digital and computational tools in the context of design and fabrication. The new trends in digital fabrication and construction industry have fundamentally impacted building envelope components design with a shift in emphasis from flexible structures to envelope and from form to performance. The objective of this research is to develop new prototypes for more lightweight, dynamic, possibly interactive body envelope with the contribution of digital crafting. The first wall prototype was designed and assembled in the laboratories of University of Minho using CAD and subtractive machining to produce the parts and apply physical tests to the wall. Based to that experiment the second prototype is digitally developed and generated with additive manufacturing; presenting the development process; as an attempt to build an entire envelope from printed components.

Keywords –

Digital design; Digital fabrication; Crafting; Building wall components; Component design; Rapid Prototyping

1 Introduction

Innovations in material, design, and fabrication processes are currently thoroughly researched and applied in various areas. Digital technology and digitally driven fabrication are now the norm of turning architects, designers and researchers towards new concepts of design thinking and manufacturing that subsequently lead to more advanced architecture. Digital fabrication with crafting techniques can evolve the creation of physical prototypes; evaluate the constructability, material behaviour and selection as well as aesthetic qualities. There is a strengthened and more correspondent relation between the development and fabrication process combined with a higher flexibility considering the geometry, process, and material driven design; not only in the phase of design and manufacturing but also in the final step (Lu B., Li D., Tian X. 2015).

Wide range fabrication technologies and composite materials have been developed and started to impact architecture for their high performance characteristics. The intelligent control and automation of processes break up the strong limitation of variation in material, structure and form in the traditional industrial production. Students and professionals design with three-dimensional digital tools and, through this technology, design and construction are inextricably woven together in a continuous feedback loop. Based on the principles of open source, computer numerical controlled CNC production data is distributed and further developed via the Internet and new knowledge regarding materialization is being shared. Ideally, production knowledge is shared using Creative Commons licenses and a global network of mini factories is created with these networked digital production methods.

In the realm of building components, the walls are providing primary site of innovative research and physical tests. Building partition and envelope wall components are among the elements in a building that can be improved for better performance and more integrated with the other building systems. The wall component prototype is related with the geometry, the function and the materials made up to perform the required design. One of the key innovations in the field of building construction and building physics has been the emergence of high-performance materials (Aksamija A., Snapp T., Hodge M., Tang M.2012). The criteria to estimate the potential of the technologies for their application in the wall are weight, rigidity, and load-bearing capability of the parts.

The advancements in Additive Manufacturing AM technology is proceeding towards customizing products in design, production and material selection; have hugely impacted the way 3D printing is viewed and relied upon by engineers, designers and manufacturers and lead increasingly construction evolutions. 3D

printers are nowadays substantial for experimenting prototypes and approaching the end-use production parts in hundreds of plastic, metals and other printing materials (Hager I., Golonka, A., Putanowicz, R. ICEBMP 2016).

2 Prototype Design: Digital Design and Crafting

Building designs and prototypes are not born out only digitally, but they can be realized digitally and to come to exist in faster time and with more accuracy. With the aid of computer aided design (CAD) and computer-aided manufacturing (CAM) technologies rapid developments have broad in building design, construction practices and rapid prototyping. Digital design is the early step of the work that provides CAD mother model. Digital processes starts with analyzing the information data structurally for all parts of the prototype to prepare them for CAM software, the second step is translating the analyzed information to command the fabrication machines to produce the physical modeling either on-site or in the factory; this workflow is known as "File to Factory". The focus of the technology descriptions will lay on the methods to produce components from different materials that contribute to a wall partition.

The fabricating processes due to the manufacturing methodology can be categorized as: subtractive manufacturing (CNC) and additive manufacturing (3d printing). Both are considered active tools for Rapid prototyping.

2.1 Subtractive Manufacturing

Subtractive manufacturing also known as CNC machining, involves the process of removing a specified surface or volume of material from solids and also milling axially; by using cutting devices; either by electro-, chemically- or mechanically-reductive also advanced CNC (multi-axis milling).

In axially constrained devices, the piece of material that is milled has one axis of rotational motion such as lathes. There are millings of three-dimensional solids that have the ability to raise or lower the drill-bit, to move it along X, Y and Z axis, removing materials volumetrically. There are also four- and five-axis machines when milling special shapes.

From the advantages of subtractive processes, can include a wide selection of end-use materials; offer a variety of surface finishes, good dimensional control and fast with a high degree of repeatability suitable for end-use manufacture. The disadvantages are related to some material waste, and geometry restrictions; certain geometries such as a sphere as well as complex geometries Additive are still the choice.

2.2 Additive Manufacturing

The term Additive Manufacturing also referred to nowadays as synonym 'layering manufacturing' and '3d printing', a process by which digital 3D design data is used to build up geometry in layers by depositing and bonding materials one layer at a time. The AM build the geometry by depositing with the benefits of robotically controlled and free-form manufacturing. The size and speed of the adding nozzle and the design size directly affects the build time, therefore, design, size, geometry, function, material and application of the component are substantial for selecting the right technology and material for the prototype. Materials available with 3D printing technologies range in heat deflection, chemical resistance and durability and material viability greatly depends on design, application and desired product life. To determine the material and 3D printing process which will best support one application, the most appropriate materials and technologies should be considered, as mentioned on Table 1 Adapted from: https://www.protolabs.com/resources/white-papers/rapid-prototyping-processes/

Table 1. Interaction between materials and techniques on digital fabrication

Rocess	Description	Finish	Example Materials
CNC	Machined using CNC mills and lathes	Subtractive machined	Most commodity and engineering-grade thermoplastics and metals
LASER	Machined using Laser head	Subtractive machined	Wood derivatives, Cardboards, PMMA and metal plates
SLA	Laser-cured photopolymer	Additive layers of 0.05-0.15mm (typical)	Thermoplastic-like photopolymers
SLS	Laser-sintered powder	Additive layers of 0.10mm (typical)	Nylon, TPU
DMLS	Laser-sintered metal powder	Additive layers of 0.02-0.03mm (typical)	Stainless steel, titanium, chrome, aluminum, Inconel

FDM	Fused extrusions	Additive layers of 0.15-0.35mm (typical)	ABS, PLA, PC, PC/ABS, PPSU
MJF	Inkjet array selectively fusing across bed of nylon powder	Additive layers of 0.10-0.20mm (typical)	Black Nylon 12
PJET	UV-cured jetted photopolymer	Additive layers of 0.015-0.030mm (typical)	Acrylic-based photopolymers, elastomeric photopolymers
DDM	Direct extrusion	Additive layers (variable)	Concrete, clay, plaster
IM	Injection-molded typically using aluminum tooling	Molded smooth (or with selected texture)	Most commodity and engineering-grade thermoplastics, metal, and liquid silicone rubber

The selection criteria among the described technologies will be on the basis of product delivery, material ,tolerance ,cost ,quantity of product, and desired needs of product whether its speed, function or a specific material (Yadav, K., Sharma, K. R., and Anand, D. JMSME, 2015).

2.3 Digital Crafting and Material Selection

Although both Additive and Subtractive have similar workflow method but still there are notable differences. The connection of digital design and digital manufacturing can be resumed as 'Digital Crafting', which describes the combination of work techniques typical of craftsmen with computer-supported processes. The way of honoring material and its strong – but ever changing – relation to manufacturing processes leads not only to new design aesthetics but also to a new, crafting oriented way of design thinking.

The principles of digital design and manufacturing processes are rather linked to a way of craft production than industrial processes as they emphasize the qualities of the materials used and provide higher flexibility during the development and production process.

Smart materials have been applied in architecture, but rarely so that the responses give a global effect on the performance of the entire building. The materials as well as the technical equipment for AM technologies have been continuously developed since. A new market opened up that is still growing today. Choosing the right materials and techniques is substantial for creating highly customized building components.

Material-technology partnerships expanding more nowadays as material chemistry explored more as well as mechanical properties can be evaluated very precisely. As stated in the differences between additive and subtractive manufacturing, materials are defined by the technology. 3D printing transforms materials through either external heat, light, lasers or other directed energies depending on the printer type. The ability of a material's mechanical composition to react positively to a certain directed energy marries that material to a technology which can deliver the desired change.

The new trends in advancing technologies encourage products made from more environmental friendly material. The performance of materials varies and to fabrication technologies and processes the material needs to be efficient in terms of mechanical properties and design capabilities. For AM developments, materials correspond with developments in methods and machines; as the workflow also improves to achieve more benefits from materials, therefore, material selections expanded to include ecological and less harmful materials.

Smart materials have been applied in fabrication as they can just replace conventional materials been used with the advanced machines, whilst smart properties can perform additional benefits. An example of this is 3d painting with nano-particles of titanium oxide, which not only protect the surface but also reduce pollution in the surrounding environment through photo catalytic behavior.

Emerging digital processes are beginning to impact the profession of architecture in a manner similar to what has occurred in other creative/design disciplines providing new methods to evolve the practice of architectural design. The study presented two models to demonstrate the technical process used to translate digital designed models to manufacture descriptions and physical assembly.

3 Smart Building Component Design Using Subtractive Techniques

The first case study presents the research process of an innovative solution for partitions, designated as AdjustMembrane, developed within a Portuguese Foundation for Science and Technology funded research project. The proposed system is a modular non-loadbearing wall, tensioned between the pavements and ceiling slabs, which are used as anchoring elements. It allows several advantages, related with the weight reduction to achieve good sustainable indicators, such as

the reduction of construction costs, energy, and materials. It is easy to recycle and reuse, allowing easy assembling and disassembling [Mendonça, Macieira and Ramos, 2014].

This solution of non-structural partition wall is characterized by a structure in tensioned belts that serve as support for the two-stage assembly of panels with a core in fibrous material, as showed in Figure 1.

Figure 1. Component design with MDF (Laser cutter)

The core may include a grid (Figure 2) - with modules that can be subtracted or added to allow the panels to adapt to the dimensional requirements of the space to be partitioned and which at the same time serve to reinforce and give rigidity to the panel.

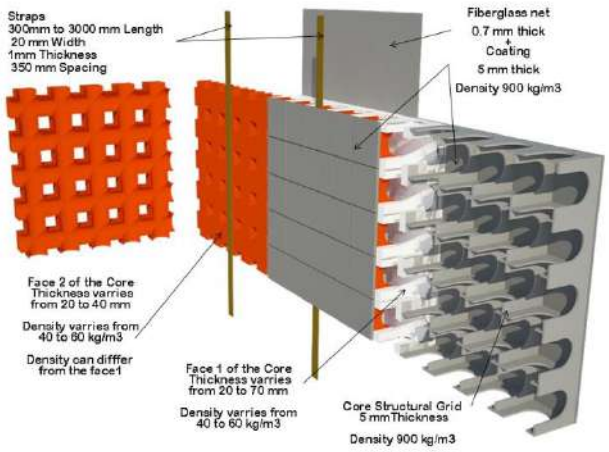

Figure 2. Prototype design and system assembly

The core of the panel solution is characterized by having vertical grooves in the interior allowing the integration of water, gas and electricity networks; the core shall consist of a material fibrous / porous so as to function at the same time as thermal and acoustic insulation of the facilities and between the various compartments.

The typological suitability required that there were a translucent variant of the study material for the partition wall. To do this, the prototype must be carried out with the application of a translucent material and performed acoustic and light transmission tests.

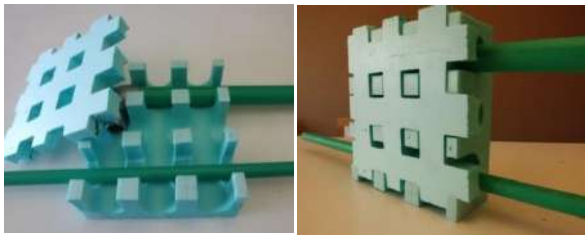

Figure 3. Component manufactured XPS (CNC hotwire cutter 2D)

4 Smart Building Component Design: Digital Fabrication and 3D Printing

The research objective is to build and develop components by conceptualizing the component assemblage and bringing it to the physical modeling with the use of 3d printing. The concept of the development is another advantage of digital fabrication when extending the future possibilities to the real scale. Although the components generated here are physically small, the study concern is how to build assembly descriptions based on real-world construction.

The most popular 3D printing manufacturing technologies can be found as PolyJet, Stereolithography (SL), Laser Sintering (LS), Fused Deposition Modeling (FDM) and Direct Metal Laser Sintering (DMLS) and more. For the study Polyjet was used for printing the component.

The aim of this case study design is to undergo the considerations of developing printing and developing the prototype through the following:

4.1 Prototype Development Process

As the study is to propose prototype development for a digitally driven fabrication framework, an exploratory model on the usability of a prototyping-process is designed. The analytical data have continued with the objectives of the first case, more flexible and manual assembling building envelopes, therefore, the

development process is considered a design to manufacturing process with Additive (Fig 3).

4.1.1 Data Preparation for Prototype By Additive Manufacturing

Data preparation is identical to other AM processes, with an exception to a supplemental post- processing step which is optimizing the generated printing path of the precipitation head so as to decrease the time of printing in addition to possible overprint of materials because of orifice proration that is on and off, by diminishing the non-printed motions of the precipitation head. A 3D MAX model was designed for the printing component, transformed as an SLT document format, slicing is performed using a coveted layer depth, a printing track is produced for each layer, and for the printing a G-Code document is manufactured.

4.1.2 Application Process

Many materials which are printed by 3D system provide biocompatible features, abilities for sterilization, licensing from FDA for skin exposure, toxicity, fire retard, heat fume, and resistance to chemical agents or other credentials that might be serious for your plan. When a material and 3D printing process is selected for the design, it will be mandatory to guarantee that your substance is capable of delivery upon these credentials.

4.1.3 Function

Stringent investigations are performed for 3 D printing substances for answering the stress types it can tolerate and the grade of the terrible environment the substance will surpass in. The fact that the material is able to act in a desirable employment depends partially on layout.

4.1.4 Geometry

As it is previously stated, substances which are printed by the 3 D technology cannot be isolated from their concordant technology. Moreover, every technology regardless of its kind (Like FDM, stereo lithography or Laser Sintering) is proficient in presenting specific geometrical fulfillments. While selecting the technology of substance and 3 D printing, dimensional tolerances, minimum feature fulfillment as well as thickness of the wall of the layout should be taken in to consideration.

The Geometry development process of the building wall component design Consider the dimensional tolerances, minimum feature execution and wall thicknesses of your design when choosing a material and 3D printing technology. The thickness for this component was 100mm.

Figure 4. The Geometry development process of the building component design

Printed designs can result in fine surface finish products with the right post-processing. Some materials may be better suited to certain post-processing methods than others – heat treating stainless steel versus post-curing a photopolymer, for example.

During the design process flexibility and sustainability of applying composite envelope configuration were assessed through Digital designing and optimization tools that can help to identify assembly and disassembly tolerances and analysis of performance objectives.

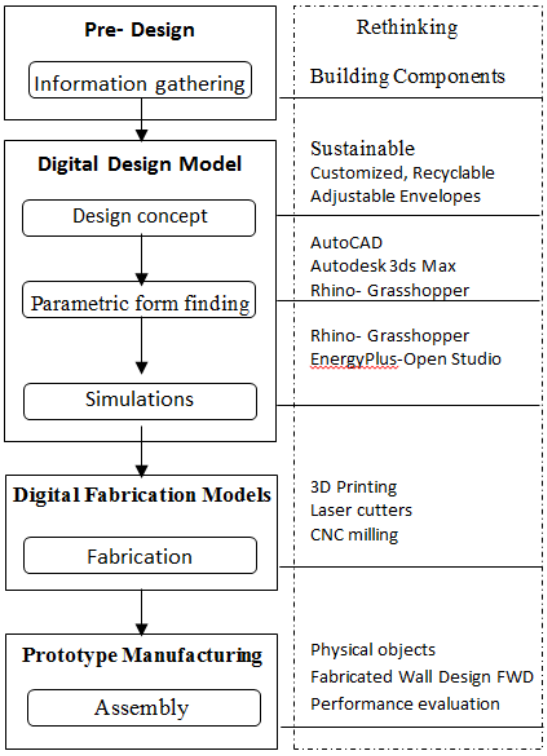

Figure 5. The development process of the building component design. Adapted from "Re-Skinning: Performance-Based Design and Fabrication of Building Facade Components" (PERKINSWILL, 2012 / VOL 04.01)

4.2 Assembly Description

The printed parts can be manually attached to become a base unit easily to connect with the printed tube bars. When combining more units, they formulate a panel, with repeating the process then a standing wall structure ready to assemble the electrical plugs and wires and also the mechanical piping. Then the system will be ready to apply panels to.

Figure 6. 3D printed component prepared for assembly

The 3D printing components will be subjected to rigorous testing in order to answer the kinds of stresses it can endure and for more future developments the components can be coded and marked with the nodes of intersection with adjacent layers of structure.

The units are designed to be fastened to each other and the final structure will be completely self-supporting and will not require secondary scaffolding. The final product is the scale of a room and is composed of 600 3D printed parts.

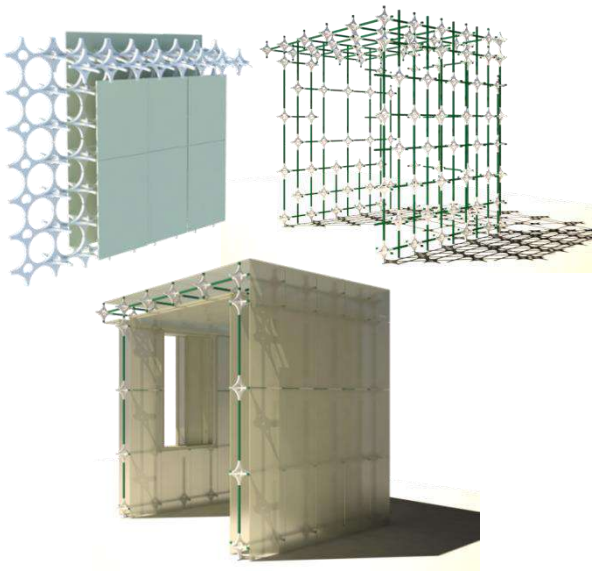

Figure 7. The FWS to be assembled, the Designed and rendered with 3cDs Max

4.3 Digital Fabrication and Performance Design

The partition wall system Adjust Membrane presents ease integration of facilities, good mechanical principles, and good acoustic properties and modularity. Experimental prototypes were executed to test the mechanical properties, the access to the placement of installations as well as the integration of the structural grid and the way of installing the partition wall. The assembly process has been tested allowing to define the expected to adjustments, in particular with regard to the connection to the structural straps.

The mechanical properties to be tested for a printed sample of a panel consisting of 3 attaching units and to determine the physical test in the Construction and Technology laboratories of Uminho, Structural links have to be more detailed and investigated, with trials and simulations. The connection between panels should be tested in prototype as well as possible coating application.

5 Conclusion

The study demonstrates the potential of digital design and fabrication, and crafting techniques to develop building envelope components to become more adjustable, flexible and sustainable. Digital design tools offer guidance in analyzing the manufacturability of the building components. The principles of digital design and manufacturing processes are rather linked to a way of craft production rather than industrial processes as they emphasize the qualities of the materials used and provide higher flexibility during the development and production process.

New developments in advanced computational tools and methods are offering unprecedented ways for design exploration and evaluations. Performance-based design that integrates simulations and environmental analysis in the design process has an advantage over traditional design methods, because it allows a certain design iteration to be evaluated against different solutions. Also, digital fabrication techniques allow for creation of physical prototypes, which can be used to evaluate constructability, material behavior and selection as well as aesthetic qualities.

Contribution of digital crafting in the generation of design and building assemblies is an integral approach in improving design process, with the direct connection to practice and research. The innovative products can be developed rapidly with digital design and fabrication of numerous representation tools and production software. Such uses of technology strengthen the ties between design and craftsmanship and motivates to a continual evolution of the field of architecture with construction

companies and universities supporting such innovative trends of research and design.

The study on typological suitability, functional and structural performance in both wall solutions presented in this paper will be subjected to more analytics, performance simulations and later experimental testing. There is a strengthened and more correspondent relation between the development and fabrication processes combined with a higher flexibility considering the geometry: in the phase of design and manufacturing but also in the final shape.

Acknowledgments

This work has the financial support of the Project Lab2PT - Landscapes, Heritage and Territory laboratory - AUR/04509 with the financial support from FCT/MCTES through national funds (PIDDAC) and co-financing from the European Regional Development Fund (FEDER) POCI-01-0145-FEDER-007528, in the aim of the new partnership agreement PT2020 through COMPETE 2020 – Competitiveness and Internationalization Operational Program (POCI).

References

[1] Aksamija A., Snapp T., Hodge M., Tang M. "Re-Skinning: Performance-Based Design and Fabrication of Building Facade Components, *Design Computing, Analytics and Prototyping"* ResearcH JournaL www.perkinswill.com 2012 / VOL 04.01

[2] Mendonça, P., M. Macieira, L. Ramos. "Lightweight adjustable partition system: Evaluation of resistance to horizontal loads and functional failure from impacts." Informes de la Construcción, 67(539):e102,2015

[3] P. Mendonça, "ADjustMEMBRANE – Membrana divisória adaptável", Materiais de Construção n.169 Ano XXXI, 2014, pp 40-42.

[4] P. Mendonça, M. Macieira, "AdjustMEMBRANE" Relatório Milestone 4, Área de Arquitetura, Universidade do Minho, Abril, 2011.

[5] Helm, Volker, Selen Ercan, Fabio Gramazio, and Matthias Kohler. "In-Situ Robotic Construction: Extending the Digital Fabrication Chain in Architecture." To be published in ACADIA 12: Synthetic Digital Ecologies. San Francisco, 2012.

[6] Hager I., Golonka, A., Putanowicz, R. "3D printing of buildings and building components as the future of sustainable construction?" International Conference on Ecology and new Building materials and products, ICEBMP 2016

[7] Hopkinson, N. and Dickens, P., "Analysis of Rapid Manufacturing - Using Layer Manufacturing Processes for Production", *Proceedings of the* Institution of Mechanical Engineers Part C: Journal of Mechanical Engineering Science, Vol. 217(1), pp.31-39, 2003.

[8] Lim, S., Le, T., Webster, J., Buswell, R., Austin, S., Gibb, A. and Thorpe, T., "Fabricating Construction Components Using Layer Manufacturing Technology", *Proceeding of Global Innovation in Construction Conference (GICC'09)*, Loughborough, UK, 13-16 September, 2009.

[9] Lu B., Li D., Tian X. " Development Trends in Additive Manufacturing and 3D Printing" Engineering 2015, 1(1): 85–89 DOI 10.15302/J-ENG-2015012

[10] Khoshnevis, Caterpillar Inc. funds Viterbi 'Print-a-House' construction technology. Contour Crafting B. 2008.

[11] Yadav, K., Sharma, K. R., and Anand, D. **"**Additive and Subtractive Manufacturing: A Review" Journal of Material Science and Mechanical Engineering (JMSME) Volume 2, Number 2; March, 2015 pp. 174-177.

[12] Z. Malaeb, H. Hachen, A. Tourbah, T. Maalouf, N.E. Zarwi, F. Hamzeh, 3D concrete printing: Machine and mix design, International Journal of Civil Engineering and Technology 6 (2015) 14–22.

[13] 3D PRINT CANAL HOUSE, available from: http://3dprintcanalhouse.com/construction-technique, (2018).

As-is Geometric Data Collection and 3D Visualization through the Collaboration between UAV and UGV

P. Kim[a], J. Park[a], and Y. K. Cho[a]

[a] School of Civil and Environmental Engineering, Georgia Institute of Technology, USA
E-mail: pkim45@gatech.edu, jpark711@gatech.edu, yong.cho@gatech.edu

Abstract –

The characteristics of dynamic construction sites increase the difficulty of collecting the high-quality geometric data necessary to achieve construction management activities. This paper introduces a new autonomous framework for 3D geometric data collection in a dynamic cluttered environment using an unmanned ground vehicle (UGV) and an unmanned aerial vehicle (UAV). This method first deploys UAV to collect photo images of a site and builds a point cloud of the 3D terrain of the site, including obstacle information. A mesh grid is then created from the UAV-generated point cloud, and simulation for laser-scan planning is conducted to determine the stationary laser-scan positions at which a mobile robot can collect data with less occluded views while capturing all crucial geometric information. Finally, optimal paths for the UGV to navigate among the estimated scan positions are generated. Promising test results regarding data accuracy and collection time show that the proposed collaborative UAV-UGV approach can significantly reduce human intervention and provide technologies for enabling construction site to be frequently monitored, updated, and analyzed for timely decision-making.

Keywords –

Mobile Robot; UGV; UAV; Point Cloud; Laser Scanning; SLAM; Path Planning

1 Introduction

Collecting accurate and complete geometric data from construction sites is essential but challenging. It is particularly crucial to obtain timely, complete, and accurate spatial information for decision-making in construction projects since inaccurate, missing, or insufficiently detailed data can lead to uncertainty in decision-making. However, the dynamic and complex properties of construction sites not only require various 3D geometric data but also increase the difficulty of efficiently and effectively collecting spatial data [1], [2]. It is also necessary to ensure that data collection activities have a minimal influence on other construction activities; interference between data collection and construction activities can cause project delays and low data quality, which results in poor decision-making and further delays [3].

Currently, the quality of 3D spatial data acquisition depends solely on the intuition or experience of the data collector. This experience-based data collection may not be practical or efficient due to the complexity of the process, which involves 3D spatial domain and the physical target placing for registration. Also, feedback is limited during the data acquisition, and registration process since the completeness of site scan is unknown until the full registration is completed. Furthermore, low-quality 3D spatial data can negatively impact effective decision-making, and duplicated data caused by largely overlapping scan ranges can result in extensive time and computational burdens for data processing. Further, it is possible that unnecessarily high-quality data may be collected for unimportant features at a job site while other geometric data necessary for making critical decisions may be missing. Therefore, a strong need exists to smoothly integrate automated jobsite inspection into the daily or weekly work cycle. If the jobsite inspection is automated, quality control measurements can be taken and reported to stakeholders automatically as well. To increase the efficiency of daily as-is data collection in the field, this study proposes a framework of the unmanned aerial vehicle (UAV)-assisted laser-scan location and path planning for an autonomous mobile robot, or unmanned ground vehicle (UGV).

2 Related Work

2.1 3D Reconstructions from UAV Images and Cooperation with UGV

Extracting 3D geometric data from the scene of interest [4] is very valuable for activities such as monitoring construction progress [5], [6] and defect analysis [7], [8]. The 3D reconstruction process has advanced dramatically due to recently developed computer vision-based technologies. One method for producing a 3D sitemap is photogrammetry. Photographs provide useful information about the construction progress that can be automatically processed and converted to 3D point clouds using Structure from Motion [7]-[9]. Due to stability and payload issues, UAVs typically use a photo camera to capture scenes and build a 3D point cloud with photogrammetry. Since a ground robot can be more easily stabilized with higher payloads than an aerial robot, it can collect a higher quality of 3D geometry data.

As a means of collecting 3D geospatial information, UAVs and mobile robots share the advantage of being able to collect geospatial information without exposing surveyors or device operators to hazardous areas. However, both technologies also have distinct disadvantages caused by their measuring positions. The ground-based measurement methods used by mobile robots have blind spots behind vertical obstacles and cannot capture horizontal surface data located higher than the robots. In contrast, UAVs generate blind spots under horizontal obstacles (e.g., roof). Furthermore, the overall accuracy of the point cloud generated by UAVs is lower than that of the ground-based generated point cloud even though UAVs possess operational advantages over the ground-based approaches regarding navigation.

2.2 Scan Planning and Autonomous Scanning

A widely used technology in many field applications, Light Detection and Ranging (LiDAR) can measure a wide area with higher resolution and accuracy compared to photographs and is generally not limited by surrounding lighting and weather conditions during its operation. However, multiple scans from different locations must be taken and registered because of limited data capture coverage and occlusions. To register multiple scans in one coordinate system, many physical targets or markers are typically pre-installed in the overlapping scan area, which requires substantial cost, labor, and time [9]. A well-designed scanning plan minimizes data collection time while capturing all required geometric information. Latimer et al. [10] have used the concept of "sensor configuration space" to automate laser-scan planning. The configuration space is a 3D volume in which specific geometric features, or "information goals," are displayed on an imaging sensor. Their algorithm clusters information goals and generates configuration spaces for each cluster. It then selects sensing locations and plans the "minimum-time" path for moving the scanner to this location. Some studies have shown that the laser-scan planning problem can be solved using as-designed models [11], [12]. However, current practices still manually collect and process the 3D point clouds of large-scale environments, which requires many scans and often results in high labor and time costs, human errors, and inconsistent data quality. Automating some or all of the data collection and registration processes can mitigate these problems.

Automatic scanning has recently gained strong interest among academics and industry technology developers. Various sizes and types of LiDAR have been equipped to vehicles and mobile or aerial robots, and the simultaneous localization and mapping (SLAM) technique has been utilized in their approaches in generating dynamic point clouds[13], [14]. In robotics, SLAM is a popular method for enabling a robot to estimate its current position and orientation from a map of the environment created by LiDAR or cameras. The problem with this approach is that most SLAM systems are commanded manually; humans must decide where to go and how to perform complete scanning of a large site [15], [16]

3 Objective

The objective of this study is to explore a methodology that carries out multiple automation including robot navigation, laser scanning, and registration of multiple point clouds collected by 3D laser scanners mounted on UGV. To achieve the research objective, the following primary tasks are proposed. First, UAV is deployed to obtain an initial 3D map of the cluttered site. Second, optimal scan locations are estimated by simulation, using a mesh grid applied to the UAV-generated map and an occupancy map generated based on the gradient value of the terrain. Finally, the optimal navigation path is determined from among the simulated scan locations. The overall framework of the proposed approach is shown in Figure 1.

4 Methodology

4.1.1 System Architecture

In this study, a UAV (DJI Mavic Pro) equipped with a 1/2.3" complementary metal-oxide semiconductor sensor and a hybrid LiDAR system mounted on the Ground Robot for Mapping Infrastructure (GRoMI) are used, as shown in Figure 2. The two major parts of GRoMI are a laser scanning system and a mobile

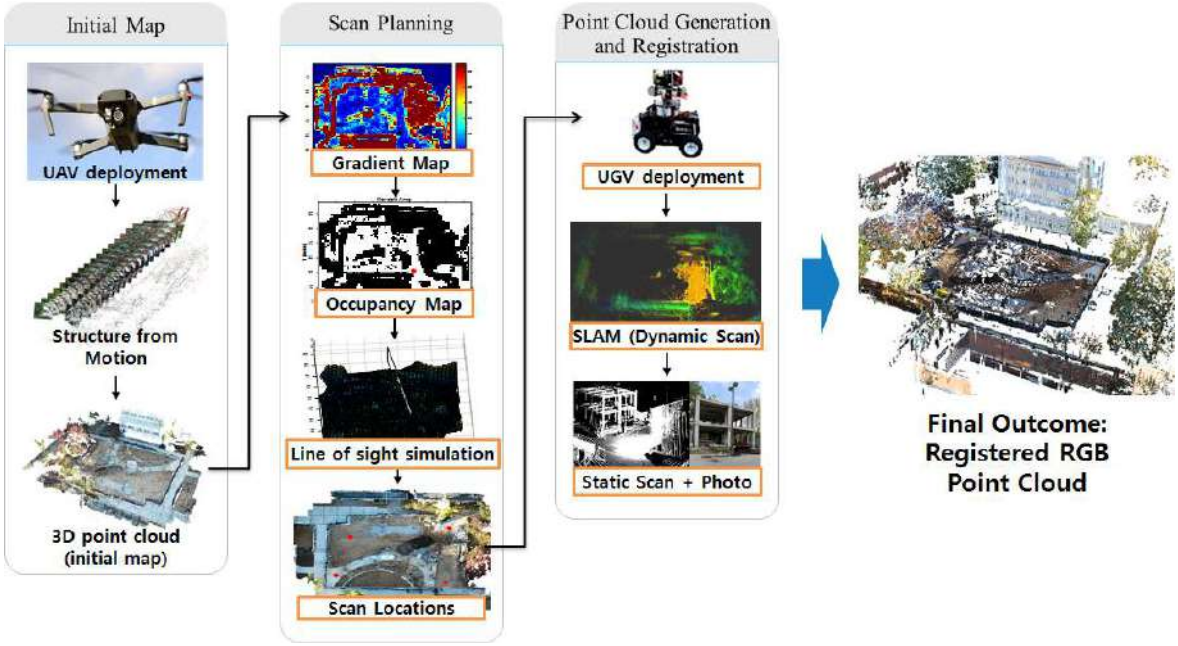

Figure 1. The overall framework of the collaborative UAV-UGV data collection and visualization

platform. The upper laser scanning system includes four vertically mounted 2D SICK line laser scanners to collect 3D mapping information. A horizontally mounted 2D line laser scanner is to estimate the robot's location and pose information on a 2D plane and a regular digital camera to obtain the RGB data of the scenes. The lower mobile platform system, used primarily for navigation, has object avoidance sensors, an IMU, and a navigation camera. The robotic system offers the following functionalities: 1) point-cloud data acquisition while the robot is moving; 2) RGB data collection through a DSLR camera, and 3) autonomous navigation.

The proposed framework allows the robot to automatically collect the geometry data for construction progress monitoring and analysis through LiDAR-based SLAM and automatic point cloud registration methods. To avoid the potential of interfering with construction workers and other activities, the data collection has been done after daily work is completed. In addition, collecting scan data during construction work is not meaningful because the site geometry is rapidly changing and blocked by moving objects (e.g., workers and equipment). In this study, the tested environment is limited to the outdoor construction site since this approach is using UAV-generated map data as prior information for UGV's scan and path planning.

4.1.2 UAV Scan

The factors affecting the performance of the photogrammetry created from UAV include 1) ground control points (GCPs); 2) ground sampling distance (GSD); 3) overlapping ratio; and 4) image processing methods.

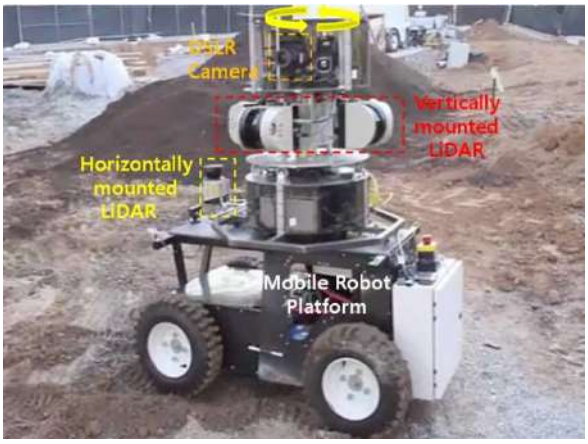

Figure 2. UAV (top) and ground robot systems (below)

Because this study is intended for autonomous 3D as-is data collection in which there is no human intervention, and GCPs were not considered. Referring to the number of pixels per unit length, GSD is a factor related to the flight level, focal length, and resolution of the camera. The GSD can be written as the following Equation (1):

$$\text{GSD} = \frac{H}{f}\,\mu \tag{1}$$

Where H is flight height above ground level (m), f is a focal length (mm), and μ is pixel size (μm). Since the GSD value directly affects the results of the photogrammetry, it is important to determine the flight altitude. The overlapping ratio also affects the accuracy of the photogrammetry. Both GSD and overlapping ratio should be determined when the flight plan is made. In this study, flight altitude was set to 30 m above ground level to determine the GSD to be 1 cm. Using the images obtained from the UAV, this study processed photogrammetric data to generate a point cloud, as shown in Figure 3.

Figure 3. UAV-generated 3D point cloud map of the construction site using image data

4.1.3 Scan-Spot Selection for the Mobile Robot

The scan planning method proposed by this study is to locate satisfactory stationary scanning locations for GRoMI by evaluating the candidate scan locations with a line-of-sight simulation of a 3D laser scanner. Considerations for selecting these locations include 1) the surface point with a large field-of-view of the surroundings with minimal obstructions; 2) the minimal overlapped area between scans; and 3) the most complete possible scan areas for the entire site. Evaluation criteria include a quantity of point data and the amount of occlusion, which differ depending on each scan location. Based on these criteria, a number of scans and data collection time can be reduced while maintaining satisfactory area coverage and level of detail. The scan-spot selection process is accomplished through the following four steps:

1) Divide the job site into cells (1 m by 1 m each) and compute the gradient between neighbor cells for each cell,
2) Create a 2D gradient map and an occupancy map to find the movable area at a site,
3) Run a line-of-sight simulation for every candidate scan location cell and count how many points and how few occlusions can be achieved, and
4) Find candidate scan locations where more point-cloud data and less occlusion can be obtained.

These four steps are described in detail below.

A. Gradient Map Generation

The first stage of the scan planning process requires obtaining an initial 3D terrain model of the target site. In general, it is difficult to use existing or as-designed 3D data because as-is site conditions are generally different from the existing information. Therefore, the UAV-generated point cloud is used as a guidance map to compute the scan locations and to generate a navigation path for GRoMI. The gradient-based map is used to simulate a series of scan views for the robotic scanning system at all scan locations before GRoMI conducts any data acquisition tasks. At first, the UAV-generated point cloud of the construction site is divided into 1 m by 1 m cells. Gradients between neighbor cells are then computed. Figure 4 demonstrates the gradient map of a test site. It can visualize which cells are flattened, tilted or occupied by obstacles. The blue color area is relatively flat with a small gradient value where the mobile robot can be better balanced horizontally for laser scanning, and the red color area is relatively inclined with a more considerable gradient value where the mobile robot should avoid.

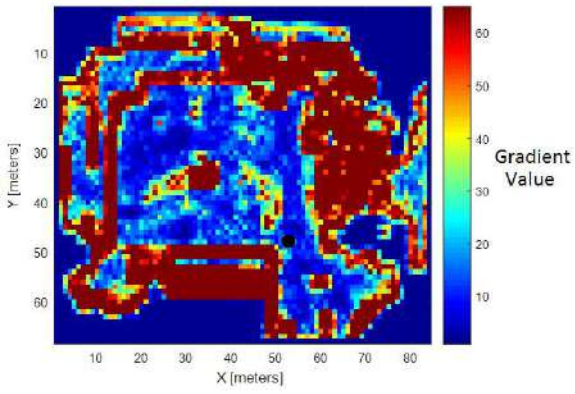

Figure 4. Gradient map of a test site

B. Occupancy Map for Candidate Scan Locations

Based on the generated gradient map, the movable and flat areas in the site are defined by setting a specific gradient threshold value. The movable area is the place where GRoMI can move around because the area has a relatively small gradient value, and it is used for path planning for GRoMI. A reference point is required for selecting optimal locations. This study uses the starting position of GRoMI as the reference point. Figure 5 shows the occupancy map of the movable areas, while GRoMI's initial location is shown as a small red dot in the target site. Occupancy means whether the obstacle is present at each cell.

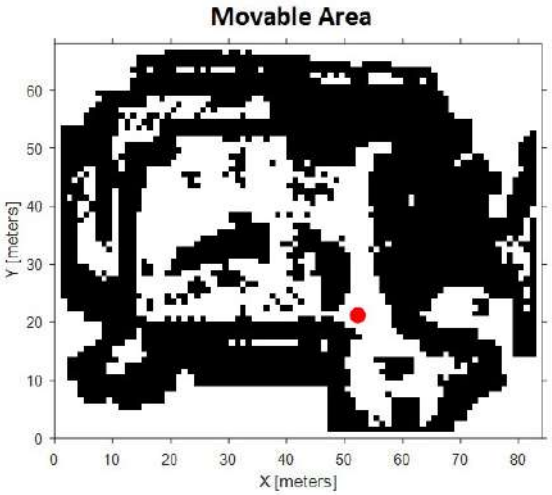

Figure 5. Occupancy map for the movable area

C. Line-of-Site Simulation

The next step is to compute the visibility of each candidate scan location. The ray tracing algorithm [17] is used to calculate the line-of-sight visibility. At first, the mesh grid is created from the UAV-generated point cloud. The 3D ray tracing for each laser line is then simulated. It is possible to find the cross points between laser lines and contour of the terrain. These points can be classified into two groups. The first is the simulated laser points, which are the minimum distance points from the specific scan location, has one point per laser line. The others are occluded points. This simulation lists the scan locations with the maximum number of points from the laser scanner and the minimum number of occlusion points. In addition, the greedy cover algorithm [18] is utilized to select an approximation for the optimal number of scan locations necessary to cover the entire site. It chooses the scan location that can see the largest amount of the boundary and then continues selecting the scan locations to cover the remaining area from the potential viewpoints. This process repeats until either the entire site has been covered or the iteration reaches the approximation for the optimal number of scans.

D. Find Satisfactory Scan Locations

The scan planning simulation calculates the number of laser points and occlusion points during the previous steps. Among these locations, removing some of the scan locations within a specific distance is required to minimize the overlapped area caused by the redundancy. The specific distance differs depending on the size of the target site; a 10 m distance is used for our test bed. After the simulation, four of the optimized scan locations were estimated as shown in red dots in Figure 6.

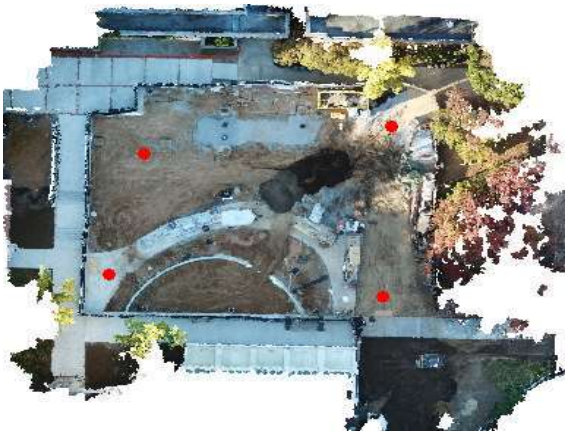

Figure 6. Identified scan locations from the scan planning simulation with UAV's point cloud (top view)

4.1.4 Automatic Registration of Scans

The laser-scan data from the horizontal LiDAR is used by the Hector SLAM algorithm to estimate the position and orientation of GRoMI on the horizontal plane. The Hector SLAM algorithm, developed by Kohlbrecher et al. [19], is employed in this study to perform laser-scan matching between the laser scans and progressively built maps to estimate the robot's postures and planar maps of the environment. In addition, the SLAM-driven localization approach is used to automatically register the point clouds obtained from each stationary scan location [20].

5 Results

In this study, a real-world construction site at the Georgia Tech campus was selected as a cluttered environment for the test. Three devices, UAV, GRoMI, and a commercial laser scanner, were used to build 3D point clouds of the site. To generate a 3D point cloud,

UAV used the photogrammetry technique, and a commercial laser scanner used sphere targets for point

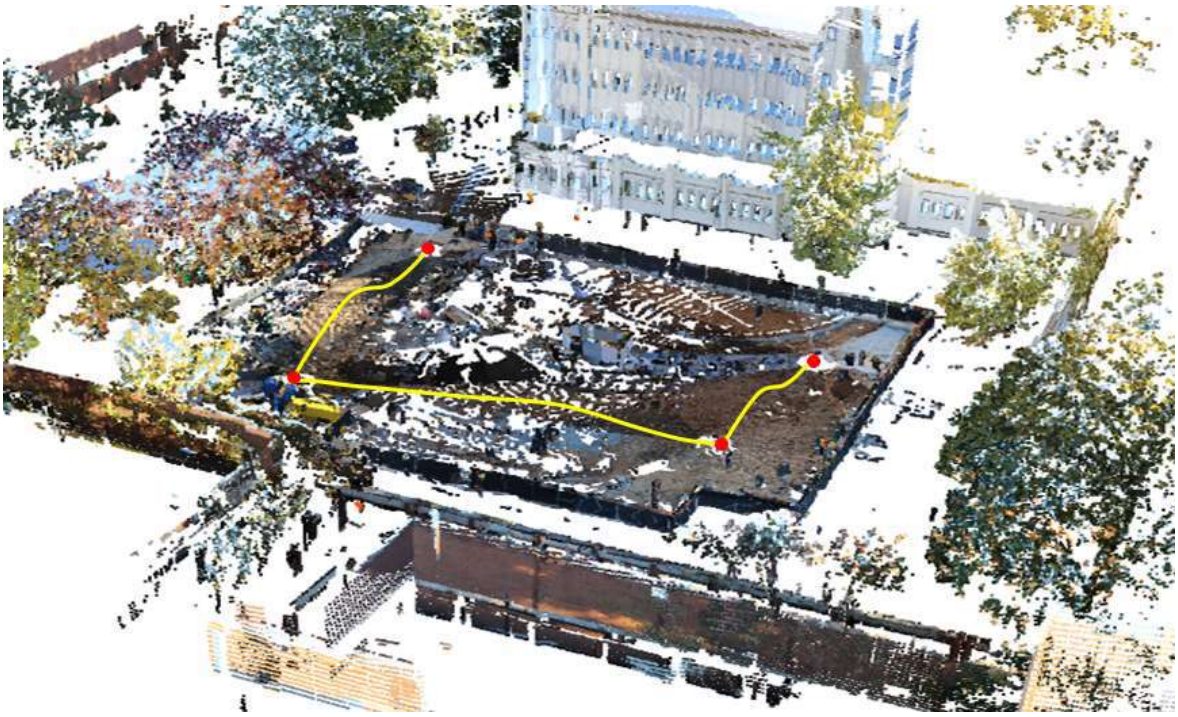

Figure 7. Registered 3D point cloud of the test site and GRoMI's scan and moving paths

cloud registration. As previously described, GRoMI conducted the SLAM-based automatic registration. Figure 7 shows the automatically registered RGB point clouds of the target site made by GRoMI.

Table 1. Error assessment

	GRoMI
Mean absolute error (MAE)	1.97 cm
Root mean square error (RMSE)	2.31 cm

Table 2. Required time from data collection to registration

	GRoMI	Commercial laser scanner
Pre-processing	35 min	10 min
Operation	30 min	40 min
Post-processing	0 min	40 min

In this study, the commercial laser scanner is considered the ground truth to measure the registration error of the registered point cloud collected by GRoMI since the terrestrial laser scanner has the highest accuracy of ±3 mm. As shown in Table 1, the mean absolute error (MAE) between the GRoMI and commercial laser scanner point clouds is 1.97 cm, and the root mean square error (RMSE) is 2.31 cm; MAE is an average distance between two point cloud sets, and RMSE is a standard deviation between two data sets.

Table 2 shows the required time to build a 3D registered point cloud with each device. The pre-processing includes the UAV's scanning time and path-planning processes for GRoMI and a target placing and laser preparation time for the commercial laser scanner. Operation refers to the data collection process with each device, and post-processing is the point-cloud registration process. During the 35 min of pre-processing for GRoMI, 10 min of UAV operation, 20 min of point-cloud generation, and 5 min of scan planning are included. The clear advantage of using GRoMI with UAV is the shortened processing and operation time. A commercial laser scanner has slightly higher accuracy but requires significantly more time than GRoMI for the target relocation and manual point clouds registration. Also, it cannot guarantee the complete scan of the job site since selecting scan locations is based on human intuition. Conversely, the advantage of using GRoMI is the planning scan locations and paths created by using a UAV-generated point cloud. Thus, it can realize more favorable results. Also, it does not need post-processing (registration) because it is registered automatically using the robot localization data (i.e., SLAM). Therefore, the proposed aerial mobile robot-based autonomous data acquisition approach resulted in higher time and cost efficiencies compared with the traditional terrestrial LiDAR-based data acquisition method.

6 Discussion and Conclusion

In general, effective mobile robot path planning for unknown and clustered environments is challenging because no a priori information of site conditions exists. To overcome these problems, this paper introduces an autonomous method for 3D point-cloud generation through the collaboration between UAV and UGV. From the test results, both commercial laser scanner and UGV yielded satisfactory accuracy. However, the proposed method, with UGV (GRoMI), is more effective in post-processing for point-cloud registration using the SLAM-driven robot localization data. The advantages of using the proposed approach over traditional methods include (1) to automate the point-cloud acquisition process by finding the robot's preferred scan locations and planning navigation paths with the aid of UAV's site map; (2) to remove redundant scans and reduce time and cost for data collection; (3) to reduce missing areas of the target site; and (4) to automatically register multiple scans.

The proposed framework enables mobile robots to robustly and effectively collect high-quality site data, thereby enhancing site inspection and monitoring capabilities and reducing necessary time and cost. Since the robot can frequently update the geometric information of a site, it can be used for several construction management applications including virtual site access from remote places, progress monitoring, defect management, safety, legal dispute, supply chain management, as-built BIM, and more.

However, the implementation of the proposed method is still limited by its dependence on UAV's generated map data. As such, pre-processing for the proposed approach requires more time than the traditional 3D scanning process. For future study, the current robotic approach should be further investigated for cases when UAV data is not available (e.g., indoor construction). In this case, the robot must be able to itself estimate preferred scan locations.

7 Acknowledgment

The work reported herein was supported by a grant (18CTAP-C144787-01) funded by the Ministry of Land, Infrastructure, and Transport (MOLIT) of Korea Agency for Infrastructure Technology Advancement (KAIA) and by the United States Air Force Office of Scientific Research (Award No. FA2386-17-1-4655). Any opinions, findings, and conclusions or recommendations expressed in this material are those of the authors and do not necessarily reflect the views of MOLIT and the United States Air Force. Their financial support is gratefully acknowledged.

References

[1] Y. Cho, C. T. Haas, K. Liapi, and S. V Sreenivasan, "A framework for rapid local area modeling for construction automation," *Autom. Constr.*, vol. 11, no. 6, pp. 629–641, 2002.

[2] Y. K. Cho and C. T. Haas, "Rapid geometric modeling for unstructured construction workspaces," *Comput. Civ. Infrastruct. Eng.*, vol. 18, no. 4, pp. 242–253, 2003.

[3] G. B. Dadi, P. M. Goodrum, K. S. Saidi, C. U. Brown, and J. W. Betit, "A case study of 3D imaging productivity needs to support infrastructure construction," *ASCE Constr. Res. Congr.*, pp. 1052–1062, 2012.

[4] C. Wang and Y. K. Cho, "Smart scanning and near real-time 3D surface modeling of dynamic construction equipment from a point cloud," *Autom. Constr.*, vol. 49, pp. 239–249, 2015.

[5] F. Bosche and C. T. Haas, "Towards Automated Retrieval of 3D Designed Data in 3D Sensed Data," *ASCE J. Comput. Civ. Eng.*, pp. 648–656, 2007.

[6] S. El-omari and O. Moselhi, "Automation in Construction Integrating 3D laser scanning and photogrammetry for progress measurement of construction work," *Autom. Constr.*, vol. 18, pp. 1–9, 2008.

[7] B. Akinci, F. Boukamp, C. Gordon, D. Huber, C. Lyons, and K. Park, "A formalism for utilization of sensor systems and integrated project models for active construction quality control," *Autom. Constr.*, vol. 15, pp. 124–138, 2006.

[8] J. Chen and Y. K. Cho, "Point-to-point Comparison Method for Automated Scan-vs-BIM Deviation Detection," in *2018 17th International Conference on Computing in Civil and Building Engineering*, 2018.

[9] P. Kim, Y. K. Cho, and J. Chen, "Target-Free Automatic Registration of Point Clouds," in *33rd International Symposium on Automation and Robotics in Construction (ISARC 2016)*, 2016, vol. Auburn, US, pp. 686–693.

[10] E. Latimer, D. Latimer, R. Saxena, C. Lyons, L. Michaux-Smith, and S. Thayer, *Sensor space planning with applications to construction environments*. IEEE, 2004.

[11] M. K. Reed and P. K. Allen, "Constraint-based sensor planning for scene modeling," *IEEE Trans. Pattern Anal. Mach. Intell.*, vol. 22, no. 12, pp. 1460–1467, 2000.

[12] C. Zhang, V. S. Kalasapudi, and P. Tang, "Rapid data quality oriented laser scan planning for dynamic construction environments," *Adv. Eng. Informatics*, vol. 30, no. 2, pp. 218–232, 2016.

[13] P. Kim, J. Chen, J. Kim, and Y. K. Cho, "SLAM-Driven Intelligent Autonomous Mobile Robot Navigation for Construction Applications," in *Advanced Computing Strategies for Engineering*, 2018, pp. 254–269.

[14] P. Kim, J. Chen, J. Kim, and Y. K. Cho, "SLAM-Driven Intelligent Autonomous Mobile Robot Navigation for Construction Applications," in *In Workshop of the European Group for Intelligent Computing in Engineering*, 2018, pp. 254–269.

[15] I. Toschi, P. Rodríguez-Gonzálvez, F. Remondino, S. Minto, S. Orlandini, and A. Fuller, "Accuracy evaluation of a mobile mapping system with advanced statistical methods," *Int. Arch. Photogramm. Remote Sens. Spat. Inf. Sci. - ISPRS Arch.*, vol. 40, no. 5W4, pp. 245–253, 2015.

[16] D. Borrmann, R. Heß, H. R. Houshiar, D. Eck, K. Schilling, and A. Nüchter, "Robotic mapping of cultural heritage sites," *Int. Arch. Photogramm. Remote Sens. Spat. Inf. Sci. - ISPRS Arch.*, vol. 40, no. 5W4, pp. 9–16, 2015.

[17] D. D. Lichti and P. Eng, "Ray-Tracing Method for Deriving Terrestrial Laser Scanner Systematic Errors," *J. Surv. Eng.*, vol. 143, no. 2, p. 6016005, May 2017.

[18] S. Parthasarathy, "A Tight Analysis of the Greedy Algorithm for Set Cover," *J. Algorithms*, vol. 25, no. 2, pp. 237–254, 1997.

[19] S. Kohlbrecher, O. Von Stryk, J. Meyer, and U. Klingauf, "A Flexible and Scalable SLAM System with Full 3D Motion Estimation," *Proc. 2011 IEEE Int. Symp. Safety,Security Rescue Robot.*, vol. Kyoto,Japa, no. November 1-5, pp. 155–160, 2011.

[20] P. Kim, J. Chen, and Y. K. Cho, "SLAM-driven robotic mapping and registration of 3D point clouds," *Autom. Constr.*, vol. 89C, pp. 38–48, 2018.

Web-based Deep Segmentation of Indoor Point Clouds

Z.H. Chen[a], E. Che[b], F.X. Li[a], M.J. Olsen[b], and Y. Turkan[b]

[a]School of Electrical Engineering and Computer Science, Oregon State University, United States
[b]School of Civil and Construction Engineering, Oregon State University, United States
E-mail: chenzeh@oregonstate.edu, chee@oregonstate.edu, Fuxin.Li@oregonstate.edu, Michael.Olsen@oregonstate.edu, Yelda.Turkan@oregonstate.edu

Abstract –

Deep learning and neural networks have empowered many tasks including semantic segmentation and image classification. Recently, novel neural networks were proposed that could directly process three-dimensional (3D) point clouds. In this paper, we present a software tool incorporating a variety of measuring tools to analyze and validate raw point cloud data while enabling an interactive segmentation of point clouds using deep learning. One of the primary advantages of implementing deep learning for point cloud segmentation is that it enables feature extraction to be learned through neural networks based on a large amount of data. Our software tool allows users to visualize 3D point cloud data sets containing millions of points in standard web browsers and process 3D point clouds using deep segmentation with deep neural networks. The interaction tool can assist with distinguishing structural buildings elements from non-structural objects in a given dataset.

Keywords –

Point cloud; Deep learning; Web-based interaction

1 Introduction

Point clouds are three-dimensional (3D) models that consist of points compared with other 3D model representations, such as meshes, volumetric models, and depth maps. Point clouds are obtained by scanning the real world using an 3D imaging method such as laser scanning (light detection and ranging, lidar) or photogrammetry. Point cloud data can be transformed into other 3D model representations and products by further processing, modeling, and analysis.

Point cloud data can be utilized in a variety of applications, such as construction progress monitoring, building structural analysis, and generation of 3D models. In addition, point clouds are also widely used in real-time perception applications such as the use of lidar perception in autonomous driving vehicles or robotic SLAM (simultaneous localization and mapping) systems. For most of these applications, point clouds are typically treated as raw data, which requires it to be processed and analyzed to extract useful information.

Building Information Modeling (BIM) is a process involving the generation and management of digital representations called "Building information models" (BIMs), which are files which can be extracted, exchanged or networked to support decision-making regarding a building or other built asset. It is also enabling its users to share and compare their models seamlessly throughout the whole lifecycle of their project, from planning to demolition. It offers a variety of benefits including prevention of data loss from one phase to another, as well as improved visualization and coordination between different trades involved in a project. BIM implementation in the construction industry has increased exponentially in the last decade. Scan-to-BIM is a process of 3D laser scanning a physical space or site to create an accurate digital representation through BIM. This representation can be used for design, progress tracking or project evaluation. The data collection in Scan-to-BIM helps eliminate human error that may occur otherwise when using traditional surveying methods and it enables collection of a high volume of data over a short amount of time. Next, the scanning data (i.e. point cloud) need to be shared with the project team; this is done most commonly by importing the data into the project's common data environment (CDE), which enables the team members to analyze, visualize and model the point cloud. This end-to-end approach delivers more detailed and accurate information about a project and enables one to verify the progress of the work in an objective manner.

Different applications usually employ different approaches to extract features from point clouds. Point features often encode certain statistical properties of the points, are designed to be invariant to certain transformations, and can be classified as intrinsic or extrinsic parameters. They can also be categorized as local features and global features. For a specific task, it is nontrivial to find the optimal feature combination. Deep learning can provide end-to-end training which automates the feature extraction process by learning from existing point cloud data, and could significantly reduce

data complexity for modeling and data analysis in an automated Scan-to-BIM framework.

In the big data era, WebGL and server framework over web browsers has become increasingly popular. Such architectures are supported over a standard browser, and enables developers, artists, companies, researchers to share their data with a wider audience and access their work on any device in any place without the need of installing additional software.

Furthermore, the widespread use of neural networks demands high-performance computational resources, (e.g., multi-core CPUs and GPUs), especially when users are required to work remotely without powerful computing resources. Web-based client-to-server communication architecture and the application of deep learning on the server side allow users to work remotely with massive 3D data regardless of the device they use. Currently, several web-based services, such as Sketchfab and Potree allow users to upload, share and view content without any knowledge about the underlying 3D modeling and geometry mechanics. But to our knowledge no deep learning service have existed.

This paper introduces a prototype web-based end-to-end point cloud processing toolbox that is capable of loading and viewing point cloud data. Furthermore, it is capable of applying neural network semantic scene segmentation and annotating point clouds. This work is expected to be a basic building block to a complete Scan-to-BIM framework.

2 Related Work

2.1 Web-based Massive Point Cloud rendering

Potree [15], a web-based renderer for large point clouds, allows users to view data sets with billions of points, obtained from sources such as lidar or photogrammetry, in real time in standard web browsers. The focus of Potree is on large point clouds, and its measuring tools allow users to visualize, analyze and validate raw point cloud data without the need for a time-intensive and potentially costly meshing step.

PointCloudViz server [19] and the corresponding web client are commercial services by Mirage Technologies, which complement their free desktop lidar viewer.

The streaming and rendering of billions of points in web browsers, without the need to load large amounts of data in advance, is achieved with a hierarchical structure that stores subsamples of the original data at different resolutions. A low-resolution version is stored in the root node and with each level, the resolution gradually increases. The structure enables Potree to neglect regions outside the view frustum, and to render distant regions at a lower level of detail.

ShareLIDAR [16] is a multi-resolution point cloud renderer with hosting service. Its notable features include illumination through normals, an orthographic top view, a sectioning (height-profile) tool and the adjustment of point sizes. However, it loads data in smaller tiles that do not cover the whole data set, which results in a large empty space within the display while the user waits for the data to stream in.

2.2 Point Cloud Feature Extraction

3D point clouds are typically processed using point cloud features that are customized for specific tasks. Point features often encode certain statistical properties of points that are usually classified as intrinsic or extrinsic parameters of transformations, or they are categorized as local and global features.

2.3 Deep Learning for Processing Large Scale Point Clouds

Deep learning is a recent technique used for point cloud processing. Previous research on 3D Convolutional Neural Networks (CNN) convert 3D point clouds to 2D images or 3D volumetric grids. Qi et al. [18] and Hang et al. [9] developed methods that project 3D point clouds or shapes into several 2D images, and then apply 2D CNN for classification. Although these approaches have achieved great results for shape classification and retrieval tasks, they cannot be extended for high-resolution scene segmentation tasks. [22, 9, and 6] presented approaches that voxelize point clouds into volumetric grids by quantization and then apply 3D CNN. These approaches are constrained by the volumetric resolution of the 3D point cloud; further, the computational cost of 3D convolutions is a significant disadvantage, especially when processing very large point clouds. [11] improves the resolution significantly by using a set of unbalanced octrees where each leaf node stores a pooled feature representation. Kd-networks [4] compute the representations in a feed-forward bottom-up fashion on a Kd-tree with a certain size. In a Kd-network, the input number of points in the point cloud needs to be the same during training and testing, which unfortunately does not hold for many tasks.

In [8], an effective feature learning method called PointNet is introduced that directly applies the raw data without preprocessing the point clouds. Point clouds are simple and unified structures and are easier to learn from compared to meshes or other types of 3D models.

2.3.1 Building Information Modeling

Building Information Modeling (BIM) is both a technology and a process that results in easer collaboration between involved parties by using a virtual

3D model of a structure. From the technology perspective, BIM is an object-oriented database that hosts both geometric and non-geometric information such as material types, costs, and scheduling. BIM has been adopted at a growing rate in the construction industry. It is used for a variety of tasks including design coordination (commonly known as clash coordination/detection), constructability analysis, and 3D/4D analysis, amongst others.

Both geometric and non-geometric data stored in BIM should be well defined when developing the BIM model. BIM data is typically stored online on a data cloud to manage and share information among members of a team working on the same project as well as to avoid the potential complications that may arise from the use of models that are not up-to-date.

One of the objectives of the system proposed in this paper is to ensure that it can assist users with model visualization and data management, which are essential for data collaboration and vital to the success of BIM.

2.3.2 System Design

To overcome the weaknesses inherent in previous point cloud processing and visualization approaches, this study aims to provide an efficient data management and visualization solution with a user-friendly interface.

Figure 1 illustrates the major nodes for achieving the goal with their individual function.

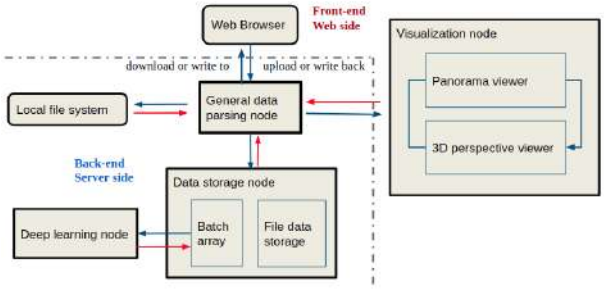

Figure 1. Data flow in the major functionality module of the proposed system

The system can be divided into the front-end and the back-end. The front-end provides the user interaction interface and enables visualization of point clouds using three different approaches. The front-end interaction interface performs several operations, including storing and parsing data into the designated format, which are sent to the back-end. Data parsing is automatically determined by the "General Data Parsing Node". Figure 1 shows that files can be uploaded into the system online or directly by the administrator in the server's file system. After the data processing is complete, the user can download the results or the data that have been processed (such as an intermediate file that is parsed in a different format, a semantic segmentation result, or a 2D panoramic image).

The general data parsing node is one of the core modules of the proposed system. It enables to use different file formats for the input file.

The use of an intermediate file makes sure that for each function module, the input format requirement is not the main hindrance to data flow through the system. This also enables all modules to use the most appropriate file format in order to decrease possible programming difficulties and compatible language problems. The intermediate file communication method ensures the system focuses on the portability and reusability and achieves low coupling, which is convenient for further development and reusing of the code.

After the data been parsed by the "General Data Parsing Node", the formed data will be stored in the data storage node. The data herein has been parsed into two structures. The first structure is in 2D array panorama form, which lists the point cloud information in a 2D array structure following a 2D panorama image sequence that can be traced back to each of the scanners that is used to acquire data. The second structure is in a batch array format, from which we can directly transfer to the neural network in order to train the network for further improvement or simply calculate the semantic segmentation result with the point cloud data from a single scan by going through the forward propagation. We will discuss how data are formed in all these intermediate files in detail in the next section.

The highlight of this system is our "Deep Learning Node", which is an abstract interface that can trigger deep learning related algorithms and trained neural networks obtained in a run. In our extendable system, the neural network model can be changed when desired. Researchers can replace or upgrade the model when they want to have a different model architecture of a network in order to improve the performance, or have a new model that can work on a different task.

Another highlighted feature in this system is the "Visualization Node", which provides a method to visualize the raw data and the analyzed result applies on the raw data views. The panorama viewer and the 3D perspective viewer provide two different ways for users to visualize the point cloud data and task results. The Panorama viewer provides the ability to show the raw data as a panoramic image with original color or by the instance segmentation result processed by the Norvana [2] algorithm. It provides several useful tools that can assist with the organization of the point cloud data and enables users to perform annotation operations on panorama image directly through a canvas. The 3D perspective viewer provides the basic visualization window for viewing the point cloud model in 3D from different perspectives.

2.3.3 Deep Semantic Segmentation of Point Clouds

In this work, the PointNet [8] architecture is utilized in the deep learning function node (Figure 2). The structured batch array, which contains the information per point in an indoor point cloud scene, will be fed to the proposed network. Each point has 9 attributes, including X, Y, Z, R, G, B, and 3D normalized location with respect to the room (from 0 to 1).

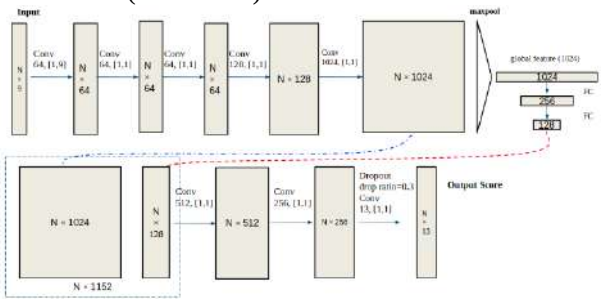

Figure 2. The network architecture based on PointNet baseline structure

The architecture contains 3 consecutive, multiple layer perceptions (MLP). In our implementation, we use an equivalent form of convolutional filters with a size of 1×1 instead.

After the feature learning, resulting in 1024 new point features, we apply a max-pooling layer to down-sample and aggregate these point features into global features. We then make the global features pass through a fully connected (FC) layer to aggregate to 128 features. These 128 features, which are tiled to the same dimension as the number of points, are then concatenated with the previous N×1024 features. After the next several convolutional layers that are similar to previous operations, we obtain the output score of a 13-dimensional array after the softmax layer.

2.3.4 Showcase and Functionality Introduction

The operation with user friendly interaction will lead user to go through the whole pipeline that finish their task step by step.

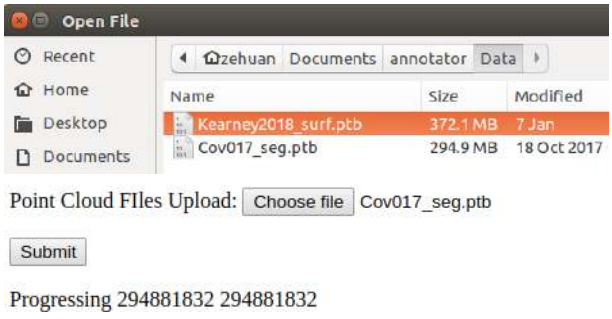

Figure 3. File select (top) and file upload (bottom) interfaces

Figure 3 explains the very first step where a user uploads a data file to the server, and then internally the file parsing node on server side will reformat the data.

After data has been reformatted, the panorama image viewer will pop up and show a panoramic image with original color and with three buttons to allow the following operations: image rotation operations, "show instance segmentation," and "show semantic segmentation."

Figure 4. Panoramic image view

The result of the instance segmentation will show up and generate the canvas overlay on the original color image. The instance segmentation results were generated according to the algorithm [2] using test data collected from a building (Covell Hall) at Oregon State University main campus. This panoramic image is shown with photographic color in different image fuse ratio (opacity). The interface also includes the panel to show which color block indicates which class ID. In that case, people can easily access the classification result directly from the algorithm and perform manual annotation, or refine the result. The user can further improve the automated results of the algorithm or annotate the dataset with a real ground truth classification result and feed it into deep neural network.

Figure 5. Panoramic image view with colormap overlay representing the instance segmentation results obtained using Norvana algorithm

2.3.5 Instance Segmentation

The classification and segmentation algorithm are the

core operation module in our system. Norvana, introduced in [2] is a highly efficient and novel approach to segment point clouds. Segmentation is a common procedure of post-processing to group the point cloud into a number of clusters to simplify the data for the sequential modelling and analysis needed for most applications. Norvana rapidly segments laser scan data based on edge detection and region growing. The algorithm computes incidence angles and then performs normal variation analysis to separate silhouette edges and intersection edges smooth surfaces. A modified region growing algorithm groups the points lying on the same smooth surface. The proposed method efficiently exploits the gridded scan pattern utilized during acquisition of laser scanning data from most sensors and takes advantage of parallel programming to process approximately 1 million points per second. Moreover, the proposed segmentation does directly not require estimation of the normal at each point, which limits the errors in normal estimation propagating to segmentation. Figure 6 shows an example scan segmented by Norvana.

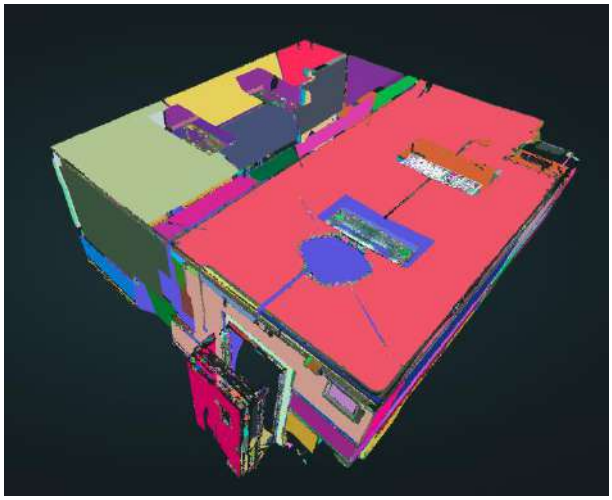

Figure 6. Norvana segmentation results in 3D perspective view via Potree

Along with the appearance of the 2D panorama with instance segmentation overlay and tools, the 3D viewer of the instance segmentation result is also shown (Figure 6). Orbit navigation with mouse and keyboard are supported. This viewer is powered by a Nested octree data structure. Points are rendered in hierarchal order to minimize the use of computational resources and avoid crashing the browser.

Table 1. Indoor object classes

Structural classes		Non-structural classes	
Column	Wall	Door	Window
Ceiling	Floor	Bookcase	Board
Beam		Chair	Sofa
		Table	Clutters

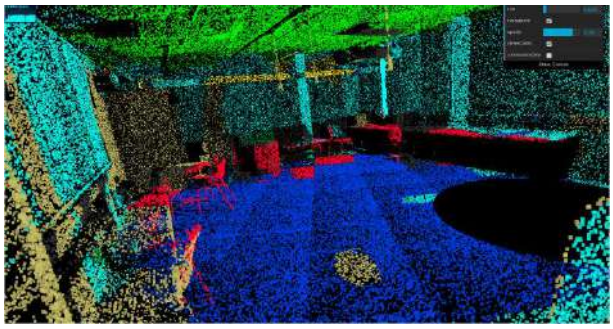

Figure 7. Original semantic segmentation result showing all classes

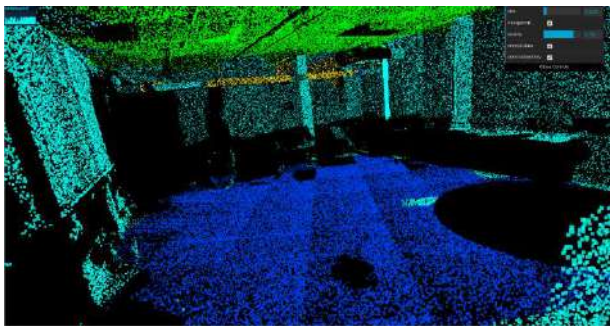

Figure 8. The scene after the semantic filter application to remove the non-construction class objects in the point cloud

3 Experiment

This section details the experiment conducted on the S3DIS (3D Semantic Parsing of Large-Scale Indoor Spaces) dataset that is visualized on the 3D viewer and segmented using deep neural network [1].

The S3DIS dataset (Figure 9) is composed of five large-scale indoor areas from three different buildings, each covering approximately 1900, 450, 1700, 870 and 1100 square meters (total of 6020 square meters). These areas show diverse properties in architectural style and appearance, including office areas, educational and exhibition spaces, conference rooms, personal offices, restrooms, open spaces, lobbies, stairways, and hallways.

One of the areas includes multiple floors, while all the other areas include only one floor. All the point clouds are automatically generated without any manual intervention using the Matterport scanner.

The dataset contains 3D scans of six different areas including 271 rooms. Each point in the scan is annotated manually with one of the semantic labels from the 13 categories (chair, table, floor, wall, etc., and clutter). We can further distinguish these 13 classes as a structural object (e.g., floor, ceiling wall, etc.) or a non-structural object (e.g., table, sofa, door, etc.). With the tag of different classes, we can visualize the two main clusters

(structural vs. non-structural, Figure 7) or view individual classes (or combination) via checking each class of interest (Figure 8).

The training data points are split room by room, and the rooms were split into blocks with 1m x 1m area. Then the segmentation algorithm in PointNet was trained to predict point classes of each block. Each point is represented by a 9-dimensional vector of XYZ, RGB and normalized location as to the room (from 0 to 1). For training, 4096 points were randomly selected from each block on-the-fly. After training, all the points in the testing dataset are tested on.

The precision-recall curve of the segmentation is calculated for both construction structure and non-construction structure points (Figure 9). This result is transferred from original 13-class semantic segmentation for each point into binary classification.

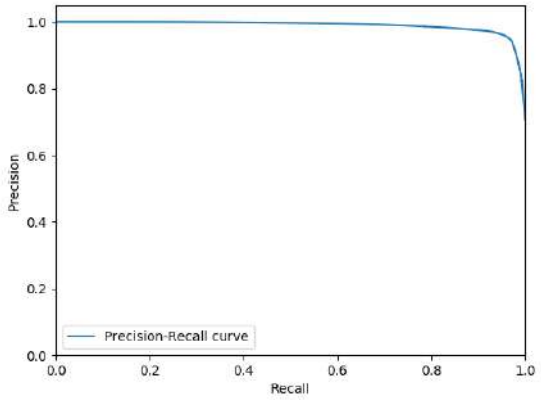

Figure 9. Precision-Recall curve for structural and non-structural objects classification in the S3DIS dataset

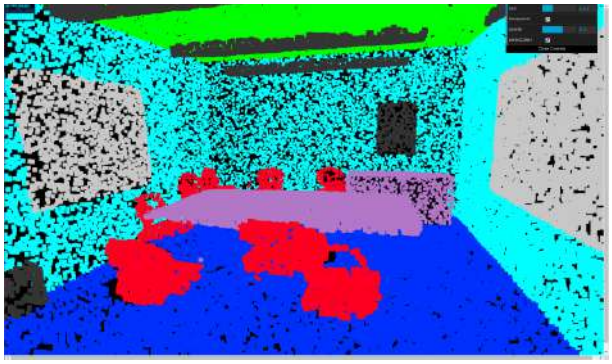

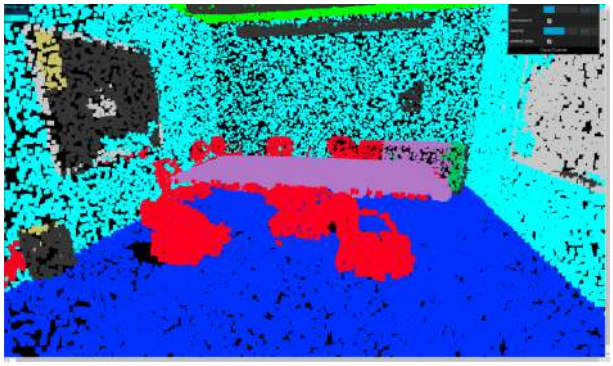

Figure 10. Conference room scene in S3DIS dataset. The ground truth semantic labelling result (top), and the prediction result (bottom) in 3D perspective viewer.

Figures 10-12 present three different point clouds of indoor scenes, selected from the S3DIS dataset. Each figure contains ground truth semantic labeling and the prediction results showing different classes.

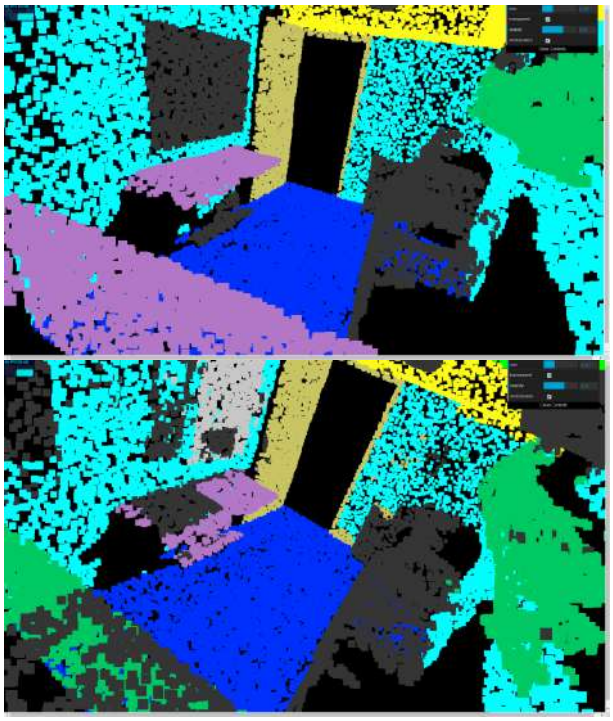

Figure 11. Copy room scene in S3DIS dataset. Top view shows the ground truth, and the bottom view shows the prediction labelling result

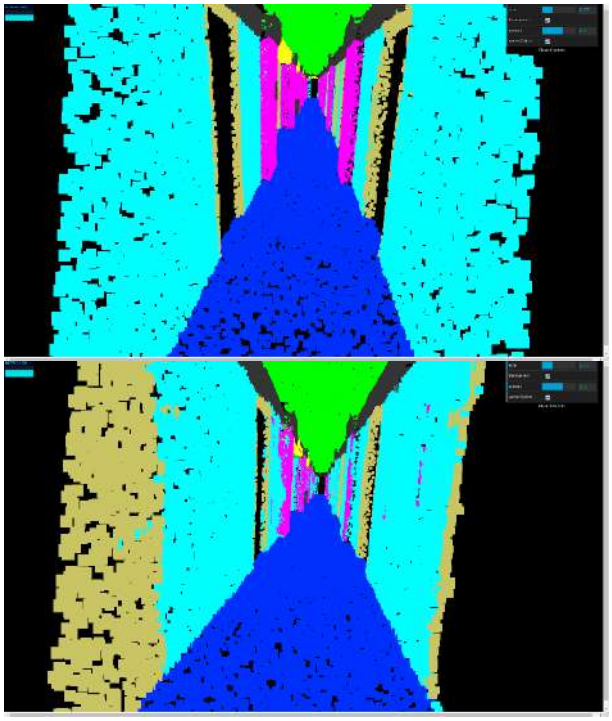

Figure 12. The ground truth (top), prediction result (bottom)

In Figure 10, the board and the clutter were slightly mismatched since the white board and the paint (belong to clutter class) could not be differentiated by the segmentation algorithm. However, tables and chairs were classified correctly with very little mismatch using PointNet.

In Figure 11, in the copy room scene, semantic labeling was performed with high accuracy. However, there were still some mismatches. For example, the table was mismatched with the part of ceiling on the bottom-left corner of the figure.

In Figure 12, a hallway scene is presented. This scene does not contain many corners or small objects. Thus, the segmentation of walls, floor and ceiling were done successfully. The figure also demonstrates that the segmentation prediction result is very close to the ground truth.

4 Conclusion and Future work

This paper presented a system that is capable of rendering 3D point clouds with millions of points real time in standard web browsers. It uses intermediate data storage format and data stream parsing to ensure that the proposed system is compatible with different file formats. In other words, it can process data regardless of the input file format and the neural network architecture. Furthermore, utilization of asynchronous mechanism and recall function during the front-end step dramatically reduces the total data download / visualization time and improve the runtime speed. The general file storage node and multiple view approach enable the system to render raw point cloud data in different representations, including panoramic and 3D viewer. To achieve a better visual quality, methods such as a multi-layer canvas interaction interface was implemented in order to increase the computing efficiency and to enable visualization and input interaction process in parallel.

Deep semantic segmentation results obtained from indoor scene point cloud data obtained from the S3DIS dataset are also presented, where each point in the dataset was labeled as structural and non-structural classes.

In future work, the point cloud rendering efficiency of the system will be improved, and other interaction tools including the synchronous correspondence of two viewers will be added. Furthermore, point cloud selection tools should be added to the 3D perspective viewer. Another issue that needs to be addressed in future work has to do with filling the empty spaces, i.e. “holes”, after filtering out the non-construction objects. More efficient point cloud semantic segmentation algorithms and network architecture could also be applied to the more recent PointConv [22] architecture.

Acknowledgements

Contributions by co-authors Che and Olsen were funded by the National Science Foundation (Award CMMI-1351487).

References

[1] Iro Armeni, Sasha Sax, Amir R Zamir, and Silvio Savarese. Joint 2d-3d-semantic data for indoor scene understanding. arXiv:1702.01105, 2017.

[2] Che, E. and Olsen, M.J. Multi-scan segmentation of terrestrial laser scanning data based on normal variation analysis. *ISPRS Journal of Photogrammetry and Remote Sensing*, 143:233-248, 2018.

[3] URL:https://www.khronos.org/registry/webgl/specs/1.0/ [Online; accessed 22-Oct-2018].

[4] Roman Klokov and Victor Lempitsky. Escape from cells: Deep kd-networks for the recognition of 3d point cloud models. In Computer Vision (ICCV), 2017 IEEE International Conference on, pages 863–872. IEEE, 2017.

[5] matplotlib.org. Choosing Colormaps. https://matplotlib.org/users/colormaps.html#grayscale-conversion, 2015. [Online; accessed 28-Dec 2018].

[6] Daniel Maturana and Sebastian Scherer. Voxnet: A 3d convolutional neural network for real-time object recognition. In Intelligent Robots and

Systems (IROS), 2015. IEEE/RSJ International Conference on, pages 922–928. IEEE, 2015.

[7] Overview and Comparison of Features. https://github.com/PointCloudLibrary/pcl/wiki/Overview-and-Comparison-of-Features, 2015. [Online; accessed 28-Oct-2018].

[8] Charles R Qi, Hao Su, Kaichun Mo, and Leonidas J Guibas. Pointnet: Deep learning on point sets for 3d classification and segmentation. Proc. Computer Vision and Pattern Recognition (CVPR), IEEE, 1(2):4, 2017.

[9] Charles R Qi, Hao Su, Matthias Nießner, Angela Dai, Mengyuan Yan, and Leonidas J Guibas. Volumetric and multi-view cnns for object classification on 3d data. In Proceedings of the IEEE conference on computer vision and pattern recognition, pages 5648–5656, 2016.

[10] Charles Ruizhongtai Qi, Li Yi, Hao Su, and Leonidas J Guibas. Pointnet++: Deep hierarchical feature learning on point sets in a metric space. In Advances in Neural Information Processing Systems, pages 5099–5108, 2017.

[11] Gernot Riegler, Ali Osman Ulusoy, and Andreas Geiger. Octnet: Learning deep 3d representations at high resolutions. In Proceedings of the IEEE Conference on Computer Vision and Pattern Recognition, volume 3, 2017.

[12] Radu Bogdan Rusu, Nico Blodow, and Michael Beetz. Fast point feature histograms (fpfh) for 3d registration. In Robotics and Automation, 2009. ICRA'09. IEEE International Conference on, pages 3212–3217. Citeseer, 2009.

[13] Radu Bogdan Rusu, Zoltan Csaba Marton, Nico Blodow, and Michael Beetz. Learning informative point classes for the acquisition of object model maps. In Control, Automation, Robotics and Vision, 2008. ICARCV 2008. 10th International Conference on, pages 643–650. IEEE, 2008.

[14] M Schutz. Potreeconverter-uniform partitioning of point cloud data into an octree, 2014.

[15] Markus Sch¨utz. Potree: Rendering large point clouds in web browsers. Technische Universit¨at Wien, Wiede´n, 2016.

[16] URL: https://www.sharelidar.com/ [accessed 22-Oct-2018].

[17] URL: https://sketchfab.com/ [accessed 22-Oct-2018].

[18] Hang Su, Subhransu Maji, Evangelos Kalogerakis, and Erik Learned-Miller. Multi-view convolutional neural networks for 3d shape recognition. In Proceedings of the IEEE international conference on computer vision, pages 945–953, 2015.

[19] Mirage Technologies. PointCloudViz Server. http://server.pointcloudviz.com/, 2015. [Online; accessed 22-Oct-2018].

[20] URL: https://threejs.org/, 2015. [accessed 22-Oct-2018].

[21] Oriol Vinyals, Samy Bengio, and Manjunath. Kudlur. Order matters: Sequence to sequence for sets. arXiv preprint arXiv:1511.06391, 2015.

[22] Wenxuan Wu, Zhongang Qi, and Li Fuxin. Pointconv: Deep convolutional networks on 3d point clouds. arXiv preprint arXiv:1811.07246, 2018.

[23] Zhirong Wu, Shuran Song, Aditya Khosla, Fisher Yu, Linguang Zhang, Xiaoou Tang, and Jianxiong Xiao. 3d shapenets: A deep representation for volumetric shapes. In Proceedings of the IEEE conference on computer vision and pattern recognition, pages 1912–1920, 2015.

Ontology for Logistics Requirements on a 4D BIM for Semi-Automatic Storage Space Planning

J. Weber[a], J. Stolipin[b], M. König[a], and S. Wenzel[b]

[a]Chair of Computing in Engineering, Ruhr-University Bochum, Germany
[b]Department of Organization of Production and Factory Planning, University of Kassel, Germany
E-mail: jan.m.weber@rub.de, jana.stolipin@uni-kassel.de, koenig@inf.bi.rub.de, s.wenzel@uni-kassel.de

Abstract –

Well-coordinated construction site logistics are important for the efficient assembly of large-scale plants. Delays in logistics have a negative impact on assembly processes and vice versa. Incorrect storage or improper transport can lead to damage to the sensitive plant components. All relevant logistical constraints must therefore be systematically analyzed, assessed and evaluated during the planning of construction site and assembly processes. For this purpose, precise knowledge of the logistical requirements of each individual component is very important. Nowadays this information is not available in digital form and must be elaborately compiled and evaluated manually. The logistical requirements are also essential for the planning of processes. So-called 4D models are already being created and used in plant construction, but storage and transport processes on the construction site are only rudimentarily taken into account. In general, the 4D models only describe the construction process. In order to better investigate and plan construction site logistics using 4D models, the logistical requirements must be identified, classified, generated for each plant component and made available digitally. Therefore, an ontology for the description of logistic boundary conditions and requirements is presented in this paper. The focus is on large-scale plant engineering and the special storage and transport conditions of the various components. The ontology is also a knowledge base to identify which information is required for the planning of construction site logistics and which may need to be added. Then, for example, semi-automatic allocation of storage space can be calculated, an analysis of the utilization of transport equipment can be carried out or the impact on the assembly processes can be determined.

Keywords –

Logistics requirements; Ontology; 4D BIM; Site layout planning; Plant construction

1 Introduction

A precisely coordinated logistics system is important for the efficient and cost-effective handling of projects in large-scale plant construction. This is particularly important as very sensitive and large components are usually transported and stored in plant construction. Planning includes the selection, design, dimensioning and optimization of processes, material flows and resources. Depending on the complexity of the large-scale plant, many different boundary conditions must be considered in the project-specific planning of construction site logistics. The planning and control of construction site logistics for such large-scale projects are not sufficiently supported by digital planning tools. Nowadays, this requires extensive project experience. If transport and storage conditions are not correctly analyzed and adhered to, this not only leads to delays in assembly, but also to damage to the sensitive system components. In the worst case, elaborate rework or complete disassembly is necessary.

Digital models have also been used for several years in large-scale plant construction for the planning and prefabrication of plant components. However, the digital models are hardly used on site. Even if system components are visualized on the construction site with the help of mobile devices, there is currently no IT-based support for planning and controlling the logistical processes on the construction site in detail. On-site transport, storage and detailed intermediate steps cannot be analyzed, checked and visualized with existing concepts and solutions. Certain information for the precise planning and control of logistics is already available based on the digital model. However, the information available is insufficient and must be systematically supplemented.

In our approach, we examine the required logistics information and describe it formally and evaluably in the Web Ontology Language (OWL) format. This ontology is linked to the information of a 3D Building Information Model (BIM) to generate logistics information for the specific component or assembly task.

2 Related Work

The planning of construction projects is generally associated with uncertainties, because the customer-specific engineering and construction of large-scale plants fundamentally differ from stationary series production. In addition to technical and structural limits, organizational project specifications, such as production steps, construction phases or resource disposition as well as logistical boundary conditions in particular are relevant aspects. Gutfeld et al. (2014) [1] describe the problems and deficits of project management in plant construction and present a method for simulation-based and logistically integrated project management in plant construction. Nowadays, the construction schedule is manually created by project managers based on their experience. The assumptions they made during the planning phase can prove to be disadvantageous in the actual construction process. This is not only due to delays in the delivery of materials, but may also be due to difficulties during assembly. A number of aspects can affect project plans, such as weather, lack of storage spaces or limited resources [2]. Therefore, a subsequent, continuous review and, if necessary, adjustment of the schedules is required. Until now, the focus of the project managers has been on the delivery dates and the duration of the assembly processes. Logistics on the construction site itself has received little attention so far. Usually, logistics processes are regulated spontaneously on site. This leads to unnecessary delays due to lack of suitable storage areas and continuous material search.

The construction industry is currently experiencing a change to a digital construction planning process mainly with the help of BIM. The BIM method is used to provide necessary information of a specific building project starting from the planning phase up to facility maintenance with the help of an intelligent 3D-Model. This is achieved by expanding the geometrical information (3D) of the model with additional information. A BIM-model can be used for visualization, fabrication drawings, code reviews, forensic analysis, facilities management, cost estimating, conflict, interference and collision detection and construction sequencing. During the whole construction process, an up-to-date as-built BIM-model helps keep an overview of the construction site and to avoid incorrect planning that may cause interferences of different trades. These interferences generally cost time, which leads to higher costs due to additional wage costs or contractual fines because of delay [3]. The Industry Foundation Classes (IFC) provide a comprehensive and standardized data model for the vendor-neutral exchange of digital building models. A significant advantage of IFC is that digital model objects can be dynamically extended by any additional information [4].

To implement an integrated digital planning, the site layout also needs to be integrated into BIM-models. A BIM-based site layout planning not only provides 3D models of site equipment, where 2D site layout plans can easily be derived from, but also considers scheduling information. The linking of building elements or construction equipment with activities of a time schedule is called a 4D model. The main purpose is the visualization and analysis of the construction processes and the temporally variable construction site equipment [5]. The use of 4D-BIM promotes communication and enables a uniform understanding between all project participants. Variant assessment tests provide support in procurement with material lists and material calculations. The planned progress can be represented at any time during the construction project and delays can be seen by comparison with an as-built model. This also supports the analysis of work processes.

An essential aspect of BIM is the linking of building elements with other external information for a certain application. Which information is linked or added under which conditions can be defined using a higher-level ontology. An ontology describes a hierarchy of concepts (class and subclass) linked by relationships, adding appropriate axioms to express relationships between concepts and limit their interpretation. Furthermore, ontologies can be used to describe a common vocabulary of terms and the specification of their meaning for the knowledge area [6]. Special ontologies have already been developed in various research approaches in the construction industry. Zhang and Issa (2012) use an ontology to extract specific information from a BIM-model [7]. El-Gohary et al. (2010) show a concept of a domain ontology for supporting knowledge-enabled process management and coordination across various stakeholders, disciplines, and projects [8]. Kim et al. (2009) use an ontological consistency checking for design coordination in BIM [9]. Lee et al. (2015) create an ontology model for supporting information handling of off-site automatic prefabrication and on-site assembly [10]. In order to achieve the target of just-in-time (JIT) production and lean construction, Xiong et al. (2018) use the Process Specification Language (PSL) based ontology to unify the process information from multiple planning software applications [11]. Pedro et al. (2017) use an ontology for linking and sharing Job Hazard Analyses (JSA), safety rules and training contents for construction safety [12]. For the controlling of construction site logistics, it is important to have (near) real-time data to confirm the planned schedule. Therefore, Isaac (2016) reviewed existing scheduling methods and compared their outputs with the data provided by automated monitoring technologies. He proposes ways in which scheduling methods can be enriched in order to better support real-time monitoring and control processes [13]. One of the key integration gateways between BIM and ontology is represented by the ifcOWL and ifcWoD [14]. These ontologies allow the publication

of IFC-based building models using the Resource Description Framework (RDF) data model.

3 Methodology

An essential requirement for planning and control in large-scale plant construction is the systematical description of all logistical constraints according to the specific project. There are different requirements for different plant components and parts. Certain components must be specially stored and transported. Suitable storage areas and transport aids have to be available for this purpose. This information must be systematically recorded, documented and made available digitally in advance. In our concept describes below, the logistical requirements are described flexibly and they are reusable with the help of an ontology. In large-scale plant construction, the focus lies on sensitive and costly plant components. The components are usually prefabricated and partly pre-assembled. Afterwards, the components are transported to the construction site. The next step is often an intermediate storage. On international construction sites, most problems arise during this intermediate storage and corresponding transport.

For typical plant components and projects in large-scale plant construction, our ontology covers all essential logistical boundary conditions. Complex dependencies between the components, means of transport and logistic influencing variables are modelled. The ontology is thus a formally ordered representation of a set of concepts and the relationships between them. The ontology is used to provide expert knowledge on logistic processes on construction sites in a digitized and formal form for planning and control. Furthermore, ontologies contain inference and integrity rules, i.e. rules on conclusions and on ensuring compliance.

We worked out company-specific requirements by analyzing the results of surveys on the topic of logistics and assembly planning for small medium-sized (SME) companies by means of expert interviews and case study analyzes. Here, other companies were also involved in individual discussions in order to record project and product-specific boundary conditions regarding organization, technology, personnel, quality and safety measures and country-specific regulations to be observed. In addition, requirements regarding the content of a digital planning and management of the construction logistics are included. At the same time, it is being examined how and to what extent product-specific restrictions must be formulated.

It is assumed that a digital model of the plant and the site equipment as well as associated and linked assembly processes for the individual components are available (see Figure 1). The existing digital models (4D-BIM including construction site layout) are imported and evaluated. This means that the components, storage areas, transport aids, processes and other boundary conditions are extracted. The ontology is used to classify the various objects and to conclude the associated logistical requirements. Therefore, every object needs to provide the standard properties, inter alia, family, type, identifier and dimensions. With the help of manual inputs via a user interface, logistics information, respectively logistics requirements per component, can be edited as well as extended and later used for planning and controlling on-site logistics.

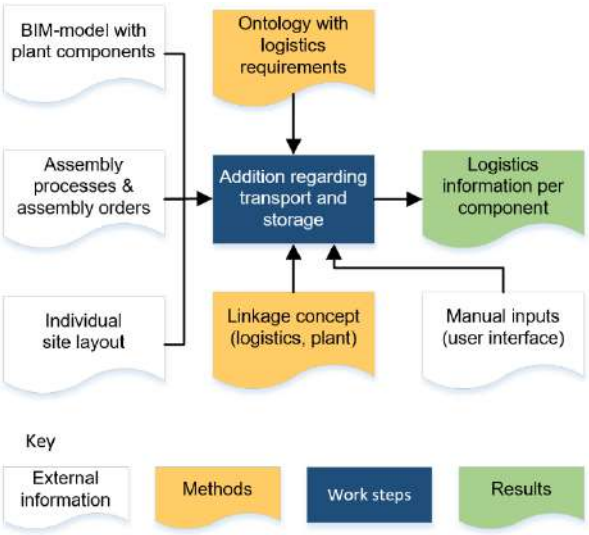

Figure 1. Methodology overview

4 Ontology for Logistics Requirements

When planning onsite-logistics, it is important to consider the specific requirements of the plant components. For space and cost reasons, not all components can be stored in secure areas. Therefore, the use of different types of storage areas is appropriate. Secure areas should be provided for very sensitive or very valuable components. Such components are typically present particularly in large-scale plant construction. Components that cannot be mounted directly after delivery (e.g. due to delays in the assembly of previous components) must be secured accordingly. Other components, which are sensitive to environmental influences such as dust, sunlight, cold or moisture, must be stored in closed storage areas. However, if components are to be protected from rain and direct sunlight only, a covered area will be a sufficient storage location.

If components react very sensitively to external influences, they will be specially packaged. The disadvantage

of packaging is that often special transport aids are requires and more waste is produced. In this case, the disposal areas must be enlarged or reorganized accordingly. The construction site layout must also be analysed and taken into account in detail. For example, it must be determined which transport routes and areas are available. Figure 2 shows a typical layout of a construction site in large-scale plant construction.

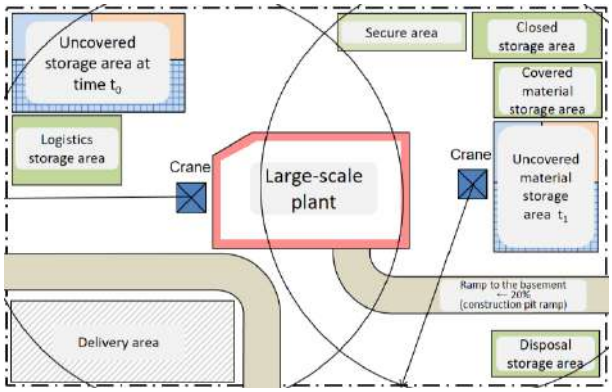

Figure 2. Construction site layout with typical logistical elements

In connection with the storage location, the logistical requirements of the components must also consider that they can be reached and equipped in a time-effective manner (e.g., only components of the same type may be stacked). The range of the cranes must also be taken into account. It should be noted, for example, that a direct crane operation from the truck to the covered storage areas might not be possible due to the roofing. For the affected components, lift trucks, or forklifts must be available on delivery, as well as suitably qualified personnel. In some cases, roof elements of the storage areas must also be removed for the delivery of large, heavy equipment requiring appropriate storage. JIT delivery should be preferred for such components.

During transport and storage of components on the construction site, the following information must be observed:

- package size (number of components per package),
- weight,
- packaging dimensions,
- permissible temperature range,
- permissible (air) humidity range,
- shock sensitivity,
- permitted change of position,
- stackability,
- fragility,
- legal requirements,
- hazardous content,
- just-in-time priority,
- assembly order.

For a valid planning of logistics processes, it is important to have the necessary project-relevant information available. This information can also be used to optimize logistics processes on the construction site. The logistical requirements should therefore be known at an early stage. The exact definition of the logistics processes (transport and storage at the construction site) depends not only on the components of the large-scale plant, but also on the delivery dates, assembly processes and other conditions at the construction site. In order to optimize assembly and logistics processes, planners must be provided with project-relevant information in the right quality at the right time. BIM is a suitable method for storing

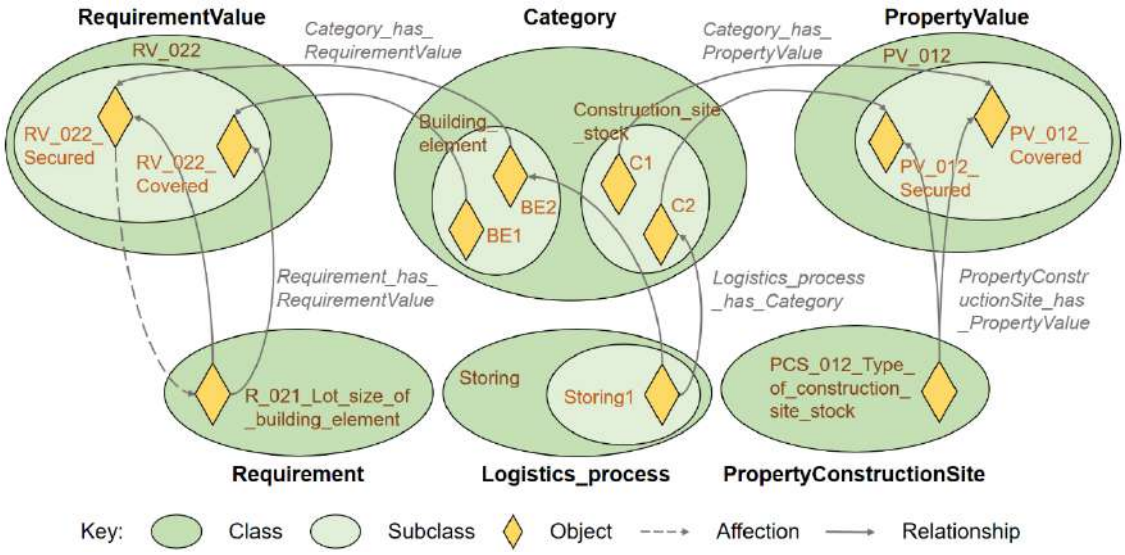

Figure 3. Detail of the basic structure of the developed ontology

this information and making it available to all parties involved. For the planning of logistics processes in large-scale plant construction, requirements for components, construction site equipment, etc. were examined and confirmed with the help of an interview study.

The ontology is mainly designed to support the planning of construction site logistics. For this purpose, existing information in the form of BIM-models of the objects of the plant to be built, the necessary assembly processes and scheduled resources are analyzed based on the ontology and are supplemented by necessary logistical information. The ontology provides a basis for summarizing requirements for the planning of logistics processes on the construction site in large-scale plant construction. In its semantic structure, the planning-relevant information on requirements, prerequisites for site equipment and planning objects (see Figure 3, class *Category* with *Construction_site_stock*, *Building_element* etc.) can be linked, represented and saved. The class *Requirement* contains a list of possible logistical requirements.

Currently ca. 20 pre-defined requirements are available. The characteristics of these requirements are described in the *RequirementValue* class. The individual components relevant to planning (such as *Assembly_group*, *Assisting_tool*, *Building_element*, *Construction_site_stock*, *Control*, *Data*, *Means_of_transport*, *Staff*, *Structure*, *and Working_environment*) are described in the *Category* class. The processes to be planned (*Assembly_process* and *Logistics_process* with *Search*, *Storing* and *Transport* subclasses) are defined in the *Process* class. They are assigned to certain properties in relation to the construction site facilities (*PropertyConstructionSite*), whereby the values of these properties are also assigned in a class called *PropertyValue* is defined. The list *PropertyConstructionSite* with the properties and their characteristics can also be extended. To compare the requirements with a digital model, the class *Sources* is defined with subclasses *BIM* and *Calculations*.

The ontology editor *Protégé 5.2* [15] was used to develop the ontology. The hierarchy of the ontology is shown in Figure 4. The *RequirementValue* and *PropertyValue* classes were created to group the possible characteristics of the properties and requirements. They group the values into individual numbered types (subclasses) and display their possible values in the form of objects (see Figure 4).

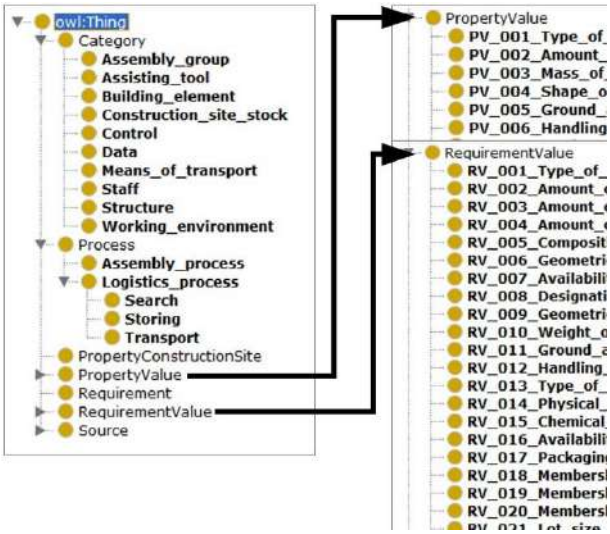

Figure 4. Classes *RequirementValue* and *PropertyValue*

With the help of the proposed ontology, the information relevant for planning can be linked and visualized in the *Protégé* editor with the help of *OntoGraf* (see Figure 5). This visualization helps to understand and verify the ontology.

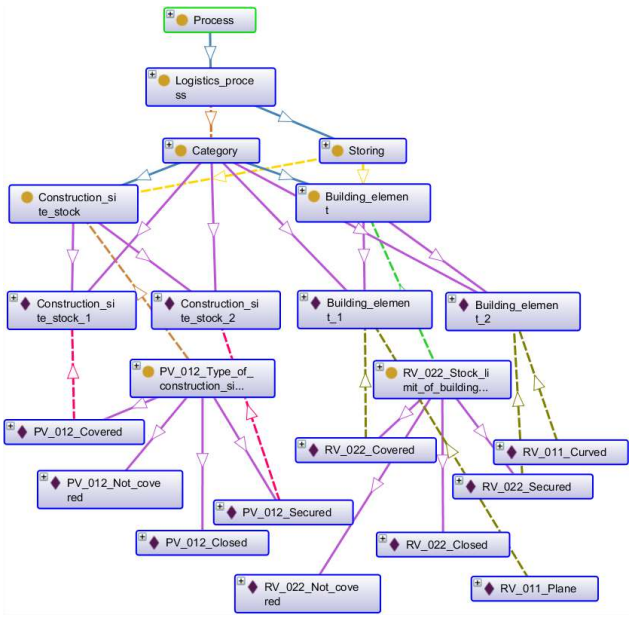

Figure 5. Graphical representation of the ontology in OntoGraf

Figure 6 shows how the limitations of a component (to be stored only in a covered place) influence the storage process. The associated storage process can therefore only be planned considering this requirement. For this purpose, the conditions on the construction site must be examined with regard to a covered storage area and the storage of the component in such a storage area must be planned. Afterwards, the corresponding relationship is set according to this relationship.

Figure 6. Classes *Requirement* and *PropertyConstructionSite*

5 Evaluation of the Ontology

The proposed ontology can be used in the BIM-based planning of site logistics processes to share knowledge about site logistics. This ontology will assist project participants in two areas. First, it will help to identify and classify the requirements for planning individual processes, as the user may not have enough logistics knowledge to fully incorporate this information into BIM-models. Second, it will help to analyze the information from a BIM-model in relation to logistics planning and assign it to the processes to be planned. These two cases are explained in the following sections using the proposed ontology. The queries are created with the *Protégé 5.2* tool.

5.1 Case 1 - Ontology to Read the Requirements for Planning the Individual Processes

When creating BIM-models, these requirements can be incorporated into the model in the form of planning-relevant information. For this purpose, a checklist can be created using the ontology in order to check such planning-relevant information in the model.

Simple ontology queries can be performed in *Protégé 5.2* using either a DL query or a SPARQL query. SPARQL is a query language for RDF, i.e. a query language for databases capable of retrieving and editing data stored in RDF format [16]. Table 2 shows an extract of the result of the SPARQL query shown in Table 1 that retrieves *Requirements* relevant to logistics planning. This list of planning-relevant information can be used as a checklist.

Table 1. SPARQL query for requirements

```
PREFIX bimlog: <http://www.semantic-web.org/user/ontologies/2018/12/bimlog#>
SELECT ?Requirement
WHERE { ?Requirement a bimlog:Requirement}
order by asc(str(?Requirement))
```

Table 2. Results of SPARQL query for requirements

Requirement
R_001_Type_of_assembly_group
…
R_008_Designation_of_building_element
…
R_010_Weight_of_building_element
…
R_039_Transmission_speed
…
R_051_Priority_of_task
…
R_060_Lot_size_of_building_element
…

5.2 Case 2 - Analysis of Information from BIM-Models in Relation to logistics Planning

If the information on the individual category classes (e.g. *Building_element*) from BIM-models is integrated into the ontology, the missing information can be analyzed and supplemented.

Table 3 shows the SPARQL query where components are retrieved, their requirement values are queried and restricted to the referring requirements of warehouse or transport restrictions (see Table 4).

Table 3. SPARQL query for Building_element and RequirementValue

```
PREFIX bimlog: <http://www.semantic-web.org/user/ontologies/2018/12/bimlog#>
SELECT ?Building_element ?Stock_limit
WHERE {
?Building_element a bimlog:Building_element.
?Building_element bimlog:Category_has_requirementValue ?Stock_limit.
?Stock_limit a bimlog:RV_022_Stock_limit_of_building_element}
```

Table 4. Results of SPARQL query for Building_element and RequirementValue

Building_element	Stock_limit
Building_element_2	RV_022_Secured
Building_element_1	RV_022_Covered

Queries can be carried out to obtain further information on transport and storage on the construction site, to find out where the construction elements are stored on the construction site and by which means of transport they can be transported. It is also possible to add new recommendations to the requirements according to use. For example, it is also possible to define automatic recommendations to support the decisions of project planners.

In our approach, we used the 4D-BIM software ceapoint desiteMD to import an IFC-format building model. As shown in Figure 7 information based on the developed ontology can help to visualize specific elements for the logistics planning.

Figure 7 shows two states of the visualization. In the upper screenshot, the entire plant is shown at the time t_1, in the lower screenshot, however, the object properties are used to highlight and to show only all the components in question. In this sample model, these are the bolts, queried by their amount and *Weight_of_building_element*. The advantage of the visualization in this example is the quick recognition of a possible storage position for short transportation paths of these small but numerous elements. Furthermore, possible logistical problems or potentially vulnerable components can be identified. For each element, IFC 3D Models only provide standard properties e.g. name, dimensions, material and identifier, while the ontology database only provides general logistics information, independent of individual elements.

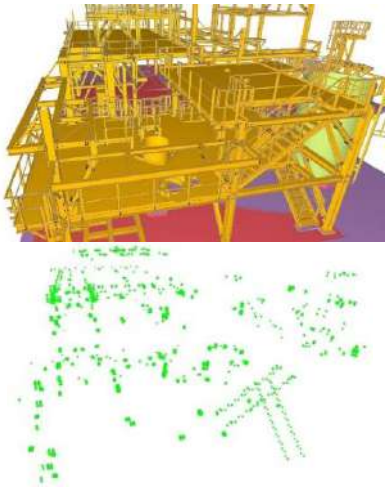

Figure 7. Highlighted consumable building components

To receive the specific logistics information for each element the information of the ontology database and the IFC 3D-model need to be linked as shown in Figure 8.

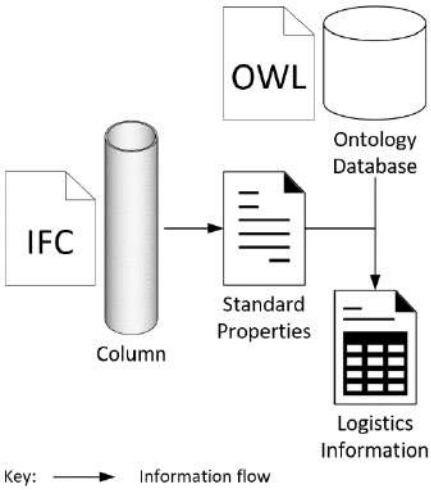

Figure 8. Receiving and linking logistics information

The link between the IFC and the OWL format may be established e.g. with the software *ceapoint desiteMD* via JavaScript and the help of the *Apache Jena RDF API* (Application Programming Interface).

6 Conclusion & Outlook

The definition of the specific requirements and the development of the ontology with the support of the surveyed companies creates the methodical prerequisite for semantically combining logistics, assembly and product descriptions to ensure a standardization and transferability of the results. This approach enables companies to

identify gaps in their planning to ensure smoother operation, to improve processes to reduce costs and save time on the job site.

Today, there are no commercial solutions on the market or scientific approaches available to implement a BIM-based logistics model. Therefore, new ground is broken with the conceptual work carried out in our approach. Based on the results of this work, software solutions can be developed for the coupling of IFC models and OWL ontologies. Based on our methodology, comprehensive databases can be created and will support project managers and planners to plan their construction schedules and to ensure a smoother progress of the projects. These databases can be continually supplemented, so that these knowledge bases grow gradually and require only fewer adjustments in future projects. Furthermore, the component information could also be extended by empirical values for the assembly time, thus ultimately enabling semi-automatic scheduling, taking into account all logistical requirements on the construction site.

Acknowledgements

The results presented in this paper originated in the joint research project "BIMLog - BIM-Based Logistics Planning and Control in Large-Scale Plant Construction" of the University of Kassel and the Ruhr University Bochum. The Industrial Collective Research (IGF) Operation (19720 N) of the Bundesvereinigung Logistik e.V. (BVL) was funded via the Industrial Research Associations (AiF) under the program for the promotion of the IGF by the German Federal Ministry for Economic Affairs and Energy (BMWi) based on a resolution by the German Bundestag.

References

[1] Gutfeld T., Jessen U., Wenzel S., Laroque C. and Weber J. A technical concept for plant engineering by simulation-based and logistic-integrated project management. In *Proceedings of the Winter Simulation Conference*, Savanah, GA, USA, 2014.

[2] Castro-Lacouture D., Süer G. A., Gonzalez-Joaqui J. and Yates J. K. Construction Project Scheduling with Time, Cost, and Material Restrictions Using Fuzzy Mathematical Models and Critical Path Method. *Journal of Construction Engineering and Management*, (10):1096–1104, 2009.

[3] Khoshnava S. M., Ahankoob A., Preece C. and Rostami R. Potential application of BIM in construction dispute and conflict. In *Management in Construction Research Association Postgraduate Conference*, Universiti Teknologi Malaysia Kuala Lumpur, 2012.

[4] buildingSMART e.V. IFC Introducion. Online: https://www.buildingsmart.org/about/what-is-openbim/ifc-introduction/, Accessed: 28/01/2019.

[5] Borrmann A., König M., Koch C. and Beetz J. *Building Information Modeling: Technology Foundations and Industry Practice*. Springer Vieweg, Wiesbaden, 2015.

[6] Guarino N. Formal ontology in information systems. In *Proceedings of the first international conference*, Trento, Italy, 1998.

[7] Zhang L. and Issa R. R. Ontology-based partial building information model extraction. *Journal of computing in civil engineering*, (6):576–584, 2012.

[8] El-Gohary N. M. and El-Diraby T. E. Domain ontology for processes in infrastructure and construction. *Journal of Construction Engineering and Management*, (7):730–744, 2010.

[9] Kim H. and Grobler F. Design coordination in building information modeling (BIM) using ontological consistency checking. *Journal of computing in civil engineering*, (27):410–420, 2013.

[10] Lee S., Isaac S. and Bock T. An Ontology for Process Information Modeling. In *Proceedings of the 32nd ISARC*, Oulu, Finland, 2015.

[11] Xiong W., Yang J., Wang Z., Hu H., Xu F. and Zhang J. Improving Supply Chain Communications for Off-Site Construction Using Process Specification Language. In *Proceedings of the 35th International Symposium on Automation and Robotics in Construction (ISARC)*, Taipei, Taiwan, 2018.

[12] Pedro A., Lee D. Y., Hussain R. and Park C. S. Linked Data System for Sharing Construction Safety Information. In *Proceedings of the 35th International Symposium on Automation and Robotics in Construction (ISARC)*, Taipei, Taiwan, 2018.

[13] Isaac S. Real-time Schedule Control. In *Proceedings of the 33rd International Symposium on Automation and Robotics in Construction (ISARC)*, Auburn, AL, USA, 2016.

[14] Pauwels P. and Terkaj W. EXPRESS to OWL for construction industry: Towards a recommendable and usable ifcOWL ontology. *Automation in construction*, (63):100–133, 2016.

[15] Stanford. The Protégé Ontology Editor and Knowledge Acquisition System. Online: http://protege.stanford.edu/index.html, Accessed: 04/01/2019.

[16] W3C. SPARQL Query Language for RDF. Online: https://www.w3.org/TR/rdf-sparql-query, Accessed: 04/01/2019.

Integrating Social Sustainability in Value Stream Mapping: Panelized Post-Disaster Temporary Housing Case Study

M. Mora[a], B. Akinci[b], and L.F. Alarcón[c]

[a]Fundación Vivienda, Chile / Civil and Environmental Engineering, Carnegie Mellon University, USA
[b]Civil and Environmental Engineering, Carnegie Mellon University, USA
[c]Department of Engineering and Construction Management, Pontificia Universidad Católica de Chile, Chile
E-mail: mimora@ing.uchile.cl, bakinci@cmu.edu, lalarcon@ing.puc.cl

Abstract –

The Triple Bottom Line (TBL) framework defined by Elkington in 1998 [1] proposed three aspects of sustainability: economical, environmental and social. However, several researchers have observed that further studies are needed to guide people and companies on how to achieve sustainable development. Specifically, many gaps are found in trying to implement social sustainability in processes within companies. This study aims to contribute to the integration of social sustainability in processes, with a specific focus on companies that fabricate and deliver post-disaster temporary housing. Our study is based on Value Stream Mapping (VSM) methodology, which previous research studies have identified as one of the main lean methodologies to analyze and identify waste in processes. Existing approaches based on VSM only attempted to integrate social sustainability of internal stakeholders into it. The research described in this paper aims to extend previous studies by integrating social sustainability of external stakeholders in companies' processes using VSM methodology. The analyzed system is the fabrication and delivery of panelized post-disaster temporary housing solutions where the post-disaster context is used to identify processes as well as internal and external stakeholders. Subsequently stakeholders' expectations and indexes that relate them with the outcomes of companies' processes are defined using existing research studies on social impact and on disaster management. Then, a model is proposed to integrate social sustainability of external stakeholders on VSM methodology. Finally, the proposed model is tested within an existing NGO that fabricates and delivers panelized post-disaster temporary housing in Chile.

Keywords –

Social sustainability; Value stream mapping; Lean and Sustainability; Post-disaster temporary housing; Panelized housing

1 Introduction

In 1987, the World Commission on Environment and Development (WCED) established by United Nations, proposed the most accepted definition of sustainable development: "sustainable development is development that meets the needs of the present without compromising the ability of future generations to meet their own" [2]. However, as several researchers have stated, further studies are needed to guide people and companies on how to achieve sustainable development [3-10]. Then, in order to propose guidance on achieving sustainable development, Elkington in 1998 [1] proposed the Triple Bottom Line (TBL) framework defining three trends on sustainability: economic, environmental and social. Where economic sustainability aims for long-term business profits (including costs of products, services, programs, etc.); environmental sustainability aims for the preservation of natural ecosystems [1] and social sustainability aims for supporting and fostering long-term human and society´s well-being [1].

The research described in this paper aims to contribute to the integration of social sustainability in processes of fabrication and delivery of panelized post-disaster temporary housing. Therefore, only the social sustainability aspect of TBL will be analysed within the disaster management context.

Most of the existing studies on social sustainability focus on supporting strategic decisions within companies, and limited research studies have focused on guiding processes' managers in process design towards social sustainability. Also, limited studies considered social sustainability within disaster management context, specifically for activities, such as fabrication and delivery of post-disaster temporary housing. The main objective of the research described in this paper is to contribute to the evaluation of existing fabrication and delivery processes of panelized post-disaster housing from social sustainability perspective. To achieve that objective, the research team focused on integrating social sustainability

into the Value Stream Mapping tool (VSM), which a well-known methodology to analyse processes is.

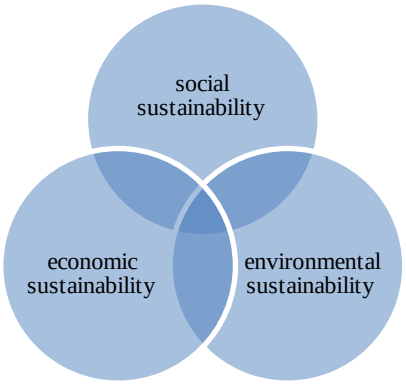

Figure 1. TBL diagram based on Elkington, 1998

2 Research Methodology

As it was stated before, the research presented in this paper aims to integrate social sustainability in the processes of fabrication and delivery of panelized post-disaster temporary housing using Value Stream Mapping methodology. This research builds on and extends prior studies on social impact, value stream mapping and post-disaster activities. In order to propose a plausible model for the integration of social sustainability, the post-disaster temporary housing context is used to define the system, participant stakeholders, as well as relevant indexes towards social sustainability. Finally, the proposed model was tested in a real scenario, the 2017 fire that affected Chile where 305 post-disaster temporary houses were built by the NGO Fundación Vivienda [11]. The results of the proposed model in the case study are shown and analysed in this paper.

3 State of the Art

Previous researchers have identified several interest topics in social sustainability. These topics are based on Elkington' social sustainability definition and aim to simplify and focus social sustainability analysis (see Colantonio 2009 research [4] for further social sustainability topics analysis). This research focuses only on Well-being of people and Basic needs (such as housing and food) topics. Therefore, the following sections summarize the state of the art of research studies that are relevant for these topics and this research.

3.1 Social Sustainability and Social Impact

Social sustainability has been studied in several fields, however, most of the developed methodologies have focused on the social impact of projects, programs and policies, hence they have not aimed to measure social sustainability contribution of processes [12-14]. Most of these methodologies aim for development agencies and NGOs, such as the Social Life Cycle Assessment methodology (S-LCA), defined in the "Guidelines for Social Life Cycle Assessment of Products" published by the United Nations Environment Programme (UNEP) in 2009 [15-16]. This is one of the most accepted social impact methodologies, it is based on the structure of the Environmental Life Cycle Assessment methodology defined on the ISO 14044 and aims to provide a roadmap for social impact assessment of products.

Several previous studies have summarized and compared social impact methodologies and/or performed case studies. For example, Costa & Pesci (2016) [17] reviewed 12 different social impact models used by academics and practitioners. They focused on identifying stakeholders and defining metrics, and concluded that metrics have to be based on the relationship between stakeholders and the analyzed organization. Moreover, the research team stated that stakeholders' point of views have to be considered to define social impact metrics. In another study Dubois-Iorgulescu (2018) [18] performed 33 case studies to understand how a system's boundaries were defined in different situations. They found that most of the case studies assessed social impact at top management level and only few of them (three) assessed social impact at process level. Dubois-Iorgulescu (2018) [18] study also focused on identifying a cut-off criteria to dismiss unconnected elements in product chains. They detected that almost half of the analyzed case studies did not present clear definitions to include or exclude elements in particular systems.

Few studies have developed approaches to integrate social impact on processes. For example, Baumann et al. (2013) [19] examined the production of airbag systems and concluded that is better to adapt Environmental Life Cycle Assessment methodology (E-LCA) instead of S-LCA methodology to measure social impact of processes. The research team argued that social indexes and categories defined in S-LCA are unclear along the life-cycle, therefore they cannot be used in different life cycle stages [19]. In another study, Feschet et al. (2013) [20] studied how changes in the banana industry of Cameroon affected GDP and life expectancy using the Preston curve, which defines a relationship between GDP and life expectancy. This study concluded that multi-criteria analysis with several impact categories and stakeholders is needed to draw more accurate and stronger social impact conclusions [20]. In another study, Jorgensen et al. (2010) [21] attempted to analyze the social impact of particular choices among processes. In order to do it, the study defined two different scenarios: a baseline scenario, and a test scenario with changes incorporating some implemented management decisions. Although this study is an starting point, the research team only focused on the

social impact on the workers of the company and did not include external stakeholders in the analysis [21].

3.2 Social Sustainability in Value Stream Mapping

Several previous studies have identified synergies between lean and sustainable practices [15, 22-30]. However, most of the approaches have focused on the environmental part of sustainability and only few have focused on the social part. Moreover, as stated in the study done by Martínez-Jurado & Moyano-Fuentes (2014) [30], within which they reviewed 58 articles from 1990 to 2013 approaches targeting their lean and social sustainability integration have been developed only during the last few years [29-30].

Since VSM has been identified as one of the main lean methodologies to analyze processes [15][30], most of the previous approaches that integrate lean and social sustainability are based on VSM methodology. For example, the study done by Helleno, de Moraes, & Simon (2017) [31] aimed to integrate VSM with social and environmental sustainability in manufacturing processes in Brazil. They identified social and environmental indexes through a comprehensive literature review and tested them in three factories: a cosmetic products mill, a thermoplastic products mill and an alumninium appliances mill. Although the study integrated social sustainability in manufacturing processes using VSM, the impact on the community was only assessed using the domestic rate of production against the total products available in the market. Therefore, no other stakeholder expectations were included to assess social sustainability of the processes.

Another example is found in Faulkner & Badurdeen (2014) [28] study, within which the research team developed the sustainable value stream mapping methodology (Sus-VSM) to integrate social sustainability in VSM. They started reviewing methods that aimed to integrate sustainability in processes but found that none of the nine reviewed methods included specific social sustainability metrics. As in Helleno, de Moraes & Simon (2017) [31] study, they also recognized that different metrics are needed for different industries, therefore their focus was on defining generic social metrics that can be applied in several specific industries. However, the proposed social metrics only addressed physical work within processes and work environment inside the mills. Hence, only internal stakeholders were considered and no social sustainaibility assessment was done for external stakeholders.

In further studies related to Sus-VSM, Brown, Amundson, & Badurdeen (2014) applied Sus-VSM on three manufacturing contexts with different products and production volumes. They identified that several challenges arise when different system descriptions and boundaries are considered. Hence, they concluded that case studies from different industries are needed to define comparable parameters and generalize metrics. Although this study provided insights about the applicability of Sus-VSM, it did not extend the social sustainability metrics defined by Faulkner & Badurdeen (2014) [28].

3.3 Social Sustainability in Post-Disaster

As it was identified at the beging of this section, one of the social sustainability topics is people's basic needs. In a post-disaster context, the most accepted minimum standard for basic needs was defined by the Sphere Handbook, a standard that is meant to by used during disaster response and was developed by the International Red Cross and a group of NGOs involved in humanitarian aid [37]. This standard identifies the following basic needs areas: water supply, sanitation and hygiene, food security, nutrition, shelter and settlement and health [37]. Since this research is based on the post-disaster temporary housing context, only studies focusing on shelter and settlement assessment after a disaster are considered. However few literature exist in this context and only two studies were found, the first of them is Johnson (2007) [32] research that analyzed particular temporary housing projects after the 1999 earthquakes in Turkey. In this post-disaster situation, the Turkish government gave rental stipends to some of the affected people, but also built 40,621 emergency housing on 136 settlements nearby the affected cities. Johnson's analysis was done at the project level and his study provided the analysis of four projects: two of them lead by the government and two lead by NGOs. The analyses were done using the Logical Framework Analysis approach (logframe), an approach promoted by the US Agency for International Development (USAID) to define stakeholders' roles and to plan activities to achieve defined goals or impacts [12]. Although Johnson's (2007) study [32] identified the impacts of projects' objectives, the analysis was done at a project-level and no process was included. Furthermore, the study did not identify all of the stakeholders who participated in the project and hence did not analyze the impacts of the projects to all of the stakeholders. For example, in one of the projects the NGO Action by Churches Together was in charge, but their objectives specific processes objectives, such as construction times or local materials used, were not included in the study.

Another study that focused on post-disaster temporary housing is Mora & Akinci (2018) research [11], which is the starting point of the research described in this paper. This study focused on measuring the social impact of innovation in processes of fabrication and delivery of post-disaster temporary housing. The research team adapted S-LCA methodology to identify the system, participating stakeholders and their objectives, and to identify processes. Through a case study based on data

from NGO Fundación Vivienda in the post-disaster situation generated by 2017 fire in Chile, the research team identified social impacts that can be influenced by the processes of fabrication and delivery of post-disaster temporary housing. Then, they analyzed the innovations done in the case study and proposed indexes to measure the social impacts. However, the research team only used S-LCA definitions to define the indexes and they did not include any other social sustainability or impact methodology.

4 Integrating Social Sustainability in VSM in Post-Disaster Temporary Housing Context

4.1 System Definition

There are several examples of temporary housing approaches around the world, Wagemann (2012) [33] identified 53 different types of temporary housing for post-disaster contexts implemented only from 2001 to 2011 [33]. These designs have been proposed by several architects and organizations and one of the first identified approaches was proposed in 1944 by Jean Prouvé to support temporary housing for refugees [33-34]. More recent architects have been working in this topic, like Shigeru Ban that have successfully implemented emergency housing since 1995 in diverse post-disaster contexts [35]. Other proposals and designs are from the governmental side, for example in Chile temporary housing is regulated by the National Office of Emergency (ONEMI). This governmental office defined the minimum surface, insulation and fire-resistance rating for the envelope, as well as transportation and installation requirements for the temporary housing used in Chile [36].

Although sometimes the terms shelter and temporary housing are interchanged, there is a clear distinction between them. The most accepted definitions of these terms were provided by Quarantelli in 1995 [38]:

- *Emergency shelter:* Refers to short period accommodation (most of the times only overnight) outside its own home immediately after the occurrence of a disaster. For example, a friend´s house can be considered as an emergency shelter.
- *Temporary shelter:* Refers to short period accommodation (days to months) during post-disaster. For example, a tent or a rented apartment can be considered as a temporary shelter.
- *Temporary housing:* Refers to long period accommodation (months or years) used until people can return to a permanent house. For example FEMA trailers used after Katrina 2005 in New Orleans can be considered in this category [39].
- *Permanent housing:* Refers to permanent accommodation (years). It can be a repaired house or a new one.

All of these approaches aim to resume normal life after a disaster [37], the former two accommodations aim for short time periods after a disaster, while the latter two accommodations aim for long periods [38]. Documented examples of post-disaster accommodations are found in Johnson (2007) [32] study, where people first moved to tents (temporary shelter), then to temporary housing and then to permanent housing. In another documented example, after the 8.5 Richter scale earthquake in Chile people moved directly from emergency shelters to temporary housing and then to permanent housing [40].

The research described in this paper focuses on temporary housing and external stakeholders, therefore only activities and external stakeholders involved in the fabrication and delivery of temporary housing are studied. Moreover, the temporary housing system analyzed in this research is a sub-area of disaster management, which aims to reduce the impact of disaster on communities and encompasses the management of pre-disaster and post-disaster stages [41]. Additionally, four stages can be identified in any disaster management strategy: mitigation, preparedness, response and recovery [41-44]. Preparedness and mitigation are pre-disaster activities, and response and recovery are post-disaster activities [37]. This research narrows the analyzed system to the fabrication and delivery of post-disaster temporary housing in response and recovery stages.

Several stakeholders, such as governments, local and international NGOs, private contractors, communities and final users are involved in each one of the disaster management activities. Although their final goal for disaster management is the same, specific objectives can vary amongst them. For example, private companies could aim to provide standardized low-cost solutions while NGOs could aim to provide community-based solutions [45]. Moreover, several strategies exist to implement post-disaster housing reconstruction. According to Barenstein (2006) [46], who analyzed reconstruction approaches after the earthquake of Gujarat, India, the differences between post-disaster housing strategies are: location (of the new house), funding (for materials and labor), fabrication (of the new house), delivery (of the new house) and on-site construction. For example, in an owner-driven strategy, affected families can be in charge of financing a solution, while in a subsidiary or a contractor-driven approach externals, such as NGOs or governments, provide financial assistance to the affected families [46].

The research described in this paper is based on a subsdiary approach, hence, the housing solution is financed, fabricated, delivered and built on-site by externals, who are not families that are affected by a disaster. This research also considers that new housing solutions are installed where houses were prior disaster.

4.2 Identification of Stakeholders

While previous studies narrowed the integration of social sustainability in VSM to internal stakeholders, the research presented in this paper aims to include external stakeholders when integrating social sustainability in VSM. However, the internal or external classification of the stakeholders is not straightforward and depends on the analyzed system. In the context of post-disaster temporary housing construction, previous studies identified the following participating stakeholders during response and recovery: affected families; NGOs and donor agencies; local and national governmental agencies; housing suppliers and housing on-site builders [32] [37] [47]. Therefore, since this research only focuses on the fabrication and delivery processes of panelized post-disaster housing, internal stakeholders are those in charge of the fabrication and delivery processes of the housing, while external stakeholders are the ones that receive the outcome (post-disaster temporary housing) including intermediates and final user.

Then, since this study is based on a subsidiary approach, we considered as external stakeholder the stakeholders that are funding labor and materials as well as the stakeholders in charge of on-site construction (including those that coordinate on-site construction) and final user of the housing solution. For example, in a governmental subsidiary approach, government funds labor and materials while fabrication, delivery and on-site construction can be performed by private contractors or NGOs.

4.3 Identification of Relevant Social Sustainability Indexes

As it has been described in previous sections, most of previous studies proposed social sustainability indexes for internal stakeholders. Only Helleno, de Moraes & Simon (2017) [31] proposed social sustainability indexes to assess an external community. However, the indexes proposed by them are not applicable to the system defined in this research since their indexes were defined for mass consumption products in a regular context. Then, in order to propose suitable indexes to assess social sustainability for external stakeholders in a post-disaster temporary housing context, several methodologies that have aimed to assess social sustainability were studied and summarized in Table 1.

Table 1. Summary of social sustainability indexes from social impact methodologies and studies

Methodology or study	Stakeholder	Qty. of indexes
Social Life Cycle Assessment [48]	- Workers - Consumer - Local Community - Society - Value chain	No indexes were proposed
Global Reporting Initiative (GRI) [49]	- Workers - Consumer - Local Community - Society - Value chain	58 21 18 11 54
Social Vulnerability index [50]	- Local Community	11
Fontes et al. (2018) [51]	- Workers - Consumers - Local Community	No indexes were proposed
Jorgensen et al. (2010) [21]	- Local community	4
Lagarde & Macombe (2014) [52]	- Local community	6
Feschet et al. (2013) [20]	- Society	1
Baumann et al. (2013) [19]	- Society	8
Handbook for emergencies [53]	-Consumer	7

Although several social sustainability indexes were identified in this research, not all of them allow social sustainability assessment of external stakeholders in the defined post-disaster temporary housing system. Moreover, from all the identified indexes, only the following indexes can be estimated using information from the processes of fabrication and delivery of post-disaster temporary housing and provide information to guide processes' managers in process design towards social sustainability.

1. *Percentage of products and services assessed for improvement:* This index is from Global Reporting Initiative (GRI) [49] and it enables the assessment of the ratio of processes that have been re-designed towards social sustainability. Therefore, it assesses internal processes and provides information to processes' managers.
2. *Total number of incidents for noncompliance of regulations:* This index is also from GRI [49] and it allows the assessment of how many stakeholder requirements have not been fulfilled towards social sustainability. Therefore, it assesses internal processes and provides information to processes' managers.
3. *Content of substances that can cause environmental or social impact:* This index is also from GRI [49] and it enables the identification of products that can negatively impact social sustainability of external stakeholder. Therefore, it assesses internal processes and provides information to processes' managers.
4. *Demand fulfillment:* This index is based on the Handbook for emergencies [53] and Mora & Akinci' study [11] and it enables the assessment of the speed

of the delivery of the solution towards social sustainability. Therefore, it assesses internal processes and provides information about external stakeholders that oversee on-site construction, on-site coordination and final users to processes' managers.

5. *On-time arrivals:* This index is based on [53] and [11] studies and allows the assessment of the arrival expectation of the stakeholders. Therefore, it assesses internal processes and provides information about external stakeholders that oversee on-site construction, on-site coordination and final users to processes' managers.

4.4 Integrating System, Stakeholder and Social Sustainability Indexes to VSM

Value stream are the processes or actions required in a plant or company to produce a product from raw material and deliver it to a customer [54]. Therefore, Value Stream Mapping (VSM) is a plot of all of the processes and information flows to fabricate a product within a given company or plant. This plot allows decision-makers to analyse the current state of the production and to define a "future state" (or desired state) of the flow and processes [54]. In the research described in this paper, we modelled only processes and information flows that relate fabrication and delivery of post-disaster temporary housing with the identified external stakeholders and that can be assessed by the proposed indexes.

Based on the stated definitions of system, stakeholders and indexes, Figure 2 shows a generic model developed to integrate social sustainability for external in VSM for the subsidiary approach of post-disaster temporary housing. The arrows between the stakeholders indicate there is a relationship between them, however, these relationships can change among different scenarios, therefore the direction of the double-headed arrows must be defined in the analyzed scenario.

The main difference between the proposed model and the regular VSM model and also with Sus-VSM model proposed by Faulkner & Badurdeen (2014) [28] is that the proposed model considers multiple external stakeholder receiving the product while previous models considered only one external stakeholder receiving the product. This modification enables the identification of all the participant external stakeholders as well as their expectations on the outcome. In the context of the research presented in this paper, this modification aims to represent all the participant external stakeholders and their expectations towards social sustainability in the subsidiary approach of the fabrication and delivery of post-disaster temporary housing.

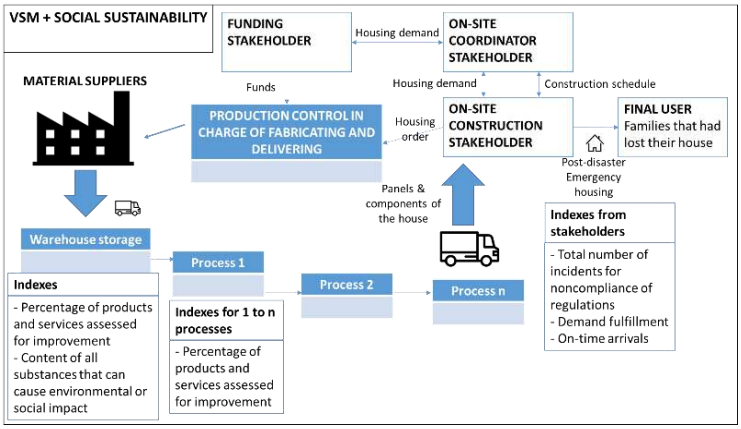

Figure 2. Generic model for social sustainability integration of external stakeholders in VSM

5 Case Study: Panelized Post-Disaster Temporary Housing Processes at Fundación Vivienda, Chile

The proposed model was tested with the NGO Fundación Vivienda in Chile. Specifically, data from the 2017 Fire in Chile from Mora & Akinci (2018) study (11) and on-site interviews were used to feed and test the model. In this event, Fundación Vivienda was in charge of fabricating and delivering the houses and the external stakeholders were:

6. *Funding:* NGO TECHO-Chile (data from interviews with NGO's director of operation)
7. *On-site coordination:* Local governments [11]
8. *On-site construction:* NGO TECHO-Chile [11]
9. *Final user:* Families who had lost their house [11]

Based on the identified external stakeholders and the identified process within Fundación Vivienda, Figure 3 shows our proposed model applied to this case study. Additionally, changes to the fabrication and delivery processes were documented in Mora & Akinci (2018) study [11], therefore the proposed indexes can be calculated for an initial state (before the changes were applied) and for a future state (Figure 3). The calculated indexes are shown in Table 3 and they enabled the comparison between the initial and the final state of the system.

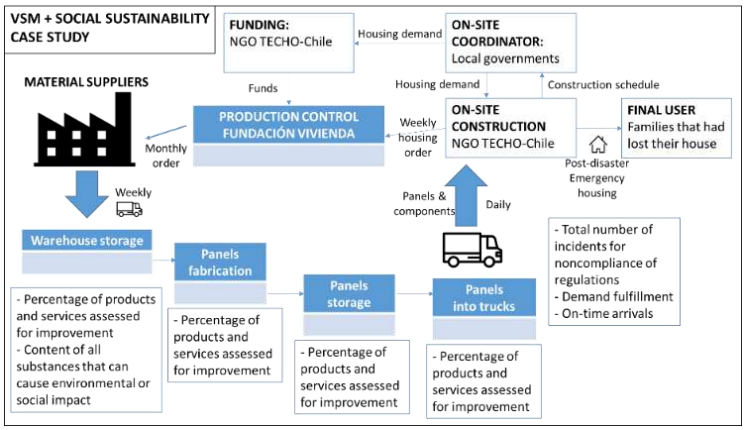

Figure 3. Proposed model to integrate social sustainability in VSM applied in 2017 Fire in Chile case study

Table 3. Summary of indexes of initial and final state of the processes and information flow in the case study

Index	Initial state	Final state
Percentage of products and services assessed for improvement	0%	100%
Total number of incidents for noncompliance of regulations	0%	9.8%
Content of substances that can cause environmental or social impact	0	0
Demand fulfillment	75%	84%
On-time arrivals	66%	92%

6 Case Study Discussion

The case study demonstrated that the model proposed in this research can enable social sustainability assessment of external stakeholders in VSM. As it has been stated, this was not possible in previous VSM approaches because they only considered one final user of the outcome, but the model proposed in this research enabled the representation of the several stakeholders that exist between the factory (that is fabricating and delivering the outcome) and the final user. For example, in this case study, NGO TECHO-Chile was an external stakeholder although it was not the final user of the outcome.

Moreover, when changes were done to the processes, the indexes proposed in the model enabled social sustainability assessment of external stakeholders. This is important to processes' managers because the comparison between the indexes of an initial and final state enables the social sustainability evaluation of the changes. Also, the proposed indexes enabled internal processes evaluation towards social sustainability of external stakeholders. For example, the index "percentage of products and services assessed for improvements" indicates whether the company is improving products and services towards maximizing its social sustainability contribution to external stakeholders. Another proposed index is "total number of incidents for noncompliance of regulations" which can assess whether changes done impacted the compliance of the outcome according to the external stakeholders' requirements. In this case study the changes done increased this index, which means that some of the changes negatively impacted the social sustainability expectations of the external stakeholders.

Another proposed index that assessed company' processes towards social sustainability is the "content of substances that can cause environmental or social impact" index. In this case study, the company was not using harmful substances or products in its process flow, therefore this index is 0, and must be supported.

Finally, "demand fulfillment" and "on-time arrivals" indexes represent the social sustainability expectation about the outcome of the NGO TECHO-Chile and affected families. A 100% index means that changes done to the fabrication and delivery processes were fulfilling social sustainability expectation of these external stakeholders. In this case, when comparing initial and final states, a positive change in the indexes is noticeable, which means that the changes done to the processes maximized social sustainability of external stakeholders.

It is important to mention that the model proposed in this research is based on a subsidiary reconstruction approach to build post-disaster temporary housing, therefore housing solutions were financed, fabricated, delivered and built on-site by people or companies that are not the families affected by a disaster. Then, further studies are needed to validate the model with other reconstruction approaches, such as the owner-driven approach.

7 Conclusions

The model proposed in this research aims to contribute to the integration of social sustainability assessment of external stakeholders in VSM in a post-disaster temporary housing context. In order to do it, the proposed model enables the evaluation of existing processes towards integrating social sustainability perspective of external stakeholders into processes. Moreover, the proposed model enables the integration of additional external stakeholders and not only the final user of the outcome. This external stakeholder's integration enables the addition of different stakeholders' expectations on the outcome, towards social sustainability in VSM. Also, in order to integrate these expectations, the research presented in this paper defined specific indexes that were tested in a case study and demonstrated their suitability to

integrate social sustainability's point of view into processes.

Moreover, the case study used to test the model demonstrated that the proposed model with the proposed indexes can be applied in a subsidiary approach to fabricate and delivery post-disaster emergency housing. The case study also demonstrated that the proposed indexes enabled the integration of external stakeholders' social sustainability point of view within existing processes of fabrication and delivery of the housing solutions. Finally, the calculated indexes also enabled the assessment of changes done to processes towards social sustainability. Therefore, the model and indexes proposed in this research are valuable to processes' managers for process design towards social sustainability of external stakeholders.

8 Perspectives

This study was useful to understand what social sustainability indexes are useful in a post-disaster temporary housing system and how they can be included in VSM. However, only stakeholders that received the outcome of the processes were considered, hence other stakeholders have to be studied in detail as well. Moreover, surveys with statistical validity must be done to evaluate social sustainability indexes' relevance to its associated stakeholders.

References

[1] J. Elkington, Cannibals with forks, Gabriola Islands BC: New Society Publishers, 1998.

[2] World Commission on Environment and Development, "Our Common Future," United Nations, Geneva, 1987.

[3] C. Gimenez, V. Sierra and J. Rodon, "Sustainable operations: their impact on the triple bottom line," *International Journal of Production Economics*, pp. 149-159, 2012.

[4] T. Gladwin, T.-S. Krause and J. Kennelly, "Beyond eco-efficiency: Towards socially sustainable business," *Sustainable Development*, pp. 35-43, 1995.

[5] K. Yongvanich and J. Guthrie, "An Extended Performance Reporting Framework for Social and Environmental Accounting," *Business Strategy and the Environment*, pp. 309-321, 2006.

[6] G. Broman and K.-H. Robert, "A framework for sustainable development," *Journal of Cleaner Production*, pp. 17-31, 2017.

[7] M. Missimer, K.-H. Robert and G. Broman, "A strategic approach to social sustainability - Part 2: a principle-based definition," *Journal of Cleaner Production*, pp. 42-52, 2017.

[8] K.-H. Robert, "Tools and concepts for sustainable development, how do they relate to a general framework for sustainable development, and to each other," *Journal of Cleaner Production*, pp. 243-254, 2000.

[9] A. Mejias, E. Paz and J. Pardo, "Efficiency and sustainability through the best practices in the logistics social responsibility framework," *International Journal of Operations & Production Management*, pp. 164-199, 2016.

[10] M. Radu, "Empirical study on the indicators of sustainable performance - the sustainability balanced scorecard, effect of strategic organizational change," *Sustainability and Organizational Change*, pp. 451-469, 2012.

[11] M. Mora and B. Akinci, "Measuring the Social Impact of Innovation in the Fabrication and Delivery of Post-Disaster Temporary Housing – 2017 Fire in Chile Case Study," in *Construction Research Congress 2018: Safety and Disaster Management*, New Orleans, 2018.

[12] Center for International Development and Training, "Tools for development: A handbookfor those engaged in development activity," University of Wolverhampton, Wolverhampton, 2003.

[13] Hivos, Theory of change thinking in practice, The Hague: Hivos, 2015.

[14] J-PAL, "Introduction to Evaluations," 11 01 2018. [Online]. Available: https://www.povertyactionlab.org/research-resources/introduction-evaluations.

[15] C. M. Dües, K. H. Tan and M. Lim, "Green as the new lean: how to use lean practices as a catalyst to greening your supply chain," *Journal of Cleaner Production*, pp. 93-100, 2013.

[16] E. Staniskiene and Z. Stankeviciute, "Social sustainability measurement framework: The case of employee perspective in a CSR-committed organisation," *Journal of cleaner production*, pp. 708-719, 2018.

[17] E. Costa and C. Pesci, "Social impact measurement: why do stakeholders matter?," *Sustainability accounting management and policy journal*, pp. 99-124, 2016.

[18] A.-M. Dubois-Iorgulescu, A. K. Bernstad Saraiva, R. Valle and L. Mangia Rodriguez, "How to define the system in social life cycle assessments? A critical review of the state of the art and

identification of needed developments," *International Journal of Life Cycle Assessment,* pp. 507-518, 2018.

[19] H. Baumann, R. Arvidsson, H. Tong and Y. Wang, "Does the producion of an airbag injure more people than the airbag saves in traffic? Opting for an empirically based approach to Social Life Cycle Assessment," *Journal of Industrial Ecology,* pp. 517-527, 2013.

[20] P. Feschet, C. Macombe, M. Garrabé, D. Loeillet, A. Rolo Saez and F. Benhmad, "Social Impact Assessment in LCA using the Preston pathway. The case of banana industry in Cameroon," *Internationa Journal of Life Cycle Assessment,* pp. 490-503, 2013.

[21] A. Jorgensen, M. Finkbeiner, M. Jorgensen and M. Hauschild, "Defining the baseline in social life cycle assessment," *International Journal of Life Cycle Assessment,* pp. 376-384, 2010.

[22] R. Florida, "Lean and Green: The move to environmentally conscious manufacturing," *California Management Review,* pp. 80-105, 1996.

[23] P. Kleindorfer, K. Singhal and L. Van Wassenhove, "Sustainable Operations Management," *Production and operations management,* pp. 482-492, 2005.

[24] G. Fliedner and K. Majeske, "Sustainability: The new lean frontier," *Production and inventory management journal,* pp. 6-13, 2010.

[25] M. Taubitz, "Lean, green & safe. Integrating safety into lean, green and sustainability movement," *Professional safety,* pp. 39-46, 2010.

[26] I. Nahmens and L. Ikuma, "Effects of Lean Construction on Sustainability of modular homebuilding," *Journal of architectural engineering,* pp. 155-163, 2012.

[27] A. Brown, J. Amundson and F. Badurdeen, "Sustainable value stream mapping (Sus-VSM) in different manufacturing system configurations: application case studies," *Journal of cleaner production,* pp. 164-179, 2014.

[28] W. Faulkner and F. Badurdeen, "Sustainable Value Stream Mapping (Sus-VSM): methodology to visualize and assess manufacturing sustainability performance," *Journal of Cleaner Production,* pp. 8-18, 2014.

[29] J. A. Garza-Reyes, "Lean and green - a systematic review of the state of the art literature," *Journal of cleaner production,* pp. 18-29, 2015.

[30] P. J. Martínez-Jurado and J. Moyano-Fuentes, "Lean Management, Supply chain management and sustainability: A literature review," *Journal of Cleaner Production,* pp. 134-150, 2014.

[31] A. L. Helleno, A. de Moraes and A. Simon, "Integrating sustainability indicators and lean manufacturing to assess manufacturing processes: Application case studies in Brazilian industry," *Journal of cleaner production,* pp. 405-416, 2017.

[32] C. Johnson, "Impacts of prefabricated temporary housing after disasters: 1999 earthquakes in Turkey," *Habitat International,* pp. 36-52, 2007.

[33] E. Wagemann, "Dissertation: Transitional accommodation after disaster. Short term solutions for long term necessities," University of Cambridge, Cambridge, 2012.

[34] ArchDaily, "The paradoxical popularity of JeanProuvé's Demountable houses," 14 12 2018. [Online]. Available: https://www.archdaily.com/782589/the-paradoxical-popularity-of-jean-prouves-demountable-houses.

[35] Shigeru Ban Architects, "Works | Disaster relief projects," 14 12 2018. [Online]. Available: http://www.shigerubanarchitects.com/works.html#disaster-relief-projects.

[36] ONEMI, "Requerimientos Técnicos - Viviendas de Emergencia ONEMI," ONEMI, Santiago, 2015.

[37] Sphere Project, "Sphere Handbook: Huanitarian Charter and Minimum Standards in Humanitarian Response," Practical Action Publishing, Rugby, CV, 2011.

[38] E. L. Quarantelli, "Patterns of sheltering and housing in US disasters," *Disaster Prevention and Management: An International Journal,* pp. 43-53, 1995.

[39] L. Garofalo and D. Hill, "Prefabricated Recovery: Post-disaster housng component production and Delivery," *Without a hitch: new directions in prefabricated architecture,* pp. 64-71, 2008.

[40] M. Comerio, "Housing Recovery in Chile: A Qualitative Mid-program review," Pacific Earthquake Engineering Research Center, Berkeley, 2013.

[41] IFRC, "Disaster management and risk reduction: strategy and coordination," International Federation of Red Cross and Red Crescent Societies, 2010.

[42] United Nations, "Hyogo Framework for action 2005 - 2015: Building the Resilience of Nations and Communities to Disasters," World Conference on Disaster Reduction, Hyogo, 2016.

[43] FEMA, "FEMA Incident Management and Support Keystone," FEMA, 2011.

[44] Habitat for Humanity, "The Forum: Promoting dialogue among Habitat for Humanit´s worldwide partners," Habitat for Humanity, Americus, GA, 2012.

[45] C. Johnson, "Impacts of prefabricated temporary housing after disasters: 1999 earthquakes in Turkey," *Habitat International*, pp. 36-52, 2007.

[46] J. Barenstein, "Housing reconstruction in post-earthquake Gujarat," Humanitarian Practice Network, London, 2006.

[47] R. Sarkar, "Post-earthquake reconstruction - in context of housing," *Advances in Geosciences*, pp. 91-104, 2006.

[48] UNEP, Guidelines for Social Life Cycle Assessment of products, Ghent: UNEP/SETAP Life Cycle Initiative, 2009.

[49] GRI, Global Reporting Initiative Standards, GRI, 2016.

[50] S. Cutter, B. Boruff and L. Shirley, "Social vulnerability to environmental hazards," *Social Science Quarterly*, pp. 242-261, 2003.

[51] J. Fontes, P. Tarne, M. Traverso and P. Bernstein, "Product social impact assessment," *International journal of life cycle assessment*, pp. 547-555, 2018.

[52] V. Lagarde and C. Macombe, "Designing the social life cycle of products from the systematic competitive model," *International Journal of Life Cycle Assessment*, pp. 172-184, 2014.

[53] UNHCR, "Handbook for emergencies," United Nationas High Commissioner for Refugees, Geneva, 2007.

[54] M. Rother and J. Shook, Learning to see. Value Stream Mapping to add value and eliminate muda, Brookline, Massachusetts: The Lean Enterprise Institute, 1999.

An Experimental Investigation of the Integration of Smart Building Components with Building Information Model (BIM)

K. Afsari[a], L. Florez[b], E. Maneke[c], and M. Afkhamiaghda[a]

[a] School of Construction Management Technology, Purdue University, USA
[b] Department of Architecture and Built Environment, Northumbria University, UK
[c] Department of Computer Graphics Technology, Purdue University, USA
E-mail: kafsari@purdue.edu , laura.florez@northumbria.ac.uk, emaneke@purdue.edu , mafkhami@purdue.edu

Abstract –

Building Information Modeling (BIM) is a methodology to digitally represent all the physical and functional characteristics of a building. Importantly, in smart buildings smart components that are enabled with sensing and actuation need to be modeled accurately within the BIM model. This data representation needs to include multiple status of the smart component based on their performance to guide the design and construction process. However, currently there is not a clear methodology or guideline on how to embed smart components in the BIM model. Visualization techniques have been developed based on CAD technology to integrate smart components in the building model but these techniques have not been applied to BIM environment. To accurately model smart components, the component must be more than a single status representation and must contain complete and accurate dynamic data of the smart component. In this research, data properties, visualization techniques, and categorization of smart components is investigated. Then, through an experimental investigation, nine smart components across five building disciplines are modeled and embedded in a BIM model of a smart space. The model includes parameters that facilitate the data representation of the smart components. Data properties, data organization, and simulation of the smart component within the building model is explained. Challenges and future research is discussed.

Keywords –

Smart components; BIM; Smart buildings; Sensors; Actuators

1 Introduction

Smart buildings are buildings that consist of several types of interconnected smart technologies and smart components that enable the building to run based on the data collected by the smart components. This data can enable the increased sustainability, occupant experience, financial performance, operational efficiency, and prestige of smart buildings [1]. To enable the design of smart buildings, development of the 3D model of the building and planning for context-aware design of such smart environment is critical for designers [2].

On the other hand, Building Information Modeling (BIM) is a methodology that utilizes a set of software tools and processes for facilitating the creation and use of the digital representation of the physical and functional characteristics of a building. BIM models are intelligent data-rich sources of building data that can be used through the lifecycle of a building to analyze buildings and inform design, construction, and maintenance decisions [3]. In fact, smart technologies can be embedded in building spaces and components, using smart objects to enhance the performance of the building. However, there is a lack of studies on how BIM can accurately represent smart objects and the data within the design and construction of smart buildings. There is no clear guideline on how to model smart components, how to accurately embed the required data within the BIM model, and how to organize the data associated with the smart components within the BIM model. There is a need to develop BIM use cases to indicate how smart objects can be modeled and embedded within the BIM model [4].

Importantly, smart technologies and components need to be integrated with BIM to accurately model and analyze smart components within smart buildings [4]. BIM can help the design and construction process with the opportunity to integrate smart components from the design phase as well as the post-construction and operation of the building while providing a data repository for the users and for its for maintenance [2,4]. Therefore, this research investigates how BIM can be used in the development of smart buildings during the

design process and how smart objects can be embedded with organized data in the BIM model to guide the process of design and construction of smart buildings. The objective of this study is to investigate how data properties of smart objects can be integrated in BIM models embedding sensing and actuation data. This paper will first study the ways smart component properties can be captured. Next, existing visualization techniques and simulation strategies for smart components is discussed. Then, the study investigates the different categories of smart components and within an experiment, the study develops BIM models of multiple building disciplines of a given space in a use case scenario to discuss how smart components with required data can be embedded in the BIM model.

2 Smart Components Data Properties

Smart environments operate through a sensing and actuating paradigm. A smart environment requires sensors to collect data and to communicate with smart components. The microprocessors analyze the data received from the sensors and command the actuators to respond accordingly. The actuator then uses the sensor data to complete their actions. Recently this paradigm has shifted from a wired sensing and actuating connection to an Internet of Things (IoT) approach. Internet of Things is a technology to create a network of interconnected objects that do not require human interference to perform tasks. These tasks can fall into the three main categories of sensing, analytics, and visualization [5]. There has been studies on how to embed smart objects in the BIM model of a smart building. Zhang et al. [4] embedded smart components in a Revit model to later work with a facility management tool they developed for energy management functions. They specifically integrated the smart components so that they can be exported to Industry Foundation Classes (IFC) to enable interoperability through open BIM standard. Their approach uses (1) Revit's IFC shared parameter specifying IFCSensorType to indicate the sensor type within an IFC entity (2) element property in the smart component family for the actuator, for the type of smart object, and for the mark tag of an individual smart object. Their work provides a data exchange interface for their developed facility software through mapping the smart object's family property parameters to IFC text, then, to their facility software interface and also, the smart device through using three main data as output, input and control [4]. Their study does not specify the structure of the object properties in the family level and it does not contain types of smart components other than smart objects for energy management systems. Also, their framework relies on the IFC within EXPRESS technology and P21 encoding (STEP-file) which parses the IFC files, it created a disconnected environment [6] with the source of data in the BIM model that relies on exporting and importing files. The work by Dave et al. [7] has developed a web based solution called Otaniemi3D that can integrate smart devices with the BIM data to provide information about energy usage, occupancy, and user comfort. They have exported the BIM model to a static IFC file essentially for the data regarding spaces in the building. They do not add the smart component and all the required properties of the smart component to the original BIM model (in Revit). Instead, they remodel the Revit file to add sensor data through IFC shared parameters using IfcSensorType to specify the type of sensor (e.g. TEMPRETURESENSOR). Then, they load the IFC file into IFCOpenShell to visualize the model then translate it to the final web formats to be transferred to Otaniemi3D environment running on a web browser. They also mentioned that during the data translation process, IfcSensorType and IfcSpaces data are either missing or incorrectly mapped which is not fully fixed and automated as they describe [7]. There is currently a lack in knowledge of how to model smart components integrating required data properties through the design and construction process and how to visualize smart components data in the BIM model, especially pertaining to data regarding sensors, actuators, microprocessors and components with more than one status.

3 Visualization of Smart Components

Crigliano [8] developed a QCAD extension as a systematic approach to appropriately allocate and install sensor nodes in an indoor environment. These sensor nodes are essential to smart environments to ensure that smart components receive data upon which to act. The 2D modeled environment allows the layout of sensor nodes to be adequately visualized.

Su and Huang [2] proposed a Visualization System of Context-aware Application Scenario Planning (VS-CaSP) and developed a visualization tool for non-technology users. VS-CaSP allows designers to quickly plan and construct 3D environments through rule-based and 3D visualization techniques. While the system is functional and claimed to be easy-to-use, it is based on CAD and its functionalities need to be extended to fulfill the needs of a BIM Model. Additionally, the rule expressions need to be evaluated to ensure the representation of more complex requirements in smart buildings. In this study some of the recommendations in the study by Su and Huang [2] is used and extended to BIM modeling and smart component parameters in the use case development.

3.1 Simulation Techniques

Agent-Based Modeling (ABM) is a simulation approach to model complex, interacting systems of

agents. Components are modeled agent by agent or interaction by interaction. ABM is distinguishable by its emphasis on modeling the agent's heterogeneity and the emergence of self-organization. It has a bottom-up approach, thus the system's behavior emerges from how individual heterogeneous agents interact with each other and their environment based on defined rules. These features offer a way to model systems with agents, who can learn and adapt from other agents [9], to assess how their interactions affect the system.

Discrete Event Simulation (DES) is another simulation approach that mimics system behavior. DES tracks the system's state during a length of time using a collection of state variables. The system's state can only change instantaneously and these changes are referred to as events [10]. ABM and DES can be useful as they can reflect the dynamic nature of smart components and capture complicated behavior, dependencies and interrelationships [11, 12]. Although a simulation approach can be an effective technique, this is only possible if the simulation tool is integrated with the BIM authoring tool.

4 Categorization of Smart Components

Smart objects function based on sensing and actuation and they consist of sensors, microprocessors and actuators in order to connect with the surrounded environment in the building so that they can react accordingly [13, 14]. Sensors read the real-time status of the environment and pass the input as a signal through a network for processing [15]. Sensors and actuators each act as a node in a Wireless Sensor Network (WSN) which can have the ability to work with other systems and devices such as the occupancy feedback system. Table 1 shows the different criteria which can be used for the categorization of smart objects.

Sensors can be categorized based on various criteria, many researchers [16,17] have classified sensors based on their type and parameter they read from the outside environment (e.g. vibration, humidity, pressure etc.). However, a lot of other factors such the environment needs and complexities, [17], the phase of the project lifecycle [18, 19], and area of usage in buildings [16, 18] affect the criteria for categorization of sensors. As sensors receive information from their surroundings, they send the data as an electronic signal to the actuators, and actuators take action accordingly [14]. This makes the interaction and sequence of data transfer between sensors and actuators critical in the way they respond to the changes in their surrounded environment. As Liu et al. [19] have demonstrated, the sequence and type of data transfer can lead to different networks and systems, in addition, the type of output data from each sensor defines how the smart object would respond to the environment.

Table 1. Criteria for categorization of smart components

Categorization Criteria	Example Categories
Sensor Type	Thermal Humidity Acoustic RFID Motion Light Vibration Pollution Pressure Flow Rate Plug Load Devices Fire Smoke
Speed Needs	Static Mobile Embedded
Building Phase	Construction Plan and Design Construction Safety Management Site Facility and Material Management Site Environment Construction Process Management Structural Inspection Re- Structure & Expansion
Areas of Usage in Building	HVAC System Information and transformation (e.g. sensing floors, high rise elevators) Safety and Security (e.g. biometric authentication access) Maintenance and Facility Management Modeling Building Occupancy IT Equipment Openings (window, door) Status
Component Type	Blinds Door Windows Electrical Devices Lights Fan Heater Boiler Urinals Water closet Facade
Building Discipline	Architectural Mechanical Electrical Structural
Connection & Data Exchange	Periodic Conditional Timeout Interrupt
Output Data	Booleans Binary (e.g. Yes/No, Occupy/Empty) Continuous Range of Values

A threshold is defined for smart objects which they

respond accordingly to that predefined value. According to Weng and Agarwal [16], these conditions contains a broad range of variables such as binary statements, Booleans, as well as continuous range of values. This study specifically investigates the BIM modeling in the design and construction phase with regard to capturing these conditions within the data properties of the smart components.

5 An Approach to Information Modeling of Smart Components

This study focuses on integrating smart components within BIM models and it was undertaken in two phases as explained below.

5.1 Study Phase

This research informed decisions on how to represent smart components and the data that the smart components would need to contain through the study of the current status of the modeling of smart components, previous work on smart components and smart technology. Then, to categorize smart components and parameters, all investigated smart components as well as their parameters and modeling requirements were listed and then went through a selection process to determine which smart components would be modeled in the experiment. The overarching study process is depicted in Figure 1.

Figure 1. Overarching study process

5.2 Modeling Phase

For the next step, to integrate smart components with the BIM model an experiment was designed for this empirical study and a use case was developed to represent the BIM model of the building in the experiment. A prototype was developed as the use case to integrate selected smart components. The model will be explained in more details in the following sections.

For the development of smart components and embedding them in the BIM model, the study first investigated several smart technologies as well as capabilities of the selected space within the use case. Then, nine smart components from five building disciplines were selected to be modeled and integrated in the BIM model. As mentioned in section 4, among categorization criteria for smart components, this study uses "Building Discipline" criteria to categorize and arrange the information regarding the smart components. Then, data properties were added to the developed smart components to represent the capabilities and data inputs and outputs received by the smart components. The data properties are provided for both sensing and actuating. Table 2 shows the list of selected smart components in this study and their object properties based on sensor parameters and actuator parameters.

Table 2. List of Modeled Smart Components and Their Object Parameters

Category	Smart Object Name	Sensor Parameters	Actuator Parameters
Architectural	Door	Occupant's Presence Temperature	Position Angle
	Window	Humidity Luminance Occupancy Temperature	Opening Distance
Electrical	Security Alarm	Surveillance Status Security Code Occupancy Windows Doors Lights	Alarm Status
	Smart Plug	Timer Load	Status
Mechanical	Duct Static Pressure Sensor	Resistance	Status
	Air Handling Unit	Temperature Humidity Occupancy	Status
Structural	Structural Deflection Monitoring	Strain	Compression Force Tension Force
Fire Protection	Fire Detection Sensor	Smoke Detection CO2 Detection Temperature	Resident Notification Fire Department Notification Sprinkler Activation
	Sprinkler	Sprinkler Sensor	Status

For all of these smart components there are two additional properties as the "sensor type" and "actuator type" that is integrated as well. These smart components are used in the buildings with the means of providing occupant comfort, reducing energy consumption, and providing safety [1]. For example, fire protection is considered as one of the most important safety issues in

the buildings as it can lead to damage and fatality, therefore it is of vital importance to have an immediate notification system for the occupants. Many researchers [20,21] have used sensors capable of detecting any high rising amount of smoke, heat, or CO2 gas in the environment. Once the sensor detects any abnormal presence of these parameters in the environment, the input from sensors then goes to the actuator. Depending on the system design, the actuator parameter can be simple alarm system for notifying the occupants and the fire department all the way to activating sprinklers for preventing the fire from spreading [21]. Smart plug is another object integrated in this study. Shutting down any unnecessary or unused electronic is considered as one of the methods to reduce the electricity consumption of the building. In light of this subject, Weng and Agarwal [16] have suggested tracking the plug load of electronic devices, using this method, systems such as lighting and IT equipment which are not being used by occupants can be easily spotted and be turned off. For places such as offices or schools, where the occupant's system usage is predictable and follows a certain schedule, one can use timer sensors to turn off equipment in a specific time [22]. For the structural discipline in this study, a Structural Deflection Monitoring (SDM) system in embedded for monitoring dynamic deflection of columns and beams. In this system, the Long-gauge fiber Bragg grating (LG-FBG) sensors can measure average strain over a certain length [23] and accordingly when needed, the actuator will apply compression or tension force measured in kips.

The next step is digital development of building using BIM authoring tools. In this study we use Autodesk Revit. A medical waiting room was developed as the use case. In this research, the use case was selected within a commercial building. This part of the study allows a space to be developed with the integration of smart components into the building performance. By limiting the use case to one space within the building, the focus is on the smart components and their parameters as opposed to general building performance. This also allows for the ability to generalize the study findings upon completion of this one scenario. In fact, the prototype used for this study is a one story steel structure, 1300 square foot commercial waiting room facility with a front desk space. Each building disciple was housed in a separate model before being linked together using Revit linked features. Modeled building disciplines included architectural, structural, mechanical, electrical, and fire protection.

Next, is embedding smart components in the building. The BIM model was created considering the following sub-models: architectural, structural, mechanical, electrical, and fire protection. Each smart component categorized in Table 2 was embedded in the building model of its corresponding discipline as shown in Figure 2. Figure 3, 4 and 5 illustrate the BIM model data set developed as the prototype in this study.

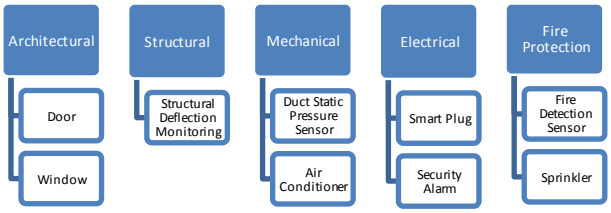

Figure 2. Building disciplines and smart components in the prototype

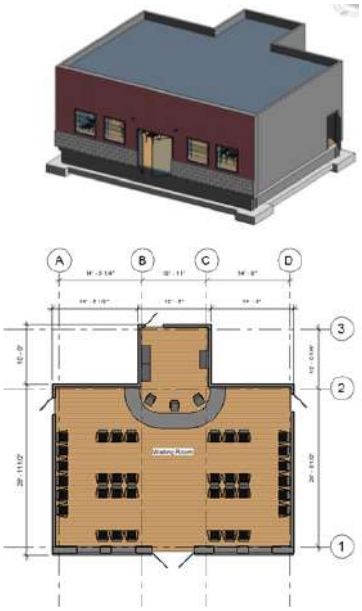

Figure 3. Top: merged BIM model; bottom: first floor architectural plan

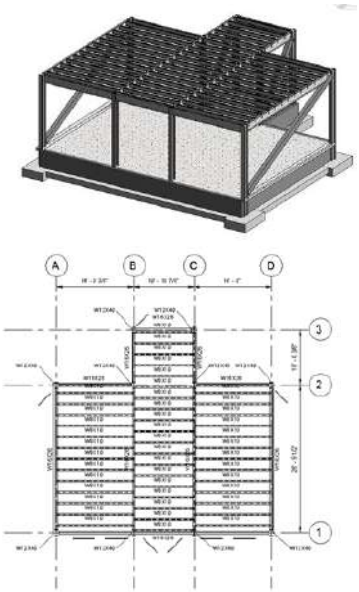

Figure 4. Top: structural BIM model; bottom: first floor framing plan

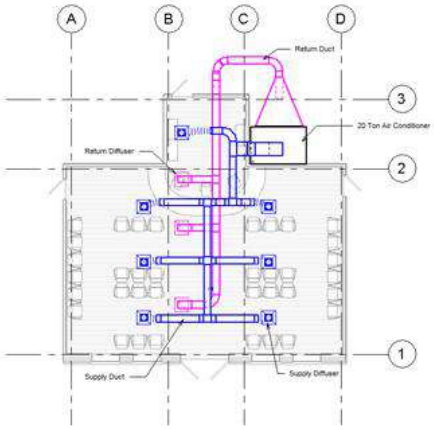

Figure 5. Mechanical ductwork floor plan

6 Results

One of the challenges regarding the integration of smart components with the BIM model of the smart building is the static nature of current BIM authoring tool which limits the data representation of smart components with multiple status in a dynamic environment. In this study, nine smart components across the five different building disciplines were modeled. Component parameters were developed based on the literature study in the initial study phase. In order to represent the parametric behavior of the smart components and most importantly to capture multiple status of the smart components to inform the design and construction process, experimental equations were used to represent the interrelations of the sensor and actuator. Experimental equations for the parameters of the nine smart component are shown in Table 3.

For each smart component a parametric object is modeled and all the parameters and equations are embedded in the model. For instance, for the automatic door a parametric one panel door was modeled. Standard attributes such as height, width, and thickness were used to model the door. Other parameters involving the integrated smart technology including sensor type, actuator type, and opening angle were assigned to the door. To enable the data representation of the automatic door capabilities, parameters were added for presence and temperature. The presence parameter was assigned an integer of 0 or 1, where 0 designates no presence detected and 1 designates presence detected. Similarly, the temperature parameter was assigned an integer of 0 or 1, where 0 designates the temperature is within the specified range and 1 designates the temperature is outside of the specified range. An experimental equation was developed such that the opening angle of the door was controlled by the presence and temperature parameters, Angle = (Presence x 45 degrees) + (Temperature x 45 degrees). Based on inter-related sensor-actuator rules [2] this methodology has enabled the data representation of automatic door data in the BIM model to inform the design and construction process with multiple status of the smart object.

Table 3. Simulation equations for smart components

Component - Actuator	Equation	Sensor Numerical Associations	Conditions
Door - Angle	= (Presence * 45) + (Temperature * 45)	**Presence:** 0 = no presence detected, 1 = presence detected **Temperature:** 0 = below or at temperature, 1 = above temperature	
Window - Opening Distance	= (Humidity + Luminance + Temperature) x Occupancy	**Humidity:** 0 – outside of threshold 1 – within threshold **Luminance:** 0 – outside of threshold 1 – within threshold **Occupancy:** 0 – no occupants detected 1 – occupants detected **Temperature:** 0 – outside of threshold 1 – within threshold	**Opening Distance:** 0 – window is closed 1+ – window is open
Security Alarm – Alarm Status	if Surveillance Status = 1, (Occupancy + Windows + Doors + Lights) x Security Code	**Surveillance Status:** 0 – inactive 1 – active **Occupancy:** 0 – no occupants detected 1 – occupants detected **Windows:** 0 – windows closed 1 – windows open **Doors:** 0 – doors closed 1 – doors open **Lights:** 0 – lights off 1 – lights on **Security Code:** 0 – code entered 1 – code not entered	**Alarm Status:** 0 – alarm is inactivated 1+ alarm activated
Smart Plug - Status	= Timer x Load	**Timer:** 0 – inactive 1 – active **Load:** 0 – inactive 1 – active	**Smart Plug Status:** 0 – off 1 - on
Duct Static Pressure Sensor - Duct Status	= Resistance	**Resistance:** 0 – outside of threshold 1 – within threshold	**Duct Status:** 0 – duct is not in use 1 – duct is in use
Air Handling Unit - Status	= (Temperature + Humidity) x Occupancy	**Temperature:** 0 – outside of threshold 1 – within threshold **Humidity:** 0 – outside of threshold 1 – within threshold **Occupancy:** 0 – no occupants detected 1 – occupants detected	**Air Conditioner Status:** 0 – off 1+ – on
Structural Deflection Monitoring- Compression Force	= Strain	**Strain:** 0 – outside of threshold 1 – within threshold	**Compression Force:** 0 – force applied 1 – force not applied
Fire Detection Sensor – Resident Notification	= Smoke Detection + CO2 Detection	**Smoke Detection:** 0 - smoke under threshold 1 - smoke over threshold **CO2 Detection:** 0 - CO2 under threshold 1 - CO2 over threshold	**Resident Notification:** 0 – not activated 1+ – activated.
Fire Detection Sensor – Fire Department Notification	= Smoke Detection + CO2 Detection	**Smoke Detection:** 0 - smoke under threshold 1 - smoke over threshold **CO2 Detection:** 0 - CO2 under threshold, 1 - CO2 over threshold	**Fire Department Notification:** ≤1 – not activated 2+ - activated
Fire Detection Sensor - Sprinkler Activation	= Smoke Detection + CO2 Detection	**Smoke Detection:** 0 - smoke under threshold 1 - smoke over threshold **CO2 Detection:** 0 - CO2 under threshold 1 - CO2 over threshold	**Sprinkler Activation:** ≤1 – not activated 2+ - activated
Sprinkler - Status	= Sensor Activation	**Sensor Activation:** 0 - no/off 1 - yes/on	**Sprinkler Status:** 0 – sprinklers are off, 1 – sprinklers are on

Also, an air handling unit was modeled in the way that its parameters such as temperature, humidity, and occupancy were added to the component. The temperature parameter was assigned an integer of 0 or 1, where 0 designates the temperature is within the specified range and 1 designates the temperature is outside of the specified range. The humidity parameter was assigned an integer of 0 or 1, where 0 designates the humidity is

within the specified range and 1 designates the humidity is outside of the specified range. The occupancy parameter was assigned an integer of 0 or 1, where 0 designates no occupancy detected and 1 designates occupancy detected. An experimental equation was developed such that the on/off status of the air handling unit was controlled by the temperature, humidity, and occupancy parameters while Status = (Temperature + Humidity) x Occupancy thus can inform the design and construction process. Figure 6 shows the family parameters modeled in Revit for the smart air handling unit developed in this study.

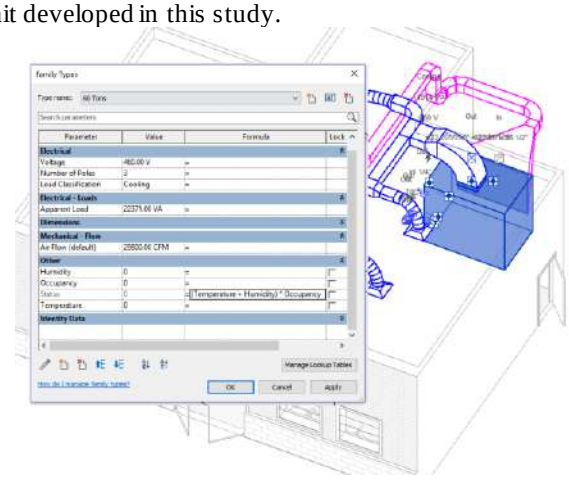

Figure 6. Family parameters for the smart air handling unit

Once the parameters and equations have been established for each of the components in the model (see Table 3), these can be integrated into a simulation model. The simulation model takes two types of input information. The first type of input is the components' parameters obtained from the smart components data properties. The second type of input is the value range of a parameter, which depicts the status from the low-start point of the first event to the last-finish point of the last event in the process. To represent the behavior of the system, the simulation model considers the components (with its parameters) as agents and model these to capture their interactions and dependencies. The model may also adjust probability distributions to the parameters of the smart components, which defines the status of the component. By modelling agents, the simulation phase aims to predict the smart components' values that will serve as inputs for the actuator. The input to the simulation phase includes the probability distributions of the components' values (with the maximal status for each parameter), which allow generating multiple scenarios using random numbers drawn from the probability distributions. Additionally, the model can also estimate the parameters by fitting probability distributions. Fitting methods allow selecting the parameters that produce the best fit to the collected data. With this fitted distributions, it is possible to replicate the components' values.

The results from the simulation model can then be integrated to the BIM authoring tool to digitally represent the smart components and better manage information to guide the process of design and construction of smart buildings. With the information collated from the simulation model into the BIM tool, it is expected that a rich data file can be produced for optimizing the facilities management process. The reader is referred to [24] for a detailed description on how to integrate information and create COBie (Construction Operations Building Information Exchange) data for the facilities management process. COBie data comes directly from the building information. This information is collected, stored and linked (using COBie) and COBie deliverables become the monitor and decision support documents to be updated and managed.

7 Discussion and Conclusion

This study investigated the data properties of smart components with the purpose to be embedded in the BIM model while capturing smart components conditions with required sensing and actuation to inform the design and construction process. Future research will study data flow and interaction of smart components in the BIM model and smart devices. In this study, several smart components were modeled with their corresponding parameters to enable their accurate representation and data capabilities. While these smart components can hold relevant data, this data must be embedded manually for each component individually as parameters are not identical among the components. Future research should evaluate the effectiveness of the smart component data representations created in this study.

Other modeling challenges pertained to visualization. While the opening angle of a door can easily be seen as the inputted data changes, actuations such as air handling unit status are harder, if not impossible, to visualize. Instead, one must look at the data parameters to determine the component's status in a dynamic smart environment. Similarly, developing equations that simulated the components' actuations proved challenging. As several sources of sensor data affect the component's actuations, the interrelations of the data needs to be captured while creating the data representation. Future research should evaluate simulation equations to more accurately represent the interconnected inputs and behaviors of the various smart components. To accomplish this, future work may look toward integrating computational solutions and if/then rule principles into the BIM smart framework. BIM software systems such as Revit are currently a static methodology that does not lend itself to depicting smart components that constantly read, evaluate, and respond

to their environment. Hence, the manual input of device data is necessary in current BIM solutions. As such, future solutions should turn toward BIM enabled with simulation strategies to integrate smart components representation with the building model.

References

[1] Brown, S., Karnatz, K., & Knight, R. A comprehensive look at the intelligent building. Consulting Specifying Engineer, 53(3): 54-58. 2016.

[2] Su, J., & Huang, C. An easy-to-use 3D visualization system for planning context-aware applications in smart buildings. Computer Standards & Interfaces, 36(2): 312-326. 2014.

[3] Teicholz, P. BIM for Facility Managers. John Wiley & Sons: Hoboken, NJ, USA. 2013.

[4] Zhang, J. C., Seet, B. T., & Lie, T. Building Information Modelling for smart built environments. Buildings, 5(1): 100-115. 2015.

[5] Gubbi, J., Buyya, R., Marusic, S., & Palaniswami, M. Internet of Things (IoT): A vision, architectural elements, and future directions. Future Generation Computer Systems, 29(7): 1645-1660. 2013.

[6] Afsari, K. Standard-based Data Interoperability of the Building Information Model in Cloud. In Proceedings of the 54th ASC Annual International Conference, April 18-21, Minneapolis, MN. 2018.

[7] Dave, B., Buda, A., Nurminen, A., & Främling, K. A framework for integrating BIM and IoT through open standards. Automation in Construction, 95: 35-45. 2018.

[8] Cirigliano, A. Toward Smart Building Design Automation: Extensible CAD Framework for Indoor Localization Systems Deployment. IEEE Transactions on Computer-Aided Design of Integrated Circuits & Systems, 37(1): 133-146. 2018.

[9] Macal, C. M., & North, M. J. Tutorial on agent-based modelling and simulation. Journal of Simulation, 4(3): 151-162. 2010.

[10] Jacob, M. Discrete event simulation. Resonance, 18(1): 78-86. 2013.

[11] Siebers, P. O., MacAl, C. M., Garnett, J., Buxton, D. & Pidd, M. (2010). Discrete-event simulation is dead, long live agent-based simulation. Journal of Simulation, 4(3), pp. 204–210.

[12] Sargent, R. G. (2015). An introductory tutorial on verification and validation of simulation models, In Yilmaz, L. et al. (eds) Proceedings of the 2015 Winter Simulation Conference. Huntington Beach, CA, USA: IEEE, pp. 1729–1740

[13] Kortuem, G., Kawsar F., Sundramoorthy V., and Fitton D. Smart objects as building blocks for the internet of things. IEEE Internet Computing 14(1): 44-51. 2010.

[14] De Farias C., Soares H., Pirmez L., Delicato F., Santos I., Carmo L., Souza J., Zomaya A., and Dohler M. A control and decision system for smart buildings using wireless sensor and actuator networks. Transactions on Emerging Telecommunications Technologies, 25(1):120-135, 2014.

[15] De Guglielmo, D., & Anastasi, G. Wireless sensor and actuator networks for energy efficiency in buildings. In Second IFIP Conference on Sustainable Internet and ICT for Sustainability (SustainIT 2012). IEEE. 2012.

[16] Weng, T. and Agarwal Y. From buildings to smart buildings—sensing and actuation to improve energy efficiency. IEEE Design & Test of Computers. 29 (4): 36-44. 2012.

[17] Essa, I. A. Ubiquitous sensing for smart and aware environments. IEEE personal communications 7(5): 47-49. 2000.

[18] Arampatzis, T., Lygeros, J., & Manesis, S. A survey of applications of wireless sensors and wireless sensor networks. In Intelligent Control, Proceedings of the 2005 IEEE International Symposium on Mediterrean Conference on Control and Automation: 719-724. IEEE. 2005.

[19] Liu Z., and Deng Z. A Systematic Method of Integrating BIM and Sensor Technology for Sustainable Construction Design. In Journal of Physics: Conference Series, 910(1). IOP Publishing, 2017.

[20] Silva B., Fisher R.M., Kumar A., Hancke, G.P. Experimental link quality characterization of wireless sensor networks for underground monitoring. IEEE Trans. Ind. Inform. 11:1099–1110. 2015.

[21] Saeed, F.; Paul, A.; Rehman, A.; Hong, W.H.; Seo, H. IoT-Based Intelligent Modeling of Smart Home Environment for Fire Prevention and Safety. J. Sens. Actuator Netw. 7(11). 2018.

[22] Gandhi, P., & Brager, G. S. Commercial office plug load energy consumption trends and the role of occupant behavior. Energy and Buildings, 125: 1-8. 2016.

[23] Hong W, Qin Z, Lv K, Fang X. An Indirect Method for Monitoring Dynamic Deflection of Beam-Like Structures Based on Strain Responses. Applied Sciences. 8(5):811. 2018.

[24] Florez, L., & Afsari, K. Integrating facility management information into building information modelling using COBie. In 35th International Symposium on Automation and Robotics in Construction and International AEC/FM Hackathon: The Future of Building Things (pp. 832-839). 2018.

Semantic Segmentation of Sewer Pipe Defects Using Deep Dilated Convolutional Neural Network

M.Z. Wang[a] and J.C.P. Cheng[a]

[a] Department of Civil and Environmental Engineering, The Hong Kong University of Science and Technology, Hong Kong, China
E-mail: mwangaz@connect.ust.hk, cejcheng@ust.hk

Abstract –

Semantic segmentation of closed-circuit television (CCTV) images can facilitate automatic severity assessment of sewer pipe defects by assigning defect labels to each pixel in the image, from which defect types, locations and geometric information can be obtained. In this study, a deep convolutional neural network (CNN), namely DilaSeg, is developed based on dilated convolution for improving the segmentation of sewer pipe defects including cracks, tree root intrusion and deposit. Sewer pipe CCTV images are extracted from inspection videos and are annotated to be used as the ground truth labels for training the model. DilaSeg is constructed with dilated convolution for producing feature maps with high resolution. Both DilaSeg and the state-of-the-art model, fully convolutional network (FCN), are trained and evaluated on the annotated dataset using the same hyper-parameters. The results of the experiments indicate that the proposed DilaSeg improved the segmentation accuracy significantly compared with FCN, with 18% of increase in mean pixel accuracy (mPA) and 22% of increase in mean intersection over union (IoU) with a fast detection speed.

Keywords –

Dilated convolution; Convolutional neural network (CNN); Semantic segmentation; Sewer pipe defect; Defect segmentation; Visual inspection

1 Introduction

Sewer pipe defects such as cracks, root intrusions through the pipe joints and the deposits inside the pipe are major causes of pipe deterioration, leading to serious consequences e.g. around 23,000 to 75,000 sanitary sewer overflows (SSOs) occurred every year in the United States, causing concerns for the environment and human life [1]. Therefore, discovering and repairing pipe defects at an early stage is significant to prevent sewer system deterioration such that severe consequences can be avoided. Currently, visual inspection techniques such as closed-circuit television (CCTV) are widely utilized for sewer pipe inspection. As the manual assessment is time-consuming, error-prone and subjective, computer vision techniques are studied for defect classification, defect detection and semantic segmentation. Defect detection and classification can inform inspectors of defect type and relative locations in the image. However, automated assessment of defect severity has been rarely studied, although it is important for arranging maintenance activities. Semantic segmentation can facilitate defect severity assessment by providing the defect type, location and geometric information for each pixel.

Semantic segmentation traditionally relies on classifiers such as Support Vector Machines (SVMs) or probabilistic graphical models e.g. Markov Random Fields (MRFs) and Conditional Random Fields (CRFs) for modelling pixel relationships [2], which all require handcrafted feature descriptors. In recent years, deep learning based models such as fully convolutional network (FCN) are developed by learning rich features automatically and have achieved the state-of-the-art performance [3]. However, the consecutive convolution and pooling implementations in previous deep learning models down-sampled the feature maps by a large factor and generate feature maps of low resolution. Such severe spatial information loss results in obscure segmentation for detailed structures or object boundaries after up-sampling. Therefore, the objective of this study is to improve sewer pipe defect segmentation by proposing a deep CNN model, namely DilaSeg, based on normal convolution, dilated convolution and bilinear interpolation. The proposed model is constructed to extract important features by normal convolution, improve the feature map resolution by dilated convolution, refine the segmentation for object with multiple scales by multi-scale dilated convolution and upsample the feature maps using bilinear interpolation. Sewer pipe images with three types of defects are collected and annotated to train both the proposed model and FCN. Model performance is

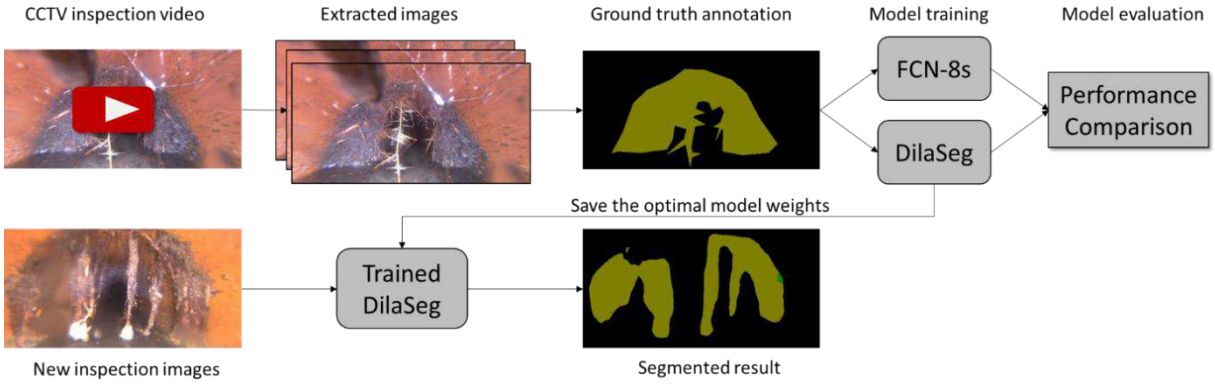

Figure 1. The workflow of sewer pipe defect segmentation using deep learning models

2 Related Work

Computer vision techniques are studied to facilitate the automatic interpretation of visual sewer inspection results. Previous studies have focused on the classification and detection of sewer pipe defects from CCTV images using image processing techniques e.g. morphological operations, histograms of oriented gradients (HOG) and SVMs [4]. More recently, deep learning is applied to address limitations of conventional methods by learning rich features automatically with convolutional neural networks (CNNs). A CNN based model was proposed for classifying multiple sewer pipe defects from CCTV images [5] and a region-based CNN method has been proposed for identifying and locating defects with bounding boxes on sewer pipe images [6]. So far, segmentation of pipe images mainly focuses on pipe components such as joints or segmenting single types of defects using image processing techniques [7]. There are limited studies on the segmentation of multiple pipe defects of sewer pipes, which could provide important references for evaluating the defect severity.

In conventional semantic segmentation, feature extractors such as HOG or scale-invariant feature transform (SIFT) are designed to extract expressive features, based on which small patches of the input image are extracted and classified using local classifiers like random decision forest or SVMs [8]. However, small spatial windows often lead to noisy prediction and require high computational cost. MRFs and CRFs have been widely applied for semantic segmentation [9] by modelling the correlations between variables and incorporating the context knowledge. The main limitation of MRFs and CRFs is that features are obtained from conventional classifiers which are designed for particular cases, during which expertise and efforts are needed. On the contrast, FCN is one breakthrough semantic segmentation deep learning model with higher accuracy than traditional approaches. FCN is developed by transforming the fully connected layers of typical CNNs into convolutional layers and developing a deconvolutional layer for upsampling feature maps [3]. Based on the FCN, many variant networks are proposed, utilizing the architecture of a typical CNN as the "encoder" for generating feature maps and focusing on the development of "decoder" for upsampling images [10]. However, the feature maps generated by FCN and other similar models are of low resolution and predictions are coarse due to the huge spatial information loss during downsampling process.

3 Methodology

3.1 Workflow of Sewer Pipe Defect Segmentation Using Deep Learning Models

As shown in Figure 1, the workflow of implementing deep learning models for segmenting sewer pipe defects mainly includes: (1) extract image from CCTV inspection videos; (2) pre-process and annotate images with different colors for each defect as ground truth labels; (3) build the model architecture and train the model using the annotated images; (4) evaluate and compare the proposed model with the state-of-the-art model; (5) save the best model and apply for new images. Among all the steps in the workflow, the model architecture has great influence on the segmentation performance while the model evaluation provides metrics on the performance. Details of the model and the evaluation are introduced in the following sections.

3.1.1 Architecture of the Proposed DilaSeg

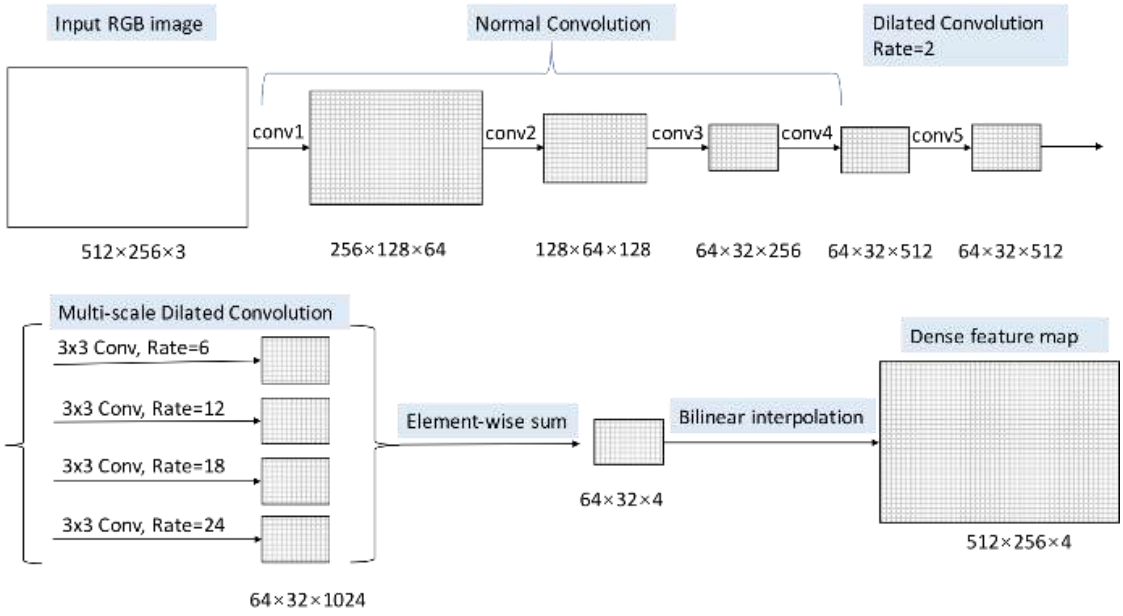

Figure 2. Brief architecture of DilaSeg for generating dense feature maps

To address the problem of large spatial information loss in previous deep learning models, DilaSeg is proposed to improve the feature map resolution and to produce dense feature maps. As shown in Figure 2, the dense feature maps are obtained mainly through (1) normal convolution, (2) dilated convolution, (3) multi-scale dilated convolution and (4) bilinear interpolation. After obtaining the dense feature maps, softmax function is applied for calculating the loss and producing the predicted labels for each pixel.

(1) Normal convolution

During the normal convolution, each image is fed into the network as a three-channel array and a certain number of filters are assigned with random weights at the model initialization stage. In the convolutional layer, the dot product of filters and the convolved image patch is calculated and added with a bias value get the convolution result. In the activation layer, the convolution result is fed into an activation function called Rectified Linear Units (ReLU) so as to add non-linearity to the model. The max-pooling layer is applied after the activation layer, during which only the maximum value in the covered feature map patch is remained to the next layer. The function of the max-pooling is to reduce the spatial dimension of the feature maps such that the computational cost will not exceed the capability. The process of performing a stack of convolution, ReLU and max pooling layers consecutively can be regarded as a down-sampling process, after which the obtained feature maps are of low resolution and may lead to difficulties in the later map upsampling process. Therefore, the resolution of feature maps is controlled through setting different zero padding layers around the feature maps in this study. In the end, the original images are only downsampled by a factor of 8, which is smaller than that by using other networks such as FCN and hence prevents large spatial information loss.

(2) Dilated convolution

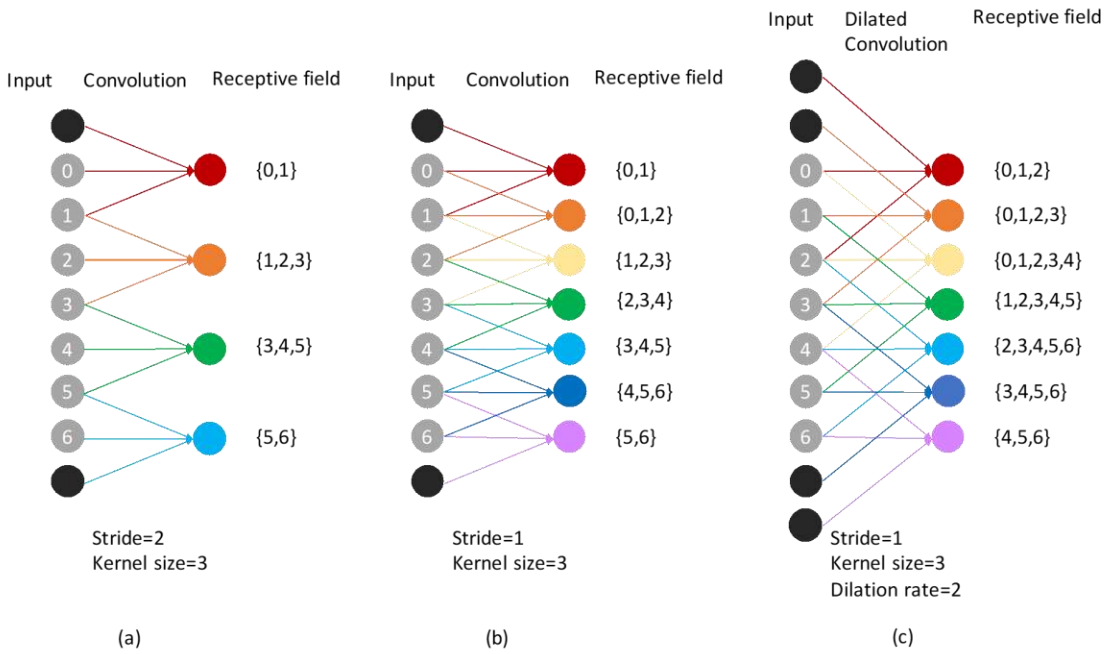

Figure 3. Example of normal convolution and dilated convolution

Another method to prevent too much resolution loss of feature maps is using smaller stride values during the convolution process. For example, the feature map resolution is increased in Figure 3 (b) compared with Figure 3 (a) as the stride value is decreased from 2 to 1. Nevertheless, one limitation of applying small stride values is that the receptive field (i.e. the area convolved by the filters with respect to the original input) is still small, which means there is not much global information incorporated during the learning process. Therefore, dilated convolution [11], is applied in the proposed model such that feature map resolution is improved and the receptive field is enlarged, but the parameter number will not increase. The dilated convolution filters can be treated as normal filters filled with certain number of holes (zeros), which is indicated by the dilation rate. Filters with dilation rate of *k* means that there are *(k-1)* zeros inserted among each consecutive columns or rows of original filters. Specially, filters with dilation rate of 1 are the same with normal filters. Consequently, the scope of the convolved pixels of the original input (i.e. receptive field) is increased while the number of parameters remains the same with that of using normal filters. For example, Figure 3 (c) with the dilation rate of 2 increases the map resolution to the same density as (b) while the receptive field becomes larger, which enables more contextual information involved.

(3) Multi-scale dilated convolution

During segmentation, when aspect ratio of objects is different, convolution using the fix-sized filters only extract features from objects with certain scale while omitting features of different scale objects. Similar case exits for the segmentation of sewer pipe defects, considering different scales of the sewer pipe defects, e.g. scale of cracks is similar to long and thin rectangle while deposits tend to have square scale. Therefore, multi-scale dilated convolution layers are added in the developed model. Specifically, dilated convolution with 4 different dilation rates i.e. {6,12,18,24} is performed in parallel to generate feature maps respectively, the process of which is similar to convolution using filters of different sizes. With the aim not to reduce the feature map resolution, zero padding layers are applied according to the dilation rate of each layer. The feature map values from the four parallel layers are summed pixel-by-pixel and the fused results are used for the final interpolation.

(4) Bilinear interpolation

After the parallel dilated convolution, the generated feature maps are upsampled using bilinear interpolation, which is a common method used for upsampling. As shown in Figure 4, on the feature map to be upsampled, the value of each pixel is known. With the information of both location and values two pixels, the value of pixels in a certain location between them can be calculated through linear interpolation. Similarly, the value of pixels at other positions can also be obtained. For example, based on the known coordinates of all the pixels on the feature map, the value of pixel e can be obtained through the P_a and P_b while P_f can be calculated from P_c and P_d. In the end, P_g is obtained

using P_e and P_f. By repeating this process, the feature map can be upsampled to the original resolution with values for each pixel.

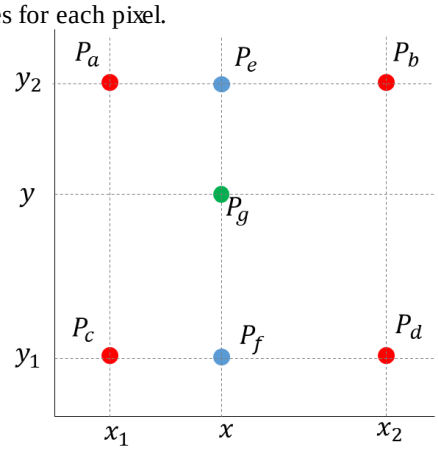

Figure 4. Example of bilinear interpolation

3.2 Model Evaluation

The proposed model is designed for real-time defect segmentation, the model implementation and computational cost should be feasible for on-site inspection while the segmentation accuracy should also be satisfying.

3.2.1 Accuracy

The four indices in [12] are used for measuring segmentation accuracy. As shown in Figure 5, assume the total class number is $k+1$ (including k objects and 1 background class), p_{ij} is the number of pixels of class i but assigned with class j and can be treated as false positives. p_{ji} can be interpreted as false negatives while p_{ii} represents true positives. Circle A represents the total number of pixels of class i, i.e. $t_i = \sum_{j=0}^{k} p_{ij}$. Circle B represents all the pixels predicted to be class i and the intersection C between A and B represents all the true positives.

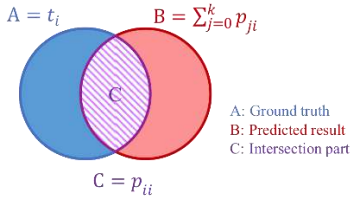

Figure 5. Graphical representation of the predicted results and ground truth

(1) Pixel accuracy (PA)

PA is the simplest evaluation by calculating the ratio of pixels correctly classified over the total number of pixels.

$$PA = \frac{\sum_{i=0}^{k} p_{ii}}{\sum_{i=0}^{k} t_i} \tag{8}$$

(2) Mean pixel accuracy (mPA)

mPA is calculated based on the pixel accuracy for each class, by computing the ratio of correctly predicted pixels over the total pixel amount in each class and taking the average value for all the classes.

$$mPA = \frac{1}{k+1}\sum_{i=0}^{k} \frac{p_{ii}}{t_i} \tag{9}$$

(3) Mean intersection over union (mIoU)

IoU is the dominant metric for evaluating segmentation accuracy and is calculated by taking the ratio of the intersection between predicted results and ground truth labels over the union between these two sets. The intersection is the true positives while the union is the sum of false positives and false negatives and subtracted by true positives. mIoU is obtained by taking average value of the IoUs for all the classes.

$$mIoU = \frac{1}{k+1}\sum_{i=0}^{k} \frac{p_{ii}}{t_i + \sum_{j=0}^{k} p_{ji} - p_{ii}} \tag{10}$$

(4) Frequency weighted intersection over union (fwIoU)

As the percentage of pixels belonging to each class may be different in the training dataset, evaluating the accuracy considering pixel occurrence frequency is also important.

$$fwIoU = \frac{1}{\sum_{i=0}^{k}\sum_{j=0}^{k} p_{ij}}\sum_{i=0}^{k} \frac{p_{ii} t_i}{t_i + \sum_{j=0}^{k} p_{ji} - p_{ii}} \tag{11}$$

3.2.2 Computational Cost

The computational cost is a significant evaluation aspect to ensure a desired segmentation speed for real-time segmentation of sewer pipe defects. The computational cost of the models is evaluated for the inference stage using the segmentation speed as well as the training stage using training duration and model convergence performance. Compared with training stage, evaluation of the inference stage is more important as the inference speed affects the real-time performance of the model.

4 Experiments and Results

To validate the proposed models for sewer defect segmentation, experiments are conducted to evaluate

FCN-8s and the DilaSeg in terms of accuracy and computational cost.

4.1 Experiment Dataset and Implementation Details

Images containing three types of defects i.e. cracks, deposits and tree root intrusions are extracted from CCTV inspection videos of sewer pipe inspection company in the United States. 90% of 1510 annotated images are used for training (1,359 images) and 10% are for testing (151 images). The annotation files are generated through LabelMe [13] by plotting the polygon along the boundary of each defect. All the pixels inside the same polygon are assigned with the same defect class. In the end, each defect is annotated with different colors and the background is set to be black. Caffe [14] is one common library for building deep learning models. As the functions of the dilated convolution are not included in the initial Caffe, source code of Caffe was revised and recompiled for training the proposed model. All the segmentation models are trained on Ubuntu system with Intel® Core™ i7-6700 CPU @ 3.40GHz × 8 and GPU of GeForce GTX 1080. During each training iteration, images are fed into the network with a mini-batch of 16, to reduce GPU memory requirement and improve the training efficiency. The "poly" learning rate is applied with a base learning rate of 0.01, momentum of 0.9 and weight decay of 0.005. Each model is trained using the re-compiled Caffe for 50,000 iterations and saved every 500 iterations to evaluate their accuracy on validation dataset.

4.2 Experiment Results

4.2.1 Accuracy

As shown in Figure 6 (a), the pixel accuracies of the two models follow a similar trend, i.e. within a certain number of iterations, PA increases with the increase of training iteration. The increase is obvious during first few thousand iterations and gradually becomes small in the later training period. Finally, the PA reaches a plateau and no longer yields increase. The point where the model reaching the plateau indicates the convergence of the model and is different for each model depending on the convergence speed. The DilaSeg has higher PA values than FCN-8s, indicating the effectiveness of dilated convolution.

As shown in Figure 6 (b), the mPA values of both models are increasing during the training process. Although FCN-8s has a more obvious increase trend, DilaSeg achieved much higher mPA value than FCN-8s. As shown in Figure 6 (c), in terms of values of mIoU, the overall varying situation is similar to PA and mPA, with an increase at first and reaching a plateau in the end. The mIoU values of FCN-8s also increase with the training iterations, but the overall mIoU values are much lower than the proposed model. The mIoU values of DilaSeg are higher than FCN-8s during the whole training process, which reflecting the stronger capability of the developed model for segmentation. The fwIoU values which considers the pixel occurrence frequency when calculating IoU are shown in Figure 6 (d). Almost during the whole training, the fwIoU values of DilaSeg are higher than FCN-8s.

The best accuracy values of the two models are shown in Table 1. It can be seen that accuracies in terms of the four indices obtained using DilaSeg are higher than FCN-8s. The developed model improved the segmentation accuracy largely, especially with 18% of increase in mPA and 22% of increase in mIoU using DilaSeg.

Some of the segmentation results are analysed. As shown in Figure 7 (a) and (b), for crack segmentation, FCN-8s can approximately provide the locations but cannot detect the correct defect type. One reason is that the model cannot recognize the defect type due to the color similarity between the cracks and other defects.

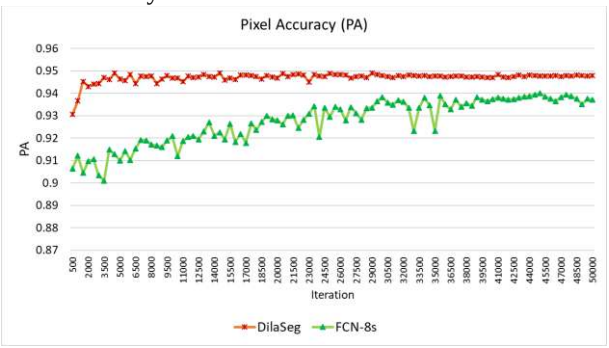

(a)

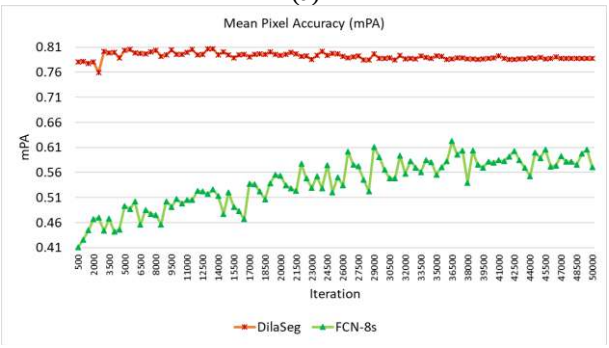

(b)

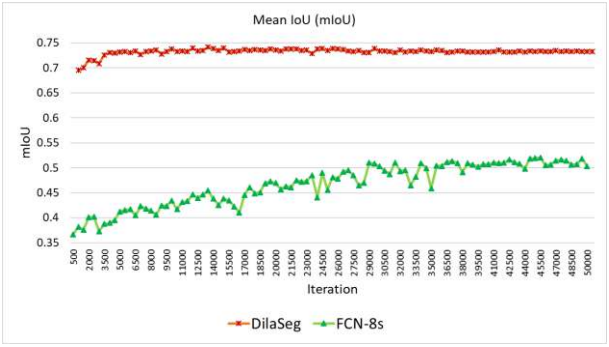

(c)

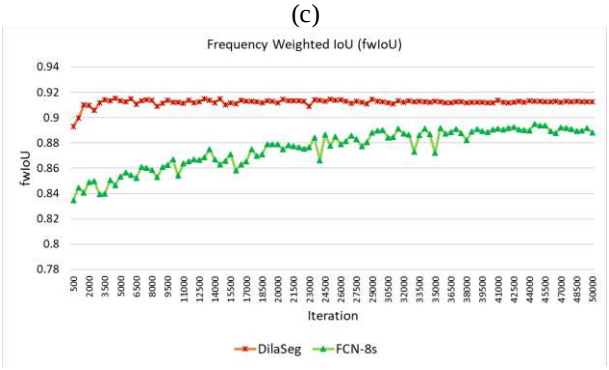

(d)

Figure 6. Accuracy of the two models for segmentation of sewer pipe defects

The DilaSeg performed better than FCN-8s, with segmentation of more parts of cracks, although some cracks are not segmented completely. In terms of deposit and tree root, FCN-8s achieved better results compared with segmenting cracks. However, segmentation of deposit and tree root are mixed with each other as shown in Figure 7 (c) and some defects are not segmented completely as shown in Figure 7 (d). On the contrary, DilaSeg is capable of segmenting both deposit and tree root much better with fewer mixed segmentation cases. In addition, more areas of the defects can be segmented by DilaSeg and more complete segmentation results can be provided as shwon in Figure 7 (e).

Table 1. Accuracy of the two models

	FCN-8s	DilaSeg
PA	0.939	0.949
mPA	0.623	0.807
mIoU	0.521	0.742
fwIoU	0.895	0.915

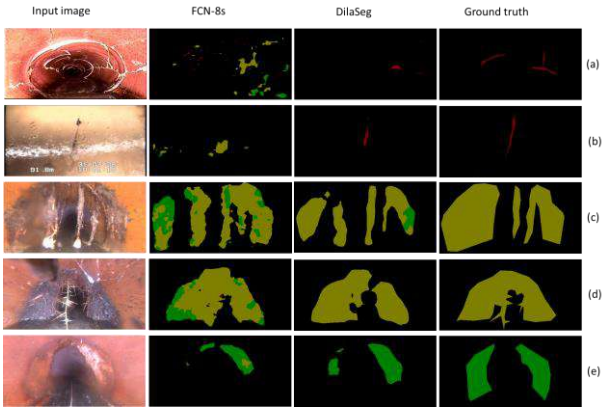

Figure 7. Examples of segmentation results (red color represents cracks, lime color represents roots and green color represents deposit)

4.2.2 Computational Cost

The computational cost of the two methods is evaluated using the detection speed (i.e. the time taken for detecting each image), training duration (in hours) and converge iteration (i.e. the number of iterations taken for the model to obtain convergence). The training duration and converge iteration indicate the difficulty for training the model to achieve desired performance while the detection speed reflects the possibility of real-time segmentation. As shown in Table 2, although the training process of DilaSeg is longer than FCN-8s, the detection speed of DilaSeg is relatively faster during model inference. In addition, the training loss of DilaSeg is dropping quickly within the first few thousand iterations and achieved a plateau at around 15,000 iterations, as shown in Figure 8 (a). However, the loss of FCN-8s was much higher and was dropping at a quite slow rate during the whole process, achieving a converging point after 45,000 iterations. The training loss trend reflects the proposed model can learn image features and optimize weights more efficiently.

Table 2. Computational cost of the two models

	FCN-8s	DilaSeg
Detection speed (s/image)	0.352	0.265
Training duration (h)	3.417	17.405
Converge iterations	45000	15000

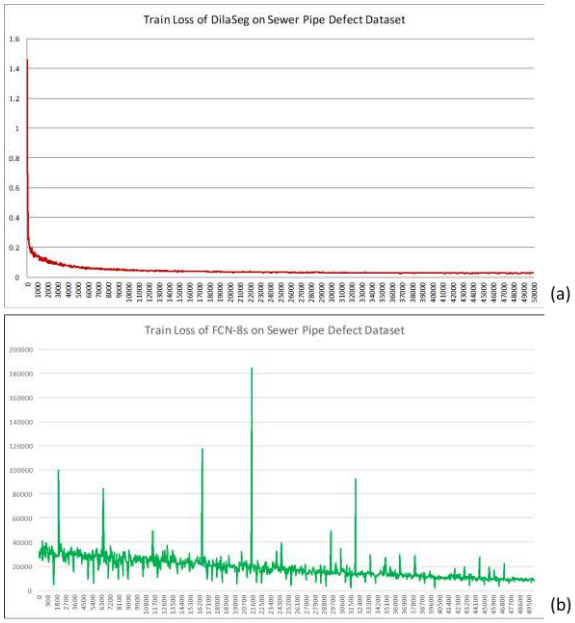

Figure 8. Training loss of DilaSeg and FCN-8s

5 Conclusion and Future Work

Computer vision techniques are attracting attention for automatic interpretation of sewer inspection results. Previous studies mainly focus on classifying and locating defects in images, which cannot provide information about the severity level of different defects. In addition, the requirement of the practical implementation of models on CCTV robots, e.g. the computational cost is rarely considered. This study aims to obtain the segmentation of three different types of sewer pipe defects i.e. crack, deposit and tree root, from CCTV inspection images to facilitate real-time severity assessment in the future.

To address the problem of large information loss during the down-sampling process of most previous deep learning models such as FCN, a new model called DilaSeg is developed in this study for semantic segmentation based on dilated convolution to increase feature map resolution. The proposed model is featured for performing several modules to obtain dense segmentation results, including normal convolution, dilated convolution, multi-scale dilated convolution as well as bilinear interpolation. Important features are extracted using the normal convolution and the feature maps are down-sampled due to consecutive convolution and max-pooling. Dilated convolution is implemented to prevent too much spatial information loss, which is also applied for objects with different scales through multi-scale dilated convolution. In the end, the feature maps are upsampled to original scale using bilinear interpolation. Experiments demonstrate that compared with FCN-8s, DilaSeg improved segmentation accuracy significantly in terms of all the evaluation indices. Especially, there is 18% of increase in mean PA and 22% of increase in mean IoU. Furthermore, the inference of the DilaSeg is faster than FCN-8s, which indicates the advantage of the proposed model for real-time application. Regardless of the improved accuracy, there are still some negative segmentations, possible reasons and potential solutions need to be validated in the future.

References

[1] EPA, Report to Congress on Impacts and Control of Combined Sewer Overflows and Sanitary Sewer Overflows, 2004.

[2] A. Arnab, S. Zheng, S. Jayasumana, B. Romera-Paredes, M. Larsson, A. Kirillov, B. Savchynskyy, C. Rother, F. Kahl, P.H.S. Torr, Conditional Random Fields Meet Deep Neural Networks for Semantic Segmentation: Combining Probabilistic Graphical Models with Deep Learning for Structured Prediction, IEEE Signal Process. Mag. 35 (2018) 37–52. doi:10.1109/MSP.2017.2762355.

[3] E. Shelhamer, J. Long, T. Darrell, E. Shelhamer, T. Darrell, J. Long, T. Darrell, E. Shelhamer, T. Darrell, Fully Convolutional Networks for Semantic Segmentation, Proc. IEEE Conf. Comput. Vis. Pattern Recognit. (2015) 3431–3440. doi:10.1109/CVPR.2015.7298965.

[4] M.R. Halfawy, J. Hengmeechai, Automated defect detection in sewer closed circuit television images using histograms of oriented gradients and support vector machine, Autom. Constr. 38 (2014) 1–13. doi:10.1016/j.autcon.2013.10.012.

[5] S.S. Kumar, D.M. Abraham, M.R. Jahanshahi, T. Iseley, J. Starr, Automated defect classification in sewer closed circuit television inspections using deep convolutional neural networks, Autom. Constr. 91 (2018) 273–283. doi:10.1016/j.autcon.2018.03.028.

[6] J.C.P. Cheng, M. Wang, Automated detection of sewer pipe defects in closed-circuit television images using deep learning techniques, Autom. Constr. 95 (2018) 155–171. doi:10.1016/j.autcon.2018.08.006.

[7] S. Iyer, S.K. Sinha, Segmentation of pipe images for crack detection in buried sewers, Comput. Civ. Infrastruct. Eng. 21 (2006) 395–410. doi:10.1111/j.1467-8667.2006.00445.x.

[8] M. Thoma, A Survey of Semantic Segmentation, CoRR. (2016) 1–16. http://arxiv.org/abs/1602.06541.

[9] P. Krähenbühl, V. Koltun, Efficient Inference in Fully Connected CRFs with Gaussian Edge Potentials, Proc. 30th Int. Conf. Int. Conf. Mach. Learn. - Vol. 28. (2012) 513–521. doi:10.1.1.760.9549.

[10] V. Badrinarayanan, A. Kendall, R. Cipolla, SegNet: A Deep Convolutional Encoder-Decoder Architecture for Image Segmentation, IEEE Trans. Pattern Anal. Mach. Intell. 39 (2017) 2481–2495. doi:10.1109/TPAMI.2016.2644615.

[11] M. Holschneider, R. Kronland-Martinet, J. Morlet, P. Tchamitchian, A Real-Time Algorithm for Signal Analysis with the Help of the Wavelet Transform, in: J.-M. Combes, A. Grossmann, P. Tchamitchian (Eds.), Wavelets. Inverse Probl. Theor. Imaging, Springer Berlin Heidelberg, Berlin, Heidelberg, 1990: pp. 286–297.

[12] A. Garcia-Garcia, S. Orts-Escolano, S. Oprea, V. Villena-Martinez, J. Garcia-Rodriguez, A Review on Deep Learning Techniques Applied to Semantic Segmentation, (2017) 1–23. http://arxiv.org/abs/1704.06857.

[13] A. Torralba, B.C. Russell, J. Yuen, LabelMe: Online Image Annotation and Applications, Proc. IEEE. 98 (2010) 1467–1484. doi:10.1109/JPROC.2010.2050290.

[14] Y. Jia, E. Shelhamer, J. Donahue, S. Karayev, J. Long, R. Girshick, S. Guadarrama, T. Darrell, Caffe: Convolutional Architecture for Fast Feature Embedding, in: Proc. 22Nd ACM Int. Conf. Multimed., ACM, New York, NY, USA, 2014: pp. 675–678. doi:10.1145/2647868.2654889.

Information Exchange Process for AR based Smart Facility Maintenance System Using BIM Model

S.W. Chung[a], S.W. Kwon[b], D.Y. Moon[a], K.H. Lee[a], and J.H. Shin[a]

[a]Department of Convergence Engineering for Future City, SungKyunKwan University, Republic of Korea
[b]School of Civil, Architectural Engineering and Landscape Architecture, Sungkyunkwan University, Republic of Korea (corresponding author)
E-mail: suwanx@nate.com, swkwon@skku.edu, yoshy17@nate.com, kiwijoa@skku.edu, kyup@skku.edu

Abstract –

In this study, we propose information exchange process for the effective integration of building information modeling (BIM) into an augmented reality (AR)-based smart facilities maintenance (SFM) system. The proposed SFM system refers to a system that combines technologies such as AR and IoT sensors in the field maintenance work. This requires the acquisition of data from various sources followed by transformation of these data into an appropriate format. Construction operation building information exchange (COBie) is widely used as a means to effectively integrate and utilize information for maintenance. Therefore, SFM system has a requirement attribute information system with reference to COBie. But this information should be linked to the maintenance work procedures in the actual use case scenario and it is necessary to define the information exchange process. To solve this problem, we uses the following methods to enable SFM system development with applications for BIM and AR technologies in the FM of the building sector of public facilities. First, it analyzes the previous studies on BIM-based maintenance works and AR technology. Second, it divides the SFM work process utilizing the BIM-based COBie system, and it defines the COBie data required for each work phase. Third, it develops a scenario-based business process modeling notation (BPMN) for the SFM system prototype. Finally, it proposes an implementation method of SFM system architecture.

Keywords –

Building information model; Facility maintenance; Augmented reality; Business process modeling notation

1 Introduction

1.1 Background and Objectives of the Research

One of main purposes of facility management (FM) is to realize the expected asset value by maintaining or complementing qualities of facilities planned in the design phase and secured in the construction phase. FM phase accounts for the longest proportion in the building life cycle, and the cost consumed in this phase occupies 85% of the life cycle cost (LCC) [1]. Facility information generated in the design and construction phases is utilized as basic implementation data of the facility management system (FMS) for effective and systematic operation and maintenance, but it takes a considerable amount of time and money to implement basic data in the FMS through defining and verifying the required information in the operation and maintenance phases. To resolve difficulties in current FMS implementation process, building information modeling (BIM) technology has been introduced, which can act as an alternative system to systematically and efficiently operate and maintain the facilities. BIM is structured with objects, attributes, and relationships. Since all attributes and relationships are defined based on objects, BIM can manage the required information for operation and maintenance by function, space, and use purpose.

Building owners and facility maintenance mangers have an opportunity to reduce a large amount of cost during a much longer maintenance period than that of design or construction phase by utilizing BIM-based information. However, although utilization of BIM information in the facility maintenance phase has many advantages, BIM information has not yet been utilized in on-site maintenance work. This is because a variety of information required for facility maintenance has not been defined, and, in many cases, this information is not included in BIM-based design.

To solve this problem, a large number of studies have been conducted to develop a system to transfer BIM information generated over the design and construction phases into the facility maintenance phase. As a result, data exchange format called construction operation building information exchange (COBie) was developed by public institutions, which took project ordering tasks of major facilities in the USA.

Meanwhile, AR technology has been utilized in various areas, such as product review and production system design. More recently, with the advancement of smart devices, users can now employ AR more easily than ever before. The construction industry is also actively introducing on-site facility data visualization and real-time collaboration features by utilizing AR technology. However, few studies have been conducted on the utilization of AR technology in the maintenance phase as compared to the design and construction phases, even though economic benefits would be the largest in terms of LCC.

Thus, as one of the few studies on SFM for automation management and efficient execution of facility maintenance, this study aims to discuss the current trend of BIM and AR technology; it measures of how to link information and proposes an AR-based SFM system. In addition, this study sets the COBie system as a benchmarking target—which has been developed as a system prototype in the USA and is now widely recognized in the world—to define the required information exchange process for implementation.

1.2 Study Method and Procedure

This study uses the following methods to enable SFM system development with applications for BIM and AR technologies in the FM of the building sector of public facilities. First, it analyzes previous studies on BIM-based maintenance works and AR technology. Second, it divides maintenance work process utilizing a BIM-based COBie system, and it defines COBie data required for each work phase. Third, it develops a scenario-based business process modeling notation (BPMN) for the SFM system prototype. Finally, it proposes an implementation method of SFM system architecture.

2 Analysis of Previous Studies

2.1 Building Maintenance Using BIM

When BIM is applied in the maintenance phase, it can be utilized in analysis data for the purchase procurement of machine equipment, control systems, and other products; it can also check whether all systems are correctly operating after buildings are complete, which is the advantage of BIM to the maintenance phase. It can also act as an interface for sensors; it can remotely operate the management of facilities and provide real-time monitoring of control systems through providing accurate information about space and systems [2]. BIM for FM provides a manual for building users, which can help to locate models visually, such as facilities, attachments, and furniture. BIM also supports contingency plans, security management, and scenario planning [3]. As described above, several studies have been conducted actively to show the advantages of a BIM application to FM.

A study by Yu developed a data model, Facility Management Classes (FMC), which can extract required information from Industry Foundation Classes (IFC) for information compatibility of BIM data into FM [4]. A study by Mendez R. proposed functions that can be utilized by BIM in the maintenance phase; the study developed a web-based prototype to improve the utilization of BIM information [5]. East and Brodt developed a data exchange format called COBie based on a spreadsheet to solve inefficiencies due to unnecessary information in maintenance among information sets created during the design and construction phases [6]. A study by Burcin defined a level of BIM recognition in the maintenance phase through expert interviews, applicable areas, required data, and processes to implement BIM successfully [7]. Lee et al. attempted to improve a facility maintenance system through benchmarking the COBie system, and Choi et al. conducted a study to implement a FM system for sewage treatment based on the COBie [8][9].

One study proposed software architecture to integrate BIM with geographic information system (GIS)-based FMS effectively [10]. Another study proposed integrating BIM-based Mechanical, Electrical, and Plumbing (MEP) information in the operation and maintenance phases [11].

Most of the previous studies on FM utilizing BIM focus on the interoperability with FM system and a measure to link data produced during design and construction phases as well as a direction to application of BIM to FM systems and commercialization has been chosen.

2.2 Utilization of AR Technologies in Building Industry

The trend of utilizing AR technology in building industry has showed that earlier studies focused on the analysis of applicability of virtualization technology Hammad presented the applicability of AR technology to field works of infrastructure, and Koo considered the development of a wireless technology-based, AR-applied system in terms of display, tracking, and servers. Afterward, a study on the presentation of an AR system

prototype for the inspection of steel column construction was conducted [12] [13].

For studies on AR authoring tools, AR modeling through capturing and rendering of exterior structures in real time and 3D modeling can be found. A tool called "Tinmith" was manufactured to interact between users and AR directly [14]. Moon et al. implemented an AR prototype that can select the position of a tower crane appropriately in a high-rise building construction site and conducted a verification procedure through actual building drawings [15].

More recently, studies on the application of AR to building maintenance have been conducted in various ways. A study by Bae et al. proposed a novel method that supported on-site construction and facility management works by documenting on-site problems and progress visually by on-site staff and by making recent project information accessible as a form of AR overlay [16]. Another study proposed a natural marker-based AR framework that can support facility managers digitally when they search FM items or perform maintenance and repair works [17]. Kwon et al. proposed a SFM system that improved existing maintenance work; thy studied a novel maintenance work process and an implementation method to apply AR technology [18].

The analysis results of previous studies have showed that the utilization of AR technology in the building industry has enabled efficient construction management by recognizing design drawings intuitively by users. Four-dimensional (4D) BIM based on existing virtual environments has lacked reflection about the actual construction site conditions. Thus, if AR technology that reduces a cognitive resistance is applied to maintenance sites, its value and utility would be significant in terms of productivity improvements.

3 SFM and COBie System

3.1 Overview of SFM

A SFM system proposed in this study aims to support tasks of workers and managers by introducing Internet of things (IoT)/VR/AR technologies to existing on-site maintenance works. The base data to combine the new technologies are BIM data. To do this, a study on improved process of sequential and repetitive task elements was conducted by applying AR/VR technologies to existing maintenance tasks [18].

Data such as drawings, historical information, and related documents stored in a distributed manner in the facility maintenance tasks are linked and integrated with BIM data to overcome the limitations of simple repetitive tasks and inefficient data utilization.

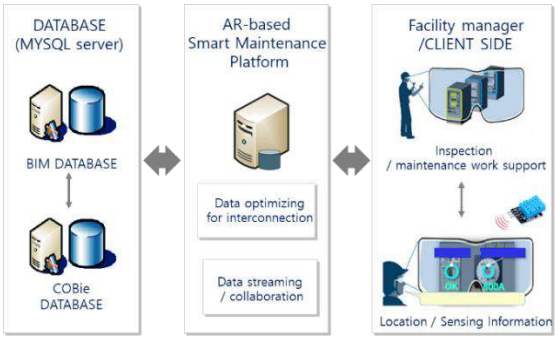

Figure 1. Configuration of proposed system

As shown in Figure 1, variably distributed data can be gathered, and each request can be processed as a hub through the AR-based smart maintenance platform, which manages the facility management database in the center. This study's scope is limited to building interior constructions (floor, wall, ceiling, window, door etc.) among the maintenance target facilities.

3.2 SFM Work Process

A BIM attribute information and the historical management information required by task units in the maintenance work may be different from each other. To define the information clearly and store them in a database for the utilization of AR visualization, task units were classified based on maintenance work scenarios.

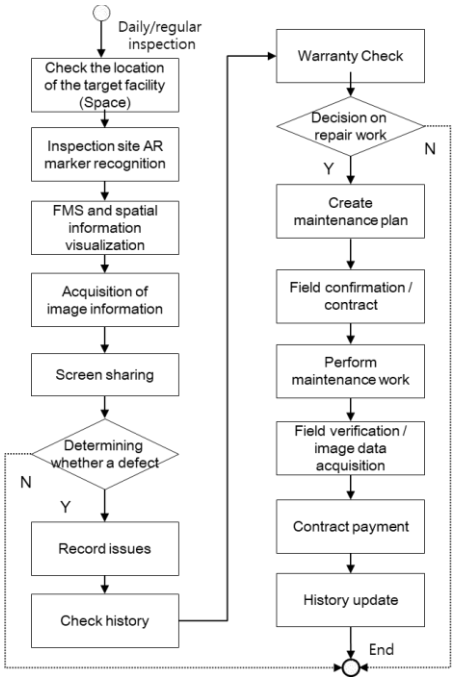

Figure 2. Scenario-based workflow

As shown in Figure 2, an on-site inspector checks the inspection-required facility location and recognizes the AR marker attached to the inspection target space in the daily inspection task scenario. Inspection-required members and checklists in the corresponding space are visualized through the markers by which the inspector can perform visual inspection and photo shooting. In this process, video information through the inspector's camera is shared in real time so that various decision-making participants can judge together whether there are defects or not. If decision making determines that there is a defect through the inspection, historical information, such as installation, warranty, and management companies, is visualized, and the status information can be sent to the corresponding companies directly from the site. After this, a maintenance manager decides whether repair work is needed. If repair work is done, task-related guidance and progress are monitored in the construction process, and stored in the FMS.

The core technologies of AR visualization in this process are the following: 1) AR-based surveillance task support technology, 2) 3D information plus AR overlaying technology, and 3) 3D data conversion technology for AR/VR.

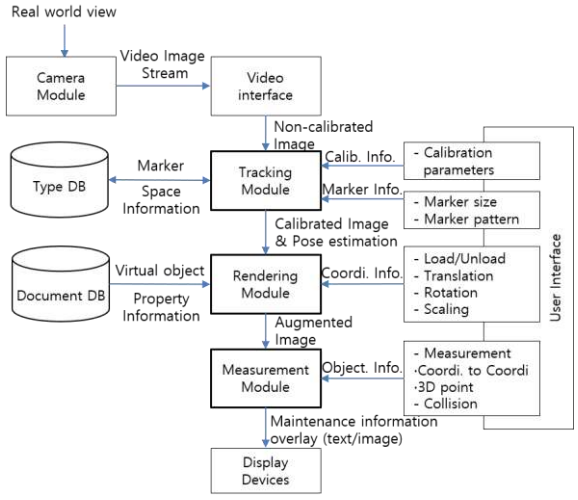

Figure 3. AR visualization process in inspection work

3.3 Definition of the COBie System

To implement the AR-based smart maintenance process proposed in this study, COBie is benchmarked and utilized. COBie is an information exchange data format based on a spread sheet jointly developed by public institutions that take project orders of major facilities in the USA led by the US army corps of engineers. It was developed as a means to replace a large amount of documents related to facility management at the time of completing the construction of a project. COBie includes definitions and formats of information required during the maintenance phase among a BIM information created in a series of phases during construction projects: planning, design, construction, operation, and maintenance.

Table 1. COBie data sheets and contents by phase

Phase	Sheet	Contents
All	Contact	People and Companies
	Document	All applicable document references
	Attribute	Properties of referenced item
	Coordinate	Spatial locations in box, line, or point format
	Issue	Other issues remaining at handover.
Early Design	Facility	Information on Facilities and Standards
	Floor	Vertical levels and exterior areas
	Space	Spaces
	Zone	Sets of spaces sharing a specific attribute
	Type	Types of equipment, products, and materials
Detailed Design	Component	Individually named or schedule items
	System	Sets of components providing a service
	Assembly	Constituents for Types, Components and others
	Connection	Logical connections between components
	Impact	Economic, Environmental and Social Impacts at various stages in the life cycle
O&M	Spare	Onsite and replacement parts
	Resource	Required materials, tools, and training
	Job	PM, Safety, and other job plans

As presented in Table 1, COBie consists of 18 data sheets, and the related detailed contents can be expanded through expandable templates. In the data sheets that can be utilized in the whole phases of construction projects, contract-related items of construction participants, drawings, coordination systems, and building completion-related issues are included. In the initial design phase, facility information

and floors, spaces, and material types are included, and in the detailed design phase, the connection of all members and assembly, system configurations, processes, and costs are added. In operation and maintenance (O&M) phase, replacement and repair items and required resources and tasks are included. In addition, COBie is configured to expand the required attribute information constantly.

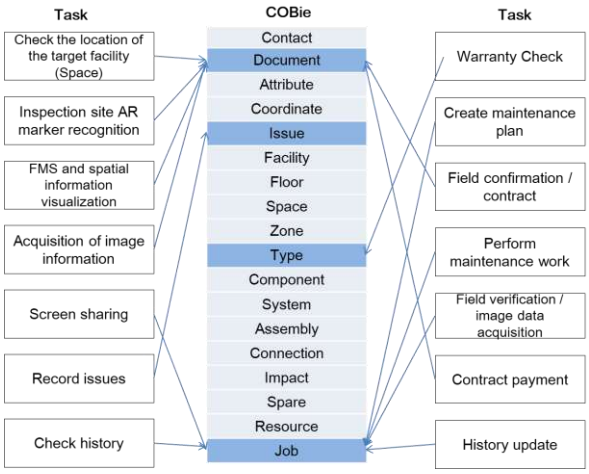

Figure 4. Smart maintenance tasks and COBie data mapping

All of these data sheets are not needed in the COBie system definition, which were required for the previously proposed maintenance work by the scenarios, but it is important to utilize only minimum information considering the link between attribute information and data lightweight, which are essential for AR visualization. Thus, the information required for the previously proposed maintenance work by the scenarios and COBie data sheets was mapped. This process was conducted through prior literature reviews and through interviews and surveys with on-site maintenance workers, as shown in Figure 4.

Through this process, document, issue, type, and job data sheets were found to include attribute information required for the on-site maintenance work. However, excessive attribute information was required in the document and job sheet among these four data sheets, and unnecessary information was also included depending on maintenance work participants. Thus, warranty and plan data sheets were additionally created and used for optimization of AR-based visualization information.

Table 2. COBie data sheet for field maintenance

Sheet	Contents
Document	Submittals and approvals, DWG.
Issue	Other issues remaining at maintenance
Type	Types of equipment, products, materials, model, Warranty data
Job	PM, Safety, and other job plans

Contents included in the newly added warranty data were the product names of the interior finish materials, repair (warranty) responsible companies, contact details, and warranty-related document information. Through this information, which companies are responsible can be identified when defects occur, and requests for repair can be achieved rapidly. A plan data contains information that is utilized when maintenance construction occurs, which includes construction progress status, follow-up tasks, and next maintenance inspection date.

4 Information Exchange Process to Implement the Prototype

4.1 Smart Maintenance BPMN

To implement a prototype of an AR-based, on-site support module for the SFM on the basis of maintenance scenarios proposed in this study, a BPMN, including the current status of data input and output, is required. BPMN is a visualized notation method to represent business processes. It is developed to notate a message flow between activities over a time flow in the process. BPMN that defines and represents the data inputs and outputs required in the maintenance work process, based on daily inspection scenarios, is shown in Figure 5.

Most of the 3D models and attribute information of the inspection-required objects are extracted from a BIM information and stored in a database as COBie Excel sheets. Here, the additionally required attribute information is AR market information, inspection date, and warranty period, which requires a manual input process by the maintenance manager or supplier.

The most important thing in the utilization of BIM in maintenance work is to clarify the definitions of requirements and use cases. Thus, the proposed BPMN facilitates detailed implementation of smart maintenance use case.

between users and managers who use the AR system.

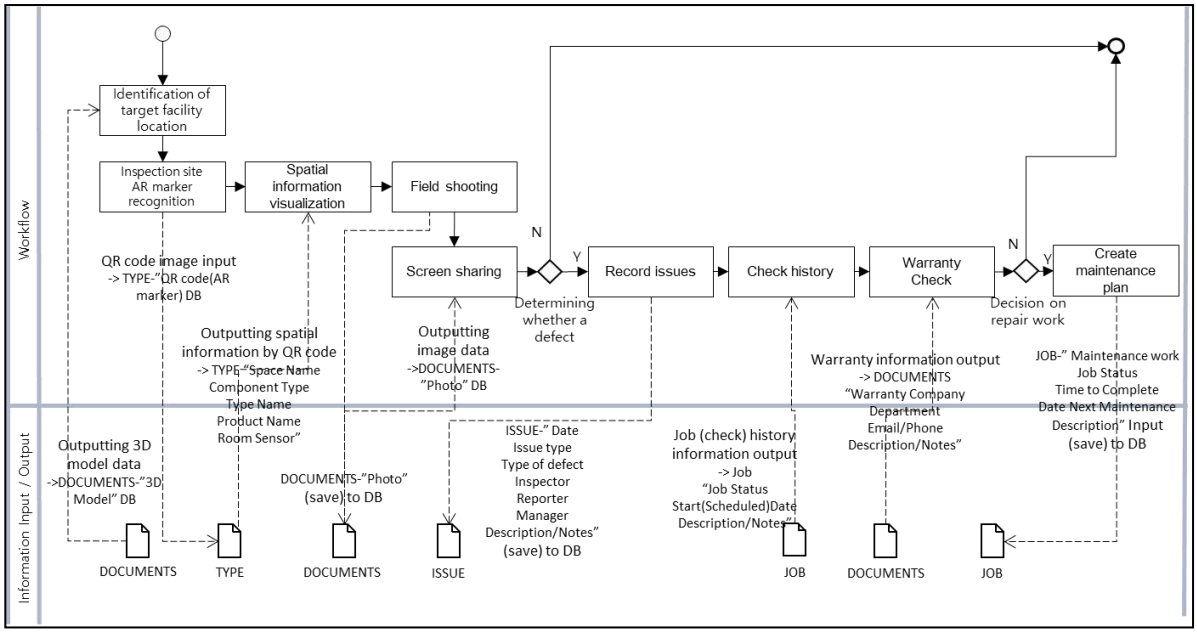

Figure 5. Daily / regular maintenance scenario based BPMN

4.2 Functional Screen Configuration and UI

Basically, an AR system consists of a camera, an image converter, tracking, and a video background render. A camera component helps efficient delivery to the camera frame. A camera frame is provided automatically according to the device, depending on image format and size. Once markers are recognized through the HMD camera, users define the targets that will be observed through the AR via the pixel format conversion. Targets defined in the database configured with COBie system monitors objects through the tracking module. After detected object's status is identified, the 3D virtual objects are modeled, and information is provided on the display. Auxiliary information about augmented 3D virtual object in display is managed by the web-based FMS and augmented through XML. In web service application, auxiliary information about augmented objects was composed of a management system and two-way communication systems. The auxiliary information management system was configured to provide various pieces of information rapidly to users and overcome the existing problem, which only showed 3D object augmentation. Two-way communication system was configured to provide information in real time—which was not provided by the auxiliary information management system—through two-way communication

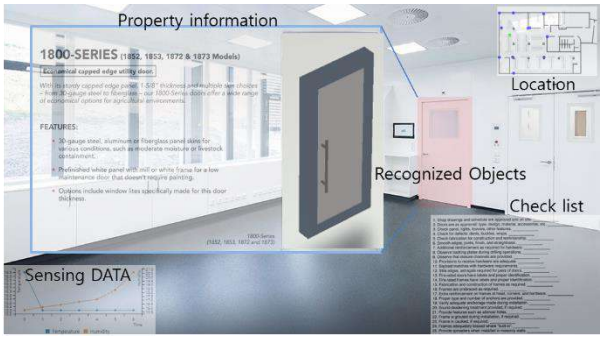

Figure 6. Example of AR-based SFM system UI

UI in the AR application, which emphasizes interaction functions through real world, requires different designs from those of existing mobile applications. Most mobile devices utilized in site are smart phones and tablets, which support a touch-based interface. However, since on-site maintenance support application proposed in this study targeted HMD devices, existing touch-based operations cannot be used. Thus, controls through gesture or voice recognition are needed, which require more user-friendly and intuitive UI. Consequently, menu button items were removed, and required attribute information was laid out on the lower side of the screen. Since augmented reality interacts with the real world, visualized information supports a transparency control function to project the real world.

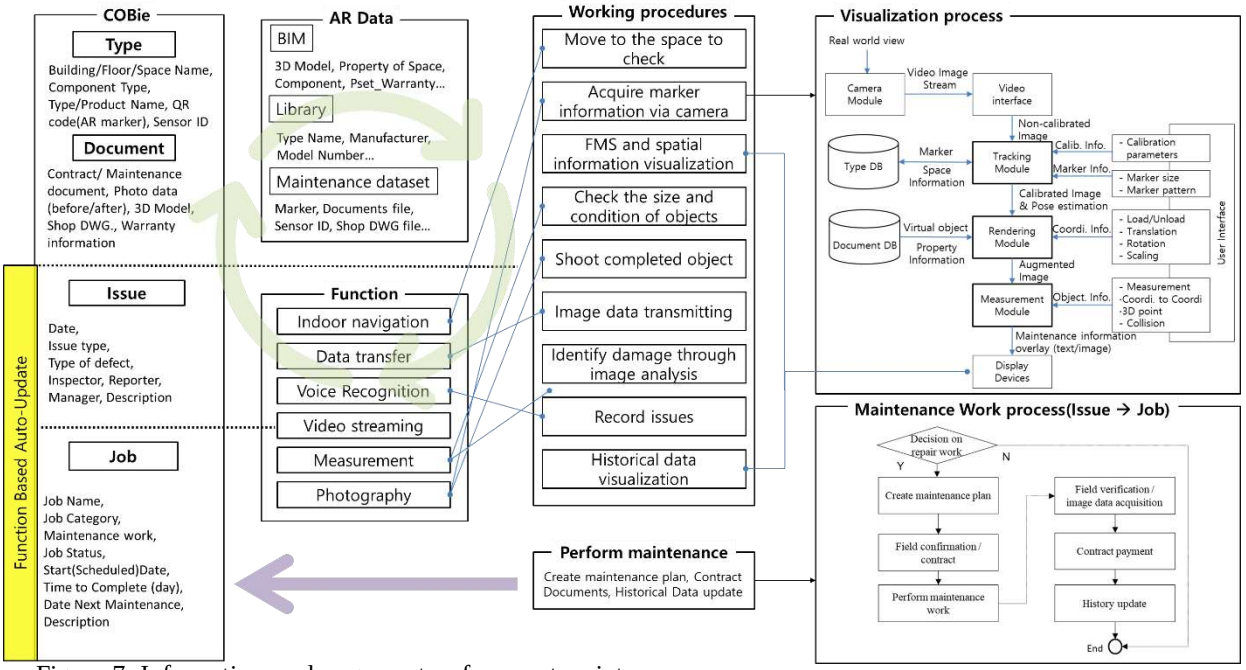

Figure 7. Information exchange system for smart maintenance

This feature excludes obstacles in the view when workers move or perform works, and it helps to verify the worker's location by positioning a navigation map inside the building on the right upper side of the screen. Figure 6 shows the example of the screen configuration of the prototype implementation, in which site inspector visualizes specification information about door. Information about supplier expert who supplied door, information about temperature and humidity of room, and information about interior finish inspection can be found in the lower side of the screen. An inspector observes target facility, such as door, window, wall, and column, and can record inspection results about inspection items through checklist.

4.3 Definition of SFM System Information Exchange System

Entire information exchange process of the SFM System described above is shown in Figure 7. Preliminary data use BIM data at handover. BIM information at this stage includes more detailed information of the space and the interior finishing material, and the space information and the property information of the space are used in conjunction with COBie. Among the information required for AR visualization, 3D model shape information does not work directly from BIM, so it is processed through information processing and optimization, and additional information necessary for maintenance is also included at this time. Basic information required before performing all these operations is stored in the Type and Document sheets of the COBie data.

After that, procedure of performing the work by the site inspector is moved to the site, the marker recognition, the space and absence information are visually confirmed, and the result of inspection is automatically transmitted. In order to recognize the AR marker information and visualize necessary information, modules needed are tracking / rendering / measurement module and implemented through separate API. In addition to the AR visualization function, there is an additional need for indoor navigation, data transmission, voice recognition, video streaming, automatic measurement and photo shooting functions, which are linked to each stage of operation.

When inspection is completed, the result information is stored in COBie's issue sheet, and it is used when maintenance work is in progress. As the maintenance work progresses, newly generated contract information is automatically saved in the Job Datasheet again, and COBie repeats this process and updates it.

5 Conclusions

This study proposed that data exchange procces through data item configuration and functional definition to apply AR technology to on-site maintenance works in a BIM-based SFM system.

As a result, this study determined that when maintenance and management information are configured based on the COBie system, interoperability in various software environment can be ensured. In addition, if AR visualization technology of maintenance information through overlay with real site circumstances

is utilized, it can enable rapid information sharing about on-site working conditions and decision making. Furthermore, the utilization of BIM datasets generated in design and construction phases is meaningful in terms of utilization BIM data throughout the whole life cycle.

However, since the study scope was limited to filed inspection works, the study results cannot be applied to all maintenance works in general. This study also needs some feedback through user satisfaction surveys regarding the proposed system development and UI configuration. For a future study, a technology that can visualize the information of complex facilities which cannot be identified visually should be developed through AR technology by expanding the maintenance target to mechanical, electrical, and plumbing in addition to the interior finish.

Acknowledgment

This research was supported by a grant (19AUDP-B127891-03) from the Architecture & Urban Development Research Program funded by the Ministry of Land, Infrastructure and Transport of the Korean government.

References

[1] Teicholz, E. Overview and current state of FM technology. FACILITY MANAGEMENT—AN, 2004.

[2] Sacks, R., Eastman, C., Lee, G., & Teicholz, P. BIM Handbook: A Guide to Building Information Modeling for Owners, Designers, Engineers, Contractors, and Facility Managers. John Wiley & Sons, 2018.

[3] Jieun, K., Hyunsang, C., Taewook, K. Derivation of System Requirements and Implementation of System Framework for BIM-based Urban Facility Maintenance System. Journal of the Korean Content Association, 14(4):397-406, 2014.

[4] Yu, K., Froese, T., & Grobler, F. A development framework for data models for computer-integrated facilities management. Automation in construction, 9(2):145-167, 2000.

[5] Mendez, R. O. The building information model in facilities management. PhD Thesis. Worcester Polytechnic Institute, 2006.

[6] East, W. E., & Brodt, W. BIM for construction handover. Journal of Building Information Modeling, 28-35, 2007.

[7] Becerik-Gerber, B., Jazizadeh, F., Li, N., & Calis, G. Application areas and data requirements for BIM-enabled facilities management. Journal of construction engineering and management, 138(3):431-442, 2011.

[8] Lee, S. G., & Yu, J. H. Prerequisites to utilize BIM (Building Information Modeling) for Facility Management. Journal of the Korea Facility Management Association, 8(1):27-39, 2013.

[9] Choi, J. H., & Um, D. Y. A study on the feasibility of COBie to the wastewater treatment plant. Journal of the Korean Society of Civil Engineers, 34(1):273-283, 2014.

[10] Kang, T. W., & Hong, C. H. A study on software architecture for effective BIM/GIS-based facility management data integration. Automation in Construction, 54:25-38, 2015.

[11] Hu, Z. Z., Tian, P. L., Li, S. W., & Zhang, J. P. BIM-based integrated delivery technologies for intelligent MEP management in the operation and maintenance phase. Advances in Engineering Software, 115:1-16, 2018.

[12] Hammad, A., Garrett, Jr, J. H., & Karimi, H. A. Potential of mobile augmented reality for infrastructure field tasks. In Applications of Advanced Technologies in Transportation pp. 425-432, 2002.

[13] Koo, B., Choi, H., & Shon, T. Wiva: Wsn monitoring framework based on 3D visualization and augmented reality in mobile devices. In International Conference on Smart Homes and Health Telematics pp. 158-165, Springer, Berlin, Heidelberg, 2009.

[14] Piekarski, W., & Thomas, B. H. Tinmith-mobile outdoor augmented reality modelling demonstration. In Proceedings of the 2nd IEEE/ACM International Symposium on Mixed and Augmented Reality pp. 317, IEEE Computer Society, 2003.

[15] Moon, S. Y., Yun, S. Y., Kim, H. S., & Kang, L. S. Improved Method for Increasing Maintenance Efficiency of Construction Structure Using Augmented Reality by Marker-Less Method. Journal of The Korean Society of Civil Engineers, 35(4):961-968, 2015.

[16] Bae, H., Golparvar-Fard, M., & White, J. Rapid image-based localization using clustered 3d point cloud models with geo-location data for aec/fm mobile augmented reality applications. In Computing in Civil and Building Engineering, pp. 841-849, 2014.

[17] Koch, C., Neges, M., König, M., & Abramovici, M. Natural markers for augmented reality-based indoor navigation and facility maintenance. Automation in Construction, 48:18-30, 2014.

[18] Chung, S. W., Kwon, S. W., Moon, D.Y., & Ko, T. K. Smart Facility Management Systems Utilizing Open BIM and Augmented/Virtual Reality. In 35th International Symposium on Automation and Robotics in Construction, 2018

A Framework Development for Mapping and Detecting Changes in Repeatedly Collected Massive Point Clouds

S. Yoon[a], S. Ju[a], S. Park[a], and J. Heo[a]

[a]Department of Civil and Environmental Engineering, Yonsei University, Seoul, Korea
E-mail: yoonssa@yonsei.ac.kr, jsh4907@yonsei.ac.kr, parksangyoon@naver.com, jheo@yonsei.ac.kr

Abstract –

On a construction site, progress deviations can cause fatal damages to the project and stakeholders. Therefore, accurately monitoring and managing the construction environment is essential. Efficiently detecting and recognizing the changes will be the key factor for monitor and management goals. In this research, we present a framework for detecting and recognizing changes in repeatedly collected, massive 3D point cloud data from a mobile laser scanning system. The framework mainly consists of three parts; 1) mapping system; 2) analysis system; 3) Hadoop platform. Collecting point clouds is repeatedly executed to detect the changes over different time epochs. For collecting point cloud data, a mobile laser scanning system was developed based on Robot Operating System (ROS). Detecting changes between repeatedly collected point clouds have been processed based on Hadoop platform. Finally, detected changes are then implemented to a semantic mapping process which is based on deep learning. Developed framework have potential for wide application in massive point cloud data processing, construction site monitoring, street level change detection, and facility management.

Keywords –

Mobile laser scanning (MLS); ROS; Deep learning; Change detection; Hadoop

1 Introduction

Due to the remarkable developments of sensor technologies and processing algorithms for point cloud data acquisition and registration, mapping over large spaces became more accessible than ever before. Over the last few decades, research groups focused on formulating a metric map, within which the mapping system explores the area without any information and gets self-localized using, Simultaneous Localization and Mapping (SLAM) techniques. The next step in mapping technology is the ability to produce maps directly understandable by humans, semantic mapping, which consequently integrates the robots into human environments [1].

From civil engineering perspective, metric and semantic maps from various data sources have been applied to environmental monitoring [2], building change detection ([3], [4]), disaster management ([5], [6]) and construction/infrastructure monitoring ([7]–[10]). The above mentioned applications share a primary analysis technique which is 3D change detection. 3D change detections has growing demands and possibilities for applications in environmental and civil engineering fields [11].

Despite the recent developments and possibilities, huge size of 3D point cloud data often leads to system slowdown or failure [12]. To overcome the issues, [13] and [14] introduced a distributed system to process point cloud data in a high memory cloud computing environment. However, it was costly to set the hardware environment. [14], [15] and [16] introduced a general solution for point cloud data processing based on Hadoop. In terms of cost, Hadoop had advantages, however, studies had limitations on analytic operations. Most previous studies mostly handle well-constructed data or operate on incompletely constructed data for distributed computing frameworks. Also, previous studies carry out research on only a small fraction of the whole process from beginning to the end.

In this research, practical framework including point cloud acquisition to point cloud management and analysis was conducted. The contributions of this paper is as follows: (1) ROS based 3D mapping system, which consists of three 2D Laser Range Finders (LFR) was introduced; (2) Hadoop based massive point cloud analysis system, which interacts with users using web interface was developed; (3) Deep learning algorithm was applied for point cloud based semantic segmentation and the feasibility was verified.

2 Integrated Framework Design

Our integrated framework consists of three main parts. Firstly, the mapping system based on ROS, automatically and repeatedly achieves metric maps. Second, analysis

system detect changes from collected metric maps. Additionally, semantics were provided to the detected changes based on deep learning algorithm. Lastly, detecting changes and visualizing point clouds has been operated upon developed Hadoop platform.

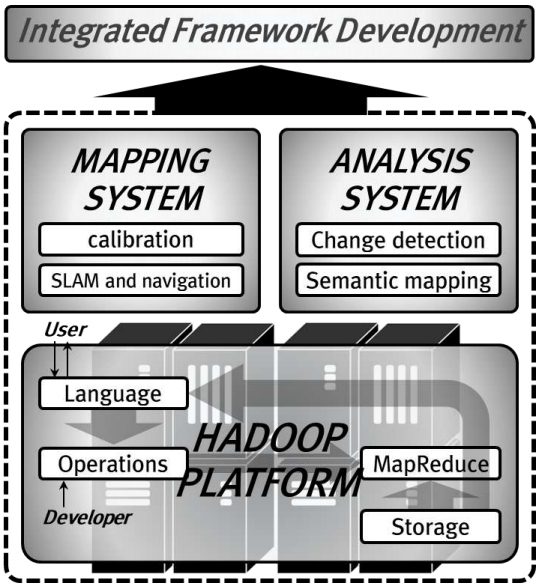

Figure 1. Integrated framework architecture

2.1 Design of Mapping System

The ROS platform is extensively used in this research since it can simply interconnect multiple programming languages and machines in seamless way. Due to this fact, ROS is the most popular robotics platform. It provides a set of tools, libraries and drivers in order to help developing robot applications, also with hardware abstraction [17]. In this research, the mapping system is based on ROS using packages for collecting data from sensors, constructing map from data and navigating through the map.

The mapping system is equipped with three 2D LFRs (UTM-30LX, Hokuyo, Osaka, Japan). It provides a scanning range of 270° with angular resolution of 0.25°. It can measure distances up to 60 meters, but without guaranteed reliability. One full scan cycle lasts for 25 milliseconds, which supplies a 40Hz measurement frequency. Pioneer 3DX mobile robot from ActivMedia Robotics, provides a stable platform for LRF sensors (Figure 2).

Over past decades, the number of SLAM algorithms were developed and the performance of the algorithms were compared . Popular SLAM algorithms such as GMapping [18], Karto SLAM [19], Hector SLAM [20], and Google Cartographer [21] were compared each other with diverse approaches ([22]–[26]). Evaluation results on every paper indicates that Google Cartographer delivers most accurate and precise results compare to others. Therefore, in this research Google Cartographer was used to construct the map, which is a robust solution on most input sequences. Cartographer provides real-time SLAM in 2D and 3D across multiple platforms and sensor configurations. It is a graph-based solution which stores a map of environment as associations for nodes and edges. Nodes represent a submap which has been created using scans, and edges represent transformations between corresponding submaps.

Using previously constructed map and navigation stack from ROS, the mapping platform autonomously navigates the given environment safely based on proper operation. The Adaptive Monte Carlo localization (amcl) [27] package was used to localize the platform itself in the previously constructed map. Additionally, the 'move_base' package [28], which links the global and local planner together, was used to accomplish navigation tasks. Standard A* path planning algorithm was used for global path planning and Dynamic Window Approach (DWA) [29] was used for local path planning. To perform navigation task efficiently, essential goal point needs to be set for our system. To achieve the goal points, morphological skeletonization [30] was applied in the 2D occupancy grid map. Among the exported candidate points from skeletonization, the goal points for the navigation stack was selected manually.

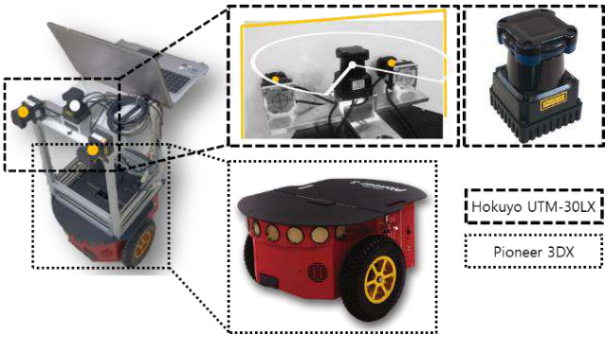

Figure 2. Mapping platform

2.2 Design of Analysis System

Semantic mapping explains the surrounding environment with various components, provides intuitive understanding of the situation to humans and bridges the gap between robots and humans. This could improve efficiency on conventional applications in infrastructure monitoring fields, since it can reduce the human labor on manually giving attributes to geometric information.

Recent developments in autonomous driving and robotics applications accelerate the necessity of point clouds semantic mapping. However, the development stage for point cloud is far behind image segmentation using Convolutional Neural Networks (CNNs). There

have been only a few studies related to semantic mapping with 3D point datasets.. PointNet [31] and PointNet++ [32] are the pioneers in this area which introduces efficient and flexible ways to deal with point cloud data.

In this study, PointNet++ was implemented to analyze the geometric point cloud data. PointNet++ processes a set of points sampled in a metric space in a hierarchical manner. It first partitions the set of points into overlapping local regions by the distance metric of the underlying space. As well as extracts local features capturing fine geometric structures from small neighborhoods; such local features are further grouped into larger units and processed to produce higher level features. This process is repeated until algorithm obtains the features of whole point cloud data. PointNet++ presents more robust result regardless of the density [32].

2.3 Design of Hadoop Platform

The overall architecture of our Hadoop platform with the three main layers is depicted in figure 3. The framework consists of 3 layers: (1) Storage layer; (2) Operation layer; (3) Interactive layer. The storage layer is optimized by indexing techniques to accelerate the Hadoop Map-Reduce applications. The operation layer is equipped with two powerful modules including "Change Detection" and "3D Geometric Model" for efficient monitoring. In this study, only change detection module was used. More details for 3D geometric model will be introduced in our future paper. Lastly, The Interactive layer enables users to approach a distributed computing model on Hadoop without requiring deeper related knowledge.

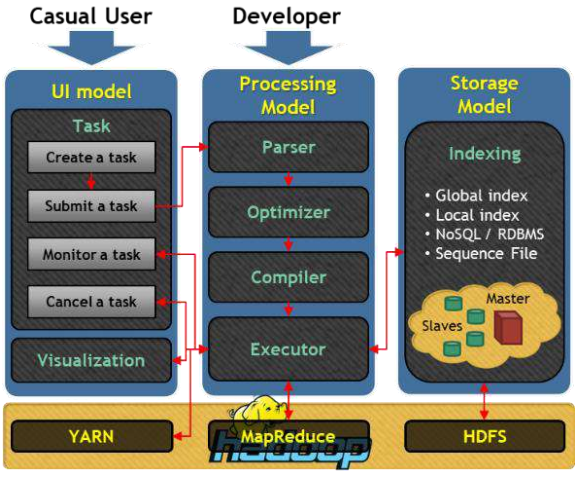

Figure 3. Hadoop platform architecture

3 Implementation and Experiment

The overview of this research is as follows.

- Using the mapping platform 3D point cloud map was constructed.
- Based on the pre-constructed map, mapping system navigates the manually defined goal points automatically and constructs another map.
- Change detection was processed based on Hadoop platform between 2 maps.
- Semantic segmentation was implemented to detected changes.

3.1 Mapping System Experiment

3.1.1 Calibration

Calibration is the process of estimating the parameters that need to be applied to correct actual measurements to their true values. According to the parameter types, calibration also can be divided into intrinsic and extrinsic forms. This research assumes that the intrinsic sensor calibration is completed and focuses on the extrinsic calibration of multiple LRF sensors to identify the rigid transformation from each sensor frame to the platform body frame.

Figure 4(b) shows three 2D LRFs in the mapping system and the configurations of the three coordinate systems. The middle LRF is mounted horizontally, other two LRFs are mounted vertically to scan the profiles of the surrounding environments. For carrying out the calibration, the double-deck 3D calibration facility was developed as shown in figure 4(c). The alignment errors usually are computed by least squares using a set of target points captured from the scanners. Since this research is not focused on calibration, further information about the least squares system equation and experimental results can be referred from [33].

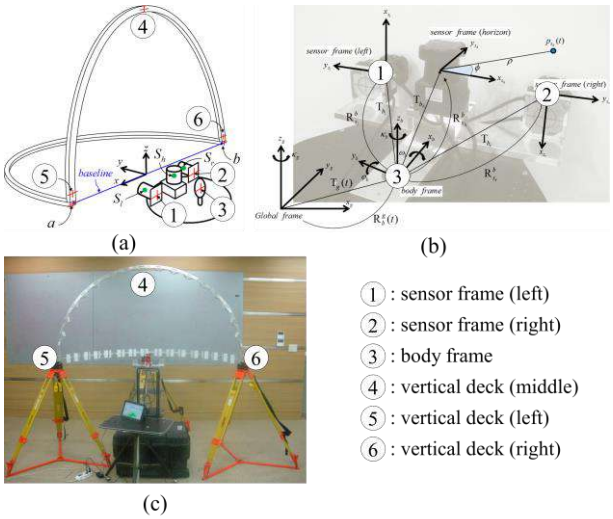

Figure 4. Double-deck calibration facility

3.1.2 SLAM and Navigation

The implementation of Google cartographer SLAM was conducted in seminar rooms and corridors in the Engineering building at Yonsei University. Map was built twice in the same location with intentionally caused changes. Figure 5 shows two types of intentionally caused changes, which is newly added space and added furniture in existing space. Figure 5(a) is an added seminar room which can be seen in the left part of the figure 6(b). Additionally, chairs were added in figure 5(b) which were located in middle of the corridor as shown in figure 6(b). Figure 6 shows the map where high intensity values are represented bright.

To build the second map, consecutive goal points were manually selected among the junctions from the skeletonization result of pre-constructed map. Figure 7(a) shows the skeletonized result, and red dots in figure 7(b) shows the path consists of manually selected goals.

(a) (b)

Figure 5. Added environments in the second map

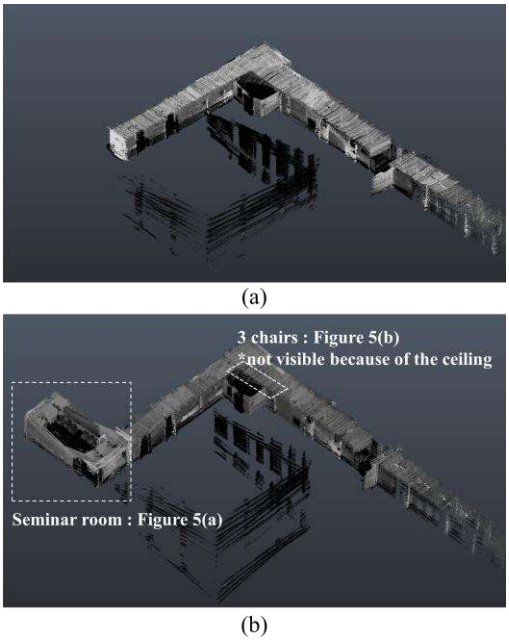

(a)

(b)

Figure 6. (a) First map; (b) Second map

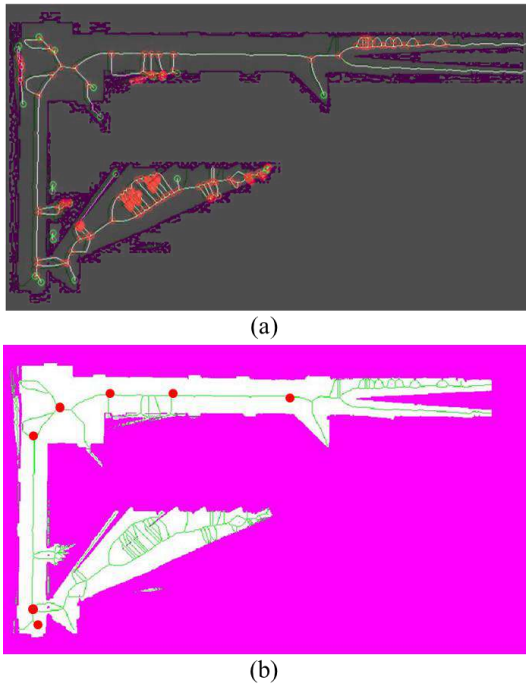

(a)

(b)

Figure 7. (a) Skeletonization results; (b) manually selected goal points (red dots)

3.2 Analysis System Experiment

3.2.1 Change Detection

Change detection between two maps were processed based on the Hadoop operation layer. The Hadoop cluster was configured with 8 nodes of the same capacity, i.e. Intel Core i5-2300 2.80GHz*4, 16GB memory.

Figure 8 shows the two maps and change detection result, using the web User Interface (UI) based on Hadoop platform. Detail explanation for the WebUI will be in our future paper. The red and green part represents the first and second map respectively. Blue dots are the parts which have been detected as a change. Developed platform can simply upload and overlay different point clouds and visualize them. The detailed description for the change detection algorithm is introduced in section 3.3.

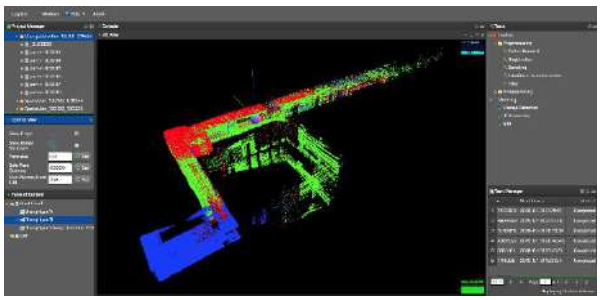

Figure 8. Change detection result in webUI

3.2.2 Semantic Mapping

For training the model for point cloud segmentation for semantic scene labeling, the Stanford Large-Scale 3D Indoor Spaces Dataset (S3DIS) [34] was used. The dataset was acquired using Matterport scanners in 6 areas for 271 rooms. 13 classes were annotated to each point. The model was trained using S3DIS from area 1-5 and tested using area 6. The overall per-point accuracy of the trained segmentation model was 83.4%. Per-point accuracy compares the predicted label and real label for each point.

Trained model was implemented to the map which was detected as a change between the first and second map from mapping system. To evaluate the accuracy of the semantic segmentation result, annotations were manually assigned to each point in the map. Figure 9 shows the semantic segmentation result for seminar room.

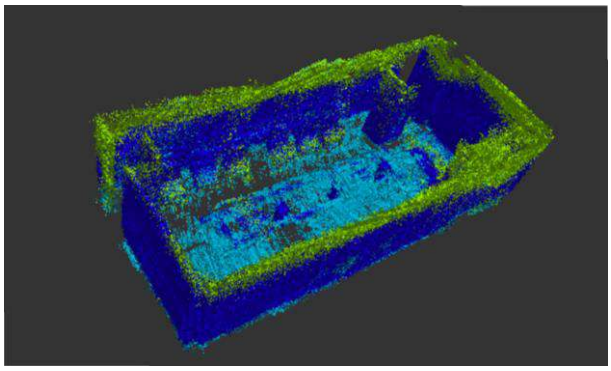

Figure 9. Semantic mapping result (point cloud)

Table 1. Semantic mapping accuracy

Overall accuracy	72.76%
classes	IoU
Ceiling	0.502
Wall	0.721
Floor	0.527
Door	0.050
Chair	0.000
Table	0.000

Overall per-point accuracy for experimental data was 72.76%. IoU in Table 1 stands for Intersection over Union, which is calculated by equation (1).

$$IoU_i = \frac{TP_i}{FP_i + FN_i + TP_i} \quad (1)$$

Where TP is the true positives FP is the false positives FN is the false negatives and i stands for each class such as ceilings, wall etc.

In figure 9, ceiling points were colored in deep green, wall points in blue, floor points in sky blue and doors in pink but not visible in the figure. As listed in table 1, table and chairs were not detected. Firstly, the top surface of the table was not collected enough in our data, since the height of the table top and the sensor was similar. Secondly, there were too many sensor noise for chair data. Compared to the S3DIS training dataset, the data acquired from our mapping system contains more noise since it was acquired while moving through the environment and no additional process were conducted after acquiring. To segment the movable objects, such as table, chair, sofa, bookcase and boards, further improvements are necessary for the mapping system.

3.3 Hadoop Platform

To optimize the storage layer in the Hadoop platform, Sort-Tile-Recursive (STR) algorithm [35] was applied to construct a global index. STR groups nearby points in each minimum bounding rectangle (MBR) which does not exceed 128MB. After constructing a global index, an Octree local index is also implemented on each block.

Based on the storage layer, change detection was tested for the operation. Change detection is based on a soft-join algorithm which is an application of point-to-point change detection in a distributed system (Figure 10).

The interactive layer was developed based on web UI. Interface provides simple access to users and visualizes massive point cloud data directly from Hadoop, which is useful for analytical processes.

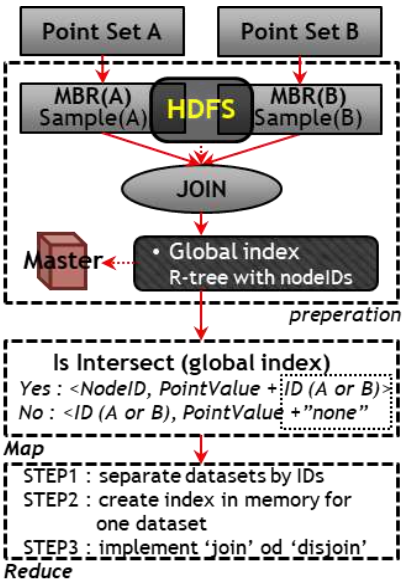

Figure 10. Change detection on Hadoop platform

4 Conclusion

An integrated framework for processing massive point cloud data was introduced in this research. It is

consisting of three main parts: mapping system; analysis system; and Hadoop platform, for the integrated framework developed as a prototype. However, this comprehensive system is a pioneer work related to massive point cloud data producing and processing. Future works for this prototype version will be focused on each system. For mapping system, additional sensors which can provide more information, should be implemented. Also, navigation algorithms will be improved for fully automated system. For analysis system, change detection process need to be focus on algorithm perspective, since it is now focused managing massive point cloud data. Applied semantic mapping process will also be included in the process more practically.

Acknowledgement

This work was supported by the National Research Foundation of Korea (NRF) grant funded by the Korea government (Ministry of Science and ICT) (NRF-2018R1A2B2009160).

References

[1] K. Charalampous, I. Kostavelis, and A. Gasteratos, Recent trends in social aware robot navigation: A survey. *Rob. Auton. Syst.*, vol. 93, page 85–104, 2017.

[2] M. Jaboyedoff, T. Oppikofer, A. Abellan, M.H. Derron, A. Loye, R. Metzger and A. Pedrazzini, Use of LIDAR in landslide investigations: a review. *Nat. hazards*, vol. 61, no. 1, page 5–28, 2012.

[3] S. Nebiker, N. Lack, and M. Deuber, Building change detection from historical aerial photographs using dense image matching and object-based image analysis. *Remote Sens.*, vol. 6, no. 9, page 8310–8336, 2014.

[4] R. Qin, X. Huang, A. Gruen, and G. Schmitt, Object-based 3-D building change detection on multitemporal stereo images. *IEEE J. Sel. Top. Appl. Earth Obs. Remote Sens.*, vol. 8, no. 5, page 2125–2137, 2015.

[5] K. Choi, I. Lee, and S. Kim, A feature based approach to automatic change detection from LiDAR data in urban areas. *Int. Arch. Photogramm. Remote Sens. Spat. Inf. Sci*, vol. 18, page 259–264, 2009.

[6] M. Gerke and N. Kerle, Automatic structural seismic damage assessment with airborne oblique Pictometry imagery. *Photogramm. Eng. Remote Sens.*, vol. 77, no. 9, page 885–898, 2011.

[7] D. Rebolj, N. Č. Babič, A. Magdič, P. Podbreznik, and M. Pšunder, Automated construction activity monitoring system. *Adv. Eng. informatics*, vol. 22, no. 4, page 493–503, 2008.

[8] A. Braun, S. Tuttas, A. Borrmann, and U. Stilla, Automated progress monitoring based on photogrammetric point clouds and precedence relationship graphs. in *Proceedings of the International Symposium on Automation and Robotics in Construction*, vol. 32, page 1., Oulu, Finland, 2015.

[9] K. Han, J. Lin, and M. Golparvar-Fard, A formalism for utilization of autonomous vision-based systems and integrated project models for construction progress monitoring. In *Proceedings of Autonomous and Robotic Construction of Infrastructure Conference*, Iowa, USA, 2015.

[10] S. Siebert and J. Teizer, Mobile 3D mapping for surveying earthwork projects using an Unmanned Aerial Vehicle (UAV) system. *Autom. Constr.*, vol. 41, page 1–14, 2014.

[11] R. Qin, J. Tian, and P. Reinartz, 3D change detection – Approaches and applications. *ISPRS J. Photogramm. Remote Sens.*, vol. 122, page 41–56, 2016.

[12] J. Jung, S. Hong, S. Yoon, J. Kim, and J. Heo, Automated 3D wireframe modeling of indoor structures from point clouds using constrained least-squares adjustment for as-built BIM. *J. Comput. Civ. Eng.*, vol. 30, no. 4, page 4015074, 2015.

[13] J. W. Hegeman, V. B. Sardeshmukh, R. Sugumaran, and M. P. Armstrong, Distributed LiDAR data processing in a high-memory cloud-computing environment. *Ann. GIS*, vol. 20, no. 4, page 255–264, 2014.

[14] V. Pajić, M. Govedarica, and M. Amović, Model of Point Cloud Data Management System in Big Data Paradigm. *ISPRS Int. J. Geo-Information*, vol. 7, no. 7, page 265, 2018.

[15] C. Wang, F. Hu, D. Sha, and X. Han, Efficient LiDAR point cloud data managing and processing in a hadoop-based distributed framework. *ISPRS Ann. Photogramm. Remote Sens. Spat. Inf. Sci.*, vol. 4, page 121, 2017.

[16] Z. Li, M. E. Hodgson, and W. Li, A general-purpose framework for parallel processing of large-scale LiDAR data. *Int. J. Digit. Earth*, vol. 11, no. 1, page 26–47, 2018.

[17] M. Quigley *et al.*, ROS: an open-source Robot Operating System. in *ICRA workshop on open source software*, vol. 3, no. 3.2, page 5, Kobe, Japan, 2009.

[18] G. Grisettiyz, C. Stachniss, and W. Burgard, Improving grid-based slam with rao-blackwellized particle filters by adaptive proposals and selective resampling. in *Proceedings of IEEE International Conference on Robotics and Automation*, page

2432-2437, Barcelona, Spain, 2005.

[19] Karto SLAM, ROS package. accessed Nov, 2016. [online], wiki.ros.org/slam karto

[20] S. Kohlbrecher, J. Meyer, T. Graber, K. Petersen, U. Klingauf, and O.V. Stryk, Hector open source modules for autonomous mapping and navigation with rescue robots. in *Robot Soccer World Cup*. Springer, 2013.

[21] W. Hess, D. Kohler, H. Rapp, and D. Andor, Real-time loop closure in 2D LIDAR SLAM. in *Robotics and Automation (ICRA)*, page 1271–1278, Stockholm, Sweden, 2016.

[22] H. A. Lauterbach, D. Borrmann, R. Heß, D. Eck, K. Schilling, and A. Nüchter, Evaluation of a backpack-mounted 3D mobile scanning system. *Remote Sens.*, vol. 7, no. 10, page 13753–13781, 2015.

[23] R. Yagfarov, M. Ivanou, and I. Afanasyev, Map Comparison of Lidar-based 2D SLAM Algorithms Using Precise Ground Truth. in *International Conference on Control, Automation, Robotics and Vision (ICARCV)*, page 1979–1983, Singapore, 2018.

[24] J. M. Santos, D. Portugal, and R. P. Rocha, An evaluation of 2D SLAM techniques available in robot operating system. in *Safety, Security, and Rescue Robotics (SSRR)*, page 1–6, Linkoping, Sweden, 2013.

[25] A. Filatov, A. Filatov, K. Krinkin, B. Chen, and D. Molodan, 2D SLAM quality evaluation methods. in *Open Innovations Association (FRUCT)*, page 120–126, Helsinki, Finland, 2017.

[26] K. Krinkin, A. Filatov, A. yom Filatov, A. Huletski, and D. Kartashov, Evaluation of Modern Laser Based Indoor SLAM Algorithms. in *Conference of Open Innovations Association (FRUCT)* page 101–106, Jyväskylä, Finland, 2018.

[27] D. Fox, W. Burgard, F. Dellaert, and S. Thrun, Monte carlo localization: Efficient position estimation for mobile robots. In *AAAI/IAAI*, vol. 1999 no. 343–349, page 2, Orlando, USA, 1999.

[28] Navigation, ROS package. accessed Mar, 2013. [online], wiki.ros.org/navigation

[29] D. Fox, W. Burgard, and S. Thrun, The dynamic window approach to collision avoidanc. *IEEE Robotics & Automation Magazine*, no. 4.1, page 23-33, 1997.

[30] E. R. Dougherty, An Introduction to Morphological Image Processing (Tutorial Texts in Optical Engineering. *DC O'Shea, SPIE Opt. Eng. Press. Bellingham, WA, USA*, 1992.

[31] C. R. Qi, H. Su, K. Mo, and L. J. Guibas, Pointnet: Deep learning on point sets for 3d classification and segmentation. In *Proceeding of Computer Vision Pattern Recogniton*, vol. 1, no. 2, page 4, Honolulu, Hawaii, 2017.

[32] C. R. Qi, L. Yi, H. Su, and L. J. Guibas, Pointnet++: Deep hierarchical feature learning on point sets in a metric space. In *Advances in Neural Information Processing Systems*, page 5099–5108, California, USA, 2017.

[33] J. Jung, J. Kim, S. Yoon, S. Kim, H. Cho, C. Kim and J. Heo, Bore-sight calibration of multiple laser range finders for kinematic 3D laser scanning systems. *Sensors*, vol. 15, no. 5, page 10292–10314, 2015.

[34] I. Armeni, S. Sax, A. R. Zamir, and S. Savarese, Joint 2d-3d-semantic data for indoor scene understanding. *arXiv Prepr. arXiv1702.01105*, 2017.

[35] S. T. Leutenegger, M. A. Lopez, and J. Edgington, STR: A simple and efficient algorithm for R-tree packing. In *Conference on Data Engineering*, page 497–506, Birmingham, UK, 1997,

Development of the Simulator for Carrying a Lifted Load in Large Plant Construction

Y. Mori[a], M. Wada[a], S. Maki[a], and S. Tsukahara[a]

[a]Hitachi Plant Construction, Ltd., Japan
E-mail: yoshihito.mori.vx@hitachi.com, masaomi.wada.rv@hitachi.com, sayuri.maki.jz@hitachi.com, satoshi.tsukahara.nm@hitachi.com

Abstract –

Large plant construction has numerous works, and the proportion of hoisting operations in the total construction work is high. In the hoisting operations, many things should be considered to keep the operations safe, and the work steps of the hoisting operations are planned by considering them. However, it is difficult for novice construction workers to understand the work steps with conventional two-dimensional drawings. Thus, to have those workers understand it well, we developed the hoisting-operation simulator considering the physical behavior of a load in conjunction with 3D viewer and physics engine. The simulator can visualize the work steps as three-dimensional animation. Moreover, by associating the simulator with mixed reality technology, we developed the system superimposing the 3D animation on reality space via head mount display. Experiments verify that the 3D animation of a load moves with the vibration due to the inertial force and that the 3D animation generated by the simulator is superimposed in the work site.

Keywords –

Simulator; Mixed reality; three-dimensional measurement

1 Introduction

Large plant construction has numerous works, and in particular, the proportion of hoisting operations in the total construction work is high. In the hoisting operations, many things should be considered to keep the operations safe. When a load is hoisted in a narrow work site, the clearance between the load and the surrounding equipment should be considered. In addition, considering the forces of each lifting point (i.e., the placement of lifting tools) is also important. According to those information, the work steps of the hoisting operations are planned. In conventional planning, work steps were determined with two-dimensional drawings. However, novice construction workers take time to understand the details in the 2D drawings. In fact, the proportion of the novice construction workers in the total workers increases due to the decrease of skilled construction workers. For the reason, it is imperative to develop the system that make the novice construction workers understand the work steps of hoisting operations.

In recent years, some examples of using three-dimensional design software and 3D viewer have been reported to make construction workers understand their works. In particular, Building Information Modeling (BIM) associating information of design, construction and maintenance with the 3D model of buildings is used to various construction works [1]. As examples of recent BIM, Zhang et al. developed safety checking platform that detects the opening in a 3D model and automatically places guardrails for preventing fall-related accidents [2]. Sugimoto et al. developed a simulation system for quantitatively evaluating the validity of crane-deployment plans by integrating 3D models and a time dimension [3].

Moreover, Augmented Reality (AR) and Mixed Reality (MR) (i.e., a technology superimposing computer-generated objects on a reality space) has been promoted to use in construction works. Singh et al. indicated that AR has the important role in automating the site layout planning on construction projects [4]. Yeh et al. proposed a wearable device that can project the construction drawings and related information to on-site space [5]. Riera et al. reported the implementation and evaluation of an AR application to the education of building engineering [6]. On the other hand, as examples of recent MR, Ammari and Hammad developed a BIM-based system to facilitate on-site data collection and to support inspectors in evaluating building elements via MR [7]. Chalhoub and Ayer reported that using MR reduced the time required to understand the design of electrical conduit and led to fewer errors during the assembly process as compared to using traditional 2D drawings [8].

As above, many BIM and AR/MR technologies have been developed in order to make construction workers

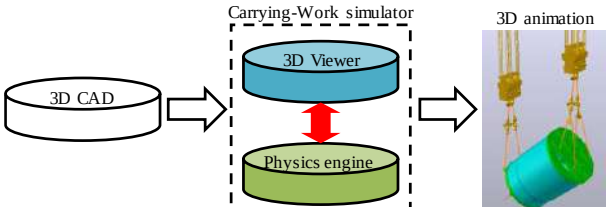

Figure 1. System flowchart of the animation application

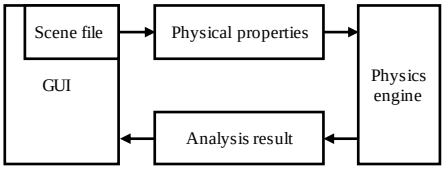

Figure 2. System diagram of the 3D viewer and the physics engine

understand their works. However, Most of them are not specialized in hoisting operations. Specifically, the physical behavior such as the vibration of a lifted load are not considered in the conventional BIM and a computer-generated lifted load including the physical behavior are not superimposed in conventional AR/MR. Hence, we have developed applications focusing on hoisting operations.. The features of the applications are as follows.

1) It creates 3D animations considering the physical behavior of a lifted load in conjunction with 3D viewers and physics engines.

2) It calculates forces applied to lifting points to define the position of lifting points and lifting tools.

Furthermore, we devised a system associating the above applications with MR technology. The features of this system are as follows.

3) It superimposes the 3D animation created by 1) to the reality space.

This paper is structured as follows. Chapter 2 gives the overview and method diagram of 1) and 2). Chapter 3 explains the overview and method diagram of 3). Chapter 4 presents the results of experiments to verify some proposed applications and systems. Finally, Chapter 5 concludes the paper.

2 Applications for Hoisting Operations

2.1 Animation Application Considering the Physical Behavior of a Lifted Load

In order to plan the hoisting operations for a lifted load considering physical behavior, we have developed the application that cooperates physics engines with by using the Application Programming Interface (API) of 3D viewers. Figure 1 shows the system flowchart of the application. Herein, this application is Hoisting

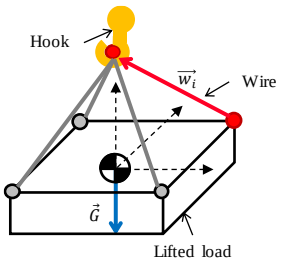

Figure 3. Configuration diagram of multi-point

Operation simulator (HO simulator).

First, the 3D model of a lifted load is made by 3D CAD. In order to perform the physical calculation on the 3D viewers, the center of gravity (the pink cube in Fig. 1) and the lifting points (the orange cube in Fig. 1) are incorporated in the 3D model.

Next, the 3D hoisting-operation animation is generated by using physics engines. Figure 2 shows the system diagram of the 3D viewer and the physics engine. The scene file is loaded into the 3D viewer's graphical user interface (GUI). Then, physical properties (e.g., the mass of each element in the model, friction coefficient and restitution coefficient) and the constraint condition are defined in the scene file. The defined file is handed over to the physics engine, and the analysis result is feedback to the GUI. These systems make it possible to generate the 3D animation considering the physical behavior and the planning of hoisting operation is performed more efficiently.

2.2 Force-Calculation Algorithm of Each Lifting Point

In the hoisting operation of large equipment into a work site, "multi-point lifting" is often used. The multi-point lifting is the method that carries a lifted load with many lifting tools. By using the multi-point lifting, the forces of lifting tools decrease and the attitude of the lifted load is more stable than single-point lifting. When using this method, the calculation of accurate forces of each lifting point and the selection of proper lifting tools are important.

Figure 3 shows the configuration diagram of multi-point lifting. Herein, F_i is the force of the lifting point, $\overrightarrow{w_i}$ is the three-dimensional vector from the lifting point to the hook, m is the mass of the lifted load, and g is the gravitational acceleration. The number i is numbered from No. 1 to No. n counterclockwise. The equation of motion of Fig. 3 is given as

$$[\overrightarrow{w_1} \quad \cdots \quad \overrightarrow{w_n}] \cdot [F_1 \quad \cdots \quad F_n]^T = [0 \quad 0 \quad mg]^T \tag{1}$$

$$\Rightarrow \vec{W} \cdot \vec{F} = \vec{G},$$

where the size of $\vec{W}$ is 3 × n, the size of $\vec{G}$ is 3 × 1, and

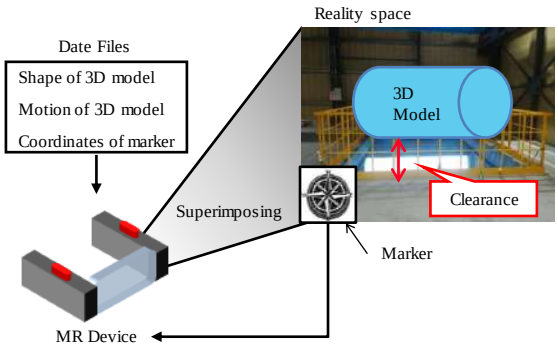

Figure 4. System diagram to superimpose 3D animations

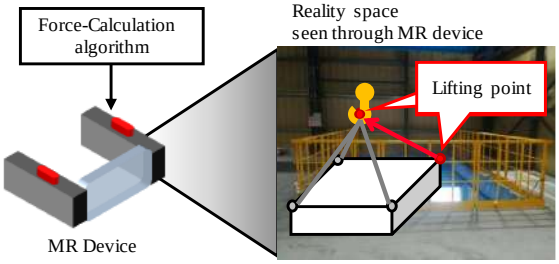

Figure 5. System diagram to calculate the forces of each lifting point

the size of $\vec{F}$ is 1 × n. Thus, when n is larger than 3, Eq. (1) is defined as an overdetermined equation system and general physics engines cannot calculate solutions accurately.

Therefore, we developed an algorithm that can calculate the forces of each lifting point even equations are overdetermined. Herein, this application is the Force-Calculation algorithm (FC algorithm). In the algorithm, a redundant equation is solved by regarding when the sum of root square of $\vec{F}$ is the minimum as the solution of Eq. (1). The solution of Eq. (1) is derived as

$$\vec{F} = \vec{W}^T \cdot \left(\vec{W} \cdot \vec{W}^T\right)^{-1} \cdot \vec{G} \quad (2)$$

By Eq. (2), the forces of each lifting point in the multi-point lifting are calculated.

3 System Combining the Applications with MR Technology

As noted in Chapter 2, the HO simulator can generate 3D hoisting operations animations. However, it is desirable to explain how the hoisting operations is performed at a work site to managers and workers in order for them to appreciate the hoisting operation. In addition, the 3D animations are likely to interfere with the equipment in the plant because the work site does not always correspond with a map of that. Taking these matters into consideration, the application that can display the 3D animations in realty space is indispensable. Thus, the system that superimposes 3D animation on reality space by utilizing Mixed Reality (MR) technology is developed. Figure 4 shows the diagram of the proposed system.

First, the shape date of the 3D model, the motion date of the 3D animation generated by the HO simulator, and the coordinate date of a two-dimension marker model on the 3D viewer are stored in a HMD.

Next, a marker is set at the coordinate position defined in the 3D viewer. The marker is photographed by the RGB camera mounted on the HMD, and is recognized in the device. The initial position and direction to superimpose the 3D animation is defined. After recognizing the marker, the position of HMD itself in the reality space is defined by using the image data acquired by the monocular camera, and the animation is accurately superimposed according to the relative position between the marker and the device itself. At the same time, the surrounding environment seen through the HMD is meshed. Therefore, the 3D animation can be superimposed at an initial position in the reality space even a HMD wearer moves in the reality space. Moreover, in order to review the same scene as necessary, the system supports rewind, temporary stop, and frame-by-frame playback (rewind). Furthermore, the system supports measuring the distance between the 3D animation and the surrounding object (e.g., floor surface and wall) in the real space since the three-dimensional reality space where the HMD exists is meshed.

In addition, by combining the FC algorithm in Section 2.2 with the MR technology, the system that grasp the forces of each lifting point in a work site can be realized as shown in figure 5. Since the distance from a lifting point to a hook can be measured, the vector $\overrightarrow{w_i}$ is determined. Therefore, the forces are calculated by the equations (1) and (2).

4 Verification Testing

4.1 Verification of Animation Application and Superimposition System

Experiments were performed to verify the HO simulator and the superimposition system. Figure 6 shows a 3D work site model of the experiments. The beam (length: 8.0 m, weight: 1.8 t) was lifted by an overhead crane and carried from the first floor to the second floor through the aperture (dimension: 6.0 m×4.0 m). The beam and the overhead crane were connected by chain blocks and the attitude of the beam can be arbitrarily changed by hoisting the chain blocks. In the carrying experiments, the following things should be considered.

1) The attitude and the carrying path of the beam for

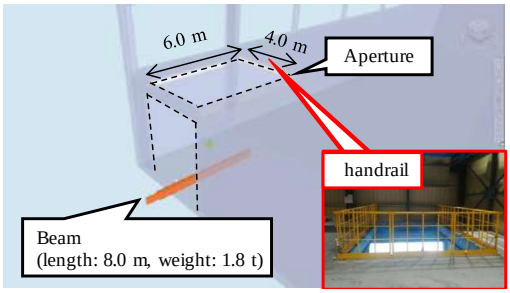

Figure 6. 3D work site model of the experiments

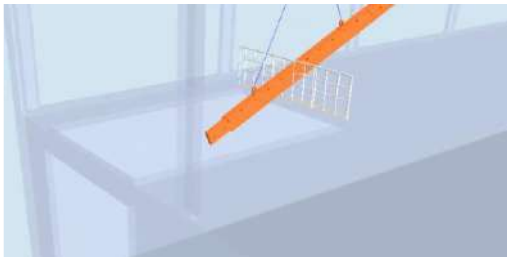

Figure 7. One scene cut out from the 3D animation

Fig. 8 3D animation superimposed on the work site

it to pass through the narrow aperture.

2) The clearance between the handrail (dimension: 4.0 m×1.3 m) around the aperture and the beam.

3) The collision between the second floor and the beam due to the vibration of the beam while carrying.

In order to examine these matters, the hoisting operations was planned with the HO simulator by using a beam model and the work site model. In addition, the 3D animation of the work was superimposed on the work site. Herein, in order to check the superimposed animation either on the 1st floor or the 2nd floor, markers were set at the positions indicated by the red letters in Fig. 6.

Figure 7 shows one scene cut out from the 3D animation. The 3D animation shows that the beam moves with the vibration due to the inertial force. Moreover, the 3D animation also shows that the magnitude of the vibration is changed by the influence of the length of the chain block. By realizing this vibration, checking the collision between the beam and the second floor is performed more realistically.

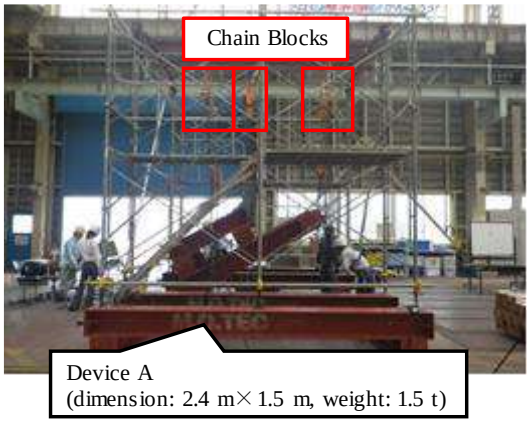

Figure 9. Equipment for the verification experiment of the Force-Calculation

The result of superimposing the 3D animation on the work site is shown in Figure 8. The RGB camera of the HMD successfully authenticated the marker and the 3D model of the beam is superimposed on the 1st floor. Then, it was confirmed that the 3D animation was superimposed at the initial position even when the HMD wearer moved due to the self-localization function of the HMD. Also, the same motion as the motion created on the HO simulator was superimposed in the work site.

4.2 Verification of Force-Calculation Algorithm

An equipment for a verification experiment is shown in Figure 9. The attitude of a device A (dimension: 2.4 m ×1.5 m, weight: 1.5 t) was changed by operating the length of six chain blocks. The angle between the bottom surface of the device A and the ground surface was changed from 0 degree to 60 degree. Forces of each lifting point were measured with load cells (i.e. total number of load cells is 6) and the angle was measured with a digital angle sensor attached on the bottom surface of the device A. The measured results were compared with analyzed results from the algorithm in Section 2.2. The analysis was conducted under same conditions as the ones in the experiment.

Figure 10 is a side view of the device A at 0 degree and 60 degree, and Table 1 and 2 show measured results and analyzed results under each degree. Table 1 and 2 also include relative errors based on the analysis values. The difference between the measured results and the analyzed results is ± 10% or less at each hanging point. Therefore, the effectiveness of the algorithm is verified.

5 Conclusion

In order to improve secure the safety of hoisting

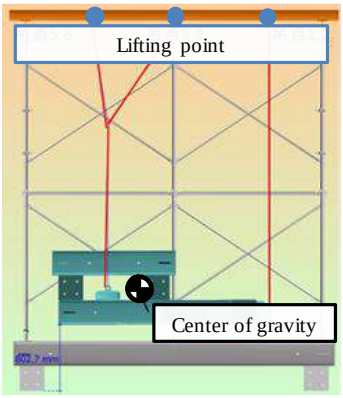

1) 0 degree.

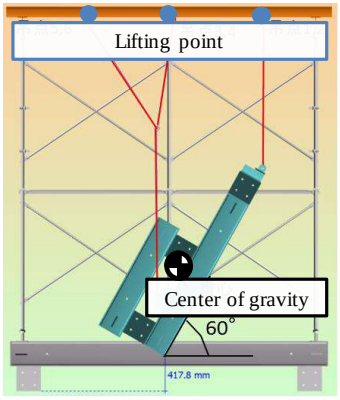

2) 60 degree.

Figure 10. Attitude of a device A at each degree

operations, the paper proposed an application for planning a hoisting operations. Furthermore, in order to have construction workers understand the plan of hoisting operations, the paper proposed a system associating the applications with MR technology. From the results of verification testing, we got the following conclusion.

1) The application that creates 3D animations considering the physical behavior of a lifted load was developed. The application was realized by cooperating physics engines with Application Programming Interface (API) of 3D viewers. The application make it easy to check the clearance between a lifted load and the equipment in a plant and to plan an appropriate hoisting operation procedure.

2) The system that superimposes 3D animations to reality space was developed. The system was realized by using MR HMD that includes many sensors. The system make it possible to predict the dangerousness of a hoisting operations at a work site.

3) The application that calculates forces applied to each lifting point was developed. The application can calculate the forces of each lifting point even a simultaneous equation is redundant. The application make it easy to define the position of each lifting point and lifting tools.

Table 1. Comparison of measured forces and calculated forces at 0 degree

Number of Lifting point	Measured Force [N]	Calculated Force [N]	Error [%]
1	1200	1300	8
2	1200	1300	8
3	205	220	7
4	205	220	7
5	5200	5030	3
6	5200	5030	3

Table 2. Comparison of measured forces and calculated forces at 60 degree

Number of Lifting point	Measured Force [N]	Calculated Force [N]	Error [%]
1	1175	1297	10
2	1175	1297	10
3	1550	1430	8
4	1550	1430	8
5	4000	3866	3
6	4000	3866	3

References

[1] Porwel, A. & Hewage, K. N. Building Information Modeling (BIM) partnering framework for public construction projects. *Automation in Construction*, 31: 204-214, 2013.

[2] Zhang, S., Teizer, J., Lee, J., Eastman, C. M., Venugopal, M. Building Information Modeling (BIM) and Safety: Automatic Safety Checking of Construction Models and Schedules. *Automation in Construction*, 29: 183-195, 2013.

[3] Sugimoto, Y., Seki, H., Samo, T., & Nakamitsu, N. Methods for Simulating Crane-Deployment Plans Used in Construction of Nuclear Power Plants. In *32nd International Symposium on Automation and Robotics in Construction*, pages 1-8, Oulu, Finland, 2015.

[4] Singh, A. H., Suthar, V., & Delhi, V. S. K. Augmented Reality (AR) Based Approach to Achieve an Optimal Site Layout in Construction Projects. In 34th *International Symposium on Automation and Robotics in Construction*, pages 1-8, Taipei, Taiwan, 2017.

[5] Yeh, K-C., Tsai, M-H., & Kang, S-C. On-Site Building Information Retrieval by Using Projection-Based Augmented Reality. *Journal of*

Computing in Civil Engineering, 26 (3): 342-355, 2012.

[6] Riera, A. S., Redondo, E., Fonseca, D., & Navarro, I. *Construction Processes Using Mobile Augmented Reality: A Study Case in Building Engineering Degree*. Vol 206. Springer, Berlin, Heidelberg, 2013

[7] Ammari, K. E. & Hammad, A. Collaborative BIM-Based Markerless Mixed Reality Framework for Facilities Maintenance. In *Proceedings of the 2014 International Conference on Computing in Civil and Building Engineering*, pages 657-664, Orlando, Florida, 2014.

[8] Chalhoub, J. & Ayer, S. K. Using Mixed Reality for electrical construction design communication. *Automation in Construction*, 86: 1-10, 2018.

Digital Twinning of Existing Bridges from Labelled Point Clusters

R.D. Lu[a] and I. Brilakis[a]

[a]Department of Engineering, University of Cambridge, United Kingdom
E-mail: rl508@cam.ac.uk, ib340@cam.ac.uk

Abstract –

The automation of digital twinning for existing bridges from point clouds has yet been solved. Whilst current methods can automatically detect bridge objects in points clouds in the form of labelled point clusters, the fitting of accurate 3D shapes to detected point clusters remains human dependent to a great extent. 95% of the total manual modelling time is spent on customizing shapes and fitting them to right locations. The challenges exhibited in the fitting step are due to the irregular geometries of existing bridges. Existing methods can fit geometric primitives such as cuboids and cylinders to point clusters, assuming bridges are made up of generic shapes. However, the produced geometric digital twins are too ideal to depict the real geometry of bridges. In addition, none of existing methods have evaluated the resulting models in terms of spatial accuracy with quantitative measurements. We tackle these challenges by delivering a slicing-based object fitting method that can generate the geometric digital twin of an existing reinforced concrete bridge from labelled point clusters. The accuracy of the generated models is gauged using distance-based metrics. Experiments on ten bridge point clouds indicate that the method achieves an average modelling distance smaller than that of the manual one (7.05 cm vs. 7.69 cm) (value included all challenging cases), and an average twinning time of 37.8 seconds. Compared to the laborious manual practice, this is much faster to twin bridge concrete elements.

Keywords –

Digital twin; BrIM; BIM; Point cloud data; IFC

1 Introduction

The United States (US) and United Kingdom (UK) spend a lot of money every year ($12.8 billion and £4 billion, respectively) to address deteriorating bridges and maintain their road networks. The reasons behind these massive costs are in part because bridge owners face a major challenge with structuring and managing the data needed for rapid maintenance and retrofit of their assets. The data available in Bridge Management Systems (BMS) does not meet the standard of information needed for sound decision-making. There is a need for at least 315,000 bridge inspections per annum across the US and the UK, given the typical two-year inspection cycle [1] [2]. Visual inspection is still the most common form of condition monitoring. The resulting condition information from visual assessment is then entered into a BMS, such as the AASHTOWare (US) or the NATS (UK). However, these BMSs are geared primarily to make system-wide prioritization decisions based on high-level comparisons of condition data. They do not assess the actual condition of a particular bridge component and of a particular location of the component. Having a Geometric Digital Twin (gDT) would be quite useful for this purpose as texture and damage information can then be properly integrated with the geometry at the component-level of the virtual 3D representation of a bridge. However, bridge owners today do not create such gDTs for existing bridges in the maintenance stage [3]. The following text reviews the current practice of digital twinning using point clouds, i.e. the process to acquire a gDT for an existing asset. This explains why the gDT implementation is so limited.

Major vendors such as Autodesk, Bentley, Trimble and ClearEdge3D, etc. provide the most advanced digital twinning software solutions. For example, ClearEdge3D can automatically extract pipes in a plant point cloud as well as specific standard shapes like valves and flanges from industry catalogues followed by fitting built-in models to them through a few clicks and manual adjustments. This means ClearEdge3D can realize a certain degree of automation. However, ClearEdge3D can only recognize and fit point cloud subparts with standardised shapes such as rectangular walls, pipes, valves, flanges, and steel beams, based on an industry specification table. Other commercial applications do not automate object detection nor arbitrary shape fitting. Fitting accurate 3D shapes to individual point clusters is challenging because the set

of allowable primitives is limited in most software applications. Reinforced concrete (RC) bridge components usually have complicated shapes, containing skews and imperfections, and cannot be simply fitted using idealized generic shapes. Modellers must manually create an accurate solid form to fit each point cluster as none of the existing software packages can do this automatically. Although modelling software such as Revit provides fine flexibilities that allow users to design a shape in a freeform manner (via Revit's

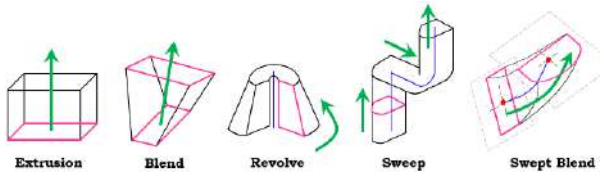

Figure 1. Forms available in Revit family

Family editor) (Figure 1), 95% of the total modelling time is spent on customizing shapes and fitting them to point clusters [4].

2 Research Background

Unlike building geometries which are defined in a grid system, real-world bridge geometries are more complex, which are defined with curved alignments, vertical elevations, and varying cross-sections. Extensive manual effort is required for practitioners to manually customize 3D accurate models to fit the underlying bridge components in arbitrary shapes in point clouds. We define "fitting" in this context as leveraging computer graphic techniques to form the 3D shape of a point cluster, a subpart of a point cloud. The 3D shape is approximate in the sense that it describes the geometry or the shape of a point cluster to produce its digital 3D representation to an acceptable quality based on the specific required level of detail.

2.1 Fitting Techniques

There is no universal solution to describe an object. How to choose a representation mainly depends on (1) the nature of the object being modelled, (2) the particular modelling technique that we choose to use, and (3) the application scenario where we bring the object to life. Existing shape representation methods can be categorized into four groups: Implicit Representation, Boundary Representation, Constructive Solid Geometry, and Swept Solid Representation. We review each of these in the following texts.

2.1.1 Implicit Representation

One solid modelling approach is based on the representation of 3D shapes using mathematical formulations, i.e. implicit functions. Common implicit surface definitions include, but are not limited to:

Table 1. Common implicit surfaces

Shape	Equation
Plane	$ax + by + cz = d$
Sphere	$x^2 + y^2 + z^2 = r^2$
Ellipsoid	$(\frac{x}{r_x})^2 + (\frac{y}{r_y})^2 + (\frac{z}{r_z})^2 = 1$

Given that only a very limited number of primitives can be represented exactly by algebraic formulations, implicit functions are of limited usefulness when modelling bridge objects. There is a trade-off between the accuracy of the representation and the bulk of information used for shapes that cannot be represented by mathematical formulations. We present three other basic modelling types: Boundary Representation (B-Rep), Constructive Solid Geometry (CSG), and Swept Solid Representation (SSR), in the following texts.

2.1.2 Boundary Representation (B-Rep)

Boundary Representation (B-Rep) is a method to describe shapes using their limits. The model represented using B-Rep is an explicit representation, as the object is represented by a complicated data structure giving information about each of the vertices, edges, and loops and how they are joined together to form the object. The geometry of a vertex is given by its (x, y, z) coordinates. Valero et al. [5] developed a method to yield B-Rep models for indoor planar objects (walls, ceilings and floors). Valero et al. [6] then upgraded their method to detect more objects in an indoor environment. Both Tessellated Surface Representation (TSR) and Polygon/Mesh Representation (PR/MR) can be considered as B-Rep types. A final model of TSR or PR/MR, is represented as a collection of connected surface elements. Oesau et al. [7] leveraged a graph-cut formulation to reconstruct a synthetic building point cloud into a mesh-based model. Representing an object using polygonal facets or mesh is the most popular representation in computer graphics. However, there are some problems with polygon mesh models: 1) Level of detail. High resolution could be unduly complex. An option is to reduce the polygon resolution without degrading the rendered presentation. But by how much? 2) Missing data, i.e. occlusions. Large occluded regions are hardly smoothed. Thus, PR/MP does not guarantee that a group of polygons facets can form a closed mesh model. 3) No sense of volume. It is difficult to extract geometric properties such as the radius of a cylindrical column on a mesh representation.

2.1.3 Constructive Solid Geometry (CSG)

Constructive Solid Geometry (CSG) is a high-level volumetric representation that works both as a shape representation and a record of how an object was built

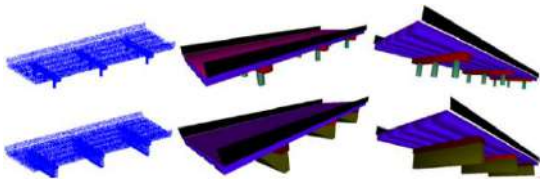

Figure 2. Fitted IFC entities in synthetic bridge point clouds (Zhang et al., 2014)

up [8]. The final shape can be represented as the combination of a set of elementary solid primitives, which follow a certain "logic". The primitives can be cuboids, cylinders, spheres, cones, and so on. When building a model, these primitives are created and positioned, then combined using Boolean set operators such as union, subtract, intersect and so on. Xiao and Furukawa [9] introduced an algorithm called "inverse CSG" to reconstruct large-scale indoor environments with a CSG representation consisting of volumetric primitives. However, this method uses only cuboids as volumetric primitives, assuming that they are the most common shapes found in indoor walls. Zhang et al. [10] (Figure 2) designed a classifier from surface primitive features to classify both infrastructure components (pier, beam, deck etc.) and 3D shape entities labels (cuboid, cylinder, sheet etc.) However, this method is tailored for idealized or simplified topology designs that do not consider the real geometries of bridge components. For example, a real sloped slab with varying vertical elevation cannot be simply modelled by a single sheet.

2.1.4 Swept Solid Representation (SSR)

Swept Solid Representation (SSR) or Extrusion is a representation of model which creates a 3D solid shape by sweeping a 2D profile that is completely enclosed by a contour line along a specific path. The sweeping line could be a straight line perpendicular to the contour surface, or it could be a curve in 3D space. Ochmann et al. [11] presented a method to reconstruct parametric 3D building models from indoor point clouds. Laefer & Truong-Hong [12] introduced a kernel-density-estimated-based method to identify the cross-sections of steel beams in point clouds. A cross-section is matched to one real steel type from a steel standard library and is extruded along the alignment.

2.2 Industry Foundation Classes (IFC)

2.2.1 IFC and MVD

IFC provides a set of definitions for all object element types encountered in the construction sector and a text-based structure for storing those definitions in a data file, based on an open data exchange standard, i.e. the IFC schema. It defines three basic components for modelling constructions: objects, relationships, and properties. An object is an abstract super-type entity, *IfcObject*, structured in an order hierarchy. An instance of the entity is used to represent a real-world object. The concept of relationships is the objectified relationship, *IfcRelationship*, relating different objects to each other, and the property definition, *IfcPropertyDefinition*, is the generalization of all characteristics and context information that can be added to an object. Ji et al. [13] introduced an extension to the IFC-Bridge format, providing a means of interchanging parametric bridge models. They describe in detail the necessary entities introduced to define parameters and capture dimensional and geometric constraints. Likewise, Amann et al. [14] suggested a generalized alignment model that can be extended with cross sections to describe a road body. This model can be further used for other product data models of linear infrastructure contractions, such as tunnels, roads, and bridges.

IFC is huge and defines a detailed schema of roughly 800 data types for representing building objects, their relationships, and associated lifecycle information. Specific uses of IFC have been narrowed to smaller subsets using a fraction of the data definitions, called Model View Definitions (MVD). The SeeBridge research team compiled an Information Delivery Manual (IDM) [16] to ensure that the final bridge DT would be sufficiently semantically meaningful to provide most of the information needed for subsequent bridge repair, retrofit and rebuild work.

2.2.2 IFC Geometric Representation

The section represents the most important IFC geometry representations. According to Borrmann et al. [15], all geometry representations in IFC data model can be grouped into four classes: Bounding Boxes, Curves, Surface models, and Solid models.

Specifically, bounding Boxes can be represented using *IfcBoundingBox*. Bounding Boxes are highly simplified geometric representation for 3D objects that are usually used as placeholders. *IfcBoundingBox* is defined by a placement corner point and dimensions of the three sides as a cuboid. *IfcCurve* and its subclasses *IfcBoundedCurve*, *IfcLine*, and *IfcConic* can be used to model line objects. Freeform curved edges (i.e. splines) and curved surfaces are required to model complex geometries. Surface models are used to represent composite surfaces comprised of sub-surfaces. They can be curved surfaces, such as NURBS surfaces or flat surfaces, such as mesh. *IfcTriangulatedFaceSet* can be used to represent the tessellated surfaces, i.e. polygons with an arbitrary number of edges, or triangular mesh. TSR cannot represent curved surfaces ideally but approximate them into triangular facets. In this case, the curved surface can be described using a finer mesh size, if accuracy is a concern. Specifically, *IfcBSplineSurface* can be used for representing curved surfaces. One

classic way to generate 3D objects as solid models is through CSG. *IfcCsgPrimitive3D* and its subclasses such as *IfcBlock*, *IfcRightCircularCylinder*, *IfcSphere*, and so on can be used. However, the use of CSG is very limited due to the fact that the use of primitives is very restrictive. By contrast, SSR is widely used for creating 3D objects in IFC. Possible representations include but not limited to the classes summarized in the following. In general, IfcSweptAreaSolid and its subclasses *IfcExtrudedAreaSolid*, *IfcRevolvedAreaSolid*, *IfcFixedReferenceSweptAreaSolid*, and IfcSurfaceCurveSwptAreaSolid can be used to present extruded solids. A closed profile *IfcArbitraryClosedProfileDef* is necessary for this representation. When using *IfcExtrudedAreaSolid*, the ExtrudedDirection is defined so that *IfcArbitraryClosedProfileDef* can be extruded along the direction. When using *IfcRevolvedAreaSolid*, both ExtrudedDirection and axis are defined so that *IfcArbitraryClosedProfileDef* can rotate around the axis up to a given angle. Then, *IfcFixedReferenceSweptAreaSolid* allows the extrusion to be done along any curve in space through the attribute Directrix. That is to say, the profile is extruded along a specific axis defined by the attribute FixedReference. By contrast, *IfcSectionedSpine* and *IfcSweptDiskSolid* are two representations working in a different but similar way. Detailed descriptions can be found in [15].

Among existing 3D object fitting work, almost all methods are used for generating building or industrial elements, such as walls, ceilings, floors, and standardized industrial elements. These objects are simply represented as extruded planes elements, cuboids, cylinders, and extruded steel beams. The gDT generation for existing RC bridges is almost missing in the literature. The problem of fitting 3D solid models in IFC format to real bridge point clusters has yet to be addressed. No effective method can reconstruct bridge point clusters into 3D IFC objects. In addition, no standardized metric is available for the quantitative evaluation of a gDT.

3 Proposed Method

3.1 Scope

Our method focuses on four types of bridge components: slab, pier, pier cap, and girder, in typical RC slab and beam-slab bridges. These two types of RC bridges represent 73% existing and 86% planned future bridges in the UK. These four types of components represent the most important and the most detectable structural components in the two types of bridges.

3.2 Overview

A definition of the level of detail (LOD) for gDT generation of existing infrastructure is missing in the literature. We use the LOD specification suggested by BIMForum as guidance. Table 2 illustrates an example of the interpretation of the LOD for a highway bridge component: a concrete precast girder.

The inputs of the proposed method are the four types of labelled point cluster. The outputs are two IFC files, containing various *IfcObjects* making up a bridge gDT and corresponding to two different LOD: LOD 200 and LOD 250—300. We define the LOD 250 as a LOD that is higher than LOD 200 but may not necessarily totally reach LOD 300. Figure 3 illustrates the workflow of the proposed method, which consists of two major steps: Step 1, geometric feature extraction of point clusters; Step 2, *IfcObjects* fitting to the extracted features. We use the MVD proposed by Sacks et al. [16], which proposes a binding to the IFC4 Add2 standard for exchanging bridge DTs.

3.3 LOD 200 gDT generation

We use TSR to create the Oriented Bounding Box (OBB) for each point cluster. The reason to choose TSR is because the OBB of a point set is a parallelepiped of 12 edges, 8 vertices and 6 faces. TSR is an explicit way to present an OBB. The parallelepiped geometry can be represented using the tessellated geometry model through *IfcShapeRepresentation*, expressing it as a triangulated tessellation. The coordinates of each vertex are provided by an index into an ordered list of Cartesian points *IfcCartesianPointList3D*. We introduce the property set *Pset_BoundingBoxProperties*, in which the method adds the attributes such as the length, width, and height of each OBB and composes them into an *IfcPropertyset*.

Table 2. LOD specification for highway bridge precast structural girder

LOD	Interpretation	Schema
200	Elements are generic placeholders. Any information derived from LOD 200 elements must be considered approximate.	
300	The quantity, size, shape, location, and orientation of the element as designed can be measured directly from the model.	

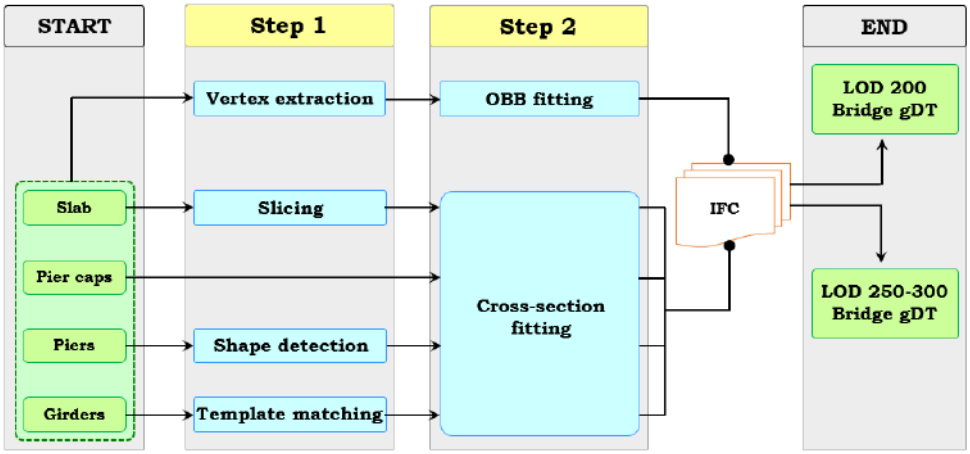

Figure 3. Workflow of the proposed IFC object fitting method

3.4 LOD 250 – 300 gDT Generation

Solid extrusions are preferred wherever possible if the cross-section in each slice model is deemed to be constant.

3.4.1 Slab – *IfcSlab*

Real-world bridges are neither straight nor flat. To circumvent or be compatible with the existing constraints of road geometry, many highway bridges carrying roads are on a curved alignment and the supporting structure follows that curved alignment. We use a similar but not identical slicing method to that proposed in [17] to slice the deck slab into J slices. The slicing does not take a parallel pattern but is rather oriented along the normal direction of the slab curved alignment. According to Kobryń [18], a circular curve is assumed to be the horizontal alignment of bridges investigated in this research. We then project the deck slab point cluster onto the XY-plane followed by fitting it with a unique second-degree polynomial to derive the parabola of the deck slab alignment. Next, we compute the tangent, slope, and normal at each interpolant of the parabola. The deck slab is then segmented along the direction of the normal of each interpolated position into J slices (Figure 4).

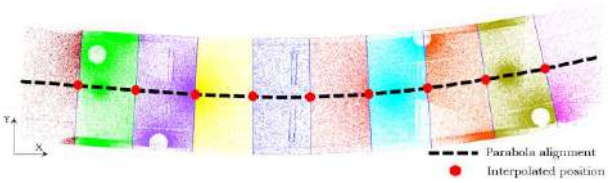

Figure 4. Deck slab slicing

Then, the problem of modelling the whole deck slab is transformed into modelling each straight slab slice assuming each slice is straight along the tangent direction and the cross-section of each slice is constant. For each slice, we rotate the slice around the Z-axis:

$$\begin{bmatrix} x' \\ y' \\ z' \\ 1 \end{bmatrix} = \begin{bmatrix} \cos(-\varphi_j) & \sin(-\varphi_j) & 0 & 0 \\ -\sin(-\varphi_j) & \cos(-\varphi_j) & 0 & 0 \\ 0 & 0 & 1 & 0 \\ 0 & 0 & 0 & 1 \end{bmatrix} \cdot \begin{bmatrix} x \\ y \\ z \\ 1 \end{bmatrix} \quad (1)$$

where the rotated angle φ_j is the angle between the normal direction of the alignment of the slice j and the global Y-axis. The updated points (x', y', z') are used to define the cross-section of each slice and descripted using a 2D α-shape. Each hull of the α-shape is represented as a 2D Cartesian point *IfcCartesianPoint*. A profile *IfcArbitraryClosedProfileDef* is used and the slab slice geometry is then represented using an extruded geometry model through *IfcExtrudedAreaSolid* and *IfcShapeRepresentation*, expressing it as a Swept Solid. The ExtrudedDirection is defined using the tangent direction of the mid-point of each slice. We introduce the property set *Pset_SlabSliceProperties*, in which the method can add the attributes of each slab slice.

3.4.2 Pier Cap – *IfcBeam*

Similar to how the slab slice is extruded, when modelling a pier cap point cluster, we project its points onto the XY-plane. We then use 2D α-shape to describe the projected contour such that each hull is stored in a 2D Cartesian point *IfcCartesianPoint* followed by mapping the contour with a list of *IfcPolyLine* objects. Like the slab slice, a pier cap is also represented as a Swept Solid through *IfcArbitraryClosedProfileDef* and *IfcExtrudedAreaSolid*.

3.4.3 Pier – *IfcColumn*

Piers can take many configurations. The shape of a pier is defined by the shape of its cross-section. To

simplify the problem, we group pier shapes into 3 classes: Shape 1 – Circular, Shape 2 – Quadrilateral, and Shape 3 – Others. Unlike simplified scenarios and synthetic data, real objects embedded in point clouds are similar to hand-drawn geometric shapes that usually contain imperfections or distortions. To tackle this challenge and identify the cross-section shape of a pier, we use a fuzzy-logic-based shape descriptor. We project a pier point cluster points onto the global XY-plane followed by calculating the perimeter of the projected points (denoted P_{ch}) and the bounded area (denoted A_{ch}). We then compute the area of the enclosing rectangle, i.e., the 2D oriented-bounding-box (denoted A_{er}) and the area of their largest-quadrilateral (denoted A_{lq}). if ${P_{ch}}^2/A_{ch} \cong 4\pi$, then the cross-section is a circle; else if $A_{ch}/A_{er} \cong A_{lq}/A_{er} \cong 1$, then the cross-section is a rectangle; Otherwise, the cross-section takes another shape. Similarly, cylindrical pier is represented using *IfcExtrudedAreaSolid* and *IfcShapeRepresentation*, expressing it as a Swept Solid. Attributes such as Position, Direction, Diameter, and Length. Then, stacked representation is used to approximate the overall pier shape through multiple slice models for quadrilateral and other piers (Figure 5).

Figure 5. An RC bridge point cloud (L) and the stacked representation (R)

3.4.4 Girder – *IfcBeam*

The girders studied in this research are assumed precast as the majority of existing and planned future RC slab and beam-slab bridges in the UK select precast elements. We suggest a template matching method to find the best-match girder type in existing precast bridge beam catalogues. We use three criteria to specify the girder type in each span: 1) Span length *sl*; 2) Girder bottom flange b_f; and 3) Web depth *d*.

We use the span length *sl* to narrow down a possible range of girder types. Then, the averaged girder flange b_f and the web depth *d*, computed using [17] can select a specific girder from the range of girders. Next, we store each of the cross-section feature point of the identified girder in *IfcCartesianPoint*. A 2D profile *IfcArbitraryClosedProfileDef* is used to describe the profile. Similarly, the girder is represented as a Swept Solid.

4 Experiments

4.1 Ground Truth Data and Results

We used the 10 bridge point clouds collected in [17] to conduct our experiments. The raw data is available at: http://doi.org/10.5281/zenodo.1233844. We also manually generated two sets of models *GT A* and *GT B* (Table 3), which serve as ground truth data:

GT A: The four types of bridge components in this set of models were represented using their tightest cuboids (average modelling time: 0.92 hours). They are used to compare against the automated generated LOD 200 gDTs.

GT B: The four types of bridge components in this set of models were represented within their precise dimensions (average modelling time: 27.6 hours). They are used to compare against the automated generated LOD 250-300 gDTs.

We implemented the proposed method on Gygax (https://github.com/ph463/Gygax/) as two different classes according to the suggested two different model resolution on a desktop computer (CPU: Intel Core i7-4790K 4.00GHz, Memory: 32GB, SSD: 500GB).

Table 4 demonstrates the results of the automated gDTs: LOD200 gDTs and LOD250-300 gDTs. Compared to manual modelling times, the average modelling time 10.2 seconds for LOD200 and 37.8 seconds for LOD 250-300, are trivial. We only demonstrate 4 bridge results due to limited space.

4.2 Evaluation

4.2.1 Evaluation of LOD 200 gDTs

We computed the volume and the centroid of each GT cuboids (gtBBox) Vol_{gt} and C_{gtBBox} and the automated ones Vol_{auto} and C_{autoBBox}. Denote E_{dc} and FVR are the Euclidean distance and false volume ratio between each C_{gtBBox} and the corresponding C_{autoBBox}.

$$\text{FVR} = \frac{|Vol_{auto} - Vol_{gt}|}{Vol_{gt}} \quad (2)$$

We also computed the point-to-point (P2P) distance, which is Euclidean distance between each vertex of the automated gDT and that of the GT one of each component of each bridge. The averaged $\overline{\text{P2P}}$ of all the 10 bridges was 23 cm (Table 5).

Table 5. Comparison of LOD 200 gDTs and *GT A*

	E_{dc} (m)	FVR (%)	P2P (m)
Bridge 1	0.06	17.6	0.23
Bridge 4	0.17	10.8	0.19
Bridge 7	0.23	24.1	0.35
Bridge 9	0.18	16.1	0.30

Table 3. Manual modelling *GT A* and *GT B*

	Bridge 1	***Bridge 4***	***Bridge 7***	***Bridge 9***
GT A	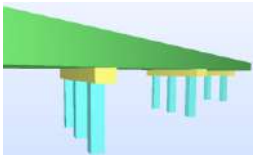	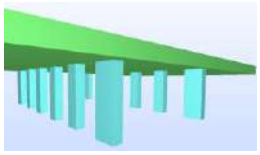	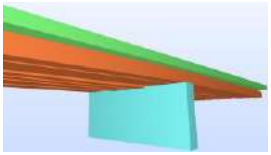	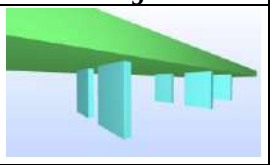
Time (h)	1.1	1.5	1.75	0.5
GT B	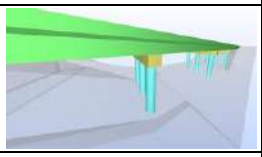	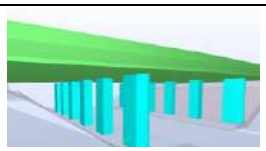	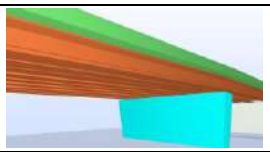	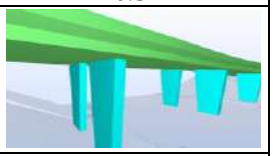
Time (h)	50.2	25.9	26.6	20.1

Table 4. LOD 200 gDTs & LOD 250 – 300 gDTs

	Bridge 1	***Bridge 4***	***Bridge 7***	***Bridge 9***
LOD200 gDT	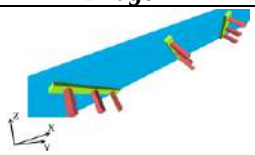	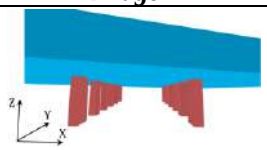	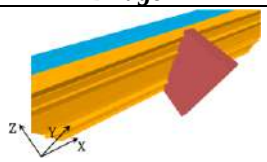	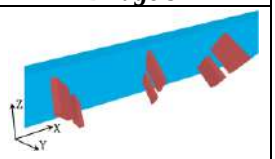
Time (s)	10.1	9.5	8.2	10.0
LOD250 -300 gDT	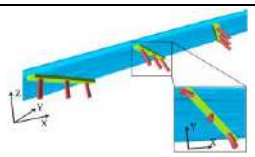	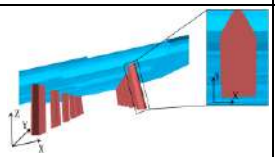	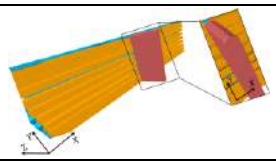	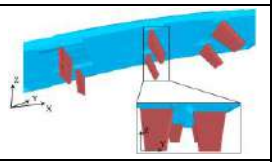
Time (s)	25.5	58.1	31.1	37.3

4.2.2 Evaluation of LOD 250 – 300 gDTs

We used a cloud-to-cloud (C2C) distance evaluation to detect changes between *GT B* and the automated ones. To do so, we first converted the *GT B* and the automated gDTs into .obj files followed by random sampling dense points from the generated polygons. Then, both sampled bridge point clouds (denoted GT and Auto) were compared against the reference point cloud, which is each bridge's original point cloud (denoted Real). We followed a local distance strategy to compute a local model Q. A quadratic model is used to fit neighbouring points in the reference point cloud to a surface (radius=0.3m) so that the average local distance from a compared point cloud α to a reference point cloud β is:

$$\overline{\mathrm{dist}} = \frac{1}{n}\sum_{i=1}^{n} \min\{d(q_i, Q)\}, \quad (3)$$

where q_i is a point of the compared point cloud α that is not on the model Q. Then, the estimated C2C distance between the two clouds is the bigger one of the mutual $\overline{\mathrm{dist}}$:

$$\mathrm{C2C} = \max(\overline{\mathrm{dist}}_{\alpha/\beta}, \overline{\mathrm{dist}}_{\beta/\alpha}). \quad (4)$$

An automated gDT is deemed better modelled if its C2C (denoted $\mathrm{C2C_{Auto}}$) is smaller compared with that of the manual model (denoted $\mathrm{C2C_{GT}}$) and vice versa (Table 6).

5 Conclusions

This paper presents an object fitting method able to generate gDTs of existing RC bridges in IFC format, using the four types of point clusters making up the bridge. Compared to the manual modelling process, the proposed method was more consistent, less liable to human errors. The gDTs were evaluated using distance-based quantitative metrics. Most of the automatically generated gDTs were better than the manually generated ones in terms of spatial accuracy. The overall $\overline{\mathrm{C2C}}_{\mathrm{Auto}}$ of 10 bridges gDTs was 7.05 cm while the $\overline{\mathrm{C2C}}_{\mathrm{GT}}$ was 7.69 cm. This value was down to 5.6 cm for $\overline{\mathrm{C2C}}_{\mathrm{Auto}}$ while 7.0 cm for $\overline{\mathrm{C2C}}_{\mathrm{GT}}$, if we didn't take two large distances (*Bridge 7* & *9*) into account. Last, the modelling time was also drastically reduced.

Table 6. Comparison of C2C between *GT E* PCD and Auto PCD against Real PCD

Bridge 1		***Bridge 4***	
$C2C_{GT/Real}$	$C2C_{Auto/Real}$	$C2C_{GT/Real}$	$C2C_{Auto/Real}$
4.0 cm	4.3 cm	7.3 cm	9.4 cm
	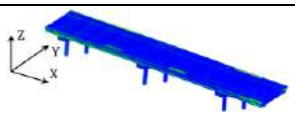	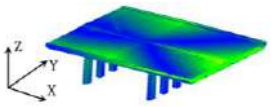	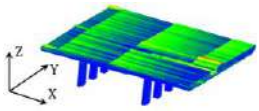
Bridge 7		***Bridge 9***	
$C2C_{GT/Real}$	$C2C_{Auto/Real}$	$C2C_{Real/GT}$	$C2C_{Auto/Real}$
15.7 cm	12.5 cm	9.8 cm	5.6 cm
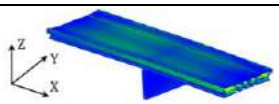	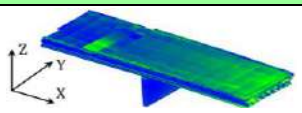	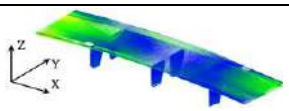	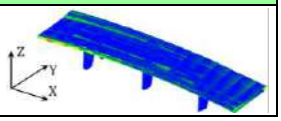

Acknowledgements

This research is funded by EPSRC, EU Infravation SeeBridge project and Trimble Research Fund. We thank their support.

References

[1] ASCE. (2017). 2017 Report Card for America's Infrastructure, Bridges. *ASCE*.

[2] Network Rail. (2015). Network Rail Bridge List.

[3] Buckley, B., & Logan, K. (2017). The Business Value of BIM for Infrastructure 2017. *Dodge Data & Analytics*, 1–68.

[4] Lu, R., & Brilakis, I. (2017). Recursive Segmentation for as-is Bridge Information Modelling. LC3

[5] Valero, E. et al., (2016). Semantic 3D Reconstruction of Furnished Interiors Using Laser Scanning and RFID Technology. *Jr of Comp in Civil Eng*.https://doi.org/10.1061/(ASCE)CP.1943-5487.0000525

[6] Valero, E., Adán, A., & Cerrada, C. (2012). Automatic Method for Building Indoor Boundary Models from Dense Point Clouds Collected by Laser Scanners. *Sensors*. https://doi.org/10.3390/s121216099

[7] Oesau, S., Lafarge, F., & Alliez, P. (2014). Indoor scene reconstruction using feature sensitive primitive extraction and graph-cut. *ISPRS*. https://doi.org/10.1016/j.isprsjprs.2014.02.004\

[8] Deng et al., (2016). Mapping between BIM and 3D GIS in different levels of detail using schema mediation and instance comparison. *Aut in Constr*, https://doi.org/10.1016/j.autcon.2016.03.006

[9] Xiao, J., & Furukawa, Y. (2014). Reconstructing the World's Museums. *International Jr of Computer Vision*, https://doi.org/10.1007/s11263-014-0711-y

[10] Zhang et al., (2014). Automatic Generation of As-Built Geometric Civil Infrastructure Models from Point Cloud Data. In *Comput in Civil and Building Eng*, pp. 406-413

[11] Ochmann et al., (2016). Automatic reconstruction of parametric building models from indoor point clouds. *Computers & Graphics*, https://doi.org/10.1016/j.cag.2015.07.008

[12] Laefer, D. F., & Truong-Hong, L. (2017). Toward automatic generation of 3D steel structures for building information modelling. *Auto in Constr*. https://doi.org/10.1016/j.autcon.2016.11.011

[13] Ji et al., (2013). Exchange of Parametric Bridge Models Using a Neutral Data Format. *Journal of Computing in Civil Engineering*. https://doi.org/10.1061/(ASCE)CP.1943-5487.0000286

[14] Amann et al., (2015). Extension of the upcoming IFC alignment standard with cross sections for road design. *ICCBEI*.

[15] Borrmann et al., (2018). Industry Foundation Classes: A Standardized Data Model for the Vendor-Neutral Exchange of Digital Building Models. https://doi.org/10.1007/978-3-319-92862-3_5

[16] Sacks et al. (2018). SeeBridge as next generation bridge inspection: Overview, Information Delivery Manual and Model View Definition. *Aut in Constr*. https://doi.org/10.1016/j.autcon.2018.02.033

[17] Lu, R., Brilakis, I., & Middleton, C. (2018). Detection of Structural Components in Point Clouds of Existing RC Bridges. CACAIE. https://doi.org/10.1111/mice.12407

[18] Kobryń, A. (2017). *Transition Curves for Highway Geometric Design*. *Springer Tracts on Transportations and Traffic* (Vol. 14). Cham: Springer International Publishing.

Improved Tag-based Indoor Localization of UAVs Using Extended Kalman Filter

N. Kayhani[a,b], A. Heins[b], W.D. Zhao[b], M. Nahangi[a,b], B. McCabe[a], and A.P. Schoellig[b]

[a] Department of Civil and Mineral Engineering, University of Toronto, Canada.
[b] University of Toronto Institute for Aerospace Studies (UTIAS), Canada.
E-mail: navid.kayhani@mail.utoronto.ca, adam.heins@mail.utoronto.ca, wenda.zhao@mail.utoronto.ca, m.nahangi@utoronto.ca, brenda.mccabe@utoronto.ca, schoellig@utias.utoronto.ca

Abstract –

Indoor localization and navigation of unmanned aerial vehicles (UAVs) is a critical function for autonomous flight and automated visual inspection of construction elements in continuously changing construction environments. The key challenge for indoor localization and navigation is that the global positioning system (GPS) signal is not sufficiently reliable for state estimation. Having used the AprilTag markers for indoor localization, we showed a proof-of-concept that a camera-equipped UAV can be localized in a GPS-denied environment; however, the accuracy of the localization was inadequate in some situations. This study presents the implementation and performance assessment of an Extended Kalman Filter (EKF) for improving the estimation process of a previously developed indoor localization framework using AprilTag markers. An experimental set up is used to assess the performance of the updated estimation process in comparison to the previous state estimation method and the ground truth data. Results show that the state estimation and indoor localization are improved substantially using the EKF. To have a more robust estimation, we extract and fuse data from multiple tags. The framework can now be tested in real-world environments given that our continuous localization is sufficiently robust and reliable.

Keywords –

Unmanned aerial vehicles (UAV); Building Information model (BIM); Indoor navigation; Autonomous flight; Visual inspection; Construction automation; Extended Kalman filter (EKF)

1 Introduction

Due to their capabilities, unmanned aerial vehicles (UAVs) are increasingly being employed for various purposes and in many industries, such as the construction industry. UAVs are able to function in unsafe and inaccessible locales that may be hazardous for humans. In addition, they provide maneuverability and perspective advantages over ground robotic platforms, which is an asset, particularly in multi-story buildings. A UAV can be equipped with various sensors to further enhance the data and insight acquisition. Thus, these features can enhance the collection of informative data in congested and dynamically changing construction environments. For instance, the inspection and monitoring of under-construction buildings [1], progress tracking and assessment [2] [3], site surveying [4], quality control [5], civil infrastructure condition assessment [6][7], and safety inspections [8] are among the broad applications of UAVs in the construction industry.

UAVs can be programmed such that they perform their tasks autonomously. To accomplish autonomous missions, the UAV must be able to navigate a collision-free path and be aware of its pose in the operating environment at any point in time. Autonomous robots in outdoor environments may take advantage of robust external sources of localization such as the Global Positioning System (GPS). However, GPS connectivity in highly congested urban areas with a dense distribution of high-rises (i.e., urban canyons) may be challenging even outdoors. Similarly, localization remains a real challenge in indoor environments.

1.1 Indoor Localization

A robust indoor localization system aims to continuously estimate the pose of one or more mobile agents in an indoor environment in real-time, given that the environment's map is available. Such a system has to not only be accurate, but also be financially, energy, space, and time efficient. It also needs to suitably cover the area. Several methods have been investigated to address this problem in the past decade. These state-of-the-art studies have mostly relied on localization systems based on radio-frequency identification (RFID) [9], ultra-wideband (UWB) [10][11], wireless local area networks (WLAN) [12], inertial measurement units (IMU) [13],

and machine vision [14]. In the construction sector particularly, RFID [15][16][17], UWB [18], IMU [19][20], and machine vision [21][22] are among the most commonly employed types of indoor localization systems.

However, not all the aforementioned systems may be suitable in the case of autonomous indoor flight during construction. For instance, due to the limited UWB signal communication range, dense network infrastructure may be needed. Metallic materials, such as piping and wall framing, may interfere with the radio frequency based systems including UWB [23] and RFID [24]. Non-line-of-sight (NLOS) propagation conditions may induce error in UWB [10], while IMU-based estimates may drift [19]. The most important concern in this regard, however, is insufficient localization accuracy of these systems [20] for autonomous UAV navigation. Although machine-vision-based localization methods such as motion tracking systems (e.g., Vicon systems) provide accurate estimates, they are an impractical solution for this application because they impose extra costs, logistics, complexity, and distraction to the construction site.

1.2 Visual Fiducial Markers

Visual fiducial markers, such as ARTag [25], AprilTag [26][27], and CalTag [28], are artificial landmarks consisting of patterns. They are designed to be easily recognized and robustly distinguished from one another and among other features in a natural scene when they are placed in an environment. Fiducial markers have been frequently used in augmented reality applications for camera pose estimation (e.g., ARTag [25]). AprilTag markers are passive square-shaped payload tags with an external black border and a binary internal code. Unlike QR (quick response) codes, AprilTag markers contain a small information payload. Therefore, they can be quickly detected and localized even when they are rotated or located in different lighting conditions. Indeed, AprilTag markers are two-dimensional barcodes that provide 6-DOF camera position estimation, and are cost-effective in that they can be printed on a standard printer [26]. AprilTag markers have also been found to be robust for indoor localization and object tracking in various mobile robotics applications [27]. AprilTag has different marker family types. The difference between the types are twofold: (1) the number of bits and (2) the minimum Hamming distance. The Hamming distance between two tags is defined as the number of positions at which the corresponding bits are different. For instance, an AprilTag of "Tagn^2hm" refers to an $n \times n$ array (n^2-bit) marker with a minimum Hamming distance of m between any two markers.

1.3 Extended Kalman Filter (EKF)

Since the position estimates and measurements are imperfect and prone to error, prediction and noise reduction algorithms are critical to enhancing these estimates. By minimizing the mean of the squared error, the Kalman filter [29] estimates the past, present, and even future state of a process using an efficient recursive approach [30]. However, since the Kalman filter (KF) is limited to linear systems, it is not able to solve non-linear localization problems. The EKF linearizes non-linear systems so that it can address non-linear localization problems [30][31].

1.4 Summary

In short, this paper presents the implementation of an EKF for improving the estimation module of the previously developed GPS-denied indoor localization framework using AprilTag markers [22]. In this study, it is shown that a probabilistic approach to the data fusion of multiple markers and the IMU using an EKF can substantially improve the estimation accuracy. Given that the 3D coordinates of the fiducial markers are also identified in the building information model (BIM), a camera-equipped UAV can recognize its pose relative to these artificial fiducial markers and then calculate its global location.

2 Overview of Prior Work

To develop a system for indoor localization of UAVs equipped with an onboard camera, the authors previously proposed a framework [22] using AprilTag markers. As illustrated in Figure 1, the calibration of the on-board camera is first undertaken to ensure that the measurements are accurate. The Robotics Operating System (ROS) package for camera calibration is used to estimate the camera parameters. Next, based on the mission plans and the critical locations that are supposed to be monitored by the UAV, the number and the corresponding location of tags are identified using the BIM model. Tags are then generated and the corresponding coordinates are assigned to them.

With the tags placed in the indoor construction environment, the UAV can be localized relative to the tags. Given that the global locations of the tags are available based on the BIM, the UAV's local coordinates can be translated to global coordinates. The authors reported the results of an experimental study designed to verify and validate the performance of the proposed framework. In this regard, the study investigated the impact of four critical parameters, namely, tag size, tag placement orientation, UAV distance from a single tag, and angle of view.

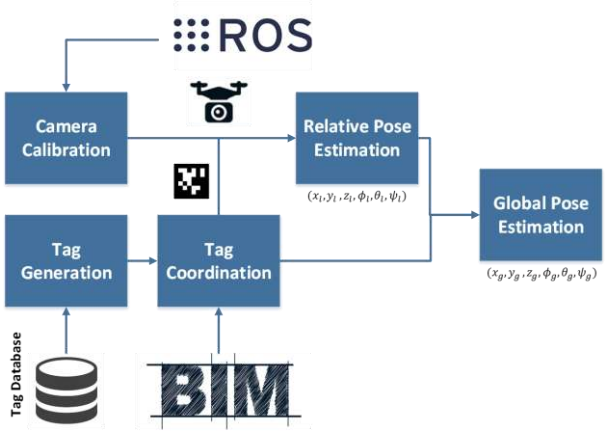

Figure 1. Indoor localization framework overview

That research also identified a number of factors that require further investigation to achieve a more robust indoor localization system. As all sensor measurements contain systematic and random errors, reducing or eliminating these errors is required to improve UAV pose estimation and reduce instability. It is intuitive that data from more sources of information can improve our measurements. Thus, to enhance the estimation process of the previously developed indoor localization framework [22], a standard extension of the KF [29] is used in this study.

In the previously developed method, the UAV used a single-tag detection algorithm. This algorithm only took measurements from a single designated tag at any given time. If this tag was not visible, the algorithm would estimate the UAV's location based solely on the less-reliable IMU measurements. In other words, the previously developed single-tag UAV localization method (hereafter the ST method) produced estimates based on only a single tag or the on-board IMU.

In the EKF method proposed in this work, however, the estimation process accounts for all available measurement data. It can be divided into two steps. The first step is the *prediction step*, which produces a predicted location based on the previous location and IMU data. The prediction is then updated in the *correction step*, where tag data is fused in to produce an overall estimate. This estimate is then used as the previous location during prediction in the next time step, and so on. By so doing, instead of switching back and forth between the IMU and the tag-based localization in different situations, we will combine the information from the IMU and all the visible tags. This multi-tag UAV localization method using EKF is hereafter called the MT method. This process will be investigated further in the next section.

3 The Extended Kalman Filter

Extensions of the KF are able to overcome the linearity limitation of the algorithm and enable the state estimation of nonlinear systems. Generally, the KF algorithm contains two steps: the prediction step and the correction step. In the prediction step, the current state ($\boldsymbol{x_k}$) is estimated based on the previous estimated state ($\boldsymbol{x_{k-1}}$) and the system inputs ($\boldsymbol{u_{k-1}}$) considering a random Gaussian noise ($\boldsymbol{w_{k-1}}$) when using a prediction model ($\boldsymbol{f}(.)$) (See Eq. 1). The estimates are then updated using the measurement model ($\boldsymbol{g}(.)$), which also has random Gaussian noise ($\boldsymbol{v}$). (See Eq. 2)

$$x_k = f(x_{k-1}, u_{k-1}, w_{k-1}) \quad (1)$$

$$y_k = g(x_k, v_k) \quad (2)$$

A simplified dynamic model is used in which the UAV is modeled as a rigid body double integrator system with discretization time step ΔT. An EKF is then employed to first fuse the captured data from the IMU and AprilTag markers and then estimate the UAV's desired state in terms of position, velocity, and orientation. Thus, the state vector that we intend to estimate is defined as $\boldsymbol{x} := [\boldsymbol{p}^T \quad \boldsymbol{v}^T \quad \boldsymbol{q}^T]^T$, where 3D vectors $\boldsymbol{p}, \boldsymbol{v}$ and quaternion $\boldsymbol{q}$ are representative of the UAV's position, velocity and orientation, respectively.

IMU measurements are treated as the input data for the prediction model, which is responsible for propagating the state from one time step $(k-1)$ to the next (k). The process noise of this step is modelled by independent zero-mean Gaussian distributions. The prediction step ends up with a *prior* estimate of $\boldsymbol{x}$, $\check{\boldsymbol{x}}_k$.

In the measurement model, because the position and orientation of all the tags are available, the relative position and orientation of the UAV with respect to all visible tags is measured at each time step *k*. The measurement noise is modeled as an independent zero-mean Gaussian distribution. Based on this model, the *prior* estimation $\check{\boldsymbol{x}}_k$ is updated. The final result of these two steps will be the *posterior* estimate of the state $\hat{\boldsymbol{x}}_k$. This algorithm is implemented based on the EKF ROS node, *ekf_localization_node*.

By so doing, we are able to continuously fuse data from multiple sources, namely, the on-board IMU and visible tags, providing a more robust system than the previous work.

4 Experimental Design and Setup

To study the MT method proposed in this study, an experimental setup is designed. AprilTag markers of type *36h11* are placed at six locations, which are also identified in the BIM (see Figure 2). Corresponding

coordinates are then easily extracted from the BIM. A Vicon motion capture system is employed as the ground truth to verify and validate the algorithm. By so doing, we are able to compare the results under varying experimental conditions using two methods (i.e., ST and MT). The UAV used in this study is a Parrot Bebop 2 in its default configuration and equipped with a camera and an onboard IMU. The overhead Vicon system is also used for control.

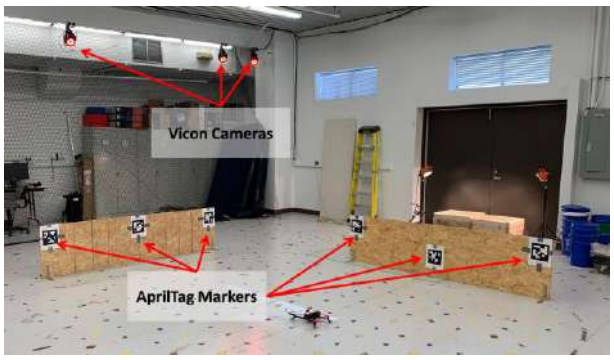

Figure 2. Experimental setup; six AprilTag markers with known coordinates, Parrot Bebop 2 UAV, and overhead Vicon camera system which tracks the motion of the UAV in the laboratory. The Vicon system is considered as the ground truth baseline in this study.

In these experiments, four trajectory scenarios are planned to investigate the dynamic performance of the proposed MT method.

1. *Straight line trajectory*. In the first scenario, a straight line trajectory is designed to investigate the impact of the distance from tags on the pose estimation accuracy. Although the MT method is able to fuse data from multiple sources, previous research [22] showed that the robustness of the tag detection process significantly drops when the distance increases. Thus, the whole pose estimation process potentially becomes more prone to noise and error. As a result, it is important to investigate the performance of the EKF in this situation. To do so, we run the planned scenario and assess the performance of these two methods relative to the ground truth Vicon measurement.

   As illustrated in Figure 3, the UAV starts its motion at a point 4.5m from panel B, which contains three tags. It moves 3m toward the panel at a rate of 0.86 m/s and finishes at a point 1.5m from the panel. In this scenario, all three tags on the panel B are used for the measurement process in the MT method. However, the middle tag is the only tag used in the ST method.

2. *Vertical line trajectory*. To investigate the impact of the angle of view on the MT method, a similar experimental setup is used, as shown in Figure 3. In this case, the UAV takes off from *O(0.0, 0.0, 0.0)* facing panel B, rises to the starting position of *Start(0.0, 0.5, 0.5)* and goes upward to *Finish(0.0, 0.5, 2.0).*

3. *Horizontal line trajectory*. To study the impact of the angle of view, the UAV takes off from *O(0.0, 0.0, 0.0)* facing panel B, and moves to its starting position of *Start(-1.5, 1.0 ,0.5).* It then goes sideward to *Finish(1.5, 1.0 ,0.5).* In this scenario, the ST method uses the nearest tag, and the MT method fuses pose data from of all the visible tags.

4. *A mixed trajectory*. Finally, a combination of the aforementioned trajectories is planned to provide insight into the overall performance of each method in more realistic circumstances. In this scenario, the UAV takes off from *O(0.0, 0.0, 0.0)* facing panel A (see Figure 3). The planned trajectory contains all of the other scenarios and a rotational motion.

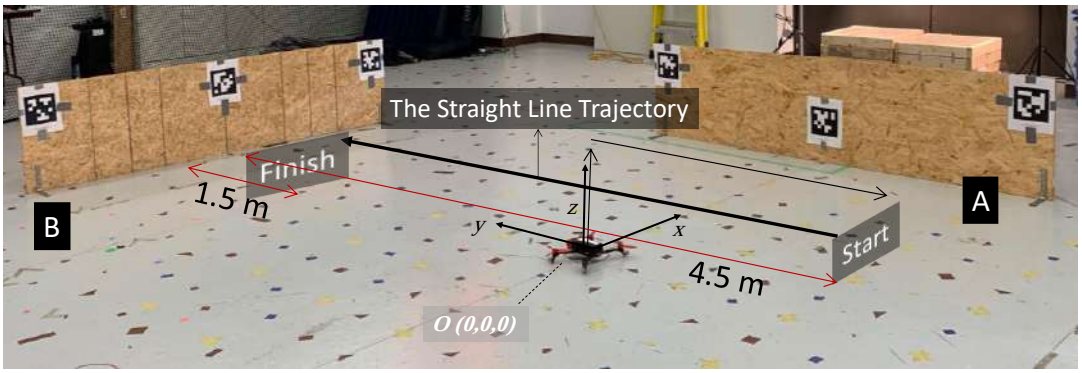

Figure 3. The experimental setup for scenario one; the performance of the methods are investigated at varying distances in the shown straight path. The UAV takes off from the *O(0.0, 0.0, 0.0)* while facing panel B. It flies its path from *Start(0.0, -1.5, 0.0) to Finish(0.0, 1.5, 0.0).*

5 Results and Discussion

The experimental scenarios are designed to evaluate the performance of the MT method in indoor localization of UAVs using AprilTag markers. The aim is to show that this approach makes the prior framework more reliable in real world ever-changing construction environments. To do so, the localization results of the MT and ST methods are compared to the ground truth system. To assess the pose estimation results, the root-mean-square error (RMSE) is used as a quantitative indicator of error reduction. Figures are provided to offer a visual insight of the estimation reliability and show the fluctuations and errors.

First, the impact of distance from tags is investigated while the UAV automatically flies based on the programmed scenario. Figure 4 illustrates in 2D the performance of the UAV in the first scenario. In this scenario, the UAV flies from *Start(0,-1.5,0.5)* to *Finish(0,1.5,0.5)*. The top and bottom graphs in Figure 4 show the performance of estimation using the MT and ST methods, respectively. The Vicon system, as a ground truth system, depicts the actual path taken by the UAV.

In both cases, localization accuracy increases as the UAV gets closer to the tags. However, the estimation error and fluctuation is significantly improved using the EKF in the MT method. In the ST method, where the EKF is not used, localization varies approximately -1m to +0.6m from ground truth whereas the EKF was able to reduce this variation to a range of -0.2m to +0.6m. Thus, it is clear that the MT estimation is smoother and converges toward the ground truth measurements more quickly and at a distance further from the tags. Therefore, it performs more reliably compared to the other method used in the previous study.

To better understand the multidimensional components of the errors, the Euclidean distance between the 3D positions estimated by two methods and the ground truth system also calculated. The results are shown in Figure 5. Here, the MT method performs not only considerably better than the ST method, but also robustly in distances less than 3 meters. Numerically, the RMSE values for the global position estimates using the ST and the MT methods are 0.35 m and 0.20 m respectively. This further supports the finding that MT significantly enhanced our estimations.

Although the proposed framework is not significantly sensitive to the changes in yaw angle and view angle [22], the second and third scenarios are tested to compare the methods' performances. Figure 6 (A) and (B) respectively compare the ground truth measurement of X value in the third scenario with ST and MT estimates. Figure 6 (A) and (B) show that the MT estimates are smoother and more reliable in comparison with the ST estimates.

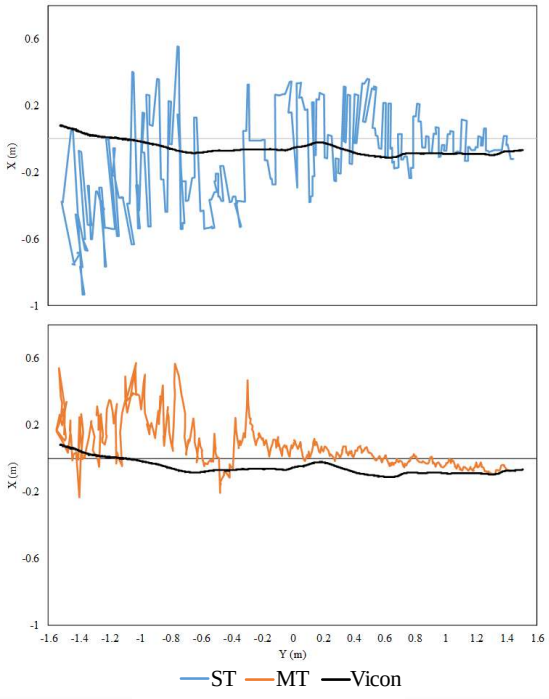

Figure 4. The plan view of the UAV's performance in Scenario 1 and the corresponding estimates: One-dimensional error in the pose estimation of the UAV while it decreases its distance from the tags.

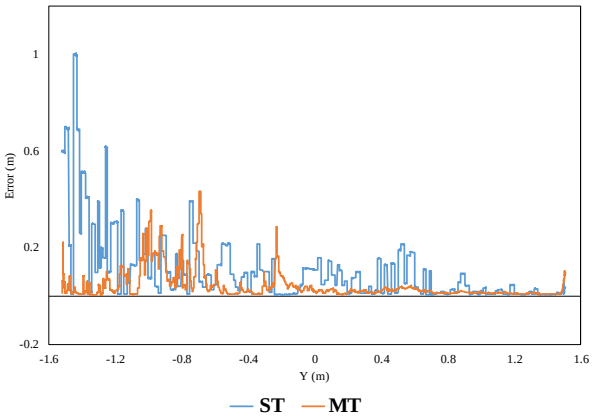

Figure 5. Position estimated error for the ST and the MT methods in Scenario 1

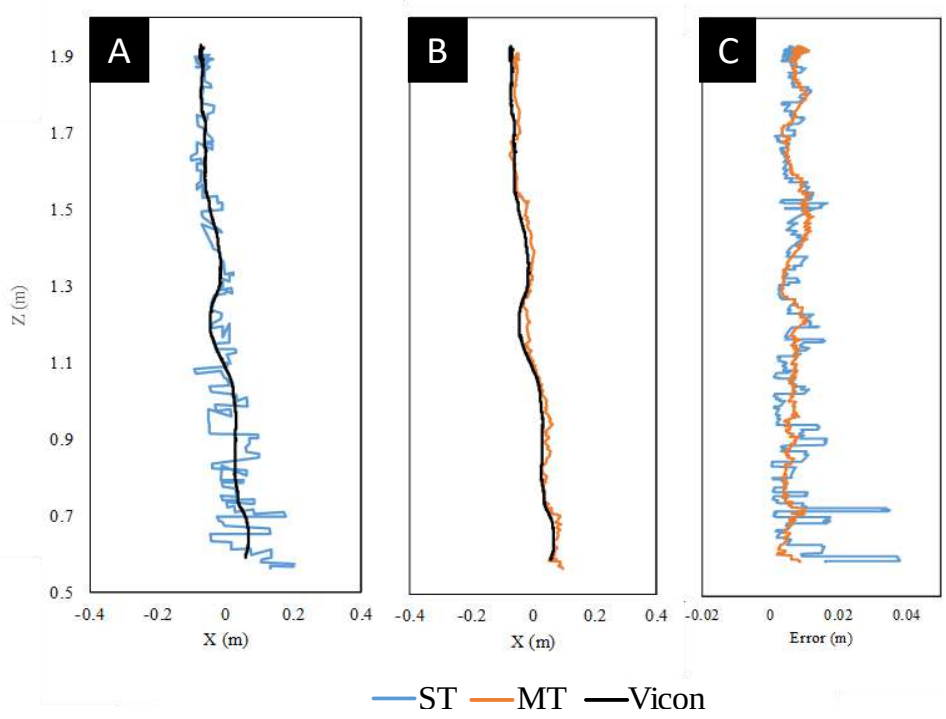

Figure 6. The second scenario: (A) estimated X value using the ST method; (B) estimated X value using the MT method; (C) error for two methods.

The error in Figure 6 (C) is defined as the Euclidian distance between the 3D positions estimated by two methods and the ground truth system. Even though the magnitude of the error is not large, Figure 6 (C) also confirms that the MT method not only performs noticeably more smoothly than the ST method, it also more reliably estimates the UAV's position.

Finally, to evaluate the performance of the proposed improvement in a real indoor construction environment, a full trajectory is tested in the fourth scenario. The estimated and ground truth positions of the UAV within the planned trajectory are plotted in Figure 7. The MT method is able to mitigate localization instability of the UAV by dramatically reducing the estimation error relative to the ST method. This is especially evident when compared in the same graph as shown in Figure 7. In this challenge, the UAV rotates from an orientation facing panel A to one facing panel B (Figure 3). There are some time steps in which the UAV is not able to see any tags, and therefore, the estimate is extremely noisy and unreliable, as evidenced by the ST method estimation performance in area A of the figure. Importantly, the MT method remains smoother and closer to the ground truth in this area.

In short, the overall performance of the MT method is significantly better than the ST method, because it estimates the ground truth position with fewer fluctuations and errors. To measure how these measurement errors are distributed, the RMSE is calculated. The RMSE can provide an overall insight about the performance of these two methods in the global pose estimation of the UAV. The RMSE for the ST method is 0.18m and for the MT method is 0.07m. Thus, it confirms that the MT method successfully improves our pose estimation in all the investigated scenarios.

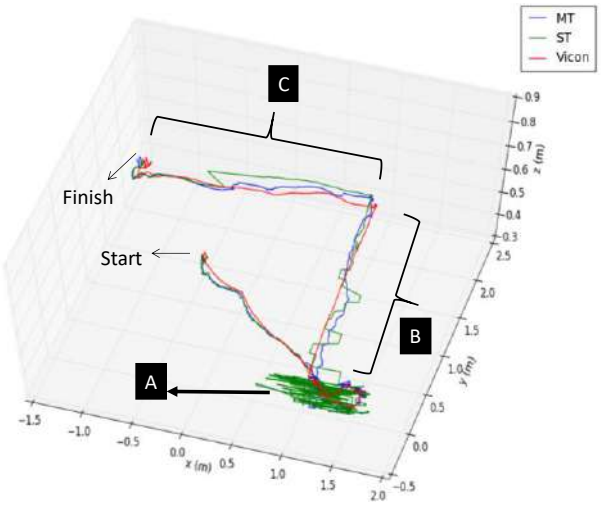

Figure 7. The performance of the methods in the fourth scenario; a planned mixed trajectory

6 Summary and Conclusion

To improve the state estimation process of the previously developed indoor localization framework of UAVs using AprilTag markers (i.e., ST), this study presented the implementation of an EKF (i.e., MT). By using an EKF, not only are we able to improve the estimation process by accounting for uncertainty, but we are also able to fuse data from two sources, namely, multiple tags and the onboard IMU. To evaluate the performance of the MT method within our framework, an experimental study was designed. Four scenarios were implemented, and pose estimation was done using both the ST and MT methods. The experimental results confirmed that the MT method successfully improves our pose estimation in all investigated scenarios. In other words, the estimated path using the MT method is smoother with less errors relative to the ground truth Vicon system. Thus, this approach improves upon our prior framework by making it more reliable for use in real-world and in ever-changing construction environments.

Future work includes using this method to provide state estimates for the control system. To this end, we need to conduct additional analyses and tests and further improve the performance of the state estimation module. For instance, in the proposed MT method, the EKF treats all the visible tags equally. However, localization data extracted from different tags may have different uncertainties (e.g., data associated with closer tags are generally more reliable than farther tags). These improvements should be implemented before any real-world tests are conducted.

Acknowledgment

Sincere support from The Natural Science and Engineering Research Council (NSERC) grant number RGPIN-2017-06792 is greatly appreciated. The arthurs are also thankful to those who participated in this study and supported the research project.

References

[1] Roca D, Lagüela S, Díaz-Vilariño L, Armesto J, Arias P. Low-cost aerial unit for outdoor inspection of building façades. *Automation in Construction*. 2013.

[2] Hamledari H, McCabe B, Davari S, Shahi A, Rezazadeh Azar E, Flager F. Evaluation of Computer Vision- and 4D BIM-Based Construction Progress Tracking on a UAV Platform. *6Th Csce/Asce/Crc Int Constr Spec Conf.*, 2017.

[3] Lin JJ, Han KK, Golparvar-Fard M. A Framework for Model-Driven Acquisition and Analytics of Visual Data Using UAVs for Automated Construction Progress Monitoring, *Computing in Civil Engineering*, 2015.

[4] Siebert S, Teizer J. Mobile 3D mapping for surveying earthwork projects using an Unmanned Aerial Vehicle (UAV) system. *Automation in Construction*, 2014.

[5] WANG F, CUI J-Q, CHEN B-M, LEE Comprehensive UAV Indoor Navigation System Based on Vision Optical Flow and Laser FastSLAM. *Acta Autom Sin.*, 2013.

[6] Ham Y, Han KK, Lin JJ, Golparvar-Fard M. Visual monitoring of civil infrastructure systems via camera-equipped Unmanned Aerial Vehicles (UAVs): a review of related works. *Vis Eng.*, 2016.

[7] Ellenberg A, Branco L, Krick A, Bartoli I, Kontsos A. Use of Unmanned Aerial Vehicle for Quantitative Infrastructure Evaluation. *J Infrastruct Syst.*, 2015.

[8] Gheisari M, Irizarry J, Walker BN. UAS4SAFETY: The Potential of Unmanned Aerial Systems for Construction Safety Applications. In: *Construction Research Congress*, 2014.

[9] Liu T, Yang L, Lin Q, Guo Y, Liu Y. Anchor-free backscatter positioning for RFID tags with high accuracy. In*: Proceedings - IEEE INFOCOM.*, 2014.

[10] Witrisal K, Meissner P. Performance bounds for multipath-assisted indoor navigation and tracking (MINT). *IEEE Int Conf Commun.*, 2012.

[11] Yassin A, Nasser Y, Awad M, et al. Recent Advances in Indoor Localization: A Survey on Theoretical Approaches and Applications. *IEEE Commun Surv Tutorials.*, 2017.

[12] Deasy TP, Scanlon WG. Stepwise algorithms for improving the accuracy of both deterministic and probabilistic methods in WLAN-based indoor user localisation. *Int J Wirel Inf Network*, 2004.

[13] Zhang R, Hoeflinger F, Gorgis O, Reindl LM. Indoor localization using inertial sensors and ultrasonic rangefinder. *Int Conf Wirel Commun Signal Process WCSP 2011*. 2011.

[14] Liang JZ, Corso N, Turner E, Zakhor A. Image based localization in indoor environments. *Proc - 2013 4th Int Conf Comput Geospatial Res Appl COMGeo* 2013.

[15] Motamedi A, Soltani MM, Hammad A. Localization of RFID-equipped assets during the operation phase of facilities. *Adv Eng Informatics.*, 2013.

[16] Razavi SN, Moselhi O. Automation in Construction GPS-less indoor construction location sensing. *Automation in Construction*, 2012.

[17] Costin AM, Teizer J. Fusing passive RFID and BIM for increased accuracy in indoor localization. *Vis*

Eng. 2015.
[18] Shahi A, Aryan A, West JS, Haas CT, Haas RCG. Deterioration of UWB positioning during construction, *Automation in Construction*, 2012.
[19] Taneja S, Akcamete A, Akinci B, Garrett JH, Soibelman L, East EW. Analysis of Three Indoor Localization Technologies for Supporting Operations and Maintenance Field Tasks. *J Computing in Civil Engineering*, 2012.
[20] Ibrahim M, Moselhi O. Inertial measurement unit based indoor localization for construction applications. *Automation in Construction*, 2016.
[21] Baek F, Ha I, Kim H. Augmented reality system for facility management using image-based indoor localization. *Automation in Construction*, 2019;99
[22] Nahangi M, Heins A, McCabe B, Schoellig A. Automated Localization of UAVs in GPS-Denied Indoor Construction Environments Using Fiducial Markers., *Proceedings of the 35th ISARC, Berlin, Germany)*, 2018.
[23] Xiao J, Zhou Z, Yi Y, Ni LM. A Survey on Wireless Indoor Localization from the Device Perspective. ACM *Comput Surv*., 2016.
[24] Mainetti L, Patrono L, Sergi I. A survey on indoor positioning systems. *22nd Int Conf Software, Telecommun Comput Networks, SoftCOM*, 2014.
[25] Mainetti L, Patrono L, Sergi I. A survey on indoor positioning systems., *22nd Int Conf Software, Telecommun Comput Networks, SoftCOM*, 2014.
[26] Fiala M. ARTag , a fiducial marker system using digital techniques., Proceedings - *IEEE Computer Society Conference on Computer Vision and Pattern Recognition (CVPR)*, 2005.
[27] Olson E. AprilTag: A robust and flexible visual fiducial system. *Proc - IEEE Int Conf Robot Autom.*, 2011.
[28] Wang J, Olson E. AprilTag 2: Efficient and robust fiducial detection. *IEEE Int Conf Intell Robot Syst.*,2016.
[29] Atcheson B, Heide F, Heidrich W. CALTag : High Precision Fiducial Markers for Camera Calibration., *In VMV*, vol. 10, pp. 41-48. 2010.
[30] Kalman RE. A New Approach to Linear Filtering and Prediction Problems, *Journal of basic Engineering* 82, no. 1 (1960): 35-45, 1960;
[31] Welch G, Bishop G. An Introduction to the Kalman Filter., *University of North Carolina at Chapel Hill, 2001 (Lesson Course).* 2006:1-16.
[32] Moore T, Stouch D. A Generalized Extended Kalman Filter Implementation for the Robot Operating System., *IAS*, 2014.

Live Data Visualization of IoT Sensors Using Augmented Reality (AR) and BIM

W. Natephra[a] and A. Motamedi[b]

[a] Department of Architecture, Faculty of Architecture Urban Design and Creative Arts, Mahasarakham University, Thailand
[b] Department of Construction Engineering, École de technologie supérieure, Montreal, Quebec, Canada
Email: worawan.ne@msu.ac.th, ali.motamedi@etsmtl.ca

Abstract –

Recently, the integration of Building Information Modeling (BIM) technology and Virtual and Augmented Reality (VR/AR) technologies during the operation and maintenance phase has been increasingly adopted. There has also been a surge of interest in the exploitation of Internet of Things (IoT) for constructed facilities, in the form of wireless networks connecting physical objects (e.g., sensing devices, facility assets, equipment, etc.). Recent IoT systems offer data management and visualization solutions. However, to improve issues such as safety and indoor comfort conditions for facilities, most of the existing IoT deployment do not benefit from the enriched digital representations of BIM and its graphical visualization capabilities. Although the integration of sensor data with BIM models has been investigated in academia, storing such real-time data in a standard and structured manner remains to be further investigated. This research aims to visualize live environmental data collected by IoT agents in the AR environment built upon existing BIM models. In our case study, the environmental data, such as indoor air temperature, light intensity, and humidity are captured by sensors connected to Arduino microcontrollers. Sensor reading are then stored in the BIM model and visualized in both the BIM platform and the AR application in a real-time manner.

Keywords –

BIM; sensors; thermal comfort; Augmented Reality; Arduino; Internet of Things (IoT); Visualization

1 Introduction

Since the emergence of Internet of Things (IoT) paradigm, numerous IoT architectures have been deployed to support indoor environmental monitoring and management. Many of those architectures are deployed and used for maintaining optimal comfort conditions with the aid of live streams of sensor data. IoT sensors can provide real-time feedback to building occupants about their surrounding physical environments. This information will be of great value since indoor conditions have a huge influence on the quality of their well-being.

Choosing an appropriate method for sensor data visualization is important as it may help users to intuitively understand and work with the data faster and easier [1]. Conventionally, static visualization techniques are used to interpret the meaning of captured data by turning data into various graphical forms (e.g., line graphs, charts, bar graphs, scatter plots, and maps). However, such static visualization techniques have certain constraints. For example, they can only allow certain data types to be presented and they are unable to present the real-time sensor data, such as indoor/outdoor air temperature, relative humidity, and air-flow rate. Provision of such information will be of essential importance for making prompt decisions for tackling building problems more proactively. As the complexity of relationships between various sources of data increases and the size of datasets continues to grow, 2D static visualization methods become less helpful and such methods need to be improved [2, 3]. In addition, static visualizations significantly suffer from the lack of the capability for representing live data interactively, thereby prohibiting interactive tasks [2].

A number of previous studies have proposed the development of various visualization methods, which allow for faster and more interactive data representation. Kim et al. (2017) [2], developed VisAR system which offers interactivity with static data visualization using Augmented Reality (AR). Sicat et al. (2018) [4] developed data visualization applications for extended reality (DXR), a toolkit for immersive visualization of building data based on Unity development platform. An immersive data visualization embedded in DXR system was developed to present data with interactive 2D or 3D visualizations. Hosokawa et al. (2016) [5] developed a

virtual reality (VR) system to visualize the air flow rate and temperature for an HVAC system by integrating BIM, Computational Fluid Dynamics (CFD) software (i.e., OpenFOAM) data, and VR.

In addition, other methods have been proposed to improve data visualization and facilitate decision-making throughout building lifecycle. For example, Motamedi et al. (2014) [6] investigated a knowledge-assisted BIM-based visual analytics approach for failure root-cause detection. In the mentioned study, BIM is integrated with other sources of FM knowledge (such as fault-tress) and inspection data to provide customized visualizations. Such visualizations assist technicians to utilize their cognitive and perceptual reasoning for problem-solving purposes. In an another study, Natephra et al. (2017) [7] proposed a method to integrate BIM and thermographic images together with environment sensing data in order to visualize spatio-temporal thermal data of building surfaces to support the assessment of indoor thermal comfort. Based on the previous studies, preprocessing of data is a crucial step before proceeding to incorporate digital models into virtual environments. To the best of our knowledge, effective methods for generating visualizations of live data streams for immersive environments are currently missing within the existing body of knowledge.

On the other hand, IoT and real-time sensing technologies are being increasingly used and applied in various platforms to enhance quality of life [8]. Vaccari (2015) [9] stated that IoT enables data streaming from network-connected devices to be delivered and transformed into other types of information to be included in virtual simulations.

Research efforts to integrate IoT and BIM for creating platforms to facilitate various processes in the architecture, engineering, construction and facilities management (AEC/FM) industry have already started. Dave et al. (2018) [10] developed Otaniemi3D platform, which integrates the BIM model of a campus and its corresponding environment data with IoT sensors. The system was used to monitor energy usage, occupancy and user comfort. Pasini et al. (2016) [11] presented a framework for connecting BIM with IoT for operating cognitive buildings. IoT sensors and BIM virtual models were integrated to track the behavior of occupants and provided an opportunity to predict building performance. Previous studies on the integration of BIM and IoT are mainly focused on automating the transfer of sensor information to BIM models [8]. However, when integrating BIM and IoT, in addition to data transfer, special attention must be also paid to the visualization of sensor data. Generating appropriate and targeted visualizations helps stakeholders better comprehend sensor outputs and eventually make better decisions.

In a board sense, BIM refers to a digital transformation of information throughout the building lifecycle [12]. The integration of IoT systems with BIM models remains a great challenge, though, it offers potential benefits for operation and facility management [13]. Integrating BIM and sensor data facilitates measuring environment parameters, such as comfort conditions. Although such integration has been investigated in recent research projects, storing real-time sensor readings and visualizing calculated comfort-related parameters have not been explored sufficiently. To respond to the aforementioned research gaps, this research presents a novel method for live sensor data visualization. In particular, an AR-based visualization technology has been used for indoor comfort condition monitoring. This paper presents a framework for integrating BIM information and IoT sensor data to support visualization of live data streams.

A number of Arduino-based sensing devices have been used to capture real-time values of comfort parameters including, air temperature, humidity, and light intensity. The sensor data are then transferred from Arduino units to BIM and then stored in the BIM file using visual programming. The developed virtual charts are provided with a real-time display of sensor readings in a dedicated AR application. Autodesk Revit, Unreal Engine, and a number of plugins for scripting in those environments were used in our developed prototype system.

2 Proposed Methodology

The proposed architecture for AR live sensor data visualization is an integrated framework for storing IoT sensor data in BIM models, as well as visualizing sensor information in an AR environment for monitoring indoor conditions and assessing indoor thermal comfort. The proposed system provides a real-time measurement and representation of physical environmental variables influencing the experience of indoor environment. Moreover, it provides occupants and facility technicians an ability for identifying problematic issues with indoor conditions in a real-time manner while moving within the facility. The proposed system utilizes a marker-based localization scheme for AR registration. The AR system can visualize the measured values of environmental conditions by augmenting corresponding virtual charts each of which assigned to a predefined maker. The detection of markers triggers the display of the charts on a real-world scene. The system works on the basis of a seamless connectivity between various sources of real-time sensing data, an existing BIM model, and an immersive AR environment. The realization of the proposed framework consists of five steps (as shown in Figure 1). The first step is to install IoT sensors to collect real-time data about environmental variables (e.g., indoor

air temperature, humidity, and light intensity). Localization markers are also installed at this step. The second step is to create a BIM model of the facility and to identify the locations of the markers in the BIM model. The locations of the markers and sensors in the model correspond to their real-world placements. In this step, the BIM model together with the location information of markers and sensors are transferred to a game environment. In the third step, sensor readings are transferred by an IoT controller (Arduino in our prototype system) to the BIM server and are stored in the BIM database. In the fourth step, an effective connection is established for allowing a seamless flow of sensor data to the game engine environment. For this purpose, this study takes advantages of visual scripting features of selected game engine. For our experiment, four types of virtual charts have been created for displaying comfort-related parameters in the game environment. These charts are assigned to represent data about indoor air-temperature, humidity, light intensity, and thermal comfort chart which shows acceptable range of air temperature and humidity values according to the Predicted Mean Vote (PMV) method [14]. The virtual charts are registered with respect to the markers' locations. The predefined markers allow accurate registration of the virtual charts for the AR experience. In the last step, the live sensor data and the result of the indoor thermal comfort assessment are visualized in an AR application in a handheld device.

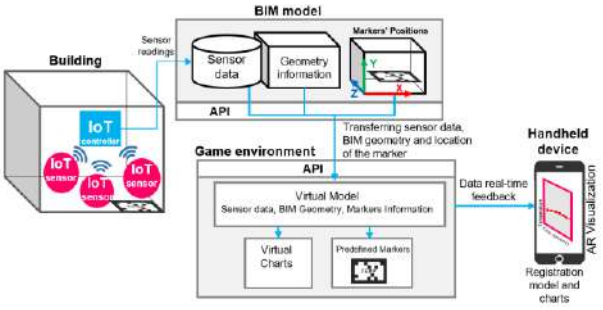

Figure 1. Overview of the proposed framework

3 Prototype system

Figure 2 shows the steps of using the developed prototype system. It follows the steps presented in the previous section. First, a BIM model is created using a BIM authoring application, and sensors devices are installed to collect environment data. Autodesk Revit (Version 2017) is used to create the BIM model of an existing building in our experiment. As mentioned previously, our prototype system uses a marker-based AR localization method. Hence, coordinates of the markers are defined in the BIM model. Environmental data (i.e., indoor air temperature, relative humidity, and light intensity level) is captured using sensors compatible with Arduino microcontrollers. The physical markers are then placed in the facility according to their assigned positions (Figure 2a). The sensor readings are then automatically stored in the BIM model. In order to store sensor readings in the model, a software application is developed using Dynamo, which is a visual programming environment for Revit (Figure 2b). The locations of markers are transferred to the game engine from the BIM model. The third step is to connect sensor readings to the game environment. Unreal Engine is used as the game authoring environment in our prototype system (Figure 2c). In this step, sensor readings are linked to the game environment using visual scripting feature of Unreal Engine. The live stream of sensors in the game engine is maintained using the developed tool. In the fourth step, virtual charts are created in Unreal Engine to represent the measured parameters of the physical environment (Figure 2d). In the fifth step, the sensor readings are visualized in the AR environment. The virtual charts are developed to display real-time data plot of sensor data in AR visualization agents (e.g., smartphone). To display virtual charts, the markers in each room need to become readily visible to the camera. The system then detects the location and the orientation of the smartphone relative to the marker and visualizes the appropriate virtual chart (Figure 2e). Users can quantitatively analyze the environmental condition and assess the indoor thermal comfort based on the PMV method by checking the charts in the AR environment (Figure 2f).

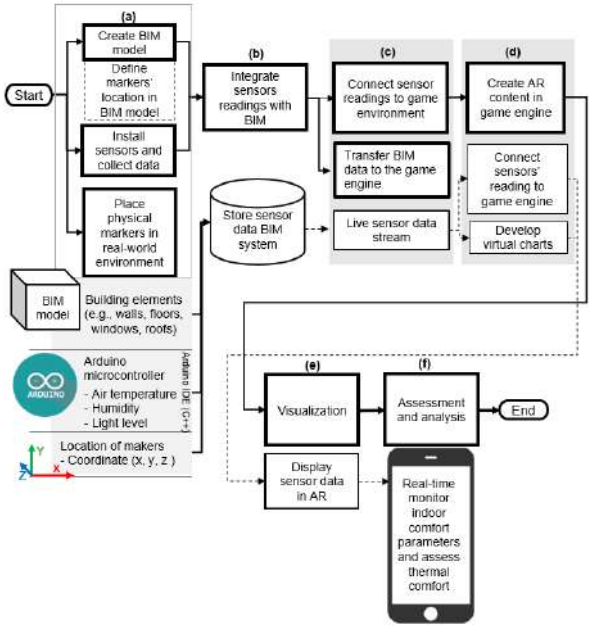

Figure 2. Process flow for integrating IoT sensors and BIM with AR

Figure 3 shows the user interface of our developed prototype system. The initial interface includes a scanning tool (Figure 3a). A marker is used to represent different environmental sensor outputs at once (Figure 3b). Once the smartphone camera recognizes the coordinates of the detected markers, the virtual charts augment the scene (Figure 3c).

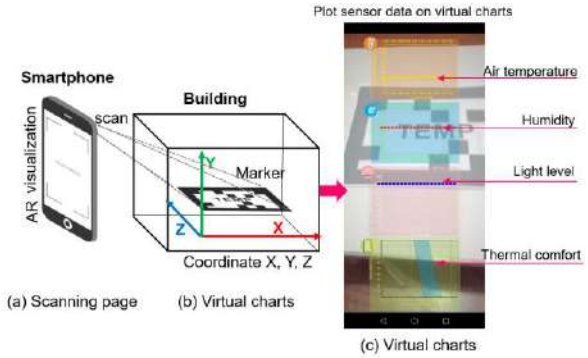

Figure 3. Screenshot of the prototype system

4 Case study

A case study for monitoring indoor comfort-related parameters was implemented using our developed application. To evaluate the capabilities of our prototype system, an apartment on the 7th floor of an existing residential building at Mahasarakham University was selected as an experimentation area. The apartment has two bedrooms with a living and kitchen areas, as shown in Figure 4. The environmental data was captured in the winter (December) from 9 a.m. to 6 p.m.

4.1 BIM modeling and installation of environmental sensors

Autodesk Revit version 2017 was used to create the BIM model of the case study. The markers were placed in the center of each room at a height of 1m from the floor (Figures 4a). For each room, specific visual charts to present related environmental parameters were associated to the corresponding marker. Three measurement points for capturing indoor air temperature, relative humidity, and light intensity were chosen at the level of 1m above from the floor (Figure 4b). Arduino Uno with its compatible sensor, (i.e., DHT11) were used to measure indoor air temperature and the percentage of relative humidity. Temperature range of the chosen sensor is from 0 to 50 °C, with ±2°C accuracy. Humidity range of the sensor is 20- 90% RH, with ±5% RH accuracy. Light intensity of the case study was measured by Photoresistor sensors. The sensors were set to collect data with time intervals of 1 second.

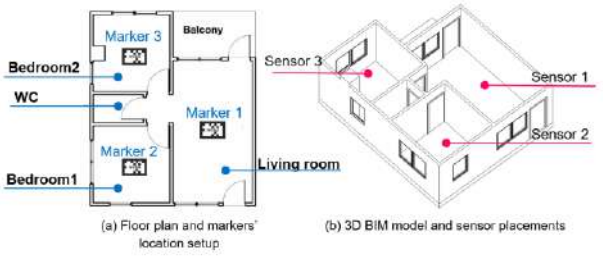

Figure 4. Experimentation room, makers' and sensors placements

DHT11 environmental sensor modules were connected to Arduino Uno microcontroller (Figure 5a). DHT 11 provides digital signal outputs of relative humidity and temperature. Arduino Integrated Development Environment (IDE) was used to build the code uploaded to the physical board. DHTLib library was installed to Arduino IDE to collect humidity and temperature readings. In this experiment, pin signal of the sensor was connected to a digital port of the Arduino board to read data output from the sensor. To measure the light intensity, photoresistor sensor modules are installed on Arduino boards. Analog pin A0 was used to read value of lighting level. Once the procedure to upload the developed code to Arduino boards is done, sensors start to capture readings. The code used to setup and run sensors for measuring the specified comfort parameters is shown in Figure 5b. Three variables are measured and displayed in the serial monitor (Figure 5c). The outputs of temperature, humidity, and light intensity level readings were represented in Celsius (C), percentage (%) and Lux (lx), respectively.

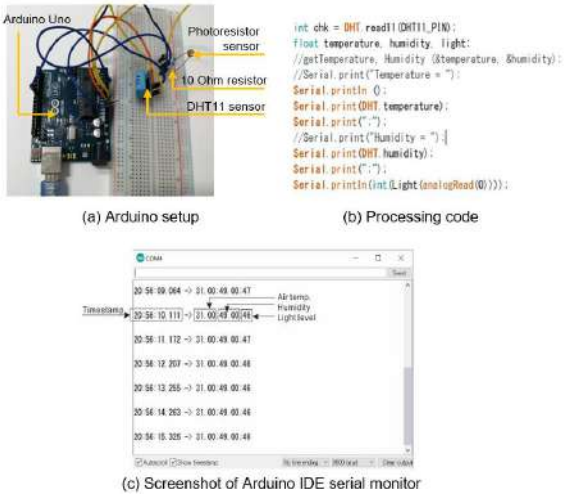

Figure 5. Circuit board setup, processing codeand sensor reading outputs

4.2 Sensor reading, BIM, and game engine integration

The procedure of connecting sensor readings with BIM is shown in Figure 6. First, DHT11 and photoresistor sensors were interfaced with Arduino board (Figure 6a). After uploading the developed code to the board, environmental parameters (i.e., air temperature, humidity, and light intensity level) were captured and the outputs of sensor data were displayed on the serial monitor console (Figure 6b). In order to transmit sensor readings from Arduino Uno to BIM, Firefly plugin provided in Dynamo (a BIM visual programming tool) was used (Figures 6c and 6d). To link Arduino sensor outputs with Unreal Engine, UE4Duino2 was used (Figure 6e). This plugin makes it possible for the Unreal Engine to retrieve data from Arduino in real-time. The user interface for representing sensor data in AR is created using Unreal Engine (version 4.20) (Figure 6f). Google ARCore, a plugin for Unreal Engine and an Android smartphone was utilized to build the AR application (Figure 6g).. Consequently, the AR live data visualization in smartphone can be performed. Consequently, the AR live data visualization in smartphone can be performed.

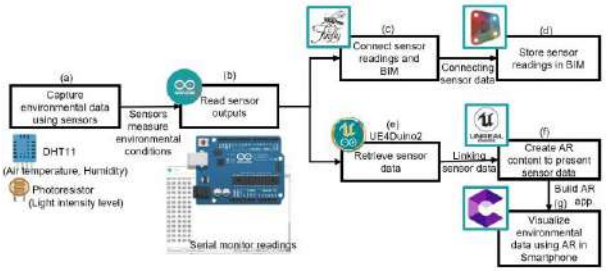

Figure 6. Sensor readings transfer to BIM and game engine

4.3 Connecting IoT sensor outputs with virtual chart in game engine

In order to visualize the measured values from IoT sensor readings, virtual chart widgets were created in Unreal Engine using Kantan Charts, a simple Unreal Motion Graphics (UMG) chart plugin. To monitor environment variables in real-time, Time Series Plot charts were used to represent the sensor outputs containing environmental information over the specified time intervals (Y-axis presents value of the measured values of environment parameters, X-axis presents time, in seconds). Cartesian Plot chart was used for real-time representation of indoor thermal comfort (Y-axis presents value of the measured relative humidity values, X-axis presents dry bulb temperature value).

4.4 Creating AR application using Unreal Engine

Our prototype application was run on an Android smartphone. In this experiment, the handheld device to support ARCore was a Huawei Y9 2019 (Android 8.1). To setup target markers in the AR application, the locations of the marker were obtained from the BIM model. The target images were imported to the Unreal Engine and added as a data asset using *GoogleARCoreAugmentedImageDatabase* and *GoogleARCoreSessionConfig*. To allow the AR content to be built and target image to be tracked by a smartphone, *Start ARCore Session* node was used. The created data asset was added in the configuration input.

4.5 Storing data in BIM and data visualization in AR

To store sensor data in BIM, readings were retrieved using Firefly visual programming plugin. Figure 7 shows sensor readings in Dynamo. Sensor readings along with their timestamp were saved as text file (Figure 8a), which can be used for tracking operation history for further indoor condition analytics. Figure 8b shows an example of the environmental data output visualization using the developed system.

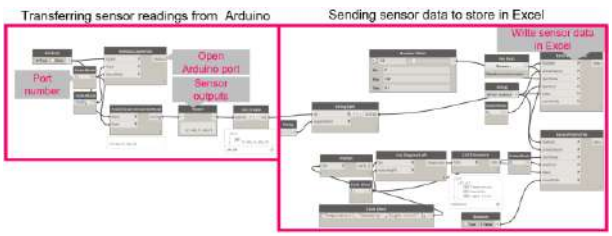

Figure 7. Screenshot of visual script for connecting sensor reading to BIM

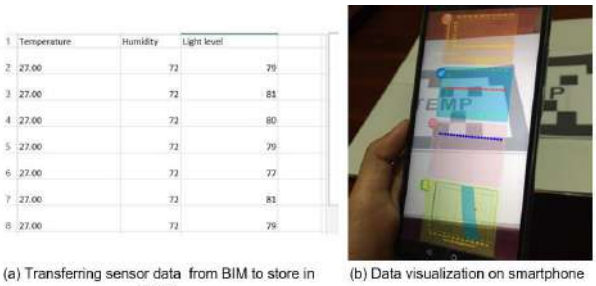

(a) Transferring sensor data from BIM to store in Excel

(b) Data visualization on smartphone

Figure 8. Example of sensor outputs

5 Conclusions and future work

This paper presented a method for developing a live sensor data visualization of indoor comfort variables using AR technology. According to the real-world experiments reported in this study, integration of BIM, IoT-driven environmental sensing, and AR based visualization provides the opportunity for real-time monitoring of comfort-related parameters and indoor comfort condition tracking. The system also provides the possibility for the assessment of those indoor environmental variables that have significant effect on indoor comfort. The proposed system can assist users in the identification of problems in a real-time manner. The information collected about indoor environmental conditions can be stored within the BIM database to be further analyzed for knowledge discovery from historical data about the facility indoor conditions.

For the delivery of AR experiences, an AR application was designed and developed with the aid of marker-based localization method. The results demonstrated that the sensor data retrieved from Arduino Uno can be successfully transferred to the BIM model, and sensor outputs were also successfully integrated with the game environment. To build the AR application, Google ARCore plugin for Unreal Engine and ARCore for smartphone were used. In our prototype system, the developed AR application was able to successfully deliver the augmentation of the real-time sensor data in the form of virtual charts on a smartphone.

Some challenges need to be addressed in our future works, such as improving the system to assess thermal and visual comforts by integrating other sensors including, air-flow rate, infrared radiations, noise, and air quality. Additionally, calculating other variables necessary for comfort assessments (e.g. MRT) will be added. Regarding the visualization method, in order to provide a greater level of immersion for users, integrating the prototype system with other Mixed Reality (MR) solutions should be developed. The interaction between users and the virtual environment can also be improved by adding an ability to move the AR objects in the AR application. Further, investigating methods to use the developed system for other use cases in facility management, training, and design processes should be investigated. Further research should also focus on improving the system to automatically track the current environment conditions and push alerts to occupants' personal digital devices and warn them about the prospective causes of the detected undesirable comfort conditions. Finally, a method to use BIM as a central storage of sensor data which is connected to the AR system will be developed.

Acknowledgement

The authors would like to acknowledge the assistance provided by Mr. Mehrzad Shahinmoghadam in writing this paper by providing constructive comments.

References

[1] Richter, C. (2009). Visualizing Sensor Data. *Trends in Information Visualization*, 1–21.

[2] Kim, T., Saket, B., Endert, A., & MacIntyre, B. (2017). VisAR: Bringing Interactivity to Static Data Visualizations through Augmented Reality, *arXiv:1708.01377*.

[3] Olshannikova, E., Ometov, A., Koucheryavy, Y., & Olsson, T. (2015). Visualizing Big Data with augmented and virtual reality: challenges and research agenda. *Journal of Big Data*, 2(1), 1–27.

[4] Sicat, R., Li, J., Choi, J. Y., Cordeil, M., Jeong, W. K., Bach, B., & Pfister, H. (2018). DXR: A Toolkit for Building Immersive Data Visualizations. *IEEE Transactions on Visualization and Computer Graphics*, (c).

[5] Hosokawa, M., Fukuda, T., Yabuki, N., Michikawa, T., & Motamedi, A. (2016). Integrating CFD and VR for indoor thermal environment design feedback. In *Proceedings of the 21st International Conference of the Association for Computer-Aided Architectural Design Research in Asia (CAADRIA)*, Hong Kong. pp. 1–10.

[6] Motamedi, A., Hammad, A., & Asen, Y. (2014). Knowledge-assisted BIM-based visual analytics for failure root cause detection in facilities management. *Automation in Construction*, 43, 73–83.

[7] Natephra, W., Motamedi, A., Yabuki, N., & Fukuda, T. (2017). Integrating 4D thermal information with BIM for building envelope thermal performance analysis and thermal comfort evaluation in naturally ventilated environments. *Building and Environment*, 124, 194–208.

[8] Chang, K.-M., Dzeng, R.-J., & Wu, Y.-J. (2018). An Automated IoT Visualization BIM Platform for Decision Support in Facilities Management. *Applied Sciences*, 8(7), 1086.

[9] Vaccari, A. (2015). How Virtual Reality Meets the Industrial IoT. https://wiki.aalto.fi/download/attachments/109392027/How-VR-meets-IIoT.pdf

[10] Dave, B., Buda, A., Nurminen, A., Främling, K., A framework for integrating BIM and IoT through open standards, *Automation in Construction*. 95 (2018) 35–45.

[11] Pasini, D., Mastrolembo Ventura, S., Rinaldi, S., Bellagente, P., Flammini, A., Ciribini, A.L.C.,

Exploiting internet of things and building information modeling framework for management of cognitive buildings, *IEEE 2nd International Smart Cities Conference: Improving the Citizens Quality of Life (ISC2)*, 2016.

[12] Eastman, C., Teicholz, P., Rafael, S., & Liston, K. (2008). *BIM Handbook*. New Jersey: John Wiley & Sons, Inc.

[13] Teizer, J., Wolf, M., Golovina, O., Perschewski, M., Propach, M., Neges, M., & König, M. (2017). Internet of Things (IoT) for integrating environmental and localization data in Building Information Modeling (BIM). In *proceedings of the 34th International Symposium on Automation and Robotics in Construction (ISARC 2017)*, pp 603–609.

[14] Fanger, P.O., *Thermal Comfort, Analysis and Applications in Environmental Engineering*, McGraw-Hill, New York, 1972.

An Image Augmentation Method for Detecting Construction Resources Using Convolutional Neural Network and UAV Images

S. Bang[a], F. Baek[b], S. Park[a], W. Kim[a], and H. Kim[a]

[a]Department of Civil and Environmental Engineering, Yonsei University, South Korea
[b]Industrial Technical Laboratory, Yonsei University, South Korea
E-mail: bangdeok@yonsei.ac.kr, fbeak@yonsei.ac.kr, somin109@yonsei.ac.kr, wontkim@hotmail.com, hyoungkwan@yonsei.ac.kr

Abstract –

Images acquired by UAV can be analyzed for resource management on construction sites. However, analyzing the construction site images acquired by UAV is difficult due to the characteristics of UAV images and construction site images. This paper proposes an image augmentation method to improve the performance of an object detection model for construction site images acquired by UAV. The method consists of three techniques: intensity variation, image smoothing, and scale transformation. Experimental results show that the method can improve the performance of the detection model (Faster R-CNN) by achieving a recall and a precision of 53.08% and 66.76%, respectively. With future studies, the method is expected to contribute to UAV-based resource management on construction sites.

Keywords –

Image augmentation method; Faster R-CNN; UAV; Resource management

1 Introduction

Previous studies have been conducted to analyze the images acquired by Unmanned Aerial Vehicle (UAV) for on-site construction management [1,2]. UAV is advantageous in acquiring images on a wide area in a short time, unlike closed-circuit television (CCTV). The use of UAV is more effective in large-scale construction sites where daily monitoring is difficult to perform. For generating managerial information on construction sites, it is necessary to recognize construction resources such as workers, construction equipment, and materials. The information on construction resources can be used for safety assessment, productivity analysis, and material tracking.

The object detection methods using image processing and machine learning algorithms have been proposed for construction resources [3-5]. Although previous studies have shown excellent performance in resource detection on construction sites, it is difficult to directly apply them to analyzing construction site images acquired by UAV, as shown in Figure 1. First, the quality of the images varies due to the diverse conditions such as the flight situation of UAV, external illuminations, and weather conditions. Second, vibration in UAVs makes the acquisition of blurred images frequent. Third, the same object is recognized as a different size based on the UAV position.

Image detection models should be trained from datasets with a large number of labeled data for improving their generalization capability. In general, a dataset composed of construction site images acquired by UAV is extremely inconsistent because it has both characteristics of construction site images and UAV images. Therefore, the dataset requires a large number of labeled data reflecting various situations. However, the publicly available image data in the construction industry are scarce, unlike datasets consisting of millions of images with labels, i.e., ImageNet Large Scale Visual Detection Challenge (ILSVRC) dataset [6], COCO dataset [7], and Open Images dataset [8]. Kim et al. [3] released the dataset of 2,920 construction equipment images including dump truck, excavator, loader, mixer truck, and roller; however, its size is not big enough compared to the datasets in computer vision domain. Furthermore, it is difficult to find publically available datasets of construction site images acquired by UAV.

We propose an image augmentation method that increases the number of training images while preserving the labels of construction site images acquired by UAV. For solving the aforementioned challenges regarding the UAV images, three image augmentation techniques (intensity variation, image smoothing, and scale transformation) are applied to each

Figure 1. Examples of construction site images acquired by UAV

training image. Our datasets consist of 10 classes: workers, four types of materials (tarpaulin, rebar, H-beam, concrete pipe), and five types of equipment (drilling equipment, crane truck, excavator, concrete truck, and dump truck). The faster region-based convolutional neural network (Faster R-CNN) proposed by Ren et al. [9] is used for construction resource detection. To validate the effectiveness of the proposed method, we compare the detection performances between the Faster R-CNN trained with the 593 images and the network trained with the augmented 11,800 images. The experimental results show that the proposed method is effective in augmenting the training dataset for significantly improved detection results in the UAV images.

2 Related Works

Many researchers have proposed vision-based object detection methods for construction resources such as workers, materials, equipment, and buildings at construction sites. Golparvar-Fard et al. [10] presented a computer vision-based method for equipment action detection. A Support Vector Machine (SVM) classifier used in the method recognized and localized equipment actions using the features of Histogram of Oriented Gradients (HOG). Park and Brilakis [11] proposed a detection method for construction workers in video frames. They used background subtraction to detect moving objects and used HOG features and an SVM classifier to extract objects like human-shape and used a hue, saturation, and value (HSV) color histogram and k-Nearest Neighbors (k-NN) to detect workers. Kim and Chi [4] presented a method for tracking construction equipment using functional integration of a detector and a tracker. They focused on solving the problem that the target equipment could be occluded due to its dynamic movements and site conditions. Hamledari et al. [12] suggested a computer vision-based algorithm for detecting the components of an interior partition. The partition including studs, electrical outlets, insulation, and three states for drywall sheets (installed, plastered, and painted) was detected by using image processing and machine-learning algorithms such as Otsu algorithm, k-mean clustering, and SVM. Kim et al. [13] proposed a data-driven scene parsing method to recognize the whole area of construction site images. The methods classified not only the construction resources such as workers, equipment, material, and structures, but also the background such as ground, sky, and tree.

The object detection methods using a convolutional neural network (CNN) have shown promising performances in computer vision tasks. These methods use the feature-maps extracted from the convolutional layer for finding candidate regions in which objects may exist. Girshick et al. [14] proposed the regions with convolutional neural network (R-CNN), which was known for the first attempt at implementing a CNN for object detection. In this network, the candidate regions extracted by using a selective search method [15] was input into the pre-trained AlexNet [16]. Girshick [17]

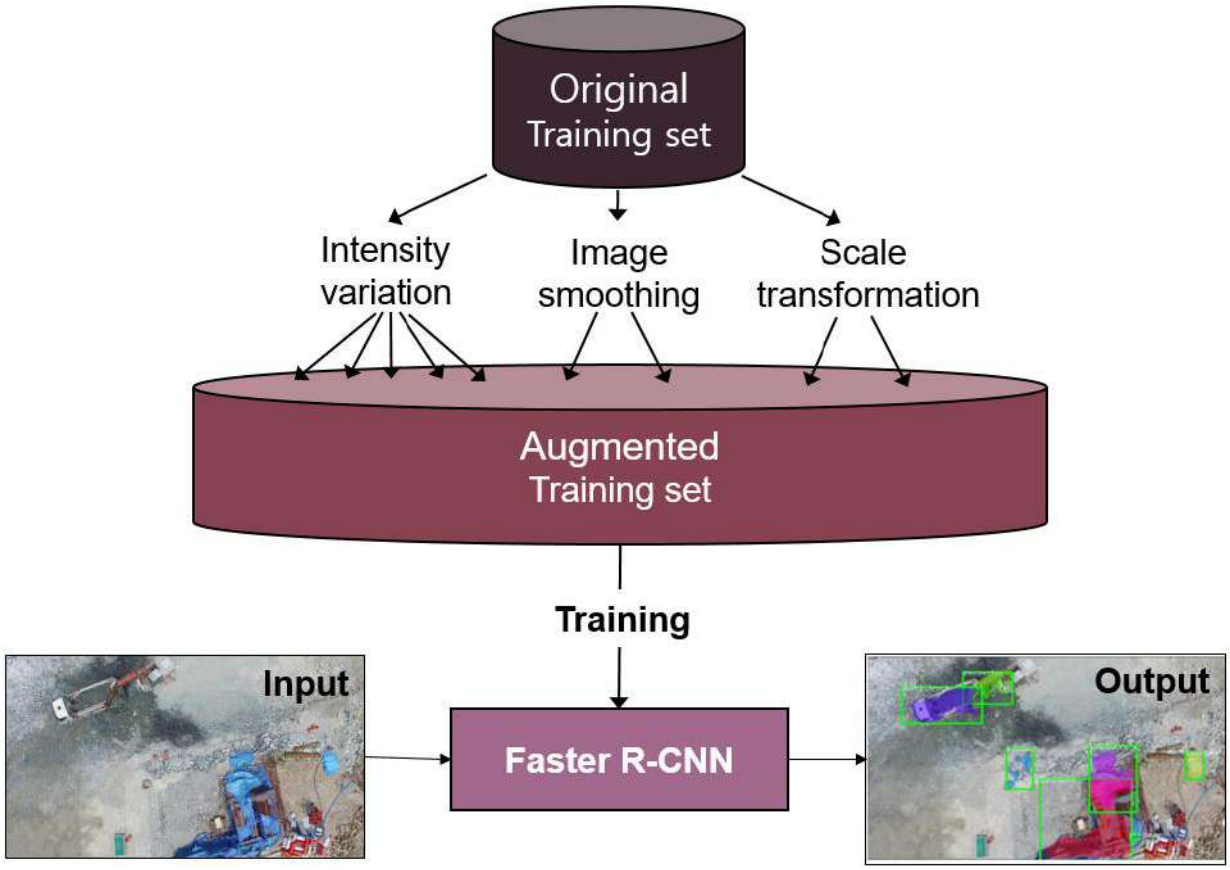

Figure 2. Overview of the image augmentation method

proposed Fast R-CNN to directly input the target image into the pre-trained AlexNet, unlike R-CNN. However, two networks (R-CNN, Fast R-CNN) took tens of seconds for processing an image because these networks used the selective search method to exhaustively generate bounding boxes regardless of aspect ratio and scale. To solve this problem, Ren et al. [9] proposed Faster R-CNN to perform the region proposal by adding a region proposal network (RPN) instead of using selective search methods. The RPN moved nine different size sliding windows on the feature-map obtained from the CNN and generated several bounding boxes with the expectation values indicating the probability that an object exists. This attempt has led Faster R-CNN to achieve promising performance in object detection.

CNN has been recently used successfully in construction resource detection. Kim et al. [3] proposed a method to detect construction site equipment using a region-based fully convolutional network (R-FCN). The R-FCN showed outstanding performance, achieving 96.33% mean average precision in identifying construction equipment. Kim et al. [18] proposed an integrated method of simulation and CNN-based monitoring for an earthmoving process in a tunnel. The CNN was successfully used for detection of excavator and dump truck with a 99.09% average precision.

3 Image Augmentation Method with Faster R-CNN

An UAV-based resource management strategy on construction sites can be developed using a CNN, which has shown outstanding performances in object detection. Although UAV can efficiently acquire a large amount of data, the quality of construction site images acquired by UAV varies greatly depending on UAV flight situations and outdoor environments. Furthermore, it is difficult to obtain a sufficient number of labeled images due to the lack of publically available dataset in the construction industry. In this context, image augmentation techniques are required to generate training images with preserving label information.

In this paper, we address three variables of construction site images acquired by UAV. The first variable is illumination changes due to ambient light exposure. The time of day, weather condition, and light exposure can affect the intensity of images. The second

variable is image quality change due to the vibration of UAV. Unlike other image collection devices such as CCTV, hand-held camera, and smartphone camera, UAV is likely to generate blurred images due to its continuous moving. The third variable is scale change in images due to the difference in flight height of UAV. The same visual data can be recorded as different sizes in different images depending on the distance between the construction site and the UAV.

Considering the three variables, we apply three image augmentation techniques: intensity variation, image smoothing, and scale transformation. Intensity variation is a technique to add or subtract the same value to all pixel in original images. Image smoothing is a technique to generate blurred images by applying a Gaussian filter to original images. In the case of the two techniques, we use the same label information as that of original images because the position of objects in augmented images does not change. Scale transformation is a technique to generate images using 2D scale transformation while preserving the aspect ratio of original images. In the case of third technique, the label information indicating the bounding box coordinates of objects are adjusted in accordance with the scale change of images. The following image augmentation techniques allow generating a sufficient number of training images in reflecting the characteristics of the construction site image acquired by the UAV. Figure 2 shows the framework of the proposed method.

4 Experimental Study

The effectiveness of the proposed methodology was validated through experiments. All experiments were conducted on the Ubuntu 16.04 operating system with GTX 1080 Ti GPU and an Intel Core i7-7700 processor, using the Python programming language and Tensorflow. The experimental dataset consists of 703 images collected at five construction sites. Among them, 593 were used as training images, and the remaining 110 were used as test images. We defined the construction resources as the 10 classes. The proposed method was used to generate 11,860 additional training images based on the 593 original images. Table 1 shows the parameters of three techniques. Figure 3 shows examples of the prediction results, and Table 2 summarizes a comparison of the performances. Because both methods learned the same network (Faster R-CNN), the computational speed at which the network processes images and detects construction resources is the same. The experimental results show that the image augmentation method improve the detection accuracy of the Faster R-CNN on construction site resources.

Table 1. The parameters of three techniques

Technique	Parameters
Intensity variation	(adding value) -60, -30, 0, 30, 60
Image smoothing	(σ value of Gaussian filter) 0, 1
Scale transformation	(scale factor) 0.8, 1.0

Table 2. Result evaluation on the dataset and computational speed

Method	Precision	Recall
Faster R-CNN trained with 593 images	39.10%	68.65%
Faster R-CNN trained with 11,860 augmented images	53.08%	66.76%

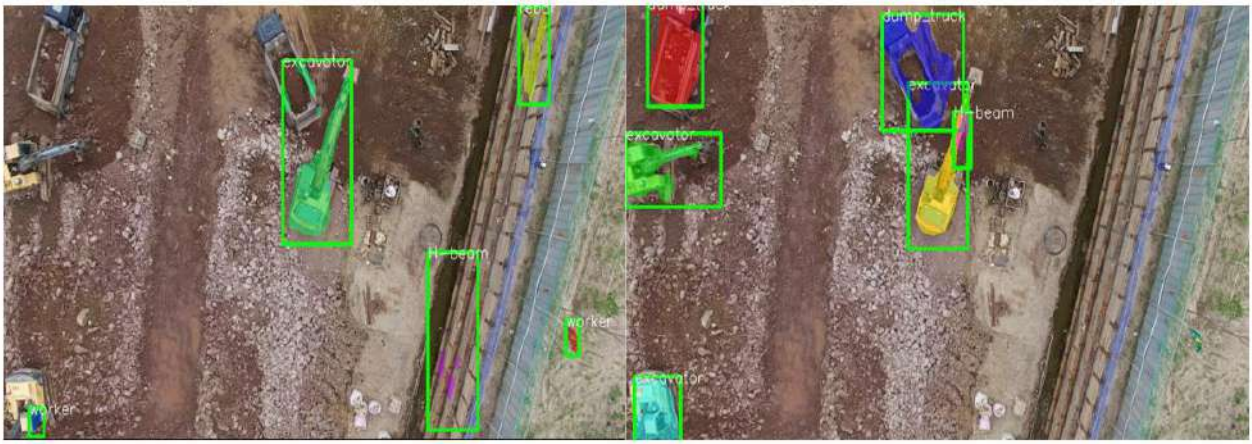

(a) (b)

Figure 3. Comparison of construction resource detection results using Faster R-CNN: (a) a detection result without our method; (b) a detection result with our method

5 Conclusion

This paper proposes an image augmentation method for UAV-based resource management on construction sites. The proposed method consists of three image augmentation techniques: intensity variation, image smoothing, and scale transformation. Faster R-CNN, one of the CNNs achieving promising results in object detection, was used for validating the method. Of the 703 construction site images acquired by UAV, 593 were used to train Faster R-CNN, and the remaining 110 were used to test the network. The Faster R-CNN trained with 11,860 training images augmented by the method showed a recall of 53.08% and a precision of 66.76%, which is superior to the performances of the trained network without this method. However, this study has the following limitations. First, it is difficult to improve the ability to detect new objects in terms of shape or color, which do not exist in the training dataset. Second, since contextual information between objects and backgrounds are not generated, it is difficult to successfully detect objects in the images having a different context from training dataset. Future researches are needed to improve the detection performance for practical implications in construction sites.

Acknowledgement

This work was supported by the National Research Foundation of Korea (NRF) grant funded by the Ministry of Science and ICT (No. 2018R1A2B2008600) and the Ministry of Education (No. 2018R1A6A1A08025348).

References

[1] S. Bang, H. Kim, H. Kim, UAV-based automatic generation of high-resolution panorama at a construction site with a focus on preprocessing for image stitching, Automation in Construction 84 (2017) 70-80.

[2] S. Siebert, J. Teizer, Mobile 3D mapping for surveying earthwork projects using an Unmanned Aerial Vehicle (UAV) system, Automation in Construction 41 (2014) 1-14.

[3] H. Kim, H. Kim, Y.W. Hong, H. Byun, Detecting Construction Equipment Using a Region-Based Fully Convolutional Network and Transfer Learning, Journal of Computing in Civil Engineering 32 (2) (2017) 04017082.

[4] J. Kim, S. Chi, Adaptive detector and tracker on construction sites using functional integration and online learning, Journal of Computing in Civil Engineering 31 (5) (2017) 04017026.

[5] E.R. Azar, Construction equipment identification using marker-based recognition and an active zoom camera, Journal of Computing in Civil Engineering 30 (3) (2015) 04015033.

[6] O. Russakovsky, J. Deng, H. Su, J. Krause, S. Satheesh, S. Ma, Z. Huang, A. Karpathy, A. Khosla, M. Bernstein, Imagenet large scale visual recognition challenge, International journal of computer vision 115 (3) (2015) 211-252.

[7] T.-Y. Lin, M. Maire, S. Belongie, J. Hays, P. Perona, D. Ramanan, P. Dollár, C.L. Zitnick, Microsoft coco: Common objects in context, European conference on computer vision, Springer, 2014, pp. 740-755.

[8] A. Kuznetsova, H. Rom, N. Alldrin, J. Uijlings, I. Krasin, J. Pont-Tuset, S. Kamali, S. Popov, M. Malloci, T. Duerig, The Open Images Dataset V4: Unified image classification, object detection, and visual relationship detection at scale, arXiv preprint arXiv:1811.00982 (2018).

[9] S. Ren, K. He, R. Girshick, J. Sun, Faster R-CNN: towards real-time object detection with region proposal networks, IEEE Transactions on Pattern Analysis & Machine Intelligence (6) (2017) 1137-1149.

[10] M. Golparvar-Fard, A. Heydarian, J.C. Niebles, Vision-based action recognition of earthmoving equipment using spatio-temporal features and support vector machine classifiers, Advanced Engineering Informatics 27 (4) (2013) 652-663.

[11] M.-W. Park, I. Brilakis, Construction worker detection in video frames for initializing vision trackers, Automation in Construction 28 (2012) 15-25.

[12] H. Hamledari, B. McCabe, S. Davari, Automated computer vision-based detection of components of under-construction indoor partitions, Automation in Construction 74 (2017) 78-94.

[13] H. Kim, K. Kim, H. Kim, Data-driven scene parsing method for recognizing construction site objects in the whole image, Automation in Construction 71 (2016) 271-282.

[14] R. Girshick, J. Donahue, T. Darrell, J. Malik, Rich feature hierarchies for accurate object detection and semantic segmentation, Proceedings of the IEEE conference on computer vision and pattern recognition, 2014, pp. 580-587.

[15] J.R. Uijlings, K.E. Van De Sande, T. Gevers, A.W. Smeulders, Selective search for object recognition, International journal of computer vision 104 (2) (2013) 154-171.

[16] A. Krizhevsky, I. Sutskever, G.E. Hinton, Imagenet classification with deep convolutional neural networks, Advances in neural information processing systems, 2012, pp. 1097-1105.

[17] R. Girshick, Fast r-cnn, Proceedings of the IEEE international conference on computer vision, 2015, pp. 1440-1448.
[18] H. Kim, S. Bang, H. Jeong, Y. Ham, H. Kim, Analyzing context and productivity of tunnel earthmoving processes using imaging and simulation, Automation in Construction 92 (2018) 188-198.

A New UAV-based Module Lifting and Transporting Method: Advantages and Challenges

J. O. Choi[a] and D. B. Kim[b]

[a]Department of Civil and Environmental Engineering and Construction, University of Nevada, Las Vegas
[b]Department of Mechanical Engineering, University of Nevada, Las Vegas
E-mail: jinouk.choi@unlv.edu, dongbin.kim@unlv.edu

Abstract –

The modular construction technique is the one key technology that can substantially advance the competitiveness of the construction industry. However, the industry is having difficulty creating an optimum environment for broader and more effective use of modularization due to one key barrier: implementing a modular construction technique, that is, shipping modules from the fabrication shop to the build site. Multiple issues are potentially challenging to overcome, such as module size and center of gravity, rigging, tie-down, site access, site congestion, and transportation regulations, as well as the availability of local heavy lift equipment. The researchers propose to implement drones as a way to address module transportation challenges and innovative logistics of modules. The primary research objectives are to innovate logistics with a new drone-based module lifting/transporting method, consisting of a drone lifting/transporting a module from below, similar to a pallet. In this paper, the researchers present key challenges and potential advantages, which have been identified from a manual test flight of the new method, with a drone lifting/transporting an acrylic cube box from below. The key challenges identified from the manual test flight are 1) limited payload, 2) limited power supply, 3) dynamic properties of a module; 4) agility/instability of unmanned aerial systems (UAS), and 5) regulations. Through the use of the drone-based module method, the researchers expect that lifting/transporting times and costs can be significantly reduced, eventually diminishing total installation costs, and expediting the overall construction process. This study will lead to the development of a drone-based module transportation framework for practitioners in the construction industry.

Keywords –

Modular construction; Modularization; UAS; Drone; Logistics; Module transportation; Lifting

1 Introduction

Modular construction is a manufacturing and installation technique that specializes in exporting site-based development to an offsite location. The modular construction technique has been utilized for centuries. Yet, in the past, modular construction was limited to lower levels of modularization. Moreover, many modular projects failed to achieve expected levels of performance or full benefits due to poor planning, poor management, late scope commitment, design changes, union jurisdictional problems, and/or module shipping failure. However, thanks to the advancement of robotics, information technology (IT), and Building Information Modeling (BIM) technologies, as well as an increased awareness of green construction and lean principles, the modular construction technique has rapidly evolved. This has enabled practitioners to plan and manage a modular project better, fabricate modules more precisely, and apply the modular technique to bigger and more complicated projects. It is now evident that practitioners and researchers in the construction industry recognize the value of modular construction. The potential of the modular construction technique will continue to grow [1] as the productivity growth of fabrication shops increase [2].

An inevitable disadvantage of the modular construction technique, compared to the conventional stick-build method, and one key barrier to implementing this technique is shipping modules to the build site and lifting/placing modules at final installation locations [3–6]. Multiple issues, such as module size and center of gravity, rigging, tie-down, site access, site congestion, onsite storage areas, transportation rules, regulations, delivery time restrictions, traffic, and local heavy lift equipment availability can potentially add costs for module transport and lift [3,6]. If the construction industry can innovate module logistics and shipping processes, the industry may accomplish broader and more effective use of modularization.

For the first time, the researchers propose to implement drones as a way to address module transportation challenges and innovative logistics (lifting/transporting) of modules. The primary research objectives are to innovate logistics with a new drone-based module lifting/transporting method, consisting of a drone lifting/transporting a module from below, similar to a pallet. In this paper, the researchers present key challenges and potential advantages identified from the literature review, as well as a manual test flight of a new drone-based module lifting/transporting method, with a drone lifting/transporting an acrylic cube box (a module) from below.

2 Methods

This research process for this paper is as follows: 1) problem identification with the process of module logistics; 2) extensive literature review on modular construction and drone applications; 3) development of a new method of a drone lifting/transporting a module from below; 4) fabrication of a prototype unmanned aerial vehicle (UAV); and 5) manual test flight of the new UAV-based module lifting/transporting method. Detailed research steps are described below.

First, the researchers identified the need for innovation of module logistics in modular construction in order to accomplish more effective uses of modularization. One of the researchers' past findings showed that one key barrier to implementing the modular construction technique is shipping modules to sites and lifting/placing modules at final installation locations [3,4]. Additionally, executing a preliminary transportation evaluation based on a full understanding of module limitations is the most critical success factor (CSF) for modularization [1].

Second, to define the research problem clearly and to find gaps in the existing knowledge, the researchers conducted a review of the literature on modular construction methods as well as drones. In this paper, the researchers summarized the current applications of drone in the construction industry and the challenges of module transportation.

Third, the researchers proposed and developed a method of implementing drones as a way to address module transportation challenges and innovative logistics (lifting/transporting) of modules. To better understand the new method's potential and challenges, the researchers developed/fabricated a small-scale prototype and tested it. The details of the proposed method, the development process of the prototype, and the specifications of the prototype can be found in the Results and Discussion section.

Finally, the researchers conducted a manual test flight of the new UAV-based module lifting/transporting method, with a drone lifting/transporting an acrylic cube box (a module) from below. A discussion of the identified potential and challenges are summarized below.

3 Results and Discussion

An unmanned aerial vehicle (UAV) is defined as:

> "an aircraft which is designed or modified, not to carry a human pilot and is operated through electronic input initiated by the flight controller or by an onboard autonomous flight management control system that does not require flight controller intervention." [6, p.7]

While flying robots/aircraft are commonly referred to as UAVs, a term, unmanned aerial systems (UAS) (typically referred to as *drones*), is used to indicate the entire infrastructure, systems, and human-machine interfaces required for autonomous operation [8]. UAS are classified as fixed-wing UAS (FW-UAS) and rotary-wing UAS (RW-UAS). FW-UAS tend to use the most power efficient flying principles, while RW-UAS are tailored to increased maneuverability and stationary vertical flight [8]. This research implements an RW-UAS, as it has higher maneuverability and stationary vertical flight ability.

3.1 Current Applications of Drone in the Construction Industry

Currently, drones have been deployed in [8]:

1. remote sensing – pipeline spotting, power line monitoring, volcanic sampling, mapping, meteorology, geology, agriculture, unexploded mine detection, pipeline risk assessment and repair, power line maintenance, real-time mapping, crop care and mine defusing;
2. disaster response – chemical sensing, flood monitoring, wildfire management, infrastructure repair, flood mitigation, and wildfire fighting;
3. surveillance – law enforcement, traffic monitoring, coastal and maritime patrol, border patrols, crowd control, traffic redirection, and inspection of maritime and trucking containers;
4. search and rescue – assessing the care and delivering first-aid support;
5. image acquisition – inspecting industrial and civil structures, and conducting maintenance work tasks;
6. communications;
7. transportation – small- and large-cargo transport and passenger transport; and
8. payload delivery – firefighting or crop dusting.

Numerous researchers have demonstrated drone applications in the construction industry as well, such as

drones to assemble structures (proof-of-concept) [9,10], with manipulators [11–15], and to probe and repair civil infrastructure [16,17]. Lindsey et al. [9] and Willman et al. [10] demonstrated proof-of-concept of workpiece pickup and drop-off (with self-connect, using magnets or pre-machined joints) to defined locations. Some researchers are equipping RW-UAS with manipulators to illustrate more dexterous tasks like inserting, screwing, and removing workpieces [11–15]. Darivianakis et al. [16] and Marconi et al. [17] have presented drones that can physically probe bridges, pipelines, and power lines to repair and replace parts. These efforts led to the inspection of a real power plant boiler using a multirotor vehicle and tightly integrated visual-inertial algorithms [18]. Many practitioners have also shown interest and participated in large consortia to implement drones in the construction industry (e.g., Petrobot Project [19], Aerial Robotics Cooperative Assembly System [20], European Robotics Challenges [21], ARGOS Challenge [22]).

3.2 The Current State-of-the-art of Heavy Aerial Lifting by Drone

Scientists in the UAS domain have demonstrated a system like a flying taxi, which will be commercially available shortly. EHANG 184 has test-flown successfully in Dubai in 2017; it is designed to carry a 100 kg payload for 25 minutes [23]. The Boeing company just conducted first test flight with their Air-Taxi prototype design in January 2019. The specifications are not open to the public yet, but they are planning to launch air-taxis operating in Los Angeles, and Dallas Texas by 2023 [24]. Lastly, Bell Helicopter unveiled a full-scale air taxi concept in 2019 at Las Vegas. The concept is designed to carry one pilot and four passengers [25]. The current state-of-the-art of heavy aerial lifting is described in table 1.

Table 1. The Current State-of-the-art of Heavy Aerial Lifting by Drone

Name	**EHANG 184**[23]	**Boeing Air Taxi**[24]	**Bell NEXUS**[25]
Test Flown	2017	2019	N/A
Weight	260 Kg	N/A	2720 kg
Capacity	100 Kg Payload 1 passenger No pilot	2~4 passengers No pilot	272 kg Payload 1 pilot, 4 passengers
Flight Range & Speed	Time: 25 minutes Speed: 100 km/h	Range: 80 km	Range: 240 km Speed: 240 km/h

Considering the speed of recent technological advancements of UAS, as scientists have demonstrated, a system like a flying taxi will be commercially available shortly, a drone will be available for heavy aerial lifting in the near future.

3.3 Problem Identification with the Process of Module Transportation

Compared to the conventional stick-build method, the process of module transportation, including rigging, lifting, and installation is unique to the modular construction method. According to two recent surveys [4,26], this process was selected as one key barrier to implementing the modular construction technique. There are many issues related to modules that need to be considered, such as design/fabricate/install strategies, module type, number of modules (one box or multiple assemblies), contract, supply chain, transportation restrictions (length, height, width, and weight), and critical constraints (water access, road access, and overhead obstructions) [1]. Additional issues, such as module size and center of gravity, rigging, tie-down, site access, site congestion, onsite storage area [27], can be potentially additive and more difficult to overcome for transporting and lifting modules. Proper engineering, planning, and project support are required for a successful module transport effort. However, planning module transportation is a very complex task [28]. Because many municipalities, counties, and townships have their own restrictions, without an experienced shipping and traffic coordinator, transport is not easy to manage [29]. In particular, transportation restrictions determine maximum module sizes [30,31] and that fact can impede the implementation of modularization.

3.4 A New UAV-based Module Lifting/ Transporting Method

The researchers propose a new method (hereafter known as *the new UAV-based module lifting/ transporting method*) of *a drone lifting/transporting a module from below* like a pallet, as illustrated in **Error! Reference source not found.**, to replace the traditional modular transportation process.

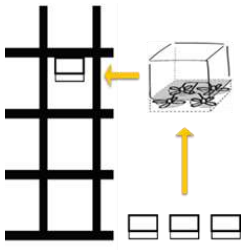

Figure 1. The new UAV-based module lifting/

transporting method

As Figure 1 illustrates, in this study, the researchers focus on transporting and lifting a cube shape, light building/facility module (i.e., HVAC and utility skids) with one UAS.

3.5 Development of a Prototype UAV

To test-and-evaluate the UAV-module, the off-the-shelf component Q450 V4 glass fiber frame is selected. The UAV-module consists of a Pixhawk autopilot controller and four 920kv (RPM/V) brushless motors fitted with 9.5-inch propellers. The selected battery (3-cell, 2.2 A, 11.1 V lithium poly) yields a UAV that can carry up to a 4.5 kg payload. The size of the UAV-module is 0.45m by 0.45m. A cubic-foot sized acrylic box was chosen for transportation. Lastly, a 3D printer is used to customize a suitable holder for the battery and acrylic cube box (Fig. 2). The UAV-module is manually deployed by FrSky Taranis X9D plus a transmitter (Fig. 3).

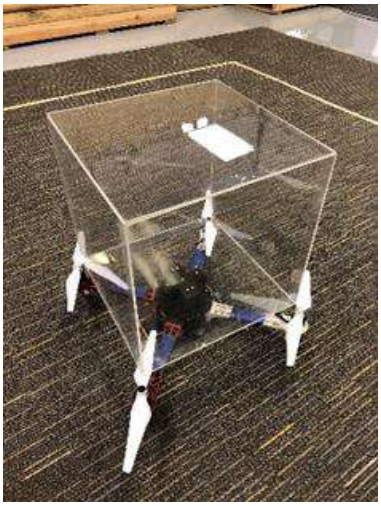

Figure 2. Prototype UAV with an acrylic cube box (a module)

Figure 3. Prototype in-flight testing

3.6 Manual Test Flight

The researchers conducted a manual test flight of the new UAV-based module lifting/transporting method, with a drone lifting/transporting an acrylic cube box (a module) from below (see Figure 3). The key challenges that have been identified from the manual test flight are 1) limited payload, 2) limited power supply, 3) dynamic properties of a module, 4) agility/instability of UAS, and 6) regulations.

First, there is a significant gap between a current drone's payload capability and a typical module's weight. Scientists in the UAS domain have demonstrated a system like a flying taxi [23–25,32], which will be commercially available shortly. However, a module's weight can be heavier than a drone's current maximum payload capacity. The second key issue is the power supply of a drone. Currently, with an 11 Volt, 2.2 Ampere Lithium-Polymer (Li-Po) Battery, a typical hobby quadcopter Q450 can only fly about 15 mins and lift 4.8kg, including the parts. As the flight duration is negatively correlated with the weight of the drone and module, the new UAV-based module lifting/transporting method may able to fly for only a few minutes without an improvement of the battery. Due to these weight and size restrictions, the choice of sensors, processors, and algorithms also impose technical and scientific challenges [8,33].

Third, the dynamic properties of the module, such as length, height, width, weight, and center of gravity, introduce additional technical and scientific challenges for implementation of the new UAV-based module lifting/transporting method. The manual test flight revealed that with the current flight control system, it is very difficult to manually adjust and control the UAV when the center of gravity of the module is not in the center. This issue leads to the problem of enhanced instability of the UAS. A UAS itself is very agile, which means that it is continuously moving and cannot be stopped to acquire sensor readings. For the new method, as the center of gravity of a module is not always in the center, additional technical and scientific challenges are imposed. To solve the instability issues, new algorithms and autonomous navigation systems are needed.

Finally, regulations related to drone application are key barriers to the new method. Regulations are needed for multiple reasons, such as safety, security, and privacy. Currently, the Federal Aviation Administration (FAA) requires the registration of all different UAV types for all purposes. Additionally, some purposes require certifications, training, and permits. For successful implementation of the new method, several requirements must be met: 1) overcome all of the issues and challenges addressed above; 2) demonstrate its application in terms of capability and reliability; 3) obtain advanced permits.

The high maneuverability and stationary vertical

flight ability of RW-UAS give engineers the potential to innovate the module logistics. The test flight demonstrates that the module transportation process can be significantly reduced through the implementation of the new UAV-based module lifting/transporting method. With the new method, once HVAC modules arrive on a jobsite, the modules can be transported directly to the installation location, without a need for the workers to set up or hook the modules into a module lift frame or spreader bars. Moreover, there is no need for scissor/boom lifts, tower cranes, forklifts, or transporters. Due to these reasons, the UAV-based module method can reduce transportation, lifting times, and costs significantly, eventually diminishing total installation costs and expediting the overall construction process.

4 Conclusion

The process of module transportation, rigging, lifting, and installation is unique to the modular construction method, one of the critical barriers to implementing the modular construction technique and executed inefficiently by practitioners. If the process is innovated, the construction industry will achieve broader and more effective use of modularization. Recently, drones have drawn increasing attention from researchers and others in the construction industry due to rapid advancements in related technologies and applications.

The key challenges that have been identified from the manual test flight are:

1. limited payload;
2. limited power supply;
3. dynamic properties of a module;
4. agility/instability of UAS; and
5. regulations.

However, if these challenges can be overcome through the use of the UAV-based module method, transportation times, lifting times, and costs can be significantly reduced, eventually diminishing total installation costs, and expediting the overall construction process. This innovative method will help the industry to overcome key barriers of modular construction: site access problems, site congestion issues, and the limited availability of local heavy lift equipment.

To make this new method application viable to the industry, the development of new batteries, motors, and propellers may require the next level of advancement (increasing size and capacity of motors and propellers, and changing power sources) in order to lift heavy modules. The researchers believe substantial efforts are necessary in the future to solve these issues. However, as scientists in the UAS domain have demonstrated, a system like a flying taxi, which will be commercially available shortly, can be solved within five years, considering the speed of recent technological advancements.

This study will lead to the development of a drone-based module transportation framework for practitioners in the construction industry, including but not limited to, general contractors, module fabricators, and module transporters.

5 Acknowledgments

The researchers would like to thank Dr. Paul Oh, Lincy Professor for Unmanned Aerial Systems at the University of Nevada, Las Vegas for his invaluable advice in this research.

References

[1] O'Connor J.T., O'Brien W.J. and Choi J.O. Critical Success Factors and Enablers for Optimum and Maximum Industrial Modularization. *Journal of Construction Engineering and Management*. 140(6):04014012, 2014.

[2] Eastman C.M. and Sacks R. Relative Productivity in the AEC Industries in the United States for On-Site and Off-Site Activities. *Journal of Construction Engineering and Management*, 134(7):517–26, 2008.

[3] Choi, J.O., O'Connor J.T., and Kim T.W. Recipes for Cost and Schedule Successes in Industrial Modular Projects: Qualitative Comparative Analysis. *Journal of Construction Engineering and Management*, 142(10):04016055, 2016.

[4] National Institute of Building Sciences (NIBS). 2014 Off-Site Construction Industry Survey. Washington, DC. 2014.

[5] Choi J.O. Links between Modularization Critical Success Factors and Project Performance. Ph.D. Diss. The University of Texas at Austin. 2014.

[6] O'Connor J.T., O'Brien W.J. and Choi J.O. Industrial Project Execution Planning: Modularization versus Stick-Built. *Practice Periodical on Structural Design and Construction*, :12, 2015.

[7] Nonami K., Kendoul F., Suzuki S., Wang W., and Nakazawa D. Autonomous Flying Robots. Springer Japan, Tokyo. 2010.

[8] Leutenegger S., Hürzeler C., Stowers A.K., Alexis K., Achtelik M.W., Lentink D., Flying Robots. *Springer Handbook of Robotics*, Springer International Publishing, Cham. p. 623–70 2016.

[9] Lindsey Q., Mellinger D. and Kumar V. Construction with quadrotor teams. *Autonomous Robots*, Springer US. 33(3):323–36, 2012.

[10] Willmann J., Augugliaro F., Cadalbert T., D'Andrea R., Gramazio F. and Kohler M. Aerial

Robotic Construction towards a New Field of Architectural Research. *International Journal of Architectural Computing*, SAGE Publications London, England. 10(3):439–59, 2012.

[11] Korpela C., Orsag M. and Oh P. Towards valve turning using a dual-arm aerial manipulator. *Intelligent Robots and Systems (IROS 2014), 2014 IEEE/RSJ International Conference On*, IEEE. p. 3411–6 2014.

[12] Korpela C., Orsag M., Danko T., Kobe B., McNeil C., Pisch R. Flight stability in aerial redundant manipulators. *Robotics and Automation (ICRA), 2012 IEEE International Conference On*, IEEE. p. 3529–30 2012.

[13] Danko T.W., Chaney K.P., and Oh P.Y. A parallel manipulator for mobile manipulating UAVs. *Technologies for Practical Robot Applications (TePRA), 2015 IEEE International Conference On*, IEEE. p. 1–6 2015.

[14] Fumagalli M., Naldi R., Macchelli A., Carloni R., Stramigioli S. and Marconi L. Modeling and control of a flying robot for contact inspection. *Intelligent Robots and Systems (IROS), 2012 IEEE/RSJ International Conference On*, IEEE. p. 3532–7 2012.

[15] Keemink A.Q.L., Fumagalli M., Stramigioli S. and Carloni R. Mechanical design of a manipulation system for unmanned aerial vehicles. *Robotics and Automation (ICRA), 2012 IEEE International Conference On*, IEEE. p. 3147–52 2012.

[16] Darivianakis G., Alexis K., Burri M. and Siegwart R. Hybrid predictive control for aerial robotic physical interaction towards inspection operations. *2014 IEEE International Conference on Robotics and Automation (ICRA)*, IEEE. p. 53–8 2014.

[17] Marconi L., Naldi R. and Gentili L. Modelling and control of a flying robot interacting with the environment. *Automatica*, Pergamon. 47(12):2571–83, 2011.

[18] Nikolic J., Burri M., Rehder J., Leutenegger S., Huerzeler C. and Siegwart R. A UAV system for inspection of industrial facilities. *2013 IEEE Aerospace Conference*, IEEE. p. 1–8 2013.

[19] PETROBOT. Petrobot Project. On-line: http://petrobotproject.eu/, Accessed: 07/07/2018.

[20] ARCAS. ARCAS Project. On-line: http://www.arcas-project.eu/, Accessed: 07/07/2018.

[21] EuRoC. European Robotics Challenges. On-line: http://www.euroc-project.eu/, Accessed: 07/07/2018.

[22] TOTAL. ARGOS Challenge. On-line: http://www.argos-challenge.com/en, Accessed: 07/07/2018.

[23] EHANG. EHANG 184. On-line: http://www.ehang.com/ehang184/, Accessed: 13/03/2019.

[24] Stewart J. BOEING'S FLYING TAXI PROTOTYPE TAKES TO THE AIR. On-line: https://www.wired.com/story/boeing-air-taxi-uber/, Accessed: 13/03/2019.

[25] Kikin D. CES 2019: Bell unveils a prototype of the Nexus convertiplane. On-line: https://beam.land/aviation/ces-2019-bell-unveils-a-prototype-of-the-nexus-convertiplane-1904, Accessed: 13/03/2019.

[26] Choi J.O., Chen X.B., and Kim T.W. Opportunities and challenges of modular methods in dense urban environment. *International Journal of Construction Management*, 2017.

[27] Akagi K., Yoshida M., Murayama K. and Kawahata J. Modularization Technology in Power Plant Construction. *10th International Conference on Nuclear Engineering*, Arlington, Virginia, USA. p. 641–7 2002.

[28] Jumbo_Shipping. Start of the first shipments for Pluto LNG project. On-line: http://www.yourindustrynews.com/news_item.php?newsID=12057, Accessed: 06/10/2010.

[29] Jameson P. Is modularization right for your project? *Hydrocarbon Processing*, 86(12):47–53, 2007.

[30] Deemer G.R. Modularization Reduces Cost and Unexpected Delays. *Hydrocarbon Processing*, 75(10):143, 1996.

[31] Pan W., Dainty A.R.J. and Gibb A.G.F. Establishing and Weighting Decision Criteria for Building System Selection in Housing Construction. *Journal of Construction Engineering and Management*, 138(11):1239–50, 2012.

[32] Moon M. Dubai tests a passenger drone for its flying taxi service. On-line: https://www.engadget.com/2017/09/26/dubai-volocopter-passenger-drone-test/, Accessed: 07/07/2019.

[33] Kim D. and Oh P.Y. Toward Lab Automation Drones for Micro-plate Delivery in High Throughput Systems. *2018 International Conference on Unmanned Aircraft Systems (ICUAS)*, IEEE. p. 279–84 2018.

Window-Warping: A Time Series Data Augmentation of IMU Data for Construction Equipment Activity Identification

K.M. Rashid[a] and J. Louis[a]

[a]School of Civil and Construction Engineering, Oregon State University, USA
E-mail: rashidk@oregonstate.edu, joseph.louis@oregonstate.edu

Abstract –

Automated, real-time, and reliable equipment activity identification on construction sites can help to minimize idle times, improve operational efficiencies, and reduce emissions. Many previous efforts in activity identification have explored different machine learning algorithms that use time-series sensor data collected from inertial measurement units mounted on the equipment. However, machine learning algorithms requires large volume of training data collection from the field, as inadequate and smaller amounts of data results in model overfitting. This study proposes an automatic and real-time activity recognition framework by using data from multiple IMUs attached to equipment's moving and articulated parts. In doing so, first a time-series data augmentation technique called *window-warping* (WW) is introduced to generate synthetic training data from a smaller volume of field-collected data. Two supervised machine learning algorithms, artificial neural network (ANN), and K-nearest neighbour (KNN) were trained and evaluated using the augmented training data to identify equipment activity. The developed data augmentation methodology is validated using a case study of an earthmoving excavator. The results show the potential for using time-series data augmentation in training machine learning algorithms for construction equipment activity recognition using minimal data collected from the field.

Keywords –

Data augmentation; Activity recognition; Time series; Construction equipment; Machine learning; IMU

1 Introduction

Automated, and real-time activity recognition of construction equipment plays an important role in construction operation analysis by enabling productivity monitoring [1-2], preparation of input for near real-time simulation [3–5], and automated cycle-time analysis [2-6]. It is also a key necessity for real-time safety applications on the construction site [7–9] and for automating environmental assessments [11-12]. Equipment activity identification can also enabled several applications in AR/VR visualization [12–15]. Despite being a necessary component for all the aforementioned applications, activity identification in construction site has historically been a manual effort. The manual approach of observing, recording, and analysing an equipment's action is prone to human error and requires excessive time, effort, and cost. In order to overcome these shortcomings, past efforts have investigated vision-based, as well as inertial measurement unit (IMU)-based activity recognition frameworks to automatically identify the activities that are performed by construction equipment in real-time or near real-time. Previous efforts in IMU-based frameworks have mostly used a single IMU attached to the equipment's cabin in order to capture the vibration of the equipment [9–11]. The vibration data were then used to train different machine learning algorithms that then classified an equipment actions. However, training machine learning algorithms requires a large volume of initial training data, which can be challenging to acquire from an active construction site due to the cost and effort inherent in such an endeavour that requires equipment and their operators to perform tasks that are extraneous to the work involved with their operation. Collecting data from an equipment during the course of its regular operations results in data that needs to be manually labelled and data that is non-uniformly distributed over the various activities that the equipment could be performing. These factors result in low-quality training data that result in poor performance of the training algorithm. Moreover, a small volume of training dataset poses a challenge in identifying a higher number of activities performed by the equipment as it creates an imbalance in the dataset. This paper describes a means for increasing the amount of training data for machine

learning algorithms for equipment activity identification by using the technique of data augmentation.

In the machine learning domain, specifically in object recognition, handwriting recognition, and speech recognition, data augmentation is a popular technique to generate synthetic training data when only small training sets are available [17]. By augmenting training data, errors of the classifiers due to variance can be reduced. The issue of model overfitting due to a dearth of learning examples can be overcome by introducing synthetic data generated by data augmentation. Even though literature is rife with examples that have applied data augmentation techniques for images, handwriting, and speech, data augmentation of time series data for classification purposes has not be fully explored yet.

This paper thus presents a real-time and automatic activity recognition framework for construction equipment using augmented data from multiple IMUs that mounted to articulated parts of the equipment. A time series data augmentation technique called *window-warping* (WW) is introduced to generate synthetic training data, thereby eliminating the need for obtaining large volume of field data. The developed framework is validated by carrying out a case study using an excavator from an actual earthmoving site.

This paper is organized as follows. First, a review of the state-of-the-art in IMU-based construction equipment activity recognition and data augmentation is provided to set the context for this research and highlight research gaps. Then, the methodology section discusses the main components of the proposed framework. Next, the results of the case study are presented. Finally, the results and main contribution of this work is summarized along with the limitations and future directions of this research.

2 Related Work

The framework presented in this paper consists of an activity recognition platform for construction equipment using multiple IMUs and a time-series data augmentation technique. This section provides a comprehensive literature review in IMU-based equipment activity recognition and data augmentation techniques in classification.

2.1 IMU-based Equipment Activity Recognition

IMU-based approaches for equipment activity recognition leverage the location and/or the vibration of the equipment in order to identify its activity at a specific time. El-Omari and Moselhi (2011) [18], and Ergen et al. (2007) [19] proposed a framework combining radio frequency identification (RFID) and global positioning system (GPS) technology for automated localization and tracking of construction equipment. Vahdatikhaki and Hammad (2014) [5] enhanced the performance of equipment state-identification approach by adopting a multi-step data processing framework combining location and motion data. Song and Eldin (2012) [20] developed an adaptive real-time tracking of equipment operation based on their location to improve the accuracy of project look-ahead scheduling. Although location-based operation tracking can identify the state and operation of construction equipment at a coarse level (e.g., *idle* and *busy* states), it is incapable of classifying the activities performed by equipment when it is stationary. Such limitations of location-based operation tracking have inspired researchers to explore the feasibility of both independent [10] and smartphone embedded [9 - 10] inertial measurement units (IMUs) for automated equipment activity recognition. Ahn et al. (2015) [10] used a low-cost accelerometer mounted inside the cabin of an excavator to collect operational data from an earthmoving worksite. Several classifiers were tested to classify three different states (i.e., engine-off, idle, and busy) of an excavator. Mathur et al. (2015) [6] utilized smartphone-embedded accelerometer by mounting it inside an excavator cabin to measure various activity modes (e.g., wheel base motion, cabin rotation, and arm movement) as well as duty cycles. Akhavian and Behzadan (2015) [16] adopted a similar approach by attaching a smartphone to the cabin of a front-end loader to collect accelerometer and gyroscope data during an earthmoving operation, upon which several classification algorithms (i.e., ANN, DT, KNN, LR, SVM) were tested. Their study also investigated the impact of different technical parameters such as level of details, segmentation window size, and selection of features on the performance of different classification algorithms. The same approach and technical parameters were further extended for construction workers [21].

2.2 Data Augmentation for Classification

Numerous data augmentation techniques have been tried and tested in computer vision [24–28] and speech recognition domain [29–31]. Charalambous and Bharath (2016) [24] introduced a simulation-based methodology which can be used for generating synthetic video data and sequence for machine/deep learning gait recognition algorithms. D'Innocente et al. (2017) [22] proposed an image data augmentation technique which zooms on the object of interest in an image and simulates the object detection outcome of a robot vision system. The goal of this paper was to bridge the gap between computer and robot vision, utilizing data augmentation. Most of the advanced object recognition algorithms utilizes various image augmentation techniques on images, such as flipping, rotating, scaling, cropping, translating, adding Gaussian noise etc. in order to generate synthetic data for

training and testing machine/deep learning algorithms [25,26,30]. Moreover, in the speech recognition domain, studies have applied techniques such as vocal tract length normalization [27-28], speech rate, and frequency-axis random distortion [27], label-preserving audio transformation [29] to improve the performance of learning algorithms.

Despite the frequent implementation of data augmentation techniques in the computer vision and speech recognition domains, data augmentation in time series classification have not been deeply investigated yet [31]. Guennec et al. (2016) [32] proposed two time series data augmentation techniques; window slicing, and window-warping to train a convolutional neural network (CNN). In order to reduce the variance of a classifier, Forestier et al. (2017) [17] introduced dynamic time warping (DTW) for time series classification. Um et al. (2017) [31] proposed the most comprehensive set of time series data augmentation techniques in order to monitor Parkinson's disease patients using wearable sensors.

2.3 Research Gaps and Point of Departure

Several machine learning approaches in IMU-based activity recognition for construction equipment have been explored in the recent past. Machine learning models usually benefit from larger training dataset because small and inadequate training data leads to model overfitting [33]. Moreover, small training dataset prevents a classification algorithm from learning parameters for identifying a higher number of classes due to an imbalance in data [16]. Furthermore from a practical standpoint, collecting large volume of IMU data from equipment operating in active construction sites poses challenges related to cost, time, and effort. In order to overcome these challenges, this paper aims to develop an equipment activity recognition framework which uses augmented training data, decreasing the effort of collecting large volume of field data. In doing so, a time-series data augmentation technique named *window-warping* (WW) is developed.

3 Methodology

The general architecture of the designed framework for data augmentation and classification is presented in Figure 1. In this methodology, accelerometer and gyroscope data are collected from multiple IMUs attached to different articulated elements of the equipment. The raw data is first divided into training and test data. The raw training data are used for data augmentation. The raw and augmented training data are combined together to train the machine learning algorithms. The trained models are then evaluated using the test data, separated at the beginning of the data processing.

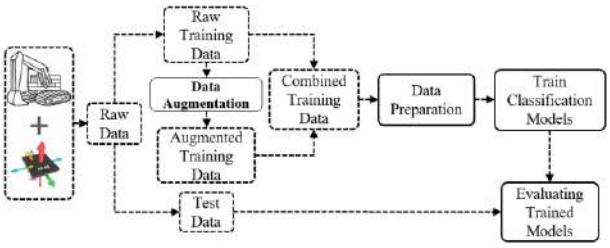

Figure 1. Developed framework for data augmentation and classification model

The following sections discusses the methodological details of data augmentation and model training.

3.1 Data Augmentation Using Window-Warping (WW)

Data augmentation can be regarded as an insertion of prior knowledge about the invariant properties of the data against certain transformations. The resulting augmented data can cover an unknown input space, prevent model overfitting, and increase the generalization capability of the classification model [31]. It is well known in the computer vision arena that minor changes (or augmentations) of the image in terms of jittering, scaling, warping, and rotating do not change the data labels as they can happen in real world observations. But not all data augmentation techniques implemented in computer vision domain are applicable to time-series data augmentation. This study utilizes a time-series specific data augmentation technique named *window-warping* (WW). Figure 2 provides a visualization of the WW augmentation technique proposed in this research. This data augmentation technique is implemented by warping the time-series data of each activity by speeding it up or down. This technique is logical in context of this research as the construction equipment can perform any specific

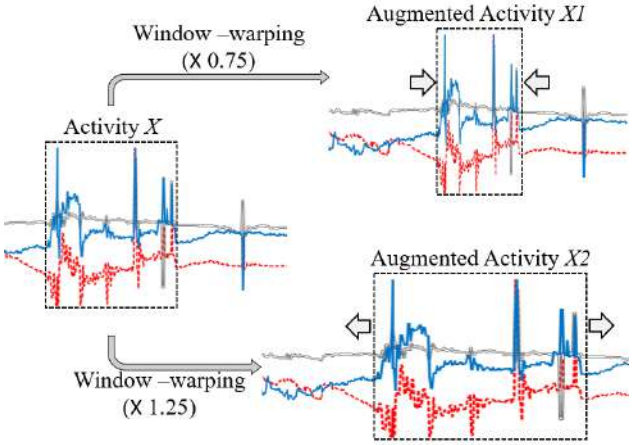

Figure 2. Window-warping (WW) data augmentation

activity at slightly different speeds. Thus, synthetic data

can be generated, which generalizes IMU data for different operational speeds of the equipment. In this paper, warping ratios of $1/2$, $3/4$, 1.25 and 1.5 were considered. In other words, the raw training data are speeded up to 1.25, and 1.5 times and slowed down up to $1/2$, and $3/4$ times. Figure 2 illustrates the WW technique with warping ratio $3/4$ (top), and 1.25 (bottom) for a specific activity *X*, which generates two augmented activities; *X1*, and *X2*. Applying four different warping ratio, training data are increased 5-fold, considering raw training data as 1-fold. This method generates training data of different lengths, which cause difficulties in training the machine learning algorithm. This issue is dealt with segmenting all training data (i.e., raw training data and augmented training data) with sliding window technique of fixed length and 50% overlap. More specifics about the data preparation and classification model training are discussed in following section.

3.2 Data Preparation

The data preparation step of the methodology includes data segmentation and feature extraction from the field-collected data. A single data point of the IMU sensor does not provide useful information about the activity of the equipment, since it just represents a momentary position of the equipment, similar to a snapshot image. In contrast, the activities of equipment consists of sequential motions distributed over a period of time, similar to a sequence of images or a video. Thus, data streams containing individual data points are segmented into data windows (i.e., consecutive time-series data points). In this paper, data windows of 1 second fixed length is considered with a 50% overlap between adjacent windows. After segmenting the time-series data into windows, a set of time-domain statistical features are extracted from each window. These features represent the pattern of the signal in the corresponding window and are eventually used as inputs in the classification algorithms. In this paper, 12 statistical features are extracted from each window, and they *are mean, maximum, minimum, standard deviation, mean absolute deviation, interquartile range, skewness, kurtosis* and, *4th order autoregressive coefficients*. Using these features as inputs, classification models are trained as discussed in the next section.

3.3 Training and Evaluation of Classification Model

Activity recognition frameworks are developed using both supervised and unsupervised classification models. However, since supervised learning algorithms provide better performance for equipment activity recognition [34], a network-based learning algorithm, *Artificial Neural Network* (ANN), and a distance based classification algorithm, *K-Nearest Neighbour* (KNN), are considered for training. Both ANN and KNN models are trained using the combined (raw and augmented) training data. After each model is trained, they are evaluated with the test data, which were separated from the raw data before the data augmentation phase. The performance of the model is evaluated using *accuracy*, *precision*, *recall*, and *F-1 score*. Confusion matrices are also generated in order to analyse inter-activity confusion of the trained model. The following section discusses the results of the case study carried out in this research, using motion data captured from an excavator.

4 Case Study and Results

In the case study, three IMUs were attached to the bucket, stick, and boom of an excavator. The excavator was operating on an earthmoving site, loading trucks with soils and levelling the ground. In addition to IMU data, video data were also collected for 2 hours for labelling purpose. The entire operation of the excavator was divided into 9 different classes: *Engine Off, Idle, Scooping, Dumping, Swing Loaded, Swing Empty, Moving Forward, Moving Backward*, and *Ground Levelling*. Raw data from the IMUs were labelled using the video, with numeric numbers (1 to 9) being assigned for each activity. Next, the raw data was separated into training and testing data with 50-50 ratio. Raw training data were used for the *window-warping* (WW) data augmentation, generating 4-fold augmented training data (with warping ratio of $1/2$, $3/4$, 1.25, and 1.5), thus increasing the volume of the training data 5- fold (4-fold augmented data plus raw training data). Table 1 summarizes the number of instances of each of the activity in raw and augmented dataset in the case study.

Table 1. No. of instances of raw and augmented data

		No of Instances				
Label	Act. Name	Raw data	Raw testing data	Raw training data	Augmented training data (4-fold)	Combined training data (5-fold)
1	Eng. off	166	83	83	332	415
2	Idle	34	17	17	68	85
3	Scooping	78	39	39	156	195
4	Dumping	81	40	41	162	203
5	Swi. Loaded	80	40	40	160	200
6	Swi. Empty	87	43	44	174	218
7	Mov. For.	5	2	3	10	13
8	Mov. Bac.	7	3	4	14	18
9	Grnd. Level.	17	8	9	34	43

For example, *Scooping* activity happened total 78 times during data collection, 39 of them were separated for testing, and 39 for training. 39 training instances were used for 4-fold WW augmentation, generating total 195 training instances for *Scooping*. Next, two supervised classifiers (i.e., ANN, and KNN) were trained for 9 classes of activities using combined 5-fold training data. Finally, the models were tested using the 50% raw test

data.

Figure 3 and Figure 4 illustrates the effect of WW data augmentation by comparing the use of 1-fold raw training data vs. 5-fold combined training data. From both the figures, we see that training the models with 5-fold augmented data improves their performance substantially from just training with raw training data. For example, the accuracy, precision, recall, and F-1 score of KNN improves from 51.7% to 97.9%, 49.5% to 96.4%, 44.2% to 96.8%, and 45.6% to 96.6% respectively by training the model with augmented data. It can also be observed that, improvement in the performance indices (i.e., accuracy, precision, etc.) is higher for KNN than ANN.

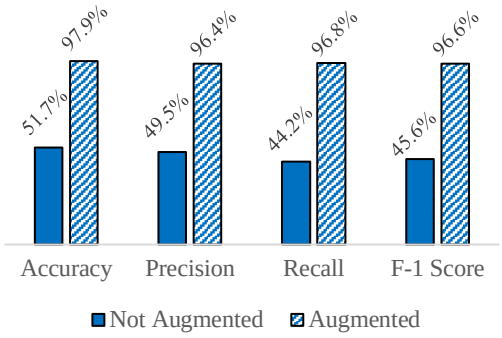

Figure 3. Performance measures of KNN

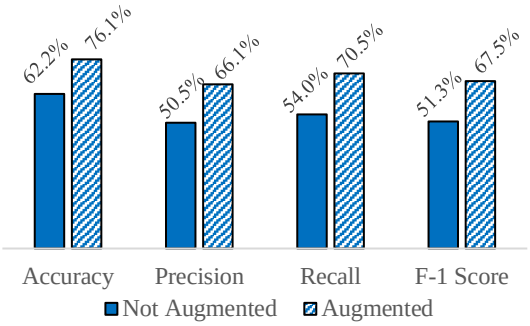

Figure 4. Performance measures of ANN

Next, a sensitivity analysis was conducted using different volume of training dataset (e.g., 1-fold, 2-fold, etc.) for the model training. KNN was trained with raw training data (i.e., 1-fold), 2-fold, 3-fold, 4-fold, and 5-fold augmented training data. Figure 5 illustrates that F-1 score of KNN increases with the volume of augmented training data. We see that KNN performs best for 5-fold training data, and worst for 1-fold training data.

Figure 6, and Figure 7 are confusion charts of KNN with 1-fold, and 5-fold training data, respectively. The confusion charts are generated to explore the improvement of inter-class confusion of the trained

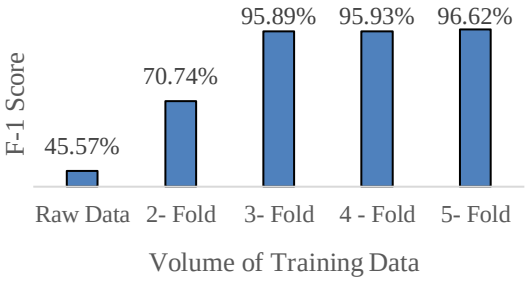

Figure 5. Performance of KNN for different volume of training data

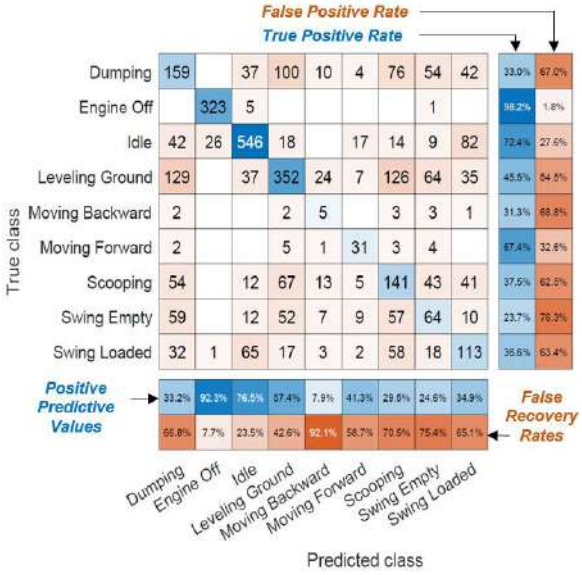

Figure 6. Confusion chart of KNN with 1-fold training data

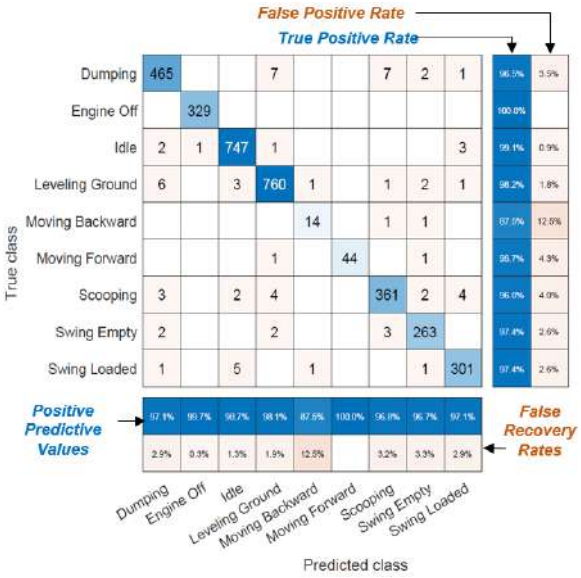

Figure 7. Confusion chart of KNN with 5-fold training data

model before and after data augmentation is implemented. Training the model without any augmented data (Figure 6) results in significantly higher percentages of error. Moreover, the KNN confuses in predicting activities with similar type of signal patterns such as, *Moving Forward* and *Moving Backward*, *Swing Empty* and *Swing Full*, *Scooping* and *Ground Levelling*, *Dumping* and *Ground Levelling* etc. On the other hand, error of the model decreases significantly while augmented data is used for the training (Figure 7). Also, the KNN can successfully identify similar kind of activities.

5 Conclusions and Future Work

Automated and accurate recognition of construction equipment's activity can help to improve productivity, safety, fuel use, and overall management and monitoring of the construction operations. To this end, this study presents an activity recognition framework for construction equipment using multiple IMUs. Moreover, as machine learning algorithms performs better for large volume of training data, a time series data augmentation technique, *window-warping* (WW) is proposed to generate synthetic training data. The methodology was validated using a comprehensive dataset collected from an excavator from a real construction site. The result of this study shows significant improvement in classifier's performance while using augmented training data. Specifically, data augmentation results in 51% and 16.2% increase in F-1 score for KNN, and ANN respectively. This indicates the potential of adopting data augmentation methods in equipment activity recognition which eliminates the necessity of collecting large volume of data from the field.

Future works of this study include testing the methodology for multiple types of equipment, such as loader, hauler, dump truck etc. Moreover, other types of time series data augmentation techniques will be explored to see their effect on the classification algorithms. Deep learning methods such as, convolutional neural network (CNN), recurrent neural network (RNN) will also be explored to analyse time series sequences for higher accuracy.

References

[1] Ahn, C. R., Lee, S., and Peña-Mora, F. (2015). "Application of Low-Cost Accelerometers for Measuring the Operational Efficiency of a Construction Equipment Fleet." Journal of Computing in Civil Engineering, 29(2), 04014042.

[2] Akhavian, R., and Behzadan, A. H. (2013). "Knowledge-Based Simulation Modeling of Construction Fleet Operations Using Multimodal-Process Data Mining." Journal of Construction Engineering and Management.

[3] Akhavian, R., and Behzadan, A. H. (2015). "Construction equipment activity recognition for simulation input modeling using mobile sensors and machine learning classifiers." Advanced Engineering Informatics, 29(4), 867–877.

[4] Akhavian, R., Brito, L., and Behzadan, A. (2015). "Integrated Mobile Sensor-Based Activity Recognition of Construction Equipment and Human Crews." Conference on Autonomous and Robotic Construction of Infrastructure, (Krassenstein).

[5] Brain, D., and Webb, G. (1999). "On the effect of data set size on bias and variance in classification learning." Proceedings of the Fourth Australian Knowledge Acquisition Workshop, 117–128.

[6] Carbonari, A., Giretti, A., and Naticchia, B. (2011). "A proactive system for real-time safety management in construction sites." Automation in Construction, Elsevier B.V., 20(6), 686–698.

[7] Charalambous, C. C., and Bharath, A. A. (2016). "A data augmentation methodology for training machine/deep learning gait recognition algorithms." 1–12.

[8] Cheng, T., and Teizer, J. (2013). "Real-time resource location data collection and visualization technology for construction safety and activity monitoring applications." Automation in Construction, Elsevier B.V., 34, 3–15.

[9] D'Innocente, A., Carlucci, F. M., Colosi, M., and Caputo, B. (2017). "Bridging between computer and robot vision through data augmentation: A case study on object recognition." Lecture Notes in Computer Science (including subseries Lecture Notes in Artificial Intelligence and Lecture Notes in Bioinformatics), 10528 LNCS(figure 2), 384–393.

[10] Ding, J., Chen, B., Liu, H., and Huang, M. (2016). "Convolutional Neural Network with Data Augmentation for SAR Target Recognition." IEEE Geoscience and Remote Sensing Letters, 13(3), 364–368.

[11] Dong, S., and Kamat, V. R. (2013). "SMART: scalable and modular augmented reality template for rapid development of engineering visualization applications." Visualization in Engineering, 1(1), 1–17.

[12] El-Omari, S., and Moselhi, O. (2011). "Integrating automated data acquisition technologies for progress reporting of construction projects." Automation in Construction, Elsevier B.V., 20(6), 699–705.

[13] Ergen, E., Akinci, B., East, B., and Kirby, J. (2007). "Tracking Components and Maintenance History within a Facility Utilizing Radio Frequency Identification Technology." Journal of Computing

in Civil Engineering, 21(1), 11–20.

[14] Forestier, G., Petitjean, F., Dau, H. A., Webb, G. I., and Keogh, E. (2017). "Generating synthetic time series to augment sparse datasets." Proceedings - IEEE International Conference on Data Mining, ICDM, 2017–Novem, 865–870.

[15] Golparvar-Fard, M., Heydarian, A., and Niebles, J. C. (2013). "Vision-based action recognition of earthmoving equipment using spatio-temporal features and support vector machine classifiers." Advanced Engineering Informatics.

[16] Le Guennec, A., Malinowski, S., and Tavenard, R. (2016). "Data Augmentation for Time Series Classification using Convolutional Neural Networks." 2nd ECML/PKDD Workshop on Advanced Analytics and Learning on Temporal Data.

[17] He, K., Zhang, X., Ren, S., and Sun, J. (2016). "Deep Residual Learning for Image Recognition Kaiming." ((ed.), Oxford, U.K., Pergamon Press PLC, 1989, Section 3, p.111–120. (ISBN 0–08–036148–X)), 1–9.

[18] Jaitly, N., and Hinton, G. E. (2013). "Vocal Tract Length Perturbation (VTLP) improves speech recognition." Proc. ICML Workshop on Deep Learning for Audio, Speech and Language.

[19] Kim, H., Ahn, C. R., Engelhaupt, D., and Lee, S. H. (2018). "Application of dynamic time warping to the recognition of mixed equipment activities in cycle time measurement." Automation in Construction, 87, 225–234.

[20] Ku, K., Tech, V., Mahabaleshwarkar, P. S., and Tech, V. (2011). "Bulding Interactive Modeling for Construction Education in Virtual Worlds." Journal of Information Technology in, 16(13), 189–208.

[21] Liang, M., and Hu, X. (2015). "Recurrent convolutional neural network for object recognition." Proceedings of the IEEE Computer Society Conference on Computer Vision and Pattern Recognition, 07-12-June-2015(Figure 1), 3367–3375.

[22] Louis, J., and Dunston, P. (2016). "Platform for Real Time Operational Overview of Construction Operations." Construction Research Congress ASCE, 2039–2049.

[23] Louis, J., Dunston, P. S., and Martinez, J. (2014). "Simulating and Visualizing Construction Operations using Robot Simulators and Discrete Event Simulation." Sixth International Conference on Computing in Civil and Building Engineering, 1179–1184.

[24] Mathur, N., Aria, S. S., T, A., Ahn, C. R., and Lee, S. (2015). "Automated Cycle Time Measurement and Analysis of Excavator's Loading Operation Using Smart Phoen-Embedded IMU Sensors." Proceedings of the 2015 International Workshop in Civil Engineering, June 21-23, 2015, Austin, Texas, 2015-(January), 730.

[25] Naoyuki Kanda, R. T. and Y. O. (2013). "ELASTIC SPECTRAL DISTORTION FOR LOW RESOURCE Research Laboratory , Hitachi Ltd ." 309–314.

[26] Radford, A., Metz, L., and Chintala, S. (2015). "Unsupervised Representation Learning with Deep Convolutional Generative Adversarial Networks." 1–16.

[27] Rashid, Khandakar, M., Datta, S., and Behzadan, Amir, H. (2017). "Coupling risk attitude and motion data mining in a preemtive construction safety framework." Proceeding of the 2017 Winter Simulation Conference, 4220–4227.

[28] Rashid, K. M., and Behzadan, A. H. (2018). "Risk Behavior-Based Trajectory Prediction for Construction Site Safety Monitoring." Journal of Construction Engineering and Management, 144(2), 04017106.

[29] Schlüter, J., and Grill, T. (2013). "Exploring Data Augmentation for Improved Singing Voice Detection With Neural Networks."

[30] Song, L., and Eldin, N. N. (2012a). "Adaptive real-time tracking and simulation of heavy construction operations for look-ahead scheduling." Automation in Construction, Elsevier B.V., 27, 32–39.

[31] Song, L., and Eldin, N. N. (2012b). "Adaptive real-time tracking and simulation of heavy construction operations for look-ahead scheduling." Automation in Construction.

[32] Um, T. T., Pfister, F. M. J., Pichler, D., Endo, S., Lang, M., Hirche, S., Fietzek, U., and Kulić, D. (2017). "Data Augmentation of Wearable Sensor Data for Parkinson's Disease Monitoring using Convolutional Neural Networks."

[33] Vahdatikhaki, F., and Hammad, A. (2014). "Framework for near real-time simulation of earthmoving projects using location tracking technologies." Automation in Construction.

[34] You, S., Kim, J. H., Lee, S. H., Kamat, V., and Robert, L. P. (2018). "Enhancing perceived safety in human–robot collaborative construction using immersive virtual environments." Automation in Construction, Elsevier, 96(March 2017), 161–170.

Comparative Study of Experienced and Inexperienced Operators with Auto-controlled Construction Machine

T. Hashimoto[a] and K. Fujino[a]

[a]Public Works Research Institute, Minamihara, Tsykuba-shi, Ibaraki-ken, 305-8516, Japan
E-mail: t-hashimoto@pwri.go.jp, fujino@pwri.go.jp

Abstract –

In the Japanese construction industry, it is predicted that during the next ten years, more than a million veteran technicians will retire, and a sudden shortage of experienced technicians will be inevitable. One way of countering this problem now being considered is the use of robotics technology to support inexperienced operators. To develop such systems, it is important to first quantitively compare differences of the working efficiency, working quality, operating methods etc. between experienced operator and inexperienced operator.

Hence, experiments were performed to compare how experienced operators and inexperienced operators execute base course material grading work using a motor grader. During the experiments, the time required to complete the work, and the finished height at a pitch of 1 m were measured in order to quantitatively identify working efficiency and working quality. To clarify operating methods, the line of sight of the operators during work was measured. Moreover, similar comparative experiments were performed with the introduction of MC to verify its impact on experienced and inexperienced operators.

Keywords –

Construction machine; Experienced operator; Inexperienced operator; Machine control

1 Introduction

In recent years, the number of young people entering the Japanese construction industry has been decreasing, and the veteran workforce is aging [1] (Figure 1). It is predicted that during the next ten years, more than a million veteran technicians will retire, and a sudden shortage of experienced technicians will be inevitable. The same patterns have appeared among construction machine operators, and a sudden shortage of experienced operators is predicted. One way of countering this problem now being considered is the use of robotics technology to support inexperienced operators. This means using robotics technology to perform some aspect of construction machine operation to assist inexperienced operators so that they can execute work at the same performance level as experienced operators. As a robotics technology that automates some of the operational work, machine control (MC) has already been introduced in motor graders and bulldozers [2][3]. MC refers to a system

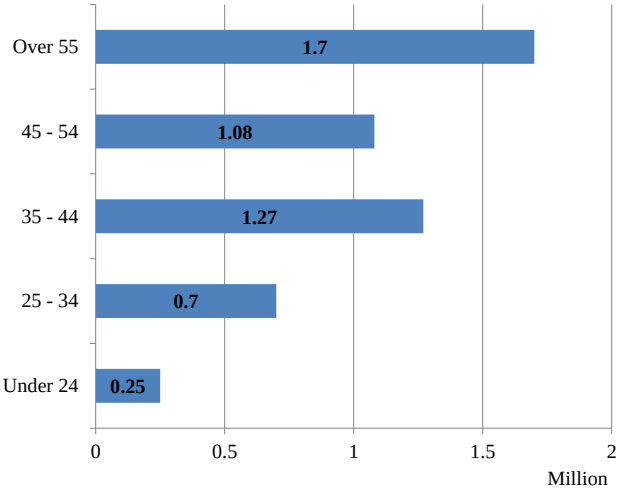

Figure 1. Labour force population by age group in construction industry (2015)

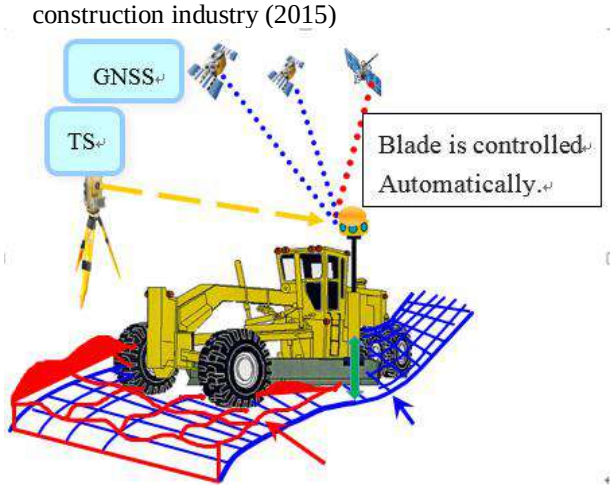

Figure 2. Machine control (MC)

that uses Total Station (TS), Global Navigation Satellite System (GNSS), etc. to identify the position of a construction machine, and calculates the discrepancy between the design value and the actual position of the working device (blade, etc.) so that the working device is automatically controlled in real time to remain in a position that conforms to the design value (Figure 2 [2]). It is presumed that expanding this kind of robotics technology to other types of machines and other types of work would be an effective measure of countering the future shortage of experienced operators. To develop such systems, it is important to first quantitively compare differences of the working efficiency, working quality, operating methods etc. between experienced operator and inexperienced operator. However, while differences between these two classes of operators have been partially verified, for excavation by hydraulic excavators for example [4][5], these differences have not yet been quantitatively confirmed. In order to evaluate the present state of MC and develop it further, it is important to also clarify the effects of MC on working efficiency, working quality, and on the operators. No studies that quantitatively clarify such effects of MC have been conducted.

Hence, experiments were performed to compare how experienced operators and inexperienced operators execute base course material grading work using a motor grader. During the experiments, the time required to complete the work, and the finished height at a pitch of 1 m were measured in order to quantitatively identify working efficiency and working quality. To clarify operating methods, the line of sight of the operators during work was measured with reference to the line of sight measurements used in the field of automated driving [6][7]. Moreover, similar comparative experiments were performed with the introduction of MC to verify its impact on experienced and inexperienced operators.

2 Outline of the Experiments

2.1 Outline of the Experiments

A subgrade with a width of 6 m and total length of 65 m (straight: 45 m, curved: 20 m) was prepared, and a motor grader was used to experimentally grade the base course material (M40) so as to generate a 30 cm thick layer on the subgrade. Each operator used the same motor grader (KOMATSU DG655) to perform the work, once without MC ("normal operation"), and once with MC ("MC operation"). The view of the experiment is shown in Figure 3.

2.2 Operators

The ten operators shown in Table 1 performed the experiment. Operators A, B, C, and D were experienced operators with at least 15 years of experience, and operators E, F, G, H, I, and J were inexperienced operators with less than 10 years of experience.

2.3 Measurement of the Data

The following data were collected:

(1) Working time: time from the start of each work

Figure 3. The view of the experiment

Table 1. Operator

	age	Year of experience	
A	57	35	Experienced Operator
B	52	33	
C	37	17	
D	36	16	
E	31	9	Inexperienced Operator
F	30	8	
G	24	6	
H	24	2	
I	23	5	
J	22	1	

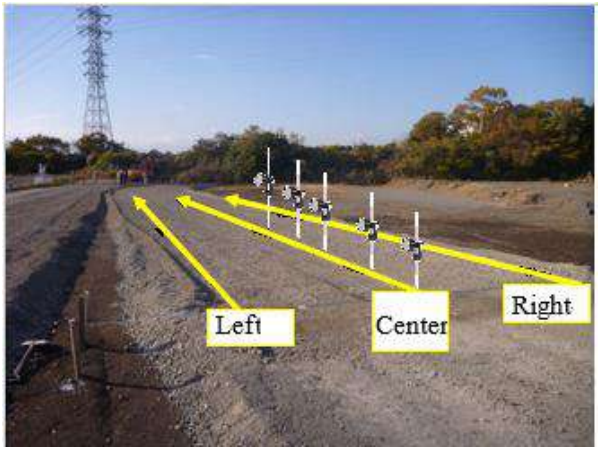

Figure 4. Finished height measuring points

until the height at the measurement points (every 10 m) was within 1 cm of the designed height (Japanese standard).

(2) Finished height: height at a pitch of 1 m along three measurement lines—center, right, and left—after completion of the work, measured by TS (Figure 4).

(3) Operator's line of sight: operator's line of sight during the work. This measurement was taken with an eye tracking system (NAC, EMR-9, Figure 5), and only during the operation of operators A, C, E, G, and H.

(4) Operator's heart rate: the heart rate of each operator during work was measured by a heart rate monitor (EPSON, SF-850, Figure 6) , and only during the operation of operators A, C, E, G, and H.

3 Results of the Experiments

3.1 Working Time

Figure 7 shows the average actual working times of experienced operators and inexperienced operators for normal and MC operation. The actual working times include only the time spent grading, and do not include time spent backing up, or measurement time.

According to Figure 7, in the case of normal operation, the working time of inexperienced operators is approximately 1.8 times that of experienced operators, which shows that the working efficiency of inexperienced operators is much lower than that of experienced operators. For this reason, it can be surmised that the future shortage of experienced operators will have a serious impact on the construction industry, and that it is necessary to implement countermeasures such as the introduction of robotics technology.

In the MC operation, working time of inexperienced operators was approximately 40% shorter than it was when they performed normal operation, while the working time of experienced operators was almost the same for normal operation and MC operation. For this reason, it can be inferred that MC had a considerable effect on inexperienced workers, and that introducing MC could enable inexperienced operators to work at a working efficiency equal to that of experienced operators. Meanwhile, there was almost no difference between the normal operation working time and MC operation working time of experienced operators, revealing that MC had little impact on the experienced operators.

3.2 Finished Height

As an example of the results, Figures 8 and 9 show the measurements of finished heights for operator D (an experienced operator) and operator J (an inexperienced operator). The horizontal axis of the figure represents the working length (total length: 65 m) and the vertical axis represents the difference between the measurement data and designed (target) height.

Figures 8 and 9 show that it is possible to estimate working quality based on the discrepancy between

Figure 5. Eye tracking system

Figure 6. Heart rate monitor

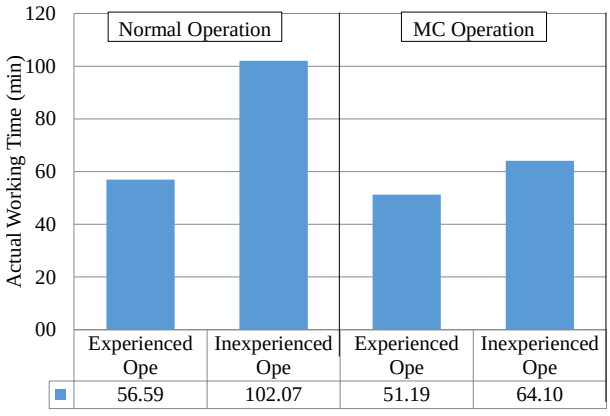

Figure 7. Actual working times

actual height and target height. It can be presumed that the working quality of the normal operation by operator D is better than that by operator J, and that the working quality for the MC operation by operator D and that by operator J are not very different.

To quantitatively represent working quality, all the finished height measurement data obtained for experienced operators and for inexperienced operators are represented by frequency polygon (frequency line graphs) in Figures 10 and 11. The figures also indicate the standard deviations.

According to Figures 10 and 11, in the case of

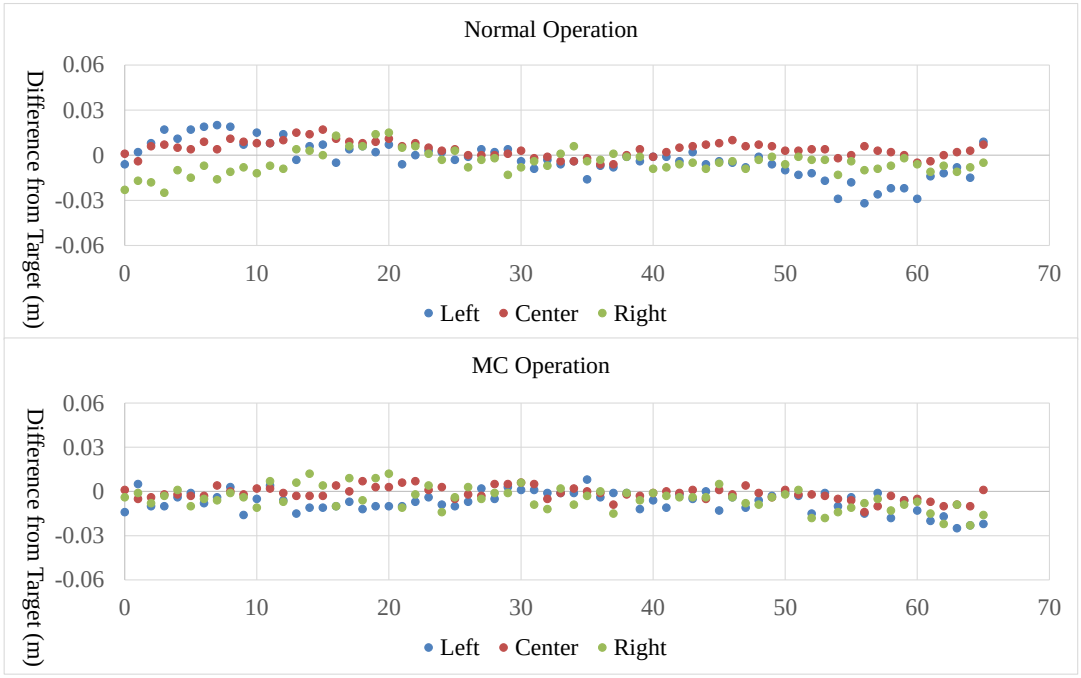

Figure 8. Finished height of operator D (experienced operator)

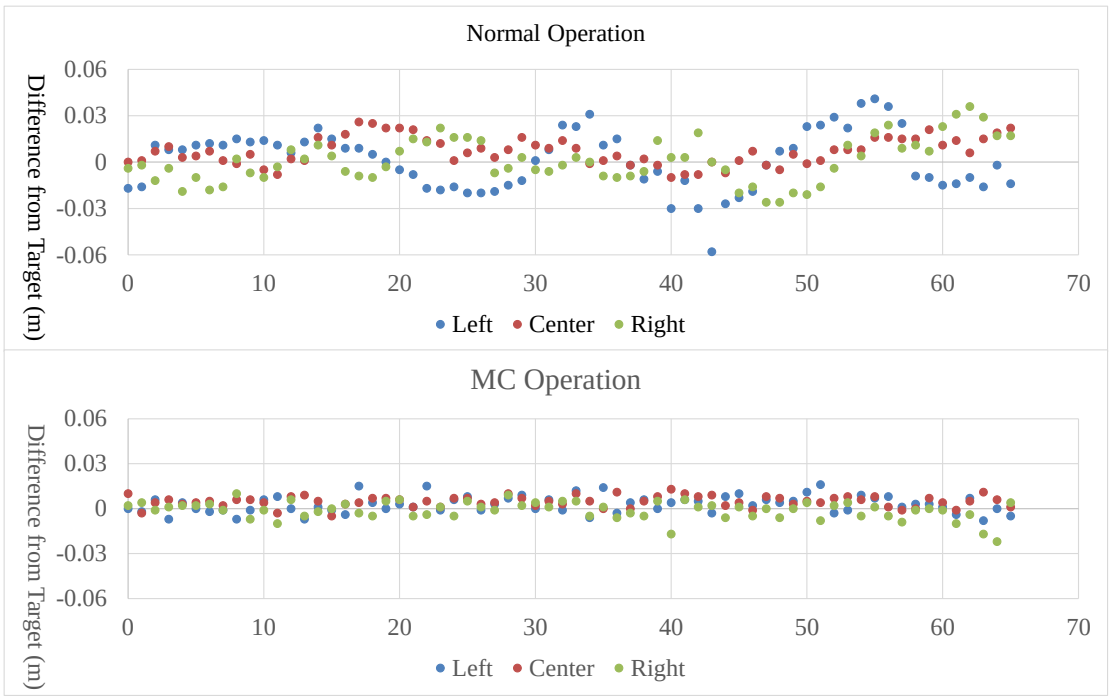

Figure 9. Finished height of operator J (inexperienced operator)

normal operation, the standard deviation of inexperienced operators is approximately double that of experienced operators, indicating that the working quality of inexperienced operators is much lower than that of experienced operators. For this reason, it can be stated that, as shown by the working time results in the previous section, the future shortage of experienced operators will seriously impact the construction industry, requiring countermeasures in the future, such as those based on robotics technology.

The standard deviation of inexperienced operators in MC operation was approximately 50% lower than it in normal operation, while the standard deviations of experienced operators in normal operation and MC operation were almost equal. Similar to the working time results shown in the previous section, this reveals that MC has a considerable effect on inexperienced operators, and that introducing MC could enable inexperienced operators to work with an working quality equal to that of experienced operators. While the effects of MC on experienced operators would be minimal.

3.3 Line of Sight of Operators

In order to organize the line-of-sight analysis data, the view of the operator is divided into three as shown in Figure 12, "near (the blade)", "forward," and "other" (outside the range of Figure 12, at monitors, etc.). And the time ratio of looking at each is shown in the Figure 13. Unfortunately, line-of-sight data during MC operation for operators C and G could not be obtained.

According to Figure 13, in the case of normal operation, the percentage of time that operators A and C (experienced operators) were watching "near (the blade)" were about 70%. On the other hand, that of operators E, G, and H (inexperienced operators) were 80% and 90%. From this, it is presumed that the inexperienced operators concentrated primarily on the area "near (the blade)" that was grading the base course material, and could not identify the state of the surroundings, but that the experienced operators paid attention to the area ahead, permitting them to predict the course the machine would travel smoothly and work high-quality.

In the MC operation case, the percentage of time that operators E and H (inexperienced operators) paid attention to the area "near (the blade)" fell substantially. This presumably occurred because, thanks to MC, they did not have to pay much attention to the blade operation, giving them opportunity to observe the

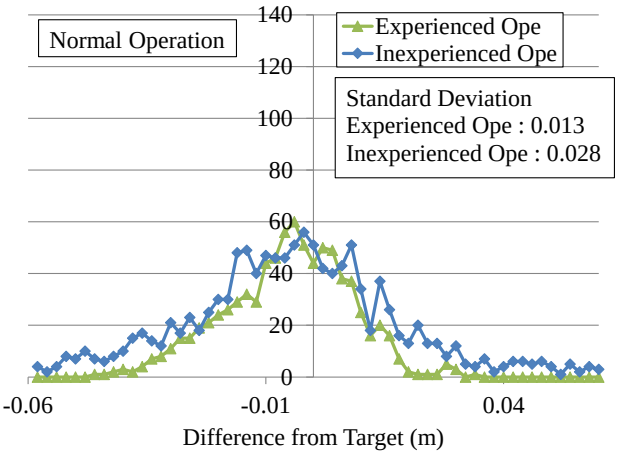

Figure 10. Frequency polygon of finished height data in normal operation

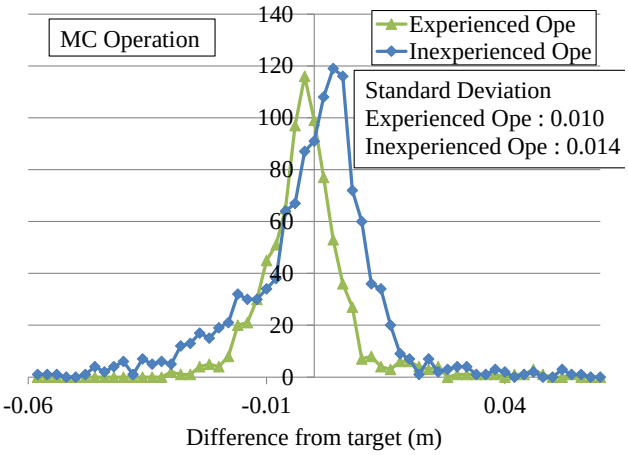

Figure 11. Frequency polygon of finished height data in MC operation

Figure 12. Operator's view

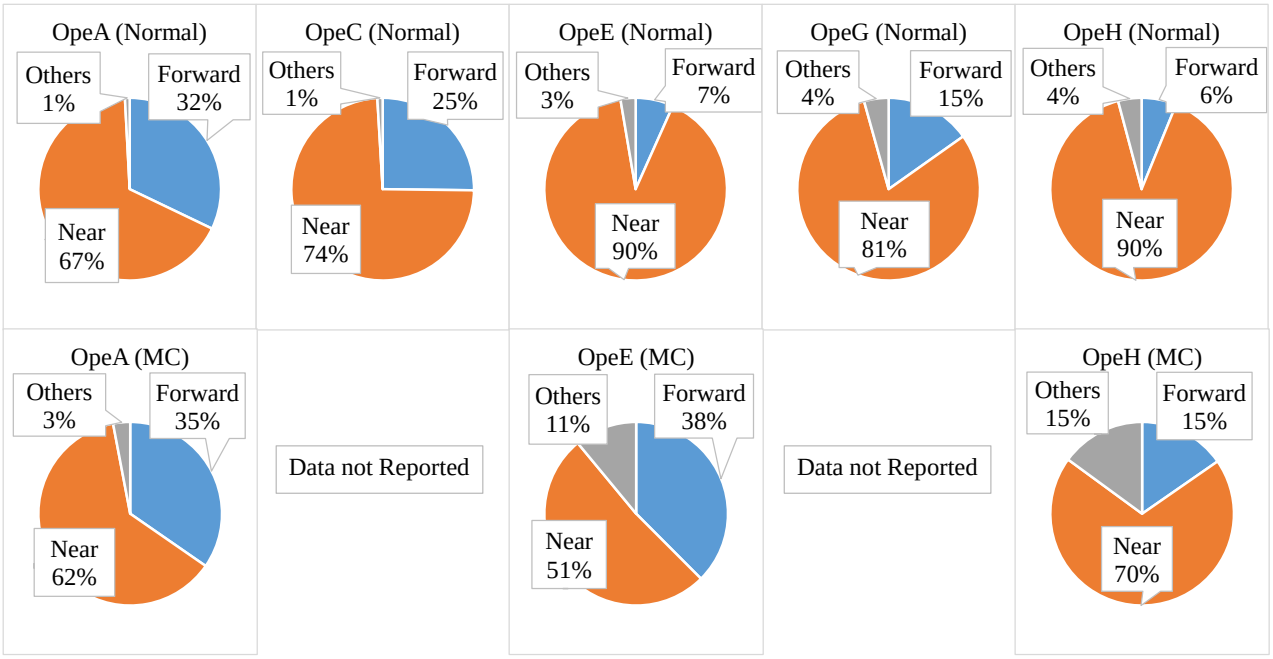

Figure 13. Time rate of looking

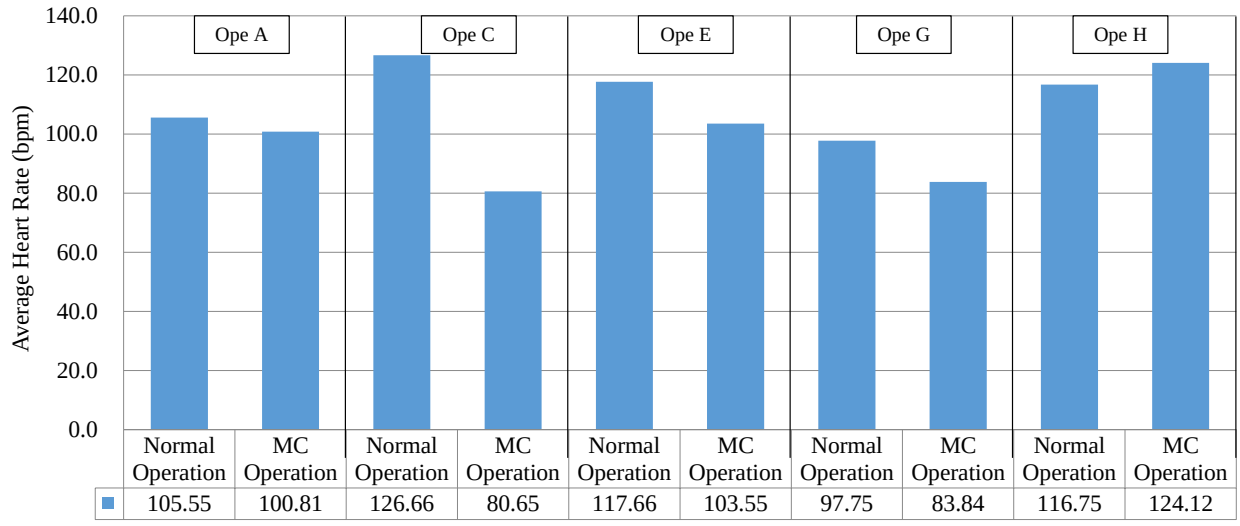

Figure 14. Average heart rate during operation

surroundings. For this reason, it can be stated that the introduction of MC would not only permit inexperienced operators to smoothly perform high-quality work, but it would also permit safer operation as they pay more attention to the surrounding conditions.

Meanwhile, it also shows that like working time and finished height, the line of sight of experienced operators would not be greatly affected by MC.

3.4 Heart Rate During Operation

To verify the effects of MC on operator mental burden, operator's heart rate during operation was measured. The average heart rate during operation are shown in Figure 14.

According to Figure 14, during MC operation, the average heart rate of all operators except operator H were lower than they were during normal operation. It is difficult to draw a conclusion based solely on heart rate, but results suggest that the introduction of MC could lower the mental burden of both experienced and inexperienced operators.

4 Summary

This study compared the working result of experienced operator and inexperienced operator when grading base course material using a motor grader. And also this verified the impacts that MC would have on both operators too. The results illustrated the following points:

(1) In the case of normal operation, the working time and finished height standard deviations of inexperienced operators are approximately double those of experienced operators, revealing that the working efficiency and working quality of inexperienced operators are much lower than those of experienced operators. This shows that the future shortage of experienced operators will have a serious impact on the construction industry, and that it is necessary to implement countermeasures such as the introduction of robotics technology.

(2) According to the line-of-sight analysis results, inexperienced operators concentrated only on the area "near (the blade)" that was grading the base course material, and thus they could not observe the surrounding conditions, experienced operators paid attention to the area ahead of the machine and predicted its travel path to smoothly perform high-quality work.

(3) MC had a considerable impact on the working time, finished height standard deviations, and line of sight of inexperienced operators, and the introduction of MC could permit inexperienced operators to achieve working efficiency, working quality, and safety equal to that of experienced operators.

(4) In the case of experienced operators, on the other hand, MC had only minimal effect on working time, finished height standard deviation, and operator line of sight.

(5) Introducing MC could lower the mental burden on both experienced and inexperienced operators.

The aging of experienced technical workers, and the oncoming shortage of these workers in Japan's construction industry poses serious challenges. This study has clearly shown that if the situation remains unchanged, it is highly likely that the construction industry will be seriously impacted. It has been confirmed that the use of MC or other robotics technology would be an effective way to counter these problems. In the future, we wish to continue conducting research intended to introduce robotics technology in machines other than motor graders. And also we wish to research to fully automate these machines instead of automating only some machine operations.

References

[1] Japan Federation of Construction Contractors. Handbook of Construction Industry 2016. p.19, 2016.

[2] TOPCON. Machine control system mechanism. On-line:https://www.topcon.co.jp/en/about/ business /positioning/mc/ , Accessed: 26/11/2018.

[3] Trimble Grade Control for Motor Graders. On-line : https://construction.trimble.com/products-and-solutions/grade-control-motor-graders , Accessed: 26/11/2018.

[4] Sakaida Y. Yamamoto H. Shao H. Nozue A. and Yanagisawa Y. Analysis of Skillful Hydraulic Excavator Operation. *Symposium on Construction Robotics in Japan*, Vol.11, pp.263-270, 2008.

[5] Miyata K. Skill Transfer Method for Construction for Construction Machine Operators. *Symposium on Human Interface in Japan*, p.1442, 2007.

[6] Seya Y. Nakayasu H. and Miyoshi T. A study on visual search strategies in driving by an eye movement analysis. *IEICE Technical Report*, Vol.107, No.369, pp.125-130, 2007.

[7] Underwood G. Chapman P. Brocklehurst N. Underwood J. and Crundall D. Visual attention while driving: sequences of eye fixations made by experienced and novice drivers. *Ergonomics*, Vol.46, No.6, pp.629-646, 2003.

Design, Modelling and Simulation of Novel Hexapod-Shaped Passive Damping System for Coupling Cable Robot and End Effector in Curtain Wall Module Installation Application

M. Taghavi[a], T. Kinoshita[a], and T. Bock[a]

[a]Department of Architecture, Chair of Building Realization & Robotics, Technical University of Munich, Germany
E-mail: meysam.taghavi@br2.ar.tum.de, taku.kinoshita@tum.de, thomas.bock@br2.ar.tum.de

Abstract –

The application of robotics in the construction industry has been growing recently. However, it suffers from the lack of construction dedicated systems. The industry is characterised largely by designers and researchers scrambling to adapt systems from other industries and trying to apply them to the construction industry. In the application of Curtain Wall Module (CWM) installations, "HEPHAESTUS" is a European founded project that is engaged in designing a Cable Driven Parallel Robot (CDPR) automatic system capable of 1 mm positioning accuracy. It can perform other tasks such as drilling on the building by using a dedicated Modular End Effector (MEE). Conventional CWM installation from the outside of the building can be done in the case of 15 m/s wind but, to be competitive, the automatic cable robot system should be able to perform the task in similar outdoor situations. However, the cable robot – like other mechanical systems – has a specific stiffness which means that it could move slightly in the event of an external load such as wind, depending on the exerted load and stiffness. This movement should not be transferred to the final tool (e.g. the driller) while it's performing tasks on the building. To prevent or minimise the effect of the external load on the final tool in the chain of the mechanically connected system, a damping system should therefore exist. This paper introduces the novel hexapod-shaped passive damper. The damping system will be mathematically modelled and simulated using the Matlab Simscape software. The simulation results give logical consequences on the design. The designed damper and model can be used in other applications or dimensions with some simple modifications.

Keywords –

Construction robotics; Design; Modelling; Simulation; Passive damper; Hexapod; Cable robot; Façade installation

1 Introduction

The construction industry plays a crucial role all over the world. In many countries, it supports the economy, the development of other industries and helps maintain high employment rates [1], [2]. However, some tasks at construction sites involve dangers and risks and, in addition to this, need performance improvements. As a consequence of these challenges, the study of automatic construction robotics has recently been growing [3], [4] and [5].

The installation of a Curtain Wall Module (CWM) is one of such instances where high labour effort is required. This task involves several hazards for manual workers because it is performed on the outer edges and top floors of incomplete buildings. In addition, this operation is time consuming as it requires a lot of attention for completion. Therefore, automatic installation of curtain walls is required on grounds of safety and productivity [6].

This study is part of the HEPHAESTUS project [7], which was founded by the European Union. The focus of the project is on the installation of a Curtain Wall Module (CWM) as it is considered to be a high risk, yet critical, construction task [8]. The Cable Driven Parallel Robot (CDPR) moves on the face of a building and carries the CWM, while the Modular End Effector (MEE) works on the CDPR platform to set the brackets which are needed in advance for the installation of the CWM [9].

Excessive vibration from the CDPR caused by live loads like wind load could prevent the MEE from functioning properly while performing tasks such as drilling. Therefore, a damping system is necessary. A damping system is crucial because, when the frequency of vibrations from external forces is the same as the natural frequency of the structure, the structure may collapse like the Tacoma Narrows Bridge in 1940. Globally, there are many different kinds of damping systems. For example, a Tuned Mass Damper (TMD)

consists of a mass, a spring and a viscous damper, and is used to reduce the amplitude of vibration of a structure caused by environmental forces or other factors. The largest and heaviest TMD is situated in the Taipei 101 skyscraper in Taiwan [10], [11]. There are other ways to classify damping systems: passive, semi-active and active [12]. The passive damper does not need an energy input, i.e. electricity. On the other hand, the active damper has actuators that require a high quantity of energy to function. The semi-active damper has variable dampers that require less energy than the active damper. The passive damper is less efficient than the active damper; however, it is cheaper and less complex. An example of an active damper that is in use is an active stabiliser for the CDPR which was developed by (Lesellier et al, 2018)e [13].

A hexapod-shaped spring-damper was applied in this paper as a passive damping system, which is represented by the Stewart Platform [14]. A hexapod is a 6-DOF robotic parallel manipulator. Although it is light and compact, it has a large payload. A hexapod is used in many other fields of study [15] such as milling machines, flight simulators or in medical science.

In this paper, first the design of a hexapod-shaped spring-damper between a cable robot and an MEE is proposed and modelled. Next, the analysis of the kinematics and dynamics of that model and simulation in Matlab® is presented. Finally, a conclusion is derived from the results that were obtained.

2 Passive Damper Design

In the application of the HEPHAESTUS project, a fully constrained cable-driven parallel robot (CDPR) [8] exists on one end and on the other end there is a Modular End Effector (MEE) [9] which is gripped to the side of the building when in operation. Between these two mechanical components, there is a passive damper that was designed as shown in Figure 1.

For the tasks of the MEE to be performed with precision on the building, it is required that its base remains stable throughout the duration of the task.

Figure 2 shows the connection in a simplified manner, for example, the CDPR connection to the building and the ground are shown with just one connection and spring whereas, in reality, it consists of 6-9 cables providing the stiffness and damping in six dimensions including three translational and three rotational. As demonstrated in [16] and [17], studies have been carried out in this area. On the design of the CDPR, the stiffness could be one of the design parameters. Put simply, the higher stiffness means stronger cables, motor and gearboxes, which is one of the design constraints.

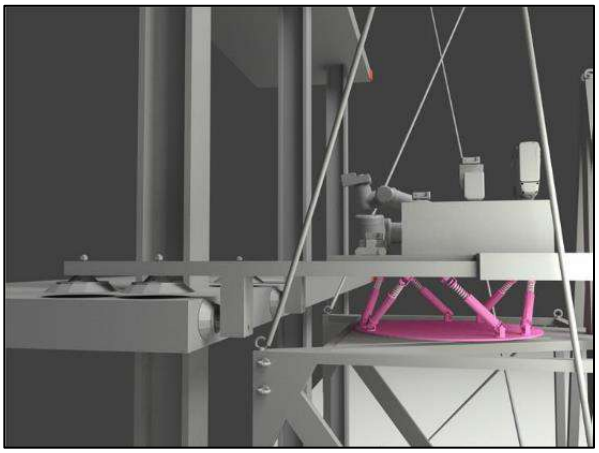

Figure 1. Hexapod-shaped damping system between the MEE and CDPR

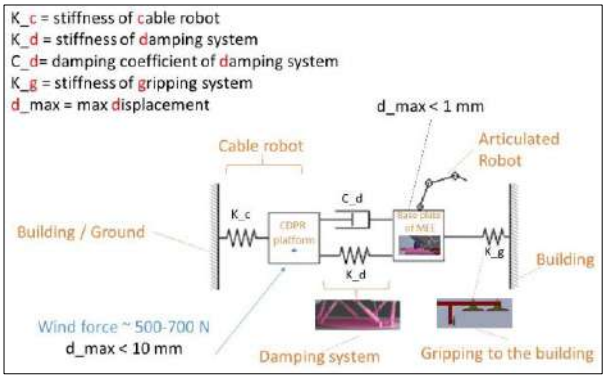

Figure 2. The chain of systems mechanically coupled

For the application of the HEPHAESTUS project, it is considered that the maximum displacement of the CDPR platform is less than 10 mm in the case of a wind force of 700 N which is caused by a 15 m/s wind speed on the CWM with a size of 150×350 cm. The relationship between these parameters can be seen using the following equation from [18]:

$$\boldsymbol{F}_W = \boldsymbol{p}_d A = \frac{1}{2}\rho v^2 A \quad (1)$$

where $\boldsymbol{F}_W$ = wind force (N), A = surface area (m^2), $\boldsymbol{p}_d$ = dynamic pressure (Pa), ρ = density of air (kg/m^3), and v = wind speed (m/s). ρ is equal to 1.2 kg/m^3at 20° C. $\boldsymbol{F}_W$ is an estimation of the force, caused by the pressure acting on a surface. The surface slows the air and the dynamic energy in the wind is transformed into pressure. Here, the drag force is not considered.

This research focuses solely on the damping system of the chain shown in Figure 2. The final goal of the design is to keep the maximum displacement of the MEE base to less than 1 mm, while keeping the displacement of the "connection point of MEE and

CDPR" other end to a maximum of 10mm. To do so, a model of the damper is required, which is the main subject of this paper. The model is generic, which means that the dimensions (size of the linear cylinder as well as the diameter of the upper and lower plate of the damper) and physical characteristics (mechanical properties e.g. damping and spring coefficient of each linear axis) could be adjusted based on the output requirements which is the maximum displacement.

In the following sections, the mathematical model of the design, together with the dynamic model and simulation in the Matlab® Simscape™ program, are explained.

2.1 Mathematical Modelling

Mathematical modelling of hexapods has been performed in previous researches. Forward kinematics and inverse kinematics have also been studied, as can be seen in [19] and [20]. Although there are researches about the dynamics of the active hexapod e.g. [21] and [22], few studies exist that focus primarily on the dynamics of the passive hexapod. In the passive hexapod model, the following equation can be established:

$$\boldsymbol{f} = -\boldsymbol{K}(\boldsymbol{l} - \boldsymbol{l}_r) - \boldsymbol{C}\dot{\boldsymbol{l}} \qquad (2)$$

where, $\boldsymbol{f}$ is the 6×1 vector of forces exerted at the bottom of the strut from each strut; $\boldsymbol{K}$ and $\boldsymbol{C}$ are the 6×6 matrices containing the stiffness and damping of each strut respectively; $\boldsymbol{l}$ is the 6×1 vector of the strut lengths; $\boldsymbol{l}_r$ is the constant 6×1 vector of the relaxed strut lengths.

Then, the force P and the moment M about the tool point position are given by:

$$\begin{bmatrix} P_x \\ P_y \\ P_z \\ M_x \\ M_y \\ M_z \end{bmatrix} = -\begin{bmatrix} u_{1x} & u_{2x} & u_{3x} & u_{4x} & u_{5x} & u_{6x} \\ u_{1y} & u_{2y} & u_{3y} & u_{4y} & u_{5y} & u_{6y} \\ u_{1z} & u_{2z} & u_{3z} & u_{4z} & u_{5z} & u_{6z} \\ J_{1x} & J_{2x} & J_{3x} & J_{4x} & J_{5x} & J_{6x} \\ J_{1y} & J_{2y} & J_{3y} & J_{4y} & J_{5y} & J_{6y} \\ J_{1z} & J_{2z} & J_{3z} & J_{4z} & J_{5z} & J_{6z} \end{bmatrix} \boldsymbol{f} \qquad (3)$$

where, $\boldsymbol{u}_i = [u_{ix} \quad u_{iy} \quad u_{iz}]$ is the unit vector of the ith strut; $\boldsymbol{J}_i = \boldsymbol{u}_i \times \boldsymbol{b}_i$; $\boldsymbol{b}_i$ is the vector from the centre of the base body to the attachment point of the ith strut. Figure 3 shows a schematic of a mathematical model of the hexapod described above.

This Mathematical model relates the forces $\boldsymbol{f}$ at the bottom of each strut to the forces P and the moments M at the centre of the top plate (tool point position). The mathematical model is introduced here to give the reader an understanding of how the dynamic system works within the theoretical framework of the paper.

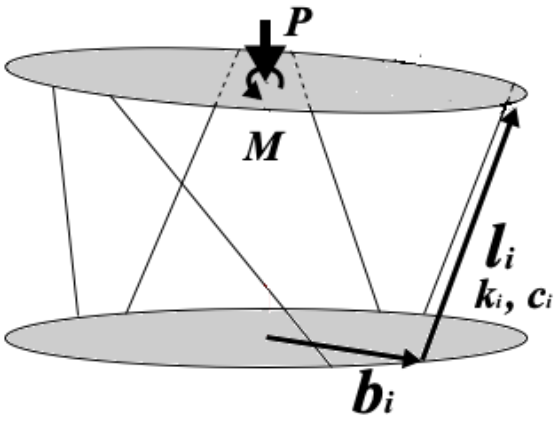

Figure 3. The mathematical model of the hexapod

2.2 Simscape™ Model in Matlab®

For simulation by the Simscape™ environment of Matlab® software, the CAD model in AUDODESK® INVENOR® software is first created and then imported to Simscape Multibody™. The relation and assembly constraints were carefully selected to automatically drive to a Simscape™ proper joint. The material and weight of the physical part were selected so as to resemble stainless steel, the material that the component will most probably be made out of. Once they are all imported, the Simscape™ model was edited to most closely resemble what the system is like in reality. Figure 4 shows the first level of the multibody diagram.

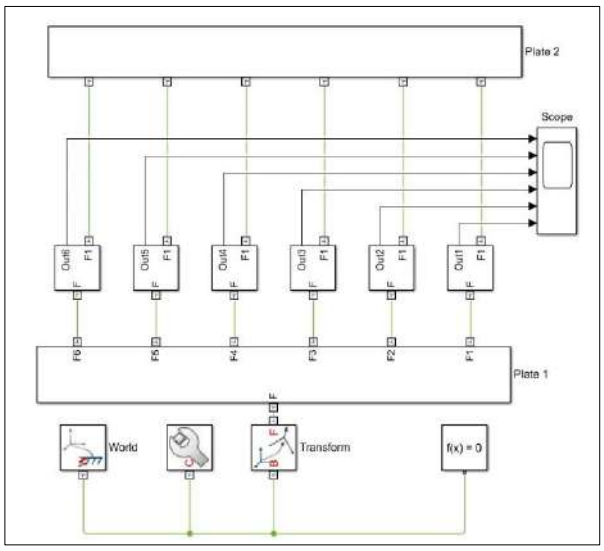

Figure 4. The first level of the multibody diagram

As shown in Figure 4, there are two plates which have between them six spring-damper cylinders. A scope module is also inserted to show the result of the

simulation which is, in this paper, the position of each cylinder. Although several results could be extracted from this model, e.g. the force on each cylinder and the speed of each of them, their positions in this model are shown as an illustration. It would be possible for one to extract more results from this model.

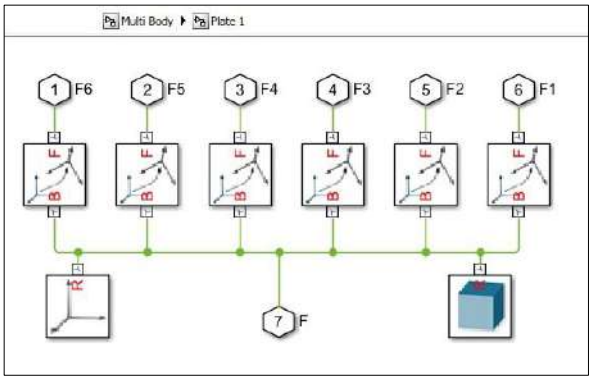

Figure 5. The lower plate of the multibody diagram

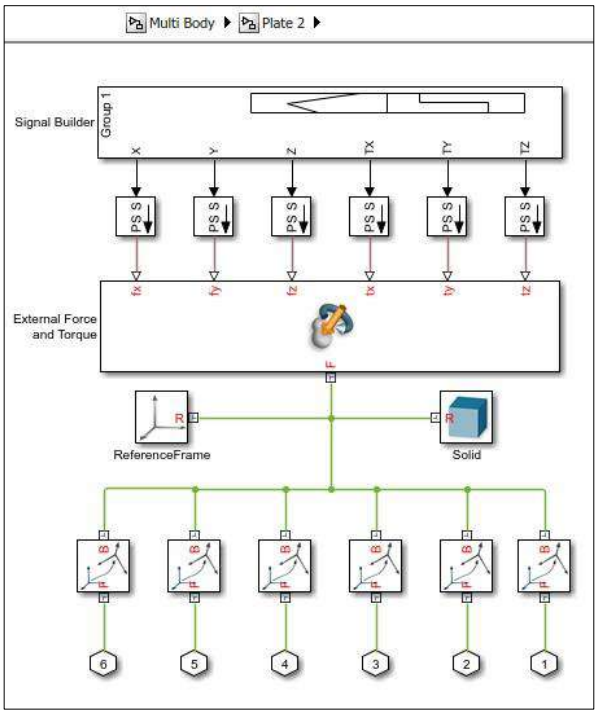

Figure 6. The upper plate of the multibody diagram

In this model, it is considered that the lower body is fixed, as shown in Figure 5, and that the upper body is free to move. Sample forces and torques are applied on the upper body in all directions. The diagram of the upper plate is shown in Figure 6. The purpose of this model is to provide a demonstration on how the model works in general.

Each of the spring-damper cylinders is modelled in Simscape™ with a set of revolute joints and one cylindrical joint as shown in Figure 7. In the properties of the cylindrical joint, the spring and damping coefficient, together with the equilibrium point of the cylinder, could be identified. In this example, the spring factor or stiffness of the damping system is considered to be 31,200 N/m and the damping coefficient of each cylinder is considered to be 2,250 N.s/m which is in the same range of suspension systems as automobiles, which are also considered in [23]. Automobiles are chosen since they are widely used and show that the model works with any conventional spring-damper system. The value is also not unlike off-road motorbike damping systems, which is another example of equipment that is widely used [24].

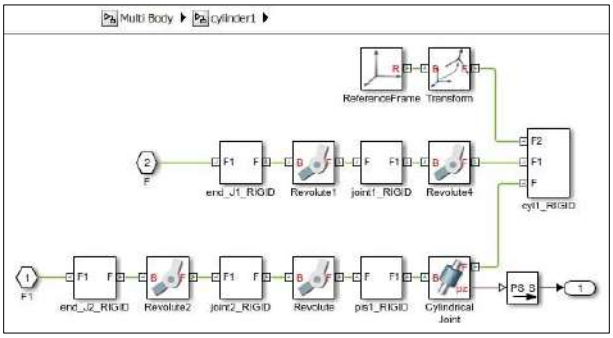

Figure 7. The cylinder level of multibody diagram

The characteristics of the sample damper are shown in Table 1 and the details of the simulation parameters are explained in the simulation results section. As previously explained, the dimensions and mechanical properties could easily be changed in the model, and the dynamic behaviour of the new model could then be established. For future development in the HEPHAESTUS project, the CDPR should be added to one plate on one end and, on the other end, the system that grips to the building.

Table 1. Damper characteristics

Property of item	Nomenclature	Value
Upper bound of cylinder movement	l_0	0.04 m
Lower bound of cylinder movement	l_m	-0.04 m
Spring factor of each cylinder	31,200	N/m
Damping coefficient of each cylinder	2,250	N.s/m

2.3 Simulation Results

For the simulation, one set of sample forces and torques is applied on the upper plate (representing, for example, the wind load applied to the CDPR and the effect it has on the damping system) since the lower plate is considered fixed to the ground (which represents the MEE gripped to the building). These loads are chosen for illustration purposes only; one can edit the input in the model and analyse the simulation results for specific loads. The applied forces are shown in Figure 8.

For the Y axis, a load of 700 N calculated using equation 1 is considered, even though in reality, by using the CDPR, not all of this wind load will be transferred to the MEE.

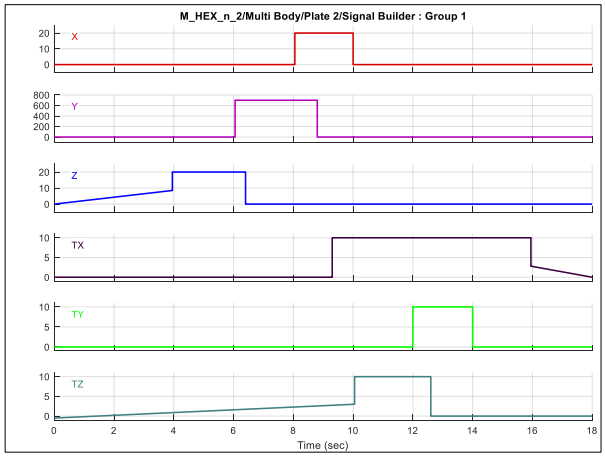

Figure 8. Input forces [N] and torques [N.m] signals

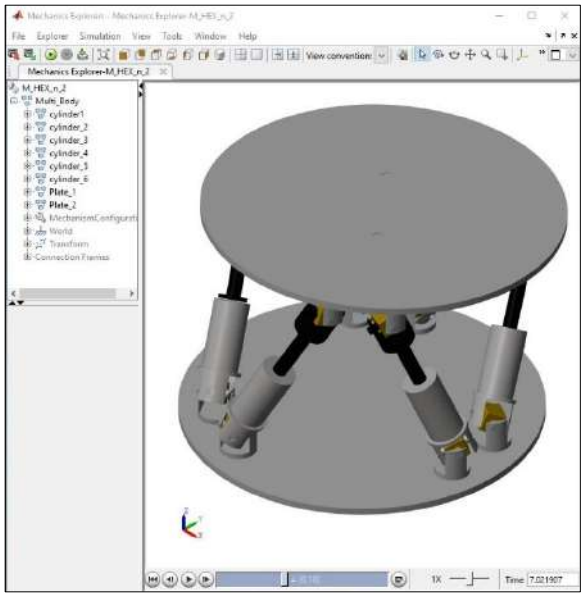

Figure 9. Mechanics explorer windows showing the simulation at the moment: time = 7.02 s

In the Matlab® Simscape™ model, under mechanism configuration, the linearisation delta is set to 0.001. "The linearisation delta specifies the perturbation value that is used to compute numerical partial derivatives for linearisation" [25]. The other solver configuration, the ODE solver, is set to "auto" mode in Matlab®, as this leads to the best matching results. g, the acceleration due to gravity, is considered as 9.80665 m/s^2 in the model configuration. In the solver configuration, filtering time is considered to be 0.001 s and consistency tolerance is considered equal to 1e-09.

As a visual result, in the *Mechanics explorer* window of Simscape™, the movement of the whole damper is also simulated. Figure 9 shows a screenshot of the *Mechanics explorer* windows at the moment: time = 7.02 s.

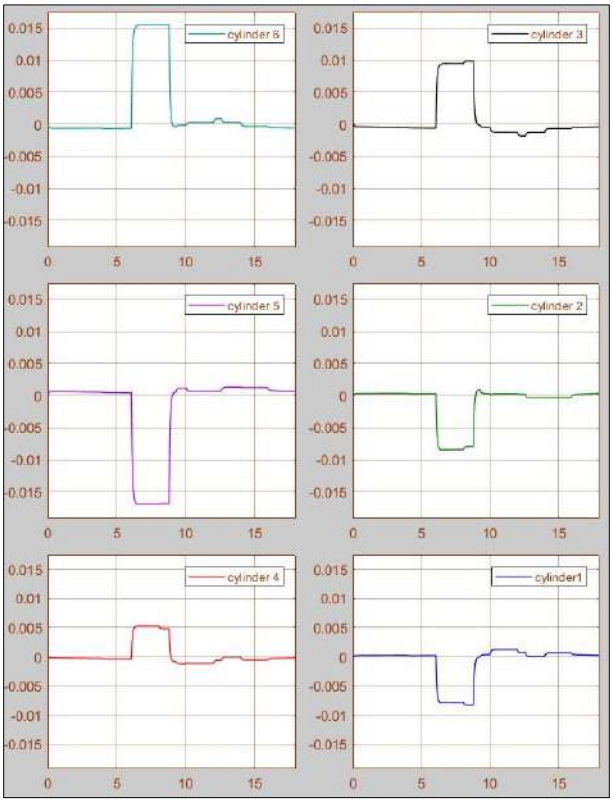

Figure 10. Output of cylinder position in Y axis [m] regarding the time in X axis [s]

As a result, the dynamic characteristics and movements of each cylinder could be drawn in a SCOOP module. It is possible to extract the forces and speeds on each joint. In this paper, only the position of each cylinder (spring-damper) is shown in Figure 10.

3 Conclusion

In this paper, a novel damper for passive damping of

a Modular End Effector mounted on a CDPR has been introduced. If a MEE and CDPR are directly coupled, excessive vibrations from the CDPR (caused by e.g. wind) may render the MEE unable to effectively fulfil some of its tasks (e.g. drilling). This problem calls for the installation of a novel damping system to reduce these effects. The system consists of a hexapod-shaped spring-damper placed between a MEE and CDPR. A mathematical model and Matlab® Simscape™ model are introduced and a simulation has been performed. The displacement of each cylinder is shown; however, other output data such as the forces and speeds on each joint could be extracted from the model for analytical purposes, which are not shown in this paper.

Although the initial design was for the CWM installation application, the model is generic and the characteristics of the mechanical system can be chosen freely. This entails the system can be used in other applications as well.

For future development of the CWM installation with CDPR and MEE, one can add the CDPR stiffness model on top of this model. This approach will be explored together with some other partners of the HEPHAESTUS project. In addition, to make the dynamic model presented in this paper for the damper more precise, one could perform some laboratory tests to optimise the Simscape model; this will be carried in the next steps of the project.

Acknowledgement:

This project has received funding from the European Union's Horizon 2020 research and innovation programme under grant agreement No 732513.

References

[1] Finkel G. *The Economics of the Construction Industry*. Routledge, 1997.

[2] Ball M. *Rebuilding Construction (Routledge Revivals)*. Routledge, 2014.

[3] Bock T. The future of construction automation: Technological disruption and the upcoming ubiquity of robotics. *Automation in Construction*, 59:113–121, 2015.

[4] Feng C. Xiao Y. Willette A. McGee W. and Kamat V.R. Vision guided autonomous robotic assembly and as-built scanning on unstructured construction sites. *Automation in Construction*, 59:128–138, 2015.

[5] Linner T. Pan M. Pan W. Taghavi M. Pan W. and Bock T. Identification of Usage Scenarios for Robotic Exoskeletons in the Context of the Hong Kong Construction Industry. In *Proceedings of the 35th ISARC conference*, pages 40–47, Berlin, Germany, 2018.

[6] Yu S.N. Lee S.Y. Han C.S. Lee K.Y. and Lee S.H. Development of the curtain wall installation robot: Performance and efficiency tests at a construction site. *Autonomous Robots*, 22(3):281–291, 2007.

[7] HEPHAESTUS WEB PAGE. About the prpject. On-line:http://www.hephaestus-project.eu/, Accessed: 19/12/2018.

[8] Taghavi M. Iturralde K. and Bock T. Cable-driven parallel robot for curtain wall modules automatic installation. In *Proceedings of the 35th ISARC conference*, pages 396–403, Berlin, Germany, 2018.

[9] Taghavi M. Heredia H. Iturralde K. Halvorsen H. and Bock T. Development of a Modular End Effector for the installation of Curtain Walls with cable-robots. *Journal of façade design and engineering*. 6(2):001-008, 2018.

[10] A&H Custom Machine. Taipei 101 Tuned Mass Damper. On-line: http://www.ahcustom.com/featured_projects/damping_system.html, Accessed: 19/12/2018.

[11] Tuan A.Y. and Shang G.Q. Vibration control in a 101-storey building using a tuned mass damper. *Journal of Applied Science and Engineering*, 17(2):141–156, 2014.

[12] Segla S. and Reich S. Optimization and comparison of passive, active, and semi-active vehicle suspension systems. *12th IFTOMM world congress, France*, 18–21, 2007.

[13] Lesellier M. Cuvillon L. Gangloff J. and Gouttefarde M. An active stabilizer for cable-driven parallel robot vibration damping. In *Proceedings of the IEEE/IROS conference*, pages 5063–5070, Madrid, Spain, 2018.

[14] Stewart D. A Platform with Six Degrees of Freedom. In *Proceedings of the Institution of Mechanical Engineers*, 180(1):371–386, 1965.

[15] Patel Y.D. and George P.M. Parallel Manipulators Applications-A Survey. *Modern Mechanical Engineering*, 2:57–64, 2012.

[16] Khajepour A. and Behzadipour. S. Stiffness of Cable-based Parallel Manipulators With Application to Stability Analysis. *The journal of mechanical Design, ASME*, 128(1):303-310, 2006.

[17] Nguyen D.Q. and Gouttefarde M. Stiffness Matrix of 6-DOF Cable-Driven Parallel Robots and Its Homogenization. Book. *Advances in Robot Kinematics*. Springer, 2014.

[18] Engineering ToolBox, (2011). Wind Velocity and Wind Load. online: https://www.engineeringtoolbox.com/wind-load-d_1775.html , Accessed 22/01/2019.

[19] Ji P. and Wu H. A closed-form forward kinematics solution for the 6-6P Stewart platform. *IEEE Transactions on Robotics and Automation*, 17(4):522–526, 2001.
[20] Jakobovic D. and Jelenković L. The forward and inverse kinematics problems for stewart parallel mechanisms. *CIM 2002 Computer Integrated Manufacturing and High Speed Machining - 8th International Scientific Conference on Production Engineering*, II-001-II012, 2002.
[21] Chen Y. and Mcinroy J.E. Decoupled Control of Flexure-Jointed Hexapods Using Estimated Joint-Space Mass-Inertia Matrix. *Brain and Cognition*, 32(2):273–344, 1996.
[22] McInroy J.E. and Hamann J.C. Design and control of flexure jointed hexapods. *IEEE Transactions on Robotics and Automation*, 16(4):372–381, 2000.
[23] Malmedahl G.A. Analysis of Automotive Damper Data and Design of a Portable Measurement System. *Thesis*, The Ohio State University, Department of Mechanical Engineering, Center for Automotive Research, 2005.
[24] Zanarini A. and Brugnoni E. Frequency analysis of a motorbike under motion conditions. In *ISMA2012-USD2012 Conferences, Volume: Multi-Body Dynamics and Control*, Leuven, Belgium, 2012.
[25] MathWorks®, (2017). Mechanism Configuration library (R2017b) Simscape™, From software's Help. Accessed: 22/01/2019.

Computer Vision Techniques in Construction, Operation and Maintenance Phases of Civil Assets: A Critical Review

S. Xu[a], J. Wang[a,b], X. Wang[a,c], and W. Shou[a]

[a]Australasian Joint Research Centre for Building Information Modelling, Curtin University, Australia
[b]School of Architecture and Built Environment, Deakin University, Australia
[c]Chongqing University Industrial Technology Research Institute, China
E-mail: Shuyuan.xu@postgrad.curtin.edu.au, jun.wang1@curtin.edu.au, xiangyu.wang@curtin.edu.au, wenchi.shou@curtin.edu.au

Abstract –

Throughout the life cycle of civil assets, construction, operation and maintenance phases require monitoring to assure reasonable decision makings. Current methods always involve specially-assigned personnel conducting on-site inspections, which are work-intensive, time-consuming and error-prone. Computer vision, as a powerful alternative to manual inspection, has been extensively studied during the past decades. On the basis of existing summary papers, this paper reviews a wide range of literatures, including journal articles, conference proceedings and other resources. Current applications of computer vision during construction, operation and maintenance stages of civil structures are concluded, with a special focus on operation and maintenance phase. This review aims to provide a comprehensive insight about the utilization of computer vision in civil engineering and an inspiring guidance for future research.

1 Introduction

In construction, operation and maintenance phases of civil assets' life cycle, monitoring is required for reasonable resource allocation and decision making. To be specific, monitoring of construction sites paves way for progress tracking, quality control, safety assurance and productivity analysis. When it comes to in-service structures, understanding of their current situations can help engineers to determine repair, retrofit and replace plans. Traditional methods always involve specially-assigned personnel conducting on-site inspections, during which physical measurements can impose extensive workload and potential danger to inspectors [1]. Such manual inspection processes are also time-consuming and prone to the biased judgement of inspectors. Alternatively, the development of reality capture technology and image processing techniques facilitate the utilization of computer vision in Architecture, Engineering & Construction and Facility Management (AEC & FM) industry. As an interdisciplinary field, computer vision aims to generate human-like understanding from digital images or videos, and thus attracts focused attention from researchers worldwide. Numerous studies have been done and impressive progress has been achieved. This paper goes through computer vision's applications in construction, operation and maintenance stages of built assets in a large scale, with a focus on recent researches that are published after existing review papers [2, 3].

The structure of this paper is as follows. Section 2 illustrates research methods. Section 3 presents analysis results and in-depth discussions about current researches. Section 4 provides envisions for future work.

2 Research Methods

2.1 Data Collection

Aiming to obtain a comprehensive insight about vision-based practices in civil engineering, the research started with initial searching and scanning in both web search engine, google scholar, and academic databases such as ScienceDirect and IEEE Xplore. Direct search method based on title, abstract and keywords was employed to collect a wide range of literatures, so as to form a fundamental concept about how computer vision is combined with civil engineering. "Computer vision", "civil engineering" and other related terms such as "machine vision" were search keywords. Different types of literature including journal articles, conference proceedings, even book sections were collected and reviewed. Apart from the relevance, publishing date was regarded as another sift criteria. The emergence of this topic was largely facilitated by the development of computer science and image processing techniques, thus the time limit was set to year 2000 to exclude unrelated studies. After the initial stage of review, top journals embodying high-quality articles in this field were

identified, some (but not all) of which are: Computer-Aided Civil and Infrastructure Engineering, Automation in Construction, Advanced Engineering Informatics, Journal of Computing in Civil Engineering and IEEE. Key authors who made advanced contributions to this field were also recognized. Existing review papers were referred to and set as a time mark for further selection of data. Focused search was then conducted centring on the above-mentioned journals and authors. In total, 71 papers were collected and analysed (Figure 1), including 54 journal articles, 16 conference proceedings and 1 book section. EndNote X7 was used for data storage, management and citations.

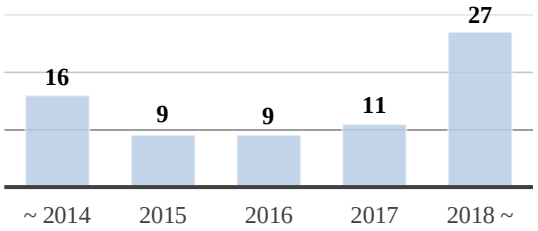

Figure 1. Chronological distribution of articles

2.2 Data Analysis

Preliminary data analysis was completed during data collection by scanning titles and abstracts, followed by context analysis, a typical method for qualitative data analysis. Regarding the application scenarios of computer vision, the literature was divided into two blocks: one that focused on construction phase and the other on operation and maintenance phase. Papers in two parts were then analysed separately. Excel tables were created for note takings while reviewing, with critical information and peculiar contributions of each article highlighted. Notable information included the main purpose of application, area of use, equipment demand, methodology, outcome quality, and future agenda. A comparison was made based on the systematic review.

3 Results and Discussions

Current applications of computer vision in civil engineering are categorized into two groups: (1) construction phase and (2) operation and maintenance phase in structure's life cycle.

3.1 Computer Vision in Construction Phase

Due to an early start of computer vision on construction sites, a thorough research in this area has been developed in the last decade. Summaries and overviews are available in existing literatures [2].

The utilization of computer vision technology in construction jobsites can be categorized into four classes regarding the main purpose of application, namely progress monitoring, quality control, operational productivity analysis [4-7] (which is to what extent onsite resources are being utilized) and safety assurance [8-12]. Combination of multiple purposes was achieved in some researches [13, 14]. Apart from fatality prevention, there is another safety concern named occupational health assessment, referring to [15]. Seo, J., et al. integrated vision-based human kinematics data to biomechanical analysis, so as to evaluate the risk of musculoskeletal disorders faced by workers when conducting lifting tasks.

One important constitution in a vision-based monitoring system is object detection. Typical methods follow two sequent steps, feature extraction and object classification. The most frequently employed image descriptors include, but are not limited to, shape-based features like edges [16] and texture-based ones like Histogram of Oriented Gradients (HOG), which is a local spatio-temporal feature particularly suitable for action recognition. Extracted features are then fed into classifiers for object recognition. In addition to traditional classification algorithms like support vector machine (SVM), deep learning techniques, e.g. faster region-based convolutional neural network (faster R-CNN) in [11], are rising up in recent studies. Its core part is an artificial neural network (ANN) as an analysis kernel during object recognition, categorization and other information extraction [17]. Luo, H., et al. [6] presented a three-stream CNN dealing with RGB images, optical flow images and grayscale images, separately, then fused the results together to identify workers' states in reinforcement installing activities.

Another core task in job sites involves the tracking of detected construction entities (i.e. workforce and equipment). Xiao, B. and Z. Zhu [18] summarized and compared 15 2D tracking methods in past studies regarding the outcome quality (i.e. overlap score and centre location error), highlighting the superiority of methods using sparse representations and generative classification algorithms. The 2D tracking results are then transformed into 3D space through triangulation to gain trajectories of the target, for example, crane jib [19] and excavators [16].

Subsequently, activity recognition of either workers [6, 9] or equipment (especially excavator and dump trunk in earthmoving operations [4], and cranes [19]) constitutes the next level of image processing, allowing the detection of un-safe behaviour and understanding of onsite situations. Moving personnel and equipment were monitored in [20] and by fuzzy inference, potential dangers like struck-by accidents were evaluated in a numerical way for an efficient safety management. Luo, X., et al. [21] managed to identify 20 activity patterns in sites assisted by prior knowledge (i.e. whether two

certain objects cooperate in an activity and their proximity). Similar relevance information was adopted in [5] for interactive analysis of individualized action recognition. Both one-to-one- and group-level analysis led to a precision of 91.27% in situation understanding.

Combination of computer vision and other state-of-the-art technology is also emerging. For example, Jeelani, I., et al. [10] utilized eye-tracking techniques to obtain workers' viewing patterns, which was then integrated into a computer-vision-based localization system to indicate workers' ability to recognize onsite hazards.

3.2 Computer Vision During Operation and Maintenance Phase

The utilization of computer vision in structural health monitoring (SHM) and performance evaluation has been increasingly studied in recent years. Such a scheme can positively contribute to a reasonable management of construction resources, leading to a sustainable built environment. Koch, C., et al. [3] concluded the achievements and challenges faced in this field and since then, notable improvements have been accomplished.

3.2.1 Reality Capture Technology

For data acquisition, two main reality capture techniques include laser scanning and photogrammetry, where point clouds and images/ videos are input and analysed, respectively. Aiming to lower inspection cost, digital imaging was favoured in the literature. 49 out of 51 studies extracted information from photos or video frames, most of which relied on consumer-grade devices like digital single-lens reflex (DSLR) camera [22-25], action camera [26], video camcorder [27], existing closed-circuit television (CCTV) [28], or even smart phone cameras [29-32]. Un-manned Aerial Vehicle (UAV) [33] or flying robot [34] can be utilized to mount cameras to free workers from hand-held cameras and on-site tour for inspection. To note, Dorafshan, S. et al. [35] studied the robustness of crack detection in steel bridges against various camera specifications. Three types of cameras, i.e. Nikon COOLPIX L830, DJI Mavic and GoPro Hero 4, were tested, indicating different crack-to-camera distance requirement for a desirable result.

3.2.2 Image Processing Algorithms

A typical computer vision-based defect detection method involves four levels of image processing, namely image pre-processing, segmentation, feature extraction and pattern recognition. Satisfactory segmentation results can lead to a high accuracy of detection, which, in most cases, was ensured by the use of thresholding-based segmentation algorithms. Defect detection leverages similar features as job-site monitoring, covering edges, diverse interest points, region proposals (especially in R-CNN algorithms), HOG, gradient magnitude and orientation, entropy, and even colour-based ones. Edge detection dominates in previous studies, and Qizhen, H. et al. [36] concluded two classes of edge detection algorithms: ones dependent on first-order derivative, i.e. image gradient, and ones based on second-order derivatives.

In higher-level image processing, deep learning algorithms have gained popularity as mentioned. The form of the core network, ANN, evolves from CNN [37, 38], fully convolutional neural network (FCN) [39], fast R-CNN [29], to faster R-CNN [24, 28]. Along with the superiority to eliminate multi-step image processing, such algorithms are further supported by acceptable performances and adaptability to diversified structures and defect types.

3.2.3 Area of Use

In real life, defect inspection and condition assessment procedures are carried out both regularly (routine inspection) and after disasters.

- Post-disaster inspection

Past work for post-disaster inspection focuses on damaged reinforced concrete (RC) columns due to their critical role to resist lateral seismic loads. Lattanzi, D., et al. [40] established relationship between visual defects (e.g. cracks and spalls) and the maximum experienced displacement of concrete bridge columns for post-earthquake condition assessment. The peak drift estimated through machine learning regression models can facilitate triage evaluation. Similarly, German, S., et al. [41] first adopted computer vision algorithms (e.g. edge detection, region-growing detection, thresholding, etc.) to identify and measure cracks and spalling on RC columns, based on which, a framework for vision-based structural analysis is completed.

- Routine inspection

The allocation of past researches in different areas of use is shown as Figure 2.

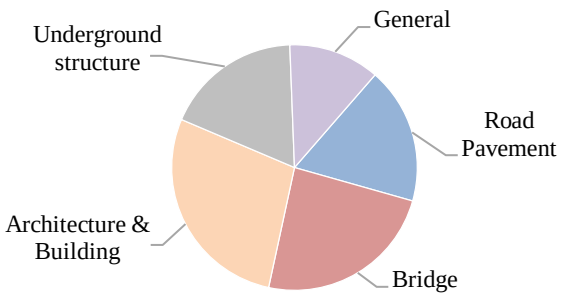

Figure 2. Literature distribution (area of use)

Comparatively, a wider range of civil structures are studied in routine inspection, and an almost even distribution is shown. The aging problem of architectures and buildings attracts the most attention (making up 28% of the literature). 12 out of 51 studies focus on the health of bridges. Roadways (asphalt pavements in particular) and Underground structures (including sewer pipes [28, 42], tunnels [38, 43, 44] and subway system [17]) are also frequently studied fields, accounting for 9 out of 51 papers equally. Different from the majority of studies, Kamal, K., et al. [45] classified various knot defects in wood structures.

There are about 12% researchers developing their proposals in a general scale, testing on laboratory specimen [46] and existing point cloud datasets [47], and aiming to tackle prevailing or critical challenges encountered during applications.

3.2.4 Defect Types

Figure 3 illustrates the allocation of past work in various defect detection.

Cracks appeal the most intensive studies by far, accounting for more than 35% of the literature. Among them, 17 articles study on concrete structures, 3 researches target fatigue cracks on steel structures and 5 papers recognize cracks on road pavement. Around a quarter of past work focus on displacement, based on which structural vibration properties (e.g. natural frequency and mode shapes [48]) are further retrieved. Pothole, as a distress peculiar to roadways, are recognized in 3 out of 51 papers. Other defects include cavities [29, 49], spalling [50], rebar exposure [29, 50], moisture marks on subway structures [17], loosened bolts [44], etc.

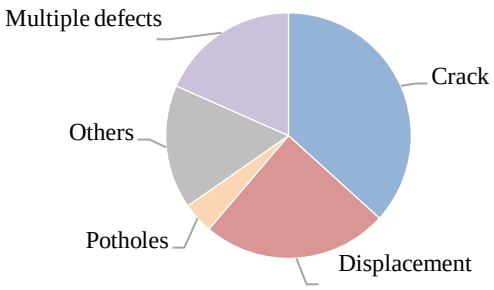

Figure 3. Literature distribution (defect types)

In addition, a few of studies (nearly 20%) recognize multiple defects [51] and cover more damage patterns, such as deposits, tree root intrusions and water infiltrations on pipes [28], steel corrosion, bolt corrosion and steel delamination on general structures [24].

Particularly, artificial markers or specific objects (e.g. lane marker, manhole and patches on roadways) on the asset were utilized to clarify novel methods in [52].

3.2.5 Level of Detection Details

To what extent computer vision can benefit maintenance decision making is fully dependent on the level of detail of the inspection results. The outcome of a computer-vision-based inspection system develops from the mere detection of defects' presence, classification of multiple damages, defect localization, to numerical measurement of critical properties. The progress so far is shown in Table 1. And detailed achievements in each category are illustrated below.

Table 1. Current research progress

Level of detail / Defect type	Defect detection		Defect property retrieval
	presence	localization	
Crack	[23-25, 30, 33, 34, 37, 53-55]	[28]	[22, 39, 56-59]
Pothole		[60, 61]	
Spalling			[50]
Cavity		[49]	
Moisture marks			[17]
Displacement		-	[26, 27, 46, 48, 62-65]
Dynamic responses		-	[66]

Note: The grey area means that this level of defect details has been successfully retrieved using computer vision techniques in the literature (with relevant references listed), while blank area means that few researches included the extraction of such information so far.

- Classification. Identification across defect types were realized in [31] to classify pothole, longitudinal-transversal cracks, and fatigue cracks on pavement. Other researches define category based on damage severity (major/ minor cracks in [42]), defect features (crack orientation in [56]), or different maintenance demand (sealed or ordinary cracks in [67]).
- Localization. Several researches locate the defect-included bounding box in the identified image [28, 60, 61], requiring further processing to gain their positions in global coordination. Additional devices

are deployed as supplementary, such as GPS [31], infrared camera and laser range finder for cavity localization on roadways [49].

- Property quantification. For crack measurement, its length, orientation, max width and mean width are extracted either through skeletonizing operations in static images [39, 68] or by tracking surface discontinuities in video streams [22]. Properties of spalling area, i.e. its length and depth, are obtained by analyzing the region with exposed longitudinal reinforcement [50]. The severity of wet marks on subway structures is quantified in terms of the area's percentage [17]. Displacements are retrieved in almost all relevant researches. One notable improvement is that early studies rely on manually-created markers [64] or speckle created by a laser pointer [66], while recent work achieve target-free inspection using "key points" [63, 69] on structures. Another progress is multi-point displacement measurement using multiple synchronized low-cost cameras [26] or a multithread active camera with Galvano-mirror [48]. Displacements can be further converted to natural frequencies through the Fast Fourier Transform (FFT) [63].
- Structural analysis. Limited research manages to complete this step with vision-based defect information. Post-earthquake fragility curves of RC columns were generated in [41], indicating structural damage states and estimated retrofit cost. Davoudi, R. et al. [32] estimated structural load levels of RC beams and slabs based on crack patterns. Combination with other technology like robotics [58] further facilitates this process.

4 Conclusions and Future work

This paper presents an overview about the applications of computer vision in civil engineering. Researches in construction sites start early and form a relatively mature system, and there are considerable advances in defect property retrieval for existing civil assets. However, challenges remain in this field and promising future work on the basis of current achievements is demonstrated as below.

Currently, vision-based defect information is underutilized due to the lack of relationship between visual data and structural responses. Thus, the integration and utilization of defect information in structural analysis so as to facilitate maintenance decision makings is in the future agenda.

Another task is to establish an enlarged dataset for computer vision. For construction phase, images with a wider range of personal protective equipment (PPE) [8], construction entities, and their activity patterns [11] should be collected. As for operation and maintenance stage, images containing more defect patterns under various environmental conditions can largely contribute to this field. Such enlarged datasets can be used to train classifiers for higher detection accuracy and achieve comprehensive monitoring of both construction sites and aging structures.

Robustness of analysis results against adverse factors encountered during data acquisition should be tested and improved. In jobsites, though effects of various illumination, varying object-to-camera distances, and different levels of occlusion on the accuracy of object tracking have been studied [7], further evaluation concerning other uncertainties, like shadows, should be included in future work. Similar envision applies to in-service assets, even if the impacts of surrounding lighting conditions on crack detection have been assessed [35].

For practical considerations, real-time analysis is desired. In routine inspections, real-time defect recognition and feedback to inspectors are enabled by the simplification of image capturing devices [31]. The leverage of Graphics Processing Unit (GPU) can further shorten computation time. However, when faced with cluttered construction sites and existence of various deterioration patterns, further improvements are in need.

In the future, combination with other advanced technology is encouraged. The utilization of deep learning methods has been proved efficient. Data-driven algorithms also facilitate the vison-based condition assessment [32] , calling for more multidisciplinary applications. Moreover, devices like GPS providing additional information for vision-based system also deserve consideration.

Acknowledgement

This work was sponsored by the Australian Research Council Linkage discovery project [grant number DP170104613], and a research project SEBnrc 2.64: Unlocking Facility Value through Lifecycle Thinking.

References

[1] Institution, T.B.S. BS 8210:2012: Guide to facilities maintenance management. BSI Standards Limited, 2012.

[2] Yang, J., M.-W. Park, P.A. Vela, and M. Golparvar-Fard, Construction performance monitoring via still images, time-lapse photos, and video streams: Now, tomorrow, and the future. Advanced Engineering Informatics, 2015. **29**(2): p. 211-224.

[3] Koch, C., K. Georgieva, V. Kasireddy, B. Akinci, and P. Fieguth, A review on computer vision based defect detection and condition assessment of concrete and asphalt civil infrastructure. Advanced Engineering Informatics, 2015. **29**(2): p. 196-210.

[4] Golparvar-Fard, M., A. Heydarian, and J.C. Niebles, Vision-based action recognition of earthmoving equipment using spatio-temporal features and support vector machine classifiers. Advanced Engineering Informatics, 2013. **27**(4): p. 652-663.
[5] Kim, J., S. Chi, and J. Seo, Interaction analysis for vision-based activity identification of earthmoving excavators and dump trucks. Automation in Construction, 2018. **87**: p. 297-308.
[6] Luo, H., C. Xiong, W. Fang, P.E.D. Love, B. Zhang, and X. Ouyang, Convolutional neural networks: Computer vision-based workforce activity assessment in construction. Automation in Construction, 2018. **94**: p. 282-289.
[7] Park, M.-W., A. Makhmalbaf, and I. Brilakis, Comparative study of vision tracking methods for tracking of construction site resources. Automation in Construction, 2011. **20**(7): p. 905-915.
[8] Wu, H. and J. Zhao, An intelligent vision-based approach for helmet identification for work safety. Computers in Industry, 2018. **100**: p. 267-277.
[9] Han, S. and S. Lee, A vision-based motion capture and recognition framework for behavior-based safety management. Automation in Construction, 2013. **35**: p. 131-141.
[10] Jeelani, I., K. Han, and A. Albert, Automating and scaling personalized safety training using eye-tracking data. Automation in Construction, 2018. **93**: p. 63-77.
[11] Fang, W., L. Ding, H. Luo, and P.E.D. Love, Falls from heights: A computer vision-based approach for safety harness detection. Automation in Construction, 2018. **91**: p. 53-61.
[12] Fang, Q., H. Li, X. Luo, L. Ding, H. Luo, and C. Li, Computer vision aided inspection on falling prevention measures for steeplejacks in an aerial environment. Automation in Construction, 2018. **93**: p. 148-164.
[13] Wang, Z., H. Li, and X. Zhang, Construction waste recycling robot for nails and screws: Computer vision technology and neural network approach. Automation in Construction, 2019. **97**: p. 220-228.
[14] Soltani, M.M., Z. Zhu, and A. Hammad, Framework for Location Data Fusion and Pose Estimation of Excavators Using Stereo Vision. Journal of Computing in Civil Engineering, 2018. **32**(6): p. 04018045.
[15] Seo, J., R. Starbuck, S. Han, S. Lee, and T.J. Armstrong, Motion Data-Driven Biomechanical Analysis during Construction Tasks on Sites. Journal of Computing in Civil Engineering, 2015. **29**(4): p. B4014005.
[16] Yuan, C., S. Li, and H. Cai, Vision-Based Excavator Detection and Tracking Using Hybrid Kinematic Shapes and Key Nodes. Journal of Computing in Civil Engineering, 2017. **31**(1): p. 04016038.
[17] Dawood, T., Z. Zhu, and T. Zayed, Computer Vision-Based Model for Moisture Marks Detection and Recognition in Subway Networks. Journal of Computing in Civil Engineering, 2018. **32**(2): p. 04017079.
[18] Xiao, B. and Z. Zhu, Two-Dimensional Visual Tracking in Construction Scenarios: A Comparative Study. Journal of Computing in Civil Engineering, 2018. **32**(3): p. 04018006.
[19] Yang, J., P. Vela, J. Teizer, and Z. Shi, Vision-Based Tower Crane Tracking for Understanding Construction Activity. Journal of Computing in Civil Engineering, 2014. **28**(1): p. 103-112.
[20] Kim, H., K. Kim, and H. Kim, Vision-Based Object-Centric Safety Assessment Using Fuzzy Inference: Monitoring Struck-By Accidents with Moving Objects. Journal of Computing in Civil Engineering, 2016. **30**(4): p. 04015075.
[21] Luo, X., H. Li, D. Cao, F. Dai, J. Seo, and S. Lee, Recognizing Diverse Construction Activities in Site Images via Relevance Networks of Construction-Related Objects Detected by Convolutional Neural Networks. Journal of Computing in Civil Engineering, 2018. **32**(3): p. 04018012.
[22] Kong, X. and J. Li, Vision-Based Fatigue Crack Detection of Steel Structures Using Video Feature Tracking. Computer-Aided Civil and Infrastructure Engineering, 2018. **33**(9): p. 783-799.
[23] Yeum, C.M. and S.J. Dyke, Vision-Based Automated Crack Detection for Bridge Inspection. Computer-Aided Civil and Infrastructure Engineering, 2015. **30**(10): p. 759-770.
[24] Cha, Y.-J., W. Choi, G. Suh, S. Mahmoudkhani, and O. Büyüköztürk, Autonomous Structural Visual Inspection Using Region-Based Deep Learning for Detecting Multiple Damage Types. Computer-Aided Civil and Infrastructure Engineering, 2018. **33**(9): p. 731-747.
[25] Jahanshahi, M.R. and S.F. Masri, Adaptive vision-based crack detection using 3D scene reconstruction for condition assessment of structures. Automation in Construction, 2012. **22**: p. 567-576.
[26] Lydon, D., M. Lydon, J.M.d. Rincón, S.E. Taylor, D. Robinson, E. O'Brien, and F.N. Catbas, Development and Field Testing of a Time-Synchronized System for Multi-Point Displacement Calculation Using Low-Cost Wireless Vision-Based Sensors. IEEE Sensors Journal, 2018. **18**(23): p. 9744-9754.
[27] Yang, Y. and X.B. Yu. Real time measurement of the dynamic displacement field of a large-scale

arch-truss bridge by remote sensing technology. in 2016 IEEE SENSORS. 2016.

[28] Cheng, J.C.P. and M. Wang, Automated detection of sewer pipe defects in closed-circuit television images using deep learning techniques. Automation in Construction, 2018. **95**: p. 155-171.

[29] Li, R., Y. Yuan, W. Zhang, and Y. Yuan, Unified Vision-Based Methodology for Simultaneous Concrete Defect Detection and Geolocalization. Computer-Aided Civil and Infrastructure Engineering, 2018. **33**(7): p. 527-544.

[30] Varadharajan, S., S. Jose, K. Sharma, L. Wander, and C. Mertz. Vision for road inspection. in IEEE Winter Conference on Applications of Computer Vision. 2014.

[31] Tedeschi, A. and F. Benedetto, A real-time automatic pavement crack and pothole recognition system for mobile Android-based devices. Advanced Engineering Informatics, 2017. **32**: p. 11-25.

[32] Davoudi, R., G.R. Miller, and J.N. Kutz, Data-driven vision-based inspection for reinforced concrete beams and slabs: Quantitative damage and load estimation. Automation in Construction, 2018. **96**: p. 292-309.

[33] Aliakbar, M., U. Qidwai, M.R. Jahanshahi, S. Masri, and W. Shen. Progressive image stitching algorithm for vision based automated inspection. in 2016 International Conference on Machine Learning and Cybernetics (ICMLC). 2016.

[34] Dhule, J.J., N.B. Dhurpate, S.S. Gonge, and G.M. Kandalkar. Edge Detection Technique Used for Identification of Cracks on Vertical Walls of The Building. in 2015 International Conference on Computing and Network Communications (CoCoNet). 2015.

[35] Dorafshan, S., R.J. Thomas, and M. Maguire, Fatigue Crack Detection Using Unmanned Aerial Systems in Fracture Critical Inspection of Steel Bridges. Journal of Bridge Engineering, 2018. **23**(10): p. 04018078.

[36] Qizhen, H. and Z. GuoLong. On image edge detection method. in 2011 International Conference on Electrical and Control Engineering. 2011.

[37] Zhang, A., K.C.P. Wang, B. Li, E. Yang, X. Dai, Y. Peng, Y. Fei, Y. Liu, J.Q. Li, and C. Chen, Automated Pixel-Level Pavement Crack Detection on 3D Asphalt Surfaces Using a Deep-Learning Network. Computer-Aided Civil and Infrastructure Engineering, 2017. **32**(10): p. 805-819.

[38] Makantasis, K., E. Protopapadakis, A. Doulamis, N. Doulamis, and C. Loupos. Deep Convolutional Neural Networks for efficient vision based tunnel inspection. in 2015 IEEE International Conference on Intelligent Computer Communication and Processing (ICCP). 2015.

[39] Yang, X., H. Li, Y. Yu, X. Luo, T. Huang, and X. Yang, Automatic Pixel-Level Crack Detection and Measurement Using Fully Convolutional Network. Computer-Aided Civil and Infrastructure Engineering, 2018. **33**(12): p. 1090-1109.

[40] Lattanzi, D., G.R. Miller, M.O. Eberhard, and O.S. Haraldsson, Bridge Column Maximum Drift Estimation via Computer Vision. Journal of Computing in Civil Engineering, 2016. **30**(4): p. 04015051.

[41] German, S., J.-S. Jeon, Z. Zhu, C. Bearman, I. Brilakis, R. DesRoches, and L. Lowes, Machine Vision-Enhanced Postearthquake Inspection. Journal of Computing in Civil Engineering, 2013. **27**(6): p. 622-634.

[42] Sinha, S.K., P.W. Fieguth, and M.A. Polak, Computer Vision Techniques for Automatic Structural Assessment of Underground Pipes. Computer-Aided Civil and Infrastructure Engineering, 2003. **18**(2): p. 95-112.

[43] Attard, L., C.J. Debono, G. Valentino, and M. Di Castro, Vision-based change detection for inspection of tunnel liners. Automation in Construction, 2018. **91**: p. 142-154.

[44] Cha, Y.-J., K. You, and W. Choi, Vision-based detection of loosened bolts using the Hough transform and support vector machines. Automation in Construction, 2016. **71**: p. 181-188.

[45] Kamal, K., R. Qayyum, S. Mathavan, and T. Zafar, Wood defects classification using laws texture energy measures and supervised learning approach. Advanced Engineering Informatics, 2017. **34**: p. 125-135.

[46] Ferrer, A.D.D., E.E. Escalante, S.R.J. Barbosa, and S.L.C. Suarez. Material deformation estimation with Computer Vision methods. in 2015 20th Symposium on Signal Processing, Images and Computer Vision (STSIVA). 2015.

[47] Khaloo, A. and D. Lattanzi, Robust normal estimation and region growing segmentation of infrastructure 3D point cloud models. Advanced Engineering Informatics, 2017. **34**: p. 1-16.

[48] Aoyama, T., L. Li, M. Jiang, K. Inoue, T. Takaki, I. Ishii, H. Yang, C. Umemoto, H. Matsuda, M. Chikaraishi, and A. Fujiwara, Vibration Sensing of a Bridge Model Using a Multithread Active Vision System. IEEE/ASME Transactions on Mechatronics, 2018. **23**(1): p. 179-189.

[49] Yamaki, K., K. Matsushima, and O. Takahashi. Road deformation detection based sensor fusion. in 2017 9th International Conference on Information Technology and Electrical Engineering (ICITEE). 2017.

[50] German, S., I. Brilakis, and R. DesRoches, Rapid entropy-based detection and properties measurement of concrete spalling with machine vision for post-earthquake safety assessments. Advanced Engineering Informatics, 2012. **26**(4): p. 846-858.

[51] Makantasis, K., E. Protopapadakis, A. Doulamis, N. Doulamis, and C. Loupos. Deep convolutional neural networks for efficient vision based tunnel inspection. in Intelligent Computer Communication and Processing (ICCP), 2015 IEEE International Conference on. 2015. IEEE.

[52] Sultani, W., S. Mokhtari, and H. Yun, Automatic Pavement Object Detection Using Superpixel Segmentation Combined With Conditional Random Field. IEEE Transactions on Intelligent Transportation Systems, 2018. **19**(7): p. 2076-2085.

[53] Cha, Y.J., W. Choi, and O. Büyüköztürk, Deep learning‐based crack damage detection using convolutional neural networks. Computer‐Aided Civil and Infrastructure Engineering, 2017. **32**(5): p. 361-378.

[54] Yokoyama, S. and T. Matsumoto, Development of an automatic detector of cracks in concrete using machine learning. Procedia engineering, 2017. **171**: p. 1250-1255.

[55] Zhang, L., F. Yang, Y.D. Zhang, and Y.J. Zhu. Road crack detection using deep convolutional neural network. in Image Processing (ICIP), 2016 IEEE International Conference on. 2016. IEEE.

[56] Lins, R.G. and S.N. Givigi, Automatic Crack Detection and Measurement Based on Image Analysis. IEEE Transactions on Instrumentation and Measurement, 2016. **65**(3): p. 583-590.

[57] Jahanshahi, M.R., S.F. Masri, C.W. Padgett, and G.S. Sukhatme, An innovative methodology for detection and quantification of cracks through incorporation of depth perception. Machine Vision and Applications, 2013. **24**(2): p. 227-241.

[58] Menendez, E., J.G. Victores, R. Montero, S. Martínez, and C. Balaguer, Tunnel structural inspection and assessment using an autonomous robotic system. Automation in Construction, 2018. **87**: p. 117-126.

[59] Protopapadakis, E., K. Makantasis, G. Kopsiaftis, N. Doulamis, and A. Amditis. Crack Identification Via User Feedback, Convolutional Neural Networks and Laser Scanners for Tunnel Infrastructures. in VISIGRAPP (4: VISAPP). 2016.

[60] Azhar, K., F. Murtaza, M.H. Yousaf, and H.A. Habib. Computer vision based detection and localization of potholes in asphalt pavement images. in 2016 IEEE Canadian Conference on Electrical and Computer Engineering (CCECE). 2016.

[61] Yousaf, M.H., K. Azhar, F. Murtaza, and F. Hussain, Visual analysis of asphalt pavement for detection and localization of potholes. Advanced Engineering Informatics, 2018. **38**: p. 527-537.

[62] Luo, L. and M.Q. Feng, Edge-Enhanced Matching for Gradient-Based Computer Vision Displacement Measurement. Computer-Aided Civil and Infrastructure Engineering, 2018. **33**(12): p. 1019-1040.

[63] Fukuda, Y., M.Q. Feng, Y. Narita, S. Kaneko, and T. Tanaka, Vision-Based Displacement Sensor for Monitoring Dynamic Response Using Robust Object Search Algorithm. IEEE Sensors Journal, 2013. **13**(12): p. 4725-4732.

[64] Zeinali, Y., Y. Li, D. Rajan, and B. Story. Accurate structural dynamic response monitoring of multiple structures using one CCD camera and a novel targets configuration. in Proceedings of the 11th International Workshop on Structural Health Monitoring, Palo Alto, CA, USA. 2017.

[65] Lattanzi, B.J.A.K.a.D., Tracking Structural Deformations via Automated Sample-Based Point Cloud Analysis, in Computing in Civil Engineering 2017 : Information Modeling and Data Analytics. 2017.

[66] Park, K., M. Torbol, and S. Kim, Vision-Based Natural Frequency Identification Using Laser Speckle Imaging and Parallel Computing. Computer-Aided Civil and Infrastructure Engineering, 2018. **33**(1): p. 51-63.

[67] Zhang, K., H.D. Cheng, and B. Zhang, Unified Approach to Pavement Crack and Sealed Crack Detection Using Preclassification Based on Transfer Learning. Journal of Computing in Civil Engineering, 2018. **32**(2): p. 04018001.

[68] Zhu, Z., S. German, and I. Brilakis, Visual retrieval of concrete crack properties for automated post-earthquake structural safety evaluation. Automation in Construction, 2011. **20**(7): p. 874-883.

[69] Khuc, T. and F.N. Catbas, Completely contactless structural health monitoring of real-life structures using cameras and computer vision. Structural Control and Health Monitoring, 2017. **24**(1): p. e1852.

Monitoring and Alerting of Crane Operator Fatigue Using Hybrid Deep Neural Networks in the Prefabricated Products Assembly Process

X. Li[a], H.L. Chi[a], W.F. Zhang[b], and Q.P. Geoffrey Shen[a]

[a]Department of Building and Real Estate, The Hong Kong Polytechnic University, China
[b]Ocean University of China, China
E-mail: shell.x.li@polyu.hk, hung-lin.chi@polyu.hk, zhangwenfeng@stu.ouc.edu.cn, geoffrey.shen@polyu.hk

Abstract –

Crane operators fatigue is one of the significant constraints should be monitored. Otherwise, it may lead to inefficient crane operations and safety issues. Recently, many deep neural networks have been developed for fatigue monitoring of vehicle drivers by processing the image or video data. However, the challenge is to distinguish the slight variations of facial features among still and motion frames (e.g., nodding and head tilt, yawning and talking). It can be exacerbated in the scenarios for crane operators due to their constant head moving to track the loads' position and recurrent communication (talking) with crane banksman. In contrast to previous approaches, which models spatial information and traditional temporal information for sequential processing, this study proposes a hybrid model can not only extract the spatial features by customized convolutional neural networks (CNN) but also enrich the modeling dynamic motions in the temporal dimension through the deep bidirectional long short-term memory (DB-LSTM). This hybrid model is trained and evaluated on the very popular dataset NTHU-DDD, and the results show that the proposed architecture achieves 93.6% overall accuracy and outperform the previous models in the literature.

Keywords –

Fatigue monitoring and alerting; Deep learning; Crane operator; Prefabricated construction

1 Introduction

In prefabricated construction, the prefabricated products become more and more complicated for assembly, with the evolution from components (light-weight, e.g., facade) and modules (large and heavy, e.g., volumetric precast bathroom) to pre-acceptance integrated units (larger and heavier, e.g., completed with finishes, fixtures, and fittings) [1]. Given this course of prefabricated products evolution, cranes, with their excellent transportation capacity, perform a decisive role in the assembly of prefabricated products by lifting them vertically and horizontally [2]. To achieve smooth crane operations, the crane operators should not only have enough physical strength but also be agile in the hearing, eyesight, and reflexes. As such, the operations and judgment of the crane operator will be a crucial factor for safety and productivity particular in the construction site of Hong Kong due to the high level of congestion and dynamics. However, the fatigue or drowsiness has been identified as the critical constraint in disturbing the operator's operations and judgment, which leads to the decreased attentiveness and vigilance, as well as casualties by collisions or falling loads [3,4]. In addition, Tam and Fung [3] revealed that around 60.5% of the crane operators would continue to work even feeling fatigue due to the long working hours (tight construction schedule) and about 52.6% of the crane operators are lack of breaks due to the inconvenient and narrow workspace (inconvenience of frequent in and out). Thus, automatically monitoring and warning the fatigue can provide timely support for crane operators, site superintendents and safety directors to make the scientific shifts and breaks.

Although there are seldom studies on developing fatigue monitoring and warning systems for the crane operator, numerous objective approaches have been proposed for detecting the fatigue or drowsiness of vehicle drivers from vehicle trajectory [5], physiological signal [6], and facial expression [7]. The first two approaches in crane operation can measure the fatigue by several parameters such as trolley movement speed, loads path deviation, jib rotation speed, heart rate, electroencephalogram (EEG), electrooculogram (EOG), electromyogram(EMG), and electrocardiogram (ECG). These two methods have shown a good accuracy when monitoring physical fatigue of vehicle drivers. However, crane operation trajectory may be affected by other factors (e.g., operation errors due to inexperience, inefficient communication with site signaller) and the physiological signal should be collected by an annoying

and invasive way to crane operators. Thus, monitoring the fatigue reflected by facial expressions (e.g., eye state, yawning, nodding) can be a more convenient, fast-speed and cost-effective approach. This kind of approach can analyze the facial features extracted from the videos/images of crane operators, and it performs a high accuracy after the boosting of various deep neural networks as it facilitates the computer to learn by itself for capturing the key features. For example, Zhang et al. [8] adopted the convolutional neural network (CNN) to detect the yawning by using the features in nose region instead of mouth area due to the head turnings of vehicle drivers. However, it is still difficult to distinguish easy-to-confuse fatigue states, such as blinking and closing eyes. Huynh et al. [9] provided a more practical solution with the 3D-CNN by considering the broader features on the face and temporal information (sequence of video frames). However, it is still a challenge to distinguish the fatigue states with long-term dependencies, such as yawning and talking. Guo and Markoni [10], and Lyu et al. [11] improved the learning model on the temporal information by integrating CNN with Long Short-Term Memory (LSTM) network, which is a type of recurrent neural network (RNN) that can distinguish the states with long-term dynamical features over sequential frames. However, the potential of CNN-LSTM is far from being fully exploited in the domain of driver/operator fatigue monitoring. The primary limitation in previous studies on CNN-LSTM in fatigue monitoring is that the long-term dependencies of periodic fatigue behavior (e.g., distinguish nodding and head tilt along with loads movements, yawning and talking) are learned from positive-sequence video frames considering only forward dependencies, while backward dependencies learned from reverse-order frames has never been explored that means some useful information may be missed.

To address this issue for improving the accuracy in monitoring and alerting of crane operator fatigue, this study develops a hybrid deep neural network by integrating CNN with deep bidirectional LSTM (DBLSTM) network. The specific objectives of this study are: (1) to accurately detect and align the facial regions with critical fatigue features; (2) to extract the effective facial fatigue features on single-frame images; (3) to distinguish the fatigue state by mining bidirectional temporal clues of sequential features.

2 Literature Review

Crane operator executes the repetitive lift tasks under the fatigue state in a complex construction environment may lead to catastrophic casualties as same as the vehicle drivers. There are apparent signs that suggest an operator/driver is fatigue, such as repeatedly yawning, inability to keep eyes open, swaying the head forward, face complexion changes due to blood flow [12]. As the facial features of operator/driver in a fatigued state are significantly different from that of the conscious state, the real-time monitoring the operator/driver's face by the camera can be an efficient, non-invasive and practical approach to alert the drowsiness and avoid the accidents [13]. PERCLOS (percentage of eyelid closure over the pupil over time) is a reliable measure to monitor the fatigue [14]. In addition, numerous machine learning-based approaches have also been applied to fatigue monitoring. For example, Mbouna et al. [15] developed an approach to extract the visual features from the eyes and head pose of the drivers, and then support vector machines (SVMs) was used to classify the fatigue levels. Choi et al. [16] trained the hidden Markov models (HMMs) to model the temporal behaviors of head pose and eye-blinking for identifying whether the driver is drowsy or not. However, these approaches relied on hand-crafted features which have shown limited efficacy in real-time monitoring and can be inaccurate when driver/operator wear the sunglasses or under considerable variation of illumination conditions [17]. Concurrently, features learned from unlabelled data based on the deep neural networks such as the convolutional neural network (CNN) have been proved to have a significant advantage over hand-crafted features in real-time monitoring of fatigue [14].

CNN is the class of deep and feed-forward neural networks that involves three main elements including local receptive fields, shared weights, and spatial or temporal pooling [18]. The process of fatigue monitoring and alerting by CNN is the same as other machine learning-based methods that can be shown in Figure1. The previous studies regarding fatigue monitoring and alerting by using CNN related models have also been summarized in Table 1. CNN was first applied to fatigue monitoring as the features extractor of static facial fatigue images by Dwivedi et al. [19]. Then, Zhang et al. [8] used the CNNs as both face and nose detectors to show their performances that are quite better than the conventional face detectors such as AdaBoost and WaldBoost with Haar-like features. To achieve real-time fatigue monitoring, Reddy et al.[20] utilized multi-task cascaded CNN with the compression technique to achieve a faster fatigue recognition than existing models of VGG-16 and AlexNet at a reasonable accuracy rate. As the fatigue states are dynamic (e.g., yawning, nodding) and it is difficult to distinguish whether the driver/operator is yawning or talking when only capturing their open mouths, a 3D CNN was proposed to capture the motion information of numerous adjoining frames from videos, and 3D filters

(kernel) were adopted to extract spatiotemporal features [9]. Furthermore, Part et al. [17] integrated three existing CNN-based models including AlexNet, VGG-FaceNet, and FlowImageNet in terms of their efficiency in the extraction of image features, facial features, and temporal features. However, these methods can only extract features with fixed temporal length, and the 3D convolution processes may spend numerous resources and time to impede the real-time monitoring.

Long Short-Term Memory networks (LSTMs) has been proved to be effective in learning long-term temporal dependencies by solving the exploding and vanishing gradient problems that is a Gordian knot for the traditional recurrent neural network (RNN) [21]. And an LSTM comprises typically a cell and three gates (input,output, and forget). The cell can remember values over arbitrary time intervals, and the gates control the information flow out and into the cell. Thus, the integration of CNN and LSTM can be an alternative in fatigue monitoring and alerting. Several studies have adopted CNN to extract frame-level features and then feed them into LSTM to extract the temporal features for determining whether fatigue or not. And several refinement techniques help them achieve the high accuracy such as reducing the hidden layer of LSTM [10], noisy smoothing in post-processing [22], and alignment technology to learn the most critical fatigue information [11]. However, to improve the accuracy, all information included in time series data should be entirely employed. The frames of video are sequentially fed into an LSTM that lead to an information flow with positive direction from time step t-1 to t along the chain-like structure. Therefore, the LSTM can only utilize the forward dependencies, and it is very likely that valuable information is filtered out or not efficiently passed through the chain-like gated structure [23]. Thus, it may enrich the temporal features by considering the backward dependencies. Moreover, the facial expressions of fatigue can be periodical and regular, and even short-term periodicity such as nodding can be detected. Learning the periodicity of time series data, particularly for recurring fatigue patterns, from both forward and backward temporal information can improve the performance of fatigue monitoring and alerting. However, to the authors' knowledge, few studies on crane operator fatigue monitoring considered the backward dependencies. To fill this gap, a deep bidirectional LSTM (DB-LSTM) is integrated into the CNN to form the architecture of fatigue monitoring and alerting system.

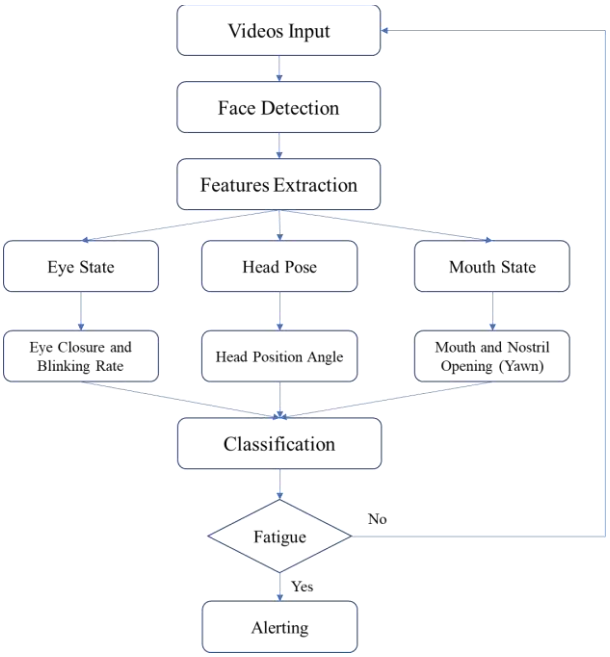

Figure 1. The machine learning-based process of facial fatigue monitoring and alerting

Table 1. The summary of studies by using deep neural networks for fatigue monitoring

Research	Techniques	Database	Accuracy
Dwivedi et al.2014	CNN, Viola and Jones algorithm	Customized	78%
Zhang et al. 2015	CNN, Kalman filter with track-learning-detection (TLD)	YawDD	92%
Huynh et al. 2016	3D CNN, Gradient Boosting	NTHU	87.46%
Park et al. 2016	AlexNet, VGG-FaceNet, FlowImageNet	NTHU	73.06%
Shih and Hsu, 2016	VGG-16, LSTM	NTHU	85.52%
Reddy et al. 2017	Multi-Task Cascaded CNN,	Customized	89.50%
Guo&Markoni, 2018	MTCNN,VGG-11,LSTM	NTHU	84.85%
Lyu et al. 2018	Multi-granularity CNN, LSTM	NTHU	90.05%

3 Proposed Solution

Figure 2 shows the architecture of the proposed hybrid deep neural networks, which comprises three steps and each step maps to a specific model. Firstly, the multi-task cascaded convolutional networks (MTCNN) are adopted as the face detector to locate and align the facial area in each frame of the video. Secondly, the customized CNN model is designed to extract facial

fatigue features from individual-frame images. Finally, a sequence of features within a specific time interval is fed into DB-LSTM to model the temporal variation of fatigue. And the Gaussian smoothing is adopted to reduce the noise and improve the fatigue monitoring performance. Each step of the proposed method is detailed in the following sections.

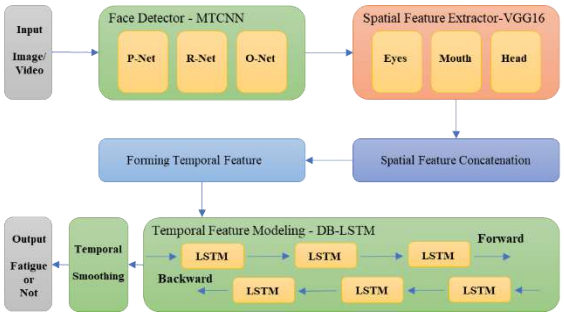

Figure 2. The architecture of the hybrid deep neural networks for fatigue monitoring and alerting

3.1 Face Detection

Precisely detecting and aligning the facial area of crane operator from an image is very critical to achieve efficient extraction of facial fatigue features and fatigue recognition. One of the famous face detectors proposed by Viola and Jones, [24] uses Haar-Like features and AdaBoost to train cascading classifiers, which achieves high detection rate in a real-time manner. However, previous studies have proved and indicated that the accuracy and efficiency of this face detector might reduce with large variations of facial regions [9,16]. These challenges could be exacerbated for face detection and alignment during crane operations in the real-world situations, such as the large pose variations of the operator who should change pose along with the moving loads, extreme lightings or darkness in operation cabin, and occlusions in front of the face. To fill this gap, the multi-task cascaded convolutional networks (MTCNN) proposed by Zhang et al., [25] shows the significant performance improvement in both accuracy and efficiency compared with other face detectors. This study adopts MTCNN to conduct the face detection and face alignment tasks with several stages. Firstly, the input images with various scales should be resized to build an image pyramid. Secondly, a shallow CNN (P-Net) with the input size of 12×12 to fast generate the candidate facial windows that are calibrated based on the bounding box regression vectors, and the highly overlapped candidates are fused by using non-maximum suppression (NMS). Thirdly, a complex CNN (R-Net) with the input size of 24×24 is adopted to reject the non-facial candidates with the same process of calibration and fusion. Finally, a more powerful CNN (O-Net) with the input size of 48×48 is applied to refine the results and produce five landmark points including positions of left-eye, right-eye, nose, left-lid-end, and right-lip-end.

3.2 Spatial Features Extraction

The objective of the features extraction is to learn a CNN-based spatial-domain feature extraction model E for capturing fatigue features F from the individual facial images I. As the feature extraction model E would go through each individual image in I, the extracted F should be general and robust to different input noises. Thus, this study chooses VGG-16 as our basic model which has achieved good performance in various datasets of image recognition [26]. On the basis of original VGG-16, several improvements are conducted to balance the efficiency and accuracy for extracting fatigue feature in a real-time condition. Figure 3 demonstrates the improved VGG-16 architecture V. The original VGG-16 which includes 13 convolutional layers (grouped into Conv 1-5), 5 max-pooling layers (pool 1-5), and 3 fully connected feedforward network layers. However, the input of this study has a smaller size image (64×64 RGB images) than the original VGG-16 (224×224 RGB images), which means the number of parameters can be reduced by using smaller fully connected (Fc) network layers (Fc-6, Fc-7, binary classifier) to avoid over-fitting in the improved VGG-16. Given the input to the improved VGG-16 is a fixed-size 64×64×3 face image, the features both in max pooling 5 and max-pooling 3-4 can be used to obtain the discriminative representation. This considers the fact that forward layers of CNN include more detailed information, while the backward layers summarize the global information. This improvement can be beneficial for improving the accuracy of extracting the small region features that are easily ignored by max-pooling, such as the eyes. To this end, a 1×1 convolutional layer is applied into each of pool 3-5 to approximate the Fc 6 by generating three vectors with the same depth (e.g., 256 in this study). This approximation strategy can not only reduce the number of parameters of Fc layers but also facilitate the Fc layers to extract fatigue-related features by pooling operation automatically. The pooled vectors are concatenated to feed into Fc 7 with fewer parameters to extract the more critical features, which forms the F.

To enable the faster and stable training process in generating the feature extraction model E with good generalization, another improvement for VGG-16 is to use Batch Normalization (BN) [27]. BN is a kind of feature scaling technique that can normalize the sample mean and variance of hidden units before or after the process of activation functions over mini-batch data.

This normalization process helps lessen the internal covariate shift for allowing using the larger learning rates. Meanwhile, the mini-batch including various samples may lead to randomness, which can reduce the risk of over-fitting. In this study, there are 5 BN layers placed before max-pooling layer and Fc layer. Lastly, a binary classifier is placed after Fc7 to predict the fatigue score Y. Given both Y and ground truth label L ϵ {0,1}, the cross-entropy loss function with the Adam optimizer is adopted to minimize the loss. If the Y is larger than 0 and is close to 1, the fatigue degree of the input is higher, and vice versa.

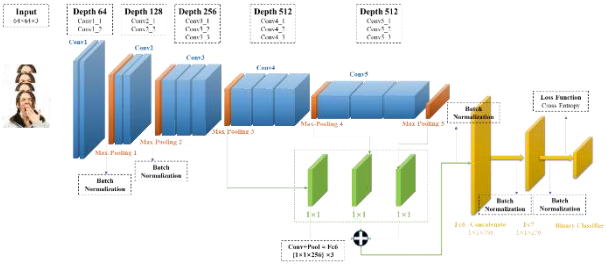

Figure 3. The architecture of CNN-based spatial-domain feature extraction model

3.3 Temporal Features Extraction

Although the feature extractor E has already enabled to predict the fatigue score of each frame based on the spatial features, sometimes it is still hard to discriminate the slight dynamic variations that have strong temporal dependencies such as yawning and talking. Therefore, it can be meaningful to consider both backward and forward information in the sequential frames. To this end, the deep bidirectional long short-term memory (DB-LSTM) is applied to model the temporal features F. DB-LSTM can process the sequential data from two directions by two separate hidden layers and then feed them into the same output layer. The outputs of forward and backward layers (as shown in Figure 4(b)) are both computed by using the basic structure of standard LSTM, See Figure 4.

DB-LSTM has a memory cell to save the state vector which is the sequence of the past or future input data. The current state can be updated on the basis of the current input, output, and the previous state saved in that "cell." DB-LSTM has a gated structure which allows the network to forget the previous state saved in cells or to update the latest state based on the new input data. At time t, the input gate vector, forget gate vector, output gate vector and the state of the memory cell can be denoted as it, ft, ot, and ct respectively. then ct can be updated by the equation (1)-(6).

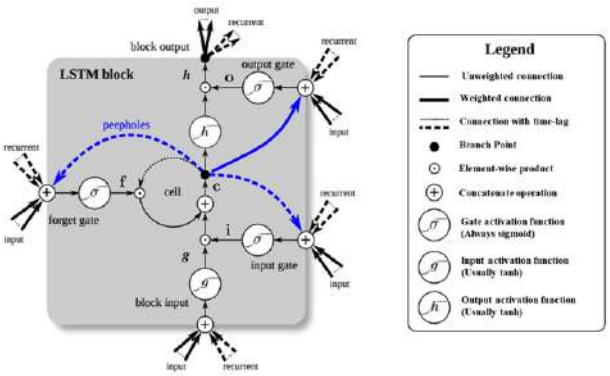

Figure 4 (a). The structure of the standard LSTM [28]

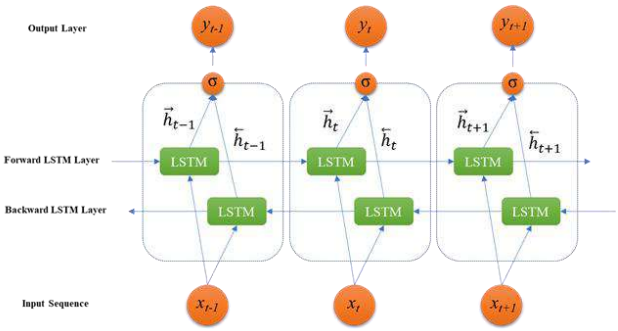

Figure 4 (b). The architecture of the DB-LSTM

$$i_t = \sigma_i(W_{xi}x_t + W_{hi}h_{t-1} + b_i) \quad (1)$$

$$f_t = \sigma_f(W_{xf}x_t + W_{hf}h_{t-1} + b_f) \quad (2)$$

$$o_t = \sigma_o(W_{xo}x_t + W_{ho}h_{t-1} + b_o) \quad (3)$$

$$g_t = tanh(W_{xc}x_t + W_{hc}h_{t-1} + b_c) \quad (4)$$

$$c_t = f_t \odot c_{t-1} + i_t \odot g_t \quad (5)$$

$$h_t = o_t \odot tanh(c_t) \quad (6)$$

Where x_t is the input and σ is the gate activation function, which usually is the sigmoid function. g_t is the state update vector that has activation function ''tanh'' (hyperbolic tangent function) and is computed from the input of the current state and previous state. Forget gate f_t allows the LSTM to forget its previous memory cell c_{t-1} or further memory cell c_{t+1}, and the output gate o_t adopts a transformation to the current memory cell to produce the hidden state h_t. For three gates, the gate can accept the input vector only if the gate value is 1 and reject the input vector when the gate value is 0. Weight matrices $\boldsymbol{W}$ and biases $\boldsymbol{b}$ are the trained parameters. $\odot$ indicates the element-wise product with the gate value. Then, the vector $\boldsymbol{Y_t}$ in feature sequence $\boldsymbol{F}$ is the

concatenated vector by combining the outputs of forward and backward processes as follows:

$$Y_t = \vec{h}_t \oplus \overleftarrow{h}_t \qquad (7)$$

Where $\oplus$ represents the concatenate operation.

In this study, each video can be randomly sampled as the training data by dividing it into numerous video clips with fixed length 50. The DB-LSTM temporal network includes 64 hidden units to predict the refined fatigue score $\boldsymbol{Y_t}$ of each frame (t=1,…,50). The cross-entropy loss function with the Adam optimizer is still applied to minimize the loss.

In the previous stages, both spatial network (CNN) and temporal network (DB-LSTM) are applied to predict the fatigue score of each frame. However, there are still certain noises during the testing on the validation set. In order to achieve a better performance of accuracy, the post-processing techniques including Gaussian smoothing, moving mean/median filtering can be adopted to "smoothing" the predicted fatigue scores.

4 Results and Conclusions

Figure 5 demonstrates the average loss among 20 videos of the training set (orange line), and the evaluation set blue line). The spatial features extraction model E already achieves 85.82% accuracy of fatigue even though its prediction is merely based on a single frame. Figure 6 represents the comparison of DB-LSTM and LSTM on accuracies and convergent performance in the evaluation set. The temporal network LSTM models the temporal variation of the fatigue status, and thus improves the accuracy of fatigue to 92.20%. It is worth noting that a longer clip length T during testing achieves higher accuracies. Finally, after adopting DB-LSTM, it achieves 93.60 % accuracy.

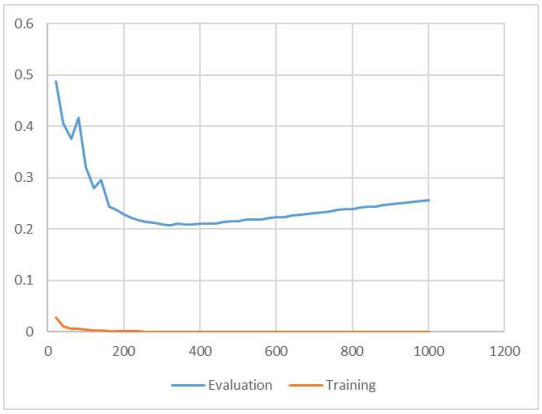

Figure 5. Loss curve of DB-LSTM for both training set and evaluation set

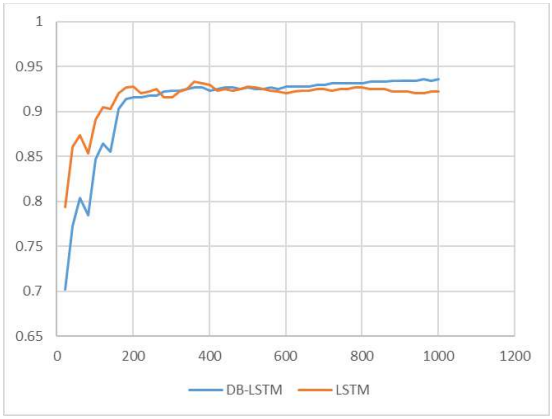

Figure 6. The comparison of DB-LSTM and LSTM on accuracies and convergent performance in the evaluation set

Table 3 represents the average F1 scores and accuracies on the evaluation set. In term of accuracy, the proposed hybrid neural network works pretty well under the sunglasses scenario (98.82%) and Non-Glasses scenario (95.41%). In terms of F1 score, the balanced F1 score among all scenarios shows that the proposed method does not make a biased prediction.

Table 3. Average F1 scores and accuracies for different scenarios

	F1-Score	Accuracy	Number of clips
Night_nonglasses	0.8080	0.8800	125
Night_glasses	0.6061	0.8839	112
Glasses	0.9617	0.9440	125
Non_glasses	0.9655	0.9541	109
Sunglasses	0.9870	0.9882	170
All	0.9286	0.9360	641

This study proposes a hybrid neural network to monitor and alert the fatigue status of the crane operator on the videos. The improvements and contributions in this study are threefold: (1) expand the vehicle driver drowsiness detection to the crane operator fatigue monitoring and alerting; (2) to detect and align the face, and extract the spatial features, the customized CNN is developed based on the baseline models which have excellent performance; (3) a deep bidirectional LSTM (DB-LSTM) is developed by considering both forward and backward dependencies to model the temporal pattern, which can learn compositional representations in space and time. The experiment results indicate that the effectiveness of the proposed hybrid neural network in comparison with several state-of-the-art methods. Further improvements and extensions can be made based on this study. Firstly, the dataset for crane operators should be established instead of using datasets

from the vehicle drivers. Additionally, devising more powerful features by combining multiple signals such as ECG, human audio, other physiological signals can be considered to achieve better accuracy and efficiency in fatigue monitoring.

Acknowledgments

This research was supported by National Key R&D Program of China (No.2016YFC070200504).

References

[1] Han, S. H., Hasan, S., Bouferguène, A., Al-Hussein, M., & Kosa,J. Utilization of 3D visualization of mobile crane operations for modular construction on-site assembly. *Journal of Management in Engineering*, *31*(5), 04014, 2014.

[2] Chi, H. L., Chen, Y. C., Kang, S. C., & Hsieh, S. H. Development of user interface for teleoperated cranes. *Advanced Engineering Informatics*, *26*(3), 641-652, 2012.

[3] Tam, V. W., & Fung, I. W. Tower crane safety in the construction industry: A Hong Kong study. *Safety Science*, *49*(2), 208-215, 2011.

[4] Marquez, A., Venturino, P., & Otegui, J. Common root causes in recent failures of cranes. *Engineering Failure Analysis*, 39, 55-64. 080,2014.

[5] Thiffault, P., & Bergeron, J. Monotony of road environment and driver fatigue: a simulator study. *Accident Analysis & Prevention*, *35*(3), 381-391, 2003.

[6] Borghini, G., Astolfi, L., Vecchiato, G., Mattia, D., & Babiloni, F. Measuring neurophysiological signals in aircraft pilots and car drivers for the assessment of mental workload, fatigue, and drowsiness. *Neuroscience & Biobehavioral Reviews*, *44*, 58-75, 2014.

[7] Ji, Q., & Yang, X. Real-time eye, gaze, and face pose tracking for monitoring driver vigilance. *Real-time Imaging*, *8*(5), 357-377, 2002.

[8] Zhang, W., Murphey, Y. L., Wang, T., & Xu, Q. (2015, July). Driver yawning detection based on deep convolutional neural learning and robust nose tracking. In *Neural Networks (IJCNN), 2015 International Joint Conference on* (pp. 1-8). IEEE.

[9] Huynh, X. P., Park, S. M., & Kim, Y. G. Detection of driver drowsiness using the 3D deep neural network and semi-supervised gradient boosting machine. In *Asian Conference on Computer Vision* (pp.134-145). Springer, Cham, 2016.

[10] Guo, J. M., & Markoni, H. Driver drowsiness detection using the hybrid convolutional neural network and long short-term memory. *Multimedia Tools and Applications*, 1-29, 2018.

[11] Lyu, J., Yuan, Z., & Chen, D. Long-term multi-granularity deep framework for driver drowsiness detection. arXiv preprint arXiv:1801.02325, 2018.

[12] Ngxande, M., Tapamo, J. R., & Burke, M. Driver drowsiness detection using behavioral measures and machine learning techniques: A review of state-of-art techniques. In *Pattern Recognition Association of South Africa and Robotics and Mechatronics (PRASA-RobMech), 2017*(pp. 156-161). IEEE, 2017.

[13] Shi, S. Y., Tang, W. Z., & Wang, Y. Y. A Review on Fatigue Driving Detection. In *ITM Web of Conferences* (Vol. 12, p. 01019). EDP Sciences, 2017.

[14] Zhang, F., Su, J., Geng, L., & Xiao, Z. Driver fatigue detection based on eye state recognition. In *Machine Vision and Information Technology (CMVIT), International Conference on* (pp. 105-110). IEEE, 2017.

[15] Mbouna, R. O., Kong, S. G., & Chun, M. G. Visual analysis of eye state and head pose for driver alertness monitoring. IEEE transactions on intelligent transportation systems, 14(3), 1462-1469, 2013.

[16] Choi, I. H., Jeong, C. H., & Kim, Y. G. Tracking a driver's face against extreme head poses and inference of drowsiness using a hidden Markov model. *Applied Sciences*, *6*(5), 137, 2016.

[17] Park, S., Pan, F., Kang, S., & Yoo, C. D. Driver drowsiness detection system based on feature representation learning using various deep networks. In *Asian Conference on Computer Vision* (pp. 154-164). Springer, Cham, 2016.

[18] LeCun, Y., & Bengio, Y. Convolutional networks for images, speech, and time series. *The handbook of brain theory and neural networks*, *3361*(10), 1995.

[19] Dwivedi, K., Biswaranjan, K., & Sethi, A. Drowsy driver detection using representation learning. In *2014 IEEE International Advance Computing Conference (IACC)*(pp. 995-999).

[20] Reddy, B., Kim, Y. H., Yun, S., Seo, C., & Jang, J. Real-time Driver Drowsiness Detection for Embedded System Using Model Compression of Deep Neural Networks. *Comput. Vis. Pattern Recognit. Work*, 2017.

[21] Hochreiter, S., & Schmidhuber, J. Long short-term memory. *Neural Computation*, *9*(8), 1735-1780, 1997.

[22] Shih, T. H., & Hsu, C. T. MSTN: a multistage spatial-temporal network for driver drowsiness detection. In *Asian Conference on Computer Vision* (pp. 146-153). Springer, Cham, 2016.

[23] Cui, Z., Ke, R., & Wang, Y. Deep Bidirectional and Unidirectional LSTM Recurrent Neural

Network for Network-wide Traffic Speed Prediction. *arXiv preprint arXiv:1801.02143*, 2018.
[24] Viola, P., & Jones, M. Robust real-time face detection. In *null* (p. 747). IEEE, 2001.
[25] Zhang, K., Zhang, Z., Li, Z., & Qiao, Y. Joint face detection and alignment using multitask cascaded convolutional networks. *IEEE Signal Processing Letters*, *23*(10), 1499-1503, 2016.
[26] Simonyan, K., & Zisserman, A. Very deep convolutional networks for large-scale image recognition. *arXiv preprint arXiv:1409.1556*, 2014.
[27] Ioffe, S., & Szegedy, C. Batch normalization: Accelerating deep network training by reducing internal covariate shift. *arXiv preprint arXiv:1502.03167*, 2015.
[28] Greff, K., Srivastava, R. K., Koutník, J., Steunebrink, B. R., & Schmidhuber, J. LSTM: A search space odyssey. *IEEE transactions on neural networks and learning systems*, *28*(10), 2222-2232, 2017.

Automatic Floorplan Generation of Living Space for Simulating a Life of an Elderly Resident Supported by a Mobile Robot

C. Jiang[a] and A. Mita[b]

[a]Graduate School of Science and Technology, Keio University, Japan
[b]Department of System Design Engineering, Keio University, Japan
E-mail: canjiang@keio.jp, Mita@keio.jp

Abstract –

A mobile robot follows a resident and grabs his/her health condition using a Kinect sensor. The 3D environment of the robot's working space has a huge impact on the design and operation of the mobile robot in two aspects: (1) it defines movements of the resident; (2) it affects the view and trajectories of the robot. This paper proposes an efficient and lightweight floorplan generator which automatically samples 2D semantic floorplans. With the height function, generated floorplans can be converted to diverse 3D indoor scenes. Secondly, based on a floorplan, movements of the resident during a period can be generated automatically with his/her activity schedule. Generated 3D scenes with resident movements will be used to evaluate how indoor spaces affect the design and operation policies of the mobile watching robot. The diversity of scenes with movements has two benefits: (1) providing massive data to constitute a training set for machine learning algorithms; (2) various scenes can be classified for finding statistical conclusions.

Keywords –

Floorplan; Automatic simulation; Mobile robot; Elderly people living alone; Design; Operation policy

1 Introduction

The elderly population around the world is steadily increasing. The estimated number of people aged 65 years and older was 524 million in 2010 and is forecasted to increase to 1.5 billion by 2050. [1] Most elderly people preferred to live with family members, but the proportion of them choosing to live alone has shown an increase in recent years. [2] For elderly people, living alone is associated with elevated mortality, a study undertaken it shortened survival by 0.6 years. [3] Although elderly people living alone would benefit from nursed by specialized agents, the shortage of global aged care workforce makes this difficult.

However, recent improvements in robotic, AI and IoT technologies provide some options to address this challenge. For example, monitoring systems were integrated into smart houses. Generally, there are two schemes to grip the health condition of elderly people by using: (1) wearable sensors, such as wearable inertial sensors [4]; (2) stationary sensors, such as cameras [5], passive infrared (PIR) sensors [6, 7], pressure-based item sensors and magnetic door sensors [7]. Secondly, mobile robots were used to support the independent elderly. These robots mainly observed the state of resident, their functions included fall detection [8] and human activity recognition (HAR) [9, 10], and they had additional functions such as interaction, object grasping, entertainment and floor-clean [8].

We focus on using a mobile robot, e-bio (Figure 1a), to monitor the health condition of elderly independent residents with a Kinect V2 sensor. Figure 1b shows the robot tracking people and observing his walking pattern in a studio apartment. Our robot focuses on resident monitoring and omits the functions like interaction and grasping, which reduces its size and degree of freedom. The advantage is that our robot is more economical and affordable for consumers, but the lower and fixed watching view of the Kinect sensor is more vulnerable to indoor obstacles such as furniture when the robot is tracking people and planning its trajectories.

Therefore, some issues regarding our robot need to be addressed, such as:

- Will the robot work well when monitoring an elderly resident?
- How should we adjust the height of the robot and the fixed angle of the Kinect sensor in different indoor scenes to balance its tracking performance and manufacturing cost?
- What operation policies should the robot use for its purpose?

We plan to address these issues by simulation, so

indoor environments and elder people's movements and activities should be simulated as preconditions. Instead of researching few cases, our aim is to obtain statistical results from diverse indoor scenes, the finalized framework of this study is shown in Figure 2.

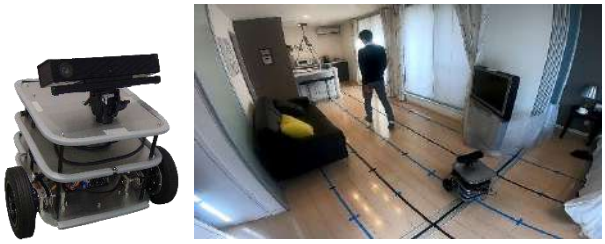

a) b)

Figure 1. Our robot and its utilization: (a) e-bio, (b) e-bio tracks people

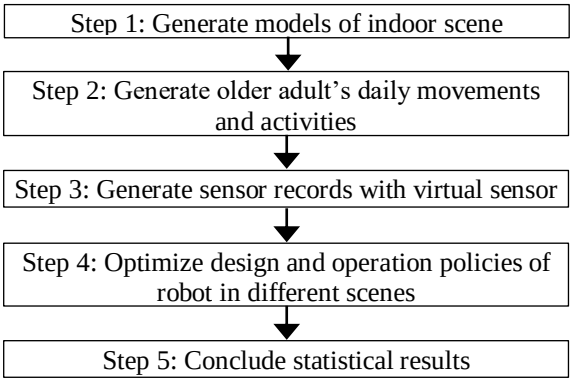

Figure 2. Framework for general study

This paper proposes a generator to automatically produce diverse floorplans for studio apartments, which addresses the primary challenge of Step 1 of the framework. Section 3 describes the basic rules and methodology to generate floorplan; Section 4 details the performance of the generator; Section 5 describes how to convert a floorplan to 3D scene and how to generate resident's paths based on the floorplan.

2 Related Works

2.1 Simulation of Smart House

In recent years, many smart house simulators were proposed because building real smart house test beds was expensive and time consuming. These simulators generated testing data for different purposes such as optimizing the arrangement of house components and sensors [11], human activity recognition [12], ubiquitous application testing [13] and location-based service testing [14].

These simulators enabled smart house designers to verify their ideas and plans. However, they had two shortages: (1) models of house were built manually, (2) virtual residents repeated a predefined schedule or were controlled by users.

To handle the second shortage, Lee et al. [15] proposed a smart house simulator with an automatic virtual resident. This simulator used a motivation-driven behavior planning method to force the resident to interact with the house. During simulation, resident's motivations such as hunger, thirst, and the need to study were generated. However, users still need to build the house model. Furthermore, this simulator did not meet our demands because the virtual resident did not imitate the elderly. The actions and movements of the elderly are slower than the average level and some of them may fall down or suffer from dementia. We should consider these situations in our simulation.

2.2 Floorplan Generation

Floorplan is a 2D semantic map which shows the relationships between physical features of the architecture such as rooms, doors and furniture. Automatic floorplan generation is necessary for our research.

There are two main steps to generate a complete floorplan: (1) deciding the relationships between rooms, (2) placing furniture inside the rooms.

In aspect of the first step, Hahn et al. [16] focused on the interior generation of a large building. They divided the floor into room clusters with parallel hallways. However, the room clusters were regular rectangles and most rooms were the same size. Mirahmadi et al. [17] divided a rectangle house into rooms using Squarified Treemap algorithm. They decided the areas of each room and sorted the areas in descending order, which was the input for the algorithm. This generator is unstable because of the limitation of the algorithm, the areas must be decided carefully. Ma et al [18] generated floorplans based on topological relationship between rooms. They input a topological map and all room blocks, then combined the blocks based on the map. But this generator can not avoid gaps between blocks.

In aspect of the second step, Anderson et al [19] automated desk layouts for diverse offices. Tutenel et al [20] proposed a layout solver which places furniture according to rules defined by users. Users could set rules such as "place X instances of class Y" and "place as many objects of class Z as possible". Henderson et al [21] proposed a data-driven, probabilistic, generative model for room layouts. This model learned statistics from 250, 000 room models designed by human.

For future studies, we hope to develop an efficient and lightweight floorplan generator for residences; the

generators mentioned before do not meet all our demands.

3 Floorplan Generation

Our laboratory's robot has been tested in a studio apartment shown in Figure 3. [22] Different from most dwellings, studio apartments have a large main room where the elderly can sleep, cook and watch TV.

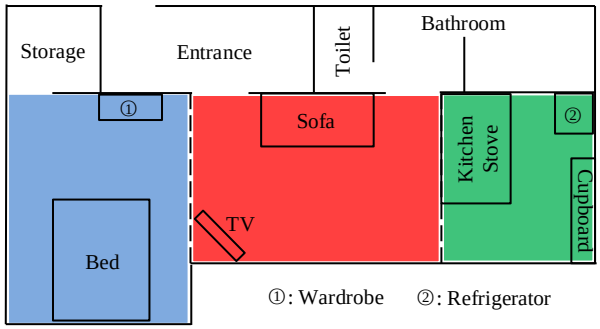

Figure 3. Studio apartment in the test

In Figure 3, the studio apartment includes a main room, entrance, toilet, bathroom and storage. The main room was the working space of our robot, we divide the room into three zones according to the furniture inside them: resting zone (blue area), living zone (red area) and cooking zone (green area). There are no physical boundaries between zones, resident passes through the virtual boundary (black dashed lines) to enter another zone. The walls of the house are represent by black solid lines, and gaps represent doors.

When placing furniture in the main room, normal procedure is: (1) deciding shape and size of the room, (2) dividing room into zones, (3) placing furniture into each zone. But a reverse thinking, deciding size of all zones first and then combining them into the room, has two advantages: (1) The room's shape is usually not a regular rectangle, but the shapes of zones always are; (2) In the future, we will research the dwelling owning separate bedroom, livingroom and kitchen, the reverse method will be more extensive.

3.1 Generation Rules

The desired floorplan describes 2D semantic information of additional rooms, zones, furniture, doors and walls. Additional rooms include a toilet and bathroom, Zones are the working space of virtual robot, which include the resting zone, living zone and cooking zone. There are three classes of furniture:

- Resting furniture includes bed, wardrobe, writing desk-chair set and nightstands.
- Living furniture includes dining table set and sofa-TV set. The dining table pairs one to four chairs.
- Cooking furniture includes kitchen stove, cupboard, refrigerator, wash machine and trash bin.

Each furniture is only inside its corresponding zone. Doors include the entrance, toilet door and bathroom door. The entrance connects zones with external areas (other rooms not in the model or outside of the house). Walls are the boundaries of additional rooms and the union of zones (no walls in the boundaries between zones).

The rules in Section 3.1.1 and 3.1.2 define the size of each element and topological relationship between them.

3.1.1 Rules about Size

In reference to the London Housing Design Guide [23], seven rules are proposed to balance realism and efficiency of our generator.

SR 1. The sizes of the toilet and the bathroom are 0.6 × 1.2m and 1.8 × 1.2m. The 1.2m-long sides are wing sides. The remaining sides are face side and rear side, respectively.

SR 2. The lengths of all sides of all zones are multiplies of 0.2m.

SR 3. The aspect ratios of all zones are less than 2.

SR 4. The area of the resting zone, A_R, is in ($8m^2$, $16m^2$). The area of the living zone is in ($12m^2$, $24m^2$) and ($1.2A_R$, $1.8A_R$). The area of the cooking zone is in ($6m^2$, $12m^2$) and ($0.6A_R$, $0.9A_R$).

SR 5. The furniture size candidates are listed in Table 1.

SR 6. When sampling the size of a furniture item, the area of the zone impacts the generator. Appearance of large furniture in large zones occur with a higher possibility.

SR 7. The lengths of doors are 0.6m.

3.1.2 Rules about Topology

There are seven rules about the topology of generated floorplans:

TR 1. The toilet must connect with the bathroom along one of its wing sides (SR 1). The same with the bathroom.

TR 2. The toilet can connect with the living zone and the cooking zone, the bathroom can connect with the living zone and the resting zone. They connect with zones along their rear sides (SR 1).

TR 3. The toilet and bathroom may be inside or outside of the zones to which they are connected.

TR 4. The generated floorplan must include the resting zone, may include either the living zone or cooking zone or both. The topology candidates of zones are

Table 1. Furniture size candidates

Furniture	Candidate sizes (m)	Furniture	Candidate sizes (m)
Bed	2.1 × 0.9, 2.1 × 1.2, 2.1 ×1.5, 2.1 × 1.8	Writing desk-chair set	1.0 × 1.0, 1.2 × 1.0
Wardrobe	0.6 × 0.6, 0.8 × 0.6, 1.0× 0.6, 1.2× 0.6	Nightstand	0.4 × 0.4
Dining table	0.8 × 0.8, 1.0 × 0.8, 1.2× 0.8, 1.4× 0.8, 1.6 × 0.8	Writing desk	1.0 × 0.5, 1.2 × 0.5
Sofa-TV set	3.0 × 0.9, 3.0 × 1.4, 3.0 × 1.9	Chair	0.4 × 0.4
Kitchen stove	0.6 × 0.6, 1.2 × 0.6, 1.8 × 0.6	Refrigerator	0.6 × 0.6
Cupboard	1.0 × 0.5, 1.2 × 0.5, 1.5 × 0.5	Wash machine	0.6 × 0.6
Sofa	0.9 × 0.8, 1.4 × 0.8, 1.9 × 0.8	Trash bin	0.6 × 0.3
Furniture	Candidate sizes (m)		
TV table with TV	0.6 × 0.4, 0.8 × 0.4, 0.8 × 0.6, 1.0 × 0.4, 1.0 × 0.6, 1.2 × 0.4, 1.2 × 0.6		

Table 2. Topology candidates of zones

Type	1	2	3	4	5
Topology	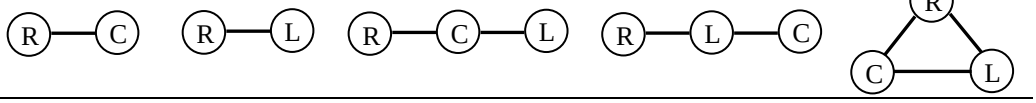				

listed in Table 2, where ®, © and © represent the resting zone, the living zone and the cooking zone, respectively.

TR.5 There are two relationships between a furniture and walls, against a wall or not. A writing desk-chair set and dining table set are not against a wall, all others are against a wall.

TR 6. A furniture item is at least 0.6m away from any other furniture items and doors.

TR 7. The entrance can appear in any wall except in the toilet's and bathroom's walls. The toilet door and bathroom door appear in the middle of the face wall (SR 1) of the corresponding room.

3.2 Methodology

A sample floorplan is generated in three steps: (1) placing zones and additional rooms, (2) generating walls and doors, (3) placing furniture inside each zone.

3.2.1 Placing Zones and Additional Rooms

As the resting zone must be included (*TR 3*), we first sample its size based on *SR 2* to *4* and set the center of the zone to the origin of the coordinate system. We then sample a topology from Table 2 and combine zones and additional rooms based on sampled topology and *TR 1* and *2*. The toilet's and bathroom's size are defined by *SR 1*. To achieve realism and avoid gaps in the floorplan, we should align connected zones and additional rooms.

Figure 4 shows the principles of the alignment. In Figure 4a, when a zone parallels the resting zone (topology 1-4 in Table 2), it must at least be aligned with a short side of the resting zone, and its connected side must be equal to or 1.2m shorter or longer than the long side of the resting zone (1.2m is the length of toilet and bathroom wing sides). Figure 4b, 4c and 4d show that when the living zone is perpendicular to the resting and cooking zones (topology 5 in Table 2), it must connect with the aligned sides of these two zones along its long side. One of its short sides must be aligned with an edge of the union of the resting and cooking zones or exceed or fall short of the 1.2m edge.

3.2.2 Generating Walls and Doors

After placing the toilet and bathroom, it is easy to generate the toilet and bathroom doors with *TR 7*, and the walls are also easy to define. We then sample a wall to place the entrance. The entrance appearing in a wall shorter than 2.0 m or longer than 4.0 m occurs with a higher possibility due to *TR 6* (most furniture items are against a wall). The entrance should be placed close to one end of the wall rather than in the middle for the same reason.

3.2.3 Placing Furniture Inside Each Zone

After sampling the size of a furniture item, we place it inside its corresponding zone by determining the coordinate of its center as shown in Figure 5. In Figure 5a, *dx* and *dy* are the distances between a furniture item and the boundaries of the zone (black solid lines), the black dashed lines represent possible placements of the furniture item's center, for furniture against a wall (*TR 5*), $dx = dy = 0$m. Besides, we must consider *TR 6*, so the effects of other furniture and rooms are described as obstacle areas shown in Figure 5b, where the yellow rectangle represent a furniture item, room or connected zone (to keep distance from furniture inside the zone), *f* is the minimal distance between the yellow rectangle

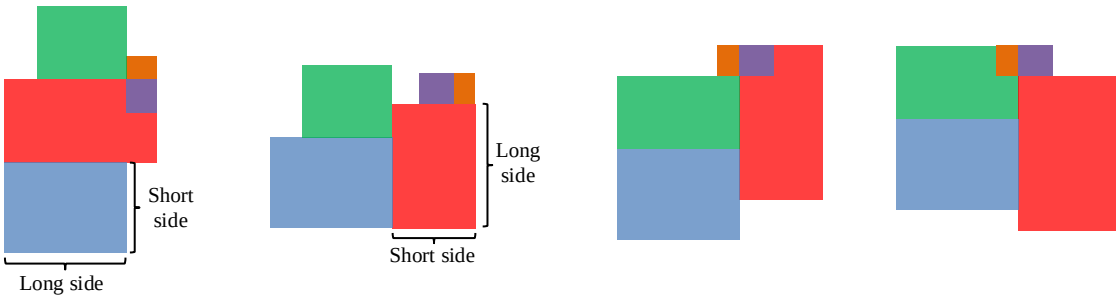

Figure 4. Principles of alignment (resting zone is blue, living zone is red, cooking zone is green, toilet is orange and bathroom is purple): (a) alignment when zones are parallel to resting zone, (b, c and d) alignment when living zone is perpendicular to resting and cooking zones

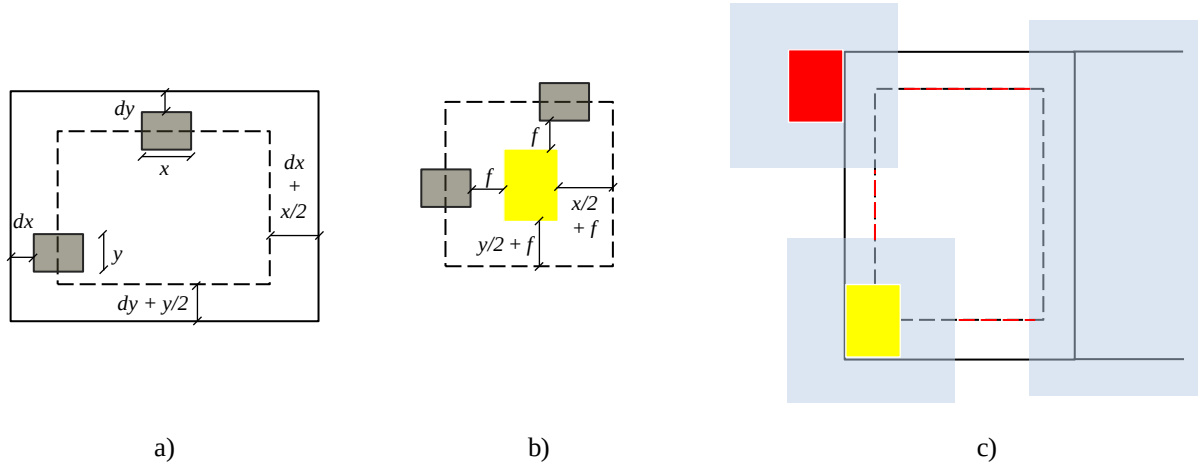

Figure 5. Methodology of placing furniture item inside a zone: (a) possible placements without considering obstacles, (b) obstacle area (b) possible placements considering all obstacles

and the furniture (if the yellow rectangle is a zone, f = 0.3m, otherwise, f = 0.6m). The possible places of the furniture item's center is in the relative complement of black dashed lines in the union of all obstacle areas (Figure 5c).

Therefore, all furniture items are placed by following the procedure below:

1. *List original obstacles including rooms and other zones which are connected with this zone;*
2. *For a furniture item to be placed, sample its size based on SR 5 and 6;*
3. *Considering the furniture can be placed horizontally or vertically, we determine x and y;*
4. *Calculate all obstacle areas;*
5. *If the furniture item is not against a wall, sample dx and dy, otherwise dx = dy =* 0;
6. *Calculate possible placements of the furniture item according to* Figure 5;
7. *Decide the furniture item's placement;*
8. *Add the placed furniture item to the obstacles list and go back to step 2.*

4 Generation Results

The generator is built using Python3. For showing generated floorplans, we sample 1000 times, of which 966 succeeded. The 34 failure cases are caused by the fact that living zones are too small to place the sofa-TV set. All successful samples are shown in this website [24]. We picked two generated floorplans randomly shown in Figure 6. In Section 5, we will describe how to convert a floorplan to 3D indoor scene and how to generate resident's paths with both of them.

We also test the performance of our generator on Intel(R) core(TM) i7-7770 CPU @ 3.60GHz. The generator works 1 million times on average 435.5 seconds with a 96% successful ratio. In the average 959311 successful samples, there are only average 49.2 same floorplans.

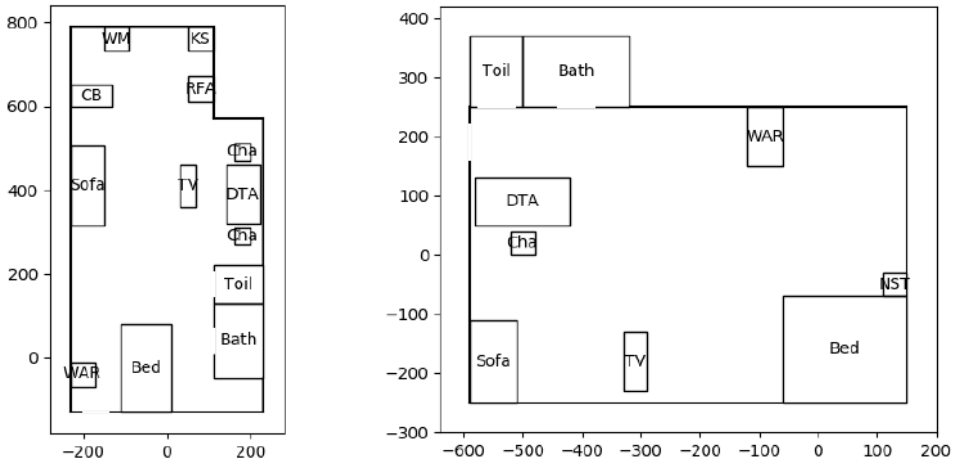

Figure 6. Two generated floorplans (unit: cm, WAR: wardrobe, NST: nightstand, DTA: dining table, CHA: chair, KS: kitchen stove, CB: cupboard, RFA: refrigerator, WM: wash machine, Toil: toilet, Bath: bathroom)

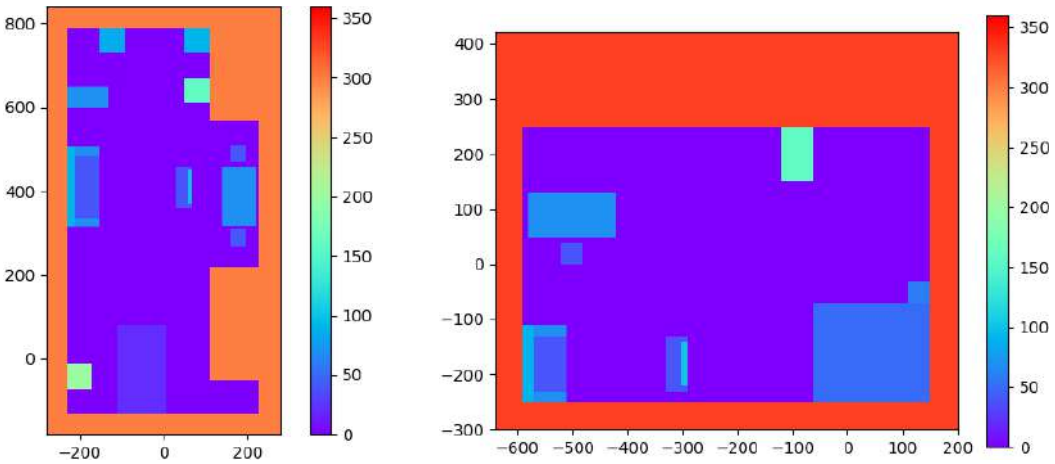

Figure 7. Height functions of two generated houses (unit: cm)

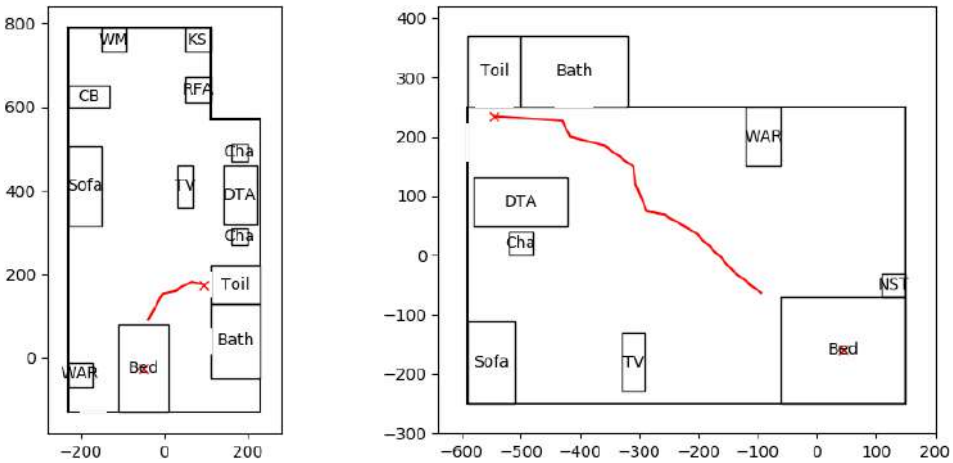

Figure 8. Generated resident's paths from bed to toilet (unit: cm)

5 Utilization of Floorplans

With a floorplan, we can produce a 3D indoor scene with the height function and generate the paths of resident if we know the start and destination points.

5.1 3D Indoor Scene Generation

The 3D scene of a room can be described as a 2D semantic map with the height function if we assume that 3D models of the furniture inside the room are simplified as a combination of cubes. We assume the floor is in the $\boldsymbol{z} = 0$ plane of the 3D coordinate system. For furniture items, their height functions equal the heights of their upper surfaces (we assume all of their lower surfaces are in the $\boldsymbol{z} = 0$ plane). For the floor, its height function is equal to 0. For the toilet, bathroom and external areas, their height functions are equal to the floor height of the house.

After sampling the floor height and heights of all the furniture, the 3D indoor scene is defined. Figure 7 shows the 3D scenes of the two virtual houses with their height functions.

5.2 Resident's Path Generation

Using Rapidly exploring Random Tree Star (RRT*) algorithm, the paths for the resident from the bed to toilet are generated in Figure 8. It reveals that the floorplan has a huge impact on resident's paths, the two paths shown in Figure 8 are quite different despite the fact that they have semantically the same starting point and destination. In the future, we will try different algorithms to generate paths for a more realistic simulation.

6 Summary

A small mobile robot is an amazing option for monitoring the health condition of elderly people living alone. However obstacles inside the house such as walls and furniture may obstruct the robot from tracking resident and disturb its observation. Therefore, it is necessary to optimize the design and operation policies of the robot considering the influence of the indoor space. We hope evaluate the influence and optimization by simulation.

This paper proposes an automatic floorplan generator as a first step in our simulation. This generator is efficient and lightweight, which produces diverse and realistic floorplans. With the generated floorplans, indoor 3D scenes are defined after sampling the floor heights and heights of furniture items. Moreover, the paths of the resident moving from starting points to destinations can be generated.

For the next step, we will generate a resident's daily activities and movements in different indoor 3D scenes. This requires studying daily activities schedules of the elderly and the characteristics of elderly pedestrians. With the schedule, we know when the elderly do some activities, when they move and the starting points and destinations of the movements. With the study of elderly pedestrians, we can grasp the position of body joints during his/her movement, these information will be useful in the simulation.

We will then simulate a virtual robot with a Kinect sensor, and produce virtual sensor records. Finally, we will evaluate the influence of indoor spaces and optimize the robot's design and operation policies based on produced models and sensor records.

In these studies, diverse indoor scenes will help us draw statistical conclusions compared with only researching limited indoor spaces. Massive sensor records are also necessary for machine learning algorithms. These are advantages of our floorplan generator.

Acknowledgement

This research was partially supported by JSPS KAKENHI 18H00968 and the Japanese Government (Monbukagakusho: MEXT) Scholarship. We would also like to sincerely express our appreciation to Mr. Wang Xiao of Southeast University, China, for introducing us to some references about studio apartment design.

References

[1] National Institutes of Health. Global health and aging. On-line: https://www.who.int/ageing/publication/global_health.pdf, Accessed: 28/12/2018.

[2] Pimouguet C., Rizzuto D., Schön P., Shakersain B., Angleman S., Lagergren M., Fratiglioni L. and Xu W.; Impact of living alone on institutionalization and mortality: a population-based longitudinal study, *European Journal of Public Health*, 26(1): 182–187, 2016.

[3] Thang, L.; Living Independently, Living Well: Seniors Living in Housing and Development Board Studio Apartments in Singapore. On-line: http://www.fas.nus.edu.sg/srn/archives/55785, Accessed: 15/11/2018

[4] Vuong N., Chan S., Lau C., Chan S., Yap P., and Chen A.; Preliminary results of using inertial sensors to detect dementia-related wandering patterns. In *Proceedings of 37th Annual International Conference of the IEEE Engineering in Medicine and Biology Society (EMBC)*, page 3703-3706, Milan, Italy, 2015.

[5] Chen D., Bharucha A., and Wactlar H.; Intelligent

video monitoring to improve safety of older persons. In *Proceedings of 29th Annual International Conference of the IEEE Engineering in Medicine and Biology Society*, page 3814-3817, Lyon, France, 2007.

[6] Gochoo M., Tan T., Velusamy V., Liu S., Bayanduuren D. and Huang S.; Device-Free Non-Privacy Invasive Classification of Elderly Travel Patterns in a Smart House Using PIR Sensors and DCNN, *IEEE Sensors Journal*, 18(1): 390-400, 2018.

[7] Das B., Cook D., Krishnan N., and Schmitter-Edgecombe M.; One-class classification-based real-time activity error detection in smart homes, *IEEE Journal of Selected Topics in Signal Processing*, 10(5): 914-923, 2016.

[8] Fischinger D., Einramhof P., Konstantinos P., Wohlkinger W., Mayer P., Panek P., Hofmann S., Koertner T., Weiss A., Argyros A. and Markus Vincze M.; Hobbit, a care robot supporting independent living at home: First prototype and lessons learned, *Robotics and Autonomous Systems*, 75(A): 60-78, 2016.

[9] Do H., Pham M., Sheng W., Yang D. and Liu M, RiSH: A robot-integrated smart home for elderly care, *Robotics and Autonomous Systems*, 101: 74-92, 2018

[10] Duckworth, P., Gatsoulis Y., Jovan, F., Hawes, N., Hogg, D. and Cohn, A. Unsupervised Learning of Qualitative Motion Behaviours by a Mobile Robot, In *Proceedings of the 2016 International Conference on Autonomous Agents & Multiagent Systems*, page 1043-1051, Singapore, Singapore, 2016

[11] Park J., Moon M., Hwang S. and Yeom K., CASS: A Context-Aware Simulation System for Smart Home, In *Proceeding of 5th ACIS International Conference on Software Engineering Research, Management & Applications*, page 461-467, Busan, South Korea, 2007.

[12] Bouchard, K., Ajroud, A., Bouchard, B., and Bouzouane, A; SIMACT: A 3D Open Source Smart Home Simulator for Activity Recognition. In *Proceedings of the Advances in Computer Science and Information Technology: AST/ UCMA/ ISA/ ACN 2010 Conferences*, page 524-533, Miyazaki, Japan, 2010.

[13] Nishikawa H., Yamamoto S., Tamai M., Nishigaki K., Kitani T., Shibata N., Yasumoto K. and Ito M.; UbiREAL: Realistic smarspace simulator for systematic testing, *Lecture Notes in Computer Science*, 4206: 459–476, 2006.

[14] Yang Y., Wang Z., Zhang Q. and Yang Y.; A time based Markov model for automatic position-dependent services in smart home, In *Proceeding of 2010 Chinese Control and Decision Conference*, page 2771–2776, Xuzhou, China, 2010.

[15] Lee W., Cho S., Chu P., Vu H., Helal S., Song W., Jeong Y., Cho K.; Automatic agent generation for IoT-based smart house simulator, *Neurocomputing*, 209: 14-24, 2016.

[16] Hahn E., Bose P., and Whitehead A.; Persistent realtime building interior generation, in *Proceedings of the 2006 ACM SIGGRAPH symposium on Videogames, ser. Sandbox '06*, page 179-186, New York, USA, 2006.

[17] Mirahmadi M. and Shami A.; A Novel Algorithm for Real-time Procedural Generation of Building Floor Plans. On-line: https://arxiv.org/abs/1211.5-842, Accessed: 04/10/2018.

[18] Ma C., Vining N., Lefebvre S. and Sheffer A.; Game level layout from design specification, Computer Graphics forum, 33(2): 95-104, 2014.

[19] Anderson C., Bailey C., Heumann A. and Davis. D; Augmented space planning: Using procedural generation to automate desk layouts, *International Journal of Architectural Computing*, 16(2): 164-177, 2018.

[20] Tutenel T., Bidarra R., Smelik, R and Kraker K.; Rule-based layout solving and its application to procedural interior generation, In *Proceeding of CASA workshop on 3D Advanced Media in Gaming and Simulation*, Amsterdam, Netherlands, 2009.

[21] Henderson P., Subr K. and Ferrari V.; Automatic Generation of Constrained Furniture Layouts, On-line: https://arxiv.org/abs/1711.10939, Accessed: 04/10/2018.

[22] Ogawa A. and Mita A.; Performance of a Sensor Agent Robot in a Real Living Environment for Monitoring in Houses, In *Proceeding of International Conference on Smart, Sustainable and Sensuous Settlements Transformation*, page 35-40, Munich, Germany, 2018.

[23] London Development Agency, London Housing Design Guide, On-line: https://www.london.gov-.uk/sites/default/files/interim_london_housing_design_guide.pdf, Accessed: 08/12/2018.

[24] https://github.com/Idontwan/Studio-Apartment-Generator/tree/master/Sample%20Layout

Infographics on Unmanned Dozer Operation

S. Nishigaki[a] and K. Saibara[b]

[a]Mazaran, Co., Ltd., Japan
[b]Kick Co., Lt., Japan
E-mail: sleepingbear@c2mp.com, saibara@c2mp.com

Abstract –

As for unmanned dozer operation, this study aims development on infographics to reduce likely mental stress burden to operators in the remote-control room. First of all, this paper introduces problems in unmanned construction and the purpose of this study. Secondly, actor-critic based construction control system is described, which generates infographics. Thirdly, point on construction system is presented, which gathers readings from onboard smartphone for dozer in real-time manner. Fourthly, lesson learned from examples of infographics are reported; Finally, concluding remarks and future works are mentioned.

Keywords –

Unmanned construction; Infographics; Actor-Critic; Loading surface displacement; Underground stress

1 Problems and Purpose

Basically, operators can feel their realistic sensation of their own machine's behaviour based on the seat of the pants under their operations, e.g., distance and clearance perception using front views, possible motion space, and speed, acceleration, jerk, jolting, rattling, rolling, pitching, and yawing of the machine body, and so on. Handling joysticks to operate a machine, either directly or remotely, is an inherently eye-hand coordination task. The eye-hand coordination means to control eye movements with hand movements, and to handle joysticks along with the use of proprioception of the hands, or vice versa, as processing visual representation of the situational views.

Considering unmanned operation, however, the operators handle the joystick controllers to operate construction machines remotely in narrow field of views produced by camera-monitor system at the control room. Here, the operator receives a visual representation of the situational views from the camera monitor, process it, and select an action by handling the joysticks. Although, the operators have to make a decision instantaneously on do's and don'ts in their operations, it is sometimes difficult to ensure line-of-sight for or visuospatial perspective taking to location and movement direction of their machines or positions of their targets. Then they have to mentally translation, rotation and scaling between different frames of references to [1]:

(1) Orient the different sets of information into the same of reference, and

(2) Understand the relationships between the sets of information.

Therefore, the unmanned construction asks the operators to acquire extensive trainings and broad experiences on problem-solving skills. The skilled operators of these kinds are imperative for the unmanned construction. In Japan, however, there are very few skilled operators, and most of them are aged people.

Overcoming these sort of problems, it is significant and requisite to compensate their realistic sensation in order to enhance spatial awareness, in other words, conscious awareness of actions. To do so, we have been and are doing research and development on infographics pertaining to construction state, and trying to build actor-critic based construction control system, which could provide the operators with the infographics in a timely manner. The infographics are a visual representation of construction profile with graphics, numerical tables, quantitative evaluation indexes, and early precautionary messages, which are inferred from outputs of spatiotemporal analysis models built in the critic component as explained later. The construction profile is defined as a set of data to vision characteristics of phenomena being generated along with construction in progress and indexes to show the patterns [2]. The infographic makes it possible for the operators to quickly grasp the essential insights on construction situation at a glance.

As is well known, an unmanned construction process is separated into several operations such as excavation, loading, hauling, unloading, filling, dozing, compacting, slope shaping, etc., which are sometime independently and at other time interactively performed by different operators. Focusing on dozer operation, included in the unmanned construction process, this paper reports research and development on infographics to compensate operator's realistic sensation. Dozer operation presented here is remotely dozing and compacting to build retaining embankment as countermeasures to additional landslide.

First, this paper describes overview of actor-critic based construction control system, which handles readings and derive relevant infographics from a data set of readings. Secondly, lessons learned from examples of infographics are reported. Finally concluding remarks and future works are presented.

2 Overview of Actor-Critic Based Construction Control System

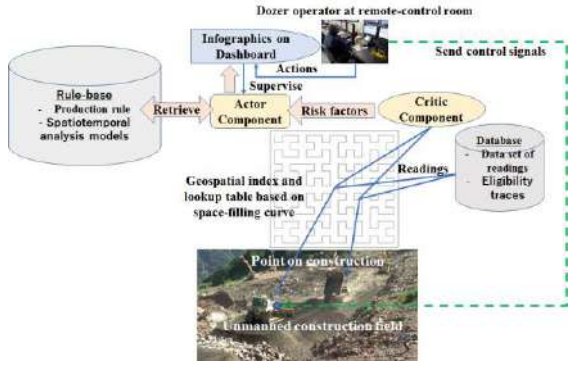

Figure 1. Schematic view of actor-critic based construction control System

The actor-critic based construction control system is largely classified into construction machine, points on construction (hereafter called POC), operator at the remote-control room, rule-base, database, actor-critic architecture, and dashboard as shown in Figure 1.

2.1 Points on Construction (POC)

POC takes sensor-based event detection approach to track construction machines and to automatically and real-timely gather a data set of readings related to events occurred by unmanned construction operations as shown in Figure 2 [3].

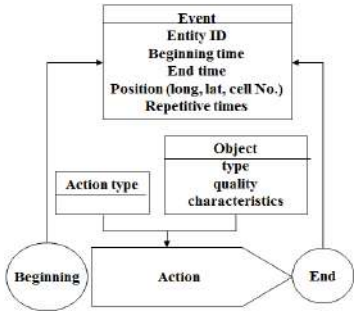

Figure 2. Image of sensor-based event detection approach

In this approach, the beginning and end of action could be automatically detected by sensors built in smart phone (e.g., 3-axial accelerometer, 3-axial angular velocity meter, GPS receiver, and communication module), and otherwise recognized by a button pressed event, that is, pushing predetermined function key on the smart phone by operator. Unmanned construction machine has on-board smart phone whenever it is being operated. And then, the smart phone automatically sends the data set of readings via the Internet to store them into the database. Readings gained from the POC consist of time, longitude, latitude, direction, speed, 3-axis acceleration, 3-axis angular velocity, and son.

2.2 Operator

Operator here includes not only machine operator but also resident engineers and experts in unmanned construction. The operator can supervise the actor by inputting previous setting into the dashboard. The previous setting consists of sampling frequency, various elements of machines, thresholds for discriminations, local coordinates and bounded box of construction area, positions of landmarks (i.e. spots of digging, loading and unloading, waypoints on haulage route), and numerical targets of construction works such as digging, hauling, dozing, the order of priority to select the if-then rule inside the actor, and so on.

Construction site area is expanded by quadrangular work cells with geospatial indexes, which are labelled by the unique number that defines cell's position in order of cell vertices in sequence of space-filling curve, that is, Hilbert curve. This is conversion between positions on the Hilbert curve and local coordinates in geometric range of construction area. The labelled work cells build an index structure that enables us to retrieve information effectively and efficiently.

The operator can choose spots containing the point of interest from the work cells to be controlled, e.g., loading spot, haulage route, dumping spot, embanking spot, compartments of concrete placement, hazards latent in construction area, dangerous phenomena, and so forth.

2.3 Critic Component

The critic fetches the readings sent from on-board sensors built in smart phone, calculates risk factors and propagates them towards the actor. The risk factors consist of:

(1) Descriptive statistics as to running speed, 3-axis acceleration, 3-axis angular velocity;

(2) Composition value of 3-axis acceleration gained by

$$force = \sqrt{ax^2 + ay^2 + az^2} \quad (1)$$

where force: composition value, ax: lateral acceleration, ay: longitudinal acceleration, and az: vertical

acceleration;
(3) Values of jerks: The jerk is the first-order difference of consecutive data elements in time series;
(4) Change-points in mean and variance of the values of jerks;
(5) Run length: The run length in this study is defined as a continuous sequence of repeated upward or downward values in many consecutive data elements;
(6) Distance: distance travelled, distance to other machines and landmarks;
(7) Attitude of machine gained by applying complementary filter to 3-axis acceleration and 3-axis angular velocity;
(8) Dozing area and density; and
(9) Progress rate.

2.4 Actor Component

Largely speaking, actor component includes two mechanisms as follows:
(1) Production rule (If-then rule <state, action, strength>)

This rule associates a condition (if) with an action (then); The rule states what action to perform when a condition is true; The strength indicates firing priority (i.e. rank, utility, severity, probability, cost, etc); The production rule is chosen based on the order of priority predefined by the operator; and
(2) Eligibility trace

Eligibility trace is a temporary record of the occurrence of an event, such as the visiting of a state or the taking of an action, and so on; The eligibility trace marks the memory parameters associated with the event as eligible for undergoing learning changes.

The actor component incorporates spatiotemporal analysis models to analyse the risk factors. These models are applied to:
(1) Visualize travelling trajectory of construction machines, and to show interference among work lines,
(2) Calculate jerks of running speed and to detect occurrence spots of sudden acceleration and rapid deceleration
(3) Calculate composition values of 3-axis acceleration and the jerks, and to calculate frequency of impacts and free-falls and then to show rugged sections or damaged spots on haulage road,
(4) Calculate distances to other machines and any landmark,
(5) Apply complementary filter to 3-axis acceleration and 3-axis angular velocity and then gain attitude of machine, and to show probable turnover and sliding,
(6) Grasp dozing trajectory and to calculate the constructed area, and more to show the progress gauge of the operation,
(7) Grasp compacting trajectory and the compacted density,
(8) Calculate loading surface displacement after dozing and show the time-series changes,
(9) Calculate underground stress below dozing and show the time-series changes, and
(10) As for acceleration and angular velocity in time series, detect change-points in the mean and the variance and to find the trend by counting the run length.

The actor produces list-wise infographics with early precautionary messages, and forwards them to the dashboard. The early precautionary messages inform operator of the phenomena prognosticated from the risk factor. The early precautionary messages are composed of:
(1) Objective: description of the infographic's objective;
(2) Hazard clarified: dangerous behaviour or phenomena identified by the built-in spatiotemporal analysis models, for examples,

1) Dangerous proximity during operating machine when entering into the proximate area of 100 m range from other machine or dangerous spots like those;
2) Dangerous operation:
   a) Sudden acceleration or rapid deceleration, when the jerk value of travelling speed gets larger than the predefined threshold value;
   b) Turnover risk when finding trend for machine body to lean to crosswise or longitudinal direction and value of rolling or pitching more than 15 degrees; and
   c) Defect productivity warning when finding
      - Run length of key performance indicator (hereafter called KPI) changes in time series more than the threshold "7";
      - Any shift in the mean and the variance of KPI; and
      - Actual progress behind the planned baseline.

(3) Early precaution
Referring to ANSI Z535,5 definitions, the levels of precaution are set as follows:

1) Danger: indicate an extreme hazardous situation which, if not avoided, will result in death or serious injury,
2) Warning: indicate a hazardous situation which, if not avoided, is liable to result in death or serious injury, to decrease one's productivity, or to end degradation of construction quality,
3) Caution: indicate a hazardous situation which, if not avoided, is likely to result in minor or moderate injury, to decrease productivity, or to end degradation of construction quality, and
4) Notice: address current practices that are not related to the above hazards.

2.5 Dashboard

A dashboard is a visual display on screen of smart phone, PC or other device that are installed at the

control room or the operators hold. Information displayed on the dashboard is consolidated and arranged on a single screen so that infographics can be monitored at a glance.

2.6 Database and Rule-based Database

Database and rule-based are web-based cloud systems. The database stores a data set of readings. Infographics and early precautionary messages generated by the actor component are displayed the dashboard, and stored in the database. Also, the eligibility trace data is stored in the database. The rule-base stores if-then rule and spatiotemporal analysis models that the actor component uses.

3 Lesson Learned from Examples of Infographics

This chapter reports examples of the infographics that show images of the exploratory spatiotemporal visualizations with wrap-up of lesson learned. The wrap-up of lesson learned is composed of objectives, hazard clarified, dangerous operation identified, early precautionary message, and reflective description on lesson learned.

3.1 Data Set Used to Generate Examples of Infographics

In order to generate examples of infographics, we utilized a data set of readings with respect to remote-controlled dozing and compacting operations applied to build retaining embankments as countermeasures to further large-scale landslide. The data set of readings was obtained from sensors, such as 3-axis accelerometer, 3-axis angular velocity meter, digital compass, GPS receiver, which were built in the on-board smartphone for the dozer. The data set utilized here is structured of meta data and variables as follows:
(1) Machine id
(2) Number of original obs.: 12013
(3) Sampling frequency: 4 HZ
(4) Measurement start time: "2017-03-09 08:24:00 JST"
(5) Measurement end time: "2017-03-09 16:25:00 JST"
(6) Analysis object: 3000 obs. of 11 variables (dd: num Time: POSIXct, long: num, lat: num, speed: num, ax: num, ay: num, az: num, gx: num, gy: num, gz: num)
The observations of analysis object here were chosen from the original observations at random sampling with replacement.

3.2 Travelling Trajectory

Spatiotemporal trajectory of dozing and compacting is shown in Figure 3.

Wrap-up of lesson learned from Figure 5 is listed below.
(1) Objectives: Visualization of travelling, dozing, compacting, and time lapsed
(2) Hazard clarified: None
(3) Dangerous operation identified: None
(4) Early precautionary message: Notice
(5) Reflective description on lesson learned:

By Figure 5, we will be able to explore existential changes in spatial and thematic properties of travelling, dozing, and compacting, and also the time lapsed. This trajectory is plotted along with the vertical time axis and with locations on two-dimensional plane of longitude and latitude coordinates. Stopped and/or idling states of machine are dotted vertically along with the time axis. It can be seen from Figure 5 that the stopped and/or idling time is short during dozing and compacting operations. Total distance travelled here was 6030.622 m.

Furthermore, this infographic can be utilized for a fleet management of several machines, such as backhoes, crawler carriers, dozers, and vibration rollers, and so on. If dotted marks should be plotted at the same time and at the same position, the machine works related to the dotted marks are liable to be interfered with each other. As far as possible, it is desirable for these dotted marks to be plotted at the different start time and then in parallel with each other.

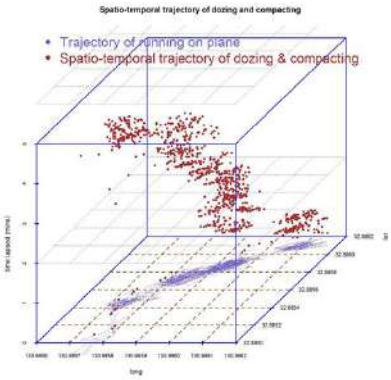

Figure 3. Spatiotemporal trajectory of dozing and compacting (Slate blue dashed line: "running trajectory on plane"; Brown dot "spatiotemporal trajectory of running along with the axis of time")

3.3 Safety Control

It is significant and required to compensate operator's realistic sensation, when remotely operating machine at dangerous spots, for example, at the steep slope, at the ridge of steep cliff, etc. In addition, spatial awareness is very important for operators to infer and understand the present and future surroundings of their own machines and to watch oneself in the work space.

In order to compensate operators' realistic sensation

and evoke their spatial awareness, it would be significant to provide them with physical cues related to appearance and posture of machine body, which would enhance their diagnostic and prognostic capabilities to reflect on their own unsafe behaviour

Examples containing to spatiotemporal visualization of unsafe behaviour and potential hazards are presented below.

3.3.1 Occurrence Spots of Sudden Acceleration and Rapid Deceleration

Upper 95% and lower 5% points in the jerk distribution of running speed are used as the threshold to detect occurrence spot of sudden acceleration and rapid deceleration, and then the if-then rules are shown below:

If (the jerk of speed >= the upper 95%-point value), then it is presumed that sudden acceleration occurred at the longitude and latitude; and
If (the jerk of speed < the lower 5%-point value) then it is presumed that rapid deceleration occurred at the longitude and latitude.

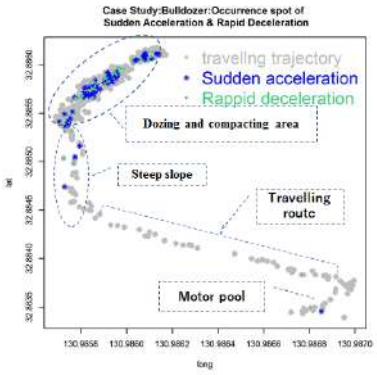

Figure 4. Occurrence spots of sudden acceleration and rapid deceleration while running

Wrap-up of lesson learned from Figure 4 is listed below.
(1) Objectives: Detection of occurrence spots of sudden acceleration and rapid deceleration while running.
(2) Hazard clarified: Many sudden accelerations and rapid decelerations were found.
(3) Dangerous operation identified: It is liable to evoke traffic accident, and degradation of quality as to surface and subsurface soil.
(4) Message: Warning
(5) Reflective description on lesson learned:
Many sudden accelerations and rapid deceleration were found at the dozing and compacting area. It is presumed that the dozing and compacting might be rough or harsh operations, which are liable to trigger disturbing and stirring the ground surface. It might involve risk of quality degradation of the surface and subsurface ground. Many sudden accelerations were found when climbing at steep slope,. Conversely, some rapid decelerations were found when descending.

3.3.2 Detection of Rugged Sections or Damaged Spots on Site

It is more likely to find phenomena of impacts and free-falls at rugged sections or damaged spots. Nevertheless, operators could not easily envisage any hazard latent in a narrow field of view from camera-monitor system at the control room without any background information on unmanned earthwork process.

The if-then rules to identify levels of impact and free-fall are shown as follows:

If (2G<=the 3-axis acceleration composition value) then it is presumed that strong impact occurred at the longitude and the latitude;
If (1.4G =< the 3-axis acceleration composition value & the composition value<2G) then it is presumed that somewhat strong impact occurred at the longitude and the latitude;
If (1.2G=< the 3-axis acceleration composition value & the composition value<1.4G) then it is presumed that impact occurred at the longitude and the latitude; and
If (the 3-axis acceleration composition value<0.7G) then it is presumed that free-fall occurred at the longitude and the latitude.

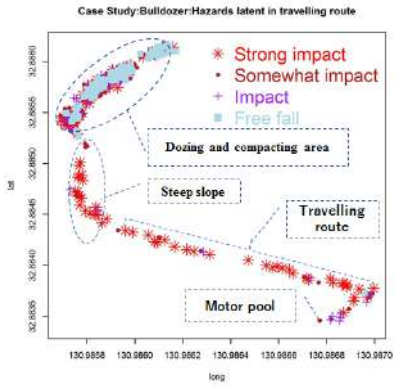

Figure 5. Existing of impacts and free-falls on site

It would be helpful and significant for operators at the control room to see severe dangerous spots with coloured marks, and to watch the early precautionary messages on the screen of their smart phone or PC, when approaching to the severe dangerous spots.

Wrap-up of lesson learned from Figure 5 is listed below.
(1) Objectives: Detection of rugged sections or damaged spots on site.
(2) Hazard clarified: Many strong impacts, and impacts were found everywhere. Furthermore, There were many

occurrences of free-falls in dozing and compacting area.
(3) Dangerous operation identified: Remote operation of dozer might be poorly handled and harsh. There would be otherwise many rugged sections or damaged spots latent in the whole area of the construction.
(4) Message: Alert
(5) Reflective description on lesson learned:
It can be confirmed in Figure 5 that there are many impacts and free-falls within dozing and compact area, and many strong impacts were found everywhere on the travelling route. The former phenomena indicate that dozing and compacting is rough or harsh operations, which are likely to trigger disturbing and stirring the ground surface. It is likely to result in traffic accident, degradation of quality as to surface and subsurface soil. The latter phenomena indicate the travelling route might be severe uneven.

3.3.3 Detection of Probable Turnover and Sliding

It aims to prevent a dozer from accidents of rollover, slide and falling. The method here largely forks the two:
(1) Find signals of turnover, slither, or skid of the machine body, and then issue early precautionary messages, and
(2) Visualize phenomena of rolling, pitching, and vacillation of the machine body in order to prognosticate likely dangerous sections and spots latent in the travelling route to the work zone.

More concretely, both the 3-axis acceleration and 3-axis angular velocities are captured by sensors built in the onboard smart phone, calculated by a complementary filter, and then rolling and pitching of machine body are visualized in time series. Moreover, if and when finding both of run-length more than "7" in the time series of rolling and pitching and the values more than 15 degrees, and then the occurrence places denote dangerous sections and spots latent in the travelling route to the work zone. Figure 6 shows dozer attitude in time series.

Wrap-up of lesson learned from Figure 6 is listed below.
(1) Objectives: Finding dangerous sections and spots latent in the access road to the work zone.
(2) Hazard clarified: None
(3) Dangerous operation identified: None
(4) Early precautionary message: None
(5) Reflective description on lesson learned:
It can be shown from Figure 6 that there are not dangerous sections and spots latent in the access road to the work zone, no matter whether rough or harsh operations

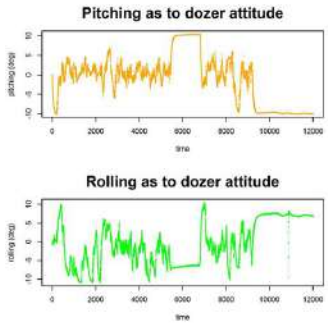

Figure 6. Dozer attitude in time series and the histogram

3.4 Productivity Control

Figure 7 shows dozing trajectory and the area, and the progress gauge of the operation. The progress gauge represents progress rate to the target value.

Kernel density estimation is a nonparametric method for estimation of probability density functions. An axis-aligned bivariate normal kernel is utilized to estimate the dozed area.

Wrap-up of lesson learned from Figure 7 is listed below.
(1) Objectives: Visualization of dozing trajectory and the area, and progress rate of the operation.
(2) Hazard clarified: None
(3) Dangerous operation identified: None
(4) Early precautionary message: None
(5) Reflective description on lesson learned:
Dozing and compacting are being operated as scheduled.

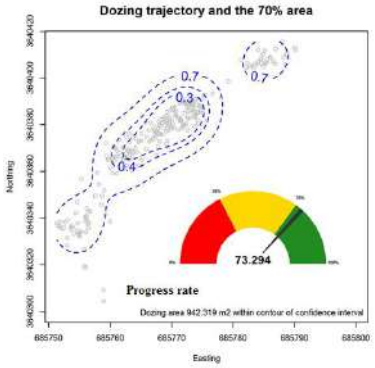

Figure 7. Dozing trajectory and the area, and progress rate of the operation

3.5 Quality Control

3.5.1 Compacting Trajectory and the Compacted Density

Weighted Kernel density Estimate method is utilized to visualize compacting trajectory and the compacted density, where the weight is impulse values. Figure 8 shows compacting trajectory and the compacted density.

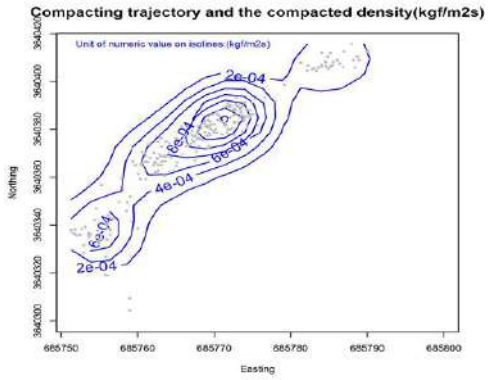

Figure 8. Compacting trajectory and the compacted density

Wrap-up of lesson learned from Figure 8 is listed below.
(1) Objectives: Visualization of compacting trajectory and the compacted density.
(2) Hazard clarified: None
(3) Dangerous operation identified: None
(4) Early precautionary message: None
(5) Reflective description on lesson learned:
Compaction is filled in all the required area.

3.5.2 Grasp of Loading Surface Displacement

Nonlinear dynamical behavior as to loading surface displacement consists of transient term and stationary term.

If the damping ratio ζ<1, the former is given as

$$x(t) = \exp(-\xi\omega_0 t)\frac{v_0}{\omega}\sin\omega t \quad , \qquad (2)$$

where v0 is the running speed. The latter is expressed as

$$x(t) = A\sin(\omega t - \phi), \qquad (3)$$

$$A = \frac{x_{st}}{\sqrt{(1-\lambda^2)^2 + 4\xi^2\lambda^2}}, \qquad (4)$$

$$\tan\phi = \frac{2\xi\lambda}{1-\lambda^2}, \quad \text{and} \qquad (5)$$

$$\lambda = \sqrt{1-\zeta^2} \quad , \qquad (6)$$

where x_{st} is static displacement.

Relationship between the damping ratio ζ and the logarithmic decrement δ is expressed as

$$\delta = \frac{2\pi\xi}{\sqrt{1-\xi^2}} \quad , \qquad (7)$$

If and when the damping ratio ζ <<1,

$$\delta \cong 2\pi\xi \qquad (8)$$

In addition, the relationship between the natural frequency ω_0 and the damped natural frequency ω is presented by the following equation.

$$\omega = \omega_0\sqrt{1-\zeta^2} \quad . \qquad (9)$$

The natural frequency can be obtained from the zero-crossing rate of the 3-axis composition values in time series. And then, the damped natural frequency is calculated.

In this study, the logarithmic decrement δ is obtained from the jerk of the 3-axis composition value. First, Empirical Mode Decomposition (EMD) is applied to the jerk, and then we can obtain the 5-th intrinsic mode function (IMF). This sifting process is shown on the left in Figure 9. We could find carriers with amplitude decay envelope in the close-up of 5-th IMF on the right in Figure 9.

By finding local extrema (e.g., maxima and minima), the logarithmic decrement δ can be obtained and then the damping ratio ζ can be given.

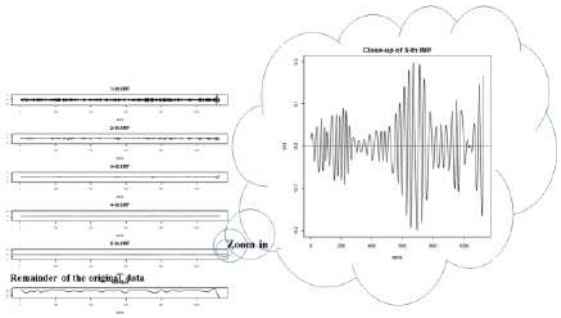

Figure 9. Sifting process of the EMD

Figure 10 shows changes in the loading surface displacement. The solid blue line and the dashed green line are local polynomial regression and the 95% confidence interval, respectively, in the upper illustration of Figure 10. Change points as to the mean and variance of the loading surface displacement in the lower illustration of Figure 10.

Wrap-up of lesson learned from Figure 10 is listed below as follows.
(1) Objectives: Visualization of the loading surface displacement.
(2) Hazard clarified: None
(3) Dangerous operation identified: None
(4) Early precautionary message: None
(5) Reflective description on lesson learned:
Phenomena of spreading fill materials and stepping on them is continuously repeated. The fill material here is lime-stabilized andosol. Unexpected event in this operation is not occurred.

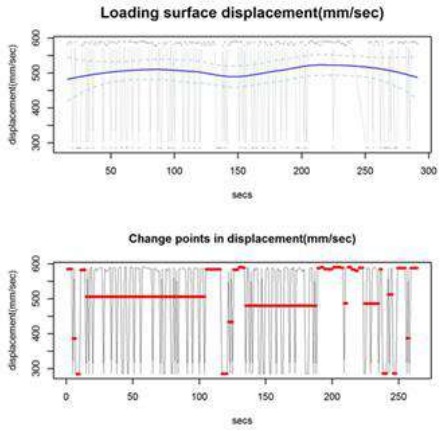

Figure 10. changes in the loading surface displacement

3.5.3 Visualization of Underground Stress

Steinbrenne's stress solution is shown as follows [4]:

$$\sigma_z = \frac{2p}{\pi}\left[\frac{abz}{D}\frac{a^2+b^2+2z^2}{D^2z^2+a^2b^2} + \sin^{-1}\frac{ab}{\sqrt{a^2+z^2}\sqrt{b^2+z^2}}\right] \quad (9)$$ and

$$D^2 = a^2 + b^2 + z^2 \quad , \quad (10)$$

where σ_z is stress at the depth z, the shoe width is 2a, the shoe length 2b, and p is impulse per unit of area.

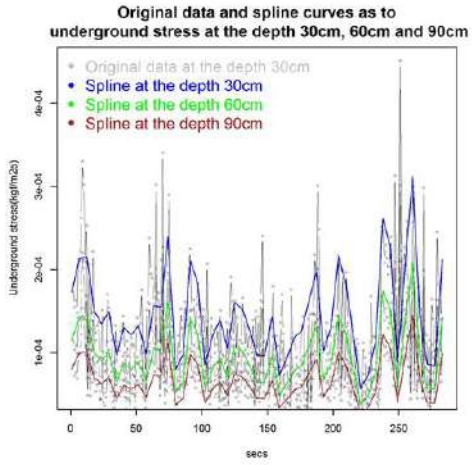

Figure 11. Underground stress in time series

Wrap-up of lesson learned from Figure 11 is listed below.

(1) Objectives: Visualization of the l Underground stress in time series.
(2) Impact clarified: None
(3) Hazard identified: None
(4) Message: None
(5) Reflective description on lesson learned:

Although the waveforms of those underground stresses have almost same shape, the deeper its position is, the smaller the stress value become. Besides the smaller the dispersion gets.

4 Concluding Remarks

The infographics play role in the following matters:
(1) Feedback of physical cues related to machine behaviour,
(2) Spatiotemporal visualization of hazards latent in in-situ earthwork process,
(3) To pick a set of building block of information at the right level of abstraction,
(4) To provide oneself with the opportunities to reflect on their own bearings as facing their own works at hand,
(5) To take timely and quickly correct actions based on detailed visibility of appearances and motions of mobile entities in a whole unmanned construction process, and accordingly, and
(6) To reduce likely mental stress burden to oneself in the remote-control room.

Taken together, these enhancements of conscious awareness of actions would be able to provide operators with the opportunities to reflect on their own bearings as facing their own works at hand.

References

[1] Brian P. DeJong, J. Edward Colgate, Michael A. Peshkin. Improving teleoperation: Reducing mental rotations and translations, Proceedings of the 2004 IEEE International Conference on Robotics & Automation, pp.3708-3714, 2004, On line: http://peshkin.mech.northwestern.edu/publications/2004_Dejong_ImprovingTeleop.pdf, Accessed: 15/08/2018.

[2] Shigeomi Nishigaki, Hitoshi Sugiura, Teiji Takamura, et al. Study on framework of construction profile for collaborative and intelligent construction, Journal of Applied Computing in Civil Engineering Vol.14, 2005.

[3] Shigeomi Nishigaki, Katsutoshi Saibara, et al. Points on construction, 25th ISARC 2008, pp.796-803, 2008.

[4] Hamilton Cray. Stress Distribution in Elastic Solids, Research Assistant in Soil Mechanics, Graduate School of Engineering, Harvard University, On line: ttps://www.issmge.org/uploads/publications/1/44/1936_02_0041.pdf, Accessed: 15/08/2018.

Formulation of the Optimization Problem of the Cyber-Physical Diagnosis System Configuration Level for Construction Mobile Robots

A. Bulgakov[a], T. Kruglova[b], and T. Bock[b]

[a]Institute of Mechatronic and Robotic in Construction, Southwest State University, Kursk, Russia
[b]Institute of Mechatronic, Platov South-Russia State Polytechnic University, Novocherkassk, Russia
E-mail: a.bulgakow@gmx.de, tatyana.kruglova.02@mail.ru, thomas.bock@br2.ar.tum.de

Abstract –

This article studies the development of a cyber-physical prediction diagnosis system for electric drives of the construction robots. The structure of the five level diagnosis cyber-physical system is described. The optimization problem with the configuration level of the cyber-physical diagnostic system is formulated.The problem of determining the optimal trajectory for a mobile construction robot taking into account the wear of its electric drives is presented. As an example, a construction four wheels mobile robot with a differential drive is considered. The task of the robot is the alignment of the construction site, which involves its sequential bypass. From the standpoint of wheels drives wear, the trajectory is considered optimal if the robot makes approximately equal number of right and left side turns. To design a mathematical model for optimal trajectory determination, graph theory and probabilistic algorithms is proposed. The presented model does not take into account the soil structure and the working space inclination.

Keywords –

Cyber-physical diagnosis system; Building robots; Electric drives; Optimal trajectory; Wear

1 Introduction

Reliable construction work entails the need for continuous monitoring of the technical condition of all its actuators with further optimization of their mode of operation and consequently of the entire technological process as a whole. This can be achieved by using a technical condition monitoring system built into the robot's end-effectors, which continuously measures parameters and analyzing the information obtained and determining the current and future technical condition, and optimizing the parameters of the object's operation mode. Implementation of this approach assumes the integration of computing resources into physical processes, i.e. application of cyber-physical systems [1]. In such systems includes, sensors, mechanical equipment and information systems are connected during all stages of the life cycle and interact with each other using standard Internet protocols. This allows to predict and adapt to changes in operating conditions and technical condition of the equipment. The structural scheme of the cyber-physical predicting diagnosing system of the construction robot is shown in Figure 1.

The cyber-physical predicting diagnosis system has five levels: connecting, conversion, cloud, cognition and configuration [2].

At the “Connection” level, an effective set of diagnostic parameters and the sensors for its measurement are selected. The sensors should be designed for self-connection and self-monitoring of the state of the object.

At the "Conversion" level, the values of diagnostic parameters are measured and their necessary transformations in the case predicting diagnostic methods.

Storage and processing of large amounts of diagnostic information is carried out in cloud servers. This will allow the information flow and communication between the drives of various construction robots. Based on that, the optimization of the technological process starts taking into account the state of a separate actuating element.

At the “Cognition” level, methods of diagnosing and forecasting the technical condition of construction robots drives are chosen [3].

These methods must meet the following requirements:

– the possibility of assessing the technical state in real time; minimum composition of the measured parameters;
– the absence of complex bulky measuring equipment installed on the drive housing, which can affect the operation of process equipment;
– possibility to use on a moving object with high humidity and dustiness; applicable for DC and AC motors;
– the ability to automatically analyze the measured parameters;

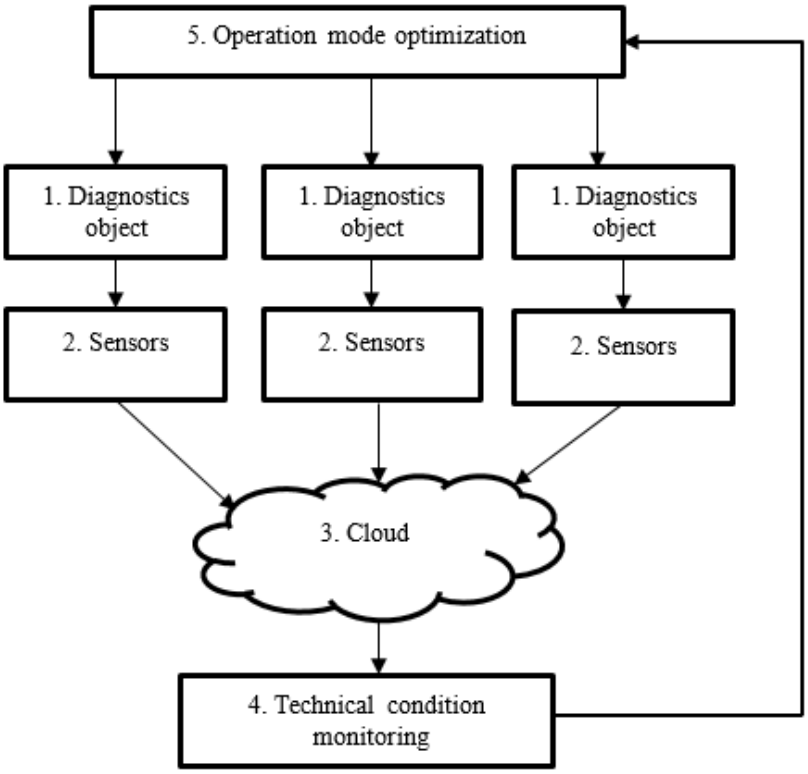

Figure 1. Cyber-physical system of the technical condition prediction diagnosis for electrical drives: 1– Intelligent connection level; 2–Data conversional level; 3–Cloud level; 4–Cognitive level; 5– Configuration level

– the ability to distinguish a malfunction from a change in operating mode; the ability to record and store diagnostic results in a cloud server and to provide the user with an Internet protocol.

The results of diagnostics and forecasting are presented to users and transmitted to the mathematical model of the object for further optimization of the robot operation mode.

At the "Configuration" level, the operation of the diagnostics object is optimized.

Construction robots operate in complex non-deterministic conditions with high alternating loads in conditions of high humidity and dust. Their drives are often installed on a mobile base, which imposes significant requirements for the choice of methods and means of diagnosis such as:

– minimum composition of the measured parameters;
– the absence of complex bulky measuring equipment installed on the drive housing, which can affect the operation of process equipment;
– the automatically analyze the measured parameters.

Analysis of the majority of electrical and mechanical faults of the electrical drive can be detected by monitoring the supply and capacitive current, which can be measured without the use of special sensors.

For the "Cognition" level, a method for diagnosing electric drives of building robots has been obtained [4], which makes it possible, without using expensive measuring instruments, to determine their current state of failure, a malfunction from changing the operating mode. This will increase the efficiency of such robots and the quality of construction operations.

The main part of the cyber-physical system is the "Configuration" level. It implements the task of optimizing the work of construction robots according to the results of diagnosing the technical condition of their electric drives.

After the technical condition of each electric drive of a construction robot is determined, it is necessary to optimize the operating mode of robots in order to increase the equipment life. Significant impact on the electric motor life have loading conditions during operation. The diagnosis will significantly extend the uptime of the electric drive and all equipment as a whole. To solve the increasing the reliability of the electric motor problem separate from the object where it is installed without taking into account the operation of all other mechanisms is impossible. Therefore, this problem should be solved in a group

of drives of an object operating in a certain technological process.

As an example, consider a mobile construction robot used to level the construction site. Tit have four independent electric drives, which are a mechatronic module "motor-wheel" [5]. The task of the robot is to handle rough terrain of a given geometry. In this case, the choice of the trajectory of the robot should be carried out in such a way that the wear of the drives of its wheels was minimal.

2 Robot Wear Model

Consider a model of a four-wheeled mobile robot with a differential drive (Fig. 2). It is assumed that the robot is driven in one of three ways:

1) using the wheels D^1 and D^2 (front wheel drive);
2) using the wheels D^3 and D^4 (tasks drive);
3) using all four wheels simultaneously (all-wheel drive).

The preferred option for controlling, all-wheel robot drives, since the life of the wheel drive is consumed evenly. However, in the event of a failure of one of the engines, the control system can be returned to the front or rear wheel drive.

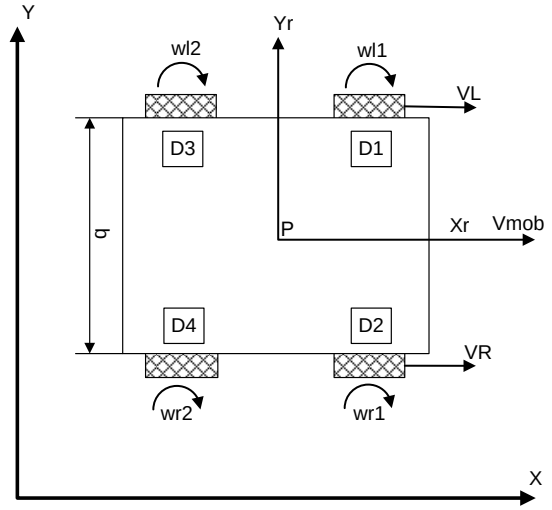

Figure 2. Model of a four-wheeled mobile robot with differential drive

A complete failure of a mobile robot will be considered to be options for working on the right or the left pair of drives (D^1 and D^3 or D^2 and D^4 in Figure 1) or on any one drive, as this leads to a situation of uncontrolled movement of the robot and unreasonable wear of working engines. The degree of wear of the robot is the sum of the degrees of wear of the drives of each wheel when performing a single technological operation t_i (1).

$$P(t_i) = p^1 + p^2 + p^3 + p^4, \qquad (1)$$

where p^1, p^2, p^3, p^4 is the degree of wear when performing a single technological operation of the drives D^1, D^2, D^3 and D^4, respectively.

The wear of the electric drive of each wheel is determined as a function of three arguments (2):

k_{ground} – the soil properties variable (takes on the values: 1 - smooth hard soil, 2 - smooth loose soil, 3 - uneven loose soil);

t_{fun} – the electric drive mode operation variable (0 - passive, 1- "full drive" mode, 2 - active front or rear drive mode);

M_{turn} – the additional motor load variable in a turn (for drives D^1 and D^3 - the right turns, for D^2 and D^4 - the left turns).

$$\begin{cases} p^1 = f(k^1_{ground}, t^1_{fun}, M^1_{turn}), \\ p^2 = f(k^2_{ground}, t^2_{fun}, M^2_{turn}), \\ p^3 = f(k^3_{ground}, t^3_{fun}, M^3_{turn}), \\ p^4 = f(k^4_{ground}, t^4_{fun}, M^4_{turn}). \end{cases} \qquad (2)$$

3 The Optimization Problem Formulation

For experiments in the proposed model of wear, the following restrictions are introduced:

1) the robot moves on a horizontal working space (Z=const);

2) the robot moves at approximately constant speed (V=const).

The trajectory of the robot is selected depending on the configuration of a specific construction site. Examples of their forms are shown in Fig. 2

t_0	t_1	t_2	t_3
t_4	t_5	t_6	t_7
t_8	t_9	t_{10}	t_{11}
t_{12}	t_{13}	t_{14}	t_{15}

a)

t_0	t_1	t_2	
t_3	t_4		
t_5	t_6	t_7	
t_8	t_9	t_{10}	t_{11}
t_{12}		t_{13}	t_{14}

b)

Figure 3. The examples of the construction robot working space

The robot working space being processed is divided into n segments so that each of them uniquely defines the limits of a single technological operation t_i (i = 1..n) .

For processing of construction sites (Fig. 3), it is necessary to set a complex trajectory of movement taking into account the wear of its electric motors.

The task of the robot is to fully implement the technological process (performing all its technological stages) so that the total wear of P_0 electric drives is minimal (3):

$$P_0 = \sum_{i=1}^{n} P(t_i) \to \min . \quad (3)$$

The wear P_0 is assumed to be minimal when it is evenly distributed between the drives D^1, D^2, D^3 and $D^4$is accepted. It is possible to reach with the minimum difference between the right ($M_{turn(R)}$) and left ($M_{turn(L)}$) turns (4):

$$\sum M_{turn(R)} - \sum M_{turn(L)} \to \min . \quad (4)$$

If for a particular construction site all its n segments are represented as the corresponding graph *T (V, E)*, the set of vertices *(V)* uniquely corresponds to the field segments, and the set of edges *(E)* logically defines possible transitions between adjacent segments (technological operations), then the mathematical problem of synthesizing the effective trajectory $G(P_0)$ for processing the construction site can be represented as follows (5) [6,7]:

$$G(P_0) = \left\{ t_i \,\middle|\, f(t) = \sum_{i=1}^{n} P(t_i) \to \min, i = 1...n \right\},$$
$$Z = \text{const}, \quad (5)$$
$$V = \text{const}.$$

The graph representation options for partitioning the working space of the robot (Fig. 3) are shown in Figure 4 accordingly.

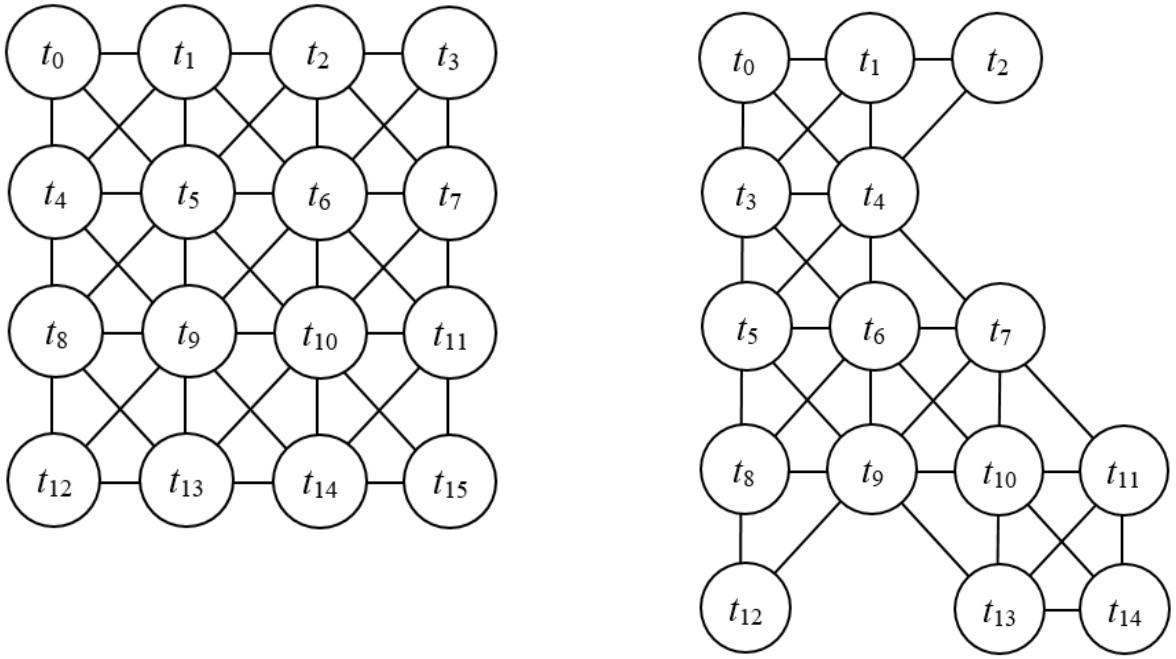

a) b)

Figure 4. Variants of the graph representation of the robot workspace

Possible solutions for the cases considered from Fig. 3a and Fig.3,b are followed:

– $G(P_0) = \{t_0, t_1, t_2, t_3, t_4, t_5, t_6, t_7, t_8, t_9, t_{10}, t_{11}, t_{12}\}$

– $G(P_0) = \{t_0, t_1, t_2, t_3, t_4, t_5, t_6, t_7, t_8, t_9, t_{10}, t_{11}, t_{11}\}$

To demonstrate the turns within the selected trajectories the turn matrixes $G(M_{turn})$ is defined,

where 0 - turn within t_i (not performed),

1 - right turn $(M_{turn(R)})$,

2 - left turn $(M_{turn(L)})$.

Then the matrix $G(M_{turn})$ for each of the four previously defined trajectories will take the following form:

1st trajectory:

$G(M_{turn})$ = {0,0,0,1,1,0,0,2,2,0,0,1,1,0,0,0};

2nd trajectory:

$G(M_{turn})$ = {0,0,1,1,2,0,0,2,2,1,1,0,2,2,0}).

The selected trajectory can be considered optimal from the standpoint of minimizing engine wear if the

number of left and right turns for the indicated options of trajectories $G(P_0)$ approximately coincides.

For solving the formulated problem and the need to solve it based on probabilistic algorithms (for example, agent metaheuristics). [8-10]

4 Conclusion

In this paper, the design of a cyber-physical system for diagnosing and predicting the technical condition of electric drives of construction robots is presented. Furthermore, the structure of the cyber-physical system consisting of five levels is defined and the work of each system level is also described. The optimization problem with the configuration level of the cyber-physical diagnostic system is formulated. The problem of determining the optimal trajectory for a mobile construction robot taking into account the wear of its electric drives is presented. From the standpoint of wheels drives wear, the trajectory is considered optimal if the robot makes approximately equal number of right and left side turns. To design a mathematical model for optimal trajectory determination, graph theory and probabilistic algorithms is proposed. The presented model does not take into account the soil structure and the working space inclination.

References

[1] Giese H., Rumpe B., Schätz B. and Sztipanovits J. Science and Engineering of Cyber-Physical Systems. *Dagstuhl Seminar 11441, Dagstuhl Reports:* 1(11) 1–22, 2012.

[2] Horvath I., Rusak Z., Albers A., Behrendt M. Cyber-physical systems: Concepts, technologies and implementation principles in Tools and Methods of Competitive Engineering Symposium. *TMCE,* 19–36, 2012.

[3] Bulgakov A., Kruglova T., Bock T. A cyber-physical system of diagnosing electric drives of building robots. *ISARC 2018*, 16-23, 2018

[4] Bulgakov A., Kruglova T., Bock T. Synthesis of the AC and DC Drives Fault Diagnosis Method for the Cyber-physical Systems of Building Robots. *IPICSE 2018*, (251), 2018.

[5] Bishop R. The mechatronics handbook *The University of Texas at Austin Austin, Texas* 1229, 2002.

[6] Moiseeva R., Samigullina R., Bazhenov N., Yu N. Zatsarinnaya Problems of Improving the Reliability of Electric Machines. *Bulletin of Kazan Technological University*, 3(17) 117-119, 2014

[7] Mokhov V., Turovsky F., Turovskaya E. Mathematical statement and interpretation of a variant of the problem of discrete optimization on a temporal graph. *ICIEAM*, 9, 279-283, 2016

[8] Kubil V., Mokhov V., Grinchenkov D. Modeling the Generalized Multi-Objective Vehicle Routing Problem Based on Costs. In *Proceedings of the 6th International Conference on Applied Innovations in IT*, 2018.

[9] Kubil V., Mokho V. On the issue of the application of swarm intelligence in solving the problems of transport logistics. *Problems of modernization of engineering education in Russia*. 140-144, 2014.

[10] Turovskaya E., Mokhov V., Kuznetsova A.. Simulation of the process of optimal placement of goods in the self-service warehouse based on evolutionary search algorithms. *Engineering Bulletin of Don*. 28(1), 56, 2014.

Ontology-Based Knowledge Modeling for Frame Assemblies Manufacturing

S. An[a], P. Martinez[a], R. Ahmad[b], and M. Al-Hussein[a]

[a] Department of Civil and Environmental Engineering, University of Alberta, Canada.
[b] Laboratory of Intelligent Manufacturing, Design and Automation (LIMDA), Department of Mechanical Engineering, University of Alberta, Canada.
E-mail: san3@ualberta.ca, pablo1@ualberta.ca, rafiq.ahmad@ualberta.ca, malhussein@ualberta.ca

Abstract –

As modular construction becomes popular, an increasing number of products are prefabricated in an offsite construction environment. While improving the productivity and efficiency of construction-oriented production, it also raises the complexity of process planning. Although the specifications of a product are fully defined by Building Information Models (BIM), no information is provided on how construction products are manufactured and assembled. This paper proposes an ontology-based approach aimed to link construction-oriented product assemblies and manufacturing resources using manufacturing operations. By identifying intersections of connecting members of a product assembly, feasible manufacturing methods and resources are determined based on expert knowledge and machine configurations. The proposed approach is validated using a wood frame assembly.

Keywords –

Building information modeling; Ontology modeling; Offsite construction; Construction automation; Construction manufacturing

1 Introduction

Modular and panelized construction have been promoted and recognized globally as advanced construction techniques for commercial and high-rise residential buildings in the last decade. Thus, an increasing number of buildings are manufactured using off-site construction methods: first, wall panels are prefabricated in an indoor facility; then, shipped on-site for installation. Offsite construction is becoming increasingly popular as it improves productivity of the construction process, reduces material waste, and yields better quality products [1, 2]. With the growing interest in modular construction, industrial automated machines have been developed to satisfy such needs. A prototype was designed at the University of Alberta for automatic light-gauge steel framing [3].

In industry, the current practice of introducing new construction products to an existing or new facility consists of the following procedures: (1) a 3D model of the desired product assembly is generated using the Building Information Model (BIM) specifications; (2) then, it is analyzed by product engineers to determine the manufacturing process (or processes) required and to select the appropriate machines necessary to accomplish such tasks; (3) the machinery is finally analyzed for installation in the indoor facility (i.e., layout design, safety requirements).

The vision of the 4th industrial revolution describes the realization of smart factories, where a higher flexibility and adaptability of production systems is achieved [4]. The challenge arises when deciding if a new assembly can be manufactured in the existing production line or if one or more machines must be commissioned to make a new product assembly. Although BIM models provide information on what the final product assembly would be, it does not offer the benefit of hindsight as to how it is manufactured and assembled. Such challenges are often overcome by engineering experience. As a result, no link between machinery, manufacturing processes and construction product assemblies in the knowledge domain exists. To shorten the decision-making effort in determining machine eligibility, a relationship between product assemblies, manufacturing procedures, and machines needs to be established.

The objective of this study is to create knowledge models that represent components of a manufacturing domain with a special focus on the manufacturing of product assemblies. An ontology-based model is proposed to communicate between three knowledge domains: the 3D BIM model of a desired product assembly, its necessary manufacturing steps, and the key attributes of the machines used for manufacturing. A wood frame assembly is used as a case study.

2 Related Work

Relating product information to the manufacturing domain exists in the machining industry. Computer Aided Process Planning (CAPP) is the use of computer technology to aid in the process planning of a product in manufacturing [5]. CAPP is used to interpret product design data by recognizing features on a part and translating them into manufacturing operation instructions [6]. CAPP has been proven to be successful in providing process planning to manufacture a designed part. The challenges of using CAPP in manufacturing construction-oriented products arise due to the complexity of the products, which usually involves assembling individual parts.

Extracting information from BIM models is the first step involved in fabricating and inspecting the quality of construction-oriented products. Malik et al. successfully extracted product specifications from BIM models and generated safe tool-paths for moving carriages in an automated framing machine [7]. Martinez et al. proposed a vision-based system for pre-inspection of steel frame manufacturing. The proposed approach provides real-time inspection of steel frame assemblies by comparing real frame assembly with manufacturing information from the BIM model [8].

In typical manufacturing processes, knowledge modeling has successfully enabled decision making systems to be defined for such purposes [9]. However, a link between construction-oriented products and construction machinery is yet to be properly defined. Gruber defined ontology as "an explicit and formal specification of a conceptualization" [10]. Ontology is used for various reasons. First, ontologies offer interoperability of information from various knowledge domains; second, ontologies support consistency checking and reasoning; third, concepts used in product and manufacturing domains can be represented by defining classes and properties of the ontology in an intuitive way [11]. A proposal named MASON (MAnufacturing's Semantics ONtology), proposed by Lemaignan et al., created a common semantic net in the manufacturing environment using ontologies for general purposes [12]. This approach successfully related product specifications (entities) and manufacturing related resources using operations. MASON sets the foundation to link construction-oriented products to the manufacturing environment.

Ontologies have been proven useful in extracting information from BIM for practical use. Zhang et al. proposed an ontology-based model to relate on-site construction safety management with job hazards of construction activities. By linking tasks, methods, and the job hazards involved in construction activities, the developed automated system provides a significantly more efficient and formalized job hazard analysis [13]. Liu et al. proposed an ontology-based semantic approach that successfully extracts construction-oriented quantity take-off information. Using this approach, construction practitioners can readily obtain and visualize the relevant information from complex BIM models [11].

3 Methodology

By integrating the work proposed by Lemaignan et al. and Liu et al., this paper proposes an ontology-based semantic approach to relate construction-oriented product assemblies to machineries in a production line that is responsible for manufacturing the products. Extending the methodologies proposed by Liu et al. by using a MASON-based approach to the manufacturing

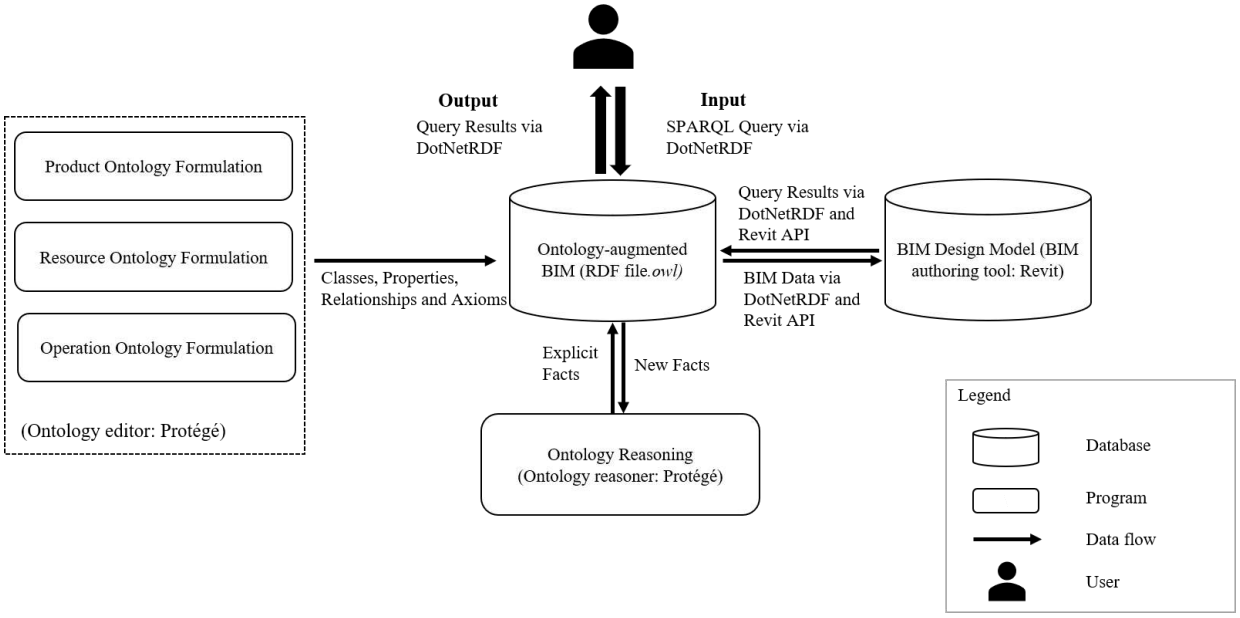

Figure 1. System architecture

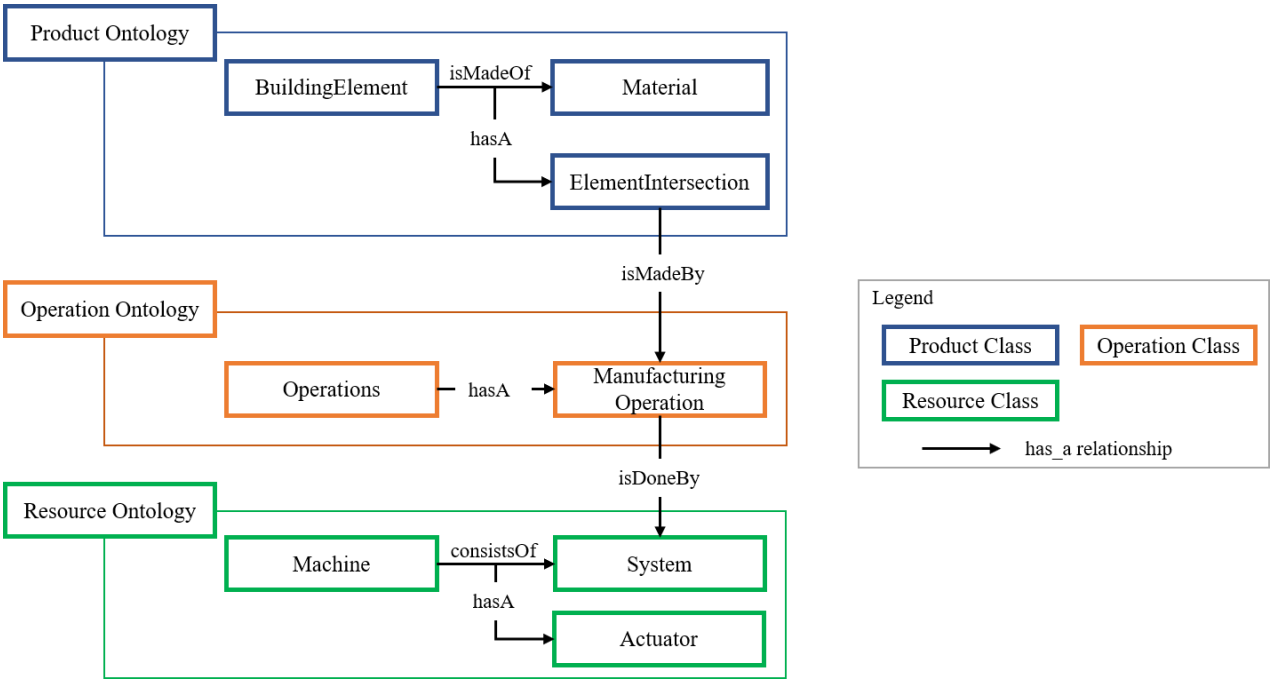

Figure 2. Product, operation and resource ontology models

domain, the proposed system architecture is shown in Figure 1. Three knowledge domains (manufacturing resource, operation, and product) need to be incorporated to build the ontology-augmented BIM model. Each knowledge model is simplified in Figure 2. Protégé, an open source ontology editor and reasoner, was used to build the ontology model using the following steps: (1) Entity class is created to specify construction-oriented products; (2) Resource class is used to describe manufacturing machineries to be used to fabricate and assemble the products; (3) Operation class is then built to relate entities and resources. Once the knowledge domains are constructed, machine eligibilities can be determined.

Using the approach proposed in MASON, classes will be used to define the product, operations and manufacturing domains. Attributes of classes are specified using "Data properties". The relationship between classes are captured using "Object properties". Instances of classes are modeled using "Individuals" [12].

3.1 Product Ontology Formulation

First, the class *Product* containing information from BIM is modeled. BIMs are digital representations of physical and functional characteristics of a facility and contain all the physical information related to a product [14]. In terms of the construction of a building element using machines, the following information will be used to allocate manufacturing resources: material, dimension, and intersection between elements. All machines have limitations as to the material to be processed and the dimension of a product. Since a product assembly is typically made using multiple basic elements, intersections of these elements also place constraints on how the product assembly may be constructed. An intersection is defined as the interface between any two or more members to be connected. Since an intersection is dominantly affected by the product material, each intersection is specific to each type of product. For wood frames, intersections are identified based on 3 criteria: (1) single or double plates/studs; (2) either it is at a corner (LConnection) or inside the frame (TConnection); (3) horizontal or vertical. Six intersections are identified using the above criteria and are denoted by specific notations:

Table 1. Intersections in wood frames

Intersection Type	Notation
Stud_Plate_LConnection	SP_L
Stud_Plate_TConnectionVertical	SP_TV
Stud_Plate_TConnectionHorizontal	SP_TH
Stud_DoublePlate_LConnection	SDP_L
Stud_Stud_Connection	SS
Stud_DoublePlate_TConnectionHorizontal	SDP_TH
Stud_DoublePlate_TConnectionVertical	SDP_TV

Since manufacturing processes depend on the material and the intersections of each product assembly, they must be defined in the ontology model. As an

example, Figure 3 shows the class hierarchy of wood element intersections.

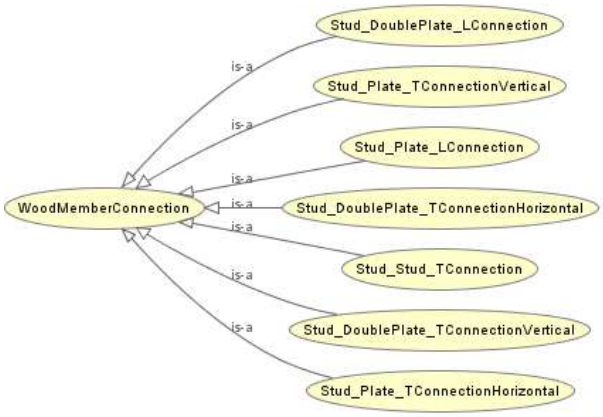

Figure 3. WoodMemberConnection class hierarchy

3.2 Resource Ontology Formulation

Similar to the product model, the resource ontology is also modeled. Although resources consist of multiple categories, only machine resources need to be considered as far as machine eligibility is concerned. A construction manufacturing machine consists of several systems that carry out manufacturing operations. For example, a nailing system in a wood framing machine can shoot nails into the wood frame to create a permanent connection. In this model, the class *Resource* that consists of subclasses *Machine* and *Actuator* are created. Under the class *Machine*, several sub-classes of various machines are created. Systems of certain machines are specified under each *Machine* sub-class. The *Machine* resource ontology model is shown in Figure 4.

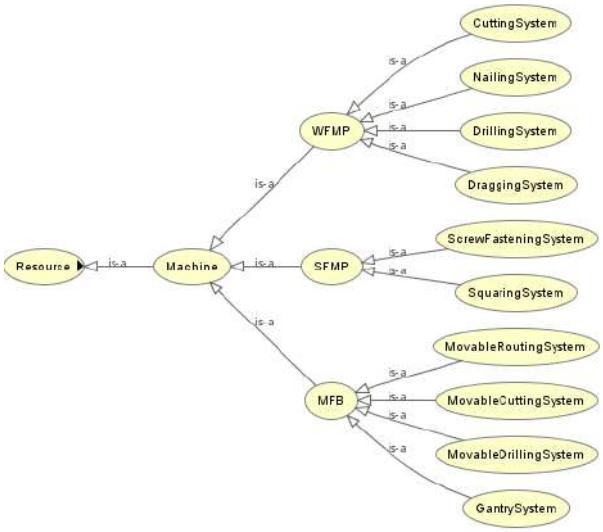

Figure 4. Resource ontology model

3.3 Operation Ontology Formulation

As mentioned before, the BIM model does not include information pertaining to how a product assembly is fabricated. Therefore, manufacturing operations need to be analyzed to form a relationship between product entities and machine resources. Since a product assembly is typically made of several members, intersections of these members require certain manufacturing method(s) to secure these elements. In addition to joining materials, some locations also require the addition and/or removal of materials. These locations, along with intersections, are defined in the BIM model and categorized into classes of connections defined in the *Product* model. Each category of intersection requires specific manufacturing method(s). Therefore, based on the type of connections identified, the manufacturing operation is determined.

In the *Operation* ontology model, the class *ManufacturingOperation* is created to identify feasible product assembly construction methods. By establishing relationship "isMadeBy" between the class *Product* and *ManufacturingOperation*, the system now has clear knowledge about how a product assembly can be constructed. The ontology model of *Operation* is shown in Figure 5.

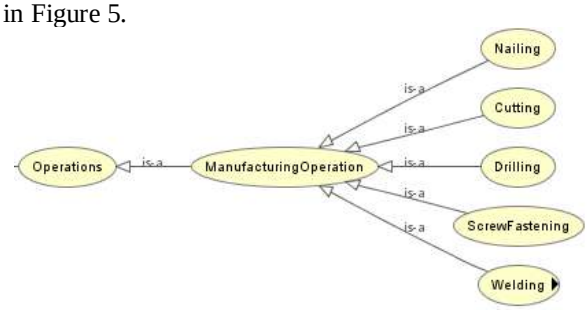

Figure 5. Operation class hierarchy

4 Results and Discussion

In this section, the proposed methodology is validated with a wood framing wall. The advantages and limitations of using ontology models to relate product, manufacturing resources, and operation are also discussed.

4.1 Case Study

A wood frame is to be modelled and studied. The panel is 20 ft (approximately 6 m) long and 10 ft (approximately 3 m) high and is made of 2x6 (38 mm x 150 mm) wood timbers of various length. The frame contains a window and a door component. Note that a single plate is used for the footer and double plates are used for the header. The frame is shown in Figure 6 below.

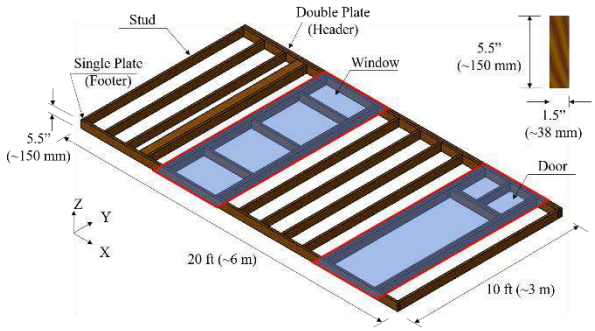

Figure 6. 3D representation of the wood frame case study

First, using the given information, material and dimensions are identified. Next, the possible types of intersections are recognized: stud-to-stud intersections and stud-to-plate intersections. Plates are wood members along the x-axis and studs are the rest of the members. As shown in the product ontology model, all the possible intersections of product assembly of wood framing wall are modeled as sub-properties under the object property "isMadeBy". Since it is a group of properties of the element intersection which requires manufacturing operations, the domain of "isMadeBy" is *ElementIntersection* and the ranges are within *ManufacturingOperations*. This relationship is represented in Figure 7.

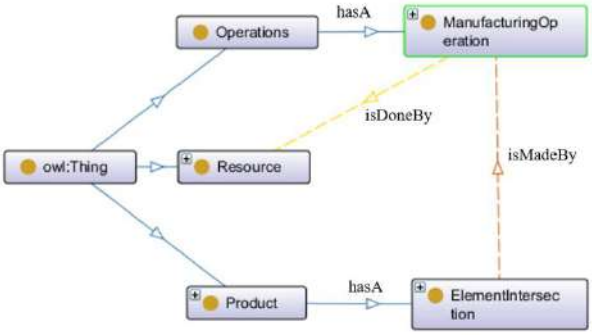

Figure 7. Class wood member intersections

For this wood frame, all types of intersections are identified and matched to the ontology model. These types of intersections are annotated in Figure 8 and are tabulated in Table 2. Note that an integer that follows the letters in the Identifier column represent a specific instance of corresponding wood members.

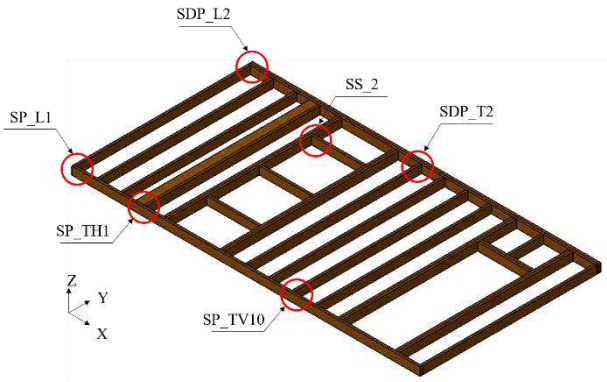

Figure 8. Intersections identified from provided wood frame

Table 2. Connections in wood frame panel

Intersection Type	Identifier
Stud_Plate_LConnection	SP_L1
Stud_Plate_TConnectionVertical	SP_TV10
Stud_Plate_TConnectionHorizontal	SP_TH1
Stud_DoublePlate_LConnection	SDP_L2
Stud_Stud	SS2
Stud_DoublePlate_TConnection	SDP_T2

To represent knowledge of the manufacturing machine domain, resource ontology is modeled for further analysis. As an example, the Wood Framing Machine Prototype (WFMP) built at the University of Alberta is used for this case study. It is a semi-automated framing machine designed to build wood frames. The prototype consists of four independent systems: cutting, dragging, drilling, and nailing. These systems are modeled in Protégé as shown below in Figure 9. Note that WFMP has not equipped with decision-support system to this point. The knowledge of the machine, however, will lead to development of decision-support system in the future.

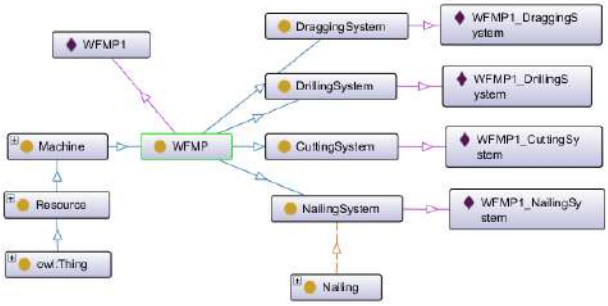

Figure 9. Systems of the WFMP

After knowing element intersections and systems of the machine, the relationship among product assemblies and machine domains can be established by analyzing the manufacturing operations needed to make such product assemblies. Based on expert knowledge, wood

members with intersections presented in Table 2 should be joined using screw fastening or nailing. In the ontology model, this knowledge is embedded in the object property "isMadeBy": the domain consists of element intersections and the ranges contain feasible operations. As an example, a sub-property "SDP_LConnection" of "isMadeBy" is defined in Figure 10.

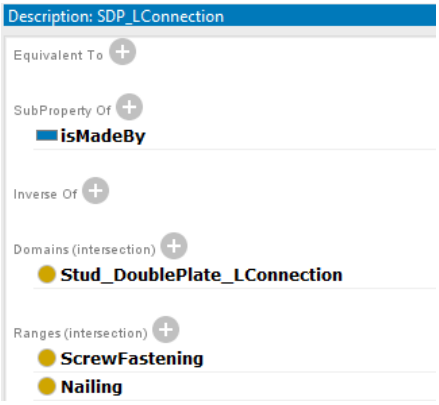

Figure 10. Object properties of SP_LConnection

Analyzing all the intersections in the wood frame, only screw fastening and nailing operations are feasible options for creating permanent connections. Since nailing is more popular for connecting wood timbers in North America, the only manufacturing process required for building this panel is the nailing operation. This result agrees with current industry practice for framing a wood panel.

4.2 Discussion

As shown in the case study, ontology models can not only represent knowledge of construction-oriented product assemblies and machine resources in detail, but also form a relationship between these knowledge domains. Using the product assembly information such as material, dimension, and intersections exported from The BIM model, appropriate manufacturing operations are suggested by the knowledge model. This requires building ontology models for both the product to be built and assembled, and the potential machines to be used to make such product.

A number of advantages are observed after having the knowledge model. First, a machine's capacity fabricate certain construction-oriented products can be determined by analyzing the manufacturing processes required to complete the product assembly. Second, if one machine cannot fulfill the manufacturing requirement, a well-defined model will suggest the appropriate manufacturing activities, such as a combination of machines, to fabricate the product. In addition, the ontology model built in the case study can easily be expanded to a related field. For example, machine logic, actuators, and sensors can be modeled and integrated to the existing model. As a result, a data exchange will be initiated between physical systems such as product assemblies and machines, which will accelerate product fabrication and simplify the modifications to existing production lines if needed.

However, certain limitations are also observed. Building knowledge models is extremely time consuming. A machine cannot decide or suggest manufacturing activities without sufficient knowledge from all relevant knowledge domains. In fact, ontology formulations need to cover all manufacturing resources in a production line. It is common that a product assembly is made by a series of activities and it is not feasible for a single machine to have all the functionalities required. The sequence by which a product assembly is made must be determined in addition to the specific manufacturing operations required. Therefore, future work is needed to address:

1. A more detailed ontology formulation that includes machines of the entire production line and encompasses material cost and manufacturing time estimation;
2. The sequence by which a product must be assembled (process planning of manufacturing processes);
3. The machine-product interaction within a production line has yet been defined.

5 Conclusion

Since the BIM model does not provide information regarding how products are to be fabricated, ontology models are used to bridge the knowledge gap. By building knowledge models for product, operation and machine, the relationship between product and machine is formed. Using expert knowledge, the required manufacturing operations are determined by identifying the intersections in a product assembly.

Once the manufacturing system is equipped with knowledge, it is possible to determine if a machine can manufacture a certain product, even though this is not the main focus of this study. Future more, it can further suggest additional manufacturing activities needed to complete the product in the case where one machine can only fulfill part of the fabrication requirements. In this case, combinations of machines need to be used to make the product. In future work, the proposed approach can be extended to all the machines in a factory to address this issue.

References

[1] N. Malik, R. Ahmad and M. Al-Hussein, "Investigating the effects of reduced technological constraints on cycle time through simulation modelling for automated steel wall framing," in *Modular and Offsite Construction (MOC) Summit*, HollyWood, 2018.

[2] R. M. Lawson and R. G. Ogden, "'Hybrid' light steel panel and modular systems," *Thin-Walled Structures*, vol. 46, no. 7-9, pp. 720-730, 2008.

[3] E. Tamayo, M. Bardwell, A. Qureshi and M. Al-Hussein, "Automation of a Steel Wall Framing Assembly," in International Structural Engineering & Construction Conference (ISEC), Valencia, 2017.

[4] J. Lee, H. Davari, J. Singh and V. Pandhare, "Industrial Artificial Intelligence for industry 4.0-based manufacturing systems," Manufacturing Letters, vol. 18, pp. 20-23, 2018.

[5] W. D. Engelke, How to Integrate CAD/CAM Systems: Management and Technology, CRC Press, 1987.

[6] X. Zhou, Y. Qiu, G. Hua, H. Wang and X. Ruan, "A feasible approach to the integration of CAD and CAPP," *Computer-Aided Design*, vol. 39, no. 4, pp. 324-338, 2007.

[7] N. Malik, R. Ahmad and M. Al-Hussein, "Generation of safe tool-paths for automatic manufacturing of light gauge steel panels in residential construction," *Automation in Construction*, vol. 98, pp. 46-60, 2019.

[8] P. Martinez, R. Ahmad and M. Al-Hussein, "A vision-based system for pre-inspection of steel frame manufacturing," *Automation in Construction*, vol. 97, pp. 151-163, 2019.

[9] R. Ahmad, S. Tichadou and J.-Y. Hascoet, "A knowledge-based intelligent decision system for production planning," The International Journal of Advanced Manufacturing Technology, vol. 89, no. 5-8, pp. 1717-1729, 2017.

[10] T. R. Gruber, "Toward principles for the design of ontologies used for knowledge sharing," *International Journal of Human-Computer Studies*, vol. 43, no. 5-6, pp. 907-928, 1995.

[11] H. Liu, M. Lu and M. Al-Hussein, "Ontology-based semantic approach for construction-oriented quantity take-off from BIM models in the light-frame building industry," *Advanced Engineering Informatics*, vol. 30, no. 2, pp. 190-207, 2016.

[12] S. Lemaignan, A. Siadat, J.-Y. Dantan and A. Semenenko, "MASON: A Proposal For An Ontology Of Manufacturing Domain," in *Proceedings of the IEEE Workshop on Distributed Intelligent Systems: Collective Intelligence and Its Applications*, 2006.

[13] S. Zhang, F. Boukamp and J. Teizer, "Ontology-based semantic modeling of construction safety knowledge: Towards automated safety planning for job hazard analysis (JHA)," *Automation in Construction*, vol. 52, pp. 29-41, 2015.

[14] "National Building Information Model Standard-United States," National Institute of Building Sciences, 16 October 2016. [Online]. Available: https://web.archive.org/web/20141016190503/http://www.nationalbimstandard.org/faq.php#faq1. [Accessed 29 October 2018].

[15] B. T. Zhong, L. Y. Ding, H. B. Luo, Y. Zhou, Y. Z. Hu and H. M. Hu, "Ontology-based semantic modeling of regulation constraint for automated construction quality compliance checking," *Automation in Construction*, vol. 28, pp. 58-70, 2012.

Measuring and Positioning System Design of Robotic Floor-tiling

T.Y. Liu[a], H.X. Zhou[a,b], Y.N. Du[b], and J.P. Zhao[b]

[a]College of Engineering, China Agricultural University, China
[b]School of Mechanical-Electronic and Vehicle Engineering, Beijing University of Civil Engineering and Architecture, China
E-mail: perc_lty@126.com, perc_zhx@126.com, perc_dyn@126.com, perc_zjp@126.com

Abstract –

The research of floor-tiling robots aiming to replace the artificial floor tile installation, which is a trend in the development of construction automation. Modular design of the robotic floor-tiling system used embedded PC as the main controller, which has several advantages, such as reliable system performance, convenient modular communication, and simple function improvement. The measuring and positioning system of robotic floor-tiling consists of multiple subsystems. The task calls of each subsystem are allocated in real time through control flow and control algorithms. Feasibility of the measuring and positioning system is proved by test run and the future works are discussed.

Keywords –

Robotic floor-tiling; Control system; Embedded PC; Modular design

1 Introduction

Floor-tiling is a project in the construction industry that is labor intensive, highly repetitive, and testable to the skills and body of workers [1]. There are large quantities of tiles to be consumed and an increasing trend every year all over the world [2]. The environment of floor-tiling process is fully filled with mud, dust, noise, and vibration. Workers will squat or kneel on the floor when installing tiles [3]. If we rely entirely on the workers to set such large quantities of tiles, it will cost a lot of manpower and labor time, also can be physically harmful to workers [4]. Therefore, developing robotic floor-tiling to replace artificial floor tile installation will play a key role in the future of construction industry [5].

To use robotic floor-tiling instead of manual floor-tiling, the robot system must have the advantages in floor-tiling process such as higher efficiency, better quality, lower cost, and so on [6].

In the following of this section, the process of artificial floor-tiling is analyzed first, and then a floor-tiling robot system frame that can fulfill measuring and positioning function is designed.

1.1 Artificial Floor-Tiling Process Analysis

Thinset tiling method is one of the most widely used method in the current floor-tiling. Thinset tiling is also called dryset or drybond tiling [7], it uses a blend of cement, fine sand, and a unique blend of special additives to install tiles on an even substrate surface [8]. Fig.1 shows the thinset tiling process, this method can be described as the following steps [9]:

1. Level substrate by self-leveling epoxy or self-leveling cement.
2. Hold a notched trowel at a slight angle, push down and away to spread the thinset mortar to substrate surface or to tile's back evenly and following the same direction.
3. Set tiles and spacers, plug wedge into spacer to leveling tiles.
4. Repeat thinset spreading, tile setting, spacer setting and tile leveling till all tiles are installed, then grout joints and further clean the room.

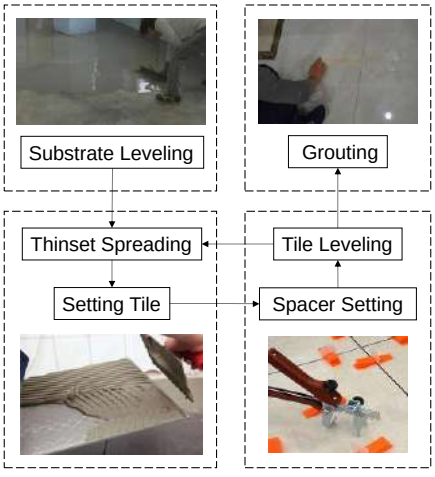

Figure 1. Process chart for thinset tiling

Thinset tiling has the following advantages compared to traditional thick-bed tiling:

- Less steps and easy operation.
- Lower cost and higher efficiency.
- Stronger bonding strength.
- Use less material and save more space.

Therefore, a floor-tiling robotic measuring and positioning system frame is designed based on thinset tiling method.

1.2 Frame Design of Floor-Tiling Robot System

The measuring and positioning system is the most critical component of the floor-tiling robot. By analyzing the artificial floor-tiling process, the measuring and positioning system can be divided into several subsystems to realize the precise placement of tiles [10]. Fig. 2 shows a general floor-tiling robot's measuring and positioning frame diagram, it basically consists of the following subsystems [11]:

- HMI (Human Machine Interface), which is the medium for information interaction between the control system and the operator.
- The main controller, which is responsible for sending control commands to and receiving statuses from the slave controllers of the subsystems.
- The mobile platform system, which is a crucial part of the floor-tiling robot to achieve a wide range of operations.
- The actuator system and robotic arm system, which contribute to the grabbing and placing of tiles.
- The sensor system, which is the key part of the floor-tiling robot, in order to implement measurement and carry out positioning functions when tiling.

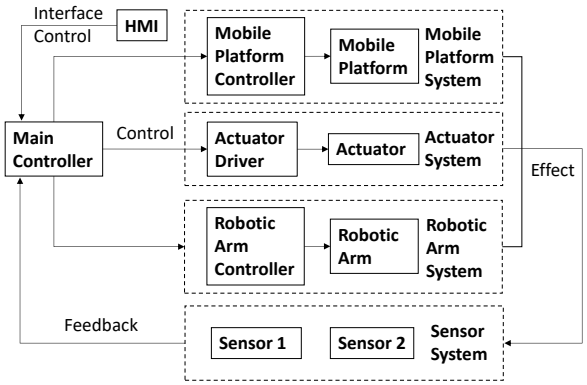

Figure 2. General floor-tiling robot's measuring and positioning system frame diagram

2 Hardware Platform Design

In this section, the hardware part of each subsystem is built according to the previous general floor-tiling robot's measuring and positioning system frame diagram, and the communication of the whole hardware platform is established through various communication modules [12].

2.1 Subsystems

According to the suitable measuring and positioning method used by the floor-tiling robot, the system is divided into the following five subsystems, which are introduced separately.

2.1.1 Point Laser Measurement System

The point laser measurement system contains two sets of measurement modules. Two sensor heads mounted on the end tool can measure one edge of a tile at the same time, and obtain relative position deviation data. Precise positioning function is achieved through position correction algorithm.

As shown in Figure 3, IL-300 is used as sensor head, which has 30 micron repeatability, ±0.25% F.S linear accuracy, 300mm reference measurement distance, and the measuring range is 160 to 450 mm from the laser head. The IL-1000 and IL-1050 are used as amplifiers, and the two amplifiers are plug-in connected to save connection cables and space. The DL-EN1 communication module is used to transmit laser measured data.

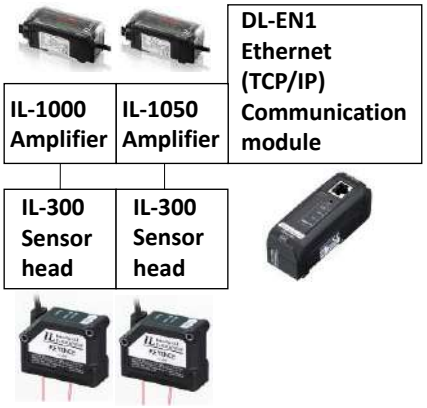

Figure 3. Point laser measurement system frame diagram

2.1.2 Pneumatic System

The using of pneumatic system with the suction cup is the most suitable method for grasping and placing

tiles or other flat objects.

As shown in Figure 4, four suction cups with a diameter of 25mm are used for the pneumatic system to grab and place 300mm×300mm tiles with the weight of about 2 kilograms after calculation and selection. The assembled vacuum generator can monitor the air pressure in real time and control it by switching the supply valve and destruction valve. The air source uses an air compressor and a filter valve is installed at the outlet to clean the air to prevent dust from clogging the vacuum generator.

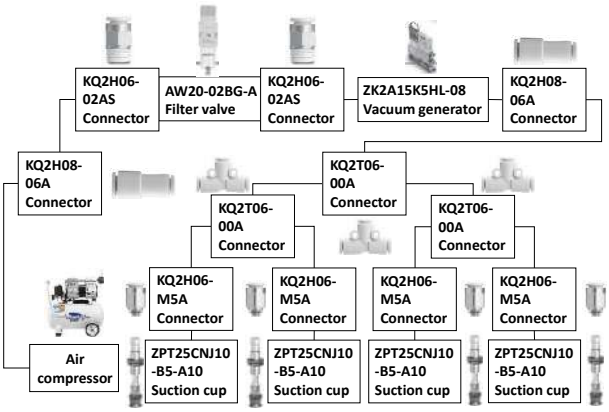

Figure 4. Pneumatic system frame diagram

2.1.3 Main Controller and Terminal System

The German Beckhoff modular products are used for the main controller and terminal system, which have the characteristics of reliable performance, fast transmission rate and convenient installation and disassembly.

As shown in Figure 5, the embedded PC is used as the main controller, which most of the algorithms are compiled and written into. The embedded PC coordinates the work of each subsystem controller. The power system can provide a stable 24V DC power supply, which can not only supply power to the embedded PC, but also support the power requirements of other subsystems. The subsequent terminals are responsible for information interaction with the communication modules of each subsystem, and the multiple subsystems are combined into a complete measuring and positioning system design of robotic floor-tiling.

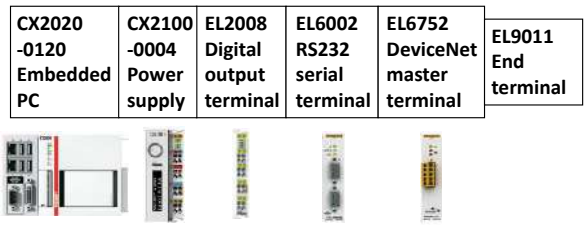

Figure 5. Main controller and terminal system

frame diagram

2.1.4 Robotic Arm System

Figure 6 is the robotic arm system frame diagram. The Yaskawa industrial robot products are used in the robotic arm system. The GP7 industrial robot has six axes of freedom and a load of 7 kilograms, which can meet the requirements of tile measuring and positioning. Each action of the robotic arm is programmed by the teaching programmer and written into the YRC1000micro control cabinet. MOTOPLUS software is used to write the protocol for the data exchange between the control cabinet and the Beckhoff embedded PC, the protocol is programmed on the computer and eventually written into the control cabinet.

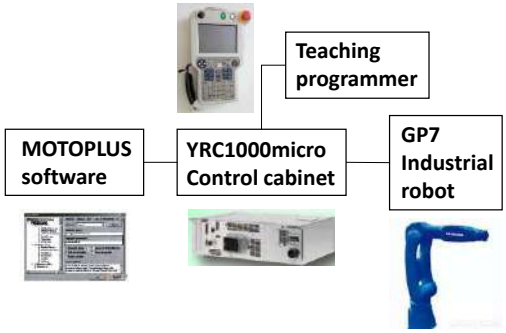

Figure 6. Robotic arm system frame diagram

2.1.5 Mobile Platform System

The mobile platform has a load capacity of 200kg, Figure 7 shows the mobile platform system frame diagram. The mobile platform system uses an STM32-based control board. The movement program in the control board sends drive commands to the four servo drives. Each servo drive drives a servo motor connected to a Mecanum wheel for rotation. The Mecanum wheel is one kind of omnidirectional wheel. The mobile platform based on the Mecanum wheel has a minimum turning radius of 0mm, it is flexible in movement and can move laterally. And the control board is equipped with a wireless module, the mobile platform can be controlled through the remote control.

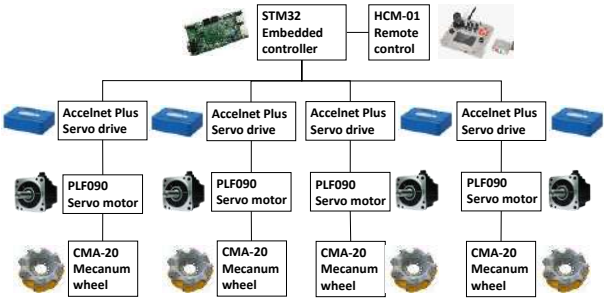

Figure 7. Mobile platform system frame diagram

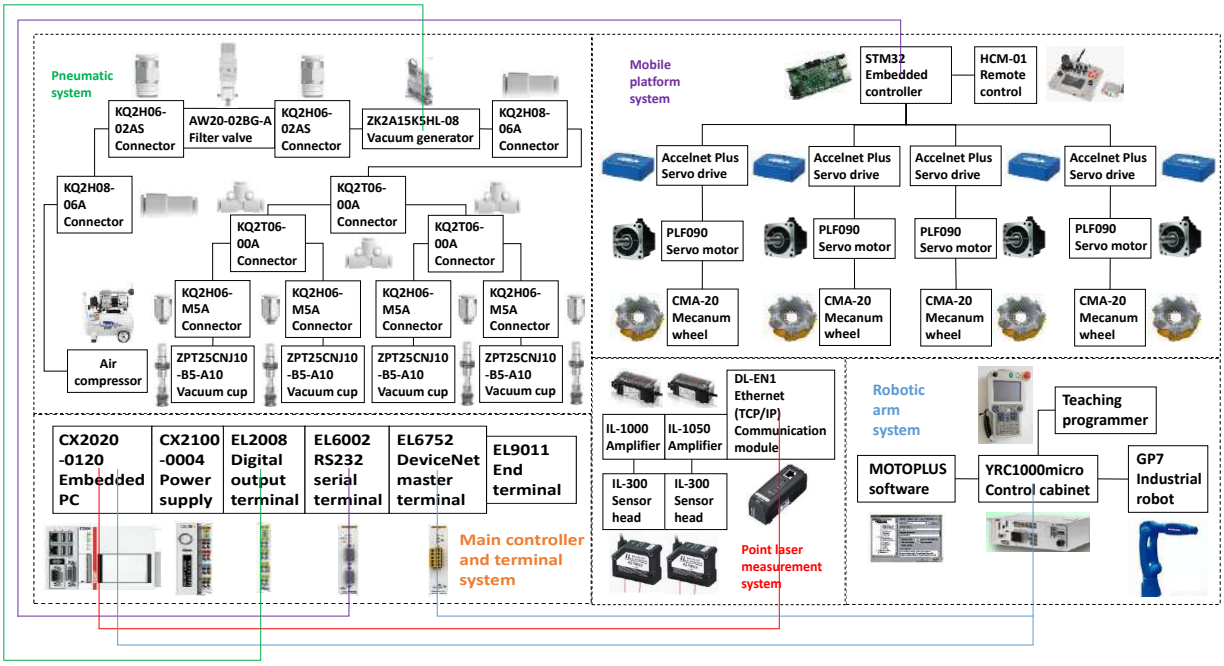

Figure 8. Measuring and positioning system's module communication frame diagram

2.2 Module Communication

As shown in Figure 8, there are several ways to communicate between subsystems.

The main controller controls the vacuum generator in the pneumatic system by EL2008 digital output terminal, and supply valve and destruction valve in the vacuum generator is controlled by the digital output, the communication cable is indicated in green.

Communication between the main controller and the point laser measurement system is realized by Ethernet TCP/IP, and TCP/IP has the advantage of reliable data transmission. The communication cable between the CX2020-0120 embedded PC and the DL-EN1 is indicated in red.

The main controller and terminal system and the mobile platform system is realized by serial port RS232. RS232 is one of the most commonly used serial communication methods, which is suitable for data transmission in non-real-time application conditions. The communication cable between the EL6002 serial terminal and the STM32 embedded controller is indicated in purple.

There are two communication ways between the main controller and terminal system and the robotic arm system. One is the Ethernet TCP/IP, which is used for robotic pose transmission, and the other is the fieldbus DeviceNet. The DeviceNet has the characteristic of high real-time performance, which is used for the transmission of motion commands sent to the robot by the main controller. Both communication cables are indicated in blue.

3 Software Environment Establishment

After the hardware platform of the robotic floor-tiling system is built, the software environment should be established in the system. The software design can be completed in three steps. The principle of tile measuring and positioning is analyzed firstly. Then, the task assignment is performed to figure out which tasks each subsystem needs to complete in a complete measuring and positioning process. Last, the control flow is developed so that each task can proceed in the order.

3.1 Tile Measuring and Positioning Principle

Figure 9 shows the schematic of tile measuring and positioning. Firstly, the end tool picks up the tile 2 and moves along the yellow arrow. When the laser spot of one point laser sensor moves from the ground to the tile 1 and another sensor head's laser spot still shoot on the ground, the end tool will slightly rotate along the orange arrow and continue to move along the yellow arrow until both laser spots shoot on the tile 1's edge. The good parallelism of the gap between two tiles is achieved by this method.

Secondly, the end tool moves back and forth along the green arrow, so that the two laser sensors can measure the range between the two red lines on the tile 1 and determine the placement position of the tile 2. In this way, the good linearity of a row tiles can be achieved.

In the process of measuring and positioning, the good levelness of the end tool is guaranteed by a

gyroscope mounted on the end tool. And the relative position of the tile 2 to the end tool can also be calculated through the two laser sensors data. When laying the second row of tiles, the same method can be used for measuring and positioning by rotating the end tool 90 degrees clockwise.

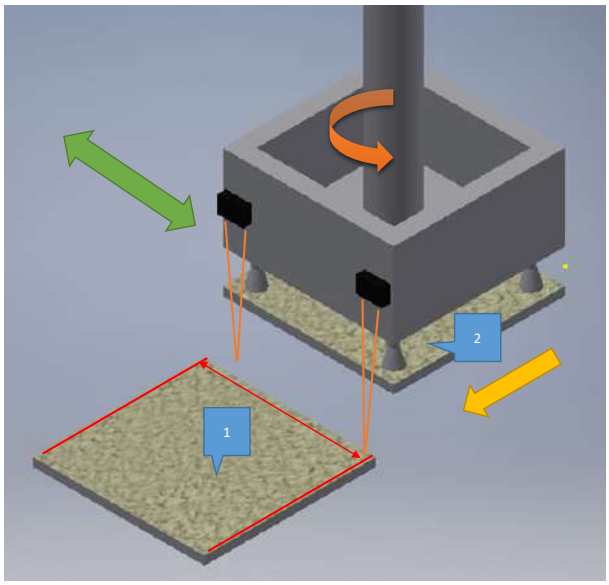

Figure 9. Tile measuring and positioning schematic

3.2 Task Assignment

According to the tile measuring and positioning principle. The process of robotic floor-tiling is divided into the following tasks to complete:

- Reference tile measuring.
- Reference tile calculation.
- Tile picking.
- Tile measuring.
- Tile calculation.
- Target position calculation.
- Tile placing.
- Return to starting point.
- Mobile platform movement.

3.3 Control Flow

The control flow is the actual flow and order of instructions and data between subsystems in the measuring and positioning process for several tasks. Figure 10 is the control flow chart of measuring and positioning process, for example in reference tile measuring task, the main controller sends movement instruction to the robotic arm. By the control flow, system tasks can be executed correctly and orderly.

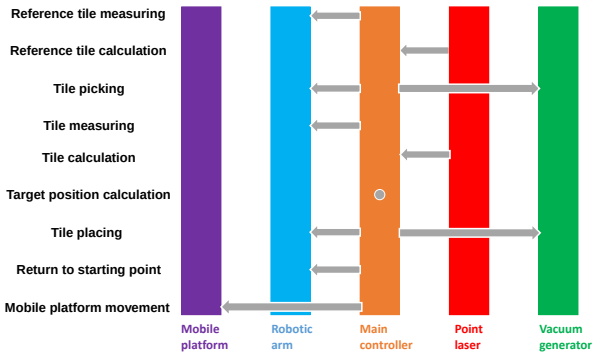

Figure 10. Control flow chart of measuring and positioning process

4 System Test and Results

Before the measuring and positioning test of the robotic floor-tiling, it is necessary to adjust the jump value of the point laser sensors. The jump value of the point laser sensor is the basis for recording the posture of the robotic arm which includes 6 parts: X, Y, Z, Rx, Ry, and Rz in the Cartesian coordinate system. And when the laser spot moves from the upper edge to the lower edge of the tile or reversed, the hopping signal generated by the point laser sensor will cause the robot to automatically record the current posture as a reference value for the test. In this test, the laser sensor has an optimum jump value of 4.2 mm.

Figure 11. Measuring and positioning test of robotic floor-tiling

The measurement and positioning test of the tile is shown in Figure 11. After placing the reference tile, the robotic arm continuously sets 10 tiles according to the position of the reference tile, and the posture of robotic arm will be recorded. Comparing the actual position with the theoretical standard position of the 10 tiles estimated from the reference tile position, the data results can be obtained in Table 1. The linear deviation range is within 0.5mm, and the rotation deviation range is within 0.2°. Results meet test expectations.

Table 1. Tile position deviation in measuring and positioning test

Tile number	X deviation (mm)	Y deviation (mm)	Z deviation (mm)	Rx deviation (°)	Ry deviation (°)	Rz deviation (°)
1	0.420	0.339	0.194	0.125	0.112	0.157
2	0.376	0.491	0.104	0.112	0.194	0.171
3	0.108	0.110	0.178	0.123	0.146	0.120
4	0.466	0.191	0.266	0.123	0.107	0.121
5	0.217	0.151	0.261	0.135	0.195	0.152
6	0.379	0.240	0.339	0.181	0.119	0.140
7	0.175	0.124	0.499	0.165	0.109	0.163
8	0.124	0.173	0.154	0.171	0.140	0.155
9	0.479	0.205	0.483	0.196	0.136	0.191
10	0.258	0.396	0.485	0.199	0.102	0.126

5 Conclusions and Future Works

This paper describes a design of measuring and positioning system for robotic floor-tiling. This system uses embedded PC as the main controller to exchange data with subsystems through various communication terminals. In the system, the main controller communicates with the robot controller via Ethernet TCP/IP and DeviceNet field bus, which can ensure the correctness and real-time of data transmission. And the connection between the main controller and the point laser measurement system is also Ethernet TCP/IP which can ensure the reliable measuring data transmission. RS232 serial port is used to control mobile platform that can save costs and meet non-real-time communication requirements. And digital output is simple and efficient enough to control the opening and closing of the supply valve and the destruction valve in the vacuum generator. The test shows the measuring and positioning system has a high precision. And this system can be seemed as the basis for the subsequent research of the floor-tiling robot.

In future works, the point laser sensors need to be replaced by other sensors, and the measuring and positioning principle also need to be improved cause the low process efficiency. More subsystems need to be added to complement the functionality of the entire robotic floor-tiling system.

References

[1] Navon, R. Process and quality control with a video camera, for a floor-tilling robot. *Automation in construction*, 10(1):113-125, 2000.

[2] Baraldi, L., & by ACIMAC, M. M. E. S. World production and consumption of ceramic tiles. AMERICA, 1(9.2):7-7, 2016.

[3] Lichtenberg, J. The development of a robot for paving floors with ceramic tiles. *Proceedings of the 20th International Association for Automation and Robotics in Construction*, 85-88, Eindhoven, Holland, 2003.

[4] Apostolopoulos, D., Schempf, H., & West, J. Mobile robot for automatic installation of floor tiles. *In Proceedings of IEEE International Conference on Robotics and Automation*, pages 3652-3657, 1996, April.

[5] Wong, J. K., Li, H., & Wang, S. W. Intelligent building research: a review. *Automation in construction*, 14(1):143-159, 2005.

[6] Baharudin, M. E. Development of Automatic Floor Tile Laying Machine. Universiti Sains Malaysia, 2007.

[7] TCNA.(n.d.). Thick-Set/Thick-Bed. Online: http://www.tcnatile.com/faqs/71-thick-setthick-bed.html.

[8] C-Cure (n.d.). ThinSet 911, dry-Set Portland Cement Mortar. Online: https://www.c-cure.com/doc/ds/ds_thinset911.pdf

[9] FloorsTransformed. (n.d.). Applying The Thinset Mortar. Online: http://www.Floors-transformed.com/thinsetmortar.html

[10] King, N., Bechthold, M., Kane, A., & Michalatos, P. Robotic tile placement: Tools, techniques and feasibility. *Automation in Construction*, 39:161-166, 2014.

[11] Vähä, P., Heikkilä, T., Kilpeläinen, P., Järviluoma, M., & Gambao, E. Extending automation of building construction—Survey on potential sensor technologies and robotic applications. *Automation in Construction*, 36:168-178, 2013.

[12] Chatila, R., & De Camargo, R. F. Open architecture design and inter-task/inter module communication for an autonomous mobile robot. *In Proceedings of IEEE International Workshop*, pages 717-721, 1990, July.

3D Human Body Reconstruction for Worker Ergonomic Posture Analysis with Monocular Video Camera

W. Chu[a], S.H. Han[a], X. Luo[b], and Z. Zhu[c]

[a] Department of Building, Civil and Environmental Engineering, Concordia University, Canada
[b] Department of Architecture and Civil Engineering, City University of Hong Kong, Hong Kong
[c] Department of Civil and Environmental Engineering, University of Wisconsin - Madison, USA
E-mail: monian0627@gmail.com, sanghyeok.han@concordia.ca, xiaowluo@cityu.edu.hk, and zzhu286@wisc.edu

Abstract –

In the modular construction industry of Canada, workers experience awkward postures and motions (reaching above shoulder, back bending backward, elbow/wrist flex, etc.) due to improper workstation designs. The awkward postures often lead to worker injuries and accidents, which do not only reduce the productivity but also increases the production cost. Therefore, the ergonomic posture analysis becomes essential to identify, mitigate and prevent the awkward postures of workers when workstation designs are changed. This paper proposes a novel framework to conduct the worker ergonomic posture analysis through the 3D reconstruction of human body from the video sequences captured by a monocular camera. The framework consists of four components: tracking worker of interest; detecting worker joints and body parts; refining 2D worker pose; and generating 3D human body model. The human body model generated from the framework could be used to estimate the joint angles of the workers to identify whether their postures meet the ergonomic requirements. The proposed framework has been tested on real construction videos, and the test results showed its effectiveness.

Keywords –

Joints detection; Body parts detection; 3D reconstruction; and Ergonomic posture analysis

1 Introduction

The modular construction has gained significant interest in recent years. According to the annual report from the modular building institute, the gross revenue in the modular construction industry in 2016 was roughly $3.3 billion in North America, which was increased by more than 60% from the year of 2015 [1]. Compared with the traditional, onsite construction, the factory-controlled processes in the modular construction provides the benefits of generating less material waste and reducing potential site disturbances [2]. They mitigate the adverse weather impacts on the project and faster the construction schedule [3]. Also, the factory controlled working environments are supposed to be safer for the workers involved.

However, workers' awkward postures are often noticed in several modular construction workshops [4]. These awkward postures might be due to the improper workstation designs in the factory controlled working environments. As shown in Figure 1, the workbenches are not high enough. Then, the workers have to bend their backs forward and strain their necks in order to reach materials and tools. The foot pedals in the machines are set too close. As a result, the workers have to bend their backs backward in order to reach the pedals. Sometimes, the workers are required to lift the materials from one spot to another over their shoulders, twist their wrists and elbows, and kneel or crouch to complete their assigned tasks in the production lines.

Figure 1. Awkward postures of the workers in modular production lines

The awkward postures easily lead to work-related musculoskeletal disorders [5, 6]. For example, the frequent kneeling will cause workers' pain and strain in their low backs and knees, which pose a high risk of developing muscle and joint problems. The musculoskeletal disorders hurt the health of the workers

and result in the absenteeism [6]. Also, they impact the employers simultaneously. Additional time and efforts must be spent on handling the lost-time and disabling injury claims with high compensations; and the workflow in the production lines are delayed [7]. New workers need to be hired to replace the injured ones, which might not always be easy.

In order to reduce the occurrences of the work-related musculoskeletal disorders, the employers in the modular construction workshops are encouraged to conduct the Physical Demand Analysis (PDA) [8]. PDA is a systematic procedure to help the employers quantify and evaluate the physical and environmental demands of a job [9]. One important step in the Physical Demand Analysis is to measure the frequency of the body posture of a worker in a job, such as percentage of the worker's back forward or backward; and then identify any potential ergonomic risk for the worker from the measurements

Traditional measures heavily rely on direct manual observations and self-reporting [10], which are easy to implement with little costs associated in the workshops. However, the manual observations and self-reporting are subjective; and the measurement results are always error-prone [11]. Recently, the idea of attaching physical sensors or tags on the worker's body to record their motions, postures and even muscle activity in the work to indicate whether the muscle is fatigue [12, 13]. The sensors can provide the accurate measurements, but their implementation cost is high. Also, it is not widely acceptable by the workers in practice, who are not willing to wear these sensors and tags during the work [14].

An alternative solution is to use digital video cameras that could be set up in the workshops by the employers. This paper combined different computer vision techniques and proposed a novel framework that relies on the video from one monocular camera to reconstruct the 3D human body of a worker. The framework consists of four main components. First, the worker of interest in the video sequences is identified through the visual tracking. Then, the 2D joints and body parts of the worker are detected. The detected joints and body parts are combined to refine the worker's 2D pose in the video sequences. The 3D human body model is further generated by matching the model with the refined 2D pose in the video sequences. This way, the 3D posture and joint angles of the worker could be estimated for the corresponding ergonomic posture analysis.

The proposed framework has been implemented in Python 2.7 with the support of GPU (Graphic Processing Unit) computing. It was tested with the videos of two real working scenarios. The first video was recorded in the production line of the Fortis LGS Structures Inc., where a worker was cutting and transporting boards. The second one was provided by Alwasel et al. [15], where a worker was laying masonry units. The test results from both scenarios showed that the framework could generate the 3D human bodies of the workers of interest and obtain their joint angles effectively and efficiently. Moreover, the joint angle information could be further input to existing ergonomic posture analysis tools, such as 3D Static Strength Prediction Program (3DSSPP) [16], to identify whether the postures of the workers meet the ergonomic requirements.

2 Related Work

This section first provides a holistic view on the techniques available for ergonomic posture analysis and their limitations. Then, 2D and 3D human pose estimation methods in the field of computer vision are presented. The 2D pose estimation methods are reviewed, since they are the solid foundation to most of existing 3D pose generation methods.

2.1 Ergonomic Posture Analysis

Existing techniques available for ergonomic analysis can be classified into the categories of self-reporting, manual observation, sensor-based direct measurement, and vision-based analysis. Self-reporting is to collect the data from worker diaries, interviews, and web-based questionnaires [10] to conduct the ergonomic analysis. It is straightforward to implement in a wide range of workplaces and appropriate for surveying large numbers of workers at low cost. However, it was found that the self-reporting data were not always precise and/or reliable [11]. Also, the levels of comprehension and question interpretation may increase the difficulty, when adopting the self-reporting in practice [17].

Manual observation mainly relies on experienced experts to record the body postures of the workers in a workplace to conduct the ergonomic analysis. Several tools have been designed and developed to facilitate the observations and evaluation of ergonomic risk factors, such as Ovako Working Posture Analysing System (OWAS) [18]. The observation produces the minimal disturbances to the workers, which makes it applicable in various working environments. On the other hand, the manual observation results are error-prone due to the influence from the subjective judgement of the experts.

Sensor-based direct measurement is to complement or replace the self-reporting or manual observation. A wide range of direct measurement sensors have been developed, and they are directly attached to the workers to improve the measurement accuracy. For example, the Lumbar motion monitor (LMM) [12] was developed to assess the risk of the worker' low back injury. The

electromyography (EMG) [13] was used to study the muscle exertions. Also, the retroreflective markers were attached on the worker bodies. This way, the 3D motion of the joints and body segments of the workers could be tracked with infrared cameras [19]. The measurements with sensors and/or markers are accurate and detailed. However, the workers complain about the physical requirement of attaching sensors and/or markers on the bodies, and not willing to wear them in practice [14].

The vision-based analysis tried to capture the joint motions of the workers and assess their body postures in a marker-less way. For example, Diego-Mas and Alcaide-Marzal [20] computerized the OWAS and processed the RGB-D data from a Microsoft Kinect camera to identify the risk level of each recorded posture. Ray and Teizer categorized the ergonomic or non-ergonomic body postures captured by a Kinect camera with a predefined set of rules [21]. Both methods solely focused on the classification of simple postures, such as lifting and crawling, in the indoor environments.

In addition to the Microsoft Kinect cameras, video cameras are also adopted. For example, in the method of Han and Lee [22], they extracted and matched the visual features of a worker in 2D video frames and then the worker's 3D skeleton can be extracted through the triangulation. This way, the unsafe actions could be detected by comparing the skeleton with pre-trained motion templates and skeleton models.

Compared with sensor-based direct measurement, the vision-based analysis does not have to physically tag workers, which makes it more acceptable in the workplaces. However, the vision-based analysis mainly relies on the data from the range or video cameras to approximate the joint motions of the workers. The accuracy and robustness of such approximation are always affected by environmental factors. Any illumination change, occlusions, and/or far shooting distance might lead to the vision-based analysis inaccurate and non-robust. So far, several methods were proposed to improve the accuracy and robustness of the vision-based ergonomic analysis.

2.2 2D Human Pose Detection

A classical method for 2D pose detection refers to the use of a pictorial structural (PS) model, in which the spatial relationships between various body parts are represented with kinematics priors. One example of the PS models is a tree-like structure, which was adopted by Lan and Huttenlocher [23] in their work of determining the human body pose. Andriluka et al. [24] combined the PS model with a strong human body part detector to make the human pose detection more generic. In addition, the mixture of the deformable parts model (DPM) was also introduced [25]. The introduction of DPM extended the application scope of the PS models, but it requires the substantial computations.

Recently, the 2D human pose detection has been significantly advanced with Deep Learning technologies. For example, DeepPose [26], the first method for human pose estimation with Deep Neural Networks (DNNs), was built on a 7-layered convolutional neural network (CNN). It formulated the pose detection as a joint regression problem and each joint could be directly regressed from a full image [26]. Pfister et al. [27] created the Flow ConvNets to detect 2D human poses, which benefitted from video temporal contexts to improve the pose estimation performance. Also, researchers developed the convolutional pose machines (CPM) [28] and stacked hourglass [29], both of which estimated the human pose without the need of an explicit human body model.

The methods described above have been used only for single-person pose estimation. They typically fail when multiple persons are captured into one image or video frame. This issue was overcome in the method of DeepCut [30], but the computational intensity is high. Its upgraded version, DeeperCut [31], was introduced to adapt to the newly proposed residual network for body part extraction. This way, the computation is reduced significantly and the robustness to the human body pose detection is maintained.

2.3 3D Human Pose Generation

The generation of 3D human pose from 2D images or videos is still one of the promising and popular research directions. Existing methods could be divided into two categories: i.e. multi-view vs. monocular view, depending on the number of video cameras adopted. Multi-view methods were inspired by human vision and infer a 3D human pose from two or more cameras [32]. The main mechanism is to obtain the 2D pose in each camera view first, and then reconstruct the 3D skeletal pose from the 2D poses [33].

Compared with the multi-view methods, it is much challenging to generate the 3D human pose with the monocular view methods. The methods tried to recover the depth information by creating a relationship between the 2D visual features (e.g. silhouette) and 3D skeletal pose [34]. This relationship could even ben learned with deep learning technologies, such as Vnect [35], which regressed 2D and 3D poses jointly through a CNN-based pose prior with Kinematic skeleton fitting. Moreover, Federica et al. [36] described how to automatically generate the 3D pose of a human body as well as its 3D shape from a single unconstrained image.

3 Research Objective

The monocular view methods for 3D human pose

generation are supposed to achieve better performance in terms of the cost-effectiveness and wide-range applicability for ergonomic posture analysis. However, they have not been well studied yet. It is still necessary to improve the 3D pose generation accuracy before the methods could be adopted in practice. One important aspect for improvement is to locate the body joints in the images or videos more precisely, considering that the locations of the body joints are directly related to body angles calculation for the ergonomic analysis.

The main objective of this research is to investigate whether it is possible to improve the 3D pose generation accuracy with the integration of existing computer vision techniques. A novel framework is proposed here for the 3D reconstruction of human poses with one monocular video camera. The overview of the framework is illustrated in Figure 2. Under the framework, the worker of interest is first tracked visually in the video sequences, and represented as a rectangular bounding box. Then, the 2D joints and body parts of the worker are detected. Based on the detection results, the 2D pose of the worker is refined and the 3D human body model is further generated by matching the model with the refined 2D pose in the videos. The joint angles are computed based on the 3D joint coordinates to serve as the input for the ergonomic posture analysis. The proposed framework is expected to function in real modular construction scenarios, which could help to identify the awkward and improper postures of the workers in modular construction workshops.

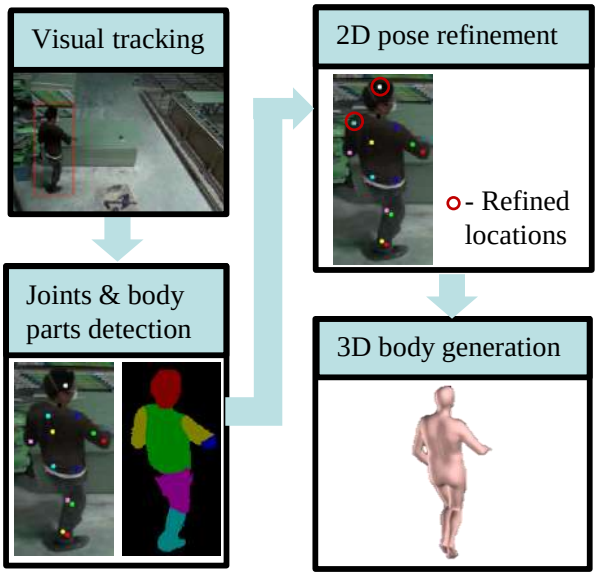

Figure 2. Overview of the proposed framework

4 Research Methodology

4.1 Visual Tracking

Visual tracking here is to locate the worker of interest along the consecutive video sequences. It could narrow down the image region with the less irrelevant background information contained for processing. Here, the CNN-based tracking algorithm *MDNet* [37] was selected due to its significant performance on the human-tracking challenge competition. It is worth noting that the tracking results need to be appropriately resized, since the accuracy of the pose estimation is easily affected by the image size. The size of 150 (width) x 350 (height) pixels was adopted in this study, based on the previous finding that the human pose detection could always perform well, when the standing height of the persons was scaled at around 340 pixels in the images [31].

4.2 Joints and Body Parts Detection

The resized visual tracking results are further processed to detect the worker's joints and body parts. Here, the joint detection is conducted by the DeeperCut algorithm [31]. It could identify a total of 14 joints from their corresponding heat maps, where the probability of each pixel in the image region to be a joint is indicated.

As for the body parts detection, the Deeplab v2 method [38] is modified to have the method only detect 6 body parts, i.e. head, torso, upper /lower arm and upper/lower leg, instead of 24 detailed body parts shown in the Pascal-Person-Part dataset [39]. Moreover, the reliability of the body part detection results is evaluated with the heatmaps produced by the DeeperCut algorithm [31]. A detected body part is considered reliable only when it has a high probability of containing a joint (larger than 0.2 in this research study). For example, the detected head body part is reliable when its probability of containing the head joint is high. The high probability does not mean that it must include the head joint.

4.3 2D Pose Refinement

The joints detected in the previous step compose an initial pose for the 3D reconstruction later. However, this initial pose is not always accurate. This is mainly because each joint is not located perfectly at the joint detection stage. For example, it is highly possible that a left shoulder joint is located on the right shoulder area instead of the left one. Therefore, the initial pose from the joint detection needs to be refined by combining the joint and body part detection results.

The refinement first checks whether the initial joints lie in their corresponding body parts. If not, the joints are relocated in the body parts based on the confidence

values of the body part regions in the heat maps. For example, if the initial head joint does not lie in the head part, then it is relocated in the head part region. The position where the highest confidence value to be the joint point in the head part area is selected. If the initial joints lie in their corresponding body parts, the refinement is then conducted on a case-by-case basis. For example, the head joint will be preferred in the top of the head part area. More details for the adjustment of the joints with the body part detection results could be found in the authors' recent work [40].

4.4 3D Human Body Reconstruction

Based on the refined 2D pose, the 3D human body of the worker of interest is reconstructed. Here, the generative Skinned Multi-Person Linear (SMPL) model [41] is adopted in the reconstruction process. The SMPL model could represent a wide variety of natural 3D human poses with body joints and shapes [41]. Following the workflow of Bogo et al. [36], these 3D poses are projected onto the camera view and compared with the refined 2D pose from the previous step. The one that optimally matches to the refined 2D pose is selected as the final reconstruction result.

The joint angles are further calculated from the reconstructed 3D human body. There are a total 14 joint angles under the consideration: clavicle (left and right), upper arm (left and right), lower arm (left and right), hand (left and right), upper leg (left and right), lower leg (left and right), and foot (left and right). Each joint angle is described both horizontally and vertically. These joint angles could be input into the 3DSSPP program [16] with other work-related information (e.g. external loads, worker's gender, age, height and weight), and assess the risk factors that may produce excessive physical loads on the worker's body.

5 Implementation and Results

5.1 Implementation and Tests

The proposed framework has been implemented in the Python 2.7 environment. It runs under the Ubuntu 16.04 LTS operation system and relies on the support of the GPU computing from an NVIDIA Titan Xp. Two real scenarios were selected to test the framework. In the first scenario, the video was collected from the production line of the Fortis LGS Structures Inc., where the worker was cutting boards in a sheathing table. The second scenario was provided by Alwasel et al. [15]. The worker in the scenario was laying concrete masonry units. He is also equipped with a motion capture suite with the attachment of 17 sensors to record his joint angles during the work.

5.2 Results

Figure 3 showed an example of the results from the first test scenario. Figure 3a illustrated the visual tracking of the worker of interest, where the red bounding box indicated the tracking result. Figure 3b indicated the detection of worker's body parts, which were represented with different colors. Figure 3c showed the refined locations of the 2D joints through the combination of the joints and body parts detection. Figure 3d was the final 3D human body reconstructed from the refined 2D joints.

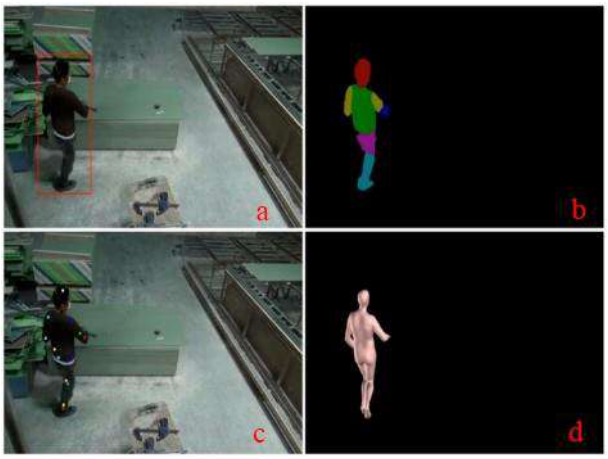

Figure 3. Results from the first test scenario

Figure 4 showed the examples of the results from the second test scenario. In the figure, the reconstructed 3D human body was placed beside the worker in the video sequences, in order to compare their visual similarity. It could be seen that the reconstructed 3D human body generally reflect the worker's posture during the work. Also, the human body could be generated, even when the worker experienced partial occlusions. In Figure 4c, both worker's head and arm were occluded, the human body was still reconstructed through the references from other visible 2D joints.

Moreover, the joint angles estimated from the 3D human body were compared with the sensory data from the motion capture suite in the second test scenario. The suit has the sampling rate of 125 Hz, and the video was captured at 25 frames per second. Therefore, the sensory data from the motion capture suite were down sampled for the frame-by-frame comparison.

Table 1 summarized the estimation error for each joint type. It could be seen that the minimum error (4.5°**)** occurs on measuring the horizontal angle of the lower arm joint. The maximum error (45.2°**)** occurs on measuring the horizontal angle of the upper leg joint. The errors for the remaining horizontal and vertical joint angles range from 10.0° to 28.0°**.** In average, the measurement error is around 17.5°**.**

Figure 4. Results from the second test scenario

Table 1. Estimation error for each joint type

Joint Type	Horizontal Angle	Vertical Angle
Clavicle	11.7°	13.2°
Upper Arm	15.9°	10.0°
Lower Arm	4.5°	10.8°
Hand	14.2°	10.1°
Upper Leg	45.2°	20.2°
Lower Leg	14.2°	20.7°
Foot	19.4°	28.0°

6 Discussion

The errors for measuring the joint angles may come from several aspects. First, the joint definitions in the SMPL model and the measurement from the motion capture suites are not one-on-one matching. The SMPL model has defined 24 joints, while the motion capture suite measured a total of 28 joint data. Therefore, those close to the joint definitions in the SMPL model were selected for the comparison, which may introduce the measurement errors.

Also, the occlusions affect the joints and body parts detection, as well as the quality of the 3D human body generation. Therefore, they may increase the joint angle measurement errors. Figure 5 illustrated the frame-by-frame comparison of the horizontal angle measurements for the lower arm from the 3D human body and motion sensory data in the second test scenario. The worker's head and arm were severely occluded from the 234th to the 388th video frames. As a result, the difference of the joint angle measurement fluctuated significantly during the occlusion period, as shown in Figure 5.

Also, the 2D pose refinement played an important role on the quality of the 3D human body reconstruction. In order to highlight its effectiveness, the pose similarity is calculated and compared for the 3D human bodies generated with and without the refinement step. It was found that the refinement improved the horizontal and vertical measurements of the pose similarity by 7.0% and 2.1%.

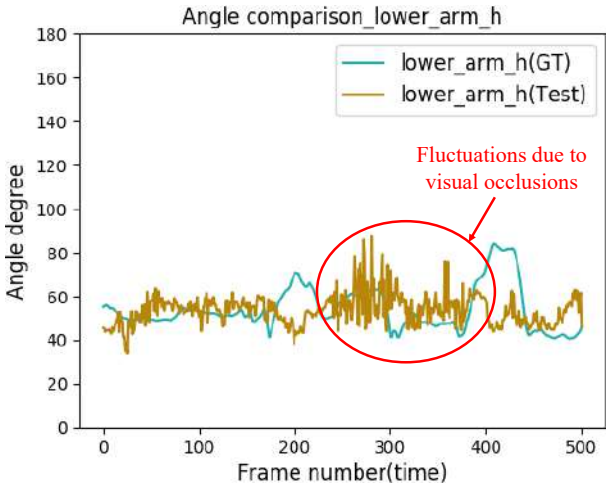

Figure 5. Comparison of the horizontal joint angle measurements for lower arm

7 Conclusions and Future Work

This paper presented an integrated framework for the 3D reconstruction of human body from the videos captured by monocular video cameras. The framework includes four main components: visual tracking, joints and body parts detection, 2D pose refinement, and 3D human body generation. The 3D human body generated from the framework could be used to estimate the body joint angles. This information could be input into the ergonomic posture analysis tool, 3DSSPP, to evaluate the risk factors that the worker may experience in a job.

The proposed framework was tested in two real scenarios. The joint angles of the 3D human body from the framework were also compared with the sensory data directly captured by a motion capture suite. The comparison results indicated that the average error for measuring joint angles was around 17.5°. The error for measuring the horizontal angle of the lower arm was as low as 4.5° and the error for measuring the horizontal angle of the upper leg reached up to 45.2°.

Future work will focus on reducing the errors of joint angle measurements. The temporal continuity in consecutive video frames and the worker's silhouettes in the video frames will be considered. They may improve the accuracy of joints and body parts detection and 3D human body reconstruction in the framework. This way, the joint angle measurement from the 3D

human body could be more accurate.

Acknowledgement

This research study was financially supported by the National Science and Engineering Research Council of Canada (NSERC) and the NVIDIA GPU Grant Program. Any opinions, findings, and conclusions expressed in this paper are those of the authors and do not necessarily reflect the views of the funding agencies. Also, the authors would like to thank the support of Dr. C. Haas and Dr. A. Alwasel from the University of Waterloo, Dr. S. Lee from the University of Michigan and their research teams. They kindly provided the videos and the sensory data as ground truth in the second test scenarios.

References

[1] Modular Building Institute, Permanent Modular Construction: Annual Report, Online: http://www.modular.org/documents/document_publication/mbi_sage_pmc_2017_reduced.pdf, Accessed: 04/ 2018.

[2] InnovativeModular Solutions, The sustainability of modular construction: reduce. Online: https://blog.innovativemodular.com/sustainability-modular-construction-reduce, Accessed: 01/2019.

[3] Modular building insitute, What is modular construction? Online: http://www.modular.org/htmlpage.aspx?name=why_modular Accessed: 01/2019.

[4] Inyang, N.I., A framework for ergonomic assessment of residetnal construction tasks. *Ph.D. Thesis*, University of Alberta, 2013.

[5] Canadian Centre for Occupational Health and Safety, Worker-related Musculoskeletal Disorders. Online: https://www.ccohs.ca/oshanswers/diseases/rmirsi.html Accessed: 01/2019

[6] Simoneau, S., St-Vincent, M., and Chicoine, D. Worker-related musculoskeltal discorders – a better understanding for more effective prevention. Online: https://www.irsst.qc.ca/media/documents/PubIRSST/RG-126-ang.pdf Accessed: 01/2019

[7] Hinze, J. and Appelgate, L.L. Costs of construction injuries." *Journal of construction engineering and management*, 117(3): 537-550.

[8] Li, X., Fan, G., Abudan, A., Sukkarieh, M., Inyang, N., Gül, M., El-Rich, M., and Al-Hussein, M. Ergonimics and physcial demand analysis in a construction manufacturing facility. In: *Proceedings of 5th International/11th Construction Special Conference*, Vancouver, British Columbia, June 810, 2015, 231-1:10

[9] Occupational Health Clinics for Ontario Workers Inc. Physical demands analysis (PDA). Online: https://www.ohcow.on.ca/ Accessed 01/2019

[10] Dane, D., Feuerstein, M., Huang, GD., Dimberg, L, Ali, D., and Lincoln, A. "Measurement properties of a self-report index of ergonomic exposures for use in an office work environment." *Journal of Occupational and Environmental Medicine*, 2002, 44(1): 73-81.

[11] David, GC. Ergonomic methods for assessing exposure to risk factors for work-related musculoskeletal disorders. *Occupational medicine*, 2005, 55(3): 190-199.

[12] Marras, WS. and Granata, KP. Spine loading during trunk lateral bending motions. *Journal of biomechanics*, 1997, 30(7): 697-703.

[13] Ning X., Zhou J., Dai B., and Jaridi, M. The assessment of material handling strategies in dealing with sudden loading: the effects of load handling position on trunk biomechanics. *Applied ergonomics*, 2014, 45(6): 1399-1405.

[14] Yu, Y., Li, H., Yang, X., and Umer, W. Estimating construction workers' physical workload by fusing computer vision and smart insole technologies. In: *Proceedings of the 35th International Symposium on Automation and Robotics in Construction*, Berlin, Germany, July 20-25, 2018, paper-247.

[15] Alwasel, A., Sabet, A, Nahangi, M., Haas, C.T., and Abdel-Rahman, E. Identifying poses of safe and productive masons using machine learning. *Automation in Construction*, 84(2017): 345-355.

[16] Center for Ergonomics, University of Michigan, 3DSSPP Software, Online: https://c4e.engin.umich.edu/tools-services/3dsspp-software/ Accessed: 01/2019

[17] Spielholz, P., Silverstein, B., Morgan, M., Checkoway, H., and Kaufman, J. Comparison of self-report, video observation and direct measurement methods for upper extremity musculoskeletal disorder physical risk factors. *Ergonomics*, 2001, 44(6): 588-613.

[18] Karhu O, Kansi P, and Kuorinka I. Correcting working postures in industry: a practical method for analysis. *Applied ergonomics*, 1977, 8(4): 199-201.

[19] Richards, J.G. The measurement of human motion: A comparison of commercially available systems. *Human movement science*, 1999, 18(5): 589-602.

[20] Diego-Mas. J.A, and Alcaide-Marzal J. Using Kinect™ sensor in observational methods for assessing postures at work. *Applied ergonomics*, 2014, 45(4): 976-985.

[21] Ray S.J, and Teizer J. Real-time construction worker posture analysis for ergonomics training. *Advanced Engineering Informatics*, 2012, 26(2):

439-455.

[22] Han, S.U, and Lee, S.H. A vision-based motion capture and recognition framework for behavior-based safety management. *Automation in Construction*, 35(2013): 131-141.

[23] Lan, X. and Huttenlocher, D.P. Beyond trees: Common-factor models for 2d human pose recovery, In: *Proceedings of the 10th International Conference on Computer Vision*, IEEE, 2005, 1: 470-477.

[24] Andriluka, M, Roth, S., and Schiele, B. Pictorial structures revisited: People detection and articulated pose estimation. In: *Proceedings of the IEEE Conference on Computer Vision and Pattern Recognition*, 2009.: 1014-1021.

[25] Felzenszwalb, P.F, Girshick, R.B., McAllester, D., and Ramanan, D., Object detection with discriminatively trained part-based models. *IEEE transactions on pattern analysis and machine intelligence*, 2010, 32(9): 1627-1645.

[26] Toshev, A., and Szegedy, C. Deeppose: Human pose estimation via deep neural networks In: *Proceedings of the IEEE conference on computer vision and pattern recognition*. 2014: 1653-1660.

[27] Pfister, T., Charles, J., and Zisserman, A. Flowing convnets for human pose estimation in videos. In: *Proceedings of the IEEE International Conference on Computer Vision*. 2015: 1913-1921.

[28] Wei, S.E., Ramakrishna, V., Kanade, T, and Sheikh, Y. Convolutional pose machines. In: *Proceedings of the IEEE Conference on Computer Vision and Pattern Recognition*. 2016: 4724-4732.

[29] Newell, A., Yang, K., and Deng, J. Stacked hourglass networks for human pose estimation. In: *Proceedings of the European Conference on Computer Vision. Springer*, Cham, 2016: 483-499.

[30] Pishchulin, L., Insafutdinov, E., Tang S, Andres, B., Andriluka, M., Gehler, P., and Schiele, B. Deepcut: Joint subset partition and labeling for multi person pose estimation. In: *Proceedings of the IEEE Conference on Computer Vision and Pattern Recognition*. 2016: 4929-4937.

[31] Insafutdinov, E, Pishchulin, L., Andres, B., Andriluka, M., and Schiele, B. Deepercut: A deeper, stronger, and faster multi-person pose estimation model. In: *Proceedings of the European Conference on Computer Vision*. 2016: 34-50.

[32] Trucco, E, and Verri, A. *Introductory techniques for 3-D computer vision*. Prentice Hall, 1998.

[33] Hofmann, M., and Gavrila, D.M. Multi-view 3d human pose estimation combining single-frame recovery, temporal integration and model adaptation. In: *Proceedings of the IEEE Computer Vision and Pattern Recognition*, 2009, 2214-2221.

[34] Atrevi, D.F., Vivet, D., Duculty, F., Emile, B. A very simple framework for 3D human poses estimation using a single 2D image: comparison of geometric moments descriptors. *Pattern Recognition*, 2017, 71: 389-401.

[35] Mehta, D, Sridhar, S, Sotnychenko, O, Rhodin, H., Shafiei, M., Seide, H.P., Xu, W., Casas, D., and Theobalt, C. Vnect: Real-time 3d human pose estimation with a single rgb camera. *ACM Transactions on Graphics*, 2017, 36(4): 44.

[36] Bogo, F., Kanazawa, A., Lassner, C., Gelher, P., Romero, J., and Black, M.J. Keep it SMPL: Automatic estimation of 3D human pose and shape from a single image. In: Proceedings of *European Conference on Computer Vision*. 2016: 561-578.

[37] Nam, H. and Han, B. Learning multi-domain convolutional neural networks for visual tracking. In: *Proceedings of the IEEE Conference on Computer Vision and Pattern Recognition*. 2016: 4293-4302.

[38] Chen, L.C, Papandreou, G., Kokkinos I, Murphy, K., and Yuille, A.L. Deeplab: Semantic image segmentation with deep convolutional nets, atrous convolution, and fully connected crfs. *IEEE transactions on pattern analysis and machine intelligence*, 2018, 40(4): 834-848.

[39] Chen, X., Mottaghi, R., Liu, X., Fidler, S., Urtasum, R. and Yuille, A. Detect what you can: Detecting and representing objects using holistic models and body parts. In: *Proceedings of the IEEE Conference on Computer Vision and Pattern Recognition*. 2014: 1971-1978.

[40] Chu, W. Han, S.H., and Zhu, Z. Devlopment of Human Pose using Hybrid Motion Tracking System. In: Proceedings of the 18th International Conference on Construction Applications of Virtual Reality, Nov. 22-23, 2018, Auckland, New Zealand

[41] Loper, M., Mahmood, N, Romero J, Pons-Moll, G., and Black, M.. SMPL: A skinned multi-person linear model. *ACM Transactions on Graphics*, 2015, 34(6): 248.

Dispersed Cyber-Physical Coordination and Path Planning Using Unmanned Aerial Vehicle

A. Bulgakov[a], D. Sayfeddine[b], T. Bock[c], and S. Emelianov[a]

[a]Institute of Mechatronic and Robotic in Construction, Southwest State University, Kursk, Russia
[b]Institute of Mechatronic, Platov South-Russia State Polytechnic University, Novocherkassk, Russia
[c]Chair for Building Realisation and Robotics, Technical University of Munich, Germany
E-mail: a.bulgakow@gmx.de, tatyana.kruglova.02@mail.ru, thomas.bock@br2.ar.tum.de, esg@mail.ru

Abstract –

In recent years, drones have been used exclusively for military missions, but with the advent of new characteristics in UAV technology, more industries are now moving to add this new element to their practices. Engineers and analysts use UAVs to monitor projects, scan the ground, find out its dimensions and reduce the incidence of costly errors. The Drones improved the world over the next years and its use becomes a general trend in all areas, including industrial. Technology can be said to have a way of breaking down barriers and making impossible. The emergence and spread of a technological event is one of the key features that ensure the continuation of technological progress, and also guarantees us the creation of best products that the future holds. In this paper, we analyze a close coordination between dispersed cyber-physical system parts; aiming to mount pre-casted concrete pergola sections on rooftop of a building. The system consist of a manipulating robotized crane, moving the sections of pergola to the top level and positioning them according to a predefined shape. For better positioning of the sections, the trajectory of the manipulating system, in terms of lifting altitude, and two-dimensional positioning, is coordinated using unmanned aerial vehicle.

Keywords –

Cyber-physical system; UAV; Robot path planning

1 Introduction

In the past few years, the importance of unmanned aerial vehicles can be clearly defined in different techno-social fields. The application of autonomous systems is not anymore strictly related to military applications. Nowadays, unmanned platforms are used in medical, construction, rescue and cinematography business. Despite the relative success and the development of market share, the integration of these platforms in our quotidian life cycle is endangered by physical isolation of these solutions from direct contact with end-users, the absence of regulations and laws and relatively late development in human-machine interfaces.

Focusing on the UAV, the challenges are more serious than the ground-based autonomous platforms. The reason might be the importance of skies in military and civil aspects. Hence, the integration of the UAV in day-to day applications is limited due to the aforesaid reasons.

Pertaining to the construction market, the presentation of UAV is limited to photogrammetry and BIM. Researches about these topics are plenty: bridges, light poles, high-rise building and facades inspections are some of them.

In this paper, we would like to take the discussion further more and use the aerial capabilities of the UAV to guide and lead trajectory planning for dispersed cyber-physical system, the goal of which is to install heavy-weight roof mounted pergola.

This research will be composed in three main paragraphs:

- Description of the cyber physical system;
- Odometric approach and calculations of trajectory planning;
- Formation of control tasks and generation of results.

2 Dispersed Cyber-Physical System

By cyber-physical system, we understand the concept of reliable fusion between computational and physical platform embedded within the same body [1], however, enabling better interaction capabilities with the surrounding (world and human operator) though many modalities and processes. In light of that, the terms of interaction, integration and enhancement are

key areas where the research of cyber physical systems is occurring.

Traditionally, the physical system is a consolidated system and not dispersed over selected area. Recently, with the introduction of Internet of things (later IoT), the probability of designing distributed physical systems became achievable, as it overcame the disadvantages of radio systems and the huge cost related to GPS and GLONASS integration in navigation platforms, which made these solution not optimal techno-commercially. In this paper, we introduce the cyber-physical system consisting of the following levels:

- Aerial: a UAV scanning the roof and generating the positioning tasks for the subsequent component of the pergola;
- Cybernetic: analyzing the video-input of the UAV and generating trajectory for the manipulator using visual odometry algorithm;
- Ground: a Mobile robotic crane, receiving the coordinates from the cyber system and performing the laying-out of the pergola blades.

A concept of the solution is illustrated in fig.1 according to which, the UAV will dictated the following parameters as a potential control task to the cybernetic system: the swing angle ϕ, the luff angle θ, the hoist elevation h and the mobility across axis OX and OY, which can be replaced by the angle formed by the hoist and the luff axis [10].

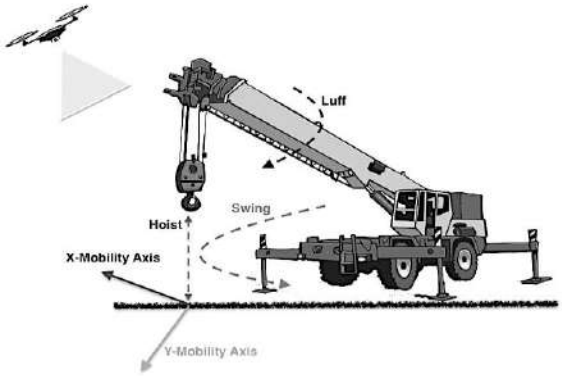

Figure 1. Concept of dispersed cyber-physical system

3 Trajectory Identification

3.1 Optical Odometry

The task of global planning is to fly through checkpoints [2]. This approach has already been applied in determining the position of the UAV and managing altitude using color or shape identification [9]. The difference between the proposed algorithm and the known control methods using machine vision algorithms is that for autonomous localization, the autopilot determines the distance traveled by calculating the rotor speed and rotation axis and establishes the relationship between the pixel system and the associated coordinate reference system (Body-axis). Usually, to determine the location of the UAV, information from the global localization system and the onboard sensors are used. Here, it is proposed to solve the problem using a machine vision and the method of optical odometry, which allows determining the location and orientation of the movement based on the sequence of optical information (images) in each time step. Figure 2 shows the relation between different references systems.

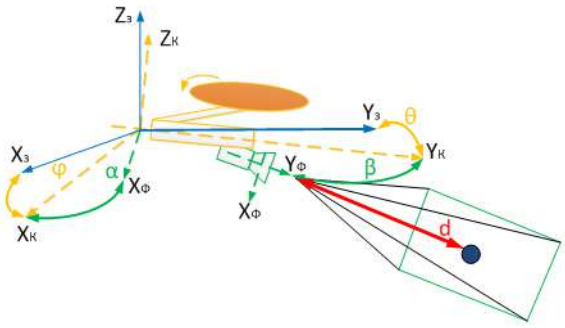

Figure 2. Axis and reference systems

To change the UAV position in relation to the Earth, using camera frames, it is necessary to find geometric relationships between different coordinate reference systems. We consider AR DRONE as UAV, which has a diaphragm deviation diagonally within 64 degrees. Using the laws of trigonometry, we obtain the angles of vertical and horizontal deviations, equal to 43.18 degrees and 51.62 degrees, respectively. The definition of the angles of inclination of the UAV with respect to the fixed axis of coordinates, and the roll, pitch and flight altitude, which are needed to determine the position of the camera in relation to the Earth are as follows: the aperture deviates by 51.62 degrees from the horizontal coordinate system i.e. from the origin of the roll angle (φ), therefore, the deviation of the projection of the image on the horizontal axis of the diaphragm can be computed according to equation (1):

$$\varphi = (51.62 - \alpha), \quad (1)$$

Where $\alpha -$ is the horizontal polar angle in the aperture coordinate system. In the same way we find the vertical projection by the formula:

$$\theta = (43.18 - \beta), \quad (2)$$

Where $\beta -$ vertical polar angle in the aperture coordinate system.

A geometrical representation of the deviation of the diaphragm from a fixed coordinate system is presented in Figure 3.

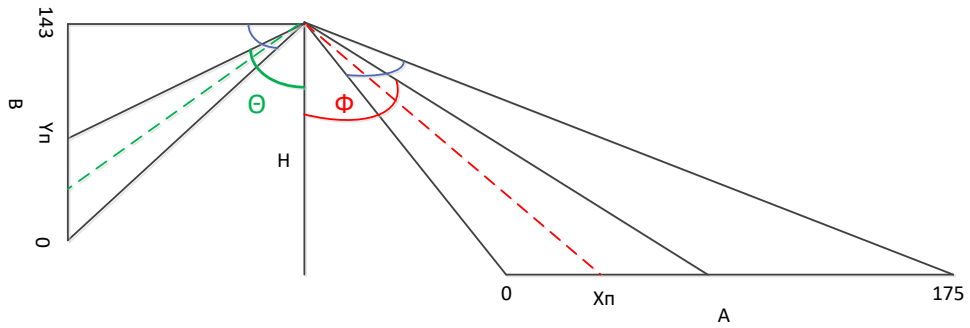

Figure 3. Geometric relationship between the associated coordinate system and the camera reference system

The distance from the camera to a specific coordinate (Earth-axis) is computed using the following equations

$$d(x) = H_{\text{г}} = H * \tan(\varphi + \alpha); \quad (3)$$

$$d(y) = H_{\text{B}} = H * \tan(\theta + \beta), \quad (4)$$

Using equations (3) and (4), we can identify the transformation formulas between different reference systems.

$$\begin{cases} X_{\text{п}} = \frac{x}{\Pi x}.\cos\left(\arctan\left(\frac{H_B}{H_{\text{г}}}\right)\right) \\ Y_{\text{п}} = \frac{y}{\Pi y}\sin\left(\arctan\left(\frac{H_B}{H_{\text{г}}}\right)\right) \\ \rho_x = \sqrt{{X_{\text{п}}}^2 + {Y_{\text{п}}}^2} * \cos\left(\arctan\left(\frac{H_B}{H_{\text{г}}}\right)\right) \\ \rho_y = \sqrt{{X_{\text{п}}}^2 + {Y_{\text{п}}}^2} * sin(\arctan\left(\frac{H_B}{H_{\text{г}}}\right)) \end{cases} \quad (5)$$

Where $X_{\text{п}}$ and $Y_{\text{п}} -$ are the pixel coordinates, x and $y -$ are the body axis coordinate and ρ_x and ρ_y are the angular pixel coordinates.

3.2 Minimum Jerk Trajectory

The pixel coordinates calculated in equation (5) has to be fed to the crane as a desired trajectory for its manipulator. In light of that, the obtained coordinates and rotational angels have to be transformed to metric again in terms of swing and luff angles, elevation and 2D mobility. We will assume that the height of the building is known and the influence of the wind is negligible; hence the elevation parameter will be considered as an input value and the dragging coefficient of the pergola blades will be neglected aerodynamically.

The remaining four parameters can be directly correlated with received by computing equation (5) and interchanging equivalence. The difficulty remains in generating a trajectory that achieve minimum jerk to the manipulator as it might cause risks, false positioning of the moved piece and possible abortive works [5,6]. To achieve an optimal trajectory to the manipulator, the movement will be posed and solved as quadratic programming using multi-segment Chebyshev orthogonal collocation for transcription.

Using the two dimensional Chebyshev-Gauss collocation method to obtain possible numerical solution of differential equation by partially is differentiating it in time and discretizing it using finite difference method [4]. Taking into consideration that the trial or candidate trajectories $f_k(x)$ will be set on homogenous Dirichlet boundary conditions [3], the approximate solution can be presented in the following equation

$$U^N(x,t) = \sum_{k=0}^{N} a_k(t)\, f_k(x) \quad (6)$$

In the collocation approach, the differential equation has to be satisfied by the approximate solution at the collocation points in the assigned domain [8]. The derivative at each node can be found by multiplying the value at any Chebyshev point by a differentiation matrix.

3.3 Results

Implementing the equations in sections (3.1) and (3.2), and running the quadratic programming listing on Matlab, the result of multi-segment trajectory simulation based on the aforementioned modeling constraints is depicted in Figure 4.

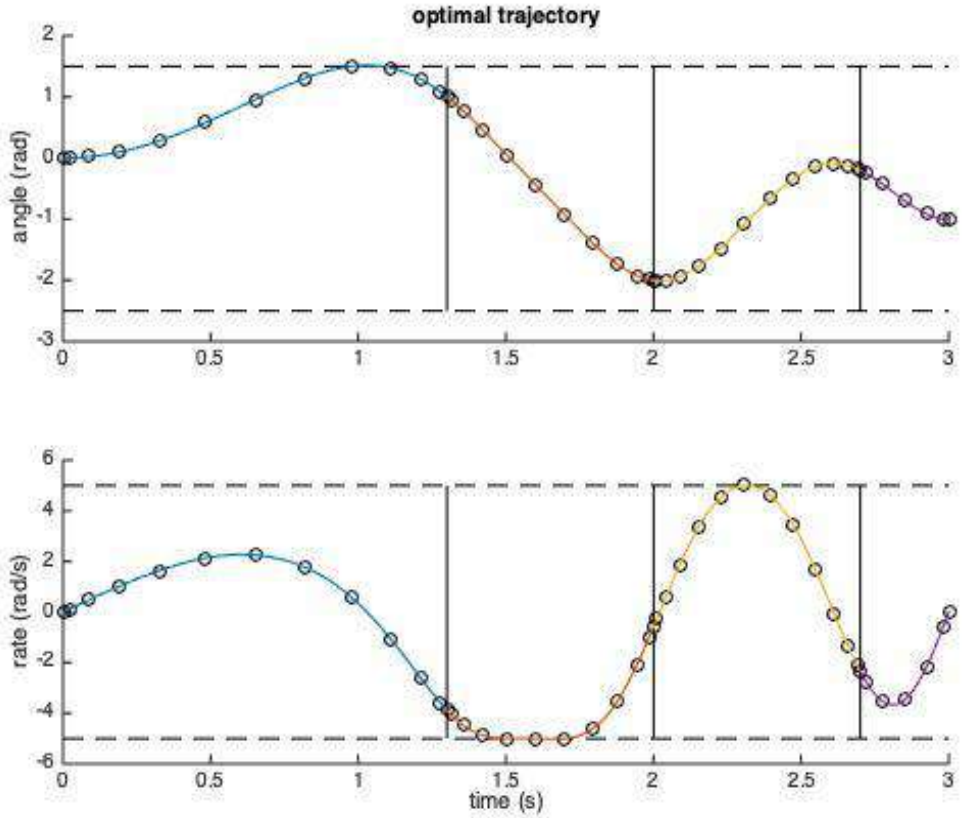

Figure 4. Results of multi-segment trajectory

In figure 4, we can clearly see, that the trajectory is passing by all the Chebyshev node points, where the initial an final velocity rated in rad/s is zero and the angle of the final trajectory is almost negligible.

By applying the same concept to the both sections of the manipulator, with specific boundaries and input trajectory, we can see that the arm end-effector holding the bald is travelling smoothly, on the doted lines, shown in Figure 5, taking into consideration for joint 1 and 2, the initial velocity is zero (starting point of lifting task), and the resultant final velocity of the end-effector is also zero rad/s, which corresponds to discharge of the manipulator after laying task.

4 Conclusion

This paper presented an operational simulation of dispersed cyber-physical system performing a lifting and disposing pergola blades on certain rooftop of a building. The system consisted of UAV, the task of which is to analyze the surrounding and generate an optimal trajectory to a robotic manipulator (crane) considered as a Chebyshev orthogonal collocation points based on optical odometry. The task was formulated as a quadratic programming problem. The obtained results endorsed the theoretical approach and showed that both the joints of the lifting crane have followed the optimal trajectory, passing by all Chebyshev points with minimum jerk considering that the initial velocity of the joints is zero and the final velocity should be obtained zero rad/s with minimum to zero overshooting angles.

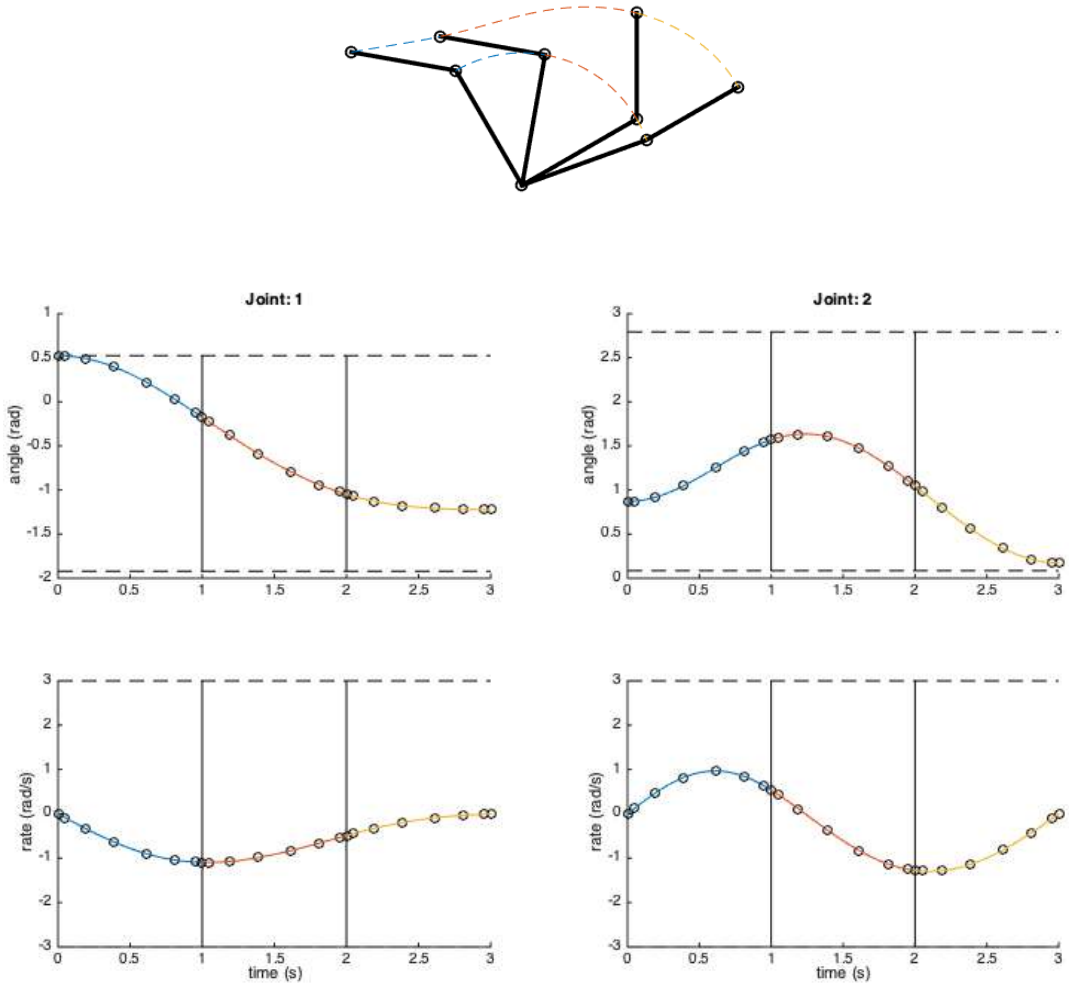

Figure 5. Minimum-Jerk Trajectory of the robotic manipulator corresponding to Chebyshev nodes

References

[1] Rajhans A. et al. An architectural approach to the design and analysis of cyber physical systems. *3rd International workshop on multi-paradigm modeling.*

[2] Sayfeddine D. Translated from Russian – UAV online agent tracking using geometric approach. *International Scientific Conference*, Vol.2, 2009, pp. 109-112.

[3] Cheng, A. and Cheng D.T. *Heritage and early history of the boundary element method, Engineering Analysis with Boundary Elements*, 29, 268–302.

[4] Sameeh M. et Chebyshev al. Collocation Method for Parabolic Partial Integrodifferential Equations. *Advances in Mathematical Physics*, Volume 2016, Article ID 7854806, 7 pages.

[5] Kyriakopoulos K.J. et al. Minimum jerk for trajectory planning and control. *Robotica. Cambridge University Press*. Volume 12, Issue 2, pp. 109-113.

[6] Amirabdollahian F. et al. Minimum jerk trajectory control for rehabilitation and haptic applications. In *Proceedings 2002 IEEE International Conference on Robotics and Automation.*

[7] Cheuprasert K. et al. A Chebyshev-Gauss collocation method for the numerical solution of ordinary differential equations. *J. Sci. Technol.* 39 (3), 383-397, 2017.

[8] Yixin L. Introduction to spectral methods.

[9] Kemper M. and Fatikow S. "Impact of center of gravity in quadrotor helicopter controller design," in Proc. *4th IFAC-Symposium on Mechatronic Systems*, (Heidelberg, Germany), 2006.

[10] Upadhay A. et al. UAV-Robot relationship for coordination of robots on a collision free path. *International conference on robotics and smart manufacturing (RoSMa2018)*, pp. 424-431.

Design and Development of Drill-Resistance Sensor Technology for Accurately Measuring Microbiologically Corroded Concrete Depths

N. Giovanangeli[a], L. Piyathilaka[a], S. Kodagoda[a], K. Thiyagarajan[a], S. Barclay[b], D. Vitanage[b]

[a]iPipes Lab, Centre for Autonomous Systems, University of Technology Sydney, Australia.
[b]Sydney Water Corporation, Parramatta, New South Wales, Australia.
E-mail: Karthick.Thiyagarajan@uts.edu.au (Corresponding Author)

Abstract -

Microbial corrosion of concrete is a severe problem that significantly reduces the service life of underground sewers in countries around the globe. Therefore, water utilities are actively looking for in-situ sensors that can quantify the biologically induced concrete corrosion levels, in order to carry out preventive maintenance before any catastrophic failures. As a solution, this paper introduces a drill-resistance based sensor that can accurately measure the depth of the microbiologically corroded concrete layer. A prototype sensor was developed and evaluated in laboratory test conditions. The lab experiments proved that the developed sensor has the ability to measure the depth of the microbiologically corroded concrete with millimeter level of accuracy. Additionally, the sensor can also locate and accurately measure the size of concrete aggregates as well as potential cracks, effectively creating a sub-surface 'scan' of the concrete at the targeted point of interest. Therefore, providing valuable extra information for assessing the condition of the sewer concrete.

Keywords -

Concrete, corrosion, drill resistance, measuring, sensor, sewer.

1 Introduction

Reinforced concrete sewers undergo significant microbiologically induced corrosion caused by sulphuric acid producing bacteria, particularly in countries with warm climate conditions. This sewer concrete corrosion leads to sewer pipe deterioration and consequential structural failures by incurring losses that are estimated to be in the order of billions of dollars per year worldwide.

Furthermore, microbial corrosion of concrete increases the likelihood of catastrophic structural failures that can cause not only detrimental damage/harm to urban-dense populations but also irreversible damage to the surrounding environment. The annual cost of corrosion for drinking water and sewer systems in the United States alone is about USD36 billion [1] including maintenance, rehabilitation, and replacement. In the United Kingdom, the total replacement cost of sewer mains was estimated to be 104 billion pounds [2] whilst in Germany, the rehabilitation cost for sewer concrete corrosion was estimated to be 100 million Euros [3]. In addition, the rehabilitation of sewer concrete pipes cost AUD40 million annually in Australia [4]. Therefore, sewer corrosion is a significant problem worldwide which needs to be identified promptly, so water utilities can intervene and carryout the the necessary maintenance before any catastrophic failure [5].

A key parameter that water utilities use for decision making in sewer infrastructure maintenance is the estimation of the Remaining Service Life (RSL) of the sewer pipe, which is often estimated by measuring the depth of the remaining intact concrete left to the reinforcement bars. RSL gives an estimation of how many years the sewer can be used without further rehabilitation. In general, sewer wall corrosion rates are very slow (could be less than a millimeter per year) and hence, depth of the microbiologically corroded concrete layer needs to measured precisely to accurately estimate the RSL. However, due to the non-homogeneous nature of concrete combined with the harsh conditions of a sewer pipeline, particularly with extremely high humidity and acidity, conventional sewer monitoring sensors are prone to malfunctions [6, 7], struggle to reliably and accurately measure the depth of the microbiologically corroded concrete in field conditions. The most conventional way for measuring the depth of the corroded concrete is done by taking core samples from the sewer walls, which is a time consuming process and expensive endeavour. Additionally, prolonged exposure to sewer environments poses serious occupational health and safety issues for the workers in the sewers [8]. Hence, wastewater managing utilities are looking for innovative sensing technologies which can assess the level of the microbial induced corrosion of concrete accurately and quickly so the required maintenance can be carried out promptly.

Over the years, there have been remarkable strides in developing drill-technology capable of operating in challenging conditions. Drills are often perceived to be destructive tools, yet we often overlook that there are many precise and delicate micro-invasive applications for drills, such as in brain surgery or orthopaedic repair.

Drill-resistance based measuring methods are a useful sensing option for differentiating non-homogeneities in a given material as the mechanical drilling component guarantees penetration through the material. Unfortunately, due to the misconceived destructive nature associated with drills, this sensing approach has not been so widely adopted in the past. However, the unique ability to accurately characterize many materials at various given depths (i.e. whether the material at a certain unit of depth is hard or soft) below the surface in real-time makes drill-resistance based measuring an excellent candidate for developing a sensor technology that can accurately measure the depths of corrosion in concrete for both human operator and autonomous robotic applications.

Previously, drill-resistance based sensors have been developed for sampling the ring-growth pattern in tree-trunks [9, 10, 11], which was later evolved into using the sensing approach to measure decay in trees - substituting the use of X-ray as result of several advantages such as simplicity, portability, and accessibility in comparison. Later on, drill-resistance based sensing was adapted for assessing the strength of fire-damaged concrete [12, 13] yet it was not until early this decade drill-resistance based sensing was developed for measuring the decay in natural stone and marble as part of conservation projects of irreplaceable cultural heritage monuments and buildings [14]. Whereas this paper will go into the design and development of a prototype, which is the first of its kind to demonstrate accurate depth of the boundary layer between corroded and intact concrete, even with the presence of hard aggregates within the relatively soft corroded layer. The sensor can provide a scan of any corroded concrete target area in real-time without any need for calibration or advanced/heavy post-processing.

2 Background

2.1 Concrete Corrosion

Figure 1 shows the microbiologically induced corrosion process inside sewer system. Sulphate-producing bacteria that reside in sewage produce dissolved H_2S in wastewater under anaerobic conditions. This dissolved H_2S is released as a gas phase due to turbulence in the wastewater as it flows down the pipeline. In general, surface pH of newly installed sewer concrete pipes ranges approximately between 12-13. When the pH value falls to 9, the bacteria begin to colonize on the concrete surface [16]. The chemoautotrophic bacterium that exists on the sewer concrete surface oxidizes the gas phase H_2S into biogenic sulphuric acid H_2SO_4, which reacts with the cementitious material of concrete leading to concrete corrosion [17, 18]. The corrosion process transforms the effected concrete into calcium sulfide, commonly known as gypsum - a soft brittle material whose presence introduces focused areas of strength loss in a structure. In addition, gypsum is moderately water soluble - the combination of a soft brittle gypsum under structural load in a highly humid environment makes the gypsum layer prone to breaking off with the subsequent material loss in the pipeline structure, leading to structural failure if left untreated.

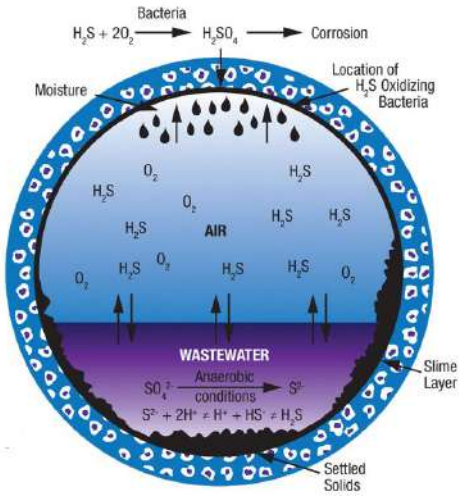

Figure 1. Sewer Corrosion Process [15].

2.2 Conventional NDT Sensing Modalities

Conventional Non-Destructive Testing (NDT) sensing systems like Ground-Penetrating-Radar (GPR) and ultrasound sensors are widely used for detecting concrete defects like delamination in concrete civil infrastructure. Therefore, these sensors have the potential for detecting the depth of the boundary layer between the microbiologically corroded concrete and intact concrete. However, use of these sensors for detecting microbiologically corroded concrete in sewer environment is challenging. The GPR signal measurements can be potentially affected by the moisture conditions of the exposed sewer surface [19], and the ultrasound techniques need sound coupling with the sewer wall [20], making it practically challenging to use on uneven rough surfaces of the sewer pipes. Besides direct measurements, predictive models have been developed for estimating the corrosion throughout the sewer network. Quality of such model prediction rely on the data supplies by the sensors [21, 22, 23, 24].

2.3 Drill-Resistance Sensing

Drill-resistance is an unconventional sensing approach in the sense that it is an integration of multiple sensors functioning in parallel but also that the main principles of drill-resistance based measurements are based on mechan-

ical principles rather than physical phenomena. There is a direct correlation between the reaction force exerted on the drill-bit and drill-bit penetration per drill-bit revolution [25]. Therefore, the penetration rate of the drill (Δd_p) and the drill speed (ω_d) must be kept constant in order for the reaction force per ongoing depth measurement to show an accurate and valid representation of the material being drilled. Assuming those parameters are kept constant, the hard material will exert a higher reaction force on the drill-bit compared to a softer material as more energy is required for penetrating into the harder material per unit distance per drill-bit revolution.

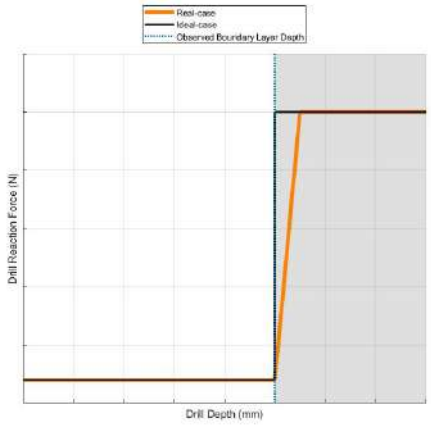

Figure 2. Boundary layer identification between two different materials based on force-depth readings: The point where there is a significant change in force-depth gradient signifies a different material at that corresponding drill-depth.

Figure 2 shows a simplified example of the measured thrust (reaction) force acting through the drill-bit per increment in drill depth whilst drilling through two different material layers. The depth where there is significant change in the force-depth gradient signifies a different material at that depth. Maximising the drill-bit penetration per drill-bit revolution (or $\Delta d_p : \omega_d$ ratio) will cause the force-depth readings to become closer to the ideal case (i.e. creates a sharper force-depth gradient) - making significant points of inflection, and therefore, boundary layers easier to identify. Consequently, doing so can increase wear on the drill-bit and reduce its effectiveness to cut through material [26]. In addition, it can also increase the likelihood of exceeding the load capacity rating of any force-measurement sensors embedded in the drill assembly. Alternatively, reducing the $\Delta d_p : \omega_d$ ratio scales down the reaction forces acting on the drill as the drill-bit is removing material significantly faster than it is penetrating material - consequently reducing the sensitivity to changes in force due to changes in material, leading to losses in accuracy as well as operation time due to the subsequently slower penetration rate.

3 Drill-Resistance Prototype Development

In this design iteration, a stand-alone drill-resistance prototype was developed with a modular design to carry out a vast array of tests with controlled concrete lab samples. This prototype is capable of drilling depths up to 120mm without any need for physical interaction/bracing from a human or robotic operator. This decision was made to ensure result validity and repeatability of measurements under various test cases. Figure 3 shows the overall breakdown of the prototype, which consists of an off-the-shelf cordless drill that was reverse-engineered into a custom 3D-printed housing - allowing the drill to be fitted with a load-cell for thrust force measurements, and an independently driven lead-screw for controlling the penetration rate.

The prototype works by using the lead-screw to push the drive plate at a constant rate which in turn achieves a constant penetration rate for the drill assembly into the concrete. As a result, the reaction force along the drill axis is transfered along the drill assembly, allowing this force to be measured by the load-cell sub-assembly. Simultaneously, the linear position of the drill assembly along the drill axis is measured using a linear potentiometer - thus allowing a measured drill-reaction-force to be linked to its corresponding drill depth at its given instance in time. Therefore, allowing the ongoing force-depth readings to be acquired as the drill penetrates the concrete - showing the changes in material and building a subsurface 'scan' of the targeted corroded concrete area in real-time as demonstrated in Figure 4.

4 Methodology

This paper focuses on tests with controlled concrete lab-samples with gypsum layers with and without aggregates as shown in Figure 5. A fixed high-speed drill setting (1200 rpm) is used to maintain a low penetration rate to drill speed ratio whilst using a 5mm diameter tungsten-carbide masonry drill-bit. In addition, no hammer drilling was used in the reported experiments in order to see if it is possible to acquire accurate results without the risk of propagating micro-stress cracks [27].

The first main experiment uses the concrete lab-sample with a 20 (±1)mm layer of gypsum without any aggregates on top of a 30mm layer of intact concrete. The Drill-Resistance prototype is placed on top of the target sample and the depth where the drill-bit meets the surface of the lab sample is recorded for reference. For example, the drill is measured to have moved 42mm from its starting

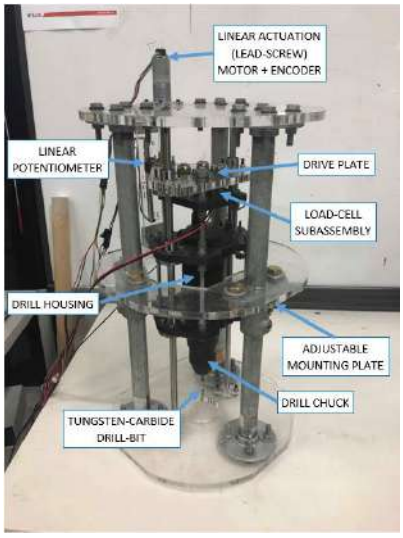

Figure 3. Drill-resistance system prototype design.

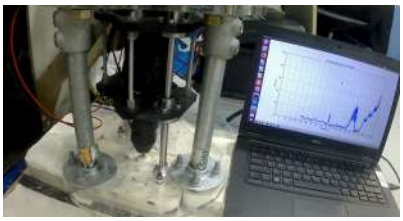

Figure 4. Drill-Resistance real-Time force-depth readings of a concrete lab sample with the presence of aggregates.

Figure 5. Concrete lab samples - 20mm gypsum layer with no aggregates (right) and 30mm gypsum layer with 10mm aggregates (left).

Algorithm 1 Boundary Layer Depth algorithm

$i = 2$ ▷ Start index at 2nd data point to ensure a (i-1) and (i+1) data point
$d_m = \infty$ ▷ Set large initial value for measured depth
while $i \leq (n-1)$ **do** ▷ where n is the sample size
  $F\dot{D}(i) = (F(i+1) - F(i-1))/(2\Delta d)$ ▷ calculate gradient
  $F\ddot{D}(i) = (F(i+1) - 2F(i) + F(i-1))/(\Delta d^2)$
  if $F\dot{D}(i) \geq \alpha \wedge F\ddot{D}(i) \geq \beta$ **then** ▷ significant increase check
    if $d(i) < d_m$ **then**
      $d_m = d(i)$ ▷ Records first depth of significant force increase
$D_B = d_m - d_s$ ▷ Boundary layer depth w.r.t surface

position (i.e. drill depth = 0mm) when the drill-bit comes into contact with the surface of the concrete. The drill is then reset back into its starting position before engaging both the drill and linear actuating motors to drill into the concrete sample and observe the force-depth readings in a controlled manner. The drill is retracted once the force-depth real-time plot shows there has been an increase and then plateau, signifying the hard intact concrete layer has been reached and slightly penetrated. This experiment was designed to investigate the Drill-Resistance prototype's ability to accurately distinguish the boundary layer between a homogeneous soft gypsum and hard concrete depth from the surface. In addition, this experiments tests an algorithm that was developed for autonomously measuring the depth of the boundary layer between a homogeneous gypsum layer and intact concrete. The pseudocode for autonomous boundary layer depth measurement of no-aggregate gypsum is given in Algorithm 1.

The second experiment is a repeat of the first experiment except the concrete lab-sample has a 30 (±1)mm gypsum layer with 10mm aggregates present to investigate the Drill-Resistance prototype's ability to accurately distinguish the boundary layer with hard obstructive material present, similar to those in corroded layers of concrete. Finally, the third experiment is a variant of the second by adjusting certain lengths in the prototype (such as the adjustable mounting plate - refer to Figure 3) - causing reference lengths to change, thereby altering the surface relative to the drill depth. For instance, initially the drill came into contact with the surface at 42mm relative to the starting position of the drill - the linear potentiometer mounting position is shifted 10mm along the drill axis and away from the concrete surface - now the surface relative to the drill depth becomes 52mm. This experiment was added to see if the surface could be detected by only allowing the linear actuator motor to run, such that when the static drill-bit meets the surface, a sudden force spike would be registered at the corresponding depth. This information could then be used as a marker for identifying the surface relative to the drill depth within the force-depth readings rather than recording this reference value separately before drilling. If successful, this allows all relevant information to be contained in one data set (i.e. the force-depth readings) for easier interpretation of results. Thus, streamlining the operation for users measuring the depth of the boundary layer relative to the surface of the material being drilled.

5 Experimental Results

5.1 Drilling Without Aggregates

Initial assessment of Drill-Resistance prototype readings through the no aggregate gypsum layer concrete lab sample shows remarkable accuracy in measuring the depth of the boundary layer between the gypsum and concrete layer (see Figure 6). The surface relative to the drill depth was measured at 59mm, therefore with a 20mm gypsum layer, the drill depth of the boundary layer of the lab sample would be expected at 79mm. The point at which the force-depth readings exhibit a significant increase can be observed at a drill depth of 78mm, which would result in a measured boundary layer depth of 19mm from the surface with an error of -1mm.

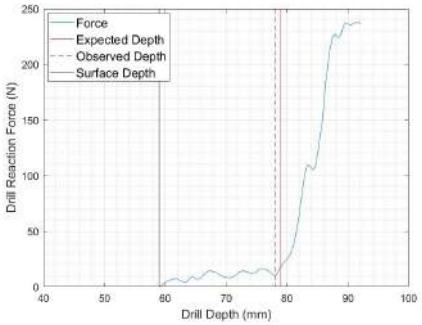

Figure 6. Drill-Resistance prototype force-depth readings of concrete with 20mm gypsum layer with no aggregates present: Increase and plateau in force can be observed to begin at 78mm drill depth, indicating the boundary layer - the surface was recorded at 59mm drill depth resulting in a measured gypsum layer depth of 78 - 59 = 19mm from the surface.

Figure 7 shows the developed Boundary Layer Depth algorithm being applied to the 'No-aggregate gypsum' experimental results from Figure 6. The calculated boundary layer depth of 19.45mm (+0.55mm error from the expected 20mm depth) is more precise than the observed depth of 19mm, thereby demonstrating a proof-of-concept towards autonomously measuring the boundary layer depth correctly and accurately.

5.2 Drilling With Aggregates

Experimental results of the Drill-Resistance prototype through a 30mm gypsum layer with 10mm aggregates consistently reveal the depth of the boundary layer between the gypsum and concrete layer. The surface relative to the drill depth was measured at 58mm, therefore with a 30mm gypsum layer, the drill depth of the boundary layer of the lab sample would be expected at 88mm. The Drill-Resistance prototype force-depth readings shown in Figure 8 detects

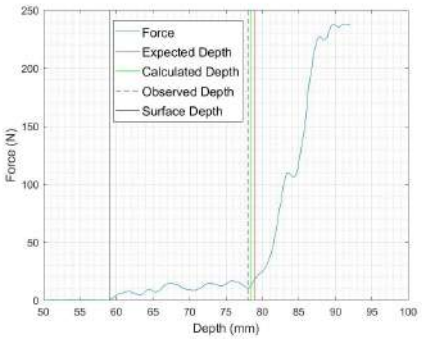

Figure 7. Boundary Layer Depth algorithm applied to the 'No-aggregate gypsum' lab sample data. The resulting calculated boundary layer depth was 19.45mm from the surface compared to an observed depth of 19mm

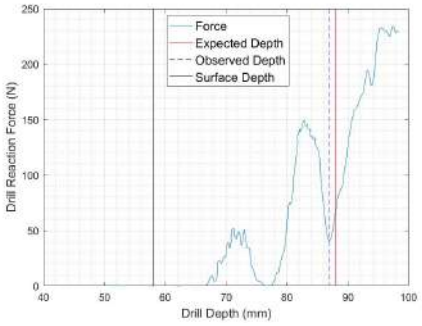

Figure 8. Drill-Resistance prototype force-depth readings of concrete with 30mm gypsum layer with 10mm aggregates present - boundary layer observed at 87mm despite going through two aggregates at 66-76mm and 78-88mm. The surface was recorded at 58mm drill depth, resulting in a measured gypsum layer depth of 87 - 58 = 29mm from the surface.

an aggregate via the force increase at 66mm and 78mm drill depth and respective force decrease at 76mm and 88mm (thus validating 10mm aggregate sizes). A larger force is observed to begin and plateau at 87mm which indicates the concrete layer has been reached, indicating a boundary layer depth of 29mm from the surface resulting in -1mm error.

Another Drill-Resistance prototype measurement was taken from where an aggregate was visible to the surface on the same concrete lab sample, where such a harder material on the surface would reflect most ultrasound or GPR signals before reaching the gypsum itself, let alone the boundary layer. Before this sample was taken, a replacement drill-bit that was 3mm shorter was installed, resulting in a change in the measured surface relative to drill depth to become 55mm. Figure 9 shows reaction

force on the drill rise and fall at 55mm (surface) and 64mm drill depth respectively. The low forces observed between drill depths 64mm and 85mm signifies the soft gypsum material. The sharp force increase observed at 85mm signifies the boundary layer was reached, which matches the expected boundary layer drill depth, measuring a 30mm boundary layer depth from the surface.

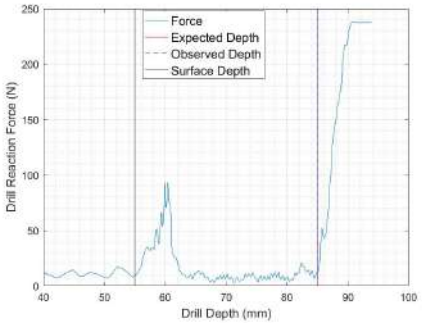

Figure 9. Drill-Resistance prototype force-depth readings of concrete with 30mm gypsum layer with 10mm aggregates present - boundary layer detected at 85mm despite an aggregate (55-64mm) at the surface (55mm) - resulting in a measured gypsum layer depth of 85 - 55 = 30mm from the surface.

5.3 Surface Detection

Figure 10 and Figure 11 demonstrate the Drill-Resistance prototype can also be used to detect the surface relative to the drill depth as in Figure 10, which shows the surface to be detected at drill depth 53mm, resulting in an expected boundary layer drill depth of 83mm. A 10mm aggregate is detected at 71mm drill depth as seen by the increase in drill reaction force which then subsides at 81mm drill depth, followed by a larger increase in force observed starting at 84mm drill depth, resulting in a measured boundary layer depth of 31mm from the surface (+1mm error). Similarly, Figure 11 records a surface detection at 51mm, prompting an expected boundary layer depth of 81mm for the given 30mm gypsum layer. A 10mm aggregate can be observed between 69mm and 79mm drill depth followed by a force increase and plateau at 81.5mm, resulting in a measured boundary layer depth of 30.5mm from the surface (+0.5mm error).

6 Discussion

All the experiments were conducted within the iPipes Lab facility. Gypsum layered samples were fabricated as an alternative to the real corroded layer [28] for the preliminary sensor evaluation. The gypsum layer brittleness is similar to corroded concrete. After assessing

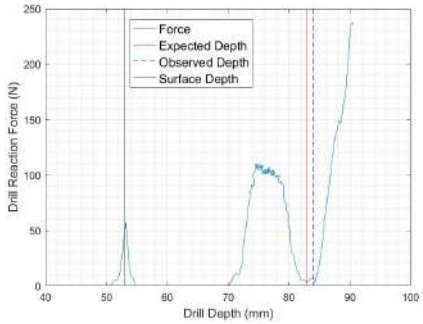

Figure 10. Drill-Resistance prototype force-depth readings of concrete with 30mm gypsum layer with 10mm aggregates present - surface (53mm), aggregate (71-81mm) and boundary layer (84mm) all mapped in this one data set. The measured boundary layer is 84 - 53 = 31mm from the surface.

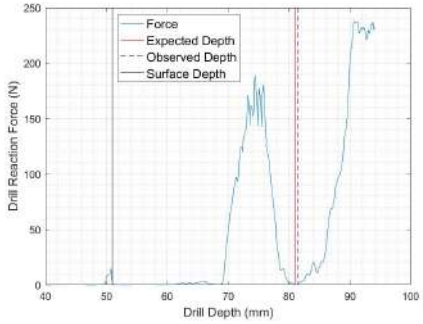

Figure 11. Drill-Resistance prototype force-depth readings of concrete with 30mm gypsum layer with 10mm aggregates present - surface (51mm), aggregate (69-79mm) and boundary layer (81.5mm) all mapped in this one data set. The measured boundary layer is 81.5 - 51 = 30.5mm from the surface.

all experimental results, the maximum deviation in observed/measured boundary layer depth from the expected boundary layer depth was 1mm regardless if aggregates were/were not present in the gypsum layer of the concrete lab sample being analysed. We must disclose that during the final experiment with regards to surface detection, there were observed instances of mechanical compliance along the drill axis (i.e. the drill could slightly move freely along its axis) because of frequent ongoing tests. This behaviour can be observed in the beginning of Figure 10 and Figure 11 where although the drill was in contact with the surface, there was slack in the mechanism that would allow the drive plate (and therefore linear potentiometer) to still move a few more millimeters – resulting in a 'wind up' of force across a small distance. Hence, the true surface relative to drill depth is when the force

asymptotically increases with no increase in drill depth. In addition, allowing the drill mechanism to wind-up the reaction force at the surface removes the mechanical compliance whilst drilling into the concrete, thereby eliminating the error in the force-depth readings as a result of mechanical error. We must also highlight that the concrete lab sample fabrication/curing process has a ±1mm tolerance when pouring/layering the concrete and gypsum into the mould. Hence a 20mm or 30mm gypsum layer could range between 19-21mm and 29-31mm respectively. Therefore, the maximum error in results of 1mm reflects exactly this sizing tolerance of the depth/thickness of the gypsum layer (boundary layer depth), making the force-depth readings an entirely valid pin-point subterranean 'scan' of a gypsum-concrete section – with the potential for sub-millimetre accuracy.

The results from the first experiment, shown in Figure 6 demonstrate the Drill-Resistance prototype can accurately measure the depth of a boundary layer between a soft homogeneous material and hard non-homogeneous material respectively from the surface with millimetre accuracy compared to NDT sensors such as ultrasound or GPR. However, in the case of the second experiment, the presence of large aggregates either obstructs conventional NDT sensors from detecting boundary layers or inhibits their ability to do so accurately and reliably. Whereas the Drill-Resistance prototype can penetrate through these large, hard aggregates – providing force-depth readings like the ones shown in Figure 8 and Figure 9 that provide a complete/detailed 'scan' of the gypsum layer; not only revealing the boundary layer depth between gypsum and concrete within 0-1mm error but also revealing/validating the depth and thickness of the aggregates themselves. Furthermore, not having the drill running before coming into contact with the surface in the final experiment shows the Drill-Resistance prototype can also detect the surface relative to itself – making it an entirely self-sufficient sensor with no need for reference/calibration values such as material density or signal velocity or in this case, surface depth relative to drill depth, to be known prior to using the sensor to find and measure the boundary layer depth. The Drill-Resistance prototype can be placed over any point and drill accordingly to provide an accurate real-time force-depth 'scan' of the subsurface.

7 Conclusion and Future Work

This paper introduced a novel drill-resistance based sensor for detecting the depth of the concrete affected by microbial corrosion. According to our knowledge, this is the first instant that such a sensor was developed and verified. Several lab experiments were carried out to validate the sensor measurements on carefully prepared lab samples. The lab experiments revealed the developed drill-resistance sensor is capable of measuring the corroded concrete depths with mm accuracy. In addition, the sensor has the ability to accurately identify aggregate location which could be useful in evaluating concrete structures.

In the future, the developed prototype can be miniaturized based on the requirements of the sewer operators and lab testing will be done on the corroded samples obtained from the Sydney based sewer.

Acknowledgment

This publication is an outcome from the project "Development of sensor suites and robotic deployment strategies for condition assessment of concrete sewer walls" funded by the Sydney Water Corporation.

References

[1] Gerhardus H Koch, Michiel PH Brongers, Neil G Thompson, Y Paul Virmani, and Joe H Payer. Corrosion cost and preventive strategies in the united states. Technical report, 2002.

[2] Great Britain. Office of Water Services. *Maintaining Water and Sewerage Systems in England and Wales: Our Proposed Approach for the 2004 Periodic Review*. Office of Water Services, 2002.

[3] W Kaempfer and M Berndt. Polymer modified mortar with high resistance to acid to corrosion by biogenic sulfuric acid. In *Proceedings of the IXth ICPIC Congress, Bologna, Italy, 14th*, pages 681–687, 1998.

[4] Sydney Water. *Annual expenditures 2012/2013 Report*. 2014.

[5] K Thiyagarajan and S Kodagoda. SMART monitoring of surface temperature and moisture content using multisensory data fusion. In *2015 IEEE 7th International Conference on Cybernetics and Intelligent Systems (CIS) and IEEE Conference on Robotics, Automation and Mechatronics (RAM)*, pages 222–227, 2015.

[6] Karthick Thiyagarajan, Sarath Kodagoda, Linh Van Nguyen, and Ravindra Ranasinghe. Sensor Failure Detection and Faulty Data Accommodation Approach for Instrumented Wastewater Infrastructures. *IEEE Access*, 6:56562 – 56574, 2018.

[7] K. Thiyagarajan, S. Kodagoda, and L.V. Nguyen. Predictive Analytics for Detecting Sensor Failure Using Autoregressive Integrated Moving Average Model. In *12th IEEE Conference on Industrial Electronics and Applications*, pages 1923–1928, Siem Reap, 2017. IEEE.

[8] Karthick Thiyagarajan and Sarath Kodagoda. Analytical Model and Data-driven Approach for Concrete Moisture Prediction. In *33rd International Symposium on Automation and Robotics in Construction (ISARC 2016)*, pages 298–306, Auburn, 2016. IAARC.

[9] Frank Rinn. Basics of typical resistance-drilling profiles. *West Arborist Winter*, pages 30–36, 2012.

[10] Frank Rinn, F-H Schweingruber, and E Schär. Resistograph and x-ray density charts of wood. comparative evaluation of drill resistance profiles and x-ray density charts of different wood species. *Holzforschung-International Journal of the Biology, Chemistry, Physics and Technology of Wood*, 50(4):303–311, 1996.

[11] Tiemo Kahl, Christian Wirth, Martina Mund, Gerhard Böhnisch, and Ernst-Detlef Schulze. Using drill resistance to quantify the density in coarse woody debris of norway spruce. *European Journal of Forest Research*, 128(5):467–473, 2009.

[12] Roberto Felicetti. The drilling resistance test for the assessment of fire damaged concrete. *Cement and Concrete Composites*, 28(4):321–329, 2006.

[13] Kishor S Kulkarni, Subhash C Yaragal, KS Babu Narayan, and Harsha Vardhan. Assessment of thermally deteriorated concrete by drilling resistance test and sound level1. *RUSSIAN JOURNAL OF NONDESTRUCTIVE TESTING*, 53(11), 2017.

[14] Emilio Valentini, Alessio Benincasa, Piero Tiano, Fabio Fratini, and Silvia Rescic. On site drilling resistance profiles of natural stones. *Personal communication*, 2008.

[15] Steve Barclay. Corrosion Protection of Sydney Water's Sewer Assets Using Sulfalock Higel, 2014.

[16] P Wells, Robert E Melchers, et al. Microbial corrosion of sewer pipe in australia–initial field results. In *18th International Corrosion Congress Proceedings November*, 2011.

[17] Lehua Zhang, Peter De Schryver, Bart De Gusseme, Willem De Muynck, Nico Boon, and Willy Verstraete. Chemical and biological technologies for hydrogen sulfide emission control in sewer systems: a review. *Water Research*, 42(1):1–12, 2008.

[18] K Thiyagarajan, S Kodagoda, and N Ulapane. Data-driven machine learning approach for predicting volumetric moisture content of concrete using resistance sensor measurements. In *2016 IEEE 11th Conference on Industrial Electronics and Applications (ICIEA)*, pages 1288–1293, 2016.

[19] S Laurens, JP Balayssac, J Rhazi, G Klysz, and G Arliguie. Non-destructive evaluation of concrete moisture by gpr: experimental study and direct modeling. *Materials and structures*, 38(9):827–832, 2005.

[20] DM McCann and MC Forde. Review of ndt methods in the assessment of concrete and masonry structures. *NDT & E International*, 34(2):71–84, 2001.

[21] Karthick Thiyagarajan. *Robust Sensor Technologies Combined with Smart Predictive Analytics for Hostile Sewer Infrastructures*. PhD thesis, 2018.

[22] K Thiyagarajan, S Kodagoda, R Ranasinghe, D Vitanage, and G Iori. Robust sensing suite for measuring temporal dynamics of surface temperature in sewers. *Scientific Reports*, 8(1), 2018.

[23] K Thiyagarajan, S Kodagoda, and J K Alvarez. An instrumentation system for smart monitoring of surface temperature. In *2016 14th International Conference on Control, Automation, Robotics and Vision (ICARCV)*, pages 1–6, 2016.

[24] Karthick Thiyagarajan, Sarath Kodagoda, Linh Van Nguyen, and Sathira Wickramanayake. Gaussian Markov Random Fields for Localizing Reinforcing Bars in Concrete Infrastructure. In *2018 Proceedings of the 35th International Symposium on Automation and Robotics in Construction*, pages 1052–1058, Berlin, 2018. IAARC.

[25] Tudor F Dumitrescu, Giovanni LA Pesce, and Richard J Ball. Optimization of drilling resistance measurement (drm) user-controlled variables. *Materials and Structures*, 50(6):243, 2017.

[26] Marisa Pamplona, Mathias Kocher, Rolf Snethlage, and Luís Aires Barros. Drilling resistance: overview and outlook [bohrhärtemessungen: Übersicht und ausblick]. *Zeitschrift der Deutschen Gesellschaft für Geowissenschaften*, 158(3):665–679, 2007.

[27] Roberto Felicetti. Combined while-drilling techniques for the assessment of deteriorated concrete cover. In *7th International Symposium on Nondestructive Testing in Civil Engineering-NDT-CE*, volume 9, pages 369–376. Citeseer, 2009.

[28] Understanding Concrete Sewer Pipe Corrosion - Fact Sheet for Sewer Pipe Corrosion. Technical report.

A Real-Time 4D Augmented Reality System for Modular Construction Progress Monitoring

Z.Y. Lin[a], F. Petzold[b], and Z.L. Ma[c]

[a]Department of Architecture, Technical University of Munich, Germay
[b]Department of Architecture and Informatics, Technical University of Munich, Germay
[c]Department of Civil Engineering, Tsinghua University, China
E-mail: mazl@tsinghua.edu.cn

Abstract –

Construction monitoring plays a vital role in modular construction practice, since faulty installation of individual parts could incur significant delays and extra cost to the project, modular construction eagerly requires a real time progress monitoring. Previous researchers tended to get as-built site data back at first, like making cloud points model or taking photos, and then use it to compare with as-designed BIM model. Such an approach cannot find any potential problem before it happens and will still bring unexpected economic loss and schedule delay. In converse thinking, this paper developed a real time 4D AR system for modular construction progress monitoring, which uses the as-designed AR model to compare with the as-built site, in which a markerless AR registration method is established to link the 4D BIM data with the as-built ones directly. In addition, mock up components are used as a scale model to validate the system. The result indicated that, the system can facilitate users to avoid possible errors by giving helpful assembly sequence monitoring and powerful tool for schedule control.

Keywords –

Construction progress monitoring; Modular construction; 4D BIM; Augmented reality

1 Introduction

Construction progress monitoring has been regarded as a critical successful factor in a construction project. Timely construction progress monitoring brings efficacious manner and helpful decision-making to management team members such as construction manager and on-site supervisors. In a modular construction project, every unit gets its own assembly sequence and position, any wrong assembly would definitely bring project delay and extra cost for rework. Thus, compared with onsite project, real-time construction progress monitoring between as-planned and as-built progress is much more important to modular construction.

1.1 BIM in Construction Progress Monitoring

Building Information Modelling (BIM) can be expected to help the management team in a modular construction project to make decision for assembly sequence simulation and work plan control before constructing. It has been proved that 4D BIM (3 dimensions digital model with timeline) gives effective support for construction scheduling and site monitoring by updating onsite data and comparing with 4D BIM models (Hamledar et al., 2017). Another method via using 4D BIM in concert with 3D data obtained by remote-sensing technology was proposed, in which continuous scanned data are obtained and compared with BIM model, but it assumed that there is no deviation from original construction plan (Kim et al., 2013). Partial point cloud device equipped in construction workers' protection helmets was also used for continuous construction progress monitoring, and the device can get as-built 4D BIM model which can be compared with 4D as-designed BIM model to check current progress status, but it needs workers to go through project site to collect data, and it is possible to miss cloud point data of some corners (Zoran et al., 2018). Also photos taken by UAV can be used to make cloud points model for progress monitoring, comparison between as-built and as-planned is visualized via using a corresponding point cloud and source image with re-projected geometry (Braun et al., 2018).

1.2 AR in Construction Progress Monitoring

On the other hand, Augmented Reality (AR), which adds computer generated objects into real world images, links 4D BIM data with real construction site and bring systemic and comprehensive progress monitoring and control (Lee et al., 2006). 4D progress simulation could

be overlaid on time-lapsed photographs via AR, such augmented photographs with 4D AR (AR contents show future work overlay on 3D objects in real world) simulation could compare discrepancies between the as-planned model and the as-built model in a consistent platform. However, the comparison was static and could not give real-time response. (Golparvar-Fard et al., 2009). In addition, augmented reality combined with 4D BIM could be used for automated operation-level construction progress monitoring, where onsite workers take daily photos and built 4D AR model which can detect materials to infer the actual state of progress. Nevertheless, this method needs taking many photos to build 3D point cloud model (Kevin et al., 2014). Further, a framework for cloud-based augmented reality using real time information for construction progress monitoring was proposed, which creates an automated real-time bidirectional flow between construction site and planning office, but it still need passive data acquisition at the first step (Soman et al., 2017).

1.3 Limitations in Previous Research

Previous researches by using BIM method or AR method do improve construction progress monitoring and schedule control, but they tend to get the as-built data from construction site as first step and then compared with as-designed 4D BIM. Thus, management team members only find discrepancy after it happened. Such lagging method cannot be used for finding potential problems and conducting real time construction site monitoring. In addition, construction workers still have to spend long time on data acquisition like photo taking or spend high cost for laser scanning device. There is a totally different situation for modular construction. Modular construction, in which all units are produced in manufacturing factory then assembled on construction site in a planned sequence, and have shorter schedule than onsite construction in similar volume. Moreover, any wrong assembly will definitely cause schedule delay and extra cost for rework. So real-time progress monitoring system avoiding wrong assembly before error happens is required by modular construction.

In order to improve modular construction progress monitoring and solve problems mentioned above, this study aims to develop a prototype by integrating real time AR and 4D BIM. To achieve our research goal, we focus on three questions: how to link 4D BIM with construction site directly via AR content, how to check modular components assembled in correct position and unit, and how to ensure modular components assembled in right sequence and date. In following text, workflow of this system and AR registration method will be introduced at first. Next we demonstrate what functions this system has and how it works step by step for progress monitoring. Finally we give discussion and conclusion about our system.

2 Method

2.1 Workflow

The as-designed 4D BIM data of modular components contains: 1) 3D information such as shape, size and floor; 2) 4D information like sequence and date. Firstly all the 4D BIM information related to construction progress monitoring is imported into this real-time 4D AR system via screen display, 3D BIM information is transferred into such AR registration part, which refers to the alignment of spatial properties (Schmalstieg et al., 2016). Meanwhile 4D BIM information is be restored into AR database for progress monitoring. Afterwards target position at as-built construction site will be located according to AR registration method, so construction management team is able to use displayed 4D AR content to compare as-built status in real world. The workflow of the 4D AR progress monitoring system for modular construction is shown in Figure 1.

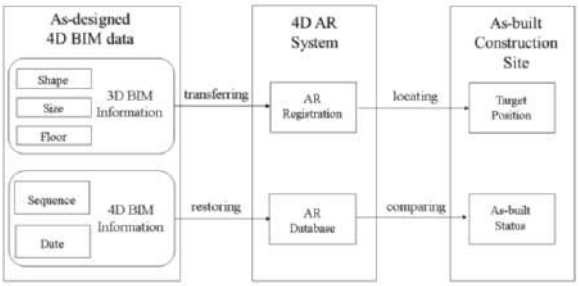

Figure 1. Workflow of 4D AR construction progress monitoring system

2.2 AR Registration Method

Fiducial makers are usually used for AR representation, however there are many limitations of marker-based AR on construction site, e.g. AR representation is easily failed by partial occlusion (João et al., 2018). Compared to marker-based AR, markerless AR method, in which any part of the real environment can be tracked in order to place virtual objects, is suggested for construction engineering (João et al., 2018). Even markerless AR methods can support construction process, currently major types of common markerless AR representation rely on features recognition (Teichrieb et al., 2007). As progress goes on, features for AR registration are always changed because site scenes keep changing, which means common markerless AR methods cannot show AR content

seamlessly and there are still limitations for AR uses on construction sites. In those cases construction progress monitoring is still hysteretic and unexpected loss may still exist.

To give real time monitoring, construction site, 4D BIM and AR content should be linked with each other. In the described concept we use another markerless AR registration method related to relative coordinate system between objects and camera. There are two concepts in BIM model: 1) Project Base Point, which defines the origin (0, 0, 0) of the project coordinate system and becomes reference point for measurements across the site; and 2) Survey Point, which identifies a real-world location near the model and defines the origin of the survey coordinate system to provide a real-world context for the model. We coincide Project Base Point and Survey Point in a same origin and build up the World Coordinate System which is related to real-world objects, then every point of a modular unit gets its own coordinate. If there is a real fixed monocular camera facing to objects in real world, then every point of this camera will also get its own coordinate. Such fixed camera could be put on crane mast, which is helpful to determine its position and simulate in BIM model. We make this real camera into a simplified computation model named Pinhole Camera Model in computer vision area and choose camera's optical center as origin to build a new coordinate system, which is called Camera Space in computer vision area. Because there is no object deformation between the two coordinate systems, we can transfer every unit's coordinate in World Coordinate System to Camera Space by rigid transformation. Through this method, AR content representation is registered by relative coordinate to camera space instead of any marker or feature, so that AR content can be linked with real construction site directly. Even there are people, machines or scaffolding in the camera image, AR content will not be affected. Fig.2 shows relationship between these two coordinate systems, a rotation matrix R and an offset vector $\vec{T}$ makes object transfer coordinate systems, and AR content of objects was shown by Camera Space.

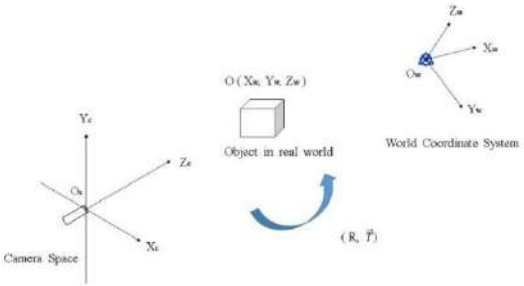

Figure 2. Relationship between world coordinate system to camera space

The equation for coordinate system transformation is shown in Eq.1. (X_c, Y_c, Z_c) means object's coordinates in Camera Space, (X_w, Y_w, Z_w) means object's coordinate in World Coordinate System. R means rotation matrix and $\vec{T}$ means offset vector. By using this transformation method, there is no change of objects' shape and size, objects shown in screen will reflect actual views in real world.

$$\begin{bmatrix} X_c \\ Y_c \\ Z_c \\ 1 \end{bmatrix} = \begin{bmatrix} \boldsymbol{R} & \boldsymbol{T} \\ 0^T & 1 \end{bmatrix} \begin{bmatrix} X_w \\ Y_w \\ Z_w \\ 1 \end{bmatrix} \quad (1)$$

3 System Development

To verify the method mentioned above, we developed a prototype system. This progress monitoring system, developed for construction project management team, represents AR content at beginning and use as-designed AR content to compare with as-built site status in real time. The system developed 3 function modules: 1) 4D Date Module, this module restores date information of 4D BIM, users can choose and see finished work and planned work in different dates through AR; 2) 3D BIM Module, in this module 3D BIM information like shape, size, etc. is transferred into AR content, we use 3D AR overlay as target position which is ensured by such AR registration method, then modular units will be moved and matched with AR overlay; and 3) 4D Sequence Module, in this module we release 4D assembly sequence via 4D AR animation, it gives both progress monitoring and navigation to construction area. In next part we will express details about how to use these function modules step by step. BIM software Revit and game engine Unity3D is used for AR prototype system development. A modular BIM model and mock up components are used for demonstration, shown in Figure 3.

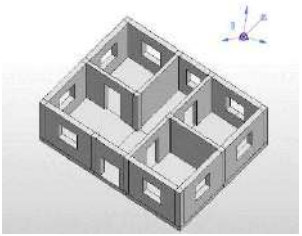

(1) BIM model with World Coordinate System

(2) Mock up components

Figure 3. BIM model and mock up model

To simulate real construction situation, we used a tripod as crane mast and an Android pad as fixed camera and monitoring screen. Such prototype is shown in Figure 4.

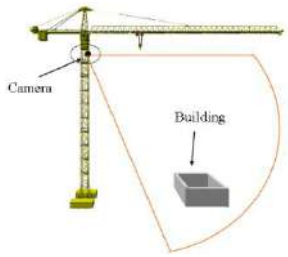

(1) Fixed camera on crane mast

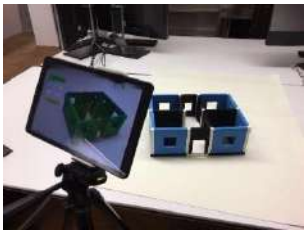

(2) Simulation by tripod and Android pad

Figure 4. Prototype of this AR system

4 Case Study Based on a Mock Up

To show how this prototype works, we use a case study based on a mock up here. The mock up, consists of several components like floorslabs, walls and columns in one floor, is used as a modular construction project. Then we use an Android pad fixed on a tripod to simulate camera on crane. This system works on assembly process, users just need fix the camera and click some AR buttons. By using this system, users can check whether every unit is assembled in right position, sequence and date. There are three main steps to use it: (1) Date Selection; (2) Real Objects Match; and (3) 4D AR Animation. In following text we will give details about how to use our system step by step.

4.1 Step 1: Date Selection

The first step is choosing date in 4D Date Module. After starting our system, users can choose date to represent AR content of date information via a dropdown menu. On such AR user interface, *Project Button* in initial scene shows the final construction project status and different construction dates. Day Task scene (*Day 01, Day 02, Day 03 Buttons*) shows finished work in previous days via yellow overlay and intraday work via green overlay. Click *Return Project Button* will leave current date scene and come back to initial project scene, which helps users check AR data between different dates. In the presented case, initial start scene shows the completed status of modular BIM model in white opacity, Day 02 scene includes finished floorslabs in yellow overlay and planned columns in green overlay, shown in Figure 5.

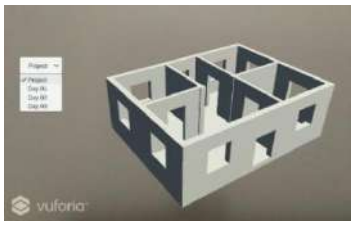

(1) Project button and day task button

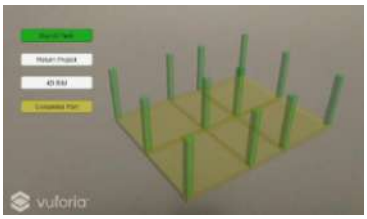

(2) Day 02 task scene

Figure 5. Different buttons and scenes

4.2 Step 2: Real Objects Match

Second step is to match real objects with green AR overlay. AR content is represented before components' match. There are 4 match scenarios in our system: 1) Match before construction, this scenario presents works of first day, in which there is only green overlay in this scenario because no component is assembled before construction; 2) Match with finished work and planned work, in this scenario finished work has been matched with yellow overlay, planned work will be matched with green overlay; 3) Match with intraday work, this scenario only shows intraday work via green overlay, which can give intuitive combination between real objects and planned work; 4) Match with completed project, in this scenario all the components have been assembled, green overlay is still existed because last modular component is moved to match with green

overlay. Every match scenario is related to 3D BIM Module. If a real modular component matches with green overlay perfectly in shape and size, such unit is assembled in right position. By this function, users can check whether a real modular unit is put on right position while it is close to assembly point. Besides if a real unit is deviated or missed from corresponding AR overlay, a construction error happened and users can adjust construction plan immediately. Different match scenarios are displayed in Figure 6.

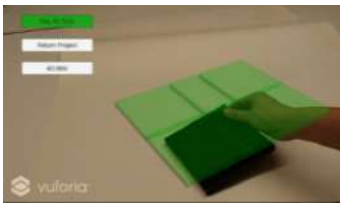

(1) Match before construction

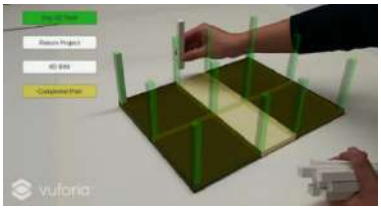

(2) Match with finished work and planned work

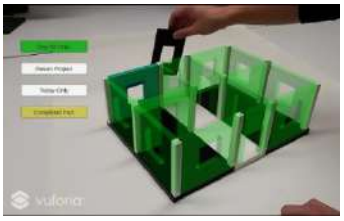

(3) Match with intraday work

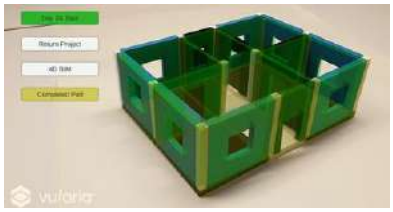

(4) Match with completed project

Figure 6. As-built objects match with as-designed AR content

4.3 Step 3: 4D AR Animation

In order to give real-time monitoring and navigation of intraday work, the last step to use our AR system is 4D AR animation. Another 4D BIM information, sequence, is also linked with real construction site directly through 4D Sequence Module, shown in Figure 7. *4D BIM Button* shows 4D live animation on its own date scene, in which previous work represented by yellow overlay is also displayed for comparison. Such animation shows assembly sequence extracted from construction schedule plan. By touching *Today Only Button*, AR monitoring system only represent 4D live animation on that date, which match with real world objects precisely and intuitively. Through this progress monitoring function, construction management team can check intraday assembly sequence conveniently. If a modular component follows assembly sequence in 4D AR animation, such unit is assembled in right sequence. By this function, users can check whether a modular unit is assembled in correct sequence while it is close to assembly point.

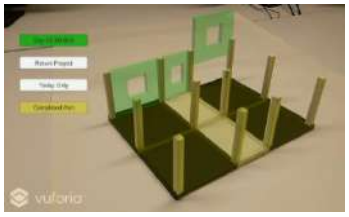

(1) BIM 4D animation with finished work

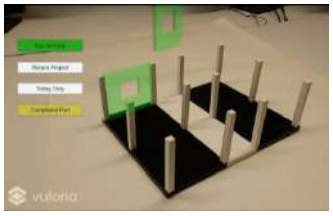

(2) Today Only animation

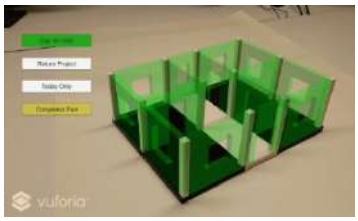

(3) Final 4D match

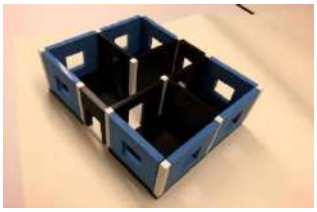

(4) Assembled modular components

Figure 7. 4D assembly sequence monitoring

5 Discussion and Conclusion

This paper proposed a real time 4D AR system for modular construction progress monitoring. Also we

introduced workflow of this system, AR registration method this system used, what function modules it has and how this system works step by step. By using a markerless AR registration method represented by relative coordinate and a fixed monocular camera, BIM 3D data like shape, size and floor can be linked with construction site directly. Objects in real world match precisely with AR content. Additionally 4D BIM information such as date and sequence can be restored in AR database and released as live animation, which can give helpful support to progress monitoring and work schedule check. This AR system, targeting at nature of modular construction, can help construction management team avoid potential schedule problems before construction work start. Besides this system make it easier for users to check whether every component is assembled in correct position and sequence. Construction management team will have better construction schedule control and decision making through our AR system, which can both save money and time for a modular construction project. In the future work, we will have a further development of real-time communication function between construction management team and crane operator to avoid wrong assembly of modular components.

References

[1] Braun A., Tuttas S., Stilla U., Borrmann A. (2018). "BIM-Based Progress Monitoring". In *Building Information Modeling: Technology Foundations and Industry Practice*. Springer, Cham, Germany.

[2] Hesam Hamledari; Brenda McCabe; Shakiba Davari; and Arash Shahi. (2017). "Automated schedule and progress updating of IFC-based 4D BIMs." *Journal of Computing in Civil Engineering*. 31(4).

[3] Kim, C., Son, H. and Kim, C. (2013). "Automated construction progress measurement using a 4D building information model and 3D data." *Automation in Construction*. 31, 75–82.

[4] Kevin K. HAN and Mani GOLPARVAR-FARD. (2014). "Automated Monitoring of Operation-Level Construction Progress Using 4D BIM and Daily Site Photologs." *Construction Research Congress*, Atlanta, Georgia, May 19-21.

[5] Lee, S. and Peña-Mora, F. (2006). "Visualization of Construction Progress Monitoring." *Joint International Conference on Computing and Decision Making in Civil and Building Engineering*. 2527-2533, Montréal, Canada, June 14-16.

[6] Mani Golparvar-Fard; Feniosky Peña-Mora; Carlos A. Arboleda; and SangHyun Lee. (2009). "Visualization of Construction Progress Monitoring with 4D Simulation Model Overlaid on Time-Lapsed Photographs." *Journal of Computing in Civil Engineering*. 23(6), 391-404.

[7] Paulo Silva, João & Lima Severino, Monte & Gomes, Paulo & Márcio, Neto & Bueno, Marcio & Teichrieb, Veronica & Kelner, Judith & Santos, Ismael. (2018). "APPLICATIONS IN ENGINEERING USING AUGMENTED REALITY TECHNOLOGY." ResearchGate, < https://www.researchgate.net/publication/265562985_APPLICATIONS_IN_ENGINEERING_USING_AUGMENTED_REALITY_TECHNOLOGY> (2018).

[8] Schmalstieg D. and Höllerer T. (2016). "Chapter 3, Chapter 5 and Chapter 6". *Augmented Reality: Principles and Practice*. Addison-Wesley, Boston, USA.

[9] Soman R.K. and Whyte J. K. (2017). "A Framework for Cloud-Based Virtual and Augmented Reality using Real-time Information for Construction Progress Monitoring." *Lean and Computing in Construction Congress (LC3)*, 835-842, Heraklion, Greece, July 4-7.

[10] Teichrieb, V., Lima. J., Apolinário, E., Farias, T., Bueno, M., Kelner, J., & Santos, I. (2007). "A survey of online monocular markerless augmented reality." *International Journal of Modeling and Simulation for the Petroleum Industry*. 1, 1-7.

[11] Zoran Pučko, Nataša Šuman, Danijel Rebolj. (2018). "Automated continuous construction progress monitoring using multiple workplace real time 3D scans." *Advanced Engineering Informatics*. 38, 27-40.

Development of an Eye- and Gaze-Tracking Mechanism in an Active and Assisted Living Ecosystem

A. Liu Cheng[a,b], N. Llorca[b,c], and G. Latorre[d]

[a]Faculty of Architecture and the Built Environment, Delft University of Technology, Delft, The Netherlands
[b]Facultad de Arquitectura e Ingenierías, Universidad Internacional SEK, Quito, Ecuador
[c]Escuela de Arquitectura, Universidad de Alcalá, Madrid, Spain
[d]Centro de Educación Continua, Escuela Politécnica Nacional, Quito, Ecuador
E-mail: a.liucheng@tudelft.nl, nestor.llorca.arq@uisek.edu.ec, galoget.latorre@epn.edu.ec

Abstract –

This paper details the development of an open-source eye- and gaze-tracking mechanism designed for open, scalable, and decentralized Active and Assisted Living (AAL) ecosystems built on Wireless Sensor and Actuator Networks (WSANs). Said mechanism is deliberately conceived as yet another service-feature in an on-going implementation of an extended intelligent built-environment framework, one motivated and informed by both Information and Communication Technologies (ICTs) as well as by emerging Architecture, Engineering, and Construction (AEC) considerations. It is nevertheless designed as a compatible and subsumable service-feature for existing above-characterized AAL frameworks. The eye- and gaze-tracking mechanism enables the user (1) to engage (i.e., open, shut, slide, turn-on/-off, etc.) with a variety of actuable objects and systems deployed within an intelligent built-environment via sight-enabled identification, selection, and confirmation; and (2) to extract and display personal identity information from recognized familiar faces viewed by the user. The first feature is intended principally (although not exclusively) for users with limited mobility, with the intention to support independence with respect to the control of remotely actuable mechanisms within the built-environment. The second feature is intended to compensate for loss of memory and/or visual acuity associated principally (although not exclusively) with the natural aging process. As with previously developed service-features, the present mechanism intends to increase the quality of life of its user(s) in an affordable, intuitive, and highly intelligent manner.

Keywords –

Intelligent built-environments; Active and assisted living; Wireless sensor and actuator network; Internet of things; Adaptive architecture

1 Introduction

The eye- and gaze-tracking mechanism detailed in this paper is situated within the *Active and Assisted Living* / *Ambient Assisted Living* (AAL) discourse [1–4]. Its objective is to enable the user (1) to open, shut, slide actuable windows and doors as well as to turn lights on or off within an intelligent built-environment via sight-enabled identification, selection, and execution; and (2) to extract and display personal identity information from recognized familiar faces viewed by the user. Although this mechanism is designed to be compatible with existing AAL or AAL-pertinent ecosystems and frameworks (e.g., *CASAS* [5], *The Aware Home* [6], *PlaceLab* [7]; and more recently in the last three years: *eServices* [8], *REACH* [9], *WITS* [10], etc.), it is deliberately designed as a service-feature in an ongoing implementation of an intelligent built-environment framework inspired by what Oosterhuis has called a *Society of Home*, where users and their surrounding objects / systems communicate and thereby instantiate a home of *Internet of Things and People*; as well as a *Society of Building Components*, where the intelligent built-environment's objects / systems act, react, and interact computationally as well as physically [11] towards user well-being. In order to realize this *Society of Home*, emerging trends in *Architecture, Engineering, and Construction* (AEC) research laboratories in academia and industry—such us robotic fabrication, computational design and optimization, etc.—are considered in conjunction with *Information and Communication Technologies* (ICTs) as well as allied and resulting technical services that typically dominate the AAL discourse. This dual consideration, while adopted from the early stages of conception and design, ascertains mutual complementarity [12] between ICTs and AEC features where neither requires retrofitting from or to the other. In such an intelligent built-environment, both ICTs and AECs features serve to enhance—in conjunction—the user's quality of life.

The eye- and gaze-tracking mechanism's first objective / feature intends principally (although not exclusively) to assists users with limited mobility to control remotely actuable mechanisms within the built-environment. The second objective / feature intends to compensate for the user's loss of memory and/or visual acuity—with respect to recognition of familiar faces—associated principally (although not exclusively) with the natural aging process. That is to say, these two features serve as extensions of the user's physical and mental capabilities (with respect to the described contexts and scopes) in a way that enables the user to retain a degree of independence otherwise impossible without technical and technological assistance. This is in line with current trends where *Computer Vision* is integrated into assistive services and solutions (see, for example, [13]).

The present mechanism is deployed within an inherited *Wireless Sensor and Actuator Network* (WSAN) [14]. This WSAN's ecosystem is highly heterogenous in architecture, communication protocols, and network topology. Some of its nodes are embedded in the physical environment, while others are embedded in ambulant systems or in wearable devices. Capitalizing on the different levels of integration within the built-environment, all nodes work in conjunction to instantiate and to sustain a variety of intelligent service-features. Some service-features are strictly computational in character, while others involve computation and physical action, reaction, interaction as input or output; some are completely localized (i.e., dependent strictly and solely on the local network) while others are either hybrid (i.e., relying on services present both in the local network as well as in distributed cloud-based services) or based entirely on free cloud-based services via their corresponding *Application Program Interfaces* (APIs). The hardware of the eye- and gaze-tracking mechanism is embedded in a wearable device, which works together with architecture-embedded nodes and systems, as well as with a variety of communication protocols, to instantiate the above-mentioned features. In order to center on the discussed mechanism, the systems and subsystems implemented in the inherited WSAN are presupposed without delving into their description and functionality details.

This paper consists of four main sections. Section 2 details the *Concept and Approach*, where the system is described and the implementation scope is defined. Section 3 explains the *Methodology and Implementation*, where the software and hardware implementations are described and the sequence of operation is detailed. Finally, Section 4 presents the *Results* that validate the present *proof-of-concept* implementation and provides a discussion on limitations, further work, and conclusions.

2 Concept and Approach

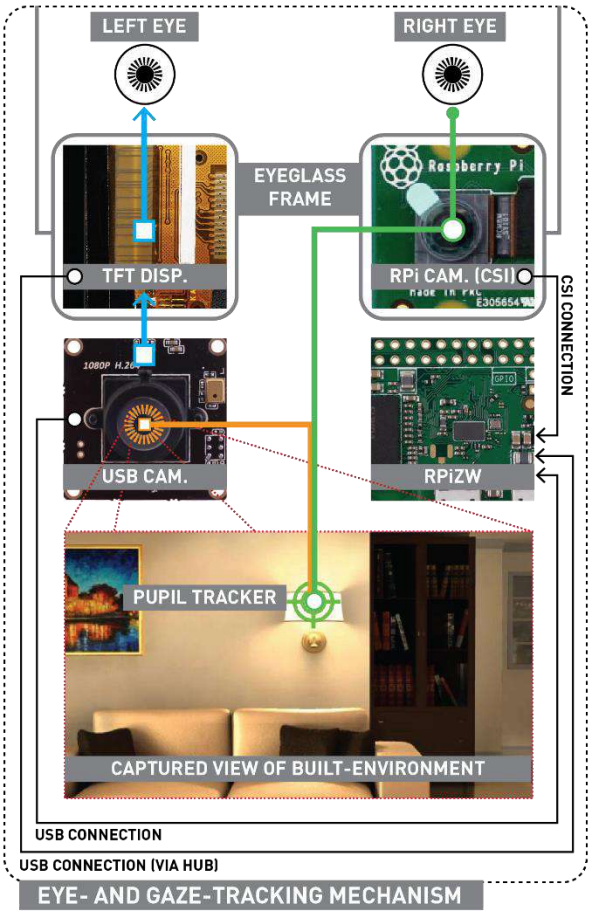

Figure 1. Concept and system architecture of the eye- and gaze-tracking mechanism

The eye- and gaze-tracking mechanism integrates the following hardware components into a generic eyeglass frame: a (i) Raspberry Pi Zero W (RPiZW); (ii) generic USB TFT Display; (iii) generic USB Camera (USBCam); (iv) and a CSI Raspberry Pi Camera v. 2.1. (RPiCam). The RPiCam is used to track the movement of the pupil corresponding to the right eye, while the USBCam captures the environment viewed and projects this scene back to the left eye via the TFT Display with a real-time update frequency. The position of the pupil is mapped on top of the captured scene, and gaze-tracking is enabled by analyzing the position of the pupil—and its movements—in relation with recognizable objects captured in the scene (see Figure 1). The following recognizable objects are presently defined: a (1) sofa, (2) wall-light, (3) window, (4) ceiling-light, (5) bookcase, (6) lamp, (7) wall-art, and (8) a dining table (see Figure 2, *Bottom*). This represents a generic sampling of objects contained in a given built-environment, where some actuate and others do not.

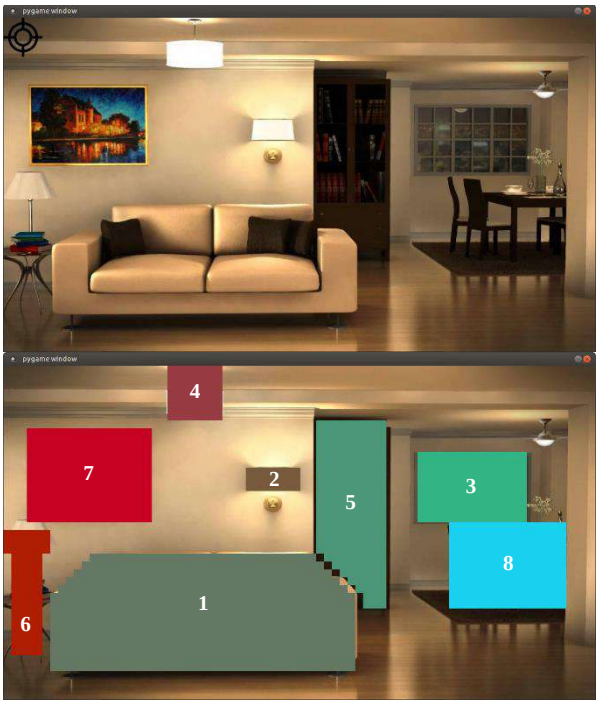

Figure 2. Top: Captured-gaze of generic sample built-environment. Bottom: Object-boundaries overlaid on top of objects represented. Both generated with PyGame.

In this implementation, the engagement with actuable objects and systems (e.g., doors, windows, lights, etc.) is limited to their generic virtual representation (see Figure 2, *Top*). That is, while previous implementations have required the building of physical representations in real-scale, the present development only requires confirmation of engagement at a software level to ascertain its functionality. Accordingly, a black-box approach is adopted with respect to the other subsystems of the inherited WSAN. In this manner, the present mechanism is said to actuate a window, a door; or to turn on/off a light, etc., if the user is detected to be engaging with a given object / system and the eye- and gaze-tracking mechanism does indeed respond by sending a signal to actuate or to turn on/off.

A caveat on the architecture / built-environment used as the captured scenes in this implementation: the type of architecture displayed intends to represent an average contemporary built-environment. As such, it is meant as a neutral representation, and not as an illustration of the type of environments to be generated by considering both ICTs and emerging AEC features. Nevertheless, as simple and reduced as representation as it may be, it does serve to illustrate the functionality of the present mechanism in a variety of existing AAL or AAL-compatible built-environments.

As mentioned at the beginning of this section, the position of the tracked pupil is overlaid with frequently updated captured scenes. When the eye-target symbol representing the location of said pupil lands on a non-defined region, its color remains black and no actuation options appear on the display (see Figure 2, *Top*). The eye-target symbol changes color whenever the system detects that it has entered any of the eight defined regions. N.B.: entering a region occurs when the overlap between the eye-target symbol's area and a given object's defined region is greater than 50% of the symbol's overall area—that is, when the majority of the symbol representing the eye is inside a given object's region.

If the eye-target symbol's color turns red (see Figure 3), the console outputs confirmation of recognition of viewed object while warning that no actuations are associated with said object—as Kolarevic points out, an adaptive environment is more appropriately conceived as one containing both high-tech. and low-tech. objects [15], where the former are actuatable while the latter are fixed. If, however, the eye-target symbol's color turns green (see Figure 4, *Wall* and *Wall-Light*), the console confirms object recognition and provides a list of actuation options associated with said object. The user is able to select any of the available actuation options by looking at it (i.e., by moving the eye-target symbol to sit on top of the preferred option) and then blinking twice to confirm selection and trigger actuation execution (i.e., sending a confirmation signal to the responsible node via which the actuatable object is controlled). Finally, if the eye-target symbol's color turns yellow (see Figure 4, *Wall-Art*) the console confirms object recognition and outputs a series of options pertaining not to physical actuation but to other kinds of engagement, namely information finding about the object, etc.—for example, in Figure 4, *Wall-Art*, which represents the user looking at a generic instance of wall-art, options to find information about said art on the web or to take, store, and share a picture of it are outputted by the console.

This first feature concerns the recognition of actuatable and static objects and systems within the built-environment. In addition to this feature, and as mentioned in the *Introduction*, the mechanisms is equipped with a second feature that concerns the extraction of information corresponding to recognized familiar faces. In this second feature, recognized human faces—that is, faces that have already undergone *Machine Learning* (ML)-based training for identity recognition for a given user—are also a *de facto* defined region. If the eye-target symbol enters this region, the console outputs previously stored information about the recognized person (see Figure 5). Since this region is not of the same class as the previously listed eight regions corresponding to the actuatable / static objects

in the present generic built-environment, the eye-target symbol disappears to give way to a rectangular boundary that contains the recognized face. This change of representation explicitly distinguishes identified and viewed non-human and human objects. As illustrated in Figure 5, the probability of recognition of a face is overlaid on top of the captured scene. Accordingly, in this particular figure, the user is informed that the viewed person is "Alejandra" with a 77.98% probability—for simplicity, any probability higher than 75% is accepted as accurate in this implementation.

The console portion of the figure (Figure 5, *Bottom*) shows multiple console outputs, each of which represents the processing of a new instance of a captured scene. In this particular figure, it may be appreciated how the prediction probability fluctuates depending on lighting conditions, distance, etc. Nevertheless, all shown instances correctly and strongly indicate that the person viewed is "Alejandra". Furthermore, in addition to successful prediction probabilities, the console also outputs other useful and pertinent information in order to compensate for loss of memory and/or visual acuity. For example, in this figure, the mechanism informs the user that this is "Alejandra", and that she is: "24 years old"; an "Architecture student"; the user's "daughter-in-law"; and the wife of "Luis Francisco", who may be presumed to be the user's son. All this information pertaining to this familiar face are previously stored for the user and will naturally differ from user to user. In the present setup, only a small set of data (i.e., Full name, Age, Profession, etc.) is provided to illustrate the mechanism's functionality. However, the amount and type of data may be added or removed depending on the user's preference and/or need. The principal purpose of this second feature is to enable to user to always recognize the people in her/his immediate surroundings.

3 Methodology and Implementation

3.1 Eye- and Gaze-Tracking for Object Actuation

The eye- and gaze-tracking mechanism as a means to engage actuatable objects / systems is implemented via two Python programs: (1) *main_eye_detector.py* and (2) *pygame_window.py*. The first (built with *OpenCV* and *Numpy*) is responsible for identifying and tracking the pupil; while the second (built with *Sys* and *PyGame*) is responsible for generating and/or displaying the representation of a given captured built-environment scene. It is in this latter that the regions corresponding to the eight actuatable / static objects are defined; and where the overlapping between eye-target symbol and the defined objects' boundary is calculated.

3.2 Eye- and Gaze-Tracking for Human Identity Recognition

The component of the eye- and gaze-tracking mechanism responsible for human identity recognition depends on the inherited facial-identity and -expression mechanism previously developed by the authors [16]. In the previous work as with the present, the facial identity recognition component is implemented in the local network via Google Brain®'s *TensorFlow*™ [17]. That is, TensorFlow™ is installed in the RPiZW's *Raspbian* operating system and its cloud-based services are implemented via Python. The implementation of this service has two phases. In the first phase, and during execution of its *Multi-task Cascaded Convolutional Networks* (MTCNN) face detection model, the camera captures a given subject's face from different positions, orientations, and angles. All the people to be added to the eye- and gaze-tracking mechanism's users circle of familiar faces must undergo this phase. The second phase is the actual real-time execution of facial recognition, following the successful acquisition of analysed and stored faces from the first phase.

4 Results and Conclusion

With respect to the object actuation feature (see Section 3.1) of the present mechanism, three volunteers (with varying ages) (see *Acknowledgements*) in addition to the authors tested its functionality and performance via the following five steps:

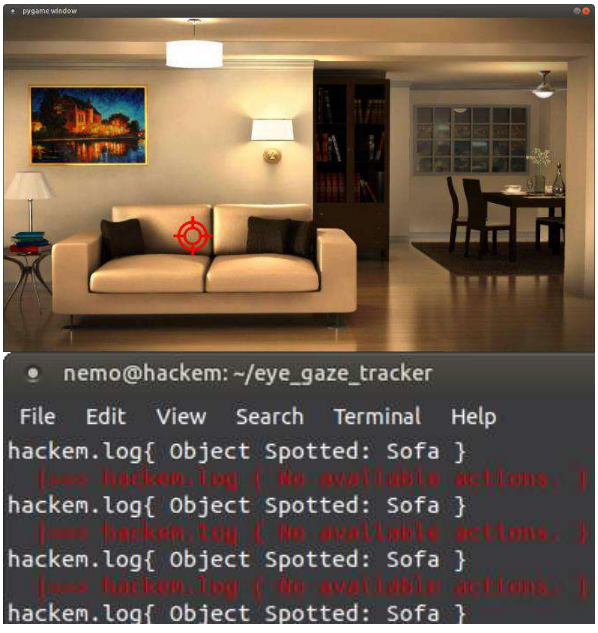

Figure 3. Pupil detected on object *Sofa*, with no available actuations.

1. At initialization of *PyGame*'s represented captured-scene, the eye-target symbol first appears in the upper-left corner. The user then moves her/his pupil in question (i.e., right-eye's pupil) and blinks twice over defined objects in order to first calibrate the eye-tracking component.
2. Once the eye-tracking component is calibrated the user is directed to look at the *window*, at which point the eye-target symbol changes colors to green, and the console first recognizes the actuatable object and the outputs the available actuation options: *open* or *close* (see Figure 4, *Window*). The user selects *open* and a confirmation of a corresponding execution signal sent is ascertained—the same, *mutatis mutandis*, for *close*.
3. The user is then instructed to look at the *sofa*, which is a non-actuating / fixed object that is nevertheless recognized. At this point the eye-target symbol turns red to indicate that no available actuation options exist for this object (see Figure 3).
4. The user's attention is turned to the *wall-art*, which is a non-actuatable object yet is nevertheless an object associated with non-physical actions. That is, after the eye-target symbol turns yellow (to indicate that the object in question is neither actuatable or fixed with no available options), the user is given the choice *to search for more information on the art online* or *to take, store, and share a picture of the art* (see Figure 4, *Wall-Art*). The user is instructed to engage in both, and a corresponding confirmation signal is ascertained.
5. Finally, the user is instructed to look at any of the light fixtures (see Figure 4, *Wall-Light*). Any of these fixtures present the user with two options: *turn on* or *turn off*. The user is instructed to engage in both, sequentially, and corresponding confirmation signals are ascertained.

Again, and as mentioned in Section 2, the present setup has its actuations act on virtual representations of generic objects found in an average built-environment. For the scope of the present implementation, it is only necessary to ascertain that a confirmation signal is sent to a respective enabling-node (enabling of the window, the lights, etc.) in order to demonstrate the successful functionality of the present *proof-of-concept*. In all of the above five steps mentioned, corresponding confirmation signals were indeed ascertained.

In the present setup, only three types of responses / options have been considered: (1) actuatable object (green eye-target); (2) static object (red eye-target); and (3) static object associated with non-physical actions (yellow eye-target). However, other possible responses / options may be envisioned for subsequent iterations of this feature of the mechanism.

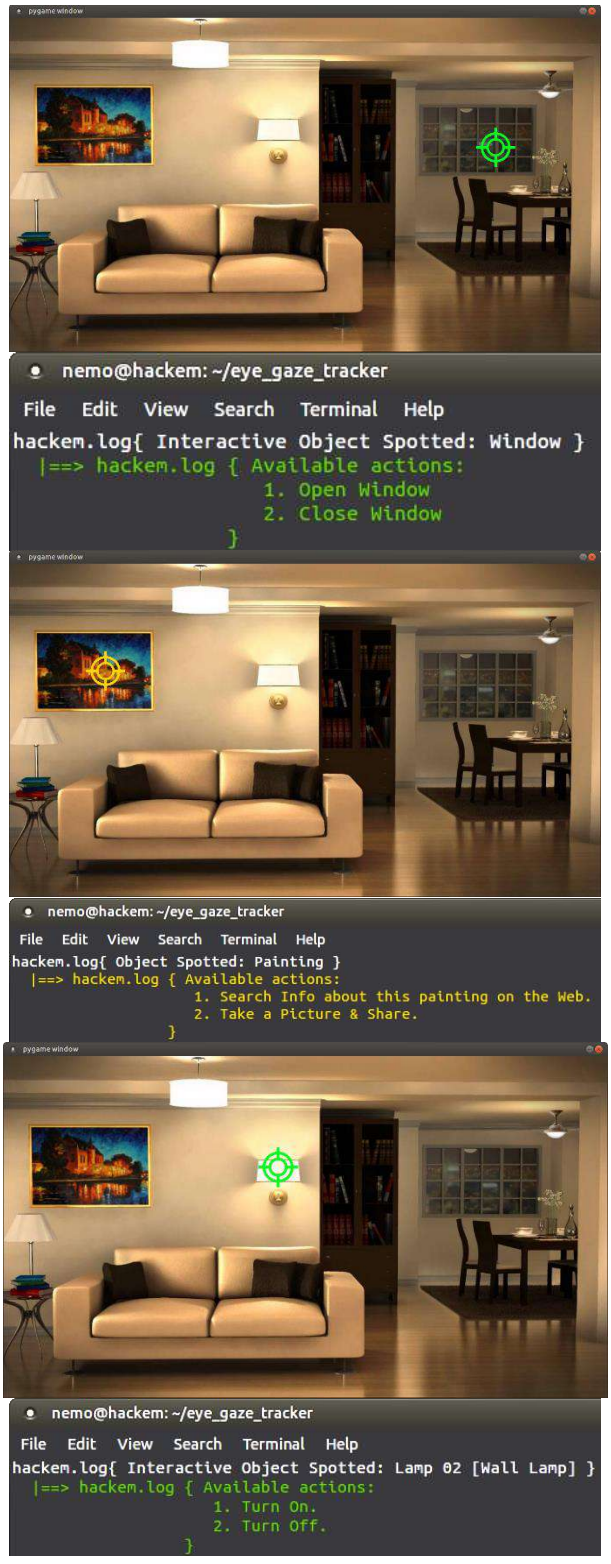

Figure 4. Top-to-Bottom: Pupil on object *Window* (green target/text); *Wall-Art* (yellow target/text); and *Wall-Light* (green target/text).

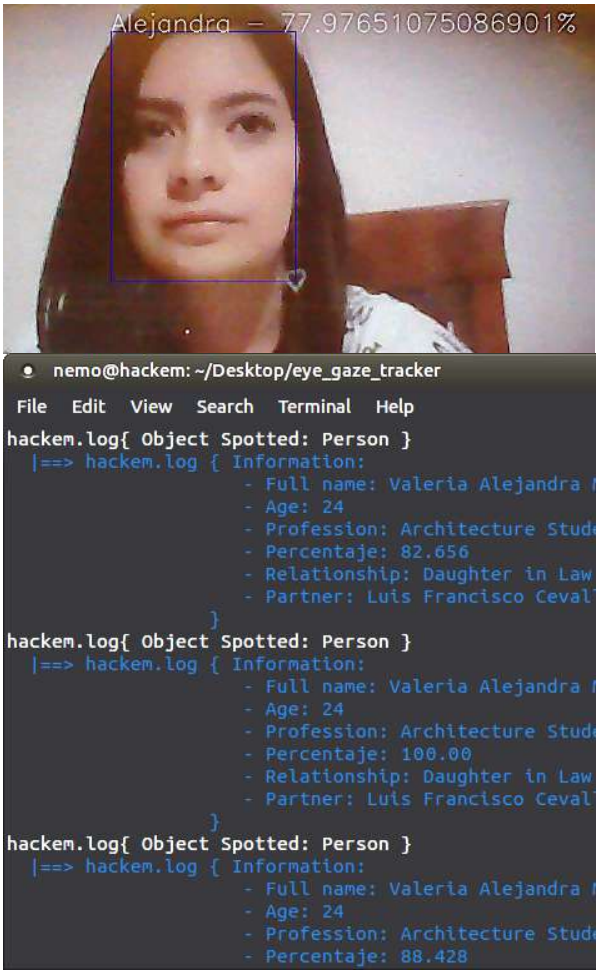

Figure 5. Recognition of a familiar face and corresponding output of associated information pertaining to the identified person.

With respect to the human identity recognition feature (see Section 3.2) of the present mechanism, a database of recognizable faces was first established, followed by a sequence of trials by the same three volunteers and the authors to gauge the feature's human identity recognition capabilities. The feature performed as expected, where the prediction accuracy probabilities were consistently above 70%.

In this paper an eye- and gaze-tracking mechanism has been presented. Said mechanism enables the user (1) to engage (i.e., open, shut, slide, turn-on/-off, etc.) with a variety of actuable objects and systems deployed within an intelligent built-environment via sight-enabled identification, selection, and confirmation; and (2) to extract and display personal identity information from recognized familiar faces viewed by the user. As with previously developed service-features, the present mechanism intends to increase the quality of life of its user(s) in an affordable, intuitive, and highly intelligent manner. Although the present setup is limited and not yet ready for widespread adoption (being in a *Technology Readiness Level* [18] of 5), the detailed *proof-of-concept* implementation's validated functionality and performance indicates further potential for development, which is presently being undertaken. Furthermore, in order to explore facial recognition alternatives in order to enhance the efficiency—with respect to the performance of the local network—of the mechanism, a subsequent version of the eye- and gaze-tracking mechanism is being implemented with *Keras* [19].

Acknowledgement

The authors acknowledge the kind assistance that the following people provided during the implementation and trials of the detailed mechanism: Steffany A. Cevallos G., Nelson B. Solano Y., and Jonathan G. Díaz A.

References

[1] Dimitrievski, A., Zdravevski, E., Lameski, P., and Trajkovik, V. A survey of Ambient Assisted Living systems. Challenges and opportunities. In *Proceedings, 2016 IEEE 12th International Conference on Intelligent Computer Communication and Processing (ICCP). Cluj-Napoca, Romania, September 8-10, 2016*. IEEE, pages 49–53, Piscataway, NJ, 2016. DOI=10.1109/ICCP.2016.7737121.

[2] Flórez-Revuelta, F. and Chaaraoui, A. A., Eds. Active and Assisted Living: Technologies and Applications. Healthcare technologies series, volume 6. The Institution of Engineering and Technology, Stevenage, UK, 2016.

[3] Grzegorzek, M., Gertych, A., Aumayr, G., and Piętka, E. Trends in Active and Assisted Living - Open hardware architecture, Human Data Interpretation, intervention and assistance. *Computers in biology and medicine*, volume 95: 234–235, 2018.

[4] Byrne, C., Collier, R., and O'Hare, G. A Review and Classification of Assisted Living Systems. *Information*, volume 9, 7: 182, 2018.

[5] Rashidi, P. and Cook, D. J. Keeping the Resident in the Loop. Adapting the Smart Home to the User. *IEEE Trans. Syst., Man, Cybern. A*, volume 39, 5: 949–959, 2009.

[6] Kidd, C. D., Orr, R., Abowd, G. D., Atkeson, C. G., Essa, I. A., MacIntyre, B., Mynatt, E. D., and Starner, T. The Aware Home: A Living Laboratory for Ubiquitous Computing Research. In

Proceedings of the Second International Workshop on Cooperative Buildings, Integrating Information, Organization, and Architecture. Springer Verlag, London, UK, 1999.

[7] Intille, S. S., Larson, K., Tapia, E. M., Beaudin, J. S., Kaushik, P., Nawyn, J., and Rockinson, R. Using a Live-In Laboratory for Ubiquitous Computing Research. In *Pervasive Computing*. Springer Berlin Heidelberg, pages 349–365, Berlin, Heidelberg, 2006.

[8] Marcelino, I., Laza, R., Domingues, P., Gómez-Meire, S., Fdez-Riverola, F., and Pereira, A. Active and Assisted Living Ecosystem for the Elderly. *Sensors (Basel, Switzerland)*, volume 18, 4, 2018.

[9] European Union's Horizon 2020 Research and Innovation Programme. REACH: Responsive Engagement of the Elderly promoting Activity and Customized Healthcare. *(Grant agreement No 690425.)*. On-line: http://reach2020.eu. Accessed: 20/04/2017.

[10] Yao, L., Sheng, Q. Z., Benatallah, B., Dustdar, S., Wang, X., Shemshadi, A., and Kanhere, S. S. WITS. An IoT-endowed computational framework for activity recognition in personalized smart homes. *Computing*, volume 100, 4: 369–385, 2018.

[11] Oosterhuis, K., 2014. Caught in the Act. In *ALIVE. Advancements in adaptive architecture*, M. Kretzer and L. Hovestadt, Eds. Applied Virtuality Book Series v.8. Birkhäuser, Basel/Berlin/Boston, pages 114–119.

[12] Milgrom, P. R. The economics of modern manufacturing: technology, strategy, and organization. *The American Economic Review*, volume 80, 3: 511–528, 1990.

[13] Leo, M. and Farinella, G. M., Eds. Computer Vision for Assistive Healthcare. Elsevier, 2018.

[14] Liu Cheng, A. and Bier, H. Extension of a High-Resolution Intelligence Implementation via Design-to-Robotic-Production and -Operation strategies. In *Proceedings of the 35th International Symposium on Automation and Robotics in Construction (ISARC) 2018*, pages 1005–1012, Berlin, Germany, 2018.

[15] Kolarevic, B., 2014. Outlook. Adaptive Architecture: Low-Tech, High-Tech, or Both? In *ALIVE. Advancements in adaptive architecture*, M. Kretzer and L. Hovestadt, Eds. Applied Virtuality Book Series v.8. Birkhäuser, Basel/Berlin/Boston, pages 148–157.

[16] Liu Cheng, A., Bier, H., and Latorre, G. Actuation Confirmation and Negation via Facial-Identity and -Expression Recognition. In *Proceedings of the 3rd IEEE Ecuador Technical Chapters Meeting (ETCM) 2018*, 2018.

[17] TensorFlow™. An open source machine learning framework for everyone, 2018. On-line: https://www.tensorflow.org/. Accessed: 20/04/2018.

[18] European Association of Research and Technology Organisations. The TRL Scale as a Research & Innovation Policy TOOL. *EARTO Recommendations*, 2014. On-line: http://www.earto.eu/fileadmin/content/03_Publications/The_TRL_Scale_as_a_R_I_Policy_Tool_-_EARTO_Recommendations_-_Final.pdf. Accessed: 07/01/2015.

[19] Keras®. Keras: The Python Deep Learning Library, 2019. On-line: https://keras.io/. Accessed: 10/01/2019.

Improvement of Automated Mobile Marking Robot System Using Reflectorless Three-Dimensional Measuring Instrument

T. Tsuruta[a], K. Miura[a], and M. Miyaguchi[a]

[a]Research and development institute, Takenaka corporation, Japan
E-mail: tsuruta.takehiro@takenaka.co.jp, miura.kazuyuki@takenaka.co.jp, miyaguchi.mikita@takenaka.co.jp

Abstract –

In previous study we have already reported fully automated mobile marking robot system in construction site for streamlining marking work that is currently carried out manually. However, marking accuracy and efficiency were not satisfied compared to those of construction worker, further improvement was desired. This paper is the second report of the system. The purpose of this paper is to improve the marking performance of the system. The proposed system consists of a reflectorless three-dimensional measuring instrument and a mobile marking robot. The former accurately directs a measuring laser and measures a distance to the robot. The latter is a mobile robot which has a marking device and a special positioning sensor. It is important to navigate the marking robot to the designated marking position quickly and correctly. Two self-positioning estimation method is combined. The robot position is roughly estimated by the wheel odometry method during movement. On the other hand, it is accurately measured by the combination of a three-dimensional measuring instrument and the special positioning sensor just before drawing a mark on the floor. The marking device draws the mark exactly on the designated position based on the deviation between the designated position and the measured robot position. This paper describes the mechanism of proposed system and some experimental results. It also shows improvement of the marking performance compared to previous prototype.

Keywords –

Marking; Mobile robot; Reflectorless three-dimensional measuring instrument

1 Introduction

In Japan, a shortage of construction workers has become a major social issue. In 2015, the number of construction workers was about 73% of what it had been at its peak in 1997. Therefore, improvement of productivity in construction work is an urgent issue. In the construction process, marking work is indispensable. Before installing building material such as dry walls, free access floors and anchor bolts, construction workers have to draw marks and lines on the floors, walls, ceilings, and so on in construction site. They mean positions for installing building materials. In a big building construction, the number of marks and lines is more than thousands and it is currently carried out manually. Therefore, there is a great need for improving efficiency of the marking work.

The progress of surveying technology in recent years is remarkable. Some measuring instruments such as laser scanner and total station are already being used at construction site. Prior studies on the efficiency improvement for the marking work by using these instruments have already been reported. They are roughly divided into researches on support technology aimed at improving efficiency of marking manually [1-3] and those on automated marking robots [4-6]. If this work is fully automated with marking robots, construction workers will be able to concentrate on installing building materials and productivity will increase.

Several studies on automated mobile marking robot have already been done. Inoue et al. reported a system that combines a marking robot having a cross-mark stamp and a total station [4,5]. It is roughly navigated a designated marking position by using a laser range finder and its position and orientation is measured by the total station. After that, it stamps a cross mark accurately on the designated position. “Laybot” developed by DPR construction [6] can draw lines for installing drywalls on a floor. Its position is also measured by using a total station. Kitahara et al. reported a system that combines a marking robot having a XY plotter and a total station [7]. In the system, an operator of the system moves the marking robot to a marking position with operation of a remote controller. The total station measures its position and orientation and the mobile robot draws arbitrary figure on a floor based on the measured position.

All of them mentioned above need a total station that can collimate and track prism. However, this kind of the total station is generally very expensive. In author's view point the total station occupies most of the system cost. On the other hand, a reflectorless three-dimensional measuring instrument that does not track and collimate prism is less expensive. Cost is a very important factor for wide spread use of the marking robot system. Therefore, we propose a marking robot system with the reflectorless three-dimensional measuring instrument. As a first step, we intended to automate the marking work for installing free access floors. In our previous study, we reported a performance of a prototype system [8] [9]. The marking robot automatically moves to designated positions and draws cross marks in sequence. These marks mean positions where pedestal bases of free access floors are installed. We succeeded in marking 182 positions automatically in a 6m x 6.5m working area in construction site. Average deviation between drawn mark and designated position was 2.3 mm and average time required for marking a single position was 98 second. However, marking accuracy and efficiency were not satisfied compared to those of construction worker. Further improvement is desired in the working area, the time required for marking and the marking accuracy.

In this study, new marking robot system was developed. Two self-positioning estimation method is combined to improve marking performance. The wheel odometry method is used during movement. The combination method of the three-dimensional measuring instrument and the special positioning sensor is used just before drawing a mark on the floor.

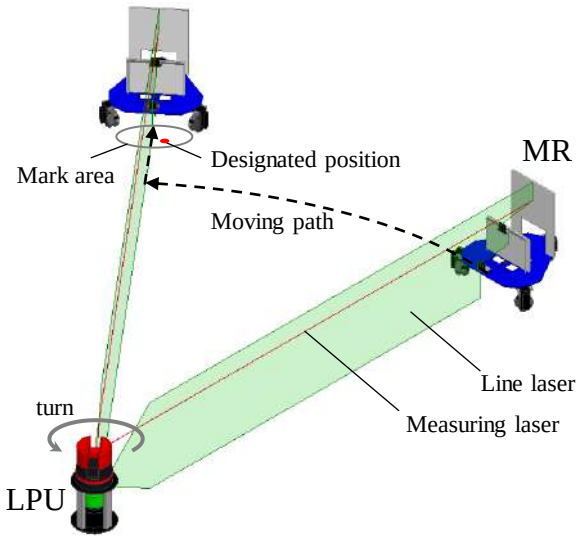

Figure 1. Outline of the marking flow using previous marking robot system

2 Proposed Marking Robot System

2.1 Problems in Previous Prototype

In our previous study, we proposed a line laser tracking navigation method using a laser positioning unit (LPU) and a marking robot (MR). As shown in Figure 1, the MR tracks a rotating line laser generated from the LPU in order to move to a designated position. The MR has two couples of screen and camera to detect the laser line projected on the screen. This method has two problems that deteriorate marking performance. First, when the MR is far from the LPU, the line laser light projected in the screen becomes weak and it is difficult to detect the laser line from a captured image. This is the reason that limits the working area and deteriorates the marking accuracy. Second, tracking path is a combination of the traveling on the circular path and straight path. This means that the MR does not move on the shortest path. Thus long time was required for moving to the designated position. For these reason we concluded that the usage of the line laser deteriorated the marking performance.

2.2 Automated Marking Flow

In order to improve marking performance, we stop using the line laser. The proposed system consists of a marking robot (MR) and a three-dimensional measuring instrument (3D-MI). The MR automatically moves to a marking position and draw marks on the floor. The moving path is a straight line connecting the current position and next designated position. The MR moves to the designated marking position by the combination of a straight traveling and a spin turn as shown in Figure 2. Two self-positioning estimation method is combined. The MR position is roughly estimated by the wheel odometry method during movement. On the other hand, it is accurately measured by the combination method of the 3D-MI and a special positioning sensor attached on the MR just before drawing a mark on the floor.

The 3D-MI is used for measuring the MR position and orientation. Like a motor driven total station, the horizontal and vertical axes of the 3D-MI can be motorized. This can direct a measuring laser parallel to the floor in the direction of the designated marking position and measure the distance to an object on which the laser spot is projected. Although it cannot collimate and track reflector such as prism target, it is less expensive than a motor driven total station used in previous studies already reported [4-7].

The MR is a two wheel differential drive robot with a caster wheel. A marking device is attached to the MR base flame. It is similar with a XY plotter. By controlling the marking device, an arbitrary mark, figure or character can be drawn on the floor. Furthermore, the MR has the

special positioning sensor. It is a key device for measuring MR position and orientation accurately with reflectorless 3D-MI. The detailed measuring mechanism will be described in section 2.3.

In construction site, some benchmarks are already drawn on the floor just before installing building material. The coordinate of the 3D-MI in a construction site coordinate system Σw is calculated by resection. The coordinates of the target marks to be drawn on the floor in the Σw are set based on the floor plan. Automated marking is operated by repeating following steps as shown in Figure 3.

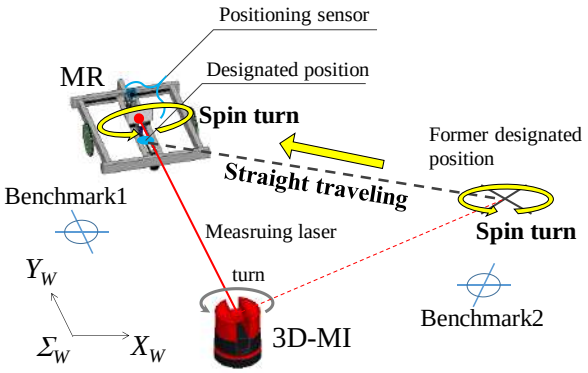

Figure 2. Move to the next designated position

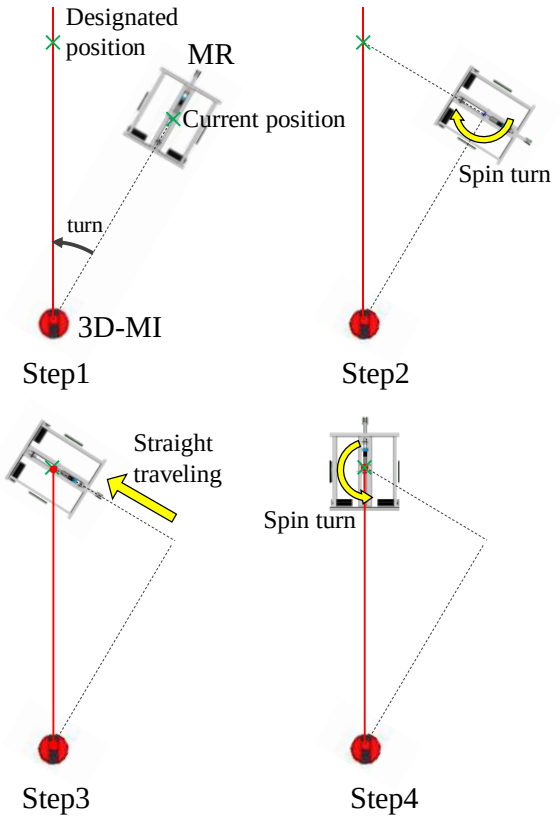

Figure 3. Automated marking flow

Step1: The 3D-MI directs the measuring laser parallel to the floor in the direction of the next designated position.

Step2: The MR makes spin-turn so that the orientation of the MR corresponds to the direction of the next designated position. The turning angle is estimated by the wheel odometry method.

Step3: The MR travels straight so that the MR reaches the next designated position. The traveling distance is also estimated by the wheel odometry method.

Step4: The MR makes spin-turn so that the positioning sensor is perpendicular to the measuring laser. After spin-turn, the MR position is not exactly on the next designated position. The MR position and orientation are accurately measured by the combination of the 3D-MI and the positioning sensor. The marking device is controlled based on the deviation between the measured position and the designated position so that a figure could be drawn exactly on the designated position.

2.3 Mechanism of the Marking with High Precision

The MR position is measured with combination of the 3D-MI and the positioning sensor. The positioning sensor consists of a light diffusion plate and a camera as shown in Figure 4. The measuring laser form the 3D-MI hits on the light diffusion plate. The 3D-MI measures the distance to the light diffusion plate. On the other hand, the camera captures an image of the laser spot projected on the light diffusion plate. The laser spot centroid is measured by an image processing described in section 2.5. After that, the positioning sensor moves y_f in the Y_R axis direction in the robot coordinate system Σ_R as shown in Figure 5. After that, the distance to the light diffusion plate and the laser spot centroid are measured again. By using these measured values before and after moving the positioning sensor, orientation α is calculated as below.

$$\alpha = tan^{-1}\left(\frac{x_{c0} - x_{c1}}{y_f}\right) \quad (1)$$

Here,

Δy: The displacement of the positioning sensor

x_{c0}: The x-coordinate of the laser spot centroid in the Σ_R before moving the positioning sensor

x_{c1}: The x-coordinate of the laser spot centroid in the Σ_R after moving the positioning sensor

From the geometry relation as shown in Figure 6, the MR coordinate in the Σ_w x_{MR} and y_{MR} are calculated following equation.

$$x_{MR} = x_p + r_0 cos\theta_l - x_{c0} cos\phi \quad (2)$$

$$y_{MR} = y_p + r_0 sin\theta_l - x_{c0} sin\phi \quad (3)$$

$$\phi = \theta_l - \frac{\pi}{2} - \alpha \quad (4)$$

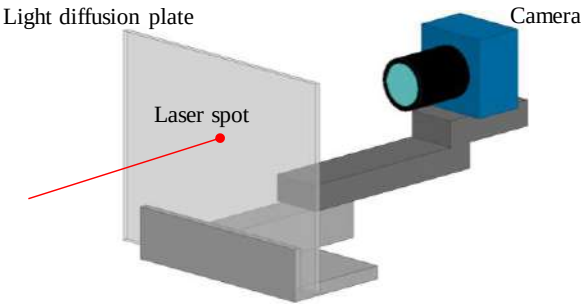

Figure 4. The positioning sensor

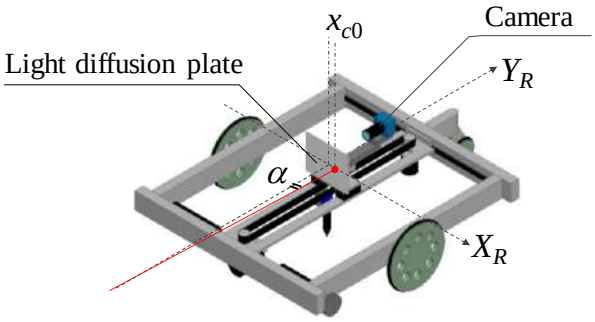

(a) Before moving the positioning sensor

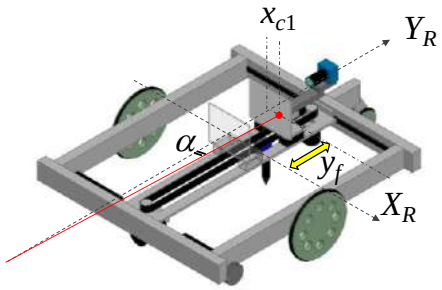

(b) After moving the positioning sensor

Figure 5. Before and after moving sensor

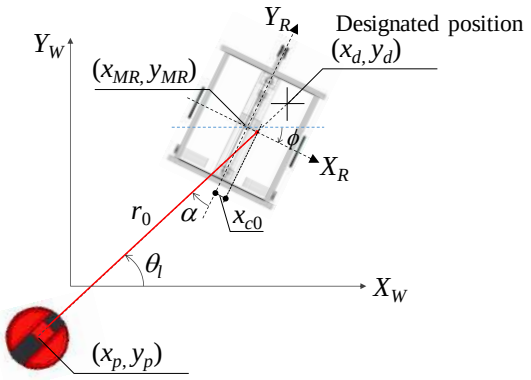

Figure 6. Explanation for calculating the x_{MR} and y_{MR}

Here,

r_0: The distance to the light diffusion plate from the 3D-MI before moving the positioning sensor

(x_p,y_p): The x and y-coordinate of the 3D-MI in the Σ_w

θ_l: An angle of the measuring laser to the X_W axis

ϕ: An angle of the X_R axis to the X_W axis

In proposed system, we prepare the figure to be drawn on the floor as a g-code data. It is commonly used in numerical control manufacturing such as milling and 3D printing. In this code, the start and end point coordinates of a line segment are defined. By controlling the movement of the marking pen based on this code, the figure can be drawn on the floor. In order to draw a designated figure exactly on the designated position with correct orientation, we need to rotate and translate the figure. The transformed coordinate of the point defined in the g-code data is calculated following equation (5). The values used in this equation are already calculated in equation (2)-(4).

$$\begin{pmatrix} p_t \\ q_t \\ 1 \end{pmatrix} = \begin{pmatrix} cos\phi & sin\phi & x_d - x_{MR} \\ -sin\phi & cos\phi & y_d - y_{MR} \\ 0 & 0 & 1 \end{pmatrix} \begin{pmatrix} p \\ q \\ 1 \end{pmatrix} \quad (5)$$

Here,

(p_t,q_t): Transformed coordinate in g-code data

(p,q): Original coordinate defined in g-code date

(x_d,y_d): The x and y-coordinate of the designated position in the Σ_w.

2.4 Component of the Marking Robot System

A photograph of the MR without controller is shown in Figure 7. Representative specifications such as external dimensions are shown in Table 1. As described in section 2.2, the MR is a two wheels differential drive robot with a caster wheel. The marking device is installed at the flame. The marking device consists of the XY movement stage and the pen unit which can move the marking pen in vertical direction by servo motor. By controlling the marking device, arbitrary figure can be drawn on the floor. The positioning sensor consisting of a camera and a light diffusion plate is also attached on the XY movement stage, thus it can move in the X_R and Y_R direction. On the other hand, a photograph of the 3D-MI is shown in Figure 8. Representative specifications such as some accuracies are shown in Table 2. System block diagram for proposed system is shown in Figure 9. Computer installed on the MR controls motor drivers for the vehicle and the XY plotter. Image processing on the captured image is also performed by the computer. 3D Disto is controlled by the computer through Wi-Fi communication.

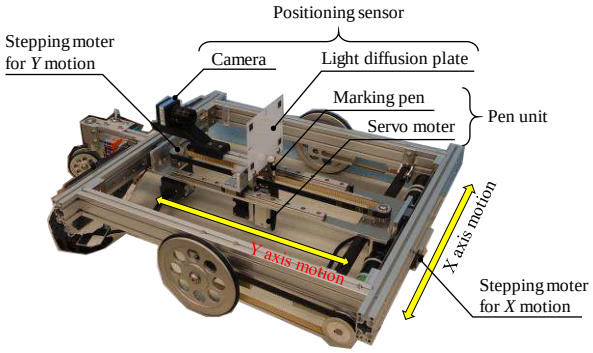

Figure 7. The MR without controller

Table 1. Specification of the MR

Item	Specification
Dimension(mm)	678x450x400
Weight(kg)	17
Power supply	lithium-ion battery

Figure 8. The 3D-MI

Table 2. Specification of the 3D-MI

Item	Specification
Manufacture / Model	Leica geosystems / 3D Disto
Accuracy of angle Measurement (Hz/V)	5”
Tie distance accuracy specified at 20 °C	Approx. 1mm at 10 m Approx. 2mm at 30 m Approx. 4mm at 50 m

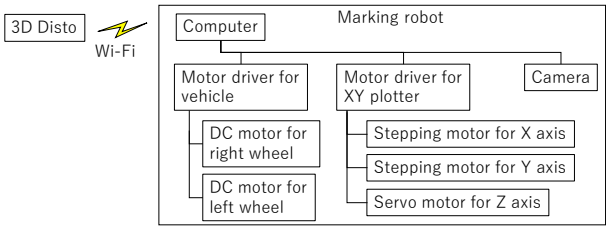

Figure 9. Block diagram for marking robot system

2.5 Detection Method of the Laser Spot

Since captured image includes the lens distortion and perspective distortion, they are removed by the same method previously reported [8]. Figure 10 shows images before and after removing these distortions. From this

(a) Before removing the distortion (b) After removing the distortion

Figure 10. Images before and after distortion removal

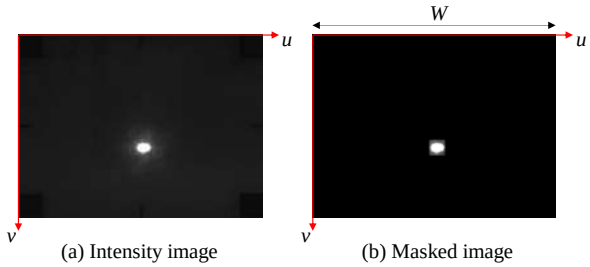

(a) Intensity image (b) Masked image

Figure 11. Images for measuring x_c

distortion-removed image, the position of the laser spot is measured. An intensity image as shown in Figure 11 (a) is obtained by averaging pixel intensity of red, green and blue channel image. On the other hand, a binary image is obtained from the intensity image by setting proper threshold level. Temporary laser spot position is obtained as the intensity center of gravity in the binary image. After that, the masked image as shown Figure 11 (b) is obtained by setting the pixel intensity to zero except for the 40 x 40 pixels centered on the temporary laser spot position in the intensity image. The horizontal camera coordinate of the laser spot, u_{max} is calculated as the intensity center of gravity in this masked image. The x_c, which is the x-coordinate of the laser spot centroid in the Σ_R is obtained from Equation (6).

$$x_c = -(\frac{u_{max}}{N_H} - 1/2)W \quad (6)$$

Here,

N_H: Number of the horizontal pixel

W: Width of the image (See figure 10)

This image processing is mainly implemented by OpenCV 3.1 and conducted by the computer.

3 Experiment

3.1 Performance of the Marking Area

In order to evaluate the performance of the marrking area, fundamental experiment was executed. The experimental layout is shown in Figure 12. The MR automatically drew cross mark from Position A to J in order. The distance between two adjacent positions was 2 m. After marking, the coordinates of the every cross

mark center were measured by using a total station. Figure 13 shows Δr_w in each designated position respectively. Here, Δr_w is the deviation between marked position and designated marking position. Position J was 22.47m apart from the 3D-MI. The MR could automatically move to the position 22.47m apart from the 3D-MI and mark with an accuracy of within 1mm or less.

3.2 Performance of the Marking for Free Access Floor

In order to evaluate the marking performance for free access floor, a basic automated marking test was executed. The experimental layout is shown in Figure 14. In the 3m x 3m test area, we set 49 designated marking positions which were grid intersections at intervals of 0.5m. They imitated positions for installing pedestal bases of free access floors. The MR marked from Position A0 to G6 in order. After that, we measured all deviations in the same way described in the previous section.

Figure 15 shows the frequency distributions of Δr_w. Summarized result is shown in Table 3. For the purpose of comparison, the results obtained from previous system [9] are also summarized together. All of the marked positions are within less than 3mm deviation. However this result was obtained in the experiment in the test area which is not the construction site. Further evaluation in construction site is needed. The time required for per position was improved from 98 seconds to 33 seconds. In proposed system, the MR can move on the shortest path from current position to next designated position. As a result, the MR could perform automated marking faster than previous prototype.

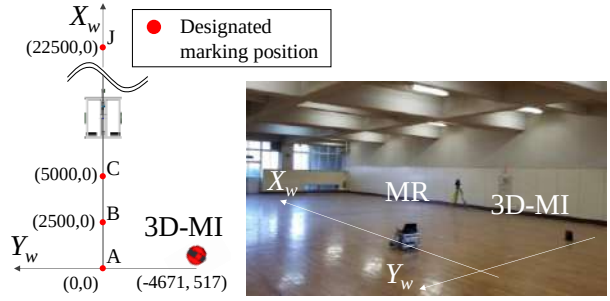

(a) Experimental layout (b) View of the test

Figure 12. Experimental layout for evaluating marking area

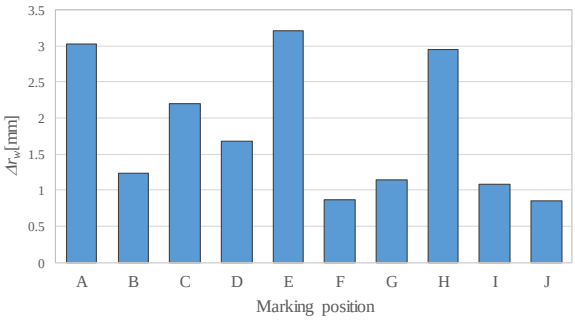

Figure 13. The Δr_w in each designated marking position

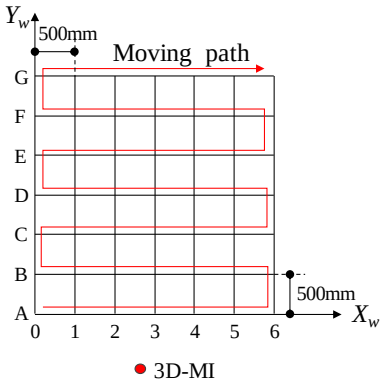

Figure 14. Experimental layout for evaluating marking for free access floor

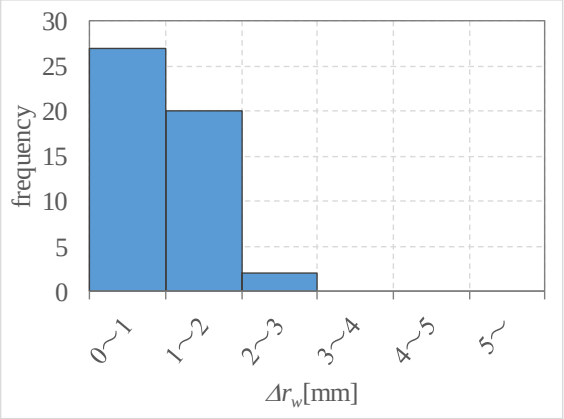

Figure 15. Frequency distribution of deviation between designated marking position and marked center

Table 3. Summarized result of the marking accuracy

Item	Proposed system			Previous system		
	Δx_w	Δy_w	$\sqrt{\Delta x_w{}^2 + \Delta y_w{}^2}$	Δx_w	Δy_w	$\sqrt{\Delta x_w{}^2 + \Delta y_w{}^2}$
Average deviation(mm)	0.6	0.5	1.0	1.7	0	2.3

Standard deviation (mm)	0.5	0.7	0.5	1.9	1.4	1.6
Maximum deviation (mm)	2.1	1.6	2.1	9.5	4.5	10.2
Percentage where deviation is within 3mm (%)		100			77	

4 Conclusion

In order to improve the efficiency of construction work, we have developed a fully automated mobile marking robot system. In this study, we obtained following conclusion.

- Proposed system is cost effective since it uses a reflectorless three-dimensional measuring instrument which cannot collimate and track prism.
- The MR automatically could move to the position 22.47m apart from the 3D-MI and mark with an accuracy of within 1mm or less. Previous studies did not reported marking area.
- Proposed system improved the marking performance compared to previous system. Average deviation was 1.0 mm. This result was comparable to that reported by Inoue et al. [5], and worse than that reported by Kitahara et al. [7]. Though the number of measured points in their study was 10 or less.
- Average time required for single marking for installing the pedestal bases of free access floors was 33 seconds. It is about 1/3 of that of the previous system. Ohmoto et al reported it took 2 minutes in their study [10]. In the case of 100 square meter marking, proposed system can finish all the marking about 4 hours.

Proposed system currently has some limitations.

- Since the MR cannot detect and avoid obstacles, it is available only in areas without obstacles. We can solve this limitation by using sensor such as laser range finder or bumper sensor.
- Some previous study reported floor inclination affected the marking accuracy [5], [7]. The MR does not measure its own tilt. Thus proposed system is effective in plane area. The inclination angle can be measured by tilt sensor. We can correct the marking position by measured value.

Since we only tested proposed system in a test field, we have to confirm the marking performance in construction site. In this study we reported the result of drawing cross mark for free access floor. If we change the figure to be drawn, the MR can draw arbitrary figure. We are now preparing the automated marking test for dry partition walls in construction site. Marking work for dry partition walls is more complicated than that for free access floors. We consider automated marking for dry partition wall with robot system is more effective for improving productivity.

In proposed system, we have to set the marking positions manually from a floor plan. This work is very laborious. Therefore, we need to develop a tool for making marking position data directly from CAD data.

Acknowledgement

The authors thank Dr. Eiji Koyanagi and Mr. Masayuki Miyashige from Mobile Robot Research Corporation LTD for their cooperation in the development of this mobile marking robot system.

References

[1] Shintaro Sakamoto, Hiroki Kishimoto, Kouetu Tanaka and Yukiteru Maeda. 3D Measuring and Marking System for Building Equipment: Developing and Evaluating Prototypes. *Proceedings of the 26th International Symposium on Automation and Robotics in Construction*, 131-138, Austin, USA, 2009

[2] Shintaro Sakamoto, Naruo Kano, Takeshi Igarashi, Hiroki Kishimoto, Hirohiko Fujii, Yuji Oosawa, Kentarou Minami and Kousei Ishida. Laser Marking System Based on 3D CAD Model. *Proceedings of the 28th International Symposium on Automation and Robotics in Construction*, 64-69, Seoul, Korea, 2011.

[3] Shintaro Sakamoto, Naruo Kano, Takeshi Igarashi, Hiroyuki Tomita. Laser Positioning System Using RFID-Tags. *Proceedings of the 29th International Symposium on Automation and Robotics in Construction*, Eindhoven, The Netherlands, 2012.

[4] Fumihiro Inoue, Satoru Doi and Eri Omoto. Development of High Accuracy Position Making System Applying Mark Robot in Construction Site. *SICE Annual Conference 2011*, 2413-2414, Tokyo, Japan, 2011.

[5] Fumihiro Inoue and Eri Omoto. Development of High Accuracy Position Marking System in Construction Site Applying Automated Mark Robot. *SICE Annual Conference 2012*, 819-823, Akita, Japan, 2012.

[6] DPR construction, 'Laybot Shows Promise in Speed and Accuracy', 2013 [Online]. Available: https://www.dpr.com/media/news/2013 [Accessed: 22- Feb- 2018]

[7] Takashi Kitahara, Kouji Satou and Joji Onodera.

Marking Robot in Cooperation with Three-Dimensional Measuring Instruments. *Proceedings of the 35th International Symposium on Automation and Robotics in Construction*, 292-299, Berlin, Germany, 2018.

[8] Takehiro Tsuruta, Kazuyuki Miura and Mikita Miyaguchi. Development of automated mobile marking robot system for free access floor. *Proceedings of the 35th International Symposium on Automation and Robotics in Construction*, 622-629, Berlin, Germany, 2018.

[9] Takehiro Tsuruta and Mikita Miyaguchi. Evaluation of the automated marking system by cooperative operation of multiple robots (in Japanese), *The 18th Symposium on Construction Robotics in Japan*, O4-1.

[10] Eri Ohmoto, Fumihiro Inoue and Satoru Doi. Marking System applying Automated Robot for Construction Site (in Japanese), Reports of the Technical Research Institute Obayashi-Gumi Ltd, No76, 1-7, 2012

A Mask R-CNN Based Approach to Automatically Construct As-is IFC BIM Objects from Digital Images

H.Q. Ying[a] and S. Lee[a]

[a]Department of Civil Engineering, The University of Hong Kong, Hong Kong
E-mail: u3004315@connect.hku.hk, sanghoon.lee@hku.hk

Abstract –

Various image-based building object recognition approaches have been developed to create as-is Building Information Models (BIMs) of existing buildings. However, existing approaches generally rely on human-designed features to automatically or semi-automatically recognize building objects, which makes them sensitive to input images and difficult to extend to new building objects. Furthermore, when constructing object geometries, most of these approaches are limited to rectangular or pre-defined surface shapes. To address these limitations, this study presents a human-designed features-free, shape constraints-free and fully automatic approach to construct as-is BIM objects from images of a building. This approach adapts Mask R-CNN, a deep convolutional neural network, to automatically recognize and segment building objects with arbitrary shapes (i.e., surface boundary shapes) from images. The segmented objects, characterized by object types and pixel masks, are further geometrically fitted to construct surface geometries. Finally, the constructed building objects are defined in the Industry Foundation Classes (IFC) data format. Three types of building objects (i.e., walls, doors, and lifts) are used in this study. Total 430 images containing these objects collected from the interiors of 4 university buildings are used to train and test the Mask R-CNN model. The test results show that the trained model is accurate and robust to recognize and segment all the three types of building objects. Furthermore, the feasibility of the proposed approach is preliminarily validated by successfully extracting IFC building objects from an image.

Keywords –

As-is BIM object; IFC; Image-based modeling; Deep learning; Mask R-CNN

1 Introduction

As-is building information models (BIMs) are characterized by containing up-to-date building information that can be used to support effective operations and maintenance of existing buildings [1, 2]. In the current practice, creating such a BIM remains a laborious, time-consuming, and costly process [1, 3]. Recent studies have focused on developing automatic approaches to create as-is BIMs. Although considerable progress has been made by exploring approaches that consume 3D point clouds [4], image-based modelling approaches have received increasing attentions. Compared to point clouds-based approaches that usually rely on a laser scanner to collect the data, image-based approaches have significant advantages in the conveniences, efficiency and cost of as-is data collection [1, 5].

Image-based as-is BIM creation generally consists of four steps [1, 6, 7]: (1) data collection, to capture images of a building and/or corresponding "location" data; (2) object recognition and construction, to recognize building objects and extract their geometries from the images; (3) geometry merging, to align constructed building objects in a common coordinate system; and (4) semantic enrichment and as-is BIM generation, to add required semantic information and save the enriched model in a specific data format (e.g., IFC or gbXML). Among these steps, the second step plays a foremost and challenging role. Most of existing approaches in this step rely on carefully hand-crafted features to recognize building objects. The commonly used features include colors [8], textures [8], edges [9], shapes [8, 10, 11], and so on. Unfortunately, these appearance-related features could vary under different environments (e.g., lighting conditions, and camera positions and poses) and/or be affected by uninterested objects (e.g., decorations and small devices that commonly exist in building interiors) in the images. Thus, these approaches are often sensitive to input images and usually require a manual pre-processing to remove noises from the input images or make the features required in downstream detection processes to be more easily extractable. Furthermore, for every new building object, corresponding detection features need to be additionally designed, which largely limits the

scalability of these approaches. In addition, when constructing object geometries, most of these approaches are limited to rectangular and pre-defined (e.g., arch) shapes. As an effort to address the first limitation, Lu et al. [12] developed a neuro-fuzzy based system, which can robustly recognize five types of building objects (i.e., beams, columns, windows, doors, and walls) in complex environments with few appearance features. However, this system is also a hand-crafted features – based approach and does not address the latter two limitations. Moreover, the system is semi-automatic. To recognize objects in an image, considerable manual efforts are required, including drawing the ground line and the ceiling line first and then orderly clicking the corners of the target objects to be recognized.

To address the aforementioned limitations, this study aims to develop a fully automated (i.e., without manual pre-processing of input images and human intervention in the algorithmic process), scalable (i.e., human-designed features-free), and shape constraints-free approach to construct as-is IFC BIM objects from digital images of existing buildings. This approach is based on Mask R-CNN [13], a deep neural network, to recognize and segment building object instances from images. In the remainder of this paper, the principles of Mask R-CNN are introduced first. Then the proposed approach is explained. Next, the implementation of the approach as well as a simple experiment is detailed, followed by the conclusion and discussion of future work.

2 Mask R-CNN for Instance Segmentation

In the computer vision community, instance segmentation refers to detect all interested objects in a given image while also precisely segmenting each instance [13]. It combines two classical computer vision tasks [14]: object detection, which aims to detect interested object instances and return their spatial locations (e.g., via a bounding box) with their category labels; and semantic segmentation, which aims to classify each pixel into a predefined object category list without differentiating object instances.

In the past several years, deep learning techniques have driven significant advances in various computer vision tasks including instance segmentation [14]. Compared to conventional recognition models that consume human-designed features, deep neural networks are powerful as they automatically learn important features from training data themselves [15]. Among various types of deep neural networks, Mask R-CNN surpassed prior state-of-the-art instance segmentation results [13]. It was developed based on another two powerful baseline deep neural frameworks, Faster R-CNN for object detection [16] and Fully Convolutional Network (FCN) for semantic segmentation [17], respectively. Figure 1 shows a high-level Mask R-CNN architecture.

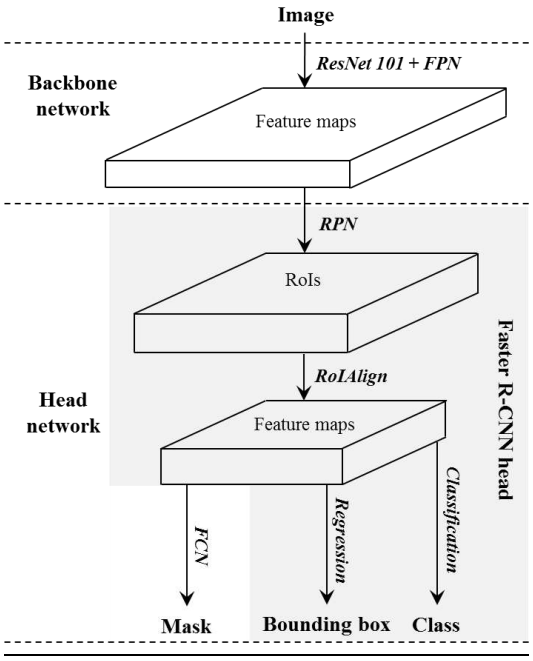

Figure 1. High-level Mask R-CNN architecture based on He et al. [13] and Ren et al. [17].

The Mask R-CNN architecture consists of two connected modules: a backbone network and a head network. The convolutional backbone network is used to extract feature representations from an input image. Then the produced feature maps are fed to the head network for succeeding three parallel tasks, namely object classification, bounding box regression and instance mask prediction. According to He et al. [13], the backbone of Mask R-CNN can achieve excellent gains in both accuracy and speed by combining ResNet [18] and Feature Pyramid Network (FPN) [19]. For the head network, Mask R-CNN was mainly designed by extending the Faster R-CNN head (see the blocks with grey background in Figure 1). The Faster R-CNN head for object detection includes two stages. In the first stage, a Region Proposal Network (RPN) is implemented on top of feature maps produced by the backbone network to propose candidate object bounding boxes (i.e. Region of Interests (RoIs)). In the second stage, high-level features are extracted from each RoI, and then object classification and bounding-box regression are performed. In this stage, Mask R-CNN adds a mask prediction branch, which is a small FCN on top of a feature map, and is parallel with existing classification and bounding box regression branches.

In this study, Mask R-CNN is adapted to achieve a fully automatic building object segmentation from images of buildings. Due to the automatic feature learning ability, Mask R-CNN based building object recognition is expected to be robust to various and complex environmental conditions, and to be scalable to customized building object types. Furthermore, Mask R-CNN allows predicting pixel-accurate masks of objects in images, which provides the potential of constructing building objects with arbitrary-shape surfaces.

3 The Proposed Approach

The proposed approach aims to automatically extract IFC building objects from images of existing buildings to support as-is BIM construction. It consists of three modules (see Figure 2): building objects recognition and segmentation, building object geometry construction, and IFC BIM object generation.

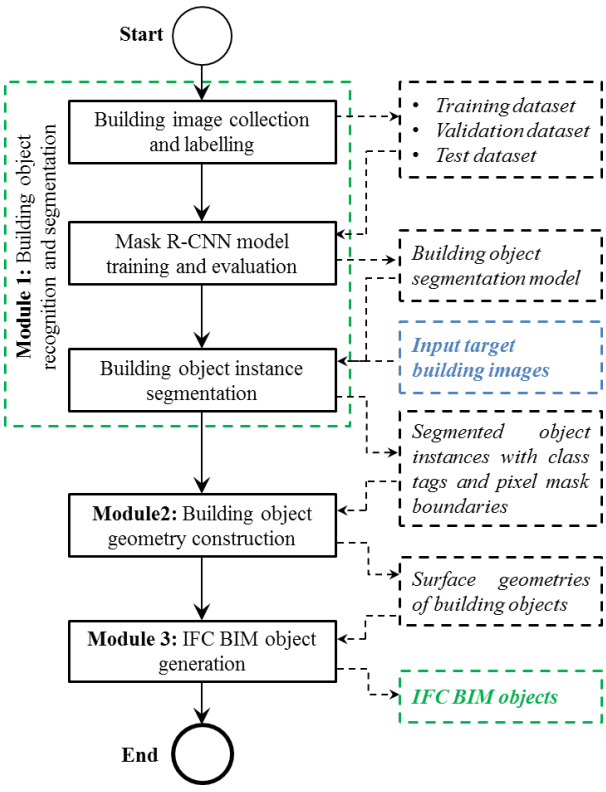

Figure 2. The proposed approach

3.1 Module 1: Building Object Recognition and Segmentation

This module takes building images as an input and produces a list of object instances segmented from each image. Each output instance consists of an object class and a mask boundary of the instance in the image. To link the pixel dimensions with real-world dimensions for object surface construction in the next module, a ruler with a known length (e.g., 1 meter) is used as a reference object in each image. Specifically, this module contains three successive steps: building image collection and labelling (Section 3.1.1), Mask R-CNN model training (Section 3.1.2), and building object instance segmentation (Section 3.1.3).

3.1.1 Building Image Collection and Labelling

Building images (most images, if not all of them, should contain the reference ruler) are collected and labeled to fit the Mask R-CNN model for building object segmentation. To ensure the generalization and the robustness of the model, images of building objects in diverse environmental conditions (e.g., building facades and building interiors, various lighting conditions, and spaces with various usages) need to be considered. Images can be conveniently collected by using handheld digital cameras or smartphones. For each image, all the building objects and the ruler (if present) need to be manually annotated by outlining their masks and adding corresponding class tags. In this study, images are annotated by the "VGG Image Annotator" web tool [20].

3.1.2 Mask R-CNN Model Training and Evaluation

The whole labeled image dataset is randomly split into the following three subsets: a training subset, a validation subset, and a test subset. The Mask R-CNN model is trained based on the image – annotation pairs in the training subset. The goal of the training is to find optimal weight parameters of Mask R-CNN that can map the training images to corresponding annotations with minimal loss. According to He et al. [13], the loss function of Mask R-CNN is defined as a multi-task loss (L) which refers to the sum of the classification loss (L_{cls}), the bounding-box loss (L_{box}), and the mask loss (L_{mask}). Details of L_{cls} and L_{box} can be found in Girshick [21] and details of L_{mask} in He et al. [13]. The validation subset is used to inspect the training process to minimize overfitting. Generally, various training strategies involving the configurations of hyperparameters need to be implemented to obtain an optimal model. For a trained model (i.e., with minimal training loss on the premise of minimal overfitting) obtained under a specific training strategy, it is further evaluated with the test subset. The model that can accurately and robustly segment building objects and the ruler in the test subset is identified and used in the downstream processes.

3.1.3 Building Object Instance Segmentation

Once the Mask R-CNN model is well trained, it can perform the building object segmentation on input

images. Although the model could segment building objects captured in various camera poses, the input images are required to be captured right in front of the target building objects to construct their surface geometries as accurate as possible in Module 2. For the same reason, each input image should contain a well-placed (i.e., vertically or horizontally) ruler (the same ruler used in the training process). By using the scikit-image package (http://scikit-image.org/), the boundary of the predicted mask of each segmented object instance is extracted as a polygon consisting of pixel points in image coordinates.

3.2 Module 2: Building Object Geometry Construction

This module takes the pixel-level mask polygons of objects generated from Module 1 as an input, and produces the surface geometries of objects in two steps: shape extraction (Section 3.2.1) and coordinate transformation (Section 3.2.2).

3.2.1 Shape Extraction

The pixel-level mask polygon of an object is in great detail in terms of shape representation. This step simplifies the shape representation by detecting corner pixels, and then constructing boundary edges (see the example in Figure 3).

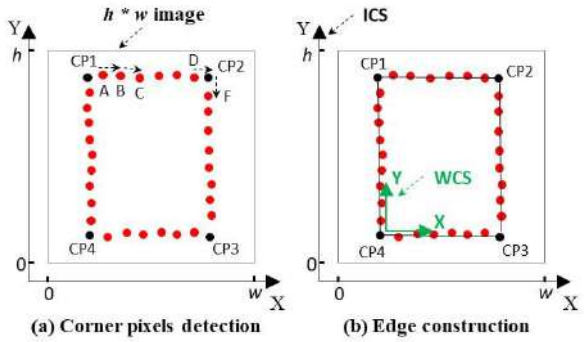

Figure 3. Object shape extraction from a segmented mask

A corner pixel refers to the pixel shared by two adjacent edges to be constructed. Corner pixels are detected by the following procedure. First, for any two adjacent pixels in a mask polygon, the direction vector from one pixel to the other is computed. Second, the angle between two adjacent direction vectors is calculated. Each angle involves a group of three successive pixels. When an angle is larger than a pre-set threshold (e.g., 10 degrees), the corresponding second pixel is recognized as a corner pixel (see CP1, CP2, CP3, and CP4 in Figure 3(a)). Once all the corner pixels are detected, an edge is constructed by fitting two adjacent corner pixels and other pixels between the two corner pixels with a line segment or a circular arc. These two geometric primitives are used in this study is because they are common in representing building object shapes and easy to be processed. As a result, the object shape can be extracted and approximately represented by the constructed edges.

3.2.2 Coordinate Transformation

This step transforms the extracted object shapes represented in an image coordinate system (ICS) into a world coordinate system (WCS), which is used to define the objects' geometries with real dimensions. In each image, objects (e.g., a wall and its hosting openings) on a common plane are assigned with a common WCS. The WCS of an object is set up by taking the lower left point as the origin and keeping x-axis and y-axis of the ICS (see Figure 3 (b)). In this manner, the transformation only involves a translation. To calculate the real dimensions of building objects, the segmented ruler with a known length (i.e., 1m) is used to calculate the pixel dimension by:

$$d_p = \frac{1}{\sqrt[2]{(x_{r_CP1} - x_{r_CP2})^2 + (y_{r_CP1} - y_{r_CP2})^2}} \quad (1)$$

Where (x_{r_CP1}, y_{r_CP1}) and (x_{r_CP2}, y_{r_CP2}) refers to the image coordinates of two endpoint pixels of a long edge of the segmented ruler instance, respectively.

Then for any $\boldsymbol{P}$ (x_{imag}, y_{imag}), its world coordinates (x_{world}, y_{world}) can be computed by

$$\begin{bmatrix} x_{world} \\ y_{world} \end{bmatrix} = d_p \times \begin{bmatrix} x_{image} - x_{o_image} \\ y_{image} - y_{o_image} \end{bmatrix} \quad (2)$$

Where $(x_{o_{imag}}, y_{o_imag})$ refers to the image coordinates of the origin of the world coordinate system.

Since each extracted shape is defined by a combination of line segments and/or circular arcs, the transformation of a shape essentially refers to transform all relevant geometric primitives into the corresponding WCS. For a line segment, its two endpoints are transformed via Equation (2). For a circular arc defined by a center, a radius, two trimming points and an arc direction, the center and the two trimming points need to be transformed via Equation (2).

3.3 Module 3: IFC BIM Object Generation

This module defines the constructed building objects as IFC objects. For each building object, only the visible sections of surfaces (i.e., exposed to a space or the outdoors) are constructed. Thus, the IFC concept of space boundary (SB) (i.e., IfcRelSpaceBoundary) [22], which defines the surface partition of a building object that bounds a space or contacts outdoors, is proper to

store the constructed information. Figure 4 shows the IFC entities and data structure used to define a SB in the IFC4 specification. To be more specific, each building object is defined by an IfcRelSpaceBoundary instance. To store the object type information, this instance references a building element instance that matches the type via the attribute "RelatedBuildingElement". For example, for a wall object, an IfcWallStandardCase instance is created and linked to the IfcRelSpaceBoundary instance via that attribute. The object surface geometry is defined by the IfcRelSpaceBoundary instance via the attribute "ConnectionGeometry" (see Figure 4). It is noteworthy that the created IFC SB instances do not constitute a valid IFC model as other IFC instances (e.g., IfcProject, IfcSite, IfcBuilding and IfcSpace) required by the IFC4 specification are not yet included. All the missing instances can be automatically inferred and added by using the semantic enrichment approach developed by Ying et al. [6].

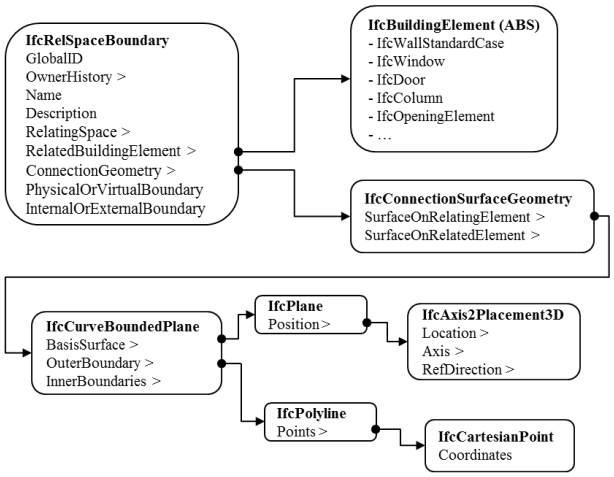

Figure 4. Instantiation diagram to define a space boundary in IFC4 schema

4 Implementation and Experiment

A prototype system implementing the proposed approach was developed in multiple programing languages. Module 1 was implemented in Python. Module 2 and Module 3 were implemented in C#. In the rest parts of this section, the implementation details of Mask R-CNN for building object segmentation are first elaborated and then a preliminary experiment of the entire approach is presented.

4.1 Mask R-CNN Model Implementation

4.1.1 Dataset Preparation

The authors created a 2D image dataset to train a Mask R-CNN model for building object segmentation. The dataset includes 430 images from interiors of 4 multifunctional buildings in the University of Hong Kong with significantly different decoration designs (see some examples in Figure 5). All the images were captured by a smartphone and their sizes are 3024×4032. The dataset also includes the ground truth annotation of each building object contained in each image. The authors randomly split the annotated dataset into three sub datasets: 80% (344 images) for training, 10% (43 images) for validation, and 10% (43 images) for testing. Table 1 shows the number of building object instances in each sub dataset. In this test, only three types of building objects (i.e. walls, doors and lifts) and a reference ruler were considered. Other objects such as columns, beams and windows will be taken into account later.

Figure 5. Varieties of collected building interior images in the dataset

Table 1. The number of building objects in each dataset

Dataset	Wall	Door	Lift	Ruler
Training dataset	599	443	34	99
Validation dataset	68	49	6	11
Test dataset	73	53	2	12

Whole dataset	740	545	42	122

4.1.2 Training

The authors implemented the Mask R-CNN model using an open-source package built on Keras and Tensorflow developed by Matterport [23]. ResNet-101 + FPN are used as the backbone network. Parameters of the sub models of the Mask R-CNN (e.g., ResNet-101, FPN, RPN, FCN etc.) are left in default settings in Matterport's implementation, which basically follows the suggestions in He et al. [13]. It is noteworthy that all the input images (3024×4032) are automatically resized as 1024×1024 for training in the Matterport's implementation. Instead of training the model from scratch, the authors used the weights of a pre-trained Mask R-CNN model on MS COCO (http://cocodataset.org/#home) to initialize the model. In addition, to make the resulting model more robust, a set of image argumentation operations (e.g., horizontal flipping and Gaussian blurring) were randomly used to introduce variety in the training images. The model was trained on a desktop with 61GB RAM and a NVIDIA Tesla K80 GPU with 12 GB memory. The training process consists of two stages. In the first stage, only the head layers that do not use pre-trained weights from MS COCO are trained to adapt the building object segmentation task. In the second stage, all layers are trained to fine-tune the weights to achieve the best performance. The authors set the batch size of 2, the learning momentum of 0.9, and the weight decay of 0.0001 for both training stages, and the learning rate of 0.001 for the first stage and the learning rate of 0.0001 for the second stage. The authors adopted an early stopping strategy to minimize overfitting with the validation dataset. The model was trained with 60 epochs to record the full learning curve. Finally, the model trained at the 50th epoch was selected as the model began to get overfitting after 50 epochs (i.e., the validation loss began to increase).

4.1.3 Assessment

The performance of the trained model was evaluated with the hold-out test dataset from two aspects: (1) the object classification accuracy, which aimed to evaluate the performance of the model in terms of building object and ruler recognition; and (2) the object segmentation accuracy, which aimed to evaluate the performance of the model in terms of the instance mask generation. A positive classification of an instance is acknowledged if the following two criteria are satisfied: (1) the predicted mask of the instance has an overlap with the ground truth; and (2) the predicted class of the instance is correct. Table 2 shows the overall classification accuracy and the object-level classification accuracy with precision and recall. The results show that the trained model can accurately and robustly recognize the building objects and the reference ruler.

Table 2. Classification accuracy of the trained model on the test dataset

		P	N	Precision	Recall
Wall	T	72	0	97.3%	100%
	F	2	0		
Door	T	48	0	100%	90.6%
	F	0	5		
Lift	T	2	0	100%	100%
	F	0	0		
Ruler	T	11	0	100%	91.7%
	F	0	1		
Overall	T	133	0	98.5%	95.7%
	F	2	6		

Note: P – Positive; N – Negative; T – True; F – False; Precision = TP / (TP + FP); Recall = TP / (TP + FN).

For the segmentation accuracy evaluation, the authors use the metric called mAP (the mean of average precision values of all classes), which is commonly used in computer vision community to evaluate the performance of an object detector. Given that the quality of a predicted mask would have a significant effect on corresponding surface construction, the authors set a large threshold value - 0.75 - of IoU (Intersection over Union: the ratio between the intersection and the union of the predicted mask and the ground truth mask of an instance) for the mAP computation. The mAP $^{IoU = 0.75}$ of the trained model on the test dataset reaches 0.912, which indicates that the trained model can generate effective masks.

4.2 Experiment

A new image (i.e., not in the dataset used for the Mask R-CNN model training, validation and testing) taken in an interior space at night, as shown in Figure 6(a), is used to validate the feasibility of the proposed approach. The image mainly contains three building objects, a reference ruler, as well as a noisy object – the emergency exit sign. The three building objects (from left to right in Figure 6 (a)) includes a wall showing a small surface region, a wall showing the entire surface, and a door showing the entire surface. The latter two are the target building objects to be constructed. Figure 6(b) – (f) shows the whole flow of generating interested IFC objects from the image by the proposed approach. In Figure 6 (b), all three building objects and the ruler are correctly segmented by the trained Mask R-CNN model. Then the two target building objects are further distinguished from the segmented wall instance with a partial surface region, and proceed to the downstream

steps with the ruler to construct surface geometries (see Figure 6(c) – (e)). Finally, two corresponding IFC objects are successfully generated (see Figure 6(f)).

Regarding the geometry construction accuracy in the result, the areas of the constructed wall surface and door surface are 8.69 m^2 and 4.78 m^2 respectively. Compared to the real values (measured with a laser range finder), 7.97 m^2 for the wall and 4.184 m^2 for the door, the errors are +9% and +13.97% accordingly. As seen in Figure 6, these errors are mainly caused from the imperfection in the reference ruler placement and its segmentation (Figure 6(b)) as well as the process of determining building object shapes from the extracted mask boundaries (from Figure 6(c) to Figure 6(d)). In future, the Mask R-CNN model needs to be improved to generate more accurate masks for segmented objects.

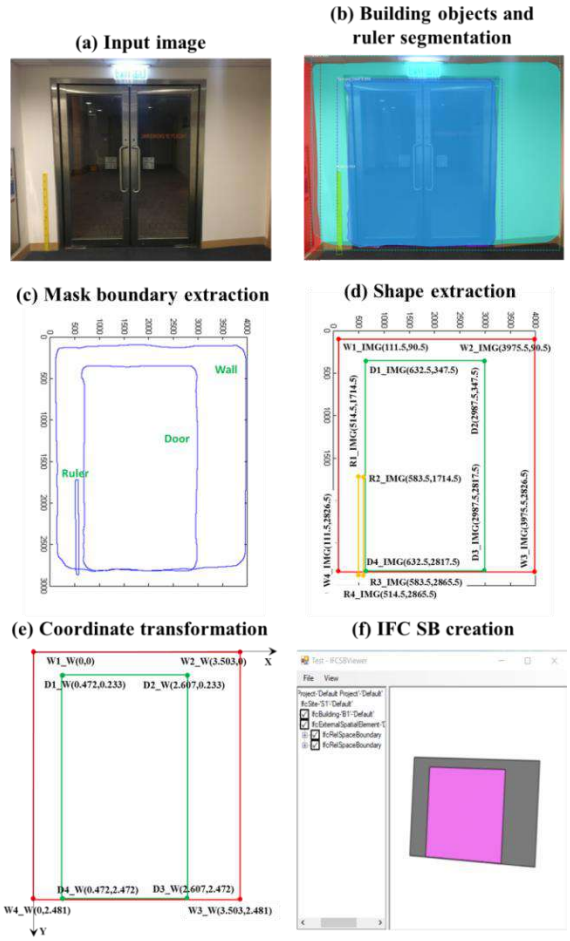

Figure 6. The flow of processing an image by the proposed approach

5 Conclusion and Future Work

In this study, a fully automatic approach is presented to construct IFC building objects from digital images of existing buildings. Unlike previous image-based approaches that rely on human-designed features to recognize building objects, the proposed approach automatically learns important features from training data themselves to segment building object instances. This makes the approach to be robust in various building indoor conditions, and to be efficiently scalable to customized building object types. Furthermore, the approach is able to construct building objects with complex surface shapes. The proposed approach was implemented with three modules: Mask R-CNN based building object recognition and segmentation, building object geometry construction and IFC BIM object generation. 430 images containing three types of building objects (i.e., walls, doors, and lifts) were collected and used to train and test the Mask R-CNN model. The test results show that the trained Mask R-CNN model can accurately and robustly recognize the three types of building objects and the reference ruler (with average precision of 98.5% and average recall of 95.7%), and can generate effective masks for the recognized building object and ruler instances (with mAP $^{IoU = 0.75}$ of 0.912). Based on the trained Mask R-CNN model, the feasibility of the entire approach was examined by successfully extracting IFC BIM objects from an image, while the geometry construction accuracy still has room for further improvement. It is expected that the approach can be useful for researchers and practitioners to develop semantically rich as-is BIMs of existing buildings.

In future, the approach will be further improved in the following aspects. First, the Mask R-CNN model will be improved to generate more accurate masks of segmented objects to support accurate surface geometry construction. Second, the size of the image dataset will be increased with more images from different environments (e.g., building exteriors) and different building types (e.g., residential buildings and commercial buildings) to improve the performance and enhance the generalization of the Mask R-CNN model. Other common building objects such as windows, beams, columns, and curtain walls will be included. Third, more flexible and accurate dimension measurement method (e.g., photogrammetry technique) will be introduced to address the constraint on input image capturing (i.e., taking images right in front of target building objects). Finally, the performance of the proposed approach will be further examined by more case studies.

Acknowledgement

The work described in this paper was supported by a grant from the Research Grants Council Early Career

Scheme of the Hong Kong Special Administrative Region, China (Project No. HKU 27203016).

References

[1] Lu Q. and Lee S. Image-based technologies for constructing as-is building information models for existing buildings. *Journal of Computing in Civil Engineering*, 31(4), p.04017005, 2017.

[2] Becerik-Gerber B., Jazizadeh F., and Li N., et al. Application areas and data requirements for BIM-enabled facilities management. *Journal of Construction and Engineering Management*, 138(3): 431-442, 2011.

[3] Tang P., Huber D., Akinci B., Lipman R. and Lytle A. Automatic reconstruction of as-built building information models from laser-scanned point clouds: A review of related techniques. *Automation in construction*, 19(7): 829-843, 2010.

[4] Pătrăucean V., Armeni I., Nahangi M., Yeung J., Brilakis I., and Haas C. State of research in automatic as-built modelling. *Advanced Engineering Informatics*, 29(2): 162-171, 2015.

[5] Bhatla A., Choe S.Y., Fierro O., and Leite F. Evaluation of accuracy of as-built 3D modeling from photos taken by handheld digital cameras. *Automation in Construction*, 28: 116-127, 2012.

[6] Ying H., Lu Q., Zhou H., and Lee S. A framework for constructing semantic as-is building energy models (BEMs) for existing buildings using digital images. In *Proceedings of 35th International Symposium on Automation and Robotics in Construction*, pages 309-316, Berlin, Germany, 2018.

[7] Ying H., Zhou H., Lu Q., Lee S., and Hong. Y. Semantic Enrichment of As-is BIMs for Building Energy Simulation. In: Mutis I., Hartmann T. (eds) *Advances in Informatics and Computing in Civil and Construction Engineering*, pages 733-740, Springer, Cham, 2019.

[8] Oskouie P., Becerik-Gerber B., and Soibelman L. Automated recognition of building façades for creation of As-Is Mock-Up 3D models. *Journal of Computing in Civil Engineering*, 31(6), p.04017059, 2017.

[9] Zhu Z. and Brilakis I. Concrete column recognition in images and videos. *Journal of Computing in Civil Engineering*, 24(6): 478-487, 2010.

[10] Neuhausen M. and König M. Automatic window detection in facade images. *Automation in Construction*, 96: 527-539, 2018.

[11] Cao J., Metzmacher H., and O'Donnell J., et al. Facade geometry generation from low-resolution aerial photographs for building energy modeling. *Building and Environment*, 123: 601-624, 2017.

[12] Lu Q., Lee S., and Chen L. Image-driven fuzzy-based system to construct as-is IFC BIM objects. *Automation in Construction*, 92: 68-87, 2018.

[13] He K., Gkioxari G., Dollár P., and Girshick R. Mask R-CNN. In *Proceedings of International Conference on Computer Vision*, pages 2980-2988, Venice, Italy, 2017.

[14] Liu L., Ouyang W., Wang X., Fieguth P., Chen J., Liu X., and Pietikäinen M. Deep learning for generic object detection: A survey. *arXiv preprint arXiv:1809.02165*, 2018.

[15] LeCun Y., Bengio Y. and Hinton G. Deep learning. *Nature*, 521(7553): 436, 2015.

[16] Ren S., He K., Girshick R., and Sun J. Faster R-CNN: Towards real-time object detection with region proposal networks. In *Proceedings of Advances in neural information processing systems*, pages 91-99, Montreal, Canada, 2015.

[17] Long J., Shelhamer E., and Darrell T. Fully convolutional networks for semantic segmentation. In *Proceedings of the IEEE Conference on Computer Vision and Pattern Recognition*, pages 3431-3440, Boston, USA, 2015.

[18] He K., Zhang X., Ren S., and Sun J. Deep residual learning for image recognition. In *Proceedings of the IEEE Conference on Computer Vision and Pattern Recognition*, pages 770-778, Las Vegas, USA, 2016.

[19] Lin T.-Y., Doll´ar P., Girshick R., He K., Hariharan B., and Belongie S. Feature pyramid networks for object detection. In *Proceedings of the IEEE Conference on Computer Vision and Pattern Recognition*, Honolulu, USA, 2017.

[20] Dutta A., Gupta A. and Zisserman A. VGG Image Annotator (VIA). Online: http://www.robots.ox.ac.uk/~vgg/software/via/, Accessed: 18/1/2019.

[21] Girshick R. Fast R-CNN. In *Proceedings of the IEEE International Conference on Computer Vision*, pages 1440-1448, Santiago, Chile, 2015.

[22] BuildingSMART. IfcRelSpaceBoundary. Online: http://www.buildingsmart-tech.org/ifc/IFC4/final/html/schema/ifcproductextension/lexical/ifcrelspaceboundary.htm, Accessed: 18/1/2019.

[23] Waleed Abdulla. Mask R-CNN for object detection and instance segmentation on Keras and TensorFlow. Online: https://github.com/matterport/Mask_RCNN, Accessed: 15/11/2018.

Using Scan-to-BIM Techniques to Find Optimal Modeling Effort; A Methodology for Adaptive Reuse Projects

M. Esnaashary Esfahani[a], E. Eray[a], S. Chuo[a], M.M. Sharif[a], and C. Haas[a]

[a]Department of Civil and Environmental Engineering, University of Waterloo, Canada
E-mail: mesnaash@uwaterloo.ca

Abstract –

With increased computing power to render 3D models and affordability of as-built data acquisition technologies, new techniques for enhancing the quality of pre-project planning of adaptive reuse projects can be investigated. The main objective of this research is to present a decision making methodology to select the optimum effort using 3D as-built point clouds to develop a BIM of an existing building. Three value proposition and risk reduction areas are investigated: (1) dimensional, (2) material, and (3) disassembly. To measure the cost and value of developing models with corresponding value propositions, a small case study is conducted. Three different Model Detail Levels (MDL) are defined for adaptive reuse projects, and corresponding models are developed for each of them. The value of each model is considered based on its ability to provide information about dimension, materials, and fixtures within an existing building. The cost of the scan-to-BIM process includes costs of purchasing 3D acquisition device, buying BIM modeling software license, scanning and registration, and developing BIM using scan-to-BIM techniques.

Keywords –

Adaptive reuse; Value of information; Pre-project planning; Scan-to-BIM; Modeling; Existing buildings

1 Introduction

Having a successful project or receiving the best outcome from a project has always been a goal of engineers and project managers. In general, a project is successful when it meets all of its goals and expectations and when all of the stakeholders (e.g. owners, consultants, contractors, suppliers, end-users, community, etc.) achieve their requirements individually and collectively [1]. The Construction Industry Institute (CII) conducted extensive research and concluded that improving the planning process during the early stages of a project lifecycle would be more effective and cheaper in order to improve a project's outcome, as opposed to later stages [2]. Planning during the early stages of a project life cycle is called pre-project planning and is defined as, "the process of sufficient strategic information with which owners can address risk and decide to commit resources to maximize the chance for a successful project" [3]. Pre-project planning would be more effective and ensures higher probability of having successful design, construction, and operation phases, depending on the efforts that have been dedicated to completely define the details of a project's scope [4]. Scope definition is considered as defining the vague and uncertain areas such as area and site investigation, existing brownfields, weather conditions, safety and security regulations that will be used during the detailed design, construction, and operation phases.

Gathering information is the first step of defining details of a project's scope. There are several pre-project planning tools that help a project team (owners, engineers, architects, contractors, investors, and developers) to know which type of information is needed. However, there is not any clear decision making methodology regarding the process and prioritization of information gathering. The methods and technologies to obtain information, the cost and value of each method, the amount of risk reduction, and finally the optimal amount of information are the steps that must be addressed through further research.

The objective of the adaptive reuse approach is revitalizing old and obsolete buildings and returning them to the use cycle. Therefore, as-built condition of an existing building is one of the most important information categories for defining project scope of an adaptive reuse project. However, obtaining useful as-built dimensions of an old existing building can be costly. Typically, either as-built drawings are not available, or they might be inaccurate [5]. Lack of updated as-built drawings brings more uncertainty to the adaptive reuse projects that causes financial loss and time delay during design and construction phases. Thus, it is necessary to provide updated as-built information during pre-project planning and before authorizing a project for the detailed design and construction phase.

Using 2D surveying tools and software is the common way to create as-built drawings of an existing building [6]. However, there are drawbacks associated

with this method of as-built data collection, such as high level of error, long time of surveying, difficulties of obtaining details of building's fixtures and facilities, difficulties of converting the 2D surveying information to the 2D drawings, and complexity of interpreting the 2D drawings. On the other hand, usage of advanced software and technologies that have 3D surveying and drawing capabilities can support the process of developing more exact and less complex as-built drawings. In addition, 3D as-built drawings can provide more information regarding the existing conditions of a building to the project team.

The objective of this paper is to fill the mentioned knowledge gap by presenting a decision making methodology for finding the optimal amount of effort in the data collection and modeling step in adaptive reuse projects. This methodology will be presented by conducting a case study to select the optimum effort required in the 3D data acquisition step (laser scanning and structured lighting has been utilized) and to develop a 3D as-built BIM (Building Information Model – defined and described in more detail in section 2.5 of this paper) of an existing building. The method, which has been used in this case study to obtain as-built information, can be generalized to find the optimal amount of information about other project scope elements.

2 Literature review

2.1 Adaptive Reuse

There are numerous definitions for "adaptive reuse" in the literature. In this research, adaptive reuse is accepted as the process of extending the useful life of a historic, old, obsolete, and derelict building, considering new usage compatible with historic background, new socio-cultural demands, political and environmental regulations of a building's location and applicable building codes, maximizing the reuse and retention of existing structures and fabrics, and improving financial performance and economic viability of buildings [7], [8]. Since adaptive reuse specially deals with old and historic building restoration, UNESCO defines it as a respectful process to the form, character, structure, and historic integrity of buildings, while finding an appropriate use for them [9].

Extending building useful lives, preserving natural resources, reducing waste production, controlling negative impacts of old buildings, satisfying new demands, and preserving cultural, historical and social aspects of a building are among the most important key drivers of the adaptive reuse approach [10]. Hence, adaptive reuse is a novel sustainable approach to fulfill previously mentioned key drivers.

2.2 Uncertainty and Information

In the project management literature, uncertainty is used as a general concept and is defined as the degree of deviation between actual outcomes of an event from its predicted outcomes. In fact, uncertainty is the effect of lack of knowledge and information about an event. There is an inverse relationship between information and uncertainty level [11]. Providing more information increases the knowledge of the project team about the project and consequently enhances the project predictability and decreases its uncertainty. Although providing more information has the mentioned values, it also adds to the cost of the project. Thus, there is a practical limit to the amount of information needed to reach a reasonable level of uncertainty. As long as the marginal expected value of working with more information (lower uncertainty) is positive, and the cumulative expected value of working with more information is higher than the expected value of working without any information (higher uncertainty), it is reasonable to collect information and reduce uncertainty.

In other words, collecting information more than this limit will decrease the net value, because after the limit point, the rate of information gathering cost would be higher than value enhancement. This limit will differ from scope element to scope element and project to project. So, it is up to the project team to come up with the limit of information for each scope element according to the specific project. Or, where information is fuzzy, applying the 80:20 rule works well, and here we identify ways of prioritizing so that rule can be observed.

2.3 LOD and Other Methods

The project design phase involves an iterative process in which the final product is achieved after several changes and improvements. In construction projects, be it a new project or an adaptive reuse project, design progress starts with conceptual drawings, and a fully coordinated construction model is created after many iterations. While design evolves from conceptual drawing to ready for construction model, details of the model elements and model disciplines become more mature and accurate. In this iterative process determining the detail level of the design is a complicated problem. In the literature there are several frameworks proposed to determine the detail levels of the model elements and model disciplines. One of the known frameworks that focuses on design details of the model elements is the Level of Detail (LOD) framework.

The LOD framework is created in 2005 by VICO Software Ltd. to track cost estimates of the projects, and later it was adopted by the American Institute of Architects (AIA). After AIA improved the LOD framework into specific levels, the meaning of the LOD

acronym was changed to "Level of Development", and in 2008 the definition of different LOD levels were released. AIA defined five LOD levels (LOD 100, LOD 200, LOD 300, LOD 400, and LOD 500) for model elements in a Building Information Model. According to the "AIAE202-2008 BIM Protocol Exhibit" contract document, LOD 100 refers to the conceptual drawing of a model element which shows its area, height, volume, and location, while LOD 500 means that the model element has reached its as-built version, and it would include useful information for operations and facility management phases of a project [12]. However, it is important to note that, there is no defined total LOD or LOD of the whole model. LOD definitions are created for single model elements on a design model [13]. Figure 1 represents five different LOD versions of a steel framing column model element according to the BIM Forum's 2018 LOD Specifications [14].

Figure 1. Representation of different LOD Levels of Steel Framing Column (Source: [14])

CII's Model Maturity Index (MMI) definitions are an example of a framework that can be used for determining the design detail level of a design model and design progress by focusing on information added to the related model disciplines [15]. In 2017, CII published a new set of definitions that is called MMI, and a toolkit called Model Maturity Risk Index to measure modelling progress and productivity in building projects. CII provided these definitions and related tool for 12 disciplines including; Piping, Structural, Instrumentation, HVAC, Equipment, Civil, Electrical, Fire Protection, Layout, Foundations, Buildings, and P&IDs in building type of projects. Defined MMI levels follow similar sequence with LOD levels. There are seven different MMI levels for each modeling discipline varying between Generic Model to Facility Management information added as-built model. Similar to LOD, there is no such total MMI of whole model, these definitions are developed for disciplines in the model.

Inspired by the concepts of LOD and MMI, the Model Definition Level (MDL) is defined in this study to emphasize that there are different effort levels regarding the scan-to-BIM process, which may lead to different value levels.

2.4 3D Acquisition

2.4.1 Laser Scanning

Three-dimensional laser scanning named LiDAR (Laser Detection and Ranging) has been introduced and used in industry since the 1970s as an advanced imaging technology. Due to the high cost and low reliability of the early devices, this technology did not spread widely until the 1990s [16]. Several technologies, such as computer, optics, and micro-chip lasers came together to form the laser scanner as a high-tech device. Laser scanners can be used to capture the geometry of a construction site accurately and quickly [17]. The output of a 3D laser scanner is a dense point cloud for which each point has three coordinate indices "X", "Y" and "Z" based on the scanner's coordinate system. In fact, the laser scanner records the 3D geometry of objects by collecting thousands or millions of points located on the objects' surfaces.

To this date, many researchers have worked on using laser scanners for tracking new construction and fabrication processes, and developing as-built models of construction sites [18]. However, there is limited research about exploiting the capabilities of laser scanner to record 3D as-built of existing buildings and collect some mandatory information to feed the design and construction of adaptive reuse projects [19]–[21].

2.4.2 Structured Lighting

A structured-light 3D scanner is a device for measuring the three-dimensional shape of an object using projected light patterns (infrared light in Microsoft Kinect and Structure IO) and a camera system [6]. The projector projects speckle patterns on the objects and the sensor calculates the distance of a point to itself. In order to use triangulation, two separate images must be captured. In terms of accuracy, the support group of Structure IO (one of the commercially available scanners, which uses structured light technology) claims that the device can achieve an accuracy of 1% of distance measured. While the accuracy of structured-lighting scanners is significantly lower than laser scanners, the ease of use and acceptable accuracy for small objects has made them an acceptable option for rudimentary modeling efforts.

2.5 Building Information Modeling (BIM)

According to international standards, Building Information Modeling (BIM) is defined as "shared digital representation of physical and functional characteristics of any built object, which forms a reliable basis for decisions" [22]. Predecessors of BIM were used for product modeling, and had wide application in the petrochemical, automotive, and shipbuilding industries [23]. BIM can be categorized as having a narrow to broad perspective, based on its capability and the amount of information contained. Narrow perspective may include 3D (building model), 4D (3D plus construction schedule), and 5D (4D plus cost calculation) models of a building.

On the other hand, BIM with broad perspective goes further and considers the energy and environmental performance of a building. As a matter of fact, the narrow and broad perspectives refer to technical and functional issues of a building, respectively [19].

Until recent years, the use of BIM had been restricted to new construction and earlier stages of the building's lifecycle [19]. However, as BIM enables project teams to precisely manage the building's information along the whole lifecycle [24], it is able to support later stages of life cycle as well. Therefore, BIM can be used to manage maintenance, renovation, deconstruction, adaptive reuse, and the stage of building end of life [25].

Although using BIM for existing buildings has many benefits, such as providing valuable as-built documentation and planning renovation or retrofit projects, research studies have indicated infrequent implementation of BIM for existing buildings. The need for high modeling efforts in order to convert collected data to a BIM, handling uncertain data and objects, and difficulties in updating the BIM of existing buildings have been the main obstacles of implementing BIM for existing buildings [19]. Thus it is valuable to focus on implementation of BIM for existing buildings and research further into this field.

3 Research Methodology

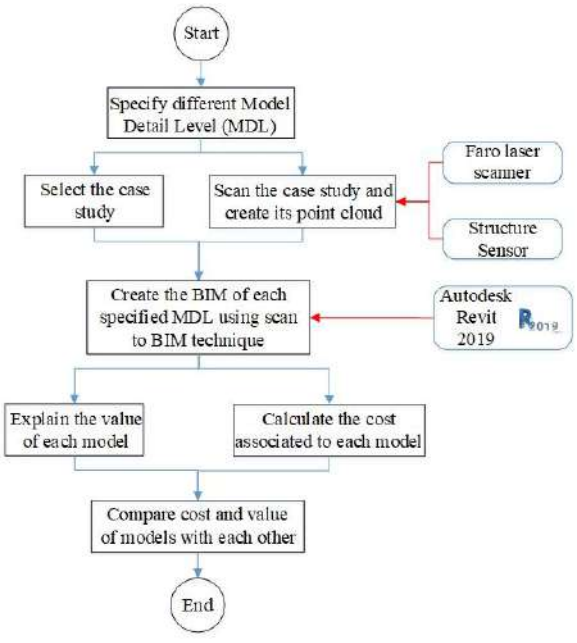

Figure 2. The overview of research methodology

3.1 Model Detail Level (MDL)

3.1.1 Value of Dimensional Information

Collecting dimensions of all physical surrounding is necessary for re-designing a space, whether in renovation or adaptive reuse projects. Furthermore, to optimize the effort required, designers try to minimize the amount of effort required in the disassembly and gutting steps (try to reuse space as much as possible). An important aspect of having a BIM of a project is instantaneous access to all dimensions, such as location of the openings (windows, doors, etc.), location of the elevators and stairs, and the area of spaces in an existing building. On projects where no prior model exists (or they are not accurate) using scan-to-BIM methods can be effective to rebuild an accurate model. As such, having access to the dimensional information resulted from the scan-to-BIM effort is considered as one of the axioms to determine how much effort shall be designated for the process. Access to dimensional information is referred to as "Dimension" and is the only existing value of information provided by MDL 1 models.

3.1.2 Value of Material Information

In addition to the dimensions, it is essential to consider the materials that have been used in an existing building for selecting the most compatible new usage with the prior one. Also, adaptive reuse seeks to fulfil the requirements of environmental sustainability. This goal will be achieved by maximizing the use of existing buildings' materials through recycling, reusing and minimizing the need for new materials. Decreasing the rate of natural resources depletion, greenhouse gas emission, and global warming effects due to lower demand for material production and transportation are benefits of using existing materials. Hence, "Material" of each component is another important type of information that must be considered for designing the adaptive reuse projects.

3.1.3 Value of Disassembly Information

In order to increase the efficiency of recycling and reusing processes, the project team needs to access more detailed information than a building's dimensions and material. Examples of detailed information include the routes of plumbing and wiring networks, location and details of electrical and mechanical facilities, location of sprinklers and smoke detection facilities, type and location of lighting, and location of a building's fixtures and furniture. These kinds of information are called "Disassembly" information, because they will help the project team to efficiently plan for disassembly, recycling and reuse the existing materials.

In this study, the LOD and MMI concepts are utilised, and a new framework that is related to the detail of a

whole design model is defined. This new framework is called Model Definition Level (MDL) and divided to three different levels based on the provided information. A BIM satisfies the requirements of MDL 1 (Dimension information) if contains the dimensional information about an existing building. The BIM will be upgraded from MDL 1 to MDL 2 (Material information) by adding material information of building's components to the model. In addition, adding disassembly information to a BIM that already satisfies the requirements of MDL 2, will upgrade this to MDL 3.

3.2 Case Study

The case study of this conference paper is the Ralph Haas Infrastructure and Sensing Analysis Laboratory, located within Engineering 3 building at the University of Waterloo.

Figure 3. The panorama picture of the case study

The objective is to develop a BIM for each specified MDL by converting the 3D point cloud of the laboratory to the BIM (scan-to-BIM technique). Two different devices including the "Faro Focus M70" laser scanner and the "Structure Sensor" (Structure IO) are used to capture the point cloud. The Faro laser scanner is a professional scanner that can capture up to 488,000 points per second. Its measurement range is between 0.6 and 70 meter, and the ranging error is 3 millimeters. Furthermore, capturing HDR pictures and applying color information to the point cloud is another advantage of laser scanners, which can be useful in the scan-to-BIM process. On the other hand, the Structure Sensor is a structured light scanner which is mounted on Apple iPad. By incorporating an IMU (inertial motion unit) and elements of SLAM (simultaneous localization and modeling), it does real-time registration and does not need manual registration to create the point cloud. Thus, the scanning process is significantly faster when Structure Sensor is used for scanning. Furthermore, the scan registration process using laser scanners requires sophisticated knowledge in post processing software.

Figure 4. Point cloud: Structure IO (left) and Faro (right)

3.3 Developed Models

The captured point clouds are used to develop BIM for each specified MDL. As seen in Figure 4, the captured point cloud using the Structure Sensor does not have enough information (point density, precision and accuracy) to recognize the openings and details of the building fixtures. Therefore, it is only feasible to use it to attain the first MDL (which only contains dimensional values). So, MDL 1 is developed using both point clouds, while MDL 2 and MDL 3 are developed based on the point cloud obtained by the laser scanner.

3.3.1 MDL 1

As explained in section 3.1.1, the first MDL includes only the overall dimensions of the building. The walls, floor, ceiling, windows, and doors are modeled to fulfill the requirements of this MDL. Elements are in the generic state and no material properties are assigned to them. Figure 5 shows the developed BIM model for this MDL using the Structure Sensor and Faro point cloud. Modeling the doors and windows was only feasible based on the Faro's point cloud.

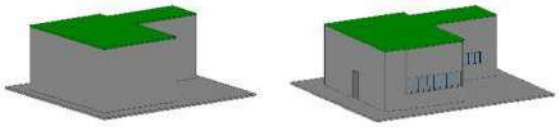

Figure 5. Developed BIM model based on Structure Sensor (left) and Faro (right)

Since a point cloud is a set of discrete points, the placement of a building's elements in the model depends somewhat on the modeller's judgment. Hence, a model's dimensions will be different for the same objects, which are modeled by different modellers. So, to investigate the effect of modellers on the dimensions of BIMs, six different modellers developed the BIMs for the first MDL, using the Structure Sensor and Faro point cloud. The wall height, floor area, and floor perimeter were extracted from each model and the mean value and standard deviation were calculated. According to the Table 1 the coefficient of variation differs from 0.84% to 3.52%, which may seem like a low value, but it is an unacceptable amount of error in absolute dimensions (up to 20 cm) from an engineering design perspective. It may be acceptable from a building operation or maintenance perspective. So, it can be observed, pending more sophisticated experiments and statistical analysis, that inconsistency between different modellers has a more significant effect on error than the type of scanner used in this case.

To compare the accuracy of the Faro laser scanner and the Structure Sensor, the true dimensions of the laboratory are measured by a laser meter. The "wall height", "floor area", and "floor perimeter" are calculated by using the true dimensions, and they are equal to 4.78m, 81.07m^2, and 44.41m, respectively. Also, the error range associated to these parameters are calculated by comparing their true values with the extracted data from the developed models. Figure 6 shows the error percentage range associated to Faro and Structure Sensor. According to this figure, the Structure Sensor dramatically underestimates the dimensions, especially for area and perimeter. On the other hand, the Faro results is closer to the true dimensions, which emphasizes its superior accuracy than Structure Sensor. The error range depends on the modeller's precision during the scan-to-BIM process. The maximum and minimum error range is related to wall height and floor perimeter modeled by Structure Sensor's point cloud, respectively. The error range associated to wall height modeled by the Structure Sensor's point cloud is higher than Faro. While the error range associated to each of the floor perimeter and the floor area is similar for Structure Sensor and Faro.

3.3.2 MDL 2

To develop the second MDL, material information is assigned to elements of the case study. The type of material is retrieved from the Faro point cloud and observations from the project's site. Also, the exact thickness of exterior walls is calculated by comparing the point cloud of the case study from inside and outside view.

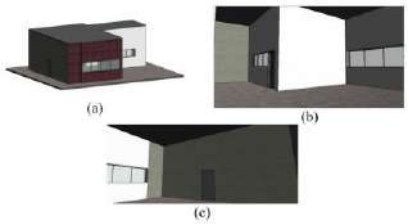

Figure 7. (a) Allocated materials to outside walls (brick cladding, concrete block, dry wall system)- (b) and (c) Allocated materials to inside walls and floor (dry wall system, concrete block, and carpet)

Table 1. The effect of having different modellers on the wall height

	Wall Height (m)		Floor Area (m^2)		Floor Perimeter (m)	
	Structure Sensor (m)	Faro Focus (m)	Structure Sensor (m^2)	Faro Focus (m^2)	Structure Sensor (m)	Faro Focus (m)
Modeller1	4.70	4.83	73.62	78.70	42.6	44
Modeller 2	4.40	4.70	76.21	81.09	42.8	44.40
Modeller 3	4.70	4.80	74.8	80.5	42.5	44.32
Modeller 4	4.90	4.90	74.70	81.5	42.7	44.6
Modeller 5	4.78	4.78	75.30	80.71	42.9	44.4
Modeller 6	4.72	4.88	70.09	75.32	41.9	43.2
Mean	4.70	4.81	74.12	79.64	42.57	44.15
Std. dev.	0.165	0.072	2.147	2.323	0.356	0.506
COV	0.0352	0.0150	0.0290	0.0292	0.0084	0.0115

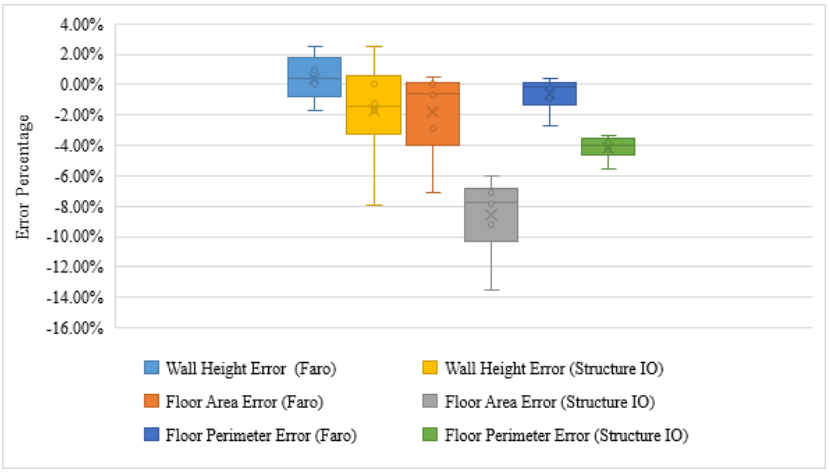

Figure 6. Error percentage ranges associated to Faro and Structure Sensor (Structure IO)

3.3.3 MDL 3

In this level, detail of plumbing, wiring network, HVAC system, and building fixtures and furniture, including their materials, are added to the BIM.

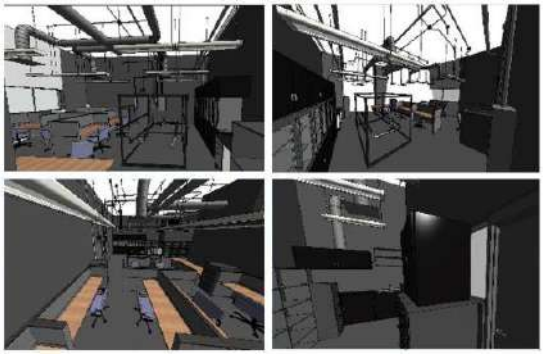

Figure 8. Developed BIM for MDL 3 based on Faro point cloud

3.4 Costs and Benefits

The cost of the scan-to-BIM process includes cost of purchasing a 3D acquisition device, license of BIM software, scanning and registering, and developing the BIM using scan-to-BIM techniques. The average renting cost of Faro M70 is CDN$650 per day. There is no renting option for Structure Sensor and it must be bought at the price of CDN$500. Also, the monthly price of an Autodesk Revit license is CDN$365.

To calculate the cost of scanning and registration, as well as developing the BIM, CDN$100 per hour is considered as the wage of an expert person. The time of completing each activity is multiplied by this wage and the outcome is the cost.

Table 4: The detail of cost calculation

Model Definition Level	MDL1	MDL1	MDL2	MDL3
Type of Scanner	Structure Sensor	Faro	Faro	Faro
3D Acquisition Device	500	650	650	650
BIM Software License	365	365	365	365
Scanning & Registration	17	200	200	200
Scan-to-BIM	33	33	67	2000
Total Cost (CDN$)	915	1248	1282	3215

4 Discussion

The cost of the scan-to-BIM process would increase as the BIM model becomes more detailed. Therefore, it depends on the needs, available budget, and project team's judgment to select which MDL is the most valuable for a project. If the project team is involved in finding a new usage for reviving a building, which is a high level of planning, an approximate estimation of buildings' dimensions might be sufficient for them. In this case, it makes sense to use Structure Sensor and MDL1, which has the lowest cost. At the end, the cost of this alternative would be lower than CDN$915, because of the salvage value of Structure Sensor (it can be sold as a second handed device).

On the other hand, selecting MDL3 will bring more value to an adaptive reuse project if the project involves detailed planning. The cost of this MDL is CDN$3,215. The capability of having exact time and cost estimation, material quantity estimation, disassembly plan, recycle and reuse plan, and design of electrical and mechanical facilities are several values that are provided by MDL3.

When the new usage was selected, and the project team is involved in high level of architectural design (e.g. assigning different spaces to different applications), the planning level is between the two-mentioned boundary level. In this case, MDL1 with Faro, or MDL2 makes more sense and provide both more value and sufficient information to the project.

5 Conclusion and Future Work

Based on the results of this research, the significance of the added value would be different from project to project and it is up to project team to decide which amount of information is optimal.

For the future plan, it is valuable to consider the losses associated to the lack of information in the planning levels and compare this to the cost of developing BIM for each MDL to make a decision in such a way that has the least cost and provides highest value to a project.

References

[1] B. V. Sanvido, A. Member, F. Grobler, K. Parfitt, M. Guvenis, and M. Coyle, "Critical Success Factor For Construction Projects," *Engineering*, vol. 118, no. 1, pp. 94–111, 1992.

[2] U. of Texas at Austin. Construction Industry Institute, G. E. Gibson, and R. Haggard, *Pre-project planning: Beginning a project the right way*. Institute, University of Texas at Austin, 1994.

[3] C. I. I. (CII)., "Pre-project planning handbook." Univ. of Texas at Austin Austin, Tex., 1995.

[4] C.-S. Cho and G. E. Gibson, Jr., "Development of a

Project Definition Rating Index (PDRI) for General Building Projects," *Constr. Congr. VI*, pp. 343–352, 2000.

[5] B. Becerik-Gerber, F. Jazizadeh, N. Li, and G. Calis, "Application areas and data requirements for BIM-enabled facilities management," *J. Constr. Eng. Manag.*, vol. 138, no. 3, pp. 431–442, 2011.

[6] B. Furht and S. Ahson, "Handbook of Mobile broadcasting DVB--H," *DMB, ISDB-T MEDIAFLO, 1st Ed. USA Taylor Fr. Gr.*, pp. 67–73, 2008.

[7] C. Langston, F. K. W. Wong, E. C. M. Hui, and L. Y. Shen, "Strategic assessment of building adaptive reuse opportunities in Hong Kong," *Build. Environ.*, vol. 43, no. 10, pp. 1709–1718, 2008.

[8] S. Conejos, C. Langston, and J. Smith, "Improving the implementation of adaptive reuse strategies for historic buildings," p. 11, 2011.

[9] E. Sugden, "The adaptive reuse of industrial heritage buildings: A multiple case studies approach," University of Waterloo, 2017.

[10] K. Dyson, J. Matthews, and P. E. D. Love, "Critical success factors of adapting heritage buildings: an exploratory study," *Built Environ. Proj. Asset Manag.*, vol. 6, no. 1, pp. 44–57, 2016.

[11] K. Samset, "Project management in a high-uncertainty situation," no. May, 1998.

[12] U. S. AIA, "Document E202TM-2008 Building Information Modeling Protocol Exhibit," *Am. Inst. Archit.*, 2008.

[13] C. Boton, S. Kubicki, and G. Halin, "The challenge of level of development in 4D/BIM simulation across AEC project lifecyle. A case study," *Procedia Eng.*, vol. 123, pp. 59–67, 2015.

[14] BIM Forum, "Level of Development Specification For Building Information Models and Data," 2018. [Online]. Available: https://bimforum.org/wp-content/uploads/2018/09/BIMForum-LOD-2018_Spec-Part-1_and_Guide_2018-09.pdf.

[15] CII Reseach Team no. 332, "Measuring Progress and Defining Productivity Metrics in Model-based Engineering.," 2017.

[16] Y. Turkan, F. Bosche, C. T. Haas, and R. Haas, "Automated progress tracking using 4D schedule and 3D sensing technologies," *Autom. Constr.*, vol. 22, pp. 414–421, 2012.

[17] G. S. Cheok, S. Leigh, and A. Rukhin, "Calibration experiments of a Laser Scanner," *NASA STI/Recon Tech. Rep. N*, vol. 2, 2002.

[18] M. Nahangi and C. T. Haas, "Automated 3D compliance checking in pipe spool fabrication," *Adv. Eng. Informatics*, vol. 28, no. 4, pp. 360–369, 2014.

[19] R. Volk, J. Stengel, and F. Schultmann, "Building Information Modeling (BIM) for existing buildings - Literature review and future needs," *Autom. Constr.*, vol. 38, pp. 109–127, 2014.

[20] J. Jung *et al.*, "Automation in Construction Productive modeling for development of as-built BIM of existing indoor structures," *Autom. Constr.*, vol. 42, pp. 68–77, 2014.

[21] A. Akbarnezhad, K. C. G. Ong, and L. R. Chandra, "Automation in Construction Economic and environmental assessment of deconstruction strategies using building information modeling," *Autom. Constr.*, vol. 37, pp. 131–144, 2014.

[22] I. S. O. Standard, "ISO 29481-1: 2010 (E), Building Information Modeling Information Delivery Manual Part 1: Methodology and Format (2010)," *Google Sch.*

[23] J. Wong and J. Yang, "Research and application of building information modelling (BIM) in the architecture, engineering and construction (AEC) industry: a review and direction for future research," in *Proceedings of the 6th international conference on innovation in architecture, engineering & construction (AEC)*, 2010, vol. 1, pp. 356–365.

[24] X. Liu, M. Eybpoosh, and B. Akinci, "Developing as-built building information model using construction process history captured by a laser scanner and a camera," in *Construction Research Congress 2012: Construction Challenges in a Flat World*, 2012, pp. 1232–1241.

[25] J. C. P. Cheng and L. Y. H. Ma, "A BIM-based system for demolition and renovation waste quantification and planning," in *Proceedings of the 14th International Conference on computing in Civil and Building Engineering (ICCCBE 2012)*, 2012.

Primitive Fitting Using Deep Geometric Segmentation

Duanshun Li[a]* and Chen Feng[b]*

[a]Department of Civil and Environmental Engineering, University of Alberta, Canada
[b]Tandon School of Engineering, New York University, United States
E-mail: duanshun@ualberta.ca, cfeng@nyu.edu

Abstract -

To identify and fit geometric primitives (e.g., planes, spheres, cylinders, cones) in a noisy point cloud is a challenging yet beneficial task for fields such as reverse engineering and as-built BIM. As a multi-model multi-instance fitting problem, it has been tackled with different approaches including RANSAC, which however often fit inferior models in practice with noisy inputs of cluttered scenes. Inspired by the corresponding human recognition process, and benefiting from the recent advancements in image semantic segmentation using deep neural networks, we propose BAGSFit as a new framework addressing this problem. Firstly, through a fully convolutional neural network, the input point cloud is point-wisely segmented into multiple classes divided by jointly detected instance boundaries without any geometric fitting. Thus, segments can serve as primitive hypotheses with a probability estimation of associating primitive classes. Finally, all hypotheses are sent through a geometric verification to correct any misclassification by fitting primitives respectively. We performed training using simulated range images and tested it with both simulated and real-world point clouds. Quantitative and qualitative experiments demonstrated the superiority of BAGSFit.

Keywords -

Geometric Segmentation; Primitive Fitting; As-Built BIM

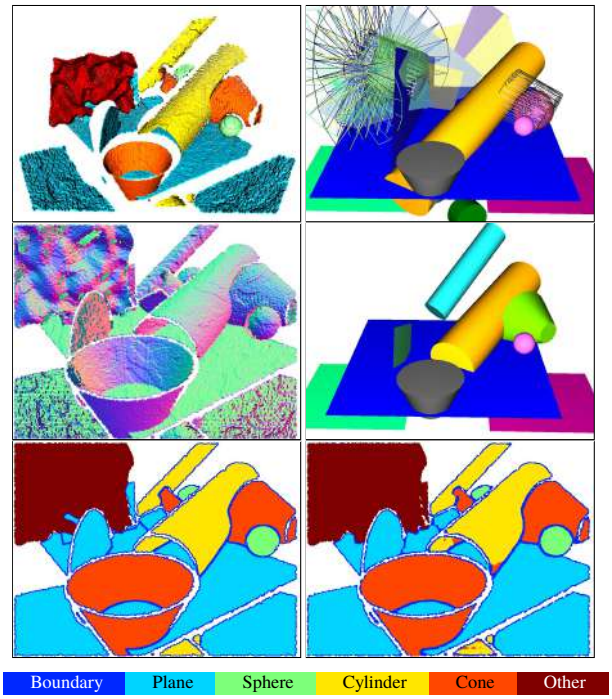

Figure 1: Primitive fitting on a simulated test range image (top left) with BAGSFit (middle right) vs. RANSAC (top right) [4]. Estimated normals (middle left) and ground truth labels (bottom left) are used to train a fully convolutional segmentation network in BAGSFit. During testing, the boundary-aware and thus instance-aware segmentation (bottom right) is predicted, and sent through a geometric verification to fit final primitives (randomly colored). Comparing with BAGSFit, the RANSAC-based method produces more misses and false detections of primitives (shown as transparent or wire-frame), and thus a less appealing visual result.

1 Introduction

The idea of decomposing a scene or a complex object into a set of simple geometric primitives for visual object recognition dates back as early as 1980s when Biederman proposed the object Recognition-By-Components theory [1], in which primitives were termed "geons". Although some real scenes can be more complicated than simple combinations of "geons", there are many useful ones that can be efficiently modeled for the purpose of as-built building information modeling [2, 3], where man-made structures are primarily composed of basic primitives. Also, it is desirable to model individual components in a building separately because they have different functions and were built with different types of material and construction methods. Separated components can then be used in building information modeling systems to carry its relevant semantic information and perform quantitative analysis.

This primitive fitting problem is a classic chicken-and-egg problem: with given primitive parameters, point-to-

*The authors contributed equally. And Chen Feng is the corresponding author.

primitive (P2P) membership can be determined by nearest P2P distance; and vise versa by robust estimation. The challenge comes when multiple factors present together: a noisy point cloud (thus noisy normal estimation), a cluttered scene due to multiple instances of a same or multiple primitive models, and also background points not explained by the primitive library. See Figure 1 for an example. The seminal RANSAC-based method [4] often tends to fit inferior primitives that do not well represent the real scene.

Different from existing work for this multi-model multi-instance fitting problem, we are inspired by human visual perception of 3D primitives. As found by many cognitive science researchers, human "observers' judgments about 3D shape are often systematically distorted" [5]. For example, when looking at a used fitness ball, many people would think of it as a sphere, although it could be largely distorted if carefully measured. This suggests that human brain might not be performing exact geometric fitting during primitive recognition, but rather rely on "qualitative aspects of 3D structure" [5] from visual perception.

Due to recent advancements in image semantic segmentation using convolutional neural networks (CNN) [6,7], it is natural to ask: whether CNN can be applied to this problem with geometric nature and find the P2P membership as segmentation on the range image without geometric fitting at all? Our answer is yes, which leads to the BAGSFit framework that reflects this thought process.

Contributions This paper contains the following key contributions:

- We present a methodology to easily obtain point-wise ground truth labels from simulated dataset for supervised geometric segmentation, demonstrate its ability to generalize to real-world dataset, and released the first simulated dataset [1] for development and benchmarking.
- We present a novel framework for multi-model 3D primitive fitting, which performs both qualitatively and quantitatively superior than RANSAC-based methods on noisy range images of cluttered scenes.
- We introduce this geometric segmentation task for CNN with several design analyses and comparisons.

Related Work Constructive Solid Geometry (CSG) and Boundary Representation (BRep) are the most common 3D representations in building information modeling (BIM) because of their simplicity and flexibility [8]. Both methods model a complex object with a collection of basic primitives. However, creating these models manually can be costly and time-consuming [9], especially for as-built modeling because the dimension of the objects are implicitly constrained by the scanned data. In [8], as-built modeling was separated into several auxiliary tasks, including geometric primitive fitting, point cloud clustering, shape fitting, and point cloud classification. The study of primitive fitting-based as-built modeling in construction mainly focus on the modeling of indoor scene with parametric planar surface [10] or industrial plant with cylinders [9,11]. Such methods lack the capability to deal with complicated buildings with planar walls, cylinder-shaped columns, cone-shaped roofs, and so on. The remaining of this section will investigate existing methods for multi-model primitive fitting.

By assuming the existence of potentially multiple classes of primitives in a scene, it is more realistic than the previous group, and thus more challenging when a cluttered scene is observed with noisy 3D sensors. Previous work with this assumption can be roughly grouped further into the following categories: *Segmentation*: Segmentation methods [12–14] segment a point cloud into individual clusters and performs classification and fitting either during the segmentation or afterwards.

RANSAC: Since the seminal work by Schnabel et al. [4], the idea of selecting sampled primitive hypotheses to maximize some scoring functions becomes a default solution to this problem. In this research, we chose this method as our baseline. In practice, the 3D sensor noise is often more structured (e.g., depth dependent noises for range images) than uniform or Gaussian in 3D as experimented in many of these papers. What really makes the problem difficult is that those noisy points belonging to other partially occluded primitive instances become outliers of the primitive to be fit at hand, causing false detections of "ghost" primitives not existed in the real scene but still with very small fitting errors and large consensus scores, e.g. the ghost cones fitted with cylinder and background points in the top right of Figure 1. More recently, prior probabilities or quality measure of the data [15,16] were used to improve the probability of sampling an all-inlier subset.

Energy Minimization: Unlike the sequential and greedy nature of RANSAC based methods, it is appealing in theory to define a global energy function in terms of P2P membership that once minimized results in desired solution [17–20]. However most of them are only shown on relatively small number of points of simple scenes without much clutters or occlusions, and it is unclear how they will scale to larger datasets due to the intrinsic difficulty and slowness of minimizing the energy function.

2 Framework Overview

Figure 2 gives an overview of the multi-model primitive fitting process by our BAGSFit framework. As introduced

[1] The dataset is available at https://github.com/ai4ce/BAGSFit.

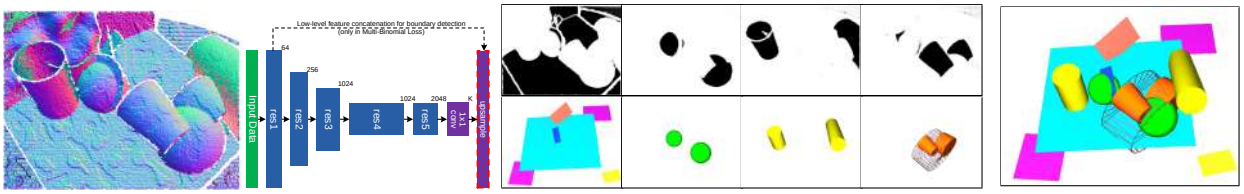

(a) CNN-based Segmentation (b) Geometric Verification (c) Fitted Primitives

Figure 2: BAGSFit overview. In 2a, a proper form of a range image, e.g., its normal map, is input to a fully convolutional neural network for segmentation. We use the same visualization style for the CNN as in [7], where each block means layers sharing a same spatial resolution, decreasing block height means decimating spatial resolution by a half, and red dashed lines means loss computation. The resulting segmentation probability maps $\mathbf{Y}_k$ (top row of 2b, darker for higher probability) for each primitive class k are sent through a geometric verification to correct any misclassification by fitting the corresponding class of primitives (bottom row of 2a). Finally, fitted primitives are shown in 2c. Without loss of generality, this paper only focuses on four common primitives: plane, sphere, cylinder, and cone.

above, the front-end of this framework (Figure 2a) mimics the human visual perception process in that it does not explicitly use any geometric fitting error or loss in the CNN. Instead, it takes advantage of a set of stable features learned by CNN that can robustly discriminate points belonging to different primitive classes. The meaning of a pixel of the output probability map (top row of Figure 2b) can be interpreted as how much that point and its neighborhood look like a specific primitive class, where the neighborhood size is the CNN receptive field size.

Such a segmentation map could already be useful for more complex tasks [21], yet for the sake of a robust primitive fitting pipeline, one cannot fully trust this segmentation map as it inevitably contains misclassification, just like all other image semantic segmentations. Fortunately, by separating pixels belonging to individual primitive classes, our original multi-model problem is converted to an easier multi-instance problem. Following this segmentation, a geometric verification step based on efficient RANSAC [4] incorporates our strong prior knowledge, i.e., the mathematical definitions of those primitive classes, to find the parametric models of the objects for each type of primitives. Note that RANSAC variants using prior inlier probability to improve sampling efficiency are not adopted in this research, because 1) they are orthogonal to the proposed pipeline; and 2) the robustness of primitive fitting is highly dependent on the spatial distribution of samples. Different from spatial consistency based methods [22, 23] mainly dealing with homography detection, in our 3D primitive fitting task, samples with points very close to each other usually lead to bad primitive fitting results [4]. Thus the potential of using the CNN predicted class probabilities to guide the sampling process, while being interesting, will be deferred for future investigations.

The advantage for this geometric segmentation task is that exact spatial constraints can be applied to detect correct primitives even with noisy segmentation results. One could use the inliers after geometric verification to correct the CNN segmentation results, similar to the CRF post-processing step in image semantic segmentation that usually improves segmentation performance.

3 Ground Truth from Simulation

Before going to the details of our segmentation CNN, we need to first address the challenge of preparing training data, because as most state-of-the-art image semantic segmentation methods, our CNN needs supervised training. To our best knowledge, we are the first to introduce such a geometric primitive segmentation task for CNN, and there is no existing publicly available datasets for this task. For image semantic segmentation, there have been many efforts to use simulation for ground truth generation. Yet it is hard to make CNNs trained over simulated data generalize to real world images, due to intrinsic difficulties of tuning a large number of variables affecting the similarities between simulated images and real world ones.

However, since we are only dealing with geometric data, and that 3D observation is less sensitive to environmental variations, plus observation noise models of most 3D sensors are well studied, we hypothesize that simulated 3D scans highly resemble real world ones such that CNNs trained on simulated scans can generalize to real world data. If this is true, for this geometric task, we can get infinite number of point-wise ground truth almost for free.

Although saved from tedious manual labeling, we still need a systematic way of generating both random scene layouts of primitives and scan poses so that simulated scans are meaningful and covers true data variation as much as possible. Due to the popular Kinect-like scanners, which mostly applied in indoor environment, we choose to focus on simulating indoor scenes. And note that this dose not limit our BAGSFit framework to only indoor situations. Given a specific type of scenes and scanners, one

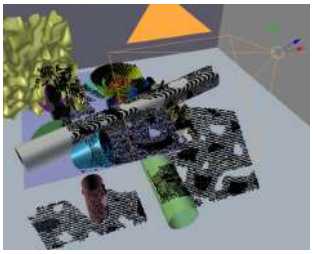

Figure 3: A simulated Kinect scan of a random scene. Black dots represents the scanned points.

should be able to adjust the random scene generation protocols similarly. Moreover, we hypothesize that the CNN is less sensitive to the overall scene layout. What's more important is to show the CNN enough cases of different primitives occluding and intersecting with each other.

Thus, we choose to randomly generate a room-like scene with 10 meters extent at each horizontal direction. An elevated horizontal plane representing a table top is generated at a random position near the center of the room. Other primitives are placed near the table top to increase the complexity. Furthermore, empirically, the orientation of cylinder/cone axis or plane normal is dominated by horizontal or vertical directions in real world. Thus several primitive instances at such orientations are generated deliberately in addition to fully random ones. For planes, two additional disk shaped planes are added to make the dataset more general. To make the training set more realistic, two NURBS surfaces (class name "Other" in Figure 1) are added, representing objects not explained by our primitive library in reality.

An existing scanner simulator, Blensor [24], was used to simulate VGA-sized Kinect-like scans, where class and instance IDs can be easily obtained during the virtual scanning process by ray-tracing. For each scene, we obtain a total number of 192 scans with varying view directions surrounding the scene. Totally 20 scenes were generated following this protocol. 18 scenes, i.e. 3456 scans, were split for training, and the other 2 scenes, i.e. 384 scans, were used for validation. Figure 3 shows the screenshot of such a scan. The test set is generated through a similar protocol, containing 20 scenes (each with 36 scans). Note that invalid points were converted to the zero-depth point avoiding computation issues.

4 Boundary Aware Geometric Segmentation

Our segmentation network (Figure 2a) follows the same basic network as described in [7], which is based on the 101-layer ResNet [25] with minor modifications to improve segmentation performance. While the semantic segmentation CNN architecture is actively being developed, there are several design choices to be considered to achieve the best performance on a given base network for our new task.

Position vs. Normal Input. The first design choice is about the input representation. Since we are dealing with 3D geometric data, what form of input should be supplied to the CNN? A naive choice is to directly use point positions as a 3-channel tensor input. After all, this is the raw data we get in reality, and if the CNN is powerful enough, it should be able to learn everything from this input form. However, it is unclear how or whether necessary to normalized it.

A second choice is to use estimated per-point unit normals as the input. This is also reasonable, because we can almost perceive the correct segmentation by just looking as the normal maps as shown in Figure 2a. Plus it is already normalized, which usually enables better CNN training. However, since normals are estimated from noisy neighboring points, one might have concerns about loss of information compared with the previous choice. And a third choice is to combine the first two, resulting in a 6-channel input, through which one might hope the CNN to benefit from merits of both.

Separate vs. Joint Boundary Detection. When multiple instances of a same primitive class occlude or intersect with each other, even an ideal primitive class segmentation can not divide them into individual segments, leaving a multi-instance fitting problem still undesirable for the geometric verification step to solve, which discounts the original purpose of this geometric segmentation. Moreover, boundaries usually contains higher noises in terms of estimated normals, which could negatively affect primitive fittings that use normals (e.g., 2-point based cylinder fitting). One way to alleviate the issue is to cut such clusters into primitive instances by instance-aware boundaries. To realize this, we also have two choices, 1) training a separate network only for instance boundary detection, or 2) treating boundary as an additional class to be segmented jointly with primitive classes. One can expect the former to have better boundary detection results as the network focuses to learn boundary features only, although as a less elegant solution with more parameters and longer running time. Thus it is reasonable to trade the performance a bit for the latter one. Note that with such a step, we could already move from category- to boundary- and thus instance-aware segmentation by region-grow after removing all instance-aware boundaries.

Handling of Background Class. When generating random scenes, we added NURBS modeling background points not explained by the four primitive classes, for a more realistic and challenging dataset. Thus we need to properly handle them in the CNN. Should we ignore back-

ground class when computing the loss, or add it as an additional class?

For all of the above design questions, we will rely on experiments to empirically select the best performing ones.

5 Geometric Verification and Evaluation

5.1 Verification by Fitting

Given the predicted probability maps $\{\mathbf{Y}_k\}$, we need to generate and verify primitive hypotheses and fit primitive parameters of the correct ones to complete our mission.

One direct way of hypothesis generation is to simply binarize the BAGS output $\{\mathbf{Y}_k\}$ by thresholding to produce a set of connected components, and fit only one k-th class primitive for a component coming from $\mathbf{Y}_k$. However, when the CNN incorrectly classify certain critical regions due to non-optimal thresholds, two instances can be connected, thus leading to suboptimal fittings or miss detection of some instances. Moreover, a perfect BAGS output may bring another issue that an instance gets cut into several smaller pieces due to occlusions (e.g., the top left cylinder in Figure 2a). And fitting in smaller regions of noisy scans usually result in false instance rejection or lower estimation accuracy. since the core contribution of this paper is to propose and study the feasibility of BAGS-Fit as a new strategy towards this problem, we leave it as our future work to develop more systematic ways to better utilize $\{\mathbf{Y}_k\}$ for primitive fitting.

In this work, we simply follow a classic "arg max" prediction on $\{\mathbf{Y}_k\}$ over each point, and get K groups of hypothesis points associated to each of the K primitive classes. Then we solve K times of multi-instance primitive fitting using the RANSAC-based method [4]. Note this does not completely defeat the purpose of BAGS. The original RANSAC-based method feed the whole point cloud into the pipeline and detect primitives sequentially in a greedy manner. Because it tends to detect larger objects first, smaller primitives close to large ones could often be missed, as their member points might be incorrectly counted as inlier of larger objects, especially if the inlier threshold is improperly set. BAGS can alleviate such effects and especially removing boundary points from RANSAC sampling is expected to improve its performance.

5.2 Primitive Fitting Evaluation

It is non-trivial to design a proper set of evaluation criteria for primitive detection and fitting accuracy, and we are not aware of any existing work or dataset that does so. It is difficult to comprehensively evaluate and thus compare different primitive fitting methods partly because 1) as mentioned previously, due to occlusion, a single instance are commonly fitted into multiple primitives, both of which may be close enough to the ground truth instance; and 2) such over detection might also be caused by improper inlier thresholds on a noisy data.

Pixel-wise average precision (AP) and AP of instances matched at various levels (50~90%) of point-wise intersection-over-union (IoU) are used for evaluating image based instance segmentation problems [26]. However, this typical IoU range is inappropriate for our problem. More than 50% IoU means at most one fitted primitive can be matched for each true instance. Since we don't need more than 50% of true points to fit a reasonable primitive representing the true one, this range is over-strict and might falsely reject many good fits: either more than 50% true points are taken by other incorrect fits, or during observation the true instance is occluded and split into pieces each containing less than 50% true points (see Figure 5 for more examples). After all, a large IoU is not necessary for good primitive fitting.

Thus, the IoU is replaced by intersection-over-true (IoT) in this problem. It indicates the number of true inliers of a predicted primitive over the total number of points in the true instance. Thus, a predicted primitive and a true instance is matched iff 1) IoT>30% and 2) the predicted primitive having the same class as the true instance. This indicates that one instance can have at most 3 matched predictions.

Based on the above matching criteria, a matched instance (if exists) can be identified for each predicted primitive. On the contrary, each true instance may have several best matching prediction candidates. To eliminate the ambiguity, the candidate that has the smallest fit error is selected as the best match. To be fair and consistent, fitting error is defined as the mean distance to a primitive by projecting all of the points in the true instance onto the predicted primitive. After the matches are found, *primitive average precision* (PAP) and *primitive average recall* (PAR) are used to quantify the primitive detection quality.

$$PAP = N_{p2t}/N_p, PAR = N_{t2p}/N_t, \quad (1)$$

where N_{p2t} is the number of predictions having a matched true instance, N_p the total number of predicted primitives, N_{t2p} the number of true instance with a best prediction, and N_t the total number of true instances, all counted over the whole test set.

6 Experiments and Discussion

6.1 Geometric Segmentation Experiments

Network Short Names. To explore answers to the questions raised in section 4, we designed several CNNs and their details with short names are listed as follows:

Table 1: Geometric segmentation evaluation. Red highlights the best along a column, and magenta for the top 3 best.

	Precision						Recall						IoU						F1						Accuracy
	BND	PLN	SPH	CYL	CON	AVE	BND	PLN	SPH	CYL	CON	AVE	BND	PLN	SPH	CYL	CON	AVE	BND	PLN	SPH	CYL	CON	AVE	
N+BO	0.944						0.820						0.781						0.877						0.964
P		0.915	0.811	0.867	0.642	0.809		0.971	0.620	0.715	0.664	0.743		0.891	0.599	0.655	0.488	0.658		0.939	0.664	0.762	0.611	0.744	0.871
N		0.979	0.915	0.934	0.727	**0.889**		**0.988**	**0.884**	0.788	**0.829**	**0.872**		**0.968**	**0.860**	0.752	0.633	**0.803**		**0.983**	**0.894**	0.826	0.734	**0.859**	**0.924**
PN		0.978	0.913	0.919	0.710	0.880		0.984	0.868	0.806	0.797	0.864		0.962	0.847	0.758	0.601	0.792		0.980	0.882	0.838	0.711	0.853	0.920
N+BAGS	0.868	0.963	0.908	0.926	**0.756**	**0.888**	0.849	0.976	0.874	**0.833**	0.821	**0.871**	0.752	0.941	0.848	**0.790**	**0.654**	**0.797**	0.858	0.969	0.884	**0.859**	**0.755**	**0.865**	0.918
N5		**0.980**	**0.917**	**0.940**	0.744	**0.895**		0.979	0.877	0.809	0.808	**0.868**		0.960	0.854	0.776	0.642	**0.808**		0.979	0.889	0.844	0.741	**0.863**	**0.940**
N5+BAGS	0.847	0.966	0.906	0.932	0.728	0.883	0.804	0.970	0.873	0.808	0.812	0.853	0.702	0.939	0.845	0.769	0.630	0.777	0.825	0.968	0.883	0.842	0.732	0.850	**0.921**

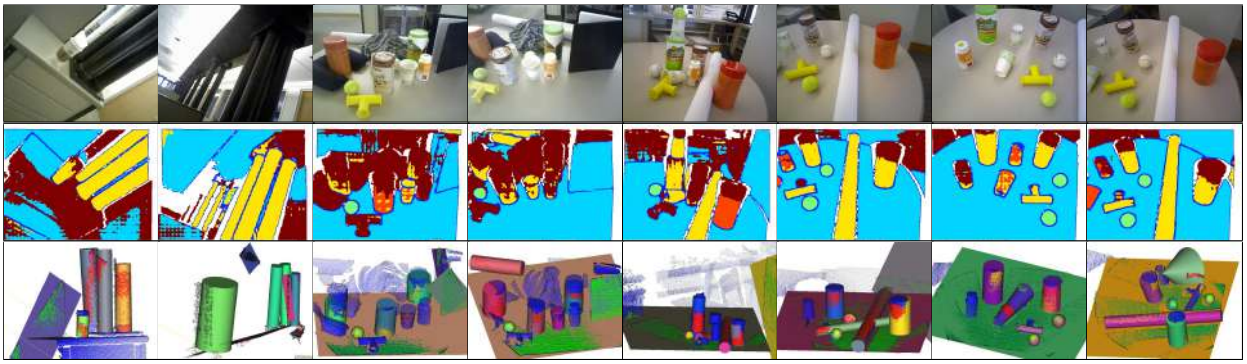

Figure 4: BAGSFit (**N5+BAGS**) on real Kinect scans. Top: RGB image of the scanned scene. Middle: segmentation results. Bottom: fitted primitives (randomly colored) rendered together with real scans.

- **P/N/PN**. Basic networks, using position (**P**), normal (**N**), or both (**PN**) as input, trained with a multinomial loss function, outputting a 4-channel *mutual-exclusive* class probability maps (i.e., each pixel's probabilities sum up to one, $K = 4$). Background class points, the NURBS, are ignored for loss computation.
- **N+BAGS**. Network trained with normal input and BAGS labels (i.e., instance-aware boundary as an additional class jointly trained, $K = 5$).
- **N5**. Same as basic network **N** except treating the background class as an additional class involved in loss computation ($K = 5$).
- **N5+BAGS**. Same as **N+BAGS** except trained using a multi-binomial manner (i.e., boundary and NURBS are two additional classes jointly trained, $K = 6$).
- **N+BO**. Same as **N** except only trained to detect boundary (i.e., a binary classifier, $K = 2$).

Implementation Details. We implemented the geometric segmentation CNNs using *Caffe* [27] and *DeepLabv2* [6]. Normals were estimated by PCA using a 5×5 window. We use meters as the unit for networks requiring position input. Instance-aware boundaries were calculated if not all pixels belong to a same instance (or contain invalid points) in a 5×5 window. Input data size was randomly cropped into 440×440 during training time, while full VGA resolution was used during test time. All of our networks were trained with the following hyper-parameters tuned on the validation set: 50 training epochs (i.e. 17280 iterations), batch size 10, learning rate 0.1 linearly decreasing to zero until the end of training, momentum 0.9, weight decay 5e-4. The networks were trained and evaluated on several NVIDIA TITAN X GPUs each with 12 GB memory, with a 2.5Hz testing frame rate.

Discussions. Evaluation results of all 12 networks on the test set of 720 simulated scans are in table 1.

1. Comparing the **P/N/PN** rows, we found that normal input turned out to be the best, and interestingly outperforming combination of both normal and position. This may be caused by the difficulty in normalizing position data for network input.
2. Comparing the **N** with **N+BAGS**, we found that adding additional boundary detection to the segmentation only have very small negative influences to the segmentation performance. This is appealing since we used a single network to perform both segmentation and boundary detection. Further comparing the **N+BAGS** with **N+BO**, we found that BAGS in fact increases the boundary recall comparing to **N+BO** that only detects boundaries.
3. Comparing the **N5** with **N**, we found that the effect of ignoring background class is inconclusive in terms of significant performance changes, which however suggests the benefit of jointly training the background class, as this enables the following steps to focus only on regions seemingly explainable by the predefined primitive library.

Just for reference, we tried SVM using neighboring 7×7 or 37×37 normals or principal curvatures for this task, and the highest pixel-wise accuracy we obtained after many

Table 2: Primitive fitting evaluation. Red highlights the best along a column, while magenta highlights the top 3 best.

	No. Primitives Fitted (N_p)					No. Matched Instance(N_{t2p})					$\frac{N_{t2p}^{all}}{N_p^{all}}$	Primitive Average Precision (PAP)					Primitive Average Recall (PAR)					Fitting Error (cm)				
	PLN	SPH	CYL	CON	ALL	PLN	SPH	CYL	CON	ALL		PLN	SPH	CYL	CON	ALL	PLN	SPH	CYL	CON	ALL	PLN	SPH	CYL	CON	ALL
ERANSAC	4596	1001	2358	3123	11078	2017	542	942	879	4380	0.395	0.453	0.541	0.402	0.286	0.403	0.500	0.432	0.403	0.443	0.456	0.915	0.324	**0.766**	0.954	0.810
P	5360	621	2242	2037	10260	2448	591	1219	944	5202	0.507	0.470	0.952	0.549	0.468	0.516	0.607	0.471	0.521	0.476	0.541	0.936	**0.248**	0.931	**0.519**	**0.759**
N	4617	961	2789	2492	10859	**2565**	**870**	1456	1254	**6145**	0.566	0.571	0.905	0.532	0.507	0.576	**0.636**	**0.693**	0.623	**0.633**	**0.640**	0.903	0.403	1.229	0.657	0.866
PN	4537	888	3172	2133	10730	2522	859	**1498**	1197	**6076**	0.566	0.572	0.967	0.480	0.570	0.577	0.625	0.684	**0.641**	0.604	**0.632**	0.903	0.397	1.196	0.628	0.852
N+BAGS	3893	845	2299	2108	9145	2279	796	1453	1149	5677	**0.621**	0.594	0.942	0.637	0.548	**0.626**	0.565	0.634	0.621	0.580	0.591	0.765	0.363	1.144	0.587	**0.768**
N5	3701	863	1874	1876	8314	2490	859	1458	**1226**	**6033**	**0.726**	**0.693**	0.995	0.793	**0.663**	**0.740**	0.617	0.684	0.624	0.619	**0.628**	0.841	0.395	1.163	0.617	0.815
N5+BAGS	3500	804	1765	1730	7799	2254	804	1397	1129	5584	**0.716**	0.654	**1.000**	**0.796**	0.658	**0.723**	0.559	0.640	0.598	0.570	0.581	**0.742**	0.367	1.096	0.555	**0.740**

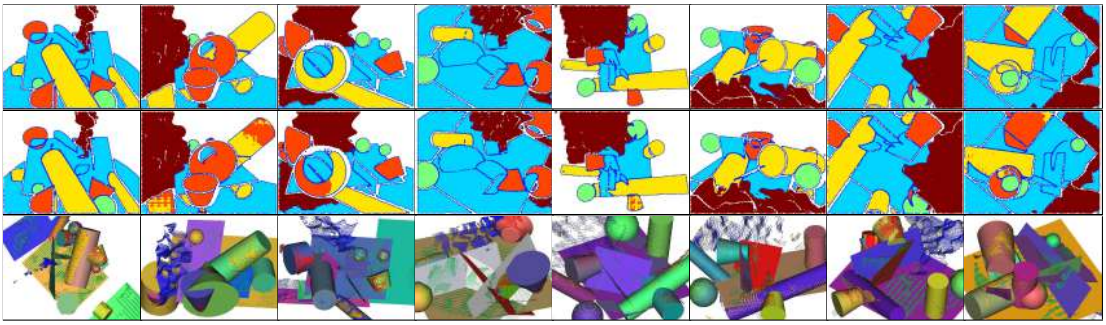

Figure 5: BAGSFit (**N5+BAGS**) on simulated test scans. Top: Ground truth labels. Middle: segmentation results. Bottom: fitted primitives (randomly colored) rendered together with real scans.

parameter tuning is only 66%.

Generalizing to Real Data. Even though we did not tune the simulated scanner's noise model to match our real Kinect scanner, Figure 4 shows that the network trained with simulated scans generalizes well to real world data.

6.2 Primitive Fitting Experiments

For fitting primitives, we used the original efficient RANSAC implementation [4] both as our baseline method (short name **ERANSAC**) and for our geometric verification.

Experiment Details. We used the following parameters required in [4] for all primitive fitting experiments, tuned on the validation set in effort of maximizing **ERANSAC** performance: min number of supporting points per primitive 1000, max inlier distance 0.03m, max inlier angle deviation 30 degrees (for counting consensus scores) and 45 degrees (for final inlier set expansion), overlooking probability 1e-4. The simulated test set contains 4033 planes, 1256 spheres, 2338 cylinders, 1982 cones, and in total 9609 primitive instances.

Discussions. Using respective network's segmentation as input to the geometric verification, the primitive fitting results were evaluated on the simulated test set and summarized in table 2 together with the **ERANSAC** baseline.

1. **ERANSAC** performance is significantly lower than most variants of BAGSFit, in accordance with our qualitative evaluation.
2. **N5** related experiments receives highest PAP scores, which is reasonable due to the recognition and removal of background classes that greatly reduce the complexity of scenes.
3. In terms of average fitting error, **N+BAGS** < **N**, **N5+BAGS** < **N5** which strongly supports the benefit of BAGS as mentioned in section 5.1.
4. **N5+BAGS** gets the lowest fitting error, benefiting from both background and boundary removal.

More results. Figure 5 shows more testing results.

7 Future Work

Our next step is to compare BAGSFit with MaskR-CNN [28], quantitatively evaluate it on real scans, and apply it in as-built BIM generation. We also plan to extend the network so it can directly predict primitive parameters.

Acknowledgment

This work was supported by Mitsubishi Electric Research Labs (MERL) and New York University. We thank Yuichi Taguchi, Srikumar Ramalingam, Zhiding Yu, Teng-Yok Lee, Esra Cansizoglu, and Alan Sullivan for their helpful comments.

References

[1] Irving Biederman. Recognition-by-components: a theory of human image understanding. *Psychological review*, 94(2):115, 1987.

[2] Pingbo Tang, Daniel Huber, Burcu Akinci, Robert Lipman, and Alan Lytle. Automatic reconstruction of as-built building information models from laser-scanned point clouds: A

review of related techniques. *Automation in construction*, 19(7):829–843, 2010.

[3] Jianxiong Xiao and Yasutaka Furukawa. Reconstructing the world's museums. *Int'l J. Computer Vision*, 110(3):243–258, 2014.

[4] Ruwen Schnabel, Roland Wahl, and Reinhard Klein. Efficient ransac for point-cloud shape detection. In *Computer Graphics Forum*, volume 26, pages 214–226. Wiley Online Library, 2007.

[5] James T Todd. The visual perception of 3d shape. *Trends in cognitive sciences*, 8(3):115–121, 2004.

[6] Liang-Chieh Chen, George Papandreou, Iasonas Kokkinos, Kevin Murphy, and Alan L Yuille. Deeplab: Semantic image segmentation with deep convolutional nets, atrous convolution, and fully connected crfs. *arXiv preprint arXiv:1606.00915*, 2016.

[7] Z. Yu, C. Feng, M. Y. Liu, and S. Ramalingam. CASENet: Deep category-aware semantic edge detection. In *IEEE Conf. on Computer Vision and Pattern Recognition*, 2017.

[8] Viorica Pătrăucean, Iro Armeni, Mohammad Nahangi, Jamie Yeung, Ioannis Brilakis, and Carl Haas. State of research in automatic as-built modelling. *Advanced Engineering Informatics*, 29(2):162–171, 2015.

[9] Soon-Wook Kwon, Frederic Bosche, Changwan Kim, Carl T Haas, and Katherine A Liapi. Fitting range data to primitives for rapid local 3d modeling using sparse range point clouds. *Automation in construction*, 13(1):67–81, 2004.

[10] Jaehoon Jung, Sungchul Hong, Seongsu Jeong, Sangmin Kim, Hyoungsig Cho, Seunghwan Hong, and Joon Heo. Productive modeling for development of as-built bim of existing indoor structures. *Automation in Construction*, 42:68–77, 2014.

[11] Joohyuk Lee, Hyojoo Son, Changmin Kim, and Changwan Kim. Skeleton-based 3d reconstruction of as-built pipelines from laser-scan data. *Automation in construction*, 35:199–207, 2013.

[12] Aleš Leonardis, Alok Gupta, and Ruzena Bajcsy. Segmentation of range images as the search for the best description of the scene in terms of geometric primitives. 1990.

[13] Zahra Toony, Denis Laurendeau, and Christian Gagné. Describing 3d geometric primitives using the gaussian sphere and the gaussian accumulator. *3D Research*, 6(4):42, 2015.

[14] Kristiyan Georgiev, Motaz Al-Hami, and Rolf Lakaemper. Real-time 3d scene description using spheres, cones and cylinders. *arXiv preprint arXiv:1603.03856*, 2016.

[15] O. Chum and J. Matas. Matching with prosac - progressive sample consensus. In *Proc. IEEE Conf. Computer Vision and Pattern Recognition (CVPR)*, pages 220–226, 2005.

[16] B. J. Tordoff and D. W. Murray. Guided-mlesac: faster image transform estimation by using matching priors. *IEEE Trans. Pattern Anal. Mach. Intell.*, 27(10):1523–1535, 2005.

[17] Hossam Isack and Yuri Boykov. Energy-based geometric multi-model fitting. *Int'l J. Computer Vision*, 97(2):123–147, 2012.

[18] Oliver J Woodford, Minh-Tri Pham, Atsuto Maki, Riccardo Gherardi, Frank Perbet, and Björn Stenger. Contraction moves for geometric model fitting. In *Proc. European Conf. Computer Vision (ECCV)*, pages 181–194. Springer, 2012.

[19] Daniel Barath and Jiri Matas. Multi-class model fitting by energy minimization and mode-seeking. *arXiv preprint arXiv:1706.00827*, 2017.

[20] Paul Amayo, Pedro Pinies, Lina M Paz, and Paul Newman. Geometric multi-model fitting with a convex relaxation algorithm. *arXiv preprint arXiv:1706.01553*, 2017.

[21] Wolfram Martens, Yannick Poffet, Pablo Ramón Soria, Robert Fitch, and Salah Sukkarieh. Geometric priors for gaussian process implicit surfaces. *IEEE Robotics and Automation Letters*, 2(2):373–380, 2017.

[22] T. Sattler, B. Leibe, and L. Kobbelt. Scramsac: Improving ransac's efficiency with a spatial consistency filter. In *Proc. IEEE Int'l Conf. Computer Vision (ICCV)*, pages 2090–2097, 2009.

[23] Kai Ni, Hailin Jin, and F. Dellaert. Groupsac: Efficient consensus in the presence of groupings. In *Proc. IEEE Int'l Conf. Computer Vision (ICCV)*, pages 2193–2200, 2009.

[24] Michael Gschwandtner, Roland Kwitt, Andreas Uhl, and Wolfgang Pree. Blensor: blender sensor simulation toolbox. *Advances in visual computing*, pages 199–208, 2011.

[25] K. He, X. Zhang, S. Ren, and J. Sun. Deep residual learning for image recognition. In *Proc. IEEE Conf. Computer Vision and Pattern Recognition (CVPR)*, 2016.

[26] Min Bai and Raquel Urtasun. Deep watershed transform for instance segmentation. *arXiv preprint arXiv:1611.08303*, 2016.

[27] Yangqing Jia, Evan Shelhamer, Jeff Donahue, Sergey Karayev, Jonathan Long, Ross Girshick, Sergio Guadarrama, and Trevor Darrell. Caffe: Convolutional architecture for fast feature embedding. In *ACM Multimedia*, 2014.

[28] Kaiming He, Georgia Gkioxari, Piotr Dollár, and Ross Girshick. Mask r-cnn. In *Proc. IEEE Int'l Conf. Computer Vision (ICCV)*, pages 2980–2988, 2017.

Employing Simulated Annealing Algorithms to Automatically Resolve MEP Clashes in Building Information Modeling Models

H.C. Hsu[a] and I.C. Wu[a]

[a]Department of Civil Engineering, National Kaohsiung University of Science and Technology, Kaohsiung, Taiwan

E-mail: F107141125@nkust.edu.tw, kwu@ nkust.edu.tw

Abstract –

Building Information Modeling (BIM) covers the whole lifecycle of a building and facilitates the coordination of activities in the design, construction, and operation stages. However, during the design stages of pre-construction, it is time-consuming for a BIM project team to resolve design clashes as they integrate models finished by individual team members into a composite master model. To effectively overcome the issue, this study proposes a computer programming system. Based on the application programming interface provided by BIM software, a simulated annealing algorithm is employed to determine the layout modifications to minimize the number of design clashes. In this paper, the mechanical, electrical and plumbing (MEP) systems in a clean room on the first floor of an integrated circuit assembly factory are used to validate the effectiveness of the proposed system. The experimental results reveal the feasibility and effectiveness of the proposed system.

Keywords –

Building information modeling; Clash resolution; Simulated annealing algorithms

1 Introduction

As building information modeling (BIM) software matures, BIM is gradually becoming conventional in both design and construction practice worldwide [1]. As first defined in the National BIM Standard–United States®, a BIM model is a digital representation of the physical and functional characteristics of a facility. As such, BIM serves as a shared knowledge resource for information about a facility, forming a reliable basis for decisions during its life cycle from inception onward [2]. In addition to helping in the design stage, BIM provides decision makers with the ability to make informed decisions across the lifecycle, in the construction stage [3], the project closeout stage [4], and the facility management stage [5]. BIM has also become a platform for project management teams to collaborate [6]. Through the digital portal provided by BIM software, team members such as architects, structural engineers, and mechanical, electrical and plumbing (MEP) engineers can collaborate on a design and share their knowledge of a construction development at the design, construction, and post-construction stages [7]. During the design stages of pre-construction, BIM models finished by team members are integrated into a composite master model, which is then tested to detect design clashes [8], The design clashes defined in [6] are 'positioning errors', where building components overlap each other when original individual designer models are merged. During the construction phase, rework caused by design clashes undetected in the pre-construction stage is usually costly. However, resolving these design clashes is a time-consuming task and is imperative to project performance [9]. Obviously, it presents a great challenge for project team members to ensure there are no clashes in a composite master model within a reasonably short time, even with the use of BIM software.

In addition to the modeling functions, BIM software provides an application programming interface (API) for users to effectively achieve multitudinous applications of BIM models. In previous studies, Mangal and Cheng [10] employed a hybrid genetic algorithm (GA) and the API provided by BIM software to develop an automatic system for the optimization of steel reinforcement in RC buildings. Lin and Lin [4] took advantage of API to propose a final as-built BIM model management system

for owners to handle the inspection, modification, and confirmation work beyond project closeout. Based on a repetitive trial-and-error procedure, Xue and Lu [11] presented a novel segmentation-free, derivative-free optimization approach that translates as-built BIMs from two-dimensional images into an optimization problem of fitting BIM components within architectural and topological constraints. Moreover, to evaluate the overall thermal transfer value of the building envelope and the cost of construction, Lim and Majid [12] developed a BIM-GA optimization method by using the functionalities of BIM software, Autodesk Revit, the iterated learning of GA, and the computer programming of PHP. In fact, their method [12] can also be achieved by directly using the API provided by Revit.

To facilitate designer to resolve the clashes, numerous emerging model collaboration systems, such as EXPRESS Data Manager and BIM 360, have been developed to make it possible to have the ability to manage the coordinated workflow required for clash resolution. However, this function still requires human intervention [15].

To automatically resolve the design clashes in a composite master model, this study developed an effectively system by using the API provided by Revit to control building components and adopting a simulated annealing (SA) algorithm [13] to implement iterated learning to simulate coordination cycles. In consideration of the fact that when some clashes are resolved, other clashes may occur, the iterated learning process of the SA algorithm is used. Heuristic optimization methods, such as GA and SA, have been extensively applied to searching the fittest solutions of combinatorial problems. Single thread processing is more efficient for design clashes resolving problem. Therefore this paper adopts SA. The related works such like Hackl, et al. [14] utilized SA to determine the optimal restoration programs for transportation networks. To tackle the search issue in BIM projects. Zeferino, et al. [16] present an efficient simulated annealing (SA) algorithm for solving a regional wastewater system planning model. Focusing on MEP systems, our program detects design clashes with their coordinates and then makes modifications to building components, such as moving or revising them, to gradually minimize the number of design clashes. In the experiment, we tested our system on a real case that occurred during the compilation of a federated BIM model for the MEP systems in the clean room in a factory. The new layout of the MEP systems could be taken as the suggested prototype for the discussion of clash resolution in the design team meeting.

The remainder of this paper is organized as follows: Section 2 introduces the simulated annealing (SA) algorithm. Section 3 explains the proposed system. Section 4 addresses the experimental data and discusses the experimental results. Finally, Section 5 provides the conclusion to this paper.

2 Simulated Annealing Algorithm

The SA algorithm proposed by Kirkpatrick and Gelatt [13] is an extension of the Monte Carlo (MC) method and is widely applied to approximating the global optimum in combinatorial problems. The name SA comes from annealing in metallurgy, wherein the states of molecular structures of a material are changed by heating and cooling. Heating and cooling the material affects both the temperature and the thermodynamic free energy. SA thus employs MC to generate random samples to simulate the states of a thermodynamic system. Unlike MC, which is a completely random method, SA has a mechanism to control the movement of molecules as the temperature decreases to make a converged learning process. The learning process of SA is briefly described in pseudocode in Figure 1.

```
// s0: a given initial state (solution)
// itermax: the maximum iteration number
// T0: a given initial temperature
function SimAnneal(s0, itermax , T0)
    s = s0; // Set current states as s0
    T = T0; // Set current temperature T as T0
    i=1; // Set the iteration number as 1
    while (i ≤ itermax)
        // Create a feasible neighbor state snew
        snew = CreateOneNeighbor(s);
        // The energy function which updates T according to
        iteration times
        T = UpdateTemperature(i, T);
        // Check if accept snew under T
        if Cost(s) ≤ Cost (snew)
            s = snew; i++;
        else
            // Giving an opportunity of accepting a worse snew
            if P(Cost(s), Cost(snew), T) ≥ Random(0, 1)
                s = snew; i++;
            end if
        end if
    end loop
    return s;
end function
```

Figure 1. The pseudocode of simulated annealing

3 The Proposed System Framework

The objective of this study was to develop an effective programming system to automatically resolve the design clashes of MEP systems when BIM models finished by individual team members are integrated into a federated BIM model. The iterated learning process of the proposed system has five steps, as shown in Figure 2. Through the API provided by Revit, attributes of building components such as types, shapes, lengths, widths, and

positions (coordinates) can be controllable and revisable, and even clash coordinates can be detected. More information about the use of the Revit API is available on the official Revit website(http://www.revitapidocs.com/). Below, we will first explain the definition of the clash list used in our system, since the clash list is the core of our system. Then the five steps in Figure 2 will be addressed.

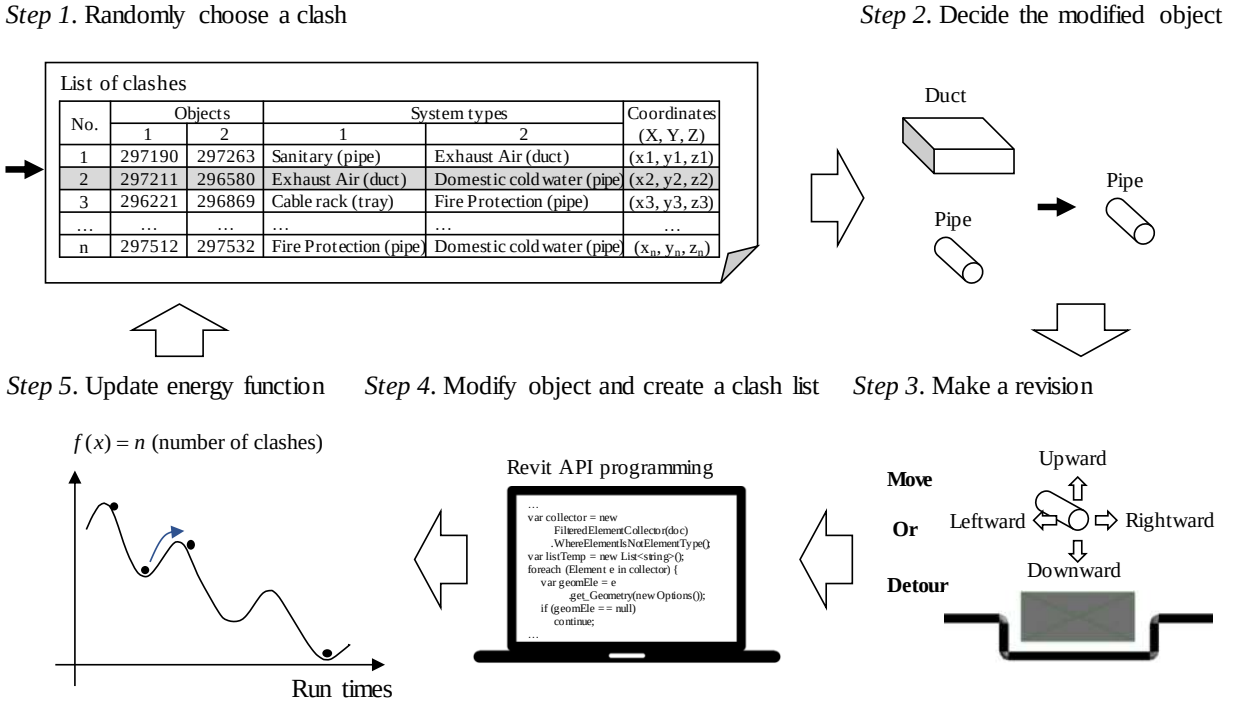

No.	Objects		System types		Coordinates
	1	2	1	2	(X, Y, Z)
1	297190	297263	Sanitary (pipe)	Exhaust Air (duct)	(x1, y1, z1)
2	297211	296580	Exhaust Air (duct)	Domestic cold water (pipe)	(x2, y2, z2)
3	296221	296869	Cable rack (tray)	Fire Protection (pipe)	(x3, y3, z3)
…	…	…	…	…	…
n	297512	297532	Fire Protection (pipe)	Domestic cold water (pipe)	(x_n, y_n, z_n)

Figure 2. The five steps in the iterated learning process of the proposed system

3.1 Definition of Clash List

The core of our system is the clash list, which is created by our programming through the Revit API, and the mission is to minimize the number of detected clashes. An example of a clash list is provided in Table 1, in which there are three main attributes: objects, systems, and three-dimensional coordinates.

Table 1. An example of a clash list used in this study

No.	Objects		System types		Coordinates
	1	2	1	2	(X, Y, Z)
1	297190	297263	Sanitary (pipe)	Exhaust Air (duct)	(x1, y1, z1)
2	297211	296580	Exhaust Air (duct)	Domestic cold water (pipe)	(x2, y2, z2)
3	296221	296869	Cable rack (tray)	Fire Protection (pipe)	(x3, y3, z3)
…	…	…	…	…	…
n	297512	297532	Fire Protection (pipe)	Domestic cold water (pipe)	(x_n, y_n, z_n)

1. The “objects” attribute shows a pair of building components whose geometric shapes intersect. The values of the objects are the identifiers (id) given by Revit.
2. The “systems” attribute lists the MEP systems to which the two intersected objects belong.
3. The “coordinates” attribute is the three-dimensional position of the clash between object 1 and object 2, plotted in three values of X-axis, Y-axis, and Z-axis. Based on a clash coordinate and the shape profiles of the two objects, our program can revise an object or decide on a moving distance of an object, or the whole system, from the original coordinates to a new position to avoid the clash.

3.2 The Operation Principles

The operation principles are used to determine which of the two objects should be modified and what revision options can be selected in a clash instance. There are two principles, the priority of systems and the available revision options. It is notable that these principles can be experience-based, case-based, or country-based.

According to the case examined in this study, the contents of the two principles are briefly described as follows:

1. Based on [13], the priority order of MEP systems and the reasons are listed in Table 2, in which parts of the system names have been revised to be consistent with the words used in Revit. For example,

if the systems of object 1 and object 2 are "Fire Protection (pipe)" and "Domestic cold water (pipe)", respectively, object 2 should be chosen for revision, rather than object 1.

2. The revision options for MEP objects are defined in Table 3, in which the circles denote the action options available for an object. For instance, "Sanitary pipe" has two possible revision actions, "Moving" and "Sloping", while "Duct" only has the "Moving" action. Note that only the revision action "Moving" is available when our system determines to execute a revision on a whole MEP system to which object 1 or object 2 belongs. Moreover, a brief description of the three revision actions are summarized in Table 4.

Table 2. The priority order for sequential comparison process (source [13] and revised in this paper)

System	Priority/special notes
Exhaust Air (duct)	Usually first due to large size of components
Supply Air (duct)	Follows HVAC Dry due to interdependence of these systems
Sanitary (pipe)	Design criteria for slope essential for system performance
Process piping	Takes the first priority if critical to manufacturing process
Fire Protection (pipe)	Most flexible routing, especially small diameter pipe
Domestic hot/cold water (pipe)	Lower priority because less difficult to re-route
Cable rack (tray)	Flexible routing within safety and architectural requirements
Control systems	Flexible routing but must limit bend radius for pneumatic tubes
Telephone/Data communications	Flexible routing but must limit bend radius for fiber optic cables

Table 3. The revision options for MEP objects

Actions	Sanitary pipe	Duct	Cable rack	Other pipes
Moving	○	○	○	○
Revising			○	○
Sloping	○			

Table 4. The descriptions of revision actions

Actions	Descriptions
Moving	Move an object or a system upward, downward, leftward, or rightward to avoid clashes.
Revising	Make a pipe or a cable rack take a roundabout way to avoid clashes.
Sloping	Adjust the slope of a sanitary pipe to avoid clashes. The minimum acceptable ratios of slopes are defined as 1:100 in USA and 2:100 in Japan. This revision action is only applicable to sanitary pipe.

3.3 The Learning Steps

In this subsection, we present the five steps in Figure 2, which are an iterated learning process in our system. Below, the details of the five steps are explained.

Step 1. Randomly select a clash instance from the clash list as a start of the current iterated learning. Suppose that the No. 2 instance in Figure 2 is chosen.

Step 2. For the selected clash instance, decide which of object 1 and object 2 should be chosen for modification according to the priority order of their systems, as mentioned in section 3.2. For the No. 2 instance, for example, since the systems of object 1 and object 2 are "Exhaust Air (duct)" and "Domestic cold water (pipe)", respectively, object 2 should be chosen for revision.

Step 3. Revise the object or its system as decided in *Step 2* through Revit API. Here, we define a parameter $\theta \in [0, 1]$ as the criterion to determine whether the revision is executed on an object or its whole system. Moreover, we also define a random seed (*rs*) drawn from a uniform distribution [0, 1] as a tester. The revision action that will be taken depends on the following conditions:

1. When $rs \leq \theta$, the modification will be made on the object. According to Table 3 and the object's system, randomly choose an action to make the modification. For example, the candidate actions for object 2 (a pipe) are "Moving" and "Revising".
2. When $rs > \theta$, the modification will be made on the object's system. Our system will then move the whole system.

After deciding to revise an object or its system, the proposed system will compute the spatial information of the object as a reference for the decision on revision actions. The spatial information is the available distance aggregated in the four directions (up, down, left, and right) of the object. First, our system calculates the minimum moving distances based on the geometric parameters of object 1 and object 2, such as the widths, lengths, and heights, and the clash coordinates obtained from the Revit API. In the example shown in Figure 3, it is better to move the pipe upward or downward rather than leftward or rightward. Then our system will compute the distances between an object and the objects of the other systems in its neighborhood and the limit of vertical clearance. In Figure 4 (a), for example, there is a grey pipe under the black pipe. If the black pipe were moved downward to avoid the original clash, a new clash between the two pipes would occur, as shown in Figure 4 (b). Accordingly, the black pipe should move farther to

avoid the new possible clash. The direction having the minimum aggregated distance is adopted for movement, and a construction tolerance (five cm in this study) is added to the aggregated distance to prevent an imprecise construction collision from being caused by insufficient distance. In this study, the action "Revising" is only applicable when the direction is determined to be up or down. Note that once an object is moved, parts of the objects in the same system, such as its branches or the object from which it branches, would need to be accordingly moved and corresponding lengths added or subtracted.

The steps from *Step 1* to *Step 3* are actually the content in the function **CreateOneNeighbor** in SA in Figure 1. The pseudo code of the function **CreateOneNeighbor** is provided in Figure 5.

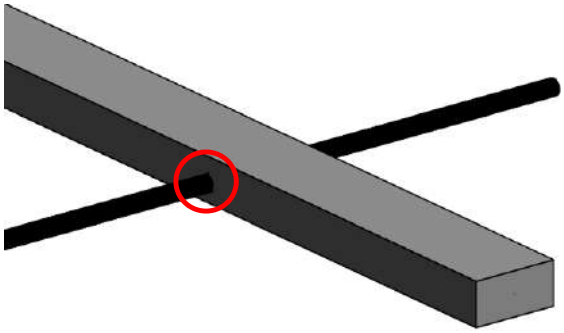

Figure 3. An example of a clash between a duct and a pipe.

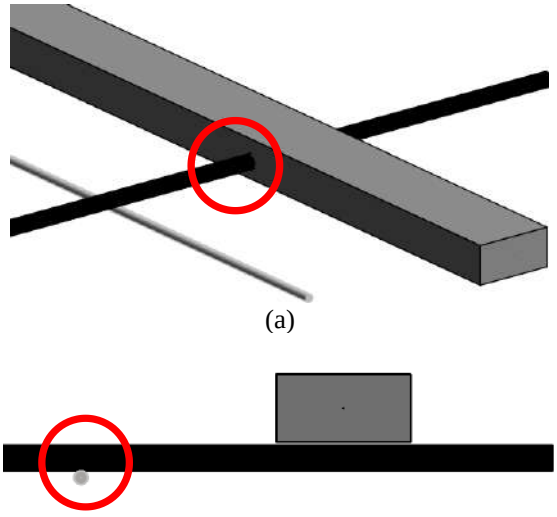

(a)

(b)

Figure 4. The diagrams of two clashes, (a) an original clash and (b) a new clash caused when the black pipe is moved downward to avoid the original clash

```
// s: a given list of clashes in the form of Table 1
function CreateOneNeighbor(s)
    c; // a randomly selected clash instance from s
    D; // the direction (up, down, left, or right)
    d; // the minimum aggregated distance
    g; // the limit of vertical clearance
    o; // the object or system that needs to be revised in c
    θ; // the criterion to decide to revise an object or a system.
    t; // the construction tolerance
    α; // the criterion to decide moving or revising
    while
        c = GetOneRandomClashInstance(s);
        o = DetermineRevisingObject(c, θ);
        // in some case, d does not exist because of g
        if IsMinDistanceExist(o, t, g, ref D, ref d);
            if D is up or down and o is object
                if Random(0, 1) ≥ α
                    Move(o, D, d);
                else
                    Revision(o, D, d);
                end if
            else
                Move (o, D, d);
            end if
            return false;
        end if
    end loop
end function
```

Figure 5. The pseudocode of creating a neighbor solution for SA

Step 4. According to the revision action decided in Step 3, a revision is executed on an object or its system and then a new list of clashes is output through our program and Revit API. This step is the function **Cost** in SA in Figure 1.

Step 5. Record the number of clashes and update the energy function to decrease temperature.

According to the operation in SA, when temperature is higher, the algorithm has a higher probability to accept a worse solution to escape from the current local area. Nevertheless, as iteration times increase, it becomes less likely that a worse solution will be accepted.

4 The Experiment

In this section, we will briefly introduce the profile of the proposed case and then discuss the experimental results.

4.1 The Proposed Case

The proposed case is the MEP systems in a clean room on the first floor of an integrated circuit (IC) assembly factory, as shown in Figure 6. The clean room has four MEP systems, as listed in Table 5, and the four MEP systems have a total of 50 Revit elements (excluding fittings). When the first MEP design models finished by team engineers were integrated into a federated BIM model, 20 clashes were detected (red circles in Figure 6).

The 20 clashes and their clash coordinates are listed in Table 6. Below, the two places marked 1 and 2 in Figure 6 are presented as examples in Figures 7 and 8, respectively, to show the clash status.

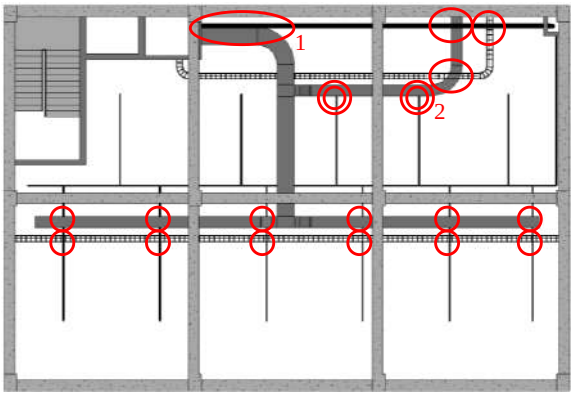

Figure 6. The floor plan of the first floor of the factory

Table 5. The MEP systems in the proposed case

Systems	System types
Supply Air	Mechanical/ Duct
Sanitary	Plumbing/ Pipe
Fire Protection (water)	Plumbing/ Pipe
Electrical	Electrical/ Cable Tray

Table 6. The clashes and their coordinates in the proposed case

No.	Objects		System types		Clash coordinates (X, Y, Z)
	1	2	1	2	
1	367903	371380	Sanitary (pipe)	Cable rack (tray)	(41.819132952, 22.539205146, 10.170603675) (41.819132952, 23.100470191, 10.170603675)
2	370451	367722	Fire Protection (pipe)	Cable rack (tray)	(-22.859319532, -8.881478564, 10.006561680) (-22.661402865, -8.881478564, 10.006561680)
3	370473	367722	Fire Protection (pipe)	Cable rack (tray)	(-8.216683959, -8.881478564, 10.006561680) (-8.018767292, -8.881478564, 10.006561680)
4	370618	367722	Fire Protection (pipe)	Cable rack (tray)	(7.923771212, -8.881478564, 10.006561680) (8.121687878, -8.881478564, 10.006561680)
5	370639	367722	Fire Protection (pipe)	Cable rack (tray)	(22.447435371, -8.881478564, 10.006561680) (22.645352037, -8.881478564, 10.006561680)
6	370660	367722	Fire Protection (pipe)	Cable rack (tray)	(35.638009583, -8.881478564, 10.006561680) (35.835926250, -8.881478564, 10.006561680)
7	370681	367722	Fire Protection (pipe)	Cable rack (tray)	(48.197120136, -8.881478564, 10.006561680) (48.395036803, -8.881478564, 10.006561680)
8	367101	367903	Supply Air (duct)	Sanitary (pipe)	(-2.216012647, 22.460462668, 9.514435696) (6.595010975, 22.460462668, 9.690656168)
9	367107	370627	Supply Air (duct)	Fire Protection (pipe)	(9.595010975, -1.361906094, 10.006561680) (12.219682891, -1.361906094, 10.006561680)
10	367130	370639	Supply Air (duct)	Fire Protection (pipe)	(22.546393704, -7.677522892, 10.006561680) (22.546393704, -6.037102945, 10.006561680)
11	367130	370660	Supply Air (duct)	Fire Protection (pipe)	(35.736967916, -7.677522892, 10.006561680) (35.736967916, -6.037102945, 10.006561680)
12	367130	370681	Supply Air (duct)	Fire Protection (pipe)	(48.296078469, -7.677522892, 10.006561680) (48.296078469, -6.037102945, 10.006561680)
13	367191	370451	Supply Air (duct)	Fire Protection (pipe)	(-22.760361198, -7.677522892, 10.006561680) (-22.760361198, -6.037102945, 10.006561680)
14	367191	370473	Supply Air (duct)	Fire Protection (pipe)	(-8.117725625, -7.677522892, 10.006561680) (-8.117725625, -6.037102945, 10.006561680)
15	369883	370599	Supply Air (duct)	Fire Protection (pipe)	(18.605084296, 12.252387737, 10.006561680)
16	369883	370700	Supply Air (duct)	Fire Protection (pipe)	(31.106234416, 12.252387737, 10.006561680)
17	369883	371780	Supply Air (duct)	Fire Protection (pipe)	(31.106234416, 12.516579798, 9.820465021)
18	369883	371812	Supply Air (duct)	Fire Protection (pipe)	(18.605084296, 12.516579798, 9.820465021)
19	369891	367695	Supply Air (duct)	Cable rack (tray)	(9.595010975, 15.232694664, 9.514435696) (12.219682891, 15.232694664, 9.514435696)
20	369908	367903	Supply Air (duct)	Sanitary (pipe)	(36.007371265, 22.819837668, 10.278903374) (37.648508636, 22.819837668, 10.311726121)

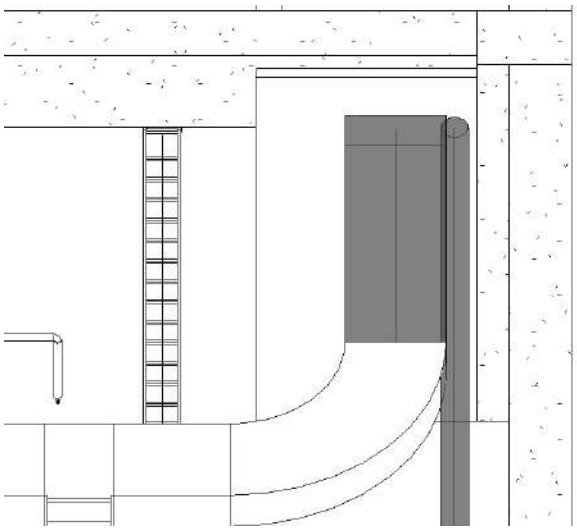

Figure 7. The clash between a duct and a sanitary pipe

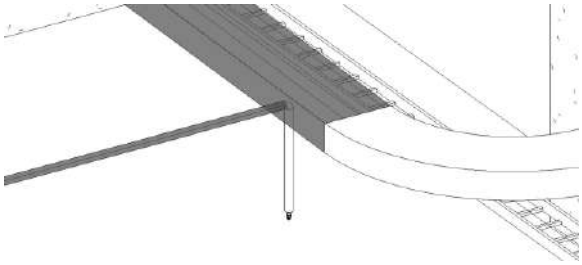

Figure 8. Two clashes between a duct and two pipes

4.2 The Experimental Results

The objective of the proposed system was to resolve the MEP clashes listed in Table 6. The strategy of this study was to set moving as the first priority, i.e., α in Figure 5 is 0.95. The experimental results are summarized in Table 7 and drawn in Figure 7.

Table 7. The details of experimental results

Runs	Clash Numbers	Time (Seconds)
1	14	4.410
2	10	5.822
3	8	5.757
4	2	5.916
5	1	5.788
6	0	5.746
		33.440

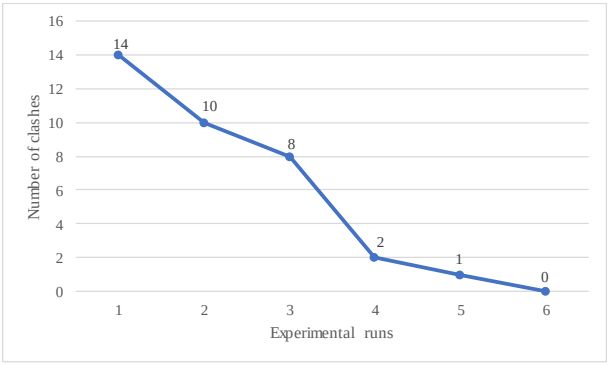

Figure 9. The trend of experimental results

As shown in Figure 9, the clashes were resolved very quickly, in 33.44 seconds. In the first run, six of the twenty clashes were resolved. Although the proposed case is rather simple, it indicates that the proposed system can provide BIM team members an initial reference for further discussions on clash resolution. For comparison with the two examples in Figures 7 and 8, the automatic resolutions are shown in Figures 10 and 11.

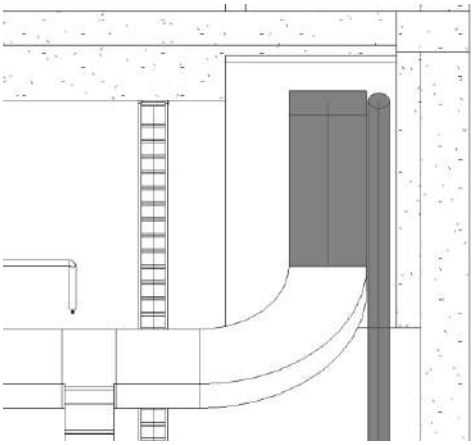

Figure 10. Automatic resolution of a clash between a duct and a sanitary pipe

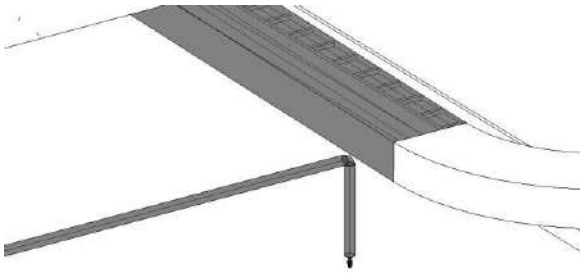

Figure 11. Automatic resolution of two clashes between a duct and two pipes

5 Conclusion

During the design stages of pre-construction, it is time-consuming for a BIM project team to resolve design clashes as they integrate models finished by individual team members into a composite master model. To automatically resolve design clashes, we designed a programming system by employing SA and API provided by Revit. In this paper, a real case of the MEP systems in a clean room in an IC-Assembly factory was employed. In the case, twenty design clashes were detected when the BIM models were merged. The case was used to evaluate the effectiveness and feasibility of the proposed system. The experimental results showed that the twenty design clashes were automatically resolved within a very short time. The revised BIM model can serve as a reference for team members in discussions of how to resolve design clashes. Although the experimental results indicated that design clashes can be automatically resolved in this way, the proposed system still needs more specific guidelines to ensure suitable revisions of building components, rather than random revisions.

References

[1] Liu, Y., van Nederveen, S. and Hertogh, M. Understanding effects of BIM on collaborative design and construction: An empirical study in China. *International Journal of Project Management, 35*(4), 686-698, 2017.

[2] States), N. N. B. S.-U. An Authoritative Source of Innovative Solutions for the Built Environment, 2015.

[3] Love, P. E. D., Liu, J., Matthews, J., Sing, C.-P. and Smith, J. Future proofing PPPs: Life-cycle performance measurement and Building Information Modeling. *Automation in Construction, 56*, 26-35, 2015.

[4] Lin, Y.-C., Lin, C.-P., Hu, H.-T. and Su, Y.-C. Developing final as-built BIM model management system for owners during project closeout: A case study. *Advanced Engineering Informatics, 36*, 178-193, 2018.

[5] Wetzel, E. M. and Thabet, W. Y. Utilizing Six Sigma to develop standard attributes for a Safety for Facilities Management (SFFM) framework. *Safety Science, 89*, 355-368, 2016.

[6] Pärn, E. A., Edwards, D. J. and Sing, M. C. P. Origins and probabilities of MEP and structural design clashes within a federated BIM model. *Automation in Construction, 85*, 209-219, 2018.

[7] Ciribini, A. L. C., Mastrolembo Ventura, S. and Paneroni, M. Implementation of an interoperable process to optimise design and construction phases of a residential building: A BIM Pilot Project. *Automation in Construction, 71*, 62-73, 2016.

[8] Bhagwat, P. and Shinde, R. Clash Detection: A New Tool in Project Management. *International Journal of Scientific Research in Science, Engineering and Technology, 2*(4), 193–197, 2016.

[9] Lee, G. and Kim, J. W. Parallel vs. Sequential Cascading MEP Coordination Strategies: A Pharmaceutical Building Case Study. *Automation in Construction, 43*, 170-179, 2014.

[10] Mangal, M. and Cheng, J. C. P. Automated optimization of steel reinforcement in RC building frames using building information modeling and hybrid genetic algorithm. *Automation in Construction, 90*, 39-57, 2018.

[11] Xue, F., Lu, W. and Chen, K. Automatic Generation of Semantically Rich As-Built Building Information Models Using 2D Images: A Derivative-Free Optimization Approach. *Computer-Aided Civil and Infrastructure Engineering, 33*(11), 926-942, 2018.

[12] Lim, Y. W., Majid, H. A., Samah, A. A., Ahmad, M. H., Ossen, D. R., Harun, M. F. and Shahsavari, F. BIM and Genetic Algorithm Optimisation for Sustainable Building Envelope Design. *International Journal of Sustainable Development and Planning, 13*(1), 151-159, 2018.

[13] Korman, T. M. and Tatum, C. B. *Development of a Knowledge-Based System to Improve Mechanical , Electrical , and Plumbing Coordination.* Paper presented at the Technical Report No. 129, Centre for Integrated Facility Engineering, Stanford University, CA, 2001.

[14] J. Hackl, B.T. Adey, N. Lethanh, Determination of Near-Optimal Restoration Programs for Transportation Networks Following Natural Hazard Events Using Simulated Annealing, Computer-Aided Civil and Infrastructure Engineering 33 (8) (2018) 618-637.

[15] M.T. Shafiq, J. Matthews, S.J.J.o.I.T.i.C. Lockley, A study of BIM collaboration requirements and available features in existing model collaboration systems, 18 (2013) 148-161.

[16] J.A. Zeferino, A.P. Antunes, M.C. Cunha, An Efficient Simulated Annealing Algorithm for Regional Wastewater System Planning, 24 (5) (2009) 359-370.

Application of Virtual Reality in Task Training in the Construction Manufacturing Industry

R. Barkokebas[a], C. Ritter[a], V. Sirbu[a], X. Li[b], and M. Al-Hussein[a]

[a]Department of Civil and Environmental Engineering, University of Alberta, Canada
[b]Department of Mechanical Engineering, University of Alberta, Canada
E-mail: rdbarkokebas@ualberta.ca, critter1@ualberta.ca, sirbu@ualberta.ca, xinming1@ualberta.ca, malhussein@ualberta.ca

Abstract –

Automation in construction manufacturing is becoming increasingly common due to the drive for higher productivity and increased quality. One important consideration in the implementation of automation is the training and maintenance of the equipment. This study proposes an approach to assess the training for assembly/disassembly and maintenance of machines developed for the construction manufacturing industry by using immersive virtual reality (VR). The application of VR allows the collection of data such as the time required to complete the task, the distance travelled, the identification of ergonomic risks (e.g., awkward body posture), and the layout effectiveness, as well as the observation of multiple users performing an identical task under laboratory circumstances. Moreover, VR significantly reduces the costs associated with real mock-ups and the time required for implementation as it allows testing machine designs in a virtual environment that mimics the machine's real operation setting. To demonstrate the proposed approach, a case study (i.e., VR experiment) is conducted. The primary objective of the case study is to use VR to assess the effectiveness of training using the VR environment for maintenance, and the complexity of the task (i.e., the amount of time needed to understand the task). The VR experiment is performed inside an office room dedicated exclusively for that purpose where participants can move freely, and interactions with the virtual environment are possible through the utilization of a headset and wireless controllers. During the experiment, information is collected both by manual observation and automatic extraction of data from the computer. Based on the analyses of the data collected, the average time to complete the task is determined, and potential areas of design improvement are identified.

Keywords –

Virtual Reality; VR; Maintenance; Automation; Training; Construction; Manufacturing;

1 Introduction

The implementation of visualization, communication, and information technologies by the construction industry has been confirmed as a powerful approach to optimize and integrate industrial processes [1]. Virtual Reality (VR), for instance, has proven to be an integrating tool that supports communication between different stakeholders as well as decision-making processes, especially during the design phase [2]. In the past years, several studies were conducted to investigate the application of VR in the construction industry, focusing on a variety of areas such as virtual prototyping [3–5], ergonomic analysis (e.g., detection of unsafe body motions and unsafe worker behaviour) [6–8], safety hazard detection [9–13], construction equipment training [14–19], and educational purposes [2,20,21].

In terms of training, VR offers the possibility of effective training while reducing significantly cost and safety risks related to mock-ups [16,22]. Investments in training strategies are essential to ensure that employees are continuously improving their skills to accurately and safely perform tasks [23]. According to Rezazadeh et al. 2011 [16], VR can assist training since, by utilizing VR, the user has the sensation, to some extent, of performing the activity as he/she would perform it in reality. Besides the mentioned capability, VR also allows users to practice how to perform a task/activity without pressure due to costs, the inability to complete the task, and risk of hazards inherent to real mock-ups [24]. In terms of the impact of the presentation medium used to provide safety training, Leder et al. [25] compare an immersive VR and a Microsoft PowerPoint presentation. Results obtained conclude that the investment on costly equipment for VR safety training is not cost-effective since Microsoft PowerPoint developed with realistic figures and scenes has a similar impact on user risk

perception and learning outcomes [25].

The application of VR technologies to educational purposes is also explored by researchers. Sampaio et al. [2] use 3D modelling techniques and VR to develop models to represent several construction processes. Based on the results obtained, it is determined that introducing 3D models and VR techniques in schools assist students to learn and prepare them to use these technologies in their professional practice. Pan et al. [20] perform a state-of-art research on the concept of VR applied to learning, training, and entertainment, and concludes that the application of VR can enhance, motivate and stimulate learners' understanding of certain events. In addition, it is identified that learners learn faster and are happier using virtual environments than they are when using conventional learning methods [20]. Goulding et al. [21] investigate the utilization of VR to provide a risk-free environment for training construction tasks. The primary goal of Goulding et al. [21] is to stimulate multidisciplinary learning between different construction professionals during the design phase, since faulty work, safety, and health issues are often caused by decisions taken in this stage.

In light of the information provided, it is noted that research has been carried out in the area of VR and the construction manufacturing industry; however, there is still a research gap on VR applications with emphasis on training, especially in terms of machine assembly/disassembly tasks. In this context, the aim of this paper is to design and test a VR experiment to evaluate how two training techniques (i.e., VR experiment and a printed instruction manual) impact the performance of a user conducting a maintenance task.

2 Methodology

This project is the first phase of a larger experiment that will test the effectiveness of VR on training in a construction manufacturing setting. This phase was done to validate the design of the experiment. The overall outline for the project can be seen in Figure 1. This paper will cover the section labelled 'experimental design and testing phase'.

2.1 Experimental Design and Hypothesis

The hypothesis to be tested by this experiment is that users carrying out a maintenance task for the first time in real life will be more successful after completing a training sequence in a virtual reality training environment than users trained by reading an instruction manual. The first run of the experiment was done to analyze the success of the experimental design in testing this hypothesis and to determine whether there were factors that had not been previously considered that should be designed for in the full run of the experiment.

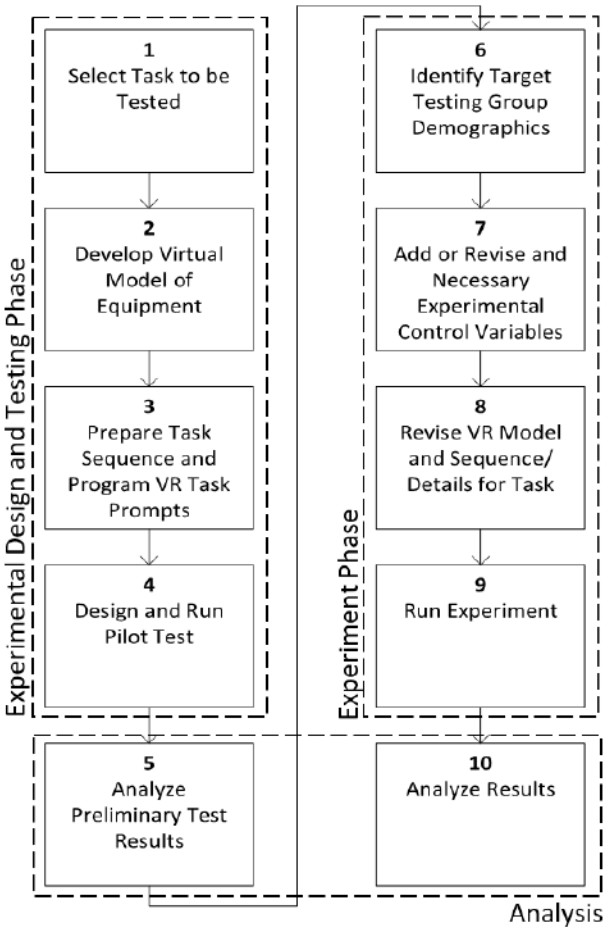

Figure 1. Project outline for testing the effectiveness of virtual reality training for tasks in construction manufacturing and equipment maintenance

2.2 Virtual Environment Design

The VR application used for this experiment was built on the Unity game engine and assets were created using 3DS Max and Photoshop. Standard game engine asset creation workflow was used including using low poly models with baked normal maps and textures to improve performance. Programming was done inside Unity using the C# language. The headset used was an HTC Vive with one hand controller and the application was run on a powerful desktop using a GTX 1080 ti video card. The active physical area of the application was 8' × 8'.

The application itself was developed by a multidisciplinary team including mechanical engineers, construction engineers, a programmer and one digital artist. The 3D model of the machine was based on

SOLIDWORKS files of the real-life machine that was built in our lab. In this way we were able to perfectly match the real life machine that was used for this experiment with the virtual one.

2.2.1 User Experience

An account of the user experience of the VR application is as follows. The user spawns facing the machine fully assembled (since it is to be disassembled first). The controller can have various tools attached to it; however, to begin, it has a placeholder for a hand. To the left of the user is a table with tools that can change the controller placeholder. This is pictured in Figure 2.

Figure 2. Tool selection in VR environment

Behind the user is a table onto which disassembled parts can be arrayed before they are put back together. This table is seen in Figure 3. The task to be performed next is highlighted in yellow, as can be seen in both Figure 3 and Figure 4, for reassembly and disassembly steps, respectively.

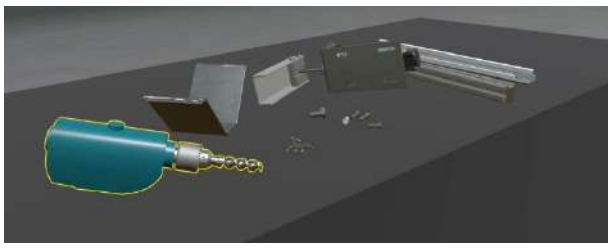

Figure 3. Prompt for the next step of assembly in the VR environment

Figure 4. Disassembly prompt with tool in the VR environment

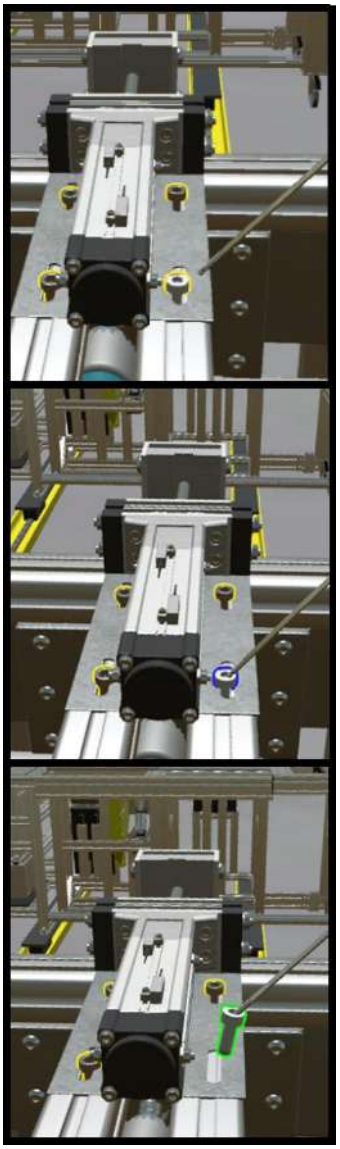

Figure 5. Sequence of colour prompts in the VR training environment

The first step is to take apart screws that connect the top clamp of the machine to the frame. Before detaching the screws, the correct tool must be selected; therefore, as the user first spawns, the tool needed to unfasten these first screws is highlighted in yellow on the table to the left of the user that contains the tools. The user must place the controller (with the hand placeholder) over this tool (that is highlighted in yellow) and activate the controller trigger button. The controller swaps the hand placeholder with the tool and now the screws of the clamp are highlighted in yellow. The user must place the tool in the correct place over one of the screws and activate the controller trigger. Now the screw is attached to the tool and can be moved away from the machine and placed on the table behind the user. When the controller is placed over any yellow part, that yellow part turns blue in order to signify that the controller is touching that part. Parts turn green when the user activates the trigger and the step is completed successfully. This sequence of colour prompts can be seen in Figure 5.

In this manner, by always highlighting the next part in yellow, by giving feedback when the controller is in the right place in blue and highlighting completed steps in green, the user always knows what to do next and whether they are doing things correctly. Over the course of the VR application the user is guided through one full disassembly and one full assembly, and, in theory, he/she would gain a solid understanding of these processes.

2.2.2 Advantages

In theory, the VR training application has the potential to be more engaging from the point of view of the user. VR enables him/her to experience the physicality of the space in relation to the physicality of their own body. In the VR environment the user can freely look to observe the machine and its parts from the same angle and point of view as they would in real life. Moreover, they have ability to reach with their hand into the space and as such they gain an understanding of their own ability to reach into various parts of the machine and to possibly make observations in regard to safety or ease of use that would be impossible to arrive at by looking at a photograph, a technical drawing or written instructions. Moreover, due to the design of the training module, the user is only ever concerned with what to do next and can focus on tasks knowing that the training module will guide them along. The experiential qualities of VR applications are unique and can lead to insights that cannot be arrived at through other means. This allows designers or industrial machinery to test user experience and behaviour in relation to machine operation in ways not previously possible.

2.2.3 Disadvantages

Disadvantages mostly revolve around technical limitations. These include the inability to observe one's body in the space. Currently most VR applications do not allow the user to observe their own hands and body. At best, it is possible to create a 3D model of the user, but even in that case there is a disconnect between one's sense of one's real body and the virtual avatar that acts as a stand-in. Moreover, our application does not account for the user's actual hands. The controller has a placeholder for those instances when the user must use their hands. This is a poor substitute, especially in a training module where using one's hands to put parts together and take them apart is the key component. In order to address this problem, the researchers would have to implement a motion capture system that accounts for hand motion. Hand motion capture is technologically challenging and an area in which advances are being attempted by specialists in that field.

2.3 Experiment Setup

The experiment was carried out in a research facility for three days. Volunteers were randomly assigned to either learn in the VR training environment or by reading an instruction manual. They were then each given six minutes to study the material or use the VR training system. A participant completing the VR training portion can be seen in Figure 6. Next, they were taken to see the physical model for the first time and were tasked with completing the same steps as they were trained. Participants were notified that they would be recorded and scored based on their ability to complete the task, but were not told how aspects of their performance would be weighted when determining their score. Additional instructions on how to perform the task (e.g., bolts do not need to be fully tightened) were given to all participants.

Figure 6. Participant completing the virtual reality training activity before the evaluation activity

2.4 Participants

In total, seventeen people participated in the experiment. Based on how they received instructions to perform the task, they were randomly (as mentioned in the previous subsection) divided into two groups: (1) VR and (2) instruction manual. The VR group had five male and four female participants, while the instruction manual group had five males and three females. All participants were part of the same research group as the authors—the majority of participants, fourteen in total, were graduate students (either master or doctoral students) and three were part of the administrative team. All participants have an engineering background with the exception of two participants, one from each group, and all were under forty years old.

2.5 Data Collection and Analysis

Once the training portion of the experiment was completed, the participants were asked to complete the task on a prototype of the machine. Participants were timed (disassembly time, reassembly time, and total time), as well as marked on the quality of the work completed. This information was used to analyze the differences between the learning methods and performance. A participant completing the last step in the assembly of the prototype machine can be seen in Figure 7.

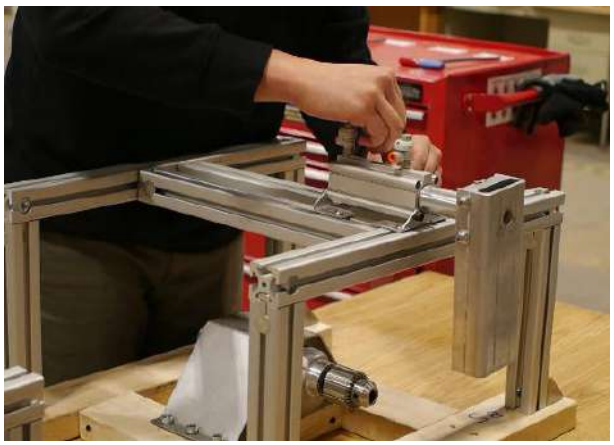

Figure 7. Participant completing the assembly of the prototype

Table 1 shows the number of participants trained in the VR environment or by reading the instruction manual split by gender and by the qualitative aspects of their performance in the experiment, including the final state of the equipment and their organization while completing the task.

Table 1. Count of participants split by training method, gender, and qualitative results

		Count	
		Virtual Reality	**Instruction Manual**
Gender	**Male**	5	5
	Female	4	3
Final State of Equipment	**Operable**	5	7
	Inoperable	4	1
Organization	**Organized**	5	7
	Unorganized	4	1

Table 2 shows the average time taken to complete the task for the participants based on their training type and results. In general, the participants trained using the VR were slower at completing the task. Another interesting observation is that the participants who were able to assemble the prototype so that it was operable again were faster than the ones who left it in an inoperable state.

Table 2. Average time to complete task split by training method, gender, and qualitative results

		Average Time (mm:ss)	
		Virtual Reality	**Instruction Manual**
Gender	**Male**	14:53	11:54
	Female	22:47	16:57
Final State of Equipment	**Operable**	16:31	12:18
	Inoperable	20:45	24:16
Organization	**Organized**	18:40	14:03
	Unorganized	18:03	12:03

3 Results and Discussion

This preliminary run of the experiment allowed for the identification of several parameters that should be identified and possibly controlled for in the next set of experiments. These parameters include the complexity of the project, the deviations from the script in the VR environment that can occur during the test, and the age, experience, and profession of the people completing the experiment.

Figure 8 shows the relationship between the time to assemble/disassemble the equipment in the test. It can

be seen that there is little to no correlation between these times for the population tested in this phase of the experiment. This may be due to the simplicity of the task and we expect to see an increased correlation to these times if the complexity of the task is increased.

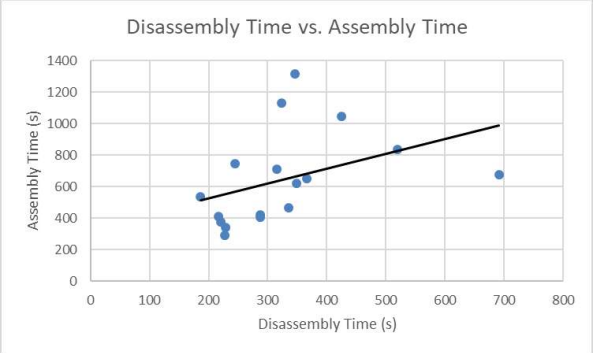

Figure 8. Test results showing the relationship between the time to disassemble and assemble the equipment for each participant

Most of the volunteers were graduate students with undergraduate degrees in engineering. This background would indicate that these volunteers are comfortable with quickly learning through demonstration or reading and analyzing problems.

The complexity of the task is another important factor to consider in the design of the experiment. The task that was used for this demonstration was relatively simple and, given some time, it can be expected that even without the training participants would be able to complete the task. This prompts a separate research question—at what level of complexity does VR training start to outperform text-based training methods, if at all?

Another important observation was the deviations from the VR script. One example of this was how some bars often fell apart when participants loosened them too much, but in the VR training the same bars could simply be slid out of the way. One of these bars can be seen in Figure 9. This prompts an important question regarding the time required to prepare the VR training and what should be included, because as the complexity of the task increases more deviations from the planned path are possible.

4 Limitations and Future Work

This investigation was limited by a relatively small number of tests, as well as by limited diversity in the test group, since all the participants were employed in an office setting and most were graduate engineering students. In the future, the experiment will be expanded to include a demographic that is more aligned with that for whom the VR training technology is to be developed.

Future testing will also be expanded to include more possible deviations from the expected scenario to increase how realistic the VR experience is for the users. Tool orientation, pressure, and level of looseness or tightness that should be accomplished in the disassembly and assembly of the prototype were also issues for the participants. There are several possible solutions to this that could be investigated, including animations of the tools when the right location is selected in the VR environment, or VR options that produce haptic feedback and allow for better tool orientation in the environment.

Figure 9. An example of one deviation from the VR script that occurred in the test

5 Conclusion

As mentioned, this experiment was done to validate the experimental design for a larger evaluation of the effectiveness of VR training on construction manufacturing and maintenance tasks, which will be continued in the future. This test will be repeated with a more applicable and diverse demographic and the task will be modified based on the results of this test. The complexity of the task will be adjusted and the ability for users of the VR to view the proper tool orientation and use will be added.

Since in this test, while the number of participants was limited, the VR users were on average slower and less successful at completing the task, it can be concluded that adding more technology to the training method may not always be necessary; however, more testing needs to be done to determine if, with an increasing task complexity and length, the VR training method may become more effective than traditional training methods.

Acknowledgement

The authors appreciate the technical writing assistance of Jonathan Tomalty and Kristin Berg. In addition, special thanks to Mingjun Zhao, for his

assistance in programming the VR sequence, Hossein Abaeian for insights during the development of 3D models in the VR environment, Anas Itani for assisting with the experiment setup, as well as to all volunteers that participated in the experiment.

References

[1] C.M. Eastman, BIM handbook : a guide to building information modeling for owners, managers, designers, engineers, and contractors, Wiley, Hoboken, N.J., 2008. http://www.loc.gov/catdir/enhancements/fy0741/2007029306-t.html.

[2] A.Z. Sampaio, M.M. Ferreira, D.P. Rosário, O.P. Martins, 3D and VR models in Civil Engineering education: Construction, rehabilitation and maintenance, Autom. Constr. 19 (2010) 819–828. doi:https://doi.org/10.1016/j.autcon.2010.05.006.

[3] H. Li, N.K.Y. Chan, T. Huang, M. Skitmore, J. Yang, Virtual prototyping for planning bridge construction, Autom. Constr. 27 (2012) 1–10. doi:https://doi.org/10.1016/j.autcon.2012.04.009.

[4] T. Huang, C.W. Kong, H.L. Guo, A. Baldwin, H. Li, A virtual prototyping system for simulating construction processes, Autom. Constr. 16 (2007) 576–585. doi:https://doi.org/10.1016/j.autcon.2006.09.007.

[5] T. Deviprasad, T. Kesavadas, Virtual prototyping of assembly components using process modeling, J. Manuf. Syst. 22 (2003) 16–27. doi:https://doi.org/10.1016/S0278-6125(03)90002-1.

[6] S. Han, S. Lee, F. Peña-Mora, Application of dimension reduction techniques for motion recognition: Construction worker behavior monitoring, in: 2011: pp. 102–109.

[7] Y. Yu, H. Guo, Q. Ding, H. Li, M. Skitmore, An experimental study of real-time identification of construction workers' unsafe behaviors, Autom. Constr. 82 (2017) 193–206. doi:https://doi.org/10.1016/j.autcon.2017.05.002.

[8] N. Inyang, S. Han, M. Al-Hussein, M. El-Rich, A VR model of ergonomics and productivity assessment in panelized construction production line, in: Constr. Res. Congr. 2012 Constr. Challenges a Flat World, 2012: pp. 1084–1093.

[9] A. Albert, M.R. Hallowell, B. Kleiner, A. Chen, M. Golparvar-Fard, Enhancing construction hazard recognition with high-fidelity augmented virtuality, J. Constr. Eng. Manag. 140 (2014) 4014024.

[10] C.-S. Park, D.-Y. Lee, O.-S. Kwon, X. Wang, A framework for proactive construction defect management using BIM, augmented reality and ontology-based data collection template, Autom. Constr. 33 (2013) 61–71. doi:https://doi.org/10.1016/j.autcon.2012.09.010.

[11] D. Zhao, J. Lucas, Virtual reality simulation for construction safety promotion., Int. J. Inj. Contr. Saf. Promot. 22 (2015) 57–67. doi:10.1080/17457300.2013.861853.

[12] H. Guo, H. Li, G. Chan, M. Skitmore, Using game technologies to improve the safety of construction plant operations, Accid. Anal. Prev. 48 (2012) 204–213. doi:https://doi.org/10.1016/j.aap.2011.06.002.

[13] B.H.W. Hadikusumo, S. Rowlinson, Integration of virtually real construction model and design-for-safety-process database, Autom. Constr. 11 (2002) 501–509.

[14] H. LI, G. CHAN, M. SKITMORE, Multiuser Virtual Safety Training System for Tower Crane Dismantlement, J. Comput. Civ. Eng. VO - 26. (2012) 638. http://login.ezproxy.library.ualberta.ca/login?url=https://search.ebscohost.com/login.aspx?direct=true&db=edscal&AN=edscal.26379679&site=eds-live&scope=site.

[15] H.-L. Chi, Y.-C. Chen, S.-C. Kang, S.-H. Hsieh, Development of user interface for tele-operated cranes, Adv. Eng. Informatics. 26 (2012) 641–652. doi:https://doi.org/10.1016/j.aei.2012.05.001.

[16] I.M. Rezazadeh, X. Wang, M. Firoozabadi, M.R. Hashemi Golpayegani, Using affective human–machine interface to increase the operation performance in virtual construction crane training system: A novel approach, Autom. Constr. 20 (2011) 289–298. doi:https://doi.org/10.1016/j.autcon.2010.10.005.

[17] J.R. Juang, W.H. Hung, S.C. Kang, SimCrane 3D+: A crane simulator with kinesthetic and stereoscopic vision, Adv. Eng. Informatics. 27 (2013) 506–518. doi:https://doi.org/10.1016/j.aei.2013.05.002.

[18] J. Xu, Z. Tang, X. Yuan, Y. Nie, Z. Ma, X. Wei, J. Zhang, A VR-based the emergency rescue training system of railway accident, Entertain. Comput. 27 (2018) 23–31. http://10.0.3.248/j.entcom.2018.03.002.

[19] L. Damiani, M. Demartini, G. Guizzi, R. Revetria, F. Tonelli, Augmented and virtual reality applications in industrial systems: A qualitative review towards the industry 4.0 era, IFAC-PapersOnLine. 51 (2018) 624–630. doi:https://doi.org/10.1016/j.ifacol.2018.08.388.

[20] Z. Pan, A.D. Cheok, H. Yang, J. Zhu, J. Shi, Virtual reality and mixed reality for virtual learning environments, Comput. Graph. 30 (2006) 20–28.

[21] J. Goulding, W. Nadim, P. Petridis, M. Alshawi,

Construction industry offsite production: A virtual reality interactive training environment prototype, Adv. Eng. Informatics. 26 (2012) 103–116. doi:https://doi.org/10.1016/j.aei.2011.09.004.

[22] R.J. Seidel, P.R. Chatelier, Virtual reality, training's future? : perspectives on virtual reality and related emerging technologies., Boston, MA : Springer, 1997., 1997. http://login.ezproxy.library.ualberta.ca/login?url=https://search.ebscohost.com/login.aspx?direct=true&db=cat03710a&AN=alb.8022922&site=eds-live&scope=site.

[23] J.L. Burati, M.F. Matthews, S.N. Kalidindi, Quality management in construction industry / Gestion de la qualité dans l'industrie de la construction, J. Constr. Eng. Manag. VO - 117. (1991) 341. http://login.ezproxy.library.ualberta.ca/login?url=http://search.ebscohost.com/login.aspx?direct=true&db=edscal&AN=edscal.4939931&site=eds-live&scope=site.

[24] X. Li, W. Yi, H.-L. Chi, X. Wang, A.P.C. Chan, A critical review of virtual and augmented reality (VR/AR) applications in construction safety, Autom. Constr. 86 (2018) 150–162. doi:https://doi.org/10.1016/j.autcon.2017.11.003.

[25] J. Leder, T. Horlitz, P. Puschmann, V. Wittstock, A. Schütz, Comparing immersive virtual reality and powerpoint as methods for delivering safety training: Impacts on risk perception, learning, and decision making, Saf. Sci. 111 (2019) 271–286. http://10.0.3.248/j.ssci.2018.07.021.

Improving the Quality of Event Logs in the Construction Industry for Process Mining

L. Chen1[a], S. Kang2[a], S. Karimidorabati3[b], and C. T. Haas4[a]

[a]Department of Civil and Environmental Engineering, University of Waterloo, Canada
[b]Gina Cody School of Engineering & Computer Science, Concordia University, Canada
E-mail: l364chen@uwaterloo.ca, s43kang@uwaterloo.ca, shahin.karimi@concordia.ca, chaas@uwaterloo.ca

Abstract –

Process mining is an emerging tool kit to discover, analyze, and improve workflows. In the construction industry, projects can be large and unique in terms of costs and durations. In such projects, commercial software that support analyses and decision making may be helpful. Process mining software allow construction companies to quickly discover benchmark workflows, conduct conformance checking, and analyze root causes. However, engineers who initially format the event logs, and users who use the event logs for analyses may not share the same knowledge or values. Due to the lack of understanding, knowledge, or experience in these respective domains, companies may not have documented the event logs in the most practical way. With the poorly structured event logs, the software may not be able to provide the most accurate analyses. Therefore, there is a need to pre-process event logs so as to improve their quality. This paper examines a case study on Engineering Change Request (ECR) in the construction industry to explain the importance of pre-processing the event logs before importing them into the commercial process mining software. For large complex projects, the improved quality of event logs will reduce confusion between engineers and analyzers and improve the accuracy of the analysis results produced by the process mining software.

Keywords –

Process mining; Event log; Pre-processing

1 Introduction

Process mining, which is a powerful tool in analyzing workflow and improving its efficiency, has been widely used in the academic fields of many different industries, such as healthcare [1] and banking [2]. Because of their standardized processes and the process mining software's ability to deal with big data, process mining has been successful in these industries. Disco, ProM, and Celonis are some example software that have been used in different research [3]–[5]. In the construction industry, the management of workflow makes the processes easier to monitor and control. Collecting and analyzing event data using data mining techniques allow people to track and validate the processes [6]. Process mining uses event logs to perform analyses on workflows. Event logs record information including Case IDs, Activities, Timestamps, and Attributes (such as people, costs, and locations). As process mining aims at utilizing information in event logs to discover, monitor, and improve processes, the quality of the data imported to the software will greatly affect the clarity and effectiveness of process mining [3].

After uploading the event logs, the commercial software creates a discovered model and conducts conformance checking, bottleneck analysis, and root cause analysis. These analyses provide meaningful insights regarding the efficiency of the existing workflow. However, when importing the event logs into the software, the software may have difficulties in analyzing the event logs, if they are poorly structured. Meanwhile, users may also have trouble in understanding the results. For example, the event logs could have ambiguous naming when multiple activities share the same activity name. Hence, there are needs to pre-process the event logs to minimize the ambiguity and enhance the understanding for the users and analyses from the software. This may include the formatting of the event log names, timestamps, and adding or deleting certain logs.

According to Suriadi et al. [3], a "high-quality" event log is defined as the one with minimal information loss, which is also valid in the context of the domain and for the analysis purpose. Resulting from manually recording the data, poor-quality event logs have missing data, incorrect data, imprecise data and irrelevant data. In this context, to clean up event logs means to address these issues by correcting the errors if possible. However, in this paper, the event logs are assumed to have all the information required, including activity names, timestamps, and attributes. A "high-

quality" event log is thus defined as a structured data that minimizes the confusion and maximizes the ease and clarity for both software and users to analyze and interpret the workflow.

This paper focuses on pre-processing event logs to improve their quality both on their format and content. An event log including 58 cases of Engineering change requests (ECR) of a mega-construction project was used as a case study. The case study elaborated on the importance of the clarity and accuracy of the activity names and timestamps of event logs. Therefore, companies should be aware of pre-processing the event logs before manipulating them if they want to take full advantage of process mining.

2 Literature Review

Construction projects can happen over a long period of time due to large scope. The planning, design, construction, and maintenance stages can take years to happen and complete. In the meantime, construction projects are prone to delays [7]. High uncertainties due to the weather, resources or changes can result in delays. Recent studies have focused on the automation of change management in construction industry to minimize the delays caused by change management [8]. The processes of construction projects have been the area that the researchers and engineers consider as important and try to standardize [9], [10]. When time is the main concern, process mining may provide suggestions by analyzing the patterns from timestamp records. Despite the fact that process mining has been introduced to other industries to minimize the delay and improve the efficiency of the workflow, few companies have adopted process mining in the construction industry. Process mining has shown potential to help in managing construction projects. Due to the long timespan of capital projects, process mining techniques, such as bottleneck analysis and root cause analysis, could be applied to project workflows to find where delays usually occur and what their causes may be. The information could be used to improve the workflow of the latter project stages. The advantage of applying process mining techniques to the same project is that it will produce more accurate results where the time, location, and human factors are most likely to remain the same.

Process mining takes event logs to automatically obtain process models and check conformance. In this case, event logs are considered as construction information whose quality will be important [11]. Moreover, event logs are the main foundation data to identify bottlenecks and deviations, suggest improvements, and predict processing time. For process mining, event logs are the raw data that need to be dealt with to construct models and analysis. The quality of the data, both form and content, is critical in order for the process mining exercise to be successful [12]. Anomalies and impurities lead to higher cost and less benefit for data processing, potentially making it less applicable to the clients [13]. Therefore, pre-processing event logs to improve their quality before conducting a process mining analysis is a necessary task. However, this pre-stage to clean the data for process mining is often overlooked because the task is considered tedious. The proper handling of potential problems and challenges of event logs should be taken care of before moving on to recording logs [14], [15]. In addition, there are also studies to find patterns after event logs are recorded and diagnose the issues afterwards [16], [17]. This paper focuses on ways to pre-process event logs before conducting further analyses, preventing potential confusion and errors. This includes activity definitions and timestamp alignment.

3 Pre-processing Event Log Framework

Although event logs existed before, how to manage and use event logs were not thoroughly investigated. This paper discusses how to improve the quality of event logs to deliver the meanings and intentions better. While there may be many overlaps, there is no consensus on how to define an event log. Therefore, suggested methodology in this paper may not be the unique path to build the data. However, this methodology will be a stepping stone especially for the construction management domain where there are various participants and activities involved throughout a process. In this section, a general framework to obtain a high quality event log is presented. An event log is a combination of "Case ID", "Activity", and "Timestamp" as the main components. Thus, clarifying these three areas of information can be beneficial.

Especially when it comes to activity names, some information can be added or simplified. In order to pursue clarification, the first task is to differentiate two different activities that share one activity name. If this step is skipped, high confusion is expected once the event log is recorded. Usually, activity names include actions. However, in construction management processes, there are many tasks with the same actions but executed by different position performers. In other words, if only actions without performers are included, overlaps may exist which can create confusion. Therefore, in this study, the form of "Action + Performer" is recommended. This way, clarity can be achieved. Note that "performer" and "user" need to be distinguished. "Performer" refers to a participant who is involved in the process, here, the ECR process. "User" on the other hand, refers to the process analyzer.

Additional information can be provided through attributes. However, in this paper, Case ID, Activity, and Timestamp are the main interests. When naming the activities, the authors recommend to use the form of "Verb" + "by/to Noun" for consistency.

The next task would be regarding timestamps. Every case has a different path from start to end. For some cases, errors exist, and completion time information does not exist. For other cases, the case is not formally closed but ends abruptly. Such cases should be treated differently so that the users can extract as much information as possible. Timestamps that receive "NULL" for the completion time by the workflow software have several reasons. First, the activity happened instantly which means the start time and end time are the same. If an activity is informational (notifications) and is automatically generated by the software, this requires no further action from the participants who get it. Second, when certain activities are not completed by the designated performer, the ECR is sent to another performer or again to the original performer automatically. When this happens, the original performer's previous activity receives a "NULL" by most workflow software such as LANA, Celonis, etc. Third, if an activity is not completed by the user before the predefined due date, the activity receives a "NULL" as the timestamp. Fourth, when the action is performed by a group of performers and there exists at least one "NULL" for the completion time, the performer who got "NULL" will receive a timeout warning. However, performers who completed the action in time may also get a timeout warning. For the timeout warning activities, the performers may again receive "NULL". Fifth, there are abort cases which includes "NULL" for the completion time. A summary on the common problems in event logs and their solutions can be seen in Figure 1.

4 Case Study

A case study was conducted to show some ways to pre-process the event logs before uploading them into the process mining software. The data used in the case study was regarding 58 cases of the Engineering Change Request (ECR) in a mega construction project. Figure 2 summarizes the problems of the raw event data that the user attained.

The first problem observed was the duplicated names. As shown in (1) in Figure 2, the activity "Change Request Participants Verification" happened twice. However, the activities were performed by different performers. This can be inferred from the fact that one was followed by "Review (Engineer)" whereas the other one was followed by "Review (Participants)". Considering the fact that "participants" were also ambiguous, the activity "Change Request Participants Verification" should be further analyzed and re-named properly.

The second problem shown in (2) was regarding the "action (performer)" format. Some activities such as "Review (Participants)" and "Approve (Engineer)" included the action performer in the brackets. However, activities such as "Rejected Notification" and "Rejected Close Out" did not include the action performer nor recipient. This is the inconsistent format mentioned in the framework.

The third problem was ambiguous definition. For example, in the raw event log, there existed confusion in "Approve (Engineer)." It turned out that this can mean both approve and reject based on each case.

The fourth problem was missing critical information, such as reasons for warnings. The fifth problem was the timestamp format. Problems shown in (6) and (7) were both regarding the "NULL" completion time. The "NULL" timestamps happened due to a couple of reasons which will be elaborated in section 4.2.

No	Activity		No	Timestamp	
	Problem	Solution		Problem	Solution
1	- Duplicated names	- Rename into different names	5	- Inconsistent format	- Consistent format
2	- Inconsistent format	- Consistent format (Action + Performer)	6	- Missing values due to instant occasion	- Data imputation (e.g. completion time = start time)
3	- Ambiguous definitions	- Remove ambiguity	7	- Missing values due to overtime or group recipients	- Data imputation
4	- Missing information	- Additional information	8	- Missing values in abandoned activities	- Ignore the missing values

Figure 1. Pre-processing event log framework

WF_ID	activitydisplayname	createddatetime	OwnershipDateTime	completeddatetime	ResponseBy	Name	CurrentStatus
216	Verify Details	3/30/11 17:59	31-03-2011 13:36	NULL	NULL	Amin	Closed
216	Verify Details	3/30/11 17:59	31-03-2011 13:36	NULL	NULL	Blake	Closed
216	Verify Details	3/30/11 23:59	31-03-2011 13:36	3/31/11 13:36	NULL	Amin	Send On
216	Change Request Participants Verification	3/31/11 1	31-03-2011 19:52	3/31/11 19:53	NULL	Amin	Send On
216	Review (Engineer)	3/31/11 19:53	01-04-2011 17:21	4/4/11 22:45	05-04-2011 23:00	Tracy	Send for Review
216	Change Request Participants Verification	4/4/11 22:45	04-04-2011 22:45	4/5/11 19:06	NULL	Tracy	Send On
216	Review (Participants)	4/5/11 19:06	07-04-2011 16:15	4/7/11 16:19	11-04-2011 22:00	Vic	Send On
216	Review (Participants)	4/5/11 19:06	05-04-2011 19:07	4/5/11 20:34	11-04-2011 22:00	Karen	Send On
216	Review (Participants)	4/5/11 19:06	06-04-2011 12:54	4/6/11 13:08	11-04-2011 22:00	Kirk	Send On
216	Review (Participants)	4/5/11 19:06	05-04-2011 23:13	4/5/11 23:16	11-04-2011 22:00	Andrew	Send On
216	Approve (Engineer)	4/7/11 16:19	09-04-2011 1	NULL	09-04-2011 19:28	Tracy	Closed
216	Approve (Engineer) Warning	4/9/11 19:28	14-04-2011 21:11	4/15/11 21:18	NULL	Tracy	Reject
216	Rejected Notification	4/15/11 21:18	NULL	NULL	NULL	Randy	Deleted
216	Rejected Notification	4/15/11 21:18	NULL	NULL	NULL	Tim	Information
216	Rejected Notification	4/15/11 21:18	NULL	NULL	NULL	Vic	Deleted
216	Rejected Notification	4/15/11 21:18	NULL	NULL	NULL	Karen	Information
216	Rejected Notification	4/15/11 21:18	NULL	NULL	NULL	Andrew	Deleted
216	Rejected Notification	4/15/11 21:18	NULL	NULL	NULL	Kirk	Deleted
216	Rejected Notification	4/15/11 21:18	NULL	NULL	NULL	Duffy	Information
216	Rejected Notification	4/15/11 21:18	NULL	NULL	NULL	Tracy	Deleted
216	Rejected Notification	4/15/11 21:18	NULL	NULL	NULL	Kevin	Deleted
216	Rejected Notification	4/15/11 21:18	NULL	NULL	NULL	Jack	Deleted
216	Rejected Notification	4/15/11 21:18	NULL	NULL	NULL	Don	Deleted
216	Rejected Notification	4/15/11 21:18	NULL	NULL	NULL	Amy	Deleted
216	Rejected Notification	4/15/11 21:18	NULL	NULL	NULL	Michael	Deleted
216	Rejected Close Out	4/15/11 21:18	15-04-2011 22:41	4/15/11 22:42	NULL	Amin	Send On
241	Verify Details	4/5/11 15:47	06-04-2011 13:26	NULL	NULL	Faisal	Closed
241	Verify Details	4/5/11 21:47	06-04-2011 13:26	4/6/11 13:27	NULL	Amin	Send On

Figure 2. Raw event logs and their problems

4.1 Activity Names

Activity names are one of the most crucial components in event logs as they tell users what happened. Therefore, it is important to name the activity names properly and clearly. This section talks about some naming issues encountered during the process mining analysis of the case study and how they were solved. These problems include duplicated names, ambiguous naming and missing information, which had caused confusion.

4.1.1 Duplicated Names

The overview of the raw data can be seen in Figure 2. From the raw data, it can be seen that in Case 216, the activity "Change Request Participants Verification" was followed by two different activities, "Review (Engineer)" and "Review (Participants)". This proves the fact that the "participants" did refer to different groups of performers. When analyzing the processes using software, the activity "Change Request Participants Verification" caused confusion as they were considered as one activity due to the same activity name.

Based on their following activities, "Change Request Participants Verification" was renamed as "Change Request Participants Verification (Engineer)" and "Change Request Participants Verification (Participants)" respectively. "Change Request Participants Verification (Engineer)" was later renamed as "Verify Senior Engineer by Coordinator" whereas "Change Request Participants Verification (Participants)" was later renamed as "Verify Engineer by Senior Engineer."

4.1.2 Activity Name Format

The data set has eighteen different activities in total as shown in Figure 3, referred as original activity names. By observation, there are four problems regarding the naming of the event logs. Firstly, the activity names started with different parts of speech. Majority of the activities started with verbs. However, activities such as "Notification Approved" and "Notification Rejected" started with nouns. After consideration, all the activities were decided to start with verbs for they indicated the actions of each activity clearly.

Secondly, some activity names included the performers / recipients involved, but some did not. For example, the activity "Approve (Engineer)" clearly indicated that the performer who approved the change was the engineer. However, the activity "Verify Detail" did not specify who was the performer that had verified the detail.

Thirdly, some activity names were ambiguous on the individuals who performed or received the action. For example, the terms "Approver" and "Participants" are ambiguous pronouns and not proper nouns that identify real roles or positions in the construction project, which also caused confusion.

Ideally, the activity names should be unique, clear and straightforward. By looking at the activity names, users should be able to know what the action was, who performed the action, and whom the action affected. To make the action clear, the activities have been structured to start with verbs. For example, the name "Notification Approved" means to send out the notification of approval to relevant recipients, although it can be

interpreted as the notification is approved to be sent out. To avoid the confusion, "Notification Approved" has been renamed as "Notify All Relevant Participants of the Approval".

No.	Original Activity Names	New Activity Names
1	Approve (Approver)	Approve/Reject by Assistant Project Manager
2	Approve (Approver) Warning	Timeout Warning to Assistant Project Manager
3	Approve (Engineer)	Approve/Reject by Senior Engineer
4	Approve (Engineer) Warning	Timeout Warning to Senior Engineer
5	Approve (Manager)	Approve/Reject by Project Manager
6	Approved (Close out)	Approved (Close out by Coordinator)
7	Change Request Draft	Initiate Engineering Change Request by Initiator
8	Change Request Participants Verification	Verify Engineer by Senior Engineer
9	Change Request Participants Verification	Verify Senior Engineer by Coordinator
10	Notification Approved	Notify Approval to All Relevant Participants
11	Notification Rejected	Notify Rejection to All Relevant Participants
12	Rejected (Close out)	Rejected (Close out by Coordinator)
13	Review (Engineer)	Review by Senior Engineer
14	Review (Engineer) Warning	Review Timeout Warning to Senior Engineer
15	Review (Participants)	Review by Engineer
16	Review (Participants) Warning	Review Timeout Warning to Engineer
17	Rework	Rework by Initiator
18	Verify Details	Verify Details by Coordinator

Figure 3. Original activity names vs new activity names

To make the action performer and recipient clear, there was an investigation on the hierarchy of the positions and roles involved. Firstly, the "Approver" is not a real position title in the construction company. It is a temporary role, and in this case, it anonymizes the person responsible and results in ambiguous information. As approvers approve and reject the engineering change request, they were identified as the assistant project managers who are at the higher position in the company with the authority to approve or reject the change requests. Note that the names of positions can be flexible, e.g. project director can be added as approver. "Participants" who reviewed the change requests were interpreted as engineers whereas "Engineer" who verified "Participants" were thus inferred as senior engineers. The summary of the original and the new performers'/recipients' names has been shown in the Figure 4.

Moreover, the activity "Approve (Approver)" could mean that Approver approved the change request, or it could also mean that Approver's action or decision was approved. To clearly differentiate the action performer from the action recipient, action performers were added to the activity names as "by someone" whereas action recipients were added to the activity names as "to someone". Realizing that Approver was the one who approved the change request, the activity "Approve (Approver)" was renamed as "Approve by Approver" which was eventually renamed as "Approve/Reject by Assistant Project Manager" as shown in Figure 3.

No.	Original Performers/Recipients Names	New Performers/Recipients Names
1	Approver	Assistant Project Manager
2	Manager	Project Manager
3	Engineer	Senior Engineer
4	Participant	Engineer

Figure 4. Original vs. new performers' / recipients' names

4.1.3 Ambiguous Activity Names

After having carefully investigated the event logs, it could be seen that some activities were not defined properly. For example, by looking at the activity name "Approve (Approver)", users might interpret it as such that the approver has approved the engineering change request. However, in the case shown in the Figure 5, "Approve (Approver)" was followed by "Rejected Notification". Hence, it could be induced that the activity "Approve (Approver)" does not necessarily mean approving. Instead, it refers to the process of making the decision on whether to approve or reject the change request. Therefore, to minimize the confusion, the activity "Approve (Approver)" was renamed as "Approve / Reject by Approver", which was later renamed as "Approve / Reject by Project Manager". Similarly, "Approve (Engineer)" was renamed as "Approve / Reject by Senior Engineer" and "Approve (Manager)" was renamed as "Approve / Reject by Assistant Project Manager." The summary of the original activity names and the new activity names can be seen in the Figure 3.

Case ID	Activity	Start Time	Completion Time	Name	Current Status
15	Change Request Draft	5-10-11 0:43	5-10-11 0:58	Amy	Submit
15	Verify Details	5-10-11 0:59	5-10-11 14:34	Faisal	Send On
15	Change Request Participants Verification	5-10-11 14:34	5-10-11 14:36	Faisal	Send On
15	Review (Engineer)	5-10-11 14:36	5-11-11 19:53	Rudy	Send for Approval
15	Approve (Approver)	5-11-11 19:54	NULL	Andrew	Closed
15	Approve (Approver) Warning	5-15-11 23:00	5-19-11 14:37	Andrew	Reject
15	Rejected Notification	5-19-11 14:38	NULL	Randy	Deleted
15	Rejected Notification	5-19-11 14:38	NULL	Rudy	Deleted
15	Rejected Notification	5-19-11 14:38	NULL	Ken	Deleted
15	Rejected Notification	5-19-11 14:38	NULL	Tim	Deleted
15	Rejected Notification	5-19-11 14:38	NULL	Vic	Deleted
15	Rejected Notification	5-19-11 14:38	NULL	Karen	Information
15	Rejected Notification	5-19-11 14:38	NULL	Kirk	Deleted
15	Rejected Notification	5-19-11 14:38	NULL	Andrew	Deleted
15	Rejected Notification	5-19-11 14:38	NULL	Kevin	Deleted
15	Rejected Notification	5-19-11 14:38	NULL	Don	Information
15	Rejected Notification	5-19-11 14:38	NULL	Jack	Deleted
15	Rejected Notification	5-19-11 14:38	NULL	Gerry	Deleted
15	Rejected Notification	5-19-11 14:38	NULL	Amy	Deleted
15	Rejected Close Out	5-19-11 14:38	5-19-11 17:18	Faisal	Send On

Figure 5. Event logs regarding "Approve (Approver)"

4.1.4 Missing Information

When investigating the event logs, there was a set of activities named with warnings. The warning events are missing values as the activity names did not indicate

which type of warnings they were. For example, these warnings could mean exceedance of costs, resources or time. The warning activities can be seen in Figure 6. In all the cases, the warning activities were followed by the normal activities without warnings. For example, the activities "Review (Engineer)" were followed by "Review (Engineer) Warning". Keeping such a relationship in mind, it was found that the warning activities happened when the participants failed to respond before the deadline. Therefore, the warnings were identified as the timeout warnings since the performers did not respond in time.

No.	Original Activity Names	New Activity Names
1	Approve (Approver) Warning	Timeout Warning to Project Manager
2	Approve (Engineer) Warning	Timeout Warning to Senior Engineer
3	Review (Engineer) Warning	Review Timeout Warning to Senior Engineer
4	Review (Participants) Warning	Review Timeout Warning to Engineer

Figure 6. Timeout warning activities

4.2 Timestamps

Timestamps are another crucial factor in event logs, which usually indicates the start time and the completion time. In this case study, timestamps included created time, ownership time and completed time as shown in Figure 2. The ownership time refers to the opening time of the tasks by the action performers. However, as there were cases when the performers had already started the work but did not open the task, the ownership time was not the actual start time. The created time was thus used as the start time as that was when the performers are supposed to begin to work on the activities.

There are two main problems for timestamps. One is the inconsistent formatting, and the other one is the "NULL" timestamps. The "NULL" timestamps happened due to three reasons: the activity happened instantly, the activity was aborted, or the performer did not manage to complete the activity before the due time and data. These cases will be further explained in the following sections.

4.2.1 Inconsistent Timestamp Format

After fixing the activity names, the timestamps were also investigated carefully. In Figure 2, it can be seen that the timestamps were documented in different format. The "createddatetime" (start time) in and the "completeddatetime" (completion time) adopted the format of "MM-dd-yy HH:mm". In contrast, the "OwndershipDateTime" (opening time) and the "ResponseBy" (deadline) adopted the format of "yyyy-MM-dd HH:mm". The inconsistency in the format caused confusion for both users and process mining software. For example, if the date is "April 10th, 2011", it will be written as "04-10-11" which could also possibly mean "October 4th, 2011" without a clear definition. To be consistent and avoid the confusion, all the timestamps were reformatted as "dd/MM/yyyy HH:mm:ss."

4.2.2 "NULL" Cases

In the event logs, some activities were triggered and completed instantly. For example, the activity "Notify Approval to All Relevant Participants" referred to the action of sending notification of approval to performers involved. This activity is merely an automated machine-based action that takes place instantly upon the approval or rejection of the ECR by an authorized performer such as Senior Engineer or Assistant Project Manager. With no further action required from the participants, "Notify Approval to All Relevant Participants" had a completion time of "NULL" as shown in Figure 7. The "NULL" timestamps were assigned values using data imputation. The completion time for "Notify Approval to All Relevant Participants" and "Notify Rejection to All Relevant Participants" were therefore changed to the same time as their start time.

Case ID	Activity	Start Time	Completion Time	Name	Current Status
1	Notify Approval to All Relevant Participants	10/03/2011 15:13:14	NULL	Randy	Deleted
2	Notify Rejection to All Relevant Participants	10/03/2011 14:50:12	NULL	Randy	Deleted
3	Verify Details by Coordinator	09/03/2011 18:02:14	NULL	Faisal	Closed
3	Review by Engineer	10/03/2011 14:12:34	NULL	Amy	Closed
3	Review Timeout Warning to Engineer	13/03/2011 23:00:01	NULL	Amy	Abort
20	Review by Senior Engineer	12/04/2011 14:22:26	NULL	Mark	Closed
32	Approve/Reject by Assistant Project Manager	11/05/2011 19:54:17	NULL	Andrew	Closed
54	Approve/Reject by Senior Engineer	02/09/2011 17:52:36	NULL	Mark	Closed

Figure 7. Activities with "NULL" completion time

"NULL" timestamps were also observed for other activities, which have been listed in Figure 7. By looking into the attributes, it was found that these activities all had the current status of either "Closed" or "Abort". The status of "Abort" indicates that the change request was cancelled and no longer proceeded. As a result, the completion time for those "Abort" activities were left blank, for they did not have a completion time.

"Verify Details by Coordinator" was one of the activities with the greatest number of "NULL" timestamps for their completion time. These cases were usually repeated again with a non-NULL completion time. From Figure 8, it was suggested that the "NULL" timestamp happened when the original performer was not able to complete the task in time. As a result, the original performer appears to have a "NULL" completion time, and another performer, authorized as the coordinator, may complete the task. The current status was thus "Closed" instead of "Send on."

Case ID	Activity	Start Time	Completion Time	Name	Current Status
1	Verify Details by Coordinator	09/03/2011 18:31:20	NULL	Faisal	Closed
1	Verify Details by Coordinator	10/03/2011 01:31:21	10/03/2011 14:15:50	Amin	Send On
2	Verify Details by Coordinator	10/03/2011 00:53:26	NULL	Faisal	Closed
2	Verify Details by Coordinator	10/03/2011 00:53:27	10/03/2011 14:14:28	Amin	Send On
3	Verify Details by Coordinator	09/03/2011 18:02:14	NULL	Faisal	Closed
3	Verify Details by Coordinator	10/03/2011 01:02:14	10/03/2011 14:00:46	Amin	Send On
4	Verify Details by Coordinator	09/03/2011 18:14:02	NULL	Amin	Closed
4	Verify Details by Coordinator	10/03/2011 01:14:02	10/03/2011 14:16:41	Faisal	Send On
5	Verify Details by Coordinator	10/03/2011 18:45:15	NULL	Faisal	Closed
5	Verify Details by Coordinator	10/03/2011 18:45:16	10/03/2011 18:59:52	Amin	Send On

Figure 8. Activity "Verify Details by Coordinator"

In the case study, there were also timeout warning activities which have been summarized in Figure 6 in Section 4.1.4. The timeout warning activities happened when the performers did not manage to complete the activities by deadline. In this case, the completion time for the normal activity was recorded as "NULL" and the normal activity was followed by a timeout warning. The solution to the timeout activities was to add up the duration of the normal activity and the timeout activity.

5 Conclusion

Process mining has great potential in the construction industry as it allows people to find out the activities causing delays, thus improving the efficiency. To make sure that process mining provides the best result, it is important to pre-process the event logs. Some of the issues with activity names are duplicated naming, ambiguous naming and missing information. These problems should be identified and fixed before the event logs are used for further analysis. Timestamps are also another critical feature of event logs. Some of the issues with timestamps are confusing format, missing values, i.e. "NULL" cases, and activities that are not completed by the deadline. The discovery of the timeout activities had triggered thoughts on conformance checking. In process mining, conformance checking is conducted between the model discovered using event logs and the target model. The difference between the discovered model and the target model, i.e. missing or inserted activities, can be considered as non-conformance. In the real world, projects usually have a deadline by which they are supposed to be completed. Hence, if the performers are not able to finish their tasks before the predefined deadlines, it should be considered as non-conformance too. This paper mainly focused on the first step of process mining, which is to pre-process the event logs extracted from the construction projects. The next step will be to use the pre-processed event logs to conduct analyses such as conformance checking, bottleneck analysis, and root cause analysis. As every industry has workflows and processes, this paper can be further generalized to all industries, not limited to the construction industry, on how to pre-process and improve the quality of event logs. With event log quality improvement, there will be less confusion for both engineers who created the event logs and users, which results in better accuracy in process mining analyses.

References

[1] E. Rojas, J. Munoz-Gama, M. Sepúlveda, and D. Capurro, "Process mining in healthcare: A literature review," *J. Biomed. Inform.*, vol. 61, pp. 224–236, Jun. 2016.

[2] C. Moreira, E. Haven, S. Sozzo, and A. Wichert, "Process mining with real world financial loan applications: Improving inference on incomplete event logs," *PLOS ONE*, vol. 13, no. 12, p. e0207806, Dec. 2018.

[3] S. Suriadi, R. Andrews, A. H. M. ter Hofstede, and M. T. Wynn, "Event log imperfection patterns for process mining: Towards a systematic approach to cleaning event logs," *Inf. Syst.*, vol. 64, pp. 132–150, Mar. 2017.

[4] W. van der Aalst, "Spreadsheets for business process management: Using process mining to deal with 'events' rather than 'numbers'?," *Bus. Process Manag. J.*, vol. 24, no. 1, pp. 105–127, Jan. 2018.

[5] M. Kebede and M. Dumas, "Comparative Evaluation of Process Mining Tools," 2015.

[6] W. van der Aalst *et al.*, "Process Mining Manifesto," in *Business Process Management Workshops*, 2012, pp. 169–194.

[7] Lo Tommy Y., Fung Ivan W., and Tung Karen C., "Construction Delays in Hong Kong Civil Engineering Projects," *J. Constr. Eng. Manag.*, vol. 132, no. 6, pp. 636–649, Jun. 2006.

[8] S. Karimidorabati, C. T. Haas, and J. Gray, "Evaluation of automation levels for construction change management," *Eng. Constr. Archit. Manag.*, vol. 23, no. 5, pp. 554–570, Sep. 2016.

[9] B. Golzarpoor, C. T. Haas, D. Rayside, S. Kang, and M. Weston, "Improving construction industry process interoperability with Industry Foundation Processes (IFP)," *Adv. Eng. Inform.*, vol. 38, pp. 555–568, Oct. 2018.

[10] B. Golzarpoor, C. T. Haas, and D. Rayside, "Improving process conformance with Industry Foundation Processes (IFP)," *Adv. Eng. Inform.*, vol. 30, no. 2, pp. 143–156, Apr. 2016.

[11] A. J. Antony Chettupuzha and C. T. Haas, "Algorithm for Determining the Criticality of Documents within a Construction Information System," *J. Comput. Civ. Eng.*, vol. 30, no. 3, p. 04015039, May 2016.

[12] R. P. J. C. Bose, R. S. Mans, and V. D. W. M.P. Aalst, "Wanna improve process mining results? :

it's high time we consider data quality issues seriously," *2013 IEEE Symp. Comput. Intell. Data Min. CIDM13 Singap. April 16-19 2013*, pp. 127–134, 2013.

[13] H. Mueller and J.-C. Freytag, "Problems , Methods , and Challenges in Comprehensive Data Cleansing," 2005.

[14] R. Conforti, M. La Rosa, and A. H. M. ter Hofstede, "Noise Filtering of Process Execution Logs based on Outliers Detection," Report, 2015.

[15] R. Sarno, W. A. Wibowo, K. Kartini, Y. Amelia, and K. Rossa, "Determining Process Model Using Time-Based Process Mining and Control-Flow Pattern," *TELKOMNIKA Telecommun. Comput. Electron. Control*, vol. 14, no. 1, pp. 349–360, Mar. 2016.

[16] C. Fernandez-Llatas, J. L. Bayo, A. Martinez-Romero, J. M. Benedí, and V. Traver, "Interactive pattern recognition in cardiovascular disease management. A process mining approach," in *2016 IEEE-EMBS International Conference on Biomedical and Health Informatics (BHI)*, 2016, pp. 348–351.

[17] C. Fernandez-Llatas, A. Lizondo, E. Monton, J.-M. Benedi, and V. Traver, "Process Mining Methodology for Health Process Tracking Using Real-Time Indoor Location Systems," *Sensors*, vol. 15, no. 12, pp. 29821–29840, Dec. 2015.

Applying an A-Star Search Algorithm for Generating the Minimized Material Scheme for the Rebar Quantity Takeoff

S. Chang[a], R.-S. Shiu[b], and I-C. Wu[a]

[a]Department of Civil Engineering, National Kaohsiung University of Science and Technology, Kaohsiung, Taiwan
[b]SINOTECH Engineering Consultants, Ltd, Taipei, Taiwan
E-mail: shen0619@nkust.edu.tw, rexshiu@mail.sinotech.com.tw, kwu@nkust.edu.tw

Abstract –

Rebar engineering is a construction method for building structures that is critical to the earthquake resistance of the entire building. The construction process and quality of rebar have always been valued by the construction industry, and it is imperative to improve the quality of reinforcement construction to reduce injuries. In recent years, Building Information Modeling (BIM) technology has been widely applied in the stages of design, operation and maintenance, but less in the construction phase. For rebar works in the construction phase, a BIM model of rebar can facilitate the development of a solution because 3D visualization of the model makes it easier to understand the problem. However, to apply the rebar BIM model to practice, it is necessary to build a model with the rebar takeoff to meet the actual construction status. Thus, how to optimize the takeoff of rebar from the completed 3D model has practical research value. This study takes the on-site construction of rebar as an example. For the main component, a BIM model is built with Tekla software to produce practical rebar takeoff plans with an A-star algorithm based on legal norms and construction feasibility that can reduce the amount of excess rebar material. It also chooses the best rebar takeoff plan to build the rebar BIM model. As a result, the relevant personnel who use the rebar BIM model can correctly solve the actual problems with the BIM model.

Keywords –

Building Information Modeling; Rebar Takeoff; A-Star Search Algorithm; Construction Phase

1 Introduction

Rebar engineering is a construction technology for a building, and it is also a safety factor of the structure. The construction industry has committed to reducing the waste of rebar under safe conditions to decrease the cost of rebar. In traditional rebar engineering, a building is constructed according to a 2D design drawing. But the designed rebar diagram cannot be directly applied at construction sites. It is necessary to perform rebar quantity takeoff to carry out rebar cutting, transportation, construction and other steps to complete the work of rebar engineering. The rebar quantity takeoff work is generally problematic for most untrained construction workers, who have insufficient planning ability and professional knowledge. Problems with incorrect material cutting or improper lashing may result in poor construction quality. Even if the reinforced concrete material is completed, it is difficult to effectively understand whether the takeoff result is the best. In recent years, the introduction of BIM in each stage of the building life cycle has become more diverse through the visualization and parameterization of Building Information Modeling (BIM). For example, a 3D model established by BIM software can quickly show design defects before construction and prevent waste in reconstruction [1]. It can be used to simulate the estimation of cash flow, including equipment, manpower and materials, during construction [2]. It is also possible to conduct conflict analysis for various types of work in advance and as a cross-domain information communication interface [3, 4]. Building Information Modeling has the capability to automate a quantity take-off, which will reduce the time and costs required to estimate a project [5]. The system using Autodesk Revit API automatically generates rebar placement plans for a building structure and labels the placement sequence of each individual bar or set of bars with ascending numbers [6]. At present, most rebar BIM models are established according to the two-dimensional map. The completed BIM model only provides a reference for the relevant personnel to easily understand the conflict positions and quantities of the entire rebar project. Therefore, it is worthwhile to create a practical rebar BIM model and to explore how to continue to use the BIM model to optimize the rebar material quantity to decrease freight, increase the correctness of rebar construction, and mitigate the problems caused by the rebar construction process. Figure 1 shows the research workflow.

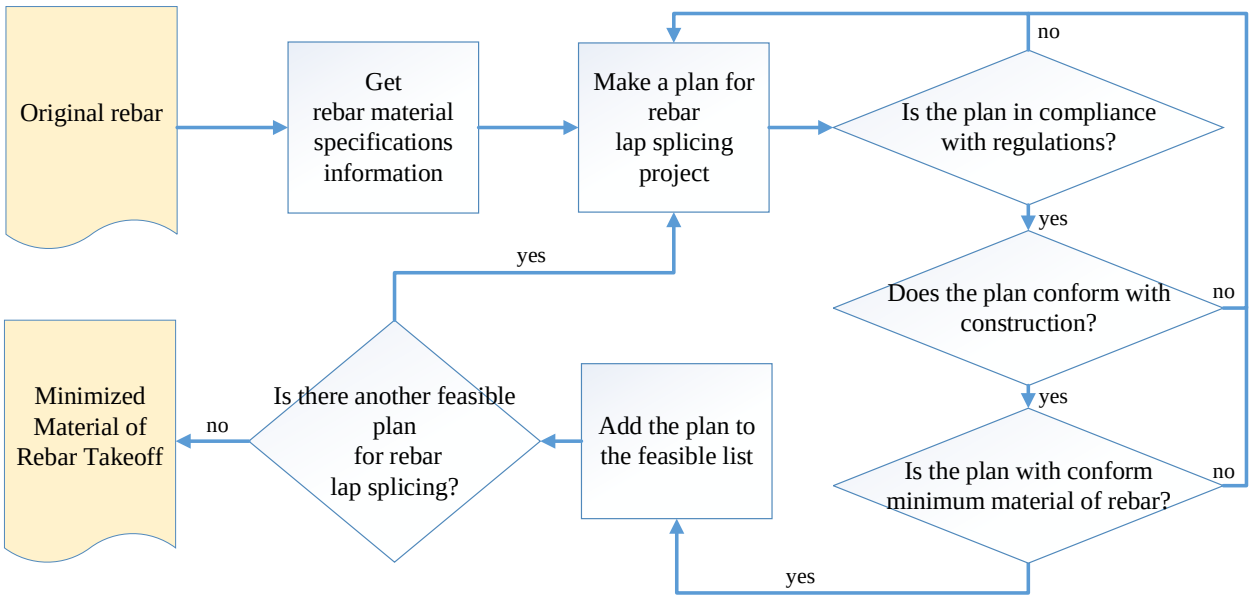

Figure 1. Research workflow

2 Application of Algorithm in Construction Engineering

Appling algorithms to solve problems in construction engineering has been discussed in related studies, which have examined using a genetic algorithm (GA) to optimize the RC beam rebar design to achieve the lowest construction cost [7]. A GA can be used to minimize the cost of RC columns in a reasonable time [8]. Also, a hybrid GA-HJ can be used to automatically generate optimized rebar under the BIM software model architecture. These studies have also solved some practical problems. The rebar cutting problem can use the Maze Problem (MP), for which the Pathfinding Algorithm is used to solve its path or shortest path. This was proposed by the Dutch computer scientist Edsger Wybe Dijkstra in 1956 [9].

Beam and column joint look like the intersection node of maze, we need consider to apply straight rebar or add a hook based on constructivity and cost analysis. According to these characteristics of problem, the A-star search algorithm used in this study is an improved algorithm based on Dijkstra's algorithm [10], which is commonly used in the movement path control of non-player characters in role-playing games. The breakpoint position of the rebar is calculated according to its logic and the construction specifications. The process is summarized as follows: Step 1: Search for the information of rebar in a structural beam and convert it to a quantized node. Step 2: Start from point A and inspect all nodes adjacent to point A. At this time, the program will consider the rebar situation such like straight or hook, only the passable nodes are placed in the open list. Step 3: Set point A as the parent node and move it from the open list to the closed list. Temporarily set each node as the parent node A in the open list and calculate their estimation function,

$$f(A) = g(A) + h(A) \quad (1)$$

where g(A) is the actual distance from the start point to the current node A; h(A) is the estimated distance from the node A to the end point. There are many ways to estimate the distance, depending on the case being explored. Step 4: Select the node with the smallest value as the current node A and move it from the open list to the closed list, while the previous parent node is temporarily called A'. Step 5: Repeat steps 2 and 3, and put the passable node adjacent to point A into the open list. If node B already exists in the list, compare the actual distance of A'→B and the actual distance of A'→A→B. If the former is less than the latter, set the node B to the next point A and repeat this step. If it is more, repeat Steps 2 to 5. Step 6: Repeat steps 2 to 5 until the endpoint is found. Once the endpoint is found, each parent node can reverse its path. When node A' is extended to node A, it determines by node A' and node 2 whether node A is lapped or not. If it is lapped, calculate the lap location and the residual material of node A, i.e., g(A). At the same time, estimate the residual material, i.e., g(A), under the possible lapping conditions with node 3 and node 4. However, if the splicing form of node A is determined, an infeasible situation may occur. For example, node A' and node 2 need to be overlapped, but node A cannot find the offset position of 60 cm so it must be straight through.

The length of node 2 plus the length of node A will be too long and difficult to construct. At this time, it is necessary to re-adjust the splicing form of node A' or 2, and then continue to complete the rebar takeoff operation as shown in Figure. 2.

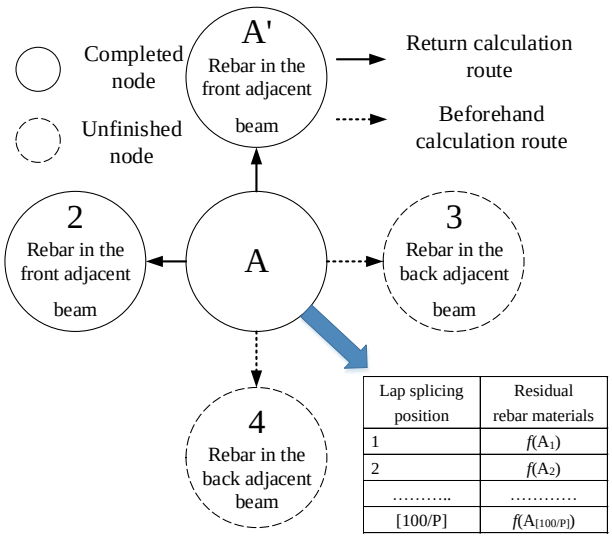

Figure 2. A-star search algorithm for rebar lap splicing scheme

3 BIM Model Combined with Algorithm for rebar takeoff

According to the structural member, the type of rebar lap splicing will be different. In this study, C# was used to program a method to calculate the minimum amount of rebar project and decide the main reinforcement splicing project to create and update the rebar BIM model. When the program needs to decide how to splice the main reinforcement, the length and location of splicing need to follow the law of the concrete construction design specifications. The splicing locations of beam members need to be located on the beam clear span L in the upper pressure zone, the range of L is between 1/4 and 3/4 of the center of the beam member, and the length of this range is 1/2 L. According to the beam clear span, the splicing method can be decided as the double-span for style 1 in Table 1 or the triple-span for style 2 in Table 1. The splicing location of a beam member needs to be located on the range of L from two sides of the beam member to 1/4 of the beam clear span, and the length of this range is 1/4 L. According to the above range, the splicing method can be decided as the cross-column lap for style 3 in Table 1. If the adjacent rebar overlaps, the overlap position can be staggered by 60 cm, as shown in style 4 of Table 1. Because multi-span continuous beam rebar lap splicing is more complicated than the single span beam in practice, the program design regulation needs to consider the following factors of adjacent beams: (A) the size of the section, (B) the quantity of the main reinforcement, (C) the location of the main reinforcement, and (D) the center line. So, in the judgment rule of the program design, the cross-sectional area dimensions (A), the rebar quantity (B), the rebar position (C), and the center line (D) of adjacent beams must be considered. The decided project is lap splicing or non-lap splicing, or anchor in the column member. This research conforms each factor to the decision tree in Figure 3. If the size of the adjacent beam section (A) is the same as the quantity of the main reinforcement, the adjacent main reinforcement can select the project of lap splicing or non-lap splicing.

Table 1. Diagram of rebar lap splicing

Lapping style	1	2	3	4
Lapping place	Beam upper	Beam upper	Beam lower	Beam upper
Rebar number	#7	#7	#7	#7
Rebar amount	7	8	6	9
3D	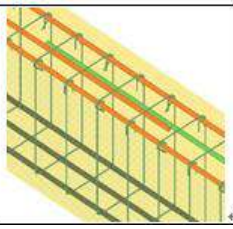	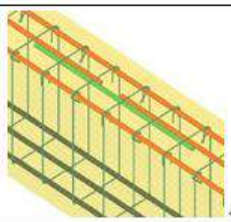	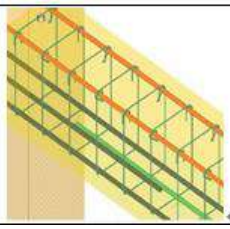	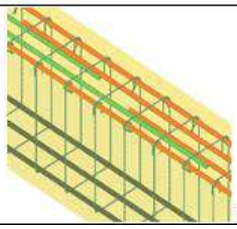

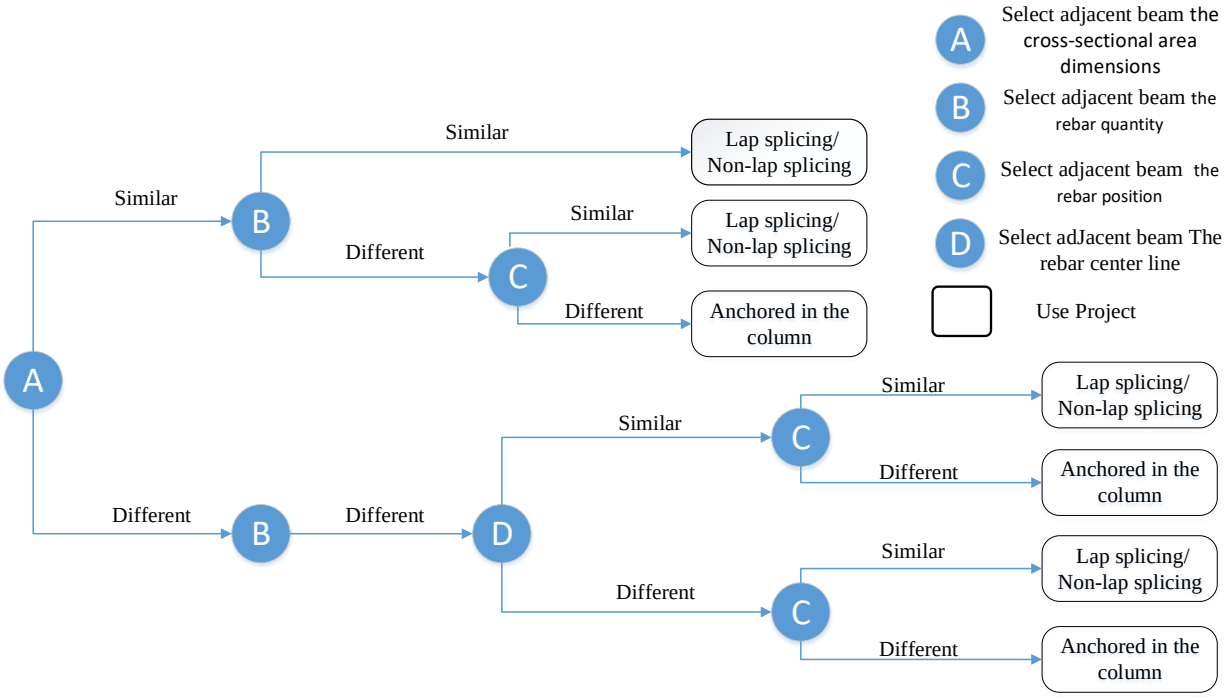

Figure 3. The decision tree about Rebar lap splicing

4 Example analysis

Consider the second floor of a three-story reinforced structure building, which consist of eleven beam members, and the double-span continuous beams are only three of them. This case is easier than most reinforced structure types. Its structural drawing and rebar model created by BIM software are shown in Fig. 4. The reinforcement situation of the multi-span continuous beam can be found by the beam number of the following structure reinforcement drawing, and this drawing can divide the reinforcement of each structure member into items such as the straight main reinforcement, which is in the top and bottom layers, the anchor in the left and right, the non-straight main reinforcement in the top layer, and the non-straight main reinforcement in the center of the bottom layer, and an Excel table can be designed. Finally, that information on reinforcement is inputted into Excel, and following the above, the rebar takeoff and quantity of rebar are calculated. The experimental results of fifty runs are listed in Table 2. Although the first run resulted in the minimum rebar remainders, the total needed rebar length is the maximum in the fifty runs. While the total length of original rebars in the twenty-seventh run is the lowest of the fifty runs, its rebar remainders are not the lowest. Accordingly, this study adopted the twenty-seventh run as the determined scheme due to the minimized material.The detailed cutting results of 3G1 and 3G2 for the twenty-seventh run are summarized in Table 3. Finally, the designer revised the rebar BIM model of structural elements, including columns, beams and walls, according to Table 3, and the results are shown in Fig. 5.

5 Conclusions

Rebar installation causes conflicts and higher costs in the construction stage of a building project's lifecycle. The A-Star search algorithm is applied to obtain the beam element rebar takeoff quantity to match the construction situation and constructability in a BIM model. According to the achievements of this study, the following conclusions can be drawn:

1. Recently, rebar takeoff model is modeled by 2D drawings, the model can not inflect the actual situation on site. Moreover, BIM model without considering rebar splicing and anchor that has the same problems with 2D drawings. Therefore, developing a practical Rebar BIM Model is importent.
2. The A star search algorithm can analyze the rebar splicing and anchor between structural elements and provide various possibilities of rebar takeoff. According to the result, engineers no longer need to operate by personal experience and can obtain the

overall information of rebar takeoff to reduce the rate of material waste and error.

3. At present, this research has only analyzed the situation of a single floor and provided a preliminary result on the rebar takeoff possibility plan. Based on this research, this topic can be extended to related research and BIM technology can be applied more widely.

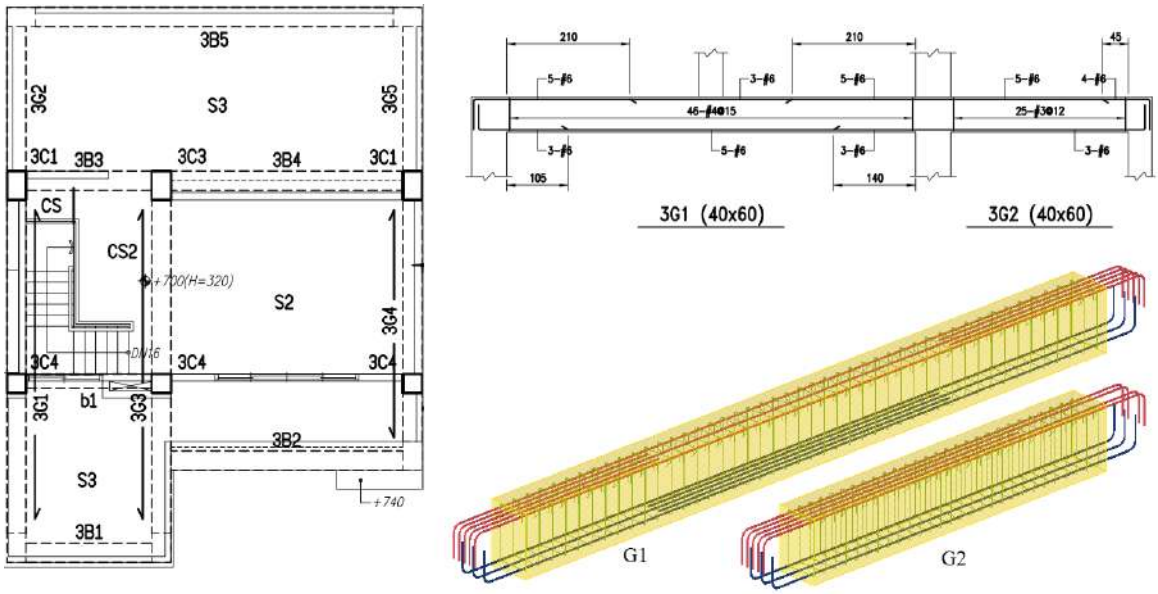

Figure 4. Beam structure and the part of the rebar BIM model

Table 2. The fifty experimental results sorted in ascending order of the cutting remainder lengths

Runs	Rebar No.	Remainders (cm)	Total lengths (cm)		Runs	Rebar No.	Remainders (cm)	Total lengths (cm)	
			Needed rebars	Original rebars				Needed rebars	Original rebars
1	#6	132.9	52167.1	52300	26	#6	264.9	51735.1	52000
2	#6	148.9	51951.1	52100	27	#6	292.9	50007.1	50300
3	#6	156.9	51843.1	52000	28	#6	264.9	51735.1	52000
4	#6	164.9	51735.1	51900	29	#6	296.9	51303.1	51600
.....			.....		.....			.....	
22	#6	212.9	51087.1	51300	47	#6	440.9	52059.1	52500
23	#6	228.9	50871.1	51100	48	#6	444.9	50655.1	51100
24	#6	240.9	52059.1	52300	49	#6	472.9	51627.1	52100
25	#6	264.9	51735.1	52000	50	#6	520.9	50979.1	51500

Table 3. The rebar takeoff results according to the twenty-seventh run

Project No	Element No	Object Sequence	Object Label	Rebar Type	Rebar No	Rebar Index	Is Splice	Has Left Anchor	Has Right Anchor	Splice Length	Splice Position	Left Length	Right Length
27	5	1	3G1	Upper	6	1	FALSE	TRUE	FALSE	0	0	814.65	0
27	5	2	3G2	Upper	6	1	FALSE	FALSE	TRUE	0	0	387.65	0
27	5	1	3G1	Upper	6	2	TRUE	TRUE	FALSE	108	422.55	559.2	363.45
27	5	2	3G2	Upper	6	2	TRUE	FALSE	TRUE	108	89.75	197.75	297.9
27	5	1	3G1	Upper	6	3	TRUE	TRUE	FALSE	108	364.35	393	529.65
27	5	2	3G2	Upper	6	3	FALSE	FALSE	TRUE	0	0	387.65	0
27	5	1	3G1	Lower	6	1	FALSE	TRUE	FALSE	0	0	814.65	0
27	5	2	3G2	Lower	6	1	FALSE	FALSE	TRUE	0	0	387.65	0
27	5	1	3G1	Lower	6	2	FALSE	TRUE	FALSE	0	0	814.65	0
27	5	2	3G2	Lower	6	2	FALSE	FALSE	TRUE	0	0	387.65	0
27	5	1	3G1	Lower	6	3	FALSE	TRUE	FALSE	0	0	814.65	0

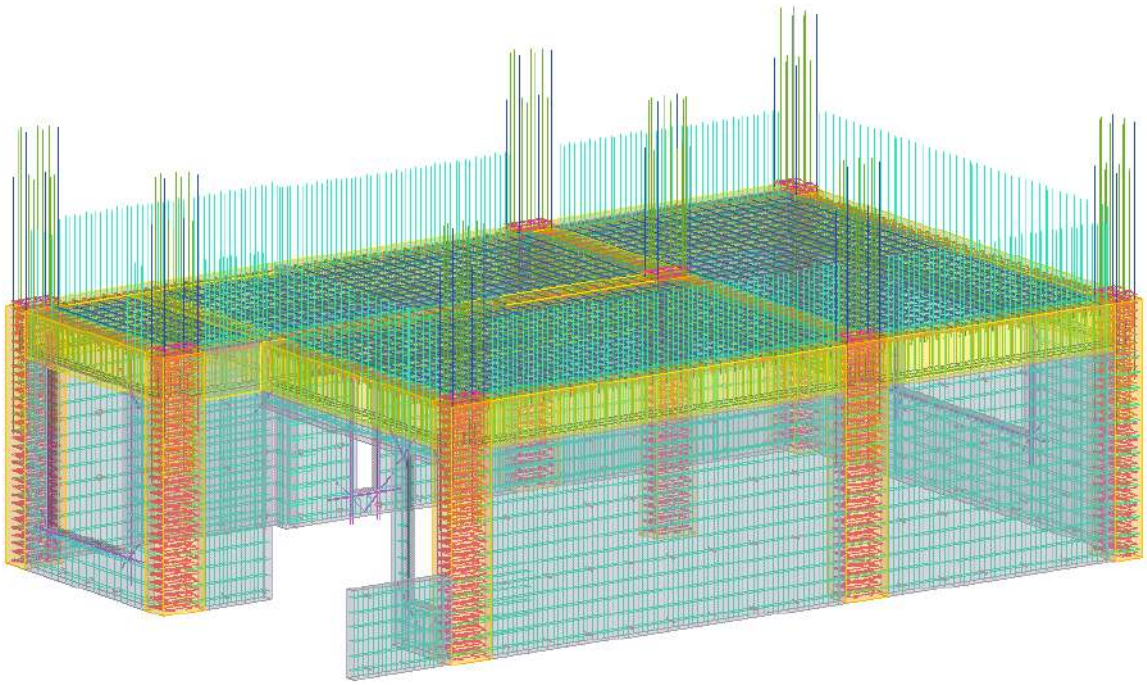

Figure 5. The rebar BIM model of the second floor

References

[1] Won J., Cheng J. C. P. and Lee G., "Quantification of construction waste prevented by BIM-based design validation: Case studies in South Korea". *Waste Management*, 49：170-180, 2016.

[2] Lu Q., Won J. and Cheng J. C. P., "A financial decision making framework for construction projects based on 5D Building Information Modeling (BIM)". *International Journal of Project Management*, 34(1)： 3-21, 2016.

[3] Lin Y. C., Chou S. H. and Wu I. C., "Conflict Impact Assessment between Objects in a BIM system". *Proceedings of the 30th International Symposium on Automation and Robotics in Construction*, Montreal, Canada, 2013.

[4] Zhang J. P., Hu Z. Z., "BIM- and 4D-based integrated solution of analysis and management for conflicts and structural safety problems during construction: 1. Principles and methodologies". *Automation in Construction*, 20(2)：155-166,2011.

[5] Sattineni A. and Bradford II R. H., "Estimating with BIM: a survey of US construction companies". *Proceedings of the 28th ISARC*, pages 564-569, Seoul, Korea, 2011.

[6] Park U-Yeol, "BIM-Based Simulator for Rebar Placement". *Journal of the Korea Institute of Building Construction*, 12(1)：98-107, 2012.

[7] Lepš M. and Šejnoha M., "New approach to optimization of reinforced concrete beams". *Computers & Structures*, 81(18)：1957-1966, 2003.

[8] Sahab M. G., Ashour A. F. and Toropov V. V., "A hybrid genetic algorithm for reinforced concrete flat slab buildings". *Computers & Structures*, 83(8)： 551-559, 2005.

[9] Dijkstra E. W., "A Note on Two Problems in Connexion with Graphs". *NUMERISCHE MATHEMATIK*, 1(1)： 269-271, 1959.

[10] Hart P. E., Nilsson N. J. and Raphael B., "A Formal Basis for the Heuristic Determination of Minimum Cost Paths". *IEEE Transactions on Systems Science and Cybernetics*, 4(2): 100-107, 1968.

Using BIM and Sensing Mats to Improve IMU-based Indoor Positioning Accuracy

C.-H. Chen[a] and I-C. Wu[a]

[a] Department of Civil Engineering, National Kaohsiung University of Science and Technology, Kaohsiung, Taiwan
E-mail: 1106312108@nkust.edu.tw, kwu@nkust.edu.tw

Abstract –

Currently, numerous approaches to Indoor Positioning Systems (IPSs), such as RSSI (Received Signal Strength Indication), fingerprint, PDR (Pedestrian Dead-Reckoning), and image recognition, have been developed. But each individual positioning method has unique drawbacks. In this study, we provide an IPS with a novel combined positioning method that applies Building Information Modelling (BIM) and Internet of Things (IoT). We employ an Inertial Measurement Unit (IMU) to track people's positions. We then utilize a BIM model that has information (semantic and geometric) and a sensing mat to eliminate IMU drift error in the positioning process. The demonstration field is a research office, and test results show that the BIM based positioning constraint can effectively filter IMU cumulative error along with time; thereby, positioning accuracy can be controlled to a range of 30cm × 30cm. In sum, this paper proposes a new positioning method that compensates for the weakness of the IMU. In the future, this system can be applied to people management, such as telecare for older adults.

Keywords –

BIM; Indoor Positioning System; IoT; IMU; Sensing Mat

1 Introduction

Building Information Modelling (BIM) is widely used in Architecture, Engineering, Construction. BIM not only contains 3d data for visualizations but also provides object geometry and attribute data for the planning, design, building, and operation and maintenance stages of a building's life cycle [1]. Currently, BIM is most often used in the early stages of the project life cycle [2]. Furthermore, person tracking and positioning have potential benefits in later stages of the project life cycle. The IPS (indoor positioning system) has been developed by researchers because the ability to locate and track people could be useful in the Operations & Maintenance (O&M) stage, such as in emergency response [3]. Multiple techniques for acquiring the positions of people have been developed. IPSs are classified into two categories: absolute tracking and relative tracking [4]. Absolute positioning systems can be further classified according to their methods, such as RSSI-based, fingerprinting-based, image-based, and floor-based methods. Both RSSI and fingerprint methods use wireless signals, namely, Wi-Fi, BLE (Bluetooth Low Energy), and magnetic fields, to compute distance, and then they utilize triangulation to acquire an estimated position of a target, or they use a pre-built signal map in an offline phase to compare online signal strength data with map data to estimate position [5]. However, these methods have some drawbacks: (1) Positioning accuracy is affected by variations in signal due to environmental changes, such as people walking or changes in furniture layout, and (2) The offline phase of the fingerprint method is a time-consuming and tedious task. Image-based methods also have some drawbacks: (1) Positioning accuracy is affected by image quality, which varies with environmental factors such as light intensity, and (2) The positioning ability is invalid when targets move out of range and multiple objects need to be tracked in several video fields of view [6]. Lastly, the floor-based method that located object (people or furniture) through measure pressure to detect object position on surface of floor, that through variation of surface pressure in every pixel of floor to know flow of people, but this method has a drawback that cannot aware specific character [7]. The relative positioning method, which uses the Inertial Measurement Unit (IMU), is widely used in personnel tracking, but the IMU has a problem of error accumulation that leads to serious drift error over time [8]. As noted above, each IPS has limitations. The objective of this paper is to propose a method that employs BIM model information and IoT technology to eliminate IMU positioning error and thereby to achieve an IPS with high accuracy and stability.

2 Methodology

To avoid the drawbacks of existing methods, we propose a positioning method that combines IoT and BIM technology to achieve high accuracy, real-time indoor positioning. The system was developed with the Revit API in the Microsoft .NET framework. The flowchart of the indoor positioning processes is shown in Figure 1.

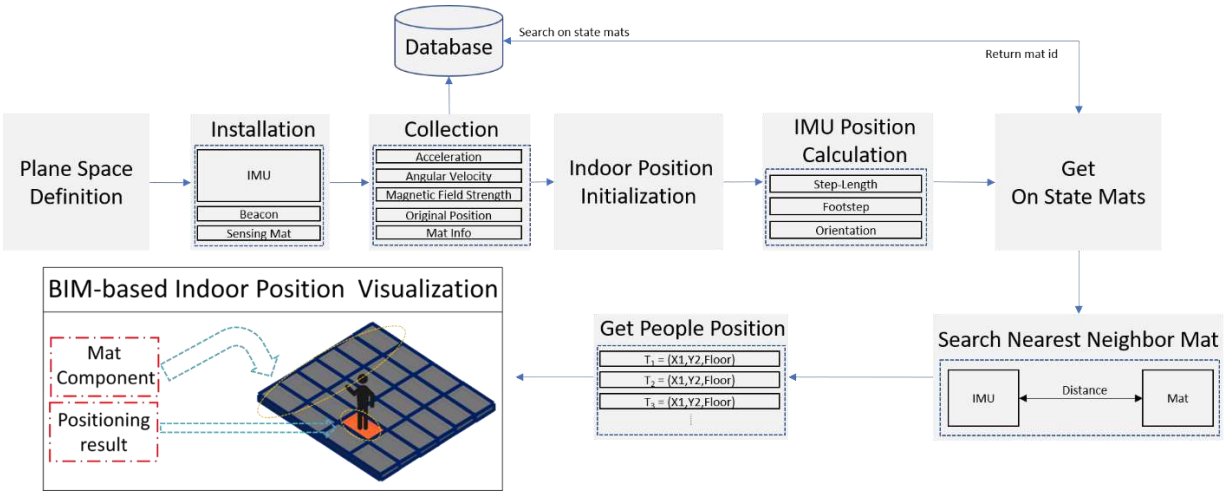

Figure 1. Research workflow of the proposed indoor positioning system.

In this process, we first defined the positioning space for demonstration and constructed a BIM model with Autodesk Revit. The model included a mat model having geometric shapes and specific parameters. Next, we installed sensing mats equal in size to the mat components in the defined space. The Beacon was installed on the door, and IMUs were worn by people. When sensor data were collected, the data of the sensing mats were output to a database. The Beacon's original position and the data on 3-axis acceleration, angular velocity, and magnetic field strength of the IMU were directly output to the positioning server. Upon receiving the original position data, the program initialized the position and utilized IMU data to calculate step-lengths, footsteps, and orientation to obtain the position of the IMU. Once the IMU position was determined, the positioning server searched for all the on-state mats in the database and got each mat id. The program also compared distances between the IMU and each on-state mat. After that, the mat at the shortest distance from the IMU was chosen as a person's position, and this position was used as a new original position for calculating the next position. Finally, the people's position results were displayed with highlights in Revit.

3 Experiment

In this chapter, we describe the entire experiment process, which is divided into four parts that are discussed separately.

3.1 Experimental site

The experimental site was in the research office of the Department of Civil Engineering at National Kaohsiung University of Science and Technology, as illustrated in Figure 2. In this experiment, we mainly focused on whether the reality sensing mat in cooperation with the BIM sensing mat component could effectively constrain IMU-based positioning error. Therefore, since positioning range was not the main topic of this study, we only used 9 block sensing mats in the experimental site.

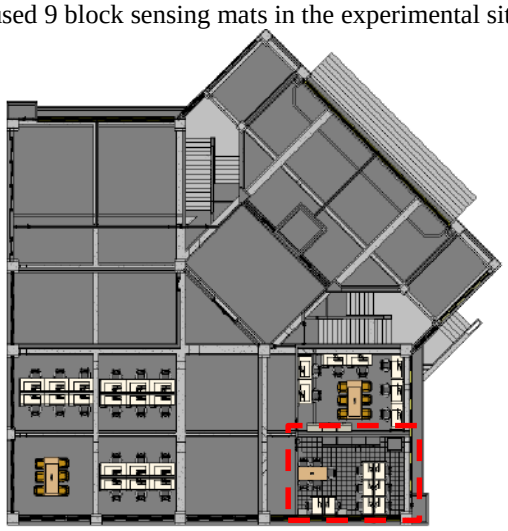

Figure 2. Experimental site

3.2 Sensor installation

The function of each sensor is shown in Figure 3.

The Beacon product model (USBeacon), which served as the original position in this study, was placed on the doorway of the room, as illustrated in Figure 4. The USBeacon is like a broadcast tower that transmits Bluetooth signals ceaselessly to provide UUID = fix, Major = 2, Minor = 2 for an IMU-based positioning system to initialize positions. These parameters stand for building, floor, and room, respectively.

In this study, IMU module is used to overcome the people Identification problem of floor-based method. The IMU product model was MPU-9250. The MPU-9250 can sense 3-axis acceleration, 3-axis angular velocity, and 3-axis magnetic field strength. The IMU device outputs necessary positioning data to the positioning server for a follow-up PDR algorithm to calculate an estimated position. In this study, the IMU was placed on the wearer's foot to easily count footsteps. An MCU (Microcontroller Unit) received raw data from the IMU sensor and the RSSI (received signal strength indicator) from the USBeacon. The MUC product model was ESP-32S. Once the ESP-32S entered the proximity detection range of the USBeacon, which was determined by RSSI value, the ESP-32S sent IMU data packets to the positioning sever via socket interface with UDP (User Datagram Protocol). UPD was used for data transmission because its transmission speed is faster than that of TCP (Transmission Control Protocol).

The sensing mat was the main feature in this study, so the relevant discussion is further divided into 4 points.

1. Composition of Sensing Mat: As shown in Figure 5, the sensing mat had a simple design using cheap materials such as sponge, cardboard, aluminum foil, and a mat. The design was inspired by button devices; the sensing mat is designed as an enormous button. The working principle of the sensing mat is 2 wires placed on the aluminum foil on the back of the mat and aluminum foil on the cardboard, respectively. When people step on the mat, the circuit is completed and the sensing mat will show an "on" state. While the sensing mat is in the "on" state, the Arduino YUN sends data to the positioning server database. To avoid accidental contact and erroneous updates, we used an elastic sponge material to separate the mat from the cardboard.
2. Figure 6 presents the installation positions of the sensing mats. We used 9 block sensing mats to verify the fusion algorithm that we proposed.
3. The sensing mat parameter design is shown in Figure 7. The parameters included UID, Room and Time respectively. "Room" indicated the room number where the sensing mat was located, "UID" was the identification number of each sensing mat, and "Time" was a timestamp for each "on" state. These parameters were used in the follow-up database search.
4. The sensing mat component design in the BIM model is shown in Figure 8. We created the UID parameter as the mapping condition for an actual sensing mat to extract coordinates from the sensing mat by UID parameter.

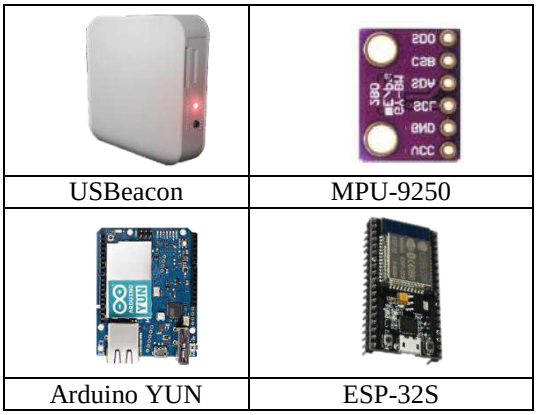

Figure 3. Sensors overview

Figure 4. The installation location of the USBeacon

Figure 5. The composition of a sensing mat

Figure 6. Sensing mat installation positions

UID	Room	Time 1
3	202	2019-01-23 22:29:44
6	202	2019-01-23 22:29:40
2	202	2019-01-23 22:29:37
4	202	2019-01-23 22:29:24
1	202	2019-01-23 22:29:21
8	202	2019-01-23 22:29:17
9	202	2019-01-23 22:29:14
7	202	2019-01-23 22:29:11
6	202	2019-01-23 22:29:09
8	202	2019-01-23 22:29:06
5	202	2019-01-23 22:29:03
4	202	2019-01-23 22:29:01
1	202	2019-01-23 22:28:58
3	202	2019-01-23 22:28:55
2	202	2019-01-23 22:28:53

Figure 7. Sensing Mat Database parameters

Figure 8. Sensing Mat component parameters

3.3 Positioning calculation

In this section, we generally introduce the IMU-based PDR algorithm and cooperation of the IMU with the BIM algorithm. Because the PDR was not a main research focus, we used an idealistic method to estimate position. The following sections describe the calculation processes for positioning.

3.3.1 IMU device position calculation

This research employed the Pedestrian Dead-Reckoning (PDR) algorithm. The PDR algorithm requires 3 positioning parameters: step length, orientation, and footsteps. In this study, we fixed step length at 30 cm. We employed Madgwick's method to obtain orientation components including roll, pitch, and yaw [9]. Lastly, we used total acceleration to count footsteps by threshold, and then we could calculate the estimated positions of the people. Figure 9 illustrates the concept of the PDR algorithm. Starting from the target's original position, the target's position at every moment is calculated as equation (1) and (2)

$$X_{k+1} = X_k + S * sin\,\theta_k \quad (1)$$
$$Y_{k+1} = Y_k + S * cos\,\theta_k \quad (2)$$

where (X_k, Y_k) is target's position at k time, S denotes the target's step length, and θ is orientation of the movement, and the θ value is as above-mentioned yaw that is from Madgwick's method, due to the position calculation is not involved three-dimension, therefore we only extract yaw as azimuth to calculate position.

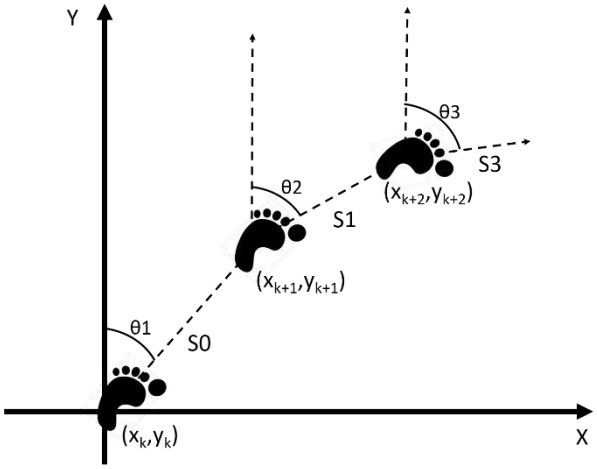

Figure 9. Pedestrian Dead-Reckoning algorithm

3.3.2 Fusion algorithm using Sensing Mat and BIM model

When the IMU device coordinates are calculated completely, we search the database for sensing mats in the "on" state. Next, we compare the sensing mat component from Revit to get a corresponding sensing mat component with the sensing mat UID parameter. Then the distance between the IMU and each sensing mat component coordinate is calculated. The process is illustrated in Figure 10. Afterwards, the sensing mat component with the shortest distance is taken as the final estimated position of the IMU. This final position is used to calculate the next position continually. Whenever the

final position of the IMU device is calculated completely, the sensing mat will be highlighted in orange. If not, the sensing mat with the final position is restored to its normal color.

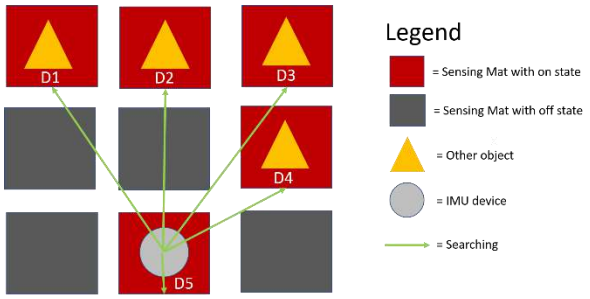

Figure 10. Searching process diagram.

3.4 Demonstration

As shown in Figure 11, we developed the IPS "Start" button in the Revit API and then defined the sensing area. When the user triggers the "Start" button, the program is launched. It starts a new thread in Revit to monitor port 3333. When a target enters the room (Room 202), the ESP-32S obtains original position information for that room, including UUID, Major, and Minor from USBeacon, and then via UDP sends a packet marked “202” to the positioning server. When the positioning server receives the original position of the target in Room 202 and starts receiving IMU sensor data of the target, the IPS will execute the indoor positioning process.

We tested some different states in the system, as shown in Figure 12. Starting in the lower right corner, the test path is shown in Figure 12 (a), (d), and (e). First, we tested the straight path state, then we tested the stretching across one block sensing mat state, and finally, we tested the diagonal path state. The results indicated that the IPS could correctly identify the position of the IMU device in the straight path, stretch across and diagonal path states.

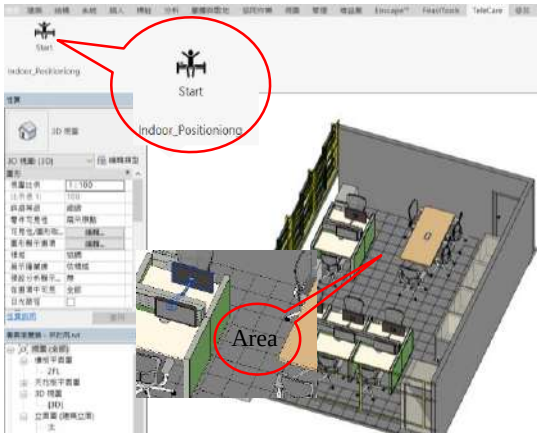

Figure 11. IPS GUI and visualization in Revit.

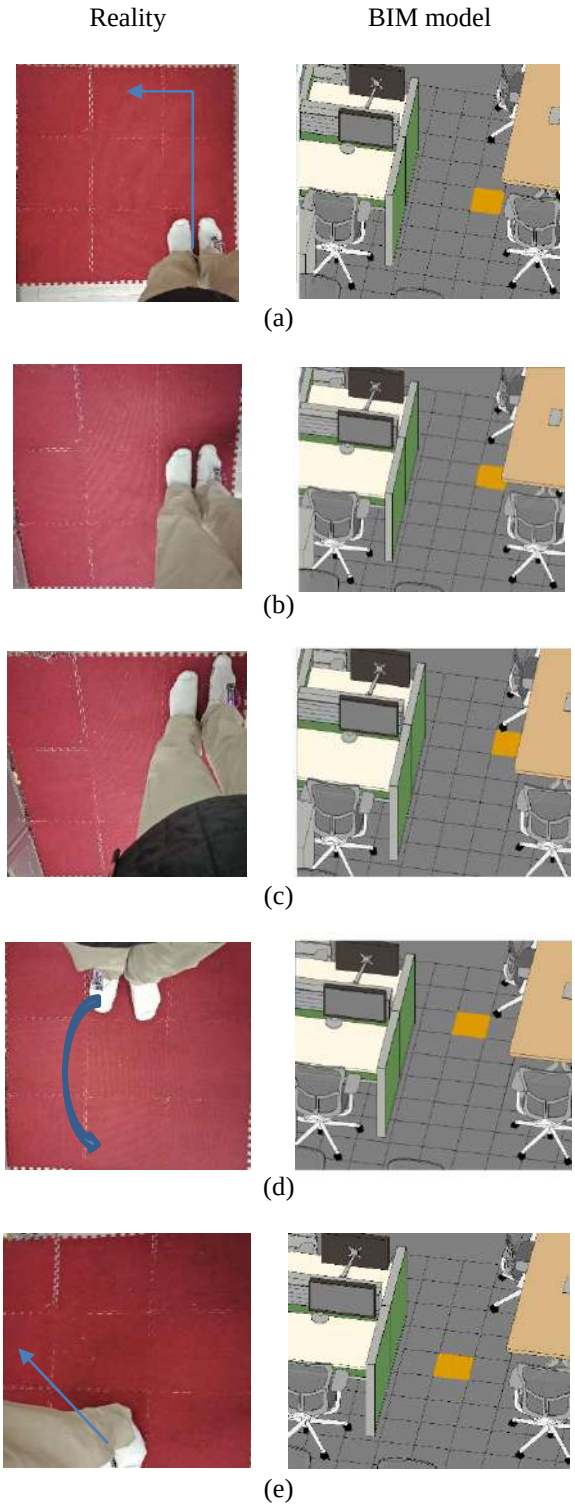

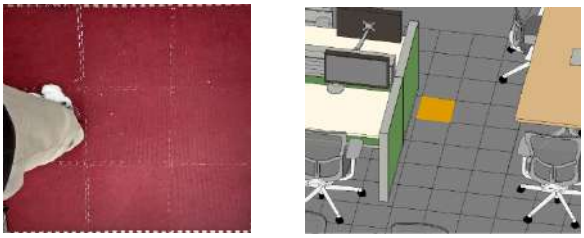

(f)

Figure 12. Test case for different walking states in Indoor Positioning System.

4 Conclusions

In this study, we used a simple method to fabricate sensing mats for use as sensors to detect the movements of people and employed a BIM model for integration and visualization to improve IMU-based positioning accuracy. The system presents these following characteristics: (1) simple materials to make sensing mats and easy installation; (2) improved accuracy to 30cm x 30cm zones; (3) a BIM model for visualizing indoor positioning data so that the user can easily know the locations of targets.

In the future, this system can integrate physiological sensors, such as heart rate sensors and blood velocity sensors, to automatically monitor people's conditions. If people have accidents, the system will notify the user or a caregiver. This idea may find application as a nursing home management system for monitoring elderly residents.

References

[1] Eastman C. and Teicholz P. and Sacks R. and Liston K. *BIM Hand book: A Guide to Building information Modelling for Owners, Managers, Designers, Engineers, and Contactors*, volume 2. John Wiley and Sons, Hoboken, NJ, USA, 2011.

[2] Eadie R. and Browne M. and Odeyinka H. and McKeown C. and McNiff S. BIM implementation throughout the UK construction project lifecycle: An analysis. *Automation in Construction*, 36:145-151, 2013. doi.org/10.1016/j.autcon.2013.09.001.

[3] Li N. and Becerik-Gerber B. and Krishnamachari B. and Soibelman L. A BIM cantered indoor localization algorithm to support building fire emergency response operations. *Automation in* Construction, 42:78-89, 2014. doi.org/10.1016/j.autcon.2014.02.019.

[4] Park J. and Chen J. and Cho Y.K. Self-corrective knowledge-based hybrid tracking system using BIM and multimodal sensors. *Advanced Engineering Informatics*, 32:126-138, 2017. doi.org/10.1016/j.aei.2017.02.001.

[5] Yim J. and Park C. and Joo J. and Jeong S. Extended Kalman Filter for wireless LAN based indoor positioning. *Decision Support Systems*, 45(4):960-971, 2008. doi.org/10.1016/j.dss.2008.03.004.

[6] Deng Y. and Hong H. and Deng H. and Luo H. BIM-based Indoor Positioning Technology Using a Monocular Camera. *Proceedings of the International Symposium on Automation and Robotics in Construction (ISARC 2017)*, pages 1030-1036, Taipei, Taiwan, 2017.

[7] Vezina R. and Lombardi M. and Pieracci A. and Santinelli P. and Cucchiara R. A general-purpose sensing floor architecture for human-environment interaction. *ACM Transactions on Interactive Intelligent Systems (TIIS)*, 5(2):1-26, 2015. doi.org/10.1145/2751566.

[8] Alvarez J.C. and Alvarez D. and López A. and González R.C. Pedestrian Navigation Based on a Waist-Worn Inertial Sensor. *Sensors (Basel)*, 12(8):10536–10549, 2012. doi.org/10.3390/s120810536.

[9] Madgwick S. An efficient orientation filter for inertial and inertial/magnetic sensor arrays. *Report x-io and University of Bristol (UK)*, 25:113-118, 2010.

Assessment of Work Efficiency of HMD Viewing System for Unmanned Construction Work

G. Yamauchi[a], T. Hashimoto[a], and S. Yuta[b]

[a]Public Works Research Institute, Japan
[b]Shibaura Institute of Technology, Japan
E-mail: yamauchi-g573bs@pwri.go.jp, t-hashimoto@pwri.go.jp, yuta@ieee.org

Abstract –

This study describes a simple head mounted display(HMD) viewing system for an unmanned construction system(UCS) and an assessment of the work efficiency using the HMD system.

The deployment of a UCS is a significant problem because majority of the construction machines are not compatible with remote operation. In this study, focusing on the deployment problem regarding the viewing system of a UCS, we developed a simple HMD type viewing system. The HMD system provides the visual information so that images are projected on the HMD in the same arrangement as conventional LCD monitor systems.

The HMD system of a hydraulic excavator was tested with respect to work efficiency in comparison with a conventional LCD system using a model task that simulates the excavation and transportation of soil. Experimental results of the model task indicate that the working efficiency of the HMD system was improved compared to the conventional LCD system.

Keywords –

Unmanned Construction Work; Teleoperation; Head Mounted Display;

1 Introduction

In recent years, natural disasters such as a sediment disaster caused by typhoons, heavy rains, earthquakes, and volcanic eruptions are increasing in Japan. Once disasters occur, construction works are conducted for reduction and restoration of the damages. In such cases, an unmanned construction system (UCS) will be used for safe construction to prevent secondary disasters [1]. A UCS is a construction system that uses a teleoperated construction machine, and an operator controls the machine from a safe place, as shown in Figure 1. It was developed to respond to the volcanic disasters occurring owing to pyroclastic and debris flows in the eruption of Mount Unzen-Fugen in 1991[2]. UCSs have been used at over 150 sites, and recently, they were utilized for construction works related to debris demolition in the 2011 East Japan Great Earthquake. the 2016 Kumamoto

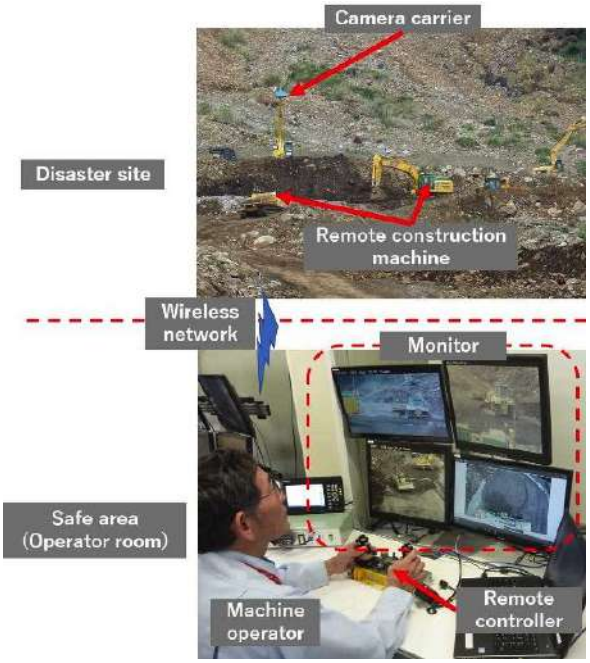

Figure 1. Unmanned construction system using conventional LCD monitors.

2 VIEWING SYSTEM OF CURRENT UCS AND ITS ISSUES

In a UCS, the operator recognizes the environment surrounding the construction machine via two types of viewing: direct viewing for a near field and non-direct viewing for a distant field. In the direct viewing system, a machine operator controls a construction machine in the near field at several tens of meters using a small and light-weight remote controller. Further, in the non-direct viewing system, a machine operator and camera operator are required to control the machine with

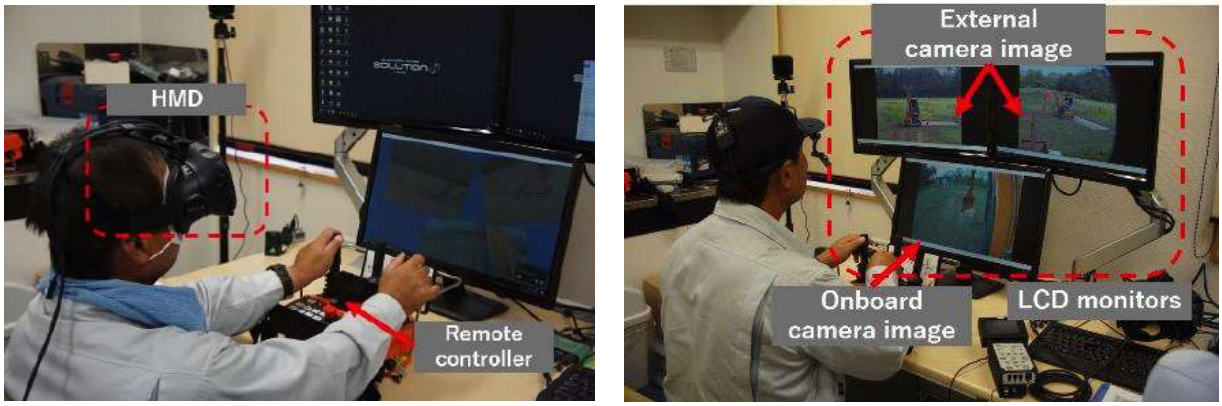

(a) HMD viewing system (b) LCD viewing system

Figure 2. Viewing system

Figure 3. Monitor layouts of HMD viewing system

limited information such as the transmitted image, which is controlled by a camera operator. The camera operator controls camera conditions such as the pan angle, tilt angle, and zoom for the machine operator. In the non-direct viewing system, cameras are usually installed on the construction machine and outside the machine to recognize a construction environment, and wireless communication systems are also installed on the machine. LCD monitors and other equipment are installed in an operator room.

A UCS realizes safe construction work in dangerous areas such as disaster sites. However, a UCS has several disadvantages such as work efficiency reduction and deployment of remote operation systems. Usually, work efficiency owing to UCS usage is approximately 50% compared to a normal manned construction work[5]. The cause of the reduction is considered the lack of information and time delay in data and image transmission. Moreover, the deployment is also a major problem because most of the construction machines are not compatible with remote operation. Furthermore, in a situation where a disaster occurs, the roads may be deteriorated, and it makes it difficult to readily set up the remote operation system.

To overcome such situations, the Japanese government developed a decomposable excavator that can be transported as small parts (3 ton) using a large helicopter. Further, rapid deployment of the remote operation system is still a problem. Several systems were proposed using additional information such as virtual reality and haptic interfaces [6][7]. These intelligent systems improve remote operation, but it is difficult to use them at disaster sites owing to the deployment problem. Teleoperation systems with the objective of rapid deployment were also proposed by [8] and [9]. However, the systems were not verified the work efficiency and effectiveness compared to the current UCS.

In this study, focusing on the deployment problem regarding the viewing system of remote construction machines, we describe a simple head mounted display(HMD) viewing system and an assessment of the work efficiency of the HMD system.

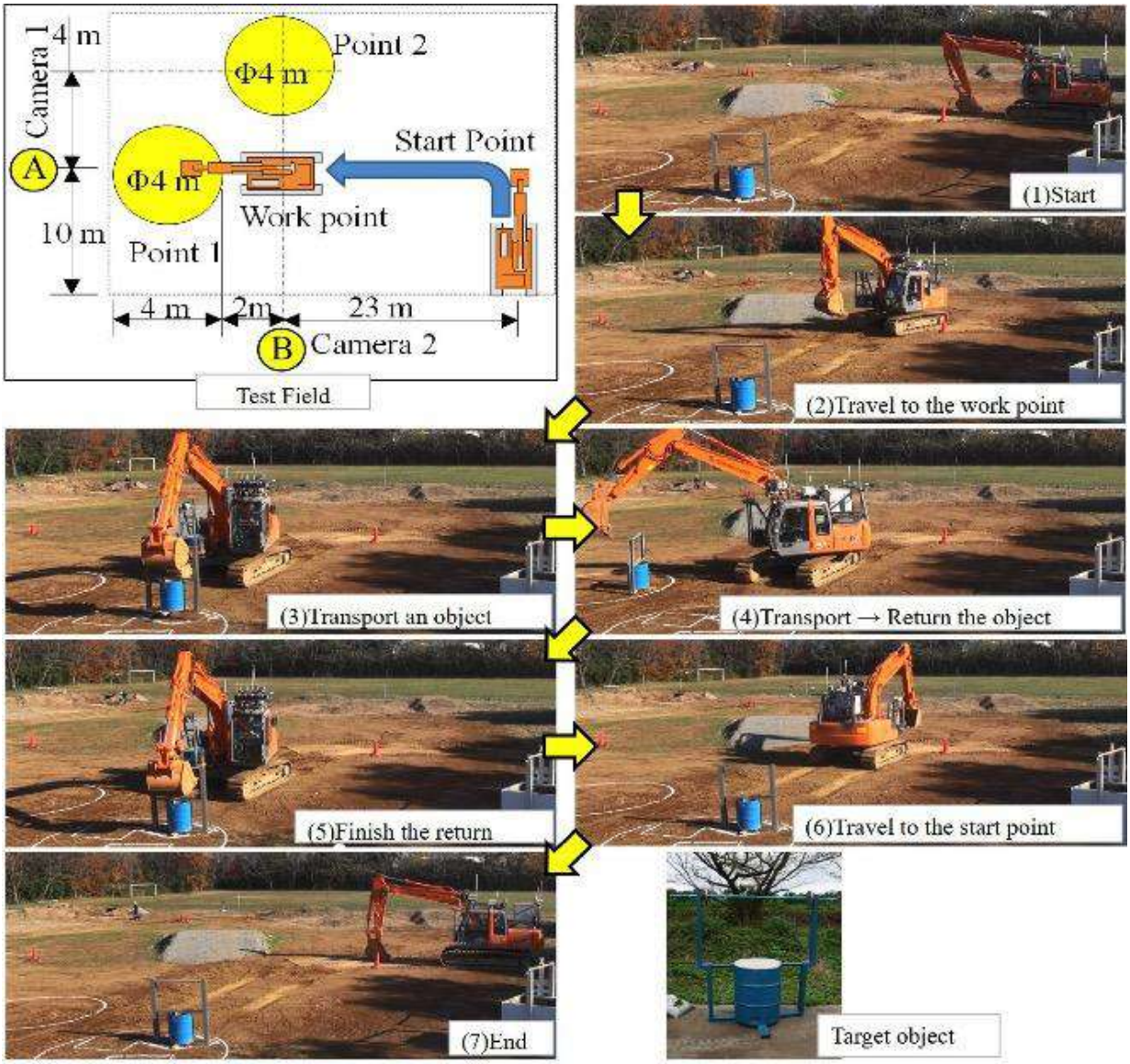

Figure 4. Overview of model task [10]

3 HMD VIEWING SYSTEM

To reduce the setup time for remote operation, we developed a HMD viewing system for the alternation of the current LCD monitor system. Figure 2 shows the HMD and LCD viewing systems, respectively. The HMD viewing system displays a similar monitor layout and similar images as the LCD system on the HMD's monitor as shown in Figure 3. The top two monitors display the image from external cameras, which are installed outside the excavator. In contrast, the bottom monitor displays the image from the onboard camera at the front of the excavator's cabin via a wireless network. The time delay of the transmitted image is approximately within 200 ms in both the HMD and LCD systems.

In addition, the manufacturer's remote controller is used to operate an excavator. The remote controller can teleoperate the excavator several hundred meters away within a delay period of 50–80 ms.

4 EXPERIMENTAL SETUP

4.1 Model task

The work efficiencies of the HMD viewing system and LCD monitor system were evaluated based on a model task. The model task was developed to evaluate

the work efficiency of hydraulic excavators in actual sites, and it simulates the traveling, excavation, and transportation of soil[10]. The model task consists of the movement job and working job. The overview of the model task is shown in Figure **4**. The scheme of the model task is described below:

1) Traveling job: the excavator moves from the starting point to the working job area

2) Working job: the excavator lifts a target object placed in a circle , transports it to another circle, and releases the target object

3) Working job: the excavator lifts the target again and transports it to the initial point

4) Traveling job: the excavator moves to the initial starting point

4.2 Experimental condition

The work efficiency was evaluated in three patterns of conditions as listed in Table 1.

Table 2 lists the specifications of the hydraulic excavator and other equipment used for the experiment. The model task was conducted in ten trials with respect to each pattern; thus, a machine operator conducts the model task using 30 trials in an experiment. The experiment was conducted by ten different machine operators. Table 3 lists the ages of the machine operators and their years of experience in using construction machines.

The camera operations were controlled by the same person. Two external cameras were installed at points A and B in the Figure 4.

Table 1. Experimental pattern

Pattern	Viewing system	Operation
1	LCD	remote
2	HMD	remote
3	Onboard	Onboard

Table 2. Specifications of equipment

Hydraulic excavator	Model	HITACHI ZX35U-5B
	Operation weight	3440 kg
	Bucket capacity	0.11 m^3
Onboard camera		SONY SNC-VB630
External camera		SONY SNC-VB630
wireless access point		icom SE-900

Table 3. Operator age and machine usage experience

Tag	Age	Year of experience
A	34	10
B	37	19
C	41	20
D	35	6
E	33	15
F	60	33
G	38	8
H	37	10
I	49	20
J	42	19

5 EXPERIMENTAL RESULTS AND DISCUSSION

The work efficiency is evaluated based on the time taken to complete the model task (i.e., cycle time). In each pattern, the previous three trials are handled as learning trials, and the last seven trials were considered as evaluation data. Figure 5 shows the average cycle time of the forward movement, working, and backward movement with respect to 10 operators. Thus, the onboard operation is executed in 129 s with a standard deviation of 10 s, the remote operation using LCD monitors is completed in 328 s with a standard deviation of 11 s, and the remote operation using the HMD is completed in 292 s with a standard deviation of 10 s. As previously reported in [11], the remote operation depends on the operator ’s skills to understand the environments near the excavator from only the image information. Therefore, the standard deviation of remote operation is larger than the onboard teleoperation, particularly in case of the working job.

The cycle time of remote operation in case of HMD was shorter than that in case of LCD monitor. It is considerable that internal and external factors exist that caused the difference of the cycle time. In this study, we focus on the learning progress and interfaces. The experiment was conducted in the order of onboard operation, remote operation using an LCD monitor, and remote operation using the HMD. Based on the learning effects, the last operation might possess a relatively short cycle time. To confirm the effects, we categorized the learning progress of both remote operations. In terms of the learning progresses in both remote operations, it is considerable that the order of the experiment pattern should affect the results.

The examples of the series of cycle times are shown in Figure 6. In this experiment, the criterion for learning progress was considered as to whether the slope of the regression line is less than -3. Based on this criterion, Table 4 lists the learning progress of each operator. The

learning of two operators (A and G) progressed continuously in both the experiments. Other operators did not seem to be affected by the order of the experiment pattern.

Further, the averages of the cycle time, except for the two operators, are 324 s and 287 s using the LCD monitor and HMD, respectively. Therefore, the influence of the learning effects was small, and it is considered that the difference in the apparatus significantly affects the cycle time.

After the experiment, we interviewed the operators regarding the problems with the HMD. Most of the operators said that it was easy to understand the situation of the excavator, but it was heavy, and it tired them easily.

6 CONCLUSION

This study compares the conventional LCD system with the HMD system regarding the change in the work efficiency owing to the visual interface in the remote control of the hydraulic excavator. The HMD system was constructed so that images are projected on the HMD in a similar arrangement as the conventional one. Experimental results regarding the working efficiency of the hydraulic excavator in model tasks were confirmed, and the efficiency of the HMD system was improved compared with the conventional one.

In terms of the visual device, compared with the conventional system, it is possible to construct a system with only a PC and HMD, and combining with the hydraulic excavator, which can be transported freely, it is possible to respond immediately in the event of a disaster.

The future task is immediate deployment of an external camera. Currently, the external cameras are assembled in the tower or via construction machines with cameras attached to the tip of the bucket called camera carrier, to provide a viewpoint from the outside while working. It is necessary to develop a system that constructs external cameras immediately on site.

Table 4. Learning progress of the model task. O means that the learning progressed (i.e., cycle time became relatively short gradually), and X means that the learning did not progress.

Tag	Remote operation using LCD monitor	Remote operation using HMD
A	O	O
B	X	X
C	X	X
D	O	X
E	O	X
F	X	X
G	O	O
H	X	O
I	X	O
J	X	O

References

[1] K. Chayama, A. Fujioka, K. Kawashima, H. Yamamoto, Y. Nitta, C. Ueki, A. Yamashita, and H. Asama, "Technology of unmanned construction system in japan," *JRM*, vol. 26, no. 4, pp. 403–417, 2014.

[2] Y. Hiramatsu, T. Aono, and M. Nishio, "Disaster restoration work for the eruption of mt usuzan using an unmanned construction system," *Advanced Robotics*, vol. 16, no. 6, pp. 505–508, 2002.

[3] E. Egawa, K. Kawamura, M. Ikuta, and T. Eguchi, "Use of construction machinery in earthquake recovery work," *Hitachi Review*, vol. 62, no. 2, pp. 136–141, 2013.

[4] T. Hashimoto, "Unmanned construction system for disaster response," *JAPAN-AMERICA Frontiers of Engineering Symposium*, 2014.

[5] T. Hashimoto, K. Fujino, and S. Yuta, "A study of the working efficiency of a remote control type hydraulic excavator," in Proceedings of International Society for Terrain-Vehicle Systems (ISTVS). Joint 19th International and 14th European-African Regional Conference.

[6] M. D. Elton, A. R. Enes, and W. J. Book, "A virtual reality operator interface station with hydraulic hardware-in-the-loop simulation for prototyping excavator control systems," in *2009 IEEE/ASME International Conference on Advanced Intelligent Mechatronics*, July 2009, pp. 250–255.

[7] H. Sulaiman, M. N. A. Saadun, and A. A. Yusof, "Modern manned, unmanned and teleoperated excavator system," *Journal of Mechanical Engineering and Technology (JMET)*, vol. 7, no. 1, 2015.

[8] M. Hutter, T. Braungardt, F. Grigis, G. Hottiger, D. Jud, M. Katz, P. Leemann, P. Nemetz, J. Peschel, J. Preisig, N. Sollich, M. Voellmy, M. Zimmermann, and S. Zimmermann, "Ibex; a tele-operation and training device for walking excavators," in *2016 IEEE International Symposium on Safety, Security, and Rescue Robotics (SSRR)*, Oct 2016, pp. 48–53.

[9] "Development of remote operation room for unmanned construction," http://www.kumagaigumi.co.jp/press/2015/pr 160324 1.html (in Japanese).

[10] M. Moteki, S. Yuta, and F. Kenichi, "The proposal of the model task for efficiency evaluation of the

construction work by remote control of a hydraulic excavator," *Journal of JCMA*, 2014.
[11] M. Moteki, S. Yuta, and K. Fujino, "Work efficiency evaluation on the human interface of the unmanned construction," *Journal of RSJ*, 2014.

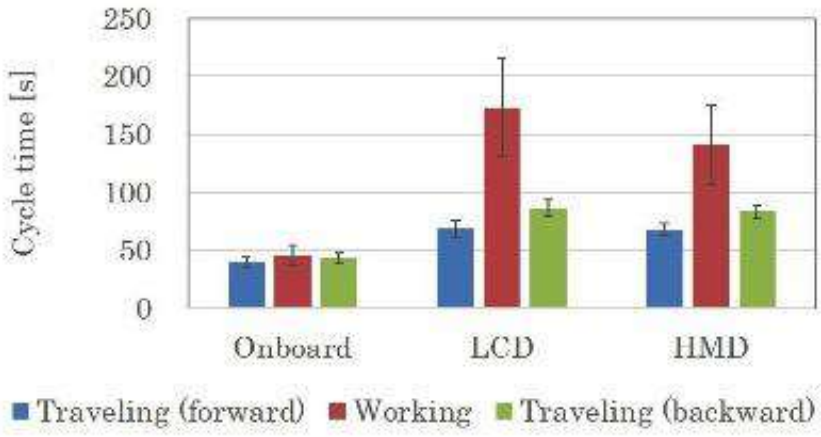

Figure 5. Average cycle time

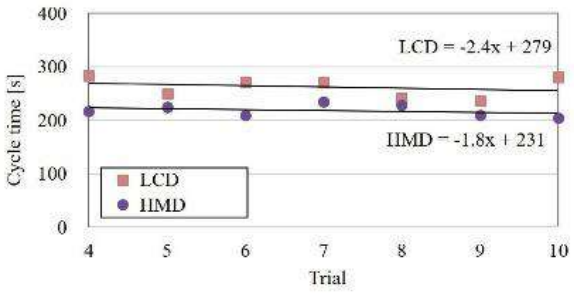

(a) Operator C result; the learnings of LCD and HMD results were not progressed.

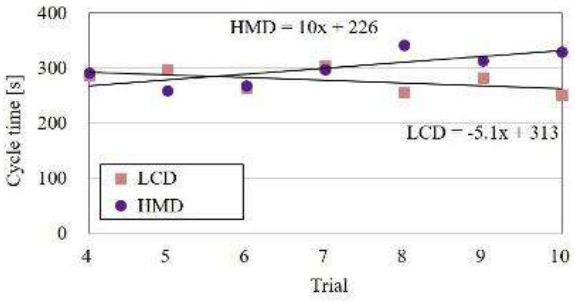

(b) Operator D result; the learning of LCD was progressed, but its HMD results was not progressed.

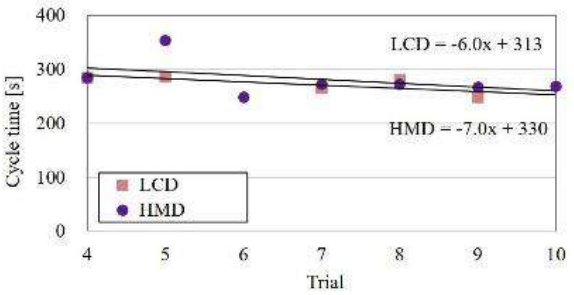

(c) Operator G result; the learnings of LCD and HMD results were progressed.

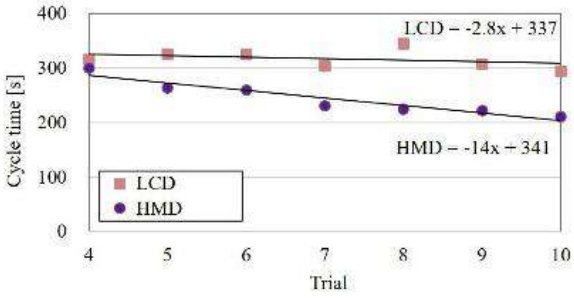

(d) Operator H result; the learning of LCD was not progressed, but its HMD results was progressed.

Figure 6. Trial series of experimental results

Using Virtual Reality Simulation for Optimizing Traffic Modes Toward Service Level Enhancements.

F. (Firas) Habbal[a], F. (Fawaz) Habbal[a], A. Al Shawabkeh[b], A. Al Nuaimi[c], and A. Safi[c]

[a]College of Business Administration, American University in the Emirates, UAE
[b]College of Business, Al Ain University of Science & Technology, UAE
[c]Ministry of Infrastructure Development, UAE
E-mail: Firas.Habbal@aue.ae, Fawaz.habbal@aue.ae, Abdallah.alshawabkeh@aau.ac.ae, Abdullah.alnuaimi@moid.gov.ae, Ammar.safi@moid.gov.ae

Abstract –

Traffic congestion and roads service level are major issue in many countries. Using technology such as simulation offers effective approach to better understanding the problem, and predict optimal solutions. This paper examines the application of Virtual reality (VR) for evaluating the roads service level of five different scenarios in UAE as new method to evaluate and enhance road service levels, as well as understanding the potential risks and costs for applying those scenarios into reality. The study will test the usefulness of VR simulation to enhance traffic service level, second creation of traffic objects to explore potential usage, third understand the interaction between users and digital objects. All hypothesis have significant impacts toward enhancing service level, and the overall findings are consistent and clear. The level of technological orientation was examined to the overall implementation. The results help understanding key issues and potential service level in development of future VR applications in roads construction.

Keywords –

Virtual realities; automation in Construction; roads service level; traffic objects enhancements.;

1 Introduction

Ministry of Infrastructure of Development in United Arab Emirates always strive to utilize the latest technology to enhance its service related to roads and infrastructure. Many scholars reviewed the use of technology to enhance construction modes and experience, construction has seen a significant increase in its productivity since using automation to analyze best practices [1]. The application of virtual reality in construction was described by Sampaio and Matins [2] to provide better understanding of how roads construction are being belt such as bridges with considering related to safety and level of service. Other scholars used virtual reality to study deeper usage of VR in maintaining complexed buildings, Grabowski and Jankowski [3] used this technology to study VR input methods using different HMD hardware setups. Roupé et al. [4] also studied the level of enhancement using VR and body movement, and stated that one of the main implications of VR body tracker is the cost of equipment's and needs a specialized team to be able to utilize this technology, Roupé et al. proved that VR body postures is able to navigate through out city modeling. This paper will study the reflect of changes in optimizing traffic modes toward level of service based on the UAE government needs and reviews. Using Virtual Reality screening methods the system will predict the level of enactments and analyze the results of the interchange with the models update.

2 Literature Review

The Virtual Reality have been used rapidly for many industries recently, and the need of to apply this technology in the construction industry became a need from both government and private sector, and the positive impact of this technology has been demonstrated in many studies [5]. Goedert et al. [6] discussed the impact of VR simulation into construction education and to provide better understanding for different scenarios of building methodologies. The main feature of VR environment is to provide immediate real time results for its applications, especially in interactive activities [7]. VR also proven that it will be great addition for other technologies to enhance understanding and performance of construction sites in addition to analyzing the development of Building Information Modelling (BIM)[8-10]. Following the mixed realities technologies which combines both VR and AR, Russell el al.[11] demonstrated the usage of mixed realities technologies to train and improve understanding of 3D modelling techniques which can

replace the traditional methods using computer – aided design (CAD). Hence, the Mixed realty technology became very acceptable by users and supports interactive visualization [12]. However, the studies related to VR actual application and its application in construction is very limited [13]. And many scholars found immersive technologies using head mounted display (HMD) can be cause errors and unpredictable results for many systematic applications [14]. Yet there are enormous need for studies to prove or to propose a successful usage technologies and to investigate or develop new methods of VR in training and analyzing results [15]. Most of construction drawings use 2D modeling, although using 2D modeling can assist specialists to determine necessary information in construction sites, it cannot interact with real time environment and more important it cannot provide enough information to build the required data. Jang [16] declared that using experimental methods using immersive technologies can enhance practical abilities to better understanding results. Additionally, virtual reality influenced by the way people do their work and provide new opportunities to better understand surrounding environment [17]. Arian and Burkle [18] virtual reality improves the understanding of real time issues in construction sites, and the successful collaboration of virtual reality with real construction sites will improve safety education through experiential learning.

3 Methodology

The analysis methodology that will be followed in evaluating the various roadway elements surveyed; interchanges, junctions, roundabouts and links. The basis of the analysis will be highway Capacity Manual (HCM) using VR scenario modeling. The Highway Capacity Manual (HCM) methodology specifies six levels of service to represent the operational characteristics of a given transportation facility. Roadway Level of service (LOS) describes the operating condition determined from the number of vehicles passing over a given segment of the roadway during a specified period of time. It is a qualitative measure of several factors which include: speed, travel time, traffic interruptions, freedom to maneuver, driver comfort, convenience, safety and vehicle operating costs. The study is based on Al Ittihad road in Sharjah – Sharjah bound.

The six levels of service which have been established as standards by which to gauge roadway performance are designated by the letters A through F and are defined as follows:

- LOS “A” – Free flow, individual users virtually unaffected by the presence of others;
- LOS “B” – Stable flow with a high degree of freedom to select operating conditions;
- LOS “C” – Flow remains stable, but with significant interactions with others;
- LOS “D” – Approaching unstable flow, freedom to maneuver is severely restricted;
- LOS “E” – Unstable flow, with volumes approaching capacity of the roadway; and
- LOS “F” – Forced flow in which the traffic exceeds the amount that can be serviced.

A Passenger Car Equivalent is essentially the impact that a mode of transport has on traffic variables (such as headway, speed, density) compared to a single car. The factors adopted in this analysis are as below:

Table 1. PCE factors

NO	Mode	PCE Factor
1	LGV	1.0
2	HGV	2.5

Signalized intersection LOS describes the operation of the intersection based on average delay per vehicle. To estimate the average vehicle delay for each intersection, average control delay per vehicle is calculated for each lane group and aggregated for each approach and for the intersection as a whole. The six levels of service are designated by the letters A through F. and are defined as follows:

- LOS “A” – Average vehicle delay 10 seconds or less;
- LOS “B” – Average vehicle delay between 11-20 seconds;
- LOS “C” – Average vehicle delay between 21-35 seconds;
- LOS “D” – Average vehicle delay between 36-55 seconds;
- LOS “E” – Average vehicle delay between 56-80 seconds; and
- LOS “F” – Average vehicle delay exceeds 80 seconds.

Unsignalized intersection LOS describes the operation of the individual movement. It is determined by the computed or measured control delay and is defined for each minor movement. LOS is not defined for the intersection as a whole. According to the HCM, six levels of service have been established, designated by the letters A through F. These levels of service levels are defined as follows:

- LOS “A” – Average vehicle delay 10 seconds or less;

- LOS "B" – Average vehicle delay between 11-15 seconds;
- LOS "C" – Average vehicle delay between 16-25 seconds;
- LOS "D" – Average vehicle delay between 26-35 seconds;
- LOS "E" – Average vehicle delay between 36-50 seconds; and
- LOS "F" – Average vehicle delay exceeds 50 seconds

This study proposes a comparison between the application of different models to study the level of enhancements to the same road for each prospective using HCM VR modelling.

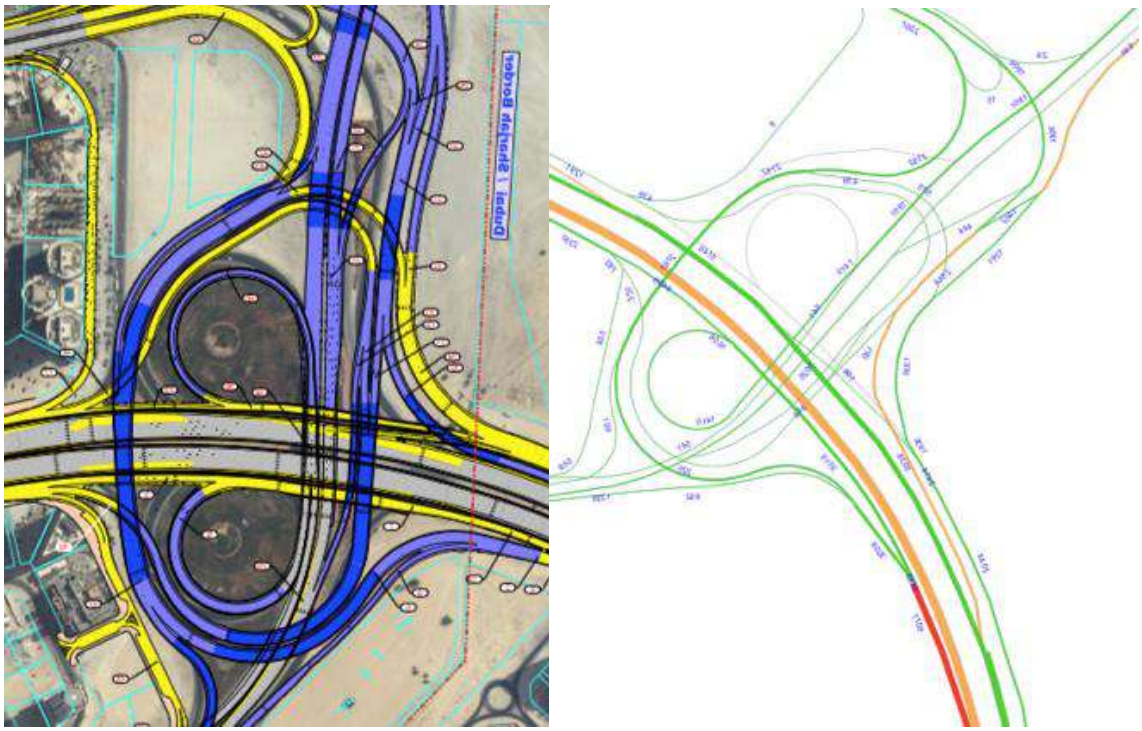

Figure 1. Screenshot for the system comparing between the Al Nahda intersection before and after utilizing VR technology

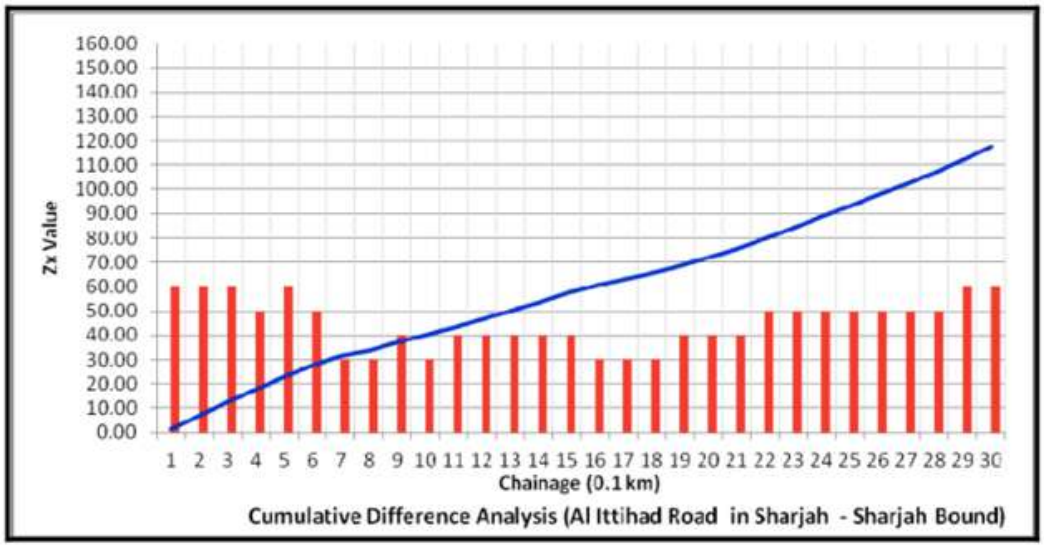

Figure 2. Cumulative difference analysis

The traffic count survey results and the analysis thereof for roadway elements surveyed. The methodology followed in the analysis is also mentioned along with the Level of Service (LOS) criteria.

4 Data analysis and discussion

Traffic count locations were discussed with the Ministry in the project early start as tabulated in the Table 2 - 3 below. The classification followed in the survey was Light Vehicles and Heavy Vehicles. Data were collected in 2018, junctions name were listed as per ministry of infrastructure development classifications.

Table 2. Existing traffic count

Junction No.	Junction type
J-1	Signalized
R/A-1	Roundabout
R/A-2	Roundabout
R/A-3	Roundabout
R/A-4	Roundabout
R/A-5	Roundabout
R/A-6	Roundabout
RIRO-1	Right In/ Right Out
RIRO-2	Right In/ Right Out
RIRO-3	Right In/ Right Out
RIRO-4	Right In/ Right Out
RIRO-5	Right In/ Right Out
I/C-1	Interchange

Table 3. Existing traffic count

Roundabout	AM		PM	
	LOS	Delay	LOS	Delay
R/A-1	E	42.8	F	70.8
R/A-2	F	236.3	F	248.2
R/A-3	C	19.6	D	31.2
R/A-4	F*	N/A	F*	N/A
R/A-5	F*	N/A	F*	N/A
R/A-6	F	296.3	F	166.5

Note: (*) Roundabout is failing due to upstream blockage

Data on vehicle classification were collected during the traffic count survey. Vehicles were classified into heavy vehicles and light vehicles. The percentages of LV and HV were calculated for two locations along Al Ittihad Road (Junction 1 and Roundabout 1), during the AM and PM peak periods. An overall summary of this vehicle classification is shown in tables (4) below.

Table 4. LV – HV percentage from traffic survey

Intersection	AM		PM	
	LV	HV	LV	HV
J-1	93.4%	6.6%	95.0%	5.0%
R/A-1	97.6%	2.4%	96.2%	3.8%
R/A-2	97.9%	2.1%	97.5%	2.5%
R/A-3	94.5%	5.5%	97.0%	3.0%
R/A-4	93.0%	7.0%	95.0%	5.0%
R/A-5	95.5%	4.5%	95.5%	4.5%
R/A-6	94.8%	5.2%	97.5%	2.5%
RIRO-1	93.8%	6.20%	95.6%	4.40%
RIRO-2	94.1%	5.90%	97.9%	2.10%
RIRO-3	92.0%	8.0%	97.2%	2.80%
RIRO-4	93.3%	6.70%	96.9%	3.10%
RIRO-5	97.7%	2.30%	95.2%	4.80%
I/C-1	95.60%	4.40%	97.10%	2.90%
I/C-2	92.0%	8.0%	93.0%	7.0%
I/C-3	95.0%	5.0%	94.7%	5.3%
L1	94.6%	5.4	97.4%	2.6%

In the experiments the above data were inserted into the VR prediction software and attributes were specified to study the level of enhancements and the influence of the proposed junctions' layouts in order to obtain future LOS based on average delay values according to the HCM methodology.

The proposed design includes upgrade of number of lanes, upgrade roundabouts to four legged and 3 legged signalized intersections, demolish flyover and replace it with four legged signalized intersection and underground tunnel, upgrade signalized intersections to flyover bridges and underground tunnels, and adding directional ramps to interchanges and eliminating key waving segments. The volumes obtained from the traffic model were used for the analysis. Table 5 tabulates the analysis results based on the recommended option and Figure 1 present the analysis summary. Based on the constructability and phasing of the project improvements two possible scenarios have been considered.

- Ultimate Scenario
- Reduced Configuration

Accordingly, for the reduced configuration scenario all tunnels in Junctions 1, 3 and 5 were removed and the traffic analysis for this option was carried out. Table 5-3 shows the analysis summary results of the reduced configuration scenario.

Table 5. LOS analysis for ultimate design scenarios

Junction #	Type of Junction	AM		PM	
		LOS	Delay	LOS	Delay
Junction 1	Signal + Tunnel	A	10	C	30.9
Junction 2	Signal	A	9.5	C	23.4
Junction 3	Signal + Tunnel	B	17.3	C	20.4
Junction 4	Signal	A	4.4	A	4.3
Junction 5	Signal + Tunnel + Bridge	C	20.9	C	25.7
Junction 6	Single point diamond Interchange	A	9.9	B	16.8
IC-1	Interchange	C	-	C	-
IC-2	Interchange	D	-	D	-
IC-3	Interchange	D	-	D	-

Table 6. LOS analysis for reduced configuration scenarios

Junction #	Type of Junction	AM		PM	
		LOS	Delay	LOS	Delay
Junction 1	Signal + Tunnel	C	23.3	F	87
Junction 2	Signal	B	14	C	30.8
Junction 3	Signal + Tunnel	B	13.4	D	40.6
Junction 4	Signal	B	13.7	A	8.4
Junction 5	Signal + Tunnel + Bridge	C	24.3	E	62.2
Junction 6	Single point diamond Interchange	B	16.4	C	21.9

It can be inferred from Table 6 that Junction 3 operates at an acceptable level of service with the reduced configuration. However, the removal of the tunnels in junctions 1 and 5 depict that the junctions do not operate at an acceptable level of service. Accordingly, the grade separations at junctions 1 and 5 are warranted.

Since Junction 3 was working at an acceptable LOS in previous experiment with the removal of the underground tunnel unlike Junctions 1 and 5, the reduced scenario comprised of the removal of the Junction 3 tunnel. Table 7 tabulates the analysis results based on the ultimate option.

Table 7. LOS analysis for ultimate design scenarios update

Junction #	Type of Junction	AM		PM	
		LOS	Delay	LOS	Delay
Junction 1	Signal + Tunnel	B	10.8	C	33.4
Junction 2	Signal	A	9.9	C	20.4
Junction 3	Signal + Tunnel	B	18.3	C	21.7
Junction 4	Signal	A	4.4	A	4.1
Junction 5	Signal + Tunnel + Bridge	C	23.5	D	42
Junction 6	Single point diamond	B	10.6	B	18.8
IC-1	Interchange	C	-	C	-
IC-3	Interchange	D	-	D	-

Table 8. LOS analysis for reduced configuration scenarios update

Junction #	Type of Junction	AM		PM	
		LOS	Delay	LOS	Delay
Junction 1	Signal + Tunnel	B	13.6	D	42.9
Junction 2	Signal	B	11.1	D	35.3
Junction 3	Signal	C	32.2	D	51.7
Junction 4	Signal	A	9.1	A	5.3
Junction 5	Signal + Tunnel + Bridge	C	26.4	D	37.7
Junction 6	Single point diamond	B	12.7	C	22.5

The analysis summary for the Ultimate Year update was carried out using the volumes obtained from the traffic model based on the proposed design is tabulated as Table 7 and 8

5 Conclusion

Many countries suffer because of traffic congestion problem. To handle it, many strategies have been followed to understand the potential risks and costs of this problem. Therefore, in this project; VR simulation has been used to evaluate the roads level of five different scenarios to obtain insights into alternate roads services to optimize roads service levels. Five different scenarios were proposed. Upgrade of number of lanes, upgrade roundabouts to four legged and 3 legged signalized intersections, demolish flyover and replace it with four legged signalized intersection and underground tunnel, upgrade signalized intersections to flyover bridges and underground tunnels, and adding directional ramps to interchanges and eliminating key waving segments.

As a result of the analysis using VR technology, two possible scenarios have been considered.

- Ultimate Scenario
- Reduced Configuration

The approach adopted in simulation is to understand and analyse service level and plan a better design in the targeted junctions. The resulting outputs can be visualized based on the attributes added into the simulations. The feedback obtained will have significant improve among the accessibility of roads optimizing.

Acknowledgment

This research is financially supported by the Ministry of Infrastructure Development in United Arab of Emirates (Contract No. 8937). and International Group of Innovative Solutions. Special thanks for the research team Engr. Marwa Al Taffag, Engr. Khulood Al Suwaidi, Engr. Abdulrahman Al Kholy

References

[1] E. Rojas, P. Aramvareekul, Is construction labor productivity really declining? J. Constr. Eng. Manag. 129 (1) (2003) 41–46.

[2] Sampaio, A. Z., & Martins, O. P. (2014). The application of virtual reality technology in the construction of bridge: The cantilever and incremental launching methods. Automation in Construction, 37, 58–67.

[3] Grabowski, A., & Jankowski, J. (2015). Virtual Reality-based pilot training for underground coal miners. Safety Science, 72, 310–314.

[4] Roupé, M., Bosch-Sijtsema, P., & Johansson, M. (2014). Interactive navigation interface for virtual reality using the human body. Computers, Environment and Urban Systems, 43, 42–50.

[5] Woksepp, S.; Olofsson, T. Credibility and applicability of virtual reality models in design and construction. Adv. Eng. Inform. 2008, 22, 520–528.

[6] Goedert, J.D.; Rokooei, S. Project-based construction education with simulations in a gaming environment. Int. J. Constr. Educ. Res. 2016, 12, 208–223.

[7] Park, C.S.; Le, Q.T.; Pedro, A.; Lim, C.R. Interactive building anatomy modeling for experiential building construction education. J. Prof. Issues Eng. Educ. Pract. 2015, 142, 04015019.

[8] Wang, X.; Truijens, M.; Hou, L.; Wang, Y.; Zhou, Y. Integrating Augmented Reality with Building Information Modeling: Onsite construction process controlling for liquefied natural gas industry. Autom. Constr. 2014, 40, 96–105.

[9] Li, X.; Wu, P.; Shen, G.Q.; Wang, X.; Teng, Y. Mapping the knowledge domains of Building

Information Modeling (BIM): A bibliometric approach. Autom. Constr. 2017, 84, 195–206.
[10] Russell, D.; Cho, Y.K.; Cylwik, E. Learning opportunities and career implications of experience with BIM/VDC. Pract. Period. Struct. Des. Constr. 2013, 19, 111–121.
[11] Russell, D.; Cho, Y.K.; Cylwik, E. Learning opportunities and career implications of experience with BIM/VDC. Pract. Period. Struct. Des. Constr. 2013, 19, 111–121.
[12] Wang, J.; Wang, X.; Shou, W.; Xu, B. Integrating BIM and augmented reality for interactive architectural visualisation. Constr. Innov. 2014, 14, 453–476
[13] Guo, H.; Li, H.; Chan, G.; Skitmore, M. Using game technologies to improve the safety of construction plant operations. Accid. Anal. Prev. 2012, 48, 204–213
[14] Kerawalla, L.; Luckin, R.; Seljeflot, S.; Woolard, A. "Making it real": Exploring the potential of augmented reality for teaching primary school science. Virtual Real. 2006, 10,163–174
[15] Wu, H.-K.; Lee, S.W.-Y.; Chang, H.-Y.; Liang, J.-C. Current status, opportunities and challenges of augmented reality in education. 2013, 62, 41–49.
[16] Jang, S.J.: The effects of integrating technology, observation and writing into a teacher education method course. 50(3), 853–865 (2008).
[17] Cheong, D.: The effects of practice teaching sessions in second life on the change in pre-service teachers' teaching efficacy. 55(2), 868–880 (2010)
[18] Arain, F.M., Burkle, M.: Learning construction project management in the virtual world: Leveraging on Second Life. J. Inf. Technol. Constr. (Special Issue: Use of gaming technology in architecture, engineering and construction) 16, 234–257 (2011)

PPEs Compliance Technology to Legalize the Automated Monitoring of Safety Standards

F. (Firas) Habbal[a], F. (Fawaz) Habbal[a], A. Al Nuaimi[b], A. Al Shimmari[b], A. Safi[b], and T. AbuShqair[b]

[a]College of Business Administration, American University in the Emirates, UAE
[b]Ministry of Infrastructure Development, UAE
E-mail: Firas.Habbal@aue.ae, Fawaz.habbal@aue.ae, Abdullah.alnuaimi@moid.gov.ae, Anwaar.Alshimmari@moid.gov.ae, Ammar.safi@moid.gov.ae, Tala.AbuShuqair@moid.gov.ae

Abstract –

Governments are always looking to monitor safety violations on construction sites. Those violations are not only causing numerous injuries and deaths to workers but also delays and subsequently costs to the project developers. In the hierarchy of control, personal protective equipment (PPE), albeit the least effective, is still one of the most visible and therefore fundamental controls to protect workers from workplace hazards. While PPE should be monitored at all times by the related authorities and project organizations, adequately trained staff and availability to monitor projects often fails short. Therefore, monitoring the right use of PPE electronically has yet to become a recommended practice for safety and health programs. This paper examines the application of legalizing smart hard hat to monitor the use of PPE among construction site workers. Using automated cameras and detection technology the PPE will be detected and analyzed. The proposed approach then automatically identifies violators and safety alerts will be issued correspondingly. The developed technology has been tested on real sites. Results from these tests were used for legalizing this technology for everyday construction application in the UAE.

Keywords –

smart hart hard hat; automation in construction; construction safety; site surveillance technology, legalization, personal protective equipment, worker rights

1 Introduction

Infrastructure development is one of the most important industry to any government and to secure this industry is a major concern for all official department, due to harsh working environment and huge amount of workers, governments are striving to maintain level of safety in any site and enforce the use or personal protective equipment among all labors, however, those personals fail to comply to those rules which lead to catastrophic incidents. According to global statistical data the rate of injuries and death in construction is almost three times higher in construction comparing to other industries [1]. This paper proposes a new method of legalizing smart hat and responds to a frequent question Why government are still using manual inspections to record PPE violations? This question reflects the vision of Ministry of Infrastructure Development in UAE and encourage using innovative technologies to reduce number of injuries and deaths caused by careless site foremen and un educated labors. The proposed technologies can fundamentally redefine government responsibilities with social responsibilities. It will also improve the usage of PPE which has not been really developed since the eighties. The construction industry has reported the highest number of casualties among different industries [2]. Many scholars and governmental reports around the world studied the fatal injuries caused by poor attention to personal safety equipment among workers [3][4]. Therefore to minimize such injuries and causalities in construction sites one of the most important strategic goal of MOID [5]. As a result monitoring workers safety has been a top priority for all governmental sectors in the world and became an important pillar to evaluate the construction sites and companies, nevertheless using technology in this matter has become an urge for its accuracy and fast respond. It is with those information enforcing smart hard hats will lead to monitor safety measures everywhere by creating live on time feed to the concern departments and control workers biometrics and to prevent potential violation. The liberty mutual Safety Index (2018) stated that top 10 causes of injuries in workplaces and those injuries amounted of almost $60 billion dollars [6] (Figure 1)

Figure 1. Top 10 causes and cost of the most disabling US workplace injuries

Workers in major cities and developed countries such as United Arab of Emirates are experiencing very safe environment and less work hazards base on very strict regulations in UAE, while employers are trying to avoid any direct or indirect fines might cause by not setting the right on site regulations and force all workers to follow the government safety regulations. According to research done by Grandview Research the market value of PPE is nearly $34 Billion in 2014 with potential growth of 7.2% [7] (Figure 2).

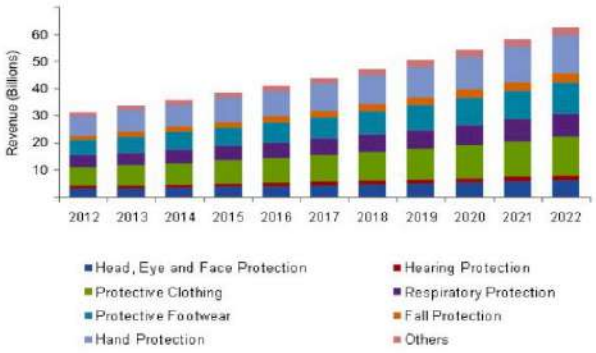

Figure 2. Potential growth of PPE market

Hard hats are designed to protect workers, resist shock, object penetrations, and electrical hazards and this only if workers are using them properly, site marshals with governmental inspectors are expecting the amount of injuries to be reduced since all workers are using the right PPEs [8], however controlling large amount of workers in big constructional sites are almost impossible every time and injuries actually are increasing and study showed that almost 47% of workers injuries are caused by not using the right PPE and no actual monitor took in place to prevent such unfortunate incidents [9]. This paper examines the effects of legalizing smart hard hats to remotely monitor any PPE violations in construction sites and using systematic tools to provide 24/7 surveillance for to detect any workers who are not using their assigned PPE or not using them properly. Studies showed that using smart hard hats for visualizing PPE usage had significant factor for reducing violations and this will lead to reduce number of fatal injuries among site workers [10].

2 Literature review

2.1 Smart Hard Hat

Using smart hard hats will satisfy the needs of safety of clients and will develop a functioning tools to keep the end users safer using the latest technology [11]. Teizer and Reynolds [12] studied the usefulness of smart hard hats to help workers avoid contact with hazard equipment using radio frequency and wireless microprocessors to warn workers once they are close to specified equipment's. Shrestha et al. [13] created a framework to visualize construction safety and detection algorithm. She used CCTV cameras and server side connection to detect workers without their PPEs. Dey S. [14] invented a smart safety gears to calibrate with smart sensors attached to wearable protection equipment, the method is to control the surroundings and measure signal based on the quantity of the element measured. Edirisinghe [15] explained the future context aware using smart sensors technologies in construction sites and real time safety. Gubbi et al. provided evidence that the world is moving to utilize latest technology in enable connectivity of day to day devices and enable IoT for better human enhancements [16] . Par el Al. [17] studied that workers in construction sites need to fulfil 2 main conditions the outline of a person and using PPEs, by using image processing technology to identify whether the person detected is a valid worker or not, In this experiment workers are identified by validating their PPEs from the image processing system can determine whether the person detected is a random person or a worker.

2.2 Image detection

Several research studied image detection for safety measures. [18] used camera features to detect different cues and facial expressions to trigger related warnings for specific incidents. Dai et al [19] developed a software which detect mobile sensors that read personal behaviour and record users action and compare collected data with typical patterns to store any unfamiliar activities. [20] addressed the power of automated visualization using 4D to analyse the relation between Virtual design construction (VDC) with Geographical location (GIS) to detect any faults or

errors among construction sites. Qi et al. proposed a tool for maintaining safety suggestion based on images collected from checking construction sites. [22] studied number of images need to be collected and frequently captured in construction sites to be detected and analysed to produce valid information about how construction sites are performing their daily tasks. Many scholars have developed visual data collection to monitor safety among construction sites using image processing, table (1) list some prior work that used image automation to detect image information.

Table 1. Level automation for image detection [22]

Application	Data Analytics
Damage Assessment	• Image Based 3D reconstruction • Image segmentation & object classification • Machine learning classification
Infrastructure inspection	• Geometric recognition • 3D image processing
Urban Monitoring	• 4D image registration • Orthophoto mapping
Road Assessment	• 3D image based
Geo hazard Investigation	• Orthophoto mapping • Visual interpretation

3 Research Methodology

The paper methodology of PPE monitoring is to collect images data from cameras attached to the smart hard hat including personal traits and PPE availability as well as recording workers face detection and automated object recognition to detect whether is the worker is using the right PPE on the right time at the assigned place as illustrated in figure (3).

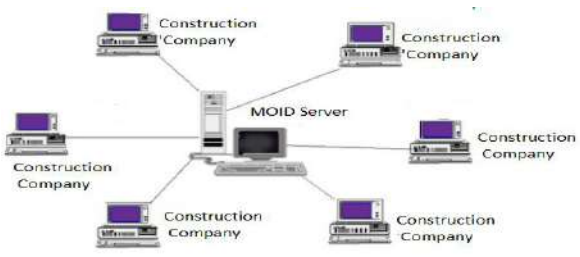

Figure 3. Framework to collect data and send data to MOID server

After the PPE checking by the cameras attached to the smart hard hat, the cameras will identify safety measures system will generate real time report and upload it to the MOID inspection portal and propose the corrective action such as site admin warnings and record fine on the contractor with incident details and visual evidence stored in database.

This paper will study the usage of smart hard hat by analysing three pillars

- Face detection to analyze if the workers already registered in MOID server for the construction site
- PPE object recognition to validate the usage of the correct and valid safety equipment
- Real time report to record all incompliance incidents and record it into MOID database and site manager.

Figure 4. Smart hard hat with detection camera

3.1 Detection device

The detection process of workers and their protective equipment's will rely on face detection and object recognition applications installed into the smart hard hat. The concept is to use the camera attached to the smart hard hat as shown on figure (4) to scan across each worker on site and store several images for each individual to read the data collected independently and analyse it based on the safety standards of MOID. This strategy has two main advantages

- Detecting worker profile: it retrieves the worker data from the database to understand his role and main job functionalities.
- Detecting equipment: over the construction sites many types of equipment should be used as per the safety standards shown on table (5) will be detected and analyzed for its existence

Table 2. List of safety standards

PPE Required	PPE required
Eye gaggles	Grinding, hammering, chopping, abrasive blasting, and punch press operations
Face Cover	Pouring, mixing, painting, cleaning, syphoning, and dip tank operations
Head and Body Cover	Building maintenance; utility work construction; wiring; work on or near communications
Feet	Construction, plumbing, smiting, building maintenance, trenching, utility work, and grass cutting
Hands	Building maintenance; utility work construction; wiring; work on or near communications

3.2 Standards Matching

The system will match serious of standards added by MOID safety department and compare it to a certain measures among construction site. The system will check the similarity and calculate the efficiency of the smart hard hat daily reports. Due to the unified design and shapes of safety equipment, the application will match the images detected on site and match it with template design stored. The template matching algorithms defined as detector (D) and true result (TR) of image detected and template matching (TM) of total image frames per second (n) and (TD) represents safety marshals detection.

$$D = tr\left(\frac{tm}{n}\right)/td\left(\frac{tm}{n}\right)$$

The algorithm will compare the use of smart hard hat detection with traditional way of inspection which use of human inspector or safety marshal to be available on site.

4 System Application

As per one epitome, construction site must be observed during working hours continuously so that workers must be saved from unforeseen situation, casualties and approach of illegal personnel on sites. Staff movement at a building site is followed utilizing electronic hardware incorporated into smart hard hat worn by supervisors at the site.

These smart Hard Hats must be manufactured observing all the requirements e.g., power for long working hours, perfectly working in any activity during construction and environment of construction sites. The smart hard is including an external hard shell joined to the inward shell adjusted to fit supervisor, must not hinder during his routine activities nor too heavy to carry all day long.

The inward shell compromising of most important technical part for smart hard hat having HD camera, environmental interaction sensors (accelerometer, gyroscope), wireless connection (sim card), power source, distress alert, geometric location, pulse measurement. Utilizing Smart Hard Hat technology we can sure to make environment safe and following MOID rules on every construction site.

As prerequisite all construction companies registered with MOID need to record their employees' data on MOID server.

Here we will choose cloud computing for efficient performance as it optimizes the computation partitioning of a data stream application between mobile and cloud to achieve maximum speed/throughput in processing the streaming data. This data storage framework is able to combine and extend multiple databases and Hadoop to store and manage diverse types of data collected from database or either by sensors and RFID readers [23].

On construction sites one or more supervisor wearing smart hard hat will be observing environment while performing his duties. Meanwhile, smart hard hat is in continuous state of detecting and monitoring workers, worn by supervisor situated at the construction site using face detection technology. Meanwhile, a broad range of high-resolution embedded cameras in combination with the development of commercial AI systems allows for a full replacement of traditional security and identification measures with face recognition and provide all above functionality with its additional features. The camera attached to the helmet is able to monitor individual, and looking beyond face recognition, to human analytics. As well as, provides face detection, identification and verification, emotion, age, gender, sentiment, ethnicity and multi-face detection, attention measurements and face grouping in real time.

As soon as human is detected by the hat, it will capture image so that his traits will be examined under the rules of MOID. Smart hard hat being powered by battery and wireless connection will capture working employee and process image on construction sites.

Firstly, the head areas are caught from human pictures. At last, with red, yellow, blue, white and non-helmet image samples, helmet identification based on image processing is used to detect whether workers are wearing helmets or not and to distinguish the shades of helmets if helmets exist. Then, Jackets will be detected due to high reflective clothing workers wear on construction sites. We propose and assess a framework for recognizing people wearing reflective apparel on construction sites by estimating their directions in 3D space under a wide scope of various light settings

during image captured process. If the employee is wearing safety helmet and jacket, it will validate the working employee and if employee is not wearing safety jacket or helmet, smart hard hat will generate alert for MOID server. An alert for MOID server must be latency free, in this regard, we present Mobile Fog, a high level programming model for the future Internet applications that are geospatially distributed, large-scale, and latency-sensitive. Upon validating employee uniform for work, smart hard hat will also recognize employee as register worker or not, again smart cameras will play the role by its powerful system to identify registered employee within fraction of Nano seconds and generate alert for MOID server dependent on the individual data got after recognition process fails.

For instance, the alert may caution MOID and specific work force that they violate rules at the building site or non-registered worker is working on site. Alternatively, workforce action might be intermittently checked and revealed as shown in figure (5).

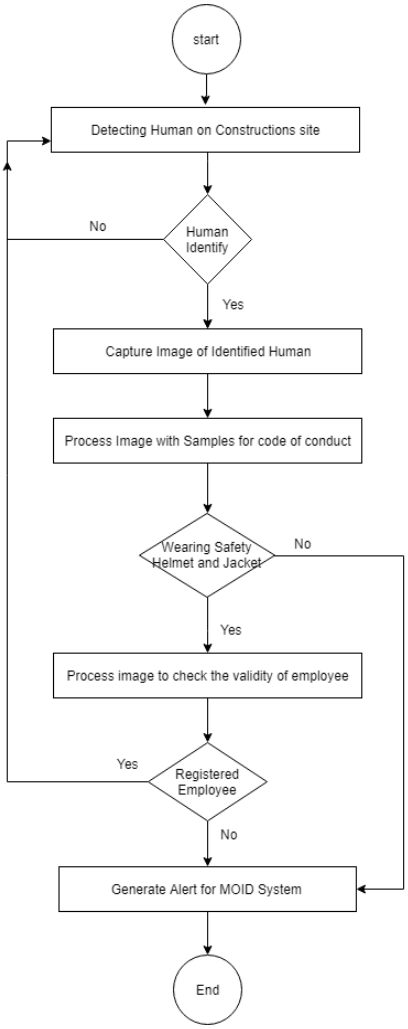

Figure 5. System notification workflow

4.1 System Reporting

The application of smart hard hat is based on wearable device (Safety helmet) which will be used by safety marshals or foreman on each site, and this will allow the user to monitor all site personal without disturbing their daily tasks. The smart helmet will keep recording all objects and human and compare all values with the stored database with the safety module.

4.2 Face detection

The technology will address the face detection using stored meta data, face images, which will be compared with the video captured. In order to communicate with the nature of images collected to a remote node from the camera arrangement. The accuracy of the face detected identify the image frame or field and include the image position. This method will use key frames to recover facial structure, and rely on image similarity which has

been collected and stored in the server. Then the image structure will refine the collected results and add the new data to the targeted database. Based on the results the hat will analyse the face detected along with geolocation of the image taken to evaluate the difference and trigger the notification command.

Figure 6. Face recognition using smart hard hat

4.3 Object Detection

The main goal of smart hard hat detection is to detect objects attached to face of the workers, this goal will check if protective equipment exist at 3 main positions on the worker body

- Focus on the upper area of the worker face
- Focus on the center area of the worker body

The results refer to the degree of the safety equipment with respect to the x-axis, the values between (-1 and 1) indicate if the PPE location is correct relatively to the body and head position. The system will store up to 8 images per second in real time, then the object detection will compare its results with the data collected from the face detection to report whether any safety violations has been registered. In case of no equipment detected a red alert will be raised and report will be generated with incident details and sent to both Ministry Safety Department and site manager.

Figure 6. Face recognition using smart hard hat

4.4 Results & findings

Based on the technology described above, the experiment was divided into two sections: (1) validating construction workers PPE using human inspectors and (2) use smart hard hat to generate safety reports, results are shown on table (3) and (4). The study included 3 sites with over 1500 worker.

Table 3. No. of violations reported per day

Sites	Smart Detection	Site Marshal
Site 1	128	85
Site 2	63	25
Site 3	176	63

As seen on table (3) site marshals are not very accurate on their safety violations reporting as workers are moving around and located in different locations, while using smart camera detection the violations are automatically detected and process time of recording and analysing the image is much faster.

Table 4. Accuracy ratio for different type of detection

Sites	Precision (%)	Speed (s)
Head	95.1	0.201
Body	97.2	0.190
Hand	87.4	0.204
Shoes	56.3	0.204

Table (4) is testing the accuracy of the whole body detection and classify the objects into four categories: head, body, hand, shoes. The result shows that the highest accuracy is the body vest detection for its clear view and because of the reflected stripes it is easy for the camera to detect, however the shoes or feet detection is showing the lowest accuracy as not all images are able to detect the lower body parts of the workers and sometimes the workers shoes are too dirty to be detected.

5 Conclusion

The technology proposed to detect safety violations involves image detection and object recognition. The implementation of the application involves smart hard hat with internet based camera attached to the hat and involves database management for the safety template comparison. The main goal of this research is to legalize the smart hard hat among construction sites by generating real time automated reports and sent to both ministry safety department and site managers, this technology will provide daily reports of safety compliance and will increase the safety awareness among workers.

The system will analyse real-time images for the construction sites and detect workers who are not complying to the safety standards by comparing images taken on sites with standardized templates added by the ministry of infrastructure to reduce number of violations and relatively reduce number of injuries reported.

6 Recommendations

In the future research studying smart hard hat with its application using IoT to generate better understanding of workers daily behaviour in order to reduce number of incompliance, this will produce more accurate data and more automated results for more accurate monitoring for registered construction sites. Additionally further study needed for the effects of data signals transmitted from the hat technology to find better and faster data collection, this study will be able to provide better data analytics should the worker face any drop of negative impact. Furthermore, market analysis to determine the demand for this technology will be also required and would create better applications.

Acknowledgment

This research is financially supported by the Ministry of Infrastructure Development in United Arab of Emirates (Contract No. 8937). and International Group of Innovative Solutions. Special thanks for the research team Engr. Marwa Al Taffag, Engr. Khulood Al Suwaidi, Engr. Abdulrahman Al Kholy

References

[1] Dong, X. S., Wang, X., & Largay, J. A. (2015). Occupational and non-occupational factors associated with work-related injuries among construction workers in the USA. *International journal of occupational and environmental health*, *21*(2), 142-150.

[2] V. Sousa, N.M. Almeida, L.A. Dias, Risk-based management of occupational safety and health in the construction industry-part 1: background knowledge, 2014. Saf. Sci. 66 75–86.

[3] US Bureau of Labor Statistics. Census of fatal occupational injuries [Internet]. Washington, DC: US Bureau of Labor Statistics; 2013 Mar Available from: http://www.bls.gov/iif/oshcfoi1.htm.

[4] Evanoff B, Dale AM, Zeringue A, Fuchs M, Gaal J, Lipscomb HJ, et al. Results of a fall prevention educational intervention for residential construction. Safety Science 2016;89:301–7.

[5] MOID strategic goals reference

[6] Liberty Mutual Research Institute. (2018). 2018 Liberty Mutual Workplace Safety Index.

[7] "Global Personal Protective Equipment (PPE) Market By Product, By End-Use Expected to Reach USD 62.45 Billion by 2022." Grandview Research. Oct. 2015. Web. 4 Mar. 2016.

[8] Occupational Safety & Health Administration, Personal Protective Equipment, 2003, https://www.osha.gov/Publications/osha3151.pdf.

[9] Y.-S. Ahn, J. F. Bena, and A. J. Bailer, "Comparison of unintentional fatal occupational injuries in the Republic of Korea and the United States," Injury Prevention, vol. 10, no. 4, pp. 199–205, 2004.

[10] K. Shrestha, P. Shrestha, D Bajracharya, E. Yfantis, "Hard-Hat Detection for Construction Safety Visualization" Journal of Construction Engineering Volume 2015, Article ID 721380, 8 pages

[11] Fyffe, D., Langenderfer, C., & Johns, C. (2016). The Smart Hard Hat.

[12] J. Teizer and M. Reynolds, Hard Hat Alerts Workers to Dangerous Equipment , The Herald Sun, 2010, http://www.teizer.com/a news 2010-08-23-HeraldSun.pdf.

[13] K. Shrestha, P. P. Shrestha, and E. A. Evangelos, "Framework development for construction safety visualization," in Proceedings of the Canadian Society for Civil Engineering An Conference, CSCE, Montreal, Canada, May-June 2013.

[14] Dey, S., Reepmeyer, G., Sengupta, A., Zhavoronkov, M., Perumal, S., & Friedman, S. (2017). U.S. Patent No. 9,686,136. Washington, DC: U.S. Patent and Trademark Office.

[15] Edirisinghe, R. (2018). Digital skin of the construction site: Smart sensor technologies towards the future smart construction site. Engineering, Construction and Architectural Management.

[16] Gubbi, J., Buyya, R., Marusic, S. and Palaniswami, M. (2013), "Internet of Things (IoT): A vision,

architectural elements, and future directions", Future Generation Computer Systems, Vol. 29 No. 7, pp. 1645-1660.

[17] M. Park, E. Palinginis, and I. Brilakis, "Detection of construction workers in video frames for automatic initialization of vision trackers," in Proceedings of the Construction Research Congress (ASCE '02), pp. 940–949, West Lafayette, Ind, USA, May 2012.

[18] M. S. Devi and P. R. Bajaj, "Driver fatigue detection based on eye tracking," in Proc. IEEE ICETET, Nagpur, Maharashtra, Jul. 2008, pp. 649 –652.

[19] J. Dai, J. Teng, X. Bai, Z. Shen, and D. Xuan, "Mobile phone based drunk driving detection," in Proc. IEEE PervasiveHealth NO PERMISSIONS, Munich, Germany, Mar. 2010, pp. 1 –8.

[20] Z. Mallasi, N. Dawood, Workspace competition: assignment, and quantification utilizing 4D visualization tools, Proceeding of Conference on Construction Application of Virtual Reality, ADETTI/ISCTE, Lisbon, 2004, pp. 13–22.

[21] J. Qi, R.R.A. Issa, J. Hinze, S. Olbina, Integration of safety in design through the use of building information modeling, Proceedings of the 2011 ASCE International Workshop on Computing in Civil Engineering, 2011, pp. 698–705.

[22] Ham, Y., Han, K. K., Lin, J. J., & Golparvar-Fard, M. (2016). Visual monitoring of civil infrastructure systems via camera-equipped Unmanned Aerial Vehicles (UAVs): a review of related works. *Visualization in Engineering*, *4*(1), 1.

[23] Milan Erdelj, Michał Król, Enrico Natalizio (2017). Wireless Sensor Networks and Multi-UAV systems for natural disaster management.

Use of Finite Element Analysis for the Estimate of Freezing & Maintenance Phase of Indirect & Direct Artificial Ground Freezing of Proposed Frozen Silt Mat, an Alternative of Timber Mat

G. M. Ali[a], M. Al-Hussein[b], and A. Bouferguene[c]

[a,b]Department of Civil & Environmental Engineering, University of Alberta, Canada
[c]Campus Saint-Jean, University of Alberta, Canada
E-mail: gmali@ualberta.ca, malhussein@ualberta.ca, ahmed.bouferguene@ualberta.ca

Abstract –

The use of heavy cranes has increased with the impact of modernized modular construction, which in turn has led to heavier modules, with weights often measured in hundreds of tons. As a result, the criticality of such lifts depends primarily upon the ground support health. The traditional approach is to make use of timber/steel mats for ground stability. The use of frozen silt (water and silt frozen mixture) as an alternative to this or to reduce the number of layers of timber mats is a novel technology that is explored in this work. For projects where this technology could be applicable, heavy construction companies will be able to avoid extensive ground preparation and reclamation by adopting this approach. The mechanical properties of frozen silt are comparable to timber mats (Coastal Douglas-fir), but are dependent upon the temperature constraint. This contribution encompasses the use of artificial ground freezing for the preparation of frozen silt matting for ground support. The required mat surface temperature is considered as −10 °C, based on the competitive mechanical properties for its practical use. The freezing process is investigated using Finite Element Analysis (FEA). Simulation is performed to obtain the bottom-up estimate of ground freezing using indirect freezing (brine chillers) and direct freezing (liquid nitrogen) for both the freezing phase and maintenance phase. The simulation is executed under three ambient temperatures (10 °C, 5 °C and 0 °C) in order to make it realistic. The results from these simulations can establish a baseline for cost estimation for the alternative crane matting solution in the form of frozen silt mat.

Keywords –

Artificial Ground Freezing, Brine Chillers, Liquid Nitrogen, Crane Mats, FEA, ANSYS Simulation

1 Introduction

Traditionally, the heavy construction industry has relied upon using cranes to build the structures needed in the field since the elements constituting these structures are generally voluminous and heavy. With off-site construction becoming the paradigm of choice for project delivery, complete projects are delivered in the form of modules, which, over the years, have become heavier as an increasing number of components are added to the skeletal modular structure during fabrication. As a result, high-capacity cranes have emerged as the fundamental equipment for the assembly of modularized power plants and refineries. Of course, as the weight of the lifting system (crane + payload) has become heavier, ground-bearing capacity analysis cannot be ignored, since failure of the ground can result in loss of life and property. Today, the traditional approach to improving the capacity of the ground proceeds in two phases: (i) ground preparation, which consists of excavating a given depth of ground that is replaced by a layer (or a mix of layers) of construction aggregates compacted; and/or (ii) addition of one, two or three layers of timber mats. This setup allows the total load of the lifting system to be appropriately distributed. With the adoption of the modular construction paradigm, the demand for crane mats has been augmented. According to market research, in 2014, the total annual mat demand in Canada was in the range of 450,000–750,000, while annual mat production in North America in 2014 was approximately 300,000–600,000, and the number of mats produced in Canada in 2014 was approximately 20,000–25,000. The matting industry increased 200% from 2009 to 2014 [6]. Nevertheless, a study by OSHA reported that, from 2000 to 2009 in the United States, approximately 12% of fatalities on construction sites were associated with crane

work. A total of 587 lives were lost as a result of 571 accidents from crane work during that period, of which 105 were crane operators, 375 were riggers, and eight were signal people. It is estimated that approximately 50 deaths were caused by "Crane Tipped Over", which is directly associated with poor ground support [22]. Interestingly, ground support technology has been largely overlooked by practitioners despite the cost and environmental impact associated with current ground capacity improvement methods. In this respect, with increasing environmental awareness, choosing a technology for a given purpose needs not only to be cost-effective but also to have a low impact on the environment. Using the same characteristics, frozen soil has properties similar to the supporting structural material [1]. Considering the mechanical properties of frozen silt (water and silt frozen mixture), the novelty of using frozen silt for crane matting is a novel idea which transcends traditional constraints and helps to minimize environmental impact. The mechanical properties of frozen silt are comparable to timber matting (Coastal Douglas-fir), but are dependent upon the temperature constraint (i.e., the mechanical properties of frozen silt with the surface temperature below −10°C are comparable to Coastal Douglas-Fir). To achieve this temperature, artificial ground freezing can be used. The earliest documented application of artificial ground freezing was in a mine shaft near Swansea, South Wales, in 1862. Later, this freezing method was patented by F. H. Poetsch, in 1883 with some major improvements [18]. In 1884, excavation of a tunnel in Stockholm was aided with a frozen stabilized arch [2]. In practical usage, there are two types of ground freezing methods: indirect freezing (brine chiller) and direct freezing (liquid nitrogen). In this contribution, the Fluid Flow (Fluent) module of ANSYS (17.1) is used to estimate the usage of indirect and direct freezing for the preparation of frozen silt matting. A model of the proposed frozen mat with freezing pipes is generated and uploaded in ANSYS module. The mat model is placed on the ground to create a real case scenario. We thus create a basis for the practical and onsite application of ground freezing methods for frozen silt mat preparation. Constructed on energy equations and viscosity constraints for heat transfer between mat, ground, and air, ANSYS simulation provides the graphical representation of mat freezing with respect to time lapse. To make it realistic, the simulation is performed under three ambient temperatures (10 °C, 5 °C and 0 °C). The simulation of indirect freezing is performed by taking constant fluid flow of brine, whereas for direct freezing, three different fluid velocities are assigned. The idea is to simulate the weather condition of the north-western part of Canada. The freezing phase and the maintenance phase for the frozen silt mat are analyzed to obtain the cooling requirement in figures (numbers). For indirect freezing, the cooling requirement is in the form of the temperature difference between inlet and outlet of freezing pipes, flow of brine, and, for direct freezing, the amount of liquid nitrogen used for the freezing of the mat. The results indicate how much energy drainage is required to convert silt into frozen silt under the same boundary conditions but at different ambient temperature and different flow velocities of the cooling agent. The results are found to be favourable and comparable to the actual artificial ground freezing. The results from these simulations provide a baseline for the cost estimation for the alternative crane matting solution in the form of capital, operational, and opportunity costs for this novel alternative to the use of timber matting ground support. Based on these results, a value proposition of using frozen silt mat can be generated with better SWOT (Strength, Weakness, Opportunities & Threats) figures.

2 Research Methodology

2.1 Frozen Silt Mat Proposed Design

The first step is to provide a preliminary conceptual design for the frozen silt mat. Based on the data available, a conceptual silt mat design is initiated in this section for ANSYS heat transfer simulation. As per the dimensions of the mat (3.6449 m × 2.4384 m × 0.2032 m), eight frozen silt mats are proposed to be used for a Manitowoc 18000 Crawler Crane (see Figure 1). For analysis purposes, only the crawler crane is selected. The aim of the research presented in this paper, is to perform the simulation for the freezing process of silt mats until the surface temperature reaches or drops below −10°C.

Figure 1 shows the placement of the proposed four frozen silt mats under one track of a crawler crane. For the freezing purpose, conceptually, 10 freezing pipes are used. In the proposed layout, the pipes are placed evenly inside the soil perpendicular to the length of the mat but parallel to the crawler track. It is assumed that each pipe crosses all four mats under one crawler track. The cooling agent enters one end of these pipes and exits from the other end. For insulation purposes, the soil, cost-effective insulation on site, itself can be used as the mat cushion (insulation), where the thickness of the mat is increased to create a mat cushion (insulation) (see Figure 2).

The four silt mats combine to form one long frozen silt mat with mat cushion (insulation). The length of the whole mat (consisting of four frozen silt mats) is considered to be approximately 10.5 m, with a width of 4 m. The proposed height (0.303 m) of the mat exceeds the practical normal mat height (0.203 m). The extra height provides the mat cushion which functions as insulation. If this insulation is not provided, the surface temperature of the mat drops rapidly. A freezing

temperature of −10 °C throughout the mat is required (including the mat surface). 2″ steel pipe schedule 40 is used for the freeze pipes. These steel pipes work as a conducting material to transfer heat from the silt to the cooling agent (either brine or liquid nitrogen).

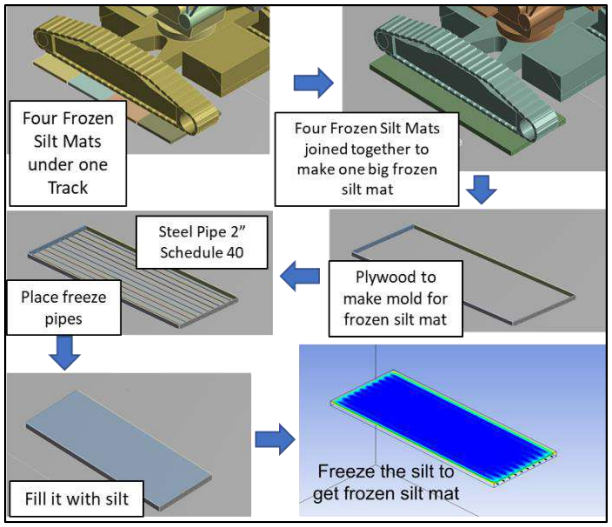

Figure 1: Proposed Frozen Silt Mat configuration

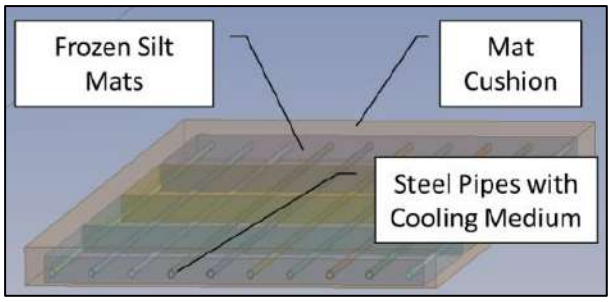

Figure 2. Mat Cushion for insulation

2.2 Mechanical Properties of Frozen Silt Mat

Mats made of frozen silt can sustain the Ground Bearing Pressure (based on the comparable mechanical properties of timber matting) if the mat temperature is below −10 °C. The mechanical properties of the frozen silt mat, it should be noted, are considered from the research done by Yang et al. (2015), and by Wilson (1982) [20][21]. The value of Young's modulus ranges from 0.7 GN/m^2 to 16.5 GN/m^2 with the temperature ranging from 0 °C to −10 °C. The dry density is found to vary from 320 kg/m^3 to 941 kg/m^3, while the water/moisture content varies from 62% to 225% [21]. Based on the above data, the compressive strength of the frozen silt varies from 1.7 MPa to 7.1 MPa [21]. For the purpose of comparison, the surface temperature of frozen silt mat is considered as −10 °C. Table 1 shows the comparison between the mechanical properties of Coastal Douglas-Fir and the proposed frozen silt mat. As can be seen, the properties of the frozen silt are found to be comparable with the timber mat made of Coastal Douglas-Fir.

Table 1. Linear mechanical properties for comparison

		Units	Coastal Douglas-Fir	Frozen Silt
1	Young's Modulus	MPa	13,400[a]	10,000[b, d]
2	Poisson's Ratio		0.449[c]	0.3[e]
3	Tensile Yield Strength	MPa	2.3[a]	5.1[d]
4	Compressive Yield Strength	MPa	5.0[a]	5.0[d]
5	Tensile Ultimate Strength	MPa	5.0[a]	5.1[d]

Sources: Data adapted from

a) Kretschmann, David. E. 2010. "Mechanical Properties of Wood, Chapter 5." In Wood Handbook, 5.1-46. U.S. Dept. of Agriculture, Forest Service, Forest Products Laboratory.
b) Wilson, Charles Ralph. 1982. "Dynamic Properties of Naturally Frozen Fairbanks Silt." Master of Science Thesis in Civil Engineering. Corvallis: Oregon State University, April 22.
c) Green, David W., Jerrold E. Winandy, and David E. Kretschmann. 1999. "Mechanical Properties of Wood." In Wood Handbook, 4.1-45. U.S. Dept. of Agriculture, Forest Service, Forest Products Laboratory.
d) Yang, Zhaohui (Joey), Benjamin Still, and Ziaoxuan Ge. 2015. "Mechanical properties of seasonally frozen and permafrost soils at high strain rate." Cold Region Science and Technology 113: 12-19. doi:doi.org/10.1016/j.coldregions.2015.02.008
e) Andersland, Orlando B., and Branko Ladanyi. 2004. Frozen Ground Engineering. New Jersey: Wiley

2.3 ANSYS Methodology

This research on frozen silt mats can be divided into two parts with respect to Finite Element Analysis (FEA):

a. heat transfer to/from proposed frozen silt mat;
b. usage of a cooling agent for the freezing of proposed silt mat for cost comparison.

ANSYS Workbench (version 17.1) is used for this research. For thermal simulation, it should be noted, "Fluid Flow (Fluent)" solver is available in ANSYS to

simulate the computational fluid dynamics (CFD) and thermal variation. The whole process is divided into 5 steps. Step 1 (Geometry Build): In this step, the geometry of the object or structure is drafted or imported from a 3D AutoCAD file. Here the lower the number of geometry parts is, the faster the ANSYS fluid flow solver can analyze and implement the mesh. As the number of parts of a geometry increases, the time required by the ANSYS solution increases exponentially. Step 2 (Generate Mesh): In this step, the model is uploaded to ANSYS Fluid Flow (Fluent) solver "Mesh". This includes meshing of the model to small elements for FEA. The type and conditions of meshing are described later in this section, where, the smaller the meshing element is, the better it is considered to be. However, the accuracy and precision must be monitored to make it workable. It is also preferable to give each surface a separately named selection. (These name selections make step 4 easier.) Step 3 (Apply Boundary Conditions): In this step, the previously determined energy equations are applied to the geometry, and thermal/viscous properties of the fluids are assigned. The interference between different body surfaces is also assigned in this step, as well as cell zone conditions. Finally, the inlet and outlet temperature and fluid velocity are assigned accordingly. Step 4 (Obtain Solution): After obtaining the geometry and assigning the required boundary conditions, the solution to the problem is initiated. The solution depends upon the solution initialization, the number of time steps, the duration of time steps, and the maximum iterations per time step. Step 5 (Display Results): The final step is to obtain the results, where fluid dynamics is the basis of these results. Heat transfer with respect to time is obtained in this step. The results can be shown in the form of graphs, colour variation, or various charts and sheets. The data can be exported to different file formats as necessary for further investigation.

2.4 Thermal Properties

For the thermal analysis, the thermal properties of the material for ANSYS simulation are tabulated in Table 2. The heat transfer occurs in the following manner: (a) heat transfer from the pipes to the cooling agent through conduction and convection, where the thermal properties and the viscosity of the cooling agent cover the estimation for heat rejection from the geometry (frozen silt mat, pipes, air, ground); (b) heat transfer from the mat to the pipes through conduction; (c) heat transfer from ground to the freezing mat, where, during the mat freezing process, the soil under the mat also is frozen with the passage of time and later functions as insulation; and (d) heat transfer from the air to the silt mat in the form of convection (2 W/m^2•K, assumption) and radiation (external emissivity 0.98, assumption) [4][19].

Table 2. Thermal properties of materials involved in frozen silt mat thermal process ANSYS analysis.

Density (kg/m^3)	C_p (j/kg•°C)	Thermal Conductivity (W/m•K)	Viscosity (Poise)
	Steel		
7,500	500	43	0
	Frozen Silt (120%)		
1,100[a]	1,360[a]	1[a]	0
	Ice		
900	2,090	0.08	0
	$CaCl_2$ (30%)		
1,318[b]	2,650[b]	0.5[c]	0.221[c]
	Liquid Nitrogen (−150°C)		
808.5[d]	2,040[e]	0.1396[e]	0.00068[f]

Sources: Data adapted from

a) Andersland, Orlando B., and Branko Ladanyi. 2004. Frozen Ground Engineering. New Jersey: Wiley.
b) OXYChem. 2018. "Calcium Chloride - A Guide to Physical Properties." OXYChem Publisher.
c) DYNALENE. 2018. "Calcium Chloride Series Brine." Dynalene.
d) Itterbeek, A. Van, and O. Verbeke. 1960. "Density of Liquid Nitrogen and argon as a function of pressure and temperature." Physica (Elsevier) 26(11): 931-938.
e) Jensen, J. E., W. A. Tuttle, R. B. Stewart, H. Brechna, and A. G. Prodell. 1980. VI - Properties of Nitrogen. Vol. 1, in BROOKHAVEN NATIONAL LABORATORY SELECTED CRYOGENIC DATA NOTEBOOK, by J. E. Jensen, W. A. Tuttle, R. B. Stewart, H. Brechna and A. G. Prodell, 45. New York: Brookhaven National Laboratory.
f) Grevendonk, W., W. Herreman, and A. De Bock. 1970. "Measurement on the Viscosity of Liquid Nitrogen." Physica (Elsevier B.V.) 46 (4): 600-604.

2.5 Freezing Methods

A standard soil freezing installation involves a refrigeration source, a distribution system, and cooling pipes for freezing of the soil (called "freeze pipes") [14]. The distribution system circulates the cooling agent (coolant for the freezing of the soil) from the refrigeration source to the freeze pipes, which extract the heat from the soil. In general, there are two main types of cooling agents: brine solution (indirect freezing) and liquid nitrogen (direct freezing).

In indirect freezing, one- or two-stage refrigeration

plants are the most commonly used refrigeration sources. They are powered by diesel or electric engines. Usually, chilled calcium chloride ($CaCl_2$) is used as a cooling agent to freeze the ground. The cooling agent is pumped through the freeze pipes, and, after withdrawing heat, returns to the unit (see Figure 3). The whole process occurs in three phases. The first phase is known as the **freezing phase**. The temperature of the brine solution increases by approximately 1°C to 2°C during this process. In this phase, the ground is frozen to achieve the required strength. The next step is to maintain the temperature of the frozen soil. This is known as the **maintenance phase**. The energy drainage required to freeze the ground, it should be noted, is greater than the energy drainage required to sustain the frozen ground [12].The final phase, known as the thaw phase, is to terminate the freezing project. In this phase, the ground is left to thaw [9].

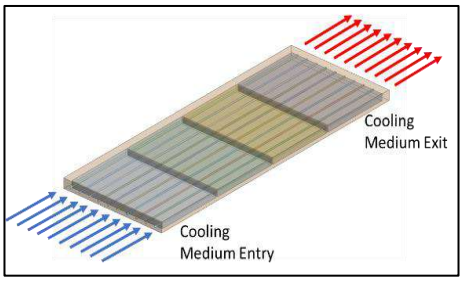

Figure 3. Cooling agent flow through mat

In direct freezing, as indicated by its name, the soil is directly cooled by the freezing agent. Primarily liquid nitrogen is used to freeze the ground in this process. It also involves three phases: the freezing phase, the maintenance phase, and the thaw phase. The coolant is supplied directly from the storage tank, and the soil/silt around each freeze pipe freezes radially. The amount of nitrogen required for the freezing is maintained by means of a temperature-sensing valve. As the valve opens, nitrogen escapes into the atmosphere at a rate that is not dangerous to the environment.

2.6 Heat Transfer Analysis Method

The data from the mat strength analysis provide the basis for the heat transfer analysis. For heat transfer analysis, ANSYS Fluid Flow (Fluent) solver is used to simulate the cooling of frozen silt mat in order to convert silt into frozen silt mat (solid). The process is summarized in the following steps:

Step 1: The mat dimensions obtained from the mat strength analysis are used to propose the design of the frozen silt mat. The freeze pipes are added to the frozen silt mat for the purpose of freezing the soil around the freeze pipes, resulting in a solid frozen silt mat. The proposed design of the mat with the addition of freeze pipes is uploaded in ANSYS Flow (Fluent) Geometry Module, and the proposed mat is placed on the soil model. The parameters of soil and the frozen silt mat are considered equal, with the exception of the differences in the internal temperature of the frozen silt after cooling and the ambient temperature of the loose soil.

Step 2: One end of the pipe is considered an inlet for the cooling agent, while the other end is the outlet for the cooling agent. For indirect freezing, $CaCl_2$ is used as the cooling agent. The velocity and temperature of the cooling agent are adjusted to obtain the heat transfer. For direct freezing, the flow of liquid nitrogen is used to monitor the freezing of the mat. The temperature of the cooling agent is adjusted as per the cooling parameters.

Step 3: The heat transfer rate along the flow of the liquid provides the heat transfer data for estimation purposes, while the cooling administered by the cooling agent is used to determine the freezing refrigeration unit for indirect freezing. For direct freezing, the amount of liquid flow provides the quantity of liquid nitrogen used for the freezing of the mat. The time required for the freezing of the mat surface is also recorded for further analysis.

Step 4: The ambient temperature and the boundary conditions are applied to the model. Prior to this, the geometry is subdivided into smaller elements by applying “meshing”. Meshing is carried out to break the whole model into small finite elements for analysis. The time steps and iterations per step are applied to the solver.

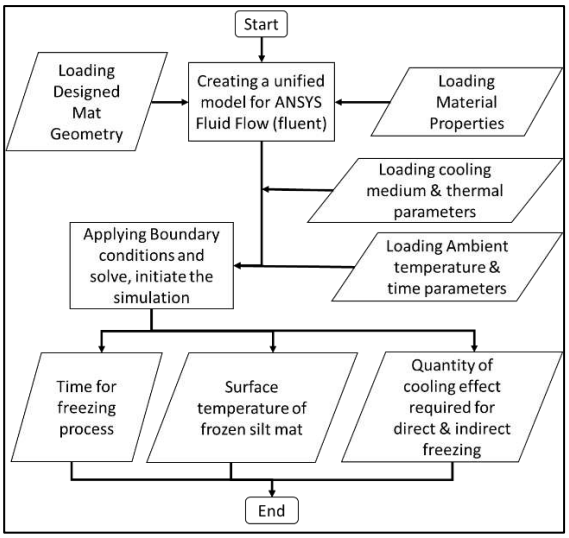

Figure 4. Flowchart for frozen silt mat freezing sequence

Step 5: The solution is uploaded to the results section of the solver, and the heat transfer with respect to time is obtained for the whole system. The surface temperature

of the mat is observed and recorded to check the feasibility of the required frozen silt mat temperature. For indirect freezing, there are three main variables obtained from this exercise: the temperature difference between inlet and outlet temperature of cooling medium; the time required for cooling; and the surface temperature of the frozen silt mat. For direct freezing, there are three main variables: the flow of liquid nitrogen; the time required for cooling; and the surface temperature of the mat.

The above-mentioned methodology is presented in the form of a data flowchart in Figure 4.

3 ANSYS Simulation

3.1 Indirect Freezing ($CaCl_2$)

Calcium chloride ($CaCl_2$) is used as a cooling agent, and its velocity is assumed to be 0.29 ft/s (0.088392 m/s). The inlet temperature of $CaCl_2$ at the start of the analysis is the same as the ambient temperature, but it drops gradually until it reaches −30.15 °C. To avoid complexity, it is assumed that the temperature drop is 5 °C over a 24-hour period (gradual). To simplify the model, the heat generated from the crane engine/crawler track is not considered. For data collection, each step is composed of 3,600 seconds, with 200 iterations, and the number of steps as 720. Hence, the total simulation time is 30 days.

The temperature of the mat surface (under the mat cushion) is recorded and plotted against time (days) in Figure 5. As per the simulation, the surface temperature of the frozen silt mat is close to −10 °C with the ambient temperature of 10 °C, and it takes 8 to 9 days to freeze the silt sufficiently to create a frozen silt mat. In the case of 5 °C ambient temperature, it takes less than 7 days to freeze, and, for 0 °C, it is less than 5 days. The surface temperature of the mat (under mat cushion) ranges between −10 °C and −15 °C for case-2 (5 °C) and it is below −15 °C in case-3 (0 °C).

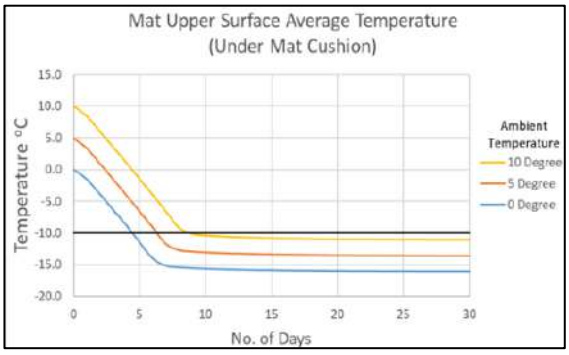

Figure 5. Mat Surface Average Temperature

The heat removal from the proposed frozen silt mat in the simulation is shown in Figure 6. The heat removal value for case-1 (ambient temperature 10 °C) is higher than in the other two case examples. The first part of the graph (the linear part) shows the freezing phase, while the later horizontal line shows the maintenance phase.

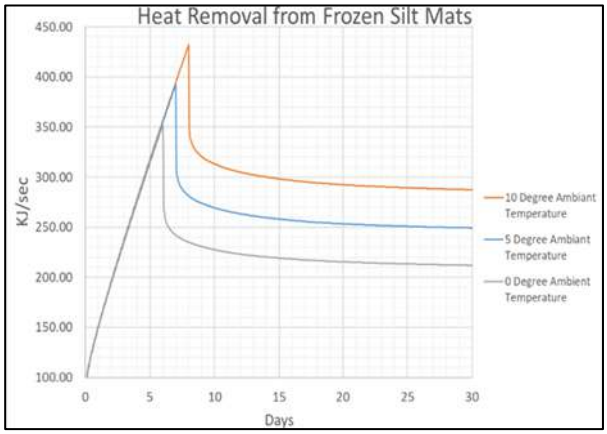

Figure 6. Heat Removal from Frozen Silt Mat

3.2 Direct Freezing (Liquid Nitrogen N_2)

Direct freezing differs from indirect freezing as discussed in section 2.5. The flow of the liquid nitrogen is the main cost driver. For ANSYS simulation purposes, three assumed cases are taken into consideration based on different flow velocities of liquid nitrogen. As per the proposed design of frozen silt mat, there are 10 pipes for each frozen silt mat. The velocity of liquid nitrogen for the outer pipes (pipe 1 and pipe 10) is taken to be constant. The velocity of liquid nitrogen for the inner pipes (pipe 2 to pipe 9) is considered variable with respect to time. Table 3 shows the details of these cases.

Each assumed case is simulated at three different ambient temperatures: 10 °C, 5 °C, and 0 °C. All the remaining parameters are similar to those described in Section 2. The use of liquid nitrogen with respect to the number of days is shown in Figure 7. The flow is found to be maximum for case-1 and minimum for case-3. With every case analyzed under each of the three ambient temperature scenarios, in total nine case examples are simulated for freezing silt mat in ANSYS.

The average surface temperature of the mat decreases rapidly due to the low temperature of liquid nitrogen as compared to brine (the boiling point of nitrogen is −195.8 °C at atmospheric pressure). It is assumed for the ANSYS simulation that the temperature of liquid nitrogen (LN_2) entering the pipe is −150 °C. Due to this low-temperature flow, the temperature of the mat material (silt) decreases rapidly. The graphical representation of the mat surface temperature with respect to time is shown in Figure 8. From this simulation exercise, case-1 is found to perform well at every ambient temperature as compared to case-2 and case-3. The

surface of the frozen silt mat reaches −10 °C faster if the use of liquid nitrogen is increased in the form of higher flow (case-1). The surface temperature for case-1 is found to be lower than that for case-2 and case-3.

Table 3. Liquid nitrogen velocity for three cases.

	Case-1	Case-2	Case-3
Outer Pipes	0.005 m/s (0.016 ft/s)	0.004 m/s (0.013 ft/s)	0.003 m/s (0.0098 ft/s)
Inner Pipes 0 to 24 hr	0.005 m/s (0.016 ft/s)	0.004 m/s (0.013 ft/s)	0.003 m/s (0.0098 ft/s)
Inner Pipes 24 to 720 hr	0.005 m/s (0.016 ft/s) linearly decreasing to 0.002 m/s (0.0056 ft/s)	0.004 m/s (0.013 ft/s) linearly decreasing to 0.0015 m/s (0.0049 ft/s)	0.003 m/s (0.0098 ft/s) linearly decreasing to 0.001 m/s (0.0033 ft/s)

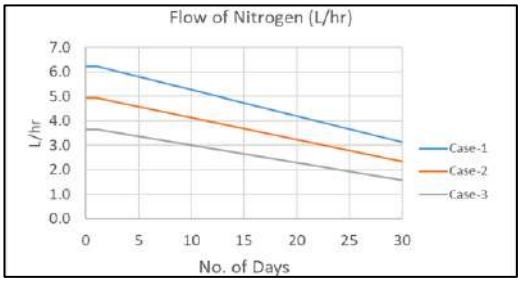

Figure 7: Liquid Nitrogen Total Flow (L/hr)

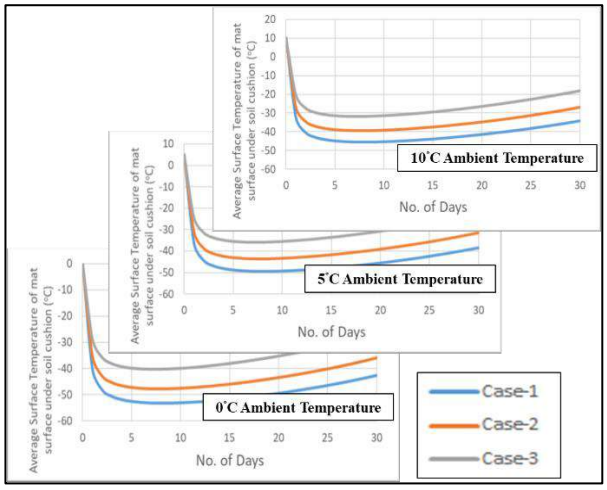

Figure 8: Average Mat Surface Temperature (Direct Freezing - Liquid Nitrogen LN_2)

4 Conclusion

- This research provides a guideline for the freezing process of frozen silt mat. The mechanical properties of frozen silt mat are found to be comparable if the surface temperature is −10 °C or below.
- The results of indirect freezing in the form of the graph representing energy drainage with respect to time are similar to the energy removal graph presented by Newman et al. (2011) [15]. The steep line represents the freezing phase while the horizontal line after the freezing phase represents the maintenance phase to maintain the temperature.
- The results also show that the freezing process in direct freezing is quicker as compared to in indirect freezing. The surface temperature reaches −10 °C in hours in direct freezing, compared to days in indirect freezing.
- This research can be used for estimating the duration of the freezing process for frozen silt mat in cold regions, as less energy drainage will be required. The frozen silt mat can be an environmentally friendly alternative for crane timber mats in some cases, but future study is required in this regard to determine the suitability of this technology.
- ANSYS can be used for the estimation of artificial ground freezing for practical use. The graphical representation of indirect and direct freezing provides a better overview of how moist soil turns into frozen ground as compared to the manual calculations of artificial ground freezing.

5 Recommendation and future aspects of the research

This research indicates that ANSYS can be used to estimate the application of artificial ground freezing methods for the preparation of frozen silt matting. Different fluid flow velocities need to be investigated to obtain a better view and understanding of the mat freezing process. But, before addressing this particular aspect, the stress comparison must be established for the frozen silt mat in accordance with the timber mats (Coastal Douglas-Fir). The physical properties must be verified using ANSYS and later by means of lab/site testing. For frozen silt mats, future research can investigate other soil types (sand, clay, loam, chalky soil, etc.) in order to establish an empirical relationship between mat surface temperature, ambient temperature, soil composition, water content, and different freezing methods. These projected figures further need to be verified by lab/site testing. The variation of Young Modulus with respect to the surface temperature on the

strength of frozen silt mat should also be investigated in detail, as well as the impact of density change on freezing methods. Density anomalies of water/ice/frozen silt with respect to ambient temperature, it should be noted, are not incorporated in this research. These anomalies and their impact on the strength of a frozen silt mat can be considered in future research. The use of mesh/reinforced bars/pulp to increase the stability and strength of frozen silt mat also needs to be studied in detail in order to arrive at a better and more progressive value proposition with respect to timber mats, both technically and financially [17].

References

[1] Andersland, O. B., & Ladanyi, B. (2004). *Frozen Ground Engineering.* New Jersy: Wiley.

[2] Cauer, W. (1885). Gefrierverfahren beim Bau eines Tunnels in Stockholm. *Zentralblatt der Bauverwaltung, No51*, 537-538.

[3] DYNALENE. (2018). Calcium Chloride Series Brine. Dynalene.

[4] Farouki, O. (1986). *Thermal properties of soils.* Clausthal-Zellerfeld, Germany: Trans Tech. .

[5] Gillard, E. (2017, 08 06). *A New Home on Mars: NASA Langley's Icy Concept for Living on the Red Planet*. (E. Gillard, Editor) Retrieved 04 23, 2018, from NASA: https://www.nasa.gov/feature/langley/a-new-home-on-mars-nasa-langley-s-icy-concept-for-living-on-the-red-planet

[6] Golden Environmental Mat Services, G. (2015). *2014 ACCESS MAT RESEARCH: PERSPECTIVES ABOUT THE INDUSTRY AND ASSET TRACKING CONCEPT.* Calgary.

[7] Green, D. W., Winandy, J. E., & Kretschmann, D. E. (1999). Mechanical Properties of Wood. In *Wood Handbook* (pp. 4.1-45). U.S. Dept. of Agriculture, Forest Service, Forest Products Laboratory.

[8] Grevendonk, W., Herreman, W., & De Bock, A. (1970, March 31). Measurement on the Viscosity of Liquid Nitrogen. *Physica, 46*(4), 600-604.

[9] Implenia. (2017, 3 3). *Ground Freezing.* Retrieved from Implenia Spezialtiefbau GmbH: http://www.spezialtiefbau.implenia.com/fileadmin/con-spezialtiefbau/prospekte/englisch/Ground_Freezing.pdf

[10] Itterbeek, A. V., & Verbeke, O. (1960). Density of liquid nitrogen and argon as a function of pressure and temperature. *Physica, 26*(11), 931-938.

[11] Jensen, J. E., Tuttle, W. A., Stewart, R. B., Brechna, H., & Prodell, A. G. (1980). VI - Properties of Nitrogen. In J. E. Jensen, W. A. Tuttle, R. B. Stewart, H. Brechna, & A. G. Prodell, *BROOKHAVEN NATIONAL LABORATORY SELECTED CRYOGENIC DATA NOTEBOOK* (Vol. 1, p. 45). New York: Brookhaven National Laboratory.

[12] Jessberger, H. L., & Vyalov, S. S. (1979). *General Report Session III: Engineering.* Amsterdam: Elsevier Scientific Publishing Company.

[13] Kretschmann, D. E. (2010). Mechanical Properties of Wood, Chapter-5. In *Wood Handbook* (pp. 5.1-46). U.S. Dept. of Agriculture, Forest Service, Forest Products Laboratory.

[14] Moretrench. (2018, 05 11). *Ground Freezing Brochure*. Retrieved 05 11, 2018, from Moretrench.com: http://www.moretrench.com/brochures/

[15] Newman, G., Newman, L., Chapman, D., & Harbicht, T. (2011). Artificial Ground Freezing: An Environmental Best Practice at Cameco's Uranium Mining Operations in Northern Saskatchewan, Canada. *Rüde, Freund # Wolkersdorfer (Editors)*, 113-118.

[16] OXYChem. (2018). Calcium Chloride - A Guide to Physical Properties. OXYChem Publisher.

[17] Perutz, M. F. (1997). *Science is not a quiet life : unravelling the atomic mechanism of haemoglobin.* Singapore: World Scientific Pub. Co.

[18] Sanger, F. J., & Sayles, F. H. (1979). Thermal and Rheological Computations for Artificially Frozen Ground Construction. *Engineering Geology, 13*, 311-337.

[19] The Engineering Toolbox. (2018). *Emissivity Coefficients of some common Materials*. Retrieved 5 2, 2018, from https://www.engineeringtoolbox.com/emissivity-coefficients-d_447.html

[20] Wilson, C. R. (1982, April 22). Dynamic Properties of Naturally Frozen Fairbanks Silt. *Master of Science Thesis in Civil Engineering*. Corvallis: Oregon State University.

[21] Yang, Z., Still, B., & Ge, Z. (2015, May). Mechanical properties of seasonally frozen and permafrost soils at high strain rate. *Cold Region Science and Technology, 113*, 12-19. doi:doi.org/10.1016/j.coldregions.2015.02.008

[22] Zhao, Q. (2011). Cause Analysis of U.S. Crane-related Accidents (Master's Thesis). Retrieved from http://ufdc.ufl.edu/UFE0042972/00001.

DEM-based Convolutional Neural Network Modeling for Estimation of Solar Irradiation: Comparison of the Effect of DEM Resolutions

J. Heo[a], J. Jung[a], B. Kim[b], and S. Han[a]

[a]Dept. of Civil and Environmental Engineering, Hanyang University, Republic of Korea
[b]Dept. of Civil Engineering, Andong National University, Republic of Korea
E-mail: heojae1234@hanyang.ac.kr, jhjung1216@gmail.com, bkim@anu.ac.kr, sanguk@hanyang.ac.kr

Abstract –

Recently, the use of solar panels has increased because of the growing demand for solar energy. To determine appropriate installation sites of photovoltaic (PV) panels, estimating the available solar energy at a certain area is important to predict the amount of power generation and planning PV plant operations. However, traditional data-driven approaches (e.g., machine learning) do not fully reflect the topographical characteristics of surrounding regions in the solar energy estimation, and the impact of data resolution (e.g., map scales) on the prediction accuracy has rarely been investigated. Thus, this paper presents a solar irradiation prediction model using a convolutional neural network (CNN) designed to process digital elevation map (DEM) images. Furthermore, an analysis of the impact of two different resolutions (i.e., 30 m and 60 m resolutions) on the model performance is also presented. A total of 25,000 DEM images are extracted from the national map of South Korea for both resolutions and then used as an input to train the CNN models. The results show that the CNN-based prediction models can be used to estimate the solar irradiation with high accuracy (e.g., mean square errors of 0.0018 and 0.0032 for 30 m and 60 m resolutions). It was also found that data resolution affects the performance of the CNN-based models. With an accurate estimation of the available solar energy at a certain site, the sites generating more power can potentially be evaluated and selected by searching a DEM on a large scale.

Keywords –

Solar energy, solar irradiation prediction, GIS, convolutional neural network

1 Introduction

Global carbon dioxide emissions from fossil fuels, which are considered to be the major cause of global warming, have been constantly increasing in the last decade: for example, by an average of 3.1 ± 0.2 GtC yr^{-1} during 2008-2017 [1]. As global warming affects human health and causes the climate change, efforts such as environment regulation, emissions trading, clean energy technology development, and deforestation reduction have been made to control and reduce the pollution. An effective approach is replacing fossil fuel with renewable energy, such as solar energy, wind energy, biofuel energy, and so on. Particularly, the use of photovoltaics (PV) has rapidly grown, nearly quadrupling over the past five years [2]. Unlike other renewable energy sources, solar energy is considered to be economical: solar cells operate for a long period, generally more than 20 years, and require low maintenance expenses [3].

To meet the increasing demand for solar energy, the prediction of solar radiation that estimates the amount of available solar energy at a certain place is a key to planning the power supply [4]. Furthermore, the accurate estimation of available solar energy allows for the optimal selection of PV installation sites, as well as the decision on PV system [5, 6]. Although various approaches to the solar energy estimation (e.g., statistical model, fuzzy logic approaches, machine learning) have been proposed and used in practice, it is still challenging to collect solar radiation data on a large scale and consider the geographical characteristic of adjacent areas in the estimation. For example, solar radiation-related data that is used to estimate available solar energy is often collected from specific observation regions. Although this approach can be suitable for general terrain, it would be hard to assume that simple linear interpolation or any estimating method for topography measurements may work well for other regions far away from the observation stations or complex terrain (e.g., mountains) [7]. Furthermore, in general, statistical methods or conventional machine learning algorithms (e.g., Bayesian networks, support vector machines) do not directly process image or map type-data with the three-

dimensional (3D) shape of an image (i.e., topography) [8]; while recent machine learning algorithms such as convolutional neural networks (CNN) are designed to keep spatial relationships among data points (e.g., pixels) in the modeling process (e.g., optimization of model parameters).

This research thus investigates the use of CNN for modeling and predicting the solar irradiation, taking into account the effect of geospatial features, including elevation, slope, aspect, shadow effect, and so on. Specifically, this paper mainly focuses on the impact of data resolutions on the prediction accuracy in order to understand the effect of map scale and geographical features on solar energy computation. The CNN model is trained with a digital elevation map (DEM) containing such topographical features and solar radiation datasets estimated in pixel levels. With the trained CNN model, performances for DEMs of 30 m and 60m resolutions are compared to evaluate the effect of data resolution.

2 Research Background

This section reviews recent studies that consider topographical features for predicting solar irradiation using machine learning techniques and statistical methods. In addition, the impact of data resolution on forecasting performance of solar irradiation is also reviewed and discussed.

2.1 Challenges in Solar Irradiation Prediction Considering the Topographical Features

Recent studies showed that the topographical features (e.g., altitude, latitude, longitude) considerably influenced the solar radiation prediction performance [7, 9, 10, 11]. For example, [7] estimated daily global solar irradiation by using solar radiation data collected on the complex mountainous terrain; it was found that the most important geographic factor to estimate global solar irradiation on complex mountainous terrain is the altitude. [9] developed the prediction model using solar radiation data observed in different regions in the model training and testing processes, showing that the solar radiation could successfully be estimated for new testing regions not used in the modeling process. Additionally, [10] evaluated geographical factors such as latitude, longitude, altitude in order to find the optimal combination of input parameters and to understand the impact of topographic features.

Overall, these previous studies provide insight into the use of data and the impact of topographical features on predicting solar irradiation by building statistical or machine learning models. Nonetheless, the models and methods proposed in the studies are mostly tested with the data collected at specific observation stations. This issue can become critical when applied to the regions far away from the study areas, where topographical characteristics can significantly be different. In this regard, further studies are still required for in-depth understanding of the topographical features in solar irradiation estimation, when the data-driven approaches are applied to large-scale areas or other areas, as pointed out in [11].

2.2 The Effect of Data Resolution on Solar Irradiation Prediction Model Performance

For machine learning or statistical methods, data resolution is another factor affecting the predicted amount of solar irradiation [12, 13]. The effect of data resolution was thus studied with a focus on the input data such as a DEM used to develop the geometry-based prediction model of solar radiation. In [12], geometry-based methods were developed using solar radiation models such as SRAD, Solei-32, and r.sun, which analyzed the components of solar radiation (e.g., direct, diffuse, and reflected) and geographic elements such as site latitude, topography, shadow cast, and so on. [12] found that the resolution change of a DEM affected the input variables of the prediction model, such as shadow effect, elevation, slope, etc., which resulted in a difference between the predicted solar radiation values and actual values. [13] also showed that a higher DEM resolution improved the performance of solar radiation models. These studies implied that the resolution of a DEM can affect the accuracy of surface angle calculations at the study area, which are the key inputs to theoretical computing of the solar radiation.

Unlike geometry-based methods, the impact of data resolution has rarely been studied for data-driven approaches that attempt to recognize patterns in the relevant data for the solar radiation prediction. It may be because machine learning methods in the previous studies [e.g., 14, 15] generally used solar radiation data (e.g., altitude, latitude, longitude, land surface temperature) produced at observation stations. In this case, the resolution of data may not be of importance for the prediction, as DEM data was not directly used for the modeling process. Consequently, the effect of data resolution still remains unknown when DEM data itself is used as an input for machine learning approaches to solar radiation estimation.

3 Method

To evaluate the effect of data resolution on machine learning-based solar energy prediction, this study builds and compares two CNN models trained with a DEM with 30m resolution and another DEM with 60 m resolution

along with the average amount of solar radiation for each DEM map of 30 by 30 pixel. Specifically, the DEMs are created with GIS datasets publicly provided by the National Spatial Data Infrastructure (NSDI) in South Korea, and the DEM that covers the entire national territory with the grid cell size of 30 m by 30 m is selected to create the DEM datasets with different resolutions, i.e., the inputs for the CNN models. Meanwhile, the output datasets, which are the estimated solar irradiation in pixel levels (e.g., a raster with 30 m by 30 m), are obtained by applying the computational estimation model presented in the authors' prior work [16]. Then, with the datasets used as an input and an output, CNN models are built and trained through the processes that minimize errors between the actual and predicted outputs. Eventually, the errors between two models with different data resolutions are compared to evaluate the effect of topographical features on the prediction performance.

3.1 Data Collection

For supervised learning, adopted in this paper, input datasets and labeled output datasets are needed to develop the CNN-based prediction model by iteratively learning the model parameters (e.g., weights) from the datasets. In building a solar irradiation prediction model, the CNN architecture consists of an input layer of a DEM image and an output layer of a solar radiation value with hidden layers between the two. The solar radiation amount for the region on each DEM image is extracted from a solar radiation image—produced by [16]—corresponding to the DEM image. In addition, two types of DEM images with 30 m and 60 m resolutions are created to assess the effect of data resolution on solar irradiation prediction. Specifically, for the inputs, DEM images (Figure 1c) are created by converting the contour map (Figure 1a) composed of group of lines joining points of the same elevation, to a triangular irregular network (TIN) (Figure 1b), which are continuous triangular facets with an empty space between contour lines representing the elevation. The generated TIN is then converted to a DEM image in a raster format (Figure 1c), which stores the elevation value at each pixel. This DEM image is eventually used as the input dataset in the CNN model for solar irradiation prediction.

On the other hand, the outputs, solar radiation data is produced by applying the computational method [16] that can estimate solar radiation values at every pixel given a DEN image. In [16], to consider topographical characteristics, a theoretical solar radiation energy model is transformed into a solar radiation model with inclined surface (Equation 1), which consists of reflected radiation (Equation 2), diffuse radiation (Equation 3), and direct radiation (Equation 4). Here, β is the surface tilt angle, ρ is the surface reflectance, and i is the incident angle. $I_{b,N}$, $I_{d,h}$ and I_h derived from [17], which are used to estimate solar radiation for a sunny day, are the radiation per unit area, the scattering radiation in the horizontal plane, and the horizontal solar radiation, respectively. Notably, to calculate the surface tilt angle (β), a tilt angle map is generated from the DEM. Consequently, when the DEM resolution changes, the tilt angle (β), reflected radiation, diffuse radiation, and even solar radiation can also change together. By applying [16], annual solar radiation is obtained as a result, and used as output datasets for the CNN modeling of solar irradiation prediction.

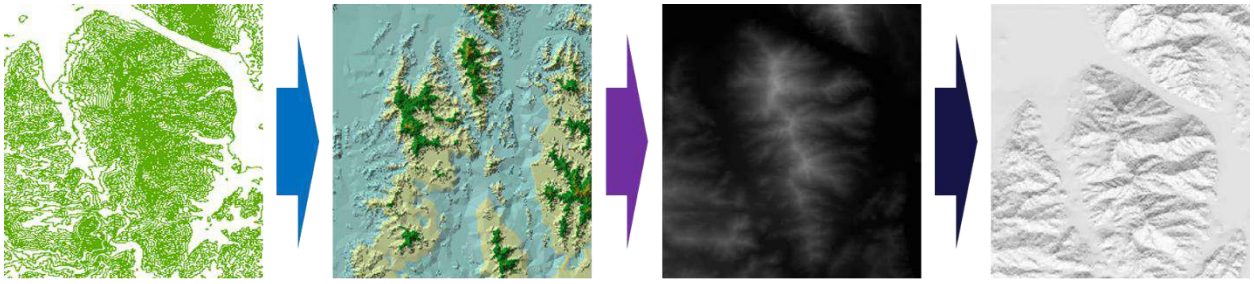

$$I_c = I_{r,c} + I_{d,c} + I_{b,c} \quad (1)$$

$$I_{r,c} = \rho I_h \sin^2(\beta/2) \quad (2)$$

Figure 1. Overview of data collection and processing: (a) contour map, (b) TIN image, (c) DEM image, and (d) solar radiation map.

$$I_{d,c} = I_{d,h} \cos^2(\beta/2) \quad (3)$$

$$I_{b,c} = I_{b,N} \cos i \quad (4)$$

In addition, when generating the two datasets (i.e., for 30 m and 60 m resolutions), the geographic map resolution is determined by the horizontal and vertical length of one pixel (i.e., a raster), which represents the size of the region covered by the information (e.g., an elevation value) in one pixel. For example, the DEM with 30 m resolutions means that one pixel covers 900 m^2 area, and in this study, total 105,000 images are extracted and generated from the national map, while the DEM with 60 m resolution means that one pixel covers 3,600 m^2 area, and total 26,145 images are obtained from the national map. For the experiment comparing two data resolutions, 25,000 images are randomly selected from both datasets for the fairness of model comparison.

3.2 Data Modeling Approach

Deep learning, such as deep neural networks (DNN), is inspired by the human brain, imitating the vast human brain network with interconnected neurons. DNN is composed of an input layer that accepts external stimuli, hidden layers that act as mediators that allow each neuron to receive and to send signals, and an output layer that responds to signals from hidden layers [18]. These processes help to identify patterns and recognize features in an unordered dataset. However, traditional neural networks have a limitation in finding patterns or features in an image because of flattening three-dimensional image data to a single dimension in the learning process [8]. For example, three-dimensional DEM image containing elevation information in each pixel is transformed onto one-dimensional data, for example, a list shape in Figure 2a. In this case, spatial relationships among pixels are ignored in the learning process, and hence topographical patterns in DEM datasets are hardly learned in predicting the solar energy. However, CNN can utilize the DEM image as a three-dimensional input as it is, and the topographical features can still be learned in the modeling process. As DEM images pass through the convolutional layers, filters in the convolutional layers extract the features in DEM images, as shown in Figure 2b. Eventually, the model parameters (i.e., weights) in hidden layers are updated in iterations, in each of which a solar irradiation value is predicted using a regression function and compared to the actual value. Therefore, the CNN-based regression is adopted to solar irradiation given a DEM, taking into account the relationship between the topographical features and solar radiation.

3.3 CNN Architecture for Solar Irradiation Prediction

The architecture of the CNN-based regression is illustrated in Figure 3. The input layer is designed to receive an input image of 30 x 30 pixels, which represents a region of 900 m x 900 m for 30 m resolution data and 1,800 m x 1,800 m for 60 m resolution data. These input images (Figure 4) are extracted from the national map without any overlap, as described in Section 3.1.

The input image representing a DEM when entered to an input layer is then sent to the following convolution layer. The first convolution layer used to extract the feature maps of the DEM image is composed in 30 x 30 x 32 dimensions, which means a DEM window size of 30 x 30 pixels with 32 filters. The size of the filter used in this study is 3 x 3. The first convolution layer is connected to an activation function, a rectified linear unit (ReLU) function that controls and determines the output of the layer, which will be sent to the following layer, as well as to a max-pooling layer that helps reduce computation and overfitting by decreasing the size of input window. For instance, the input image (i.e., 30 x 30 pixels) is reduced to an image of 15 x 15 pixels through the max-pooling layer in the first convolution layer. The second and third layers (Figure 3) have similar structure to the first one, working similarly. The second convolution layer extracts the feature maps from the data of the previous layer by using the same number of filters as the one in the first layer. However, the third convolution layer uses the 64 filters to extract the feature maps, although the second and third convolution layers are also connected to the activation function layer and

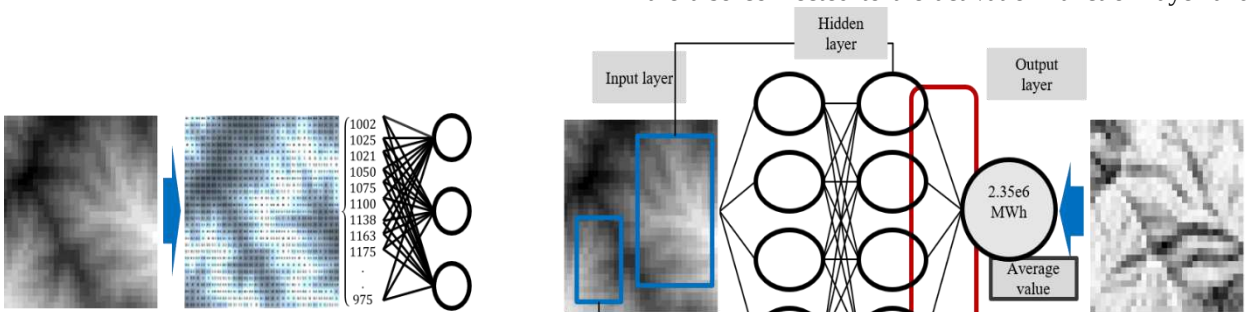

Figure 2. Overview of data modeling: (a) deep learning, and (b) convolutional neural network

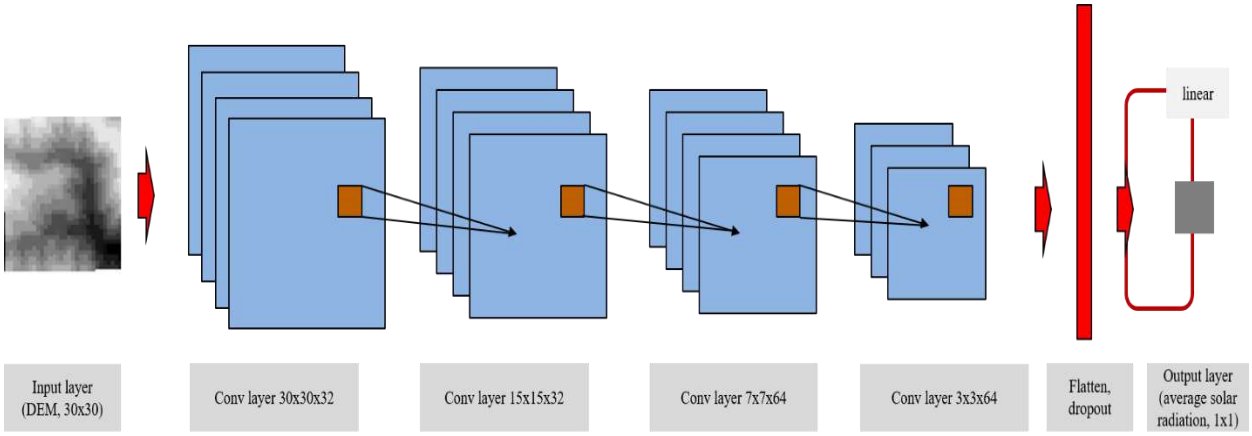

Figure 3. Architecture of convolutional neural network

max-pooling layer. The size of an input window thus decreased from 15 x 15 pixels to 7 x 7 pixels by passing the second max-pooling layer, and the size further decreased from 7 x 7 pixels to 3 x 3 pixels by passing the third max-pooling layer. The fourth layer is also a convolution layer with the same number of filters as the one in the third convolution layer, and the activation function layer; however, no max-pooling layer is included. The input data passed through the fourth layer is then sent to a dropout layer that is used to prevent the overfitting problem, and is in turn sent to a linear function layer for regression analysis (instead of a softmax function generally used for classification).

The CNN model described above is trained by using mean square error (MSE) as the loss function in the process that updates the model parameters (e.g., convolution filters) on the way that minimizes the error difference between the predicted value by the trained network and the actual solar radiation data. The MSE is defined in Equation 5, where i denotes i-th data in the dataset, and n is the number of training or testing samples in the dataset. The learning process of CNN continues in iterations until the minimum MSE, or the number of iterations a user defines, is reached. The resulting predicted value with a minimum error is compared with the actual one, and the coefficient of determination (R^2) is computed to evaluate the model performance. The value of the coefficient of determination is between 0 and 1; and for the higher correlation between the dependent variable and the independent variable, the value of coefficient of determination is closer to 1.

$$MSE = \frac{1}{n}\sum_{i=1}^{n}(actual - predicted)^2 \qquad (5)$$

In this study, the MSEs and coefficient of determination are computed for the two CNN models built for the datasets with different data resolutions, to

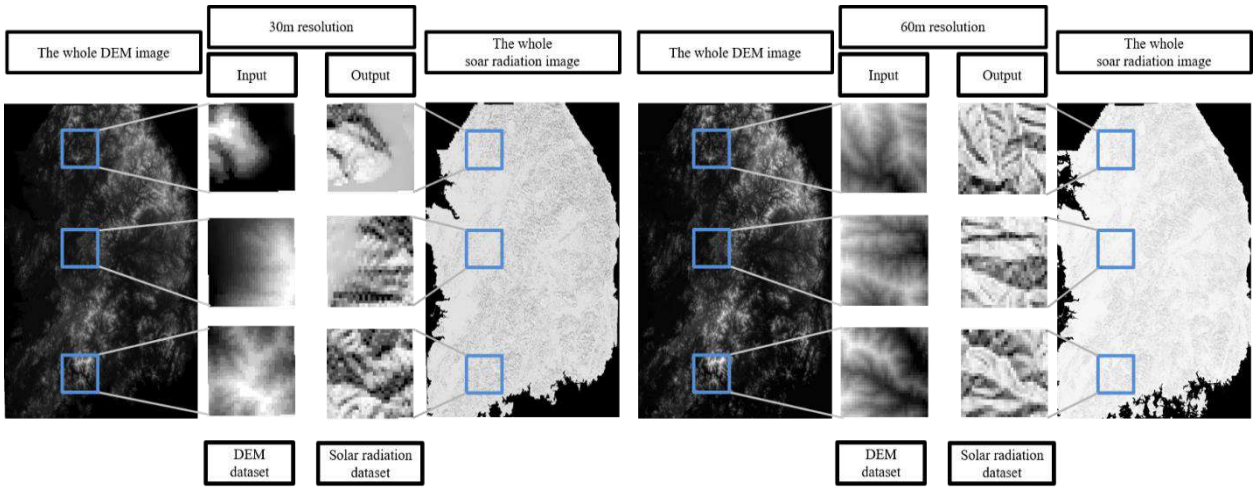

Figure 3. Overview of DEM and solar radiation datasets processing: (a) 30m resolution datasets and (b) 60m resolution datasets

assess the effect of data resolution on the solar irradiation prediction.

4 Experiment Results

Figure 4 illustrates a pair of two datasets: the DEM image and the corresponding solar radiation maps for two data resolutions. From the solar radiation map, annual mean of available solar irradiation is calculated for each map (i.e., 30 x 30 pixels), the mean value is used as an output the model attempts to predict. Particularly, the DEM image and solar radiation value are normalized as a pre-process. This normalization is adopted to prevent the poor learning caused by the wide spread of data values, and the min-max normalization method is applied for scaling the range of raw data to be [0, 1]. As a result, the raw DEM datasets for 30 m and 60 m resolutions (e.g., Figure 4a and 4b), the range of which are initially [0, 1900] and [0, 1550], respectively, are scaled to [0, 1]. The difference in the max values may happen for different DEM resolutions used to estimate the solar radiation. For example, higher-resolution data represents the elevation information more precisely than lower-resolution data [12]. This difference in data resolution affects the solar radiation data, the deviation of which between two resolutions is observed as approximately 11%.

Figures 5 and 6 present the relationship between the predicted and actual results for 30 m and 60 m resolutions, respectively. Overall, both results visually show that the predicted one is strongly correlated to the observed one with R^2 of 0.89 and 0.87.

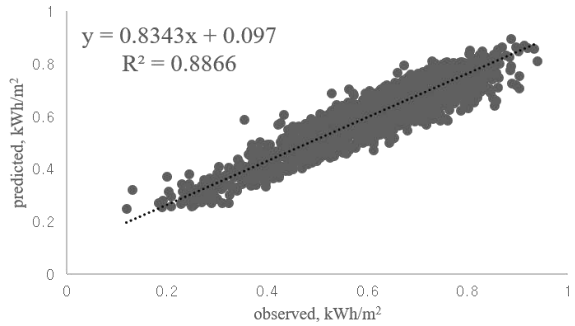

Figure 4. The plot of the relationship between the predicted and actual results for 30 m resolution

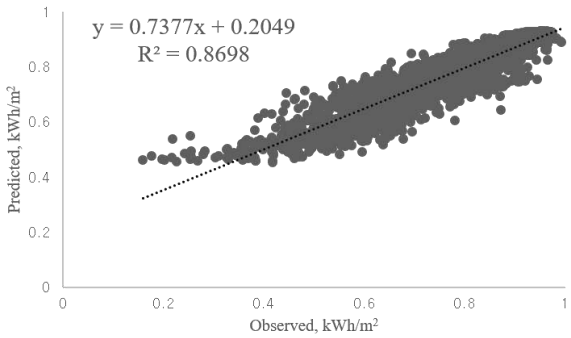

Figure 5. The plot of the relationship between the predicted and actual results for 60 m resolution

Table 1 summarizes the MSE, R^2, and MSE converted in actual units. The R^2 for 30 m resolution dataset is slightly higher than the one for 60 m resolution dataset. It is also observed that the plot of 30 m resolution (Figure 5) is slightly more uniformly distributed than the one of 60 m resolution (Figure 6). Yet, the difference caused by data resolution may not be significant in this experiment. Additionally, it is observed that the MSE value of 30 m resolution is 0.0018, while the MSE value of 60 m resolution is 0.00315. When converted in the actual units, the prediction errors of solar irradiation for 30 m and 60 m resolutions are 3,981 kWh/m^2 and 8,007 kWh/m^2, respectively. In other words, the errors from 30 m resolution data are 1.8 times and 2.0 times lower than the ones from 60 m resolution data in the MSE and MSE in actual unit, respectively. Thus, these results show that in this experiment, the solar irradiation is more accurately predicted when the data with higher resolution is used.

Table 1. Summary of the experiment results

Data resolution	MSE	R^2	MSE-in actual unit
30 m	0.0018	0.89	3,981 kWh/m^2
60 m	0.0032	0.87	8,007 kWh/m^2

5 Discussion

In this paper, CNN-based prediction is adapted to reflect the topographical features in the solar energy estimation. The results indicate that the proposed CNN-based approach produces promising results for the prediction of the solar irradiation on complex terrains or on a large scale. The CNN model learns spatial correlations among individual pixel values stored in each image (e.g., an array) during the training, and thus it can be implied that the solar irradiation is fairly affected by

the topography of a surrounding terrain. For example, the amount of solar irradiation on a surface can be significantly influenced by the shadow created by adjacent hills at high elevation. The proposed approach that can use a DEM image itself as an input thus enables us to utilize a map-type data for machine learning.

The results also reveal that, in this experiment, DEMs with higher resolution outperform ones with lower resolution when a machine learning method is applied. This result is also supported by [13], reporting that a higher DEM resolution produces more accurate results with geometry-based methods instead of machine learning applied in that study. This result may imply that when the topographical features are represented or preserved well in datasets, the solar irradiation can be better estimated, as the neural network is generally affected by the quality of image [19]. Thus, the resolution and quality of DEM inputs should be carefully selected and tested, depending on the level of accuracy required for the solar energy study.

Previous machine learning approaches have mainly focused on evaluating the geographical factors (e.g., altitude, latitude, longitude) as input variables or gathering the data related to solar energy from the meteorological observation sites. However, this study shows through the CNN modeling that geographical features can be reflected in the solar energy estimation model, and the effect of data resolution is also assessed for an CNN application. Nevertheless, there are other factors affecting the CNN performance, which should further be explored. For instance, the size of an image can have an impact on the CNN performance [20]. An input image of 30 x 30 pixel size is used in this study, but other image sizes (e.g., 60 x 60, 90 x 90) need to be studied for an in-depth understanding of the size of an area affecting the amount of solar radiation. On the other hand, the method of calculating the solar radiation used as output data can also affect the predictive performance. In this study, the mean of solar irradiations stored in a pixel level on a DEM image is used as an output the model estimates. As the solar radiation on the surface of the earth depends not only on the surface angle or the shape of the terrain but also on the position of the sun [21], specific regions with higher solar energy may exist. Thus, various regions representing the entire DEM image well (e.g., average, a top region, a middle region, top triangle shape on a DEM) should be tested to understand which part of a DEM can be better estimated with the DEM image.

6 Conclusion

This study investigates the effect of geographical features on a solar irradiation estimation model by using CNN models built based on the datasets with different data resolutions. The CNN uses DEM images in a 3D shape (e.g., an elevation value stored in x-y coordinates) as an input; thus, spatial information is still held and modelled during a learning process. Furthermore, it is found that the use of higher-resolution data can result in more accurate prediction in the experiment. Regardless of the data resolution; however, models for both resolutions produce robust estimation results (e.g., MSEs of 0.0018 and 0.0032). Thus, the CNN approach may allow for the appropriate selection of PV panel installation on a large scale. In our future study, the CNN model will be further developed to estimate the power generated at a PV panel site by investigating the CNN architecture for the use of multilayer inputs, including maps of weather conditions, which are other critical factors affecting the power generation.

Acknowledgements

This research was supported by a grant (19CTAP-C141728-02) from Technology Advancement Research Program (TARP) funded by Ministry of Land, Infrastructure and Transport of Korean government.

References

[1] Le Quéré. and Corinne. et al. Global carbon budget. *Earth System Science Data*, 10:2141-2194, 2018.

[2] BP Statistical Review of World Energy. On-line: http://bp.com, Accessed: 16/01/2019.

[3] Solar Power Advantages and Disadvantages: On-line: http://sepco-solarlighting.com, Accessed: 16/01/2019.

[4] Samanta. B. and Al Balushi. K. R. Estimation of incident radiation on a novel spherical solar collector. *Renewable energy*, 14(1-4):241-247, 1998.

[5] Escobedo and J. F. et al. Modeling hourly and daily fractions of UV, PAR, and NIR to global solar radiation under various sky conditions at Botucatu, Brazil. *Applied Energy*, 86(3):299-309, 2009.

[6] Faghih and A. K. et al. Solar radiation on domed roofs. *Energy and Buildings*, 41(11):1238-1245, 2009.

[7] Bosch. J. L and Lopez. G. et al. Daily solar irradiation estimation over a mountainous area using artificial neural networks. *Renewable Energy*, 33(7):1622-1628, 2008.

[8] Karpathy. A. Convolutional Neural Network for Visual Recognition. On-line: http://cs231n.git-hub.io, Accessed: 17/01/2019.

[9] Mohandes. M and S. R. et al. Estimation of global solar radiation using artificial neural networks. *Renewable energy*, 14(1-4):179-184, 1998.

[10] Koca. A and Oztop. H. H. et al. Estimation of solar radiation using artificial neural networks with

different input parameters for Mediterranean region of Anatolia in Turkey. *Expert Systems with Applications*, 38(7):8756-8762, 2011.

[11] Linares-Rodriguez. A and Ruiz-Arias. J. A. et al. Generation of synthetic daily global solar radiation data based on ERA-Interim reanalysis and artificial neural networks. *Energy*, 36(8):5356-5365, 2011.

[12] Liu. M and Bárdossy. A. et al. GIS-based modeling of topography-induced solar radiation variability in complex terrain for data sparse region. *International Journal of Geographical Information Science*, 26(7):1281-1308, 2012.

[13] Ruiz-Arias and J. A. et al. A comparative analysis of DEM-based models to estimate the solar radiation in mountainous terrain. *International journal of Geographical Information Science*, 23(8):1049-1076, 2009.

[14] Şahin. M and Kaya. Y. et al. Application of extreme learning machine for estimating solar radiation from satellite data. *International Journal of Energy Research*, 38(2):205-212, 2014.

[15] Şenkal. O. Solar radiation and precipitable water modelling for Turkey using artificial neural networks. *Meteorology and Atmospheric Physics*, 127(4):481-488, 2015.

[16] Jung. J and Han. S. et al. Digital Numerical Map-Oriented Estimation of Solar Energy Potential for Site Selection of Photovoltaic Solar Panels on National Highway Slopes. *Applied Energy*, 2019.

[17] Gueymard and C. A. Direct and indirect uncertainties in the prediction of tilted irradiance for solar engineering applications. *Solar Energy*, 83(3):432-444, 2009.

[18] Zaccone. G and Karim. M, R. et al. Deep learning with TensorFlow. volume 302(13). Packt, Livery Place 35 Livery Street Birmingham B3 2PB UK, 2017.

[19] Dodge. S and Karam. L. Understanding how image quality affect deep neural networks. In *Proc. Of QoMEX*, pages 1-6, Portugal, 2016.

[20] Howard and Andrew. G. Some improvements on deep convolutional neural network based image classification. On-line: https://arxiv.org/abs/1312-.5402/, Accessed 01/26/2019.

[21] Dubayah. R and Rich. P. M. Topographic solar radiation models for GIS. *International Journal of Geographical Information Systems*, 9(4):405-419, 1995.

Direct-Write Fabrication of Wear Profiling IoT Sensor for 3D Printed Industrial Equipment

M.I.N.P. Munasinghe[a], L. Miles[b], and G. Paul[a]

[a]Centre for Autonomous Systems, University of Technology Sydney (UTS), Australia
[b]UTS Rapido, UTS, Australia
E-mail: Nuwan.Munasinghe@student.uts.edu.au, Lewis.Miles@uts.edu.au, gavin.paul-1@uts.edu.au

Abstract –

Additive Manufacturing (AM), also known as 3D printing, is an emerging technology, not only as a prototyping technology, but also to manufacture complete products. Gravity Separation Spirals (GSS) are used in the mining industry to separate slurry into different density components. Currently, spirals are manufactured using moulded polyurethane on fibreglass substructure, or injection moulding. These methods incur significant tooling cost and lead times making them difficult to customise, and they are labour-intensive and can expose workers to hazardous materials. Thus, a 3D printer is under development that can print spirals directly, enabling mass customisation. Furthermore, sensors can be embedded into spirals to measure the operational conditions for predictive maintenance, and to collect data that can improve future manufacturing processes. The localisation of abrasive wear in the GSS is an essential factor in optimising parameters such as suitable material, print thickness, and infill density and thus extend the lifetime and performance of future manufactured spirals. This paper presents the details of a wear sensor, which can be 3D printed directly into the spiral using conductive material. Experimental results show that the sensor can both measure the amount of wear and identify the location of the wear in both the horizontal and vertical axes. Additionally, it is shown that the accuracy can be adjusted according to the requirements by changing the number and spacing of wear lines.

Keywords –

IIoT; Wear Sensor; Additive Manufacturing; 3D Printing; Industry 4.0

1 Introduction

Additive manufacturing, also widely known as 3D printing [1], is the process of taking information from computer-aided designs (CAD) and transforming it into a printed physical object. Additive manufacturing has passed the rapid prototyping era and is increasingly being used to manufacture finished products.

Combining Cyber-Physical Systems (CPS) and IoT in the industrial domain has led to the fourth industrial revolution (Industry 4.0), and has enabled smart production, smart products and smart services [2]. Using Internet of Things (IoT) for industrial automation is making collaboration between automation and heterogeneous devices and systems more predictable, real-time, fault-tolerant, and closed-loop [3].

Authors of this paper are working on research and development of a 3D printer to print customisable GSS for use in the mineral industry. The focus is to develop a system to print a spiral with embedded sensors, which makes it a smart product that can have its operational conditions remotely monitored. Collected data from these smart spirals can be used to optimise production output, perform condition-based maintenance, maintain worker safety, troubleshoot issues, predict future failures and improve future products.

Measuring wear in industrial components in situ provides many advantages, e.g., the ability to make informed decisions related to: (a) adaptive control of various feeds and speeds to achieve optimum production rate; and (b) planned maintenance and identification of sudden equipment failure [4]. When considering this specific application of printed spirals, it is required that wear be monitored remotely, in situ and in real-time. Such monitoring enables a measure of the amount of wear over time and the location of such wear, and hence opens the possibility of improving future prints by refining the material or printing properties. Sensors should ideally be embedded within spirals, since downtime for inspection generally requires manual intervention and production interference, and ultimately profit loss. Since GSS are used in rural locations all around the world, including Brazil, USA, South Africa, India and Australia, using an IoT solution to gather data from various remote locations is advantageous and possible. Figure 1a shows a bank of these spirals and Figure 1b depicts the relative sizes.

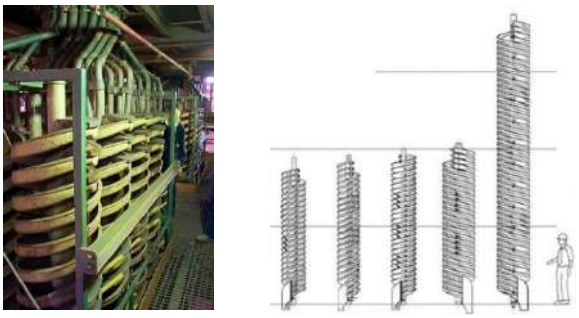

(a) (b)

Figure 1. (a) Spiral banks in the mining site; (b) Selected spiral models and relative sizes. Source: Adapted from [5].

Direct Write (DW) refers to techniques in AM to develop various electronic and functional components using different materials without using masks or subsequent etching [6].

In this paper, a novel sensor is presented, which is developed using DW methods to measure both the amount of wear and the location of wear. The main contribution is the development of a wear sensor, which can be 3D printed directly onto industrial 3D printed components using a conductive filament to monitor the linear dimension and location of wear in situ. The rest of this paper is organised as follows: Section 2 describes related work conducted in this area; Section 3 contains the methodology of development of the sensor; Section 4 presents the results of the experiments conducted, and finally, Section 5 and Section 6 provide the discussion and conclusions respectively.

2 Related Work

Additive manufacturing has evolved beyond a rapid prototyping technology, with many industries adopting AM as their primary manufacturing process [1]. The construction industry is increasingly using AM for topology optimisation, customised parts, in situ repair, and tolerance matching [7]. Additive manufacturing is also used in medical applications such as printing customised airway stents and soft prostheses [8] [9]. Due to the unique capabilities of AM, it is possible to manufacture optimised parts which would traditionally be non-trivial to produce. The benefits of AM have been utilised by the aerospace industry to improve the power to weight ratio of autonomous aerial vehicles through the manufacture of lightweight parts. [10]. Another unique advantage of AM is the ability to combine multiple parts into a single component, reducing assembly complexity. For example, General Electric developed a 3D printed fuel nozzle for their LEAP engine, a part which traditionally was made of 20 individual parts [11].

There are many different methodologies to detect wear in industrial components [4], including, optical scanning, analysing the change in product from equipment, electrical techniques, radioactive techniques, mechanical vibrations/sound analysis, temperature measurement.

Acoustic emission (AE) is the propagation of elastic waves in the range between 0.1 and 1MHz, and these waves are generated by friction [12]. Corrosion or wear will change the AE of a component. The capture and analysis of the AE can be used to identify wear in tools [13]. Douglas et al. [12] developed an AE based wear sensor for piston rings using this method.

Fritsch et al. [14] developed a vibration based wear sensor which detects micro-mechanical resonant vibrations in the low-frequency range. The sensor was developed using a micromachined silicon structure. This sensor is used to characterise vibrations from anti-friction bearings of calendar rolls mainly used in the textile industry.

Researchers have used various electrical based methods to measure wear in industrial components. Bödecker et al. [15] developed a resistance based sensor which can detect wear in the cylinders of diesel engines. Without this kind of in situ sensor, the engine must be decommissioned to inspect the engine for wear, which incurs significant resource costs. This sensor is manufactured with a conductive layer between the two insulating layers, and this conductive layer is constructed in the form of resistive loops. A change of the resistance as these loops are worn away provides a measure of wear. Ruff and Kreider [16] developed a wear sensor using vacuum deposited thin-films. The sensor package consists of two conductive layers that lie on top of the thermocouple layer separated by insulating layers. This sensor can also be used as a temperature sensor. Another thin film-based wear sensor for cutting tools developed by Holger et al. [17] uses a coating technique for the real-time measurement of wear. This sensor is also based on parallel connected electrical resistors. The wear indicator developed by Dyck et al. [18] can be used to measure a wear surface as well as the coefficient of friction for different types of coated geometries. This indicator slides a specimen material through electrical contacts to detect wear.

The proposed method for the wear sensor in this paper includes directly creating conductive traces on the material using a carbon-based composite material. There are many DW methods, with the most common ones being inkjet, aerosol jet, and photolithography methods. Le et al. [19] used inkjet-printed graphene to develop a gas sensor which can detect NH_3 and CO gasses. This sensor is a low-cost, self-powered, battery-less, wireless sensor based on radio-frequency identification (RFID) technology. Micro-scale aerosol-

jet graphene-based additive manufacturing process, which is developed by Jabari et al. [20], uses graphene ink with a particle size below 200nm, to deposit thin graphene layers. Moreover, their results show that this process is capable of printing interconnects with widths in the range of 10-90 μm and with resistivity as low as 0.018 Ω cm. Shen et al. [21] developed a temperature sensor based on extrusion DW techniques, which used a micron-level platinum layer on top of an alumina substrate to print the sensor.

In the area of DW wear sensors, Shen et al. [22] developed a high-resolution wear sensor based on parallel silver interconnects. This process requires heat treatment of the printed part to achieve full performance. In this method parallel conductive lines contain parallel resistors, and when wear occurs, conductive interconnects are progressively removed, and the resistance changes. By measuring the resistance, it is possible to identify the level of wear. Dardona et al. [6] used the same method and tested it with both printed resistors and commercial resistors (Figure 2).

One significant drawback of these methods is an inability to determine the location of wear accurately. Also, they require additional steps and technology to embed traditional resistors and to perform post-treatment of the printed parts. Therefore, the authors propose a new wear sensor design with carbon-based material, which can measure the wear as well as the location of the wear, and does not require the embedment of traditional resistors nor post-treatment.

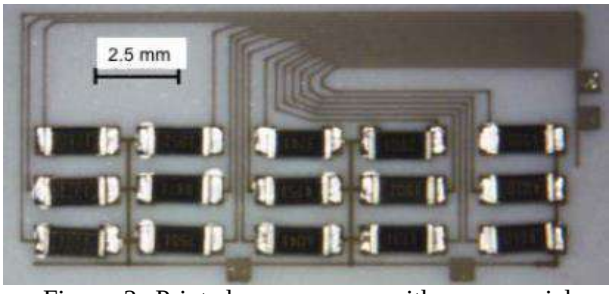

Figure 2. Printed wear sensor with commercial resistors. Source: Adapted from [6].

3 Methodology

The overall project goal is to create a large-scale printer which can 3D print a GSS. Currently, a one-third scale prototype (build volume of 220 x 1200mm) is being tested to verify the printing method. Future stages of the project will focus on constructing the full-scale eleven degrees of freedom multi-material FDM 3D printer (build volume of 700 x 2000mm). This section provides details about the materials and methodology used to develop and embed the wear profiling sensor into the printed GSS.

3.1 Design Principles

3.1.1 Conductive Filament

In order to print the conductive traces, a carbon powder blended with polylactide (PLA) is used. The volume resistivity of the moulded resin without printing is 15 Ω cm. 3D printed parts which are perpendicular to the layers along the X-Y axis have 30 Ω cm resistivity and along with the Z-axis 115 Ω cm. The nozzle temperature of the printer is 195C – 225C and heated bed temperature is in the range of 25C – 60C.

Different allotropes of carbon attracted significant interest in various types of applications in AM. The main reason is it is suitable for low-cost, large-volume applications [23]. For the developed printer project to be successful, it must be possible to produce a GSS in an equal or more economical way than traditional methods, therefore, using silver-based materials in wear sensors like Shen et al. [22] or Dardona et al. [6] is undesirable due to cost considerations. On the other hand, using carbon-based polymer composites has advantages over metal based or metal alloys. Some advantages include the lack of additional processing steps like thermal annealing, ease of printing, readily accessible technology, and longer shelf-life (years) [24].

3.1.2 Design of Printed Traces

The conductive traces shown in Figure 3 are printed using the conductive material mentioned in the previous section. The dimensions of the traces are 20x40x2mm. The number of traces can be determined based on the required wear measurement resolution. Figure 4 shows how multiple conductive layers are printed vertically aligned with each other and the intermediate insulating layers is PLA material. The number of layers can be changed according to the required wear resolution. R_X $(X = 1, \dots, 4)$ represent the resistance of each trace and $R_{LX}(X = 1, \dots, 4)$ represent total individual resistance of each layer. L_X $(X = 1, \dots, 4)$ represents the length of each trace as marked. $W_X(X = 1, \dots, 4)$ represent different locations wear can occur.

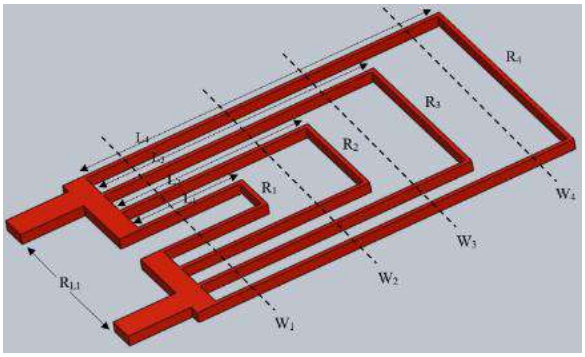

Figure 3. Printed traces in one layer.

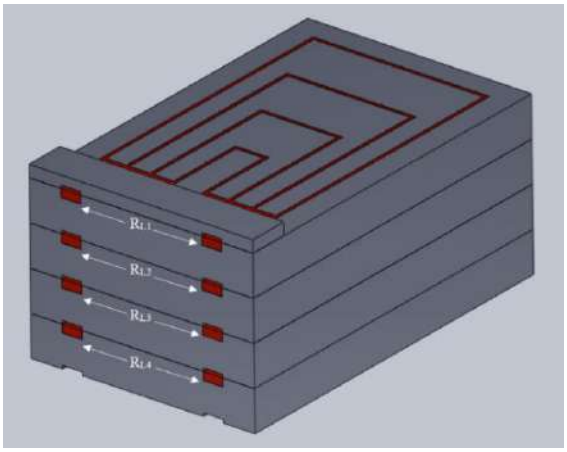

Figure 4. Printed traces in four layers.

3.1.3 Measurement and Localisation of Wear

Since all the traces in one layer are parallel with the terminals, the total resistance of the first layer can be calculated using the Equation (1). Likewise, Equation (1) applies to each trace component in each layer.

$$\frac{1}{R_{L1}} = \frac{1}{\mathrm{R}_1} + \frac{1}{R_2} + \frac{1}{R_3} + \frac{1}{R_4} \quad (1)$$

Without any wear, the resistance of the traces in all four layers will be equal. It is then assumed that wear occurs along W_2 line in layer one and is only just thick enough to cut through the first layer without reaching traces in layer 2. In this case, R_{L1} will be equal to R_1. Since the resistance of each traces are known, it is possible to predict that the wear occurs at a distance at least greater than L_1 but less than L_2. If wear occurs along with W_3line, R_{L1} will be equal to the total parallel resistance of R_1 and R_2. Then by measuring the resistance, it is possible to predict that wear occur at a distance greater than L_2 but less than L_3. Likewise, by measuring the resistance, it is possible to predict the wear location within one layer. Table 1 provides a summary of the detection of the wear locations based upon the resistance in one layer.

Table 1. Wear location and resistance in one layer.

Wear Line (W_X)	Total Resistance (R_{L1})	Wear Location (x)
W_1	∞	$x < L_1$
W_2	R_1	$L_1 < x < L_2$
W_3	$\frac{R_1R_2}{R_1+R_2}$	$L_2 < x < L_3$
W_4	$\frac{R_1R_2R_3}{R_2R_3+R_1R_3+R_1R_2}$	$L_3 < x < L_4$

The depth of the wear can be identified since the trace resistance in each layer is measured independently. Table 1 shows that in each layer, the wear distance can be estimated, which provides details of the wear profile.

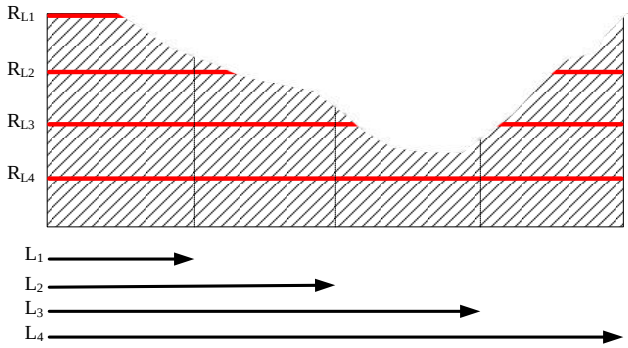

Figure 5. Cross section of the sensor with wear.

Figure 5 shows a vertical cross-section of the sensor with example wear. Table 2 summarises the possible resistance values for this wear profile and the predicted wear location.

Table 2. Wear location according to the measured resistance in each layer.

Resistance (R_{LX})	Wear Location (x)
∞	$x < L_1$
R_1	$L_1 < x < L_2$
$\frac{R_1R_2}{R_1+R_2}$	$L_2 < x < L_3$
$\frac{R_1R_2R_3R_4}{R_2R_3R_4+R_1R_3R_4+R_1R_2R_4}$	No Wear

3.2 Sensor Accuracy

The accuracy of the estimation of the wear location depends on the number of wear lines and the maximum length of the traces in each layer. Equation (2) quantifies this error and n_x is the number of lines and L is the length of the traces.

$$\Delta x = \frac{L}{n_x} \quad (2)$$

The accuracy of the amount of wear depends on the number of wear trace layers printed and the thickness of the material. Actual production sensors will not have traces on the top surface but one below the top. Equation (3) quantifies this error.

$$\Delta y = \frac{H}{n_y + 1} \quad (3)$$

where H is the thickness of the print, and n_y is the number of layers.

4 Experiment Results

4.1 Printing Process

Three printing methods were considered to produce the printed sensor: printing on a multi-material printer; printing components separately and assembling; pausing prints; and embedding printed components into print. To reduce material wastage and print time the sensor was printed separately and assembled, irrespective of the method the functionality of the sensor is the same. The main reason for selecting the assembly method was to prevent the use of a material purge tower and to remove the need to pause the print to embed components. Figure 6 shows the assembled wear sensor.

Each component was printed using the Creality CR-10, with the following print settings, layer thickness 0.1mm, layer width 0.4mm, print speed 60mm/s. The trace components were printed using Protopasta conductive filament, with a print temperature of 220 °C, bed temperature of 60 °C, 100% infill. The insulating layer was printed using PLA filament and a nozzle temperature of 185 °C, bed temperature of 60 °C, 20% infill.

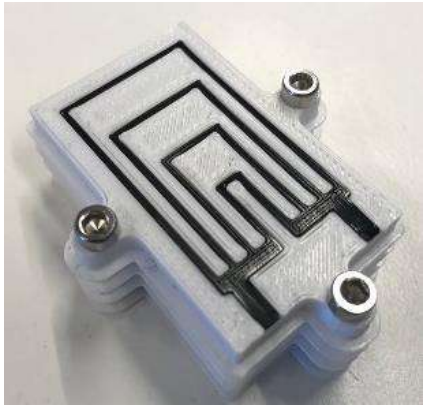

Figure 6. Printed wear sensor.

4.2 Resistance Comparison Between Multiple Prints

To determine the resistance variance across multiple conductive prints, 25 conductive traces printed as in Figure 7 and specific resistance of these traces were measured, and the standard deviation was 0.1005 kΩ. Results are shown in the graph in Figure 8, and according to the results, the resistance between multiple prints are relatively consistent.

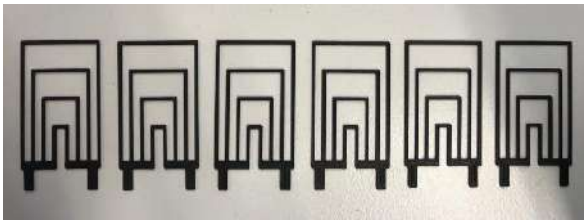

Figure 7. Multiple printed conductive traces.

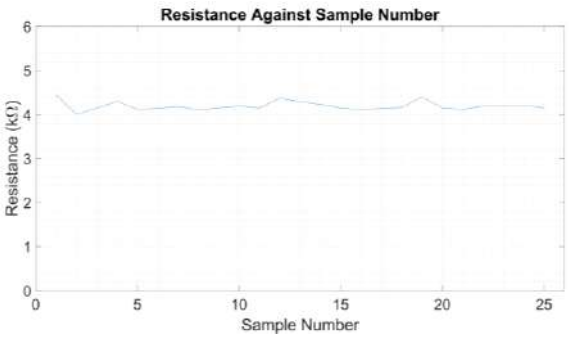

Figure 8. Total resistance against sample number.

4.3 Relationship Between Resistance and Location

The resistance values need to be determined as shown in Table 1 column 2 to identify the wear location. Printed traces were disconnected to simulate wear, as shown in Figure 9, and the resistance was measured. Results are summarised in Table 3 and the trend is shown in Figure 10.

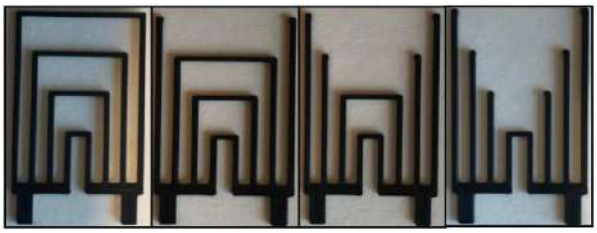

Figure 9. Resistance measurement related to different wear lines.

Table 3. Wear location and resistance in one layer

Wear Line (W_X)	Total Resistance (R_{L1} kΩ)	Wear Location (x mm)
No Wear	4.17	None
W_4	4.83	25< x < 33
W_3	5.41	17< x < 25
W_2	7.23	9< x < 17
W_1	∞	x < 9

Table 4. Predicted and actual wear locations according to the measured resistance in tested wear profiles.

Test	Resistance After Wear ($k\Omega$)				Actual Wear Line			Predicted Wear Line		
No.	R_{L1}	R_{L2}	R_{L3}	R_{L4}	Layer 1	Layer 2	Layer 3	Layer 1	Layer 2	Layer 3
1	5.45	4.82	4.29	4.10	W_3	W_4	–	W_3	W_4	–
2	5.49	5.48	5.43	4.13	W_3	W_3	W_3	W_3	W_3	W_3
3	∞	∞	4.14	4.10	W_1	W_1	–	W_1	W_1	–
4	∞	∞	7.66	4.13	W_1	W_1	W_2	W_1	W_1	W_2
5	7.20	4.18	4.11	4.16	W_2	–	–	W_2	–	–
6	7.28	7.25	4.20	4.14	W_2	W_2	–	W_2	W_2	–

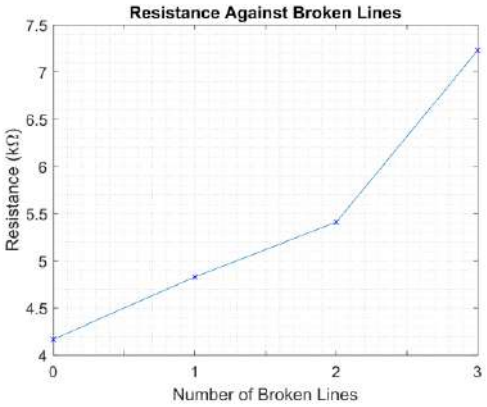

Figure 10. Resistance relative to broken wear lines.

4.4 Results with Different Wear Profiles

Table 4 summarises the test results with different wear profiles and actual and predicted wear locations. Dashes in the table represent "no wear". There was no wear for layer 4 in actual wear and predicted wear and therefore excluded from the table. Figure 11 shows different wear profiles tested. Wear location is predicted by comparing the resistance values of each layer to the values in Table 3 and selecting the closest location. In Figure 11, dash lines show the lengths of each traces (L_X) measured from left to right and W_x represents the wear line locations as in Figure 3.

According to the results above, it is evident that the proposed method provides accurate results for different wear profiles. Resistance values were measured in 25 printed traces to identify the resistance changes between multiple prints and the standard deviation was 0.1005 kΩ. Therefore, using this method as wear detection has good accuracy between multiple sensors as well.

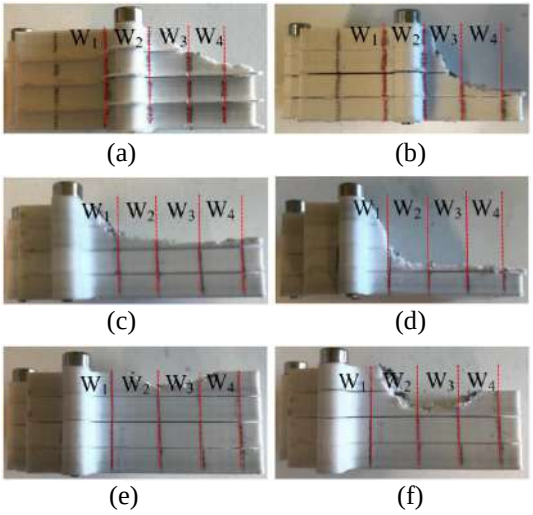

Figure 11. Wear profiles: (a) Test 1; (b) Test 2; (c) Test 3; (d) Test 4; (e) Test 5; (f) Test 6.

5 Discussion

The current design enables the measurement of the linear distance to wear values relative to one axis, parallel to W_1. These measurements can determine the wear profile relative to the datum axis, however, the tested configuration cannot determine wear profiles of the opposing side. It will be interesting to investigate the use of stacked sensors with opposing trace directions as shown in Figure 12. Such a sensor would introduce two datum axes rather than one, enabling the wear profile to be measured from either side. An additional benefit is that this configuration would allow the complete 2D cross-sectional profile of the wear area to be measured. The configuration could be extended by stacking sensors adjacent to each other, enabling a 3D map of the wear profile to be generated.

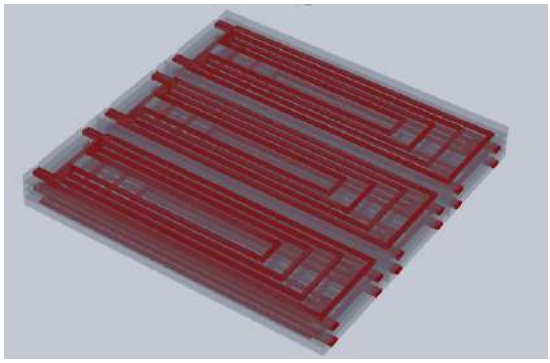

Figure 12. Suggested multi-assembly to get 3-dimensional wear profile.

6 Conclusion

The development of smart spirals, which can self-monitor operational conditions and collect data to improve future manufacturing processes, is underway. A measurement of spiral wear can help to predict its lifetime, and localising the wear provides valuable information about how to improve production. This paper has presented a novel embedded 3D printed wear sensor that can be used to measure both the location and severity of wear. The sensor is composed of printed traces using carbon-based filament, and experimental results have confirmed that real-time resistance measurements in each layer enable the location and severity of the wear to be determined accurately. By designing and printing an enhanced printed pattern it is possible to get a three-dimensional view of the wear. Future work will investigate alternative sensor configurations that will enable the wear profile to be determined in any orientation, and the integration of robustness against various wear conditions.

7 Acknowledgment

This research is supported by Innovative Manufacturing CRC (IMCRC) and Mineral Technologies.

References

[1] K. V Wong and A. Hernandez, "A Review of Additive Manufacturing," *ISRN Mech. Eng.*, vol. 2012, no. Article ID 208760, p. 10, 2012.

[2] M. Wollschlaeger, T. Sauter, and J. Jasperneite, "The Future of Industrial Communication: Automation Networks in the Era of the Internet of Things and Industry 4.0," *IEEE Ind. Electron. Mag.*, vol. 11, no. 1, pp. 17–27, 2017.

[3] H. P. Breivold and K. Sandström, "Internet of Things for Industrial Automation -- Challenges and Technical Solutions," in *2015 IEEE International Conference on Data Science and Data Intensive Systems*, 2015, pp. 532–539.

[4] N. H. Cook, "Tool wear sensors," *Wear*, vol. 62, no. 62, pp. 49–57, 1980.

[5] M. Technologies, "Gravity Separation," 2015. [Online]. Available: https://mineraltechnologies.com/process-solutions/equipment-design-selection/gravity-separation. [Accessed: 16-Jan-2019].

[6] S. Dardona, A. Shen, and C. Tokgoz, "Direct Write Fabrication of a Wear Sensor," *IEEE Sens. J.*, vol. 18, no. 8, pp. 3461–3466, 2018.

[7] D. D. Camacho *et al.*, "Applications of Additive Manufacturing in the Construction Industry – A Prospective Review," in *ISARC. Proceedings of the International Symposium on Automation and Robotics in Construction*, 2017, vol. 34, pp. 1–8.

[8] G. Z. Cheng *et al.*, "3D Printing and Personalized Airway Stents," *Pulm. Ther.*, vol. 3, no. 1, pp. 59–66, 2017.

[9] Y. He, G. Xue, and J. Fu, "Fabrication of low cost soft tissue prostheses with the desktop 3D printer," *Sci. Reports (Nature Publ. Group)*, vol. 4, p. 6973, Nov. 2014.

[10] E. P. Flynn, "Low-cost approaches to UAV design using advanced manufacturing techniques," in *2013 IEEE Integrated STEM Education Conference (ISEC)*, 2013, pp. 1–4.

[11] Y. Tadjdeh, "3D Printing Promises to Revolutionize Defense, Aerospace Industries," *Natl. Def.*, vol. 98, no. 724, pp. 20–23, Mar. 2014.

[12] R. M. Douglas, J. A. Steel, and R. L. Reuben, "A study of the tribological behaviour of piston ring/cylinder liner interaction in diesel engines using acoustic emission," *Tribol. Int.*, vol. 39, no. 12, pp. 1634–1642, 2006.

[13] L. Henrique, A. Maia, A. Mendes, W. Luiz, W. Falco, and A. Rocha, "A new approach for detection of wear mechanisms and determination of tool life in turning using acoustic emission," *Tribol. Int.*, vol. 92, no. 92, pp. 519–532, 2015.

[14] H. Fritsch *et al.*, "A low-frequency micromechanical resonant vibration sensor for wear monitoring," *Sensors and Actuators*, vol. 62, pp. 616–620, 1997.

[15] A. Bödecker, C. Habben, A. Sackmann, K. Burdorf, E. Giese, and W. Lang, "Manufacturing of a wear detecting sensor made of 17-4PH steel using standard wafer processing technology," *Sensors Actuators, A Phys.*, vol. 171, no. 1, pp. 34–37, 2011.

[16] A. W. Ruff and K. G. Kreider, "Deposited thin-film wear sensors: Materials and design," *Wear*, vol. 203, pp. 187–195, 1997.

[17] H. Lüthje, R. Bandorf, S. Biehl, and B. Stint, "Thin film sensor for wear detection of cutting tools," *Sensors and Actuators*, vol. 116, no. September 2003, pp. 133–136, 2004.
[18] T. Dyck, P. Ober-Wörder, and A. Bund, "Calculation of the wear surface and the coefficient of friction for various coated contact geometries," *Wear*, vol. 368–369, pp. 390–399, 2016.
[19] T. Le, V. Lakafosis, Z. Lin, C. P. Wong, and M. M. Tentzeris, "Inkjet-Printed Graphene-Based Wireless Gas Sensor Modules," in *Electronic Components and Technology Conference (ECTC)*, 2012, pp. 1003–1008.
[20] E. Jabari and E. Toyserkani, "Micro-scale Aerosol-jet Printing of Graphene Interconnects - ResearchGate.pdf," *Carbon N. Y.*, vol. 91, pp. 321–329, 2015.
[21] A. Shen, S. B. Kim, C. Bailey, A. W. K. Ma, and S. Dardona, "Direct Write Fabrication of Platinum-Based Thick-Film Resistive Temperature Detectors," *IEEE Sens. J.*, vol. 18, no. 22, pp. 9105–9111, 2018.
[22] A. Shen, D. Caldwell, A. W. K. Ma, and S. Dardona, "Direct write fabrication of high-density parallel silver interconnects," *Addit. Manuf.*, vol. 22, pp. 343–350, Aug. 2018.
[23] W. J. Hyun, E. B. Secor, M. C. Hersam, C. D. Frisbie, and L. F. Francis, "High-resolution patterning of graphene by screen printing with a silicon stencil for highly flexible printed electronics," *Adv. Mater.*, vol. 27, no. 1, pp. 109–115, 2015.
[24] S. W. Kwok *et al.*, "Electrically conductive filament for 3D-printed circuits and sensors," *Appl. Mater. Today*, vol. 9, pp. 167–175, 2017.

Developing Responsive Environments based on Design-to-Robotic-Production and -Operation Principles

H.H. Bier[a,b] , T. Nacafi[a], and E. Zanetti[a]

[a] Faculty of Architecture and the Built Environment, Delft University of Technology, Delft, Netherlands
[b] Dessau Institute of Architecture, Anhalt University of Applied Sciences, Dessau, Germany
E-mail: H.H.Bier@tudelft.nl, T.Nacafi@student.tudelft.nl, E.Zanetti@student.tudelft.nl

Abstract –

The development of physical and computational mechanisms aimed at augmenting architectural environments has been one of the foci of research implemented at the Faculty of Architecture and the Built Environment, Delft University of Technology (TUD) for more than a decade. This paper presents the integration of distributed responsive climate control into the built environment based on Design-to-Robotic-Production and -Operation (D2RP&O) principles. These connect computational design with robotic production and operation of buildings. In the presented case study structural elements meet load-bearing as well as functional requirements. Their spatial arrangement creates variable densities for accommodating sensor-actuators that are operating heating and cooling. This mechatronic operation relies on activity recognition for achieving responsive climate control in the built-environment.

Keywords –

Design-to-Robotic-Production and -Operation; Wireless Sensor and Actuator Networks; Responsive Environments

1 Introduction

In the past, spaces were designed to meet human needs by identifying activities for which generic spaces composed of vertical walls and horizontal floors were created. These were adapted to specific needs by furnishing. Today, technological advancements in architectural engineering [1] as well as new scientific insights into health and human comfort [2] provide the basis to design mass-customizable building components and responsive indoor climates by means of Design-to-Robotic-Production and -Operation (D2RP&O).

By connecting robotic production and operation with computational design, D2RP&O contributes to improving both manufacturing processes and performance of buildings. While, D2RO relies on sensor-actuator networks that are establishing cyber-physical mechanisms aimed at introducing responsiveness in the built-environment, D2RP facilitates designing and building such environments. Together D2RP&O establish an unprecedented feedback loop based on human-nonhuman interactions, which have properties that are not reducible to neither human nor nonhuman aspects; instead, they result from the relationships and dependencies they form.

2 D2RP&O

D2RP&O relies on hybrid componentiality. This implies that building components are cyber-physical and that their design is informed by functional, structural, and environmental requirements, while taking into consideration both passive (i.e. structural strength, thermal insulation, etc.) and active (i.e. responsive, etc.) behaviors.

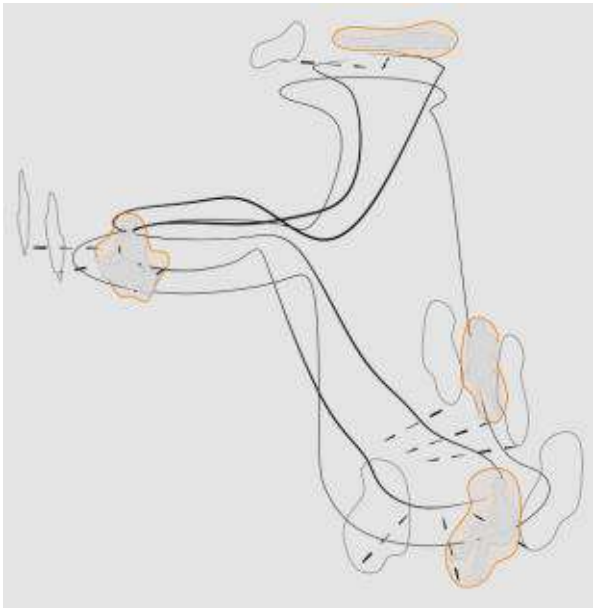

Figure 1-1. Design of the outer skin following body positions and schematic movement of activities

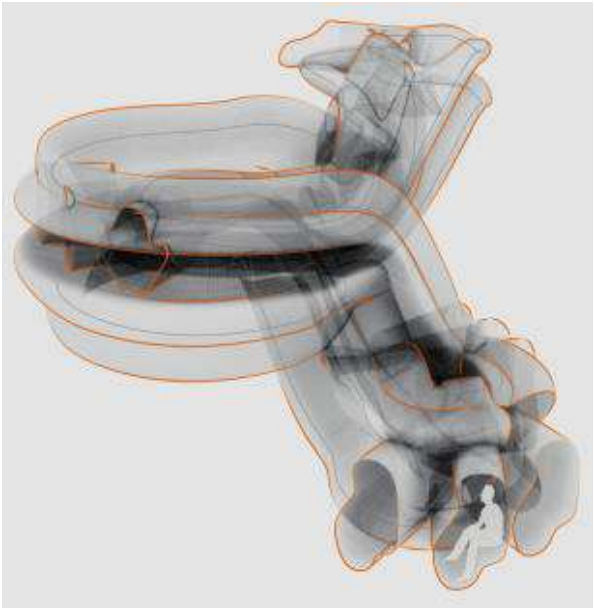

Figure 1-2. Design of spatial envelope based on mapped body positions and schematic movement of activities

In the presented case study, the focus is on the development of student housing units. Spaces are generated by mapping the movement of the human body during daily activities such as exercising, studying/working, relaxing, and sleeping. Each of these activities is described in terms of specific body positions, movement ranges, and their corresponding spatial requirements. These spatial requirements are basis for generating a schematic shape i.e. envelope onto which furnishing and climate control requirements are projected (Figure 1-1 and -2 and Figure 2). While requirements for furnishing focus on accommodating the human body during daily activities (such as seating, lying down, etc.), requirements for climate control provide distributed local comfort. Such an approach takes not only individual comfort in consideration, but also energy-efficiency, in particular when environments are inhabited or used with variable frequency.

2.1 Local Comfort and Distributed Climate Control

The proposed distributed approach to climate control is presently implemented while taking in consideration the uneven distribution and density of heat- and cold-perceiving thermo-receptors [2] in the human body. While the three areas of highest concentration of thermo-receptors are located in the head, the abdomen, and the extremities, their sensibilities vary. For example, cooling is most effective when applied to the head and the extremities [3]. Furthermore, direction of the air flow and variation of physical activity (e.g. sleeping, studying, working out, etc.) need to be considered. Such complex sometime even conflicting requirements require a locally responsive distributed approach.

The presented case study explores requirements for a student housing unit that is accommodating up to three persons at the same time. It answers the question of how the building envelope may be equipped with a set of sensor-actuators that respond to changing physiological requirements. These requirements are first mapped onto the envelope modeled from the simulated movement of the human body in space (Figure 2). Requirements vary in distribution and are effectuated by devices with various sizes. Presently considered heating devices consist of infrared lamps, whose energy is gained from photovoltaic cells integrated in the building envelope, while the cooling system employs vaporized water-streams.

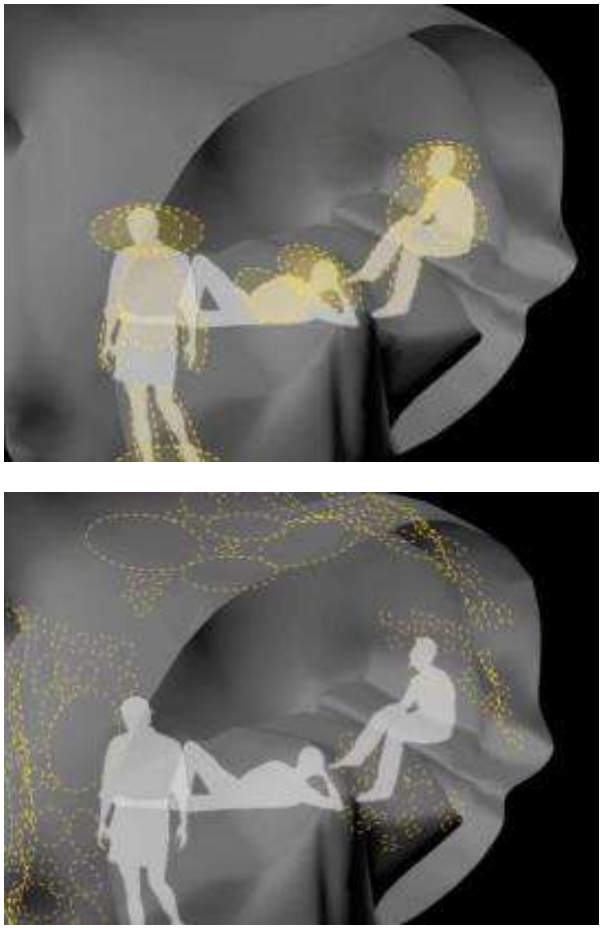

Figure 2. Mapping of physiological requirements on human body (top) and projection of local comfort requirements onto envelope (bottom)

Figure 3. Wooden beams are designed and manufactured to bend around specialized climate control components

Evaporative cooling employs jets of cold air or vapor and takes advantage of the enthalpy of vaporization [5]. The system sprinkles water onto a membrane or pad, through which air is blown. Thus, cooled vapor is created, which can be stored or delivered to the cooling devices (Figure 3). Distributed sensors gather data with respect to occupancy, temperature, humidity, etc. that is feed to the computational nodes, which in turn activate the mechanical system. Both heating and cooling systems turn on and off on demand and while these systems cannot be described as entirely off-the-shelf due to customization requirements, most of their components are already implemented in everyday life scenarios, especially open-air environments needing larger thermal control such as cafes with outdoor seating, etc.

This implementation of D2RP&O builds up on knowledge with respect to user needs [3] and wireless sensor-actuator networks for distributed climate control [4]. Such climate control functions through the use of mechanical devices that are operated by computational nodes establishing together a cyber-physical system. This distributed approach makes indoor environments adaptive and energy-efficient since vast amounts of energy required by traditional centralized climate comfort systems are saved. The novelty of the proposed system lies not in the individual components but in their synergetic operation with users based on computational feedback. This enables an immediate response to changing physiological demands. Devices are distributed and are able to rotate in three directions, in order to follow a moving person. They dynamically respond to the users' movement in space and create personalized climatic areas surrounding them.

2.2 Responsiveness and Interaction

The framework of local climate comfort requires that the building possesses the capacity of *identifying* occupants and environmental conditions in terms of temperature, humidity, etc. This is achieved through the use of architecture-embedded as well as wearable sensors i.e. smart phones.

Sensors collect data from the environment and users, which is then processed in computational nodes that activate or deactivate the distributed devices. They instantiate a responsive behavior that in a next step will be imbued with computational intelligence allowing the system to not only respond but anticipate, learn, and actively propose climatic changes by monitoring physiological and environmental data. In this implementation devices are turned on-off and rotate to track users moving in 3D space (Figure 4). The number of devices that are activated at the same time depends on climatic requirements at that time. While in this case only two kinds of devices were considered for heating and cooling, additional devices for lighting and ventilating that are combining natural and mechanical means would also need in a next step to be considered.

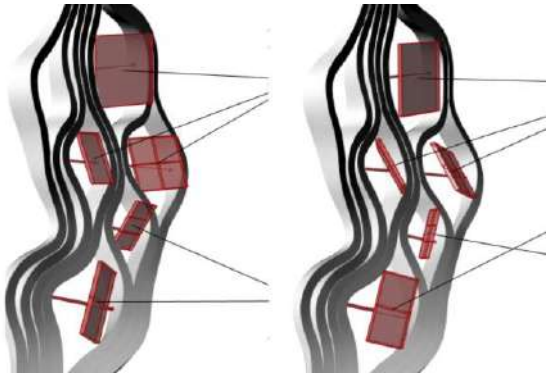

Figure 4. The infrared lamps turn on when people are approaching and rotate to follow their movement in space

2.3 Materialization

In the proposed design, the structural elements create in-between spaces to accommodate mechanical devices of varying sizes and distributions while maintaining structural integrity. Wood has been chosen because of its relative malleability allowing continuous bended beams to accommodate varying porosity requirements. Thus

beams are distributed according to structural forces and porosity requirements (Figure 3). Variation in distribution of beams is accomplished through densification and rarefication, respectively. If densification creates an increasingly compact surface, rarefication introduces porosity that accommodates windows and climate control devices.

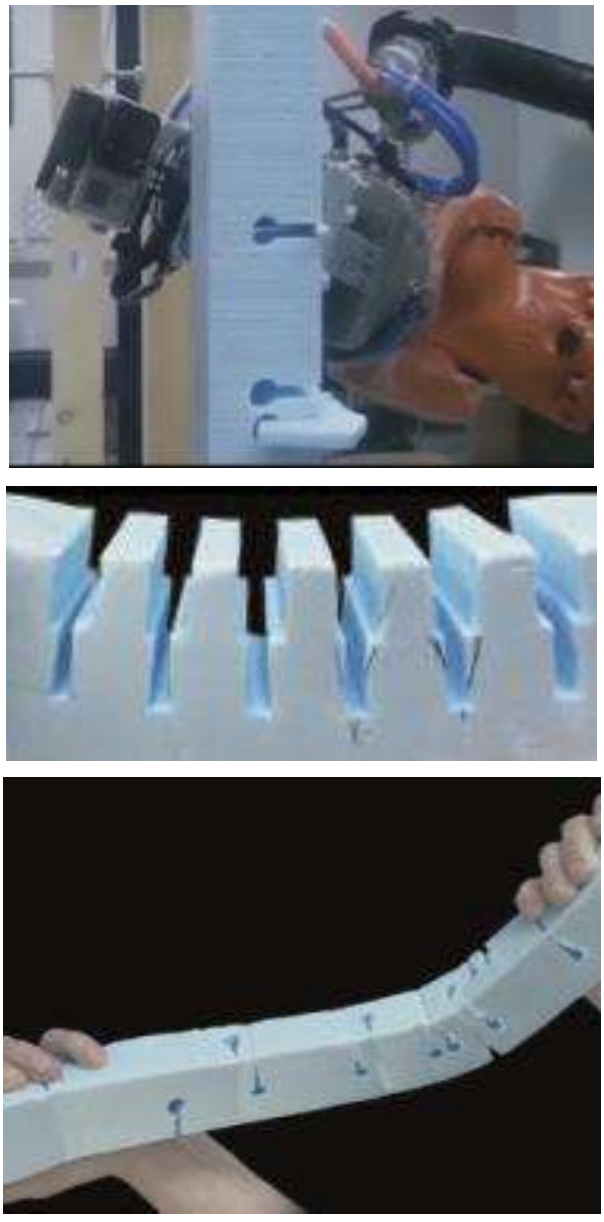

Figure 5. Materialization experiments and robotic production process involve robotic milling (top), preliminary research on the geometry of the milled section (middle) and robotically fabricated component (bottom)

Beams were manufactured using D2RP for kerf bending. This implies material removal for torqueing purposes. By milling a series of parallel cuts into the beam, a bending behavior is generated in the direction opposed to the milling direction. The assumption is that this process is a better alternative to the lengthy and wasteful approaches employing steaming and molding. Given the complexity of the design, this implementation requires extensive preliminary investigations regarding (1) the geometry of the milled sections, which directly affects the torque, (2) the distance between milled sections, which affects the bending angle and (3) the distribution on different sides in order to create torsion.

In a first step, extruded polystyrene (EPS) is introduced as a testing material. While the two materials are very different, EPS is instrumental in understanding the underlying principles and possible limits of the system (Figure 4). D2RP tests yielded relevant results in terms of precision of the computational system and the challenges of the robotic production. For instance, the higher the proximity of the milled sections is, the more the beam would start bending during the production process, resulting in imprecision or even breakage. These criteria are then fed back into the design and computational strategy, thereby establishing a loop of information exchange between the material and computational aspects of the project.

3 Methodology and Implementation

D2RP is integrated with D2RO in order to achieve hybrid architectural components that are able to respond to changing needs by employing motion and proximity recognition.

D2RP involved parametric modeling and structural simulations in Grasshopper and Karamba 3D while environmental simulations will be implemented in a next step. In terms of robotic production, a combined additive-transformative approach was carried out. The additive aspect of this approach refers to the multiple materials and components such as wood beams, mechanical devices, and building envelope that are incorporated into a hybrid whole. The transformative aspect refers to the bending of the wooden beams, which will be implemented in a next step using two robots. The process will start with first inserting a bundle of beams into a feeder. Each beam will be picked up by one of the two robots and will be transferred to a moveable spanning device with an appropriate high retaining system designed for longer beams, which will allow the robots to process the beams. The proposed bending in 3D is of interest because it is accommodating both structural and distributed climate control requirements and is particularly suitable for robotic transformative techniques. This system of bended structural elements works with spatial displacement as well as variation in

depth and width in order to meet structural requirements and accommodate user-defined requirements for illumination, ventilation, heating or cooling (Figure 6). At this stage, the design addresses only heating and cooling requirements, and physical experimentation stays at the level where beams have been only tested in EPS. Furthermore, as proof of concept, D2RO involves the use of distributed proximity and distance ultrasonic sensors, actuators (Servo Motors), and microcontrollers (Arduino Mega). While sensors detect users, the actuators turn on-off and rotate devices according to input from the microcontrollers, which have the programmed behavior to follow the movement of users.

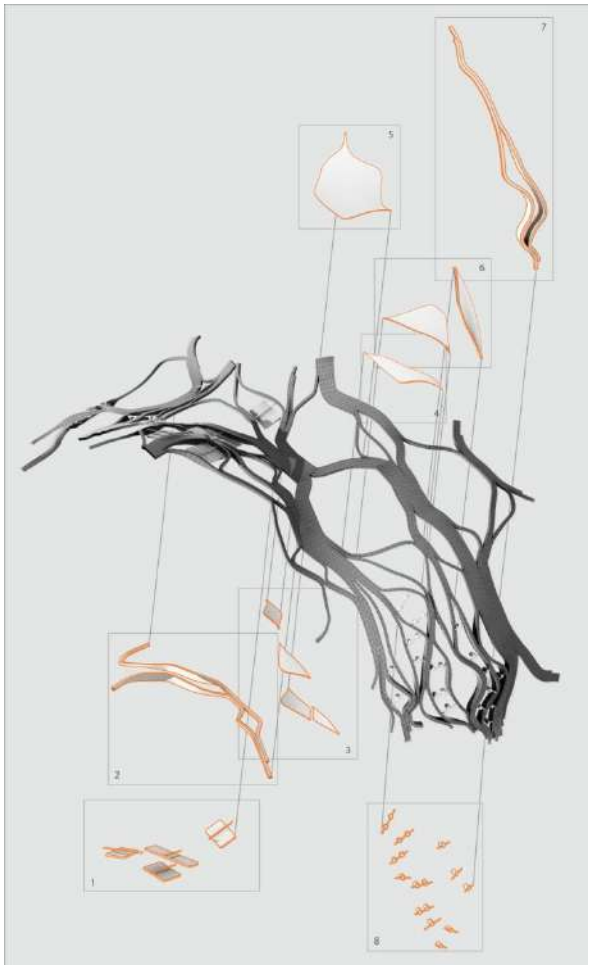

Figure 6. Fragment showing bended beams system accommodating mechatronic devices: (1) heating devices, (2) variable-depth structural elements, (3) small windows for natural illumination, (4) water storage compartment, (5) large window for illumination and views, (6) cooled-air chamber and wetted pads, (7) variable-depth structural elements, and (8) cooling devices.

4 Conclusion

The concept of the presented D2RP&O method relies on linking computational design with robotic production and operation. The implementation by means of D2RP&O of a building envelope that integrates functional, structural, and distributed local climate control requirements demonstrates the potential of this method to develop architectural spaces that accommodate a range of varying user-needs. The integration into the architectural envelope of climate control devices for local comfort using an additive and transformative D2RP approach is of particular interest because of its potential to address customization needs as well as structural- and energy-efficiency requirements. Furthermore, through the development of cyber-physical mechanisms, human capabilities in the physically built environment are extended. Even though in the present development only motion and proximity recognition are deployed, they enable the system to identify users and respond in terms of cooling and heating according to occupancy and use.

D2RP&O proves to be effective in linking computational design with robotic production and operation of buildings. It establishes human-nonhuman interactions in the built-environment, which have properties that are not reducible to those of individual components; instead, they emerge from the relationships they form. Climate control is local and customized to individual needs, where sensor-actuators respond to physiological and environmental variations. While building processes become increasingly automated, buildings evolve towards developing awareness with respect to their occupants as well as their indoor environments by interacting with both via cyber-physical mechanisms.

Acknowledgements

This paper has profited from the contribution of TUD researchers, tutors, and students as well as DIA students. It has taken advantage of two robotic labs at TUD and DIA and the expertise in D2RP&O of TUD researchers Sina Mostafavi and Alex Liu Cheng.

References

[1] H. Bier, Ed, *Robotic Building*, 1st ed.: Springer International Publishing AG, 2018.

[2] Y. Hibino, S. Hokoi, K. Yoshida, S. Takada, M. Nakajima, and M. Yamate, “Thermal physiological response to local heating and cooling during sleep,” *Frontiers of Architectural Research*, vol. 1, no. 1, pp. 51–57, 2012.

[3] P. M. Bluyssen, *The healthy indoor environment: How to assess occupants' wellbeing in buildings.* London, New York: Routledge/Taylor & Francis Group, 2014.

[4] A.Liu Cheng, H. Bier, G. Latorre, B. Kemper and D. Fischer, "A High-Resolution Intelligence Implementation based on D2RP&O strategies", in *Proceedings of the 34th International Symposium on Automation and Robotics in Construction*, 2017.

[5] B. Givoni, "Indoor temperature reduction by passive cooling systems," *Solar Energy*, vol. 85, no. 8, pp. 1692–1726, 2011.

[6] H. Bier, A. Liu Cheng, S. Mostafavi, A. Anton, and S. Bodea, "Robotic Building as Integration of Design-to-Robotic-Production and -Operation," in *Springer Series in Adaptive Environments*, vol. 1, *Robotic Building*, H. Bier, Ed. 1st ed.: Springer International Publishing AG, 2018.

An Approach to Enhance Interoperability of Building Information Modeling (BIM) and Data Exchange in Integrated Building Design and Analysis

T.V. Nguyen [a] and E. K. Amoah [b]

[a b]Mechanical & Civil Engineering Dept., Florida Institute of Technology, Melbourne, FL 32901 USA
E-mail: tnguyen@fit.edu, eamoah2015@my.fit.edu

Abstract –

Achieving high energy-efficient building designs requires conducting energy analyses iteratively starting from the conceptual stage to ensure suitable selection of building components to meet energy performance requirements. In recent years, advanced BIM capabilities have allowed designers to assimilate design and energy modeling processes geared towards improving productivity. However, there are shortcomings in many BIM platforms that circumvent effective data exchange between design/analysis models and essential data/information sources, resulting in reduced efficiency in terms of money, time and effort losses.

This paper proposes an approach to enhance data interoperability to allow seamless integration of design and energy analysis processes. The approach reviews data exchange requirements by key stakeholders in the building lifecycle and analyze how a common platform can address their needs. The paper first surveys existing BIM design and analysis software applications and various data sources to identify individual data interface formats. Autodesk Revit and USDOE EnergyPlus are examples of software tools, and ASHRAE climatic/building data are representative of a typical data source. The paper then develops use cases in which different combination of BIMs and data sources may be selected by the design team. For each use case, data exchange formats are analyzed against BIM data exchange standards to evaluate data interoperability. The objective is to identify suitable combinations of design, modeling, and data interface tools to accommodate the need of integrated design team. Finally, based on the results of the use cases, the paper recommends specific BIM tools that can accommodate the required models and data sources.

Keywords –

Data Exchange; Interoperability; Building Information model; Data Interface; Energy Modeling

1 Introduction

The AEC industry is highly diversified and there are a variety of different information systems being used in each organization. Thus, the transfer of information between different systems is and continues to be an apparent need **[1].**

One key issue in AEC industry today is ineffective information and data exchange. Poor information exchange can lead to three major problems: Costly errors in design/ construction, time wasting in making decisions and shorter life-span of design/construction projects due to poor judgement.

It is no doubt that the industry relies heavily on the use of data/information exchange between different professional disciplines for design, analysis, construction, operations and maintainace activities **[7]**. The construction industry is undergoing fundamental change, not unlike the advent of lean manufacturing in auto-making in the 1980s. A revolutionary tool called Building Information Modelling, or BIM, is the reason. BIM is rapidly transforming complex building processes -speeding project completion, lowering costs and improving overall quality at the same time. The possibilities for leveraging BIM are endless. Building Information Modelling (BIM) is currently attracting significant increased attraction of industry stakeholders with a promise of better collaboration with effective flow of data exchange resulting in higher productivity and better-quality products. The goal of this paper is to focus on identifying a suitable approach to enhance data interoperability to allow for seamless integration of design and analysis activities in building construction projects. This will result in suitable combinations of design, modeling, and data interface tools that accommodate the need of integrated design teams.

Acronyms

AEC: Architectural Engineering & Construction
AIA: American Institute of Architects
ASHRAE:American Society of Heating, Refrigeration, and Air-Conditioning Engineers
BCF: BIM Collaboration Format

COBie: Construction Operations Building Information Exchange
FM: Facilities Management
gbXML: Green Building Extensive Mark-Up Language
HVAC&R: Heating Ventilation Air Conditioning and Refrigeration
IFC: Industry Foundation Classes
IFD: International Framework for Dictionaries
IDM: Information Delivery Manuel
MEP: Mechanical Electrical and Plumbing
NBIMS: National BIM Standard-US
PDT: Product Data Template
XML: Extensive Mark Up Language
EUI: Energy Use Intensity

2 Integrated Information Exchange Process

The initiation of steady, continuous, and unambiguous performance information throughout building lifecycle is seen as a catalyst for building optimization. Stakeholders across architectural, engineering, construction (AEC) and facility management (FM) industry can share and exchange information based on the integrated information structure. For a real open process to occur, three factors need to be in place **[2]**:

a. A common data format for the exchange of information – IFC (Industry Foundation Classes),
b. Rules of which data is to be exchanged and who shall exchange them – IDM (Information Delivery Manual) and,
c. A standardized data model which is properly interpreted on each position of the exchange – IFD (International Framework for Dictionaries).

Figure 1 demonstrates the operation of the integrated information exchange structure. The structure works as a guideline for standardized data exchange. In the structure, IDM provides a universal, repeatable, reusable and verifiable collaborative methodology for initiating information exchange; IFC defines the data format of the information to be exchanged and builds the foundation for data exchange between applications. The structured information exchange framework allows preservation of meaning within different design tools.

A precise data exchange format in the BIM framework will not only lead to enhanced sustainable design and information exchange but will also bring about an increased project life-span, reduced life-cycle cost as well as fast-track design and construction turn-around time. This, when done properly, will create a win-win situation for all project stakeholders.

The subsequent sections will shed more light on how to identify suitable BIM authoring tools and data exchange formats that enable an open process and how they advance interoperability as well as generating reliable data.

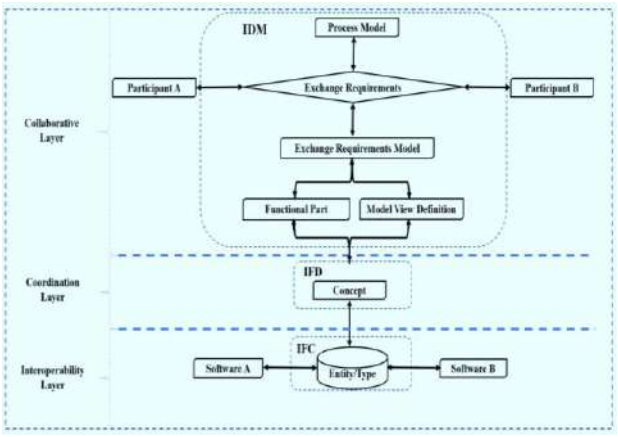

Figure 1. BIM process integrated information exchange structure

Table 1. Existing BIM authoring software application tools

BIM tool	Functionality	Phase(s)
Autodesk Revit	Building energy and carbon analysis & exchange capabilities	Conceptual & detailed design phase
Autodesk FormIt	Building energy analysis	Conceptual & detailed design phase
Revit/Archi CAD	Certification support	Conceptual & detailed design phase
Revit/Vasari	Solar studies	Conceptual &detailed design phase
Vector works	Documentation/collaboration	Conceptual design phase
AECOsim Building Designer	Documentation/collaboration	Conceptual design phase
eTakeoff Bridge	Estimating	Conceptual &detailed design phase
Archibus	Operation/work process	Detailed analysis
Assemble Insight	Support decision making	Web based solution
Tekla BIMsight	Collaboration	Check conflict at design phase
SketchUP	Exchange capabilities	Conceptual phase

3 Survey of BIM Authoring and Analysis Software Tools

There are many BIM design and analysis software application tools available in the market today and each caters to different users.

In many cases, the functionalities of different BIM software over-lapped one another requiring the users to carefully evaluate the software capabilities to ensure that the application will meet their needs. Table 1 constitutes a survey of dominant software applications available for BIM and integrated practice [3]. A brief description of functionalities and the phases of implementation/analysis are provided for information and evaluation purposes. The list is not meant to be exhaustive.

4. Data Format and Exchange Standards

Design and analysis activities in the BIM environment can leverage the wealth of data available electronically from various sources. Today, many manufacturers of building products provide BIM objects that can be imported directly into BIM applications and vice versa. Professional organizations such as ASHRAE (American Society of Refrigeration and Air-Conditioning Engineers) and AIA (American Institute of Architects) develop standards and design guidelines for the AEC industry and those can be used to support the building design and analysis process, although in most cases, much effort is required to integrate them into the BIM environment. Additionally, building codes and research data are available from government agencies such as state building commissions and USDOE (United States Department of Energy) that can be used to enhance the robustness of the design. Table 2, reviews “open standards" and BIM, non-proprietary file format and exchange protocol technologies that have been developed by public, private, and public/private entities [4]. Table 2 also provides a brief summary of different standard data exchange formats and the level of relevancy of each type of format relative to effective data transfer. The level of relevancy indicates the likelihood of the data exchange format would be used by one or more BIM software applications. As an example, BIM authoring software such as Revit and ArchiCAD have functionalities to convert BIM models into COBie, XML schemas, IFC, OmniClass, gbXML etc. There are countless number of supplies of BIM file formats out there [5, 8, 9] few of them are listed in (Table 2) for purposes of this study.

5. Data exchange use case methodology

Use cases are a useful tool in the process of evaluating interoperability of data exchange in the BIM environment. In order to capture the use case, it was necessary to first establish a set of properties by which they can be defined [6]. The data domain categories were also identified which was based on the major information contents of the Data Exchange Use Case. These include:

- The project;
- The site and the building;
- The building stores
- Spaces and their type information (space type, space intended use etc.);
- Building elements and their information (construction type) or building element material information;
- 3D – shape of the building elements (geometry) and;
- Location information of building elements.

The objects (lists) above are applicable according to general product modelling principles, the common information required that all objects should be uniquely identified (through unique ID). The main principle of the information content is that, at least the 3D-geometry data is transferred as a basic input for design analysis.

In the data exchange implementation, the data exchange representation and format for the exchange of the information is content specified. There may be alternative ways of implementing the data exchange for some information content (e.g. the internal format specific software application, default standards, or official standard).

In a specific building projects, the data exchange implementation method must be agreed upon (mostly from the early days of the project) by the stakeholders separately.

Data implementation process using the IFC specification as an example [12, 14] is described here. The description is intended to be used, firstly, by software vendors for their implementation exchange interfaces and, secondly, by the individual stakeholders to select data exchange solutions as their requirements description when the data exchange is to be implemented using IFC.

Data exchange implementation and format description procedure has been briefly explained in the ensuing sections. The use case defines only the representation and format of the implementation i.e. in which form the information should be used during data exchange transaction. The definition by which means the transfer process is done is outside the scope of the use case interpretation.

Table 2. Data format/exchange standards

Standard	Format	Efficiency Level	
		High	Low
IFC	Provides a framework for organizations to produce interoperable software to exchange information on building objects and processes to creates a language that can be shared among the building disciplined	✓	
XML	Set of rules for designing text formats to structure information. XML supports data transaction between different software applications, leading to a better way to communicate information.	✓	
gbXML	gbXML is the most widely supported data format for the exchange of building information between BIM/CAD and energy performance applications.	✓	
CIBSE -Product Data Template (PDTs)	PDTs are the source of consistent data to be used in the management of the constructed asset, allowing facilities managers to find the information they require for operation and maintenance of the facility in a structured and standardized format, improving the efficiency and productivity of the FM process, and supporting automation in the management of asset information.	✓	
COBie	Supports the sharing of data among facility management tools, such as BIM authoring tools, CMMS, and computer-aided facility management (CAFM) software. The standard eliminates the need to re-collect data, and it reduces the number of inconsistencies between similar data sets used for different purposes within a facility management organization	✓	
BIMXML	an XML schema developed to represent a simplified subset of BIM data for web services.	✓	
MVD	Model View Definition, the specification for subsets of all available BIM data to serve a stated purpose or process	✓	
IDM	Information Delivery Manual, the business case specification for exchange BIM data, including end user Exchange Requirements (ERs)	✓	
RVT	This is Autodesk's proprietary format for Revit files. These can vary significantly in size depending on the level of development. They can only be opened in Revit.	✓	
BCF	BIM Collaboration Format, an XML schema that encodes messages to enable workflow communication between different BIM (Building Information Modeling) software tools.	✓	
IFD	Describes what kind of information is exchanged by providing a mechanism that allows the creation of unique IFD IDs, to connect information from existing databases to IFC data models.		✓
PDF	Portable Document Format originally developed by Adobe for the electronic exchange of any printable document.		✓
OGC	Open Geospatial Consortium, international industry consortium for developing standards for geospatial data-enabled technologies.		✓
NWD	This is Autodesk's proprietary format for Navisworks files. NWD files are also read-only, although you may be able to save them under a new name and edit from there if the file was saved with that option enabled. These can only be open in Navisworks Freedom or Navisworks Manage.		✓
DWF/DWF	Design Web Format, originally developed by Autodesk, as a PDF alternative for CAD data/documentation.		✓
OmniClass (UniFormat Std II)	Framework for Classification of Information. A guidance document, and establishes common concepts used in building information exchange	✓	
NIBS-National BIM Guide for Owners	Serves as a shared knowledge resource for information about a facility, forming a reliable basis for decisions making during the life cycle of a facility from inception onward.	✓	

5.1. Data Exchange Implementation using IFC

The data exchange implementation using IFC is based on current release IFC4 addendum 2, publish in July 2016, as a buildingSMART final standard [12]. The Data Exchange Use Case architectural design to HVAC&R (MEP) design is closely related to the predefined IFC coordination view. The main difference is that the construction type is not supported in the coordination view.

5.2. Minimum Content of IFC Product Model

The IFC product model and specification sets some specific minimum requirements for what the information content of file-based product model IFC data exchange should be. Regarding the Use Case, the required minimum IFC product model is specified in Table 3. Separately, for the exchange of the 3D (Revit) model in figure 2 and building product model exchange sub-cases.

Table 3. The minimum IFC product model content in the two sub-case of Use Case

3D Reference model exchange	
Class	Properties
Project	-Identification and owner history -3D coordinate system -Project context and common measurement units
Site, Building & Stores	-Identification and owner's history
Building elements	-Identification and owner history -3D-shape and location
Building product model exchange	
Class	Properties
Project	-Identification and owner history -3D coordinate system -Project context and common measurement units
Site, Building and Stores	-Identification and owner
Space	Space type 3D-shape and location

5.3. IFC Data Exchange Format

IFC data exchange has two alternative formats for the exchange of some information content [14]. These formats are:

- IFC format or IFC part 21 Format, which is based on the ISO 10303 -21 standard,
- The ifcXML format, which is based on an XML Schema definition of the IFC product data model. Currently the specification is based on the IFC4 Addendum 2.

IFC implementations in commercial software application use the IFC part 21 format for IFC-based data exchange.

6. Case Study

Using Autodesk Revit, a BIM-based Architectural model is designed as a test case for this study, see Figure 2. In this example, it is assumed that the owner and architect have decided to use Autodesk Revit for the architectural design. Considering the involvement and the need of various project stakeholders, the objective is to evaluate interoperability of the data exchange in this process. EnergyPlus and Revit energy analyze are considered for energy simulation engine & tool respectively, ARCHICAD is used for structural analysis, and gbXML format was chosen as the data exchange protocol between the architectural model and analysis program.

The owner specified BIM model described below presented an opportunity to identify key interfaces between Autodesk Revit and other BIM authoring software application tools identified in Table 1, for their compatibilities in data exchange protocols.

Three of the BIM authoring tools below were selected in no order of preference for this experiment/demonstration. The authors only had in mind those BIM authoring tools which are not common and not most frequently used.

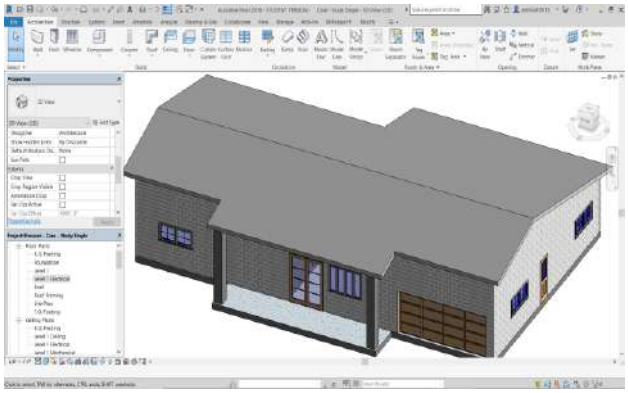

Figure 2. Sample owner specified BIM based 3D architectural model using autodesk revit

6.1. Revit/ArchiCAD Data Exchange Interface

This section discusses the GRAHISOFT ArchiCAD connection for Autodesk Revit. The Add-In improves the IFC based and bi-direction data exchange between GRAHISOFT ArchiCAD and Autodesk Revit [11,15]. The GRAHISOFT ArchiCAD connection Add-In for Auto Revit has three capabilities:

- **Improved IFC Import"** - imports IFC models to Revit using extra features that improve the

interpretation of architectural models;

- **"Link IFC"**- merges IFC models into the current Revit project as a non-editable reference;
- **"Export to ARCHICAD"** - exports Revit model elements in IFC files that are specially enhanced for use in GRAPHISOFT ARCHICAD.

To obtain the best data exchange results, it is important to ensure latest version (18.2.0 or later) of Autodesk's IFC 2018 import-export for Revit is used.

6.2. Revit/Vasari Data Exchange Interface

Project Vasari is a design tool with analysis capabilities available via cloud [13]. The problem is that, Revit/Vasari doesn't know how to pass separate conceptual masses with different building/space types to the analysis engine. There is no provision for separate buildings within the data exchange format from Revit (it is in the gbXML schema). To get around this problem, there are two options that must be considered [10, 11 13,]:

- Model the building as different masses, and run the energy analysis on each space type;
- For the initial analysis, lump the masses together and choose a building type and schedule that is the most appropriate when taken as a whole.

It is possible to make some preliminary conclusions massing and orientation from this rough analysis – and only drill down into analysis of the different space types if the analysis is not justified.

6.3. Revit/Tekla Structures Data Exchange Interface

The general collaboration/exchange with Tekla Structures to Autodesk Revit is best done on a neutral platform built for such purpose [11,16] for example, Autodesk Navisworks or Tekla BIMsight which is dedicated collaboration software with clash-checking and reporting.

Data exchange between Tekla structures and Autodesk Revit can be done using Autodesk approved IFC files through the following process:

- Export from Tekla Structures to Revit using an IFC file (Tekla > Export > IFC) from Tekla Structures,
- Import into Revit. From Revit 2015 version and later, it is possible to Insert > IFC file directly.

Where there are project co-ordinates, use Site Definition in Revit to locate the inserted Tekla Structures model correctly or use a manual model insertion point (Right click IFC model after inserting > reposition to project base point)

BIM can now be employed to co-ordinate the Structural file with the Architectural / MEP project in Revit.

7. Energy Modeling/Simulation

Kamel, E., & Memari, A. M. (2019). "Review of BIM's application in energy simulation: Tools, issues, and solutions", reviewed the challenges, issues, and shortcomings in BIM-to-BEM interoperability process (BBIP) and proposed a detailed classification for these issues and available solutions. This paper also explains how a corrective middleware, which is developed by the authors using Python, can be utilized to modify a gbXML file prior to adoption in energy simulation to resolve the issues related to building envelope in BBIP. The authors initially reviewed different types of BIM schemas such as IFC and gbXML and energy simulation tools capable of reading these files such as Green Building Studio (GBS), DesignBuilder, Integrated Environmental Solutions-Virtual Environment (IES), and OpenStudio [17]. The authors showed that not all the required data for energy simulation such as HVAC system data, schedules, and loads are exported properly to the gbXML file using Revit, and that data need to be added manually.

Autodesk Insight 360 allows architects/ designers to explore the energy impacts of different choices as they design **[11]**. Insight 360 uses EnergyPlus to calculate heating and cooling loads. It provides option of using EnergyPlus to evaluate annual energy impacts **[11]**. Insight 360 offers EnergyPlus simulations to all users through Revit and FormIt.

In figure 3, the authors developed/presented energy optimization and data transfer process framework to allow for seamless integration of design and energy modeling. The study also focused on investigating BIM authoring tools capable of providing a versatile platform for transferring all require data/file with little or no difficulty. During the first stage of the process, material specifications, construction preplanning and key decisions regarding data transfer approaches are considered. Also, the energy modeler/designer and other stakeholders come together to propose assumptions underlying the choice of building envelopes and system types at this stage. The assumptions made are used as a decision process for both design and energy simulation analysis. The authors considered EnergyPlus, gbXML and Insight 360 as the simulation engine and Revit as design tool. EnergyPlus was used to assess the initial heating and cooling loads regarding the impact of the annual energy consumption for envelopes and HVAC systems. These design and energy analysis results are to assist the stakeholders to make an inform decision. gbXML file provided us with a whole building simulation analysis result through Green Building Studio (GBS). Detailed results can be assessed, for example, Annual Energy Consumption in kWh, Energy Use Intensity (EUI) in kBtu/ft²/year, Annual Peak Energy Demand in kW, Annual Lifecycle Energy in kW etc. as indicated in the "Detailed Simulation Analysis portion of

Figure 3. The results are carefully studied, a thoughtful decision is made whether to approve the results or not. If the results are approved, the project moves to construction sage. If rejected, the updates become necessary, new assumptions and materials selection are considered. The framework for Figure 3 allows you to go back to the input stage to kick start your new materials/assumptions.

The main issue and limitation identified in the framework relates to how the key assumptions lies in the hands of the stakeholders, especially the owner who might not have enough technical know-how. If these assumptions are found to be unreasonable at the later of stage the simulation/design process, the entire energy analysis result becomes irrelevant. Fortunately, the process developed by the authors in Figure 3 makes it possible to correct any wrong assumptions made at any stage of the process. In fact, you can always go back to alter the building envelope (walls, windows or roof materials) at any time from the Specs & construction/data transfer decision stage.

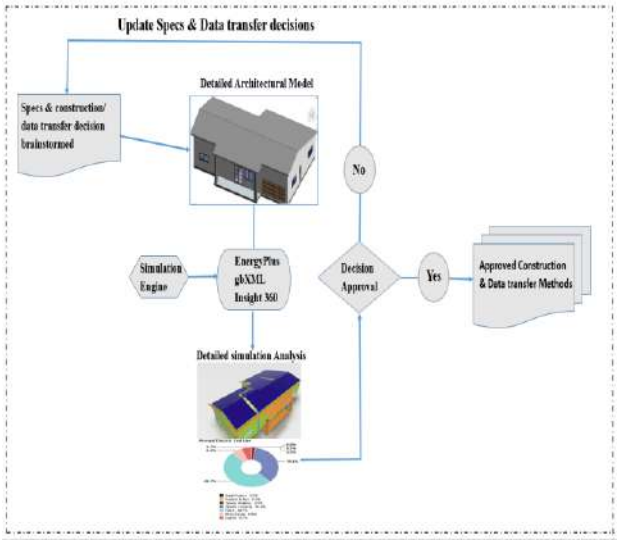

Figure 3. Data transfer decision & energy simulation process

8. Results and Discussion

Data interoperability allowing smooth integration of design and energy analysis has been investigated. The study has identified a suitable process of data exchange requirements to enable stakeholders to address their information exchange needs via a common platform.

The authors developed an integrated information exchange method, in section 2, to identify an unambiguous information sharing process throughout the building lifecycle for the industry stakeholders. The paper defined the data and information flow from IDM (Information Delivery Manual), IFD (International Framework for Dictionaries) and IFC (Industry Foundation Classes). The illustration in Figure 1 summarizes the information exchange process.

In section 3 and 4, the authors investigated several existing BIM authoring software application tools and data exchange formats, respectively. Table 1 lists the state-of the-art existing BIM software tools, their functionalities and performance phases was developed to aid decision making. Table 2 identifies data exchange formats/standards that provide guidelines to leverage data sharing electronically to minimize errors in exchange/communicating information among the team members in an ongoing project. Table 2 also ranks the efficiency level "High or Low" when selecting data exchange file/format. "High" indicates transfer with very minimal or no error while "Low" indicates substantial difficulty regarding data transfer and interpretation. The paper outlined methods for developing Use Cases with an inclusion of data exchange implementation process with IFC (Industry Foundation Classes) as an example. The properties and components that needs to be included in the IFC identified.

Finally, a case study was introduced as an example, demonstrating what constitutes an element of a building model. Autodesk Revit was used to design a BIM-based architectural model. This was used as a test case to demonstrate the data exchange interfaces with other identified BIM authoring software application tools in Table 1 (ArchiCAD, Vasari and Tekla Structures) to assist the stakeholders in making decision in relation to selecting an appropriate design and analysis BIM application tool.

Apart from Building Information Modeling (BIM) currently being adopted by the construction industry to facilitate and promote collaboration between the industry players within projects, there are ongoing deliberations and research on further digitalization and automation of the construction industry. A future research direction is to incorporate an Artificial Intelligence (AI) technology in the BIM process. This area requires more research to bring the power of artificial intelligence to assist the construction industry in tackling some challenges such as reducing design errors, enhancing greater collaboration and better software tools.

9. Recommendations

BIM-based data exchange and analysis processes are constantly evolving with emerging software products and technologies. Based on lessons learned in this study, following recommendations are proposed:

- The industry stakeholders should revolutionize the construction and engineering activities to embrace the artificial intelligence technology solution to

avoid the fast-emerging trend of technological disruption to consume the industry.

- Early collaboration among stakeholders should be made mandatory or guided by strict standards irrespective of the project size to minimize cost and save time.
- Emerging/existing software technologies should be streamlined and be made to follow a cutoff standards and regulation.
- Autodesk Revit was found to be a versatile BIM tool capable of accommodating a wide variety of design and analysis models and data sources.

10. Conclusion

This paper reviewed approaches to enhance collaboration among key stakeholders in building design and construction projects. It analyzed how a common platform could help solve the present needs of data interoperability.

Use cases were found to be a useful tool for evaluating the stakeholders' data exchange requirements, leading to the identification of appropriate software tools and data format for a specific project. Suitable combination of design, modeling, and data interface tools will help improve the project cost and schedule overruns.

The next phase of this research would be centered on using BIM to investigate into generating a comprehensive & interactive database of building data to facilitate smart designs through information to create virtual model from high-powered project data.

References

[1] Eastman, C. M., Jeong, Y.-S., Sacks, R., & Kaner, I. (2009), "Exchange Model and Exchange Object Concepts for Implementation of National BIM Standards". Journal of Computing in Civil Engineering, 24(1), 25–34. https://doi.org/10.1061/(ASCE) 0887-3801(2010)24:1(25)

[2] Zhang, J.-P, et al., (2012), "Research on IDM-based BIM process information exchange technology". In14thISCCBE.Moscow, Russia, p.8.Availableat: http://www.icccbe.ru/paper_long/0491paper_long.pdf.AuthorSurname E. *A book*, volume 2(3). The Publisher, Publication address, 2014.

[3] ASHRAE, (2009), "An Introduction to Building Information Modeling (BIM): A Guide for ASHRAE Members".

[4] AIA Knowledge Net ,2017: BIM, Standards, and Interoperability; Retrieved from: https://network.aia.org/technologyin architect turalpractice /homebimstandards

[5] Z. Creach, (2013), "The concrete construction technology newsletter article": The top five BIM file formats & how to use them; retrieved from: http://www.concrete construction .net / business s/technology/the-top-five-bim-file-formats-how-to-use-them_o

[6] McGlinn, K. et al. (2016), "Identifying Use Cases and Data Requirements for BIM Based Energy Management Processes. In CIBSE Technical Symposium. Edinburg: Heriott Watt University".

[7] G. Mayo, and R. Issa, (2014), "Processes and Standards for BIM Closeout Information deliverables for owners", In: International Conference on Computing in Civil and Building Engineering, pp. 673-680, 2014. [http://dx.doi.org/10.1061/9780784413616.08]

[8] OmniClass, (2016), The OmniClass Construction Classification System, http://www.omniclass. org/

[9] COBie, 2016. The Construction Operations Building information exchange (COBie)Guide: HTTPs://www.nibs.org/?page=bsa_cobieguide

[10] NIBS, (2016), NIBS National BIM GuidelineforOwners, https://www.nibs.org/news/254633/ Institute-Kicks-Off Effort-to-Develop-National-BIM-Guideline-for-Owners.htm

[11] Autodesk Inc., (2016), Improving Building Design Project Collaboration Using openBIM Data Exchange Standards

[12] buildingSMART International, (2016), IFC4 DesignTransfer View. http://www.buildingsmarttech.org/specifications/ifc - view - definition/ifc4 - design - transfer - view

[13] Green Building XML (gbXML) Schema Inc., gbXML Version 6.01 (2015), http://www.gbxml.

[14] BuildingSMART, (2015), retrieved from: http://www.buildingsmart-tech.org/mvd/IFC4 Add / DTV/1.0/html/

[15] GRAPHISOFT, (2017), Interoperability with Structural Disciplines: Retrieved from: http://www.Graphisoft.ArchiCAD/opinion/ structural workflow

[16] Trimble Salutation Corporation, Make Your Design Real with Tekla and Autodesk Revit: Retrieved from: https://www.tekla. com /products/tekla-

[17] Kamel, E., & Memari, A. M. (2019), "Review of BIM's application in energy simulation": Tools, issues, and solutions. Automation in Construction. ElsevierB.V.https://doi.org/10.1016/j.autcon.2018.11.008

Impact of BIM on Electrical Subcontractors

Anoop Sattineni[a] and Bradley Brock[a]

[a]McWhorter School of Building Science at Auburn University, USA
E-mail: anoop@auburn.edu; bjb0010@auburn.edu;

Abstract –

The use of BIM in the electrical subcontractor community has been increasing over the past few years. The practice of using BIM for this sector varies in many ways as compared to the design profession or the use of BIM by general contractors. This study focuses on the current state of BIM implementation among the electrical subcontractors. A literature review of the topic lead to the adoption of a qualitative methodology to study the issue. The results of the qualitative study involved semi-structured interviews with practitioners in the field. The results of the interviews found that the perception among electrical subcontractors regarding the successful use of BIM varies from the general contractor. The study lead to the identification of several key themes that govern the successful use of BIM for electrical construction. The study makes recommendations to electrical subcontractors for the successful use of BIM on projects.

Key Words: BIM; Electrical; Subcontractor; Coordination; Field Installation; Productivity;

1 Introduction

The use of Building Information Modeling (BIM) within the electrical subcontracting community continues to evolve in the United States [1]. There is an ambiguity of existing information regarding BIM usage associated with capital costs and time [1]. Returns on investment (ROI) studies often conclude that BIM is cost effective [2]. However, contrary results do exist, such as the concrete subcontractor recorded by Sawyer [3]. Sawyer [3], found that a subcontractor invested all required time and money in having a working BIM department but did not see any financial benefits. In contrast, other specialty subcontractors are mentioned within the same article and report a positive return on their investment in BIM.

Several things must be considered in the conduct of this research, the main two being time and money. Time must be considered in addition to capital costs involved. Simonian [4], conducted a survey amongst electrical specialty subcontractors. This survey revealed an ambiguity in time savings. For projects requiring BIM, more time is dedicated to creating the model and shop drawings than a two dimensional drawing method without parametric data embedded into it. However, the time put into the model decreased the amount of time required for fabrication and installation because all the details had been considered while modeling.

The time involved in coordination meetings and correcting on-site clashes must also be considered. Korman, et. al [5] outlines the traditional method of a coordination meeting and contrasts it with a coordination meeting utilizing BIM. The findings show that less time is required to resolve more conflicts when utilizing BIM throughout the coordination process. These time-saving factors also transfer into the field because more clashes between mechanical, electrical, and plumbing (MEP) systems are found utilizing BIM and are therefore prevented on the jobsite. Two main factors that are time intensive, but beyond the control of the electrical contractor, are the required level of development (LoD) and the overall area to be modeled [4].

Leite, et al [6] outlines the compounding of time required to increase a model's LoD. When progressing from a lower LoD to the next more detailed level, it may take as little as forty-five additional minutes up to eleven hours. This requirement may be beneficial to the subcontractor, especially mechanical subcontractors, for prefabrication purposes. However, if the subcontractor does not practice prefabrication, the time invested in reaching the required high LoD is virtually wasted. Therefore this factor also relates to financial benefits or detriments of BIM due to the additional modeling time potentially required.

Barlish & Sullivan [7] outline how to measure the benefits of BIM. They noted that BIM is the most helpful in heavy mechanical, electrical, and plumbing (MEP) areas. It is not uncommon for a general contractor to request a typical room to be modeled in addition to the main MEP areas throughout the building. However, general contractors do not all follow the same principles. Therefore modeling unnecessary areas to fulfill contractual requirements may also require unnecessary time.

This research is beneficial because it seeks to

provide in-depth information regarding specialty subcontractor usage of BIM in relation to time and cost. The information gained from the participating subcontractors is vital to uncovering important information in this field. The two main areas in which Simonian received the most ambiguous results directly correlates to either time or financial requirements. Additionally, this study should reveal changes since the Simonian study, conducted several years ago. Since then, BIM has been used in more projects for more applications.

This research uses a qualitative methodology by conducting semi-structured interviews with the practicing subcontractor professionals. It is imperative that those interviewed have hands-on experience with the BIM process pertaining to electrical subcontractors. In order for the results to be effective to the industry, the participants must either be directly involved in the process, or be directly affected by it. By selecting these individuals, this study uncovered detailed nuances of implementation, effectiveness, and weaknesses that individuals outside the process would not be able to provide.

2 Literature Review

Previous research has shown that BIM is used anywhere from 0% to 90% of projects [4]. A survey conducted by Azhar and Cochran [8] found that 32% of reported projects between $10 and $100 million, 55.6% of reported projects between $100 and $250 million, and 50% of reported projects more than $250 million use BIM. BIM can currently be used for visualization, clash detection, prefabrication and on-site installation [9]. An electrical subcontractor's implementation level of BIM depends on its organizational structure [10], percentage of prefabrication [11], regular contractual obligations [7], and project complexity [12].

The trade-off to BIM implementation is modeling time and estimated start-up costs. Time may be saved in the installation phase, but at least a portion of that time is used in the modeling phase. Azhar & Cochran [8] found that 67% of survey respondents reported at least some timesavings. However, they did not report where these time savings came from, or how they were justified. Azhar & Cochran [8] also found that 67% of survey respondents reported at least some cost savings. Once again, the areas in which costs were saved are not provided.

2.1 Productivity

Productivity has historically had many definitions. In order to remain consistent with previous productivity studies, this research will define productivity as: "*labor productivity = output/input = installed quantity/actual work hours*" [13, pg.2]. Park et al [13] developed a productivity comparison system revolving around cost, schedule, changes, and rework. Park et al have also defined five separate subcategories of electrical subcontractor work: electrical equipment and devices, conduit, cable tray, wire and cable, and other electrical metrics. These categories were then broken down into ten different elements: panels and small devices, electrical equipment, exposed or above ground conduit, underground duct bank or embedded conduit, cable tray, power and control cable (600 volts and below), power cable (5 to 15 kilovolts), lighting, grounding, and electrical heat tracing. These are the outputs that are compared with input costs and time to determine an electrical subcontractor's productivity. However, when considering productivity as it relates to BIM for the entire company, the overall amount of work put into a project, not simply installation, must be considered. BIM generally increases site productivity but creates additional expenses during the planning phases of a project [14]. The best two measures of productivity as regards to input are time and money [13]. Time measures the efficiency of using one process over another, and money measures the direct costs associated with using that process.

BIM models are often contractually required from electrical subcontractors for MEP coordination. BIM requirements have noticeable effects to both the time involved in a project and the money required to complete a project. These are the two most ambiguous areas of productivity input to investigate. For example, time is placed into modeling rather than fixing mistakes. Money is used to employ a modeler rather than being applied to RFI work, jobsite clashes, and change orders [4].

2.2 Level of Development

The LoD contractually required is an expensive and time-intensive item which must be investigated. The two main questions that determine the proper level of detail are where to model and what to model. When considering which parts of a project (where) to model for productivity input efficiency purposes, the electrical subcontractor needs to consider the MEP congestion within a given area. For example, certain projects may require large amounts of the electrical systems to be modeled, such as hospitals or data centers, while other buildings may only require MEP intensive rooms and a typical room, such as a dormitory. Leicht [11], conducted a case study in Pennsylvania which laid out four main factors determining required level of development, including, "*interaction with other systems, sequence of installation, prefabrication of components, and layout considerations and density of systems*" (p. 5). Barlish and Sullivan [7], conducted a case study to

determine how to measure the benefits of BIM. Within this case-study, they concluded that BIM is most helpful when utilized in heavy MEP areas such as mechanical rooms and switching rooms.

As the electrical contractor considers what to model, certain processes have an element of diminishing returns. As modeling requirements increase, the improvement to the installation process may not increase at an equal rate [11]. Additionally, Leite et al, [11] conducted a study measuring required level of detail and the returns they provided. Leite et al, found that more detailed models are considerably more helpful in coordination, but do not always increase modeling time exponentially. However, they did conclude that the level of detail should still be determined by the components' purpose and usage. Some components may be very time-consuming to model but also very easy to re-route [14]. These components would not be time or cost effective to model and should only be addressed if used for shop-drawing of pre-fabrication purposes.

Interestingly, as BIM and highly detailed models become prevalent, certain design drawings worsen [15]. In effect, the designers spend less time on the initial documents, knowing the contractors will change the initial drawings to match the installation process. This places an undue burden on the contractors to double-check existing information, fill in missing information, and eventually add all necessary installation details. Therefore the presence of accurate information received plays a heavy role in the required level of modeling detail. Finding, correcting, and replacing either missing or incorrect information is just as time-consuming as detailing existing design drawings.

Sawyer [3] conducted interviews with specialty subcontractors using BIM and discovered that in coordination meetings, what is in the model is not the problem, but what is left out may create a difficult issue to resolve and negate the efforts to conduct BIM clash detection meetings. Electrical contractors have the opportunity to either be highly efficient or sorely ineffective in the area of BIM LoD. Many areas may not require modeling and therefore should be left out for efficiency. However, certain components which are left out of the model may cause much more trouble and time to fix on the job than would have been invested in modeling it initially.

2.3 Clash Detection

BIM usage facilitates coordination through both clash detection methods and scheduling requirements. Savings in both time and money may be realized in this area through greater and more effective communication amongst specialty contractors and the general contractor if BIM is used to a proper level [14]. However it is possible to invest more than required amounts of time and finances towards coordination.

General contractors found a more efficient work process in the area of MEP coordination meetings when utilizing BIM [2]. Akinci and Kiziltas [2], conducted interviews with two different subcontractors over eight different projects and found that the coordination process took less time and was required to meet fewer times when utilizing BIM. Leicht [11], found that clashes discovered in coordination meetings revolve around three issues: the LoD required, a coordination issue, or a design issue. Akinci et al [14] also found that certain items should not be considered in clash detection. For instance, if a piece of 12/2 metal clad (MC) cable is clashing with a mechanical duct, that clash should simply be ignored. It would take much more time to model all of the MC cable in the office than it would to move the same MC cable in the field. Therefore, the ease and flexibility of installation needs to be considered when combing through clashes.

2.4 Site Installation

Site installation within the electrical subcontractor's realm operates in conjunction with the LoD translated to the jobsite. If the electrical contractor increases the model's LoD, then the site superintendents and working foremen will have more information at their disposal to properly install (output) the required components [16]. However, the translation of this information to the jobsite and the benefits thereof will vary from one company to another. It is possible that additional training is required in order to utilize the tools required to effectively translate BIM to the jobsite. Training is an additional cost and must be considered in overall company productivity. On the contrary, BIM may be just as effective for electrical subcontractors in the form of a specialized set of prints which would require no additional training.

When considering outside influences, BIM projects sometimes have a noticeable increase in the amount of information received from the Architects and Engineers [7]. The increased amount of information received helps decrease the amount of Requests for Information (RFI's) and change orders [7]. A reduced number of change orders also constitute a reduced amount of rework; rework is prevented because of fullness and transparency of information received from Architects, Engineers and coordination of subcontractors [11]. If the amount of time and money (input) placed into RFI's, change orders, and rework could be re-routed to jobsite BIM translation and prefabrication, then dollars per unit put in place would decrease due to a fullness of information. Therefore, by the definition used for this study, it will increase electrical subcontractor productivity. One study found that the implementation of BIM resulted in a reduction of time in most of the

construction stages. The largest of these reductions was found within the construction phase [17]. Almost 60% of respondents reported a 12.5% reduction in schedule duration within the construction phase of a project. This reduction is contributed to the pre-solving of installation problems and a better transfer of information from the office to the field. Amongst the pre-solving of installation problems lies the use of prefabrication for site installation.

2.5 Construction Scheduling

Another coordination issue which currently seems to work well is BIM enabled scheduling. BIM enabled schedules help visualize overlapping scheduled activities and aid in equipment coordination [2]. Barlish and Sullivan [7] also define schedule improvements as one of the most quantifiable returns for BIM usage. One way that BIM helps improve a project's schedule is that it allows for earlier coordination meetings and faster resolutions to problem [18]. Therefore, if the coordination meeting process is investigated and a preferred method of conduct is established, then the schedule could also be improved because the amount of time spent resolving MEP coordination meetings could be applied to the overall project schedule.

Additionally BIM may help the schedule by having a 4D model, time being the fourth dimension, for differing areas or pieces of work. When creating a time-loaded model, each component or groups of components have a duration imbedded. Then a schedule can be derived using the imbedded durations for a given area or activity. However, according to the survey conducted by Eadie [19], schedule automation was listed in the last three reasons to implement BIM for any given project. BIM can be used as a visualization tool which informs the general contractor which areas can be completed first so the following sequence of operations will go as smoothly as possible. This is contrasted with attaching a time-based field within each of the BIM model objects or families. As previously mentioned in the site installation section, the majority of participants utilizing BIM found a twelve and a half percent schedule reduction [17]. Therefore, when discussing BIM enabled scheduling, the current use seems to be by the general contractor to inform the proper sequence of operations, not through a time-loaded BIM model.

The results of the literature review show that the impact of BIM within any discipline is a multi-variable, fluid target. The results could change from project to project within the same company. The main areas of investigation are as follows: main factors for BIM use, level of development, clash detection process, site installation, scheduling and modeling impacts. Based on the observations of Miettinen and Paavola [20], as well as Succar [21], the isolation of external variables is virtually impossible. Therefore, a qualitatively nuanced and inductive approach should be used to study the impact of BIM implementation in the electrical subcontracting sector.

3 Methodology

This research implements an interpretive philosophy. The Interpretive philosophy allows for a more situational and flexible approach to data collection. This is necessary because electrical subcontractor productivity is affected by many variables mentioned in the literature review; moreover, those variables are affected by outside influences such as: organizational structure, project general contractor requirements, proficiency in prefabrication, owner expectations, and facility management requirements, all of which are beyond the scope of this research. Due to the outside variables it would be highly unlikely to accurately compare one electrical subcontractor's productivity for a particular project with another electrical subcontractor's productivity on a different project. An inductive approach is deemed appropriate for the purpose of this research. The research strategy implemented semi-structured interviews, as a mixed method choice for a cross-sectional study. The proposed qualitative research method allowed for personal perceptions and situational knowledge to be revealed and explored. Speaking to two current employees working as BIM modelers were used as a pilot test to aid in developing questions. The refined questions were then administered via face-to-face, phone or web meeting interviews. Data saturation for structured interviews usually occurs at twelve interviews [22]. Therefore a total of twelve candidates were interviewed. The observations recorded during the interviews were transcribed and analyzed for correlations and similarities.

The electrical subcontractors considered for interview have been contractually obligated to use BIM on more than three projects. The total number of employees can range from fifty to five hundred. The target personnel interviewed were BIM modelers, BIM coordinators, and project managers who have worked on BIM projects. Guest et al. [23] found that in a sixty participant research study, over ninety percent of all codes, and over ninety-five percent of all important codes occurred within twelve interviews. Therefore, for the purpose of this research, twelve participants were interviewed. The interview results were first transcribed then coded, using open coding techniques. The codes were further consolidated as deemed appropriate. Content analysis techniques were employed in the analysis phase of the study to comprehend the data.

4 Results & Discussion

In performing the qualitative content analysis, six main themes were found. The six themes are: Coordination, Field Issues, Electrical Software, Current Modeling Parameters, Factors for BIM Usage, and Company Factors. Each theme describes an important aspect of the Impact of BIM on Electrical Subcontractor Productivity, and was developed by grouping similar participant responses found in the data. Within each theme are important aspects and subjects which the specific theme covers. Sub-themes helped the researchers to quantify participant responses in a comparable way. The percentages displayed note how many participants mentioned a particular idea, within the same context. Each theme and corresponding sub-themes are discussed in the sections below.

4.1 Coordination

The main theme of coordination covers areas mentioned about the clash detection process and subcontractor collaboration in general. The percentage of participants' responses can be seen in Figure 1. The interviews revealed that most parties involved in the BIM process during the modeling and pre-construction phase seek out and resolve joint problems with pertinent trades. It was also noted that the person running the clash detection process, commonly called the coordination leader, is a very important party with specific responsibilities that impact the entire clash detection process.

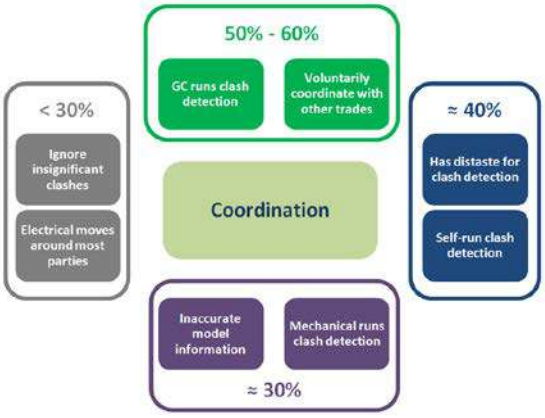

Figure 1. Coordination Qualitative Content Analysis Diagram

4.1.1 Coordination Leader

The data surrounding this topic defines coordination leader as the party responsible for combining coordination models for clash detection, running the clash detection meetings, and determining who moves how far. The majority of respondents mentioned either the GC or the mechanical contractor as being the coordination leader. Only two participants mentioned the possibility of either one taking on this role.

The participants who said the mechanical contractor had to be the coordination leader never mentioned the GC in a coordination role. When both the GC and mechanical contractor were mentioned as potential coordination leaders, the GC was preferred because they have the power to force another party to move. The main power mentioned was withholding payment until requests are met.

Another factor within the coordination role is the mentality of the subcontractors involved. In certain instances, the GC has nothing to do with the clash detection process, and it is orchestrated and run by the subcontractors entirely. Within this instance, if the GC is not viable to be the coordination leader, the mechanical contractor was deemed proprietary, the one with the most to model, the party with the most at risk, and therefore should head up the coordination. The reasoning is, "*we will have to move around them anyways*," so they may as well lead.

Less than thirty percent of participants mentioned that electrical sub-contractors commonly move around other MEP trades. Their reason given is due to code restrictions for mechanical, plumbing and sprinkler locations, versus relatively few codes dictating electrical conduit locations. Therefore, it is reasonable to assume that electrical subs move around other parties on a regular basis. No participant mentioned electrical items being proprietary or having code restrictive locations. This fact makes it even more enticing to coordinate locations with other trades, because it creates less re-work for the electrical modeler in moving obstructive items.

4.1.2 Voluntarily Coordinate with other Trades

The voluntary coordination with other trades takes place regardless of who the coordination leader is. It refers to a willingness to call, email, or otherwise contact another subcontractor you are clashing with outside of a planned coordination meeting. Voluntary coordination is connected to self-run clash detection and distaste for clash detection, as well as moving around most parties, as mentioned earlier.

The participants believe the clash must be cleared up regardless. As one participant put it, "*If we coordinate before the meeting and have a largely clash-free model before the meeting, then the meeting will take less time*" is a main thought. The modelers usually have multiple projects going at once, so the more work they can do in advance the better. Therefore, they will model, call to coordinate large items with other trades, run their own clash detection before upload, and clear up those clashes before uploading the model. This sequence cuts down on the overall coordination meeting time.

A long coordination meeting is one of the main complaints for clash detection. The complaint being that "*you cannot keep the modelers as you go through every little clash,*" coupled with "*sometimes the [coordination leader] is not looking in the proper places for clashes.*" Voluntarily coordinating with other subcontractors helps mitigate the distaste for clash detection, because that subcontractor would usually run his own clash detection, and therefore be required to spend less time in the coordination meeting and have less to fix afterwards.

4.1.3 Inaccurate Model Information

Over thirty percent complained about inaccurate model information. One major shift in modeling expectations sends a chain reaction of field re-work down the chain of subcontractors. The shift can come from modeling omissions, unexpected site conditions, or incorrectly designed components (from any of the designing engineers). This inaccurate information results in one of two things for an electrical subcontractor: either field coordinating previously modeled components (therefore rendering the modeling a waste of time), or waiting until dead last to install whatever was either omitted or incorrect. Installing last absolutely destroys productivity because a straight run turns into a plethora of offsets and ninety's to dodge all the other systems in your way. Not to mention, it needed to be done yesterday because the ceiling crew is following right behind you.

4.1.4 Ignore Insignificant Clashes

Within a clash detection meeting, the parties go through the clashes and designate who moves and how far. This note, if followed, will resolve the clash. However, every clash picked up by the clash detective is not significant. An insignificant clash would be one easily fixed in the field with little to no actual conflict. An insignificant clash would not require field re-work if not resolved. One participant mentioned that "*in a building with one thousand clashes, only about six-hundred will be significant.*" The act of going through and dismissing these clashes, according to the modelers, should be done before conducting the coordination meeting with all the trades together. Going through every clash was noted as a rookie mistake only made by inexperienced coordination leaders.

One company goes as far as saying, prior to upload, they do not even run a true clash detection in Navisworks. Instead they visually inspect what has been modeled, fix visual clashes, and continue. They took this approach because the clash detective picks up so many insignificant clashes. It is more efficient to visually inspect important clashes than wade through all the insignificant clashes.

4.2 Field Issues

BIM must be transferred to the field installation practices, or else, it is largely a wasted opportunity to achieve efficiency. If a model is created, but they coordinate in the field as if there was not a coordinated model in existence, then the modeling time and money was wasted. This theme of field issues encompasses how BIM is transferred to the field, and the effects it therefore has on the field (positive or negative). There were mostly positive reports given regarding BIM's impact on field installation. The respondent percentages and sub themes may be seen in Figure 2 below.

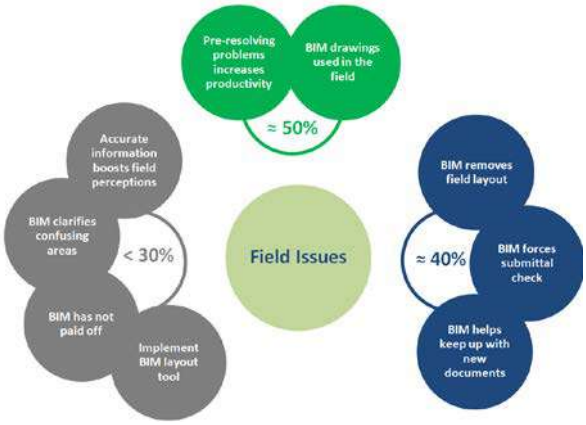

Figure 2. Field Issues Qualitative Content Analysis Diagram

4.2.1 Pre-resolving Problems Increases Productivity

The pre-resolving of problems encompasses other sub-themes mentioned within the realm of field issues. The participants primarily referred to the pre-coordinated location of large conduit runs, or laid out electrical rooms. These items in turn referred to forcing a submittal check and removing field layout. They were placed into three separate categories because they are mentioned in separate locations and help explain one another. Therefore, the following discusses the idea of field layout and submittal checks.

Field layout is the act of the electrical superintendent deciding where to run the main feeders, what can be run underground, how to fit the conduits within the tight electrical room, and discerning where the main areas of confusion will be and who could help clarify these areas. While making these decisions, the field men are staring, waiting for marching orders. This is a typical, non-BIM electrical project. With BIM, the modeler, usually under the direction of the project manager and superintendent, has pre-coordinated many of these decisions. This allows the field men to begin installing conduit according to the coordinated drawings immediately. It also allows the superintendent to focus more heavily on

the areas of contention and confusion. The field will still perform a level of layout, as far as measuring where items will go, however, the bulk of the decisions have already been made.

One of the most important processes of layout is ensuring that the installation components will fit within their designated areas. Usable square footage is precious, therefore non-usable areas, such as electrical rooms, are made as small as possible. If it is discovered in the field that a particular item, a panel, switchboard, light fixture, automatic transfer switch, or transformer, will not fit within its place, then your field men have to waste their time on a mistake that could have been avoided. It would be an easy fix if the project manager or superintendent simply double-checked the submittal sizes. However, as one participant noted, "*getting someone to back check submittal data when they are coordinating the actual installation of items every day is not an easy thing.*" The BIM modeler has an opportunity to ensure these items will fit before they are required to be installed. This is noted by modelers and project managers alike as a very important task. Three inches difference of a light fixture depth in a hospital corridor might as well be a mile.

The pre-resolving of layout and submittal items are the two main "*problems*" that BIM resolves and delivers higher productivity. As previously mentioned, these two items help describe the pre-resolution productivity boost.

4.2.2 BIM Transfer to the Field

The efficiency with which the BIM information is transferred to the field is just as important as the information itself. The respondents described a range of BIM transfer to the field including the following: giving coordinated BIM drawings, providing specialized multi-system drawings, supplying superintendents with tablets loaded with the BIM model, training and providing BIM stations for the entire electrical crew, utilizing a BIM layout tool to establish points. The main thread throughout the entire range of BIM to field transfer is the field's ability to understand and assimilate the transfer method into their workflow. That is the main reason that over fifty percent still use specialized drawings rather than BIM-loaded tablets. The companies are certain their field personnel would not know how to properly use the BIM model. Those not making BIM available to every electrician see more benefit in having the modeler supply pertinent information to the field through paper drawings. Then, if the field has requests for more information, the modeler will provide specialized drawings or model snap-shots.

For those companies that have invested in BIM training for the electricians, the implementation of a BIM layout tool has proved greatly beneficial. One modeler reported that going into the field to lay points creates a synergy between the modeler and field personnel. It brings the modeler into the reality of what is being modeled. Simultaneously, it helps the field understand the benefit of what the modeler is doing. "*BIM total station increases morale between field men and designer because the field men see the benefit of the modeler.*" Additionally, the BIM layout tool decreases the time required for certain tasks. As clearly stated in this quote, "*using the BIM total station, they laid out a floor in one day rather than two weeks.*"

The transfer of BIM information to the field is extremely important. However, that does not automatically mean an electrical contractor should train everyone, buy all new tablets, and create BIM jobsite stations. The most important thing is for the field to use and assimilate the information. Coordinated 2D drawings that are understood would be better than a frustrated crew.

4.2.3 BIM Helps Keep Up with New Documents

Construction projects, often times, release addendums and change orders throughout the duration of the pre-construction and construction phases. Having an additional person dedicated to ensuring the field has the latest and greatest information is invaluable. As noted in the software section under thematic analysis, an electrical subcontractor can be responsible for up to thirty different digital collaboration tools. It is very easy for a change to be missed, and it is crucial for the field to receive every change. Otherwise, mistakes will be corrected at the expense of the contractor. Inaccurate information is still a potential, however, an additional set of investigative eyes helps mitigate the error of outdated information.

4.2.4 BIM has not Paid Off

Two participants specifically mentioned they did not feel BIM has paid off. One performs partial modeling in-house (subbing out larger modeling jobs), and the other subs out all the BIM modeling. One participant clearly stated that "*BIM is a lot of work that just hasn't paid off.*"

The only redeeming factor for one participant is that the clash detection process gets all the trades on the same page. However, he argues it is no different than the process before modeling. Conversely, he mentions a benefit in modeling within congested or complicated areas. Therefore, someone who largely opposes the BIM process still finds benefit in modeling congested areas. However, modeling the entire building is seen as a waste of time, money, and resources, which will not pay off.

Participant ten mainly claim that BIM has not paid off due to a recent project. The project performed the

clash detection process and achieved a clash free model. Upon installation, design changes were made, which threw the "*entire model into chaos.*" Site coordination meetings were foregone by the general contractor in lieu of the coordinated model. This project was "*less coordinated than other projects without BIM.*" Primarily, the only redeeming factor of the BIM process is that it is a source for coordination drawings, which would have to be made regardless. Consistently inaccurate model information has convinced this participant that BIM has not paid off.

Therefore, the two main arguments that BIM has not paid off may be reduced to: we can coordinate most areas much faster in two dimensions, and inaccurate modeling information will ruin a project. Both of which are worthy points for further investigation.

4.3 Electrical Software

The main software dominating the electrical modeling sector are two semi-competing platforms, AutoCAD 3D and Revit. Both are owned by Autodesk, and both create geometry in three dimensions necessary for clash detection. However, only Revit is an actual BIM platform. AutoCAD 3D is a modeling program, but is not capable of having submittal data loaded into it. Figure 3 displays the percentage of participants' software preference and their opinion of electrical software in general.

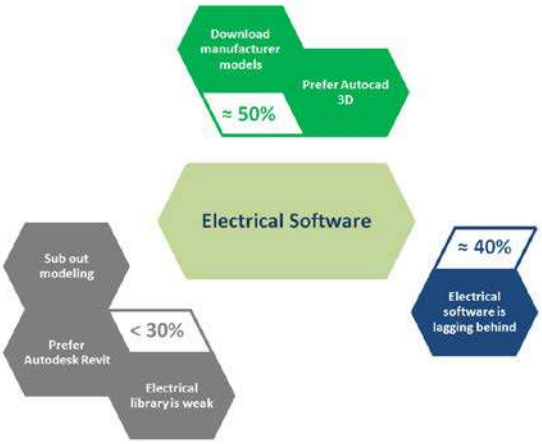

Figure 3: Electrical Software Qualitative Content Analysis Diagram

4.3.1 AutoCAD 3D Vs Revit

As shown above (Figure 3), the majority of participants prefer AutoCAD 3D over Revit. The main reason given is AutoCAD 3D is easier to use and more tailored to the electrical industry than Revit. Those who prefer Revit claim much of the same benefits that AutoCAD 3D users mention with the addition of manufacturer model download capabilities.

According to the proponents of AutoCAD 3D, it is a simpler program, with easier modeling procedures, and can be executed more quickly than Revit. According to one participant "*one of our operators went to school and was trained on Revit, and we trained him on AutoCAD MEP. He said the MEP for what we do is really better, faster, more tailored to what we do.*" AutoCAD is not a smart model and therefore does not require loads, circuits, or any submittal information. At times Revit is called for in the specifications. In these instances, usually the GC will allow the electrical contractor to model in whatever program they are most comfortable with and simply provide a particular export file type.

Of those proponents of Revit, two are modelers and one is a project manager. One modeler jumped straight from AutoCAD 2D into Revit, and has little to no experience with AutoCAD 3D. The other modeler has used both AutoCAD 3D and Revit. His main example of Revit's supremacy derives from being able to download manufacturer models and place them within the model. The project manager prefers Revit because of the ease of information retrieval. Revit can give you the length, size, fill, source, and destination from one click. This greatly helps in information retrieval in the field.

According to all the participants, a data loaded BIM model is a rare request. Therefore, both the AutoCAD 3D and Revit users are primarily modeling for in-house benefit and coordination purposes. That is why the selection of modeling software weighs more heavily to speed and ease of use.

4.3.2 Electrical Software Lagging Behind

Forty percent of participants agree that "*electrical is at the bottom of the [software] food chain.*" This is mostly in comparison to mechanical and structural contractors. The libraries are weaker, component transition is less smooth, and certain items the program may are not even electrically based. Duly noted, "*Here in a couple three years ago, the fittings the software was putting was…like using plumbing fitting or a plumbing configuration to do electrical.*"

A majority of the complaints revolved around lacking a component library. However, this was often offset by commenting on the benefit of retrieving manufacturer created components online. The other complaint was that neither AutoCAD nor Revit are actually tailored to the electrical industry. "*I can make it do what I need it to do, but there's definitely room for improvement on Autodesk's side,*" basically sums up the current standing of electrical modeling software.

One participant expounded on his contact with Autodesk in response to this room for improvement. There are opportunities to provide feedback as well as support communities. Certain support communities, at

least for Revit, are monitored by Autodesk. An Autodesk representative will try to answer operational answers, or at least note a change to be incorporated into later releases.

4.3.3 Sub-out BIM Modeling

Less than thirty percent of research participants subcontract out the BIM portion of the work. The primary reason for subbing out the BIM portion of a job is a lack of resources. Smaller companies do not have the additional resources to dedicate to BIM modeling in-house. In certain instances, there may be an in-house modeling department which will model certain sections of a project, but not the entire building. Although in-house modeling capabilities may be present, "*it is better to not tie up your own resources on very large projects.*"

4.4 Factors for BIM Usage

This main theme covers the main reasons why an electrical contractor will use BIM. The most common reason is, "because the contract requires it." However, this theme also uncovers what will be done when BIM is not required. It also helps delve into the intended primary beneficiaries of the BIM process. If BIM is not required, and certain items are modeled regardless, there is an intended beneficiary and reasoning for executing the additional work.

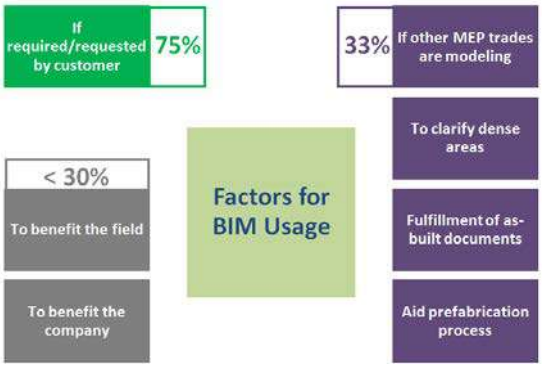

Figure 4: Factors for BIM Usage Qualitative Content Analysis Diagram

4.4.1 If Required or Requested by the Customer

The primary driving force of BIM usage within our range of participants is still the owner and or general contractor. There is over a forty percent gap between those who model when required and those who model for their own benefit. The reluctance for electrical contractors to BIM a job still exists, although most participants would say that BIM has paid off. In other words: BIM has paid off when used in the most desired way. None of the project participants mentioned modeling an entire project solely for company benefit. There are always stipulations, one of the biggest currently being, if it is required?

One of the positions among subcontractors regarding the requirement is, "*this is an additional cost I need to put into my estimate.*" This especially applies to those subbing out the BIM portion of the work. If one includes the additional overhead/subcontractor cost to use BIM on a project, while another does not include that cost the contractor not carrying additional BIM charges will have a financial bidding advantage. Based on the interviews, the BIM model may cost a small percent of the entire project. In a market where a one percent change could be the determining factor between award or dismissal, documentation of a BIM requirement is crucial.

Although the same contractor may realize benefit through the BIM process, either by reduced re-work, shorter installation durations, or more field coordination, this benefit has most likely not been incorporated into the estimating programs. No participant mentioned using the BIM model for an actual bid estimate. Additionally, many modelers mentioned receiving modeling information after the project had been awarded. Hopefully, BIM savings and costs will be integrated into the estimating process, but until then, the documented requirement for BIM will likely remain the primary determining factor for its usage amongst electrical contractors.

4.4.2 If other MEP Trades are Modeling

This reason did not come from those subbing out the BIM scope of work, only from those who primarily model in-house. "*If we are not required to BIM a project, the first thing I will do is call the mechanical sub and see if he is modeling.*" The primary purpose of modeling a project is coordination. There is no reason to model if there is no one to coordinate with. The model will be an added expense with no relevance to installation, and have no potential field benefits.

However, if the other MEP trades intend to model, especially the mechanical contractor, the potential field benefits remain. As mentioned earlier, there are instances where the general contractor does not require or monitor the clash detection process, and the trades do it anyways. In this instance the mechanical contractor will most likely take the coordination leadership role. As noted in the diagram, only one-third of participants are confident enough in their potential savings through the BIM process to proceed under these conditions.

4.4.3 Clarification of Dense Areas and Field / Company Benefit

As mentioned under the company factors theme, at least half of the participants will conduct a post-award meeting. Within this meeting, the project manager,

superintendent, estimator, and modeler will go through the project after its award. This is the meeting in which dense or potentially confusing areas will be identified for modeling. This meeting will also be the prime determinant of what exactly will benefit the field and/or company.

The primary dense area mentioned, which is also noted within the company factors theme, is the electrical room. Fitting all the gear and conduit into this room is described as "*trying to shove ten pounds of [stuff] into a five pound bag.*" Electrical rooms are the primary location where the electrical contractor will have a conflict with himself. Additionally mentioned are hospital head walls and primary corridor intersections, where multiple trades have multiple crucial components.

These are areas where questions will be left unanswered and RFI's unissued until installation. Identifying and detailing these areas before installation benefits the field by reducing re-work and limiting submittal item errors.

4.4.4 Aid the Prefabrication Process

Modeling for pre-fabrication benefit is trumped by the following factors: whether BIM is required in the documents, if other MEP trades are modeling, or if modeling is determined beneficent in the post award meeting. No participant mentioned modeling for the sole benefit of prefabrication. The noted thirty-three percent of participants went into greater modeling detail, within the areas already deemed necessary to model, if it helped the prefabrication process. Therefore, prefabrication may be aided by the modeling process, but does not drive the components modeled. In compliment, the greatest benefits of prefabrication are mentioned to be within complicated, labor intensive areas. To summarize, the areas most likely to be deemed beneficial to model, will also reap the greatest prefabrication benefits. Therefore, prefabrication does not determine components to be modeled. It is an added benefit to modeling certain components in greater detail.

4.5 Current Modeling Parameters

Current modeling parameters would be the external factors of BIM modeling set out in the construction documents. If a project is required to be BIM, there is usually a BIM execution plan within the specifications. This execution plan varies in length, from as little as, "*this is a BIM project*," up to forty pages of details and responsibilities. This plan usually covers what to model, where to upload the model, and sets certain modeling completion benchmarks. It varies depending on owners, designers, and general contractors involved. Figure 5 below displays the commonalities amongst most modeling parameters.

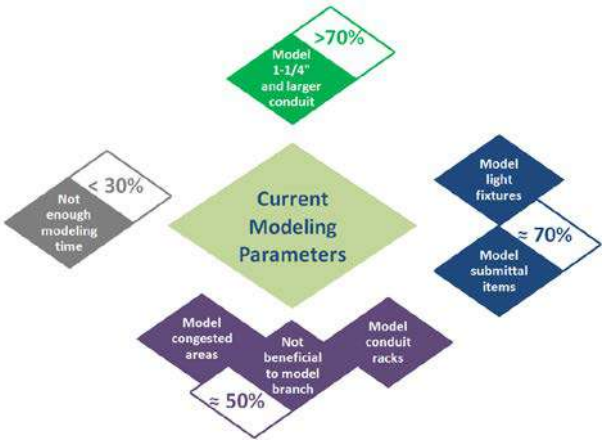

Figure 5: Current Modeling Parameters Qualitative Content Analysis Diagram

4.5.1 Model 1 ¼" Conduit and Larger

The conduit over one inch is usually associated with a project's main electrical feeds located on the single line. The single line is the diagrammatic drawing showing the main power connections between power distribution items, such as: primary power entry from the utility company, primary switchgear, 480 volt panels, transformers, 240 volt panels, uninterrupted power supplies, automatic transfer switches, and certain large pieces of equipment. The feeds are usually home runs and considerably less abundant than branch conduit.

Some participants argue that modeling any feeds smaller than two inches is ridiculous. In this instance they may negotiate modeling requirements with the general requirements. However, as noted above, over seventy percent agree that modeling feeders is a beneficial component to model. One reason is that, conduit over one inch is considerably less flexible than smaller sizes, especially over two inches. Also, the wires inside the larger conduits are usually larger and can be quite expensive per foot, as well as laborious to pull. Additionally more offsets translate into more pull boxes and wire splices which also add material and labor. As one participant said, *"I can assure you, we do not want to run 6 - 4" conduits and have to move them."* Based on other participants, that would include snaking them through other trade's obstructions.

4.5.2 Modeling Light Fixtures and Other Submittal Items

This is another area that is commonly required in the execution plan, and also accepted as beneficial by the electrical contractors. Technically, light fixtures are considered submittal items, but, within the interviews, submittal items refers to special pieces of power distribution equipment, or other bulky, specialized components with longer-than-normal lead times. These

are usually included on the single line.

The high acceptance of modeling light fixtures consists of two main factors: the ease with which light fixtures can be put into the model, and the drastic impact and cost just a few inches of light fixture depth can have on above-ceiling coordination. Concerning the modeling of the light fixtures, over fifty percent will turn to online manufacturer models. From that point, all they have to do is place and position. But once the modeling process has begun, the lighting package has already been scoped out and the electrical contractor has likely issued a letter of purchasing intent to a lighting vendor for their quoted lighting package. If the electrical contractor was in the field and a coordinated component did not fit due to a deeper than anticipated light fixture, the electrical contractor would be responsible for making it work. In other words, changing light fixtures to gain a few inches is an expensive proposition to the electrical contractor. And according to one participant, "*3-inches could make all the difference in a tight space.*"

Submittal items have the same issues as light fixtures, with added lead-time precautions. There are relatively few crucial submittal items in comparison to the entire electrical scope of work. However, unanticipated changes to these precious few items could quickly eat away profits and create labor down time. Akin to modeling light fixtures, modelers may find the manufacturer model for certain pieces of gear online. If not, it does not take much time to create a colored mass of the overall dimensions of the component and place it within the model. For about seventy percent or participants, the duration modeling lights and submittal items is time well spent.

4.5.3 Modeling Branch

The majority of conduit in a project is branch. Branch is the connection from one device to the next in a circuit. The branch wiring is fed by home runs. These are designated as diagrammatic arrows on electrical drawings which go back to one specific panel circuit. Homeruns often run parallel to each other, and, where applicable, run down a main corridor and feed into the appropriate panel.

The modelers are not completely opposed to modeling the home runs. Blocking out this space allows for a much quicker installation within the corridor because fewer offsets and splices would be required. However, the modelers agree that once the home run reaches either the first device or the intended room, the branch modeling should stop. The argument for this is twofold. First, electrical metallic conduit (EMT) and metal clad (MC) cable are very flexible items which can be diverted around most objects. Therefore, if these components are modeled, they will simply cause an irrelevant clash, because the field man can easily divert the conduit. Second, modeling branch is an extremely laborious task with virtually no field benefits. And, if a room is reconfigured, or a wall moved, the entire branch modeling process must be re-done. Simply because fifty percent mentioned that modeling branch was not beneficial does not indicate the other half see the benefit to modeling branch. In fact, only one participant voluntarily models branch for company benefit.

4.6 Company Factors

Each company has its own guidelines and best practices regarding BIM usage. These factors have been compiled into the Company Factors main theme. Figure 6 displays different actions a company may take when faced with differing levels of BIM requirements.

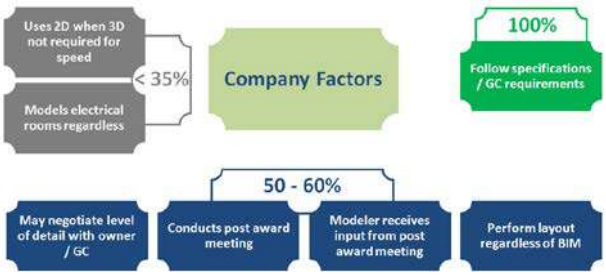

Figure 6: Company Factors Qualitative Content Analysis Diagram

4.6.1 Specifications and Negotiation

Every participant was very clear that the specification documents and GC requirements were to be completely followed. It is the contractual guarantee of the electrical subcontractor to fulfill all requirements listed within the specifications and shown on the drawings. However, there are instances where the electrical subcontractor may negotiate the terms of level of modeling detail requirements.

The possibility of negotiation hinged upon the following three factors: the severity of the initial requirements, the relationship between the electrical subcontractor and the general contractor, and the type of contractual agreement (design-bid-build or design-build). The severity of the initial requirements overrules the following two factors. For instance, if the electrical contractor is initially required to model all items down to the threaded rod, he will "educate" the owner and general contractor on this time-intensive requirement regardless of prior relationship or contractual framework. Likewise, the relationship between electrical and general contractors trumps the contractual framework; positive relationships indicate a level of trust and collaboration necessary for productive

negotiation.

In summary, the electrical subcontractor agrees to follow every item within the drawings and specifications. However, when the possibility to negotiate certain terms of the contract arises, particularly the modeling level of detail, fifty percent of the participants in this research capitalize on that chance.

4.6.2 Post Award Meeting and Modeling

A majority of participants mentioned conducting a post award meeting. This is described as a meeting between the estimator, project manager, superintendent, and BIM modeler for the electrical contractor. After being awarded the project, they will go through the drawings and specifications. The purpose of this meeting is to orient the project manager, superintendent, and BIM modeler to the project. Additionally, this meeting is an opportunity for the project team to point out complicated areas and dictate certain components to be modeled. One participant mentioned they will "*write down what would benefit the project, or what would benefit the company as far as the BIM modeling process*" during the post-award meeting. Another uses, "*forms to determine, what we are going to do on this project, what requires modeling.*" This information is then passed and explained to the BIM modeler so it can be incorporated into the final model.

4.6.3 2D Layout

As shown in figure 6, fifty to sixty percent of participants perform a level of layout regardless of BIM requirements. This layout, at a minimum, consists of drawings red-lined by the superintendent, showing where he intends to run the main components of the project. If BIM is required, the modeler will reflect the markings into the BIM model. If BIM is not required, the markings will be reflected in the 2D coordination study and taken into the field.

4.7 Conclusions

The impact of BIM on electrical subcontractor productivity is too recent to be objectively measured. Participants mention time savings and increases in coordination productivity. However, these measurements have not been completely quantified. Quantification is nearly impossible because of all the variables surrounding any given project, regardless of BIM. Location, electrical project manager, general contractor project manager, owner, electrical superintendent and crew, other subcontractors' managers, relationships with other subcontractors, and project complexity all play a part in electrical subcontractor productivity. However, certain conclusions can be made to the electrical subcontracting community, based on the findings of this research.

- The electrical subcontractor should try to operate under the GC as the coordination leader. If the GC is not willing to be coordination leader, the electrical contractor must should support the mechanical contractor to take up the role.
- Ensure there are no requirements to model items that have no impact on field installation. If required, negotiate with the parties requesting that level of detail.
- Give the field as much information as they can assimilate into their installation. Deliver the information in a format that enhances field personnel productivity.
- The primary areas of benefit with BIM are more thorough submittal checks, coordinated clash detection, and eases in field installation (due to prior coordination and layout). Perform these activities whenever possible and conduct an internal post award meeting.
- Coordinate with the other trades on system layout as much as possible before the BIM modeling process begins. This will reduce the number of clashes and modeling rework.
- When considering who to subcontract the BIM scope of work to, prioritize relationships and timeframes.
- The modeler should only model to an LoD for prefabrication if that area is required or beneficial to be modeled, regardless of prefabrication.
- Consideration to hire personnel who are modeling purposes must be given to those candidates who also possess field experience even if their software usage capability is not the best.

4.8 Future Research

This exploratory research of the impact of BIM on electrical subcontractor productivity opens the door for quantitative research in the future. The main limitation of the findings within this study is applicable due to participant size and location. It would be greatly beneficial to translate many of these findings into a widely distributed quantitative data collection medium, such as a survey.

Also, the topic of modeling timeframes seems to have the least amount of research. However, it has a great impact on coordination accuracy. It is connected with construction start dates, as well as design completion dates. The closer construction commencement edges towards design completion, the less time for underground and first floor coordination. The electrical trade is greatly impacted because the discerning what can be installed underground is largely dependent on the load requirements of the first few floors of the building. The more time between design

completion and construction, the more thorough the underground installation. As underground is one of the least expensive methods of electrical installation, this could potentially lower the overall project cost to the owner. At the very least, it would help maximize electrical subcontractor profits. Although BIM may not have sufficient research to quantify financial impacts, it has the potential to significantly change the construction industry in the future.

References

[1] Hanna, A., Boodai, F., El Asmar, M., 2013. State of Practice of Building Information Modeling in Mechanical and Electrical Construction Industries. Journal of Construction Engineering and Management 139, 04013009. doi:10.1061/(ASCE)CO.1943-7862.0000747

[2] Akinci, B., Kiziltas, S., 2010. Lessons Learned from Utilizing Building Information Modeling for Construction Management Tasks, in: Construction Research Congress 2010. American Society of Civil Engineers, pp. 318–327.

[3] Sawyer, T., 2008. Take Their Time Adoption Follows Uneven Paths. Engineering News-Record 261, 36. December.

[4] Simonian, L., 2009. Building Information Modeling for Electrical Contractors: Current Practice And Recommendations | ELECTRI International [WWW Document]. URL http://www.electri.org/research/building-information-modeling-electrical-contractors-current-practice-and-recommendations (accessed 1.7.13).

[5] Korman, T.M., Simonian, L., Speidel, E., n.d. 2008. Using Building Information Modeling to Improve the Mechanical, Electrical, and Plumbing Coordination Process for Buildings, in: AEI 2008. American Society of Civil Engineers, pp. 1–10.

[6] Leite, F., Akcamete, A., Akinci, B., Atasoy, G., Kiziltas, S., 2011. Analysis of modeling effort and impact of different levels of detail in building information models. Automation in Construction 20, 601–609.

[7] Barlish, K., Sullivan, K., 2012. How to measure the benefits of BIM — A case study approach. Automation in Construction 24, 149–159.

[8] Azhar, S., Cochran, S. 2009. Building Information Modeling: Benefits, Opportunities and Challenges for Electrical Contractors. National Electrical Contractors Association (NECA).

[9] Brown, D., 2011. Corbins Electric Powers the Region. Engineering News-Record 267, 24. September.

[10] Dossick, C., Neff, G., 2010. Organizational Divisions in BIM-Enabled Commercial Construction. Journal of Construction Engineering and Management 136, 459–467.

[11] Leicht R, M.J., 2008. Moving toward an "intelligent" shop modeling process. ITcon 13, 286–302.

[12] Korman, T.M., 2009. Rules and Guidelines for Improving the Mechanical, Electrical, and Plumbing Coordination Process for Buildings, in: Construction Research Congress 2009. American Society of Civil Engineers, pp. 999–1008.

[13] Park, H., Thomas, S., Tucker, R., 2005. Benchmarking of Construction Productivity. Journal of Construction Engineering and Management 131, 772–778.

[14] Akinci, B., James Garrett, J., Leite, F., n.d. 2009. Identification of Data Items Needed for Automatic Clash Detection in MEP Design Coordination, in: Construction Research Congress 2009. American Society of Civil Engineers, pp. 416–425.

[15] Tulacz, G., 2013. Subcontractor as Designer. Engineering News-Record.

[16] Ruwanpura, J.Y., Hewage, K.N., Silva, L.P., 2012. Evolution of the i-Booth© onsite information management kiosk. Automation in Construction 21, 52–63.

[17] Becerik-Gerber B, R.S., 2010. The perceived value of building information modeling in the U.S. building industry. IT in Construction 15, 185–201.

[18] Knapschaefer, J., 2011. Rx for Hospital Design: Models and Meetings. Engineering News-Record (New York Edition) 266, NY72. July.

[19] Eadie R, O.H., 2013. An analysis of the drivers for adopting building information modelling. IT in Construction 18, 338–352.

[20] Miettinen, R., Paavola, S., 2014. Beyond the BIM utopia: Approaches to the development and implementation of building information modeling. Automation in Construction 43, 84–91. doi:10.1016/j.autcon.2014.03.009

[21] Succar, B., 2009. Building information modelling framework: A research and delivery foundation for industry stakeholders. Automation in Construction 18, 357–375. doi:10.1016/j.autcon.2008.10.003

[22] Francis, J.J., Johnston, M., Robertson, C., Glidewell, L., Entwistle, V., Eccles, M.P., Grimshaw, J.M., 2010. What is an adequate sample size? Operationalising data saturation for theory-based interview studies. Psychology & Health 25, 1229–1245.

[23] Guest, G., Bunce, A., Johnson, L., 2006. How Many Interviews Are Enough? An Experiment with Data Saturation and Variability. Field Methods 18, 59–82. doi:10.1177/1525822X05279903

Analytic Hierarchy Process as a Tool to Explore the Success Factors of BIM Deployment in Construction Firms

S.-M. Liang[a], I-C. Wu[a], Z.-Y. Zhuang[a], and C.-W. Chen[b]

[a] Department of Civil Engineering, National Kaohsiung University of Science and Technology, Taiwan
[b] SINOTECH Engineering Consultants, Ltd., Taiwan
E-mail: f107141134@nkust.edu.tw, kwu@nkust.edu.tw, wayne@nkust.edu.tw, cwchen@mail.sinotech.com.tw

Abstract –

In the past ten years, more and more construction companies have adopted and implemented the Building Information Modelling (BIM). Government agencies have addressed the relevant technologies because the application of BIM has brought a lot of benefits to engineering. However, many companies today have neither deployed BIM technology nor confirmed their intention(s) to adopt BIM technology. This is perhaps subject to the limited knowledge about successful BIM deployments. Based on the literature and the experience of an expert, in this study, the influencing factors and a decision hierarchy are identified and developed by using Delphi method. The priority over and the relative importance of these factors and over/of those upper constructs were analysed using the analytic hierarchy process (AHP). These findings are key to enhance the decision-making process of a construction firm which wishes to introduce a BIM system.

Keywords –

Building Information Modelling; Delphi Method; Analytic Hierarchy Process (AHP); System Adoption Factors (SAF)

1 Introduction

Adopting BIM technology in an architecture, engineering, or construction (AEC) project may improve the performance of the project and bring benefit to the project. Establishing an effective BIM evaluation standard can help new users of BIM systems during deployment [1]. However, as the studied case in Taiwan, at this stage, most of the companies that have adopted BIM technology are the construction firms.

This paper studies the influencing factors which may affect a construction firm's decision on the adoption of BIM technologies for deployment and implementation. Except for analysing the priority and the relative importance of these factors, these factors are mounted under four constructs, namely, BIM system integration, BIM use, organisation (organizational factors), and project execution. The relative importance of these constructs, which is also the key knowledge that is to be explored, is also assessed.

This study progresses as follows. First, from a literature study and the expert discussions, the set of initial system adoption factors (SAFs) for BIM were determined. These SAFs are organised as a 'decision hierarchy' [2] [3]. It is a tree which includes a layer of constructs and another layer of factors, while the root of this hierarchical tree is the total decision goal (i.e., the deployment and implementation of a BIM system). Delphi Method, which is also known as the expert survey method, is used confirm the form of the decision hierarchy, with expert discussions polled.

Next, using the analytic hierarchy process (AHP), a questionnaire is designed and the expert opinions are investigated in terms of the pairwise comparison matrices. To facilitate this survey process, Expert-Choice, a computerised tool, is used as an assistant tool to validate the consistency in the data (i.e., polled opinions) and to obtain the weights (relative importance) of the factors/constructs. Finally, these factors are prioritized according to their associated weights. The key factors that influenced BIM system adoption, which is the key knowledge as desired by the decision makers (DMs), are identified. Together with other findings, the set of knowledge can serve as an important guide for any construction firm which is willing to adopt, deploy and implement the relevant technologies of BIM.

2 The Determination of the Influencing Factors Using Delphi Method

Figure 1 shows the way in which this study has applied the Delphi Method.

First, in the literature study phase, the influencing factors of BIM on BIM adoption are identified from the literature, using materials in the research field. The literature and the collected materials are also used as the

important references for subsequent study. A number of influencing factors (i.e., SAFs) are collected in this process. For example, but not limited to, Badrinath summarised a set of 454 initial SAFs [4]. Tsai et al. identified the other set of 123 SAFs, considering the whole life cycle of the building as the research subject [5][6], while in general, the life cycle of a building is mainly divided into four general stages: planning, design, construction, and operation/maintenance.

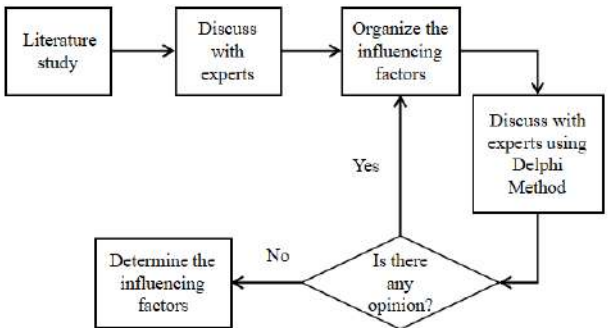

Figure 1. Determining the influencing factors

Second, it is the 'discussion with the expert' phase. The SAFs which are summarized from the literature are given by a BIM researcher in Taiwan. She is in charge of filtering the SAFs and reduce the size of the set of SAFs so that only those factors which are regarded as important for the construction firms in Taiwan are included. So after the discussions, this phase obtains a set of only 25 'initial SAFs'.

Third, the Delphi method (see the right loop in the figure) is used to confirm the obtained set of SAFs, while any addition of a new SAF or removal of an included SAF in the set is possible. The Delphi method, also known as the 'expert survey method', mainly uses communication methods to send questions that are to be discussed to the experts for consultation, to collect the opinions of all the experts, to understand these opinions by discussions and to aggregate the opinions. These aggregated opinions are once again fed back to the experts for further consultation, so their opinions are collected and aggregated more accurately. This approach gradually produces more consistent results for making a precise decision. It uses an anonymous way where the aggregated opinion maintains a general representativeness and is thus a reliable decision-making method.

In this study, through the use of the Delphi method with the experts help, eventually, two new SAFs, i.e., BIM system expansion capability and BIM technology cooperation between the construction firm and downstream subcontractors, are added to the set, but no SAF in the initial set is removed. In the opinion of the expert, the system scalability of BIM technology is very important. In addition, most of the downstream subcontractors of the construction firm will affect the performance of the BIM system owned by the construction firm itself. Therefore, finally, a total number of 27 SAFs are included and studied in this study.

3 AHP Questionnaires and Surveys

In this study, a tree-like hierarchical diagram is established, as to organise the SAFs. This is usually called a 'decision hierarchy'. This decision hierarchy includes not only a bottom layer of the SAFs, but also a middle layer of constructs, where each SAF is mounted under some construct. Thus, a decision construct may have several SAFs mounted. And, all of these constructs are further mounted under the total decision goal, which is BIM adoption.

However, as this decision hierarchy is established by the researchers of this study (see *phase 1* in Figure 2), it requires further confirmation. In this study, this is confirmed by also using the Delphi Method (see *phase 2* in Figure 2). Fortunately, the established decision hierarchy is approved by the expert when it was first established.

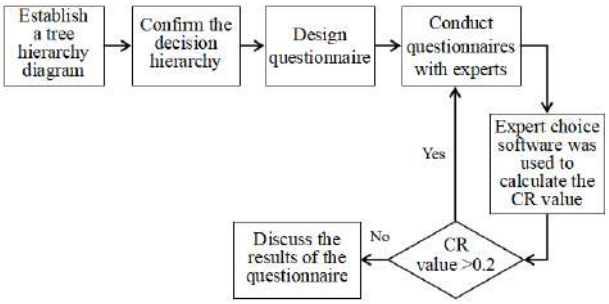

Figure 2. The workflow of AHP processes

Therefore, the confirmed decision hierarchy is used as the basis to design the questionnaires for the pairwise comparisons in the style of AHP. In the confirmed hierarchy, since there are four constructs w.r.t. the goal and there are different numbers of SAFs w.r.t. each construct, there are five questionnaires. This is exactly *phase 3* in Figure 2.

After the questionnaires are designed, they are used for the survey wherein the DM expresses his preferences in terms of pairwise comparisons. The DM is asked for more rounds of interview if the result does not pass the consistency check. This survey process is as shown in the *right part* of Figure 2.

The Analytic Hierarchy Process (AHP) [7] is mainly used for decision problems with multiple evaluation criteria. The purpose is to divide the considerations for a

complex decision problem system into several smaller parts (i.e., the constructs), where each of these smaller parts includes the observable factors (i.e., the SAFs). A decision hierarchy can help a DM to fully understand the influencing factors during decision-making, and the analysis of AHP is a method to assess the (relative) importance of these factors in terms of the results from the pairwise comparisons performed by the DM.

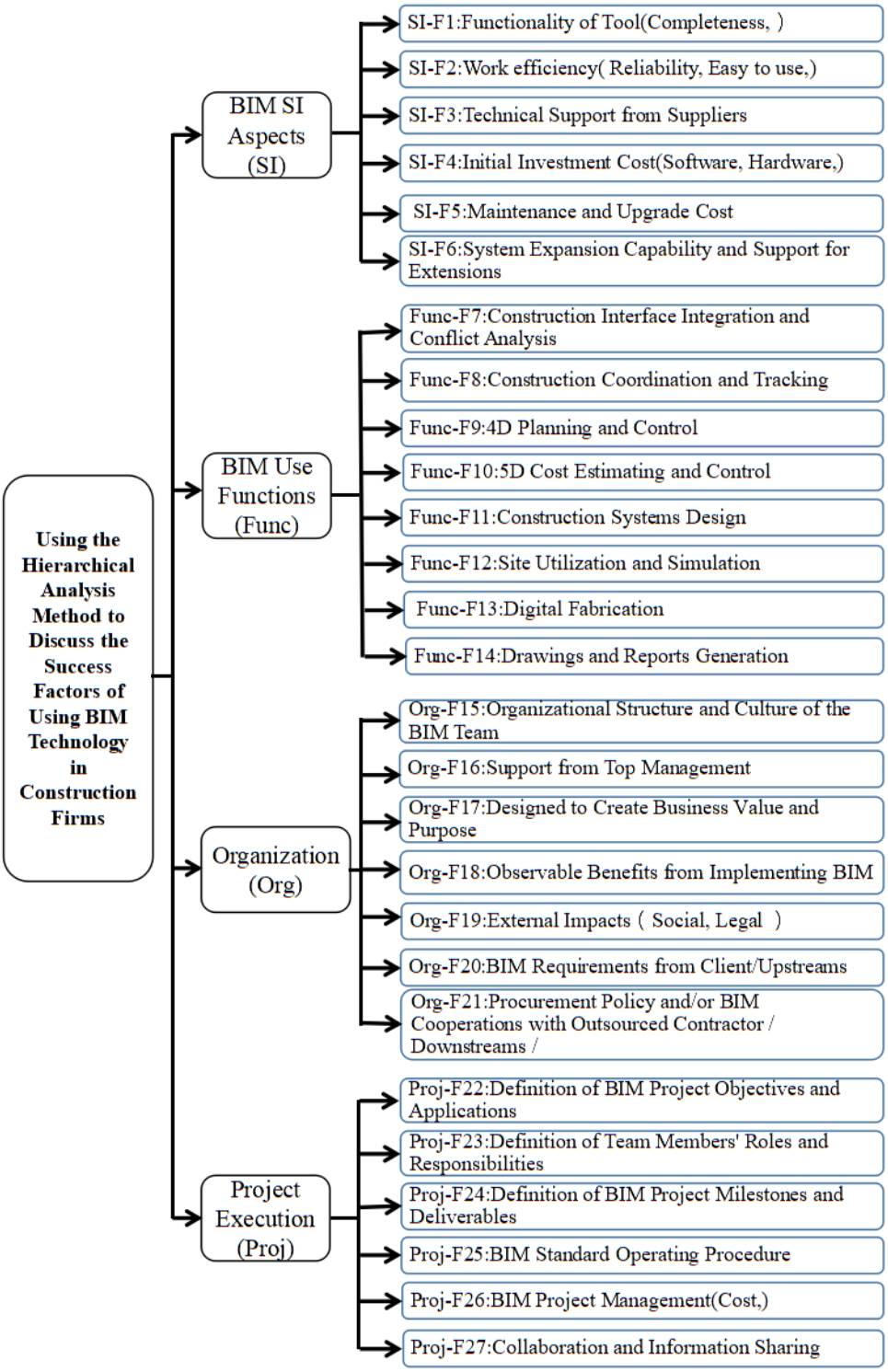

Figure 3. The decision hierarchy diagram

In this study, the decision hierarchy that is confirmed is shown in Figure 3. This hierarchy details what are to be compared pair-wisely.

For the constructs w.r.t. the total BIM adoption decision goal or the SAFs w.r.t. some construct, results from the pairwise comparisons are recorded in a 'pairwise comparison matrix'. Each element in the matrix is recorded as a level revealing the relative importance of a criterion (i.e., a construct or a SAF), C_x, against another criterion, C_y. This is a quantitative measure because the evaluation values in the matrix state the following facts (in the DM's mind): C_x is equal strong (1:1), weakly strong (3:1), strong (5:1), very strong (7:1), and absolutely strong (9:1) than C_y, so the corresponding measured values are 1, 3, 5, 7 and 9, whilst 1, 1/3, 1/5, 1/7 and 1/9 are recorded for the cases vice versa.

The survey work of this study obtain several pairwise comparison matrices in this manner, as the questionnaires that were designed based on the decision hierarchy and were answered the BIM expert had provided data to fill up these matrices. During the survey, the interviewed expert DM specified the relative importance of each pair of two criteria in the questionnaire, and such information became the data source to compose (fill in) each pairwise comparison matrix.

To validate the collected source data, Expert Choice (i.e., a decision analysis software) was used to receive the input, to compose the decision matrix, to validate the answers in terms of consistency ratio (C.R.) and as to calculate the weights of the constructs or the SAFs.

In the consistency analysis, if the C.R. value of the questionnaire was greater than 0.2, the DM was asked to fill the questionnaire once again until the C.R. of the questionnaire yielded a value less than the standard of the inconsistency threshold (C.R. value < 0.2). As in other engineering fields, Zhuang et al. [8], Schmidt et al. [9] and other scholars believe that an AHP questionnaire is acceptable when the C.R. value of a pairwise comparison matrix it infers is less than 0.2.

In this study, actually, the DM was interviewed twice (i.e., the DM was re-interviewed only once as to meet the above data validation requirement). So finally, the relative weight of each construct (w.r.t. the total BIM adoption decision goal) and the relative weight of each SAF (w.r.t. some construct) was obtained and sorted. Based on the information, eventually, the absolute weights of all SAFs were calculated and prioritised. Such knowledge is both critical and significant for a DM to understand the priority over the evaluation criteria of BIM system adoption, as to mitigate the risk of decision-making mistakes.

A mathematical review to AHP (including the data validation process based on C.R. and the determination of the weights) is provided in the subsequent subsection. Readers who are familiar with this method can skip this subsection.

3.1 A Review to AHP's Mathematical Process

In this subsection, the data validation method used based on the pairwise comparison matrix data and the determination of the SAF weights in AHP are introduced. First, the survey process of AHP compared n SAFs pair-wisely. Each of the results is the relative importance between the i-th and j-th SAFs, which can be connoted as: m_{ij}. The matrix $M = \left(m_{ij}\right)$ is the comparison matrix obtained by comparing the n SAFs pair-wisely.

By calculating the eigenvector and finding the maximum eigenvalue $\lambda_{\max}$, they are then used to evaluate whether the respondents' judgments on the pairwise comparison matrix are inconsistent, according to the following equations:

$$v_i = (\sum_{j=1}^{n} w_j m_{ij})/w_i, \text{ for all } i = 1, 2, \ldots, n \quad (1\text{-}1)$$

$$\lambda_{\max} = \frac{\sum_{i=1}^{n} v_i}{n} \quad (1\text{-}2)$$

$$C.I. = \frac{\lambda_{\max} - n}{n} \quad (2)$$

$$C.R. = \frac{C.I.}{\text{R.I.}} \quad (3)$$

where n is the number of criteria for the given decision context; the weight for the i-th criterion, w_i, has been assessed according to a known method (e.g., the following Eqs. (4)-(7)); v_i is the temporary eigenvector element used for calculating the eigenvalue, $\lambda_{\max}$; *C.I.* is the consistency index for M as can be evaluated based on $\lambda_{\max}$ and n; C.R. is the final result which is the consistency ratio that is used to assess the consistency in the pairwise relationships as revealed in M; however, the necessary denominator of Eq. (3), which is the R.I. value, is a value determined (and can be looked up in Table 1) by the dimension of square matrix, which is M; the matrix elements, m_{ij}, are the source data in matrix M, as defined previously.

Table 1. The random index (R.I.)

n	1	2	3	4	5	6	7	8
R.I.	0	0	0.58	0.9	1.12	1.24	1.32	1.41

As can be seen, when the respondent's judgment in the pairwise comparison matrix is not consistent, the values

in *M* will produce a larger value of λ_{max}. Then, the consistency index (C.I.) grows larger. So when C.I. is further divided R.I., which is the Random Index (R.I.) that can be looked up in the Table 1, the C.R. ratio will exceed the threshold that is set in the decision context (e.g., 0.2 in our study). The entire consistency analysis process presented here, which validates the source data for AHP, was proposed and proved by Saaty [7].

Second, the criterion weight vector (CWV) of the factors can be obtained, so it is possible to judge the relative importance of them by prioritizing them [8] [3]. Following from the matrix $M=\left(m_{ij}\right)$, which is the source pairwise comparison matrix that has passed the above consistency check, *M* is expanded as the following:

$$M = \begin{bmatrix} m_{11}=1 & \cdots & m_{1n} \\ \vdots & \ddots & \vdots \\ m_{n1} & \cdots & m_{nn}=1 \end{bmatrix} \quad (4)$$

The column-sums vector, *V*, of the matrix *M* is thus:

$$V = [\sum_{i=1}^{n} m_{i1} \quad \sum_{i=1}^{n} m_{i2} \cdots \sum_{i=1}^{n} m_{in}] \quad (5)$$

Dividing the elements in matrix *M* by the column-sums vector, *V*, another square matrix, *M'*, is obtained, as:

$$M' = \begin{bmatrix} m'_{11}=1/\sum_{i=1}^{n} m_{i1} & \cdots & m'_{1n}=m_{1n}/\sum_{i=1}^{n} m_{in} \\ \vdots & \ddots & \vdots \\ m'_{n1}=m_{n1}/\sum_{i=1}^{n} m_{i1} & \cdots & m'_{nn}=m_{nn}/\sum_{i=1}^{n} m_{in} \end{bmatrix} \quad (6)$$

So the row-sums vector of *M* is exactly the CWV:

$$CWV = \left[\sum_{j=1}^{n} m'_{1j} \quad \sum_{j=2}^{n} m'_{2j} \cdots \sum_{j=n}^{n} m'_{nj}\right]^{T} \quad (7)$$

The main results that are further analysed in the next section are assessed using the abovementioned mathematical process.

4 Results and Discussion

As discussed in Section 3, the questionnaire that was filled out by the DM in the second interview round passed the consistency check (i.e., the CR values of the five pairwise comparison matrices, 0.0975, 0.1805, 0.0884,0.186 and 0.0574, were all less than 0.2). In the first round of interview, because the number of SAFs w.r.t. each construct was close to 7 (i.e., human's psychological limit to make pairwise comparisons over items [10]), the difficulty of filling in the questionnaire increased and led to logical errors by the interviewees.

As shown in the Figure 4, we conclude that the DM believed that a construction firm needs to address the matters about the execution of a BIM project (43.19%) and the organisational factors (38.01%) that may influence the deployment of BIM technologies. The various aspects about the system integration (SI) matters of BIM and the BIM functions that are used can be placed in a secondary position (i.e., 14.68% and 4.13%, respectively).

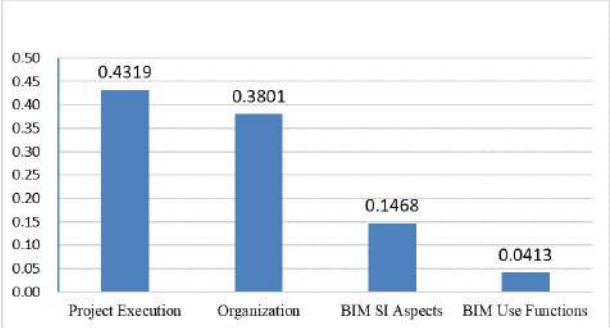

Figure 4. Relative importance of the constructs for BIM system/technologies adoption decision in a construction firm

As shown in Figure 5 to Figure 8, the SAFs for the BIM adoption decision w.r.t. the four constructs are visualised, while their ranks are also sorted according to their relative importance.

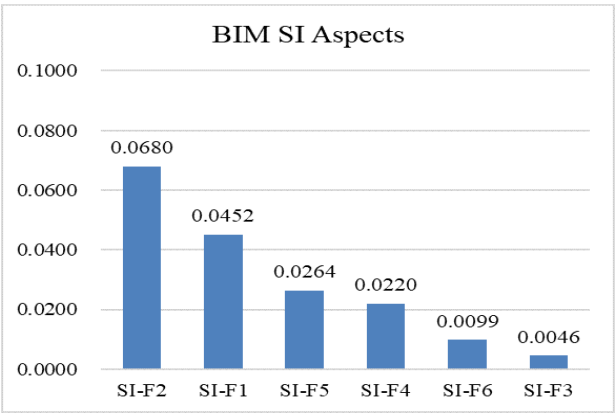

Figure 5. The weights of SAFs w.r.t the 'BIM SI' construct

The top three SAFs w.r.t the constructs are easily observed in these figures. These SAFs are not only the major factors which should be put into consideration when a construct is solely addressed during the introduction of BIM, but also the topics worthy of note in this study.

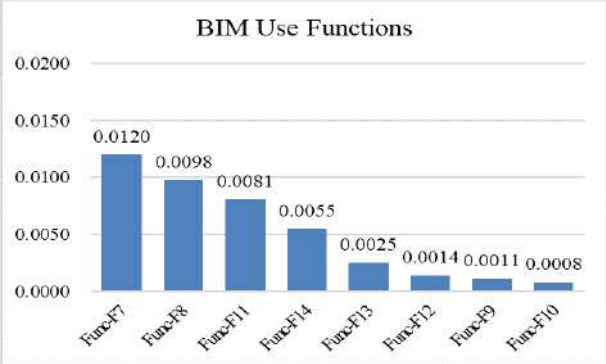

Figure 6. The weights of SAFs w.r.t. the 'BIM use functions' construct

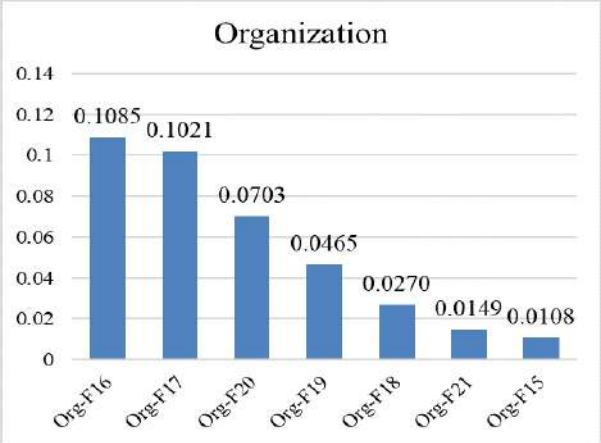

Figure 7. The weights of SAFs w.r.t. the 'organization' construct

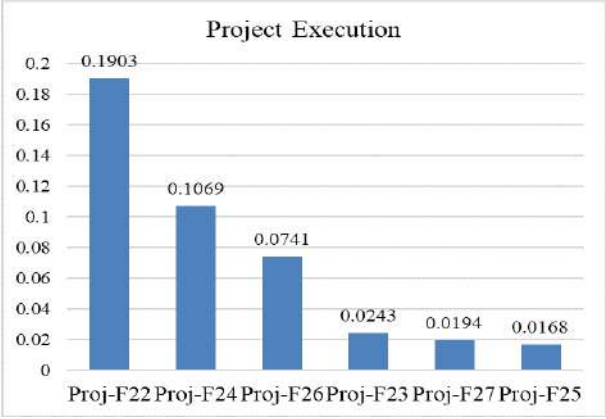

Figure 8. The weights of SAFs w.r.t. the 'project execution' construct

For example, according to the analysis, it is clearly understood that the DM believes that the three most important SAFs w.r.t. the 'BIM SI aspects' construct are the 'efficiency of BIM technology', 'software functions', and 'maintenance and upgrade costs'.

Since there are still other interesting observations which can be made for the 'top three SAFs' w.r.t. other constructs in these figures, relevant discussions are omitted here because of the space reason.

Another significant observation can also be made based on the absolute weights, rather than on the relative weights. For this sake, all of the 27 SAFs that have been confirmed using the Delphi Method are sorted and ranked all together in Table 2. Figure 9 provides a visualisation for Table 2.

It can thus be found that the top five SAFs with the highest absolute weight values are 'Proj-F22', 'Org-F16', 'Proj-F24', 'Org-F17' and 'Proj-F26' (i.e, definition of BIM project objectives and applications, supports from the top management, specification of BIM project milestones and deliverables, whether the design creates and fits business value and purpose, and finally, the BIM project management matters).

Table 2. Weight rankings for all factors

Ranking	SAFs	Weights
1	Proj-F22	0.1903
2	Org-F16	0.1085
3	Proj-F24	0.1069
4	Org-F17	0.1021
5	Proj-F26	0.0741
6	Org-F20	0.0703
7	SI-F4	0.0499
8	SI-F5	0.0465
9	SI-F2	0.0387
10	Org-F18	0.0270
11	Proj-F23	0.0243
12	SI-F1	0.0236
13	Proj-F27	0.0194
14	SI-F3	0.0186
15	Proj-F24	0.0168
16	Org-F21	0.0149
17	Func-F7	0.0120
18	SI-F5	0.0118
19	Org-F15	0.0108
20	Func-F8	0.0098
21	Func-F11	0.0081
22	Func-F14	0.0055
23	SI-F6	0.0041
24	Func-F13	0.0025
25	Func-F12	0.0014
26	Func-F9	0.0011
27	Func-F10	0.0008
Total		1.0000

In other words, the DM believes that these five SAFs play a role of impact when a decision for BIM adoption is made by the construction firms. This is the key knowledge that is discovered by this study: construction

firms should give priority to these five SAFs. When introducing a BIM system or relevant BIM technologies. The results as mentioned above are also verified and confirmed by another expert in the construction industry (than the interviewed DM during AHP investigation or the experts selected for confirming the SAFs set and the decision hierarchy during the use of the Delphi method). In this sense, in this study, works for data validation have been performed not only for the dataset itself (i.e., the C.R.-based consistency analysis), but also for the various empirical aspects from the results.

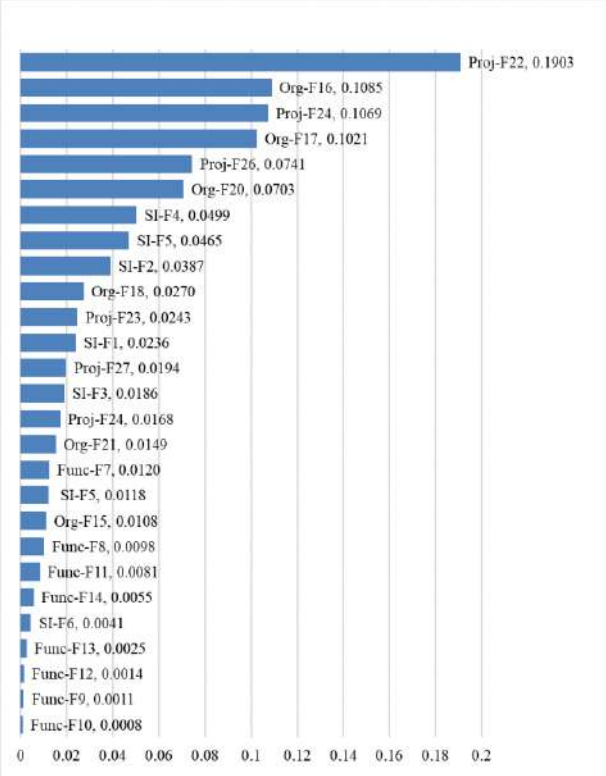

Figure 9. Prioritising the absolute weights of all SAFs

5 Conclusion

This study identified the key SAFs for the adoption of relevant BIM system and technologies and examined the relative importance of them. The initial set of SAFs deemed as important by the authors through literature study is further modified and confirmed by the expert in the construction domain of AEC, using the Delphi Method. In other words, the obtained set of the 27 SAFs consists of the major factors that are to be considered for the adoption of BIM. Given the thoroughness of the original literature review process (see also the reviewed articles [13-25]), this knowledge (i.e., the identified and confirmed set of SAFs) is important for construction firms whenever one such BIM-adoption decision is to be made.

In order to conduct the research for the influence of each SAF on the BIM-adoption decision systematically, a decision hierarchy which introduces an additional layer of constructs and organises the SAFs in a suitable manner is developed and further confirmed by also using the Delphi Method. Such knowledge (i.e., the decision hierarchy) is also a significant sub-product of this study.

The importance of the constructs and the SAFs is then assessed using AHP. The relative importance of each construct w.r.t. the total BIM-adoption decision goal is assessed and ranked. The relative importance of each SAF w.r.t. the construct on which it is mounted is also assessed and ranked. The absolute weight of each SAF is further calculated, and all absolute weights are ranked so that the relation (i.e., the absolute priority) among these SAFs is observed. These have formed another important set of knowledge for BIM-adoption in that the weights are quantitatively assessed. Since preference relations among the SAFs have been easily ordered, some interesting observations are made and the practical implications for the adoption of BIM or the decision to adopt BIM are drawn. For example, from the analysis of this study it is understood that the DM believes the most critical constructs for BIM adoption/introduction include the project execution factors and the organisational factors, which are closely related to the support from the top management. For another example, through the final absolute ranking analysis, it is understood that among the 27 SAFs, the (top five) most influential factors that may affect the expected success of BIM adoption/deployment are the objective of the BIM project, BIM project milestones, BIM project management, and whether BIM can create enterprise value and competitive advantage are important SAFs. These factors form a set of empirical knowledge which can serve as a reference for construction firms in deciding whether to deploy BIM technology or how to implement a BIM project more successfully.

Despite the fact that the results from this study are subject to the interviewee (i.e., a DM of a construction firm in Taiwan) during AHP investigations, the research framework can be generalised to surveys in other AEC domains (e.g., architecture and engineering) and/or in other countries. Not only the survey works themselves but also the possible comparisons that can be made based on the future available data across the nations would draw further more fruitful yet more insightful implications for

the whole civil engineering industry.

Moreover, despite the fact that the study has successfully identified a set of SAFs which a construction firm may think important for the 'successful deployment' of BIM, in the opposite sense, these results can also be used to understand the reasons for why there is 'reluctance' for BIM adoption, which is a fact that is often observed in the industry (to the authors' knowledge). This is also another future knowledge discovery topic worth of exploration.

Finally, given the confident results in this study, more in-depth future researches can also be expected. For example, the number of interviewees may be increased so the knowledge can be explored on a group basis, while the group/subgroup analytical methods can be introduced [2] [3], as the group-based mind-mining process [11] is a focused cognitive topic in the recent development of data-driven decision-making (DDM, or D^3M) [12]. In this sense, this study is a pilot work for subsequent studies which pertain to the decision of BIM system adoption.

References

[1] Chen K. Y. Strategic decision making framework for organisational BIM implementation. Cardiff School of Engineering, Cardiff, Wales, UK, 2015.

[2] Chi L.-P., Zhuang Z.-Y., Fu C.-H. and Huang J.-H. A knowledge discovery education framework targeting the effective budget use and opinion explorations in designing specific high cost product. *Sustainability*, 10(8): 2742, 2017.

[3] Chi L.-P., Fu C.-H., Zhuang Z.-Y., Chyng J.-P., Zhuang Z.-Y. and Huang J.-H. A post-training study on the budgeting criteria set and priority for MALE UAS design. *Sustainability*, in press, 2019.

[4] Badrinath A. C. An empirical approach to define success for BIM projects. *Doctoral Dissertation*, National Taiwan University, 2018.

[5] Tsai M.-H., Mom M. and Hsieh S.-H. Developing critical success factors for the assessment of BIM technology adoption: part I methodology and survey. *Journal of the Chinese Institute of Engineers*, 37(7): 845-858, 2014.

[6] Mom M., Tsai M. H. and Hsieh S. H. Developing critical success factors for the assessment of BIM technology adoption: part II analysis and results. *Journal of the Chinese Institute of Engineers*, 37(7): 859-868, 2014.

[7] Saaty T. L. Decision-making with the AHP: Why is the principal eigenvector necessary. *European Journal of Operational Research*, 145: 85-91, 2003.

[8] Zhuang Z.-Y. Chiang I.-J. Su C.-R and Chen C.-Y. Modelling the decision of paper shredder selection using analytic hierarchy process and graph theory and matrix approach. *Advances in Mechanical Engineering*, 9(12), 2017.

[9] Schmidt K., Babac A. Pauer F. and Damm K. Measuring patients' priorities using the Analytic Hierarchy Process (AHP) in comparison with Best-Worst-Scaling and rating cards: methodological aspects and ranking tasks. *Health Economics Review*, 6(1), 2016.

[10] Miller G. A. The magical number seven, plus or minus two: Some limits on our capacity for processing information. *Psychological Review*. 63(2): 81-97.

[11] Zhuang Z.-Y., Su C.-R. and Chang S.-C. The effectiveness of IF-MADM (intuitionistic-fuzzy multi-attribute decision-making) for group decisions: methods and an empirical assessment for the selection of a senior centre. *Technological and Economic Development of Economy*, 25(2): 322-364, 2019.

[12] Zhuang Z.-Y., Lin C.-C., Chen C.-Y. and Su C.-R. Rank-based comparative research flow benchmarking the effectiveness of AHP–GTMA on aiding decisions of shredder selection by reference to AHP–TOPSIS. *Applied Sciences*, 8(10): 1974, 2018.

[13] Lu Y. J., Wu Z. L., Chang R. D. and Li Y. K. Building Information Modeling (BIM) for green buildings: A critical review and future directions. *Automation in Construction*, 83: 134-148, 2017.

[14] Habibi S. The promise of BIM for improving building performance. *Energy and Buildings*, 153: 525-548, 2017.

[15] Song J. L., Migliaccio G. C., Wang G. B. and Lu H. Exploring the influence of system quality, information quality, and external service on BIM user satisfaction. *Journal of Management in Engineering*, 33(6), 2017.

[16] Wang T. K., Zhang Q., Chong H. Y. and Wang X. Y. Integrated supplier selection framework in a resilient construction supply Chain: An approach via Analytic Hierarchy Process (AHP) and grey relational analysis (GRA). *Sustainability*, 9(2):1-26, 2017.

[17] Won J. and Lee G. How to tell if a BIM project is successful: A goal-driven approach. *Automation in Construction*, 69: 34-43, 2016.

[18] Bryde D., Broquetas M. and Volm J. M. The project benefits of Building Information Modelling (BIM) International. *Journal of Project Management,*

31(7): 971-980, 2013.

[19] Xu H., Feng J. C. and Li S. D. Users-orientated evaluation of building information model in the Chinese construction industry. *Automation in Construction*, 39: 32-46, 2014.

[20] Barry G., Daniel H and Paula B. Does size matter? experiences and perspectives of BIM implementation from large and SME construction contractors. *In: 1st UK Academic Conference on Building Information Management (BIM)*, Northumbria University, Newcastle upon Tyne, UK, 2012.

[21] Barlish K. and Sullivan K. How to measure the benefits of BIM - A case study approach. *Automation in Construction*, 24: 149-159, 2012.

[22] Arayici Y., Coates P., Koskela L., Kagioglou M., Usher C. and O'Reilly K. Technology adoption in the BIM implementation for lean architectural practice. *Automation in Construction*, 20(2): 189-195, 2011.

[23] Azhar S. Building Information Modeling (BIM): Trends, benefits, risks, and challenges for the AEC industry. *Leadership and Management in Engineering*, 11(3), 241–252, 2011.

[24] Gu N. and London K. Understanding and facilitating BIM adoption in the AEC industry. *Automation in Construction*, 19(8): 988-999, 2010.

[25] Guillermo A. M., John C. and Agustin C. Building information modelling demystified: does it makebusiness sense to adopt BIM? *International Journal of Managing Projects in Business reviewer*, 2(3):419-434, 2009.

3D Modeling Approach of Building Construction based on Point Cloud Data Using LiDAR

B. Oh[a], Minju Kim[a], C. Lee[a], H. Cho[a], K.-I. Kang[a]

[a] School of Civil, Environmental, and Architectural Engineering, Korea University, Republic of Korea
E-mail: piuforte@korea.ac.kr, minju830@korea.ac.kr, e.chanwoo93@gmail.com, hhcho@korea.ac.kr, kikang@korea.ac.kr

Abstract –

LiDAR (Light Detection and Ranging) emerges as a mapping technology that provides fast, accurate, and reliable data with geometric representation of construction facilities. The technology has received high recognition especially since the importance of digital transformation in construction projects has been emphasized. However, the current state of 3D technologies including LiDAR encounters difficulty in recognizing and extracting accurate information on the as-built status of the buildings and construction sites. As a preliminary study for the development of a 3D architectural geometric representation of building and environment, this paper proposes a 3D modeling approach based on point cloud data obtained by LiDAR technology. This paper suggests a novel method for data acquisition on as-built status of construction sites and buildings during construction-operation phases. Furthermore, a field test has been performed for visualizing and modeling of the indoors of a residential house. The results of this paper are expected to inaugurate adaptation of LiDAR technology during the as-built process, and further implementation of digital technology after construction phase in construction projects.

Keywords –

LiDAR; 3D modeling; building construction; digital transformation; point cloud data

1 Introduction

The construction industry is no exception from the changes derived by the fourth industrial revolution [1, 2]. Despite the innate conservative responses of the construction industry to rapid changes, the importance of adopting digital transformation throughout the entire cycle of a construction project has long been emphasized [3]. In particular, the recent trends of applying BIM (Building Information Modeling) and AR/VR (Augmented/ Virtual Reality) technologies have triggered various efforts to revolutionize the productivity and efficiency of construction projects [4].

Meanwhile, several concerns have arose pointing out that the digital technology of the construction industry is mainly applied to the design stage [5, 6]. The main reason is that there exists technical limitations in recognizing multiple objects as separate entities in the interior buildings and external sites during construction and operation phases [7]. Thus, the current state of technologies encounters difficulty in recognizing and extracting accurate information on the as-built status of the facility and sites [8]. As the acquisition of as-built information of buildings is operated manually, digital gaps are occurring during the design phase and construction-operation phase [9]. In order to minimize the processing time of data handling and translation error of as-built data, it is necessary to upgrade the current state of digital technology adopted after the construction phase.

Therefore, as a preliminary study, this paper proposes a conceptual framework for the development of a three-dimensional architectural geometric representation of building construction after the design phase. The final and eventual output of the approach proposed in this study is an integrated platform of buildings and sites, of which the information on the exterior is acquired by using UAV (Unmanned Aerial Vehicle) and the interior by using LiDAR (Light Detection and Ranging). Considering the research process for deriving the final output, this paper focuses on suggesting a novel approach for data acquisition and processing of as-built status of the building using LiDAR technology.

What follows is an extensive literature review on the current state of related technologies, introduction on conceptual framework for 3D modeling based on the point cloud data obtained by LiDAR, applicability of the proposed method, and discussions.

2 Literature Review

There is no denying on the fact that digitalization in the construction industry has erupted a revolution in productivity of construction activities [10]. According to a survey, 93% of the construction industry players have

agreed that digitalization will affect every process [10, 11]. Thus, there is no lack of studies on exploration of digital technologies for application in construction projects.

2.1 LiDAR in construction phase

Regarding the usage of LiDAR as 3D laser scanner that transmits optical laser light in pulses delivers accurate real-time 3D data, most research has primarily focused on acquiring geo-spatial information [12, 13, 14]. High-precision numerical maps of forest areas and steeply sloping roads were created based on the data acquired by LiDAR, and the displacement of the slopes was determined based on numerical maps [14]. A method to automatically extract the 2D outline of a building by merging numerical aerial photographs and LIDAR data has been developed. LiDAR technology is also adopted for semi-automatically construction 2D and 3D indoor GIS maps based on point cloud data [15].

Most, if not all of those studies have focused on extracting the structure boundary of a building or roads while excluding non-structure or any spherical and curves [16, 17]. Even though few studies have attempted to apply LiDAR and point cloud technology in the construction industry, barely any research has suggested an approach for acquiring both indoor and outdoor 3D modeling information of a building. An algorithm for independent recognition and data acquisition of multiple objects with free forms – with lines, spheres, and curves – needs to be developed in order to visualize a full indoor 3D model of a building. Insofar, however, algorithms such as Douglas Peucker have been utilized mostly for extraction of boundary lines [18]. There has been hesitant implementation of digital technologies on building sites or built facilities, especially on the interior of a space with multiple objects to be recognized. This insinuates that the construction industry needs to catch up even on the building interior and sites.

2.2 3D modeling in building construction

The potential of integrating LiDAR with Building Information Modeling (BIM) for 3D modeling has been highlighted in few studies. A framework on the level of details on modeling of a building in BIM regenerated through reverse engineering has been proposed [19]. Furthermore, a semi-automatic three-dimensional modeling has been performed by dividing point cloud data into grids and extracting outlines [20]. Nevertheless, application of BIM is recognized as 'digital planning', insinuating that the technology is first utilized during pre-design and design phases. The data acquired during the two phases does not flow easily to construction and operation phases.

Considering the application of LiDAR and point cloud technology in construction projects, few research has aimed to promote reverse highly effective and efficient reverse engineering in construction industry [21, 22].

Reverse engineering, as the process of recreating the current state of information of a part without detailed information (drawings, bill of materials, required parts specification, engineering data), is mostly applied for detection and comparison between a CAD/BIM model created during pre-construction phase and as-built model created during and after construction phase [23]. Creation of an as-built model follows the process depicted on Figure 1.

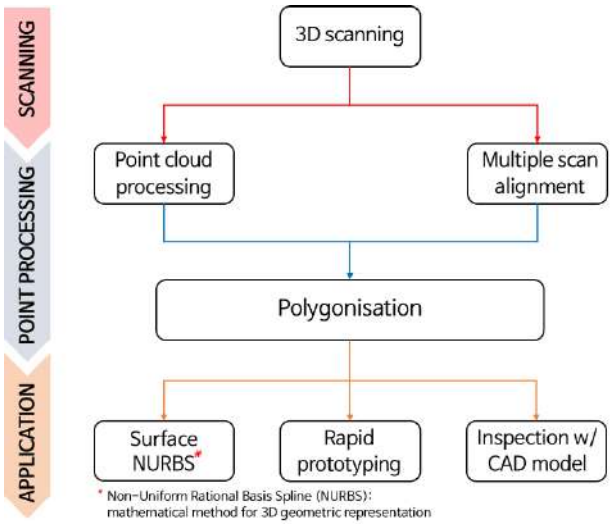

Figure 1. Process of data acquisition by LiDAR & application for reverse engineering

A three-dimensional scanning operation is performed, and then the point cloud data acquired through scanning is processed. In the case of scanning multiple targets, the merging operation of the data proceeds. After the merging work is finished, the polygonised work is applied for surface model creation, inspection with CAD model, and rapid prototyping. Throughout this process, the key element of successfully recognizing each of the multiple objects detected on the scene of scanning is developing a visualization algorithm. However, three-dimensional visualization algorithms related to construction industry are recognized as simple tools for data processing of scanning method, and the scope of application is mostly limited to earthwork construction. Most of the 3D visualization algorithms are optimized for other industries rather than the construction industry. To acquire accurate data and information on multiple objects, including structures and movable attachments, a new processing technique involving algorithms of segmenting and outlining the point cloud data are required.

3 Conceptual framework of 3D modeling approach based on LiDAR technology

As previously stated, an approach that registers, analyzes, and creates 3D models based on point cloud data delivers a reasonable source of digitalized information. To date, few studies have attempted to apply LiDAR and point cloud technology in the construction industry, but barely any research has suggested an exquisite method for acquiring 3D model of building interior with detailed information on the structure and non-structures. The current state of algorithm for visualizing data acquired as point clouds is processed for registration and surface creation. The surfaces and boundaries created by alignment of point clouds are extracted as structures of a building or infrastructure. However, a visualization algorithm that can register multiple objects independently from each other and define both the structures as well as non-structures and movable attachments is crucial for 3D modeling of an interior.

The conceptual framework of a 3D modeling approach created by point cloud data acquired by LiDAR is depicted on Figure 2.

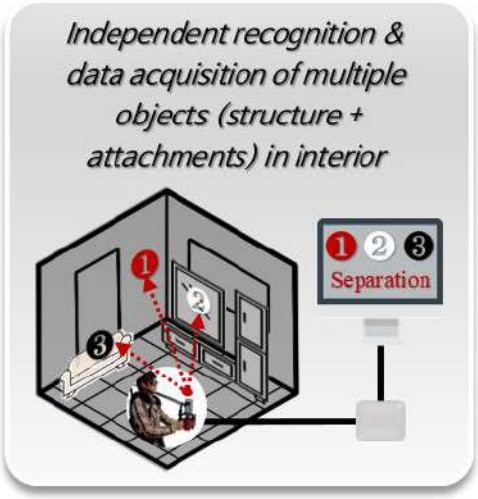

Figure 2. Conceptual approach for data acquisition

The process for ultimate modeling of building interiors based on point cloud data is defined as the following (Figure 3):

1. Data acquisition through LiDAR: 3D scanning of the interior
2. Data processing: Registration of point cloud data & segmentation by RANSAC(Random & Sampling Consensus) method, outline tracing by removing outliers & noise, surface creation based on region growing method, and input of algorithm for detection & separation of movable attachments from structures
3. Data integration & Application: Visualize the results by integrating with image processing technology, and create 3D model

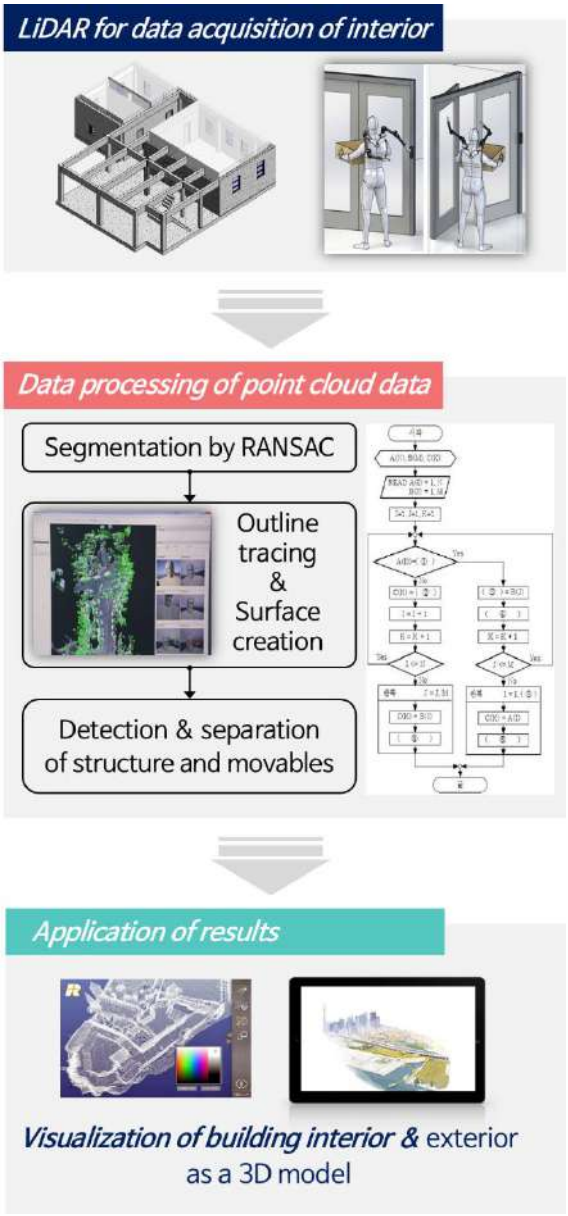

Figure 3. Process for 3D modeling based on point cloud data retrieved by LiDAR

The algorithm for segmenting the point cloud data and visualize them as three-dimensional is primarily based on RANSAC method. RANSAC is an iterative method for estimating parameters of a target model from a set of data. RANSAC is used to identify points that belong to identical planar planes from a cloud of data. Unlike the least square method, which uses all the data to

estimate the parameters of the model, RANSAC includes the process of excluding the outliers based on the hypothesis and test evaluations. The outliers are removed based on SOR (Statistical Outlier Removal) algorithm.

A sample (P) with a predetermined certain range is acquired from the entire point cloud data, and then a minimum number of data (S) is selected for estimating the parameter (θ). The model (M) is determined by the function (f_m) and parameter (θ). Considering the two equations (Eq. 1, 2) for segregating the inliers from a certain threshold (δ), the Consensus Set (CS) with outliers excluded is defined as Eq. 3.

$$P = \{d \in R^2 \mid d_1, \dots, d_n\} \quad (1)$$

$$M = \{s_n \in P \mid f_m(s_n; \theta) = 0\} \quad (2)$$

$$S(\theta) = \{d \in D \mid e(d, M) \leq \delta \quad (3)$$

The process of segmentation for exclusion of outliers from inliers is depicted on Figure 4. Among a total of 50 points (P), three points (S) are randomly selected and aligned on a surface plane. Blue points are segregated as inliers within the threshold, while green points are considered as outliers and thus eliminated.

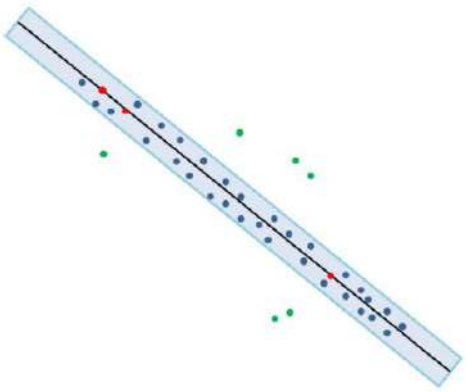

Figure 4. Process of eliminating outliers from RANSAC [20]

Point cloud data is projected under a refinement grid to verify validity for further outline tracing. During the process for outline tracing, the point cloud data is converted into a binary image using a grid as in the refinement process, and the outline is further extracted using the vectorization technique. The size of the refinement grid can be set differently according to the characteristics of the indoor environment. A cluster of planes are constructed, which results in the formulation of boundaries within 2D and 3D drawings.

When the outline extraction process ends, the binary image is inverted to extract the outline of an empty area in a segment area for visualization of the surface. At this time, the outline extraction is performed only for an empty space having an area larger than a predetermined size, and the extracted outlines are recorded in a file in the form of VRML (Virtual Reality Modeling Language). Afterwards, the point cloud data is visualized based on ICP (Iterative Closest Point) algorithm, resulting in the independent recognition of boundary structure and non-structures (movable attachments such as furniture in the interior of a building space). After the data processing phase is completed, a 3D model that provides a comprehensive information on the interior of a building and its exterior.

4 Applicability test: Results & Analysis

A field test is performed to verify the validity of the approach proposed in this study. The test was conducted mainly to secure the reliability of data acquired and processed by LiDAR technology. The interior and exterior space of a deteriorated house with all furniture properly located at its place were scanned to construct an as-built model, of which the accuracy was verified by comparing with previously completed 2D drawings. The overview of the applicability test is depicted on Figure 5.

Location:	Donae-dong, Duckyang-gu, Goyang-si, Gyeonggi-do, Korea
Area of Measurement	Basement B1 (72.48 ㎡) 1st floor (133.68 ㎡) 2nd floor (66.06 ㎡)
Number of times scanned	4 times (2 interior, 1 interior + exterior, 1 exterior)
LiDAR used	Velodyne HDL-32E

Figure 5. Overview of applicability test

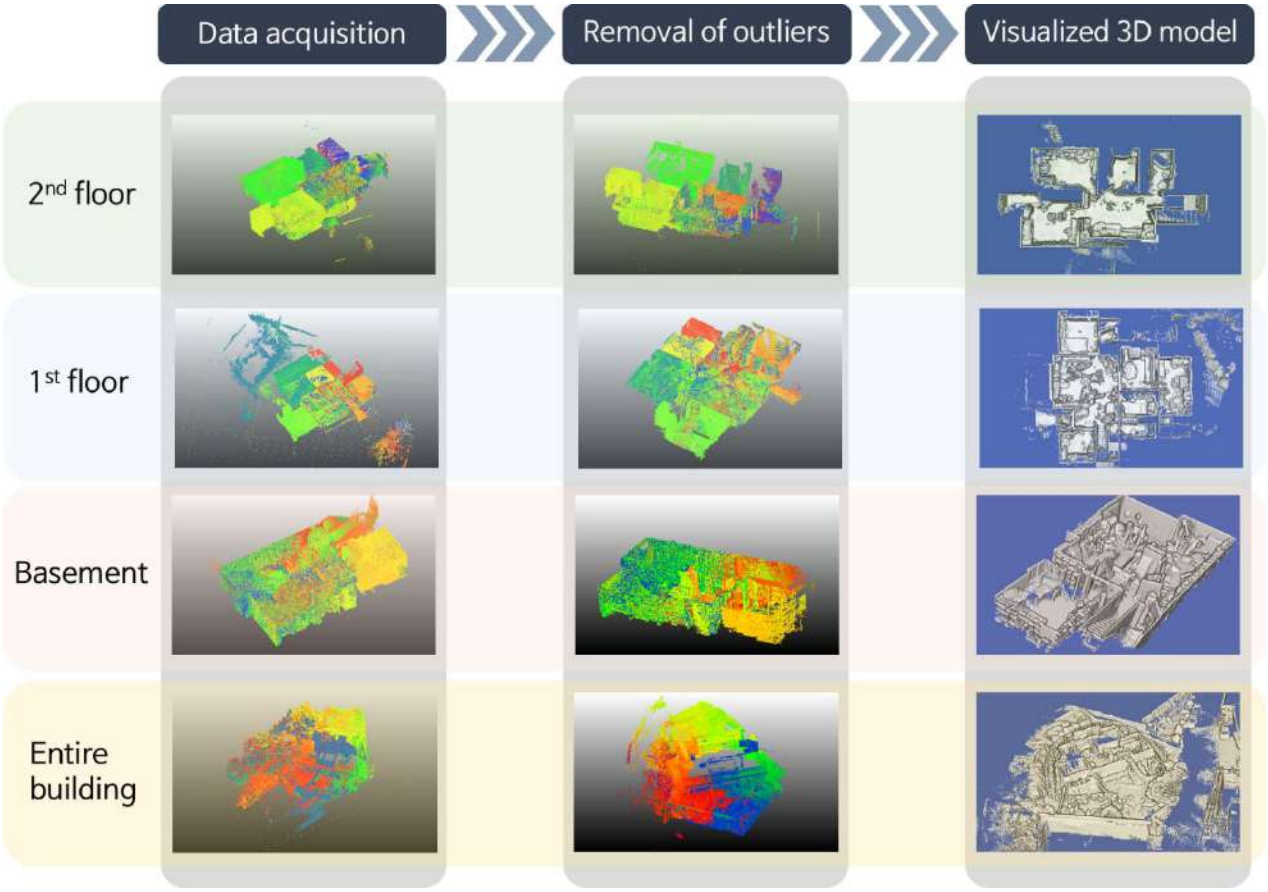

Figure 6. Results of data acquisition & processing, visualization as 3D model

The 3D scanner used for data acquisition is a backpack-type Velodyne HDL, a LiDAR scanner capable of scanning 700,000 points per second with the accuracy of 2 mm @ 200 m. The interior of the house was scanned twice; the interior was first measured from the basement to the second floor continuously at once, and then each floor was scanned separately at the second time. Also, after scanning the living room on ground floor, the scanner was moved continuously to the outside to measure the exterior. Finally, the exterior of the house, including woods, garage, and garden, was scanned. The LiDAR scanner was connected to a laptop, and thus all acquired data was accumulated on the software (Cloud Compare). Cloud Compare was used also as the software for data processing of point cloud data. As previously stated, SOR algorithm was applied within the Cloud Compare software to remove outliers, and then the processed data was visualized using ICP algorithm.

The results of acquired and processed data are depicted on Figures 6. Even though the software and applied algorithms automatically was suitable for processing the point cloud data for 3D model, some parts of the acquired data inevitable had to be modified manually. For instance, there were seven people total who conducted the field test. Five people, apart from the one who scanned the scene with the scanner while moving around and the other who held the laptop connected to the LiDAR, tried to be out of sight on the scene but were caught on some of the point clouds that were obtained after the scan. The inspectors and some of the furniture that was overlapped in some points of the scan had to be removed from the model. Additional measure are expected to be taken in case of 3D scanning.

Meanwhile, the result of data acquired on structure boundaries and non-structures is depicted on Figure 7.

As depicted on Figure 7, structure parts such as staircase, wall, and window opening are visible. All the movable items are visualized as 3D, but not easily recognizable in the current state of technology. In other words, the current 3D model simply visualizes the figures of detected object elements in three dimensions. Further studies are needed to improve precision of data processed for separating movable objects from the wall and floor of the interior. More in-depth studies are also expected to be performed for independent recognition of multiple objects.

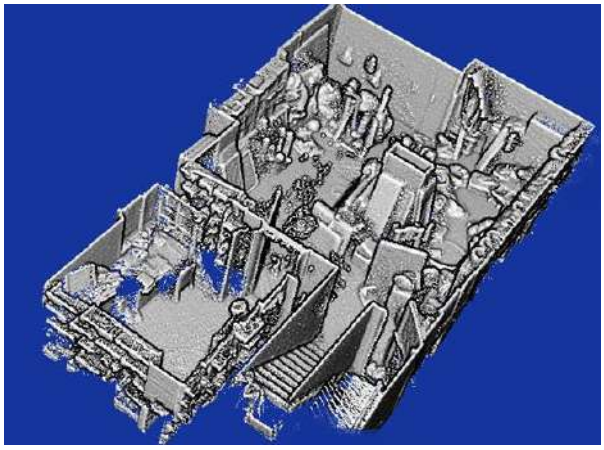

Figure 7. Scanned interior of basement

5 Conclusion

As-built data of buildings, both the exterior and interior, has been acquired manually by experts inspecting by hand using tools. However, the possibility of error arises in cases of field measurement on a manual basis, as well as the probability of safety accident occurrence. As a means to automate the data acquisition of as-built information and enhance productivity of previous work, this study proposed a novel approach for acquiring, translating, and applying as-built data retrieved under safe site conditions. The key issue of visualizing point cloud data collected by LiDAR in this study is related to the post-processing and removal of outliers for further integration with data retrieved by UAV. During this study, the outline of the building is derived through the horizontal layer division of point cloud dada based on the data acquired by LiDAR, all of which results in the creation of 3D drawings and models. In order to fully develop an automatic 3D visualization algorithm, it is necessary to consider the interference caused by the non-structure parts when setting the contour of the building. Nevertheless, the field test conducted in this study proved the possibility of adopting the novel approach in construction and operation phases.

The conceptual approach proposed in this study can provide an immediate 3D architectural geometric information visualization platform. Furthermore, the results of this study is expected to upgrade the current technology level by improving the speed and accuracy of as-built information of construction sites and buildings. Even though this paper does not address the application of UAV for measuring the exterior of buildings and the integration of retrieved data with those achieved from LiDAR, further study is expected to be conducted to visualize the conceptual framework addressed in this study.

Acknowledgment

This research was supported by the National Research Foundation of Korea (NRF) funded by the government (NSIP) (No. NRF-2018R2A4A1026027).

References

[1] A World Economic Forum. Shaping the Future of Construction: A Breakthrough in Mindset and Technology. Geneva: World Economic Forum. 2016.

[2] McKinsey Global Institute. Reinventing Construction – A Route to Higher Productivity. 2017.

[3] Fischer, M. From BIM to VDC to the Digitalization of, 2017.

[4] Woodhead, R., Stephenson, P. and Morrey, D. Digital construction: From point solutions to IoT ecosystem. Automation in Construction, 93: 35-46, 2018.

[5] Dai, Y., Gong, J., Li, Y. and Feng, Q. Building segmentation and outline extraction from UAV image-derived point clouds by a line growing algorithm. International Journal of Digital Earth, 10(11): 1077-1097. 2017.

[6] Gao, X. and Pishdad-Bozorgi, P. BIM-enabled facilities operation and maintenance: A review. Advanced Engineering Informatics, 39: 227-247, 2019

[7] Chen, J., Fang, Y., and Cho, Y. Performance evaluation of 3D descriptors for object recognition in construction applications. Automation in Construction, 86: 44-52, 2018.

[8] Shrestha, K. and Jeong, H. Computational algorithm to automate as-built schedule development using digital daily work reports. Automation in Construction, 84: 315-322, 2017.

[9] Garcia de Soto, B., Agusti-Jan, I., Hunhevicz, J., Joss, S., Graser, K., Habert, G. and Adey, B. Productivity of digital fabrication in construction: Cost and time analysis of a robotically built wall. Automation in Construction, 92: 297-311, 2018.

[10] Roland Berger Gmth, Digitalization in the construction industry, 2016.

[11] Meroschbrock, C. and Figueres-Munoz, A. Circumventing Obstacles in Digital Construction Design – A Workaround Theory Perspective, Procedia Economics and Finance, 21: 247-255, 2015.

[12] Choi, H. A study on high-precision digital map generation using ground LiDAR, The Korean Society of Industrial Application, 20(2), 125-132, 2017.

[13] Cho, H.S., Sohn, H.G., Park, H.K., and Kim, S.H.

A study for generation of facility drawing using terrestrial LiDAR, The Korean Society for Geo-Spatial Information System, 5: 73-74, 2013.
[14] Lee, I. 3D Boundary Extraction of a Building Using Terrestrial Laser Scanner. Journal of Korea Spatial Information Society, 15(1), 53-65, 2007.
[15] Feng, C., Xiao, Y., Willette, A., McGee, W. and Kamat, V. Vision guided autonomous robotic assembly and as-built scanning on unstructured construction sites. Automation in Construction, 59: 128-138, 2015.
[16] Choi, S.P., Cho, J.H., Kim, J.S. A filtering automatic technique of LiDAR data by multiple linear regression analysis. The Korean Society for Geo-Spatial Information System, 19(4), 109-118, 2011.
[17] Jung, S., Jang, H., Kim, Y., Cho, W. Automatic Building Extraction Using LIDAR and Aerial Image. The Korean Society for Geo-Spatial Information System, 13(3), 59-67, 2005.
[18] Roh, Y. An Automatic Extraction Algorithm of Structure Boundary from Terrestrial LIDAR data. Master's thesis, Kookmin University, 2008.
[19] Chae, J. and Lee, J. Definition of 3D Modeling Level of Detail in BIM Regeneration Through Reverse Engineering - Case Study on 3D Modeling Using Terrestrial LiDAR -. KIBIM Magazine, 7(4), 8-20, 2018.
[20] Hong, S.C., Jung, J.H., Kim, S.M., Hong, S.H., Heo, J., Semi-Automatic Method for Constructing 2D and 3D Indoor GIS Maps based on Point Clouds from Terrestrial LiDAR, The Korean Society for Geospatial Information System, 21(2), 99-105, 2013.
[21] Herraez, J., Carlos Martinez, J., Coll, E., Martin, M. and Rodriguez, J. 3D modeling by means of videogrammetry and laser scanners for reverse engineering. Measurement, 87: 216-227, 2016.
[22] Kwon, S. Strategy for applying of reverse engineering in construction industry. KIBIM Magazine, 5(3), 14-24, 2015.
[23] EU BIM Taskgroup. Handbook for the Introduction of Building Information Modeling by the European Public Sector. 2018.

New System Form Design Process Using QFD and TRIZ

C. Lee[a], D. Lee[a], H. Cho[a], and K.I. Kang[a]

[a]School of Civil, Environmental, and Architectural Engineering, Korea University, Republic of Korea
E-mail: changsu3005@korea.ac.kr, ldm1230@korea.ac.kr, hhcho@korea.ac.kr, kikang@korea.ac.kr

Abstract –

Current forms used in the construction site are faced with problems such as casting quality, increased labor costs and longer construction period. To solve these problems, a new system form that reflects the opinions of people who actually use it in the construction site. In this study, a new system form design process using Quality Function Deployment (QFD) and TRIZ method was proposed. It is expected that it will be possible to make an improved system form by providing a solution that combines the needs of form users and the technical elements.

Keywords –

System form; Concrete structure; Quality function deployment (QFD); TRIZ;

1 Introduction

Currently, with the buildings becoming larger and taller, reinforced concrete (RC) structures, which are advantageous in terms of usability and economics, have been increasing. Formwork is one of the most important types of reinforced concrete structure construction, accounting for 30 to 40 percent of structural construction costs and 10 percent of overall construction costs [1].

However, the form commonly used in formwork was developed approximately 40 years ago. As building construction become larger, there have been limitations such as increase of material loss rate, increase of input labor force, increase of labor cost, and defective concrete surface [2]. Therefore, it is necessary to develop a new form to solve the problem of existing forms.

Quality function deployment (QFD) is a systematic design support technique that has been used to improve the construction system [3]. The QFD method has great advantages for users because it not only translates customer requirements into technical characteristics, but also prioritizes characteristics. However, the QFD technique is accompanied by contradictory problems, and systematic analysis is needed to solve them.

A theory of creative problem solving (TRIZ) was developed to propose innovative solutions with numerous tools that enable a targeted and systematic problem-solving method [4]. Mayda and Borklu implemented a method using TRIZ to identify innovative concepts, then using QFD to meet customer's needs [5]. Hajime Yamashina et al. [5] integrated the QFD and TRIZ to analyze the customer needs by calculating the most needed technical factors and the weight of the factors. Lim et al. [3] proposed a system form design process using QFD and TRIZ. However, this was a system form design process that was limited to the table form used in skyscraper.

Therefore, this study proposed a system form design process commonly used in the construction site. The proposed system form design process reflects the needs of the customers who use the form in the field and converts them into technical characteristics. In addition, priorities of technical characteristics were determined and reflected by considering the relationship between technical characteristics.

2 Literature review

2.1 Quality function deployment

QFD is a tool used to improve product quality. It has been used successfully in assisting product developers systematically incorporate customer requirements (CRs) into engineering characteristics (ECs) to plan and manage product and process development [7]. From the interrelationships between CRs and ECs and the correlations between ECs, the main task of product planning using QFD is to determine target values of ECs to achieve higher overall customer satisfaction[8]. The House of Quality (HOQ) supports defining the relationship between CRs and ECs through comparison and analysis of data. Because of these advantages, HOQ is regarded as a QFD core element technology that reflects customer needs [9]. This is shown in Fig 1.

2.2 TRIZ

TRIZ was proposed by the Russian researcher Altshuller (1984), who was using it to solve "creative" problems, which usually have the features of paradoxical and conflicting demands [8]. TRIZ helps find

contradictions and find solutions to overcome those contradictions. In Table 1, TRIZ analyzes and summarizes 39 engineering features through the contradiction matrix, and Table 2 shows 40 innovative principles corresponding to the contradiction matrix [10].

2.3 Integration of QFD and TRIZ

QFD is a good tool to convert CRs into ECs. However, it has its limits. Applying the contradiction matrix through TRIZ to solve these limitations and provide various optimal solutions. In this study, the relationship between the results of technical characteristics and the contradiction matrix of TRIZ was as shown in Fig 2. Among the technical features derived through HOQ, technical features with negative correlation were derived and converted to 39 standard features. Repetition of this mechanism gave a reasonable understanding of the contradiction of technical features and also provided a systematic solution.

Table 1. Thirty-nine TRIZ Engineering features [10]

1. Weight of moving object	21. Power
2. Weight of stationary object	22. Loss of Energy
3. Length of moving object	23. Loss of substance
4. Length of stationary object	24. Loss of Information
5. Area of moving object	25. Loss of Time
6. Area of stationary object	26. Quantity of substance/the matter
7. Volume of moving object	27. Reliability
8. Volume of stationary object	28. Measurement accuracy
9. Speed	29. Manufacturing precision
10. Force	30. External harm affects the object
11. Stress or pressure	31. Object-generated harmful factors
12. Shape	32. Ease of manufacture
13. Stability of the object's composition	33. Ease of operation
14. Strength	34. Ease of repair
15. Duration of action by a moving object	35. Adaptability or versatility
16. Duration of action by a stationary object	36. Device complexity
17. Temperature	37. Difficulty of detecting and measuring
18. Illumination intensity	38. Extent of automation
19. Use of energy by moving object	39. Productivity
20. Use of energy by stationary object	

Table 2. Forty TRIZ innovative principles [10]

1. Segmentation	21. Hurrying
2. Separation	22. Blessing in disguise
3. Local quality	23. Feedback
4. Symmetry change	24. Intermediary
5. Merge	25. Self-service
6. Multi-functionality	26. Copying
7. Nested doll	27. Cheap disposables
8. Weight compensation	28. Mechanical interaction substitution
9. Preliminary counteraction	29. Pneumatics & hydraulics
10. Preliminary action	30. Flexible shells & thin film
11. Beforehand compensation	31. Porous materials
12. Equi-potentiality	32. Optical property changes
13. The other way around	33. Homogeneity
14. Curvature increase	34. Discarding & recovering
15. Dynamic parts	35. Parameter change
16. Partial or excessive actions	36. Phase transition
17. Dimensionality change	37. Thermal expansion
18. Mechanical vibration	38. Strong oxidants
19. Periodic action	39. Inert atmosphere
20. Continuity of useful action	40. Composite materials

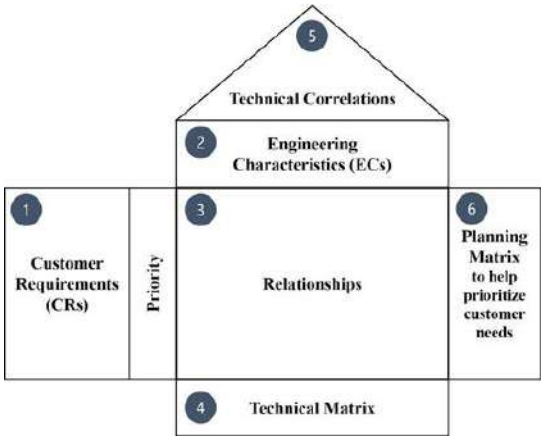

Figure 1. The House of Quality [7]

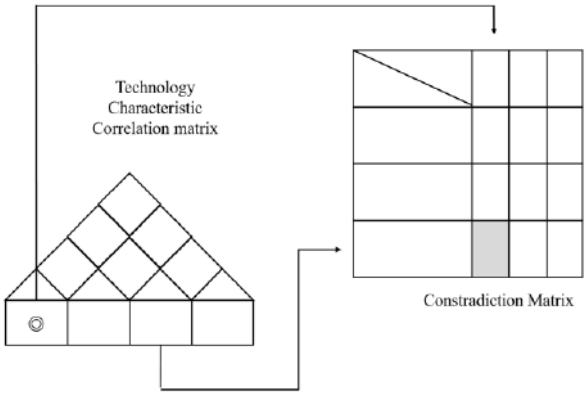

Figure 2. Mechansim of intergrating QFD and TRIZ

2.4 A case study using QFD and TRIZ

Franica et al. applied QFD and TRIZ to 3D PrinterCAD to provide innovative design methods and results in improved manufacturing processes [11].

Donnici et al. completed the QFD analysis of the hover board and suggested the solution principle to realize the hover board as urban transportation through the TRIZ method. This study demonstrated that the integration of QFD and TRIZ provides an innovative solution to the problem that has not been solved [12].

3 Proposal of Improvement System form using QFD and TRIZ

3.1 Conversion of CRs into TCs utilizing QFD

3.1.1 CRs Importance Calculation

Two interviews were conducted to derive the CRs. To collect objective CRs, the interviewees were designated as two high-rise building project directors, four formwork company presidents, and six formwork experts. The final 15 CRS were derived from the two interviews, which were as summarized in Tables 4. In order to calculate CRs significance, The IPA survey was conducted on 15 field managers in five major construction companies in Korea and 28 field workers with more than 10 years' experience. Finally, 35 surveys were completed and returned. The weighted priority of the system form CRs was determined through the IPA survey, and the overall significance related to CRs and design was classified by item. The figures from the IPA survey were translated into 100 points, which made it possible to sequence CRs importance. The three most important sequences were CR1: Easy assembly and disassembly, CR2: Reduced noise during dismantlement or assembly and disassembly, CR13: Compatible with existing formwork units. The remaining importance shown in Table4. 14 TCs was derived from the same experts and correlated them with CRs as seen in Table 3.

Table 3. Relationship between TCs and required quality

No.	Technical characteristic (TC)	Related required quality
TC1	Shape of outer frame	CR1, CR4, CR6, CR13, CR14, CR15
TC2	Weight	CR4, CR6
TC3	Size	CR1, CR4, CR13, CR14, CR15
TC4	Number of repeat uses	CR7, CR8, CR10
TC5	Shape of the inner structure	CR5, CR9, CR10
TC6	Assembly type	CR1, CR9, CR10
TC7	Installation method	CR1, CR2, CR4
TC8	Dismantlement method	CR1, CR2, CR4
TC9	Impact resistance	CR7, CR8, CR9, CR10
TC10	Allowable load	CR5, CR9
TC11	Material of panel	CR2. CR3, CR7, CR8, CR10, CR11
TC12	Material of frame	CR7, CR8, CR9, CR10
TC13	Lifting method	CR4
TC14	Structure of panel frame	CR2, CR10

3.1.2 Correlation Analysis between CRs and TCs

In this section, a correlation analysis was conducted between CRs and TCs previously classified. Correlation analysis was performed with the help of the same form developers. The degree of correlation between CRs and TCs was set to 1-low, 3-normal, 9-high. To give priority to the technical characteristics reflecting
the required quality, the absolute weight was first obtained. Absolute weight is the sum of the multiplying values of the importance index and the correlation coefficient as shown in equation (1). Equation (2) divided the absolute weight for each technical characteristic into the sum of the total absolute weight by obtaining the relative weight. The priority of each technical characteristic was judged through these two equations as shown quantitatively in Table 5.

$$\text{Absolute weight} = \sum \text{Importance Index} \times \text{Correlation coefficient} \quad (1)$$

$$\text{Relative weight} = \frac{\text{Absolute weight of technical charateristic}}{\sum \text{Absolute weights of technical characteristics}} \quad (2)$$

3.2 Required TCs Contradictions

The important required technical characteristics categorized above are contradictory to each other. To solve these contradictions, the technical characteristics that reflect the requirements were summarized as follows:

1. If the external factors (TC1, TC3) are changed to simplify the assembly and disassembly, contradictions arise in compatibility (TC6, TC7) with existing forms.

Table 4. CRs-Importance Index

No.	Category	Customer Requirement	Impor-tance Index	Rank
CR1	Constructability	Easy assembly and disassembly (it fits and fastens together with reasonable ease)	91.3	1
CR2		Reduced noise during dismantlement or assembly and disassembly	87.4	2
CR3		Easy removal from concrete	76.2	8
CR4		Efficient lifting and carrying	79.6	6
CR5	Safety	Not distorted or deflected during concrete placing	56.3	15
CR6		Reduced safety accident (struck by object)	57.7	13
CR7	Durability	High repeat use with constant module size	83.2	4
CR8		Recyclable material usage	61.4	12
CR9		Durable against falling and external impacts	64.2	10
CR10		Easy maintenance and cleaning	69.9	9
CR11	Reliability	Low thermal conductivity (low temperature sensitivity)	59.1	14
CR12		High concrete surface quality	78.8	7
CR13	Conformance	Compatible (size, height, fixing method) with existing formwork units (e.g., Euro form, Aluminum form, Skydeck)	86.7	3
CR14		Hybrid (concurrent usage) usage for vertical (wall and column) and horizontal (slab) forms	63.1	11
CR15		Provide various module sizes to minimize on-site work (filler, conventional formwork)	81.9	5

2. Changes to the base metal of the material to reduce noise (TC11, TC12) contradict the form performance (TC2, TC9, TC10).
3. Reducing the weight (TC2) for efficient operation and movement causes a contradiction in form performance (TC9, TC10).
4. Changing the fastening method to the bolt assembly (TC6) for the maintenance of the form contradict the form performance (TC9, TC10).
5. Changing the material (TC11) of the panel to improve the quality of the concrete casting contradicts the reuse rate (TC4).

3.3 Proposing a new System form using TRIZ

3.3.1 Conversion to TRIZ features

In order to present ideas using TRIZ, it was necessary to relate the technical contradictions derived above to standard features. Therefore, in this section technical contradictions that deteriorated were matched during the improvement process and standard features as shown in Table 6.

3.3.2 Apply contradiction matrix of TRIZ features

Apply contradiction matrix of TRIZ features. First, apply the contradictory standard features to the contradiction matrix and extract the intersecting items in Table 7. Next it was proposed in Table 8 with the general

Table 5. A calculation matrix for absolute & relative weights between TCs and CRs

CRs \ TCs		TC1	TC2	TC3	TC4	TC5	TC6	TC7	TC8	TC9	TC 10	TC 11	TC 12	TC 13	TC 14
CR1	91	9	9	9		9	9	9	9						3
CR2	87		9					9	9			9	9		3
CR3	76								3			9			
CR4	80	3	9	3		1		3						9	
CR5	56					3					9		9		
CR6	58	1	9	3				3	3						
CR7	83				9					9		9			
CR8	61				9							9			
CR9	64		3	1		3	9		3		9		9		3
CR10	70				9	3	9			9		9	3		3
CR11	59											9	3		
CR12	78											9			
CR13	87	9		9				3	3						3
CR14	63	1		3				3	3						
CR15	82	3		1				3	3						
Absolute weight		2207	3037	2349	1931	1473	2029	2715	2898	1378	1085	4644	2258	716	1199
Relative weight		7.38	10.15	7.85	6.45	4.92	6.78	9.08	9.69	4.61	3.63	15.52	7.55	2.39	4.01
Rank		7	2	5	9	10	8	4	3	11	13	1	6	14	12

Table 6. Conversion of Contradiction into TRIZ standard features

Contradiction	Improvement objects	Converted TRIZ features	Deteriorating objects	Converted TRIZ features
1	TC1, TC3	39. Productivity	TC6 TC7	35. Adaptability
2	TC11, TC12	31. Harmful side effects	TC2 TC10	13. Stability of object
3	TC2	39. Productivity	TC9 TC10	35. Adaptability
4	TC6	34. Repairability	TC9 TC10	14. Strength
5	TC11	27. Reliability	TC4	25. Loss of time

solutions and the improved approach to the contradictory standard feature corresponding to the intersection. Our study improved the general concrete form through the principle of contradiction matrix of TRIZ.

3.3.3 Proposal of improvement form

This study associated contradictions in the technical characteristics with standard features and applied them to the contradiction matrix to provide a systematic and logical solution to form improvement. As a solution, first, the problem of compatibility and size was solved with existing form by changing integrated form into assembly type. Second, the external frame, the inner frame, and the panel were separated to satisfy the requirements of each part, and the weight was reduced, thereby improving the working environment and improving the productivity. Third, with rubber material on the corners, the problem of damage due to impact was solved. Fourth, a very thin film was applied to the panel to facilitate detachment from concrete without using form oil. Finally, forms satisfying segmentation, composite materials, prior compensation, and flexible membranes/thin films were as shown in Table 9.

Table 7. Application of the principle of Invention of TRIZ

	2	13	14	32	25
6	–	–	–	40, 16	–
27	–	–	–	–	10, 30, 4
31	35, 22, 1, 39	–	–	–	–
34	–	2, 35	–	–	–
39	–	–	29, 28, 10, 18	–	–

Table 8. Ideal development based on general solutions of TRIZ

Contradiction	Invention principle	General solutions	Idea development
C1	1. Segmentation	Divide an object into independent parts Make an object sectional, easy to assemble/disassemble Increase the degree of fragmentation of segmentation	The form's frame could be divided into three main parts (inner, outer, and panel) to reduce the weight of forms, avoid usage of form oil, and also for ease of maintenance
C2	40. Composite materials	Change from uniform to composite (multiple) materials	Plastic-based noise-reducing materials(joint apparatus) are used
C3	40. Composite materials	Change from uniform to composite (multiple) materials	Lightweight composite material (aluminum and magnesium composite) frames could be used
C4	11. Prior compensation	Prepare emergency means beforehand to compensate for the relatively low reliability of an object	Rubber-based impact-reducing materials are used
C5	30. Flexible membranes/thin films	Use flexible shells and thin films instead of 3D structures Isolate the object from its external environment using flexible membranes	Very thin films are applied to avoid attachment of concrete

Table 9. Improvement solution according to the ideas

Idea	Improvement solution	
1. Segmentation	1	
40. Composite materials	2	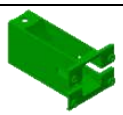
40. Composite materials	3	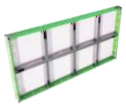
11. Prior compensation	4	
30. Flexible membranes/thin films	5	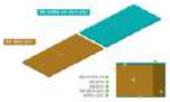

4 Conclusion

This study combined QFD and TRIZ to prioritize the technologies required by construction site system form users and to derive contradictions between their correlation and technical characteristics. It also used TRIZ contradictory metrics to provide solutions to those contradictions. The study proposed a systematic and logical system form design process that reflects the requirements of form users. The study is expected to solve the problem of compatibility with existing form by presenting the assembled form based on this system form design process. In addition, to solve the weight problem of existing form by separating external frame and panel and reducing weight. Furthermore, it will contribute to shortening the construction time, reducing the construction cost, noise and eco-friendly construction.

The systematic design process proposed in this study is expected to be applicable not only to form but also to other construction materials in construction sites. This will contribute to the reduction of the construction costs, shortening the construction time, and establishing a safe working environment.

In the future study, this process will be to make an optimal system form and conduct field test to verify form strength, concrete casting quality, noise reduction and productivity analysis. In addition, a satisfaction survey of the products produced from this study will be conducted to verify the validity of this study and conduct a complementary study of the form design process.

Acknowledgement

This research was supported by a grant (19AUDP-B106327-05) from the Architecture & Urban Development Research Program funded by the Ministry of Land, Infrastructure and Transport of the Korean Government.

References

[1] SHIN, Han-Woo, et al. A research on a comparison between the strength and weakness of each formwork methods in the core wall construction. *Journal of the Korea Institute of Building Construction*, 7.4: 153-159, 2007.

[2] LEE, Jun-hyuk. Improvement of System form using Advanced Composite Material(Doctoral thesis) . *Korea University, Seoul, Korea*, 2018

[3] LIM, Hyun-Su, et al. Design process for formwork system in tall building construction using quality function deployment and TRIZ. *Journal of the Architectural Institute of Korea Structure & Construction*, 28, 2012.

[4] TURSCH, Philipp; GOLDMANN, Christine; WOLL, Ralf. Integration of TRIZ into quality function deployment. *Management and Production Engineering Review*, 6.2: 56-62, 2015.

[5] MAYDA, Murat; BORKLU, Huseyin Riza. Development of an innovative conceptual design process by using Pahl and Beitz's systematic design, TRIZ and QFD. *Journal of Advanced Mechanical Design, Systems, and Manufacturing*, 8.3: JAMDSM0031-JAMDSM0031, 2014.

[6] YAMASHINA, Hajime; ITO, Takaaki; KAWADA, Hiroshi. Innovative product development process by integrating QFD and TRIZ. International Journal of Production Research, 40.5: 1031-1050, 2002.

[7] AKAO, Yoji; KING, Bob; MAZUR, Glenn H. *Quality function deployment: integrating customer requirements into product design*. Cambridge, MA: Productivity press, 1990.

[8] FUNG, Richard YK, et al. A fuzzy expected value-based goal programing model for product planning using quality function deployment. *Engineering Optimization*, 37.6: 633-645, 2005.

[9] LEE, Dong-min. Hybrid system formwork and AI based construction planning model for high-rise building construction(Doctoral thesis). *Korea University, Seoul, Korea*, 2019

[10] Altshuller, G. The innovation algorithm: TRIZ, systematic innovation and technical creativity. MA: Technical Innovation Center, 2000

[11] FRANCIA, D., et al. PrinterCAD: a QFD and TRIZ integrated design solution for large size open moulding manufacturing. *International Journal on*

Interactive Design and Manufacturing (IJIDeM), 12.1: 81-94, 2018.

[12] DONNICI, Giampiero, et al. TRIZ method for innovation applied to an hoverboard. *Cogent Engineering*, 5.1: 1-24, 2018.

Automated Clash Resolution of Rebar Design in RC Joints using Multi-Agent Reinforcement Learning and BIM

J. Liu [ac], P. Liu [ac], L. Feng [bc], W. Wu[bc], and H. Lan[c]

[a]School of Civil Engineering, University of Chongqing, China
[b]School of Computer Science, University of Chongqing, China
[c]Chongqing University Industrial Technology Research Institute, University of Chongqing, China
E-mail: liujp@cqu.edu.cn, pengkunliu@cqu.edu.cn, liangf@cqu.edu.cn, wuwenbo@cqu.edu.cn

Abstract –

The design of rebar in reinforced concrete (RC) structures is a mandatory stage in building construction projects. Due to the large number and complicated arrangement rules of rebar in each design code, it is impractical, labor-intensive and error-prone for designers to avoid all clashes (i.e., collisions and congestion) manually or partial automation by using computer software. Therefore, the building information modeling (BIM) technology has been employed in the present architecture, engineering, and construction (ACE) industry for clash free rebar design. However, it is worth noting that most of existing BIM based approaches are using optimization algorithms for moving components, which can only be applied for regular shaped RC structures. In particular, shapes of rebar are fixed which means the optimized path of rebar cannot bend to avoid the obstacle in current studies. Furthermore, most of the existing studies cannot meet design constraints after avoiding clash, lack automatic and intelligent identification and resolution of rebar clash for complex RC joints and frame structures.

Therefore, we present a framework towards automatic rebar design in RC frame without clashes via multi-agent reinforcement learning (MARL) system with BIM. In particular, by treating each rebar as an intelligence reinforcement learning (RL) agent, we propose to model the rebar design problem as a path-planning problem of multi-agent system. Next, by employing FALCON (A fusion architecture for learning, cognition, and navigation) with immediate evaluative feedback as the reinforcement learning engine, we design particular form of state, action, and rewards for reinforcement MARL for automatic rebar design. In addition, the design of rewards and some strategies in MARL are presented for build-ability constraints. Comprehensive experiments on one-story RC building frame have been conducted to evaluate the efficacy of the proposed framework. The obtained results confirmed that the proposed framework with MARL is effective and efficient.

Keywords –

Building Information Modeling; Reinforcement Learning; Multi-agent; Rebar Design; Clash Resolution; RC Joints

1 Introduction

Rebar design is a mandatory and important stage in reinforced concrete (RC) structures construction projects. According to Chinese design codes for RC members design (GB50010-2010), the design of rebar has to meet the seismic and the bearing capacity requirements of RC members. Besides, rebar design needs to be constructed easily, safe and cost effective. Since the rebar are densely located and the arrangement rules for rebar are extremely complex as per design codes, it is impractical, labor-intensive and error-prone for the designers to manually avoid all collisions (hard clash) or congestions (soft clash) in the RC structures even using computer software [1]. In addition, current clash detection software like Autodesk Navisworks Manage and Solibri Model Checker, have realized detection and visualization of the clash members [2]. However, the current software mainly focuses on the clash identifications of construction members after the design stage. It cannot automatically avoid the clash of the rebar or offer implementation resolution for solving clashes, which thus are lack of automatic arrangement in rebar design.

Recently, building information modeling (BIM) has been widely in the current Architecture, Engineering and Construction (AEC) industry. BIM technology allows us to represent the detailing of rebar digitally and transfer the detailing information to structural analysis software [5]. However, automated resolution of rebar clashes is lacking in the existing BIM software packages. Therefore, developing a framework for solving the problem of clash detection and resolution for automated design of rebar connects with the exiting BIM technology will be

significant value in the AEC industry.

Various researchers in the past have tried to solve the problem of the clash detection and resolution for automated design of rebar with the aid of BIM technology, in the literature, Park [3] developed a BIM-based simulator to determine the sequence of rebar placement, and the clashes of rebar were identified by a developed application programming interface. Nevertheless, it focused on the simulation of the placement sequence and the spatial clash has to be solved manually. Next, Radke *et al.* [4] proposed an identification and resolution for mechanical, electrical and plumbing (MEP) systems. The offered resolution was moving one of the two clash entities to solve spatial conflicts. In fact, design constraints were not verified after moving one object. Besides, it provided manual resolution for resolving limited types of clashes. Moreover, Wang *et al.* [2] carried out a knowledge representation for spatial conflict coordination of MEP systems. The clash knowledge representation included description, context, evaluation and management details. However, the developed presentation pattern only provided a documentation to store clash information without any clash resolution strategy for identified clashes. Mangal and Cheng [5] proposed a framework based on BIM and genetic algorithm (GA) to realize rebar design and avoid clash at RC beam-column joints. However, the proposed framework only offered clash resolution strategy for moving components by using GA and can only applied for regular shaped RC structures. In particular, the optimized path of rebar cannot bend to avoid the obstacles, which thus limits its practicability in real-world complex RC joints. The main drawbacks of existing approaches can be summarized as follows: (1) Due to the complex design codes of rebar, most of the above studies cannot meet design constraints after avoiding clash by moving one object. (2) Most of the above studies lack automatic and intelligent identification and resolution of rebar clash for real-world complex RC joints and frame structures.

In machine learning, in light of its strength, RL algorithms have achieved many important achievements in the field of complex adaptive systems such as mobile robot path planning. What's more, a MARL system can lead to greater level of adaptivity and effective problem-solving [6]. Furthermore, the clash detection and resolution problem for the rebar design can be treated as a path planning of multi-agents in order to achieve automatic arrangements and bending of rebar to avoid obstacles. The similarity between the path planning of multi-agent and the arrangement of rebar, enlightens our work in this paper. Therefore, we propose a framework via a MARL system with BIM for automatically and intelligently provide clash resolution of rebar design in RC frames. To the best of our knowledge, this is the first modeling clash detection and resolution problem for the rebar design as a path-planning of multi-agent in the literature.

In particular, the three-dimensional coordinate information of the clash free rebar is then obtained by collecting the traces of the agents, considering longitudinal tensile, longitudinal compressive and shear rebar. To evaluate the efficiency and effectiveness of the proposed MARL, comprehensive experiments about one-story RC building frame having RC beams, columns, beam-column joints and beam-beam joints, including 63 RC beams and 23 RC columns with 1120 longitudinal rebars. Lastly, the obtained results including the success rates confirm that the proposed system is effective and efficient.

The contributions of the present study can then be summarized as follows:(1) To the best of our knowledge, this is the first modeling clash detection and resolution problem for rebar design as a path-planning problem of multi-agent in the literature. (2) To achieve automatic rebar design in complex RC joints, by employing FALCON as the reinforcement learning engine, we design the particular form of state, action, and rewards for the reinforcement MARL. (3) Comprehensive experiments on one-story RC building frame are performed to verify the effectiveness of the proposed framework.

2 Preliminary

Section 2.1 introduces the basic module of reinforcement learning. In Section 2.2, we describe the formulation of multi-agent path planning for rebar clash problem at RC beam-column joints. Section 2.3 presents rebar spacing requirements for RC members.

2.1 Introduction to Reinforcement Learning

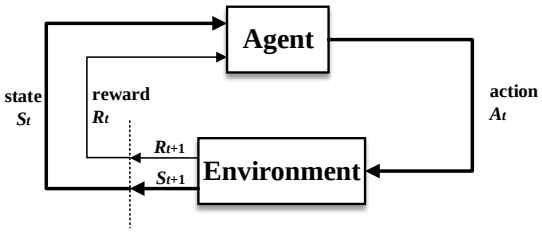

Figure 1. Basic Module of Reinforcement Learning

A multi-agent reinforcement learning (MARL) system [6] can be developed as effective tools for path planning problem-solving. RL is a natural learning paradigm to both single-agent and multiagent-agents. It creates an autonomous agent that learns and then adjusts its behavior through the action feedback (punishment and

reward) from the environment, instead of explicit teaching. Following the framework of a Markov decision process (MDP), a RL agent performs learning through the cycle of sense, action and learning [6]. In each cycle, the agent obtains sensory input from its environment representing the current state (**S**), performs the most appropriate action (**A**) and then receives feedback in terms of rewards (**R**) from the environment. It is important to note that how to turn a real-world environment into digital environment with clear reward signals is a key point to carry out RL.

2.2 Formulating Rebar Design as Path Planning of Multi-agent System

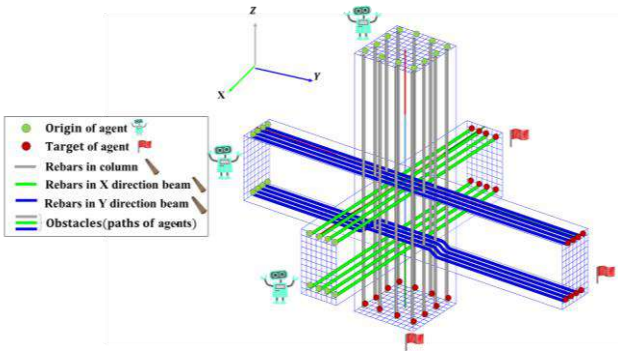

Figure 2. Problem formulation for RC beam-column joint

In particular, by treating each rebar as an intelligence reinforcement learning agent, we propose to model the rebar design problem as a path-planning problem of multi-agent system. It can be further modeled with a team of agents tasked to navigate towards defined targets safely across a RC beam-column joint that is gradually filled with obstacles which are rebars generated in the previous steps. available. In this task, the unmanned vehicle can choose one of the five possible actions, namely, up, down, forward move, left, and right at each discrete time step. The task or objective of the agent is to navigate successful through the joint towards assigned targets within the stipulated time, without hitting any obstacle. With the proposed MARL, the three-dimensional coordinates of the clash free rebar design are then obtained by collecting the traces of the agents.

Specifically, the process of rebar design in the RC beam-column joint is divided into three phases as illustrated in Figure 1: (1) In the first phase, the longitudinal rebars in the column are regarded as a group of agents from the origins navigating to the targets across the column and beam-column joint 3D environment. And there are no other obstacles (rebars) at the joint area in the first phase. (2) In the second phase, x direction beam longitudinal rebars are regarded as a group of agents and column rebars including longitudinal and shear rebars are regarded as obstacles. (3) In the third phase, y direction beam longitudinal rebars are regarded as a group of agents and rebars of column and x direction are regarded as obstacles.

2.3 Formulating Steel Rebar Spacing Requirements for RC Members and Origins and Targets for Agents

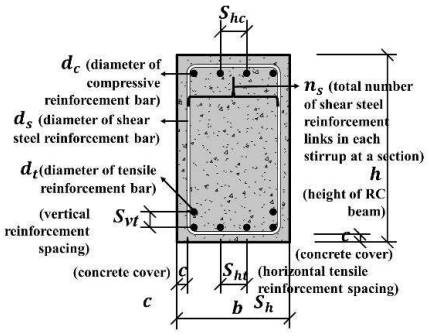

Figure 3. Spacing between rebar in an RC beam

In order to pour concrete easily and ensure the compactness of concrete around rebar, the spacings between longitudinal rebar are determined as per the provisions of GB50010-2010 (Figure 2). $S_{hc}$is horizontal compressive spacing for longitudinal compressive rebar, which is specified as $S_{hc} \geq 30$ and $\geq 1.5d_{c,max}$. In addition, S_{ht} is horizontal tensile spacing for longitudinal tensile rebar, which is specified as $S_{ht} \geq 25$ and $\geq d_{t,max}$.

N_t denotes the total number of tensile rebars, and $n_{t,min} \leq N_t \leq n_{t,max}$.

$$n_{t,min} = (b - 2 \times c)/\, S_{ht,max} \quad (1)$$

$$n_{t,max} = (b - 2 \times c)/\, S_{ht,min} \quad (2)$$

Where b denotes the width of RC beam, and c denotes the concrete cover. $S_{ht,max}$ and $S_{ht,min}$ are the maximum and minimum spacing between tensile rebars, respectively. Further, $S_{ht,max}$ and $S_{ht,min}$ are used in MARL to decide the origins of agents in each mission.

Similar to the longitudinal tensile rebar, spacing demands for compressive rebar are straight forward and require no explanation.

The calculations of spacing demands in RC column design are similar to those in RC beam design and require no explanation. The spacings between longitudinal steel reinforcement bars S_h are decided as per the provisions of GB50010-2010(Figure 3), and 50mm$\leqslant S_h \leqslant$ 300mm. Specifically, when the width of column is more than 400mm, the spacings between longitudinal rebars S_h must to be less than 200mm [1].

The origins of agents in each mission are decided by

the $S_{ht,max}$ and $S_{ht,min}$, meanwhile the targets of agents in each mission are also decided by the $S_{hc,max}$ and $S_{hc,min}$ as per the provisions of GB50010-2010, as illustrated in subsection 2.3.

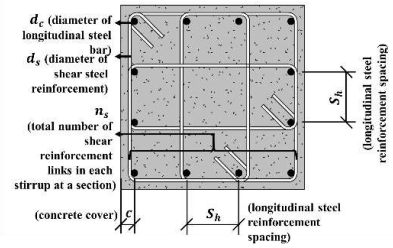

Figure 4.Spacing between rebar in an RC column

3 Proposed MARL system with BIM Solving the Path-Planning Problem for Clash Free Rebar Design

The presented framework for clash free rebar design is based on Mangal and Cheng [5] framework. The framework consists of 4 modules named (a) BIM Model Extraction, (b) Structural Analysis, (c) Structural Type Analysis, (d) Multi-Agent Reinforcement Learning System shown in Figure 5. The first three modules are clearly clarified in Mangal and Cheng [5] framework. The last module is explained in the following subsection.

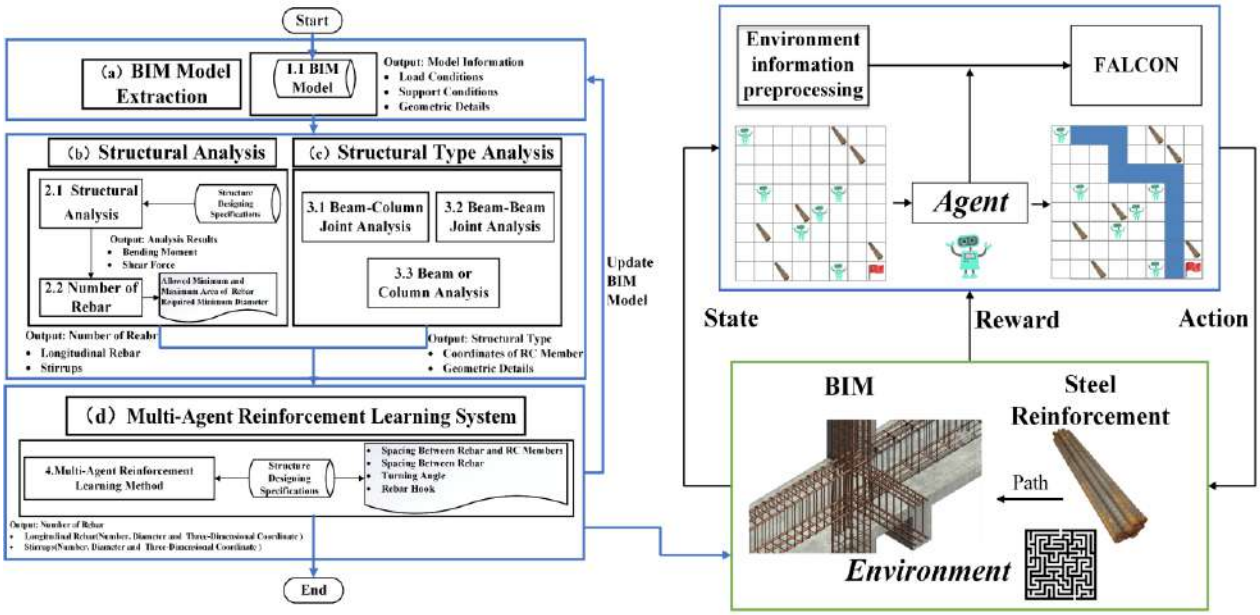

Figure 5. The presented framework for clash free rebar design via MARL with BIM.

3.1 Environment Information Pre-processing of RC Members

In addition, the RC members have to be transformed into a digital environment that is suitable for MARL system. Furthermore, we transform the BIM model of RC member into tessellated mesh environments approximating the geometry of the RC members with known boundary conditions, as illustrated in Figure 6. Then in tessellated mesh environment, a team of agents tasked to navigate towards defined targets safely.

Each tessellated mesh dimension Di of environment is the dimension of a single square mesh, which can be calculated as:

$$Di = \min(d_c \; and \; d_t) \tag{3}$$

Where d_c denotes the diameter of longitudinal compressive rebar, and d_t denote the diameter of longitudinal tensile rebar.

Therefore, the size of tessellated mesh environment Sz depends on Di and the dimension of RC members,

$$Sz = floor(D/Di) \tag{4}$$

Where D denotes the dimension of RC members, which can be length, width and height of RC members, and $floor()$ denotes the integer rounding down function in order to limit the range of Sz.

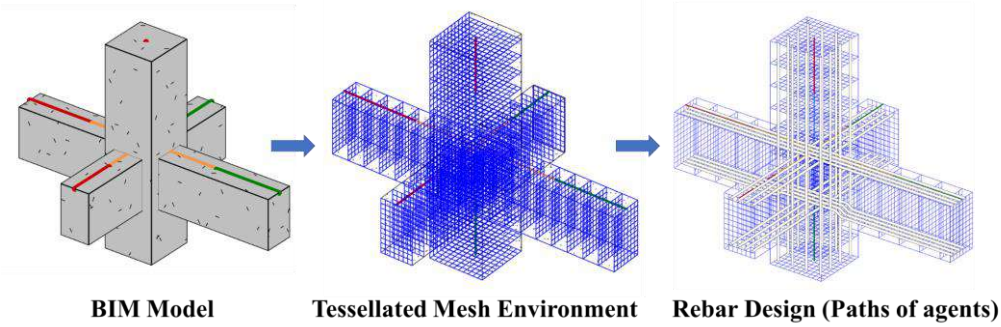

Figure 6. Environment information pre-processing of RC members

3.2 Neural Network Architecture of Each Agent

The architecture of each agent takes the form of FALCON [6], which has a three-channel neural network architecture (Figure 7), consisting of three modules: (1) State: a sensory field F_1^{c1} for saving and representing current agent states, (2) Action: a motor field F_1^{c2} for representing available actions, and (3) Reward: a feedback (reward) field F_1^{c3} for representing the internal states of an agent, as well as external feedbacks from the environment. It has a cognitive field F_2 where agents calculate the maximum expected future rewards for action at each state, which encodes a relation among the patterns in the three input channels.

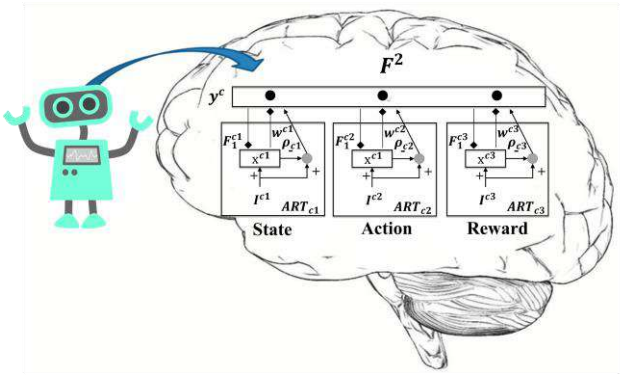

Figure 7. Neural network architecture of each agent

3.2.1 State Module

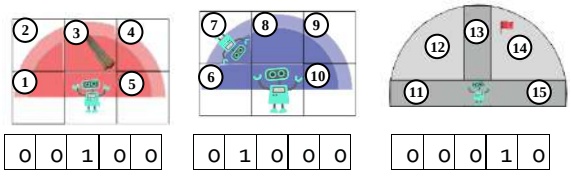

Figure 8. Illustration of states in 2D

MARL system involves numbers of agent equipped with a set of sonar sensors that has a 180° forward view. Meanwhile, input attributes of sensory (state) vector consist of obstacle (path of other agent) detection, other agent position detection and the bearing of the target from the current position. Therefore, without a priori knowledge of the three-dimensional coordinate information of the obstacle and targets, each agent is equipped with a localized view of its environment.

3.2.2 Action Module

In MARL system, the agent can choose one of the five possible actions (left, forward move, right, up and down at each discrete time step).

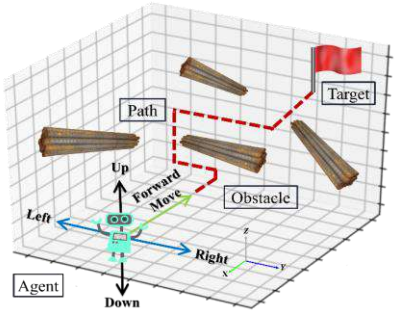

Figure 9. Illustration of five possible actions

3.2.3 Reward Module

In MARL, the design of reward, punishment and some specific strategies are presented for build-ability constraints. In particular, the reward and punishment strategies are described in Table.1:

Table 1. Reward and punishment strategies for agents.

Reward and Punishment Strategies	
Reach targets without hitting obstacles	+1.0
The distance between agents and targets decreases	+0.4
Hit obstacles (paths of other agents)	-1.0
Hit other agents	-1.0

Within the range of other agents' paths	-1.0
Run out of time	-1.0
Take actions (left, right, up and down)	-0.5
Take action (forward move)	0

A reward of +1 is given when the agent reaches the target without hitting obstacles and running out of time. A reward of +0.4 is given when the agent takes action that can get close to the target to encourage agents search for defined targets. A punishment of -1 is given when the agent hits an obstacle (paths of other agents), collides with another agent or runs out of maximum time in order to avoid clash of rebar. A punishment of -1 is given when the agent moves into the specified range (1.5 × diameter of rebar) of paths or positions of other agents, therefore the spacing demand of rebar is satisfied. A punishment of -0.5 is given when the agent takes actions including left, right, up and down in order to make sure agent to move as straight as possible, therefore the layout of rebar is most likely to be a straight line unless obstacles are encountered. A reward of 0 is also assigned when the agent moves forward and does not find the target in the maximum allowable time.

Figure 10. Illustration of multi-agent path planning including reward, punishment and mission endings in 2D

3.3 FALCON in MARL

The architecture of FALCON based on 3-channel Adaptive Resonance Associative Map (multichannel ARAM) [6], an extension of predictive Adaptive Resonance Theory (ART) networks (Figure 7).

Input vectors: Let {**S**,**A**,**R**} denote the input vector, where **S** = $(s_1, s_2, \ldots, s_n)$ denotes the state input, and s_i indicates the value of sensory input i ; **A** = $(a_1, a_2, \ldots, a_n)$ denotes the action vector, and a_i indicates a possible action i; **R** = (r) denotes the reward vector, and $r \in [-1,1]$is the reward signal value.

Activity vectors: Let x^{ck} denote the F_1^{ck}activity vector. Let y^c denote the F_2^c activity vector.

Weight vectors: Let w_j^{ck} denote the weight vector associated with the jth node in $F_2^c$for learning the input representation in F_1^{ck} . Initially, all F_2^c nodes are uncommitted, and the weight vectors contain all 1's.

Parameters: The FALCON's dynamics is determined by choice parameters $\alpha^{ck} > 0$ for $k = 1, \ldots, K$; learning rate parameters $\beta^{ck} \in [0;\ 1]$ for $= 1, \ldots, K$; contribution parameters $\gamma^{ck} \in [0;\ 1]$ for $= 1, \ldots, K$; and vigilance parameters $\rho^{ck} \in [0;\ 1]$ for $= 1, \ldots, K$.

3.3.1 From Sensory to Action

Given the state vector **S**, the system performs code competition and selects an action based on the output activities of action vector **A**. The detailed algorithm is presented below.

Code activation: Given activity vectors $x^{c1}, x^{c2}, \ldots, x^{cK}$ for each F_2^c node j, the choice function T_j^c is computed as follows:

$$T_j^c = \sum_{k=1}^{K} \gamma^{ck} \frac{|x^{ck} \wedge w_j^{ck}|}{\alpha^{ck} + |w_j^{ck}|} \quad (5)$$

Code competition: All F_2^c nodes undergo a code competition process. The winner is indexed at $J$where

$$T_J^c = \max\{T_j^c : \text{for all } F_2^c \text{ node } j\} \quad (6)$$

Action selection: The chosen F_2^c node J performs a readout of its weight vector to the action field F_1^{c2}such as

$$x^{c2} = w_J^{c2} \quad (7)$$

The chosen action a_I is then determined by

$$x_I^{c2} = \max\{x_i^{c2} : \text{for all } F_1^{c2} \text{ node } i\} \quad (8)$$

3.3.2 From Feedback to Learning

Upon receiving a feedback from its environment after performing the action a_I, the system adjusts its internal representation based on the following principles. Given a reward (positive feedback), the agent learns that an action executed in a state will result in a favorable outcome. Therefore, the system learns to associate the state vector **S**, the action vector **A**, and the reward vector **R**.

Template matching: Before code J can be used for learning, a template matching process checks that the weight templates of code J are sufficiently close to their respective input patterns. Specifically, resonance occurs if for each channel k, the *match function* m_j^{ck} of the chosen code J meets its vigilance criterion:

$$m_j^{ck} = |x^{ck} \wedge w_J^{ck}| \,/ |x^{ck}| \geq \rho^{ck} \quad (9)$$

Learning then ensues, as defined below. If any of the vigilance constraints is violated, mismatch reset occurs in which the value of the choice function T_J^c is set to 0 for the duration of the input presentation. The search process repeats to select another F_2^c node J until resonance is achieved.

Template learning: Once a node J is selected for firing, for each channel k, the weight vector $w_J^{ck}$is modified by the following learning rule:

$$w_J^{ck(new)} = (1-\beta^{ck})w_J^{ck(old)} + \beta^{ck}|x^{ck} \wedge w_J^{ck(new)}| \quad (10)$$

3.4 Proposed MARL System

Algorithm 2 Pseudo Code of MARL System

Initialization: Generate the initial *m* agents
While (a mission ending conditions are not satisfied)
For each agent
  If (agent dose not fail or not arrive the target)
    Perform FALCON algorithm
  Else
    Stop training
  End If
End For
End While

The basic steps of the proposed MARL system are outlined in Algorithm 2. In the first step, a population of *m* agents is initialized. An agent fails when hitting obstacles, exceeding 30 sense-act-learn cycles (running out of time). A mission ends when all agents fail or arrives at the target successfully. A mission will also be deemed to have failed if an agent collides with another, as depicted in Figure 10.

4 Empirical Study

4.1 The Example of Training Process in RC Beam-Column Joint by MARL

In the initial stage of mission as shown in Figure 11, agents are encouraged to explore new possibilities and try to reach defined targets without hitting obstacles or running out of time, therefore the paths of the agents looks messy, cluttered or indirect in trial 10 and 100. In the late stage of mission such as trial 500 and 1000, agents converge gradually to the global optimum and find the optimum paths for the clash free rebar design. Furthermore, along with the experimental training, the paths of agents have also gone from chaos to the gradual and orderly process of development. Finally, the global optimum of the agents' path will be selected to generate the clash free rebar design.

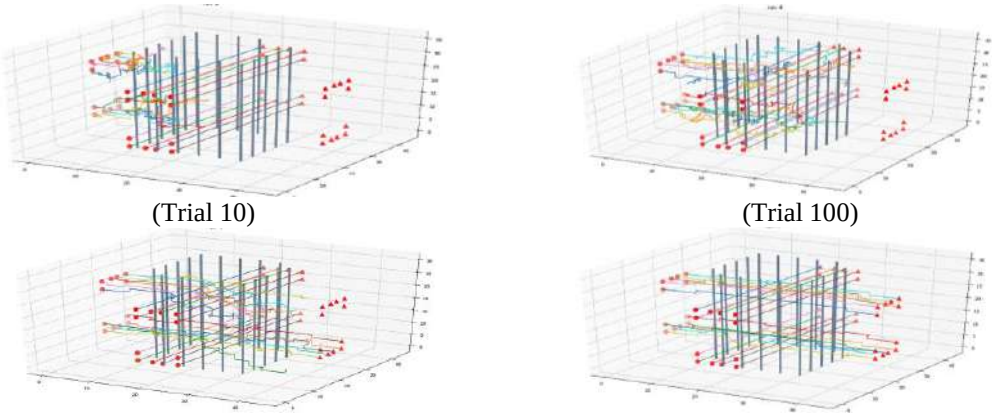

(Trial 10) (Trial 100)

(Trial 500) (Trial 1000)

Figure 11. The training process in beam-column joint by MARL

4.2 The Example of RC Frame

Figure 12. one-story frame

In this section, the empirical study is established to study the effectiveness of the proposed model. One illustrative example about one-story frame as shown in Figure 12 will be used to test the proposed model. In this tested frame, there are 63 RC beams and 23 RC columns with 1120 longitudinal rebars.

An agent having reached the target without hitting obstacles or running out of time is defined as a success. The success rate S_r can be calculated by Eq. 1:

$$S_r == \frac{1}{Nm} \times \sum_{i=1}^{N_m} \frac{N_t^i}{N_t} \times 100\% \quad (7)$$

where N_m denotes the number of total missions, N_t denotes the total number of participating agents and N_t^i stands for the number of agents that reach the targets successfully in mission i without hitting obstacles.

We analyzed the averaged success rate S_r on 40

simulations on the proposed MARL. The averaged success rates S_r presented in Figure 13 indicate that the proposed MARL successfully solving the path planning problem of rebar design after training. The design of reward, punishment and some specific strategies can satisfy build-ability constants.

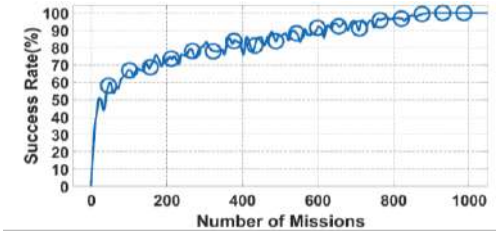

Figure 13. The success rates of MARL system

The automated 3D BIM outputs of the rebar in RC frame are given in Figure 14 and 15. Design of rebars of the RC frame are based on the result of the proposed system. It can be observed that there is no rebar clash in RC beam-column joints and frame by clash detection of the 3D BIM output.

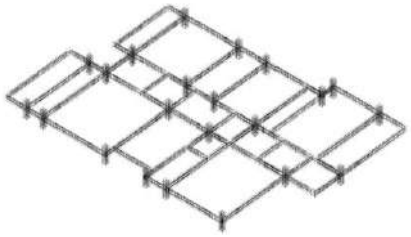

Figure 14. The simulation result of considered one-story RC frame

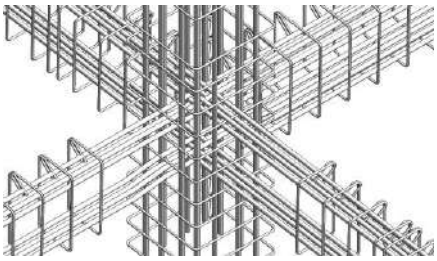

Figure 15. The simulation result of considered one-story RC frame

5 Conclusions and Future Research

In this paper, we model the clash detection and resolution problem for clash free rebar design as a path planning problem of multi-agents in order to achieve automatic arrangements and bending of rebar to avoid obstacles. Therefore, a framework via MARL system with BIM has been proposed to identify and avoid rebar spatial clash in complex RC frames. The three-dimensional coordinate information of the clash free rebar including bending of rebar is then obtained by collecting the traces of the agents. The design of reward, punishment and some specific strategies for build-ability constants are also put forward in MARL. Next, according to FALCON, the agent selects the suitable action and reaches the defined targets without hitting obstacles or running out of time. Subsequently, agents converge gradually to the global optimum along with the experimental training. Finally, the paths of agents are extracted to BIM model generating the rebar design. The simulation study in terms of the success rate have shown the effectivity and efficiency of the proposed system on the design of rebar in one-story RC frame.

However, the proposed framework via MARL system with BIM still has a few limitations. (1) It only applied for regular RC beams, columns, beam-column joints and beam-beam joints. (2) Furthermore, the system only considered the design codes GB50010-2010. Therefore, extending the system for more complex RC members or fabricated RC members and other design codes will be considered in the future work.

References

[1] Tabesh, A. Reza, and Sheryl Staub-French. Case study of constructability reasoning in MEP coordination. *Construction Research Congress 2005: Broadening Perspectives*. 2005.

[2] Wang L. and Leite F. Formalized knowledge representation for spatial conflict coordination of mechanical, electrical and plumbing (MEP) systems in new building projects. *Automation in Construction*, 64 (1): 20-26, 2016.

[3] Park U. BIM-Based Simulator for Rebar Placement. *Journal of the Korea Institute of Building Construction*, 12 (1): 98-107, 2012.

[4] Radke A., Wallmark T. and Tseng M.M. An automated approach for identification and resolution of spatial clashes in building design. In *IEEM 2009-IEEE International Conference on Industrial Engineering and Engineering Management*, pages 2084-2088, Hong Kong, 2009.

[5] Mangal, M., and Cheng, J. C. Automated optimization of steel reinforcement in RC building frames using building information modeling and hybrid genetic algorithm. *Automation in Construction*, 90, 39-57,2018.

[6] Feng, L., Ong, Y. S., Tan, A. H., and Chen, X. S. (2011, June). Towards human-like social multi-agents with memetic automaton. In *2011 IEEE Congress of Evolutionary Computation (CEC)*, pages 1092-1099, 2011.

Automated Localization of a Mobile Construction Robot with an External Measurement Device

S. Ercan[a], S. Meier[b], F. Gramazio[a], and M. Kohler[a]

[a] Department of Architecture, ETH Zurich, Switzerland
[b] Department of Mechanical and Process Engineering, ETH Zurich, Switzerland
E-mail: ercan@arch.ethz.ch, sanmeier@student.ethz.ch, gramazio@arch.ethz.ch, kohler@arch.ethz.ch

Abstract –

The localization of a robot is a crucial part of any task that involves the mobile manipulation of objects. The precise repositioning of a mobile robot within the workspace is particularly important for on-site construction in situations where the operating area is much larger than the reach of the robot arm. This research presents a localization method utilizing a generic surveying and measurement device – a robotic total station.[1] The localization of the mobile robot in reference to the total station is investigated through the positioning of a reflector prism, mounted on the robot's end-effector, at different known locations in robot's coordinate frame. Through this localization method, the opportunity to remove the reliance on fixed reference points is tested in a large-scale outdoor experiment, which would alleviate the need for a full enclosure around the mobile robot to help constrain its pose.

Keywords –

On-site construction; Localization; External measurement systems

1 Introduction

Robotic fabrication has traditionally been associated with high-tech industrial environments, where fixed positioning and constant conditions determine the role of the robot in the fabrication process. Unlike in facilities employing stationary robots, construction sites are spatially complex and unstructured, and mobile robots operating in such environments may be exposed to gradual change and unpredictable events [1]. One of the greatest challenges to the employment of robotic systems in such situations is maintaining their globally consistent localization (across a large building space), and assuring their perception of the immediate surroundings. In other words, a construction robot must "know" its own position if it is to localize itself and to manipulate its surroundings. In addition, every operation on a building site is unique in terms of the dimensions of the materials used and their range of tolerances. The methods adopted to facilitate the mobility of a construction robot on site should be sufficiently flexible to satisfy the various requirements of the building techniques and materials used. Accordingly, the two main problems can be identified as: (1) task-independent flexible global localization and positioning accuracy; and (2) task-specific local perception of the context.

This research addresses the first problem through a set of real-scale experiments in which the full potential of robot localization and positioning across a large building space is investigated using a generic surveying and measurement device of the type commonly used on construction sites. Rather than developing a task specific sensing device or technique, the goal is to explore viable methods of on-site robotic construction that do not require a full enclosure around the mobile fabrication unit. Such an In-Situ Fabricator (IF) would allow for flexibility in the production of building components larger than a workspace constrained by fixed references.

2 Background and Motivation

The mobile robot, the In-Situ Fabricator (IF), was developed within the scope of an interdisciplinary research project by Gramazio Kohler Research (GKR) and Agile & Dexterous Robotics Lab (ADRL) at ETH Zurich, in pursuit of the goal of bringing robots to the construction site. Over the last few years, IF has been successfully deployed in different projects [2], [3], exploring multiple strategies for localization. Prior to these projects, an earlier version of IF, the Echord dimRob [1], was utilized to explore localization with on-board sensors relative to its environment. The research

[1] A robotic total station allows for the remote measurement of vertical and horizontal angles and the slope distance from the instrument to a particular point.

[2], [3] focused mainly on on-board sensing and SLAM for the pose estimation of the robot end-effector to ensure minimal dependency on external sensing systems. Even though these methods proved to be successful, they came with certain limitations, such as in the achievable accuracy of the manipulator and the reliance on a full or partial enclosure around the robot to ensure reliable pose estimations.

This project explores a method in which an external tripod-based measuring system (an off-the-shelf robotic total station found commonly on construction sites, Figure 1) is employed to investigate the potential of localizing a mobile fabrication unit like IF with an external tracking strategy, without fixed reference points around the robot to help constrain the pose, thus eliminating the need for a full enclosure.

Figure 1. Setup exploring the use of an external measuring system in the form of a robotic total station for localization.

3 State of the Art

There are many methods that can be employed today for the localization of objects within a large space. The global positioning system (GPS) is used for localization on the Earth's surface, in which a network of satellites orbiting the Earth broadcast precise timing information, from which those receiving the information can calculate their position based on the timestamps of these messages. The US Department of Defence, as the developer of the system, states in [4] that the accuracy of GPS on an open field is 7.8m in the 95th percentile. A construction site, however, rarely exhibits the conditions of an open field, being mostly indoor environments, and methods that rely on GPS measurements to attain the required precision for a construction application would be more suitable for outdoor environments, such as the way the construction robotics start-up Built Robotics [5] use GPS measurements augmented with on-site base stations, fused with on-board Lidars (laser based measurements).

Recently, light detection and ranging (Lidar) devices have attracted considerable attention in the field of on-site construction involving the employment of mobile robots. Such devices measure all points in the visible environment as a point-cloud to aid localization through the use of Lidar point-cloud data, and a map of the visible environment is also needed that can either be given a priori or built simultaneously (SLAM). To exemplify, in a Mobile Robotic Brickwork project [2], an on-board laser range finder is used to scan the environment and the built structure so as to align the point-cloud data with the CAD model of the structure, and to manage the localization of IF through the creation of an enclosure around the robot to help constrain the pose.

Instead of measuring all points in the visible environment, an external measurement system, such as a robotic total station, can be used to measure the distance to a reference point – in this case, a reflector prism – in an exploration of methods to overcome limitations in positioning accuracy. A number of different approaches have been suggested involving the use of a total station for the localization of mobile robots in construction. One such approach involves placing the measurement device on the mobile hardware, which in the case of [6] was s a trolley pulled behind an asphalt paver carrying an automatic theodolite. The setup is augmented with robotic beacons placed in known locations within the surrounding environment and the theodolite rotates around its vertical axis to provide a continuous measurement of the distance to these beacons. These measurements, together with the readings from an encoder wheel on the trolley, are fused with an extended Kalman filter to obtain a position and an orientation estimate. Through the experiments conducted to date, it has been shown that an accuracy of $\pm 3cm$ in the x and y axis, $\pm 1cm$ in z and $\pm 0.1^{\circ}$ in pitch and roll were achieved in 95% of the measurements. Another approach is to mount the reflector prism on the mobile hardware, as exemplified in [7], and as adopted by construction robotics start-up N-Link with the mobile drilling robot. In such systems, two prisms are mounted on the mobile base of the drilling robot and the total station carries out sequential measurements within an environment constrained by a fixed reference point. The mobile drilling robot is then localized based on the relative distances between the prisms.

In the present project, the opportunity to remove the dependency on fixed reference points within the environment is explored. For this purpose, a reflector prism was mounted on the robot end-effector (Figure 3) to allow the measurement of the point at the location of the prism from different trajectory points (instead of the

robot base or at fixed locations within the workspace). The goal was to use these flexible points as reference points for the external measurement device (robotic total station), as a substitute for fixed reference points within the environment (Figure 2), hence allowing for building within an unconstrained space.

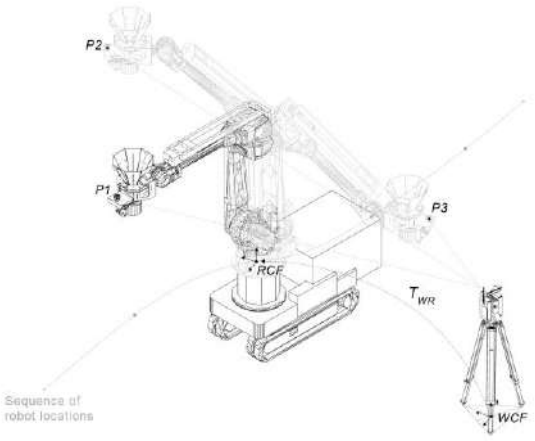

Figure 2. The substitution of "fixed reference points" with three end-effector trajectory points obtained from the mobile fabrication unit (IF).

4 Method

4.1 The setup

To localize IF using a robotic total station, a 360° reflector prism was mounted on its end effector (Figure 3), providing it with flexibility in the setting of arbitrary trajectories within the robot workspace as reference points, and ensuring a clear line of sight.

Figure 3. Reflector prism mounted on the end-effector of IF.

4.1.1 Hardware setup

A total station measures spherical coordinates (ϕ, θ, d) in an environment that is bounded by reference points, giving the precise interpolating range. The total station used in the present project was a Hilti POS 150, together with its tablet computer POC 200 and a set of $360°$ reflector prisms. The POS 150 offers distance precision of $2mm \pm 2ppm$, an angle precision of $5''(\approx 0.00139°)$ and a measurement range of $\approx 1000m$.

4.1.2 Software setup

Communication with the IF controller in the experimentation process was based on specific libraries developed previously at ETH Zurich. All developments for localization were implemented in Python, and could be easily integrated into the overall fabrication workflow (in Rhino Grasshopper), with the most basic approach to controlling the end effector being chosen (sending poses together with speed information to the robot controller). This permitted the robot end-effector, mounted with the reflector prism, to be moved sequentially to various points in the robot workspace.

4.2 Three-point Localization

In this first method, the first point is chosen by the operator of the system; the second point is then located along the robot's X-Axis at distance d; and the third point is located along the robot's Y-Axis, again at distance d. The coordinates of these points P_1, P_2, P_3, in the robot coordinate frame, are obtained directly from the robot (Figure 2). As each of these points is also measured by the total station, the coordinates, M_1, M_2, M_3, are also known within the global frame. Based on the special configuration of the points, the axes of the robot coordinate frame can be inferred directly as:

$$\begin{aligned} X &= M_1 - M_2 \\ Y &= M_3 - M_2 \\ Z &= \vec{X} \times \vec{Y} \end{aligned} \tag{1}$$

While $X, Y, Z \in \mathbb{R}^3$, to simplify the next set of computations, these vectors can be normalized as:

$$\bar{X} = \frac{X}{\|X\|}, \qquad \bar{Y} = \frac{Y}{\|Y\|}, \qquad \bar{Z} = \frac{Z}{\|Z\|} \tag{2}$$

In the next step, the origin of the robot coordinate frame is calculated. As the direction of the axis of the robot coordinate frame in the world coordinate frame is known, the origin can be extrapolated from the measurements:

$$O_w = M_2 - P_2^X * \bar{X} - P_2^Y * \bar{Y} - P_2^Z * \bar{Z} \quad (3)$$

where O_w is the origin of the robot coordinate frame in the world coordinate frame, and P_2^X, P_2^Y, P_2^Z are the x, y and z components of localization point P_2.

The transformation from the world coordinate frame into the robot coordinate frame is expressed in a homogenous transformation matrix. The $\bar{X}$, $\bar{Y}$ and $\bar{Z}$ vectors, as well as the origin O_w of the robot coordinate frame are expressed in the world coordinate frame. Deriving the homogeneous transformation matrix from the robot coordinate frame to the global coordinate frame is equivalent to calculating the change of the basis matrix:

$$T_R^W = \begin{bmatrix} \bar{X} & \bar{Y} & \bar{Z} & O_w \\ 0 & 0 & 0 & 1 \end{bmatrix} \quad (4)$$

As the transformation from the global coordinate frame to the robot coordinate frame is missing, the inverse transformation is computed by:

$$T_W^R = T_R^{W\,-1} \quad (5)$$

Therefore, for any given point Q_W the coordinates can be calculated within the robot coordinate frame by:

$$Q_R = T_W^R Q_W \quad (6)$$

4.3 Arbitrary Point Localization

When using arbitrary points for localization, there is no inherent information about the orientation of the robot coordinate frame. However, similar to the point set registration problem, the two significant sets of measurements are known to differ only in rotation and translation. For the point set registration problem a multitude of algorithms exists in [10]. As previous, the coordinates of n points P_i in the robot coordinate frame and the n measurements M_i in the global coordinate frame are derived. The sum of the deviation between localization point P_i and measurement M_i of the same point is calculated as:

$$f(O,X,Y) = \sum_{i=1}^{n} \left\| O + \underbrace{P_i^x * X + P_i^y * Y + P_i^z * (X \times Y)}_{Localization\ Point} - M_i \right\|_2 \quad (7)$$

With the addition of the constraints, the problem is defined as follows:

$$\begin{aligned} &\min_{O,X,Y} f(O,X,Y) \\ &X * Y = 0 \\ &|X| = 1 \\ &|Y| = 1 \end{aligned} \quad (8)$$

The first constraint ensures that the X-axis and Y-axis of the robot coordinate system are perpendicular; while the second and third constraints fix the length of the X-axis and the Y-axis at 1, thus simplifying the formulation of the objective function. The objective function, as well as the constraints, are both non-linear, meaning that the optimization problem falls within the realm of non-linear optimization problems. Resolving the problem using such a solver as the SciPy optimization package returns a local optimum. Although brute force methods for the global optimization of non-linear functions exist, such as basin-hopping [11], by choosing the initial guess of the robot coordinate frame close to the origin, in all of the experiments, the solver converged with the global optimum. Accordingly, the result of the optimization is the robot coordinate frame being expressed within the global coordinate frame. Similarly, the calculations explained previously in the three-point method can also be applied here to obtain the transformation matrix from the coordinate frame.

4.3.1 Point Selection

While setting up the total station, the fixed reference points are expected to bind the area in which the measurements are to be conducted (for the accurate interpolation of the targets to be measured). When using the robot as the reference point for the setup of the total station, this aspect is violated, as only points within the robot's workspace can be given as references, and after moving the robot, all points outside this workspace are measured (resulting in an extrapolation). To minimize the error introduced during the total station setup, the optimal points within the robot's workspace are to be selected, and this can be formulated as an optimization problem, as follows:

$$X = [P_1, P_2, \ldots, P_n], \qquad P_i \in \mathbb{R}^3 \quad (9)$$

$$\max_X \sum_{i=1}^{n} \|P_i\|_2^2 + \sum_{i=1}^{n} \sum_{j=i+1}^{n} \|P_i - P_j\|_2^2 \quad (10)$$

where the first part of the sum is the distance from the origin, and the second part is the distance between points. To ensure all of the points are within the robot's workspace, the following constraints are added:

$$\begin{aligned} \|P_i - (0,0,h)\|_2 &\le r, \qquad 1 \le i \le n \\ P_i^X &> 0 \\ P_i^Z &> 0 \end{aligned} \quad (11)$$

where h is the height of the arm above the ground ($h = 1m$ for IF) and r is the reach of the robot arm ($r = 2.55m$ for IF). Furthermore, the X and Z coordinates of the points are restricted to be positive – i.e. they need to be in front of IF and above the ground. The optimization problem was implemented in Python and resolved with [12].

4.3.2 Obstacle avoidance

One important aspect in the use of arbitrary points for localization is to prevent the collision of the robot arm with the structure being built. Accordingly, the heuristic algorithm used to select a point close to the desired localization point ensures that the end effector does not collide with the structure. The algorithm works as follows:

1. Set r = 10 cm
2. For each point P that does not fulfil the criteria:
    a. Set r = r + 10 cm
    b. Generate points
    c. Check criteria
    d. If all criteria are fulfilled, return point, otherwise go to step a.

Following the steps above, the points are generated as an equally spaced grid on a sphere at radius r from the original point.
In step 2c, the following criteria are checked for each point:

- $Z > 0$: Point should be above ground
- $X > 0$: Point should be in front of robot
- No collision: If the end effector is placed at the candidate point, it should not collide with the structure. A bounding box approximation of the end effector is used to provide some safety margins.
- Inside the robot's workspace: The point must be within the robot's reach.
- No obstacle between the point and robot: An obstacle between the robot base and the localization point may result in a collision with the arm.

For each iteration, the first point that fulfils all the criteria is returned.

5 Experiments

5.1 Procedure

The large-scale outdoor experiment was carried out at the Hönggerberg Campus of ETH Zurich, where the target points were evenly distributed on-site between the fixed reference points (Figure 6). The fixed reference points were used to provide a ground truth to validate the precision of the approach using the flexible references obtained from the mobile fabrication unit at arbitrary locations, and by evaluating the proposed method against the existing methods that rely on the existence of fixed references for localization.

The main goal in the experiment was to see how the errors propagated over time within the proposed flexible localization method, using different end-effector trajectory points as a reference to establish the total station (global) coordinate frame (Procedure A). To demonstrate the concept, a large-scale outdoor experiment was conducted using the "arbitrary points" method, in which two different procedures were followed (Figure 4):

- Procedure A: Setting up the total station using IF (different end-effector trajectory points) as reference (Figure 4, steps 1-4)
- Procedure B: Setting up the total station with fixed reference points on site (Figure 4, steps 1-6)

As mentioned above, Procedure B was introduced to establish a global reference frame using the fixed reference points on-site to validate the precision of Procedure A (proposed flexible localization method using different end-effector trajectory points as reference).

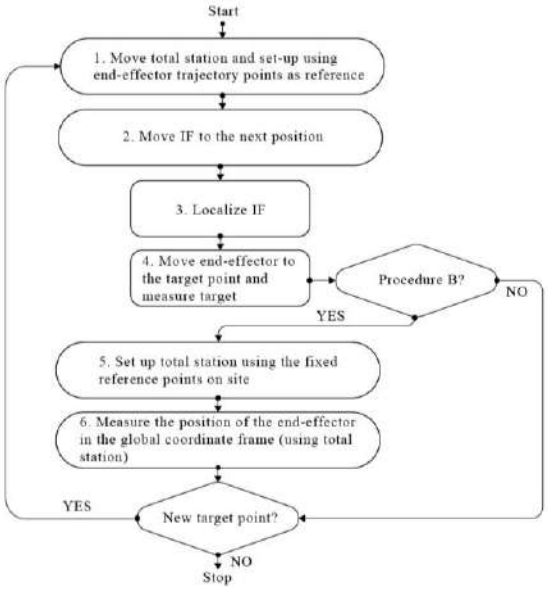

Figure 4. The full experiment flow for the acquisition of one data point.

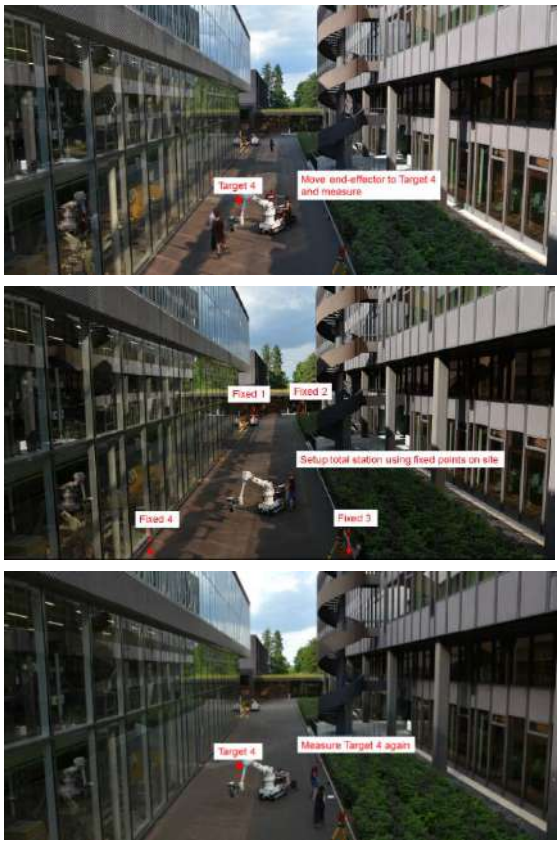

Figure 5. Steps 4, 5 and 6 of the large-scale experiment, executed for Target 4.

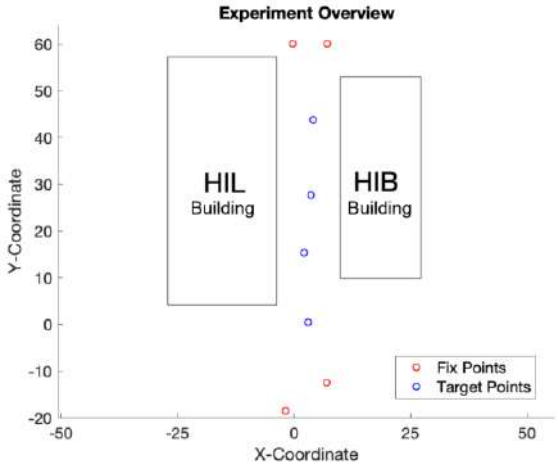

Figure 6. Large-scale outdoor experiment performed with target points distributed on site.

5.2 Results

The procedure was repeated five times for the acquisition of five data points.[2] Each cycle resulted in one measurement of the estimated target point, with the deviation from the planned target point calculated as:

$$D_i = P_i - M_i \tag{12}$$

where P_i represents the coordinates of the planned target points and M_i represents the coordinates of the estimated target points (calculated from the measurement of the end effector pose at that target point). As can be seen in Figure 7, the longer the experiment runs, the greater the deviation in the XY–plane gets, (with Procedure A, setting up the total station using IF as the reference), with an average of +-3cm and peaking at about +-7 cm at the end (Figure 7) relative to the measurements taken with Procedure B during which the ground truth is determined (for the evaluation of the proposed approach).

[2] Only four target points are marked in Figure 6. For the fifth data point, the fourth point was used a second time.

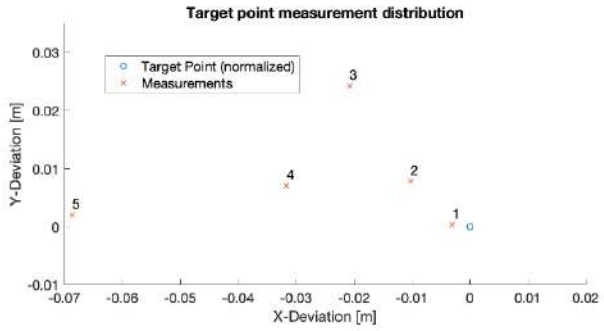

Figure 7. Deviation of the estimated points from the actual target positions in the XY-plane, at each iteration of the experiment.

6 Discussion and Future Outlook

The approach proposed in this paper aims to remove the need for fixed reference points for the localization of a mobile fabrication unit, with the intention being to address the problem of restricted workspaces in a defined enclosed area, and the possibility of building within an unconstrained space, as for on-site construction, the operating area is much larger than the reach of the robot arm. The approach makes use of an external measurement system for the evaluation of two methods: a three-point localization and an arbitrary point localization. Although the three-point localization approach lacks the required flexibility for a dynamic fabrication process, it carries a low computational cost and is easy to implement. In the arbitrary points method, the errors are minimized through the use of an optimization algorithm based on the sum of the squared distances between measurements. Furthermore, the points in this approach can be selected flexibly meaning that the robot can be prevented from colliding with the structure being fabricated. However, this method carries a high computational cost (as a non-linear optimization problem needs to be solved for each localization procedure) and is more difficult to implement. Both methods come with minor limitations, in that they require a clear line of sight from the reflector prism on the end-effector to the measurement device – in this case, the robotic total station.

All in all, the findings of the present study do not identify a single method that can be implemented for localization with external measurement systems. Such systems described in this research lack the perception component, which is needed for robotic fabrication in the context of construction sites, but target a precise pose estimation from point-to-point measurements (e.g. from the total station to the reflector prism on the end-effector). A future study could explore the possibility of merging this method with an on board-sensing system to increase the accuracy of global positioning.

Even though the method developed in this project was used in the context of a digital fabrication project, Jammed Architectural Structures [13] (Figure 8), the method is to be further investigated with a sensitivity analysis based on the precision of multiple devices. The goal is to introduce secondary devices, such as an iGPS system [14], to obtain ground truth for the validation of both the proposed localization method and the total station accuracy. The results of these experiments will be integrated into the present research.

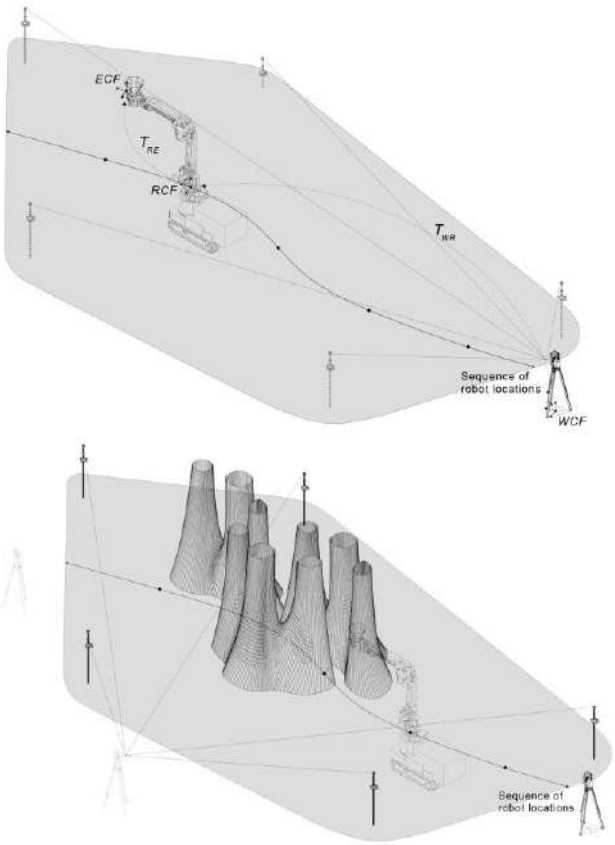

Figure 8. The method developed in this project was used in a digital fabrication project (Jammed Architectural Structures) deploying IF.

References

[1] Helm, V., Ercan, S., Gramazio, F. & Kohler, M. Mobile Robotic Fabrication on Construction Sites: dimRob*. In *Proceedings of the IEEE/RSJ International Conference on Intelligent Robots and Systems (IROS)*, 4335 - 4341. Vilamoura, Portugal, 2012.

[2] Dörfler, K., Sandy, T., Giftthaler, M., Gramazio, F., Kohler, M. and Buchli, J. Mobile Robotic Brickwork, In *Proceedings of Robotic Fabrication in Architecture, Art and Design*, Sydney, Australia, 2016.

[3] Fuentes-Pacheco, J., Ruiz-Ascencio, J., and Rendon-Mancha, J., M. Visual simultaneous localization and mapping: a survey. In *Artifical Intelligence Review*, November 2015.

[4] United States of America Department of Defense, Online: https://www.gps.gov/technical/ps/2008-SPS-performance-standard.pdf. Accessed: 07/07/2018.

[5] Built Robotics. Online: http://www.builtrobotics.com/about/. Accessed: 14/07/2018.

[6] Bouvet, D., Garcia, G., Gorham B., and Bétaille, D. Precise 3-D localization by automatic laser theodolite and odometer for civil-engineering machines. *In Proceedings of the International Conference on Robotics & Automation*, Seoul, South Korea, 2001.

[7] Halvorsen, H., Henninge, T. A., and Fagertun, K. Mobile robotic drilling apparatus and method for drilling ceilings and walls. *Patent WO2016066615A2*, 2016.

[8] Giftthaler, M., Sandy, T., Dörfler, K., Brooks, I., Buckingham, M., Rey, G., Kohler, M., Gramazio, F., Buchli, J. Mobile robotic fabrication at 1:1 scale: the In situ Fabricator. In *Construction Robotics*, 1–12, 2017.

[9] Aejmelaeus-Lindström, P., Willmann, J., Tibbits, S., Gramazio, F., Kohler, M. Jammed architectural structures: towards large-scale reversible construction. In *Granular Matter*, Robert P. Behringer, Hans J. Herrmann, 28: 1-12. Berlin, Heidelberg: Springer, 2016.

[10] Pomerleau, F., Colas, F., and Siegwart, R., A Review of Point Cloud Registration Algorithms for Mobile Robotics. In *Foundations and Trends in Robotics*, volume 4(1), 1-104, 2015.

[11] Wales, D. J., and Doye, J. P. Global Optimization by Basin-Hopping and the Lowest Energy Structures of Lennard-Jones Clusters Containing up to 110 Atoms. 1998.

[12] "SciPy.org," Online: https://docs.scipy.org/doc/scipy/reference/tutorial/optimize.html. Accessed: 06/07/2018.

[13] "Rock Print Pavilion," Online: https://vimeo.com/294086902. Accessed: 18/11/2018.

[14] Stadelmann, L., Sandy, T., Thoma, A. and Buchli, J. "End-Effector Pose Correction for Versatile Large-Scale Multi-Robotic Systems", RA-L/ ICRA 2019

Analysis of the Perceptions of Beneficiaries and Intermediaries on Implementing IPD in Indian Construction

V. P. C. Charlesraj[a] and Vatsala Gupta[a]

[a]RICS School of Built Environment, Amity University, Delhi NCR, India
E-mail: vpcharlesraj@ricssbe.edu.in, ar.vatsalagupta@gmail.com

Abstract –

Selection of appropriate project delivery system is key for project success. It also gains much importance in a fast developing economy like India where there is a greater emphasis on development of housing and infrastructure involving huge investments. The present practices of project delivery led to inefficiency and distrust among the employer, consultant, contractor, and suppliers. Integrated Project Delivery (IPD) is a project delivery approach that integrates people, systems, business structures and practices into a process that collaboratively contributes to optimise the project results. However, the adoption of IPD in Indian construction is in its formative stage due to the challenges that are faced by various stakeholders. The objective of this study is to analyse the perceptions of the beneficiaries and intermediaries in the construction sector, on these challenges. An exploratory study has been conducted among various beneficiaries and intermediaries of construction sector in India using a questionnaire survey to gain insight into the perceived challenges. It has been observed that the intermediaries and beneficiaries differ in their perceived challenges, which is also found to be significant in legal issues. An in-depth analysis also revealed that the stakeholders perceived the following challenges significantly different: *Employer's unwillingness to share consultant in the profits of the project (Finance), Resistant to change (Culture), Disengagement agreement of the parties to implement the project on time (Legal),* and *Unfamiliarity with BIM (Technical).*

Keywords –

Indian construction; Integrated Project Delivery; intermediaries

1 Introduction

India is one of the fastest growing economies in the world and construction is the second largest contributor to Indian economy. There is a consistent drive to develop housing and infrastructure in India that involves huge investments in built environment projects. However, there are inefficiencies in traditional project delivery methods used in India that hampers the progress. This also has led to distrust among the various stakeholders in the construction sector such as client, consultant, contractor, and suppliers. Integrated Project Delivery (IPD) is an alternate project delivery system that promises to overcome some of the challenges faced in traditional systems [1].

IPD is a project delivery approach that integrates people, systems, business structures and practices into a process that collaboratively contributes to optimise the project results [2][3][4]. However, the adoption of IPD in Indian construction is in its formative stage due to the challenges that are faced by various stakeholders [5]. The objective of this study is to analyse the perceptions of the beneficiaries and intermediaries in the construction sector, on these challenges. An exploratory study has been attempted among the key stakeholders to assess the critical challenges along the financial, cultural, legal and technical dimensions. Salient findings are reported in this article. It has been observed that there is a significant difference between the perceptions of the beneficiaries and intermediaries in general and the same is predominant in legal aspects of implementing IPD.

2 Literature Review

Choice of project delivery system is key in the success of a construction project. Several project delivery systems being practiced in the field of construction such as Design-Bid-Build (DBB), Design-Build (DB), Construction Manager at Risk (CM@Risk), Engineering Procurement Construction (EPC), Job Order Contracting (JOC), and Partnering & Alliancing [6]–[8]. There are challenges reported in successful implementation of these systems (lack of stakeholders' involvement in the early stages, unbalanced risk & reward sharing, lack of trust & respect, standalone decision-making, unclear project goals, ineffective communication, incompatible technology, improper organisation & leadership as found in Figure 1) [9][10][11].

IPD includes presence of all key factors of the project from outset in an integrated manner, and using their experiences and constructive cooperation in a multilateral contract to have a more successful project and participation in risk and reward for all stakeholders in project life cycle [4][12]. This technology-driven delivery method has been implemented in a number of projects at various parts of the world [1][9]. It has been reported that there are certain challenges in adoption and successful implementation of IPD[13]–[22]. The implementation of IPD in Indian construction is in its formative stage[5], [21]. All such reported challenges/barriers can be classified into four major categories: financial, legal, technical and cultural aspects [5]. 34 such factors that influence the adoption/implementation of IPD were identified from the existing literature and presented in Figure 2 [5][9][17][18], [19].

Stakeholder engagement and satisfaction is also one of the critical success factors for project delivery. It is implied that there is varied level of acceptance for IPD from difference project stakeholders [5], [23] but there is limited literature on the perspectives of the beneficiaries and intermediaries involved in the construction projects at a macro level.

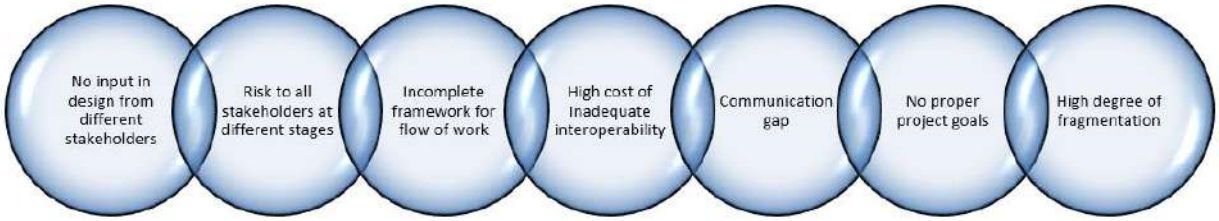

Figure 1. Challenges in Traditional Project Delivery Systems

Factors influencing the IPD adoption

Finance

F1	Compensation structure
F2	Employer's unwillingness to share consultant in the profits of the project
F3	Lack of transparency in spending done by the contractor
F4	High bids due to inexperience
F5	Confusion & Misunderstandings regarding accounting of contingency
F6	Lenders may demand 'hard pricing' for implementing IPD
F7	No specific plans for encouraging and rewarding

Legal

L1	New framework for legal practice is needed
L2	IPD contract types are not tested or understood
L3	Multiparty agreement for entire project lifecycle
L4	No insurance coverage for IPD
L5	No Dispute resolution clause
L6	Contractor's unwillingness to participate in the design phase
L7	Disengagement agreement of the parties to implement the project on time

Technical

T1	Unfamiliarity with BIM
T2	Interoperability issues
T3	Changes in the original design during construction phase
T4	Loss of focus on the aesthetic components of design due to earlier participation of other stakeholders
T5	Integration of information and knowledge management systems
T6	Early involvement of key participant
T7	Early definition of target goals without fully developed design

Cultural

C1	Lack of IPD awareness among stakeholders
C2	Training & Skill enhancement
C3	Absence or lack of respect and trust of the project parties to each other
C4	Organisation culture
C5	Resistant to change
C6	Inexperience with each other & IPD
C7	New approach take time
C8	Difficult to measure its benefits
C9	Unwillingness of employers, consultants and contractors to carry out the project in a team with common interests

Others

O1	Joint ownership of documents
O2	Who owns BIM? Who will pay for it?
O3	Shorter projects cannot spend time on organizational efforts for IPD
O4	Formation of Entity for "Real" IPD

Figure 2. Factors influencing IPD adoption

Beneficiaries are the stakeholders who are getting benefitted directly by the facilities developed; they are owners/clients, customers, developers and facility managers. The intermediaries shall include the design consultants (including architect, structural engineers, MEP engineers), project/construction managers, contractors, suppliers, etc. who are contributing to the development of the facilities (Please refer to Figure 3).

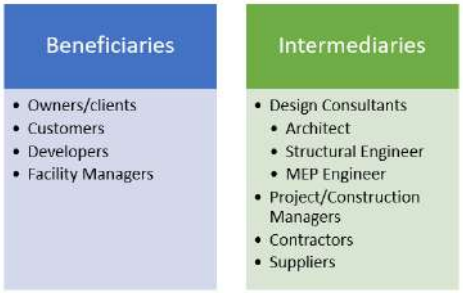

Figure 3. Beneficiaries and intermediaries in construction projects

Both beneficiaries and intermediaries would reap certain common and specific benefits when IPD is implemented. At the same time, the challenges that they face while implementing IPD also would vary due to various reasons ranging from cultural, legal, financial and technical context of the organisation. There is a need to study this characteristic of contrasting business interests of intermediaries and beneficiaries and its impact on the adoption of IPD. This would enable formulating strategies for improved adoption of IPD in construction projects.

3 Research Methodology

It has been attempted to use a questionnaire survey-based exploratory study to analyse the perceptions of beneficiaries and intermediaries on the factors influencing the implementation of IPD in Indian construction. The research methodology used is presented in Figure 4. An instrument has been designed to collect the data from the respondents (on a 5-point two-sided Likert scale; 5-Strongly Agree & 1-Strongly Disagree) on the agreement of the respondent with respect to the perceived challenges as shown in Figure 2. The respondents have been chosen using independent random sampling technique and drawn from the population of various beneficiaries and intermediaries. There were about 200 such prospective respondents invited to participate in the study and 90 responses were received (corresponding to 45% response rate). After careful scrutiny only 60 (out of 90) valid responses were used for analysis.

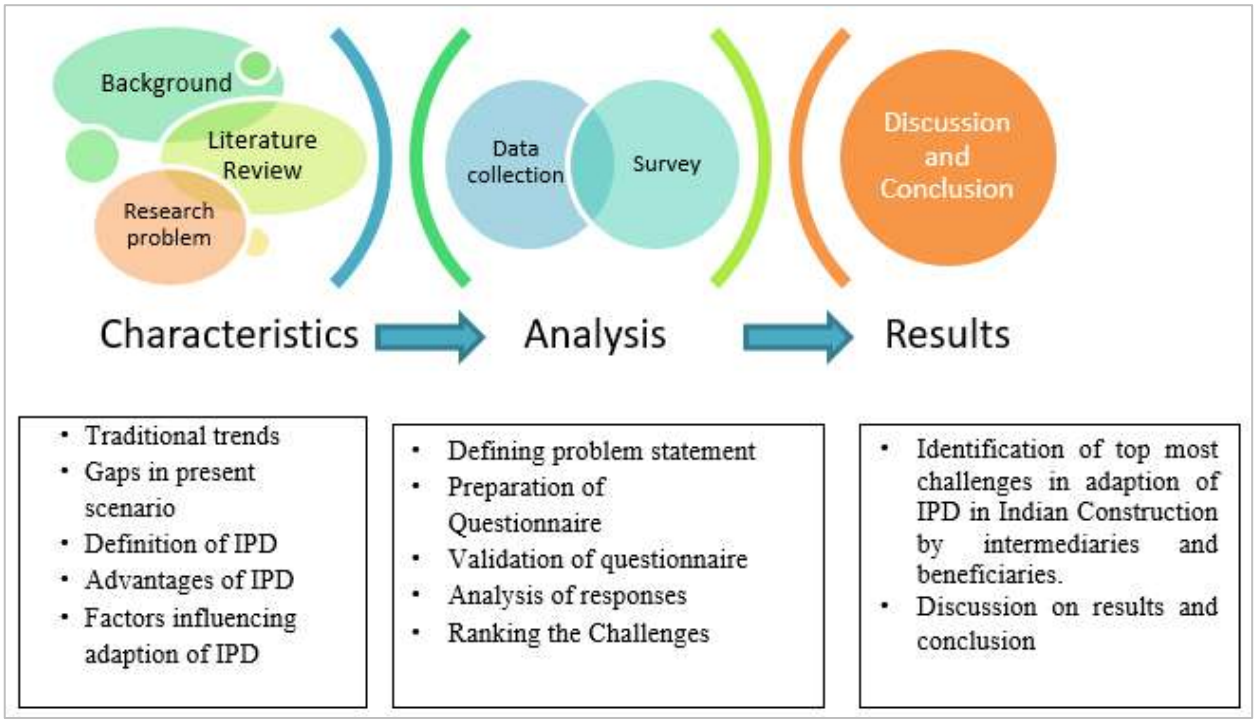

Figure 4. Research methodology

Relative Importance Index (RII) is used to prioritise the factors influencing the challenges to implement IPD.

$$RII = \frac{\sum w}{AN} = \frac{5n_5 + 4n_4 + 3n_3 + 2n_2 + 1n_1}{5N} \quad (1)$$

where

w - weighting given to each factor by the respondent, ranging from 1 to 5.

n_5 - number of respondents rated a factor as Strongly Agree;

n_4 - number of respondents rated a factor as Agree;

n_3 - number of respondents rated a factor as Neutral;

n_2 - number of respondents rated a factor as Disagree

n_1 - number of respondents rated a factor as Strongly Disagree.

A - highest weight (i.e. 5 in the study) and

N - total number of responses.

The RII ranges from 0 to 1. Higher the RII, greater the challenge.

Cronbach's Alpha has been used to measure the internal consistencyy of the instrument and reliability of data. Two-tailed t-Test (two sample unequal variance) at 5% significance level is used for hypothesis testing.

H_0: *There is no difference in perception between the Beneficiaries and Intermediaries on the relative importance of challenges in implementing IPD*

H_1: *There is difference in perception between the Beneficiaries and Intermediaries on the relative importance of challenges in implementing IPD*

4 Results and Discussion

Out of 60 valid responses, 30 belong to beneficiaries group and remaining belong to intermediaries group. The beneficiaries group respondents are primarily clients and the intermediaries consists of designers, contractors and suppliers. Sanitised data set received from all the 60 respondents is checked for reliability using Cronbach's Alpha, which is found to be 0.773. It indicates that the internal consistency of the instrument is good and the data collected using this instrument is reliable to conduct further investigation.

4.1 Overall Analysis

RII of the factors influencing the use of IPD is calculated using Equation (1) based on the responses from all the subjects. The ranking of the factors based on the RII is presented in Figure 5. It can be observed that *Lack of transparency in spending done by the contractor* is rated as the most critical challenge for the implementation of IPD in Indian construction. This can be related to the systemic characteristic of Indian construction sector, which is not highly professional and transparent that leads to lack of trust among project stakeholders. The second most rated factor is *New approach takes time*. This shows the apprehension of the stakeholders to adopt a new approach. There are three factors rated at rank three; they are:

- *Training & Skill enhancement*
- *Lack of IPD awareness among stakeholders*
- *IPD contract types are not tested or understood*

FC	Factors	RII	Rank
F3	**Lack of transparency in spending done by the contractor**	**0.81**	**1**
C7	**New approach takes time**	**0.79**	**2**
C2	**Training & Skill enhancement**	**0.76**	**3**
C1	**Lack of IPD awareness among stakeholders**	**0.76**	**3**
L2	**IPD contract types are not tested or understood**	**0.76**	**3**
T4	**Loss of focus on the aesthetic components of design due to earlier participation of other stakeholders**	**0.73**	**4**
F1	Compensation structure	0.71	5
T6	Early involvement of key participant	0.71	5
O3	Shorter projects cannot spend time on organizational efforts for IPD	0.71	5
L3	Multiparty agreement for entire project lifecycle	0.70	6
F5	Confusion & Misunderstandings regarding accounting of contingency	0.70	6
C6	Inexperience with each other & IPD	0.70	6
T3	Changes in the original design during construction phase	0.70	6
F6	Lenders may demand 'hard pricing' for implementing IPD	0.70	6
C5	Resistant to change	0.69	7
T7	Early definition of target goals without fully developed design	0.69	7
F4	High bids due to inexperience	0.69	7
C9	Unwillingness of employers, consultants and contractors to carry out the project in a team with common interests	0.69	7
L4	No insurance coverage for IPD	0.68	8
O1	Joint ownership of documents	0.68	8
C3	Absence or lack of respect and trust of the project parties to each other	0.68	8
C4	Organisation culture	0.68	8
T5	Integration of information and knowledge management systems	0.68	8
L1	New framework for legal practice is needed	0.67	9
L7	Disengagement agreement of the parties to implement the project on time	0.67	9
T2	Interoperability issues	0.67	9
O2	Who owns BIM? Who will pay for it?	0.67	9
O4	Formation of Entity for "Real" IPD	0.67	9
F7	No specific plans for encouraging and rewarding	0.67	9
L6	Contractor's unwillingness to participate in the design phase	0.66	10
F2	**Employer's unwillingness to share consultant in the profits of the project**	**0.65**	**11**
T1	**Unfamiliarity with BIM**	**0.65**	**11**
C8	**Difficult to measure its benefits**	**0.62**	**12**
L5	**No Dispute resolution clause**	**0.61**	**13**

Figure 5. Overall ranking of factors by all the respondents

As the IPD demands high skill levels for implementation, stakeholders feel that they may have to focus on training before embarking on IPD system. Also, IPD is found to be not so familiar with the stakeholders. There is also some concern about the type of contracts (typically multi-party) that are quite different from the contracts used in the traditional delivery systems. It has been observed that there is some hesitations on the use of IPD due to the fact that the early involvement of other stakeholders might have adversarial impact on the design as *Loss of focus on the aesthetic components of design due to earlier participation of other stakeholders* rated as the next big challenge.

Among the least challenging factors *No Dispute resolution clause* is found to be least critical. This may be due to the presence of such dispute resolution clauses in most of the contracts used. In addition, the following factors seems to be of less significance to the stakeholders:

- *Difficult to measure its benefits*
- *Unfamiliarity with BIM*
- *Employer's unwillingness to share consultant in the profits of the project*

This shows that BIM is gaining wider attention and the stakeholders have systems in place for performance measurement of newer project delivery systems. Also, it can be noticed that profit sharing between the consultant and the client is not reported as critical.

It has been attempted to identify the highly important factors within the categories and the results are presented below.

- Financial
  - *Lack of transparency in spending done by the contractor*
  - *Compensation structure*
- Cultural
  - *New approach takes time*
  - *Training & Skill enhancement*
  - *Lack of IPD awareness among stakeholders*
- Legal
  - *IPD contract types are not tested or understood*
  - *Multiparty agreement for entire project lifecycle*
- Technical
  - *Loss of focus on the aesthetic components of design due to earlier participation of other stakeholders*
  - *Early involvement of key participant*
- Others
  - *Shorter projects cannot spend time on organizational efforts for IPD*

4.2 Comparative Analysis

The primary objective of this study is to analyse if there is any significant difference in the perception of beneficiaries and intermediaries on the factors influencing the implementation of IPD. Hence, the RII is computed using the Equation (1) based on the responses from the respective stakeholders and the same along with the ranking is presented in Figure 6. It can be noticed that *Lack of transparency in spending done by the contractor* and *New approach takes time* have been rated as the most critical factors by both the groups. *Resistant to change* is also reported as the top critical challenge by the beneficiaries. While there is an agreement on the top two factors, difference in perception is observed in the next most critical challenge. Beneficiaries reported that *IPD contract types are not tested or understood* in contrast to the preference of the intermediaries i.e. *Lack of IPD awareness among stakeholders* and *Training & Skill enhancement* as the third most critical challenge. This implies that the beneficiaries are more concerned about the project procurement compared to the intermediaries (like designers, contractors & suppliers) are apprehensive about the development of capabilities and capacity building that are related to the cultural aspects (it may be noted that *Resistant to change*, a top rated challenge by beneficiaries is also a cultural issue). Another interesting observation is that technical factors are not figured in the top three critical challenges by both the groups. This may indicate that both the groups are confident about the technical competence.

Please refer to Figure 7 to understand the least preferred factors between the groups. While the RII of the top rated factors are closer (0.80 & 0.82 by beneficiaries & intermediaries respectively), the RII of the least rated factors are 0.57 & 0.65. This can be interpreted as the intermediaries rated the challenges higher compared to the beneficiaries. This prompted to conduct the hypothesis testing to check these differences perceived by the beneficiaries and intermediaries are significant.

4.2.1 Hypothesis Testing

The two-tailed t-Test (two sample unequal variance at 5% significance level) conducted on the means of all the categories resulted in the rejection of H_0 i.e. there is significant difference between the perceptions of the beneficiaries and intermediaries (Please refer to Figure 8 for test results). It was also noticed that the perceptions of the beneficiaries are significantly different from intermediaries on the legal aspects but not on the other three dimensions. Further, a factor level test revealed that only on the following four factors, both the groups significantly differ:

- *Employer's unwillingness to share consultant in the profits of the project* (F2)
- *Disengagement agreement of the parties to implement the project on time* (L7)

Comparison of Relative Importance of Factors Influencing IPD Adoption

		Beneficiaries		Intemediaries	
FC	**Factors**	**RII**	**Rank**	**RII**	**Rank**
F1	Compensation structure	0.70	10	0.73	6
F2	Employer's unwillingness to share consultant in the profits of the project	0.59	19	0.71	8
F3	**Lack of transparency in spending done by the contractor**	**0.80**	**1**	**0.82**	**1**
F4	High bids due to inexperience	0.64	16	0.74	5
F5	Confusion & Misunderstandings regarding accounting of contingency	0.69	11	0.71	8
F6	Lenders may demand 'hard pricing' for implementing IPD	0.67	13	0.72	7
F7	No specific plans for encouraging and rewarding	0.65	15	0.69	10
C1	**Lack of IPD awareness among stakeholders**	**0.74**	**6**	**0.77**	**3**
C2	**Training & Skill enhancement**	**0.76**	**4**	**0.77**	**3**
C3	Absence or lack of respect and trust of the project parties to each other	0.69	11	0.67	11
C4	Organisation culture	0.69	11	0.67	11
C5	**Resistant to change**	**0.57**	**21**	**0.82**	**1**
C6	Inexperience with each other & IPD	0.71	9	0.69	10
C7	**New approach takes time**	**0.79**	**2**	**0.80**	**2**
C8	Difficult to measure its benefits	0.57	21	0.67	11
C9	Unwillingness of employers, consultants and contractors to carry out the project in a team with common interests	0.71	9	0.67	11
L1	New framework for legal practice is needed	0.62	17	0.73	6
L2	**IPD contract types are not tested or understood**	**0.77**	**3**	**0.74**	**5**
L3	Multiparty agreement for entire project lifecycle	0.69	11	0.72	7
L4	No insurance coverage for IPD	0.65	15	0.71	8
L5	No Dispute resolution clause	0.58	20	0.65	13
L6	Contractor's unwillingness to participate in the design phase	0.64	16	0.67	11
L7	Disengagement agreement of the parties to implement the project on time	0.60	18	0.75	4
T1	Unfamiliarity with BIM	0.58	20	0.71	8
T2	Interoperability issues	0.66	14	0.69	10
T3	Changes in the original design during construction phase	0.69	11	0.71	8
T4	Loss of focus on the aesthetic components of design due to earlier participation of other stakeholders	0.76	4	0.71	8
T5	Integration of information and knowledge management systems	0.70	10	0.65	13
T6	Early involvement of key participant	0.73	7	0.69	10
T7	Early definition of target goals without fully developed design	0.68	12	0.71	8
O1	Joint ownership of documents	0.72	8	0.65	13
O2	Who owns BIM? Who will pay for it?	0.68	12	0.67	11
O3	Shorter projects cannot spend time on organizational efforts for IPD	0.75	5	0.66	12
O4	Formation of Entity for "Real" IPD	0.64	16	0.70	9

Figure 6. Comparison of relative importance of all the factors influencing IPD adoption by Beneficiaries and Intermediaries

BENEFICIARIES

FC	Factors	RII	Rank
F3	Lack of transparency in spending done by the	0.80	1
C7	New approach takes time	0.79	2
L2	IPD contract types are not tested or understood	0.77	3
C2	Training & Skill enhancement	0.76	4
T4	Loss of focus on the aesthetic components of design due to earlier participation of other stakeholders	0.76	4
O3	Shorter projects cannot spend time on organizational efforts for IPD	0.75	5
L7	Disengagement agreement of the parties to implement the project on time	0.60	18
F2	Employer's unwillingness to share consultant in the profits of the project	0.59	19
L5	No Dispute resolution clause	0.58	20
T1	Unfamiliarity with BIM	0.58	20
C5	Resistant to change	0.57	21
C8	Difficult to measure its benefits	0.57	21

INTERMEDIARIES

FC	Factors	RII	Rank
F3	Lack of transparency in spending done by the	0.82	1
C5	Resistant to change	0.82	1
C7	New approach takes time	0.80	2
C1	Lack of IPD awareness among stakeholders	0.77	3
C2	Training & Skill enhancement	0.77	3
L7	Disengagement agreement of the parties to implement the project on time	0.75	4
O3	Shorter projects cannot spend time on organizational efforts for IPD	0.66	12
T5	Integration of information and knowledge management systems	0.65	13
L5	No Dispute resolution clause	0.65	13
O1	Joint ownership of documents	0.65	13

Figure 7. Comparison of the most and least influencing factors as perceived by the Beneficiaries and Intermediaries

Results of Hypothesis Testing

p* (All the Categories)	0.006

CC	Categories	p*
F	Financial	0.062
C	Cultural	0.214
L	Legal	0.020
T	Technical	0.784

FC	Factors	p*	Benificiaries		Intermediaries	
			RII	Rank	RII	Rank
F2	Employer's unwillingness to share consultant in the profits of the project	0.012	0.59	19	0.71	8
L7	Disengagement agreement of the parties to implement the project on time	0.020	0.60	18	0.75	4
C5	Resistant to change	0.041	0.57	21	0.82	1
T1	Unfamiliarity with BIM	0.047	0.58	20	0.71	8

*p-value in two-tailed t-Test (two sample unequal variance) at 5% significance level

Figure 8. Results of hypothesis testing

- *Resistant to change* (C5)
- *Unfamiliarity with BIM* (T1)

It is interesting to note that the above four are from four different categories and the intermediaries rated them as on the higher side of importance compared to the beneficiaries.

5 Summary and Conclusions

IPD is gaining wider attention among the stakeholders of Indian construction. An exploratory study conducted among them revealed that *Lack of transparency in spending done by the contractor* is rated as the most critical challenge for the implementation of IPD in Indian construction and the least challenging one is *No Dispute resolution clause*. The comparative analysis between the beneficiaries and intermediaries showed that there is a significant difference in their perception but they agree on *Lack of transparency in spending done by the contractor* and *New approach takes time.* It is also evident that technical competence is not a major challenge for both the groups. It was also observed that beneficiaries significantly differ from intermediaries on the legal aspects but not on the other three dimensions viz. financial, cultural and technical. The factors on which the groups significantly differ in their perceived challenge in adopting IPD are consistently rated higher by the intermediaries.

As IPD is technology-driven, use of Blockchain and promotion of professionalism can be a possible solutions to overcome the challenges with respect to lack of transparency. In order to address the challenges such *as New approach takes time, Training & Skill enhancement* and *Lack of IPD awareness among stakeholders*, capacity & capability building among the stakeholders can be considered. Having understood the perceived challenges and the differences between these groups, the future work would include formulating strategies for addressing these issues for successful project delivery in order to meet the ambitions targets of Indian construction.

References

[1] Z. Kahvandi, E. Saghatforoush, M. Alinezhad, and F. Noghli, "Integrated Project Delivery (IPD) Research Trends.," *J. Eng. Proj. Prod. Manag.*, vol. 7, no. 2, pp. 99–114, 2017.

[2] P. Pishdad-Bozorgi and Y. J. Beliveau, "Symbiotic Relationships between Integrated Project Delivery (IPD) and Trust," *Int. J. Constr. Educ. Res.*, vol. 12, no. 3, pp. 179–192, 2016.

[3] P. Tillmann, K. Berghede, G. Ballard, and I. D. Tommelein, "Developing a Production System on IPD: Considerations for a Pluralistic Environment," *22nd Annu. Conf. Int. Gr. Lean Constr.*, vol. 1, no. 415, pp. 317–328, 2014.

[4] AIA, "Integrated Project Delivery: A Guide," *Am. Inst. Archit.*, pp. 1–62, 2007.

[5] D. Roy, S. Malsane, and P. K. Samanta, "Identification of Critical Challenges for Adoption of Integrated Project Delivery(IPD)," *Lean Constr. J.*, pp. 1–15, 2018.

[6] T. Rizk and N. Fouad, "Alternative project delivery systems for public transportation projects," *Int. J. Constr. Educ. Res.*, vol. 3, no. 1, pp. 51–65, 2007.

[7] A. S. Al Subaih, "A Framework for Implementation of IPD Principles in Oil & Gas Projects," University of Salford, 2016.

[8] S. R. Kramer and T. J. Meinhart, "Alternative Contract and Delivery Methods for Pipeline and Trenchless Projects," in *Pipeline Division Specialty Congress 2004*, 2004, pp. 285–287.

[9] B. Ghassemi, Reza; Becerik-Gerber, "Transitioning to Integrated Project Delivery : Potential barriers and lessons learned," *Lean Constr. J.*, no. January, pp. 32–52, 2011.

[10] S. A. Rahim, M. N. Mohd Nawi, and F. A. A. Nifa, "Integrated project delivery (IPD): A collaborative approach to improve the construction industry," *Advanced Science Letters*, vol. 22, no. 5–6. pp. 1331–1335, 2016.

[11] W. Collins and K. Parrish, "The need for integrated project delivery in the public sector," in *Construction Research Congress 2014: Construction in a Global Network - Proceedings of the 2014 Construction Research Congress*, 2014, pp. 719–728.

[12] M. Fischer, D. Reed, A. Khanzode, and H. Ashcraft, "A Simple Framework for Integrated Project Delivery," in *22nd Annual Conference of the International Group for Lean Construction*, 2014, pp. 1319–1330.

[13] H. W. Ashcraft Jr, "Negotiating an Integrated Project Delivery Agreement," 2001.

[14] A. R. Aslesen, R. Nordheim, B. Varegg, and O. Lædre, "IPD in Norway," in *26th Annual Conference of the International Group for Lean Construction*, 2018, pp. 326–336.

[15] S. Forero, S. Cardenas, H. Vargas, and C. Garcia, "A deeper look into the perception and disposition to integrated project delivery (IPD) in Colombia," in *Proceedings of IGLC 23 - 23rd Annual Conference of the International Group for Lean Construction: Global Knowledge - Global Solutions*, 2015, pp. 297–306.

[16] S. Gomez, G. Ballard, N. Naderpajouh, and S. Ruiz, "Integrated Project Delivery for Infrastructure Projects in Peru," in *26th Annual Conference of the International. Group for Lean Construction*, 2018, pp. 452–462.

[17] S. Korb, E. Haronian, R. Sacks, P. Judez, and O. Shaked, "Overcoming But We Are Different. An IPD Implementation in the Middle East," in *24th Annual Conference of the International Group for Lean Construction. Boston*, 2016, pp. 3–12.

[18] S. Li and Q. Ma, "Barriers and Challenges to Implement Integrated Project Delivery in China," in *25th Annual Conference of the International Group for Lean Construction*, 2017, no. July, pp. 341–348.

[19] P. J. Morton and E. M. Thompson, "Uptake of BIM and IPD within the UK AEC Industry: The Evolving Role of the Architectural Technologist," *Built Nat. Environ. Res. Pap.*, vol. 4, no. 2, pp. 275–286, 2011.

[20] F. Rached, Y. Hraoui, A. Karam, and F. Hamzeh, "Implementation of IPD in the Middle East and its Challenges," in *22nd Annual Conference of the International Group for Lean Construction (IGLC-22)*, 2014, pp. 293–304.

[21] D. Sarkar, "A framework for development of Lean Integrated Project Delivery Model for infrastructure road projects," *Int. J. Civ. Struct. Eng.*, vol. 5, no. 3, pp. 261–271, 2015.

[22] A. Townes, B. W. Franz, and R. M. Leicht, "A Case Study of IPD Team Selection," in *Engineering Project Organization Conference*, 2015.

[23] W. N. Osman, M. N. M. Nawi, F. Zulhumadi, M. W. M. Shafie, and F. A. Ibrahim, "Individual readiness of construction stakeholders to implement integrated project delivery (IPD)," *J. Eng. Sci. Technol.*, vol. 12, no. Special Issue 2, pp. 229–238, 2017.

Modelling Traffic Conditions on Fuel Use and Emissions of On-road Construction Equipment

K. Barati[a], X. Shen[a]

[a]School of Civil and Environmental Engineering, The University of New South Wales, Sydney, Australia
E-mail: Khalegh.barati@unsw.edu.au, X.shen@unsw.edu.au

Abstract –

The consumption of fossil fuels by on-road vehicles is a main source of air pollution specifically greenhouse gases (GHGs) worldwide. The construction industry, due to the use of a large number of heavy-duty equipment including haulage trucks, contributes to a significant amount of fuel consumption and consequent emissions production. Due to increasing number of vehicles on the road, traffic condition is becoming one of the main variables having a considerable impact on the fuel use and emissions of such vehicles. There is a lack of comprehensive studies in construction field quantifying the effect of road traffic on fuel use and emissions of construction equipment. This research aims to model the impact of traffic conditions on fuel use and emissions of on-road construction vehicles. The research framework is first developed to present the methodology of data collection and analysis, and then introduce the fuel use and emissions models applied in predicting the effect of traffic conditions. Three variables of driving speed, idling time and equipment stop are identified as representatives of traffic conditions, and their impacts on fuel use and emissions are quantified through conducting statistical analyses on collected field data. The achieved results found that by having more effective traffic management and planning, the fuel cost and consequent emissions can be reduced up to 9% due to the decreasing idling time of equipment. It is also indicated that by lowering the number of equipment stops, up to 0.66 l/100kW fuel is saved and up to 1.7 kg/100kW CO_2 is emitted less per each stop.

Keywords –

Construction Equipment; Traffic Condition; Fuel Use and Emissions; Construction Sector; Idling Mode; Equipment Stop

1 Introduction

The construction sector plays a significant role in fossil fuels consumption and the production of GHG pollutants. According to the Environmental Protection Agency (EPA), construction sector accounts for 1.7% of total GHG production and 6.8% of all industrial-related emissions which is ranked as the third largest GHG emitter after oil and gas, and chemical manufacturing industries [1, 2]. In addition, it is estimated that construction industry produces more than 100 million tons of carbon dioxides (CO_2) annually, and contributes to around 5% of global CO_2 emissions which is ranked as the third CO_2 emitter per utilized unit of energy after cement and steel production sectors [3]. According to the United Nation Framework Convention on Climate Change (UNFCCC), GHG emissions from construction operations account for around 6.8% of the total emissions produced by all industrial sectors [4]. The majority of fuel used and emissions produced in the construction sector is related to equipment operations. Construction equipment accounts for 45% to 48% of the total vehicular consumed fuel and emitted pollutions of all industries [5, 6]. The machinery is mainly involved in huge earthmoving operations which their emitted pollution is by far more than other vehicles. For example, the pollution production of a middle-sized loader is nearly 500 times more than that of a private car [7, 8]. Based on the report prepared by the EPA's Clean Air Act Advisory Committee (CAAAC), construction sector accounts for 6% of the light-duty vehicles (LDVs) and 17% of the heavy-duty vehicles (HDVs) while producing 32% of nitrogen oxide (NO_x) and 37% of particulate matters (PM) of all mobile source emissions [9]. In the construction projects, equipment operations and materials transportation account for the majority of fuel use and emissions production.

Improving traffic conditions can have a significant effect on decreasing the total amount of pollutions emitted by construction equipment. As an

illustration, if the idling time of construction equipment reduces by 10%, the emission of CO_2 decreases by around 0.8 million tons per year [10]. Furthermore, EPA estimates if the fuel consumed by construction equipment decreases by 10% through lowering the idling times and equipment's stop, around 5% of the entire energy used in the construction sector will be saved resulting in a reduction of 6,700 tons CO_2 production [1, 11]. The Australian Clean Energy Regulator Agency (CERA) predicts that by improving the traffic volumes and having a more effective traffic planning and control, over 3 billion liters fuel can be saved by on-road equipment involved in all industries including construction which approximately 8 million tones CO_2 is emitted less in Australia only [12].

In spite of the significance, there is a lack of comprehensive study on modelling the effect of traffic conditions of fuel use and emissions rate of on-road construction equipment as the primary strategy to improve the fuel efficiency of such vehicles. The current traffic modelling systems mainly have been developed in the transportation field take into consideration just the impact of traffic on small-sized urban vehicles. The main focuses in construction field are on engine attributes, fuel types and mechanical practices to decrease the amount of used fuel and emitted pollutions per specific trip cycle which are costly and not applicable for all equipment.

The main goal of this paper is to model the effect of traffic conditions on fuel use and emissions production of on-road construction equipment. The comprehensive research framework is first developed presenting the methodology of data collection and analysis procedure. The operational level fuel use and emissions models applied in this study for modelling traffic conditions are then briefly introduced. This research continues with developing three variables of driving speed, idling time and equipment's stop representing the road traffic volume. The fuel use and emissions production of equipment at different speeds, idling mode and per each stop are measured in the next step using the developed fuel use and emissions model and equipment's specifications.

2 Background

Traffic management is one of the main challenges of the transportation field covering all moving vehicles. Traffic is a dynamic system which needs to be precisely modelled considering all affecting parameters including operators' driving patterns, road conditions and instantaneous traffic flow rate. It seems impossible to distinguish all factors affecting traffic conditions and model their impacts. Some models focus mainly on the driving pattern of each vehicle driver known as microscopic traffic models, while others concentrate on the average effect of factors at the macroscopic level and do not consider the dynamicity of traffic [13, 14].

As one of the major applications of the traffic models, fuel use and emissions rate of vehicles can be estimated based on the traffic flow. Different studies have been conducted to model the effect of traffic conditions on fuel use and emissions rate at both microscopic and macroscopic levels [15]. Microscopic fuel use and emissions models emphasize the instantaneous measurement of traffic variables plus the vehicle's specifications. The Motor vehicle emission measurement simulator (MOVES) is an example of such models that was developed by the EPA in 2004 to estimate the fuel use and different emissions (CO, NO_x, PM, CO_2, NH_3 and SO_2) of a variety of on-road motor vehicles. This model considers numerous parameters such as vehicle specific power (VSP), and derives second-by-second data from different programs such as US I/M240 and MOBILE6 [16]. MOVES simulator models the traffic conditions and driving cycles considering speed profile and distribution of the operation modes.

On the other hand, the macroscopic models have different inputs of average speed and vehicle group [13]. As an example of this modelling approach, the comprehensive modal emission model (CMEM) was developed by the cooperation of the University of California-riverside and the University of Michigan with the sponsorship of the National Cooperative Highway Research Program (NCHRP) in 1995. The prime objective of designing this model is to estimate fuel use and emissions rate associated with the operation modes of light-duty vehicles. CMEM simulates fuel use rate taking into consideration different readily-available parameters such as operating modes and specific vehicle factors, and calibrated parameters like fuel specifications and catalyst variables [13].

In addition to the traffic controlling and planning, numerous efforts have been devoted by scholars and international agencies to developing fuel use and emissions reduction schemes in the construction field. A number of studies have sought various means of reduction schemes, such as fuel changes, equipment upgrading and operator training. Avetisyan et al. developed a decision model to reduce fuel use and GHG emissions from transportation construction projects. Using the mixed integer programming (MIP), the optimization-based technique minimizes the emissions produced by the

equipment through considering numerous parameters, e.g. machinery availability, compatibility among equipment pieces and operation conditions [3]. Kaboli and Carmichael explored the relationship between the operation cost and produced emissions in the earthmoving activities using queueing technique. They concluded that by reducing emissions produced by machinery, the operation cost would decrease as well. It was also found that the minimal unit cost of emission and project cost are coincident, and this result does not rely on the operation conditions and equipment type [17].

3 Research Framework

As Figure 1 demonstrates, this section presents the methodology adopted in this study to model the effect of traffic conditions on fuel use and emissions of on-road construction vehicles. First, three instruments of the engine data logger, portable emission measurement system (PEMS) and GPS-aided inertial navigation system (GPS-INS) were developed to collect required field data including engine load (EL), fuel use and emissions rate in each second from in-use construction equipment. As shown in Table 1, during seven days of experimentation, eight HDVs with different classes, sizes and year models were tested to cover real working conditions in practice.

After obtaining the field data through experimentation, a data processing and synchronization procedure was performed to create a centralized database of all raw data gathered from the instrument. Database files were first created for storing the data collected from each piece of equipment. Data validation was then conducted to identify potential errors in the raw data. In the next step, the data gathered by instruments were synchronized. Since instruments did not have much delay in recording data, the simultaneous speed of the vehicle measured by both devices was used as a reference for data synchronization. The PEMS data were further processed to match with the data obtained from the other two instruments. One centralized database was then created with all field data of investigated parameters synchronized. The invalid data measured by each of the devices were finally detected and removed together with the corresponding data from other instruments.

Processing and analyzing the real-time obtained data, the fuel use and emissions rate of on-road construction vehicles were then modelled through investigating the effects of operational and engine factors on fuel use and emissions. Figure 2 shows some sample processed data used for modelling fuel use and emissions.

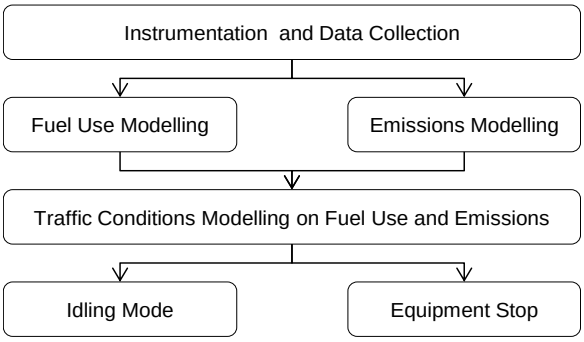

Figure 1. Research framework for modelling the effect of traffic conditions on fuel use and emissions rate of on-road construction equipment

3.1 Fuel Use and Emissions Models

The models developed in this text predict the fuel use and emissions rate of on-road construction equipment at the operation level [18]. There are numerous operational, environmental and engine parameters affecting the fuel use and emissions of equipment, but this study aims to focus on factors having a more significant effect and ignore parameters having a negligible impact. The initial analysis on the gathered raw data indicated that four operational variables of acceleration, speed, road slope and WF are the primary parameters affecting fuel use and emissions. The parameter of WF is defined as the combined weight of equipment (ton) should be carried per 100 kW of engine size [6, 20]. The combined weight refers to the total weight of the vehicle including equipment itself, trailers and payloads. Fuel type is another major factor influencing the fuel use and emissions rate. Different engine attributes also impact the fuel use and emissions including engine size, engine tier and engine age. In this study, the models consider the engine size, and estimate fuel use and emissions per kW of the engine. There are construction equipment pieces with three tiers of IV, V and VI engines in the market, but the tier V engine is currently predominant and is the main focus of this study. Engine age and maintenance conditions vary significantly from vehicle to vehicle and have minor effect of fuel use. Therefore, the parameters of engine age and maintenance have not been considered in this study at this stage. Construction equipment normally uses diesel as the primary fuel globally, and this research develops the models considering diesel fuel.

Table 1. Summary of field experimentation process conducted in this study

Day	Vehicle	Model	Engine size (kW)	Empty Weight (ton)	Payload (ton)	Experimentation Time (min)
Day 1	Six-axle Trident	2014	400	17.7	30.3	235
Day 2	Six-axle Vision	2005	350	17.6	30.9	340
Day 3	Three-axle Granite	2010	345	9.5	13	270
Day 4	Seven-axle Trident	2013	400	18.8	31.7	310
Day 5	Seven-axle Granite	2010	345	16.6	33.9	260
Day 6	Six-axle Granite	2010	345	14.5	33.5	410
Day 7	Three-axle Trident	2013	400	11	11.5	205

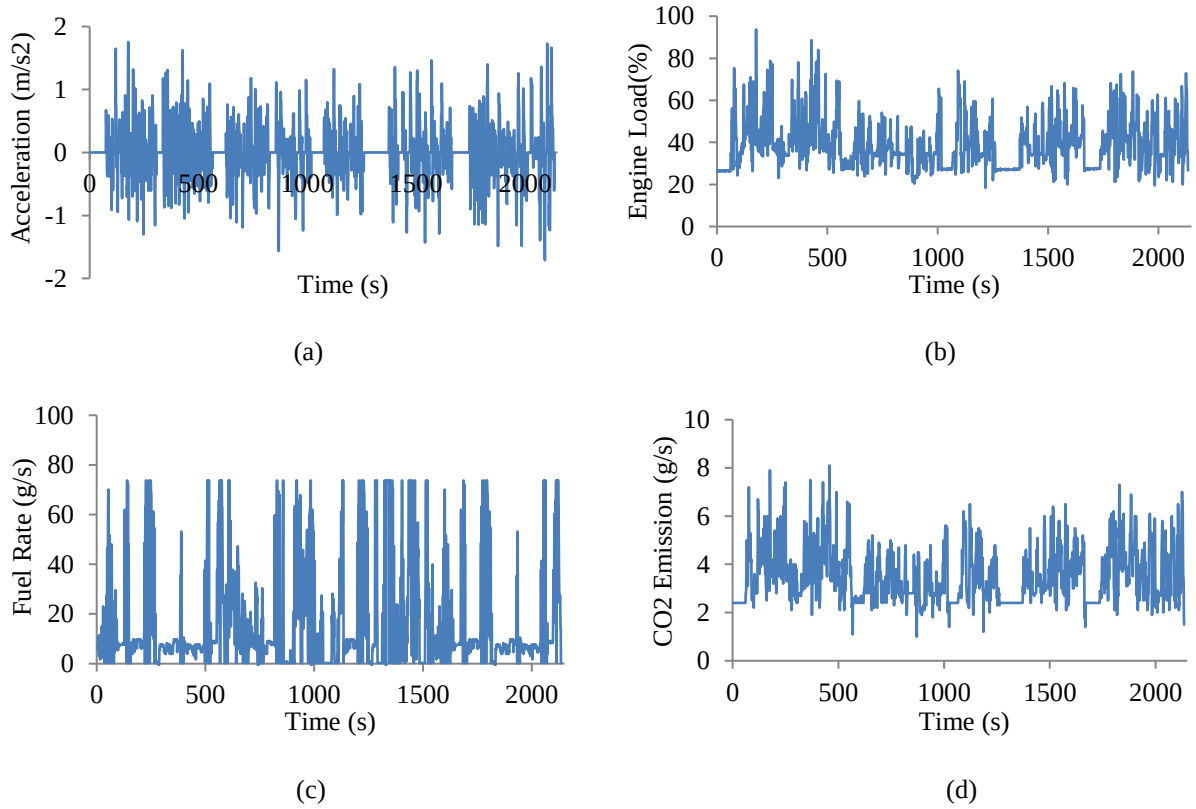

Figure 2. Samples of obtained data analyzed for developing fuel use and emissions model, (a) acceleration rate versus time, (b) engine load versus time, (c) fuel use rate versus time and (d) CO_2 emission rate versus time

In the devised models, EL acts as a critical intermediate factor bridging fuel use and emission rates with affecting operational parameters. Considering the internal specification of the engines, operational and environmental variables impact the engine power, and then engine power effects fuel use and emissions. Therefore, an intermediate parameter must be defined to link operational parameters to fuel use and emissions. Three engine variables of engine load, engine speed and manifold absolute pressure (MAP) were initially introduced as the used power of the engine, but the regression analyses on the collected data indicated that engine load is the best surrogate of the used engine power. Engine load is the percentage of used power of the engine and is defined as the ratio of the used power over the maximum available power of the engine.

The regression statistical method was the theory used in this study to develop the fuel use and emissions models. This method is more flexible compared to the other data analysis techniques. As one of the advantages, it is simple to add or remove some data after conducting an initial analysis. Using regression technique, it seems easier to find the differences among the developed relationships, and compare the results achieved from processing the data of various vehicles. Regression technique has other strong points such as level of familiarity, assumptions and use of multiple variables.

Equation (1) presents the function estimating the EL considering four factors of acceleration, road slope, driving speed and WF. As can be seen, there is a multivariable linear function between operational parameters and EL variable. Also, the constant value (C) shows the EL of equipment in idling mode which is around 20%. The coefficients of investigated factors in the developed EL model are presented in Table 2.

$$EL = (C_{AC}*AC) + (C_{SL}*SL) + (C_{SP}*SP) + C \quad (1)$$

Where:
EL: Engine load of equipment (%)
AC: Acceleration of equipment (km/h.s)
SL: Slope of the road (degree)
SP: Speed of equipment (km/h)
C_{AC}, C_{SL}, and C_{SP}: Coefficients of acceleration, road slope and driving speed parameters given in Table 1,
C: EL of equipment in idle mode which is around 20%.

The conducted ordinary least square (OLS) statistical analyses show there is a direct linear relationship between fuel use and emissions, and EL. The fuel use is around 0.02 l/kWh in idling mode (EL ≈ 20%) reaching approximately 0.12 l/kWh when the engine is fully loaded (EL ≈ 100%). CO_2 is the dominant GHG pollutant emitted by construction equipment and is the main focus of this study. CO_2 emission varies between 45 g/Kwh in idling mode to around 250 g/Kwh in full EL.

4 Modelling Traffic Conditions on Fuel Use and Emissions

Applying the presented fuel use and emission models, this section aims to model the effect of traffic conditions on fuel use and emissions of on-road construction vehicles. As discussed, traffic is a very complex dynamic phenomenon and there are numerous factors affecting traffic flow and its impact on fuel use and emissions. To simplify, three major variables of driving speed, idling time and equipment stop are distinguished and introduced as the representatives of traffic conditions in this study. There are absolutely other variables as the surrogate of traffic conditions, but these three parameters seem the most significant in the construction field. As demonstrated in the developed models, the effect of equipment speed as an operational parameter interrelated with WF has been estimated on fuel use and CO_2 emission. As indicated, by increasing the WF, the effect of speed on fuel use and consequently CO_2 emission linearly rises. In the following, the effect of idling time and stop on fuel use and CO_2 emissions are accurately estimated.

4.1 Fuel Use and Emissions in Idling Mode

Lots of operation times of construction equipment is spent in idling mode. The idling times are mainly due to traffic conditions, poor planning and low compatibility among involved equipment involved in the construction sites. As one of the factors in modelling traffic conditions, idling time of vehicles has considerable influence in fuel consumption and emissions production. It has been estimated if the idling time of construction equipment involved in construction sites decreases by 10%, CO_2 emission reduces approximately 800 million ton per year [1]. In this section, the fuel use and CO_2 emission production in idling mode of construction equipment are first estimated using developed models. Then, the additional fuel use and emissions production due to stop of on-road construction vehicles caused by traffic conditions are calculated.

Table 2. The coefficients of parameters in the EL estimation model

	WF				
Coefficients	2.75	4.5	6.5	13	14.5
C_{AC}	20.3	24.8	29.6	41.7	46.3
C_{SP}	0.20	0.25	0.31	0.42	0.47
C_{SL}	1.8	2.6	3.6	5.1	5.6

Figure 3 presents the fuel use and CO_2 emission rate of on-road construction vehicles in different operation modes. In comparison with other modes, vehicles consume much more fuel and produce much higher emissions in hauling mode due to using more power of the engine. As can be seen, the fuel use and CO_2 emission rate of construction vehicles in idling mode are 0.027 l/kWh and 0.073 kg/kWh respectively showing the high significance of lowering vehicles' idling time to reduce fuel use and emissions production. For example, by reducing the idling time of an equipment piece with the engine size of 400 kW for an hour, 10.8-liter fuel is consumed less resulting around 29 kg reduction in CO_2 production.

Figure 4 illustrates the average percentage of used fuel and emitted CO_2 in different operation modes of on-road construction vehicles. These results were achieved by analyzing collected raw data and using presented fuel use and emissions models. As shown, approximately 9% of used fuel and emissions of construction vehicles is in idling mode. This shows that by having more effective traffic management and project planning, the fuel cost and consequently emissions can be lowered up to 9%.

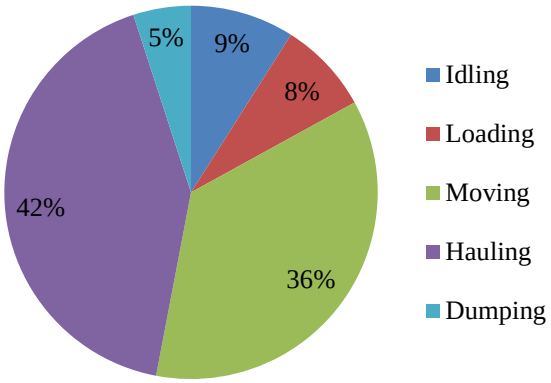

Figure 4. The average percentage of fuel use and CO_2 emission in different operation modes of on-road construction vehicles

4.2 Fuel Penalty and Extra Emissions due to Equipment's Stop

Stops of on-road construction vehicles which are mainly due to congested traffic flows or traffic lights have a considerable impact on the increase of fuel use and emissions. In this step, it is focused to investigate the effect of equipment stop on the fuel consumption and CO_2 production of on-road construction vehicles. Figure 5 indicates the additional fuel use and CO_2 emission due to the equipment's stop.

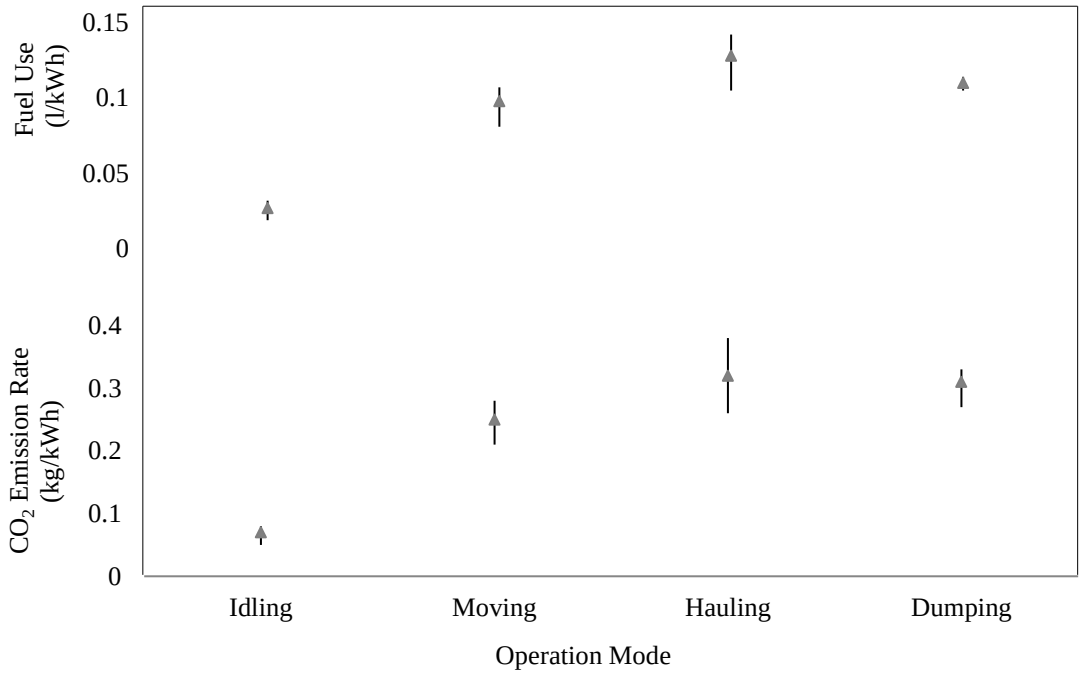

Figure 3. Comparison of fuel use and CO_2 emission of on-road construction vehicles in different operation modes

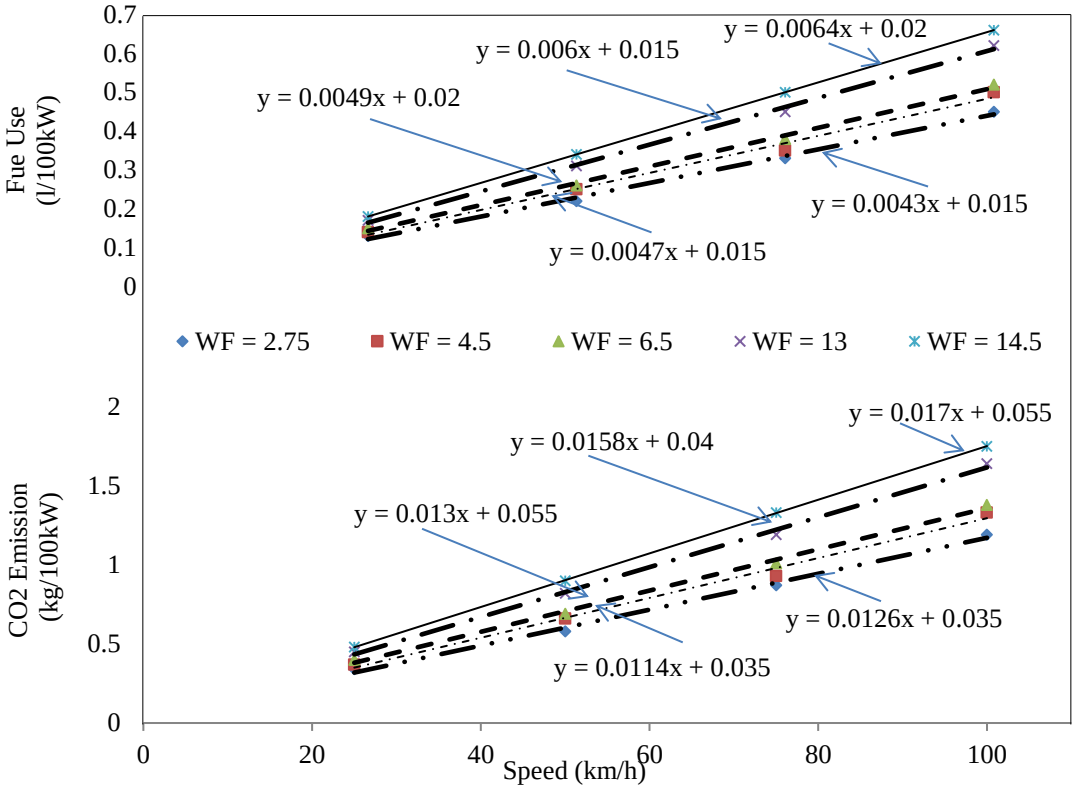

Figure 5. The fuel use and CO_2 emission due to stop of equipment with different WF values

The analyses were undertaken on various experimented equipment pieces. The effect of WF parameter was also taken into consideration in the data analysis process. In the calculations presented in Figure 4, it was assumed that during deceleration step to stop, the gas pedal is not pressed and EL is around 20% (like idling mode). Also, vehicles have three minutes stop, and then they start moving with the acceleration rate of 0.5 km/h.s to reach their previous speed. These assumptions have been made based on conducted observations, and it has been tried to simulate normal stop conditions of construction vehicles.

The equipment's speed and WF are the two main parameters influencing the additional fuel use and emissions in a stop. As shown, there is a highly-correlated direct linear relationship among vehicles' speed, WF and fuel use and emissions production. The additional fuel consumption and CO_2 emission due to stop vary from 0.13 l/100kWh and 0.35 kg/100kWh for the vehicles with the speed of 25 km/h and WF of 2.75 to 0.66 l/100kWh and 1.75 kg/100kWh for equipment with the WF of 14.5 driven with 100km/h speed. It shows the significant effect of vehicles' stop that must be considered by equipment's operators as a reduction scheme to lower fuel use and emissions at the operation level.

5 Conclusions

The construction industry is regarded as one of the major contributors to global energy consumption and GHG emissions due to the large engine size of involved equipment. Despite the significance, there is a lack of comprehensive schemes to indicate the effect of traffic conditions on extra fuel use and emissions production of construction equipment. Such guidelines can be broadly used by traffic planners and equipment operators to decrease the used fuel and emitted pollutions of construction vehicles. This research focused on modeling the effect of traffic conditions on fuel use and emissions of on-road construction equipment by analyzing collected field data and using devised fuel use and emission models.

As three prime parameters for modelling the traffic conditions, the effect of driving speed, idling time and full equipment stop on fuel use and CO_2 emission was investigated. To do so, the fuel use and CO_2 emission production of vehicles in idling operation mode were estimated using devised models. The analysis of raw data indicated that around 9% of used fuel and consequently produced CO_2 emission of construction vehicles are in idling mode showing the importance of lowering idling time

of equipment as a parameter representing traffic conditions. The impact of equipment's full stop on additional fuel use and CO_2 emission was also investigated. The achieved results indicated that by trying to have fewer stops during moving and hauling operation modes, up to 0.66 l/100kW fuel is saved and 1.7 kg/100kW CO_2 is produced less per each stop.

As the future study, this research aims to develop different fuel use and emissions reduction strategies and schemes at operational, equipment and planning level including trailer configuration, equipment's compatibility and engine upgrading to be used machinery manager, project manager and equipment worldwide as guidelines to deliver greater fuel efficiency and more sustainable operations.

References

[1] EPA. Office of Transportation and Air Quality, EPA NONROAD model updates, EPA-420-F-09-020, Ann Arbor, MI., 2009.

[2] Azzi M. Duc H. and Ha Q.P. Toward sustainable energy usage in the power generation and construction sectors-a case study of Australia. *Journal of Automation in Construction*, 59: 122-127, 2015.

[3] Avetisyan H.G. Miller-Hooks E. and Melanta S. Decision models to support greenhouse gas emissions reduction from transportation construction projects. *Journal of Construction Engineering and Management*, 138 (5): 631-641, 2012.

[4] Barati K. and Shen X. Operational level emission modelling of on-road construction equipment through field data analysis, *Journal of Automation in Construction*, (72):338-346, 2016.

[5] Lewis P. Rasdorf W. Frey C. Pang S.H. and Kim K. Requirements and incentives for reducing construction vehicle emissions and comparison of non-road diesel engine emissions data sources. *Journal of Construction Management and Engineering*, 135(5): 341-351, 2009.

[6] Barati K. and Shen X. Modelling emissions of construction and mining equipment by tracking field operations, In *Proceeding of 32nd International Symposium on Automation and Robotics in Construction and Mining*, pages 478-486, Oulu, Finland, 2015.

[7] Kaboli A.S. and Carmichael D.G. Emission and cost configurations in earthmoving operations. *International Journal of Organization, Technology and Management in Construction*, 4 (1): 393-402, 2012.

[8] Barati K. and Shen X. Comprehensive methodology for emission modelling of earthmoving equipment. In *Proceeding of 33rd International Symposium on Automation and Robotics in Construction and Mining*, pages 538-546, Auburn, United States, 2016.

[9] EPA. Clean Air Act Advisory Committee, Recommendation for reducing emissions from the legacy diesel Fleet, Washington, D.C., 2006.

[10] Barati K. and Shen X. Optimal driving pattern of on-road construction equipment for emissions reduction. *Journal of Procedia Engineering*, 180: 1221-1228, 2016.

[11] Barati K. and Shen X. Fuel use optimization of on-road construction equipment using artificial neural network. In *Proceeding of the Construction Research Congress*, pages 198-207, Louisiana, United States, 2018.

[12] Klein J. Shen X. and Barati K. Optimum driving pattern for minimizing fuel consumption of on-road vehicles. In *Proceeding of the 33rd International Symposium on Automation and Robotics in Construction and Mining*, pages 555-562, Auburn, USA, 2016.

[13] Zegeye S.K. De Schutter B. Hellendoorn J. Breunesse E.A. and Hegyi A. Integrated macroscopic traffic flow, emission, and fuel consumption model for control purposes. *Transportation Research Part C: Emerging Technologies*, 31: 158-171, 2013.

[14] Chen D. Zhang J. Tang S. and Wang J. Freeway traffic stream modelling based on principal curves and its analysis. *IEEE Transactions on Intelligent Transportation Systems*, 5(4), 246–258, 2004.

[15] Ahn K. and Rakha H. The effects of route choice decisions on vehicle energy consumption and emissions. *Transportation Research Part D*, 13(3): 151-167, 2008.

[16] EPA. Office of Transportation and Air Quality, Policy guidance on the use of MOVES for state implementation plan development, transportation conformity, and other purposes, Washington, DC, 2009.

[17] Kaboli, A.S. and Carmichael D.G. Truck dispatching and minimum emissions earthmoving. *Journal of Smart and Sustainable Built Environment*, 3(2), 170-186, 2014.

[18] Barati K. and Shen X. Weight estimation of on-road construction equipment based on operational parameters. In *Proceeding of the 34th International Symposium on Automation and Robotics in Construction and Mining*, pages 294-301, Taipei, Taiwan, 2017.

Distributed Coordination and Task Assignment of Autonomous Tandem Rollers in Road Construction Scenarios

P. Wolf[a], T. Ropertz[a], A. Matheis[a], K. Berns[a], and P. Decker[b]

[a]Robotics Research Lab, TU Kaiserslautern, Germany
[b]BOMAG GmbH, Germany
E-mail: {patrick.wolf, ropertz, a_matheis12, berns}@cs.uni-kl.de, peter.decker@bomag.com

Abstract -

Automation in construction is a highly active field of research with promising prospects for more efficient construction processes. This paper presents a novel behavior-based approach for distributed coordination of autonomous tandem rollers. Hereby, a detailed road representation and concepts for tandem roller and paver interaction as well as distributed task assignment are presented. The concept has been tested in a simulated road construction environment on the virtual B10 highway, Germany and compared to real construction data.

Keywords -

Off-Road Robotics, Behavior-Based Control, Multi-Robot Cooperation, Automated Road Construction

1 Introduction

The domain of construction industry strongly benefits from recent developments towards high-performance assistance systems and autonomous machines [1]. Complex construction tasks can be performed with higher efficiency, safety, and quality despite the continuously increasing complexity of the tasks. The area of road construction offers a high potential to profit disproportional from automation because collaborating machines have to be organized according to available time windows, their capabilities, and clearly defined tasks.

The automation of road works raise challenges subjected to the environment, infrastructure, and AI skills of smart machines. For instance, the construction environment changes permanently which challenges a robust and safe robot control. Additionally, the unstructuredness, varying environmental conditions, and fluctuating illumination affect sensor systems negatively. While it is still an open research problem, behavior-based control systems (BBS) present a promising approach to conquer these challenges. They are highly modular and run parallel components with overlapping functionality to increase robustness [2]. Also, swarm robotics are widely studied and there exist various approaches to handle the complex coordination tasks of robot interaction [3].

A prerequisite for robot interaction and collaboration is the availability of communication infrastructure. The project *Autonomous Mobile Machine Communication for Off-Road Applications* (5G-AMMCOA) funded by the German Federal Ministry of Education and Research (BMBF) focuses on the development of mobile 5G-Islands for a local, infrastructure independent communication and its impact on autonomous fleet management.

This paper presents a novel behavior-based control approach for a distributed coordination and task assignment of autonomous tandem rollers in a road construction scenario. Sect. 2 provides an overview to state of the art in autonomous road construction and multi-agent robotic systems. The integrated behavior-based control architecture serving as a base for the presented approach is introduced in Sect. 3. Then, the considered road construction scenario is described in Sect. 4. Sect. 5 introduces the formal description of a road model exploited in the control approach. The corresponding task description for tandem rollers is stated in Sect. 6. A behavior-based, distributed task assignment concept is proposed in Sect. 7. Sect. 8 presents experimental simulation results to evaluate the approach. Finally, Sect. 9 summarizes and concludes.

2 Related Work

In the recent past, there have been various research activities towards the automation of road construction and coordination of machinery. As early as 1998 the GNSS-based assistance system *AutoPave* was developed to map tandem roller trajectories on individual road segments for an improved quality and future automation [4]. Nearly twenty years later advances in automation technology promote the developments towards autonomous road construction. Control concepts have been developed to achieve an autonomous tandem roller navigation that is coordinated with a paver [5] as well as trajectory planning strategies for rolling patterns on asphalt [6]. Design concepts for future tandem rollers envisage machines without a cabin, where a fleet of robots which mimic a manned master machine is operated by a single human [7]. The *SmartSite* project targets real-time path-planning of multi-agent compactors systems [8]. Next to improvements to the overall logistic chain, a focus is directed to sensor data

exchange and adaptation to environmental changes. Subsequently, the project *Road Construction 4.0* builds upon *SmartSite*'s results and aims to further improve the intelligent control of construction processes [9].

Behavior-based and bio-inspired multi-agent systems have been well studied in the past [10]. The ALLIANCE architecture [11] presents a fault tolerant system for heterogeneous robot interaction. Each robot uses a motivational behavior to activate a task and suppress the task assignment of collaborating robots. The authors of [12] suggest a distributed swarm coordination approach which uses hybrid automata for behavior coordination through processing time- and event-based components to coordinate robots. A safety concept for robot collaboration is suggested by [13] and combines dynamic safety contracts with behavior-based control. Hereby, unsafe autonomous operations are limited through a safety cage.

3 Integrated Behavior-Based Control

The integrated behavior-based control (iB2C) architecture ([14], [15]) developed at the Robotics Research Lab (RRLab), TU Kaiserslautern, is used as the underlying software architecture for the presented approach due to its advantages concerning robustness and modularity. An iB2C behavior network consists of three main components (Fig. 1).

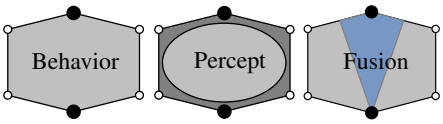

Figure 1. Main components of iB2C [15].

Standard behaviors are applied within a control context. Therefore, the complex tasks are decomposed into rather simple, but yet self-contained sub-tasks that can be implemented by individual behaviors. Thereby, partially overlapping functionality increases the system robustness, while the inherent modularity fosters reuse and extensibility. Similarly, percept behaviors are used to realize perception tasks including the data quality assessment. Competing control (perception) tasks are orchestrated by exploiting predefined fusion behaviors. All behavior components offer the same standardized interface for component coordination. Thereby, the behavior component's activity plays an important role since it represents the relevance of the component in the current system state, which can be externally adjusted via stimulation and inhibition by other modules.

4 Scenario

An important scenario which offers a lot of potential for optimizations in efficiency and quality by exploiting automation is the paving and compaction process of an asphalt layer in road construction. The road is layed out by a paver and compacted by a group of cooperating tandem rollers. To ensure a good compaction result, the rollers have to complete several tasks:

- Right behind the paver, the main compaction occurs. Rollers will compact the asphalt by applying a certain amount of passes, possibly with active drum vibration.
- Further back, rollers finish the surface statically.
- On open sides of the road, a roller has to press the edges with a special edge cutter tool.
- If a top layer is being built, a roller with a chip spreader might have to apply chip.

The process is dynamic, i.e. there is no fixed plan beforehand defining which task will be completed by whom at which time. There are several necessary events which will interfere the process during the day:

- The paver might have to slow down or stop because of a lack of material supply, caused e.g. by a traffic jam or a mixing plant failure.
- Rollers have to refill their water. Since the water tank is usually not moved during the day, the rollers have to travel back some distance to refill.
- Special jobs, like pressing the edges or seams, do not have their own dedicated machine - they are done in between.

5 Road Representation

An automated road compaction process requires a common representation for data exchange. One asphalt paver acts as the primary vehicle and stores road construction data collected during the paving process. The participating pavers collect data about the asphalt area like temperature and compaction. Collaborating rollers gather sensor readings as compaction and temperature to update already existing information. An overview of the road model is depicted in Fig. 2.

A road $\mathcal{R}$ has a set of lanes $\vec{\mathcal{L}}$ corresponding to the number of pavers. A lane $\mathcal{L}_i$ corresponds to the paver with ID i. Additionally, the road has longitudinal seams which connect and delimit lanes. A seam $\mathcal{S}_j$ is shared by

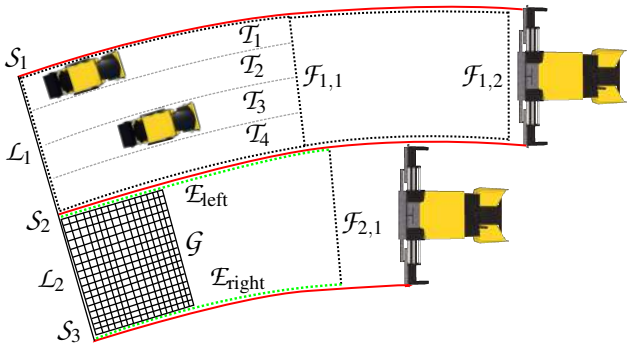

Figure 2. Road $\mathcal{R}$ with lanes $\vec{\mathcal{L}}$, seams $\vec{\mathcal{S}}$, fields $\vec{\mathcal{F}}$, edges $\vec{\mathcal{E}}$, grids $\vec{\mathcal{G}}$, and tracks $\vec{\mathcal{T}}$.

neighboring lanes. Therefore, there exists one additional seam with respect to the number of lanes

$$\mathcal{R} = \left(\vec{\mathcal{S}}, \vec{\mathcal{L}}\right), \text{ where } ||\vec{\mathcal{L}}|| = ||\vec{\mathcal{S}} + 1||. \tag{1}$$

Each road lane $\mathcal{L}_i$ contains a vector of fields $\vec{\mathcal{F}}$. Thereby, each field $\mathcal{F}_{i,k}$ has a maximum length of 25 m. It is defined as a polygon based on the paver's screed points $\vec{\mathcal{P}} = \overrightarrow{(p_{\text{left}}, p_{\text{right}})}$ during paving. Therefore, the field's width varies over time depending on the construction process. Exemplary, the minimum screed length for a BF 800 C paver is 2.55 m and 10 m maximum.

A field $\mathcal{F}_{i,k}$ contains two edges $\mathcal{E}_m$ with $m \in \{\text{left}, \text{right}\}$ and a grid $\mathcal{G}$.

$$\mathcal{F}_{i,k} = \left(\mathcal{E}_{\text{left}}, \mathcal{E}_{\text{right}}, \mathcal{G}\right) \tag{2}$$

Each edge is represented as B-spline which is appended by the respective paver's extending screed outer point p_{left} or respectively p_{right}. An edge is also a part of the corresponding seam $\mathcal{S}_j$.

The grid $\mathcal{G}$ has a resolution of $r = 10$ cm and stores construction relevant data such as the asphalt insertion time or respectively the last sensor update t_{up}, temperature estimation time t_{est}, measured stiffness c in MN/m^2, asphalt temperature T_{asph}, and asphalt temperature estimate T_{est} in °C. The temperature estimate is based on the last temperature measurement by the rollers or paver.

$$\mathcal{G}_{l,w} = \overrightarrow{\left(t_{\text{up}}, t_{\text{est}}, c, T_{\text{asph}}, T_{\text{est}}\right)} \tag{3}$$

The longitudinal grid index l depends on the current field length, while the index w on the respective paver screed width. Each grid $\mathcal{B}$ represents an detailed map of the current road section. Rollers utilize it for path planning under the consideration of the compaction effort, compaction time, temperature, and the current compaction state. Therefore, each field and respectively grid can be converted into a set of tracks $\vec{\mathcal{T}}$. A track $\mathcal{T}_n$ is a planned compaction area of a roller. Therefore the track's width depends on the area covered by a roller's drum or crab steering. For instance, the BW 154 tandem roller class has a drum width of 154 cm while BW 174 has 174 cm respectively. Additionally, the width can be extended through crab steering by 135 cm.

5.1 Temperature Model

A detailed description of asphalt cooling is provided in [16]. The most relevant parameters that influence the cooling behavior are the layer thickness λ, asphalt temperature T_{asph}, wind speed v_{wind}, and ambient temperature T_{amb}. In the previously described road representation, the asphalt layer thickness is provided by the road object $\mathcal{R}$ itself. Hereby, it is differentiated between base course, binder layer, and wearing course. The layer's thickness λ can be set as a parameter depending on the given class. This is also relevant for later compaction, vibration, and chip spreading. As mentioned before, T_{asph} is stored within the lane's grids $\mathcal{G}$. The parameters v_{wind} and T_{amb} are determined externally and set up in advance or measured by additional sensors. To estimate the temperature at time point $t_{\text{est}} = t_{\text{up}} + \Delta t$, which is Δt seconds after the actual measurement sensor measurement time t_{up}, the estimation of the temperature flow $\dot{Q}$ is exploited:

$$\begin{aligned}\dot{Q} = 7.4 + 6.39 \cdot v_{\text{wind}}{}^{\frac{3}{4}} (T_{\text{asph}} - T_{\text{amb}}) + \\ + 53.83 \cdot 10^{-9} \cdot (T_{\text{asph}}^4 - T_{\text{amb}}^4) - 680\end{aligned} \tag{4}$$

It follows

$$T_{\text{est}}\left(T_{\text{asph}}, \lambda, v_{\text{wind}}, T_{\text{amb}}, \Delta t\right) = T_{\text{asph}} - T_{\text{drop}}, \tag{5}$$

where the temperature drop T_{drop} for the duration Δt is

$$T_{\text{drop}} = \frac{\int_0^{\Delta t} \dot{Q}\, \mathrm{d}t}{2640 \cdot \lambda r^2}. \tag{6}$$

Analogous, a maximum time window until a certain temperature is reached can be determined. This is especially relevant for the asphalt compaction planning.

5.2 Asphalt Compaction

The asphalt compaction depends on different factors as asphalt composition and temperature. Furthermore, it can be differentiated between pre-, static and dynamic compaction. Additionally, the machine used for road works influences the compaction process.

Mix proportions are assumed to be constant in the following. This is also a prerequisite of the previously described temperature model, where factors like asphalt density and thermal conductivity are included as constant factors. The current asphalt temperature determines

the compaction effort and defines time frames for compaction. In general compaction should start as early as possible. The effort $\mathrm{Eff}(T)$ depends on the temperature T and is defined as

$$\mathrm{Eff}(T) = \begin{cases} T < 80\,^{\circ}\mathrm{C} & \text{too cold} \\ 80\,^{\circ}\mathrm{C} \leq T < 100\,^{\circ}\mathrm{C} & \text{stop range} \\ 100\,^{\circ}\mathrm{C} \leq T < 140\,^{\circ}\mathrm{C} & \text{optimum} \\ 140\,^{\circ}\mathrm{C} \leq T < 160\,^{\circ}\mathrm{C} & \text{start range} \\ \geq 160\,^{\circ}\mathrm{C} & \text{too hot} \end{cases} \quad (7)$$

Therefore, the duration ΔT_{stop} denotes the time until the asphalt is too cold based on the previously described temperature model.

The road's required number of transitions to achieve a feasible compaction can be estimated beforehand according to the vehicle class. It can be differentiated between static and dynamic compaction. Hereby, static compaction is used to achieve a minimum precompaction (too low compaction value) or for ironing (high compaction value). Dynamic compaction utilizes drum vibration of the roller. Usually, low and high amplitude modes are available. The low amplitude vibration is used for the wearing course and the binder layer, while the high amplitude is used for the road's base course. Additionally, there exist different tandem roller classes as for instance 4t, 7t, or 10t vehicles. Hence, the transition count and compaction amount depends on the roller class. Exemplary data is provided by [17]. In the following, the number of transitions is used to estimate the current compaction.

The optimum compaction speed is inbetween 1 and 2 m/s. This is used for scheduling of tracks based on the compaction priority. The compaction amount and compaction effort define the priority of a track $\mathcal{T}_n$ under the consideration of remaining time. Therefore fields with a low ΔT_{stop} value and low compaction amount c are prioritized high.

6 Road Construction Approach

The general road model of a specific construction site depends mainly on the available pavers. Usually, several rollers of different build types are available. Their usage and usability depends on their properties, the given construction scenario and the task requirements.

6.1 Roller Tasks

Aside from the *compaction* task itself, rollers have several other tasks to fulfill. They have a limited supply of diesel and water, which is consumed meanwhile. Due to the relevance of machine availability, *refueling* is considered as an own task and enables to remain operational even on low supplies. Additionally, resource rerouting may be required. Thereby, a roller *navigates* to a target position. Under certain conditions a roller may be *idle*, e.g during an oversupply. Hereby, it monitors the construction progress and can be requested to rejoin the fleet and actively work on another task.

6.2 Roller Skills

The larger a road construction site, the higher is the probability that there exist unequal rollers which belong to another vehicle classes or are equipped differently. Each roller has some tasks it excels at and some where it is inadequate for. In order to be able to compare rollers, different skills have to be considered. They are described as a percentage of the task feasibility, which influences a later assignment. This guarantees that a roller is able to perform a task in an adequate manner. Exemplary skills are edge compaction, chip spreading, pre-compaction, or narrow curve compaction.

6.3 Compaction Tasks

Road compaction is divided into sub-tasks which are accomplished by the rollers. An initial task is the processing of the *latitudinal seam* which provides a suitable connection to another street segment. Hereby, a roller's drum has an overlap of approximately 20 cm with the hot asphalt while the other part remains on the connected segment. A main tasks is the *track* compaction. It is also related to *longitudinal seam* processing. Each track overlaps with its neighbor for several centimeters in order to achieve an even connection. Additionally, the *ironing* of tracks is important. Final tasks are *edge compaction* and *chip spreading*. While chip spreading is essentially identical in the movement planning to track compaction, edge compaction depends mostly on the type of edge. Usually, edge processing requires a specific tool as a cutter or conical roll mounted on the vehicle. Furthermore, edges need to be driven as accurately as possible. Hence, those tasks are especially dependent on the roller's capabilities.

6.4 Compaction Strategies

The exists a variety of asphalt compaction strategies depending on the number of available rollers. In general, a single roller usually compacts a track, seam, or edge on its own. At the end of each track, a curve is driven towards the center of a seam to create a matrix within the asphalt to improve robustness.

A practical oriented swarm compaction approach is used in the following. Two rollers compact directly behind the paver, while a third roller irons a field behind. If a front roller has to leave the formation, the rear roller can catch up.

6.5 Compaction Errors

The final roads quality depends heavily on the avoidance of compaction errors. A major factor is the road's temperature since the compaction of too hot asphalt damages the surface, while too cold asphalt prevents the completion of compaction, respectively. Furthermore, the application of an unsuited roller class, e.g. too heavy vehicles, can introduce bow waves. Similarly, severe fractures may appear at the rolls edges. Also, shear forces have to be considered and sharp turns on the asphalt prevented. An insufficient bandages sprinkling may cause the material to stick on the rolls. Usually, a damaged section of the road forces a complete reconstruction and has to be prevented by all means. Therefore, error avoidance is explicitly considered during task assignment.

7 Distributed Task Assignment

Road compaction involves many vehicles which have to be coordinated accordingly. The construction process consists of many tasks that are distributed between machines. In contrast to a strict hierarchical procedure, where a master defines every task and the corresponding assignment, human workers follow a more self-determined way of task-fulfillment. In the following, a distributed approach for task assignment is proposed. Here, robots determine their suitability for a task self-directed. Each robot suggests its feasibility for a given task to an inter-robot behavior network which selects the most suited robot.

7.1 Communication of Construction Vehicles

The REACTiON architecture [18] provides a framework for robust and safe off-road navigation of commercial vehicles using a behavior-based approach. REACTiON provides basic perception and localization skills [15], as well as a low-level collision avoidance [19] to the involved robots as tandem rollers, or paver. Furthermore, a behavior-based communication approach adapts transmitted data according to the available bandwidth [20].

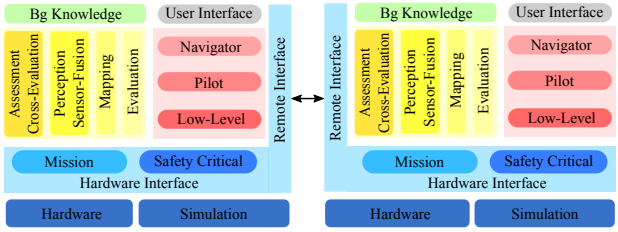

Figure 3. Robot communication using REACTiON remote interfaces.

Robot communication is realized by an extended REACTiON architecture exploiting remote interfaces (Fig. 3). Hereby, a remote interface equals a standard hardware interface. Subsequently, collaborating vehicles and transmitted sensor data can be considered as external sensors. Additionally, higher level information can be exchanged. Therefore, it is possible to span a behavior network across vehicles.

7.2 Paver Road Update and Task Assignment

The paver is the central element of the road construction process. Therefore, it manages the communication of the fleet and creates a mobile 5G-island [21]. As part of the inter-vehicle behavior network, it distributes all road construction and compaction tasks.

Fig. 4 depicts the part of the distributed BBS running on the paver. The *Perception* system provides information about the paver's *Screed* like pre-compaction, temperature, and current screed extension. *Pose* data is used to determine the exact screed location under the consid-

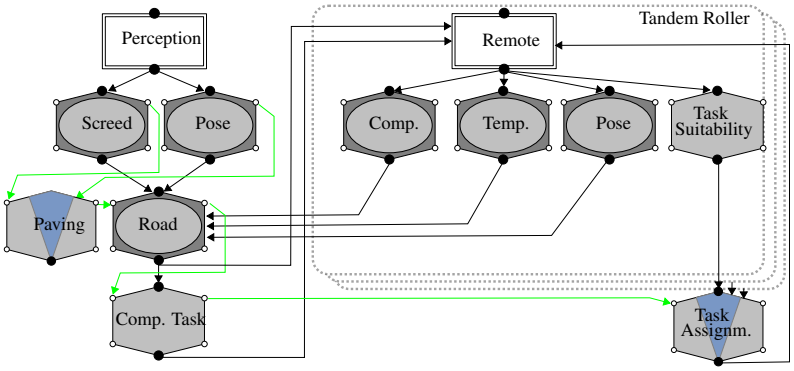

Figure 4. Paver behavior network for road model maintance and task assignment. Tandem rollers connect remotely to the paver and update road information. Task assignment uses a fusion behavior to select a roller.

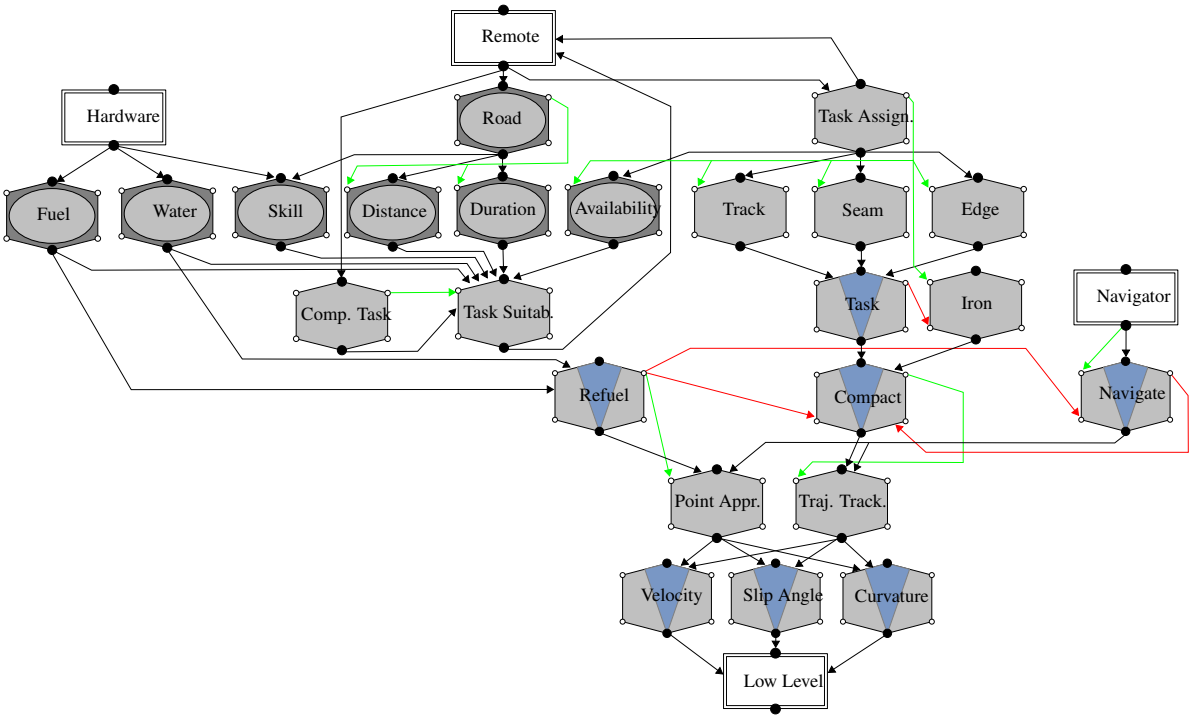

Figure 5. Tandem roller behavior network for road compaction. Properties as fuel, water level, skill, distance to a location, availability, and task duration are considered to determine the individual suitability to execute a task.

eration of localization sensor quality estimates. A *Road* model is maintained during the *Paving* process by successive updates of the paver's screed data. Additionally, collaborating tandem rollers provide road relevant data like the measured *Compaction*, *Temperature*, and the roller's *Pose* through the *Remote* interface. Compaction and temperature data update the temperature information and estimate contained by the road's grid content.

The paver determines the next *Compaction Task* which has to be performed by a roller. Hereby, a priority queue schedules the next task based on the criticality resulting from time constrains, compaction effort, and temperature. The compaction task is sent together with a task identifier to all collaborating rollers through the remote interface. Each roller responds with an estimate about its *Task Suitability* and the roller ID. The suitability is encoded within the behavior's activity and is determined individually by each roller. Thereby, factors as the current task, roller skills, fuel level, distance to the task location, and availability are considered. The *Task Assignment* uses a maximum fusion to select the best suited roller. The winner is acknowledged and adds the task to its task queue.

7.3 Tandem Roller Task Request and Execution

The task assignment among tandem rollers is a distributed process through the connected inter-vehicle behavior network. An extract of the network is depicted in Fig. 5. A roller can fulfill three main actions. It can *Refuel Fuel* or *Water*, *Compact*, or *Navigate*. The latter bases on the output of the *Navigator* interface. The vehicle is idle if there exists no activity in the network. Each of the three tasks provides either a target destination to a *Point Approach* behavior or a spline which is followed using the *Trajectory Tracking* behavior. Both navigation behaviors provide a *Velocity*, *Curvature*, and *Slip Angle* to the *Low Level* control interface.

Each roller retrieves a *Compaction Task* and the updated *Road* model from the *Remote* interface connected to the paver. Thereby, the individual *Task Suitability* is estimated under the consideration of the *Fuel* and *Water* level, as well as its *Skill* for the task based on the *Hardware* information. Additionally, the spatial *Distance* is considered to prefer tasks nearby. Furthermore, the *Duration* of a task and current *Availability* is regarded. This enables a roller to acquire an additional task when it is nearly finished with the current work. The estimate is transmitted and subsequently the *Task Assignment* behavior receives a roller ID for the outstanding task from the paver. The winning roller acknowledges and activates one compaction behavior. Accordingly, either a *Track*, *Edge*, or *Seam* compaction is executed. If there exists no specific *Task*, the roller's *Iron* behavior is active.

8 Experiments

The presented approach was tested in a virtual road construction environment. Simulated tandem rollers compacted a road and assigned tasks based on the construction process and skills. The results were compared to recorded real road construction activities.

The control software was implemented using Finroc, a C++, Java based robot control framework [22]. The scenario was simulated using the Unreal Engine 4 (UE4). Sensors were modeled to behave similar to corresponding real systems [20]. A virtual model of the B10 highway, Germany, served as the test environment, where three BW 174 roller and a BF 800 C operated (Fig. 6). Real construction data was available for comparison.

Figure 6. Road construction test on the simulated B10 highway, Germany.

The paved lane had a width of 7.5 m and length of approximately 1 km. An extract of the road as well as the asphalt cooling behavior is shown in Fig. 7. A comparison of human and robot trajectories can be seen in Fig. 8. In both trials, the lane was separated into 4 tracks. A human operator reversed after approximately 35 m, in contrast to the the autonomous systems with 25 m. The robots stayed strictly in the middle of the track and turned close to the paver. The human drivers navigated more imprecise inbetween the tracks. Additionally, the task separation differed. Real workers operated within different fields, where one roller compacted on all 4 tracks and the other roller stayed more behind. In contrast, the robots equally distributed the tracks of a field which results in a consistently distributed work-load.

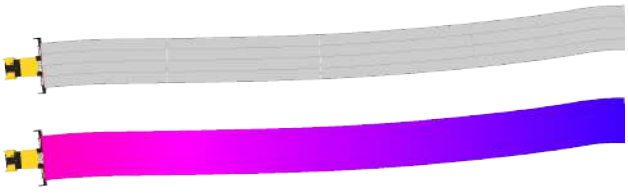

Figure 7. Extract of simulated lane of B10 highway with fields, and tracks. A temperature map shows asphalt cooling from hot (pink, 180 °C) to cold (blue, 80 °C).

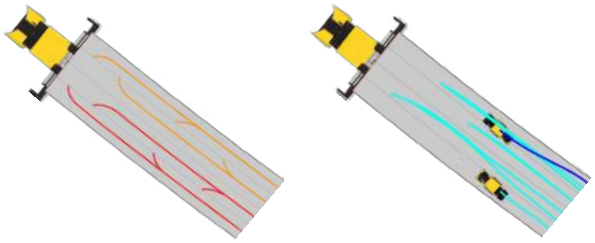

Figure 8. Simulated (orange, red) vs. human (turquoise, blue) trajectories in correlation to paved fields (gray).

9 Conclusion

This paper presented a novel approach for multi-robot collaboration in road construction. It provides an overview to the state of the art in autonomous road construction and multi-robot control. A formal road representation including layout, temperature, and compaction data is proposed. An inter-robot distributed BBS was used for task selection and assignment. Hereby, each roller competes for a task based on the suitability. The design compensates roller failures and distribute tasks accordingly. Finally, the system was tested in simulation and compared to real road construction data.

Future work targets an even more sophisticated road representation, which includes compaction errors as fractures, or bow waves. Additionally, the street model can be improved through considering more factors as different characteristics of mix proportions. Furthermore, varying asphalt supply as well as fluctuating weather conditions like wind or rain can be considered and impact on assignment and quality investigated. Finally, the concept should be tested using the real 5G-AMMCOA demonstrators.

References

[1] S. Deb. Automation and robotics based technologies for road construction, maintenance and operations. The Masterbuilder, pages 44–50, April 2013.

[2] K. Berns, K.-D. Kuhnert, and C. Armbrust. Off-road robotics - an overview. KI - Künstliche Intelligenz, 25(2):109–116, May 2011.

[3] L. Bayındır. A review of swarm robotics tasks. Neurocomputing, 172:292 – 321, 2016.

[4] B. K. Krishnamurthy, H.-P. Tserng, R. L. Schmitt, J. S. Russell, H. U. Bahia, and A. S. Hanna. AutoPave: towards an automated paving system for asphalt pavement compaction operations. Automation in Construction, 8(2):165 – 180, 1998.

[5] C. Halbrügge and B. Johanning. Automatisierte Asphaltverdichtung mit schemelgelenkten Tandemwalzen. ATZoffhighway, 8(2):56–67, Jul 2015.

[6] C. Halbrügge, B. Johanning, and A. Römer. Automatisierte Maschinenführung von Straßenwalzen. BauPortal, 4:35–37, June 2015.

[7] S. Klumpp and A. Römer. Autonome Walzen. Asphalt & Bitumen, 3:38–41, 2017.

[8] R. Kuenzel, J. Teizer, M. Mueller, and A. Blickle. SmartSite: Intelligent and autonomous environments, machinery, and processes to realize smart road construction projects. Automation in Construction, 71(Part 1):21 – 33, 2016. The Special Issue of 32nd International Symposium on Automation and Robotics in Construction.

[9] A. Ulrich, M. N. Tamo, V. Farbischewski, and M. Watermann. Autonom arbeitende Maschinen im Straßenbau. Forschungsprojekt schafft Voraussetzungen für erfolgreichen Einsatz. VDBUM Info, pages 30–33, September / Oktober 2018.

[10] H. Oh, A. R. Shirazi, C. Sun, and Y. Jin. Bio-inspired self-organising multi-robot pattern formation: A review. Robotics and Autonomous Systems, 91:83 – 100, 2017.

[11] L. E. Parker. Alliance: an architecture for fault tolerant multirobot cooperation. IEEE Transactions on Robotics and Automation, 14(2):220–240, April 1998.

[12] F. J. Mendiburu, M. R. A. Morais, and A. M. N. Lima. Behavior coordination in multi-robot systems. In 2016 IEEE International Conference on Automatica (ICA-ACCA), pages 1–7, Oct 2016.

[13] S. Müller, P. Wolf, K. Berns, and P. Liggesmeyer. Combining behavior-based and contract-based control architectures for behavior optimization of networked autonomous vehicles in unstructured environments. In K. Berns, K. Dressler, P. Fleischmann, D. Görges, R. Kalmar, B. Sauer, N. Stephan, R. Teutsch, and M. Thul, editors, Commercial Vehicle Technology 2018. Proceedings of the 5th Commercial Vehicle Technology Symposium – CVT 2018, pages 25–36, Kaiserslautern, Germany, March 13–15 2018. Commercial Vehicle Alliance Kaiserslautern (CVA), Springer Vieweg.

[14] M. Proetzsch. Development Process for Complex Behavior-Based Robot Control Systems. PhD thesis, Robotics Research Lab, University of Kaiserslautern, München, Germany, June 2010.

[15] T. Ropertz, P. Wolf, and K. Berns. Quality-based behavior-based control for autonomous robots in rough environments. In O. Gusikhin and K. Madani, editors, Proceedings of the 14th International Conference on Informatics in Control, Automation and Robotics (ICINCO 2017), volume 1, pages 513–524, Madrid, Spain, July 26–28 2017. SCITEPRESS – Science and Technology Publications, Lda.

[16] J. Wendebaum. Nutzung der Kerntemperaturvorhersage zur Verdichtung von Asphaltmischgut im Straßenbau. PhD thesis, 2004.

[17] H.-J. Kloubert. Grundlagen der Asphaltverdichtung. Verdichtungsverfahren Verdichtungsgeräte Walztechnik. Handbuch, BOMAG GmbH, Hellerwald, Germany, 2009.

[18] P. Wolf, T. Ropertz, K. Berns, M. Thul, P. Wetzel, and A. Vogt. Behavior-based control for safe and robust navigation of an unimog in off-road environments. In K. Berns at. al., editor, Commercial Vehicle Technology 2018. Proceedings of the 5th Commercial Vehicle Technology Symposium – CVT 2018, pages 63–76, Kaiserslautern, Germany, March 13–15 2018. Commercial Vehicle Alliance Kaiserslautern (CVA), Springer Vieweg.

[19] T. Ropertz, P. Wolf, and K. Berns. Behavior-based low-level control for (semi-) autonomous vehicles in rough terrain. In Proceedings of ISR 2018: 50th International Symposium on Robotics, pages 386–393, Munich, Germany, June 20–21 2018. VDE VERLAG GMBH.

[20] T. Ropertz, P. Wolf, K. Berns, J. Hirth, and P. Decker. Cooperation and communication of autonomous tandem rollers in street construction scenarios. In K. Berns at. al., editor, Commercial Vehicle Technology 2018. Proceedings of the 5th Commercial Vehicle Technology Symposium – CVT 2018, pages 25–36, Kaiserslautern, Germany, March 13–15 2018. Commercial Vehicle Alliance Kaiserslautern (CVA), Springer Vieweg.

[21] J. Kochems and H. D. Schotten. AMMCOA-Nomadic 5G Private Networks. arXiv preprint arXiv:1804.07665, 2018.

[22] M. Reichardt, T. Föhst, and K. Berns. Introducing FINROC: A Convenient Real-time Framework for Robotics based on a Systematic Design Approach. Technical report, Robotics Research Lab, Department of Computer Science, University of Kaiserslautern, Kaiserslautern, Germany, 2012.

Indoor Visualization Experiments at Building Construction Site using High Safety UAV

T. Narumi[a], S. Aoki[a], and F. Muramatsu[b]

[a]Shimizu Corporation, Institute of Technology
[b]Panasonic Corporation, Innovation Promotion Sector
E-mail: narumi@shimz.co.jp

Abstract –

Importance has been placed on improving productivity at construction sites in a recent year, reducing bitterness and repetitive work, and improving the efficiency of inspection and management work. Since buildings usually have a unique shape, efficiency improvement methods used in mass production plants had not been able to be applied, however, due to the recent progress in machine learning and robotics technology, complex works have also been becoming possible gradually. Especially at a construction site where the gross floor area is large, it is necessary to spend a lot of time for checking the status of daily situations and inspection work, and then it is often discussed as an object of efficiency improvement. There are also attempts to autonomously run the rover at a construction site, photograph the surroundings with a camera, automatically check a situation with Building Information Model (BIM), and identify the unusual part. However, the floor surface of the construction site is generally complex shape in many cases, for example reinforcing bars are exposed, it is not easy to run around. Accordingly, we focused on Unmanned Aerial Vehicle (UAV) as a means to move freely without concern the shape of the floor. There are many merits because it is possible to move in any structure as long as it is a small UAV, and it is also possible to grasp states of a high altitude that cannot be reached by a rover. Although autonomous flight of UAV is almost established outdoors, the introduction of indoor autonomous flight has not advanced yet because localization technology and object recognition technology are insufficient, and the risk of damage to people and structures due to collision and fall. There are some UAVs equipped with collision avoidance sensors, and safety is not guaranteed completely. Therefore, in this research, we developed a high safety UAV against collision and falling and conducted experiments on verifying the efficiency of inspection work and the possibility of visualization of acquired data. To ensure strong safety, a balloon type fuselage was manufactured, and collision tests and drop tests were carried out to confirm that it is incredibly safe. Besides, we performed a flight test in the indoor construction site using the UAV and demonstrated that it could be used for inspection work. Furthermore, the walkthrough view was generated from the photographed image for making daily progress management easily. As the results, it was confirmed that some works of walking around the construction site for checking would be reduced, and productivity will be improved. In the near future, we aim to collect data by autonomous flight at night when work is stopped and to create a database of daily information.

Keywords –

Construction management; Inspection; UAV

1 Introduction

The productivity of the construction site has not much changed for decades. Improvement of productivity such as reduction of repetitive work, inspection, and management optimization by cooperation with BIM, becomes an urgent issue. Since the shapes of buildings are usually individual, productivity improvement has been not natural so far. However recent drastic advancement in machine learning technology and robotics technology, even complicated works have also been becoming possible. For example, Shimizu Construction has built a Shimizu Smart Site (Fig. 1[1]) which has been running horizontal slide cranes, column welding robots, arm robot, and horizontal/vertical conveying robot autonomously with artificial intelligence (AI) and internet of things (IoT). The operation status and the work results are recorded and accumulated in real time in the management system integrated with BIM and can be confirmed at any time on the tablet screen, which leads dramatic reduction of work.

Regarding inspection work, it is necessary to spend a lot of time for checking the status of each day and detecting abnormality at construction sites where the total floor area is wide in particular. Typically, a worker is occupied by the inspection work for several hours in a day because pictures taken by a camera at each point including high-place is required. Then it is often cited as an object of efficiency improvement. Thus, there are many attempts to autonomously run a rover at a construction site, photograph and check the surroundings with cameras automatically with the building information model (BIM), and identify the abnormal part[2]. The accuracy of detecting concrete cracks and tile damage by camera imagery has been improved by using AI and machine learning techniques.

However, the floor surface of the construction site is generally in a complex shape in many cases. For instance, since the reinforcing bars are exposed, it has risks and dif-

Figure 1. Shimizu Smart Site

ficulties to walk around. Then we focused on Unmanned Aerial Vehicle (UAV), especially multirotor as a means to survey the site freely without the constraint of the shape of the floor. There are many merits because it is possible to fly any structure as long as it is a sufficiently small UAV, and it also makes possible to grasp the situation of a high altitude that cannot be reached by a rover. Autonomous flight of UAV is generally utilized Global Navigation Satellite System (GNSS), various cameras, Light Detection and Ranging (LIDAR), etc. However, GNSS can only acquire absolute position outdoors, distance accuracy from the camera is low while it is relatively easy to recognize an object, the weight of LIDAR is large while it has high distance accuracy. Although autonomous flight of UAV is usually achieved outdoors, indoor flight has a risk of damage to people and structures due to collision and fall because of the difficulty of localization technology and object recognition technology have not sufficiently developed yet. Carnegie Mellon University[3] and Pennsylvania University[4] are working on research of autonomous flight in GNSS-denied environments, and partially succeed in flying while carrying out localization and obstacle avoidance even in complex shape. Although there are some products equipped with collision avoidance sensors, these are not entirely guaranteed safety. Utilizing UAV for indoor inspection by comparing to BIM is not yet practically sufficient[5] because of the above reasons.

Therefore, in this research, we developed a quite safe multirotor against collisions and falls. Flight experiments were conducted for verifying the efficiency of inspection work and the possibility of visualizing the acquired data. To ensure reliable safety, a balloon-type fuselage was manufactured. Collision and drop tests were carried out to confirm that it was extremely safe. Since it uses injected helium gas, it also has the advantage of increasing the payload weight by buoyancy. Besides, we conducted a flight test in an indoor construction site using the multirotor and demonstrated that it could be used for inspection work. Furthermore, walkthrough view was generated from the photographed imagery which makes daily progress management easy. As a result, it will reduce the amount of walking and checking works, which means productivity considered to be further improved.

Ultimately, we plan to aggregate data by autonomous flight through the night when work is stopped and to create a database of daily information automatically in the future.

2 Method

2.1 Concept

As mentioned in the previous section, general multirotor has the risk of crash and collision, and it is not allowed under current circumstances to use it at the construction site where safety is of utmost importance. Also, if the interior is damaged before completion, time and cost will be wasted. Therefore, in any case, safety must be ensured. As a means to solve this problem, a structure having a spherical frame, a structure hanging from a spherical balloon, a method of mounting an airbag, a structure of extremely lightweight, and a way of making the UAV itself a balloon-type are conceivable. Although the spherical shell structure is lightweight, there is a risk that it may be caught by reinforcing bars or pipes at a construction site, the method of hanging from a spherical balloon is challenging to ensure mobility, the airbag has uncertainty of deployment, lightweight body has a disadvantage that cannot mount a highly accurate sensor.

Therefore we focused on balloon-type multirotor, which can overcome any of the above drawbacks. First, we confirm the flight performance using this balloon-type body. Also, experiment by changing the type of camera installed, and confirm what kind of capturing method is most beneficial to the construction site. The camera to be used is a spherical camera, infrared camera + visible camera, and a high-resolution action camera.

Since the operator must easily check the photographed image, a visualization test is performed by creating a walkthrough view of the work site for validity confirmation. In the future, we will build a system that automatically carries out everything from site photographing by autonomous flight to visualization.

2.2 Balloon-type Multirotor

The figure 2 shows the developed balloon-type multirotor. The position and attitude angles are controlled by the rotational speed of the four propellers attached to the rods. In the center of the body, communication equipment, control equipment, battery, and camera are installed. Depending on the application, the camera can be replaced

with a spherical camera, an infrared camera, an action camera, etc., and its orientation can also be changed.

As shown in the table 1, the outside body is covered with polyvinyl chloride so that both collision safety and buoyancy are acquired by injecting helium gas into the inside. Since it is a prototype, the payload that can be installed at present is as small as 0.3 kg and the flight time is as short as 10 minutes, but these can be improved by the design refinement and the advance of battery performance. The propeller noise is the same as a conventional multirotor, and the flight speed is about the same as a person's walk. Also, video transmission by wireless is also enabled. Because it is very safe against a collision, it also has the advantage that it is possible to take close-up shots when examining walls and ceilings.

Figure 2. Balloon-type Multirotor

Table 1. Specification

Size	$\phi 1.2x0.6$ m
Weight	1.6 kg
Buoyancy of helium gas	−0.3 kg
Endurance	10 min
Speed	1.0 m/s
Membrane	PVC

2.3 Time-Series Spherical Viewer

There are various ways to visualize the acquired data, such as three dimensional model generation by Simultaneous Localization and Mapping (SLAM)[6, 7], Structure from Motion (SfM)[8], a database of images by cooperation with indoor positioning system by Bluetooth beacon or ultra-wideband (UWB), fixed camera images, immersive viewing system with virtual reality (VR) headset using spherical imagery, and so on. However, as the result of our examination and hearing, we found that the walkthrough view of spherical images can be most intuitively operated and the inspection is easy. Therefore, by using commercially available Holobuilder[9], it is possible to browse by moving to the target place simply by clicking the points on the screen or clicking the position on the drawing. Additionally, since images can be saved in chronological order, it is also possible to confirm daily changes, progress, and the cause when an abnormality occurs.

3 Results

The size of the multirotor body is 1.2 m in diameter that is rather large in the present situation, and then the flight experiment was carried out at the site under construction of sufficiently large space (Fig. 3). As a component where inspection is difficult with a general rover, the diagonally below the catwalk near the ceiling was selected as the experimental location.

According to preliminary verification experiments, it was found that the body is very safe against collision and fall, and not damage the object. Additionally, depending on the environment it turned out that the multirotor was liable to disturb the attitude angle by the wind. This is thought to be due to the fact that the shape of the body is ellipsoidal, vortices are likely to occur around the periphery, and the drag coefficient is relatively large. Also, since the inertial efficiency is larger than that of general multirotor, it requires more energy to restore the attitude. The airflow due to convection was confirmed although the influx of wind was also shut out at the experimental site, it was able to stably fly by adequately tuning the attitude control parameter of the multirotor. Typically, when the aircraft is too close to a wall or object, it is likely to be sucked in because the air current is disturbed and the posture is not stable. Nevertheless, such a phenomenon did not occur in this experiment. However, due to the shape of the fuselage and the lack of performance of the propeller, the robustness of attitude stability against a wind more than 1 m/s is not enough at the moment. In the future, it is necessary to improve so that it can maintain stable attitude and position in any wind environment.

Figure 3. Inspection of Catwalk

The figure 4 is an image of a spherical camera (Ricoh Theta V). Because interval shooting is possible, we shot every 4 seconds this time. The resolution of the photo is 5376 x 2688 pix, and the weight of the body is 121 g. As shown in the figure, since the camera is attached to the upper part of the UAV, the lower one third is hidden by the balloon film surface. However, there was no problem

Figure 4. Onboard Spherical Camera

because this purpose is photographing in the upward direction, and further the camera can be attached to the lower part, and then it can be changed according to the purpose.

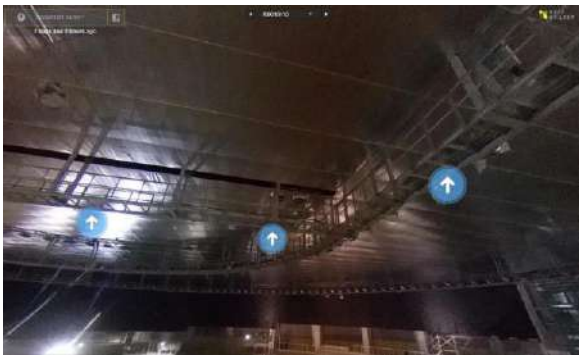

Figure 5. Walkthrough View

The figure 5 shows an example of created walkthrough view from the above spherical camera image using Holobuilder which is on-site image management software. The image can be rotated and scaled quickly, and by clicking the arrow arranged on the picture, it is possible to move to the viewpoint image from the place. By registering the position of the image on the drawing, it becomes possible to view the whole sky ball image at the viewpoint of the desired place. Furthermore, since images can be managed in time series, it is possible to manage daily progress. Also, data is managed on the cloud, and then it can be shared and edited by multiple people. It also has functions such as adding annotations, browsing from mobile devices, and distance measurement. Although it is useful software in visualization, it has a disadvantage that it requires human work such as registration of a position of an image. Recently, the software that can automatically performs localization from a movie and image extraction also appears.

Figure 6. Onboard Action Camera

The figure 6 is a captured image of a motion picture taken by action camera (GoPro Hero 6, 120 g weight). It is possible to take a picture at 4K (3840 x 2160 pix), but this time for the purpose of image processing, we shot at 2.7K (2704 x 1520 pix) using Linear View function with lens distortion removed. The image was very clear, and it was possible to grasp the state of the bolt finely and so on. It was also found out that it was possible to reconstruct the 3D model by SfM from Linear View images. However, position information such as a marker is indispensable for high-precision 3D reconstruction, however, it is not desirable to increase the amount of people's work at the construction site where the environment changes every day. It is a future subject to realize everything automatically and unattended.

The figure 7 is an image by FLIR Duo R (84 g weight) which is a combination of an infrared camera and a visible

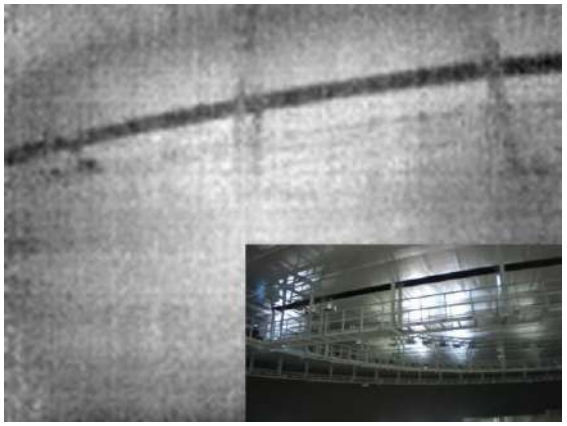

Figure 7. FLIR Infrared & Visible

light camera. As for the resolution, the infrared image is 160 x 120 pix, and the visible light image is 1980 x 1080 pix. Using SfM software such as Pix4D[10], it is possible to paste an infrared image as a texture to a three-dimensional model reconstructed by a visible light image. Researches on abnormality detection using infrared images have been actively conducted for discovering tile deterioration, concrete cracks, or estimate distortion from the temperature of the structure by utilizing artificial intelligence. The resolution of the infrared camera used this time is not sufficient, although it can distinguish a specific temperature difference.

4 Conclusion

We developed highly safe UAV and verified the performance for improvement the productivity of inspection work at a construction site. To ensure reliable safety at any time, a balloon-type multirotor was manufactured. Collision tests and drop tests were carried out to confirm that it was extremely safe. We also conducted a flight test at the construction site of the large indoor space using the multirotor and demonstrated that it could be used for inspection work using the equipped camera.

In the flight experiment of this time, The airflow due to convection was confirmed although the influx of wind was also shut out at the experimental site, stable flight was possible with adequate tuning of the attitude control parameter of the multirotor. However, it easily drifts against the wind and the attitude stability is not sufficient due to its shape of the fuselage. Therefore, future improvement of the robustness against environmental uncertainties is necessary. Also, since the size of the fuselage is slightly big at 1.2 m, it should be miniaturized to a size of less than 80 cm which can pass through the door. Further, since it is not easy to handle helium gas at all times from the viewpoint of cost and operation, it is necessary to improve so that handling can be easily performed with air injection.

Three-dimensional reconstruction by SfM using action camera images is expected, however artificial correction information such as markers is indispensable for highly accurate reconstruction currently. The situation and environment at the site that change every day, it is not desirable to increase the amount of people's work at the site, and it is a future subject to make everything automatic and unattended. Regarding infrared images, if high-resolution cameras are used to make meaningful data, there is a possibility that defects can be found by using machine learning techniques. For the whole sky ball image, we created a walkthrough view to facilitate day-to-day progress management. As the results, it was confirmed that some works of walking around the construction site for checking would be reduced, and productivity will be improved. However, although it is useful software in visualization, it has a disadvantage that it requires human work such as registration of a position of an image. The software that can automatically perform localization and extraction is needed.

In the future, we plan to aggregate data by autonomous flight through the night when work is stopped and to create a database of daily information automatically.

References

[1] M. Indo and S. Sakamoto. Next generation autonomous construction system: Shimizu Smart Site (in Japanese). *Welding technology*, Vol. 65, No. 12, pp. 45–49, 2017.

[2] H. Ardiny, S. Witwicki, and F. Mondada. Construction automation with autonomous mobile robots: A review. pp. 418–424, oct 2015.

[3] Z. Fang, S. Yang, S. Jain, G. Dubey, S. Roth, S. Maeta, S. Nuske, Y. Zhang, and S. Scherer. Robust Autonomous Flight in Constrained and Visually Degraded Shipboard Environments. *Journal of Field Robotics*, Vol. 34, No. 1, pp. 25–52, jan 2017.

[4] S. Shen, N. Michael, and V. Kumar. Autonomous multi-floor indoor navigation with a computationally constrained MAV. pp. 20–25, may 2011.

[5] J. Wang, W. Sun, W. Shou, X. Wang, C. Wu, H.-Y. Chong, Y. Liu, and C. Sun. Integrating BIM and LiDAR for Real-Time Construction Quality Control. *Journal of Intelligent & Robotic Systems*, Vol. 79, No. 3-4, pp. 417–432, aug 2015.

[6] H. Durrant-Whyte and T. Bailey. Simultaneous localization and mapping: part I. *IEEE Robotics & Automation Magazine*, Vol. 13, No. 2, pp. 99–110, jun 2006.

[7] T. Bailey and H. Durrant-Whyte. Simultaneous local- ization and mapping (SLAM): part II. *IEEE Robotics*
& Automation Magazine, Vol. 13, No. 3, pp. 108–117, sep 2006.

[8] M.J. Westoby, J. Brasington, N.F. Glasser, M.J. Hambrey, and J.M. Reynolds. ' Structure-from-Motion' photogrammetry: A low-cost, effective tool for geoscience applications. *Geomorphology*, Vol. 179, pp.300–314, dec 2012.
[9] https://www.holobuilder.com/, retrieved Jan 30th 2019.
[10] A. Murtiyoso and P. Grussenmeyer. Documentation of heritage buildings using close-range UAV images: dense matching issues, comparison and case studies. *The Photogrammetric Record*, Vol. 32, No. 159, pp.206–229, sep 2017.

Using Serious Games in Virtual Reality for Automated Close Call and Contact Collision Analysis in Construction Safety

O. Golovina[a], C. Kazanci[a], J. Teizer[a], and M. König[a]

[a]Civil and Environmental Engineering, Ruhr-University Bochum, Universitätsstrasse 150, 44801 Bochum, Germany
E-Mail: olga.golovina@rub.de, caner.kazanci@ruhr-uni-bochum.de, jochen.teizer@rub.de, koenig@inf.bi.rub.de

Abstract –

Injuries and fatalities resulting from workplace accidents remain a global concern within the construction industry. While education and training of personnel offer well known approaches for establishing a safe work environment, Serious Games in Virtual Reality (VR) is being increasingly investigated as a complementary approach for learning. They yet have to take full advantage of the inherent data that can be collected about players. This research presents a novel approach for the automated assessment of players' data. The proposed method gathers and processes the data within a serious game for instant personalized feedback. The application focuses on close calls and contact collisions between construction workers and hazards like equipment, harmful substances, or restricted work zones. The results demonstrate the benefits and limitations of safety information previously unavailable, or very hard or impossible to collect. An outlook presents work ahead for practical implementation in existing risk management processes.

Keywords –

accident investigation, close call, construction safety, equipment contact collisions, hazard, human-hazard interaction, risk prevention, serious game, situational awareness, virtual reality, workforce education and training.

1 Introduction

The original inspiration to conduct this research stems from a scientific study on construction accident investigations [1]. It found that approximately 13% of all construction workplace fatalities in the United States relate to too close contact with construction equipment or parts of it (like attached loads) [2]. While construction equipment is dangerous, other industries in engineering suffer from similar problems. As shown in Fig. 1, the location (marked with "x") of 29 coal miners killed while at work between 1984-2004 could only be determined after the tragic loss of their lives. The image depicts detail to the miners who were either remotely operating (72%, indicated by a blank circle) or maintaining (grey shaded circle or square) a continuous miner. The figure is – due to its rarity of pointing out the victim's location – regularly shown in construction safety education classes. However, current learning methods do not engage the trainees in other effective ways of self-experiencing high risk work activities. These often cannot be implemented, especially in field-based safety training where they would endanger one's life [4, 5].

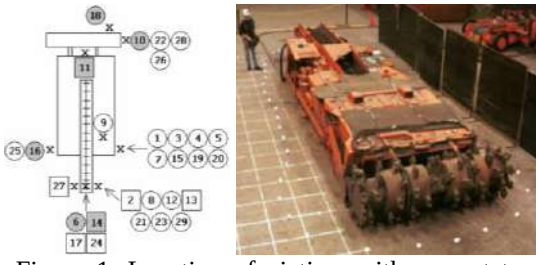

Figure 1. Location of victims with respect to a continuous coal miner (closely related industry) [3]

The novelty of the proposed approach is to provide a safe learning environment where mistakes can be made without suffering the normal consequences. The general hypothesis is that wrong judgement – whether conducted knowingly or not – can be discovered and eliminated by training early on, before it happens at the workplace [6].

Several best practices exist today to mitigate risk in organizations early, starting with a good safety culture and tight safety processes. The layers in the hierarchy of controls, however, still have to take full advantage of data that can be provided by technology during training sessions. Data mining in serious games can offer participants instant personalized feedback.

This research first designed a safe learning process, then a learning platform using serious games in virtual reality (VR). The implementation of a realistic VR environment was supported by the latest, commercially-existing head-mounted display (HMD) units and actual three-dimensional worksite models and schedules (4D) using Building Information Modeling (BIM). Several hazards related to close calls (aka. near misses) and contact collisions between construction workers,

equipment or its parts, harmful substances, and restricted zones were added to the virtual construction scene. Consequentially, close calls and contact collisions were defined based on given occupational safety and health standards. Participants with some construction experience tested the scenario individually while personal safety performance data were collected and analyzed in real-time. Instant quantitative analysis and visual safety performance information became available that is used for personalized feedback and improvement.

2 Background

For years Virtual Reality (VR) has been used for training purposes. A high number of VR applications exist in the fields of military, aviation, and medicine. For example, a serious game (defined 'serious' because of a primary purpose other than pure entertainment) helped to increase the awareness of airplane passengers in case of an emergency situation [7]. Like many studies, it evaluated two user groups (one group using the traditional approach with safety cards, the other using a serious game) based on questionnaires and pre- and exit-interviews. Studies related to construction [4-5,8-12] concluded that VR-based safety awareness training offers more engaging learning environments. Study participants also reported to favor personalized feedback over no feedback (as commonly in lectures, videos, or demonstrations) [5]. Some of the benefits of VR-based safety training are:

- presents trainees with hazards directly and realistically without compromising their own safety;
- holds the attention of trainees better than conventional classroom teaching does;
- gives trainees a measure of control in the environment, thus reinforcing learning; and
- allows trainers to repeat learning content for many participants under the same training conditions.

VR learning scenarios were criticized by some for being unsophisticated and unrealistic compared to the real world experience [12]. A reason is that creating VR scenarios is a very time-consuming task, requiring a lot of attention to fine details [5] such as programming logic, whereas [6,13-14] proposed using BIM to increase the realism level of VR scenes. While using 4D models adds additional return-on-investment to create BIM data (e.g., beyond its use in design/planning tasks or for providing visual walkthroughs), reducing motion sickness for some players, teaching people unaccustomed to computerized environment, creating multi-user environments (incl. training larger groups), and providing options to instantly record and analyze the players' behaviors seem to be challenges for realistic VR-implementations. Known limitations are:

- Although hard- and software technology are rapidly evolving, the investment of developing training materials and virtual construction scenarios is high.
- Several studies [5,10-12] claim that the gained safety knowledge of some trainees may remain at similar levels compared to standard learning approaches.

While some of the issues create needs for additional research, they remain outside the scope of this study (e.g., motion sickness and multi-user environments). This study addresses an effort towards real-time data collection and instant analysis in an immersive serious game for a more detailed construction worker-equipment close call and contact collision assessment.

3 Proposed method

This section explains noteworthy details to the research methodology, its objective and scope definition. As illustrated in Fig. 2, the developed virtual safety learning platform consists of a user (e.g., (un)skilled construction worker), a virtual construction site environment (e.g., 3D content generated from 4D models or open source libraries), scene- or object-related content (e.g., typical sounds), and soft- and hardware technology (e.g., authoring tools and head mounted displays, respectively).

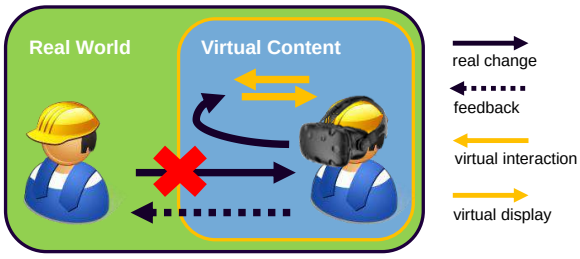

Figure 2. VR safety learning platform [15]

While a person may have previous education and experience (i.e., related to construction safety), advanced tools for automated, in depth, and personalized performance analysis and feedback are not existent in today's practice (research objective). Personal safety skills particularly to close call and contact collision detection and analysis of construction workers to hazardous equipment or restricted work areas will be tested (research scope definition). VR technology is used as it provides a safe work environment (called an experimental testbed) where humans can make mistakes without suffering the losses they would typically experience in the real world. Thus, further processing of any worthwhile information generated in the virtual world (e.g., the location of close calls or contact collisions, their frequency and types) might be applied to improve the working conditions in the real world. Since 4D-models normally exist before construction starts, such information (e.g., relations between 3D objects and

construction sequence) will be used to generate realistic virtual work environments. The following explains how VR is used to advance the analysis and control.

3.1 Visualizing and controlling

VR consists primarily of hard- and software components. While multiple commercial systems exist, this approach used the head mounted display (HMD) HTC Vive Pro (2018 Version) for visualization and control and the game engine Unity3D for authoring content. Although VR raises the immersion effect of the user, it is still challenging to achieve a high realism of VR scenes. Two controllers give a player the opportunity to interact within the virtual construction scene. The lighthouse-system tracks the head-mounted display and controller movements via the emitted infrared rays. A computer combines and finally sends data from the graphics processing unit to the displays of the virtual reality headset. To reduce latency and diminish motion sickness the refresh rate should be close to 90 Hz [14].

3.2 Processing

The second technology which was used is the gaming-engine Unity3D. While the virtual construction scenario is created in Unity3D, it offers programmers many additional functionalities like collision detection or physical handling. To use the HTC Vive tracking system in Unity3D the "steamVR"-plugin" [17] is needed. This plugin contains necessary objects like the "[CameraRig]"-object which handles the communication between the HTC Vive tracking system and the operating computer. The "[CameraRig]"-object has three child-objects: "Controller (left)", "Controller (right)" and "Camera (head)". Both of controller-objects are used to handle the player's input. They visualize the controller's position and rotation in real-time. The "Camera (head)"-object is used to show the direction of the player's view. A player uses the touchpad of the right HTC Vive controller for moving within the VR scene.

3.3 Authoring content and model functions

Construction site models from a real project and additional 3D models (e.g., equipment and materials) from the internal Unity3D Asset Store, online libraries for free share or for purchase, self-modeled models, or other sources served as content to create a serious game which was tested by players. To increase a player's immersion effect, the selection of 3D models plays a pivotal role. Compulsory to the construction scene model were models of a construction worker, a tower crane, a skid steer loader and several smaller construction objects to illustrate two restricted work areas.

Unity3D supports files with .fbx-, .dae-, .3DS-, .dxf- and .obj-extensions [17]. All selected models were converted into the file extension .fbx and made available for further use in Unity3D. They should have the same quality in order to keep the player´s experience, an realistic level. The acceptable number of polygons are preferred, because a higher number influences the computing performance negatively. Once the required models with the supported extension are fetched, they can be imported into the Unity3D-project. While recently announced plugins allow exporting/importing native building information models into Unity3D [17], this research used a self-developed approach [12] to import .IFC models directly. Via drag-and-drop the models can finally be placed into the Unity3D-scene. Within the scene the position, the rotation, and the scale-properties of the models can be adjusted using the inspector-window.

3.3.1 Construction scene

For this research, an existing building project incl. the 3D models (e.g., model of neighboring buildings, detailed site layout plan, pit model and structural model, incl. reinforced concrete walls, columns, and slabs) and the construction schedule served as the main source of information. Fig. 3 shows the resulting scene model.

Figure 3. Construction scene (isometric view)

3.3.2 Construction worker

A 3D-model of a construction worker (Fig. 4) allowed to visualize the movement of the player. The following pseudocode explains the movement in the scene.

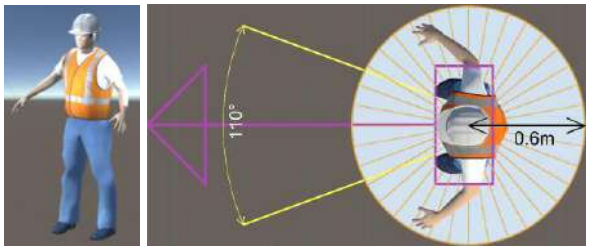

Figure 4. 3D model view of the construction worker with PPE (left); the bounding cylinder field-of-view of head-mounted display (right)

The Start-function initializes the right HTC Vive Pro controller, when the simulation starts. The Update-function checks in every frame whether the worker has pressed the right controller's touchpad. The task of this pseudo C#-script is to move the 3D-model of the worker dependent on the input of the right controller's touchpad.

Pseudocode 1: Movement of the construction worker

```
Start(){
  rightController.initialize();
}
Update(){
  if(rightController.touchpadTouched)){
    WorkerPosition += touchpadInput * movementScale;
  }
}
```

The developed approach displays two additional items (Fig. 4): (a) an arrow that visualizes the direction of the worker's field-of-view (FOV) in real-time and (b) a circular layer, defined as the safety envelope [6,18]. A player's FOV covers 114° [19] (compared to 110° of the Vive tracking system). The arrow's purpose is to give trainers or by-standers administering or observing a training session an immediate understanding which direction the player is looking at. Data collected to the FOV can further be analyzed, as explained later.

The construction worker's safety envelope has a radius of 0.6 m and represents a typical adult person's shoulder width [5]. This segmentation assists in the counting of the number and the direction of close call or contact collisions. Segments with higher counts thus explain how often and from where the worker collided with hazards.

3.3.3 Equipment

A model of a skid steer loader with operator [17] (Fig. 5) travels (for now) on a pre-scripted path within the scene. The purpose is to cause, and later help analyze model interactions from construction workers and equipment. To add further complexity to the scene, a tower crane with a moving load (Fig. 6) was added to the scene.

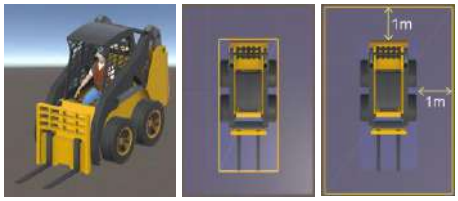

(a) (b) (c)

Figure 5. (a) 3D model of skid steer loader and operator, (b) bounding box encompassing all physical elements, and (c) 1 m-safety envelope

Figs. 5b-c further shows two different layers which are important for the close call and contact collision data recording and analysis. The first layer bounds all of the physical parts of the skid steer loader to a box. The second layer represents, according to the ISO 5006 standard, a 1 m-safety envelope to each side of this bounding box [20]. No worker is allowed to enter either area, otherwise a contact collision or a close call, respectively, is called. The crane load is also given a 1.5 m safety envelope.

Figure 6. Model of tower crane and load

3.3.4 Harmful substance, restricted work zone, and other object models

Among the many potential construction hazards are the handling of harmful substances and the prohibited entrance in restricted work zones. A gas bottle and an electric power generator (Fig. 7) were placed in the scene as representative examples. The safety envelope of the gas bottle was set to a 1 m radius. 3 security fences around the generator and a nearby wall formed a restricted work zone of 2.5 m×3 m. Despite shortcut options, no player was allowed to enter either one. The scene also consisted of a recycling container, which each player had to fill with recycling bags.

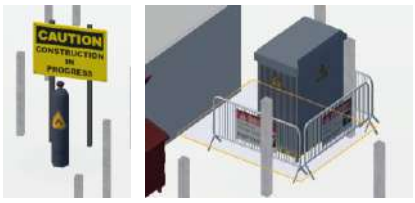

Figure 7. Models of harmful substance (left) and restricted workzone with security barriers and a shortcut option (right)

3.4 Player's mission

Each player was in the role of the construction worker. Equipped with the HMD and controller's touchpad a player traversed through the scene. Their mission was to pick, walk, and finally place 5 recycling bags, one after the other, in a nearby container. Figure 8 shows the construction scene. The gas bottle and the generator with its associated fences were placed in such way that all players had the opportunity of entering their respective safety envelopes. For example, a player may squeeze by the security fences (an obviously shorter, but more dangerous path). While completing their mission, the players further had chances to interact with the skid steer load and crane load.

3.5 Data gathering in VR

3.5.1 Close calls and contact collisions

The second pseudocode shows how to detect a close call or a contact collision between the construction worker's and the crane load's safety envelopes:

Pseudocode 2: Collision detection

```
OnCollisionEnter(){
  If(collision.name == "CraneLoadLayer"){
    CollectDataOfCollision();
    CreateCyanSphereOnGround();
  }
}
```

The OnCollisionEnter-function (provided in Unity3D) detects collisions between two objects: A pseudo C#-script attached to the construction worker's safety envelope layer checks whether it collides with, for example, the crane load's safety envelope layer. If it does, it collects timestamped data of the actual positions and speeds of the construction worker and the crane load. Simultaneously, the CreateCyanSphereOnGround-function sets a cyan colored sphere (a visual marker) at the position of the close call position in the virtual scene.

While placing a visual marker provides real-time feedback for the user (and might be helpful in sensitizing his/her behavior), it might influence the data recording in the remainder time of playing the serious game. For this reason, the option of visualizing the markers right away can be set inactive.

The developed serious game designed 6 different collision types (colors). Fig. 8 shows the visual markers obtained from participant 1 in the construction scene. As explained later in detail, it includes the trajectories of the skid steer load and the crane (both scripted, in blue and red colors, respectively) and the construction worker (participant's actual path, in green color).

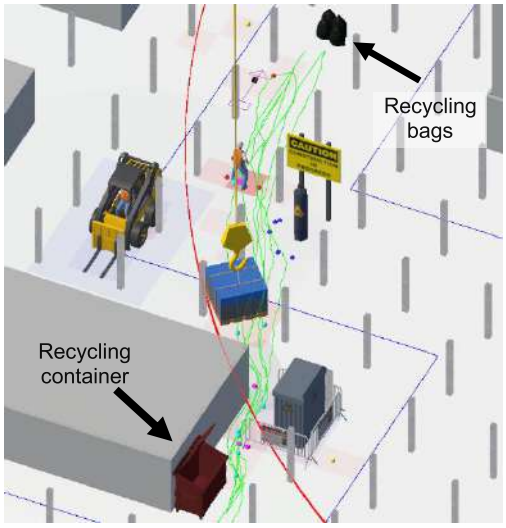

Figure 8. Various types of automatically detected close calls and contact collisions (incl. markers)

A collision point becomes red if the construction worker's safety environment layer collides with the skid steer loader's 1 m safety envelope layer (Fig. 5c). Black cubes are set to the scene's ground if the construction worker's safety envelope collides with the skid steer loader's bound box (0 m) (Fig. 5b). Every type of close call or contact collisions receives its own color (Table 1). This differentiation makes the post analysis between trainer and trainee more effective. For example, a black marker means the player made physical contact with the skid steer loader. While this may result in the real world in life-threating damage, a trainer may give a trainee special responses if such colors appear.

Table 1. Color scheme of close calls & contact collisions

Collision type	Color (Size of safety envelope)	Marker color
Construction worker (0.6m)	Skid steer loader (1m)	**Red**
Construction worker (0.6m)	Skid steer loader (0m)	**Black**
Construction worker (0.6m)	Crane load (1.5m)	**Cyan**
Skid steer loader (1m)	Crane load (1.5m)	**Yellow**
Construction worker (0.6m)	Gas bottle (1m)	**Blue**
Construction worker (0.6m)	Electric generator, Restricted work zone (0m)	**Magenta**

3.5.2 Trajectories

During the entire play time, the trajectories to each moving object are recorded. The blue and green lines, for example, show the trajectories of the skid steer loader and the construction worker, respectively. These can be visualized in real-time while playing or for later analysis (Fig. 8), for example, to reason about collision angle and speeds. The following pseudocode shows how the trajectories of objects are visualized:

Pseudocode 3: Trajectory visualization

```
Update () {
  DrawLine(oldPosition, currentPosition, green, 999);
  oldPosition = currentPosition;
  currentPosition = new Vector3(currentXPosition,
    currentYPosition, currentZPosition);
}
```

The pseudo C#-script is attached to the 3D-model of the construction worker. Its task is drawing the trajectory of the worker first using the internal Untiy3D-library (which offers the DrawLine-function). The function has the input values: 3D-vectors (oldPosition,

currentPosition), a color (green), and a number (999). The latter defines how many seconds the line should be visible. The first 3D-vector defines the start position of the line (oldPosition: the position of the last frame) and the second 3D-vector defines the end position of the line (currentPosition: current frame). Finally a green line between both positions is drawn. The 3D-vector oldPosition is updated in every frame. Analogue thereto a similar pseudo C#-script is attached to the skid steer loader and the crane load (blue and red lines, respectively).

3.5.3 Heat map, statistics and video recording

In order to visualize the location and frequency of close calls, a C#-script generates a heat map after [6,18]. The heat map is divided into equally sized squares (1 m×1 m). Each square changes its saturation from a bright to a dark (red) color as the number of close calls in the square increases. Darker colors probably refer to a location on the virtual construction site that deserves further attention and/or corrective action by responsible safety personnel. Fig.9 shows in an example the different saturation levels. A built-in bird-view camera provides at the end of each serious game a screenshot of the resulting heat map. It can be used for feedback with the player.

Figure 9. Close-up view of heat map: Increasing saturation visualizes higher number of close calls

Further functions were scripted to offer detailed insights on the whereabouts and frequency of the recorded close calls. Examples like investigation of angles and speeds were mentioned already. Every gaming session was recorded using virtually placed cameras. Such video material was used occasionally for playback, giving the participant opportunity to explain behavior or simply modify the construction site layout. Although these options exist, they were not explored in this research at this time.

4 Tests and results

The results of testing 3 participants are presented. Every participant was able to choose their own path through the construction scene to complete the task. They were first instructed on the functionality of the VR equipment and told in advance that time to complete the task is of importance. Signs to restricted work areas in the scene and the possibility of oncoming traffic (a skid steer loader and a crane load) were not explained ahead of time.

4.1 Close call and contact collision events

Within the developed serious game close calls and contact collisions occurred with static hazards: a participant (without the proper safety experience nor in possession of an adequate training certificate) was getting too close to a gas bottle (blue marker, Fig. 10a) or was entering a restricted work zone (magenta marker, Fig. 10b). The second observation shows a too close human-machine interaction. Red (Fig. 11a) and black markers (Fig. 11b) were left at the close call positions accordingly. Fig. 13 illustrates the third example of a recorded close call between the construction worker and the crane load.

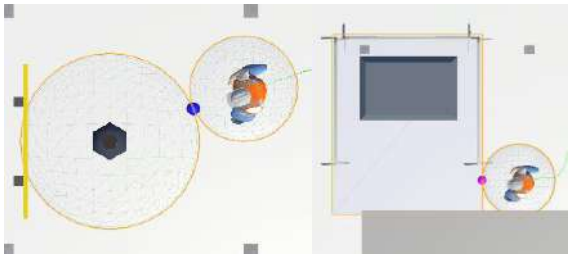

(a) (b)

Figure 10. Construction worker: (a) proximity to gas bottle and (b) entrance in restricted zone

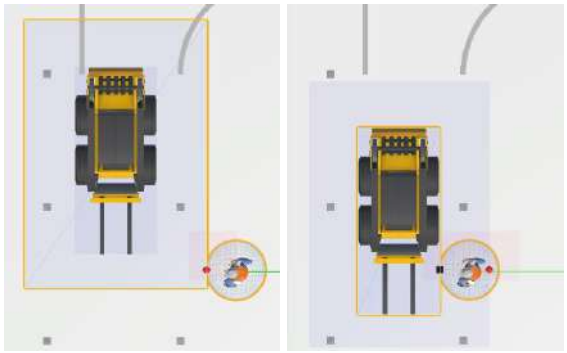

(a) Close call: t_1=120s (b) Collision: t_2=121s

Figure 11. Worker-skid steer loader close call and contact collision at two consecutive timestamps

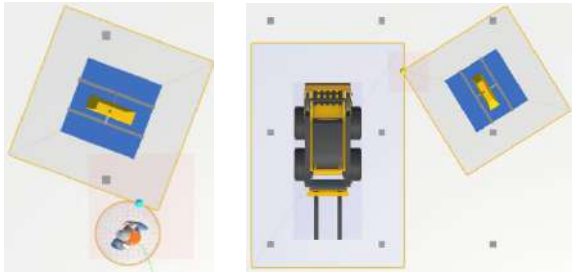

Figure 12. Close calls with crane load: construction worker (left) and skid-steer (right)

The required time for completion of the same work task by all 3 participants were 193, 298, and 177 seconds. While one might think that the number of close calls might increase with the speed a participant executing the mission, the third participant was the fastest and safest.

Table 2 summarizes the results of the independent tests. Participant 1 had by far the most close calls and was the only one who made contact collisions with the skid steer loader (4). The second participant had less, while the third had the fewest. In brief, the first test participant had 48 close calls within the 3 minutes and 13 seconds needed to complete the mission. In brief, while all participants deserve (additional or first time) safety training, the first participant should attend basic safety education (had 4 contact collisions, entered restricted work areas).

Table 2. Number of close calls

Type	Hazard	Participant			Sum / Avg
		1	2	3	
Crane	Overhead load	20	10	2	32 / 10.6
Skid steer loader	Close call (1m)	8	3	2	13 / 3.3
	Collision (0m)	4	0	0	4 / 1.3
Gas bottle	Proximity (1m)	10	0	0	10 / 3.3
Restricted work zone	Entrance	10	0	0	10 / 3.3

As explained in the introduction section, visuals are important to communicate the cause of close calls or contact collisions. Fig. 13 illustrates the precise location of each of the participants' self-made experiences. It appears that all participants in this study had such events in the front-left of the skid steer loader's driving direction. While this is quite the opposite to the equipment shown in Fig. 1, this in fact due to the scripted path of the skid steer loader (traveling only forward). Had a multi-user environment with a second or third player operating the equipment existed, the result may have looked differently.

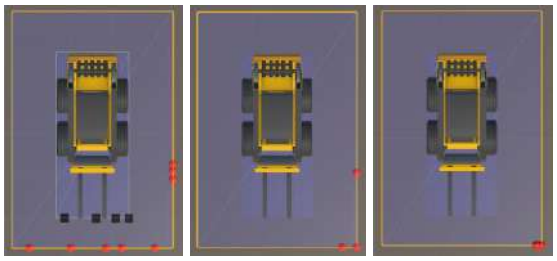

(a) Participant 1 (b) Participant 2 (c) Participant 3

Figure 13. Close call & contact collision locations

Data in Fig.14 shows the performance of the first participant over the game time. The large number of crane load swings becomes visible. Future training may point out this important safety issue still very common to many workers on construction sites (and even in this virtual game).

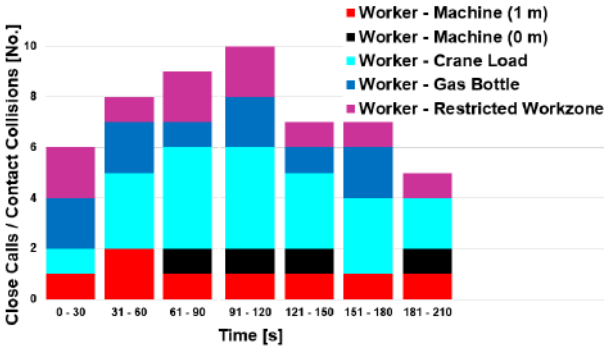

Figure 14. Close call & contact collision numbers

4.2 Heat maps

Heat maps were drawn. Fig. 15 displays the heat map of the first participant. Position and frequency of close calls and contact collision events become visible. While the other participants' heat maps were different, a site safety layout plan always could now be adjusted based on the observed 'hot spots' (arrows pointing to darker red cells). It seems in this situation that the construction worker's path collided with the skid steer loader, crane load, gas bottles and restricted work area. Skid steer loader and crane load had several close call situations as well. While some hot spots were expected (worker passing scripted equipment path), this may still result in decisions towards modifying the internal traffic control plan, for example, the installation of a guided crosswalk.

Figure 15: Heat map to test data of participant 1

5 Discussion and conclusion

Serious games in VR have been around since the late 20th century. They are applied games designed for specific purposes other than pure entertainment, however, so far hardly collect nor analyze data that is readily

available in the game engine. This study developed and tested a serious game in VR that allows a player in a role (construction worker) to immersive into a construction scene (facing hazards). It became possible to record and analyze previously unknown data to close calls and contact collision to human-hazard interactions. Several benefits and limitations were found throughout the study that will help improve further research and development. In particular the difficulty of building realistic and meaningful (multiplayer) VR scenes, the size of the test group, human-behavioral issues, and impact on existing construction workface planning and safety processes (i.e. digital tools of any kind for pre-investigative construction risk analysis and prevention) play important future roles to make any kind of VR education and training an effective tool in construction.

Acknowledgment

This research is funded by the German Federal Ministry of Education and Research (BMBF) within the "Innovations for Tomorrow's Production, Services, and Work" program as well as by the European Social Fund (ESF). The authors are responsible for the content.

References

[1] Hinze J.W. and Teizer J. Visibility-Related Fatalities Related to Construction Equipment, *Safety Science*, 49(5):709-718, 2011, http://dx.doi.org/10.1016/j.ssci.2011.01.007.

[2] US Bureau of Labor Statistics. 2011 Census of fatal occupational injuries, Washington, DC, 2013, http://www.bls.gov/iif/oshcfoi1.htm#2011.

[3] Author unkown. Remote Control Hazard Awareness, Keep out of the Turning Radius, U.S. Department of Labor (MSHA), 2004.

[4] Kassem M., Benomran L., Teizer J. Virtual environments for safety learning in construction and engineering: seeking evidence and identifying gaps for future research, *Visualization in Engineering*, Springer, 5:16, 2017, http://doi.org/10.1186/s40327-017-0054-1.

[5] Sacks R., Perlman A., Barak R. Construction safety training using immersive virtual reality. *Construction Management and Economics*, 31(9):1005–1017, 2013.

[6] Golovina O., Teizer J., Pradhananga N. Heat map generation for predictive safety planning: preventing Struck-by and near miss interactions between workers-on-foot and construction equipment, *Automation in Construction*, 71:99-115, 2016, http://dx.doi.org/10.1016/j.autcon.2016.03.008.

[7] Chittaro L., Buttussi F. Assessing Knowledge Retention of an Immersive Serious Game vs. Traditional Education Method in Aviation Safety. *IEEE Trans. on Visualization and Computer Graphics*, 21(4):529-538, 2015.

[8] Wang P. Wu P., Wang J., Chi H., Wang X. A Critical Review of the Use of Virtual Reality in Construction Engineering Education and Training, *Environment Research and Public Health*, 15(6):1204, 2018.

[9] Li X., Yi W., Chi H., Wang X., Chan A. A critical review of virtual and augmented reality (VR/AR) applications in construction safety. *Automation in Construction*, 86:150-62, 2018.

[10] Zaker R., Coloma E. Virtual reality-integrated workflow in BIM-enabled projects collaboration and design review: a case study, *Visualization in Engineering*, 6:4, 2018.

[11] Burke et al.'s. The Dread Factor: How Hazards and Safety Training Influence Learning and Performance, *Applied Psychology*, 96:46-70, 2011.

[12] Hilfert T., Teizer J., König M. First Person Virtual Reality for Evaluation and Learning of Construction Site Safety, *33rd ISARC*, 2016, https://doi.org/10.22260/ISARC2016/0025.

[13] Zhao D., Jason L. Virtual reality simulation for construction safety. Promotion. *Injury Control and Safety Promotion*, 22:1, 57-67.

[14] Bailenson J., Yee, N., Blascovih J., Beall A.C., Lundblad N., Jin M., The Use of Immersive Virtual Reality in the Learning Sciences: Digital Transformations of Teachers, Students, and Social Context, *J. Learning Practices*, 17:102–141, 2008

[15] Teizer J., Wolf M., König M. Mixed Reality Anwendungen und ihr Einsatz in der Aus- und Weiterbildung kapitalintensiver Industrien, *Bauingenieur*, Springer, 73-82, 2018, ISSN 0005-6650.

[16] Deb S., Carruth D., Sween R. Strawderman L. Garrsion T. Efficacy of virtual reality in pedestrian safety research, *Applied Ergonomics*, 65:449-460, 2017.

[17] Unity3D. https://assetstore.unity.com, 2019.

[18] Teizer J., Cheng T., Proximity hazard indicator for workers-on-foot near miss interactions with construction equipment and geo-referenced hazard areas, *Automation in Construction*, 60:58-73, 2015, http://dx.doi.org/10.1016/j.autcon.2015.09.003.

[19] Howard I.P., Rogers, B.J. *Binocular vision and stereopsis*. Oxford University Press, 1995.

[20] Teizer J., Allread B.S., Fullerton C.E., Hinze J. Autonomous Pro-Active Real-time Construction Worker and Equipment Operator Proximity Safety Alert System, *Automation in Construction*, 19(5):630-640, 2010, http://dx.doi.org/10.1016/j.autcon.2010.02.009.

Impact of BIM on Field Pipeline Installation Productivity Based on System Dynamics Modeling

L. Chen[a], P. Shi[a], and Q. Wu[a]

[a]School of Rail Transportation, Soochow University
E-mail: chenlij@suda.edu.cn, pxshi@suda.edu.cn, mmttqing@163.com

Abstract –

It is well documented that Building Information Modeling (BIM) can significantly improve project performance and productivity. Although the construction phase typically involves in the largest part of financial cost during the project life, insufficient attention has been paid in academia to quantitatively address the impact of BIM on labor productivity. This paper studies the effects of BIM on field pipeline installation productivity using system dynamics modeling. The critical impact factors of BIM on pipeline installation productivity are identified and a system dynamics model is established to map the impact mechanism and quantify the BIM impact on labor productivity. The model is applied to evaluate the pipeline installation productivity of three large scale buildings and their productivity indices are compared. The comparison shows a positive impact of BIM on pipeline installation productivity, resulting in 13~38% of increase in labor productivity dependent on different trades and project phase of BIM application.

Keywords –

Information technology impact; BIM; system dynamic modeling; field productivity

1. Introduction

Labor productivity (LP) is an important index of project performance that reflects the cost conversion efficiency of a project. As reported by the US Bureau of Labor Statistics, the construction LP has been declining in recent years mainly due to the gap between design and construction, relatively low systematic information technology (IT) application and insufficient investment of research and innovation [1]. To improve the LP of the construction industry, significant changes are required in the development of information tools and the formulation of collaborative strategies. Embedding parametric design in a 3D platform, BIM has been proposed to improve construction LP since its emergence. The past decades have seen wide application of BIM in the global construction industry.

One typical example of BIM implementation in construction is to optimize complicated utility pipeline design and coordinate the field installation. There are a large number of utility pipelines with different functions such as water supply, gas supply, electricity circulation, and ventilation in residential and commercial buildings. Design errors and collisions happen frequently in traditional 2D design [3]. Through the application of BIM to arrange pipelines in a 3D space and coordinate on-site installation, the LP of pipeline installation could

be improved from 75~240% [4]. According to statistics in China, the production value of the utility pipeline installation in 2016 is 250 billion USD accounting for 8% of the total value of construction industry. The BIM application in this field has the potential to save substantial resources and generate significant benefits. However, improper BIM application may result in negative effects, such as project shutdown or even engagement of lawsuits and claims [5]. Therefore, study on impact factors and quantify the interaction among these factors is of critical significance to ensure effective BIM implementation. Limited research has been conducted in this field.

The construction activities in the supply chain are closely related and actively interacted, but the interaction between construction tasks is difficult to elaborate in the traditional network diagram due to the nonlinear impact of these activities. System dynamics (SD) is an approach to understanding the nonlinear behavior of complex systems over time using stocks, flows, internal feedback loops, table functions. It can explain system evolution trend and describing the dynamic influence of the internal links. This paper studies the effect of BIM on the LP of complex pipeline installation based on SD modeling. The critical impact factors of BIM on pipeline installation labor productivity （PILP）are identified and a SD model is established. The model is applied to evaluate the PILP of three large scale buildings and the task-level productivity indices are compared.

Table 1. Impact factors of pipeline installation productivity

Impact Factors	Organization	Management	Technical
(1)	Collaboration Degree	Change Orders	Model Precision
(2)	BIM Execution	Quality Control	IFC Application
(3)	BIM Specialist	Plan Compliance	Data Diversity
(4)	Owner’s Support	Risk Control	Localization
(5)	Teams BIM Expertise	RFIs (Requests for Information)	Add-on Development
(6)	Project Delivery Method	Time Delay	Software Function
(7)	BIM Applications	Total Workload	Data Exchange

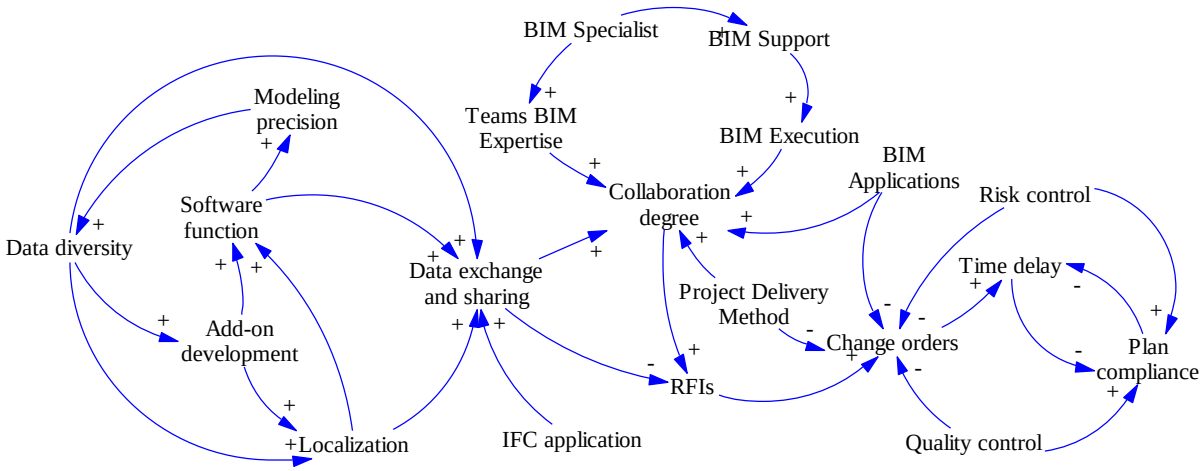

Figure 1. Overall casual loop diagram of impact factors

2. LP impact factor identification

The impact factors of BIM on PILP can be grouped into three primary categories related to the organization, management, and technical aspects of the project, respectively. Within each category, the major factors are identified as listed in Table 1. In total, 21 major impact factors are identified for further system modeling.

3. System dynamics (SD) modeling

In order to study the impact mechanism, a casual loop diagram is developed to qualitatively describe the logical causal relationship between the factors, then a stock and flow diagram is developed to quantitatively illustrate the interrelationship of variables, and the equations for deriving each variable are presented to form a SD model

.3.1 Causal loop diagram

The causal loop diagram describes the feedback structure of a complex system. It reflects the dynamic environment of a causal cycle and visualize relationship between variables and their interaction. By forming a closed feedback loop, the logical causal relationship between the factors are clarified.

The inter-relationship of the impact factors is visualized using a causal loop diagram as shown in Figure 1. By forming a closed feedback loop, the logical causal relationships among the factors impacting the BIM aided pipeline installation productivity are clarified. The factors are with both positive and negative feedbacks and different subsystems interact with each other.

.

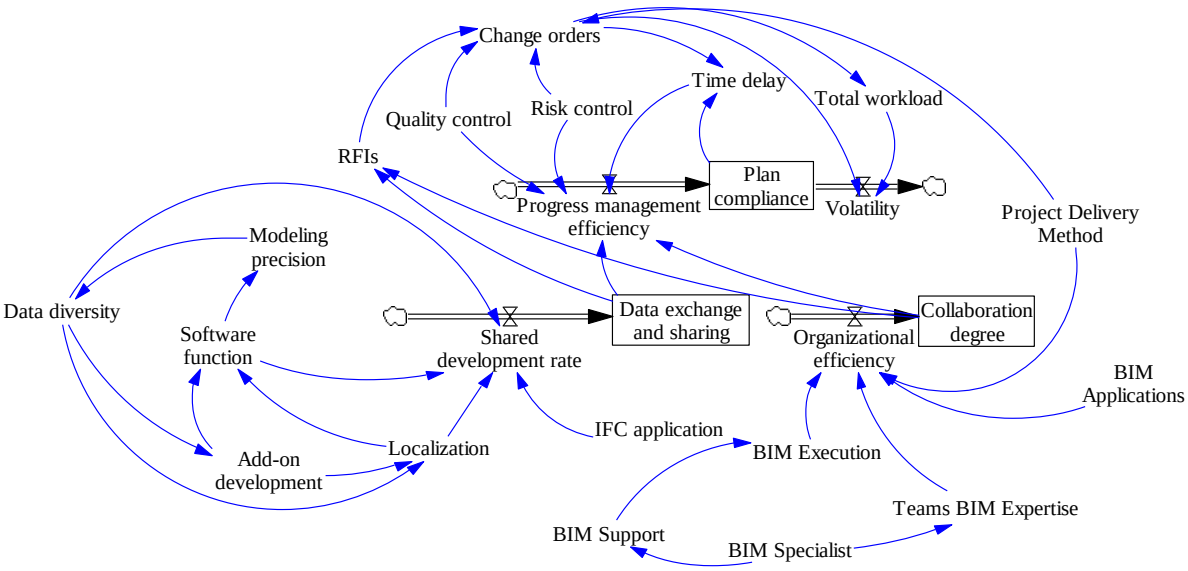

Figure 2. Stock and flow diagram of BIM impact model

3.2. Stock and flow diagram

The causal loop diagram sorts out the model effectively and analyzes the system qualitatively but it is not capable of performing quantitative analysis. The stock and flow diagram is based on the causal loop diagram to distinguish different types of variables, and thus establishing the mathematical relationship between variables. The stock and flow diagram is shown in Figure 2. The plan compliance degree directly reflects the progress control level, and ensures the implementation of the project according to the plan. Engineering changes caused by various factors lead to delay and affect the

degree of plan compliance. Measures such as quality assurance and risk control reduce engineering changes and improve plan-compliance. Data exchange and sharing degree improve the speed and effect of information transmission, enhance communication efficiency, and then increase productivity

3.3 SD Equations

Based on the variable analysis and the stock flow diagram, the level variables (L), rate variables (R) and auxiliary variables (A) that describe quantitative relationship between the impact factors are defined as follow

3.3.1 SD equation of organization subsystem

(1) Collaboration degree equation

The collaboration degree (*CO_DEGREE*) is a level variable whose value is affected by organizational efficiency (ORG_E), DT is time interval. It is defined as

L $CO_DEGREE.K = CO_DEGREE.J + DT * ORG_E$

(2) Organizational efficiency equation

The organizational efficiency (*ORG_E*) is a rate variable whose value is the sum of BIM executive, Teams BIM Expertise, project delivery method mode and BIM applications. It is defined as

R
$$ORG_E = EXCUTION + T_EXPERTISE + D_MODE + APPLICATIONS$$

The teams BIM expertise is a table function of BIM Specialists number and is defined as

A
$$T_EXPERTISE = WITH_LOOKUP(SPECIALISTS)$$

3.3.2 SD equation of technical subsystem

The data exchange and sharing degree (*D_ENJOY*) is a level variable affected by the rate of shared development.

1) Data exchange and sharing degree equation

L $D_ENJOY.K = D_ENJOY.J + DT * DEV_RATE$

2) Shared development rate equation

As a rate variable, the shared development rate (*DEV_RATE*) is the sum of data diversity, localization, software function and the application of IFC standards. It is defined as

R $DEV_{RATE} = D_DIVERSITY + D_LOCAL + FUNCTION + IFC$

The degree of localization (*D_LOCAL*) and software function (*FUNCTION*) are table functions of add-on development (*REDEV*) and are defined as

A $D_LOCAL = D_DIVERSITY + REDEV$

A $FUNCTION = WITH_LOOKUP(REDEV)$

The add-on development (*REDEV*) is a table function of data diversity and is defined as

A $REDEV = WITH_LOOKUP(RICHNESS)$

3.3.3 SD equation of management subsystem

1) Plan compliance degree equation

The plan compliance degree (*D_FOLLOW*) is a level variable whose value is positively related to the BIM based schedule management efficiency (*MAN_E*) and negatively related to the change rate (CHANGE_RATE). It is defined as

L
$$D_FOLLOW.K = D_FOLLOW.J + DT * (MAN_E - CHANGE_RATE)$$

2) Schedule management efficiency equation

The schedule management efficiency (*MAN_E*) is a rate variable that directly impacts the project compliance degree (*D_FOLLOW*). Its value is equal to the sum of risk control level (*M_RISK*) and quality assurance (*M_QUALITY*) minus time delay (*DELAY*) which is the table function of the change orders (*CHANGES*).

R $MAN_E = M_RISK + M_QUALITY - DELAY$

A $DELAY = WITH_LOOKUP(CHANGES)$

The change order (*CHANGES*) is equal to the number of information requests RFI minus the quality assurance (*M_QUALITY*) and the risk control level.

A $CHANGES = RFI - M_QUALITY - M_RISK$

3.3.4 Initial value and variable table function

According to "China Construction Industry Informatization Development report (2015): BIM depth Application and Development") and previous study [3], the initial values of variables are determined. The table function describes the nonlinear relation between some variables whose data source could be historical and literature. Data range is determined by the variation trend and the key points between variables. The interaction effect curve of variables can be obtained by the analysis of VENSIM software，the equation for the variable table function is as follow:

(1) Add-on development equation [30]：

REDEV= =WITH LOOKUP (RICHNES, ([(2000, 0)-(2500, 0.012)], (2000, 0.0101), (2030, 0.0102), (2060, 0.0103), (2090, 0.0104), (2120, 0.0105), (2150, 0.0106), (2180, 0.0107), (2210, 0.0108), (2240, 0.0109), (2270, 0.011)))

(2) Software function equation：

FUNCTION=WITH LOOKUP (REDEV, ([(0，0.4)-(0.011，0.8)], (0，0.4), (0.0102，0.402), (0.0103，0.404), (0.0104,0.406), (0.0105，0.408), (0.0106，0.41), (0.0108，0.412), (0.0109，0.414), (0.011，0.416)))

(3) Time delay equation：

DELAY=WITH LOOKUP (CHANGES, ([(0.08，0.1)-(0.126，0.33)](0.08，0.1), (0.126，0.33)))

(4) BIM level equation：

SPECIALITY=WITH LOOKUP (SPECIALIET, ([(1000, 0.026) -(4000, 0.032)], (1000, 0.026), (1500, 0.028), (2000, 0.03), (2500, 0.032), (3000, 0.034), (3500, 0.036), (4000, 0.038)))

(5) Modeling accuracy equation [29]：

PRECISION=WITH LOOKUP (FUNCTION, ([(0.4, 0.45)-(0.5, 0.6)], (0.4, 0.45), (0.41, 0.47), (0.42, 0.48), (0.43, 0.5), (0.44, 0.52), (0.45, 0.54), (0.46, 0.56), (0.47, 0.58), (0.48,0.6)))

3.4Validation

In order to test the stability of the model, three different time intervals of DT=1, 0.5 and 0. 25 are set in the three subsystem models, respectively. The initial parameter of the model is INITIAL TIME=1, FINAL TIME=15, TIME STEP=1, 0.5, and 0.25. When the interval DT is set to 0.25 and 1, the curves of collaboration degree, schedule compliance degree and data exchange and sharing ability tend to be consistent, so the model is stable to perform sensitivity analysis.

4. Significance evaluation of impact factor

Through sensitivity analysis with initial value of productivity is 0, the significance of the management factor is 0. 56, the technical factor is about0. 29, and the organizational factor is about 0.15. Significance level of each secondary impact factors and overall productivity for 3 subsystems are as follow in Table 2:

5. Case studies

5.1 Background

To evaluate the effects of BIM application, this study compares the installation LP of three cases, a five-star Intercontinental hotel adopted BIM in late construction phrase mainly for facility management, an International Conference Center, which is located next to Continental Hotel, applied BIM from early construction coordination to operation phrase, and the World Trade Square adopted BIM from design review to construction coordination and operation phase. As complexity and size is the most significant factors of projects classification. The three cases are all large-scale with complex pipeline layout, BIM implemented projects and are constructed by contractors with same qualification, such that the installation LP is comparable.

Table 2. Significance level of LP factors

Primary Factor （Significance）	Secondary Factor	Secondary Factor Significance	Significance on Productivity
Organizational Factors （0.15）	BIM Applications	0.284	0.0426
	BIM Execution	0.241	0.0362
	Teams BIM Expertise	0.154	0.0231
	BIM Support	0.148	0.0222
	Project Delivery Method	0.091	0.0136
	BIM Specialists	0.082	0.0123
Management Factors （0.56）	Quality Control	0.324	0.1814
	Change Orders	0.241	0.1350
	RFIs (Requests for Information)	0.158	0.0885
	Risk Control	0.138	0.0773
	Time Delay	0.118	0.0661
	Total Workload	0.021	0.0118
Technical Factors （0.29）	Modeling Precision	0.302	0.0876
	Data Diversity	0.238	0.0690
	Localization	0.151	0.0438
	Add-on Development	0.143	0.0414
	IFC Application	0.090	0.0261
	Software Function	0.079	0.0229

Table 3. Installation LP statistics for three projects

Installation Tasks	HVAC (m^2/man-hr)	Bracket (kg/ man-hr)	Cable trays (m/ man-hr)	Fire control (m/ man-hr)
Intercontinental Hotel	2.60	40.10	1.39	3.70
Conference Center	3.20	45.30	1.70	4.50
World Trade Square	3.60	47.57	1.86	4.74

5.2. Measurement of MEP installation site productivity

The working hours and number of workers are determined according to the records of the weekly reports and construction plan collected from 3 cases. Productivity statics of HVAC (Heating Ventilating and Air Conditioning), bracket, cable trays and fire control pipelines are calculated as

LP=Installed Quantities/Working Time

The results of the LP of the 3 cases are shown in Table 3. Table 3 shows the productivity of the four trades of the three BIM projects. Through field investigation, the conference center and World trade Square showed in higher level of quality control, change orders, BIM Execution and model precision. The installing

productivity statics reflect efficiency of working process including components assembling, connecting, erecting. Compared to the Intercontinental projects, which applied BIM in late construction phrase, early BIM utilized projects, the Conference Center and World Trade Square projects, increased LP between 13% and 38% dependent on different trades

6. Conclusions

In this paper, the critical impact factors of BIM on pipeline installation productivity are identified and a system dynamics model is established to map the impact mechanism and quantify the BIM impact on labor productivity. The model is applied to evaluate the pipeline installation productivity of three large scale buildings and the task-level productivity indices are compared. The comparison shows a positive impact of BIM on pipeline installation productivity, resulting in 13~38% of increase in labor productivity dependent on different trades and project phase of BIM application.

Acknowledgements

The presented work has been supported by the Natural Science Foundation of Jiangsu Province through grant No. BK20160320.

References:

[1]. Teicholz, P., Labor Productivity Declines in the Construction Industry: Causes and Remedies. 2004.

[2]. Dyer, B., P.M. Goodrum and K. Viele, Effects of Omitted Variable Bias on Construction Real Output and Its Implications on Productivity Trends in the United States. Journal of Construction Engineering and Management, 2012. 138(4): p. 558-566.

[3]. Chelson, D.E., The Effects of Building Information Modeling on Construction Site Productivity. 2010, University of Maryland.

[4]. Poirier, E.A., S. Staub-French and D. Forgues, Measuring the impact of BIM on labor productivity in a small specialty contracting enterprise through action-research. Automation in Construction, 2015. 58: p. 74-84.

[5]. Love, P.E.D., et al., From justification to evaluation: Building information modeling for asset owners. Automation in Construction, 2013. 35: p. 208-216.

Trajectory Prediction of Mobile Construction Resources Toward Pro-active Struck-by Hazard Detection

D. Kim[a], M. Liu[a], S. Lee[a], and V. R. Kamat[a]

[a]Department of Civil and Environmental Engineering, University of Michigan, MI, US.
E-mail: daeho@umich.edu, meiyin@umich.edu, shdpm@umich.edu, vkamat@umich.edu

Abstract –
In construction, unanticipated struck-by hazards often arise, which have resulted in a significant number of construction fatalities. To address this problem, many studies have attempted to automate proximity monitoring and struck-by hazard detection using various technologies, such as wireless sensors and computer vision methods. While this technology focuses on understanding what is happening as hazards arise, it is not equipped to detect future hazards. In impending situations, detecting current hazards may not provide enough time for workers to take evasive actions. To address this challenge this study develops a trajectory prediction model for mobile construction resources. Specifically, this study conducts hyper-parameter tuning of a deep neural network, called Social Generative Adversarial Network to develop a prediction model capable of predicting more than five seconds. Further, a test on a real construction operations data follows to validate developed models' trajectory prediction accuracy. As a result, a developed model could achieve promising accuracy: the average displacement error and the final displacement error were 0.78 and 1.27 meters, respectively. The trajectory prediction allows for detecting future hazards, which will support pro-active intervention in hazardous situations. It will ultimately contribute to promoting a safer working environment for construction workers.

Keywords –
Struck-by hazard; Pro-active intervention; Trajectory prediction; Deep neural network; Hyper-parameter tuning

1 Introduction

In construction, mainly due to unstructured and limited workspaces, unanticipated struck-by hazards involving mobile vehicle or equipment often arise, contributing to the significant number of construction fatalities [1]. According to *The Center for Construction Research and Training, United States*, from 2011 to 2015, total 925 struck-by fatalities were reported from construction [2]. The figure accounted for 24% of overall struck-by fatalities in the U.S. and was unmatched by other U.S. industries [2]. Notably, the number of struck-by fatalities rose 34% from 2010 (N=121) to 2015 (N=162) [2].

A critical element of construction safety management is "a proactive, ongoing process to recognize hazards that are present or that could have been anticipated" [3]. However, such continuous monitoring has not been viable in practice as manual observation and inspection is notoriously time-consuming, labor-intensive, and costly [4].

A major research area for this issue is attuned to automating object localization, proximity monitoring, and accordingly struck-by hazard detection. Prior research leveraged various technologies—such as wireless sensors [5-9] and computer vision methods [1, 10-11]—and made a great progress on automation of struck-by hazard detection. It is expected that the successful deployment of such technologies will allow for prompt feedback to involved workers, thereby reducing the chance of an impending collision [1, 5, 10].

However, there remains a critical challenge that has not been tackled yet: how to recognize not only current hazards but also the ones that will be present in the near future for pro-active intervention. All prior works using wireless sensors and computer vision are limited to understand what is happening. That is, these technologies are only capable of detecting current hazards because they depend on current locations of entities of interest. In many cases, however, letting a worker know "now you are in a danger" may not provide enough time for him/her to take a proper evasive action. Therefore, predicting what will happen (i.e., knowing future position of entities and detecting future hazards) is critical in the prevention of potential accidents.

As a preliminary study to address this challenge, this research examines the potential of trajectory prediction for mobile construction resources. To this end, this study develops a trajectory prediction model through hyper-parameter tuning of a deep neural network (DNN), called Social Generative Adversarial Network (GAN) [12], and conducts test on a real construction operations data to

evaluate the developed model's prediction accuracy.

2 Previous Works

Considerable research efforts have been made to automate the struck-by hazard detection in construction. Some studies applied wireless sensors—such as Radio Frequency Identification (RFID) [5-6], Magnetic Field (MF) [7], Global Positioning System (GPS) [8], and Bluetooth Low Energy (BLE) [9]—to instantly detect hazardous proximity between entities of interest. On the other hand, other studies applied deep neural networks (DNNs)-based object detection framework—such as Faster R-CNN [13], R-FCN [14], and YOLO-V3 [1]—for continuous object localization and proximity monitoring.

The previous works have made large strides in automating struck-by hazard detection. However, trajectory prediction and accordingly future hazard detection have not been tackled yet. All prior works using wireless sensors and computer vision are limited to detect current hazards. To provide enough time for workers to take a prompt evasive action, to predict what will happen, namely recognizing future position of entities and detecting future hazards, is required.

One possible solution that can address the above issue is to enable trajectory prediction, which stands for a task to predict a target's future trajectories (a set of future positions) by observing the target's moving pattern. Recently, the trajectory prediction has made a great progress with the advancement of DNNs, such as Long-Short Term Memory (LSTM) [15], Gated Recurrent Unit (GRU) [16], and social pooling layers [17], and Generative Adversarial Network (GAN) [12]. Alahi et al. 2016 [17] first presented social pooling layers-embedded LSTM architecture (called Social LSTM), which showed remarkable progress in trajectory prediction. This work demonstrated the Social LSTM can learn not only each entity's moving pattern, but also social behaviour of human in crowded settings (e.g., collision avoidance). The interconnected use of individual and social features in turn showed a great performance in trajectory prediction: predicted trajectories by the Social LSTM only had 0.72 meter displacement error on average, compared to the ground truth trajectories.

Encouraged by this progress, Gupta et al. 2018 [12] more improved the Social LSTM [17] by using GAN. This work developed unique generator and discriminator by integrating LSTM encoder-decoder and social pooling layers (Figure 1, please refer to Gupta et al. 2018 [12] for detailed information). Consequently, the strict supervision by the discriminator successfully improved the model's prediction performance: the displacement error on average was 0.58 meters.

Despite the promise, applying the trajectory prediction DNN (i.e., Social GAN) to our problem involves another challenge: how to modify the original network so that it can predict longer time-steps. Note that the published Social GAN model has 2.64 s prediction length. To provide a worker in a danger with enough time for evasive action, longer prediction and accordingly more early notice are needed.

3 Research Objective and Framework

With this background, this study conducts hyper-parameter tuning of the Social GAN [12] to develop a trajectory prediction model for mobile construction resources. In essence, the longer prediction is needed for more pro-active hazard detection. This study sets five seconds as the target to predict with the assumption that it would be enough for workers to take prompt evasive actions. Further, tests on real construction operations data are conducted so as to demonstrate the developed model's potential in real-world applications. This study follows the below framework to achieve these aims (Figure 1).

- Data collection: for the purpose of hyper-parameter tuning, ETH [18] and UCY [19] dataset widely used for trajectory prediction are used. In addition, a real construction operations data that captures interactions between construction resources is collected for the test purpose.
- Hyper-parameter tuning: training the Social GAN [12] with multiple hyper-parameter scenarios is conducted to develop trajectory prediction models capable of predicting more than 5 seconds.
- Test on a real construction operations data: the trained models then are tested on a real construction operations data for evaluation.

4 Data Collection

The more extensive data is used for training, the higher performance of a model can be reached. For the hyper-parameter tuning purpose, this study thus benchmarked two sets of human trajectory data, ETH [18] and UCY [19], which are the most widely used dataset in trajectory prediction studies [12,17]. In total, the two datasets captures four different crowded scenes and contains 1,536 human trajectories. The trajectories reflect various human-human interactions, including (i) crossing each other; (ii) collision avoidance, (iii) group forming; and (iv) dispersing [17] (A in Figure 1).

In addition, this study collected a real construction operations data for the purpose of test. UAV captured construction site videos were collected. Of these, the total of 916 sequential frames were sampled that captures interactions between a worker, an excavator, and a wheel loader (B in Figure 1). Each trajectory (i.e., a set of x-y coordinates) of the three entities were manually annotated over the whole frames and a complete

inspection ensured the validity of the annotations.

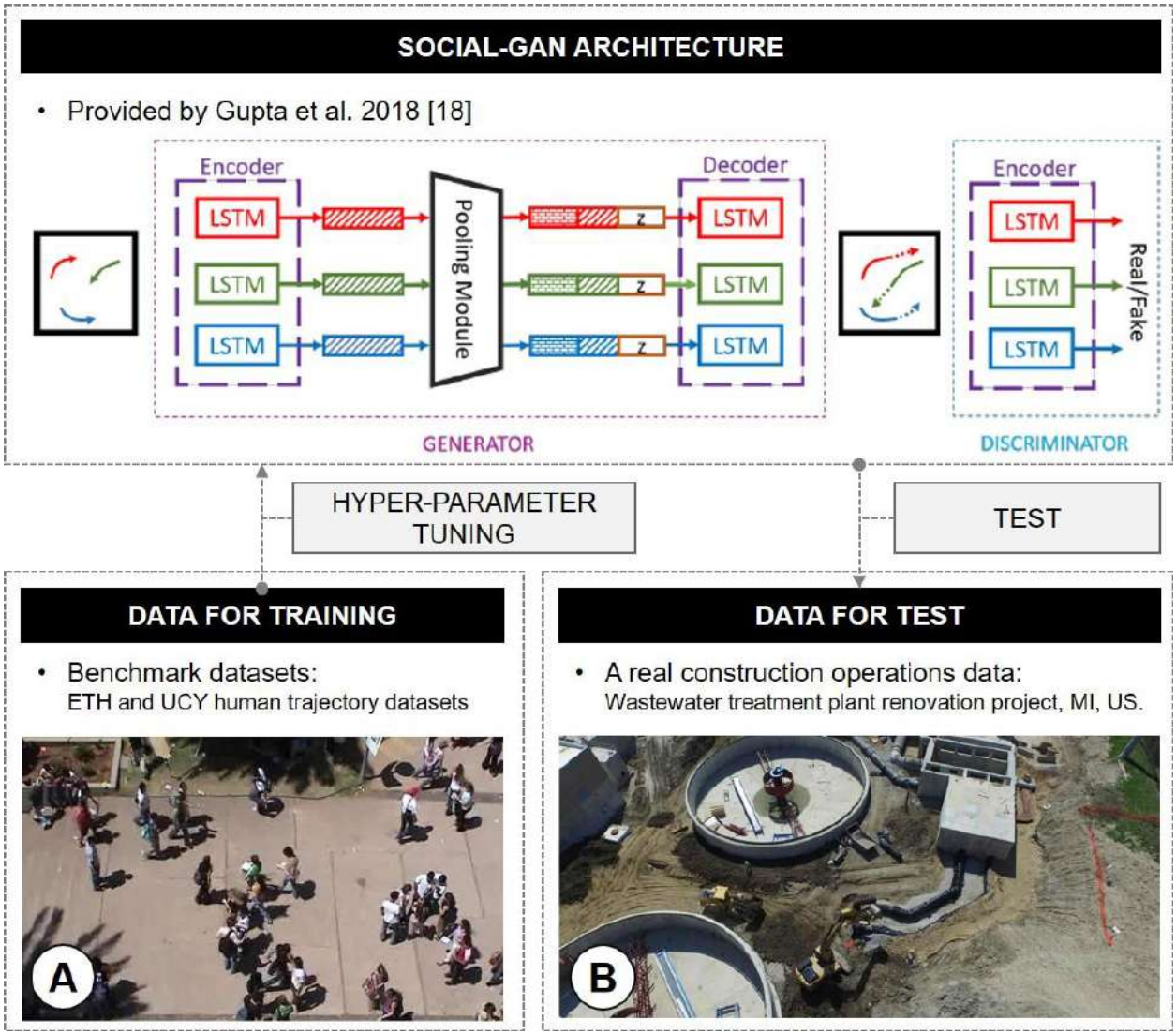

Figure 1. Research framework

5 Hyper-Parameter Tuning

To develop a long-term trajectory prediction model for construction mobile resources, this study conducted hyper-parameter tuning of the Social GAN [12].

The Social GAN has around 40 hyper-parameters that might need to be considered for successful training: batch size, number of iteration, number of epoch, model dimensions, observation length, and prediction length, to name a few. A small change in each hyper-parameter might be able to affect training and a trained model's final performance; however, examining all possible combinations is not viable as training a model with a graphical processing unit (GPU, e.g., Tesla K40c) in general takes more than five days. Hence, this study selected two important hyper-parameters, prediction and observation length, as tuning targets with the following reasons:

- Prediction length: the prediction length is the most important hyper-parameter that literally determines how many time-steps the model will predict. To achieve the prediction model capable of predicting more than five seconds, this study changed the prediction length from the default value (8 time-steps, 2.64 s) to 16 time-steps (5.28 s).
- Observation length: the observation length was selected as the second important hyper-parameter that needs to be tuned. The major input consumed for inferring a set of future trajectory in the Social GAN is a set of observed trajectory. The length of

observation is therefore bound to have a significant impact on a trained model's prediction performance. This work considered seven different observation lengths: from 8 time-steps (2.64 s) to 20 time-steps (6.6 s) with 2 time-steps interval (0.66 s).

Considering the above two hyper-parameters, total seven different tuning scenarios were established and applied in training (Table 1).

Table 1. Hyper-parameter tuning scenarios

Scenarios	Hyper parameter			
	Observation length		Prediction length	
	Time-steps	Seconds	Time-steps	Seconds
#1	8	2.64	16	5.28
#2	10	3.30	16	5.28
#3	12	3.96	16	5.28
#4	14	4.62	16	5.28
#5	16	5.28	16	5.28
#6	18	5.94	16	5.28
#7	20	6.60	16	5.28

6 Test Result and Discussion

To evaluate the trajectory prediction accuracy of the trained models on real construction settings, a test on a real construction operations data is conducted. As evaluation metrics, this study applied average displacement error (ADE) and final displacement error (FDE) that are commonly used metrics in trajectory prediction studies [12,17].

- ADE: average *L2* distance (i.e., mean square error) between ground truth and prediction over all predicted time-steps [12,17].
- FDE: distance between the predicted final destination and the ground truth destination at the end of the prediction period [12,17].

Table 2 summarizes the ADE and FDE of each trained model on the test dataset. Overall, all seven of the trained models showed promising accuracy in this test: the ADEs and FDEs for all the models were less than one meter (avg. ADE=0.88 meters) and 1.6 meters (avg. FDE=1.51 meters), respectively. Given a set of observation, predicting position of far time-step is naturally more challenging than close one. Accordingly, it was shown that the FDEs are 0.6 meters higher than the ADEs on average.

In this test, it was revealed that longer observation length does not necessarily guarantee higher accuracy. Longer observation means that the trajectory of less relevant time-steps are more consumed in the prediction. For example, in the scenario #7, not that all 20 time-steps observation are closely relevant to the future time-steps positions. The first several time-steps observation may have less relevancy to the future trajectory than the last several ones, which can be noises and have a negative impact on the model's prediction performance. In actual, the ADEs and FDEs slightly increased as observation length increased (Table 2).

It turned out that the best model for 16 time-steps prediction (5.28 s) is the one with 8 time-steps (2.64 s) observation (Table 2). This model consumes the shortest observation in the prediction, which however has the highest relevancy to the future trajectory. Consequently, this model outperformed the others and showed the most promising result: ADE=0.78 meters and FDE=1.27 meters (Table 2). Figure 2 illustrates the best model's prediction performance. Note that in this figure, green, blue, red lines stand for predicted trajectory of the worker, wheel loader, and excavator, respectively. And white circles stand for their ground truth position. As shown in Figure 2, the ground truth position of each entity well follows the predicted trajectory in process of time. This fact visually verifies validity of the predicted trajectories.

The developed model also demonstrated that it can continuously update the trajectory prediction at every 0.33 s without significant time-lag. With the use of a GPU (i.e., Tesla K40c), the model predicts three sets of trajectories for 5.28 s (16 time-steps) within 0.12 s. Then, at the next time step, 0.21 s later after completing the previous prediction, it predicts new sets of trajectories with the latest observation. That is, the model can continuously provide trajectory prediction for 5.16 s (5.28 s – 0.12 s) at every 0.33 s.

This test shows the great potential for the developed model in predicting construction mobile resources' trajectories. However, there is still room for further improvement. This study only focuses on hyper-parameter tuning, not considering fine-tuning with augmented construction data. Once an extensive dataset for construction resources' trajectory is available, this work will have another chance that can likely improve the prediction performance.

Table 2. Test result

Scenarios	Observation length	ADE (meters)	FDE (meters)
#1	80	0.78	1.27
#2	100	0.87	1.48
#3	120	0.84	1.42
#4	140	0.89	1.53
#5	160	0.89	1.54
#6	180	0.98	1.80
#7	200	0.91	1.57

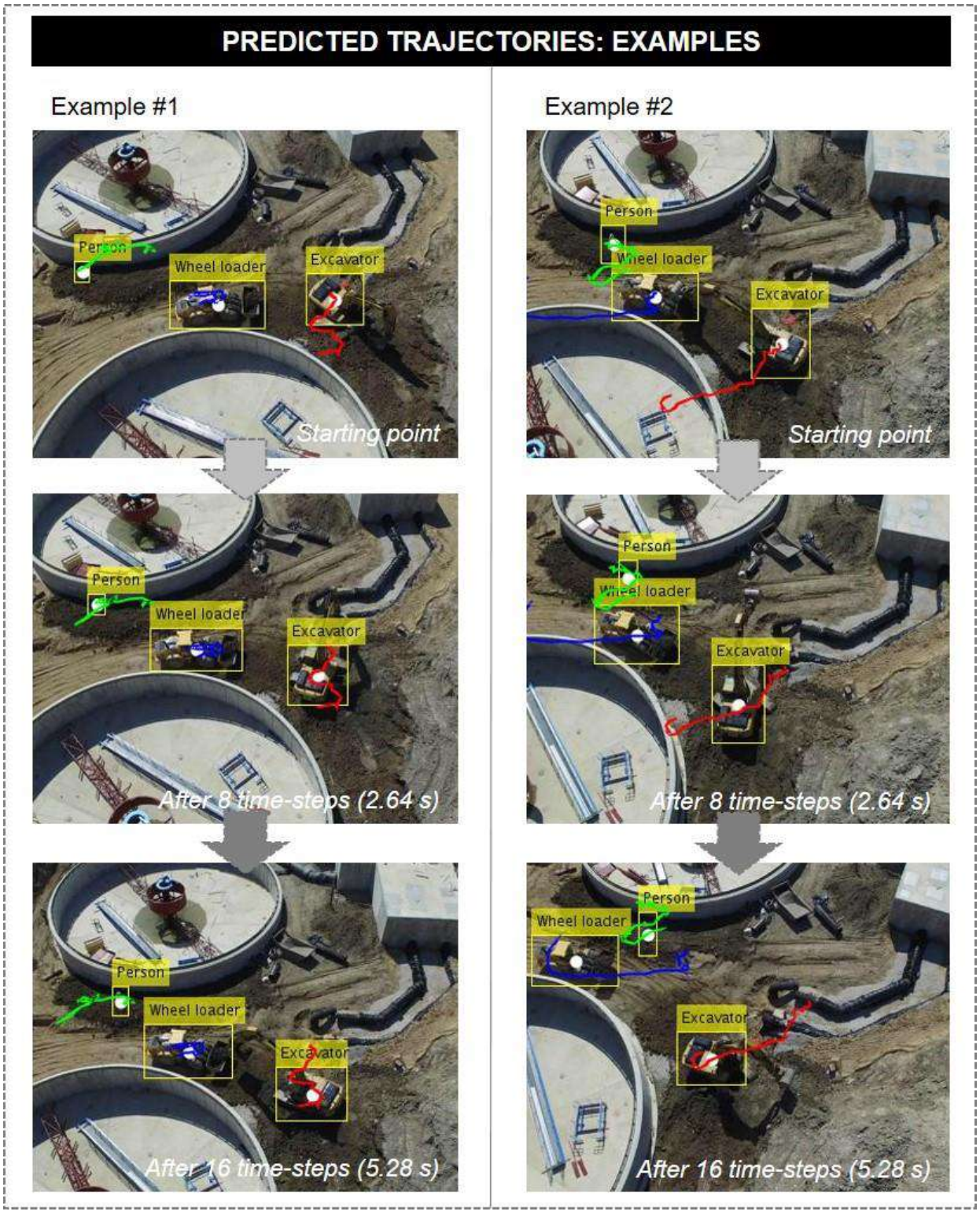

Figure 2. Predicted trajectory vs. ground truth positions

7 Conclusion

To support the pro-active struck-by hazard detection in construction, this study developed a trajectory prediction model for construction mobile resources. Specifically, this study conducted hyper-parameter tuning of a deep neural network, called Social GAN and developed a prediction model capable of predicting target's trajectory more than five seconds.

As a result, the best model (i.e., scenario #1) could achieve promising prediction accuracy: the ADE of 0.78 meters and the FDE of 1.27 meters. However, there still remain critical opportunity to improve the prediction accuracy—such as the fine-tuning with augmented construction training dataset.

With such refinement, an updated model would likely result in a more robust and accurate prediction on real construction operations data. The proposed trajectory prediction allows for detecting hazards that will be present in the near future, which will support pro-active intervention in hazardous situations. It will ultimately contribute to promoting a safer working environment for construction workers.

8 Acknowledgement

The work presented in this paper was supported financially by a National Science Foundation Award (No. IIS-1734266, 'Scene Understanding and Predictive Monitoring for Safe Human-Robot Collaboration in Unstructured and Dynamic Construction Environment'). Any opinions, findings, and conclusions or recommendations expressed in this paper are those of the authors and do not necessarily reflect the views of the National Science Foundation. Lastly, the authors wish to specially thank Weston Tanner and John McGlennon from WALSH Construction Co. for their considerate assistance in collecting onsite data.

References

[1] Kim, D., Liu, M., Lee, S., and Kamat, V.R. Remote proximity monitoring between mobile construction resources using camera-mounted UAVs. *Automation in Construction*, 99(2019):168–182, 2019.

[2] CPWR, Struck-by injuries and prevention in the construction industry. *The Center for Construction Research and Training*, 2017.

[3] OSHA, Recommended Practices for Safety & Health Programs in Construction. *Occupational Safety and Health Administration*, 2017.

[4] Bahn, S. Workplace hazard identification and management: The case of an underground mining operation. *Safety Science*, 57(2013):129-137, 2013.

[5] Teizer, J., Allread, B.S., Fullerton, C.E., Hinze, J. Autonomous pro-active real-time construction worker and equipment operator proximity safety and alert system. Automation in Construction, 19(2010):630-640, 2010.

[6] Marks, E. and Teizer, J. Proximity sensing and warning technology for heavy construction equipment operation. *Construction Research Congress 2012*, West Lafayette, IN, USA, 2012

[7] Teizer, J. Wearable, wireless identification sensing platform: Self-monitoring alert and reporting technology for hazard avoidance and training (smarthat). *Electronic Journal of Information Technology in Construction*, 20:295-312, 2015

[8] Ruff, T.M. Monitoring blind spots: A major concern for haul trucks. *Engineering and Mining Journal*, 202(12):17-26, 2001.

[9] Park, J.W., Marks, E., Cho, Y.K., and Suryanto, W. Performance test of wireless technologies for personnel and equipment proximity sensing in work zones. *Journal of Construction Engineering and Management*, 142(1): 04015049, 2016

[10] Kim, D.H., Yin, K., Liu, M., Lee, S.H., and Kamat, V.R. Feasibility of a drone-based on-site proximity detection in an outdoor construction site. *IWCCE 2017*, Seattle, WA, USA, 2017

[11] Kim, H.J., Kim, K.N., and Kim, H.K. Vision-based object-centric safety assessment using fuzzy inference: Monitoring struck-by accidents with moving objects. *Journal of Computing in Civil Engineering*, 30: 04015075, 2016

[12] Gupta, A., Johnson, J., Fei-Fei, L., Savarese, S. and Alahi, A. Social GAN: Socially Acceptable Trajectories with Generative Adversarial Networks. *IEEE Conference on Computer Vision and Pattern Recognition (CVPR)*, 2018.

[13] Fang, Q., Li, H., Luo, X., Ding, L., Luo, H., Rose, T.M., and An, W. Detecting non-hardhat-use by a deep learning method from far-field surveillance videos. *Automation in Construction*, 85(2018):1-9, 2018.

[14] Kim, H.J., Bang, S.D., Jeong, H.Y., Ham, Y.J., and Kim, H.K. Analyzing context and productivity of tunnel earthmoving process using imaging and simulation. *Automation in Construction*, 92(2018):188-198, 2018.

[15] Gers, F.A., Schmidhuber, J. and Cummins, F. Learning to forget: Continual prediction with LSTM. 1999.

[16] Chung, J., Gulcehre, C., Cho, K. and Bengio, Y. Empirical evaluation of gated recurrent neural networks on sequence modeling. *arXiv preprint arXiv:1412.3555*, 2014.

[17] Alahi, A., Goel, K., Ramanathan, V., Robicquet, A., Fei-Fei, L. and Savarese, S. Social lstm: Human trajectory prediction in crowded spaces.

Proceedings of the IEEE Conference on Computer Vision and Pattern Recognition, 961-971, 2016.

[18] Pellegrini, S., Ess, A., and Van Gool, A. Improving data association by joint modeling of pedestrian trajectories and groupings. *Computer Vision–ECCV 2010*, 452–465, 2010.

[19] Leal-Taix´e, L., Fenzi, M., Kuznetsova, A., Rosenhahn, B., and Savarese, S. Learning an image-based motion context for multiple people tracking. *IEEE Conference on Computer Vision and Pattern Recognition (CVPR)*, 2014.

Automated Monitoring of Physical Fatigue Using Jerk

L. Zhang [a], M. M. Diraneyya [b], J. Ryu [a], C. T. Haas [a], E. Abdel-Rahman [b]

[a] Civil and Environmental Engineering, University of Waterloo, Canada
[b] Systems Design Engineering, University of Waterloo, Canada
E-mail: lichen.zhang@uwaterloo.ca, mohsen.diraneyya@uwaterloo.ca, j4ryu@uwaterloo.ca, chaas@uwaterloo.ca, eihab@uwaterloo.ca

Abstract –

Construction workers are commonly subjected to ergonomic risks due to manual material handling that requires high levels of energy input over long work hours. Fatigue in musculature is associated with decline in postural stability, motor performance, and altered normal motion patterns, leading to heightened risks of work-related musculoskeletal disorders. Physical fatigue has been previously demonstrated to be a good indicator of injury risks, thus, monitoring and detecting muscle fatigue during strenuous work may be advantageous in mitigating these risks. Currently, few researchers have investigated how physical fatigue and exertion can be continuously monitored for practical use outside laboratory settings. Exercise-induced fatigue has been shown to impact motor control; thus, it can be measured using jerk, the time derivative of acceleration. This paper investigates the application of a machine learning approach, Support Vector Machine (SVM), to automatically recognize jerk changes due to physical exertion. We hypothesized that physical exertion and fatigue will influence motions and thus, can be classified based on jerk values. The motion data of six expert masons were collected using IMU sensors during two bricklaying tasks. The pelvis, upper arms, and thighs jerk values were used to classify inter- and intra-subject rested and exerted states. Our results show that on average, intra-subject classification achieved an accuracy of 94% for a five-course wall building experiment and 80% for a first-course experiment, leading us to conclude that jerk changes due to physical exertion can be detected using wearable sensors and SVMs.

Keywords –

Fatigue; Masonry; Classification; Lifting; Jerk

1 Introduction

Construction work is typically physically demanding and can result in a high number of accidents and injuries caused by fatigue. Fatigue can also have a detrimental impact on workers' judgement, productivity, and quality of work. Although accident and injury prevention has become a primary area for improvement within the construction industry, fatigue prevention and detection continue to require manual observation or self-reported subjective assessments. The inherent subjectivity of these methods has prompted the introduction of biomechanical and physiological assessments that quantify fatigue levels, thereby increasing reliability while reducing the time and human resources needed for their implementation. Despite extensive research that confirms the validity of these assessments, they can be cumbersome and or intrusive because they often require that multiple sensors and wires be attached to the worker, or need external devices that work in conjunction to worn devices. These assessments also often require tasks that involve several sequential activities or motions to be manually segmented; this is not only a time-consuming process, but it eliminates the applications of these assessments for real-time feedback and consumer use. The recent advances of inertial measurement units (IMUs) enable the automatic collection of motion data and offer several advantages over the traditional assessments, for example, they are cost-effective, non-intrusive, and wireless. This research investigates the use of support-vector machines (SVM) to automate the monitoring of physical exertion levels using jerk. The detection of high levels of exertion would allow workers to take proactive measures in mitigating adverse effects of fatigue.

2 Background

Physical fatigue refers to a decline in a muscle's ability to exert force as a result of performing a task requiring physical effort [1], [2]. Physical fatigue has been shown to result in increased risks of injury that lead to a variety of musculoskeletal disorders including lower back disorders, tendinitis, and carpal tunnel syndrome [3].

Construction work typically involves prolonged hours of physically demanding tasks, such that workers' muscles can become fatigued, resulting in a reduction in muscle strength.

Currently, there is no standard for a fatigue assessment that is universally accepted in both practical or research settings [4]. Thus, numerous objective and subjective fatigue assessments have been developed for specific industry requirement such as construction, manufacturing, and healthcare. Several work-related studies have developed or used various subjective scales and questionnaires for assessing fatigue or perceived exertion [5]–[7]. Aside from the inherent discrepancies that is expected between one's perceived fatigue and one's true level of fatigue, subjective measures are also cumbersome to implement and are not realistic for use on construction sites [8].

Previous studies have also used physiological measurements to assess the buildup of fatigue, including heart rate, oxygen consumption, and energy expenditure [9]. The downside to physiological measurements is that many factors can reduce their reliability including alcohol consumption, fitness level, and caffeine intake [10]. In laboratory settings, electromyography (EMG) is commonly used to predict muscle activity. Surface EMG (sEMG) can non-invasively assess the development of fatigue over time, however, it has low signal-to-noise ratio and are poorly correlated to fatigue for deep muscles such as at the lower back [11]–[13].

Recent advancements of wearable sensors with processing and communication capabilities, have expanded the applications of existing assessments beyond laboratory settings. Schall et al. assessed the IMU system in field-based occupational settings over an eight-hour work shift and suggested that the IMU system can achieve reasonably good accuracy and repeatability compared to the gold standard, optical motion capture systems [14]. Moreover, the light-weight and portability of wearable IMUs compared to external sensors, make them easy to attach to workers such as on construction vests, gloves, or helmet. IMUs, which combine accelerometers, gyroscopic and magnetic sensors, have been used by researchers to monitor ergonomically safe and unsafe postures during construction activities [15]–[18]. Among inertial sensors, accelerometers have been used extensively for activity recognition and studied with different body locations, number of sensors, classifiers, and feature sets [19]. Valero et al. developed an IMU system to detect unsafe postures of construction workers from motion data [20]. Ryu et al. used a single wrist-worn accelerometer-embedded activity tracker for automated action recognition [21], [22]. However, the use of wearable sensors to monitor physical exertion or fatigue during physically demanding tasks has not been studied extensively.

Physical fatigue and its impact on motor control and jerk has not been widely studied outside of clinical research. One reason is because prior to the advent of IMUs, motion capture systems that collect body segment positions must be differentiated three times in order to obtain jerk, resulting in a low signal-to-noise ratio. Jerk, the time derivative of acceleration, is typically used as a measure of motor control. In the short-term, fatigue can result in reduced motor control and strength capacity [23]. Fatigue is also manifested in increased tremor and changes in the recruitment of muscles, affecting both gross and fine motor skills. During lifting, high jerk values or a sudden change in acceleration can be felt as the change in force on the body and result in biomechanical damages over time. Two studies are notable and relevant to the current research. Maman et al. used IMU-collected motion data during simulated manufacturing tasks to determine acceleration- and jerk-based features that are predictive of fatigue occurrence [24]. Similarly, Zhang et al. used support vector machines (SVMs) to classify the occurrence of lower extremity muscle fatigue of gait [25]. These methods, however, have not assessed the feasibility of using machine learning techniques to recognize changes in jerk values during construction work.

Several methods have been used to classify human movement. Supervised classification techniques include k-Nearest Neighbour (k-NN), Support Vector Machines (SVM), Gaussian Mixture Models (GMM), and Random Forest (RF), and unsupervised classification techniques include k-means, Gaussian mixture models (GMM) and Hidden Markov Model (HMM). The focus of this work is to classify with SVM. Many studies with SVM have been reported in the field of activity recognition, although they do not focus on the study of fatigue.

In our previous work [26], we found that jerk may be used as an indicator of loss of motor control caused by physical exertion. However, the tasks were manually separated to ensure that jerk values were compared between the same action types, for examples, the motion data collected during each lifting action (pick up – transport – lay down) were segmented out from other motions such as spreading mortar. Manual segmentation of the data prevents this method from being used for real-time assessments. In this paper, we conducted two sets of analyses: 1) we tested the feasibility of analyzing jerk values using continuous motion data collected from our previous study to monitor changes in motor control, and 2) we conducted a second experiment that evaluates changes in jerk values between two identical bricklaying tasks following a series of exhausting exercises. Continuously monitoring jerk is investigated in the present study using IMU sensors and SVMs, which have been used extensively to classify human motion patterns and activities [17], [27]. Given that rested and exerted states can create unique jerk signal patterns, machine learning algorithms using motion data may be used to monitor the development of physical exertion in real-time for practical applications.

3 Methodology

3.1 Participants

The experiment was conducted at the Canadian Masonry Design Center (CMDC) indoor training facility in Mississauga, Ontario. Six male bricklayers with an average of 22 years of masonry experience were recruited for the experiment. The participants' mean (SD) stature and body mass were 179.0 (5.0) cm, 89.3 (14.1) kg, respectively. The study was approved by the Office of Research Ethics at the University of Waterloo.

In our previous work, experienced masons displayed statistically significant inter-subject differences between the rested and exerted jerk values over the duration of a bricklaying task. The statistically significant differences between experienced masons was attributed to greater inter-subject similarities compared to unexperienced masons in their learned technique and work pace. In this work, we examine both the inter- and intra-subject differences of experienced workers.

3.2 Instrumentation

The segment kinematics of the participants were collected using a wearable IMU-based motion capture suit, Noitom Perception Neuron [28]. The sampling rate of the IMUs is 125 frames per second. The full-body suit is composed of seventeen IMUs located at the pelvis, sternum, head, and both shoulders, upper arms, lower arms, hands, upper legs, lower legs, and feet. Although not all IMUs were used, all seventeen IMUs were active during the experiment due to the suit configuration. Each IMU sensor is comprised of a three-axis accelerometer, a three-axis gyroscope, and a three-axis magnetometer. Motion data was transmitted between the suit and a laptop via Wi-Fi. The sensor locations are shown in Figure 1.

3.3 Experimental Procedure

In the bricklaying experiment, jerk analysis was carried out on five body segments, namely the pelvis, the dominant and non-dominant upper arms and thighs since lifts involve whole-body work. We hypothesized that the three distinct body segments are suitable for fatigue monitoring since bricklaying requires large ranges of motion, forceful contractions, high precision from the upper and lower limbs, and frequent bending at the torso. IMU sensors have been used to study human motion in several locations. However, some studies have found that the torso is the best location to analyze movements since it reflects major motions and is close to the human body center of mass [29]. The selected body segments may also be the most suitable areas for sensor placement since they are far from external impact and from subject protective equipment.

Prior to the experiment, a calibration session was carried out to allow the Axis Neuron software to detect the placement and orientation of the sensors on the participant. The sensor-to-segment calibration was obtained using three standard postures including the A-pose, T-pose, and S-pose. Two sets of analyses were conducted. First, we tested the feasibility of analyzing jerk values using continuous motion data to monitor changes in motor control with data collected from a previous study which required workers to complete a wall building experiment. Second, we conducted an additional experiment to evaluate changes in jerk values between two identical bricklaying tasks following a series of exhausting exercises. The participants were given an hour break between the two experiments.

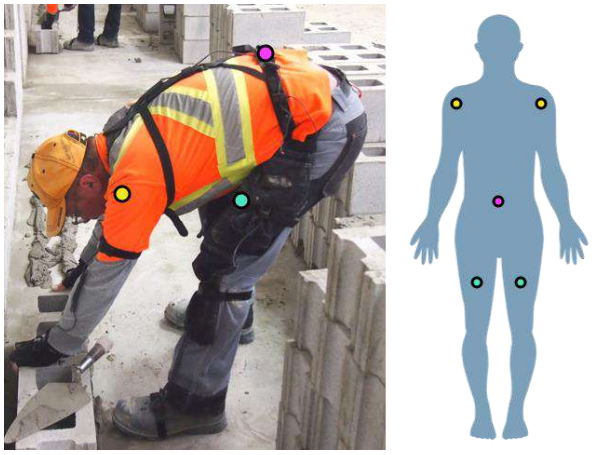

Figure 1. IMU sensor locations

3.4 Wall Building Experiment

To investigate the feasibility of using continuous motion data as an input to train SVM, we first analyzed data from our previous study [26]. Each participant was instructed to complete a pre-built lead wall shown in Figure 2(a), using forty-five concrete masonry units (CMUs) from the second to the sixth course. Each course is defined as a layer of CMUs. The CMUs were Type 1 blocks weighing 16.6 kg as detailed in Table 1. The blocks were placed in three piles approximately one meter away from the pre-built lead wall, and two panels of mortar were placed between the three block piles. The use of mortar and the requirement to meet alignment tolerances reflected field-work conditions. After the experiment, the participants were given a one-hour break before commencing the second experiment. Figure 3 shows the timeline of the tasks completed by the participants and the corresponding level of intensity measured in kg of laid CMU per minute.

Table 1. CMU block properties

Block	Weight [kg]	Dimensions [mm x mm x mm]
Type 1	16.6	390 x 190 x 100
Type 2	23.6	290 x 390 x 190
Type 3	36.1	290 x 390 x 190

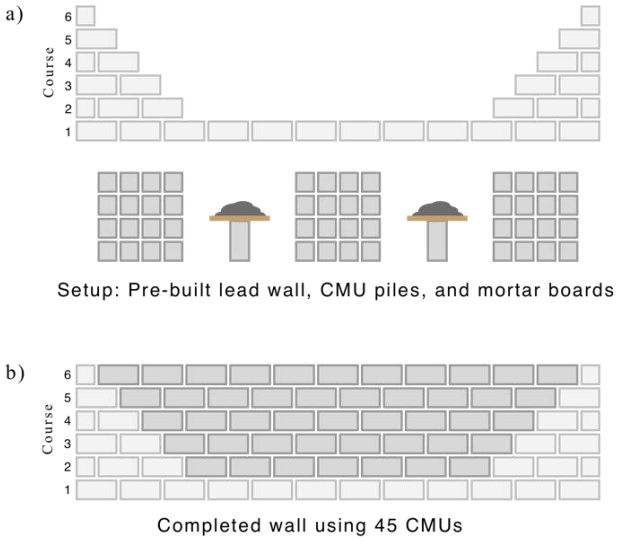

Figure 2. Experimental setup for wall building experiment

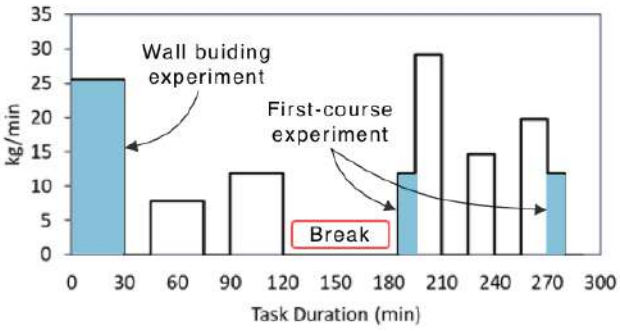

Figure 3. Timeline of task duration and intensity level in kilograms per minute

3.5 First Course Experiment

The purpose of the second experiment was to compare the jerk values of two identical tasks performed before and after an exhausting set of exercises. Each participant was instructed to build the first course of a wall using seven CMUs. The first course was selected because it imposes the greatest loading on the lower back [30]. The CMUs were Type 1 blocks weighing 16.6 kg. The blocks were placed in one pile approximately one meter away from the work space. Figure 4 shows a participant completing the bricklaying task.

After completing the first course, the participants were asked to carry out three bricklaying activities: 1) complete a wall individually using Type 2 CMUs, 2) complete a wall collaboratively using Type 2 CMUs, and 3) complete a wall collaboratively using Type 3 CMUs. In total, each participant carried approximately 1000 kg over an average of 50 minutes to complete all three bricklaying tasks. Lastly, the participants were asked to complete the first course again. Figure 5 shows the experiment sequence schematically.

Figure 4. Experimental setup for first course (top) and series of exhausting bricklaying tasks (bottom)

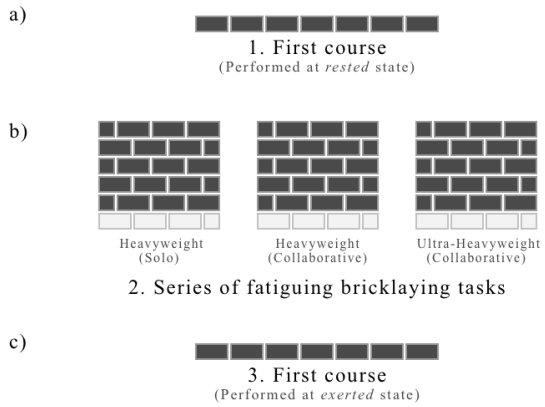

Figure 5. Building sequence for first course experiment

4 Data Analysis

Body segment accelerations collected from the IMU accelerometers were imported into MATLAB for computations. For each of the five IMU sensors, the resultant acceleration data were calculated from the Cartesian components collected from the IMU accelerometers. High frequency noise was removed using a low-pass Butterworth filter with a 10Hz cut-off frequency. Jerk was calculated as the time-derivative of the acceleration magnitude as shown in Table 2.

Table 2. Jerk calculations from Cartesian components of acceleration

	Formula
Acceleration	A_x, A_y, A_z
Resultant acceleration	$R = \sqrt{A_x^2 + A_y^2 + A_z^2}$
Resultant jerk	$J = \frac{dR}{dt}$
Jerk cost	$J = \int_{T_1}^{T_2} \left\|\frac{dR}{dt}\right\|^2 dt$

The classification is performed using predefined MATLAB functions. SVM is a supervised learning algorithm for pattern recognition and classification. Given labelled training data, the algorithm outputs an optimal hyperplane that define decision boundaries which it can then use to categorize new data points. Linear, polynomial, and Gaussian kernels were employed in the SVM classifier. During the wall building experiment, the motion data collected during the second course was labelled as 'rested' and those collected during the sixth course was labelled as 'exerted'. Likewise, during the first course experiment, the motion data collected during the first course completed at the beginning of the task was labelled as 'rested' and those collected at the end of the task was labelled as 'exerted'. Figure 6 shows the schematic to bypass the requirement for manual task segmentation.

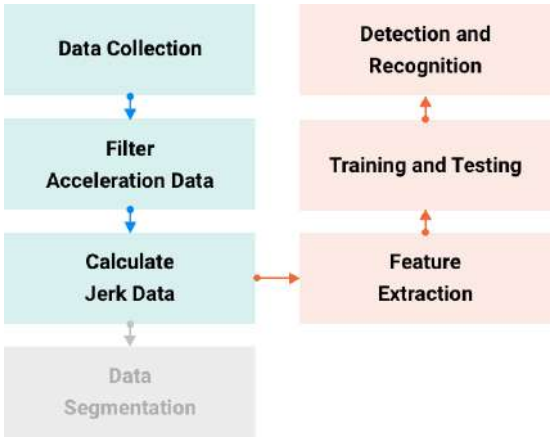

Figure 6. A schematic diagram of data processing for automatic fatigue detection

The selection of a window size has a significant impact on the classification accuracy. Wang et al. [31] conducted tests on different sliding-window sizes for activity recognition and found that accuracy decreases as window size increases. The optimal window size, however, is also dictated by what the classifier is required to classify such that the segment length is adequate to distinguish between unique signal patterns. Using a sliding window approach, multiple window sizes were tested and an overlap size of 50% was used. The window size for optimal recognition was 15 s. Features were extracted from the segmented data and characterised in both the time and frequency domains. The feature set was based solely on jerk measured in g/s and includes the following: 1) mean, the average value of acceleration data over the window; 2) standard deviation of acceleration values over the window; 3) maximum; 4) minimum; 5) jerk cost, an important measure to estimate the energy economy described by the area under squared jerk curve; and 6) dominant frequency – Fast Fourier Transform (FFT) over the window. The classification accuracies are based on all features and for all five body segments.

5 Results & Discussion

In our experiments of classifying rested and exerted states of six subjects, we considered jerk-based features extracted from five IMU sensor body locations, namely

the pelvis, and dominant and non-dominant upper arms and thighs. In the classification stage, we applied several classifiers using MATLAB. On comparing the average classification accuracy, the analysis showed that the SVM classifiers had the highest average value for both experiments, as reported in Table 3 and Table 4. A five-fold cross-validation scheme was used to evaluate the SVM classification algorithms, providing an indication of how well the learner will do when it is repeated using new data. Thus, the reported accuracy is the average accuracy over five iterations.

As expected, the SVM classification results demonstrated a significantly higher intra-subject rested/exerted classification than the inter-subject classification. For the wall completion experiment, the polynomial kernels (94%) performed better than the linear kernel (91%) to identify intra-subject rested/exerted states. For the first course experiment, the linear kernel performed similarly (80%) to the polynomial kernel (79%). The lower classifier accuracy for the first course experiment may be explained by the fact that it was completed following the first experiment. Since a sufficient amount of time is required for muscle recovery following exercise, the participants may not

Table 3. Wall completion experiment – SVM classification accuracy [%], mean, and standard deviation

SVM Kernel Function	Intra-subject							Inter-subject
	W1	W2	W3	W4	W5	W6	Mean±SD	All workers
Linear	98.0	84.1	87.0	91.1	84.6	100.0	90.8±6.8	78.5
Quadratic	98.0	87.0	89.1	95.6	94.2	100.0	**94.0±5.1**	79.2
Cubic	98.0	87.0	91.3	97.8	90.4	100.0	**94.1±5.2**	76.5
Fine Gaussian	62.7	69.6	58.7	66.7	63.5	56.7	63.0±4.8	60.1
Medium Gaussian	96.1	85.5	80.4	93.3	86.5	100.0	90.3±7.4	78.8
Course Gaussian	72.5	69.6	63.0	66.7	63.5	100.0	72.6±13.9	71.3

Table 4. First course experiment – SVM classification accuracy [%], mean, and standard deviation

SVM Kernel Function	Intra-subject							Inter-subject
	W1	W2	W3	W4	W5	W6	Mean±SD	All workers
Linear	75.4	74.0	69.1	76.6	84.6	100.0	**80.0±11.0**	62.0
Quadratic	72.3	71.4	68.1	76.6	87.2	97.1	78.8±11.2	63.0
Cubic	72.3	67.5	68.1	76.6	84.6	100.0	78.2±12.4	63.3
Fine Gaussian	52.3	59.7	61.7	51.9	56.4	60.0	57.0±4.2	57.6
Medium Gaussian	80.0	71.4	67.0	68.8	89.7	94.3	78.5±11.4	65.9
Course Gaussian	50.8	59.7	61.7	67.5	71.8	71.4	63.8±8.1	59.4

have fully recovered from the first experiment before moving onto the second experiment. Thus, the participants may have begun the second experiment in an exerted state. The participants might have also recruited an alternate group of muscles for the two collaborative lifting tasks compared to the individual lifting tasks during the first course experiment. Thus, fatigue may have built up for a different group of muscles that were not all utilized in laying the first courses. Another explanation could be that the level of intensity as measured in kilograms per minute could have affected the exertion levels developed by the participants. The intensity level was higher during the wall building experiment compared to the first course experiment; however, the series of fatiguing tasks conducted in between the two sets of first course block laying was higher in intensity.

6 Limitations and Future Work

Conclusions provided in this study should be considered in context of the limitations. First, there was no secondary measure of fatigue, thus we cannot be certain that experiments induced sufficient fatigue. Since we know that the participants had indeed exerted themselves in performing the bricklaying tasks, the classification accuracy reflects the extent to which fatigue was developed. Second, we did not consider masons with other experience levels other than expert masons. Third, due to the fact that physical exertion levels may last for several hours following physical activity, the break in between the first and second experiments may not have been sufficient for the participants to return to a rested state.

The placement of the sensors is of high importance because it can potentially affect the recognition between rested and fatigued states. Thus, future work involves a feature selection method to identify the most significant motion changes after fatigue and determine the optimal number and placements of the sensors to improve the utility of the method.

7 Conclusions

In the construction industry, fatigue can impair workers ability to safely and effectively perform their duties which negatively impacts their well-being, reduces productivity and the quality of their work, and elevates workers' compensation costs. Current workload and fatigue assessment methods, including subjective, physiological, and biomechanical assessments, can be unreliable, cumbersome, or require extensive post processing, which render them impractical for real-time assessment.

This research investigated the use of SVMs to automatically recognize changes in jerk values due to physical exertion. Motion data were collected during two bricklaying activities using IMU sensors to obtain jerk input to SVM classifiers. Inter- and intra-subject classification of rested and exerted states of six expert masons were carried out using the jerk values of the pelvis, upper arms, and thighs.

We found that changes in jerk values due to the development of fatigue can be classified by supervised machine learning techniques. On average, intra-subject classification achieved an accuracy of 94% for the wall building experiment and 80% for the first course experiment. The difference between the classification accuracy for the two experiments may be attributed to differences in task sequence and intensity level resulting in lower classification accuracy in the first-course experiment compared to the wall experiment.

The results lead us to conclude that jerk changes resulting from exertion can be assessed by wearable sensors and SVMs. The investigated method holds promise for continuous monitoring of physical exertion and fatigue which can help in reducing work related musculoskeletal injuries or other fatigue-related risks.

Acknowledgements

We would like to acknowledge the Canadian Masonry Design Centre (CMDC), Mississauga, Ontario, Canada for their considerable help in the data collection effort. The work presented in this paper was supported financially by CMDC and the Natural Sciences and Engineering Research Council of Canada (NSERC).

References

[1] A. J. Dittner, S. C. Wessely, and R. G. Brown, "The assessment of fatigue: A practical guide for clinicians and researchers," *J. Psychosom. Res.*, vol. 56, no. 2, pp. 157–170, 2004, https://doi.org/10.1016/S0022-3999(03)00371-4.

[2] B. Bigland-Ritchie and J. J. Woods, "Changes in muscle contractile properties and neural control during human muscular fatigue," *Muscle Nerve*, vol. 7, no. 9, pp. 691–699, 1984, https://doi.org/10.1002/mus.880070902.

[3] S. Gallagher and M. C. Schall, "Musculoskeletal disorders as a fatigue failure process: evidence, implications and research needs," *Ergonomics*, vol. 60, no. 2, pp. 255–269, 2017, https://doi.org/10.1080/00140139.2016.1208848.

[4] L. S. Aaronson *et al.*, "Defining and Measuring Fatigue," *Image J. Nurs. Scholarsh.*, vol. 31, no. 1, pp. 45–50, 1999, https://doi.org/10.1111/j.1547-5069.1999.tb00420.x.

[5] M. Zhang *et al.*, "Development and validation of a fatigue assessment scale for U.S. construction workers.," *Am. J. Ind. Med.*, vol. 58, no. 2, pp. 220–228, Feb. 2015, https://doi.org/10.1002/ajim.22411.

[6] D. Fang, Z. Jiang, M. Zhang, and H. Wang, "An experimental method to study the effect of fatigue on construction worker's safety performance," 2015, https://doi.org/10.1016/j.ssci.2014.11.019.

[7] A. Troiano, F. Naddeo, E. Sosso, G. Camarota, R. Merletti, and L. Mesin, "Assessment of force and fatigue in isometric contractions of the upper trapezius muscle by surface EMG signal and perceived exertion scale," *Gait Posture*, vol. 28, no. 2, pp. 179–186, 2008, https://doi.org/10.1016/j.gaitpost.2008.04.002.

[8] P. Spielholz *et al.*, "Comparison of self-report , video observation and direct measurement methods for upper extremity musculoskeletal disorder physical risk factors," *Ergonomics*, vol. 44, no. 6, pp. 558–613, 2001, https://doi.org/10.1080/00140130118050.

[9] A. Aryal, A. Ghahramani, and B. Becerik-Gerber, "Monitoring fatigue in construction workers using physiological measurements," *Autom. Constr.*, vol. 82, pp. 154–165, Oct. 2017, https://doi.org/10.1016/j.autcon.2017.03.003.

[10] L. Bosquet, S. Merkari, D. Arvisais, and A. E. Aubert, "Is heart rate a convenient tool to monitor over-reaching? A systematic review of the literature.," *Br. J. Sports Med.*, vol. 42, no. 9, pp.

709–14, Sep. 2008.

[11] P. Dolan and M. A. Adams, "Repetitive lifting tasks fatigue the back muscles and increase the bending moment acting on the lumbar spine," *J. Biomech.*, vol. 31, no. 8, pp. 713–721, 1998, https://doi.org/10.1016/S0021-9290(98)00086-4.

[12] X. Li, A. Komeili, M. Gül, and M. El-Rich, "A framework for evaluating muscle activity during repetitive manual material handling in construction manufacturing," *Autom. Constr. J.*, vol. 79, pp. 39–48, 2017.

[13] M. R. Al-Mulla, F. Sepulveda, and M. Colley, "A Review of Non-Invasive Techniques to Detect and Predict Localised Muscle Fatigue," *Sensors*, vol. 11, pp. 3545–3594, 2011, https://doi.org/10.3390/s110403545.

[14] M. C. Schall, N. B. Fethke, H. Chen, S. Oyama, and D. I. Douphrate, "Accuracy and repeatability of an inertial measurement unit system for field-based occupational studies," *Ergonomics*, vol. 59, no. 4, pp. 591–602, Apr. 2015, https://doi.org/10.1080/00140139.2015.1079335.

[15] N. D. Nath, R. Akhavian, and A. H. Behzadan, "Ergonomic analysis of construction worker's body postures using wearable mobile sensors," *Appl. Ergon.*, vol. 62, pp. 107–117, 2017, https://doi.org/10.1016/j.apergo.2017.02.007.

[16] W. Lee, E. Seto, K. Y. Lin, and G. C. Migliaccio, "An evaluation of wearable sensors and their placements for analyzing construction worker's trunk posture in laboratory conditions," *Appl. Ergon.*, 2016, https://doi.org/10.1016/j.apergo.2017.03.016.

[17] J. Chen, J. Qiu, and C. Ahn, "Construction worker's awkward posture recognition through supervised motion tensor decomposition," *Autom. Constr.*, vol. 77, pp. 67–81, 2017, https://doi.org/10.1016/j.autcon.2017.01.020.

[18] J. Ryu, L. Zhang, C. T. Haas, and E. Abdel-Rahman, "Motion Data Based Construction Worker Training Support Tool: Case Study of Masonry Work," in *35th International Symposium on Automation and Robotics in Construction (ISARC 2018), Berlin*, 2018, vol. 35, no. IAARC Publications, pp. 1079–1084.

[19] A. Mannini and A. M. Sabatini, "Machine learning methods for classifying human physical activity from on-body accelerometers," *Sensors*, vol. 10, no. 2, pp. 1154–1175, 2010, https://doi.org/10.3390/s100201154.

[20] E. Valero, A. Sivanathan, F. Bosché, and M. Abdel-Wahab, "Musculoskeletal disorders in construction: A review and a novel system for activity tracking with body area network," *Appl. Ergon.*, vol. 54, pp. 120–130, 2016, https://doi.org/10.1016/j.apergo.2015.11.020.

[21] J. Ryu, J. Seo, H. Jebelli, and S. Lee, "Automated Action Recognition Using an Accelerometer-Embedded Wristband-Type Activity Tracker," *J. Constr. Eng. Manag.*, vol. 145, no. 1, p. 04018114, 2019, https://doi.org/10.1061/(ASCE)CO.1943-7862.0001579.

[22] J. Ryu, J. Seo, M. Liu, S. Lee, and C. T. Haas, "Action Recognition Using a Wristband-Type Activity Tracker: Case Study of Masonry Work," in *Construction Research Congress 2016*, 2016, pp. 790–799.

[23] M. Björklund, A. G. Crenshaw, M. Djupsjöbacka, and H. Johansson, "Position sense acuity is diminished following repetitive low-intensity work to fatigue in a simulated occupational setting," *Eur. J. Appl. Physiol.*, vol. 81, no. 5, pp. 361–367, 2000, https://doi.org/10.1007/s004210050055.

[24] Z. Sedighi Maman, M. A. Alamdar Yazdi, L. A. Cavuoto, and F. M. Megahed, "A data-driven approach to modeling physical fatigue in the workplace using wearable sensors," *Appl. Ergon.*, vol. 65, pp. 515–529, Nov. 2017, https://doi.org/10.1016/j.apergo.2017.02.001.

[25] J. Zhang, T. E. Lockhart, and R. Soangra, "Classifying Lower Extremity Muscle Fatigue During Walking Using Machine Learning and Inertial Sensors," 2013, https://doi.org/10.1007/s10439-013-0917-0.

[26] L. Zhang, M. M. Diraneyya, J. Ryu, C. T. Haas, E. M. Abdel-rahman, and S. D. Engineering, "Assessment of Jerk as an Indicator of Physical Exertion and Fatigue," *Autom. Constr.*, 2019.

[27] V. Kellokumpu, "Human Activity Recognition Using Sequences of Postures."

[28] Noitom Ltd., "Perception Neuron," 2018. [Online]. Available: https://neuronmocap.com/. [Accessed: 11-Jun-2018].

[29] D. Rodriguez-Martin, A. Samà, C. Perez-Lopez, A. Català, J. Cabestany, and A. Rodriguez-Molinero, "SVM-based posture identification with a single waist-located triaxial accelerometer," *Expert Syst. Appl.*, vol. 40, no. 18, pp. 7203–7211, 2013, https://doi.org/10.1016/j.eswa.2013.07.028.

[30] A. Alwasel, E. M. Abdel-Rahman, C. T. Haas, and

S. Lee, "Experience, Productivity, and Musculoskeletal Injury among Masonry Workers," *J. Constr. Eng. Manag.*, vol. 143, no. 6, p. 05017003 1-13, Jun. 2017, https://doi.org/10.1061/(ASCE) CO.1943-7862.0001308.

[31] L. Wang, T. Gu, X. Tao, and J. Lu, "A hierarchical approach to real-time activity recognition in body sensor networks," *Pervasive Mob. Comput.*, vol. 8, no. 1, pp. 115–130, 2012, https://doi.org/10.1016/j.pmcj.2010.12.001.

A Real-time Path-planning Model for Building Evacuations

Farid Mirahadi[a] and Brenda McCabe[a]

[a]Department of Civil Engineering, University of Toronto, Canada
E-mail: f.mirahadi@mail.utoronto.ca, brenda.mccabe@utoronto.ca

Abstract –

Simultaneous evacuation is the most widely used evacuation strategy in buildings. However, there are other evacuation strategies that might lead to safer outcomes if selected appropriately. Different forms of evacuation result from applying time delays to phased evacuation or altering path planning. The best strategy for evacuation depends on the characteristics of the building and the circumstances of the particular emergency. A real-time evacuation path-planning model that identifies the fire hazard and proposes the best strategy of evacuation during the emergency can reduce risk and improve safety. In this paper, a model is proposed to find the safest strategy of evacuation based on the current state of the building and the emergency case. The model focuses on fire emergencies, as they are the dominant cause of fatalities in buildings compared to other types of natural and manmade disasters. The proposed model first defines a risk factor for each compartment based on the location of fire and then calculates the lowest risk path using Dijkstra algorithm. The path-planning runs on the geometric network graph (GNG), which is generated from the IFC file of the building. Furthermore, unexpected events during evacuation, e.g. another source of fire, can force the system to search for another strategy. Herein, a model is designed to monitor the building in real-time and in case of any unexpected event, changes the evacuation plan accordingly. The case study shows that the proposed model for real-time evacuation management can significantly enhance the safety level of evacuation compared to the conventional simultaneous evacuation process.

Keywords –

Evacuation; Dijkstra; Route risk index; Geometric network graph; BIM; IFC; Fire safety

1 Introduction

Decision-making and coordination for evacuation processes are normally managed by a human emergency commander. This person has to comprehend the status of the building, estimate the distribution of the residents, recognize the type and the location of the hazard, decide the best strategy of evacuation and transfer the message to occupants. The procedure gets even more complicated when the commander has to monitor the building and the evacuees during evacuation and improvise solutions for unexpected situations that differ from the forecasted plan. Such complexities in decision making, data interpretation, time constraints, and inevitable human errors highlight the benefits of using automated systems to inform the decision making processes.

Computer simulation can stochastically imitate the course of events during emergencies. Today, crowd simulation approaches make it possible to model the movements and the behaviors of residents during an evacuation. Moreover, the growth pattern of the hazard itself, in cases such as fire, can be modeled and forecasted via software applications and simulators. Such tools enable us to examine a specific building design and evaluate the safety of evacuation processes in that facility. By developing different emergency scenarios and simulating them, a computer-based decision support system can determine the best strategy of evacuation.

However, the main goal of evacuation management process is to facilitate decision making during the emergency event. It is no surprise that the real evacuation process will be different from the simulated event in some aspects. People might escape by different routes, the number and distribution of evacuees could vary, congestion could occur, or a new threat could be added to the original one. These deviations from the simulated scenario need an efficient model that performs path-planning within the tight time limits. During evacuation, there is not sufficient time for running multiple iterations of a fire simulation or a detailed crowd simulation. This highlights the need for a real-time path-planning model that responds to changes in emergency situations and promptly generates new plans that secure the safety of the occupants. For a long time, evaluation of evacuation processes has been measured based on finding plans that result in the shortest exit routes or shortest time of evacuation. However, a successful path-planning model needs to assess and rank the strategies based on the level of safety and the risks to evacuees' lives, and not only the time of evacuation.

The objective of this paper is to present a real-time path planning model for building evacuations during fire

emergency events.

2 Literature Review

The main goal of an evacuation management system is real-time path-planning of escape routes in a building. Path-planning requires a measure based on which the privilege of each specific route can be quantified. In fire emergencies, a combined temperature-smoke risk index measured by heat and smoke detectors has been used to find the optimal evacuation routes. Finally, the optimal routes were transmitted to occupants through smartphone-based devices [1]. The study did not provide enough information about the computational load, the time required for modeling, and how they addressed the challenges of using positioning techniques in indoor spaces. In another research, predictions of stochastic evacuation models were used to generate the optimal evacuation routes in real-time [2]. The framework lacked explicit attention to hazard detection and threat propagation. Dynamic exit signs were proposed for use in a smart emergency management system for tall buildings to guide evacuees towards the safest routes within a proposed geometric architecture [3]. Researchers also used information regarding ignition points, locations of trapped occupants, and locations of firefighters to help firefighters find the optimal route to access trapped person [4].

Real-time path-planning requires accurate and updated information about the physical and functional characteristics of the building. This information is collected and organized in building information model (BIM). BIM can be used to construct a door-to-room connectivity graph that facilitates path-planning in a building [5]. The interoperability of industry foundation classes (IFC) motivated researchers to extract the topological connectivity graph of the building directly from IFC data structure. This approach also uses doors to recognize the connected spaces of the building [6]. The transformation from BIM to a network graph allows the use of graph exploration algorithms for path-planning. Medial Axis Transform algorithm can also be used to produce the geometric topology network (GTN) of a building [7]. Medial axis of a polygon is the collection of all points inside the polygon having more than one closest point on the polygon's boundary.

Traditionally, the main purpose of egress design and path-planning has been to find the shortest path of evacuation. The original problem of finding the shortest path between two points has been solved based on graph exploration methods. Dijkstra algorithm is a graph search algorithm that finds the global shortest path between two nodes of a graph [8]. The cost function of the algorithm in its simplest form is based on the distance between the nodes. A* is another widely used algorithm, but instead of performing a global search, it contains a heuristic function. Similar to Dijkstra, it calculates the cost of traversed paths, while the heuristic leads the search directly towards the goal [9]. Compared to Dijkstra, the computational load of A* is much less and consequently the algorithm is faster. However, the solution is not necessarily globally optimal. In emergency management, Dijkstra has been used to find the shortest rescue path to victims [10]. A combination of BIM and Dijkstra was used for finding optimal evacuation/rescue routes [11].

The quality of evacuation processes has been primarily measured by the time of evacuation. The total evacuation time, average evacuation time of evacuees, and total evacuation time of each evacuee are some examples of this measure. However, real-time management of crowds during emergencies demands that people be guided away from the hazard along the safest possible route. In other words, finding the shortest path cannot necessarily guarantee a safe evacuation.

Route Risk Index (RRI), a risk index designed to quantify the risk of each egress route, was proposed to allow comparison between egress alternatives [12]. This index considers the length of evacuation and proximity to hazards in its calculation. Equation (1) shows the formula of RRI.

$$RRI = \int_{t=0}^{T} \frac{1}{ALET_{p(t)}}\ dt \qquad \text{Equation (1)}$$

where:

$ALET_{p(t)}$ (Available Local Egress Time) is the time it takes for a fire to reach $p_{(t)}$;

$p_{(t)}$ is the location (x,y,z) of an evacuee at time t;

T is total travel time of an evacuee from their starting location to the end of the egress route.

Given Equation (1), the risk of being at point $p_{(t)}$ is equal to 1/ALET, which is integrated over time to determine the risk for the entire evacuation path.

3 Model Development

The flowchart of the proposed model is presented in Figure 1. It is worth noting that since fire emergencies are the most frequent causes of evacuations in buildings, this model focuses on fire as the hazard. In this model, BIM is used to acquire information related to functional and physical characteristics of the facility. The BIM model is transformed to IFC data structure and geometric network graph (GNG) of the building is generated from it. It is assumed that an existing decision support system, such as EvacuSafe [12], already selected the best strategy of evacuation based on the current state of the building and the occupants at the beginning of the emergency. Such decision support system has to conclude based on precise fire simulation and crowd simulation. Here, the main goal

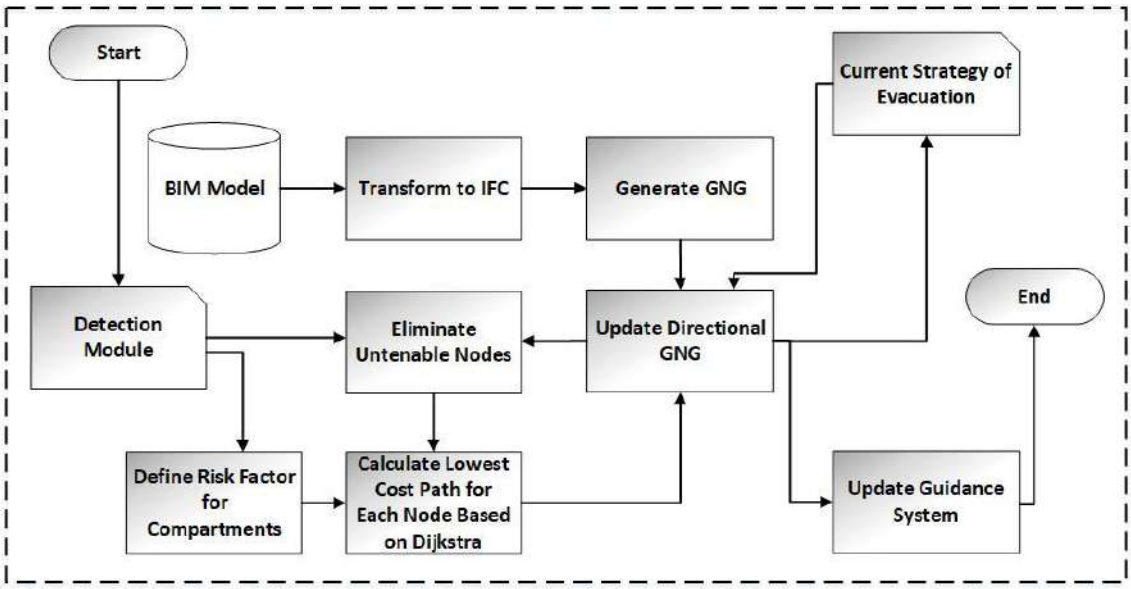

Figure 1. Flowchart of the proposed model

is to update the guidance system during the course of the emergency as the real sequence of events unfold. Fusion of the selected strategy of evacuation with the GNG of the building produces a directional network graph. Once the detection module locates the exact coordinates of the hazard, the associated node in the GNG is eliminated. A risk factor is assigned to all of the compartments/nodes in the building and Dijkstra algorithm is applied to find the updated safest path of evacuation for each node. The guidance system can then be updated.

3.1 GNG

A 3D network graph is required to represent the navigable connections between the spaces in the building. Each node stands for a space and each edge represents a connection between the spaces. This graph also has to contain information about the distances and directions of the pathways.

The graph is defined in continuous 3D space. Each node is positioned at the center of each space (room), and the length of each edge is proportional to the distance between the nodes. In order to generate this graph automatically, two sets of information are required: 1) The data related to the available connections between the spaces; and, 2) The data related to the location of each node in the space and the distance between the nodes. IFC data structure can provide this information and remain independent of a specific BIM file extension, but requires some explanation.

ifcRelSpaceBoundary was first introduced in IFC release 1.5 and was later modified in the 2X release. This entity determines the physical or virtual relationship of each space with its surrounding elements. Two attributes of this entity are *RelatingSpace* and *RelatedBuildingElement*. *RelatedBuildingElement* specifies the elements, including walls, doors or virtual elements that are immediately connected to that space. *ifcDoor* and *ifcVirtualElement* matter here. In this terminology, a virtual element is a delimiter between the rooms or spaces. This element does not exist in the built environment and its only purpose is to allow decomposition of one space into smaller segments. The IFC file is parsed and a query is run to filter the spaces sharing common virtual elements or doors. Therefore, spaces sharing the same element of these two types are connected to each other. Gradually the graph of the entire building is constructed. This graph contains information about the characteristics of all connections between the spaces.

The other element that needs to be extracted is the center of each space. *ifcSpace* has two subtypes of *IfcProductDefinitionShape* and *ifcLocalPlacement*. *ifcLocalPlacement* defines the placement of the element, i.e. space here, in the 3D space. *IfcProductDefinitionShape* describes the physical or topological representation of the product. What matters here is the footprint of the space mirrored on the navigable surface. Each space's boundaries are represented by polylines and composite curves [13]. The type of this mirrored shape on the surface combined with the information related to the coordinates of the boundaries facilitate calculation of the centroid of each space. The combination of the network graph generated from navigable connections between the spaces and the centroids of the spaces generates a GNG in which the length of edges and coordinates of nodes exactly imitates the building dimensions in reality.

3.2 Eliminate Untenable Nodes and Request Updated Path-planning

The GNG prepared in the previous step shows the navigable skeleton of the building. However, it does not present any information regarding the desired movement of the evacuees in the building. An evacuation strategy selection system, such as EvacuSafe, has the ability to select the safest strategy of evacuation based on the first signal from fire alarm system [12]. It positions the location of the hazard and then based on integrated fire and agent based crowd simulations prescribes the safest strategy for evacuation. Merging the best strategy with the GNG generates a directional GNG, which specifies the safest direction of evacuees' movements by inserting arrows on the edges of the GNG.

GNG is only the visual representation of space connections in the building. An adjacency matrix is the mathematical representation of the GNG. An adjacency matrix is an *n-by-n* matrix in which n is equal to the total number of nodes and is filled with 0 and 1 values. A value of 1 indicates that the pair of nodes are connected to each other. In the case of directional graphs, only one element of the pair is marked as 1.

Once a fire case is detected in the building, the fire alarm module sends a signal containing the location of the fire. The node in which the fire is located is eliminated from the directional GNG. As the fire expands, more nodes are eliminated. These changes in the GNG forces recalculation of the safest path for each node. Since this happens during an emergency, there is no time to redo the fire simulation or crowd simulation. As such, another algorithm is required to quickly calculate the risk of available exit paths so that the crowd can be redirected through the safest ones.

3.3 Risk Factor of Compartment

As the fire is initiated in the building, each spot in the building is subject to a level of risk. Herein, the risk factor is defined based on philosophy of RRI. As mentioned previously, 1/ALET specifies the risk of being present at each spot in the building. This risk factor is distributed based on the time that each space can stay tenable from the evidence of fire. The risk factor provides a basis to know which zones are in higher danger compared to the others. However, ALET has to be computed via fire simulation. Fire simulation is computationally heavy and cannot be performed within the tight time limits of an emergency situation. Therefore, before the emergency occurs, the initiating point of fire has to be placed at all of the compartments of the building in fire simulation, one after the other. The results of simulation reports the ALETs for all of the compartments associated with each initiating point of fire. In this way, each node of the building is assigned by a risk factor. If another fire occurs concurrently in the building, the risk factors add up in each node.

3.4 Dijkstra Algorithm

The Dijkstra algorithm is a widely used graph search algorithm in navigation and robotics. The algorithm can be modified to calculate the cost of each path instead of the number of steps taken. In this research, two factors influence the safety of evacuation. The first is the travel time of the evacuee. The second is the path's proximity to the fire. Proximity is represented by the risk factor RRI. Based on these requirements, the cost function for the traversed path between two nodes is defined in Equation 2 using the Euclidean distance algorithm.

$$f(x) = R \times \frac{\sqrt{(x_2-x_1)^2+(y_2-y_1)^2+(z_2-z_1)^2}}{\bar{V}} \qquad (2)$$

where:

x_1, y_1, z_1 are the coordinates of the start node

x_2, y_2, z_2 are the coordinates of the end node

R is the risk factor of the edge connecting node 1 to node 2

$\bar{V}$ is the average speed of evacuees

Since the risk factors were previously defined for all of the nodes, the risk factor of the edges are calculated based on the average of two connecting nodes.

In Dijkstra, the start node is tagged first. Then, the cost of travel to all the connected nodes is calculated. The node with the smallest value is tagged. Then, the cost of travel to all of its connected nodes are calculated. The cost of unvisited nodes is updated if it is less than their previous cost. This process continues until the end node is met.

Large facilities and high-rise buildings typically have multiple exit doors. Therefore, there are multiple goals in this pathfinding problem. The Dijkstra algorithm is therefore solved for multiple exit goals and the minimum of those is the final solution.

4 Case Study

A hypothetical floor plan is used for implementation of the proposed model. The upper part of Figure 2 shows an isometric view of the three floor building with three stair cases that connect each floor level. The lower part of Figure 2 shows the floor plan, which is standard for each floor. The 3 exit doors are at the bottom of each staircase.

The BIM model of the building is translated to IFC data structure. IFC file is parsed and GNG is extracted. It is assumed that an analysis has been performed and it has been concluded that the best strategy of evacuation is simultaneous evacuation. Simultaneous evacuation is the most prevalent strategy in which all of the occupants are

asked to exit at once.

Based on simultaneous evacuation, the directional graph of the building is generated and shown in Figure 3. Note that the exit doors on the ground level are shown as red circles. The length of each edge is shown in meters, and the risk factor (R) at each node is shown in blue.

In this case, occupants in each compartment on the 2nd and 3rd floors can take all three exits and the staircases are one-way downward. That is why the edges on the 2nd and 3rd floors do not have directional arrow and the edges in the staircases do.

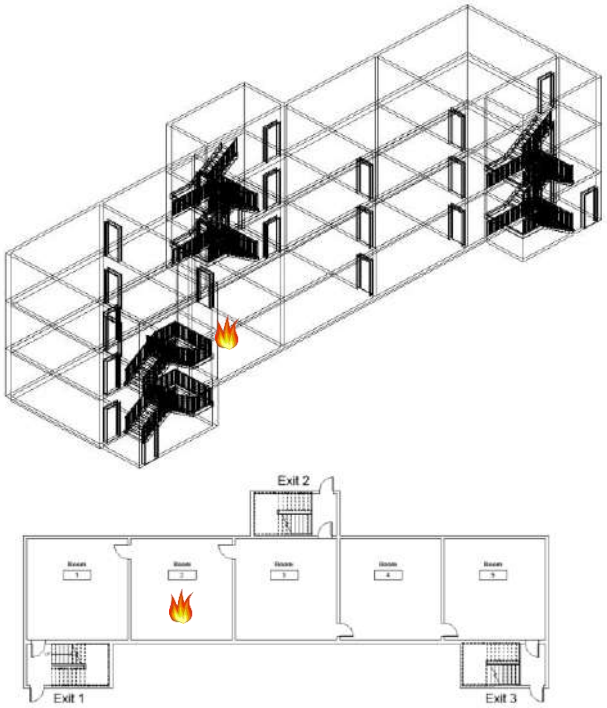

Figure 2. Isometric view and floor plan of the case study

For this research, the widely known Fire Dynamics Simulator (FDS) [14] developed by National Institute of Standards and Technology (NIST) is used to simulate the fire initiation and expansion. It is assumed that the fire-initiating element is a piece of household furniture, represented by a 1 cubic meter block of wood. The early alert of un-tenability or an approaching fire has a threshold defined by the presence of smoke that results in a visibility obstruction of 11%. Due to the computational heaviness of FDS, the fire simulations are run for a large number of scenarios during the evaluation planning stage, i.e. well before the emergency happens. Initiating point of fire is placed in all of the nodes and un-tenability times of the rest of the nodes are calculated. Simulation results are stored for access during an emergency situation.

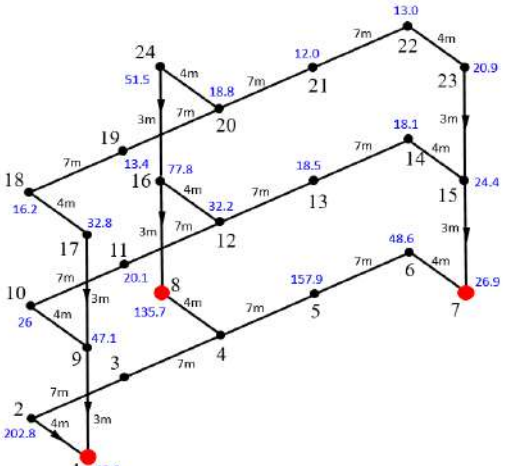

Figure 3. Directional GNG of the building with risk factors

Let's assume that the fire is initiated in node 3 on the first floor and after a specific amount of time, the fire expands. Smoke is quickly detected in node 4. It is prudent at this time to test if simultaneous evacuation is still the best strategy for evacuation.

The un-tenability condition defines ALET in Equation 1. Using this equation, the risk factor of each node is the summation of 1/ALET of the fire initiated in node 3 and node 4. The risk factor of each edge is then defined based on the average risk factor (R) of the nodes at two ends of the edge. The average speed of evacuees is assumed 1.35 (m/s) based on a study on commuters with varying genders and ages [15]. Dijkstra is later run for each node based on the cost function of Equation (2). Table 1 tabulates the result of this calculation. The 'selected route' comprises the path, as labeled in the directional GNG. The lowest cost path for each node is listed. The cost of the *shortest* path is also reported for the purpose of comparison. In 18 of the 24 nodes, the shortest path is the lowest cost path. In six cases, however, the shortest path is not the safest path. These are shown shaded in red.

For example, the lowest cost path from node 12 to an exit goes through nodes 12-13-14-15-7. Its cost is $346.5*10^{-4}$. Note that this path takes occupants to the exit at node 7 and not to the closer node 8 exit, which has a higher cost ($400.2*10^{-4}$) because it is near the fire at nodes 3 and 4. Merging the results in Table 1 with the GNG will result in the directional GNG shown in Figure 4. Note that all of the edges in the graph are now directional.

Table 1. Result of Dijkstra graph search

Node	Selected Route As per Eq.2 (Lowest Cost Path)	Cost of Selected Route ($\times 10^{-4}$)	Cost of Shortest Path ($\times 10^{-4}$)
1	1	0.0	0.0
2	2 1	372.9	372.9
3	3 2 1	Untenable	Untenable
4	4 8	Untenable	Untenable
5	5 6 7	647.5	647.5
6	6 7	112.0	112.0
7	7	0.0	0.0
8	8	0.0	0.0
9	19 1	106.6	106.6
10	10 9 1	214.9	214.9
11	11 10 9 1	334.4	870.2
12	12 13 14 15 7	346.5	400.2
13	13 14 15 7	215.0	746.7
14	14 15 7	120.0	120.0
15	15 7	57.0	57.0
16	16 8	237.3	237.3
17	17 9 1	195.3	195.3
18	18 17 9 1	268.0	268.0
19	19 18 17 9 1	344.7	913.2
20	20 21 22 23 15 7	302.1	485.1
21	21 22 23 15 7	222.2	787.2
22	22 23 15 7	157.6	157.6
23	23 15 7	107.4	107.4
24	24 16 8	380.9	380.9

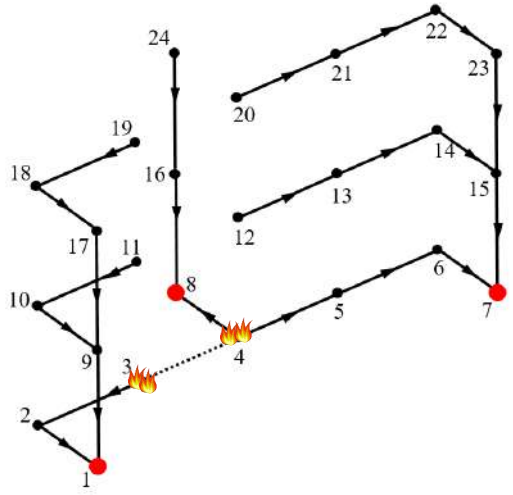

Figure 4. Resulted directional GNG from real-time path-planning model

Figure 4 graphically shows the safest evacuation routes for the current situation. Compared with simultaneous evacuation where evacuees are free to select any route, this graph recommends the evacuees in each node move away from the middle exit. It is interesting how adjacent compartments of 19-20 and 11-12 are directed to take separate egress routes. This emphasizes the point that the shortest exit path is not necessarily the safest or the most efficient option of evacuation.

The graph exploration and cost optimization of the proposed method, which must be performed during evacuation process, took less than 1.0 second on a Core i-7 dual core 2.7 GHz. This quick computation time satisfied the need for an algorithm that could reliably perform during the evacuation process. It was supported by the thorough exploration of emergency scenarios that performed during evacuation planning when the building was first occupied.

5 Conclusion

In this paper a real-time path-planning model for building evacuation was proposed. The model used IFC to automatically generate a GNG of the building. The Dijkstra method was modified and applied for exploration of the lowest cost path. The cost function of Dijkstra was defined based on combination of the proximity to the source of the fire and the length of the escape route. The risk factor representing the proximity to the source of fire was adopted from the RRI concept.

Finally, a hypothetical case study showed that the proposed model can successfully operate within tight time limits of an evacuation process. The result also showed that the conventional notion of "the shortest path is the safest path" may not always be true.

Future work in this research requires a modification to the cost function in order to include other influential factors in path-planning. Incorporating directional bias of the movements, congestion, speed variety in different zones, blockage caused by structural collapse and complexity of the routes can significantly enhance the accuracy and confidence of path-planning, which leads to a safer evacuation process.

References

[1] Lujak, M. Billhardt, H. Dunkel, J. Fernández, A. Hermoso, R. and Ossowski, S. A distributed architecture for real-time evacuation guidance in large smart buildings. *Computer Science and Information Systems*, 14(1), 257-282, 2017.

[2] Cuesta, A. Abreu, O. Balboa, A. and Alvear, D. Real-time evacuation route selection methodology for complex buildings. *Fire Safety Journal*, *91*, 947-954, 2017.

[3] Mirahadi, F., McCabe, B., Shahi, A. Smart Disaster Management System for Tall Buildings. In

Proceedings of CSCE 2017, Canadian Society of Civil Engineers, Vancouver, BC, Canada, 2017.

[4] Chou, J. S. Cheng, M. Y. Hsieh, Y. M. Yang, I. T. and Hsu, H. T. Optimal path planning in real time for dynamic building fire rescue operations using wireless sensors and visual guidance. *Automation in Construction*, *99*, 1-17, 2019.

[5] Yan W., Culp C. and Graf, R. Integrating BIM and gaming for real-time interactive architectural visualization. *Automation in Construction*, 20(4): 446-458, 2011.

[6] Eastman, C. Lee, J. M. Jeong, Y. S. and Lee, J. K. Automatic rule-based checking of building designs. *Automation in construction*, 18(8): 1011-1033, 2009.

[7] Taneja, S. Akinci, B. Garrett, J. H. Soibelman, L. and East, B. Transforming IFC-based building layout information into a geometric topology network for indoor navigation assistance. In *Computing in Civil Engineering*, 315-322, 2011.

[8] Dijkstra, E. W. A note on two problems in connexion with graphs. *Numerische mathematik*, 1(1): 269-271, 1959.

[9] Hart, P. E. Nilsson, N. J. and Raphael, B. A formal basis for the heuristic determination of minimum cost paths. *IEEE transactions on Systems Science and Cybernetics*, 4(2): 100-107, 1968.

[10] Wu, C. H. and Chen, L. C. 3D spatial information for fire-fighting search and rescue route analysis within buildings. *Fire Safety Journal*, 48: 21-29, 2012.

[11] Cheng, M. Y. Chiu, K. C. Hsieh, Y. M. Yang, I. T. Chou, J. S. and Wu, Y. W. BIM integrated smart monitoring technique for building fire prevention and disaster relief. *Automation in Construction*, 84: 14-30, 2017.

[12] Mirahadi F., McCabe B., Shahi A. IFC-centric performance-based evaluation of building evacuations using fire dynamics simulation and agent-based modeling. *Automation in Construction*, 101: 1-16, 2019.

[13] Lin Y. H., Liu Y. S., Gao G., Han X. G., Lai C. Y. and Gu M. The IFC-based path planning for 3D indoor spaces. *Advanced Engineering Informatics*, 27(2): 189-205, 2013.

[14] McGrattan, K. Hostikka, S. Floyd, J. Baum, H. R. Rehm, R. G. Mell, W. and McDermott, R. *NIST special publication, 1018-5: Fire dynamics simulator (version 5), technical reference guide.* NIST, 2007.

[15] Fruin, J. J. *Pedestrian planning and design.* Metropolitan Association of Urban Designers and Environmental Planners, 1971.

Development of an Earthmoving Machinery Autonomous Excavator Development Platform

R. Heikkilä[a], T. Makkonen[a], I. Niskanen[a], M. Immonen[a], M. Hiltunen[a], T. Kolli[a], and P. Tyni[a]

[a]Structures and Construction Technology, Faculty of Technology, University of Oulu, Finland
E-mail: rauno.heikkila@oulu.fi, tomi.makkonen@oulu.fi

Abstract –
This paper presents the initial planning phase results of excavator automation in the SmartBooms research project funded by Business Finland. Automation control is a key factor for the earth construction industry. Automation of excavators enables increased productivity and accurate adjustment of the digging work process, especially in depth control, which results in cost reductions. For design and research of excavator automation, a development platform has been planned using an E85 Bobcat 8.5 t excavator equipped with modified hydraulics and controls. Simulation and software development was selected using Matlab Simulink Realtime Desktop with SimlabIO CAN bus communications and custom code, while additional software development is performed mainly with integration of the robotics simulation software V-rep and Matlab.

Keywords –
Excavator; Automation; Development Platform; Robotic;

1 Introduction

1.1 Development trends of automatic 3D control systems for construction machinery

Over the past few years, the construction machinery, mining, and forest industries have experienced particularly vigorous development in the field of work machines and directly integrated digital processes, and in automation. Finland is currently a pioneer in the world of information modeling and automation in earthworks. The control of earthmoving machinery is based on information models that provide the necessary information for control systems in machines.

Typical automatic 3D control systems at the machinery level are (Tab. 1) for example guidance (the driver moves the machine and manages the machining blade manually on the basis of computer display information); coordinating (the driver moves the machine and manages the machining blade manually with the help of inverse kinematics), guiding (the driver moves the machine and controls some of the movements of the machining blade manually when the system is running automatically on some movements), and autonomous (operating without a driver). In the Nordic countries in particular, guidance, coordinating, and guiding 3D control systems are already widely used in the control of earthmoving machinery.

Table 1. The levels of automation for earthmoving machinery.

Level	Name	Description of the activity
0	No automation	Human operates machine
1	Remote control	Human operates remotely machine
2	Guidance	Operator supported, the operator drives manually machine and blade using computer user-interface to BIM model
3	Coordinated	Tip control, the operator moves the machine and manages the tool blade manually with the help of inverse kinematics
4	Partial automation	Controlling, the operator moves the work machine and manages the part of the tool blade manually while the system drives automatically some of the movements
5	Autonomous	Machine can operate without human driver
6	Autonomous machine swarm	Autonomous operation of work machines, interactivity and collaboration of working machines

The level of automation also depends on the type of machine. In spreader-type machines such as graders, bulldozers, and asphalt spreaders, the control systems are already actively controlling automated movements. In boom-type machines, control is generally still at the guidance level, where the driver manually controls the boom based on the control information displayed by the system. To increase the automation level in control of machines, one of the basic problems and challenges is to take account of changes in the work environment

efficiently and safely. Other machines, vehicles, and people may move into the working area of the machine, or the material to be cut or loaded in excavator work can move unpredictably. Automatic functions always require sensing and control values calculated by the computer. Verifying the condition and correctness of sensing and steering is closely related to the security review of autonomous movements.

An interesting algorithm toolbox and development platform has been introduced by Fraunhofer IOSB [1]. The purpose is to equip a variety of robotic systems with different autonomous capabilities relevant for their intended purpose with minimal adaptation effort.

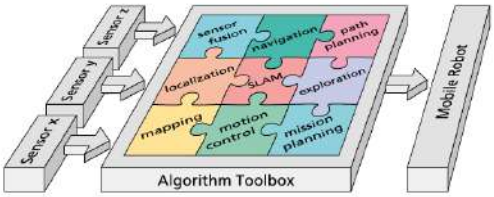

Figure 1. Fraunhofer Algorithm Toolbox for Autonomous Mobile Robots [1].

The puzzle modules of the Toolbox of Fraunhofer are mapping, localization, sensor fusion, motion control, SLAM, navigation, mission planning, exploration and path planning (Fig. 1).

1.2 Automatic control for Excavator

The excavator is a general-purpose machine on construction sites, with a high number of operating hours. The excavator has a lot of end-effectors such as buckets of different sizes, spikes, vibrators, and accessories for pipe installation, drilling, piling, stabilization, etc. The tasks are very versatile and challenging with guidance. The most typical infrastructure construction tasks are ground cutting, loading, material reception, and geometrically challenging ramp work.

The Robotics Institute at Carnegie Mellon University (USA) performed an interesting experiment with an autonomous excavator back in 1998 [2], while LUCIE by Lancaster University [3] is equally well known. The research group behind Carnagie Mellon created a model from the surrounding area and was able to find and fill a truck without the help of a human operator.

In recent years, Komatsu has been one of the most important technology drivers in the construction industry. Komatsu has already introduced an excavator control system. Novatron Ltd is currently marketing a guiding Xsite PRO system, which is the most integrated of commercial systems in the overall process of open information modeling (Open Infra BIM).

Figure 2. Commercial example: the Leica iCON iXE3 Copilot.

Figures 2 and 3 show the automation system of the Swiss Leica, where the guidance system has integrated automatic control of the level of cut of the excavator bucket, based on an angle readings by the machine control model. The Trimble Earthworks system automatically controls the lifting of the main boom according to the model, otherwise the operator manually drives the machine in the guidance model.

Figure 3 Testing the Leica machine automation system at Destia Ltd construction site in Vaala, Finland.

Figure 4. Research project in Japan by Kanamoto Ltd, on a movable humanoid remote robot for remote control.

Figure 5. Control and pilot station for more realistic remote operations.

It is particularly interesting to study and monitor the development of guidance technology in Japan, which is constantly affected by landslides due to earthquakes, typhoons, and sensitive earth material. These conditions are dangerous for workers, which is why Japan has developed and switched to a wide range of remote-controlled earthmoving machinery (Figures 4 and 5). In this case, the operators sit at a safe distance from the work site, in cabins from which they can control the heavy machinery using video connections and machine control systems. Some companies use a human robot in these systems to repeat as accurately as possible the drive movements made by the human operator in a safe cabin. However, Japan is lagging behind northern Europe in the use of information modeling based automation.

The self-propelled or self-contained excavator has been a research and development goal for quite some time. Various test systems have been tested. For example, the excavator introduced by Carnegie Mellon University in 1998 [2] was able to fill a truck platform without driver assistance, based on laser scanning. Automated excavators for construction sites have still not become mainstream, but development activities are now properly ongoing.

1.3 Aim of the research

The aim of the research and paper was to develop and experiment the new robotic development platform to the University of Oulu as well as to introduce the first results how to apply the platform for practical developments and experiments.

2 Automated Excavator Development Platform and the Experiments

The University of Oulu is developing an autonomous excavator in a SmartBooms research project funded by Business Finland. The aim of the SmartBooms project is to research and develop a new, continuously adaptable and automated control method for the boom of working machines through:

1. Developing automated control of the movements of machine and booms.
2. Use of different information models and real-time situation updating by continuous surveying.
3. Modular development enabling wide and versatile development of control applications in the earthmoving, forest, and mining industry, and installation of the control systems at the early manufacturing phase in the machinery factories
4. Applicability to product development of smart boom control systems for earthmoving, forest, and mining working machines.

2.1 Excavator and equipment

Figures 6 and 7 show the Bobcat E85 (8.5 t), which was chosen as the excavator machine by public tender. This excavator size was chosen to fit general construction sites, so it can be tested in a wide range of tasks, including road construction. It was decided to steer away from larger excavators, to make maintenance and handling

easy, while smaller excavators are not well suited to general-purpose digging and there is too little room for fitting the components and sensors needed. The machine needed to undergo a complete overhaul of the hydraulic systems, where valves were retrofitted for precise electrical control. For hydraulic control, a separate control unit was installed. To equip the excavator with a sight, a laser measuring device was installed onto the stick boom of the machine.

Figure 6. The University of Oulu's Smart Bobcat E85 Excavator.

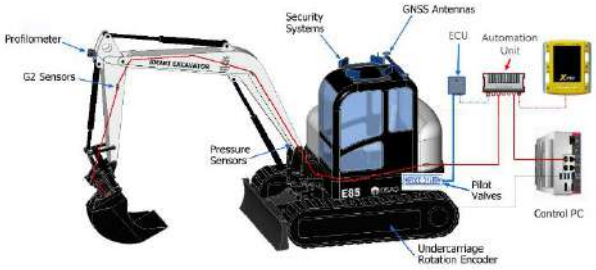

Figure 7. Components of the University of Oulu's Smart Bobcat E85 Excavator.

The basis of the sensory system are newly developed Novatron IMU G2 sensors, which can work up to 200Hz frequency. They provide accurate and precise positioning of the excavator which is good enough for automatic movements. Novatron's G2-type sensors have CAN bus-interfaced sensors. Use of CAN bus decreases the need for wiring and all sensors can be set at the same bus. Sensing accuracies and characteristics of the sensors were tested with the KUKA industrial robot (Figure 8). Dynamic and static features of previous versions of the Novatron sensors were also tested at the University of Oulu [4]. The new G2 sensors are significantly more accurate and reliable than the previous versions of Novatron sensors used widely in earthmoving work.

CAN bus is widely used in the automotive industry and various other industries. It is a low-cost device with less wiring, it works in various electrical environments, and it uses priority according to node ID [5].

Figure 8. G2 sensor testing using a KUKA robot manipulator

For global coordinates, a Trimble GNSS system is used in combination with an Xsite machine control system to provide location data. Communication between Xsite and hydraulic control is by CAN bus, while communication between machine and main level development pc is by both CAN bus and Ethernet proxy.

For safety reasons, it was decided to implement a camera system, most likely in the roof of the excavator. Laser profilometers and stereo sensors are currently selected to fit the excavator to provide data for both security and path planning. In the experiments, a new miniaturized 256x8 pixels line laser profilometer developed at University of Oulu was used.

2.2 Simulation environment

Virtual prototyping and code development testing were first intended to be performed in Matlab only, but it quickly emerged that this was not a reasonable approach, even using a Virtual Reality Toolbox. The Msc.Adams that we have successfully used previously for this purpose [6, 7, 8] was too laborious, lacked programming methods, and was too restricted to be selected. The game engine approach we have used previously in one case [9] is well suited to this task, but is quite a human resource-intensive option. After testing multiple general- and special-purpose virtual simulators, we selected the V-rep robotic simulation tool [10]. The main reasons were a) ease of use, b) light enough to run in normal laptop, and c) reasonable Matlab integration.

For non-commercial and educational use, Coppelia Robotics offers an educational license for The Virtual Robot Experimentation Platform. V-rep is a practical tool for the purpose, since it has many built-in actuators and sensors that are easily modified with scripts. That is why it requires less effort to build a functional environment compared with general tools such as Msc.Adams and Simulink. Model building in the V-rep scene editor is intuitive. Other specialist systems lack significant features such as mesh manipulation, simulation video, and multiple default physics engines. V-rep also has a wide library of miscellaneous robots, vehicles, and objects.

V-rep was chosen as a platform for the prototyping and testing of controls, and sensing of the automated excavator. Simulation parameters and movement are controlled through remote-API with external applications such as Matlab, where an inverse kinematics model and functions to operate actuators and to manipulate sensing data will be built.

With default simulation settings, V-rep simulates the tested scene (Figure 9), which simplifies the dynamic model, as represented in Figure 10, with execution times of around 40 ms for non-threaded scripts and of 10 ms for dynamic handling calculations. Because the calculation time increment is 50 ms, the calculations are somewhat faster than real time and the simulation video is rendered at around 24 frames per second. For the scene shown in Figure 10, one minute of simulation took 55 seconds running in the researcher's basic laptop. Simulation has an option for the lower accuracy and lighter calculations, as well as the customized time increment.

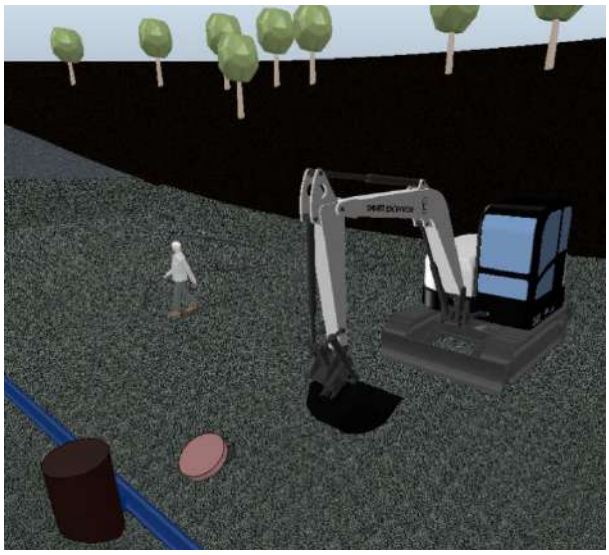

Figure 9. Test scene to study performance of the simulation software.

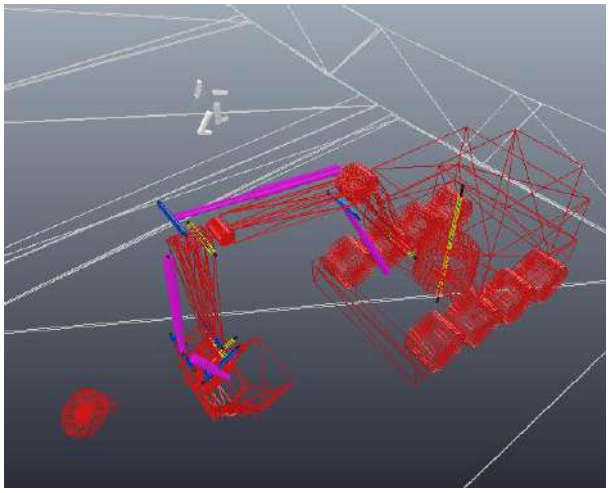

Figure 10. Simplified dynamic model for simulations.

A series of tests were performed using the robotic development platform. In the paper some observations from sensor calibrations, the use of the industrial robot as a reference model for the generation of digging trajectories i.e. control models, the first experiences of V-rep robotic development software as well as some test results of the new type of laser profilometer are reported.

3 Results

In the experiments with KUKA industrial robot, three IMU G2 sensors attached to the robot were used for real-time accurate capturing of boom and bucket movements. Actually, a kinematic sensor calibration of the G2 sensors was successfully performed using the driving paths of the robot as references. The robot was programmed to mimic real excavators digging movements to acquire data of G2 sensors repeatability, angle accuracies and effects of acceleration to the sensors data. Valuable detailed data of sensors abilities were gathered during robot measurements and will be reported later.

The first experiences of the V-rep robotic development software quite positive. The software has a good user-interface with a support of versatile robotic subroutine library, and the programming work was found to be relatively easy to execute. The accuracy and complexity of model details can slow down the real-time calculation of the program.

Experimental field tests and obtained results showed the suitability of the laser profilometer for surface changes monitoring and 3D visualization of a surface from the excavator (Fig. 11). The applied

method seems offer sufficient measurement accuracy in relation to the measurement range in work site. As the main advantages of the method the monitoring does not require expensive measuring equipment. Typical measurement materials and targets on earth construction sites seems to have sufficient reflectivity, color, and brightness of the object surfaces to be captured by the measurement system.

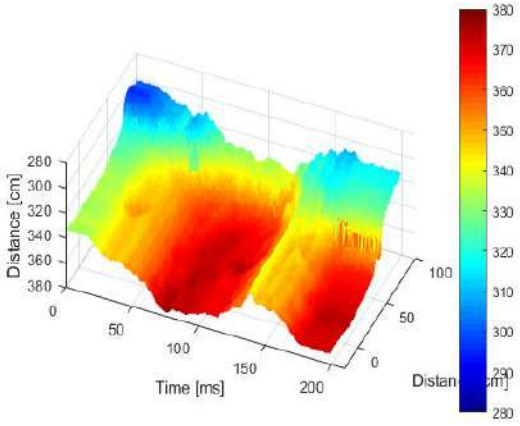

Figure 11. A pit measured by the laser profilometer from the boom of Bobcat excavator.

4 Conclusions

The SmartBooms project has created a simulation test environment and robotic development platform into University of Oulu for the development of autonomous excavation equipment. The simulation environment was a powerful tool for safely testing new concept and control algorithms. The platform utilizes also the selection of newest sensor systems with IMU G2 sensors and a solid state laser measurement system developed at University of Oulu.

The main software chosen for development was Matlab Simulink Realtime with SimlabIO integration to CAN. The main platform software is supported by many different tools, with V-rep used extensively. The physical excavator chosen through public tender is a medium-sized Bobcat E85 equipped with a Novatron Xsite machine control system.

The puzzle modules of the Toolbox of University of Oulu are so far 1) open information modelling, 2) positioning in accurate coordinate system, 3) sensor fusion, 4) motion control for machine rotation and movements of booms and bucket, 5) machine transition and navigation, 6) mission planning and work task creation, 7) path generation and 8) safety assurance.

Our goal in future work is to produce a fully autonomous excavator operating on an earth construction/excavation site according to the parameters given by the designer. In addition, the excavator algorithm must prevent the excavator from undesired and possibly destructive movements. A self-moving machine must always know what to do. The most important facilitator of autonomous control and machine learning, *i.e.* "machine intelligence", is integration into the information modeling process used by the Infra industry.

References

[1] Fraunhofer IOSB (J. Petereit & C. W. Frey) “Algorithm Toolbox for autonomous Mobile Robots”, 2017, 4 pages. https://www.iosb.fraunhofer.de/servlet/is/21022/

[2] A. Stentz, J. Bares, S. Singh, and P. Rowe, “A robotic excavator for autonomous truck loading,” Autonomous Robots, vol. 7, no. 2, pp. 175–186, 1999

[3] W. Seward, F. W. Margrave, I. Sommerville, and R. Morrey, “LUCIE the robot excavator - design for system safety.,” in Proceedings of the 1996 IEEE international conference on robotics and automation, vol. 1, Minneapolis: IEEE, 1996, pp. 936–968.

[4] M. Immonen, R. Heikkilä, and T. Makkonen, “Suitability of a Three-Axis Inclinometer to the Automated Blade Control System of Excavator,” in ISARC. Proceedings of the International Symposium on Automation and Robotics in Construction, 2015, vol. 32, p. 1.

[5] NIST, Controller Area Network (CAN) Overview, http://www.ni.com/white-paper/2732/en/ 8.1.2018

[6] T. Makkonen, K. Nevala, and R. Heikkilä, “A 3D model based control of an excavator,” Automation in Construction, vol. 15, no. 5, pp. 571–577, 2006.

[7] T. Makkonen, K. Nevala, and R. Heikkilä, “Automation of an excavator based on a 3D CAD model and GPS measurement,” in Proceedings of the 21st International Symposium on Automation and Robotics in Construction (ISARC’04), 2004.

[8] T. Makkonen and K. Nevala, “Simulating an excavator equipped with a rotating bucket—the 6 DOF system,” in OST–03 Symposium on Machine Design, ISBN, 2003, pp. 951–42.

[9] T. Makkonen, R. Heikkilä, A. Kaaranka, and K. Nevala, “Roadwork Site 3D Virtual Visualization Using Open Source Game Engine and Open Information Transfer,” in ISARC. Proceedings of the International Symposium on Automation and Robotics in Construction, 2014, vol. 31, p. 1.

[10] M. Freese, S. Singh, F. Ozaki, and N. Matsuhira, “Virtual robot experimentation platform v-rep: a versatile 3d robot simulator,” in International Conference on Simulation, Modeling, and Programming for Autonomous Robots, 2010, pp. 51–62.

Construction Data-Driven Dynamic Sound Data Training and Hardware Requirements for Autonomous Audio-based Site Monitoring

Y. Xie[a], Y.C. Lee[a], T. Huther da Costa[b], J. Park[b], J. H. Jui[c], J.W. Choi[b], Z. Zhang[b]

[a]Department of Bert S. Turner Department of Construction Management, Louisiana State University, United States
[b]School of Electrical Engineering and Computer Science, Louisiana State University, United States
[c]Division of Computer Science and Engineering, Louisiana State University, United States
[d]Louisiana Transportation Research Center, United States
E-mail: yxie21@lsu.edu, yclee@lsu.edu, thuthe1@lsu.edu, jpar132@lsu.edu, jjui1@lsu.edu, choijw@lsu.edu, doc.zhang@la.gov

Abstract –

In a dynamic construction site, sound generated by work activities and equipment operations is one of vital field data indicating construction progress, work performance, and safety issues. However, because of an enormous number of construction work types, accurate sound classification is currently limited. To address this challenge, this study proposes a schedule-based sound classification for establishing dynamic sound training data. With the schedule-based dynamic training method, this system retrieves the types of sounds of daily planned construction activities for flexibly restricting training data types of working sounds and ultimately improving the accuracy of sound classification. To reveal the implications of audio-based construction activity detection and site monitoring frameworks, this study also involves the development of a construction sound library, a hardware system, a sound classification framework, and a web-based visualization method. This proposed method is expected to play a critical role in managing a construction project by supporting site monitoring and progress analysis, and safety surveillance.

Keywords –

Schedule-based data training; Audio-based site monitoring; Audio sensor-based hardware system; Automated work activity surveillance; Machine Learning-based sound classification

1 Introduction

In the construction industry, the lack of appropriate technologies to acquire field data has been a primary obstacle to prevent real-time data collection and analyses. With the rapid development of information technology, the construction industry has been seeking for new field data acquisition and advanced analysis methods to pursue enhanced construction activity monitoring and automated field management. It is critical to allow domain professionals to manage construction activities and operations efficiently with accurate analyses and measurement of field data throughout an entire construction project, because of dynamic and complicated backgrounds of a construction project with various work activities. With the help of previous research studies of field data collection, diverse applications and monitoring technologies such as sensors- and vision-based methods have been investigated to explore their potentials and practicability in the construction industry [1, 2]. Recent studies have also identified the implications of the implementation of the audio-based site monitoring technique [3, 4]. This study states that sound data not only require less data processing weight for a data analysis than one from vision data, but also have no limitation to capture data with an unlimited level of illumination and scope [3]. Because of the diverse types of equipment, materials, and work environment, however, it is not practically feasible to establish a comprehensive sound data library covering all sound types of construction work activities in a site. To ameliorate this challenge, this study aims to establish construction schedule-based sound data training and audio-based site monitoring frameworks that dynamically develop sound training data according to daily planned work activities. This study involves the development of a construction sound library, a dynamic sound data training model, a hardware system, and a web-based sound data map visualization. To assess the proposed approach, this study has the experiment of sound classification with a real construction project schedule and illustrates improved classification accuracies with a confusion matrix.

2 Literature Review

Recent decades, diverse studies explored advanced technologies for construction field data collection and process monitoring using sensors, ultra-wide band, and computer vision-based monitoring [1, 2, 5, 6, 7]. However, vision-based monitoring is somewhat limited in tracking work activities during night time because it requires certain level of illumination and has the restricted range of a vision angle [3]. In addition, video and kinematic data are too heavy to be processed for real-time monitoring. Sound data as a new type of field data requiring less data processing weight have been explored in several studies. The execution of an audio-based approach using the support vector machine has been investigated for construction activity identification of heavy equipment [3]. The frequency domain approach was also applied to identify overlapped sounds generated by different equipment at a construction site [4]. However, these previous studies mostly focus on utilizing and improving a signal analysis, feature extraction, model training, and testing. This study has an objective to enhance sound classification accuracy by providing dynamic sound training data according to planned daily schedule.

3 Research Approach and Methodology

The primary goal of this study is to establish a schedule-based sound data library containing sound data types associated with daily planned construction activities and compare the classification result based on the schedule and that without the schedule. To identify construction activities accurately, the audio-based monitoring system requires a robust sound data library involving diverse types of work activities. Since a construction project schedule entails a detailed daily work plan including types of work activities useful for building the foundation of a site monitoring system, its data can be utilized for pre-identifying daily planned work activities and their sound types, allowing the system to flexibly retrieve sound data from an existing sound data library and establish training datasets accordingly. Figure 1 shows the research process including the establishment of a sound data library, sound classifier training, a construction activity detection framework, and a visualization interface.

To accomplish this objective, this study employs a construction schedule in the XML format extracted from a construction scheduling software. In addition, this system adopts the K-nearest neighbor (KNN) classifier for sound classification based on extracted features of selectively retrieved sound data.

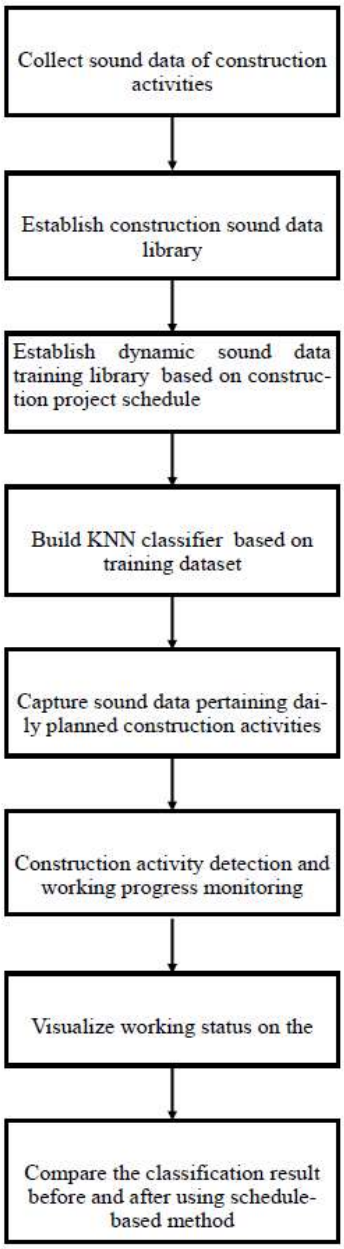

Figure 1. Framework of the methodology

With the customized XML schema, this system extracts XML-based construction schedule data including construction activities, equipment resources, and operation time from the Microsoft project, which is one of the broadly used construction scheduling software. This schedule data are imported into a framework to retrieve corresponding sound data from the established sound data library to build dynamic training datasets. The authors have already developed a sound data library that encompasses more than 100 sound data covering 15 types of construction work activities. Figure 2 shows the

process of the establishment of a dynamic training data library including schedule information retrieval, sound data extraction, and training data development. The retrieved daily schedule information is referred to build a training data library including audio files (.wav) of equipment and work activities by conducting the matching process using the filenames and the semantics of audio data. With the established schedule-based library, the input file containing daily planned work types can be interpreted to extract corresponding audio data and their features that are the imperative resources analyzed by the KNN model.

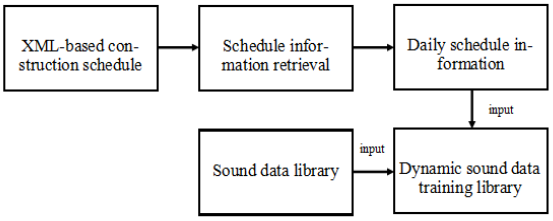

Figure 2. Establishment of dynamic sound data library

3.1 Development of a Sound Data Library

In this study, eight type sound data of construction activities including Excavating, Concrete Mixing, Compacting, Bulldozer, Hammering, Piling, Concrete Pumping and Drilling were recorded from the real bridge construction sites in East Baton Rouge, Louisiana. These sound data are divided into a short segment with bins of 2 seconds long and split into both training and testing sets. Because of the complex background and the dynamic environment of the construction site, recorded sound data of construction activities generally include noise and the classification accuracy is highly dependent on signal to noise ratio [8]. Therefore, a de-noising process is required to enhance raw sound signal data and a noise estimation algorithm [9] is adopted in this research. This algorithm is applied to reduce noise by computing the ratio of power spectrum to minimum power spectrum for each segment. If a ratio is less than one, it should be removed from original signal waves, or it can be regarded as valuable signal. The original and enhanced sound data of compacting and excavating are shown in Figure 3 and 4.

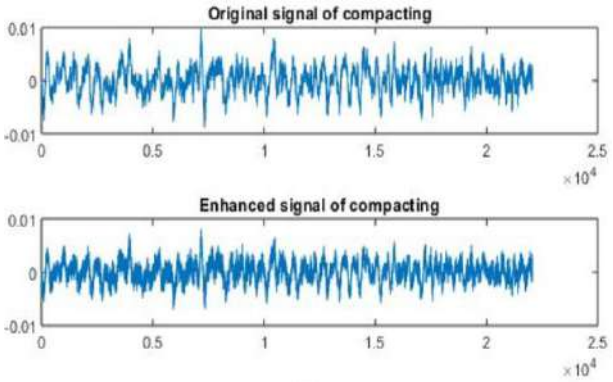

Figure 3. Original and enhanced signal of compacting

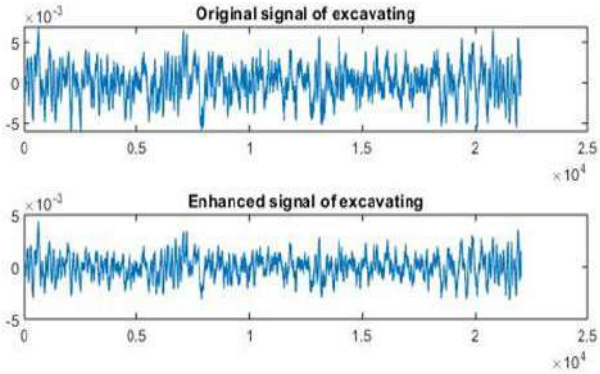

Figure 4. Original and enhanced signal of excavating

3.2 Generation of XML-based Construction Schedule Data and Training Data Library

Table 1 shows the schedule of the bridge construction project in East Baton Rouge, Louisiana, which consists of construction activities, resources, and starting and finishing time. Figure 5 illustrate the XML-based schedule data extracted from the Microsoft Project software.

Table 1. Schedule of Bridge Construction in East Baton Rouge

Construction Activities	Construction Resources	Starting Time	Finishing Time
Earth Works	Mobile excavators	2018-09-07	2018-09-20
Structural Excavation for Minor Structures	Mobile excavators	2018-09-07	2018-09-20
Fabric and Grid Reinforcing	Complete Reinforcement Cages	2018-09-11	2018-09-13
Sheeted Caissons	Pile Drivers (Rammers) and Pulling Tools	2018-09-12	2018-09-13
Sheeted Caissons	Pile Casings (linings)	2018-09-12	2018-09-13
Cast-in-Place Concrete Pile	Ready Mixed Concrete C30	2018-09-14	2018-09-17
Spreading and Compaction	Wheel loaders	2018-09-14	2018-09-20
Reinforcement Bars	Reinforcing Bars	2018-09-18	2018-09-25
Reinforcement Bars	Steel Reinforcement cutters	2018-09-18	2018-09-25
Structural Cast-in-Place Concrete Forming (steel)	Steel Forms	2018-09-26	2018-09-28
Cast-in-Place Concrete C25	Concrete truck mixer / agitator	2018-10-01	2018-10-02
Cast-in-Place Concrete C25	Concrete pumps and equipment	2018-10-01	2018-10-02
Cast-in-Place Concrete C25	Concrete vibrators	2018-10-01	2018-10-02
Cast-in-Place Concrete C25	Ready Mixed Concrete C25	2018-10-01	2018-10-02
Concrete Curing	Coatings for Concrete and Masonry	2018-10-03	2018-10-05

Figure 5. Generated XML based schedule

By referring the project schedule information, this system retrieves project-specific sound data from the pre-developed sound data library to build a dynamic training data library. To evaluate the proposed method, the research team conducted the case study using the following three construction activities in Table 1 scheduled from 2018-09-14 to 2018-09-17: Earth Works, Spreading and Compaction, and Cast-in-Place Concrete Pile. As shown in Figure 6, these schedule data are exported in the XML format from MS Project and imported into the framework to retrieve the associated sound data and generate a daily training library.

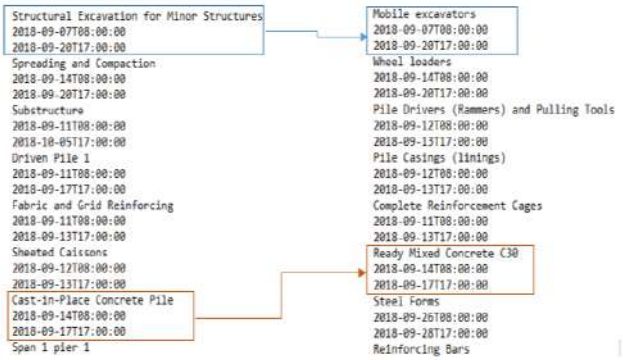

Figure 6. Schedule information retrieval

3.3 Hardware development of an audio sensor-based system

Microphones are the primary devices for capturing and recording sound data and each microphone contains a surface designed to capture audio waves. The internal circuits of a microphone should be powered to generate a sound signal and a wireless system is designed for audio signal receiving combined with the data analysis. Figure 7 shows the hardware design including a microphone, a radio frequency module (RF) including a transmitter and a receiver (nRF24L01), and a multi-track recorder (Zoom F8).

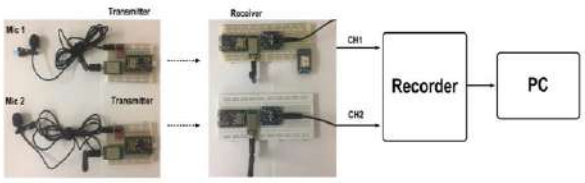

Figure 7. Hardware settings

3.4 Audio Signal Transmission and Analysis

Microphones capture surrounding sounds and transform them into electrical signals that are amplified through pre-amps making that the signals can be readable by micro-controllers. For a real-time sound signal transmission, we utilize a nRF24L01 transceiver module which is widely used in two-way radios, called walkie-talkie. In the current research, even if nRF24L01 modules work as one-way radios, the RF module can be suitable because it has an operating frequency of 2.4 GHz (ISM band) and a multichannel capability (up to 126 channels). Moreover, it can achieve a sample rate of 44 KHz with 1 Mbps data rate.

Within an available network of the RF module generally covering 1.5 miles, transmitters play a role in transferring the data sets to the receivers as shown in Figure 8. Receivers obtain the sound data in the form of digital signals. Microcontrollers select proper channels for the receivers from different channels and the digitized

sound information can be transformed into the analog signal for the 8-channel recorder. The recorder collects the sound data from the multi-channel and transfers the data to a computer for analysis as shown in Figure 9.

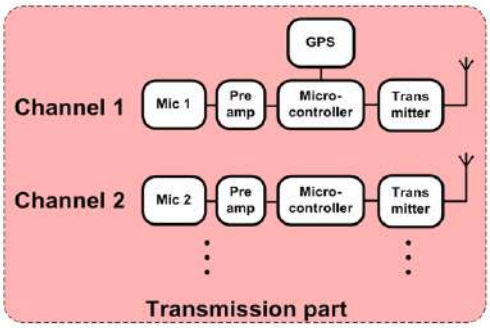

Figure 8. Sound signal transmission

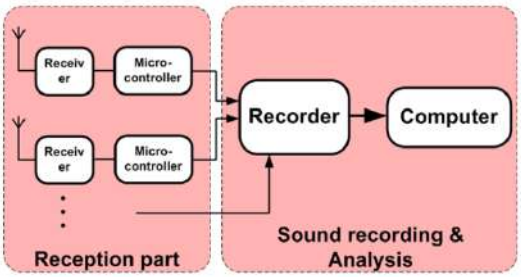

Figure 9. Sound signal receiving and analysis

3.5 Pre-processing Including De-noising, Feature Extraction, and KNN-based Sound Classification

Recorded sound data in a construction site generally contain background noise that negatively affects the accuracy of sound classification and site monitoring. Thus, this system adopts the noise estimation algorithm for de-noising, which reduces noise of a training dataset. This method computes the ratio of power spectrum to minimum power spectrum for each segment and then remove if a ratio is less than one. By using 44.1 kHz sampling frequency, this study utilized 15 distinct sets of features and in our experiments, the K nearest neighbor (KNN) algorithm achieved enough high classification accuracies, while maintaining fast execution. A set of features is required to build the KNN model. To extract the features, sound files were split in frames of 2s, from which the features shown in Table 2 were extracted to fit the KNN model. During training, each sound belongs to a defined construction activity category, as mentioned earlier. During execution, features are extracted from the recorded sound and fed to the KNN algorithm. The predicted category is found by minimizing the expected cost among the nearest neighbors of the current sample that is, by finding the nearest neighbors, shown in figure 10. When testing new audio segments, the output should be one of construction work activities or equipment operations in sound data library mentioned in section 3.1.

Table 2. Selected Sound Features

Symbol	Feature name	Number of features in the set
ZCC	Zero Crossing Count	10
VZCR	Variance of Zero Crossing Rate Ratio	1
HZCRR	High Order Zero Crossing Rate Ratio	1
RMS	Root Mean Square	10
LEF	Low Energy Frame	1
STE	Short Time Energy	1
LSTER	Low Short Time Energy Ratio	1
VLER	Variance of Low-Band Energy Ratio	1
VSFLUX	Variance Spectrum Flux	1
LFRMS	Low-Frequency Root Mean Square	1
LFZCC9	9th-order moment of LFZCC	1
SBC	Sub Band Correlation	5
HOC	High Order Crossing	8
LPC	Linear Predictive Coefficients	7
MFCC	Mel-Frequency Cepstral Coefficients	13
Total		62

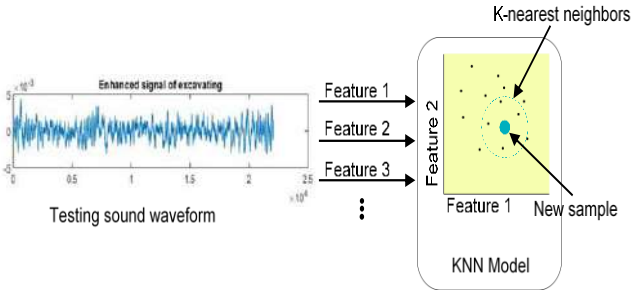

Figure 10. Predicting new sound

3.6 Construction Activity Identification and Accuracy Evaluation

By executing the fitted KNN model with daily dynamic training sound data, this study evaluates the accuracies of sound classifications before and after using the schedule-based approach. 200 short time segments (2s long) audio files of the three selected work activities are split into training and testing datasets evenly: 100 segments are the training dataset and the rest are the testing dataset. To compare the accuracies of the two scenarios without and with the integrated schedule data, the confusion matrices are adopted as illustrated in Figure 11 and 12. The classification accuracy is only 78.6% without the integration of the schedule information and 99.7% with the schedule-based dynamic training data library. These experiments clearly show that a schedule-based dynamic training framework significantly improves the accuracy of construction work sound classification.

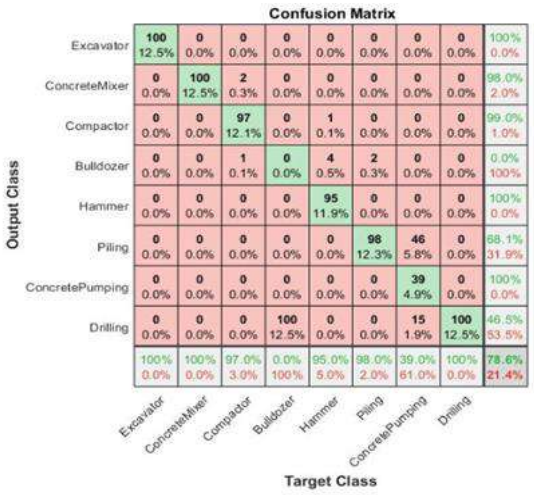

Figure 11. Classification accuracy without schedule information

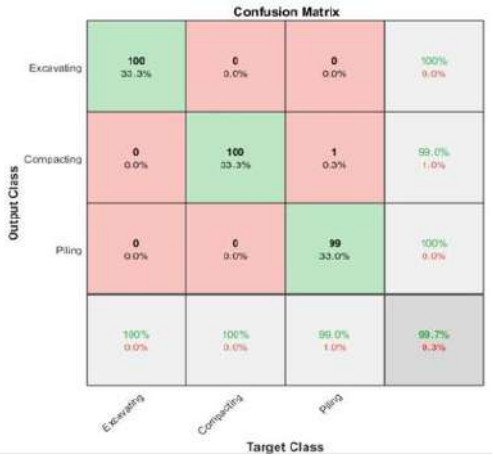

Figure 12. Classification accuracy with dynamic training data library

3.7 Web-based Visualization Map

As a visualization interface, a website has been developed to represent real-time construction work status and progress on different locations. The Web framework has been built with the Python Django framework and Leaflet is used for the base map tiles. Mapbox, ArcGIS and OSM tiles have also been integrated to the website for a better perspective of visualization data. The backend of the website is connected to a PostGreSQL database that is using the cloud Relational Database Service (RDS) from Amazon Web Services (AWS). An additional script written in Python has been used to read data from a JSON file and update the cloud database accordingly. Finally, the website has been deployed using Heroku. The website map representing site locations, job types, and working dates is shown in Figure 13.

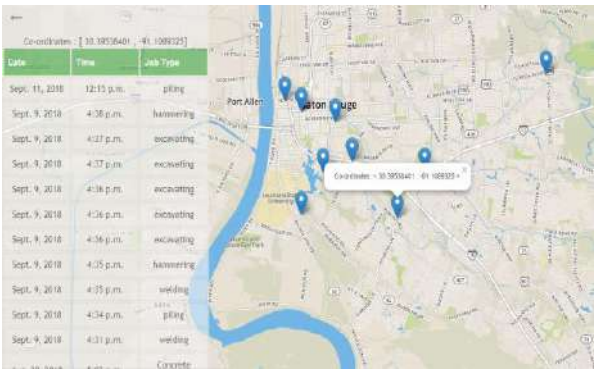

Figure 13. Construction Activity Visualization

4 Conclusion

The sound recognition technology has been adopted in diverse disciplines, but not received much attention in the construction industry. This paper proposes a schedule-based approach to improve the sound classification accuracy for providing robust construction event detection and site monitoring frameworks. As the outcomes show the significantly improved accuracy, this method is expected to be an imperative asset for diverse disciplines to develop an innovative technology that captures, analyses, and visualizes sounds of construction work and equipment in a dynamic and complicated construction site. The research results also involve new knowledge on the implications of sound recognition in the construction industry for accurately identifying working status and progress monitoring without any human effort. However, there are a few limitations identified in this research such as the insufficient size of sound data. The size of the data is not huge enough to validate the result and this research team will keep collecting sound data including various types of work activities for future research. In addition, the identification of heterogeneous sounds occurring simultaneously by using neural network is necessarily to be discussed in the next study and the recognition of sounds that do not belong to any of the categories such as the recognition of idle time will be also investigated. It is expected that the developed theoretical framework will add the innovative scientific knowledge and the new logical theory which pose significant impacts on the workflow optimization, the accurate task-performance measurement, and civil infrastructure construction projects for roads, highways, bridges, and tunnels.

5 References

[1] Teizer, J., Lao, D., & Sofer, M. (2007, September). Rapid automated monitoring of construction site activities using ultra-wideband. In *Proceedings of the 24th International Symposium on Automation and Robotics in Construction, Kochi, Kerala, India* (pp. 19-21).

[2] Cheng, T., & Teizer, J. (2013). Real-time resource location data collection and visualization technology for construction safety and activity monitoring applications. *Automation in Construction*, *34*, 3-15.

[3] Cheng, C. F., Rashidi, A., Davenport, M. A., & Anderson, D. (2016, January). Audio Signal Processing for Activity Recognition of Construction Heavy Equipment. In *ISARC. Proceedings of the International Symposium on Automation and Robotics in Construction* (Vol. 33, p. 1). Vilnius Gediminas Technical University, Department of Construction Economics & Property.

[4] Cho, C., Lee, Y. C., & Zhang, T. (2017). Sound recognition techniques for multi-layered construction activities and events. In *Computing in Civil Engineering 2017* (pp. 326-334).

[5] Brilakis, I., Fathi, H., & Rashidi, A. (2011). Progressive 3D reconstruction of infrastructure with videogrammetry. *Automation in Construction*, *20*(7), 884-895.

[6] Golparvar-Fard, M., Peña-Mora, F., & Savarese, S. (2009). Application of D4AR–A 4-Dimensional augmented reality model for automating construction progress monitoring data collection, processing and communication, ITcon Vol. 14, Special Issue Next Generation Construction IT: Technology Foresight, Future Studies, Roadmapping, and Scenario Planning, pg. 129-153.

[7] Turkan, Y., Bosche, F., Haas, C. T., & Haas, R. (2012). Automated progress tracking using 4D schedule and 3D sensing technologies. *Automation in Construction*, *22*, 414-421.

[8] Hirsch, H. G., & Pearce, D. (2000). The Aurora experimental framework for the performance evaluation of speech recognition systems under noisy conditions. In *ASR2000-Automatic Speech Recognition: Challenges for the new Millenium ISCA Tutorial and Research Workshop (ITRW)*.

[9] Rangachari, S., & Loizou, P. C. (2006). A noise-estimation algorithm for highly non-stationary environments. *Speech communication*, *48*(2), 220-231.

Applying Kanban System in Construction Logistics for Real-time Material Demand Report and Pulled Replenishment

N. Zeng[a], X. Ye[a], X. Peng[b], and M. König[a]

[a] Department of Civil and Environmental Engineering, Ruhr-University Bochum, Germany
[b]Sinohydro Bureau 14 Co., Ltd, Power Construction Corporation of China, Shenzhen, China
E-mail: ningshuang.zeng@rub.de, xuling.ye@rub.de, pxf0228@gmail.com, koenig@inf.bi.rub.de

Abstract –

Drawbacks of the absence of the flow view in the conventional construction logistics planning gain more attention. Inefficiency and wastes (e.g., on-site overstock) in the construction logistics caused by adopting an avoidance strategy is recognized. Meanwhile, the unstable labour productivity and periodic planning method cause difficulties for adopting Just-in-Time (JIT) approach in construction. As a real-time control system of a production flow with the ability of rapid and precise acquisition of facts, the Kanban system can be a solution for a pulled production and related logistics. This paper explores how to apply Kanban concept to record the material consumption, report the real-time demand and trigger a material replenishment from off-site to on-site. A methodology of designing and applying Kanban batch in the digital construction logistics with Building Information Modelling (BIM) systems or tools is proposed. A case study of an infrastructure project is carried out to address the functions and performance of a Kanban-triggered material replenishment. The results of the case study show significant savings of site storage area and construction time by applying Kanban concept in the construction logistics.

Keywords –

Kanban; Construction Logistics; Pull; Real-time Demand; Building Information Modeling

1 Introduction

For a long time, buffering is a conventional solution to prevent adverse effect of off-site material supply disruptions in the construction field [1,2]. However, it may cause problems, e.g., additional waiting time, an excessive amount of orders, overstock on-site, waste of site capacity as well as difficulty in materials and related equipment maintenance [3]. To reduce buffers and remove wastes from the construction process, lean production approaches such as Just-in-Time (JIT) are considered useful [4,5]. However, the unstable labour productivity and periodic planning method cause difficulties for adopting JIT production in the construction field.

The original Kanban system is well-known as a JIT control system, but its application is not limited to JIT production. The essence of the Kanban system is characterized as a real-time control system of a production flow with the ability of rapid and precise acquisition of facts [6]. A conventional construction logistics plan adopts a short-term demand forecast based on managers' experience and expertise. However, most information systems for construction logistics cannot capture this kind of demand forecasting results because of limited data. Developing the knowledge bases and sophisticated algorithms can help transfer the knowledge in this specific field from the person to the computer. Based on it, real-time analysis, adaptive buffering, proactive scheduling and automated decision-making for construction logistics are realizable. From an operational perspective, the equilibrium of material consumption, on-site stock, and off-site replenishment is essential for construction logistics at the current stage. To address this point, adopting the Kanban concept is helpful for information systems to capture the real-time material consumption amount and replenishment demands precisely and timely.

This paper explores how to apply the Kanban concept to record the material consumption, report the real-time demand and trigger a material replenishment from off-site to on-site. First, a literature review regarding Kanban system and construction logistics planning is conducted to trace back the theoretical foundation. Meanwhile, experiences are drawn from current construction planning practices. Afterwards, a methodology to design and apply Kanban batch in the construction logistics with 4D Building Information Modelling (BIM) systems or tools is elaborated. An infrastructure project is finally studied and simulated to address the functions and performance of a Kanban-triggered material replenishment.

2 Literature Review

2.1 Kanban System

The Toyota Motor Corporation developed the Kanban system with order cards to control production flows because the cost of adopting the computerized system was huge in the 1970s [6]. As the development and maintenance costs of information systems gradually decrease, many manufacturers implemented electronic Kanban systems. Junior and Filho (2010) did a review and classified variations of Kanban systems into systems which follow the original Kanban logic and systems which do not [7]. Systems using the original Kanban logic have the following features:

- Use of two communication signals, i.e., production and transportation signals;
- Pulled production;
- Decentralized control;
- Limited WIP, i.e., finite buffer capacity.

By comparison, variations beyond the original Kanban logic emphasize one or several following aspects:

- Variable maximum inventory level;
- Signal use modification;
- Gathering and using the information;
- Functioning;
- Materials release.

Nowadays, the manufacturing industry has adopted a series of mature production information systems or software packages using original, partially or entirely modified Kanban logic. In the AEC field, Kanban-like or Kanban-type methods are frequently mentioned in lean construction research, addressing the pull concept and visual control of construction workflows. Tserng et al. (2005) proposed a Kanban-like visual control system for project participants to manage construction supply chains [8]. Sacks et al. (2009) introduced Kanban-type pull signals in BIM-based environments to improve the transparency of construction workflows [9]. Dave et al. (2016) adopted control principles from Kanban to fulfil the visual controls in a lean construction management system using BIM [10]. However, most of the Kanban signals applied in construction serves as a visualized process status (e.g., finished, delayed or under construction), rather than the demand-driven, i.e., pull production trigger, which is the essential part of the original Kanban system.

2.2 Construction Logistics Planning

According to current practices, the construction logistics plan is generally made according to construction managers' experience and expertise. It involves an as-designed site-layout, project QTO (Quantity Take-off) and a series of periodic (e.g., daily, weekly, monthly) schedules [11]. It adopted periodic planning of material consumption, and site storage areas are configured according to the periodic consumption. Another essential feature of the current construction logistics planning is that materials and building components are treated as input or constraint of a certain construction task from a construction workflow or schedule [11]. The completion of the target construction task is the highest goal and any shortage of on-site material stock should be avoided. Therefore, problems about excessive amounts of orders, waste of site capacity and difficulty in materials maintenance etc. may occur. Two aspects should be taken into account regarding current construction logistics planning:

1. Uncertainty caused by periodic consumption, i.e., short-term demand forecast based on experience and expertise;
2. Inefficiency and wastes (e.g., on-site overstock) caused by adopting an avoidance strategy to ensure sufficient material resource for construction workflow.

Considering the aspects mentioned above, Last-Planner System (LPS) provides a pull concept using the "Should-Can-Will-Did" pattern and weekly meetings regarding construction workflows and schedules [11]. It helps to correct the deviation between as-planned and as-built progress and to reduce the uncertainty of a short-term demand forecast. Meanwhile, approaches, e.g., Advanced Work Packaging (AWP) and location-based management improve construction scheduling and workface developing [12].

From an operational perspective, the equilibrium of material consumption, on-site stock, and off-site replenishment is essential for the two aspects above. It does not emphasize the robust of the construction workflow itself but requires a clear production flow [13]. Every construction task can be treated as a discrete production, where precise real-time material consumption can be reported as evidence of future demand. It is the essence of the Kanban signal in a pulled production. Compared to LPS or AWP, the Kanban system is more appropriate to deal with material flows rather than construction workflows. The season is that the material flows are not sensitive to on-site discrete production and unstable productivity.

Simulation techniques support the analysis of material and information flows in construction. As Law described, material and information flows for analysing supply chains are suitable to be defined as a simulative system [14]. Modelling and Simulation methods e.g. discrete event simulation (DES) and agent-based simulation (ABS), have been continuously developed in

the field of the construction logistics, to analyse and optimize logistics processes and configurations [15].

The original Kanban system contains complete rules and principles, which companies, e.g., SAP (System Applications and Products) and Oracle already adopted into the ERP (Enterprise Resource Planning) system or supply chain information system. It is also possible to introduce it into BIM-platforms which adopting Industry Foundation Classes (IFC). Building models with higher LOD (Level of Development) can provide abundant detailed information for the construction logistics. For example, LOD 400 contains information required for fabrication, assembly and installation [16]. Meanwhile, 3D visualization with Model View Definitions (MVDs) is helpful for collaborative product development from design to on-site construction. Digital construction sequencing and scheduling techniques and current 4D BIM practices [17] [18] [19] provide a foundation for the adoption of the Kanban signals to report real-time material consumptions. It is essential to not only provide a visual Kanban board or tool with 3D representations but also help change a periodic and centralized construction logistics planning into a real-time demand-driven logistics management.

3 Methodology

3.1 Overview

This paper draws experiences from current construction planning practice, including the long-term planning, short-term periodic scheduling, and site storage planning [12] [17], as shown in Figure 1:

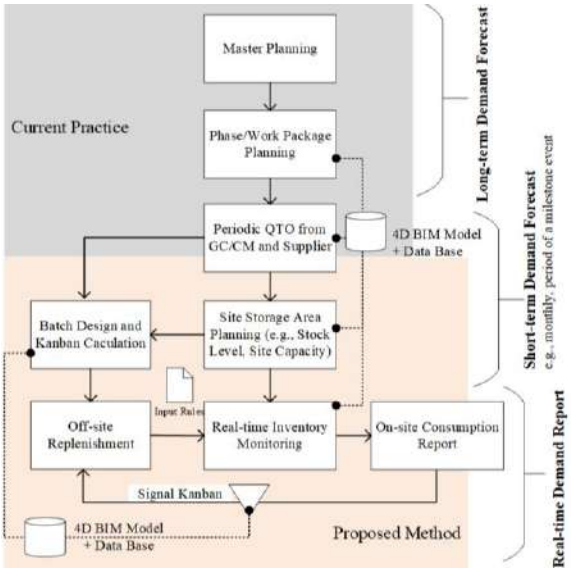

Figure 1. Logistics planning method combined with current construction planning practice

In the proposed method, the following aspects are emphasized:

Long-term demand forecast addresses the project objectives, i.e., overall cost, schedule, and quality goals. It involves mater or milestone planning, phase or work package planning, and project QTO. It follows the conventional construction project management and is conducted in the project early phase.

Short-term demand forecast addresses the periodic planning, i.e., weekly, monthly or within a milestone event's duration. The general contractor, construction manager, trade manager (if any) and suppliers work out periodic QTO documents and Kanban batch size collaboratively. These periodic QTO documents are fundamental for the on-site store area configuration.

Real-time demand report and pulled replenishment adopts the Kanban signal as the trigger of off-site replenishment. Suppliers collect Kanban signals and arrange their production and replenishment activities according to the real demand. Every material batch can be tracked along the whole process using a Kanban barcode or RFID (Radio-frequency identification) and assigned to its area. Therefore, it is possible to achieve a decentralized on-site stock monitoring.

4D BIM provides adequate LOD (level of details) building or construction component models, model-based QTO and related construction processes.

Applying the Kanban signal does not mean JIT production or zero stock. The Kanban signal is adopted as a real-time demand indicator for the off-site replenishment and site stock monitoring. It does not apply for every kind of material resource. The target material type has two features: 1) produced off-site and 2) with a certain level of site stock.

In the following sections, the critical activities in the proposed method to apply the Kanban system in construction logistics will be elaborated: 1) Kanban batch design; 2) site storage area planning and initial Kanban deployment; 3) real-time consumption record, real-time demand report and pulled replenishment.

3.2 Kanban Batch Design

The first step of introducing the Kanban system into construction logistics is to design the Kanban batch size associated with periodic QTO at the short-term demand forecast stage. This paper provides a BIM-enabled example to explain how to work out a consensual periodic QTO and Kanban batch size from both supplying and consuming sides. The collaborative workflow is presented in Figure 2:

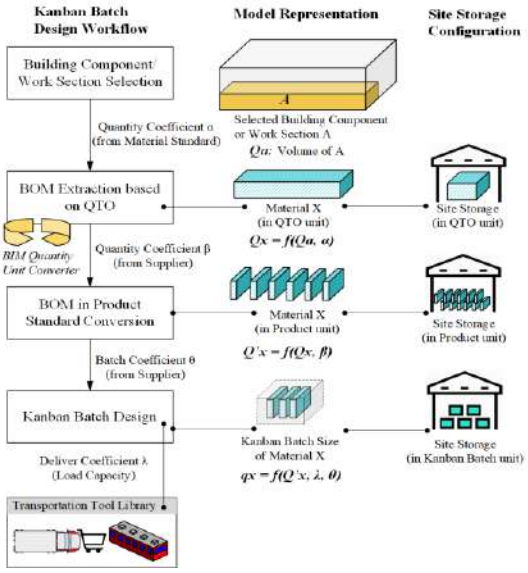

Figure 2. Workflow of Kanban batch design

Building component/work section selection: it depends on the short-term planning objectives, e.g., for a milestone event or a monthly plan. In this example, the building component or work section A is chosen, and its principal material is material X. The QTO extracted from the BIM model provides the volume of A (Qa).

Bill of Material (BOM) extraction based on QTO: according to Qa and quantity coefficient α from the material standard, the quantity of material X (Qx) can be calculated, and a BOM list can also be generated when there is more than one kind of materials.

BOM in product standard conversion: a BIM quantity unit converter (see Figure 3) is applied to convert the unit of quantity of material X from QTO into a product standard or a customized standard, which is provided by suppliers. The contractor can choose BIM objects and submit material quantity information to the calculator as an input, and suppliers can send product information to the server as another input, then a product quantity is worked out as the output.

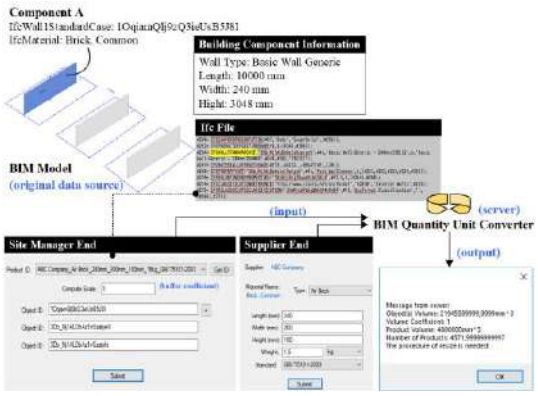

Figure 3. Example of BIM quantity unit converter

Kanban batch design: the Kanban batch size means the least lot size in the pulled material flow, e.g., a container capacity or a customized package capacity. It is the basic unit for consumption reporting, ordering, and material delivery and mainly decided according to suppliers' production (coefficient θ) and transportation (coefficient λ) conditions.

3.3 Site Storage Area Planning and Initial Kanban Deployment

An adequate initial area of site storage is crucial for the execution of the Kanban system. For a certain type of material e.g., material X (see Figure 2), GC/CM or material manager should provide total material consumption quantity (Qc) extracted from QTO and target construction duration (Tc). It is necessary to achieve an agreement about the storage duration (Ts). Besides, the non-uniform coefficient (σ), quantity-to-area convert coefficient (ε) and site utilization factor (μ) should be obtained according to technical standards. The initial area of site storage (see Equation (1)) can be calculated as:

$$S = \frac{Qc * Ts * \sigma}{Tc * \varepsilon * \mu} \quad (1)$$

Meanwhile, the supplier needs to provide the product standard or sufficient design information i.e., the quantity coefficient β (see Figure 2), to convert the initial total stock quantity from the material unit (Qs) into the product unit (Qk) (see Equation (2)). According to the initial value of stock quantity Qk and Kanban batch size qx (see Figure 2), the number of Kanban batches (N) can be further calculated (see Equation (3)):

$$Qk = f(Qs, \beta) = f(\frac{Qc * Ts * \sigma}{Tc}, \beta) \quad (2)$$

$$N = Q's/qx \quad (3)$$

3.4 Real-time Consumption Record, Demand Report and Pulled Replenishment

After the initial Kanban batches of material for the site storage are deployed on the construction site, the real-time material consumption can be recorded, and the discrete demand can be reported using Kanban signals. The information flow is illustrated in Figure 4:

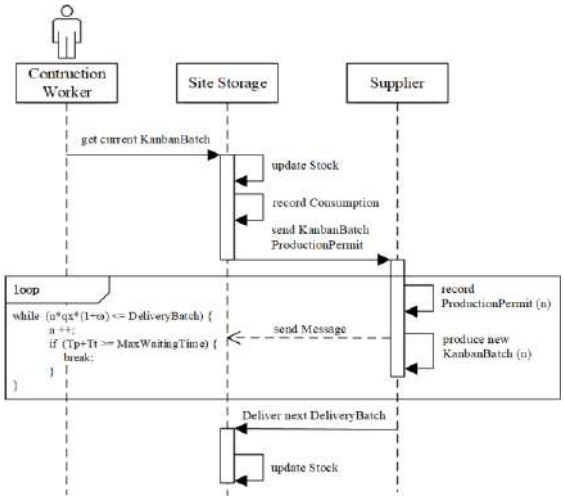

Figure 4. Information flow of real-time consumption record, demand report and pulled replenishment

Getting a KanbanBatch from site storage is a discrete event. When this KanbanBatch is taken out from the on-site storage, a production permit or an order of a new KanbanBatch is released to the supplier. It means that the supplier can know the real-time consumption of required materials. The supplier can collect discrete production orders and produces several new KanbanBatch according to his/her own delivery policy e.g., the minimum size of DeliveryBatch in this example. Meanwhile, the max waiting time of the construction site about the required KanbanBatch should be also taken into account, i.e., the MaxWaitingTime in this example. This paper adopts demand theories from Sugimori et al. (1977) [6] and adapts them into the context of construction logistics. Two discriminants for the loop of recording demands and producing new batches are set up (see Discriminant (4) and (5)):

$$n*qx/(1+\omega) \leq DeliveryBatch \quad (4)$$

$$Tp+Tt \leq MaxWaitingTime \quad (5)$$

Here:
n: number of KanbanBatch production orders;
qx: Kanban size;
ω: buffering coefficient of container/package capacity;
Tp: off-site production time;
Tt: transportation time.

The first discriminant determines how many new Kanban batches should be produced according to the collected demands and the supplier's delivery policy. The second discriminant is a constraint condition of the lead-time, i.e., production time and transportation time. However, the tolerance for lead-time is sensitive to the on-site storage buffer level, material type and flexibility of construction schedule etc., and it should be developed further.

4 Case Study

The aforementioned method is employed for controlling the on-site stock of a river remediation project. The remediation project of Tantou River is located in Shenzhen city, China. It includes six sub-projects: 1) channel improvement; 2) culvert construction; 3) desilting work; 4) sewage interception; 5) spillway tunnel and 6) flood retarding basin improvement. The engineering-procurement-construction (EPC) contractor is Power Construction Corporation of China and Sinohydro Bureau 14 Co., Ltd. manages the project.

We take the section of Furong Road (K0+000 ~ K0+050) in the culver construction sub-project (X0+000.00 ~ X1+192.021) as a case to study how to improve off-site warehousing and on-site stock configuration of culverts' main material i.e., steel bar with the type of HRB400 (16~25). In this case, we focus on applying Kanban signal to capture real-time consumption and adopt a pulled replenishment. It includes on-site storage area planning, initial stock deployment, and Kanban-triggered delivery. A BIM-enabled Kanban batch design is excluded in this case because standardized steel bars are used.

The duration of the target culvert construction section is 116 days and costs 13,862,112.17 in Chinese currency. The size of the culvert is 2.7x3.0 m and built with C25 reinforced concrete, as shown in Figure 5:

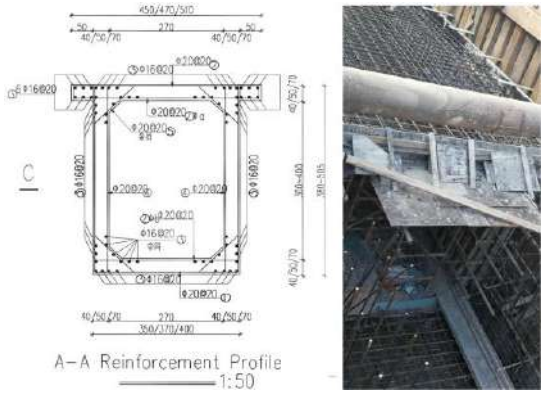

Figure 5. Culvert size and reinforcement profile

For this construction section, an off-site warehouse was set for steel bar storing and a on-site storage area with the size of 8x30 m was planned for weekly consuming. The distance of the off-site warehouse and on-site storage area was 3 km (see Figure 6). There are challenges in the storage and replenishing of steel bars:

- A large amount of steel consumption
- Unstable labor productivity
- Strict construction duration requirement
- Limited on-site storage area because the river flows through residential and commercial sectors

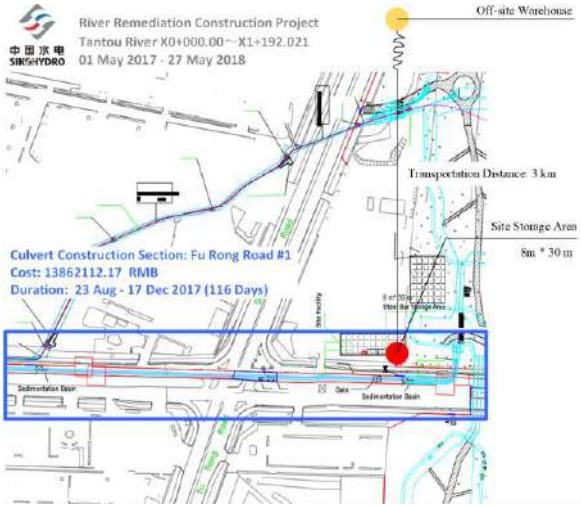

Figure 6. Project information and site layout

The site manager monitored the on-site storage of steel bars, and the replenishing plan of steel bar was delivered weekly from the off-site warehouse to the on-site storage area. Table 1 provides necessary information of steel bar site storage and replenishment. In this construction section, three problems related to site storage occurred and were reported by the site manager:

- Overstock on site in the earlier days
- Site stock shortages in the later days
- Construction delays caused by site stock shortages

Table 1. Steel bar site storage and replenishment plan

Plan Item	Number
Construction duration	60 days
Total quantity	458.83 t
Site storage area	240 m^2
Initial site stock	180 t
Weekly replenish	30 t

To study the periodic on-site storage planning and the influence of the unstable labour productivity, a simulation was conducted. We adopted a distribution triangular (0, 20, 5.01) for the daily consumption of steel bars affected by the labour productivity. It was chosen according to the historical project data. The simulation results are shown in Figure 7:

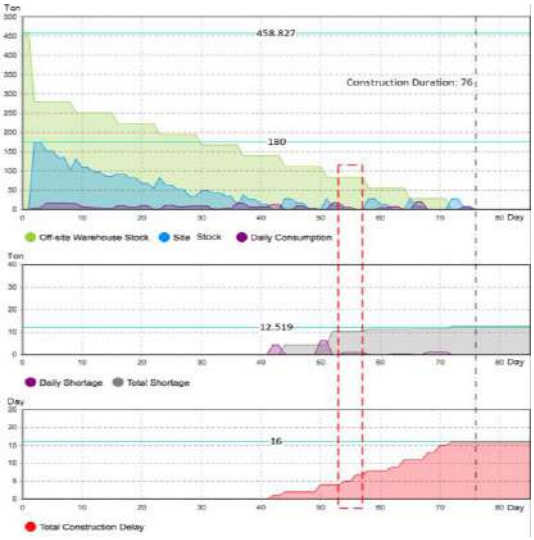

Figure 7. Simulation results of weekly replenishement

The simulation results show a construction delay of 16 days and some steel bar shortages. The results also show that, as the project progresses, even a minor shortage can lead to further delays in construction (outlined with dotted red line in Figure 7). The problem of overstock at the beginning is also obvious according to the simulation results.

To improve this situation, the Kanban signal is applied to report the real-time consumption, and another simulation was conducted. In this case, we treat the off-site warehouse as the supplier. The Kanban size design is simple in this case because standardized steel bars are used. The weight of each 12m long steel bar is 0.0145 t. A bundle with 100 steel bars is set as a package unit and its weight is 1.45 t. The Kanban batch size is designed as 20 bundles with a weight of 29 t. Table 2 shows key parameters of Kanban-triggered on-site storage and material replenishment planning:

Table 2. Parameters of Kanban-triggered replenishment

Parameter	Expression	Value
Site storage area	$S = \frac{Qc*Ts*\sigma}{Tc*\varepsilon*\mu}$	214.12 (m^2)
Initial site stock	$Q's = \frac{Qc*Ts*\sigma}{Tc} * \beta$	144 (t)
Package unit	1 Bundle = 100 steel bar	1.45 (t)
Kanban batch size	qx	29 (t) 20 (bundle)
Initial Kanban stock	N = Q's/qx	5

*Qc = 458.83; Tc = 90; Ts = 30; α = 1.40; ε = 2.5; μ = 0.6; β = 0.8.

The simulation results are shown in Figure 8. We adopt the same distribution for the daily consumption as

the weekly replenishment mode. Because of the real-time consumption report and Kanban-based delivery, all shortages and delays in the weekly replenishment (see Figure 8) mode could be avoided. Meanwhile, the initial site stock is saved from 180 t to 144 t, and the site stock maintains a stable level.

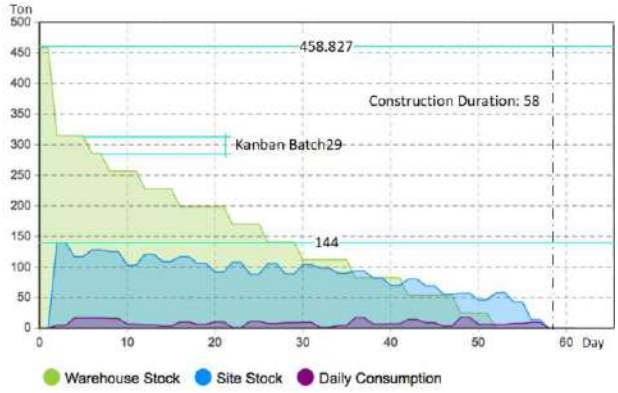

Figure 8. Simulation results of Kanban-triggered Replenishment

To explore the differences between weekly replenishment and Kanban replenishment, a comparison analysis is given in Figure 9.

Figure 9. Comparison of site stock in weekly and Kanban-triggered replenishment modes

Three distributions of steel bar daily consumption are applied: triangular (0, 15, 5.01), triangular (0, 20, 5.01) and triangular (0, 25, 5.01). In the Kanban mode, on-site stocks are stable and the total construction duration is shorter when the daily consumption level is higher. Comparatively, in the weekly replenishment mode, the on-site stock is excessive in the earlier days and insufficient in the later days. The total construction duration can be longer even when an intensive labour input is employed, as additional construction delays occur caused by stock shortages.

5 Discussion

This study was initiated to seek a driving mechanism for efficient construction logistics planning aided by information systems. Besides rethinking of the Kanban system, this paper provided implications for future construction logistics related research:

Essential Role of Digital Collaboration in Construction Logistics: based on the proposed method and the results collected from the case study, it can be stated that digital collaboration between the supplier and the construction manager plays an essential role in the construction logistics planning and monitoring. The construction logistics requires both on-site information and off-site information. Transferring site activities into off-site supply chains is a trend. It is helpful for some types of projects, for example, projects near residential areas. It means accurate and timely off-site information is indispensable for the construction logistics management. Meanwhile, suppliers need more building information for their production schedule and quality control. All these aspects indicate that an efficient digital collaboration in the construction logistics is required. With the development of industry-specialized information technology e.g., BIM and the decrease of information systems costs, it is the time to consider a digital collaboration from both the supply and construction sides. The Kanban batch design, therefore, can be more convenient with the assist of digital collaboration. This kind of digital collaboration in logistics planning can also contribute to a long-term commercial partnership.

Proactive Attitude toward Construction Logistics: there are challenges cause by the unstable labour productivity on-site and it has great effects on the construction logistics. The construction manager of the case study project reported that there were overstocks on-site in the earlier days and site stock shortages in the later days. It indicates the drawbacks of the conventional buffering approach: 1) waste site capacity; 2) ignore the influence of oncoming labour productivity peak. Applying the Kanban concept can improve current situation by collecting real-time consumptions and converting them into demands. It can ease the pressure of stock consuming after a productivity peak by a quick-respond replenishment. When a forecasting procedure of the productivity is applied, a proactive control is possible for the construction logistics. However, it is still a long way to go for a proactive logistics management aided by accurate forecasting.

6 Conclusion

Unlike the manufacturing industry, the unstable labour productivity and periodic planning method cause

barriers for adopting concepts e.g., JIT production in the construction field. The original Kanban system is well-known as a JIT control system, but its application is not limited to JIT production. In this paper, a methodology of designing and applying Kanban batch in the construction logistics with 4D BIM systems or tools was proposed. The Kanban concept was highlighted to record the material consumption, report the real-time demand and trigger a material replenishment from off-site to on-site. A case study of a river remediation project was carried out with a focus on steel bar site consumption and off-site replenishment. The simulation method was carried-out to analyse different scenarios. The simulation results presents significant savings of on-site storage area size and construction time by applying the Kanban concept. Finally, a discussion and implications were provided for future research.

More efforts will be made to integrate theory with practice regarding Kanban in the construction logistics planning and monitoring. Further studies will address complete Kanban application in the construction field and explore the real-time demand forecasting with abundant data from both on-site and off-site sides.

References

[1] O'Brien W. J., Formoso, C. T., Ruben, V. and London, K. Construction supply chain modeling: Issues and perspectives. *Construction Supply Chain Management Handbook*; CRC Press, United States, 2008.

[2] Russell, M. M., Hsiang, S. M., Liu, M. and Wambeke, B. Causes of time buffer and duration variation in construction project tasks: comparison of perception to reality. *Journal of Construction Engineering and Management*, 140(6): 1943-7862 . 2014

[3] Bankvall, L., Bygballe, L. E., Dubois, A. and Jahre, M. Interdependence in supply chains and projects in construction. *Supply Chain Management: An International Journal*, 15(5):385-393; 2010.

[4] Sacks, R., Seppänen, O., Priven, V. and Savosnick, J. Construction flow index: a metric of production flow quality in construction. *Construction Management and Economics*, 35(1-2):45-63, 2017.

[5] Childerhouse, P., Lewis, J., Naim, M. and Towill, D. R. Re‐engineering a construction supply chain: a material flow control approach. *Supply Chain Management: An International Journal*, 8(4):395-406, 2003.

[6] Sugimori, Y., Kusunoki, K., Cho, F. and Uchikawa, S. Toyota production system and Kanban system Materialization of just-in-time and respect-for-human system. *The International Journal of Production Research*, 15(6):553-564, 1977.

[7] Junior, M. L. and Filho, M. G. Variations of the kanban system : Literature review and classification. *Int. International Journal of Production Economics*, 125(1):13-21, 2010.

[8] Tserng, H. P., Lin, Y. and Lin, S. Mobile construction supply chain management using PDA and bar codes. *Computer-Aided Civil and Infrastructure Engineering*, 20(4):242-264, 2005.

[9] Sacks, R., Treckmann, M. and Rozenfeld, O. Visualization of work flow to support lean construction. *Journal of Construction Engineering and Management*, 135(12):1307-1315, 2009.

[10] Dave, B., Kubler, S., Främling, K. and Koskela, L. Opportunities for enhanced lean construction management using Internet of Things standards. *Automation in Construction*, 61:86-97, 2016.

[11] Ballard, H. G. The last planner system of production control, The University of Birmingham, 2000.

[12] Seppänen, O., Ballard, G. and Pesonen, S. Combination of last planner system and location-based management system. *Lean Construction Journal*, 43-54, 2010.

[13] Koskela, L. An exploration towards a production theory and its application to construction, VTT Technical Research Centre of Finland, 2000.

[14] 14. Law, A. M., Kelton, W. D. and Kelton, W. D. *Simulation modeling and analysis*; McGraw-Hill New York, 1991.

[15] AbouRizk, S. Role of Simulation in Construction Engineering and Management. *Journal of Construction Engineering and Management*, 136(10):1140-1153, 2010.

[16] Solihin, W. and Eastman, C. Classification of rules for automated BIM rule checking development. *Automation in Construction*, 53:69–82, 2015.

[17] Tauscher, E., Mikulakova, E., Beucke, K. and König, M. Automated generation of construction schedules based on the IFC object model. In *International Workshop on Computing in Civil Engineering 2009*, pages 666-675, Austin, Texas, United States, 2009.

[18] Chua, D. K. H., Nguyen, T. Q. and Yeoh, K. W. Automated construction sequencing and scheduling from functional requirements. *Automation in Construction*, 35:79-88, 2013.

[19] Tulke, J. and Hanff, J. 4D construction sequence planning - new process and data model. In *Proceedings of CIB-W78 24th International Conference on Information Technology in Construction*, pages 79-84, Maribor, Slovenia, 2007.

Simulating Wood-framing Wall Panel's Production with Timed Coloured Petri Nets

Fabiano Correa[a]

[a]Department of Construction, University of Sao Paulo, Brazil
E-mail: fabiano.correa@usp.br

Abstract –

The integration of design and construction processes remains, after decades of dedicated research, a great challenge. Even considering the specific context of pre-fabrication and modularization, it was just in recent years, with increasing adoption of Building Information Modeling (BIM) processes, that the challenge, albeit in a virtual environment, begins to be really addressed. With the advent of the Digitization phenomena in Construction, and the advances in Machine Learning techniques to cope with uncertainties of different natures in modelling real processes, it seems that the use of computational tools to simulate off-site production should be reconsidered. In this article, it is adopted an approach in viewing BIM as in a development stage to become an implementation of Product Lifecycle Management (PLM) for Construction. Towards this end, it is identified the lack of representation of the entire dynamics of production processes inside BIM models. The proposition of using Petri Nets with stochastic transitions to represent and simulate those processes are presented, altogether with the use of real RFID data, to adjust the model parameters, collected from a case study with a Brazilian company that pre-fabricate wood-framing houses. The probability distributions are derived based on the Mixture of Gaussians algorithm, and considers parameters of the design of wall panels – so it could be used to extrapolated performance for new designs. Following the presented approach, it is expected that, with more data, the simulation process could be a good feedback to architects in evaluating the impact of its design options in production.

Keywords –

High-level Petri Nets; Building Information Modeling; Simulation; Wood-framing

1 Introduction

In general, architects are not able to exploit design choices and its impact in production processes: they would need to specialize in each existent building system. Design is just one phase of the product development lifecycle, and through it, it will need the expertise of many different professionals. As communication between them is normally scarce and noisy, many opportunities to produce a better product is lost, and problems found later, on construction phase, could be traced back to unaided design decisions.

Computational tools have been developed to aid in this context, but there are still problems, and limitations. Even with the growing importance of information and communication technologies, the integration of design and construction processes remains, after decades of dedicated research [1], a great challenge. The situation is not different when one considers the specific context of pre-fabrication and modularization. It should be expected that in industrialized construction, similar to manufacturing industries, the use of computer-aided systems would be more common. It was just in recent years, with increasing adoption of Building Information Modeling (BIM) processes, that the challenge of integrate the processes of design and construction, albeit in a virtual environment, begins to be really addressed. And because of it, the interest in using pre-fabrication and modularization is rising again [2].

In viewing BIM as in a development stage to become an implementation of Product Lifecycle Management (PLM) for Construction [3], BIM models should resemble the idea of a digital twin, where it is possible to trade working with bits instead of atoms [4]. To use it to give to architects an advanced feedback of the impacts of planned design in production, it would be necessary to build a simulation of the production process in the factory. Although largely employed in other industries, for Construction, simulation have had more success in academic research than large use by the industry [5]. It is natural that with the advent of the Digitization phenomena in Construction, and the advances in Machine Learning techniques to cope with uncertainties of different natures in modelling real processes, it seems that the use of computational tools to simulate off-site production should enter a new cycle of development [5],

and integrate with digital information provided by BIM models.

BIM models are Product Data Models, and lacks the representation of the processes [6]. As so, there is a lack of representation of the entire dynamics of production processes inside BIM models – it is possible to create information about sequential tasks in the model; however, there is few semantic contents to that representation. As an illustration, consider IFC (Industry Foundation Classes) schema for interoperability. There is a growing presence of physical building components in the information model. However, although one could create, from basic entities, and describe construction processes, there will not be an inherent semantic in the representation. There isn't a library of processes to be used "off-the-shelf".

In this article, the proposition of using Petri Nets with timed coloured extension to represent and simulate those processes is presented, altogether with a procedure to use RFID data to adjust the model parameters. Implementation and test were done in a case study with a Brazilian company, which pre-fabricate wood-framing houses. Time representation in a coloured Petri Net is done via delays imposed to each transition. The delays are statistical, based on probability distributions. The probability distributions are derived based on the Mixture of Gaussians algorithm, and considers parameters of the design of wall panels – so it could be used to extrapolated new designs. Each type of wall panel contributes with a normal distribution, which composes the mixture distribution.

In section 2, we briefly present the mathematical formulation of Petri Nets, with extensions for time and colours (tokens are from different kinds in the simulation). Section 3 presents a proposition to derive parameters for mixture of gaussian model of the probability distribution to use in the delay of the Petri Nets. Section 4 presents the experiment that were done with the simulation of the production of wall panels in wood-framing, in a Brazilian company. And finally, section 5 summarizes the presented work, drawing some conclusions about our approach, and indicates future direction of work.

2 Petri Nets for Construction Processes Simulation

The main view about the formalism of what late became known as Petri Nets, and its potential as a model for dynamic systems was conceived in the PhD thesis of Carl Adam Petri [7].

Research in the use of Petri Nets to model asynchronous and concurrent dynamic systems, such as manufacturing systems started to appear in the scientific literature around the 80's. However, for the application of Petri Nets to real world problems, it was necessary to develop many high-level extensions of the traditional Petri Net formalism; for example, to include time, and a way to represent different kind of tokens (coloured).

2.1 Timed Coloured Petri Nets

The concept of Coloured Petri Nets was proposed by Jensen [8], as an high-level Petri Net. Following definition of Viswanadham and Narahari [9], a Coloured Petri Net is defined by the quintuple:

$$N = (P, T, C, I, O) \quad (1)$$

$$P = \{p_1, p_2, p_3, \dots, p_n\}, n > 0 \quad (2)$$

$$T = \{t_1, t_2, t_3, \dots, t_m\}, m > 0 \quad (3)$$

where: P is a finite set of places; T is finite set of transitions; such that $P \cup T \neq \emptyset$ and $P \cap T = \emptyset$.

$C(p)$ and $C(t)$ are the set of colours associated with place $p\ \varepsilon\ P$ and $t\ \varepsilon\ T$.

$$C(p_i) = \{a_{i1}, a_{i2}, \dots, a_{iu_i}\}, i = 1,2, \dots, n\ and\ u_i = |C(p_i)| \quad (4)$$

$$C(t_j) = \{b_{j1}, b_{j2}, \dots, b_{jv_j}\}, j = 1,2, \dots, m\ and\ v_j = |C(t_j)| \quad (5)$$

$I(p,t)\colon C(p) \times C(t) \to \mathbb{N}$ is an input function and $O(p,t)\colon C(p) \times C(t) \to \mathbb{N}$ is an output function.

There is also a token, a mark inside places, to represent the dynamics of the net. One transitions only occurs if there are token in every place connected to it (input set). And if a place is connected to two transitions, and both could fire, a decision should be made.

The concept of time in Coloured Petri Nets (although it could also be inserted in classic Petri Nets) has been implemented as a delay in turning available the tokens generated by a transition. Also, it is possible to employ probability distributions to model uncertainty and randomness in the time of completion of each task.

3 Learning Probability Distributions with Mixture of Gaussians

As there is the necessity to expose some parameters of the model to represent different panel designs, it was chosen to represent the probability distribution as an mixture of Gaussians, in which each Gaussian is attributed to one already monitored production of panel design.

It is expected that, with monitoring many different projects, from houses to buildings, this mixture of Gaussians could capture the intricacies and particularities of products in a company's production line and be

extrapolated to new designs. Then, it could be a source of feedback to the architect based on simulation results, and optimization.

Figure 1 represents graphically how two gaussian distributions could be used to model a multimodal histogram. It is expected that each individual wall panel design would give a specific normal distribution, and that with a large database of production of different designs, for houses and buildings, it should be relevant to predict, based on the estimated mixture of gaussians, future time delays for unseen product design.

The representation of a probability distribution using a mixture of Gaussians as a model, following Figueiredo and Jain [10], is given by:

$$p(y|\theta) = \sum_{m=1}^{k} \alpha_m p(y|\theta_m) \quad (3)$$

$$\alpha_m \geq 0, m = 1, \dots, k, and \sum_{m=1}^{k} \alpha_m = 1 \quad (4)$$

$\theta_m$are the parameters of the model to be find based on data collected.

Traditionally, it is used Expectation-Maximization algorithm to obtain the values of θ, with the formulation presented in (5):

$$\log p(\Upsilon|\theta) = \log \prod_{i=1}^{n} p\left(y^{(i)}|\theta\right) = \sum_{i=1}^{n} \log \sum_{m=1}^{k} \alpha_m p\left(y^{(i)}|\theta_m\right) \quad (5)$$

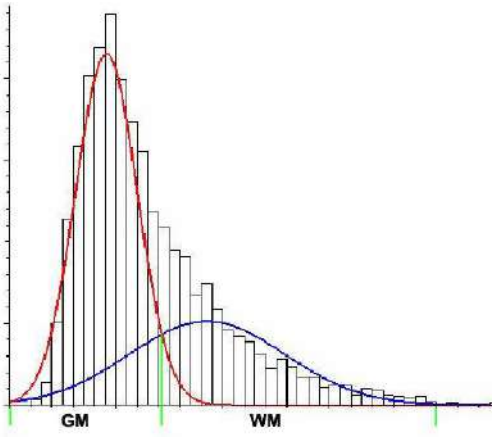

Figure 1. Representation of gaussians distributions derived from a histogram data.

4 Experiments and Results

In the last section, it was demonstrated how to obtain a probability distribution, based on data collected from real process. In our experiments, we do not achieve yet a relevant amount of data to use this methodology. The amount of data acquired is not statistically relevant but was adequate to obtain some estimation of the duration of each activity in the wall panel production, and to test the Petri Nets, and the model of a Mixture of Gaussian probabilistic distribution, as valid representations or models to use in our objective to provide a feedback of the impacts in design of alternative design decisions.

4.1 Production process at a Brazilian company of prefabricated homes in wood-framing

Production plant layout is represented in Figure 2. There are 6 working stations (identified by blue rectangles in the figure and labelled with numbers in white). The numbers represent the processing order.

Their plant is organized as a production line, without buffers. This is known in the factory as “Weinmann line”, after the Weinmann machinery bought by the company, which produces only wall panels. Floor and roof panels are produced manually, and in parallel lines (and are not represented in the figure).

The frame of each panel is composed of studs that are gathered from storage magazines (red rectangle, with an **S** in it), and from special modules (for door and window installation), which are also produced manually in another workstation.

There is a framing machine that reads the digital model and fix one component in the other, until the frame is finished – the red rectangle with the **SA** letters indicate where there is the storage and the other machine that automatically feeds the internal studs to the framing machine.

Workers bring OSB boards from storage (red rectangle with **OSB** in it) and position them with preliminary use of nails. There is another machine that cut electric and hydraulic openings in the OSB board, in both workstations 2 and 4 – represented by a blue rectangle, and a **W** letter in white for the representation of the machine itself.

Transportation between work station 2 and 3 is done by a “butterfly” table mechanism (Figure 3), allowing to work in the other side of the frame, to close it. Work station 4 is movable.

In the workstation 5, two to three workers install Tyvek film in the panel, insert the frame for windows and doors installing (the local where these frames are is represented by the red rectangle with the E letter in it), and put plasterboard – storage of plasterboard are represented by the red rectangle with the **G** letter in it. This work is also carried out in the workstation 6, so they have more space to complete these tasks in two panels.

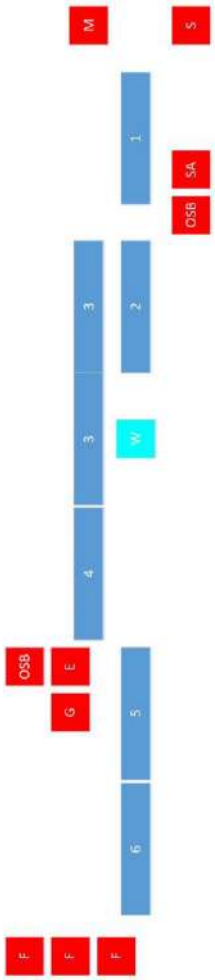

Figure 2. Rough layout of the production plant – not necessarily on scale.

Figure 3. One of the workstations ("butterfly" table) at the production plant.

After completion, the panel is moved by a crane, to temporary storage – represented by three red rectangles with the **F** letter in it.

4.2 RFID Data Collection

As stated by Mullens [11], "[q]uantitative data measuring cycle time variation and its root causes are rarely available". It is important to develop some solution to automatically capture such data. One solution could be an RFID system.

The RFID system employed to temporarily collect data at a Brazilian company was composed by three Sargas Readers from Trimble, and three antennas of 9 Db (one for each reader, although each reader could be used to gather data from two antennas – Figure 4). The maximum workable range between antenna and passive tags were estimated in 1.2 m.

Each panel received two tags, one in each of its lateral studs. The three points of time measure was: 1) immediately after the framing machine (the use of the frame machine is known by the log of the machine); 2) immediately when the panel, turned around, goes back to the main line of production; 3) Between work done in workstations 5 and 6, until the finished panel is elevated to the storage area.

Figure 4. One of the RFID Antennas temporarily installed for data collection in the factory of a Brazilian company.

During two days of collecting production data, it was possible to acquire some information about the dynamics of production for the line in general, and for each panel. However, such amount of data do not have statistic relevance to be used in estimating a global parameter for probability distribution.

It was decided to just attribute some values,

compatible with data collect, to investigate if the proposed solution, Petri Net formalism, given relevant data, could be used as original planned.

4.3 Petri Net Model of Production Line

To build a model representation of the production line of wall panels in wood-framing for the prefabrication of homes in Timed Coloured Petri Net, and to analyze its performance, it was used the software CPN Tools [12].

The resources needed for each activity were modeled by places. There were places for workers, machines, and panels along the production process. A mark in a place means that the resource is available.

The coloured sets extensions allows modelling of different panel designs (they were formatted as coloured sets of the product of an INT – order of production – and a STRING – type of each panel), and the modelling of distinct resources, such as workers and machines (defined as INT).

With the timed extension allowed, every activity in the production line was modelled with time delayed transitions, with a probability distribution composed of a mixture of gaussians. Each arc leaving a transition received a delay of a weighted sum of normal distributions such as (we opted to use only two types of gaussian to simplify, as the extension to the five different wall panels to assemble a house is straightforward):

$$F(x) = \sum_{i=1}^{5} 0.2 * normal(n_i, v_i^2) \quad (6)$$

Places representing the stages of wall panel production demanded a special treatment because an upcoming place should be empty before a previous transition is enabled – so that it not accumulate two panels in the same workstation. As a general and needed solution for this model, it was necessary to create for each pair of consecutive transitions representing work done at workstations, two additional places to avoid accumulation of more than one token in each place – that represents the panels in the workstations (Figure 5). This solution also helped in controlling the sequence of different panels to be produced.

There are 10 activities represented that were already described in previous section (we also give here the average time delays for the two gaussians employed in the simulation):

1. Frame production (time delay: 10 / 11 min);
2. OSB-one side (time delay: 7 / 6 min);
3. Cutting (time delay: 4 / 3 min);
4. Butterfly use (time delay: 4 / 3 min);
5. Electric, HVAC, Cutting, and OSB (time delay: 7 / 6 min);
6. Back to main line (time delay: 3 / 2 min);
7. Cutting-other side (time delay: 4 / 2 min);
8. Door and Windows install, Tyvek (time delay: 32 / 30 min);
9. Plaster board (time delay: 20 / 18 min);
10. To storage (time delay: 6 / 5 min);

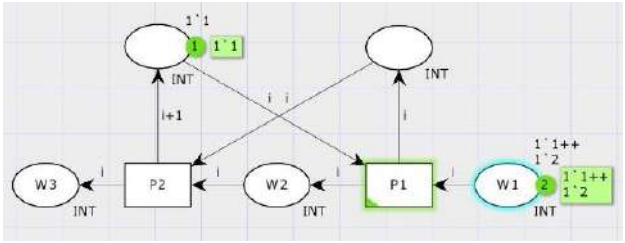

Figure 5. Modelling order of and workstation capability of production.

Figure 6 shows details of the modelling of shared resources in some workstations / activities – the model reproduces the same logic of the layout presented previously: the cutting machine receives a digital design, and it cuts small holes for electric and hydraulic use, and also there is in general one single operator to coordinate movement of wall panels and the machine that do the cutting in two different workstations – in the network. In red are highlighted two workstations (places) where cut, in both faces of the wall panel, occurs and in blue are highlighted two resources (places), operator and machine, that are divided between the workstations.

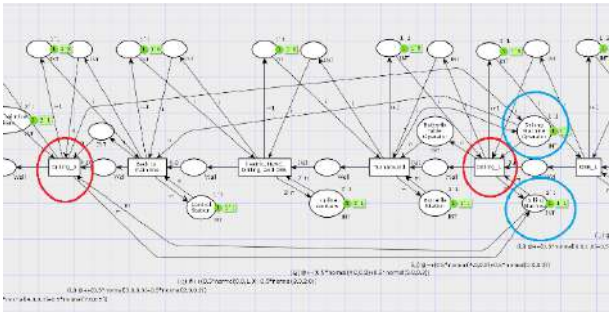

Figure 6. Detail of resources (Drilling Machine and Operator) between different workstations.

Due to the large network obtained, and the lack of space in the article, we opted to give an overview of the topology of the Petri Net, without giving more details (Figure 7).

The bottleneck of the production process is known to be work in the fifth and sixth stations, which is entirely manual, and there are a lot of work to do in it.

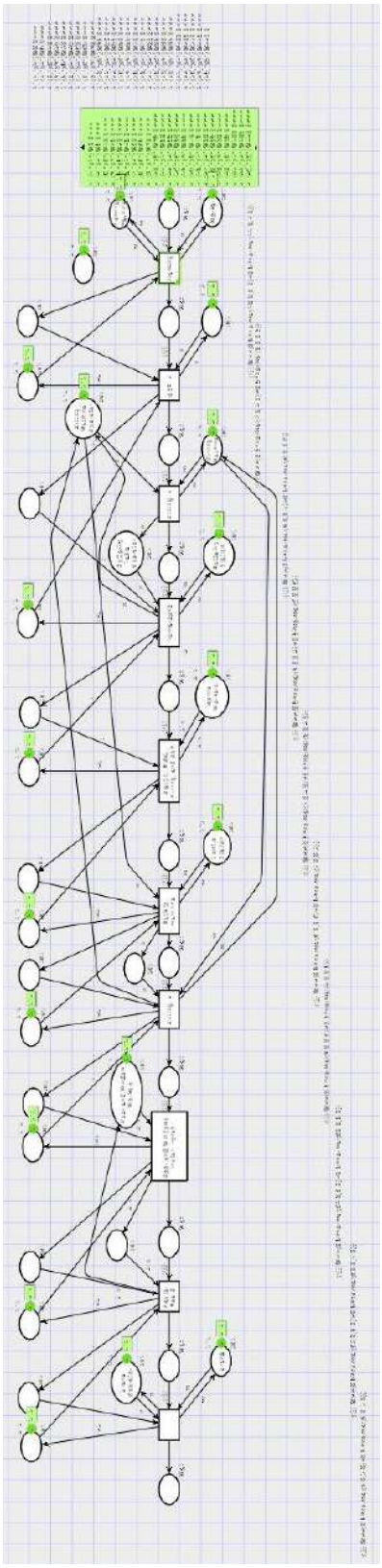

Figure 7. Timed Petri Net representing production of wall panels.

Part of the real dynamics that was not modelled was the movement of workers along different workstations to help its colleagues to keep in the TAKT time. For this, it would be necessary to model agents with decisions, and rewards.

As one example where it happens and is relevant for the dynamics, there is such a case just after the first transition with the operator of the framing machine. He works by itself until the frame is finished. The frame then moves to the next work station, and he also starts to work along two other workers, in fixing OSB boards on the frame. Based on a timed-schedule, he decides when to start a new wall panel, going back to operate the framing machine.

4.4 Results

Our experiment was developed to investigate the Timed Coloured Petri Net, as a formalism, and CPN Tools, as an implementation software, to produce a discrete-event simulation model of the production process. As a result, we could model almost every feature that appears to be relevant to our intent.

However, one behaviour would be of interest, although until the present knowledge of the authors, it is impossible to model it explicitly or directly with Petri Nets: variable time of transitions based on the number of tokens in a place representing resources, i.e., in some occasions, two to three workers are in a specific workstation, and the amount of time to complete the job depends on the size of the workforce at that moment.

The network was simulated with a production programming of 25 wall panels, in two different scenarios. In each scenario, the time delay between the beginning of production process of new panels was delayed by 5 and 10 minutes, respectively.

Table 1. Probability distribution parameters.

	1st Gaussian	2nd Gaussian
Place 1	26 ± 3	20 ± 2
Place 2	9 ± 1	7 ± 0.5
Place 3	4 ± 0.2	3 ± 0.3
Place 4		
Place 5	9 ± 1	8 ± 2
Place 6	3 ± 0.3	2 ± 0.2
Place 7	4 ± 0.3	2 ± 0.5
Place 8	40 ± 3	29 ± 8
Place 9	40 ± 5	38 ± 7
Place 10	6 ± 1	5 ± 1

The production time of each panel throughout the experiment (Table 2) was around the same time obtained in monitoring the production for two days at the plant. Results are exhibited in Table 2.

The registered times in Table 2 refer to the global

clock of the simulation (that starts at zero with the beginning of production of the first wall panel), at the time that each panel is moved to temporary storage. For each scenario, we run the network 5 times, and calculated the average time and its standard deviation.

Table 2. Results from simulating the production plant for two scenarios. The timestamp at the end of the production line is exhibited in the columns.

Type of wall panel	Global clock (s)	
	Scenario 1 (Δ10min)	Scenario 2 (Δ20min)
Type 1	129.6 ± 3.5	130.0 ± 3.4
Type 2	167.2 ± 4.5	169.6 ± 3.2
Type 3	207.7 ± 4.5	208.1 ± 3.0
Type 4	246.4 ± 5.3	246.9 ± 3.3
Type 5	283.8 ± 4.6	286.4 ± 3.6
Type 1	323.1 ± 4.5	324.7 ± 3.8
Type 2	363.0 ± 7.9	363.1 ± 4.4

Verification and validation of results from simulation were done based on comparison with real data collected with RFID system. Even if the collected data is a scarce set, it was verified that the probability distribution applied to the model was able to reproduce compatible times with the observed practice. During the simulation of one entire day of production, 8 hours of work, the behaviour of the model was similar to what was observed in the factory. Thus, it is a promising implementation of a process simulation to be further developed, towards obtain a feedback to architect of design decision on production.

5 Conclusions

The aim of the research present in this paper, was to investigate an adequate formalism to make use of different simulation models that could integrate somehow with digital information provided by BIM models.

It was presented how to use a Timed Coloured Petri Net to represent the off-site production of wall panels for wood-framing houses. The focus was in the specific plant (and processes) of a Brazilian SME. It was also presented a methodology to derive probability distributions from real data of production times collected with RFID systems. However, in the experiment we used guessed values, based on data collected, due to not have collected a representative amount of data until now – two days of data collection, including installation of equipment, and trials with regard to the position of antennas in the factory and tags in the wall panels. Through simulation of the production process, it was possible to derive TAKT time to have a balanced production.

Future goal is to be able to predict production times for new design of wall panels, and thus, to be able to give feedback to architects during design decision making process. Also, it is our intent to install RFID system in the factory, and to automatically monitor the production for one or two months in the near future. We also need to further develop the simulation model, to include stoppage of machinery due to fault, and due to maintenance to obtain a more realistic simulation model.

Acknowledgements

This work was funded by FAPESP grant #2017/03258-0. The author would also to thanks Tecverde, especially Pedro Virmond Moreira and Ivo Mitsumassa Tamura, for supporting the data collection, without their help the present work would not be possible.

References

[1] Yamazaki, Y. Integrated design and construction planning system for Computer Integrated Construction. *Automation in Construction*, 1(1):21-26, 1992.

[2] McGraw-Hill Construction, Prefabrication and Modularization, 2011.

[3] Jupp, J. R. Cross industry learning: a comparative study of product lifecycle management and building information modelling. *International Journal of Product Lifecycle Management*, 9(3):258-284, 2016. doi:10.1504/IJPLM.2016.080502.

[4] Grieves, D.M. *Virtually Perfect - Driving both lean and innovative products through Product Lifecycle Management*, Space Coast Press, 2011.

[5] AbouRizk, S. Role of Simulation in Construction Engineering and Management. *Journal of Construction Engineering and Management*, 136(10):1140-1153, 2010.

[6] Pan, W. and Langosch, K. and Bock, T. Development of the Process Information Modelling in the Construction Project: A Case Study of the ZERO-PLUS Project. In *Proceedings of the International Symposium on Automation and Robotics in Construction*, Taipei, Taiwan, 2017.

[7] Silva, M. 50 years after the PhD thesis of Carl Adam Petri: A perspective. In *Proceedings of the IFAC Workshop on Discrete Event Systems*, Guadalajara, Mexico, pages 13–20, 2012.

[8] Jensen, K. Colored Petri-Nets and the Invariant Method, *Theoretical Computer Science*, 14(3):317-336, 1981.

[9] Viswanadham, N. and Narahari, Y. Coloured Petri net models for automated manufacturing systems. In *Proceedings of the 1987 IEEE International Conference on Robotics and Automation*, Raleigh, United States of America, pages 1985–1990, 1987.

[10] Figueiredo, M.A.T. and Jain, A.K. Unsupervised learning of finite mixture models. *IEEE Transactions on Pattern Analysis and Machine Intelligence*, 24(3):381–396, 2002.
[11] M. Mullens, *Factory Design for Modular Homebuilding*, Constructability Press, Winter Park, Florida, 2011.
[12] Ratzer, A.V. and Wells, L. and Lassen, H.M. and Laursen, M. and Qvortrup, J.F. and Stissing, M.S. and Westergaard, M. and Christensen, S. and Jensen, K. CPN Tools for Editing, Simulating, and Analysing Coloured Petri Nets. In *International Conference on Application and Theory of Petri Nets*, pages 450–462, Berlin, Germany, 2003.

Spatial Efficacy of Respiration Monitoring using Doppler Radars for Personalized Thermal Comfort Assessment

W. Jung[a] and F. Jazizadeh[a]

[a]Department of Civil and Environmental Engineering, Virginia Tech, USA
E-mail: jwyoungs@vt.edu, jazizade@vt.edu

Abstract –

Recent research efforts have shown that human thermophysiological features could play a crucial role in inferring occupants' thermal comfort, which is required for comfort-aware heating, ventilation, and air conditioning (HVAC) operation. Our previous studies have demonstrated that variations of respiration, a representative human thermophysiological feature, can be non-intrusively quantified by a Doppler radar sensor (DRS). However, in pursuit of enabling human-aware rooms in buildings, in this study we have explored the impact of distance and position of the respiration monitoring system to investigate the potential of DRS systems as a ubiquitous apparatus in the real-world scenarios. Through experimental studies, respiration characteristics were evaluated in different locations and angles relative to the location of the measurement device. The measurements were carried out using a DRS system and a respiratory belt for ground truth data collection. The noise artifacts were reduced by applying the Savitzky-Golay method and Hann window, and respiration was identified by selecting the frequency component with the maximum amplitude in the typical breathing frequency range (0.1 to 0.5 Hz). Our analyses demonstrated that the signal from a cost-effective DRS technology without the use of external amplifiers could cover a range, within 1.0m longitudinally and 0.5m laterally, which is sufficient for an individual sensing given a normal office environment. It was also observed that the use of an external amplifier extends the range of the DRS sensing but at the same time accentuates the noise. Therefore, advanced noise removal methods are needed to increase the range of robust sensing. This study contributes to DRS deployment strategies for realization of comfort-aware systems.

Keywords –

Comfort-aware HVAC operation; Doppler radar; Respiration monitoring

1 Introduction

Studies have demonstrated that accounting for human dynamics in the control logic of Heating, Ventilation, and Air-Conditioning (HVAC) systems has potentials of creating satisfactory indoor environments and improving energy efficiency in buildings [1, 2]. Conventionally, the predicted mean vote (PMV) model, which has been recommended by American Society of Heating, Refrigerating, and Air-Conditioning Engineers (ASHRAE) [3], has played such a role. However, it has been shown that the generalized human-related factors in the PMV model (the met and clo units for metabolic rate and clothing insulation) could misrepresent actual occupants' dynamics [4, 5] during the operations. For example, Humphreys and Hancock [6] have shown that occupants prefer diverse thermal sensations from cold to hot, which is different from the assumption of the PMV model for thermal satisfaction at neutral state. The objective of the PMV model is to provide thermal conditioning for an environment that majority of occupants find acceptable. Therefore, the predicted thermal comfort by the PMV model, especially when a small number of occupants are present in a space, could deviate from the actual thermal comfort [7]. Hence, recent research efforts have been dedicated to proposing novel methods of adapting actual thermal perception and preferences of occupants to address the aforesaid limitations.

Motivated by the prevalence of the information and communication technologies (ICT), the starting point was the use of electronic surveys [8, 9] to digitize the process of distributing, collecting, and analysing questionnaires and facilitate the data collection process. Hence, large scale occupant comfort voting data have been conveniently collected (e.g., over 10,000 votes were collected within one year [10]), which has contributed to context-aware HVAC operational strategies. This strategy aims to offer personalized comfort zones based on occupants' thermal preferences (hereinafter, this operation is called comfort-aware HVAC operation in this study).

The difficulty of this survey-based approach comes from two aspects: (1) the need for user dedications, and (2) direct comfort quantification. Jazizadeh and Becerik-Gerber [11] have evaluated the participants' dedications in the first data collection process and through a stratified sample selection focused on users that had consistency in providing thermal feedback. Similarly, Kim, et al. [5], have emphasized on the need for users' dedications to create their comfort profiles. It has been also shown that the direct comfort quantification might not fully represent the cause and effect given that occupants' preferences vary under the same thermal conditions [12]. Therefore, when it comes to comfort inference, moderate accuracies (up to 75.0%) have been reported [5, 13]. Accordingly, the integration of physiological attributes in thermal comfort inference has gained attention [14].

Current research efforts are searching for physiological sensing systems (PSS) that can be used in practice to collect human contextual data not only for developing high-performance comfort profiles, but also for realization of comfort-aware HVAC operation. For example, Li, et al. [15] and Ranjan and Scott [16] used an infrared imaging technology for this purpose. Our previous studies have shown that Doppler Radar Sensors (DRSs) have potentials of measuring human thermoregulation states as a non-intrusive apparatus for quantification of respiration [17-19]. However, practical application of this technology calls for investigating the feasibility of the technology under realistic environmental conditions including the distance from the sensor and the direction of signal communication.

Therefore, in this study, we have explored the potential of DRS systems as a ubiquitous measurement method for thermal comfort assessment. In addition to non-intrusiveness, applicability, and sensitivity, ubiquity is one of the core attributes needed for PSS methods to be applied in control loops. Further details on these attributes could be found in the study by Jung and Jazizadeh [20]. In doing so, we conducted two experimental studies. The first focuses on assessing the effective range of a DRS system. To this end, we used two sensing set ups; (1) a minimal DRS setting (without an external amplifier) and (2) a DRS setting with an external amplifier. The subjects were sitting at multiple locations and changed the angle with respect to the DRS, and then their pulmonary activities were measured by the DRS and respiratory belt (the latter for the ground truth). By comparing the respiration extracted by two devices, we assessed the range of a DRS sensor with regard to pulmonary activity measurement. The second experimental study focuses on multi-occupant sensing. As a preliminary attempt, we sought to measure the respiration activity of two occupants in front of a single DRS.

The structure of this paper is as follows. The following section reviews the previous studies that have revealed the potentials of using respiration as a PSS methodology for thermal comfort quantification. Section 3 explains the methodology of this study, and Section 4 presents the results. The paper is concluded with contributions and limitations of this study in Section 6.

2 Previous studies

Thermal comfort is the outcome of diverse mechanisms in the human body and human thermoregulation state demonstrates the response to the ambient environment [21]. Hence, in the indoor comfort research domain, the association between human thermophysiological response and ambient temperature has been investigated for decades.

One of the main contributing mechanisms is the skin blood flow adjustment for heat dissipation regulation. The expansion of blood vessels (i.e., vasodilation) increases the heat dissipation and vice versa (i.e., vasoconstriction). These variations contribute to the skin temperature, that has been used as a well-known physiological parameter for thermal comfort quantification. To this end, given its non-intrusive nature, the infrared imaging technology has been used as a potential apparatus [15, 16]. Moreover, the feasibility of using RGB video images by employing the photoplethysmography (PPG) has been also explored [20, 22].

Another thermophysiological feature that represent thermoregulation mechanism is breathing. ASHRAE [21] mentions that metabolic rate – a collective response of the human body to the ambient environment – can be most accurately quantified by respiration. The inspired air is at ambient temperature and expired air is near the core temperature. In other words, the human body exchange heat with the surrounding environment through respiration. Despite this substantial contribution to the heat exchange between the human body and ambient environment, respiration has not been widely utilized as an attribute in thermal comfort assessment due to the difficulties, associated with its measurements. For example, a spirometer, which is a commonly used apparatus for respiration measurement, requires subjects to blow their breaths into the device, which is not a practical approach for building level measurements.

Leveraging the Doppler effect, a physical phenomenon that causes variation of frequency or wavelength, when the location of wave source or observer is moving, DRSs have been employed as a non-intrusive approach of measuring cardiopulmonary activity (i.e., periodic movements of chest and abdomen area, induced by heart rate and respiration) in the

clinical domain [23]. A DRS transmits a signal and receives a modulated signal representing the frequency and the displacement of the motion which causes the modulation. Motivated by its non-intrusiveness, we have investigated the potentials of using a DRS system as a means of quantifying human thermoregulation states. The implication of this approach is to employ this physiological response as input parameters to operate HVAC systems. The applicability and sensitivity have been demonstrated with two experimental studies for (1) two opposite temperatures (20 and 30ºC) with a 20-min acclimation time [17] and (2) transient thermal conditions (from 20 to 30ºC with no acclimation time) [18]. However, as noted the ubiquity is another critical attribute for practical use of DRS systems. Therefore, in this study, we have sought to explore whether we could use limited sensing nodes to cover a larger area in an indoor space (the primary objective) and multi-occupancy cases (the secondary objective).

These research questions have not been addressed by the previous studies, which focused on cardiopulmonary activity extraction by DRSs at a static location (0.5 m away from a DRS vertically) [24]. The data collection, respiration extraction process, and reason of having the simplest DRS setting are presented in the next section.

3 Methodology

3.1 Non-intrusive respiration extraction by Doppler radar sensors

Using the linear relationship between air volume variations and human chest and abdomen area [25], our thermoregulation state assessment approach extracts the features of pulmonary activities by using DRS systems [17]. The frequency and amplitude of DRS signals represent rates and intensity of breathing. Therefore, in our respiration quantification approach, we could infer thermoregulation states by quantifying the respiration leveraging the aforementioned features. Figure 1 shows the signal characteristics and the resultant breathing index. However, since we are interested in assessing the ubiquity attribute of the DRS systems in this study, we have solely focused on the frequency of respiration in evaluating the feasible range of measurement in quantifying the respiration activities. In doing so, four steps of post-processing methods have been utilized in analyzing the raw DRS signals: (1) applying the Savitzky-Golay smoothing filtering, (2) applying the Hanning window, (3) applying the fast Fourier transform, and (4) identifying the respiration component on the signal. The variations, derived from each step, is presented in Figure 2. The rationale behind using each step is as follows.

- The first step reduces noise and redundancy while preserving the shape and height of waveforms by the local least-squares polynomial approximations [26].
- The second step reduces the amplitude of discontinuities, caused by the digitization, by multiplying an amplitude that changes smoothly and gradually toward zero at the edges (Figure 3). Therefore, the process could result in better frequency resolution. Upon observing such discontinuities in the collected DRS datasets, we chose the Hanning window in consideration of its high applicability to different problems [27].
- The fast Fourier transform (FFT) is applied to convert a time-domain signal into the frequency-domain signal. This process helps the fourth step because the typical frequency range of respiration is often observed with a frequency less than 0.5 Hz [28]. Hence, the respiration activity can be extracted by identifying the signal that has the maximum amplitude within the aforesaid range of frequency [29].

3.2 Experimental setup

We have conducted an experimental study with three male human subjects. Their ages were 26, 31, and 33 and heights were 172, 182, and 183 cm. They declared no cardiopulmonary-related illnesses at the time of the experiment. This study was conducted upon receiving the approval of Virginia Tech's Internal Review Board (IRB) and informed consent was obtained. We used a number of experimental configurations:

1. A basic DRS sensing setup that does not use signal amplification with the first subject
2. A DRS setup that uses signal amplifier with the second subject.
3. The third configuration was focused on multi-occupant sensing, for which the second and third human subjects participated. In this configuration, we used the DRS sensing with signal amplification.

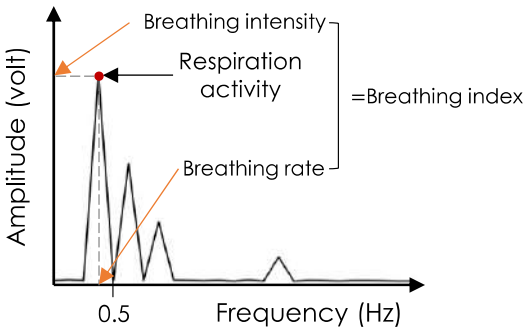

Figure 1. Features of the respiration activity

captured by DRS system.

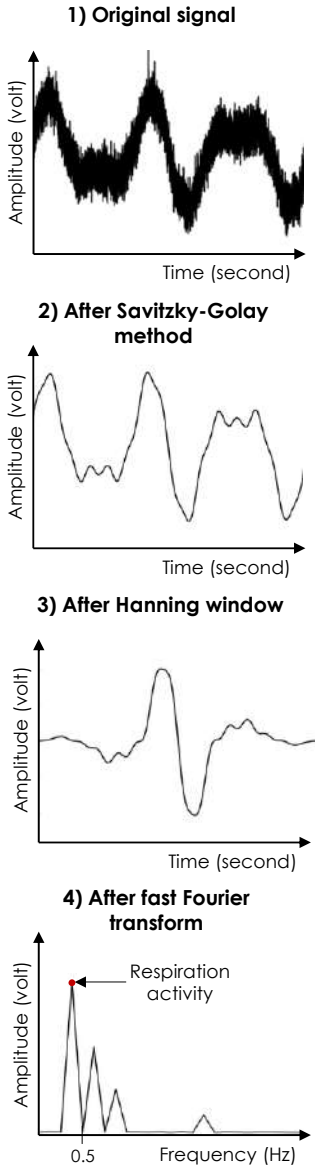

Figure 2. Respiration activity detection by using Doppler radar sensor signal (the signals are schematic representations)

For the sensing set up, we have used an RFBeam K-LC5 product as the DRS sensing system. This senor is a wide-angle sensing system – 34º vertical and 80º of horizontal beamwidths (Figure 4) – with a frequency of 24 GHz in the K-band, which is less occupied by other communication technologies. The sensing system is sensitive to subtle displacement and uses small antenna. As shown in Figure 5, the sensor dimensions are $25\times25\times6mm^3$ [30]. This product includes a built-in low noise amplifier with 10dB gain and needs 5 voltage to power on. For the external amplifier, in the second and third configuration, we used a low-noise preamplifier, SR560. We used 30dB for the amplification factor, which was empirically selected after a tuning process. We also employed a low-band pass filter with the pre-amplifier to reduce the noises caused by higher frequency components. Considering the aforesaid typical frequency of human respiration activities, we employed 3Hz for the low-band pass filtering. For data acquisition, we used a generic data acquisition card from National Instruments (NI6001) and the LabView software with a sampling rate of 1,000 per second.

We placed a DRS on a table as shown in Figure 4. The height was 0.7m (a typical table height) and the subject was sitting naturally and wearing the MLT1132 respiratory belt by ADInstrument. The belt is a transducer that produces a voltage proportional to variations in length of the belt and was used for ground truth data collection.

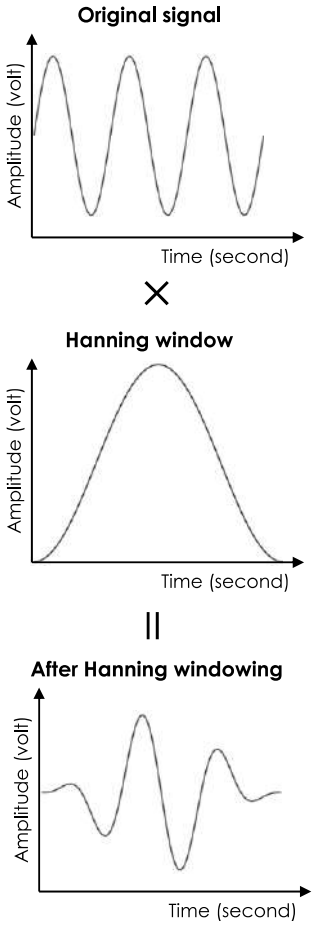

Figure 3. Applying Hanning window

For the first experimental configuration, the subject sat at multiple locations with respect to the location of the sensing system (Figure 6). With the use of external preamplifier, we presumed that a longer distance can be attempted. more distant points were examined: (1) 1.50m longitudinal and 0.50m lateral distance from the sensor and (2) 2.0m longitudinal distance from the sensor at the centreline. These locations have been highlighted with red circles in Figure 6. In each position, the subject faced different angles (from +45, +22.5, 0, –22.5 to –45º). Considering the symmetry of the sensing system, the data collection was conducted only on one side of the sensing system. Considering that DRS measures respiration activity by capturing the periodic movement of chest and abdomen area (moving back and forth), we did not consider the angle beyond ±45º. At each position and angle, we measured the subject's respiration activities for four times (each was 30 seconds of measurement – two minutes in total).

For the multi-occupancy case, which was the third configuration, two subjects were sitting in front of a DRS at 0.50m from the sensor and breathed naturally for 30 seconds.

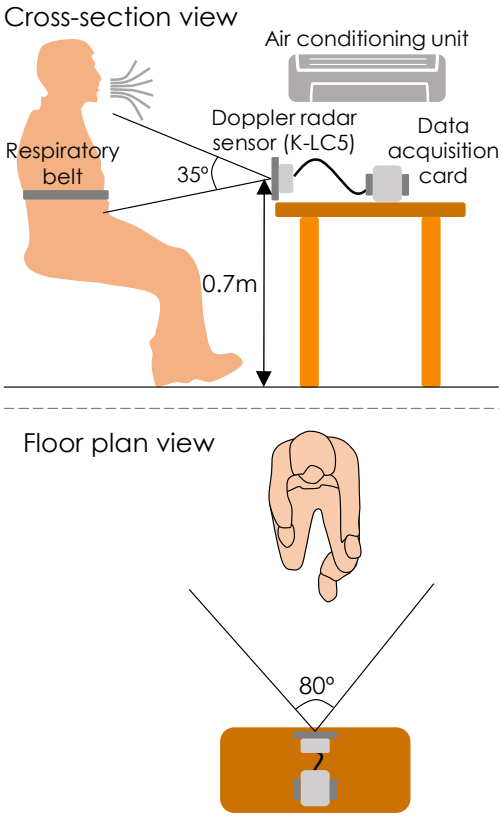

Figure 4. Cross-section and floor-plan view of the experimental set-up

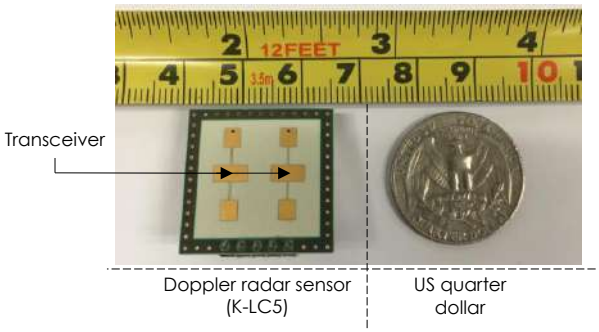

Figure 5. Doppler radar sensor used in this study

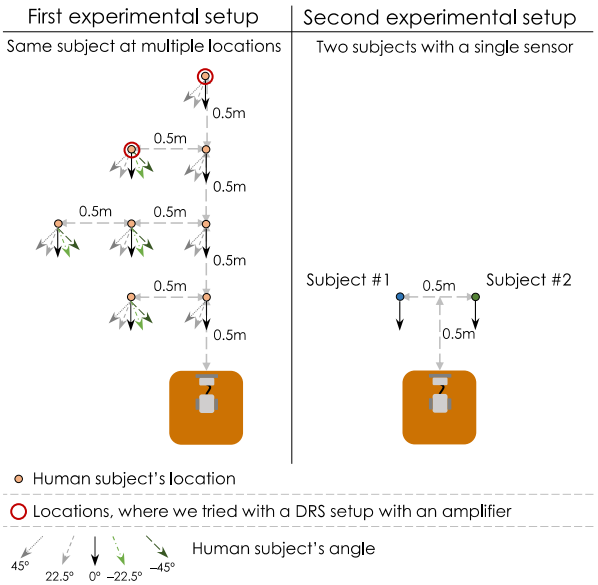

Figure 6. Subjects' locations and angles with respect to the DRS

4 Result

After collecting the raw DRS and respiratory belt data, we employed the aforesaid four steps to extract respiration activities from raw DRS data. Given that the data from belt does not contain noise we only employed the third and fourth steps on the data from that sensor. Due to the use of 30 seconds of measurements (N) with a sampling rate of 1,000 per second (F_s), the frequency resolution of FFT was $0.033Hz$ (F_s/N = 1000/30000 = 2 breathing per minute (BPM)). We compared the respiration rate from the DRS and respiratory belt data and interpreted the results using three indices: (1) there is no gap between the DRS and belt data (good), (2) the gap is equal to or below 4 BPM (moderate), and (3) the gap is more than 4 BPM (poor).

The results are shown in Table 1. Without the use of an external amplifier, the best performance was

observed when the subject was facing the DRS at a distance of 0.5m. In this position, even when the subject's position was shifted at 45 degrees, correct measurements were observed in three out of four cases. In general, as anticipated, in cases the subject was facing the DRS system sitting parallel with the radar antenna plane, the returned signal captures more pronounced movements of the chest and abdomen areas, resulting in a better performance. In addition, in cases that the subject was sitting within the 0.5 m range (both longitudinal and lateral) away from the DRS, the accuracies were fairly acceptable. The discrepancy between the DRS measurements and the ground truth data increases as the range of measurement increases. The cells with light orange color represent the poor performances.

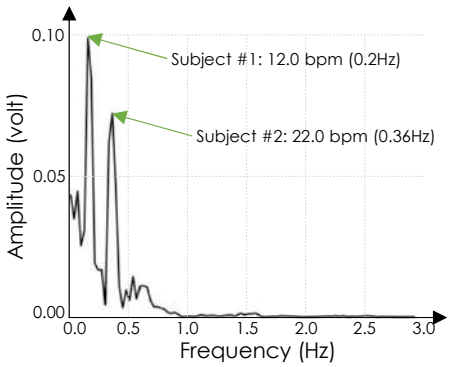

Figure 7. Results from the second experimental study

When the external amplifier was used, we could observe that the accuracy for farther ranges (or longer distances) is improved. For example, the case that the human subject was sitting in 1.0 m range (both longitudinal and lateral) away from the DRS, this DRS setup could identify breathing with fair accuracies, while the first setup fails. Even with the farthest ranges (1.5m longitudinal and 0.5m lateral, and 2.0m longitudinal), respiration activities could be quantified with fair accuracies. However, it has been observed that amplifying the DRS signal might result in lowering the overall accuracy. This is because the amplifier also amplifies the noise in the environment, often caused by subjects' subtle and spontaneous (e.g., yawning) movements.

Lastly, Figure 7 illustrates FFT output of the DRS signal for the third experimental configuration. As this graph shows, within the typical respiration frequencies two peaks are clearly located. Although limited observation, it shows that multi-occupant sensing could be potentially feasible using a single DRS system. However, more experimental studies are required for significant conclusions on multi-occupancy conditions.

5 Conclusion

This study has sought to investigate the ubiquity attribute of a non-intrusive respiration monitoring system, which has the potentials to be integrated into comfort-aware HVAC system operation. Given the recent research trends of exploring potential apparatuses of measuring human-related contextual data, this study provides insight into the feasibility of utilizing DRSs as a cost-effective and ubiquitous measurement system. The results demonstrated that, even by using a simple sensing and data processing set-up, respiration activities could be reasonably captured within the range of 1.0 m longitudinally and 0.5 m laterally. Considering the normal office environments, where occupants normally sit in a distance of 1.0 meter vertically from the computer monitor, this range can sufficiently cover an occupant. Moreover, the size of this sensor is small enough to be placed in a desk without interfering with occupants' activities. It is also noted that having an amplifier could expand the range of a DRS, but the set-up requires more advanced noise cancellation processes for precise respiration activity quantification. We have also preliminarily assessed the potential of sensing multiple people with a DRS with promising result.

One of the requirements for use of DRSs for thermoregulation state quantification is the duration of data acquisition, required for measurements. Due to the low frequency of respiration by nature, its precise measurement requires longer data collection durations. In this study, we used 30 seconds of measurements and, as a consequence, a 2-BPM resolution could be achieved with FFT. For a higher frequency resolution, a longer measurement time is necessary. As noted before, users' unintentional motions could add noise to the DRS signal and having a long measurement time increases a possibility of having noises.

Although this study used a specific product to evaluate the ubiquity attribute of a DRS, it can be used as a baseline for the future studies as we used a minimal hardware and software set-up. Accordingly, as future research, more diverse DRS set-ups can be explored with several scenarios such as expanding the testing area or having multiple DRS systems. Furthermore, the signal processing framework could be further developed. For example, in case of multi-occupancy conditions, a signal separation technique, such as independent component analysis, could be tried when similar breathing rates are captured by multiple occupants. As the results show, the proposed DRS system can also be used in vehicle air-conditioning operations considering its vicinity to the drivers. Accordingly, the outcome of this study will contribute to realization of comfort-aware HVAC operation, assisted with physiological sensing system. Another potential application includes monitoring of construction equipment operators.

Acknowledgement

This material is based upon work supported by the National Science Foundation under grant #1663513. Any opinions, findings, and conclusions or recommendations expressed in this material are those of the authors and do not necessarily reflect the views of the National Science Foundation.

Table 1. Subject's location, angle, the experimental configurations, and the three evaluation criteria: (1) BPMs from the DRS and respiratory belt are equal, (2) the gap is equal to or below 4 BPM, and (3) the gap is more than 4 BPM.

Location (m)		Angle (°)	Number of monitored cases					
			Differences between the breathing rate from ground truth and DRS-based respiration monitoring					
			Without an external amplifier			With an external amplifier		
Longitudinal	Lateral		Equal (Good)	≤4 (Moderate)	>4 (Poor)	Equal (Good)	≤4 (Moderate)	>4 (Poor)
0.5	0.0	0.0	4	0	0	0	0	4
		22.5	4	0	0	2	0	2
		45.0	3	1	0	1	2	1
0.5	0.5	–45.0	2	2	0	1	3	0
		–22.5	2	2	0	2	1	1
		0.0	3	1	0	1	2	1
		22.5	2	2	0	0	2	2
		45.0	2	1	1	0	3	1
1.0	0.0	0.0	3	1	0	1	3	0
		22.5	1	2	1	0	3	1
		45.0	1	1	2	0	2	2
1.0	0.5	–45.0	2	0	2	0	3	1
		–22.5	1	1	2	0	2	2
		0.0	0	0	4	2	1	1
		22.5	2	0	2	1	1	2
		45.0	1	0	3	0	2	2
1.0	1.0	–45.0	0	4	0	0	1	3
		–22.5	0	0	4	2	1	1
		0.0	0	0	4	1	3	0
		22.5	0	0	4	2	1	1
		45.0	0	0	4	0	2	2
1.5	0.0	0.0	1	2	1	1	2	1
		22.5	0	0	4	2	2	0
		45.0	2	0	2	0	2	2
1.5	0.5	–45.0	-	-	-	2	1	1
		–22.5	-	-	-	0	2	2
		0.0	-	-	-	1	3	0
		22.5	-	-	-	1	1	2
		45.0	-	-	-	1	1	2
2.0	0.0	0.0	-	-	-	2	1	1
		22.5	-	-	-	1	1	2
		45.0	-	-	-	0	3	1

The cells with the light orange color have the bad cases more than 3 times (75%)

References

[1] Jazizadeh, F., Ghahramani, A., Becerik-Gerber, B., Kichkaylo, T. and Orosz, M. User-led decentralized thermal comfort driven HVAC operations for improved efficiency in office buildings. *Energy and Buildings*. 70: 398-410, 2014.

[2] Erickson, V. L. and Cerpa, A. E. Thermovote: participatory sensing for efficient building HVAC conditioning. ACM, 2012

[3] ASHRAE. Thermal Environmental Conditions for Human Occupancy. ASHRAE, 2017

[4] Maiti, R. Physiological and subjective thermal response from Indians. *Building and Environment*. 70: 306-317, 2013.

[5] Kim, J., Zhou, Y., Schiavon, S., Raftery, P. and Brager, G. Personal comfort models: Predicting

individuals' thermal preference using occupant heating and cooling behavior and machine learning. *Building and Environment*. 129: 96-106, 2018.

[6] Humphreys, M. A. and Hancock, M. Do people like to feel 'neutral'?: Exploring the variation of the desired thermal sensation on the ASHRAE scale. *Energy and Buildings*. 39(7): 867-874, 2007.

[7] Yao, Y., Lian, Z., Liu, W. and Jiang, C. Measurement Methods of Mean Skin Temperatures for the PMV Model. *HVAC&R Research*. 14(2): 161-174, 2008.

[8] Jazizadeh, F., Kavulya, G., Klein, L. and Becerik-Gerber, B. Continuous Sensing of Occupant Perception of Indoor Ambient Factors. 2011

[9] Huizenga, C., Laeser, K. and Arens, E. A web-based occupant satisfaction survey for benchmarking building quality. *Indoor Air*. 1-6, 2002.

[10] Pritoni, M., Salmon, K., Sanguinetti, A., Morejohn, J. and Modera, M. Occupant thermal feedback for improved efficiency in university buildings. *Energy and Buildings*. 144: 241-250, 2017.

[11] Jazizadeh, F. and Becerik-Gerber, B. Toward adaptive comfort management in office buildings using participatory sensing for end user driven control. *Proceedings of the Fourth ACM Workshop on Embedded Sensing Systems for Energy-Efficiency in Buildings*, pages 1-8, 2012.

[12] Jazizadeh, F., Ghahramani, A., Becerik-Gerber, B., Kichkaylo, T. and Orosz, M. Human-Building Interaction Framework for Personalized Thermal Comfort-Driven Systems in Office Buildings. *Journal of Computing in Civil Engineering*. 28(1): 2-16, 2014.

[13] Ghahramani, A., Tang, C. and Becerik-Gerber, B. An online learning approach for quantifying personalized thermal comfort via adaptive stochastic modeling. *Building and Environment*. 92: 86-96, 2015.

[14] Li, D., Menassa, C. C. and Kamat, V. R. Personalized human comfort in indoor building environments under diverse conditioning modes. *Building and Environment*. 126: 304-317, 2017.

[15] Li, D., Menassa, C. C. and Kamat, V. R. Non-Intrusive Interpretation of Human Thermal Comfort through Analysis of Facial Infrared Thermography. *Energy and Buildings*. 2018.

[16] Ranjan, J. and Scott, J. ThermalSense: Determining Dynamics Thermal Comfort Preferences using Thermographic Imaging. 2016.

[17] Jung, W. and Jazizadeh, F. Non-Intrusive Detection of Respiration for Smart Control of HVAC System. 2017

[18] Jung, W. and Jazizadeh, F. Towards Integration of Doppler Radar Sensors into Personalized Thermoregulation-Based Control of HVAC. *4th ACM Conference on Systems for Energy-Efficient Built Environment (BuildSys' 17)*, Delft, The Netherlands, 2017.

[19] Jung, W. and Jazizadeh, F. Towards Non-intrusive Metabolic Rate Evaluation for HVAC control. 2018

[20] Jung, W. and Jazizadeh, F. Vision-based thermal comfort quantification for HVAC control. *Building and Environment*. 2018.

[21] ASHRAE. 2017 ASHRAE® Handbook - Fundamentals (SI Edition). American Society of Heating, Refrigerating and Air-Conditioning Engineers, Inc., 2017

[22] Jazizadeh, F. and Jung, W. Personalized Thermal Comfort through Digital Video Images for Energy-Efficient HVAC Control. *Applied Energy*. 2018.

[23] Kranjec, J., Beguš, S., Geršak, G. and Drnovšek, J. Non-contact heart rate and heart rate variability measurements: A review. *Biomedical Signal Processing and Control*. 13: 102-112, 2014.

[24] Lee, Y. S., Pathirana, P. N., Evans, R. J. and Steinfort, C. L. Noncontact Detection and Analysis of Respiratory Function Using Microwave Doppler Radar. *Journal of Sensors*. 2015: 13, 2015.

[25] Massagram, W., Lubecke, V. M. and Boric-Lubecke, O. Microwave non-invasive sensing of respiratory tidal volume. *2009 Annual International Conference of the IEEE Engineering in Medicine and Biology Society*, pages 4832-4835, 2009.

[26] Schafer, R. W. What Is a Savitzky-Golay Filter? [Lecture Notes]. *IEEE Signal Processing Magazine*. 28(4): 111-117, 2011.

[27] National Instruments. Understanding FFTs and Windowing. On-line: http://download.ni.com/evaluation/pxi/Understanding%20FFTs%20and%20Windowing.pdf, Accessed: 09/16/2018

[28] Gu, C., Li, R., Zhang, H., Fung, A. Y. C., Torres, C., Jiang, S. B. and Li, C. Accurate Respiration Measurement Using DC-Coupled Continuous-Wave Radar Sensor for Motion-Adaptive Cancer Radiotherapy. *IEEE Transactions on Biomedical Engineering*. 59(11): 3117-3123, 2012.

[29] Adib, F., Mao, H., Kabelac, Z., Katabi, D. and Miller, R. Smart Homes that Monitor Breathing and Heart Rate. pages 837-846, 2015.

[30] Yanming, X., Lin, J., Boric-Lubecke, O. and Lubecke, M. Frequency-tuning technique for remote detection of heartbeat and respiration using low-power double-sideband transmission in the ka-band. *IEEE Transactions on Microwave Theory and Techniques*. 54(5): 2023-2032, 2006.

BIM-based Automated Design Checking for Building Permit in the Light-Frame Building Industry

H. Narayanswamy[a], H. Liu[b], and M. Al-Hussein[a]

[a]Department of Civil and Environmental Engineering, University of Alberta, Canada
[b]Department of Civil and Construction Engineering, Western Michigan University, USA
E-mail: hnarayan@ualberta.ca, hexu.liu@wmich.edu, malhussein@ualberta.ca

Abstract –

Automation of the code compliance checking has been explored extensively, particularly in recent years with the emergence of building information modelling (BIM). Still, automated code compliance checking has not yet been fully realized, as there is no standardized method for rule interpretation and building model preparation for code compliance. Manual verification of design code compliance, meanwhile, requires significant effort and time and is error-prone, while uncertainty and inconsistency in assessment lead to delays in the construction process. In this paper, the development of a prototype to automate municipal bylaw and wall framing code compliance checking for residential building is presented. The building rules have been classified into three groups based on the complexity involved in translation into computer-readable format and complexity in retrieving the required information, and they are represented based on building objects, which makes the regulations easier to understand and assists in translating the regulations into a computer-readable format. By creating a model view based on the required element's parameters extracted from a model for checking purposes, the prototype application offers automated code compliance checking functionality to validate designs based on building code requirements and construction engineering specifications. The implementation of the prototype and its benefits compared to manual checking is demonstrated.

Keywords –

Building Information Modeling (BIM); Automated code compliance checking; Building permit; Building rules

1 Introduction

Technological advancements in the architectural, engineering, and construction (AEC) industry have digitized nearly every stage of the building lifecycle, and this digitization has been a significant advancement in the industry over the past several decades. In this context, building information modelling (BIM) technology has been utilized for a wide variety of applications across the building lifecycle. In particular, automated code compliance checking saw a major leap with the advent of BIM in the late nineties [1]. An automated code compliance checking system is one of the processes for verifying the design in accordance with building codes, regulations, and bylaws. For many years, authorities and researchers have been working on an automated code compliance checking process, yet it is still only a semi-automated process. Many researchers have developed applications for safety, egress, and design checking, but still no application is in use for code compliance checking, even in countries where the BIM model for the design checking process was made mandatory. Many applications have not been updated since they were first developed, and an even fewer number of those have survived. This is partially due to the fact that there is no standardized method for rule interpretation and building model preparation for code compliance.

This research develops a BIM-based automated design checking prototype, in the form of an add-on for Autodesk Revit (i.e., DCheck), for automated checking Edmonton zoning bylaws, lot design for residential houses construction, and wood framing for walls of the residential building in accordance with Alberta building code 2014 part 9. To develop the prototype, the building rules have been classified into three groups based on the complexity involved in translation into computer-readable format and complexity in retrieving the required information, and they are represented based on building objects, which makes the regulations easier to understand and assists in translating the regulations into a computer-readable format.

In the subsequent section, a review of state-of-the-art existing software and plug-in applications with respect to automated compliance checking is presented. Detailed explanations pertaining to the methodology are presented in Section 3. Section 4 illustrates the system architecture of the prototype. A case study is presented as a test-bed to verify the developed prototyped system in Section 5.

Finally, findings are summarized, particularly as they pertain to potential future research.

2 Existing Design Checking Applications

With the use of CAD tools for design purposes by AEC professionals in the 1990s, the automation of design checking has gained more interest among researchers. Exhaustive studies have been performed in automating the building code by many researchers in this field, each exploring different techniques in interpreting the rules from his or her perspective [2]. Typical examples include the development of the following: logic-based approaches for the organization of design standards [3]; computer representation of design standards [4]; and knowledge-based expert systems capable of reviewing building design [5]. An overview of software applications developed by different countries and government authorities for automated compliance of each country's building code is described in the subsection that follows and a summary is presented in Table 1.

2.1 CORENET (Singapore)

In 1995, the Building Construction Authority (BCA) of Singapore initiated CORENET (Construction and Real Estate Network) as a comprehensive network system with a series of IT systems for exchange of information between government agencies and parties involved in construction and real estate [6]. CORENET for approval process provides electronic web-based submission system incorporating in-house building plans (BP) expert system to check 2D plans for any technical irregularities with reference to the building regulations [7]. e-PlanCheck, as part of CORENET, was the first initiative developed for automated code-checking. CORENET consists of three platforms: e-submission, e-PlanCheck, and e-info. E-PlanCheck was used as a pilot project in Norway and New York with replacement of rules required by Norway and by using ICC (International Code Council) codes for New York.

2.2 DesignCheck (Australia)

DesignCheck was developed by Australian authorities for automated building code compliance for Australia, focusing on accessible design regulations [8]. In fact, code checking efforts by Australia involved development in two phases. The first phase was to assess the capabilities of existing rule checking systems to find out which would be the best one for computerization of Australian standards [8]. Both SMC and Express Data Management (EDM) were considered as possible platforms for automated code checking. EDM was considered as the more suitable one because of its ability to provide a publicly accessible definition language to represent building codes. After the first stage of checking for a feasible solution, different domain-specific knowledge can be encoded to EDM rule base and can be applied to check a building model.

2.3 Statsbygg (Norway)

The Norwegian government organization, Statsbygg, acts as the Norwegian government's key advisor in construction, building commissioning, property management and property development [9]. The CORENET e-PlanCheck system has been used for a couple of industry foundation class (IFC) based BIM building projects as an early effort by Norwegian authorities. Multiple platforms, such as e-PlanCheck, SMC (Solibir Model Checker), dRofus, and Express Data Management (EDM) model checkers were also adopted for the purpose of experimenting for finding a better checking system. "HITOS" is a BIM project managed by the Statsbygg government organization and Tromso University since 2005, for which several software applications have been used for modelling architectural, structural, MEP (mechanical, electrical and plumbing), cost estimation, and energy simulation, and an EDM model server was also used for storing and accessing the model data in IFC format [10]. dRofus as rule based system was used for spatial program validation: which acts as a database system used for managing architectural programs, technical functional requirements and equipment's for early stage planning[9]. Solibir model checker (SMC) was used for checking accessible design in the building model. SMC was developed in 2000 in Finland as quality assurance and validation tool.

2.4 International Code Council (ICC) and General Service Administration (GSA) Design Rule Checking (The United States)

GSA, an independent agency of the United States government, issued BIM-guidance in 2006, and starting in 2007, made it mandatory to have a BIM model for validation for all projects seeking permission for spatial planning projects[11]. The application uses the SMC platform and design assessment tool for extending rules, developed by Georgia Institute of Technology. The most interesting initiative in this area is SMARTcode, which was started in 2006 and handled by ICC, a US-based association that develops the master building codes for residential and commercial buildings and most institutional buildings [12]. SMARTcodes is a project for transforming natural language code into computer inter-

Table 1. Summary of typical BIM-based Automated Design Checking

Article	Checking Platform	Focus	Research Theme		
			Code representation	MVD	Checking algorithms
Khemlani 2005[13]	FORNAX	Rules in Building plans and services (Singapore)	Computer code	IFC based (FORNAX)	Object-based approach
Preidel & Borrmann 2015[14]	CodeBuilder plugin	German fire code	VCCL (visual code checking language)	VCCL graph	Flow-based visual Language
Pauwels et al. 2011[15]	Semantic web	Acoustic Performance Checking Occupational circulation rules	Semantic rule language	N3Logic rules	Semantic Web Ontology language
Martins & Monteiro, 2013[16]	LicA	Portuguese Domestic Water system	XML-based parametric tables	IFC based	Structured Query Language
Sjøgren 2007[17]	SMC (Solibri model checker)	Norway's Building accessibility rules	Parametric tables	IFC based with adding geometric data	Object-based parameters checking
Zhang et al. 2013[18]	Rule checking Process	OSHA Fall protection and safety	Parametric tables	Object-based parametric model	Object-based and logic approach
See 2008[19]	DA's SMART codes for SMC, AEC3 XABIO	United States: ICC Building code	SMART builder	IFC based	RASE
Ding et al. 2006[8]	EDM	Australian Design checking for disabled access code.	Rule-based language	IFC based using internal model schema.	Object-based approach using ExpressX language
Tan et al. 2010[20]	Rule Engine	Building Envelop (Canada)	XML based decision tables	EBIM, XML based model	Decision table
Lee et al. 2015[21]	KBIMLogic program	Korean Building code	Parametric table	Object based parametric model	Logic-based query

pretable format, and a dictionary of the properties found within the building codes have been developed in SMARTcodes. The dictionary is helpful in communication between SMARTcodes model checking system and the IFC building model [22]. The rule interpretation process is the most vital stage in automated code compliance checking, where various technologies have been investigated and employed. With so many technologies there is no standardized way for translating the complete building rules and regulations into computer-readable format. Out of many applications developed the Singapore CORENET project is an early initiative started by a government organization about 23 years ago for checking of 2D building plans submitted online for code compliance. Subsequently, the Solibri company developed an application called Solibri model-checker (SMC) for checking 2D plans around 1999. And even after over two decades since the start of the CORENET project, there has not been much progress in the development of an automated checking process. Solibri is the only commercial software available for checking some aspects of building design like clash detection, and space validation. The applications developed should provide easy way for future updates with change of building rules and regulations and should be user-friendly for continuous use of code compliance. In terms of BIM model preparation, the building models should be developed with BIM technology-enabled software with a certain level of detail (LoD). LoD is details that are included in model objects related to dimensional, special, qualitative, quantitative, and other data to support required purposes. Models should be developed with LoD 300 or more for efficient extraction of information needed for compliance checking process.

It should be noted that previous research classified design rules into four groups, based on the complexity involved in extracting the required information from the BIM model. The present research further considers the complexity of rule translation to classify rules, as the major problem in the process of automated checking is

the rule interpretation, where human-written codes are translated to computer interpretable format. However, building codes are not self-contained and make reference to many other documents. We proposed the strategies of the rule interpretation for each rule category. The translation of the human-readable natural language code into computer interpretable code is complete, only if when the logical representation of regulations gives a clear understanding of the building regulations.

3 Methodology

Figure 1 shows an overview of the process of automated design checking of building code and municipal bylaws for residential buildings. This process can be divided into four main steps [11]: (1) Rule translation, which is the interpretation of natural language building rules into computer-interpretable format; (2) BIM model preparation, which involves the design of the building model in Autodesk Revit software and creating model views from the given BIM model; (3) Rule checking, which involves the checking of the designed model with the encoded rules; and (4) Checking report, where the compliance check result is obtained.

3.1 Rule Translation

The translation of the context and content of the building code and municipal bylaws for residential buildings into a machine-readable format is one important step in the automated rule checking process. Each regulation has a different level of complexity involved in the translation into a machine-readable format. In this research, all the building rules are classified into three groups based on complexity in translation into machine-readable format and also with complexity involved in extracting the required information from the BIM model, These include (1) Easy: These are rules that are classified as easy to translate from natural human-readable language into computer-processable codes and where the information required can be directly extracted from the BIM model; (2) Intermediate: These are rules that are classified as difficult to translate and where the information required needs to be derived. The complexity level of translating these rules into computer-processable codes and getting that information from BIM model involves introducing some new attribute values for defining some properties of building objects for compliance; (3) Difficult: These are rules that are classified as needing to be simplified in order to translate them, and where the information required needs an extended data structure. Some rules need clarification depending on the building design and specifications, and some rules need the building model to be analysed to get the required value to be checked, and the information required from the BIM model is extracted using an extended data structure. Compared with previous studies in which building rules are classified into 4 groups, only based on complexity in extracting the information from BIM model, the proposed three groups make it easier to implement. This classification of building rules facilitates the development of the checking add-on software application in later stages, giving the user a clear understanding of the checking process. The

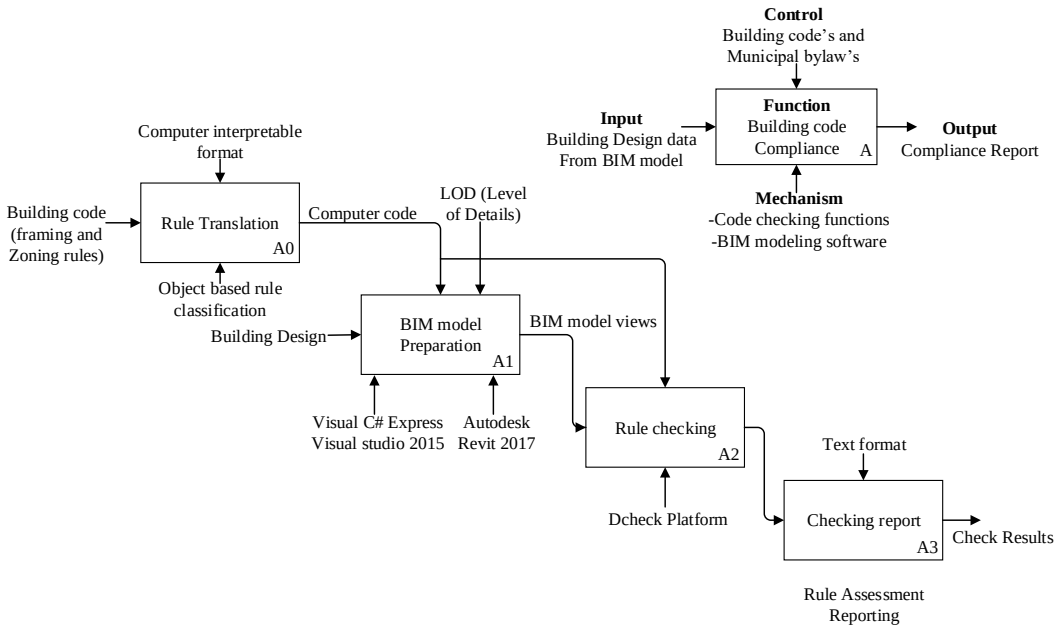

Figure 1. Methodology

representation of building codes based on building objects with conditions to be satisfied, attribute values to be driven from BIM models, and the threshold values to be checked for object-oriented representation, provides a clear understanding of building rules and makes easy for knowing the required parameter value from the model. By using this rule classification, building codes can be efficiently and comprehensively translated into computer interpretable format. In this study, an object-oriented programming language (i.e., C#) is used for compliance checking because of its flexibility and consistency in encoding building rules from the Alberta building code and municipal bylaws related to different zones in accordance with Edmonton municipal bylaws.

3.2 BIM Model Preparation

The BIM model can be defined as a digital representation of physical characteristics, such as architectural designs, and functional characteristics, like structural analysis, energy analysis, or a myriad of other simulations with semantically rich information. Building objects modelled in BIM enabled software's have parametric properties. For example, a wood stud member in the model possess types and properties like dimensions (length, width, depth), material properties, location of element member (XYZ coordinates), and so forth. The building model can be developed with level of details (LoD) above 300 for better extraction of information from a given model. Autodesk Revit provides a way to define and export extensible and interoperable BIM model data with use of Autodesk Revit's API (application program interface). The structure of APIs for exchanging information is object-based, where the geometry and properties of objects, such as name, size, location, finishes, faces and abstract information like cost, quantities, and so forth, can be accessed. In this research, C# language has been used to extract building information for compliance checking from the BIM solution, Autodesk Revit.

3.3 Rule Checking

The fundamental aspect of automated compliance checking is the information exchange from the BIM model to the rule checking platform. The checking platform (i.e. DCheck) applies a set of related rules to a model view. Prior to applying rule checking, syntactic checking of model is needed, to determine that the building model carries the properties, names, objects needed for the complete checking task. With object-based building information extraction, the geometric and functional information of objects, such as faces of building components, vertices, edges, location, and some derived information is extracted for compliance checking. Basically, mapping between the BIM model and the building rules is done by DCheck platform in this step.

3.4 Checking Report

The final step of the automated compliance checking process is to provide the user with a final compliance checking report by notifying the user checking results, such as success or failure and associated reasons and suggestions for failed regulation. This report is displayed to the user in textual format, and those building objects related to the rules which they have failed to satisfy are highlighted in the model, which helps to spot those objects and make corrections. The checking process can be run at any time during the design by the user, so it is easy for the architects or the draftspersons to check models in a parallel manner while designing.

4 Prototype Application

The automated building design checking is implemented as an add-on software application (i.e., DCheck) for the Autodesk Revit software, developed in C# language using Revit API's. Figure 2 shows the architecture of the prototyped Revit-based automated design checking software application. The inputs for the system include: (1) building design of the project and BIM model of the building intended to be constructed containing the architectural and structural framing information; (2) the project applicant information, regarding the applicant, architect's and builder information; and (3) zoning and framing information, regarding site location, plot number, type of wood used for framing and so forth. Criteria for this project are: (1) building code, in this case Alberta building code 2014 part 9, housing and small buildings, containing regulations related to framing of residential building; (2) municipal bylaws, Edmonton zoning bylaws, containing regulations related to different types of zones and residential building; (3) Level of details (LoD), development of model with LoD above 300 serves the required purpose for automation of building rules checking in this prototype.

The core processor of this prototype has main components: (1) object-based representation of building code, where building rules are represented based on the building objects so that required information from building model related to particular building object can be known clearly; (2) BIM model view definition, where required model views of BIM data for compliance checking are extracted; (3) BIM model extension, where some information which cannot be accessed directly from the BIM model needs to be derived and data structure platform extended by DCheck will provide those values; and (4) code compliance with model, where extracted information from the model will be checked

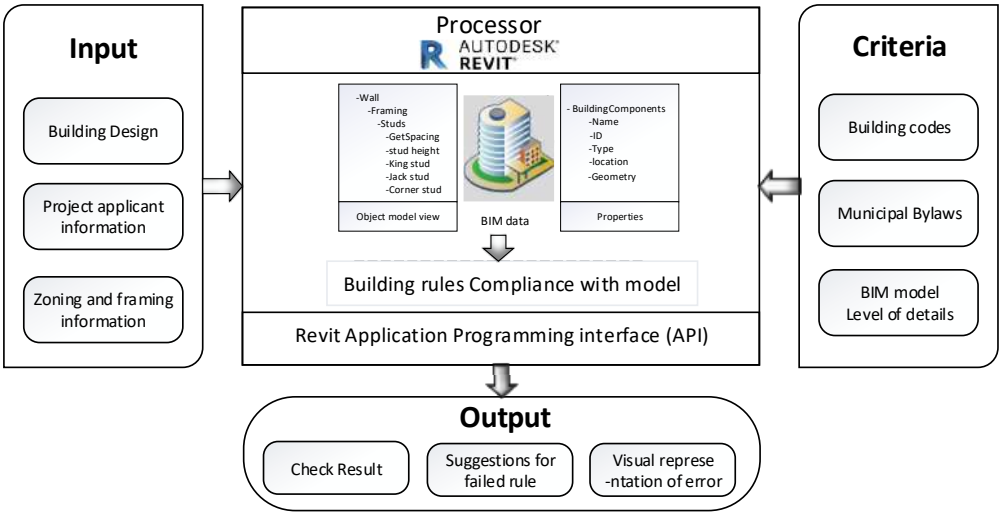

Figure 2. System Architecture

against the already-encoded building rules. These four components are compiled into Autodesk Revit as an add-on through using C# language.

5 Case Study

A residential building design has been modelled in Autodesk Revit as required, with a level of details more than LoD 300 for efficient automated-checking process. Before starting checking, users are required to provide some initial information related to the project, which is the same information house owners or contractors used to provide while submitting 2D CAD drawings for approval.

The building rules are represented based on building objects. The logical representation of rules based on building objects gives a clear understanding and provides an efficient way to accomplish the interpretation of rules into a computer-readable format. Figure 3 gives details about minimum setback distances required for different house types. Building rules from municipal bylaws like "If it is Single Detached Housing: Minimum site/ Lot Dimensions should be, Area: 250.8 m^2. Width: 7.6 m^2. Depth: 30 m^2" and so on are represented in a logical format for better understanding. As an example, the above explained rule related to lot checking can be represented as shown in Eq. (1), which represents two-dimensional matrix with threshold values to be satisfied for each type of house (j) and for different zone types (i). Where i is different residential zones present in city, j is different types of houses built in those residential zones. Finally, if the equation (2) returns the result of 1, then the rules have failed to satisfy, else it is correct.

In the City of Edmonton, there are ten different zones (Z_{bylaw}): Single Detached Residential Zone (RF1),

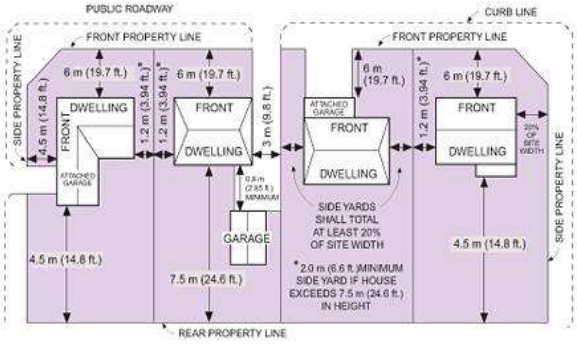

Figure 3. Illustration of Setback Distances Requirements for RF1 Zone (Adopted from City of Edmonton Website [23])

Residential small Lot Zone (RSL), Low Density Infill Zone (RF2), Planned Lot Residential Zone (RPL), Small Scale Infill Development Zone (RF3), Semi-detached Residential Zone (RF4), Residential Mixed Dwelling Zone (RMD), Row Housing Zone, Urban Character Row Housing Zone (UCRH), and Medium Density Multiple Family Zone (RF6). All the residential houses built in these zones are classified as single-detached housing (sdh), semi-detached housing (ssh), duplex housing (dh), limited group homes (lgh), garden suite (gs), secondary suits (ss), or minor home-based business (mhb).

$$i = Z_{bylaw} = \begin{bmatrix} \text{RF1, RF2, RPL, RF3, RF4,} \\ \text{RMD, Row housing zone,} \\ \text{UCHR, RF6.} \end{bmatrix}$$

$$j = HT_{bylaw} = \begin{bmatrix} \text{sdh, ssh, dh, lgh, gs,} \\ \text{ss, mhb.} \end{bmatrix}$$

$$L_{bylaw} \in M_{9X7} = A = \begin{vmatrix} \text{for i} \in 1 \dots 9 \\ \quad \text{for j} \in 1 \dots 7 \\ M_{i,j} \leftarrow [i_j] \end{vmatrix}$$

$$where, \mathrm{A} = \begin{pmatrix} \mathrm{RF1}_{sdh} & \dots & \mathrm{RF1}_{mhb} \\ \vdots & \ddots & \vdots \\ \mathrm{RF6}_{sdh} & \cdots & \mathrm{RF6}_{mhb} \end{pmatrix} \quad (1)$$

$$\text{get the user inputs:} \begin{cases} \sum Z_i = 1\ (i) \\ \sum HT_j = 1\ (j) \end{cases} \rightarrow find\ A(i,j)$$

$$\rightarrow L_{bylaw(i,j)} = \begin{bmatrix} LA^{bylaw} \\ LD^{bylaw} \\ LW^{bylaw} \end{bmatrix}$$

$$\delta_{lot} = \begin{cases} 1 & \text{if } L_{bylaw(i,j)} > L_{BIM} \\ 0 & \text{otherwise} \end{cases} \quad (2)$$

The user needs to provide the project information on housing and zoning type through the main user interface of DCheck add-on application as shown in Figure 4. By running the application for checking municipal bylaws, it provides a textual report related to compliance checking in accordance with municipal bylaws based on building design and user input (see Figure 4). The textual report displays municipal bylaws failed to satisfy with the building objects attribute name, reason for the failure and details about that rules, so that user can easily understand the error in design and make changes as suggested. Once the errors have been corrected, the user can run the checking application again. If there are no further errors in design, it will display a textual report indicating checking successful.

6 Conclusion

This study presents the automated checking of zoning regulations according to the City of Edmonton municipal bylaws related to residential zoning designs and the Alberta Building Code part 9 related to housing and small buildings for light-frame residential buildings in Autodesk Revit. The representation of the building rules based on building objects and the classification of building rules into three groups based on complexity in translation and also in complexity in extracting required information, makes it easier to understand the rules and helps to translate the rules and regulations into computer-readable format. This kind of knowledge formularization makes it easier to understand the regulation and determine the required threshold value to be checked for that building object in the model with specified conditions. This makes it easier for any changes or for the development of add-on software application for a different province or jurisdiction where the building rules are different. Also, the classification of building regulations supports the development of the extended data structure platform in a step-by-step process, which gives the user a clear understanding of the checking process with rules that are incorporated in the add-on application system.

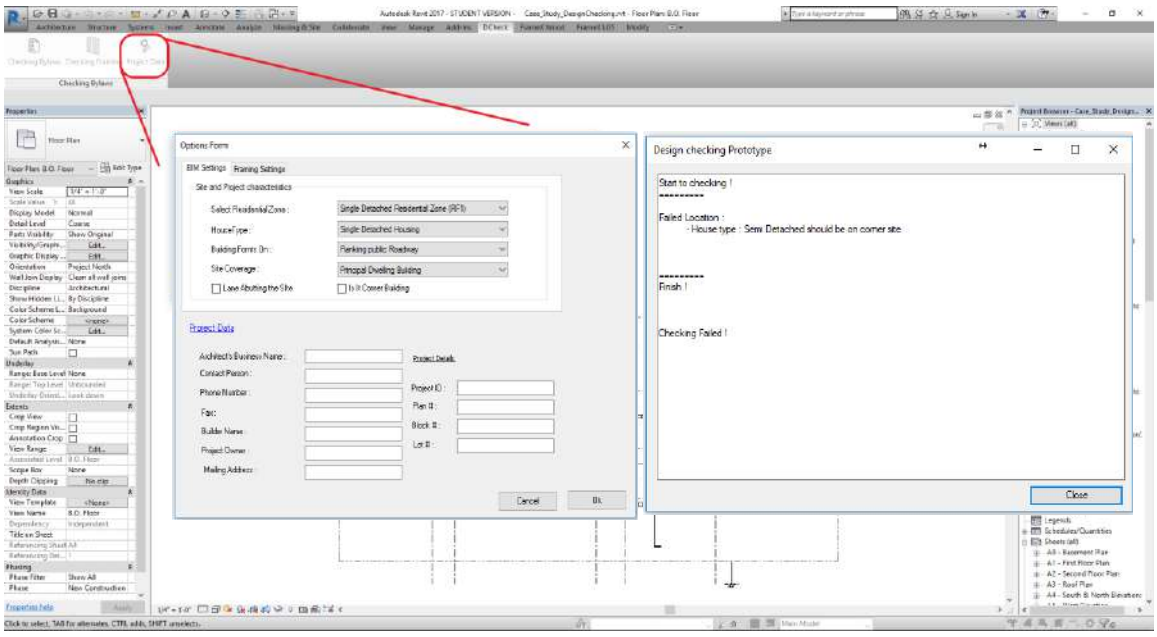

Figure 4. Graphic User Interfaces of DCheck add-on application

References

[1] C. S. Han, J. C. Kunz, and K. H. Law, "A Hybrid Prescriptive-/Performance-Based Approach to Automated Building Code Checking," *Fifth Congr. Comput. Civ. Eng.*, pp. 1–12, 1998.

[2] J. Dimyadi and R. Amor, "Automated Building Code Compliance Checking – Where is it at?," *Proc. 19th World Build. Congr. Constr. Soc. 5-9 May*, pp. 172–185, 2013.

[3] B. W. J. Rasdorf and S. Lakmazaheri, "Logic-Based Approach For Modeling Organization Of Design Standards In general , a design standard is composed of a set of provisions , where each provision defines a set of rules (constraints) that have to be satisfied in a give," vol. 4, no. 2, pp. 102–123, 1990.

[4] S. Fenves, J. Garrett, and H. Kiliccote, "Computer representations of design standards and building codes: US perspective," *Int. J. Constr. Inf. Technol.*, vol. 3, no. 1, pp. 13–34, 1995.

[5] C. L. Dym, R. P. Henchey, E. A. Delis, and S. Gonick, "A knowledge-based system for automated architectural code checking," *Comput. Des.*, vol. 20, no. 3, pp. 137–145, 1988.

[6] Global Reporting Initiative, "Construction and Real Estate," 2014.

[7] C. Preidel and A. Borrmann, "Automated Code Compliance Checking Based on a Visual Language and Building Information Modeling," *Proc. 32nd Int. Symp. Autom. Robot. Constr. 15-18 June*, pp. 256–263, 2015.

[8] L. Ding, R. Drogemuller, M. Rosenman, and D. Marchant, "Automating code checking for building designs - DesignCheck," *Coop. Res. Cent. Constr. Innov.*, pp. 1–16, 2006.

[9] "STATSBTGG website," 2018. [Online]. Available: https://www.statsbygg.no/.

[10] S. Malsane, J. Matthews, S. Lockley, P. E. D. Love, and D. Greenwood, "Development of an object model for automated compliance checking," *Autom. Constr.*, vol. 49, no. PA, pp. 51–58, 2015.

[11] "Automated compliance checking using building information models," no. September, pp. 2–3, 2010.

[12] C. Eastman, J. min Lee, Y. suk Jeong, and J. kook Lee, "Automatic rule-based checking of building designs," *Autom. Constr.*, vol. 18, no. 8, pp. 1011–1033, 2009.

[13] L. Khemlani, "CORENET e-PlanCheck : AECbytes ' Building the Future ' Article CORENET e-PlanCheck : Singapore â€™ s Automated Code Checking System CORENET e-PlanCheck : AECbytes ' Building the Future ' Article," *Design*, pp. 1–8, 2005.

[14] W. Solihin, C. Preidel, and A. Borrmann, "Towards code compliance checking on the basis of a visual programming language," *ITcon Vol. 21, Spec. issue CIB W78 2015 Spec. track Compliance Checking, pg. 402-421, http//www.itcon.org/2016/25*, vol. 21, no. 25, pp. 402–421, 2016.

[15] P. Pauwels *et al.*, "A semantic rule checking environment for building performance checking," *Autom. Constr.*, vol. 20, no. 5, pp. 506–518, 2011.

[16] J. P. Martins and A. Monteiro, "LicA: A BIM based automated code-checking application for water distribution systems," *Autom. Constr.*, vol. 29, no. 23, pp. 12–23, 2013.

[17] Sjøgren, "in Norway," 2007.

[18] S. Zhang, J. Teizer, J. K. Lee, C. M. Eastman, and M. Venugopal, "Building Information Modeling (BIM) and Safety: Automatic Safety Checking of Construction Models and Schedules," *Autom. Constr.*, vol. 29, pp. 183–195, 2013.

[19] R. See, "SMARTcodes : Enabling BIM Based Automated Code Compliance Checking AEC-ST Conference Presentation – 21-May-08 SMARTcodes : Enabling BIM Based Automated Code Compliance Checking," no. October 2007, pp. 1–7, 2008.

[20] X. Tan, A. Hammad, and P. Fazio, "Automated Code Compliance Checking for Building Envelope Design," *J. Comput. Civ. Eng.*, vol. 24, no. 2, pp. 203–211, 2010.

[21] H. Lee, S. Lee, S. Park, and J. Lee, "An Approach to Translate Korea Building Act into Computer-readable Form for Automated Design Assessment," *Proc. 32nd ISARC*, pp. 1–8, 2015.

[22] W. Solihin and C. Eastman, "Classification of rules for automated BIM rule checking development," *Autom. Constr.*, vol. 53, pp. 69–82, 2015.

[23] "City of Edmonton." [Online]. Available: https://www.edmonton.ca/residential_neighbourhoods/zoning-regulations-for-houses.aspxå. [Accessed: 15-Jan-2019].

Schedule Quality Assessment for nD Models using Industry Foundation Classes

A. Kavad[a], R. Dharsandia[a], A. Hosny[a], and M. Nik-Bakht[a]

[a]Department of Building, Civil and Environmental Engineering, University of Concordia, Canada
E-mail: ashokkavad1994@gmail.com, rahul47007@gmail.com, a_hosny@live.concordia.ca, mazdak.nikbbakht@concordia.ca

Abstract –

Schedule assessment models were created to ensure the proper development of a schedule. The checks can be categorized into scheduling-related and constructability reviews. Most of the existing automated models are targeted towards two-dimensional schedules, and not nth-dimensional, despite the emergence of building information modelling in the construction industry. The type, method and relations between stored temporal information for activities in nth-dimensional models differ than the typical two-dimensional schedules. Accordingly, this paper presents the adaptation of the existing schedule quality assessment criteria to evaluate nth-dimensional models, utilizing building information modelling and Industry Foundation Classes (IFC). The paper starts with a comprehensive review of previous assessment models, identifying the major checks performed, detailing out the needed activity information and evaluation techniques. The checks are then categorized as quantifiable and qualitative, to differentiate between the measures that can be fully automated and others which would require expert intervention. Afterwards, the paper presents the methodology for attaining the inputs required for the quantitative measures in nD models. The methodology revolves around using IFC, as a standard data model for storing building and construction data. Accordingly, a technological review was conducted of the existing nD modelling software, to view the capabilities and limitations that could affect the development of a schedule assessment model. Initial Algorithms were developed to measure the wellness of schedule properties such as activity duration, criticality levels and accuracy of relationships. These developed algorithms were then verified by testing them versus different schedules with known errors.

Keywords –

4D Modelling; Schedule health assessment; Schedule quality checks; IFC

1 Introduction

According to International Building Information Modelling (BIM) Report 2017 by National BIM Standard, 78% of Canadians think that BIM is the future for managing project information and 67% are currently using BIM in their organization. [1]. The design and construction industry are now transitioning from use of two-dimensional Computer aided designs (CAD) and paper for design to three-dimensional digital models loaded with information. The BIM usage in project is expected to continue growing sharply in coming years [2]. The emergence of BIM in construction industry has allowed for the development of nD models, which combine the 3D spatial information with time, cost, resources, etc. The development of these models has provided enhanced multi-disciplinary and constructability analysis, and more efficient communication of spatial and temporal information between project teams by visualizing the evolution of the construction works throughout the project duration, allowing for the creation of more practical time schedules [3].

The United States Government Accountability Office (GAO) reports that there is a significant relationship between good scheduling practices used early in the project life cycle and the ultimate success of the project [4]. Accordingly, extensive research has been conducted to develop metrics that evaluate the quality of schedules, from various aspects, such as the construction logic, the activity identification, adequacy of estimates durations, enough allocation of resources, ideal cash flow distribution, etc. [5] [6] [7] [8]. Additionally, these metrics have been automated via commercial software [9] [10] [11] [12]. However, despite BIM's growing popularity, these automated schedule assessment models are still configured based upon the review of schedules from the conventional planning tools. In nD models the activities' temporal information and schedule relations are stored in a different database configuration than that in the conventional planning tools (such as Primavera &

Microsoft projects), which is more complex owing to combining the spatial information in the same database. Hence, the current automated schedule assessment models cannot be used to evaluate nD models without adaptation, which is rendering the process of development of these models inefficient.

Consequently, the focus of this paper is to develop the framework that adapts the current schedule assessment metrics of conventional planning tools, to capture information and analyse the schedules directly from nD models. Furthermore, the framework is based upon the Industry Foundation Classes (IFC) format, which is an open and neutral data format, to standardize the information storage and to work with any nD modelling software in the market. IFC is defined using the ISO 10303 suite of specifications for data modelling and exchange, also known as STEP (Standard for the Exchange of Product Data) [13]. This paper presents its method for categorizing previously developed evaluation metrics to identify the potential ones for adaptation. Then, the paper presents the methodology for capturing the selected metrics from nD databases in IFC format, and the corresponding algorithms using Psuedo code. Lastly, the paper verifies the approach via a theoretical case study of a 3-story office building, where faulty schedules were created intentionally to measure the responsiveness of the algorithms.

2 Review of Previous Schedule Assessment Models

The most popular assessment model is that of the United Stated Defence Contract Management Agency (DCMA). They formulated 14 points to assess the schedule quality at both pre-construction and during construction and identified the threshold for each which are presented in Table 1 [14]. For example, to test schedule practicality, they identified metrics as: (1) logic: which stated that only 5% of the activities in the schedule are allow to not have successors nor predecessors, to ensure proper linkage, (2) leads: which stated that activities cannot have a relationship between them with a negative lag, as this leads to improper relationships, (3) hard constraints: which stated that any schedule cannot have more than 5% of its activities with hard constraints, and they tend to disrupt the paths when being misplaced, etc. Currently, these points represent the minimum checks in modern assessment models, with variant thresholds.

Table 1. DCMA 14 Metrics [14]

Metric	Description	Threshold
Logic	Activities without successors/or predecessors	< 5%
Leads	Relationships that have a negative lag	0%
Lags	Relationships that have positive lags	< 5%
Relationship Types	Finish to Start Relationships	>= 90%
Hard Constraints	Activities with Must Finish On/ Must Start On/ Start No Later Than/ Finish No Later Than	< 5%
High Float	Activities with total float greater than 44 WD	< 5%
Negative Float	Activities with total float less than 0	0 %
High Durations	Activities with Duration greater than 44 WD	< 5%
Invalid Dates	Activities with forecast dates earlier than status date or actual dates later than status date	0 %
Resources	Activities without resource loading (money/ hours)	-
Missed Tasks	Activities with actual/forecasted finish dates later than planned finish date	< 5%
Critical Path Test	Test the integrity of the critical path by introducing intentional slippage. If the delay is not proportional to the slippage, then the logic is faulty and is flagged	
Critical Path Length Index (CPLI)	(Critical Path Length + Total Float) / Critical Path Length	>= 0.95

Baseline Execution Index (BEI)	Activities completed within current reporting period / (Activities completed in previous reporting periods + Activities missing their planned finish dates)	>= 0.95

Further metrics were developed in later work after the DCMA to add more analysis for areas as the logic and resources. [8] [15], developed their assessment model, which would check the job logic by: (1) Recognizing pre-defined keywords in the activities' names (2) check for the existence of relationships between each set of keywords. For example, any activity name containing "pouring" must have predecessors with activity names containing "framework" and "rebars", and successors with activity names containing "curing". Furthermore, they developed a set of empirical rules to verify the job logic in any schedule. The empirical rules explained the expected relationship and duration ratios that activities should have with reference to the schedule. For instance, the duration for the curtain wall activities should be around 30% of the project duration, and cannot start until at least 3 floors are done with the framing works. As for resource allocation, their model compared the schedule's productivity rates with that of RS Means, flagging any activities with a deviation of over 30%. Opposing to the DCMA, their system categorized the metrics as obligatory and complementary, where the former must be satisfied, and the later measures the fitness according to a "Schedule Development Index (SDI)". The schedule fitness was considered excellent with SDI ≥800, good with 800>SDI≥500, and acceptable with SDI<500.

[5] [6] [7] developed 75 schedule requirements grouped under 5 categories: (1) General Requirements: which dealt with generic parameters, such as checking for an activity coding structure, defined calendar, etc. (2) Construction Process Requirements: which dealt with job-logic, productivity, activity duration and timing. (3) Schedule mechanics requirements: which dealt with scheduling issues as open-ended activities or relationship types (4) Cost and resource requirements: which dealt with cost and resource loading assignments. (5) Control process requirements: which dealt with validating and evaluating the schedule updates. They used the BEI and CPLI of DCMA, which are shown above in Table 1. Their model was based on user-defined thresholds for each requirement, in which graphs would be developed to display a schedule's performance (rating) under each requirement group according to the defined thresholds, where the rating is a subjective evaluation of the reviewer. The main addition in their assessment model is identifying spatial requirements under "Construction Process requirements" as having a "safe and non-congested work areas." which was done manually.

Similarly, [3] [16] and [17], developed their assessment criteria by reviewing the 4D schedule model created in ArcGIS. However, contrary to the typical metrics, their model focused mainly on the review of the job logic by manual observation of the 4D visualization to check for the adequate activity detailing and proper sequencing. Also, their model ensured that all temporal activities were assigned to at least one spatial object, based their assessment criteria on the manual visualization of 4D schedule to ensure the sequencing and constructability. Such research was based on expert judgement, with loosely defined metrics and was never automated. Till date, there doesn't exist a comprehensive model that combines temporal and spatial metrics for assessing schedule qualities, as that would require moving between more than one software and migrating the data back and forth for multiple iterations which is time-consuming.

3 Model View Definitions for Industry Foundation Classes

IFC schema is constructed of entities (or classes), the relationship between entities, and attributes, which together constitute the IFC model. An IFC model is usually big as it is a representation of all physical and non-physical elements in the project for all types of information (spatial, temporal, etc.) [18]. There are 4 standard methodologies for understanding IFC: (1) ISO 16739 for data sharing in the construction and facility management (2) International Framework for Dictionaries (IFD) ISO 12006-3 (3) Information Delivery Manual (IDM) ISO 29481-1 ISO 29481-2, and (4) Model View Definition (MVD) buildingSMART [19].

Focusing on MVDs, they represent is a subsection of the IFC schema for specific use cases. Meaning that the use of MVDs allows for extracting the necessary information only from IFC and not dealing with the entire model. This allows for faster analysis and less computational efforts. For example, when analysing schedule quality, the required information from IFC is mostly temporal information, and the size and coordinates of the physical components, with no need of material, or structural information. An MVD can help filter this information from an IFC Model. The latest IFC Schema developed by buildingSMART is IFC4 Addendum 2 with two released MVDs: Reference View and Design Transfer View, where the later is more comprehensive than the former and both contain the schedule information [20].

4 Methodology

4.1 Database Creation

Figure 1 displays the 3 steps taken to develop the nD assessment model. Stage 1 deals will the compilation of previous literature, international standards and commercial tools to create a database of 176 metrics. Each metric was tagged to its author, provided with a clear description, displays the suggested threshold (if any).

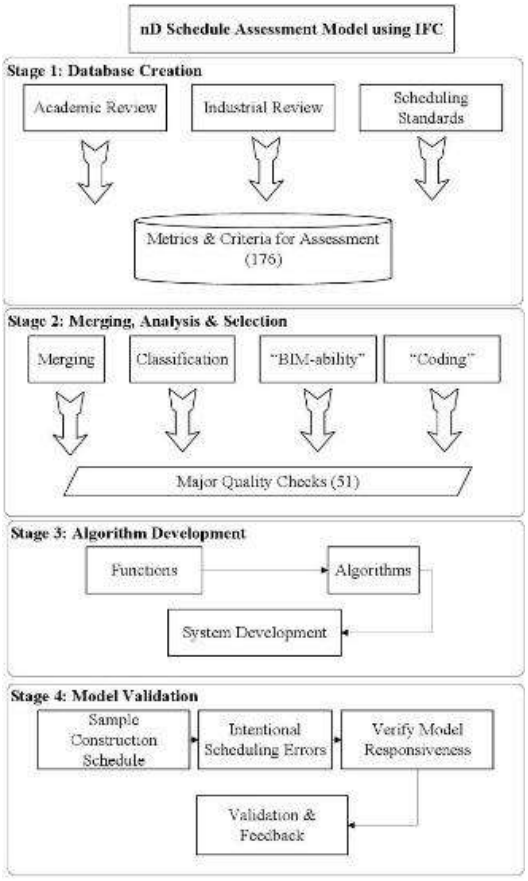

Figure 1. Methodology Procedure

4.2 Merging, Analysis & Selection

The second stage is the analysis of the database (176 metrics) which was conducted on 4 aspects: (1) Merging: to remove any duplicate checks that were suggested by more than one researcher, while maintaining the suggested threshold by each. For example, [14] suggested high duration activities metrics as shown in Table 1. This principle was also used by [8] and [7], but each defined a different threshold in their approaches. This reduced the metrics to 168. (2) Classifying the metrics as (2.1) qualitative: where 26 metrics had no clear threshold defined, and their description indicated manual expert intervention; (2.2) quantitative: where 104 metrics had clear thresholds and evaluation criteria; and (2.3) generic metrics: where 38 of the metrics had very generic description and couldn't be analysed without additional information.

As the target is developing an automated system, the focus was on the quantitative metrics, having clear guidelines for evaluation, which had 83 related to the planning (pre-construction) phase, and 21 related to the progress monitoring (construction) phase. The paper's concentration was on the metrics for the pre-construction phase. Where these were selected for further analysis of their "BIM-ability": a check to verify the existence of the required information in a BIM model exported in an IFC formatted database; and "coding potential": the ability to capture the information using a suitable MVD. This eventually led to selecting 51 metrics for the nD schedule assessment model.

4.3 Algorithm Development

Some of the selected metric required the same information, with the difference of the evaluation criteria and threshold, and hence could use the same algorithm. For example, 2 of the metrics selected were "relationships with lag" and "relationships with lead". Both shared the same evaluation criteria shown in Equation 1, where the metric depended mainly on measuring the ratio between the number of relationships (links # (Lag or Lead)) that had a lag or a lead, to the total number of relationships (Total Links #). hence, both metrics required filtering part of the part of the links with lags or leads. The only difference is the selection, for "lead' links are negative lags and "lag" links are positive lags. Accordingly, both can use the same algorithm. Subsequently, 22 unique algorithms were developed for the 51 metrics. Furthermore, these algorithms shared some global functions that were created as well.

$$Links\ \#\ (Lag\ or\ Lead)\ /\ Total\ Links\ \# \qquad (1)$$

To better explain this approach, Figures 2 and 3 shows the codes for the "total tasks" global function used in the "logic density" algorithm. The logic density is a measure of the soundness (practicality) of a schedule by finding the ratio of the number of relationships developed to the number of activities created. The threshold limit is a minimum of 2.1. To calculate this metric, the "number of links" and the "total number of activities" need to be captured. The "total number of activities' is also required in the "high-duration" metric, where the activities with a duration higher than a specified value are compared to the "total number of activities". The threshold for this measure is a maximum of 5%. Hence, a global function called "total tasks" was created to be used in both algorithms.

Total Tasks:

```
BEGIN FUNCTION TotalTasks(IfcTask,
IfcRelNests)
  ''' INPUT: IfcTask.ID(),
        IfcRelNests.RelatingObject()
        OUTPUT: TotalTasks - A list contaning all
        Tasks'''

  DECLARE LIST: A, B, TotalTasks

   FOR EACH ID IN IfcTask
      ADD IfcTask.ID to List A
    END FOR

    FOR EACH IfcRelNests.RelatingObject[ID]
      ADD IfcRelNests.RelatingObject[ID] to List B
    END FOR

    TotalTasks = List A - List B

    RETURN TotalTasks
END
```

Figure 2 "Total Task" Global Function

Logic Density

Relationships per activity or Relationship ratio or Logic Density = # of Logic links / # Total Tasks

```
BEGIN MAIN LogicDensity (IfcRelSequence,
AllowableValue = 2.1 )
  ''' INPUT: IfcRelSequence.ID()
    DECLARE LIST: TotalTasks
    DECLARE NUMBER: TotalNumberOfTask = 0,
    LogicLinks = 0

     TotalTasks = CALL FUNCTION
TotalTasks(IfcTask, IfcRelNests)
      TotalNumberOfTask = COUNT ID in
      TotalTasks
      TotalNumberOfTask = 100 *
      TotalNumberOfTask

       LogicLinks = COUNT ID in IfcRelSequence

       PRINT CALL FUNCTION
       MeasureCheck(Numerator: LogicLinks,
       Denominator: TotalNumberOfTask, value:
       AllowableValue, Condition: >, MetricName:
       "LogicDensity%=")
END
```

Figure 3. "Logic Density Algorithm"

5 Model Verification

As explained before, the developed algorithms were tested against a hypothetical case study of a 3-storey office building. The 3D model was created using Autodesk Revit. Then was imported to Synchro Pro to develop the nD model. The reason for selecting Synchro Pro over Autodesk Navisworks is because of its extra project management abilities, that enabled the storing of relationships between activities and the assigning of resources and cost loading. Additionally, Synchro Pro supports exporting nD models in IFC format [21].

A baseline schedule was developed for the model, then intentional scheduling errors were placed as alternative scenarios. An example of these errors is changing the activity duration of the foundation works to 60 working days (1,728,000 seconds) and setting the threshold for 44 working days (1,267,200 seconds). The verification was done by breaking down each algorithm into sub-sections and manually calculating the output of each section. Continuing with the "High duration" metric example, Figures 4, 5 and 6 show the breakdown of the algorithm. Step 1 (Figure 4) is to identify the attribute "ID" under "IfcScheduleTimeControl" Class with attribute "ScheduleDuration" greater than 1,267,200 seconds. The model filtered out the ID # 48719 and not # 48701 which was correct. As the # 48701 referred to a WBS level and not an activity. This output verified the functionality of the "Total Tasks" global function and the capturing process. Step 2 & 3 are to find the flagged activity's name, which is stored under "IfcTask" class. Hence, step 2 (Figure 5) is to find the "IfcTask" number under "RelatedObjects" attribute corresponding to the "IfcScheuleTimeControl ID" # 48719 under the "Time for Task" attribute in the "IfcRelAssignsTasks" Class. Lastly, step 3 (Figure 6) is to print out the "Name" attribute for the selected "ID" under "IfcTask" Class.

IfcScheduleTimeControl (41)			
ID	GlobalId	OwnerHistory	ScheduleDuration
48701	3NokVVgsH6aRUs2p$5W5_4	IfcOwnerHistory 5	1814400
48710	3gC0$xPQT7495FmP7p_$Dq	IfcOwnerHistory 5	230400
48719	3MDQqkX_969PX5xnlX79sB	IfcOwnerHistory 5	1728000
48728	0mHop__Yj1OQGrytDRxwnR	IfcOwnerHistory 5	0.00E+00

Figure 4. "High Duration" Metric: Step 1 Output

IfcRelAssignsTasks (41)		
ID	RelatedObjects	TimeForTask
48708	(1) IfcTask 48700	IfcScheduleTimeControl 48701
48717	(1) IfcTask 48709	IfcScheduleTimeControl 48710
48726	(1) IfcTask 48718	IfcScheduleTimeControl 48719
48735	(1) IfcTask 48727	IfcScheduleTimeControl 48728

Figure 5. "High Duration" Metric: Step 2 Output

IfcTask (41)			
ID	Name	TaskId	Description
48700	Office building	1	1
48709	Sub-structure	1.1	1.1
48718	Foundation	1.1.1	1.1.1

Figure 6. "High Duration" Metric: Step 3 Output

6 Limitations & Challenges

Although the use of IFC format allowed for standardization independent from any software application, yet it has presented some challenges as well. The main challenge in this study was the lack of any existing software that exports nD models in IFC format other than Synchro Pro. Moreover, Synchro Pro is based upon IFC2x2 and IFC2x3, earlier schemas than IFC4 which are not as comprehensive as IFC4. Lastly, Synchro uses a specific MVD that does not export all resource and cost assignments and hence any algorithms related to such information could not be verified. Unfortunately, the industry does not have a nD modelling software that is based on IFC4 and can utilize any of the released MVDs.

Another challenge with the use of IFC was the different methodology and definition for certain temporal information. For example, the types of tasks available in IFC are attendance, construction, demolition, dismantle, disposal, installation, logistic, maintenance, move, operation, removal, renovation [22]. However, in Synchro Pro, the activity types were level of effort (LOE), resource dependent, and time dependent. The same applies for the definitions of the milestones. Accordingly, all metrics related to these two aspects could not be verified as well.

7 Conclusion & Future Works

The paper presents a novel schedule assessment model that can evaluate the quality of the construction schedule directly from nD models, without the need to revert to the conventional planning tools. The model starts with developing a database of the assessment criteria developed by previous researchers and commercial software. Then, the criteria were merged and analysed to determine the quantifiable metrics that can be automated. Afterwards, algorithms and global functions were developed to carry out the metrics. The model was then verified via a hypothetical case study of a 3-storey office building.

This work is a genuine contribution to the body of knowledge as it opens the door for the development of new assessment metrics by utilizing the nD abilities. Hence, the future works will focus mainly on exploring such. Additionally, other future works would focus on enhancing the practicality of the developed assessment model such as (1) exploring the development of a specific MVD that would capture only the required information for assessment as the current MVDs have more information that is not used. (2) Extending the evaluation criteria to include controlling metrics that would evaluate the quality of the updated schedules. (3) validating the developed model against a real case study and receiving feedback.

8 References

[1] Royal Architectural Institute of Canada, "BIM Explained," 2016. [Online]. Available: https://www.raic.org/raic/bim-explained. [Accessed 31 October 2018].

[2] J. Steel, R. Drogemuller and B. Toth, "Model Interoperability in Building Information Modeling," *Software & Systems Modeling*, vol. 11, no. 1, pp. 99-109, 2012.

[3] V. Bansal and M. Pal, "Construction schedule review in GIS with a navigable 3D animation of project activities," *International Journal of Project Management*, vol. 27, p. 532–542, 2009.

[4] U. S. G. A. Office, *GAO Cost Estimating and Assessment Guide: Best Practices for Developing and Managing Capital Program Costs*, Washington DC, District of Columbia: GAO, 2009.

[5] M. A. Bragadin and K. Kahkonen, "Safety, space and structure quality requirements in construction scheduling," *Procedia Economics and Finance*, vol. 21, pp. 407-414, 2015.

[6] M. A. Bragadin, "Quality Driven Scheduling in Construction," Tampere University of Technology, 2018.

[7] M. A. Bragadin and K. Kahkonen, "Schedule health assessment of construction projects," *Construction Management and Economics*, vol. 34, no. 12, pp. 875-897, 2016.

[8] S. F. Moosavi and O. Moselhi, "Review of Detailed Schedules in Building Construction," *Journal of Legal Affairs and Dispute Resolution in Engineering and Construction*, vol. 6, no. 3, pp. 05014001- 1 to 9, 2014.

[9] Deltek Acumen Fuse, "Schedule Quality: 9 Industry Benchmarks for Sound Scheduling," 2018. [Online]. Available: https://www.deltek.com/~/media/infographics/schedule%20quality.ashx?la=en. [Accessed 2 June 2018].

[10] P6 Schedule Checker, "Running the “Check Schedule” Feature with P6 EPPM," 2018. [Online]. Available: http://www.projwebsite.com/publications/TechTip_Running_the_Check_Schedule_Feature_with_P6_EPPM.pdf. [Accessed 3 June 2018].

[11] XER Schedule Toolkit, "User Manual Overview & Function," 2018. [Online]. Available: https://xertoolkit.com/support/xer8-user-manual.pdf. [Accessed 3 June 2018].

[12] Schedule Inspector, "Schedule Inspector User Guide," 2018. [Online]. Available: https://www.barbecana.com/wp-content/uploads/2016/02/ScheduleInspectorUserGuide.pdf. [Accessed 4 June 2018].

[13] J. Steel, R. Drogemuller and B. Toth, "Model Interoperability in Building Information Modeling," *Software & Systems Modeling,* vol. 11, no. 1, pp. 99-109, 2012.

[14] D. C. M. A. –. D. o. Defense, *Earned Value Management System (EVMS): Program Analysis Pamphlet (PAP),* Washington DC, District of Colombia: Department of Defense , 2012.

[15] S. F. Moosavi, "Assessment and Evaluation of Detailed Schedules in Building Construction," MASc Thesis, Concordia University, Montreal, 2012.

[16] Bansal, V.K.; Pal, Mahesh, "Generating, Evaluating, and Visualizing Construction Schedule with Geographic Information Systems," *Journal of Computing in Civil Engineering,* vol. 22, no. 4, pp. 233-242, 2008.

[17] B. Garcia de Soto, A. Rosarius, J. Rieger, Q. Chen and B. T. Adey, "Using a Tabu-search Algorithm and 4D Models to Improve Construction Project Schedules," *Procedia Engineering,* vol. 196, pp. 698-705, 2017.

[18] T. Froese, "INDUSTRY FOUNDATION CLASS MODELING FOR ESTIMATING AND SCHEDULING," in *Durability of Building Materials and Components 8*, Vancouver, 1999.

[19] T. Liebich, "IFC 2x Edition 3 Model Implementation Guide," buildingSMART International Modeling Support Group, 2009.

[20] BuildingSMART, "Open Standards - the basics," 2018. [Online]. Available: https://www.buildingsmart.org/standards/technical-vision/open-standards/. [Accessed 30 October 2018].

[21] Synchro Software, "Integrations," 2018. [Online]. Available: https://www.synchroltd.com/integrations/. [Accessed 10 October 2018].

[22] BuildingSMART, "IfcTaskTypeEnum," 2018. [Online]. Available: http://www.buildingsmart-tech.org/ifc/IFC4/Add2/html/schema/ifcprocessextension/lexical/ifctasktypeenum.htm. [Accessed 15 October 2018].

A Mixed VR and Physical Framework to Evaluate Impacts of Virtual Legs and Elevated Narrow Working Space on Construction Workers' Gait Pattern

M. Habibnezhad[a], J. Puckett[a], M.S. Fardhosseini[b], and L.A Pratama[b]

[a]Durham School of Architectural Engineering and Construction, University of Nebraska-Lincoln, USA
[b]Department of Construction Management, College of Built Environments, University of Washington, USA
E-mail: mahmoud@huskers.unl.edu , jay.puckett@unl.edu, sadrafh@uw.edu, pragungl@uw.edu

Abstract –

It is difficult to conduct training and evaluate workers' postural performance by using the actual job site environment due to safety concerns. Virtual reality (VR) provides an alternative to create immersive working environments without significant safety concerns. Working on elevated surfaces is a dangerous scenario, which may lead to gait and postural instability and, consequently, a serious fall. Previous studies showed that VR is a promising tool for measuring the impact of height on the postural sway. However, most of these studies used the treadmill as the walking locomotion apparatus in a virtual environment (VE). This paper was focused on natural walking locomotion to reduce the inherent postural perturbations of VR devices. To investigate the impact of virtual height on gait characteristics and keep the level of realism and feeling of presence at their highest, we enhanced the first-person-character model with 'virtual legs'. Afterward, we investigated its effect on the gait parameters of the participants with and without the presence of height. To that end, twelve healthy adults were asked to walk on a virtual loop path once at the ground level and once at the 17th floor of an unfinished structure. By quantitatively comparing the participants' gait pattern results, we observed a decrease in the stride length and increase in the gait duration of the participants exposed to height. At the ground level the use of enhanced model reduced participants' average stride length and height. In other words, in the presence of VR legs, the level of realism significantly increases and thus results in a better virtual gait simulation. The results of this study help us understand users' behaviors when they were exposed to elevated surfaces and establish a firm ground for gait stability analysis for the future height-related VR studies. We expect this developed VR platform can generate reliable results of VR application in more construction safety studies.

Keywords –

Construction safety, virtual reality, virtual legs, extreme height, gait pattern, fall

1 Introduction

According to the annual Bureau of Label Statistics (BLS) report, the construction industry contributed more than 10 percent of all fatal occupational injuries in 2017 [1]. Falling from elevated surfaces accounted for a significant portion of these incidents. According to Hsiao and Simonov [2], the primary stated reasons for falling were slips, trips, and loss of balance based on the worker compensation descriptions and fatality investigation reports. To address the disproportional rate of fall injuries and fatalities, researchers have been focusing on the influential factors affecting postural sway and gait stability. Many of these experiments, especially those related to fear of height and flight, were expensive and dangerous [3]. Therefore, recent studies have been investigating alternative methods to conduct postural stability and fall-related experiments. They found virtual reality (VR) as an alternative solution which "offers the opportunity to bring the complexity of the physical world into the controlled environment of the laboratory [4]."

VR is "a simulation in which computer graphics are used to create a realistic-looking world" [5]. Powerful real-time interaction capability, immersion feeling, and a much more intuitive link between the computer and the user turn this technology into one of the most rapidly growing technological fields. Specifically, there are extensive areas of VR applications ranging from manufacturing design and operation management—things like prototyping, product design, planning, and simulation [6]—to training and rehabilitation [4]. VR provides the users with an immersive environment, a wide range of view, and haptic feedback, delivering a firm platform for experiment designs in a much cheaper and safer way. Despite the inherent instability induction of VR headsets [7], this new technology has been used

in numerous postural stability and fall studies due to its many above-mentioned capabilities [8–12]. Although these studies attempt to utilize VR systems to simulate the destabilizing environment with different kind of stimuli, most of the experiments did not focus on the natural ground walking locomotion in a virtual environment. Furthermore, we did not find any articles concerning the relationship between height exposure and gait stability. Most of the studies in this area have been focusing on the stationary postural sway as the dependent factor. For example, [8] compared the impact of real and virtual height on the postural stability of participants who were standing next to the edge of an elevated surface. However, they did not measure the impact of height on the gait stability of the subjects.

The proposed method of this study for measuring the gait pattern of the participants is to use a virtual environment and first-person character model enhanced with virtual legs to simulate a more realistic gait analysis on narrow, elevated surfaces. By collecting the time series data of the gait patterns from the participants' mounted trackers, this study sought to investigate potential differences between the average and variability of subjects' stride length and height due to elevation and increased realism.

2 Background

2.1 Fall. The leading cause of fatalities in the construction industry is fall, contributing to 38 percent of all fatal injuries happen every day at the construction sites[1]. Numerous research has been conducted recently to find the main reasons behind the disproportional number of fatalities associated with fall [2,13–18]. Slips, trips, and losses of balance are the most common factors contributing to falling [2,13,15]. Hsiao and Simeonov identified loss of balance as the leading cause of fall incidents. They stated that postural regulation of construction workers, especially those who work on elevated surfaces such as roofs or beams, is one of the leading factors in fall injuries and fatalities. Therefore, a closer look at the postural stability and influential factors affecting it can provide valuable insights into the fall-risk assessment.

2.2 Postural stability. Postural stability is defined as "the ability to maintain and control the body center of mass (CoM) within the base of support to prevent falls and complete desired movements [19]." Three central sensory cues for postural stability regulation are visual, vestibular, and somatosensory inputs. Compared to somatosensory and vestibular afferents triggered after the external exposure, visual input is considered a proactive mechanism of balance [2]. Paillard and Noe showed that expertise has a strong relationship with the visual input dependencies for postural regulation [20]. To accurately study the impact of visual input on the postural stability of the construction workers, we need to answer the following two questions: 1. How postural metrics can be measured, and 2. How do individuals respond to different visual perturbations affecting postural sway, especially those associated with height?

2.3 Postural metrics. Based on the definition of postural stability presented earlier, one way of measuring postural metrics is to measure the extent to which the center of the body deviates from the base (feet). Three principal reference planes are describing the anatomical motion of the body, transverse, frontal, and the median plane. The three sway directions namely frontier-posterior, mediolateral, and inferior sway happens respectively on the frontal, medial, and inferior planes. Biomechanical studies use maximum body sway (BS) in the frontier-posterior and mediolateral direction [21,22] and the root mean square of the total body velocity in frontier-posterior, mediolateral, and inferior direction [21] to measure the response of individual to different stimuli. The required data can be obtained by using the force plates or IMU sensors [23]. The other way of measuring the dynamic postural sway responses to external perturbations is to use Maximum Lyapunov exponent (Max LE) [24,25]. Lyapunov exponent directly measures the sensitivity of a dynamical system to minimal perturbations, considered to be a decent indicator of the level of chaos in the system [26]. By utilizing this method, the time series data captured by IMU sensors can then be investigated for any divergence reflecting the response of the dynamic system to the external perturbations. To efficiently find the reasons behind the postural instability of construction workers, identifying workers' responses to diverse types of external visual perturbations is of great importance. Accordingly, numerous studies have been conducted on human subjects to find out the impacts of different perturbations on the postural sway [3,19,27,28]. Interestingly, while postural stability is sensitive to the amplitude of these perturbations, the type of perturbation has far more impact on postural stability than the corresponding amplitude does [19]. Therefore, finding stimulus' characteristics is considered a critical step in fall-prevention techniques. Based on Hsiao and Simeonov critical review, the most significant environmental factors affecting postural stability are elevation, moving visual scenes, depth perception, visual ambiguity, and obstacle detection ability [2]. Since a high number of fatalities are due to falling from elevated surfaces, the current study will focus only on elevation as one of the prominent stimuli on postural stability and consequent loss of balance.

2.4 Elevation, fear of height and VR. The deficit of close visual contact due to the instigating sensory mismatch, and fear-related reactions, especially close to

edges of elevated surfaces, are the two main characteristics of elevation leading to falling [2,29]. In many gaits and postural studies related to elevation and fear of height, pseudo-environment setup and stimuli simulations are the two common procedures to investigate the impact of the factors mentioned above. However, due to versatility of VR tools in generating virtual environment and various visual stimuli, and the unsafe nature of mechanical systems in provoking postural instability, VR systems have been widely used in fear-related behavioral and psychological responses [3,8,12,28,30]. Regenbrecht et al. scrutinized the concept of "presence" and explained that VR is a powerful tool in establishing an immersive environment to convey the feeling of presence to the user [30]. Wallach and Bar-Zvi showed that people suffering from flight phobia could be treated by using VR technology [12]. With an exposure-treatment approach, Rothbaum et al. measured the level of anxiety, avoidance, and attitudes of the participants before and after treatment with VR systems [28]. The outcome of the study showed a significant difference between the self-reported results of anxiety and avoidance of height of participants treated by computer-generated exposure, before and after treatments. In 2012, Celworth et al. compared the impact of height on the postural stability and anxiety level of subjects in a real and virtual environment. They used force plates to measure the center of body frequency and subsequently the stationary balance, and electrodermal activity (EDP) to measure anxiety. By sampling 17 young adults, while minimizing the inherent VR postural instability effect [7], they showed that virtual environment (VE) could simulate the height effect on the mediolateral and anterior-posterior balance of the subjects similar to the real height effect. They concluded that VR could be a useful study and rehabilitation tool for people with balance regulation deficits associated with fear or height. Numerous studies discussed the impact of gait speed and stride length on the overall gait stability and odds of falling in humans [31]. Step and stride length measures the distance between successive points of heel contact of opposite foot and same foot correspondingly. Based on the gait stability studies, the differences between the gait cycle patterns can be good indicators of the overall gait stability performance. During a simple walk the foot will experience periodic movement, which can be represented by the spatiotemporal acceleration and deceleration values. It is assumed that for a stable gait, the acceleration values should be following similar patterns and that the changes are periodically repeated. If there is any irregularity in this cyclic pattern, it indicates that there is an external (e.g., exposure to height) or internal disturbance (e.g., unstable CoM) in the system. Previous research suggests that people have a tendency to reduce their gait stride and speed when they suffer a preexisting fear of falling [32,33]. Interestingly, a higher level of walking disorder parameters--such as gait stride variability--can be affected by the fear of height as well [32].

In the light of foregoing research, the current study will focus on analyzing the time series data obtained in various VR/non-VR scenarios by retrieving the position of the HTC Vive trackers attached to the participants' feet. Furthermore, by quantitatively comparing these time-series data, this paper aims to present the ground walking experiments in VR as a promising tool for time-series data collection in different destabilizing environments, e.g., walking on an unguarded narrow elevated surface. To this end, the first-person character model developed in Unity will be enhanced with the virtual legs, helping the subject to walk on a virtual structural-beam path close to that he would perform in reality. Afterward, the role of VR legs and height in predicting the average value and the variability of gait stride parameters will be studied. By finding differences in gait pattern of the participants across these experiments, further data analysis for obtaining postural sways such as finding MaxLE or maximum BS becomes both possible and promising.

3 Methodology

To compare the impact of height on the gait stability of the 12 volunteer participants, two different experiments were designed (see Figure 1), each with two settings: one with no VR leg, and one with VR leg enhancement (see Table 1). In all the corresponding VR experiments, we attempted to minimize the inherent postural perturbations of VR headsets by simulating a VE as a static visual scene, removing any visual and physical distractions from the virtual environment, and minimizing the VR experiments durations (Horlings et al. 2009). To reduce the VR unfamiliarity, all the participants were instructed to stand, look, and walk for few steps in the VE for 1 minute total. The VR environment was the same environment that they would experience in the other parts of the data collection. After the completion of this part, the participants were equipped with three HTC Vive trackers and an HTC Vive headset. In the first trial, the 'immersed' beam path was presented to the participants while they were able to see their virtual legs. The immersed path consists of a closed triangular polygon constructed by three connected structural beams, with no elevation (figure 1-a). The participants were instructed to walk on the path at a comfortable speed. During this trial and others that followed, the coordinates of the trackers attached to the participants' feet were retrieved with the refresh rate of 60 times per second. The procedure for the second trial was identical to the first trial except that the VR leg

enhancement was not available to the participants. In the third trial, the participants were subjected to height by locating the triangular beam path on the 17th floor of an unfinished building (figure 1-b). The virtual environment remained unchanged save for the height. Similar to the first trial, the participants were able to see their VR legs. In the last trial, the participants were asked to walk again on the same elevated path again. However, the third trial excluded virtual legs from the VR model. In other words, the participants were not able to see their virtual legs as they had been in the first and second trials.

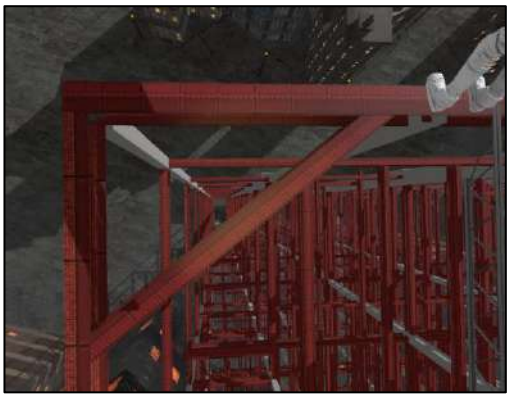

(a)

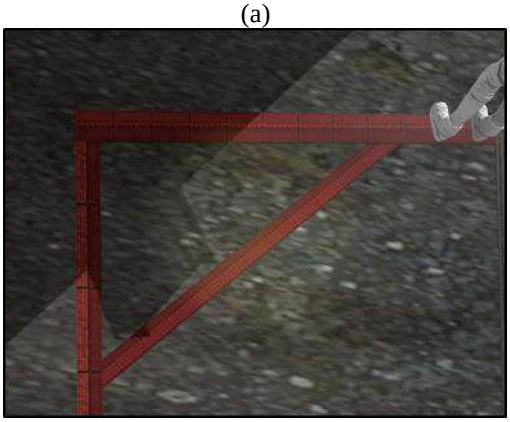

(b)

Figure 1. Two different scenarios namely, real office at the top left, the same virtual office at the bottom left, the virtual elevated path at the top right, and virtual narrow elevated path at the bottom right

Table 1. Experiment configuration

Setting	**Scenarios**	
No virtual legs	VR path on the ground	Elevated VR path
Virtual legs		

4 Results and Analysis

Gait analysis often includes the spatial and temporal measurement of a gait cycle so that the interesting factors can be inferred by comparing the differences between the measurements. Therefore, the focus of this study was on the gait parameters; namely, average speed, length of step and stride, and their variabilities. As mentioned previously, the x, y, and z coordinates of each tracker (attached to participants' feet) were recorded during each trial. Figure 2 shows a sample gait pattern plotted by using one of the participant's right tracker position dataset. The solid lines showed trials with models enhanced with virtual legs and the dashed lines showed those trials without any enhanced virtual legs. Similarly, those lines accompanied by the astride sign '*' represent trials conducted in the presence of virtual height, while those with no '*' represents trials without the presence of elevation. To study the impact of our two purposed factors—namely, height and virtual legs--we conducted series of two-tailed paired T-tests between relevant groups divided based on the presence of the focused factor. The results of the paired T-test are valid as long as the distribution of the data for each group is normal, and each participant is compared with himself/herself. To test the normality of the data, the Anderson-Darling test was performed for each comparison executed between the two paired groups (Anderson and Darling 1952). For each comparison case, the null hypothesis was not rejected. More specifically, the results of the 'normality tests' showed that the distribution of the paired groups data is normally distributed.

By statistically comparing the gait durations across all scenarios, we found out that (1) LEGS: by enhancing the participants' virtual models with virtual legs, the duration of the ground walking trials increased significantly compared to cases in which the virtual legs

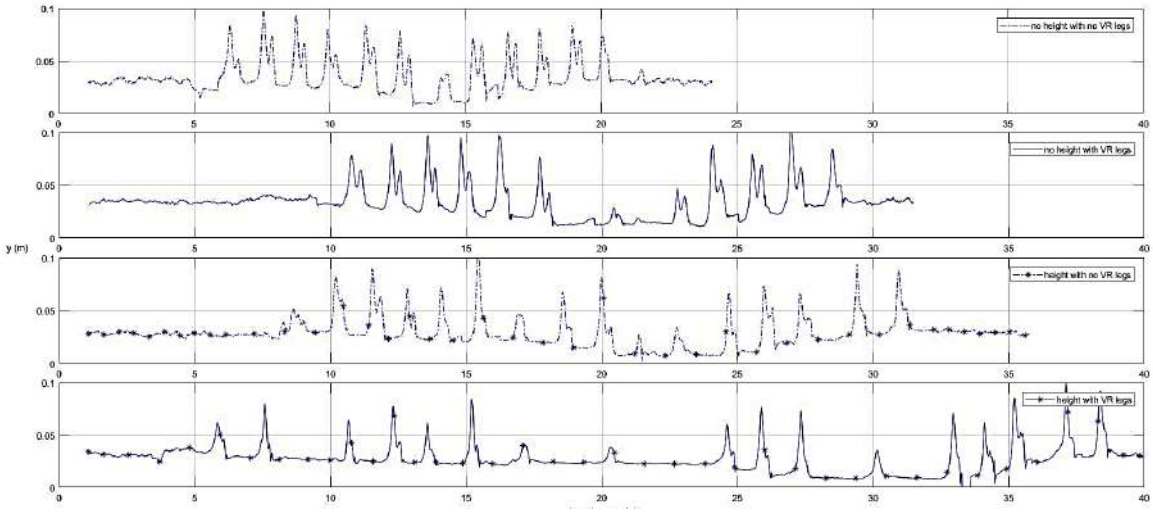

Figure 2. Comparison of the gait patterns of a sample participant during the four trials. The continues lines and those accompanied by the Astrid sign '*' represent the usage of VR legs and the presence of VR height respectively.

Table 2. Two-tail paired T test's significant level of mean differences between each pair of groups (P values)

		average		**variability (sd)**	
	Exp. Duration	stride length	stride height	stride length	stride height
no L[1] (H vs. no H)	0.0052*	0.0145	0.7609	0.6631	0.0678
L (H vs. no H)	0.0305*	0.0000**	0.6554	0.4850	0.0281*
no H(L vs. no L)	0.0004**	0.4464	0.0227*	0.2518	0.7381
H(L vs. no L)	0.2912	0.2968	0.2634	0.0884	0.7290

[1] L: VR legs, H: height
* Sig. at 0.05 level
** Sig. at 0.01 level

were not present (P value= 0.0004). Also, the paired T-test showed that the presence of VR legs noticeably decreased the average gait stride height on the non-elevated walking path. Interestingly, no significant increase in the duration of the trials performed at height was observed while the effect of virtual legs was considered, and (2) HEIGHT: while the participants were able to use their virtual legs in the manifestation of height, the average stride length of the participants decreased significantly (P value= 0.00004). Even without the virtual legs, a similar height effect was detected (P value=0.015). In addition, the duration of the trials performed with (P value=0.03) and without (P value=0.005) virtual legs was noticeably increased once the subjects were exposed to height. No prominent difference in the stride heights was detected with or without the presence of height. However, the stride height variability was meaningfully increased when the participants, equipped with the enhanced model, were subjected to height (P value=0.02).

5 Discussion and Conclusion

By analyzing the data regarding the basic spatiotemporal variables of stride length and speed, we detected a noticeable stride length difference across different scenarios. More precisely, when we focused on height as the influential factor, we observed that the number of strides significantly increased while the average stride length significantly decreased. Hence, these reductions of participants' gait speed and stride length imply that the participants attempted to walk more "carefully." The decrease in gait speed and stride length between ground and elevated walking is in line with Sheik_Nainar and Kaber's findings [34]. Also, Schniepp et al.'s experiment results [35] demonstrated the same bodily reactions from participants subject to destabilizing

environments. The decrease in stride length as a result of participants being asked to walk on the elevated path confirms Schniepp et al.'s previous results, with the only difference being a real elevated path for their experiments as compared to a VR simulation in ours.

Another interesting result was the reduction in the average stride length combined with an increase in both the average stride height and the duration of the trials once the participants had access to the enhanced VR model for the ground walking trials. In other words, with the presence of virtual legs, the participants walked on the path instead of just 'following the path.' This would imply that the use of responsive and real-time tracking virtual legs will increase the level of realism for the participants. However, a similar statistically significant result was not spotted for the elevated walking trials. The average participant's stride length did not decrease significantly (P-value=0.296). This finding perhaps indicates that height was the dominant factor here, reducing the average stride length even without the presence of the virtual legs.

Based on the result of table 2, the stride height variability was significantly affected by height as well (P-value=0.0281). The standard deviation of the stride height was lower for the data obtained from the ground walking trial with the presence of virtual legs compared to those extracted from the elevated path that also included the presence of virtual legs. This higher level of walking disorder parameters can be affected by the fear of height [32]. The thought-provoking part of these findings was that, in the absence of virtual legs, there were no significant variability differences between the two datasets pertaining to ground walking and walking on the height. Whether the cause of this phenomenon was the participants' attempts to place their feet exactly on the beam or the participants' experience of changes in their visual and vestibular systems, we cannot know for sure. However, it is quite apparent that the presence of virtual legs has an impact on the gait parameters, even for the higher level of walking disorder parameters. Therefore, we conclude that walking on the virtual structural beams without being able to look at one's virtual legs is less realistic than when someone walks with virtual legs in view.

Overall, these findings show that VR, along with the advanced virtual models, was successful in inducing the height effect on the basic spatiotemporal variables related to gait. Since these variables are essential to postural sway and gait stability measurements, the finding of the current study could be a good start in designing efficient, height-related experiments for construction workers' posture and gait assessments with fewer safety concerns. In addition, many of these virtual experiments can be integrated with other evolving construction safety studies such as eye-tracking and risk perception [36,37], cultural factors and risk perception [38], and intoxication at construction sites [39].

References

[1] Bureau of Labor Statistics Data, (2018). https://data.bls.gov/timeseries/FWU00X4XXXXX8EN00 (accessed January 10, 2019).

[2] H. Hsiao, P. Simeonov, Preventing falls from roofs: a critical review, Ergonomics. 44 (2001) 537–561. doi:10.1080/00140130110034480.

[3] C.C. Boffino, C.S. Cardoso de Sa, C. Gorenstein, R.G. Brown, L.F.H. Basile, R.T. Ramos, Fear of heights: Cognitive performance and postural control, Eur. Arch. Psychiatry Clin. Neurosci. 259 (2009) 114–119. doi:10.1007/s00406-008-0843-6.

[4] E. Keshner, Virtual reality and physical rehabilitation: a new toy or a new research and rehabilitation tool?, J. Neuroeng. Rehabil. 1 (2004) 8. doi:10.1186/1743-0003-1-8.

[5] G. Burdea, P. Coiffet, Virtual reality technology, J. Wiley-Interscience, 2003. goo.gl/W5x41J (accessed July 26, 2017).

[6] T.S. Mujber, T. Szecsi, M.S.J. Hashmi, Virtual reality applications in manufacturing process simulation, J. Mater. Process. Technol. 155–156 (2004) 1834–1838. doi:10.1016/j.jmatprotec.2004.04.401.

[7] C.G.C. Horlings, M.G. Carpenter, U.M. Küng, F. Honegger, B. Wiederhold, J.H.J. Allum, Influence of virtual reality on postural stability during movements of quiet stance, Neurosci. Lett. 451 (2009) 227–231. doi:10.1016/j.neulet.2008.12.057.

[8] T.W. Cleworth, B.C. Horslen, M.G. Carpenter, Influence of real and virtual heights on standing balance, Gait Posture. 36 (2012) 172–176. doi:10.1016/j.gaitpost.2012.02.010.

[9] S. Greffou, A. Bertone, J.-M. Hanssens, J. Faubert, Development of visually driven postural reactivity: a fully immersive virtual reality study., J. Vis. 8 (2008) 15.1-10. doi:10.1167/8.6.426.

[10] A. Mirelman, I. Maidan, T. Herman, J.E. Deutsch, N. Giladi, J.M. Hausdorff, Virtual reality for gait training: Can it induce motor learning to enhance complex walking and reduce fall risk in patients with Parkinson's disease?, Journals Gerontol. - Ser. A Biol. Sci. Med. Sci. 66 A (2011) 234–240. doi:10.1093/gerona/glq201.

[11] T. Tossavainen, M. Juhola, I. Pyykkö, H. Aalto, E.

Toppila, Virtual reality stimuli for force platform posturography, Stud. Health Technol. Inform. 90 (2002) 78–82. doi:10.3233/978-1-60750-934-9-78.

[12] H.S. Wallach, M. Bar-Zvi, Virtual-reality-assisted treatment of flight phobia, Isr. J. Psychiatry Relat. Sci. 44 (2007) 29–32.

[13] T. Abdelhamid, J. Everett, Identify Root Causes of Construction Accidents, J. Constr. Eng. Manag. 126 (2000) 52–60. doi:10.1061/(ASCE)0733-9364(2000)126:1(52).

[14] T.G. Bobick, Falls through Roof and Floor Openings and Surfaces, Including Skylights: 1992–2000, J. Constr. Eng. Manag. 130 (2004) 895–907. doi:10.1061/(ASCE)0733-9364(2004)130:6(895).

[15] J. Hinze, J. Gambatese, Factors That Influence Safety Performance of Specialty Contractors, J. Constr. Eng. Manag. 129 (2003) 159–164. doi:10.1061/(ASCE)0733-9364(2003)129:2(159).

[16] Y. Kang, S. Siddiqui, S.J. Suk, S. Chi, C. Kim, Trends of Fall Accidents in the U.S. Construction Industry, J. Constr. Eng. Manag. 143 (2017) 04017043. doi:10.1061/(ASCE)CO.1943-7862.0001332.

[17] T. Parsons, T. Pizatella, Safety analysis of high risk activities within the roofing industry., NTIS, SPRINGFIELD, VA(USA). 1984. (1984). goo.gl/Jt7t6v (accessed July 27, 2017).

[18] K. Hu, H. Rahmandad, T. Smith-Jackson, W. Winchester, Factors influencing the risk of falls in the construction industry: a review of the evidence, Constr. Manag. Econ. 29 (2011) 397–416. doi:10.1080/01446193.2011.558104.

[19] E.H. Sinitksi, K. Terry, J.M. Wilken, J.B. Dingwell, Effects of perturbation magnitude on dynamic stability when walking in destabilizing environments, J. Biomech. 45 (2012) 2084–2091. doi:10.1016/j.jbiomech.2012.05.039.

[20] T. Paillard, F. Noé, Effect of expertise and visual contribution on postural control in soccer, Scand. J. Med. Sci. Sport. 16 (2006) 345–348. doi:10.1111/j.1600-0838.2005.00502.x.

[21] J. Faubert, R. Allard, Effect of visual distortion on postural balance in a full immersion stereoscopic environment, in: A.J. Woods, J.O. Merritt, S.A. Benton, M.T. Bolas (Eds.), Proc. SPIE, Vol. 5291, p. 491-500 (2004)., 2004: pp. 491–500. doi:10.1117/12.527017.

[22] N.J. Minshew, K. Sung, B.L. Jones, J.M. Furman, Underdevelopment of the postural control system in autism., Neurology. 63 (2004) 2056–61. http://www.ncbi.nlm.nih.gov/pubmed/15596750 (accessed July 27, 2017).

[23] H. Jebelli, C.R. Ahn, T.L. Stentz, Fall risk analysis of construction workers using inertial measurement units: Validating the usefulness of the postural stability metrics in construction, Saf. Sci. 84 (2016) 161–170. doi:10.1016/j.ssci.2015.12.012.

[24] S.A. England, K.P. Granata, The influence of gait speed on local dynamic stability of walking, Gait Posture. 25 (2007) 172–178. doi:10.1016/j.gaitpost.2006.03.003.

[25] X. Qu, Effects of cognitive and physical loads on local dynamic stability during gait, Appl. Ergon. 44 (2013) 455–458. doi:10.1016/j.apergo.2012.10.018.

[26] D.L.C. Rosenstein MT, Collins JJ, A practical method for calculating largest Lyapunov exponents from small data sets, Phys D. 65 (1993) 117–134.

[27] P.M. McAndrew, J.B. Dingwell, J.M. Wilken, Walking variability during continuous pseudo-random oscillations of the support surface and visual field, J. Biomech. 43 (2010) 1470–1475. doi:10.1016/j.jbiomech.2010.02.003.

[28] B.O. Rothbaum, L.F. Hodges, R. Kooper, D. Opdyke, J.S. Williford, N. North, Effectiveness of computer generated (virtual reality) graded exposure in the treatment of acrophobia, Am. J. Psychiatry. 152 (1995) 626–628. doi:10.1176/ajp.152.4.626.

[29] T. Brandt, F. Arnold, W. Bles, T.S. Kapteyn, The mechanism of physiological height vertigo. I. Theoretical approach and psychophysics., Acta Otolaryngol. 89 (1980) 513–23.

[30] H.T. Regenbrecht, T.W. Schubert, F. Friedmann, Measuring the Sense of Presence and its Relations to Fear of Heights in Virtual Environments, Int. J. Hum. Comput. Interact. 10 (1998) 233–249. http://www.igroup.org/schubert/papers/regenbrecht_schubert_friedmann_ijhci98.pdf (accessed December 29, 2018).

[31] D.D. Espy, F. Yang, T. Bhatt, Y.-C. Pai, Independent influence of gait speed and step length on stability and fall risk., Gait Posture. 32 (2010) 378–82. doi:10.1016/j.gaitpost.2010.06.013.

[32] F. Ayoubi, C.P. Launay, A. Kabeshova, B. Fantino, C. Annweiler, O. Beauchet, The influence of fear of falling on gait variability: results from a large elderly population-based cross-sectional study., J. Neuroeng. Rehabil. 11 (2014) 128. doi:10.1186/1743-0003-11-128.

[33] M.E. Chamberlin, B.D. Fulwider, S.L. Sanders, J.M.

Medeiros, Does Fear of Falling Influence Spatial and Temporal Gait Parameters in Elderly Persons Beyond Changes Associated With Normal Aging?, 2005. https://core.ac.uk/download/pdf/85214868.pdf (accessed December 30, 2018).

[34] M.A. (Nort. C.S.U. Sheik_Nainar, D.C.S.U. Kaber B., The Utility of a Virtual Reality Locomotion Interface for Studying Gait Behavior, Hum. Factors. 4 (2007) 696–709. doi:10.1518/001872007X215773.

[35] R. Schniepp, G. Kugler, M. Wuehr, M. Eckl, D. Huppert, S. Huth, C. Pradhan, K. Jahn, T. Brandt, J. Wagner, J. Kline, T.M. Lau, Quantification of gait changes in subjects with visual height intolerance when exposed to heights, Front. Hum. Neurosci. 8 (2014). doi:10.3389/fnhum.2014.00963.

[36] M. Habibnezhad, S. Fardhosseini, A.M. Vahed, B. Esmaeili, M.D. Dodd, The Relationship between Construction Workers' Risk Perception and Eye Movement in Hazard Identification, in: Constr. Res. Congr. 2016 Old New Constr. Technol. Converg. Hist. San Juan - Proc. 2016 Constr. Res. Congr. CRC 2016, 2016. doi:10.1061/9780784479827.297.

[37] S. Boheir, S. Hasanzadeh, B. Esmaeili, M.D. Dodd, S. Fardhosseini, MEASURING CONSTRUCTION WORKERS' ATTENTION USING EYETRACKING TECHNOLOGY, in: 5th Int. Constr. Spec. Conf., Univ. of British Columbia, Vancouver, 2015. https://www.researchgate.net/publication/288516371 (accessed March 21, 2019).

[38] M. Habibnezhad, B. Esmaeili, The Influence of Individual Cultural Values on Construction Workers' Risk Perception, 52nd ASC Annu. Int. Conf. Proc. (2016). http://ascpro.ascweb.org/chair/paper/CPRT211002016.pdf (accessed October 30, 2017).

[39] M.S. Fardhosseini, B. Esmaeili, The Impact of the Legalization of Recreational Marijuana on Construction Safety, in: Constr. Res. Congr. 2016, American Society of Civil Engineers, Reston, VA, 2016: pp. 2972–2983. doi:10.1061/9780784479827.296.

Experiencing Extreme Height for The First Time: The Influence of Height, Self-Judgment of Fear and a Moving Structural Beam on the Heart Rate and Postural Sway During the Quiet Stance

M. Habibnezhad[a], J. Puckett[a], M.S. Fardhosseini[b], H. Jebelli[c], T. Stentz[a], L.A Pratama[b]

[a]Durham School of Architectural Engineering and Construction, University of Nebraska-Lincoln, USA
[b]Department of Construction Management, College of Built Environments, University of Washington, USA
[c]Department of Architectural Engineering, The Pennsylvania State University, USA
E-mail: mahmoud@huskers.unl.edu, jay.puckett@unl.edu, sadrafh@uw.edu, jebelli.houtan@gmail.com, tstentz1@unl.edu, pragungl@uw.edu

Abstract –

Falling from elevated surfaces is the main cause of death and injury at construction sites. Based on the Bureau of Labor Statistics (BLS) reports, an average of nearly three workers per day suffer fatal injuries from falling. Studies show that postural instability is the foremost cause of this disproportional falling rate. To study what affects the postural stability of construction workers, we conducted a series of experiments in the virtual reality (VR). Twelve healthy adults—all students at the University of Nebraska-Lincoln—were recruited for this study. During each trial, participants' heart rates and postural sways were measured as the dependent factors. The independent factors included a moving structural beam (MB) coming directly at the participants, the presence of VR, height, the participants' self-judgment of fear, and their level of acrophobia. The former was designed in an attempt to simulate some part of the steel erection procedure, which is one of the key tasks of ironworkers. The results of this study indicate that height increase the postural sway. Self-judged fear significantly was found to decrease postural sway, more specifically the normalized total excursion of the center of pressure (TE), both in the presence and absence of height. Also, participants' heart rates significantly increase once they are confronted by a moving beam in the virtual environment (VE), even though they are informed that the beam will not 'hit' them. The findings of this study can be useful for training novice ironworkers that will be subjected to height and/or steel erection for the first time.

Keywords –

Virtual reality, Postural sway, Height, moving structural beam, Heart rate, Construction safety

1 Introduction

The growing rate of injuries and fatalities due to falling is concerning. In 2017, more than 5147 workers died at job sites, from which 887 were fall-related accidents [1]. Unfortunately, these fall-related losses have reached to the highest level in the 26-year history of the Census of Fatal Occupational Injuries (CFOI)[2]. This fact indicates that current safety procedures, training, and precautions have not adequately limited these types of injuries and fatalities at construction sites.

Therefore, numerous research studies have been conducted to shed lights on the important predictors of falling [3]. Some studies presented risk perception of construction workers as the key driver for these incidents, suggesting that the workers' engagement in unsafe situations results in severe injuries and death [4–6]. These types of studies are valuable in investigating the risk-taking behavior of construction workers [7]. However, the factors affecting postural stability of the workers can address more fall incidents, considering scenarios in which the worker has already executed the task [8].

Postural stability is the result of an association between three main sensory cues, namely, visual, vestibular, and somatosensory systems. The foremost mission of these balance control systems is to maintain the equilibrium of the center of mass of the body against direct or indirect stimuli. Accordingly, to find the root causes of postural instability, first, one needs to discover these provoking factors. Interestingly, from the three sensory cues for postural stability regulation, visual input

is the proactive mechanism of balance, while the other two balance mechanisms of the body, triggered after the external exposure, considered reactive mechanisms. Therefore, the focus of this study would be mainly on the visual inputs as the dominant instigating factors. According to Hsiao and Simeonov, elevation, moving visual scenes, and depth perception are the most commonly visual perturbations affecting balance [8]. Not only these visual perturbations cause instigating mismatch and affect balance, but the exertion of anxiety due to the unsafe nature of these factors, especially those present at construction sites, will influence postural stability as well.

Following this rational, many studies strived to find out the extent to which anxiety (fear) impact postural regulation parameters. Interestingly, the result of these studies demonstrated that the presence of fear, especially in great extents, will negatively impact postural stability [9,10]. Notably, most of these research studies examined fear by utilizing various fear and acrophobia questionnaires. While these 'passive' questionnaires are reliable in measuring the self-judged level of anxiety, however, the need for more 'active' methods in determining the anxiety level of construction workers, subjected to fearful visual perturbations, seems necessary. Methods such as measuring variations in the facial temperature [11] the level of salivary cortisol [12], and heart rate [13] can imply the anxiety level. The latter could be misleading since many activities will impact the heart rate and diminish the reliability of the results. On the other hand, measuring heart rate is simple and inexpensive due to the ubiquity of smartwatches such as Fitbit and Apple watch. Considering the caveats above, this study attempts to investigate if heartrate variability across different trials is significantly affected by provoking visual factors.

2 Point of Departure

The current study will reinvestigate the impact of visual stimuli and fear on the postural stability through the precise and realistic simulation of the environment and virtual body parts (mixed reality). In other words, this research strives to create a virtual environment (VE) of the construction sites, in which participants will be exposed to 1. extreme height and 2. a moving structural beam directed towards participants as a part of the steel erection simulation. Also, the impact of these stimuli on the heart rate of the participant will be measured precisely. To our knowledge, very few studies utilize heart rate for these types of tasks happening at the construction sites.

3 Background

3.1 Impact of height on the visual sensory system. As previously described, one of the most prominent reasons behind slip, trip, and falling is the loss of balance. As such, finding the influential factors which trigger instability in humans, especially those working at great height, is of utmost importance. The integration of the visual, vestibular, and somatosensory sensory systems is essential in maintaining one's postural balance. Some studies suggest that visual sensory system is the dominant system in controlling the human body's postural balance [14] and essential for maintaining balance [15–17]. In addition, the visual sensory system can compensate for the lack of other balance-dependent sensory systems, vestibular and somatosensory, in the presence of visually-induced disturbances. While each sensory system's weight on the postural stability is dependent on the environmental context and goal of the study [16], the importance of visual input as the prominent indicator of postural balance alludes that study of visual perturbations should be researched more extensively. Considering one in three people has visual height intolerance [18], many studies suggest height as an important stimuli in provoking gait instability and susceptibility to falling [19–22]. Studies examining height and fear of falling have reported that the deficit of close visual contact due to the instigating sensory mismatch, and fear-related reactions, especially close to edges of elevated surfaces, are the two main characteristics of falling from an elevated surface [8,23]. Following these findings, the current study aims to explore the aforementioned instigating factors, height, and the corresponding fear, on the postural sway of the participants subjected to virtual height.

3.2 Fear of height. Fear is a bodily response to a danger or hazard in the form of emotional or physical reacts. Sometimes, these responses can be alarming, adversely influencing the humans' health and performance ranging from the reluctance of going to a dentist to changes in the gait and postural stability on elevated surfaces [24,25]. In light of the foregoing, it is important to consider fear and the fear of height (person's level of acrophobia) as leading factors influencing gait and postural stability [26]. Accordingly, in the current study, two questionnaires were presented to the participants, one for generally measuring fear and one for exclusively measuring the level of acrophobia of each subject. Although the focus of this study is on the height-related factors impacting safety, the circular contribution of visuo-vestibular to the fear and anxiety should not be ignored [21]. Coelho and Balaban stated that visuo-vestibular are not only associated with the fear of height, but also with panic and driving. Therefore, along with the acrophobia questionnaire (AQ), the famous James Geer

fear measurement scale [27] has been utilized to pinpoint the potential relationship between any of the aforementioned fear aspects to the changes in the gait and postural stability parameters. Later, it will be shown that those questions related to sharp objects, driving, and auto accident, height, airplane, roller coasters, and death, appropriately predict height while only-height related questions were incapable of addressing postural parameter changes due to height. While these self-judgmental scales possibly show the self-perceived fear, however, the consideration of physiological responses to the experiment trials can be beneficial as well. The number of heartbeats per minute (HBM) is suggested to be a good indicator of the emotional responses to the unexpected thread or danger [13]. Therefore, in this study, the HBM factor was considered to be informative and included in the data collection process.

4 Methodology

4.1 Participants. Based on the flyer approved by the institutional review board (IRB), we recruited 13 students from the University of Nebraska-Lincoln (UNL). Although randomization was considered in the recruiting process, we attempted to selectively recruit an equal number of males and females, so that the potential influential sex factor could be precisely considered. As a result, six females and seven males were selected for of this study. The average age of the volunteers was 29 years old. The participants had no previous falling experience or any problem with standing still.

4.2 Apparatuses and software. To measure the center of pressure (COP) of the participants and consequently calculate the postural sway parameters, the AMTI force plate was utilized, which is capable of accurately calculating COP based on the reaction forces of the plate. Later, by utilizing an in-house code in MATLAB, all the necessary parameters for the postural sway, and heart rate would be imported and calculated. The HTC Vive Pro headset was selected for the immersive virtual environment demonstration. We chose the Vive Pro over other brands since the resolution and display quality of the headset is believed to be higher. As for the game engine software, the Unity3D software [28] was used, so that the creation of the immersive environment and all the VR simulations such as induction of height and the moving structural beam would be easily performed. Finally, to collect the heart rate of the participants, we used a Fitbit Versa. To easily and precisely synchronize the heart rate collection with the other devices, a heart rate collector application was developed in Fitbit studio, so that the start and stop events for each trial could be triggered on the Fitbit Versa remotely from a smartphone.

4.3 Questionnaires. Prior to the experiments, to predict the participants' self-judgment fear scale, the electronic version of James Geer's questionnaire [27] was presented to each participant. In addition, to measure their level of acrophobia, participants were asked to fill out the Cohen acrophobia questionnaire (AQ) as well [29]. As mentioned before, we attempted to find out if the results of these questionnaires can be promising in predicting the physiological responses such as heart rate or postural sway, in different study setups.

4.4 Experiments. The first part of the experiment was designed to help the participants get familiar with the VR environment. The VR environment was the same environment for all parts of the data collection. To potentially improve the feeling of presence in the VR environment, the VR model was enhanced with virtual legs. To ensure that the learning curve effect would be minimal for the participants, prior to conducting the experiment, they were asked to stand, walk, and look at their virtual legs for 1 minute. The force plate was placed on a specific location in an office so that the initial standing position of the participants became the designated location in the virtual environment (VE). In the second part of the experiment, the participants were asked to stand in the center of the force plate and open their legs to the extent to which they are comfortable and most stable. After 5 seconds, the participants were asked to look at their feet once, for 2 seconds, with the least movement possible. This movement will affect the postural stability of the participants; however, they were instructed to perform the same task in the other trials. Therefore, the data collection would be consistent and not biased. This trial finished after 20 seconds. During the trial, the heart rate and COP of the participants were retrieved. After the completion of the first part, the participants were equipped with the VR headset, while they were asked to hold the initial position of their feet on the force plate. In the second trial, the same procedure as the previous trial was undertaken, however, virtually.

The participants were asked to look at their 'virtual feet' in the same way as before. To ensure that the experiment complies with that of the quiet stance postural balance, no subject was allowed to look down more than once. After 20 seconds, a moving structural beam hung from a crane wire, slowly approached the participants. The moving beam's trajectory was in line to the participant's site of view. Before the start of this trial, each participant was informed that the virtual beam will not 'hit' them and will stop 1ft away from their body. This part of the experiment took 10 seconds to finish. The last part of the experiment was almost identical to the second part of the experiment, however, this time the participants were placed on the 17th floor of an unfinished building. The VE, standing beam, moving beam, lighting, shadows, and other virtual scenes were identical to the pervious trial, except the height. Again,

before the start of this trial, all the participants were informed that the moving beam will slowly approach them and will not 'hit' or 'pass through' them. With the last 10 seconds of the moving structural beam approaching the participants, the overall duration of this part was 30 seconds.

Table 1. Experiment configuration

Scenarios					
No Height			Height		
No VR	VR - No MB	VR - MB	No VR	VR - No MB	VR - MB

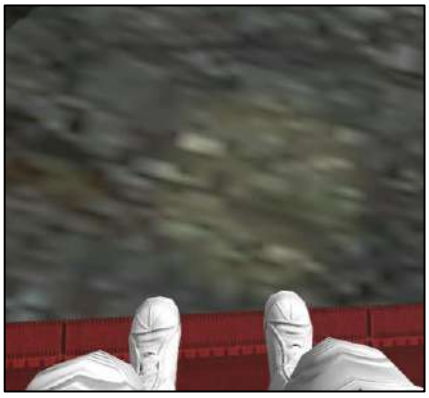

(a)

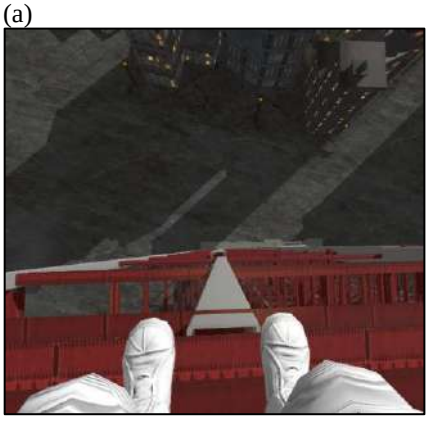

(b)

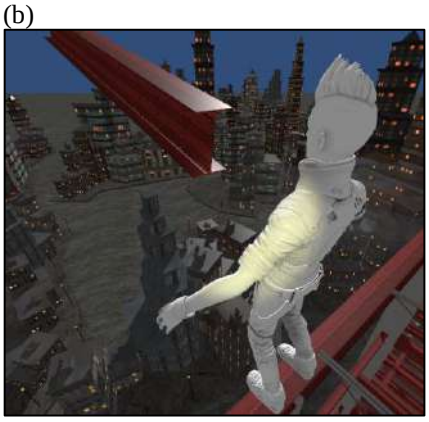

(c)

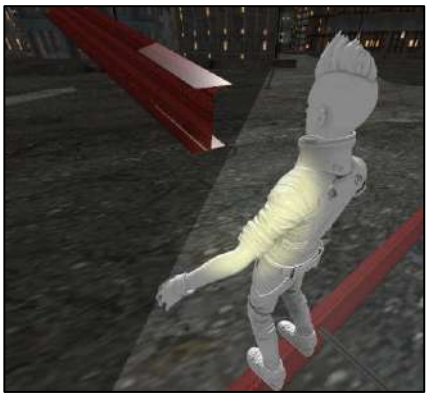

(d)

Figure 1. All the virtual scenarios in the experiments. The (a) image is no height and no MB scenario, and the (b) is height and no MB. The (c) image is no height and MB scenario, and the (d) image is height and MB.

5 Results and Analysis

All the data was imported from different text files generated throughout the experiments and then tabulated for statistical analysis. By using the MATLAB statistical toolbox, standard two-tail T-test was performed on the table of experiment results. It is important to note that the normality of the data was tested by performing the Anderson-Darling test [30] and turned out to be valid for this study. For the first part of the analysis, all the data was tabulated for a within-subject design case in which the same subjects perform in all the levels of independent variables. The result of the paired T-tests for such an analysis can be investigated in Table 2. The dependent factors were heart rate and postural parameters. The independent variables were the presence of VR, Height, MB on the ground (no height), and MB at height. Four postural parameters were considered in this research: 1. Total Excursion (TE) of the COP throughout the trial duration, 2. Root-mean-square (RMS) amplitude is representing the variability (standard deviation) of the COP displacement. 3. Maximum absolute amplitude distance of the COP traveled during the trial duration, and 4. Peak-to-Peak (PP) amplitude is expressing the maximum displacement shown between two COP points during the trial. As shown in Table 2, there was a statistically significant difference between the heart rate of the participants subject to the MB on the ground and at height with the P value of 0.00005. Based on the descriptive results, the HRMs of the participants increased by almost 10 percent. Another interesting case was the significant increase in the TE of the participants exposed to VR for the first time. Although prior to the data collection, they experienced VR, the significant increases in all the postural parameters were noticeable.

Table 2. T test's significant level of mean differences between each pair of groups (P values)

	P-values			
	Presence of VR	Height	MB (no Height)	MB (Height)
Heart rate	.190	.554	.00005**	. 00005**
Postural sway (TE)	.004**	.052*	.497	.890
Postural sway (RMS)	.066	.174	.095	.584
Postural sway (Max)	.057	.156	.112	.694
Postural sway (PP)	.017*	.084	.123	.670

* Sig. at 0.05 level
** Sig. at 0.01 level

Table 3. Descriptive standard two-tail unpaired T-test mean results for HR and RMS based on the participants' sex, fear (selective questions) and AQ

		No height			Height	
	Groups	No VR	VR - No MB	VR – MB	VR - No MB	VR – MB
Sex (HRM)	Male	83.23	82.31*	90.65*	80.74*	89.65
	Female	86.73	99.18*	111.42*	98.26*	105.98
Fear[1] (HRM)	Low[2]	85.98	87.75	98.73	87.83	98.11
	High	83.98	90.93	99.88	88.25	97.51
AQ (HRM)	Low	85.06	88.01	98.18	89.43	94.95
	High	84.90	90.66	100.43	86.65	100.68
Sex (RMS)	Female	. 000217	.000341	.000350*	.000447	.000265*
	Male	.000284	.000530	.001318*	.000588	.000845*
Fear (RMS)	Low	.000249	.000292	.000693	.000275*	.000395
	High	.000251	.000579	.001136	.000784*	.000812
AQ (RMS)	Low	.000199	.000370	.000591	.000336	.000341
	High	.000302	.000501	.001238	.000722	.000865

Besides, Table 2 demonstrates that the mean difference between the TE of the subjects collected during the quiet stance in VR on the ground and their TE during the quiet stance in VR at height was statistically significant with the P value of 0.05. In other words, the TE of the participants increased when they were subjected to height. For each trial, to measure the impact of the participants' self-judged fear values on the heart rate and postural stability, an in-between subject design was performed on the tabulated data. James Geer's fear questionnaire consists of 50 questions collected based on the empirical data and participants' reports [27]. The questions range from auto accidents, being a passenger in an airplane, and height to hypodermic needles, being alone, and crowded places. Since many of these questions may not be strongly correlated to our physiological responses at height, we conducted various test aimed to find out which of these questions best describe the fear of height. Considering Coelho and Balaban's visuo-vestibular study [21], and the result of this study, we find out that "sharp edges", "being a passenger in an airplane", "roller coasters", "death", "heights", "driving a car", and "auto accidents", are strongly in line with the visuo-vestibular predicting factors and leads to statistically significant results in our study. To account for the factor of sex, the participants were divided into two groups of male and female, respectively. The data was then sorted based on

the level of fear reported by the subjects and split into two groups of less fearful and more fearful subjects. The same procedure was undertaken for the AQ factor. The result of the unpaired T-tests on the two groups of the participants can be seen in table 3.

By focusing on the P values of the T-tests on each of the paired groups, the significant mean differences between the groups are recorded in table 3. As reported in this table, in VR with no height and the presence of MB, the male group has a statistically significant lower average HRM compared to the female group. Interestingly, the difference between the RMS of the 'fearful' and 'non-fearful' group was significant (P value = 0.023) for the same scenario, VR with MB and no height. Besides, the presence of height in VR played a key role in differentiating between the RMS of the fearful and non-fearful participants; The participants with more self-reported fear had a higher RMS mean compared to those with less self-reported fear (P-value = 0.046). A similar effect was manifested when the two male and female groups were compared concerning their HR differences during the quiet stance at height. Females had higher HR compared to males. Notably, no statistical difference was spotted between the male and female groups for RMS at height in the absence of MB. However, in the presence of MB at height, the result of T-test indicated that the mean RMS of the females was significantly higher (P value = 0.009) compared to that of males. Another important observation was the inability of AQ values in predicting the differences between the two groups of subjects separated by their levels of acrophobia.

6 Discussion and Conclusion

According to the statistical test results, the presence of a virtual environment has a substantial influence on the postural sway of the participants. Except for postural variability, RMS, almost all the other postural parameters increased for the participants who were experiencing VR for the first time. Based on similar findings of previous studies, the observed increase in the postural sway—due to the exposure to the immersive environment—was predictable [31].

Furthermore, participants were asked to 'normally' look at their feet during the quiet stance in VR with the absence of height. Due to the lower field of view of the VR headsets compared to that of a person without wearing VR headsets, participants' postural balance might have been affected. Streepey et al., pointed out this limitation as a lack of peripheral visual inputs while wearing glasses [32]. Therefore, although the existence of such a factor in the comparison between VR trial cases is unlikely, its potential impact on the presence of VR cannot be rendered negligible. As for the impact of elevated surfaces on balance, the presence of height increased subjects' postural sway. Based on the statistically significant mean differences of the participants' TE, the presence of height factor was able to predict the difference in the means with the P value of 0.05. This finding was also in line with the results of the Cleworth et al., study [33]. They suggested that the virtual height reduces the mediolateral and anterior-posterior balance of subjects similar to the real height. Remarkably, the visual stimuli in the form of a moving object increased participants heartbeat dramatically. With a P value of 0.00005 both with and without the presence of height, the MB significantly increased participants' heart rates. These findings suggest that tasks involving handling of big moving objects, e.g., steel erection, will increase the heart rate of first-time workers exposed to the great extents. This physiological response to big approaching objects should be studied more extensively since the noticeably low P-value magnifies its importance in the context of safety. On the other hand, since the participants were informed that the approaching digital beam would not 'hit' them, no statistically significant mean changes were observed for their postural parameters.

Based on the results of the unpaired T-tests, those fear questions related to driving, height, and sharp objects, derived from James Geer's fear questionnaire, powerfully predict the differences in the RMS in the presence of virtual height. Accordingly, it can be inferred that fear increases RMS, in the presence of virtual height. In other words, standing on elevated surfaces, people with higher self-judged fear values have more postural sway variability compared to those with lower fear values. Adkin et al. showed that fear of height modifies the postural sway [34]. Based on the participants' anxiety rating, they suggested that balance would be affected by the fear of height factor. Similar to our findings, they concluded that both physiological variables, such as postural balance, and psychological factors, such as anxiety, may result in postural instability.

However, to our surprise, the AQ values were not able to address any changes in the postural stability, nor were they able to explain heart rate for different scenarios during quiet stance. One explanation for the incapability of AQ to address mean differences between the corresponding groups might be because this questionnaire was designed to detect abnormalities rather than differences concerning the fear of height. Therefore, since most of the participants did not score high on this questionnaire, then they latent differences regarding fear of height was not noticeable. Following this rationale, a threshold-based categorization should be conducted on the AQ results rather than the AQ mean-based approach. Since the threshold should not be less than 2 (Likert-scale range for AQ is from 1 to 5), so that it can detect people

with acrophobia, and most of our subjects' average AQ score was less than 2, we were not able to categorize with thresholds.

With respect to subjects' gender, at height, female subjects perceived a higher level of anxiety, in the form of HR, compared to male. Also, the average HR of female participants were higher compared to that of male, when they were confronted by the moving structural beam. Another interesting result was the influence of gender on the RMS. With the P values less than 0.05, their RMS values were significantly lower than male in both scenarios with MB. Therefore, regarding bodily responses in the proximity of big moving objects, seemingly, women HR increases more than men and men's RMS increases more than women. Considered as one of the limitations of the current study, prior information regarding VR studies could influence the postural stability of the participants as their uncertainty about the experiments mixes with the expectation of being at height. This unwanted effect potentially explains the differences between the postural stability of male and female groups in VR with the absence of any visual perturbations.

References

[1] Bureau of Labor Statistics Data, (2018). https://data.bls.gov/timeseries/FWU00X4XXXXX8EN00 (accessed January 10, 2019).

[2] NATIONAL CENSUS OF FATAL OCCUPATIONAL INJURIES IN 2017, (2018). www.bls.gov/iif/oshcfoi1.htm (accessed July 9, 2018).

[3] M.S. Fardhosseini, B. Esmaeili, The Impact of the Legalization of Recreational Marijuana on Construction Safety, in: Constr. Res. Congr. 2016, American Society of Civil Engineers, Reston, VA, 2016: pp. 2972–2983. doi:10.1061/9780784479827.296.

[4] T. Abdelhamid, J. Everett, Identify Root Causes of Construction Accidents, J. Constr. Eng. Manag. 126 (2000) 52–60. doi:10.1061/(ASCE)0733-9364(2000)126:1(52).

[5] H. Mahmoud, F. Sadra, V.A. Moghaddam, E. Behzad, D.M. D., The Relationship between Construction Workers' Risk Perception and Eye Movement in Hazard Identification, in: Constr. Res. Congr. 2016, 2017. doi:doi:10.1061/9780784479827.297.

[6] S. Boheir, S. Hasanzadeh, B. Esmaeili, M.D. Dodd, S. Fardhosseini, MEASURING CONSTRUCTION WORKERS' ATTENTION USING EYETRACKING TECHNOLOGY, in: 5th Int. Constr. Spec. Conf., Univ. of British Columbia, Vancouver, 2015. https://www.researchgate.net/publication/288516371 (accessed March 21, 2019).

[7] M. Habibnezhad, B. Esmaeili, The Influence of Individual Cultural Values on Construction Workers' Risk Perception, in: 52nd ASC Annual International Conference Proceedings, 2016. http://ascpro0.ascweb.org/archives/cd/2016/paper/CPRT211002016.pdf (accessed October 30, 2017).

[8] H. Hsiao, P. Simeonov, Preventing falls from roofs: a critical review, Ergonomics. 44 (2001) 537–561. doi:10.1080/00140130110034480.

[9] C.C. Boffino, C.S. Cardoso de Sa, C. Gorenstein, R.G. Brown, L.F.H. Basile, R.T. Ramos, Fear of heights: Cognitive performance and postural control, Eur. Arch. Psychiatry Clin. Neurosci. 259 (2009) 114–119. doi:10.1007/s00406-008-0843-6.

[10] H.T. Regenbrecht, T.W. Schubert, F. Friedmann, T.W. Schubert Ifrank Friedmann, Measuring the Sense of Presence and its Relations to Fear of Heights in Virtual Environments, Int. J. Hum. Comput. Interact. 10 (1998) 233–249. doi:10.1207/s15327590ijhc1003_2.

[11] I. Pavlidis, J. a Levine, P. Baukol, Ioannis Pavlidis Honeywell Laboratories Minneapolis , MN ioannis . pavlidis @ i), honeywell . com James Levine Mayo Clinic Mayo Clinic, IEEE Trans. Biomed. Eng. (2002) 315–318.

[12] S.A. Vreeburg, F.G. Zitman, J. Van Pelt, R.H. Derijk, J.C.M. Verhagen, R. Van Dyck, W.J.G. Hoogendijk, J.H. Smit, B.W.J.H. Penninx, Salivary cortisol levels in persons with and without different anxiety disorders, Psychosom. Med. 72 (2010) 340–347. doi:10.1097/PSY.0b013e3181d2f0c8.

[13] C. Schmitz, L. Drake, M. Laake, P. Yin, R. Pradarelli, Physiological Response to Fear in Expected and Unexpected Situations on Heart Rate, Respiration Rate and Horizontal Eye Movements, J. Adv. Student Sci. 1 (2012). http://jass.neuro.wisc.edu/2012/01/Lab 602 Group 10 Final Submission.pdf (accessed December 31, 2018).

[14] M.G. Gaerlan, The role of visual, vestibular, and somatosensory systems in postural balance, 2010. http://digitalscholarship.unlv.edu/thesesdissertations (accessed December 31, 2018).

[15] M. Friedrich, H.J. Grein, C. Wicher, J. Schuetze, A. Mueller, A. Lauenroth, K. Hottenrott, R. Schwesig, Influence of pathologic and simulated visual dysfunctions on the postural system, Exp. Brain Res.

186 (2008) 305–314. doi:10.1007/s00221-007-1233-4.

[16] L.M. Nashner, C.L. Shupert, F.B. Horak, F.O. Black, Organization of posture controls: An analysis of sensory and mechanical constraints, Prog. Brain Res. 80 (1989) 411–418. doi:10.1016/S0079-6123(08)62237-2.

[17] M. Schmid, A. Nardone, A.M. De Nunzio, M. Schmid, M. Schieppati, Equilibrium during static and dynamic tasks in blind subjects: No evidence of cross-modal plasticity, Brain. 130 (2007) 2097–2107. doi:10.1093/brain/awm157.

[18] D. Huppert, E. Grill, T. Brandt, Down on heights? One in three has visual height intolerance, J. Neurol. 260 (2013) 597–604. doi:10.1007/s00415-012-6685-1.

[19] F. Ayoubi, C.P. Launay, A. Kabeshova, B. Fantino, C. Annweiler, O. Beauchet, The influence of fear of falling on gait variability: results from a large elderly population-based cross-sectional study., J. Neuroeng. Rehabil. 11 (2014) 128. doi:10.1186/1743-0003-11-128.

[20] M.E. Chamberlin, B.D. Fulwider, S.L. Sanders, J.M. Medeiros, Does Fear of Falling Influence Spatial and Temporal Gait Parameters in Elderly Persons Beyond Changes Associated With Normal Aging?, 2005. https://core.ac.uk/download/pdf/85214868.pdf (accessed December 30, 2018).

[21] C.M. Coelho, C.D. Balaban, Visuo-vestibular contributions to anxiety and fear, Neurosci. Biobehav. Rev. 48 (2015) 148–159. doi:10.1016/J.NEUBIOREV.2014.10.023.

[22] P.I. Simeonov, H. Hsiao, B.W. DotsonM, D.E. Ammons, HEIGHT IN REAL AND VIRTUAL ENVIRONMENTS, Hum. Factors J. Hum. Factors Ergon. Soc. 6 (2005) 430–438. https://journals.sagepub.com/doi/pdf/10.1518/0018720054679506 (accessed December 31, 2018).

[23] T. Brandt, F. Arnold, W. Bles, T.S. Kapteyn, The mechanism of physiological height vertigo. I. Theoretical approach and psychophysics., Acta Otolaryngol. 89 (1980) 513–23.

[24] J.R. Davis, A.D. Campbell, A.L. Adkin, M.G. Carpenter, The relationship between fear of falling and human postural control, Gait Posture. 29 (2009) 275–279. doi:10.1016/J.GAITPOST.2008.09.006.

[25] S.M. Gordon, Dental fear and anxiety as a barrier to accessing oral health care among patients with special health care needs, Spec. Care Dent. 18 (1998) 88–92. doi:10.1111/j.1754-4505.1998.tb00910.x.

[26] C.M. Coelho, G. Wallis, Deconstructing acrophobia: physiological and psychological precursors to developing a fear of heights, Depress. Anxiety. 27 (2010) 864–870. doi:10.1002/da.20698.

[27] J.H. Geer, The Development Of A Scale To Measure Fear, Behav. Res. Ther. 3 (1965) 45–53.

[28] Unity - Game Engine, (2017). https://unity3d.com/ (accessed July 29, 2017).

[29] D.C. Cohen, Comparison of self-report and overt-behavioral procedures for assessing acrophobia, Behav. Ther. 8 (1977) 17–23. doi:10.1016/S0005-7894(77)80116-0.

[30] T.W. Anderson, D.A. Darling, Asymptotic Theory of Certain "Goodness of Fit" Criteria Based on Stochastic Processes, Ann. Math. Stat. 23 (1952) 193–212. doi:10.1214/aoms/1177729437.

[31] C.G.C. Horlings, M.G. Carpenter, U.M. Küng, F. Honegger, B. Wiederhold, J.H.J. Allum, U.M. Küng, F. Honegger, B. Wiederhold, J.H.J. Allum, Influence of virtual reality on postural stability during movements of quiet stance, Neurosci. Lett. 451 (2009) 227–31. doi:10.1016/j.neulet.2008.12.057.

[32] J.W. Streepey, R. V. Kenyon, E.A. Keshner, Field of view and base of support width influence postural responses to visual stimuli during quiet stance, Gait Posture. 25 (2007) 49–55. doi:10.1016/j.gaitpost.2005.12.013.

[33] T.W. Cleworth, B.C. Horslen, M.G. Carpenter, Influence of real and virtual heights on standing balance, Gait Posture. 36 (2012) 172–176. doi:10.1016/j.gaitpost.2012.02.010.

[34] A.L. Adkin, J.S. Frank, M.G. Carpenter, G.W. Peysar, Fear of falling modifies anticipatory postural control, Exp. Brain Res. 143 (2002) 160–170. doi:10.1007/s00221-001-0974-8.

Applying Eye Tracking in Virtual Construction Environments to Improve Cognitive Data Collection and Human-Computer Interaction of Site Hazard Identification

X. Ye[a] and M. König[a]

[a]Department of Civil and Environmental Engineering, Ruhr-University Bochum, Germany
E-mail: xuling.ye@rub.de, koenig@inf.bi.rub.de

Abstract –

In the Architecture, Engineering and Construction (AEC) field, eye tracking technology is being applied more frequently in cognitive research such as hazard identification. These studies typically use eye tracking in a diagnostic way and pay less attention to the application of virtual environment. However, in virtual environment, eye tracking not only can enhance the study of the cognitive process but also improves the human-computer interaction. Therefore, this paper elaborates on how we use eye tracking devices to track 3D objects in virtual environments diagnostically and interactively. First, we analyze the existing research gaps of using eye tracking in the construction industry. Then, we follow 3D object identification, diagnostic mode and interactive mode to develop a methodology by HTC VIVE device with Pupil Labs HTC Vive Binocular Add-on based on the research gaps. Finally, an example experiment is provided to demonstrate studying hazard identification using eye tracking in construction safety. For analyzing the eye movement data from the participants, we offer the number of confirmations, the scan path and the 3D heatmap of objects in both static and dynamic construction site scenes. This paper provides an approach of applying eye tracking to gather more data in virtual environment for the future cognitive studies and explores the possibility to improve human-computer interaction using eye tracking in the construction industry.

Keywords –

Eye Tracking; Virtual Environment; Human-Computer Interaction; Site Hazard Identification

1 Introduction

The construction industry has been in an era of transformation and reorganization for years. Not only the complexity of construction projects is increasing, but also the technical challenges influence the work on the construction site. A high construction quality is to be guaranteed in even shorter time. Health and safety at work is one of the most important goals of a construction project. However, statistics on accidents at work show that workers on construction sites worldwide are exposed to higher risks than in other industries [1]. The identification of hazards on construction sites is therefore becoming increasingly important. However, hazards cannot be entirely identified on dynamic and complex construction sites since humans cannot simultaneously notice all possible hazards at once. Therefore, actions to increase the safety on construction sites include intensive training and a clear hazard identification. Whether a certain object is identified as hazard can only be determined by intensive testing. It is important, especially on complex construction sites, that hazards are identified as quickly as possible. The availability of different technologies means that these studies can now be evaluated more comprehensively, realistically and detailed.

In existing research, eye tracking is commonly used as a tool to study the cognitive process by collecting the eye movement data at the viewing direction from 2D pictures or real sites, but neglecting which particular object the viewer is looking at. In this way, even the 3D objects in real scenes have no connection with the eye movement data. Jeelani et al. [2] presents a method to facilitate the recognition of objects in the real site. As a post-recognition method, it still does not provide a connection between the eye movement and objects. In these cases, by ignoring the distance between viewer and the viewing object, viewing 3D objects will not provide more information than 2D images.

Combining eye tracking with virtual environment can easily build connection between viewer and the viewing objects. Moreover, the eye movement data collected from a digital model of a construction site can also be made available directly in a virtual environment. Using virtual reality allows a realistic representation of a complex situation on a construction site without exposing the viewer to a real danger [3].

In the context of this paper, an approach to the

systematic use of eye tracking and virtual reality for the analysis of eye movement data is presented. It will be shown how objects can be identified based on available technologies and how the data can be collected automatically. Raw eye movement data automatically generated by eye tracker are not structured, which will cause a big difficulty in data analysis. Table-format eye movement data is used in this approach to help researchers in the construction field read and analyze the data easier. Meanwhile, the data can be evaluated how long a certain object has to be viewed in order to be identified as a hazard by detecting confirmation actions from viewers and to find the scan path (sequence of fixations) of identifying these hazards. These results are a helpful basis for developing more effective markings, e.g. heatmap.

2 Related Work

Research has shown that different frequencies of eye movement give different information [4]. When continuously watching something, this behavior is called fixation; while frequently moving the eyes is considered as saccades. For example, in reading, saccades are for speed reading, while fixations are for comprehension.

Eye tracking is commonly recognized as a process of measuring the gaze direction and collecting data of human's behavior related to eye movement. Specifically, eye tracking is defined as a technique whereby the position of the eye is applied to identify gaze direction of a person at a certain dwell time and the eye movement trajectory [5]. The existing eye tracking applications could be divided into two categories: Diagnosis and Interaction [6].

In the diagnosis of eye tracking, many researchers focus on studying the cognitive process. Salvucci and Goldberg [4] give evidences of utilizing eye tracking in image scanning, driving, arithmetic and analogy. In the computer science area, Bednarik and Tukiainen [7] study program comprehension by tracking the eye movement process of programmers with different experiences reading code. Recently, Meißner and Oll [8] point out eye tracking is widely used in various academic disciplines: information search and decision making, learning, training systems, and expertise.

However, eye tracking technology could not only help studying the cognitive process, but also improve human-computer interaction. Jacob and Karn [6] state the research of human-computer interaction using eye tracking emerged in the 1980s, but the main application is in helping disabled people, e.g. eye typing. Jacob [9] deems that studying cognitive processes only involves recording and follow-up analyzing of eye movement data but has no effect on the computer interface at runtime.

Mine [10] summaries that the fundamental forms of interaction in a virtual world are movement, selection, manipulation and scaling. As one of the fundamental forms of interaction in virtual environments, selection has three steps to follow: indication of object, confirmation of selection and feedback [11].

In the construction industry, the research of studying cognitive process using eye tracking has commenced from the past few years. Among them, the safety awareness for safety training is frequently discussed [2, 12-14]. In addition to studying safety awareness, researchers use eye tracking to study the end-user satisfaction in building design [15], the 2D-construction-drawings interpretation process [16], the architectural features in building design [17] and other applications. Currently, most of the researchers use static images to study safety awareness, which cause problems since the construction site is dynamic [2, 12, 13]. Considering this limitation, Jeelani et al. [2] and Hasanzadeh et al. [13] collect eye movement data from real scenes under construction instead. However, studying cognitive processes on real construction sites has limitations. For example, it is difficult and time-consuming to build or find real sites. Moreover, it is unsafe for the participants to be in the real scene. To address all the problems above, Sacks et al. [3] suggest using virtual reality to demonstrate the construction site. Besides, they underline that using virtual construction sites is feasible, safer and more effective [3].

In summary, there are still gaps in research for the identification of hazards on construction sites:

- A large amount of eye movement data is needed in order to better study the behavior of hazard identification on different construction sites. Using eye tracking in different virtual environments can easily demonstrate different construction sites and generate many eye movement data accordingly.
- Using 2D images to firstly collect the eye movement data and then identify the objects from the images is ineffective. This problem can be solved by having interaction between eye tracker and hazards in the virtual environment.
- Construction sites are hazardous and dynamic. Using virtual environments are always safe to the workers for the cognitive study and fully demonstrate dynamic construction sites at the same time.

3 Methodology

Eye tracking technology is implemented within a virtual environment for the comprehensive study of the identification of hazards on construction sites. This

allows not only for realistic testing but also automated evaluation. The first step is to create virtual and dynamic environments of construction sites with possible hazards. On the one hand, digital planning models are used, which today can already be adopted automatically. On the other hand, special object libraries are integrated for the realization of the construction site equipment. It is important to create dynamic hazards in a virtual scene so that the hazards generated because of the dynamic situations on the construction sites can be demonstrated. The tests can then be carried out based on such virtual environments.

On the device, we use HTC Vive Binocular Add-on provided by Pupil Labs to track the eye movement and attach the Add-on to the VIVE device for tracking eye movement in virtual environment. To make the process of using eye tracking in virtual environment diagnostically and interactively manageable for researchers in the construction industry, the following concepts have been implemented in the Figure 1:

- Systematic calibration of the eye movement by Pupil Labs is for enhancing the ability of object indication based on the eye movement habit of different users.
- Recording the eye movement data with the name and dwell time of objects in certain duration as standardized output.
- Interactive selection of an object as marking a dangerous situation with the help of an external controller.

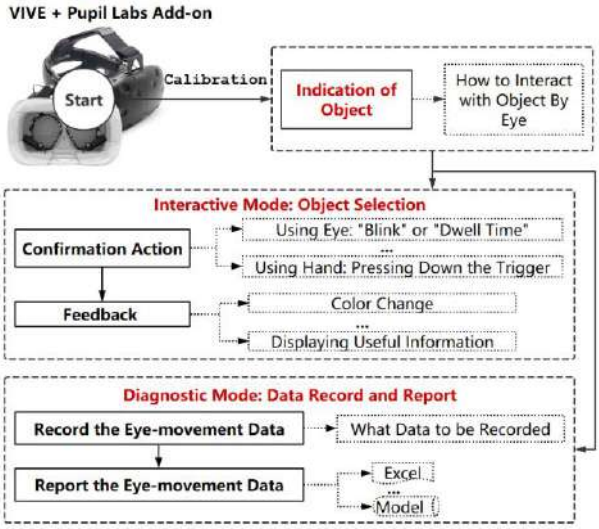

Figure 1. The workflow of methodology

In the following sub-sections, the *Indication of Object*, the *Diagnostic Mode* and the *Interactive Mode* are described in detail.

3.1 Indication of object

In the real world, to touch an object by hand, the distance to the object should be reachable. In order to realize interacting with an object by eyes in distance, we are inspired by Mine's study [10] of using laser beams or spotlights that protrudes from the user's hand and intersects objects in virtual environment. Unlike using the hand as the launch source of a laser pointer, we use the eye. One advantage of using laser pointers to indicate an object is that we can easily change the width of the laser in the virtual environment. By setting the gradient of the laser pointer, we can adjust the visual angle to enhance the accuracy of the particular object we select. Another advantage is that the laser pointer can be invisible in virtual environment by setting its transparency to 100 percent. Therefore, the laser pointer will not affect the eye movement data when studying the identification of hazards.

3.2 Diagnostic Mode: Data Record and Report

In diagnostic mode, recording the eye movement data is essential. To study cognitive processes, the dwell time of an object and process tracking (i.e., scan path) are vital. To avoid missing any important data, we recorded the object data (i.e., object ID, start time, end time and dwell time) line by line based on the eye-movement process. To make those data more intuitive, we put them into a file with a CSV-format file.

Once the laser pointer "hits" an object, we record the object ID to identify the object and the start time to know when the person starts looking at the object. When the laser pointer releases the object, we record the end time to know when the person stops looking at the object and calculate the dwell time. All those data will be outputted as a line in a table-format file. Forming such a table, we know when and how long a person looks at which object, the sequence of eye movement for objects and the individual and total time of an object.

Alternatively, collecting other eye movement data related to an object (e.g. the focusing parts, the position and the shape of the object) could form a file in another format (e.g. OBJ-format and FBX-format) as needed.

3.3 Interactive Mode: Object Selection

As input medium in interactive mode, eye movements as well as other input devices (e.g. mouse, keyboard and controller) are possible. Blink or dwell time can be used as a confirmation action [9]. In addition to using eyes, hand (e.g. pressing down the trigger of controller manually) is another option to confirm in virtual environment. Among these three options, blink as an input medium is difficult to control

[6, 9]. Therefore, in this subsection, we will discuss only the use of dwell time or pressing down the trigger to confirm the selection.

When using the dwell time, the main factor is to select a suitable duration to activate confirmation action. If the duration is too long, the user is forced to wait for a long time to confirm his/her selection. This would be unfriendly and inefficient. Furthermore, it can be difficult to identify the object. The user then looks at such an object for a longer time without wanting to select it. If so, pressing down the trigger might be a better option for a normal user (without disable). In order to allow a short reaction time, the position of the controller should be neglected. Thus, the user does not have to align the object when pressing down the trigger.

If the trigger is used, a late reaction or multiple confirmation may be possible for one-time selection. Therefore, an *isClickRecord* flag is implemented to store the recording of the selection. If the user triggers a manual confirmation, but the identification of the object by the laser pointer has just ended, a false confirmation may occur. In this case, either no or the next object will be selected. However, it is difficult to define the behavior of late reaction. Consequently, we omit the late reaction and record the confirmation action when the user is looking at the object. A multiple selection can simply be ignored, i.e. the *isClickRecord* flag is only set once and cannot be deactivated.

Without feedback, the user cannot know exactly whether the desired object is selected successfully [10]. There are different ways of giving feedback, e.g. changing the color of a selected object or showing a message to the user.

4 Example Application

To show how this methodology address the research gaps mentioned in this paper, an example application as an experiment in construction safety is designed. To introduce the experiment clearer, the *Experimental Procedure*, the *Results* and the *Discussion and Limitations* are provided in the following.

4.1 Experimental Procedure

In this experiment, two different construction-site scenes (shown in Figure 3 and Figure 4) are provided to indicate the simplicity of creating multiple scenes at the same time by the methodology. To differentiate these two scenes, the first scene is considered as a static construction-site scene and the second as dynamic with two moving vehicles. The eye-movement data collected by this method could be analyzed from three angles: *the number of confirmations*, *the scan path* and the *3D heatmap*. To make the process of the experiment intuitive for researchers, the following use case is provided in Figure 2:

- The operator provides some explanation of possible hazards in the construction site to guarantee every participant has basic knowledge about construction safety.
- After calibration, the participant can navigate through two different virtual construction sites (shown in Figure 3 and Figure 4).
- In these two scenes, a task, namely perception of the possible hazards, needs to be accomplished. Once an object is considered as a hazard, the trigger of the controller is used for confirmation.
- Every eye movement and the according confirmation action data will be recorded and reported in a CSV-format file automatically (shown in Figure 5).
- Feedback on feelings about the scenes compared with 2D images and the real construction site.

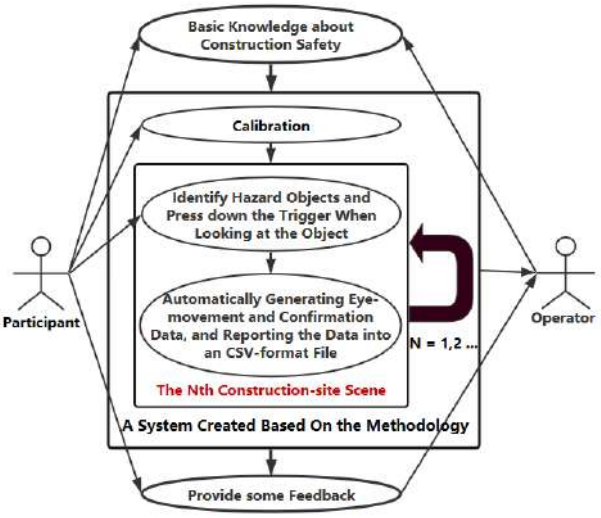

Figure 2. The use case of example application

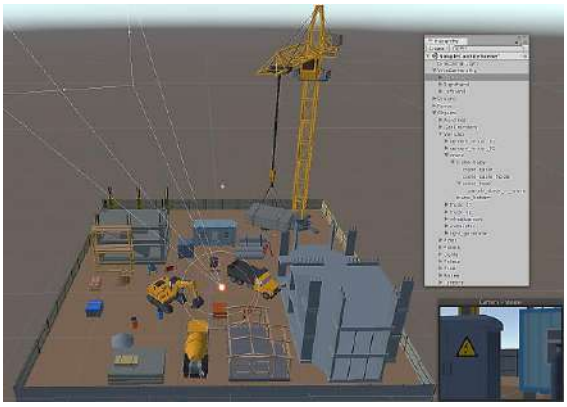

Figure 3. The static construction-site scene

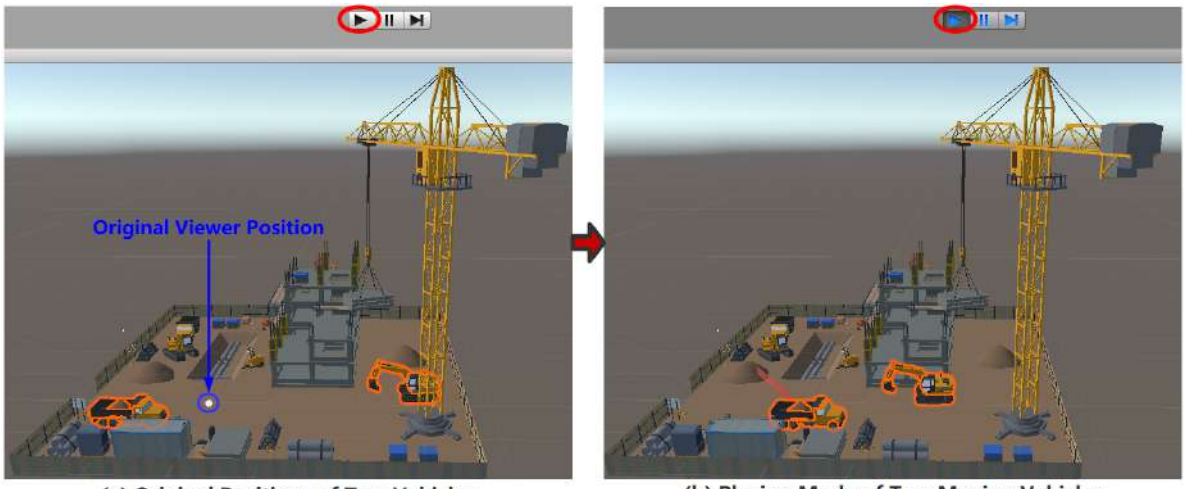

(a) Original Positions of Two Vehicles (b) Playing Mode of Two Moving Vehicles

Figure 4. The dynamic construction site scene

In the static construction-site scene, objects with some possible hazards are reachable from the original viewer position (the position of *Camera* shown in Figure 3).

In the dynamic construction-site scene (see Figure 4), two moving vehicles are hazards with the danger of hitting the participant or the participant being stuck in between. However, without moving, the two vehicles would not be hazards. Therefore, it is important to make one of the scenes dynamic in order to test if the participants can notice hazards on real dynamic construction sites.

Fourteen participants in the range of 20 to 60 years old with basic construction background are invited in the experiment. Since none of the participants had practical construction-site background, the explanation of possible hazards in the construction site (e.g. falls, stuck by objects, electrical hazards, caught-in-between and hazardous materials) was provided to guarantee each participant could find out some hazards in the scenes.

As a confirmation of selection, pressing down the trigger of controller is provided to record the time of confirmation every time the participant selects an object. However, in order to avoid affecting the awareness of the participant, we decided not to provide any feedback to the user during but after the experiment. In this case, the feedback will not affect the cognitive study. After the experiment, the 3D heatmap is generated according to the different dwell time of viewing different objects (see Figure 9). The position of the controller is neglected, but the participants must look at the object when they press down the trigger.

A sample CSV-format file is provided in Figure 5. For each participant, the *ObjectName*, the *StartTime*, the *ConfirmTime*, the *EndTime* and the *TimeDuration(ms)* are recorded based on his/her eye movement behavior and confirmation action. From the table, the number of selected hazards, the scan path of those hazards and the dwell and confirmation time of each hazard are shown.

ObjectName	StartTime	ConfirmTime	EndTime	TimeDuration(ms)
building_01	2019-01-18 14:20:40.36213		2019-01-18 14:20:40.47307	110
wheelbarrow_body	2019-01-18 14:20:40.48507		2019-01-18 14:20:40.57402	88

Figure 5. Data of one participant

4.2 Results

After collecting the eye movement data and the feedback from the fourteen participants, the number of confirmations, scan path and 3D heatmap are offered to demonstrate the data analysis based on the data we collected in the experiment.

4.2.1 Number of Confirmations

After the experiment, we realized that the recorded hazards were not always the participants expected. Since the accuracy of the approach is not high enough yet, it is worthy to calculate the accuracy rate of this approach in this experiment to evaluate the usability of this approach so far for the future cognitive study. In this evaluation, the number of missed, wrong-recorded and well-recorded confirmations with respect to each participant is shown in Figure 6. In the experiment, we did not consider the fences or the ground in the scenes as objects. Therefore, looking at fences, the ground or without objects when pressing down the trigger and a wrong use of the trigger could cause missed-recorded situation. Based on Figure 6, the missed rate and wrong rate overall and separately are calculated, and the corresponding results are in Table 1 and Table 2 to have a better evaluation about the methodology.

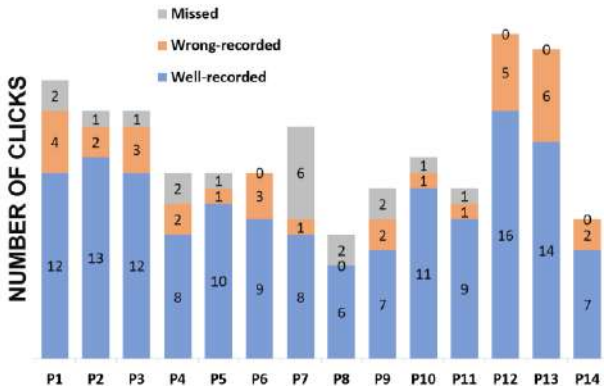

Figure 6. Histogram and table of all the results in both scenes related to confirmation action

Table 1. Rates related to the number of confirmations

Rate	Value (%)
Missed Rate	9.79
Wrong Rate	17.01

Table 2. The sum of the rates of each participant related to the number of confirmations

Participant	$R_M + R_{Wr}$ (%)	Participant	$R_M + R_{Wr}$ (%)
P1	33.33	P8	25.00
P2	18.75	P9	36.36
P3	25.00	P10	15.38
P4	33.33	P11	18.18
P5	16.67	P12	23.81
P6	25.00	P13	30.00
P7	46.67	P14	22.22

Conclusion about the accuracy of the technology cannot be drawn based on the limited number of confirmations. However, based on the rates, there are still room for improving the accuracy of the methodology.

4.2.2 Scan Path

The data collected in the experiment can tell the scan path of each participant. For example, the confirmations shown in Figure 8 were in line 110th, 112th, 113th, 120th and 129th. One sample scan path of the five selected objects is established in Table 3 based on these objects were recorded in chronological order in the data.

Table 3. Sample scan path of confirmations based on the data in Figure 8

Scene	Scan Path
Static	building_01 > fuse_box > gas_cylinder_01 > panelsstack_in_crane > cement_mixer_01_body

The corresponding selected order of the participant could be examined from the static scene (shown in Figure 7).

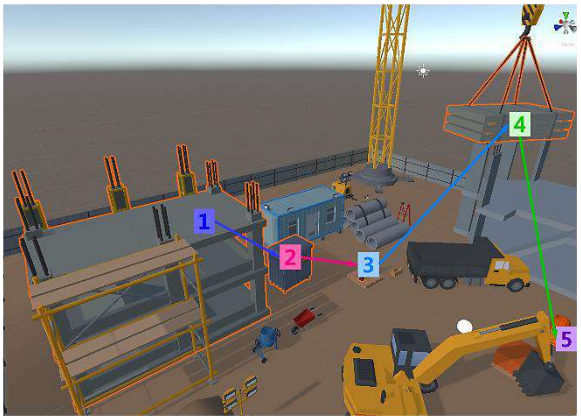

Figure 7. The sample scan path in static scene

110	building_01	2019-01-18 14:21:18.64684	2019-01-18 14:21:18.88218	2019-01-18 14:21:19.18320	536
111	building_01	2019-01-18 14:21:19.28314		2019-01-18 14:21:20.24210	958
112	fuse_box	2019-01-18 14:21:20.33093	2019-01-18 14:21:20.99223	2019-01-18 14:21:21.33884	1007
113	gas_cylinder_01	2019-01-18 14:21:21.40680	2019-01-18 14:21:22.62426	2019-01-18 14:21:25.02520	3618
114	portable_cabin	2019-01-18 14:21:25.22630		2019-01-18 14:21:27.04817	1821
115	truck_02_dump	2019-01-18 14:21:27.11513		2019-01-18 14:21:27.37127	256
116	truck_02_body	2019-01-18 14:21:27.39326		2019-01-18 14:21:27.56112	167
117	truck_02_dump	2019-01-18 14:21:27.98449		2019-01-18 14:21:28.25440	269
118	building_02	2019-01-18 14:21:28.45529		2019-01-18 14:21:28.47628	20
119	panels_stack_in_crane	2019-01-18 14:21:28.67826		2019-01-18 14:21:29.21455	536
120	panels_stack_in_crane	2019-01-18 14:21:29.25952	2019-01-18 14:21:29.54937	2019-01-18 14:21:29.88418	624
121	crane_body	2019-01-18 14:21:31.38257		2019-01-18 14:21:31.39257	9
122	crane_body	2019-01-18 14:21:31.40456		2019-01-18 14:21:31.41571	11
123	truck_02_dump	2019-01-18 14:21:31.79439		2019-01-18 14:21:32.28601	491
124	building_02	2019-01-18 14:21:32.68736		2019-01-18 14:21:32.93394	246
125	building_02	2019-01-18 14:21:32.94493		2019-01-18 14:21:32.97891	33
126	building_02	2019-01-18 14:21:33.00090		2019-01-18 14:21:33.02289	21
127	building_02	2019-01-18 14:21:33.06787		2019-01-18 14:21:33.30374	235
128	cement_mixer_01_body	2019-01-18 14:21:33.31373		2019-01-18 14:21:33.35827	44
129	cement_mixer_01_body	2019-01-18 14:21:33.39226	2019-01-18 14:21:33.89272	2019-01-18 14:21:34.11660	724

Figure 8. Data for scan path in static scene

However, in addition to the lines with confirmation data in Figure 8, the other lines tell the dwell time of each object. To make it intuitively, the concept of heatmap needs to be introduced.

4.2.3 3D Heatmap

Heatmap is frequently used in eye tracking research to visually show the dwell time of eye movement in 2D displays. However, compared to 2D heatmap, 3D heatmap will be more suitable in our approach.

3D heatmap can be generated as well by changing the colours of the objects based on the overall dwell time of each object. Based on the colour bar we designed as an example, a 3D heatmap is shown in Figure 9. By using 3D heatmap, we can visually see the overall dwell time of each object from the participants based on the changed color of those objects.

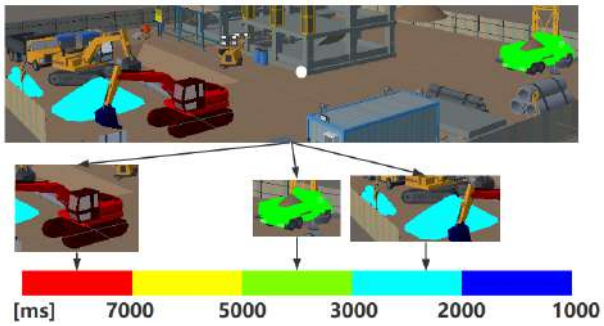

Figure 9. 3D heatmap based on the dwell time in dynamic scene

4.3 Discussion and Limitations

In this experiment, 86% of the participants agreed that standing in a virtual environment is more realistic than watching a 2D image and 100% of them felt safer than standing in the real construction site. However, from the perspective of the participants, the scenes still looked unreal. Based on the Results section, we draw a conclusion that the table data shown in Figure 5 represents human's eye movement to a large extent and can be analyzed in three different angles (i.e., *the number of confirmations*, *the scan path* and *3D heatmap*). Since the number of participants, the number of confirmation action by each participant and the number of construction-site scenes are too low, and none of them had construction-site experience, we cannot simply draw conclusions based on the data we collected. In addition, from the rates shown in Table 1 and Table 2, we know the accuracy of the method still has room for improvement.

Even though this experiment demonstrated how to address the research gaps of combining eye tracking with virtual reality in studying hazard identification as an example, it contains limitations. First, due to only two scenes used in the experiment, the diversity of data is insufficient. Second, the data were analyzed manually. Third, the results of the experiment are not convincing enough based on the inadequate number of participants. Fourth, the accuracy of the eye tracking in virtual environment could be improved by ameliorating the implemented programming algorithms. Fifth, only one possible application is provided in this experiment. Sixth, the dynamic construction-site scene cannot fully represent the dynamic construction site.

5 Conclusion and Outlook

Technological innovations are gradually changing the landscape of the construction industry. Such innovations could improve some remaining industrial issues, e.g. the on-site hazard identification. To study the hazard identification, many researchers use eye tracking technology to collect eye movement data from pictures or real construction sites. However, drawbacks e.g. the poor immersion feelings with pictures and the non-storable real site environment in a one-off project, could occur from these two ways of collecting data. For addressing those drawbacks, we provided an approach to use eye tracking in virtual environment diagnostically and interactively. By this approach, a large amount of different eye movement data could be collected. To verify our method, we conducted an example application using eye tracking in two different construction-site scenes (with static and dynamic objects respectively) to collect different eye-movement data. We analyzed the data quality of the confirmation actions of the experiment participants. We explored how to use the experimental data to generate the scan path and 3D heatmaps.

Future studies should focus more on improving the efficiency of the data collection approach and the accuracy of the collected data on the implementation (e.g. using filtering and smoothing algorithms). Efforts also should be made in digging out more possible applications in the construction industry. Meanwhile, we will focus on building more real and dynamic scenes to improve the immersion feelings and the human-computer interactivity in the demonstration of construction sites. Furthermore, after collecting abundant eye movement data from multiple types of participants in various scenes, studying the cognitive process by data mining would be a better idea to analyze the "big data".

References

[1] Sawacha E., Naoum S. and Fong D. Factors affecting safety performance on construction sites. *International journal of project management*,

17(5): 309-315, 1999.

[2] Jeelani I., Han K. and Albert A. Automating and scaling personalized safety training using eye-tracking data. *Automation in Construction*, 93: 63-77, 2018.

[3] Sacks R., Perlman A. and Barak R. Construction safety training using immersive virtual reality. *Construction Management and Economics*, 31(9): 1005-1017, 2013.

[4] Salvucci D.D. and Goldberg J.H. Identifying fixations and saccades in eye-tracking protocols. In *Proceedings of the 2000 symposium on Eye tracking research & applications*, ACM, 2000.

[5] Poole A. and Ball L.J. Eye tracking in HCI and usability research. *Encyclopedia of human computer interaction*, IGI Global, 211-219, 2006.

[6] Jacob R.J.K. and Karn K.S. Eye tracking in human-computer interaction and usability research: Ready to deliver the promises. *The mind's eye*, 573-605, 2003.

[7] Bednarik R. and Tukiainen M. An eye-tracking methodology for characterizing program comprehension processes. In *Proceedings of the 2006 symposium on Eye tracking research & applications*, ACM, 2006.

[8] Meißner M. and Oll J. The Promise of Eye-Tracking Methodology in Organizational Research: A Taxonomy, Review, and Future Avenues. *Organizational Research Methods*, 1094428117744882, 2018.

[9] Jacob R.J.K. The use of eye movements in human-computer interaction techniques: what you look at is what you get. *ACM Transactions on Information Systems (TOIS)*, 9(2): 152-169, 1991.

[10] Mine M.R. Virtual environment interaction techniques. *UNC Chapel Hill CS Dept*, 1995.

[11] Argelaguet F. and Andujar C. A survey of 3D object selection techniques for virtual environments. *Computers & Graphics*, 37(3): 121-136, 2013.

[12] Jeelani I. et al. Are Visual Search Patterns Predictive of Hazard Recognition Performance? Empirical Investigation Using Eye-Tracking Technology. *Journal of Construction Engineering and Management*, 145(1): 04018115, 2018.

[13] Hasanzadeh S., Esmaeili B. and Dodd M.D. Examining the Relationship between Construction Workers' Visual Attention and Situation Awareness under Fall and Tripping Hazard Conditions: Using Mobile eye tracking. *Journal of Construction Engineering and Management*, 144(7): 04018060, 2018.

[14] Dzeng R.J., Lin C.T. and Fang Y.C. Using eye-tracker to compare search patterns between experienced and novice workers for site hazard identification. *Safety science*, 82: 56-67, 2016.

[15] Mohammadpour A. et al. Measuring end-user satisfaction in the design of building projects using eye-tracking technology. *Computing in Civil Engineering 2015*, 564-571, 2015.

[16] Sears M., Alruwaythi O. and Goodrum P. Visualizing eye tracking Convex Hull Areas: A Pilot Study for Understanding How Craft Workers Interpret 2D Construction Drawings. *Construction Research Congress 2018*, 2018.

[17] Zou Z. and Ergan S. Where Do We Look? An Eye-Tracking Study of Architectural Features in Building Design. *Advances in Informatics and Computing in Civil and Construction Engineering*, Springer, Cham, 439-446, 2019.

Optimizing the Usage of Building Information Model (BIM) Interoperability Focusing on Data Not Tools

E. K. Amoah[a] and T. V. Nguyen[b]

[ab]Department of Mechanical & Civil Engineering, Florida Institute of Technology, Melbourne, FL 32901 USA
E-mail: eamoah2015@my.fit.edu, tnguyen@fit.edu

Abstract –

Architectural, Engineering, Construction (AEC) and Facility Management (FM) industry rely on varied expertise to achieve a highly successful project. The industry professionals in these fields require greater level of collaboration in managing the expectation of a project success. When every individual in the team uses different BIM software, it becomes stressful, time consuming and an excessive use of budgeted funds to maintain accurate design model version. It also becomes virtually impossible to controls users, compare versions and analyze different models and data. Consider a large-scale project for example, there are several teams and different professional specializations coming together, all using different BIM software's they have been tasked and making all those interoperate, multiplying the challenges in several folds.

Overall, data is extremely important, and no single firm would want to be held back by the tools they use, nor do they want to maintain various disparate software packages. This paper seeks to find optimal ways in addressing BIM interoperability with emphasis on data exchange not the tools. The study reviews number of top vendors and manufacturers website and solicit their views on BIM interoperability and how those companies deal with the challenges of providing a product that integrate well with competing industry software packages.

Keywords –
Building Information Modelling (BIM); BIM Software; Interoperability; BIM Collaboration; Data exchange

1 Introduction

1.1. Building Information Modeling (BIM)

The National Building Information Model Standard Project Committee defines BIM as "a digital representation of physical and functional characteristics of a facility. A BIM is a shared knowledge resource for information about a facility forming a reliable basis for decisions during its life-cycle; defined as existing from earliest conception to demolition" [1]. A basic premise of BIM is collaboration by different stakeholders at different phases of the lifecycle of a facility to insert, extract, update or modify information in the BIM to support and reflect the roles of that stakeholder. Use of BIM goes beyond the planning and design phase of the project, extending throughout the building lifecycle, supporting processes including cost management, construction management, project management and facility operation.

Participants in the building process are constantly challenged to deliver successful projects despite tight budgets, limited manpower, accelerated schedules, and limited or conflicting information. The significant disciplines such as architectural, structural and MEP designs should be well coordinated, as two things can't take place at the same place and time. Building Information Modeling aids in collision detection at the initial stage, identifying the exact location of discrepancies.

The BIM concept envisages virtual construction of a facility prior to its actual physical construction, in order to reduce uncertainty, improve safety, work out problems, simulate and analyze potential impacts [2]. Sub-contractors from every trade can input critical information into the model before beginning construction, with opportunities to pre-fabricate or pre-assemble some systems off-site. Waste can be minimized on-site, and products delivered on a just-in-time basis rather than being stock-piled on-site [2].

BIM can bridge the information loss associated with handling a project from design team, to construction team and to building owner/operator, by allowing each group to add to and reference back to all information they acquire during their period of contribution to the BIM model. This can yield benefits to the facility owner or operator. For example, a building owner may find evidence of a leak in his building. Rather than exploring the physical building, he may turn to the model and see

that a water valve is located in the suspect location. He could also have in the model the specific valve size, manufacturer, part number, and any other information ever researched in the past, pending adequate computing power [3]. Dynamic information about the building, such as sensor measurements and control signals from the building systems, can also be incorporated within BIM software to support analysis of building operation and maintenance [4].

BIM technology is receiving great attention in the architecture, engineering and construction (AEC) industry, and since it contains a complete set of information of the lifecycle of a structure in the form of a digital model, it is widely projected to be the technology of tomorrow. By being a comprehensive digital database, it is rapidly gaining acceptance as the preferred method of communicating the design professional's intent to the owner and project builders [5]. BIM has been traditionally used for design and its use in the construction phase has also been increasing recently. However, nowadays owners have realized the potential of BIM and insist on inheriting the BIM models for further use. The owner can benefit from the BIM model as an archive of as-built information, for purposes such as Facility Management (FM) decision making tool or repository of materials.

1.2. BIM Interoperability

Architecture, engineering, construction, and facilities management are information intensive industries, and are highly dependent upon effective information technologies. Various software and tools are used to help with the AEC/FM design and management tasks. However, currently the information is passed from one project member to the next by producing paper based or electronic documents which can only be interpreted by people. These members must also re-enter relevant information into their own professional tool. This manual data entry is a non-value adding activity, can often introduce errors into the project, and inhibits the use of better computational tools [6].

With respect to software, the term interoperability is used to describe the capability of different programs to exchange data via a common set of exchange formats, to read and write the same file formats, and to use the same protocols [7]. One common use case for software interoperability is for the customers freedom to switch from one product to another while keeping the data intact after the transfer. This is especially important for use cases where the data will stay in one system for a long time (e.g. in Computer Aided Facility Management - CAFM systems or cloud) to prevent vendor lock-in.

In the AEC industry where, one-off projects teams are assembled across different organizations, disciplines and phases you want the different discipline tools to share information with each other and you want data generated in one phase to be usable without re-entry for the next phase. This is the foundation for openBIM. You cannot have a true openBIM workflow without interoperable software. Interoperability is about freedom to work with the best in any discipline and for them to use the tools they are most comfortable and productive with.

To communicate with each other systems, need to use common data formats and communication protocols. Examples of formats are IFC, XML, JSON, SQL, ASCII and Unicode. Examples of protocols are HTTP, TCP, FTP and IMAP. When systems are able to communicate with each other using these standards they exhibit syntactic interoperability.

For BIM tools to work together we need more than just the ability to transfer information. We need the ability to transfer meaning. What is sent must be the same as what is understood. To achieve this both sides must refer to a common information exchange reference model. We need semantic interoperability. Interoperability between various software applications can be achieved in a number of ways such as: Using software that directly reads the proprietary file format contained in the BIM software application, which will be the case for a suite of software applications developed by one software vendor; using software that incorporates an Application Programming Interface (API), providing a well-developed interface between software from different providers; and using software that supports data exchange standards such as Industry Foundation Classes (IFC) format [8].

2 Industry Foundation Classes (IFC)

BuildingSMART developed Industry Foundation Classes (IFCs) as the open and neutral data format for openBIM with the aim of improving information exchange between software applications [14]. The specification of the IFC standard includes for each major and minor edition:

- the IFC Specification html documentation (including all definitions, schemas, libraries)
- the URL for the IFC EXPRESS long form schema
- the URL for the ifcXML XSD schema

The IFC specification is written using the EXPRESS data definition language, defined as ISO10303-11 by the ISO TC184/SC4 committee. It has the advantage of being compact and well suited to include data validation rules within the data specification.

The ifcXML spec is provided as an XML schema 1.0, as defined by W3C. The ifcXML exchange file structure (the syntax of the IFC data file with suffix ". ifcXML") is the XML document structure. The XML

schema is automatically created from the IFC-EXPRESS source using the "XML representation of EXPRESS schemas and data", defined as ISO10303-28 ed. 2. This ensures that both IFC-EXPRESS and ifcXML handle the same data consistently and that the *.ifc and *. ifcXML data files can be converted bi-directionally.

2.1 IFC Data File Formats and Icons

IFC data exchange has two alternative formats for the exchange of some information content [14]. These formats are:

- IFC format or IFC part 21 Format, which is based on the ISO 10303 -21 standard,
- The ifcXML format, which is based on an XML Schema definition of the IFC product

IFC data files are exchanged between applications using the formats (Table 1) and should be indicated by the published icons:

Table 1 IFC data file exchange format

Icons	Data File Format
.ifc	IFC data file using the STEP physical file structure according to ISO10303-21. The *.ifc file shall validate according to the IFC-EXPRESS specification. This is the default IFC exchange format.
. ifcZIP	IFC data file using the XML document structure. It can be generated directly by the sending application, or from an IFC data file using the conversion following ISO10303-28, the XML representation of EXPRESS schemas and data. IFC data file using the PKzip 2.04g compression algorithm (compatible with e.g. Windows compressed folders, WinZip, zlib, info-zip, etc.). It requires to have a single .ifc or *. ifcXML data file in the main directory of the zip archive.

3 Review of Comparative Building Design and BIM Software

Building design and building information modeling (BIM) software includes computer-aided design (CAD) products used commonly within the architecture and construction industries. Many of these products offer tools and libraries specifically targeted toward architectural design and construction, including mechanical, electrical, and plumbing (MEP) and building information modeling (BIM). Table 2 categorizes BIM software that offers a model-based process for designing and managing buildings and infrastructures, going beyond construction drawings to generate a digital representation of the functional properties of a facility. Other products in this category may be used for a range of CAD purposes beyond architectural design, but their rankings within this grid focus exclusively on their use as a tool in building design. The best products in Table 2 are determined by customer satisfaction (based on user reviews) and market presence (based on products' scale, focus and influence). The list is not meant to be excusive.

Table 2 Comparative Building design and BIM software

Product Name	Features
Revit	Specifically built for Building Information Modelling (BIM), Building design software for consistent model-based approach.
Vectorworks	Tackles complex ideas in 2D and 3D, refine construction details with ease and directly inside files
ARCHICAD	BIM software application for design, document and collaborate on building projects.
SketchUP	Layout, Extension Warehouse and the 3D Warehouse to design everything
Bentley	BIM Application for MicroStation, PowerDraft, and AutoCAD
Navisworks	Reviews integrated models and data with stakeholders to better control project outcomes.
BIM Object	Creates a straight path to the users of any BIM software.
IrisVR	Integrates with Revit, Rhino, SketchUP, and other 3D tools
Trimble Connect	Avenue for designers, builders, owners and operators to collaborate, share and view project information.
AECOsim Building Designer	Single building information modelling (BIM) software application for multi-discipline teams
Tekla BIMsight	Check for clashes, and share information using the same easy-to-use BIM environment.
Virtual Construction	Leverages 2D drawings and 3D BIM models for 4D model-based scheduling and 5D model-based estimating.
Konstru	Cloud-based automation platform that lets you view, edit, clean, synchronize and share model data stemming from a variety of BIM

4 Case Study

Under this section, the paper demonstrated the potentials on interoperability as well as the issues and challenges specific to the selected vendor software's in Table 2. Authors further examined views of how these vendors' deals with challenges of providing product that integrates well with other competing software's. The vendor software products that featured for the case study include;

- Bentley
- Autodesk,
- Graphisoft,
- Vectorworks,
- Konstru, and
- Trimble.

The selection is done in no order of preference. It was solely based on informational purposes and to facilitate the decision-making process for the end-users.

4.1 Bentley

Bentley provide i-models that enable users to access and share information-rich models. This can include competing solutions and varying file formats. i-models act as a container for exchanging information and conveying AECO data to the right people at the right time by breaking down issues with interoperability that have hindered the progress of infrastructure projects. Bentley is fully committed to i-models by recently launching iModel 2.0 Platform which offers a better solution for synchronizing work in infrastructure projects by managing all the change related to a project. Bentley also announced the availability of AECOsim Building Designer CONNECT Edition (Figure 1) which is Bentley's building information modeling (BIM) application designed for building projects of significant size and/or engineering complexity, and which are typically characterized by the challenges of combining vertical construction and horizontal infrastructure (like roads, railways, utilities, etc.). AECOsim Building Designer CONNECT Edition shares a comprehensive modeling environment with all of Bentley's CONNECT Edition applications. Without a comprehensive modeling environment, engineers and architects have had to struggle with complex data exchange, resulting in information loss and repeated translations, or even resort to force-fitting a BIM application beyond its intended use to model geometry, which is lacking in BIM intelligence [15].

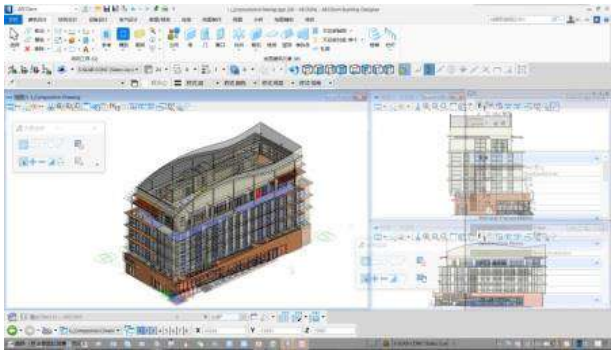

Figure 1: AECOsim Building Designer CONNECT Edition sample

4.2 Autodesk

Autodesk supports interoperability with other BIM vendor software and hardware in a variety of ways. In fact, in 2016, Autodesk and Trimble signed an interoperability agreement to benefit AEC Customers to gain greater flexibility throughout the BIM Project Lifecycle [16]. And, also signed an interoperability agreement with Bentley nearly a decade ago.

- All the BIM products have support for the IFC standard as well as other Industry Standard Formats.
- In addition, Autodesk offer direct reading of Multiple BIM formats with Autodesk Navisworks and cloud-based BIM 360 products. Navisworks is widely regarded as a key BIM interoperability solution on the market today.
- Autodesk provides its IFC software for Revit as a free open source toolkit [17].

Revit software provides certified IFC export and import based on the buildingSMART IFC 2×3 Coordination View data exchange standard. This includes architectural, structural and MEP certifications based on the buildingSMART IFC 2×3 coordination View 2.0 data exchange standard, as of March 2013 and April 2013, respectively. Revit received stage-1 IFC 2×3 Coordination View Certification in June 2006, and full stage-2 certification for Coordination View in May 2007. The IFC for Autodesk Revit 2016 contains up-to-date improvements on the default IFC import and export capabilities of Revit contributed by Autodesk and the Open Source contributors. This application also includes an alternate UI (User Interface) for the export that has extra options from the default.

While this app is not necessary for IFC support, it is recommended that users that depend on the quality of their IFC files download this app and keep it up-to-date, as new enhancements and defect fixes are added, for more information on IFC [18].

Autodesk Software with IFC support: Autodesk Revit LT, Autodesk Navisworks, Autodesk Infraworks, Autodesk BIM 360, Autodesk Robot Structure,

Autodesk Advance Steel, Autodesk Inventor, Autodesk Civil 3D. Examples of initiatives that Autodesk participates in around the world include:

- Support of the U.S General Services Administration (GSA) IFC model view definitions.
- Support of COBie via IFC and xlsx
- Autodesk BIM 360 Docs is designed to help government clients comply with the BIM Level 2 mandate in the UK [19].

Through Application Programming Interfaces (APIs) Autodesk software offerings also provide many ways to work with other BIM vendor's information. For example, when viewing BIM information from other software systems and when using 3D vector file formats for

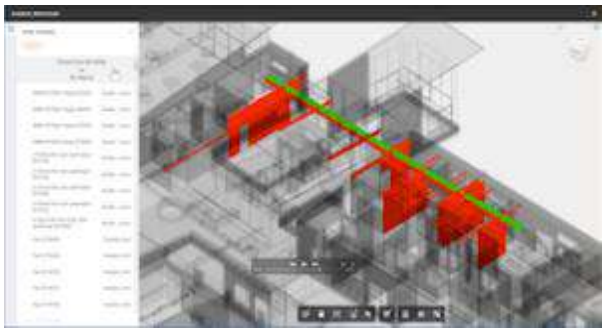

Figure 2. Autodesk BIM 360 Glue on Forge sample

detecting clash/collisions, BIM 360 Glue (Figure 2) supports the many file formats [20]:

4.3 Graphisoft

GRAPHISOFT has been involved in the development of IFC standards since 1996. The latest ARCHICAD version (21) supports the import and export of IFC 4 models including two types of the Model View Definitions, which are developed for multi-disciplinary 3D mode-exchange workflows [21]:

- IFC4 Reference View
- IFC4 Design Transfer View

ARCHICAD continues to support the former 2×3 version of IFC as well. In order to enhance model base communication, ARCHICAD also provides native BIM Collaboration Format (BCF) support in ARCHICAD. There are many other unique solutions in ARCHICAD, such as built-in collision detection, IFC model change detection or custom IFC translators that offers the best in class OPEN BIM workflow for the users (Figure 3).

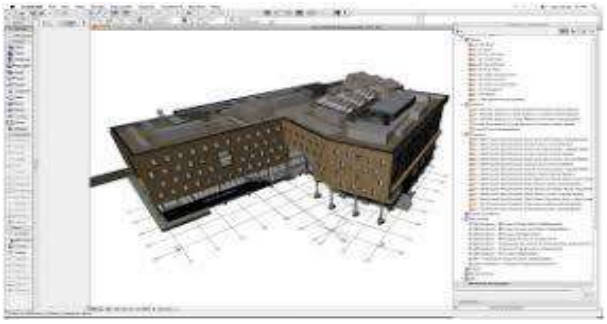

Figure 3. GRAPHISOFT ARCHICAD Sample

4.4 Vectorworks

Vectorworks provides several different methods for sharing data across a large spectrum of workflows and file formats, giving users the ability to select the best option for their needs. For BIM, where geometry and associated information are important, there is the IFC export/import, as well as ODBC. Vectorworks is also the first product to offer import of RVT and RFA files based on the Open Design Alliance (ODA) Teigha BIM software development kit. In addition, important 2D and hybrid 2D/3D workflows can be supported with PDF/3DPDF, DWF and DWG/DXF export and import. For 3D geometry-centric processes and workflows, especially around early design and building product research, Vectorworks supports import and/or export of another dozen or more file formats including 3DM, SKP/COLLADA, 3DS and a multitude of point clouds formats **[22]**.

4.5 Konstru

Konstru, a new product launched in June 2017 is a central interoperability platform that automates the exchange of BIM data between analysis & modeling software tools. Konstru supports all your favorite and most popular design and analysis tools and allows them to communicate with one another.

The product was created by structural engineers and for structural engineers, in order to make this communication possible between BIM software programs. Konstru is a quick plug-in download that allows you to upload your current projects model to their secure cloud. It's possible to exchange BIM data across multiple platforms, make necessary revisions, and visually understand everything that changed.

Konstru has an open API and modern API to allow for people have the flexibility to build their own use cases and develop apps for BIM without much programming language.

4.6 Trimble

Trimble has a philosophy that project team members

should be able to work together smoothly regardless of the tools they use in demonstrated the integrations and interoperability features across multiple solutions:

- **Trimble Connect** — a collaboration environment where everyone involved in a construction project can access and manage project data from other software packages via a cloud platform. For example, a team member using Revit can upload the .RVT file to Trimble Connect for others to view.
- **Tekla Structures** – Tekla Structures has an open approach to BIM. Through IFC, Tekla links with AEC, MEP and increasingly with plant design software. Tekla Structures effectively integrates with other AEC industry software solutions through Tekla Open API, while maintaining the highest levels of data integrity and accuracy [23]. In addition, for anyone working with AutoCAD, those CAD files can be imported and exported into and from Tekla Structures.

Tekla Structural Designer – Tekla Structural Designer was developed specifically with BIM interoperability and collaboration in mind and helps design engineers maximize collaboration with other project parties, including technicians, fabricators and architects. Its unique functionality allows users to integrate the physical design model seamlessly with Tekla Structures or Autodesk® Revit®, and to round-trip without compromising vital design data.

- Most importantly, industry stakeholders, government agencies, educational institutions and users of BIM application must be educated, to fully understand the capabilities and benefits of BIM based collaboration and building lifecycle management.
- Secondly open, vendor independent, practical BIM standards must be adopted in every country.

4.7 Case Study Evaluation Process

BIM tools that works together, ability to transfer meaning, serves as a common information exchange reference model and able to interoperate between various software application formed the basis for the authors evaluation method. Table 3 defines the vendor software products which reads directly the proprietary file format contained in the BIM software application. The authors used the vendors software product that featured for the case study analysis and ranked them against each other to determine a particular software vendor using software that incorporates using an Application Programming Interface (API), providing a well-developed interface between software from different providers. The authors also considered the software that frequently supports data exchange standards such as Industry Foundation Class (IFC) format for the evaluation. The number of meaningful data exchange transfer model/interfaces that each BIM software product could successfully perform among each other were counted. Based on the number of programming interfaces (API) and open standards file formats associated with each software products was assessed. Based on each assessment, paper ranked the software's according to the scale of "LOW to HIGH". "HIGH" indicates a product that can smoothly communicate and transfer data with less effort or difficulty while "LOW" constitute substantial difficulty in exchanging data. To broaden the support base for this analysis, the paper further took into the following considerations; the customer satisfaction – based on user reviews and market presence – based on product scale, focus and influence.

Table 3 Evaluation of BIM Product to support data interoperability

BIM Products / **Project Data Format**	**Bentley**	**Autodesk Revit**	**Vectorworks**	**Graphisoft ArchiCAD**	**Konstru**	**Trimble.**
File Extension	***dgn**	***.rvt**		*.pln	*.vmx	.dwg
Application Programming Interface (API)	i-models	Revit Open .NET API	API + Vectorscript scripting language	Geometric Description Language (GDL)	Open	FC (2x3, 4), IFCZIP
Open Standards						
• Architectural Model	XFM, ODBC	IFC, RVT, DWG, DGN, PLN, NWD	IFC	IFC, DWG, DGN	SAP2000, ETABS	IFC
• Structural	IFC	IFC,	IFC	IFC	IFC	IFC

Mode		CIS/2				
• Civil Engineering	DWG	LandXML, DWG, DGN	DWG	LandXML, DWG	DWG	IFC
• Cost Estimating	CSV, XLSX	XLSX, ODBC	ODBC	ODBC	DWG,IFC	IFC
• COBie Data	PDT	IFC, XLSX	IFC	IFC	XLSX	IFC
• Scheduling Data	P3, MPP	P3, MPP	P3, MPP	P3, MPP		IFC
• Energy Analysis	IFC, gbXML	IFC, gbXML	IFC, gbXML	IFC, gbXML	IFC,	IFC
RANKING	**Medium**	**High**	**Medium**	**Medium**	**Low**	**Low**

5 Challenges

As BIM technology and interoperability continue to evolve, every indication shows that the challenges are less about the technology but more revolves around:

- Contracted deliverables: Engineers are still producing drawings. Even those who would give up drawings in a heartbeat are likely still contractually bound to produce them for the client (usually the architect in design-bid-build contracts) as part of their deliverable. Because of this, they spend more time than is necessary working on 2D drawings. It would be worthwhile spending time on things such as value engineering and identifying potential constructability issues in a 'constructible model' and then simply sharing that model.
- Contracted responsibilities: Often referred to as Level of Development (LOD) 300, contracts typically require that engineers only produce a full set of 2D construction documents that convey the design intent. This approach is very inefficient for the owner as overall project costs can escalate due to RFIs and change management issues during construction.
- Liability. Many engineers are concerned about providing too much detail because if something goes wrong later in the project, they seem to be concerned that it could make them liable.

6 Discussion

The goal of this paper was to provide different approaches to allow for a flexible response to complicated data transfer challenges. The major issues raised in the case study readily focused on project data standards and its interoperability.

Autodesk encourages owners to use their BIM mandates to ask for the data in the native file format of the authoring tool and in IFC format [24]. Autodesk offers both open source and owned its own plug-ins for interoperability. IFC is the most often used but other methods are also useful. For example, autodesk has series of free utilities to facilitate the quality of BIM data exchanges. These consist of classification manager for Revit, COBie toolkit plugin for Revit and a model checking tool for Revit [24].

There are varieties of options, including openBIM, open sources, and host of others but the preferred standard for Bentley would be to ensure cityGML and IFC are adhere to, to deliver and share better engineering – ready models [25].

Most structural analysis programs were written before the emergence of BIM and work around centerline base wire frame model. This becomes extremely difficult if not impossible to find a perfect solution to fit-in nicely with physical modelling solution like Revit and Tekla Structures regardless of how good the link may be. Trimble has developed a structural analysis solution purposely with this problem in mind (Tekla Structural Designer). Tekla Structural Designer has a physical model and a wire frame model working together so the transfer of information and out of BIM environment is made easy [27].

buildingSMART International provides the global marketplace with the openBIM standard IFC format for BIM interoperability. It is the only open, non-proprietary data exchange standard for the building industry that is comprehensive enough to address the many workflows, processes and stakeholders involved in the design, construction and operations of a building over its entire lifecycle. Because it is an International Standards Organization (ISO) standard, like XML and HTML, anyone can build tools to read and/or write IFC data, including BIM authoring, simulation and analysis, viewing and data server platforms. IFC puts the emphasis on the data, not the tools, so important information can be transmitted regardless of source or receiver of the data. This also encourages a healthy, open marketplace for tools to give end users the best technology and value proposition for their investment. Trying to achieve the same level of BIM interoperability by only utilizing proprietary APIs is economically infeasible at the scale necessary to serve so many end users, for so many projects, in so many markets, using so many different tools [27].

There are over 200 software products by 140 plus vendors/developers across the globe that support IFC data exchange for their customers, irrespective of their country of practice. buildingSMART also has a software certification program to verify the technical capability of applications to read and/or write IFC data. This certification program includes IFC2x3 support and has recently started on the new IFC4 standard. To date, 22 different applications, including major market applications from the Nemetschek Group, Trimble and Autodesk, have been certified to exchange IFC2x3 files. Efforts by five vendors, including Vectorworks, are already underway to certify on IFC4 exchanges [28].

7 Recommendation

The market is changing and so are the requirements for managing data throughout the project lifecycle in AEC industry. Digitization and cloud-based services are the trends resonating with all industry players, who want to make data talk to other data platforms. In this regard, stakeholders must embrace the change through:

- digital platforms, and understand the changing context of BIM information,
- organizations need to ensure this information can be interoperable but resolute in order to better connect distributed teams.

Though technical capability of BIM interoperability and other tool interfaces has improved significantly over the past decade, end-user's knowledge and ability to leverage that capability needs to improve as well. Many times, the biggest obstacle to BIM data exchange is the end users' lack of understanding the best practices in their tools for creating good BIMs, neglecting set up of good, consistent data exchange requirements and processes with collaborators and not knowing how to utilize the data exchange commands in their tools for the best results.

Data exchange standard technology also, needs to improve continuously, improving the IFC data exchange transfer results for project teams.

The authors data interface analysis evaluation gives credence to fact that, Autodesk Revit is more versatile BIM tool capable of accommodating a wide variety of design interfaces for data exchanges among other software products, scoring "HIGH" in the rankings in Table 3.

8 Conclusion

From the search and analysis conducted across the interfaces of almost all the software products, each vendor firm is drifting towards cloud services. Autodesk for example, is pushing heavily for cloud services and cloud central model management, so each project team member could readily access changes and updates from their project data irrespective of their location. Based on this paradigm shift, the authors believe cloud is the future for interoperability and collaboration. The could services does not only offer powerful processing potential but also data distribution and accessibility by enabling a connected data environment.

It will be far-fetched to say technology that is holding back BIM interoperability. It is being held back by contractual issues. One simple solution would be to execute more projects as Design-Build projects rather than Design-Bid-Build. That way, it is in everyone's interest to share information to compress construction schedules. Some structural engineers are adopting what is being termed, 'HD BIM' techniques or offering 'Construction Services' as part of their service – this is another way of eliminating some of these contractual issues. Also, in all situations, it would be ideal on all projects to implement a true BIM execution plan that states who will create a model, to what LOD and how it will be utilized.

References

[1] National BIM Standard - United States, (2007-2015), National Institute of Building Sciences

[2] Smith, Deke (2007). "An Introduction to Building Information Modeling (BIM)" (PDF). Journal of Building Information Modeling

[3] Leite, Fernanda; Akinci, Burcu, (2012). "Formalized Representation for Supporting Automated Identification of Critical Assets in Facilities during Emergencies Triggered by Failures in Building Systems". Journal of Computing in Civil Engineering.

[4] Liu, Xuesong; Akinci, Burcu, (2009). "Requirements and Evaluation of Standards for Integration of Sensor Data with Building Information Models". In Caldas, Carlos H.; O'Brien, William J. Computing in Civil Engineering. pp. 95–104.

[5] Alireza G., Vineet R. K., (2013). Evaluation of Industry Foundation Classes for Practical Building Information Modeling Interoperability

[6] Froese, T. (2003). Future Directions for IFC-Based Interoperability. ITcon Vol. 8, Special Issue IFC - Product models for the AEC arena.

[7] Johan x., (2016). What Interoperability Really Means in BIM Context. Retrieved from: https:// www.bimmodel.co/single-post/2016/09/05/What-Interoperability-really-means-in-a-BIM-context

[8] Gayer, A. (2009). BIM Power: Interoperability. Structure magazine, October edition.

[9] BIM Maturity Matrix, (2015). Retrieved from: http://www.bimframework.info/2013/12/bim-maturity-index.html

[10] Hutchinson, A., & Finnemore, M. (1999). Standardized process improvement for construction enterprises. Total Quality Management, 10, 576-583.

[11] Jaco, R. (2004). Developing an IS/ICT management capability maturity framework, Proceedings of the 2004 annual research conference of the South African institute of computer scientists and information technologists on IT research in developing countries. Stellenbosch, Western Cape, South Africa: South African Institute for Computer Scientists and Information Technologists.

[12] Paulk, M. C., Weber, C. V., Garcia, S. M., Chrissis, M. B., & Bush, M. (1993). Key Practices of the Capability Maturity Model - Version 1.1 (Technical Report): Software Engineering Institute, Carnegie Mellon University.

[13] SUCCAR, B. (2010). The five components of BIM performance measurement. Paper presented at the CIB World Congress, Salford, United Kingdom. http://bit.ly/BIMPaperA4

[14] "IFC Overview summary — Welcome to buildingSMART-Tech.org". Retrieved: http:// www.buildingsmart-tech.org/specifications/ifc-overview.

[15] Mercer A. (2017): Bentley's AECOsim Building Designer CONNECT Edition Surmounts the

Challenges of BIM Scalability for Major Projects. Retrieved from: https://www.bentley.com /en/about-us/news/2017/september/18/aecosim-building-designer-connect-edition
[16] Autodesk and Trimble Sign Agreement to Increase Interoperability. Retrieved: news. autodesk .com/2016-06-14-Autodesk-and-Trimble-Sign-Agreement-to-Increase-Interoperability
[17] IFC for Revit (2014 -2018). Retrieved from: https://sourceforge.net/projects /ifc exporter/
[18] buildingSMART, (2016). Retrieved from: http://buildingsmart.org or the Revit wiki http://help.autodesk.com/view/RVT/2016/ENU/?guid=GUID-6708CFD6-0AD7-461F-ADE8-6527423EC895).
[19] Autodesk and UK BIM Level 2 Mandate Retrieved from: http://thebuildingcoder. typepad. com /files/autodesk_and_uk_bim_level_2_mandate.pdf.
[20] Sullivan J. (2016), Business Development Manager, Autodesk: Application Programming Interfaces
[21] GRAPHISOFT (2017). Step up your BIM! Retrieved from: http://www.graphisoft.com /info/ news/press releases/archicad-21-step-up-your-bim.html
[22] Vectorworks (2017). Transform the World Design with Vectorworks, Retrieved from: http://www.vectorworks.net/2017.
[23] Trimble Solutions Corporation, Make Your Design Real with Tekla and Autodesk Revit; retrieved from: https://www.tekla.com/us/products/tekla-structures/tekla-interoperability-autodesk-revit-products.
[24] Autodesk (2016), BIM Interoperability Tool; Retrieved from: https://www.biminteroperabilitytools.com/
[25] Bentley (2017), Solutions for Architecture and Engineering; Retrieved from: https://www. Bentley. com /en/solutions/project-delivery/architecture-and-engineering.
[26] Trimble (2016), Tekla Structural Designer Integration with Tekla Structures; Retrieved from: https://t eklastructuraldesigner.support.tekla.com/system/files/integration-between-tekla-structural-designer-and-tekla-structures.pdf
[27] Vectorworks (2016), IFC Format Interoperability; Retrieved from: http://app-help. Vectorworks. net /2016/eng/VW2016_Guide/IFC/IFC_Format_Interoperability.htm
[28] GRAPHISOFT (2018), OPEN BIM Program Structural Workflows MEP Workflows; Retrieved from:http://www.graphisoft.com/archicad/open_bim/open_bim_program/

Digital Terrain Modeling Using AKAZE Features Derived from UAV-Acquired, Nadir and Oblique Images

H. Kim[a], H. Son[a], and C. Kim[a]

[a]Department of Architectural Engineering, Chung-Ang University, South Korea
E-mail: kkhs1127@cau.ac.kr, hjson0908@cau.ac.kr, changwan@cau.ac.kr

Abstract –

During construction, digital terrain models based on images from unmanned aerial vehicles (UAVs) are useful, as they rapidly provide data for objective volume calculations that can be used to monitor in-progress earthworks. As many curved objects are present on construction sites and as construction materials and equipment can provide partial obstructions, nadir images alone is not adequate to generate accurate digital terrain models during the earthwork phase, thus, it is necessary to acquire both nadir and oblique images. However, it is difficult to extract features from oblique images to determine accurate locations using the traditional method from photogrammetry software, the scale-invariant feature transform (SIFT) algorithm. This study proposes a method for generating accurate digital terrain models of construction sites based on the accelerated KAZE (AKAZE) algorithm using a combination of nadir and oblique UAV images. The proposed method consists of the following steps: 1) feature extraction and matching based on the AKAZE algorithm; 2) three-dimensional (3D) point cloud generation based on the results of the feature matching; and 3) digital terrain model generation based on the resulting 3D point cloud and on the GPS information for the corresponding locations of each ground control point (GCP). Validation of the proposed method involves 100 oblique UAV images of the actual construction site's in-progress earthworks. The experimental results indicate that the AKAZE algorithm can be applied to generate an accurate digital terrain model by extracting and matching features to ensure the accuracy of the edges and corners. Based on these results, the proposed method can be expected to provide accurate volume calculations from a generated digital terrain model, which can enable monitoring of the earthwork phase.

Keywords –

AKAZE; Digital Terrain Model; Earthwork; Oblique Images; Photogrammetry; UAV

1 Introduction

3D digital terrain models are used in fields such as traffic, geology, and archeology, but they are especially common in the construction industry, where they can rapidly provide data for objective volume calculations that can be used to monitor in-progress earthworks. The role of the digital terrain model is regarded as increasing because of the need to periodically monitor the continual terrain changes of the construction site. However, for such digital terrain models to be effectively used in construction project, an approach is needed that can both model the terrain rapidly to provide periodic updates and accurately represent the terrain.

In the construction industry, terrestrial laser-scanning surveys are widely used in digital terrain modeling because of their high accuracy (e.g., [1–3]). However, these surveys' data acquisition is not efficient enough to provide periodic updates because, for each area of the construction site, the laser scanner needs to be moved and installed multiple times before the data can be acquired; this is time consuming and requires at least two people. These surveys also have the disadvantage of being difficult to use on terrain with severe drop-offs and/or inclines. In recent years, digital terrain modeling through the use of photogrammetry based on images from UAVs has gained popularity due to the evolution of UAV technology, which is now possible to improve stability and to allow longer flight time. This approach allows for the fast and easy acquisition of images for a large area, including for terrain with severe variations.

Several researchers have attempted to generate digital terrain models for construction sites using UAV nadir images (e.g., [4,5]) or a combination of UAV and ground images [6]. Previous studies have shown that digital terrain modeling using UAV images has the potential to rapidly generate digital terrain for a large area. However, image-acquisition or -processing methods from other industries are inadequate to be used

in construction site without considering the unique characteristics of construction-site terrain [4–6].

Construction sites often have severe terrain variations, and various construction materials and equipment can partially obstruct terrain in the images. In this environment, using nadir and oblique images together (rather than nadir type alone) increases the vertical accuracy of a digital terrain model [7]. Several UAV manufactures (e.g., Leica Geosystems, Pictometry International, and Microsoft) have developed camera sensors that can acquire both nadir and oblique images from four directions, thus solving the obstruction problem. Accordingly, several researchers (e.g., [8–10]) have attempted to generate digital terrain models using nadir and oblique images in combination. The most commonly used feature-extraction and -matching algorithm in photogrammetry software—SIFT algorithm [12], which is employed in Agisoft's PhotoScan and Pix4D's Pix4Dmapper—is suitable for matching parallel nadir images. This is because the SIFT algorithm performs well when matching two images that have been acquired at different distances [12]; in this scenario, it can extract the features of the edges and corners. On the other hand, the SIFT algorithm has a limited ability to accurately extract features when matching two images that have been acquired from different angles [11]. It is still necessary to consider which feature-extraction and -matching method—when considering construction sites' terrain characteristics—will generate the most accurate digital terrain model from nadir and oblique images.

The aim of this study is to propose a method for using nadir and oblique UAV images to generate accurate digital terrain models of construction sites based on the AKAZE algorithm. This paper is organized as follows. Section 2 reviews the studies on digital terrain modeling based on UAV images in the construction industry. Section 3 introduces the proposed method, and Section 4 provides analysis of the experimental results. Finally, Section 5 describes the conclusions and includes suggestions for future research.

2 Literature Review

Several researchers (e.g., [4–6]) have attempted to generate digital terrain models for construction sites based on UAV-based nadir image acquisition. Sibert and Teizer [4] and Hugenholtz et al. [5] used UAV flight-plan software provided by manufacturers (e.g., DJI and Intel) in addition to commercial photogrammetry software. The UAV flight-plan software developed by the UAV industry provides the ability to acquire images while maintaining a constant overlap ratio at a certain height. The resulting images can be used to generate digital terrain models using photogrammetry software. Sibert and Teizer [4] used the UAV flight-plan software to collected nadir images from a height of 30 m and then applied commercial photogrammetry software (Agisoft's PhotoScan) to generate a digital terrain model of a construction site. Hugenholtz et al. [5] used AutoGrid's Aeryon Labs flight-plan software to acquire nadir images from a height of 100 m and then applied commercial photogrammetry software (MosaicMill's EnsoMOSAIC) to generate a digital terrain model. In general, commercial photogrammetry software generates digital terrain models based on the SIFT feature-extraction algorithm [12]. Bügler et al. [6] acquired both aerial and ground images and used them to generate a digital terrain model using open-source VisualSFM software [13], which is also based on the SIFT algorithm. The resulting digital terrain model and the activity status of the construction equipment based on video analysis provided information on equipment productivity. In summary, image-acquisition and -processing methods from other industries are inadequate to be used in construction without first considering the characteristics of construction sites' terrain [4–6]). Thus, it is still necessary to consider—based on construction sites' terrain—which method of feature extraction is most appropriate for generating accurate digital terrain models from UAV images.

3 Methodology

3.1 Image Acquisition

In this study, the images were acquired using DJI's UAV Matrice 100 and Zenmuse Z3 camera, with the point-of-interest function from DJI's Ground Station Pro software used to plan the image-acquisition flight. The flight path had a 90% overlap ratio, using angles of −75°, −60°, −45°, and −30°. This resulted in four flight paths. Each flight path followed a hemispherical orbit with a radius of 30 m around the target terrain; in all, 100 images of 4,000 × 3,000 resolution were acquired.

Figure 1 illustrates the difference between regions for rough terrain when using the nadir images alone (Figure 1[a]) and when using nadir and oblique images simultaneously (Figure 1[b]). As shown in Figure 1(a), when using only nadir UAV images for digital terrain modeling, obstructions can be occurred in areas of severe drop-offs and/or inclines [4,5]. On the other hand, as shown in Figure 1(b), when both nadir and oblique images are used, obstructed areas can be revealed.

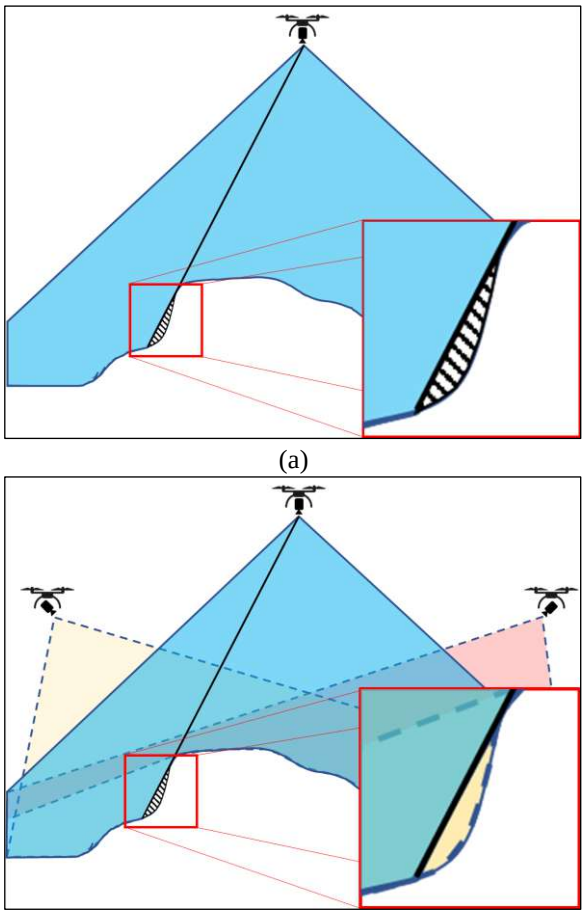

(a) (b)

Figure 1. Image-acquisition approaches: (a) nadir images alone and (b) both nadir and oblique images

3.2 Image Processing

Nadir and oblique images are based on different distances to the same object, as shown in Figure 2. For this reason, the same object appears on a different scale in these images. Under these conditions, determining accurate locations in all images is important because they affect the accuracy of the resulting digital terrain model. The SIFT algorithm that is often used in commercial photogrammetry software applies the Laplacian of Gaussian method, which uses differences between images (after blurring with a Gaussian filter) to extract the same features of an object that is seen from various scales. Equal-sized masks are used on the images of multiple scales to extract the features that are relevant to determining the edges and corners; this process helps identify the corresponding features for the same objects at various distances. However, the Gaussian filter can result in blurred edges and corners, which makes it difficult to extract accurate locations of features [14].

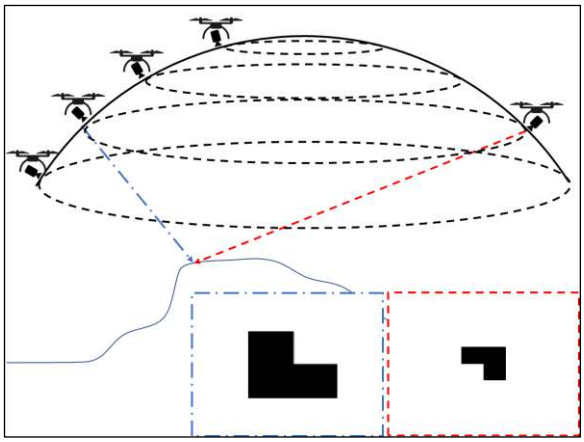

Figure 2. Changes in the scale of the same object in images acquired from different angles

To handle the problem of constructing nonlinear scale space to find the corresponding features for the same object from images obtained at multiple distances, the KAZE algorithm using a nonlinear diffusion filter was proposed by Alcantarilla et al. [14]. The nonlinear diffusion filter is advantageous because the edge information is preserved rather than blurred as it is processed in the Gaussian filter (e.g., [14–16]). Figure 3 shows an image of the GCP placed on the terrain, and the GCP's edges are distinctive in the image.

Figure 3. An example of a UAV image obtained at the actual earthwork site

Figure 4 shows the results of applying the Gaussian filter and the nonlinear diffusion filter, respectively, to Figure 3. Figure 4(a) shows the result of applying the Gaussian filter to construct the scale space in the SIFT

algorithm, and this process blurred edge information from the original image. Figure 4(b) shows an example of applying the nonlinear diffusion filter. During the construction of the scale space, the distinctive edges in the image were retained without sacrificing the object's edges. Unlike the SIFT algorithm, this property leads to the identification of exact position of objects' edges and corners at various scales using such scale spaces [14–16]. This study employed the AKAZE [17] algorithm, which uses the same nonlinear diffusion filter as the KAZE algorithm but improves the processing speed.

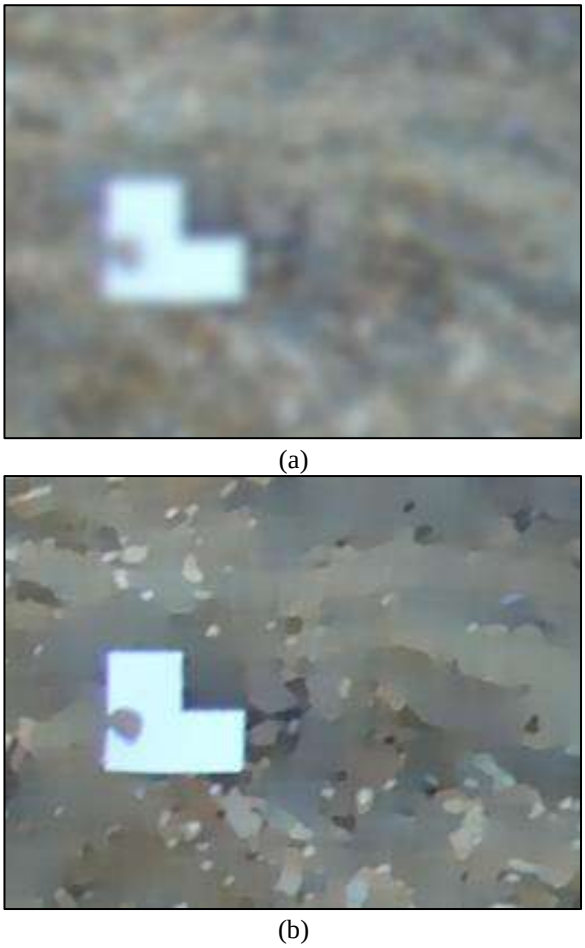

(a)

(b)

Figure 4. Example of applying (a) Gaussian filter and (b) nonlinear diffusion filter

3.3 3D Terrain Model Generation

Once the features have been extracted from a pair of images, the features from the same locations are matched using the random sample consensus algorithm and transformed into a 3D point clouds. When the position of the extracted feature is more accurate, so too is its corresponding 3D point. A 3D point cloud is then generated based on the extracted feature-matching results of 100 images. In this process, the SIFT and AKAZE algorithms are applied using OpenCV3.4.0 connected to OpenMVG [18]—open-source photogrammetry software—by applying defualt parameters. Then, the digital terrain model is generated using OpenMVS, which is an open-source method for generating dense point clouds and mesh models from 3D point cloud recalibrated through the bundle-adjustment process; this position of the resulting 3D point cloud is based on the GPS information of the corresponding locations of each GCP.

4 Experiments

This section provides a description of the results for each step of the experiment. The experiment was performed at an actual highway construction site with in-progress earthworks in Asan-si, Chungcheongnam-do, South Korea. The target area for generating the digital terrain model included bumpy terrain. The UAV acquired images of the target area using a hemispherical flight path.

4.1 Performance Measures

To evaluate the accuracy of the generated 3D point cloud, the values of X, Y, and Z at each check point (CP) derived from the dense point cloud are compared with GPS information measured at the site. The dense point cloud generated by registering GPS information corresponding to each GCP location contains CPs to be used for evaluation, which are not used in georeferencing, and the values of X, Y, and Z in each CP can be derived using CloudCompare. The measures used for evaluation are four values of root mean square error (RMSE), which represent the error for each axis and the overall error in the 3D space. The equations for the four measures are as follows.

$$\mathrm{RMSE_x}=\sqrt{\frac{\sum_{i=1}^{n}\left[\left(X_{pi}-X_{qi}\right)^2\right]}{n}} \quad (1)$$

$$\mathrm{RMSE_y}=\sqrt{\frac{\sum_{i=1}^{n}\left[\left(Y_{pi}-Y_{qi}\right)^2\right]}{n}} \quad (2)$$

$$\mathrm{RMSE_z}=\sqrt{\frac{\sum_{i=1}^{n}\left[\left(Z_{pi}-Z_{qi}\right)^2\right]}{n}} \quad (3)$$

$$\mathrm{RMSE_{xyz}}=\sqrt{\frac{\sum_{i=1}^{n}\left[\left(X_{pi}-X_{qi}\right)^2+\left(Y_{pi}-Y_{qi}\right)^2+\left(Z_{pi}-Z_{qi}\right)^2\right]}{n}} \quad (4)$$

where n is the number of CPs and X_{pi}, Y_{pi}, and Z_{pi} are the X, Y, and Z coordinates derived from the 3D point cloud for the i_{th} CP. X_{qi}, Y_{qi}, and Z_{qi} are X, Y, and Z coordinates of GPS information for the i_{th} CP measured at the site. A smaller value for each measure means the 3D point cloud is generated closer to the actual site.

4.2 Results and Discussion

The resulting nadir and oblique images produced a digital terrain model through feature extraction and matching; the resulting point cloud was generated based on GPS information for each GCP. Figure 5 compares the results of the matching features for the SIFT and AKAZE algorithms based on two oblique images acquired from the construction site. The point at the end of each line represents the location of the feature.

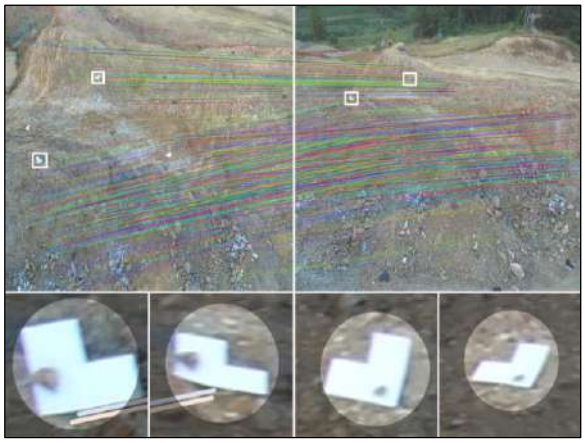

(a)

(b)

Figure 5. Comparison of the feature-extraction and -matching results for (a) the SIFT algorithm and (b) the AKAZE algorithm

The feature-matching result of the AKAZE algorithm in Figure 5(b) was more accurate than the SIFT algorithm in Figure 5(a) in terms of the edges and corners. Figure 6(a) shows a 3D point cloud that was generated using the AKAZE algorithm. The extracted features have two-dimensional location values. Through triangulation based on the camera locations, a single point with a 3D location value can be computed. Finding accurate locations for the edges and corners in each image can reduce errors in the point cloud, thus enabling better matching between pairs of images and improving the accuracy of the resulting digital terrain model. Because the resulting point cloud is generated only using feature matching without GPS information, it is necessary to register GPS information to improve accuracy. Figure 6(b) shows a dense point cloud with GPS information. In Figure 6(b), each pair of a white point and a tag represents where the CP is located.

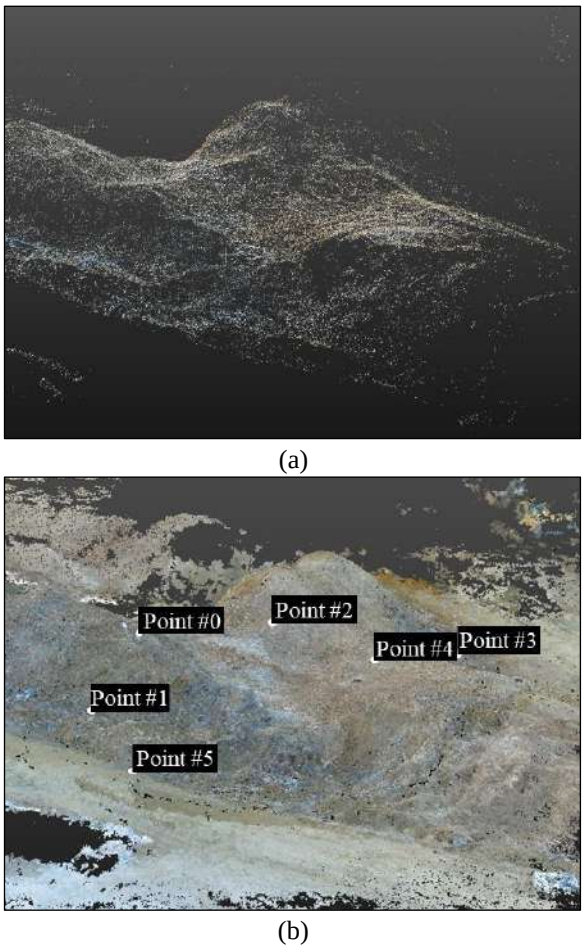

(a)

(b)

Figure 6. (a) 3D point cloud generated from images using the AKAZE algorithm and (b) dense point cloud based on feature points

Table 1 summarizes the comparison of errors of 3D point cloud generated by the two algorithms. The 3D point cloud generated by applying the AKAZE algorithm showed smaller error values than that generated by applying the SIFT algorithm for all four measures. In other words, the results indicate that a more accurate 3D point cloud was generated when the AKAZE algorithm was applied.

Table 1. Comparison of errors of 3D point cloud generated by various algorithms

Measures (m)	SIFT	AKAZE
$RMSE_x$	0.044	**0.012**
$RMSE_y$	0.116	**0.108**
$RMSE_z$	0.053	**0.038**
$RMSE_{xyz}$	0.053	**0.032**

Figure 7 shows a digital terrain model that is generated from the same dense point cloud from Figure 6. The digital terrain model is then generated, with open-source code (OpenMVS) as the basis for the dense point cloud and the mesh model. The resulting model is based on accurate feature locations, which were extracted using the AKAZE algorithm and which thus are expected to have higher accuracy than those produced using the SIFT algorithm.

Figure 7. Digital terrain model generated using the proposed method

5 Conclusion

In this study, the AKAZE algorithm was employed to generate an accurate digital terrain model from nadir and oblique UAV images. The results indicate that the features extracted using the AKAZE algorithm are more accurate than those extracted using the SIFT algorithm. This difference implies that the proposed method can generate more accurate digital terrain models than can be generated through conventional method. The model generated by the proposed method can be used to provide quantitative measurements, which can be applied for more accurate construction-site volume calculations. Future research will apply the algorithms based on stable affine invariant features and compare the 3D reconstruction performance in terms of accuracy.

Acknowledgments

This research was supported by Basic Science Research Program through the National Research Foundation of Korea (NRF) funded by the Ministry of Education (NRF- 2018R1D1A1B07049846).

References

[1] Jaselskis, E. J., Gao, Z., & Walters, R. C. Improving transportation projects using laser scanning. *Journal of Construction Engineering and Management* 131(3):377–384, 2005.

[2] Du, J. C., & Teng, H. C. 3D laser scanning and GPS technology for landslide earthwork volume estimation. *Automation in Construction* 16(5):657–663, 2007.

[3] Slattery, K. T., Slattery, D. K., & Peterson, J. P. Road construction earthwork volume calculation using Three-dimensional Laser Scanning. *Journal of Surveying Engineering* 138(2):96–99, 2011.

[4] Siebert, S., & Teizer, J. Mobile 3D mapping for surveying earthwork projects using an unmanned aerial vehicle (UAV) system. *Automation in Construction* 41:1–14, 2014.

[5] Hugenholtz, C. H., Walker, J., Brown, O., & Myshak, S. Earthwork volumetrics with an unmanned aerial vehicle and softcopy photogrammetry. *Journal of Surveying Engineering* 141(1):06014003, 2014.

[6] Bügler, M., Borrmann, A., Ogunmakin, G., Vela, P. A., & Teizer, J. Fusion of photogrammetry and video analysis for productivity assessment of earthwork processes. *Computer-Aided Civil and Infrastructure Engineering* 32(2):107–123, 2017.

[7] James, M. R., & Robson, S. Mitigating systematic error in topographic models derived from UAV and ground-based image networks. Earth Surface Processes and Landforms 39(10):1413–1420, 2014.

[8] Fernández-Lozano, J., & Gutiérrez-Alonso, G. Improving archaeological prospection using localized UAVs assisted photogrammetry: An example from the roman gold district of the Eria river valley (NW Spain). *Journal of Archaeological Science Reports* 5:509–520, 2016.

[9] Agueera-Vega, F., Carvajal-Ramirez, F., Martínez-Carricondo, P., López, J. S. H., Mesas-Carrascosa, F. J., García-Ferrer, A., & Pérez-Porras, F. J. Reconstruction of extreme topography from UAV structure from motion photogrammetry. *Measurement* 121:127–138, 2018.

[10] Rusnák, M., Sladek, J., Kidová, A., & Lehotský, M. Template for high-resolution river landscape mapping using UAV technology. *Measurement* 115:139–151, 2018.

[11] Yu, G., & Morel, J. M. ASIFT: An algorithm for fully affine invariant comparison. *Image Processing on Line* 1:11–38, 2011.

[12] Lowe, D. G. Distinctive image features from scale-invariant keypoints. *International Journal of Computer Vision* 60(2):91–110, 2004.

[13] Wu, C. VisualSFM: A visual structure from motion system. Online: http://ccwu.me/vsfm/, Accessed: 27/01/2019.

[14] Alcantarilla, P. F., Bartoli, A., & Davison, A. J. KAZE features. In *Proceedings of the European Conference on Computer Vision*, pages 214–227, Berlin, Heidelberg, 2012.

[15] Fortun, D., Bouthemy, P., & Kervrann, C. Optical flow modeling and computation: A survey. *Computer Vision and Image Understanding* 134:1–21, 2015.

[16] Gastal, E. S., & Oliveira, M. M. Oliveira. Domain transform for edge-aware image and video processing. *ACM Transactions on Graphics* 30(4), 2011.

[17] Alcantarilla P. F., Nuevo J., and Bartoli A. Fast explicit diffusion for accelerated features in nonlinear scale spaces, In *Proceedings of the British Machine Vision Conference*, 2013.

[18] Moulon, P., Monasse, P., Perrot, R., & Marlet, R. OpenMVG. Online: https://openmvg.readthedocs.io/en/latest/#, Accessed: 27/01/2019.

Deep-learning for Occupancy Detection Using Doppler Radar and Infrared Thermal Array Sensors

M. Abedi[a], and F. Jazizadeh[b]

[a] Charles Edward Via. Department of Civil and Environmental Engineering, Virginia Tech, US
E-mail: jazizade@vt.edu

Abstract –

An accurate, real-time monitoring of the occupancy state of each space is a necessity for applications such as energy-aware smart buildings. In this paper, we have studied the feasibility of using Doppler Radar Sensors (DRS) and Infrared Thermal Array Sensors (ITA) to build an effective occupancy detection framework. The proposed sensor types are cost-effective and protect the privacy of the occupants. We have utilized Deep Neural Networks (DNN) to analyze the sensor data without any need for specialized feature extraction that is necessary for classical machine learning approaches. The results are indicative of the feasibility and the reliability of using both sensor types for detection of the occupancy state. While a threshold-based approach reached an average accuracy of 84.3% and 86% for the DRS and ITA sensors respectively, DNN models were able to achieve average accuracies of 98.9% and 99.96% for the DRS and ITA sensors respectively, thereby demonstrating the feasibility and success of the proposed framework.

Keywords –

Doppler Radar Sensor; Infrared Thermal Array Sensor; Deep Learning; Deep Neural Network

1 Introduction

In the US, residential and commercial buildings are responsible for 39% of the total energy consumption [1]. About 8% of the total electricity consumed in residential and commercial buildings is used for lighting [2]. Heating, Ventilations, and Air Conditioning (HVAC) systems, being responsible for the consumption of 40% of total energy used by the building sector, are also considered to be a major consumer of energy [3]. The combination of these figures underlines the necessity of the notion of energy-aware "smart buildings".

The nature of the relationship between the demand for HVAC and lighting in the environment (e.g. a room) and the state of occupancy of the environment, has given rise to a growing demand for effective occupancy detection technologies. Several smart HVAC control frameworks rely directly on information regarding the occupancy state of the environment for control purposes [4,5]. Occupancy-based control of the lighting system has also been the subject of research studies [6] and has been widely adopted in practice. The potential for energy saving by enabling occupancy-based control of building systems has been estimated to be as high 25% [7] for HVAC systems and 50% [8] for lighting systems.

A necessary condition for the realization of the true potential of occupancy-based smart control of building operations, is the development of accurate and robust sensing frameworks, easily deployable in a variety of environments. Two of the traditional sensing frameworks for detection of occupancy are such technologies as Passive Infrared sensors (PIR) [9], and image-based technologies [10,11]. However, the PIR sensing framework has been known to suffer from high error rates [12]. PIR sensors require an unobstructed view of the occupant to function and their ability to detect the occupant deteriorated with the increase in distance-to-target [13]. Moreover, the ability of PIR sensors to detect the occupant relies on the existence of a temperature contrast between the occupant and the surrounding environment, thereby resulting in a performance loss in warmer room environments [14]. The mechanism of detection of the occupant for PIR sensors relies on measuring the changes in the temperature contrast of the monitored area, as created by movements of the occupant. Thus, the performance of the PIR sensor is predicated on clear occupant movements, rendering the sensor insensitive to more subtle movements by occupants' body parts.

An alternative to PIR sensors is the image-based sensing technology. In particular, video-camera-based occupancy detection frameworks are considered to be an effective alternative to PIR sensors. However, implementation of these technologies is accompanied by considerable privacy concerns. As such, researchers have endeavored to propose alternative sensing technologies to address deficiencies of the traditional approaches while respecting occupant privacy.

One type of sensors that we have evaluated in this

paper with regards to their applicability for occupancy detection purposes are Doppler Radar Sensors (DRS). DRS sensors rely on motion for detection of the state of the occupancy. DRS sensors can detect the existence of the motion by measuring the change in the frequency of the reflected wave as a result of target motion. However, unlike PIR sensors, DRS sensors are capable of detecting subtle movements of the body such as rotation of the occupants' head, movement of the occupants' hands and arms, and even pulmonary activities, thereby resulting in higher accuracy and reliability.

Another sensor type that has been subject to investigation in the present paper is the Infrared Thermal Array (ITA) sensor. While ITA sensors have been prevalently present in the market, until recently there was a gap in the production resolution of these sensors and the users had to choose between an affordable sensor resolution of up to 64 pixels (8×8 or 4×16) or opt for high resolution sensors at an approximate cost of $200 [15] per sensor. However, in early months of 2018, mid-resolution (32×24) ITA sensors (e.g. model name: MLX90640 [16]) at an affordable cost of under $50 have been introduced to the market. These sensors present a unique opportunity for utilization in an occupancy detection framework as the resolution/cost balance has become reasonable enough to allow for such applications. While our original intention was to build a framework that would utilize both sensors simultaneously to reduce individual error-rates, the high accuracy of each individual sensor convinced us to evaluate them separately.

For the proposed sensing setup to be operationally feasible, the framework must be augmented with an effective data analysis algorithm. By defining a binary state of occupancy for the room, the problem of occupancy detection becomes one of binary classification. Within the multitude of well-established classification algorithms, we have opted to utilize a Deep Neural Network (DNN) model for analysis of sensor data. Utilization of DNN models will allow us to obviate the need for feature-extraction step thereby resulting in an autonomous data analysis framework.

2 Literature Review

Given the growing demand for energy-efficient smart buildings, researchers have endeavored to propose a multitude of occupancy monitoring frameworks consisting of various sensor types and data-analysis strategies.

One of the well-studied sensor types for indoor occupancy monitoring are Passive Infrared (PIR) sensors. PIR sensors measure the infrared light emitted from the object and detect the movements of the source of emission. However, these sensors are not sensitive to subtle and slow movements, which diminishes their capacity to perform as a presence sensor. As such, researchers have endeavored to rectify the aforementioned limitation by means of algorithmic developments and augmentation with other sensor types. For instance Pedersen, et al. [17] have augmented PIR sensors with additional noise, CO_2, Volatile Organic Component (VOC), humidity, and temperate sensors to monitor the state of occupancy of a room. In another study, Dodier, et al. [18] have proposed a belief network approach to analyze the data coming from a network of PIR sensors.

Video cameras have also been used for occupancy detection (mostly occupancy counting) and monitoring. For instance, Hoover and Olsen [10] and Fleuret, et al. [19] have used video cameras to enable tracking of occupied spaces within a room. While implementations of camera-based occupancy detection methods have proven to be accurate [20], utilization of cameras is accompanied by privacy considerations. As such, researchers have endeavored to propose sensing frameworks that are both accurate and compliant with privacy expectations.

Doppler Radar Sensors (DRS) have been studied by researchers as an alternative to traditional occupancy detection frameworks. Like PIR sensors, DRS sensors also detect the motions in their field of view, however, their ability to detect very subtle movements such as those created by pulmonary activities, allows DRS sensors to circumvent some of the important limitations of PIR sensors. Lurz, et al. [21] have demonstrated the feasibility of using DRS sensors for occupancy detection in an experiment that emulated human respiration by means of a linear stage at a distance of 2 m from the sensor. Yavari, et al. [22] have used DRS sensors to detect occupancy by relying on extraction of pulmonary and cardiovascular signatures in the DRS signal while the occupant was either at rest or was moving at different activity levels. One limitation of their study was the constant 1.5 m distance between the radar and the occupant. In the present paper, we have sought to extend the investigation of the capability of DRS sensors to measure occupancy throughout the room without preset conditions such as restricting occupant distance from the sensor to enable room-level service. We have used wide-angle DRS sensors, installed at the ceiling to monitor the state of occupancy in a typical office room.

Another sensor type that has presented a potential for occupancy detection is the Infrared Thermal Array Sensor (ITA). Beltran, et al. [7] utilized an ITA sensor with the resolution of 8×8 to monitor room occupancy state and then used the knowledge of occupancy to more efficiently control the HVAC system operations thereby achieving an annual energy saving rate of 25%. The

algorithms utilized in the aforementioned study [7] for the interpretation of the ITA sensor outputs are K-Nearest Neighbor (KNN), Linear Regression, and an Artificial Neural Network. In another study, Tyndall, et al. [23] used an ITA sensor with the resolution of 4×16 to estimate the state of occupancy inside the room. The algorithms used for analysis of data consist of a number of standard classification algorithms such as Support Vector Machine, and KNN [23].

Recent industry advancements have given rise to semi-high resolution ITA sensors at an affordable price of approximately $50 (e.g. MLX90640 [16] with a resolution of 32×24). This development could result in an increased potential for utilization of ITA sensors for non-intrusive occupancy-monitoring applications. As such, in this paper we have evaluated the performance of the MLX90640 [16] sensor for real-time monitoring of the occupancy state in a typical office room environment. Additionally, by implementing a Deep-Learning solution for the analysis of sensor data we have eliminated the feature extraction step, thereby rendering the data analysis step autonomous.

3 Methodology

Presented in this section is the discussion of two aspects of the occupancy detection framework. In the first part we have discussed the overview of the sensing framework. In the subsequent section, the data analysis and occupancy inference approach have been discussed.

3.1 Sensing System Setup and Data Acquisition

As noted, in this study, we have investigated the potential of two distinct sensor types for occupancy detection applications. The first sensor type is the Doppler Radar Sensor (DRS). We have used the RFBeam K-LC3 [24] wide angle doppler transceiver. With dimensions of 25×25 mm and a weight of 5 g the K-LC3 DRS sensor is a cost-effective and practical solution for occupancy detection. Another desirable feature of the selected sensor model is the wide field of view (132º×138º), which allows for coverage of larger areas, compared to other sensor models with narrower fields of view. In Figure 1, the coverage area for the DRS sensor (as well as the ITA sensor) that has been installed in a typical US office room (7.5×4 m) is presented. The sensor is assumed to have been installed on the ceiling with the height of 2.75m (9ft) which is typical in the US. The coverage area has been calculated such that it at least captures the parts of the occupant's body at or under the desk level (0.8 m from the floor), i.e. occupant's hands, lower torso, and legs. As seen in Figure 2., we have installed the DRS sensor on the ceiling close to the air-vent. The DRS sensor has been connected to a SR 560 preamplifier [25] to amplify the output signal by a gain factor of 5×10^4. The amplifier also filters out the frequency content above 1kHz since the frequency content above that threshold is highly unlikely to have been generated due to the motions of the human subject. This sampling rate also helps avoid aliasing error due to possible presence of high-frequency signals associated with the existing equipment in the room (e.g. computer fans and HVAC).

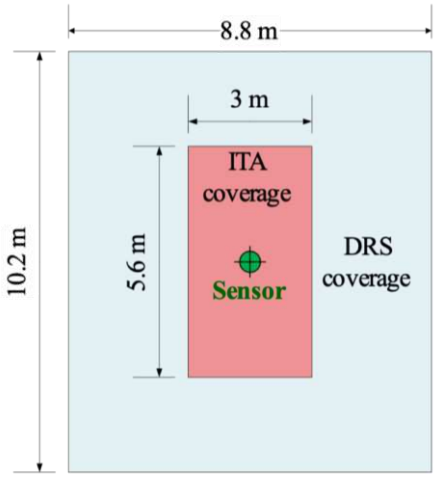

Figure 1. Space covered by each sensor type

Figure 2. Sensors installed (ITA sensor on the left and DRS sensor on the right)

For data acquisition, we used a National Instrument USB-6001 Multifunction I/O Device [26] to record the amplified signal at a sampling rate of 1kHz. The signal was processed through a zero-phase notch filter to remove the frequency harmonic contents, associated with powerline-noise (i.e. 60 Hz, 120 Hz, …). These frequencies in the signal are usually generated due to the existence of AC powerlines (60 Hz) in the vicinity of the setup.

The second sensor type is the MLX90640 [16] Infrared Thermal Array (ITA) sensor. This ITA sensor has a field of view of 110º×75º divided into 32×24 pixels respectively, where each pixel reads the average

temperature of the objects, covered in the view-window of that pixel. We have used a Raspberry Pi 3 [27] computer for data acquisition from the ITA sensor through the I2C serial protocol. We have installed the ITA sensor on the ceiling, close to the air vent as can be seen in Figure 2. The transfer of sensor readings to the on-site computer is done through wire-less connection.

3.2 Occupancy Inference Framework

Each data-point, acquired through our experiments, consists of a 10-second DRS signal @1kHz and a single ITA sensor temperature reading. The DRS data is represented as a time-series and the ITA sensor output is a 2D thermal image. Additionally, each data-point has a binary label (0,1) that determines the state of the occupancy during the 10 second interval associated with each data-point. Through this description, the task of occupancy detection has become one of binary classification (i.e. unoccupied, occupied).

In this study, we have investigated two different occupancy inference methods for the classification problem. In pursuit of an unsupervised method of inference, similar to methods commonly used for PIR sensors, the first approach is a threshold-based decision tree method, that has been used to establish a base-line. Thus, if at any point in time, the DRS time-series exceeds a certain threshold (regardless of the signal amplitude sign), the model will output a positive occupancy state for the room and vice versa. Similarly, if the temperature reading at any of the ITA sensor's output pixels exceeds a certain threshold, the model will output a positive occupancy state for the room and vice versa. The threshold has been selected by using a decision tree of depth 1. The implementation of the decision tree was performed by utilizing the Scikit-Learn [28] library in python 3.65.

As the second class of inference method, we have proposed and evaluated a Deep Neural Network (DNN) solution for the task of occupancy inference based on sensor data. Utilization of a DNN model brings about a number of advantages. Firstly, by utilizing the Deep Learning model, we obviate the need for specialized feature extraction, because the task of feature extraction in a DNN model is performed automatically by the initial layers. Moreover, combining information of fundamentally different nature (in our case a DRS time series and an ITA 2D temperature array) is a relatively effortless task to achieve using DNN models, and it does not require further feature engineering. The structure of the DNN, used for analysis of the DRS time series is as presented in Table 1. Given the high number of trainable parameters in DNNs, there is often a need for a large training data-set to facilitate training and avoid overfitting. However, in some real-world applications such as ours, the size of the data-set is limited. As such, we have opted to use two Dropout layers with a dropout rate of 50% to help avoid overfitting of the model to the training data. The loss function used for training of the model is the 'binary cross-entropy' measure, which is a common choice for binary classification problems.

Table 1. DNN structure for analysis of DRS data with 223,481 trainable parameters.

Layer Type	Layer Size / Drop Rate	Filter Size	Activation Function
Conv1D	128	7	Relu
MaxPool1D	-	2	-
Conv1D	64	6	Relu
MaxPool1D	-	2	-
Conv1D	32	5	Relu
MaxPool1D	-	2	-
Conv1D	16	4	Relu
MaxPool1D	-	2	-
Conv1D	8	4	Relu
MaxPool1D	-	2	-
Flatten	-	-	-
Dropout	50%	-	-
Dense	64	-	Relu
Dropout	50%	-	-
Dense	32	-	Relu
Dense	1	-	Sigmoid

As shown in Table 1, the initial layers consist of relatively large 1D convolutional layers with larger filter sizes. The concatenation of convolutional layers with a shrinking size through the depth results in a phenomenon, through which the first layers are trained to perform generic feature extraction with lesser relevance to the data labels and more relevance to the input data itself. Conversely, the subsequent layers have more and more relevance to the label information. As such, after training the model, one could freeze the initial feature extraction layers, and reuse them for other models, thereby reducing the computational cost of training the new models. This is another helpful feature of DNNs that allows multiple models to share a common body of knowledge. This is an important feature of the model toward generalizability. In occupancy detection, unsupervised models with high accuracy and reliability are preferred.

In Table 2, the structure of the DNN used for analysis of ITA sensor output has been presented. Similar to the previous model, we have utilized Dropout layers to avoid overfitting to the training data. The initial layer of this model can also be used for transfer-learning purposes to obviate the need to re-train feature-extraction layers in a new DNN model. Similarly, the loss function has been chosen to be 'binary cross-entropy'.

Table 2. DNN structure for analysis of ITA data with 70,433 trainable parameters

Layer Type	Layer Size / Drop Rate	Filter Size	Activation Function
Conv2D	64	(3,3)	Relu
MaxPool2D	-	(2,2)	-
Conv2D	32	(3,3)	Relu
MaxPool2D	-	(2,2)	-
Flatten	-	-	-
Dropout	50%	-	-
Dense	64	-	Relu
Dropout	50%	-	-
Dense	32	-	Relu
Dense	1	-	Sigmoid

Both models have been implemented by utilizing the Keras [29] library with the TensorFlow [30] backend. Before feeding the data to the model, we have subtracted the mean from the ITA sensor readings. This has been done in order to stabilize the model and also to break possible time dependent relationships among data-points, since data-points that have been recorded close to each other could have a similar mean temperature reading. Thus, the ITA readings become temperature differentials rather than actual temperature readings. An example of these readings has been presented in Figure 3.

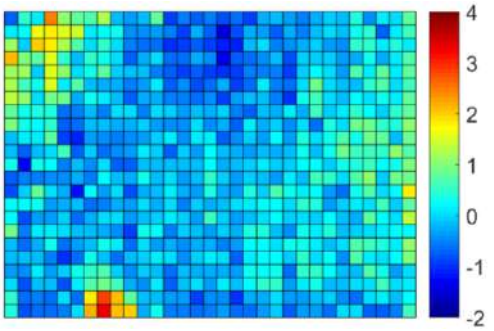

(a) The room is occupied

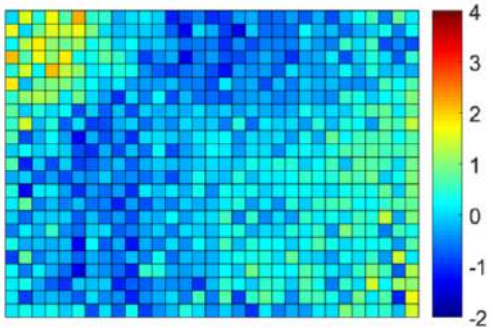

(b) The room is unoccupied

Figure 3. Temperature differentials (°C)

As can be seen in Figure 3, in both the occupied and unoccupied case, the upper left corner is warmer than the average. This is due to the presence of a personal computer at the corresponding location, which serves as a thermal noise. In Figure 4 an example of DRS sensor readings has been presented.

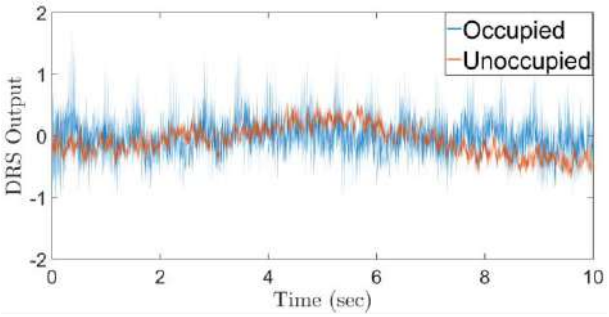

Figure 4. DRS sensor reading

Given that DRS sensor readings for both occupied and unoccupied cases were mostly in the [-1,1] range, no normalization was deemed necessary.

4 Results

In order to train the model to detect the state of occupancy in the environment, we need to provide the model with a data-set that includes both occupied and unoccupied states. The data associated with an unoccupied state, have been collected during the weekend. As for data associated with a positive state of occupancy, the human subject has sat at two different locations within the field of view of the ITA sensor.

The acquired dataset for this study consists of 1000 data-points, where each data-point contains an ITA sensor reading and 10 seconds of DRS signal (but only one sensor's reading will be given to each model, i.e. either DRS or ITA). In 500 of these cases, the room was unoccupied and in the other 500 cases the room was occupied. The evaluation of the models was performed through a 3-fold cross-validation. As noted, a simplified, threshold-based model was initially used to establish a baseline against which the performance of the DNN model is to be compared. In training of all models, the loss function has penalized equally against both false-positive and false-negative error types. In future studies, the loss function should be modified so as to take into account the relative importance of the two error types for the intended application.

The threshold-based model used to analyze the DRS signal has achieved an average accuracy of 84.3%. By contrast, the DNN model used for the analysis of the DRS signal has achieved an average accuracy of 98.9%. The training process of the model consisted of 10

epochs (batch size of 10) with a total elapsed time of 8 minutes on an Intel Xeon E5-1620 V4 CPU [31].

The threshold-based model for the analysis of the ITA sensor resulted in an average accuracy of 86%. By contrast, the DNN model has been able to reach an average accuracy of 99.96%. Training of DNN model used for analysis of ITA sensors consisted of 15 epochs (batch size of 10) with a total elapsed time of 6 seconds on an Intel Xeon E5-1620 V4 CPU [31].

In order to investigate the performance of the DNN model used for analysis of ITA sensor data, we retrieved the activation values of each layer (on the trained model) when the data-point associated with Figure 3.(a) was passed to the model. The filters in a convolutional layer seek to learn a pattern within the input data, and the activation values associated with each filter layer represents the level of a match that exists between a given input data and the pattern that the particular filter has learned. If the pattern of interest for that particular filter exists in certain areas of the data, the activation values for those areas will be higher. In Figure 5, we have presented the activation outputs for two of the filters in the third layer of the DNN model used for analysis of ITA data, i.e. the Conv2D layer with the size of 32.

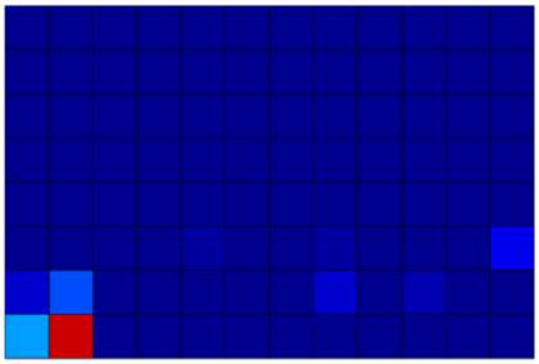

(a)

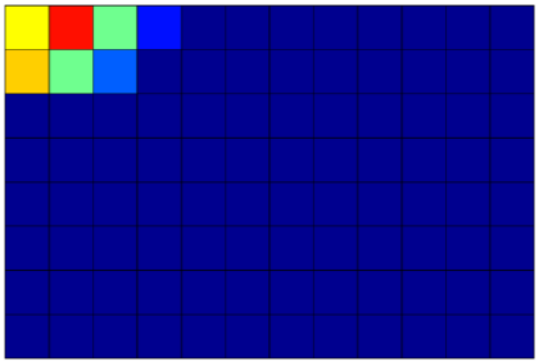

(b)

Figure 5. Activation outputs from two filters in the third layer of the DNN model (i.e Conv2D with the layer size of 32)

By comparing Figure 5.(a) with Figure 3.(a), it becomes apparent that the filter associated with these activation values has been trained to exclusively extract the thermal signatures of a human occupant since the activation values are high at the area associated with the location of the occupant. Interestingly, comparison of Figure 5.(b) with Figure 3.(a) reveals that the filter associated with these activation values has been trained to exclusively learn the thermal signature of the environmental noises (in this case the heat emissions from a personal computer in the environment). The mechanism of learning to detect both the noise and the actual occupant-related signatures in the data could be responsible for the high accuracy of the DNN model.

5 Limitations and Future Work

One limitation of this study was the limited size of the train and test data-sets. Moreover, the results are limited to experiments under a single environmental setting (i.e. one room and one occupant). In our future research we will evaluate the potential of the proposed framework under a multitude of experimental settings. Moreover, we will be investigating the potential of the proposed framework to count the number of occupants within each room.

Another line of research which will be the subject of our future studies is the potential to jointly learn from multiple sensor types to achieve synergistic combinations. For instance, in a room with occasionally high thermal noise, the DRS data could help reduce the possible errors in the performance of the ITA-based system. Similarly, if the degree of non-occupant related activities increases to a level that it would affect the performance of the DRS sensor, the information from ITA sensor could compensate for the possible increase in the DRS-based occupancy detection system's error rate.

6 Conclusion

A reliable and accurate occupancy detection framework is in high demand for realization of such applications as smart buildings. In this paper, we have proposed a framework for the detection of indoor occupancy based on cost-effective Doppler Radar Sensors (DRS) and cost-effective high-resolution Infrared Thermal Array Sensors (ITA). We have presented a Deep Neural Network solution for the analysis of the sensor data. We have further evaluated the performance of the framework by conducting real-work experiments in a typical office room. In order to establish a base-line for the performance of the proposed framework, we utilized a simplified threshold-based approach. The threshold-based approach achieved

an average accuracy of 84.3% and 86% for the DRS and ITA sensors respectively. The proposed DNN framework has demonstrated an accuracy of 98.9% via the DRS sensor and 99.96% via the ITA sensor.

Acknowledgement

This material is based upon work partially supported by the National Science Foundation under grant #1663513. Any opinions, findings, and conclusions or recommendations expressed in this material are those of the authors and do not necessarily reflect the views of the National Science Foundation.

References

[1] U.S. Energy Information Administration. How much energy is consumed in U.S. residential and commercial buildings? On-line: https://www.eia.gov/tools/faqs/faq.php?id=86&t=1 Accessed: 24/01/2019

[2] U.S. Energy Information Administration. How much electricity is used for lighting in the United States? On-line: https://www.eia.gov/tools/faqs/faq.php?id=99&t=3 Accessed: 24/01/2019

[3] Department of the Environment and Energy of the Australian Government. HVAC factsheet - Energy breakdown On-line: https://www.energy.gov.au/publications/hvac-factsheet-energy-breakdown Accessed: 24/01/2019

[4] Agarwal Y. and Balaji B. and Gupta R. and Lyles J. and Wei M., Weng T. Occupancy-driven energy management for smart building automation. In *Proceedings of the 2nd ACM Workshop on Embedded Sensing Systems for Energy-Efficiency in Building*, pages 1-6, Zurich, Switzerland, 2010,

[5] Nikdel L. and Janoyan K. and Bird S.D., Powers S.E. Multiple perspectives of the value of occupancy-based HVAC control systems. *Building and Environment*, 129:15-25, 2018

[6] Zou H. and Zhou Y. and Jiang H. and Chien S.-C. and Xie L., Spanos C.J. WinLight: A WiFi-based occupancy-driven lighting control system for smart building. *Energy and Buildings*, 158:924-938, 2018

[7] Beltran A. and Erickson V.L., Cerpa A.E. ThermoSense: Occupancy Thermal Based Sensing for HVAC Control. In *Proceedings of the 5th ACM Workshop on Embedded Systems For Energy-Efficient Buildings*, pages 1-8, Roma, Italy, 2013,

[8] Dubois M.-C., Blomsterberg Å. Energy saving potential and strategies for electric lighting in future North European, low energy office buildings: A literature review. *Energy and Buildings*, 43 (10):2572-2582, 2011

[9] Kaushik A.R., celler B.G. Characterization of Passive Infrared Sensors for Monitoring Occupancy Pattern. In *2006 International Conference of the IEEE Engineering in Medicine and Biology Society*, pages 5257-5260, 2006,

[10] Hoover A., Olsen B.D. A real-time occupancy map from multiple video streams. In *Proceedings 1999 IEEE International Conference on Robotics and Automation (Cat. No.99CH36288C)*, pages 2261-2266 vol.2263, 1999,

[11] Bhatia B. and Oates T. and Xiao Y., Hu P. Real-time identification of operating room state from video. In *Proceedings of the 19th national conference on Innovative applications of artificial intelligence - Volume 2*, pages 1761-1766, Vancouver, British Columbia, Canada, 2007,

[12] Srinivasan S. and Pandharipande A., Caicedo D. Presence detection using wideband audio-ultrasound sensor. *Electronics Letters*, 48 (25):1577-1578, 2012

[13] Hodges L. Ultrasonic and Passive Infrared Sensor integration for dual technology user detection sensors.

[14] Beckwith D., Hunter-Zaworski K. Passive pedestrian detection at unsignalized crossings. *Transportation Research Record: Journal of the Transportation Research Board*, (1636):96-103, 1998

[15] FLIR Systems Inc. Lepton LWIR Micro Thermal Camera Module On-line: https://www.flir.com/products/lepton/?model=500-0763-01 Accessed: 24/01/2019

[16] Melexis. Far infrared thermal sensor array (32x24 RES) On-line: https://www.melexis.com/en/product/MLX90640/Far-Infrared-Thermal-Sensor-Array Accessed: 24/01/2019

[17] Pedersen T.H. and Nielsen K.U., Petersen S. Method for room occupancy detection based on trajectory of indoor climate sensor data. *Building and Environment*, 115:147-156, 2017

[18] Dodier R.H. and Henze G.P. and Tiller D.K., Guo X. Building occupancy detection through sensor belief networks. *Energy and Buildings*, 38 (9):1033-1043, 2006

[19] Fleuret F. and Berclaz J. and Lengagne R., Fua P. Multicamera People Tracking with a Probabilistic Occupancy Map. *IEEE Transactions on Pattern Analysis and Machine Intelligence*, 30 (2):267-282, 2008

[20] Tomastik R. and Narayanan S. and Banaszuk A., Meyn S. Model-Based Real-Time Estimation

of Building Occupancy During Emergency Egress. pages 215-224, Berlin, Heidelberg, 2010,

[21] Lurz F. and Mann S. and Linz S. and Lindner S. and Barbon F. and Weigel R., Koelpin A. A low power 24 GHz radar system for occupancy monitoring. In *2015 IEEE Radio and Wireless Symposium (RWS)*, pages 111-113, 2015,

[22] Yavari E. and Jou H. and Lubecke V., Boric-Lubecke O. Doppler radar sensor for occupancy monitoring. In *2013 IEEE 13th Topical Meeting on Silicon Monolithic Integrated Circuits in RF Systems*, pages 216-218, 2013,

[23] Tyndall A. and Cardell-Oliver R., Keating A. Occupancy Estimation Using a Low-Pixel Count Thermal Imager. *IEEE Sensors Journal*, 16 (10):3784-3791, 2016

[24] RFbeam Microwave GmbH. K-LC3 Wide Angle Doppler Transceiver On-line: https://www.rfbeam.ch/product?id=6 Accessed: 24/01/2019

[25] Stanford Research Systems. Low Noise Voltage Preamplifier On-line: https://www.thinksrs.com/products/sr560.html Accessed: 24/01/2019

[26] National Instruments. USB-6001 Multifunction I/O Device On-line: http://www.ni.com/en-us/support/model.usb-6001.html Accessed: 24/01/2019

[27] The Raspberry Pi Foundation. Raspberry Pi 3 On-line: https://www.raspberrypi.org/products/raspberry-pi-3-model-b-plus Accessed: 24/01/2019

[28] Pedregosa F. and Varoquaux G. and Gramfort A. and Michel V. and Thirion B. and Grisel O. and Blondel M. and Prettenhofer P. and Weiss R., Dubourg V. Scikit-learn: Machine learning in Python. *Journal of machine learning research*, 12 (Oct):2825-2830, 2011

[29] Chollet F. Keras: The python deep learning library. *Astrophysics Source Code Library*, 2018

[30] Abadi M. and Barham P. and Chen J. and Chen Z. and Davis A. and Dean J. and Devin M. and Ghemawat S. and Irving G., Isard M. Tensorflow: a system for large-scale machine learning. pages,

[31] Intel Corporation. Intel® Xeon® Processor E5-1620 v4 On-line: https://ark.intel.com/products/92991/Intel-Xeon-Processor-E5-1620-v4-10M-Cache-3-50-GHz- Accessed: 24/01/2019

Towards Mobile Projective AR for Construction Co-Robots

Siyuan Xiang, Ruoyu Wang, Chen Feng*

Tandon School of Engineering, New York University, Brooklyn, NY 11201, USA

E-mail: {siyuan, ruoyuwang, cfeng}@nyu.edu

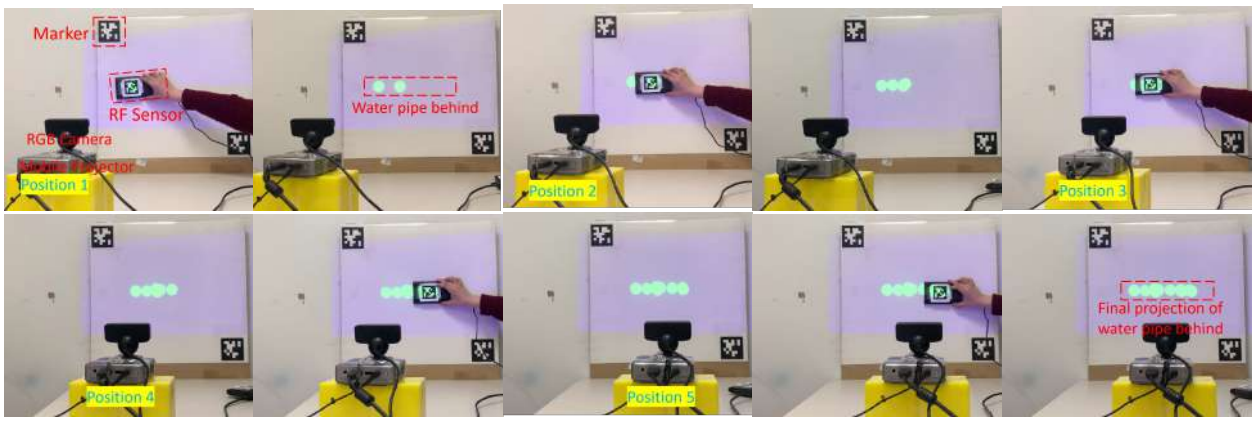

Figure 1. An assistive application of MPAR. An occluded utility is detected and visualized on the fly by projecting the detection results back onto the wall via a moving RF sensor. MPAR enables consistent visualization even after the projector changed its pose. The whole process can be seen in the video at: https://youtu.be/xvNBy$_C$0h3s.

Abstract -

The construction industry has been suffering from both low labor productivity growth and safety issues, due to the increasing project site complexities and the lack of skilled labors. As a potential technical solution, Augmented Reality (AR) has been studied to reduce the cognitive workloads in construction job sites by visualizing task-related information in the direct context of the workspace and operations. Instead of using helmets/goggles that may decrease users' field of views, we advocate mobile projectors for AR (MPAR), and propose a camera-projector system to ensure consistent AR projection even if the projectors may change poses when installed on mobile platforms such as human workers or even construction collaborative robots (co-robot). By obtaining the projector's pose relative to the projection plane (e.g., a wall or panel on construction site) via composing a series of homography transformations in this system, we could determine how to warp virtual information (images or 3D models) for desired projections, no matter whether human observers' head poses are needed. We demonstrate the effectiveness of the method using two construction AR applications: displaying occluded as-planned or as-built facility information behind a mock-up wall.

Keywords -

Projector-based AR; Camera-Projector System; Pose Estimation; Mobile Co-Robots

1 Introduction

The construction industry has been labeled as hazardous [1, 2] and susceptible to casualties and economic losses [3, 4]. Occupational Safety and Health Administration(OSHA) provides statistical data to state that the fatal injury rate in the construction industry is higher than the national average in any other industries in the US [5]. Many research works have been done to improve construction safety. Also, according to McKinsey [6], the construction industry has an intractable productivity problem and there is a large room to improve project efficiency and boost value. Therefore, higher construction productivity has become another pursuit of the construction industry. By blending task-related information directly in real context, AR technology offers the potential to increase construction safety and efficiency with easier access to retrieve on-site information [7]. One trend is integrating AR technology with Building Information Modeling (BIM) [7–11]. Their research works focused on employing AR as a visualization tool to display as-planned BIM information in the context of the real environment in architectural visualization, facility management, construction education, and other construction-related fields. Another trend is to design a mobile augmented reality (MAR) system for architectural, engineering, construction and facility management (AEC/FM), BIM information retrieval and construction education [12–15].

However, conventional AR has several limitations that could be potentially problematic for construction/civil applications. Unlike AR for gaming or education, which is operated in a relatively simple and safe environment, restricted field of view of conventional helmet-based AR will reduce the amount of environmental information available to people [16, 17] and may cause fatal injuries to construction workers. Kawano et al. [18] reported that in their survey of using HoloLens (a pair of head-mounted smart glasses developed and manufactured by Microsoft) to train the construction team during the assembly process, in order to get a full view of the assembly site, workers have to move head instead of moving eyes naturally. Wearing AR devices may also cause distraction and reduce situational awareness, raising concerns about safety [19]. For tablet-based AR, the technology is relatively mature, however, it produces less immersive user experience [20] which could also impede the application of AR technology in the construction field. Also, for many tasks other than monitoring/inspection, workers cannot hold a tablet while working on the tasks.

The objective of this research is to develop a mobile projector-based AR technology to increase the safety and efficiency of the construction industry by enriching the information on the real construction site while avoiding the drawbacks of conventional AR. Our contributions are listed as follows:

- We introduce related projective geometry theory as fundamentals for our method.
- We design MPAR, a camera-projector system that can augment task information directly onto a physical workspace.
- Our MPAR system can be either independent or dependent on the observer's pose.
- We test MPAR in an assistive application that projects positions of occluded utilities behind a wall using an RF-image sensor.

2 Related Work

There have been some researches on introducing AR technology to construction. However, projector-based AR technology that can somehow overcome the drawbacks of conventional AR, has not received much attention. To realize AR technology using a projector, we need to dive into mobile AR technology and other related work, such as projective AR system's math model and pose estimation.

AR in construction. Kamat et al. [21] discussed an HMD/glass-based AR method for assessing the building damage caused by earthquake. Their method superimposes the previously stored building information onto the real structure and computes the difference between the two views. Bae et al. [12] proposed a tablet-based AR system for smartphone users to query 3D virtual information onsite. Their system reconstructs the camera pose by matching feature points of a photo and pre-stored point cloud, thereby obtaining the user's position. Mevza et al. [22] focused on implementing a BIM-based AR system to improve the performance of digital materialization. Their method feeds the mobile AR system with pre-generated AR model converted from BIM.

Projector-based AR. Given the above-mentioned limitations of using conventional AR, we propose to use projector-based AR for our applications. Projector-based AR is not a completely new idea, it has been proposed and used in many areas. For example, assisting human-robot interaction [23], augmenting details for cultural heritage artifacts [24], improving user's gaming experience [25], etc. Benko et al. [26] combined HMD AR display with view-dependent projection to improve user experience. However, their method needs wearable devices, which produces the same problems as we mentioned above. Also, superimposing stereoscopic views onto monoscopic projections is still a challenging work. Our method only focuses on projector-based AR technology so that these problems can be avoided. Lindlbauer et al. [27] developed a framework for combing shape-changing interface with projection mapping, while we assume that our work is performed on a plane of constant shape. Different from all these methods above, our work aims at rendering the 2D frames of objects on the correct position they projected onto the wall.

Methods for Projector-based AR. Since the projector is mobile, we need projector's math model and pose estimation. As Tatsumoto et al. [28] presented in their work, the robot can project the image to any specified location by detecting the marker placed in the environment previously. Chadalavada et al. [29] showcased their work aiming at improving the robot's ability to communicate with human by projecting internal state information through a projector. One important part of their work is to find the relationship between the real world vehicle path and OpenGL frame to render the image. While their work [28, 29] required to calibrate camera-projector system ahead for a precise physical pinhole camera model, our work directly computes the homography transformation matrix between camera and projector to pass the geometry relationship between the two. Boroomand et al. [30] proposed a method that can compensate for distortion of the projected image caused by an uneven projection plane. In order to improve picture projection accuracy, we use two markers of known physical coordinates for precision control.

3 Mobile Projective AR

Our method realizes AR using a camera-projector system to ensure a consistent projection during the process,

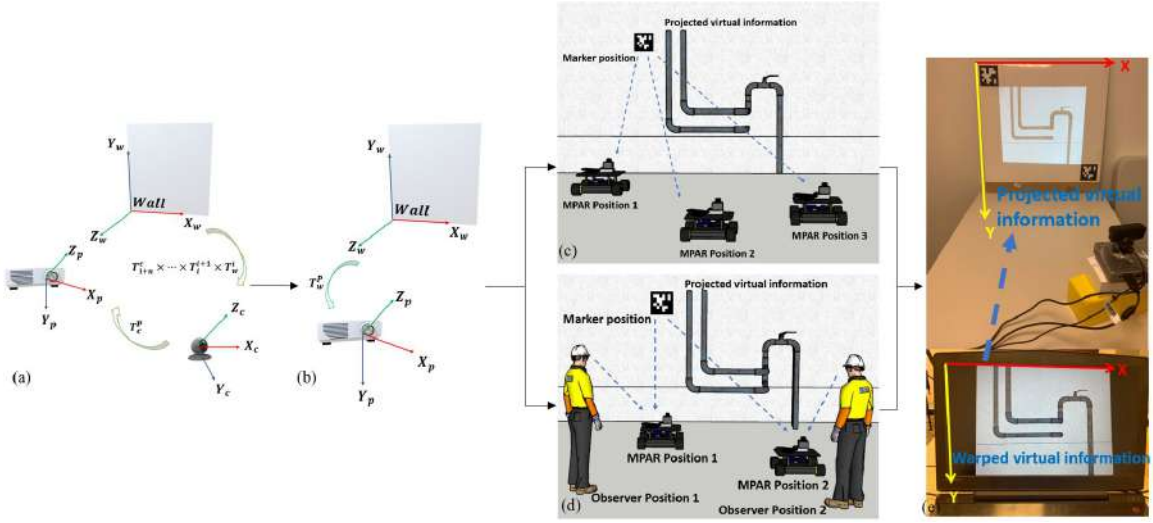

Figure 2. MPAR pipeline. (a) Pose representation and estimation. (b) Composition of projection matrix. (c) observer-independent system. (d) observer-dependent system. (e) Projection of the warped virtual information.

even if the projector might be moved due to various reasons (e.g., to enlarge/move the field of view, to make room for co-workers, etc.). Figure 2 depicts two categories of the MPAR system, one is observer-independent and the other is observer-dependent. The observer-independent MPAR system does not need to know where the observer is (we assume the position of the observer's head represents the position of the observer) while the observer-dependent MPAR system requires for the observer's position. For both systems, we first estimate and represent the pose of the projector in the world coordinate system by passing homography matrices between components in the system; then, according to the projector's pose, the projection matrix from the projector to the target projection plane can be estimated. Therefore, the observer-independent MPAR system could project the excepted virtual information onto the projection plane. For the observer-dependent MPAR system, the observer's location needs to be known before the projection phase. In this section, we will provide a general formulation of our method.

3.1 Pose Representation and Estimation

It is necessary to estimate the pose of the projector relative to the world coordinate system, so we can determine how to warp the virtual information (image or 3D model) for displaying the desired content on the projection plane without geometrical distortion. We developed a camera-projector system to estimate the pose of the projector via vision-based perception. By passing sequential transformations from the world coordinate system via the camera and other possible intermediate coordinate systems to the projector coordinate system, the pose of the projector in the world coordinate system could be calculated. The transformation from a coordinate system to b coordinate system can be represented by a matrix T_a^b. We express the transformation matrix from the world coordinate system to the projector coordinate system as:

$$T_w^p = T_c^p T_N^c \prod_{i=1}^{N-1} T_i^{i+1} T_w^1 \tag{1}$$

Here, w represents the world coordinate system, p represents the projector coordinate system and c represents the camera coordinate system. N is the total number of intermediate coordinate systems. T_i^{i+1} is the transformation from the ith intermediate coordinate system to the $(i+1)$th intermediate coordinate system. To register the position of the MPAR system, either the marker-based method or the markerless method could be used [31, 32]. Markerless AR is usually more flexible than marker-based AR for not requiring marker installation. But there are several reasons that still favor marker-based solution on several circumstances.

Why use markers? First, the markerless technology usually requires abundant visual features in the environment and there is a trade-off between precision and efficiency when applying this method to realistic job sites [33]. Second, our method is effective in indoor environments, no matter whether the projection plane has discriminative visual features or not. While marker-less AR might sometimes lose track for features. Besides, by using markers, it is more reliable to determine the location of the projection plane in the world coordinate system than without markers. Nevertheless, similar to recent works [34, 35] that integrate markers into structure from motion systems,

our on-going work is combining the marker-less solution with marker-based one in MPAR system.

For marker-based AR, the relative pose can be represented by a translational vector and a rotational vector [36]. However, camera calibration is required if poses are represented in this way [32], which may cause inconvenience and complexity, thereby affecting AR application in industry.

To avoid the aforementioned drawbacks, we utilize marker-based AR. Besides, instead of using translational and rotational vectors, we choose to use homography to represent the pose, since all components in the system, such as projection plane, image plane, and makers are planar objects. Homography transformation matrix is an invertible non-singular 3×3 projective matrix which can map the corresponding points from one plane to another plane [37]. Using homography does not require camera calibration. Therefore, the pose of the projector in the world coordinate system can be represented in the form of homography:

$$H_w^p = H_c^p H_N^c \prod_{i=1}^{N-1} H_i^{i+1} H_w^1 \tag{2}$$

where we represent homography transformation between a and b coordinate systems as H_a^b. Given the pose of the projector in world coordinate system, if $\mathbf{x}_w$ are the homogeneous coordinates of a point on the projection plane in world coordinate system, then the coordinates on the projector's image plane should be:

$$\mathbf{x}_p = H_w^p \mathbf{x}_w \tag{3}$$

According to H_w^p, virtual information which needs to be projected can be converted to a warped image. By sending the warped image to the projector, the virtual information can be projected to the correct locations in the world coordinate system.

3.2 Observer-Independent MPAR

In the multi-person collaborative site, the projected information will be shared by multiple workers and designers, so the projected information should not change with the position of one person. Therefore, the previously proposed methodology, equation 3 could be used for the displaying purpose.

3.3 Observer-Dependent MPAR

In contrast to observer-independent MPAR, the projected content of an observer-dependent MPAR system is related to the observer's position. This feature is important when the worker or designer on the site is moving while observing a 3D virtual model. To establish an observer-dependent MPAR system, either static projector(s) or mobile projector(s) can be used.

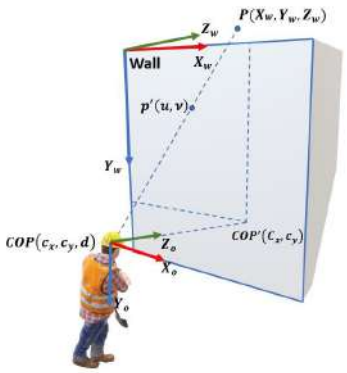

Figure 3. Illustration for computing a projected point in the observer-dependent MPAR.

For the observer-dependent MPAR system using static projectors, the pose of the projector relative to the world coordinate is known. Therefore, the virtual information can be projected directly without computing the series of homography transformation matrices. We can only focus on the impact of human location on the overall system. Equation 4 links the three-dimensional coordinates of the object to the corresponding projected two-dimensional coordinates by the observer's location.

$$s \begin{bmatrix} u \\ v \\ 1 \end{bmatrix} = \underbrace{\begin{bmatrix} d & 0 & c_x & 0 \\ 0 & d & c_y & 0 \\ 0 & 0 & 1 & 0 \end{bmatrix}}_{\text{projective}} \underbrace{\begin{bmatrix} 1 & 0 & 0 & -c_x \\ 0 & 1 & 0 & -c_y \\ 0 & 0 & 1 & d \\ 0 & 0 & 0 & 1 \end{bmatrix}}_{\text{world to observer}} \begin{bmatrix} X_w \\ Y_w \\ Z_w \\ 1 \end{bmatrix} \tag{4}$$

Figure 3 establishes the world coordinate system and the observer coordinate system. The observer's location COP, the virtual point's location P and its projection on the wall P' have also been defined. For proper projection, we first convert the coordinates of the object from the world coordinate system to the observer coordinate system. For this conversion, since the corresponding coordinate axes of the two coordinate systems have the same direction, the rotation matrix is a 3×3 identify matrix; the translation vector is $(-c_x, -c_y, d)$, related to the observer's location. To apply the transformation matrix to the homogeneous coordinates of $P(X_w, Y_w, Z_w)$, the rotation and translation matrix should be combined as the world to observer matrix in equation 4. Then the object's coordinates $P'(u, v, 1)$ in the world coordinate system plane can be obtained by multiplying the projective matrix in equation 4. s is a scaling factor.

The observer-dependent MPAR system using mobile projectors is complicated and comprehensive in taking

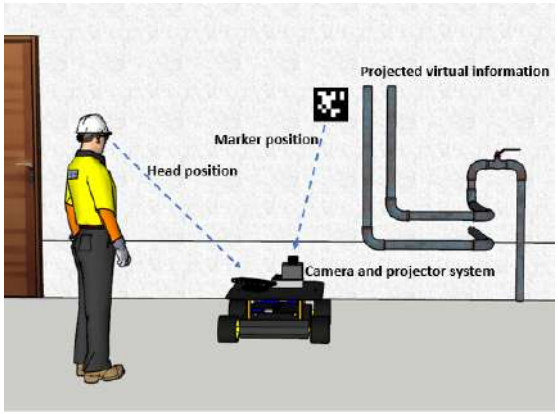

Figure 4. Illustration of observer-dependent MPAR.

both observer's location and projectors' mobility into consideration. The methodology of this system can be realized as a combination of the aforementioned methodologies. Figure 4 shows the schematic of the observer-dependent MPAR system. Knowing the position of the observer (COP), the coordinates of the virtual point being projected onto the projection plane P' can be calculated by equation 4. Then according to equation 3, coordinates of P' on the warped image can be calculated.

4 Applications

It is important that designers and workers can see building/facility information in the exact location during the construction process. For example, in the maintenance or inspection process, workers can evaluate the quality of the building by comparing the appearance of the on-site building with the as-designed building information projected onto the site. Based on the aforementioned MPAR methodology, our first task is to project as-designed building/facility information to where they are located.

Our task 2 is to detect the object behind the wall, visualize and save the detected RF signal based on the framework of MPAR methodology. In practice, workers can set up the markers in an unknown construction site for renovation work. After settling down the MPAR system, they should be able to employ the Walabot to detect the hidden objects and visualize them in real time. Moreover, they can save the detected signal to BIM database for future information retrieval. Task 2 is a prototype for such work, and its result can be seen in Figure 1.

Since in last section, we have provided a general formulation of our proposed method, in this section, we will show two applications which realize our method.

4.1 Projection of As-Designed Building Information

Some assumptions should be made before the implementation of task 1. First, it is reasonable that we have access to as-designed building information and its location in the world coordinate system. Also, since our pose estimation method is based on detecting optical markers, the projection area is within the control range defined by markers, so the physical coordinates of the building information that our task can project need to be within the control area.

System Setup. For computing homography matrix, AprilTag, a robust visual fiducial system [38] is utilized to detect correspondences in two coordinate systems [39, 40]. By placing markers on the wall, the world coordinate can be defined. As Figure 5 shows, a RGB camera is fixed on the ultra short throw projector. Also, a laptop is utilized as a mobile workstation for computing homographies and displaying the virtual information.

Related Transformations:

Wall to Camera. For this part, we first set up the two markers on the wall, as can be seen in Figure 5, to define the world coordinate system, which is a 2D coordinate system on the wall plane. Then we measure the physical coordinates of four corners for each marker. Also, the on-board camera captures an image which contains the two markers. The image coordinates of eight corners can be automatically measured. Then the homography from world coordinate system to the camera's image coordinate system H_w^c can be calculated using Direct Linear Transformation (DLT).

Camera to Projector. In addition to capturing the physical markers on the wall, the RGB camera is also set up to capture the projected marker. An image of a marker is sent to the projector to make it being projected on the wall. Then the RGB camera takes an image of the projected marker on the wall. The corners of the projected marker are automatically measured in the captured image and the input image. According to the corresponding corners, homography from camera's image coordinate system to projector's image coordinate system H_c^p can be calculated.

Wall to Projector. After obtaining H_w^c and H_c^p, H_w^p can be calculated according to equation 2. Then the warped image sent to the projector can be obtained according to equation 3.

Result. As we can see in Figure 5, suppose the plumbing is located in the control area defined by the markers, though the projector is moving, the projected information remains at the same specified location.

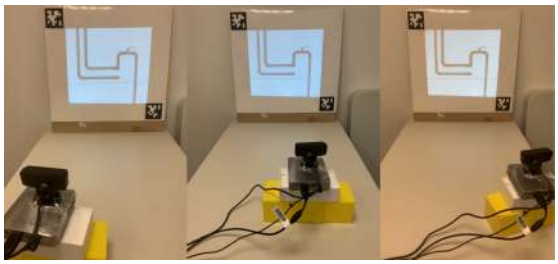

Figure 5. Observer-Independent MPAR for as-designed building information

4.2 Projection of Occluded Building Information

Specific Image Warping Representation. Unlike the previous application, which needs to find homography transformation from world coordinate system to projector coordinate system, this application aims to project the sensed RF image to the correct location on the wall. Therefore, homography from the sensed image coordinate system to the projector's image coordinate system H_i^p needs to be calculated:

$$H_i^p = H_c^p H_s^c H_i^s \tag{5}$$

H_c^p, H_s^c, H_i^s represent the homography transformation from camera's image to projector's image, Walabot sensor's coordinate system to camera's image and sensed RF image to Walabot sensor's coordinate system respectively. To better visualize the detected RF image, we rendered a circle, centered on the location of object being detected, on the 21×21 pixel sensed RF image. According to H_i^p, we could warp the RF image such that it can be projected properly on the projection plane.

Since the projector's pose is changing during the projection process, we should warp the image of the previous frame to align with the projector's pose of the current frame and fuse all images together to get a global image for projection.

System Setup. In addition to the camera-projector system used in the previous application, Walabot, a handheld 3D-imaging device was utilized for detecting the RF signal of the object behind the mock wall. Since it is difficult to directly detect the pose of the Walabot sensor plane, we attached a marker on the Walabot to detect its position.

Related Transformations:

Image to Sensor. The homography transformation matrix H_i^s is pre-defined since we specified the physical sensing arena in the sensor coordinate system and image size in the digital image coordinate system. We can calculate H_i^s by using the corresponding four corners in both two coordinate systems.

Sensor to Camera. To compute the transformation matrix between the sensor coordinate system and the projector coordinate system, we attached an optical marker on the opposite side of the sensor plane, whose center coincides with the surface's center in z axis, as can be seen in Figure 1. By capturing the four corners of the marker, we could compute the homography H_t^c between the tag and the RGB camera. For the transformation between the sensor plane and the marker plane, we can easily measure the the thickness of Walabot, which represents the translational vector between sensor plane and tag plane. Since homography transformation matrix does not contain the translational information explicitly, we need to use affine matrix for geometry transformation. By decomposing the homography transformation matrix H_t^c with the RGB camera's intrinsic matrix, we can obtain the affine matrix which contains the rotational and translational information between the tag and the camera; adding the translational vector allows us to get the affine transformation matrix between sensor plane and the RGB camera. Then we can compose the homograhpy matrix H_s^c with the camera's intrinsic matrix.

Camera to Projector. This part of implementation is the same as the previous application.

With these homogaphy matrices obtained, we could calculate the homography transformation between project the warped image of each frame onto the projection plane properly.

Two Frame Image Fusion. Since the projector is moving during the scanning process, we need to fuse the previous frame image to the current frame image such that H_i^p is always representing the current homography transformation matrix between image coordinate system and projector coordinate system. The homography between two frames can be calculated by solving DLT problem using the optical markers' points captured by the RGB camera in two frames. After knowing the homography transformation matrix between two frames, we can warp the previous image using equation 3 and fuse it with the current image.

Result. By sending the fused image to the projector, we can visualize the water pipe behind the mock wall. As can be seen in Figure 1, our result shows that even the projector's pose changed during the scanning process, our system could still augment the occluded water pipe consistently.

5 Conclusions

In this paper, we proposed MPAR, a camera-projector AR system which ensures a consistent projection even when the device might be moving during the AR process. In our two applications, by composing a series of homographies modeling poses between components in the system, it is possible to warp the virtual information in the projector coordinate system and display it on the projection plane as desired.

Limitations and Discussions. There are some limitations in our proposed method. Limited by the image brightness of the projector, the result of our method might be affected by the sunlight outdoors. Also, since our method uses optical markers for detecting feature points, it might cause extra workload for setting up these markers. The method might even become invalid in a large-scale scenario due to the inability to detect the markers.

Another limitation is that our MPAR system does not provide an as immersive environment as helmets/goggles (see-through based AR). Yet we believe that the restricted field of views will cause safety concerns for the construction industry, which could be a more serious problem compared to the less immersive user experience.

Future Work. Some future work needs to be done to produce a more general and reliable MPAR system. One work is to calibrate the projector to obtain the intrinsic matrix, thus we could know the pose of the projector as long as we know the extrinsic matrix of the projector. This frees us from acquiring the image of the projected marker. Also, we believe that by projecting the virtual information on uneven surfaces using 3D cameras, the MPAR system could be applied to more scenarios. Another important work we need to conduct is quantitative evaluation. It is important to evaluate how accurate our method is, and we should also explore some possible factors that might affect the accuracy of our method.

6 Acknowledgment

Siyuan Xiang gratefully thanks the IDC Foundation for its scholarship.

References

[1] Kurt M Lundeen, Vineet R Kamat, Carol C Menassa, and Wes McGee. Scene understanding for adaptive manipulation in robotized construction work. *Automation in Construction*, 82:16–30, 2017.

[2] Evan Nadhim, Carol Hon, Bo Xia, Ian Stewart, and Dongping Fang. Falls from height in the construction industry: a critical review of the scientific literature. *International journal of environmental research and public health*, 13(7):638, 2016.

[3] LY Ding and C Zhou. Development of web-based system for safety risk early warning in urban metro construction. *Automation in Construction*, 34:45–55, 2013.

[4] Ying Zhou, LY Ding, and LJ Chen. Application of 4d visualization technology for safety management in metro construction. *Automation in Construction*, 34:25–36, 2013.

[5] OSHA. Worker Safety Series, 2018. [Online; accessed 1-Jan-2019].

[6] McKinsey Global Institute. Reinventing construction: A route to higher productivity, 2017.

[7] Xiangyu Wang, Martijn Truijens, Lei Hou, Ying Wang, and Ying Zhou. Integrating augmented reality with building information modeling: Onsite construction process controlling for liquefied natural gas industry. *Automation in Construction*, 40:96–105, 2014.

[8] Chan-Sik Park, Do-Yeop Lee, Oh-Seong Kwon, and Xiangyu Wang. A framework for proactive construction defect management using bim, augmented reality and ontology-based data collection template. *Automation in Construction*, 33:61–71, 2013.

[9] Xiangyu Wang, Peter ED Love, Mi Jeong Kim, Chan-Sik Park, Chun-Pong Sing, and Lei Hou. A conceptual framework for integrating building information modeling with augmented reality. *Automation in Construction*, 34:37–44, 2013.

[10] Yi Jiao, Shaohua Zhang, Yongkui Li, Yinghui Wang, and BaoMing Yang. Towards cloud augmented reality for construction application by bim and sns integration. *Automation in construction*, 33:37–47, 2013.

[11] Masoud Gheisari and Javier Irizarry. Investigating human and technological requirements for successful implementation of a bim-based mobile augmented reality environment in facility management practices. *Facilities*, 34(1/2):69–84, 2016.

[12] Hyojoon Bae, Mani Golparvar-Fard, and Jules White. High-precision vision-based mobile augmented reality system for context-aware architectural, engineering, construction and facility management (aec/fm) applications. *Visualization in Engineering*, 1(1):3, 2013.

[13] Javier Irizarry, Masoud Gheisari, Graceline Williams, and Bruce N Walker. Infospot: A mobile augmented reality method for accessing building information through a situation awareness approach. *Automation in Construction*, 33:11–23, 2013.

[14] Arezoo Shirazi and Amir H Behzadan. Design and assessment of a mobile augmented reality-based information delivery tool for construction and civil engineering curriculum. *Journal of Professional Issues in Engineering Education and Practice*, 141(3):04014012, 2014.

[15] Marianna Kopsida and Ioannis Brilakis. Markerless bim registration for mobile augmented reality based inspection. In *ICCCBE2016, Osaka, Japan*, pages 6–8, 2016.

[16] Robert Xiao and Hrvoje Benko. Augmenting the field-of-view of head-mounted displays with sparse peripheral displays. In *Proceedings of the 2016 CHI Conference on Human Factors in Computing Systems*, pages 1221–1232. ACM, 2016.

[17] Andrew Maimone, Douglas Lanman, Kishore Rathinavel, Kurtis Keller, David Luebke, and Henry Fuchs. Pinlight displays: wide field of view augmented reality eyeglasses using defocused point light sources. In *ACM SIGGRAPH 2014 Emerging Technologies*, page 20. ACM, 2014.

[18] Noel Kawano, Ryan Theriot, Jack Lam, Eric Wu, Andrew Guagliardo, Dylan Kobayashi, Alberto Gonzalez, Ken Uchida, and Jason Leigh. The destiny-class cybercanoe–a

surround screen, stereoscopic, cyber-enabled collaboration analysis navigation and observation environment. *Electronic Imaging*, 2017(3):25–30, 2017.

[19] Sunwook Kim, Maury A Nussbaum, and Joseph L Gabbard. Augmented reality âĂIJsmart glassesâĂİ in the workplace: industry perspectives and challenges for worker safety and health. *IIE transactions on occupational ergonomics and human factors*, 4(4):253–258, 2016.

[20] Dingtian Yan and Huosheng Hu. Application of augmented reality and robotic technology in broadcasting: a survey. *Robotics*, 6(3):18, 2017.

[21] Vineet R Kamat and Sherif El-Tawil. Evaluation of augmented reality for rapid assessment of earthquake-induced building damage. *Journal of computing in civil engineering*, 21(5):303–310, 2007.

[22] Sebastjan Meža, Žiga Turk, and Matevž Dolenc. Component based engineering of a mobile bim-based augmented reality system. *Automation in construction*, 42:1–12, 2014.

[23] Michael D Coovert, Tiffany Lee, Ivan Shindev, and Yu Sun. Spatial augmented reality as a method for a mobile robot to communicate intended movement. *Computers in Human Behavior*, 34:241–248, 2014.

[24] Brett Ridel, Patrick Reuter, Jeremy Laviole, Nicolas Mellado, Nadine Couture, and Xavier Granier. The revealing flashlight: Interactive spatial augmented reality for detail exploration of cultural heritage artifacts. *Journal on Computing and Cultural Heritage*, 7(2):6, 2014.

[25] Brett Jones, Rajinder Sodhi, Michael Murdock, Ravish Mehra, Hrvoje Benko, Andrew Wilson, Eyal Ofek, Blair MacIntyre, Nikunj Raghuvanshi, and Lior Shapira. Roomalive: magical experiences enabled by scalable, adaptive projector-camera units. In *Proceedings of the 27th annual ACM symposium on User interface software and technology*, pages 637–644. ACM, 2014.

[26] Hrvoje Benko, Eyal Ofek, Feng Zheng, and Andrew D Wilson. Fovear: Combining an optically see-through near-eye display with projector-based spatial augmented reality. In *Proceedings of the 28th Annual ACM Symposium on User Interface Software & Technology*, pages 129–135. ACM, 2015.

[27] David Lindlbauer, Jens Emil Grønbæk, Morten Birk, Kim Halskov, Marc Alexa, and Jörg Müller. Combining shape-changing interfaces and spatial augmented reality enables extended object appearance. In *Proceedings of the 2016 CHI Conference on Human Factors in Computing Systems*, pages 791–802. ACM, 2016.

[28] Kenji Tatsumoto, Satoshi Iwaki, and Tetsushi Ikeda. Tracking projection method for 3d space by a mobile robot with camera and projector based on a structured-environment approach. *Artificial Life and Robotics*, 22(1):90–101, 2017.

[29] Ravi Teja Chadalavada, Henrik Andreasson, Robert Krug, and Achim J Lilienthal. That's on my mind! robot to human intention communication through on-board projection on shared floor space. In *European Conference on Mobile Robots (ECMR)*, pages 1–6, 2015.

[30] Ameneh Boroomand, Hicham Sekkati, Mark Lamm, David A Clausi, and Alexander Wong. Saliency-guided projection geometric correction using a projector-camera system. In *Proc. IEEE Int'l Conf. Image Processing (ICIP)*, pages 2951–2955, 2016.

[31] Feng Zhou, Henry Been-Lirn Duh, and Mark Billinghurst. Trends in augmented reality tracking, interaction and display: A review of ten years of ismar. In *Proceedings of the 7th IEEE/ACM International Symposium on Mixed and Augmented Reality*, pages 193–202, 2008.

[32] Eric Marchand, Hideaki Uchiyama, and Fabien Spindler. Pose estimation for augmented reality: a hands-on survey. *IEEE transactions on visualization and computer graphics*, 22(12):2633–2651, 2016.

[33] Elisa Ziegler. *Real-time markerless tracking of objects on mobile devices*. PhD thesis, Citeseer, 2009.

[34] Chen Feng, Vineet R Kamat, and Carol C Menassa. Marker-assisted structure from motion for 3d environment modeling and object pose estimation. In *Construction Research Congress 2016*, pages 2604–2613, 2016.

[35] Joseph DeGol, Timothy Bretl, and Derek Hoiem. Improved structure from motion using fiducial marker matching. In *Proc. European Conf. Computer Vision (ECCV)*, pages 273–288, 2018.

[36] Mohammad Nahangi, Adam Heins, Brenda Mccabe, and Angela Schoellig. Automated localization of uavs in gps-denied indoor construction environments using fiducial markers. 07 2018.

[37] Richard Hartley and Andrew Zisserman. *Multiple view geometry in computer vision*. Cambridge university press, 2003.

[38] Edwin Olson. Apriltag: A robust and flexible visual fiducial system. In *Proc. IEEE Int'l Conf. Robotics and Automation (ICRA)*, pages 3400–3407. IEEE, 2011.

[39] Chen Feng and Vineet R Kamat. Augmented reality markers as spatial indices for indoor mobile aecfm applications. In *CONVR*, pages 235–24, 2012.

[40] Chen Feng. Camera marker networks for pose estimation and scene understanding in construction automation and robotics. 2015.

Implementing Collaborative Learning Platforms in Construction Management Education

R. Tayeh[a], F. Bademosi[a], and R.R.A. Issa[a]

[a]M.E. Rinker, Sr. School of Construction Management, University of Florida, USA
E-mail: ralph.tayeh@ufl.edu, mofoluwaso@ufl.edu, raymond-issa@ufl.edu

Abstract –

Over the last few decades, the investments in more complicated construction projects, involving multiple disciplines and different teams, have increased the need for more complex communication means. The purpose of communication methods is to ensure higher levels of coordination between project participants (owners, architects, engineers, contractors, suppliers, etc.). Adequate communication brings many benefits to a project, such as improved team performance due to information exchange, increased knowledge of other participants' skills or their availability. Building Information Modelling (BIM) has the ability to aggregate information on construction projects and facilitate the design, construction, and facility management processes. Therefore, including BIM classes in construction management education is of utmost importance for the success of students. Moreover, introducing cloud collaboration to these classes helps students better understand the collaborative aspect of the construction industry. The purpose of this paper is to study the benefits of Autodesk Next Gen BIM 360 brought to a graduate BIM class. Students of this class were divided into groups and asked to model the different disciplines of a project using Autodesk Revit© while collaborating the project on Next Gen BIM 360. At the end of the semester, students reported the benefits and drawbacks of Next Gen BIM 360. The benefits included the ease of use of the platform, better communication of ideas and concerns using Next Gen BIM 360 cloud services, real-time collaboration opportunities, and model coordination on the cloud.

Keywords –

BIM; Next Gen BIM 360; Collaboration; Construction; Education

1 Introduction

The construction industry is very dependent on information exchange between project stakeholders, as communication is imperative for the success of construction projects. The structure of the industry is very much fragmented, and it involves numerous data-intensive processes through the lifespan of projects [1]. Typically, massive amounts of data which need to be continuously updated and synchronized are generated across the entire lifecycle to achieve better project outcomes [2]. Seeing as construction projects comprise complex activities interconnected with these vast amounts of data, collaboration between team members is highly essential to ensure successful completion of these projects. However, seamless collaboration and information exchange continue to be a challenge for the industry despite great efforts dedicated to understanding and improving these processes [3]. With the advancements in information technology, the construction industry has gradually shifted towards more collaborative working practices based on BIM. Collaboration is a process of teamwork and information dispersion through communicating, coordinating, networking, and exchanging in order to maximize the group effort of the project stakeholders [4].

In recent years, collaboration technologies have evolved through research efforts to increase the efficiency of information communication. The utilization of cloud-based technologies to realize the integration of all project phases has increasingly grown to be a widespread practice in project management, making the communication of more cumbersome information probable [4]. Through the use of these collaborative technologies, long-distance communication is made possible, and project stakeholders are not confined to an actual workstation next to each other. Consequently, collaboration, communication, and teamwork skills are ever more crucial in the construction workforce today [5]. Thus, there is an opportunity for institutions of higher learning

to incorporate collaborative learning into their curricula in order to equip students with essential employability skills and to also enhance their engagement in the classroom. This paper explores the use of Autodesk Next Gen BIM 360 as a collaborative learning platform in construction management education to enhance the learning experience of students.

2 Literature Review

2.1 BIM in Education

BIM is an intelligent three-dimensional model-based process capable of combining the dispersed information shared between project stakeholders [6]. For this reason, BIM has been customarily implemented on construction projects to address several of the problems confronting the industry such as budget overruns, contingencies in schedule forecasts, safety, and overall quality of the project [7]. In the last few years, BIM has been used as a collaborative platform in projects to magnify the quota of data shared between the various parties involved in construction. Taking into account the high potentials of BIM and the several advantages to its implementation on construction projects, the technology can be employed as an educational tool in institutions of higher learning. For instance, construction jobsites can be virtually incorporated into classrooms with computer-generated models hosted in virtual environments that simulate design and construction processes. With BIM-based instructional techniques, educators are capable of equipping students in the architecture, engineering, construction, and operations (AECO) fields with the required skills and abilities necessary to complete construction tasks successfully, by eliminating inadequacies from the lack of practical exposure to real-time jobsite situations [8]. Computer and information technologies significantly impact the skills and educational successes of students as they foster collaboration between instructors and students, ultimately enhancing problem-solving and inquiry skills in the students [9].

Additionally, some government protocols require that public construction projects are commissioned with BIM, leading to a rise in demand of BIM specialists in the construction workforce. As a result, several approaches to encourage institutions of higher learning to integrate BIM into the curricula of both undergraduate and graduate courses [10, 11, 12]. Research has shown that BIM can be implemented as an instructional tool for a variety of construction activities such as the operation of construction machinery, occupational health and safety, logistics planning, jobsite training, and project coordination and visualization [13, 1, 14, 15, 9].

2.2 Collaborative Learning

As established, BIM processes are multidisciplinary and require seamless collaboration and information exchange between all project stakeholders. In the construction, context collaboration can be defined as a harmonious team-based setting in which every member understands and values the contribution of others, as well as their role and responsibilities [16]. However, there is often the problem of ensuring the various disciplines, trades and companies collaborate amicably which poses an obstacle to channeling the full potentials of BIM [17]. Several researchers have tackled the issues facing BIM-enabled projects in maintaining collaboration through the lens of technology, while others consider the issue to be that of human behavior [17, 18]. Following the human behavior school of thought, the integration of collaboration philosophies into BIM courses in institutions of higher learning has been suggested as a practical solution to hostile teamwork situations in the industry [18, 19]. In the context of construction management education, collaboration can be defined as a shared, interactive process that requires the involvement of two or more participants, working collectively to attain results not easily achievable individualistically [20]. This process is commonly referred to as collaborative learning.

Collaborative learning often incorporates team-based, project-based, and problem-based learning methods in which students work together in small teams to achieve a common objective [15]. Collaborative projects characteristically simulate actual construction projects and processes with the goal of solving problems more efficiently in order to ensure better outcomes [21]. During the process, students are trained to be good listeners to their team members, as well as to regard the ideas of others with respect and uphold equivalent decision-making authority [22]. Several collaborative learning platforms can be utilized in classrooms to make the learning, designing and executing process easier [5]. Three-dimensional modeling platforms and information communication technologies can be employed to impart a clearer understanding and visualization of designs and models, and to improve communication among the students [18]. For the purpose of this study, Autodesk Next Gen BIM 360 was the platform used to facilitate collaborative learning in a construction management program.

2.3 Autodesk Next Gen BIM 360

Autodesk BIM 360 is as a cloud service that aims to connect the construction project lifecycle. BIM 360 improves construction project delivery processes by providing the tools required to evoke informed-decision making as the platform emphasizes the importance of

well-structured data that is continuously kept up-to-date [23]. BIM 360 is an inclusive project management program intended for the construction industry. Since its introduction into the industry in 2010, the portfolio expanded as a group of products designed to support construction workflows from pre-construction through handover and operations through the BIM 360 Docs, BIM 360 Glue, BIM 360 Field, and BIM 360 Plan services [24]. However, each of these services fundamentally functions as isolated products, creating a non-unified platform for communicating and sharing information.

However, at present, the BIM 360 platform has evolved from a set of separate solutions to a construction management platform that offers a more integrated, workflow-focused, "one-product" experience, called the Next Gen BIM 360. The Next Gen BIM 360 platform features a single, common data platform that allows easy access to all project information from anywhere in BIM 360 [24]. Drawings, models, and files uploaded during the design phase can be carried into the construction phase to support requests for information (RFIs), submittals, inspections and more. The platform also features a powerful insight and analytics layer that includes interactive dashboards and reporting, for informed decision making and predictive analysis. The services included in the Next Gen BIM 360 portfolio are Document Management, Design Collaboration, Model Coordination, Field Management, Project Management, and Cost Management [24].

The cloud-based platform endeavors to optimize project delivery schedules and budget while ensuring that industry standards, safety regulations, and project specifications are adhered to. The software empowers managers by allowing them to coordinate staff actions, implement workable schedules, improve communication between teams and companies, resolve issues and non-conformities; all of these in a digitalized environment with real-time information. One of the significant advantages of Next Gen BIM 360 is the fact that the software is flexible enough to accommodate different sizes and scopes of construction projects, which is one of the prime reasons for choosing the platform as a collaborative learning platform for this study.

3 Methodology

3.1 Use of Autodesk Next Gen BIM 360 in the Classroom

For the purpose of this study, the data collected is based on a sampling of students enrolled in the M.E. Rinker, Sr. School of Construction Management at the University of Florida (UF). The Construction Information Systems class offered by the Center for Advanced Construction Information Modeling (CACIM) was the class selected for the implementation of this study, which is a graduate level class covering virtual design and construction (VDC) technologies. The first eight sessions of the class demonstrate modeling concepts in Autodesk Revit®, where students are asked to complete architectural, structural, and mechanical models of a medium-scale commercial building. The remaining eight sessions of the class expound on the use of BIM for scheduling, estimating, point layouts, and visualization. In addition to the class assignments, students are expected to complete a team project which entails developing BIM models using original blueprints of educational buildings.

Since the Fall 2016 semester, the Autodesk BIM 360 has been incorporated in the class for collaboration; however, in the Fall 2018 semester, the class transitioned to the Next Gen BIM 360 platform. The study was conducted over two semesters, with participants from the Fall 2018 and Spring 2019 semesters. The breakdown of the sample size is shown in Table 1 with 47 students participating in this study. Using the Next Gen 360 platform, specifically the Document Management, Design Collaboration, Model Coordination, and Project Management modules, students had the chance to explore the multi-disciplinary coordination, clash detection, BIM data, and document management functionalities of the platform. Most importantly, the different team members were able to co-author BIM models on a single Revit® file. At the end of the semester, students were asked to evaluate the usefulness of the Next Gen BIM 360 platform, and rate their experience using the tools to collaborate and communicate.

Table 1. Study sample size

Semester	Number of Study Participants
Fall 2018	18
Spring 2019	29

3.2 Workflow

One of the class deliverables is a final project in which the class is divided into groups of four or five. Each group was given a set of two-dimensional drawings and asked to model the architectural, structural, and mechanical components of the building.

The first task for the students was to upload the drawings to Next Gen BIM 360 Document Management. In Document Management, students were able to organize the drawings into folders, and create templates that can automatically detect the sheets' numbers and names. Moreover, Document Management can

automatically detect sections and callouts on the drawings, and create hyperlinks to facilitate the navigation of large sets of drawings.

The next task required of the team project was to initiate the project on the cloud using Next Gen BIM 360 Design Collaboration. Students also created worksets to control the level of permission and the ownership of elements in the model. This facilitated the modeling process as students had the ability to grant or deny editing requests placed by other team members, which guaranteed the correct placement of the elements in the model.

During the modeling process, students also used Next Gen BIM 360 Project Management to communicate issues and RFIs. Students were able to place pushpins on the drawings and submit RFIs to the class instructor related to the drawings. Once the RFI is reviewed by the instructor, all team members were able to see the response. The Issues functionality was also used for communication among team members themselves.

Finally, before the final submission of the model, students used Next Gen BIM 360 Model Coordination. Model Coordination automatically creates clash detection tests from the models saved on the cloud. Moreover, similar clashes are grouped to facilitate the review process. Students used these clash groups to coordinate the model better and resolve clashes between the different disciplines of the project.

During the semester, a questionnaire was developed and distributed to the class. The questionnaire was a short survey that asked the following questions:

1. What did you like best about the Autodesk Next Gen BIM 360 tools?
2. What did you dislike about the Autodesk Next Gen BIM 360 tools?
3. How would you rate your experience using the Autodesk Next Gen BIM 360 tools on a scale of 1 to 5, 5 being best?

4 Results and Discussion

4.1 Benefits of Autodesk Next Gen BIM 360

At the end of the semester, students were asked to evaluate the usefulness of Next Gen BIM 360, and discuss how it enhanced their construction management education. Based on the responses of the study participants, the benefits of the Autodesk Next Gen BIM 360 tools can be categorized into six as shown in Table 2, all of which center on enhanced collaboration and communication.

Table 2. Responses of students to the benefits of Autodesk Next Gen BIM 360

Benefits	Frequency n = 47	Percentage of total
Ease of use	40	85%
Real-time collaboration	45	96%
Single data repository	38	81%
Central project collaboration	47	100%
Design review	41	87%
Model coordination	40	85%

The percentages of the responses of the participants in summarized in Figure 1.

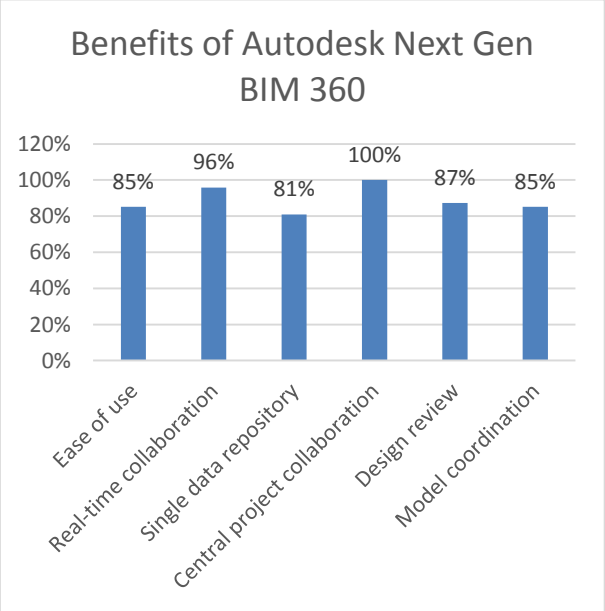

Figure 1. Benefits of Autodesk Next Gen BIM 360

4.1.1 Ease of Use

The Next Gen BIM 360 platform is a user-friendly platform that did not require any extensive knowledge of cloud-based services. Some of the feedback from the students regarding the ease of use of the platform include:

- The platform is relatively easy to use and is getting more and more integrated as a coordination tool.
- The simplicity of use for people with little or no computer knowledge.
- The easy access to the website and ease of use was a big benefit.

4.1.2 Real-Time Collaboration

With the Next Gen BIM 360 platform, students were able to work remotely and still collaborate with their team members from their different locations. Some of the feedback from the students regarding the benefit of long-distance collaboration include:

- It is perfect for working remotely from home.
- It fostered a connection with team members even though we worked mostly from different locations.
- Next Gen BIM 360 enabled real-time updating of models and documents.

4.1.3 Single Data Repository

The Next Gen BIM 360 platform now centralizes all project data in a single data repository connecting all workflows from design to construction to operations. Some of the feedback from the students regarding the single data repository feature of the platform include:

- It is an excellent depository to compile all the project information in one place.
- Having relevant project information readily accessible in the cloud was helpful.
- A significant benefit is having information available in the cloud and having the ability to collaborate with others in the cloud.
- The concept of a single bank of all the project information and to have a well-structured process in place for checking, reviewing and approving the information is appreciated.
- Autodesk Next Gen BIM 360 improves sharing and storing of documented files.
- One centralized location where all project information is kept was essential.

4.1.4 Central Project Communication

With the Next Gen BIM 360 platform, communication with other team members can be easily achieved in the BIM 360 environment without the need for email. Some of the feedback from the students regarding the benefit of central project communication include:

- Communication was improved by BIM 360.
- BIM 360 solved countless communication errors between all the members of the team.

4.1.5 Design Review

Using the Document Management Module, students could create markups on design sheets, make comments as well as publish both the mark-ups and comments for other team members to see and respond accordingly. Also, Document Management made it easy to publish design sets by converting models into individual two-dimensional sheets that could be measured and calibrated. Some of the feedback from the students regarding the benefit of design review include:

- Being able to make markups and issues and share them with team members, as well as keep a record of them.
- Creating mark-ups and issues on the sheets is a significant benefit.
- Easy to upload 3D models with sheet generated files easily extracted sheets.
- Title block data is automatically scanned and extracted when uploading pdf files and also comes with an automatic zoom of sheet title, sheet numbers, and sheet names.
- Having the ability to review and analyze the information is a powerful tool.

4.1.6 Model Coordination

With the Model Coordination module, students were able to automate the BIM coordination process, making it quicker to identify and resolve problems between the different disciplines. Some of the feedback from the students regarding the model coordination feature include:

- It is a great collaboration tool that makes problem-solving much easier through model coordination processes.
- The ability to coordinate and solve problems much sooner than usual without using BIM 360.
- It is excellent for viewing models as it quickly highlights any problems or clashes.
- The comparison tool is useful for visualizing model changes.
- It sped up the review process by almost half the time.

4.2 Drawbacks of Autodesk Next Gen BIM 360

As with all emerging software, the Autodesk Next Gen BIM 360 is not without a few technical difficulties that can be improved. The students were also asked to evaluate the limitations of the Next Gen BIM 360 platform. Based on the responses of the study participants, the top five drawbacks of the Autodesk Next Gen BIM 360 tools is shown in Table 3.

Table 3. Responses of students to the limitations of Autodesk Next Gen BIM 360

Benefits	Frequency n = 47	Percentage of total
Slow speed	47	100%
Time consuming to sort documents	30	64%
Issues cannot be assigned to more than one person	40	85%
Problematic issues tracking	25	53%
Working with worksets is delicate	40	85%

The analysis of the responses indicated that:

- Out of the 47 respondents, 100% mentioned the slow upload and download speed to and from the cloud platform as a significant limitation.
- In the Document Management module, 64% of the respondents indicated the lack of a feature that highlights the most recently updated documents as a limitation, as it makes it time-consuming to sort through several sheets.
- The inability of users to assign an issue to more than one person at a time was indicated by 85% of the respondents as a limitation.
- Of the 47 respondents, 53% stated that the issues tracking functionality in the Model Coordination module is problematic.
- Of the 47 respondents, 85% stated that working with worksets in the Design Collaboration module is delicate as a team member can change the properties of elements assigned to worksets of other team members without permission.

4.3 Experience using the Autodesk Next Gen BIM 360 Platform

The last question of the questionnaire was designed to evaluate the experience the students had with using the Autodesk Next Gen BIM 360 Platform. The experience of the students were rated on a Likert scale ranging from poor to excellent. The results of the responses to this question are summarized in Table 4. Out of the 47 respondents, 4% indicated that they had a moderate experience using the Autodesk Next Gen BIM 360 tools, 21% indicated that they had a good experience using the platform, while 75% of the students stated that they had an excellent experience using the Autodesk Next Gen BIM 360 platform.

Table 4. Frequency and percentages of the experience of participants

Experience using Autodesk Next Gen BIM 360	Frequency n = 47	Percentage of total
Very poor	0	0%
Poor	0	0%
Moderate	2	4%
Good	10	21%
Excellent	35	75%

5 Conclusion

With construction projects becoming more complex and multidisciplinary, the amount of information exchanged between project stakeholders has increased the need for more advanced collaboration and communication technologies. BIM and cloud-based collaborative platforms can aggregate the dispersed information and enhance communication between project stakeholders. In addition to their use in the construction industry, collaborative platforms can also be employed in education to improve the learning experience of construction management students.

This paper explored the use of Autodesk Next Gen BIM 360 as a collaborative learning platform in a Construction Information Systems graduate class. In Fall 2018, 18 students reported the benefits of Next Gen BIM 360 and how it helped them collaborate and communicate with their team members for successful completion of their final project. The students highlighted the ease of use, real-time collaboration opportunities, single data repository, central project communication, design review capabilities, and model coordination as significant benefits of Next Gen BIM 360. However, the platform is not without a few technical difficulties that must be improved upon for a better experience.

References

[1] Eastman C. et al. *BIM handbook: A guide to building information modeling for owners, managers, designers, engineers and contractors*, Wiley, New Jersey, 2011.

[2] Hooper M. and Ekholm A. A pilot study: Towards BIM integration - An analysis of design information exchange and coordination. In *Proceedings of the CIB W78 2010: 27th International Conference*, pages 1-10, Cairo, Egypt, 2010.

[3] Staub-French S., Forgues D., Iordanova I., Kassaian A., Abdulaal B., Samilski M., Cavka

H.B., and Nepal M. *Building information modelling "Best practices" Project report. An investigation of "best practices" though case studies at regional, national, and international levels*, 2011.

[4] Alreshidi E., Mourshed M., and Rezgui, Y. Requirements for cloud-based BIM governance solutions to facilitate team collaboration in construction projects. *Requirements Engineering*, 23(1): 1-31, 2018.

[5] Clevenger C.M., Valdes-Vasquez R., and Abdallah M. Implementing a collaboration activity in construction engineering education. In *New Developments in Engineering Education for Sustainable Development*, pages 35-44, Springer, Cham, 2016.

[6] Jacoski C. and Lamberts R. The lack of interoperability in 2D design — a study in design offices in Brazil. *J. Inf. Technol. Constr.*, 12(17): 251–260, 2007.

[7] Gallaher M. P., O'Connor A. C., Dettbarn J. L., and Gilday L. T. Cost analysis of inadequate interoperability in the U.S. capital facilities industry. *National Institute of Standards and Technology*, Gaithersburg, MD, 2004.

[8] Lu W., Peng Y., Shen Q., and Li H. Generic model for measuring benefits of BIM as a learning tool in construction tasks. *J. Constr. Eng. Manag.*, 139(2): 195–203, 2013.

[9] Behzadan A. H. and Kamat V. R. Integrated information modeling and visual simulation of engineering operations using dynamic augmented reality scene graphs. *J. Inform. Technol. Constr.*, 16: 259–278, 2011.

[10] Sacks R. and Barak R. Teaching building information modeling as an integral part of freshman year civil engineering education. *J. Prof. Issues Eng. Educ. Pract.*, 136(1): 30-38, 2010.

[11] Dossick C.S., Lee N., and Foleyk S. Building information modeling in graduate construction engineering and management education. *Computing in Civil and Building Engineering*, 2176-2183, 2014.

[12] Woldesenbet A., Ahn C., Kim H.-J., and Rokooei S. Faculty learning community 3D (FLC) for BIM education in a multidisciplinary school. *Architecture and Engineering Institute*, 39-48, 2017.

[13] Fox S. and Hietanen J. Interorganizational use of building information models: potential for automational, informational and transformational effects. *Constr. Manage. Econ.*, 25(3): 289–296, 2007.

[14] Sacks R., Treckmann M., and Rozenfeld O. Visualization of work flow to support lean construction. *J. Constr. Eng. Manage.*, 135(12): 1307–1315, 2009.

[15] Becerik-Gerber B., and Kensek K. Building information modeling in architecture, engineering, and construction: emerging research directions and trends. *J. Prof. Issues Eng. Educ. Pract.*, 136(3), 139–147, 2010.

[16] Hughes D., Williams T., and Ren, Z. Differing perspectives on collaboration in construction. *Construction Innovation*, 12: 355-368, 2012.

[17] Merschbrock C., Hosseini M. R., Martek I., Arashpour M., and Mignone, G. Collaborative role of sociotechnical components in BIM-based construction networks in two hospitals. *Journal of Management in Engineering*, 34:05018006, 2018.

[18] Emmitt S. and Ruikar K. Collaborative design management, London Routledge, 2013.

[19] Baradi K., Oraee M., Hosseini M. R., Tivendale L., and Pienaar, J. Teaching collaboration in tertiary BIM education: A review and analysis.

[20] Salmons J. *Taxonomy for online collaboration: Theory and practice in e-Learning*. Hershey: IGI Global, 2011.

[21] Levi D. *Group dynamics for teams*, SAGE Publications, Inc, 2013.

[22] Forsyth D. R. *Group dynamics*. Boston, MA: Cengage Learning, 2010.

[23] Autodesk, Inc. Autodesk BIM 360. On-line: https://bim360.autodesk.com/, Accessed: 01/05/2019.

[24] Davison M. The BIM 360 "next gen" platform. On-line: http://blogs.autodesk.com/bim360-roadmap/bim360-priorities/, Accessed: 01/05/2019.

Quantifying Remoteness for Construction Projects Using Nighttime Satellite Imagery and Machine Learning

P. Zangeneh[a], H. Hamledari[b], and B.Y. McCabe[a]

[a] Department of Civil & Mineral Engineering, University of Toronto, Canada
[b] Department of Civil and Environmental Engineering, Stanford University, United States of America
E-mail: p.zangeneh@mail.utoronto.ca, hesamh@stanford.edu, brenda.mccabe@utoronto.ca

Abstract –

Remoteness, although a subjective concept, has indispensable consequences. It can support decision-makers in quantifying risks and feasibilities of developing newly discovered mineral deposits, resilience planning and evaluation of accessibility challenges of remote communities, or support agency budget allocations for much-needed services. Developing a remoteness index typically involves merging spatial and temporal data from a variety of incompatible sources such as topographical, census, and travel cost and duration. This paper presents a novel method for generating a measure of remoteness for any geographical location based on the nighttime satellite imagery. This continuous measure, herein referred to as Nighttime Remoteness Index (NIRI), is generated using machine learning-based models that link the intensity and statistical features of nighttime lights to remoteness; the predictive model is trained and validated using the nighttime satellite imagery and the Accessibility Remoteness Index for Australia (ARIA). This method does not require local data; hence, it is not limited by political jurisdictions or geographic boundaries. The NIRI is developed by using multivariate adaptive regression splines, and support vector machines regressions, after examining several other machine learning techniques. The NIRI maps of Australia and North America are developed based on the validated models.

Keywords –

Remoteness; Accessibility; Resource Projects; Resilience; Nighttime Satellite Imagery; Machine Learning; GeoTIFF

1 Introduction

Remoteness is a relative term. It is defined as "situated far from the main centers of population; distant" [1]. Remote could be used to refer to the fringes of a megacity that have sparse access to public transit or medical aid or to an uninhabited corner of the earth that has rarely seen human activity. Remoteness can be highly subjective, and its labeling can be controversial as it might have social, economic, technical, or political implications associated with it. These challenges may result in inherent biases that can hamper the objective measurement of remoteness.

The quantification of remoteness can assist decision makers in many domains, including 1) risk quantification for construction and industrial projects; 2) the resiliency assessment for communities and their underlying infrastructure; 3) policy making and research regarding resource allocation, public projects, and accessibility to essential services.

First, quantifying remoteness helps in risk assessments of large construction projects. The choice of location is particularly crucial for industrial projects due to their specific demands for skilled labor, material, and equipment [2]. The prevalence of remote projects is on the rise due to several factors. For natural resources projects, the depletion of conventional and accessible deposits has urged explorations in ever distant areas. Infrastructure projects are proposed to connect inaccessible communities and emerging markets to population hubs and open waters. Renewable energy projects such as hydroelectric dams and wind farms are built to harness clean but distant potentials. Quantifying the remoteness risk is an important step in assessing the overall risk of such projects, and in determining their development feasibility. Remote projects suffer from cost overrun, schedule slippage, and operability problems respectively 30%, 29%, and 70% more [3]. The distance to economic hubs represents access challenges to skilled trades and determines the safety and productivity implications of shift rotations that have employees work for several weeks followed by weeks-long leaves. Remoteness also affects access to raw materials, the most suitable modes of transportation, and access to markets or downstream treatments for the products of such remote projects. In this context, remoteness is a measure of vulnerability in adhering to the schedule and budget that make such developments economically feasible.

Second, with ever-growing implications of climate

change and extreme weather effects, understanding remoteness is crucial in creating expert systems for resiliency assessment and planning for remote communities and infrastructures. Physical remoteness is an inherent quality of cities, townships, and communities and plays a major role in assessing their resiliency and vulnerability [4]. A quantification of remoteness can benefit mitigation strategies and response plans for natural disasters. For example, remoteness can function as an input to regional multi-severity casualty estimations [5] or similar vulnerability functions.

Third, accessibility is the inverse of remoteness and while distinct in their perspective, the two are highly correlated [6]. Accessibility reflects the proximity to population centers that have the capacity to provide healthcare, education, and other essential services. Quantifying remoteness and accessibility is essential in policy making and budget allocation for public projects, including public health, education, and infrastructure projects. For example, a measure of remoteness was used to guide the eradication of malaria in Lao People's Democratic Republic. The study's success prompted its extension for achieving similar disease eradication goals and improving overall health in Vanuatu, and the Solomon Islands [7].

Approaches to the development of remoteness and accessibility indices are data intensive, mostly based on census and transportation data that takes a long time to collect and require specific strategies based on the range of their policy implications. Therefore, their applicability and scope are usually limited to certain spatial or temporal contexts due to the restricting nature of their input data and its level of aggregation. For example, an index developed to facilitate policy making on a national level may not be valid at the community level due to the loss of resolution. Remoteness indices are also typically developed for a specific jurisdiction, ranging from local to national, but rarely crossing national borders due to data ownership and compatibility. Even adjoining countries have difficulty comparing accessibility indices since there exists no standard method for their development.

As such, a *universal continuous remoteness index*, developed from a readily available source of data, that is applicable to different geographical, spatial, and temporal contexts can be utilized in a multitude of situations and be of utmost value.

1.1 Objective and Scope

Nighttime satellite imagery is an independent and readily available data source, and it can be used to understand the distribution and the growth of populations over time. The objective of this paper is to examine the potential of nighttime satellite imagery to measure remoteness and to build a continuous remoteness index that can be calculated for any location, and for any time.

Sections 2 and 3 review the related efforts on quantifying remoteness and elaborate on the nighttime satellite data used for the development of the remoteness index introduced in this work. Section 4 discusses the methodology used to develop the proposed nighttime remoteness index (NIRI), while sections 5 and 6 discuss the results, their validity, and finally the conclusions.

2 Approaches to Quantifying Remoteness

The proximity of human settlements to economic hubs is an important factor for countries with large land masses and only moderate populations as they strive to provide essential services to their residents. Two such countries are Canada and Australia who rank 222nd and 228th respectively out of 233 countries with respect to population density in 2018 [8].

Australia is a global leader in the study of proximity for practical purposes. One of the earliest of such studies was an index to distinguish the remoteness of rural areas created by associating population data with grid sections of the national map [9]. The index was based on the distance of the center of each grid to the center of the nearest populated grid. A contour map was drawn reflecting discrete categories of remoteness and accessibility. The remoteness index was later upgraded and named as the Australian rural, remote & metropolitan areas (RRMA) classification [6]. Both indices were criticized due to the subjectivity and the effect of the grid layouts on the index values assigned to specific regions.

In 1998, the continuous Accessibility Remoteness Index for Australia (ARIA) was created using census data to define population centers [10]. Travel times were incorporated in ARIA by overlaying the ground transportation network of roads and highways. This allowed the index to classify a region's accessibility to general practitioners, pharmacies, cardiovascular services, scientific grants, and urban infrastructure. As the index is linked to government funding policies, there was some concern about the fairness and reliability of some of the classifications. Although ARIA was calculated as a nominal index, the published version summarized it as discrete contour maps comprising five remoteness categories. In this way, the impact of moving a line could appear tremendous for communities on or near those boundaries.

A set of indices for remoteness and accessibility was developed for Canadian townships to measure and compare their accessibility to health, retail, and financial services [6]. It largely followed the ARIA methodology but instead of using the driving distance, the indices were scaled by the most affordable mode of transportation to reach the fundamental services. This accounted for the lack of year-round road networks and the local practices

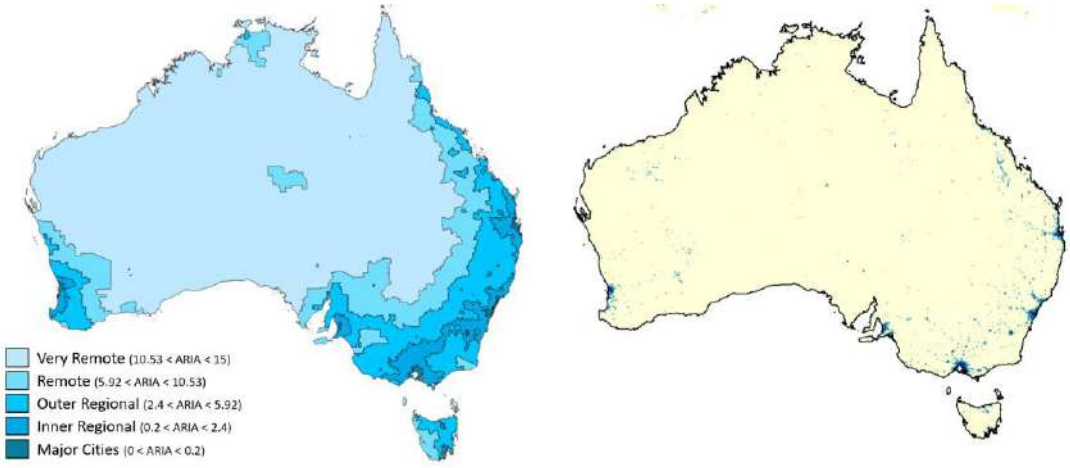

(a) (b)

Figure 1: a) The target variable: ARIA Map of Australia for 2011 [11,12]. b) The predictor: Average stable nighttime lights from satelite imagary of Australia in 2011 [13]. (both figures are reconstructed).

of using travel modes that better suited the region.

3 Nighttime Satellite Imagery

Satellite images are breathtaking and pique our imagination. They contain immense data and have great potential to provide us with valuable information. At first glance, the images can estimate electrification rates if coupled with population data [14]. More generally, they serve as a proxy for human development. Images can be compared over time to understand growth patterns in locations around the world [14].

Economic growth can be seen as the expansion of lighted centers, reductions in the dark spaces between centers, and as the increased intensity of lights in highly urbanized centers. Where reliable statistical data are unavailable, using nighttime imagery to estimate economic indicators [15] and socio-economic factors has proved accurate and effective [16].

Development can also be viewed as a measure of economic equality. With this perspective, the Night Light Development Index (NLDI) [16] measures the intensity of nighttime lights and their distribution and forms a Gini coefficient versus the distribution of the population. In effect, the resulting Gini coefficient interprets the comparative wealth of the neighborhoods without the use of monetary measures of wealth. Significant correlations were found between the NLDI and other data-intensive development factors such as the Human Development Index (HDI), Human Security Index (HSI), and electrification rates. While NLDI provides a spatial depiction of development in a country, it does not reflect an area's proximity to developed centers.

Shifts in economic activity have also been identified using nighttime imagery. The discovery of minerals in one area in Madagascar was made evident by the dramatic appearance and growth of nighttime lights in the area over a period of 5 years. The lights resulted from the development of mining facilities, local commerce, and communities to support workers. The mine was also identified to be the cause of the dimming of light intensity and slowed economic activity at a town further away [17].

Although the use of satellite nighttime imagery has many successes, some shortcomings have been discovered. In mapping global economic activities, satellite nighttime imagery methods were unable to account for activity that did not generate light, such as agriculture [19]. Along the same theme, regional cultural or operational practices, such as restricting the use of outdoor lights at night, can affect the results if the analysts are not aware of local practices. Although nighttime satellite lights are a reliable source for comparative analysis within similar regions, methods to validate findings are helpful in identifying such shortcomings.

4 Nighttime Remoteness Index (NIRI)

This work uses machine learning techniques to develop a predictive model linking the intensity and statistical features of the nighttime satellite data to remoteness. A model is trained to map a feature vector extracted from the nighttime satellite data (i.e., the predictor, or the independent variable) to the ARIA remoteness values (i.e., the target, or the dependent variable). The predictions of this model are further used to develop a continuous remoteness index, herein referred to as the nighttime satellite imagery (NIRI) for any given geographical location. NIRI maps the degree of remoteness to a nominal scale between 0 to 100, with

0 being the least remote, and 100 being the most remote point in the spatial context where NIRI is developed. The NIRI is independent of national boundaries and the data collection and integration challenges often related to local jurisdictions. Using the satellite data available for different time periods, NIRI can be automatically adjusted to reflect remoteness for a given temporal context, and it can be utilized to study changes in remoteness over time.

The majority of work was done in R programing language by taking advantage of Raster library. The maps are developed using ArcGIS® software. The following sections respectively elaborate on 1) the nature and the format of the input nighttime data; 2) the feature engineering and the choices regarding the mathematical representation of the input data in formulating the predictor variables; 3) calculating the target variable; 4) the predictive modeling process, mapping the predictors to target variables; and 5) the generation of NIRI based on the prediction results.

4.1 Predictor Variable: Nighttime Satellite Imagery

National Oceanic and Atmospheric Administration's National Geophysical Data Center (NOAA) published nighttime satellite imagery data annually from 1992 to 2013. Two data sets are available. The average lights data are calculated as the average readings during the year. Readings affected by clouds, moonlight, sunlight, aurora, and glare are excluded. The average stable lights data are further adjusted to exclude temporary light effects caused by, for example, wildfires and visual background noise. The data are available in 8-bit quantized georeferenced tagged image file format (GeoTIFF) as 30-arc-second resolution maps from -180 to 180 degrees Longitude and -65 to 75 degrees Latitude. GeoTIFF is an image file embedded with metadata, such as the reference coordinate system and pixel resolution, and spatial or georeferenced data in the form of pixel parameters [20] [20].

4.2 Feature Engineering

For any location on the map, a feature vector is generated for the purpose of training and testing the predictive models; a series of statistical features and summary statistics are extracted from the nighttime satellite data and in the neighborhood of a given location. This neighborhood is defined by a radius, the size of which can have important implications on the final index. The perceived remoteness of a location will vary depending on the region size and the distance in the context of major construction projects. For example, a site located more than 200km from a populated area can be considered remote in North America but perceived as relatively less remote in Africa [3]. A continuous remoteness index shall be sensitive to absolute distance from populated areas.

Therefore, this paper uses multiple neighborhood sizes to calculate the feature vector; individual feature vectors are calculated for four different influence radii of 100km, 300km, 500km, and 1000km, and they are concatenated together. The feature extraction process is further adjusted to reflect the proximity of open waters, ensuring that the model is expressive to the coastlines. This is intended to take into account the effect of open waters on the summary statistics of a given location; for example, while two locations may have similar readings on the nighttime satellite data, their corresponding remoteness indices can differ based on proximity to open waters.

4.3 Target Variable

In the next step, the target variables are calculated. Because Australia has established a robust and long-term record of indexing remoteness and accessibility, ARIA was used for this purpose. ARIA is published as contour maps, dividing Australia into five classes based on the measure of remoteness (see Figure 1) [11]. For any location, the target variable can be considered as either, first, the remoteness class (e.g., "very remote", that can be extracted from the ARIA map), or second, the actual nominal value of remoteness (ranging from 0 to 15 in the case of ARIA). The former formulates a classification problem that links the predictor variable (i.e., readings from the nighttime satellite images, see section 4.2) to their corresponding class of remoteness. This does not allow for introducing a continuous index that accounts for the gradient changes in remoteness. The latter choice results in a regression problem; and hence, allows the development of NIRI as a continuous index. However, nominal ARIA values are only known for the classes' borders from the overall map. The latter was used in this paper.

4.4 Predictive Modeling

The feature vectors and the target variables are passed to a machine learning model; several algorithms from regression-based modeling techniques were used for the purpose of predicting the target variable using the predictors, including the linear regression, the multivariate adaptive regression splines (MARSplines), the support vector machines regression (SVR), and the k-nearest-neighbor regression. Several validity tests were performed on the prediction results including the stratified random resampling and a non-random geographic split test. The residuals were carefully investigated to avoid overfitting and modal behaviors.

Moreover, an iterative model tuning campaign was carried forward to optimize the behavior of the models based on various definitions of cost parameters.

4.5 NIRI Development

The predictive models map the intensity and the statistical features of the nighttime data to the ARIA index. In this step, the model predictions are normalized across the geographical context for which the NIRI maps are being developed (e.g., across the entire map of Australia). The normalization allows for the resulted NIRI to specify the remoteness of any point at a value between 0 and 100, reflecting the relative remoteness of that location within its spatial context. This also allows for comparison of NIRI values between geographical locations, and it makes NIRI applicable to all regions.

When expanding the use of NIRI to other regions, the index shall be normalized based on the context of the region in question. It must be separately developed for countries with major cultural and geographic differences. This is due to the different mechanism of illuminating cities and population settlements across the globe, the geographic and cultural differences, among others [17].

5 Validation and Discussion

To train and test the predictive models, more than 7000 data points were selected on the region borders of the ARIA map (i.e., where the nominal value of remoteness is known). The feature vectors were calculated for all these locations using the process described in section 4.2.

The accuracy of the models is established by performing several validity tests, including the geospatial half split test; the ARIA map is split in two halves; the models are trained on one half, and they are used to predict the remoteness values in the other half. The best performing model is used to predict remoteness and develop the NIRI maps based on the normalization steps described in Section 4.5.

5.1 Results

Among the trained models, the SVR achieved the highest coefficient of determination, R^2=0.94 while, MARSplines produced similar results with R^2=0.93. Both models performed reliably in terms of the residuals. The non-random geographic split test, using Eastern Australia data to train and Western Australia data to test posed the highest challenge to coefficients of determination, however, it resulted in R^2=0.85 and R^2=0.84 for SVR and MARSplines, respectively. The SVR produced slightly less normally distributed residuals for the geographic split test in comparison to MARSplines, and hence, MARSplines is less prone to overfitting and more appropriate for these data. Therefore, MARSplines is chosen as the best performing model and is used hereafter to create the NIRI maps using the procedure described in section 4.5.

Figure 2 and 3 show the NIRI maps of Australia and North America, generated using MARSplines model and the nighttime satellite data of 2011. Figure 4 shows the superimposition of NIRI contours (iso-remote lines), on the average stable lights of North America for 2011. NIRI envelopes the light clusters normal to the direction of remoteness gradient from population centers to remote areas with great accuracy.

5.2 Discussion

The spacing of the corresponding grid to build the index determines the resolution of the ultimate NIRI map and has an immediate effect on its accuracy as well as the computation time. The triangulation error increases as the resolution of the grid increases, subjecting the corresponding maps to both random and systematic errors. More importantly, larger grids mean that each point represents a larger area. This increases the occurrence of index locations that do not represent their areas. To examine the sensitivity of the grid size on the accuracy of the map, analysis was performed to identify the potential systematic and random impacts on the results. Figure 5 plots the average and standard deviation of NIRI for a region in the southeast of Australia encompassing Sydney and Melbourne for four grid sizes ranging from 0.2 to 1.2 degrees. The random error disappears as the average and the standard deviation of the index start to converge in grid sizes below 0.8 degrees. Therefore, depending on the size of the coverage area, the desired resolution, and the computational power available, a grid size of 0.8 degrees or smaller produces reliable results.

Because NIRI is a continuous index, it allows establishing remoteness contours at any interval and for any region. Once the models are built to link the nighttime satellite imagery to remoteness as the target variable based on Australia data, the same models can be used to compute NIRI for other regions of the world. This extends the use of the index to a variety of applications. Once the model is run, the relative remoteness difference between any two points can be measured for risk assessment and other purposes.

NIRI can be used to better understand and quantify the resiliency of communities and their underlying infrastructure. In the case of infrastructure resiliency, NIRI can be used as an additional factor to improve mitigation strategies for natural disasters [21]. Combining an understanding of remoteness and accessibility with casualty estimations can optimize the use of the limited resources in the face of natural disasters such as earthquakes, tsunamis, and hurricanes.

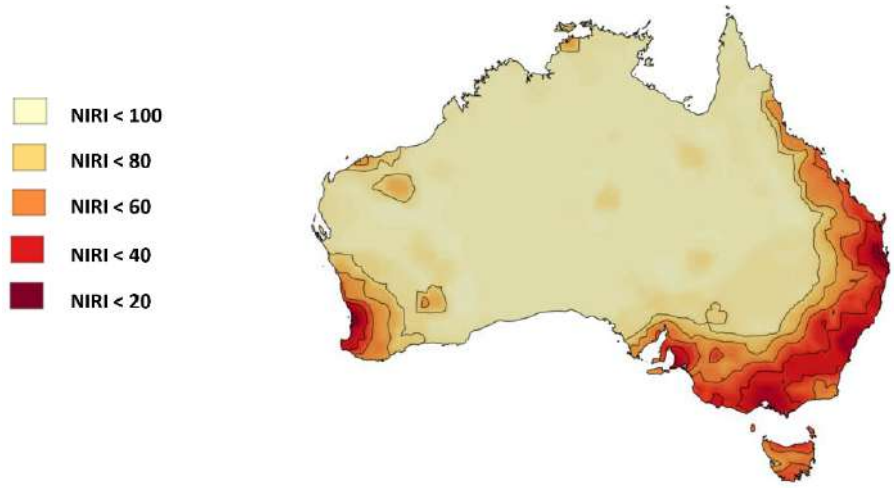

Figure 2: NIRI Map of Australia for 2011

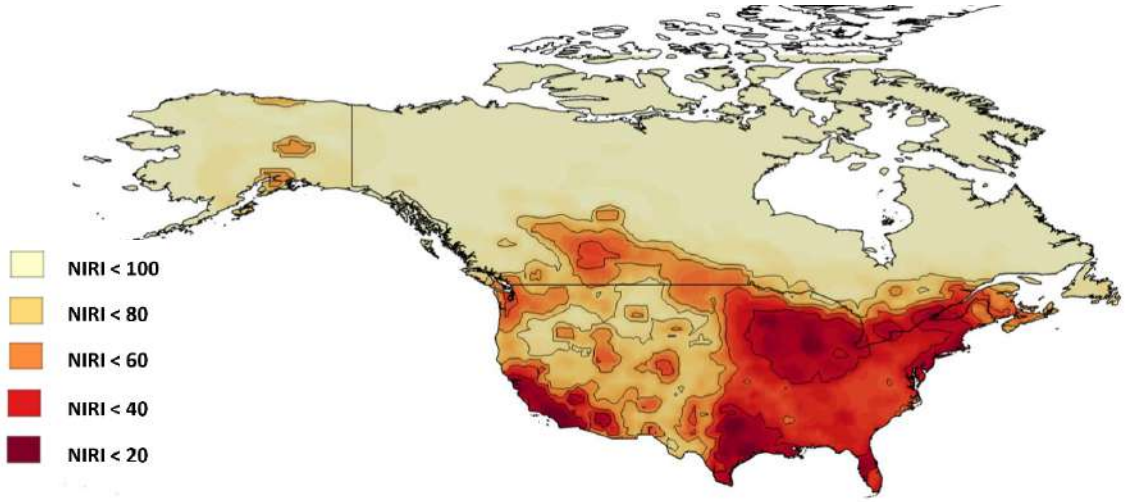

Figure 3: NIRI Map of North America for 2011

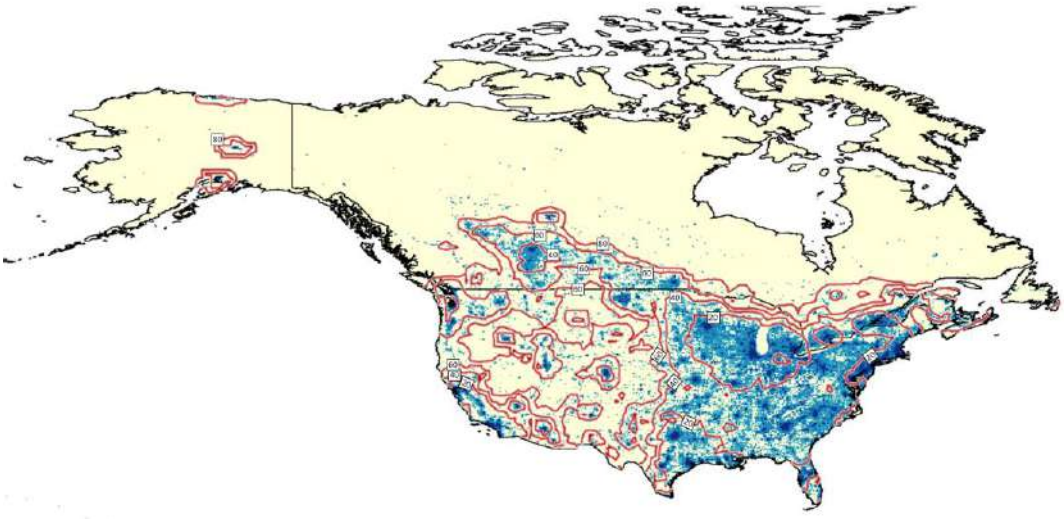

Figure 4: NIRI Contours (Iso-Remoteness Lines) Superimposed on Average Stable Nighttime Lights of North America for 2011

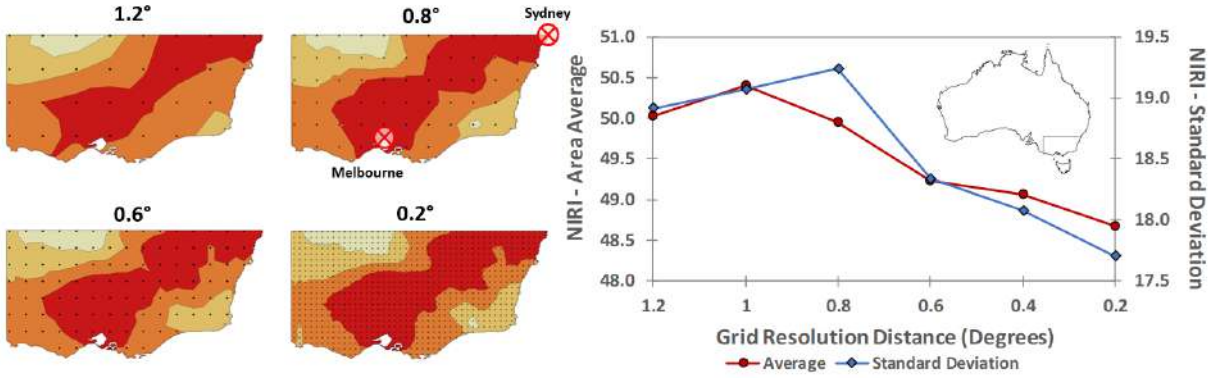

Figure 5: Grid Spacing Sensitivity Analysis Results

Regional remoteness indices were directly utilized in vulnerability analysis of road networks for south east Australia [22], such frameworks and programs can be expanded to any other part of the world by utilizing NIRI. Several models are proposed to forecast damage and severity for seismic events. For instance, NIRI can be a direct input to regional multi-severity casualty estimations [5] and Earthquake vulnerability functions [23] to calibrate those models for physical location characteristics. Previous studies have linked remoteness to both resiliency and vulnerability of communities and proposed adaptation pathways to consequences of climate change and extreme weather events to those communities [4]. NIRI can quantify remoteness for implementation of such strategies.

Moreover, NIRI can help in research applications at a variety of economic and social sciences' fronts. Satellite data in general [24], and nighttime satellite imagery in particular [15~19] have been effectively used in several studies to explore various economic outcomes including poverty. Separate studies have established links between the prevalence of poverty and remoteness characteristics of communities [25]. NIRI can be utilized effectively as an input to such models to better understand similar phenomena.

6 Conclusions

Remoteness is hard to measure, yet it is a crucial factor in determining the success and feasibility of large international projects and assessing the resiliency and vulnerabilities of remote communities. The existing means of quantifying remoteness require extensive data collection and are based on the integration of multiple data sources. A global measure of remoteness is needed that is not limited in terms of its applicability to different geographical contexts and time periods. This paper proposes a novel method that exploits the readily available nighttime satellite data for developing a continuous measure of remoteness that is not limited to local jurisdictions or certain borders. While most research on nighttime satellite imagery has been focused on the characteristics of illuminated clusters and its relationship with human development, this paper links the lack of such light clusters to remoteness.

In this study, the nighttime satellite imagery proved to accurately predict a multidimensional composite index of remoteness. The nighttime data is used as a predictor of remoteness and to create a continuous remoteness index, NIRI, that describes remoteness and its directional gradient with great accuracy for a variety of risk and resiliency assessment tasks.

NIRI can be developed across different regions and as well in time. Although this paper only used 2011 data to establish the predictive model, the index can be developed using nighttime satellite imagery of other points in time. This allows NIRI to measure the changes of remoteness not only across regions but also across time.

Acknowledgments

We benefited from comments of Murray Pearson and Nick Mason in formulizing the index to best suit practical risk assessment procedures of large construction projects. The project is funded by Hatch Ltd. and Natural Sciences and Engineering Research Council (NSERC) of Canada grant CRDPH 491877-15.

References

[1] English Oxford Living Dictionaries. Oxford University Press. On-line: http://en.oxforddictionaries.com/definition/remote/, Accessed: 29/12/2018.

[2] Barrie, D.S. and Paulson, B.C. *Professional construction management*. McGraw-Hill. New York, United States of America, 1984.

[3] Merrow, E.W. *Industrial megaprojects: concepts, strategies, and practices for success*. John Wiley &

Sons, Inc., Hoboken, New Jersey, United States of America, 2011.

[4] Maru, Y. T., Smith, M. S., Sparrow, A., Pinho, P. F., & Dube, O. P. A linked vulnerability and resilience framework for adaptation pathways in remote disadvantaged communities. *Global Environmental Change*, *28*(1):337-350. 2014.

[5] Ceferino, L., Kiremidjian, A., Deierlein, G. Probabilistic Model for Regional Casualty Estimation due to Building Damage Following and Earthquake. *The ASCE-ASME Journal of Risk and Uncertainty in Engineering Systems*, 4(3), 2018.

[6] Alasia A., Bédard F., Bélanger J., Guimond E., Penney, C. *Measuring remoteness and accessibility- A set of indices for Canadian communities.* Reports on Special Business Projects. Statistics Canada Catalogue 18-001-X, Ottawa, Canada, 2017.

[7] Beaver C., Pontifex S., Zhao Y., Marston L., and Bobogare A. Applications of a remoteness index: funding malaria programs. *International Journal of Geoinformatics* 7(1):15-19, 2011.

[8] Statistics Times. Countries by Population Density On-line: http://statisticstimes.com/ demographics/countries-by-population-density.php/, Accessed: 29/12/2018.

[9] Faulkner H. and French S. Geographic remoteness: conceptual and measurement problems. *Bureau of Transport Economics*, *Reference Paper* (54), Canberra, Australia, 1983.

[10] Department of Health. The Accessibility Remoteness Index of Australia (ARIA). On-line: http://www.health.gov.au/internet/publications/publishing.nsf/Content/ARIA-Review-Report-2011/, Accessed: 29/12/2018.

[11] ARIA. The Accessibility/Remoteness Index of Australia (ARIA). On-line: https://www.adelaide.edu.au/hugo-centre/spatial_data/aria/, Accessed: 29/12/2018.

[12] ArcGIS. Accessibility/Remoteness Index of Australia. On-line: https://www.arcgis.com/home/item.html?id=23e8510c40fa4b4e8c700e59048ba5fb/, Accessed: 29/12/2018.

[13] Earth Observation Group, EOG. Global Radiance Calibrated Nighttime Lights. On-line: https://www.ngdc.noaa.gov/eog/dmsp/download_radcal.html/, Accessed: 29/12/2018.

[14] Elvidge C., Safran J., Tuttle B., Sutton P., and Cinzano P. Potential for global mapping of development via a nightsat mission. *GeoJournal* 69(1-2):45–53, 2007.

[15] Chen X. and Nordhaus W.D. Using luminosity data as a proxy for economic statistics. *Proceedings of the National Academy of Sciences* 108(21):8589-8594, 2011.

[16] Elvidge, C.D., Baugh, K.E., Anderson, S.J., Sutton, P.C., and Ghosh, T. The Night Light Development Index (Nldi): A Spatially Explicit Measure of Human Development from Satellite Data. *Social Geography* 7(1):23-35, 2012.

[17] Henderson, J.V., Storeygard, A., and Weil, D.N. Measuring Economic Growth from Outer Space. *American Economic Review*, 102(2):994-1028, 2012.

[18] Ghosh T., Anderson S., Elvidge C., and Sutton P. Using Nighttime Satellite Imagery as a Proxy Measure of Human Well-Being. *Sustainability* 5(12):4988-5019. 2013.

[19] Ghosh, T., Powell, R.L., Elvidge, C.D., Baugh, K.E., Sutton, P.C., and Anderson, S. Shedding Light on the Global Distribution of Economic Activity, *The Open Geography Journal*, 3(1):147-160, 2010.

[20] Berrick, S. GeoTIFF. On-line: https://earthdata.nasa.gov/user-resources/standards-and-references/ geotiff/, Accessed: 29/12/2018.

[21] Bocchini, P., Frangopol, D. M., Ummenhofer, T., & Zinke, T. Resilience and sustainability of civil infrastructure: Toward a unified approach. *Journal of Infrastructure Systems*, *20*(2), 2013.

[22] Taylor, M.A. Remoteness and accessibility in the vulnerability analysis of regional road networks. *Transportation research part A: policy and practice*, *46*(5):761-771. 2012.

[23] Noh, H., Kiremidjian, A., Ceferino, L., So, E. Bayesian Updating of Earthquake Vulnerability Functions with Application to Mortality Rates. *Earthquake Spectra*, 33(3), 2017.

[24] Jean, N., Burke, M., Xie, M., Davis, W. M., Lobell, D. B., & Ermon, S. Combining satellite imagery and machine learning to predict poverty. *Science* 353(6301), 2016.

[25] Partridge, M. D., & Rickman, D. S. Distance from urban agglomeration economies and rural poverty. *Journal of Regional Science*, *48*(2):285-310, 2008.

BIM-based Decision Support System for Concrete Formwork Design

R. Romanovskyi[a], L. Sanabria Mejia[a], and E. Rezazadeh Azar[a]

[a] Department of Civil Engineering, Lakehead University, Canada
E-mail: rromanov@lakeheadu.ca, lsanabri@lakeheadu.ca, eazar@lakeheadu.ca

Abstract –

The type and quantities of formwork system are necessary information for construction process of a concrete-framed building and the solution to this problem usually lays on the shoulders of specialized consulting firms or contractor's engineering department. These calculations are generally performed using available procedures and guidelines. The conventional formwork design process is manual and time-consuming, which requires considerable experience and attention to details. The emergence of building information modeling (BIM) in the AEC industry has allowed automation of many time-consuming tasks through application of object-oriented 3D modeling. In this project, a system was developed to automate formwork design process for the concrete-framed buildings. This method first extracts required data for the formwork design from the building information model of the project, which includes concrete elements' dimensions, quantities, and spatial information. It then applies formwork design rules and a database of modular formworks to determine dimensions and type of the formwork for each element. This system demonstrated promising performance in automation of formwork design in two test models.

Keywords –

Formwork design; Construction; Automation; Building Information Modelling; Reinforced Concrete

1 Introduction

Formworks are auxiliary structure made of wood, metal or composite materials; which serve to temporarily maintain shape, geometric dimensions, position in space, surface texture, and solidity of the structures that are made of shapeless or bulk materials, namely fresh concrete [1]. Formwork (also called shuttering) systems typically consist of forming elements, supporting structures, and fasteners [2]. After hardening of the concrete, formwork elements are usually removed (called detachable formwork), but there are also permanent formwork systems which are not removed and become a part of the main structure [3]. Both of these systems are widely used in modern concrete construction [1], but the removable formworks are more common and are classified based on their function, design, and material. Formwork systems for various structural members are slightly different from each other. For example, column formworks include struts whereas props are used for beams and slabs construction [1].

Traditional timber formwork systems are known for ease of fabrication and installation, and economical benefits in small construction. Aluminum and steel formworks usually cost more than wooden systems and are used in large-scale and high-precision construction. Moreover, these formworks can be used multiple times and they are more efficient for fast installation and removal of formwork, which in turn reduce the cost of form working after each use [3].

Conventional formwork design is a time-consuming and heuristic process, and is often based on the skill and experience of the engineers [4], and strength and the quantity are the main parameters in the design of a formwork system [2, 3]. A well-designed formwork system contributes to the quality, and timely and cost-effective construction of a reinforced-framed concrete building [1, 3]. Designing of a concrete structure and its formwork system are usually carried out separately, where the structural engineers design the concrete structure, and then the contractor designs a formwork for each element based on the dimensions and geometry of that component [5]. Therefore, development of automated formwork design tools would assist site engineers with the process of determining a suitable formwork system.

Earlier research efforts summarized best practices for design of a formwork system and proposed step-by-step guides and specific tables to speed up the process of formwork design [6]. Later, a Fuzzy logic-based model was proposed to assist site engineers in selection of a suitable vertical formwork system [7]. In addition, a

mathematical formwork design method integrated with formwork operation layout planning demonstrated promising performance in high-rise building construction [8].

The multifaceted capabilities of the BIM have encouraged the use of this platform in the design and planning of on-site construction processes. The abilities of BIM to generate, store, share, and reuse information of building components are useful for repetitive tasks such as document generation, visualization, and quantification [9]. Application of BIM for different analysis, such as construction energy analysis [16], planning of construction processes [17, 18], and cost estimation [19], could reduce human errors of manual processes. Therefore, later efforts employed building information modelling to improve formwork design and planning processes. For example, a rule-based model was developed to assess the constructability of the horizontal formworks [10]. A cascade method was proposed which extracts required data (such as quantity take-off and construction phases) from the BIM model and uses them to design a formwork system for the project [5]. Industry Foundation Classes (IFC) schema was employed to optimize formwork design of concrete walls in building construction [11]. Later, a method was proposed to increase the proportion of the modular forms to increase formwork efficiency [12].

In addition to the formwork design, BIM-based data could be used to estimate labor productivity in formwork operations [13], and to determine required consumption of formwork systems [20]. These research efforts, however, did not present customizable approaches. In particular, most of these systems used a certain type of modular formwork system and did not search among various modular alternatives, and also did not investigate traditional timber formwork systems.

This paper presents a customizable system which was developed using a visual programming environment to extract data of cast-in-place concrete elements form BIM model and then designs a formwork system using a database of modular formworks from different suppliers. Upon the user request, this system is able to design traditional timber formwork for the concrete elements.

2 Methods

The workflow of this method is presented in Figure 1. It extracts certain attributes of the cast-in-place concrete elements, which are identified based on the corresponding codes, such as type and reference level. Then the system calculates pressure of the concrete based on the dimensions of each element. Afterwards, the system selects formwork elements based on the preference of the user between modular and wooden formwork systems. It should be noted that the system is only able to process prismatic elements rectangular cross-sections. Following subsections discuss the modules of this system.

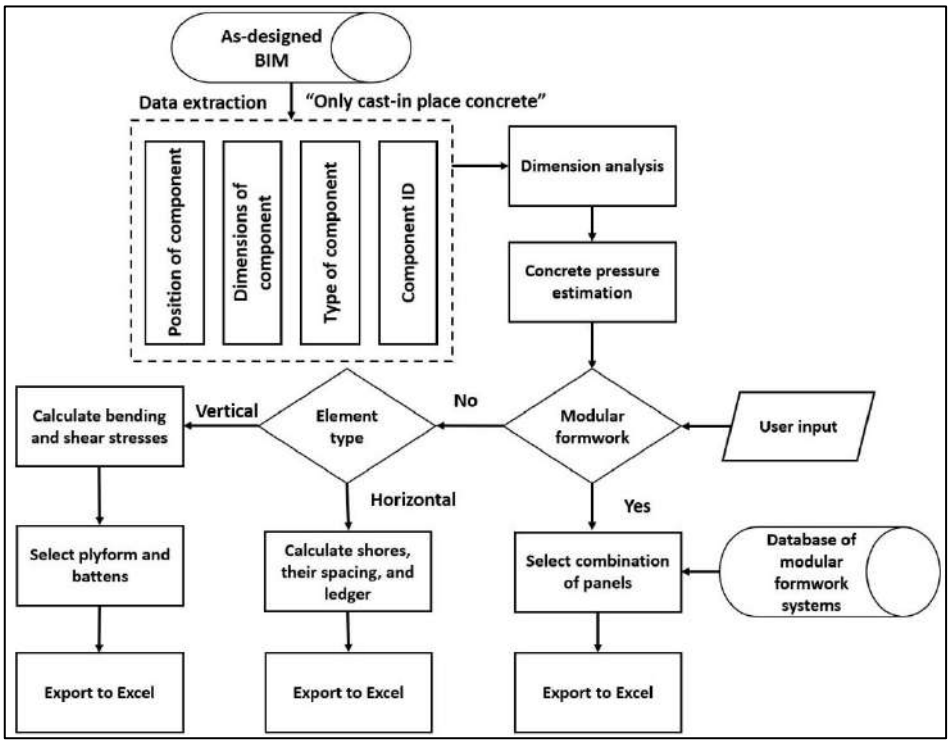

Figure 1. Workflow of the proposed system

2.1 Data Extraction

Dynamo environment [14] was used to automate the data extraction process. Dynamo is a visual programming and open-source platform for automated interaction with BIM models, which has the ability to extract various attributes of building elements.

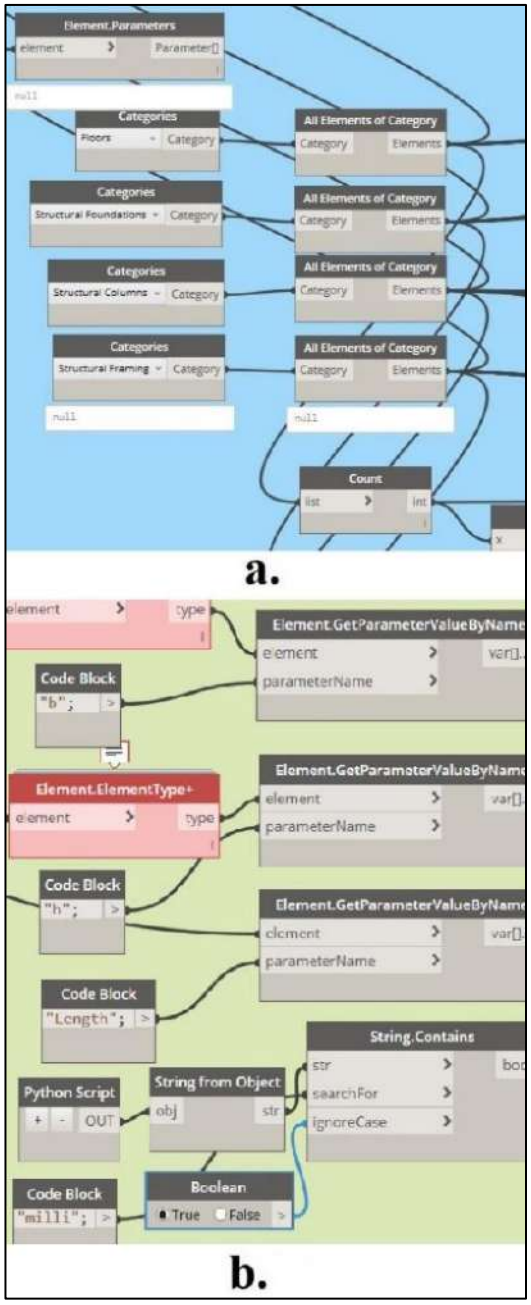

Figure 2. Data extraction using Dynamo functions: a) selection of elements of interest; b) selection of the target attributes

This module extracts the following data for each concrete element: dimensions (width, depth, height), ID (e.g. gridlines), type (e.g. column, beam, slab, foundation), and its level. Figure 2.a depicts a small part of this script which uses "Categories" and "All Elements of Category" to select all elements in the target categories, and then "Code Block" and "Element.GetParameterByValueName" are employed to extract the attributes of interest. For example, Figure 2.b shows a part of the script used the extract dimension of the columns.

2.2 Concrete Pressure Estimation

2.2.1 Vertical Load Estimation

There are two main types of vertical loads: 1) Dead loads include weight of fresh concrete, rebars, and the formwork; 2) Live loads consist of the weight of equipment, workers, and other related items. Based on the guidelines in ACI 347R-14 [15], the live load should not be less than 2.4 kPa (assuming no motorized cart is used) and the unfactored combined load (dead + live) should be more than 4.8 kPa (6.0 kPa in case of using motorized carts).

2.2.2 Lateral Pressure Estimation

Lateral concrete pressure depends on the dimension of concrete elements. The lateral pressure exerted on the formwork walls (see Figure 3), which was estimated based on the guidelines provided in ACI 347R-14 [15]. The lateral pressure of the fresh concrete depends on a few main factors, namely slump and temperature of the concrete and rate of concrete pouring. Two conditions were implemented in this system which should be selected by the user based on the properties of the concrete and pouring conditions. Equation 1 should be used for high slump concretes (greater than 17.8 cm) and concretes with deep vibration (greater than 122 cm), which simply calculates the equivalent hydrostatic pressure of the concrete. The lateral pressure for other cases is calculated using Equation 2. These equations were implemented in the Dynamo environment using "Python Script" node, which enables development of customized functions within the Dynamo platform.

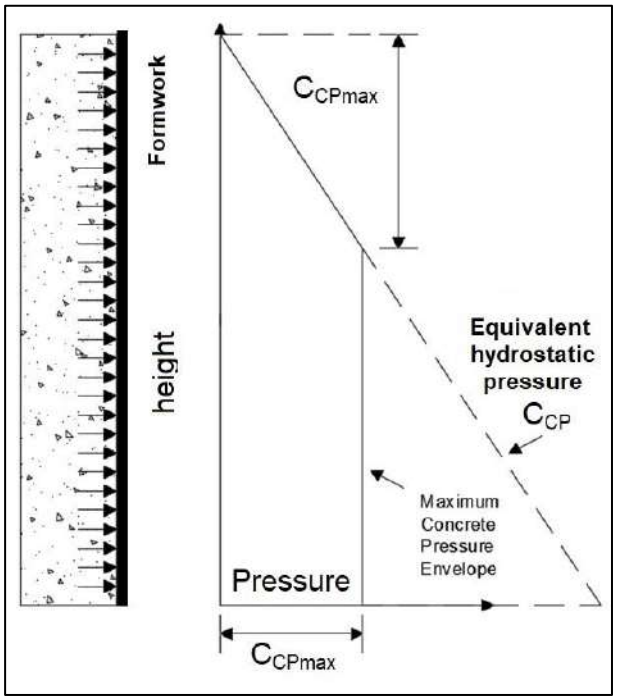

Figure 3. Schematic view of the lateral concrete pressure [15]

$$C_{CP} = \text{wh} = \rho gh \quad (1)$$

$$C_{CPmax} = C_c C_w [150 + \frac{900R}{T}] \quad (2)$$

Where C_{CP} is the equivalent hydrostatic pressure, w is unit weight of fresh concrete, h is the height of the element, C_{CPmax} is the maximum concrete pressure, C_C is chemistry coefficient, C_W is unit weight coefficient, R is the rate of placement ft/h (m/h), and T is the temperature of fresh concrete °F (°C).

2.3 Modular Formwork Design

Lists of modular formwork systems from four manufacturers were created. These lists include name of the manufacturer, admissible load (Kg/sq.m), width, and length of the available panels by each manufacturer (see Figure 4). Selection of formwork panels for concrete elements is carried out by a special "Python Script" node, which requires a number of inputs, including the name of the manufacturer, admissible load of the formwork panels in kg/sq.m, list of available panel dimensions for that formwork system, and the dimensions of concrete element.

When the system analyzes a vertical element (e.g. columns), the length corresponds with the vertical axis, and 0 to +0.30 m tolerance is accepted for this dimension. The same tolerance is applied for the side formworks of horizontal elements, namely beams. If there are more than one manufacturer for an element, then the program will eventually select the type that has appeared the most in all of the solutions. It is also possible to include unit cost of each type; thus, the system determines the lowest cost option.

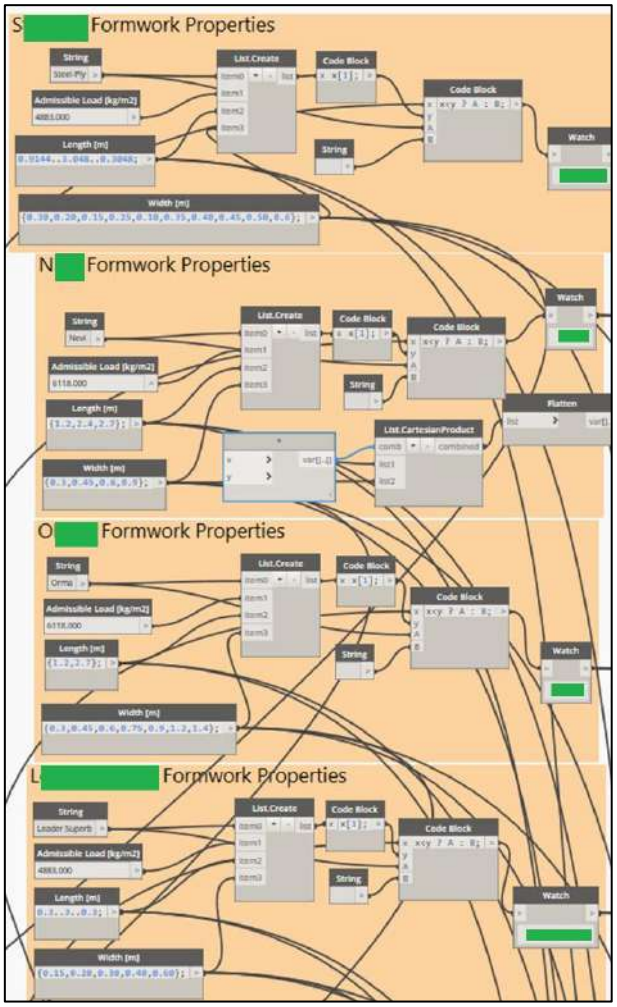

Figure 4. Lists of formwork systems from four manufacturers (names are covered)

The system identifies width (w in Figure 5) and length (l in Figure 5) as the smaller and larger dimensions of each formwork surface, respectively. The panel selection process iterates over the list of available dimensions from the manufacturers lists (using for loops) to find combinations that completely cover each formwork surface. It should be mentioned that this algorithm only uses panels from a same manufacturer to create a combination. This process is illustrated in Figure 5.

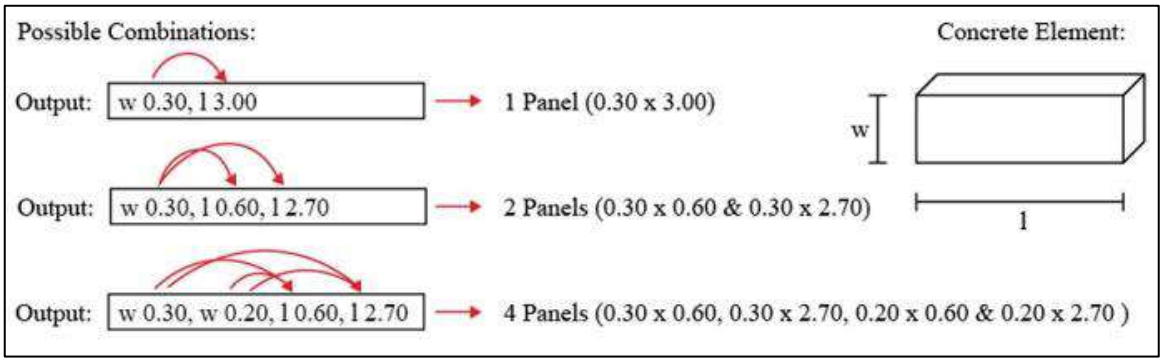

Figure 5. A sample workflow for selection of a panel combination

2.4 Conventional Timber Formwork Design

If the user chooses timber formwork option, the system calculates formwork elements based on whether they are vertical or horizontal.

2.4.1 Vertical Elements

The lateral concrete pressure acts against the plyform, which is supported with vertical wood battens laid flat. The plyform panels must transfer lateral pressure to the adjacent vertical wood battens. There are different types of wooden formwork products with different mechanical and physical (e.g. moisture content) properties, and dimensions, but a small number of options was used in this prototype. The plyform must have adequate strength to transfer the pressure with supports spacing up to 18 cm. The main criteria for selection of the plyform and battens is to pass the allowable bending and shear stresses. The calculations were implemented according to the design procedures available in [3].

In this approach, the system starts with a plyform with the smallest thickness, and if it fails, then it tries the next thickness until it reaches the allowable stresses. The same approach is used for the battens.

2.4.2 Horizontal Elements

This part of the system calculates three main items: shore spacing for the bottom part, ledger spacing, and shore design. These calculations were implemented according to the procedures provided in [1].

The shore spacing is calculated based on the bending due to the vertical loads and the bending capacity of the bottom surfaced two sides (S2S) lumber. The ledger spacing is also calculated based on allowable stress of the selected (surfaced on 4 sides) S4S ledgers and the stresses due to concrete load. Then based on the spacing of the shores, the applied load on each shore is calculated and compared against the allowable load of the unbraced shores.

2.5 Exporting Results

At the end, generated results are organized and exported to MS Excel for presentation. This process is implemented using a series of nodes, namely "Excel.WriteToFile" function. This way, the system arranges formwork information in a tabular format with all the necessary parameters such as element ID, level, family type, dimensions, and the proposed panel combinations and manufacturer.

3 Case Study

A five-story and four-story reinforced concrete-framed buildings were modelled in the Autodesk Revit environment. Isolated footings were used for foundation and beams and slabs were used for the flooring systems. Figure 6 depicts a 3D view of the five-story building model.

Figure 6. A 3D view of the test model

Figure 7 presents a sample of the results generated for modular formwork in the Excel environment. All the mentioned properties are organized and presented for the user.

Column ID	Column Base Level	Family Name	Column Width [m]	Column Depth [m]	Column Height [m]	Concrete Volume [m3]	Formwork System: L
T-1	Base Level : Ground	300 x 300mm	0.3	0.3	3.000103381	0.270009304	w 0.30, l 0.60, l 2.70
U(-648)-1	Base Level : Ground	300 x 300mm	0.3	0.3	3.000103381	0.270009304	w 0.30, l 0.60, l 2.70
U(-648)-3	Base Level : Ground	300 x 300mm	0.3	0.3	3.000103381	0.270009304	w 0.30, l 0.60, l 2.70
U-6	Base Level : Ground	300 x 300mm	0.3	0.3	3.000103381	0.270009304	w 0.30, l 0.60, l 2.70
U-9	Base Level : Ground	300 x 300mm	0.3	0.3	3.000103381	0.270009304	w 0.30, l 0.60, l 2.70
U(-648)-11	Base Level : Ground	300 x 300mm	0.3	0.3	3.000103381	0.270009304	w 0.30, l 0.60, l 2.70
U(-648)-12	Base Level : Ground	300 x 300mm	0.3	0.3	3.000103381	0.270009304	w 0.30, l 0.60, l 2.70
T-12	Base Level : Ground	300 x 300mm	0.3	0.3	3.000103381	0.270009304	w 0.30, l 0.60, l 2.70
S-12	Base Level : Ground	300 x 300mm	0.3	0.3	3.000103381	0.270009304	w 0.30, l 0.60, l 2.70
R-12	Base Level : Ground	300 x 300mm	0.3	0.3	3.000103381	0.270009304	w 0.30, l 0.60, l 2.70
Q-12	Base Level : Ground	300 x 300mm	0.3	0.3	3.000103381	0.270009304	w 0.30, l 0.60, l 2.70

a.

Beam Reference Level	Family Name	Beam Width [m	Beam Height [m	Beam Length [m	Concrete Volume [m3]	Bottom L	Sides L
Reference Level : Level 1	400x500mm (reg)	0.4	0.5	4.5	0.9	w 0.40, l 1.50, l 3.00	w 0.40, w 0.40, l 1.50, l 3.00
Reference Level : Level 1	400x500mm (reg)	0.4	0.5	3.6	0.72	w 0.40, l 0.60, l 3.00	w 0.40, w 0.40, l 0.60, l 3.00
Reference Level : Level 1	400x500mm (reg)	0.4	0.5	2.031474108	0.406294822	w 0.40, l 1.80, l 0.30	w 0.40, w 0.40, l 1.80, l 0.30
Reference Level : Level 1	400x500mm (reg)	0.4	0.5	2.031474108	0.406294822	w 0.40, l 1.80, l 0.30	w 0.40, w 0.40, l 1.80, l 0.30
Reference Level : Level 1	400x500mm (reg)	0.4	0.5	6.0	1.2	w 0.40, l 3.00, l 3.00	w 0.40, w 0.40, l 3.00, l 3.00
Reference Level : Level 1	400x500mm (reg)	0.4	0.5	8.129	1.6258	w 0.40, l 3.00, l 3.00, l 2.1	w 0.40, w 0.40, l 3.00, l 3.00, l 2.10

b.

Figure 7. Sample tabular output: a) sample columns; b) sample beams

In addition, these formwork data can be imported in the Revit environment and saved as a parameter for the corresponding case-in-place concrete objects, and then be visualized for each element. Figure 8 displays a sample of a formwork combination added to the BIM model in Revit environment.

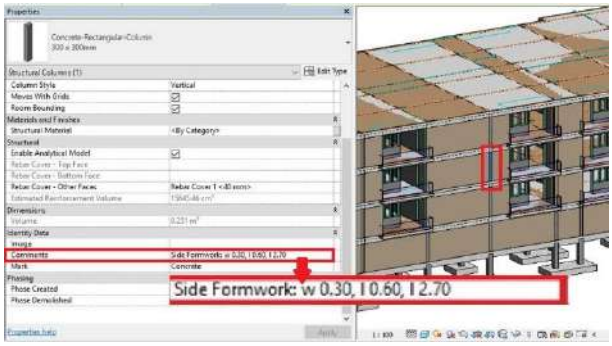

Figure 8. Sample of a formwork combination added to the BIM model

The system was also tested in designing of a conventional timber formwork. For this purpose, a simple BIM model, containing four columns and four beams, was used. Figure 9 shows the result for one of the column formwork designs (the results are drawn manually).

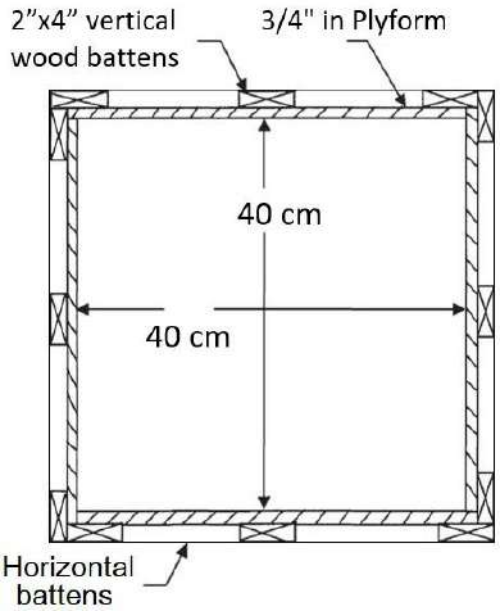

Figure 9. Cross-section of the wooden formwork for a 40x40 cm column

The results of this method and its modules was assessed to validate its performance. First, the outputs of the data extraction part were compared against the BIM models, where no difference was found. Second, the concrete pressure estimation correctly estimated vertical and lateral pressures. Next, selected panel combinations were validated, in which the system was able to provide a sufficient combination for each element; however, the results do not necessarily represent an optimized combination. Because this system does not consider form working state of other concrete elements and the availability of formworks. Moreover, performance of

this system is limited to prismatic elements with rectangular cross-sections and further expansion is needed to analyze curved elements and the concrete components with irregular shapes and openings.

4 Conclusion

Formwork systems are essential part of cast-in-place concrete construction and automated design of formwork systems could improve this design process by saving time, and enhanced visualization and documentation. This research paper proposed a BIM-based decision support system to design modular and conventional wooden formwork systems for concrete-framed buildings. This system was implemented in the Dynamo platform, which extracts required data of cast-in-place concrete elements, and then calculates concrete pressure on the formwork surfaces. It finally tries different panel combinations to obtain a sufficient combination for each concrete element. This system demonstrated promising performance to facilitate formwork design processes in concrete construction, and the same data extraction and analysis could be used to develop automated tools for similar problems. The future research will focus on the analysis of irregular shapes, and also will investigates optimization of the formwork systems by considering overlapping and succeeding formwork activities.

References

[1] Aghayere A. O. and Limbrunner G.F. *Reinforced Concrete Design 8th ed.*, Pearson, Boston, MA, USA, 2014.

[2] Nunnally S.W. *Construction Methods and Management, 7th ed.*, Pearson, Upper Saddle River, NJ, USA. 2007.

[3] Peurifoy R. L. and Oberlender G.D. *Formwork for Concrete Structures 4th ed.*, McGraw Hill, New York, NY, USA, 2011.

[4] Kim K. and Teizer J. Automatic design and planning of scaffolding systems using building information modeling. *Advanced Engineering Informatics*, 28(1): 66-80, 2014.

[5] Mansuri D., Chakraborty D., Elzarka H., Deshpande A. and Gronseth, T. Building information modeling enabled cascading formwork management tool. *Automation in Construction*, 83: 259-272, 2017.

[6] Ringwald R. C. Formwork Design. *Journal of Construction Engineering Management*, 111(4): 391-403, 1985.

[7] Elbeltagi E. E., Hosny O. A., Elhakeem A., Abdelrazek M. E. and El-Abbasy, M. S. Fuzzy logic model for selection of vertical formwork systems. *Journal of Construction Engineering and Management*, 138(7): 832-840, 2012.

[8] Kim T., Lim H., Lee U. K., Cha M., Cho H. and Kang K. I. Advanced formwork method integrated with a layout planning model for tall building construction. *Canadian Journal of Civil Engineering*, 39(11): 1173-1183, 2012.

[9] Lu W., Peng Y., Shen Q., and Li H. Generic model for measuring benefits of BIM as a learning tool in construction tasks. *Journal of Construction Engineering and Management*, 139(2): 195-203, 2013.

[10] Jiang L. and Leicht R. M. Automated rule-based constructability checking: Case study of formwork. *Journal of Management in Engineering*, 31(1): A4014004. 2015.

[11] Hyun C., Jin C., Shen Z. and Kim H. Automated optimization of formwork design through spatial analysis in building information modeling. *Automation in Construction*, 95: 193-205, 2018.

[12] Lee C. and Ham S. Automated system for form layout to increase the proportion of standard forms and improve work efficiency. *Automation in Construction*, 87: 273-286, 2018.

[13] Lee J., Park Y. J., Choi C. H. and Han C. H. BIM-assisted labor productivity measurement method for structural formwork. *Automation in Construction*, 84: 121-132, 2017.

[14] Dynamo, Open-source Dynamo for BIM. On-line: http://dynamobim.org/, Accessed: 15/01/2018.

[15] ACI 347R-14: Guide to Formwork for Concrete, American Concrete Institute, MI, USA, 2014.

[16] Zhou H. and Rezazadeh Azar E. BIM-based Embodied Energy Assessment of Building Structural Systems. *Journal of Built Environment Project and Asset Management*, 9(1): 2-14, 2019.

[17] Sigalov K. and König M. Recognition of process patterns for BIM-based construction schedules. *Advanced Engineering Informatics*, 33: 456-472, 2017.

[18] Wang Z. and Rezazadeh Azar E. "BIM-based Draft Schedule Generation in Reinforced Concrete-framed Buildings." *Construction Innovation: Information, Process, Management*, http://www.emeraldinsight.com/1471-4175.htm, 2019.

[19] Lee S. K., Kim K. R., and Yu J. H. BIM and ontology-based approach for building cost estimation. *Automation in construction*, 41: 96-105, 2014.

[20] Wu K., García de Soto B., Zhang, F. and Adey B. T. Automatic Generation of the Consumption for Temporary Construction Structures Using BIM: Applications to Formwork. In Proceedings of the 35th ISARC, 72-79, 2018.

Deep Learning Detection for Real-time Construction Machine Checking

B. Xiao[a] and S.-C. Kang[a]

[a]Department of Civil & Environmental Engineering, University of Alberta, Canada
E-mail: bxiao2@ualberta.ca, sckang@ualberta.ca

Abstract –

Construction sites require many efforts to be well organized due to the complicated tasks and various construction machines. Recently, computer vision technology has gained success in the construction research field. By deploying single or multiple cameras, we can extract construction information from videos and then help the project manager to understand what happened in real-time. This paper presents a method of checking construction machine status automatically by cameras. We assume that the camera is installed in a high position, which provides clear views for the whole site. This research focuses on extracting the machine information from videos, comparing with construction schedule and feedbacking to project manager for further decision making. In the preliminary stage, a deep learning detector has been employed for detecting active construction machines. Meanwhile, a construction image dataset has been organized for training deep learning models precisely and robustly. This dataset also helps to promote this method to generalized construction scenarios. Comparing the number of active machines of video and the expected number of machines from the schedule, the project manager will get real-time feedback and alerts when missing construction machines. In the future steps, we will develop a method to understand construction activities from videos and highlight important activities automatically. Once the reliable method has been developed, it will benefit the project manager to monitor construction sites from an easier way.

Keywords –

Construction Machine; Computer Vision; Deep Learning

1 Introduction

Construction machines have participated the most of construction activities, and they are essential for any construction processes [1]. Properly using and monitoring of machines contributes to the economy, speed, and quality of projects. It is difficult to track the working machine status, especially in a large construction site. The traditional way of monitoring construction machine is employing a worker to record the information and report to project manager each day. Manually checking of machines is tedious, time-consuming, error-prone, and not safe [2].

Furthermore, the recorded information cannot be feedbacked to the project manager for making a real-time decision. Recently, computer vision technology has succeeded in medical imaging, human-computer interaction and autonomous driving [3]. This technology also shows great potential in construction management. In this paper, we present a method of automatically checking construction machines from the video stream.

By deploying the camera in a high position of construction sites, such as the crane boom and existing high-rise buildings, the camera captures the entire footprint of construction sites. In this research, we have developed a method to extract machine active status from the video stream and comparing the number of active machines with the project schedule. The deep learning detection algorithm YOLOv3[4] has been employed to extract machine category and position from videos. A construction image dataset has been built with the purpose of training deep learning models. Until now, 5,000 images have been collected and manually labeled for construction object detection. This dataset will be kept developing in order to train deep learning detectors and make these methods generalized in more construction scenarios. Then the expected number of active machines can be extracted from project schedules. The comparison results will be summarized in the active chart and feedback to project managers in real-time.

This method benefits project managers and enables them to monitor construction machine status more

directly. If any machine is missing when compared with the planned schedule, the project manager will be notified immediately and they can coordination among construction crews to figure out the problem. The machine active information can be recorded every day for documentation purpose. In the future, we will focus on how to understand construction activates from videos, highlight essential moments for project managers, and help them control the project schedules. A user interface will be designed to display essential information and enable users to search their interested information.

2 Literature Review

In this section, recent studies on object detection methods are reviewed. Then, applications of computer vision technology in construction management are presented. At the end, the evaluation criteria which are widely used has been introduced.

2.1 Development of Object Detection

Object detection refers to detecting instances of semantic objects of certain classes from digital images and videos [5]. The sliding-window paradigm has a successful history in classic object detection, which applies classifier on dense image grid. Viola and Jones [6] have introduced boosted detectors into face recognition. The HOG (Histograms of oriented gradients) [7] provides effective features to pedestrian detection. DPMs [8] are based on part-based deformable models and had achieved the best performance on PASCAL VOC dataset [9] before the introduction of deep learning models.

Recently, the Convolutional Neural Networks (CNNs) methods become the dominant in object detection. The CNNs detector has two categories, which are two-stage detector and one-stage detector. In two-stage detectors, the first stage generates a bunch of candidate regions which may contains expected instances, and the second stage employs classifier to filter all instances into categories. R-CNN [10] has adopted AlexNet [11] and SVM [12] into the second stage and achieved higher performance on VOC dataset. R-CNN has been enhanced in boost precision and speed recently [13], [14].One-stage detectors do not have the first stage of generating candidate regions.

One-stage detectors, such as YOLO and SSD [15], have excellent performance in speed. Recent researches have shown the two-stage detectors perform better in accuracy than one-stage detectors, while one-stage detectors are much fast. Although, recent work shows that two-stage detectors can be faster by reducing the input image resolution and proposal regions [16], one-stage detectors are the better choice for real-time applications. All object detection methods have faced a large class imbalance problem in training, which means these detectors evaluated thousands of candidate regions per image but only a few of them contain objects. The focal loss [17] has been introduced to figure out this problem and allow us training deep learning detectors effectively.

2.2 Applications in Construction

There are many researches and applications that have been developed in construction management with the assisting of computer vision technology. The applications can be categorized as productivity estimation and safety control. For productivity estimation, Weerasinghe and Ruwanpura [18] tracked construction resources with the purpose of reducing waste. Rezazadeh and Brenda [2] have developed an automated method to detect dirt-loading cycles in earth moving tasks. Xiao and Zhu [19] have compared fifteen tracking algorithms in construction scenarios in order to identify the most efficient algorithm. Yang et al. [20] have employed Gaussian background subtraction to detect crane jibs and then make sure the crane operates in good environment.

Construction has become one of the most unsafe industries because of the high risks exist. According to previous study [21], there was more than 2500 annual deaths accompanied in construction sector from 1994 to 2014 in China. Computer vision technology is able to help safety management from comprehensive ways [22]. Han and Lee [23] have developed a system to detect workers and machines. This system protect workers from potential collisions from video streams. Deploying multiple cameras in construction sites can reconstruction 3D clouds of workers, which tracks worker motion precisely [24]

2.3 Evaluation Criteria

Evaluation criteria is important to estimate detectors. Precision and recall are the most common criteria for object detection [25]. Precision refers to the fraction of correct instances among all retrieved instances, while recall means the fraction of correct instances among total ground truth instances. Figure 1. shows the definition of True Positive (TP), False Positive (FP), False Negative (FN), and True Negative (TN). The precision and recall can be then defined as follows.

$$Precision = \frac{TP}{TP+FP} \quad (1)$$

$$Recall = \frac{TP}{TP+FN} \quad (2)$$

Mean average precision (mAP) is another metric that measures the performance of CNN detectors [26]. mAP is the average of maximum precisions at different recalls. The average precision can be calculate as the

average of precisions in 11 recall levels, which from 0.0 to 1. The formula has been defined as follow. The mean average precision is the average of AP in each object class. In this study, we will use mAP to evaluate the deep learning detector.

$$AP = \frac{1}{11}\sum_{r\in\{0.0,0.1,\ldots,1\}} AP_r \quad (3)$$

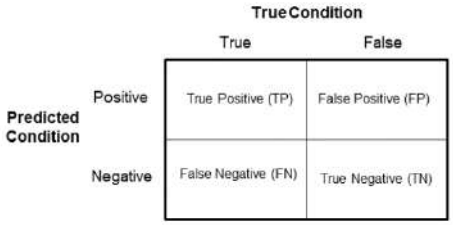

Figure 1. Definition of true positive, false positive, false negative, and true negative

3 Methodology

Figure 2. illustrates the overview of the methodology of machine status checking pipeline. There are four main parts of this method, which are building the dataset, training YOLOv3, detection and visualization, and feedback. In this section, we will introduce each part in details.

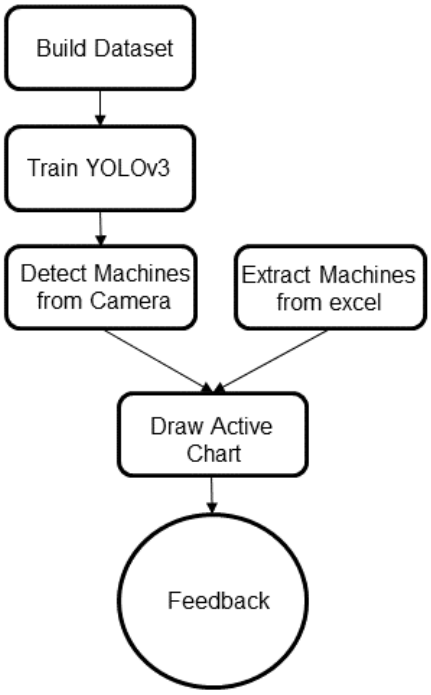

Figure 2. Overview of methodology

3.1 Build Dataset

The biggest challenge for deep learning detection is the limited data. The sufficiently large number of data helps the deep learning model robust and generalized. Since the proposed method will employ the deep learning detector and there not exists construction detection dataset, we have worked on building a new construction image dataset, which contains common construction machines. Over 200 construction videos, which come from YouTube channels, real construction projects, and other datasets, have been collected. 5000 images have been extracted and manually labeled to build this dataset. The entire dataset is divided into training set and testing set, while 80% of images in training set and 20% of images in testing set. In this dataset, there are four types of construction equipment, which are truck, excavator, loader, and backhoe. It shows that 22% of instances in our dataset contain have the size smaller than 5% of the whole image, while 25% of instances have the larger size than the 60% of the entire image. This distribution shows our dataset has both close-up equipment images and bird-view images. A large number of images helps to train deep learning models and generalize into common construction scenarios.

3.2 Training YOLOv3

YOLOv3 is a one-stage state-of-art detector with extremely fast speed. YOLOv3 has shown excellent in COCO dataset [26] with the mAP of 0.553. In this study, the image input size is 416x416 and this algorithm can process 30 images in one second. Compared with some two-stage detectors, the performance of YOLOv3 is slightly low, but the speed is much faster and that is important for real-time applications. The construction detection dataset from the previous step is used for training YOLOv3, which takes 12 hours for the training process. The mAP of YOLOv3 on our testing set is 0.87 from an overall view, where the AP is 0.71 in the truck category, 0.93 in excavator category, 0.91 in loader category, and 0.93 in backhoe category. The validation result shows YOLOv3 fits well in our dataset and could be used in other construction videos.

3.3 Detection and Visualization

This part refers to three steps of methodology in Figure 2, which are detecting machines from the camera, extracting machines from excel and drawing the active chart. In the detection stage, the image stream captured from cameras will be put into YOLOv3 model in real time. The detected images with bounding box will show to users for visualizing the object detection (Figure 3). The detection performance directly effects the overall performance of the entire system. The detected

information, which includes the number of each category of machines, sent to the next step for drawing the active chart.

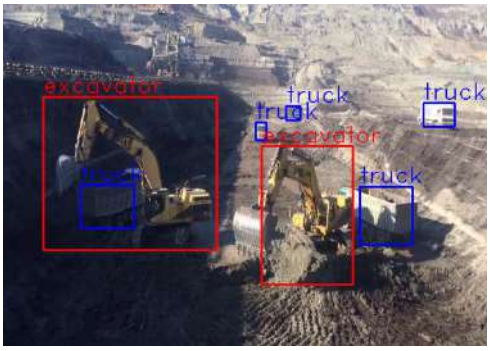

Figure 3. An example of detected images

The excel file of project schedule has been parsed to extract the machine numbers during this time. The information extracted from an excel schedule can be specific to one hour by one hour. The active chart will be drawn to visualize the number of machines active from the camera and construction schedule. Figure 4 shows an example of active chart, which is monitoring excavators and trucks. In the active chart, the jet colormap represents the number of machines, and the horizontal axis represents the time.

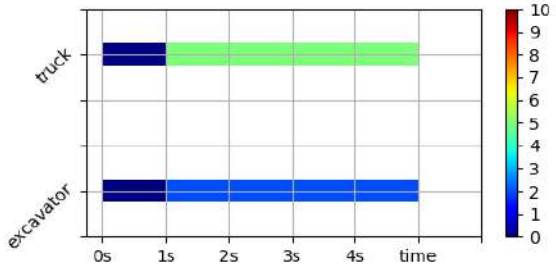

Figure 4. Active chart of describing machine amount

3.4 Feedback

The active chart shows the real-time machine status in construction sites. In each hour or few minutes, the checking system summarizes the active machine chart in this term and saves in local files. The system will notify users with a short sentence, such as "2 trucks and 1 excavator are missed at 14:00pm", when there is a mismatch of detected and scheduled information. The historical information of missing equipment will also be recorded including the timestamp, machine category, missing numbers to local files. This feedback process supports the project manager to document construction activities and active machine status. These files saved with original videos for further purpose. This system expected to help project managers generate construction logs for documentation purpose.

4 Results and Discussion

The construction machine checking system has implemented by Python and C language. All training and detection process was running on an NVIDIA 1080Ti GPU. The testing video has the duration of one hour, which recorded the earthmoving activity. The monitoring object is excavator and trucks. The expected machine number has been manually set up in the excel file, and the number changes every ten minutes. The detection result updated 25 times in each second and the active chart updated by seconds.

To evaluate our system, we use success rate (SR) to describe the performance. Construction sites are slowly moving, and we decided to check the machine numbers in every minute. If the detected machine number is the same as the ground truth from this frame and the feedback information is correct, it will give a positive sign in this minute. Otherwise, it will give a negative sign in this minute. The SR is calculated as Equation 4. The test precision is 95%, which means the machine checking system succeeded 57 times in one-hour test video.

$$SR = \frac{\sum Positive\ Sign}{60} \quad (4)$$

In this study, it found that deep learning detection is robust when well-developed image dataset provided. In computer vision community, there exists some detection dataset such as VOC and COCO. These dataset helps researchers to evaluate new algorithms and applications. It is necessary to build a public image dataset in construction research field, which will benefit the whole community. Since deep learning methods have huge potential in the construction automation field. Detecting all construction objects from images allows us to understand what happened in sites. For project managers, filtering useful information and visualize help them to monitor construction activities and decide in real-time.

Visualization is another concern in construction management. Effective visualization improves the sites communication and help experts understand what happened in construction sites. Since construction sites are always disordered, managers cannot extract useful information directly even with the assistance of cameras, visualized information provided key information to managers to support real-time decision making. Visualization in construction provides an efficient way to training junior workers and engineers.

5 Conclusion

This paper presents a system of checking construction machines automatically from video streams and construction schedule. Cameras deployed in construction sites provide clear views for the whole site and activities. The machine checking system extracts machine information from videos by using deep learning detector YOLOv3. Then it compares detected results and expected number from schedule excel file to feedback to project manager for further decision making. In order to train a general model, a construction image dataset has been built in this study.

In the future steps, the authors will work on developing a method to understand construction activities from videos and highlight important activities automatically. In addition, the authors will keep expanding the construction image dataset.

References

[1] Nunnally, Stephens W. Construction methods and management. Upper Saddle River, NJ: Pearson Prentice Hall, 2007.

[2] Rezazadeh Azar, Ehsan, Sven Dickinson, and Brenda McCabe. "Server-customer interaction tracker: computer vision–based system to estimate dirt-loading cycles." Journal of Construction Engineering and Management 139, no. 7 (2012): 785-794.

[3] Szeliski, Richard. Computer vision: algorithms and applications. Springer Science & Business Media, 2010.

[4] Redmon, Joseph, and Ali Farhadi. "Yolov3: An incremental improvement." arXiv preprint arXiv:1804.02767 (2018).

[5] Hjelmås, Erik, and Boon Kee Low. "Face detection: A survey." Computer vision and image understanding 83, no. 3 (2001): 236-274.

[6] Viola, Paul, and Michael Jones. "Rapid object detection using a boosted cascade of simple features." In Computer Vision and Pattern Recognition, 2001. CVPR 2001. Proceedings of the 2001 IEEE Computer Society Conference on, vol. 1, pp. I-I. IEEE, 2001.

[7] Dalal, Navneet, and Bill Triggs. "Histograms of oriented gradients for human detection." In Computer Vision and Pattern Recognition, 2005. CVPR 2005. IEEE Computer Society Conference on, vol. 1, pp. 886-893. IEEE, 2005.

[8] Felzenszwalb, Pedro F., Ross B. Girshick, and David McAllester. "Cascade object detection with deformable part models." In Computer vision and pattern recognition (CVPR), 2010 IEEE conference on, pp. 2241-2248. IEEE, 2010.

[9] Everingham, M., Van Gool, L., Williams, C.K., Winn, J. and Zisserman, A., 2010. The pascal visual object classes (voc) challenge. International journal of computer vision, 88(2), pp.303-338.

[10] Girshick, R., Donahue, J., Darrell, T. and Malik, J., 2014. Rich feature hierarchies for accurate object detection and semantic segmentation. In *Proceedings of the IEEE conference on computer vision and pattern recognition* (pp. 580-587).

[11] Krizhevsky, Alex, Ilya Sutskever, and Geoffrey E. Hinton. "Imagenet classification with deep convolutional neural networks." In *Advances in neural information processing systems*, pp. 1097-1105. 2012.

[12] Cortes, Corinna, and Vladimir Vapnik. "Support-vector networks." *Machine learning* 20, no. 3 (1995): 273-297.

[13] Girshick, Ross. "Fast r-cnn." In Proceedings of the IEEE international conference on computer vision, pp. 1440-1448. 2015.

[14] He, Kaiming, Xiangyu Zhang, Shaoqing Ren, and Jian Sun. "Spatial pyramid pooling in deep convolutional networks for visual recognition." In *European conference on computer vision*, pp. 346-361. Springer, Cham, 2014.

[15] Liu, W., Anguelov, D., Erhan, D., Szegedy, C., Reed, S., Fu, C.Y. and Berg, A.C., 2016, October. Ssd: Single shot multibox detector. In *European conference on computer vision* (pp. 21-37). Springer, Cham.

[16] Huang, Jonathan, Vivek Rathod, Chen Sun, Menglong Zhu, Anoop Korattikara, Alireza Fathi, Ian Fischer et al. "Speed/accuracy trade-offs for modern convolutional object detectors." In *IEEE CVPR*, vol. 4. 2017.

[17] Lin, T.Y., Goyal, P., Girshick, R., He, K. and Dollár, P., 2018. Focal loss for dense object detection. *IEEE transactions on pattern analysis and machine intelligence*.

[18] Weerasinghe, IP Tharindu, and Janaka Y. Ruwanpura. "Automated data acquisition system to assess construction worker performance." In Construction Research Congress 2009: Building a Sustainable Future, pp. 61-70. 2009.

[19] Xiao, Bo, and Zhenhua Zhu. "Two-Dimensional Visual Tracking in Construction Scenarios: A Comparative Study." Journal of Computing in Civil Engineering 32, no. 3 (2018): 04018006.

[20] Yang, Jun, Patricio Vela, Jochen Teizer, and Zhongke Shi. "Vision-based tower crane tracking for understanding construction activity." Journal of Computing in Civil Engineering 28, no. 1 (2012):

103-112.
[21] He, Xueqiu, and Li Song. "Status and future taqsks of coal mining safety in China." Safety Science 50.4 (2012): 894-898.
[22] Guo, Hongling, Yantao Yu, and Martin Skitmore. "Visualization technology-based construction safety management: A review." Automation in Construction 73 (2017): 135-144.
[23] Han, SangUk, and SangHyun Lee. "A vision-based motion capture and recognition framework for behavior-based safety management." Automation in Construction 35 (2013): 131-141.
[24] Brilakis, Ioannis, Man-Woo Park, and Gauri Jog. "Automated vision tracking of project related entities." Advanced Engineering Informatics 25.4 (2011): 713-724.
[25] Davis, Jesse, and Mark Goadrich. "The relationship between Precision-Recall and ROC curves." In Proceedings of the 23rd international conference on Machine learning, pp. 233-240. ACM, 2006.
[26] Lin, Tsung-Yi, Michael Maire, Serge Belongie, James Hays, Pietro Perona, Deva Ramanan, Piotr Dollár, and C. Lawrence Zitnick. "Microsoft coco: Common objects in context." In European conference on computer vision, pp. 740-755. Springer, Cham, 2014.

A comparison of TLS-based and ALS-based techniques for Concrete Floor Waviness Assessment

N. Puri[a] and Y. Turkan[b]

[a]PhD Student, School of Civil and Construction Engineering, Oregon State University, Corvallis, OR 97331
[b]Assistant Professor, School of Civil and Construction Engineering, Oregon State University, Corvallis, OR 97331
E-mail: purin@oregonstate.edu, yelda.turkan@oregonstate.edu

Abstract –

Laser scanning-based techniques have been applied for checking the dimensional tolerances of concrete elements. Several studies utilized Terrestrial Laser Scanning (TLS) for measuring concrete floor waviness. The results of those efforts have shown that accurate floor waviness information can be obtained using TLS. Unmanned Aerial Vehicles (UAVs) mounted with cameras and 3D laser scanning sensors, referred to as Airborne Laser Scanning (ALS) hereafter, have versatile applications in construction, such as surveying, progress control, 3D modelling and inspections. As-built data collection for dimensional quality assessment can be a potential application of such technology. In particular, the application of ALS for assessing the waviness of concrete slabs warrants further exploration. This study presents the results of a comparative analysis of floor waviness measurement results obtained using ALS and TLS-based technologies. Continuous Wavelet Transform (CWT) is applied to the depth map derived from both point cloud datasets to obtain waviness information. Comparable results are obtained for the CWT scales of 30, 60 and 75. Detailed discussions on how the results can be improved are presented. The analysis of the accuracy of results obtained using ALS advances its application in the field of dimensional quality assessment.

Keywords –

TLS, ALS, Continuous wavelet transform, Depth map, Point cloud, Dimensional quality control, tolerance compliance

1 Introduction

The geometric dimensions of as-built concrete elements often fail to comply with the tolerances specified in the as-designed plans [1]. The factors that contribute toward such discrepancies include lack of attention to details included in the project specifications, low accuracy and precision issues that occur during the construction of elements, and the misinterpretation of information provided in the project specifications. Consequently, increasing tolerance accumulation may affect the aesthetics of concrete elements, affects the correct placement of adjacent concrete elements and negatively affects the structural health of components in severe cases [2]. Construction quality control inspectors collect data related to the quality of on-going construction for effectively designing solutions to correct any defects or discrepancies that are present on concrete surfaces. Thus, dimensional quality assessment ensures that constructed elements accurately reflect the dimensions and locations specified in the contract documents. For concrete floors, this is one of the most significant processes constituting the overall construction process. For instance, constructed floors that do not meet appropriate flatness and waviness requirements negatively affect the operation of Very Narrow Aisle (VNA) trucks in warehouses. Furthermore, the undesired waviness present on the floor surface can affect the racking height of such vehicles, and consequently, the static lean which ultimately may cause these vehicles roll over [3–5].

Existing methods commonly used in the industry such as the Straightedge Method, the F-number method (ASTM E1155)[6] and the Waviness Index (WI) method (ASTM 1486) share the common drawback as they yield sparse as-built measurements. In addition, the data collection process is time and labor intensive, given that the floor surface area in warehouse construction projects easily exceed 4,000 m^2 [3–5]. The method proposed in [3] utilizes a framework that uses lidar-based point clouds and the Continuous Wavelet Transform (CWT) to overcome these disadvantages and provides a novel framework for measuring floor waviness. This framework was further developed to process 2D as built information in the form of depth maps, as opposed to 1D survey lines derived from TLS-based point clouds to impart waviness information of newly constructed concrete slabs. This study focuses on performing a comparative analysis of the floor waviness

results obtained using point cloud data collected with a TLS and a lidar sensor mounted UAV. The method of comparison presented in this study uses waviness detection results from TLS point clouds as ground truths, and relies on recall and precision rates to determine the accuracy of waviness results obtained using ALS point clouds.

2 Related Work

Lidar technology has a wide range of applications in the civil engineering industry, such as quantifying erosion rates and surface deformation [7], to landslide inventorying and assessing hazards [8], structural health monitoring [9–12], road roughness quantification [13–17] and survey and maintenance of historic buildings [18–20]. In the construction industry, lidar is primarily used for as-built documentation that supports progress tracking [3]–[7], facility management [8]–[13], dimensional quality control [3–5,32–34] in construction projects. In the area of dimensional quality control, lidar technology is commonly used for acquiring as-built data, owing to its ability to capture millions of points with mm-level accuracy. The acquired data is processed with the help of a multitude of algorithms, based on the desired applications. Few of the applications include assessing the flatness of the exterior facades using a color map derived from TLS point clouds [35], visualizing the elevation differences across a floor using elevation map generated from point cloud data [36] and assessing the dimensional compliance of concrete elements using BIM and TLS-based point cloud data [37]. Lidar-based point clouds, with the application of the Continuous Wavelet Transform (CWT), were also used in the assessment of floor waviness in [3,4]. The study in [3] demonstrated the efficacy of applying the two-dimensional CWT (2D CWT) to lidar-based point cloud data for assessing the waviness of concrete surfaces. The comparative analysis between results obtained using the framework and those obtained using the Waviness Index (WI) method showed that the framework accurately identifies regions on the floor where surface waviness of different characteristics exist. The framework utilized TLS-derived point cloud data for assessing the surface waviness of concrete floors.

Unmanned Aircraft Systems (UAVs) are exponentially gaining popularity for collecting as-built data from construction sites. UAVs mounted with photographic cameras, thermal cameras and lidar sensors or “pucks” have been widely used for survey data collection. Compared to TLS, UAV-mounted lidar sensors are capable of collecting data from large survey areas in a non-intrusive manner with limited occlusions [38,39]. For instance, a person standing in front of the laser scanner can create a larger obstruction during data collection using TLS, compared to ALS. Moreover, using TLS for collecting as-built data from working surfaces may hinder on-going operations and may interrupt workers on the surface. Thus, the objective of this paper is to compare the results of floor waviness obtained using point clouds derived from TLS and ALS. The framework proposed in [3,5] will be used for obtaining surface waviness results.

3 Analysis

3.1 Data Collection and Preprocessing

The data was collected from a newly constructed floor of a lecture hall under the Magruder Hall Expansion project in Corvallis, OR. Figure 1. shows the region of interest, and its surface area was approximately 140 m2. The Leica P40 scanner was setup in two locations across the floor. After registering the two scans, the spatial resolution of the output point cloud was approximately 5 mm within a range of 10 m. The Riegl miniVUX was used for obtaining the ALS point cloud. The UAV mounted with the lidar sensor was flown at a constant height of approximately 60 m above the surface of the ground, making two passes over the area of interest. It is assumed that the beam divergence is constant throughout the flight. The spatial resolution of the output point cloud collected from the UAV system was approximately 5 cm.

Figure 1. The region of interest is marked in orange.

3.2 Data Processing

The framework developed in [3] was used to process the data obtained from TLS and ALS. The obtained point clouds from the TLS and ALS systems were imported into a commercial point cloud processing software to remove scans corresponding to workers

working on the floor and various construction debris. A depth map is developed using triangulation-based linear interpolation on a grid with regular intervals of 1 cm. This process generated a map showing z-coordinates at each query point, where each query point is represented by the intersection of lines on the x-y plane of the grid. CWT, using the Mexican Hat wavelet as the mother wavelet, was applied to the depth map at different scales. To simplify the analysis, only five scales were chosen for the CWT: 15, 30, 45, 60 and 75. The five scales correspond to the five undulation periods in the WI method: 2, 4, 6, 8 and 10 ft, respectively. The correspondence between the WI index values and the CWT scales are shown in Table 1.

Table 1**.** Waviness Index values and corresponding continuous wavelet transform scales [3][4]

Characteristic period (T) [cm]	CWT scale (a)	Waviness Index (k values)
61	15	1
121.9	30	2
182.9	45	3
243.8	60	4
304.8	75	5

3.3 CWT Results

The surface waviness results obtained for the TLS- and ALS-based point clouds, for scales 15, 30, 45, 60 and 75, are shown in Figure 2, Figure 3, Figure 4, Figure 5 and Figure **6**, respectively. The peaks detected for the CWT responses for these five scales are presented.

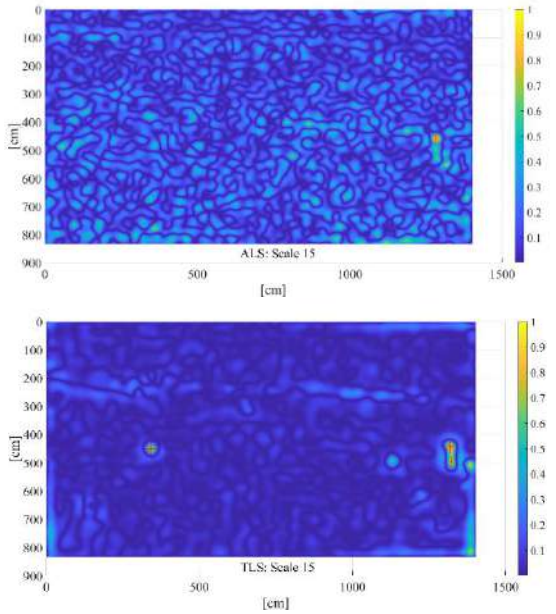

Figure 2. The results of the CWT analysis at scale 15 with peak detection (red asterisk) for the ALS (top) and TLS point clouds (bottom)

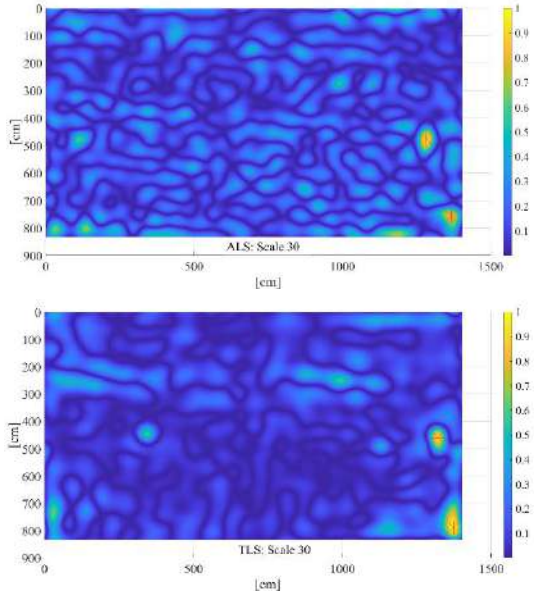

Figure 3. The results of the CWT analysis at scale 30 with peak detection (red asterisk) for the ALS (top) and TLS point clouds (bottom)

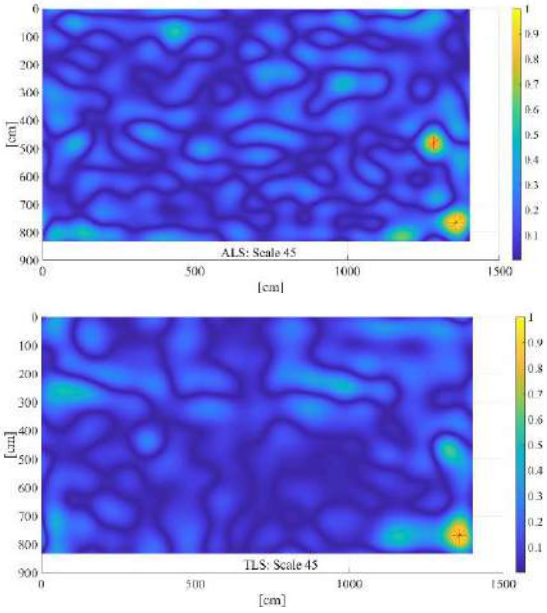

Figure 4. The results of the CWT analysis at scale 45 with peak detection (red asterisk) for the ALS (top) and TLS point clouds (bottom)

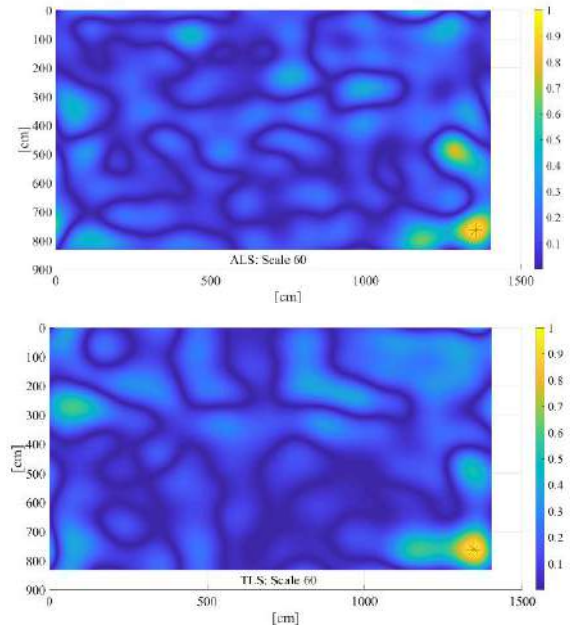

Figure 5. The results of the CWT analysis at scale 60 with peak detection (red asterisk) for the ALS (top) and TLS point clouds (bottom)

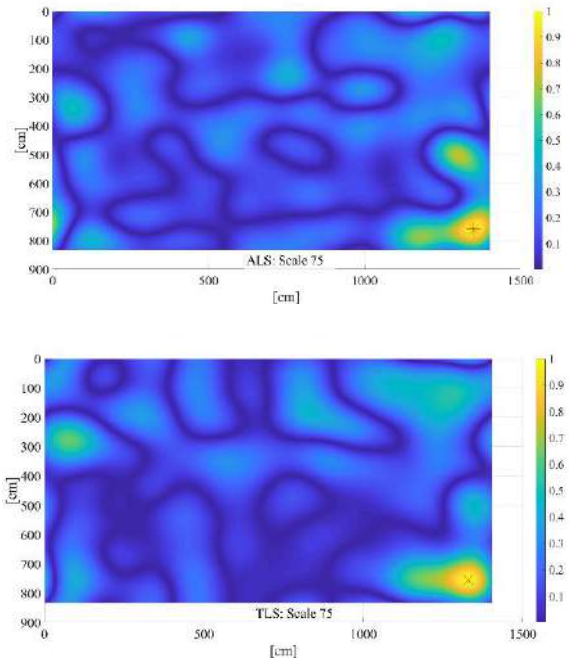

Figure 6. The results of the CWT analysis at scale 75 with peak detection (red asterisk) for the ALS (top) and TLS point clouds (bottom)

As shown in Figure 2, Figure 3, Figure 4,Figure 5, and Figure **6**, peak responses for the CWT coefficient values lie 10% below the maximum value. The location of these peak responses for each of the five scales are used for our analysis.

The waviness results obtained from the TLS-based point clouds are used as ground truth for measuring the performance of the ALS-based point clouds for generating the waviness results. The convention of true positives (TP), true negatives (TN), false positives (FP) and false negatives (FN) that applies to the peak detection problem in our study is shown in Table 2. The number of true positives, true negatives, false positives and false negatives are shown in Table 3.

Table 2. Convention of the true positive, true negative, false positive and false negative for peak detection

	Peak present (TLS)	**Peak absent (TLS)**
Peak detected (ALS)	TP	FP
Peak not detected (ALS)	FN	TN

Table 3. Total number of true positives (TP), true negatives (TN), false positives (FP) and false negatives (FN)

Scales	**TP**	**TN**	**FP**	**FN**	**Actual number of peaks (TLS based)**
15	1	0	0	2	3
30	2	0	0	0	2
45	1	0	1	0	1
60	1	0	0	0	1
75	1	0	0	0	1

In the TLS based results, for scale 15, the ground truth shows that there are 3 peaks that correspond to undulations having a characteristic period of 61 cm. Only one of those peaks are detected in the waviness results derived from the ALS point cloud. For scale 30, two peaks that correspond to the characteristic period of 121.9 cm were detected in both the TLS and ALS based results. At scale 45, one peak corresponding to 182.9 cm was obtained in the TLS and two peaks in the ALS based results. Similarly, for scales 60 and 75, 1 peak corresponding to the characteristic period of 304.8 cm was detected in both the TLS and ALS based results. Table 4 shows the correspondence between the waviness detection results obtained using TLS and ALS using precision and recall rates for the five scales selected in this study.

Table 4**.** Recall, precision and accuracy rates

Scales	**15**	**30**	**45**	**60**	**75**
Recall	33%	100%	100%	100%	100%
Precision	100%	100%	50%	100%	100%

Accuracy	33%	100%	100%	100%	100%
F-Score	0.5	1	0.67	1	1

The surface waviness results for scales 60 and 75 using the TLS and ALS based point clouds are comparable. For scale 45, a false positive was detected near [1283 cm, 481 cm]. The same region near the TLS was inspected and no peak was found. The CWT response at that region for the ALS based results was 0.8816, and 0.1674 for the TLS. This discrepancy might be attributed to the difference in the z-values shown in the depth maps of the TLS and ALS point clouds. The TLS based depth map shows the elevation at [1283 cm, 481 cm] to be approximately 2.8 cm and the ALS based depth map shows 1.75 cm. Although the TLS and ALS scans were collected almost simultaneously, there were workers actively working on the work surface. This may be due to dynamic changes resulting from moving objects or debris on the floor surface. Another reason may be due to the low resolution of the ALS point cloud. For scale 15, the results are not comparable to each other. A possible reason could be that using TLS-based high-resolution point cloud helped detect undulations of a lower characteristic period (61 cm) accurately. The lower resolution ALS-based point cloud may have failed to capture those undulations. While generating the depth map, the z-coordinates are smoothed out to a higher degree if there were fewer neighbouring points present around the query points.

4 Discussions and Conclusions

The efficacy of using ALS-derived point clouds for detecting surface waviness of concrete floors was examined. Using the UAV mounted with lidar can help quality control inspectors to non-intrusively collect as-built point cloud from concrete slabs. The analysis of the CWT results show that the surface waviness detection results are not comparable for scales 15 and 45. The analysis showed comparable results for detecting the undulations corresponding to scales of 30, 60 and 75. In summary, one of the possible reasons for discrepancies in the two results is the difference in the resolution of both point clouds. The resolution of the TLS based point cloud was approximately 10 times better than that of the ALS based point cloud. The other reason could be due to the misalignment of both point clouds. The targets placed on the ground were visible in the TLS data, but were not clearly visible in the ALS point clouds. Two solutions are proposed: 1) Flying the UAV closer to the ground: The lower the aircraft flies, the smaller the lidar footprint diameter will be, which results in a higher density of points per scanning area. Decreasing the lidar footprint is essential for detecting small changes in elevation across the surfaces. A good option would be flying under 15 m. 2) Increase the number of passes: An increase in the number of passes will improve the resolution quality of the point cloud.

Future work will focus on examining the number of passes required to obtain a point cloud resolution that is comparable to that obtained using a TLS. In addition, the impact of the altitude difference for obtaining the desired resolution and capturing the small changes in elevation across the floor will be examined. Furthermore, the differences in the z-coordinates of the depth map resulting from the application of other interpolation methods will be evaluated.

5 Acknowledgements

The authors would like to thank Chase Simpson from Oregon State University and Jake Dafni from the NHERI RAPID Experimental Facility at the University of Washington for their help in collecting the data using the UAV and for preprocessing the data. The authors would also like to thank John M. Doty, the project manager, Scott Cach and the Fortis team for their help and cooperation throughout the data collection process.

6 References

[1] D.K. Ballast, Handbook of Construction Tolerances, Second, John Wiley & Sons, 2007.

[2] N. Puri, Y. Turkan, Toward Automated Dimensional Quality Control of Precast Concrete Elements Using Design BIM, WIT Transactions on The Built Environment. 169 (2017) 203–210.

[3] N. Puri, E. Valero, Y. Turkan, F. Bosché, Assessment of compliance of dimensional tolerances in concrete slabs using TLS data and the 2D continuous wavelet transform, Automation in Construction. 94 (2018) 62–72. doi:10.1016/j.autcon.2018.06.004.

[4] F. Bosché, B. Biotteau, Terrestrial laser scanning and continuous wavelet transform for controlling surface flatness in construction – A first investigation, Advanced Engineering Informatics. 29 (2015) 591–601. doi:10.1016/j.aei.2015.05.002.

[5] E. Valero, F. Bosché, Automatic Surface Flatness Control using Terrestrial Laser Scanning Data and the 2D Continuous Wavelet Transform, (2016) 2016.

[6] ASTM, Standard Test Method for Determining FF Floor Flatness and FL Floor Levelness Numbers (Metric 1, Astm. 96 (2015) 7–14. doi:10.1520/E1155M-96R08.2.

[7] M.J. Olsen, J.C. Allan, G.R. Priest, Movement and Erosion Quantification of the Johnson Creek, Oregon, Landslide through 3D Laser Scanning, in:

GeoCongress 2012: State of the Art and Practice in Geotechnical Engineering, 2012: pp. 3050–3059.

[8] B.A. Leshchinsky, M.J. Olsen, K. Hall, Enhancing Landslide Inventorying, Hazard Assessment and Asset Management Using Lidar, (2015).

[9] X. Xu, H. Yang, I. Neumann, Concrete crack measurement and analysis based on terrestrial laser scanning technology, Sens. Trans. J. 186 (2015) 168–172.

[10] M.J. Olsen, F. Kuester, B.J. Chang, T.C. Hutchinson, Terrestrial laser scanning-based structural damage assessment, Journal of Computing in Civil Engineering. 24 (2009) 264–272.

[11] Y. Turkan, S. Laflamme, L. Tan, Terrestrial Laser Scanning-Based Bridge Structural Condition Assessment, (2016).

[12] Y. Turkan, J. Hong, S. Laflamme, N. Puri, Adaptive wavelet neural network for terrestrial laser scanner-based crack detection, Automation in Construction. 94 (2018) 191–202. doi:10.1016/j.autcon.2018.06.017.

[13] A. Alhasan, D.J. White, K. De Brabanter, Wavelet Filter Design for Pavement Roughness Analysis, Computer-Aided Civil and Infrastructure Engineering. 31 (2016) 907–920. doi:10.1111/mice.12242.

[14] A. Alhasan, D.J. White, K. De Brabanterb, Automation in Construction Continuous wavelet analysis of pavement pro fi les, 63 (2016) 134–143. doi:10.1016/j.autcon.2015.12.013.

[15] A. Alhasan, D.J. White, K. De Brabanter, Spatial pavement roughness from stationary laser scanning, International Journal of Pavement Engineering. 18 (2017) 83–96. doi:10.1080/10298436.2015.1065403.

[16] P. Kumar, P. Lewis, C.P. Mcelhinney, A.A. Rahman, An algorithm for automated estimation of road roughness from mobile laser scanning data, Photogrammetric Record. 30 (2015) 30–45. doi:10.1111/phor.12090.

[17] A. Chin, M.J. Olsen, D. Ph, A.M. Asce, Evaluation of Technologies for Road Profile Capture, Analysis, and Evaluation, J. Surv. Eng. 141 (2015) 1–13. doi:10.1061/(ASCE)SU.1943-5428.0000134.

[18] E. Valero, F. Bosché, A. Forster, Automatic segmentation of 3D point clouds of rubble masonry walls, and its application to building surveying, repair and maintenance, Automation in Construction. 96 (2018) 29–39. doi:10.1016/j.autcon.2018.08.018.

[19] E. Valero, F. Bosché, A. Forster, L. Wilson, A. Leslie, Evaluation of historic masonry--Towards greater objectivity and efficiency, Heritage Building Information Modelling. Taylor & Francis. (2017).

[20] S. Fai, K. Graham, T. Duckworth, N. Wood, R. Attar, Building Information Modelling and Heritage Documentation, XXIII CIPA International Symposium, Prague, Czech Republic. (2011). doi: http://dx.doi.org/10.1136/adc.2010.183327.

[21] Y. Turkan, F. Bosche, C.T. Haas, R. Haas, Automated progress tracking using 4D schedule and 3D sensing technologies, Automation in Construction. 22 (2012) 414–421. doi:10.1016/j.autcon.2011.10.003.

[22] Y. Turkan, F. Bosche, C.T. Haas, R. Haas, Tracking Secondary and Temporary Concrete Construction Objects Using 3D Imaging Technologies, Computing in Civil Engineering. (2013) 749–756. doi:10.1017/CBO9781107415324.004.

[23] A. Braun, S. Tuttas, A. Borrmann, U. Stilla, Automated progress monitoring based on photogrammetric point clouds and precedence relationship graphs, Proceedings of the 32nd International Symposium on Automation and Robotics in Construction and Mining. (2015) 274–280.

[24] A. Braun, S. Tuttas, A. Borrmann, U. Stilla, A concept for automated construction progress monitoring using BIM-based geometric constraints and photogrammetric point clouds, Journal of Information Technology in Construction (ITcon). 20 (2015) 68–79.

[25] C. Kim, H. Son, C. Kim, Automated construction progress measurement using a 4D building information model and 3D data, Automation in Construction. 31 (2013) 75–82. doi:10.1016/j.autcon.2012.11.041.

[26] S. Kiziltas, Technological Assessment and Process Implications of Field Data Capture Technologies for Construction and Facility/Infrastructure Management, 13 (2008) 134–154.

[27] F. a Al-shalabi, Y. Turkan, a Novel Framework for BIM Enabled Facility Energy Management – a Concept Paper, (2015) 1–8.

[28] Roper, K., & Payant, The facility management handbook. (2014)

[29] B. Becerik-Gerber, F. Jazizadeh, N. Li, Application areas and data requirements for BIM-enabled facilities management, And Management. 138 (2011) 431–442. doi:10.1061/(ASCE)CO.1943-7862.0000433.

[30] P. Teicholz, BIM for Facility Managers, Wiley, Hoboken, NJ, 2013.

[31] L.Y. Liu, A.L. Stumpf, S.S. Kim, F.M. Zbinden, Capturing as-built project information for facility

management, in: Computing in Civil Engineering, 1994: pp. 614–621.
[32] M.-K. Kim, Q. Wang, J.-W. Park, J.C.P. Cheng, H. Sohn, C.C. Chang, Automated dimensional quality assurance of full-scale precast concrete elements using laser scanning and BIM, Automation in Construction. 72 (2016) 102–114. doi:10.1016/j.autcon.2016.08.035.
[33] F. Bosché, Automated recognition of 3D CAD model objects in laser scans and calculation of as-built dimensions for dimensional compliance control in construction, Advanced Engineering Informatics. 24 (2010) 107–118. doi:10.1016/j.aei.2009.08.006.
[34] M.K. Kim, J.C.P. Cheng, H. Sohn, C.C. Chang, A framework for dimensional and surface quality assessment of precast concrete elements using BIM and 3D laser scanning, Automation in Construction. 49 (2015) 225–238. doi:10.1016/j.autcon.2014.07.010.
[35] M.C. Israel, R.G. Pileggi, Use of 3D laser scanning for flatness and volumetric analysis of mortar in facades, 9 (2016) 91–106.
[36] P. Tang, B. Akinci, D. Huber, Characterization of three algorithms for detecting surface flatness defects from dense point clouds, IS&T/SPIE Electronic Imaging. 7239 (2009) 72390N–72390N. doi:10.1117/12.805727.
[37] F. Bosché, E. Guenet, Automating surface flatness control using terrestrial laser scanning and building information models, Automation in Construction. 44 (2014) 212–226. doi:10.1016/j.autcon.2014.03.028.
[38] M.J. Olsen, J.D. Raugust, G.V. Roe, Use of Advanced Geospatial Data, Tools, Technologies, and Information in Department of Transportation Projects, 2013. doi:10.17226/22539.
[39] R.A. Vincent, M. Ecker, others, Light detection and ranging (LiDAR) technology evaluation., 2010.

Comparison of Virtual Communication Environment for Remote BIM Model Review Collaboration

T.H. Wu[a], F. Wu[a], S.C. Kang[b], and H.L. Chi[c]

[a] Department of Civil Engineering, National Taiwan University, Taiwan
[b] Department of Civil and Environmental Engineering, University of Alberta, Canada
[c] Department of Building and Real Estate, The Hong Kong Polytechnic University, Hong Kong
E-mail: f00521611@ntu.edu.tw, ilohoo@caece.net, sckang@ualberta.ca, hung-lin.chi@polyu.edu.hk

Abstract –

Remote building information modeling (BIM) model review collaboration is the trend in the architecture, engineering, and construction (AEC) industry. Virtual communication environment is a key factor in a successful collaboration. However, the proper environment has yet to be fully revealed. Therefore, this study aims to identify the effective environment. We identified the environment with three main types and then proposed and developed the corresponding environment namely BIM-based, PC-based virtual BIM reviewer (VBR), and VR-based VBR. A user test has been conducted to evaluate their performance and task loading in finding issues and reaching consensus. In the test, the participants were asked to find four kinds of issues and determine the top five issues and their solutions. The result shows that in finding issues, the average of issues they found in BIM-based, PC-based VBR, and VR-based VBR are 6.57, 9.77, and 9.91. The performance of PC-based VBR and VR-based VBR are no significant difference ($\alpha = 0.461462$) but both of them are significantly better than BIM-based ($\alpha = 0.000339$ and 0.004431). However, the averages of task loading in finding issues are 899.50, 813.84, 807.00 with no significant difference. In reaching consensus, the averages of seconds they used are 740.67, 682.93, and 724.40 with no significant difference. However, the averages of task loading in both of PC-based VBR ($\mu = 721.00$) and VR-based VBR ($\mu = 718.10$) are significantly lower than BIM-based ($\mu = 867.00, \alpha = 0.009610$ and 0.013879). In overall, both PC-based VBR and VR-based VBR have better performance in finding issues and lower task loading in reaching consensus.

Keywords –

Remote collaboration; Virtual communication environment; BIM model review

1 Introduction

The beginning of remote collaboration can be considered starting from the offshoring and outsourcing of services that emerged in the late 1980s and early 1990s [1]. With the rapid development of information and communications technology reduces the barriers of remote collaboration, remote collaboration has become the trend in many industries. In the AEC industry, there are also many construction teams consist of engineers and architects located in different regions or countries requires remote collaboration. For instance, the Oakland Bay Bridge is manufacturing in China and fabricating in the United States [2], Taiwan High Speed Rail Project consists of many experts from different countries including Taiwan, Britain, Denmark, India, and other countries [3], and Taiwan Taoyuan International Airport Terminal 3 is also a remote collaboration example that is joint contracted by Taiwan, Britain, and Hong Kong companies.

BIM is a novel approach in the AEC industry [4]. The concept of BIM is being a data center that integrates geometric and functional information during the building life-cycle. The information will be represented in a visualized 3D model for project participants to use. BIM supports strong spatial cognition and abundant information that can reveal most the of design issues in the early design stage through BIM model review, which is a repeated design process reviews visualized information model from various aspects, such as design, construction, specification, and safety, to decipher a proper solution [5].

Remote BIM model review collaboration is the trend in the AEC industry [6]. However, the existing common virtual communication environments, such as Skype, Hangout, Join.me, Zoom, Sococo, etc., can only help users review BIM models with a shared screen-view controlled by one of the users. This is easy to build the virtual communication environment but hard to provide the senses of teamwork and immersive exploration.

Without both of them will reduce the effectiveness of remote BIM model review collaboration. Some researchers mention that virtual avatar [7-10] and virtual reality [11] will solve these problems, but they are more focused on finding issues rather than reaching the consensus of final solutions. Although we know the communication environment is a key factor in a successful collaboration [12]. However, the proper communication environment has yet to be fully revealed.

2 Research Goals

This study aims to identify effective communication environments for BIM model review collaboration with following goals: (1) identify the main types of virtual communication environment; (2) propose and develop these communication environments; (3) evaluate their performance and task loading in finding issues and reaching consensus.

3 Virtual Communication Environment

In this study, we classified virtual communication environment types by two factors: the flexibility of exploration and the degree of immersive. The flexibility of exploration consists of passive exploration and proactive exploration. The degree of immersive consists of semi-immersive and full-immersive. Therefore, we have four kinds of type: (1) Type I: a passive exploration with semi-immersive; (2) Type II: a passive exploration with full-immersive; (3) Type III: a proactive exploration with semi-immersive; and (4) Type IV: a proactive exploration with full-immersive. Four types of virtual communication environment are listed in Table 1.

Table 1. The types of virtual communication environment

		The flexibility of exploration	
		Passive	Proactive
The degree of immersive	Semi-	Type I	Type III
	Full-	Type II	Type IV

In the existing common approaches to implementing these four types. It often uses screen-sharing-based to implement passive exploration and virtual-avatar-based to implement proactive exploration. Regard to the semi-immersive and full-immersive will often be implemented on PC devices and VR devices respectively. However, Type II is not reasonable and will not be practiced due to the dizziness issue. If users fully immersive themselves into a virtual environment but the view is controlled by others, it will cause serious dizziness to them. Moreover, in the existing VR technology, most of them already provide a virtual avatar for each user no matter it is visible or not. Therefore, this study will only focus on discussing Type I, III, and IV. We proposed and developed three environments to the Type I, III, and IV namely BIM-based, PC-based VBR [13], and VR-based VBR [13] respectively. The reviewing tool, conference tool, display device, control device, etc. they used are listed in Table 2.

Table 2. The implementation of the three main types

	BIM-based	PC-based VBR	VR-based VBR
Reviewing tool	Revit 2016	VBR (PC)	VBR (VR)
Conferencing tool	Sococo	Sococo	Sococo
Exploration type	Screen-sharing	Virtual-avatar	Virtual-avatar
Display device	Screen	Screen	VR goggles
Control device	Keyboard and mouse	Keyboard and mouse	VR controllers and VR goggles
Communication device	Microphone and headphone	Microphone and headphone	Microphone and headphone

3.1 BIM-based Environment

The BIM-based environment allows users to review BIM models by a reviewing tool, Revit 2016. Users can navigate and manipulate the models in Revit 2016 by keyboard and mouse. They can communicate with each other through a conferencing tool, Sococo. They will use microphones, headphones, and screen-sharing in Sococo. Users using the BIM-based environment is shown in Figure 1.

Figure 1. Users using the BIM-based environment

3.2 PC-based VBR Environment

The PC-based VBR environment allows users to review BIM models by a reviewing tool, VBR (PC). Users can navigate and manipulate the models in VBR (PC) by keyboard and mouse. They can communicate with each other through a conferencing tool, Sococo. They will only use microphones and headphones in Sococo. They do not use the screen-sharing through Sococo since they can directly interact with each other in a virtual environment through VBR (PC) by their own avatars. Users using the PC-based VBR environment is shown in Figure 2.

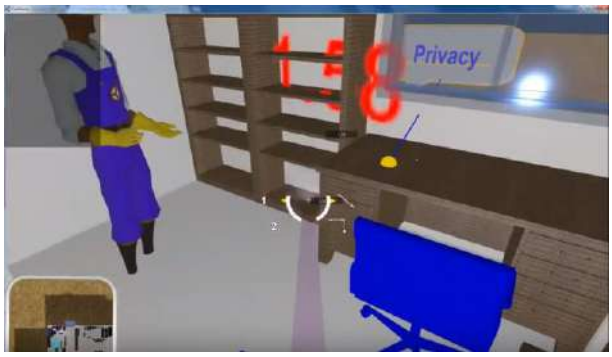

Figure 2. Users using the PC-based VBR environment

3.3 VR-based VBR Environment

The VR-based VBR environment allows users to review BIM models by a reviewing tool, VBR (VR). Users can navigate and manipulate the models in VBR (VR) by VR goggles and controllers. They can communicate with each other through a conferencing tool, Sococo. They will also only use microphones and headphones in Sococo and directly interact with each other in a virtual environment through VBR (VR) with their own avatars. Users using the VR-based VBR environment is shown in Figure 3.

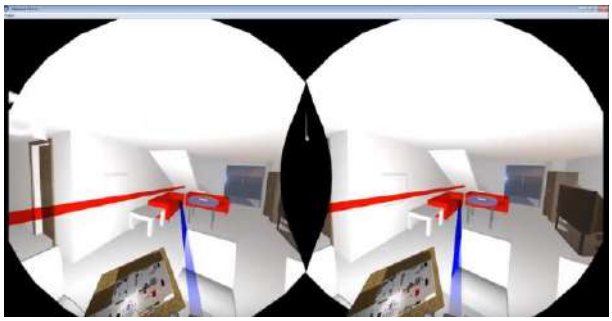

Figure 3. Users using the VR-based VBR environment

4 Evaluation

This study designed a Space Feasibility Inspection test to evaluate the performance and task loading of BIM-based, PC-based VBR, and VR-based VBR in finding issues and reaching consensus. We used Revit 2016 to build an example BIM model with four kinds of issues: usability, safety, privacy, and others. This model is a common living space including one living room, one dining room, one kitchen, one bathroom, one study room, one bedroom with bathroom, and one balcony. One example of the usability issue is that the height below the stair is too short that users are not comfortable to use the sofa. One example of the safety issue is that the table and the chair are too close to the fence. Once someone climbs on, he will be exposed to the falling danger. One example of the privacy issue is that the sliding door window would be better to have a curtain for privacy. Regarding other issues, one example of other issues is a construction problem. It is better to locate both bathrooms next to each other. So it will only require one piping space.

There are four phases in this test. The pre-phase has 3 minutes for demographics questionnaire. Then, the first phase is finding issues. It has 5 minutes for explanation and practicing, 12 minutes for finding issues, and 5 minutes for task loading questionnaire. After the first phase, the second phase is reaching consensus. It has 5 minutes for explanation and practicing, 12 minutes for reaching consensus, and 5 minutes for task loading questionnaire. Finally, the post-phase has 5 minutes for overall post-questionnaire and 8 minutes for an interview discussion. The flow-chart of this experiment is listed in Table 3.

Table 3. The procedure of user test

Phase	Description	Time (Minutes)
Pre-phase	Demographics questionnaire	3
1st phase: Finding issues	Explanation and practicing	5
	Finding issues	12
	Task loading questionnaire	5
2nd phase: Reaching consensus	Explanation and practicing	5
	Reaching consensus	12
	Task loading questionnaire	5
Post-phase	Post-questionnaire	5
	Interview discussion	8

In this test, we random recruited 90 participants and separate them into 45 groups, each environment has 15 groups and each group has 2 participants. The participants know each other before they come to the experiment to prevent the communication barriers caused by they are not familiar with each other.

At the beginning of this experiment, two participants and two research assistants meet in the same room. While all members arrive, one participant and one research assistant will go to room A. The others will go to room B. They do the same thing in the two different rooms. In the pre-phase, the research assistants will guide the participants to fill out the demographics questionnaires.

Next, the research assistant will explain the control manners of reviewing tools (Revit 2016 / VBR) and the task (finding issues) in the first phase within 5 minutes. Participant has 12 minutes to find issues as many as possible. After 12 minutes, the research assistants will guide the participants to fill out task loading questionnaires of finding issues.

Then, the research assistants will guide the participants to use a conferencing tool (Sococo) to communicate with each other. After 5 minutes of practicing, they were asked to list the top 5 issues they want to solve and also negotiate the proper solution within 12 minutes. They are also required to fill out the task loading questionnaires of reaching consensus.

Finally, they will turn off the conferring tool and fill out the overall post-questionnaires. After that, the research assistants will ask questions we designed and other questions related to the participants' 1st phase and the 2nd phase behaviors.

5 Results and Discussions

In the test, we measured (1) the average issues they found in finding issues (Table 4); (2) the average task loading in finding issues (Table 5); (3) the average time they used in reaching consensus (Table 6); and (4) the average task loading in reaching consensus (Table 7).

In the finding issues phase, the performance of PC-based VBR ($\boldsymbol{\mu = 9.77}$) and VR-based VBR ($\boldsymbol{\mu = 9.91}$) are no significant difference ($\boldsymbol{\alpha = 0.461462}$) but both of them are significantly better than BIM-based ($\boldsymbol{\mu = 6.57, \alpha = 0.000339 \text{ and } 0.004431}$). We further compared the performance in usability, safety, privacy, and other aspects of PC-based VBR and VR-based VBR. The results show that PC-based VBR is better in safety and privacy issues. VR-based VBR is better in usability and other issues. It may be caused by that VR-based VBR supports full-immersive experience enhancing participants more focus on simulating whether space is convenient for use. Regarding the averages of task loading in finding issues are 899.50, 813.84, 807.00 with no significant difference. We further compared the task loading in mental demand, physical demand, temporal demand, performance, effort, and frustration. All of them are no significant differences in mental demand and frustration. VR-based VBR has the greatest loading in physical demand ($\boldsymbol{\mu = 94.17}$) and is significantly higher than BIM-based ($\boldsymbol{\mu = 31.17, \alpha = 0.012771}$) and PC-based VBR ($\boldsymbol{\mu = 41.67, \alpha = 0.033628}$). But VR-based VBR has the lowest loading in performance ($\boldsymbol{\mu = 104.00}$) and is significantly lower than BIM-based ($\boldsymbol{\mu = 177.67, \alpha = 0.001412}$) and PC-based VBR ($\boldsymbol{\mu = 158.50, \alpha = 0.023266}$). VR-based VBR also has the lowest loading in effort ($\boldsymbol{\mu = 114.00}$) and is significantly lower than BIM-based ($\boldsymbol{\mu = 189.33, \alpha = 0.001212}$) and PC-based VBR ($\boldsymbol{\mu = 158.00, \alpha = 0.023981}$). The loading in temporal demand decreases from BIM-based to PC-based VBR and then to VR-based VBR. Among them, BIM-based and VR-based VBR have significant differences ($\boldsymbol{\alpha = 0.008672}$).

Table 4. The average issues they found in finding issues

Finding issues	BIM-based	PC-based VBR	VR-based VBR
Usability	3.83	4.77	5.77
Safety	1.40	2.70	1.97
Privacy	0.97	1.53	1.30
Other	0.37	0.77	0.87
Overall	6.57	9.77	9.91

Table 5. The average task loading in finding issues

Task loading in finding issues	BIM-based	PC-based VBR	VR-based VBR
Mental demand	247.17	236.67	269.83
Physical demand	31.17	41.67	94.17
Temporal demand	176.67	138.50	106.17
Performance	177.67	158.50	104.00
Effort	189.33	158.00	114.00
Frustration	77.50	80.50	118.83
Overall	899.50	813.84	807.00

In reaching consensus, the averages of seconds they used are 740.67, 682.93, and 724.40 with no significant difference. However, the averages of task loading in both of PC-based VBR ($\boldsymbol{\mu = 721.00}$) and VR-based VBR ($\boldsymbol{\mu = 718.10}$) are significantly lower than BIM-based ($\boldsymbol{\mu = 867.00, \alpha = 0.009610 \text{ and } 0.013879}$). We further compared the task loading in mental demand, physical demand, temporal demand, performance, effort, and frustration. All of them are no significant

differences in effort and frustration. PC-based VBR has the lowest loading in mental demand ($\boldsymbol{\mu = 185.67}$) and is significantly lower than BIM-based ($\boldsymbol{\mu = 249.83, \alpha = 0.017308}$). PC-based VBR also has the lowest loading in physical demand ($\boldsymbol{\mu = 47.17}$) and is significantly lower than VR-based VBR ($\boldsymbol{\mu = 88.00, \alpha = 0.032764}$). VR-based VBR has the lowest loading in temporal demand ($\boldsymbol{\mu = 138.33}$) and is significantly lower than BIM-based ($\boldsymbol{\mu = 220.83, \alpha = 0.008720}$) and PC-based VBR ($\boldsymbol{\mu = 212.33, \alpha = 0.015529}$). VR-based VBR also has the lowest loading in performance ($\boldsymbol{\mu = 99.50}$) and is significantly lower than BIM-based ($\boldsymbol{\mu = 147.00, \alpha = 0.032007}$).

Table 6. The time they used in reaching consensus

	BIM-based	PC-based VBR	VR-based VBR
Seconds	740.67	682.93	724.40

Table 7. The task loading in reaching consensus

Task loading in reaching consensus	BIM-based	PC-based VBR	VR-based VBR
Mental demand	249.83	185.67	227.97
Physical demand	74.17	47.17	88.00
Temporal demand	220.83	212.33	138.33
Performance	147.00	111.83	99.50
Effort	142.50	128.67	125.63
Frustration	32.67	35.33	38.67
Overall	867.00	721.00	718.10

To sum up, both PC-based VBR and VR-based VBR have better performance in finding issues and lower task loading in reaching consensus. In addition, we found that VR-based VBR has the lowest loading in temporal demand no matter in 1st phase or 2nd phase. It may be caused by that participants already immersive themselves into the virtual environment. They can use less time to adapt and realize the example BIM model and then use more time to conduct the tasks we assigned.

6 Conclusions

This study aims to identify effective communication environments for remote BIM model review collaboration. We identified and implemented three kinds of virtual communication environment: BIM-based, PC-based VBR, and VR-based VBR from two factors: the flexibility of exploration and the degree of immersive. A user test with 90 participants was conducted for evaluating their performance and task loading in finding issues and reaching consensus. The result shows that in finding issues, PC-based VBR ($\mu = 9.77, \boldsymbol{\alpha = 0.000339}$) and VR-based VBR ($\mu = 9.91, \boldsymbol{\alpha = 0.004431}$) are significantly greater than BIM-based ($\mu = 6.57$). Among them, PC-based VBR is better in finding safety and privacy issues and VR-based VBR is better in finding usability and other issues. The averages of task loading in finding issues are no significant difference in overall. However, VR-based VBR has the lowest loading in temporal demand, performance, and effort but has the highest loading in mental demand, physical demand, and frustration. The result shows that in reaching consensus, PC-based VBR and VR-based VBR can use less time to reach consensus than BIM-based but are no significant difference. However, the averages of task loading in both of PC-based VBR ($\mu = 721.00$) and VR-based VBR ($\mu = 718.10$) are significantly lower than BIM-based ($\mu = 867.00, \alpha = 0.009610$ and 0.013879). PC-based VBR has the lowest loading in mental demand and physical demand. In overall, both PC-based VBR and VR-based VBR have better performance in finding issues and lower task loading in reaching consensus.

References

[1] Olsen, K. Productivity Impacts of Offshoring and Outsourcing: A Review, OECD Science, Technology and Industry Working Papers, No. 2006/01, OECD Publishing, Paris, 2006. https://doi.org/10.1787/685237388034.

[2] Barboza, D. Bridge comes to San Francisco with a made-in-China label. On-line: http://www.nytimes.com/2011/06/26/business/global/26bridge.html?_r=0, Accessed: 31/01/2019.

[3] Schroepfer, T. Global Design Practice: IT-based Collaboration in AEC-projects. In *Proceedings of 1st International Conference on Digital Architecture and Construction*, pages 69–76, 2006.

[4] Eastman, C., Teicholz, P., Sacks, R., Liston, K. *BIM Handbook: A Guide to Building Information Modeling for Owners*, 2nd edn. John Wiley and Sons, Hoboken, 2011.

[5] Wu, F., Wu, T.H., Hsu, C.W., Kang, S.C. Virtual Building Information Modeling Reviewer. In *Proceedings of 15th International Conference on Construction Applications of Virtual Reality* (ConVR), Banff, Canada, 2015.

[6] Hosseini, M.R., Chileshe, N., Zuo, J., Baroudi, B. Adopting Global Virtual Engineering Teams in AEC Projects: A Qualitative Meta-analysis of Innovation Diffusion Studies. *Constr. Innov*, 15(2):151–179, 2015. https://doi.org/10.1108/CI-

12-2013-0058

[7] Fruchter, R. Transformative 3D Immersive Collaboration Environment in Support of AEC Global Teamwork. In *Proceedings of International Conference on Computing in Civil and Building Engineering*, pages 1425–1432, 2014.

[8] Anderson, A.K., Dossick, C.S. Avatar-model Interaction in Virtual Worlds Improves Distributed Team Collaboration through Issue Discovery. In *Proceedings of International Conference on Computing in Civil and Building Engineering*, pages 793–800, 2014.

[9] Anderson, A.K., Dossick, C.S., Azari, R., Taylor, J.E., Hartmann, T., Mahalingham, A. Exploring BIMs as Avatars: Using 3D Virtual Worlds to Improve Collaboration with, Models. Construction Research Congress 2014, American Society of Civil Engineers, pages 179–188, 2014.

[10] Anderson, A.K.: Visualization, Communication, and Copresence: Using Building Information Model in Virtual Worlds, Doctoral dissertation, University of Washington, Seattle, 2015.

[11] Dunston, P.S., Arns, L.L., Mcglothlin, J.D., Lasker, G.C., Kushner, A.G. An Immersive Virtual Reality Mock-up for Design Review of Hospital Patient Rooms. *Intelligent Systems, Control and Automation: Science and Engineering*, 48:167–176. (2011).

[12] Dossick, C.S., Homayouni, H., Lee, G. Learning in Global Teams: BIM Planning and Coordination. *Int. J. Autom. Smart Technol*, 5(3):119–135, 2015. https://doi.org/10.5875/ausmt.v5i3.916

[13] Wu, T.H., Wu, F., Liang, C.J., Li, Y. F., Tseng, C.M., and Kang, S.C. A Virtual Reality Tool for Training Global Engineering Collaboration. *Universal Access in the Information Society*. 1–13, 2017.

Efforts to Unmanned Construction for Post-disaster Restoration and Reconstruction

S. Kitahara [a], Y. Nitta [b], and S. Nishigaki [c]

[a] Fellow, Kumagaigumi Co,Ltd, Japan
(Chairperson, Disaster and Accident Sub-committee, Construction Robot Committee, JSCE, Japan)
[b] Team Leader, Advanced Technology Research Team, Public Works Research Institute, Japan
(Deputy Chairperson, Disaster and Accident Sub-committee, Construction Robot Committee, JSCE, Japan)
[c] CEO, Kick, Japan
(Member, Disaster and Accident Sub-committee, Construction Robot Committee, JSCE, Japan)
E-mail: skitahar@ku.kumagaigumi.co.jp, nitta-y573bs@pwri.go.jp, sleepingbear@c2mp.com

Abstract –

This paper presents largely severe natural disasters had happened in Japan, and efforts to unmanned construction until now. First, problems in responses to post-disaster restoration and reconstruction are reported. Secondly, are described demonstration of ultra-long-distance unmanned construction and the requirements for the deployment. Thirdly, this paper presents research and development on autonomous crawler carrier. Finally, concluding remarks and further works are reported. In addition, are proposed levels of promising applicability of robots in responses to post-disaster restoration and reconstruction.

Keywords –

Post-disaster, Unmanned construction system, Situational Awareness, Ultra-long-distance, Autonomous crawler carrier

1 Introduction

Japan is located in the Circum-Pacific Mobile Belt and Japanese archipelago, which are formed on the complex crusts. Accordingly, we are always facing and fearing natural disasters such as typhoons, unexpected strong and sudden tempest, and then deadly flash floods, earthquakes, volcanic activity, slope failures, landslides, avalanche of earth, fire of petrochemical complex, nuclear power station accident, and so on. Largely severe natural disasters have recently occurred in Japan are listed below.

(1) The 1995 Hanshin-Awaji Earthquake,
(2) The 2004 Mid Niigata Prefecture Earthquake,
(3) The 2011 off the Pacific coast of Tohoku Earthquake with the Fukushima daiichi nuclear power station accident,
(4) The 2016 Kumamoto Earthquakes, and
(5) The 2018 Hokkaido Eastern Iburi Earthquake.

Now, we need consider countermeasures against largely severe natural disasters. When facing dangerous situations in post-disaster restoration and reconstruction, in order to avoid any secondary disasters, we inevitably demand unmanned construction.

This paper reports efforts to unmanned construction for post-disaster restoration and reconstruction, which have been and are being discussed in the disaster and accident sub-committee, construction robot committee, JSCE in Japan. As for post-disaster restoration and reconstruction, this sub-committee plays a role in:

(1) Finding out applicability of unmanned construction system,
(2) Analysis of examples of the unmanned construction systems responded to natural disasters and accidents,
(3) Investigating advanced technology applicable to develop future unmanned construction systems,
(4) Guidance to put the future unmanned construction systems in practice,
(5) Informing the public widely of the achievements of these, and utilizing them to society, and
(6) Proposal of levels of promising applicability and objectives of research and development on construction robots.

The discussions in this sub-committee here will make it possible for researchers, engineers, and users to have a shared awareness of efficiency index and applicability level, performance to be the goal, state-of-the-art to be attained, and so forth, in responses to post-disaster restoration and reconstruction. Moreover, it will contribute to the research and development on robotics for post-disaster restoration and reconstruction.

This paper is organized as follows. First, this paper presents problems that we have to face when conducting unmanned construction. Secondly, this paper reports issues and future directions pertaining to ultra-long-distance remote-control unmanned construction system.

Thirdly, efforts to research and development on autonomous crawler carrier are described. Finally, are reported concluding remarks, further works, and proposal of the promising applicability in levels of responses to post-disaster restoration and reconstruction.

2 Problems

In response to post-disaster restoration and reconstruction, construction machines are often remotely controlled to remove earth and rocks at the steep slope on the left and at the ridge of steep cliff on the right as shown in Figure 1. As mentioned above, when facing dangerous situations, in order to avoid any secondary disasters, we inevitably demand unmanned construction system.

Figure 1. Works at the ridge of steep cliff and at the steep slope

Handling joysticks to operate construction machines, either directly or remotely, is an inherently eye-hand coordination task. The eye-hand coordination task means to control eye movements with hand movements, as processing the situational views to handle joysticks. Considering unmanned operation, however, the operators handle their joystick controllers to operate construction machines remotely in narrow field of views produced by camera-monitor system at the control room. Problems here include machine operability, difficulty in a task at hand, performances limited by bearings of operators in their behavioural frameworks, and continuous or intermittent mental workload on them. The continuous or intermittent mental workload might be caused by communication with latency, narrow field of view, different reference frames without realistic sensation, and so forth. Although, the operators have to make a decision instantaneously on do's and don'ts in their operations, it is sometimes difficult to ensure line-of-sight for location and movement direction of their machines, positions of and clearance from surroundings of the machine and the target. Then they have to mentally translation, rotation and scaling between different frames of references in Figure 2.

As shown in Figure 3, however,

(1) Just by images from on-board cameras, it is difficult to grasp shape of work target,

(2) Just by images from fixed cameras, it is almost impossible to understand the whole of situations on site, and so,

(3) It is required to have functions to adjust coordinates of the entire of work site.

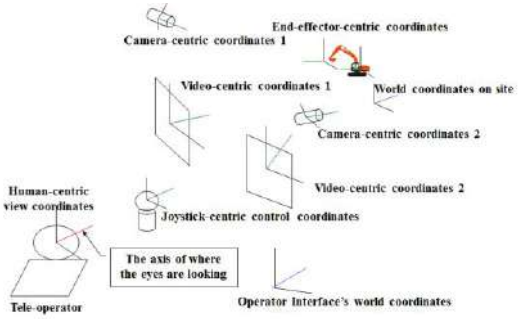

Figure 2. Different reference frames

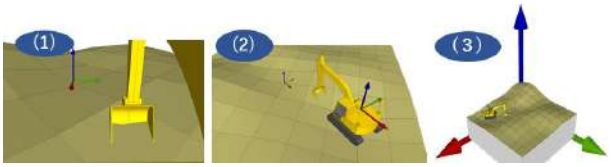

Figure 3. Images from camera

Therefore, the unmanned construction requires that operators indispensably acquire extensive trainings and broad experiences on problem-solving skills pertaining to:

(1) Different viewpoint control,
(2) Spatial locations and positioning,
(3) Figuring out and completing the given task at a hand in real-time manner.
(4) Endurance of continuous or intermittent workload
(5) Scale ambiguity
(6) Rate of motion, and
(7) Loss of peripheral vision with retention of central vision, which is liable to result in a constricted circular tunnel-like field of vision.

The skilled operators are imperative for the unmanned construction operation. In Japan, however, there are very few skilled operators, and most of them are aged people.

Therefore, it is very important and significant to provide the operators with physical cues related to behaviour of construction machines, in order to compensate for their realistic sensations, which operators would feel when directly operating their machines, and to increase their consciously and situationally spatial awareness, which enable them to infer and understand the present and future surroundings of remotely controlled machines and watch oneself in their work space.

3 Ultra-long-distance Remote-control Unmanned Construction

When the 2011 off the Pacific coast of Tohoku Earthquake occurred, the Ministry of Land, Infrastructure, Transport and Tourism of Japan (hereafter called MLIT) conducted demonstration tests on ultra-long-distance remote-controlled operation of unmanned construction machines, in March of that year, at the foothills of Mt. Unzen. This demonstration tests aim to prepare for future large-scale volcanic disasters [1], [2]. Figure 4 shows Demonstration tests network. The experiment yard is shown in Figure 5, and the mobile relay station in Figure 6.

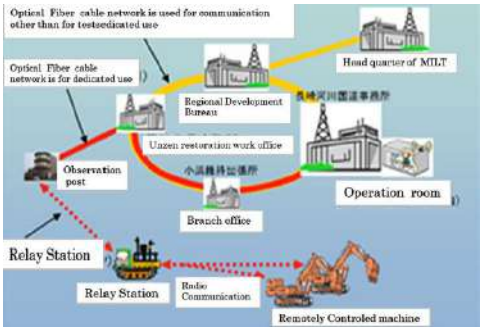

Figure 4. Demonstration tests network in ultra-long-distance remote-controlled operation of unmanned construction machines

Figure 5. Experiment yard for demonstration tests

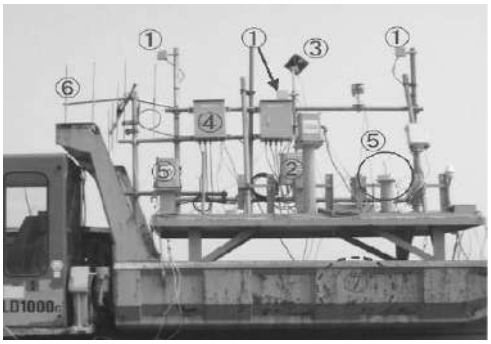

Figure 6. Mobile relay station for demonstration tests

The devices shown in Figure 6 are explained as follows:

① Directional patch antenna for wireless LAN (IEEE802.11),
② Wireless LAN (IEEE802.11) master unit 5GHZ,
③ 25GHZ low power radio device,
④ RS232C 422-LAN converter,
⑤ Specified low power radio station (429MHz),
⑥ Public broadband communication antenna, and
⑦ Public broadband communication device.

Communication latency, and image degradation in ultra-long-distance remote-control machines might make it difficult to figure out and complete the given task at a hand in real-time. And then it is easily conceivable to decrease the work efficiency. Moreover, the machines are highly liable to collide with each other.

The purposes of the demonstration tests are described below.

(1) Evaluation of capability (e.g., data-carrying capacity, latency) of various communication methods as follows:
  1) Long-distance communication (from control room to relay station on site), and
  2) Local communication on site.

(2) Analysis of operating environment and operator's bearings related to:
  1) Influence by communication latency, and image degradation,
  2) Maintenance of construction machines (refuelling, maintenance, etc.), and
  3) Operator's skill (operating envelope, proficiency, etc.).

(3) Comparison and verification experiments with respect to:
  1) Operator's proficiency (skilled, unskilled) and
  2) Operational envelope limited by image communication latency and degradation.

The demonstration tests used actual construction machines and an optical fibre cable network for the first time in Japan, and demonstrated the applicability of remote-control operation technologies to ultra-long-distance unmanned construction machines. The machines here were remotely operated from a remote-control room 30 km away. Are also demonstrated that the communication system, combined with wireless mesh LAN, simultaneously transmitted high-definition 1 Mbps images from 20 cameras. Then hydraulic excavators could be operated with a high degree of accuracy. In addition, are verified the transmission capabilities of alternative long-distance communication such as public broadband communications, long-distance wireless LANs, satellite communications, etc. in this demonstration tests.

3.1 Operator's Qualification

Operators with different level proficiency (e.g., skilled, unskilled) participate in this comparison

and verification experiments, which have been done in demonstration tests. These experiments conducted are outlined in the following subsections

3.1.1 Climbing Over a Large Bump

Each of the skilled and unskilled operators remotely controls a backhoe with 1.2 m^2 bucket for one-cycle of a series of the following operations as shown in Figure 5.
(1) Level down a fill with two meters in height and the inclined part 45 degrees, and
(2) Build a runway and climb the fill
Operators' hacks learned from the above operations are summarized below.
(1) It was observed that the unskilled operator's cycle time runs 1.9 times longer than the skilled operator's one.
(2) When not using a camera car, the difference between the two has spread to 2.3 times.
(3) On the other hand, in case of boarding operations, the unskilled operator's cycle time runs 1.8 times longer than the skilled operator's one
(4) Putting the cycle time of boarding operation equal to one, the unskilled operator took a work time to complete the task from 2.0 to 3.6 times of the one.

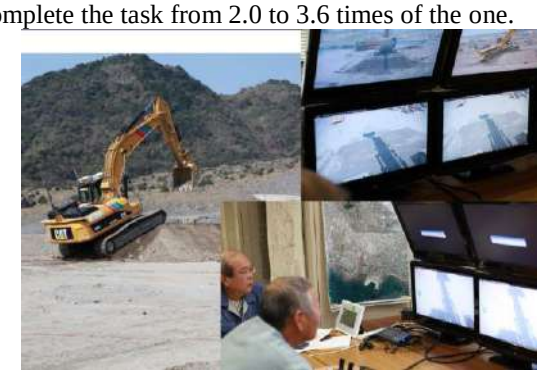

Figure 5. Climbing over a large bump

3.1.2 Travelling as Avoiding Obstacles

The three colored corns are installed in a 40 m interval of running path. In addition, three concrete blocks are placed at the running path. The backhoe zigzags between the three colored corns. The backhoe is planned to stop and scoops the three objects of concretes in the middle of running. The experiment shows the following results.
(1) The unskilled operator's cycle time runs 1.5 times longer than the skilled operator's one.
(2) In case of boarding operations, the unskilled operator's cycle time runs 1.7 times longer than the skilled operator's one.
(3) If image latency occurred, the difference between the two has decreased.

3.1.3 Pseud-refueling Operation

Aiming to unmanned maintenance, pseud-refueling works by remotely controlling a backhoe was conducted as shown in Figure 6 and Figure 7. It could be seen from this experiment that
(1) If and when camera images of the refueling hose and the refueling neck are intersecting perpendicularly, it becomes easier to position the refueling hose and to adjust its height direction, and
(2) Although it is required to improve the filler neck, the current method in this experiment could be more than enough put it in practice.

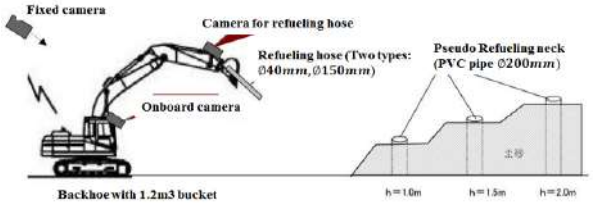

Figure 6. Image of pseud-refueling operation

Figure 7. Pseud-refueling scene

3.2 Operational Envelope Limited by Image Communication Latency and Degradation

Concerns about ultra-long-distance communication are latency and degradation of images, and presence or absence of camera cars. As arbitrarily changing conditions of images from monitors, the skilled operator has remotely operated a backhoe with a hydraulic breaker as shown in Figure 8.

Figure 8. Backhoe with a hydraulic breaker

This aims to confirm influences and operability of remote control to the following works.
(1) Travelling, grasping and placing boulders, and turning by the backhoe.
(2) Crushing boulders by the hydraulic breaker.

Accordingly, it was were confirmed that allowable delay time was less than 1.5 seconds in rough works and one second in precise works.

3.3 Lesson Learned from Demonstration

The lesson learned from these demonstration tests are outlined below.

3.3.1 Availability of Wireless LAN Method （IEEE802.11j）

The confirmed availabilities of wireless LAN method are listed below.
(1) Time delay of operational data with video communication via optical fiber network and wireless LAN is less than 1 second even if the communication distance is more than 80km.
(2) High resolution of six images per one channel of wireless LAN can be transmitted simultaneously and stably.
(3) The transmission delay long-distance wireless LAN is less than about 1 second. Communication intermittent might be occurred under the condition of the large amount of data transmission (e.g.,1.5 Mbps), that's why dropping frames of image data transmitted might happen. If the number of cameras is less, that is, volume of data transmitted is less, it might be available.
(4) The transmission amount of wireless LAN is large, but the communication sneak performance is poor.
(5) Image transmission capability
The wireless LAN is able to stably transmit 6 images per channel in case of quick changes (one image: 1.5~3.0 Mbps/30 fps), and 10 images per channel (one image: 1.0~1.5 Mbps/30 fps) in case of little changes.

3.3.2 Communication within Construction Site

In case of usage of wireless LAN and specified low power radio, it is limited to about 10 units of construction machines, in order to prevent communication interference. In this demonstration, both the image system signal and the operation system signal could be handled without hindrance. When using wireless LAN (IEEE802.11j) and specified low power radio, the each reaching distances was about 230 m. It might be promising to use low-latency type codec in wireless LAN method in future.

3.3.3 Possibility of Public Broadband Communication

The public broadband communication shows superior communication sneak performance with about 70 degrees at location where there are impenetrable hills, buildings and the like. According to narrowness of the bandwidth, image degradation, dropping frames of image, and so on, it is difficult to concurrently use image system signal. Boom or arm of backhoe might cut radio waves off sometimes. The communication sneak performance might be valid at a place with poor visibility.

3.3.4 Long-distance Communication Method

Allowable limit of transmission delay to operators is up to about 2 seconds. In ultra-long-distance communication method more than 30 km, the transmission delay is less than 0.8 seconds. When combining wireless LAN (one channel/IEEE802.11j) and optical fiber, transmission delay of operation data was less than 100 msec.

Although optical fiber communication is applicable to unmanned construction, it is necessary to carefully consider the usage environment and conditions.

3.3.5 Inmarsat Satellite Communication System

The transmission capacity is 64 kbps, and the 8-second delay occurred. If and when the usage is limited to emergency applications with fewer amount of data, it is likely that this system works well for control system.

3.3.6 Startup of Communication and Unmanned Construction Systems

To sum up the participants' opinions, it might take four days to arrange the orders and shipping pertaining to equipment such as remote-control room, relay stations, allocations of unmanned construction machines, and forth. Moreover, it might take one day to set up them, and moreover one day to take their test runs. Considering examination of new technologies, however, it shall take ten days to do so.

4 Efforts to Post-disaster Reconstruction at Aso Bridge District

4.1 Efforts Up till Now [3]

The 2016 Kumamoto Earthquakes are in a series of earthquakes, which are a foreshock earthquake observed at 21:26 on April 14, 2016 with a magnitude 6.5 at a depth of about 11 kilo meters, and then main shock earthquake with a magnitude 7.3 observed at 1:25 on April 16, 2016 with a magnitude 7.3 at a depth of about 12 kilo meters.

It was heavily damaged around the centre of Mashiki, where the earthquakes with a Japanese scale, that is seismic intensity of 7 (hereinafter called Shindo) occurred two times. Moreover, earthquakes with more than Shindo 1 were observed 4,481 times as of April 13,

2016, including seven earthquakes more than Shindo 6 lower.

After the earthquakes, 172 deformations of river embankments such as cracks and subsidence were confirmed in relatively larger river system under control of MLIT. Approaching the verge of rainy season, urgent restoration works were required without a moment's delay

MLIT has carried out urgent restoration works 24 hours a day on 11 relatively larger deformation points in 172 damaged points of river embankments, and worked it out and accomplished the restorations on May 9 before the rainy season in 2016. In addition, considering causes of the damages, methods of restoration and monitoring on the situation of restoration, full-scale restoration works have been done on 52 points required to restore and accomplished by the end of May before rainy season in 2017.

Slope failures and landslide by these earthquakes shredded major transportation routes and then it was transport impossible everywhere. These damages made it difficult to rescue and transport emergency supplies, and moreover to take measures for livelihood rehabilitation. Accordingly, MLIT had urgently restored roads within about 1 week after the disasters, which had been essential for lifesaving and indispensable to transport relief supplies.

The scale of the large-scale landslide at Aso bridge district run up about length 700 meters and about width 200 meters, and the sediment discharge was estimated about 500,000 cubic meters. Many crown cracks and terrace scarps occurred on the head of the landslide. Since the post failure ground surface was steep slope, there was a danger of further collapse caused by rainfall or aftershock.

Since it was the most important task to avoid any secondary disaster under the above circumstance, the latest unmanned construction technologies, which are leveraged the knowledge and results obtained from the demonstration tests as mentioned before, were introduced into the rehabilitation works, as monitoring and sensing movement of the post failure ground surface and the surrounding.

The works commenced on May, 2016. Firstly, as considering what kind of works are possible in the landslide area, building approaching path to the crown of the landslide started in order to construct retaining embankment.

Since sediment in the area destructed by landslide had high soil moisture content, it was forced to move forward to consolidate the surface and subbase of the approaching path as stirring and mixing soil amendment and additive in situ. Subsequently, a full-fledged construction of retaining embankment could commence in July of that year, where was utilized unmanned construction system with multiplexing of connected devices with high-speed and wide-bandwidth data transmission as shown in Figure 9. This unmanned construction system made it possible to remotely operate up to 14 construction machines at the same time and to build retaining embankment. Moreover, this system enabled us to do rounding and remove large boulders at the crown of the landslide, and to remove soil at the post ground surface. Accordingly, urgent construction works could be completed to avoid secondary disaster.

Figure 9. Bird's eye view of unmanned construction conducted at Aso bridge district

Because the danger of secondary disaster is reduced, currently, manned works have been and are being implemented to build permanent fix works such as protection net and inserting rebar.

5 Research and Development on Autonomous Crawler Carrier

5.1 Supposition and Purpose

To achieves a less burden on operators mentally, we have been and are doing research and development on autonomous crawler carrier utilized for material haulage. It is supposed that autonomous construction machines might cause new mental strain on operators, such that, as expecting nothing happens, waiting for something might happen. Then, it is worth providing operators with infographics pertaining to construction machine's behaviour. The infographics include figures, evaluation indexes and messages as to operability, safety and productivity. The infographics give operators opportunity to prognosticate something that might happen.

5.2 Experiments at the institute of technology

Experiments as to operability of a crawler carrier and driving performance of the autonomous crawler carrier developed were conducted at the institute of technology, Kumagaigumi, Co., Ltd. Objectives of the experiments are as follows:

(1) Comparison of operabilities between boarding operation and remote-control of a crawler carrier, and

(2) Confirmation of driving performance of the autonomous crawler carrier developed.

5.3 Field test on at Aso bridge district

The field test on autonomous operation of crawler carrier to haul soil removed at the mountainside was conducted. These crawler carrier was remotely controlled at loading and unloading spots and automatically run through the haulage road.

Examples of the infographics shows the following hazards latent in the haulage road:

(1) Many impacts and free-falls in Figure 10 show the surface of the haulage route is rough and uneven;

(2) Figure 11 shows sudden acceleration occurred uphill and rapid deceleration downhill and both sudden acceleration and rapid deceleration at the waypoint of turnaround, and

(3) Attitude of machine body, however, was stable as shown in Figure 12.

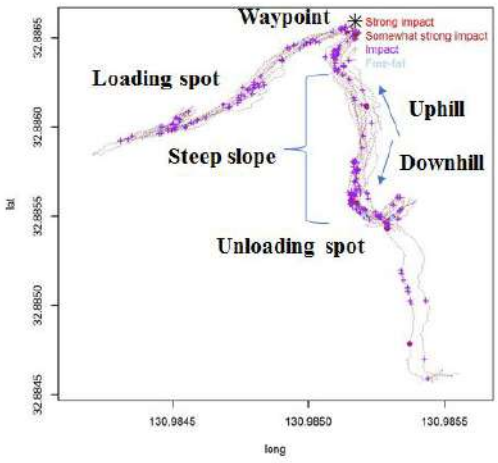

Figure 10. Impact and free fall latent spots occurred in the haulage road

These infographics are visualizing the spatiotemporal behavior of the autonomous crawler carrier, and help the operators to prognosticate hazards. These infographics could enhance their spatial awareness, which would be able to provide the operators with the opportunities to reflect on their own bearings as facing their own works at hand, to reduce likely stress in remote-control operations of construction machines. Furthermore, it would be possible to take timely and quickly correct actions based on detailed visibility of appearances and motions of the autonomous crawler carrier in a whole unmanned construction process.

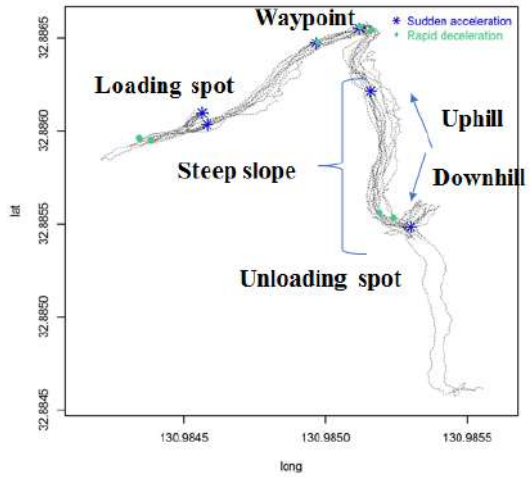

Figure 11. Sudden acceleration and rapid deceleration spots occurred in the haulage road

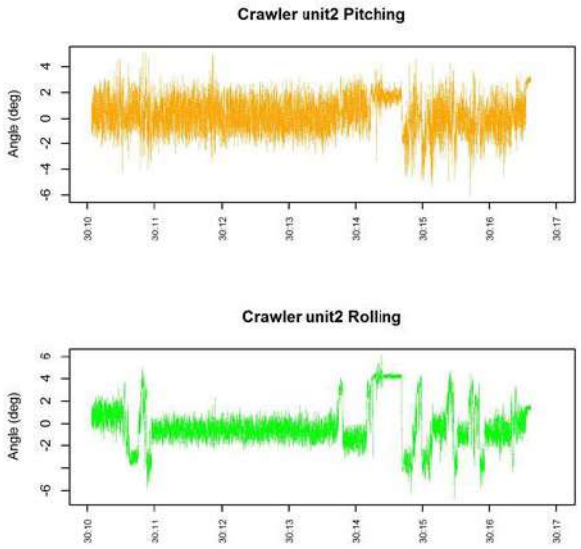

Figure 12. Attitude of machine body

6 Remarks, Further Works and Proposal

This paper presents largely severe natural disasters happened in Japan until now, problems in responses to post-disaster restoration and reconstruction, demonstration tests of ultra-long-distance unmanned construction and the requirements for the deployment, the research and development on autonomous crawler carrier.

Considering the participants' opinions, tasks to be resolved for practical use are listed below.
(1) Unmanned refueling, lubricant oil supply, and machinery maintenance.
(2) Preventive maintenance techniques for inspection and maintenance.
(3) To ensure durability of on-board communication devices.
(4) Autonomous system adjustments such as setup of devices, change of IP address, and so on.
(5) Operator training system to develop skilled operators.
(6) To build communication system suitable for peculiarities of post-disaster restoration and reconstruction site.
(7) Procurement management of construction machines and devices suitable for unmanned construction.

Providing operators with perpendicularly intersecting images of objects, it will become easier to position the object and to adjust its height direction. More arbitrary viewpoints on the monitor, however, are liable to increase new mental workload to memorize and understand simultaneously. It is desirable to develop functions that enable operator to easily accommodate mentally translation, rotation and scaling between different frames of references.

Although automation of construction machines will decrease mental workload on operators, it will produce new mental workloads to carefully watch unexpected occurrences of unsafe events, and cooperative states of several autonomous machines. It is desirable to develop service planning and executing diagram and functions to control complement of remote-control machines, autonomous machines and computer devices operating together for construction.

In future, when unmanned construction system would be deployed in various kinds of remotely dexterous operation in close proximity to other, for examples, approaching to the target (e.g., inspection, repair, monitoring another one), positioning or repositioning dangerous materials, connecting an object with other, grasping and stacking sandbags or gabions, inserting nozzle into a fuel filler port for replenishment, and so on. Then, it is desirable to find the better way to control micro manipulation by remote-control operation.

Finally, following discussions on construction robots at the disaster and accident sub-committee, we propose the following levels of promising applicability of robots in responses to post-disaster restoration and reconstruction.
Level 1: It could be remotely controlled to monitor and investigate within disaster-stricken location.
Level 2: It could propel oneself within disaster-stricken location to complete simple works.
Level 3: It could propel oneself within disaster-stricken location and then remotely controlled to complete complex works. and
Level 4: In combination of autonomous and remote-control operations, it could smoothly complete sophisticate works.

Considering these levels, we are going to do research and development on the further tasks to be resolved.

References

[1] Kazuhiro Chayma, Yasushi Nitta, et al. Technology of Unmanned Construction System in Japan, J. of Robotics and Mechatronics, Vol.25, No.4, 2014.

[2] Yasushi Nitta, Osamu Matsuo, Shigeo Kitahara, et al. A study of the application of ultra-long-range remote-controlled construction technology - A summary of ultra-long-range remote control experiment in Mt. Fugen in Unzen – (in Japanese), On line: http://www.actec.or.jp/documents/study(13th%20symposium).pdf, Accessed:05/01/2019.

[3] Naoto Yamagami, Shigeo Kitahara. The 2016 Kumamoto Earthquake and the Restoration Work Using the Advanced Unmanned Construction Technology, On-line http://interpraevent2018.jp/pdf/Keynote/KN-7_20180913.pdf, Accessed:05/01/2019.

Service Level Evaluation of Florida's Highways Considering the Impact of Autonomous Vehicles

A. Mahdavian[a], A. Shojaei[b], and A. Oloufa[c]

[a] Department of Civil, Environmental and Construction Engineering, University of Central Florida, FL, U.S.
[b] Building Construction Science, College of Architecture, Art & Design, Mississippi State, U.S.
[c] Professor, Department of Civil, Environmental and Construction Engineering, University of Central Florida, U.S.
E-mail: Amirsaman@knights.ucf.edu, Shojaei@caad.msstate.edu, Amr.oloufa@ucf.edu

Abstract –

Automated vehicles (AV) are undergoing development at a remarkable pace and have the potential to revolutionize the existing transportation system. The ASCE [1] evaluated the United States' infrastructure as a D+ grade. Moreover, they predicted radical infrastructure investment gaps in the surface transportation sector in the upcoming years. Some new urbanized regions might require new highways. Meanwhile, many other highways are reaching the end of their service life and will need significant repairs or even replacement. However, this seems to be unrealistic to happen until having a high market penetration of Fully Connected and Autonomous vehicles on the road to benefit from the capacity expansion benefits. Regarding the funding related issues of highway construction in the U.S. and the emergence of AVs, having a better understanding of the future's traffic status is a must. This study investigates the impact of autonomous vehicles on Florida's district five of I-95 highway traffic including three counties: Flagler, Volusia, and Brevard. This research is the first study to develop a fusion model considering the impact of both traffic flow and capacity adjustments based on the literature review to forecast the traffic from 2020 to 2040 by considering the increasing AV market penetration. The proposed approach provides a more realistic plan for government agencies and private investors, and as a result, significant savings financially and resource-wise can be achieved. The findings of the study confirm that autonomous vehicles will increase traffic flow and capacity, and the increase in flow is higher than the increase in capacity.

Keywords –

Autonomous Vehicles; Traffic Flow and Capacity; Long-term Planning; Highway

1 Introduction

Civil infrastructure systems are an integrated system of engineered systems and people within an ecological context. It is critical to keep resiliency of these complex systems in mind during their design, operation, and maintenance to ensure their efficient operation. Differing perspectives are required to understand the system dynamics of such complex systems correctly to achieve effective and stable operation. Highway Infrastructures constitute an economically vital form of transportation infrastructure. They have the potential to contribute to the productivity and economic growth of states economies. ASCE gave U.S. infrastructure a D+ in 2017. They also predicted radical investment gaps in the highway sector. Mobility is the lifeblood of our cities and a crucial aspect of urban life. U.S. automobile incidents are mostly related to human errors and the US petroleum use for road transportation corresponds to approximately 60% of the total U.S. petroleum consumption. Moreover, the average commuter gets delayed 38 hours per year due to traffic congestion. By revolutionizing the nature of personal mobility and removing the need for passengers to be in the car at all times, AVs have the potential to dramatically affect roadway usage and the built environment to yield urban spaces that are safer, more efficient, and attractive. As a result, there is a possibility that the highways that are under construction or soon their construction will commence could be obsolete by the time that they become operational due to the impact of the autonomous vehicles on effective road-capacity and shared mobility travel behavior. However, the chance of occurrence of this scenario is slim before having a high market penetration of fully Connected Autonomous Vehicles (CAVs) on the road to fully take advantage of the capacity expansion benefits.

Then again, the number of trips increases substantially due to various disruptive forces such as the increased population, increased urbanization, increased vehicle miles traveled (VMT) for AV cars as a result of easier trips, and, new consumers such as children, disabled and senior people. Truck-related travels also have a pivotal role in transportation planning as their impact on the transportation system could also be significant which in turn would affect the overall infrastructure costs. There is a positive relationship between the size of the economy and truck VMT. The size of the U.S. economy is expected to double from 2017 to 2045 which will lead to the continuous expansion of truck VMT reflecting increased productivity and population.

Even though several studies have investigated the impacts of Connected and Autonomous Vehicles (CAVs) adoption on travel behavior, much remains to be explored regarding the different ways in which upcoming disruptive forces such as CAVs, urbanization, and, the increasing population could affect the highway infrastructure level of service and their respective cost and benefit streams for the stakeholders. Considering the impact that these forces can have on the societies' quality of life, postponing decision making and quantifying their impact to the time when a significant number of CAVs are operating, and higher urbanization occurs, would be most likely too late for any remedial actions. CAVs in all likelihood will have the most significant and earliest impacts on highway capacity and traffic volume. The number of trips increases substantially due to the mentioned disruptive forces. Impact of increased congestion on the economy decreases the reliability of transportation facilities, increases vehicle operation cost, increases environmental and safety costs, and, deteriorates the roadway conditions. In this study, first, appropriate scenarios based on the literature review are devised and used to project the traffic flow. Then, the capacities of the selected highways are adjusted by considering the market penetration of AVs. Lastly, it is shown that which highways will operate under, at, or over capacity. The output of this study will eventually help long-term planning for infrastructures in Florida. Moreover, this study can be used by policymakers and researchers as an input in disaster management and planning for resilient communities.

2 Literature Review

This study applies a data-driven model to examine the impact of AVs on Florida's district five I95 highway traffic, analyzing the effect under different scenarios considering the increasing AV market penetration. The market penetration of the AVs and the corresponding travel consequences in future are of great interest to researchers and companies. Also, if AVs enter new vehicle markets in the 2020s, it will be the 2040s or 2050s before most vehicles can be Connected and autonomous driving of level four and five [16]. The market penetration assumptions used in this study is based on the literature review [15] and is summarized in Table 1. Two pessimistic and optimistic market penetration scenarios are defined for each specific time being studied in this modeling based on the [15].

Table 1. Optimistic and pessimistic CAV market penetration

2020		2025	
Pessimistic	Optimistic	Pessimistic	Optimistic
0%	10%	10%	20%
2030		2035	
Pessimistic	Optimistic	Pessimistic	Optimistic
15%	30%	30%	40%
2040			
Pessimistic	Optimistic		
35%	45%		

Highways' characteristics should improve to increase its capacity to be able to adjust CAVs in the traffic system [7]. Studies revealed that the capacity of the network could grow two to four time more than current capacity, based on the CAV fleet size [7, 22]. Improvements in the network capacity are the result of the enhanced reliability of travel time, the precision of CAV controls and the communication features [27]. [19] estimated that decreased headways could nearly double or triple roadway capacity. VMT increase concerning road capacity is 30% to 60% (short-term) and 60% to 100% (long-term). [23] also predicted that vehicle-to-vehicle (V2V) coordination of adaptive cruise control could improve capacity by 21% with 50% of all vehicles using this technology, or up to 80% capacity expansion with a 100% coordinated vehicle fleet based on empirical examination.

Due to the new category of users, vehicle automation can improve the mobility of currently underserved populations, namely, those with travel restrictive medical conditions, and seniors. Speculation based studies by different authors show that AVs would add some trips to the traffic network by providing mobility for disabled people and children [27]. [3] speculated that level four vehicles (fully automated) would considerably increase the number of trips because it provides mobility for those groups which are not able to drive using conventional vehicles. AVs could be especially transformative for one group of people in particular: those who are physically incapable of driving. [19] estimated 10% to 14%, [8] estimated

14%, Brown et al. estimated (40%), and [10] estimated 10% to 20% increase in VMT due to the new categories of users. CAV can also increase empty vehicle travel while dropping off or Picking up travelers, or during waiting to be called. It is argued that it is more reasonable for a car to drive around than to pay parking charges [24]. Furthermore, experts predict that there will be an increase in goods delivery by AVs on the roads as well.

Regarding the ownership, total travel effects will depend on the extent that households move from owning to sharing vehicles. Changes to shared mobility lead to a decrease in overall vehicle travel. It is not clear that AVs increase or reduce total vehicle travel. Lovejoy, [14] predicted that Households tend to significantly decrease their vehicle travel, by 25-75%, when they move from owning a vehicle to sharing it. Regarding safety, it is claimed that because human error is the reason for 90% of crashes. Autonomous vehicles full adoption will decrease crash rates and costs associated with insurance companies by 90% [9].

3 Methodology

The research includes the application of input-output modeling technique to conduct a traffic analysis on I-95 Highway in district five of Florida Department of transportation, counties of Flagler, Volusia, and Brevard. Weighting method is used to have a normalized Annual Average Daily Traffic (AADT) for all the segments of each county calculated by FDOT Hybrid model from 2020 to 2040, recently developed by the forecasting engineering team. In this study, the sections of the FDOT final report in 2015 are being used. There are 38 stations in total defined for the Highway I-95 in District five. Each station has information regarding the state road no., start, and end of the segment, length, level of service and so forth. [11] used systems dynamics modeling to generate three scenarios that describe the possible negative and positive outcomes of the broad adoption of AVs. They defined three scenarios to predict the future's impact of AV adoption on traffic. Likely profits include cheaper and safer travel by car, with enhanced mobility for those who do not have access. They also consider the ownership behavior of the passengers. Figure 1 illustrates the summary of the parameters used in this research for adjusting traffic volume and capacity. In this study, the optimistic and pessimistic thresholds are chosen to be used as special cases due to the suggested model by [15] regarding the AV market penetration. In the modeling procedure, the traffic capacity is adjusted by the method proposed by [17]. The inputs and outputs of this study presented in Table 2. The inputs data include the FDOT's traffic-related data and the literature information to build the fusion model regarding the various studies in this modeling. Moreover, this study includes six outputs as shown in Table 2.

Table 2. Inputs and outputs of the model

Inputs	
FDOT's Inputs	Traffic Flow Forecast Data (Average Annual Daily Traffic)
	Traffic Capacity information
Literature's input	Impacts of AV on Traffic Flow and Capacity

Outputs	
Outputs 1	Fusion Model, Defined Scenarios base on the impacts of AV on Traffic
Outputs 2	Impact of New categories of users on V/C Ratio
Outputs 3	Impact of Shared or Private Ownership on V/C Ratio
Outputs 4	Impact of Time Gaps-Capacity on V/C Ratio
Outputs 5	Impact of Behavioral Scenarios (Base-Disruptive-Adaptive) on V/C Ratio
Outputs 6	Impact of Construction scenarios on V/C Ratio

This study uses the input-output modeling technique to conduct a series of scenario analysis. Scenario analysis is the process of evaluating potential future events through the consideration of feasible alternatives, though, not equally likely, states of the world. Figure 1 shows the assumptions regarding different scenarios of the model based on the literature review that accounts for adjustments for traffic flow and capacity.

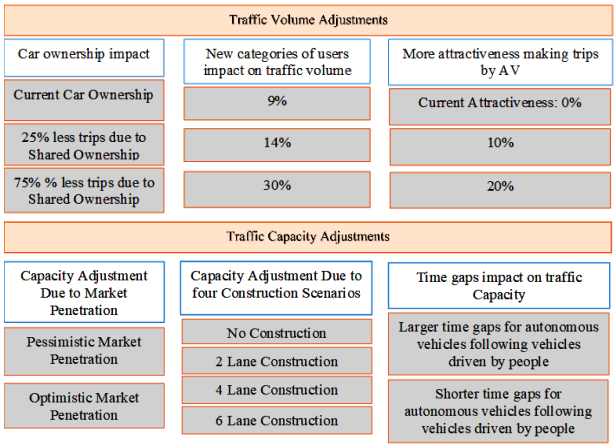

Figure 1. Traffic volume and capacity parameters

assumptions in this study.

4 Results

There are five pivotal aspects related to volume/capacity ratio (V/C) discussed in this section. Namely, the impact of new categories, the shift of the ownership, large and short time gaps, three different behavioral scenarios, and constructing of new lanes based on the Volume/Capacity (V/C) ratio.

Table 3 shows the assumptions and traffic information data regarding the study of the impact of various new categories of users on volume/capacity ratio. This study assumes a pessimistic market penetration of autonomous vehicles. Moreover, the impact of shared ownership and the attractiveness of having more trips by AV is not considered.

Table 3. Information regarding the data and the assumptions used in Figure. 2

County	Brevard County
I-95 segment #	15
Market penetration	Pessimistic
Variable under study	Impact of New categories of users
Variable's impact 1	0%
Variable's impact 2	9%
Variable's impact 3	14%
Variable's impact 4	30%
Impact of Shared or private ownership	0%
Impact of More attractiveness of making trips by AV	0%

The impact of new categories of user increase from 3% in 2025 to 18% in 2040 considering four different scenarios on the V/C ratio is depicted in Figure 2. The results show that the difference between the V/C ratio increases between different scenarios as the time passes. It is evident that higher percentage new user scenarios (more evident for the 30% scenario) start departing from the baseline earlier. The growing distance between the scenarios shows that there is a critical need for federal government to pass limiting laws (Licencing) to manage the probable new users efficiently to avoid lower service level and high congestion level. Furthermore, this study did not consider the children under 18, a tech-savvy market that mobility service start-ups are already tapping, in the calculations which have the potential to worsen the traffic congestion.

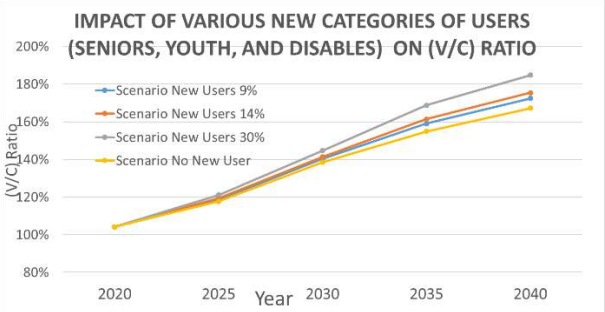

Figure 2. Impact of new categories of users on (V/C) ratio.

Table 4 shows the assumptions and traffic information data regarding the study of the impact of shared and private on volume/capacity ratio. This study assumes an optimistic market penetration of autonomous vehicles. Moreover, the impact of shared ownership and the attractiveness of having more trips by AV is not considered.

Table 4. Information regarding the data and the assumptions used in Fig. 3

County	Brevard County
I-95 segment #	15
Market penetration	Optimistic
Variable under study	Impact of Shared Ownership
Variable's impact 1	0%
Variable's impact 2	25%
Variable's impact 3	75%
Impact of New categories of users	0%
More attractiveness of making trips by AV impact	0%

Figure 3 shows the crucial impact of the shift of the ownership from private cars to shared mobility on the service level of the highway. It can be inferred that shared ownership can significantly increase the service level of the highway and delay the overflow of the highway. For instance, %75 shared ownership would delay the overflow of the highway by six years. CAVs are a naturally attractive type of transportation. The results from figure 3 stresses the importance of planning to encourage people using different kinds of shared mobility as the primary transportation means.

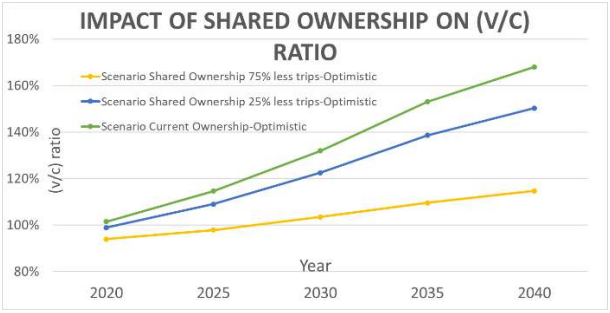

Figure 3. Impact of various shared car ownership on (V/C) ratio.

Table 5 shows the assumptions and traffic information data regarding the study of the impact of larger and shorter time gaps for autonomous vehicles following vehicles driven by people on volume/capacity ratio. This study assumes both pessimistic and optimistic market penetration of autonomous vehicles. Moreover, the impact of shared ownership and the attractiveness of having more trips by AV is also included.

Table 5. Information regarding the data and the assumptions used in Fig. 4

County	Brevard County
I-95 segment #	15
Market penetration	Pessimistic & Optimistic
Variable under study	Impact of Time Gaps of AV Following Vehicles driven by People
Variable's impact 1	Shorter Time Gaps in Optimistic Scenario
Variable's impact 2	Larger Time Gaps in Optimistic Scenario
Variable's impact 3	Shorter Time Gaps in Pessimistic Scenario
Variable's impact 4	Larger Time Gaps in Pessimistic Scenario
Impact of New categories of users	14%
Impact of Shared or private ownership	25%
Impact of More attractiveness of making trips by AV	20%

Figure 4 depicts the impact of large and short time gaps on the capacity regarding both optimistic and pessimistic market penetration. The mentioned time gap can have a 20% impact on (V/C) ratio in 2040. Automated technologies allow shorter headways between the vehicles, which in turn have the potential to increase the capacity of the freeway network and reduce traffic delays significantly. But it is important to remember that small market penetration rates of automated vehicles do not lead to noticeable capacity increase. The potential benefits are likely to be realized at higher penetration into the traffic mix. As a result, it is a crucial variable to consider in modeling for further studies.

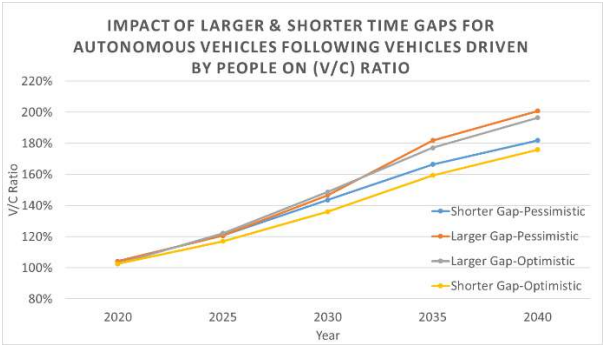

Figure 4. Impact of large and short time gaps for autonomous vehicles following vehicles driven by people on capacity.

Table 6 shows the assumptions and traffic information data regarding the study of the impact of different behavioral scenarios on the volume/capacity ratio. This study assumes an optimistic market penetration of autonomous vehicles. Moreover, the effect of variously shared ownership, the attractiveness of having more trips by AV and the new categories of users is considered.

Table 6. Information regarding the data and the assumptions used in Fig. 5

County	Flagler County
I-95 segment #	5
Market penetration	Optimistic
Variable under study	Behavioral Scenarios
Impact of Time Gap regarding the capacity adjustments	Shorter Time Gaps

Variable's impact 1, **Baseline Scenario**	Variable's impact 2, **Adaptive Scenario**	Variable's impact 3, **Disruptive Scenario**	
9%	9%	30%	New users
0%	75%	0%	Shared or private ownership
0%	0%	20%	More attractiveness

Figure 5 illustrates the impact of three different

behavioral scenarios of the future on the (V/C) ratios. As shown in that figure, the gap between the disruptive scenario and the adaptive or baseline scenario exceeds as passing the time. The gap between the scenarios is showing a critical issue of how proper planning and taking essential measures ahead regarding the adaptive scenario can delay or even enhance the traffic status. Figure 6 shows the threshold (Maximum and Minimum) range of the possible scenario of the future.

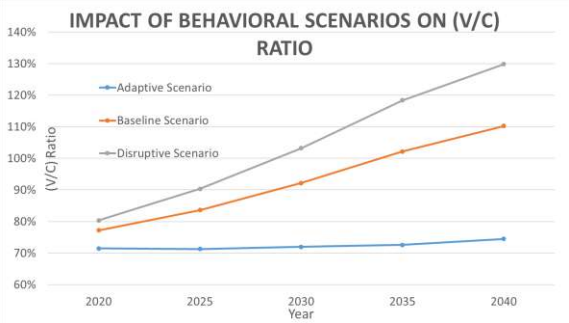

Figure 5. Impact of different behavioral scenarios on (V/C) ratio.

Table 7 shows the assumptions and traffic information data regarding the study of the impact of construction scenarios on the volume/capacity ratio. This study assumes an optimistic market penetration of autonomous vehicles. Moreover, the effect of variously shared ownership, the attractiveness of having more trips by AV and the new categories of users is considered.

Table 7. Information regarding the data and the assumptions used in Fig. 6

County	Brevard County
I-95 segment #	15
Market penetration	Optimistic
Variable under study	Impact of Construction Scenarios
Variable's impact 1	No Lane Construction
Variable's impact 2	2 Lane Construction%
Variable's impact 3	4 Lane Construction%
Variable's impact 4	6 Lane Construction
Impact of New categories of users	14%
Impact of Shared or private ownership	25%
Impact of More attractiveness of making trips by AV	20%

Figure 6 illustrates the impact of constructing new lanes on the (V/C) ratio. As shown, in 2030 there is a need to build two new lanes to have under capacity status, but if instead, four lanes are constructed, the issue will be solved until 2040. It is evident that as the number of lanes increases the impact on the V/C ratio decreases. In other words, the first extra two lanes would provide more utility compared to the next extra lanes. This figure can also be used as a tool to find the optimized time of adding more lanes to the highway not to face congestion issues.

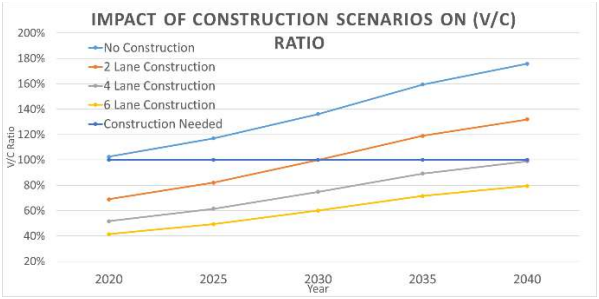

Figure 6. Impact of construction scenarios on (V/C) ratio.

5 Conclusion

This study presents a comprehensive analysis of finding the impact of connected and autonomous vehicles on traffic flow and capacity. This research is develops a fusion model considering the impact of both traffic flow and capacity adjustments based on the literature review. This research not only contributes to the body of knowledge in the transportation field by conducting a comprehensive study to develop a fusion model considering the impact of both traffic flow and capacity adjustments based on the literature review for the highways, but also has important practical applications in managing the investment measures of government agencies and private investors. The insight into the upcoming highway construction needs, with a focus on understanding the disruptive impact of CAVs on highways' performance provided by this study, would improve the resiliency of transportation systems. The findings of the study confirm that connected and autonomous vehicles will increase both traffic flow and capacity, and the increase in flow is higher than the increase in capacity. Shared ownership of passenger vehicles has been found to mitigate the traffic flow. The growth in projected demand for AVs will not be accommodated by a similar increase in the capacity that currently exists, resulting in even greater congestion of the market penetration of AVs. The time to plan the infrastructure necessary for smooth deployment of AVs and avoid congestion due to the projected traffic flow is passing. Meanwhile, the proposed approach provides a more realistic plan for

government agencies and private investors, and as a result, significant savings financially and resource-wise can be achieved. Based on the preliminary results presented in this paper, it can be concluded that federal and local governments should take a proactive approach and began to act. It is a critical issue to think ahead and plan to use limited resources efficiently. Researchers can further investigate the impact of the involved parameters on the emerging technologies to address the upcoming challenges. The directions for future research includes considering the impact of urbanization in dense cities around the world. Some States, due to their logistics and critical location, are subject to facing hurricanes, wildfires, heat waves and other natural disasters, especially regarding the severe climate change predictions, studying the impact of this parameter on the necessary highway infrastructure for the emergency evacuation situations is a must. Moreover, assessing AV impact's sensitivity to different shared use, Public Transportation behavior and urban sprawl growth are also required in better realizing the impact of AVs on the highways' service level.

References

[1] ASCE (American Society of Civil Engineers). Roads Final report, 2017.

[2] Ahmadi, N., Shahandashti, M., Comparative empirical analysis of temporal relationships between construction investment and economic growth in the United States, 2017.

[3] Anderson, J. M. Autonomous Vehicle Technology, a Guide for Policy Makers. RAND Transportation, Space and Technology Program, 2014.

[4] Bierstedt, J., A. Gooze, C. Gray, J. Peterman, L. Raykin, J. Walters. Effects of Next-generation Vehicles on Travel Demand and Capacity: FT Think, 2014.

[5] Brown A., J. Gonder and B. Repac, An Analysis of Possible Energy Impacts of Automated Vehicle, in Road vehicle Automation, Lecture Notes in Mobility pp. 137-153, DOI: 10.1007/978-3-319-05990-7_13, *Springer International Publishing Switzerland*, 2014.

[6] Bilal, M., et al. Big Data in the construction industry: A review of present status, opportunities, and future trends, *Advanced Engineering Informatics*, 2016.

[7] Childress, S., Nichols, B., Charlton, B., Coe, S., Using an activity-based model to explore possible impacts of automated driving. *Presented at 94th Annual Meeting of the Transportation Research Board, Washington DC*, 2015.

[8] Corey, D., Estimating potential increases in travel with autonomous vehicles for the non-driving, elderly and people with travel-restrictive medical conditions, *Transportation Research Part C: Emerging Technologies*, 2016.

[9] Fagnant, D, J. and K. M. Kocleman, preparing a Nation for Autonomous Vehicles, opportunities, barriers and recommendations, Report Prepared for eno Center for Transportation, 2013.

[10] Fagnant, D.J., Kockelman, K., Preparing a nation for autonomous vehicles: opportunities, barriers and policy recommendations. *Transp. Res. Part A* 77, 167–181, 2015.

[11] Gruel, W. and Stanford, J. Assessing the long-term effects of autonomous vehicles: a speculative approach. *Paper presented at the European Transport Conference. Frankfurt*, Germany: Association for European Transport, 2015.

[12] Jerath, K., S. N. Brennan. Analytical Prediction of Self-Organized Traffic Jams as a Function of Increasing ACC Penetration, IEEE Transactions on Intelligent Transportation Systems, vol.13, (4), pp. 1782–1791, 2012.

[13] Kesting, A., M. Treiber, D. Helbing. Enhanced intelligent driver model to access the impact of driving strategies on traffic capacity, Philosophical transactions, 2010.

[14] Lovejoy K, Handy S and Boarnet MG. Impacts of car sharing on passenger vehicle use and greenhouse gas emissions. Technical Background Document, California Environmental Protection Agency, 2013.

[15] Litman, T., Autonomous Vehicle Implementation Predictions, Implication for Transport Planning. Victoria Transport Policy Institute, 2014.

[16] Litman, T., Autonomous Vehicle Implementation Predictions Implications for Transport Planning, Victoria Transport Policy Institute, 2018.

[17] Maurer, M., J. C. Gerdes, B. Lenz, H. Winner, Autonomous Driving, Technical, Legal and Social Aspects, Berlin, Heidelberg: Springer Berlin Heidelberg, 2016.

[18] Motamedi dehkordi, N., Hartmann, M., Impact of Automated Vehicles on Capacity of the German Freeway Network, ITS World Congress Montreal, 2017.

[19] Rodier, C., The Effects of Ride Hailing Services on Travel and Associated Greenhouse Gas Emissions, UC Davis Institute for Transportation Studies, 2018.

[20] Sadat Lavasani Bozorg, A., Potential Implication of Automated Vehicle Technologies on Travel Behavior and System Modeling, FIU, PhD Dissertation, 2016.

[21] Shelton, J., S. Samant, J. Wagner, G. Goodin, E. Seymour, T. Lomax. Revolutionizing Our

Roadways, Modeling the Traffic Impacts from Automated and Connected Vehicles in a Complex, Congested Urban Setting: Transportation Policy Research Center, 2016.

[22] Shladover, S., D. Su, X. Y. Lu. Impacts of Cooperative Adaptive Cruise Control on Freeway Traffic Flow, *Transportation Research Record: Journal of the Transportation Research Board*, vol. No. 2324, 2012.

[23] Shladover et al., Modeling cooperative and autonomous adaptive cruise control dynamic responses using experimental data, California PATH Program of the Institute of Transportation Studies, University of California, Richmond, CA 94804, 2013.

[24] Sivak, M., Schoettle, B., Influence of Current Non-drivers on the Amount of Travel and Trip Patterns with Self-Driving Vehicles. University of Michigan Transportation Research Institute, 2015.

[25] Vander Werf, J., S. Shladover, M. Miller, N. Kourjanskaia. Effects of Adaptive Cruise Control Systems on Highway Traffic Flow Capacity, *Transportation Research Record: Journal of the Transportation Research Board*, vol.1800, pp.78–84, 2002.

[26] Van Arem, B., C. J. G. van Driel, R. Visser. The Impact of Cooperative Adaptive Cruise Control on Traffic-Flow Characteristics, *IEEE, Transaction on Intelligent Transportation*, 2006.

[27] Wallace, R. and G. Sillberg. Self-Driving Cars: The Next Revolution. Center for Automotive Research. Transportation System Analysis Group, 2012.

Study of Construction-Oriented Structural Connectors for a Temporary Bridge

Y.-Y. Yang[a], C.-M. Chang[a], S.-C. Kang[b], and F.-Y. Yeh[c]

[a]Department of Civil Engineering, National Taiwan University, Taiwan
[b]Department of Civil and Environmental Engineering, University of Alberta, Canada
[c]National Center for Research on Earthquake Engineering, Taiwan
E-mail: yybenjamin.yang@gmail.com, changcm@ntu.edu.tw, sckang@ualberta.ca, fyyeh@narlabs.org.tw

Abstract –

Temporary bridges are indeed of need after a critical disaster due to the connectivity and efficient assembly. However, the conventional structural design of these temporary bridges may be limited by the construction requirements. In this study, a new type of structural connectors is developed and beneficial for more effectively assembling ability of temporary bridges. In this development, a construction-oriented design procedure is initiated from a conceptual design and verified by an in-house, small-scale model. This conceptual connector is then modified and analyzed by sophisticated software and finally fabricated for the full-scale use. This design has a bolt-free feature and allows rotational assembly workability. The structural analysis and virtual 3D simulation are conducted to numerically verify the state-of-the-practice connector. The results from the numerical simulation imply the possibility to employ the proposed connector for a temporary bridge.

Keywords –

Bolt-free connectors; Rotational assembly workability; Temporary bridges; Construction-oriented design procedure

1 Introduction

A temporary bridge is indeed of need after a critical disaster because this structure resolves the disruptive transportation of residents and associated resources. In past, the temporary bridge designed by Yeh's team [1] was built up much faster than a commonly used temporary bridge, i.e., a culvert bridge. As analyzed from the construction video in Figure 1. Construction video of a temporary bridge. and in Table 1. Analysis of the temporary bridge construction., the erection of a glass-fiber-reinforced-polymer (GFRP) girder module costed a lot of time and human resources. The construction of the temporary bridge required five workers to adjust the orientation and alignment of this bridge module for assembly and connection. In addition, the workers had to stay at the end of the incomplete bridge structure and to accomplish the assembly, raising a concern about the worker safety. The connection between each bridge module required hundreds of bolts, resulting in tremendous manpower demands. Thus, this task should be improved by a more efficient assembly approach.

Figure 1. Construction video of a temporary bridge.

Table 1. Analysis of the temporary bridge construction.

Structural component	Task	Time[min.]/ labors/difficu-lty [1-10]
Steel segment A	Assembly	15/16/3
Steel segment B	Assembly	15/16/3
Steel segment C	Assembly	15/16/3
H-tower	Assembly	20/14/3
GFRP segment 1	Assembly	20/10/4
GFRP segment 2	Assembly	20/10/4
GFRP segment 3	Assembly	20/10/4
GFRP segment 4	Assembly	20/10/4

GFRP segment 5	Assembly	20/10/4
Steel segment A	Erection	10/7/4
Steel segment B	Erection	10/7/4
Steel segment C	Erection	10/7/4
Steel bridge panel	Installation	30/6/3
H-tower	Erection	20/15/6
GFRP 1	Erection	15/16/8
GFRP 1	Steel cable fastening	15/18/4
GFRP 2	Erection	20/16/8
GFRP 2	Steel cable fastening	20/18/4
GFRP 3	Erection	25/16/8
GFRP 3	Steel cable fastening	20/18/4
GFRP 4	Erection	30/16/8
GFRP 4	Steel cable fastening	20/18/4
GFRP 5	Erection	30/16/10
GFRP bridge panel	Installation	120/6/3

To achieve effective construction, some structural connectors featuring quick assembly and reduced manpower demands were developed. In 1994, the ATLSS system was developed to automate the beam-to-column assembly [2]. This system consisted of a quick-assembly connector and a cable-driven Stewart platform equipped on a crane. Due to expensively required equipment, the ATLSS system needed to be improved with respect to economic feasibility for the construction industry nowadays [3]. In contrast, ConXtech was a technique that provided structural connectors for quick assembly with specific constraints [4]. The ConXtech protected workers from potential risks because the working time on the assembly of structural components (e.g., workers staying at a high position) was reduced. Similarly, Kim *et al.* developed an automated beam-to-column assembly method by integrating special connectors, guiding ropes, and two developed guiding machines [5]. In addition, Liang *et al.* developed a self-rotating hook block that allowed assembling a steel beam to a steel column based on Quicon [6] connection design [7]. All these developments are directed to expedite assembly process without inducing risky manpower in construction.

In this research, the objective is to develop and design a new construction-oriented structural connector for a temporary bridge. In this development, a construction-oriented design procedure is initiated from a conceptual design and verified by an in-house, small-scale model. This conceptual connector is then modified and analyzed by sophisticated software and finally fabricated for the full-scale use. This design has a bolt-free feature and allows rotational assembly workability. The structural analysis and virtual 3D simulation are conducted to numerically verify the state-of-the-practice connector.

2 Construction-oriented structural connector design

A construction-oriented design workflow for the structural connector is proposed in this section. The workflow was iteratively improving the connector design based on a design concept described in the section as well. The section also elaborates the geometry formation.

2.1 Design workflow

Five steps were identified in the workflow in Figure 2. The design workflow for a structural connector. Step 1 is to target a structural component to redesign. The temporary bridge was constructed by connecting bridge segments. We planned to redesign the original connectors between bridge segments for quick bridge assembly. In the Step 2, by taking advantage of existing machineries we proposed possible construction methods. In the research, we aimed to use a mobile crane to assemble a temporary bridge. The following is Step 3 creating an original connector design based on the selected construction method. Finally Step 4 iteratively refines the design by the results of 3D simulation, 3D printed prototype, and finite element analysis.

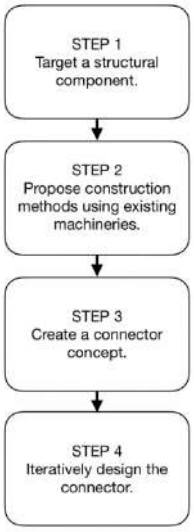

Figure 2. The design workflow for a structural connector.

2.2 Conceptual connectors and requirements

The initial connection concept was formed by a connecting mechanism and an erection method (see Figure 3. The initial connection concept). The connecting mechanism was a gravity-triggered assembly with a designed connector. When the attached connector is adjusted to the designed position a structural component applies the self-weight to finish the connection. Afterwards, the bridge segment would be temporarily fixed for workers finalizing the rest connections. The erection method was that a mobile crane lifts one end of the structural component, transports the component to where the attached connector was being placed at the designed position, and finally the crane releases the load to trigger the assembly of two structural components. Moreover, the structural behavior of the structural connector was also considered in the connection concept. The connection design must resist two axial forces, a torsional force, and a shear force. Additionally, the designed connector was attached onto the top of the connecting face of the bridge segment, and a pin-hole connection was at the bottom of the connecting face. Therefore, the designed connector and the pin-hole connection can resist negative moments and positive moments respectively.

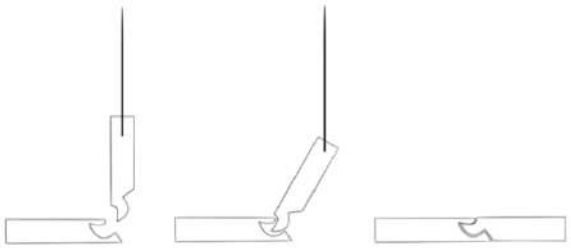

Figure 3. The initial connection concept.

2.3 Connector geometry

The workability, the strength, and the manufacturability are three major factors influencing each generation of the connector design. Because there is no definite approach to consider all major factors in a design iteration, we refined the connector design by means of divide-and-conquer approach in each design iteration. For example, although the initial connection concept met the requirements of the workability and the strength, the connection remained a challenge of producing the female connector. Therefore, for this challenge, we only focused on the production of the connector, not on the workability and the strength. We reformed the connector geometry, and the connector became the assembly of producible pieces as Figure *4*. The reformed connector. Testing the workability of connector design can be easily executed by virtual 3D simulation with physics engine and 3D printing technology. In a macro perspective, the virtual 3D simulation can simulate the assembly of the bridge segment with the designed connector. The virtual simulation helps the designer obtain the big picture of the connector application in temporary bridge construction. In contrast, the 3D printing technology can identify the problems of production from a micro perspective. Take the study for example, the tolerance and the 3D model to produce could be adjusted by taking the 3D printed prototype as a reference. The structural behavior of the designed connector can be efficiently analyzed by Finite Element Method. The manufacturability verification of the designed connector is taking the technical constraints of manufacture into the design consideration.

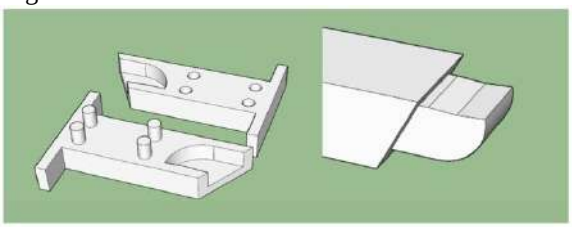

Figure 4. The reformed connector.

3 Results

This section shows the finalized connector design and two feasibility tests including a virtual assembly simulation and a structural analysis.

3.1 Finalized connector design

The final design of the connection was formed by a male connector and a female connector (see Figure 5. The finalized connector design (a) male connector, (b)

female connector). Each of both was constituted of two same designed plates and an end plate. When connecting to the female connector the joint at the top of the male connector attaches onto the groove on the top of the female connector. As a result, the male connector may rotate about the joint and then complete the connection.

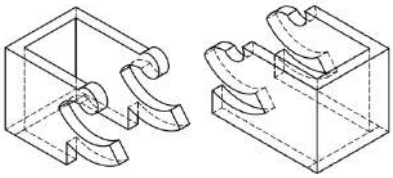

Figure 5. The finalized connector design (a) male connector, (b) female connector.

3.2 Virtual assembly simulation

We simulated the connection process in a virtual environment (see Figure 6. The virtual assembly simulation). A designed connector was attached to the bridge segment. The assembly simulation only tested the designed connection while there would be five other pin-hole connections between two bridge segments in an actual case. The simulation indicated that the alignment of the bridge segment directly influenced the operation to succeed the connection. Once the female connector and the male connector were not placed on the same plane, the connection would be stuck until the male connector was adjusted to be on the same plane of the female connector.

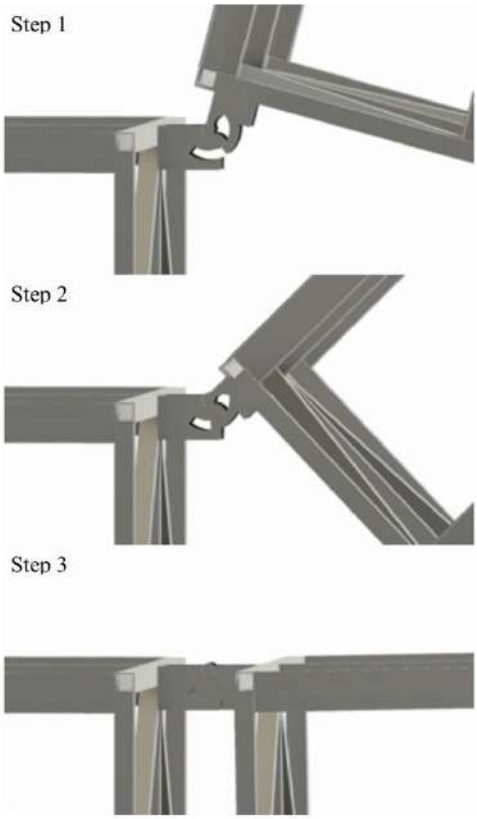

Figure 6. The virtual assembly simulation.

3.3 Results of structural analysis

We conducted four structural analyses using finite element method. Each analysis applied the designed load of the connection between bridge segments and defined the end plate of the female connector as a fixed end. The results showed the Von Mises stress.

(1) The compression test result in Figure 7. The compression test result represented that the weakest occurred at the upper part of the connection.

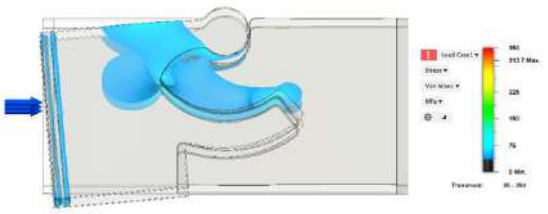

Figure 7. The compression test result.

(2) The tension test result in Figure 8. The tension test result showed that the weakest area occurred around the turning point of two discontinuous curves.

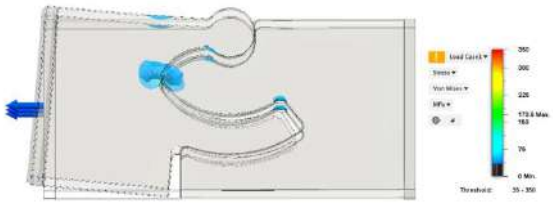

Figure 8. The tension test result.

(3) The torsion test result in Figure 9. The torsion test result showed perfect resistant to the designed torsion.

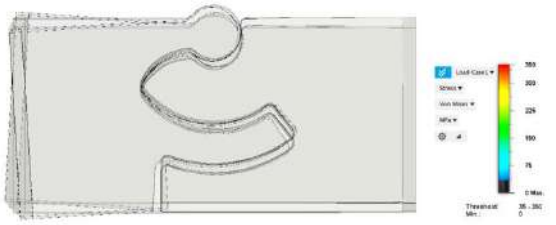

Figure 9. The torsion test result.

(4) The shear test result in Figure 10. The shear test result represented that the joint was weakest part when applying the designed load on the top surface of the male connector.

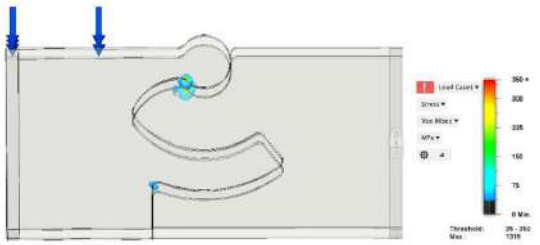

Figure 10. The shear test result.

4 Conclusion

This study proposed and designed a new type of structural connectors featuring bolt-free and rotational-assembly connection. This connector was derived from a conceptual design in the viewpoint of construction convenience and fabricated through a 3D printer. The workability of this connector was numerically and experimentally verified using a 3D manipulation platform and a small-scale model, respectively. Before turning this connector for the real-world use, the productivity and mechanics were also discussed and analyzed. Therefore, this new type of structural connectors was ready for a temporary bridge and will be experimentally evaluated in the future study.

References

[1] Yeh, F.-Y., et al., *A novel composite bridge for emergency disaster relief: Concept and verification.* Composite Structures, 2015. 127(Supplement C): p. 199-210.

[2] Vincent Viscomi, B., W.D. Michalerya, and L.-W. Lu, *Automated construction in the ATLSS integrated building systems.* Automation in Construction, 1994. 3(1): p. 35-43.

[3] Viana, D.D., I.D. Tommelein, and C.T.J.E. Formoso, *Using Modularity to Reduce Complexity of Industrialized Building Systems for Mass Customization.* 2017. 10(10): p. 1622.

[4] Renz, B., *Innovative Connections*, in *Modern Steel Construction. AISC: Chicago USA August*. 2005.

[5] Kim, C.-W., et al., *Advanced Steel Beam Assembly Approach for Improving Safety of Structural Steel Workers.* Journal of Construction Engineering and Management, 2016. 142(4).

[6] *The Steel Construction Institute: Quicon® design guide to BS 5950-1*. 2005 [cited 2018 15 March]; Available from: http://www.newsteelconstruction.com/wp/quicon-design-guide-to-bs-5950-1/.

[7] Liang, C.-J., S.-C. Kang, and M.-H. Lee, *RAS: a robotic assembly system for steel structure erection and assembly.* International Journal of Intelligent Robotics and Applications, 2017.

Through-Wall Object Recognition and Pose Estimation

Ruoyu Wang[a], Siyuan Xiang[a] Chen Feng[a]*, Pu Wang[b], Semiha Ergan[a], Yi Fang[a]

[a]Tandon School of Engineering, New York University, Brooklyn, NY 11201, USA
[b]Mitsubishi Electric Research Labs (MERL), Cambridge, MA 02139, USA
E-mail: {ruoyuwang, siyuan, cfeng, semiha, yfang}@nyu.edu, pwang@merl.com

Abstract -

Robots need to perceive beyond lines of sight, e.g., to avoid cutting water pipes or electric wires when drilling holes on a wall. Recent off-the-shelf radio frequency (RF) imaging sensors ease the process of 3D sensing inside or through walls. Yet unlike optical images, RF images are difficult to understand by a human. Meanwhile, in practice, RF components are often subject to hardware imperfections, resulting in distorted RF images, whose quality could be far from the claimed specifications. Thus, we introduce several challenging geometric and semantic perception tasks on such signals, including object and material recognition, fine-grained property classification and pose estimation. Since detailed forward modeling of such sensors is sometimes difficult, due to hidden or inaccessible system parameters, onboard processing procedures and limited access to raw RF waveform, we tackled the above tasks by supervised machine learning. We collected a large dataset of RF images of utility objects through a mock wall as the input of our algorithm, and the corresponding optical images were taken from the other side of the wall simultaneously as the ground truth. We designed three learning algorithms based on nearest neighbors or neural networks, and report their performances on the dataset. Our experiments showed reasonable results for semantic perception tasks yet unsatisfactory results for geometric ones, calling for more efforts in this research direction.

Keywords -

Through-Wall Imaging; Object Recognition; Pose Estimation; Deep Learning

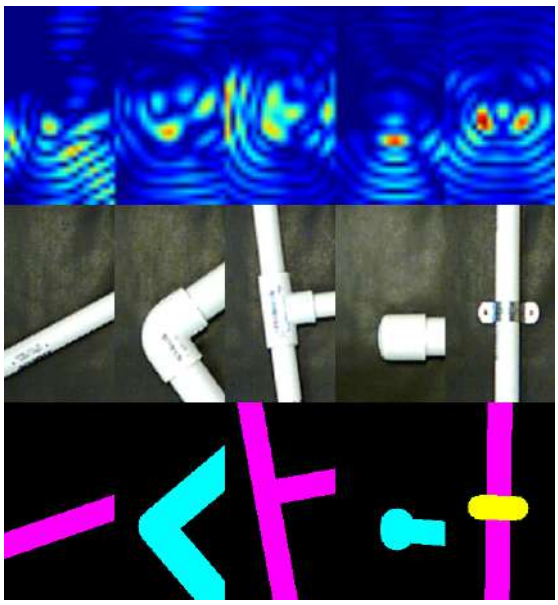

Figure 1. Overview of our problem. The first row are Walabot-returned 3D radar images (sliced at 1cm-depth for visualization) through a wooden board over the device. The second row are photos taken from the opposite side of the wooden board over Walabot. The third row are visualizations of geometric and semantic information of PVC pipe components estimated by our method. Different classification results are best viewed in color.

1 Introduction

It is often necessary to detect or even recognize the occluded objects on job sites for safety reasons. Ground penetrating radar (GPR) system has been applied for subsurface object detection. For example, GPR system can be used to survey the geological information on the construction site to predict potential construction safety hazards [1]. Signal detected by GPR can also be fused with other data. Li et al. [2] proposed a method to survey and visualize underground utilities by integrating the pre-processed GIS data with GPR signal, whose location is determined by RTK GPS.

Besides GPR, through-wall imaging techniques are widely used in fields such as fire protection, hostage rescue, flaw detection, and building construction. It is especially useful to estimate the content and structure beyond line-of-sight during maintenance and renovation. Abdel et al. [3] reviewed the state-of-the-art techniques of location and condition assessment for underground water pipelines. By employing radio frequency (RF) sensors, a through-wall imaging system can extract information through obstructions, which is impossible by using conventional line-of-

*Chen Feng is the corresponding author.

sight sensors, such as optical cameras or LIDAR.

With the development of RF sensors and signal processing algorithms, many through-wall imaging techniques have been proposed. Ahmad et al. [4] provided a method of digital beam-forming to capture 3D images behind a single uniform wall. Zhuge et al. [5] have created a real-time 3D near-field imaging algorithm with the application of Fast Fourier Transform (FFT) for 2-D multiple-input-multiple-output (MIMO) sensor array. By implementing their methods, a 3D image of object reflectivity can be formed with high accuracy and computational efficiency. In 2017, Karanam et al. [6] used WiFi router and WLAN card mounted on two UAVs to get the 3D image of an area surrounded by brick walls. These techniques are well designed in the phase of signal processing and imaging, with clearly defined forward sensor models and wave propagation model. Besides, to get higher resolution images, their antenna arrays are relatively large. In Zhuge's method, the self-designed antenna array is 0.54 m wide along both azimuth and elevation directions [5], and in Ahmad's method, their simulated antenna array can reach 2.4m [4]. Such large antenna arrays are less portable for mobile robotics applications. Also, as far as we are aware of, not much research has been done for multi-class object recognition from through-wall images.

As we mentioned before, through-wall imaging techniques benefit from increasingly accessible inexpensive off-the-shelf RF sensors. Walabot, a portable UWB-based (ultra-wideband) sensor developed by Vayyar Imaging Ltd, can provide API for users to capture 3D RF images. It has about the same size as a cell phone, drawing power and sending data through a single USB cable. Thus it can be easily incorporated in mobile robotic applications. However, due to commercial reasons, some key parameters of the Walabot sensor model are unknown to users, so detailed forward modeling of the sensor's physical process and its calibration is either impractical or cost-inefficient. Besides, the small aperture size causes low ambiguity resolution, resulting in ripple-like artifacts in the signal, as shown in the top of Figure 1. In practice, RF components are often subject to hardware imperfections (e.g., the phase noise of oscillators and mixers, nonlinear distortion from RF amplifiers, mutual coupling between antennas [7, 8]), resulting in distorted RF images, whose quality is far from the claimed specifications in user manuals. This distortion may be more severe for low-cost RF imaging systems [9]. Therefore, objects are difficult to be recognized intuitively by humans from these 3D images.

Fortunately, with the help of machine learning, some categorical and geometric information of objects could still be restored from raw 3D images, such as material, size, shape, and pose, etc. Moreover, these utility objects, such as PVC (polyvinyl chloride) pipe components, have important fine-grain attributes including thickness and contents (full of water or empty). They are all crucial for the aforementioned construction applications. The bottom of Figure 1 illustrates several results of our method based on the Convolutional Neural Network (CNN).

We highlight the contribution of our paper as follows:

- We introduce several challenging geometric and semantic tasks for better understanding and utilizing RF-based through-wall images, including materials recognition, fine-grained property classification and pose estimation.
- We propose to use machine learning methods to address the above tasks while bypassing detailed RF sensor modeling and electromagnetic wave propagation modeling that is sometimes inaccessible to end users, which showed promising results.
- We develop methods for efficiently collecting a large number and variety of through-wall images using an off-the-shelf RF sensor, with ground truth automatically generated from machine vision.
- We will make our dataset publicly available to stimulate more research in this direction.

2 Related Work

As previously mentioned, there are many research works aimed at image formation from RF signals. However, another branch of research is focused on extracting information from radar images or even raw signals. Among those, there are some works on RF object recognition and pose estimation, which is closely related to this paper.

Object Recognition. Yeo et al. [10] trained a random forest classifier for object recognition using handcrafted statistical features from raw signals. Their method has been tested for object classification, transparent material classification, and body part classification. Their method reaches over 90% accuracy on all three tasks. However, their method was not implemented with obstructions between the sensor and targets. Avrahami et al. [11] developed an activity recognition method through a cashier's counter, using a Walabot sensor, which is the same sensor used in our paper. Their method projects the 3D images sensed by Walabot to 2D plane, then extracts handcrafted statistical features for classification. By using an SVM classifier, their method reaches 90.5% accuracy. Zhao et al. [12] used RF signals reflected from a person's body to recognize one's emotion by extracting the person's heartbeats. Their method reaches comparable accuracy to on-body ECG monitors. All these above methods need handcrafted feature extractions. Wang et al. [13] proposed a method for gesture recognition using Google Soli [14], based on deep learning. However, Soli is a dedicated and customized millimeter wave radar system, which operates at a much higher frequency than Walabot, thus has a

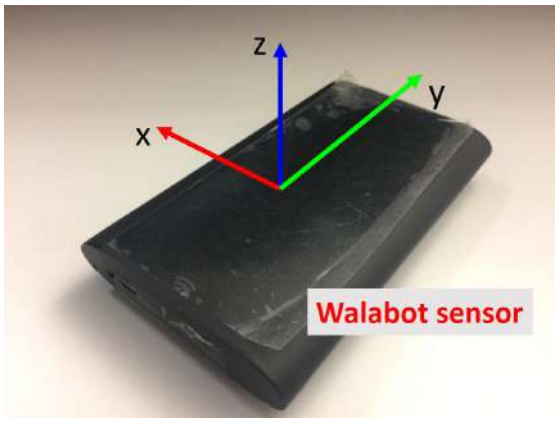

Figure 2. Walabot Coordinate System. The z axis is towards the object being detected.

higher spatial resolution. Also, there were no obstructions between the sensor and the target in their work.

Pose Estimation. Pose estimation from optical sensors has been studied for a long time [15–17]. However, pose estimation from RF sensors currently has not attracted a lot of research attention. Adib et al. has done a lot of work on pose estimation using RF sensors. In 2014, Adib et al. [18] proposed a 3D motion tracking system, WiTrack, which can track the 3D motion of a human, and estimate the direction of a pointing hand. Then they [19] presented the RF-Capture system, which can track the limbs of a human body. Most recent research on pose estimation from RF signal is from Zhao et al. [20]. In this paper, they create a deep neural network approach that estimates human 2D poses through the wall. Our work is inspired by this line of research, yet our focus is on construction robotics applications that require a different set of semantic and geometric perception tasks.

3 Method

3.1 Sensor Introduction

Walabot is an ultra-wideband MIMO array that operates at frequency 3.3-10 GHz. The model used in this research has 18 antennas. The coordinate system is defined as illustrated in Figure 2. The sensing arena used in our experiment is -5 to 5 cm in x direction, -9 to 9 cm in y direction and 1 to 10 cm in z direction. The resolution is set to 0.5 cm. In this case, the raw 3D image sensed by Walabot is a tensor of dimension $37 \times 21 \times 19$.

3.2 Dataset Design

Our dataset is designed for two tasks. The first task is material-based classification and pose estimation for linear objects. In this task, we set 5 classes of objects made from different materials. They are all common in-wall structures, including cable, wooden stud, steel pipe, PVC pipe, and background. The pose estimation task is designed only for 3 classes of straight objects: cable, wooden stud, and steel pipe. For PVC pipes, multiple shapes of pipe components are considered, and their pose estimation is designed in the second task.

The second task is more fine-grained compared to the first one, which focuses only on PVC pipes. This task contains multi-label classification and pose estimation. The PVC pipe components are classified from three aspects:

- **Thickness.** We use two types of PVC pipes in our experiment, one is 1/2" thick, the other is 1" thick. We use binary labels on these two types of pipe.
- **Content.** The PVC pipes are either full of water or empty, which is another binary classification problem.
- **Shape.** The PVC pipe components in the sensing arena are classified as 5 shapes: straight, elbow, tee, end and strap. Different shapes of objects have different ways of pose parameterization, as Figure 3 shows. It is worth to mention that, for straight components, two translational parameters x and y are enough to characterize the pose. For other types of components, two translational parameters x, y and one rotational parameter θ are used to characterize the pose. The specifications of our dataset are listed in the experimental part. For straight components, the pose is described by the coordinates of the foot of the perpendicular from the original point to the line. For elbow components, the pose is described by the coordinates of the intersecting point of the two pipes, and the angle of the angular bisector. For tee components, the pose is described by the coordinates of the intersecting point, and the angle of the pipe which constitute the vertical part of letter T. For end component, the pose is described by the coordinates of the center of the cap, and the angle of the ray away from the cap. For the strap component, the pose is described by the coordinates of the strap and the angle of the perpendicular line. The pose of the straight components also applies in task 1.

Note that we currently ignore situations when multiple objects appear simultaneously in the sensing arena, and only focus on RF images of a clean background, which is not very uncommon in practices.

3.3 Data Collection

Figure 4 shows our data collection system. The wooden board here serves as the mock wall's shell. Walabot is

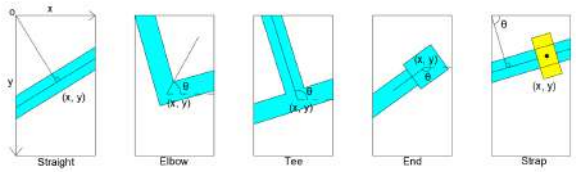

Figure 3. The definition of pose for 5 shapes of PVC pipe components.

placed right under the wooden board. Objects are placed on the upper surface of the wooden board with different poses against a black background. The camera takes photos of the objects, and synchronously, Walabot records the data it sensed from below the board. The photos are warped to the cross-section of the upper surface and the sensing arena using a homography prior to any processing. This allows us to also employ the cross-modal data annotation strategy like in [20]. But we do not need a pre-trained deep neural network to get the object poses from a camera. Instead, we developed a simple marker-based approach to track object poses from a camera, which is very robust under our controlled lab environment. This method is based on estimating the skeletons of color tapes. Figure 5 shows the procedure of pose estimation from color tapes.

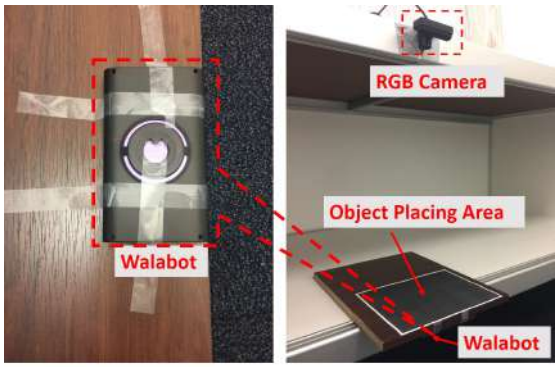

Figure 4. Cross-modal Data Collection System. RGB camera is placed above the object placing area with a black background while Walabot is placed under the object placing area (on the other side of the wooden board). Therefore, RF signals and images of the object can be collected simultaneously. The left image shows the bottom view of the Walabot in the right image.

Color Statistics. The tape is placed against the background, then the mean RGB value of pixels on the color tape and standard deviation of the distances of pixels on the color tape to the mean RGB value is calculated respectively.

Find Color Tape. For each pixel on the image taken by the camera, calculate the distance to the mean RGB value. If the distance is less than a certain threshold times the standard deviation, this pixel is classified as that color. In this case, the mask of color tape is created. Small holes on the mask are closed by morphological operations.

Figure 5. Ground truth pose generation. From left to right: Warped image, detected red mask, detected green mask, green and red tape skeletons estimation. The pose of corresponding objects can be calculated according to the skeleton of color tapes.

Skeleton Extraction. For the color tape mask image, detect line segments using LSD [21]. Merge the two longest line segments by averaging their closest end points. The merged new line segment is regarded as the skeleton of the color tape. The pose of the object is then calculated according to the new segment.

3.4 Baseline and Proposed Methods

To show the superiority of our proposed CNN-based method, we compared it with two baseline methods based on K-Nearest Neighbors (KNN) and Multi-Layer Perceptron (MLP) in all classification tasks respectively. The two baseline methods need hand-craft features, which come from Principal Component Analysis (PCA). Unlike the two baseline methods, our proposed CNN-based method does not need hand-craft features. Instead, the features are learned by the neural network.

PCA+KNN: We stretch the 37×21×19 tensor to a 14763 dimension vector. We use PCA to reduce its dimension to 5. Then a KNN classifier is applied to these 5-dimensional vectors.

PCA+MLP: We use PCA to reduce the tensor to 10 dimensions. There are 3 hidden layers in our MLP classifier with 20, 40 and 20 neurons respectively. The number of neurons in the output layer depends on the classification task.

CNN: Our CNN-based method has a share-weight structure. The input tensor is treated as a 19-channel image. After 5 interleaved 3×3 convolution layers and 2×2 max pooling layers, the tensor is reduced to a 512-dimension vector. Then this vector is sent to different sub-networks for different purposes. In task 1, the vector

is sent to a classification sub-net which predict the materials and a regression sub-net which estimate the poses of straight objects. In task 2, the vector is sent to three classification sub-nets which predict the thickness, content, and shape of the object, and a regression sub-net which estimates the poses of different PVC pipe components. The total loss function is the weighted sum of the losses of each sub-net. The total loss functions for the two tasks are formulated as following (**w** is the set of learnable network parameters):

Task 1:

$$J(\mathbf{w}) = -\frac{1}{N}\sum_{i=1}^{N}(\sum_{c=1}^{5} \underbrace{y_c^{(i)} \log \hat{p}_c^{(i)}}_{\textbf{classification loss}} + C_i\lambda_0 \underbrace{\|\mathbf{x}_i - \hat{\mathbf{x}}_i\|^2}_{\textbf{translational loss}}) \tag{1}$$

Task 2:

$$\begin{aligned} J(\mathbf{w}) = -\frac{1}{N}\sum_{i=1}^{N}(\sum_{l=1}^{3}\sum_{c=1}^{K_l} \underbrace{{}^{l}y_c^{(i)} \log {}^{l}\hat{p}_c^{(i)}}_{\textbf{classification loss}} \\ + \lambda_0 \underbrace{\|\mathbf{x}_i - \hat{\mathbf{x}}_i\|^2}_{\textbf{translational loss}} + C_i\lambda_1 \underbrace{D(\theta_i, \hat{\theta}_i)^2}_{\textbf{rotational loss}}) \end{aligned} \tag{2}$$

Here, c represents different classes; N is the number of training samples; y, $\mathbf{x}$, and θ are the ground truth values for label, translational vector, and rotational angle respectively; $\hat{p}$, $\hat{\mathbf{x}}$, and $\hat{\theta}$ are the predicted values for class probability, translational vector, and rotational angle respectively, which are functions of $\mathbf{w}$. λ_0 and λ_1 are weight coefficients of the translational and rotational loss, and both of them are hyperparameters. In task 1, $C_i = 0$ when the ith sample is "no object" or PVC pipe, in other cases, $C_i = 1$. In task 2, $C_i = 0$ when the shape of the ith sample is straight, in other cases, $C_i = 1$. We use circular distance for angular loss, since θ is in [-π, π), the loss should be their shortest distance on a circle. $D(\theta, \hat{\theta}) = |\theta - \hat{\theta}|$, when $|\theta - \hat{\theta}| < \pi$. $D(\theta, \hat{\theta}) = 2\pi - |\theta - \hat{\theta}|$, when $|\theta - \hat{\theta}| >= \pi$.

4 Experiments

For both of the two tasks, our CNN based method is trained 500 epochs with batch size of 10. λ_0 and λ_1 are both set to 10. We choose Adam optimizer with learning rate 0.0001. The confusion matrix and accuracy are calculated to evaluate the performance of classification. Root Mean Square Error (RMSE) is used to characterize the accuracy of pose estimation. Compared to the two baseline methods, PCA+KNN and PCA+MLP, our CNN based method shows better performance in overall accuracy for all experiments. Furthermore, the CNN based method is more efficient than the PCA+KNN method, without storing training data for prediction.

4.1 Material Classification and Pose Estimation

Figure 6 shows the classification result of task 1. Bkg., Cb., S.P., W.S., P.P. represent background, cable, steel pipe, wooden stud and PVC pipe respectively. The overall accuracy of our CNN based method far exceeds the other two methods, especially for the classification result of Cb.. Classification accuracy on all 5 classes exceeds 95%. For pose estimation, Figure 10 shows that our CNN-based method can achieve the overall error around 1.3 cm in both x and y directions on relatively large experimental objects. The translational error of pose estimation for straight objects in our experiment is 1.8 cm. For all types of objects, steel pipes have the highest pose estimation accuracy, due to their high reflectivity to RF waves.

4.2 Thickness, Content, Shape Classification and Pose Estimation

Figure 7, 8, 9 show our thickness, content and shape classification results for task 2 respectively.

In the thickness classification experiment, our CNN based method outperforms the other two methods, with an overall 0.90 accuracy, while the accuracy of the PCA+KNN method and PCA+MLP method is 0.66 and 0.75 respectively.

For content classification, our PCA+MLP baseline method has overall 0.92 accuracy, slightly lower than the CNN based method, whose overall accuracy is 0.98. The relatively high accuracy of the CNN based method showcases that our algorithm is quite suitable for content classification. Besides, the high reflectivity of water makes the signals very distinguishable between full and empty PVC pipes.

However, even using the CNN-based method, our experimental result of the overall accuracy of the shape classification is not satisfying, compared to material, content and thickness classification, with only 0.82 of accuracy overall. We think it might be caused by noise generated during the scanning process. Either pre-processing the RF signals to filter out noise or using larger training dataset might improve our experimental result.

Figure 11 shows the result of the pose estimation for the 5 shapes of PVC pipe components. Notice that straight shaped object does not need any rotational parameter to represent its pose, thus the rotational error ϵ_θ is not estimated in our experiment result. The overall error in x axis and y axis is 1.0 cm and 1.5 cm respectively. The translational error is 1.8 cm and the rotational error is 47.6 degree. Note that for all shapes of objects, error in x-axis is always smaller than the error in y-axis, which could be due to the arrangement of antennas of the sensor. Compared to translational error, rotational error is very large. The source of error could come from the noise of

Overall Accuracy: 0.78 Overall Accuracy: 0.85 Overall Accuracy: 0.98

Figure 6. Material Classification Confusion Matrix. 120, 119, 120, 120, 402 training data for Bkg., Cb., S.P., W.S., P.P. (background, cable, steel pipe, wooden stud ,and PVC pipe), respectively.

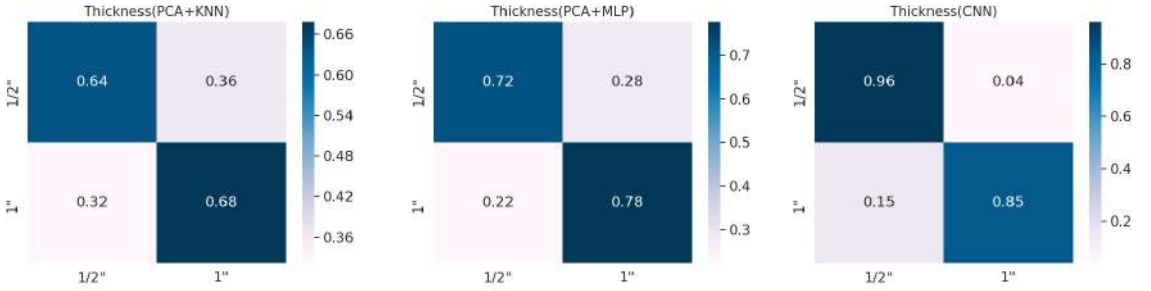

Overall Accuracy: 0.66 Overall Accuracy: 0.75 Overall Accuracy: 0.90

Figure 7. Thickness Classification Confusion Matrix. 200 and 202 training data for 1/2" thick and 1" thick PVC pipe respectively.

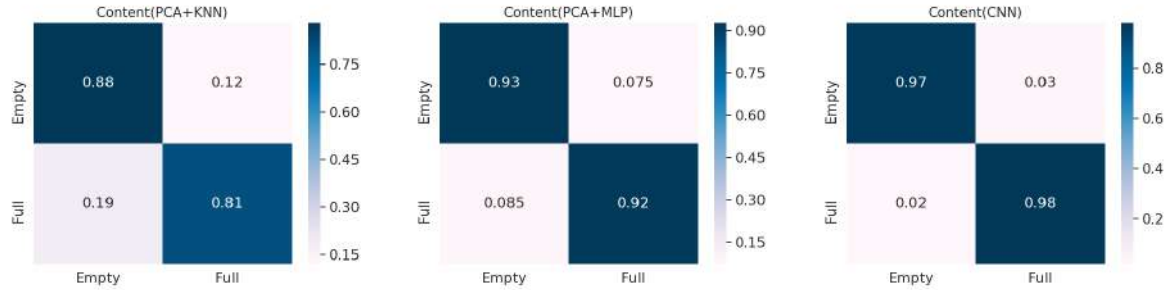

Overall Accuracy: 0.85 Overall Accuracy: 0.92 Overall Accuracy: 0.98

Figure 8. Content Classification Confusion Matrix. 200 and 201 training data for PVC pipes empty of water and filled with water respectively.

the signal, or the sensor's non-sensitivity to rotation.

5 Conclusions

In this paper, we explored the feasibility of using a CNN-based method for through-wall object recognition and pose estimation. With the CNN-based method, we could achieve very high performance on material, thickness, content classification for common in-wall structures. Our proposed method shows a large potential of application in construction industry.

Limitations and Discussions. However, there are some limitations in our proposed method. For the shape classification of five different PVC pipes, the overall accuracy is not satisfying, which calls for more efforts in this research direction. As discussed in the experimental part, we would

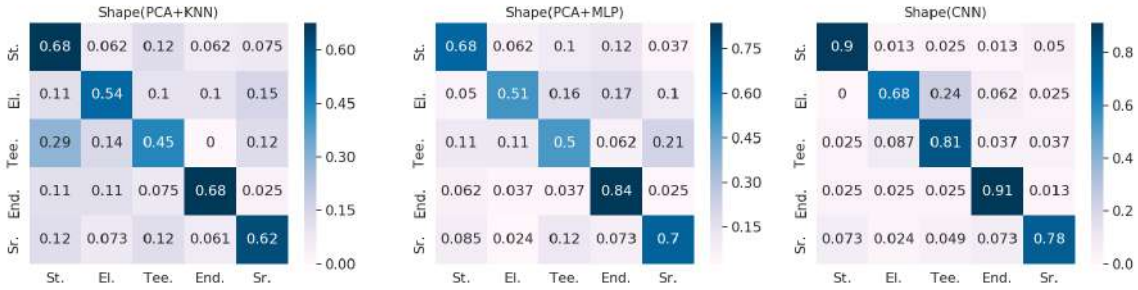

Overall Accuracy: 0.59 Overall Accuracy: 0.64 Overall Accuracy: 0.82

Figure 9. Shape Classification Confusion Matrix. 80 training data for shape Sr., End., Tee., El. respectively, and 82 training data for St..

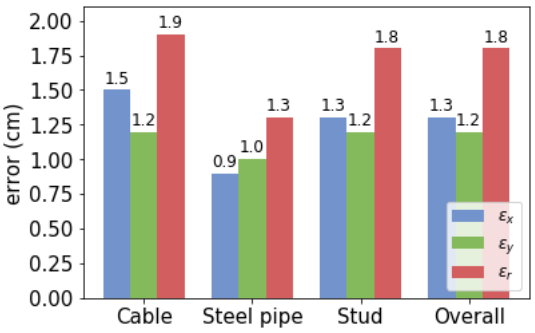

Figure 10. Pose estimation accuracy for Task 1. ϵ_x is the RMSE in x-axis, and ϵ_y is the RMSE in y-axis. Translational error $\epsilon_r = \sqrt{\epsilon_x^2 + \epsilon_y^2}$.

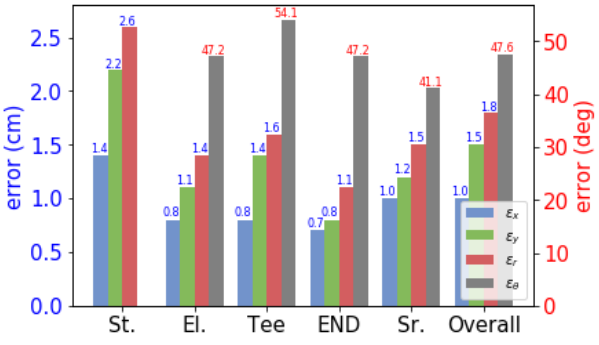

Figure 11. Pose estimation accuracy for Task 2. Translational error is defined the same as in task 1, and rotational error ϵ_θ is RMSE of θ. St., El., Tee, END, and Sr. represents straight, elbow, tee, end, and strap shape respectively.

test two possible solutions, filtering out noise or using a larger dataset, to improve the shape classification result in the future.

Future Work. One future work we are aiming towards is a useful application that can generate a detailed plumbing map behind a wall. We believe by generating such plumbing map, the designers and workers can retrieve the object information in the wall more easily.

References

[1] Xinjian Tang, Weizhong Ren, Tao Sun, and Zhicheng Zhang. Rock structures analysis from gpr radargram based on music method. In *Advanced Ground Penetrating Radar (IWAGPR), 2017 9th International Workshop on*, pages 1–4. IEEE, 2017.

[2] Shuai Li, Hubo Cai, and Vineet R Kamat. Uncertainty-aware geospatial system for mapping and visualizing underground utilities. *Automation in Construction*, 53:105–119, 2015.

[3] Mostafa Abdel-Aleem, Claude C Chibelushi, and Mansour Moniri. Multisensor data fusion for the simultaneous location and condition assessment of underground water pipelines. In *2011 International Conference on Networking, Sensing and Control*, pages 416–421. IEEE, 2011.

[4] Fauzia Ahmad, Yimin Zhang, and Moeness G Amin. Three-dimensional wideband beamforming for imaging through a single wall. *IEEE Geoscience and remote sensing letters*, 5(2):176–179, 2008.

[5] Xiaodong Zhuge and Alexander G Yarovoy. Three-dimensional near-field mimo array imaging using range migration techniques. *IEEE Transactions on Image Processing*, 21(6):3026–3033, 2012.

[6] Chitra R Karanam and Yasamin Mostofi. 3d through-wall imaging with unmanned aerial vehicles using wifi. In *Proceedings of the 16th ACM/IEEE International Conference on Information Processing in Sensor Networks*, pages 131–142. ACM, 2017.

[7] Cheng-Po Liang, Je-hong Jong, Wayne E Stark, and Jack R East. Nonlinear amplifier effects in communications systems. *IEEE Transactions on Microwave Theory and Techniques*, 47(8):1461–1466, 1999.

[8] Thomas H Lee and Ali Hajimiri. Oscillator phase noise: A tutorial. *IEEE journal of solid-state circuits*, 35(3):326–336, 2000.

[9] Emil Bjornson, Michail Matthaiou, and Mérouane Debbah. Massive mimo systems with hardware-constrained base stations. In *IEEE International Conference on Acoustics, Speech and Signal Processing (ICASSP)*, pages 3142–3146. IEEE, 2014.

[10] Hui-Shyong Yeo, Gergely Flamich, Patrick Schrempf, David Harris-Birtill, and Aaron Quigley. Radarcat: Radar categorization for input & interaction. In *Proceedings of the 29th Annual Symposium on User Interface Software and Technology*, pages 833–841. ACM, 2016.

[11] Daniel Avrahami, Mitesh Patel, Yusuke Yamaura, and Sven Kratz. Below the surface: Unobtrusive activity recognition for work surfaces using rf-radar sensing. In *23rd International Conference on Intelligent User Interfaces*, pages 439–451. ACM, 2018.

[12] Mingmin Zhao, Fadel Adib, and Dina Katabi. Emotion recognition using wireless signals. In *Proceedings of the 22nd Annual International Conference on Mobile Computing and Networking*, pages 95–108. ACM, 2016.

[13] Saiwen Wang, Jie Song, Jaime Lien, Ivan Poupyrev, and Otmar Hilliges. Interacting with soli: Exploring fine-grained dynamic gesture recognition in the radio-frequency spectrum. In *Proceedings of the 29th Annual Symposium on User Interface Software and Technology*, pages 851–860. ACM, 2016.

[14] Jaime Lien, Nicholas Gillian, M Emre Karagozler, Patrick Amihood, Carsten Schwesig, Erik Olson, Hakim Raja, and Ivan Poupyrev. Soli: Ubiquitous gesture sensing with millimeter wave radar. *ACM Transactions on Graphics (TOG)*, 35(4):142, 2016.

[15] Alexander Toshev and Christian Szegedy. Deeppose: Human pose estimation via deep neural networks. In *Proceedings of the IEEE conference on computer vision and pattern recognition*, pages 1653–1660, 2014.

[16] Alejandro Newell, Kaiyu Yang, and Jia Deng. Stacked hourglass networks for human pose estimation. In *European Conference on Computer Vision*, pages 483–499. Springer, 2016.

[17] Zhe Cao, Tomas Simon, Shih-En Wei, and Yaser Sheikh. Realtime multi-person 2d pose estimation using part affinity fields. *arXiv preprint arXiv:1611.08050*, 2016.

[18] Fadel Adib, Zachary Kabelac, Dina Katabi, and Robert C Miller. 3d tracking via body radio reflections. In *NSDI*, volume 14, pages 317–329, 2014.

[19] Fadel Adib, Chen-Yu Hsu, Hongzi Mao, Dina Katabi, and Frédo Durand. Capturing the human figure through a wall. *ACM Transactions on Graphics (TOG)*, 34(6):219, 2015.

[20] Mingmin Zhao, Tianhong Li, Mohammad Abu Alsheikh, Yonglong Tian, Hang Zhao, Antonio Torralba, and Dina Katabi. Through-wall human pose estimation using radio signals. In *The IEEE Conference on Computer Vision and Pattern Recognition (CVPR)*, June 2018.

[21] Rafael Grompone Von Gioi, Jeremie Jakubowicz, Jean-Michel Morel, and Gregory Randall. Lsd: A fast line segment detector with a false detection control. *IEEE transactions on pattern analysis and machine intelligence*, 32(4):722–732, 2010.

Schedule Uncertainty Analysis System Framework to Manage and Allocate Historical Data for Industrial Construction Project

I. Yoon[a], H.-S. Lee[a], M. Park[a], J.G. Lee[a], and S.-S. Jung[a]

[a]Department of Architecture and Architectural Engineering, Seoul National University, South Korea
E-mail: yoon92411@snu.ac.kr, hyunslee@snu.ac.kr, mspark@snu.ac.kr, potgus@snu.ac.kr, tjs6191@snu.ac.kr

Abstract –

Many project managers and researchers have emphasized the importance of considering uncertainty in the scheduling of EPC projects, and perform stochastic analysis when preparing a schedule to reflect uncertainties of duration for project activities. In this case, the uncertainty of the individual activity duration is treated as probabilistic variables, and this probability should be estimated based on previous project experience and data. To use past project data for probabilistic schedule analysis of planned schedules, the schedule information of past project should be stored and managed systematically, and the analysis should be based on the relevant past project data. Existing schedule analysis tools are focused on the analysis process, and there is a lack of consideration on how to manage and apply the past project data needed for the schedule analysis. Therefore, this paper proposes a system framework that enables probabilistic schedule analysis, which automatically supports the process of identifying and allocating corresponding past project activities for estimating activity durations of a planned schedule. We propose a data model and system framework that reflects defined issues and the requirements. The framework is composed of 4 modules: As-built schedule data storage module, a planned schedule input module, a historical data allocation module, and uncertainty analysis module. It is expected that the proposed system framework will contribute to overcoming the difficulties of data management for collection and planned schedule analysis in practice.

Keywords –

Schedule Analysis; Probabilistic Analysis; Uncertainty; System Framework; Data Model

1 Introduction

In the construction industry, many mega-projects are delivered in the form of EPC contracts. In the early stages of the EPC project development, the project scope is unclear, because the EPC contractors are responsible for the design, procurement, and construction phases. This implies the uncertainty of the management factor such as cost and schedule is much larger than other construction projects. In particular, scheduling is critical for successful project management when considering the size, participants, and scope of EPC project [1,2], and the scheduling for initial project planning should be done with careful consideration of the uncertainty.

Many project managers and researchers have emphasized the importance of uncertainty considerations in the scheduling of EPC projects [3,4], and perform stochastic analysis when preparing a schedule to reflect uncertainties of duration for project activities. For scheduling of EPC project schedule, a planned schedule is prepared, which consists of hundreds, or even thousands, of activities. In this case, the uncertainty of the individual activity duration is treated as probabilistic variables, and this probability should be estimated based on previous project experience and data [5,6].

To use past project data for probabilistic schedule analysis of planned schedules, the schedule information of past project should be stored and managed systematically, and the analysis should be based on the relevant past project data. The reliability of the schedule analysis depends on the appropriateness of the utilized data and should select relevant information of past project activities should be selected to corresponding activities of the planned schedule. In this process, it is difficult to allocate the appropriate past information on the planned schedule due to the unclear project scope at the initial stage of the project, the difficulty of activity identification from a past project, inconsistency in resource and productivity to be put into each activity of EPC projects. Such problems indicate that the process of applying past project data to the probabilistic schedule analysis is a process that requires multiple

decision-making, and it is impossible to allocate the past data to all activities of planned schedule in the same way.

To support the process of managing past project data and probabilistic schedule analysis, various methodologies and software have been developed and utilized for project scheduling. However, existing tools are focused on the analysis process, and there is a lack of consideration on how to manage and apply the past project data needed for the schedule analysis.

Therefore, this paper proposes a system framework that enables probabilistic schedule analysis, which automatically supports the process of identifying and allocating corresponding past project activities for estimating activity durations of a planned schedule. First, we investigated the precedent methods and studies for probabilistic schedule analysis to define challenging issues of project schedule analysis and the system requirements. And we propose a data model and system framework that reflects defined issues and the requirements.

2 Literature Review

In this chapter, the authors review uncertainty analysis technique to identify required data structure of the system and previous approaches about data structure for schedule data management.

2.1 Required data structure for uncertainty information

To deal with uncertainty of activity duration quantitatively, a probabilistic approach was generally used for schedule analysis. Monte-Carlo Simulation (MCS) is the most popular tool for probabilistic analysis. In case of scheduling, MCS is possible to be performed by considering activity duration as a random variable. During each iteration in the MCS process, values of random variables are determined from a specific range, probability distribution in other words [7]. Therefore, the reliability of result from uncertainty analysis depends on how to estimate the probability distribution of each activity.

According to previous studies and project management body of knowledge (PMBOK), which is recognized as a fundamental rule of project management around the world, if historical data exists sufficiently, high accuracy duration estimation is possible [5]. However, most of the researches [6,8–10] apply probability distribution to activity by expert judgment like three-point distribution due to lack of data availability. Therefore, for reliable results of analysis, it is an important issue how to develop data structure which is able to enhance data availability.

2.2 Previous Efforts for Improving Data Availability

Generally, a schedule includes work breakdown structure (WBS) information which has a hierarchical structure. Therefore, how to develop standard WBS has been an important topic in the area of construction data management. The approach for developing standard structure of WBS was based on the expectation that it could allocate the past performance information to the planned schedule of the new project if a company manages all projects with single standard WBS. Although the hierarchical structure has advantages in terms of management in practice, it has disadvantages such as difficulty in representing various perspectives and levels of detail [11]. To overcome these limitations, facet-classification model with facet concept emerged [12], and work package model was also proposed, which is improved based on the facet-classification model. Work package model expresses the structure of information divided into Where, What, How, and Who. Cho et al. [11] proposed a 5W1H model by improving abovementioned concepts.

These efforts can be categorized as a project-

Table 1. Comparisons of project-oriented data structure and activity-oriented data structure

Contents	Previous Approach	Proposed Approach
Concept	Project-oriented data structure	Activity-oriented data structure
Description	If the schedules based on a standard data structure, duration data can be allocated to new schedule just by collecting past project schedules.	Add past performance to the database through separate tasks after project execution
Advantage	If the standard is appropriate, no extra effort is required to collect and allocate schedule data.	-Flexible configuration of the purpose and type of data -Little effort is required to accumulate new data after initial database construction.
Disadvantage	If the characteristics of the each project are significantly different, there is difficulty in establishing the standard.	-The allocation process is cumbersome.

oriented data structure. In other words, previous researches try to establish a data model which is possible to utilize when a project schedule is created based on the fixed data structure. However, it is hard to ensure applicability in project schedule management practice with the project-oriented concept. Due to the different characteristics of every individual project, especially in case of mega-project, a more detailed breakdown of WBS or work package makes it hard to establish a standard data structure for multiple projects. To address the issues, this research proposes activity-oriented data structure to manage and to allocate historical data efficiently. Table 1 summarizes advantage and disadvantage of both approaches.

3 Data Model

Data for probabilistic schedule analysis can be acquired from past project schedule which contains actual data. However, data collection for certain purpose cannot be performed without purpose-built designed data model. The fact that the project manager has some past schedule files does not mean he or she can analyze schedule with historical data. So systemically structured database is essential to manage and allocate historical data to the planned schedule. A data model is an abstract model to represent data relationship and flow so that the reader can understand actual data better. The main objective of the data model is to enhance understanding of data structure and to provide access to the appropriate source to improve accessibility [13,14].

Fig. 1 shows developed logical entity relationship diagram of the proposed data model to represent activity-oriented data structure. Project and activity table in the figure indicate as-built schedules information. Resource table does not mean the type of resource, but the resource that has performed the actual project. Therefore, even if the same welder has two different activities, it would have two different resource ID. Information in the resource table is limited to labour in this research.

The duration information and the productivity information table on the right side of the figure indicate the storage type of data with a specific purpose. For example, if the A/G filed pipeline welding is to accumulate data on productivity, it is generated by assigning one data code to the Duration Information table. Whenever the information in the data-resource table is accumulated one by one, the values of productivity information such as the number of data, mean or max value of data are continuously changed. The tables in blue dotted line on figure represents the link of accumulated data to activity or resource information. These two tables are filled with information by the user's direct information allocation. However, when the work package information operates to allocate other data and activities, the query is configured so that no data is inserted to facilitate later retrieval.

Also, activity, resource and each information table have attributes to the work package. The name of these attributes may vary depending on the user or project. This is because the way and perspective of managing projects differ by person, project, or company. Through this database development, it directly supports the as-built schedule data storage module and the historical data allocation module of the system framework.

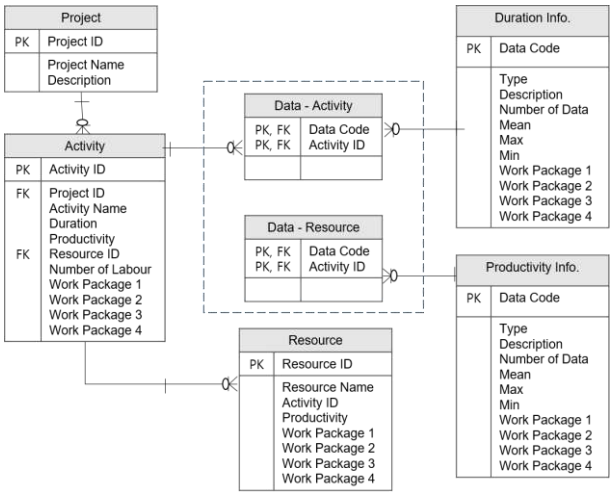

Figure 1. Proposed Data Model

4 System Framework

This chapter introduces the system framework to manage historical schedule data and to analyze the planned schedule with stored data. Each content of the system framework will be described respectively with modules and use case of the system. The prerequisite for using the system is that both as-built schedules and the planned schedule should use the same work package. The work package, which is meant here, is a high-level facet, such as a discipline (e.g. civil, architecture, mechanics) and phase (e.g. engineering, procurement, construction), so that even if the characteristics of the project are different, it can be shared by various projects. The work package is the basis for enhancing the usability of the storage and allocation modules to be described in the following chapters. Fig 2 shows the system framework developed in this research and each module of the system.

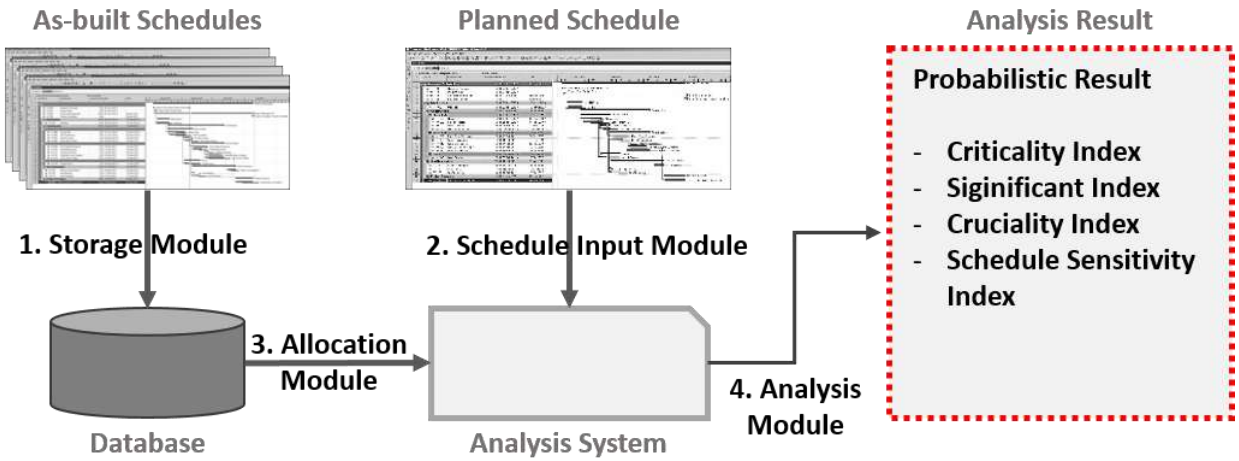

Figure 2. System framework for probabilistic schedule analysis

4.1 As-built Schedule Data Storage Module

After the project finished, the project manager has to store as-built schedule in the system. Storage module supports this process based on the data model developed in the previous chapter. In this module, the user stores the tasks of the as-built schedule in the database. In this process, the related data codes are retrieved through the work package and are selected. At this point, the user needs to decide whether to save the activity in duration table or to save in productivity table. For example, some activity or procurement tasks in engineering are often difficult to estimate for reliable productivity. Therefore, the reliability of the database can be improved by making such a selection directly by the user.

4.2 Planned Scheduled Input Module

In general, the EPC project schedule is developed and managed in Primavera or MS project. Therefore, to enhance a practical application, the system has to include a module that enables a connection with the existing schedule management system. Planned schedules generally include the following four information: activity, dependency, resource, and resource allocation. Both Primavera and MS project provides an ability to export this information as excel format. And we can easily convert excel to CSV (comma-separated variables) format. Based on imported these 4 CSV files, the system creates a simulation model of the project. This simulation model generation automation process is a modification of research in Jung et al. [15].

4.3 Historical Data Allocation Module

Although the planned schedule is input in the system, it doesn't mean appropriate historical data is allocated to each activity in the planned schedule. Therefore, users have to retrieve relevant historical data in as-built schedules. Utilizing the attributes of the work package of the previously defined data model, users can find the data codes associated with each activity of the planned schedule. Data codes can be used to search for past related activities and to use the entire or some data inherent in the data code for the analysis.

After allocating historical data for activities of the planned schedule, the system is ready for MCS. It means that system can generate a probability distribution from historical data. From statistics information of historical data, the system can generate cumulative distribution(CDF) function, inverse cumulative distribution function(ICDF) in order. By entering a random number in the range between 0 and 1 into ICDF, a value according to the probability distribution can be obtained.

4.4 Uncertainty Analysis Module

Through the process described in the first three chapters mentioned above, the planned schedule entered into the system is ready to be analyzed based on historical data. When MCS is performed, virtual schedules are generated by the number of times of simulation. The statistics of these schedules can be used to create an indicator of how the activity's uncertainty affects the schedule planned schedule. There are following four popular indicators in previous researches: criticality index, significant index, cruciality index and schedule sensitivity index [16–18]. Based on the theoretical concept and the system framework, it is

possible to provide these indicators to the user as simulation results.

5 Conclusions

This research proposed a system framework that supports the process of storing information on past schedules in a database and linking them with planned schedules. Also, this study proposed a required data model for the proposed approach. It is expected that the proposed system framework will contribute to overcoming the difficulties of data management for planned schedule analysis in practice.

There are still following limitations in the proposed framework. Most of them depend on heuristic tasks in the storage module and an allocation module. For the usability of the proposed system framework, future study is needed to explore the possibility of automation and implementation. Also, since the system is not yet implemented, the applicability and effectiveness of the proposed system framework should be validated after developing and testing a system prototype.

Acknowledgements

This work was supported by the Technology Innovation Program (10077606, To Develop an Intelligent Integrated Management Support System for Engineering Project) funded by the Ministry of Trade, Industry & Energy (MOTIE, Korea).

References

[1] Gepp M., Hellmuth A., Schäffler T. and Vollmar, J. Success factors of plant engineering projects. *Procedia Engineering*, 69:361–369, 2014.

[2] Yeo K.T. and Ning J.H. Integrating supply chain and critical chain concepts in engineer-procure-construct (EPC) projects. *International Journal of Project Management*, 20(4):253–262, 2002

[3] Alsakini W., Wikström K., and Kiiras J. Proactive schedule management of industrial turnkey projects in developing countries. *International Journal of Project Management*. 22(1): 75–85, 2004.

[4] Wang P. and AbouRizk S.M. Large-scale simulation modeling system for industrial construction. *Canadian Journal of Civil Engineering*, 36(9):1517–1529, 2009.

[5] PMI. PMBoK Guide: A Guide to the Project Management Body of Knowledge. 2013.

[6] Tokdemir O.B., Erol H., and Dikmen I. Delay Risk Assessment of Repetitive Construction Projects Using Line-of-Balance Scheduling and Monte Carlo Simulation. *Journal of Construction Engineering and Management*, 145(2): 04018132, 2019

[7] Goodarzi E., Ziaei M., and Lee T.S. Monte Carlo Simulation. Introduction to Risk and Uncertainty in Hydrosystem Engineering. Springer, Dordrecht, 2004.

[8] Schexnayder C., Knutson K., and Fente J. Describing a Beta Probability Distribution Function for Construction Simulation. *Journal of Construction Engineering and Management*, 131(2):221–229, 2005.

[9] Barraza G.A. Probabilistic Estimation and Allocation of Project Time Contingency. *Journal of Construction Engineering and Management*, 137(4): 259–265, 2011.

[10] Choudhry R.M., Aslam M.A., Hinze J.W., and Arain F.M. Cost and Schedule Risk Analysis of Bridge Construction in Pakistan: Establishing Risk Guidelines. *Journal of Construction Engineering and Management*, 140(7): 04014020, 2014.

[11] Cho, D., Russell, J.S., and Choi, J. Database Framework for Cost, Schedule, and Performance Data Integration. *Journal of Computing in Civil Engineering*, 27(6): 719–731, 2013.

[12] Kang L.S. and Paulson B.C. Adaptability of Information Classification Systems for Civil Works. *Journal of Construction Engineering and Management*, 123(4):419–426, 1997.

[13] Steeve Hoberman. Data modeling made simple. Technics Publications, Bradley Beach, NJ, 2005.

[14] Ji S., Park M., Lee H., Ahn J., Kim N., and Son B. Military Facility Cost Estimation System Using Case-Based Reasoning in Korea. *Journal of Computing in Civil Engineering*, 25(3):218–231, 2010.

[15] Jung M., Park M., Lee H.S., and Chi S. Multimethod Supply Chain Simulation Model for High-Rise Building Construction Projects. *Journal of Computing in Civil Engineering*, 32 (3):1–12, 2018.

[16] Vanhoucke M. Using activity sensitivity and network topology information to monitor project time performance. *Omega*, 38(5):359–370, 2010.

[17] Vanhoucke M. On the dynamic use of project performance and schedule risk information during project tracking. *Omega*, 39(4):416–426, 2011.

[18] Elmaghraby S.E. On criticality and sensitivity in activity networks. *European Journal of Operational Research*, 127(2):220–238, 2000.

A Methodology for Indoor Human Comfort Analysis Based on BIM and Ontology

W. Chen[a], K. Chen[a], V.J.L. Gan[a], and J.C.P. Cheng[a]

[a]Department of Civil and Environmental Engineering, The Hong Kong University of Science and Technology, Hong Kong, China
E-mail: wchenau@connect.ust.hk, kchenal@connect.ust.hk, jganaa@connect.ust.hk, cejcheng@ust.hk

Abstract –

In the operations and maintenance (O&M) stage of a building, thermal comfort and acoustic comfort are essential for the health and productivity of occupants. There are many complaints about the indoor human comfort in office buildings due to inappropriate indoor temperature or noise. Building information modeling (BIM) technology is an efficient means for helping facility managers to capture complete information from the design and construction stages and deliver this valuable information to the operation stage. In addition, WELL building standard is a performance-based system for monitoring, measuring, and certifying metrics of the environment of buildings that impact human wellbeing and health. It is potential that leveraging environment condition data and BIM data to improve the indoor human comfort level based on WELL building standard. However, there is a lack of study on improving the indoor human comfort level using BIM technology and WELL building standard.

Therefore, this study proposes the methodology of applying BIM technology and WELL standard to improve the thermal comfort and acoustic comfort. BIM provides geometric and semantic information for different BIM engineering analysis software to simulate comfort zones in office buildings. Ontology engineering approach is adopted to establish the knowledge and relationship among observation data from sensor network, occupant behavior, indoor human comfort index, and indoor human comfort situation. Ontology can address the information interoperability among these different domains. In addition, an illustrative example is studied to verify the feasibility of the proposed methodology. The results indicate the methodology can be applied to evaluate the indoor human comfort based on thermal comfort and acoustic comfort index. Finally, some recommendations are given to facility managers to improve the indoor human comfort level.

Keywords –

Acoustic Comfort; Building Information Modeling; Ontology Approach; Thermal Comfort; WELL Building Standard

1 Introduction

The physical factors related to human comfort in office buildings includes temperature, acoustics, air quality, layout and lighting [1]. Thermal comfort is essential for the places where people work and live. 11% of the office buildings met the acceptable criteria based on a survey in USA in 2006 [2]. Six essential variables influence the thermal comfort of human beings, such as radiant temperature, metabolic rate, humidity, dry bulb temperature, air speed, and clothing or other insulation [2]. Moreover, other psychological parameters also have a large role in affecting the level of thermal comfort, for example, individual expectations. People feel different comfortable levels when they are in the same condition. It means thermal comfort is subjective. Currently, a new standard, WELL building standard [3], supports an approach combining many strategies to handle the occupant issues related to thermal comfort.

The sound in the building environment, especially in open plan offices, is the major source of complains from occupants [4]. The noise and sound have a big influence on occupants' working motivation [5], behavior, and intellectual performance [6], which indicates that the optimization of the sound has a high priority. The speaking in acoustic aspect in the office is a complicated case and it is relevant to human comfort and working efficiency. Not only physical properties and acoustic descriptor, but also the condition of environments can determine the acoustic comfort. The objective of WELL building standard is to enhance the satisfaction, social interaction, and productivity, by

reducing exterior noise intrusion and indoor noise level [3].

Based on many studies [4] [5], acoustic comfort and thermal comfort are of importance in the office buildings. When the acoustic in the room cannot meet the criteria of acoustic standard, it has bad influence on the people's satisfaction, the emotion, and physical activities. However, a methodology to study the indoor human comfort in the operations and maintenance (O&M) stage is lacking. Moreover, they rarely studied the trade-off between thermal comfort and acoustic comfort.

Currently, a new technology can be applied to simulate the indoor building environment, building information modelling (BIM). BIM is defined as "a digital representation of the building process and is used to facilitate the exchange and interoperability of information in digital format" [7]. BIM can be used to monitor the indoor thermal condition and acoustic condition combining with sensor technology, which are useful for the automated evaluation and analysis of human comfort based on WELL standard. BIM supports different types of engineering analyses (e.g. thermal comfort and acoustic comfort analysis), which are helpful for improving the building operations in terms of human comfort [8]. BIM can improve data interoperability and collaboration between different participants and different engineering software to facilitate the human comfort analysis process [8].

The human knowledge can be conveted to a machine-readable knowledge in explicit format using ontology [9]. Ontology contains three main aspects, classes (entities/ concepts), properties or attributes of the classes or entities, and the relationships between entities or attributes. A knowledge base consists of the ontology combining with classes, properties and relationships. Ontology enables people to reuse the existing knowledge in different domains, and ontology also provide prototyping and sufficient details of knowledge in many domains [10]. Some researchers have leveraged ontology approaches to solve the information interoperability problem in the AEC/FM industry, such as Chen et al. [11] developed an ontology-based method and addressed the information interoperability between facility management and BIM. Moreover, an ontotology method is developed by Adeleke & Moodley [12], which aimed to monitor and control the indoor environment for a real case in Durban, South Africa.

This paper focuses on the problem of improving indoor human comfort, especially in acoustic and thermal comforts. This study explored the trade-off between acoustic comfort and thermal comfort. It leveraged BIM technology and ontology approach to improve the indoor human comfort level. In Section 3, a novel methodology to analyse the thermal comfort and acoustic comfort is proposed based on BIM and ontology engineering. The final recommendations in Section 4 will benefit the renovation and decoration of office buildings.

2 Research Background and Related Work

2.1 Indoor Human Comfort Standard

Currently, there are many standards related to indoor human comfort. Standards; EN-ISO 7730: 2005 [13], ASHRAE55-2013 [14], Fanger's Model of thermal comfort is a refer of EN 15251: 2007 [15]. However, only physiological reactions are considered in the Fanger's model for the physical aspects in the indoor environment. Thermal comfort means the level of satisfaction when people feel the heating level of the indoor or outdoor environment. Thermal comfort in various levels of humidity and temperature in different seasons is defined in ISO 7730:2005 standard [13].

Based on thermal comfort checklist [13], there are serval indexes for thermal comfort assessment are includes in the thermal comfort checklist, such as metabolic rate, humidity, air temperature, air movement, radiant temperature, and changes to the environment. EN 15251:2007 standard [15] entitled "Indoor Environmental Input Parameters for Design and Assessment of Energy Performance of Buildings". Thermal environment, acoustics, indoor air quality, and lighting are designed for indoor conditions and for setting limits, which ensures the Energy Performance of Buildings Directive do not compromise the comfort of occupants in the pursuit of energy reduction.

The new section "Open plan offices" of the standard ISO 3382 [16] "Measurement of room acoustic parameters" was released in 2012. It describes innovative measures for the acoustic condition qualification with a high correlation of the sound environment in the subjective perception. The third section of ISO 3382 summarized that the distance dependent qualities are the suitable acoustic measurement in open offices, for example, sound pressure level, spatial decay rate, and distraction distance.

However, these standards are not comprehensive to evaluate the indoor human comfort. WELL building standard is a performance-based system for monitoring, measuring, and certifying metrics of the environment of buildings that impact human wellbeing and health [3].

The WELL building standard seven aspects of wellness, i.e., Air, Light, Comfort , Nourishment, Water, Fitness, and Mind [3]. The development of WELL Certified™ leads to a good environment of buildings and helps people to enhance the sleep, mood, fitness, nutrition, performance and comfort of the occupants. WELL building standard aims to implement technologies, programs, and strategies and encourage the active lifestyles, healthy as well as reducing the opportunity of appearance of harmful pollutants and chemicals [3].

2.2 Study on Thermal Comfort and Acoustic Comfort

Noise is an unpleasant aspect of the indoor or outdoor environment as the commonly experienced. The influence of noise on human comfort w studied in many years. Physiological responses to acoustic stimulation studied by Candas and Dufour [17] showed that the vasoconstriction is affected by high noise level, and it may increase the metabolic rate of human and muscle tension. Santos and Gunnarsen [18] claimed that two or more parameters of indoor environment are relevant to the optimal levels of human comfort. They studied the trade-off between temperature and noise considering the parameters of the window opening or draft. The outcomes show that the decrease of 1 °C in operative temperature has the same effect of decreasing of approximate 7 dB in noise level. They claimed that the noise from HVAC system can reduce occupants' willingness to lower the temperature in a warm environment. Another finding, that the change in noise level of 3.9 dB has the same effect on human comfort when changing 1 °C in operative temperature (in a range of 23 – 29 °C), was proposed by Clausen & Carrick [19].

Moreover, many researchers have studied on the comfort-based control of HVAC system. A neural network was applied to come up with a thermal comfort based on HVAC system control in study Liang and Du [20]. A predictive thermal comfort model is introduced to the controlling using HAVC systems by Freire, Oliveira [21]. However, people paid little on the negative effects of HVAC system in acoustic comfort level. Some survey results were described by Reffat and Harkness [22], and they found that acoustic comfort has the equal importance of thermal comfort for the occupants in office buildings. Many occupants have to suffer from the noise from HVAC system, because the mechanical system is unavoidable and the reinstalling of HVAC system costs high. Frontczak and Wargocki [23] studied on multiple sensations and they found that the acoustic comfort and thermal comfort are the most essential parameters for human sensations.

The control of acoustic and thermal comfort affects to the multiple comforts, and people have studied this topic for many years. Even though people studied the acoustic performance, the coverage of room ceiling and the effect of HVAC system, such as Machner [24]. They indicated the different materials of ceiling have different influence on the acoustic comfort and thermal comfort. A few of researchers studied the trade-off between thermal comfort and acoustic comfort. The big problem is that there is lack of study on the trade-off between acoustic and thermal comfort for the design and control of HVAC system.

3 Methodology

3.1 Proposed Methodology

This study has drawn from various research areas, including BIM engineering software, WELL building standard, wireless sensor network for indoor human comfort management, and ontology engineering. The methodology includes the following four aspects:

(1) The geometric and semantic information from BIM models is used for indoor human comfort simulation and analysis.

(2) The various sensing networks and sensing devices are applied to monitor the indoor environment.

(3) BIM engineering software are implemented to simulate the indoor thermal comfort zones and acoustic comfort zones.

(4) Ontology approach is adopted to prototype the knowledge of indoor human comfort management and occupant behavior interaction. Ontology approach is also applied to provide information from sensor network for indoor human comfort management.

The information process of the proposed methodology for indoor human comfort analysis is illustrated in Figure 1. In the process, the geometric information of BIM models is extracted into CAD files, such as .dwg files, .dxf files, and .sat files. These files are available for BIM engineering analysis software, including Autodesk CFD and COMSOL Multiphysics [25].

When using these two software for indoor comfort evaluation, the first step is to identify materials of building structures and main components, because different materials have different influences on thermal comfort and acoustic comfort [24]. For example, the noise level from HVAC system when the ceiling is made of baffle is higher than the noise level from HVAC system when the ceiling is made of master matrix. Similarly, the materials of wall, floor, furniture, door, and window are identified.

In the second step, the space function of each room are determined based on usage situation. The sensor data obtained from ontology schema of indoor human comfort, for instance, temperature setting in HVAC system, and noise from outside, are as the parameter input and boundary setting of BIM engineering analysis software.

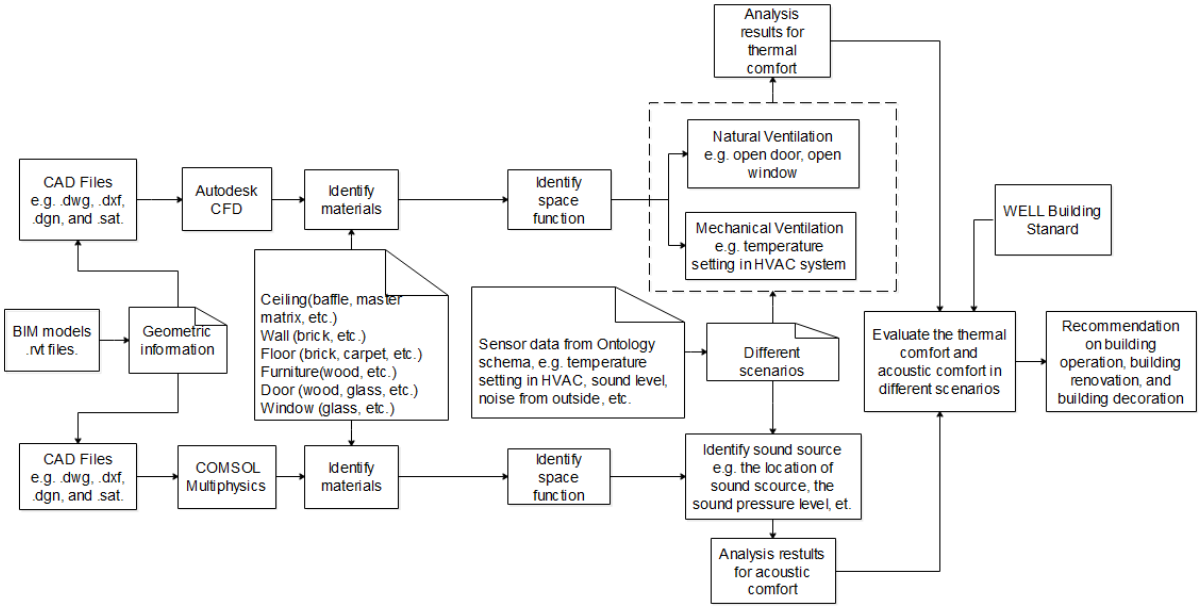

Figure 1. The information process of proposed methodology for indoor human comfort analysis

In the third analysis step, several scenarios (natural ventilation or mechanical ventilation, door open or window open, exterior noise or internally generated noise) are determined to simulate the thermal comfort and acoustic comfort. The simulation results are analysed to evaluate the indoor human comfort level based on WELL Standard. Finally, some recommendations are given for facility managers to improve building operations, building renovation, and building decoration.

3.2 Criteria of Thermal Comfort and Acoustic Comfort

In this paper, the criteria of thermal comfort and acoustic comfort in WELL standard are studied based on [14, 26], and the Indoor Air Quality Certification Scheme in Hong Kong [27]. Table 1 illustrates the requirement of acoustic comfort index based on WELL standard, while Table 2 shows the requirement of thermal comfort index.

Table 1. The requirement of acoustic comfort index

Index	The Requirement of Index	Standard
Exterior noise intrusion	Average sound pressure level from outside noise intrusion <50 dBA.	WELL Standard
Internally generated noise	Open office spaces and lobbies < 40 dBA; Enclosed offices < 35 dBA; Conference rooms and breakout rooms: <30 dBA	WELL Standard
Reverberation time	Conference rooms: 0.6 s Open workspaces: 0.5 s	WELL Standard
Sound masking	Open workspaces: 45 - 48 dBA. Enclosed offices: 40 - 42 dBA	WELL Standard

Table 2. The requirement of thermal comfort index

Index	The Requirement of Index	Standard
Ventilation effectiveness	CO_2 < 800 ppm	WELL Standard
Air flush	Indoor temperature > 15 °C Relative humidity < 60%.	WELL Standard
Humidity control	30% <Relative humidity < 50%	WELL Standard
Air quality monitoring and feedback	20 < Indoor temperature < 25.5; 40 < Relative humidity < 70 Air speed < 0.3 m/s; CO_2 < 800 ppm CO < 1.7 ppm; PM 10 < 20 ug/m3 NO2 <40 ug/m3; O3 < 50 ug/m3	Indoor Air Quality Certification Scheme 2003
Ventilated thermal environment	Air speed > 0.2 m/s, 1.0 met < Metabolic rates < 1.3 met; 0.5 clo < Clothing insulation < 1.0 clo	ASHRAE Standard 55-2013 Section 5.3

Natural thermal adaptation	Clothing insulation < 0.7 clo 1.0 met < Metabolic rates < 1.3 met 0.5 clo < Clothing insulation (Icl) < 1.0 clo 10°C < Outdoor temperature < 33.5 °C 19 °C < Floor surface temperatures< 29 °C	ASHRAE Standard 55-2013 Section 5.4

3.3 Ontology Implementation

This paper adopts ontology approach to represent the main concept of indoor human comfort management, as shown in Figure 2. The developed ontology provides representation support for the actions/ activities of the occupant, the observations of sensors in the indoor environment and the description of building environment [28]. The observations of sensor give the measurement values of sensor in certain properties (e.g., air quality, sound level, humidity, temperature, and CO_2 concentrations) of the environment. While the description of environment provides data or information such as features in the office buildings, types (e.g., type of ceilings), and quantities (e.g., number of windows), etc. Figure 2 illustrates the main concepts of the developed of indoor human comfort ontology.

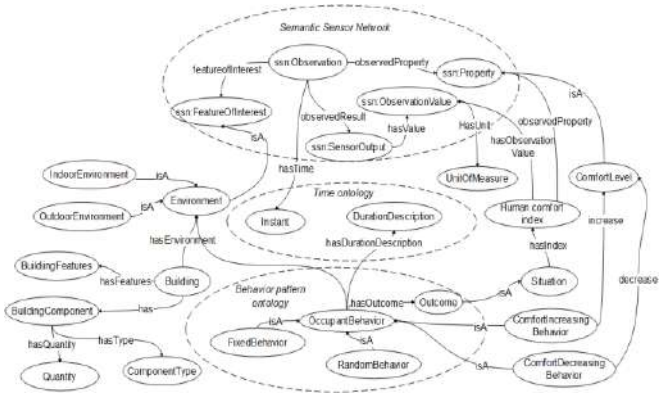

Figure 2. The main concepts of the developed indoor human comfort ontology

In the ontology schema, reasoning-based ontology can automatically determine the indoor acoustic comfort index and thermal comfort index. Sensor data is used to evaluate the proposed ontology, and the condition date can be queried from ontology for analysing the human comfort situations and determine control actions. This ontology schema enables the support for data representation and ontology reasoning on both occupant actions and the observations of sensor for indoor human comfort analysis. The ontology also represents the semantic indoor human comfort index regarding to thermal comfort and acoustic comfort.

The Unified Modelling Language (UML) diagram can represent the information in the proposed ontology schema. The office includes the space and the occupant. The office has two situations: occupied and empty. The number of occupants is one important factor to evaluate the human comfort. In order to monitor the environment condition of the office space, the temperature sensor, humidity sensor, CO_2 sensor, and sound sensor to monitor the value of each comfort index. The space has quantity of sensors, semantic type of various sensors, and different units of sensor values. For example, there are five temperature sensors in one specific office and the unit of temperature is " °C ". Similarly, there is one sound sensor in this office. The parameter of the sound sensor is acoustic pressure level and the value of acoustic pressure level is 35 dB. The UML diagram of data representation for sensors is illustrated in Figure 3, as follows.

Based on the ontology approach, the adequate sensor measurements for indoor human comfort are represented in the proposed ontology schema. It provides representation and reasoning services to analyse indoor human comfort situations based on measurements and WELL building standard. It determines human actions/ behavior to reduce the influence from bad environment. In the case, we will evaluate the proposed indoor human comfort ontology to test sensor data and query it for different situations relevant to each of scenarios.

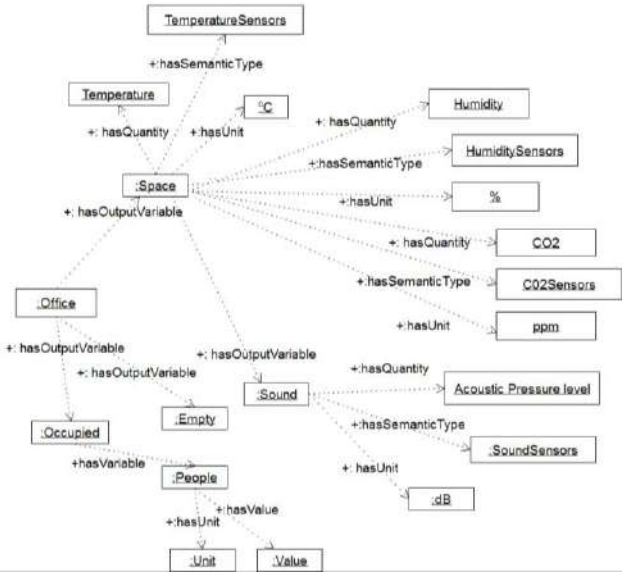

Figure 3. The data representation of sensor information for human comfort management

3.4 Using BIM Authoring Software to Evaluate Indoor Human Comfort

Different BIM-based engineering analysis software are incorporated in the proposed framework in order to

evaluate and improve indoor human comfort level based on WELL standard. For example, Autodesk CFD can be applied for indoor thermal analysis, and COMSOL Multiphysics is used for noise impact assessment. Specifically, the application procedure of using BIM-based engineering analysis software to evaluate and improve indoor thermal comfort and acoustic comfort in buildings is illustrated as follows.

(1) The inputs include geometric information (e.g. length, area) and semantic information (e.g. quantity, materials) from BIM models.

(2) The inputs include real-time data (e.g., temperature, humidity, CO_2, noise from outside) obtained from ontology schema of sensor network.

(3) Reports and code from other resources, such as building operation records, are used to set different scenarios for simulation and evaluation.

(4) The inputs are used in BIM engineering software for different types of engineering analysis (such as acoustic impact analysis and indoor thermal analysis). For example, the indoor noise, layout of one room, material of ceiling and wall can be used in COMSOL Multiphysics to simulate indoor acoustic comfort zone.

4 Illustrative Example

4.1 Case Background

In order to validate the proposed methodology, two conference rooms in the academic building of HKUST are used as the example to illustrate the methodology. The layout of two conference rooms is shown in Figure 4. The ceiling is made of baffle and the wall is made of concrete. X door, Y door, Z door and one wall of right room are made of glass, indicated in Figure 4. The left room is open office space and right room is enclosed offices.

Assume there are eight people speaking around two tables (highlighted in blue in Figure 4) in left room in this case. The sound source is internally generated noise, defined from the surface of two tables. The parameter setting in COMSOL Multiphysics is as follows: walls of two rooms are sound hard boundary. The density of air is 1.25 kg/m3 and the speed of sound is 343 m/s. The sound frequency of internally generated noise is 90HZ. The glass doors are open.

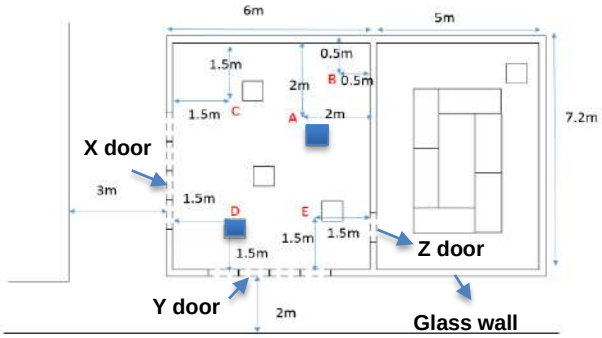

Figure 4. The layout of two conference rooms

The BIM model of two conference rooms is built using Autodesk Revit 2018, as shown in Figure 5. According to the methodology in Figure 1, the BIM model is successfully transferred into COMSOL Multiphyiscs software for acoustic comfort simulation.

Figure 5. BIM model in Revit

4.2 Simulation Results

The sound simulation result is illustrated in Figure 6a and Figure 6b. The sound pressure level in left room ranges from 45 dB to 55 dB. The sound pressure level in right room is less than 40 dB. Based on WELL standard, open office lobbies and spaces are occupied regularly and/or contain workstations, and the noise criteria in maximum level is 40 dB [3]. The maximum noise criteria of the enclosed offices is 35 dB [3]. Therefore, the sound pressure level in these two conference rooms are higher than the maximum noise criteria. People feel very noisy when there are eight people speaking. The glass door should be closed if they have meeting in left room. Otherwise, the bad influence will affect the normal work in near offices and the lobby.

Apart from the acoustic effect of people speaking, in order to validate acoustic comfort and thermal comfort without people in different situations, two scenarios are designed: (1) HVAC system is on and (2) HVAC system is off. Sensing devices are used to detect the thermal comfort and acoustic comfort index in four testing points, A, B, C, and D. The values of comfort index in four testing points are obtained from the designed ontology schema, and the values are shown in Table 3.

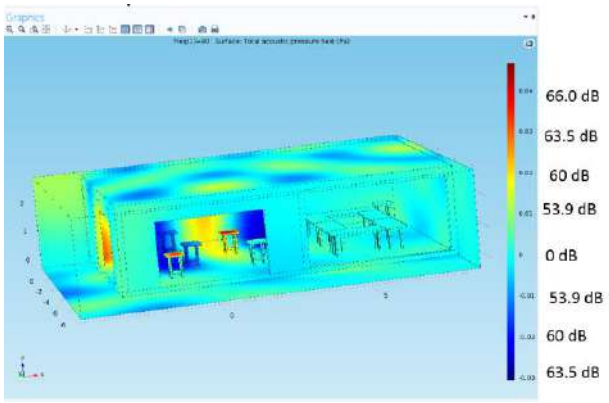

Figure 6a. The overall sound simulation results

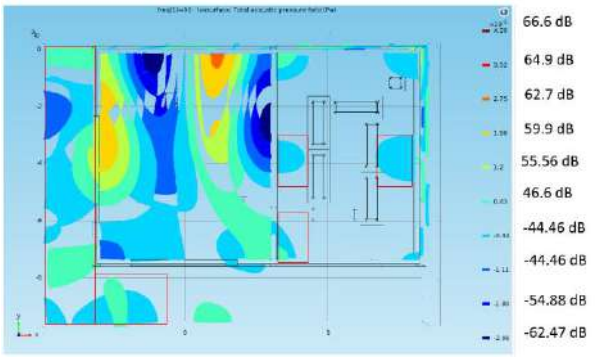

Figure 6b. The plan view of sound simulation results

According to thermal comfort index in Table 2, when temperature is more than 20 °C and less than 25.5 °C, relative humidity is 30% to 50%, and CO_2 is below 800 ppm, occupants feel comfortable [3].

When the HVAC system is off, temperature values in four testing points (A, B, C, and D) are slightly higher than 25 °C, which is near the maximum value. Humidity is 62.2% to 63.2% and CO_2 is from 542 ppm to 651 ppm. Humidity is higher than the acceptable level, and CO_2 is within the acceptable limits. The exterior noise is around 42.3 to 45.2 dB, which is higher than the maximum criteria of 40. Therefore, in this situation, occupants feel a little hot, moist and a bit noisy.

Table 3. The value of thermal comfort index

Testing point	**A**	**B**	**C**	**D**
Index	HVAC System Off			
Temperature (°C)	25.3	25.1	25.1	25.5
Humidity (%)	62.8	63.2	62.9	62.2
CO_2 (ppm)	544	651	561	542
Sound pressure level (dB)	43.6	45.2	42.5	42.3

Index	HVAC System On				
Temperature (^{o}C)	22.6	21.5	22.4	23.5	↓
Humidity (%)	50.5	50.6	47.2	45.6	↓
CO_2 (ppm)	533	533	537	521	↓
Sound pressure level (dB)	50.5	50.6	47.2	45.6	↑

When the HVAC system is on with setting the outlet temperature 20 ^{o}C, the indoor temperature decreases to 21.5~23.5 ^{o}C. Simultaneously, the humidity reduces to 45.6~50.6% located in acceptable area and CO_2 concentration decreases to 521~537 ppm. This indicates occupants would feel more comfortable than the former situation. However, the noise from HVAC system though baffle ceiling increases the sound pressure level by 3~7dB. If occupants prefer to reducing the temperature level rather than reducing noise level, they would feel more comfortable when the HVAC is on. Otherwise, they would feel more comfortable when the HVAC is off.

5 Conclusions

Thermal comfort and acoustic comfort are essential for the productivity and health of occupants in the O&M stage of a building. This paper leverages the advantages of BIM technology and ontology engineering approach to study indoor human comfort. A novel methodology is proposed to analyse the thermal comfort and acoustic comfort based on BIM technology and WELL Building Standard.

The process of methodology is explained in detail in this paper. BIM provides geometric and semantic information and information interoperability function for different engineering analysis software to simulate comfort zones in office buildings. In addition, ontology schema is developed to represent the knowledge of sensor observation domain and indoor human comfort managemnt domain. Ontology approach addresses the information interoperability problem between sensor data and indoor human comfort management. Finally, an illustrative example is studied to verify the feasibility of the proposed methodology. The results indicate that the methodology can be successfully applied to evaluate the indoor thermal comfort and acoustic comfort based on BIM and ontology approach.

References

[1] Bodin Danielsson, C. The Office-An Explorative Study: Architectural Design's Impact on Health, *Job Satisfaction & Well-being*, 2010, KTH.

[2] Huizenga, C., Abbaszadeh, S., Zagreus, L., and Arens, E. A. Air quality and thermal comfort in office buildings: results of a large indoor environmental quality survey. 2006.
[3] Standard™, W.B., WELL v2™ pilot-The next version of the WELL Building Standard™. 2018. On-line: https://v2.wellcertified.com/v/en/overview Accessed: 11/12/2018.
[4] Jensen, K.L. Acoustical quality in office workstations, as assed by occupant surveys. *Indoor Air*, 2005: p. 2401-2405.
[5] Evans, G.W. and D. Johnson. Stress and open-office noise. *Journal of applied psychology*, 2000. 85(5): p. 779.
[6] Weinstein, N.D. Effect of noise on intellectual performance. *Journal of Applied Psychology*, 1974. 59(5): p. 548.
[7] Eastman, C.M., Teicholz, P., Sacks, R. and Liston, K. *BIM handbook: A guide to building information modeling for owners, managers, designers, engineers and contractors*. 2011: John Wiley & Sons.
[8] Bahar, Y., Pere, C., Landrieu, J. and Nicolle, C. A thermal simulation tool for building and its interoperability through the building information modeling (BIM) platform. *Buildings*, 2013. 3(2): p. 380-398.
[9] Gruber, T.R. Toward principles for the design of ontologies used for knowledge sharing? *International journal of human-computer studies*, 1995. 43(5-6): p. 907-928.
[10] Niknam, M. and S. Karshenas. A shared ontology approach to semantic representation of BIM data. *Automation in Construction*, 2017. 80: p. 22-36.
[11] Chen, W., K. Chen, and J.C. Cheng. Towards an Ontology-based Approach for Information Interoperability Between BIM and Facility Management. *in Workshop of the European Group for Intelligent Computing in Engineering*. 2018. Springer.
[12] Adeleke, J.A. and D. Moodley. An ontology for proactive indoor environmental quality monitoring and control. in *Proceedings of the 2015 Annual Research Conference on South African Institute of Computer Scientists and Information Technologists*. 2015. ACM.
[13] ISO, E., *7730: 2005*. Ergonomics of the thermal environment-Analytical determination and interpretation of thermal comfort using calculation of the PMV and PPD indices and local thermal comfort criteria, 2005.
[14] ASHRAE55-2013. Thermal comfort Conditions for Human Occupancy, *ASHRAE*. Atlanta, 2013.
[15] EN, C., 15251-2007. Criteria for the indoor environment including thermal, indoor air quality, light and noise. *Brussels: European Committee for Standardization*, 2007.
[16] ISO, E. ISO 3382 Acoustics -- Measurement of room acoustic parameters -- Part 3: Open plan offices. 2012.
[17] Candas, V. and A. Dufour. Thermal comfort: multisensory interactions? *Journal of physiological anthropology and applied human science*, 2005. 24(1): p. 33-36.
[18] Santos, A. and L.B. Gunnarsen. Optimizing linked pairs of indoor climate parameters. *in Indoor Air 99*. 1999.
[19] Clausen, G., Carrick, L., Fanger, P.O., Kim, S.W., Poulsen, T. and Rindel, J.H. A comparative study of discomfort caused by indoor air pollution, thermal load and noisec. *Indoor Air*, 1993. 3(4): p. 255-262.
[20] Liang, J. and R. Du. Thermal comfort control based on neural network for HVAC application. in Control Applications, *2005. CCA 2005. Proceedings of 2005 IEEE Conference on*. 2005. IEEE.
[21] Freire, R.Z., G.H. Oliveira, and N. Mendes. Predictive controllers for thermal comfort optimization and energy savings. *Energy and buildings*, 2008. 40(7): p. 1353-1365.
[22] Reffat, R.M. and E.L. Harkness. Environmental comfort criteria: weighting and integration. *Journal of performance of constructed facilities*, 2001. 15(3): p. 104-108.
[23] Frontczak, M. and P. Wargocki. Literature survey on how different factors influence human comfort in indoor environments. *Building and Environment*, 2011. 46(4): p. 922-937.
[24] Machner, R. Thermal comfort in office buildings in line with a new German acoustic guideline. *Energy Procedia*, 2015. 78: p. 2881-2886.
[25] COMSOL. COMSOL Multiphysics Modeling Software. 2018.
[26] ASHRAE62.1-2013. Ventilation for Acceptable Indoor Air Quality.
[27] QualityManagementGroup, I. Indoor Air Quality Management Group , A Guide on Indoor Air Quality Certification Scheme for Offices and Public Places. 2003.
[28] Adeleke, J. A., & Moodley, D. (2015, September). An ontology for proactive indoor environmental quality monitoring and control. *In Proceedings of the 2015 Annual Research Conference on South African Institute of Computer Scientists and Information Technologists* (p. 2). ACM.

Pavement Crack Mosaicking Based on Crack Detection Quality

Y. Yoon[a], S. Bang[a], F. Baek[b], and H. Kim[a]

[a]Department of Civil and Environmental Engineering, Yonsei University, Republic of Korea
[b]Industrial Technical Laboratory, Yonsei University, Republic of Korea
E-mail: yeosanyoon92@yonsei.ac.kr, bangdeok@yonsei.ac.kr, fbaek@yonsei.ac.kr, hyoungkwan@yonsei.ac.kr

Abstract –

A vehicle-mounted video camera, which is one of low-cost off-the-shelf devices, can be used economically for pavement crack monitoring. The pavement frames obtained by the video camera can be merged to form a mosaic image, from which road distress information can be extracted. However, quality of crack detection in the frames is different from one another. The different level of crack detection quality should be considered for accurate construction of crack mosaic. This paper proposes a new pavement crack mosaicking method based on quality of crack detection in each frame. A convolutional neural network is suggested as a way to evaluate the quality of crack detection in the video frames. The proposed method showed a promising mosaicking performance compared to other existing methods.

Keywords –

Convolutional Neural Network; Crack Detection Quality; Pavement Crack Mosaicking; Vehicle-mounted Camera

1 Introduction

Cracking is an important factor in evaluating pavement surface condition [1]. A crack can allow water to enter the pavement and cause potholes to develop. Because potholes can damage vehicles [2], it is crucial to perform pavement monitoring and timely maintenance [3]. Pioneering studies were conducted for automatic crack detection in 1990s [4,5,6]. Ever since, various inspection devices have been used for automatic pavement crack detection research, including a ground penetrating radar (GPR) [7], an unmanned aerial vehicle (UAV) [8], laser scanners [9], infrared spectrometers [10], and a red green blue depth (RGB-D) sensor [11]. Low-cost off-the-shelf devices have also been used for pavement crack detection research; examples include smartphones [12,13,14] and vehicle-mounted cameras [15,16,17].

There are several advantages to using a vehicle-mounted video camera, which is one of the low-cost off-the-shelf devices, for pavement monitoring. By using a device already installed in a general vehicle, it is not necessary to purchase an additional experimental device for data acquisition. Obtaining data with multiple vehicles can allow large areas to be observed in a short time. A pavement that is too long to be covered by a single image can be observed by making a mosaic from successive video frames [18,19]. However, quality of crack detection is different frame by frame. For generation of the mosaic from video data, the different level of crack detection quality should be considered.

In this paper, we propose a new pavement crack mosaicking method based on crack detection quality in images. A convolutional neural network plays a major role to evaluate the crack detection quality of each frame. The methodology and experiments are explained in Chapters 2 and 3, respectively, followed by conclusions in Chapter 4.

2 Proposed Methodology

Convolutional neural network (CNN), which has shown encouraging performance in recent years [20], was used for image data processing in this paper. An encoder-decoder network based on ResNet [21], which is the winner of ImageNet Large Scale Visual Recognition Challenge 2015 (ILSVRC2015), was used for the pixel-wise crack detection; the network was the preprocessing step for this study. An input image size for the crack detection network was 1920 x 1080. Input images were collected from a vehicle-mounted camera. The dataset consisted of 427 and 100 images for training and testing, respectively. Ground truth crack binary images were made by manual labelling. Pre-trained weights learned with ImageNet data were used as the initial weights of the crack detection network.

2.1 Crack Detection Quality Prediction

The core of the proposed method is a crack detection quality prediction network (CDQ-Net). The CDQ-Net calculates a crack detection quality (CDQ) of each frame. An f1-score calculated by the crack detection network is considered as the CDQ of a frame. The CDQ-Net consists of convolutional layers, a global average pooling layer, and fully connected layers. Raw input images (2560 x 1440) obtained from a vehicle-mounted camera included non-road area. By eliminating the non-road area, the amount of computation could be reduced. On the raw input images, only the road area were extracted to result in the image size of 1536 x 540. At the convolutional layers, the filter size and the stride were 7 x 7 and 4, respectively.

The motivation why the CDQ-Net is a shallow network and includes a big filter size and stride is as follows. Most of crack shapes are thin lines, which are expected to be more related to low-level features than high-level features. Low-level features are easy to be generated by a shallow network. The vehicle-mounted camera has a high resolution (2560 x 1440) compared with many applications with ImageNet (256 x 256). If a 3 x 3 filter is used, as in a typical CNN model, it may be difficult to capture a long line feature such as cracks. A relatively larger filter sizes and strides can be appropriate for the purpose of this study.

To avoid overfitting problems, batch normalization is adopted right after each convolution and before activation. The activation function is ReLU [22]. Dropout at 50% was applied to each fully connected layer. The number of channels in each convolutional layer is determined to be similar to ResNet [21]. The number of channels in the first convolutional layer is 64 and the number of channels in the second convolutional layer is 128. In the same way as above, the number of channels in a convolutional layer is twice the number of channels in the previous convolutional layer. Except for the last fully connected layer, each fully connected layer has the same number of neurons as the number of channels in the last convolutional layer. The number of neurons of the last fully connected layer is 1 because the output of the CDQ-Net should be a single scalar value.

2.2 Pavement Crack Mosaicking

Mosaicking pavement crack information from consecutive video frames was conducted in the following steps. A CDQ of each frame was calculated by the CDQ-Net. A crack probability, which is the output just before binarization, was obtained for each pixel of a frame through the crack detection network. An example of a crack probability image is shown in Figure 1. The crack probability image, which is an oblique-view image, was transformed into a top-view image. Consecutive crack probability images were then overlapped based on the geometric relationships, which is explained in the next paragraph. Crack probabilities of overlapped pixels corresponding to a specific pixel location were weighted averaged according to the CDQ of each frame. The weighted averaged crack probability is the crack probability of the mosaic. Next, a binary crack mosaic image was derived from the crack probability mosaic image based on a specific threshold value. The optimal threshold value was to maximize a mean of f1-scores for binary crack detection of multiple mosaic images. An example of a pavement crack mosaic is shown in Figure 2.

The geometric relationship between two consecutive frames was calculated in the following steps. Oblique-view frames obtained by a vehicle-mounted camera were first transformed into top-view frames. A top-view frame included lane markings on both sides. The center curve in the previous top-view frame was then estimated based on the lane markings. Geometric relationship candidates between the two consecutive frames were derived according to the position and tangential angle of the center curve. The optimal geometric relationship was finally selected when the mean squared intensity difference between the two consecutive frames was minimum.

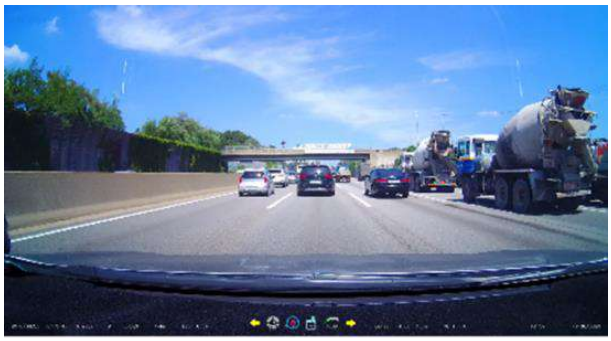

(a) An image obtained by a vehicle-mounted camera

(b) A crack probability image derived from the upper image

Figure 1. An example of pixel-wise crack probability prediction

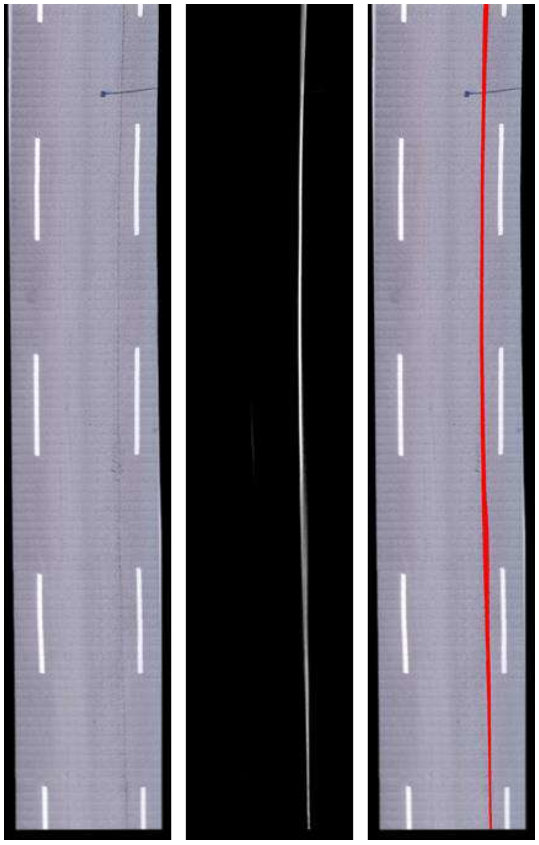

Figure 2. An example of pavement crack mosaicking (from left to right: pavement mosaic, weighted averaged crack probability mosaic, and binary crack mosaic)

3 Experiments and Results

The experimental environment was as follows. All of the image data were obtained by a dash-board camera Qrontech LK-919 QAD. The fps (frames per second) was 30 and the resolution was 2560 x 1440. Experiments were performed in a desktop with GeForce GTX 1080 Ti GPU and Intel Core i7-7700 CPU. The operating system of the desktop was Ubuntu 16.04.

3.1 Crack Detection Quality Prediction

The number of convolutional layers and the number of fully connected layers were changed to find the optimal CDQ-Net structure. The image dataset consisted of 270, 66, and 83 images for training, validation, and testing, respectively. Ground truth binary crack images were made by manual labelling. A CDQ of each frame was calculated through the crack detection network. Epochs were 500 for a majority of the CDQ-Nets, but larger epochs were used when the value of the loss function did not converge sufficiently in the validation process. Batch size was fixed to 4. The network with the lowest MAE (Mean Absolute Error) was chosen as the optimal CDQ-Net. The optimal CDQ-Net consisted of four convolutional layers and one fully connected layer. The experimental results are summarized in Table 1.

Table 1. MAE and epochs of various CDQ-Net structures: MAE (Epochs)

No. of convolutional layers \ No. of fully connected layers	1	2	3
2	8.61% (2000)	11.01% (1000)	9.99% (3000)
3	10.30% (500)	8.59% (1000)	10.98% (2000)
4	8.26% (500)	8.59% (500)	8.95% (1500)
5	10.11% (500)	10.01% (500)	10.72% (500)

The proposed CNN model was compared with a representative CNN model, the ResNet, in terms of its capability to predict the CDS. For the direct comparison, the experimental environment was set to the same conditions. Pre-trained weights learned with ImageNet data were used as the initial weights of ResNet50 [21]. In terms of MAE and duration for training, CDQ-Net's performance was superior to ResNet50. The experimental results are summarized in Table 2.

Table 2. MAE and duration on CDQ-Net and ResNet50

Performance	CDQ-Net	ResNet50
MAE (Epochs)	8.26% (500)	9.23% (1000)
Duration (Unit)	0.39 (hours)	9.77 (hours)

3.2 Pavement Crack Mosaicking

The proposed method for pavement crack mosaicking was tested using LOOCV (Leave-One-Out Cross-Validation) [23]. In the LOOCV, one mosaic image was selected for testing, while the others were selected for the determination of the optimal threshold value. The threshold value was selected to binarize each pixel of the test mosaic image into crack or non-crack category. Based on the ground truth images, the performance was measured by the f1-score. This process was repeated for every mosaic image of the dataset. In the end, the f1-scores were averaged to provide a scalar value of

performance.

The performance of the proposed method was compared with two intuitively obvious methods: overwriting and accumulating. The overwriting method is to use the crack information of the new frame to its fullest extent, ignoring the crack information of the existing mosaic. The accumulating method is to conserve every crack information of the existing mosaic to result in the OR operation with the new information. The two methods were measured by the average f1-score.

The experimental dataset for pavement crack mosaicking consisted of five videos. Each video has 90 frames. The ground truth binary crack mosaic images were made by manual labelling. In terms of f1-score for crack detection, the performance of the proposed pavement crack mosaicking method was superior to the other mosaicking methods. The experimental results are summarized in Table 3. Examples of pavement crack mosaicking results are shown in Figure 3.

Table 3. Performance of the crack mosaicking methods

Mosaicking method	Precision	Recall	F1-score
CDQ	0.5175	0.6748	0.5838
Overwriting	0.8251	0.2634	0.3969
Accumulating	0.3427	0.8543	0.4870

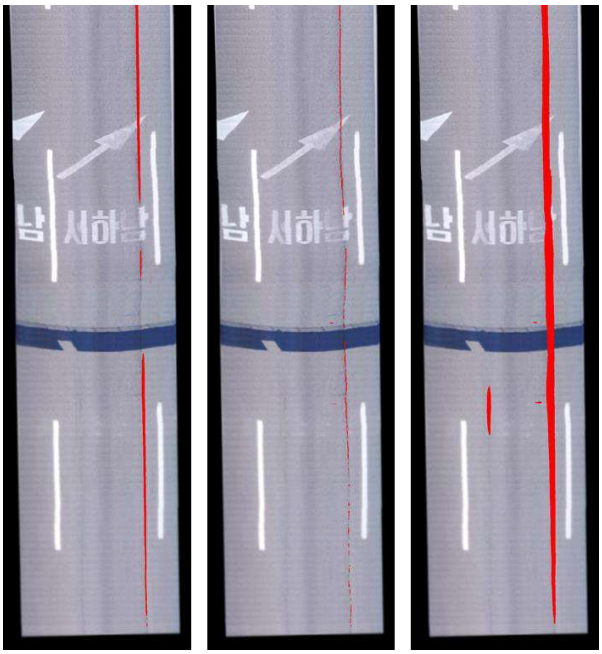

Figure 3. Examples of pavement crack mosaicking results (from left to right: CDQ based method, overwriting method, and accumulating method)

4 Conclusions

This paper presented the pavement crack mosaicking method based on crack detection quality. The proposed network, which is to predict a crack detection quality of each frame, performed better than ResNet50. The proposed pavement crack mosaicking method, which is based on the crack detection quality of each frame, showed better performance than the two intuitively obvious methods: overwriting and accumulating. The proposed method, when strengthened by a large number of crack image data, is expected to produce a significantly improved mosaic map of pavement cracks.

Acknowledgement

This work was supported by the National Research Foundation of Korea (NRF) grant funded by the Ministry of Education (No. 2018R1A6A1A08025348) and by the National Research Foundation of Korea (NRF) grant funded by the Ministry of Science and ICT (No. 2018R1A2B2008600).

References

[1] Tong Z., Gao J., Han Z., and Wang Z. Recognition of asphalt pavement crack length using deep convolutional neural networks. *Road Materials and Pavement Design*, 19(6):1334–1349, 2018.

[2] Akagic A., Buza E., and Omanovic S. Pothole detection: An efficient vision based method using RGB color space image segmentation. In *40th International Convention on Information and Communication Technology, Electronics and Microelectronics (MIPRO)*, pages 1104–1109, Opatija, Croatia, 2017.

[3] Walker D. Understanding asphalt pavement distresses – five distresses explained. On-line: http://asphaltmagazine.com/understanding-asphalt-pavement-distresses-five-distresses-explained, Accessed: 26/01/2019.

[4] Haas C., and Hendrickson C. Computer-based model of pavement surfaces. *Transportation Research Record*, 1260: 91–98, 1990.

[5] Haas C. Evolution of an automated crack sealer: a study in construction technology development. *Automation in construction*, 4(4): 293–305, 1996.

[6] Kim Y. S., Haas C. T., and Greer R. Path planning for machine vision assisted, teleoperated pavement crack sealer. *Journal of Transportation Engineering*, 124(2): 137–143, 1998.

[7] Tong Z., Gao J., and Zhang H. Recognition, location, measurement, and 3D reconstruction of concealed cracks using convolutional neural

networks. *Construction and Building Materials*, 146: 775–787, 2017.

[8] Zakeri H., Nejad F. M., and Fahimifar A. Rahbin: A quadcopter unmanned aerial vehicle based on a systematic image processing approach toward an automated asphalt pavement inspection. *Automation in Construction*, 72: 211–235, 2016.

[9] Guan H., Li J., Yu Y., Chapman M., and Wang C. Automated road information extraction from mobile laser scanning data. *IEEE Transactions on Intelligent Transportation Systems*, 16(1): 194–205, 2015.

[10] Miraliakbari A., Hahn M., and Maas H. G. Development of a multi-sensor system for road condition mapping. In *The International Archives of Photogrammetry, Remote Sensing and Spatial Information Sciences*, 40(1): 265–272, Denver, United States, 2014.

[11] Jahanshahi M. R. Jazizadeh, F., Masri S. F., and Becerik-Gerber B. Unsupervised approach for autonomous pavement-defect detection and quantification using an inexpensive depth sensor. *Journal of Computing in Civil Engineering*, 27(6): 743–754, 2012.

[12] Mertz C., Varadharajan S., Jose S., Sharma K., Wander L., and Wang J. City-wide road distress monitoring with smartphones. *In Proceedings of 21st World Congress on Intelligent Transport Systems (ITSWC)*, pages 1–9, Michigan, United States, 2014.

[13] Zhang L., Yang F., Zhang Y. D., and Zhu Y. J. Road crack detection using deep convolutional neural network. In *Proceedings of International Conference on Image Processing (ICIP)*, pages 3708–3712, Arizona, United States, 2016.

[14] Bang S., Park S., Kim H., Yeo-san Y., and Kim, H. A deep residual network with transfer learning for pixel-level road crack detection. In *Proceedings of the 35th International Association for Automation and Robotics in Construction (ISARC)*, pages 753–756, Berlin, Germany, 2018.

[15] Radopoulou S. C., Brilakis I., Doycheva K., and Koch C. A framework for automated pavement condition monitoring. In *Proceedings of the 2016 Construction Research Congress (CRC)*, pages 770–779, San Juan, Puerto Rico, 2016.

[16] Yan W. Y., and Yuan X.-X. A low-cost video-based pavement distress screening system for low-volume roads. *Journal of Intelligent Transportation Systems*, 22(5): 376–389, 2018.

[17] Park S., Bang S., Kim H., and Kim H. Patch-based crack detection in black box road images using deep learning. In *Proceedings of the 35th International Association for Automation and Robotics in Construction (ISARC)*, pages 757–760, Berlin, Germany, 2018.

[18] Geiger, A. Monocular road mosaicing for urban environments. In *IEEE Intelligent Vehicles Symposium*, pages 140–145, Xi'an, China, 2009.

[19] Sikirić I., Brkić K., and Šegvić S. Recovering a comprehensive road appearance mosaic from video. In *33rd International Convention on Information and Communication Technology, Electronics and Microelectronics (MIPRO)*, pages 755–759, Opatija, Croatia, 2010.

[20] Gu J., Wang Z., Kuen J., Ma L., Shahroudy A., Shuai, B., Liu T., Wang X. Wang G. Cai J., and Chen T. Recent advances in convolutional neural networks. *Pattern Recognition*, 77: 354–377, 2018.

[21] He K., Zhang X., Ren S., and Sun J. Deep residual learning for image recognition. In *Proceedings of the IEEE conference on computer vision and pattern recognition (CVPR)*, pages 770–778, Las Vegas, United States, 2016.

[22] Nair V., Hinton G. E. Rectified linear units improve restricted boltzmann machines. In *Proceedings of the 27th international conference on machine learning (ICML-10)*, pages 807–814), Haifa, Israel, 2010.

[23] Stone M. Cross-validatory choice and assessment of statistical predictions. *Journal of the royal statistical society*. Series B (Methodological), 36(2): 111–147, 1974.

VBUILT: Volume-based Automatic Building Extraction for As-Built Point Clouds

M.K.Masood[a], A.Pushkar[b], O.Seppänen[a], V.Singh[a], and A.Aikala[a]

[a]Department of Civil Engineering, Aalto University, Finland
[b]Department of Civil and Environmental Engineering, Carnegie Mellon University, U.S.A
E-mail: mustafa.khalidmasood@aalto.fi, apushkar@andrew.cmu.edu, olli.seppanen@aalto.fi, vishal.singh@aalto.fi, antti.aikala@aalto.fi

Abstract –
Monitoring the progress of a large construction site manually is a challenging task for managers. By collecting visual data of the site, many monitoring tasks can be automated using machine vision techniques. In this work, we study a new method of collecting site data, which is through crane camera images used to create 3D point clouds. The technology is cost-effective and enables automatic capturing and transmission of on-site data. To automatically extract buildings from the as-built point clouds, we present VBUILT, which uses 3D convex hull volumes to identify building clusters. Experimental results on 40 point clouds collected over four months on a large construction site show that the proposed algorithm can identify building clusters with 100% accuracy.

Keywords –
Building extraction, crane cameras, convex hull, progress monitoring

1 Introduction

Machine vision is revolutionizing the construction industry by allowing real-time and autonomous inspection of construction projects to replace laborious and error-prone manual methods. We can now capture as-built information in the form of 3D point clouds, which can be used for construction progress monitoring [1]-[3], quality control [4], structural damage assessment [5]-[6], heavy equipment planning [7] and safety management [8]-[9].

Point clouds are typically acquired using light detection and ranging (LiDAR) due to their high accuracy. However, laser scanners are not suited to capturing large spaces due to the high number of scans required. In fact, the time, cost and labour needed for accurately capturing an entire construction site using a laser scanner would be prohibitive. Large areas are surveyed using Airborne LiDAR, which includes the significant expense of a piloted airplane carrying specialist laser scanning equipment [10]. Besides, Airborne LiDAR produces a distant view of the site that is not suited for close-range analysis.

An alternative is the use of photogrammetric point clouds. For a large construction site, these can be created from images captured using cameras mounted on Unmanned Aerial Vehicles (UAVs) (a.k.a. drones). But UAVs have a few limitations, such as the need for flight permissions [11], image quality deterioration due to vibrations caused by weather and the difficulties in camera pose estimation with the continuous position changes of the UAV [12].

In this paper, we study a promising new approach to capture as-built information of a construction site, which is the use of photogrammetric point clouds created from crane camera images. Crane cameras offer the advantage that they are already present on construction sites and no flight permissions are required as in the case of UAVs. Their installation and operation is low-cost and convenient.

The crane camera solution used in this work was developed by Pix4D [13]. The 3D point clouds are created automatically every day and stored on the cloud. In this work, we analyse data collected on a large construction site in Finland.

We focus specifically on the problem of automatically extracting buildings from the construction site point clouds. Removing the non-building elements from a multi-building point cloud can enhance alignment with the BIM model for progress measurement, but this is beyond the scope of this paper. Our work builds on the workflow reported in the literature for automatic building extraction from airborne LiDAR data.

Our contributions are as follows:

- To the best of our knowledge, we are the first to study the potential of point clouds generated from crane cameras for automated progress monitoring.
- This is also the first work that addresses the

problem of automatic building extraction on a multi-building construction site.
- We introduce the use of 3D convex hull volumes to identify buildings on the point cloud.

The rest of the paper is organized as follows: Section 2 discusses related work on automatic building extraction, crane cameras and convex 3D hulls. Section 3 describes the crane camera data collection. Section 4 describes the VBUILT algorithm. Section 5 presents the results and discussion. Section 6 lays out the conclusions and future work.

2 Related Work

An illustrative example of the automatic building extraction workflow for airborne laser scanning (ALS) point clouds was presented by Sampath and Shan [14]. They performed ground extraction using a slope-based 1D bi-directional filter. Then, they applied a region-growing algorithm to cluster individual buildings. They set the dimensions of the moving window to incrementally more than twice the point spacing, which in a LiDAR point cloud differs in the across and along scan directions. They also set a minimum point count threshold to identify non-building clusters. Wu et al. [15] fused LiDAR data with image data to extract the boundary lines of buildings. They used a triangulated irregular network (TIN) progressive densification filtering method to extract ground points. Widyaningrum et al. [16] used a generalization of the convex hull called the alpha-concave hull [17] to do two-dimensional boundary tracing.

An excellent review of building extraction techniques for ALS point clouds is presented in [18] which categorizes all the reported techniques into three categories: i) 2D building outline extraction; ii) 3D model reconstruction of buildings and iii) 3D roof contour extraction.

Our problem differs from the reported works in a number of ways. First, we intend to extract the actual as-built point cloud of a specific building, rather than to construct a 3D model from 2D segments. Secondly, a region-growing algorithm such as the one used in [14] discards non-building clusters based on point count. That is, from the points that remain after ground extraction, those clusters that have less than a certain number of points are discarded as being possibly vehicles or trees. This method is not suitable for construction sites, where non-building clusters (corresponding to large equipment, for example) may also have a high point count. Thirdly, the reported works do not perform building identification. Our problem requires that after extraction, the buildings be labeled. Fourthly, our data is a photogrammetric point cloud obtained from crane camera images.

Additionally, we choose to use a variation of RANdom SAmple Consensus (RANSAC) called M-estimator SAmple and Consensus (MSAC) for separating ground and non-ground points. This algorithm was proposed by [19], who showed that changing the cost function of RANSAC to score inliers on how well they fit the data improves the robust estimation with no additional computational burden.

A recent work [20] used crane camera images for updating the 3D crane workspace on a construction site. However, the crane camera images were used to modify a laser-scanned point cloud, which had to be manually captured. Point clouds generated automatically from the crane camera images were not considered.

Another recent work [21] used the area of 3D convex hulls to automatically map discontinuity persistence on rock masses. However, to the best of our knowledge, the use of 3D convex hull volumes for building extraction has not been reported.

3 Data collection and description

The data was collected on the site of the Tripla project located in Helsinki, Finland, which includes a shopping centre, hotel, housing and offices. The total area of the site is 183,000 floor square meters. Our focus in this work is on three buildings of the site, whose as-designed model along with the building labels is shown in Figure 1(a). Two independent cameras were mounted on the jib of a tower crane. Images were taken automatically when the crane would begin operation and then transferred to the Pix4D Cloud, where they were converted to 2D maps and 3D models.

The dataset consists of 40 as-built point clouds corresponding to weekdays spanning August 17th, 2018 to November 23rd, 2018. The as-built point cloud for day 40 is shown in Figure 1(b). Twenty point clouds contain building A only (due to B and C not being captured by the crane cameras), while twenty others contain multiple buildings as described in Table 1.

Table 1. Description of point cloud data

Available data	No. of point clouds
Single-building data (A only)	20
Multi-building data	
A,B only	1
A,C only	10
A, B and C	9

By default, the point clouds are georeferenced, with an average point density of the order of 1000 points/m^3, except for point cloud 40, which has an average point

density of 37,233 points/m^3. However, for 13 point clouds between August 29th, 2018 and September 17th, 2018, the image geotags were not detected and thus the output coordinate system was arbitrarily set. Therefore, the point cloud could not be scaled and the resulting point density is of the order of 3 points/m^3. We subsequently refer to these point clouds as 'non-georeferenced'.

Figure 2(a) shows the front-view of Building A. The holes in the data are due to the portion of the building being out of the field-of-view of the camera. Figure 2(b) shows the top view of the building, which shows the formwork being laid. This is the clearest data of the building available.

4 Building extraction using VBUILT

In this section, we explain the VBUILT algorithm. Our objective is to extract the 3D point cloud of a specific building on the site to be used for further analysis, such as construction progress tracking.

Our solution is to extract the ground plane using MSAC, then cluster the non-ground point cloud based on Euclidean distance, followed by an analysis of the 3D convex hull volumes of each cluster.

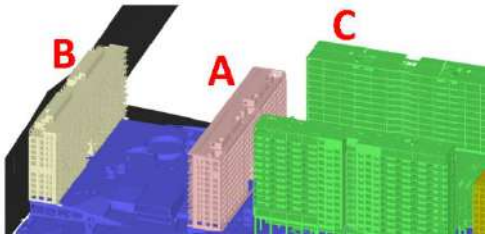

(a)

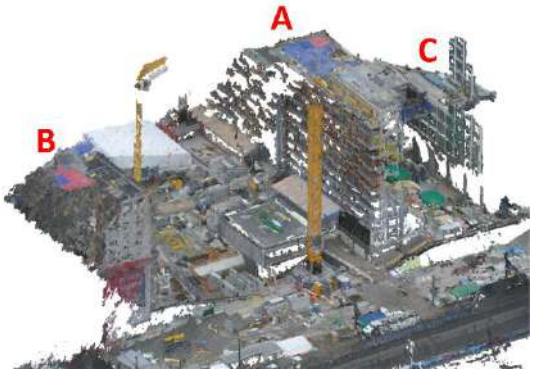

(b)

Figure 1. (a) As-designed model of the Tripla site with building labels A, B and C; (b) As-built point cloud of the Tripla site for day 40 (November 23rd, 2018)

(a)

(b)

Figure 2. Manually extracted point cloud of building A: (a) front-view and (b) top-view

4.1 MSAC-based ground extraction

Let the set of construction site point clouds be $S=\{S_1, S_2, \ldots S_D\}$, where D=40 and each point cloud $S_i=\{s_1, s_2, \ldots s_N\}$, $S_i \in R^3$. First, we downsample the point cloud for faster processing using grid average downsampling, which merges points within a 3D grid by averaging their locations and colours.

Next, we need to separate the ground and non-ground points. For this, we implement the MSAC algorithm using the in-built MATLAB function *pcfitplane*, which we explain subsequently. We specify three parameters for the MSAC algorithm:

- the reference vector ($\mathbf{n_r}$) (the *orientation constraint*).
- the maximum absolute angular distance (denoted as θ_{max}) between the normal vector of the plane hypothesis ($\mathbf{n_h}$) and the reference vector.
- the threshold d_{max}, which is the maximum distance between an inlier point and the fitted plane.

For ground plane extraction, $\mathbf{n_r}$ should be set normal to the xy plane. Then, the algorithm checks if the angular distance between $\mathbf{n_r}$ and $\mathbf{n_h}$ (denoted as θ) is less than θ_{max}. If not, the plane hypothesis is discarded and a new one is considered. Otherwise, the MSAC algorithm proceeds to calculate the following cost function:

$$C^j = \sum_{i=1}^{N} \rho_i \quad (1)$$

where j is the iteration number and the robust error term ρ is defined as follows:

$$\rho = \begin{cases} |d| & if\ |d| < d_{max} \\ d_{max} & if\ |d| \geq d_{max} \end{cases} \quad (2)$$

If C_{j+1} is less than C_j, the $(j+1)_{th}$ model is taken as the best model found so far. Every time the best model is updated, the maximum number of iterations is set to k, which is defined as follows:

$$k = \frac{log(1-p)}{log(1-w^n)} \quad (3)$$

where p is the desired confidence level (set to 0.99 as per standard practice) that at least one point in the plane hypothesis is an inlier, w is the probability that a single point is an inlier and n is the number of points needed to define the model (which for a plane, as in our case, is 3).

For the georeferenced point clouds, θ_{max} and d_{max} were selected as 5° and 5 m, respectively, based on the intuition that the ground plane is only slightly inclined with respect to the xy plane. For the non-georeferenced point clouds, due to the smaller point cloud density, d_{max} was set to a higher value (40).

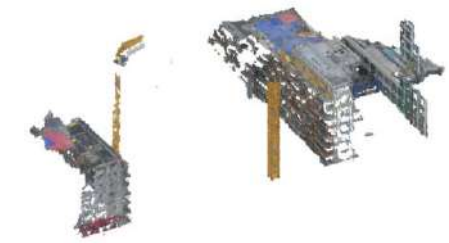

(a)

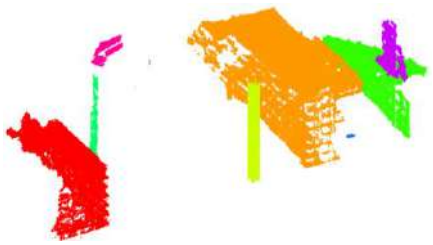

(b)

Figure 3. (a) Ground removed using MSAC; (b) Euclidean-distance based clusters

Note that the ground in the as-built point cloud contains many more points than the top floors of the buildings, thus yielding more inliers and a smaller cost (see Equation (1)). This is why the top floors are not mistaken for the ground by the algorithm.

Once the ground plane is identified, we remove the portion of the point cloud below it by checking the dot product of each point with the plane. If the dot product is negative, the point is below the plane. In other words, for a point $s_i=(x_i, y_i, z_i)$ and the ground plane parameters a_g, b_g, c_g and d_g, if $a_g x_i + b_g y_i + c_g z_i + d_g < 0$, then s_i is a below-ground point and is removed. Finally, the ground plane is removed from the point cloud. Figure 3(a) illustrates the ground-removal for Day 40.

4.2 Euclidean distance-based clustering

With the ground and below-ground points removed, the task now is to cluster the point cloud. We do this using a Euclidean distance criterion. For every point $s_i=(x_i, y_i, z_i)$ and $s_j=(x_j, y_j, z_j)$, the Euclidean distance between the points is as follows:

$$d_{ij} = \sqrt{(x_i - x_j)^2 + (y_i - y_j)^2 + (z_i - z_j)^2} \quad (4)$$

If d_{ij} is less than a distance threshold δ, then s_i and s_j are in the same cluster. We set δ =1 (and δ =5 for the non-georeferenced point clouds) as a reasonable estimate of the separation between intracluster and extracluster points. We refer to the clusters as the set C^d. The results of the clustering are shown in Figure 3(b).

4.3 Building identification using convex hull volumes

A convex hull of a set of points is the smallest convex set that contains all the points. In this paper, we describe the creation of a 3D convex hull based on the Quickhull algorithm, upon which the MATLAB function *convhull* is based. Note that *convhull* uses a more robust (albeit proprietary) strategy for coping with imprecision than the approach outlined in Section 4 of the original Quickhull paper [22], but otherwise the implementation is standard.

Starting with a 3D set of points, Quickhull first builds an initial hull from four points. Ideally, this tetrahedron should be maximal, which can be accomplished by first finding the maximum and minimum points along the X, Y and Z axes, then finding the furthest point from the line segment made by the first two points, then finding the furthest point from the plane made by the first three points. Once the initial hull is created, the point from the remaining set (not used in the initial hull) which is farthest from the hull is set as the *eye point*. Those faces of the hull that lie above the

eye point (as determined by a simple plane test) are called visible faces, while those that lie below it are non-visible faces. The edges that connect visible with non-visible faces together constitute the horizon. To determine the horizon, a flood-fill approach is used. The algorithm starts from a visible face, and then travels across an edge to a neighbouring face. If the neighbouring face is also visible, the algorithm travels further across an edge until a non-visible face is encountered, at which point the offending edge is marked as being part of the horizon. Then, the algorithm returns to the last visible face and continues traveling across another edge. This process continues until the algorithm returns to the original visible face. Once all the horizon edges are found, the eye point is connected to it and thus the hull is extended. This process continues till no face remains with a point outside it.

Our use of convex hull volumes is based on the intuition that buildings are typically more voluminous than non-buildings on a construction site, especially a large site such as the one we are considering. As we shall demonstrate, this intuition is supported by our dataset. For example, Table 2 shows the convex hull volumes for C^{40}.

Table 2. Convex hull volumes of clusters

Cluster #	Convex hull Volume	Cluster-type (Manually labeled)
1	749.2316	Building
2	318.9671	Building
3	169.1460	Building
4	10.4517	Non-building
5	7.2664	Non-building
6	3.9378	Non-building
7	3.7009	Non-building
8	0.1131	Non-building
9	0.1000	Non-building
10	0.1000	Non-building

Note that the building clusters are much larger than the non-building clusters. This motivates us to define a quantity called the *relative volume* (v_R) as follows:

$$(v_R{}^i)_d = \frac{(v_{abs}{}^i)_d}{(v_{max})_d} * 100 \qquad (5)$$

where $v_{abs}{}^i$ is the convex hull volume for cluster i and v_{max} is the largest convex hull volume for the set of clusters under consideration (i.e. for day d). Figure 4 shows the smallest building cluster and the largest non-building cluster for each day based on the v_R values of the clusters. The figure shows a considerable separation between building and non-building clusters. As Figure 4(a) shows, for the single-building data, the building cluster is always the largest and maintains a significantly higher v_R value than the largest non-building cluster for each day. In fact, the mean of the relative volumes of the largest non-building clusters is 9.68%. For the case of multi-building point clouds (Figure 4(b)), the mean of the relative volumes of the largest non-building clusters is 4.72%, while that of the smallest building cluster is 37.35%.

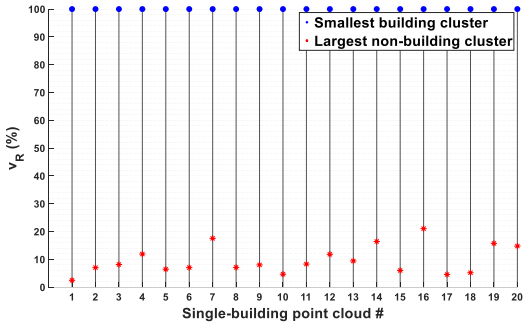

(a)

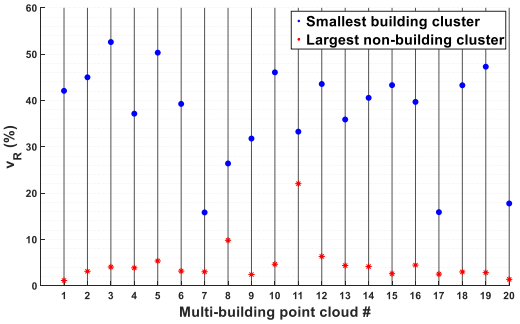

(b)

Figure 4. Comparison of smallest building cluster and largest non-building cluster for (a) single-building point clouds and (b) multi-building point clouds

Based on these insights, we outline the following strategy for extracting the building clusters:

- For the single-building data, the cluster with the largest v_R value is the building.
- For the multi-building data, a cluster with v_R less than 15% is a non-building cluster. Additionally, we impose the maximum possible buildings on the site (3 in our case) as a constraint.

The algorithm finally divides the point cloud into

two sets, *BuildingClusters* and *NonBuildingClusters*. The results are presented in the next section.

In order to label the extracted buildings, we consider the relative v_R values of the three buildings, but this approach is not fully demonstrable due to some limitations in our dataset, as is discussed in the next section.

5 Results and discussion

5.1 Classification: building vs non-building clusters

We define the classification accuracy as being 100% for a particular day if the set *BuildingClusters* contains the actual buildings available on the original construction site point cloud. The achieved accuracy is 100% for all 40 point clouds, i.e. building and non-building clusters are successfully separated for the entire dataset. Figure 5 shows the building-only point cloud obtained for day 40.

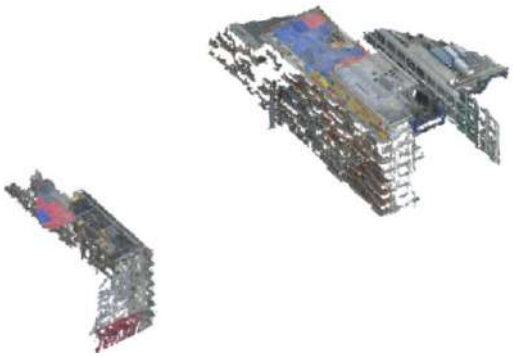

Figure 5. Building-only point cloud for day 40

5.2 Building labeling

In our dataset, building A always has the largest v_R value and it can therefore be labeled with 100% accuracy for the entire dataset. However, only a small segment of buildings B and C is captured by the crane cameras. The size of these segments varies inconsistently due to the varying positions of the crane cameras. Thus, a volume comparison cannot be consistently applied to these buildings until they are captured more completely. In other words, more complete data is required to label these buildings according to their relative v_R values.

5.3 Departure from convexity: effect of the *α-radius*

A convex hull is a specific case of an *alpha shape*, which is a polytope with a parameter called the *α-radius* that defines how tightly the boundary fits around the shape [23]. A convex hull results when the α-radius is infinity. In our specific case, using the convex hulls was more suitable due to the nature of a convex hull to "wrap around" the object, thus ignoring false cavities in the point cloud clusters resulting from the crane camera not capturing a portion of the site. An alpha shape, on the other hand, tends to "wrap into" the cavities of the point cloud clusters, resulting in a smaller boundary volume that does not approximate the actual volume of the building well. This is illustrated in Figure 6. We suggest this phenomenon might generalize to any point cloud with missing regions being subjected to boundary volume analysis. Additionally, using convex hull volumes obviates the need to find a suitable alpha radius, as was done in [24] for example.

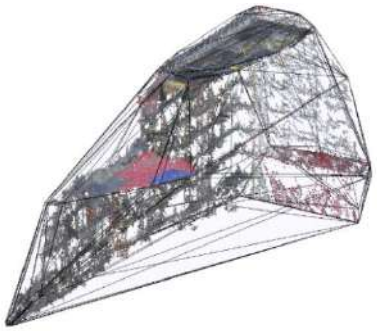

(a)

(b)

Figure 6. Illustration of (a) convex hull (*α-radius*=∞) and (b) alpha shape with lower radius

5.4 Crane cluster outlier

Figure 4(b) shows that for multi-building point cloud

11, the largest non-building cluster has a v_R value of 22%, which is a clear outlier. Visualizing this cluster shows that the large volume comes from the presence of a crane in the cluster, as is shown in Figure 7. When we manually remove this crane from the cluster, the v_R value of the cluster reduces to 4.44%. Note that the maximum building number constraint we imposed deals with this outlier effectively, which is why this cluster is correctly classified as a non-building cluster despite being above the 15% v_R threshold.

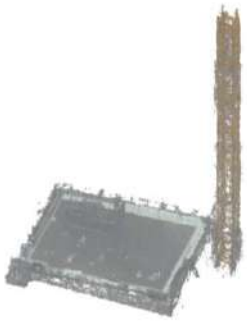

Figure 7. Outlier cluster for multi-building point cloud 11 (day 29/40) with v_R=22%

6 Conclusions and future work

Crane cameras are a convenient and cost-effective alternative to laser scanners and UAVs for visually capturing an entire construction site. In this work, we did a preliminary study on the potential of crane camera point clouds for automatic progress monitoring. We addressed the problem of automatically extracting buildings from the crane camera point clouds. We presented an algorithm called VBUILT which is based on the intuition that building clusters have larger 3D convex hull volumes than non-building clusters. We found that our dataset supports this intuition, showing a large separation between the relative volumes of building and non-building clusters. By utilizing this separation, VBUILT was able to correctly identify the building clusters for all 40 point clouds in the dataset. We also successfully labeled one building which is captured relatively well by the crane cameras, but would require better data of the other buildings to demonstrate the effectiveness of the relative volume strategy for multi-building labeling.

An important insight from our work was that convex hull volumes capture the volumes of building clusters with missing regions more effectively than alpha shapes with lower radii due to the tendency of the latter to wrap into the empty regions of the cloud. We thus recommend the consideration of the convex hull over alpha shapes for such volume-based analyses of incomplete point clouds.

The algorithm successfully dealt with an outlier non-building cluster by imposing a maximum building number constraint. However, in order to prevent such outliers altogether, an automatic crane removal algorithm can be developed in future work, possibly by leveraging on the high slenderness ratio and the uniform colour of the cranes.

The proposed algorithm worked successfully with both georeferenced and non-georeferenced point clouds, the latter constituting about 32% of our dataset. In future work, we will study why georeferencing fails for some point clouds and how we can address the problem.

The point clouds generated from crane cameras give a good overview of the site and high quality views of the top portions of the buildings where the laying of formwork and rebar can be observed. Thus, in future work, we intend to use the building point clouds obtained through VBUILT to infer the progress of formwork and rebar. Also, the crane camera point clouds contain holes in the building façade regions. More studies are needed to truly gauge the effectiveness of this portion of the point clouds for progress monitoring. Therefore, in the future, we intend to match the building-only point cloud with the as-designed Building Information Model (BIM) of the site to study the extent to which progress and deviations can be measured.

Acknowledgements

We thank YIT for providing the data for this study. The work was supported by the Reality Capture research project funded by Business Finland, Aalto University and a consortium of 5 companies.

References

[1] F. Bosché, M. Ahmed, Y. Turkan, C. T. Haas and R. Haas. The value of integrating Scan-to-BIM and Scan-vs-BIM techniques for construction monitoring using laser scanning and BIM: The case of cylindrical MEP components. *Automation in Construction*, vol. 49, pp. 201-213, 1 2015.

[2] C. Kim, H. Son and C. Kim. Automated construction progress measurement using a 4D building information model and 3D data. *Automation in Construction*, vol. 31, pp. 75-82, 5 2013.

[3] Y. Turkan, F. Bosche, C. T. Haas and R. Haas. Automated progress tracking using 4D schedule and 3D sensing technologies. *Automation in*

Construction, vol. 22, pp. 414-421, 3 2012.

[4] B. Akinci, F. Boukamp, C. Gordon, D. Huber, C. Lyons and K. Park. A formalism for utilization of sensor systems and integrated project models for active construction quality control. *Automation in construction*, vol. 15, pp. 124-138, 2006.

[5] J. Fernandez Galarreta, N. Kerle and M. Gerke. UAV-based urban structural damage assessment using object-based image analysis and semantic reasoning. *Natural hazards and earth system sciences*, vol. 15, pp. 1087-1101, 2015.

[6] C. Koch, S. G. Paal, A. Rashidi, Z. Zhu, M. König and I. Brilakis. Achievements and challenges in machine vision-based inspection of large concrete structures. *Advances in Structural Engineering*, vol. 17, pp. 303-318, 2014.

[7] D. Moon, S. Chung, S. Kwon, J. Seo and J. Shin. Comparison and utilization of point cloud generated from photogrammetry and laser scanning: 3D world model for smart heavy equipment planning. *Automation in Construction*, vol. 98, pp. 322-331, 2 2019.

[8] J. Seo, S. Han, S. Lee and H. Kim. Computer vision techniques for construction safety and health monitoring. *Advanced Engineering Informatics*, vol. 29, pp. 239-251, 4 2015.

[9] H. Kim, K. Kim and H. Kim. Vision-Based Object-Centric Safety Assessment Using Fuzzy Inference: Monitoring Struck-By Accidents with Moving Objects. *Journal of Computing in Civil Engineering*, vol. 30, p. 04015075, 7 2016.

[10] K. Johnson, E. Nissen, S. Saripalli, J. R. Arrowsmith, P. McGarey, K. Scharer, P. Williams and K. Blisniuk. Rapid mapping of ultrafine fault zone topography with structure from motion. *Geosphere*, vol. 10, pp. 969-986, 2014.

[11] S. Cardot. Crane Camera Site Surveying. *Gim International-the worldwide magazine for Geomatics*, vol. 31, pp. 31-33, 2017.

[12] S. Bang, H. Kim and H. Kim. UAV-based automatic generation of high-resolution panorama at a construction site with a focus on preprocessing for image stitching. *Automation in Construction*, vol. 84, pp. 70-80, 12 2017.

[13] [Anonymous]. Pix4D Launches Crane Camera Solution for Construction Industry. *Gim International-the worldwide magazine for Geomatics*, vol. 30, p. 7, 2016.

[14] A. Sampath and J. Shan. Building boundary tracing and regularization from airborne LiDAR point clouds. *Photogrammetric Engineering & Remote Sensing*, vol. 73, pp. 805-812, 2007.

[15] J. Wu, S. Jie, W. Yao and U. Stilla. Building boundary improvement for true orthophoto generation by fusing airborne LiDAR data. *Joint Urban Remote Sensing Event*, 2011.

[16] E. Widyaningrum, R. C. Lindenbergh, B. G. H. Gorte and K. Zhou. Extraction of building roof edges from lidar data to optimize the digital surface model for true orthophoto generation. *ISPRS - International Archives of the Photogrammetry, Remote Sensing and Spatial Information Sciences*, vols. XLII-2, pp. 1199-1205, 5 2018.

[17] S. Asaeedi, F. Didehvar and A. Mohades. Concave hull, a generalization of convex hull. *Theoretical Computer Science*, vol. 702, pp. 48-59, 11 2017.

[18] I. Tomljenovic, B. Höfle, D. Tiede and T. Blaschke. Building Extraction from Airborne Laser Scanning Data: An Analysis of the State of the Art. *Remote Sensing*, vol. 7, pp. 3826-3862, 3 2015.

[19] P. H. S. Torr and A. Zisserman. MLESAC: A New Robust Estimator with Application to Estimating Image Geometry. *Computer Vision and Image Understanding*, vol. 78, pp. 138-156, 4 2000.

[20] J. Chen, Y. Fang and Y. K. Cho. Real-Time 3D Crane Workspace Update Using a Hybrid Visualization Approach. *Journal of Computing in Civil Engineering*, vol. 31, p. 04017049, 9 2017.

[21] A. Riquelme, R. Tomás, M. Cano, J. L. Pastor and A. Abellán. Automatic Mapping of Discontinuity Persistence on Rock Masses Using 3D Point Clouds. *Rock Mechanics and Rock Engineering*, vol. 51, pp. 3005-3028, 5 2018.

[22] C. B. Barber, D. P. Dobkin and H. Huhdanpaa, .The quickhull algorithm for convex hulls. *ACM Transactions on Mathematical Software*, vol. 22, pp. 469-483, 12 1996.

[23] H. Edelsbrunner and E. P. Mücke. Three-dimensional alpha shapes. *ACM Transactions on Graphics (TOG)*, vol. 13, pp. 43-72, 1994.

[24] R. C. Santos, M. Galo and A. C. Carrilho, Building boundary extraction from lidar data using a local estimated parameter for alpha shape algorithm. *ISPRS-International Archives of the Photogrammetry, Remote Sensing and Spatial Information Sciences*, vols. XLII-1, pp. 127-132, 9 2018.

Robotic Fabrication of Nail Laminated Timber

H. Hasan[a], A. Reddy[b], and A. TsayJacobs[b]

[a]Perkins+Will Research, Boston, USA
[b]Perkins+Will Research, Los Angeles, USA
E-mail: Hakim.Hasan@perkinswill.com,
Anish.Reddy@perkinswill.com, Andrew.TsayJacobs@perkinswill.com,

Abstract –
Robotics, mass timber, and parametric design are all key technologies that are underutilized in construction. To fully take advantage of these new technologies requires a rethinking of the entire process from design to construction. The Greenbuild Pavilion represents a new construction workflow, in which a digital parametric model is communicated directly to a robot fabricator. The robot, equipped with various tools, can manipulate dimensional lumber into complex geometries with industrial precision. This workflow has the potential to drastically improve the sustainability, quality, cost, and time of construction.

Keywords –
Robotic Fabrication; Nail Laminated Timber; Mass Timber; Automated Construction; Digital Fabrication; Architectural Robotics; Advanced Timber Structures, Sustainable Structures.

1 Introduction

Perkins + Will's Building Technology Lab was able to leverage its previous research into mass timber and robotic fabrication, combining expertise across offices in a year-long effort. Hakim Hasan, from Perkins+Will Boston, and Anish Reddy, from the Los Angeles office, fabricated a pavilion in modules (using 2,451 individual pieces of wood and 10,828 nails) over 54 hours at Autodesk's Technology Center in Boston. It was then shipped to Chicago and assembled at the Greenbuild Expo, where it stole the show with its curved geometry and massive scale, topping out at 4.26 meters tall and 6 meters wide.

The success of the pavilion marks a major step forward for sustainable applications of robotics. Because it is a post-and-beam mass timber structure, the pavilion's workflow could be applied to a structure as tall as 18 stories. The use of wood allows for a renewable, widely-available material to displace steel or concrete and reduce a building's carbon footprint. The use of robotics allows for buildings to be delivered faster and more precisely. Moving forward, Perkins + Will seeks to implement these workflows into its projects, ensuring a better final product for its customers.

1.1.1 Problem Statement:

Robotics, mass timber, and parametric design are all key technologies that are underutilized in construction. To fully take advantage of these new technologies requires a rethinking of the entire process from design to construction.

Cross-laminated timber (CLT) has become more popular in recent years, with most innovation (led by companies like Katerra[1]) centering around providing orthogonal modules that can be prefabricated off-site and quickly assembled on-site. The International Code Council recently adopted new language for 2020 that would permit high-rise construction with CLT (and other related mass timber assemblies) up to 18 stories. These developments feed into a burgeoning demand for sustainable, efficient, and dense structures in the current real estate market.

Robotic fabrication has the potential to allow more complex assemblies with mass timber than are typically produced in a factory. Recent research into robotic fabrication with wood has focused on dome structures (ICDE/ITKE Research Pavilion 2015[2]) or typical balloon framing (DFAB House[3]), which do not translate easily the high-rise industry. For robotics to become economically viable in construction, it must take advantage of economies of scale and be able to produce mass timber assemblies.

2 The Robotic Setup

The robotic setup is a 6-axis ABB IRB 4600-40/2.55 mounted on an ABB IRBT 4004 external linear track yielding 7 degrees of freedom. The robot is operated at a speed of 2 metres per second and has a Maximum reach of 2.55m from the base of the robot, and when mounted

on the external linear axis, the range is extended across 9 meters with a position repeatability RP of 0.06 mm and a path repeatability of 0.28mm.

2.1.1 The Tools

5 tools are equipped with ATI automatic tool changers allowing for the robot to quickly switch from one to the other. The changeable tools are mounted to a shared base to allow for easy repositioning. These tools include:

- A custom-made spring-actuated suction gripper for gripping wood with a max payload of 20kg.
- A Modified Fasco Lignoloc Coil Nailer shooting a magazine of 150 wooden nails. (Tool Not Used throughout the entire Process)
- A Modified Dewalt Pneumatic Nail gun with a 300-nail magazine shooting 63.5mm nails
- An Air-cooled milling spindle equipped with a 12.7mm end mill with a max rpm of 24000.
- A Modified Dewalt Circular Saw with 177.8mm Diameter Blade

An alignment slide constructed to serve as a constant reference obtaining the physical gripping center of each piece of lumber. A Schunk pneumatic gripper with stepped grips was floor mounted to function as a work holding as each Lumber is processed. Using the suction gripper, there were limitations to the weight and imprecisions for vertical placing of members as there is a 1.5 mm of movement due to the spring actuation. The circular saw was limited in the max perpendicular cutting depth of 63.5mm. When using the pneumatic nail gun, in order to have a successful fire meant that the nozzle has to be fully pressed up against and perpendicular to the lumber.

2.1.2 The Robot Work Cell

The work envelope measures 4.26 meters wide by 12.22 meters long and is enclosed by 2.43 meters tall polycarbonate walls seen in Figure 2. Laid out in a linear fashion, the cell has two doors positioned at opposite ends, the first being for material loading and unloading to and from the cell and the other for general access. Each door is tied into a safety control system of the robot and activates an emergency stop if faults during robot operation. Inside of the cell starting from the loading door on the right, is a pallet positioning marker located on the floor to indicate the approximate placement of the pallet of boards. This allows the operator to quickly and accurately position the pallet in place. Next to the pallet is the lumber alignment slide where every piece of lumber picked by the robot is dropped on the slide and re-picked from its centre. Positioned next to the slide, all the robot end effectors are resting in their appropriate holders and all mounted to a shared base. The work holding is fastened to the floor next to the tools with a transparent Plexiglas wall acting as a barrier to protect the tools from dust and other objects during the milling and mitering process. Next to the work holding is the build platform where the pieces of lumber are placed and the build-up process occurs. The platform measures 1.5 meters by 4.5 meters dictating the maximum building area of the robot. At the end and outside of the cell is the operator viewing and control desk.

Figure 2

2.1.3 Selecting the Wood Grade

There were a series of investigations in attempt to select the right species and grade for the robotic process. Out of all the various species available at the local Boston lumberyards, Douglas fir was the preferred choice in terms of surface finish and density but it was prohibitive due to its relatively high cost. Our solution was to side on a low cost approach using the lowest grade Spruce-Pine-Fir (SPF) framing lumber as it is readily available and is a popular construction material. Our robotic setup was constructed to tend both 2x4 (38.1 x 88.9mm) and 2x6 (38.1 x 139.7mm) dimensional lumber at a maximum length of 1.21 meters, however we limited the design to using only 2x4 (38.1 x 88.9mm) Lumbers with a maximum length of 1.21 meters and a minimum of 0.3 meters.

2.2 Design Scripting

Various surface-based forms were explored within the 10’x20’ envelope of the booth at the exposition, with the basic theme of a Core (two Columns and a Beam) and Shell (Ground Floor, Upper Floor, Exterior Wall, Interior Surface). Grasshopper was used to divide the surfaces, modeled in Rhinoceros 3d into its individual elements and generate.

Figure 1
Rendering of Design

A nailing pattern needed to connect them. The application of textures to the digital model was also automated using the Human plugin for Grasshopper. Wood textures were mapped to each individual piece along its length (slightly shifted each time to maintain a natural feel. Primary parameters of Grasshopper Shell geometry script, used to divide the surface into its individual elements:

- Board Thickness
- Board Width
- Maximum Board Length
- Minimum Board Length

Using the Grasshopper Core geometry script, surfaces of Core are divided into curve Contours every Board Thickness along the y axis. Contours are divided into point Nodes (limited to Maximum Board Length). Nodes are connected by lines of Primary Rails. Rectangular profiles matching the Board Thickness and Board Width are extruded along the resulting linear Input data provided by the design outputs are sorted by type and subsequently by assembly. These inputs are:

- Lumber Geometry (Optional)
- Lumber Center Plane
- Lumber Center Lines
- Lumber Left and Right Miter Lines
- Dowel Points
- Lumber Lengths
- Nail Points

geometry and mitered at intersections. Lumber Geometry is organized by build order.

Primary parameters of Grasshopper Core nail script, used to generate a nailing pattern:

- Nail Offset from Ends
- Nail Offset from Center
- Nail Spacing

Using the Grasshopper Shell nailing script, two Nail Endpoints are identified for every Primary Rail, moved by the Nail Offset from Ends along the length from both endpoints. Two nails are offset by the Nail Spacing diagonally from the Nail Endpoint and assigned to each Primary Rail. Two nails are offset at the opposite diagonal (to avoid conflicts between layers) from the Nail Endpoint and assigned to the Primary Rails in the next layer. Two Nail CenterPoint are identified for every Primary Rail, moved by the Nail Offset from center both ways along the length from the CenterPoint. Two nails are offset by the Nail Spacing diagonally from the Nail CenterPoint and assigned to each Primary Rail. Two nails are offset at the opposite diagonal (to avoid conflicts between layers) from the Nail CenterPoint and assigned to the Primary Rails in the next layer finally, all nails are assigned to geometry and organized by build order as NailPoints.

2.3 Robotic Process

A program script was developed that converts outputs from the design script into a fabrication process and outputting robot-readable commands for its execution. The Software used for these processes are; Rhinoceros 3d (modelling), Grasshopper (scripting), Machina Plugin (robot communication), and ABB Robot Studio (simulation). An accurate 3d model of the robot cell was created for a visual understanding of the workspace of the robot.

OBJECTIVE:	ROBOT SUBROUTINE:	IMAGE:
1. Get Lumber From Pallet	- Pick Up Suction Gripper - Turn On Vacuum - Pick Lumber from Pallet*	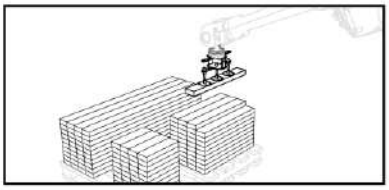
2. Align Lumber	- Place Lumber on Slide - Release Vacuum - Apply Vacuum - Pick Lumber from Slide*	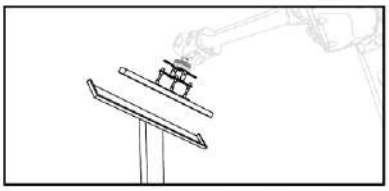
3. Clamp Lumber	- Open Work Holding - Place Lumber in Work Holding - Close Work Holding - Release Vacuum - Return Suction Gripper	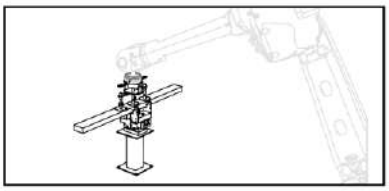
4. Miter Lumber	- Pick Up Circular Saw - Turn On Circular Saw - Miter Left and Right Ends* - Turn Off Circular Saw - Return Circular Saw	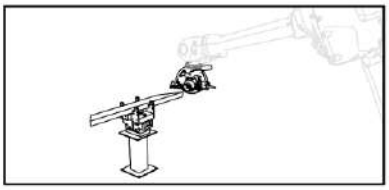
5. Mill Dowel Hole	- Pick Up Milling Spindle - Turn On Milling Spindle - Mill Dowel Hole* - Turn Off Milling Spindle - Return Milling Spindle	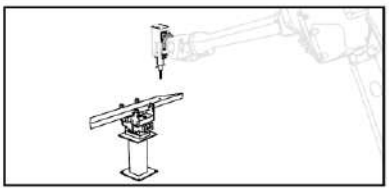
6. Get Lumber from Clamp	- Pick Up Suction Gripper - Turn On Vacuum - Move to Work Holding - Open Work Holding	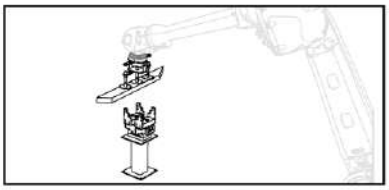
7. Place Lumber on Platform	- Place Lumber on Platform* - Release Vacuum - Return Suction Gripper	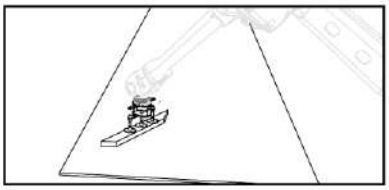
8. Nail Lumber	- Pick Up Nail Gun - Nail Lumber* - Return Nail Gun	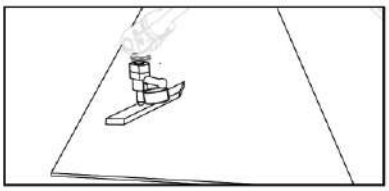

* Subroutines with variable target parameters

The first part of the script generates 3 stacks of lumber on a pallet. The stacks are 1 foot, 2 feet, and 4 feet in length from which the robot will pick each piece of lumber from. The output design data is then oriented and centered to build platform, this gives the viewer a visual understanding of the geometry which will be built. A series of sub routines were programmed outlining the overall fabrication process. This is depicted in Figure 2.

2.4 Manual Assembly

Apart from the maximum 1.5m x 4.5m x 1.4m build volume on the platform, transportation, manual handling, and assembly logistics were factored which limited the size of what each module could be. These constraints are that no module should be heavier than 200 lbs., its two smallest dimension not exceed 4 feet and 7 feet, and its longest length not greater than 16ft. This ensured that every module fabricated by the robot could be lifted by two people onto flat dollies loaded into a moving truck and erected on site without any heavy machinery involved. Every module was fabricated with ½ inch dowel holes that corresponded with its neighbouring module this aided in precisely aligning modules together and then subsequently fastened with screws for additional security. This simple modular technique was created to allow for non-skilled labour to easily assemble complex components with basic hand tools.

2.5 Results

The parametric workflow was critical to managing the complex data of the 2,154 individual pieces. The relational nature of the digital model allowed for this large amount of data to be flexible, changing as real-world tests affirmed or rejected our initial assumptions. In the robotic script, Machina was a useful tool to seamlessly compile fabrication instructions from Grasshopper into robot-readable code, simulate robot movement in ABB Robot Studio and subsequently sending that data in real time to the robot for execution. This allowed for real-time modifications to the design as changes arise.

2.5.1 Fabrication with Robots

Despite the automated nature of this process, there were a few manual processes involved prior to fabrication and post fabrication. The 800 boards supplied from the lumber yard came in 2.43 meter lengths and required cutting them down to 1.2, 0.6, and 0.3 meter lengths using a standard chop saw. With two people involved, the time to process all 800 boards was approximately 7.5 hours. These lumber pieces had to be stacked in a pile on pallets and place in the robot cell for retrieval by the robot.

2.5.2 Jointing and Planing

In initial testing, the lumber was jointed and face planed to ensure a squared rectangular profile and a smooth surface finish. This made all boards, regardless of their natural inconsistencies, uniform and guaranteed proper suction when being gripped by the suction gripper. The jointing and face planing of all 800 boards would have been time consuming and labour intensive, taking over 42 hours to complete. This approach was abandoned and instead the focus was to engineer a more robust gripping system to accommodate for the natural inconsistencies of the unprocessed wood. Special webbed suction cups from Schmalz were used that would then compartmentalize the suction over the surface of the Lumber for better adhesion. In tandem an air ejection system had to be integrated to release the boards when being placed due to the high suction (101 kPa) generated by the vacuum pump.

Figure 4

2.5.3 Quality Control

A visual inspection of the Lumbers were done when stacking them on pallets. Features that would disqualify a Lumber from being placed on the stack are significant warping, large splits, and loose knots. Splits and knots that run through or around the centre top face of the Lumber tends to create a leak in the vacuum cups and is likely to fall when being handled by the robot. Warped Lumbers however can be used in the process by cutting them down to 1 foot lengths, but unless factored in, it can affect the consistent aggregation of Lumbers. After

quality controlling all 800 boards the unusable percentage was a surprising 2.25 percent, less than anticipated.

2.5.4 Calibration

In order to utilize the high precision of the industrial robot, every tool was carefully measured in and calibrated of optimal performance. Each tool's TCP (Tool Center Point) was measured in with an accuracy of 0.01mm-0.03mm. Starting with the suction gripper, it went through a series of iterations varying the suction cup types, gripping vacuum pressure, and quick release mechanisms. As for the Fasco Lignoloc nailer, it was working normally when running at a reduced robot speed of 250mm/s but stopped working when attempting to run at 700mm/s. This was mainly because the air flow rate we were supplying was too low for the speed we were moving. This cause a rupture inside the tool rendering it unsuitable to continue use in the process. Pressed with time, we had to resort to using the standard Dewalt nailer with steel nails. The initial approach to cutting the ends of each lumber was using a milling spindle. This was to allow the flexibility of cutting beyond straight miters. The process was too slow and there was no need to cut the ends other than straight miters. The milling spindle however was appropriately used to position the dowel holes. Mitering the ends of the boards was done with a ripping blade on the circular saw. The maximum speed of cut was 90mm/s while still have a good cut finish.

2.5.5 Speed of Fabrication

Every portion of the fabrication was gradually sped up to its maximum capabilities without affecting performance or quality. On average the processing of each board takes 1 minute 20 seconds from the point of picking up the board to nailing it in place. For a total of 2,154 members, total fabrication time amounted to 54 hours.

2.5.6 Assembly Evaluation

Laser scanning was used to verify the constructed geometry against the design model. The robotically-constructed modules were accurate to 1mm precision, while the completed assembly, done by hand, were accurate to within 75mm. This further advances the notion that robotic fabrication should extend into the assembly process, allowing its inherent precision to carry through to the constructed building. Figure 3

Figure 3

Comparison of laser scan of constructed pavilion (wood texture) and digital design model (in red). All geometry was verified to be within a 75mm tolerance.

2.6 Conclusions

The success of the pavilion marks a major step forward for sustainable applications of robotics. Because it is a post-and-beam mass timber structure, the pavilion's workflow could be applied to a structure as tall as 18 stories.

The use of wood allows for a renewable, widely-available material to displace steel or concrete and reduce a building's carbon footprint. The use of robotics allows the resulting assemblies to be infinitely varied and optimized with millimetre precision. The direct nature of communication between a digital model and a robot allows for a seamless translation from an imagined design to constructed reality. Moving forward, Perkins + Will seeks to implement these workflows into its projects, ensuring a better final product for its clients.

2.7 Future Research

Future research will seek to build on this workflow and seek ways to implement them into real projects. Because of the experimental nature of the project, the workflow was somewhat imprecise. Wood is a natural material and no two pieces of lumber are alike. The project used generous tolerances to finish within the deadline.

There are two ways this research can continue: non-structural elements and structural elements. Non-structural elements would generally use the same workflow, with adaptations for specific forms and connection types. Structural elements, however, must be built to more exacting standards, and will most likely

require sensors feeding data back to the digital model, allowing the model to adapt to the shape of the actual lumber given. Machine learning could be used to optimize nailing patterns by understanding and analyzing the grain of the wood.

2.8 Acknowledgements

This research was funded by the Perkins+Will Building Technology Lab and supported by the following partners: Autodesk Technology Center Boston, Fasco, SMC, Dewalt, Komodo Fire Shield, Faro.

2.9 References

[1] Krammer M. *Robotic Fabrication in Architecture Art and Design*, Individual Serialism through the use of Robotics in the Production of Large-Scale Building Components. pages 461–467, Sydney, Australia, 2016.

[2] Glenn, Deborah Snoonian, and Deborah Snoonian Glenn. "Katerra Announces New Products for the Design and Construction Industry." Architectural Record RSS, Architectural Record, 22 Feb. 2019, www.architecturalrecord.com/articles/13925-katerra-announces-new-products-for-the-design-and-construction-industry.

[3] Mairs, Jessica, and Jessica Mairs. "Robotically Fabricated Pavilion by University of Stuttgart Students." Dezeen, Dezeen, 28 June 2016, www.dezeen.com/2016/05/05/robotically-fabricated-pavilion-university-of-stuttgart-students-plywood-icd-itke/.

[4] "SPATIAL TIMBER ASSEMBLIES." DFAB HOUSE, dfabhouse.ch/spatial_timber_assemblies/.

Design of a Robotic Software Package for Modular Home Builder

C.-H. Yang[a], T.-H. Wu[b], B. Xiao[a], and S.-C. Kang[a]

[a]Department of Civil and Environmental Engineering, University of Alberta, Canada
[b]Department of Civil Engineering, National Taiwan University, Taiwan
E-mail: chenghsuan@ualberta.ca, f00521611@ntu.edu.tw, bxiao2@ualberta.ca, sckang@ualberta.ca

Abstract –

This paper is sharing an on-going project about the design of a software package, tentatively coined as RS4B, for the builders of modularized construction. The shortage of labour resources and safety awareness issues have become the emerging problems in the construction industry. As the price of robots gradually decreases within these years, it is a promising direction to integrate robotic technology with the construction process to bring better productivity. However, shifting the long-term labour-based process to the robot-based process is not a simple task. Therefore, this research designed an assisted software package for filling the gap between the conventional process and robotic process. Four kinds of software were proposed in this research with their required functions and user interfaces design. With such an assisting tool, builders of modular home manufacturing will be able to extract information from the existing BIM model and transfer the information for the robot control.

Keywords –

Modular homes; Industrial robots; Robotic construction

1 Introduction

This research focuses on the design of an assisting software package for robotic modular home manufacturing. A modular home is a building that produced using factory-built modules instead of site-built [1, 2]. It is an innovative method that uses large, three-dimensional, and off-site manufactured modules to build a home [3]. Within these years, the modular home building has been widely utilized in North America, especially residential buildings, due to its high efficiency and low construction cost [4]. Although advance in the process can bring improvements to the industry, such a construction method has no significant improvement in productivity [5]. It is because the modular home manufacturing process still relies on labour works. The entire process may cost 202 labour hours in average for a single modular, including subassembly, module-built, interior work, and wrapping and shipping [6].

As the elevation of labour shortage and safety awareness, it is critical for builders to develop advanced construction methods for reducing the usage of labours. According to the Canadian Federation of Independent Business (CFIB)'s report, construction industries holds the second highest job vacancies rate (3.6%) in the first quarter of 2018 in Canada [7]. The severe shortage issue can bring serious issues to construction productivities. Besides, construction safety is another increasing issue in the industry. During 2014 to 2016, fatalities happened in the construction industry account for 23.81% of all industries in Canada [8]. Therefore, it is an urgent and promising direction for the industry to reduce the requirement of human involvements.

Recently, studies have been conducted for implementing the industrial robot into the manufacturing process of buildings for dealing with the labour shortage issue meanwhile increasing the productivity of the process. However, shifting the long-lasting labour-based process to robot-based is not a simple task. There are still challenges and constraints remain unsolved before implementing into the industry, such as insufficient education program for basic robot control training, no research environments for the development of new construction method, and lack of well-developed assisting software. Therefore, this research proposes the design of an assisting software package for filling the gap between conventional construction to robotic construction. The following section will include a literature review for identifying both the opportunities and challenges of utilizing industrial robots into the building industry, the research objective, and the design of the software package respectively.

2 Robots in Modularized Construction

As the growth of robot technology and decreasing of robot price, it is a promising direction to develop robotic and internet of things (IOTs) solutions to reduce labours in the job site, and meanwhile increasing the productivity of the construction industry. According to Statista - The Statistics Portal, the price of industrial robots drops 28% in the past ten years [9]. Industrial robots, such as robot arms, have been widely utilized in the manufacturing industry for complex, repetitive, and tedious tasks for years [10]. However, in the field of construction, the application of industrial robots is now infancy and still has a long way to go. In fact, in 2017, 83% of construction companies had not implemented robots into their working process [11].

Recently, research about robotic construction has been conducted for reducing the gap between labour-based and robot-based process. For instance, Khoshnevis used additive manufacturing process for large-scale construction [12]. Skibniewski and Hendrickson identified the benefits of using robots for the on-site surface finishing work [13]. The "In-situ Fabricator" was developed by ETH Zürich for the rebar work of a double-curved concrete wall [14, 15]. García de Soto et al. conducted an experiment for comparing the productivity performance of ETH Zürich's robotic method with the conventional process [16]. The results showed that robotic construction method could have higher productivity when facing a complex wall.

Although utilizing robots for repetitive building tasks has been proven for having higher efficiency than conventional methods [17], there are still challenges for implementing such technologies into the building manufacturing process. This research concluded three major issues should be overcome.

- **Thousands of components:** Unlike the manufacturing industry, the building contains thousands of components for assembly. Therefore, how to breakdown the original design to manufacturable components with considering the capacity of robots may be one of the most critical issues. The robotic assembly plan should be well organized and designed for such a huge number of components.
- **Complex building regulations:** In the industry of construction, the most important but difficult task is to meet the building regulations, such as structural regulations, connection regulations, or shipment regulations. Some of the regulation is hard for the robot. An assembly planner which is able to check if the design fits the regulation automatically is thus important.
- **Numerous unique robot motions:** The building component is more complicated than other mechanical components. The robot may need to place different types of studs for different types of frames, nailing or wielding for connection, and installing different kinds of objects like windows, doors, or Mechanical, Electrical, Plumbing (MEP) systems. Therefore, a well-designed robotic motion planner with intelligent algorithms which can automatically generate related robotic motions should be developed.

3 Research Objectives

This research aims to propose a blueprint of an assisting software package, tentatively coined as Robot Studio for Builders (RS4B). RS4B is designed to extract the information from the existing building information model (BIM), and transfer the information for robot control. Such a software package should be able to deal with the large amounts of building components meanwhile considering the building regulations and the robot motions simultaneously. The design of the RS4B will list the functions of the tool and propose a prototype of the user interface.

4 Design of RS4B

This research designed a software package for assisting the builder to link the original design (BIM) with robot controls. The package contains four software: *BIM Exporter*, *Assembly Planner*, *Robot Simulator*, and *Motion Planner*. With the four software, builders are supposed to be able to breakdown the buildings into the modular, panel, and assembly components. Such software is expected to be an assisting tool for the future building industry with robot-assisted workflow. The following subsections will describe the designed function and user interface of each software respectively.

4.1 BIM Exporter

BIM Exporter is designed to subsect the entire building into components, extract the geometrical information and generate the robot-manufacturable models of the building component. It should assist the builder to retrieve the geometric information of building components from the complete building information models. The software will help dissect the digitized 3D models and export the building components to be manufactured by robots. *BIM exporter* should divide a BIM model into building components such as walls, roofs, floors, and stairs, with their geometric properties. The exported data will be linked with the original BIM model to assist the builders to figure out where the building component in the BIM model.

Figure 1 illustrates the design of the main interface

of BIM Exporter. Four major functions will be included in the software. (1) BIM model import: The users will import common BIM models such as Autodesk Revit (.rvt), Bentley Microstation (.dgn), Graphisoft ArchiCAD (.pln), and other models in IFC format (.ifc). The software should be able to read the file and import to the associated database. The imported BIM model will be represented on the user-interface. (2) Components breakdown: *BIM Exporter* will subsect the whole building into components. The users can view the breakdown details for each component. They are able to click the component in the breakdown structure to see the isolated 3D view of the component. (3) Components classification: *BIM Exporter* will intelligently classify the objects by type and size. The similar objects can be manufactured by similar robotics working packages. With the classification, the users are easier to export similar objects as groups to reduce the efforts for the following steps. (4) Geometric information extraction: *BIM Exporter* will extract the geometric information for all the building components to be assembled by robots. The models are stored in a cloud database which allows better management and flexible usage in the following steps.

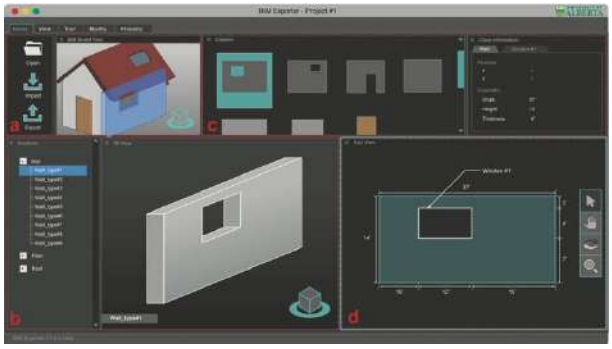

Figure 1. The designed interface of *BIM Exporter*. (a) imported BIM model (b) breakdown structure and isolated 3D view (c) classifications and their detailed information (d) geometric information of the component.

4.2 Assembly Planner

Assembly Planner aims to assist the builders to plan the assembly details of each component exported by *BIM Exporter* for robot manufacture. The assembly details include the frame layouts of each component, the temporary supporting layout for robot assembly, and the optimal sequence of assembly. The software should have an intelligent algorithm to automatically generate the suggested assembly sequences by considering the building regulations, geometrical constraints, and physical limitations.

Figure 2 illustrates the preliminary design of the main interface. Five major functions will be included in the software. (1) Components import: The users can import the building components to be manufactured by robots. The components' breakdown structure will be displayed in the left-hand side. (2) Regulations import: The users can import the regulations and the association between components and regulations will be linked. After regulations import, the software would be able to generate the default framing layout automatically considering the building regulations. (3) Components framing layout: *Assembly Planner* should allow the users to refine the default framing layout through framing toolkits. Different type of components requires different elements for framing. They can replace the different dimension of elements to satisfy the required structural strength and under the geometrical constraints. (4) Temporary supporting layout: The users can also plan the temporary supporting layout. The temporary supporting will be placed by robot arm before assembly. The physics limitations will be considered to ensure the support can keep the frame stable during assembly. (5) Assembly sequence planning: *Assembly Planner* should provide an intelligent algorithm to plan the manufacture in an efficient assembly sequence. The users can also refine the sequence by adding any other consideration and determining the weighting to reflect different scenarios.

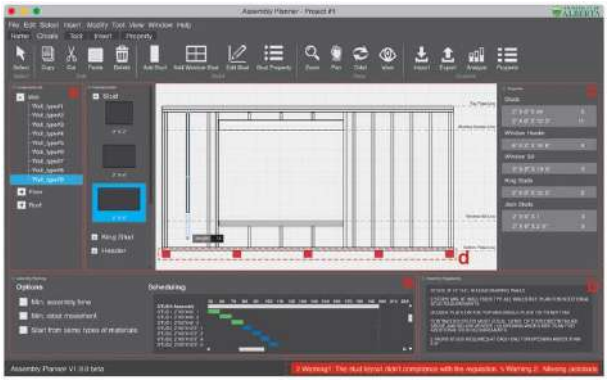

Figure 2. The designed interface of Assembly Planner. (a) components to be manufactured (b) regulations import (c) framing toolkits (d) temporary supporting layout (e) sequence planning.

4.3 Robot Simulator

Robot Simulator should provide the detailed simulation for the entire work sequence of robots, including material preparation, move, assemble as well as the working layout. In the robotic development or application, the simulator is often used to simulate a

robot's movement without depending on the actual machine. With the simulator, the builders can optimize the work sequence of robots without wasting time and cost. In some commercial simulator, it even allows the simulated movement to be directly transferred onto the physical robot without modifications.

Figure 3 illustrates the design of the main interface. The interface contains six major functions. (1) Assembly layout and schedule import: *Robot Simulator* allows the users to directly import the assembly layout and work schedule created by *Assembly Planner*. The builders can import the 3D models with detailed geometry properties, the temporary support layout, and the assembly schedule. (2) Animation-based robot programming: The software allows the users to drive the robot using time-based animation tools. The users can operate the robot through keyframing motion, velocity and acceleration tuning, motion blending, and more. The operations can be exported as either animation files or robot commands codes. (3) Built-in robot models: *Robot Simulator* provides several built-in robot models for the users. The robot's rig and post-processors, external axes, configurations, and I/Os are all extensible. With the flexibility of robot models, the users can control most brands of industrial robots in the simulator. (4) Inverse Kinematic/ Forward Kinematic robot control: The users are allowed to manipulate the robot through either Forward or Inverse Kinematic method. (5) Collisions and singularities warning: The collisions and singularities will automatically detect through an embedded algorithm. Whenever the collision or singularity is detected, the simulator will highlight on the model to warn the users. (6) Robot commands export: The software can output the operation able robot code after the users sets the movement of the robot. The real robot can directly be actuated without further programming by inputting the exported code from Robot Simulator.

Figure 3. The designed interface of Robot Simulator. (a) assembly layout and schedule import (b) animation-based robot programming (c) built-in robot models (d) FK/IK robot control (e) collisions and singularities warning (f) robot commands export.

4.4 Motion Planner

Motion Planner aims at autonomously optimizing the robotic movement to a more efficient assembly process. Motion planning is the process of breaking down the robot trajectories into discrete motions that considers both the constraints of surroundings and the limitations of the robots. Robots have been widely implemented in the manufacturing industry for high-repetitive tasks. Since building components usually consist of complex and large elements, it is essential to have an intelligent motion plan for the manipulators to interact with the surroundings safely and efficiently finish the task.

Figure 4 illustrates the design of the main interface. Six major functions are included in the software. (1) Back-end algorithm: An algorithm with features of inverse kinematics, collision detection, and singularity avoidance which considers the working space, joints limits, and speed of actuators will be utilized. Through implementing artificial intelligence, the developed algorithm can autonomously optimize the paths generated from the *Robot Simulator*. (2) Front-end fine-tune panel: The software will offer a fine-tune panel for the users to adjust the auto-generated paths. The users can change the manipulation time, add the path constraints, and modify the workspace's specifications. (3) Robot trajectories generation: The software will illustrate the image of the simulation in action with motion planning on the user-interface. This feature details the configuration of joints and links of the robot, which enables the users to check the designed movement through an intuitive way. (4) Data recording and visualization: The flexion and extension angle of the robot's joints will be recorded. The data streams can display the time-graph of each joint as well as combined to form x/y-graphs. The users can easily use those graphs for assistant them to fine-tune the planning result. (5) Connection with real robots: The optimized robot movements can directly export and output as the real robot's commands. *Motion Planner* provides the robot codes for KUKA and ABB, two major robot arms solutions globally. The user can also add the preferred robot language, such as Python, Pascal, C#/.NET, and more, through the open-sourced development environment. (6) Extensible functions: The software is designed with modularity. The users are allowed to reconfigure the interface, create the planning templates, integrate external sensors, and so on. The users can easily optimize the robot's motions by using the designed features as well as customized settings.

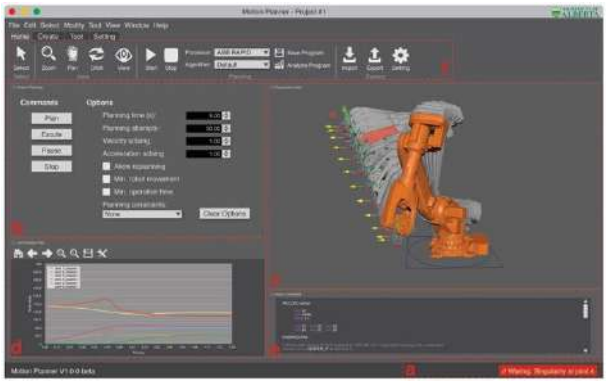

Figure 4. The designed interface of Motion Planner. (a) back-end algorithm; (b) front-end fine- tune panel (c) robot trajectories generation (d) data recording and visualization (e) connection with real robot (f) extensible functions.

RS4B is designed mainly for helping the builder to link the original design to the robotic control. The builder can follow the step-by-step process to discrete the building components, generate the assembly plan, and actuate the robots. With the help of such a software package, the builder who usually has insufficient knowledge and skills might be able to fast and easily implement robots into the manufacturing process.

5 Conclusion

This paper shared an on-going project of developing a robotic software package for the modular home builder. This research designed a four-software package for reducing the threshold of linking the conventional process and robotic manufacturing. The package includes a BIM exporter, an assembly planner, a robot simulator, and a robot motion planner. With such a package, the builder will be able to link the BIM design with robot control thus realizing the robotic process. However, two more details also need to be figure out before realizing the robotic process. One is the development of building design policy for robotic manufacturing. The design policy should also be improved with the consideration of robotic manufacturing to fit the capacity of robots for increasing both efficiency and productivity of the process. The other one is the design of the robotic factory. It may include the design of the robot gripper, the workstation, the assembly line layout, and the circulation. This research will consider these two tasks as the future works. The robotic process is estimated to be realized within the following five years. Implementing robots for modular homebuilding can be expected as the first step to lead the whole industry toward robotic construction.

References

[1] Carlson, D. O. (1995). Automated Builder: Dictionary/encyclopedia of Industrialized Housing. Automated Builder Magazine, Publications Division, CMN Associates.

[2] Gianino, A. (2005). The Modular Home. Storey Pub.

[3] Nasereddin, M., Mullens, M. A., & Cope, D. (2007). Automated simulator development: A strategy for modeling modular housing production. *Automation in Construction*, 16(2), 212–223. https://doi.org/https://doi.org/10.1016/j.autcon.2006.04.003

[4] Diekmann, J., Balonick, J., Krewedl, M., & Troendle, L. (2019). Measuring Lean Conformance. *International Group of Lean Construction 11th Annual Conference Virginia Tech*, Blacksburg, Virginia, USA.

[5] Zhang, J., Eastham, D. L., & Bernold, L. E. (2005). Waste-based management in residential construction. *Journal of Construction Engineering and Management*, 131(4), 423–430. https://doi.org/10.1061/(ASCE)0733-9364(2005)131:4(423)

[6] Mullens, M. A. (2011). Factory Design for Modular Homebuilding: Equipping the Modular Factory for Success. Constructability Press.

[7] The Canadian Federation of Independent Business (2018). Help Wanted: Private sector job vacancies, Q1 2018. https://www.cfib-fcei.ca/en/research-economic-analysis/help- wanted- private-sector-job-vacancies. (Accessed: Dec. 20, 2018).

[8] Association of Workers' Compensation Boards of Canada. 2014-2016 National Work Injury, Disease and Fatality Statistics. http://awcbc.org/wp-content/uploads/2018/03/National- Work-Injury-Disease-and-Fatality-Statistics-Publication-2014-2016-May.pdf. (Accessed: Dec. 20, 2018).

[9] Statista - The Statistics Portal. Worldwide sales of industrial robots from 2004 to 2017 (in 1,000 U.S. dollars). https://www.statista.com/statistics/264084/worldwide-sales-of-industrial- robots/ (Accessed: Dec. 20, 2018).

[10] Rüßmann, M., Lorenz, M., Gerbert, P., Waldner, M., Justus, J., Engel, P., & Harnisch, M. (2015) "Industry 4.0: The Future of Productivity and Growth in Manufacturing Industries," *Boston Consulting Group 2015.*

[11] Statista - The Statistics Portal. Degree of robotic process automation/digital labor implementation in U.S. engineering and construction companies as of 2017. https://www.statista.com/statistics/805207/degree-of-technological-adoption-in-us- engineering-and-

construction-companies-2017/. (Accessed: Dec. 20, 2018).
[12] B. Khoshnevis (2004). Automated construction by contour crafting—related robotics and information technologies, *Automation in Construction*, 13(1) 5–19, http://dx.doi.org/10.1016/j.autcon.2003.08.012.
[13] Skibniewski, M., & Hendrickson, C. (1988). Analysis of robotic surface finishing work on construction site, *Journal of Construction Engineering and Management*, 114(1), 53–68. https://doi.org/10.1061/(ASCE)0733-9364(1988)114:1(53).
[14] Hack, N., Lauer, W., Gramazio, F., & Kohler, M. (2015). Mesh Mould: robotically fabricated metal meshes as concrete formwork and reinforcement, *Proceedings of the 11th International Symposium on Ferrocement and 3rd ICTRC International Conference on Textile Reinforced Concrete*, Aachen, Germany.
[15] Giftthaler, M., Sandy, T., Dörfler, K., Brooks, I., Buckingham, M., Rey, G., Kohler, M., Gramazio, F., & Buchli, J. (2017). Mobile robotic fabrication at 1: 1 scale: the in situ fabricator. *Construction Robotics*, 1–12, http://dx.doi.org/10.1007/s41693-017-0003-5.
[16] García de Soto, B., Agustí-Juan, I., Hunhevicz, J., Joss, S., Graser, K., Habert, G., & Adey, B. T. (2018). Productivity of digital fabrication in construction: Cost and time analysis of a robotically built wall. *Automation in Construction*, 92, 297–311. https://doi.org/10.1016/j.autcon.2018.04.004.
[17] Najafi, F. T., Fu, X. (1992). Economic evaluation of robots in construction. *9th International Symposium on Automation and Robotics in Construction (ISARC)*, Tokyo, Japan, 1992, http://dx.doi.org/10.22260/ISARC1992/0027.

Implementation of an Augmented Reality AR workflow for Human Robot Collaboration in Timber Prefabrication

O. Kyjanek[a] , B. Al Bahar [b] , L. Vasey[a], B. Wannemacher [b], and A. Menges[a]

[a]Institute for Computational Design and Construction, University of Stuttgart, Germany
[b]ITECH Masters Program, University of Stuttgart, Germany
E-mail: ondrej.kyjanek@icd.uni-stuttgart.de, Lauren.Vasey@icd.uni-stuttgart.de,

Abstract –

In this paper, we present a set of enabling technologies developed for the KUKA Innovation Award to facilitate Human Robot collaboration targeted for the architecture, engineering and construction (AEC) sector. Critically, little progress has been made in the usability of user interfaces for industrial robots [1]. We targeted our investigation explicitly towards human-robot collaboration (HRC) in wood based prefabrication production. Although wood is a sustainable material with abundant processing possibilities, it is also a material system where process knowledge remains critically important, making highly automated workflows unfeasible and inefficient.

We propose an interactive fabrication process where a user such as a construction worker could wear an augmented reality head mounted display (ARHMD) as an interface to plan robotic trajectories, influence production sequencing, and view superimposed diagnostic feedback. We describe necessary system components including a robotic workcell consisting of a KUKA LBR iiwa, flexFELLOW mobile platform, a Robotiq 2-finger gripper and a custom platform and material feeding station. In addition, we describe a communication framework and set of protocols connecting a CAD digital design environment, a user interface (UI) for Microsoft HoloLens, a ROS server for backend path planning and coordination, and a 3D graphical web interface for downstream visualization of construction status. We conclude with an outlook on enabling technologies for human-robot collaboration in construction, and the importance of increasing digital integration and accessibility in characteristic production workflows through accessible and intuitive digital interfaces.

Keywords –

Human-robot Collaboration; Timber Construction Prefabrication; Robotic Fabrication; Augmented Reality; Digitalized Construction; Hardware-Software Interoperability

1 Introduction

The construction industry stands to benefit tremendously by increased digitization and automation [2,3]. Extensive progress has been made, primarily in research contexts, in the development of nonstandard material systems enabled through digital and computational workflows connected to physical and precise production equipment including industrial robots. However, there still remains a lack of transfer of these developments into typical production chains and construction processes.

Though there are many factors which have hindered the importation of robotics into construction, one reason is the need for human level dexterity and cognition due to the unstructured nature of construction tasks. In prefabrication workflows, where production occurs in a more structured setting, there is still often a need for human intervention in response to material inconsistencies. Existing timber construction methods and construction systems rely on the expertise, craftsmanship, and dexterity of human workers, favouring a "human-in-the-loop" production chain over highly automated production. Thus one way to increase efficiency and productivity is to facilitate collaborative human and robot workflows, where digital mechanisms and enabling interfaces can orchestrate safe exchanges of tasks.

1.1 Research Aim

Thus the aim of the project is to develop a set of technologies to facilitate an interactive human-robot collaborative workflow for the construction industry: where a user such as a construction worker with limited background knowledge in robotic programming, can interact with a robot system through an augmented reality (AR) interface. To investigate this question, a proof-of-concept fabrication system for human-robot

collaboration is developed. In the developed workflow, production and assembly tasks alternate between a human user and the robot system in the construction of an architecture scale non-standard wooden construction system. Additional communication mechanisms increase interoperability with secondary devices and monitoring platforms.

2 Context

2.1 Challenges in Adapting Robotics in Construction

Much has been written about the construction industry's reluctance to embrace both digitalization and robotic technologies. Reasons given include the compartmentalization of the construction industry [4], interoperability of software for different services, and lack of accessibility of robotic technology as barriers for application. A standard fabrication systems including the well-known six axis industrial arm, developed for the domain of manufacturing, is additionally known to be ill suited for unstructured environments such as a construction site. In addition, historically, robots developed with specific use for the construction industry were primarily focused on narrowly automating single tasks, rather than automating many different tasks within a singular production workflow [5].

Though redesigning building systems for the contingencies and constraints of automation through integrated co-design processes is one long term solution, this project focused in particular on HRC as a means to accelerate automation of the construction industry in the short term.

2.2 Human-Robot Collaboration

Human-robot collaboration as defined in TS/ISO 15066:2016 is an operation where a human worker and a purposely designed robot system can perform tasks in a defined collaborative space concurrently during a production operation. From a technical point of view, this definition means mainly that the motor drives are powered (moving or in safe operational stop) and brakes are not applied even when the robot or its workpiece is in close proximity or even in a physical contact with a human.

However, manufacturing applications with standard industrial robotic arms pose serious danger to human workers and have to be equipped with additional safety components for a safe HRC which decrease the flexibility of the system and increase the setup costs. To overcome this problem an entirely new type of industrial robot arm and controller emerged in past years that can limit the collision forces and thus prevent harm to human body in the event of a contact. Though collaborative robots were developed initially with different target applications and domains, their safety in proximity to humans makes it possible to implement them in fundamental research where collaborative workflows are necessary. Construction sites, which are inherently unstructured, and existing construction systems that rely on human cognition and expertise, make the AEC sector an ideal domain for human robot collaboration.

While the issue of safety is an elementary part of HRC it is only one layer of behaviors needed for successful collaboration [6]. From a broader perspective collaboration does not involve only physical behavior of the involved agents but also their cognitive states [7] as well as optimal form of human-robot communication frameworks.

In this context, the proposed system focuses mainly on the design of appropriate interfaces between a human operator and the robot system resulting in a higher level of behavioral cooperation while limiting physical human-robot interaction. The system also involves only simple cognitive functionality and focuses more on increased integration and interoperability through a set of digital mechanisms connecting design and production.

Similarly, the topic of safety is addressed by others [8,9] and it is not focused in this paper.

2.2.1 Automation in Timber Construction

There are various reasons for the recent rapid advancement and relevance of HRC within the construction industry. The two main reasons are:

- The need to address the growing demand of product customization instead of standardized mass-production.
- Importance of increasing competitiveness of small and medium-sized enterprises (SMEs) that must usually rapidly adapt production to new products in small batches.

Typical construction industry projects can be characterized as a one-of-a-kind production with a fragmented supply chain (i.e. many different contractors involved) that are being fabricated mainly on-site [10]. In Germany, where this project was based, in particular more than 88% of the construction market is formed by companies with up to 19 employees. Timber construction and carpentry companies in Germany have those numbers even higher with more than 96% of the companies having up to 19 employees [11].

Timber construction has however several key features and differences that increase the chances of the industry to adopt novel automation strategies. Those features are especially:

- High level of off-site prefabrication in a controlled

environment
- Short required technological brakes during the production (e.g. glue setting)
- Easy to machine and assemble materials

2.2.2 HRC in Timber Construction

The Level of Automation (LoA) in timber construction is relatively high in the earlier stages of the prefabrication chain where the material is being shaped and trimmed by various CNC and power tools. On the other hand, the subsequent assembly stages that require higher flexibility and human knowledge are still largely manual.

Standard automation strategies developed as a result of flow production demands are not suitable for the dynamic batch and job production within timber construction prefabrication which requires flexibility. HRC applied towards prefabrication presents an opportunity to increase the automation and productivity of timber prefabrication by combining the human knowledge and dexterity (e.g. screw fastening) with the advantages of industrial robots (e.g. precise positioning).

2.3 User Interfaces for Fabrication and Construction

User interfaces (UIs) for industrial robots have hardly made as much progress as UIs in other comparable industries [12]. Thus increasing the ability for non-expert users to interact with a robot was a key motivation for this project, and a key feature which could arguably allow robots to more readily infiltrate the construction industry.

It has already been demonstrated in previous work that well designed human-machine interfaces (HMIs) and background computational coordination have potential for coordinating multiple users in complex building processes; within HMI research just-in-time instructions provided through wearable devices could provide the necessary instructions for non-expert users to engage successfully with robots towards the production and assembly of architecture-scale structures [13].

The advantage of using AR, in addition to screen based interfaces, lies in the ability to overlay digital information over the real-world environment where and when necessary while interacting in real-time using physical and virtual controls. In addition, production statistics and information, assembly sequences as well as machine feedback and control can become more accessible with less training, less preparation time and pre-programming, and also capable of real time updates in response to detected system changes.

State-of-the-art ARHMDs have obvious traits which prohibit their deployment as a universal device for all interface needs, in particular their high cost, short battery life, and limited field-of-view, making it advantageous to develop compatible secondary screen based interfaces.

2.4 AR Applications in the AEC Sector

Several projects have investigated the use of AR in the architectural context. Already in the mid 90´s researcher visualized invisible infrastructure like load bearing columns and their structural analysis using a head worn display [14]. In more recent research, Fazel and Izadi used a head mounted display to guide the manual construction of complex architectural freeform modules [15]. Object interaction and projection-based AR was used to design and robotically transform a seemingly random material system out of melting wax [16]. Newly available plugins developed for computer-aided design (CAD) environments, including Fologram [17], suggest increased opportunities for AR displays as devices which can enable direct three-dimensional feedback superimposed on reality from a digital CAD model.

At the time of submission, limited research has been conducted using AR together with robotic manipulators for the domain of AEC. Fazal and Izadi state in their conclusion that the use of AR can be beneficial for controlling robotic systems [ibid.]. We saw a gap of research where multiple hardware and software technologies could be combined into one system, fabrication workflow, and experience, particularly addressing the need to for robotic interfaces to be compatible with customizable one-off production processes.

3 Methods

3.1 Robotic Workcell and Fabrication Setup

The hardware includes the LBR iiwa robot mounted on a flexFELLOW trolley, a Robotiq 2-finger gripper as an end-effector, a custom-built wood magazine for standard wood stock, a Microsoft HoloLens ARHMD, and a Bosch cordless impact driver for screwing.

The final structure is divided into fabricable building groups called in the context of this research “sub-assemblies”. The fabrication of each sub-assembly takes place on top of an assembly pedestal (Fig. 1). During the exhibition, the robot is moved manually along the pedestal to enable increased reach, though improving robot localization would be a next step in development. Each completed sub-assembly is moved by hand into its predefined position within the final structure, where it is connected to its neighbours with screws.

Figure 1. Robotic workcell and demonstration setup with the assembly pedestal.

3.1.1 Construction System and Computational Process

Though the wooden beams have standardized lengths for simplified implementation in an exhibition setting, the proof-of-concept construction system has the important characteristic of unique rather than standard positions of all the elements, necessitating precise positioning and digital integration. This initial design geometry is generated in CAD software Rhinoceros utilizing a generative design tool and visual scripting language Grasshopper.

Several additional software environments are used for their relative strengths; thus it is critical to establish conventions for interoperability between multiple software environments. To meet this aim, each element in the initial design file and database is given a unique identifier, indicating its assembly number, row and column position.

The driving system principles for the collaborative process are that users execute tasks requiring process knowledge and dexterity, while the robot is used for precise positioning. The HoloLens is deployed as the main HMI and control layer through which this user can plan, dispatch and manipulate robotic path planning in real-time, while also getting live feedback about the current construction status and the state of the robotic system. After selecting a part for fabrication, the path is previewed in the HoloLens. On dispatch, the robot takes an element from the magazine, places it precisely according to the digital model, and then holds the part until the user fasten parts together with screws.

3.1.2 ROS Engine and Communication Network

The core of the system is built using the Robot Operating System (ROS) [18] framework that provides the required communication layer. The ROS server is responsible to manage the CAD geometry, receive and publish robot positions and targets, collect robotic status data, keep track of the fabrication progress, plan robotic paths, and receive commands from the ARHMD and forward them for execution.

The core ROS server achieves this functionality with several features:

- A digital twin of the system that manages system states and real-time environment data
- Path planner based on the ROS package MoveIt! [19]
- Set of ROS nodes that serve as a bridge between the ROS environment and the Java environment of the KUKA Sunrise controller. The bridge nodes are responsible for sending planned actions and receiving real-time robot and gripper data using Google Protocol Buffers (Protobuf).
- Websocket server based on the rosbridge_suite ROS package that provides communication with the components of the system outside of the ROS environment (ARHMD, web-browsers etc.).

Additional important components outside of the ROS framework are:

- MongoDB database for storing the symbolic representation of the CAD geometry.
- Web server that serves as a graphical web interface using the Autodesk Forge Viewer APIs for supervisory visualization of the system data-
- Microsoft HoloLens ARHMD running a user interface build with Unity 3D.
- Rhinoceros+Grasshopper generative design environment able to stream the CAD data in real-time.
- A robot controller running the KUKA Sunrise.OS stack allowing the operation of the KUKA LBR iiwa manipulator.

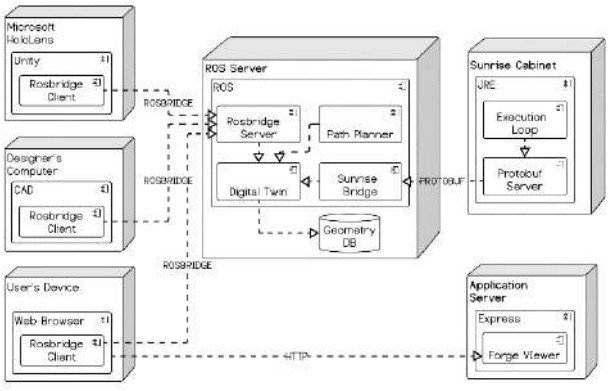

Figure 2. System deployment diagram.

3.1.3 Path Planning

The ROS-based motion planning framework MoveIt! is used for path planning (Fig. 3). Using this framework, it is possible to develop advanced pick-and-place behaviors to be able to precisely position the building elements. These behaviors consider the parameter space of the grasping position of the elements to further enlarge the workspace of the manipulator. By using the current state of the system and its limitations (e.g. arm joint limits) and the known position and shape of the already assembled structure it is possible to plan a collision-free path of the arm. The actual sequence of joint values is calculated using the RRT-Connect [20] single-query algorithm, proving to be a good compromise between the quality of the result and the speed of the calculation for holonomic robotic manipulators with 7DOF.

The "plan" button, selected through the ARHMD, triggers a regeneration and preview of a valid robotic motion. After the user's confirmation, the planned path is sent to the robot controller for execution as a discrete set of joint values.

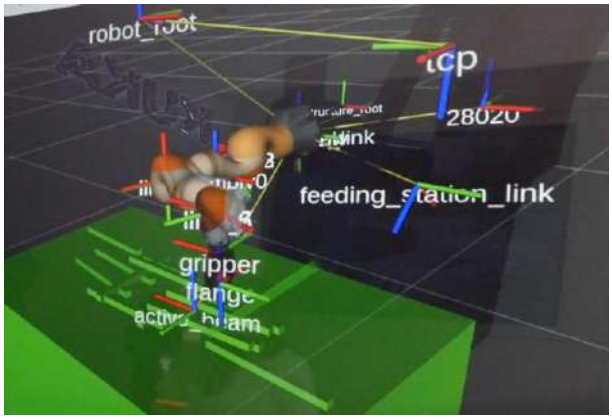

Figure 3. MoveIt! path planning scene with collision meshes visualized with the ROS 3D visualizer Rviz.

3.2 AR Interface

The Microsoft HoloLens ARHMD is used for its built-in stable simultaneous localization and mapping (SLAM) capability as well as for its self-contained nature (i.e. not needing a physical connection to an external device). The Unity 3D game engine is used to develop the AR interface for its integration and compatibility with the Microsoft HoloLens. The interface is kept rudimental and integrates the HoloLens gesture-based input system, by which the user can select and interact with the virtual superimposed content. This feature allows the user to use the UI elements such as virtual toggles and buttons. The robot main actions can be triggered through buttons, labelled as "PLAN" and "EXECUTE", virtually anchored above the selected element that is highlighted yellow (Fig. 4). The "PLAN" button triggers a generation of a robotic path while the "EXECUTE" button triggers the planned movement by uploading a sequence of joint values to the robot controller through the ROS server for execution. If the robot already performs a movement in the time of an upload of a new path the current movement is interrupted, and the newer path is executed instead.

In this UI system diagnostics about the robotic system can also be selectively previewed or overlaid directly on 3D objects including the robot or the production pedestal. The live torques on each axis for example can be displayed.

Lastly a static heads-up display (HUD) is designed in the top part of the AR field of view that displays the more abstract system data and as well as general information such as the overall construction progress percentage or the number of the current sub-assembly.

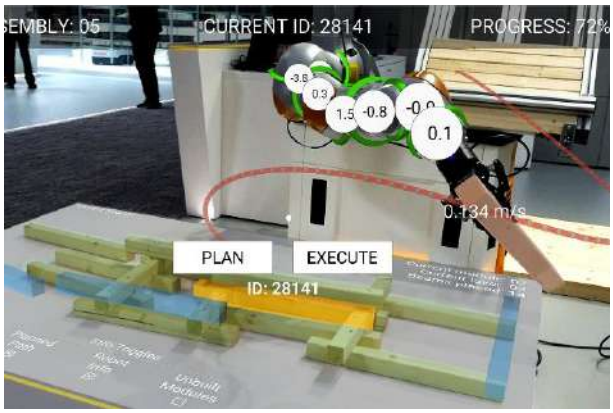

Figure 4. AR view visualizing buttons for selecting, planning, and executing robotic instructions as well as superimposed diagnostic feedback data.

3.2.1 Display Pipeline for Web Visualization

It is well-known that project management is a key component of any complex building process, and multiple concurrent production, finishing, and logistic processes ultimately affect project timelines and need to be considered simultaneously. To provide a scalable solution for unidirectional process supervision, a web user interface is integrated into the overall system communication system. This web interface additionally serves to complement some of the shortcomings of AR, in particular, its higher price and limited battery life are disadvantages which limit the deployment of AR as a universal interface for all needs. The web viewer application was developed using NODE.js and Autodesk Forge Viewer APIs. The application can be executed in any modern web browser and thus it creates

a ubiquitous and low-cost solution.

The core of the web application is a geometric scene loaded and displayed in a local web browser client utilizing the Autodesk Forge Viewer API and the WebGL cross-browser JavaScript library three.js. The preloaded scene view already has the robot model as well as the full fabrication model with naming conventions. In this preloaded model, each wooden strut element exists twice, once in its fabrication position and once in its final position. After initialization and loading events, the client browser references a json file that describes what had been already assembled and subsequently updates the scene accordingly. At the same time the browser establishes a TCP/IP communication through the WebSocket protocol to the previously described rosbridge_suite running on the ROS server. The client browser subsequently subscribes to various ROS topics and starts updating the scene. On a successful part place event, the visibility of the geometry in the scene changes from hidden to visible. Any remote user is therefore able to observe the actual fabrication updates and system data in real-time.

4 Results and Discussion

This project and exhibition successfully established a set of tools for facilitating human and robot collaboration in wood construction through enabling AR interfaces. In additional, critical system components in communication protocols were established and verified, including a communication workflow connecting multiple customizable CAD design environments to ROS through common developed data structures. Arguably, one of the core contributions of the project is the achievement of interoperability between multiple software platforms and hardware devices, particularly in the communication between ROS and the Microsoft HoloLens, which had been achieved in precedent projects only in a limited way. The project also demonstrated and achieved a process specific interface for robotic control, and demonstrated increased digital integration by propagating fabrication data downstream into secondary platforms and digital representations.

The advantages of untethered and therefore unrestricted movement and the easy marker less localization setup was extremely advantageous in the environment of a live demonstration on the Hannover fair. The limited battery life of around two hours, plus the reduced computational power of the HoloLens required an extra amount of effort for optimizing the performance which is for a proof of concept project hindrance. Furthermore, the inside-out tracking principle of the HoloLens is based on a spatial mesh mapping of the environment in combination with the data from the on-board inertial measurement unit (IMU). The highly dynamic environment of the ever-changing visitor crowd on the fair was causing an interference in localization resulting in a positional drift that impaired the AR-experience. However, with the rapid development of the AR technologies, these difficulties will arguably be eliminated in future AR-Devices.

While RRT-Connect proved to be a very robust and versatile planning algorithm for the application, its random sample-based nature sometimes resulted in an unsuccessful path when the solution space got smaller. Thus using it in isolation does not circumvent the need to make good kinematic decisions about where the robot should be placed relative to the workbench, to ensure that a viable path will be found. Furthermore, the lack of a well-defined cost function for the robot path proved to be an obstacle for the reproducibility of the robot movements as well as for planning an optimized movement.

4.1 Next Steps

This exhibit was not evaluated by the same metrics by which an interface would be evaluated in the context of HMI research: whereby efficiencies of production workflows with and without the HoloLens could be compared quantitatively. However, it was possible to gain qualitative feedback by visitors who came to the exhibit, predominately users who have extensive experience with programming robots. A next step towards evaluating the usability of the interface would be to test a novice user to interact with a defined objective, where the success of the interface could be measured by whether or not the user could accomplish a predetermined objective without supervision.

The technical implementation could have been improved by more robust localization of the HoloLens: users walking in front the interface was enough for the on-board SLAM to lose its position. A viable option would be the integration of a low frequency external outside-in localization system in parallel that would allow to correct the positional drift or a marker based optical approach that can be additionally used to automatically synchronize the position of the workpiece and the robot arm in a common world coordinate system of the HoloLens.

The presented system also clearly lacked higher cognitive functionality. Simple cognitive cooperation patterns such as joint attention could be highly beneficial in making the HRC scenario more efficient as well as rendering the robot more approachable and lifelike. Without such cognitive features it is hard to imagine that the robot system would become a real co-worker to its human counterpart.

In addition, any of the failures that happened during the course of the exhibition can be attributed to an error in communication, resulting in an incorrect system state,

or digital twin model, in one of the environments. These errors could be circumvented by increasing the ability for the human user to enter into the system when an unexpected error occurred. For example, if a part was not loaded in the magazine and was therefore not actually placed.

4.2 Outlook

This project proposed and investigated enabling interactive and interface technologies which can facilitate a more rapid advancement and utilization of robotic fabrication in building prefabrication production chains by increasing accessibility, digital integration, and usability. Simultaneously, the limitations of the project, particularly the limited reach and payload of the KUKA LBR iiwa, point to other technological developments which could accelerate robotic building production processes. In particular, there is a need for collaborative robots designed for the domain of AEC, with specifications including increased reachability, higher payloads, as well as locomotion systems for moving on a difficult terrain.

4.3 Acknowledgements

This project was executed as a demonstrator for the research project: Human-Robot Collaboration in Timber Construction at the Institute for Computational Design and Construction (ICD) at the University of Stuttgart, with funding provided by Forschungsinitiative Zukunft Bau, Bundesinstitut für Bau-, Stadt- und Raumforschung (BBSR). Additional researchers on this project included Oliver David Krieg.

This project was additionally developed as a finalist application for the KUKA Innovation Award 2018 competition. The organizer provided the robotic workcell, on a donation basis, as well as travel funding and a training for researchers.

Additional funding was obtained by Autodesk to support the use of Forge APIs for web based services. The work conceptually built upon the ITECH master's thesis at the University of Stuttgart by Benedikt Wannemacher, *Augmented Manufacturing* from 2017. His continued research was supported in parallel at the chair for Experimentelles und Digitales Entwerfen und Konstruieren under the direction of Professor Philipp Eversmann.

Student researchers, Samuel Leder and Rebeca Duque Estrada, supported the project.

5 References

[1] Aryania A, Daniel B, Thomessen T, Sziebig G (2012) New trends in industrial robot controller user interfaces. In: 2012 IEEE 3rd International Conference on Cognitive Infocommunications (CogInfoCom). IEEE, Kosice, Slovakia, pp 365–369

[2] T. Bock, The future of construction automation: Technological disruption and the upcoming ubiquity of robotics, Automation in Construction. 59 (2015) 113–121. doi:10.1016/j.autcon.2015.07.022.

[3] G. Carra, A. Argiolas, A. Bellissima, M. Niccolini, M. Ragaglia, Robotics in the Construction Industry: State of the Art and Future Opportunities, in: Taipei, Taiwan, 2018. doi:10.22260/ISARC2018/0121.

[4] M.N. Mohd Nawi, N. Baluch, A.Y. Bahauddin, Impact of Fragmentation Issue in Construction Industry: An Overview, MATEC Web of Conferences. 15 (2014) 01009. doi:10.1051/matecconf/20141501009.

[5] T. Bock, T. Linner, Construction Robots: Elementary Technologies and Single-Task Construction Robots, Cambridge University Press, Cambridge, 2016. doi:10.1017/CBO9781139872041.

[6] De Luca A, Flacco F (2012) Integrated control for pHRI: Collision avoidance, detection, reaction and collaboration. In: 2012 4th IEEE RAS & EMBS International Conference on Biomedical Robotics and Biomechatronics (BioRob). IEEE, Rome, Italy, pp 288–295

[7] Fiebich A, Nguyen N, Schwarzkopf S (2015) Cooperation with Robots? A Two-Dimensional Approach. In: Misselhorn C (ed) Collective Agency and Cooperation in Natural and Artificial Systems. Springer International Publishing, Cham, pp 25–43

[8] Flacco F, De Luca A (2013) Safe physical human-robot collaboration. In: 2013 IEEE/RSJ International Conference on Intelligent Robots and Systems. IEEE, Tokyo, pp 2072–2072

[9] P. Tsarouchi, A.-S. Matthaiakis, S. Makris, and G. Chryssolouris (2017) On a human-robot collaboration in an assembly cell. In: Int. J. Comput. Integr. Manuf., vol. 30, no. 6, pp. 580–589

[10] P. Švarný and M. Hoffmann (2018) Safety of human-robot interaction through tactile sensors and peripersonal space representations. In: Č. Šašinka; A. Strnadová; Z. Šmideková & V. Juřík, (eds) 'Kognice a umělý život XVIII [Cognition and Artificial Life XVIII]', Flow, z.s., pp. 73-75.

[11] J. Meiling (2010) Continuous Improvement and Experience Feedback in off-site Construction: Timber-framed Module Prefabrication. Luleå University of Technology.

[12] Aryania A, Daniel B, Thomessen T, Sziebig G (2012) New trends in industrial robot controller user interfaces. In: 2012 IEEE 3rd International Conference on Cognitive Infocommunications (CogInfoCom). IEEE, Kosice, Slovakia, pp 365–369

[13] Lafreniere B, et al (2016) Crowdsourced Fabrication. In: Proceedings of the 29th Annual Symposium on User Interface Software and Technology - UIST '16. ACM Press, Tokyo, Japan, pp 15–28

[14] Webster, A., Feiner, S., Macintyre, B., Massie, W., Krueger, T.: Augmented Reality in Architectural Construction, Inspection, and Renovation. Proceedings of 1996 ASCE Congress on Computing in Civil Engineering (1996)

[15] Fazel, A., Izadi, A.: An interactive augmented reality tool for constructing free-form modular surfaces. Automation in Construction (2018). doi: 10.1016/j.autcon.2017.10.015

[16] Johns, R.L.: Augmented Materiality. Modelling With Material Indeterminacy. In: Gramazio, F., Kohler, M., Langenberg, S. (eds.) FABRICATE. Negotiating design & making, pp. 216–223. UCL Press, London (2017

[17] G. Jahn, C. Newnham, N. Berg, and M. Beanland (2018) Making in Mixed Reality. In: Recalibration: On Imprecision and Infidelity

[18] M. Quigley et al. (2009) ROS: an open-source Robot Operating System. In: ICRA Work. open source Softw., vol. 3, no. 3.2, p. 5

[19] Ioan A. Sucan and Sachin Chitta. MoveIt!. [Online] Available: http://moveit.ros.org

[20] J. J. Kuffner and S. M. LaValle (2004) RRT-connect: An efficient approach to single-query path planning. In: Proceedings 2000 ICRA. Millennium Conference. IEEE International Conference on Robotics and Automation. Symposia Proceedings (Cat. No.00CH37065), 2004, vol. 2, no. Icra, pp. 995–1001.

Case Study on Mobile Virtual Reality Construction Training

M. Wolf[a], J. Teizer[a], J.-H. Ruse[a]

[a] Ruhr-University Bochum, Universitätsstraße 150, 44801 Bochum, Germany
E-Mail: mario.wolf@rub.de, jochen.teizer@rub.de, jan-hendrik.ruse@rub.de

Abstract –

Recent surveys among construction firms found, a majority has a hard time filling craft worker/hourly positions and salaried jobs. Among the ways they are trying to create more is in-house training. However, existing learning methods have been lagging effectiveness or are outdated. New approaches, like mobile virtual reality, are being investigated. In this paper, the authors describe their approach to a low cost virtual reality training that offers personalized feedback for trainees or workers. The developed approach utilizes elements of gamification for motivational purposes. While the training requirements were gathered in dialogue with leading companies in the construction and engineering industry sectors, the research conducted focused on prototyping and testing the novel learning concept. As a result, the authors developed a mobile virtual reality application that utilizes the Google Daydream SDK that runs on Google Cardboard, Samsung Gear VR, Oculus Go or compatible other inexpensive devices. The application was tested and evaluated by industry representatives. An outlook provides the path forward in research and development.

Keywords –

digitalization, construction safety, personalized feedback, virtual reality, virtual trainings, workforce education and training.

1 Introduction

The construction and engineering industries face several major hurdles at this time. While construction workplace accidents account for a significant number of fatalities and injuries [1] that consequentially lead to a loss in productivity, engineering in general faces another problem: a severe shortage of skilled labor [2].

Over the past decades, researchers and practitioners have attempted to understand and mitigate the underlying precursors of accidents in construction [3,4]; with some success the accident rates dropped until they recently started rising again [5]. Among other ways, hazard recognition is one of the first steps in effective safety management [6-8]. However, results on the effectiveness across the globe have shown that up to 50% of construction hazards remain unrecognized despite that training and certification are provided [6-12]. Among the contributing factors for such poor hazard awareness are worker's paying attention on their task, ignoring predominantly some types of hazards, and having low capabilities in "visual search". Latter means the initial detection and then identification of hazards is a very challenging human task [13]. It is particularly difficult considering that construction sites are very complex and dynamic, where one worker's attention to all the present details can often be overwhelming.

Examples of such work environments are building and industrial construction sites or larger vs. smaller work spaces. No or no recent training, no or unclear tool box meetings before work begins, imprecise work station preparation, and inadequate site conditions or staffing are some of the most common reasons that challenge worksite safety behavior. The recent example of a partial refinery explosion shows, unsafe work preparation, unclear instructions, or using the wrong tools for the wrong task can result in a tragedy [14].

The objective of this study is to leverage mobile virtual reality construction training. The preliminary research effort designed training in two virtual environments: hazard detection in a virtual building construction site and a flange training scenario in a virtual training center of a chemical plant operation. The next section presents a brief background on safety training and flange coupling. This is followed by an explanation of the virtual gaming environment that was created and tested. Results are shown and an outlook of future work is presented.

2 Background

Safety is a major concern in the construction industry. Besides numerous other approaches on hazard awareness, training has one of the highest positive impact factors in reducing fatalities. In the literature as well as in the praxis exist several different teaching formats, such as self-, hands-on-, supervised- learning. Generally, the level of awareness aimed at implies knowledge on possible hazards and safety regulations. These are strictly defined in most countries, like in Germany by the BG Bau [15],

an official organization responsible for establishing and enforcing construction safety rules.

While workers in the chemical industry are constantly confronted with the installation or maintenance of piping and the respective connections, these works can only be executed once normed guidelines and instructions are followed [16-17]. Problems arise or continue to exist if no or only limited trainings for executing work tasks are provided. This may happen less in the chemical industry because training has been part in their core business processes. The fragmented construction industry though has a continuous problem with adequate workforce training.. There, knowledge on safety and health is hardly ever refreshed in greater depth once primary education as an apprentice has ended [5]. For this reason, several researchers started investigating new methods, particularly on using Virtual Environments (VE's) for hazard awareness [6,18-19,20]. Although a full scientific validation of VE for safety education and training is a very challenging task considering that mature practical solutions seem far to be reached, all of these approaches claim that VE will provide safe and more effective training, at reduced time and cost. An additional example is, the right way to work with flange connections in the chemical industry is typically taught on a single day and is usually viewed by the trainers and trainees as a basic training. But especially larger diameter flange connections can challenge work crews, so that an adaptive VR training and instruction guide could help workers build confidence and provide readily available knowledge in handling the materials and the necessary tools.

3 Requirements and general setup

As mentioned in the introduction, this paper focuses on testing the limits of mobile virtual reality for two different scenarios with very specific requirements. To avoid the accumulation of inert knowledge, the authors want to use immersive virtual reality technology to enhance the experience for the trainee. This offers a safe way to confront the trainees with realistic representations of hazards without exposing them to real dangers.

One of the most relevant requirements, in context of this paper, is the ability to use the trainings on mobile virtual reality devices. Mobile VR devices like the Oculus Go cost around 200 €, with more advanced hardware (Lenovo Mirage Solo, Oculus Quest, etc.) costing around 400 €. This is significantly less than an equally usable stationary VR setup, which costs anywhere from 2000 to 4000€. Low cost and ease of use are centerpieces of mobile VR hardware. These advantages seem highly appreciated by training organizations or departments who need to equip higher numbers of training staff with such technology.

The aim is to offer explorative, immersive experiences at minimal costs. Both virtual trainings aim at a maximum of 15 minutes working time.

As with most virtual surroundings, the visualization of the desired scenes must be believable with a realistic scale between the user and her/his surroundings. As photorealism in the virtual reality cannot be achieved with the limited computing performance of existing mobile devices, the focus is on creating a visually-sound context for the training scenarios.

The first virtual construction safety awareness training orients itself on the regularities from the German Social Accident Insurance (DGUV) and its subdivision for the building trades (BG Bau) [15]. The second scenario is the virtual flange training, which is based on German norms and guidelines for the handling of flange connections [16].

3.1 Virtual safety awareness training

The objective of the scenario was to provide a scene that must show a realistic and valid construction site. Embedded in the scene are typical hazards that can and must be avoided in the real world. To accommodate the scene for regular use in training and to offer some variety, the total amount of hazards must exceed the number of hazards in each session, with an automated, random selection applied at the start of the training. Hazards must be identifiable by the user, preferably by pointing at them and then selecting them with the controller. Head mounted devices (HMD) provide such instruments that even allow for data gathering and post-analysis which and when a hazard was selected.

The user must have full locomotion in the scene to reach all parts of the virtual construction site. When coming closer than the typical safe distance for a particular non-identified hazard – granted the user has line-of-sight – the user needs to be informed that the concerning hazards was not detected and is therefore marked as failure. The safe distance of each hazard depends on the type of hazard and should be automatically applied.

The virtual construction safety awareness training application must record user- and session-specific datasets consisting of the current scene configuration (number of randomly selected hidden hazards with their IDs) and the user's actions in the scene (total time, full completion yes/no, total number of corrected hazards, specific listing of the hazards, their status and association with German safety training regulations). The exact documents considered for the creation of hazards must be at least BG Bau A021 (fire safety), A062 (flammable substances), A064 (pressured gas tanks), B100-1 (work-at-height), B132-1 (ladders), B161-1 (load handling), B172 (electrical equipment), B173 (mobile generators), B181 (excavators) and B202 (hand tools) and each

hidden hazard must specify the associated document for later analysis.

3.2 Virtual flange training

The virtual flange training's purpose is to teach and train both patterns of valid screw-fastening on flange-couplings (cf. DIN 1591-4) for novices and experienced work crews. The training must be flexible enough to train on a variety of flange couplings ranging from small (8 screws, DN20) to big (24 screws, DN400).

The virtual flange training is supposed to offer two separate modes. The first mode aims at teaching novices the usage of both the standard crosswise and the alternative pattern of fastening the flange's screws (Fig. 1). In this teaching mode, each step taken should be marked as either correct or incorrect to provide immediate feedback. The trainee must be able to access help functions to learn about the general guideline for the chosen approach [16] and optionally which screw to fasten next. In this training environment, the trainee should not be able to move around freely but be allowed to concentrate on the task at hand. Therefore, the flange should be placed floating in a frontal view to mimic the depiction in the guidelines.

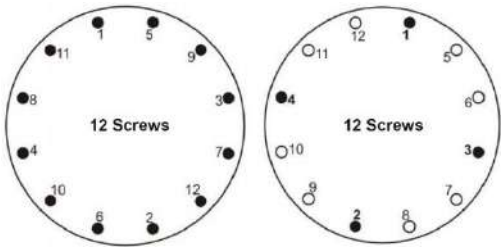

Figure 1. Standard crosswise pattern (left) and alternative pattern (right) [16]

The second "open training" scenario should offer less help, free locomotion and a realistic scenario with a flange connection of two pipes stacked vertically. This should force the trainee to change her/his position and viewing angle similarly to the movement necessary in the real world. The immersion of the trainee in the scene was improved and an option to use the controller in a movement like a ratchet was offered optionally.

The virtual flange training application must record user- and session-specific datasets consisting of the current configuration (e.g., number of screws, choice of training mode, method of fastening), the total amount of time till full completion, the achieved score and the total amount, type and time of occurrence of errors made during the training. Before each training session, the trainee was made aware of the recording, putting her/him under pressure to concentrate on quality and timely completion of the assigned tasks. The different kinds of errors that can occur in this scenario are described in Table 1.

Table 1. Registered events in the flange training application

No.	Error Description
1	User specified the wrong torque number
2	Selected screw was already fastened in the current turn
3	Selected screw is not opposing to the last
4	Selected screw is not one of the two screws orthogonal to the axis connecting the first two screws
5	Wrong sequence in the last step of the standard cross-wise pattern (i.e. not clockwise)
6	Wrong starting point in the last step of the alternative pattern
7	Wrong sequence in the last step of the alternative pattern (i.e. not clockwise)
8	Wrong combination of method and nominal diameter

4 Prototypical implementation

For the preliminary evaluation, the authors implemented two mobile virtual reality applications using the Unity3D Engine and a Samsung S8 in a Google Daydream Headset with its accompanying controller. To run the application on Google Cardboard, Samsung Gear VR, Oculus Go or compatible devices, the Google Daydream SDK was used. In each scenario, the rotational head tracking enables the trainee to look around in the scene, while interaction and movement via virtual teleportation as locomotion method is handled with the controller.

4.1 Virtual safety awareness training

The authors created a virtual construction site in the Unity3D Editor (Fig. 2, top), which has over 70 possible hazards from which each training set is drawn. When looking directly at the controller, tooltips (Fig. 2, bottom) show up to inform the user about the total time in the scene, the amount of found and left hidden hazards in the scene and the button's functions (identify hazard and teleportation).

For each training session, a new set of hazards is selected from the "hazard pool" and all non-selected hazards are "non-existent" in this very training session. The algorithm for the process is displayed in Table 2. As the number of implemented hazards is known (70) and the amount of targeted hazards per scene is known (between 10 and 25), all that is needed to set up an individual scene is a random number *i* to generate. The goal for the trainee is to find all hazards in the construction site, but no further assistance (i.e., highlighting when hovering over objects in the scene) is given.

Table 2. Algorithm for the construction safety training

Step	Description
1	Generate a random number *i* between 10 and 25
2	Generate “”"-many random numbers between 1 and 70 with no doublets allowed
3	Hide all hazards
4	Show all hazards where the generated numbers match the hazard’sIDs

Fig. 3 shows screenshots taken from the user’s perspective when looking at unsafely stacked cable spools and an unsecured falling hazard (Fig. 3, left). When the user identifies the hazard via point&click using the controller, the hazards is resolved, and the desired (safe or healthy) situation is revealed (Fig. 3, right).

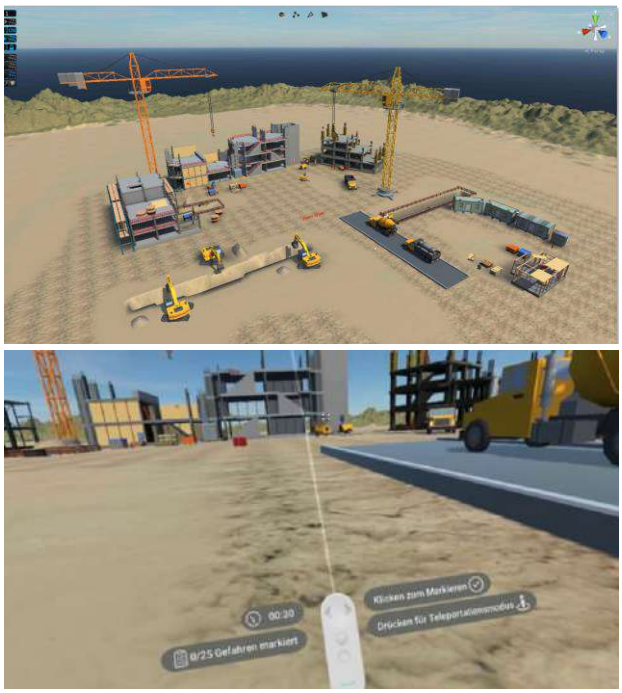

Figure 2. Screenshots with overview over the created construction scene (top) and the user’s perspective using the application (bottom)

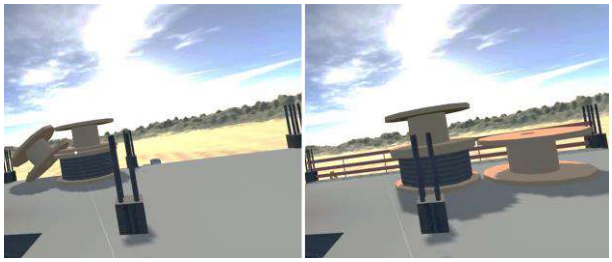

Figure 3. Close calls with crane load: contruction worker (left) and skid-steer loader (right)

4.2 Virtual flange training

The virtual flange training must implement both methods (standard and alternative) of fastening flange connections specified in the German Industrial Standard (DIN 1591-4). For that matter two different algorithms were implemented in C# and used in the training scenes to check a trainee’s input. Table 3 shows the algorithm for the standard method. In short, the standard pattern consists of three rounds with different torque figure. In each round a set of four screws is fastened, starting with two opposing screws and going to the pair of screws that are orthogonal to the first two. This crosswise pattern continues until all screws are fastened with the current torque figure. After a full pass of all three steps, the guideline specifies an “unlimited” amount of clockwise repetitions until each screw passes with 100% torque. In our algorithm a single pass is sufficient.

Table 3. Algorithm for the standard method in the flange training application

Step	Description
1	Start with 30%, 60% and 100% torque
2	Select random screw (< current max. torque)
3	Select opposing screw to the first screw
4	Select one of the two screws orthogonal to the axis connecting the first two screws
5	Select opposing screw to the third screw
6	Repeat steps 2-5 until no screw is left < current max torque
7	Repeat with next torque level starting at step 1
8	Select each screw, starting at screw one and following a clockwise path

Table 4. Algorithm for the alternative method in the flange training application

Step	Description
1	Start with 20%, 60% and 105% torque
2	Select random screw (< current max. torque)
3	Select opposing screw to the first screw
4	Select one of the two screws orthogonal to the axis connecting the first two screws
5	Select opposing screw to the third screw
6	Repeat with next torque level starting at step 1
7	Select each screw, starting at screw one and following a clockwise path

Table 4 shows the algorithm for the alternative method. It is important to note that the DIN-standard specifies the alternative method invalid for nominal flange diameters of less than 200 mm. In consequence to that, once a “smaller” training flange is selected and the alternative method is used, the current try is considered a failure. The alternative method is basically a single

crosswise pattern with different torque figures, followed by clockwise fastening with the highest torque figure. Analogue to the standard pattern, the theoretically unlimited number of repetitions until the final torque figure is met is reduced to exactly one in the algorithm.

Each algorithm can be used in each of the two training modes. As the novice mode is supposed to offer a great amount of support functions, the authors created the scene and Graphical User Interface (GUI) as seen in Fig. 4. The user starts at the trainee position (Fig. 4, No. 1) with a frontal view of a flange connection (Fig. 4, No. 2) of a specified size. The score panel shows the current number of correct steps and the score for this session (Fig. 4, No. 3). In the option and help menu (Fig. 4, No. 4) the user can switch between help for individual methods and switch on the help and instruction panel (Fig. 4, No. 5). In the scene configuration menu (Fig. 4, No. 6) the user can set up the size of the flange, the preferred method and the optional "manual ratcheting". Locomotion is disabled in this mode, so that the trainee is surrounded by (optional) information, with her/his task in front.

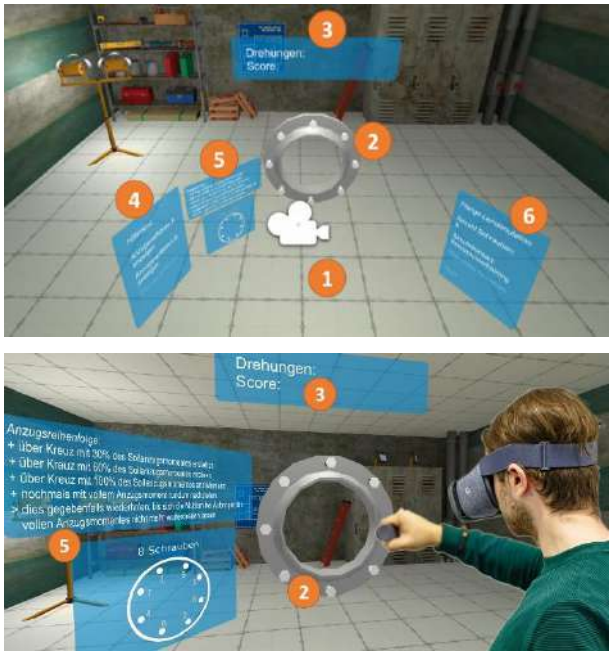

Figure 4. Screenshots with overview over the created scene (top) and the user's perspective (image overlay) using the application (bottom)

Instead of the strict nature and learning-based novice mode, the open training mode offers free locomotion (identical to the construction site scene) and more naturally placed interaction elements. The trainee starts at a standard position (Fig. 5, No. 1), with the task in front of him. The vertical piping elements with the flange connection needs to be fastened (Fig. 5, No. 2). It can be configured with the scene configuration menu (Fig. 5, No. 4), just as the frontal flange view in the novice scene. The idea behind this is, that when handling the flange connection of rather large piping, the task becomes harder, as the exactly opposing screw is not that easy to find. The score panel for the current session is fixed to the opposing wall (Fig. 5, No. 3).

The task in this scene is to choose a flange size, start wrenching and use either the standard or the alternative pattern to fulfill the task. Once the route for a particular method is set after choosing the 5th screw, every error lessens the score.

Figure 5. Screenshots with overview over the created scene for the open training

5 Results to demonstration and testing

The prototypical applications were demonstrated at an interdisciplinary internal workshop for experts for digitalization of learning environments and didactics in engineering at the Ruhr-University Bochum, Germany. Many of the attendees had long-term construction or engineering industry experience. They were asked about their opinion after testing either or both of the applications.

On the positive side, the experts mentioned the ease of use due to the nature of the light headsets and the easy way to understand locomotion. The comic-like graphics were easy to understand too and offered not much distraction, while being clear enough to offer orientation and recognition.

Concerning the construction site safety training the experts suggested, instead of revealing the ideal solution for each found hazard, the trainee could be asked to choose from several different suggested solutions. This would offer a better possibility to verify the trainee's deeper understanding.

Data gathered from three exemplary users show what kind of insight instructors can get, when preparing feedback based on virtual trainings. Table 5 lists some of the gathered data, with hazards subdivided by their according BG Bau rules like A021 or B100-1. As one can see, user 1 seems to be at ease with the recognition of hazards in a construction environment with a good time and full completion. Users 2 and 3 did not finish on time, but user 3 found all but one hazard. As the full XML data log contains timestamps for all events, a graphical

timeline could reconstruct the events within the training. That would reveal that User 3 was as fast as User 1, but didn't look up to check the load hanging from the crane till the time ran out.

In both applications, the experts found the trainings to be interesting and challenging, while the technical representation left some things to be desired. To address these concerns, performance enhancing measures will need to take place before a larger survey can be conducted. Also, future participants will need to get a precise introduction to the applications and tasks, as the applications are not self-explanatory enough and the overpowering nature of VR to first-time users might hinder this further.

Table 5. Data collected from three exemplary users in the construction hazard awareness training

	Participant		
	1	**2**	**3**
Timestamp	**11/01/2019 15:02:34**	**11/01/2019 15:34:04**	**11/01/2019 16:01:58**
Total time [min]	8:05	15:00	15:00
Full completion	Yes	No	No
Hazards in scene	19	12	17
Correctly detected	19	10	16
A021	1 of 1	1 of 1	1 of 1
A062	3 of 3	1 of 2	3 of 3
A064	2 of 2		2 of 2
B100-1	2 of 2	2 of 2	3 of 3
B132-1	3 of 3	1 of 1	
B161-1	1 of 1	1 of 1	0 of 1
B172	1 of 1	1 of 1	2 of 2
B173	3 of 3	1 of 1	3 of 3
B181	1 of 1	1 of 1	
B202	2 of 2	1 of 2	2 of 2

6 Conclusion and outlook

This study described a novel approach towards a low-cost virtual reality training that offers individual feedback for trainees or workers. The approach utilized elements of gamification for motivational purposes. With requirements gathered in dialogue with industry leading companies and based on research conducted at the Ruhr-University Bochum the concept at hand successfully created and tested a prototype. While the results are preliminary the authors have shown the complexity of creating virtual reality experiences based on existing safety-related regulations.

In case of the presented applications, the far smaller scenes of the virtual flange training contains more complex interaction elements. Its dynamic algorithms also offer a varying degree of difficulty.

In the rather large construction site scene, the algorithms are based on many elements and regulations. A simple hit or miss strategy which was particularly easy to implement might be enhanced in the future by providing immediate feedback on the hazard type. Similarly, allowing false positive errors might strengthen a trainee's attention to be careful about selections.

In brief, our future work will combine the presented approaches for work place safety and actual work tasks. This will enhance the experience with further interactive elements like dynamic non-player characters and vehicles. The idea is to offer a holistic construction site representation with varying tasks to perform, to lessen the impact of the acclimation time users usually need to accept and cope with their immergence into a virtual environment. Another research topic in this context is the increase or decrease of learning quality due to the immersion in virtual reality. As the applications were created with Unity 3D, a reference group will test the same applications and 3D contents in a non-immersive standard PC configuration. Structured may replace opinion-based surveys.

References

[1] OSHA: Commonly Used Statistics, https://www.osha.gov/oshstats/commonstats.html (accessed January 31, 2019).

[2] Karimi, H., Taylor, T.R.B., Goodrum, P.M., Analysis of the impact of craft labour availability on North American construction project productivity and schedule performance, *Construction Management and Economics*, 35(6):368-380, 2017.

[3] Mitropoulos P., Abdelhamid T.S., Howell G.A. Systems model of construction accident causation, *Journal of Construction Engineering and Management*, 131: 816–825, 2005.

[4] Rajendran S., Gambatese, J.A. Development and Initial Validation of Sustainable Construction Safety and Health Rating System, *Construction Engineering and Management*, 135: 1067–1075, 2009.

[5] Teizer J. Right-time vs. real-time pro-active construction safety and health system architecture, *Construction Innovation: Information, Process, Management*, 16(3): 253-280, 2016, http://dx.doi.org/10.1108/CI-10-2015-0049.

[6] Sacks R., Perlman A., Barak R. Construction safety training using immersive virtual reality, *Construction Management and Economics*, 1005–1017, 2013.

[7] Albert A., Hallowell, M.R., Kleiner, B.M. Enhancing Construction Hazard Recognition and Communication with Energy-Based Cognitive Mnemonics and Safety Meeting Maturity Model: Multiple Baseline Study, *Construction Engineering*

and Management, 140:4013042, 2014.
[8] Carter G., Smith S.D. Safety Hazard Identification on Construction Projects, *Construction Engineering and Management*, 132: 197-205, 2006.
[9] Bahn, S. Workplace hazard identification and management: The case of an underground mining operation, Safety Science. 57 (2013).
[10] Namian, M., Albert A., Zuluaga C.M., Jaselskis, E.J. Improving Hazard-Recognition Performance and Safety Training Outcomes: Integrating Strategies for Training Transfer, *Construction Engineering and Management*. 142: 4016048, 2016.
[11] Haslam R.A., Hide S.A., Gibb A.G.F., Gyi D.E., Pavitt T., Atkinson, S., Duff A.R. Contributing factors in construction accidents, *Applied Ergonomics*, 36: 401–415, 2005.
[12] Perlman, A., Sacks R., Barak, R. Hazard recognition and risk perception in construction, *Safety Science*, 64: 13–21, 2014.
[13] Mitroff S.R., Biggs A.T. The Ultra-Rare-Item Effect: Visual Search for Exceedingly Rare Items Is Highly Susceptible to Error, *Psychological Science*, 25: 284–289, 2014.
[14] Mannheimer Morgen. https://www.morgenweb.de/mannheimer-morgen_dossier,-basf-explosion-_dossierid,17.html (Accessed January 31, 2019).
[15] BG Bau. https://www.bgbau.de/service/angebote/medien-center/die-wichtigsten-informationen-auf-einen-blick/ (Accessed January 31, 2019).
[16] VCI. Leitfaden zur Montage von Flanschverbindungen in verfahrenstechnischen Anlagen, Verband der chemischen Industrie e.V., 2016.
[17] DIN 1591-4, Beuth-Verlag, https://www.beuth.de/de/norm/din-en-1591-4/171986785 (Accessed January 31, 2019).
[18] Lin K.Y., Son J.W., Rojas E. A Pilot Study of A 3D Game Environment for Construction Safety Education, *ITCON*, 16: 69-84, 2011.
[19] Albert A., Hallowell M.R., KLeiner B., Chen A., Golparvar-Fard, M., Enhancing Construction Hazard Recognition with High-Fidelity Augmented Virtuality, *Construction Engineering and Management*, 140(7), 2014.
[20] Hilfert T., Teizer J., König M. First Person Virtual Reality for Evaluation and Learning of Construction Site Safety, 33rd International Symposium on Automation and Robotics in Construction, Auburn, Alabama, USA, 2016, https://doi.org/10.22260/ISARC2016/0025.

Simulating Extreme Points of Crane by Robot Arm in Virtual Reality

Kuan-Lin Chen [a], King-Ho Tsang [b] , Yao-Yu Yang [b] and Shih-Chung Kang [c]

[a]Department of Civil and Construction Engineering, National Taiwan University of Science and Technology, Taiwan
[b]Department of civil engineering, National Taiwan University, Taiwan
[c]Department of Civil & Environmental Engineering, University of Alberta, Canada

E-mail: m10705504@mail.ntust.edu.tw, b06501082@ntu.edu.tw, yyben@caece.net, sckang@ualberta.ca

Abstract –

Crane simulations are necessary for selecting a proper type of crane for an erection task in a construction project. However, simulating the motion of a specific crane is hardly realized because modelling a specific crane is complex. Thus, by taking advantage of a robot arm with multiple degrees of freedom, our goal is to simulate any type of retractable crane and boom crane virtually. The developed simulation process can help identify constraints of the robot arm and transform the configuration between the robot arm and a selected crane. In the experiment, by applying the developed simulation process we used a virtual robot arm to simulate a virtual retractable crane in one of the tasks of crane operator exam. The comparison of the endpoint paths of the crane and the robot arm showed the feasibility of the method. Furthermore, the method can be applied to the real robot arm for selecting a proper type of crane for the erection tasks. The erection tasks can also be easily simulated physically with a robot arm in a scaled construction site.

Keywords –

Simulation, Extreme point, Robot arm, Crane

1. Introduction

1.1. Background

In recent years, various types of cranes are used in all walks of life, especially mobile crane has high mobility and a wide range of operation suitable for many sites. Research discussed the boom control of mobile cranes, such as Autonomous Beam Assembly System [1] or Crane Operation [2] so on and so forth.

However, due to the complex kinematics and low mobility of the crane, the crane operation is difficult. There are lots of restrictions including the size of the site, the safety of the area around the site, crane rental etc. Therefore, in the past, the 3D model technology was used to simulate in advance and observe the movement behavior of the crane in the virtual space as a reference for decision-making. [3] In this paper, the method of using a virtual robot arm to simulate the extreme points motion of a crane is presented.

1.2. Crane Simulators

With the rapid development of visualization technology, many 3D simulation tools have been developed. However, these simulations in the virtual environment are limited by the software and cannot fully consider all the influencing factors, resulting in errors between the simulated objects and the reality. Especially in the erection tasks, the movement of the hanging object will be affected by complex natural factors, so the simulation results may not be accurate.

This study focuses on the use of a virtual robot arm as a tool to simulate the extreme points of crane. There are four advantages of this method. First, the researchers are able to accurately simulate any point and path. Second, the method could simplify the process for researchers to operate the crane and make research more efficient. Third, the axis of horizontal rotation and elevation are combined into one single axis. The last but not the least, the results of these simulations can be observed by actually operating the robot arm to observe the physical changes of the hanging object.

1.3. Research goal

We use the robot arm in the virtual environment to simulate the extreme point motion of the crane. This method enables operators to simulate the endpoint path of the crane before actually operating the crane. Different

from the direct simulation of the crane, the robot arm can achieve high simulation accuracy and clearly record the coordinates of each endpoint in the path, freely control the speed of movement, and the simulated movement can be actually implemented in the robot arm. This information can be used as a reference for operator decisions.

Notation
k: The ratio of maximum length of robot arm and crane boom
μ: The distance between the hoist of crane to the origin in coordinates system
R_{max} : The maximum length of robot arm.
r_{max} : The maximum length of crane boom.
r_i: The initial length of crane boom
θ_i: The initial azimuthal angle (horizontal rotation angle) of crane boom
ϕ_i: The initial polar angle of crane boom
r_T: The terminal length of crane boom
θ_T : The terminal azimuthal angle (horizontal rotation angle)
ϕ_T: The terminal polar angle
Δr: The change of length of crane boom
$\Delta\theta$: The change of azimuthal angle (horizontal rotation angle)
$\Delta\phi$: The change of polar angle
PTP: Point-To-Point form
$i(x_i, y_i, z_i)$: The initial 3D Cartesian coordinates (input of robot arm)
$T(x_T, y_T, z_T)$: The terminal 3D Cartesian coordinates (input of robot arm)

2. Methodology

After analyzing the relationship between a crane and a robot arm, the methodology is organized as follow:

2.1. Operation process for simulation

We developed an operation process, that included input, analysis, transformation, simulation, output five parts to determine whether hoisting paths between robot arm and crane were the same or different for the developed simulation.

2.1.1. Simulation steps

First, we input the model of a crane and a robot arm, the coordinates of hoisting path in crane. Second, we calculate the effective simulation range of the crane and the robotic arm to ensure that the simulation path is feasible. After that, the 3D Cartesian coordinates input data of robot arm are collected. Third, simulation software is used to test the result whether the paths of the crane and the robot arm are the same. Finally, if the hoisting path in the simulation is the same as the crane, the robot arm simulates complete. Otherwise, the method restarts and repeats the steps repeats.

Figure 1. Simulation process

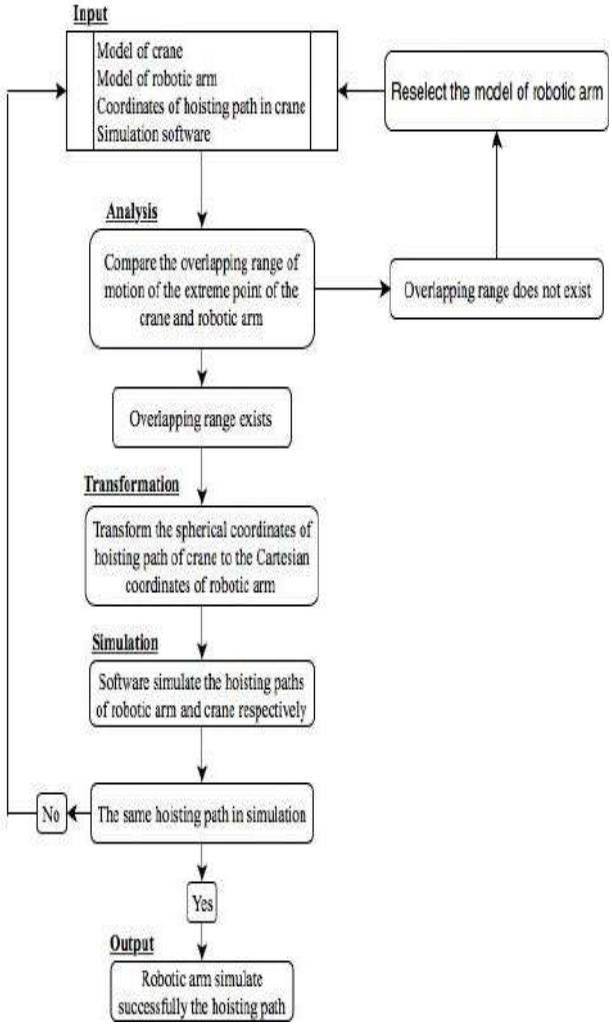

2.2. Constraint identification and assumptions

Six constraints are identified and eight assumptions regarding geometry and numerical calculation are established in this section.

2.2.1. Constraint identification

Robot arm

The upper sheave of the robot arm must be perpendicular to the ground. The form of extension and retraction of robot arm are not the same as the crane. Furthermore, one robot arm only simulates one mobile crane at each time.

Crane

The crane has two angles to be considered. The first one is the range of the elevation angle of crane: $\mathbf{0°} \leq \boldsymbol{\phi} \leq \boldsymbol{\phi_{max}}$(determined by the model of the crane). The other one is the range of the horizontal rotation angle of crane: $\mathbf{0°} \leq \boldsymbol{\theta} \leq \mathbf{360°}$.

2.2.2. Assumptions

Crane

Only mobile crane situation is considered. The pivot of the crane is fixed at the origin. The hook and cable of the crane are ignored. The factors of natural environment such as wind and personal factors such as the experience in operating crane are ignored. Moreover, any two of values of ϕ, θ, r change at the same time at most.

Both robot arm and crane

Robot base rotation center and pivot of crane's boom are the origins in the coordinates system. The swinging of extreme points of the crane and the swinging of the crane do not be considered. Furthermore, the motion of extreme points of the crane and the robot arm are analyzed since the extreme point is the main point we focus. Regarding the problem of the deformation of the boom and the robot arm, we assume that the deformation caused by the weight of the object can be ignored.

2.3. Configuration transformation

We derived the configuration transformation model between a retractable crane and a robot arm from their kinematic model. It consists of two parts. The first part is proportional scaling, that the virtual robot arm and crane are the same length of simulation to find their effective range of motion. In the second part, the endpoint motion of the crane is simplified into a triangular coordinate relationship, and the conversion formula is obtained by using the trig function and polar coordinate:

2.3.1. Proportional scaling

According to the model information provided by the government, the simulation condition of the equivalent ratio can be achieved through proportional conversion. The variational constant (1) is obtained by using the longest distance that can be reached by the lifting arm of the crane and the longest distance that can be reached by each axis of the robot arm at the initial Angle.

$$k = \frac{R_{max}}{r_{max}} \tag{1}$$

2.3.2. Conversion formula

The relationship between the rotation Angle of each axis of the robot arm and its motion posture in space is calculated based on forward and inverse kinematics [4]. As a tool to simulate the endpoint's path of the crane, we ensure that the A5 axis remains horizontal and that the changes in the intermediate axes are not considered. Therefore, the motion posture of the robot arm is simplified into a trig function to take the starting point and ending point of the motion of the robot arm. And it is necessary to consider that the pivot of crane and Rotation is different.

The spatial coordinates of x, y and z in the simulated environment are obtained by the transformation between the polar coordinate system and Cartesian coordinate system. As shown in figure 2, formula (2), (3) and (4) are used to calculate the initial point $i(x_i, y_i, z_i)$ of the robot arm movement in the 3D simulated environment.

$$x_i = k(r_i \sin\phi_i - \mu)\cos\theta_i \tag{2}$$
$$y_i = k(r_i \sin\phi_i - \mu)\sin\theta_i \tag{3}$$
$$z_i = kr_i \cos\phi_i \tag{4}$$

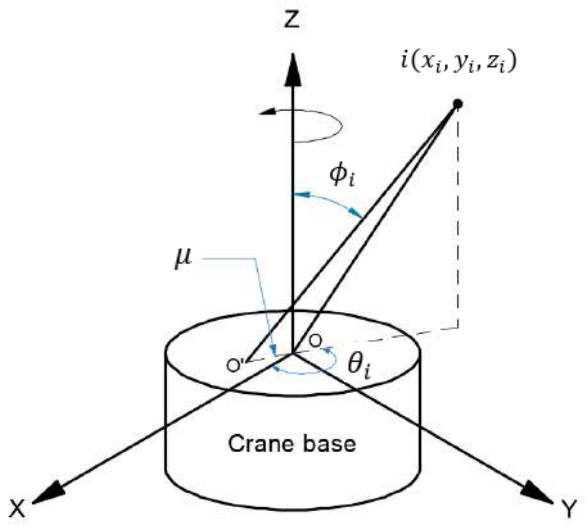

Figure 2. The initial point of the simulation

After obtaining each coordinate in the simulated space, formulas (5), (6) and (7) are used to calculate the length of the mechanical arm, horizontal rotation Angle and elevation Angle.

$$r_T = (r_i + \Delta r) \tag{5}$$
$$\theta_T = (\theta_i + \Delta\theta) \tag{6}$$
$$\phi_T = (\phi_i + \Delta\phi) \tag{7}$$

As shown in figure 3, equations (8), (9) and (10) can be used to calculate the extreme point to be simulated by the virtual robot arm.

$$x_T = kr_T \sin\phi_T \cos\theta_T \quad (8)$$
$$y_T = kr_T \sin\phi_T \sin\theta_T \quad (9)$$
$$z_T = kr_T \cos\phi_T \quad (10)$$

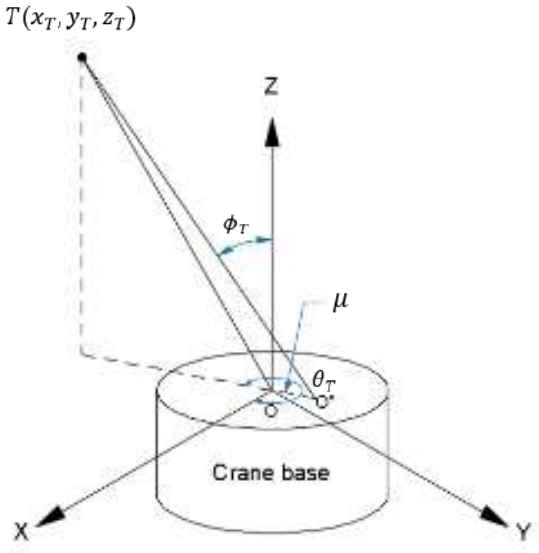

Figure 3. The end point of the simulation

Figure 4. 2D Effective simulation range

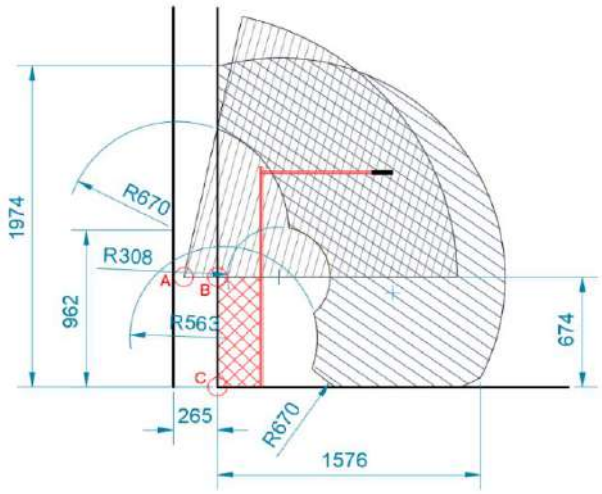

Point A: The pivot of crane
Point B: The center of Rotation
Point C: The simulated pivot of virtual robot arm
Red Area: The shape of a robot arm

Considering the crane and robot arm can rotate horizontally, 3D graphics software is used to display a complete 3D effective simulation range, as shown in figure 5.

3. Results

3.1. Analysis of crane and robot arm

At the present research stage, we combine the horizontal rotation of the crane and the pivot of the crane as a single pivot in the virtual robot arm for subsequent simulation to find out the effective simulation range between the virtual robot arm and the crane. Finally, the crane operator exam is taken as an example to verify the accuracy of the virtual robot arm simulating the motion of the crane extreme points.

We first analyze the motion path of the robot arm and the crane, and then compare them together. First, we assume that the robot arm is always horizontal and does not rotate at the A5 axis, and the motion range of the robot arm is not lower than the ground plane. For the crane part, it has two different Pivot Points and the height of the crane itself must be considered. The length of the crane arm is then converted to the ratio, and the effective simulation range of the two is calculated by 2D drawing software. According to figure 4, the inclined area at two different angles is shown. The sector is the movable range of the lifting arm of the mobile crane model RT-100, and the other irregular block is the movable range of the robot arm model KR16s.

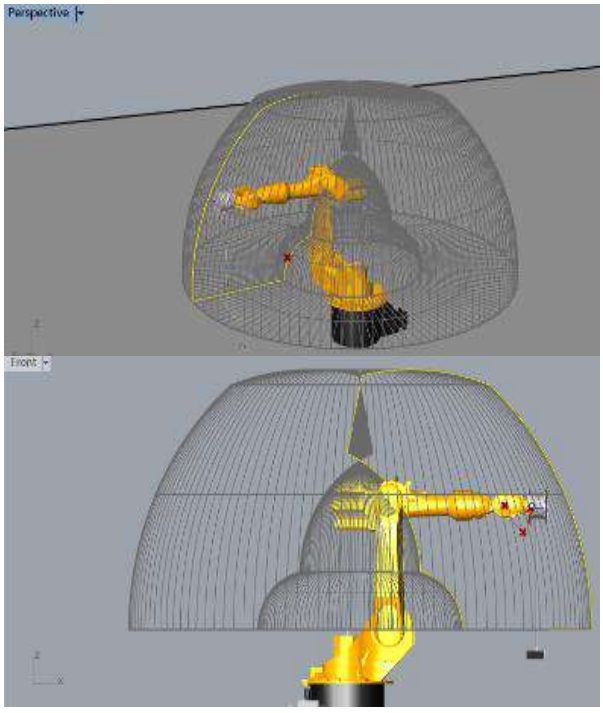

Figure 5. 3D Effective simulation range

3.2. Calculation process and simulation

According to the driving test of a mobile crane in Taiwan, we used the operation test path of the crane in the game engine, and recorded the extreme points of the boom in the space of the Coordinate points. In addition to the path, we also operate according to some examination regulations, including the following:

1. The crane is fixed in the rotation center.
2. The starting point of the crane is at point S, and the hanging object is about 2 meters high from the ground.
3. During the operation, follow the running path, pass the obstacles in sequence and return to the starting point.
4. During hoisting, the hanging object should not touch the ground.

Simulation results of crane operating model RT100 in the game engine are shown in figure 6. The red line in the space represents the route of the technical examination for the crane driver's license.

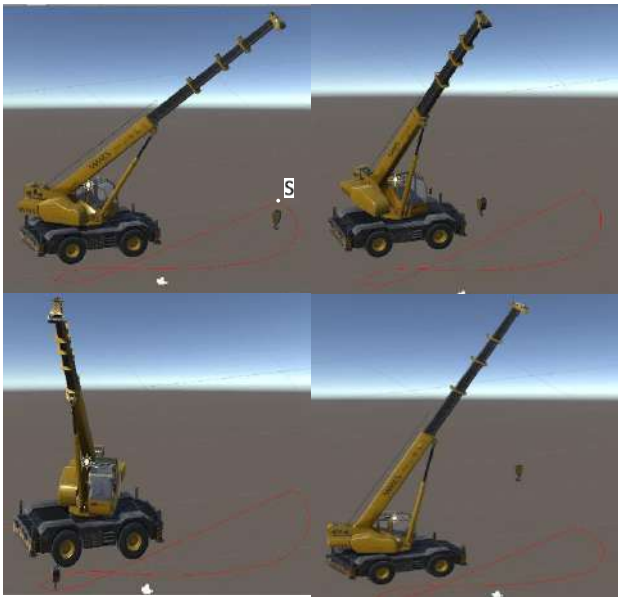

Figure 6. The crane simulates the process of the path

Next, move these Coordinate points as the crane simulates to another 3D software that can simulate a robot arm. In figure 7, you can see that the simulated path consists of red points. Some Coordinate points may appear in an area that cannot be simulated, and we can use scaling to adjust the range to be simulated. During the simulation process, it is necessary to ensure that the pose of the end of the virtual robot arm is the same as the crane. We also record the points that the end of the virtual robot arm passes through.

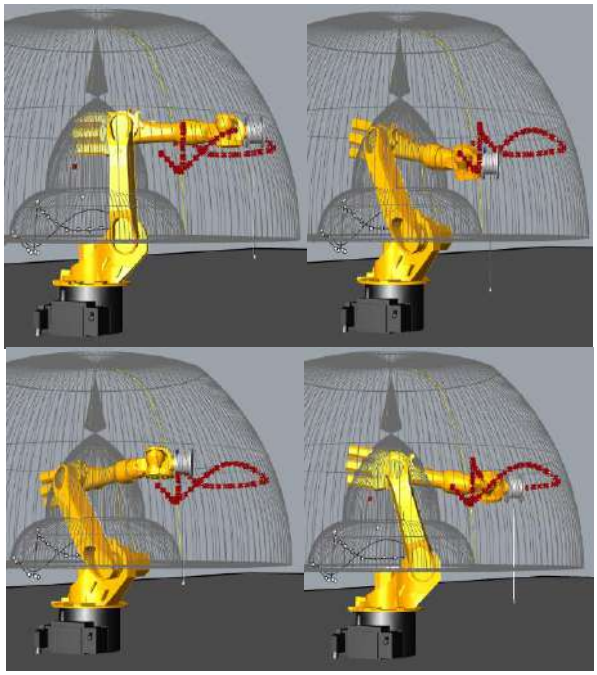

Figure 7. The virtual robot arm simulates the process of the path

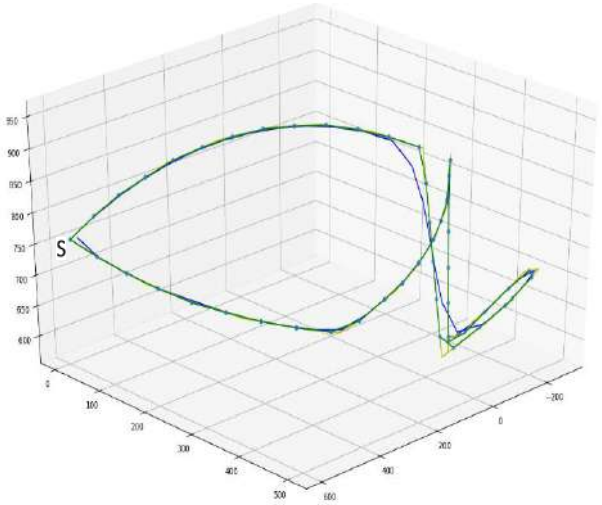

Figure 8. Comparison of simulated path results

We tested two different ways of simulations. The first is to use a curve made up of points as the simulation path, while the other is to use a straight line made up of points. In figure 8, we compare the simulated paths using 50 points. The yellow line represents the path of the crane. The blue lines represent curved paths of points, while green lines represent straight paths of points. Next, we increase the number of points on the straight path to 100

and compare again, as shown in figure 9.The red line represents the results of the robot arm simulation.

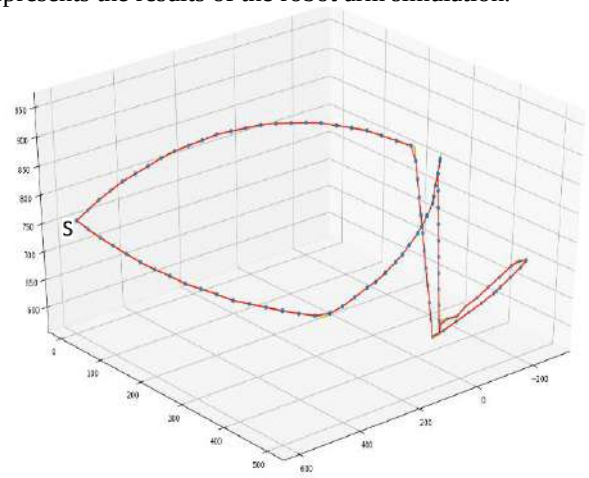

Figure 9. Increase the number of points to simulate

For the 2D plane, we compared the curves, straight lines, and lines with 100 points of simulation paths.

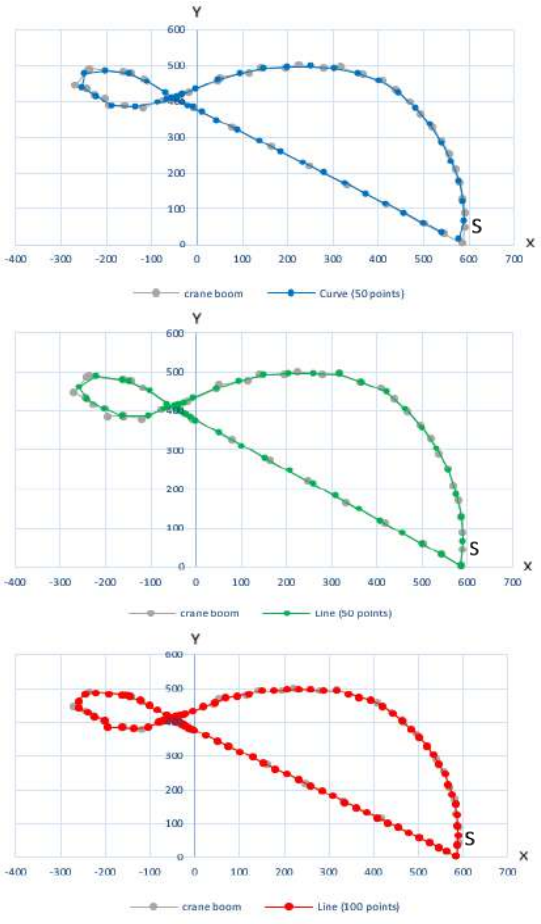

Figure 10 and figure 11 are the X-Y plane and the X-Z plane, respectively.

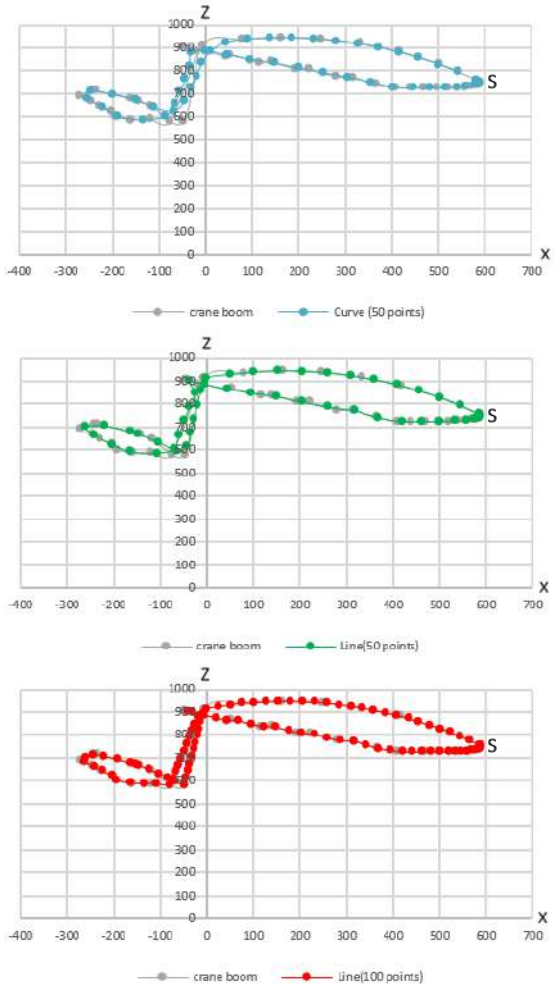

Figure 10. Comparison of coordinate point paths in X-Y plane

Figure 11 Comparison of coordinate point paths in X-Z plane

4. Discussion

We obtained the effective simulation range based on the motion limit of the crane model rt-100 and the robot arm model K 16 RS and found that some coordinate points of the crane extreme points converted from UNITY could not be simulated by the robot arm. The reason is that we are scaling with the longest length, resulting in some points near the shortest length to be outside the effective range. In order to focus on the virtual robot arm to simulate the movement of the extreme point of the crane, the coordinates are all within the range of simulation through scaling.

During the simulation of extreme point paths, we

observed several things. If the same number of coordinate points are used for simulation, the curve path will produce a large error, while the line path will be more accurate. And when the number of simulation points is increased to 100, the accuracy of the path simulated by the robot arm can be improved. At the same time, we find that even if the number of simulation points is increased to 100, there will still be some errors when the extreme points path of the crane suddenly changes. For example, when the extreme points of a crane crashes or falls suddenly or shifts up and down. However, in the real hoisting operation, the speed of the crane movement will affect the swinging posture of the suspension. [5] Therefore, in order to simulate the real crane movement with the robot arm, the speed must also be considered. In this study, the path of the crane extreme points is analysed. Future study will discuss the time factor.

5. Conclusion and future works

Selecting an improper type of crane for a construction project may significantly increase the erection cost. In order to select a proper type of crane, crane simulation is one of the effective methods. However, simulating multiple types of crane requires multiple types of crane models which are always lacking. We developed a simulation method with a 6-degree-of-freedom robot arm using the developed process. The simulation processes include the identification of simulation constraints and the configuration transformation between a robot arm and the crane. One of the erection tasks selected from the crane operator exam was applied to the simulations with a virtual crane and a virtual robot arm respectively. Despite the kinematic constraints for the robot arm simulating the crane, the motion paths of the extreme points of the crane and the arm are highly similar. Only with the same robot arm, the application of the method can simulate the retractable crane and the boom crane regardless of its size and detailed specification. In future work, we will take into account the problem of boom deformation and test configuration transformation with actual mobile crane and robot arm operating on site and in R-lab. In addition, we will find general configuration transformation to test the situation of the movement of the crane and the swing of hook in all crane models.

References

[1] Baeksuk Chu, Kyungmo Jung, Youngsu Chu, Daehie Hong, Myo-Taeg Lim, Shinsuk Park, Yongkwun Lee, Sung-Uk Lee, Min Chul Kim, Kang Ho Ko. *Robotic automation system for steel beam assembly in building construction*, International Conference on Autonomous Robots and Agents. 2009: Wellington, New Zealand.

[2] Kelvin Chen Chih Peng, William Singhose, Semir Gessesse, David Frakes. *Crane operation using hand-motion and radio frequency identification tags*, International Conference on Control and Automation. 2009: Christchurch, New Zealand.

[3] SangHyeok Han, Shafiul Hasan, Mohamed Al-Hussein and Kamil Umut Gökçe. *Simulation of mobile crane operations in 3D space*, Winter Simulation Conference. 2012, Berlin, Germany.

[4] Masahiro Izumi, Hiroaki Seki, Yoshitsugu Kamiya, and Masatoshi Hikizu. *Automatic hook crane with robot arm*.2011: Karon Beach, Phuket, Thailand.

[5] Kamal A. F. Moustafa1 A. M. Ebeid. *Nonlinear Modeling and Control of Overhead Crane Load Sway*. Journal of Dynamic Systems Measurement and Control ,1998. 120(4)

Development of Classification Model for the Level of Bid Price Volatility of Public Construction Project focused on Analysis of Pre-Bid Clarification Document

Y.E. Jang[a], J.S. Yi[a], J.W. Son[a], H.B. Kang[a], and J. Lee[a]

[a]Department of Architectural and Urban Systems Engineering, Ewha Womans University, South Korea
E-mail: jsyi@ewha.ac.kr

Abstract –

The purpose of this paper is to classify the level of formation of the bid price by using the type of uncertainty inherent in the bid document as a variable. To this end, the research examined the factors of the project related to the bid price presented in the previous study. Next, the pre-bid clarification document, which can be used to check the uncertainty of the bid documents, is used as a surrogate variable. Through these input variables, this research implemented two kinds of models using four algorithms: one predicts the level of bid price with uncertainty of bid document and the other predicts the level of bid price without uncertainty of bid documents. As a result, the model that predicts the level of the bid price reflecting the uncertainty of the bid document shows about 24 percent better performance than the model that predicts the bid price without reflecting the uncertainty of the bid document.

Keywords –

Risk Management, Bid Price Risk, Bid Price Volatility, Uncertainty of Bid Document, Pre-Bid Clarification, Bid Price Average, Bid Price Range, Machine Learning (ML), Classification Model, Public Construction Project

1 Introduction

Contracts for construction projects are made through competitive bidding. Bidding is a method of concluding a contract with a bidder who offers the most favourable content, that is, generally the lowest price, by letting multiple bidders submit applications with their price. Therefore, the most important issue for the bidder is how much the bid price should be presented [12]. This is because the bid price affects the likelihood that the bidder will be able to obtain a satisfactory profit from the project, as well as the likelihood that the bidder will be able to win the project.

Since the construction contract is concluded by contracting to implement the construction object through mutually agreed price based on the information given prior to the contract, which means bid document, the price required for the implementation of the construction object is also based on the bid document. Since the bid document can be operative as a contract document after the contract is concluded, bidders will thoroughly review the bid document from the bidding stage. In other words, the bid document serves as a substantive basis document for the bidders to calculate the bid price.

The bid document is a fundamental and essential communication tool between the client and the bidder. If the content of the bid document is uncertain, the intention of the construction object may become ambiguous and cause a mistake during construction phase [8], which may lead to construction rework, disputes and claims.

Understanding the uncertainty of the bid document can therefore enhance mutual communication among stakeholders and ultimately encourage the clients (i.e., owners) to improve the quality of the bid document [9]. In the United States, a system is in place to address such uncertainties in the bid document through a system that encourages bidders to inquire to their owners during the pre-bid clarification on the uncertainties inherent in the bid document and responds to them.

Bid price may be expressed in many ways, but generally it can be expressed as follows:

$$B_i = C_i(1 + M_i) \quad (1)$$

C_i means the total project cost of the project that bidder i expects, and M_i means the markups that bidder i internally reflect by analysing the project's uncertainty, or risk [1]. In other words, the result M_i reflecting the uncertainty in the bidding stage is included in the bid price B_i, which cause increase of total bid price. Conversely, if the uncertainty decreases, the bid price is determined at a lower level. In particular, a project that eliminates the uncertainty of bid document through the

pre-bid clarification procedure has been studied to form a bid price at a level more stable than the other projects [14].

Risk management is carried out throughout the lifecycle of the project, but initial preemptive risk management is crucial in that risk management at the bidding stages minimizes the damage that will occur at the later stages of the project [8]. Failure of risk analysis at the bidding stage is one of the root causes of project failure, which can cause significant damage to bidders and construction industry as well as project failure [15].

However, due to the many uncertain factors to be considered in predicting risk, it is difficult for bidders to offer bid prices that simultaneously satisfy satisfactory profits and the likelihood of winning a project [10]. In particular, there is a growing need to eliminate risks at the bidding stage of larger construction projects that involve relatively more uncertainty [18]. This uncertainty ultimately increases the price of the project [16], but due to the difficulty in figuring out the level of risk within a limited amount of time during the bidding process of the construction project, bidders have difficulties in determining the bid price as well as difficulty in deciding whether to participate in the bid [7].

For this reason, in practice, rather than predicting a reasonable level of risk in deciding whether to participate in a bidding for a construction project, it relies on subjective factors such as experience, speculation, and intuition. In other words, there is a need for a decision support tool that can be utilized by practitioners who have difficulties in accurate price predicting due to many factors affecting the bid price.

Therefore, this study considers uncertainty that can be observed in pre-bid clarification document as surrogate variable (i.e. proxy variable) in order to measure uncertainty in bid document and compares the level of performance of the bid price prediction between the model including that proxy variable and the model without it.

2 Theoretical Backgrounds

2.1 Risk Management of Construction Project

According to the PMBOK (Project Management Body Of Knowledge), risk management research can be said to consist of 1) Risk Identification, 2) Risk Assessment, and 3) Risk Plan and Control. Risk assessment can be defined as an estimate of the potential impact of an uncertain factor on a project based on an understanding of this uncertainty [4]. However, due to the difficulty of considering too many variables to be considered, and too much time to be taken into account, risk assessment studies in practice as well as in risk assessment remain qualitative [2]. Although the most important prerequisite for quantitative analysis is to obtain real data [22], existing risk management studies have mainly focused on higher-level risk factors, and these studies have the problem that it is difficult to identify the results through actual data.

2.2 Factors Affecting Bid Price in Preliminary Studies

Construction projects can be divided into building, transportation, and various types of plant depending on the characteristics of the construction object. Among them, although construction and transportation are relatively different in size (e.g., construction (20.2%), transportation (25.6%)), the difference is not significant. In previous risk management research, rather than dividing building and transportation, there was a considerable case in which the risks of construction projects were covered in a comprehensive manner.

However, since the data analyzed by this study is the transportation project data, the risk factor list is extracted from the total of 5 studies including the study using the transportation project data in the preceding research. Seven variables were selected by matching whether the variables corresponded to the same or inclusive relation.

In this study, 5 prior risk management studies were used to extract risk factors for model input variable selection. Risk factors extracted from each study were presented in Table 1.

Table 1. Risk factors from literature review

No.	Risk Factors
1 (Chan and Au 2009)	Poor employer's reputation to honor payment on time; Amount of liquidated damages being higher than expected; Poor financial capability of the employer; Very tight contract period; Non-ideal project cash flow; Large portion of works subcontracted to nominated subcontractors; Low intensity of work; High degree of difficulty; Onerous contract conditions and rigid specifications; Possibility to have public objections
2 (El-Mashaleh 2012)	Project type; Project size; Quality of bid documents; Terms of payment; The contract includes an "adjustment for changes in cost" sub-clause; Cash flow requirements of the project; Availability of labor required for the project; Availability

	of materials required for the project
3 (Agnieszka and Edyta 2013)	Availability of equipment required for the project; Promote the reputation of the firm; Improve the experience of firm's personnel; Increase the possibility of building a long-term relationship with the client; Identity of the client; Financial capability of the client; Reputation of the client regarding his commitment of making timely payments; Influence of the client in making recommendations in the construction market; Reputation of the consultant regarding his independence in making "fair determinations" between the contracting parties; Amount of work currently at hand; Current financial standing of the firm; Availability of other projects in the market
4 (Dominic and Simon 2014)	Type of work; Past experience with similar projects; Contract documents; Owner's reputation; Value of the project; Need of work; Current involvement in other projects; Size of the project; Profits from similar past projects; Time of project duration; Criteria of bid selection
5 (Delaney 2018)	Location of the project; Time for the preparation of the bid; Possible subcontractors; Necessity for specialized equipment; Degree of complexity of works

The variables extracted from previous studies are as follows (Table 2).

Table 2. Factors affecting bid price in preliminary studies

No.	Factors
1	Number of bidders
2	Working days
3	Engineer's estimate
4	Project location
5	Bid preparation days
6	Project type

In Chapter 5, these variables are included in the training dataset in Model 1 and 2 so that both can predict the volatility level of the bid price.

2.3 Pre-Bid Clarification Document

Bidders are provided with bid document by which they obtain the desired construction object at the bidding stage. Bidders will carefully examine the bid document from the bid announcement date to the start date of the bid, and then determine the bid price. In this way, the bid document describes the criteria and procedures for the design, construction method, material, and quality inspection to complete the construction object. Since the bid documents themselves are contractually valid, bid documents may be used as a basis for making important judgments when claims and disputes arise in the future. If the risk factors included in the bid document cannot be reviewed in advance, it may become a factor of future project costs. Therefore, it is very important to analyse the uncertainty of bid documents in terms of risk management [14].

If the bidders believe that there is a problem due to uncertain contents of the bid documents during the pre-bid clarification process, they can ask the owner to review the contents. In other words, pre-bid clarification is a process in which a bidder inquires to the owner if the content of the bid document provided by the owner (e.g., construction contract, design document such as plans, special conditions of construction contract) is unclear [14]. The owner who receives the query from the bidder generally has an obligation to respond within a fixed period. If the query determines that there is a problem with the bid document, he or she will issue an amendment document, which is called addendum, instead of simply responding. Thus, the elimination of uncertainty in bid documents through pre-bid clarification can reduce the occurrence of abnormally low bidding prices and winning prices [19], the New York State Office of General Service, [17]) proposed the policy making process of inquiry and response process of Pre-bid clarification document in the bidding system of construction project as follows:

PRE-BID INQUIRY & RESPONSE POLICY

Background

The pre-bid inquiry and response process is important and beneficial for both the bidder and OGS. It helps to ensure more accurate contractor estimates and bids and fewer ambiguities. Providing consistent responses to prospective bidders also helps to avoid or minimize contract change orders, claims and disputes.

Therefore, considering that the risks presented in the pre-bid clarification documents address uncertainties arising from all kinds of bid documents, the pre-bid clarification document is used as a proxy for uncertainty of bid document in the bidding phase of the project. In the pre-bid clarification document, the following is a table summarizing the five common types of contents that affect the bid price. In Chapter 5, the variables that

can be extracted according to these types (Table 2) are constructed and reflected in Model 2 and compared with Model 1.

Table 3. Types affecting bid price in pre-bid clarification document

No.	Type and example
1	BI 1. Discrepancy (Mutual contradiction) ***Example (Unsolved)*** ***Inquiry #34:*** *Comparing Layout drawing L-1 (pg 17) with pavement elevation plan C-1 (pg 37), the dimensions of the Alhambra Ave EB on-ramp (right) are not the same. Please clarify or re-issue correct drawings.* ***Response #2:*** *Please bid per current documents.*
2	BI 2. Error ***Example (Solved)*** ***Inquiry #10:*** *Please check the State Quantity regarding Bid item 35 Rubber HMA – GAP?* ***Response #2:*** *Quantities have been verified. Bid per current contract documents.*
3	BI 3. Omittance ***Example (Solved)*** ***Inquiry #4:*** *The Special Specifications require the installation of some plants and the irrigation. The irrigation plans shows two truck standpipe. It is safe to assume that there no water at this location either water must be truck or water must be developed.* ***Response #3:*** *Correct, the contractor is responsible for bringing water to the site. Water cannot be developed at the site, such as installing a well to capture underground water.*
4	BI 4. Insufficient information ***Example (Unsolved)*** ***Inquiry #58:*** *`?* ***Response #2:*** *Please bid per current contract documents.*
5	BI 5. Alternative information ***Example (Unsolved)*** ***Inquiry #113:*** *We are requesting clarification on the requirements for Uniaxial Geogrid specified under Section 88–1.02R Uniaxial Geogrid. Specification requires a punched and drawn polypropylene uniaxial geogrid with minimum ultimate tensile strength of 7600 lb/ft. Review of available uniaxial geogrid products indicates no manufacturer supplies polypropylene uniaxial geogrid. We are requesting Caltrans to allow uniaxial geogrid with minimum ultimate tensile strength of 7600 lb/ft meeting the requirement of Section 88–1.02D(1) and geogrid shall have a regular and defined open area with an open area of 50 to 90 percent. Geogrid shall be manufactured from high tenacity polyester (PET) or high density polyethylene (HDPE).* ***Response #2:*** *Any proposal not specifically identified in the bid documents will only be considered by the Engineer after contract award. Please bid per the current contract documents.*

3 Machine Learning

Machine learning can be roughly divided into two types, one is prediction method that derives regression equation as statistical analysis, and the other is classification method which determines the category of data. The bid price volatility level classification model that predicts the level of actual bid price after learning data by using machine learning needs a proper classification algorithm. In this study, four classification algorithms were used for the model: Decision Tree (Tree), Support Vector Machine (SVM), K-Nearest Neighbor (KNN), and Neural Net (NN).

The classification algorithm using Tree algorithm is a methodology commonly used in machine learning. It aims at generating a model that predicts the level of an output variable based on several input variables. Tree generally has merit that it can be understood only by a brief description. In addition, compared with other techniques, there is no need to process the data, so the data pre-processing procedure is simple, and the processing speed is fast, so that it can be applied stably to a large dataset. However, the Tree model is very sensitive to the initial settings, which can lead to different results each time [13]. In addition to this, there is a disadvantage that it is difficult to solve a complicated classification problem such as XOR operation with the Tree algorithm.

SVM is one of a kind of machine learning and is a supervised learning model for pattern recognition and data analysis. It is mainly used for classification. Given a set of data belonging to either of the two levels, the SVM algorithm creates a non-stochastic binary linear classification model that determines to which level new data belongs based on a given set of data [20]. The SVM algorithm finds the boundary with the largest width. SVM can be used in nonlinear classification as well as linear classification. In order to perform nonlinear classification, it is necessary to map the given data to the high dimensional feature space. In order to this efficiently, a kernel trick is used. The learning effect of SVM is known to be very good among classification algorithms, and it is useful for classification of proteins in the field of medicine.

KNN is one of the representative classification algorithm used in machine learning. It categorizes data into a principle that weights neighbors' contributions so that the closer the neighbors contribute more to the average than the farther neighbors. For example, the most common weighting scheme is to give each neighbor a weight of *1/d* when d is the distance to the neighbor. This principle allows KNN to classify data effectively, but it can be very sensitive to the local structure of the data. This is called 'Majority Voting', and this phenomenon occurs when the level distribution is biased. In other words, more frequent levels of data tend to dominate the prediction of new data because more frequent levels of data tend to be the majority of

the K Nearest Neighbors [11].

The NN algorithm, also known as the Artificial Neural Network, is a classification algorithm that can be useful for learning highly complex data. The main advantage of the NN algorithm is that it can learn from the observed data and produce the desired approximate function. In order to utilize this NN algorithm, it is necessary to set the connection pattern between the neurons of the other layers, the learning process of updating the weight of the connection, and the activation function of converting the weight input of the neuron into the activation output. The NN algorithm belongs to Deep Learning among the machine learning. It can solve complex problems such as XOR problem, and it is generally known that it has high performance in classification.

4 Data

In order to classify the bid price volatility level through the analysis of the bid data, this study selected the public construction project in transportation ordered by Caltrans, California, USA as analysis data.

There are various types of private standard contracts used worldwide, such as the International Federation of Consulting Engineers (FIDIC), Joint Contracts Tribunal (JCT), New Engineering Contract (NEC), and American Institute of Architects (AIA). In Caltrans' case, Federal-Aid Construction Contracts (FHWA-1273) is used as the standard contract terms when they carry out a general project. Unlike private projects, the contract conditions of these public projects are used without any modification of special conditions in most cases. This means that the construction project from Caltrans uses a bid document that does not deviate significantly from the standard. These standardized contracts and the bid documents that contain them will not only reduce the influence of numerous factors affecting the bid price, but also the nature of the bid documents, as described in the scope of this study, it is believed to be effective in examining the impact of uncertainty in the bid documents on the risk measurement indicators.

The California State Department of Transportation is a very large ordering organization in the United States, and it has about 450 civil engineering works each year based on its strong economic power. According to the State Transportation By The Numbers: A Compendium of State Summaries, a statistical survey conducted by the US Department of Transportation, the California State of California is a large administrative area that accounts for about 4.3 percent of the US territory. 281,617 km of roads and 8,521 km of trains, (US Department of Transportation 2015). The US State Department of Transportation is investing $ 1.7 billion annually in infrastructure to reorganize aging facilities and build new facilities, accounting for about 10 percent of the US Department of Transportation's overall budget, the largest figure in the nation's 50 states. Therefore, the California Department of Transportation has thousands of standardized construction project data that have been carried out to facilitate data collection and analysis. However, due to the long experience of ordering and project management knowledge, the uncertainty of bid documents of the California State Department of Transportation is estimated to be relatively small compared to other ordering organizations. If the uncertainty of these bid documents decreases, I think it may be a little difficult to see the relationship and its effectiveness.

In addition, the California State Department of Transportation's bidding process includes a Pre-bid clarification process that eliminates the uncertainty of the bid documents through the bid question and answer process. In addition to the Pre-bid clarification document generated during this process, and that the data are in accordance with the purpose and characteristics of this study.

5 Datamining: Modelling

There are two models to be implemented in this study:

- Model 1: Implemented with input variables NOT including uncertainty of bid document related
- Model 2: Implemented with input variables including uncertainty of bid document related

Therefore, this Chapter deals with specifying the input, output, and output variable classes required to implement these two models.

5.1 Input Variables

The input variables to be used in the model consisted of the variables related to the bid price derived from the preliminary studies and the variables related to the uncertainty of the bid document (Table 4).

Table 4. Model input variables

Model	Input variable
1	▪ Number of bidders ▪ Working days ▪ Engineer's estimate ▪ Project location ▪ Bid preparation days ▪ Project type
2	▪ Number of bidders ▪ Working days

- Engineer's estimate
- Project location
- Bid preparation days
- Project type
- Number of unsolved BI. 1
- Number of unsolved BI. 2
- Number of unsolved BI. 3
- Number of unsolved BI. 4
- Number of unsolved BI. 5
- Number of unsolved BI Total
- Solved ratio
- Number of addenda

5.2 Output Variable and Class Designation

The output variable of the model should be a risk measure of the bid price. In this study, the following two risk measures were used: Bid Average Risk and Bid Range Risk.

5.2.1 Bid Average Risk

Bid Average Risk is the ratio of the average price which can be considered the agreed bidding price to the project's base price (engineer's estimate), which measures the risk and can be expressed as follows:

$$Bid\ Average\ Risk = \frac{Average\ Bid\ Price}{Engineer's\ Estimate} \quad (2)$$

For example, if the bid price of project A and B are both \$10 billion and each average bid price of project A and B is \$10 billion and \$13 billion, the Bid Average Risk of Project A and B are 1.1 and 1.3 respectively. And for project B, bidders are expecting more risk.

5.2.2 Bid Range Risk

Bid Range Risk refers to the difference between the maximum bid price and minimum bid price as a result of the bid compared to the engineer's estimate, and it can be expressed as follows:

$$Bid\ Range\ Risk = \frac{Max\ Bid\ Price - Min\ Bid\ Price}{Engineer's\ Estimate} \quad (3)$$

Since the difference between the maximum and minimum bid price is also affected by the project size, the risk cannot be determined simply by measuring difference between the maximum and minimum bid prices. For example, in a project with \$10 billion and a project with \$1 billion of engineer's estimate, the difference between max and min bid price is all the same at \$2 billion, but the difference between the uncertainties of the two projects cannot be considered same.

Therefore, it is appropriate to compare the difference between max and min bid price against the project's base price, in this study, which is regarded as engineer's estimate.

5.2.3 Output Variable and Class Designation

According to the above discussion, the output variables of Models 1 and 2 are shown in Table 5.

Table 5. Model output variables

Model	Output variable
1	▪ Bid Average Risk ▪ Bid Range Risk
2	▪ Bid Average Risk ▪ Bid Range Risk

The classification model predicts the class divided by a certain criterion rather than the value of these output variables themselves. For this purpose, the level of each output variable is specified and their classes are designated based on a certain criterion (Table 6).

Table 6. Class designation

Output variable	Class	Range	Ratio
Bid Average Risk	++	≥ 1.1	25%
	+	≥ 1.0 and < 1.1	27%
	-	≥ 0.9 and < 1.0	26%
	--	< 0.9	22
Bid Range Risk	++++	≥ 0.27	25%
	+++	≥ 0.2 and < 0.27	23%
	++	≥ 0.13 and < 0.2	24%
	+	< 0.31	28%

6 Results

This Chapter discusses the implementation of the models in accordance with Chapter 5. The following table shows the accuracy of the algorithms and output variables of Models 1 and 2 (Table 7), where the accuracy is a predicted ratio of the total data, and the expression is as follows:

$$\text{Accuracy (\%)} = \frac{Number\ of\ correct\ predictions}{Total\ number\ of\ predictions} \quad (4)$$

Table 7. Accuracy of classification models by algorithms

Algorithm	Accuracy (%)			
	Model 1		Model 2	
	Bid Average Risk	Bid Range Risk	Bid Average Risk	Bid Range Risk

Tree	31.5	34.3	61.7	60.6
SVM	34.6	40.5	59.5	60.5
KNN	32.8	36.1	58.4	56.1
NN	37.5	42.5	63.9	65.8

First, according to the Table 7, it was showed that the prediction accuracy of the model slightly differs according to the algorithm. The NN showed the highest accuracy in all cases, followed by SVM, KNN, and Tree, although with a few exceptions.

Second, the bigger difference is between Model 1 and Model 2. In Model 1, mean accuracy is somewhat low at 36.22%. In Model 2, which includes variables related to uncertainty of bid documents, mean accuracy is 60.81% as shown in Table 7.

Third, there was a difference in the accuracy depending on the output variables. Except for only two cases in Model 1 and Model 2, both models showed better performance in predicting Bid Range Risk than Bid Average Risk.

7 Conclusion

Although it is important to manage risk at the initial stage of the construction project, that is, at the bid stage, there are many cases where it fails to calculate the appropriate bid price because it is not done properly. In particular, the bid document is one of the important risk factors in the bid phase because it contains many uncertainties in the document due to the characteristics of the one - time construction project. However, since it is difficult to analyze all of the uncertain risk factors affecting the bid price in a short time, in business, it relies on the experience of practitioners or experts in predicting bid prices, and many studies have focused on qualitative solutions to risk management. Quantitative solutions are also based on statistical techniques based on virtual data or expert questionnaires rather than based on actual bid data, which has limitations in verification. In other words, there is a lack of empirical analysis of the effect between the uncertainty of the bid document and the actual bid price.

In order to meet both the need for decision support tools that can be used to calculate the final bid price in business and the academics' need for risk management research based on actual bid data, this research has developed a model to classify the bid price volatility level for the project bid data. The bid price volatility to be considered in this paper means the average of the bid price and the range of the bid price over the engineer's estimate. In order to reflect the uncertainty of bid documents, which were previously regarded as uncontrollable risk, the research sought to improve the accuracy of the classification model by using pre-bid clarification document as a proxy variable.

First, variables that can be obtained from the bid data were extracted and variables with high contribution were chosen by analyzing 13 previous researches related to risk factors. After that, 14 variables were identified as input variables in the model through the numeralization or categorization of the variable data.

Pre-bid clarification document analysis showed that the project with high uncertainty of bid documents formed a relatively higher average of bid prices than those without, and the range of bid prices was relatively broad. This confirms that the uncertainty of the bid document affects the bid price.

In order to examine whether the information related to the uncertainty of the bid documents gives better results in terms of accuracy in classifying the level of volatility of bid prices, a classification model that includes 8 variables related to uncertainty of bid documents and a classification model that does not include those variables were developed and accuracy of both models were compared. As a result of the analysis, the model that reflects the uncertainty of the bid documents showed accuracy of 63.9% for the average bid price and 65.8% for the range in bid price volatility level classification, whereas the model that does not reflect the uncertainty of the bid documents showed accuracy of 37.5% for the average bid price and 42.5% for the range in bid price volatility level classification. Consequently, it is confirmed that the result is better when the information related to the uncertainty of the bid document is reflected.

This study ultimately has the following contributions. In the bidder 's view, the bid price should be calculated to increase the likelihood of winning the project and to guarantee the profit of the project within the limited bid preparation time. The bidder will have the opportunity to fix or strategically change their bid price by comparing their bid price with the bid price average and range of the current project predicted through the cases of the past projects. In other words, the results of this study can be used as a more reasonable decision support tool that bidders can use when determining the bid price based on actual bid data. In addition, from the view of the owner, it can be expected that unnecessary design change and increase of project cost will be reduced by contracting with the bid price which fully reflects the result of the risk analysis including uncertainty of the bid price. Moreover, the bid document is a document that the owner provides to the bidder. The result of this study that the uncertainty of the bid document affects the bid price suggests the positive effect of providing bid document with high quality.

Although the actual bid price is calculated on the basis of the actual bid documents containing the contents for the purpose of construction, there has been

a limit to the difficulty in analyzing the actual bid data as the risk management research conducted based on the higher level of qualitative risk factors. This study has significance in that variables were obtained from the actual bid data, and implies that the level of risk management research has deepened to the detail level based on the actual bid documents by reflecting uncertainty of bid document through pre-bid clarification document as a proxy variable, consequently providing the foundation of research that can make more effective risk management risk studies.

8 Acknowledgements

This research was supported by Basic Science Research Program through the National Research Foundation of Korea (NRF) funded by the Ministry of Education (NRF-2018R1D1A1A09083708).

Also, this research was supported by Basic Science Research Program through the National Research Foundation of Korea (NRF) funded by the Ministry of Science, ICT and Future Planning (No. NRF-2016R1A2B4015977).

9 References

[1] Abotaleb, I. S., & El-adaway, I. H. (2016). Construction bidding markup estimation using a decision theory approach. *Journal of Construction Engineering and Management*, 143(1), 04016079.

[2] Ahmad, I., & Minkarah, I. (1988). Questionnaire survey on bidding in construction. *Journal of Management in Engineering*, 4(3), 229-243.

[3] Chan, E. H., & Au, M. C. (2009). Factors influencing building contractors' pricing for time-related risks in tenders. *Journal of Construction Engineering and Management*, 135(3), 135-145.

[4] Chua, D. K. H., & Li, D. (2000). Key factors in bid reasoning model. *Journal of Construction Engineering and Management*, 126(5), 349-357.

[5] Chua, D. K. H., Li, D. Z., & Chan, W. T. (2001). Case-based reasoning approach in bid decision making. *Journal of construction engineering and management*, 127(1), 35-45.

[6] Delaney, J. W. (2018). *The Effect of Competition on Bid Quality and Final Results on State DOT Projects* (Doctoral dissertation, State University of New York at Buffalo).

[7] Dikmen, I., Budayan, C., Talat Birgonul, M., & Hayat, E. (2018). Effects of Risk Attitude and Controllability Assumption on Risk Ratings: Observational Study on International Construction Project Risk Assessment. *Journal of Management in Engineering*, 34(6), 04018037.

[8] Doloi, H. (2012). Cost overruns and failure in project management: Understanding the roles of key stakeholders in construction projects. *Journal of construction engineering and management*, 139(3), 267-279.

[9] Duzkale, A. K., & Lucko, G. (2016). Exposing uncertainty in bid preparation of steel construction cost estimating: II. Comparative analysis and quantitative CIVIL classification. *Journal of Construction Engineering and Management*, 142(10), 04016050.

[10] El-Mashaleh, M. S. (2012). Empirical framework for making the bid/no-bid decision. *Journal of Management in Engineering*, 29(3), 200-205.

[11] Kashyap, D., & Misra, A. K. (2013, July). Software development cost estimation using similarity difference between software attributes. *In Proceedings of the 2013 International Conference on Information Systems and Design of Communication* (pp. 1-6). ACM.

[12] KPMG International. (2015). *Global Construction Survey 2015*. Climbing the curve.

[13] Laurent, H., & Rivest, R. L. (1976). Constructing optimal binary decision trees is NP-complete. *Information processing letters*, 5(1), 15-17.

[14] Lee, J., & Yi, J. S. (2017). Predicting Project's Uncertainty Risk in the Bidding Process by Integrating Unstructured Text Data and Structured Numerical Data Using Text Mining. *Applied Sciences*, 7(11), 1141.

[15] Maemura, Y., Kim, E., & Ozawa, K. (2018). Root Causes of Recurring Contractual Conflicts in International Construction Projects: Five Case Studies from Vietnam. *Journal of Construction Engineering and Management*, 144(8), 05018008.

[16] Miller, R., & Lessard, D. R. (2008). *Evolving strategy: risk management and the shaping of mega-projects*. Cheltenham: Edward Elgar.

[17] OGS. (2018, December 3). *Pre-bid inquiry & response policy*. Retrieved from https://online.ogs.ny.gov/dnc/contractorconsultant/esb/prebidinquiryresponsepolicy.asp

[18] Priemus, H., Flyvbjerg, B., & Van Wee, B. (2008). *Decision-making on mega-projects*. Edward Elgar Publishing.

[19] Trost, S. M., & Oberlender, G. D. (2003). Predicting accuracy of early cost estimates using factor analysis and multivariate regression. *Journal of Construction Engineering and Management*, *129*(2), 198-204.

[20] Vapnik, V. (2013). *The nature of statistical learning theory*. Springer science & business media.

[21] Williams, T. P., & Gong, J. (2014). Predicting construction cost overruns using text mining,

numerical data and ensemble classifiers. *Automation in Construction*, 43, 23-29.
[22] Winch, G. M. (2010). *Managing construction projects*. John Wiley & Son.

Construction Payment Automation through Smart Contract-based Blockchain Framework

H. Luo[a], M. Das[a], J. Wang[b], and J.C.P. Cheng[a]

[a]Department of Civil and Environmental Engineering, the Hong Kong University of Science and Technology, Hong Kong
[b]Australasian Joint Research Centre for Building Information Modeling, Curtin University, Australia
E-mail: hluoaf@connect.ust.hk, moumitadas@ust.hk, Jun.Wang1@curtin.edu.au, cejcheng@ust.hk

Abstract –

A construction contract facilitates payments through the supply chain by integrating people, activities, and events throughout the project period through obligations, permissions, and prohibitions in its terms and conditions. The management of payments is a manual process and is more difficult in the case of construction projects as different stakeholders at different levels of the project organizational structure are bound by different contracts. Moreover, payments are strongly affected by the lack of clarity in the definitions of the obligations, responsibilities, and liabilities of various stakeholders in construction contracts. This intensifies disputes and causes delays in construction payments leading to additional expenditure, cash flow problems, and lack of trust. Therefore, to address these problems, we propose a methodology to automate construction payments by formalizing them into smart contracts and executing on a decentralized blockchain based framework. We formalize the payment logic that binds the prohibitions and liabilities associated with financial commitments, such as interim payments on completion of tasks in a construction project, and convert it into a computer-executable code. A framework based on blockchain is used to host this smart contract and to automate actions such as the triggering of payments after achieving consensus among the relevant project stakeholders. This framework also address the conditions required for the security of information in construction projects, such as confidentiality and information integrity in a multi-party environment. The proposed framework is demonstrated through a case-based scenario.

Keywords – Blockchain; Smart Contracts; Construction Projects; Interim Payments

1 Introduction

Construction projects often suffer from payment problems. Due to the adversarial working relationships of different stakeholders, and the complexity and uncertainty of the construction environment in Hong Kong construction projects, the outstanding payment amount was reported to be over HK$20 billion in 2015[1]. The solution to payment problems in construction projects greatly depend on the execution of construction contracts, which regulates the behaviour of the stakeholders by holding them accountable through commitments, prohibitions, obligations, and liabilities. It is the foundation for information management, claims, and payments, and therefore is a key to successful project completion. However, the execution of construction contracts is a complex process and faces many challenges, such as delays in payment [2]. A contract is said to have been breached or halted in cases such as defaulting on payment due to lack of funds or disputes on unsatisfactory quality of work. These problems escalate due to the ambiguity of language in the identifying responsibility, authority, and prohibitions described in the contracts. Moreover, the process of contract management is slow due to the fact that consensus among stakeholders is required for decision making. Achievement of consensus is preceded by several levels of approval from the stakeholders from various organizations, and therefore an immutable audit trail must be kept in order to prevent any disputes in the future. Previous research proposed measures to improve construction contract management. For example, standard construction contracts have been proposed by many countries and regions as references for contract formalization for specific types of construction projects, such as the FIDIC contract [3]. However, standard construction contracts focus on the improvement of the contract structure and are still difficult to interpret by individuals who are not lawyers by profession. To simplify contract management, e-contracts have been proposed. E-contracts are created by analysing relationships between the contract participants and contractual information, followed by modelling traditional textual contract in xml format [4]. However,

current applications of e-contracts are mainly found in electronics trade, where the complexity of relationships between parties, obligations, and activities is simpler compared to that in construction contracts. Therefore, a framework that improves the current state of construction contract management by addressing the challenges due to complexities and inherent nature of the construction industry is required. In this paper, we propose a blockchain based framework to facilitate semi-automatic contract execution and consensus achievement for the construction industry. Blockchain was selected for the proposed framework because it possesses the following characteristics: (1) information sharing among multiple parties; (2) information updating among multiple parties; (3) verification/approval at several levels [5].

The general architecture of blockchain is comprised essentially of a shared ledger. Every participant in a blockchain stores a local copy of this ledger in his/her database. The integrity of information in each local copy is maintained as they can be altered only upon achieving consensus by the majority of the participants. Information security and integrity is ensured through cryptographic techniques and consensus mechanisms. In general, there are three types of blockchain - public blockchain, private blockchain, and permissioned blockchain. A public blockchain network is open for anyone to join and host information. The BOPTI project utilized Ethereum, a well-known public blockchain platform, to issue their cryptocurrency, attracting customers through the reward mechanism [6]. Unlike public blockchains, private blockchains have a closed network and is owned by one controller. For example, it is especially useful for a closed network of banks. The private blockchain system has been used to store construction-related transactions by SiteSense software [7]. However, the construction industry may require access control mechanisms to allow or reject participants joining certain transactions. Therefore, a permissioned blockchain is most suitable for construction projects. In a permissioned blockchain, participants can join by invitation and require access rights to read or write from the blockchain, therefore adapting to the intrinsic feature of decentralization in the construction industry and the complexity of construction contracts. Thus, we propose a permissioned blockchain based framework to formalize and execute smart contracts. Our methodology includes contract formalization and a framework for automated contract execution. The methodology is supported by a case-based scenario that demonstrates its key features and advantages, such as information integrity, security, and transparency.

2 Methodology

In this study, a framework is proposed to automate payments in construction projects by formalizing construction contracts into smart contracts. The contract is executed on a blockchain based decentralized framework which supports the achievement of consensus for decision making based on the conditions of the smart contract. The methodology is divided into two parts - (1) contract formalization and (2) contract execution.

2.1 Contract Formalization

In this section, we describe our methodology for converting construction contracts into smart contracts for automatic interim payment. Construction contracts (such as HKGCC [9]) were studied to identify the general concepts of construction contracts, such as parties and activities and the logic relating them. Based on this study, data representation for smart construction contracts and the formalization of logic was done. The methodology for contract formalization as follows:

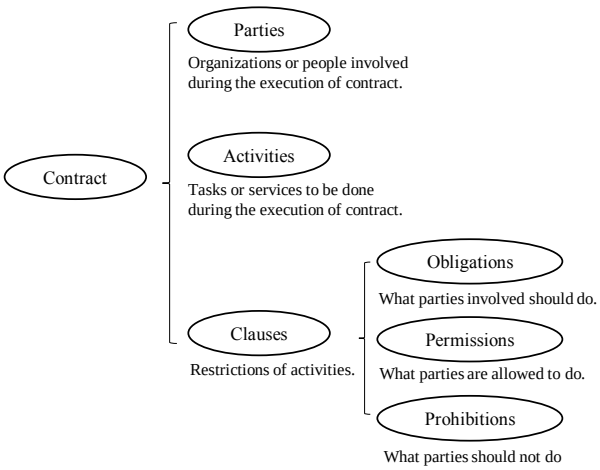

Figure 1. General structure of a construction contract

1) As shown in Figure 1, data representation for smart construction contracts was developed. Contract clauses were analyzed and key concepts were extracted, such as parties, activities, triggering events, conditions, actions, and resultant events.
2) Construction contracts were studied to identify and formalize the logic for executing smart contracts. For example, the relationship among parties and the sequence in which they are supposed to execute their responsibilities were identified. The parties involved in a construction contract for interim payment are

the contractor, inspector, quantity surveyor, engineer, and employer.

During the payment process, the obligation of a contractor is to submit an application with supplementary documents and to the initiate interim payment procedure. The inspector is supposed to check the correctness of all quantities claimed by the contractor followed by the quantity surveyor who is responsible for checking the correctness of the valuation in the payment claim and so on as shown in Figure 2.

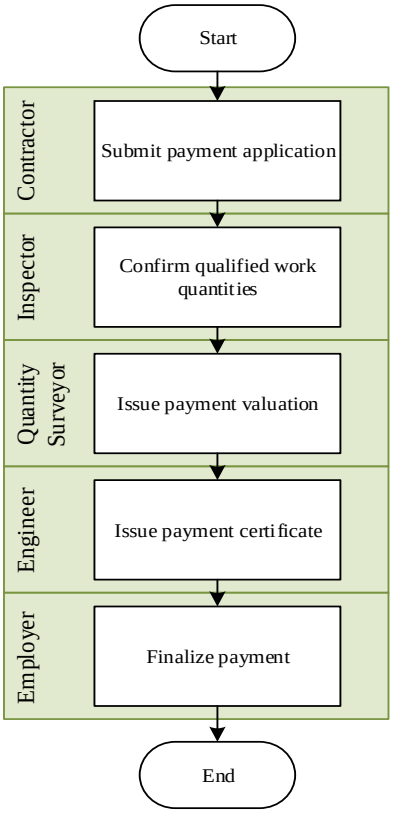

Figure 2. The sequence of activities and participants for interim payment

At the end of this process, interim payment should be triggered. This logic was converted into pseudocode and then into executable code using JavaScript. The conversion process is illustrated with an example scenario in Section 4.

2.2 Automated Contract Execution

The execution of the smart contract is done through a permissioned blockchain based framework and has two parts – (1) A automated consensus process based on pre-defined conditions of the smart contract and (2) a manual process which requires an input from the authorized stakeholder. In a blockchain based framework, information is stored in the two data models – one is for recording transactions which represents the action done by the authorized stakeholder, called the ledger, and another data model, called the asset model, is for checking and recording current values of construction data assets such as tasks and payments. All the project participants store the same construction information in their local asset data models and ledgers. The asset model is based on the transactions recorded in the ledger. The ledger is the actual backbone of blockchain which is an unmodifiable cryptographically linked storage structure, and therefore is a trusted source of information.

At the beginning of the contract execution process, a project participant, for example a contractor in this case, submits a request for payment. When the transaction of payment application is received by the following project participant which is the inspector in this case, the process of automatically achieving consensus begins. The incoming data is stored locally with every participant in a pre-defined data model, from where it is evaluated by the smart contract. Smart contracts are executed automatically to check pre-defined conditions of standard prohibitions and obligations (as discussed in Section 2.1). These pre-defined conditions check the validity of the incoming request by assessing information such as price, quantity of material, and other construction information against information such as historical records of payment and variations, stored in their local asset model. Consensus is achieved when all participants either approve or disapprove the proposed request according to the results of executing the smart contract on their local systems. After consensus on the correctness of a transaction is achieved, the transaction is added to the blockchain. This transaction contains information on who approved what (for example, who approved the payment application, quantity checking, and quality inspection results and so on), along with a timestamp, and is digitally signed by all the participants. Meanwhile, the asset model is be updated according to the transaction, which becomes the reference for validating later transactions. After this, the control is passed for manual input to the next project participant (which is quantity surveyor, as shown in Figure 3). It is to be noted that there is manual and automated consensus at each level of approval. During the manual approval part, the authorized participant has the right of approval or refusal based on existing information from the local asset model. The approver may also check other information manually, such as through on-site inspection, and may use his/her professional judgement to make a decision. After that, the decision is manually inputted by approver. The execution progresses through a series of manual inputs and automatic consensuses till the end of the approval process is reached. At every

stage, actions on construction data are recorded by transaction models in the blockchain ledger, which is unalterable. Therefore, at a later stage such information can be used for audit trail for identifying a defaulting participant or the responsible person for a project delay.

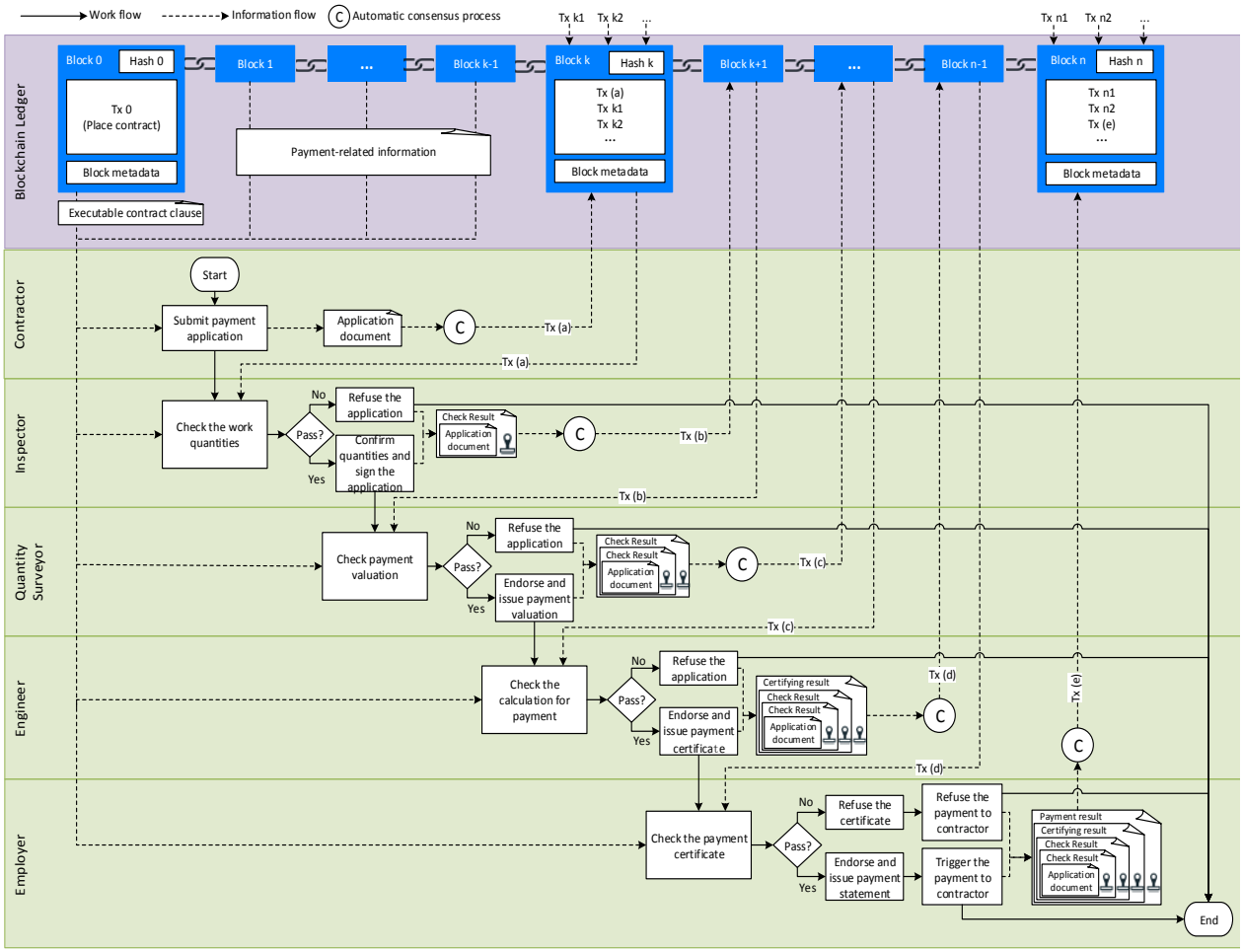

Figure 3. The semi-automatic blockchain based framework for interim payment

3 Contract Security Protection

In this section, we discuss the security related features of the proposed framework, which allows participants to come to a common consensus with verified endorsement in a secure fashion, without having to meet face-to-face. To do this, the framework implements blockchain based cryptographic protocols for the authenticity of participants and authenticity of data during transfer, and data confidentiality. This means that it ensures that only authorized participants are allowed to exchange information, that data is not altered during transmission between two participants, and sensitive project information is kept private. The proposed cryptographic protocol and hash functions ensure authenticity of the participants and authenticity of data during transfer. The private-key public-key is a type of asymmetric encryption where plain data is encrypted with a key, but is decrypted with its respective key pair. Hashing

however facilitates robust one-way encryption of plain text into encrypted text. Hash functions are collision free, which means that for a particular plain text, there a unique corresponding encrypted text. In our framework, in order to securely achieve endorsement and consensus, a participant, say A calculates the hash value of a message to be exchanged. After that, A signs (encrypts) the hash value of the message with a private key that is only known to him, as shown below.

$$signature_A = \mathrm{Pr}_{\mathrm{k_A}}(hash(message)) \quad (1)$$

The participant A, then broadcasts the concatenation of the original message and signature in the format, "$Encrypted(message \,||\, signature_A)$" to

every other participant on the blockchain framework. The participants at the receiving end can confirm that the message has been sent by A only if they can decrypt the signature with the corresponding publicly available key of A. Furthermore, the message is be confirmed to be unaltered during transfer, if calculation of the $hash(message)$ performed at the receiver's end is the same as that sent as a part of $signature_A$ by the sender, A. It is to be noted that this is done only to ensure the authenticity of the participants and data during transfer having nothing to do with data confidentiality. Data confidentially is implemented by separately encrypting the message itself in the first place with a different key available only to the project participants. Thus, only the parties within the permissioned blockchain network have the key to decrypt the message after they have ensured the authenticity of the users and data during transfer.

4 Example Scenario

In this section, an example scenario is demonstrated for describing the feasibility and key properties of the proposed methodology. Hyperledger [10] is used to set up the permissioned blockchain network for the involved parties in a construction project. The example scenario is based on the clauses related to interim payment from the General Conditions of Contract for Term Contracts for Civil Engineering Works in Hong Kong (HKGCC) [9]. Different parties have different obligations and responsibilities in the interim payment process (shown in Figure 2). These responsibilities and obligations are guided by clauses of HKGCC (as shown in step 1 of Figure 4) which have been transformed into machine executable logic to realize interim payments.

Contract execution is demonstrated in Figure 5. The contractor initiates the payment process with a manual input comprising information such as payment application ID, total payable amount, tasks and material quantity and passes control to the automatic consensus process (designated by "C" in Figure 5). The first consensus process checks the condition such as whether the claim is submitted or not. If successful, a transaction (as shown by Tx(a)) is written to the blockchain ledger. As can be seen from the data representation of the transaction, information such as price and quantity of materials, submission time and the record of associated parties are recorded and are immutable. Therefore, in a subsequent transaction at any time in the future, information from this transaction can be drawn by the smart contract. For example, as shown in Figure 5, checking the quantity of material is one of the checks for achieving consensus at a particular stage of approval. This check is designed (in the smart contract) to pull quantity data from the transactions (Tx(a) in this case) stored in the blockchain ledger. Since this framework allows standards checks to be performed against the data stored in the blockchain, it can be assured that these checks are always evaluated against authentic data. There is no scope for altering this data even by hacking into the system. If such attempts are made, a trail of the same will be left in the blockchain (due to use of cryptographic protocols such as Merkle Tree in the inherent design of blockchain).

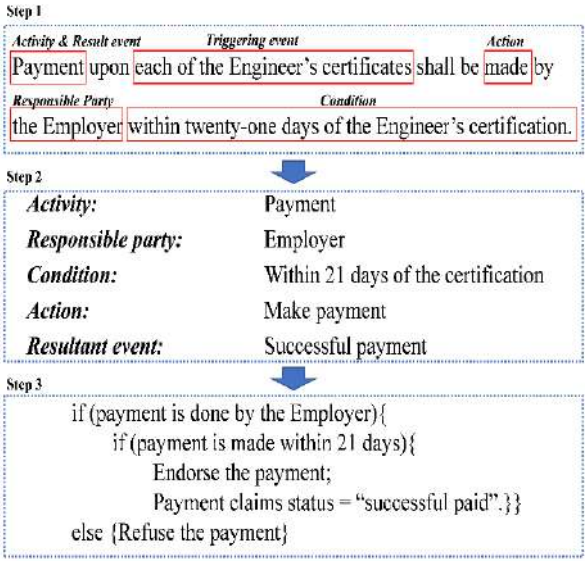

Figure 4. An example illustrating formalization and representation of smart contracts

5 Conclusion

Construction contracts regulate the behavior of the stakeholders in a construction project. Effective construction contract management protects the interests of all stakeholders, decreases the possibility of construction delay, and ensures smooth construction progress. In this research, a blockchain-based smart construction contract framework is proposed for semi-automatic execution of construction contracts for interim payments. A data representation for a smart contract is developed based on traditional textual contracts. This representation models contractual conditions into obligations, prohibitions, and actions, which can be read and executed automatically. By leveraging blockchain technology, a framework for executing this smart contract is developed which caters to the requirements of sequential approval process in a decentralized environment, such as that of the construction industry. A customized semi-automatic consensus mechanism is developed to facilitate interim payments through the blockchain framework. This mechanism regulates the sequence and conditions of

approval by stakeholders such as engineer, architect, and owner by automatically providing them with necessary information at the time of approval. It furthermore removes the scope of fraudulent approval by individual stakeholders as the consensus mechanism sends the result of individual approval to all the stakeholders on the platform.

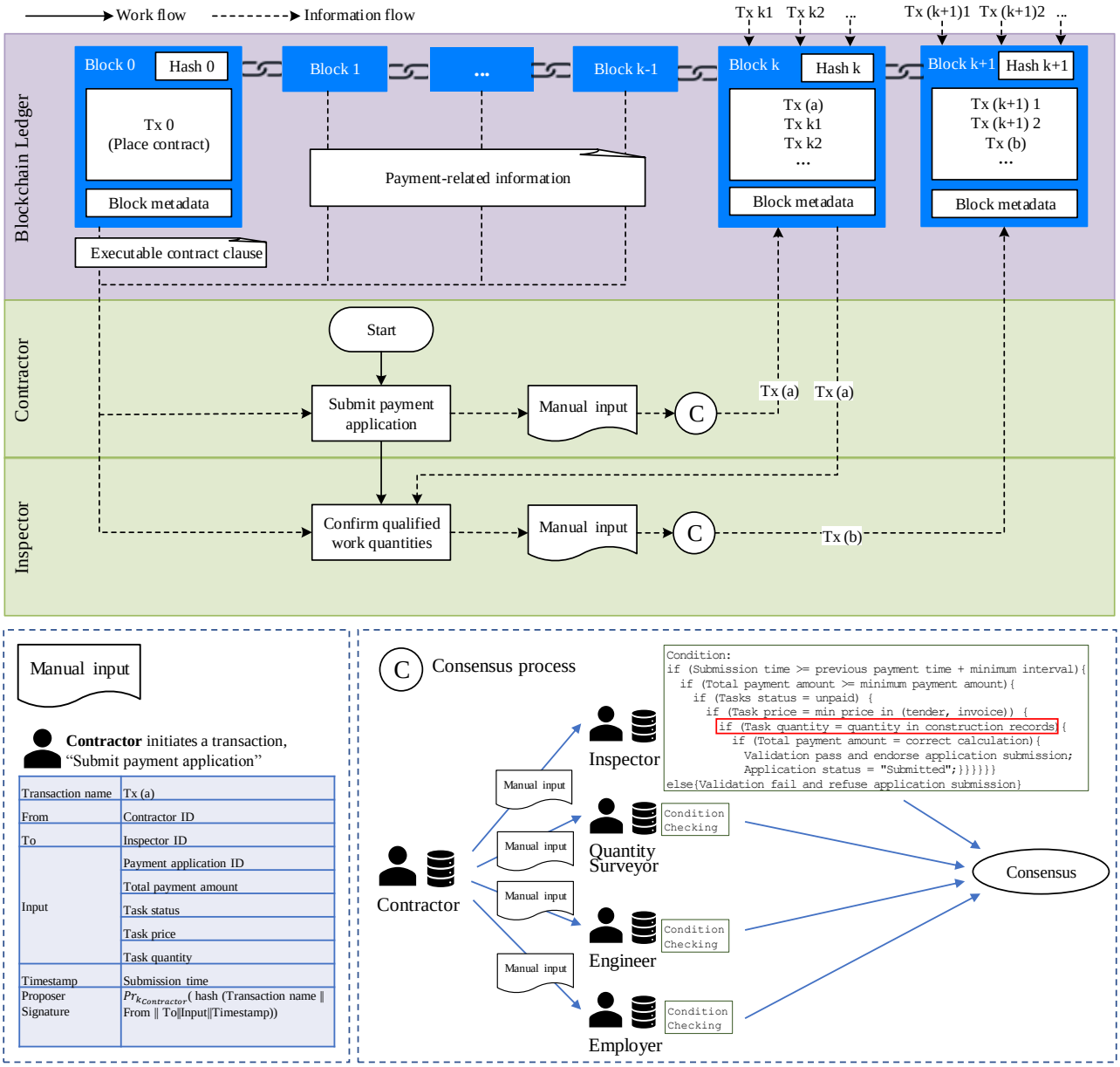

Figure 5. The example scenario illustrating blockchain-based smart contract for interim payments

All these stakeholders thereupon automatically check that result against certain pre-set rules, on their individual machines and communicate back their decisions across the group. Therefore, an approval is legitimized only when it has the collective endorsement from all the stakeholders. The record of this approval is thereupon stored on the blockchain ledger, which is inherently immutable, and therefore is secure against malicious alteration. Along with this, the proposed framework implicitly deploys cybersecurity measures to authenticate users through

public-private key encryption protocol. Presently in this research, the conditions of traditional contracts have been manually modelled into that of a smart contract by following a procedural approach. In

future, automatic development of smart construction contracts will be explored through technologies such as Natural Language Processing and Machine Learning. The scope of data representation will also be extended from interim payments to other technically feasible areas of construction contracts. The construct of the smart contract code in this paper is similar to that of e-contracts, but deployed on a secure distributed framework and regulated by a customized consensus. However, it has further potential to function as a fully enforceable contract management system through integration with resources such as BIM, which will be explored in the future. The performance of such smart contracts will also be studied in more complex scenarios such as that with various levels of project organizational structure spread across a construction supply chain.

References

[1] Development Bureau of Hong Kong SAR. Proposed Security of Payment Legislation for the Construction Industry - Consultation Document. , 2015.

[2] Davison B. and Sebastian R. J. The relationship between contract administration problems and contract type. *Journal of Public Procurement*, 9(2):261–285, 2009.

[3] Bunni N. G. The FIDIC forms of contract. Blackwell Pub, 2005.

[4] Cardoso H. L. and Oliveira E. A contract model for electronic institutions. In *Coordination, Organizations, Institutions, and Norms in Agent Systems III.*, pages 27–40, 2008.

[5] Davis, S., Arslanian, H., Fong, D., Watkins, A., Gee, W., and Cheung, C.Y. PwC's Global Blockchain Survey 2018, 2018.

[6] BOPTI – The first crypto currency dedicated to construction industry. On-line: https://bopti.io/,

[7] Intelliware Technologies Inc. How SiteSense® uses Blockchain for Construction Transactions. , 2017.

[8] Indukuri K. V. and Krishna P. R. Mining E-contract Documents to Classify Clauses. In *Proceedings of the Third Annual ACM Bangalore Conference*, 2010.

[9] The Government of The Hong Kong SAR. General Conditions of Contract for Term Contracts for Civil Engineering Works. , 2002.

[10] Androulaki E., Barger A., Bortnikov V., Cachin C., Christidis K., Caro A. De, Enyeart D., Ferris C., Laventman G., Manevich Y., Muralidharan S., Murthy C., Nguyen B., Sethi M., Singh G., Smith K., Sorniotti A., Stathakopoulou C., Vukolić M., Cocco S. W., and Yellick J. Hyperledger Fabric: A Distributed Operating System for Permissioned Blockchains. In *Proceedings of the Thirteenth EuroSys Conference*, pages 30:1-3:15, 2018.

Government Open Data and Sensing Data Integration Framework for Smart Construction Site Management

C. M. Lee[a], W. L. Kuo[a], T. J. Tung[a], B. K. Huang[a], S. H. Hsu[a], and S. H. Hsieh[a]

[a]Department of Civil Engineering, National Taiwan University, Taipei, Taiwan
E-mail: d05521012@g.ntu.edu.tw, paultom30@gmail.com, tungtzujan@gmail.com, pc0065666@caece.net, b02501030@gmail.com, shhsieh@ntu.edu.tw

Abstract –

This paper proposes a cloud-based data management framework that integrates open data from the government and monitoring data from construction site sensors. The integrated data can be consumed by artificial intelligence for smart construction project management, e.g. schedule control, resource arrangement and workers' safety. The framework includes two major parts: one is the IoT (Internet of Things) sensors and edge computing devices for collecting data from a construction site; the other one is a cloud database with Autodesk Forge for managing 3D Building Information Modeling (BIM) model information and government open data. In addition, web-based management interface and information dashboard for desktop computers and App software for hand held devices are provided for users to easily manage, query, and visualize the integrated data. Because weather and environmental conditions often affect management of a construction site, the proposed framework is prototyped for a feasibility test to see how the integration of Taiwan government open weather/environmental data and construction site monitoring data can be implemented and helpful for construction site management.

Keywords –

BIM; Construction; Data Integration; Internet of Things; Edge computing; Data distribution Service

1 Introduction

In recent years, through popular application of Building Information Modeling (BIM), a good foundation has been laid for construction management to integrate digital construction and sensor technology for achieving lean construction with better efficiency [1]. The potential applications include site design, material inventory control, transportation vehicles scheduling, construction machinery and equipment management, remote structural health monitoring and progress checking [2], especially for risk control of large scale construction projects [3]. To monitor real-time construction progress and avoid construction hazards, the use of various kinds of sensors to collect data for management analysis in the construction sites is getting popular and even become necessary [4]. Furthermore, Taiwan's labor law always concerns the construction workers' health and safety and has increasing restrictions for the workers to be exposed to extreme weather conditions and hazard environmental conditions, e.g. PM2.5 air pollution. In India, excessive PM10 concentration produced during construction was studied and it was found that the health condition of workers is related the air pollution Index. Workers at sites with less precautionary measures suffer more with respiratory illness than those at sites with more safety measures against air pollution [5]. Besides the labor law issues, the everyday weather and environmental conditions on the construction site can affect working productivity of workers and indirectly impact the construction schedule. Although project managers can always refer to the national weather report to get the measured and predicted data for the city or the district where the site is located, they may need more precise and higher resolution data on the site for better decision making on project scheduling or resources arrangement. With some monitoring systems implemented, when the system detects an abnormal situation based on the comparison between real-time data from the site sensors and historical data accumulated in the database, the project managers will receive an alert message through their hand held devices for them to quickly adjust the resources accordingly to avoid extra cost due to law violation or schedule delay. On the other hand, government open data may be very useful for construction site management. For example, for those sites in the seismic zone, early earthquake warning messages published by the government agency can help to reduce disasters due to strong earthquake. For those construction sites beside the ocean areas, the project managers may benefit from the information provided by an early-alert ocean wave system for optimal resources utilization and risk control [6].

To assist construction project managers for smart site management, this paper proposes a cloud-based data management framework to facilitate integration of

government open data and construction site monitoring data.

Based on the framework, a prototype BIM-based Smart Site Assistant (called BSSA) platform was implemented and tested for proof of concept. The prototype BSSA platform used Autodesk Forge as 3D BIM cloud database to manage digital construction site and integrated weather open data from Civil IoT Taiwan services (https://ci.taiwan.gov.tw/index_ne.aspx) as a testing and demonstration example for integrated application of government open data. The data collected by the various kinds of IoT sensors, such as vibration, PM10/2.5, and temperature sensors, installed in the construction site are gathered by edge computing control boxes through the DDS (Data Distribution Service) network protocol and stored into MariaDB database on a web-based server.[7] To ease the real-time management and access of needed data for the project manager, a web-based data management Graphical User Interface (GUI) and information dashboard are designed for desktop computers and an App software is designed for mobile hand-held devices. The rest of this paper will discuss the design of the framework and the implementation of the platform in more details.

2 The Framework

Figure 1 illustrates the system framework for the BSSA platform, which can be divided into three main parts, including data collection hardware devices in construction site, web-server for data management and applications for data visualization. First, different type of IoT sensors are needed at construction site for collecting site conditions, such as temperature, humidity, wind speed, air quality (PM10/PM2.5), ground water level, etc. These sensors data are collected and sent to edge computing devices (e.g. one per one floor) via Bluetooth, RS485 or RS232 interface. The edge computing devices communicate to each other using the DDS protocol to achieve low-latency, high-throughput data communications and one selected device is responsible for uploading collected data to the web server through network.

The second part is a web server for data management which uses Autodesk Forge for 3D BIM model data management (including basic project information) and MariaDB database to store the construction site sensing data and government open data from the Civil IoT Taiwan services. To compliment open data provided by the Civil IoT Taiwan services, which provide broad range but low resolution data, various kinds of sensors are needed to collect weather and environmental status data for the construction site.

The final part is data management GUI and APP software for users to effectively manage and access contents from the web server using desktop computers or hand-held devices.

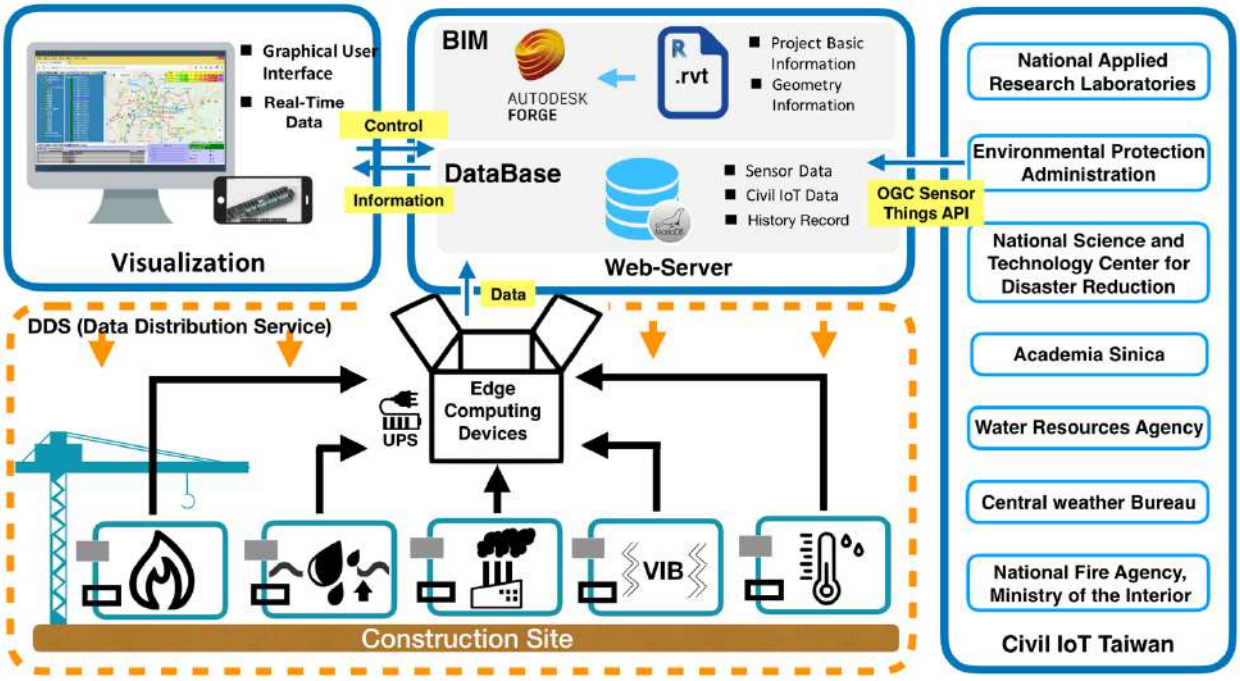

Figure 1. System Framework of the BIM-based Smart Site Assistant (BSSA) Platform

3 Prototype and Demonstration

With the rapid development and application of IoT and big data technologies, more and more government agencies have published their data as open data for public goods, especially environmental monitoring data, including temperature, humidity, air quality, precipitation, wind speed, river and ground water levels data and so on. In this work, the BSSA platform collects real-time environmental data from Civil IoT Taiwan services using OGC Sensor Things API (http://www.opengeospatial.org/ogc/markets-technologies/swe). However, the data in Civil IoT Taiwan database not only are multifarious but also come from various sources. Data filtering and integration are needed to increase their usability and reliability for construction management. Also, there are data collected through sensors installed on the construction site for a project manager to monitor the progress and various conditions of the construction, e.g. structural safety, air quality, etc. In the BSSA platform, a data management GUI is designed with the use of MariaDB, an open-source relational database management system, to help users to select and integrate data. Also, Autodesk Forge is employed for managing 3D BIM model data of the construction site. The BIM model is often built by Revit, one of the most popular building modelers, and uploaded by the user to the Forge cloud. The platform connects the model to the related environmental data and provides a viewer on the website for data visualization. In addition, mobile app software is designed for on-site project managers to easily retrieve and visualize data for decision making.

3.1 Data management GUI and information dashboard

Figure 2 illustrates the three-level data management scheme designed in the BSSA platform. The first level includes basic functions for users, such as historical data query, real time data and event alert and getting government open data. The second level includes operations for users to manipulate data in the database. The database in the third level integrates two types of data, open data (such as Civil IoT Taiwan) and local data (Edge Computing data). The central data management GUI includes six blocks, namely A, B, C, D, E, F (see Fig.3). Block A shows environmental data from the Civil IoT Taiwan database which orders contents by government administrative areas (i.e. cities, provinces, counties, etc.). There are construction sites under each area and users may connect to those sites to quickly access the surrounding environmental information. Block B provides links to all governmental sensors' data with a scroll down menu. Block C uses Google Map API to lay down different sensors' locations on map by transforming the coordinate system from WGS84 to TWD97 to help users understand better the sensor

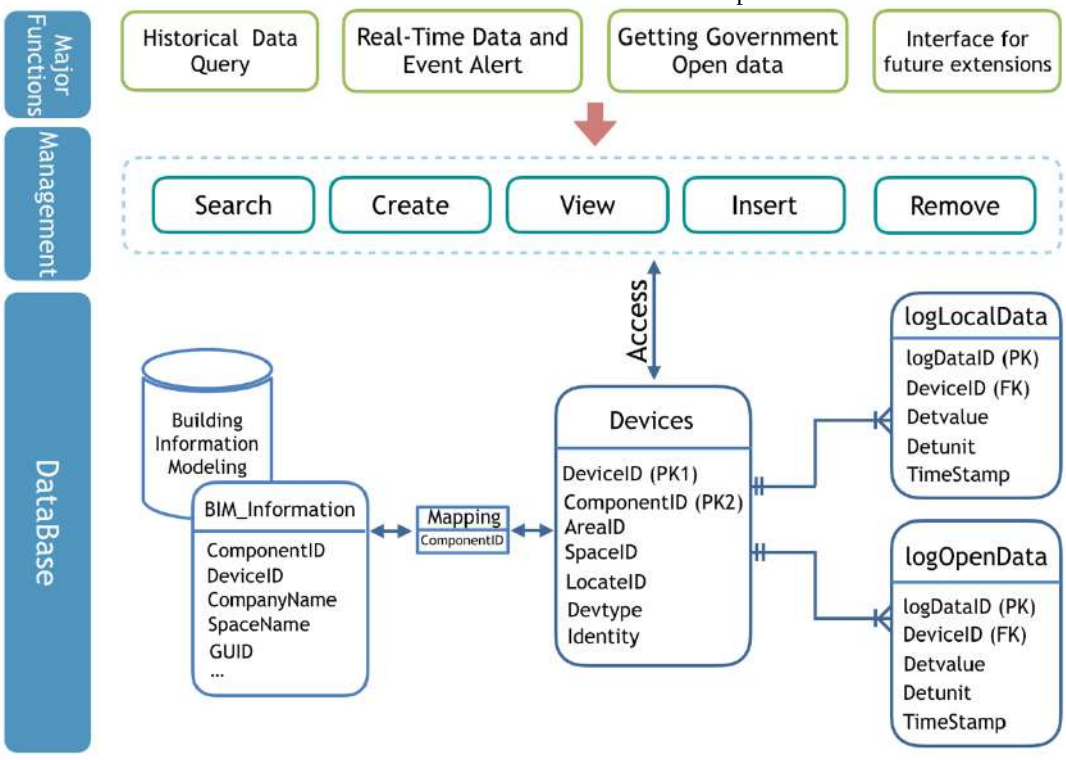

Figure 2. Data Management

locations and improve data readability. Block D records the logs of all system activities for system and data security. Block E shows the real-time data plots from the selected data source so that the user can monitor if the data remain within the normal range. This block provided the capability functions of prediction or historical data review. Block F reports the current overall status of the construction site based on all of the available data.

The dashboard interface for construction site status is shown in Fig.4, which has three blocks. Block "a" is an online building model viewer allowing users to query information about building objects and check the construction schedule. Also, the user can easily visualize the locations of the sensors in the model. Block "b" plots history data for the selected sensor, shows the location of the construction site on Google Earth, and the overall index of site conditions for construction tasks. Block "c" shows the navigation tools for viewing the model and its attributes, and users can use them to modify, explore and query more information from the model.

3.2 App software for information query

The design of an App software for the platform is for helping site managers to quickly find and visualize needed information. The App connects to the web server built by Forge and put the building model on the frontpage (see the block a in Fig.5(a)). Moreover, the block b on the frontpage is associated with environmental data. When any abnormal value of the monitoring data is detected, the user is alarmed (see the block b in Fig. 5(a)) and the level of impact by different environmental properties is visualized by colors. If the users need more detailed information, they can use the menu provided (see Fig.5(b)) to get the information. In addition, Fig. 6 shows the page displaying detailed information on some environmental aspects.

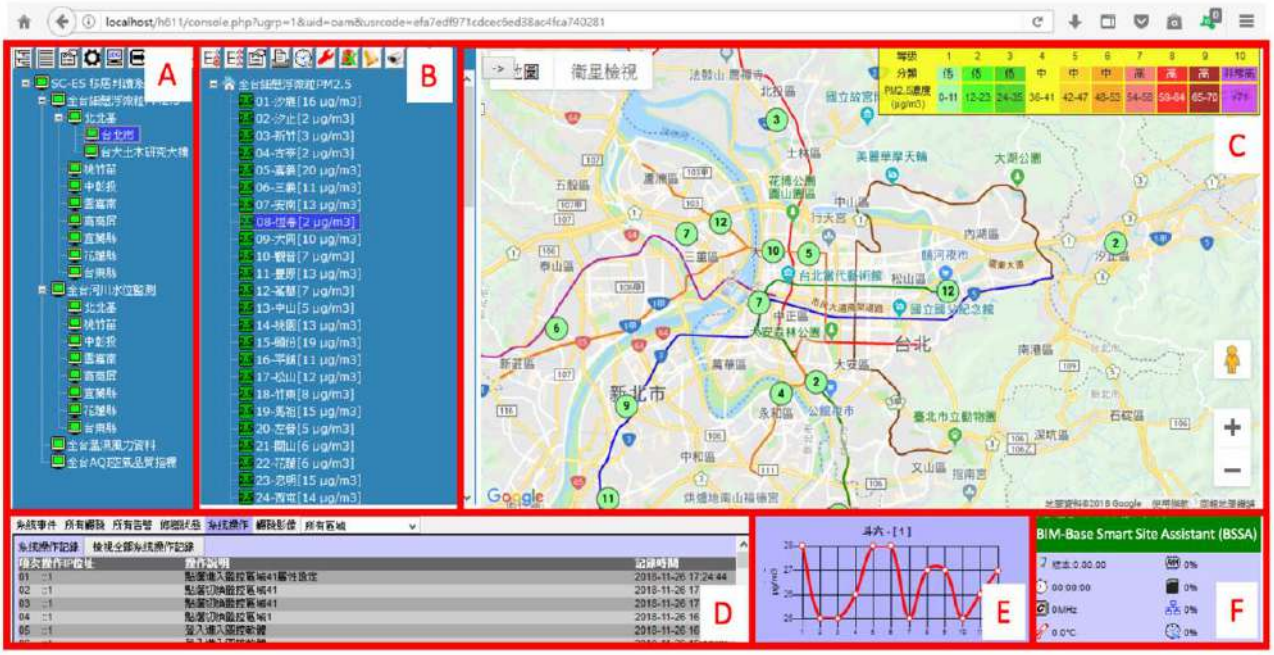

Figure 3. GUI for Central Control Management

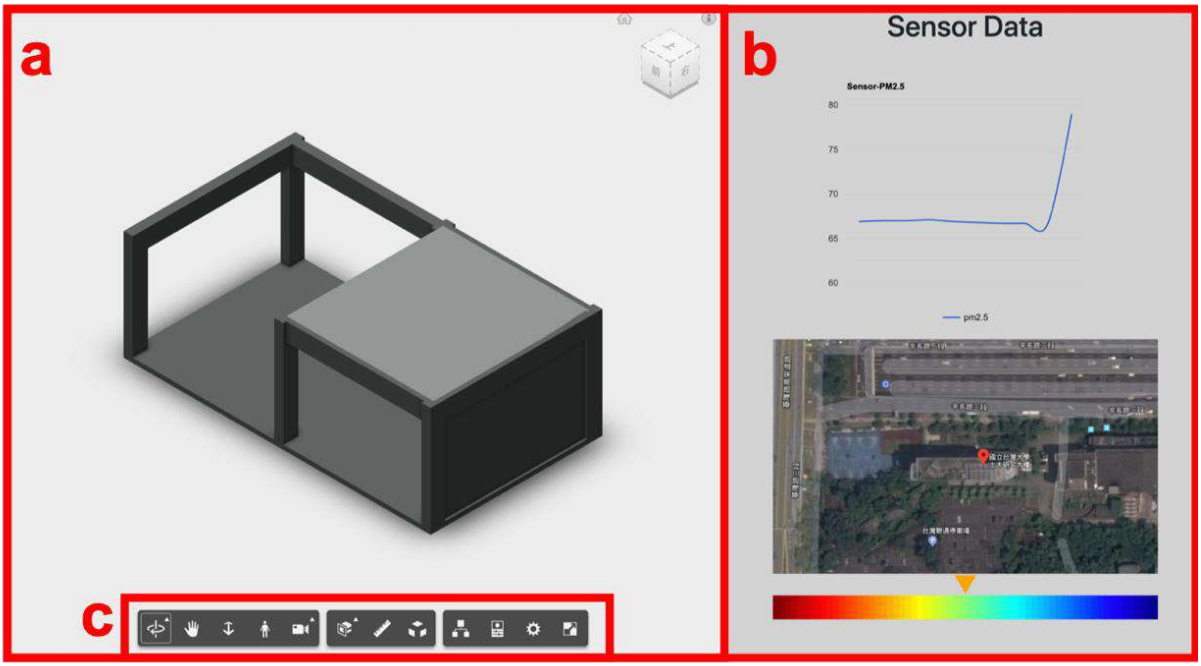

Figure 4. Construction Site Status Dashboard

(a) APP GUI - Frontpage

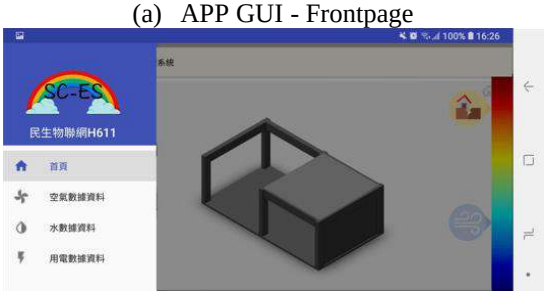

(b) APP Menu Interface

Figure 5. App User Interfaces

Figure 6. Data Screen

3.3 Platform Demonstration

The demonstration of the platform can be summarized by 6 steps (see Fig. 7):

Step 1: From the GUI provided by the central control page, the user can select first the construction site from the map and its nearby sensor data from the catalogue of government open data (e.g.

those from Civil IoT Taiwan database). Then, the system will display the data retrieved on screen using a data synchronization engine.

The user may use the Google map interface to interactively examine the sensors and retrieve their monitoring data with colour indicators for easy identification of the conditions detected by the sensors.

Step 2: The user may zoom in and out the location of a construction site and examine the sensors around the site and their data.If the user selects the location icon of the construction site from the map, the platform displays the BIM model of the site on the screen.

Step 3: The user may select a specific data source (e.g. monitoring sensors) for detailed examination of its data. The source can be either from the Civil IoT Taiwan services or one of those sensors installed on the construction site. With the data from all related sources and sensors, the data-analysis engine of the platform provides analyzed data for the site manager to make decision on construction management tasks.

Step 4: When the platform detects abnormal data, it alerts the user to take proper actions.

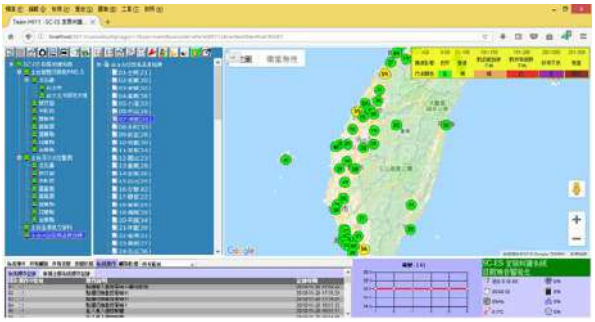

Step 1. Central Control Page

Step 2. Zoom Into the Construction Site

Step 3. Sensors' Data

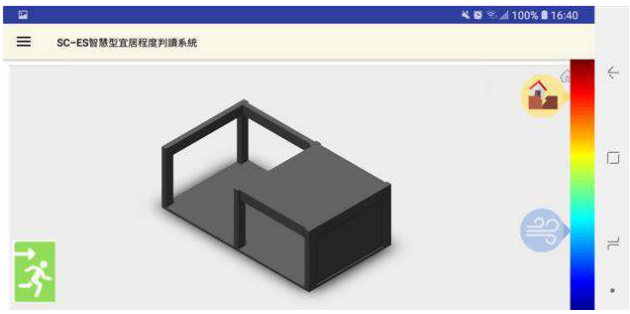

Step 4. APP GUI - Alarm

Figure 7. Prototype System Demonstration

4 Conclusion

This paper presents an effort on designing a cloud-based data management framework for integrating government open data and local monitoring sensor data for construction site management. The framework consists of two major parts: one for managing local sensing data with IoT sensors and edge computing devices; while the other one for managing 3D BIM model information and government open data with a cloud database and a web server. A BIM-based platform for facilitating smart site management has been prototyped based on the framework. Although the present effort is just a preliminary one and requires more work on the development and testing of the prototype platform, the preliminary results have shown promising feasibility of the proposed framework for assisting smart construction site management.

Acknowledgement

This research is supported by the Ministry of Science and Technology under project No. MOST107-2221-E-002-058-MY2. Special thanks go to Mr. Zhi-Min Peng of Iecont Technology Inc., Mr. Jin-Xian Wu of Mitac, Mr. Xing-Wu Tung of ITRI, Mr. Shi-Tong Huang of ITRI,

and Kai-Jen Liu of NTU for providing valuable guidance and assistance.

References

[1] Liu, Z. and Deng, Z. A Systematic Method of Integrating BIM and Sensor Technology for Sustainable Construction Design. *Journal of Physics*: Conference Series, 910(1): 012071, 2017.

[2] Kim, C., Son, H., and Kim, C. Automated Construction Progress Measurement Using a 4D Building Information Model and 3D Data. *Automation in Construction*, 31: 75-82, 2013.

[3] Jia, G., Ni, X., Chen, Z., Hong, B., Chen, Y., Yang, F., and Lin, C. Measuring the Maturity of Risk Management in Large-scale Construction Projects. *Automation in Construction*, 34: 56-66, 2013.

[4] Kim, S., Shin, Y., and Kim, G. Case Study on the Maintenance of a Construction Monitoring Using USN-based Data Acquisition. *The Scientific World Journal*, 879308, 2014.

[5] Singh, R., Ahmad, K., Jakhwal, D. C., and Kumar, M. S., Impact of Air Quality on Human Health in the Vicinity of Construction Sites in Delhi-NCR. International Journal of Engineering Research and Applications, 4(8): 18-26, 2014.

[6] Diaz-Hernandez, G., Losada, I. J., and Mendez, F.J. Improving Construction Management of Port Infrastructures Using an Advanced Computer-based System. *Automation in Construction*, 81:122-133, 2017.

[7] Kochovski, P. and Stankovski, V. Supporting Smart Construction with Dependable Edge Computing Infrastructures and Applications. *Automation in Construction*, 85: 182-192, 2018.

Review of BIM-centred IoT Deployment: State of the Art, Opportunities, and Challenges

M. Shahinmoghadam[a] and A. Motamedi[a]

[a]Department of Construction Engineering, École de technologie supérieure, Montréal, Canada
E-mail: mehrzad.shahin@gmail.com, ali.motamedi@etsmtl.ca

Abstract –

Thanks to the digital representations provided through Building Information Modeling (BIM), successful adoption of emerging digital technologies have been increasingly reported within the constriction and facility management research community. On the other hand, the number of research studies exploiting the principles of the Internet of Things (IoT) to enhance automation and control for the existing construction and facility management systems has been increasing within the last decade. By realizing the ample opportunities that can be seized through a combination of IoT and BIM, researchers have started to explore the potential benefits of BIM-centered IoT deployments. In this light, this paper aims to report the sate-of-the-art research trends for creating integration between BIM and IoT. To this end, relevant studies have been carefully reviewed to highlight the previously used sensing technologies, IoT communication protocols, BIM-centered middleware components and their ultimate application scenarios. Moreover, some of the key opportunities available through technological advancements in both IoT and BIM disciplines, along with the major open challenges threatening successful implementation of IoT-enabled BIM systems are highlighted in order to provide suggestions for future research directions.

Keywords –

Building Information Modeling (BIM), Internet of Things (IoT), Sensing technologies, BIM-centered IoT, Facility management, Construction 4.0

1 Introduction

Within the last few decades, successive waves of technological advancements have brought about the rise of the so-called 4th industrial revolution. The ultimate vision of this revolutionary movement is to blur the boundaries between physical and digital environments. The internet of things (IoT) plays a pivotal role in shaping this revolution. IoT can be viewed as networks of interconnected objects (e.g. sensors, actuators, machines, etc.) allowing real-time communications between those objects as well as communication with computer applications. Such a connectivity could significantly enhance automation and remote control of "things". Since sensors and actuators are increasingly improving in terms of power, cost, and size, more and more industries are encouraged to deploy IoT solutions [1]. The Architecture/Engineering/Construction and Facilities Management (AEC/FM) industry has been no exception to this emerging trend. Yet, according to a recent industry report published by World Economic Forum [2], this sector has been markedly slow to find its way into the mainstream of the 4th industrial revolution. This is, for the most part, due to legacy IT systems and highly fragmented nature of the construction industry.

Recently, the emergence of Building Information Modeling (BIM) has boosted hopes for expediting shifts towards a digital era for the construction industry. We have been witnessing a proliferation of research efforts for BIM during the last two decades. On the other hand, a brief look at the latest research trends reveals that there exists a growing interest among researchers to explore the potential values of the integration between IoT-driven solutions and BIM. As two emergent and fast developing technological breakthroughs, IoT and BIM offer countless opportunities for enhancing the current status of the AEC/FM industry. Evidently some of their key benefits cannot be easily achieved by approaching them separately. In this light, the research community has started paying an increasing attention to the integration of BIM and IoT. Consequently, the number of proposed BIM-centered system architectures built upon the principles of Industry 4.0, IoT, and Cyber-Physical Systems (CPS) has been rapidly growing.

This paper reviews those previous studies that have been conducted with the particular purpose of creating fusion between IoT and BIM in AEC/FM settings. By conducting this literature review, the authors pursue three main objectives: (i) identifying commonly used IoT enabler technologies that have been successfully combined with BIM-centered middleware and their

corresponding domain applications, (ii) Investigating key opportunities currently available to be exploited for increasing the benefits of IoT-enabled BIM systems, and (iii) highlighting the current and future challenges for designing effective orchestrations of BIM and IoT deployment for the construction industry.

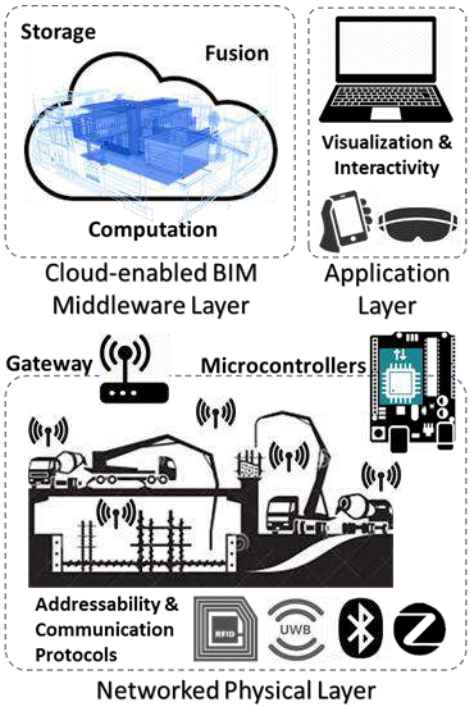

Figure 1. Conceptual framework of generic BIM-centered IoT architecture

2 Methodology

As the primary objective of this review article was set to put the current and future issues related to IoT-enabled BIM architectures into a broad perspective, the authors followed the principles of writing a narrative literature review [41]. The narrative overview presented here does not include the critique for each study reviewed. The following provides the reader with the delineation of how the present review has been conducted.

The main sources of information for this review have been selected by searching through two reputable electronic research databases namely as Science Direct, and, ASCE Library. The Google Scholar search engine was also used to ensure a reasonable breadth of potential articles. Accordingly, the three main high impact journals which together account as the primary source for the majority of the reviewed articles were: Automation in Construction, Advanced Engineering Informatics, and, Journal of Construction Engineering and Management. Moreover, in order to benefit from the knowledge in the electrical and electronics engineering domain and to bring a balanced perspective to the research issues regarding IoT development, IEEE Xplore database was also used.

The search keywords fall into two main groups each related to one of the main concepts of our primary interest. The terms within the first group which referred to the notion of BIM were: "Building Information Modeling", "BIM", and "BIM tools". The keywords within the second group indicating to IoT were: "Internet of Things", "IoT", "Cyber-Physical Systems", "Sensors", "Wireless Sensor Networks", "WSN", "Sensing devices", and "Remote sensing". Different combinations of keywords from both groups were used to find articles relevant to BIM-centered IoT architectures.

Finally, the main selection criteria applied to include/exclude searching results from the review was to make sure that the research efforts reported in the searched studies have been dedicated to the creation of a seamless integration between BIM platforms and sensing devices/networks. Respectively, the selection process was done by carefully and critically reading the methodology (or architecture description) sections of the papers found within the databases. The publication time spectrum of the final candidate studies to be included in our review spans between 2011 and January of 2019.

3 State-of-the-art Research Trends

In order to create a shared sense of what is intended by "BIM-centered IoT deployment" in this paper, we present a broad definition of it on the basis of various definitions of IoT provided in [3]: remote sensing and control of physical objects within a construction site or an existing facility through seamless communication of real-time data with BIM as the unifying framework. In that sense, for the search terms used for this review, in addition to "Internet of Things", other relevant terms such as "Cyber-Physical Systems" and "Wireless Sensor Networks" have been considered in combination with "BIM". Hence, frameworks such as those presented in [4] and [5] which bear close correspondence to the aforementioned definition have been included in our review, though no explicit indication has been made in them to the IoT concept. Moreover, the reader should bear in mind that among existing studies with the main theme of BIM-centered IoT exploration, this review mainly deals with the most recently published ones. A conceptual framework for the generic BIM-centered IoT deployment scenario is shown in Figure 1. As it can be seen, the framework is basically divided into three main

layers. The following is a summary of the state-of-the-art research trends for the architecture of our interest. Selected studies for this review are presented by taking into account the essential elements of the three layers depicted in Figure 1.

3.1 Networked Physical Layer

This layer consists of a network of physical entities which could be prefabricated building components [6], construction machinery [7], facility assets [8], [42], construction wearables [9], etc., as well as various sensor devices. Such connected entities are basically capable of communicating data with each other and to the edge of the network (to an IoT gateway for instance) in a real-time manner. In a broad sense, this layer is responsible for collecting information about physical objects and their surroundings and transferring the information to the BIM-centered middleware layer for further processing. This is done with the aid of one or more sensing technologies embedded within the network architecture. The choice for the appropriate sensing technology used in this layer depends on various factors such as the type of information that is of interest to be collected and transmitted, the rate of power consumption, implementation cost, required communication range, etc. Collected information can be about environmental conditions in construction workspaces [9], real-time location of construction workers [10], motion and orientation of building components [11], or any other useful data which could enrich the BIM model for future use. The information collected within the network is then transmitted over one or more communication medium (IoT protocols). A quick glimpse of previous proposals reveals that RFID-enabled short range communication has been the most frequent option for communicating IoT data to the BIM-centered layer. This is no surprise since RFID has been traditionally a key technology used for bringing physical objects into the digital realm through a short-range point-to-point wireless communication. Additionally, RFID tags attached to physical objects can act as distinct identifiers of those objects making them addressable within the network. Most recently, an extensive review of RFID-enabled BIM systems has been appeared in [12]. Hence, for this review we tried to include other studies that have exploited sensing technologies other than RFID and the interested reader is referred to the mentioned study for deeper insights about RFID-enabled BIM architectures. One of the emergent IoT-enablers which appears to be gaining in a rising popularity among researchers is Bluetooth Low Energy (BLE) technology, also known as Bluetooth Smart. The seminal work of Park et al. [10] is one of the pioneering examples of integrating a BIM-based system with BLE sensors used for fostering real-time location-awareness of construction workers. More recently, Teizer et al. [9], made the case for BIM-based visualizations of data about environmental conditions and workers' location in a real-time manner, with the aid of BLE beacons installed to their hard hats. Zigbee [13], is another emergent wireless communication standard famously known by its low-cost and low-power consumption rates. In [14], for the purpose of environmental monitoring of working conditions in confined spaces, researchers have developed a prototype of self-updating BIM system consuming sensor data coming from TelosB mote based sensor network which works on IEEE 802.15.4 standard (the basis for the Zigbeee specification). Another application of Zigbee-based sensor networks has been reported in [15]. In that study, the sensor network has been integrated with a multi-agent software system capable of interacting with BIM models on the basis of IFC schema to support facility management. The low data rate of indoor thermal comfort monitoring has convinced the researchers in [16] to choose Zigbee as the appropriate wireless technology for receiving and sending temperature and humidity readings to be imported into the BIM-based model of subway spaces. Despite the increasing number of studies exploiting recent sensing technologies, RFID still remains as the dominant technology used in combination with BIM systems. More discussion of opportunities available through advancements in WSNs and emergent protocols for network-based communications is given in the coming sections.

3.2 BIM-centered Middleware Layer

The main responsibility of this layer is to receive the information collected from the previous layer to be aggregated with BIM models. As depicted in Figure 1, this layer is expected to deliver three main functionalities namely as: storage, data fusion, and computation. For storage, sensor readings must be linked to a database which can be separated from or integrated with the BIM database. Since a typical IoT deployment most often encompasses multiple and heterogeneous sensing nodes, a communication medium will be needed for aggregating the multiple streams of sensor readings. To this end, an IoT gateway must be set up in order to acquire sensor datasets and prepare them to be processed and conveyed to the BIM model. As most of the reported deployments in previous studies are prototype systems, the most frequent medium used as an IoT gateway has been personal computing devices such as laptops or smartphones. In [12] for instance, with the help of an android application a smartphone was turned into an RFID-to-BIM gateway. Nevertheless, for real-world production implementations cheaper and less power-consuming computing devices such as Raspberry

pi microprocessors used in [17] will be the ideal choice for the IoT gateway. Parallel with data storage, developing intelligent data fusion algorithms will be of high importance for the realization of an effective integration of IoT and BIM data. An effective data fusion scheme allows for making sense of sensor readings streaming from multiple sources, and also dealing with almost inevitable imperfections in sensor data. Although provision of such fusions will ultimately result in producing more accurate and consistent sensing data to be aggregated in BIM models, it has not been adequately investigated within the previous studies. One of the few examples in this respect can be found in [18] where a knowledge-based approach consisting of pre-defined rules has been taken to create fusion between data coming from Bluetooth beacons and motion sensors with building's geometric information. Obviously, an intelligent information fusion requires some computational power which will be provided through the third main functionality of the middleware layer: computation or data processing. It serves for data integration, automated decision-making, and action-invoking on the basis of information received from the networked physical layer and a pre-established knowledge layer. Such computational power is also essential to a proper responding to the queries raised in the application layer.

3.3 Application Layer

This layer provides BIM-based visualizations of sensing data and an end-user access to the information contained in the BIM model that has been enriched with IoT data. The most significant feature of such data access is that the needed information is retrieved in a real-time manner. This layer makes it possible for end-users to seamlessly interact with the physical layer objects through a digital interface linked to IoT actuators/microcontrollers in the networked physical layer. Actuation could be done automatically from computation module in the middleware, asked from the user for confirmation at the application layer's interface, or triggered manually by the end-user at the application layer. Various digital devices such as personal computers, smart mobile devices, and wearable computers, can provide BIM-based visualizations and the interface between the end-user and the IoT-enabled BIM system.

Since, BIM models are typically responsible for IoT data visualizations, any computing device capable of running the BIM authoring software will be a potential medium for enabling BIM visualizations that have been augmented by real-time sensing data. For example, an Ultra-Mobile Personal Computer showing the 3D BIM-model and sensor-based visualization of construction objects has been used in [7]. In [4], results of indoor localization estimations over location sensing data were visualized in a BIM authoring tool available on any computing device. By integrating fire simulations and real-time feedback information streaming from IoT sensors about the fire scene conditions, a BIM-based fire visualization and warning system for rescue planning has been realized in [19]. Another similar example of IoT visualizations in BIM software can be found in [9].

There are several application areas that have been investigated in previous studies for BIM-centered IoT architectures. Safety management has been one of the most frequent application areas reported for both construction and facility management. Accordingly, a significant portion of previous relevant studies have attempted at combining BIM-based architectures with sensor-based safety monitoring systems. In [7] for example, researchers developed a tower crane navigation system which is capable of visualizing lifted objects in the context of 3D BIM models of the under-construction building and its surroundings. Other studies have been published with the main focus on fire related safety issues [17], [19], [4]. There have been also studies investigating construction workers' safety through real-time monitoring of construction working conditions [14], [9]. Most recently, interesting application scenarios have been proposed in the context of construction 4.0. For instance, with respect to intelligent decision making for construction activities (site planning, workflow logic, etc.), application of cyber-physical systems has been proposed for enabling real-time communications among BIM-based virtual models, physical construction entities, and pre-existing knowledge bases [20], [21]. Prefabricated construction is another interesting area that researchers have contributed to by integrating BIM with sensing technologies. In [22], by developing an IoT-enabled platform established upon a BIM-based infrastructure, RFID- and GPS-based information made it possible to improve real-time traceability and visibility of the construction progress, physical building information, and cost related data in a prefabricated construction settings. Similar attempts have been reported in [23], [6], [17]. Finally, when it comes to operating facilities, energy use management and indoor comfort monitoring have been the most recurrent domain applications [16], [24], [25].

4 Opportunities

One of the most promising possibilities of the IoT solutions combined with BIM systems is that it paves the road towards creating more realistic "digital twins" for the built environment. Generally speaking, a digital twin is responsible for imitating the dynamic behavior

of a given physical system. Although various technical definitions of digital twin already exist within the literature, we have adapted the one which is of our particular interest on the basis of the definition provided in [26]: a virtual representation of building components, construction processes and maintenance operations through the streams of real-time data throughout the facility lifecycle, enabling understanding, learning and reasoning about various aspects of that facility.

Through provision of digital representations of facilities' physical characteristics and functionalities, BIM models have paved the road for realization of such "digital twins". By drawing an analogy between BIM and Product Lifecycle Management in the manufacturing industry, Woodhead et al. [27] indicated that strong ties can be expected between BIM and Industry 4.0. Real-world examples of such ties have been most recently reported. In [11] for instance, researchers have been able to provide a digital twin of hoisting operations in underground construction through BIM representations standing for the virtual model of hoisting and various IoT sensing devices fulfilling real-time communications between the physical and cyber twins. Another example is a prototype of RFID-enabled BIM system presented in [8] which could be deemed as a digital twin of inspection and maintenance tasks for building assets. The evolution of BIM along with the advances in Artificial Intelligence and real-time analytics can unlock profound possibilities for the creation of digital twins with enhanced predictive capabilities for the built environment [27].

Finally, thanks to an unprecedented amount of data about building components, indoor environmental conditions, construction resources, assets, etc., that can be collected and integrated with BIM models for further processing, BIM-based immersive technologies can be more effectively deployed for AEC/FM applications. In other words, the more realistically digital twins are created for construction sites or operating facilities, the more enhanced and rich immersive experiences can be provided accordingly. Since many successful implementations of BIM-based immersive solutions such as Augmented and Virtual reality have been reported within the last two decades [28], the combination between BIM and IoT can significantly improve the effectiveness of such immersive experiences with the aid of real-time sensing data aggregated to BIM elements.

As an emerging technology, IoT can be viewed as a fast progressing filed of technology. As it was mentioned in section 3, application of RFID technology as a primary enabler of IoT has been proliferated within the existing body of knowledge. Nonetheless, owing to the continuous advancements in IoT, especially in wireless communication technologies, new opportunities are open for designing novel architectures of IoT-enabled BIM systems. Although the number of studies investigating relatively recent communication protocols such as BLE is increasing, the research community has been slow to adopt more recent advancements such as Zigbee and Lora. Hence, future research should pay more attention to this issue because such advancements most often offer new features and tackle some of the existing limitations. For the case of Zigbee for instance, the technology has already demonstrated an enormous potential for replacing traditionally used communication technologies for enabling indoor automation such as WiFi, by delivering similar functionalities at a fraction of cost and power consumption. Additionally, plenty of opportunities can be seized through developing hybrid architectures which exploit different IoT technologies within a single architecture. One prospective scenario in this regard can be explained as follows: while Zigbee will be an excellent choice for those indoor applications requiring low-rate data transitions (indoor comfort monitoring for example), it will not fulfil the requirements of the applications used in construction job-sites which generally require long range data communications. This is where adding a Lora-based module can properly address the limitation of Zigbee for long range communications. A review of Lora-based communications has been most recently reported in [29]. In summary, more experimental research should be conducted in the future to explore the potential benefits of integrating BIM systems with standalone or hybrid solutions based on emerging IoT-enabler technologies.

One of the major technological breakthroughs that has hugely contributed to the success of IoT is cloud computing. The integration of cloud computing and IoT promises new directions for both business and research [30]. Cloud computing also has made significant positive impacts on BIM. Therefore, it can be expected that the combination of cloud-enabled BIM with IoT could unlock ample opportunities for the construction industry. Such opportunities have been already realized by researchers in the construction sector for enabling more efficient procedures for storage, fusion and processing of IoT data. The cloud server used in [10] for example, has enabled a real-time communication of safety-related contextual information between a BIM-based hazard detection system and mobile devices of project participants. The generic concept of the IoT-cloud-BIM intelligent system has been thoroughly discussed in [31]. A cloud-based IoT platform has also been proposed in [23] for improving the leanness of prefabricated construction. Other examples in this regard can be found in [32], [17], and [33].

5 Challenges

IoT currently faces many challenges in general as an emerging and progressing technology. On the other hand, an effective adoption of BIM for AEC/FM has its own challenges as well. Hence, it can be expected that not only challenges facing IoT and BIM remain to be addressed individually, but also new challenges could rise when the integration of the two is considered.

Security is one of the most significant challenges for the IoT in general. IoT security can be broadly described as making sure that information about physical objects and properties collected from the networked layer is transmitted to the pre-assigned destinations. Encryption which has been the key approach to the Internet security can be also used for establishing secure communications between IoT nodes. However, currently available encryption methods are not adequately efficient to be used for addressing the IoT security [34]. In addition to security, privacy is another important issue in IoT. Generally speaking, IoT privacy deals with the ownership issues of data collected form the physical layer. In the context of IoT-enabled BIM solutions, privacy issues could constitute serious impediments to the proliferation of such systems. This is mainly due to the fact that the construction industry is fragmented in nature and different parties are typically engaged within it. From a business standpoint, aggregation of real-world data into BIM models could give rise to serious conflicts about data ownership rights between stakeholders since the construction sector has been traditionally reluctant to embrace the open data sharing culture. For instance, most of the constructor companies prefer not to share productivity-related data about their workers and machinery with other project participants (client, consultants, etc.), because it might help them for making financial claims. All in all, despite the fact such issues play a major role in shaping shifts towards digital construction and maintenance of facilities, the number of existing studies that put security and privacy issues at the center of attention for BIM and IoT integration are extremely low. Recent technological advancements in the internet security, such as Blockchain technology promises new opportunities for addressing such issues for IoT-enabled BIM systems. In this regard, Ye et al [35] have presented a theory named "Cup-of-Water" which suggests the application of Blockchain technology to securely and transparently preserve IoT data in BIM models during the whole life cycle of buildings.

In addition to challenges which are generally applicable to any IoT deployment, there exists other challenges which are specific to the BIM-centered IoT deployments. For instance, one of the main challenges of creating a seamless integration between BIM and IoT is to fill the gap between currently used schemas for BIM data representation such as IFC, and various IoT standards used for representing sensor data. To date, some attempts have been made to address this issue. Although IFC representations can greatly facilitate interoperability between various BIM platforms, mapping sensor data to IFC objects will be challenging if standardized IFC export guidelines and corresponding web parsers are not placed within the architecture in advance [36]. This issue has made the case for creating more semantically enhanced versions of IFC schema to provide the required readiness for integrating sensor readings with BIM models. In [8] for instance, the EXPRESS-based model of IFC schema has been edited manually to make allowance for interrelating BIM entities with RFID data. On the other hand, distributed and heterogeneous sources of IoT data streaming from the physical layer also urge the need for more semantically enriched IoT and BIM data representation schemas if an advanced information fusion is required. In this light, applications of formal data and knowledge representation methods have been proposed within the previous studies. In some studies such as those reported in [15], [20], and [37], researchers have attempted to exploit the formal representation capability of formal ontologies to address the sensor data integration with digital models of buildings. Most recently, results coming from real-world experimentations in [36] confirms that the open BIM paradigm holds the promise of improving the interoperability of IoT-enabled BIM deployments. Moreover, Semantic Web [38], Linked Sensor Data initiatives such as the SSN ontology [39], and Linked Building data initiatives such as ifcOWL [40] will open the door to more machine-understandable description of IoT data and more interoperable BIM-centered architectures.

6 Conclusion

This review article reported on the recent studies deploying BIM-centered IoT architectures in AEC/FM disciplines. The state-of-the-art research trends were highlighted in three main respects. First, previously used sensing technologies and network communication protocols were introduced. Next, key components of a BIM-centered middleware for an effective IoT-enabled implementation were discussed. Finally, those application areas that have reportedly benefitted from such fusion in the past, were also identified in this review.

The integration between BIM and IoT offers huge potentials for fundamentally altering the ways by which construction activities and maintenance of operating facilities are currently done. The primary promise of an IoT-enabled BIM solution is to bridge the real world construction sites and operating facilities to digitally

represented models. This could remarkably contribute to joining the mainstream of the paradigm shift toward digital construction era through the possibility of creating more realistic digital twins of construction job sites and operating facilities. Such digital twins can also improve the effectiveness of utilizing other digital technologies such as virtual and augmented reality for the built environment. In the light of technological advancements in IoT networking, wireless communications and the emergence of innovative breakthroughs such as cloud computing and the Blockchain technology, more and more opportunities will be available to be exploited for enhancing the usefulness of IoT-enabled BIM systems in practice.

As this review showed, there exists a significant gap between current research efforts done and unlocking the full potential of IoT-enabled BIM systems to move towards a more digitally-enabled construction and facility management paradigm. Since the integration between IoT and BIM is still in its early stages, much research is still required to be done in order to overcome the current and future challenges. This includes but is not limited to adding more intelligent information fusion algorithms, knowledge representation and inference capabilities, and developing open standards and platforms that secure information exchange and ubiquitous compatibility across various BIM environments. Moreover, the fragmented nature of the construction industry which involves participation of different role players urges for more profound investigations over security and privacy issues for IoT-enabled BIM deployments. This will encouragingly increase the willingness of industry practitioners to take steps towards such seamlessly connected solutions.

By grasping the available opportunities and overcoming the key challenges mentioned in this review, it can be expected that more and more leaders within the construction industry will be encouraged to fully embrace digital transformation and put steps towards this inevitable entirely new paradigm.

References

[1] Da Xu, L., W. He, and S. Li. Internet of things in industries: A survey. *IEEE Transactions on industrial informatics*, 10(4): p. 2233-2243, 2014.

[2] World Economic Forum. Shaping the Future of Construction: Inspiring innovators redefine the industry. On-line: https://www.weforum.org/reports/shaping-the-future-of-construction-inspiring-innovators-redefine-the-industry, Accessed: 01/01/2019

[3] Gubbi, J., et al. Internet of Things (IoT): A vision, architectural elements, and future directions. *Future generation computer systems*, 29(7): p. 1645-1660, 2013.

[4] Li, N., et al. A BIM centered indoor localization algorithm to support building fire emergency response operations. *Automation in Construction*,. 42: p. 78-89, 2014.

[5] Costin, A., N. Pradhananga, and J. Teizer. Passive RFID and BIM for real-time visualization and location tracking. *In Construction Research Congress: Construction in a Global Network*, 2014.

[6] Zhong, R.Y., et al. Prefabricated construction enabled by the Internet-of-Things. *Automation in Construction*, 76: p. 59-70, 2017.

[7] Lee, G., et al. A BIM-and sensor-based tower crane navigation system for blind lifts. *Automation in construction*, 26: p. 1-10, 2012.

[8] Motamedi, A., et al. Extending IFC to incorporate information of RFID tags attached to building elements. *Advanced Engineering Informatics*, 30(1): p. 39-53, 2016.

[9] Teizer, J., et al. Internet of Things (IoT) for Integrating Environmental and Localization Data in Building Information Modeling (BIM). *In ISARC: Proceedings of the International Symposium on Automation and Robotics in Construction*, 2017..

[10] Park, J., K. Kim, and Y.K. Cho. Framework of automated construction-safety monitoring using cloud-enabled BIM and BLE mobile tracking sensors. *Journal of Construction Engineering and Management*, 143(2): p. 05016019, 2016.

[11] Zhou, C., et al. Cyber-physical-system-based safety monitoring for blind hoisting with the internet of things: A case study. *Automation in Construction*, 97: p. 138-150, 2019.

[12] Xue, F., et al. Linking radio-frequency identification to Building Information Modeling: Status quo, development trajectory and guidelines for practitioners. *Automation in Construction*, 93: p. 241-251, 2018.

[13] Zigbee Alliance. On-line: *https://www.zigbee.org/*, Accessed: 01/01/2019

[14] Riaz, Z., et al. CoSMoS: A BIM and wireless sensor based integrated solution for worker safety in confined spaces. *Automation in construction*, 45: p. 96-106, 2014.

[15] Dibley, M., et al. An integrated framework utilising software agent reasoning and ontology models for sensor based building monitoring. *Journal of Civil Engineering and Management*, 21(3): p. 356-375, 2015.

[16] Marzouk, M. and A. Abdelaty. Monitoring thermal comfort in subways using building information modeling. *Energy and Buildings*, 84: p. 252-257, 2014.

[17] Cheng, M.-Y., et al. BIM integrated smart

monitoring technique for building fire prevention and disaster relief. *Automation in Construction*, 84: p. 14-30, 2017.

[18] Park, J., J. Chen, and Y.K. Cho. Self-corrective knowledge-based hybrid tracking system using BIM and multimodal sensors. *Advanced Engineering Informatics*, 32: p. 126-138, 2017.

[19] Chen, X.-S., C.-C. Liu, and I.-C. Wu. A BIM-based visualization and warning system for fire rescue. *Advanced Engineering Informatics*, 37: p. 42-53, 2018.

[20] Fang, Y., N. Roofigari-Esfahan, and C. Anumba. A Knowledge-Based Cyber-Physical System (CPS) Architecture for Informed Decision Making in Construction. *In Construction Research Congress*, 2018.

[21] Srewil, Y., A. Ismail, and R.J. Scherer. A Method to Integrate Virtual-Physical Construction Environment in Framework of CPS Approach. *In Smart SysTech 2016; European Conference on Smart Objects, Systems and Technologies*, 2016.

[22] Li, C.Z., et al. An Internet of Things-enabled BIM platform for on-site assembly services in prefabricated construction. *Automation in Construction*, 89: p. 146-161, 2018.

[23] Xu, G., et al. Cloud asset-enabled integrated IoT platform for lean prefabricated construction. *Automation in Construction*, 93: p. 123-134, 2018.

[24] McGlinn, K., et al. Usability evaluation of a web-based tool for supporting holistic building energy management. *Automation in Construction*, 84: p. 154-165, 2017.

[25] Arthur, S., H. Li, and R. Lark. The Emulation and Simulation of Internet of Things Devices for Building Information Modelling (BIM). *In Workshop of the European Group for Intelligent Computing in Engineering*, Springer, 2018.

[26] National Infrastructure Commission. Data for the Public Good. NIC Report 2017. On-line: http://www.nic.org.uk/publications/data-public-good/, Accessed: 01/01/2019

[27] Woodhead, R., P. Stephenson, and D. Morrey. Digital construction: From point solutions to IoT ecosystem. *Automation in Construction*, 93: p. 35-46, 2018.

[28] Li, X., et al. A critical review of virtual and augmented reality (VR/AR) applications in construction safety. *Automation in Construction*, 86: p. 150-162, 2018.

[29] Chen, Y. and D. Han. Water quality monitoring in smart city: A pilot project. *Automation in Construction*, 89(1): p. 307-316, 2018.

[30] Botta, A., et al. Integration of cloud computing and internet of things: a survey. *Future Generation Computer Systems*, 56: p. 684-700, 2016.

[31] Han, C. and Ye, H. A Novel IoT-Cloud-BIM Based Intelligent Information Management System in Building Industrialization. *In ICCREM*, 2018.

[32] Fang, Y., et al. Case study of BIM and cloud–enabled real-time RFID indoor localization for construction management applications. *Journal of Construction Engineering and Management*, 142(7): p. 05016003, 2016.

[33] Teizer, J. and T. Cheng. Proximity hazard indicator for workers-on-foot near miss interactions with construction equipment and geo-referenced hazard areas. *Automation in Construction*, **60**: p. 58-73, 2015.

[34] Whitmore, A., A. Agarwal, and L. Da Xu. The Internet of Things—A survey of topics and trends. *Information Systems Frontiers*, 17(2): p. 261-274, 2015.

[35] Ye, Z., et al. Cup-of-Water theory: A review on the interaction of BIM, IoT and blockchain during the whole building lifecycle. *In ISARC 2018-35th International Symposium on Automation and Robotics in Construction and International AEC/FM Hackathon: The Future of Building Things*, 2018.

[36] Dave, B., et al. A framework for integrating BIM and IoT through open standards. *Automation in Construction*, 95: p. 35-45, 2018.

[37] Sørensen, K.B., P. Christiansson, and K. Svidt. Ontologies to support RFID - Based link between virtual models and construction components. *Computer - Aided Civil and Infrastructure Engineering*, 25(4): p. 285-302, 2010.

[38] Berners-Lee, T., J. Hendler, and O. Lassila. The semantic web. *Scientific American*, 284(5): p. 34-43, 2001.

[39] Compton, M., et al. The SSN ontology of the W3C semantic sensor network incubator group. *Web semantics: science, services and agents on the World Wide Web*, 17: p. 25-32, 2012.

[40] Beetz, J., J. Van Leeuwen, and B. De Vries. IfcOWL: A case of transforming EXPRESS schemas into ontologies. *Ai Edam*, 23(1): p. 89-101, 2009.

[41] Green, B. N., Johnson, C. D., and Adams, A. Writing narrative literature reviews for peer-reviewed journals: secrets of the trade. *Journal of chiropractic medicine*, 5(3), 101-117, 2006.

[42] Motamedi, A., and Hammad, A. Lifecycle management of facilities components using radio frequency identification and building information model. *Journal of Information Technology in Construction (ITCON)*, 14(18), 238-262, 2009.

Automatic Key-phrase Extraction to Support the Understanding of Infrastructure Disaster Resilience

X. Lv[a] , S.A. Morshed[b] and L. Zhang[c]

[a] Florida International University, 10555 West Flagler Street, EC 2956, Miami, FL 33174
[b] Florida International University, 10555 West Flagler Street, Miami, FL 33174
[c] Florida International University, 10555 West Flagler Street, EC 2935, Miami, FL 33174
E-mail: xulv@fiu.edu, smors005@fiu.edu, luzhang@fiu.edu

Abstract –

Preventing natural disasters from causing substantial social-economic damages relies heavily on the disaster resilience of the nation's critical infrastructure. According to the National Academy of Sciences, research on understanding and analyzing the disaster resilience of our infrastructure systems is a "national imperative". To address this need, this paper proposes an automatic keyphrase extraction methodology to extract relevant phrases on disaster resilience from documents in infrastructure domain. In developing the proposed methodology, a document collection including research papers and public reports are prepared. Noun phrases are first extracted from every sentence in the collection and form the candidates for keyphrases following a filtering procedure. Each candidate phrase is then represented as a global semantic vector and a local semantic vector. To select relevant phrases on disaster resilience, a semantic similarly measure is proposed to incorporate the semantics of candidate phrases in both the general and infrastructure domain. Ten physical resilience concepts from a pre-developed community resilience hierarchy is selected as the target concepts to evaluate the performance of the proposed methodology. When evaluated on the document collection, the proposed methodology achieved 66% of precision at top 20 extracted keyphrases on average.

Keywords –

Infrastructure disaster resilience; Automatic keyphrase extraction; Natural language processing

1 Introduction

Preventing natural disasters from causing substantial social-economic damages relies heavily on the disaster resilience of the nation's critical infrastructure. U.S. National Academies has defined resilience as "the ability to prepare and plan for, absorb, recover from, and more successfully adapt to adverse events" [1]. At present, United States is in dire need of resilient infrastructure systems as its physical infrastructure is aging and deteriorating. On this context, a report published by the National Academy of Sciences has defined the research on understanding and analyzing the disaster resilience of our infrastructure systems as a "national imperative" [1]. To facilitate infrastructure disaster resilience, one major prerequire is to understand disaster resilience in a more explicit and deep manner. Existing research typically provides conceptual or theoretical framework that identifies some key characteristics (e.g., robustness, redundancy) of disaster resilience without directly linking them to more detailed and specific concepts. There is, thus a need to analyze the vast amount of text documents (e.g., reports, papers, news articles) on disaster resilience to facilitate a better understanding on the definition, interpretation and classification of disaster resilience in the infrastructure domain.

To address this need, this paper proposes a methodology that automatically extracts keyphrases about disaster resilience from documents in the infrastructure domain. Extracted keyphrases can provide highly condensed and valuable summary of disaster resilience in the infrastructure domain. The proposed methodology and the extracted keyphrases could facilitate the information and knowledge management of disaster resilience, such as the preparation and development of disaster recovery/resilience guidance manuals, and the retrieval of disaster recovery/resilience best management practices. The remainder of the paper discusses about the background and knowledge gaps, presents our proposed methodology, and analyzes the experimental results.

2 Background and Knowledge Gaps

Automatic keyphrase extraction is the process of selecting important and topical phrases from the body of

a document [2]. Keyphrase extraction starts with identifying a list of candidate phrases using some heuristics rules, which rely on syntactic features like part of speech tags, and/or statistical features like the frequency of n-grams [3]. There are commonly two different approaches to determine which candidates are correct keyphrases: supervised and unsupervised approaches. Supervised approaches utilize supervised machine learning algorithms to learn how to extract keyphrases from pre-labeled training documents and formulate the keyphrase extraction task either as a text classification problem or a sequence labeling problem [3]. For example, John et al. [4] presented a multi-feature supervised automatic keyphrase extraction system which uses a combination of statistical, linguistic, syntactic, semantic, and topic-based features with a Random Forest classifier. Zhang et al. [5] proposed a deep recurrent neural network (RNN) model that jointly extracts and ranks keyphrases from tweets based on keywords and context information.

As labeled training documents can be hard to obtain, unsupervised approaches have also been widely adopted, which commonly identify keyphrases using graph-based ranking method or topic-based clustering method [3]. For example, Liu et al. [6] proposed the topical PageRank (TPR) model, which decomposes traditional PageRank into multiple topic-specific PageRanks and extracts keyphrases based on their importance scores to different topics. Mahata et al. [7] proposed the Key2Vec model which trains multi-word phrase embeddings as thematic representation of scientific articles and ranks extracted keyphrases using theme-weighted PageRank algorithm.

Despite the above-mentioned research efforts, two major knowledge gaps for automatic keyphrase extraction have been identified: (1) most of the research works focus on extracting keyphrases from scientific papers or social media posts and have not yet been evaluated on public reports. Public reports are documents developed by public agencies such as department of transportation, metropolitan planning organization, and emergency management department. Public reports provide us an opportunity to understand the view of disaster resilience from public agencies perspective; (2) most of the existing works rank the importance of candidate phrases based on statistical and document structure features, which has limited capability to incorporate the semantics of candidate phrases into the evaluation process.

3 Proposed Automatic Keyphrase Extraction Methodology

To address the above-mentioned knowledge gaps, the paper proposes an automatic keyphrase extraction methodology that extracts relevant phrases on disaster resilience concepts from documents in infrastructure domain. In preparing the document collection, public reports developed by important agency stakeholders during the infrastructure planning and design process were collected in addition to scientific papers. When identifying keyphrases for disaster resilience concepts, a semantic similarity measure is proposed to capture the semantics of candidate phrases in both the general and infrastructure domain. The proposed methodology includes six primary tasks: data collection, data preparation, reference hierarchy selection, candidate phrase extraction, and keyphrase ranking.

3.1 Data Collection

To create a document collection, the keyphrase "infrastructure disaster resilience" was used to search for scientific papers and public reports from search engines including Google and Google Scholar. The titles of the public reports and scientific papers collected are shown in Table 1 and 2. In total, the document collection contains 11 public reports developed by 8 agencies, and 8 scientific papers. For each paper or report, the original pdf file was first converted to a txt file. Only the textual contents in the main body were kept excluding the figures, table of contents, references, and appendix.

3.2 Data Preparation

To prepare for the implementation of keyphrase extraction, each document in the collection is divided into individual sentences based on sentence boundaries, such as period, question mark, and exclamation mark. Each sentence is further divided into individual tokens (e.g., words and punctuations), and every word is converted into its lowercase form. Lemmatization is then conducted to remove inflectional endings of a word, and return its base or dictionary form, which is known as the lemma. For example, after the lemmatization, the words "rebuilds", "rebuilt", and "rebuilding" would all be transformed into their lemma "rebuild".

3.3 Reference Hierarchy Selection

In order to identify keyphrases relevant to disaster resilience, a reference concept hierarchy is used to provide additional semantic information for the keyphrase ranking process. As there is no existing concept hierarchy available for the infrastructure disaster resilience, the community disaster resilience hierarchy (taxonomy) developed by Taeby and Zhang [8] was selected due to its similarity to the domain. As shown in Figure 1, the selected reference hierarchy includes 29 practices (R1 – R29) to enhance the disaster

resilience in residential communities.

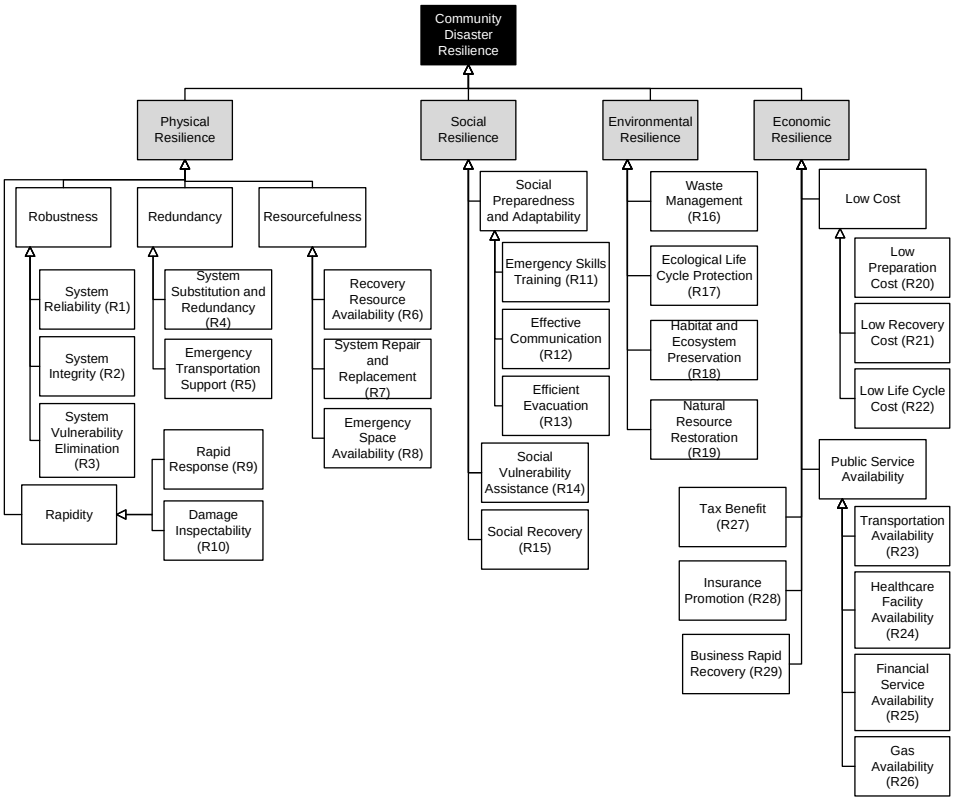

Figure 1. Community disaster resilience hierarchy [8]

Table 1. Public reports in the document collection

Public report	Reporting agency
• A Charrette on Florida's Future New Corridors	• Florida Department of Transportation (FDOT)
• Assessing Criticality in Transportation Adaptation Planning	• Federal Highway Administration (FHWA)
• Assessment of Key Gaps in the Integration of Climate Change Considerations into Transportation Engineering	• FHWA
• Community Impact Assessment: A Quick Reference for Transportation	• FHWA
• FHWA Climate Resilience Pilot Program - Alaska DOT	• Alaska DOT and FHWA
• FHWA Climate Resilience Pilot Program - Michigan DOT	• Michigan DOT and FHWA
• FHWA Climate Resilience Pilot Program - Oregon DOT	• Oregon DOT and FHWA
• MnDOT Flash Flood Vulnerability and Adaptation Assessment Pilot Project	• Main DOT
• Performance Report FDOT 2017	• FDOT
• Post disaster redevelopment plan	• Florida Department of Community Affairs • Florida Division of Emergency Management
• Post Hurricane Sandy Transportation resilience Study in	• FHWA

NY NJ Con

Table 2. Scientific papers in the document collection

Scientific paper
• A Framework to Quantitatively Assess and Enhance the Seismic Resilience of Communities
• A review of definitions and measures of system resilience
• Critical Infrastructure, Interdependencies, and Resilience
• Fostering resilience to extreme events within infrastructure systems Characterizing decision contexts for mitigation and adaptation
• Resilience and Sustainability of Civil Infrastructure Toward a Unified Approach
• Resilience of Critical Infrastructure Elements and Its Main Factors
• Review on resilience in literature and standards for critical built-infrastructure
• Robustness, Adaptivity, and Resiliency Analysis

3.4 Candidate Phrase Extraction

The Stanford CoreNLP toolkit [9] is used to extract all the noun phrases in each sentence from the collection. The following actions are then adopted to filter the extracted noun phrases:

- Remove the starting token of a noun phrase, if it (1) is a determiner (e.g., "a", "the", "this", and "that"); (2) is a number; or (3) belongs to a standard list of English stop word
- Remove all single-word noun phrases
- Keep only the unique phrases

After the filtering procedure, the resultant noun phrases form the list of candidate phrases. For example, for the sentence "these critical facilities include water and power lifeline, acute-care hospital, and organization that have the responsibility for emergency management at the local community level", the candidate phrases extracted are "critical facility", "water and power lifeline", "acute-care hospital", "emergency management", and "community level".

3.5 Keyphrase Ranking

To select phrases relevant to disaster resilience, a candidate phrase p_i is first represented as a global semantic vector $\widehat{V_i}$ and a local semantic vector V_i. A semantic vector is a real-valued vector of features that characterizes the meaning of a candidate phrase. A global semantic vector represents the contexts in which the candidate phrase appears in the general domain corpus. The global semantic vector is the weighted aggregation of the global word embeddings of its terms.

$$\widehat{V_i} = \{\cup_{j=1}^{m} w_j \hat{E}(t_j)\} \quad (1)$$

As per Equation (1), $\hat{E}(t_j)$ is the global word embedding for term t_j, w_j is the weight term of t_j, and m is the total number of terms in phrase p_i. For each term, the global word embedding is obtained from the pre-trained Fasttext embeddings on Wikipedia [10]. An entropy-based weight is adopted to accommodate terms with different contribution to the semantics of a candidate phrase. As per Equation (2) [11], $P(t_j|D_B)$ is the probability of the term t_j appears in the background sentences, and $P(t_j|D_T)$ is the probability of the term t_j appears in the thematic sentences. To differentiate thematic sentences from the background sentences, a set of keywords represent the concepts from the reference hierarchy was created. If the sentence contains any of the pre-defined keywords, it would be considered as a thematic sentence, otherwise a background sentence. When forming the global semantic vectors, common terms (words have similar probabilities to appear in both background and thematic sentences) would have lower weights and distinctive terms (words have very different probabilities to appear in background and thematic sentences) would have higher weights.

$$w_j = -P(t_j|D_B)\log\left(P(t_j|\,D_B)\right) - P(t_j|D_T)\log\left(P(t_j|\,D_T)\right) \quad (2)$$

A local semantic vector represents the contexts in which the candidate phrase appears in the domain-specific corpus. For a candidate phrase p_i, its local semantic vector V_i is defined in Equation (3), where $E(p_i)$ is the multi-word phrase embedding directly obtained using Fasttext embedding model [10] trained on the document collection. During the training process, a candidate phrase is treated as a single token and added to the vocabulary of the embedding model, a multi-word phrase embedding can thus be obtained directly without aggregating embeddings from term level.

$$V_i = E(p_i) \quad (3)$$

To select the keyphrases relevant to disaster resilience, a semantic similarity measure is proposed to incorporate the semantics of candidate phrases in both the general and infrastructure domain. For a candidate phrase pi and a concept c_k in the reference hierarchy, their semantic similarity $SS(p_i, c_k)$ is defined in Equation (4), where $\hat{S}(p_i, c_k)$ is the global similarity and $S(p_i, c_k)$ is the local similarity.

$$SS(p_i, c_k) = \hat{S}(p_i, c_k) + S(p_i, c_k) \quad (4)$$

The global similarity measures the semantic similarity between pi and c_k in general domain. As per

Equation (5), the global similarity $\hat{S}(p_i, c_k)$ is defined as the cosine similarity between $\hat{V}_i$ and $\hat{V}_k$, which are the global sematic vectors of p_i and c_k respectively.

$$\hat{S}(p_i, c_k) = \frac{\hat{V}_i * \hat{V}_k}{||\hat{V}_i|| * ||\hat{V}_k||} \quad (4)$$

The local similarity between pi and c_k measures their semantic similarity in the infrastructure domain. As per Equation (6), the local similarity $\hat{S}(p_i, c_k)$ is defined as the cosine similarity between V_i and V_k, which are the local sematic vectors of p_i and c_k, respectively.

$$S(p_i, c_k) = \frac{V_i * V_k}{||V_i|| * ||V_k||} \quad (5)$$

3.6 Evaluation

All the bottom-level sub-concepts (R1 - R10) under physical resilience were selected as the target concepts for evaluating the proposed keyphrase extraction methodology. For each target concept, the top 20 ranked keyphrases were extracted based on their semantic similarities. The authors then evaluated each extracted keyphrase and determined its relevance to the target concept based on the majority votes. The performance of the proposed methodology was then evaluated using precision at top 20, which is defined as the ratio of the number of relevant keyphrases over the top 20 ranked keyphrases.

Table 3. Performance of the proposed methodology

Disaster resilience concepts	Precision at top 20	Example keyphrases
• System reliability (R1)	85%	• system robustness, utility system
• System integrity (R2)	55%	• building integrity, structural integrity
• System vulnerability elimination (R3)	65%	• direct vulnerability reduction, vulnerability assessment
• System substitution and redundancy (R4)	50%	• power supply redundancy, structural redundancy
• Emergency transportation support (R5)	15%	• emergency transportation lifeline safety plan, public transportation emergency relief program
• Recovery resource availability (R6)	75%	• recover service, traditional disaster recovery funding
• System repair and replacement (R7)	100%	• rapid repair technology, housing repair
• Shelter availability (R8)	30%	• emergency shelter, special need shelter
• Rapid response (R9)	100%	• emergency response time, emergency response personnel
• Damage inspectability (R10)	85%	• damage evaluation, damage detection technology

4 Experimental Results and Analysis

For each target concept, the performance of the keyphrase extraction and two example keyphrases extracted are shown in Table 3. The average precision at top 20 for robustness (R1, R2, R3), redundancy (R4, R5), resourcefulness (R6, R7, R8) and rapidity (R9, R10) concepts are 68%, 33%, 68%, and 93% respectively. The proposed methodology extracted much fewer relevant phrases on redundancy concepts compared with on other concepts. This indicates that the redundancy concepts are less domain-specific and have a high level of ambiguity. For example, the concept "emergency transportation support" has the lowest precision at top 20 (15%) among the 10 target concepts evaluated. Many phrases related to transportation system are falsely extracted as keyphrases, such as "mass transportation system", and "key transportation infrastructure". On the other hand, concepts "system repair and replacement", and "rapid response" achieved 100% of precision at top 20 because of the less ambiguity they have in the infrastructure domain. Overall the proposed methodology achieved 66% of precision at top 20 extracted keyphrases on average.

5 CONCLUSION AND FUTURE WORK

This paper presents an automatic keyphrase extraction methodology to identify relevant phrases on disaster resilience from documents in infrastructure domain. In developing the proposed methodology, each candidate phrase is represented as a global semantic vector and a local semantic vector. A semantic similarity measure is proposed to incorporate the semantics of candidate phrases in both general and infrastructure domain. When evaluated on the document collection, the proposed methodology achieves 66% on average in terms of precision at top 20 extracted keyphrases.

In the future work, the authors will continue to improve the current work in four directions: (1) conduct surveys or focus-group meetings with experts on infrastructure disaster resilience to further validate the keyphrases extracted; (2) evaluate the proposed methodology on more disaster resilience concepts with larger document collection; (3) investigate how the extracted keyphrases are similar or different between scientific papers and public reports; (4) explore how the extracted keyphrases could facilitate the automatic construction of disaster resilience ontology or taxonomy.

References

[1] NRC (National Research Council). Disaster resilience: A national imperative. Washington, DC: National Academies Press, 2012.

[2] Peter Turney. 2000. Learning algorithms for keyphrase extraction. Information Retrieval, 2:303–336.

[3] Hasan KS, Ng V. Automatic keyphrase extraction: A survey of the state of the art. In Proceedings of the 52nd Annual Meeting of the Association for Computational Linguistics, (1):1262-1273, 2014.

[4] John AK, Di Caro L, Boella G. A supervised keyphrase extraction system. In Proceedings of the 12th International Conference on Semantic Systems, 57-62, 2016.

[5] Zhang Q, Wang Y, Gong Y, Huang X. Keyphrase extraction using deep recurrent neural networks on Twitter. In Proceedings of the 2016 Conference on Empirical Methods in Natural Language Processing: 836-845, 2016.

[6] Zhiyuan Liu, Wenyi Huang, Yabin Zheng, and Maosong Sun. Automatic keyphrase extraction via topic decomposition. In Proceedings of the 2010 Conference on Empirical Methods in Natural Language Processing, 366–376, 2010.

[7] Mahata D, Kuriakose J, Shah RR, Zimmermann R. Key2Vec: Automatic Ranked Keyphrase Extraction from Scientific Articles using Phrase Embeddings. In Proceedings of the 2018 Conference of the North American Chapter of the Association for Computational Linguistics: Human Language Technologies, (2): 634-639, 2018.

[8] Taeby, M. and Zhang, L. Exploring Stakeholder Views on Disaster Resilience Practices of Residential Communities in South Florida. Natural Hazards Review, 20(1): 04018028, 2018.

[9] Manning, C. D., Surdeanu, M., Bauer, J., Finkel, J., Bethard, S. J., and McClosky, D. The Stanford CoreNLP Natural Language Processing Toolkit. In Proceedings of 52nd Annual Meeting of Association for Computing Linguistic: System Demonstrations, 55-60, 2014.

[10] Bojanowski P, Grave E, Joulin A, Mikolov T. Enriching word vectors with subword information. Transactions of the Association for Computational Linguistics, 5:135-46, 2017.

[11] Aggarwal, C.C. and Zhai, C. Mining text data. Springer Science & Business Media, 2012.

Artificial Intelligence Techniques to Support Design and Construction

A. Mohammadpour[a], E. Karan[b], and S. Asadi[c]

[a] School of Polytechnic, Purdue University Fort Wayne, United States
[b] Department of Applied Engineering, Safety & Technology, Millersville University, United States
[c] Department of Architectural Engineering, Pennsylvania State University, United States
E-mail: atefeh@purude.edu, Ebrahim.Karan@millersville.edu, sxa51@psu.edu

Abstract –

In recent years, researchers have relied heavily on data (historical and real-time) and digital solutions to support informed decisions. Consequently, data analysis has become an integral part of the design and construction process. Researchers spend a tremendous amount of time cleaning, organizing, and understanding the data. Artificial Intelligence (AI) can be used to help overcome human limitations in processing and enriching large volumes of data from a variety of sources. AI can encompass millions of alternatives for various design and project delivery solutions and ultimately improve project planning, construction, and maintenance and operation process. AI can be a solution to the severely under-digitized Architecture, Engineering, and Construction (AEC) industry, however, there are two challenges with respect to creating intelligent agents in AEC; (1) finding appropriate ways of gathering information from the environment and transforming them into internal context, and (2) selecting an appropriate AI technique to succeed in decision-making based on the relevant knowledge about the environment. This study focuses primarily on the second challenge by looking at potential applications of AI in AEC. The AI techniques in AEC can generally be classified into two main areas: (1) decision making methods and algorithms, and (2) learning methods. Regarding the first area, search methods and optimization theories are used when there is enough information to tackle decision-making and the problem is solved by the selection of the best action (with regard to some constraints and criteria) from a set of alternatives. The learning methods, on the other hand, are further classified into knowledge-based, reasoning, and planning methods (to learn how to adapt to changing conditions), learning probabilistic methods (e.g. Bayesian learning), and machine learning (e.g. supervised learning, reinforcement learning).

Keywords –

Artificial Intelligence Techniques; Artificial Intelligence Applications; Architecture, Engineering, and Construction Industry

1 Introduction

Artificial Intelligence (AI) is no longer a science fiction. AI is used advantageously in different industries such as healthcare, agriculture, finance, and banking industries. AI is already embedded in our lives in a wide range of applications such as Siri, Google search, smartphone, and Amazon recommendations. People might even not realize that they are using AI in their daily life. AI uses computer processing techniques to complete tasks that need human intelligence for learning or problem solving to make human-like decisions [1]. As a result, AI performs tasks faster and with a higher level of accuracy [2]. AI is transforming all segments of numerous industries. For example, in the agriculture industry, AI can help farmers know when to plant, water, harvest, or to produce more food and less waste [3]. In the healthcare industry, AI can analyze complex medical data and also help in real-time decision-making [4]. In the banking and finance industry, AI can enhance financial cyber-security to a higher level and prevent potential fraud [5].

Architecture/Engineering/Construction (AEC) is moving toward increased automation to enhance productivity and safety. Like many other industries, the AEC industry is struggling to find analysts who can make informed decisions that require computationally intensive data processing fast enough or in real-time. AI can offer exceptional benefits to increase automation in the construction industry and can be integrated into different phases of a project during its lifecycle. It is important to note that AEC is behind other industries in advancing new technologies and implementing AI solutions [6]. Forward-thinking project managers consider AI applications to enhance productivity,

increase profits, and advance safety in their construction projects [7]. Data is the fuel of AI techniques which is produced and collected throughout the life cycle of construction projects. The collected data in each phase of a construction project, including feasibility, planning and design, construction, and operation and maintenance, can be used to feed AI techniques. Construction data are the documentation that every project collects in different forms such as requests for information, drawings, photos of the job site, change orders, contracts, list of stakeholders, communications among stakeholders, and safety issue logs [8].

AI can be used to help overcome human limitations in processing and enriching large volumes of data from a variety of sources. AI can encompass millions of alternatives for various design and project delivery solutions and ultimately improve project planning. The ultimate aim of this study is to make AI part of the AEC's digital journey. AI is basically any device (or system) that perceives its environment and takes actions that maximize its chance of successfully achieving its goals. After gathering information from the environment and transforming them into an internal context (perception), we should select an appropriate AI technique to succeed in decision-making based on the relevant knowledge about the environment (action). The information presented in this study will be used to understand potential applications of decision making and learning methods in the AI domain and thus to select the AI technique best suited to the problem at hand.

After this introduction, an overview of AI and related techniques is presented. This is followed by the applications of AI in AEC, particularly in order to support design and construction. The next section presents new opportunities and challenges for the use of AI in AEC. Finally, conclusions and recommendations are presented.

2 Overview of AI Techniques

Although it may not be scientifically accurate to classify AI techniques and algorithms into two main areas of decision making, i.e. methods/algorithms and learning methods, such classification enables researchers and practitioners, without a lot of AI and machine learning knowledge, to apply these techniques to their problems. The following sections will discuss each area separately. Search methods and optimization theories are used when we have enough information to tackle decision-making and the problem is solved by the selection of the best action (with regard to some constraints and criteria) from a set of alternatives. Examples include linear programming, genetic algorithms, and ant colony optimization.

Ant colony optimization algorithm is a simple mathematical procedure and probabilistic technique that simulate the shortest and most efficient route for solving computational problems through graphs in a way that is also used within an ant colony [9]. Artificial bee colony algorithm is also a nature-inspired optimization technique that mimics and simulates intelligent behavior of honey bees [10].

Genetic algorithm is inspired by the natural theory of evolution that can be used to solve large optimization problems such as a pre-processing technique to select the best function/attribute subsequent to trying iteration after iteration under a given set of requirements [11].

Linear programming techniques involve optimizing a quantity with a mathematical method to determine the best feasible solution with a set of constraints presented in the form of linear programming problems [12].

Teaching-learning based optimization is an efficient optimization method which is a population-based method. The population includes a cluster of learners and the quality of the instructors influence the outcome of the students based on their performances or grades [13].

Local search algorithms are a heuristic approach to solve a problem by using a number of solutions while applying local changes to find an optimal solution [14].

Game theory is the study of human being in a strategic setting that can be used to solve more difficult problems when there are at least two or more players collaborating or competing to accomplish a task. To have a game, the outcome of players might depend on how they play based on the rules and solution concepts [15].

Stochastic models have a probability-based approach and are used when the environment is not perfectly predictable and decisions are partly influenced by the user's feedback and the regulations, standards, and guidelines. The random variations used in stochastic models are observed and collected through historical data for a specified period of time by using time-series techniques [16].

Bayesian networks gain an understanding of a problem and anticipate the results of intervention when some data are missing. Bayesian networks are considered when using some data in combination with prior knowledge [17].

Meanwhile, hidden Markov models are similar to statistical Markov models with hidden or unobserved states. When decision making can be modeled as sequential decision problems in uncertain environments, decision-making algorithms such as Markov decision processes can be used [18].

The learning methods, on the other hand, are further classified into knowledge-based, reasoning, and planning methods (to learn how to adapt to changing

conditions), learning probabilistic methods (e.g. Bayesian learning), and machine learning (e.g. supervised learning, reinforcement learning, and unsupervised learning).

A knowledge-based system (KBS) is a form of AI which is based upon reasoning that uses a knowledge-base to support decision-making and solving problems more efficiently. KBS includes seizing the knowledge and problem-solving methodology with relation to real world problems with a particular domain of knowledge [19]. In another approach, case-based reasoning (CBR) substitutes cases for rules. Cases are solutions to existing problems that a case-based system would apply to new problems. [19] described the CBR as a cycle including the four REs: 1) RETRIEVE the most similar case(s); 2) REUSE the case(s) to attempt to solve the problem; 3) REVISE the proposed solution if necessary; 4) RETAIN the solution as part of a new case.

Machine learning is the study of mathematical and statistical models, algorithms, and applications of artificial intelligence that machines use to improve their performance by learning and improving from their experience. Machine learning and deep learning are subsets and core of AI (shown in Figure 1).

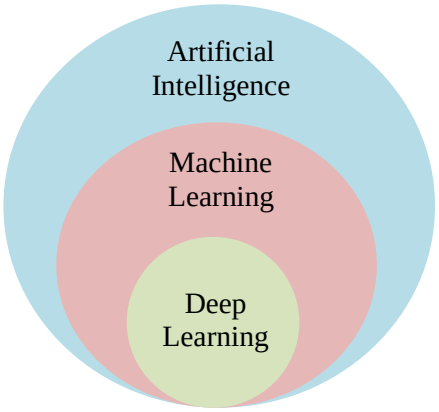

Figure 1. AI, Machine Learning, and Deep Learning

Machine learning technologies are helping computers to learn from data while thinking like a human and imitating the human brain. This became possible because of very powerful computers, availability of online data, large investment of businesses in AI, smarter algorithms, and revolution in programming. Deep learning covers a broader spectrum of machine learning methods using supervised, semi-supervised, and unsupervised techniques. In a supervised machine learning method, a machine learns from known quantities as an input that then maps an output as a future judgment. In an unsupervised technique, a machine learns from using data that is not labeled, classified, or categorized. The machine learns through the process without guidance.

3 AI Applications in AEC

In about 50% of the time, typical construction projects are behind schedule or over budget with many ongoing issues, many conflicts, numerous RFIs (Request for information), and frequent change orders [20]. Imagine having an intelligent assistant to provide help during building construction. AI has already started to change the conventional construction industry compared to the way that buildings used to be designed, constructed, and operated. AI applications can be used for many purposes, including those which have not yet been devised. Imagine the role of AI when machines provide assistance to a construction team by using algorithms. Alternatively, AI systems can collect and organize data related to projects for a project team to be used during all phases of a project like the job Watson did. Watson provides patient information to doctors in a new way to help them make better decisions related to their diagnosis.

AI can provide extra insights into data that a construction team cannot or that will take a longer time and might be processed with lower accuracy because of human errors. Construction robots can perform routine tasks that are performed by construction workers, such as a mason's job of bricklaying for a masonry project. Utilization of robots in the construction industry can be beneficial to accomplishing the job faster without the need for a break during the work or going for vacations which significantly increase productivity and efficiency. These robots enhance quality, precision, and safety while also reducing waste. Construction projects are unique in nature and can be complicated. Meanwhile, the construction industry struggles with skilled workers shortages, and the emergence of new technologies provides tremendous benefits to enhance productivity in construction and to bridge the gaps and helps the construction team with their tasks. AI works well with automation and does not get tired or make mistakes, unlike workers.

Most importantly, AI helps with projects' records. In the past, all of the construction team used paper records to save project data or used a blackboard to record information during a meeting, keep notes or create to-do lists. With all of this existing information, it was still hard to keep track of information properly and to stay on the same page with other co-workers. The use of the data being collected through mobile devices in combination with AI makes the information available, reliable, accessible, and consistent. It helps the project team to mine the information and see patterns in data that are not otherwise evident. The following examples

discuss various ways in which AI can help construction with automation through access to resources such as data.

3.1 Drones

Drones are one type of mobile robots that became a powerful innovation for the construction industry by being employed in surveying, inspection, aerial images and photography, and project monitoring and controlling. Each type of drone can be equipped with a variety of technologies and equipment, and more importantly, offers the opportunity to include AI. Drones can be controlled remotely or equipped with AI techniques to provide solutions for image detection and processing. Drones can be used for monitoring and maintaining purposes as they can provide views from a different vantage point and provide on-demand support to construction workers in their daily activities.

A drone can also be used as a first-responder at a job site for construction hazards as well as search and rescue operations including finding safety violations [21]. Project monitoring and controlling is another important area in which drones are transforming construction projects to the next level. Not only they can monitor projects, report progress, and spot problems, drones can also work together, exchange information, and collaborate in a real-time manner to complete their tasks. They can provide pictures with high resolutions to monitor projects in real-time. Drones can become the eyes of project engineers and project managers by providing vision in situations that are costly, require travel, and are challenging or hazardous. Finally, drones can determine different kinds of damage during any disaster.

3.2 Construction 3-D Printing

Construction 3-D printing includes the applications of different technologies that use 3-D printing to fabricate buildings or components of construction projects with different materials, such as cement, concrete, foam, and polymer. Construction 3-D printing has a variety of applications in the construction industry including residential, commercial, and industrial buildings, bridges, and infrastructure. 3-D printing of construction-scale projects offers design-driven construction process where the design determines the final product with a lower labor cost, shorter project duration, and making possible complex designs with the required functionality [22].

This technology has gained popularity in recent years within the construction industry. Adding AI to construction 3-D printing lets the printer create an object and then learns from the process to improve it. In addition, the use of 3-D printing was further promoted after NASA announced 3D-printed habitat competition for Mars.

3.3 Safety 4.0

With the trend of automation in construction, the internet of things (IoT), and cloud computing and cloud-based data exchange, it is necessary to take construction safety to the next level to be compatible with the new work environment. Safety 4.0 refers to conducting safety in a smart work environment or the way future safety will be practiced. With the merging of AI applications into the construction industry and shifts from conventional safety methods, safety management systems and inspections are used by project team members through using new technology, and field personnel becomes part of the decentralized safety program.

With real-time access to all of the safety information, there is no need to look for paper-based blueprints or going back to the office to look for a report. Safety 4.0 enhances communication among the project team members, specialty contractors, and stakeholders. Safety 4.0 enables team members to have access to real-time safety data. This can enhance the quality of data that can be used for AI techniques offering for the use of reporting accidents, forecasting potential incidents, or near misses. By having all the safety data, information, and report in hand, conducting regular safety meetings at the job site is made easier.

Smart wearable equipment or personal protective equipment (PPE) are developed in a way that is connected to the internet or other devices to provide real-time data while decreasing the exposure to construction safety hazards and sending automatic notifications [23]. Smart PPE can provide unlimited opportunities for field workers. For example, smart communication devices that can be connected to safety hard hats or face shields to facilitate communication in a noisy work environment can minimize hazard exposure. With all of these new technologies and AI applications, data can be transformed and adapted for safety to industry 4.0.

3.4 Autonomous Vehicles

Autonomous vehicles or self-driving cars can play an important role in construction projects. For example, some manufacturing companies have already developed heavy equipment for dozing and hauling for earthmoving projects that are able to provide 3-D pictures of the earth. As automation in construction becomes more practical, the use of autonomous vehicles that can be equipped with AI technology, robotic solutions, and sensors, enable construction equipment to operate without drivers and with better communication.

The equipment can be operated remotely and with all of the advancement in technology, it has the potential to increase productivity, efficiency, and safety and to be more cost-effective.

3.5 Generative Design

Generative design refers to a design process that employs AI techniques that generate several numbers of iterative designs according to the possibilities and constraints provided. Generative design can be used in AEC during the design process to empower the architects and designers particularly throughout the conceptual design process. Employing AI techniques by using algorithms to formulate project requirements generates design solutions and navigates them into the detailed design process. Recently, Autodesk [24] used the same approach as conceptual research and conducted the generative design approach to perform space planning. For space planning, several constraints such as building orientation, area, size of windows, daylight, and HVAC design criteria were considered in the developed algorithm.

Generative design augments architects and designers' capability and combines it with the cloud computations and machine learning to provide new solutions for clients. It enhances the ability of architects and designers to exceed current challenges during the design phase.

3.6 Risk Mitigation and Control

The use of AI applications for risk mitigation and control in construction projects is useful even with unstructured data. Cognitive analytics such as natural language processing (NLP), offers advanced algorithms to process unstructured data. Most of the generated data related to risk identifications are unstructured and it is beneficial to use cognitive analytics to leverage proactive risk identification in projects. With cognitive analytics, known and unknown risk identification can become more accurate.

3.7 Smart Sensor

In construction projects, smart sensors provide a unique role in facilitating IoT. Installing smart sensors at the job site creates continuous data collection that can be used for different purposes. For example, if there are any toxic substances or physical agents such as chemical substances or high-level noise above the permissible exposure limit in the environment, the sensors can sound an alarm and inform workers for evacuation. The sensors will be helpful for measuring air quality at the job site or in confined spaces. The real-time data collection and alarm can be shared with other people in the office such as the project manager, superintendent, or safety manager. The report can be developed automatically based on the data if AI techniques are used. Sensors can mitigate risks and issues and keep the job site safer.

To understand how the AI can be used in AEC, some of the AI applications during different phases of construction projects are summarized in Table 1.

4 Opportunities and Challenges for the Use of AI in Design and Construction

The rise of AI and machine learning in the construction industry has facilitated the construction process. It created and resulted in a more efficient and productive manner in managing the projects. This can be attributed to its application in any stage from design to pre-construction to construction to operation and maintenance. Recent advancement in technological solutions that integrates AI-powered algorithms has helped key players to tackle some of the challenges including cost and schedule overruns and safety concerns. However, in spite of the high return on investment and significant management interest in AI solutions, few construction companies and owners have the capability to employ them. One of the main challenges in implementing AI faced by these companies is the lack of critical mass data. AI is based on learning from past activities, decisions, and performances which requires a significant amount of data to train it. The other issue is the tremendous restrictions on data sharing and data ownership.

Therefore, the largest construction companies are potentially able to benefit more from AI applications in the near future. On the other side, some of the AI solutions that encourage the construction industry to adopt it are as follows: 1) project schedule optimizers which include millions of alternatives to improve project planning, 2) image recognition and classification to evaluate video data collected at the job site to determine the unsafe areas or behaviors, 3) analytical platforms to collect and assess the real-time data from various sensors installed at the job site to help project managers implement real-time solutions. Even though the construction industry is behind with technology adoption compared to other industries, now is the time to act and secure a place at the cutting-edge of implementing AI solutions and techniques into the sector.

5 Conclusions

The adoption of AI is slowly progressing in some areas of AEC, but there is still a long way to go. This study focused on identifying and leveraging synergies

between AI techniques and AEC with the aim of providing a better understanding of potential applications of AI and making AI part of AEC's digital journey. In order to provide a vision of some of the AI applications in AEC, an overview of some of the AI techniques is first explained and then application of AI specifically in AEC is summarized. This enables us to understand the potential applications of AI methods in the AEC domain. There are new ways to incorporate AI into the construction process to help the workforce become more efficient. The trend has already started and it will accelerate when using AI becomes more feasible.

Table 1. Summary of AI Applications in AEC

Construction Project Phases	Construction Activities	AI Applications	Notes
Feasibility Study			
	Collect historical information, process, and procedure	Pattern recognition	Apriori algorithm [26]
	Identify initial stakeholders	ANN	
	Identify feasible options Understand business case Develop project objectives	Neural Networks Fuzzy Cognitive Maps Genetic Algorithms Bayesian Models	Neural Networks, Fuzzy Cognitive Maps, Genetic Algorithms, Bayesian Models can be used as critical success factors identification [27]
Planning			
	Collect project requirements, constraints, and assumptions	Neural Networks Fuzzy Cognitive Maps Genetic Algorithms Bayesian Models	Neural Networks, Fuzzy Cognitive Maps, Genetic Algorithms, and Bayesian Models can be used as critical success factors identification [27]
	Determine standards and codes	Stochastic models	Cognitive computing and strategies can be used to develop stochastic models [16, 25]
	Identify risks	Cognitive analytics	Natural language processing (NLP) offers advanced algorithms to process unstructured data.
	Develop project management plan	ANN	Management by algorithm
	Define scope	ANN	
	Develop schedule	ANN	ANN can be used to optimize project duration. The mathematical model is developed based on the project network diagram, resource leveling, and time-cost trade-offs [30].
	Estimate cost and determine budget	ANN CBR	ANN and CBR can be used as a project cost optimizers to optimize the project's cost. The mathematical model is developed based on the project network diagram, resource leveling, and time-cost trade-offs [29, 30].
	Plan resource management Estimate activity resources	Generic Algorithms CBR ANN	GA can be used to search for an optimum solution for resource allocation and leveling integrated with time–cost trade-off model, resource model, and resource leveling model [29, 30].
	Perform qualitative and quantitative risk analysis and plan risk responses	CBR	Risk Mitigation

Design			
	Schematic design/rough sketches Refining the design	Generative Design	Kiviat diagram, better known as a spider diagram [24].
Construction			
	Construct the project according to the design	CBR	CBR can be used during the construction phase [28].
	Manage stakeholder engagement	CBR	CBR will be helpful for resource engagement and management [28].
	Safety	Image recognition and classification	Classify safety issues to the fatal four. Pictures and video data collected at the job site can help to identify unsafe worker behavior.
Maintenance & operation			
	Maintenance and operation of the project	ANN GA CBR	ANN, GA, and CBR can be used to assist the diagnosis and monitoring during the maintenance and operation phase [28, 30, 31].

References

[1] Russell, S. J., & Norvig, P. Artificial intelligence: a modern approach. Malaysia; *Pearson Education Limited*, 2016.

[2] Redmon, J., Divvala, S., Girshick, R., & Farhadi, A. You only look once: Unified, real-time object detection. *In Proceedings of the IEEE conference on computer vision and pattern recognition* (pp. 779-788), 2016.

[3] Abbasi, A. Z., Islam, N., & Shaikh, Z. A. A review of wireless sensors and networks' applications in agriculture. *Computer Standards & Interfaces*, 36(2), 263-270, 2014.

[4] Koh, H. C., & Tan, G. Data mining applications in healthcare. Journal of healthcare information management, 19(2), 65, 2011.

[5] Fethi, M. D., & Pasiouras, F. Assessing bank efficiency and performance with operational research and artificial intelligence techniques: A survey. *European journal of operational research*, 204(2), 189-198, 2010.

[6] Oesterreich, T. D., & Teuteberg, F. Understanding the implications of digitisation and automation in the context of Industry 4.0: A triangulation approach and elements of a research agenda for the construction industry. *Computers in Industry*, 83, 121-139, 2016.

[7] Leite, F., Cho, Y., Behzadan, A. H., Lee, S., Choe, S., Fang, Y., Akhavian, R., & Hwang, S. Visualization, information modeling, and simulation: Grand challenges in the construction industry. *Journal of Computing in Civil Engineering*, 30(6), 04016035, 2016

[8] Fellows, R. F., & Liu, A. M. Research methods for construction. *John Wiley & Sons*, 2015.

[9] Dorigo, Marco, and Gianni Di Caro. Ant colony optimization: a new meta-heuristic. *In Proceedings of the congress on evolutionary computation-CEC99*, vol. 2, pp. 1470-1477. IEEE, 1999.

[10] Karaboga, D. and Akay, B. A comparative study of artificial bee colony algorithm. *Applied mathematics and computation*, *214*(1), pp.108-132, 2009.

[11] Davis, Lawrence. Handbook of genetic algorithms, 1991.

[12] Gass, Saul I. Linear programming. *Encyclopedia of Statistical Sciences* 6, 2004.

[13] Rao, R.V., Savsani, V.J. and Vakharia, D.P. Teaching–learning-based optimization: a novel method for constrained mechanical design optimization problems. *Computer-Aided Design*, *43*(3), pp.303-315, 2011.

[14] Kanungo, T., Mount, D.M., Netanyahu, N.S., Piatko, C.D., Silverman, R. and Wu, A.Y. A local search approximation algorithm for k-means clustering. *Computational Geometry*, *28*(2-3), pp.89-112, 2004.

[15] Camerer, C.F. Behavioral game theory: Experiments in strategic interaction. *Princeton University Press*, 2011.

[16] Müller, Alfred, and Dietrich Stoyan. *Comparison methods for stochastic models and risks*. Vol. 389. New York: Wiley, 2002.

[17] Nielsen, T.D. and Jensen, F.V. *Bayesian networks and decision graphs*. *Springer Science & Business Media*, 2009.

[18] Elliott, R.J., Aggoun, L. and Moore, J.B. *Hidden Markov models: estimation and control* (Vol. 29). Springer Science & Business Media, 2008.

[19] Aamodt, A. and Plaza, E. Case-based reasoning: foundational issues, methodological variations and system approaches, Al Communications, 7 (1), 39-59, 1994.

[20] Well built company. Why Construction Projects Fall Behind Schedule. On-line: http://www.wellbuiltco.com/blog/6112017-2, Accessed: 25/01/2019

[21] Irizarry, J., Gheisari, M. and Walker, B.N., 2012. Usability assessment of drone technology as safety inspection tools. *Journal of Information Technology in Construction (ITcon)*, *17*(12), pp. 194-212.

[22] Tay, Y.W.D., Panda, B., Paul, S.C., Noor Mohamed, N.A., Tan, M.J. and Leong, K.F., 2017. 3D printing trends in building and construction industry: a review. *Virtual and Physical Prototyping*, *12*(3), pp. 261-276.

[23] Podgorski, D., Majchrzycka, K., Dąbrowska, A., Gralewicz, G. and Okrasa, M., 2017. Towards a conceptual framework of OSH risk management in smart working environments based on smart PPE, ambient intelligence and the Internet of Things technologies. *International Journal of Occupational Safety and Ergonomics*, *23*(1), pp.1-20.

[24] Autodesk. Generative Design Applied on Buildings. On-line: https://autodesk.typepad.com/bimtoolbox/2017/06/generative-design-applied-on-buildings.html, Accessed: 25/01/2019

[25] Scholz, R.W., 2012. *Cognitive strategies in stochastic thinking*(Vol. 2). Springer Science & Business Media.

[26] Inokuchi, A., Washio, T. and Motoda, H., 2000, September. An apriori-based algorithm for mining frequent substructures from graph data. In *European Conference on Principles of Data Mining and Knowledge Discovery* (pp. 13-23). Springer, Berlin, Heidelberg.

[27] Martínez, D.M. and Fernández-Rodríguez, J.C., 2015. Artificial intelligence applied to project success: a literature review. *IJIMAI*, *3*(5), pp.77-84.

[28] Yau, N.J. and Yang, J.B., 1998. Case-based reasoning in construction management. Computer-Aided Civil and Infrastructure Engineering, 13(2), pp.143-150.

[29] de Soto, B.G. and Adey, B.T., 2016. Preliminary resource-based estimates combining artificial intelligence approaches and traditional techniques. Procedia engineering, 164, pp.261-268.

[30] Li, H. and Chen, Z., 2007. *Environmental management in construction: A quantitative approach*. Routledge.

[31] Niu, G., 2017. *Data-Driven Technology for Engineering Systems Health Management*. Springer.

Frequency Sweep Based Sensing Technology for Non-destructive Electrical Resistivity Measurement of Concrete

S. Wickramanayake, K. Thiyagarajan, S. Kodagoda & L. Piyathilaka

iPipes Lab, Centre for Autonomous Systems, University of Technology Sydney, Australia.
E-mail: Karthick.Thiyagarajan@uts.edu.au (Corresponding Author)

Abstract -

Electrical resistivity is an important parameter to be monitored for the conditional assessment and health monitoring of aging and new concrete infrastructure. In this paper, we report the design and development of a frequency sweep based sensing technology for non-destructive electrical resistivity measurement of concrete. Firstly, a sensing system prototype was developed based on the Wenner probe arrangement for the electrical resistivity measurements. This system operates by integrating three major units namely current injection unit, sensing unit and microcontroller unit. Those units govern the overall operations of the sensing system. Secondly, the measurements from the developed unit were compared with the measurements of the commercially available device at set conditions. This experimentation evaluated the measurement performance and demonstrated the effectiveness of the developed sensor prototype. Finally, the influence of rebar and the effect of frequency on the electrical measurements were studied through laboratory experimentation on a concrete sample. Experimental results indicated that the electrical resistivity measurements taken at a closer proximity to the rebar had its influence than the measurements taken away from the rebar in the ideal set condition. Also, the increase in electrical resistivity to the increase in frequency was observed, and then the measurements show lesser variations to higher frequency inputs.

Keywords -

Concrete, electrical resistivity, frequency effects, frequency sweep, infrastructure, infrastructure health monitoring, non-destructive, rebar effects, sensor.

1 Introduction

Robotics play a significant role in the condition assessment of water utility assets for evaluating the integrity of pipelines [1]. Although robotic platforms are used for moving inside the pipelines, the key aspect to non-destructive measurements is the development of reliable sensors [2, 3, 4, 5]. In this context, this paper presents the design and development of a sensing system that can be used on the moving robotic platforms inside pipelines for infrastructure health monitoring applications.

The work reported in this paper is motivated by the concrete corrosion problem that wastewater utility faces globally [6]. The losses due to corrosion related problems are estimated to be in the order of millions of dollars worldwide [7]. Presently, the water utilities uses a predictive modelling approach to estimate the corrosion throughout the sewer network [8]. However, such models rely on the quality of sensor data [9, 10]. Surface moisture data is one of the parameter inputs used for improving the prediction of the model [11, 12]. Our previous investigations had studied the behaviour of concrete moisture conditions and the electrical resistivity measurements, where we employed direct current based electrical resistivity measurements [13] and through invasive approach [14]. Upon in-situ calibration, the electrical resistivity measurements can be used to determine the concrete moisture condition. However, reliable measurement of electrical resistivity is vital for the application motivated.

In this work, we aim to develop a alternating current based sensing system for accurate measurements of concrete electrical resistivity. In this regard, this paper proposes a frequency sweep based technology for non-destructive electrical resistivity measurement of concrete. The major contributions are:

- Development of a physical unit for measuring the concrete electrical resistivity, where the desired frequency can be set in the unit to perform measurements or a frequency sweep can be performed. Then, the measured readings can be stored in the system's data acquisition unit and visualized through the graphical user interface (GUI).

- Performance evaluation of the developed system was conducted by using a commercially available device's measurements as the benchmark readings. This evaluation demonstrates the effectiveness of the proposed system.

- Influence of rebar location and the effects of frequency levels on the electrical resistivity measurements were studied through the laboratory experimentation on a fabricated concrete sample.

For the readers, the rest of this paper is structured as follows: Section 2 describes the development of the sensing system. Section 3 presents the experimental results with analyses and finally, Section 4 concludes the paper by highlighting the key outcomes and future prospects.

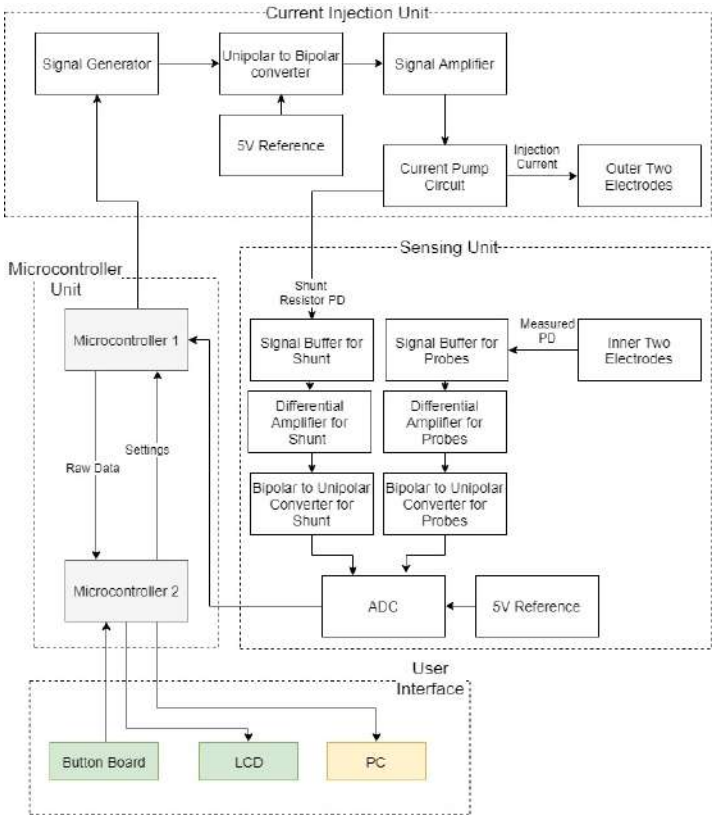

Figure 1. Hardware block diagram.

2 Development of the Sensing System

2.1 Sensing Principle

The Wenner probe method [15] is used to measure the surface resistivity of the material being tested. It uses four electrodes; outer two electrodes inject an alternating current to the surface while the inner two electrodes measure the potential difference. The principle is true for both DC current and AC Current, but there are some drawbacks when using the DC current. Applying a DC current on to the test material will cause macroscopic polarization, which will create an artificial DC potential on the surface. This will cause the measured potential difference to be inconsistent. This was eliminated by injecting a bipolar AC current in the form of a square wave or a sine wave. The alternating polarity of the injected current will prevent the material from generating an artificial DC potential.

The potential difference measured from the inner two probes and the known injected current can be used to compute the resistance of the material by using the Ohm's Law. The electrical resistivity of the material depends on the resistance and the probe spacing. Therefore, the calculated resistance and the distance between the probes can be used to compute the resistivity of the material based on the Equation (1).

$$ER = 2\pi a \frac{V}{I} \tag{1}$$

where ER is the measured electrical resistivity, a=38mm is the spacing between the electrodes, V is the measured potential difference and I is the applied current.

A major component of this design is the ability to vary the frequency of the injected current. The frequency of the injected current affects the penetration depth of the current. Lower frequencies will allow the current to penetrate deeper into the material than the higher frequencies. This characteristic behaviour can be used to determine the resistivity values at certain depths of the material being tested. The developed sensor will allow the user to perform a frequency sweep by setting the maximum and the minimum limits and the stepping frequency. During the frequency sweep, the resistivity is measured simultaneously at the set intervals.

2.2 Design of Sensing System

The three main components in designing the sensing system are the current injection unit, sensing unit and the micro-controller unit. The block diagram in Figure 1 shows the information flow through each of the major components of the system.

2.2.1 Current Injection Unit

The current injection unit produces a constant bipolar alternating current with a variable frequency. To generate this current, we used a Howland current pump circuit. The ideal Howland current pump circuit is essentially a voltage controlled current source, which can generate a constant current regardless of the load resistance. This is achieved by changing the voltage across the load accordingly to keep the current through the load constant. However, when the resistance of the load is too high, the voltage required to keep the current constant at the required amount will be higher than the input voltage to the circuit. In such situation, the current across the load will be lower than the expected value. This requires the current to be constantly monitored using a shunt resistor to prevent any errors in the resistivity measurements. The current output of the the Howland current pump circuit can be calculated using the Equation (2), where I is the injected current, V_{in} is the input voltage and R_s is the shunt resistance.

$$I = \frac{V_{in}}{R_s} = \frac{15}{60000} = 250\mu A \tag{2}$$

The output current, which will be injected into the test surface was kept very small in the range of micro-amperes due to several reasons. A lower current eliminates the heat generation on the surface from the injected current, which will cause the resistivity readings to alter. The power loss over transmitting wires is also minimized and any shock hazard from persons coming in contact with the current probes will also be eliminated by using a smaller current.

For producing the alternating current, we have used the analog devices AD9850 Signal Generator IC to generate the square wave. It is an integrated chip that uses advanced Direct Digital Synthesizer (DDS) technology coupled with a high speed 10-bit DAC to produce a sine wave. This sine wave is connected to a square wave using an internal comparator. The frequency of the signal can be digitally programmed for up to 125MHz with an accuracy of 0.3Hz. The signal generated from the AD9850 IC is unipolar with the signal alternating between 0V and 5V. The Wenner probe methodology requires a bipolar alternating current to produce the accurate results without generating any artificial potential differences. To achieve this, we have used a uni-polar to bipolar converter, which was designed using a differential op-amp configuration. After identifying the required gain and the offset of the differential amplifier, we came up with the transfer function in Equation (3) for the unipolar to bipolar converter, where V_{out} is the output voltage and V_{in} is the input voltage.

$$V_{out} = 2 \times V_{in} - 5V \tag{3}$$

The signal output from the uni-polar to bipolar converter has an amplitude of ±5V which is not sufficient for measuring resistivity using the Wenner probe method. The signal was amplified using a non-inverting op-amp configuration to an amplitude of ±15V. The op-amp used in the amplifier circuit had to have the rail-to-rail feature to allow the op-amp to output voltages equal to the supply voltage of ±15V.

2.2.2 Sensing Unit

The sensing unit measures the potential difference between the inner two probes of the Wenner array configuration. The potential difference generated in the inner two probes was first passed through a signal buffer circuit and then converted to a measurable value using a differential amplifier, which is then converted back to a uni-polar signal to be measured by the ADC. There is a high impedance difference between the ADC and the electrodes, which had to be taken into consideration when designing the sensing unit. It is also necessary to isolate the sensing unit with the current injection unit to prevent any errors in the measurements due to the common ground terminals. Those issues were addressed by using the signal buffer circuits. The buffer circuits used were voltage buffer amplifiers, which converts the high output impedance of the sensing electrode to a low impedance output to match the impedance of the ADC. The buffer amplifiers also prevented the sensing unit from loading the sensing electrodes and interfering with the current waves created in the test surface. In addition, they were used while measuring the voltage across the shunt resistors due to the same reasons. The circuit schematic in Figure 2 shows the buffer circuit used between the sensing electrodes and the ADC.

The ADC that we used in the sensing unit was the Microchip MCP3008 10-bit ADC. This ADC contains four pseudo differential channels, which are sufficient as this system requires only two differential inputs for the sensing electrodes and the shunt resistor. The voltage output from the buffer circuits was fed through a differential amplifier before being read by the ADC. Since this ADC accepts only a uni-polar input, the measured potential, which is a bipolar signal has to be converted back to a unipolar signal before being fed in to the ADC. The ADC will be powered using a regulated 5V supply and the the reference voltage needed by the ADC will be supplied using a voltage reference circuit consisting of a LM4040 reference voltage IC.

2.2.3 Microcontroller

The microcontroller is the central unit of the system, which manages all the other components. An Arduino Micro for the microcontroller was utilized as it supports SPI and I^2C communication protocol, which is required to communicate with the other components of the system.

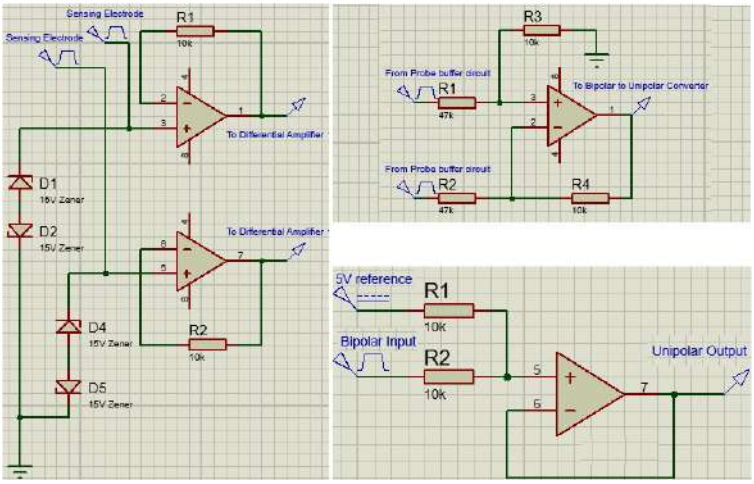

Figure 2. (Left) Signal buffer circuit schematic of the sensing electrodes. (Top Right) Differential amplifier circuit schematic of the sensing electrodes. (Bottom Right) Bipolar to unipolar converter.

The ADC needs to operate constantly without any interruptions during the measurement process. Therefore, it requires the Arduino connected with the ADC not to be interrupted during data logging. To carry out measurements and data logging at the same time, it is necessary to use a second Arduino to handle the data logging and the user interactions. This enables the results to be displayed in real-time while the device is in operation.

2.3 Operating System

The microcontroller programming of the system was carried out using the Arduino IDE and the GUI was designed and implemented using the Matlab software. The software was designed to produce useful information by processing the raw data, so that the user can interpret the measured readings easily to determine the health conditions of the structure under investigation. The control unit of this system consists of two microcontroller boards, which contains two different sets of programming instructions. The unit containing the first microcontroller board is referred to as the 'Sensor board' while the unit containing the second microcontroller is referred to as the 'UI board'

The sensor board was programmed to receive the system settings from the user including the information about the required frequency sweep and the data logging. The user information is then used to start the current injection unit, which injects a current though the outer two probes of the sensor. The potential difference measured by the inner two probes is then captured using the ADC in the sensor board. The UI board consists of the buttons, which are used to change the settings of the system and also, a LCD screen to display the settings and the real-time resistivity measurements. The raw data captured from the sensor board is passed on to the UI board for processing and to be presented to the user. The data received from the sensor board is the AC signal, which has been converted to a unipolar signal from the bipolar to unipolar converter. This signal is then converted back to a bipolar signal using software and sent though a set of filters and then, processed to plot a graph of resistivity against the frequency. The digital reading will be shown in the LCD of the UI board and plots for greater data visualization will be shown in a GUI on a computer connected to the sensor via USB. Figure 3 shows the overall software flow.

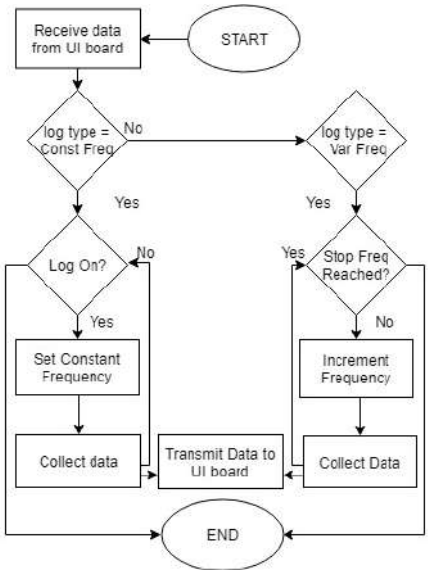

Figure 3. Overall software flow diagram.

2.4 Graphical User Interface for Visualization

The system can be connected to a computer via a USB that allows the results to be visualized graphically through the GUI, which was designed by using the Matlab software (R2016a version), and it interacts with the hardware through serial communication. The GUI allows real-time monitoring of the data and also the system can be completely controlled from the GUI rather than the hardware buttons. The resistivity values will be displayed in the system's GUI along with the frequency of the injected current. The system is programmed to plot the real-time measurements for better visualization of the resistivity variations during the frequency sweep. Further, the GUI offers an option to filter the data to remove any noise signals produced by the sensor. In addition, the GUI can also be used to easily save the logged data into a computer as a .csv or a .txt text file for comprehensive analysis. Figure 4 shows a screenshot of the GUI.

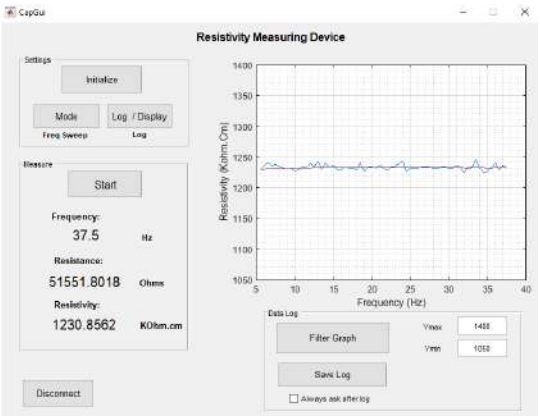

Figure 4. The GUI of the developed system.

2.5 Electrodes Arrangement and Enclosure Design

For the electrical resistivity measurement of concrete, the electrodes are required to be in contact with the test surface. A stainless steel 316-grade material bolts were chosen as electrodes mainly because of the reason that they highly resist in corrosive and high humidity environments, and has a good electrical conductivity. The electrodes were housed in a 3D printed enclosure containing a spring mechanism, which allows the electrodes to be pressed on the test surface firmly to allow maximum surface contact. Figure 5 shows the electrode arrangement with housing.

The main circuits including the micro-controller, signal generator, current pump circuit and all the other circuits were housed inside a plastic enclosure as shown in Figure 6, with cut-outs for the buttons, LCD display, power jack, USB port and the mini-DIN type connector that connects the circuits enclosure with the electrodes.

Figure 5. (Left) Assembled electrode arrangement. (Right) Electrode with spring mechanism.

Figure 6. Enclosure of the computing unit.

3 Experimental Results

3.1 Measurement Performance Evaluation

In this performance evaluation, we have utilized a commercially available electrical resistivity meter (Resipod, PCTE) [16] for the purpose of measurement comparison with the developed unit. The commercial device injects a current of 250μA at a frequency of 40Hz during measurements. To represent an identical test condition, we have set our developed system to produce a current of 250 μA at a frequency of 40Hz. A concrete sample having 10 cm thickness was fabricated and a rebar having 1cm diameter was embedded at 2cm distance from the top surface. Using both the devices, five sets of readings were taken on the concrete samples at each location and similar measurements were taken at varying horizontal distances to the rebar as shown in Figure 7.

Table 1 tabulates the electrical resistivity measurements

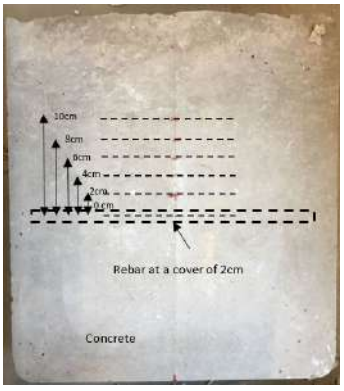

Figure 7. The concrete sample used for testing with embedded rebar and measurements were taken at 2cm spacing away from the rebar up to 10cm.

from the commercial device and the developed unit. It can be observed that the mean absolute error (MAE) for the measurements taken in different horizontal distances is less than 1 kΩcm, which indicates the effective measurement performance of the developed unit.

Table 1. Measurement Performance Evaluation

Horizontal distance to the rebar (cm)	Mean electrical resistivity from Resipod (kΩcm)	Mean electrical Resistivity from developed unit (kΩcm)	Mean absolute error (kΩcm)
0	3.27	3.20	0.07
2	8.83	9.63	0.80
4	10.9	10.07	0.83
6	13.2	12.5	0.7
8	16.23	16.17	0.06
10	17.9	17.83	0.07

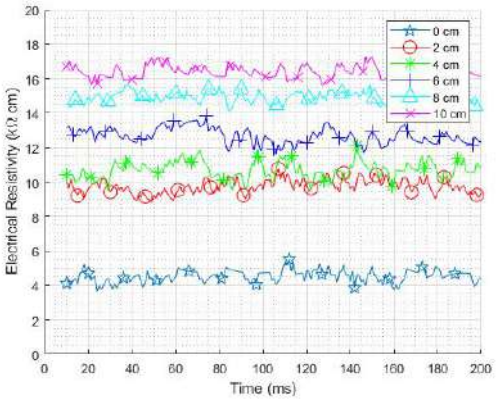

Figure 8. Resistivity vs Time graph, with the first measurement taken directly above the rebar (0cm) and last measurement at 10cm away from rebar.

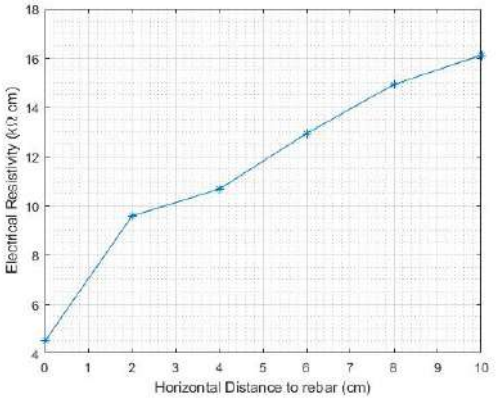

Figure 9. Resistivity vs Horizontal distance to rebar.

3.2 Influence of Rebar Location

In order to study the influence of rebar location on the electrical resistivity measurements, an experimentation was conducted on a concrete sample that has rebar at a known depth. In this experiment, the current of a constant frequency of 80Hz was injected to the surface of the concrete sample and the resistivity was calculated using the measured potential difference. A frequency of 80Hz was chosen as it is low enough to cause a variation in resistivity due to the rebar, which is located 2cm below the concrete surface. The sensor is prone to noise signals during measurements. Therefore, the resistivity readings were taken for a period of time so that an average can be obtained to minimize any error from the noise. The plot in Figure 8 shows the measurements taken on the concrete sample while moving 2cm horizontally from the rebar between each measurement.

A mean value for the resistivity was obtained by generating a line of best fit for the measurements during the 200ms interval. The constant frequency of 80Hz allowed the current to penetrate into the test material upto a certain depth and produce current flux lines. The rebar in the concrete affects the generated current flux lines, which will result in differences in the measured potential difference. The plot in Figure 9 shows the change in resistivity against the sensor distance to rebar, where we can observe that the resistivity increases as the sensor distance to rebar increases. This shows that rebar has an influence on electrical resistivity measurements taken at closer proximity.

3.3 Effect of Frequency on Measurements

The frequency of the injected AC current affects the penetration depth of the current flux generated from the outer two probes of the Wenner probe array. An experimentation was conducted, where the frequency sweep was carried out in the frequency range of 1Hz to 1.8KHz with the resolution of 2Hz. Measurements were taken on a concrete sample of 2cm rebar cover and the developed sensing unit was moved 2cm away between each set of measurements. The changes in resistivity measurements were plotted against the increase in frequency as shown in Figure 10 in order to analyze the effects due to the frequency sweep of the injected current.

It can be observed from the Figure 10 that there is an increase in resistivity as the frequency increases between 1Hz to approximately about 150Hz on the measurements taken with the sensor directly above the rebar (0cm), and similar trend was was observed with measurements taken at 2cm, 4cm, 6cm, 8cm and 10cm away from the rebar. This variation is due to the changes in the penetration depth as the frequency of the injected current changes and

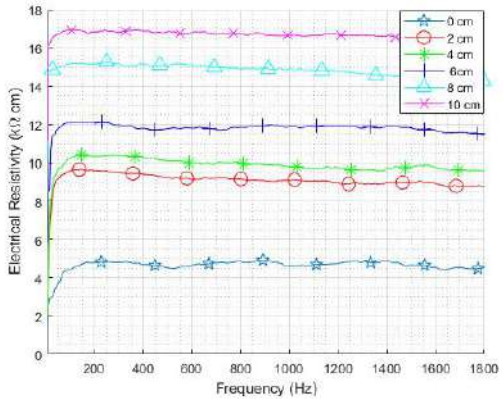

Figure 10. Resistivity variations for frequency changes on a concrete sample with 2cm rebar cover, with the first measurement taken directly above the rebar (0cm) and moving 2cm away from the rebar between each measurement until 10cm.

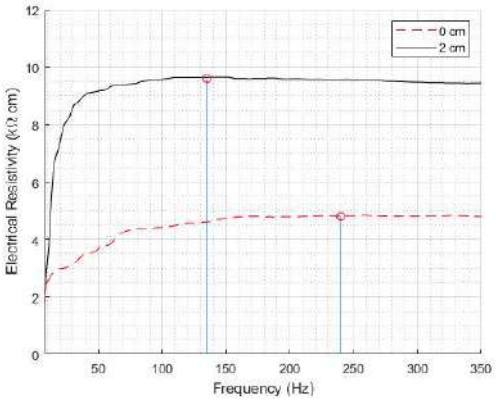

Figure 11. Resistivity versus Frequency graph for the concrete sample with 2cm rebar cover, with 0cm and 2cm plot, close up view that shows the point at which the resistivity converges to lesser variations.

the influence due to the presence of rebar in the region of interest of the sensing unit.

The current at lower frequencies has a larger wavelength, which allows for greater penetration. This enables more current flux lines to be created in the concrete, which increases the number of current flux lines interfering with the rebar. This causes the potential difference measured by the inner two probes of the developed unit to be smaller, which translates to a smaller resistivity measurement. Approximately, above 150KHz frequency, the resistivity readings shows less variations. When the frequency is greater than a certain value, the penetration power of the injected current is too low to penetrate deep enough into the rebar, which eliminates the influence on the resistivity due to the rebar.

The point at which the resistivity measurements starts to exhibit less variations is earlier when the sensor is 2cm away from the rebar than when it is directly above the rebar, as shown in Figure 10 and Figure 11. This is due to the variation of the distance between the sensor and the rebar. When the sensor was moved over 4cm away from the rebar, a less change of resistivity was observed, because of the reason that the rebar position is now away from the maximum penetration range.

4 Summary and Future Prospects

In this paper, we have presented the developments of a frequency sweep based sensing technology for non-destructive concrete electrical resistivity measurements. From the reported work, the key highlights include:

- Development of a sensor prototype for measuring the electrical resistivity of concrete and data acquisition.
- Measurement results indicated that the MAE between the developed unit and commercial device is less than 1 kΩcm, which demonstrates the effectiveness of the prototype.
- Effect of the rebar on the electrical resistivity measurement was studied. Experimentation results showed that the measurements taken at closer proximity to the rebar has lower values than the measurements taken at different distances away from the rebar.
- Effect of the frequency sweep on the electrical resistivity measurement was studied. Measurement results displayed that there is an increasing trend in the electrical resistivity measurements with the increase in frequency approximately upto 150Hz and then for higher frequencies, lesser variations in the electrical resistivity was observed.

In the future, the reported sensing system will be improved by integrating with wireless data transfer feature, and can be employed for real-world applications motivated in [17, 18].

References

[1] Jaime Valls Miro, Nalika Ulapane, Lei Shi, Dave Hunt, and Michael Behrens. Robotic pipeline wall thickness evaluation for dense nondestructive testing inspection. *Journal of Field Robotics*, 35(8):1293–1310, 2018.

[2] K Thiyagarajan, S Kodagoda, and J K Alvarez. An instrumentation system for smart monitoring of sur-

face temperature. In *2016 14th International Conference on Control, Automation, Robotics and Vision (ICARCV)*, pages 1–6, 2016.

[3] Nalika Ulapane, Alen Alempijevic, Jaime Valls Miro, and Teresa Vidal-Calleja. Non-destructive evaluation of ferromagnetic material thickness using Pulsed Eddy Current sensor detector coil voltage decay rate. *NDT and E International*, 100:108–114, 2018.

[4] Jean Kyle Alvarez and Sarath Kodagoda. Application of deep learning image-to-image transformation networks to GPR radargrams for sub-surface imaging in infrastructure monitoring. In *Proceedings of the 13th IEEE Conference on Industrial Electronics and Applications, ICIEA 2018*, pages 611–616, 2018.

[5] Nalika Ulapane, Linh Nguyen, Jaime Valls Miro, Alen Alempijevic, and Gamini DIssanayake. Designing a pulsed eddy current sensing set-up for cast iron thickness assessment. In *Proceedings of the 2017 12th IEEE Conference on Industrial Electronics and Applications, ICIEA 2017*, pages 901–906, 2018.

[6] Tony Wells, Robert Melchers, Antony Joseph, Phil Bond, Dammika Vitanage, Heriberto Bustamante, John De Grazia, Thomas Kuen, John Nazimek, and Ted Evans. A collaborative investigation of the microbial corrosion of concrete sewer pipe in Australia. In *OzWater-12 AustraliaâĂŹs National Water Conference and Exhibition, May*, pages 8–10, 2012.

[7] K Thiyagarajan and S Kodagoda. SMART monitoring of surface temperature and moisture content using multisensory data fusion. In *2015 IEEE 7th International Conference on Cybernetics and Intelligent Systems (CIS) and IEEE Conference on Robotics, Automation and Mechatronics (RAM)*, pages 222–227, 2015.

[8] Jianjia Zhang, Bin Li, Xuhui Fan, Yang Wang, and Fang Chen. Corrosion prediction on sewer networks with sparse monitoring sites: A case study. In *Lecture Notes in Computer Science (including subseries Lecture Notes in Artificial Intelligence and Lecture Notes in Bioinformatics)*, 2018.

[9] K. Thiyagarajan, S. Kodagoda, and L. Van Nguyen. Predictive analytics for detecting sensor failure using autoregressive integrated moving average model. In *Proceedings of the 2017 12th IEEE Conference on Industrial Electronics and Applications, ICIEA 2017*, pages 1926–1931, 2018.

[10] Karthick Thiyagarajan, Sarath Kodagoda, Linh Van Nguyen, and Ravindra Ranasinghe. Sensor Failure Detection and Faulty Data Accommodation Approach for Instrumented Wastewater Infrastructures. *IEEE Access*, 6:56562–56574, 2018.

[11] Karthick Thiyagarajan, Sarath Kodagoda, Ravindra Ranasinghe, Dammika Vitanage, and Gino Iori. Robust sensing suite for measuring temporal dynamics of surface temperature in sewers. *Scientific Reports*, 8(1):16020, 2018.

[12] B. Li, X. Fan, J. Zhang, Y. Wang, F. Chen, S. Kodagoda, T. Wells, L. Vorreiter, D. Vitanage, G. Iori, D. Cunningham, and T. Chen. Predictive Analytics Toolkit for H2S Estimation and Sewer Corrosion. In *OZWater*, Sydney, 2017. Australian Water Association.

[13] K Thiyagarajan, S Kodagoda, and N Ulapane. Data-driven machine learning approach for predicting volumetric moisture content of concrete using resistance sensor measurements. In *2016 IEEE 11th Conference on Industrial Electronics and Applications (ICIEA)*, pages 1288–1293, 2016.

[14] Karthick Thiyagarajan and Sarath Kodagoda. Analytical Model and Data-driven Approach for Concrete Moisture Prediction. In *33rd International Symposium on Automation and Robotics in Construction (ISARC 2016)*, pages 298–306, Auburn, 2016. IAARC.

[15] W. Morris, E. I. Moreno, and A. A. Sagüés. Practical evaluation of resistivity of concrete in test cylinders using a Wenner array probe. *Cement and Concrete Research*, 1996.

[16] Resipod Surface Resistivity Meter. *www.forconstructionpros.com*, 2011.

[17] Karthick Thiyagarajan. *Robust Sensor Technologies Combined with Smart Predictive Analytics for Hostile Sewer Infrastructures*. PhD thesis, University of Technology Sydney, 2018.

[18] Karthick Thiyagarajan, Sarath Kodagoda, Linh Van Nguyen, and Sathira Wickramanayake. Gaussian Markov Random Fields for Localizing Reinforcing Bars in Concrete Infrastructure. In *2018 Proceedings of the 35th International Symposium on Automation and Robotics in Construction*, pages 1052–1058, Berlin, 2018. IAARC.

3D Printing Architectural Freeform Elements: Challenges and Opportunities in Manufacturing for Industry 4.0

M. Niemelä[a], A. Shi[a], S. Shirowzhan[a], S.M.E. Sepasgozar[a], and C. Liu[a]

[a]Faculty of Built Environment, University of New South Wales Sydney, Australia
E-mail: Marjo.niemela@unsw.edu.au, anqi.shi@student.unsw,edu,au, S.shirowzhan@unsw.edu.au, Samad.sepasgozar@gmail.com, liuchang1126@outlook.com

Abstract –
Three-dimensional (3D) printing, as one of the additive manufacturing (AM) technologies, is transforming the design and manufacture of products and components across a variety of disciplines, however, architectural design and the construction industry have only recently begun to adopt these technologies for construction purposes. AM is considered one of the core technological advances in the paradigm shift to Industry 4.0 (the fourth industrial revolution). This term used to describe digitization and automation of the manufacturing environment and is widely recognized as a disruptive technology that could transform architectural design and the construction industry. The potential advantages of 3D printing in the construction sector are significant. They include not only improved environmental and financial resource efficiencies, but also, the capacity to produce complex customized designs for aesthetic and structural applications.

As the cost of building houses continues to rise, it is crucial to find innovative ways to build houses efficiently and cost effectively. The earliest records of 3D printing date back to the 1980's and many industries—from manufacturing to medicine—were early adopters of the technologies resulting in many significant technological advances in those sectors from organ printing to aircraft fabrication. Currently available 3D printing technologies can be adopted for building construction and this paper discusses the applications, advantages, limitations and future directions of 3D printing as a viable solution for affordable house construction with a focus on printing architectural freeform elements.

3D printing offers a new and innovative method of house construction. For this study, an analytical, as well as a numerical model were specifically designed for 3D printing. Previous studies conducted found that the construction of a 3D printed truss-like roof in a cement mixture with high-density polyethylene (HDPE), spanning the entire structure, was structurally feasible in the absence of steel reinforcements. These results led us to investigate the feasibility of 3D printing an entire house without the use of reinforcements. Investigations were also performed on comparing flat-roof and arch-roof structures and found that whilst maximum tensile stresses within flat-roof would cause the concrete truss structure to fail, the HDPE cement mix in an arch-roof structure had reduced the maximum tensile stresses to an acceptable range to withstand loadings. At the time of writing this paper, several 3D printing techniques could be adopted for the purposes of 3D printing an entire house, and the team believes that future adaptations of existing technologies and printing materials could eliminate the current limitations of 3D printing and become common practice in house construction.

Keywords –
3D printing; design; architectural freeform elements; construction, Fusion 360 Software; G-code; human-interface, Industry 4.0.

1 Introduction

There is a growing trend in architectural design and the construction industry to adopt Industry 4.0 and utilize additive manufacturing processes for building construction. Applying 3D printing in design and construction provides potential advantages as infinite forms and shapes, including large sized elements, can be created in-situ on congested or difficult to access construction sites.

The terms additive manufacturing and 3D printing both refer to the process of creating an object by sequentially adding build material in successive cross sections, or layer upon layer deposition. 3D printing also includes the hardware, machine control systems and software as well as the peripheral accessories which may

be required for producing objects during a building cycle [1]. The blueprint for the form is from a digitally constructed model created in 3D modelling software such as Fusion 360, Rhinoceros, Revit or a multitude of other 3D modelling software packages.

3D printing is the fabrication of objects through the deposition of a material using a 3D printing technology, or type of mechanism

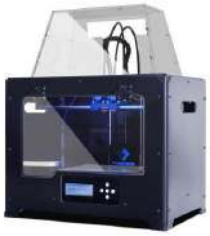

with a print head and nozzle [1]. AM technologies include gantry systems, suspended platforms, and mobile rotating manipulators with an extension arm. The gantry system is the most commonly adopted technology by manufacturers of model size fused deposition

modelling (FDM) 3D printers such as MakerBot and FlashForge.

Whilst this system works effectively in laboratories, for in situ construction scale 3D printing, gantry systems have limitations akin to those of pre-fabricated houses in that they require transportation and installation of heavy infrastructure, which, in turn also can limit the size of the build envelope. Contour Crafting completed a proof of concept at full house scale 3D print in the United States in 2001.

The term "cable-suspended platform" is used for 3D printing technologies that consists of an end-effector that is manipulated by automated motors via multiple cables attached to a rigid frame. The flexibility within well-engineered frame design means that the cable-suspended platform frees up the size of the build envelope and can be constructed from light-weight materials that are assembled on site. Being lightweight and delivered in parts this system can be less expensive to transport to site but requires expertise for assembly.

Mobile rotating manipulators comprise of a rotating arm on a central base. Apis Cor in Russia was the first company to develop a mobile 3D printer for the construction industry and claims to have successfully printed a 37m² house on site in 24 hours at a cost of US$10,134. The Apis Cor has a reach of 8500mm from a central manipulator with 360° rotation and a maximum height of 3100mm. Due to its large build envelope and low cost of materials, the mobile rotating manipulator system in the form of the Potterbot Scara (Selective Compliance Assembly Robot Arm) XLS-2 clay printer was selected as the most appropriate 3D printing technology for conducting laboratory-based experiments for this study.

Previous studies have generally looked at 3D printing specific geometrical shapes such as wall segments, cubes and vertically extruded curves. Many recently completed 3D printed projects—such as Contour Crafting in the United States, Apis Cor in Russia, and Winsun in China—have provided evidence that the 3D printing of houses can be realised at various scales including 3D printing simple geometry houses at full scale. However, an under developed area in 3D printing in construction is the production of architectural freeform elements (AFE) including extreme slopes, angels and complex curves. This paper aims to create several AFEs and discusses the challenges of creating these models in a laboratory. The paper aims to identify different factors of attainable AFEs from a practical perspective. Many previous studies and built full sized projects focused on producing simple vertically extruded geometries but further investigation is required to find out what are the possible challenges and opportunities of creating AFEs at different scales and sizes.

Researchers in the field of aerospace and manufacturing have demonstrated that 3D printing can reduce costs, but limited investigations have been undertaken to support the assumption that savings will also apply in the construction industry [2]. However, it is still appropriate to hypothesize that utilizing 3D printing can reduce costs for aesthetic and structural applications in the construction industry. Another motive to apply 3D printing technology within the construction Industry is the potential for increased safety. The construction industry has been shown to have a higher rate of fatality, injury and illness than any other sector [3]. So whilst traditional construction may appear straightforward from two-dimensional (2D) drawings, building any kind of freeform or complex curvature structure requires formwork and much skilled labor. The proposed solution and a focus of this study is to minimize and simplify the level of human-interface and human-machine or robot interaction to enable 3D printing technologies to become safe, cost effective and accessible tools in the construction industry.

2 Research Method and Data

This study is a laboratory-based investigation. We designed nine architectural freeform models and scaled them to be fabricated as models in a laboratory. A total of 56 samples were created in the lab, and overall running time of printing was approximately 30 hours. A 3D Potterbot XLS-2 (Scara) clay printer (see Fig.1) was used for the experiments as it is able to print large models in continuous flow system of layer deposition.

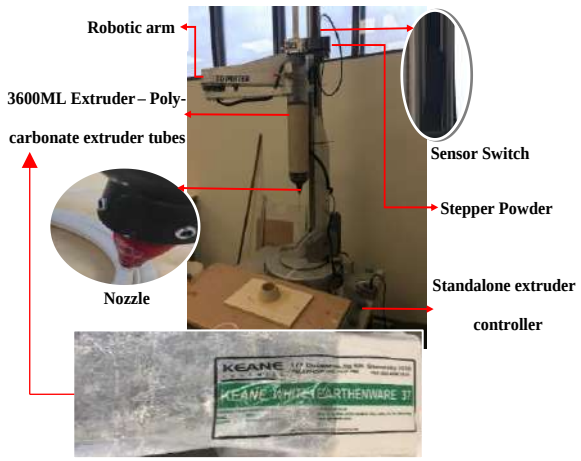

Figure 1. 3D potterbot SLX-2 (Scara) using clay for lab experiments.

The 3D potterbot SLX-2 (Scara) in its seventh series of development has evolved from the previous syringe extrusion method to a mechanical screw system. Earlier Potterbot technologies therefore required a clay and water mix which meant prints could not handle otherwise normal overhangs and did not have good success with achieving significant height.

The material used for this study is clay with no water added, which is suitable for a range of objects from very small to large, even hand applications. The study found that after the initial investment cost of the Potterbot equipment, this technology and material combination can be an efficient and inexpensive option for education and research testing.

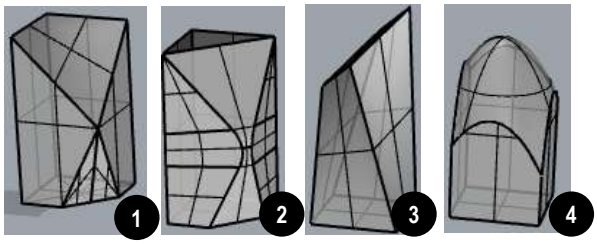

Figure 2. Selected AFE designed models of 4 to 7 for experimentations

Figure 3 shows four models, namely column (M4), column radian (M5), column slope (M6), and column dome (M7). Other models from M1 to M9 are shown in Figure 7. These models can be classified into two groups in terms of design: i) basic models ii) complex or curvature models (e.g. M4 to M7). The software used for these models are Fusion 360 and Simplify3D, which are recommended as compatible programs with the 3D printer Potterbot (XLS-2 Scara robot, 2018).

Models can be designed in any 3D modelling software and saved as STL files which are then imported into Simplify3D for layer slicing, making them them ready to print. The slicing process translates 3D models into instructions the printer understands by generating the G-code programming language, the required numerical code (NC) for motion control of the Potterbot. Any changes to scale or size of the object can be made in Simplify3D software before generating the G-code.

3 Experimentations and Failure Modes

Studies were conducted to verify the accuracy of the 3D printed output compared with the digitally produced model. The 30-degree column models were created on Fusion 360 modelling software (see Fig.1). The build envelope dimensions designed for the columns are 100mm x100mm x 120mm.

Table 1. A summary of software used evaluation.

Advantage	Limitations
Fusion 360	
(i) Cloud enabled collaboration platform can create a variety printable models including organic/complex models more naturally using both NURBS or T-Splines; (ii) Capacity to import models created on other software like Rhino or Revit and then edit specific sections; (iii) Capacity to export as STL file format which can be read directly by 3D slicing printing software like Cura and Simplify3D.	(i) Designing a building model has limitations because Fusion 360 is more suitable smaller objects (ii) It is relatively new software platform with kinks and issues but is constantly being updated and improved;
Simplify3D	
(i) Compatible with hundreds of different 3D printers; (ii) Can provide a pre-print simulation of model printing actions; (iii) Controls and communicates extruder information like speed and print time.	(i) Some aspects of 3D printer XLS-2 Scara robot motion are not possible to control / predict such as the start point of the extruder for a print; (ii) No free version of Simplify3D is available.

According to all the printed output dimension data, the 20-degree column physical model is the most accurate production of the designed model measuring 99mm x 97cm x120mm. This was more accurate than the 0-degree column output. The models with the most serious deformations are the 30-degree column and 45-degree column. Another factor for future analysis is the impact of increased human presence in proximity to the machine as the models with the most serious defamations correlated with an increase in the number of people present in the lab and in close proximity to the machine, at the time of print.

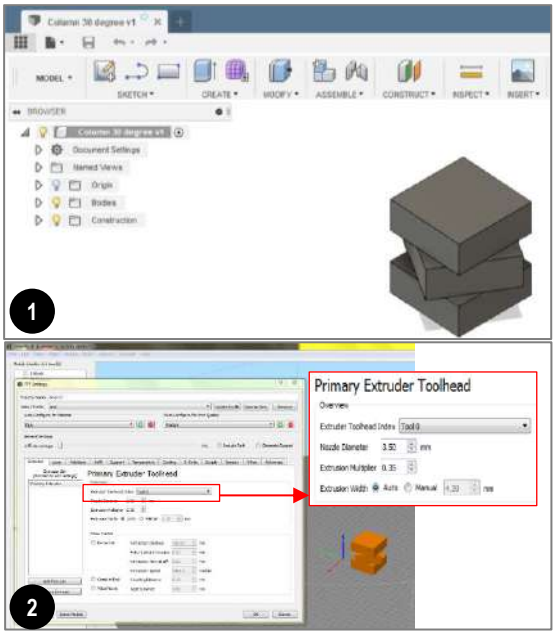

Figure 3. Processing the file in different programs: (1) Fusion 360; (2) Simplifiy3D with 30-degree column.

.

```
; G-Code generated by Simplify3D(R) Version 4.0.1
; Dec 5, 2018 at 10:56:58 AM
; Settings Summary
;   processName,Potterbot Final
;   applyToModels,30 Column
;   profileName,Potterbot Final 3mm
;   profileVersion,2018-11-07 09:55:04
;   baseProfile,Default
;   printMaterial,PLA
;   printQuality,Medium
;   printExtruders,
;   extruderName,Primary Extruder
;   extruderToolheadNumber,0
;   extruderDiameter,3.5
;   extruderAutoWidth,1
;   extruderWidth,4.2
;   extrusionMultiplier,0.35
;   extruderUseRetract,0
;   extruderRetractionDistance,150
;   extruderExtraRestartDistance,0
;   extruderRetractionZLift,0
;   extruderRetractionSpeed,5400
```

Name of the printable model.

Nozzle Diameter shown in Figure 3 (2).

Figure 4. A sample of G-code for model 8 (i.e. 30-degree column).

The 3D potterbot SLX-2 (Scara) robot can be fitted with with a variety of nozzle sizes ranging from 1mm to 25mm. The study models were printed using the 3.5mm diameter nozzle. The nozzle size in an important consideration before producing G-code (see figure 4) as various object designs are contingent on factors such as overall dimensions, level of detail required and angle of slope. Waste material is another consideration and clay loads can be loaded appropriate for the object size. The maximum build envelope height for XLS-2 Scara robot is 1828mm diameter and 1143mm Z height. It can be customized to print 2743mm diameter and 2590mm Z height.

Table 2. Selected causes of failure modes.

Models size/Scale	Failure
Appearance Designed Model 4	The start point of the extruder is hard to predict. The first layer printed outside the area of the intended base board. (see Fig.7 (1))
All 9 models	The size of the model is limited by extruder printing information such as the Nozzle Diameter in fig.5 and G-code in fig.6 for 30-degree column.
Squares, Rectangles and Arches	Due to the pressure in the extruder, the machinery cannot stop printing the clay resulting in wasted materials. (see Fig.7 (2) & (3)).
Appearance Designed Model 2 (100%)	The Shape structure changed as the size and scale of the models was modified. Same design, original size (left) collapsed, but the half size (right) printed successfully (see Fig.7 (5) & (6)).
Column models	The shape of the design is limited as the clay is soft and cannot stand by itself (see Fig.7 (9)).
All 9 models	The surface finish can be affected by the air bubbles, material may have flaws (see Fig.7 (11)).
All 9 models	Shrinkage and cracking occurred damaging the model. (see Fig.7 (12)).
Priming edge and the first layer of all models.	The start layers do not work well. The first layer is compressed, possibly caused by the height of the nozzle or the uneven moisture level of the board. The board is not flat due to the difference in water absorption (see Fig.7 (7)).
Square, Rectangle and Arches.	Due to mechanical errors the machine stopped working for three times during printing of simple shape models (Square, Rectangle and Arches).

Figure 7 shows all relevant images of the failure models. In order to observe the effect of slope in failures of the 3D printed models, the angle of the surface was changed from 0-degree to 60 and 80-degree for M8 and M9 respectively.

In the column-slope model (M6), the top section has

a collapse trend from 80% to 120%. The middle section of the sample with the scaled model of 120% (i.e. 20% larger sized printed) collapsed and cracked.

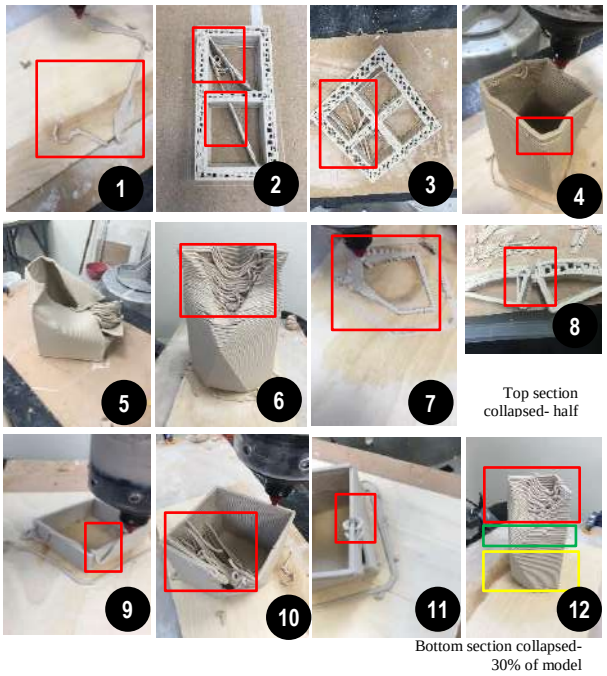

Figure 7. Selected 3D printed of failed models.

Table 3. The frequency of the issues during the 3DP process for 56 models.

The Issues during the 3D printing process	Frequency
Small Air bubbles.	44
Large Air bubbles and flaws (Fig.7 (11)).	41
One edge is wider, and the opposite is thinner due to one board moisture inconsistency (Fig.7 (7)).	8
The structure of rectangles and squares changed after scaling 130% of original size. (Rectangles and squares, Fig 7 (2)).	6
The top section collapsed for Column (M1) and Column Slope (M3) (see Fig.7 (6)).	6
Preparation time is much longer due machinery faults, generally issues getting the nozzles ready.	5
Total completion time is longer as G-code created for motion programming of machinery is inefficient.	4
The bottom section bent, and the clay path distorted for Column (M1) (see Fig.7(12)).	4
The paths distorted on top section for Column (M1) and Column Slope (M3) (see Fig.7(6)).	4
The model begins to collapse as the nozzle deposits clay a little further outside its intended path for Column (M3) (Fig.7 (4)).	3
The paths do not form a circle only a line for Column (M1) (see Fig.7(6)).	3
The center parts started printing for Column Radian (M2) (see Fig.7 (10)).	3
The machinery hardware stops working for a while	3
The path in the center at this layer cut off during the printing process for Column (M1) (see Fig.7 (6)).	2
The top paths distortion is more severe than before for Column (M1) (see Fig.7(12)).	2

The diameter of the cylinder is proposed as 10cm in models; however, the diameter in the 3D printed model with 0-degree is 96mm. Observation shows that the collapse starts at a layer with 20-degree slope in the cylinder (M8). Because the 60-degree cylinder shape is more like a triangle, which is the most robust shape in construction, the base diameter is smaller than the 45-degree cylinder and the same with the 20-degree cylinder's base diameter.

Table 4. Shrinkage Table after 7 daysfor 14 models in different slope.

Models code	Average shrinkage in each side
Cylinder 0 slope	2.56%
Cylinder 10 degree	3.16%
Cylinder 20 degree	6.39%
Cylinder 30 degree	5.10%
Cylinder 45 degree	9.70%
Cylinder 60 degree	12.51%
Column 0 degree	3.50%
Column 10 degree	4.35%
Column 20 degree	4.11%
Column 30 degree	2.96%
Column 45 degree	3.26%
Column 60 degree	2.68%
Column 70 degree	3.18%
Column 80 degree	5.56%

Note: Base on the laboratory personnel experience, the normal shrinkage rate should around 10%.

4 Results

Table 4 shows the descriptive analysis of the models. It shows that the mean time per layer for the models varies from 0.27 to 2.85 minutes.

An analysis of variance (ANOVA) test was employed to examine whether the differences of means are significant or not. Figure 5 shows the means for each model.

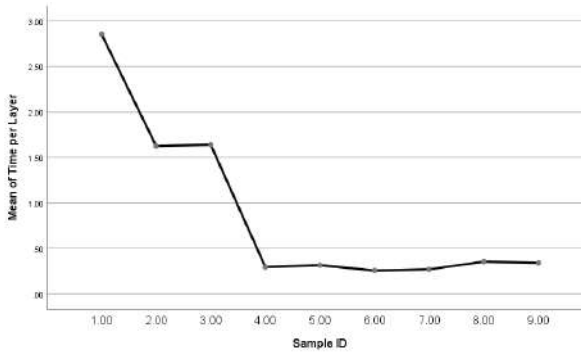

Figure 5. Mean for time per layer for all eight models.

The analysis shows that there was a statistically significant difference between models 1, 2 and 3 with all other models (e.g. from 1 to 8) except 2 and 3 as determined by one-way ANOVA ($F(8,47) = 20.782$, $p = 0.000$). The Tukey post hoc test was applied and showed that the time per layer to complete the first model was statistically significantly higher than all other models (2.85 ± 0.91 min, $p < 0.003$). The time was second highest for model 2 (1.63 ± 0.66 min, $p < 0.019$), and model 3 (1.64 ± 0.59 min, $p < 0.04$). There was no statistically significant difference between model samples of the model 2 and 3 ($p = 1.000$). There was no statistically significant difference between all models 4, 5, 4, 7, 8 and 9 with each other ($p = 1.000$).

Table 5. Descriptive analysis for time per layer.

M	N	Mean	Std. Deviation	95% Confidence Interval		Minimum	Maximum
				Lower	Upper		
1	12	2.86	0.91	2.28	3.43	1.61	4.27
2	12	1.63	0.67	1.20	2.05	0.66	2.63
3	6	1.64	0.59	1.02	2.26	0.91	2.58
4	3	0.30	0.04	0.20	0.39	0.26	0.34
5	3	0.32	0.05	0.20	0.43	0.27	0.36
6	3	0.26	0.04	0.15	0.36	0.22	0.30
7	3	0.27	0.05	0.15	0.39	0.22	0.32
8	6	0.35	0.04	0.31	0.40	0.30	0.42
9	8	0.34	0.02	0.33	0.36	0.32	0.36
T	56	1.28	1.14	0.98	1.59	0.22	4.27

Note to table: M refers to model, N refers to the number of layers per model, Mean refers to the time spent for each layer, T refers to Total.

5 Discussion

3D printing has been used in manufacturing for many years, but whilst its adoption into the construction industry has been slow, it is currently a growing area of development for building construction. Previous studies have generally investigated potential materials and their properties for 3D printing as well as adapting or designing 3d printing technologies for effective delivery on construction sites. However, investigations into combining complex geometries and construction by 3D printing have received less attention.

The potential advantages of 3D printing in construction are significant. They include not only not only increased efficiencies pertaining to financial and environmental resources but, also, the capacity for mass customization of designs to meet aesthetic, functional and structural purposes. Previous studies and realized 3D printed houses have shown the potential for minimization of construction waste from precise material deposition and eliminating the need for of formwork. Previous studies have also shown the potential for increased safety on construction sites. However, many factors need to be addressed before 3D printing can be fully utilized for complex shapes in construction. They include further research into material properties to a attain structurally stable material, not just for longevity but crucially, during printing. Challenges for 3D printing include material setting time, stability during printing, deformation, shrinkage and bonding between layers. Material behaviours require further investigation under a range of conditions to achieve a robust material that can take structural load during and after printing.[4].

This study examined the capability of 3D printing for producing complex geometries. Key factors such as shrinkage, time per layer or speed and material wastage were examined in the laboratory. We faced several challenges during the production of different models. The limitation during the laboratory experimentation was the lack of control of the machine by the user. These types of factors are very important on a real construction sites, when a worker needs to change specific dimensions, angles or position of the nozzle. To address this issue, we would recommend human-printing collaboration strategy, which helps human and 3D printers to work side by side to complete the construction of the item or structure.

Construction sites are not predictable and rarely flat and even surfaces or environments and so many adjustments are required to address issues such as slope of site, humidity and environmental factors like wind.

This study will be replicated with a variety of materials and model designs not with the intention of creating the ideal environment for 3D printing but by addressing the issues in their application on real construction sites.

Model designs can play an important role in creating feasible structural shapes to understand and predict how material properties change with curvature and slope of surfaces. However, other factors should be further investigated such as the volume of waste materials, total cost including the operation cost, optimization of nozzle path, and material properties such as brittleness of clay

and concrete. Another issue is increasing the level of automation of the entire process from design to construction.

In line with some of previous findings in different contexts [5,4,6,7], several limitations of the 3D printer were observed in our experiments. The PotterBot XLS-2 Scara was not able to generate digital data in terms of motion speed, volume of clay used and total length or volume of the printed layers. The process of 3D printing, from digital modelling in CAD programs to converting to machine instruction G-code in a CAM program, and operation of hardware requires vastly different skill-sets and knowledge than is common in current construction practices. CAD modelling software packages, with the exception of relatively costly Rhinoceros 3D Modelling package with plug-in RhinoCam, CAD platforms cannot directly communicate with 3D printers and intermediary Computer Aided Modelling (CAM) programs are required to convert vector based data to G-code to communicate with the machine, meaning that currently available software packages do not allow automation or real-time response between digital modelling and 3D printing. However, many advantages were also observed. 3D printing provides the possibility for continuous construction, not limited to working hours or visibility during sunlight with minimal supervision. Another further positive observation was the low level of noise produced during the 3D printing process which was negligible compared to that of construction sites. As predicted in numerous previous studies, the perceived and assessed safety level of using the PotterBot was of much lower risk level than for other common construction methods and has the potential to reduce injuries and fatalities in the construction industry.

6 Conclusions

This study aimed to examine the capability of 3D printing to produce complicated geometric and volumetric designs. Eight models were designed and 56 models were created in the laboratory by a 3D printer called PotterBot XLS-2 Scara robot. The entire production process was carefully observed and several factors including material setting time, stability during printing, possible unsupported material overhang, deformation, shrinkage and bonding between layers. for all 56 models were recorded. The results show that the first three models are significantly different than the last four models. In addition, the studies show that the waste material and motion path can be challenging for models with complicated designs. The key contribution of the paper is to compare several complicated models to measure how curvature and unique models can affect potential construction practices for creating complex curves and forms on construction sites without the need for formwork or reinforcements.

As discussed, future studies will continue to focus on adapting 3D printing processes, currently suitable for controlled lab environments, to real construction sites with a focus on automating and simplifying the process to enable the adoption of 3D printing into house construction.

7 References

[1] A.C.F.o.A.M. Technologies, A.C.F.o.A.M.T.S.F.o. Terminology, Standard terminology for additive manufacturing technologies, ASTM International, 2012. ISSN.

[2] S. You, J.-H. Kim, S. Lee, V. Kamat, L.P. Robert Jr, Enhancing perceived safety in human–robot collaborative construction using immersive virtual environments, Automation in Construction 96 (2018) 161-170.

[3] Y.W.D. Tay, B. Panda, S.C. Paul, N.A. Noor Mohamed, M.J. Tan, K.F. Leong, 3D printing trends in building and construction industry: a review, Virtual and Physical Prototyping 12 (3) (2017) 261-276. https://doi.org/10.1080/17452759.2017.1326724

[4] P. Wu, J. Wang, X. Wang, A critical review of the use of 3-D printing in the construction industry, Automation in Construction 68 (2016) 21-31.

[5] M. Sakin, Y.C. Kiroglu, 3D Printing of Buildings: Construction of the Sustainable Houses of the Future by BIM, Energy Procedia 134 (2017) 702-711.

[6] F. Tahmasebinia, M. Niemelä, S. Ebrahimzadeh Sepasgozar, T. Lai, W. Su, K. Reddy, S. Shirowzhan, S. Sepasgozar, F. Marroquin, Three-Dimensional Printing Using Recycled High-Density Polyethylene: Technological Challenges and Future Directions for Construction, Buildings 8 (11) (2018) 165.

[7] G. Ma, L. Wang, Y. Ju, State-of-the-art of 3D printing technology of cementitious material—An emerging technique for construction, Science China Technological Sciences 61 (4) (2018) 475-495.

Teaching Robots to Perform Construction Tasks via Learning from Demonstration

C. J. Liang[a], V. R. Kamat[a,b] and C. C. Menassa[a]

[a]Department of Civil and Environmental Engineering, University of Michigan, USA
[b]Robotics Institute, University of Michigan, USA
E-mail: cjliang@umich.edu, vkamat@umich.edu, menassa@umich.edu

Abstract –

Robots are expected to be widely used on future construction sites to assist human workers in the performance of repetitive physically-demanding tasks. Unlike typical manufacturing assembly lines, where parts are delivered to robots and workers in stationary workstations, construction robots and human workers must accumulate all necessary resources and repeatedly navigate to desired assembly locations on-site to perform useful work. The condition of such resources and the geometry of the environment are constantly changing and generally unstructured. As a result, the motion trajectories of any robot arms cannot be programmed beforehand. The robots must define the trajectory based on the encountered workspace geometry. Learning from Demonstration (LfD) methods have the potential to be used in teaching robots specific skills through human demonstration such that the robots can repeat the same process in different conditions. In this research, we explore the LfD method to teach robots to perform repetitive but geometrically adaptive construction tasks of installing suspended ceiling tiles within pre-assembled ceiling grids. The developed method translates the work context from the set of training videos demonstrated by humans to the target scene, then applies the reinforcement learning method to generate the policy for the robot to perform the subsequent ceiling tile installation. The first phase of the proposed method, i.e., the context translation model, is implemented and evaluated by characterizing whether robot-installed ceiling tiles are successfully moved to the grid area. The experiments demonstrate promising results that show the applicability of the LfD method in teaching robots to perform geometrically-adaptive construction tasks.

Keywords –

Robot Learning from Demonstration; Computer Vision; Autoencoder; Ceiling Tile Installation

1 Introduction

Human-robot and co-robot collaborative teams are broadly envisioned to be deployed on future construction sites [1]. The construction industry accounts for 4.3% of GDP in the U.S. [2] and is predicted to reach over 1.4 trillion U.S. dollars in volume by 2021, and $15.5 trillion worldwide by 2030 [3]. Construction is the economic locomotive of the society, whose competitiveness is affected by speed and quality of the construction process. However, the construction industry is confronting major issues of the aging workforce and the lack of skilled labor [44]. The U.S. labor force growth is forecasted to be lower than 0.5% by 2030 due to demographic transition [4]. The average age of the construction worker in the U.S. is 43 years old, and the younger generation is reluctant to enter the construction industry [5] due to its dangerous and demanding working environment, which causes a significant decrease in the employment-population. As a result, applying co-robots to assist or relieve human workers from hazardous, dangerous, and repetitive construction tasks has emerged as a key prospect to help mitigate issues faced by the construction industry [6–9].

According to Manzo et al. [10], approximately 50% of the construction tasks can be automated and may potentially replace nearly 2.7 million construction workers with robots by 2057. The human workers will work alongside robots or supervise them on the future construction site. By applying robots on construction sites, the human workers will switch their duty to perform the planning and cognitive tasks as supervisors, and train the robots to perform the repetitive physical work.

Similar to the manufacturing assembly line setting, the construction process is performed by several repetitive basic tasks [11,12], as shown in Figure 1. Take suspended ceiling tile installation process as an example: workers have to measure the ceiling tile layout, maneuver and position the tile, place the tile, and inspect the alignment. However, unlike the manufacturing environment, the construction site is an unstructured and

dynamic environment [45]. The robots have to understand the environment, and then plan and execute the task accordingly. They need to navigate to the next assembling location as well, which makes it impossible for robots to perform the exact same task repeatedly [13].

Figure 1. The construction process involves repetitive tasks with different objects, such as ceiling tile installation, the tiles are maneuvered and placed repetitively at different locations.

On the other hand, construction projects are unique and unidentical. The loose tolerances and the relatively low quality control of the construction project causes each workpiece to be not strictly identical with each other and requires additional adjustments or improvisation on-site. Even though the workpieces such as tiles are designed to be the same size, the actual pieces may not be the same. Therefore, construction robots must learn how to plan and execute the construction process while overcoming the general uncertainty of the environment and the workpieces they handle.

2 Robot Learning from Demonstration

When training the human worker to perform a task, the human will learn the task by observing the demonstration from experts and practicing the action. The practical knowledge will be absorbed during the practice. Thus, similar to the human learning procedure, the Learning from Demonstration method (LfD) [14,15] can be utilized for co-robots to learn the collaborative task. One approach is imitation learning, where the agent attempts to clone the behavior of the expert [16]. Inverse reinforcement learning (IRL), on the other hand, estimates a reward function based on the expert's demonstration [17,18], then utilizes the learned reward function to obtain the policy. Existing demonstration methods include visual demonstration [19–23], force demonstration [24–26], visual and force demonstration [27,28], and trajectory demonstration [29–35].

First, the visual demonstration methods utilize several or limited video clips of expert's demonstration [36–38]. These methods usually apply to move, push or place simple and light objects, which is not suitable for the construction process, that require handling complex and heavy objects of various geometries. Second, the force demonstration methods are done by force sensors attached to robots and human experts. The robot will learn the contact force on the object and try to replicate the same action. These methods have only been demonstrated on simple tasks such as bolting or unscrewing bottle caps. They do not consider the environment and only try to repeat the action.

Third, the trajectory demonstration methods utilize demonstrating trajectory from expert to train the robot, such as driving simulation or path planning. One of the examples is the kinesthetic demonstration [25], where the robot is dragged by the human to finish the task while memorizing the trajectory. However, these methods require sufficient trajectory data from experts, which is difficult to obtain on construction sites. Finally, the visual and force demonstration methods combine the advantage of both methods to teach the robot to manipulate or grasp objects [28]. For construction tasks, in addition to visual observation, the workers have to feel the haptic or force feedback from the object and react accordingly, yet the existing visual and force demonstration methods only consider the pose of the human instead of the objects.

The objective of this research is to investigate the robot Learning from Demonstration method (LfD) [36] and evaluate the feasibility of applying LfD for teaching construction tasks to co-robots. The trained robots can collaborate with human workers while the human workers focus on the planning and cognitive tasks on the future construction site. The suspended ceiling tiles installation is used as the target construction process to describe the developed methods. The video of the human worker performing the tile installation is recorded in the laboratory and utilized to train the robot. The pose of the object, i.e., ceiling tile, and the target location, i.e., suspended grid, are extracted and tracked in the training video, then encoded as knowledge for the robot to learn. The success rate of the robot performance evaluates the learned skill of the robot.

3 Construction Task Learning

The method for learning the construction task is adapted from a context translation and imitation method by Liu et al. [36]. The practical knowledge of the skill is extracted from the training video as context and translated to the target scene. The robot can further learn the results of the translation through reinforcement learning method [39]. The detailed problem definition of the construction task and the context translation method are discussed in the following sections.

3.1 Problem Definition and Assumption

When teaching a robot to perform a specific task, the knowledge, or context, from the expert's demonstration must be defined in order to let the robot know what information needs to be tracked and absorbed, as well as how to determine the action to take for achieving the task. The context ω can be defined as the pose of the object and expert, the viewpoint of the camera, the condition of the environment, or the target location. In this research, we assume the camera is fixed in two different viewpoints, and the task is to perform in the same environment in order to reduce the complexity.

The demonstration of the task is defined as [36] (1):

$$\begin{bmatrix} D_1 \\ D_2 \\ \vdots \\ D_n \end{bmatrix} = \begin{bmatrix} O_0^1 & O_1^1 & \cdots & O_T^1 \\ O_0^2 & O_1^2 & \cdots & O_T^2 \\ \vdots & \ddots & & \vdots \\ O_0^n & O_1^n & \cdots & O_T^n \end{bmatrix} \quad (1)$$

where O_t is the observation at time t, which is generated from the Partially Observable Markov Decision Process (POMDP) [40]. The probability observation distribution $p(O_t|s_t, \omega_i)$, dynamics $p(s_{t+1}|s_t, a_t, \omega_i)$, and the policy of the expert $p(a_t|s_t, \omega_i)$ are utilized to define the POMDP, where s_t and s_{t+1} are the current and next state (e.g., unknown Markovian state), a_t is the action of the agent (e.g., maneuvering direction), and ω_i is the i-th context (e.g., pose of the ceiling tile, viewpoint). The context is unknown to the robot learner. Since the robot learner might try to track the mismatch context from the demonstration (e.g., follow the pose of the ceiling tile but consider as the pose of the expert), the context ω_i is assumed to be sampled independently and the robot learner has fixed context ω_l sampled from the same distribution [36].

Due to the undetermined feature of the context variables, the robot learner cannot know whether the context from the demonstration is the same as the context in their learning domain. This can be overcome by applying the context translation model [36] to translate the context from the source to the target, then defining the reward function based on the tracked context feature for reinforcement learning method, such as Trust Region Policy Optimization (TRPO) [41] or Deep Deterministic Policy Gradient (DDPG) [42], to learn the policy. The source and the target demonstrations are defined as follows (2)(3):

$$D_s = [O_0^s \quad O_1^s \quad \cdots \quad O_T^s] \quad (2)$$

$$D_t = [O_0^t \quad O_1^t \quad \cdots \quad O_T^t] \quad (3)$$

where D_s is the demonstrations from the unknown context of source video, and D_t is from the unknown context of target video. After training with sufficient examples, the context translation model is capable of translating the new demonstration D_n into the robot learner's context ω_l so that the robot can track and learn the feature.

3.2 Context Translation Model

The objective of the context translation model is to learn the translation function that can translate the source demonstration $D_s = [O_t^s]$, $t = 0,1,...T$ to the target context ω_t with the first observation O_0^t in the target demonstration D_t, that is, the first frame of the target demonstration video. The full translation function is defined as (4):

$$M(O_t^s, O_0^t) = (\hat{O}_t^t)_{trans} \quad (4)$$

where $(\hat{O}_t^t)_{trans}$ represents the translated observations in the robot learner's context.

The context translation model is constructed by several encoders, decoders, and autoencoders [43], which includes a source encoder $En_s(O_t^s)$, a target first observation encoder $En_t(O_0^t)$, and a target context decoder $De_t(z_{trans})$, as shown in Figure 2. On the left side is the framework of translating the source observations to the target observation through the translation function $T(z_s, z_t) = z_{trans}$, where z_s, z_t and z_{trans} represent the features of the encoded source, target, and translation. The loss function for training the translation is defined as L_2-norm (5):

$$L_{trans} = \left\| (\hat{O}_t^t)_{trans} - O_t^t \right\|_2^2 \quad (5)$$

Since the unknown context is translated from source to target, the features need to train on the target video in order to ensure the consistency of the feature representation between the encoder En_s and decoder De_t. The right side of Figure 2 is the framework of the autoencoder for training the En_s and De_t with a reconstruction loss, which is defined as (6):

$$L_{rec} = \left\| De_t(En_s(O_t^t)) - O_t^t \right\|_2^2 \quad (6)$$

The next step is to align the feature representation of the autoencoder with features z_{trans}. The loss function for the alignment is defined as (7):

$$L_{align} = \| z_{trans} - En_s(O_t^t) \|_2^2 \quad (7)$$

3.3 Network Architecture

The network of the encoder and decoder is illustrated in Table 1. In the encoder network, four convolutional layers with different filter size and stride followed by two linear layers with the size of 100 and 0.5 dropout are applied to the training video frame. In the decoder

network, one linear layer with 0.5 dropout followed by four deconvolutional layers with different filter size and stride are applied to the translated feature. All the convolutional and deconvolutional layers are followed by LeakyReLu activation function with 0.2 leak except the last deconvolutional layer in the decoder. The filter size of the linear layer in the decoder is dependent on the size of the input image. Batch normalization is applied to the network. The input image is cropped to size of 48 by 48 pixels for training and testing.

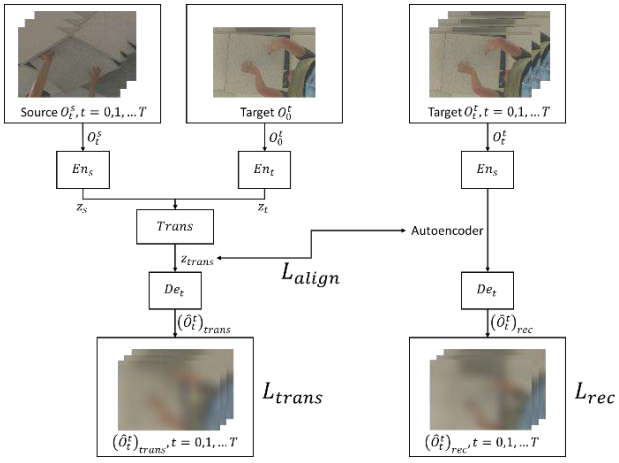

Figure 2. Architecture of the context translation model.

Table 1. Network architecture of the encoder and decoder.

Type	Layer	Filter size	Stride	Other
Encoder	Conv	32	1	LeakyReLu leak = 0.2
	Conv	16	2	
	Conv	16	1	
	Conv	8	2	
	Linear	100	n/a	Dropout = 0.5
	Linear	100	n/a	
Translation function	Linear	100	n/a	Dropout = 0.5
Decoder	Linear	*	n/a	Dropout = 0.5
	Deconv	16	½	LeakyReLu leak = 0.2
	Deconv	16	1	
	Deconv	32	½	
	Deconv	3	1	n/a

*Depends on the size of the input image

3.4 Reward Function for Robot Learning

After the source context is translated to the target observation, a reward function must be defined for the robot to learn the policy through reinforcement learning method. The reward function contains a feature tracking reward function (8):

$$\hat{R}_f(O_t^l) = -\left\| En_s(O_t^l) - \frac{1}{n}\sum_i^n T(z_s, z_t) \right\|_2^2 \quad (8)$$

and an image tracking reward function [36] (9):

$$\hat{R}_i(O_t^l) = -\left\| O_t^l - \frac{1}{n}\sum_i^n M(O_t^s, O_0^t) \right\|_2^2 \quad (9)$$

where $En_s(O_t^l)$ encodes the learner's observation O_t^l to z_l. Finally, the total reward function is defined as (10):

$$\hat{R}(O_t^l) = \hat{R}_f(O_t^l) + \omega \hat{R}_i(O_t^l) \quad (10)$$

where ω represents the weight.

4 Experiments

In order to evaluate the feasibility of applying the robot LfD method for construction tasks, the ceiling tile installation demonstration video was collected in the laboratory and utilized to train the context translation model. The performance of the model was evaluated by the success rate of the installation task.

4.1 Implementation and Training Details

The context translation model was implemented by modifying the original network using TensorFlow. A total of 55 videos were utilized to train the network, and 20 initial observations were used as the testing data, i.e., first frame of the video as the starting point for testing. In the demonstration video, the camera was set up at two fixed viewpoints for reducing the complexity, as shown in Figure 3. The network was trained by ADAM optimizer with learning rate 10^{-4} and the loss function described above.

Figure 3. Example of the ceiling tile installation demonstration video with two different camera viewpoints.

4.2 Results

We use the success rate to evaluate the performance of the context translation model on the ceiling tile installation. The success metric is defined as whether the final distance between the ceiling tile and the target grids is within a predefined threshold. After the source context is translated to the target scene, we identified the final location of the ceiling tile and the grid, then determined whether they were within the predefined threshold in order to calculate the success rate. Figure 4 is an example of the demonstration source video of ceiling tile installation. The human worker demonstrates how to install the ceiling tile.

Figure 5 shows examples of the target observations with two different viewpoints (iso view and bottom view). The target observation is the first frame of the demonstration video, which is utilized for translating the context from the source video. Figure 6 shows the results of the translated scene. The top row is the successful result, and the bottom row is the unsuccessful result. The red rectangle represents the ceiling tile, and the green rectangle represents the target grid. The distance between the ceiling tile and the grid is over the predefined threshold; thus it is determined as unsuccessful result. We compare the success rate of the translation with the different type of viewpoint, as shown in Table 2. The success rate of the bottom view is 25%, and the iso view is 43%. The overall success rate is 35%.

Figure 4. Example of a source video of ceiling tile installation.

Figure 5. Example of target observations, which is the first frame of the video.

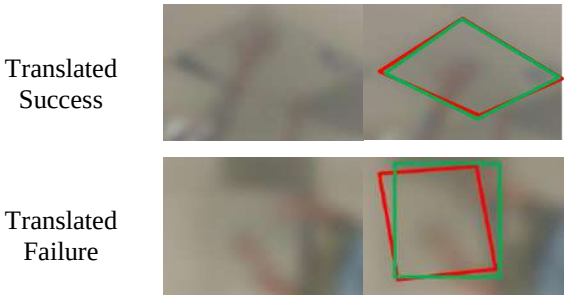

Figure 6. Results of the translated scene. Top - successful result; Bottom - unsuccessful result. Red rectangle represents the ceiling tile, and the green rectangle represents the target grid.

Table 2. Success rate of the translated result.

Viewpoint	Success	Failure	Success rate
Bottom view	2	6	25%
Iso view	5	7	42%
Overall	7	13	35%

In comparison with the Liu et al. [36], where they used the context translation model to teach the robot to ladle almonds into a frying pan and sweep the almonds into a dustpan, the success rate is 66% with 60 training videos of the almonds pouring and 75% with 100 training videos of the almonds sweeping. Thus, the performance can be improved by providing more demonstration videos. In addition, the bottom view has a lower success rate since most of the trajectories of ceiling tile installation are vertical types and the bottom view cannot provide sufficient information. This can be addressed by avoiding the vertical type viewpoint.

5 Conclusion and Future Work

In this research, we proposed and evaluated a Learning from Demonstration (LfD) method to train the construction robot to perform repetitive construction tasks, in which we utilized the ceiling tile installation as the target task. We adopted a visual LfD method, i.e., the context translation model, for our application. The context translation model only uses the visual demonstration as input to train the robot. The model is trained on a set of ceiling tile installation demonstration videos. The results showed that the model could translate the work context from the source video to the target observation with acceptable success rate when using the iso camera view, which can further apply the reinforcement learning method for robots to determine the control policy. In ongoing work, we are collecting more demonstration videos from new viewpoints. We are also implementing the reinforcement learning method for robots to learn and perform the policy.

References

[1] You S., Kim J.-H., Lee S., Kamat V.R. and Robert L.P. Enhancing perceived safety in human–robot collaborative construction using immersive virtual environments, *Automation in Construction*. 96:161–170, 2018.

[2] Statista. U.S. construction industry - statistics & facts. Online: https://www.statista.com/topics/974/construction/, Accessed: 12/11/2018.

[3] GCP and Oxford Economics. Global construction 2030. Online: http://www.globalconstruction2030.com/#products, Accessed: 19/11/2018.

[4] Harris K., Kimson A. and Schwedel A. Labor 2030: the collision of demographics, automation and inequality. Online: https://www.bain.com/insights/labor-2030-the-collision-of-demographics-automation-and-inequality/, Accessed: 2/1/2019.

[5] Belton P. Why robots will build the cities of the future. Online: https://www.bbc.com/news/business-46034469, Accessed: 19/11/2018.

[6] Lundeen K.M., Kamat V.R., Menassa C.C. and McGee W. Scene understanding for adaptive manipulation in robotized construction work. *Automation in Construction*, 82:16–30, 2017.

[7] Liang C.-J., Lundeen K.M., McGee W., Menassa C.C., Lee S. and Kamat V.R. Stacked hourglass networks for markerless pose estimation of articulated construction robots. In *Proceedings of the 35th International Symposium on Automation and Robotics in Construction*, pages 1–7, Berlin, Germany, 2018.

[8] Liang C.-J., Kang S.-C. and Lee M.-H. RAS: a robotic assembly system for steel structure erection and assembly. *International Journal of Intelligent Robotics and Applications*, 1(4):459–476, 2017.

[9] Liang C.-J. and Kang S.-C. Development of a steel beam hauling system for automatic steel beam assembly. In *Proceedings of the 2014 International Conference on Computing in Civil and Building Engineering*, pages 1295–1302, Orlando, FL, USA, 2014.

[10] Manzo J., Manzo F. and Bruno R. The potential economic consequences of a highly automated construction industry. Online: https://midwestepi.files.wordpress.com/2018/01/the-economic-consequences-of-a-highly-automated-construction-industry-final.pdf, Accessed: 30/12/18.

[11] Everett J.G. and Slocum A.H. Automation and robotics opportunities: construction versus manufacturing, *J. of Construction Engineering and Management*, 120(2):443–452, 1994.

[12] Kamat V.R. and Martinez J.C. CEPM4: comparison of simulation-driven construction operations visualization and 4D CAD. In *Proceedings of the 34th Conference on Winter Simulation: Exploring New Frontiers*, pages 1765–1770, San Diego, CA, USA, 2002.

[13] Lundeen K.M., Kamat V.R., Menassa C.C. and McGee W. Autonomous motion planning and task execution in geometrically adaptive robotized construction work. *Automation in Construction*, 100:24–45, 2019.

[14] Argall B.D., Chernova S., Veloso M. and Browning B. A survey of robot learning from demonstration. *Robotics and Autonomous Systems*, 57(5):469–483, 2009.

[15] Zhu Z. and Hu H. Robot learning from demonstration in robotic assembly: a survey. *Robotics*, 7(2):17, 2018.

[16] Schaal S. Is Imitation Learning the Route to Humanoid Robots? *Trends in Cognitive Sciences*, 3(6):233–242, 1999.

[17] Ng A.Y. and Russell S.J. Algorithms for inverse reinforcement learning. In *Proceedings of the International Conference on Machine Learning*, pages 663–670, San Francisco, CA, USA, 2000.

[18] Levine S., Popovic Z. and Koltun V. Nonlinear inverse reinforcement learning with gaussian processes. In *Advances in Neural Information Processing Systems*, pages 19–27, Granada, Spain, 2011.

[19] Acosta-Calderon C.A. and Hu H. Robot imitation: body schema and body percept. *Applied Bionics and Biomechanics*, 2(3-4):131–148, 2005.

[20] Finn C., Yu T., Zhang T., Abbeel P. and Levine S. One-shot visual imitation learning via meta-learning. In *Proceedings of the 1st Annual Conference on Robot Learning*, pages 357–368, Mountain View, CA, USA, 2017.

[21] Kalashnikov D., Irpan A., Pastor P., Ibarz J., Herzog A., Jang E., Quillen D., Holly E., Kalakrishnan M., Vanhoucke V. and Levine S. Scalable deep reinforcement learning for vision-based robotic manipulation. In *Proceedings of The 2nd Conference on Robot Learning*, pages 651–673, Zurich, Switzerland, 2018.

[22] Kim B., Farahmand A., Pineau J. and Precup D., Learning from limited demonstrations. In *Neural Information Processing Systems*, pages 9, Lake Tahoe, NV, USA, 2013.

[23] Krishnan S., Fox R., Stoica I. and Goldberg K. DDCO: discovery of deep continuous options for robot learning from demonstrations. In *Proceedings of the 1st Annual Conference on Robot Learning*, pages 418–437, Mountain View, CA, USA, 2017.

[24] Abu-Dakka F.J., Rozo L. and Caldwell D.G. Force-based variable impedance learning for robotic manipulation. *Robotics and Autonomous Systems*. 109:156–167, 2018.

[25] Calinon S., Guenter F. and Billard A., On learning the statistical representation of a task and generalizing it to various contexts. In *Proceedings of the 2006 IEEE International Conference on Robotics and Automation*, pages 2978–2983, Orlando, FL, USA, 2006.

[26] Li W. and Fritz M. Teaching robots the use of human tools from demonstration with non-dexterous end-effectors. In *Proceedings of the IEEE-RAS 15th International Conference on Humanoid Robots*, pages 547–553, Seoul, South Korea, 2015.

[27] Calandra R., Owens A., Upadhyaya M., Yuan W., Lin J., Adelson E.H. and Levine S. The feeling of success: does touch sensing help predict grasp outcomes? In *Proceedings of the 1st Annual Conference on Robot Learning*, pages 314–323, Mountain View, CA, USA, 2017.

[28] Edmonds M., Gao F., Xie X., Liu H., Qi S., Zhu Y., Rothrock B. and Zhu S.-C. Feeling the force: Integrating force and pose for fluent discovery through imitation learning to open medicine bottles. In *Proceedings of the 2017 IEEE/RSJ International Conference on Intelligent Robots and Systems*, pages 3530–3537, Vancouver, BC, Canada, 2017.

[29] Abu-Dakka F.J., Nemec B., Kramberger A., Buch A.G., Krüger N. and Ude A., Solving peg-in-hole tasks by human demonstration and exception strategies. *Industrial Robot: An International Journal*, 41(6):575–584, 2014.

[30] Peternel L., Petrič T. and Babič J. Robotic assembly solution by human-in-the-loop teaching method based on real-time stiffness modulation, *Autonomous Robots*, 42(1):1–17, 2018.

[31] Piot B., Geist M. and Pietquin O. Boosted bellman residual minimization handling expert demonstrations. In *Proceedings of the ECML PKDD 2014*, pages 549–564, Nancy, France, 2014.

[32] Ravichandar H., Salehi I. and Dani A. Learning partially contracting dynamical systems from demonstrations. In *Proceedings of the 1st Annual Conference on Robot Learning*, pages 369–378, Mountain View, CA, USA, 2017.

[33] Savarimuthu T.R., Buch A.G., Schlette C., Wantia N., Roßmann J., Martínez D., Alenyà G., Torras C., Ude A., Nemec B., Kramberger A., Wörgötter F., Aksoy E.E., Papon J., Haller S., Piater J. and Krüger N. Teaching a robot the semantics of assembly tasks. *IEEE Transactions on Systems, Man, and Cybernetics: Systems*. 48(5):670–692, 2018.

[34] Tanwani A.K. and Calinon S., Learning robot manipulation tasks with task-parameterized semitied hidden semi-markov model. *IEEE Robotics and Automation Letters*. 1(1):235–242, 2016.

[35] Wang G.-F., Fang Z. and Li P. Shaping in reinforcement learning by knowledge transferred from human-demonstrations of a simple similar task, *Journal of Intelligent & Fuzzy Systems*. 34(1):711–720, 2018.

[36] Liu, Y., Gupta A., Abbeel P. and Levine S. Imitation from observation: learning to imitate behaviors from raw video via context translation. In *Proceedings of the 2018 IEEE International Conference on Robotics and Automation*, pages 1118–1125, Brisbane, Australia, 2018.

[37] Shukla N., He Y., Chen F. and Zhu S.-C. Learning human utility from video demonstrations for deductive planning in robotics. In *Proceedings of the 1st Annual Conference on Robot Learning*, pages 448–457, Mountain View, CA, USA, 2017.

[38] Xie A., Singh A., Levine S. and Finn C. Few-shot goal inference for visuomotor learning and planning. In *Proceedings of The 2nd Conference on Robot Learning*, pages 40–52, Zurich, Switzerland, 2018.

[39] Sutton R.S. and Barto A.G. *Reinforcement learning: an introduction*, MIT Press, Cambridge, MA, 2018.

[40] Kaelbling L.P., Littman M.L. and Cassandra A.R. Planning and acting in partially observable stochastic domains. *Artificial Intelligence*. 101(1):99–134, 1998.

[41] Schulman J., Levine S., Abbeel P., Jordan M. and Moritz P. Trust region policy optimization. In *Proc. of International Conference on Machine Learning*, pages 1889–1897, Lille, France, 2015.

[42] Lillicrap T.P., Hunt J.J., Pritzel A., Heess N., Erez T., Tassa Y., Silver D. and Wierstra D. Continuous control with deep reinforcement learning. In *Proc. of the 4th International Conference on Learning Representations*, San Juan, Puerto Rico, 2016.

[43] Vincent P., Larochelle H., Bengio Y. and Manzagol P.-A. Extracting and composing robust features with denoising autoencoders. In *Proceedings of the International Conference on Machine Learning*, pages 1096–1103, Helsinki, Finland, 2008.

[44] Behzadan A. H., Iqbal A. and Kamat V. R. A collaborative augmented reality based modeling environment for construction engineering and management education. In *Proceedings of the Winter Simulation Conference (WSC)*, pages 3568-3576, Phoenix, AZ, USA, 2011.

[45] Akula M., Lipman R. R., Franaszek M., Saidi K. S. Cheok G. S. and Kamat V. R. Real-time drill monitoring and control using building information models augmented with 3D imaging data. *Automation in Construction*. 36: 1–15, 2013

Applying Augmented Reality Technique to Support On-site Rebar Inspection

H.W. Hsu[a], S.H. Hsieh[a]

[a]Department of Civil Engineering, National Taiwan University, Taipei, Taiwan
E-mail: r05521605@ntu.edu.tw, shhsieh@ntu.edu.tw

Abstract –

Rebar inspection plays an essential role during construction phases to assure the safety of the construction. Usually, inspectors use 2D drawings and tape measures to inspect rebars. However, the effectiveness of the inspection is greatly hindered by indirect three-dimensional information in 2D drawings and visual obstruction of measuring by rebars, especially when the structural elements become more complicated. To address these issues, this paper proposes an Augmented Reality (AR) approach to assist rebar inspection, which includes a framework of inspecting rebars with AR models. An experiment on stirrup inspection is conducted to evaluate the benefits of the AR approach by comparing with the traditional method. The result of the experiment indicates that the AR approach takes shorter time for inspection but with less precision.

Keywords –

Augmented Reality; Rebar inspection; On-site inspection

1 Introduction

The inspection work is one of the most important parts during construction phases. This process assures the quality of construction. In most construction projects, rebars account for a great part of the construction inspection among all the inspected elements. The efficiency of rebar inspection works is influenced by two main factors. The first one is indirect 3D information retrieval from 2D drawings. 2D drawings are still commonly used in most construction projects but do not present 3D information clearly, often leading to information missing. The other one is the measuring tool used for length measurement. Mostly, inspectors use tape measures to check whether the rebar is in accordance with the 2D drawings. However, the tape measures need to be aligned to the specific rebar, which is probably obstructed by other rebars.

Augmented Reality (AR), a technique which allows the user to superimpose virtual information on the real environment, has showed its potential to be applied in the field of architecture, engineering and construction industry [1]. Webster et al. pointed out that AR could be used to provide an inspection guide for inspectors without the use of drawings [2]. Therefore, AR becomes a promising solution to address the aforementioned issues and an AR-based rebar inspection approach was developed in this research to improve the efficiency of rebar inspection. A case study was conducted to evaluate the feasibility of the approach.

2 Literature Review

Many attempts have been made with the purpose of inspection based on AR. Chung et al. [3] conducted an experiment on thickness inspection of manufactured parts, using the instruction and sequences in forms of manual, computer-aided and AR-aided methods. The experiment was taken at fixed location to ensure the superimposition of AR information. The results showed that different forms of information did not affect the accuracy apparently; however, the completion time of AR-aided method was faster than others. Moreover, the augmented information was unaffected by the part shape complexity, proving the benefits of conveying information to inspectors. Shin and Dunston [4] developed an AR prototype system for steel column inspection, including the deviation of position and plumbness. For tracking the deviation of position, the users had to manually move and rotate the virtual model to match the real one and the system would report the value of deviation. Compared to the use of total stations, the AR approach showed time-saving advantage but lost a little precision. However, the system was said to be lab-based and not yet developed for on-site inspection applications. In 2017, Zhou et al. [5] applied marker-based AR techniques for the inspection of tunneling construction. Markers were used as the coordination of the virtual segment models during the inspection of the segment displacement. Similarly, the AR-based method took less time than the conventional measuring method and met the precision requirements. However, the number of the attached markers would be a problem in

practice.

Learning from some design of AR inspection methods in previous research [4-5], this research proposes a marker-less AR-based approach that uses model-based superimposition of the virtual and real objects for rebar inspection.

3 AR-based Rebar Inspection Framework

3.1 The Framework

This research proposes an AR-based rebar inspection framework for solving current on-site rebar inspection issues. It consists of three main modules: motion tracking module, inspection module, and interaction module, as illustrated in Figure 1.

First, we need to have the Building Information Modeling (BIM) models of the on-site structural elements constructed during the design phase. Then, these BIM models are transformed into AR models which retain necessary geometry and non-geometric information for specific inspection items of rebars. Second, inspectors use devices like a mobile phone equipped with video camera to capture the on-site scene and target rebar. To fix the virtual coordinates of rebars while the camera is moving, the motion tracking module, which uses the feature descriptor technique from Google ARCore, increases the precision of position and rotation calculated by the Inertial Measurement Unit (IMU) in devices [6]. This process includes the transformation of global coordinates, camera coordinates, screen coordinates, virtual coordinates, and virtual camera coordinates, which are mainly derived from the pose estimation technique [7]. Besides, ARCore offers the function of detecting real horizontal planes from the photo images. This function is used for anchoring the virtual rebar objects on the real ground plane and minimizing the inaccuracy caused by the IMU.

After that, the user is able to retrieve information from the models, adjusts its position, switches layers of objects, and annotates problems through the interaction module. Last, the inspection module allows the user to transform the target rebar model into a simplified form used for inspection. The forms are based on the type of rebar and the items that are going to be inspected. This process prevents the inspector from the visual obstacle of the whole virtual model, which supports the inspector to focus on one item to be checked. Because of the length limitation of this paper, only the inspection module will be discussed in detail with the case of stirrups in the next section.

3.2 Inspection Module

For proper use of the AR models in the inspection work, the inspection module transforms the rebar model into different forms based on the types of the structural elements and rebars. In this research, we consider four main types of structural elements in the inspection module: columns, beams, slabs, and walls. Columns and beams have columnar rebar combination in their structure; in contrast, walls and slabs have planar rebar combination. This research concludes the BIM model parameters for general rebar inspection of these four elements, as illustrated in Figure 2. Columns and beams consist of main bars, stirrups and tie bars. The parameters of the main bar are size, length, hook length, and splice length. Stirrups and tie bars have the same parameters that are size, spacing, and total number. As for walls and slabs, the rows of rebars have two directions, and each row has its parameters which are size, spacing, and total number.

Considering the complexity and size of the rebar model, this research adopted only some of these parameters for prototyping, as showed in Figure 2. This

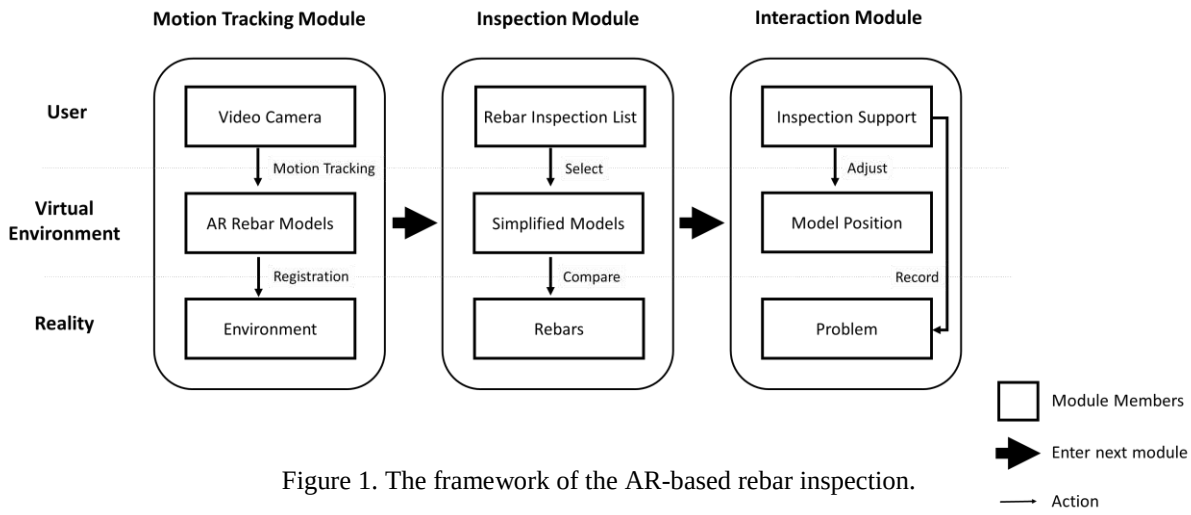

Figure 1. The framework of the AR-based rebar inspection.

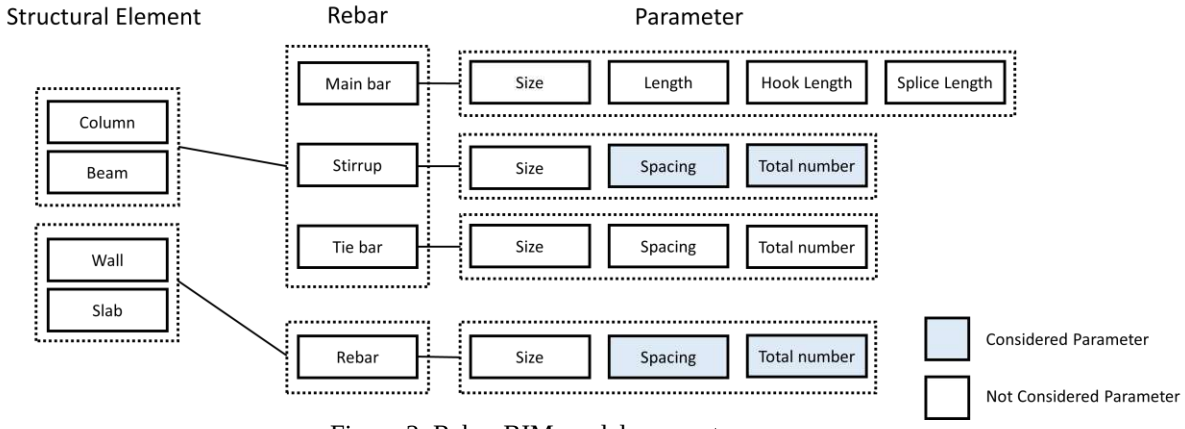

Figure 2. Rebar BIM model parameters.

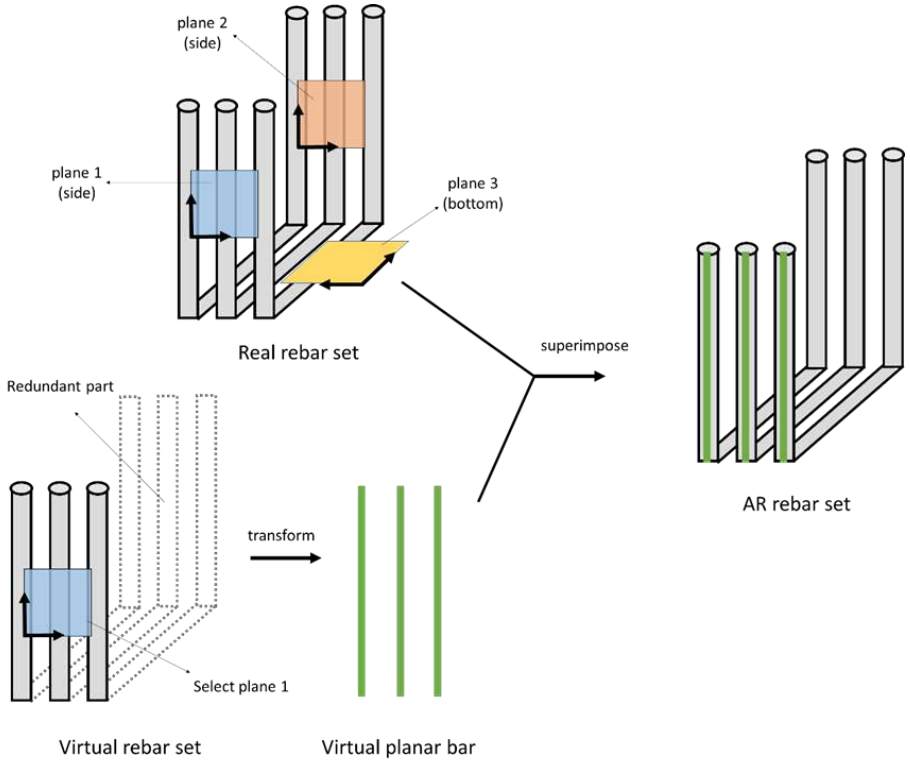

Figure 3. Spacing inspection for rebar sets.

form of AR model is called spacing check which is used for checking the spacing between the stirrups, rebars of walls and rebars of slabs. The size parameter was not used in the inspection on amount and spacing. Besides, this inspection can be implemented on each of the planes on rebar set as shown in Figure 3. Thus, this research transforms the original rebar into a planar bar on the plane facing the inspector. By doing this, the redundant part of the rebar model can be removed, remaining the planar bar representing the center line of the rebar.

When inspectors determine to check the spacing and amount of a specific rebar set, the first rebar in the rebar set will be used for duplication of the rest rebars in the form of planar bar objects. Each of the clones shifts a spacing distance along the same side plane of the rebar set. Through comparing the augmented planar bar with the real rebar, the inspector can check whether the real rebar is far from the correct position where the corresponding planar bar aligns or the rebar set has the wrong total number of rebars.

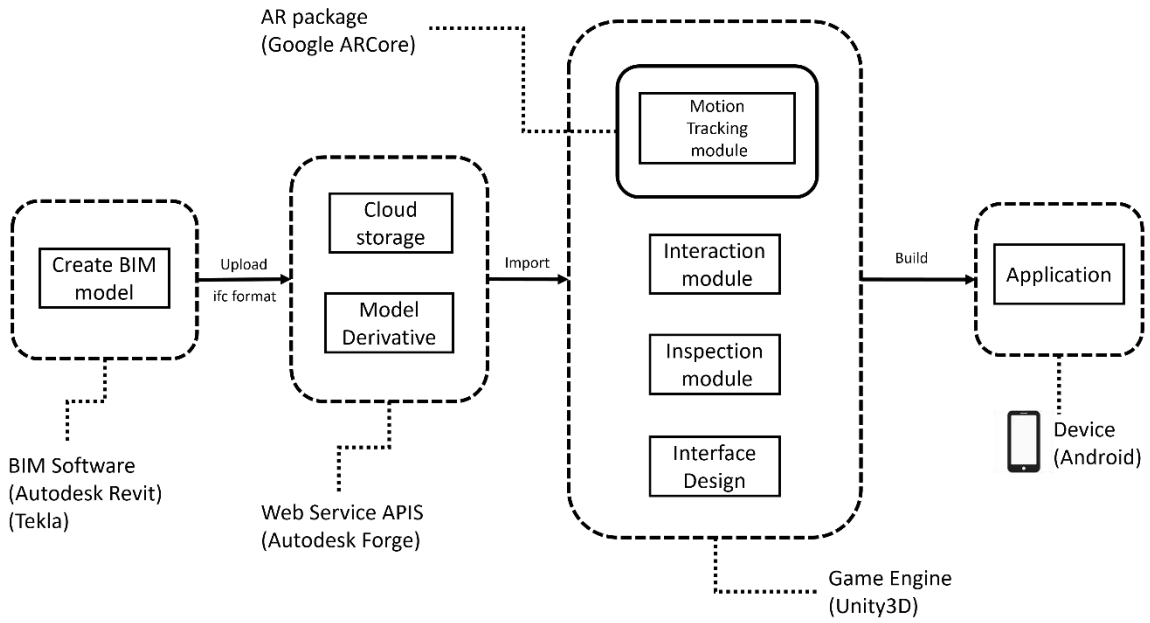

Figure 4. Application setup of the AR-based rebar inspection workflow.

4 Case Study

A case study was conducted to investigate the benefits of the proposed AR approach on stirrup inspection. The implementation of a prototype application system, the setup of experiments in the case study, and the results are discussed in this section.

4.1 Application Setup

To implement the AR rebar inspection framework, different software and packages have been adopted in this research. The process from input to output can be divided into four parts as illustrated in Figure 4. First, Autodesk Revit and Tekla are used as BIM model authoring software to create BIM models. Then, the models are exported to the format of Industry Foundation Classes (IFC) files because of the format's high interoperability. Second, the IFC files are uploaded to the cloud storage of Forge, which is a cloud-based developer tool from Autodesk Inc. Next, to import the model to the Unity 3D game engine, this research uses Forge AR/VR Toolkit to transform the BIM models into Unity 3D game objects that retain both the geometry and information from the original models. Third, this research uses C #, which is an object-oriented language based on the .NET framework, to program AR rebar inspection modules in Unity 3D. To build the AR environment, the Unity package from Google ARCore is adopted. Finally, the application is built on the device powered by the Android operating system.

4.2 Experiment Setup

To test the usability of the application prototype, this research adopted a precast beam as the target. The rebar model was created with Autodesk Revit according to its 2D drawings from the precast factory. In that process, the detail of the rebar model was simplified in order to decrease the data size. The finished model is showed in Figure 5.

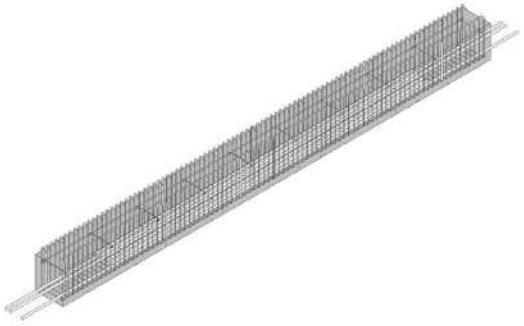

Figure 5. Test BIM model of a precast beam.

The total length of the precast beam is 9,190 mm, and the width by depth is 600 mm x 674 mm. The parts of the rebar tested with the inspection module are stirrups. The total number of the stirrups is 92, and its spacing is 100mm. The center-to-center distance can be expressed as (45 x 100 + 1 x 30 + 45 x 100). To match the model effectively, the origin point in the game engine is set to be in front of the beam section.

After the model was built, an experiment was conducted to evaluate the benefits of the AR approach. The subject was a civil engineer working in a precast factory and having good experiences in inspecting the rebars of precast structural elements. The task for the engineer was to inspect the total number and spacing of the stirrups using both the traditional manual method and the AR method with an Android phone. The inspection standards of both methods were judged by the inspector. The manual method for measuring stirrup spacing is to count the number within a section of one meter. Normally, inspectors sample two sections for inspection; on the contrary, the AR method inspects stirrups one by one. The picture of the stirrup is shown in Figure 6.

Figure 6. Stirrups of the precast beam.

4.3 Results and Discussions

The results of the experiment are shown in Figure 7, where t0 is the duration for the setup, t1 is the duration for the stirrup inspection, and sum is the total duration, which is the summation of t0 and t1.

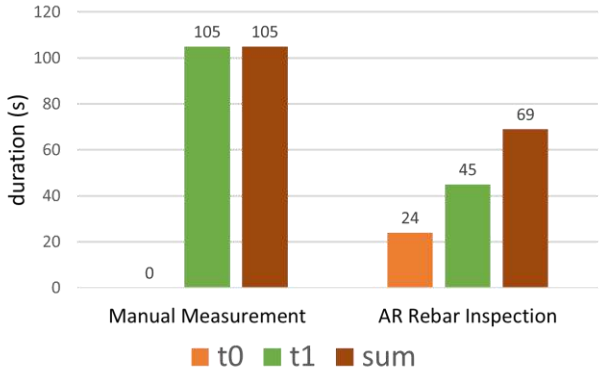

Figure 7. The duration of the manual measurement and AR rebar inspection in the experiment

At first, this research assumes that the setup time for manual measurement is zero because the tape measure and 2D drawings are handy for the inspectors. Thee setup duration for the AR approach is the time for matching the virtual model and the real rebar set. The snapshots of this process are shown in Figure 8. In this case, the inspector adjusts the model from each of the x, y, and z axis one by one to complete the matching task, which takes most of the time in this duration.

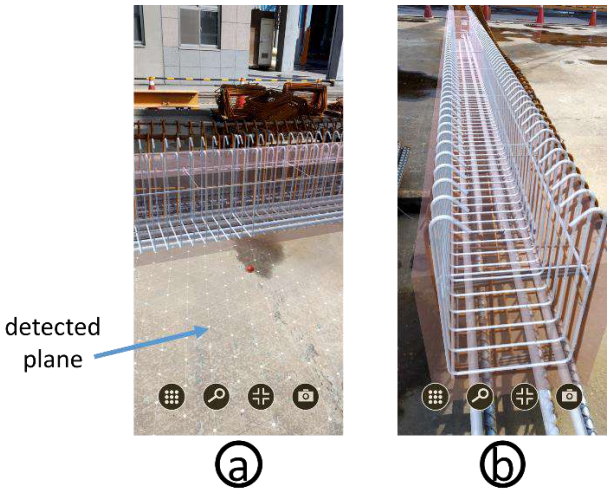

Figure 8. Snapshots of the AR-supported rebar inspection application in the setup duration. (a) Virtual rebar registration. (b) Position adjustment

As for t1, Figure 7 shows that the AR-supported spacing inspection for the stirrup takes much less time than the manual method. In the manual measurement method, the inspector counted the total number of stirrups, and then took two sections to inspect spacing, taking 65 seconds and 40 seconds, respectively. On the other hand, the AR method took almost half of the time to finish the inspection task because inspection on the number and spacing were carried out concurrently as showed in Figure 9. The correct amount of the stirrups can be easily checked. If the deviation between the real stirrups and the virtual planar bars becomes too big during the inspection, inspectors can easily infer that the total number of stirrups is not correct.

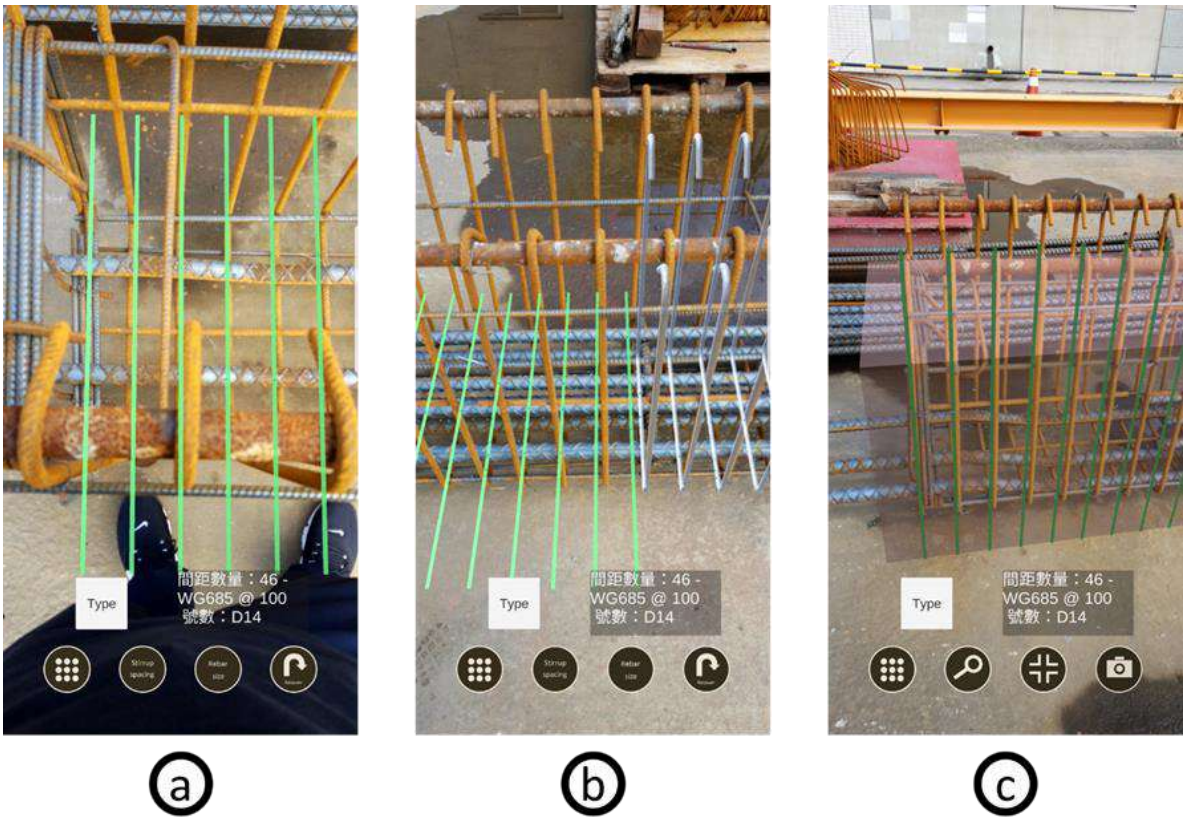

Figure 9. Snapshots of the AR-supported rebar inspection application in spacing inspection task. (a) On the left side of the stirrups, planar virtual bars are superimposed well on the bottom part of the stirrups. (b) In the middle of the stirrups, stirrups have a little deviation from the planar virtual bars. (c). The orientation of the planar virtual bars is changed to superimpose vertically on the front side of the stirrups

5 Conclusion

This research investigated an AR approach for assisting rebar inspection. The approach devised a framework that includes three main modules to facilitate the inspection task. A proof-of-concept experiment was conducted to validate the framework, especially the inspection module. The experimental results showed that the AR approach was 50% faster than the traditional approach in spacing inspection and with sufficient accuracy, proving the potential of using AR for rebar inspection.

However, it should be noted that some conditions have been controlled in the inspection test. For the tracking module, the quality of images captured from different environments may affect the accuracy of the tracking. In the experiment of stirrup inspection, the spacing is a constant, which cannot sufficiently prove the practicability of the inspection module in the AR approach. The user better faces right toward the side plane of the target stirrup so that the AR inspection would not be affected by viewing angles. Also, a proper distance from the target stirrup for the AR approach should be defined but needs further investigation.

There are still rooms for improvement on the proposed AR approach for rebar inspection. The experiment was conducted on a precast beam in a precast factory and the design of the inspection module has not considered all possible real circumstances in rebar inspection. For example, the structural elements in construction sites may be different from the tested one. Also, more inspection items like hooks can be considered in the future work.

References

[1] H. L. Chi, S. C. Kang, and X. Wang. Research trends and opportunities of augmented reality applications in architecture, engineering, and construction. *Automation in Construction*, 33:116–122, 2013.

[2] A. Webster, S. Feiner, B. Macintyre, W. Massie,

and T. Krueger. Augmented Reality in Architectural Construction, Inspection, and Renovation. *Proceedings of the Third ASCE Congress on Computing in Civil Engineering*, Anaheim, CA, USA, 1996

[3] K. H. Chung, J.P. Shewchuk, and R. C. Williges. An Application of Augmented Reality to Thickness Inspection. *Human Factors and Ergonomics in Manufacturing & Service Industries*, 9(4):331–342, 1999.

[4] D. H. Shin and P. S. Dunston. Evaluation of Augmented Reality in Steel Column Inspection. *Automation in Construction*, 18(2):118–129, 2009.

[5] Y. Zhou, H. B. Luo, Y. H. Yang. Implementation of Augmented Reality for Segment Displacement Inspection during Tunneling Construction. *Automation in Construction*, 82:112–121, 2017.

[6] Google ARCore Fundamental Concepts, https://developers.google.com/ar/discover/concepts, Accessed: 12/12/2018

[7] H. Kato and M. Billinghurst. Marker Tracking and HMD Calibration for a Video-Based Augmented Reality Conferencing System. *Proceedings of the 2nd IEEE and ACM International Workshop on Augmented Reality (IWAR'99)*, pages 85–94, San Francisco, CA, USA, 1999.

Developing a Workflow for Cloud-based Inspection of Temporary Structures in Construction

C. Liu[a], S. Shirowzhan[a], and S. M. E. Sepasgozar[a]

[a]Faculty of Built Environment, the University of New South Wales, Sydney 2052, Australia
E-mail: liuchang1126@outlook.com, samad.sepasgozar@gmail.com

Abstract –

Temporary structures are used during construction and removed after construction. It is necessary to inspect these structures in terms of quality and stability in an automated manner. However, the storage and sharing of inspection data of temporary structures is a problem because most of them have not been included in Building Information Modelling. A cloud-based platform provides a possibility to improve the workflow of data collection and sharing the real-time information with different stakeholders. Hence, to address these issues, this paper aims to develop a workflow to monitor the temporary objects and share them through a cloud accessible to multiple users for safety management.

There is a need to measure the structure heights especially scaffolds during construction. However, traditional inspection methods like tape measurement and recording 2D images on site are tedious practices and sometimes not possible. This paper applied advanced 3D, 360 and action cameras for data collection. Two case studies have been selected. The accuracy of measurement and performance of the proposed workflow were evaluated. First, the initial results of this ongoing study show that implementing the proposed workflow is highly efficient. Second, the comparison of the results with the current practice demonstrates that the workflow can be used for estimating area and quality of certain objects in medium sized buildings. Third, the initial field experimentations reflect that the accuracy of this method depends on the complexity of sites. In conclusion, the developed workflow provides a new opportunity to site engineers to record objects and share information with head offices for further processes and updating information models off site.

Keywords –

3D building modelling; Photo modelling; cloud-based construction data analysis; virtual inspection; Temporary structure; Safety management

1 Introduction

According to "Safe work Australia" report from 2014 to 2015, construction is the third highest industry in serious incidents with 12,575 serious claims [1]. Thus, safety monitoring should be the first priority in construction. As a part of safety monitoring, checking quality of temporary structures is indispensable. For example, construction fencing should be fixed in order to not hurt people in windy and rainy days. However, Engineers usually ignore quality inspection of temporary structures because they will be removed after construction. This may result in serious incidents. For instance, scaffolding has collapsed on the playground of a primary school in Cardiff and frightened children due to lack of safety monitoring [2]. Hence, temporary structures should be checked constantly to ensure the safety in construction [3].

Although 3D-based safety monitoring and quality inspection is applied in construction, it cannot be used for temporary structure in most cases. This is because 3D information of temporary structures is always lack and not included in 3D Building Information Modelling (BIM). Moreover, data collection and transmission is an important task in safety monitoring of temporary structures. Conventional visualization collection methods for data collection are 2D image collection and taking periodical notes in situ. It is usually time-consuming to give data from one partner to another with these methods, and data loss can easily happen if no effective data recording and management method is provided. Thus, it is necessary to provide a feasible and cost saving 3D-based approach for information transferring and inspection of temporary structures.

Cloud computing provides a possibility of automated storing and sharing data of temporary structure conveniently and quickly. It is a type of technology using communication devices such as tablets, laptops and mobile photos to transfer information [4]. Receivers can know the updated information immediately via cloud computing. Related research has been operated. For instance, Matthews, et al. [5]

proposed a new process of progress management based on cloud-based BIM platform for real-time monitoring of a reinforced concrete structure. In this method, the contractor's site engineers can report the process daily using iPad. The project planners and other industry partners can see this real-time progress based on cloud-based BIM in office. Zou, et al. [6] developed a cloud-based information and communication system for safety management in infrastructure. They wrote a web page to connect a Google Drive for data storage shared to all partners. Although these research projects can improve communication and collaboration of different partners of construction projects, few of these visualization methods record temporary structures.

Virtual Reality (VR) provides better understanding of space to clients and contractors which can enhance collaboration such as revising design together [7]. For example, Paes, et al. [7] improved understanding of architectural components by designing an 3D immersive environment, and testers preferred to understand information in VR compared with 2D drawings. Hence, this paper will add VR technology to enhance information understanding for individuals who have no access to real construction sites.

Several digital cameras are applied in construction and civil engineering. 3D, 360 and action cameras are three types of digital cameras. 3D camera provides depth of image, which can create 3D scenes via structure light with stereo sensing or time-of-light sensing [8]. Traditional stereo cameras have two or more lenses to obtain 3D images. Time-of-light cameras project electromagnetic or other wave and record the time from projection to sensor received the reflected wave. 360 camera, also known as omnidirectional camera, is the camera having a field of view that covers approximately the entire sphere. It can be used in building engineering [9] and help to build surveillance system in construction site [10]. Action camera is designed for recording action process with low-cost, portable and high-resolution features.

This paper aims to present a workflow of recording temporary objects using advanced cameras and share the data in a cloud accessible to multiple users. It intends to utilize and evaluate visualisation technologies and investigate their applications in construction. It first introduces background of inspection of temporary structures. Second, the workflow with related methods is presented. Thereafter, challenges and opportunities of technologies are discussed from a practical sense.

2 Methodology

This paper presents a novel workflow for temporary structure inspection including data collection by advanced cameras and process and storage on cloud to make it available for multiple users.

Using advanced cameras, the developed workflow was employed to assist in real time communication for safety management. The whole workflow includes four main steps shown in Figure 1. First, collecting data with advanced cameras. Second, creating 3D models and 2D pano images. Third, inspecting the temporary structures including measuring dimension and adding markers. Finally, displaying scenes in a cloud-based platform with VR headset. Details are introduced as follows.

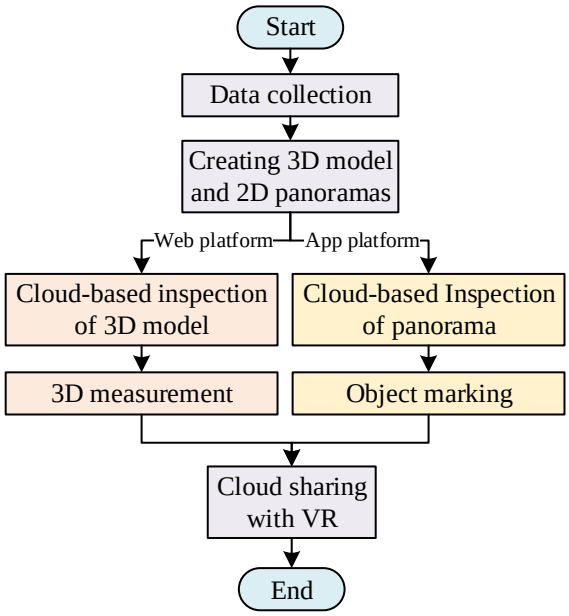

Figure 1. Developed workflow for the proposed experimentations.

2.1 Case Studies for Experimentation

The experimentation has been carried out in two places. The first place is Quadrangle Building construction site in the University of New South Wales (UNSW). Figure 2 (a) shows the plan view of the construction site from 3D model. The part in the red polygon is the construction site. Temporary objects in this scenario are mainly construction fences shown in Figure 2 (b).

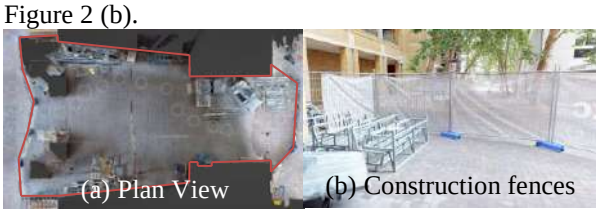

Figure 2. Quadrangle Building construction site.

The second place is a panel installation construction site with temporary objects such as unfinished panel installation shown in Figure 3 (b). The red rectangle in Figure 3 (a) is the location for data collection.

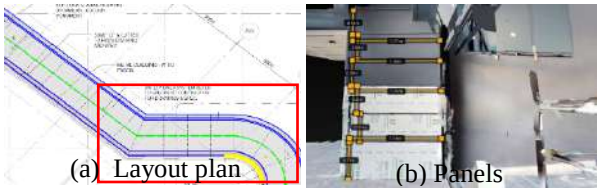

Figure 3. Panel construction site.

2.2 Data Acquisition Methods with Creating Models and Panorama

3D, 360 and GoPro cameras were used for image data collection. 2D camera is a traditional method for recording image data of temporary structures, which is considered as reference compared with other advanced cameras in this paper.

The first tool used for data collection is 3D camera. The structure light 3D camera in this paper can obtain panoramas with its self-contained App. It has an infrared light projector on the left side, an infrared light sensor on the right and an RGB camera in the middle. The projector and sensor create 3D models and the RGB camera creates the 2D panoramas. Thus, this paper uses it scan panoramas and collect 3D data of the site. A corresponding App of the camera is used for remote control. Data collection from 3D camera is shown in Figure 4.

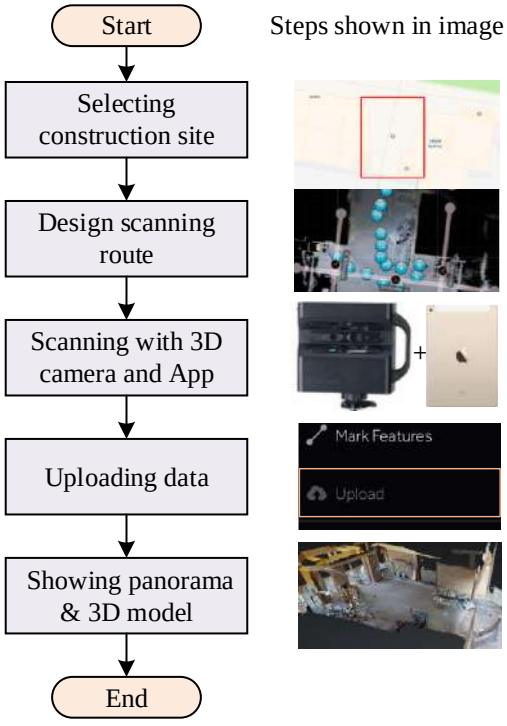

Figure 4. Steps of 3D camera data collection.

The second tool is a 360 camera shown in Figure 5. It is applied to record 2D panoramas of objects in construction site. It is small and portable with two fisheye lenses. The tripod under the lenses can help to fix the camera. Besides, a corresponding App in smart photo or tablet can aid to camera remote control. In order to compared with other cameras, the locations of 360 camera are the same as the locations of 3D camera. Thus, quality of pano images from 3D and 360 cameras can be compared, which helps site engineers to choose which device is more suitable for their construction projects. Data collection of 360 camera is quick and easy. Operators only need to tap the button for taking photos or recording videos on the device. If remote control is required, the corresponding App can be connected to the camera and operators can control the camera even a few meters away.

The third camera is a type of action camera, GoPro. GoPro has already been applied in civil engineering for displacement monitoring [11] and heritage reconstruction [12]. In this paper, GoPro is carried on with a headset by the authors to record the progress of the workflow from data collection to VR display. It is an advanced waterproof camera with wide angle lens shown in Figure 6. It is only around five hundred grams, so it is light enough to be carried on. Thus, it is widely used under the water, hiking and other sports. One of the most attractive functions is its anti-shake function, which is better than most traditional 2D cameras. This is the reason that this paper chooses GoPro to record videos other than ordinary 2D cameras.

Figure 5. 360 camera.

Figure 6. GoPro camera.

3D models will be created automatically by the 3D camera company after the collected data is uploaded by the operator. It could help to reduce modelling time. Besides, data of panoramas and 2D videos do not to be processed, so they can be shown directly in cloud-based platform. 3D models and panoramas can be seen in the website after automatically data process.

2.3 Inspection of structures

Two platforms for data from 3D and 360 cameras respectively are applied in this paper shown in Figure 1. One is an online website for inspection data from 3D camera. The other is an App for panoramas from 360 camera that can be used in tablet and smart phone. Section 2.3.1 introduces measurement based on 3D models operated on the website. Section 2.3.2 explains

how to inspect panorama in this App.

2.3.1 3D Model Measurement

Dimension measurement in construction is usually by tape measure or laser scanning. Tape measurement is easy but has limitations. For example, it cannot be used for measuring height of scaffoldings in tall buildings and it takes long time to measure of objects [13]. Besides, although laser scanning spends less time and has higher accuracy, the device is expensive and requires high professional operation to process the scanned data. Laser rangefinder is easy to measure and cheaper than laser scanner, but it is arduous and can only be worked in situ. It is also necessary to calibrate the laser rangefinder regularly, which takes workers time. Thus, this paper attempts to apply offsite 3D model measurement in construction. After obtaining 3D models from section 2.2, operators need to log on the website of the 3D camera company. Then, they can measure the distance from 3D models directly.

The measurement is compared with tape measure which is reference. The accuracy of the method is calculated by Relative Error and Root mean square deviation (RMSE) [14]. The equations are:

$$\text{Relative Error} = \frac{s_1 - s_2}{s_2} \quad (1)$$

$$\text{RMSE} = \sqrt{\frac{\sum_{t=1}^{T}(s_1 - s_2)^2}{T}} \quad (2)$$

T represents total times of measurement. s_1 means distance measured from 3D model. s_2 means distance from tape measurement. The results reflect the difference of measurement based on 3D model and tape. If the number is small, it means the difference is small. Thus, it could be judged that the method has a high accuracy.

2.3.2 Marking Objects

After taking photos by 360 camera, panoramas of temporary structures can be marked by every partner in the App. Thus, it is easy to communicate with each other using this App. Three main steps are included in adding markers. First, 360 photos should be imported into this App. Second, tapping the screen. The screen will show options including Talk+Draw, Markerup, Create Link, Comment and Insert Image. Users can choose what they need and even record their voice in this 360-view scene. After choosing an option, users can add their markers. Other users will see the changes and markers immediately if the data is revised by one user.

2.4 Panorama Shown in VR Headsets

The processed data from the two cloud-based platforms can both be shown in VR headset, which can provide visual experience to users. After logging in the platforms, the operator can choose certain accounts to access to data. Thus, engineers can share the space to multiple users and protect data that can only be seen by certain persons. It is convenient for site engineers recording temporary objects and checking construction conditions. It also provides an easy way for different offsite partners to realise and discuss danger and errors.

For the web platform for 3D camera data, VR experience can be achieved by clicking white circle button in the scene to move forward or backward. Users can see virtual scene as if they are in reality.

In order to show 3D spaces in VR headset, the user need to operate three steps after turning on the headset shown in Figure 7. The first step is logging in the website in VR headset. Next, selecting one of the scanned spaces and tapping VR button. Then, the left button in VR headset screen is the option that operators need to tap for this VR headset.

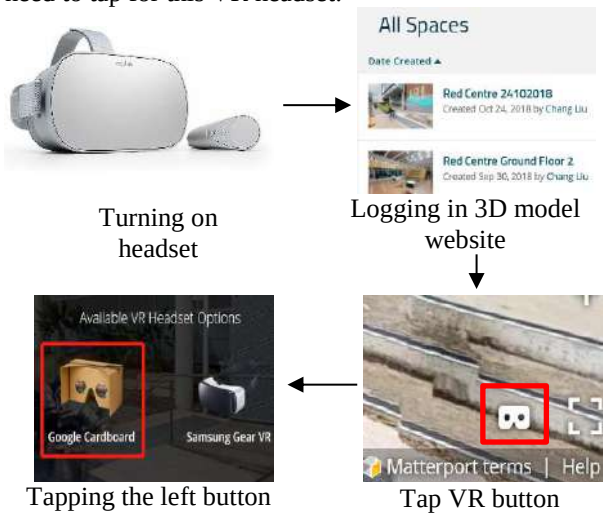

Turning on headset

Logging in 3D model website

Tapping the left button

Tap VR button

Figure 7. Showing 3D spaces with VR headset.

3 Results and Findings

3.1 Comparison of Results from Advanced Cameras and 2D Camera

The processed data results are listed in Table 1. 3D camera can create both 3D models, 2D images and 2D pano images. The quality of 2D images from 3D camera is the same as the quality of panoramas collected from 3D camera because the panoramas are merged from those 2D images. Besides, both 3D and 360 can create wider range 2D images than 2D camera. After comparing the data, the authors found that the quality of panoramas from 3D camera is the same as quality of images from 2D camera and is higher than panoramas from 360 camera, but data collection of 3D camera

spent more time than 360 camera.

Table 1. Results from different devices.

Device	Processed data	Measurement available	Marking available
3D camera	3D models, 2D images and panoramas	Yes	Yes
360 camera	Panoramas and videos	No	Yes
2D camera	2D images	No	Yes

Moreover, process recording videos from GoPro have deformation at edges shown in Figure 8. The left walls in Figure 8 (b) is not a straight line, while Figure 8 (a) can show straight line taken by the 3D camera. Besides, the recording area of GoPro is larger than 2D camera but smaller than 360 camera because it only has one fisheye lens and cannot show panoramas.

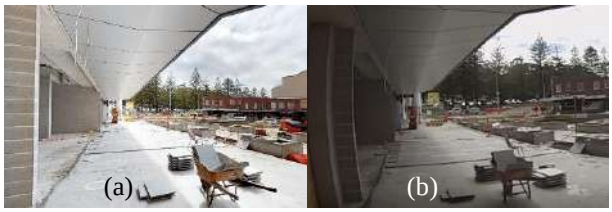

Figure 8. Images from 3D camera and GoPro; (a) 3D camera; (b) GoPro.

Based on results, it can be concluded that the accuracy of 3D models from 3D camera is enough for ordinary inspection of temporary structures. However, due to environment and device limitation, thin objects are hard to be scanned by 3D camera. That may be reason of accuracy of the first place is lower than that of the second. 360 camera is more convenient and portable than 3D camera.

As for video recording, 360 cameras can record the changes in all directions, which has the largest recording area, but the pixel of image in videos is not as high as 2D camera. The chosen 3D camera in this paper cannot record videos.

The authors in this paper created twenty-two models. The average data processing time of the models is less than one day. The time mainly depends on the area of the scanned place. The larger area needs more time.

As introduced in 2.2, after creating 3D models and 2D pano images from captured data, results can be shared in cloud-based platforms. In order to inspect 3D models, partners in a certain construction project should log in a web page designed by the 3D camera company to see the models directly. Besides, measured distance based on 3D models and panoramas collected by 3D camera can also be inspected on the webpage which is introduced in section 2.3.1. Th authors found that the change of the view from 3D model to 2D pano image can be operated easily by clicking different buttons.

Although panoramas from 3D camera can be seen from the aforementioned webpage, panoramas from 360 camera needs another platform to be observed. The platform is an App which can be downloaded both in smart phone and tablet. The App can show 2D images and panoramas but not 3D models. Since the App can show all construction site views from different directions, it is easy to help offsite engineers to inspect construction site situation. The authors in this paper imported the data from 360 camera and conventional 2D camera to the App to create over twenty spaces. The data was collected every week and showed that the construction process can be shown directly by the image recording. Partners can add markers easily based on the attempt by the authors which is introduced in section 2.3.2.

3.2 Inspection of Structures from Results

3.2.1 Comparison of 3D Model Measure and Tape Measure

The authors measured length and height of the fences based on 3D models of the first construction site and results are listed in Table 2. Table 3 lists results from wall panel construction site. Figure 3 (b) shows the measurement of panels based on 3D models. All the results measured based on 3D models are compared with the referenced tape measure results. The relative error and RMSE for analysing error are also listed. It needs to mention that relative error results keep three decimal and RMSE results keep one decimal in Table 2 and 3.

Table 2. Results from Quadrangle Building.

Width (cm)	Tape (cm)	Relative error	RMSE (cm)	Length (cm)	Tape (cm)	Relative error	RMSE (cm)
238	233	0.021		178	177	0.006	
231	233	0.009		181	177	0.023	
226	233	0.030	4.0	187	177	0.056	9.5
233	233	0.000		195	177	0.102	
232	233	0.004		180	177	0.017	

RMSE of width and length of fences shown in Table 2 are 4cm and 9.45cm respectively. The results showed that the accuracy of measurement from 3D models are enough if the requirement of accuracy is not very high. Thus, it could help engineers to decrease measurement time for height of floors even buildings.

Table 3. Results from wall panels.

Object	Place	Dimension (cm)	Tape (cm)	Relative error	RMSE (cm)
Width of Wall panel 1	Left side	59.0	58.0	0.017	0.9
		57.0	58.0	0.017	
		57.0	58.0	0.017	
		58.0	58.0	0.000	
		58.0	58.0	0.000	
		58.0	58.0	0.000	
		58.0	58.0	0.000	
		56.0	58.0	0.034	
	Right side	58.0	58.0	0.000	
		58.0	58.0	0.000	
		58.0	58.0	0.000	
		57.0	58.0	0.017	
		58.0	58.0	0.000	
		58.0	58.0	0.000	
		58.0	58.0	0.000	
		60.0	58.0	0.034	
		57.0	58.0	0.017	
Length of Wall panel 1	Right side	177.0	177.0	0.000	1.6
		177.0	177.0	0.000	
		176.0	177.0	0.006	
		174.0	177.0	0.017	
Length of Wall panel 2	Left side	75.0	77.5	0.032	1.5
		76.0	77.5	0.019	
	Right side	77.0	77.5	0.006	
		77.0	77.5	0.006	

The results in Table 3 show that relative error is low for the second construction site, and RMSE is even no more than two centimetres. Thus, It could be stated that the accuracy of measurement results from the second place are better than those from the first place. This may due to the shape of measured objects. As aforementioned, the 3D camera in this paper is hard to collect data of thin objects. Steel tubes and iron wires on the measured fences in the first place may not be captured by this 3D camera, so the loss of thin object data may influence the accuracy of measurement. The detected objects in the second place are panels whose data are easier to be captured, so their collected data are more accurately than data from Quadrangle Building.

Although there are other methods for fast and accurate measurement of distance such as a laser rangefinder, these methods suffer from the following problems. First, lack of demonstration of real time data to other partners off site in a construction project is a main problem. Second, they will be time consuming and labour intensive if construction workers miss measurement of an area. Third, the difficulty of measurement between two points in case of existence of an obstacle cannot resolved now. Fourth, inability to store data results in the users have to record them manually. Visualising the measured distances by these methods in a digital environment is either impossible or inaccurate with time consuming operations.

Compared with the conventional measuring method, the major advantages of our proposed workflow are to overcome all these problems through automatically storing and sharing accurate 3D data in a cloud-based real time platform.

As for updating indoor 3D models specially for as-built BIM models, measuring floor height is time consuming and labour intensive. This becomes more difficult when the floor height is high such as the height of floors in shopping centres. Our method in automatic measurement of indoor buildings would be of high importance to deal with the problems of lacking time and budget for updating the as-built 3D models. It could also help to increase safety because construction workers do not need to stand in a high space to measurement dimension and height. The third benefit is that it can help to save labour because traditional methods may spend one hour while this method spends only ten minutes for data collection of the same place. However, the limitation is that the data obtained from 3D camera is hard to build 3D models of small or thin objects like thin tubes. The measurement of them cannot be operated.

3.2.2 Marking Objects from 360 Camera Data

Our method is easy to check the progress of construction. Engineers can see how much work has been done via cloud-based 360 views. In order to simulate communication of different partners in a construction project, several markers are added in the cloud-based App as shown in Figure 9. The markers will only show up when fingers tap them, so they do not block items in a construction site panorama. Based on the time of adding markers, the authors find that operating this function in the platform is quick and convenient. Voices, notes and markers can all be shown in one 360 view scene from different accounts that have access to the platform. Thus, different partners can share information quickly with others in this project. It can help to adjust the design during construction and warn dangerous area in time for optimizing construction management with providing effective communication for partners.

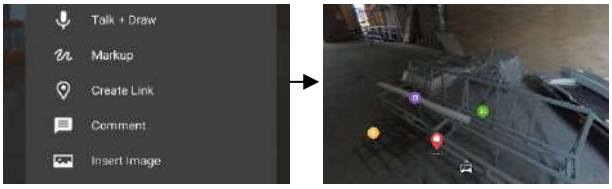

(a) Choosing one option (b) Adding markers

Figure 9. Markers in panorama.

3.3 Visualization

VR headset can access to data from both two cloud-based platforms, which helps to have a better understanding of construction environment. After processing all data, the authors invite testers to inspect VR scenes of the two places with VR headset. Based on the feedbacks from testers, VR scenes from both two places can help to understand information in construction site, which is better than 2D drawings. The quality of images in VR from both 3D and 360 cameras are high enough for inspection, while 3D camera images own higher pixels than 360 camera data. Engineers can inspect and discuss construction site situation in office shown in VR headset. Thus, they do not need to check the space in situ. What they need to do is only add markers, and then on-site construction workers can know the problems and dangers immediately shown in the cloud-based platform. One limitation is that some testers had headache or uncomfortableness of eyes if carrying on VR headset for a long time, so it is better to inspect not in a much long time.

Game engine is common for building 3D environment in VR. Operators can revise 3D models, add items and even add animation in game engine, which can provide a more vivid virtual environment than current cloud-based platform. This paper attempted to import 3D models into game engine to provide a virtual environment to multiple users in certain construction project. It can provide more options to revise models compared with cloud-based platforms, but it cannot share information in real time. In this paper, processed 3D models are imported in Blender, an open source game engine. Since the built 3D models can be downloaded in .obj format from cloud-based platform, Blender can read this format and show the models. However, after importing the data of the construction site, the model is shown without texture (see Figure 10 (a)). Figure 10 shows the comparison in different platforms. Based on it, it could be stated that 2D panorama has the highest pixel. Although Figure 10 (a) and (b) are from the same 3D model, Figure 10 (b) is clearer than Figure 10 (a). This may due to the .obj format has data loss besides texture loss.

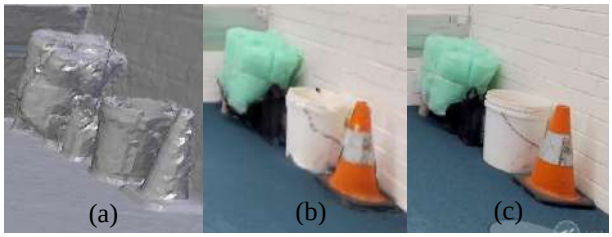

Figure 10. One scene in different platforms; (a) 3D model in Game engine; (b) the original 3D model in cloud-based platform; (c) Panorama.

4 Conclusion

This paper proposed a cloud-based recording and storing 3D data workflow of temporary structures for security purposes in construction. The novelty of the workflow is to provide a method of measuring and storing temporary structures data in a fast and safe way, because workers do not need to climb ladders or allocate a labour to observe and produce inspection reports in the construction site. The measurement results were evaluated based on computational error analysis methods relative error and RMSE. The results show that the accuracy of measurement is enough for inspection, so different partners can participate safety management off site in a cloud-based platform by inspecting information from construction site. Time latency would be eliminated, and efficiency of safety management can increase, because the time of transmitting data could decrease with the workflow.

Challenges and opportunities of temporary structure data sharing from advanced cameras for construction safety management have been identified with the several attempts in this paper. First, the cloud-based platforms in this paper can show 2D images, 2D pano images and 3D models. They provide more information than traditional safety management methods because traditional image methods only record ordinary 2D images. Based on the results of case studies, the accuracy of 3D model is enough for ordinary inspection. Thus, different partners can share information in real time. Second, in order to help engineers to measure dimensions off site, there is an attempt to inspect temporary structures based on 3D models and panoramas, which contains dimension measurement and marking addition. It needs to mention that the data that is hard to be obtained by tape measure such as height of a floor or the dimension of a wall can be measured in this workflow, so the workflow can save labour and time. Third, the workflow adds VR experience, which is few applied in safety management at the current stage. Based on the feedbacks from testers, VR can simulate the construction environment, so different partners can walk in VR environment by tapping the button to have a better standing of on-site situation and locations of construction objects in a construction project. It would be convenient to discuss and revise arrangement and method for construction. Although the workflow can realize cloud-based inspection without VR, the understanding would be as clear as the workflow with VR. Thus, VR is an important part in this workflow.

This study discussed significant potential benefits of the advanced cameras. However, the limitation of the study is that information of 3D models and panoramas are shared in two different cloud-based platforms. Besides, thin objects have not been shown in 3D models clearly because of the technological limitation of

devices. Future work should consider how to integrate information from all resources to be shown in only one platform. Selecting a type of advanced camera for inspection of thin objects is suggested Besides, adding animation and items in game engine for cloud-based publication could be a direction for future work. Moreover, there is another direction is that integrating 3D modelling with BIM to add temporary objects in BIM. It can help to provide more building information.

References

[1] Australia SW. Number of Serious Claims by Industry 2000–01 to 2014–15. Online: https://www.safeworkaustralia.gov.au/statistics-and-research/statistics/disease-and-injuries/dis ease-and-injury-statistics-industry

[2] CIOB. Firm Fined after Scaffolding Collapses onto Primary School. *Construction Manager*,2019. Online: http://www.constructionmanagermagazine.com/news/firm-fined-after-scaffolding-collapses-primary-sch/

[3] Liu X., Song Y., Yi W., Wang X., and Zhu, J. Comparing the Random Forest with the Generalized Additive Model to Evaluate the Impacts of Outdoor Ambient Environmental Factors on Scaffolding Construction Productivity. *Journal of Construction Engineering and Management*, 144 (6): 04018037, 2018.

[4] Wong J., Wang X., Li H., and Chan G. A Review of Cloud-based BIM Technology in the Construction Sector. *Journal of Information Technology in Construction*, 19: 281-291, 2014.

[5] Matthews J., Love P.E., Heinemann S., Chandler R., Rumsey C., and Olatunj O. Real time Progress Management: Re-engineering Processes for Cloud-based BIM in Construction. *Automation in Construction*, 58: 38-47, 2015.

[6] Zou P.X., Lun P., Cipolla D., and Mohamed S. Cloud-based Safety Information and Communication System in Infrastructure Construction. *Safety Science*, 98: 50-69, 2017.

[7] Paes D., Arantes E., and Irizarry J. Immersive Environment for Improving the Understanding of Architectural 3D Models: Comparing User Spatial Perception between Immersive and Traditional Virtual Reality Systems. *Automation in Construction*, 84: 292-303, 2017.

[8] Du H., Henry P., Ren X., Cheng M., Goldman D.B., Seitz S.M. and Fox D. RGB-D Mapping: Using Depth Cameras for Dense 3D Modeling of Indoor Environments. In *Proceedings of the 13th international conference on Ubiquitous computing*, Beijing, China, 2011.

[9] Felli F., Liu C., Ullah F., and Sepasgozar, S. M. Implementation of 360 Videos and Mobile Laser Measurement Technologies for Immersive Visualisation of Real Estate & Properties. In *Proceedings of the 42nd AUBEA Conference 2018: Educating Building Professionals for the Future in the Globalised World*, pages 294-304, Singapore, 2018.

[10] Yang X., Li H., Huang T., Zhai X., Wang F., and Wang C. Computer‐Aided Optimization of Surveillance Cameras Placement on Construction Sites. *Computer‐Aided Civil and Infrastructure Engineering*, 33: 1110-1126, 2018.

[11] Lydon D., Lydon M., Taylor S., Del Rincon J. M., Hester D., and Brownjohn J. Development and Field Testing of a Vision-based Displacement System using a Low Cost Wireless Action Camera, *Mechanical Systems and Signal Processing*, 121: 343-358, 2019.

[12] Fiorillo F., Limongiello M., and Fernández-Palacios B.J. Testing GoPro for 3D Model Reconstruction in Narrow Spaces. *Acta Imeko*, 5: 64-70, 2016.

[13] Lyu H.M., Shen S.L., Zhou A., and Yang J. Perspectives for Flood Risk Assessment and Management for Mega-City Metro System. *Tunnelling and Underground Space Technology*, 84: 31-44, 2019.

[14] Sepasgozar S.M., Forsythe P., and Shirowzhan S. Evaluation of Terrestrial and Mobile Scanner Technologies for Part-Built Information Modeling. *Journal of Construction Engineering and Management*, 144(12): 04018110, 2018.

Towards Rule-Based Model Checking of Building Information Models

C. Sydora[a] and E. Stroulia[a]

[a] Department of Computing Science, University of Alberta, Canada
E-mail: csydora@ualberta.ca, stroulia@ualberta.ca

Abstract –

Designing a building, so that it adheres to all the relevant applicable constraints imposed by construction codes to cultural preferences to the owners' styles and aesthetics, can be a daunting task, requiring many laborious hours of review and modification. Given the increasing adoption of Building Information Modeling (BIM) in the design process, automated model checking is a pragmatic approach to expeditiously identifying errors that may otherwise cause issues later in the building phase. A variety of methods have been proposed, but they are opaque regarding the rules they consider, and they do not allow users to edit these rules. In this paper, we describe a simple, yet extendible, language for specifying building rules and a method for evaluating these rules in the context of a BIM instance, in order to assess the compliance of the building with these rules.

Keywords –

Building Information Modeling (BIM); Design Constraints; Rule Checking

1 Introduction

Building Information Modeling (BIM) has become a key part of the design and management process for Architecture, Engineering, and Construction (AEC). It supports the 3D visualization and design of buildings, while also making explicit the non-geometric properties of, and relationships between, objects. While this is extremely useful and valuable information for the domain experts, it can be an overwhelming amount of data for bigger buildings with complex models. Each additional object in the model implies multiple new relationships between this new object and existing objects, which increase exponentially as the final model takes form. The process of designing buildings can be a complex and error-prone task, given the attention that needs to be paid to each design consideration. Mistakes can be made if a designer is not aware of the ramifications of their design choices and, unless identified early, they can lead to inefficiencies and potentially excessive additional costs in the future [1].

Checking a BIM model against a set of design rules has been a major topic in BIM research for over a decade, and yet no broadly available solutions exist to support rules from a variety of sources, such as governing agencies, handbooks, and builders. While some model-checking software systems exist, they either require that their users possess a strong software-programming knowledge to configure them with rules of interest, or they are black boxes, not configurable at all. Since it is unlikely that all stakeholders will ever be able to agree on a single immutable set of rules, applicable to all buildings, these products are fundamentally limiting the wider adoption of automated model-checking of buildings. Other attempts at automated model checking have taken the Natural Language Processing (NLP) approach, aiming at automatically transforming rules from human-readable specifications into programmatic executable code. While these methods have many benefits in terms of ease of use, there is usually far too much leniency in the written language, which makes it impossible to process automatically and accurately; as a result, these methods are fundamentally limited in their capacity to capture the requirements around compliance checking.

Our methodology is grounded in the intuition that there can be no effective "one-size-fits-all" approach to the problem [2]. In fact, we suggest that model checking be organized around different levels, appropriate for the level of programming expertise of the stakeholder checking the model. Moreover, all levels of experience should be able to work on a single open platform and use the Application Programmable Interface (API) that they feel most comfortable with. This is because there is a trade-off between the complexity of the rules, the expressiveness of the language used to specify them, and the ease of use. While some rules may require intricate functions that can be difficult to formulate, a substantial portion of rules can be described using simple logic and standard geometric relations.

In this paper, we describe a simple, easy to use, logic-based language for describing rules. Our language

is expressive enough to cover a wide array of rules, and we argue that, in principle, it can be extended to broaden its coverage.

The rest of this paper is organized as follows. We first outline some of the previous approaches in the related work in Section 2. Our methodology is described in Section 3. Section 4 contains discussion points on our methodological assumptions and how the language and rules fit in the larger picture. Concluding remarks are in Section 5.

2 Related Work

Solibri. When researching compliance-checking tools, Solibri Model Checker (SMC) [3] is frequently as one of the few tools specifically built for the purpose of checking BIM models. SMC takes as input a building model in form of the BIM industry standard of Industry Foundation Classes (IFC) [4]. While the available rulesets, initially from the Norwegian Statsbygg handbook [5], can be modified by the end user (by combining rule sets and deleting rules), there is limited support for editing rules in the form of changing the parameters (but not the form) of the provided rules. Additionally, there are a few rule templates that can be manipulated, however, full customization of rules can only be done through the SMC API, which is not open.

There are a number of research papers that report how different checks might be implemented using the available rule templates [6], [7], and [8]; however, these are black-box approaches and it is impossible to comment on their accuracy, efficiency, generality and expressiveness.

Country-Specific Implementations. Model-checking tools have been implemented for the purpose of evaluating requirements of governing bodies, with differing levels of success. Singapore's CORENET ePlanCheck has been noted as the most successful implementation, since, at one point, it was mandatory as part of the government's building requirement legislation [9]. In Australia, DesignCheck [10] was built on the Express Data Manager (EDM) Model Server but, to the best of the authors' knowledge, it has since lost support. The General Services Administration (GSA) in the United States mandates that their project models be checked with rules implemented within SMC [9].

BIM API. While not specifically model-checking tools, BIM editors, such as Autodesk Revit [11] and Graphisoft ArchiCAD [12], provide APIs (the former public while ArchiCAD's requires permission) that allow access to the model's internal structure and object database and therefore, can, in principle, be used for model checking. This requires a high level of programming knowledge even for the simplest checks. To address this challenge, some tools have been developed to perform the same functionality in a visual environment. These include tools such as Autodesk Dynamo [13], which works on the Revit platform, and Rhino Grasshopper [14]. These two tools are both graph-based visual editors that have some scripting available - Dynamo's scripting being in Python rather than C# as the Revit API.

BIMServer [15], an opensource IFC model repository platform, has a model-checking plugin, however, it requires direct coding in JavaScript. The scripts are then linked to the model for execution. This also requires programmatic coding knowledge and a strong understanding of the IFC vocabulary and syntax.

Semantic Web Ontologies. More recently, there has been a conceptual shift in model-checking approaches, given the emergence of semantic-web technologies. Specifically, newer methods have worked with extendable IFC based ontologies of the BIM model to query for design flaws. While this technology can be useful in extending the data schema, the query languages require a steeper learning curve. The basics of this approach are outlined in [16].

Natural Language Processing (NLP). As we mentioned in the introduction, attempts have been made to parse natural-language rules from design handbooks and regulation texts. While such approaches could potentially simplify the rule-creation process, many of the natural-language rules lack the clarity and unambiguity required to be directly parsed without any human intervention or interpretation.

One of the more commonly cited approaches in this vein is that of Hjelseth who used a four-sentence component classification to parse natural language rules, namely Requirement, Applicability, Selection, Exception (RASE) [17] [18]. Another use of NLP has been to identify information from rules that is missing or may need to be added to models [19].

Rule-Checking Languages. The Building Environment Rule and Analysis Language (BERA) [20] was developed as a domain-specific programming language for model checking. The concept is built on providing model-checking capabilities without the need for precise knowledge of general-purpose programming languages [21]. However, the language derives heavily from Java which may be difficult for non-programmers and it is built on the Solibri IFC engine, and therefore is still quite opaque.

Visual Programming Languages (VPL). Some approaches have taken the Rule Languages one step

Natural Language Rule:	**ModelCheck Language:**
Dishwasher must be a minimum of 21" from a corner.	∀ a = IfcDishwasher ϵ ModelObjects ∀ b = IfcCorner ϵ ModelObjects (Distance(a, b)>=21INCH)) True=>Pass; False => Error

Figure 1. An example of a design rule in natural language converted to our rule language. Note that in IFC, there is not type *IfcDishwasher* or *IfcCorner* and the Distance function is not explicitly defined as a relation property. These three elements exemplify the three proposed extensions of our language namely Virtual Objects (*IfcCorner*), implicit geometric object relations (Distance), and expansion of the BIM object type hierarchy (*IfcDishwasher*).

farther by adding a visual component to them, in the same sense that Dynamo is a visual language for Revit's API. This is intended to allow for more complex rules to be created without adding the need to code programming. Check-mate [22] first introduced this as a very simple puzzle-based interface that allowed connecting pieces that together would form a structured rule, however, the expressiveness of this language is limited. The Visual Code Checking Language (VCCL) took a node-based approach, calling it a "white-box" approach with the available nodes to be extendable as the project matures [23], although, to the best of our knowledge, geometric properties and relations cannot be expressed, unless precalculated as properties.

3 Methods

Our methodology for rule checking follows the four-stage process outlined by [9]: (i) Rule interpretation, (ii) Model preparation, (iii) Rule execution, and (iv) Reporting. The following subsections outline our approach to each stage.

3.1 Rule Interpretation

In our work, we have opted to work with a custom, structured rule language approach. As many rules are inherently logic-based and BIM can be viewed as a database for building properties and relationships, our language derives much of its structure from mathematical logical reasoning and database languages, such as Structured Query Language (SQL). As Niemeijer et al. [22] suggested, it is easy to see the similarity between a statement "*For every x in Real Numbers…*" in mathematics with "*For every Window…*" in building regulations. As BIM is a collection of 3D objects, their properties and the relationships among them, we define a model as a set of objects and a set of relationships. Therefore, similar to SQL, our rule language expresses queries on two sets or tables (the FROM element) and determining the result (the SELECT element) of a logical expression (the WHERE element). The exact implementation does not use a specific database query language; we simply use SQL to illustrate our rule language. Figure 1 describes one example of a how a rule can be interpreted from natural language to our proposed rule language.

3.2 Model Preparation

Data in IFC is structured in a highly complex manner as an objects' mesh representation can take the form of extruded solid, Boundary Representation (BREP), or their combinations. This implies that, before the rules can be evaluated, the BIM data must first be transformed into structural objects that support efficient geometric calculations. Similar to [24], our method parses the model into an internal object structure that includes a global triangulated mesh, a local triangulated mesh, and a global bounding box that contains the direction and dimensions of the object in 3D space; a mesh being a series of vertices grouped into sets of three forming triangular boundary faces. Every object with type nested under *IfcElement* is extracted and placed in the set of objects that can be checked.

Once all the IFC objects have been read, our method constructs and adds to the model several different types of Virtual Objects (VOs) which, we define as objects that represent complex, multi-object relationships. By this definition, some VO types are already included in the IFC vocabulary, such as *IfcSpace* and *IfcSite* for example, nested under *IfcSpatialElement*. We extend this list of possible VOs to include *IfcCorner*, as shown in Figure 1, which is the connection between *IfcWall* objects. VOs have geometric bounds and therefore are represented internally much like *IfcElements*. The major difference between the two is that VOs are created based on *IfcElements* and thus depend on them, whereas *IfcElements* have no strict dependence relations.

Properties of objects and object relations are the

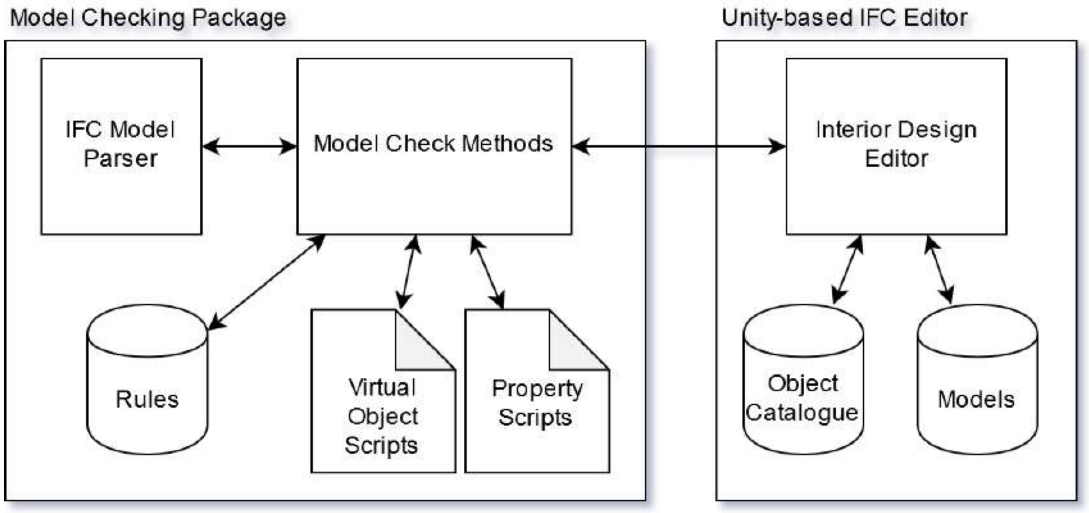

Figure 2. Current implementation of the IFC editor and model checking package.

underlying items being checked by the rules. However, these must be implicitly calculated from the model's geometric data. The geometric properties of objects, such as "Width" and "Height" for example, can be calculated directly on the object's mesh, while geometric-relation properties, such as "Distance" and "Overlap", must be derived from calculations between the two object meshes.

3.3 Rule Execution

All geometric properties and VOs are calculated on a need-to-know basis, thereby intertwining it with the model preparation. As an example, the distance between two objects of a certain type is not calculated unless it is necessary for a rule. Once calculated, it is cached, and can be reused as necessary, until the complete set of rules has been evaluated and the building model-checking is complete.

An interesting challenge is how to archive the computations performed, i.e., the VOs and the relations among objects, in support of the complete model-checking process. In principle, there are two choices: (a) they may be saved with the building model itself, or (b) they may be saved in a separate data structure but with references to the building model.

Should the VOs and properties be saved to the model, it would be necessary to develop a management process to remove the results of individual rule evaluations as the objects to which the rules apply are modified. For instance, if the "Distance" relation property was calculated but the dishwasher has been moved in the new model version, then the original "Distance" property should be removed and recalculated if required.

If the building model editor is capable of flagging the objects that have been modified since the last model check, the model check could recalculate the VOs and properties that depend on those modified objects. This would theoretically expediate the subsequent model checks.

The safer, more conservative, choice is to assume the building model has not been checked previously and that all VOs and properties must be newly calculated and, if existing, then overwritten by the new values. This is the current practice in our prototype, however, we are currently investigating the most efficient way to save and flag changes in our editor.

3.4 Reporting

Finally, all results need to be relayed back to the end user or application. This is returned in the form of an object set, along with the rules that have been evaluated relevant to those objects, and the result of the rule evaluation. While returning all results is important, the reports may also be narrowed down to only the failed rule instances. This allows the client application to parse the result information, graphically display the objects that failed the rule, and display the rule information including the error level of the rule.

4 Discussion

As validation for the proposed research, we have created a prototype model-checking .NET library, as seen in Figure 2.

The library is used by an in-house Unity-based IFC editor of building interiors that is currently capable of

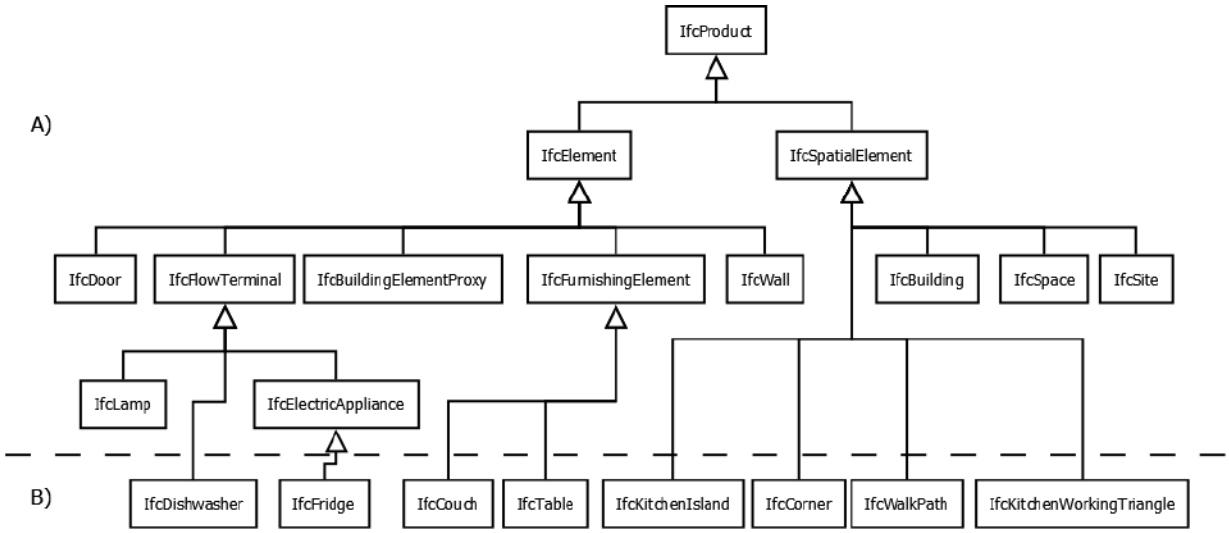

Figure 3. A) IFC object types above the dashed line represent a subset of the current IFC4 schema. B) IFC object types under the dashed line indicate sample extensions to the IFC hierarchy; those under *IfcSpatialElement* representing VOs that would be created implicitly from the existing model *IfcElements*.

reading an IFC file, displaying the model in 3D, and enabling a user to review an object catalogue and add *IfcSystemFurnitureElements* to the IFC model.

The underlying IFC model can be passed to the model-checking method, which is currently configured with an initial rule set, provided by our industrial partner. The rules in this initial set were specified in our language, and subsequently implemented into source code used by the model-checking module. The implementation process is currently manual, but we have developed a library of basic functionalities for computation of VOs and numerous geometric functions (i.e., for calculating object height and width, and distance between objects) and we are currently working on a model-driven method for automatically transforming rules into source code relying on this library.

After execution, the model-checking method returns the results for each of the rules. A rule result includes a pass/fail boolean as well as each instance of the set of objects that were checked against for the particular rule and the result of that instance.

For example, for the rule in Figure 1, an object set instance would be *dishwasher1* and *corner1*, which would have an instance result of pass/fail. The rule result is the collective result of the ANY/ALL/NONE of each object instance and their corresponding instance results. The IFC editor is therefore able to highlight the instances where an object fails a particular rule. The VO meshes are also accessible and can optionally be displayed in the IFC editor.

Since the majority of these rules deal with furnishings and appliances, there is an additional stage in the model preparation that is required but not yet implemented. In addition to restructuring the object representations into our mesh objects, we also believe the object type hierarchy within the IFC schema needs to be extended. Furniture and appliance items typically fall somewhere within either *IfcFurnishingElement*, *IfcFlowTerminal*, or *IfcBuildingElementProxy*, with each of these being the leaf or the second lowest level of the hierarchical tree. While it is possible to add a property to each object that states explicitly the object type (as in the current implementation), we believe more specific IFC types, such as *IfcCouch*, *IfcFridge*, etc. are required. Additionally, this hierarchy should be extendable such that new types defined later should be included. Figure 3 demonstrates a subset of the IFC4 [25] schema with examples of additional object types.

For the purpose of this study, we used the object name to determine automatically whether an object can be categorized, however, the onus is on a more intelligent BIM editor to infer the most specific type of the object, beyond *IfcElement*. It is also imperative that objects do not fall under multiple categories or are compositions of multiple other objects. For instance, difficulties can arise when a collection of objects, such as multiple chairs surrounding a table, are modeled as a single object. Therefore, good modeling practices should be adhered to the largest extent possible.

Other issues encountered included the direction of the objects not always being standardized in IFC, or at least by the BIM editors that export the models. Therefore, relationship properties such as behind and in

front of, which appear frequently in our rules, would occasionally return erroneous values. We see this as an error in the object design, since from an end user viewing the model, this error would not be visually apparent.

Finally, while we acknowledge there are many possible design rules and that they often come in the form of large, text-based documents, we believe that future iterations of these rule documents should be made in tandem with the rule language rules. This would both ensure that text-based rules can in fact be quantified and calculated and that automated rule check results are as the rule creator intended. The use of NLP may help expediate this process but our belief is the onus should be on the rule creator to interpret and test rules as they produce them.

5 Conclusion

In this paper, we have provided a brief introduction to our rule-specification language and a model-checking method able to evaluate rules in this language on IFC building models. Our work aims to connect many concepts put forward in previous model-checking approaches. Several building model-checking approaches exist, each with its own advantages and shortcomings. We therefore believe that providing an extensible framework to enable different rule sets to be expressed and evaluated against different BIM objects should each be supported. Each rule, regardless of method used for its specification (logical, mathematical expressions, or SQL operations on data), should be executable in the same process such that future applications can take advantage of model checking. For instance, we believe model checking can be a useful integration into generative design, which for runtime optimization would require rules sequences to be reprioritized. This will be created in latter iterations of the project and will be implemented as part of the grander scheme of a BIM service framework.

6 Acknowledgements

This work was supported by an NSERC CRD grant entitled “Development of cloud-based collaborative BIM modelling software”.

7 References

[1] Lopez, R., and Love, P. E. Design error costs in construction projects. *Journal of construction engineering and management*, 138(5):585-593, 2011.

[2] Solihin, W., and Eastman, C. Classification of rules for automated BIM rule checking development. *Automation in Construction*, 53:69-82, 2015.

[3] Solibri. Online: https://www.solibri.com/ Accessed: 30/01/2019.

[4] BuildingSMART. Online: https://www.buildingsmart.org/ Accessed: 30/01/2019.

[5] Statsbygg BIM Manual, Version 1.2.1(SBM1.2.1). Online: https://www.statsbygg.no/files/publikasjoner/manualer/StatsbyggBIM-manual-ver1-2-1eng-2013-12-17.pdf Accessed: 30/01/2019.

[6] Jiang, L., and Leicht, R. M. Automated rule-based constructability checking: Case study of formwork. *Journal of Management in Engineering*, 31(1):A4014004, 2014.

[7] Lee, Y. C., Eastman, C. M., and Lee, J. K. Automated Rule-Based Checking for the Validation of Accessibility and Visibility of a Building Information Model. In *Computing in Civil Engineering 2015*, pages 572-579, 2015.

[8] Getuli, V., Ventura, S. M., Capone, P., and Ciribini, A. L. BIM-based code checking for construction health and safety. *Procedia Engineering*, 196:454-461, 2017.

[9] Eastman, C., Lee, J. M., Jeong, Y. S., and Lee, J. K. Automatic rule-based checking of building designs. *Automation in Construction*, 18(8):1011-1033, 2009.

[10] Ding, L., Drogemuller, R., Rosenman, M., Marchant, D., and Gero, J. Automating code checking for building designs-DesignCheck. *Clients Driving Construction Innovation: Moving Ideas to Practice. CRC for Construction Innovation*, pages 1-16, 2006.

[11] Revit. Online: https://www.autodesk.com/products/revit/overview# Accessed: 30/01/2019.

[12] ArchiCAD. Online: https://www.graphisoft.com/archicad/? Accessed: 30/01/2019.

[13] Dynamo. Online: https://www.autodesk.com/products/dynamo-studio/overview Accessed: 30/01/2019.

[14] Grasshopper. Online: https://www.grasshopper3d.com/ Accessed: 30/01/2019.

[15] BIMServer. Online: http://bimserver.org/ Accessed: 30/01/2019.

[16] Pauwels, P., and Zhang, S. Semantic rule-checking for regulation compliance checking: An overview of strategies and approaches. In *32rd international CIB W78 conference*, pages 619-628, Eindhoven, Netherlands, 2015.

[17] Hjelseth, E., and Nisbet, N. Capturing normative

constraints by use of the semantic mark-up RASE methodology. In *Proceedings of CIB W78-W102 Conference*, pages 1-10, 2011.

[18] Hjelseth, E. Converting performance based regulations into computable rules in BIM based model checking software. *eWork and eBusiness in Architecture, Engineering and Construction: ECPPM*, pages 461-469, 2012.

[19] Zhang, J., and El-Gohary, N. M. Extending building information models semiautomatically using semantic natural language processing techniques. *Journal of Computing in Civil Engineering*, 30(5):C4016004, 2016.

[20] Lee, J. K. Building environment rule and analysis (BERA) language and its application for evaluating building circulation and spatial. *PhD diss., Georgia Institute of Technology*, 2011.

[21] Lee, J. K., Eastman, C. M., and Lee, Y. C. Implementation of a BIM domain-specific language for the building environment rule and analysis. *Journal of Intelligent & Robotic Systems*, 79(3-4):507-522, 2015.

[22] Niemeijer, R. A., De Vriès, B., and Beetz, J. Check-mate: automatic constraint checking of IFC models. *Managing IT in construction/managing construction for tomorrow*, pages 479-486, 2009.

[23] Preidel, C., and Borrmann, A. Automated code compliance checking based on a visual language and building information modeling. In *Proceedings of the International Symposium on Automation and Robotics in Construction (ISARC)*, Oulu, Finland, 2015.

[24] Solihin, W., Dimyadi, J., Lee, Y. C., Eastman, C., and Amor, R. The Critical Role of the Accessible Data for BIM Based Automated Rule Checking System. In *LC3 2017: Proceedings of the Joint Conference on Computing in Construction (JC3)*, pages 53-60, Heraklion, Greece, 2017.

[25] Industry Foundation Classes Release 4 (IFC4) Documentation. Online: http://www.buildingsmart-tech.org/ifc/IFC4/final/html/ Accessed: 30/01/2019.

Smart Construction Monitoring for Disaster Prevention Based on Spatial Information and GNSS/USN/IoT

S. Yeon[a], C. Yeon[a]

[a]Semyung University, South Korea

Abstract –
The monitoring technique by combination of the measurement method with the fine precision of the sensor collecting the satellite-based information that can determine the displacement space, is available to a variety of diagnostic information. The measurement method by a GNSS with the sensors is being requested. The progress of natural disasters by various environmental factors and the surroundings is occasionally caused. Such attempts are carried out nationally by distributed torsional displacement of the terrain and facilities. The various sensors and instruments track to diagnose this spatial information. Such information contains the precise displacement of the main facilities and the first reference point in the Geospatial or more three-dimensional available map and location information using the installed sensors or the like bridges and tunnels produced by a USN/IoT change at any time. Each sensor installed on the facility is to collect and integrate the precise positioning and environmental factors. In other words, Combining of the various positioning analysis of mm-class for the facility of main area observed is to be required constantly in real time information of the USN/IoT environment sensors and to be able to utilize such information as a precisely fine positioning information for the precisely fine displacement of the semi-permanent main facilities. It's to be one of the efficient information management. In this study, for the installation of the receiving system, relatively easy access is available to the USN/IoT base line positioning for the target bridges. Transmitting hourly from the received data is also executed in real time using the wireless Wi-Fi/Bluetooth bridges and related facilities to automatically process a fine position displacement. The results obtained from a method can be analyzed by real-time monitoring for a large structure or facilities to disaster prevention.

Keywords –
GNSS, USN, IoT, Construction Disaster Monitoring, Spatial Information

1. Background

It is gradually increasing exposure to the risks to the deformation of the structure aging facilities and increasing natural disasters and unpredictable global warming is a quote that greatly increased the demand for diverse emergency management system to prepare for this in advance. Nationwide construction of bridges and dams, very high buildings, factories, etc. into aging of the various structures are those widely distributed it is happening largely a problem of the collapse and demolition level each year and requires a rational management technique to solve them. While such solutions are increased significantly in recent years various disasters dam, reservoir, pre-diagnosis and safe repair for several facilities and maintenance work on the embankment and has been actively conducted. Nationwide 50-year-old reservoir and the situation that primarily carry out maintenance and ground reinforcement for some areas judged dangerous by the structural diagnosis of the levee, or not monitoring for understanding the ongoing changes and the displacement statement of the situation to be done.

Using a variety of test and measurement equipment in order to check the ongoing security situation, the related building facilities in real-time of 24-hour data acquisition in less mm, combined with the USN/IoT environment factors to be sent through the wireless network. As a

result, the obtained data in real-time by diagnosing the conditions of the various irrigation risk reinforcement for the main structure of the facility is expected for repairs and disaster prevention measures and for support to be capable of preventing and prevention of various disasters and accidents in advance. It can be applied to new emergency management techniques demonstrated.

2. Research Contents and Methods

This study sets up a system to select a three-point displacement of the existing bridge. A GNSS goes into the access and acquisition to the target desired. In case of Bangwha Bridge (1000m) in han-river that station is opened in a few years ago, the real-time receiving from the wireless transmission of data is possible for repair of dams and bridges to the related facilities by the fine displacement measurement and analysis process. The obtained GPS data relays information and data transmitted wirelessly about a geospatial information infrastructure irrigation (dams, reservoirs, embankments) the fine-motion and displacement in the 24-hour real-time on those as well most of them will measure the displacement behavior of the corresponding repair facility during a certain period and do not always identified as dangerous situation. In this study, the corresponding facilities receive GNSS satellite signals that can observe the whole region in real time, and the displacement and behavior characteristics of the structure.

Measurement of the occurrence to sudden displacement as well as a fine long-term trends is both enable to the continuous measurement and the web-based service that you can check where you want it. Also, to minimize the measurement error due to weather conditions and poor GNSS environmental factors, you can take the reinforcement work, safety measures, etc. against the preventive measures due to the long-term trend analysis of measurement results and measuring the abrupt behavior of displacement. For example, the pre-set emergency and alert set up are possible.

But the GNSS method has a disadvantage in that it can only track the displacement of a precise base line over a long period of time. Therefore, the measuring method with an accelerometer is still preferred. Recently, with the development of smart sensor technology, a small mote is applicable and is able to be installed in a place where environmental factors such as changes of temperature, humidity, vibration, illuminance, fine dust, carbon monoxide, nitrogen and wind intensity etc. are desired. In other words, while tracking the fine positional displacement due to GNSS, it is possible to simultaneously monitor by the USN / IoT sensors collecting the changes of the related values at the same time and analyzing how the constructed facilities can be displaced and collapsed from external natural factors and disasters (Fig.2).

Figure 1. GNSS measurement at the bridge using VRS in Korea

Figure 2. GNSS results after processing

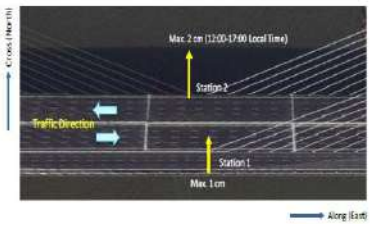

Figure 3. GNSS baseline confirm and 3D axis monitoring

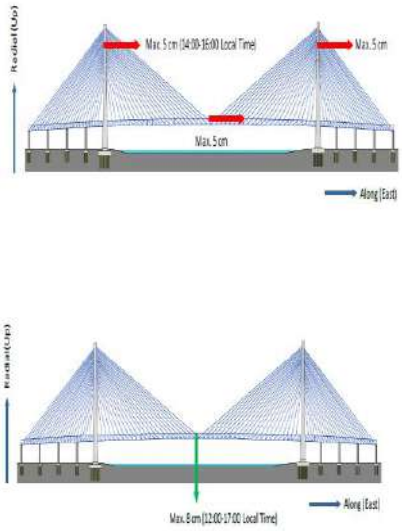

Figure 4. Test diagram at the bridge design sites

In case of bridges, there may be some variation depending on the measurement day and time. However, in case of the east and the west (X) and the north and the south (Y), traffic volume, traffic direction, wind strength, temperature and humidity, it can be seen that the repetitive displacements are continuing and the repetitive displacements occur in the vertical direction as well (Fig.4).

3. Construction Site Measurement

Type of slopes and the displacement of existing structures to install the GPS device and the receiver on the main point are suspected. The neighborhoods of the ground to install on a safe place for reference stations to the exact point by correcting the position information over the other party are received at various points (Stations) for continuously collecting the position information. The old structure continuously observed at least for three months in a year in order to make a fine displacement. The behavior of bridge structures are treated by tracking the displacement. Thus, in this study the relatively easy access to Cheongpung Bridge of Jecheon to install a GPS subject to the GNSS and the related data is transmitted using the wireless Wi-Fi in real time and the received data to the research laboratories hourly. The results from the corresponding Bridges to process fine positional displacement in real time are monitored and analyzed. The related GPS data is measured by calculating in a manner as to post-treatment such as by incomplete installation of the wireless Wi-Fi. Tracking the vibration changes in this case is tried on a valley river near Jecheon of selecting the iron bridge piers after two years of the demolition plan of Chuo-ku railroad track that run for decades over when there are no traffic of trains and the measurement of vibration by a sensor based on the IoT to diagnose conditions was performed for the test (Fig.6).

USN sensor and IoT sensor board are fabricated to collect the environmental factors such as temperature, humidity, roughness, carbon dioxide and nitrogen in the vibration displacement of railroad bridge over 50 years. The observation points for the real-time measurement are located with a wireless communication router. In addition, the environmental condition of the main facilities such as general roads and railways can be known so that they can be used in a fused manner. However, in the case of the expressway, a survey vehicle is applied for real time checking and the video imaging in the location information with various sensors.

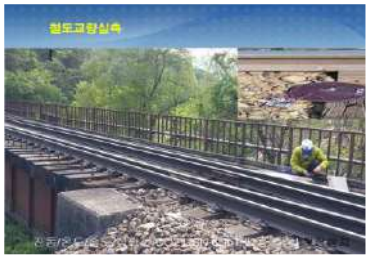

Figure 5. Measurement devices for inspection of road condition on the express way

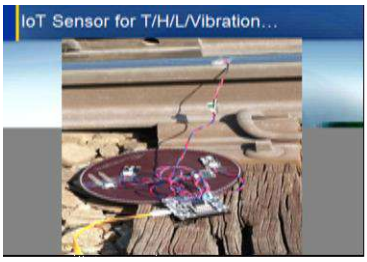

Figure 6. Measurement results from IoT on the railway bridge point

4. Results

Development and application of advanced technology that can monitor the precise displacement and the behavior of the terrain and structures with GPS and GNSS approach is one of a research fields that has a lot of attentions at nations, so its utilization is very extensive national government agencies and the academic practicality to receive much attention from research is a high technology research. Therefore, it provides the proposal studies to the Korea Research Foundation and of the disaster prevention research and support for national projects in this study. In addition, the practical application technology plan, precise safety diagnostics and prevention of observations are expected to be utilized in the corresponding areas that require a multidisciplinary.

As a result of attempting automatic matching of information that can be delivered in real time to environment sensor on the basis of digital information of object internet and remote sensing image, it is found that temperature, humidity, It is possible to integrate practical application technologies by collecting and analyzing the illuminance, carbon dioxide, nitrogen, moisture ratio, noise vibration, etc. simultaneously in real time using the wireless IoT / USN sensors.

In the near future, it is expected to be used in various fields requiring safety diagnosis and disaster prevention of medium to large-sized structures requiring precise displacement observation.

For the construction safety and disaster prevention, it is necessary to monitor the continuous state displacement by the smart sensor in addition to the periodical diagnosis of the construction structure. In recent years, the lifetime of the construction material may be changed due to the increase of environmental pollutants. It would be desirable to use a smart sensor appropriately. As we confirmed by applying in this study, it will be possible and necessary to collect desired data in real time by combining satellite sensors and various environmental sensors rather than past survey tools and methods.

5. References

[1] Bond, Dannetsch, Fleteur, “An Evaluation of Shape Accel Array(SAA) for performance of Dam Monitoring”, Canadian Geotechical Conference Conpedndiuml 2006.

[2] Boulis, C. C. Han, and M.B. Srivastava, “Design and Implementation of a Framework for Programmable and Efficient Sensor Networks”, In The First International Conference on Mobile Systems, Applications and Services (MobiSys), San Francisco, CA, 2003.

[3] USN System Using Zigbe X, Hanbaek Tech. Lab., ISBN 978-89- 90758-12-5, 2012.

[4] Sang-ho Yeon, “Development for Precision Positioning and Fine Displacement Monitoring Based on GNSS”, JIBC 2016.

[5] Sang-ho Yeon, “The application technology of 3D spatial information by integration of aerial photo and laser data”, The Korea Contents Association, ICCC2008, Vol.6 No.2, pp193-197.

[6] Sang-ho Yeon(2010), “A Study on the Application Technique of 3-D Spatial Information by Integration of Aerial Photos and Laser Data”, Journal of Korea Society for Surveying and Photogrammetry, 28(3), pp.385-392.

[7] Sang-ho Yeon, Young-wook Lee(2013),“Implementation of Ubiquitous based Construction Site Management System”, II BC. 13(2), pp239-244.